

26th Annual Conference European Society for Biomaterials



31st August – 3rd September 2014

BT Convention Centre
King's Dock, Liverpool



Final Programme

<https://twitter.com/ESB2014>

<http://m.youtube.com/user/ESB2014Liverpool>

ESB 2014



it's liverpool



Anton Paar



ebers



SCANCO MEDICAL



LIFECORE
BIOMEDICAL



Testing • Research • Consulting

www.rms-foundation.ch



JOURNAL
OF
THE ROYAL
SOCIETY
Interface



ELSEVIER



BOSE
Better products



IOP Publishing



Table of Contents

Welcome

A Warm Welcome from the Conference President	4
ESB President's Address	5

Acknowledgements

Sponsors	7
Local Organising Committee	8
International Advisory Committee	8

Conference-Related Events

Book Signings	9
---------------	---

Conference Information

Venue	10
Registration	10
Poster Sessions	10
Podium Presentations	10
Rapidfire Presentations	11
Wi-fi	11
Travel	11
Prizes	12
Certificates of Attendance	12
Social Programme	13
Awards	14
Plenary Speakers	15
Award Presentations	20
YSF Entrepreneurship Workshop	23
Fellows of Biomaterials Symposium	27
Translational Research Symposium	23
UK Society for Biomaterials (UKSB) Annual Meeting	31
Materials for the Future - University of Liverpool Outreach Event	32
Venue Maps	33
Programme at a Glance	36
Exhibitors	40

Oral Programme 49

List of Poster Presentations 75

YSF Rapidfire Presentation Schedule 102

Abstracts

ESB Oral Presentations	109
UKSB Oral Presentations	446
ESB Posters and Last Minutes Posters	468
UKSB Posters	989

Index of Authors 999



A Warm Welcome from the Conference President



Welcome to the ESB 2014 and Liverpool. Thank you to everyone that has contributed to putting together our varied, exciting and thought provoking programme of open paper sessions, symposia and social events. For me, the purpose of the ESB annual meeting is to have a real place and point in our busy research lives to come together and “cut to the chase”. In a multidisciplinary applied subject such as ours that stands as a keystone of the knowledgebase for future medicine to provide for healthy ageing and independent living, it is more important than ever to meet as a community (“scientific family”) and present and discuss first-hand what we have done, what worked and what did not.

We’ve provided everything you need; the infrastructure, the timetable and the facilities so you can focus and concentrate on presenting and discussing the detail, the issues and the future. Enjoy yourselves, work hard we’ve a lot to do to realise our collective potential.

OUR future health needs us..... 16% of the population is born disabled, 84% at birth aren’t disabled yet! If nothing else kills us on our journey through life, we will all age (more or less graciously) and with that comes, to put it bluntly disabilities. Mankind as a society can’t afford for each of us to live longer and become increasingly disabled and more dependant. We as Biomaterials Scientists can address this, all of us know we can, the question is how fast can we do it? It’ll be faster together.

A handwritten signature in black ink, appearing to read 'John Hunt'.

Conference President: John Hunt



ESB President's Address

Dear all,

It is almost metronomic, is it not, the time with which the UK community hosts the ESB annual conference; London 2001, Brighton 2007 and this year another iconic city in Britain, Liverpool.

I have been reflecting on the trajectory of our Society in the last few years with its constant travelling from Country to Country. The Council has been changing its members, the conference delegates have been growing in numbers reaching out to colleagues around the world and opening its doors to an increasing number of young scientists.

But what's about our scientific progress? What's about the life of our patient's? What's the understanding or even the simple perception that the public, industry and policy makers have of us scientists and the work we do? Well! We may see the glass half full or half empty, but this is not the point. Interpreting and analysing the present it is important, but it is more important to set the vision for the future of our work as individual scientists, research groups, national societies and of course as ESB. And for scientists the vision for the future has to be ambitious, pioneering new ways of thinking, rooted in the service of our patients.

An honest, balanced assessment (I hope you share it) tells us that in all these years our biomaterials have reached significant achievements. Just to mention few of our exciting attainments, we have entered the world of the nano-scale, we have enabled the regeneration of tissues and developed theranostics. At the same time, the translation of this innovation is lacking behind partly because of our mistakes, certainly because of the constraints of the current political and economic environment. As ESB we have been working hard to improve the service and support to all our members, but we recognise that still a lot can be and has to be done for you and for your research. We look forward to explaining our plans at our General Assembly.

In this respect, I feel that the organisers of the ESB2014 have built a programme that is thought-provoking and challenging. Prof John Hunt and his colleagues have welcome us to Liverpool with a clear message that makes us thinking about the past while looking towards an ambitious future. The choice of the plenary and keynote speakers will bring on stage some of the best scientists of our generation. The translation day will help us assess the socio-economical impact of our innovation. Through presentations, chairing of sessions and their independently-organised workshops, the Young Scientist Forum will promote new ways of thinking and communicating.

I look forward to all this with great excitement and optimism. I congratulate Prof John Hunt for choosing such a fantastic venue and for structuring such a diversified programme. On behalf of the whole ESB Council I express my deepest gratitude to him and to his team for their kind hospitality and social programme.

Finally, I wish you all a great time in Liverpool where you will see old friends and meet new ones; a time when you will inspire and be inspired, a time of excitement for your research, and a time of new hopes for our patients.



ESB President: Matteo Santin



Acknowledgements

Platinum Sponsor: GSK Ltd



GSK

St Georges Avenue
Weybridge
Surrey
KT13 0DE
United Kingdom

Mobile: +44 7920 568 730
Tel: +44 1932 82 2136
Johnathan.s.earl@gsk.com
www.gsk.com

GSK is one of the world's leading research-based pharmaceutical and healthcare companies. Our mission is to improve the quality of human life by enabling people to do more, feel better and live longer.

Sponsors of the Translational Research Symposium:



Testing • Research • Consulting
www.rms-foundation.ch



Committees

Local Organising Committee

President: John Hunt

Technical Director: Nick Rhodes

Nick Bryan

Judith Curran

Theun van Veen

Rui Chen

Shirley Rawlings

Michael Loughran

Christopher Battersby

Fanrong Pu

International Advisory Committee

Eben Alsberg (US)
Luigi Ambrosio (IT)
Conrado Aparicio (US)
Anthony Atala (US)
Mario Barbosa (PT)
Rolando Barbucci (IT)
Yves Bayon (F)
Serena Best (UK)
Nicolas Blanchemain (FR)
Aldo Boccaccini (DE)
Marc Bohner (CH)
Assunta Borzacchiello (IT)
Adrian Boyd (UK)
Daniel Bracewell (UK)
Gerben Brans (NL)
John Brash (CA)
Darren Burke (UK)
Neil Cameron (UK)
José Carlos Rodríguez-Cabello (ES)
Roberto Chiesa (IT)
Joseph Chinn (US)
Michael Cross (DE)
Guy Daculsi (FR)
Matt Dalby (UK)
Joost de Bruijn (NL)
Claudio De Luca (IT)
Sanjukta Deb (UK)
Kenny Dalgarno (UK)
Aránzazu del Campo (DE)
Maria del Rocio Herrero Vanrell (ES)
Lynn Dennany (UK)
Lucy Di-Silvio (UK)
Denis Dowling (IE)
Nicholas Dunne (UK)
Ken Fantom (UK)
Paolo Ferruti (IT)
Roberto Giardino (IT)
Florelle Gindraux (FR)
Manuela Gomes (PT)

Enrique Gomez-Barrena (ES)
Isabel Goñi (ES)
Julie Gough (UK)
Pedro Granja (PT)
Dirk Grijpma (NL)
Bernd Grimm (NL)
George Grobe (US)
Thilak Gunatillake (AU)
Marilo Gurruchaga (ES)
Antonio H. de Aza (ES)
Pamela Habibovic (NL)
Vasif Hasirci (TR)
Paul Hatton (UK)
Anthony Hollander (UK)
Anita Ignatius (DE)
Julian Jones (UK)
Kazunori Kataoka (JP)
Paul Kemp (UK)
Garry Kerch (LV)
Ali Khademhosseini (US)
Cay Kielty (UK)
James Kirkpatrick (DE)
Sotiris Korossis (DE)
Damien Lacroix (UK)
Gaétan Laroche (CA)
Andrew Lloyd (UK)
Diego Mantovani (CA)
Jose Manuel Cervantes Uc (MX)
Alexandra Marques (PT)
Ivan Martin (CH)
Dimosthenis Mavrilas (GR)
Brian Meenan (UK)
Gordon Meijs (AU)
Claudio Migliaresi (IT)
Véronique Migonney (FR)
Carmen Mijangos Ugarte (ES)
Yannis Missirlis (GR)
Antonella Motta (IT)
Bert Müller (CH)

Huang Nan (CN)
John Nicholson (UK)
Teruo Okano (JP)
Abhay Pandit (IE)
Carlos Peniche (CU)
Josep Planell (ES)
Arnau Plau (ES)
Stefan Przyborski (UK)
Malcolm Purbrick (UK)
Buddy Ratner (US)
Mike Raxworthy (UK)
Heinz Redl (AT)
Carolina Reinhard (DE)
Rui Reis (PT)
Geoff Richards (CH)
Lawrence Salvati (US)
Paul Santerre (CA)
Matteo Santin (UK)
Etienne Schacht (BE)
Francesco Serino (IT)
Kevin Shakesheff (UK)
Alina Sionkowska (PL)
Neil Smart (UK)
Chris Sutcliffe (UK)
Yasuhiko Tabata (JP)
Maria Tanzi (IT)
Pentti Tengvall (SE)
Joanne Tipper (UK)
Klemens Trieb (AT)
Hasan Uludag (CA)
Gianluca Vadalà (IT)
Edward Valstar (NL)
Michel Vert (FR)
Jerome Werkmeister (AU)
Ceri Williams (UK)
David Williams (US)
Yan Yan Shery Huang (UK)

Book Signings at ESB2014

Professor David Williams

Essential Biomaterials Science

The latest book written by Professor David Williams, has just been published. You can meet the author and examine display copies of *Essential Biomaterials Science* in the coffee and lunch breaks after his talk on Monday 1st September in the exhibition / poster area of Hall 2 stand 142. The book is available from the publisher Cambridge University Press, www.cambridge.org, ISBN 9780521899086.

Copies purchased from the publisher and brought to conference may be signed by Professor Williams.



Please click on the image to the left to download a 20% discount coupon. Print out the coupon and bring it with you to the conference to receive a 20% discount.

Professor Larry Hench

Boing Boing the Bionic Cat

The award-winning *Boing-Boing the Bionic Cat* series of children's books written by Professor Larry Hench will be available for purchase and signing by the author during the meeting. Professor Hench will be in attendance at the stand on 2/9/14 from 11:00-14:00 for a dedicated session of book signing. You can meet the author and examine display copies in the coffee and lunch breaks in the exhibition / poster area of Hall 2 stand 64. A limited number of books will be brought to the conference (and the publisher will only be able to accept cash or cheques) but you may guarantee books at a special delegate rate by pre-ordering (credit cards accepted) from the publisher here: <http://www.canofwormsenterprises.co.uk/goldaward>

Online orders will be available to pick up and be signed by Professor Hench at the conference.

Conference Information

Venue

The Liverpool ESB2014 Conference will be hosted at ACC Liverpool, which combines the Liverpool Echo Arena and BT Convention Centre. ACC Liverpool is a unique facility – the only interlinking arena and convention centre complex under one roof in Europe. The Convention Centre and Arena stand in an iconic building on Liverpool's world famous Mersey waterfront, next to the Grade I listed Albert Dock, home to Tate Liverpool, the Beatles Story and numerous bars and restaurants. The address of the venue is:

BT Convention Centre (within ACC, Liverpool)
Kings Dock
Liverpool Waterfront
L3 4FP
Tel: +44 (0)151-475 8888

Registration

Registration will take place in the BT convention centre galleria Saturday-Wednesday. The registration desk will open:

Saturday August 30 th	14:00 - 18:00	<i>The Speaker Preview Room will be open from 13:00</i>
Sunday August 31 st	07:30 - 19:00	
Monday September 1 st	07:30 - 19:30	
Tuesday September 2 nd	07:30 - 18:30	
Wednesday September 3 rd	07:30 - 17:00	

Poster Sessions

Poster sessions will take place during lunch breaks 12:30-13:30 in addition to a designated poster viewing between 18:00-19:30 on Monday 1st September; presenters are encouraged to stand by their posters during these times. Recommended poster size is A0 (90cmx120cm) in portrait format. If you would like to take your poster away please remove it before the beginning of the closing ceremony. Poster boards will be numbered, please refer to the abstract book for the location of your poster board.

Podium Presentations

Presentation format for standard oral presentations is 12 minutes plus 3 minutes to respond to questions, which will be strictly controlled by the session chair(s). Speakers are asked to upload their presentations in the speaker preview room (Room 7) at least half a day prior to their scheduled talk. The use of personal computers to display talks in the presentation rooms is not permitted.

Rapid Fire Presentations

Rapid Fire Presentations will take place in Hall 2. Timings will be strictly controlled to a 90 second presentation and 30 seconds to address a single question, there is no maximum slide limit. Presentations must be uploaded in the speaker preview room (Room 7) at least half a day prior to your allocated slot, and use of personal laptops is not permitted.

Wi-Fi

Free Wi-Fi is provided throughout the conference venue, a password is not required. The Wireless Network Connection name is *Free_Wifi*

Travel

The ESB2014 team has coordinated a number of discounted travel options for its delegates which should be [booked through the travel section of the ESB2014 website](#).

Taxi: We have negotiated a discounted rate with INTX Liverpool Executive Chauffeur Service, from £20 per journey for a single passenger from Liverpool Airport. You can book and pay for transfers to and from both Liverpool and Manchester Airports online.

Coach: We have organized free coach transfers from Manchester and Liverpool airports on 30th August and 3rd September to the BT Convention Centre. For the 30th August, coaches will leave each airport on the hour starting at 12pm with the last one leaving at 7pm. For the return journey on the 3rd September, coaches will leave the BT Convention Centre hourly starting at 4pm with the last one leaving at 7pm. Delegates wishing to use this free service need to book by following the instructions online.

Train: We have negotiated a fare reduction of 20% on Virgin Trains advance fares in standard and first class from London to Liverpool for delegates, but these must be booked through the ESB2014 website using the password *Bio2014* which is case-sensitive.

If you have been unable to take advantage of these travel options, getting to the venue is straight forward.

From Liverpool John Lennon Airport

Bus: Bus stops are located on Speke Hall Avenue which is a short walk from the airport exit. Take bus numbers 82A or 500 and disembark at Liverpool Albert Dock, both routes have an approximate journey time of 30 minutes. The convention centre is approximately a 5 minute walk from here.

Taxi: There is a taxi rank located immediately outside the airport exit. A taxi into Liverpool city centre or the convention centre directly will take around 20 minutes.

From Manchester Airport

Train: Trains from Manchester Airport train station depart to Liverpool Lime Street station approximately every 30 minutes, with a journey time of around 1 hour. From Liverpool Lime Street station the convention centre is around a 20 minute walk across the city centre.

Taxi: There are several taxi ranks throughout Manchester airport. A taxi into Liverpool city centre or the convention centre directly will take around 45 minutes.

Travel to the venue by car

From the North: Leave the M6 at junction 26 and follow signs for M58 Liverpool. Follow to end of M58 and then take signs for A59 Liverpool. Continue to follow Liverpool City Centre until picking up signs for the Albert Dock. BT Convention Centre's car park is signposted Waterfront on the city wide 'available spaces' signage.

From the South: Leave the M6 at junction 21A and take the M62 to Liverpool. At the end of the M62 follow signs for Liverpool City Centre along Edge Lane, following signs for the Albert Dock.

For Sat Nav users, please use the postcode L3 4BX or enter the city as 'Liverpool' and the road name as 'Queen's Wharf'.

Parking

For conference parking, please use the multi-storey car park directly adjacent to the conference centre (£10 per 24 hours).

Prizes

The Four Best Student Oral Presentations

Winners will be notified during the closing ceremony and receive €200 and a certificate. The candidate must be a student (with a letter from their supervisor), be the presenting author of the presentation and must have had an abstract that was accepted during the official abstract submission process. The candidate should indicate on the registration form if they wish to be considered for the award. Prizes will be awarded during the closing ceremony.

The Four Best Student Poster Presentations

Winners will be notified during the closing ceremony and receive €150 and a certificate. The candidate must be a student (with a letter from their supervisor), be the presenting author of the presentation and must have had an abstract that was accepted during the official abstract submission process. The candidate should indicate on the registration form if they wish to be considered for the award. Prizes will be awarded during the closing ceremony.

Certificates of Attendance

Certificates of attendance can be provided after the event at the delegate's request. If you would like a certificate of attendance please email the conference secretary by 30th September 2014 and your certificate will be sent to you by email, or request one at the registration desk.

Social Programme

Welcome Reception - Open to All Delegates and Exhibitors

Sunday 31st August, 18:30-20:30, BT Convention Centre

The welcome reception will take place at the convention centre after the first day of exciting scientific sessions; attendance is included in your registration fee.

YSF Hard Days Night Social Event - Ticket Only

Sunday 31st August, 19:30-late, Liverpool ONE Bridewell

The YSF will be hosting a social event at Liverpool ONE Bridewell, formerly a prison; this venue is situated in the heart of Liverpool's city centre and a short walk from the nightlife of Liverpool's famous Mathew Street and Concert Square. Tickets for this event can be purchased online during registration and will include food, drinks and live music, but be quick as tickets are limited.

Chairpersons Dinner - Invitation Only

Monday 1st September, 19:30-22:00, Liverpool Tate Gallery

The chairperson's dinner will be held at the Liverpool Tate Gallery, one of the most important collections of Modern Art in Europe, located at Liverpool's historic Albert Dock.

Gala Dinner - Ticket Only

Tuesday 2nd September, 19:30 reception for 20:00 dinner, Convention Centre

The ESB2014 gala dinner will be at the convention centre. Tickets can be purchased during registration. If you have not purchased a ticket online but would like to attend the gala dinner, please speak to one of the local organising committee at the registration desks.

Food and Drink during the conference

The conference registration fee includes morning coffee breaks, a hot fork buffet lunch and traditional afternoon tea during the conference.

Excursions / Accompanying Person Trips

Liverpool Football Club open top bus tour

Take an open top bus tour to Anfield stadium, home of the famous Liverpool Football Club via a narrated tour of some of Liverpool's historic landmarks. Tours depart from the Pump House entrance to the Albert Dock, 5 minutes walk from the conference centre. For more information visit the ESB2014 website.

The Beatles Story Museum

Located in the Albert Dock Complex the Beatles Story Museum tells the story of the worlds original Boy band! A discount voucher of 20% has been negotiated for every ESB delegate which are available by request.

Walking Tours of Liverpool

Interested in the cultural history of Liverpool? Then you can go on one of two walking tours: the Bluecoat cultural walk, and the Bluecoat literary walk. Or possibly visit the Tate Art Gallery at Albert Dock. Click the image to the right for further details.



Awards

George Winter Award – Sunday 31st August, 09:00

Guy Daculsi, *University of Nantes*: Biography on page 20

The ESB Council will choose an International Scientist who has contributed significantly to the knowledge in the field of biomaterials and/or the material controlled or influenced reactions within the host body through basic, experimental and/or clinical research. The work concerned and the results must have been published. This award is established to recognise, encourage and stimulate outstanding research contributions to the field of biomaterials and is presented annually during the Biomaterials conference of the Society, and consists of a certificate, a plaque and a refund of the registration fee and travelling expenses to the conference.

Jean Leray Award – Sunday 31st August, 17:30

Lorenzo Moroni, *University of Twente*: Biography on page 21

This award is established to recognize, encourage and stimulate outstanding research contributions to the field of biomaterials by young scientists. It will be presented annually during the Biomaterials conference of the Society, and consists of a certificate, a plaque, a refund of the registration fee and travelling expenses to the conference and a cash prize. The nominee should not be older than 40 years at the close of nomination and should be not more than 8 years post-doctoral. Furthermore, the nominee must have contributed to the knowledge in the field of biomaterials and/or the material controlled or influenced reactions within the host body through basic, experimental and/or clinical research. The nominee needs neither to be a member of the European Society for Biomaterials nor a citizen of a European country.

International Award – Wednesday 3rd September, 13:30

James Anderson, *Case Western Reserve University, Cleveland, Ohio*: Biography on page 22

The International Award is a prestigious recognition by the ESB of scientists who have generally spent their career outside Europe, who have a widely recognised, high scientific profile, and have made major contributions to the field of biomaterials. The awardee will have shown strong evidence of collaborations with members of our scientific community in Europe throughout their career.

Plenary Speaker Biographies

David Williams

Wake Forest Institute of Regenerative Medicine

Monday 1st September, 08:00 – 09:00, Hall 1



Professor Williams has had 45 years' experience in the science of biomaterials, medical devices and tissue engineering. During his career he has published over 30 books and 400 papers; his latest book, *Essential Biomaterials Science* will be published by Cambridge University Press in June 2014. He has been Editor-in-Chief of *Biomaterials*, the world's leading journal in this field since 2000. He has received the major awards from the US, European and Indian Societies of Biomaterials including the Founders Award of the US Society for Biomaterials in 2007, and he received the prestigious *Acta Biomaterialia* Gold Medal in 2012. In 1999 he was elected as a Fellow of the Royal Academy of Engineering in recognition of his contributions to Engineering in Medicine. He is currently global President of the Tissue Engineering & Regenerative Medicine International Society (TERMIS).

Professor Williams left the University of Liverpool, UK, in 2007, where he had been Head of Clinical Engineering, Director of the UK Centre for Tissue Engineering and Pro Vice Chancellor. While retaining the title of Emeritus Professor at Liverpool, he is currently Professor and Director of International Affairs, Wake Forest Institute of Regenerative Medicine, North Carolina, USA. In addition, he is a Visiting Professor in the Christiaan Barnard Department of Cardiothoracic Surgery, Cape Town, South Africa, a visiting Professorial Fellow at the Graduate School of Biomedical Engineering, University of New South Wales, Australia, a guest professor at Tsinghua University, Beijing, and Advisory Professor at Shanghai Jiao Tong University, China and the National University of Singapore. He is Visiting Chair Professor of Biomedical Materials, Taipei Medical University, Taiwan, and a Visiting Professor at Sree Chitra Tirunal Institute for Medical Sciences and Technology, Thiruvananthapuram, India. In Cape Town, with Professor Peter Zilla, the current Christiaan Barnard Professor of Surgery, he has formed a company that will produce low cost high technology medical devices that can be used with minimally invasive procedures to treat young adults in sub-Saharan Africa, who currently have no therapies available.



Stephen Minger

GE Healthcare

Monday 1st September, 14:30 – 15:30, Hall 1



Stephen received his PhD in Pathology (Neurosciences) in 1992 from the Albert Einstein College of Medicine in New York City. After post-doctoral work in CNS gene therapy, neural transplantation and neural stem cell biology at UCSD with Professor Fred “Rusty” Gage, he was appointed a Lecturer in Biomolecular Sciences at King’s College London in 1998., Senior Lecturer in Stem Cell Biology in 2005 and was Director of the Stem Cell Biology Laboratory from 2002 until joining GE in 2009.

Over the past 20 years, Stephen’s research group has been at the forefront of human stem cell research. In 2002, together with Professor Peter Braude and Dr Susan Pickering, his team was awarded one of the first two licenses granted by the UK Human

Fertilisation and Embryology Authority for the derivation of human embryonic stem cells and his group was the first to deposit a human ES cell line into the UK Stem Cell Bank. Stephen was also one of the first two groups in the UK to be granted a research license by the HFEA in 2008 to pursue Somatic Cell Nuclear Transfer to generate “hybrid human embryos” for research into genetic forms of neurodegenerative conditions. He was actively involved with the UK Department of Health and with the Minister for Public Health in the consultation with both Houses of Parliament that led to the passage of the Human Embryo Bill of 2009 and the inclusion of new forms of animal-human embryos within primary legislation.

Stephen was the Stem Cell Expert and a Member of the UK Gene Therapy Advisory Committee at the Department of Health from 2006-2012 and was the Focal Point for Regenerative Medicine, Drug Discovery and Modernisation of Traditional Chinese Medicine in China for the UK Department of Business, Innovation and Skills from 2006-2009. He has also been a an external consultant and reviewer to the European Commission Framework Programs since 2003, a member of the Grants Working Group of the California Institute of Regenerative Medicine since 2004, and is a member of the Board of Directors of the Canadian Centre for the Commercialisation of Regenerative Medicine.

In the summer of 2013, Stephen was appointed Chief Scientist for Cellular Sciences, GE Healthcare Life Sciences, and is now responsible for long-term global research strategy for technology development in cell therapy, regenerative medicine, cellular technologies, *in vivo* diagnostic imaging and molecular pathology/personalised medicine.

Dietmar Hutmacher

Queensland University of Technology

Tuesday 2nd September, 08:00 – 09:00, Hall 1



Professor Dietmar W. Hutmacher is the Chair of Regenerative Medicine at the Institute of Health and Biomedical Innovation of Queensland University of Technology, where he leads the Regenerative Medicine Group, a multidisciplinary team of researchers including engineers, cell & molecular biologists, polymer chemists, material scientists, clinician scientists, and veterinary surgeons. Prof Hutmacher has extensive expertise in bioengineering, tissue engineering and regenerative medicine and more recently he was not only among the pioneers but also developed outstanding track record in two new cutting edge research areas namely “in vitro disease models” and “development of humanized mice models via the translation of tissue engineering platform technologies”. Currently, this work in the Hutmacher laboratory has a focus on cancer research.

Prof Hutmacher’s international standing and impact on the field are illustrated by his publication record (more than 240 journal articles, edited 10 books, 30 book chapters and more than 450 conference papers) and citation record (more than 12,000 citations, h-index 54).

Awards and funding: In 2011, Prof Hutmacher was awarded the prestigious Australian Research Council Future Fellowship and in 2012 he was elected to join the highly esteemed International College of Fellows Biomaterials Science and Engineering, and received the Australasian Society for Biomaterials and Tissue Engineering (ASBTE) for Research Excellence Award. In 2012 he was elected by his peers to become one of the 23 founding members of the International Fellows of Tissue Engineering and Regenerative Medicine Society. This group provides leadership and vision for the Society with more than 3000 members. He holds since 2006 an Adjunct Professorship at the Georgia Institute of Technology (GTECH) and he was awarded in 2011 the highly prestigious Hans Fischer senior Fellowship at the Technical University Munich (TUM). Over the past 15 years in academia, Prof Hutmacher has been a lead Investigator, co-investigator or collaborator in grants totalling more than AUD 50 million, including support from the National Institutes of Health – USA, Australian Research Council, National Health and Medical Research Council – Australia, European Union, DFG, and philanthropic and industry support.



Molly Shoichet

University of Toronto

Tuesday 2nd September, 13:30 – 14:30, Hall 1



Dr. Molly Shoichet holds the Tier 1 Canada Research Chair in Tissue Engineering and is Professor of Chemical Engineering & Applied Chemistry, Chemistry and Biomaterials & Biomedical Engineering at the University of Toronto. She is an expert in the study of Polymers for Drug Delivery & Regeneration which are materials that promote healing in the body. Dr. Shoichet has published over 450 papers, patents and abstracts and has given over 275 lectures worldwide. She currently leads a laboratory of 25 researchers and has graduated 115 researchers over the past 18 years. She founded two spin-off companies from research in her laboratory and is actively engaged in translational research.

Dr. Shoichet is the only person to be a Fellow of Canada's 3 National Academies: the Canadian Academy of Sciences of the Royal Society of Canada, the Canadian Academy of Engineering, and the Canadian Academy of Health Sciences. She is the recipient of many prestigious distinctions including: the Canada Council for the Arts' Killam Research Fellowship, NSERC's Steacie Fellowship, CIAR's Young Explorer's Award (to the top 20 scientists under 40 in Canada), Canada's Top 40 under 40TM, the Society for Biomaterials' Clemonson Award, and International Fellows of Tissue Engineering and Regenerative Medicine. In 2011, Dr. Shoichet was appointed to the Order of Ontario, Ontario's highest honour, and recognized as a Fellow of the American Association for the Advancement of Science.

In 2013, Dr. Shoichet's contributions to Canada's innovation agenda and the advancement of knowledge were recognized with the QEII Diamond Jubilee Award. Before being recruited to the University of Toronto in 1995, Dr. Shoichet worked at CytoTherapeutics Inc. on encapsulated cell therapy. Dr. Shoichet received her S.B. from the Massachusetts Institute of Technology in Chemistry (1987) and her Ph.D. from the University of Massachusetts, Amherst in Polymer Science and Engineering (1992).

Larry Hench

Florida Institute of Technology College of Engineering

Wednesday 3rd September, 08:00 – 09:00, Hall 1



Larry Hench, University Professor of Biomedical Engineering in the Florida Institute of Technology College of Engineering, has been awarded the highly acclaimed international 2014 Acta Biomaterialia Gold Medal Award. The award recognizes excellence in research and development in the field of biomaterials. Professor Hench, who is also director of the Florida Tech Center for Medical Materials and Photonics, specializes in bio-ceramics and is a member of the National Academy of Engineering (NAE).

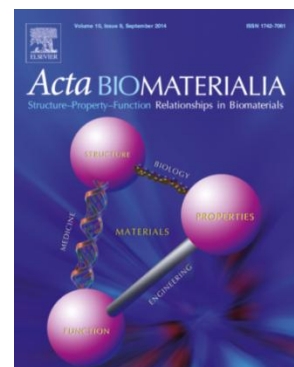
Born in Ohio in 1938, Dr. Hench received his bachelor's degree in 1961 and doctoral degree in 1964 in ceramic engineering from The Ohio State University. After 32 years on the faculty, Hench retired from the University of Florida as Emeritus Professor to join Imperial College, University of London, as chair of ceramic materials. There, he co-founded and co-directed the Tissue Engineering and Regenerative Medicine Centre for 10 years.

Discoveries made by Hench and his colleagues in the 1980s and 1990s have resulted in numerous Federal Drug Administration (FDA) approvals. In the mid-'80s the FDA approved the use of bioactive glass devices to reconstruct the ossicular chain (part of the middle ear) and restore hearing. A subsequent FDA approval led to bioactive glass implants to replace teeth, maintain jaw stability and repair maxillo-facial bone defects. In the '90s the FDA approved the use of a particulate form of bioactive glass that led to regenerating new bone to repair bone defects caused by periodontal disease. Numerous FDA approved applications in orthopedic surgery include repair of bone defects following revision surgery of failed hip and knee prostheses, and spinal repair.

Larry Hench, who has dedicated more than 45 years to his work, has earned many international awards, published 800 research papers, 30 books and has 32 U.S. patents. Twelve companies have been founded based upon technology created in Hench's laboratories and the commercial products have led to numerous advanced technology awards. He is also an author of a series of children's books featuring Boing-Boing the Bionic Cat and educational materials such as workbooks, experiment books and hands-on kits to stimulate interest in science, engineering, technology and mathematics (STEM).



Following the plenary lecture, Larry will be awarded with the *Acta Biomaterialia Gold Medal*. Click on the image to the right for further details



Sunday 31st August, 09:00 – 09:30, Hall 1



Professor Daculsi is Director of Research class Exceptional at INSERM, National Institute for Medical Research and Director of the SC3M Electron Microscopic, Microimaging and Microcharacterization Center of Nantes University. His work has mainly focused on the process of mineralization and developing models for the mineral phase of calcified tissues.

In 1984, Guy Daculsi made a thematic change to Biomaterials, and particularly Bioceramics. He directed research on calcium phosphate synthesis to model mineralization, but also to develop substitute materials for calcified tissues, particularly calcium phosphate. He was a pioneer in this field in France, developing an original concept of artificial bone; the Biphasic Calcium Phosphate Concept.

In 1989, Guy Daculsi created the Nantes University Research Centre on Calcified Tissues and Biomaterials. The activity of the laboratory was supported by INSERM and the CNRS. After 16 years of management of the research center for Materials of Biological Interest, the laboratory became UMR INSERM U791, Laboratory Osteoarticular and Dental Tissue Engineering.

He developed a theme of original research relevant to the physio-pathology of calcified tissues at the level of mineral phases, particularly degradation and dissolution by specialized cells. These studies and models are associated with design, development and study of mineral phases used as synthetic bone and dental substitutes.

His International contributions to Bioceramics and Bone substitutes has been recognized at a major scientific distinction IUSBSE (International Union of Societies for Biomaterials Science and Engineering) of the 8th World Congress on Biomaterials in 2008.

During the World Biomaterials Congress in 2008, he was awarded Fellow of the world federation of Biomaterials scientific societies (Fellow in Biomaterials Science and Engineering, FBSE). Guy Daculsi served on the executive Board of ESB, before being Chair of the 20th ESB in 2006.

Sunday 31st August, 17:30 – 18:00, Hall 1



Dr Moroni studied Biomedical Engineering at the Polytechnic University of Milan, Italy, and Nanoscale Sciences at Chalmers Technical University, Sweden. In 2001, he visited the lab of Professor Luke Lee at University of California Berkley, where he worked on microfabrication technologies for tissue engineering applications. He received his Ph.D. (cum laude) in 2006 at University of Twente on 3D scaffolds for cartilage and osteochondral regeneration, for which he was awarded the European doctorate award in Biomaterials and Tissue Engineering from the European Society of Biomaterials (ESB). In 2007, he worked at Johns Hopkins University as a post-doctoral fellow in the Elisseeff lab, focusing on hydrogels and stem cells. In 2008, he was appointed the R&D director of the Musculoskeletal Tissue Bank of Rizzoli Orthopedic Institute in Bologna, Italy, where he investigated the use of stem cells from alternative sources for cell banking, and the development of novel bioactive scaffolds for bone and cartilage regeneration.

From 2009 till 2014, he joined again the University of Twente, where he worked as an assistant professor until 2013 and as an associate professor thereafter in the Tissue Regeneration department within the MIRA institute for Biomedical Technology and Technical Medicine. Since 2014, he holds an associate professor position at the MERLN Institute for Technology Inspired Regenerative Medicine of Maastricht University. His research group interests aim at developing new biofabrication technologies to generate libraries of 3D scaffolds able to control cell fate. Since 2012, he has been a board member of the Young Scientist Forum of the ESB and co-chairman of the “Biofabrication” thematic group within the Tissue Engineering and Regenerative Medicine Society. In 2013, he was also elected to the editorial board of the journal “Biofabrication”. He is also a co-founder of the biotech company Screvo B.V., which is committed to the production of animal implantable 3D high through-put screening systems.

Wednesday 2nd September, 13:30 – 14:30, Hall 1



Dr. Anderson is a Distinguished University Professor and Professor of Pathology, Macromolecular Science and Engineering, and Biomedical Engineering at Case Western Reserve University. In addition, he is a practicing pathologist in the Department of Pathology, University Hospitals Case Medical Center.

James M. Anderson received his Ph.D. at Oregon State University in 1967, his M.D. degree from the Case Western Reserve University School of Medicine in 1976, and did his Anatomic Pathology residency at the Institute of Pathology of University Hospitals of Cleveland. Following the completion of his residency, he joined the faculty of the Institute of Pathology at Case Western Reserve University. Throughout his career James Anderson has received many honors and awards such as a NIH MERIT Award, the Elsevier

Biomaterials Gold Medal Award, the Honoris Causa Degree by the University of Geneva and the 2013 Acta Biomaterialia Gold Medal, amongst others.

He is a founding member of the Society for Biomaterials and the Controlled Release Society and serves as a consultant to the NIH, FDA, and ISO, and is an elected member of the Institute of Medicine National Academy and the National Academy of Engineering. He is the Editor-in-Chief of the Journal of Biomedical Materials Research-Part A. Dr. Anderson has worked in the area of biomaterials, medical devices, and prostheses for the past 40 years and his current activities range from the clinical pathology evaluation of retrieved implants from humans to fundamental studies of cellular interactions with biomaterials.



Symposia

The ESB 2014 Conference will feature a number of symposia:

- YSF Entrepreneurship Workshop
- Fellows of Biomaterials
- Antimicrobials, Biofilms & Surfaces
- The Meaning of Surface Charge for Biomaterial Characterization
- European Orthopaedic Research Society (EORS)
- Translational Research
- UK Society for Biomaterials (UKSB) Annual Meeting
- Women in Science & Engineering
- Advances in Bioactive Glasses

These symposia will run alongside the normal scientific session and are open to every delegate of the ESB 2014 conference. No prior registration is necessary.

YSF Entrepreneurship Workshop

Entrepreneurship – an Academic and Industrial Perspective

31st August 2014, 13.30 – 16.00

Symposium Organizers: Lorenzo Moroni (University of Twente), Sandra Van Vlierberghe (University of Gent), Anna Wistrand (KTH Royal Institute of Technology)

The workshop will give a flavour of what it takes to create spin-off companies from innovative research activities that take place at Universities, as well as in Industry. Talks will span from personal experiences in facing the challenges of setting up a spin-off, to the availability of educational programmes and important points to consider when applying for patents.

The afternoon has an extensive spectrum of experienced experts in entrepreneurship. Invited speakers include:

- Dirk Grijpma (University of Twente)
- Dietmar Hutmacher (Queensland University of Technology and Technical University of Munchen)
- Jens Thies (DSM, The Netherlands)
- Chris Sutcliffe (University of Liverpool)
- Alex Sim (AMSBIO Ltd)
- Chris Unsworth (Business Gateway, University of Liverpool)



Dirk Grijpma

Dirk Grijpma is Professor in Biomaterials Science and Technology at the University of Twente. He also holds a part-time position at the University Medical Center Groningen. His expertise is in the synthesis and properties of resorbable polymeric materials for use in medical devices, tissue engineering and in the delivery of relevant biological compounds, and the interaction of these materials and devices with cells and tissues.

Current research includes the development of advanced microstructures by photo-polymerization of functionalized degradable oligomers in stereolithography and research programmes on the tissue engineering of cardiac muscle and blood vessels, and the synthesis and processing of composite materials for fracture reconstruction in maxillofacial surgery.

Pre-designed anisotropic architectures based on biologically active materials are being developed to engineer musculoskeletal and cardiovascular tissues in bioreactors under conditions that mimic the natural environment. His research includes the synthesis and characterization of large arrays of materials and their evaluation by high-throughput methods, which will likely lead to the discovery of novel materials that perform unexpectedly well in their interaction with cells and tissues.

His research interests are: resorbable polymers for medical applications, structure-property relationships in polymers, tissue engineering, bioreactor technology, drug delivery, ring opening polymerization, photo-polymerization and stereolithography. He is author of more than 180 scientific publications and holds 13 patents. He is editorial board member of Biomaterials, Acta Biomaterialia and of the Journal for Applied Biomaterials and Biomechanics. Prof. Grijpma co-founded Medisse (www.medisse.com), a company developing medical implants based on poly(trimethylene carbonate). Medisse's lead product is FlexiSurge® Adhesion Barrier, a resorbable membrane that prevents the occurrence of postoperative adhesions. He was elected Fellow Biomaterials Science and Engineering (FBSE) in 2008.



Dietmar Hutmacher

Professor Dietmar W. Hutmacher is the Chair of Regenerative Medicine at the Institute of Health and Biomedical Innovation of Queensland University of Technology, where he leads the Regenerative Medicine Group, a multidisciplinary team of researchers including engineers, cell & molecular biologists, polymer chemists, material scientists, clinician scientists, and veterinary surgeons. Prof Hutmacher has extensive expertise in bioengineering, tissue engineering and regenerative medicine and more recently he was not only among the pioneers but also developed outstanding track record in two new cutting edge research areas namely "in vitro disease models" and "development of humanized mice models via the translation of tissue engineering platform technologies". Currently, this work in the Hutmacher laboratory has a focus on cancer research

Prof Hutmacher's international standing and impact on the field are illustrated by his publication record (more than 240 journal articles, edited 10 books, 30 book chapters and more than 450 conference papers) and citation record (more than 12,000 citations, h-index 54).

Awards and funding: In 2011, Prof Hutmacher was awarded the prestigious Australian Research Council Future Fellowship and in 2012 he was elected to join the highly esteemed International College of Fellows Biomaterials Science and Engineering, and received the Australasian Society for Biomaterials and Tissue Engineering (ASBTE) for Research Excellence Award. In 2012 he was elected by his peers to become one of the 23 founding members of the International Fellows of Tissue Engineering and Regenerative Medicine Society. This group provides leadership and vision for the Society with more than 3000 members. He holds since 2006 an Adjunct Professorship at the Georgia Institute of Technology (GTECH) and he was awarded in 2011 the highly prestigious Hans Fischer senior Fellowship at the Technical University Munich (TUM). Over the past 15 years in academia, Prof Hutmacher has been a lead Investigator, co-investigator or collaborator in grants totalling more than AUD 50 million, including support from the National Institutes of Health – USA, Australian Research Council, National Health and Medical Research Council – Australia, European Union, DFG, and philanthropic and industry support.



Jens Thies

Jens Thies received his PhD from Heriot Watt University in Edinburgh, under the supervision of Professor Ian Cowie, in 1998. Subsequently he undertook a post-doctoral position at DSM Research in the field of Rotaxanes. In 2000 he joined David Tirrell's groups at Caltech as a visiting post-doctoral researcher, investigating recombinant protein engineering. He then joined DSM Research and initiated the functional coating platform, launching several products mainly in DSM's Advanced Surface and Medical Coatings businesses. He is currently responsible for Research, Technology and Development of DSM Biomedical's Drug Delivery business globally. Jens also holds an Executive Masters in Business Innovation from TiasNimbas Business School.



Chris Sutcliffe

Dr Chris Sutcliffe is widely acknowledged as one of the world's leading research academics in additive layer manufacturing. He has been associated with flexible manufacturing methods since 1999 when he joined the Department of Manufacturing Engineering at the University of Liverpool. Here, along with academic colleagues he was a founder member of the original EPSRC-funded IMRC working in a range of fields including laser-processing using short pulse duration lasers, cold gas dynamic manufacturing, stereolithography of anatomical phantoms, selective laser sintering of medical devices, the production of controlled release oral dosages and selective laser melting.

He is now recognised as an expert in the field of selective laser melting; in particular, in the design of production manufacturing equipment and the development of next generation orthopaedic, trauma, spine and CMF implants for which he holds base technology and device design patents which have been licensed internationally. As an academic, he has been an investigator on 34 manufacturing research projects, 17 as PI totalling over £11 M in funding. He has extensive industrial experience including being R&D Director at MTT Technologies where he was, prior to its 2011 purchase by Renishaw, responsible for the delivery of a £2.5m portfolio of EU, TSB, EPSRC and company-funded projects. Dr Sutcliffe therefore has considerable experience in the management and delivery of large scale, multi-partner, multi-disciplinary research projects. He has worked with other universities, and has experience of leading and managing collaborative projects with partners such as Heriot Watt, Cambridge, Manchester, Cranfield, Nottingham, Bath, Edinburgh, Sheffield, Cambridge and Glyndwr Universities.

Dr Sutcliffe has built a research group at the University of Liverpool with a strong international reputation in manufacturing particularly in the development of orthopaedic devices in close collaboration with industrial partners. Dr Sutcliffe plays a strong role in the development of the academic activities of the School of Engineering playing a leading role in the development of manufacturing teaching, learning and design.



Alex Sim

Alex Sim is the Founder and CEO of AMS Biotechnology (Europe) Ltd. Alex, graduated from Strathclyde University as a Molecular Biologist prior to completing a postgraduate degree in Marketing. He has been involved in translating cutting edge life science technology into successful revenue generating products for 30 years. With Amersham International (now GE) he led the team that developed Hybond and was involved in the commercialisation of multiple technologies that have had direct impact on genomics and proteomics.

In 1988, Alex founded AMS Biotechnology (AMSBIO). Since then he has raised venture funding, sold a variety of companies and continues to contribute to the success of small innovative SMEs. AMSBIO provides specialist biotools including tissues, stem cells, and cell based assays in addition to tailored screening services that are increasingly being performed as 3D assays. Very recent initiatives include the establishment of new laboratories in Biocity near Glasgow and the opening of the company's North American headquarters in Cambridge, Massachusetts, where Alex now spends much of his time.



Chris Unsworth

Chris was appointed IP Manager at the University of Liverpool in January 2011 where he is responsible for the exploitation of the University's IP. Over the period since 2011 Chris developed and implemented many of the new structures and procedures that now comprise Liverpool IP. Chris also manages all relationships with the University's licensees and spin-out companies.

Chris first came to the University in 2006 to run NeoCare Ltd a spin-out created to exploit chromatic algorithm patents developed in the University's engineering department. Following his exit from NeoCare Chris held a succession of roles managing; the University's POC fund, a £1.3m TSB project with Unilever in the field of high shear mixing, the establishment and operation of the £2.8m Knowledge Centre for Material Chemistry before being appointed as the Business Manager for Science in 2010.

Chris has a background in industrial management. Following a first degree in Chemistry and Fuel Technology he worked for the National Coal Board for five years as Fuel Technologist. In 1986 Chris graduated with an MBA from Manchester Business School from where he joined Dorman Smith Switchgear as Business Development Manager. Over the next twenty years he held a variety of positions as Managing Director in operating companies run by groups such as BICC, GEC Alsthom, Hanson Electrical and Scholes.

Fellows of Biomaterials Symposium

The Race Between Engineering and Biology in Replacing Human Tissues

31st August 2014, 13.30 – 16.00

Symposium Chair: Joachim Kohn, Rutgers University

The chair will define this challenge, a take vote of the audience. There will then be six 15 minute talks from a panel of current FBSE fellows:

- **Barbara Boyan**
- **Rui Reis**
- **Abhay Pandit**
- **Cristina Tanzi**
- **John Kao**
- **David Williams**

who will expound, sometimes controversially, their own points of view about the challenge. Following the talks there will be a Q & A session and finally a vote of the audience.

This symposium is open to all conference delegates.

Translational Research Symposium

Progressing Innovations from the Bench to Bedside

2nd September 2014, 09:00 – 18:00

Symposium Organizers: Yves Bayon, Marc Bohner, David Eglin & Paul-Henri Vallotton

The path leading to commercialization – from promise to actual delivery, from prototype to useful product – is scattered with great challenges and hurdles:

- **Financing**
- **Intellectual property** (*i.e.* patentability, freedom to operate)
- **Legal agreements** with partners and services/research contractors
- **Regulatory environment** driven by FDA, CE mark – notified bodies, EMEA...
- **Manufacturing process** and its validation
- **Clinical trial design**
- **Relationships with national/regional healthcare authorities**
- **Healthcare reimbursement policies.**

On the other hand, the latest generations of biomaterials, are becoming more and more sophisticated, such as combination products and smart materials may face the limitations of standard *in vitro* and *in vivo* evaluation techniques. Regulatory agencies continuously raise the quantity of requested information for any new submitted devices: purity and characterization, safety and performance evaluation, mechanism of action, *etc.* In these respects, academia and industries may increasingly be partners throughout the full cycle of the commercial development of new biomaterial concepts and technologies.

Ideas often start on pieces of paper and a test tube on the basis of basic science research, in academic and institutional laboratories, with the support of public and philanthropic research grants. Talented scientists drive these ideas and projects through various stages of early development that mostly result in significant scientific achievements, illustrated by publications in peer-reviewed journals and, less often, by patent filings.

Many of the new biomaterial concepts and technologies, when carefully evaluated, may have benefit for patients and the public. But this further requires rigorous complementary research development activities to advance new concepts and technologies to the patients and the public: *e.g.* preclinical proof of concept and performance evaluation by *in vivo* animal studies, extensive biocompatibility studies to be performed according to international standards and in GLP (Good Laboratory Practice) conditions, safety and performance evaluation in expensive human clinical trials with appropriate product type (formulation, device *etc.*).

New concepts and technologies are generally percolated to life and progress through the early incubation phase, often showing proof-of-concept and the full promise of potentially innovative products. But, most translational efforts die here and there are multiple financial, scientific and sociological reasons for this phenomenon.

Given the increasing links between academic research and industry globally, the ESB 2014 conference includes this Translational Research Symposium. This will bring together leading Tier one companies in the medical device markets, small and medium enterprises and entrepreneurial

academics who can share their experiences on taking biomaterials technologies to commercial endpoints.

The Symposium will focus on *'Progressing innovations from bench to bedside'*. It will be richly illustrated by testimonies of leading biomaterials & medical device industries, start-up & SME entrepreneurs and academics, in the business exploitation and commercial translation of biomaterial related concepts and ideas, for now and to the 2020+ horizon. The main goal of the programme is to highlight the key factors leading to, or impairing successful translation. Specifically the industry will include three sessions:

- 1) The Industry Translation Process & 2020 Horizon – Invited speakers (*e.g.* DePuy, Covidien).
- 2) Academic management innovation & Academic spin-offs testimonies – Invited speakers and Panel discussion with selected industries, entrepreneurs & academics.
- 3) Forum for sharing translation initiatives – Abstract submission, Q&A with a mixed panel of industrials, entrepreneurs and academics.

This event will be of interest to a wide audience from large medical device producers to academics and entrepreneurs and promoters of biomaterial technologies for medical applications. The programme includes significant time for networking during coffee breaks and lunch. The Symposium feature the following speakers:

- Geoff Richards (AO Research Foundation, Davos);
- Andrea Montali (Depuy Synthes)
- Lars Neumann (Materialise NV, Leuven)
- Philip Procter (Medical Device Industry Consultant)
- Kevin Shakesheff (University of Nottingham and Regentec)
- John Fisher (University of Leeds)
- Michel Thérin (Covidien, Lyon)
- Iain McDougall (Taragenyx, UK)



Lars Neumann

Dr Lars Neumann is a business development manager at Materialise NV, Belgium with specific focus on software for biomedical engineering.

Lars received his doctoral degree in 2012 in Physics from ICFO – The Institute of Photonic Science in Barcelona. His research interests focussed on improving optical imaging techniques for biological systems by custom shaping of laser light fields through the application of nanotechnology. After his doctoral degree, Lars moved to Germany and engaged in the creation and optimisation of R&D project and process management in the automobile industry.

As a physicist curious for new technologies, Lars became interested in additive manufacturing, also known as 3D Printing, and the opportunities that the technology offers especially in biomedical engineering. The human body is one of the most individual systems we can imagine, yet most of our tools and devices are off the shelf and not customised.

At Materialise, Lars focusses on the principle of “Engineering on Anatomy” within the Mimics Innovation Suite and its applications in patient-specific biomedical engineering and science. In his role as business development manager, he is responsible for the academic users of the Mimics Innovation Suite worldwide. Lars is in charge of Materialise’s developing educational programme in Engineering on Anatomy and involved in several European Union funded research projects with academic and industrial partners.



Kevin Shakesheff

Professor Kevin Shakesheff is Director of the UK Regenerative Medicine Platform Hub for Acellular Technologies. His independent scientific career began at the Massachusetts Institute of Technology under a NATO fellowship following a PhD and his qualification as a register pharmacist. His inventions and scientific breakthroughs have resulted in over 170 peer-reviewed full papers that have been cited more than 5500 times to date, the establishment of 2 successful companies, the submission of 13 patent application families and numerous international awards. He currently holds a prestigious European Research Council Advanced Grant within an active research portfolio of more than £7 million.

In addition, he has taken a leading role in shaping interdisciplinary research in the UK through continued membership of senior policy and grant awarding committees. In 1997 he founded, with Dame Julia Polak, the Tissue and Cell Engineering Society (TCES). In 2013 he became a Royal Society Wolfson Merit Award Holder. He is a member of the Medicines and Healthcare Products Regulatory Authority (MHRA) Biologicals and Vaccines Expert Advisory Group, co-Director of the EPSRC Centre for Innovative Manufacturing Centre in Regenerative Medicine, Lead of the Research Councils UK India Science Bridge in Biopharmaceuticals and a Member of the Department of Health’s Modernising Pharmacy Careers Programme. He is a Sub-Panel Member for the UK’s Research Excellence Framework (REF) for 2014. In 2011 he was made a Fellow of the Royal Pharmaceutical Society and in 2013 a Fellow of the Society of Biologists. In 2014 he was selected as one of the 10 most inspirational scientists in the UK by the Engineering and Physical Sciences Research Council (RISE Leader Award).





John Fisher

Professor John Fisher CBE is the deputy Vice Chancellor of the University of Leeds and Director of the Institute of Medical and Biological Engineering.



UK Society for Biomaterial (UKSB) Annual Meeting

2nd-3rd September 2014

Event Chair: Sanjukta Deb, Kings College London

The UK Society for Biomaterials (UKSB) is honoured to be holding its annual meeting as a set of sessions within the ESB meeting. The society is dedicated to nurturing early career and post-doctoral researchers within the UK and providing a platform for dissemination of their research, networking and career progression. At each annual conference in addition to best postgraduate poster and oral presentations, a President's Prize and the Alan Wilson Prize are awarded. The President's Prize aims to recognise outstanding contributions to the UK Biomaterials field, and this year we are delighted to announce that the prize has been awarded to Professor Shelia MacNeil who will be presenting her award lecture in Room 4 on Tuesday 2/9/14 at 09:30. In addition Professor Paul Hatton has been awarded the Alan Wilson prize, which recognises excellent research in the dental biomaterials field, and will be presenting his lecture in Room 4 on Tuesday 2/9/14 at 14:30. The UKSB will also be introducing Dr Manus Biggs who has been selected to receive the Larry Hench Young Investigator Award, which will be presented to him in the Bioactive Glass Symposium in Room 3 on Wednesday 3/9/14 at 14:30, and where he will present his research.

Materials for the Future – University of Liverpool Outreach Event

1st September 2014, 16.00 – 19.30

Event Chair: John Hunt, University of Liverpool

This outreach event will introduce a series of world-expert speakers who will present some of the issues for providing new materials, in a sustainable manner, to meet the needs of an ageing and ever-increasing population. The speakers will provide insight into how new research is providing diverse material solutions such as nano-medicines, stem cell therapies, and high performing next generation medical implants. Delegates will include the ESB 2014 delegation and then also University of Liverpool academics, alumni, industry partners, and civic leaders. The afternoon will showcase world-leading research from the University of Liverpool. The schedule of talks is:

- **Anthony Hollander**, University of Liverpool
- **Steve Rannard**, University of Liverpool
- **Chris Sutcliffe**, University of Liverpool
- **Raphael Levy**, University of Liverpool
- **Stephen Minger**, GE Healthcare
- **Molly Shoichet**, University of Toronto
- **Joachim Kohn**, Rutgers University
- **David Williams**, Wake Forest Institute of Regenerative Medicine

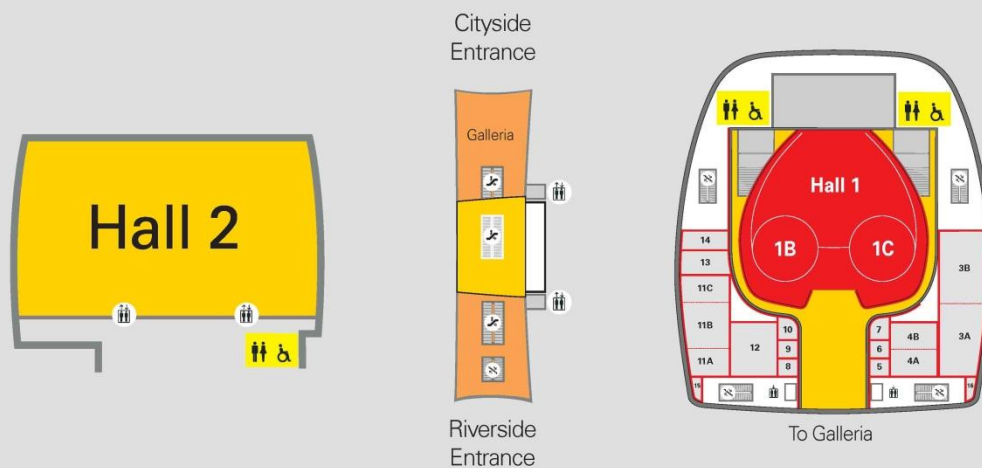
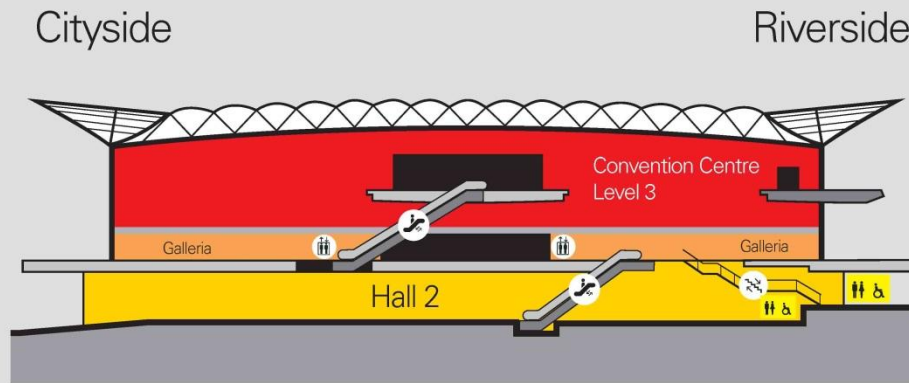
Click the image on the right to download further details








BT Convention Centre Map



BT Convention Centre

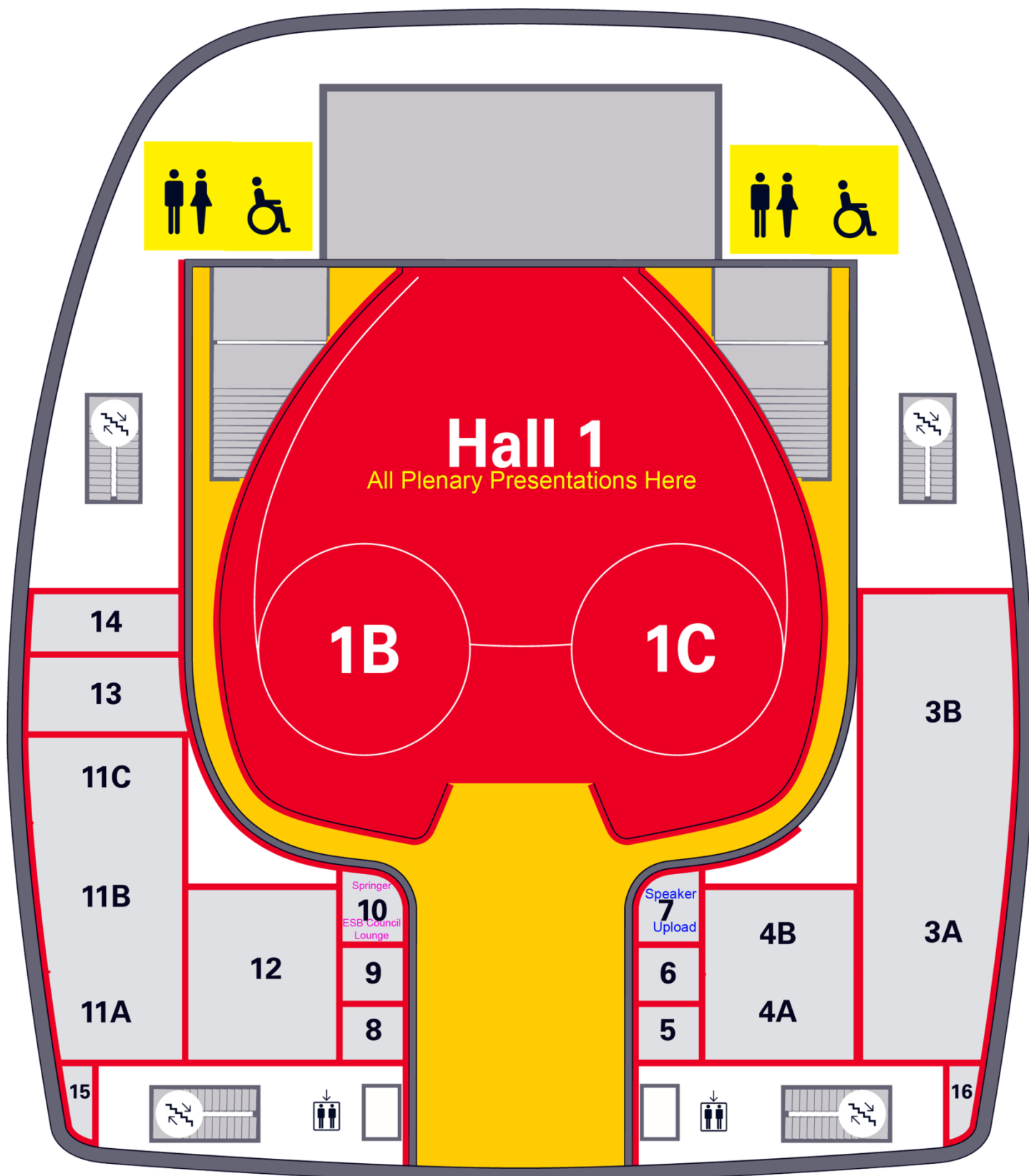


Key

-  Lift
-  Escalator
-  Stairs
-  Male/Female Toilets
-  Disabled Toilets



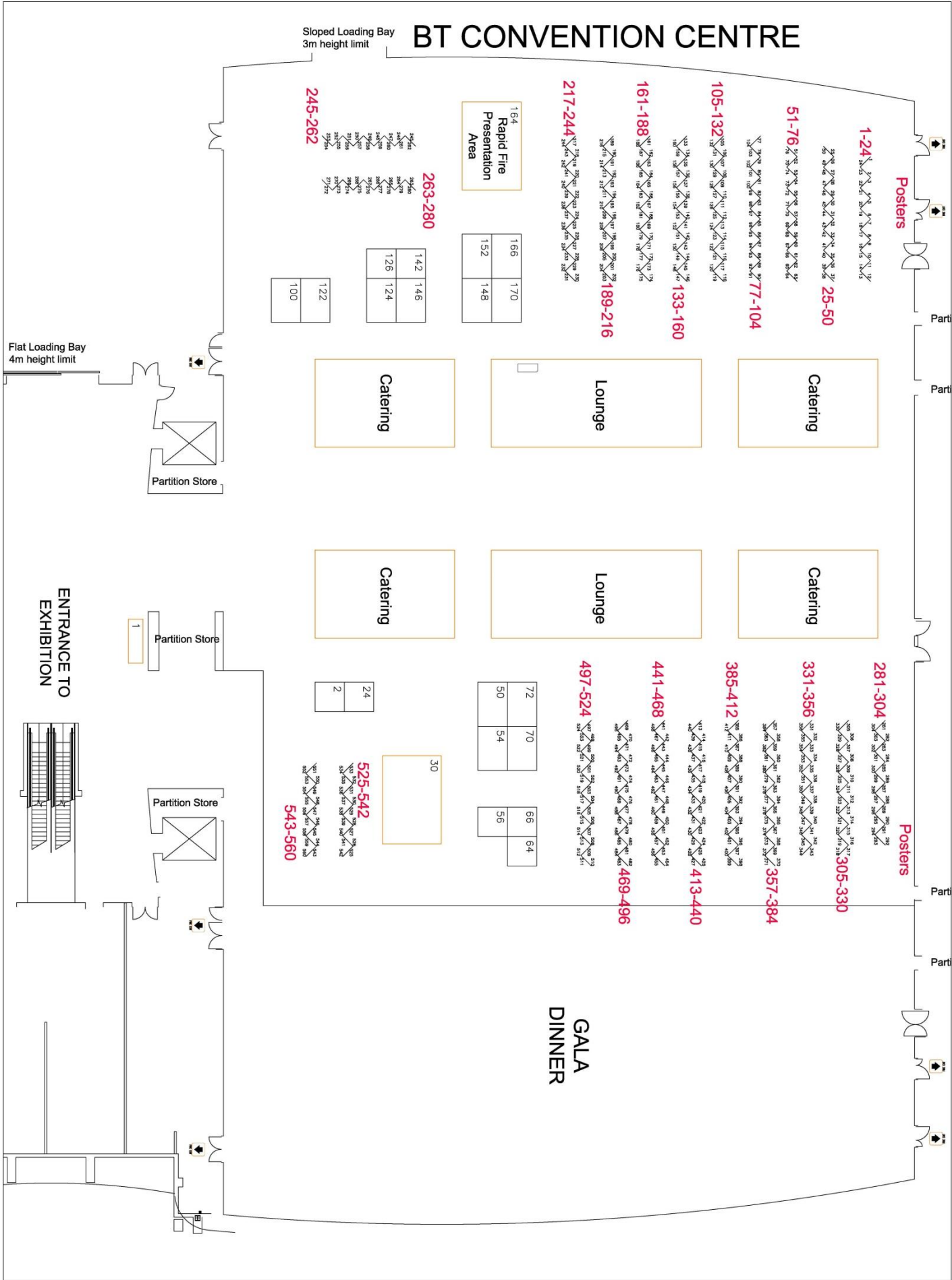
Layout of Rooms on Level 3 – All oral sessions (except RapidFire)



Speaker Preview Room and presentation upload: Room 7

Oral presentations: Hall 1, Room 1B, Room 1C, Room 3, Room 4 & Room 11

Layout of Hall2, Exhibition Hall – Posters, breaks & lunches



	Auditorium, Hall 1	Room 3	Room 11	Room 1B	Room 1C	Room 4	Exhibition Area	Room 7
8	Registration begins at 07:30 within the ACC							Presentation uploads and Speaker Preview: Open from 07:30
9	George Winter award: Guy Daculsi							
10	Biomaterials I	1-1: Whitford	2-1: Bacakova	3-1: Sayin	4-1: Wich	5-1: Rasoul		
		1-2: Gonçalves	2-2: Ataol	3-2: Seo	4-2: Van Den Berghe	5-2: Aljabo		
		1-3: de Cogan	2-3: Takata	3-3: Indrani	4-3: Aksoy	5-3: Shah		
		1-4: Satyam	2-4: Mohd-Isa	3-4: Bryan	4-4: Samal	5-4: Borget		
Morning Coffee Break with posters in Exhibition Hall							Exhibition Hall open at 10:30. Hang posters from 10:30-12:30. Posters and exhibition open until 19:00	
11	Biomaterials II	6-1: Mosser	7-1: Yoshizawa	8-1: Tseng	9-1: Zelikin	10-1: Gómez-Florit		
6-2: Kusrini		7-2: Yamano	8-2: Dursun	9-2: Paik	10-2: Tessarolo			
6-3: Campagnolo		7-3: Lyu	8-3: Workman	9-3: Hamid	10-3: Almuhamadi			
6-4: Bishop		7-4: Altuntas	8-4: Milthorpe	9-4: van der Vlies	10-4: Qasim			
12		6-5: Gomes	7-5: Chatzinikolaïdou	8-5: Prosser	9-5: Hasegawa	10-5: Ewais		
6-6: Biggs		7-6: Dong	8-6: Notingher	9-6: Novio	10-6: Ashworth			
13	Lunch & posters, in Exhibition Hall						YSF Rapidfire poster session I	
14	Symposium: Fellows of Biomaterials	11-1: Joachim Kohn: Intro of panelists	YSF: Introduction					
		11-2: Initial vote	12-1: Dirk Grijpma					
		11-3: Barbara Boyan	12-2: Dietmar Hutmacher					
		11-4: Rui Reis	12-3: Jens Thies					
11-5: Abhay Pandit		12-4: Chris Sutcliffe						
11-6: Cristina Tanzi		12-5: Alex Sim						
11-7: John Kao		12-6: Chris Unsworth						
11-8: David Williams								
11-9: Panelist Q&A and discussion								
11-10: Vote, conclusion								
15								
16	Afternoon Tea with posters, in Exhibition Hall							
17	EDA awards	Award presentations						
		14-1: Pedro Costa						
		14-2: Silvia Bidarra						
		14-3: Cecilia Granéli						
		14-4: Hanna Tiainen						
14-5: Leonardo Ricotti								
	Jean Leray award: Lorenzo Moroni							
18	Opening Ceremony							
19							Welcome Reception	
20								
21	YSF Event (Ticket only)							
22+								

	Auditorium, Hall 1	Room 3	Room 11	Room 1B	Room 1C	Room 4	Exhibition Area	Room 7						
8	Plenary Lecture: David Williams						Exhibition Hall open at 08:00. Posters and exhibition open until 19:30							
9	15-1: Yang 15-2: Ou 15-3: Ikeda 15-4: Kootala	Biomaterials III 16-1: Ullm 16-2: Pompe 16-3: Inubushi 16-4: Taguchi 16-5: Walschus 16-6: Hintze	Cardiovascular I: TECAS-ITN 17-1: Kömez 17-2: Boccaccini 17-3: Loy 17-4: Horakova 17-5: Marcolin 17-6: Goor	Imaging I 18-1: Tondera 18-2: Jumeaux 18-3: Gonçalves 18-4: Koole 18-5: Garon 18-6: Garric	Symposium: Antimicrobials 19-1: Kao 19-2: Wilcock 19-3: Rimmer 19-4: Gultekinoglu 19-5: Jones 19-6: Flores									
10	15-5: Wolf-Brandstetter 15-6: Castillo													
Morning Coffee Break with posters in Exhibition Hall														
11	20-1: Farbod 20-2: Tallia 20-3: Lara-Sáez 20-4: Behrens					Biomaterials IV 21-2: Monaco 21-2: Delcassian 21-3: Le Saux 21-4: Kerdjoudj 21-5: Bernstein 21-6: Oliveira			Cardiovascular II: TECAS- 22-1: Feng 22-2: Ryan 22-3: Piegat 22-4: Guler 22-5: Brubert 22-6: Freudenberg	Symposium: Surface Charge 23-1: Körner 23-2: Lorenzetti 23-3: Espanol	Symposium: Antimicrobials 24-1: Golda-Ceça 24-2: Aubert-Viard 24-3: Leong 24-4: Fukushima 24-5: Unosson 24-6: Percival			
12	20-5: Sheafi 20-6: Fraioli													
Lunch & posters, in Exhibition Hall												YSF Rapidfire poster session II	Presentation uploads and Speaker Preview: Room 7 Open from 08:00	
13														
14	ESB General Assembly													
15	Plenary Lecture: Stephen Minger													
Afternoon Tea with posters, in Exhibition Hall														
16	John Hunt: Intro 25-1: Hollander 25-2: Rannard 25-3: Sutcliffe	Biomaterials V 26-1: Ban 26-2: Schmitt 26-3: Gao 26-4: Pinto 26-5: Pires 26-6: Tanga 26-7: Wong 26-8: Brugmans	Symposium: EORS 27-1: Choy 27-2: Braga 27-3: Mustafa 27-4: Castaño 27-5: Gowland 27-6: Jing 27-7: Qiao 27-8: Li	Drug Delivery III 28-1: Ganesan 28-2: Nagahama 28-3: Wang 28-4: Gilde 28-5: Panseri 28-6: Moriyama 28-7: Aiertza 28-8: Chao	Keynote Lecture 29-1: Li 29-2: Ryabenkova 29-3: Feng 29-4: Wendt 29-5: Demitri 29-6: Ishikawa 29-7: San Roman	Symposium: Antimicrobials, biofilms 30-1: George 30-2: Li 30-3: Salmeron-Sanchez 30-4: Irwin 30-5: Khan 30-6: Nottelet 30-7: Prokopovich 30-8: Bergmann								
17	25-4: Levy John Hunt: Summary & Intro of experts 25-5: Stephen Minger													
18	25-6: Molly Shoichet 25-7: Joachim Kohn 25-8: David Williams Summary							Poster Session, in Exhibition Hall					YSF Rapidfire poster session III	
19														
20														
21	#													
22+														

	Auditorium, Hall 1	Room 3	Room 11	Room 1B	Room 1C	Room 4	Exhibition Area	Room 7	Room 13	Room 14
8	Plenary Lecture: Dietmar Hutmacher						Exhibition Hall open at 08:00. Posters and exhibition open until 19:30			
9	Biomaterials VII: Bioglass 31-1: Brauer 31-2: Christie 31-3: Greasley 31-4: Alm	Symposium: Translational 32-1: Richards 32-2: Montali 32-3: Neumann	Tissue Engineering III 33-1: Satyam 33-2: Hayes 33-3: Scaglione 33-4: Wan 33-5: Qazi 33-6: Wandrey	Bone III 34-1: Ohtsuki 34-2: Picard 34-3: Yamaguchi 34-4: Nakamura 34-5: Kerdjoudj 34-6: Vasconcelos	Keynote Lecture 35-1: Dalby 35-2: Van Vlierberghe 35-3: Alakpa 35-4: Bersini 35-5: Sorkio	Welcome: UKSB President UKSB President's Prize: 36-1: Sheila McNeil				
10	31-5: Haaparanta 31-6: Balasubramanian									
	Morning Coffee Break with posters in Exhibition Hall									
11	Biomaterials VIII: Bioglass 37-1: Connell 37-2: Hasan 37-3: Martin 37-4: Philippart	Symposium: Translational 38-1: Proctor 38-2: Shakesheff 38-3: Fisher	Tissue Engineering IV 39-1: Mauquoy 39-2: Vueva 39-3: Vallejo-Giraldo 39-4: Blanquer 39-5: Koivisto 39-6: Maazouz	Bone IV 40-1: Satu�� 40-2: Bannerman 40-3: Mechiche Alami 40-4: Rodr��guez-Lorenzo 40-5: Kruppke 40-6: Hadjicharalambous	Stem Cells IV 41-1: Guillem-Marti 41-2: Hess 41-3: Werner 41-4: Genchi 41-5: D'Sa 41-6: Nazhat	Keynote Lecture 42-1: Wong 42-2: Dugan 42-3: Moronkeji 42-4: Campagnolo 42-5: Rutledge				
12	37-5: Lopez 37-6: Ding									
13	Lunch & posters, in Exhibition Hall						YSF Rapidfire poster session IV	Presentation uploads and Speaker Preview: Room 7 Open from 08:00	Springer: JMS:MiM Editorial Board meeting. Invite only	ICF-BSE Fellows Annual meeting. Invite only
14	Plenary Lecture: Molly Shoichet									
15	Biomaterials IX 43-1: Miyazaki 43-2: Ahmed 43-3: Walsh 43-4: Birdi	Symp: Translational 44-1: Therin 44-2: McDougall	Tissue Eng V 45-1: Pandis 45-2: Criscenti 45-3: Bax 45-4: Shirosaki	Clinical I 46-1: Vashaghian 46-2: Gorgieva 46-3: Linti 46-4: Mizuta	Stem Cells V 47-1: Neves 47-2: Kok 47-3: Mano 47-4: Shariatzadeh	Alan Wilson Prize: 48-1: Paul Hatton				
	Afternoon Tea with posters, in Exhibition Hall									
16	Biomaterials X: Bioglass 49-1: Li 49-2: Aro 49-3: Albeshti 49-4: Chen 49-5: Solanki 49-6: Engel 49-7: Abou Neel 49-8: Jell	Symposium: Translational Research 50-1: Vestberg 50-2: Vardar 50-3: Mansourian 50-4: Mogosanu 50-5: Gr��mare 50-6: Chen 50-7: Bloebaum 50-8: Aston	Tissue Engineering VI 51-1: Oliveira 51-2: Finne-Wistrand 51-3: Brunelli 51-4: Garziano 51-5: Sohler 51-6: Kluger 51-7: Babo 51-8: Jensen	Clinical II 52-1: Navarro 52-2: Spazierer 52-3: Kehoe 52-4: Borzacchiello 52-5: Gon��alves 52-6: Rosa Aguilar 52-7: Far�� 52-8: Bosworth	Biomaterials XI: Hydrogels 53-1: Auz��ly-Velty 53-2: Halacheva 53-3: Melchels 53-4: Wieduwild 53-5: Mao 53-6: Chen 53-7: Wieringa 53-8: Kayabolen	54-1: de Cogan 54-2: Kasbekar 54-3: Tronci 54-4: Gallagher 54-5: Trzcinska UKSB AGM				
17									Elsevier: Biomaterials Editorial Board meeting. Invite only	
18										
19										
20										
21	Gala dinner (Ticket only)									
22+										

	Auditorium, Rm 1	Room 3	Room 11	Room 1B	Room 1C	Room 4	Exhibition Area	Room 7
8	Plenary Lecture: Larry Hench						Exhibition Hall open at 08:00. Posters and exhibition open until 14:00. Posters MUST be removed by 14:00	
9	Symposium: Women in Sci 55-1: Natesan 55-2: Huang 55-3: Ashworth 55-4: Anwar	Symposium: Bioactive Glass 56-1: Salinas 56-2: Jones 56-3: Frantzen 56-4: Lindfors	Biomaterials XII 57-1: Keriquel 57-2: Moreau 57-3: Anselme 57-4: de Wild 57-5: Nelson 57-6: Chen	Tissue Engineering VII 58-1: Silva 58-2: Fermor 58-3: Pandit 58-4: Shepherd 58-5: Kamata 58-6: Ronan		UKSB V Keynote Lecture 59-1: Akhtar 59-2: McLister 59-3: Reardon 59-4: Popov 59-5: Tanner		
10								
	Morning Coffee Break with posters in Exhibition Hall							
11	Symposium: Women in Sci 60-1: Curran 60-2: Gonzalez 60-3: McNamara 60-4: Posadowska	Symposium: Bioactive Glass 61-1: Boccaccini 61-2: Nedelec 61-3: Hatton 61-4: Wu	Keynote Lecture 62-1: Deng 62-2: Barata 62-3: Larsen 62-4: Gelinsky 62-5: D'Amora	Tissue Engineering VIII 63-1: Corté 63-2: Larranagae 63-3: Galea 63-4: Aktürk 63-5: Gautrot 63-6: Ghanaati		UKSB VI 64-1: Gough 64-2: Prosser 64-3: Andrews 64-4: Blaker UKSB Closing ceremony & intro to Hench awardee		
12	Symposium: Women in Sci 60-5: Kubok 60-6: Paredes	Symposium: Bioactive Glass 61-5: Vallittu 61-6: Pou						
13	Lunch & posters, in Exhibition Hall						YSF Rapidfire poster session V	
14	International Award Presentation: James Anderson							
15	Biomaterials XIV 65-1: Covarrubias 65-2: Min 65-3: Novoa-Carballal 65-4: Teixeira 65-5: Iwasaki 65-6: Mano	Hench Awardee 66-1: Biggs 66-2: Miller 66-3: Gentleman 66-4: Langford 66-5: Obata 66-6: Cormack 66-7: Hanna 66-8: Hill 66-9: Law 66-10: Hanna 66-11: Li 66-12: Macon	Biomaterials XV 67-1: Weiss 67-2: Osypova 67-3: Lewandowska-Szumiel 67-4: Hyde 67-5: Barros 67-6: Bosworth			Bone V 68-1: Wyszomirska 68-2: Engel 68-3: Diez-Escudero 68-4: Cholas 68-5: Golozar 68-6: Pasang		
16	Closing Ceremony, Travel/Conference awards							
17								
18								
19								
20								
21								
22+								

Exhibitors

Anton-Paar – Stand 122



Anton Paar GmbH

Anton-Paar-Str. 20
A-8054 Graz
Austria
Tel: +43 (0) 316 257-0
Fax: +43 (0) 316 257-257
info@anton-paar.com

Anton Paar Ltd

Unit F, The Courtyard
St Albans
AL4 0LA
Tel: +44 (0) 1992 514730
info.gb@anton-paar.com
www.anton-paar.com

Anton Paar produces high-precision measuring and laboratory instruments for industry and research. It is the world leader in the field of Rheometry and in the measurement of Density and Concentration. Other areas of specialty are: Viscometry, Polarimetry, Refractometry, Microwave Sample Preparation & Synthesis, Chemical and Mechanical Surface and Nanostructure Analysis.

IOP Publishing – Stand 1

IOP Publishing

IOP Publishing

Temple Circus
Temple Way
Bristol BS1 6HG
Tel: 0117 929 7481
Email: bmm@iop.org
<http://iopublishing.org>
Representative: Paul MacBeath

IOP Publishing provides a range of journals, magazines, websites, books and services that enable researchers to reach the widest possible audience for their research. Visit our stand at ESB to pick up your free copies of *Biomedical Materials* and *Biofabrication*, read the latest research published in our journals and find out what IOP Publishing can offer to our authors.

Bruker – Stand 148



Bruker UK Ltd

Banner Lane
Coventry
CV4 9GH
Tel: 024 7685 5200
Fax: 024 7646 5317
sales@bruker.co.uk
www.bruker-microct.com
Representative: Nick Corps

Sales and service of analytical instrumentation

Scanco Medical – Stand 170

SCANCO MEDICAL

SCANCO Medical

Fabrikweg 2
Bruttisellen 8306
Switzerland
Tel: +41 44 805 9815
Fax: +41 44 805 9801
lfalco@scanco.ch
www.scanco.ch
Representative: Lisa Falco

SCANCO Medical offers a wide range of microCT scanners for specimen and preclinical as well as clinical use (HR-pQCT). These systems are supplied with high-end computing equipment and sophisticated analysis and visualization soft-ware to provide the most comprehensive and industry-leading imaging solutions. SCANCO Medical also offers scanning, analysis and consulting services for a wide range of applications.

BioNavis – Stand 66



BioNavis Oy Ltd
Elopellontie 3C
33470 Ylöjärvi
Finland
Tel: +358 10 271 5030
info@bionavis.com
www.bionavis.com

BioNavis Multi-Parametric Surface Plasmon Resonance (MP-SPR) is a novel approach to the half-a-century old optical SPR phenomenon. SPR has been predominantly used for biomolecular interaction analysis but now MP-SPR broadens the application range also to biophysical studies, such as measurements of absolute refractive indices and formed layer thicknesses, biomaterial studies, such as ceramic and polymer coating characterizations (i.e. CaP, SiO₂, cellulose, polystyrene) as well as biocompatibility studies.

BioPharma – Stand 124



Biopharma Process Systems Ltd

Biopharma House
Winnall Valley Road
Winchester
Hants SO23 0LD
Tel: +44 (0) 1962 841092
www.biopharma.co.uk

The Biopharma Group provides a range of products and services to the pharmaceutical and biotech industries. Our expertise is in freeze-drying and our extensive range means we have equipment suitable for any application. Our dedicated laboratory also offers a range of services in freeze drying including formulation and cycle development.

BOSE-Electroforce – Stand 30



BOSE – ElectroForce Systems Group

Bose Limited, Bose House
Quayside, Chatham Maritime
Chatham, Kent ME4 4QZ
Tel: +44 (0) 3330 142545
Fax: +44 (0) 3330 142501
Electroforce_europe@bose.com
www.bose-electroforce.com

Bose Corporation is a leading supplier of materials testing and durability simulation instruments to research institutions, universities, medical device companies, and engineering companies worldwide. Bose® ElectroForce® test instruments help customers design better products and get them to market faster. Proprietary linear motors developed by Bose are at the heart of ElectroForce instruments, and they provide exceptional performance and energy-efficiency without compromising either.

Bose test instruments provide exceptional dynamic performance and precision for a variety of testing applications, including characterization of engineered materials, soft tissues and biomaterials; biomechanical testing and tissue growth solutions; fatigue testing of components used in industrial and consumer applications; and durability simulation of medical devices, including stents, endovascular grafts, and orthopaedic implants.

Cam Bioceramics – Stand 56



Cam Bioceramics

Zernikedreef 6
Leiden 2333 CL
The Netherlands
Tel: +31 628 740030
Fax: +31 71 524 0650
www.cambioceramics.com
Representative: Ralf-Peter Herber, PhD

Cam Bioceramics is a contract manufacturer of orthobiologic calcium phosphates. Cam Bioceramics develops, engineers and manufactures Orthobiologic Calcium Phosphates to meet our customers' specification. Product range includes: calcium phosphate powders, porous granules, dense granules, shapes or blocks. Cam Bioceramics is ISO13485 certified.

LACTEL® Absorbable Polymers – Stand 2



DURECT Corporation/LACTEL® Absorbable Polymers

PO Box 530, 95014, USA
Tel: 00 1 205.620.0025
Fax: 00 1 408.865.1406
absorbables@direct.com
www.absorbables.com
Representative: John Gibson

At the forefront of biomaterial production is LACTEL® Absorbable Polymers, the first commercial supply of biodegradable polyesters in the U.S. For decades we have supplied GMP excipients for biomaterial use world-wide. At our new, state-of-the-art facility in Birmingham, Alabama we continue to pioneer commercial-scale production of medical-grade polymers.

EBERS Medical Technology SL – Stand 100



EBERS Medical Technology SL

Calle Romero 29, Nave 13
Poligono Empresarium
La Cartuja Baja, Zaragoza, Spain
Tel: +34 876 013826
Fax: +34 876 013826
pmoreo@ebersmedical.com
www.ebersmedical.com
Representative Name: Dr Pedro Moreo

Design, manufacture and commercialization of 3D cell culture and tissue engineering bioreactors, microfluidic devices for cell culture and drug testing and oxygen sensors based on optical technology.

EnvisionTEC – Stand 146



EnvisionTEC GmbH
Brüsseler Str. 51
D-45968 Gladbeck, Germany
Tel: +49-2043-9875-0
Fax: +49-2043-9875-99
info@enviontec.de
www.enviontec.com
Representative: Rüdiger von Bernum

A world leader in Rapid Prototyping and Manufacturing equipment with an expert multi-disciplinary team, EnvisionTEC has produced the most reliable Rapid Prototyping system in the world. With a decade of experience in Tissue Engineering, Envision-TEC's widely accepted 3D-Bioplotter system successfully facilitated numerous in-vitro and in-vivo experiments and publications.

Plasma Biototal Ltd – Stand 24



P L A S M A B I O T A L L I M I T E D

Plasma Biototal Ltd is a leading supplier of Hydroxylapatite (HA) coating services for orthopedic device manufacturers and manufacturers of ceramic materials for grafting products, composites and other advanced biomaterials to over 20 countries worldwide. Externally audited to requirements for international standards ISO 13779:2008, 13175:2012, and for quality systems ISO 13485, 9001, and ASTM standards.

Plasma Biototal Ltd

Unit 1-5 Meverill Road Industrial Estate
Whitecross Road
Tideswell
Derbyshire SK17 8PY
Tel: +44 (0)1298 872348
www.plasma.biototal.com

Royal Society of Chemistry – Stand 166



Royal Society of Chemistry

Thomas Graham House
Science Park
Milton Road
Cambridge CB4 0WF
UK
Tel: +44 (0)1223 420066
Fax: +44 (0)1223 423623
booksales@rcs.org
www.rsc.org

The Royal Society of Chemistry is the largest organisation in Europe for advancing the chemical sciences. Supported by a world-wide network of members and an international publishing business, our activities span education, conferences, science policy and the promotion of chemistry to the public. The Royal Society of Chemistry's high quality books programme covers the breadth of the chemical sciences, ranging from the highly specialised to educational textbooks and popular science titles.

Royal Society Publishing – Stand 70



Royal Society Publishing (The Royal Society)

6-9 Carlton House Terrace
London
SW1Y 5AG
UK
Tel: +44 (0)20 7451 2633
<http://royalsocietypublishing.org>
Representative: Ruth Milne

The Royal Society journals regularly publish high quality content in the area of biomaterials. For more information about the scope and editorial procedures of our journals, please come and have a chat with our representative Ruth Milne at booth number 70. Alternatively, visit our website at <http://royalsocietypublishing.org>

Spraybase-Profector Life Sciences – Stand 54

Spraybase - Profector Life Sciences



The logo for Spraybase® features the word "Spraybase" in a stylized, cursive-like font with a registered trademark symbol (®) to its upper right.

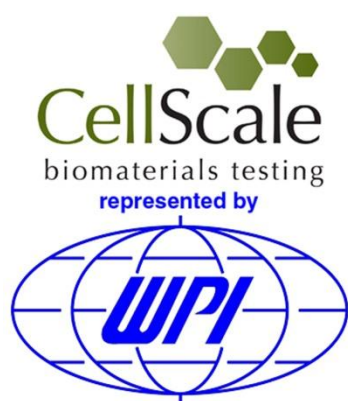
Electrospinning and Electrospaying Instruments

Value | Versatility | Expertise

1.08 Callan Building
NUI Maynooth
Kildare
Ireland
Tel: +353-85-7085045
ghendy@profector.com
www.spraybase.com

Spraybase® is the world's first integrated instrument that enables electrospinning and electrospaying technologies for life sci-ence applications. The Spraybase® instrument offers a complete solution to users investigating electrospaying and electrospin-ning applications. Spraybase® instrument can be used to form colloids and fibers of varying shape and size depending on your application.

WPI/Cell-Scale – Stand 172



World Precision Instruments / Cell-Scale

1 Hunting Gate
Hitchin
Herts
SG4 0TJ
Tel: +44 (0)1462 424700
Fax: +44 (0)1462 424701
idavies@wpi-europe.com
<http://www.wpi-europe.com/solutions/biomaterial-testing.aspx>
Representative: Dr. Ian Davies

Cell Scale mechanical test systems are specifically designed for characterizing the material properties of biomaterials. With integrated features such as image capture and analysis, media chambers, and a range of gripping mechanisms, their biaxial and micro-scale compression test systems are capable of generating high quality test data from day one.

Biomomentum Inc. – Stand 50



Biomomentum Inc.

970 Michelin, Suite 200
Laval, Quebec, H7L 5C1
Canada
Tel: (450) 677-2299
info@biomomentum.com
www.biomomentum.com
Representative: Martin Garon

Biomomentum specializes in providing solutions for testing biomaterials and cartilage. The Mach-1™ is a multiple-axis mechanical tester capable of performing compression, tension, shear, and torsion tests for the precise characterization and mechanical stimulation of cartilage and other soft tissue and materials. Among other functionalities, the Mach-1™ can be used to automatically map the mechanical properties of full articular cartilage surfaces in indentation. The Arthro-BST™ is a hand-held medical device used in conjunction with arthroscopy for the non-destructive measurement of compression-induced streaming potentials of articular cartilage. A benchtop version of this device is available for ex vivo use. Biomomentum also offers biomechanical testing services.

Elsevier



ELSEVIER

Elsevier is a world leading provider of scientific, technical and medical information, products and services. We publish high-impact articles across the whole of materials science, in bio-materials and polymers, in ceramics and composites, in alloys and compounds, in metals and in new materials for energy applications. We publish around 20,000 articles per year across our entire list and work globally with some of the best minds in the field to lead our journals. To support our program, we also run successful conferences such as *Frontiers in Polymer Science*, *Hybrid Materials*, *Nano Today*, *Materials Today Asia* and *NuMat: Nuclear Materials*.

Cook General Biotechnology



At Cook General BioTechnology, LLC, we're dedicated to advancing the science and practical application of processing, storage, and manufacturing of cells and tissues to empower new cell-based medical therapies. CGBT is proud to offer Stemulate™ to academic, medical centers, and industry partners. Stemulate™ is a substitute for fetal bovine serum (FBS) or serum free culture media. Its advantages include no risk of animal pathogen transmission, superior mesenchymal stromal cell growth kinetics (at 5% concentration) as well as reliable batch-to-batch consistency and performance.

Lifecore Biomedical – Stand 126



Lifecore is a leader in hyaluronan supply for commercial and research markets. These include applications in ophthalmology, orthopaedics, tissue engineering, aesthetics etc. Lifecore also offers Corgel® BioHydrogel and CellMate® hyaluronan-based 3D culture materials. Lifecore also has extensive experience in contract manufacturing.

Request a quotation: Rebecca Sebansky (Rebecca.sebansky@lifecore.com)

Elsevier Science and Technology

The Boulevard
Langford Lane
Kidlington
Oxford
OX5 1GB
www.elsevier.com

Cook Medical

O'Halloran Road
National Technology Park
Limerick
Ireland
www.cookgbt.com

Lifecore Biomedical LLC
3515 Lyman Blvd Chaska
MN 55318-3051
USA
Tel: +1 952 368-6321
Fax: +1 952 368 4728
www.lifecore.com

Official journal
of the European Society
for Biomaterials (ESB)



Journal of Materials Science: Materials in Medicine

New features in 2014:

- Rapid Communications
- Clinically Focused Translational Research Section
- Young Investigator-Mentor Program to Foster Development of Scientific Review Skills

Reach 8,000 institutions worldwide and millions of desktops. Free online to all ESB members.

Visit us at springer.com

A08088

The annual conference of the European Society for Biomaterials

27th European Conference on Biomaterials



www.esb2015.org

ESB 2015

30 August–3 September
Kraków, Poland





The organizers of the 10th World Biomaterials Congress (WBC) which will be held in Montreal May 18-22, 2016 welcome you to meet us at our booth at this European Society for Biomaterials meeting and to visit our website <http://www.wbc2016.org/> . The venue for the event is the Montreal Convention Center, located in the heart of downtown Montreal, just a minutes walk from the historic Old Montreal. We cordially invite you to participate in this exciting event as active organizers, reviewers, exhibitors and/or presenters. We encourage you to share your latest findings in science and technology of Biomaterials with others by submitting a paper, organizing a symposium session or sharing your ideas with us. Please feel free contact any of the four co-chairs for the conference or the conference office at info@wbc2016.org .

Key Dates

Call for Symposia: will open on September 15, 2014: New Frontier topics only; proposals for topics that are covered by the Scientific Sessions below will not be considered.

Call for Abstracts: will open on May 15, 2015

Contact

WBC2016 Montreal

Booth 412

607 Notre-Dame

St-Lambert, QC, Canada

J4P 2K8

Phone: 450-550-3488 ext 114

Fax: 514-227-5083

Email: info@wbc2016.org

Biomaterials I Hall 1, 09:30 - 10:30

Chairs: Wim De Jong, National Institute for Public Health and the Environment
Matteo D'Este, AO Foundation
Felicity de Cogan, University of Birmingham

- 09:30 1-1 **A Viscoelastic, Anisotropic, Hyperelastic Model of the Human Cornea**
Charles Whitford, Natasha Movchan and Ahmed Elsheikh
School of Engineering, University of Liverpool, UK
- 09:45 1-2 **Bacterial Cellulose as a Support for the Growth of Retinal Pigment Epithelium**
S. Gonçalves, J. Padrão, J. Silva, I. Rodrigues, H. Girão, F. Dourado and L. Rodrigues
Center of Biological Engineering, University of Minho, Portugal
- 10:00 1-3 **Nanosomes: Novel Drug Delivery Vehicles to treat Glaucoma**
F. de Cogan, L. Hill, P. Morgan-Warren, J. O'Neill, A. Peacock, R. Scott and A. Logan
School of Clinical and Experimental Medicine, University of Birmingham, UK
- 10:15 1-4 **Emulation of Extracellular Matrix for the Development of Human Corneal Stromal Substitute**
Pramod Kumar, Abhigyan Satyam, Xingliang Fan, Brian Rodriguez, Yuri Rochev, Michael Raghunath, Abhay Pandit and Dimitrios Zeugolis
Network of Excellence for Functional Biomaterials, National University of Ireland, Galway, Ireland

Tissue Engineering I Room 3, 09:30 - 10:30

Chairs: Miguel Gama, Minho University
Ferry Melchels, University Medical Center Utrecht
Hugo Oliveira, Inserm U1026, Biotis

- 09:30 2-1 **Nanostructured Materials for Tissue Engineering: Nanofibres, Nanoparticles and Nanofilms**
Lucie Bacakova
Department of Biomaterials and Tissue Engineering, Academy of Sciences of the Czech Republic, Prague
- 09:45 2-2 **Fabrication of Silk Fibroin and High Methoxyl Citrus Pectin(HMP) Based 3D Scaffolds for Bone Tissue Engineering**
Sibel Ataoğlu, Dilek Keskin, Akın Akdağ, Ayşen Tezcaner
Department of Biomedical Engineering, Middle East Technical University, Ankara, Turkey
- 10:00 2-3 **Regulation of Chondrocyte Spheroid Size using Proline-containing Periodic Peptides**
N. Takata, Y. Morita, Y. Hirano, Y. Futaki and E. Nakamachi
Graduate School of Life and Medical Sciences, Doshisha University, Japan
- 10:15 2-4 **Hyaluronic Acid Based-Hydrogels Attenuate Inflammatory Receptor and Neurotrophins in IL-1 β Induced Inflammation Model of Nucleus Pulposus Cell Cultures**
Isma-Liza Mohd-Isa, David Tiernan, Akshay Srivastava, Peter Rooney and Abhay Pandit
Network of Excellent Functional Biomaterials, National University of Ireland, Galway, Ireland

Stem Cells I Room 11, 09:30 - 10:30

Chairs: Barbara Boyan, Virginia Commonwealth University
Tugba Dursun, Middle East Technical University
Jerome Sohler, Centre National de la Recherche Scientifique

- 09:30 3-1 **Osteogenic Activity of Adipose Derived Stem Cells on Micropatterned Collagen-Fibroin Blend Films**
E. Sayin, E. T. Baran, V. Hasirci
Department of Biotechnology, Middle East Technical University, Turkey
- 09:45 3-2 **Regulation of Mesenchymal Stem Cell Differentiation by Changing the Molecular Structure of Supramolecular Surfaces**
Ji-Hun Seo, Sachiro Kakinoki, Tetsuji Yamaoka and Nobuhiko Yui
Institute of Biomaterials and Bioengineering, Tokyo Medical and Dental University, Japan
- 10:00 3-3 **Cell Viability and Cell Attachment of Mesenchymal Stem Cells on Hydroxyapatite/Alginate S. crassifolium Composite Scaffolds**
Decky J. Indrani, Ismail Dilogo, Yuyus Kusnadi
Department of Dental Materials Science, University of Indonesia
- 10:15 3-4 **The Development and Translation of a Cell Capture Technique for Cell Therapies, Diagnostics and Research**
Nicholas Bryan, Damian Bond, Christopher Stanley and John Alan Hunt
Clinical Engineering, Institute of Ageing and Chronic Disease, University of Liverpool, UK

Chairs: Giorgio Soldani, IFC-CNR

Kambiz Farbod, Radboud University Medical Center

Coline Jumeaux, Imperial College London

- 09:30 4-1 **Dynamic Polysaccharide-based Carrier Systems for the Delivery of Biotherapeutics**
Denise N. Bamberger and Peter R. Wich
 Institut für Pharmazie und Biochemie, Johannes Gutenberg-Universität Mainz, Germany
- 09:45 4-2 **Amphiphilic Graft Polyester-g-polysaccharide Copolymers for Sustained Drug Release**
L. Martellotto, J. Buisson, H. Van Den Berghe, J. Coudane
 Artificial Biopolymers Department, University Montpellier 1, France
- 10:00 4-3 **Micro and Nano Systems in Medical Applications**
Vasif Hasirci, Eda Ayse Aksoy and Nesrin Hasirci
 Middle East Technical University, Chemistry Dept, Ankara, Turkey
- 10:15 4-4 **Fibrin-based Microsphere Reservoirs for Delivery of Neurotrophic Factors**
Juhi Samal, *Ellis Dowd and Abhay Pandit*
 Network of Excellence for Functional Biomaterials, National University of Ireland, Galway, Ireland

Dental Biomaterials I Room 1C, 09:30 - 10:30

Chairs: Judith Curran, University of Liverpool

Anas Aljabo, University College London

Sabeel Valappi, University of Liverpool

- 09:30 5-1 **Synthesis and Evaluation of a Novel POSS-PEG-PLA Hydrogel for Periodontal Applications**
David K. Wang, Srinivas Varanasi, David J.T. Hill, Anne L. Symons, Andrew K. Whittaker and Firas A. Rasoul
 Australian Institute for Bioengineering and Nanotechnology, University of Queensland, Brisbane, Australia
- 09:45 5-2 **Effects of Calcium Phosphate and an Adhesion Promoting Monomer on Strength, Degree of Conversion and Adhesion of Dental Composites**
Anas Aljabo and *Anne Young*
 Biomaterials and Tissue Engineering, University College London, UK
- 10:00 5-3 **The Bone-Implant Interface – Nano-Osseointegration of Functionally Loaded, Nano-Textured, Human Dental Implants**
Furqan A. Shah, *Bengt Nilson, Rickard Brånemark, Peter Thomsen, Anders Palmquist*
 Department of Biomaterials, University of Gothenburg, Sweden
- 10:15 5-4 **Morphology, Surface Chemistry and Mechanical Properties of Commercial Guided Tissue Regeneration Membranes**
Pascal Borget, *Paul G. Rouxhet and Eric Rompen*
 Unité de Chimie des Interfaces, Université Catholique de Louvain, Belgium

Chairs: Wim De Jong, National Institute for Public Health and the Environment
Matteo D'Este, AO Foundation
Felicity de Cogan, University of Birmingham

- 11:00 6-1 **Dense Fibrillated Collagen Transparent Matrices as Artificial Corneas?**
Aurelien Tidu, Djida Ghoubay, Barbara Lynch, Céline De Sousa, Frank Wendel, Jean-Marc Allain, Vincent Borderie, Gervaise Mosser
Sorbonne Université, Paris, France
- 11:15 6-2 **Cytotoxicity of Terbium-Crown Ether Complex Against Acanthamoeba sp. - A Causative Agent for Eye Keratitis**
Eny Kusriji, Fatimah Hashim, Dewi Tristantini, Nurfatin Solehah Bustaman and Nakisah Mat Amin
Department of Chemical Engineering, Faculty of Engineering, Universitas Indonesia
- 11:30 6-3 **Biodegradable Nanoneedles for Intracellular Sensing of Enzymatic Activity**
Ciro Chiappini, Paola Campagnolo, Carina Almeida, Lesley Chow, Molly M. Stevens
Department of Materials, Imperial College London, UK
- 11:45 6-4 **Biosurface Induced Protein Manipulation for Measurement of Dynamic Platelet Function**
D. Bishop, J. Cowman, E. Dunne, D. Kenny, A. Boyd and B. Meenan
Nanotechnology and Integrated Bioengineering Centre, University of Ulster, UK
- 12:00 6-5 **Targeted Gene Delivery into Peripheral Nervous System Mediated by Trimethyl Chitosan Nanoparticles**
Carla Pereira Gomes, Aida Varela-Moreira, Maria Gomez-Lazaro, Michael Leitner, Andreas Ebner, Peter Hinterdorfer, Ana Paula Pêgo
Instituto de Engenharia Biomédica, Universidade do Porto, Portugal
- 12:15 6-6 **Nanoscale Neuroelectrode Modification Through Self-Assembly of Block Copolymers**
Parvaneh Mokarian-Tabari, Catalina Vallejo-Giraldo, Marc Fernandez-Yague, Cian Cummins, Michael A. Morris and Manus J.P. Biggs
Network of Excellence for Functional Biomaterials, National University of Ireland, Galway

Tissue Engineering II Room 3, 11:00 - 12:30

Chairs: Miguel Gama, Minho University
Ferry Melchels, University Medical Center Utrecht
Hugo Oliveira, Inserm U1026, Biotis

- 11:00 7-1 **Stimulation of Angiogenesis by Growth Factor-free Porous Adhesive Films Made by Hexanoyl Group Modified Gelatin**
Keiko Yoshizawa, Temmei Ito, Ryo Mizuta and Tetsushi Taguchi
Graduate School of Pure and Applied Science, University of Tsukuba, Japan
- 11:15 7-2 **Development of PLLA/BTO Nanofiber Sheet for Bone Tissue Engineering**
A. Yamano, Y. Morita and E. Nakamachi
Graduate School of Life and Medical Sciences, Doshisha University, Japan
- 11:30 7-3 **Preparation and Characterization of PHBV Porous Nanofibers**
Lan-Xin Lyu, Ning-Ping Huang and Ying Yang
State Key Laboratory of Bioelectronics, Southeast University, China
- 11:45 7-4 **Fabrication and Characterization of Carbon Nanotube Membranes for Neural Tissue Engineering**
Sevde Altuntas, Buket Altınok, Belma Aslım, Fatih Buyukserin
Micro and Nanotechnology Graduate Program, TOBB Univ. of Econ. & Technology, Ankara, Turkey
- 12:00 7-5 **A Degradable Chitosan-graft-poly(ϵ -Caprolactone) Copolymeric Biomaterial Supports the Growth of Wharton's Jelly Mesenchymal Stem Cells for Soft Tissue Engineering**
Amalia Skarmoutsou, Costas Charitidis, Maria Kaliva, Charalampos Pontikoglou, Maria Vamvakaki, Maria Chatzinikolaïdou
Department of Materials Science and Technology, University of Crete, Greece
- 12:15 7-6 **Application of Natural BMP Modulators on Bone Tissue Engineering**
Guo-Chung Dong and Chun-Hsu Yao
Institute of Biomedical Engineering and Nanomedicine, National Health Research Institutes, Taiwan

Stem Cells II Room 11, 11:00 - 12:30

Chairs: Barbara Boyan, Virginia Commonwealth University
Tugba Dursun, Middle East Technical University
Jerome Sohler, Centre National de la Recherche Scientifique

- 11:00 8-1 **Substrate-Mediated Nanoparticle/Gene Delivery to MSC Spheroids and the Applications in Peripheral Nerve Regeneration**
Ting-Chen Tseng and Shan-hui Hsu
Institute of Polymer Science and Engineering, National Taiwan University, Taipei, Taiwan
- 11:15 8-2 **Influence of Inner Organization of Nerve Guide on Rat Bone Marrow Stem Cells (rBMSCs)**
T. Dursun, D. Yücel, V. Hasırcı
BIOMATEN, Middle East Technical University Center of Excellence in Biomaterials and Tissue Engineering, Ankara, Turkey
- 11:30 8-3 **Designing 3D Cell Niches Exploiting Peptide Self-Assembly**
Victoria L. Workman, Aline F. Miller and Alberto Saiani
School of Materials, University of Manchester, UK
- 11:45 8-4 **Effect of Zinc-Containing Tricalciumphosphate (ZnTCP) on Growth and Osteogenic Differentiation of Mesenchymal Stem Cells**
Joshua Chou, Jia Hao, Hirokazu Hatoyama, Besim Ben-Nissan, Bruce Milthorpe, Makoto Otsuka
Advanced Tissue Regeneration and Drug Delivery Group, University of Technology Sydney, Australia
- 12:00 8-5 **High-Throughput Quantitative Chondrogenic Assay for Stem Cell Differentiation**
Amy Prosser, Colin Scotthford, Virginie Sottile, and David Grant
Division of Materials Mechanics and Structures, University of Nottingham, UK

- 12:15 8-6 **Advances in Raman Micro-Spectroscopy for Label-free Monitoring Differentiation of Stem Cells In-Vitro**
Ioan Notingher
 School of Physics and Astronomy, University of Nottingham, United Kingdom

Drug Delivery II Room 1B, 11:00 - 12:30

- Chairs:** Giorgio Soldani, IFC-CNR
 Joana Magalhaes, Instituto de Salud Carlos III
 Coline Jumeaux, Imperial College London
- 11:00 9-1 **Substrate Mediated Enzyme Prodrug Therapy**
A.N. Zelikin
 Department of Chemistry, Aarhus University, Denmark
- 11:15 9-2 **Mesoporous SiO₂-ZnO-plex: Mechanistic Approach, Complex of Nanoparticles of SiO₂-ZnO with DNA for Therapeutic Applications**
 Vijay Bhooshan Kumar, Koushi Kumar, Yitzhak Mastai, Aharon Gedanken, Pradip Paik
 School of Engineering Sciences and Technology, University of Hyderabad, India
- 11:30 9-3 **Estimation of Drug Loading Efficiency in Microspheres by “Shake Flask” Method**
 C. Y. Tham, Z. A Abdul Hamid, Z. Ahmad, H. Ismail
 School of Materials and Mineral Resources Engineering, Universiti Sains Malaysia, Seri Ampangan, Malaysia
- 11:45 9-4 **Suzuki Coupling-Functionalized Boronic Acid Nanoparticles for Drug Delivery**
André J. van der Vlies and Urara Hasegawa
 Graduate School of Engineering, Osaka University, Japan
- 12:00 9-5 **Polymeric Micelles for Hydrogen Sulfide-Based Therapy**
Urara Hasegawa, André J. van der Vlies
 Graduate School of Engineering, Osaka University, Japan
- 12:15 9-6 **Amorphous Coordination Polymer Particles. From Basic Macromolecular Science to Theranostic Applications**
F. Novio, F. Nador, K. Wnuk, M. Borges and D. Ruiz-Molina
 Centro de Investigación en Nanociencia y Nanotecnología, Consejo Superior de Investigaciones Científicas, Bellaterra, Spain

Dental Biomaterials II Room 1C, 11:00 - 12:30

- Chairs:** Judith Curran, University of Liverpool
 Anas Aljabo, University College London
 Sabeel Valappi, University of Liverpool
- 11:00 10-1 **Potential Use of 7-dehydrocholesterol Coated Titanium Surfaces for Soft Tissue Integration of Dental Implants**
Manuel Gómez-Florit, María Satué, Joana M. Ramis and Marta Monjo
 Group of Cell Therapy and Tissue Engineering, University of the Balearic Islands, Spain
- 11:15 10-2 **Studying Interaction between Oral Mucosa and Titanium by SEM in Humans**
Francesco Tassarolo, Cristiano Tomasi, Federico Piccoli, Iole Caola, Patrizio Caciagli and Giandomenico Nollo
 Bruno Kessler Foundation, Trento, Italy
- 11:30 10-3 **Synthesis and Characterisation of Novel Diopside Glass-Ceramics for Dentistry**
J. Almuhamadi, N. Karpukhina and M. Cattell
 Institute of Dentistry, Queen Mary University of London, UK
- 11:45 10-4 **Functionally Graded Guided Tissue Regenerative (GTR) Membrane for Periodontal Lesions**
S Qasim, R Delaine-Smith, A. Rawlinson, I. Rehman
 Materials Science and Engineering Department, University of Sheffield, UK
- 12:00 10-5 **Bioactivity Investigations with Calcia Magnesia Based composites**
 Emad Ewais, Amira Moustafa, Karoline Pardun, Kurosch Rezwan
 Advanced Materials Department, Central Metallurgical R&D Institute, Cairo, Egypt
- 12:15 10-6 **Characterisation of Partially-Demineralised Dentine is a Prerequisite for Remineralisation Studies**
Eleanor Ashworth, Cheryl Miller, Christopher Deery and Nicolas Martin
 School of Clinical Dentistry, University of Sheffield, UK

Chair: Joachim Kohn, Rutgers University

The Race between engineering and biology in replacing human tissues.

The chair will define this challenge, a take vote of the audience. There will then be 6, 15 minute talks from a panel of current FBSE fellows:

- 14:00 **Barbara Boyan**, Virginia Commonwealth University
- 14:15 **Rui Reis**, University of Minho
- 14:30 **Abhay Pandit**, National University of Ireland Galway
- 14:45 **Cristina Tanzi**, Politecnico di Milano
- 15:00 **John Kao**, University of Wisconsin - Madison
- 15:15 **David Williams**, Wake Forest Institute of Regenerative Medicine

who will expound, sometimes controversially, their own points of view about the argument.

Following the talks there will be a Q & A session and finally a vote of the audience.

YSF Entrepreneurship Workshop Room 3, 13:30 - 16:00

Chairs: Lorenzo Moroni, University of Twente
Sandra Van Vlierberghe, University of Gent
Anna Wistrand, KTH Royal Institute of Technology

The workshop will give a flavour of what it takes to create spin-off companies from innovative research activities that take place at Universities, as well as in Industry. Talks will span from personal experiences in facing the challenges of setting up a spin-off, to the availability of educational programmes and important points to consider when applying for patents.

The afternoon has an extensive spectrum of experienced experts in entrepreneurship:

- 13:35 **Dirk Grijpma**, University of Twente
- 14:00 **Dietmar Huttmacher**, Queensland University of Technology and Technical University of Munchen
- 14:25 **Jens Thies**, DSM, The Netherlands
- 14:50 **Chris Sutcliffe**, University of Liverpool
- 15:10 **Alex Sim**, AMSBIO Ltd
- 15:35 **Chris Unsworth**, Business Gateway, University of Liverpool

European Doctoral Awards Hall 1, 16:30 - 17:30

Chair: Dirk Grijpma, University of Twente

- 16:30 **Award presentations**
Dirk Grijpma
University of Twente, the Netherlands
- 16:40 14-1 **Periodontal Regeneration by Combining Melt Electrospinning With Fused Deposition Modelling and Cell Sheet Technologies**
Pedro Costa
Technische Universität München, Germany
- 16:50 14-2 **Development of a Pro-Angiogenic Cell-Delivery Vehicle Based on RGD-Alginate Hydrogels**
Silvia Bidarra
University of Porto, Portugal
- 17:00 14-3 **The Osteogenic Potential of Human Mesenchymal Stem Cells - Connections to Inflammation and Infection**
Cecilia Granéli
University of Gothenburg, Sweden
- 17:10 14-4 **Influence of Sintering Conditions on the Properties of Porous TiO₂ Bone Scaffolds**
Hanna Tiainen
University of Oslo, Norway
- 17:20 14-5 **Biomaterials for 2D and 3D Bio-Hybrid Robotic Devices**
Leonardo Ricotti
Scuola Superiore Sant'Anna, Italy

Chairs: Liang Yo Yang, Taipei Medical University
Oscar Castaño, Institute for Bioengineering of Catalonia
Thomas Miramond, Biomatlante

- 09:00 15-1 **Self-Healing Hybrid Nanocomposites Based on Bisphosphonated Hyaluronan and Calcium Phosphate Nanoparticles for Bone Regeneration**
Reza Nejadnik, Xia Yang, Matilde Bongio, Hamdan S. Alghamdi, Jeroen J.J.P. van den Beucken, Marie C. Huysmans, John A. Jansen, Jöns Hilborn, Dmitri Ossipov and Sander C.G. Leeuwenburgh
Department of Chemistry-Ångström, Uppsala University, Sweden
- 09:15 15-2 **Development of Novel LZ-8 protein-Containing Porous Composite Sponge Scaffold for Biomedical Applications: Biocompatibility Evaluation and an Animal Study in Rabbit**
Chia-Yin Chen, His-Jen Chiang, Li-Hsiang Lin, Keng-Liang Ou
Graduate Institute of Biomedical Materials and Tissue Engineering, Taipei Medical University, Taiwan
- 09:30 15-3 **Phase Constitution and Heat Treatment Behaviour of Ti-Mn-Sn Beta Type Alloys**
Masahiko Ikeda, Masato Ueda and Mitsuo Niinomi
Department of Chemistry and Materials Engineering, Kansai University, Japan
- 09:45 15-4 **Hyaluronic Acid Bound Bisphosphonates As A Novel Therapeutic Strategy For Osteoporosis**
Sujit Kootala, Dmitri Ossipov, Xia Yang, Yu Zhang and Jöns Hilborn
Department of Chemistry/Polymer Chemistry, Uppsala University, Sweden
- 10:00 15-5 **Influence of Anchor Strand Related Parameters on Immobilized Amount and Hybridization Efficiency in a Nucleic Acid-based Immobilization System for Titanium Implants**
Cornelia Wolf-Brandstetter, Jan Michael, René Beutner, Bernd Schwenzer, Henning Schliephake, Dieter Scharnweber
Institute of Materials Science, TU Dresden, Germany
- 10:15 15-6 **Functional Octapeptide Hydrogel to Bone Repair Applications**
Luis Castillo, Alberto Saiani, Julie Gough and Aline Miller
Manchester Interdisciplinary Biocentre, University of Manchester, UK

Biomaterials III Room 3, 09:00 - 10:30

Chairs: Dietmar Hutmacher, Queensland University of Technology
Rui Reis, University of Minho
Patrik Stenlund, SP Technical Research Institute of Sweden

- 09:00 16-1 **Pro-inflammatory Response to Novel Gelatin-based Biomaterials with Tailorable Mechanical Properties in vitro**
Sandra Ullm, Anne Krueger, Tim P. Gebauer, Axel T. Neffe, Christoph Tondera, Andreas Lendlein, Friedrich Jung, Jens Pietzsch
Institute of Radiopharmaceutical Cancer Research, Helmholtz-Zentrum Dresden-Rossendorf, Germany
- 09:15 16-2 **Dissecting the Regulating Cues of the Extracellular Matrix in Macrophage Plasticity**
Katja Franke, Liv Kalbitzer, Jiranuwat Sapudom, Ulf Andereg, Sandra Franz and Tilo Pompe
Institute of Biochemistry, Universität Leipzig, Germany
- 09:30 16-3 **Carbon Monoxide Releasing Nanoparticles**
Ryosuke Inubushi, André J. van der Vlies, Hiroshi Uyama and Urara Hasegawa
Graduate School of Engineering, Osaka University, Japan
- 09:45 16-4 **Effect of Hydrophobic Groups on the Bonding Strength of Cod-Derived Gelatins-Based Tissue Adhesives**
Tetsushi Taguchi, Temmei Ito, Ryo Mizuta, Keiko Yoshizawa
Biomaterials Unit, National Institute for Materials Science, Japan
- 10:00 16-5 **Examination of Local and Systemic Inflammatory and Immunological Reactions Following Implantation of Jellyfish Collagen Matrices in Rats**
Uwe Walschus, Susanne Meyer, Silke Lucke, Andreas Hoene, Udo Meyer, Michael Schlosser
Department of Medical Biochemistry and Molecular Biology, University Medical Center Greifswald, Germany
- 10:15 16-6 **Sulfated Hyaluronan Derivatives Interfere with TGF- β 1 Signalling**
V. Hintze, A. van der Smissen, S. Samsonov, L. Huebner, S. Rother, D. Scharnweber, S. Moeller, M. Schnabelrauch, M. T. Pisabarro, U. Andereg
Max Bergmann Center of Biomaterials, Technische Universität Dresden, Germany

Cardiovascular I: TECAS-ITN Room 11, 09:00 - 10:30

Chairs: Dimosthenis Mavrilas, University of Patras
Petra Mela, RWTH Aachen

- 09:00 17-1 **Vascular Network Generation in Hyaluronic Acid by Micromolding and Photoimmobilization of Fibronectin**
A. Kömez, E. T. Baran, N. Hasirci, V. Hasirci
Department of Biotechnology, Middle East Technical University, Turkey
- 09:15 17-2 **Collagen(I)-Poly(Glycerol Sebacate)/Poly(Butylene Succinate-Dilinoate) Fibrous Scaffolds for Cardiac Tissue Engineering**
Marwa Tallawi, David C. Zebrowski, Aga Kozłowska, Mirka El Fray, Felix B. Engel, Aldo R. Boccaccini
Institute of Biomaterials, University of Erlangen-Nuremberg, Germany
- 09:30 17-3 **Tri-Culture of Vascular Cells Promotes Vascular Tissue Remodeling**
Caroline Loy, Lucie Levesque, Jayachandran Kizhakkedathu, Diego Mantovani
Lab for Biomaterials and Bioengineering, Laval University, Quebec, Canada
- 09:45 17-4 **Nanofibrous Vascular Grafts Releasing Nitric Oxide**
Jana Horakova, Connor McCarthy, Megan Frost, Jeremy Goldman, David Lukas, Petr Mikes
Department of Nonwovens and Nanofibrous Materials, Technical University of Liberec, Czech Republic

- 10:00 17-5 **Electrospun Silk Fibroin/Gelatin Composite Tubular Matrices as Scaffolds for Small Diameter Blood Vessel Regeneration**
Chiara Marcolin, Valentina Catto, Federica D'Agostino, Serena Bertoldi, Silvia Farè, Maria Cristina Tanzi
 Department of Chimica, Materiali e Ingegneria Chimica "G. Natta", Politecnico di Milano, Italy
- 10:15 17-6 **Design and synthesis of supramolecular biomaterials for in-situ cardiovascular tissue engineering**
Olga JGM Goor, Geert C van Almen and Patricia YW Dankers
 Institute for Complex Molecular Systems, Eindhoven University of Technology, The Netherlands

Imaging I Room 1B, 09:00 - 10:30

Chairs: Julie Gough, University of Manchester
 Gavin Jell, University College London
 Alfredo Ronca, National Research Council of Italy

- 09:00 18-1 **Tissue Response and Degradation of Novel Gelatin-Based Biomaterials in vivo: Insights from Small Animal Multimodal Imaging**
Christoph Tondera, Sandra Ullm, Sebastian Meister, Tim P. Gebauer, Axel T. Neffe, Andreas Lendlein, Jens Pietzsch
 Institute of Radiopharmaceutical Cancer Research, Helmholtz-Zentrum Dresden-Rossendorf, Germany
- 09:15 18-2 **Systemically Injected Gold-Silica Hybrid Nanovectors for Combined Cancer Therapy and Imaging**
Coline Jumeaux, Ciro Chiappini, Rona Chandrawati, Matthew Hembury, Glenna L. Drisko, Cédric Boissière, Clément Sanchez, Alexandra Porter, Molly M. Stevens
 Department of Materials, Imperial College London, London
- 09:30 18-3 **Superparamagnetic Iron Oxide Nanoparticles Stabilized by Dextran Nanogel: New Nanomagnetogel as Contrast Agent for Magnetic Resonance Imaging. Biodistribution**
Catarina Gonçalves, Yoann Lalatonne, Liliana Melro, Giorgio Badino, Miguel Ferreira, Laurence Motte, Carlos Geraldès, José Alberto Martins, F. M. Gama
 Centre for Biological Engineering, Minho University, Braga, Portugal
- 09:45 18-4 **A Non-Toxic Additive to Introduce X-Ray Contrast into Poly(lactic acid)s**
Leo H. Koole, Daniel G. Molin and Yujing Wang
 Department of Biomedical Engineering, Maastricht University, The Netherlands
- 10:00 18-5 **Novel Technique to Map the Biomechanical Properties of Entire Articular Surfaces Using Indentation to Identify Early Osteoarthritis-like Regions**
Sotcheadt Sim, Anik Chevrier, Martin Garon, Eric Quenneville and Michael D. Buschmann
 Biomomentum Inc., Canada
- 10:15 18-6 **Polymer Coating for in vivo MR Visualization of Tissue Reinforcement Prostheses**
X. Garric, S. Blanquer, O. Guillaume, V. Letouzey, L. Lemaire, F. Franconi, R. DeTayrac, J. Coudane
 IBMM, Artificial Biopolymers Group, Montpellier, France

Antimicrobials, Biofilms and Surfaces Symposium, part 1 Room 4, 09:00 - 10:30

Chairs: Steven Percival, Scapa Healthcare
 Sara Svensson, University of Gothenburg
 Kenny Omoniala, De Montford University

- 09:00 19-1 **s. Aureus Evades Leukocyte Antimicrobial and Mesenchymal Stromal/stem Cell Immunomodulatory Functions**
David Antonio Cantu, Warren E. Rose, Peiman Hematti, Weiyan John Kao
 School of Pharmacy, University of Wisconsin-Madison, USA
- 09:15 19-2 **Preparation and Characterisation of an Antibacterial Silver-doped Nanoscale Hydroxyapatite Paste**
Caroline Wilcock, Monazza Fatima, Piergiorgio Gentile, Graham Stafford, Cheryl Miller, Yulia Ryabenkova, Guenter Möbus, Paul Hatton
 Centre for Biomaterials and Tissue Engineering, University of Sheffield, UK
- 09:30 19-3 **Comparisons of the Properties of Linear and Highly-Branched Poly(N-isopropyl acrylamide) with Ligands that Bind Bacteria**
P. Teratanatorn, R. Hoskins, J. Shepherd, K. Swindells, T. Swift, L. Swanson, S. MacNeil, I. Douglas, S. Rimmer
 University of Sheffield, UK
- 09:45 19-4 **Nanoscale Characterization of Cationic Polymeric Brushes and Bacterial Interactions Probed by Force Microscopy**
Merve Gultekinoglu, Yoo Jin Oh, Memed Duman, Peter Hinterdorfer and Kezban Ulubayram
 Faculty of Pharmacy, Hacettepe University, Turkey
- 10:00 19-5 **Effect of pH and Biofilm Formation on Extracellular Matrix Synthesis in Normal and Chronic Wound Fibroblasts**
Eleri M Jones, Steven Percival, Peter Clegg, John A Hunt and Christine A Cochrane
 Institute of Ageing of Chronic Disease, University of Liverpool, UK
- 10:15 19-6 **Hybrid Material (Chitosan Hydrogel/Bioceramic) Loaded with Ciprofloxacin or Simvastatin for Bone Reconstruction**
Claudia Flores, Jean Christophe Hornez, Feng Chai, Gwenaél Raoul, Juergen Siepmann, Joel Ferri, Bernard Martel, H. Frederic Hildebrand, Nicolas Blanchemain
 INSERM U1008, Biomaterials Research Group, University Lille 2, France

Chairs: Liang Yo Yang, Taipei Medical University
Oscar Castaño, Institute for Bioengineering of Catalonia
Thomas Miramond, Biomatlante

- 11:00 20-1 **Development of Bisphosphonate-functionalized Gelatin Nanoparticles for Application in Colloidal Hydrogels for Bone Regeneration**
K. Farbod, J.A. Jansen and S.C.G. Leeuwenburgh
Department of Biomaterials, Radboud University Medical Center, The Netherlands
- 11:15 20-2 **Tough Silica/PCL Hybrid Materials for Tissue Regeneration**
F. Tallia, L. Russo, L. Gabrielli, L. Cipolla, J.R. Jones
Department of Materials, Imperial College London, UK
- 11:30 20-3 **New Gelatine Functionalized Hybrid Sol-gel Coatings for Titanium Implants**
I. Lara-Sáez, M. Martínez-Ibáñez, S. Barros, A. Coso, J. Franco, M. Gurruchaga, J. Suay, I. Goñi
Biomaterials and Tissue Engineering Center, Universitat Politècnica de València, Spain
- 11:45 20-4 **On the Applicability of Magnesium-containing Layered Double Hydroxides as Novel Implant Coating Materials**
Marc D. K. Kieke, Andreas Weizbauer, Franziska Duda, M. Imran Rahim, Philip Dellinger, Stefan Budde, Thilo Flörkemeier, Julia Diekmann, Nils K. Prenzler, Muhammad Badar, Peter P. Müller, Hansjörg Hauser, Sabine Behrens, Kai Möhwald, Friedrich Wilhelm Bach, Hans J. Maier, Thomas Lenarz, Henning Windhagen, Peter Behrens
Institute for Inorganic Chemistry, Leibniz University of Hannover, Germany
- 12:00 20-5 **Fatigue Characterization of Two Bone Cements Tested Using Various Methods over a Range of In Vitro Stress Amplitudes**
E.M. Sheafi and K.E. Tanner
School of Engineering, University of Glasgow, UK
- 12:15 20-6 **Functionalization of Titanium Surfaces with $\alpha\beta 3$ and $\alpha 5\beta 1$ Integrin Selective Peptidomimetics: Influence on Osteoblast-like Cell Behavior**
Roberta Fraioli, Florian Rechenmacher, Stefanie Neubauer, José María Manero, Javier Gil, Horst Kessler, Carlos Mas-Moruno
Biomaterials, Biomechanics and Tissue Engineering Group, Universitat Politècnica de Catalunya, Spain

Biomaterials IV Room 3, 11:00 - 12:30

Chairs: Dietmar Hutmacher, Queensland University of Technology
Rui Reis, University of Minho
Patrik Stenlund, SP Technical Research Institute of Sweden

- 11:00 21-1 **Impact of Different Sterilization Methods on the Structure, Biodegradation and Cell Response of Collagen Scaffolds Designed for Peripheral Nerve Regeneration**
Graziana Monaco, Rahmat Cholas, Luca Salvatore, Marta Madaghiele, Alessandro Sannino
Department of Engineering for Innovation, University of Salento, Italy
- 11:15 21-2 **Artificial Immune Synapses; Nanoscale Control of Immune Cell Activation**
D. Delcassian, D. Depoil, D. Rudnicka, M. Liu, D. M. Davis, M. L. Dustin and I. E. Dunlop
Department of Materials, Imperial College London, UK
- 11:30 21-3 **New Approaches to Control the Host Response to Gold-based Biomaterials**
Guillaume Le Saux, Annabelle Tanga, Laurent Plawinski, Sylvain Nlate, Jean Ripoché and Marie-Christine Durrieu
Institute of Chemistry & Biology of Membranes & Nanoobjects (UMR 5248), Université Bordeaux, France
- 11:45 21-4 **Influence of Hyaluronic Acid Molecular Weight on the Biocompatibility of Chitosan/Hyaluronic Acid Multilayer Film**
Jing Jing, Aurélie Moniot, Céline Mongaret, Saad Mechiche-Alami, Romain Reynaud, Frédéric Velard, Sophie C. Gangloff, Loic Jerry, Fouzia Boulmedais and Halima Kerdjoudj
EA 4691 "Biomatériaux et inflammation en site osseux", Université de Reims Champagne-Ardenne, France
- 12:00 21-5 **Cytotoxicity of Functionalized Ggraphene to Osteoblast-like Cells**
Anke Bernstein, Dirk Heinrich, Norbert P. Südkamp, Hermann O. Mayr, Michael Seidenstücker, Ralf Thoman, Markus Stürzel, Rolf Mülhaupt
Department of Orthopedic and Trauma Surgery, Albert Ludwig University of Freiburg, Germany
- 12:15 21-6 **Subcutaneous Evaluation Of a Novel Pro-angiogenic Biomaterial For In Situ Bone Tissue Engineering Applications**
Hugo Oliveira, Nadege Sachot, Sylvain Catros, Sylvie Rey, Oscar Castano, Joëlle Amedee, Elisabeth Engel
Inserm U1026, Tissue Bioengineering, University Bordeaux Segalen, France

Cardiovascular II: TECAS-ITN Room 11, 11:00 - 12:30

Chairs: Dimosthenis Mavrilas, University of Patras
Petra Mela, RWTH Aachen

- 11:00 22-1 **Gene Targeting Nanoparticles to Mediate Proliferation and Migration of Human Vascular Endothelial Cells**
Yakai Feng, Juan Lv, Jing Yang and Changcan Shi
School of Chemical Engineering and Technology, Tianjin University, China
- 11:15 22-2 **Developing Multi-layered Vascular Grafts from a Novel Collagen and Elastin Biomaterial**
Alan J. Ryan, Fergal J. O'Brien
Tissue Engineering Research Group, Royal College of Surgeons in Ireland
- 11:30 22-3 **Elastomeric Biomaterials of Enhanced Microbiological and Mechanical Performance for Heart Assisting Devices**
A. Piegat, M. Piatek-Hnat, Z. Staniszewski, R. Kustosz, M. Gonsior, M. El Fray
West Pomeranian University of Technology, Szczecin, Poland
- 11:45 22-4 **Supercritical Carbon Dioxide (sc-CO₂) Assisted Decellularisation of Aorta**
Selcan Guler, Pezhman Hosseinian, Esin Akbay, Mehmet Ali Onur, Halil Murat Aydin
Bioengineering Division, Hacettepe University, Ankara, Turkey

- 12:00 22-5 **Hemocompatibility Assessment of Uncoated and Heparin Coated Styrenic Block Copolymers for Cardiovascular Applications**
Jacob Brubert, Joanna Stasiak, Geoff Moggridge and Hans Peter Wendel
 Department of Chemical Engineering and Biotechnology, University of Cambridge, UK
- 12:15 22-6 **Capillary Morphogenesis of Primary Endothelial Mono- and Co-cultures in starPEG-Heparin Hydrogels for Controlled Vascularization**
Uwe Freudenberg, Karolina Chwalek, Mikhail V. Tsurkan, and Carsten Werner
 Leibniz Institute of Polymer Research Dresden (IPF), Max Bergmann Center of Biomaterials, Dresden, Germany

Meaning of Surface Charge for Characterisation Symposium Room 1B, 11:00 - 12:30

Chairs: Christine Körner, Anton Paar GmbH

- 11:00 23-1 **The Zeta Potential as Indicator for Solid Surface Charge**
Christine Körner and Thomas Luxbacher
 Anton Paar GmbH, Austria
- 11:30 23-2 **Zeta Potential: a Useful Tool to Interpret the Hydrothermally Treated Titanium Behaviour as Biomaterial**
Martina Lorenzetti, Thomas Luxbacher, Spomenka Kobe and Saša Novak
 Department of Nanostructured Materials, Jožef Stefan Institute, Ljubljana, Slovenia
- 12:00 23-3 **The Role of Porosity on the Z-Potential of Calcium Phosphate Cements**
Montserrat Espanol, Gemma Mestres, Thomas Luxbacher and Maria-Pau Ginebra
 Department of Materials Science and Metallurgical Engineering, Technical University of Catalonia, Spain

Antimicrobials, Biofilms and Surfaces Symposium, part 2 Room 4, 11:00 - 12:30

Chairs: Steven Percival, Scapa Healthcare
 Sara Svensson, University of Gothenburg
 Kenny Omoniala, De Montford University

- 11:00 24-1 **The Effect of Surface Oxygen Functional Groups on Parylene C Biocompatibility - Comparison of MG-63 Cells Adhesion and Bacteria Strains Attachment**
M. Góda-Cepa, M. Brzychczy-Włoch, K. Envall, A. Kotarba
 Faculty of Chemistry, Jagiellonian University, Krakow, Poland
- 11:15 24-2 **Coating Nonwoven Polyester Textile Antibacterial Wound Dressing**
François Aubert-Viard, Oumaira Rahmouni, Adeline Martin, Feng Chai, Nicolas Tabary, Christel Neut, Bernard Martel and Nicolas Blanchemain
 INSERM U1008, Biomaterial Research Group, University Lille 2, France
- 11:30 24-3 **Keratinocyte and Fibroblast Adhesion on an Antibacterial Peptide Surface Coating**
A. Leong, M. Willcox
 School of Optometry and Vision Science, UNSW, Sydney, Australia
- 11:45 24-4 **Blood Compatible Antimicrobial Polymers with Degradable Backbone**
K. Fukushima, K. Kishi, Y. Inoue, C. Sato, A. Sasaki and M. Tanaka
 Department of Polymer Science and Engineering, Yamagata University, Japan
- 12:00 24-5 **Combinatorial Approach to Composition-Structure-Property Relationships in an Antibacterial Ag-Ti Thin Film**
Erik Unosson, Daniel Rodriguez, Ken Welch, Håkan Engqvist
 Department of Engineering Sciences, Uppsala University, Sweden
- 12:15 24-6 **Biofilms Bioreactors: An Infection concern in Medical Devices and biomaterials**
Steven L Percival, Rebecca Booth and Sean Kelly
 Institute of Ageing and Chronic Disease, University of Liverpool, UK

Materials for the Future: University of Liverpool Outreach Event Hall 1, 16:00 - 19:30

Chair: John Hunt, University of Liverpool

This outreach event will introduce a series of world-expert speakers who will present some of the issues for providing new materials, in a sustainable manner, to meet the needs of an ageing and ever-increasing population. The speakers will provide insight into how new research is providing diverse material solutions such as nano-medicines, stem cell therapies, and high performing next generation medical implants. Delegates will include the ESB 2014 delegation and then also University of Liverpool academics, alumni, industry partners, and civic leaders. The afternoon will showcase world-leading research from the University of Liverpool. There will be a series of talks from:

- 16:10 **Anthony Hollander**, University of Liverpool
- 16:25 **Steve Rannard**, University of Liverpool
- 16:40 **Chris Sutcliffe**, University of Liverpool
- 16:55 **Raphael Levy**, University of Liverpool
- 17:40 **Stephen Minger**, GE Healthcare
- 18:05 **Molly Shoichet**, University of Toronto
- 18:30 **Joachim Kohn**, Rutgers University
- 18:55 **David Williams**, Wake Forest Institute of Regenerative Medicine

Biomaterials V Room 3, 16:00 - 18:00

Chairs: James Anderson, Case Western Reserve University
Veronique Migonney, Université Paris XIII
Gloria Huerta-Angeles, Contipro Pharma

- 16:00 26-1 **Formation of Multicellular Spheroids on Arrayed Microwells with Microstructure**
Masahito Ban, Yuuya Kogi
Graduate School, Nippon Institute of Technology, Japan
- 16:15 26-2 **The Role of CD68-Positive Macrophages in the Biocompatibility of Biomaterials a Peritoneal Adhesion Prevention Model**
Christoph Brochhausen, *Volker H. Schmitt*, *Andreas Mamilos*, *Constanze N. E. Planck*, *Bernhard Krämer*, *Taufiek K. Rajab*, *Helmut Hierlemann*, *Heinrich Planck*, *C. James Kirkpatrick*
Institute of Pathology, University Medical Centre Mainz, Germany
- 16:30 26-3 **Swelling Gradients of Multilayers Mediate Directional Cell Migration**
Lulu Han, *Zhengwei Mao*, *Jindan Wu*, *Yang Guo*, *Tanchen Ren*, *Changyou Gao*
MOE Key Laboratory of Macromolecular Synthesis and Functionalization, Zhejiang University, China
- 16:45 26-4 **Improvement of Graphene Nanoplatelet Biocompatibility by Surface Oxidation**
Artur Pinto, *Carolina Gonçalves*, *Daniela Sousa*, *Agostinho Moreira*, *Inês Gonçalves*, *Fernão Magalhães*
LEPABE, Faculdade de Engenharia, Universidade do Porto, Portugal
- 17:00 26-5 **Ibuprofen-Loaded Scaffolds for Spinal Cord Injury Regeneration – Targeting RhoA at the Lesion Site**
Liliana R Pires, *Cátia DF Lopes*, *Daniela N Rocha*, *Luigi Ambrosio*, *Mónica M Sousa*, *Ana Paula Pêgo*
INEB – Instituto de Engenharia Biomédica, Universidade do Porto, Portugal
- 17:15 26-6 **A Role for Platelet CD154 in the Foreign Body Reaction to Biomaterial**
Annabelle Tanga, *Sébastien Lepreux*, *Julien Villeneuve*, *Nelly Bordeau*, *Christian Combe*, *Alexis Desmoulière*, *Shahram Ghanaati*, *Jean Ripoche*
INSERM U1026, Bordeaux University, France
- 17:30 26-7 **The Mechanical Behavior and Biocompatibility of Polymer Blends for Patent Ductus Arteriosus (PDA) Occlusion Device**
Ying Ying Huang, *Yee Shan Wong* and *Subbu S. Venkatraman*
School of Materials Science and Engineering, Nanyang Technological University, Singapore
- 17:45 26-8 **Hydrolytic and Oxidative Degradation of Electrospun Supramolecular Biomaterials: In Vitro Degradation Pathways**
M. Brugmans, *S. Sontjens*, *M. Rubbens*, *A. Nandakumar*, *A. Bosman*, *T. Mes*, *H. Janssen*, *C. Bouten*, *F. Baaijens* and *A. Driessen-Mol*
Xeltis B.V., Eindhoven, The Netherlands

European Orthopaedic Research Society Symposium Room 11, 16:00 - 18:00

Chairs: Geoff Richards, AO Foundation
Thomas Miramond, Biomatlante
Sujit Kootala, Uppsala University

- 16:00 27-1 **Incorporation of RANKL Promotes Osteoclast Formation and Osteoclast Activity on β -TCP Ceramics**
J. Choy, *C.E. Albers*, *K.A. Siebenrock*, *S. Dolder*, *W. Hofstetter*, *F.M. Klenke*
Department of Clinical Research, University of Bern, Switzerland
- 16:15 27-2 **Calcium Phosphate Graft Substitute: When the Impact of Innovation is in the Form Rather Than Content**
Francisco Braga, *Antonio Carlos da Silva*, *Sérgio Allegrini*, *Cyro Ottoni*
CCTM/IPEN, CNEN, Brazil

- 16:30 27-3 **EPA-Coated Implants Promote Osteoconduction in White New Zealand Rabbits**
Ammar Mustafa, Christie Lung, Jukka Matinlinna
ISF Consultancy Hospital (Lekhwiya), Doha, Qatar
- 16:45 27-4 **Tailored Ca²⁺ Release in Hybrid Fibrous Scaffolds for Efficient Osteo- and Angiogenesis**
Oscar Castaño, Nadège Sachot, Elena Xuriguera, Elisabeth Engel, Josep A. Planell, Jeong-Hui Park, Guang-Zhen Jin, Tae-Hyun Kim, Joong-Hyun Kim and Hae-Won Kim
Institute for Bioengineering of Catalonia, Barcelona, Spain
- 17:00 27-5 **The Wear and Biological Activity of Antioxidant UHMWPEs in Total Hip Replacements**
Nic Gowland, Sophie Williams, John Fisher, Joanne L Tipper
Institute of Medical & Biological Engineering, University of Leeds, UK
- 17:15 27-6 **Chitosan-Hyaluronic Acid Based Porous Scaffold for Bone Regeneration**
Jing Jing, Jérôme Josse, Céline Mongaret, Saad Mechiche-Alami, Romain Reynaud, Dominique Laurent-Maquin, Sophie C. Gangloff, Frédéric Velard and Halima Kerdjoudj
EA 4691 "Biomatériaux et inflammation en site osseux", Université de Reims Champagne-Ardenne, France
- 17:30 27-7 **Superficial Zn-Doping into Biomaterials is Better than Bulk Doping**
Yugin Qiao and Xuanyong Liu
State Key Laboratory of High Performance Ceramics and Superfine Microstructure, Shanghai Institute of Ceramics, China
- 17:45 27-8 **Assessment of the Biodegradability of Ultrafine PCL Fibers Reinforced Calcium Phosphate Cement**
Yi Zuo, Boyuan Yang, Fang Yang, Qin Zou, Jidong Li, *Yubao Li* and J.A.Jansen
Research Center for nano Biomaterials, Sichuan University, China

Drug Delivery III Room 1B, 16:00 - 18:00

- Chairs:** M Cristina Tanzi, Politecnico di Milano
Yan Yan Shery Huang, University of Cambridge
Alfredo Ronca, National Research Council of Italy
- 16:00 28-1 **Biocomposites Containing Collagen, D-Amino Acids and Phytosome Nanoparticles as Drug Carriers and Tissue Engineering Scaffolds**
Krishnamoorthy Ganesan, Thotappalli Parvathaleswara Sastry, Asit Baran Mandal and Mukesh Doble
CSIR-Central Leather Research Institute, Tamil Nadu, India
- 16:15 28-2 **Supramolecular Anticancer Nanostructures Formed via Self-Assembly of Curcumin Amphiphiles**
Koji Nagahama, Naho Oyama and Takayuki Kumano
Department of Nanobiochemistry, Konan University, Japan
- 16:30 28-3 **Silica/Collagen Nanocomposites for Local and Sustained Release of Therapeutic Biomolecules**
Xiaolin Wang, Christophe Hélaré and Thibaud Coradin
Sorbonne Université, Paris, France
- 16:45 28-4 **Biomimetic Thin Films as Reservoirs for BMP-2**
Flora Gilde, Raphael Guillot, Laure Fourel, Ofelia Maniti, Thomas Boudou, Corinne Albigès-Rizo and Catherine Picart
UMR 5628 (LMGP), Grenoble Institute of Technology, France
- 17:00 28-5 **Novel Tool in Nanomedicine: Completely Biocompatible and Biodegradable Superparamagnetic Hydroxyapatite Nanoparticles**
S. Panzeri, M. Montesi, M. Sandri, E. Savini, M. Iafisco, A. Adamiano, M. Ghetti, G. Cenacchi, A. Tampieri
Institute of Science and Technology for Ceramics, National Research Council, Faenza (RA), Italy
- 17:15 28-6 **Antioxidant Delivery for Inhibition of Angiogenesis**
Masaki Moriyama, Stéphanie Metzger, Martin Ehrbar, André J. van der Vlies, Hiroshi Uyama and Urara Hasegawa
Graduate School of Engineering, Osaka University, JAPAN
- 17:30 28-7 **Design of Biodegradable pH-Responsive Microgels as Targeted Drug Delivery System**
Miren K. Aiertza, Pablo Casuso, Adrián Pérez-San Vicente, Hans-Jürgen Grande, Germán Cabañero, Irida Loinaz and Damien Dupin
Biomaterials Unit, IK4-CIDETEC, Spain
- 17:45 28-8 **A Biotemplating Approach Using the Marine Diatom for Fabricating Drug Delivery Reservoirs**
J. Chao, Y. Lang, A. Abdul-Rahman, M. Biggs, A. Pandit
Network of Excellence for Functional Biomaterials (NFB), National University of Ireland, Galway, Ireland

Biomaterials VI Room 1C, 16:00 - 18:00

- Chairs:** Mario Barbosa, University of Porto
Paul Santerre, University of Toronto
Pedro Granja, University of Porto
- 16:00 29-1 **Effect of Mesoscale Structure on the Properties of Composite Scaffold: from Micro to Nano**
Limei Li, Yi Zuo, Jidong Li, and *Yubao Li*
Research Center for nano Biomaterials, Sichuan University, China
- 16:30 29-2 **Factors Influencing Injectability of Nano-Hydroxyapatite Paste: a Rheological Behaviour**
Yulia Ryabenkova, Guenter Moebus, Paul V Hatton, Cheryl A Miller
Department of Materials Science and Engineering, University of Sheffield, UK
- 16:45 29-3 **Designing Biodegradable and Biocompatible Crosslinked Film from Polycarbonate Urethane and Zwitterionic Polynorbornene as Cell Growth Substrate**
Yakai Feng, Musamir Khan, Juan Lv, Jing Yang and Gregory Tew
School of Chemical Engineering and Technology, Tianjin University, China

- 17:00 29-4 **Periodic Mesoporous Organosilica (PMO) Coatings for Biomedical Applications**
Natalja Wendt, Mandy Jahns, Nina Ehler, Sabrina Schlie, Boris Chichkov, Peter Behrens
 Institut für Anorganische Chemie, Leibniz Universität Hannover, Germany
- 17:15 29-5 **Polymer Based Scaffolds with Microwave Induced Porosity**
 Antonella Giuri, Vincenzo Maria De Benedictis, Maria Grazia Raucci, *Christian Demitri*, Alessandro Sannino
 Department of Engineering for Innovation, University of Salento, Lecce, Italy
- 17:30 29-6 **Fabrication of Carbonate Apatite Coated Calcite and its In Vivo Evaluation**
Kunio Ishikawa, Kanji Tsuru, Melvin L. Munar, Masako Fujioka-Kobayashi, Youji Miyamoto
 Department of Biomaterials/Faculty of Dental Science, Kyushu University, Japan
- 17:45 29-7 **Polysaccharide Based Nanocarriers for Antioxidants**
 Ornella Bossio, Laura G. Gómez-Mascaraque, Mar Fernández-Gutiérrez, Blanca Vázquez-Lasa, *Julio San Román*
 Institute of Polymer Science and Technology, CSIC, Madrid, Spain

Antimicrobials, Biofilms and Surfaces Symposium, part 3 Room 4, 16:00 - 18:00

Chairs: Steven Percival, Scapa Healthcare
 Kazuki Fukushima, Yamagata University
 Alma Akhmetova, Nazarbayev University

- 16:00 30-1 **Effect of Kassinin and Collagen Fibrils on Cell Spreading and De-adhesion Dynamics**
Edna George, Pradeep Kumar Singh, Samir Maji and Shamik Sen
 Department of Bioscience & Bioengineering, Indian Institute of Technology (IITB), India
- 16:15 30-2 **Fast Acting Antibacterial 45S5 Bioglass® Scaffolds Reinforced with Gelatin/Genipin for Bone Tissue Engineering**
Wei Li, Hui Wang, Seema Agarwal and Aldo Boccaccini
 Institute of Biomaterials, University of Erlangen-Nuremberg, Germany
- 16:30 30-3 **Living Biointerfaces Based on Non-Pathogenic Bacteria to Direct Cell Function**
 Aleixandre Rodrigo-Navarro, Patricia Rico, Anas Saadeddin, Andres J. Garcia, *Manuel Salmeron-Sanchez*
 Division of Biomedical Engineering, University of Glasgow, UK
- 16:45 30-4 **Self-Disinfecting Urinary Biomaterials: pH-Triggered Quinolone Release for Prevention of Catheter-Associated Urinary Tract Infections**
 Colin P. McCoy, *Nicola J. Irwin*, Christopher Brady, Louise Carson, David S. Jones, Sean P. Gorman
 School of Pharmacy, Queen's University Belfast, UK
- 17:00 30-5 **Apatite Promoting, Low Modulus Composite Bone Cements with Low Heat Generation upon Set and High Subsequent Antibacterial Release**
Muhammad Adnan Khan, Anne Young
 UCL, Eastman Dental Institute, London
- 17:15 30-6 **Toward Potent Antibiofilm Degradable Medical Devices: Generic Methodologies for the Surface Modification of Polylactide**
Benjamin Nottelet, Carla Sardo, Sarah El Habnoui, Xavier Garric, Vincent Darcos, Jean-Philippe Lavigne, Gennara Cavallaro and Jean Coudane
 Institute of Biomolecules Max Mousseron (IBMM - CNRS UMR 5247), Université Montpellier I, France
- 17:30 30-7 **Controlled Release of Gentamicin from Gold Nanocarriers**
 Stefano Perni and *Polina Prokopovich*
 School of Pharmacy and Pharmaceutical Sciences, Cardiff University, UK
- 17:45 30-8 **Plasma Nanofilm as Biocompatible and Antibacterial Coating for Biomaterials**
Michael Bergmann, Sebastian Lickert, Loic Ledernez, Gregory Dame and Gerald Urban
 Department of Microsystems Engineering, Albert-Ludwigs-University of Freiburg, Germany

Chairs: Paul Hatton, University of Sheffield
Maria Grazia Raucci, National Research Council of Italy
Marco Lopez, University of Marburg

- 09:00 31-1 **Fluoride-Containing Bioactive Glasses – from Structure to Cell Compatibility**
D. S. Brauer, E. Gentleman, R. G. Hill and N. Karpukhina
Otto Schott Institute of Materials Research, Friedrich Schiller University Jena, Germany
- 09:15 31-2 **Atomic Structure of Mg-Based Metallic Glasses for Biomedicine**
Jamieson Christie
Department of Chemistry, University College London, K
- 09:30 31-3 **Bioactive Glass Nanoparticles for Therapeutic Applications and Incorporation into Hybrids for Bone Regeneration**
Sarah Greasley, Jesse V. Jokerst, Sanjiv S. Gambhir, Alexandra E. Porter, Julian R. Jones
Department of Materials, Imperial College London, UK
- 09:45 31-4 **Antitumor Efficacy of Radioactive Holmium (166Ho) Containing Silica Sol-gel Glass Granules on Osteosarcoma (MG-63) and Breast Cancer (MCF-7) Cells in Vitro**
Riku Alaranta, Jessica J Alm, Kaisa Lehtimäki, Heimo Ylänen, Tapio Ollonqvist and Hannu T Aro
Orthopaedic Research Unit, University of Turku, Finland
- 10:00 31-5 **Hybrid PLGA/Bioactive Glass Fiber Scaffolds for Bone Tissue Engineering**
Anne-Marie Haaparanta, Timo Lehtonen, Ville Ellä, Peter Uppstu, Markus Hannula, Ari Rosling and Minna Kellomäki
Biomaterials and Tissue Engineering Group, Tampere University of Technology, Finland
- 10:15 31-6 **Development of Novel 45S5 Bioglass® Scaffolds with Fibrous Surface Morphology using Electroflooding Technology for Bone Tissue Engineering**
Preethi Balasubramanian and Aldo R Boccaccini
Institute of Biomaterials, University of Erlangen-Nuremberg, Germany

Translational Research Symposium, part 1 Room 3, 09:00 - 10:30

Chairs: Marc Bohner, RMS Foundation
David Eglin, AO Foundation
Yves Bayon, Covidien

- 09:00 32-1 **Translation of Science to the Clinic: Where Preclinical Research Fits in the Model**
R. Geoff Richards
AO Research Institute Davos, Switzerland
- 09:30 32-2 **Innovation and Product Development in a Changing Regulatory and Socio-economical Environment**
Andrea Montali
DePuy Synthes Biomaterials R&D, Oberdorf, Switzerland
- 10:00 32-3 **Development of Dedicated Tools for Personalization of Medical Devices**
Lara Vigneron, Daniel Daryaie, Sebastian De Boodt, Lars Neumann
Biomedical Engineering Department, Materialise NV, Belgium

Tissue Engineering III Room 11, 09:00 - 10:30

Chairs: Guy Daculsi, University of Nantes
Pamela Habibovic, University of Twente
Nina Parmar, University College London

- 09:00 33-1 **Modulation of Cell Microenvironment Using Macromolecular Crowding: A Self Assembly Approach Towards In Vitro Organogenesis**
Abhigyan Satyam, Pramod Kumar, Xingliang Fan, Yury Rochev, Lokesh Joshi, Héctor Peinado, David Lyden, Benjamin Thomas, Brian Rodriguez, Michael Raghunath, Abhay Pandit and Dimitrios Zeugolis
Network of Excellence for Functional Biomaterials, National University of Ireland Galway, Ireland
- 09:15 33-2 **Collagen Plasma Treatment of Poly-(ether-ether)-ketone for Improved Cell Attachment**
Jessica S Hayes, Declan M Devine, Mary Murphy
Orthobiologics, Regenerative Medicine Institute, National University in Galway, Ireland
- 09:30 33-3 **PCL/HA Functional Gradient Scaffold for Osteochondral Tissue Engineering Applications**
Alessandra Marrella and Silvia Scaaglione
National Research Council (CNR), IEIT Institute, Italy
- 09:45 33-4 **Self-assembled Peptide Gels for Intervertebral Disc Tissue Engineering**
Simon Wan, Alberto Saiani, Stephen Richardson, Julie Gough
School of Materials, University of Manchester, UK
- 10:00 33-5 **Utilizing Multifunctional Alginate Scaffolds for the Regeneration of Skeletal Muscle Defects in a Rat Crush Trauma Model**
Taimoor Qazi, Matthias Pumberger, Tobias Winkler, Sven Geißler, David Mooney, Georg Duda
Julius Wolff Institute, Charité - Universitätsmedizin Berlin, Germany
- 10:15 33-6 **Engineering Hydrogel Polymer Networks for Cell Microencapsulation and Xenotransplantation**
Françoise Borcard, Redouan Mahou, Virginia Crivelli, Elisa Montanari, Raphael P. H. Meier, Yannick Müller, Annalena Bollinger, Carmen Gonelle-Gispert, Jörg D. Seebach, Raphael Plüss, Sandrine Gerber, Léo Bühler, Christine Wandrey
Institut d'Ingénierie Biologique et Institut des Sciences et Ingénierie Chimiques, Ecole Polytechnique Fédérale de Lausanne, Switzerland

Chairs: Keng-Liang Ou, Taipei Medical University
Serena Best, University of Cambridge
John Choy, University of Bern

- 09:00 34-1 **Development of Osteoconductive Organic-Inorganic Hybrid Materials Based on Calcium Silicates**
Chikara Ohtsuki, Toshiki Miyazaki and Masakazu Kawashita
Graduate School of Engineering, Nagoya University, Japan
- 09:15 34-2 **Formation of hybrid materials based on calcium phosphate deposit on carbon fiber scaffold**
Q. Picard, S. Delpeux, J. Chancolon, N. Rochet, F. Fayon, F. Warmont, S. Mikhalovski, S. Bonnamy
CRMD, CNRS, University of Orléans, France
- 09:30 34-3 **Strontium Ion Release from Bioactive Ti Alloys with Ca enriched-Surface Layer**
Seiji Yamaguchi, Tomiharu Matsushita and Tadashi Kokubo
Department of Biomedical Sciences, Chubu University, Japan
- 09:45 34-4 **Cell-to-cell Communications of Osteocytes with Bone Marrow Cells on Ceramic Biomaterials**
Miho Nakamura, Teuvo Hentunen, Jukka Vääräniemi, Jukka Salonen, Naoko Hori and Kimihiro Yamashita
Institute of Biomaterials and Bioengineering, Tokyo Medical and Dental University
- 10:00 34-5 **Critical Bone Defect Filling with Chitosan/Hydroxyapatite Hybrid Scaffolds in Rats**
Valérie Brun, Christine Guillaume, Julien Braux, Richard Gouron, Romuald Mentaverri, Saad Mechiche Alami, Sylvie Bouthors, Dominique Laurent-Maquin, Sophie C. Gangloff, Halima Kerdjoudj, Frédéric Velard
EA 4691 BIOS, University of Reims Champagne-Ardenne, France
- 10:15 34-6 **Fibrinogen Implants for Bone Regeneration: Short- and Long-Term In Vivo Responses**
Daniel M. Vasconcelos, Raquel M. Gonçalves, Susana G. Santos, Catarina R. Almeida, Inês Odila, Marta I. Oliveira, Nuno Neves, Andreia M. Silva, António C. Ribeiro, Elisabeth Seebach, Katharina L. Kynast, Thomas Niemietz, Wiltrud Richter, Meriem Lamghari, Mário A. Barbosa
INEB, University of Porto, Portugal

Stem Cells III Room 1C, 09:00 - 10:30

Chairs: Molly Shoichet, University of Toronto
Manuel Salmeron-Sanchez, University of Glasgow
Anna Guildford, University of Brighton

- 09:00 35-1 **Nanoscale Control of Mesenchymal Stem Cells**
Matthew J Dalby, P Monica Tsimbouri, Laura McNamara, Enateri Alakpa, Lesley-Anne Turner, Rebecca McMurray, Louisa CY Lee, Jingli Yang, Habib Nikukar, Gabriel Pemberton, Terje Sjoström, Peter Childs, Jugal Sahoo, Vineetha Jayawarna, Christopher West, Karl Burgess, Stuart Reid, Bo Su, Maggie Cusack, Nikolaj Gadegaard, Rein V Ulijn, RM Dominic Meek, Bruno Peault, Richard OC Oreffo
Centre for Cell Engineering, University of Glasgow, UK
- 09:30 35-2 **Photo-Crosslinkable Biopolymers Targeting Stem Cell Differentiation: the Candidature of Gelatin**
Ine Van Nieuwenhove, Sandra Van Vlierberghe, Winnok De Vos, Achim Salamon, Kirsten Peters and Peter Dubruel
Polymer Chemistry and Biomaterials Group, Ghent University, Belgium
- 09:45 35-3 **Investigating the "Bone-Shell Divide": Pearl Oyster Shell Topography as a Means of Directing Stem Cell Behaviour**
Enateri V. Alakpa, Matthew J. Dalby and Maggie Cusack
Centre for Cell Engineering, University of Glasgow, UK
- 10:00 35-4 **Generation of 3D Functional Microvascular Networks with Mural Cell-Like Human Mesenchymal Stem Cells in Microfluidic Systems**
S. Bersini, J. Jeon, RD Kamm and M. Moretti
IRCCS Istituto Ortopedico Galeazzi, Milan, Italy
- 10:15 35-5 **Atmospheric Pressure Plasma Treatment Increases the Attachment and Maturation of Human Pluripotent Stem Cell Derived Retinal Pigment Epithelial Cells on Biodegradable Polymeric Electrospun Scaffolds**
A. Sorkio, P. Porter, K. Juuti-Uusitalo, B. Meenan, H. Skottman and G. Burke
BioMediTech, University of Tampere, Finland

UKSB I: Welcome & President's Prize Room 4, 09:00 - 10:30

Chairs: Adrian Boyd, University of Ulster
Colin Scothford, University of Nottingham

- 09:00 **Welcome and Introduction to the UKSB Annual Meeting**
Sanjiv Deb
King's College London, UK
- 09:30 36-1 **The Drive for Simplicity in Delivering Cells to the Clinic - Clever Cells and Dumb Scaffolds**
Sheila MacNeil
Department of Materials Science & Engineering, University of Sheffield, UK

Chairs: Paul Hatton, University of Sheffield
 Maria Grazia Raucchi, National Research Council of Italy
 Muhammad Hasan, Dalhousie University

- 11:00 37-1 **Functionalising Natural Polymers with Alkoxysilane Coupling Agents for Tissue Engineering Applications**
Louise S Connell, Frederik Romer, Oliver Mahony, Mark E Smith, John V Hanna and Julian R Jones
 Department of Materials, Imperial College London, UK
- 11:15 37-2 **Composition-Structure-Property Relationships for Strontium Borate Glasses for Biomedical Applications**
Muhammad Sami Hasan and Daniel Boyd
 Department of Applied Oral Sciences, Dalhousie University, Halifax, NS, Canada
- 11:30 37-3 **Unravelling the Structure of Bioglass® through the Application of Diffraction Techniques**
Richard Martin
 School of Engineering & Aston Research Centre for Healthy Ageing, Aston University, UK
- 11:45 37-4 **Surface Functionalisation of Sol-Gel-Based Bioactive Glass Scaffolds for Drug Delivery**
A. Philippart, A. M. Beltrán, L. Pontiroli, C. Vitale-Brovarone, E. Spiecker and A. R. Boccaccini
 Institute of Biomaterials, University Erlangen-Nürnberg, Germany
- 12:00 37-5 **In Vitro Assessment of 3D Printed Wollastonite – Apatite-Based Glass Ceramic Biomaterials**
M.A. Lopez-Heredia, A. Zocca, C. Gomes, J. Günster, R. Gildenhaar, P. Colombo and C. Knabe-Ducheyne
 Dept. of Experimental Orofacial Medicine, Philipps University, Marburg, Germany
- 12:15 37-6 **Fabrication and Characterization of Electrospun PHB/PCL/Sol-gel Derived Glass Hybrid Scaffolds**
Yaping Ding, Teresa Müller, Judith A. Roether, Dirk W. Schubert, Aldo R. Boccaccini
 Institute of Polymer Materials, University of Erlangen-Nuremberg, Germany

Translational Research Symposium, part 2 Room 3, 11:00 - 12:30

Chairs: Marc Bohner, RMS Foundation
 David Eglin, AO Foundation
 Yves Bayon, Covidien

- 11:00 38-1 **Development of a Competitive Calcium Phosphate Cement in a Crowded Marketplace**
Philip Procter
 Medical Device Industry Consultant, Divonne les Bains, France
- 11:30 38-2 **The Commercial and Clinical Challenges and Opportunities for Advanced Materials in Regenerative Medicine**
Kevin M Shakesheff
 School of Pharmacy, University of Nottingham, UK
- 12:00 38-3 **Stratification and Personalisation of Biomaterials and Medical Devices in Musculoskeletal Disease**
John Fisher
 Institute of Medical and Biological Engineering, University of Leeds, UK

Tissue Engineering IV Room 11, 11:00 - 12:30

Chairs: Guy Daculsi, University of Nantes
 Pamela Habibovic, University of Twente
 Nina Parmar, University College London

- 11:00 39-1 **Layer-by-Layer Assembly of Collagen and Fibronectin for Tissue Engineering Applications**
Sara Mauquoy and Christine Dupont-Gillain
 Institute of Condensed Matter and Nanosciences (IMCN), Université Catholique de Louvain, Belgium
- 11:15 39-2 **Alginate-Silica Hybrid Hydrogels Through Covalent Coupling with APTES**
Yuliya Vueva, Siwei Li, Frederik Romer, John V. Hanna, Julian R. Jones
 Department of Materials, Imperial College London, UK
- 11:30 39-3 **The Effects of Current Density on the Morphology, Electrochemical and Biological Characteristics of Poly(3,4ethylenedioxythiophene): Poly(styrenesulfonate) (PEDOT-PSS) Conducting Films**
Catalina Vallejo-Giraldo, Abhay Pandit, Manus Jonathan Paul Biggs
 Network of Excellence for Functional Biomaterials (NFB), National University of Ireland, Galway, Ireland
- 11:45 39-4 **Biomimetic Scaffolds for Annulus Fibrosus Regeneration**
Sébastien B.G. Blanquer, Arjen W.H. Gebraad, Suvi P. Haimi, Susanna Miettinen, André A. Poot and Dirk W. Grijpma
 Dept. of Biomaterials Science and Technology, University of Twente, Enschede, The Netherlands
- 12:00 39-5 **Development of Bioamine Cross-linked Gellan Gum Hydrogels as Soft Scaffolds for Neural Tissue Engineering**
J. Koivisto, Sh. Teymouri, J.E. Parraga, T.O. Ihalaainen, K. Aalto-Setälä, M. Kellomäki
 Laboratory for Biomaterials and Tissue Engineering, Tampere University of Technology, Finland
- 12:15 39-6 **Thermoresponsive Self-Setting Calcium Phosphate Pastes for Minimally Invasive Surgery and Solid Freeform Fabrication**
Yassine Maazouz, Edgar Montufar, Julien Malbert, Maria-Pau Ginebra
 Dept. Materials Science and Metallurgical Engineering, Technical University of Catalonia, Barcelona, Spain

Chairs: Keng-Liang Ou, Taipei Medical University
Matteo Santin, University of Brighton
John Choy, University of Bern

- 11:00 40-1 **Cholecalciferol Synthesized After UV-Activation of 7-Dehydrocholesterol onto Titanium Implants Inhibits Osteoclastogenesis In Vitro**
María Satué, Joana M. Ramis and Marta Monjo
Group of Cell Therapy and Tissue Engineering, University of the Balearic Islands, Spain
- 11:15 40-2 **Mapping Phase Changes in Brushite Cements**
A. Bannerman, R.L. Williams and L.M. Grover
School of Chemical Engineering, University of Birmingham, UK
- 11:30 40-3 **Biomaterial Induced Bone Nodules without Medium Supplements**
S. Mechiche Alami, J. Hemmerlé, F. Boulmedais, J. Josse, P. Schaaf, S.C. Gangloff, F. Velard, D. Laurent-Maquin, H. Kerdjoudj
EA 4691 "Biomatériaux et inflammation en site osseux", Université de Reims Champagne-Ardenne, France
- 11:45 40-4 **Fibronectin Loaded Hydroxyapatite for Reduced Healing Time on Osteoporotic Rabbit Bone**
Javier Quintana-Plaza, Luis M. Rodríguez-Lorenzo
Polymeric nanomaterials and Biomaterials/ICTP-CSIC, Madrid, Spain
- 12:00 40-5 **Mineralization of Phosphate Prestructured Gelatine – Bulk Preparation and Characterization as Bone Substitute**
Benjamin Kruppke, Hartmut Worch and Thomas Hanke
Max Bergmann Center of Biomaterials, Technische Universität Dresden, Germany
- 12:15 40-6 **Adhesion, Growth and Differentiation of Pre-osteoblasts on Novel Porous Magnesia- and Yttria-Stabilized Zirconia Ceramics**
Chrystalleni Hadjicharalambous, Vladimir Promakhov, Svetlana Buyakova, Sergey Kulkov and Maria Chatzinikolaïdou
University of Crete, Dept. of Materials Science and Technology, Heraklion, Greece

Stem Cells IV Room 1C, 11:00 - 12:30

Chairs: John Kao, University of Wisconsin-Madison
Manuel Salmeron-Sanchez, University of Glasgow
Anna Guildford, University of Brighton

- 11:00 41-1 **Mesenchymal Stem Cell Response to Covalent Functionalized Recombinant Fibronectin Fragments onto New Titanium-Niobium-Hafnium Alloy**
C. Herranz-Díez, J. Guillem-Martí, F.J. Gil, J.M. Manero
Biomaterials, Biomechanics and Tissue Engineering Group, Technical University of Catalonia (UPC), Spain
- 11:15 41-2 **Combined Stimulation with Defined Extracellular Matrices and Pulsed Electrical Fields Enhance Osteogenic Differentiation of Human Mesenchymal Stem Cells**
R. Hess, P. Lee, A. Jaeschke, H. Neubert, T. Henker, V. Hintze, S. Moeller, M. Schnabelrauch, D. A. Hart, H.-P. Wiesmann, D. Scharnweber
Institute of Materials Science / Max Bergmann Center of Biomaterials, TU Dresden, Germany
- 11:30 41-3 **Influence of Surface Curvature on Human Mesenchymal Stromal Cell Migration and Differentiation**
M. Werner, S. Blanquer, S. Haimi, D. Grijpma, A. Petersen
Dept. of Biomaterials Science and Technology, University of Twente, Netherlands
- 11:45 41-4 **Zinc Oxide Nanorod Interaction with Rat Mesenchymal Stem Cells**
Giada Graziana Genchi, Antonella Rocca, Virgilio Mattoli, Barbara Mazzolai and Gianni Ciofani
Istituto Italiano di Tecnologia, Pontedera, Italy
- 12:00 41-5 **Engineering Substrate Topography and Chemistry to Control Mesenchymal Stem Cell Function**
Mohammed Khattak, John Hunt and Raechelle A. D'Sa
Centre for Materials and Structures, University of Liverpool, UK
- 12:15 41-6 **Gel Aspiration-Ejection Fabricates Anisotropic Injectable Dense Collagen Gels with Controlled Microstructure for Regenerative Medicine**
Showan N. Nazhat, Neysan Kamranpour, Mark James-Bhasin, Amir K. Miri, Chiara E. Ghezzi and Benedetto Marelli
Department of Mining and Materials Engineering, McGill University, Canada

UKSB II Room 4, 11:00 - 12:30

Chairs: Adrian Boyd, University of Ulster
Colin Scothford, University of Nottingham

- 11:00 42-1 **Harnessing Scanning Probe Nanolithographies for Cell and Molecular Biology**
Lu Shin Wong
Manchester Institute of Biotechnology, University of Manchester, UK
- 11:30 42-2 **Photochemical Functionalisation and Patterning of Diamond-Like-Carbon for Electronic Neural Interfaces**
James Dugan and Frederik Claeyssens
Department of Materials Science and Engineering, University of Sheffield, UK
- 11:45 42-3 **Impact Testing of Skin: Overcoming the Stratum Corneum Barrier for Microneedle Application**
Kikelomo Moronkeji, Simon Todd, Ahmed Elsheikh and Riaz Akhtar
School of Engineering, University of Liverpool, UK
- 12:00 42-4 **Exploring the Cell-Nanoneedle Interface**
Ciro Chiappini, Jonathan O. Martinez, Enrica De Rosa, Paola Campagnolo, Ennio Tasciotti, Molly M. Stevens
Department of Materials, Imperial College London, UK
- 12:15 42-5 **Strategies to Enhance the Cellular Response to Bioactive Surfaces**
L. Rutledge, L. Randolph, I. Mutreja, B. Meenan, A. Boyd
NIBEC, University of Ulster, Belfast, UK

Chairs: Aldo Boccaccini, University of Erlangen-Nuremberg
Gavin Jell, University College London
Kiruthika Natesan, Plymouth University

- 14:30 43-1 **Bone-like Apatite Deposition on Chemically Synthesized Collagen in Simulated Body Environment**
Toshiki Miyazaki, Jin Furui and Yuki Shirosaki
Graduate School of Life Science and Systems Engineering, Kyushu Institute of Technology, Japan
- 14:45 43-2 **In Vivo Study of Resorbable Phosphate Glass fibre Reinforced Composite Bone Fracture Repair Plates**
I. Ahmed, A. Qureshi, A.J. Parsons, C.A. Scotchford, B.E. Scammell, C.D. Rudd
Division of Materials, Mechanics and Structures, University of Nottingham, UK
- 15:00 43-3 **Marine Inspired Biosilica-Filled Hydrogels for Hard Tissue Repair**
Pamela Walsh, Susan Clarke, Iossif Strehin, Phillip Messersmith
School of Chemistry & Chemical Engineering, Queen's University, Belfast, UK
- 15:15 43-4 **Elucidating the Biological Role of Soluble Silicon in Early Bone Mineralisation**
Gurpreet Birdi, Richard M. Shelton, James Bowen, Pola Goldberg Oppenheimer and Liam M. Grover
School of Chemical Engineering, University of Birmingham, UK

Translational Research Symposium, part 3 Room 3, 14:30 - 15:30

Chairs: Marc Bohner, RMS Foundation
David Eglin, AO Foundation
Yves Bayon, Covidien

- 14:30 44-1 **Innovation and Product Development – Example of a leading medical device company**
Yves Bayon, Michel Thérin
Covidien – Sofradim Production, Trevoux, France
- 15:00 44-2 **Launching and Building a Science-Based Business**
Iain McDougall
Taragenyx Ltd, UK

Tissue Engineering V Room 11, 14:30 - 15:30

Chairs: Nicolas Blancheman, University of Lille 2
Wan Ting Sow, Nanyang Technological University
Anja Thiebes, RWTH Aachen

- 14:30 45-1 **Chitosan-Silica Hybrids for Biomedical Applications**
Christos Pandis, Estela Pérez Roman, Sara Trujillo, Christos Chatzimanolis-Moustakas, Sotiria Kripotou, Apostolos Kyritsis and José Luis Gómez Ribelles
Physics Department, National Technical University of Athens, Greece
- 14:45 45-2 **Triphasic Scaffolds for the Regeneration of the Bone-Ligament Interface**
G. Criscenti, A. Di Luca, A. Longoni, P. S. B. de Sousa and L. Moroni
Department of Tissue Regeneration, University of Twente, The Netherlands
- 15:00 45-3 **Cellular Responses to Elastin-Collagen Composite Scaffolds**
D. Bax, C. Grover, P. Lee, R. Farndale, A. Weiss, S. Best, R. Cameron
Department of Materials Science and Metallurgy, University of Cambridge, UK
- 15:15 45-4 **Chitosan-Siloxane Porous Scaffold for Nerve Reconstruction**
Yuki Shirosaki, Satoshi Hayakawa, Akiyoshi Osaka, José D. Santos, Ana C. Mauricio, Stefano Geuna
Frontier Research Academy for Young Researchers, Kyushu Institute of Technology, Japan

Clinical I Room 1B, 14:30 - 15:30

Chairs: Sheila McNeil, University of Sheffield
Assunta Borzacchiello, National Research Council of Italy
Pradip Paik, University of Hyderabad

- 14:30 46-1 **Nano-spun Meshes as Scaffolds for Regeneration and Stiffness Remodelling of Pelvic Floor Soft Tissues**
Mahshid Vashaghian, A. Ruiz Zapata, B. Zandie Doulabi, T.H. Smit
Obstetrics & Gynaecology, VU University Medical Center, Amsterdam, The Netherlands
- 14:45 46-2 **Coating of Polypropylene Mesh with Micro-Structured Gelatine as Potential Biomimetic Composite for Active Hernia Treatment**
Selestina Gorgieva, Maja Kaisersberger Vincek and Vanja Kokol
Institute for Engineering Materials and Design, University of Maribor, Slovenia
- 15:00 46-3 **Bioresorbable Polymer Based Novel Quick Vascular Closure Device (QVCD)**
Carsten Linti, Michael Doser, Sven Oberhoffner, Erhard Müller, Monika Renardy, Bernd Neumann, Hans-Peter Wendel
Institut für Textil- und Verfahrenstechnik Denkendorf, Germany
- 15:15 46-4 **Hydrophobically Modified, Cod-Derived Gelatins-Based Surgical Sealants Strongly Adhere onto Blood Vessel under Wet Condition**
Ryo Mizuta, Temmei Ito, Keiko Yoshizawa, Mikio Kajiyama, Toshimasa Akiyama, Katsuhiro Kamiya, Tetsushi Taguchi
Graduate School of life and Environmental Science, University of Tsukuba, Japan

Chairs: Matteo Santin, University of Brighton
 Raechelle D'Sa, University of Liverpool
 Elisabeth Engel, Institute for Bioengineering of Catalonia

- 14:30 47-1 **In situ-forming Pectin Hydrogels as Cell Delivery Systems**
SC Neves, DB Gomes, A Sousa, SJ Bidarra, P Petrini, L Moroni, CC Barrias, PL Granja
 INEB - Instituto de Engenharia Biomédica, Universidade do Porto, Portugal
- 14:45 47-2 **Double Layer Nanofiber Sandwich System in Effective Delivery of Growth Factors for Osteogenic Differentiation**
P. S. Gungor-Ozkerim, E. I. Bektas, A. S. Sarac, G.T. Kose, F.N. Kok
 Molecular Biology Genetics and Biotechnology Programme, Istanbul Technical University, Turkey
- 15:00 47-3 **Patient-Customizable Scaffolds with Nano/Microenvironments Rich in Human Platelet's Lysate and Marine-Origin Polysaccharides for Bone Formation Induction**
Sara M. Oliveira, Rui L. Reis, João F. Mano
 3B's Research Group – Biomaterials, Biodegradables and Biomimetics, University of Minho, Portugal
- 15:15 47-4 **Effect of Cyclic Compression on Osteogenesis of Self-Assembled Collagen-Cell Seeded Microspheres**
Maryam Shariatzadeh, Cécile M. Perrault, Damien Lacroix
 Institute for in silico Medicine, University of Sheffield, UK

UKSB III: Alan Wilson prize Room 4, 14:30 - 15:30

Chairs: John Nicholson, University of Greenwich
 Riaz Akhtar, University of Liverpool

- 14:30 48-1 **The Effect of Extrinsic Tooth Bleaching Agents on Restorative Dental Materials: A Review**
Paul Hatton
 School of Clinical Dentistry, University of Sheffield, UK

Biomaterials X: Bioglass Hall 1, 16:00 - 18:00

Chairs: Aldo Boccaccini, University of Erlangen-Nuremberg
 Muhammad Hasan, Dalhousie University
 Marco Lopez, University of Marburg

- 16:00 49-1 **Ultra-thin Bioglass Fibres with Controlled Structures for Biomedical Applications**
Yangyang Li, Ding Zhao, Binbin Li, Qihong Zhang, Yike Fu, Mingwei Chang, Xiang Li
 Department of Materials Science and Engineering, Zhejiang University, China
- 16:15 49-2 **Serious Adverse Event of Woven Fabrics Made of Bioactive Glass Fibres of the Na₂O-K₂O-MgO-CaO-B₂O₃-P₂O₅-SiO₂ System in the Rabbit Spinal Fusion Model**
Janek P. Frantzen, Jessica J. Alm, Petteri Lankinen, Niko Moritz, Matias Røytta, Hannu T. Aro
 Orthopaedic Research Unit, University of Turku, Finland
- 16:30 49-3 **Towards Promoting Ability of Glass Ionomer Cements to Remineralise**
R. Albeshti, A. Bushby and N. Karpukhina
 Institute of Dentistry, Queen Mary University of London, UK
- 16:45 49-4 **The Retarding Effect of Zinc Oxide on Dissolution and Apatite Formation of a Fluoride Containing Bioactive Glass**
Xiaohui Chen, Priyen Shah, Mohammed Mneimne, Robert G. Hill and Natalia Karpukhina
 School of Dentistry, University of Manchester, UK
- 17:00 49-5 **Hypoxia Mimicking Glasses For Use As Chronic Wound Dressings**
AK Solanki, H Autefage, J Penide, F Quintero, J Pou, JR Jones, MM Stevens
 Department of Materials, Imperial College London, UK
- 17:15 49-6 **Bioactive glasses: Instructive Biomaterials to Control Cell Microenvironment**
Elisabeth Engel, Aitor Aguirre, Nadege Sachot, Oscar Castaño, Arlyng Gonzalez, Miguel A. Mateos-Timoneda, Soledad Pérez-Amodio, Josep A. Planell
 Biomaterials for Regenerative Therapies Group, Institute for Bioengineering of Catalonia, Barcelona, Spain
- 17:30 49-7 **Setting Kinetics and Micromechanical Properties of Flax Fibres Reinforced Restorative Glass Ionomers**
Ensanya A. Abou Neel, Wojciech Chrzanowski, Anne M. Young
 Division of Biomaterials, King Abdulaziz University, Jeddah, Saudi Arabia
- 17:45 49-8 **Hypoxia Mimicking Bioactive Glasses for Chronic Wound Healing**
Maria Azevedo, Siwei Li, Wai Ho, Alex Burns, Luara Schoenewolf, Chris Nayar and Gavin Jell
 Division of Surgery & Interventional Science, University College London, UK

Translational Research Symposium, part 4 Romo 3, 16:00 - 18:00

Chairs: Marc Bohner, RMS Foundation
 David Eglin, AO Foundation
 Yves Bayon, Covidien

- 16:00 50-1 **Non-Invasive and specific Attachment of Hernia Mesh by Click Chemistry**
R. Vestberg, M. Guerin, A. Radlovic, O. Lefranc, S. Ladet
 Covidien, Trévoux, France
- 16:15 50-2 **Tubular Compressed Collagen Scaffolds Cultured in a Novel Flow-Bioreactor System for Ureter/Urethra Tissue Engineering Application**
Elif Vardar, Eva-Maria Balet, Hans Mattias Larsson, Jeffrey A. Hubbell and Peter Frey
 Institute of Bioengineering, École Polytechnique Fédérale de Lausanne, Switzerland

- 16:30 50-3 **Making Medical Stent in the Way of Laser Spot Welding of Stainless Steel Wires L316**
Delaram Mansourian, Mahyar Fazeli and Jamshid Aghazadeh Mohandesi
Department of Material Science and Metallurgy Engineering, AmirKabir University of Technology, Iran
- 16:45 50-4 **Towards an Implantable Bioreactor: Synthesis and Surface Modification Strategy for a Soft Tissue Engineered Elastomer**
D-E. Mogosanu, J. Vanfleteren, P. Dubruel
Polymer Chemistry and Biomaterials Research Group, Ghent University, Belgium
- 17:00 50-5 **Development of an Original Model to Investigate Cell Communication in Bone Tissue Engineering**
A. Grémaré, A. Aussel, R. Bareille, J. Guerrero, J. Amedee, D. Le Nihouannen
Bioingénierie Tissulaire, U1026, University of Bordeaux, France
- 17:15 50-6 **Fabrication of Porous Titanium Scaffolds by Stack Sintering of Microporous Titanium Spheres Produced with Centrifugal Granulation Technology**
Hongjie Chen, Xiangdong Zhu, Yujia Fan, Xingdong Zhang
National Engineering Research Center for Biomaterials, Sichuan University, China
- 17:30 50-7 **Essential Model for Determining Biomaterial Attachment in Total Joint Replacement**
R. Bloebaum, N. Abdo, R. Olsen, A. Hofmann, J. Chalayan
George E. Wahlen Department of Veterans Affairs, Salt Lake City Health Care System, USA
- 17:45 50-8 **Incorporation of Polyelectrolyte Complexes into Alginate Hydrogels and their Effect on the Alginate Matrix**
R. Aston, T. Klein, G. Lawrie and L. Grøndahl
School of Chemistry and Molecular Biosciences, The University of Queensland, Australia

Tissue Engineering VI Room 11, 16:00 - 18:00

Chairs: Nicolas Blanchemain, University of Lille 2
David Shepherd, University of Cambridge
Anja Thiebes, RWTH Aachen

- 16:00 51-1 **Tissue Engineered Silk-fibroin Scaffolds for Meniscus Regeneration**
Joana Silva-Correia, Hélder Pereira, Le-Ping Yan, Ana Leite Oliveira, João Espregueira-Mendes, Joaquim Miguel Oliveira and Rui Luís Reis
3B's Research Group - Biomaterials, Biodegradables and Biomimetics, University of Minho, Portugal
- 16:15 51-2 **Design Functionalized Polyesters and Widen the Applicability in Porous Degradable 3D Scaffolds**
Anna Finne-Wistrand, Jenny Undin and Ann-Christine Albertsson
Department of Fibre and Polymer Technology, KTH Royal Institute of Technology, Sweden
- 16:30 51-3 **Investigation of the Role of Shear Stress and Compression Stimuli on Cell Seeded PCL Scaffolds**
M. Brunelli, C. M. Perrault, D. Lacroix
Institute for in silico medicine, University of Sheffield, UK
- 16:45 51-4 **Engineered Dermal Micro-Tissues For Bottom-Up Tissue Engineering And TOC Applications**
A. Garziano, F. Urciuolo, G. Imparato, P. Netti
University of Naples Federico II, Italy
- 17:00 51-5 **Jet-Sprayed 3D Nanofibrillar Environment Decreases Myofibroblastic Activation**
Halima Rabehi, Romain Debret, Pascal Sommer, Dominique Sigaud-Roussel, Jérôme Sohier
Laboratory of Tissue Biology and Therapeutic Engineering (LBTI), CNRS, Lyon, France
- 17:15 51-6 **Fatty Tissue Equivalents – Build Up with Mature Adipocytes in a Gelatin Hydrogel**
Birgit Huber, Eva Hoch, Günter Tovar, Kirsten Borchers, Petra J. Kluger
Fraunhofer Institute for Interfacial Engineering and Biotechnology, Stuttgart, Germany
- 17:30 51-7 **Development of Photocrosslinkable Hyaluronan Hydrogels with Platelets lysates for Tissue Regeneration**
Ricardo Leandro Pires, Pedro S. Babo, Rui L. Reis and Manuela E. Gomes
3B's Research Group - Biomaterials, Biodegradables and Biomimetics, University of Minho, Portugal
- 17:45 51-8 **Poly(vinyl alcohol) Physical Hydrogels as Functional, Biodegradable Matrices for Tissue Engineering**
Bettina E. B. Jensen, Katrine Edlund, Anton A. A. Smith, Leticia Hosta-Rigau, Brigitte Städler and Alexander N. Zelikin
Department of Chemistry, Aarhus University, Denmark

Clinical II Room 1B, 16:00 - 18:00

Chairs: Sheila McNeil, University of Sheffield
Assunta Borzacchiello, National Research Council of Italy
Jacob Brubert, University of Cambridge

- 16:00 52-1 **Calcium Concentrations for the Development of New Bioactive Dressings to Improve Skin Wound Healing**
Claudia Navarro, Soledad Pérez-Amodio, Josep A. Planell and Elisabeth Engel
Institute for Bioengineering of Catalonia (IBEC), Barcelona, Spain
- 16:15 52-2 **Swelling and Sealing Properties of a Novel Hemostatic Biomaterial**
Daniel Spazierer, Paul Slezak and Heinz Gulle
Baxter Innovations GmbH, Vienna, Austria
- 16:30 52-3 **A Pilot Renal Artery Embolization Study: Evaluation of "Imageable" Embolic Microspheres using Hybrid (Landrace Yorkshire) Farm Pigs**
Sharon Kehoe, Robert Abraham, Charles Daly, Daniel Boyd
ABK Biomedical Inc., Halifax NS, Canada
- 16:45 52-4 **Optimizing Properties of Bioadhesive Systems using Fermentation Derived Human Albumin**
Assunta Borzacchiello, Luisa Russo, Birgitte M. Malle, Sara Poulsen, Luigi Ambrosio
Institute of Polymers, Composites and Biomaterials, National Research Council, Naples, Italy

- 17:00 52-5 **Nanoengineered Biomaterials to Fight Gastric Infection: Exploring the Glycan-Adhesin Specific Interaction**
Inês C. Gonçalves, Ana M. S. Costa, A. Magalhães, Celso A. Reis, M. Cristina L. Martins
INEB - Instituto de Engenharia Biomédica, Universidade do Porto, Portugal
- 17:15 52-6 **Highly Selective Nanoparticles Based on Vitamin E Derivatives for the Treatment of Cancer**
Raquel Palao, Maria Rosa Aguilar, Mar Fernandez, Juan Parra, Carolina Sánchez, Ricardo Sanz, Julio San Roman
Department of Polymeric Nanomaterials and Biomaterials, ICTP-CSIC, Madrid, Spain
- 17:30 52-7 **Enhancing In Vitro and In Vivo Viability and Functionality of Pancreatic Islets Through a Gelatine-Based Hydrogel**
Serena Bertoldi, Simona Marzorati, Rita Nano, Lorenzo Piemonti and Silvia Faré
Dept. of Chemistry, Materials, and Chemical Engineering "G. Natta", Politecnico di Milano, Italy
- 17:45 52-8 **Long-term Degradation of Electrospun Poly(ϵ -caprolactone) Fibre Yarns In Vivo: A 12-month Study**
Lucy A Bosworth, Richard Wong, Marie A O'Brien, Jason K Wong, Duncan A McGruther and Sarah H Cartmell
School of Materials, University of Manchester, UK

Biomaterials XI: Hydrogels Room 1C, 16:00 - 18:00

Chairs: Luigi Ambrosio, National Research Council of Italy
Dirk Grijpma, University of Twente
Joana Magalhaes, Instituto de Salud Carlos III

- 16:00 53-1 **Design of Biomimetic Cell-Interactive Substrates using Hyaluronic Acid Hydrogels with Independently Tunable Stiffness and Biochemical Ligand Density**
Jing Jing, Marc R. Block and Rachel Auzély-Velty
Centre de Recherches sur les Macromolécules Végétales (CERMAV-CNRS), Grenoble, France
- 16:15 53-2 **Injectable Biocompatible and Biodegradable pH-Responsive Hollow Particle Gels Containing Poly(acrylic acid): The Effect of Copolymer Composition on Gel Properties**
S. Halacheva, D. Adlam, T. Freemont, J. Hoyland and B. Saunders
Institute for Materials Research and Innovation, University of Bolton, UK
- 16:30 53-3 **Dual Hydrogel System for Bioprinting of Strong Tissue Constructs**
Ferry Melchels, Wouter Dhert, Dietmar W. Huttmacher and Jos Malda
Department of Orthopaedics, University Medical Center Utrecht, The Netherlands
- 16:45 53-4 **Physical Hydrogels Based on Peptide Oligosaccharide Interaction**
Robert Wieduwild, Mikhail Tsurkan, Carsten Werner and Yixin Zhang
B CUBE Center for Molecular Bioengineering, Technische Universität Dresden, Germany
- 17:00 53-5 **The Physical Properties of Particles Dominate Cellular Uptake and Subsequent Influences on Cell Functions**
Zhenqwei Mao, Weijun Liu, Pengfei Jiang, Dahai Yu, Xiangyan Zhou, Changyou Gao
MOE Key Laboratory of Macromolecular Synthesis and Functionalization, Zhejiang University, China
- 17:15 53-6 **The Size Effect of PLGA Microspheres on the Controlled-release of Fluorescein Isothiocyanate-Dextran as a Model for Targeting Synovial Macrophages in Vitro**
Rui Chen, Colette Redmond, John Innes and John A. Hunt
Clinical Engineering, Institute of Ageing and Chronic Disease, University of Liverpool, UK
- 17:30 53-7 **Hybrid Hydrogel/Fiber Construct for Neural Engineering Applications**
P.A. Wieringa, R. Pinho, S. Micera, R. van Wezel, L. Moroni
MIRA, University of Twente, The Netherlands
- 17:45 53-8 **Decellularized Matrix /Fibroin Injectable Hydrogels for Vascularized Adipose Tissue**
Alisan Kayabolen, Dilek Keskin, Ferit Avcu, Andac Aykan, Fatih Zor and Aysen Tezcaner
Department of Biomedical Engineering, Middle East Technical University, Turkey

UKSB IV Room 4, 16:00 - 18:00

Chairs: John Nicholson, University of Greenwich
Riaz Akhtar, University of Liverpool

- 16:00 54-1 **Synthetic Defensins: Novel Antibacterial Agents for Surface Attachment**
Felicity de Cogan, Richard Williams, Anna Peacock, Artemis Stamboulis, Liam Grover, Robert Scott & Ann Logan
School of Clinical and Experimental Medicine, University of Birmingham, UK
- 16:15 54-2 **Development of Decellularised conjunctiva for Ocular Surface Reconstruction**
Shivani Kasbekar, Rosalind Stewart, Stephen Kaye, Rachel Williams and Paul Rooney
Department of Eye and Vision Science, University of Liverpool, UK
- 16:30 54-3 **Highly Swollen and Compressible Photo-Activated Collagen Hydrogels**
Giuseppe Tronci, Colin A. Grant, Neil H. Thomson, Stephen J. Russell, David J. Wood
Nonwovens Research Group, University of Leeds, UK
- 16:45 54-4 **Mechanical and Cytotoxic Evaluation of a Novel Hydrogel with Potential Application as a Corneal Bandage**
Andrew Gallagher, Don Wellings and Rachel Williams
Department of Eye and Vision Science, University of Liverpool, UK
- 17:00 54-5 **Linking Antimicrobial Peptides with the Surface of Metallic Implants**
Zuzanna Trzcińska, Anna Peacock and Artemis Stamboulis
Biomaterials Group, University of Birmingham, UK
- 17:15 54-6 **UKSB AGM**
Sanjukta Deb
King's College London, UK

Chairs: Elizabeth Tanner, University of Glasgow
Claudia Loebel, AO Foundation
Monica Golda-Cepa, Jagiellonian University

- 09:00 55-1 **Reinforcement of Sol-Gel Processed Calcium Phosphate Cement using Functionalised CNTs**
K. Natesan, H. R. Le, C. Tredwin, R. Handy
School of Dentistry, University of Plymouth, UK
- 09:15 55-2 **Dynamics of Filopodium-Like Protrusion and Endothelial Cellular Motility on 1-D Extracellular Matrix Fibrils**
Niannan Xue, Cristina Bertulli, Amine Sadok, Yan Yan Shery Huang
The Institute of Cancer Research, London, UK
- 09:30 55-3 **The Importance of Interconnectivity for Cell Invasion and Percolation through Collagen Scaffolds**
J. Ashworth, P. Buxton, T. Hart, S. Best and R. Cameron
Cambridge Centre for Medical Materials, University of Cambridge, UK
- 09:45 55-4 **Novel Continuous Plastic Flow Synthesis of Phase Pure Nano-Sized Hydroxyapatite**
Aneela Anwar, Jawwad A. Darr
Clean Materials Technology Group, University College London, UK
- 10:00 55-5 **The Effects of Ascending and Descending Strain Rate on the Mechanical Properties of Canine Cranial Cruciate Ligaments**
Rosti Hama Rashid, Brendan Geraghty, Ahmed Elsheikh and Eithne Comerford
School of Engineering, University of Liverpool, UK

Bioactive Glass Symposium, part 1 Room 3, 09:00 - 10:30

Chairs: Julian Jones, Imperial College London
Richard Langford, University of Cambridge

- 09:00 56-1 **Larry's Influences: from Bioactive Glasses to Scaffolds for Tissue Engineering and Nanoparticles for Drug Delivery**
M. Vallet-Regí, A. Salinas and D. Arcos
Dpt. Química Inorgánica y Bioinorgánica, Universidad Complutense de Madrid, Spain
- 09:30 56-2 **Bioactive Glasses: from Hensch to Hybrids**
Julian R. Jones
Department of Materials, Imperial College London, UK
- 10:00 56-3 **Clinical Use of S53P4 Bioactive Glass in Neurosurgery – Case Reports of Tumor Surgery, Infected Cervical Spine and Mucopyelocoele of the Frontal Sinuses**
Janek Frantzén
Department of Neurosurgery, Turku University Hospital, Finland
- 10:15 56-4 **Bioactive Glass S53P4 in the Treatment of Osteomyelitis – Multicenter Study**
Nina Lindfors, Carlo Romano
Helsinki University Central Hospital, Finland

Biomaterials XII Room 11, 09:00 - 10:30

Chairs: James Kirkpatrick, University of Mainz
Giulia Gigliobianco, University of Sheffield
Gloria Huerta-Angeles, Contipro Pharma

- 09:00 57-1 **In Vivo and In Situ Bioprinting of Cells and Biomaterials to Guide Tissue Repair**
Virginie Keriquel, Sylvain Catros, Sophia Ziane, Reine Bareille, Murielle Rémy, Samantha Delmond, Benoit Rousseau, Joëlle Amédée, Fabien Guillemot and Jean-Christophe Fricain
Inserm U1026, Université Bordeaux Segalen, France
- 09:15 57-2 **In Vivo Evaluation of Bone Integration of Poly(Vinyl-Alcohol) Hydrogel Fibers for Ligament Reconstruction**
D. Moreau, A. Villain, M. Bachy, D.N. Ku, D. Hannouche, H. Petite and L. Corté
Centre des Matériaux Pierre-Marie Fourn, Mines Paristech, France
- 09:30 57-3 **Understanding Nuclear Deformation Capacity of Cancer Cells Thanks to Micropillared Surfaces**
Florent Badique, Melanie Eichhorn, Jürgen Rühe, Oswald Prucker, Jean-Noël Freund and Karine Anselme
Mulhouse Materials Science Institute (IS2M), Université de Haute-Alsace, France
- 09:45 57-4 **Fatigue Behaviour of Selective-Laser-Melted Nickel-Titanium Scaffolds**
Therese Bormann, Bert Müller, Waldemar Hoffmann, David Wendt and Michael de Wild
Institute of Medical and Analytical Technologies, University of Applied Sciences Northwestern Switzerland, Muttenz
- 10:00 57-5 **3D Printed Silica- Gelatin Hybrid Tissue Scaffolds**
Maria Nelson, Siwei Li, Oliver Mahony, Molly M. Stevens, Gowsihan Poologasundarampillai, Kamel Madi, Peter D. Lee, Julian R. Jones
Department of Materials, Imperial College London, UK
- 10:15 57-6 **Tailoring Crimp Patterns of Electrospun Fibers by Using Thermal Shrinkage**
H. Chen, D. Baptista, J. Crispin, D. Saris, H. Fernandes, C.A. van Blitterswijk, R. Truckenmuller, L. Moroni
Department of Tissue Regeneration, University of Twente, The Netherlands

Chairs: Matthew Dalby, University of Glasgow
Abhay Pandit, National University of Ireland Galway
Wan Ting Sow, Nanyang Technological University

- 09:00 58-1 **Real Time Analysis of the Enzymatic Digestion of Chondroitin Sulfate: Role of the Sulfation Pattern**
Carla Silva, Ramon Novoa-Carballal, Rui Reis and Iva Pashkuleva
3B's Research Group – Biomaterials, Biodegradables and Biomimetics, University of Minho, Portugal
- 09:15 58-2 **Development and Characterisation of a Decellularised Bovine Osteochondral Biomaterial for Cartilage Repair**
Hazel Fermor, Serena Russell, Sophie Williams, John Fisher and Eileen Ingham
Faculty of Biological Sciences, University of Leeds, UK
- 09:30 58-3 **An Injectable Silk-in-Silk System for Enhanced Proteoglycan Production**
Sumit Murab, Akshay Shrivastava, Juhi Samal, Alok Ranjan Ray, Sourabh Ghosh, *Abhay Pandit*
Network of Excellence for Functional Biomaterials, National University of Ireland, Galway, Ireland
- 09:45 58-4 **Anatomically Shaped, Collagen-Fibre Reinforced Device for Meniscal Repair**
Jennifer Shepherd, Daniel Howard, Siddhartha Ghose, Simon Kew, John Wardale, Ruth Cameron, Serena Best
Department of Materials Science and Metallurgy, University of Cambridge, UK
- 10:00 58-5 **"Nonswellable" Hydrogel without Mechanical Hysteresis**
Hiroyuki Kamata, Ung-il Chung and Takamasa Sakai
Department of Bioengineering, University of Tokyo, Japan
- 10:15 58-6 **A Collagen-Based Multimodal Delivery System Provides Therapeutic Factors as well as Physical Support for Treatment of Spinal Cord Injury in the Rat**
R. Ronan, H. Kraskiewicz, B. Breen, T. Sargeant, A. Pandit, S. McMahon
Network of Excellence for Functional Biomaterials, National University of Ireland, Galway, Ireland

UKSB V Room 4, 09:00 - 10:30

Chairs: Julie Gough, University of Manchester
Raechelle D'Sa, University of Liverpool

- 09:00 59-1 **Characterising the Micro- and Nano-mechanical Properties of Ageing and Diseased Soft Tissues**
Riaz Akhtar
Centre for Materials and Structures, University of Liverpool, UK
- 09:30 59-2 **Nanotubular Titania topography combined with amorphous calcium phosphate chemistry induces direct osteoblastic differentiation in mesenchymal stem cells**
Robert McLister, Mura McCafferty, George Burke, Brian J. Meenan
Biomaterials and Tissue Engineering Group, University of Ulster, Belfast, UK
- 09:45 59-3 **Microwave-assisted Synthesis of Calcium Phosphate Nanobiomaterials with Controlled Morphology**
P.J.T Reardon, J. Huang, J. Tang
Department of Chemical Engineering and Mechanical Engineering, University College London, UK
- 10:00 59-4 **A Dual Porosity Construct for Osteochondral Modelling and Repair**
Alexander A. Popov, George Roberts, David M. Grant, Colin A. Scotchford and Virginie Sottile
Wolfson Centre for Stem Cells, Tissue Engineering & Modelling, University of Nottingham, UK
- 10:15 59-5 **Radiological Assessment of Bioengineered Bone in a Muscle Flap for Reconstruction of a Critical-Size Mandibular Defect**
Randa Al-Fotawei, Edward Odell, Kurt Naudi, Matthew J. Dalby, *K. Elizabeth Tanner*, J McMahon, Ashraf Ayoub
Glasgow Dental Hospital & School, UK

Chairs: Elizabeth Tanner, University of Glasgow
Claudia Loebel, AO Foundation
Monica Golda-Cepa, Jagiellonian University

- 11:00 60-1 **Enhanced Control of Stem Cell Responses by Sub-Micron Material Parameters**
John Hunt, Rui Chen Sandra Fawcett, Judith Curran
Centre for Materials and Structures, University of Liverpool, UK
- 11:15 60-2 **Synthesis, Properties and In Vitro Toxicity of Magnetic Ferrite Nanoparticles**
Juan Sojo, Pier Bombilli, Kareem Noris, Gema Gonzalez
Centro Ingeniería de Materiales y Nanotecnología, Caracas, Venezuela
- 11:30 60-3 **Osteogenic Micro-Nanopatterned Titania for Orthopaedics**
Laura E. McNamara, T Sjöström, P Herzyk, RMD Meek, B Su, MJ Dalby
Centre for Cell Engineering, University of Glasgow, UK
- 11:45 60-4 **Hydrogel-Based Injectable Systems for the Local Delivery of Sodium Alendronate - In Vitro Evaluation with Osteoblast- and Osteoclast-Like Cells**
Urszula Posadowska, Martin Parizek, Elena Filova, Krzysztof Pietryga, Lucie Bacakova, Elzbieta Pamula
Faculty of Materials Science and Ceramics, AGH – University of Science and Technology, Krakow, Poland
- 12:00 60-5 **Bio-Corrosion Behaviour of Chosen Magnesium Alloys from the Mg-Zn-Ca System**
Katarzyna Kubok and Lidia Litynska-Dobrzynska
Department of Functional and Structural Materials, Polish Academy of Sciences, Poland
- 12:15 60-6 **Biofunctionalization of CoCr Alloy for Bone Tissue RepARATION**
Virginia Paredes, Emiliano Salvagni, Enriquez Rodríguez, José M. Manero
Antonio Nariño University (UAN), Colombia

Bioactive Glass Symposium, part 2 Room 3, 11:00 - 12:30

Chairs: Julian Jones, Imperial College London
Richard Langford, University of Cambridge

- 11:00 61-1 **Bioactive Glasses to Stimulate Angiogenesis**
Alejandro Gorustovich, Aldo R. Boccaccini
Institute of Biomaterials, University of Erlangen-Nuremberg, Germany
- 11:15 61-2 **Porosity Engineering in Bioactive Glasses: a Sol-Gel Approach**
J. Soulié, J. Lao, E. Jallot, J.M. Nedelec
Laboratoire des Matériaux Inorganiques, Clermont Université, Clermont-Ferrand, France
- 11:30 61-3 **Bioactive Glass-Ionomer Cements for Bone Tissue Regeneration**
Paul V. Hatton, Altair Contreras, Felora Mirvakily, Yulia Ryabenkova, Ian Brook, Aileen Crawford, Robert Moorehead, Andrew Rawlinson, Christine Freeman, Ian M. Reaney and Cheryl Miller
Bioengineering & Health Technologies Research Group, University of Sheffield, UK
- 11:45 61-4 **Well Ordered Mesoporous Bioactive Glasses for Bone Tissue Engineering and Drug Delivery**
Chengtie Wu
State Key Laboratory of High Performance Ceramics and Superfine Microstructure, Shanghai, China
- 12:00 61-5 **Glass Fiber-Reinforced Composite Cranial Implant with Bioactive Glass**
Pekka K. Vallittu
Department of Biomaterials Science and Turku Clinical Biomaterials Centre, University of Turku, Finland
- 12:15 61-6 **Bioglass Transformations by Laser Assisted Techniques**
F. Lusquiños, J. del Val, R. Comesaña, F. Quintero, A. Riveiro, M. Boutinguiza, J.R. Jones, R.G. Hill, J. Pou
Applied Physics Department, Universidade de Vigo, Spain

Biomaterials XIII Room 11, 11:00 - 12:30

Chairs: James Kirkpatrick, University of Mainz
Damien Lacroix, University of Sheffield
Giulia Gigliobianco, University of Sheffield

- 11:00 62-1 **Cell Behaviour Affected by Properties of Electrospun Nanofibers**
Yan Wei, Wentao liu, Xuehui Zhang, Xuliang Deng
Department of Geriatric Dentistry, Peking University, China
- 11:30 62-2 **Two-Photon Polymerization as a High-Resolution Tool to Control Surface Structure of Polymeric Biomaterials at Micro- and Nanoscale**
David Barata, Paulo Dias, Clemens A. van Blitterswijk and Pamela Habibovic
Department of Tissue Regeneration, University of Twente, Enschede, The Netherlands
- 11:45 62-3 **Facile Photochemistry Enables Protein and Cell Micropatterning in Open and Closed Polymer Systems**
Esben Kjær Unmack Larsen, Morten Bo Mikkelsen and Niels B. Larsen
Department of Micro- and Nanotechnology, DTU Nanotech, Technical University of Denmark
- 12:00 62-4 **3D Plotting of Biopolymer-Based Hollow and Core/Shell Structures**
Ashwini Rahul Akkineni, Yongxiang Luo, Tilman Ahlfeld, Anja Lode, Michael Gelinsky
Centre for Translational Bone, Joint and Soft Tissue Research, Technische Universität Dresden, Germany
- 12:15 62-5 **Magnetic PCL-Based Nanocomposites for Soft/Hard Tissue Regeneration**
Ugo D'Amora, Teresa. Russo, Roberto De Santis, Antonio Gloria, Monica Sandri, Anna Tampieri, L. Ambrosio
Institute of Polymers, Composites and Biomaterials, National Research Council of Italy

Chairs: Matthew Dalby, University of Glasgow
David Shepherd, University of Cambridge
Kiruthika Natesan, Plymouth University

- 11:00 63-1 **Artificial Ligaments From Poly(Vinyl Alcohol) Hydrogel Fibers**
L. Corté, G. Zhang, F. Detrez, S. Cantournet, J.S. Bach and D.N. Ku
Centre des Matériaux Pierre-Marie Fourt, Mines-Paris Tech, France
- 11:15 63-2 **Bioactivity of Medium Chain Length Polyhydroxyalkanoate Scaffold for Soft Tissue-Engineering Applications**
Aitor Larrañaga, Jorge Fernández, Carmen Ronchel, José L. Adrio, Jose-Ramon Sarasua
Department of Mining-Metallurgy and Materials Science, Polymat, University of the Basque Country, Spain
- 11:30 63-3 **Bioinspired Composites: Link between Alignment Control, Platelets Content and Mechanical Properties**
Laetitia Galea, A. Studart, Thomas Graule and Marc Bohner
Skeletal Substitutes Group, RMS Foundation, Switzerland
- 11:45 63-4 **Development and Characterization of Bilayered Scaffolds Incorporated with Gold Nanoparticles as Potential Skin Substitutes**
Ömer Aktürk and Dilek Keskin
Department of Engineering Sciences, Middle East Technical University, Turkey
- 12:00 63-5 **Multi-Scale Geometric Control of Mechano-Transduction and Cell Behaviour Using Polymer Brushes**
John Connelly, Jenny Malmström, Duncan Sutherland and J. E. Gautrot
Institute of Bioengineering, Queen Mary University London, UK
- 12:15 63-6 **Is the Presence of Multinucleated Giant Cells Within the Implantation Bed of Natural-Based Biomaterials Physiological? Assessment of In Vitro and In Vivo Screening of Three Different Porcine Collagen Membranes by Means of Multichamber Three-Dimensional Systems**
Shahram Ghanaati, Carlos Mota, Mike Barbeck, Patrick Booms, Robert Sader, Clemens van Blitterswijk, Lorenzo Moroni, C James Kirkpatrick
Institute of Pathology, University Medical Center of the Johannes Gutenberg University Mainz, Langenbeckstraße 1, 55101 Mainz, Germany

UKSB VI Room 4, 11:00 - 12:30

Chairs: Julie Gough, University of Manchester
Raechelle D'Sa, University of Liverpool

- 11:00 64-1 **The Effect of a RF/DC Magnetron Sputtered Coating on the Dissolution Behaviour and Osteoblast Response to an Mg-Y-RE Alloy**
Natasha A Bhuiyan, Robert Thornton, Joseph Robson, Julie E Gough
Material Science Centre, University of Manchester, UK
- 11:15 64-2 **Novel Biomimetic Scaffolds for Osteochondral Repair**
Amy Prosser, Leander Poocha, Gerhard Hildebrand, Klaus Liefeth, Colin Scotchford, Virginie Sottile and David Grant
Division of Materials Mechanics and Structures, University of Nottingham, UK
- 11:30 64-3 **Investigation into the Ability to Accurately Mimic Natural Extracellular Matrix using Artificial Electrospun Scaffolds**
Kirstie Andrews
School of Engineering, Manchester Metropolitan University, UK
- 11:45 64-4 **Bioactive and Highly Porous Nanofibres via Solution Blow Spinning and their Formation into Macroporous Scaffolds**
Eudes Leannon, Ana Leticia Braz, Isaque Jerônimo, Aldo R. Boccaccini, Showan N. Nazhat, Eliton S. Medeiros, Jonny J. Blaker
School of Materials, Manchester University, UK
- 12:00 64-5 **UKSB Closing Ceremony**
Sanjukta Deb
King's College London, UK

Chairs: Abhay Pandit, National University of Ireland Galway
Adrian Boyd, University of Ulster
Jacob Brubert, University of Cambridge

- 14:30 65-1 **In Vitro Bioactivity and Cell Differentiation Properties of Nanobioceramics with Different Nanostructure**
Cristian Covarrubias, Fabiola Arroyo, Consuelo Balanda, Isabel Celhay, Juan P. Rodríguez, Ana M. Pino, Carla Urrea, Mario Díaz, Miguel Neira, Pablo Caviedes
Laboratorio Nanobiomateriales, Facultad de Odontología, Universidad de Chile
- 14:45 65-2 **The Modelling of Self-Inflating Tissue Expanders**
X. Min and J. T Czernuszka
Department of Materials, University of Oxford, UK
- 15:00 65-3 **Protein Nano-Carriers from Clicked Glycosaminoglycan Block Copolymers**
Ramon Novoa-Carballal, Carla Silva, Stephanie Möller, Matthias Schnabelrauch, Rui L. Reis and Iva Pashkuleva
3B's Research Group – Biomaterials, Biodegradables and Biomimetics, University of Minho, Portugal
- 15:15 65-4 **Treatment of a Degenerative/Pro-Inflammatory Intervertebral Disc Organ Culture with Chitosan/Poly-γ-Glutamic Acid Nanoparticles Carrying and Anti-Inflammatory Drug**
Graciosa Q. Teixeira, Catarina L. Pereira, Hans-Joachim Wilke, Anita Ignatius, Mário A. Barbosa, Cornelia Neidlinger-Wilke, Raquel Goncalves
Institute of Biomedical Engineering (INEB), Universidade do Porto, Portugal
- 15:30 65-5 **Detection of C-Reactive Protein using Highly Dispersible Gold Nanoparticles Bearing Phospholipid Block Copolymers**
Yasuhiko Iwasaki, Toshihiro Kimura, Masaki Orisaka, Hideya Kawasaki, Tatsuro Goda and Shin-ichi Yusa
Faculty of Chemistry, Kansai University, Japan
- 15:45 65-6 **Antibody Coated Microparticles to Fabricate Functional 3D Constructs in Combination with Cells**
C. A. Custódio, V. E. Santo, M.B. Oliveira, M. E. Gomes, R. L. Reis, J. F. Mano
3B's Research Group – Biomaterials, Biodegradables and Biomimetics, University of Minho, Portugal

Bioactive Glass Symposium, part 3 Room 3, 14:30 - 17:45

Chairs: Julian Jones, Imperial College London
Richard Langford, University of Cambridge

- 14:30 66-1 **Regulating Cellular Function Through Physicomechanical Engineering of the Nanobiointerface**
Manus Biggs, Shalom Wind, Matthew Dalby & Abhay Pandit
Network of Excellence for Functional Biomaterials, National University of Ireland, Galway, Ireland
- 15:00 66-2 **The Response of Mesenchymal Stromal Cells to Strontium-Substituted Bioactive Glasses**
M. Santocildes-Romero, P. Hatton, R. Goodchild, A. Crawford, I. Reaney and C. Miller
School of Clinical Dentistry, The University of Sheffield, UK
- 15:15 66-3 **Unsupervised Techniques Unexpectedly Highlight Steroid Biosynthesis in the Global Response of Human MSC to Strontium-Substituted Bioactive Glasses**
H. Autefage, E. Gentleman, E. Littmann, M. Hedegaard, T. von Erlach, M. D. O'Donnell, M. Hedegaard, D. Winkler, M. M. Stevens
Craniofacial Development and Stem Cell Biology, King's College London, UK
- 15:30 66-4 **Application of FIBSEM and XRM to Study the Occlusion of Dentine Tubules From a Calcium Sodium Phosphosilicate Bioactive Glass (NovaMin™)**
Richard Langford, Jonathan Earl and Arno Merkle
Cavendish Laboratory, University of Cambridge, UK
- 15:45 66-5 **Osteoblast-Like Cell Reactions to Soluble Silicate Ions Released from Bioactive Glass and Siloxane-Containing Vaterite**
Akiko Obata, Norihiko Iwanaga, Hirotaka Maeda and Toshihiro Kasuga
Graduate School of Engineering, Nagoya Institute of Technology, Japan
- 16:00 66-6 **Atomic-scale Models of the Water-Bioactive Glass Interaction**
Antonio Tilocca and Alastair N Cormack
Inamori School of Engineering, Alfred University, USA
- 16:15 66-7 **Applications of solid state NMR to the characterisation of bioactive glasses**
Z. Lin, Julian R Jones, John V Hanna and Mark E Smith
Department of Physics, University of Warwick, Coventry, UK
- 16:30 66-8 **Chloride Containing Bioactive Glasses**
Robert Hill, Natalia Karpukhina and Xiaojing Chen
Dental Physical Sciences, Barts and The London, UK
- 16:45 66-9 **Solid-State NMR Study on Strontium-Substituted 45S5 Bioglass**
Kie Fujikura, Natalia Karpukhina, Akiko Obata, Toshi Kasuga, Della S. Brauer, Robert G. Hill and Robert V. Law
Imperial College London, Department of Chemistry, UK
- 17:00 66-10 **Structural Evolution and Phase Formation During Synthesis of Phosphate-Containing Sol-Gel Derived Bioactive Calcium Silicate 58S Glasses**
John V. Hanna, B. Yu, Claudia Ionescu, Julian R. Jones and Mark E. Smith
Department of Physics, University of Warwick, Coventry, UK
- 17:15 66-11 **Nano/Micro Structured Bioglasses Synthesized via Sol-gel and Electrohydrodynamic (EHD) Approaches**
Yangyang Li, Ding Zhao, Binbin Li, Qihong Zhang, Yike Fu, Juan Wang, Mingwei Chang, Zhaohui Ren, Xiang Li
Department of Materials Science and Engineering, Zhejiang University, China

- 17:30 66-12 **A Unified In Vitro Evaluation for Apatite-Forming Ability of Bioactive Glasses and their Variants**
Anthony L. B. Maçon, Taek B. Kim, Esther Valliant, Katherine Goetschius, Richard Brow, Delbert Day, Alexander Hoppe, Aldo Boccaccini, Il-Yong Kim, Chikara Ohtsuki, Tadashi Kokubo, Akiyoshi Osaka, Maria Vallet-Regi, Daniel Arcos, Leandro Fraile, Antonio Salinas, Alexandra Teixeira, Yuliya Vueva, Rui Almeida, Marta Miola, Chiara Vitale-Brovarone, Enrica Verne and Julian Jones
 Department of Materials, Imperial College London, UK

Biomaterials XV Room 11, 14:30 - 16:00

Chairs: Nicholas Dunne, Queen's University Belfast
 Derfogail Delcassian, Imperial College London
 Damien Lacroix, University of Sheffield

- 14:30 67-1 **Role of Stromal Vascular Fraction from Adipose Tissue in Association with a Phosphocalcic Scaffold to Regenerate Bone in Irradiated Area**
Florent Espitalier, Audrey Théry, Pauline Bléry, Jérôme Guicheux, Paul Pilet, Sophie Sourice, Pierre Weiss, Olivier Malard
 INSERM U791, Center for Osteoarticular and Dental Tissue Engineering, University of Nantes, France
- 14:45 67-2 **Design of Stimuli-Responsive Film Trough Layer-by-Layer Assembly for the Control of Protein Adsorption**
A. Osypova, C.M. Pradier, C. Jérôme, J. Landoulsi, S. Demoustier-Champagne
 Institute of Condensed Matter and Nanoscience (IMCN), Université Catholique de Louvain (UCL), Belgium
- 15:00 67-3 **Tissue Engineering Creates New Basis for Scientific Research in Cell-Biomaterial Interaction**
Malgorzata Lewandowska-Szumieł, Slawomir Ruminski, Katarzyna Walenko, Barbara Ostrowska, Wojciech Swieszkowski
 Department of Histology and Embryology, Medical University of Warsaw, Poland
- 15:15 67-4 **Wear and Friction of PEEK and CFR-PEEK Materials for Cervical Total Disc Replacement Bearings**
Ksenija Vasiljeva, Phil Hyde, John Fisher, Richard Hall
 University of Leeds, UK
- 15:30 67-5 **Nanofiber-Based Biomaterials Used to Direct Cellular Responses Associated with Epithelial-Mesenchymal Transition**
Raquel C. Barros, Edith Gelens, Menno de Jong, Roel Kuijer, Theo G. van Kooten
 Department of Biomedical Engineering, University Medical Center Groningen, University of Groningen, The Netherlands
- 15:45 67-6 **Characterising the Effects of Different Sterilisation Techniques on Electrospun Fibre Scaffolds**
Lucy A Bosworth and Sarah H Cartmell
 School of Materials, The University of Manchester, UK

Bone V Room 4, 14:30 - 16:00

Chairs: John Nicholson, University of Greenwich
 Elisabeth Engel, Institute for Bioengineering of Catalonia
 Kambiz Farbod, Radboud University Medical Center

- 14:30 68-1 **Novel Electric Discharge Assisted Mechanical Milling method as a mean of biomaterials synthesis in the Al-Zr-O system**
M. Wyszomirska, A. Calka, D. Wexler
 Mechanical, Material & Mechatronic, University of Wollongong, Australia
- 14:45 68-2 **Biofabrication of Osteochondral Grafts Via 3D Printing of Cell-Laden Microcarriers in a Gelatin Methacrylamide/Gellan Gum Bioink**
Riccardo Levato, Jetze Visser, Josep A. Planell, Elisabeth Engel, Jos Malda, Miguel A. Mateos-Timoneda
 Institute for Bioengineering of Catalonia, Barcelona, Spain
- 15:00 68-3 **Controlled and Reliable Carbonation of Low Temperature Calcium Phosphates**
Anna Díez-Escudero, Montserrat Espanol, Yassine Maazouz and Maria-Pau Ginebra
 Department of Materials Science and Metallurgical Engineering, Technical University of Catalonia, Spain
- 15:15 68-4 **Characterization and Biocompatibility of a Collagen/Hydroxyapatite-Microsphere Composite Scaffold for Bone Regeneration**
Rahmat Cholas, Sanosh Kunjalukkal Padmanabhan, Francesca Gervaso, Gayatri Udayan, Graziana Monaco, Alessandro Sannino and Antonio Licciulli
 Department of Engineering for Innovation, University of Salento, Italy
- 15:30 68-5 **PEO Physicochemical Modification of Novel Low-modulus β -Ti Alloys Shows Comparable Cellular Behaviour to Commercial α - and ($\alpha+\beta$)-Ti Alloys**
Mehdi Golozar, Constantin-Edi Tanase, Roger A. Brooks and Serena M. Best
 Cambridge Centre for Medical Materials, University of Cambridge, UK
- 15:45 68-6 **Machining of Metallic Biomaterials: Comparison between Co-Cr-Mo and Ti-Al-Nb Alloys**
Timotius Pasang, Mamoru Takahashi, Daiki Shinohara, Patrick Conor, Kiyoshi Tanaka and Osamu Kamiya
 Department of Mechanical Engineering, AUT University, Auckland, New Zealand

Poster Presentation Programme

- P1 Mechanical Properties of Zirconia 3-Unit Fixed Dental Prostheses Machined on a CAD/CAM System**
Carlos Nelson Elias, Heraldo Elias Salomão dos Santos, Claudinei dos Santos
 Instituto Militar de Engenharia, Brazil
- P2 Nano-Crystallite TCP Synthesized by Mechanical Activation To Use Tissue Engineering**
Hassan Gheisari Dehsheikh, Ebrahim Karamian
 Department of Material Engineering, Islamic Azad University, Isfahan, Iran
- P3 Hyperbranched Poly(β -Amino Ester) for High Performance Gene Delivery**
Dezhong Zhou, Wenxin Wang
 Charles Institute of Dermatology, University College Dublin, Ireland
- P4 Optimisation of Macromolecular Crowding Conditions for Enhanced Extracellular Matrix Deposition *in vitro***
Diana Gaspar, Abhay Pandit, Dimitrios Zeugolis
 Network of Excellence for Functional Biomaterials, National University of Ireland, Galway, Ireland
- P5 Enhanced Extracellular Matrix Deposition and Maintenance of Mesenchymal Stem Cell Phenotype *In Vitro* using Macromolecular Crowding and Low Oxygen Tension**
D. Cigognini, P. Kumar, A. Satyam, C. Sanz-Nogués, T. O'Brien, A. Pandit and D. Zeugolis
 Network of Excellence for Functional Biomaterials, National University of Ireland, Galway, Ireland
- P6 Synthesis and characterization of novel bioglass-ceramic $\text{CaO-Na}_2\text{O-SiO}_2\text{-P}_2\text{O}_5\text{-ZrO}_2\text{-TCP}$ by sol-gel processing**
Parisa Eslami, Giovanni Baldi, Valentina Faso
 Ce. Ri. Col Research Center of Colorobbia Italia, Italy
- P7 WITHDRAWN**
- P8 Interconnected porous calcium phosphate forming cement consisting of α -TCP foam granules and calcium phosphate acidic solution**
Khairul Anuar Shariff, Kanji Tsuru, Kunio Ishikawa
 Department of Biomaterials, Kyushu University, Japan
- P9 Antithrombogenic Surface on Poly(ether ether ketone) Prepared by Self-initiated Photoinduced Graft Polymerization of 2-Methacryloyloxyethyl Phosphorylcholine**
Kazuhiko Ishihara, Masayuki Kyomoto, Tetsuji Yamaoka, Sachiro Kakinoki
 Department of Materials Engineering, The University of Tokyo, Japan
- P10 Development of bioengineered designer scaffolds for full thickness skin wound healing**
Naveen Kumar
 Division of Surgery, Indian Veterinary Research Institute, Uttar Pradesh, India
- P11 Synthesis and *In Vitro* Biocompatibility of Carbonated Hydroxyapatite for Bone Tissue Engineering Application**
Yanny M. Baba Ismail, Oana Bretcanu, Kenneth W. Dalgarno, Alicia J. El Haj
 Institute for Science and Technology in Medicine, Keele University, Stoke-on-Trent, UK
- P12 Modification of Magnesium Coated Titanium Surfaces to Control Its Corrosion Rate**
O. Mazmanoglu, S. Onder, F. N. Kok, K. Kazmanli, M. Urgan
 Molecular Biology Genetics and Biotechnology Programme, Istanbul Technical University, Turkey
- P13 Dip TIPS as a Novel Process for Preparation of Anisotropic Channeled Porous Polymer Scaffolds for Guided Tissue Engineering Applications**
Naresh Kasoji, Dana Kubies, Marta M. Kumorek, Lud'ka Machová, Jan Kríž, Daniel Jiráček, Eva Fabryová, František Rypáček
 Institute of Macromolecular Chemistry, Academy of Sciences of Czech Republic, Prague
- P14 Different cryogel architectures as basis for 3D cell culture of prostate cancer cells**
Anne Baecker, Bettina Goeppert, F.J. Gruhl
 Karlsruher Institute of Technology, Germany
- P15 Rapid screening of potential biomedical zirconium alloys with 1 wt. % alloy additions**
F.Y. Zhou, Y.F. Zheng
 Center for Biomedical Materials and Engineering, Harbin Engineering University, China
- P16 Iron Oxide Colloids as hyperthermia agents**
Paula Soares, Isabel Ferreira and João Paulo Borges
 Department of Materials Science, FCT-UNL, Caparica, Portugal
- P17 Biodegradable Shape Memory Polymer Composite for Endovascular Embolization**
Yee Shan Wong, Subbu S. Venkatraman, Kiang Hiong Tay, Wei Min Huang and William R. Birch
 School of Materials Science and Engineering, Nanyang Technological University, Singapore
- P18 Analysis of PVA- hydrogels loaded with propolis for burn healing application**
Renata N. Oliveira, Regis Rouze, Brid Quilty, Gloria D.A. Soares, Rossana M.S.M. Thiré and Garrett B. McGuinness
 Department of Materials and Metallurgical Engineering, Federal University of Rio de Janeiro, Brazil
- P19 Bone regeneration in human bone defect by octacalcium phosphate collagen composite**
Tadashi Kawai, Shinji Kamakura, Keiko Matsui, Yuji Tanuma, Seishi Echigo, Osamu Suzuki and Tetsu Takahashi
 Division of Oral and Maxillofacial Surgery, Tohoku University Graduate School of Dentistry, Japan
- P20 Biological performance of injectable octacalcium phosphate-hyaluronic acid composites on bone augmentation**
Kentaro Suzuki, Takahisa Anada, Tatsuya Miyazaki, Naohisa Miyatake, Masami Hosaka⁴ Hideki Imaizumi, Eiji Itoi and Osamu Suzuki
 Division of Craniofacial Function Engineering, Tohoku University Graduate School of Dentistry, Japan

- P21 Mathematical Design and Experimental Evaluation of Borate Based Glass Ionomer Cements (GICs): Towards Predicting Antibacterial Efficacy and Ion Release**
X.F. Zhang, H. O'Shea, D. Boyd
Department of Applied Oral Sciences, Dalhousie University, Canada
- P22 Pre-osteoblast cell responses on phosphate and calcium co-immobilized titanium**
Sunarso, Riki Toita, Kanji Tsuru, Kunio Ishikawa
Department of Biomaterials, Kyushu University, Japan
- P23 Nanohybrid Approach to Create Cell-Compatible Degradable Copolymer Thermogels as Cell Delivery Carriers**
Naho Oyama and Koji Nagahama
Department of Nanobiochemistry, Konan University, Japan
- P24 Self-assembly of PEI Modified Biodegradable Complex Micelles as Gene Transfer Vector for Proliferation of ECs**
Juan Lv, Jing Yang, Xuefang Hao and Yakai Feng
School of Chemical Engineering and Technology, Tianjin University, China
- P25 Ultrasonic non-invasive monitoring of the mechanical properties of collagen vascular scaffolds in bioreactors**
Bernard Drouin, Ramiro M. Irastorza and Diego Mantovani
Laboratory for Biomaterials and Bioengineering, Laval University, Quebec City, Canada
- P26 Scaffold and tissue engineering by self-assembly therapies for tendon repair**
Dimitrios Zeugolis
Network of Excellence for Functional Biomaterials (NFB), National University of Ireland, Galway
- P27 Characterization of PCL based nano/micro fibrous scaffold for Bone Tissue Engineering**
Izabella Rajzer, Elżbieta Menaszek
Department of Mechanical Engineering Fundamentals, University of Bielsko-Biała, Poland
- P28 Mechanism of Electrodeposition of Poly(Ethylene Glycol) to Titanium Surface**
Takao Hanawa, Osamu Fukushima, Yusuke Tsutsumi, Hisashi Doi and Maki Ashida
Institute of Biomaterials and Bioengineering, Tokyo Medical and Dental University, Japan
- P29 Effects of Combination of Biomaterial and Stem cell Implants on the Hard and Soft Tissue of Experimental Animals**
Mara Pilmane, Andrejs Skagers, Ilze Salma, Sandris Petronis, Dagnija Loca, Janis Locs
Institute of Anatomy and Anthropology, Riga Stradins University, Latvia
- P30 Several drugs and model molecules controlled release studies from nanometric vesicles of polymer-lipid complexes**
Virginia Saez-Martinez, Anisa Mahomed, Brian J. Tighe
Biomaterials Research Unit, Aston University, Birmingham, UK
- P31 Modification of PVC catheters with a binary graft of PEGMA and AAc to improve their biocompatibility**
L. Islas, G. Burillo
Instituto de Ciencias Nucleares, Universidad Nacional Autonoma de México
- P32 Antibiotic-loaded silica nanoparticles/collagen composite hydrogels with prolonged antimicrobial activity for wound infection prevention**
Christophe Hélyar, Gisela S. Alvarez, Andrea M. Mebert, Xiaolin Wang, Thibaud Coradin and Martin F. Desimone
Materials and Biology Team, University Pierre and Curie, Paris, France
- P33 Fibroin reinforced calcium phosphate cement**
Martha Geffers, Jürgen Groll, Uwe Gbureck
Department of Functional Materials in Medicine and Dentistry, University of Würzburg, Germany
- P34 Influence of heat treatment and additives of alkali substituted calcium phosphate cements on their properties**
Martha Geffers, Laura Straub, Jürgen Groll, Uwe Gbureck
Department of Functional Materials in Medicine and Dentistry, University of Würzburg, Germany
- P35 Development of an in situ culture-free screening test for the rapid detection of Staphylococcus aureus within healthcare environments**
Adam Le Gresley, Alex Sinclair, Lauren E. Mulcahy, Lynsey Geldeard Samerah Malik and Mark D. Fielder
Pharmacy and Chemistry, Kingston University, London, UK
- P36 New Technology Based on Combination of Cryogel and Nanoparticles for Wound Management**
Timur Saliev, Gulsim Kulsharova, Alma Akhmetova, Talgat Nurgozhin, Ray D.L. Whitby and Sergey Mikhaylovsky
School of Engineering, Nazarbayev University, Kazakhstan
- P37 Rapid Patterning of 1-D Collagenous Topography as an ECM Protein Fibril Platform for Image Cytometry**
Niannan Xue, Xia Li, Cristina Bertulli, Zhaoying Li, Atipat Patharagulpong, Amine Sadok, Yan Yan Shery Huang
Department of Engineering, University of Cambridge, UK
- P38 Control of Bone Conduction on Pure Titanium by Surface Modification**
Masato Ueda, Masahiko Ikeda, Richard Langford, Jeremy Skepper, Ruth E. Cameron and Serena M. Best
Faculty of Chemistry, Kansai University, Japan
- P39 Modification Of Electrospun Nanofibrous Scaffold By Ink-Jet Printing**
Izabella Rajzer, Monika Rom, Elżbieta Menaszek
Department of Mechanical Engineering Fundamentals, University of Bielsko-Biała, Poland
- P40 WITHDRAWN**
- P41 Chelate Bonding Mechanism of a Novel Magnesium Phosphate Bone Cement**
Theresa Christel, Martha Geffers, Susanne Christ, Jürgen Groll and Uwe Gbureck
Department for Functional Materials in Medicine and Dentistry, University of Würzburg, Germany
- P42 Biocompatibility and Solubility of Calcium Doped Magnesium Phosphate Cement Granules**
Theresa Christel, Martha Geffers, Susanne Christ, Uwe Klammert, Berthold Nies, Andreas Höß, Jürgen Groll and Uwe Gbureck
Department for Functional Materials in Medicine and Dentistry, University of Würzburg, Germany

- P43 Study and design of RGD-Self-assembling peptide hydrogels**
Deidda Graziano, Mitraki Anna
 Materials Science Department, University of Crete, Heraklion, Greece
- P44 Structure and Properties Study of Calcium Apatites**
Y. Gao, R.V. Law, N. Karpukhina, R.G. Hill
 Department of Chemistry, Imperial College London, UK
- P45 Development and study of poly(butylene succinate)/chitosan/hemp fiber fully biodegradable composites**
Z. Terzopoulou, V. Nikolaidis, D. Bikiaris, E. Athanassiadou, E. Papadopoulou
 Department of Chemistry, Aristotle University of Thessaloniki, Greece
- P46 Effect of Albumin Adsorption on MC3T3-E1 and RAW264.7 Cell Response to Hydroxyapatite and α -Alumina**
Masakazu Kawashita, Jumpei Hayashi, Tada-aki Kudo, Hiroyasu Kanetaka, Zhixia Li, Toshiki Miyazaki, Masami Hashimoto
 Graduate School of Biomedical Engineering, Tohoku University, Japan
- P47 New Insights into the Control of 3D Architecture and Porosity in Collagen Scaffolds for Tissue Engineering**
K. M. Pawelec, A. Husmann, S. Best, R. Cameron
 Cambridge Centre for Medical Materials, University of Cambridge, UK
- P48 Characterization and cytocompatibility of nanocellulose films**
K.Hua, D.O. Carlsson, M. Strømme, A. Mihranyan, N. Ferraz
 Nanotechnology and Functional Materials, Uppsala University, Sweden
- P49 L-Lactide, D-Lactide and ϵ -caprolactone or δ -valerolactone based terpolymers for application in the medical field**
J. Fernández, A. Larrañaga, A. Etxeberria and J. R. Sarasua
 Department of Mining-Metallurgy Engineering and Materials Science, University of the Basque Country, Bilbao, Spain
- P50 WITHDRAWN**
- P51 Ionic liquid-doped and *p*-NIPAAm-based temperature responsive copolymer: Extraordinary entrapping and releasing behaviors of BSA at 38-42 °C**
Jae-won Seo, Ueon Sang Shin
 Institute of Tissue Regeneration Engineering, Dankook University, South Korea
- P52 Synthesis of a Bifunctional Silver-containing Biocomposite**
Anna A. Ivanova, Roman A. Surmenev, Maria A. Surmeneva, Timur Mukhametkaliyev, Kateryna Loza, Oleg Prymak, Matthias Eppler
 Department of Theoretical and Experimental Physics, National Research Tomsk Polytechnic University, Russia
- P53 Osteoinduction and survival of human osteosarcoma MG-63 cells on nanoporous hydroxyapatite scaffolds**
M. Beaufils-Hugot, F. Burgio, S. Stevanovic, P. Chavanne, O. Braissant, P. Gruner, R. Schumacher, U. Piolet
 FHNW, University of Applied Sciences and Arts of Northwestern Switzerland, Muttenz
- P54 Protein Adsorption onto Polymer-based Nanocarriers for Vaccine Delivery**
Nitesh Kunda, Gillian Hutcheon and Imran Saleem
 School of Pharmacy and Biomolecular Sciences, Liverpool John Moores University, UK
- P55 Surface functionalization of electro-spun Poly(L)Lactic Acid scaffolds with heparin to induce angiogenesis**
Giulia Gigliobianco, Sabiniano Roman, Chuh K. Chong and Sheila MacNeil
 Kroto Research Institute, University of Sheffield, UK
- P56 Neuronal growth on nano-pillar substrates**
Nahoko Kasai, Rick Lu, Touichiro Goto, Yoshiaki Kashimura, Azusa Oshima and Koji Sumitomo
 NTT Basic Research Laboratories, Atsugi, Japan
- P57 Biodegradable and Bioadhesive Hemostatics Comprising Polymer Complex Gel and Chitosan**
Tomoko Ito, Masazumi Eriguchi and Yoshiyuki Koyama
 Japan Anti-tuberculosis Association, Shin-Yamanote Hospital, Japan
- P58 The Effect of Water Saturation on the Compressive Properties of Calcium Sulphate Dihydrate**
J Koh, A López, B Helgason and S Ferguson
 Institute for Biomechanics, ETH-Zürich, Switzerland
- P59 Flexural Properties of Calcium Sulphate Dihydrate and Dicalcium Phosphate Dihydrate: Potential Role of Degradation with Water Saturation**
J Koh, B Helgason and S Ferguson
 Institute for Biomechanics, ETH-Zürich, Switzerland
- P60 Osteoconductivity of Super Hydrophilic Valve Metals and Titanium Alloys**
Kensuke Kuroda and Masazumi Okido
 EcoTopia Science Institute, Nagoya University, Japan
- P61 WITHDRAWN**
- P62 Evaluation of Dense Collagen Matrices as Wound Dressing for the Treatment of Foot Diabetic Ulcers**
Christophe Hélar, Gervaise Mosser, Aicha Abed, Didier Letourneur, Liliane Louedec, Thibaud Coradin, Marie Madeleine Giraud-Guille and Anne Meddahi-Pellé
 Materials and Biology Team, University Pierre and Curie, Paris, France
- P63 Electrodeposition of Nanostructured Zinc Oxide on Zinc with Potential for Bioresorbable Medical Devices**
M. Alves, C. Santos, M. J. Carneizim and F. Montemero
 Instituto Superior Técnico, Universidade Técnica de Lisboa, Portugal
- P64 Mechanical Strength and Microstructure of Biomedical Beta-type Ti Alloy Subjected to Fine Particle Bombarding**
Toshikazu Akahori, Yurie Oguchi, Tomokazu Hattori, Hisao Fukui, and Mitsuo Niinomi
 Faculty of Science and Technology, Meijo University, Japan

- P65 Stoichiometric Control for Hydroxyapatite Thin Film Prepared by Pulsed Laser Deposition Technique**
Hiroaki Nishikawa, Ryota Yoshikawa
Faculty of Bio-Oriented Science and Technology, Kinki University, Japan
- P66 The Influence of PBS and Lactic acid on vacuum-sintered bodies of a novel apatite for artificial bone and tooth**
Kenichi Tamura and Tomohiro Uchino
College of Engineering, Nihon University, Japan
- P67 Sol-gel assisted preparation of collagen hydrolysate scaffold: A Novel biomaterial for the treatment of chronic wounds**
Sathesh Kumar Ramadass, Sathiamurthi Perumal and Balaraman Madhan
Central Leather Research Institute, Tamil Nadu, India
- P68 Stress and Deformation in a Sutured Tendon Repair; an *in silico* Model**
S D Rawson, L Margetts, J K F Wong and S H Cartmell
School of Materials, University of Manchester, UK
- P69 Chemically cross-linked peptide-based hydrogels with potential biomedical applications**
M.A. Elsayy, A. Smith, A.F. Miller and A. Saiani
School of Materials, University of Manchester, UK
- P70 Calcium phosphate spheres incorporated into PMMA cement for enhanced antibacterial properties**
Tao Qin, Alejandro López, Caroline Öhman, Håkan Engqvist, Cecilia Persson, Wei Xia
Department of Engineering Sciences, Uppsala University, Sweden
- P71 MP-SPR New characterization method for interactions and ultrathin films**
Annika Jokinen, Niko Granqvist, Willem M. Albers and Janusz Sadowski
BioNavis Ltd., Finland
- P72 A Dimensionless Number for Electrospinning**
William W. Sampson
School of Materials, University of Manchester, UK
- P73 Acidic pH resistance of grafted chitosan on dental implant**
Doris M. Campos, Bérengère Toury, Mélanie D'Almeida, Ghania N. Attik, Alice Ferrand, Pauline Renoud and Brigitte Grosgeat
UFR d'Odontologie, Université Claude Bernard Lyon, France.
- P74 Ex vivo osteo-chondral organ culture**
Andrea Schwab, Jenny W Reboredo, Heike Walles
Tissue Engineering & Regenerative Medicine, University Hospital Wuerzburg, Germany
- P75 3D powder printing of structured TCP/Alginate scaffolds for bone tissue engineering**
Miguel Castilho, Jorge Rodrigues, Inês Pires, Barbara Gouveia, Manuel Pereira, Claus Moseke, Jürgen Groll, Uwe Gbureck, Elke Vorndran
Instituto Superior Técnico, Universidade de Lisboa, Portugal
- P76 Surface modification of Ti-6Al-4V alloy controlling OCP nucleation by electron cyclotron resonance plasma oxidation**
Hiroshi Masumoto, Mayumi Oikawa, Yusuke Oori, Takahisa Anada, Osamu Suzuki and Keiichi Sasaki
Frontier Research Institute for Interdisciplinary Sciences, Tohoku University, Japan
- P77 Evaluation the Cellular Behavior on Poly Lactic-co-Glycolic Acid - Gelatin Scaffolds by Electrospinning Method**
Farnaz Ghorbani, Haniyeh Nojehdehyan, Ali Zamanian
Biomedical Engineering Department, Islamic Azad University, Tehran, Iran
- P78 Conducting Polymer Platform for Anti-Cancer Drug Delivery**
K. Krukiewicz, T. Jarosz, J.K. Zak, M. Łapkowski, P. Ruskowski, T. Bobkiewicz-Kozłowska, B. Bednarczyk-Cwynar
Department of Physical Chemistry and Technology of Polymers, Silesian University of Technology, Poland
- P79 Stability of self-assembled hyaluronan polymeric micelle cores in aqueous solutions and whole human blood**
Daniela Šmejkalová, Kristina Nešporová, Jana Šógorková, Pavlína Halamková, Jaroslav Novotný, Jakub Syrovátka, Gloria Huerta-Angeles
Contipro Pharma, Dolní Dobrouč, Czech Republic
- P80 Extracellular matrix proteins regulate Adipose Derived Mesenchymal Stem Cells and Amniotic Fluid Stem Cells attachment and proliferation: utility for tissue and organ regeneration**
Anna Bajek, Joanna Olkowska, Natalia Gurtowska, Tomasz Drewa
Department of Tissue Engineering, Nicolaus Copernicus University, Bydgoszcz, Poland
- P81 Development of a new biomaterial based on Hyaluronan and oleic acid for drug delivery applications**
Gloria Huerta-Angeles, Martin Bobek, Daniela Šmejkalová, Kristina Nešporová and Vladimír Velebný
Contipro Pharma, Dolní Dobrouč, Czech Republic
- P82 Imaging of Biofilm Removal on Titanium and Glass by Dental Instruments**
E. Pecheva, N. Vyas, R.L. Sammons and A.D. Walmsley
School of Dentistry, University of Birmingham, UK
- P83 Poly (ϵ -lysine) dendrons as modulators of quorum sensing in *Pseudomonas aeruginosa***
Rahaf Issa, Steve Meikle, Stuart James and Ian R. Cooper
School of Pharmacy and Biomolecular Sciences, University of Brighton, UK
- P84 Comparative Osteogenesis of Calcium Silicate Cement and Calcium Phosphate Cement**
Shinn-Jyh Ding and Shu-Ching Huang
Institute of Oral Science, Chung Shan Medical University, Taichung, Taiwan
- P85 A study on PLLA/MWCNT nanocomposites compatibilized with pyrene-end-functionalized PLLA**
I. Martínez de Arenaza, M. Obarzanek-Fojt, J. R. Sarasua, E. Meaurio, F. Meyer, J. M. Raquez, P. Dubois and A. Bruinink
Materials Biology Interactions, EMPA, St Gallen, Switzerland
- P86 Microgels Immobilizing Eudragit Nanoparticles for Indomethacin Release**
Mihaela Nicoleta Holban, Anca Niculina Cadinoiu, Elena Folescu and Vasile Burlui
Acad. Ion Haulica Research Institute, Apollonia University of Iasi, Romania

- P87 Design of Biomimetic Fibronectin Fragment Used in Multi-layer Film Coating for Tissue Engineering**
C. Dridj, B. Miladi, G. Bœuf, A. Elmarjou, S. Changotade, F. Poirier, D. Lutowski, A. Elm'selmi
Laboratoire de Biologie Moléculaire, Ecole de Biologie Industrielle, France
- P88 Effect of increasing alanine content in self-assembling FEK octapeptides**
Andrew Smith, Stephen Boothroyd, Aline F. Miller and Alberto Saiani
School of Materials and Manchester Institute of Biotechnology, University of Manchester, UK
- P89 Structural alterations in the dura mater after exposure to clinically relevant CoCr nanoparticles. An organ culture approach**
Papageorgiou Iraklis, Abberton Thomas, Fuller Martin, Tipper Joanne L, Fisher John, Ingham Eileen
Institute of Medical & Biological Engineering, University of Leeds, UK
- P90 New Materials with Antibacterial Action of Functionalized Au Nanoparticles and Ga³⁺ Ions**
Mario Kurtjak, Marija Vukomanović and Danilo Suvorov
Advanced Materials Department, Jožef Stefan Institute, Slovenia
- P91 Biomimetic mineralization of early caries lesions with a self-assembling peptide**
Sabrina Stevanovic, Lucy Kind, Iwona Dziadowiec, Bert Müller, Uwe Pieses
Institute of Chemistry and Bioanalytics, University of Applied Sciences and Arts Northwestern Switzerland
- P92 Bacterial Adhesion and Biofilm Formation Reduced by the Immobilization of hLf1-11 Peptide onto Titanium Surface: A Comparison Study between Direct and ATRP based Covalent Immobilization**
Maria Godoy-Gallardo, Carlos Mas-Moruno, Kai Yu, Jose M. Manero, Javier Gil, Jayachandran N. Kizhakkedathu, Daniel Rodríguez
Department of Material Science, Technical University of Catalonia, Spain
- P93 A Preliminary Examination of Composition-Property Relationships for Methotrexate-Loaded Germanium-Based Glass Ionomer Cements**
Lauren Kiri, Daniel Boyd
School of Biomedical Engineering, Dalhousie University, Canada
- P94 PEI – Starch Nanospheres for siRNA based Gene Silencing Therapy for Cancer**
Berke Bilgenur Kandemir, Bülent Özpolat, Gamze Torun Köse, Vasif Hasirci
Middle East Technical University, Department of Biotechnology, Ankara, Turkey
- P95 Intracellular delivery system based on acylated hyaluronan**
Kristina Nešporová, Jana Šógorková, Lucie Vištejnová, Daniela Šmejkalová, Hana Kolářová, Vladimír Velebný
Contipro Biotech, Czech Republic
- P96 In vivo Investigations of the Early Stages of Bone Healing with Microdialysis**
Yvonne Foerster, Claudia Rentsch, Stefan Kalkhof, Martin von Bergen, Stefan Rammelt
University Centre of Orthopaedics and Trauma Surgery, University Hospital Carl Gustav Carus, Dresden, Germany
- P97 Characterization of Oxygen Plasma-treated Dental All-Ceramic Zirconia**
Hsiang Kao, Chung-Kai Wei and Shinn-Jyh Ding
Institute of Oral Science, Chung Shan Medical University, Taichung, Taiwan
- P98 High throughput screening of hMSC response to algorithm generated micro-topographies**
Frits F.B. Hulshof, Bernke J. Papenburg, Roman K. Trückenmuller, M. Hulsman, Natalie Fekete, Shantanu Sing, Clemens A. van Blitterswijk, Anne E. Carpenter, Dimitrios Stamatialis, Jan de Boer
Department of Tissue regeneration, University of Twente, Enschede, The Netherlands
- P99 On the Biocompatibility of UV Pre-irradiated Hydrothermally Grown TiO₂-coatings**
Martina Lorenzetti, Giulia Bernardini, Katja Trinkaus, Iztok Dogsa, Thomas Luxbacher, Katrin Susanne Lips, Annalisa Santucci, Reinhard Schnettler, David Stopar, Saša Novak and Spomenka Kobe
Department of Nanostructured Materials, Jožef Stefan Institute, Ljubljana, Slovenia
- P100 Fabrication of Tissue Engineering Scaffolds from Poly(ester-anhydride) by Projection Stereolithography**
Harri Korhonen, Pekka Lehtinen, Jouni Partanen, Jukka Seppälä
Laboratory of Polymer Technology, Aalto University, Finland
- P101 Immobilization Strategies to Functionalize Tantalum Surfaces with Cell-Adhesive Peptides: Physicochemical and Biological Characterization**
Carlos Mas-Moruno, Beatriz Garrido, Daniel Rodríguez, Elisa Ruperez, F. Javier Gil
Biomaterials, Biomechanics and Tissue Engineering Group, Universitat Politècnica de Catalunya, Spain
- P102 Novel sol-gel synthesis of (P₂O₅)₅₀-(CaO)₃₀-(Na₂O)₁₅-(Fe₂O₃)₅ glasses for biomedical application**
Farzad Foroutan, Nora de Leeuw and Jonathan Knowles
Division of Biomaterials and Tissue Engineering, University College London, UK
- P103 Development of novel nanofunctionalised glass ionomer cements containing chlorhexidine-hexametaphosphate nanoparticles: mechanical properties and method of incorporation**
Candice A Bellis, James A Holder, Dominic J O'Sullivan, Michele E Barbour
Oral Nanoscience, UK Kempton
- P104 Evaluation of the effect of polymer content on drug release and mechanical strength of a Geopolymer ER Formulation for opioid drugs**
Bing Cai, Håkan Engqvist, Susanne Bredenberg
Division for Applied Materials Science, Uppsala University, Sweden
- P105 Poly(butylene succinate) nanocomposites containing strontium hydroxyapatite nanorods for tissue engineering applications**
M. Nerantzaki, Z. Terzopoulou, E. Roumeli, D. Papageorgiou, D. Bikiaris, J. Will, J. Hum, A. Hoppe, J.A. Roether, A.R. Boccaccini
Chemistry Department, Aristotle University of Thessaloniki, Greece

- P106 New N-(2-carboxybenzyl)chitosan hybrid biocomposites for scaffolds applications**
M. Nerantzaki, Z. Terzopoulou, M. Mavidou, D.N. Bikiaris, M.D. Anastasopoulou, M.A. Karakassides, A.R. Boccaccini
 Chemistry Department, Aristotle University of Thessaloniki, Greece
- P107 Release of Propranolol hydrochloride from Polyethyleneglycol Modified Lactone Polymers**
Sanja Asikainen, Minna Malin and Jukka Seppälä
 Research Group of Polymer Technology, Aalto University, Finland
- P108 Titanium oxide coated cobalt-chromium-molybdenum; improving the osteogenic response of mesenchymal stem cells *in vitro***
N Logan, A Cross, S Collins, A Trayner, I Parkin, L Bozec and P Brett
 Biomaterials and Tissue Engineering, University College London, UK
- P109 Autophagy Modification by Intracellular Controlled Release of Rapamycin**
Junpei Nagata, Makoto Matsui and Yasuhiko Tabata
 Department of Biomaterials, Kyoto University, Japan
- P110 Bioactive orthopaedic devices for the local delivery of Gentamicin Sulfate preventing nosocomial infections**
Loïc Pichavant, Hélène Carrié, Laurent Plawinski, Valérie Héroguez and Marie-Christine Durrieu
 Laboratoire de Chimie des Polymères Organiques, Université de Bordeaux, Pessac, France
- P111 Design of a new composite structure based on resorbable synthetic and natural polymers for anterior cruciate ligament reconstruction**
Coline Pinese, Xavier Garric, Benjamin Notellet, Jean Coudane, Christian Gagnieu
 Artificial Biopolymers department, Montpellier I University, France
- P112 Impact of silver-coated wound dressings on bacteria biofilm viability for the prevention of skin infections**
Federica Paladini, Cinzia Di Franco, Angelica Panico, Gaetano Scamarcio, Alessandro Sannino, Mauro Pollini
 Dhitech Scarl, Lecce, Italy
- P113 Characterization of Antibacterial Nano-Silver Coated Hydrogel Fibers for Biomedical Applications**
Riccardo Raho, Fiorella Anna Lombardi, Federica Paladini, Sandro Boccarella, Alessandro Sannino, Mauro Pollini
 Department of Engineering for Innovation, University of Salento, Lecce, Italy
- P114 Optimization of Silicone as Implant Material for the Application in the Middle Ear: Incorporation of Functionalized Nanoporous Silica Nanoparticles**
Tanja Heemeier, Mandy Jahns, Songül Noyun, Laura Doniga-Grivat, Silke Besdo, Peter Behrens
 Institute for Inorganic Chemistry, Leibniz University of Hannover, Germany
- P115 Temporary implant surfaces equipped with an anti-adhesive plasma fluorocarbon polymer film**
Birgit Finke, Holger Tetrich, Henrike Rebl, J. Barbara Nebe, Rainer Bader, Uwe Walschus, Michael Schlosser, Klaus-Dieter Weltmann, Jürgen Meichsner
 Leibniz Institute for Plasma Science and Technology, Greifswald, Germany
- P116 Biocompatible Conductive Coatings based on Carbon Nanotubes**
Niklas Burblies, Katharina Kranz, Athanasia Warnecke, Peter Behrens
 Institute of Inorganic Chemistry, Leibniz Universität Hannover, Germany
- P117 Installing multifunctionality on titanium with RGD-decorated polymeric nanocapsules: Towards new osteointegrative therapies**
Pau Rocas-Alonso, Mireia Hoyos-Nogués, Josep Rocas, Fernando Albericio, José M. Manero, Javier Gil, Carlos Mas-Moruno
 Institute for Research in Biomedicine, Barcelona, Spain
- P118 Improvement of Electrode Surfaces for Biomedical Applications by Nanoporous Platinum Coatings**
Kim D. Kreisköther, Nina Ehlert, Natalja Wendt, Hans-Christoph Schwarz, Athanasia Warnecke, Katharina Kranz, Peter Behrens
 Institute of Inorganic Chemistry, Leibniz Universität Hannover, Germany
- P119 Vancomycin loaded bioactive orthopaedic devices preventing infections**
Hélène Carrié, Loïc Pichavant, Laurent Plawinski, Gilles Amador, Valérie Héroguez and Marie-Christine Durrieu
 Laboratoire de Chimie des Polymères Organiques, Université de Bordeaux, Pessac, France
- P120 Amidation via DMTMM: A New and Efficient Method for Hyaluronan Biomaterials Preparation**
Matteo D'Este, Mauro Alini, David Eglin
 AO Research Institute Davos, Switzerland
- P121 Silver nano-coatings on silk sutures for the prevention of surgical infections**
De Simone Serena, Gallo Anna Lucia, Paladini Federica, Sannino Alessandro, Pollini Mauro
 Dhitech Scarl, Lecce, Italy
- P122 Functionalisation of polyurethane films using YIGSR poly(ϵ -lysine) linked dendrons to manipulate the human mesenchymal cell response**
Anna Guildford, Nicola Contessi, Mariagemiliana Dessi, Steve Meikle, Serena Bertoldi, Silvia Fare, Maria Cristina Tanzi and Matteo Santin
 School of Pharmacy and Biomolecular Sciences, University of Brighton, UK
- P123 WITHDRAWN**
- P124 Synthesis and Characterization of Chitosan/Hydroxyapatite Biocomposite Scaffolds for Potential Bone Repair Applications**
Vitor César Dumont, Nádia S. Vieira Capanema, Alexandra A. Piscitelli Mansur and Herman Sander Mansur
 Center of Nanoscience, Nanotechnology and Innovation-CeNano²I, Federal University of Minas Gerais, Brazil
- P125 Synthesis of morphology controlled calcium phosphate nanobiomaterials for biomedical applications**
P.J.T. Reardon, J. Huang, J. Tang
 Department of Chemical Engineering and Mechanical Engineering, University College London, UK

- P126 Dextran as a Versatile Scaffold for Hydrogel Formation with Hyaluronic Acid**
Nick Dibbert, Bastian Dieter, Gerald Dräger and Andreas Kirschning
 Institute of Organic Chemistry, Leibniz University Hannover, Germany
- P127 Adsorption of Col I on poly(NaSS) grafted Ti6Al4V surfaces improves MC3T3-E1 osteoblast-like cells mineralization**
Helena Felgueiras and Véronique Migonney
 Laboratory of Biomaterials and Specialty Polymers, Université Paris XIII, France
- P128 Enhancement of integrin-mediated cell attachment by pre-adsorbed model proteins on poly(NaSS)-functionalized Ti6Al4V substrates: a QCM-D study**
Helena Felgueiras, Sven Sommerfeld, N. Sanjeeva Murthy, Joachim Kohn and Véronique Migonney
 Laboratory of Biomaterials and Specialty Polymers, Université Paris XIII, France
- P129 Predicting Change in Constitutive Behaviour of Degrading Polymers**
Hassan Samami, Jingzhe Pan
 Department of Engineering, University of Leicester, UK
- P130 Nitric oxide releasing polyester blends for topical skin vasodilation**
Victor Baldim and Marcelo Ganzarolli de Oliveira
 Institute of Chemistry, University of Campinas, Brazil
- P131 Structural Integrity Assessment of a Polymer-based Knee Implant**
Y. Fong, P. Reed, F. Pierron and M. Browne
 Bioengineering Science Research Group, University of Southampton, United Kingdom
- P132 Fabrication of hydroxyapatite thin film with entirely c-plane surface**
Masanobu Kusunoki, Yasuhiro Sakoishi, Katsuya Asano, Naoki Fujita, Takayuki Makino, Daisuke Oka
 Faculty of Biology-Oriented Science and Technology, Kinki University, Japan
- P133 A Parametric Study of a Mathematic Model for Degradation of Bioresorbable Polymers**
X. Chen and J. Pan
 Department of Engineering, University of Leicester, UK
- P134 Patient Specific Implants Using a Novel Rapid Template Approach**
A. Chan, P. Boughton, J. van Gelder, N. Young and A. Ruys
 Biomedical Engineering, University of Sydney, Australia
- P135 Use of Ivory to Assess Composite Dentine Bonding**
Saad Liagat, Paul Ashley, Laurent Bozec, Anne Young
 Eastman Dental Institute, University College London, UK
- P136 Preparation of Porous Titanium-Polyglycolide Composites**
Nobuyuki Hayashi, Shun Kojima, Masato Ueda, Masahiko Ikeda, Kenji Doi, Kazuki Hanami, Shigeo Mori, Hisashi Kitagaki, Shuntaro Terauchi
 Graduate School of Science and Engineering, Kansai University, Japan
- P137 Mechanical Properties and Surface of Ultrafine Grained Titanium for Dental Implants**
Carlos Nelson Elias, Daniel J. Fernandes, Jochen Roestel
 Instituto Militar de Engenharia, Brazil
- P138 Preparation and Characterization of Novel Composite Agarose Films for Wound Healing**
Alma Akhmetova, Matthew Illsley, Timur Saliev, Talgat Nurgozhin, Sergey Mikhailovsky and Iain Allan
 Department of Translational Medicine, Longevity and Global Health, Nazarbayev University, Kazakhstan
- P139 New approaches for the local prevention and treatment of fragilized osseous sites using doped-calcium phosphate cements**
C. Mellier, V. Schnitzler, E. Verron, F. Fayon, C. Despas, A. Walcarius, N. Rochet, J.-C. Scimeca, O. Gauthier, J.-M. Boulter, B. Bujoli and P. Janvier
 Pres L'Unam, CNRS UMR 6230, Nantes, France
- P140 Robotic Deposition of 3D Scaffolds Using β -tricalcium Phosphates Inks for Bone Regeneration**
Raquel Costa Richard, Renata Nunes Oliveira, Rossana Mara da Silva Moreira Thiré
 Department of Materials Engineering, Federal University of Rio de Janeiro, Brazil
- P141 Evaluation of Bone Replacement Materials in a Rabbit Cranial Defect Model using MicroCT and Hard Tissue Histology**
Gerlind Schneider and Dirk Linde
 Department of Otorhinolaryngology, Friedrich Schiller University Hospital, Jena, Germany
- P142 A New Analytical Model of GAAS MESFET With Different Laws of Mobility**
Y. Saidi, Z. Fares
 Department of Physics, Mentouri University, Constantine, Algeria
- P143 Tailoring the Interfacial Adhesion of Anodised TiO₂ Nanotubes on Ti-6Al-4V Alloy for Medical Implants**
U. Danookdharree, H. R. Le, R. Handy and C. Tredwin
 School of Marine Science and Engineering, University of Plymouth, UK
- P144 Nano-sized α -tricalcium phosphate for bone cement**
L. Vecbiskena, L. Altomare, L. De Nardo, R. Chiesa
 Institute of Biomaterials and Biomechanics, Riga Technical University, Latvia
- P145 Single Cell Tracking of Haematopoietic Stem Cells in 3D Biomimetic Gradients**
Michael Ansorge, Jiranuwat Sapudom, Tilo Pompe
 Institute of Biochemistry, Universität Leipzig, Germany
- P146 Electrochemical dissolution of stainless steel endodontic files fractured in the middle and apical thirds of the root canal**
Caroline Amaral, Fabiola Ormiga and José Ponciano Gomes
 Department of Metallurgy and Materials, Federal University of Rio de Janeiro, Brazil

- P147 Photochemical nitric oxide release from a Flutamin derivative incorporated in Pluronic F127 hydrogel**
Patricia Taladriz-Blanco and Marcelo G. de Oliveira
 Institute of Chemistry, University of Campinas, Brazil
- P148 Electrospun Human Hair Keratin Matrices Affect Human Fibroblast Behavior Through Topographical Cues**
Wan Ting Sow and Kee Woei Ng
 School of Materials Science and Engineering, Nanyang Technological University, Singapore
- P149 Release Kinetics of Gentamicin, Moxifloxacin, Vancomycin, and Colistin from Gelatin Micro- and Nanospheres**
J. Song, J. Odekerken, D. Löwik, T. Welting, F. Yang, J. Jansen and S. Leeuwenburgh
 Department of Biomaterials, Radboud University Medical Centre, The Netherlands
- P150 Atmospheric Plasma Surface Modification of Electrospun Poly(L-Lactic Acid): Effect on Mat Properties and Cell Culturing**
Laura Calzà, Vittorio Colombo, Luisa Stella Dolci, Andrea Fiorani, Maria Letizia Focarete, Matteo Gherardi, Romolo Laurita, Anna Liguori, Santiago David Quiroga, Paolo Sanibondi
 Department of Industrial Engineering, Università di Bologna, Italy
- P151 Development and characterization of a tridimensional intestinal model to study protein drugs absorption**
Carla Pereira, Francisca Araújo, Pedro L. Granja, Bruno Sarmento
 Instituto de Engenharia Biomédica, University of Porto, Portugal
- P152 Antifouling coatings of poly(ethylene glycol) on titanium for dental implants**
Judit Buxadera-Palomero, Sergi Torrent, Cristina Calvo, F. Javier Gil, Cristina Canal, Daniel Rodríguez
 Biomaterials, Biomechanics and Tissue Engineering group, Technical University of Catalonia, Barcelona, Spain
- P153 Hierarchical Structure of Multicomponent Polysaccharide-Based ECM Mimetics**
Ortal Levi, Guy Hochbaum and Ronit Bitton
 Department of Chemical Engineering, Ben-Gurion University of the Negev, Israel
- P154 Scavenging effect of Trolox released from brushite cements**
Gemma Mestres, Carlos F Santos, Lars Engman, Cecilia Persson, Marjam Karlsson Ott
 Department of Engineering Sciences, Uppsala University, Sweden
- P155 Thermomechanical properties and bioactivity of silicone hybrids containing inorganic biomedical fillers**
I.-G. Athanasoulia, S.P. Vasilakos, P.A. Tarantili, Tr. Papadopoulos
 Dental School, University of Athens, Greece
- P156 Kartogenin Conjugated Chitosan-Nano/Microparticles for the Intra-Articular Osteoarthritis Treatment**
Mi Lan Kang, Ji Yun Ko, Ji Eun Kim, Gun Il Im
 Department of Orthopedics, Dongguk University, Ilsan Hospital, Korea
- P157 Composition-Property Relationships for Lanthanum-Borate Glasses**
K. O'Connell, H. O'Shea, Muhammad Hasan, D. Boyd
 Department of Biological Sciences, Cork Institute of Technology, Ireland
- P158 Osteogenic Differentiation of AdMSCs on 17 β -Estradiol Releasing Chitosan-Hydroxyapatite Scaffolds**
Gülseren İrmak, T. Tolga Demirtaş, Damla Altındal, Mert Çalış, Menemşe Gümüşderelioğlu
 Bioengineering Department, Hacettepe University, Turkey
- P159 Understanding the Physiochemical Interactions between Denture Adhesives and the aqueous phase**
S. Gill, B.J Tighe, N. Roohpour, C. Jeffrey
 Biomaterials Research Unit, Aston University, Birmingham, UK
- P160 New approach of biomaterial design to enhance osteogenesis at the interface bone/implant**
Ibrahim Bilem, Pascale Chevallier, Laurent Plawinski, Eli Sone, Gaétan Laroche, Marie-Christine Durrieu
 Laboratory of Surface Engineering, Laval University, Canada
- P161 Development of nanostructured silicone copolymers to deliver antimicrobials to treat human infected wounds**
S Finnegan, S Rimmer, S Macneil, S Percival
 Department of Chemistry, University of Sheffield, UK
- P162 Development of new approaches to fabricate scaffolds for deep zone engineered articular cartilage**
Anne Canning, Paul Roach, Ying Yang, James Richardson
 Institute of Science and technology, University of Keele, UK
- P163 Adhesives and their role in the reduction of HCAI, skin and wound infections**
Steven L Percival, Rebecca Booth and Sean Kelly
 Institute of Ageing and Chronic Disease, University of Liverpool, UK
- P164 The utilisation of poloxamer as a model to study the complexicity of biofilms and antimicrobial efficacy in biomaterials**
Steven L Percival, Rebecca Booth and Sean Kelly
 Institute of Ageing and Chronic Disease, University of Liverpool, UK
- P165 The use of the MBEC assay for quantitative and qualitative investigation of biofilm forming isolates isolated from biomaterials**
Rebecca Booth, Sean Kelly and Steven L Percival
 Scapa Healthcare, Manchester, UK
- P166 Physical and chemical characteristics of adhesives for application on the skin**
Sean Kelly, Rebecca Booth and Steven L Percival
 Scapa Healthcare, Manchester, UK
- P167 The role of adhesives in biofilm prevention**
Steven L Percival, Rebecca Booth and Sean Kelly
 Institute of Ageing and Chronic Disease, University of Liverpool, UK

- P168** **Silicone adhesives and their use in skin and wound care**
Sean Kelly, Rebecca Booth and Steven L Percival
Scapa Healthcare, Manchester, UK
- P169** **A Computer Model for Polymer Degradation in the Presence of Acidic Drug**
K. Sevim and J. Pan
Department of Engineering, University of Leicester, UK
- P170** **In vitro degradability, bioactivity and cell responses to mesoporous magnesium silicate for bone regeneration**
Jie Wei, Zhaoying Wu, Han Guo, Changsheng Liu
Key Laboratory for Ultrafine Materials, East China University of Science and Technology, P.R. China
- P171** **Macromolecular crowding maintains tenogenic phenotype ex vivo**
Kyriakos Spanoudes, Abhigyan Satyam, Abhay Pandit, Dimitrios Zeugolis
Network of Excellence in Functional Biomaterials, National University of Ireland, Galway
- P172** **Effect of cooling rates after casting and subsequent Solution Treatment on Microstructure and Mechanical Strength of Dental Silver Alloys with different Cu contents**
Tomoya Yasuda, Toshiyazu Akahori, Yushi Hoshiya, Tomokazu Hattori, Hisao Fukui
Graduate School of Science and Technology, Meijo University, Japan
- P173** **Change in Microstructure and Mechanical Strength of Substitution Material for Dental Precious Alloys Fabricated by Solidification under Various Conditions**
Yushi Hoshiya, Toshiyazu Akahori, Tomoya Yasuda, Tomokazu Hattori, Hisao Fukui
Graduate School of Science and Technology, Meijo University, Japan
- P174** **Morphological Control of Layered Double Hydroxide Crystals as Drug Carrier by Organic Molecules with Carboxyl Group**
Taishi Yokoi, Sota Terasaka and Masanobu Kamitakahara
Graduate School of Environmental Studies, Tohoku University, Japan
- P175** **Properties of β -TCP based Calcium Phosphate Cement using mechano-chemical process**
J. Y. Bae, Y. Ida, K. Sekine, F. Kawano and K. Hamada
Department of Biomaterials and Bioengineering, University of Tokushima, Japan
- P176** **Evaluation of osteoinductive properties of different combinations of macroporous biphasic ceramic (MBCP+™), simvastatin, total bone marrow cells and rhBMP-2 in a rat subcutaneous induced membranes model**
Erwan de Monès, Silke Schlaubitz, Reine Bareille, Chantal Bourget, Pascal Borget, Guy Daculsi, Marlène Durand, Jean-Christophe Fricain
Bioingénierie Tissulaire, Université Bordeaux, France
- P177** **Development and Characterization of Thermally Responsive PluronicF127-Chitosan-Kartogenin Conjugates Based Dual Drug Delivery System**
Mi Lan Kang, Ji Yun Ko, Ji Eun Kim, Gun Il Im
Department of Orthopedics, Dongguk University Ilsan Hospital, Korea
- P178** **Transduction of Tissue-specific Transcription Factor Protein as a Tool for Tissue Engineering**
Masayasu Mie, Shinya Hashimoto, Mami Kaneko and Eiry Kobatake
Department of Environmental Chemistry and Engineering, Tokyo Institute of Technology, Japan
- P179** **Construction of Multifunctional Proteins by Integration of Scaffolds and Growth Factors**
Eiry Kobatake and Masayasu Mie
Department of Environmental Chemistry and Engineering, Tokyo Institute of Technology, Japan
- P180** **Gel-in-Gel extrusion of cells for soft and hard tissue construction**
Erkan Türker Baran and Vasif Hasirci
Center of Excellence in Biomaterials and Tissue Engineering, Middle East Technical University, Turkey
- P181** **Real-time monitoring of chondrocyte activity by electrical impedance measurement**
R. Mizota, Y. Morita and E. Nakamachi
Graduate School of Life and Medical Sciences, Doshisha University, Japan
- P182** **Dynamic Hardness Evaluation of Two Phases of Au-xPt-8Nb Alloys for MRI-artifact-free Biomedical Devices**
S. Inui, E. Uyama, E. Honda and K. Hamada
Institute of Health Biosciences, University of Tokushima, Japan
- P183** **Electrospun fleeces fabricated from new biodegradable polyurethanes and evaluation of their use as tissue engineering scaffolds for adipose-derived stem cells**
Thorsten Laube, Alfred Gugerell, Ralf Wyrwa, Johanna Kober, Torsten Walter, Sylvia Nürnberger, Elke Grönniger, Simone Brönneke, Maike Keck, Matthias Schnabelrauch
Biomaterials Department, INNOVENT eV, Jena, Germany
- P184** **Design, Synthesis and Development of a Self-Assembled Polymeric Nanoparticle System for Gene Delivery**
Li-yen Wong, Ernst Wolvetang, Justin Cooper-White
Tissue Engineering and Microfluidics Laboratory, University of Queensland, Brisbane, Australia
- P185** **Biological Properties of an Acellular Xenogeneic Tendon Graft following Chemical and Irradiation Sterilisation**
J H Edwards, J Fisher and E Ingham
Institute of Medical and Biological Engineering, University of Leeds, UK
- P186** **Improved early cell adhesion on bioinert ceramics by alkaline phosphatase immobilization**
Alieh Aminian, Bahareh Shirzadi, Laura Treccani and Kuroschi Rezwan
Advanced Ceramics, University of Bremen, Germany
- P187** **Thermoresponsive Hydrophobic Copolymer Brush for Cell Separation by Multi-Step Temperature Change**
Kenichi Nagase, Yuri Hatakeyama, Tatsuya Shimizu, Katsuhisa Matsuura, Masayuki Yamato, Naoya Takeda, Teruo Okano
Tokyo Women's Medical University, Japan

- P188 A Novel Biological Polyester Based Wet Spun Scaffold for Bone Tissue Engineering**
Ayşe Selcen Alagoz, Jose Carlos Rodriguez-Cabello, Nesrin Hasirci, Vasif Hasirci
 Department of Biological Sciences, Middle Eastern Technical University, Turkey
- P189 Development of novel hydroxyapatite-chitosan porous 3D scaffolds for biomedical applications**
Dimitris Tsiourvas and Triantafillos Papadopoulos
 Department of Biomaterials, School of Dentistry, University of Athens, Greece
- P190 Controlled release of drugs from innovative multi-layered biodegradable coating on polymeric orthopaedic implants**
Nerea Argarate, Beatriz Olalde, Garbiñe Atorrasagasti, Jesus Valero, Sandra Carolina Cifuentes, Rosario Benavente, Marcela Lieblich, Jose Luis González-Carrasco
 Networking Research Centre on Bioengineering, Biomaterials and Nanomedicine, Spain
- P191 Study on calcium silicate / zein scaffold implanted in vivo by synchrotron radiation-based X-ray Imaging**
Han Guo, Jie Wei, Changsheng Liu, Tiqiao Xiao
 Shanghai Institute of Applied Physics, CAS, P R China
- P192 Fabrication and Characterization of Gelatin-based Polyurethane Vascular Graft for Tissue-engineering Applications**
Paola Losi, Enrica Briganti, Luisa Mancuso, Alice Gualerzi, Tamer Al Kayal, Simona Celi, Silvia Volpi, Giacomo Cao, Giorgio Soldani
 Laboratory of Biomaterials & Graft Technology, Institute of Clinical Physiology, Massa, Italy
- P193 Controlling the Delivery of Vascular Endothelial Growth Factor and Platelet Derived Growth Factor**
Laura Kelly, Laura Platt, Sheila MacNeil, Paul Genever, Tim Chico, Stephen Rimmer
 Department of Chemistry, University of Sheffield, UK
- P194 Cell Behaviour on Self-assembled Nanohole Arrays on Type 316L Stainless Steel Formed by Anodic Process**
Sayaka Miyabe, Yushi Fujinaga, Hiroaki Tsuchiya and Shinji Fujimoto
 Division of Materials and Manufacturing Science, Osaka University, Japan
- P195 Strontium-substituted CaP bone cements for the treatment of osteoporotic bone defects**
Matthias Schumacher, Arne Helth, Anja Lode, Anne Bernhardt, Anja Henß, Marcus Rohnke, Seemun Ray, Ulrich Thormann, Volker Alt and Michael Gelinsky
 Centre for Translational Bone, Joint and Soft Tissue Research, Technische Universität Dresden, Germany
- P196 Mesoporous bioactive glass/CaP bone cement composites as drug delivery system**
Matthias Schumacher and Michael Gelinsky
 Centre for Translational Bone, Joint and Soft Tissue Research, Technische Universität Dresden, Germany
- P197 The influence of PEG/PCL ratio on properties of PU/ β -TCP composites for orthopaedic applications**
Piotr Szczepańczyk, Kinga Pielichowska, Jan Chłopek
 AGH University of Science and Technology, Department of Biomaterials, Kraków, Poland
- P198 Effect of fibre reinforcement on the crystallinity of PEEK for articular joint implants**
Marco Regis, Simonetta Fusi, Michele Pressacco, Marco Zanetti and Pierangiola Bracco
 R&D Department, Limacorporate, Italy
- P199 Effect of surface roughness on the biocompatibility of $\text{Ti}_{40}\text{Zr}_{10}\text{Cu}_{38}\text{Pd}_{12}$ bulk metallic glass**
Andreu Blanquer, Anna Hynowska, Carme Nogués, Elena Ibáñez, Maria Dolors Baró, Jordi Sort, Eva Pellicer and Lleonard Barrios
 Dept. Biologia Cellular, Fisiologia i Immunologia, Universitat Autònoma de Barcelona, Spain
- P200 Plasma assisted production of residual solvent free PLLA electrospun scaffolds**
V. Colombo, D. Fabiani, M.L. Focarete, M. Gherardi, C. Gualandi, R. Laurita, M. Zaccaria
 Department of Industrial Engineering, Università di Bologna, Italy
- P201 Fabrication of Stable Biocatalytic Networks for the Cascadable Manufacture of Fine Chemicals**
Christopher Hickling, Helen Toogood, Alberto Saiani, Nigel Scrutton and Aline Miller
 Chemical Engineering and Analytical Sciences, Manchester Institute of Biotechnology, University of Manchester, UK
- P202 Crosslinked albumin hydrogel as adhesion barrier to prevent postoperative fibrosis**
Burkhard Schlosshauer, Dominic Stadel, Elke Rist, Helmut Wurst, Jürgen Mollenhauer, Erich K. Odermatt
 NMI Natural and Medical Sciences Institute, Reutlingen, Germany
- P203 Local Inflammatory Tissue Response After Implantation of Electrospun Polylactide Fiber Meshes With and Without Plasma-Polymerized Allylamine in Rats**
Andreas Hoene, Matthias Schnabelrauch, Ralf Wyrwa, Birgit Finke, Silke Lucke, Uwe Walschus, Michael Schlosser
 Department of Surgery, University Medical Center Greifswald, Germany
- P204 Differentiation of Macrophage Involvement in Tissue Regeneration Following Implantation of Biodegradable Matrices in Rats**
Silke Lucke, Uwe Walschus, Andreas Hoene, Jens-Wolfgang Pissarek, Matthias Schnabelrauch, Michael Schlosser
 Department of Medical Biochemistry and Molecular Biology, University Medical Center Greifswald, Germany
- P205 In vitro and in vivo osteoinductive potential of polycaprolactone-based bioactive composite scaffold fabricated via additive manufacturing technology**
Patrina S. P. Poh, Dietmar W. Hutmacher, Boris M. Holzapfel, Molly M. Stevens and Maria A. Woodruff
 Institute of Health and Biomedical Innovation, Queensland University of Technology, Australia
- P206 PLA-Glass Composites For Bone Tissue Engineering**
João S. Fernandes, Ricardo A. Pires, Rui L. Reis
 3B's Research Group, University of Minho, Guimarães, Portugal
- P207 Stability of Peptide Hydrogels in Cell Culture Conditions**
I. Nawi, V. L. Workman, A. M. Smith, A. F. Miller and A. Saiani
 School of Materials & Manchester Institute of Biotechnology, The University of Manchester, UK

- P208 Guiding bone cells with surface patterned nano-calcium phosphate**
Gillian Munir, Mohan J. Edirisinghe, Lucy Di Silvio, Miriam Rafailovich and Jie Huang
 Department of Mechanical Engineering, University College London, UK
- P209 The Potential Role of Statins in the Regeneration of Osteoporotic Tissue and the Use of Star Degradable Polymers for Controlled Local Delivery**
Jason Burke, Sarah Cartmell, Nicola Tirelli
 Institute of Inflammation & Repair, University of Manchester, UK
- P210 Effective Cellular Uptake of Exosomes Using Cationic Lipids and pH-sensitive Fusogenic Peptide**
Ikuhiko Nakase
 Nanoscience and Nanotechnology Research Center, Osaka Prefecture University, Japan
- P211 Borates-loaded Biomaterials to trigger Cell Differentiation**
P. Rico, A. Rodrigo-Navarro, M. Salmerón-Sánchez
 Center for Biomaterials and Tissue Engineering, Universitat Politècnica de València, Spain
- P212 Animal Experiment on In-vivo Galvanic Corrosion of SUS316L and Ti-6Al-4V. Observation of tissue reaction at 52 weeks after implantation**
Y. Kato, A. Ito, T. Hattori, T. Akahori, N. Kimata, K. Sato
 Dept. of Materials Science and Engineering, Meijo University, Nagoya, Japan
- P213 The degradation relationship between mechanical and in vitro testing of a phosphate glass fibre composite**
R. J. Colquhoun and Prof K.E. Tanner
 Department of Biomaterials, University of Glasgow, UK
- P214 Animal Experiment on In-vivo Galvanic Corrosion of SUS316L and Ti-6Al-4V. Surface observation and EPMA element mapping analysis**
A. Ito, Y. Kato, T. Hattori, T. Akahori, N. Kimata, K. Sato
 Dept. of Materials Science and Engineering, Meijo University, Nagoya, Japan
- P215 Nanoscale Roughness Influences on Cell Proliferation**
Prabhjeet Kaur Dhillon, Ajay Kumar, Shalmoli Bhattacharyya and Subhendu Sarkar
 Department of Physics, Indian Institute of Technology Ropar, Punjab, India
- P216 Role of Fibronectin assembly in Mesenchymal Stem Cell differentiation**
P. Rico, H. Mnatsakanyan, M. Salmerón-Sánchez
 Center for Biomaterials and Tissue Engineering, Universitat Politècnica de València, Spain
- P217 Graphene oxide and 4-arm-PPO-PEO composite hydrogels for injectable biomedical applications**
Yunki Lee, Jin Woo Bae, and Ki Dong Park
 Department of Molecular Science and Technology, Ajou University, Suwon, Republic of Korea
- P218 pH-Mediated Surfactant Release in the Development of Self-Sterilising Urinary Biomaterials**
C. P. McCoy, J. L. Trotter, N. J. Irwin, L. Carson, D. S. Jones
 School of Pharmacy, Queen's University Belfast, UK
- P219 Silica Beads Grafted with Thermoresponsive Cationic Copolymer Brush Possessing Quaternary Amine Group for Effective Thermoresponsive Ion-exchange Chromatography**
Kenichi Nagase, Mike Geven, Saori Kimura, Jun Kobayashi, Akihiko Kikuchi, Yoshikatsu Akiyama, Dirk W. Grijpma, Hideko Kanazawa and Teruo Okano
 Institute of Advanced Biomedical Engineering and Science, Tokyo Women's Medical University, Japan
- P220 Thermo-Responsive Nano-Structured Surface Modulates Cell Adhesion and Detachment**
Yoshikazu Kumashiro, Morito Sakuma, Masamichi Nakayama, Nobuyuki Tanaka, Kazuo Umemura, Masayuki Yamato and Teruo Okano
 Institute of Advanced Biomedical Engineering and Science, Tokyo Women's Medical University, Japan
- P221 Reciprocating Sliding Friction of Polyvinyl Alcohol Hydrogels as Articular Cartilage Substitutes**
Takashi Hayami, Koji Morimoto, Yoshihiro Kimura, Noriyasu Hirokawa and Tadashi Shibue
 Faculty of Biology-Oriented Science and Technology, Kinki University, Japan
- P222 Comparison of Inverse-opal and Salt-leached Silk Fibroin Scaffolds for Bone Tissue Engineering**
Marianne Sommer, Jolanda Vetsch, Jessica Leemann, Ralph Müller, Sandra Hofmann and André Studart
 Department of Materials, ETH Zurich, Switzerland
- P223 Towards Biocompatible Medical Devices: Modification of Polymer and Metal Surfaces**
J. Buchholz, C. Hess, A. Kirschning, L. Möller, M. Pflaum, S. Schmeckebeier, M. Stiesch, B. Wiegmann, A. Winkel, G. Dräger
 Institute of Organic Chemistry, Gottfried Wilhelm Leibniz Universität Hannover, Germany
- P224 Evaluation of network and pore morphology of self-assembling peptides for biomimetic therapy**
Franziska Koch and Uwe Piele
 ICB/Nanotechnology, University of Applied Sciences, Muttentz, Switzerland
- P225 Morphological Gradients for Protein-Adsorption and Blood-Interaction Studies**
Rebecca P. Huber, Katharina Maniura-Weber, Nicholas D. Spencer
 Department of Materials, ETH Zurich, Switzerland
- P226 An Innovative Intraocular Lens Surface Functionalization to Control Posterior Capsular Opacification**
Yi-Shiang Huang, Virginie Bertrand, Dimitriya Bozukova, Christophe Pagnouille, Edwin De Pauw, Marie-Claire De Pauw-Gillet and Marie-Christine Durrieu
 Institut Européen de Chimie et Biologie, University of Bordeaux I, Pessac, France
- P227 Optical Projection Tomography as a Tool for Visualizing Hydrogels Microstructures**
A. M. Soto, J. Koivisto, J. E. Parraga, J. Silva-Correia, J. M. Oliveira, R. L. Reis, M. Kellomäki, J. Hyttinen, E. Figueiras
 Computational Biophysics and Imaging Group, Tampere University of Technology, Finland

- P228 Adsorption Profiles of Inflammatory Cytokines by Activated Carbon Beads and Monoliths for Haemoperfusion**
Alma Akhmetova, Sergey Mikhailovsky, Timur Saliev, Talgat Nurgozhin
Department of Translational Medicine, Nazarbayev University, Kazakhstan
- P229 Evaluation of short-term degradation of bicomponent electrospun fibres via AFM analysis**
Marica Marrese, Vincenzo Guarino, Valentina Cirillo, Luigi Ambrosio
Institute for Polymers, Composites and Biomaterials, National Research Council of Italy, Naples, Italy
- P230 Optimization of titanium foam scaffold with bioactive surface obtained by chemical treatment**
Cristina Caparrós, Mónica Ortiz-Hernandez, Meritxell Molmeneu, Miquel Punset, Jose Antonio Calero, F. Javier Gil
Biomaterials, Biomechanics and Tissue Engineering Group, Technical University of Catalonia, Barcelona, Spain
- P231 Application of Central Composite Design to Evaluate the Effect of Dry-Spinning Parameters on Poly (ϵ -caprolactone) Fibers Properties**
B. Azimi, P. Nourpanah, M. Rabiee, M. G. Cascone, A. Baldassare, S. Arbab, L. Lazzeri
Department of Textile Engineering, Amirkabir University of Technology, Tehran, Iran
- P232 Gentamicin-Loaded Microparticles Immobilized on Porous Scaffolds for Prevention of Biomaterials-Related Bone Infections**
Urszula Posadowska, Malgorzata Krok-Borkowicz, Lucja Rumian, Elzbieta Pamula
Faculty of Materials Science and Ceramics, AGH – University of Science and Technology, Krakow, Poland
- P233 Investigating Mesenchymal Stem Cell Self-Renewal on Nanotopography**
L.C.Y. Lee, L.A. Turner, N. Gadegaard, S. Yarwood, R.M.D. Meek, M.J. Dalby
Centre for Cell Engineering, University of Glasgow, UK
- P234 Elastomeric Polycaprolactone scaffold for cardiovascular tissue engineering**
Shraddha Thakkar, Anita Mol Driessen and Frank Baaijens
Soft Tissue Biomechanics & Tissue Engineering, Eindhoven University of Technology, the Netherlands
- P235 New Injectable Elastomeric Materials for Hernia Repair and their Biocompatibility in vitro and in vivo**
J. Skrobot, L. Zair, W. Ignaczak, M. Ostrowski, M. El Fray
Division of Biomaterials and Microbiological Technologies, West Pomeranian University of Technology, Szczecin, Poland
- P236 Corrosion resistance assessment of NiTi alloys in 0.9% NaCl solution**
Camila Dias dos Reis Barros (Camila Barros) and José Antônio da Cunha Ponciano Gomes (Ponciano Gomes)
Department of Metallurgy and Materials Engineering, Federal University of Rio de Janeiro, Brazil
- P237 Supermacroporous Cryogels for Bioligand Binding**
Ganesh Ingavle, Yishan Zheng, Carol Howell, Irina Savina and Susan Sandeman
Biomaterials and Medical Devices Research Group, University of Brighton, UK
- P238 Modification of nanofiber scaffold by biologically active substances and study of biocompatibility**
Mária Hnátová, Monika Michliková, Jana Dragúňová, Dušan Bakoš
Faculty of Chemical and Food Technology, Slovak University of Technology, Bratislava, Slovakia
- P239 Pre-clinical Evaluation of Additive Manufactured Surfaces for Orthopaedic Applications**
Grace Stevenson, John Haycock, Sarrawat Rehman, James Hunt and Edward Draper
JRI Orthopaedics Ltd, Sheffield, UK
- P240 Central Venous Catheters Functionalised with Chlorhexidine-Hexametaphosphate Nanoparticles for Prolonged Anti-Biofilm Efficacy**
Helena Grady, Sarah Maddocks, Rachel Dommert, Rikke Meyer, Mira Okshevsky, Andrew Collins, Sameer Rahatekar, Michele Barbour
Bristol Centre for Functional Nanomaterials, University of Bristol, UK
- P241 Preliminary data on sol-gel silicate glasses containing magnesium and zinc for dental tissue regeneration**
G. Theodorou, E. Kontonasaki, L. Papadopoulou, N. Kantiranis, G. Zachariades, O.M. Goudouri, A. R. Boccaccini, K.M. Paraskevopoulos, P. Koidis
Department of Physics, Aristotle University of Thessaloniki, Greece
- P242 Material-driven fibronectin networks: modulating the degree of fibrillogenesis**
Hayk Mnatsakanyan, Aarón Maturana Candelas, Alexandre Rodrigo-Navarro, Patricia Rico, José Antonio Gómez Tejedor, Manuel Salmerón-Sánchez, Roser Sabater i Serra
Center for Biomaterials and Tissue Engineering, Universitat Politècnica de València, Spain
- P243 WITHDRAWN**
- P244 Development of Biodegradable Virus and miRNA Eluting Stent Technology**
Hannah Stepto, Keith Oldroyd, Lee Cronin, Andrew H Baker
College of Medical Veterinary and Life Sciences, University of Glasgow, UK
- P245 Composite bone cement to improve the primary stability of orthodontic mini-screws**
Alberto Lagazzo, Fabrizio Barberis, Elisabetta Finocchio, Cristian Restano, Marco Capurro
Department of Civil, Chemical and Environmental Engineering, University of Genoa, Italy
- P246 Characteristics and Cytocompatibility of Novel Borophosphate Glasses**
Chenkai Zhu, Ifty Ahmed, Xiaoling Liu, Andy Parsons, Jingsong Liu, Chris Rudd
Division of Materials, Mechanics and Structures, University of Nottingham, UK
- P247 Gelatin/Chitosan Microspheres for a Modulated Drug Delivery System**
Costantino Del Gaudio, Valentina Crognale, Pierluca Galloni, Domenico Ribatti, Alessandra Bianco
Department of Enterprise Engineering, University of Rome "Tor Vergata", Italy
- P248 Design of Multi-Component Artificial Extracellular Matrices and their Effects on Cells Relevant to Wound Healing**
S. Rother, S. Thönes, J. Salbach-Hirsch, S. Moeller, M. Schnabelrauch, U. Anderegg, L. C. Hofbauer, V. Hintze, D. Scharnweber
Max Bergmann Center of Biomaterials, TU Dresden, Germany

- P249 Nanowires on Ti-6Al-4V for Creation of Antimicrobial Orthopaedic Implant Surfaces**
Terje Sjöström, Angela Nobbs and Bo Su
 School of Oral & Dental Sciences, University of Bristol, UK
- P250 Evaluation of In Vitro Cytocompatibility of Alginate-Gelatin Crosslinked Hydrogels**
Bapi Sarker, Raminder Singh, Judith A. Roether, Rainer Detsch, Iwona Cicha and Aldo R. Boccaccini
 Institute of Biomaterials, University of Erlangen-Nuremberg, Germany
- P251 Osteoblastic Differentiation Induced by Bioactive Glass-Ceramic Surfaces**
E.P. Ferraz, P.T. de Oliveira, M.M. Beloti, M.C. Crovace, O. Peitl-Filho, A.L. Rosa
 School of Dentistry of Ribeirão Preto, University of São Paulo, Brazil
- P252 Effect of surfaces properties on bone differentiation in composite scaffolds**
Vincenzo Guarino, Marica Marrese, Francesca Veronesi, Paola Torricelli, Monica Sandri, Anna Tampieri, Milena Fini, Luigi Ambrosio
 Institute of Polymers, Composites and Biomaterials, National Research Council of Italy, Naples
- P253 Controlling Mechanical Properties of Electrospun Gelatin Scaffolds**
Kaido Siimon, Paula Reemann, Uno Mäeorg, Martin Järvekülg
 Institute of Physics, University of Tartu, Estonia
- P254 Nanoscale Imaging and Quantitative Nanomechanical Characterization of Biomaterials by Atomic Force Microscopy**
Rob Field, Alex Winkel, Elmar Hartmann, Torsten Mueller, Florian Kumpfe, Joerg Barner
 JPK Instruments Ltd, Cambridge, UK
- P255 Transfer of CVD Graphene onto Polymer Substrates: Implications to Blood-Contacting Surfaces**
Gordon Xiong, Antonio Castro Neto, Cleo Choong
 School of Materials Science and Engineering, Nanyang Technological University, Singapore
- P256 Contribution of new analgesic or antibacterial properties on an implant for parietal refection: an in vitro and in vivo evaluation**
Nicolas Blanchemain, Guillaume Vermet, Stephanie Degoutin, Feng Chai, Christel Rousseaux, Christel Neut, Bernard Martel, Frederic Hildebrand
 INSERM U1008, Biomaterial Research group, University Lille 2, France
- P257 Novel nano-particular calcium phosphate and carbonate phases made by electro-migration technique. A component of silica/collagen based bone replacement materials**
Benjamin Kruppke, Christiane Heinemann, Sascha Heinemann, Anne Keroué, Maria Jäger and Thomas Hanke
 Max-Bergmann-Centre of Biomaterials, Technische Universität Dresden, Germany
- P258 In-situ Synthesized Silver Nanoparticles in Silk Fibroin Nanofibers: Effect of Fibroin Morphology on Ag⁺ Release Kinetics**
Semih Calamak, Eda Ayse Aksoy, Nusret Ertas, Ceren Erdogan, Meral Ozalp, Kezban Ulubayram
 Graduate Department of Nanotechnology and Nanomedicine, Hacettepe University, Ankara, Turkey
- P259 Sustained Release of Azithromycin from an Electrospun Polycaprolactone Membrane for Guided Tissue Regeneration**
Asha Mathew, Cedryck Vaquette, Dietmar Hutmacher and Saso Ivanovski
 Tissue Engineering and Regenerative Medicine, Griffith University, Australia
- P260 Functional Characterisation of SDF-1 α GAG Binding Variants**
Nydia Panitz, Lars Baumann, Stephan Theisgen, Daniel Huster and Annette G. Beck-Sickinger
 Institute of Biochemistry, University Leipzig, Germany
- P261 Polystyrene Sodium Sulfonate Grafted Electrospun Membrane for Applications in Guided Bone Regeneration**
C. Vaquette, V. Migonney, S. Ivanovski, D. Hutmacher
 Institute of Health and Biomedical Innovation, Queensland University of Technology, Australia
- P262 Chlorhexidine-based Antimicrobial Nanoparticles as a Coating for Dental Implants**
Natalie Wood, Howard Jenkinson, Dominic O'Sullivan, Sean Davis and Michele Barbour
 Bristol Centre for Functional Nanomaterials, University of Bristol, UK
- P263 PEGylation as a method of modification of collagen-elastin based scaffolds for tissue engineering**
Joanna Skopinska-Wisniewska, Anna Bajek, Justyna Sitkowska, Alina Sionkowska
 Faculty of Chemistry, Nicolaus Copernicus University, Torun, Poland
- P264 Gelatin Biofunctionalization of Poly(L-Lactide-co-Glycolide) Surfaces by Post-Plasma Grafting of AEMA**
Malgorzata Krok-Borkowicz, Olga Musial, Paulina Kruczala, Timothy Douglas, Sandra Van Vlierberghe, Peter Dubruel, Elzbieta Pamula
 Department of Biomaterials, AGH University of Science and Technology, Krakow, Poland
- P265 Osteoinductive effects of simvastatin loading on mesoporous silica and titania nanoscaled thin films**
Miriam López-Álvarez, Vanesa López-Puente, Jorge Pérez-Juste, Julia Serra, Isabel Pastoriza-Santos, Pío González
 New Materials Group, University of Vigo, Spain
- P266 Chitosan-catechol/graphene nanocomposite for biosensing applications**
Peter Sobolewski, Magdalena Pilarz, Malgorzata Aleksandrak, Ewa Mijowska, Jacek Podolski, Mirosława El Fray
 Division of Biomaterials and Microbiological Technologies, West Pomeranian University of Technology, Szczecin, Poland
- P267 Fabrication of microparticles and patterned substrates for directing stem cell growth**
Y. Yang, L. Glennon-Alty, A. Ahmed, L. Qian, P. Murray, D. Bradshaw and H. Zhang
 Department of Chemistry, University of Liverpool, UK
- P268 Selenium-doped calcium phosphate coatings on titanium implants with inhibition properties on cancerous osteoblasts**
Cosme Rodríguez-Valencia, Miriam López-Álvarez, Julia Serra, Pío González
 Department of Applied Physics, University of Vigo, Spain

- P269 Effects of stirring condition and fluid perfusion on the in-vitro degradation of calcium phosphate cement**
Jie An, J.G.C.Wolke, S.C.G.Leeuwenburgh, J.A.Jansen
 Department of Biomaterials, Radboud University Medical Center, The Netherlands
- P270 Ultrastructural features of mesenchymal stem cells in calcium alginate hydrogel during osteogenic differentiation by means of FIB-SEM**
Jakub Grzesiak, Krzysztof Marycz, Agnieszka Śmieszek, Anna Siudzińska
 Electron Microscopy Laboratory, Wrocław University of Environmental and Life Sciences, Poland
- P271 High Throughput Production and Analysis of Tissue Engineering Scaffolds prepared using Combinatorial Chemistry**
Erwin Zant, Maarten M. Blokzijl, Dirk W. Grijpma
 Department of Biomaterials Science and Technology, University of Twente, The Netherlands
- P272 Relationship between physical properties and biological response in tyrosine-derived polyarylates explored by association rules**
Daniela C. Soto and Loreto M. Valenzuela
 Department of Chemical and Bioprocess Engineering, Pontificia Universidad Católica de Chile
- P273 Generation of functional oxygen groups on parylene C for enhanced biocompatibility: LDI-MS investigations**
M. Golde-Cepa, N. Aminlashgari, M. Hakkarainen, K. Envall, A. Kotarba
 Faculty of Chemistry, Jagiellonian University, Krakow, Poland
- P274 Controlled Drug Delivery From Bioresorbable Magnesium Orthopaedic Implants**
Jessica A. Lyndon, Ben J. Boyd and Nick Birbilis
 Department of Materials Engineering, Monash University, Australia
- P275 Effect of Different Crosslinking Treatments on the Physical Properties of Collagen-based Scaffolds**
Luca Salvatore, *Deborah Pedone*, Emanuela Calò, Valentina Bonfrate, Marta Madaghiele
 Department of Engineering for Innovation, University of Salento, Italy
- P276 Degradation and mechanical properties of biodegradable PLGA film**
Reyhaneh Neghabat Shirazi, Yury Rochev, Peter McHugh
 Mechanical and Biomedical Engineering, National University of Ireland, Galway
- P277 Temporal Analysis of Dissolution By-Products and Genotoxic Potential of Spherical Zn-Si Bioglass: "Imageable beads" for Transarterial Embolization**
Muhammad Sami Hasan, Sharon Kehoe and Daniel Boyd
 Department of Applied Oral Sciences, Dalhousie University, Halifax, Canada
- P278 A modular flow-chamber bioreactor as a tool for the analysis of degradable materials**
Frank Feyerabend, Ralf Pörtner and Regine Willumeit
 Institute of Materials Research, Helmholtz-Zentrum Geesthacht, Germany
- P279 Use of a PTMC-PEG-PTMC coated PTMC film as a postoperative adhesion barrier**
Vincent Verdoold, Ruben R.M. Vogels, Kevin W.Y. van Barneveld, Nicole D. Bouvy and Dirk W. Grijpma
 MIRA Institute for Biomedical Technology and Technical Medicine, University of Twente, The Netherlands
- P280 Comparison of Sr-substituted Hydroxyapatite Obtained of Various Precursors through Neutralization Reaction: Characterisation at the Bulk and Particle Level**
L. Stipnice, K. Salma-Ancane and L. Berzina-Cimdina
 Institute of General Chemical Engineering, Riga Technical University, Latvia
- P281 Hybrid Multi-layered Coatings for Surface Functionalization of Magnesium alloys for biomedical applications**
Laura Córdoba, Christophe Hély, Thibaud Coradin, Fátima Montemor
 Instituto Superior Técnico, Technical University of Lisbon, Portugal
- P282 Degradation in the Jar: Optimising the *in vitro* enzymatic degradation of collagen-based devices**
Ayélén L. Helling, Eleni Tsekoura, Gerard Wall, Yves Bayon, Abhay Pandit, Dimitrios Zeugolis
 Network of Excellence for Functional Biomaterials, National University of Ireland, Galway
- P283 Composite Collagen/Bioceramics Strips, Plugs for Bone Filling Defect Repair: A Comparative Study**
Thomas Miramond, Thibaut Galtier, Guy Daculsi, Pascal Borget
 Inserm UMRS 791, Université de Nantes, France
- P284 Development of Artificial Stem Cell Microenvironments for Tissue Engineering Applications**
Ilida Ortega Asencio, Sheila MacNeil, Aileen Crawford, Paul Hatton, Frederik Claeysens
 School of Clinical Dentistry, University of Sheffield, UK
- P285 Fabrication of dispersible nanocrystals of bioceramics via a modified Pechini method under non-stoichiometric condition**
Yuko Omori, Masahiro Okada, Shoji Takeda, Naoyuki Matsumoto
 Graduate School of Dentistry, Osaka Dental University, Japan
- P286 Titanium with Nanotopography Drives Mesenchymal Stem Cells to Osteoblast Differentiation through miR-4448, -4708 and -4773 Downregulation**
R.B. Kato, B. Roy, F.S. de Oliveira, E.P. Ferraz, P.T. de Oliveira¹, M.Q. Hassan, A.L. Rosa, *M.M. Beloti*
 School of Dentistry of Ribeirão Preto, University of São Paulo, Brazil
- P287 Semi-interpenetrating polymer networks (SIPNs) incorporating polygalacturonic acid as biocompatible materials for implantable medical devices**
A. O' Carroll, C. McCoy and *L. Carson*
 School of Pharmacy, Queen's University Belfast, UK

- P288 In Vivo Assessment of Titanium Devices loaded with gentamicin in a methicillin-resistant *Staphylococcus aureus* Rabbit Osteomyelitis Experimental Model**
Gilles Amador, Loic Pichavant, Hélène Carrié, Laurent Plawinski, Valérie Héroguez, Cédric Jacqueline and Marie-Christine Durrieu
 Faculté de Médecine, Université de Nantes, France
- P289 Radially Aligned Collagen Scaffolds for Deterministic 3D Models of Cancer Migration**
Anke Husmann, Jonathan Campbell, Samuel Troughton, Robert Hume, Christine J. Watson and Ruth Cameron
 Department of Materials Science and Metallurgy, University of Cambridge, UK
- P290 Recombinant Production of Antimicrobial Spider Silk for Wound Dressing Materials**
L. Nilebäck, R. Jansson and M. Hedhammar
 Department of Anatomy, Physiology and Biochemistry, Swedish University of Agricultural Sciences, Sweden
- P291 Sol-Gel Hybrids with RAFT-Polymerised Branched Methacrylate Copolymers as Organic component for Tissue Engineering**
Justin Chung, Anthony Maçon, Theoni Georgiou, Julian R. Jones
 Department of Materials, Imperial College London, UK
- P292 In vitro Evaluation of a Novel Injectable Thermo-Responsive Polymeric Hydrogel for the Delivery of Self-Assembly Peptide Nanoparticles Containing an Osteoconductive Agent**
S. Pentlavalli, P. Chambers, A. Massey, M. O'Doherty, H. McCarthy and N. Dunne
 School of Mechanical and Aerospace Engineering, Queen's University Belfast, UK
- P293 Design of Drug-immobilized Polylactide-graft-Poly(ethylene glycol) as a Temperature-Responsive Injectable Polymer for Controlled Release of Low-molecular-weight Water Soluble Drugs**
Yuichi Ohya, Masay Umezaki, Yasuyuki Yoshida, Akihiro Takahashi and Akinori Kuzuya
 Department of Chemistry and Materials Engineering, Kansai University, Japan
- P294 Localized Corrosion Behaviour of Stainless Steel and Titanium Based Hard Tissue Implants**
Ilven Mutlu and Enver Oktay
 Metallurgical and Materials Engineering Department, Istanbul University, Turkey
- P295 Degradation of Calcium-Phosphate Based Glasses Controlled by TiO₂ Addition**
A. M. B. Silva, J. M. Oliveira, M. H. V. Fernandes
 Centre for Research in Ceramics and Composite Materials, University of Aveiro, Portugal
- P296 Comparison of UV and EDC Cross-linking on Mechanical Properties of Collagen-based Scaffolds for Myocardial Tissue Engineering**
Natalia Davidenko, Carlos Schuster, Ruth Cameron, Serena Best
 Department of Materials Science and Metallurgy, University of Cambridge, UK
- P297 Electrochemical Corrosion Behaviour of Highly Porous Beta-Type Ti-Nb-Cu Alloy**
Ilven Mutlu
 Metallurgical and Materials Engineering Department, Istanbul University, Turkey
- P298 Recombinant Affinity Silk for Presentation of Active Protein Domains**
R. Jansson, N. Thatikonda, P.-Å. Nygren, M. Hedhammar
 Department of Anatomy, Physiology and Biochemistry, SLU, Sweden
- P299 One-pot synthesis of hybrid biocompatible hydrogels based on methacrylamide gelatin and polyacrylamide**
A. Serafim, C. Tucureanu, D. Petre, D.M. Dragusin, A. Salageanu, S. Van Vlierberghe, P. Dubruel, I.C. Stancu
 University Politehnica of Bucharest, Romania
- P300 Bactericidal and cell compatible titanium surfaces with TiO₂ nanowires**
T. Diu, M. Ryadnov, N. Faruqi, B. Lamarre, H. Jenkinson and B. Su
 School of Oral and Dental Sciences, University of Bristol, UK
- P301 Precise Hyaluronan-tyramine synthesis for tailored cellular microenvironments**
Claudia Loebel, Matteo D'Este, Mauro Alini, Marcy Zenobi-Wong and David Eglin
 AO Research Institute Davos, Switzerland
- P302 Hyaluronic Acid-Coated Chitosan Nanoparticles: the Influence of Hyaluronic Acid Presentation**
Arianna Gennari, Erwin Hohn, Abdulaziz Almalik, Nicola Tirelli
 Institute of Inflammation and Repair, University of Manchester, UK
- P303 Real-time Monitoring of DNA Plasmid Interactions with Poly (ε-lysine) Dendrons using Optical Waveguide Lightmode Spectroscopy (OWLS)**
Steve Meikle, Valeria Perugini, Mariagemiliana Dessi, Wanda Lattanzi, Enrico Pola, Giandomenico Logroscino, Gary Phillips, Matteo Santin
 School of Pharmacy and Biomolecular Sciences, University of Brighton, UK
- P304 The Atomic-Scale Structure of Bio-Resorbable Glasses: Na₂O:P₂O₅**
David Pickup, Robert Moss, Jenni Vibert and Robert Newport
 School of Physical Sciences, University of Kent, UK
- P305 Preparation and characterization of Sr, Zn, Si and Fe-doped hydroxyapatite nanoparticles**
Zhitong Zhao, Montserrat Espanol, Maria-Pau Ginebra
 Department Materials Science and Metallurgy, Technical University of Catalonia, Spain
- P306 Endothelization and thrombogenicity response of CoCr alloy nano depth patterns for cardiovascular stents**
R. Schieber, M. Fernández-Yagüe, M. Hans, M. Díaz-Ricart, G. Escolar, F. Javier Gil, F. Mücklich, M. Pegueroles
 Materials Science Department, Universitat Politècnica de Catalunya, Spain
- P307 Cell Spraying Approach *in vitro* for Coating of Respiratory Tissue Engineered Constructs**
A. L. Thiebes, S. Albers, S. Jockenhoevel and C. G. Cornelissen
 Helmholtz-Institute, RWTH Aachen University, Germany

- P308 Biodegradable hyper-branched tissue adhesives for meniscus tears**
Agnieszka I. Bochyńska, Tony G. van Tienen, Gerjon Hannink, Pieter Buma, Dirk W. Grijpma
 Department of Orthopaedics, Radboud University Nijmegen Medical Centre, The Netherlands
- P309 WITHDRAWN**
- P310 Impact of Surface Treatment on the Properties of Dental Implant Materials**
M. Murphy, R. Lindsay, A. Thomas and N. Silikas
 School of Materials, University of Manchester, UK
- P311 Monodisperse microspheres loaded with gentamicin dioctyl sodium sulfosuccinate for the treatment of orthopaedic infections**
Gert-Jan A. ter Boo, Dirk W. Grijpma, Geoff Richards, Fintan T. Moriarty and David Eglin
 AO Foundation, Davos, Switzerland
- P312 Retention of Myoblast Differentiation Capacity in 3D Culture on TIPS Microspheres**
Nina Parmar, Richard Day
 Applied Biomedical Engineering Group, University College London, UK
- P313 Corrosion behaviour of beta titanium alloys containing zirconium for dentistry**
J. Fojt, L. Joska, A. Bernatikova and J. Malek
 Department of Metals and Corrosion Engineering, Institute of Chemical Technology in Prague, Czech Republic
- P314 Surface modification of Ti-surfaces by alginate polyelectrolyte layers**
Dana Kubies, Ognen Pop-Georgievski, Eliška Mázl-Chánová, Josef Zemek, Neda Neykova, Roman Deminachuk, Milan Houska, Elena Filová, Lucie Bačáková, František Rypáček
 Institute of Macromolecular Chemistry, Academy of Sciences of the Czech Republic
- P315 Hydrophobic quaternized chitosan for efficient nanoparticle formation and transfection of therapeutic oligonucleotides**
Pedro M.D. Moreno, Joyce C. Santos, Carla P. Gomes, Aida Varela-Moreira, Artur Costa, Francisco Mendonça, Ana P. Pêgo
 Instituto de Engenharia Biomédica, Universidade do Porto, Portugal
- P316 In Vitro Response of Human Osteoprogenitor Cells to Cross-Linked Poly(Lactide-co-Caprolactone) Dimethacrylate for Bone Repair**
Laura Brown, Jessica Gwynne, David Shepherd, Leander Poozca, Gerhard Hildebrand, Klaus Liefeth, Roger Brooks, Serena Best
 Department of Materials Science & Metallurgy, University of Cambridge, UK
- P317 Drug delivery carriers based on two functionalized spider silk proteins: a novel approach for cancer therapy**
Anna Florcza, Katarzyna Jastrzebska, Andrzej Mackiewicz, Hanna Dams-Kozłowska
 NanoBioMedical Centre, Adam Mickiewicz University, Poznan, Poland
- P318 Controlling Intramembranous Bone Mineralisation using a Bone Tissue Engineering Approach**
Anthony J. Deegan, Halil M. Aydin, Bin Hu, Sandeep Konduru, Jan H. Kuiper, Ying Yang
 Institute of Science and Technology in Medicine, Keele University, UK
- P319 Generation of electrospun yarns for use as tissue engineered blood vessel scaffolds**
Richard O'Connor and Garrett B. McGuinness
 Centre for Medical Engineering Research, Dublin City University, Ireland
- P320 Injectable Thermo-responsive Hyaluronan Hydrogel in a Rabbit Osteochondral Defect Model**
D. Eglin, M. D'Este, I. Dresing and M. Alini
 AO Research Institute Davos, Switzerland
- P321 Modification of Porcine Pericardium with Low-Energy Non-thermal Electron Beam**
Jessy Schönfelder, Eberhard Spörl, Richard Funk, Christiane Wetzler
 Fraunhofer Institute for Electron Beam and Plasma Technology, Germany
- P322 Developing a Method for Tracking and Quantifying Metallic Particle Internalisation**
Hayley Floyd, Janet Lord, Edward Davies, Owen Addison, Hamid Dehghani, Liam Grover
 School of Chemical Engineering, University of Birmingham, UK
- P323 Endothelialization of gas exchange membranes to provide antithrombogenicity**
A. Wenz, K. Linke, M. Schandar, F. Metzger, E. Novosel, J. Schneider, P. Kluger
 Institute of Interfacial Process Engineering and Plasma Technology, University of Stuttgart, Germany
- P324 Influence of TCP Content on Chitosan Agglomerated Scaffold Properties**
Martyna Kucharska, Katarzyna Walenko, Małgorzata Lewandowska-Szumieł, Tomasz Brynk, Tomasz Ciach
 Biomedical Engineering Laboratory, Warsaw University of Technology, Poland
- P325 In-situ Charge Formation on Hydroxylapatite Coatings**
L. Pluduma, K. A. Gross, H. Koivuluoto, P. Vuoristo, M. Kylmälahti, A. Bystrova, Yu. Dekhtyar
 Institute of Biomaterials and Biomechanics, Riga Technical University, Latvia
- P326 Preparation and Characterization of Porous Hydroxyapatite Based Microcarriers for Cell and Drug Delivery**
Merve Guldiken, Sibel Ataoğlu, Caner Durucan, Can Özen, Dilek Keskin and Ayşen Tezcaner
 Department of Biotechnology, Middle East Technical University, Ankara, Turkey
- P327 In Vitro studies to measure the inflammatory response of crosslinked poly(lactide-co-caprolactone) dimethacrylate scaffolds**
David Shepherd, Laura Brown, Leander Poozca, Gerhard Hildebrand, Klaus Liefeth, Roger Brooks, Serena Best
 Department of Materials Science and Metallurgy, University of Cambridge, UK
- P328 A comparison of two approaches to the formation of antibacterial surfaces: doping with bactericidal element vs drug loading**
I.V. Batenina, D.V. Shtansky, Ph.V. Kiryukhantsev-Korneev, A.N. Sheveyko, N.Yu. Anisimova and N.A. Gloushankova
 National University of Science and Technology "MISIS", Russia

- P329 Investigation of Factors Influencing Deposition of Nanocomposite Coating onto Open Cell Foams using Layer-by-Layer Assembly: Design of Experiment Approach**
Monika Ziminska, Helen McCarthy, Nicholas Dunne and Andrew Hamilton
School of Mechanical & Aerospace Engineering, Queen's University Belfast, UK
- P330 In-vivo response of a novel Ti-Ta-Zr-Nb alloy for medical implants**
Patrik Stenlund, Omar Omar, Ulrika Brohede, Susanne Norgren, Lena Emanuelsson, Jukka Lausmaa, Peter Thomsen and Anders Palmquist
BIOMATCELL VINN Excellence Center of Biomaterials and Cell Therapy, Sweden
- P331 Adipose derived stem cells cultured in 2D and 3D settings for the use in bone tissue engineering**
Claudia Kleinbans, Inga Satller, Lena Schmohl, Jakob Barz, Thomas Schiestel, Günter Tovar, Petra J. Kluger
Institute for Interfacial Process Engineering and Plasma Technology, University of Stuttgart, Germany
- P332 Bioengineered spider silk spheres as anti-cancer drug carriers**
Katarzyna Jastrzebska, Anna Florczak, Yinnan Lin, Rosalyn Abbott, Andrzej Mackiewicz, David L. Kaplan, Hanna Dams-Kozłowska
NanoBioMedical Centre, Adam Mickiewicz University, Poznan, Poland
- P333 Aligned electrospun PLGA fibres reinforcing tubular small intestine submucosa**
Omaer Syed, Richard Day, Jonathan Knowles
Eastman Dental Institute, University College London, UK
- P334 Hyaluronic Acid Regulation of Cytokine Secretion, GAG Production and Permeability in Urothelial Cells**
Peadar Rooney, Akshay Srivastava, Leo Quinlain, Abhay Pandit
Network of Excellence for Functional Biomaterials, National University of Ireland, Galway
- P335 Nanohelical Shape and Periodicity dictate Stem Cell Fate**
R. K. Das, O. F. Zouani, G. Kemper, L. Plawinski, C. Labrugère, R. Oda and M-C. Durrieu
Institute of Chemistry & Biology of Membranes & Nanoobjects, Université Bordeaux, Pessac, France
- P336 Controlling the Modulus of Gellan Gum Hydrogels for Inkjet Printing Cell Culture Substrates**
Sam Moxon & Alan M Smith
Department of Pharmacy, University of Huddersfield, UK
- P337 Nano-Micro Architectural Hybrid Composite Scaffold for Bone Tissue Engineering**
Prabhash Dadhich, Bodhisatwa Das, Pavan Kr. Srivas, Pallabi Pal, Sabyasachi Ray, Santanu Dhara
School of Medical Science and Technology, Indian Institute of Technology Kharagpur, India
- P338 Bioactive and Highly Porous Nanofibres via Solution Blow Spinning**
Jonny J. Blaker, Eudes Leonnan, Ana Letícia Braz, Isaque Jerônimo, Aldo R. Boccaccini, Juliano E. Oliveira, Eliton S. Medeiros, Showan N. Nazhat
Materials Science Centre, Manchester University, UK
- P339 The Reciprocal Relationship between Pore Size and Crosslinking, and Their Impact on Porous Scaffold Strength**
S. Ali Poursamar, Alexander N. Lehner, A.P.M. Antunes
Institute for Creative Leather Technology, University of Northampton, UK
- P340 Tuning the 3D Architecture of Gelatin Hydrogel-PLLA Combination Scaffolds**
Jasper Van Hoorick, Marica Markovic, Aleksandr Ovsianikov, Tristan Fowler, Oskar Hoffmann, Peter Dubrue and Sandra Van Vlierberghe
Polymer Chemistry & Biomaterials Research Group, Ghent University, Belgium
- P341 Fine-Tuning Self-Assembling Peptide Hydrogels for Cell Culture Applications**
Laura Szkolar, Alberto Saiani, Aline F Miller, Julie E Gough
School of Materials, University of Manchester, UK
- P342 Sol-Gel Dip-Coating for Immobilization of Poly (ϵ -lysine) Dendrons on Biomaterials Surfaces for Regenerative Medicine Applications**
Maria Elena Verdenelli, Steve Meikle, Matteo Santin, Roberto Chiesa
Department of Chemistry, Materials and Chemical Engineering, Politecnico di Milano, Italy
- P343 Characterization of Silicone-polycarbonate-urethane/PDMS based Material for Polymeric Heart Valves**
Marianna Asaro, Tamer Al Kayal, Silvia Volpi, Paola Losi, Simona Celi, Mattia Glauber, Giorgio Soldani
National Council of Research, Institute of Clinical Physiology, Massa, Italy
- P344 Study of the effect of SLS manufacturing parameters on the porosity of PHB scaffolds for tissue engineering**
Tatiana F. Pereira, Bruna N. Teixeira, Sara C Marques, Marcelo F. Oliveira, Izaque A. Maia, Jorge V. L. Silva, Gutemberg G. Alves, Marysilvia F. Costa, Rossana M. S. M. Thiré
Programa de Engenharia Metalúrgica e de Materiais, Federal University of Rio de Janeiro
- P345 Assessment of the Corrosion Behaviour and Cytocompatibility of a Nano-fluorided Coating Obtained by Simple Chemical Conversion on AZ31 Biodegradable Mg Alloy**
Emerson Alves Martins, Dorota Artymowicz, Kwangchul Shin, Andrey I. Shukalyuk, Roger C. Newman
Department of Chemical Engineering and Applied Chemistry, University of Toronto, Canada
- P346 Mechanical Response of Calcium Phosphate Bioceramics**
D.E. Mouzakis, S.P. Zaoutsos, S. Rokidi, N. Bouropoulos
Department of Mechanical Engineering, Technological Educational Institute of Thessaly, Larissa, Greece
- P347 Bacterial Cellulose Based Electrospun Scaffolds for Bone Tissue Engineering**
Deniz Atila, Ayten Karataş, Dilek Keskin, Ayşen Tezcaner
Department of Engineering Sciences, Middle East Technical University, Ankara, Turkey
- P348 WITHDRAWN**
- P349 The Influence of Porosity and Pore Shape of PCL Electro-spun Nano-fibrous Meshes on Macrophage Activation**
Kieran P. Fuller, Colm O'Dowd, Abhay Pandit, and Dimitrios Zeugolis
Network of Excellence for Functional Biomaterials, National University of Ireland, Galway

- P350 Production and Characterization of a Chitosan Coating on Titanium with Silver Nanoparticles**
Daniel Rodríguez, María Godoy-Gallardo, Marc Avilès, Montserrat Español, F. Javier Gil
 Biomaterials, Biomechanics and Tissue Engineering group, Technical University of Catalonia, Barcelona, Spain
- P351 Photo-crosslinkable and biopolymer-based inks for inkjet-bioprinting of artificial cartilage**
Eva Hoch, Achim Weber, Günter E.M. Tovar and Kirsten Borchers
 Institute for Interfacial Process Engineering, University of Stuttgart, Germany
- P352 A Bioreactor-based 3D Culture System for skeletal Muscle Engineering in Fibrin Scaffolds**
Philipp Heher, Christiane Fuchs, Johanna Prüller, Babette Maleiner, Josef Kollmitzer, Dominik Rünzler, Andreas Teuschl, Susanne Wolbank and Heinz Redl
 Trauma Care Consult, Vienna, Austria
- P353 WITHDRAWN**
- P354 Functionalization of Polyurethane Substrates with Dendrons for Stem Cell Culture**
Nicola Contessi, Serena Bertoldi, Steven Meikle, Anna Guildford, Silvia Farè, Matteo Santin and Maria Cristina Tanzi
 Department of Chemistry, Materials and Chemical Engineering "G. Natta", Politecnico di Milano, Italy
- P355 Quantification of Volume and Size Distribution of Internalised Calcium Phosphate Particles and Their Influence on Cell Fate**
Richard Williams, Midhat Salimi, Gary Leeke, Paula Mendes, Liam Grover
 School of Chemical Engineering, University of Birmingham, UK
- P356 Functional PEPM-A-HA cryogels for drug conjugation and cartilage integration**
Joana Magalhaes, Luis Rojo del Olmo, Lara M. Nieto Couce, Julio San Roman and Francisco J. Blanco
 CIBER in Bioengineering, Biomaterials and Nanomedicine, Spain
- P357 Biaxial stretching of poly(L-lactide) tubes for improvement of mechanical properties**
A. Løvda, J. Wenzel Andreasen, L. Pilgaard Mikkelsen, K. Agersted, K. Almdal
 Department of Micro- and Nanotechnology, Technical University of Denmark
- P358 Controlled IL-2 Delivery from Novel Photocured Biodegradable Poly (decane-co-tricarballoylate) Elastomers**
Husam M. Younes and Mohammad Shaker
 Pharmaceuticals and Polymeric Drug Delivery Research laboratory, Qatar University, Doha
- P359 Incorporation of Elastin Enhancement Agents on Nano-scale Fibers**
F. Damanik, C. van Blitterswijk, J. Rotmans and L. Moroni
 Department of Tissue Regeneration, University of Twente, The Netherlands
- P360 Mineralized Porous Pullulan Microcarriers for Bone Tissue Engineering**
Hazal Aydoğdu, Dilek Keskin, Ayşen Tezcaner, Erkan Türker Baran
 Biomedical Engineering, Middle East Technical University, Turkey
- P361 Interaction Study between Functionalised Si-Nanoparticles and Colon Carcinoma Cells for Theranostic Applications**
Helena Montón, Colin Moore, Antonio Aranda-Ramos, Vladimir Gubala, Arben Merkoçi, Carme Nogués
 Department Biologia Cellular, Fisiologia i Immunologia, Universitat Autònoma de Barcelona, Spain
- P362 Expression of Bone Markers in Pre-Osteoblastic Cells Grown on Titanium Surface with Nanotopography**
L. M. S. de Castro-Raucci, L. N. Teixeira, P.T. de Oliveira, A. L. Rosa, M.M. Beloti
 School of Dentistry of Ribeirão Preto, University of São Paulo, Brazil
- P363 A novel method to measure the primary stability of dental implants and orthodontic screws**
Fabrizio Barberis, Alberto Lagazzo, Stefano Benedicenti, Marco Migliorati, Marco Capurro
 Department of Civil, Chemical and Environmental Engineering, University of Genoa, Italy
- P364 Development of novel tamponades to treat retinal detachments**
Victoria Kearns, Robert Poole, Albert Caramoy and Rachel Williams
 Department of Eye and Vision Science, University of Liverpool, UK
- P365 Ambient Temperature Patterning of Bioactive Deposits on Curved Metallic Substrates For Orthopaedic Implants**
A. Nithyanandan and M. Edirisinghe
 Mechanical Engineering, University College London, UK
- P366 Effect of Substrate Geometry on Mineralization and Cell Proliferation of Calcium Phosphate Ceramics**
E.R. Urquía Edreira, Astghik Hayrapetyan, J.G.C. Wolke, J.A. Jansen, J.J.J.P. van den Beucken
 Department of Biomaterials, Radboud University Nijmegen Medical Center, The Netherlands
- P367 Bone mineralization in Zebrafish embryos treated with Silicon ions**
M. Montazerolghaem, L. Nyström, H. Engqvist and M. Karlsson Ott
 Department of Engineering Sciences, Uppsala University, Sweden
- P368 PolyHIPE-based porous microparticles for bone tissue engineering**
T. Paterson, C. Sherborne, R. Owen, S. Puwun, G. Reilly, F. Claeysens
 Department of Materials Science and Engineering, University of Sheffield, UK
- P369 Retrieval Analysis of Titanium – Nitride Coated Femoral Heads Articulating Against Polyethylene**
Łukasz Łapaj, Justyna Wendland, Adrian Mróz, Jacek Markuszewski, Tomasz Wiśniewski
 Department of General Orthopaedics, Musculoskeletal Oncology and Trauma Surgery, Poznan University of Medical Sciences, Poland
- P370 Investigation of Ion Exchange between Silicate-substituted Bone Graft Substitutes and Cell Culture Media and the effect on Osteoblast-like Cell Response**
N. K. Chana, S. C.F. Rawlinson and K. A. Hing
 School of Engineering and Materials Science, Queen Mary University of London, UK

- P371 Highly Reinforced Bioactive Glass – Gellan Gum Composite Hydrogels For Biomedical Applications**
Ana Gantar, Rok Kocen and Saša Novak
 Department for Nanostructured materials, Jožef Stefan Institute, Slovenia
- P372 In vitro testing of osteoinductivity and osteoconductivity of titanium alloys with nanostructured surface for orthopaedic applications**
E. Jablonská, J. Lipov, J. Fojt, L. Joska, T. Ruml
 Department of Biochemistry and Microbiology, Institute of Chemical Technology, Prague, Czech Republic
- P373 Influence of collagen cross-linking on fibroblast and macrophage response**
Luis M. Delgado, Abhay Pandit, Dimitrios I. Zeugolis
 Network of Excellence for Functional Biomaterials, National University of Ireland, Galway
- P374 Preparation of chitosan nanowires and their application to hemostasis**
Ying-Chiang Ho and Yi-Chang Chung
 Institute of Biotechnology, National University of Kaohsiung, Taiwan, ROC
- P375 Mobilization of Mesenchymal Progenitor Cells to Improve Bone Healing**
P.S. Lienemann, A.S. Kivelioe, S. Metzger, S. Höhnle, A. Roch, O. Naveiras, A. Sala, V. Milleret, F. E. Weber, W. Weber, M.P. Lütolf, M. Ehrbar
 Department of Obstetrics University Hospital, Zürich, Switzerland
- P376 Modification of polylactide surfaces with PLA-b-PEO nano-colloids**
Eliska Mazl Chanova, Ognen Pop-Georgievski, Marta Maria Kumorek, Ludka Machova and Frantisek Rypacek
 Institute of Macromolecular Chemistry of the Academy of Sciences of the Czech Republic, Prague
- P377 Local Delivery of Alendronate and Bone Remodelling in Rat Models**
Necati Harmankaya, Johan Karlsson, Anders Palmquist, Mats Halvarsson, Martin Andersson and Pentti Tengvall
 Department of Biomaterials, Sahlgrenska Academy at University of Gothenburg, Sweden
- P378 Localized cell differentiation with BMP-2 in a PEG scaffold using a streptavidin linker**
S. Metzger, P. S. Lienemann, C. Ghayor, M. Karlsson, F. E. Weber, W. Weber, M. Ehrbar
 Department of Obstetrics, University Hospital Zurich, Switzerland
- P379 Plasma Spraying of Zinc Substituted Hydroxyapatite**
David Shepherd, Roger Brooks and Serena Best
 Department of Materials Science and Metallurgy, University of Cambridge, UK
- P380 Candida glabrata in mouthwash -coated endotracheal tubes: antibiofilm activity by electronically scanning microscopy**
Danielle Bezerra Cabral, Evandro Watanabe and Denise de Andrade
 Fundamental Nursing, University of São Paulo at Ribeirão Preto, Brazil
- P381 Simple Silver Deposition Strategy for Antibacterial Titanium Implants**
Kennedy Omoniala, David Armitage, Susannah Walsh
 Leicester School of Pharmacy, De Montfort University, Leicester, UK
- P382 Assessment of the bioactivity of gold doped hydroxyapatite-polyvinyl alcohol nanocomposites**
Amany Mostafa, Hassane Oudadesse and Mayyada El Sayed
 Biomaterials Department, National Research Centre, Cairo, Egypt
- P383 Haemocompatibility of Citrate Stabilised Gold Nanoparticles**
Brian G. Cousins, Niloofar Ajdari & Alexander M. Seifalian
 Centre for Nanotechnology & Regenerative Medicine, University College London, UK
- P384 Vitronectin Tunes The Biological Activity Of Material-Driven Fibronectin Matrices**
M. Cantini, K. Gomide, C. González-García, and M. Salmerón-Sánchez
 Biomedical Engineering Research Division, University of Glasgow, UK
- P385 Investigation on Mechanical Loading of Hydrogels for Cartilage Tissue Engineering**
Stefanie Biechler, Sandy Williams and Ruochong Fei
 Bose Corporation, ElectroForce Systems Group, Eden Prairie, USA
- P386 Biological Performance of Cell-Laden Methacrylated Gellan Gum Hydrogels**
Joana Silva-Correia, Mariana B. Oliveira, João F. Mano, Joaquim M. Oliveira and Rui L. Reis
 3B's Research Group, University of Minho, Guimarães, Portugal
- P387 Melt Electrospinning Of PCL/Bioactive Glass Composites In Direct Writing For Highly Ordered Scaffolds For Non-Load Bearing Defects**
Keith A. Blackwood, Nikola Ristovski, Sam Liao, Nathalie Bock, Jionguy Ren, Giles T.S. Kirby, Roland Steck, Molly M. Stevens, Maria A. Woodruff
 Institute of Health & Biomedical Innovation, Queensland University of Technology, Brisbane, Australia
- P388 Material-driven fibronectin fibrillogenesis promotes growth factor binding and stem cell differentiation**
V. Llopis-Hernández, M. Cantini, P. Rico, M. Tsimbouri, A. García, M. Dalby, M. Salmerón-Sánchez
 Division of Biomedical Engineering, University of Glasgow, UK
- P389 Design, Development and Characterization of Novel Polyacrylates to direct Kidney Progenitor / Stem Cell Differentiation**
Isabel Hopp, Rachel Williams, Simon Dixon, Patricia Murray
 Institute of Translational Medicine, University of Liverpool, UK
- P390 Antibacterial Polyurethane Surfaces: Modification with Chitosan by Covalent Immobilization**
Filiz Kara, Eda Ayse Aksoy, Serpil Aksoy and Nesrin Hasirci
 Center of Excellence in Biomaterials and Tissue Engineering, Middle East Technical University, Turkey
- P391 Catechol-Chitosan/Genipin Hydrogel as Mucoadhesive Buccal Drug Delivery System**
J. Xu, S. Strandman, J. Zhu, J. Barralet and M. Cerruti
 Department of Mining and Materials Engineering, McGill University, Montreal, Canada

- P392 Inflammatory Response to Magnesium Based Biodegradable Implant Materials**
Maria Costantino, Bérengère Luthringer, Regine Willumeit
Helmholtz-Zentrum Geesthacht, Zentrum für Material- und Küstenforschung, Germany
- P393 Surface modification of poly(D,L-lactic acid) scaffolds for orthopedic applications: a biocompatible, non-destructive route via diazonium chemistry**
H. Mahjoubi, J. Kinsella, M. Murshed and M. Cerruti
Materials Engineering, McGill University, Montreal, Canada
- P394 Bioactive glass for treatment of tooth hypersensitivity during or after treatment with bleaching**
Nataša Drnovšek, Kaja Križman, Sebastjan Perko, Saša Novak
Department for Nanostructured Materials, Jožef Stefan Institute, Slovenia
- P395 Selenium-containing hydroxyapatites – spectroscopic studies**
J. Kolmas, E. Oledzka and M. Sobczak
Department of Inorganic and Analytical Chemistry, Medical University of Warsaw, Poland
- P396 Determination of metallic biomaterials susceptibility to crevice corrosion**
L. Joska, J. Fojt, A. Bernatíkova
Department of Metals and Corrosion Engineering, Institute of Chemical Technology in Prague, Czech Republic
- P397 Characterization of Poly (Lactic-co-Glycolic Acid) / Poly (Isoprene) Blend for Application in Tissue Engineering**
Douglas Ramos Marques, Luis Alberto dos Santos, Sarah Harriet Cartmell, Julie Elizabeth Gough
Materials Science Centre, University of Manchester, UK
- P398 Calcium phosphate nanoparticles carrying BMP-7 plasmid DNA induce osteogenic differentiation in MC3T3-E1 pre-osteoblasts**
Chrystalleni Hadjicharalambous, Viktoriya Sokolova, Diana Kozlova, Matthias Epple and Maria Chatzinikolaïdou
Department of Materials Science and Technology, University of Crete, Heraklion, Greece
- P399 Synthesis and *in vitro* Bioactivity of Cu and Zn doped sol-gel- silicate bioactive glasses**
J. Bejarano, H. Palza, P. Caviedes
Department of Chemical Engineering and Biotechnology, University of Chile
- P400 A pH-responsive polymer-based drug-delivery platform demonstrating intracellular siRNA target-gene knockdown**
D Roebuck and R Chen
Department of Chemical Engineering, Imperial College London, UK
- P401 Using Simulation to Predict the Thermomechanical behaviour Of the Hydrogel Matrix Applied in Drug Delivery System**
Nirina Santatriniaina, Dominique Pioletti, Lalaonirina Rakotomanana, Mohandrea Nassanjan and Arne Vogel
Mathematical Research Institute, University of Rennes, France
- P402 Using Bioactive Scaffolds to synthesise an *in vitro* 3D Bone Model for Implant Testing**
G. Tetteh, I. U. Rehman and G. C. Reilly
Kroto Research Institute, University of Sheffield, UK
- P403 Bis-urea based supramolecular materials for tissue engineering**
Samaneh Kheyrrooz, Patricia Y.W. Dankers, Rint P. Sijbesma
Laboratory for Macromolecular and Organic Chemistry, Eindhoven University of Technology, The Netherlands
- P404 Biomaterialized hydroxyapatite nanocrystals/graphene oxide as filler for bone tissue engineering**
Maria Grazia Raucci, Daniela Giugliano, Angela Longo, Stefania Zeppetelli, Gianfranco Carotenuto and Luigi Ambrosio
Institute of Polymers, Composites and Biomaterials, National Research Council of Italy, Naples
- P405 Effects on growth and osteogenic differentiation of mesenchymal stem cells by the strontium-added sol-gel hydroxyapatite gel materials**
Maria Grazia Raucci, Daniela Giugliano, M.A. Alvarez-Perez, C. Demitri and Luigi Ambrosio
Institute of Polymers, Composites and Biomaterials, National Research Council of Italy, Naples
- P406 Development of Nerve Guide Scaffold with a Microstructured Intraluminal**
Atefeh Mobasser, Alessandro Faroni, Julie Gough, Giorgio Terenghi, Adam Reid
School of Materials, University of Manchester, UK
- P407 From Bench to bedside: realization of a bioartificial, wearable lung assist device**
Esther Novosel, Annika Wenz, Kirsten Borchers, Markus Schandar, Jörg Schneider, Georg Matheis, Petra Kluger
Novalung GmbH, Heilbronn, Germany
- P408 Gelatin/hydroxyapatite multicomponent system with a modulate biological signals**
Daniela Giugliano, Maria Grazia Raucci and Luigi Ambrosio
Institute of Polymers, Composites and Biomaterials, National Research Council of Italy, Naples
- P409 Osteogenic differentiation induced by biomaterialized gelatin scaffold**
Daniela Giugliano, Maria Grazia Raucci and Luigi Ambrosio
Institute of Polymers, Composites and Biomaterials, National Research Council of Italy, Naples
- P410 Implantable biocomposite based radical oxygen species scavengers as a therapeutic strategy to manage age related macular degeneration**
Marta O. Freitas, Ana S. Neto, B. Moreno, E. Chinarro and Ana P. Pêgo
Instituto de Engenharia Biomédica, Universidade do Porto, Portugal
- P411 Soft Matrices vs. Hard Minerals: Biomimetic Morphogenesis of Calcium Phosphate in Lyotropic Liquid Crystals**
Wenxiao He and Martin Andersson
Department of Chemical and Biological Engineering, Chalmers University of Technology, Sweden
- P412 Development of titanium alloy-based scaffold by 3D printing for bone tissue engineering**
Pavan Kumar Srivas, Kausik Kapat, Prabhsh Dadhich
Indian Institute of Technology Kharagpur, West Bengal, India

- P413 Mechanical-stress-assisted rapid cell sheets recovery from poly(*N*-isopropylacrylamide) grafted PDMS surfaces**
Yoshikatsu Akiyama, Miki Matsuyama, Naoya Takeda, Masayuki Yamato and Teruo Okano
 Institute of Advanced Biomedical Engineering and Science, Tokyo Women's Medical University, Japan□
- P414 The Oceans as a Source and as an Inspiration for Biomaterials Development: Some key examples**
Tiago H. Silva, Alexandre A. Barros, Ana L.P. Marques, Ana Rita C. Duarte, Gabriela S. Diogo, Joana Moreira-Silva, Lara L. Reys, Simone S. Silva, Rui L. Reis
 3B's Research Group, Guimarães, Portugal
- P415 Development and Characterization of Lithium-Releasing Silicate Bioactive Glasses for Bone Repair**
Valentina Miguez-Pacheco, A. Malchere, J. Chevalier and Aldo Boccaccini
 Institute of Biomaterials, University of Erlangen-Nuremberg, Germany
- P416 Effect of magnesium extract on osteoblastic progenitor cells differentiation**
Bérengère J.C. Luthringer, Lili Wu, Frank Feyerabend, Arndt F. Schilling, Regine Willumeit
 Structural Research on Macromolecules, Helmholtz-Centre Geesthacht, Germany
- P417 Fabrication of bilayer nano/microfibrous scaffold for skin tissue engineering**
Pallabi Pal, Pavan Kumar Srivas, Prabhaskar Dadhich, Bodhisatwa Das, Santanu Dhara
 School of Medical Science & Technology, Indian Institute of Technology Kharagpur, West Bengal, India
- P418 Chemical Guiding of Magnetic Nanoparticles in Dispersed Media Containing Poly(methylmethacrylate-co-vinylpyrrolidone)**
Myriam G. Tardajos, Inmaculada Aranaz, Carlos Elvira, Helmut Reinecke, Erhan Piskin, Alberto Gallardo
 Polymer Chemistry and Biomaterials Group, Ghent University, Belgium
- P419 Influence of Surface Roughness Parameters on MG63 Cell Viability: Studies on Laser Microtextured Ti6Al4V Surfaces**
Sumanta Mukherjee, Partha Saha, Santanu Dhara
 Mechanical Engineering Department, Indian Institute of Technology Kharagpur, India
- P420 Extended Release Drug Layer for POSS-PCU Cardiac Stents**
Megan Livingston and Alexander Seifalian
 Division of Surgical and Interventional Sciences, University College London, UK
- P421 Practical Application of Whole Slide Imaging in Biomaterial Science**
C. Brochhausen, H. B. Winther and C. J. Kirkpatrick
 Institute of Pathology, University Medical Centre, Mainz, Germany
- P422 Cryostructured hierarchical scaffolds with zonal biochemistry and anisotropic porosity for biomimetic in situ cartilage tissue engineering**
Kai Stuckensen, Jenny Reboredo, Andrea Schwab, Uwe Gbureck, Heike Walles and Jürgen Groll
 Department for Functional Materials in Medicine and Dentistry, University of Würzburg, Germany
- P423 Additive Manufactured 3D Scaffolds with Tailorable Surface Topography by a Single-Step Method**
SC Neves, C Mota, CC Barrias, PL Granja, L Moroni
 Instituto de Engenharia Biomédica, Universidade do Porto, Portugal
- P424 Biodegradable Biopolymer and Calcium Phosphate Composites Manufactured via Impregnation Method**
Marina Sokolova, Janis Locs
 Rudolfs Cimdins Riga Biomaterials Innovations and Development Centre, Riga Technical University, Latvia
- P425 Collagen IV and Fibroblasts as Supportive Factors in Angiogenesis Performed in a Perfusion Bioreactor Setup**
Franziska Kreimendahl, Stefan Weinandy, Julia Frese, Michael Vogt and Stefan Jockenhoevel
 Tissue Engineering and Textile Implants, RWTH Aachen University, Germany
- P426 Asymmetric Biodegradable Scaffolds for Vascular Tissue Engineering**
Patrycja Domalik-Pyzik, Anna Morawska-Chochół, Jan Chłopek, Elżbieta Menaszek, Izabella Rajzer
 Department of Biomaterials, AGH University of Science and Technology, Krakow, Poland
- P427 Biodegradation studies on some magnesium alloys without Al for biomedical application**
Iulian Antoniac, Florin Miculescu, Aurora Antoniac and Ana-Iulia Blajan
 Department Materials Science and Engineering, University Politehnica of Bucharest, Romania
- P428 Glucose sensitive gelation of hydrogel based on hyaluronan-tyramine conjugate**
Lenka Kohutová, Martin Pravda, Julie Bystroňová, Lucie Wolfová, Vladimír Velebný
 Contipro Biotech s.r.o., Dolní Dobruč, Czech Republic
- P429 Surface modification of injectable microspheres for cell therapy applications**
Abdulrahman Baki, Omar Qutachi, Toby Gould, Emily Overton, Kevin Shakesheff and Cheryl Rahman
 Drug Delivery and Tissue Engineering Department, University of Nottingham, UK
- P430 Photocrosslinkable divinyl-fumarate poly-ε-caprolactone for stereolithography application**
A. Ronca, S. Ronca, G. Forte, A. Gloria, R. De Santis, L. Ambrosio
 Institute for Polymers, Composites and Biomaterials, National Research Council of Italy, Napoli, Italy
- P431 Novel radiopaque UHMWPE sublamina wires in a growth-guidance system for the treatment of early onset scoliosis: feasibility in a large animal model**
Alex Roth, Rob Bogie, Paul Willems, Lodewijk van Rhijn, Jacobus Arts
 Department Orthopaedic Surgery, Maastricht University Medical Centre, the Netherlands
- P432 3D Plotting of hydrogels based on fibrillar collagen to create scaffolds with defined inner and outer architecture**
Anja Lode, Kristin Faulwasser, Sophie Brüggemeier, Birgit Hoyer, Hagen Baltzer, Michael Meyer, Claudia Winkelmann, Frank Sonntag, Michael Gelinsky
 Centre for Translational Bone, Joint and Soft Tissue Research, Technische Universität Dresden, Germany

- P433 Porous bioactive glass foam scaffolds: Comparison of 3 compositions**
Amy Nommeots-Nomm, Aine Delvin, Naomi Todd, Robert Law, Hua Geng, Christopher Mitchell, Peter D. Lee, Julian R. Jones
 Department of Materials, Imperial College, London, UK
- P434 Biodegradable nanoparticles coated with hyaluronic acid for targeted and sustained drug delivery to tumors**
Laura Mayol, Marco Biondi, Luisa Russo, Carla Serri, Assunta Borzacchiello, Luigi Ambrosio
 Institute of Polymers, Composites and Biomaterials, National Research Council, Naples, Italy
- P435 Human bone marrow as a unique source of both microvascular endothelial cells and mesenchymal stem cells for vascularised bone tissue engineering**
Julien Guerrero, Hugo de Oliveira, Sylvain Catros, Robin Siadous, Reine Bareille, Mohammed Derkaoui, Didier Letourneur, Joelle Amédée
 Inserm, U1026 Tissue Bioengineering, University of Bordeaux, France
- P436 Effect of Calcium Phosphate Ceramics Substrate Geometry on Mineralization and Cell Organization and Differentiation**
E.R. Urquía Edreira, A. Hayrapetyan, J.G.C. Wolke, J.A. Jansen, J.J.J.P. van den Beucken
 Department of Biomaterials, Radboud University Medical Center, The Netherlands
- P437 Biomechanical & morphological analysis of blend polymeric electrospun scaffolds for Cardiovascular Tissue Engineering**
Alexandros Repanas, Birgit Glasmacher and Dimosthenis Mavrilas
 Laboratory for Biomechanics & Biomedical Engineering, University of Patras, Greece
- P438 Biological interaction between a novel Sr-substituted bone cement and mesenchymal stem cells**
M. Montesj, M. Dapporto, S. Panseri, S. Sprio, A. Tampieri
 Institute of Science and Technology for Ceramics, National Research Council, Faenza, Italy
- P439 In vitro study of the combined effect of hydroxyapatite nanoparticles and lactoferrin in bone homeostasis**
Monica Montesj, Silvia Panseri, Michele Iafisco, Alessio Adamiano, Anna Tampieri
 Institute of Science and Technology for Ceramics, National Research Council, Faenza, Italy
- P440 Fabrication of De-epithelialized Amniotic Membrane/Silk Nanofibre Scaffolds for Skin Tissue Engineering**
Shaghayegh Arasteh, Somaieh Kazemnejad, Mohammad Mehdi Akhondi, Hamed Heidari-Vala, Afsaneh Mohammadzadeh, Sahba Mobini
 Reproductive Biotechnology Research Centre, Avicenna Research Institute, ACECR, Iran
- P441 Bioprinting of vasculature at cell-compatible conditions**
Jing Yang, Kevin Shakesheff
 Division of Drug Delivery and Tissue Engineering, University of Nottingham, UK
- P442 Creating albumin-binding nanostructured surfaces using a thrombin-inhibiting peptide**
Sidónio C. Freitas, Sílvia Maia, Ana C. Figueiredo, Paula Gomes, Pedro J.B. Pereira, Mário A. Barbosa, M. Cristina L. Martins
 Instituto de Engenharia Biomédica, Universidade do Porto, Portugal
- P443 Electrochemical deposition of calcium phosphate coatings on Ti6Al4V substrate**
Richard Drevet, Nader Ben Jaber, Ahmed Tara, Joël Faure and Hicham Benhayoune
 Université de Reims Champagne-Ardenne, France
- P444 Soft-matrices based on keratin/alginate for regenerative medicine**
Raquel Silva, Raminder Singh, Bapi Sarker, Judith A. Roether, Iwona Cicha, Joachim Kaschta, Dirk W. Schubert, Rainer Detsch and Aldo R. Boccaccini
 Department Materials Science and Engineering, University of Erlangen-Nuremberg, Germany
- P445 In Vitro Evaluation of Nanohydroxyapatite Biocompatibility in 2D vs 3D Cell Culture Systems**
Aileen Crawford, Abigail Pinnock, Veronika Hruschka, Heinz Redl, Paul V Hatton, Cheryl A Miller
 Bioengineering & Health Technologies Research Group, University of Sheffield, UK
- P446 Engineering of Staple Electrospun Fibres for Biodegradable Nanocomposites by Particle Enhanced Ultrasonication**
E. Mulky, G. Yazgan, K. Maniura-Weber, R. Luginbuehl, G. Fortunato, A. M. Buehlmann-Popa
 Chemistry & Biology, RMS Foundation, Switzerland
- P447 Electrochemically grown mesoporous titania layers**
Sureeporn Uttiya, Daniele Contarino, Sonja Prandi, Maria Maddalena Carmasciali, Ranieri Rolandi, Maurizio Canepa, Ornella Cavalleri
 Department of Physics, University of Genova, Italy
- P448 Characterisation of DNA Interactions with Cationic Polymer Brush**
Mahentha Krishnamoorthy and Julien Gautrot
 School of Engineering & Materials Science, Queen Mary, University of London, UK
- P449 Physicochemical Characterization and In Vitro Hemolysis Evaluation of UV Poly(ethylene glycol) Hydrogels**
M. Flores-Reyes, J. Flores-Estrada, M.V. Dominguez-Garcia, M.S. Camarillo-Romero, M.V. Flores-Merino
 Research Center in Biomedical Science, UAEM, Mexico
- P450 Gold-Containing PMMA Microspheres. A Route to New Highly Radiopaque Cements for Vertebroplasty**
Leo H. Koole, Ketie Saralidze, Eva Jacobs, Alex Roth, and Paul Willems
 Department of Biomedical Engineering, Maastricht University, The Netherlands
- P451 3D Direct Laser Writing of Biomimetic Structures for Osteogenesis Enhancement**
Attilio Marino, Carlo Filippeschi, Barbara Mazzolai, Virgilio Mattoli, Gianni Ciofani
 Center for Micro-BioRobotics, Istituto Italiano di Tecnologia, Pontedera, Italy
- P452 Understanding material properties of 3D poly(ϵ -caprolactone)-based ternary composite scaffolds responsible for highly improved colonization by Human Bone Marrow Mesenchymal Stem Cells**
J. Idaszek, A. Bruinink, J. Rębiś, V. Zell, W. Świąszkowski
 Faculty of Materials Science and Engineering, Warsaw University of Technology, Poland
- P453 The vascularization of porous calcium phosphate ceramics: an in vitro and in vivo study**
Ying Chen, Xiangdong Zhu, Yujiang Fan, Xingdong Zhang
 National Engineering Research Center for Biomaterials, Sichuan University, People's Republic of China

- P454 Thermal Ageing Effect on the Micromechanical Properties of Fiber-Reinforced Composites for Orthopaedic Applications**
Radek Sedláček, Tomáš Suchý, Karel Balík, Zbyněk Sucharda, Zdeněk Padovec
 Department of Mechanics, Biomechanics and Mechatronics, CTU in Prague, Czech Republic
- P455 Fabrication of a Bone Graft Substitute based on a Pre-set Bioactive Glass-Ionomer Cement**
Altair Contreras, Paul V. Hatton, Ian Brook, Abigail Pinnock and Cheryl A Miller
 Bioengineering & Health Technologies Research Group, University of Sheffield, UK
- P456 In vivo Response of Biodegradable Biphasic 3D Printed Scaffolds for Bone Tissue Engineering**
S. Ghanaati, M Barbeck, T. Serra, P. Booms, R. Sader, J. A. Planell, M. Navarro, C. J. Kirkpatrick
 Institute of Pathology, University Medical Center of the Johannes Gutenberg University Mainz, Germany
- P457 Cobalt alloy specific regulation of bone remodelling via HIF: a cause of aseptic orthopaedic implant failure?**
Yutong Li, Johannes Staufenberg, Jay Mashari, Divyahline Logitharajah and Gavin Jell
 Division of Surgery & Interventional Science, University College London, UK
- P458 Trimethyl Chitosan-Based Nanoparticles Intracellular Trafficking and Transfection: a Bioimaging Study**
Aida Varela-Moreira, Carla Pereira Gomes, Maria Gomez-Lázaro, Pedro Miguel Moreno, Ana Paula Pêgo
 Instituto de Engenharia Biomédica, Universidade do Porto, Portugal
- P459 Electrospun Polyvinylpyrrolidone Nanocomposites Mesh with Silica-coated Magnetic Nanoparticles**
Rebecca Zhiyu Yuan, Jian Ping Fan and Jie Huang
 Department of Mechanical Engineering, University College London, UK
- P460 WITHDRAWN**
- P461 Laser surface modification of anodically grown oxide of titanium for biomedical applications**
Diego Pedreira de Oliveira, Laís Tereza Duarte, Adriano Otuka, Claudemiro Bolfarini
 Departamento de Engenharia de Materiais, Federal University of São Carlos, Brazil
- P462 Fibrin-Hyaluronic Acid Interpenetrating Network Hydrogel with Improved Fibrin Stability**
Yu Zhang, Philipp Heher, Sujit. Kotala, Heinz Redl, Jöns Hilborn and Dmitri Ossipov
 Department of Chemistry-Ångström, Uppsala University, Sweden
- P463 Effect of Preconditioning on 70S30C Bioactive Glass Foam Structure and Protein Adsorption**
Gowsihan Poolagasundarampillai, Peter D Lee, Dave Clark, Julian R Jones
 Department of Materials, Imperial College, London, UK
- P464 Synthesis and Characterization of Silicate Glasses with the Sol-Gel Process Containing ZnO or SrO**
G. Theodorou, E. Kontonasaki, K. Chrissafis, L. Papadopoulou, N. Kantiranis, T. Zorba, K.M. Paraskevopoulos, P. Koidis
 Department of Physics, Aristotle University of Thessaloniki, Greece
- P465 Mechanical Stabilisation of Non-Toxic Collagen Fibres for Tendon Repair**
Anna Sorushanova, India Sweeny, Abhay Pandit, Dimitrios Zeugolis
 Network of Excellence for Functional Biomaterials, National University of Ireland, Galway, Ireland
- P466 Cell Osteogenic Function Enhancement and Selective Apoptosis by Hydroxyapatite Nanoparticles**
Fangzhu Qing, Zhe Wang, Yanfei Tan and Xingdong Zhang
 National Engineering Research Center for Biomaterials, Sichuan University, P. R. China
- P467 Low Temperature Aqueous Precipitation of Nanocrystalline Hydroxyapatite Containing Strontium and Magnesium for Biomedical Application**
Kristine Salma-Ancane, Liga Stipniece and Liga Berzina-Cimdina
 Rudolfs Cimdins Riga Biomaterials Innovation and Development Centre, Riga Technical University, Latvia
- P468 Controlled release of nucleic acid to enhance bone regeneration**
Bita Sedaghati, Alexander Ewe, Achim Aigner, Michael C. Hacker, Michaela Schulz-Siegmund
 Pharmaceutical Technology, University of Leipzig, Germany
- P469 Determination of Anti-Cancer and Anti-Bacterial Efficacy of Selenium Doped Hydroxyapatite Coating on Titanium Alloy**
Bengi Yilmaz, Zafer Evis, Aysen Tezcaner and Sreeparna Banerjee
 Department of Biomedical Engineering, Middle East Technical University, Turkey
- P470 Microfluidic neuronal circuitry – towards therapies for Huntington’s disease**
Munyaradzi Kamudzandu, Paul Roach and Rosemary A. Fricker
 Institute for Science and Technology in Medicine, Keele University, UK
- P471 Nanoscale Analyses of *Parawixia bistriata* Synthetic Spider Silk Fibres**
Valquíria A Michalczechen-Lacerda, Giovanni R Vianna, André M Murad, Luciano P Silva, Elibio L Rech
 Department of Cell Biology, University of Brasília, Brazil
- P472 Characterization and *In Vitro* Testing of Calcium Phosphate Coatings on Dense and Porous Substrates**
Alexandre Antunes Ribeiro, Roseli Marins Balestra, Mônica Calixto de Andrade, Emanuela Prado Ferraz, Adalberto Luiz Rosa, Paulo Tambasco de Oliveira, Marize Varella de Oliveira
 Powder Technology Laboratory, National Institute of Technology, Brazil
- P473 Synthesis and Characterization of Novel Chitosan Hydrogels for Biomedical Applications**
Krzysztof Pazdan, Kinga Pielichowska, Jan Chłopek
 Department of Biomaterials, AGH University of Science and Technology, Kraków, Poland
- P474 Silver Nanoparticles Modified Titanium for Medical Implants**
Barbara Szaraniec, Magdalena Oćwieja, Marta Kujda and Bartosz Piec
 Department of Biomaterials, Faculty of Materials Science and Ceramics, AGH – University of Science and Technology, Poland
- P475 Synergistic Reinforcement of Poly(e-caprolactone)/Gelatin Nerve Tissue Engineering Scaffolds by Graphene Oxide Nanosheets**
S. Soltanian-Zadeh, Z. S. Ghazali, M. Rabiee, F. Moztarzadeh, M. Mozafari
 Biomedical Engineering Department, Amirkabir University of Technology, Tehran, Iran

- P476 Mechanical reinforcement of chitosan-poly(lactic-co-glycolic) acid scaffolds by 58S bioactive glass**
Katayoun Nazemi, Fathollah Moztarzadeh, Masoud Mozafari
 Biomedical Engineering Department, Amirkabir University of Technology, Iran
- P477 Co-culture of human monocytes and mesenchymal stem cells in order to simulate the bone remodelling processes**
Claudia Kleinhans, Freia Schmid, Franziska Schmid, Petra J. Kluger
 Institute for Interfacial Process Engineering and Plasma Technology, University of Stuttgart, Germany
- P478 Electrospun Poly(ϵ -caprolactone)/Gelatin Scaffold Electrophoretically Coated with Graphene Oxide for Nerve Tissue Engineering**
Z.S. Ghazali, S. Soltanian-Zadeh, F. Moztarzadeh, M. Mozafari
 Biomedical Engineering Department, Amirkabir University of Technology, Iran
- P479 Morphometry of bone tissue around endossal implantation of Hap/TCP granules and autologous mesenchymal cells in rabbits with experimental osteoporosis**
Aleksandrs Grishulonoks, Vita Zalite, Inese Cakstina, Arvids Jakovlevs, Andrejs Skagers
 Department of Oral and Maxillofacial Surgery, Riga Stradins University, Latvia
- P480 A Study On 45S5 Bioglass® Foam Dissolution**
V. Melli, L.-P. Lefebvre, L. Altomare, L. De Nardo
 Dipartimento di Chimica, Materiali e Ingegneria Chimica G. Natta, Politecnico di Milano, Italia
- P481 Biocompatibility of Poly High Internal Phase Emulsion Scaffolds prepared using Stereolithography**
Atra Malayeri, Ilida Ortega, Frederik Claeyssens, Colin Sherborne, Neil R Cameron, Paul V. Hatton
 School of Clinical Dentistry, University of Sheffield, UK
- P482 Implantable hybrid composite for reducing inflammation in age related macular degeneration**
E. Chinarro, L. Pires, Ana P. Pêgo and B. Moreno
 Instituto de Cerámica y Vidrio, CSIC, Madrid, Spain
- P483 Hypoxia inducible factor-1 α (HIF-1 α) stabilization for enhanced cell and tissue construct survival**
Wai Ho, Barry Fuller and Gavin Jell
 Division of Surgery and Interventional Science, University College London, UK
- P484 Practical fixation issues of multifunctional bioresorbable miniplates for osteotomies**
Karol Gryń, Anna Morawska-Chochół, Barbara Szaraniec, Magdalena Ziąbka, Jan Chłopek
 Department of Biomaterials, AGH University of Science and Technology, Krakow, Poland
- P485 Dynamic Surfaces for Stem Cell Differentiation and Retention of Stem Cell Phenotype**
Laura E. McNamara, Jemma N. Roberts, Jugal Sahoo, Karl V. Burgess, Jake Hay, Hilary Anderson, Richard O.C. Oreffo, Rein Ulijn and Matthew J. Dalby
 Centre for Cell Engineering, University of Glasgow, UK
- P486 Cytotoxicity control of SiC nanoparticles introduced into polyelectrolyte multilayer films**
Aldona Mzyk, Roman Major, Bogusław Major
 Institute of Metallurgy and Materials Science, Polish Academy of Sciences, Poland
- P487 Effects of Plasma Electrolytic Oxidation Treatment of Titanium and Titanium-Niobium-Zirconium alloys on Leucocyte Inflammatory Response and Human Osteoblast Mineralization**
Constantin-Edi Tanase, Mehdi Golozar, Kim Hoenderdos, Serena M. Best, Roger A Brooks
 Division of Trauma & Orthopaedic Surgery, Addenbrooke's Hospital, University of Cambridge, UK
- P488 Development of new bioactive phosphate-based glasses and study of the particle size effects on osteoblasts response for bone implant applications**
Martin Stefanic, Xiang Zhang
 Lucideon Ltd., Stoke-on-Trent, UK
- P489 Backside wear in fixed-bearing total knee arthroplasty : the effect of liner locking mechanism and surface roughness of tibial tray**
Łukasz Łapaj, Jacek Markuszewski, Justyna Wendland, Adrian Mróz, Jacek Kruczyński
 Department of General Orthopaedics, Musculoskeletal Oncology and Trauma Surgery, Poznan University of Medical Sciences, Poland
- P490 Paraffin versus frozen sectioning in the histologic evaluation of biomaterial implants – a pilot study**
Volker H. Schmitt, Christoph Brochhausen, Dominic Schwarz, Christine Tapprich, Andreas Mamilos, Helmut Hierlemann, Heinrich Planck, C. James Kirkpatrick
 Institute of Pathology, University Medical Centre, Johannes Gutenberg-University Mainz, Germany
- P491 WITHDRAWN**
- P492 Composition-Property Relationships for Gallium-Borate Glasses**
K. O'Connell, H. O'Shea, Muhammad Hasan, D. Boyd
 Department of Oral Sciences, Dalhousie University, Canada
- P493 RF-Magnetron Sputter Deposited Cap-Based Coatings on the Surface of Titanium**
Maria A. Surmeneva, Roman A. Surmenev, Oleg Prymak, Matthias Epple, Irina I. Selezneva
 Department of Theoretical and Experimental Physics, National Research Tomsk Polytechnic University, Russia
- P494 Electrochemical Surface Treatment for Making Antibacterial Porous Oxide Layer on Ti**
Yusuke Tsutsumi, Naofumi Niizeki, Peng Chen, Maki Ashida, Hisashi Doi, Kazuhiko Noda and Takao Hanawa
 Institute of Biomaterials and Bioengineering, Tokyo Medical and Dental University, Japan
- P495 Imaging the structure, dissolution, and bone ingrowth into Bioactive Glass scaffolds**
Peter D. Lee, Taek Bo Kim, Wouter van den Bergh, Hua Geng, Sheng Yue, Christopher Mitchell, Julian Jones
 School of Materials, University of Manchester, UK

- P496 Bioactive hydrogels supporting angiogenesis produced by EB-irradiation**
Bozena Rokita, Slawomir Kadlubowski, Piotr Komorowski, Bogdan Walkowiak, Janusz M. Rosiak
 Institute of Applied Radiation Chemistry, Technical University of Lodz, Poland
- P497 Nanostructured Organic Layers via Polymer Demixing to Control Mesenchymal Stem Cell Response**
Mohammed Khattak, John Hunt and Raechelle A. D'Sa
 Department of Musculoskeletal Biology, Institute of Ageing and Chronic Disease, University of Liverpool, UK
- P498 Role of Gallium doped phosphate-based glasses in the Management of Periodontitis**
Bernadette Lackey, Rohan Sahdev, Quentin Nunes, Tahera Ansari, Susan Higham, David Fernig, Sabeel Valappil
 Department of Health Services Research, University of Liverpool, UK
- P499 Antibacterial TiO₂ nanotubes incorporated with silver nanoparticles**
Zhijun Guo and Li Zhang
 Research Center for Nano-biomaterials, Sichuan University, China
- P500 Bone Nodule Formation by Osteoblast-Like Cells Incubated with a Novel Silane Modification of Glass**
Sandra Fawcett, Nicholas Rhodes, John Hunt and Judith Curran
 Department of Musculoskeletal Biology, University of Liverpool, UK
- P501 Manufacturing of AZ91D Implants with Micro-Scale Features by Powder Metallurgy Route**
Aydin Tahmasebifar, Said Murat Kayhan, Zafer Evis, Yusuf Usta and Muammer Koç
 Engineering Sciences, Middle East Technical University, Turkey
- P502 Nerve Tissue Engineering Using Blends of Polyhydroxyalkanoates**
L.R. Lizarraga-Valderrama and Ipsita Roy
 Faculty of Science and Technology, University of Westminster, London, UK
- P503 Polyethyleneimine-iron oxide hybrid nanomaterials – structure and biocompatibility**
Roxana Mioara Piticescu, Laura Madalina Popescu, Alexandrina Burlacu, Ana-Maria Rosca, Eugeniu Vasile, Andrea Danani
 Laboratory of Nanostructured Materials, National R&D Institute for Non-ferrous and Rare Metals, Romania
- P504 Regulation of Sclerostin Expression by ATP and PTH at Different Stages of Human Bone Development**
Osman M Azuraiddi, Peter J Wilson, Nicholas P Rhodes and James A Gallagher
 UK Centre for Tissue Engineering, Department of Musculoskeletal Biology, University of Liverpool, UK
- P505 Hemocompatible Biomaterial Based on Fibrin Coatings**
Ondřej Kaplan, Tomáš Riedel, Milan Houska, and Eduard Brynda
 Department of Biomaterials and Bioanalogous Systems, Academy of Sciences of the Czech Republic, Prague
- P506 Inflammation-modulating biomaterial impacts neutrophil-monocyte juxacrine and paracrine regulation**
Hannah Caitlin Cohen, Tyler Jacob Lieberthal, W. John Kao
 Pharmaceutical Sciences Division, School of Pharmacy, University of Wisconsin-Madison, USA
- P507 A Heterotypic Microfluidic Model of PDAC Microenvironment for Investigating Stroma-Tumor Interactions and Therapeutic Evaluations**
Cole Drifka, Kevin Eliceiri, Agnes Loeffler, Sharon Weber, W. John Kao
 Department of Biomedical Engineering, University of Wisconsin, Madison, USA
- P508 Enhanced migration of Mesenchymal stem cell spheroids towards glioma**
Smruthi Suryaprakash, Hon Fai Chan and Kam W Leong
 Department of Biomedical Engineering, Duke University, USA
- P509 Feasibility study of developing mosaic and tissue engineering pulmonary valved conduits**
Xiufang Xu, Jinhui Ma, Wenbin Li, Haiping Guo, Sheng Wang, Haifeng Shi, Yi Xin, Xuejun Ren, Zifan Zhou
 Department of Cardiac Surgery, Beijing Anzhen Hospital, Capital Medical University, China
- P510 A Novel Soft Tissue Model for Biomaterial-Associated Infection and Inflammation – Bacteriological, Morphological and Molecular Observations**
Sara Svensson, Margarita Trobos, Maria Hoffman, Birgitta Norlindh, Sarunas Petronis, Jukka Lausmaa, Felicia Suska and Peter Thomsen
 Department of Biomaterials, Sahlgrenska Academy at University of Gothenburg, Sweden
- P511 Pore Structure and Imaging of Collagen- and Elastin-based Scaffolds for Vascular Grafts**
H. Frank, J. Shepherd, S. Best, R. Cameron
 Department of Materials Science and Metallurgy, University of Cambridge, U
- P512 Sustained Release of Naproxen Sodium from Electrospun Aligned PLLA/PCL Scaffold for Tendon Tissue Regeneration**
Yuan Siang Lui, Mark P. Lewis, Joachim Say Chye Loo
 School of Materials Science and Engineering, Nanyang Technological University, Singapore
- P513 Analysis of cells proliferation after dynamic culture on cross-linked synthetic collagen peptide based microcarriers**
M. La Marca and Suzan van Dongen
 Fujifilm Manufacturing Europe, The Netherlands
- P514 Cell Response on the Ti-15Mo alloy Surface after Nanotubes Growth**
Ana Paula Rosifini Alves Claro, André Luiz Reis Rangel, Nathan Trujillo, Ketul C. Popat
 Materials and Technology Department, University of Estadual Paulista, São Paulo, Brazil
- P515 Elaboration of degradable PCL-based shape memory materials**
Thomas Defize, Raphaël Riva, Jean-Michel Thomassin, Michaël Alexandre, Bernard Gilbert and Christine Jérôme
 Center for Education and Research on Macromolecules, University of Liege, Belgium
- P516 Surface immobilization of a green fibronectin-like protein onto cold plasma modified polystyrene substrates**
O. M. Ba, A. Ponche, O. Gallet, P. Marmey, A.C. Duncan, K. Anselme
 Institut de Science des Matériaux de Mulhouse, UMR CNRS 7361, France
- P517 Peptide-Polysaccharide Based Injectable Hydrogel for Sustained Delivery of Active Agents**
Cem Bayram, Ekin Çelik and Emir Baki Denkbaş
 Chemistry Department, Aksaray University, Turkey

- P518 Characterisation of Freeze-Dried Collagen-Fibrinogen Constructs**
Jennifer Shepherd, Charlotte Rasser, Serena Best, Ruth Cameron
 Department of Materials Science and Metallurgy, University of Cambridge, UK
- P519 Nanosized grooves controlling neuronal cell-organization and axonal outgrowth for cochlear implant optimization**
Alexey Klymov, Joost te Riet, John A Jansen and X Frank Walboomers
 Department of Biomaterials, Radboud University Medical Center, Nijmegen, The Netherlands
- P520 The effectiveness of tetra sodium EDTA as an anti-biofilm agent for use in biomaterials**
Steven L Percival and Peter Kite
 Institute of Ageing and Chronic Disease, University of Liverpool, UK
- P521 Composite scaffolds from gelatin and elastin-like block polypeptides for tissue engineering**
Duc H. T. Le, Tatsuya Okubo, Ayae Sugawara-Narutaki
 Department of Chemical System Engineering, The University of Tokyo, Japan
- P522 Pelvic Floor Repair Materials Releasing Vitamin C to Promote Extracellular Matrix Production**
Naside Mangir, Anthony J Bullock, Sabiniano Roman, Nadir Osman, Christopher Chapple, Sheila MacNeil
 Department of Materials Science Engineering, University of Sheffield, UK
- P523 Synthetic collagen peptide based microspheres/ hydrogel hybrid system for bone growth factor delivery**
L. de Miquel, G. van Osch and S.G.J.M. Kluijtmans
 Fujifilm Life Sciences, Tilburg, the Netherlands
- P524 Development of a Novel Composite Polymer Material to Facilitate Regeneration of Chronic Non-Healing Wounds**
Alma Akhmetova, Matthew Illsley, Timur Saliev, Gulsim Kulsharova, Talgat Nurgozhin, Sergey Mikhailovsky, Iain Allan
 Department of Translational Medicine, Longevity and Global Health, Nazarbayev University, Kazakhstan
- P525 The effect of amphiphilic and anionic β -sheet peptides on blood clotting**
Ziv Azoulay and Hanna Rapaort
 Avram and Stella Goldstein-Goren Department of Biotechnology Engineering, Ben-Gurion University of the Negev, Beer - Sheva, Israel
- P526 Processing and Mechanical Properties of Biodegradable β TCP-15Fe15Mg Composites**
Sanjaya K. Swain, Irena Gotman, Elazar Y. Gutmanas
 Department of Materials Science and Engineering, Technion, Haifa, Israel
- P527 Economical Production of Medium Chain Length Polyhydroxyalkanoates**
Yiangos Psaras
 Faculty of Science and Technology, University of Westminster, London, UK
- P528 A New Method to Rapidly Retrieve Encapsulated Cells from Alginate Hydrogels using Pyrophosphate**
David C. Bassett and Pawel Sikorski
 Department of Physics, Norwegian University of Science and Technology, Norway
- P529 Stable Electrospun Hyaluronan Matrices: Production and In Vitro Characterization for the Evaluation as Skin Substitute**
Annalisa La Gatta, Marcella Cammarota, Antonella D'Agostino, Agata Papa, Stefano Guido, Chiara Schiraldi
 Department of Experimental Medicine, Second University of Naples, Italy
- P530 Collagen and PNIPAM Hydrogels: An Injectable Solution to Repair the Knee**
Amanda Barnes, J Lapworth, Mark Coles, Stephen Rimmer and Paul Genever
 Biomedical Tissue Research Group, University of York, UK
- P531 WITHDRAWN**
- P532 Antimicrobial efficacy and biocompatibility of silver-including nanocomposite carbon coatings**
Dorota Bociaga, Piotr Komorowski, Witold Jakubowski, Anna Jędrzejczak, Anna Olejnik
 Division of Biomedical Engineering and Functional Materials, Lodz University of Technology, Poland
- P533 The Impact of Serum, Plasma, and Platelet-Rich Plasma Derived After Exposure to Exercise, Altitude and Recombinant Human Erythropoietin (rHuEpo) on Mesenchymal Stem Cells**
C. Coombs, P. Watt, A. Guildford, G. Bruinvels, Y. Pitsiladis
 Brighton Centre for Regenerative Medicine, University of Brighton, UK
- P534 Towards a 3-Dimensional Model of Neural Tissue with Integrated Recording Sites**
H. Lancashire, C. Pendegrass, A. Vanhoestenbergh and G. Blunn
 Institute of Orthopaedics and Musculoskeletal Science, University College London, UK
- P535 Indirect Prototyped Polyurethane Urea Scaffolds for Cardiac Tissue Engineering**
Roberto Hernandez-Cordova, Donna A Mathew, Alberto Ceballos-Villanueva, Hugo J Carrillo-Escalante, Araida Hidalgo-Bastida, Fernando Hernandez-Sanchez
 Manchester Metropolitan University, UK
- P536 RF Magnetron Sputtering of Multicomponent Ion Doped Phosphate Glasses**
Bryan Stuart, M. Gimeno-Fabra, D. Grant, I. Ahmed and J. Segal
 Department of Mechanical, Materials and Manufacturing Engineering, University of Nottingham, UK
- P537 Manufacture of Bioresorbable Fibre Reinforced Composites for Fracture Fixation Devices**
Fernando Barrera Betanzos, Miquel Gimeno-Fabra, Joel Segal, David Grant and Ifty Ahmed
 Department of Mechanical, Materials and Manufacturing Engineering, University of Nottingham, UK
- P538 Development of a Soft Tissue in vitro Model for Ameloblastoma**
T. Eriksson, S. Fedele, R. Day, V. Salih
 Eastman Dental Institute, University College London, UK
- P539 Porous Electrospun PCL fibres for Osteo-Differentiation**
Selene Alcantara-Barrera, Zandra Flores, Ricardo Vera-Graziano, Alfredo Maciel-Cerda, L. Araida Hidalgo-Bastida
 Manchester Metropolitan University, UK

P540 Atomic Layer Deposition of Silver on High Aspect Ratio Structures for Medical Implants

Zahra Golrokhi

Department of Materials Science and Engineering, University of Liverpool, UK

P541 Characteristics and Cytocompatibility of Novel Borophosphate Glasses

Chenkai Zhu, Ifty Ahmed, Xiaoling Liu, Andy Parsons, Jingsong Liu, Chris Rudd

Division of Materials, Mechanics and Structures, University of Nottingham, UK

YSF Rapidfire Presentation Programme

Rapidfire Session I Hall 2, Sunday 31st August 12:30 - 13:30

Chairs: Nicholas Bryan, University of Liverpool
Theun van Veen, University of Liverpool
Lorenzo Moroni, University of Twente
Sandra van Vlierberge, University of Gent
Anna-Finne Wistrand, KTH Royal Institute of Technology

- 1-1 Carlos Elias**
Mechanical Properties of Zirconia 3-Unit Fixed Dental Prostheses Machined on a CAD/CAM System
- 1-2 Sandra Fawcett**
Bone Nodule Formation by Osteoblast-Like Cells Incubated with a Novel Silane Modification of Glass
- 1-3 Annika Jokinen**
MP-SPR New characterization method for interactions and ultrathin films
- 1-4 Prabhjeet Kaur Dhillon**
Nanoscale Roughness Influences on Cell Proliferation
- 1-5 Kasai Nahoko**
Neuronal growth on nano-pillar substrates
- 1-6 Annabelle Chan**
Patient Specific Implants Using a Novel Rapid Template Approach
- 1-7 Stéphanie Metzger**
Mobilization of Mesenchymal Progenitor Cells to Improve Bone Healing
- 1-8 Febriyani Damanik**
Incorporation of Elastin Enhancement Agents on Nano-scale Fibers
- 1-9 Helena Grady**
Central Venous Catheters Functionalised with Chlorhexidine-Hexametaphosphate Nanoparticles for Prolonged Anti-Biofilm Efficacy
- 1-10 Gloria Huerta-Angeles**
Development of a new biomaterial based on Hyaluronan and oleic acid for drug delivery applications
- 1-11 Natalie Wood**
Chlorhexidine-based Antimicrobial Nanoparticles as a Coating for Dental Implants
- 1-12 Matteo Gherardi**
Plasma assisted production of residual solvent free PLLA electrospun scaffolds
- 1-13 Irina Batenina**
A comparison of two approaches to the formation of antibacterial surfaces: doping with bactericidal element vs drug loading
- 1-14 Lorena del Rosario Lizarraga Valderrama**
Nerve Tissue Engineering Using Blends of Polyhydroxyalkanoates
- 1-15 Ąukasz Ąapaj**
Backside wear in fixed-bearing total knee arthroplasty : the effect of liner locking mechanism and surface roughness of tibial tray
- 1-16 Danielle Cabral**
Candida glabrata in mouthwash -coated endotracheal tubes: antibiofilm activity by electronically scanning microscopy
- 1-17 Prabhhash Dadhich**
Nano-Micro Architectural Hybrid Composite Scaffold for Bone Tissue Engineering
- 1-18 Diego de Oliveira**
Laser surface modification of anodically grown oxide of titanium for biomedical applications
- 1-19 Matteo D'Este**
Amidation via DMTMM: A New and Efficient Method for Hyaluronan Biomaterials Preparation
- 1-20 Ting Diu**
Bactericidal and cell compatible titanium surfaces with TiO₂ nanowires
- 1-21 Cyrine Dridi**
Design of Biomimetic Fibronectin Fragment Used in Multi-layer Film Coating for Tissue Engineering
- 1-22 Matthias Schumacher**
Strontium-substituted CaP bone cements for the treatment of osteoporotic bone defects
- 1-23 Farzad Foroutan**
Novel sol-gel synthesis of (P₂O₅)₅₀-(CaO)₃₀-(Na₂O)₁₅-(Fe₂O₃)₅ glasses for biomedical application
- 1-24 Giulia Gigliobianco**
Surface functionalization of electro-spun Poly(L)Lactic Acid scaffolds with heparin to induce angiogenesis
- 1-25 Daniela Giugliano**
Gelatin/hydroxyapatite multicomponent system with a modulate biological signals
- 1-26 Chris Hickling**
Fabrication of Stable Biocatalytic Networks for the Cascadable Manufacture of Fine Chemicals



- 1-27 Isabel Hopp**
Design, Development and Characterization of Novel Polyacrylates to direct Kidney Progenitor / Stem Cell Differentiation
- 1-28 Shihoko Inui**
Dynamic Hardness Evaluation of Two Phases of Au–xPt–8Nb Alloys for MRI-artifact-free Biomedical Devices
- 1-29 Wai Ho**
Hypoxia inducible factor-1 α (HIF-1 α) stabilization for enhanced cell and tissue construct survival
- 1-30 Eva Hoch**
Photo-crosslinkable and biopolymer-based inks for inkjet-bioprinting of artificial cartilage

Rapidfire Session II Hall 2, Monday 1st September 12:30 - 13:30

Chairs: Nicholas Bryan, University of Liverpool
Theun van Veen, University of Liverpool
Lorenzo Moroni, University of Twente
Sandra van Vlierberge, University of Gent
Anna-Finne Wistrand, KTH Royal Institute of Technology

- 2-1 Kai Stuckensen**
Cryostructured hierarchical scaffolds with zonal biochemistry and anisotropic porosity for biomimetic in situ cartilage tissue engineering
- 2-2 Miguel Castilho**
3D powder printing of structured TCP/Alginate scaffolds for bone tissue engineering
- 2-3 Monica Montesi**
Biological interaction between a novel Sr-substituted bone cement and mesenchymal stem cells
- 2-4 Marta Alves**
Electrodeposition of Nanostructured Zinc Oxide on Zinc with Potential for Bioresorbable Medical Devices
- 2-5 Wan Ting Sow**
Electrospun Human Hair Keratin Matrices Affect Human Fibroblast Behavior Through Topographical Cues
- 2-6 Joanna Idaszek**
Understanding material properties of 3D poly(ϵ -caprolactone)-based ternary composite scaffolds responsible for highly improved colonization by Human Bone Marrow Mesenchymal Stem Cells
- 2-7 Monika Ziminska**
Investigation of Factors Influencing Deposition of Nanocomposite Coating onto Open Cell Foams using Layer-by-Layer Assembly: Design of Experiment Approach
- 2-8 David Shepherd**
In Vitro studies to measure the inflammatory response of crosslinked poly(lactide-co-caprolactone) dimethacrylate scaffolds
- 2-9 Constantin Edi Tanase**
Effects of Plasma Electrolytic Oxidation Treatment of Titanium and Titanium-Niobium-Zirconium alloys on Leucocyte Inflammatory Response and Human Osteoblast Mineralization
- 2-10 Erwin Zant**
High Throughput Production and Analysis of Tissue Engineering Scaffolds prepared using Combinatorial Chemistry
- 2-11 Jie An**
In vitro degradation of calcium phosphate under static and dynamic conditions
- 2-12 Khairul Shariff**
Interconnected porous calcium phosphate forming cement consisting of α -TCP foam granules and calcium phosphate acidic solution
- 2-13 Shraddha Thakkar**
Elastomeric Polycaprolactone scaffold for cardiovascular tissue engineering
- 2-14 Annika Wenz**
Endothelialization of gas exchange membranes to provide antithrombogenicity
- 2-15 Patrycja Domalik-Pyzik**
Asymmetric Biodegradable Scaffolds for Vascular Tissue Engineering
- 2-16 Hannah Stepto**
Development of Biodegradable Virus and miRNA Eluting Stent Technology
- 2-17 Smruthi Suryaprakash**
Enhanced migration of Mesenchymal stem cell spheroids towards glioma
- 2-18 Laura Szkolar**
Fine-Tuning Self-Assembling Peptide Hydrogels for Cell Culture Applications
- 2-19 Patricia Taladriz**
Photochemical nitric oxide release from a Flutamin derivative incorporated in Pluronic F127 hydrogel
- 2-20 Eva Urquia Edreira**
Effect of Substrate Geometry on Mineralization and Cell Proliferation of Calcium Phosphate Ceramics

- 2-21 Chenkai Zhu**
Characteristics and Cytocompatibility of Novel Borophosphate Glasses
- 2-22 Alma Akhmetova**
Preparation and Characterization of Novel Composite Agarose Films for Wound Healing
- 2-23 Yoshikatsu Akiyama**
Mechanical-stress-assisted rapid cell sheets recovery from poly(N-isopropylacrylamide) grafted PDMS surfaces
- 2-24 Anthony Deegan**
Controlling Intramembranous Bone Mineralisation using a Bone Tissue Engineering Approach
- 2-25 Costantino Del Gaudio**
Gelatin/Chitosan Microspheres for a Modulated Drug Delivery System
- 2-26 Luis M Delgado**
Influence of collagen cross-linking on fibroblast and macrophage response
- 2-27 Anna Guildford**
Functionalisation of polyurethane films using YIGSR poly(ϵ -lysine) linked dendrons to manipulate the human mesenchymal cell response
- 2-28 Richard Drevet**
Electrochemical deposition of calcium phosphate coatings on Ti6Al4V substrate
- 2-29 Anke Husmann**
Radially Aligned Collagen Scaffolds for Deterministic 3D Models of Cancer Migration
- 2-30 Gulseren Irmak**
Osteogenic Differentiation of AdMSCs on 17 β -Estradiol Releasing Chitosan-Hydroxyapatite Scaffolds

Rapidfire Session III Hall 2, Monday 1st September 18:00 - 19:30

Chairs: Nicholas Bryan, University of Liverpool
Theun van Veen, University of Liverpool
Lorenzo Moroni, University of Twente
Sandra van Vlierberge, University of Gent
Anna-Finne Wistrand, KTH Royal Institute of Technology

- 3-1 Claudia Loebel**
Precise Hyaluronan-tyramine synthesis for tailored cellular microenvironments
- 3-2 Urvashi Danookdharree**
Tayloring the Interfacial Adhesion of Anodised TiO₂ Nanotubes on Ti-6Al-4V Alloy for Medical Implants
- 3-3 Anne Castilho**
Different cryogel architectures as basis for 3D cell culture of prostate cancer cells
- 3-4 Luisa Islas**
Modification of PVC catheters with a binary graft of PEGMA and AAc to improve their biocompatibility
- 3-5 Frits Hulshof**
High throughput screening of hMSC response to algorithm generated micro-topographies
- 3-6 Anna Liguori**
Atmospheric Plasma Surface Modification of Electrospun Poly(L-Lactic Acid): Effect on Mat Properties and Cell Culturing
- 3-7 Candice Bellis**
Development of novel nanofunctionalised glass ionomer cements containing chlorhexidine-hexametaphosphate nanoparticles: mechanical properties and method of incorporation
- 3-8 Miriam Flores Merino**
Physicochemical Characterization and In Vitro Hemolysis Evaluation of UV Poly(ethylene glycol) Hydrogels
- 3-9 Cristina Martins**
Creating albumin-binding nanostructured surfaces using a thrombin-inhibiting peptide
- 3-10 Navinderpal Kaur Chana**
Investigation of Ion Exchange between Silicate-substituted Bone Graft Substitutes and Cell Culture Media and the effect on Osteoblast-like Cell Response
- 3-11 Nick Dibbert**
Dextran as a Versatile Scaffold for Hydrogel Formation with Hyaluronic Acid
- 3-12 Marco Regis**
Effect of fibre reinforcement on the crystallinity of PEEK for articular joint implants
- 3-13 Osamu Suzuki**
Biological performance of injectable octacalcium phosphate-hyaluronic acid composites on bone augmentation
- 3-14 Bapi Sarker**
Evaluation of In Vitro Cytocompatibility of Alginate-Gelatin Crosslinked Hydrogels
- 3-15 Jacobus Arts**
Novel radiopaque UHMWPE sublaminar wires in a growth-guidance system for the treatment of early onset scoliosis: feasibility in a large animal model

- 3-16 Linda Vecbiskena**
Nano-sized α -tricalcium phosphate for bone cement
- 3-17 Amany Mostafa**
Assessment of the bioactivity of gold doped hydroxyapatite-polyvinyl alcohol nanocomposites
- 3-18 Anja Lena Thiebes**
Cell Spraying Approach in vitro for Coating of Respiratory Tissue Engineered Constructs
- 3-19 Ana Soto de la Cruz**
Optical Projection Tomography as a Tool for Visualizing Hydrogels Microstructures
- 3-20 Jiyoung Bae**
Properties of β -TCP based Calcium Phosphate Cement using mechano-chemical process
- 3-21 Keith Blackwood**
Melt Electrospinning Of PCL/Bioactive Glass Composites In Direct Writing For Highly Ordered Scaffolds For Non-Load Bearing Defects
- 3-22 Bing Cai**
Evaluation of the effect of polymer content on drug release and mechanical strength of a Geopolymer ER Formulation for opioid drugs
- 3-23 Ross Colquhoun**
The degradation relationship between mechanical and in vitro testing of a phosphate glass fibre composite
- 3-24 Jennifer Edwards**
Biological Properties of an Acellular Xenogeneic Tendon Graft following Chemical and Irradiation Sterilisation
- 3-25 Shahram Ghanaati**
In vivo Response of Biodegradable Biphasic 3D Printed Scaffolds for Bone Tissue Engineering
- 3-26 Simrone Gill**
Understanding the Physiochemical Interactions between Denture Adhesives and the aqueous phase
- 3-27 Munyaradzi Kamudzandu**
Microfluidic neuronal circuitry – towards therapies for Huntington's disease
- 3-28 Lauren Kiri**
A Preliminary Examination of Composition-Property Relationships for Methotrexate-Loaded Germanium-Based Glass Ionomer Cements
- 3-29 Alexandra LÄ, vdal**
Biaxial stretching of poly(L-lactide) tubes for improvement of mechanical properties
- 3-30 Sepeedah Soltanian-Zadeh**
Synergistic Reinforcement of Poly(ϵ -caprolactone)/Gelatin Nerve Tissue Engineering Scaffolds by Graphene Oxide Nanosheets
- 3-31 Sabrina Stevanovic**
Biomimetic mineralization of early caries lesions with a self-assembling peptide
- 3-32 Piotr SzczepaÄ, czyk**
The influence of PEG/PCL ratio on properties of PU/ β -TCP composites for orthopaedic applications
- 3-33 Gert-Jan ter Boo**
Monodisperse microspheres loaded with gentamicin dioctyl sodium sulfosuccinate for the treatment of orthopaedic infections
- 3-34 Masato Ueda**
Control of Bone Conduction on Pure Titanium by Surface Modification
- 3-35 Hayley Floyd**
Developing a Method for Tracking and Quantifying Metallic Particle Internalisation
- 3-36 Arianna Gennari**
Hyaluronic Acid-Coated Chitosan Nanoparticles: the Influence of Hyaluronic Acid Presentation
- 3-37 Zahra Sadat Ghazali**
Electrospun Poly(ϵ -caprolactone)/Gelatin Scaffold Electrophoretically Coated with Graphene Oxide for Nerve Tissue Engineering
- 3-38 Monika GoÄ, da-CÄ™pa**
Generation of functional oxygen groups on parylene C for enhanced biocompatibility: LDI-MS investigations
- 3-39 Zhijun Guo**
Antibacterial TiO₂ nanotubes incorporated with silver nanoparticles
- 3-40 Rahaf Issa**
Poly (ϵ -lysine) dendrons as modulators of quorum sensing in Pseudomonas aeruginosa

Rapidfire Session IV Hall 2, Tuesday 2nd September 12:30 - 13:30

Chairs: Nicholas Bryan, University of Liverpool
Theun van Veen, University of Liverpool
Lorenzo Moroni, University of Twente
Sandra van Vlierberge, University of Gent
Anna-Finne Wistrand, KTH Royal Institute of Technology

- 4-1 Patrik Stenlund**
In-vivo response of a novel Ti-Ta-Zr-Nb alloy for medical implants



- 4-2 Louisa Lee**
Investigating Mesenchymal Stem Cell Self-Renewal on Nanotopography
- 4-3 Pau Rocas-Alonso**
Installing multifunctionality on titanium with RGD-decorated polymeric nanocapsules: Towards new osteointegrative therapies
- 4-4 Thomas Miramond**
Composite Collagen/Bioceramics Strips, Plugs for Bone Filling Defect Repair: A Comparative Study
- 4-5 Nina Parmar**
Retention of Myoblast Differentiation Capacity in 3D Culture on TIPS Microspheres
- 4-6 Romain Schieber**
Endothelization and thrombogenicity response of CoCr alloy nano depth patterns for cardiovascular stents
- 4-7 Satiesh kumar Ramadass**
Sol-gel assisted preparation of collagen hydrolysate scaffold: A Novel biomaterial for the treatment of chronic wounds
- 4-8 Judit Buxadera-Palomero**
Antifouling coatings of poly(ethylene glycol) on titanium for dental implants
- 4-9 Katarzyna Jastrzebska**
Bioengineered spider silk spheres as anti-cancer drug carriers
- 4-10 Maria Godoy-Gallardo**
Bacterial Adhesion and Biofilm Formation Reduced by the Immobilization of hLf1-11 Peptide onto Titanium Surface: A Comparison Study between Direct and ATRP based Covalent Immobilization
- 4-11 Pinese Coline**
Design of a new composite structure based on resorbable synthetic and natural polymers for anterior cruciate ligament reconstruction
- 4-12 Kristina Nešporová**
Intracellular delivery system based on acylated hyaluronan
- 4-13 Thomas Defize**
Elaboration of degradable PCL-based shape memory materials
- 4-14 Anne Canning**
Development of new approaches to fabricate scaffolds for deep zone engineered articular cartilage
- 4-15 Maryam Montazerolghaem**
Bone mineralization in Zebrafish embryos treated with Silicon ions
- 4-16 Sibel Ataol**
Preparation and Characterization of Porous Hydroxyapatite Based Microcarriers for Cell and Drug Delivery
- 4-17 Sam Moxon**
Controlling the Modulus of Gellan Gum Hydrogels for Inkjet Printing Cell Culture Substrates
- 4-18 Matthew Murphy**
Impact of Surface Treatment on the Properties of Dental Implant Materials
- 4-19 Pallabi Pal**
Fabrication of bilayer nano/microfibrous scaffold for skin tissue engineering
- 4-20 Sreekanth Pentlavalli**
In vitro Evaluation of a Novel Injectable Thermo-Responsive Polymeric Hydrogel for the Delivery of Self-Assembly Peptide Nanoparticles Containing an Osteoconductive Agent
- 4-21 Urszula Posadowska**
Gentamicin-Loaded Microparticles Immobilized on Porous Scaffolds for Prevention of Biomaterials-Related Bone Infections
- 4-22 Jae-won Seo**
Ionic liquid-doped and p-NIPAAm-based temperature responsive copolymer: Extraordinary entrapping and releasing behaviors of BSA at 38-42 °C
- 4-23 Laura Brown**
In Vitro Response of Human Osteoprogenitor Cells to Cross-Linked Poly(Lactide-co-Caprolactone) Dimethacrylate for Bone Rep
- 4-24 Jason Burke**
The Potential Role of Statins in the Regeneration of Osteoporotic Tissue and the Use of Star Degradable Polymers for Controlled Local Delivery
- 4-25 Doris Campos**
Acidic pH resistance of grafted chitosan on dental implant
- 4-26 Xinpu Chen**
A Parametric Study of a Mathematic Model for Degradation of Bioresorbable Polymers
- 4-27 Aileen Crawford**
In Vitro Evaluation of Nanohydroxyapatite Biocompatibility in 2D vs 3D Cell Culture Systems
- 4-28 Eva Jablonska**
In vitro testing of osteoinductivity and osteoconductivity of titanium alloys with nanostructured surface for orthopaedic application
- 4-29 Okan Mazmanoglu**
Modification of Magnesium Coated Titanium Surfaces to Control Its Corrosion Rate
- 4-30 Samaneh Kheyrrooz**
Bis-urea based supramolecular materials for tissue engineering

Rapidfire Session V Hall 2, Wednesday 3rd September 12:30 - 13:30

Chairs: Nicholas Bryan, University of Liverpool
Theun van Veen, University of Liverpool
Lorenzo Moroni, University of Twente
Sandra van Vlierberge, University of Gent
Anna-Finne Wistrand, KTH Royal Institute of Technology

- 5-1 Franziska Koch**
Evaluation of network and pore morphology of self-assembling peptides for biomimetic therapy
- 5-2 Reyhaneh Neghabat Shirazi**
Degradation and mechanical properties of biodegradable PLGA film
- 5-3 Bita Sedaghati**
Controlled release of nucleic acid to enhance bone regeneration
- 5-4 Mario Kurtjak**
New Materials with Antibacterial Action of Functionalized Au Nanoparticles and Ga³⁺ Ions
- 5-5 Jessy Schönfelder**
Modification of Porcine Pericardium with Low-Energy Non-thermal Electron Beam
- 5-6 Yuichi Ohya**
Design of Drug-immobilized Polylactide-graft-Poly(ethylene glycol) as a Temperature-Responsive Injectable Polymer for Controlled Release of Low-molecular-weight Water Soluble Drugs
- 5-7 Laura Madalina Popescu**
Polyethyleneimine-iron oxide hybrid nanomaterials – structure and biocompatibility
- 5-8 Iraklis Papageorgiou**
Structural alterations in the dura mater after exposure to clinically relevant CoCr nanoparticles. An organ culture approach
- 5-9 Yanny Marliana Baba Ismail**
Synthesis and In Vitro Biocompatibility of Carbonated Hydroxyapatite for Bone Tissue Engineering Application
- 5-10 Agnieszka Bochynska**
Biodegradable hyper-branched tissue adhesives for meniscus tears
- 5-11 Marina Beaufils-Hugot**
Osteoinduction and survival of human osteosarcoma MG-63 cells on nanoporous hydroxyapatite scaffolds
- 5-12 Julian Bejarano**
Synthesis and in vitro Bioactivity of Cu and Zn doped sol-gel- silicate bioactive glasses
- 5-13 Abdulrahman Baki**
Surface modification of injectable microspheres for cell therapy applications
- 5-14 Sandra Rother**
Design of Multi-Component Artificial Extracellular Matrices and their Effects on Cells Relevant to Wound Healing
- 5-15 Sunarso -**
Pre-osteoblast cell responses on phosphate and calcium co-immobilized titanium
- 5-16 Shelley Rawson**
Stress and Deformation in a Sutured Tendon Repair; an in silico Model
- 5-17 Franziska Kreimendahl**
Collagen IV and Fibroblasts as Supportive Factors in Angiogenesis Performed in a Perfusion Bioreactor Setup
- 5-18 Katarzyna Krukiewicz**
Conducting Polymer Platform for Anti-Cancer Drug Delivery
- 5-19 Inger Martinez de Arenaza**
A study on PLLA/MWCNT nanocomposites compatibilized with pyrene-end-functionalized PLLA
- 5-20 Laura McNamara**
Dynamic Surfaces for Stem Cell Differentiation and Retention of Stem Cell Phenotype
- 5-21 Elias Mulky**
Engineering of Staple Electrospun Fibres for Biodegradable Nanocomposites by Particle Enhanced Ultrasonication
- 5-22 Kathleen O'Connell**
Composition-Property Relationships for Lanthanum-Borate Glasses
- 5-23 Ali Poursamar**
The Reciprocal Relationship between Pore Size and Crosslinking, and Their Impact on Porous Scaffold Strength
- 5-24 Maria Grazia Raucci**
Effects on growth and osteogenic differentiation of mesenchymal stem cells by the strontium-added sol-gel hydroxyapatite gel materials
- 5-25 Deborah Roebuck**
A pH-responsive polymer-based drug-delivery platform demonstrating intracellular siRNA target-gene knockdown
- 5-26 Virginia Saez-Martinez**
Several drugs and model molecules controlled release studies from nanometric vesicles of polymer-lipid complexes
- 5-27 Ayse Selcen Alagoz**
A Novel Biological Polyester Based Wet Spun Scaffold for Bone Tissue Engineering

- 5-28 Deniz Atila**
Bacterial Cellulose Based Electrospun Scaffolds for Bone Tissue Engineering
- 5-29 Victor Baldim**
Nitric oxide releasing polyester blends for topical skin vasodilation
- 5-30 Ibrahim Bilem**
New approach of biomaterial design to enhance osteogenesis at the interface bone/implant

ESB

ORAL PRESENTATIONS

A Viscoelastic, Anisotropic, Hyperelastic Model of the Human Cornea

Charles Whitford^{1*}, Natasha Movchan² and Ahmed Elsheikh^{1,3}

^{1*}School of Engineering, University of Liverpool, UK, whitford@liv.ac.uk

²Department of Mathematical Sciences, University of Liverpool, UK

³National Institute for Health Research (NIHR) Biomedical Research Centre, Moorfields Eye Hospital NHS Foundation Trust and UCL Institute of Ophthalmology, London, UK

INTRODUCTION

Numerical simulation of the cornea's mechanical performance has led to improvements in the design of diagnostic and corrective procedures for degenerative visual conditions such as Keratoconus¹. Accurate simulations require close representation of in-vivo conditions including the tissue's response to strain. The main contribution to mechanical stiffness is provided by the collagen fibrils embedded within the stroma. Over recent decades the accuracy of simulations has improved significantly with developments in fibril anisotropy representation^{2,3}. Wide angle x-ray scattering (WAXS) characterised microstructural relationships and identified that stiffness increased with fibril density⁴. In this paper, we present a constitutive model which represents stromal viscoelasticity, hyperelasticity, shear stiffness, regional variation of collagen fibril anisotropy and density, through-thickness fibril density and angular distribution, fibril cross-linking, extra-fibrillar matrix and age-related stiffening. The model has been calibrated with an extensive experimental database providing representative numerical parameters.

EXPERIMENTAL METHODS

Experimental data from 128 human donor eyes has been used in this study. The data includes WAXS data on fibril anisotropy and density, second harmonic-generated cross-section images leading to through-thickness angular distribution of fibrils, and both tissue shear and inflation tests which provided measurements of deformation vs. loading relating to stress-strain behaviour. Visual representation of the anisotropic and density relationships within the model is provided in Figure 1.

Material representation has been developed as a constitutive model based on continuum mechanics theory. This model was incorporated within finite element analysis (FEA) for the non-linear finite element solver Abaqus/Standard 6.13. Numerical parameters have been derived through an inverse analysis approach to represent the cornea at ages 40-100 years.

RESULTS AND DISCUSSION

The results simultaneously represent multiple loading scenarios (shear & inflation) and multiple strain-rates with the differences between numerical predictions and experimental data remaining below 5%.

Table 1. Tangent modulus/stiffness (E) at a selection of locations within the cornea. Values represent the stiffness at 0.02 logarithmic strain and a slow strain-rate. Key: Vertical (V), Diagonal (D), Latitudinal (La), Longitudinal (Lo) and Shear (S); reference location numbers found in Fig. 1.

Location reference	1	2	3	4	5	6	7	8	9	10	1
E(KPa)	979	541	959	894	1171	490	459	584	669	494	30
Direction	V	D	La	La	La	Lo	Lo	Lo	La	Lo	S

These results quantify previous observations which reported that the mechanical response of the cornea is significantly affected by its microstructural arrangement and viscoelastic behaviour.

CONCLUSION

Consideration of the microstructure of the stroma has improved the accuracy of numerical simulations of the mechanical behaviour of the cornea. The introduction of combined viscoelastic and anisotropic representation has particular benefit when modelling surgery, microstructure scarring, and high-speed tonometers such as the Ocular Response Analyzer and the Corvis. Work is being extended to represent the behaviour of the human sclera. While this model has been developed to represent the cornea, the methodology is adaptable for other collagenous soft tissues.

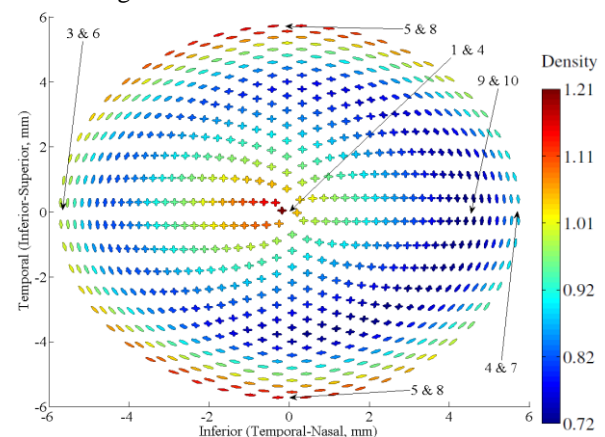


Figure 1. Output from numerical simulation representing the regional variation of fibrils across the cornea. Anisotropic weighting for each angle at each integration point was combined to form individual plots of local distribution. Directional related stiffness is a combination of the local anisotropic distribution and density. Numbered arrows are used for reference in Table 1.

REFERENCES

- Roy A. *et al.*, Exp Eye Res, 2011, 52(12):9174-87
- Pinsky P. *et al.*, J Cataract Refract Surg, 2005, 31:136-45
- Petsche *et al.*, Biomech Model Mechan, 2013, 12(6):1101-13
- Boote *et al.*, IOVS, 2003, 14:2941-48

Bacterial Cellulose as a Support for the Growth of Retinal Pigment Epithelium

S. Gonçalves^{1*}, J. Padrão¹, J. Silva¹, I. Rodrigues², H. Girão², F. Dourado¹ and L. Rodrigues¹

¹Center of Biological Engineering, University of Minho, Portugal, sarammg@deb.uminho.pt

^{2*}Center of Ophthalmology and Vision Sciences, IBILI-Faculty of Medicine, University of Coimbra, Portugal

INTRODUCTION

Age-related macular degeneration (AMD) is the leading cause of blindness among the elderly in industrialized countries¹⁻². Healthy stem cell derived retinal pigment epithelium (RPE)—like cells delivered as an integer epithelial sheet on a carrier substrate, represent a promising approach for RPE replacement in AMD²⁻⁴. An optimal substrate should simulate RPE natural microenvironment and maintain its phenotype, allow nutrient flow or biodegrade rapidly, among others^{2,4}. Bacterial cellulose (BC) is an interesting biomaterial for tissue regeneration applications, presenting unique structural and mechanical properties, biocompatibility, non-toxicity, high hydrophilicity, transparency and permeability for gas and fluid exchange⁵⁻⁸. In this work, we evaluated if RPE cells were able to adhere and proliferate on BC, to assess its feasibility as a novel substrate for RPE transplantation. BC substrates were also characterized according to surface and bulk properties relevant for this application. BC surface was modified via surface acetylation and polysaccharide adsorption, using chitosan and carboxymethyl cellulose, to obtain different surface profiles (ABC, CBC and CMBC) that affect differently RPE cell response^{9,10}.

EXPERIMENTAL METHODS

BC was produced in static cultures of *Gluconacetobacter xylinum*. Water contact angles were measured using the sessile drop method to assess surface hydrophobicity. Diffusion experiments were performed to evaluate substrate permeation. Substrates with known permeability (reference) were used to enable comparison and the solutes used were PEG 35 and 300 kDa. BC substrates were analysed for endotoxin using the limulus amebocyte lysate test. HTERT-RPE1 cells were seeded in BC and tissue culture polystyrene (TCP) at a density of 40 000 cells/cm². Cell viability and proliferation were evaluated using the MTS assay and LIVE/DEAD fluorescence microscopy after 3, 7, and 14 days.

RESULTS AND DISCUSSION

BC, CBC and CMBC presented a similar hydrophilic degree with contact angles ranging from 20 to 25°. ABC substrates decreased surface hydrophilicity to 65°. The permeation coefficients of permeable substrates were 4.2×10^{-6} and 3.8×10^{-6} cm²/s, for PEG 35 and 300 kDa, respectively. BC substrates presented permeation coefficients in the range $2.5 - 3.4 \times 10^{-6}$ and $1.3 - 2.2 \times 10^{-6}$ cm²/s, for PEG 35 and 300 kDa, respectively. The differences observed among permeable and BC substrates were not significant suggesting that BC is permeable and allows fluid transport. Substrates remained stable for up to 3 months

although some swelling was observed with 5, 2, 6 and 8 times its dry weight in water for BC, ABC, CBC and CMBC substrates, respectively. The endotoxin levels measured for BC, ABC, CBC and CMBC substrates were 34.0 ± 11.7 , 4.4 ± 0.4 , 31.8 ± 2.7 and 26.6 ± 17.9 mEU/device, respectively. These levels are much lower than the limit of 20 EU/device, established by the FDA for medical devices¹¹. Through viability assays it was possible to observe the formation of a cell monolayer in TCP after 7 days. Similarly, cell monolayers were observed in ABC substrates after 14 days. The other modified BC substrates presented lower initial cell adhesion, however with similar proliferation rates as in ABC. The unmodified BC showed low initial cell adhesion and no cellular proliferation.

CONCLUSION

BC modification was essential for the adhesion and proliferation of hTERT-RPE1 cells. ABC substrates showed improved properties comparing to the other modified substrates, with less swelling and lower levels of endotoxins and hydrophilicity that lead to a better initial cell adhesion. Therefore, BC seems to be an interesting substrate for RPE adhesion and proliferation. However, other studies should be performed to further confirm BC feasibility as substrate for RPE transplantation. Additionally, alternative surface modifications can be considered to further improve cell adhesion, such as the adsorption of specific proteins.

REFERENCES

1. Ambati J. *et al.*, S. Ophthalmology. 48:257-93, 2003;
2. Binder S. *et al.*, Prog Ret Eye Res. 26:516-54, 2007;
3. Liu Z. *et al.*, Biomaterials. 35:2837-50, 2014; 4. Carr A.F. *et al.*, Trends in Neuroscience. 36:385-95, 2013; 5. Fu L. *et al.*, Biomaterials. 92:1432-42, 2013; 6. Chang C. and Zhang L., Carbohydrate Polymers. 84:40-53, 2011; 7. Czaja W.K. *et al.*, Biomacromolecules. 8:1-12, 2007; 8. Bodin A., Comprehensive Biomaterials. 2:405-10, 2011; 9. Kim D. *et al.*, Cellulose. 9:361-7, 2002; 10. Orelma *et al.*, Biomacromolecules. 12:4311-8, 2011

ACKNOWLEDGMENTS

The authors acknowledge the Portuguese Foundation for Science and Technology (FCT, Portugal) for the financial support provided by research grants SFRH/BD/63578/2009, SFRH/BD/ 64901/2009 and SFRH/BPD/64958/2009 for Sara Gonçalves, Jorge Padrão and João Silva, respectively. The authors also acknowledge the projects PEst-OE/EQB/LA0004/2013, PEst-OE/EQB/LA0023/2013 and RECI/BBB-EBI/0179/2012 (number: FCOMP-01-0124-FEDER-027462), co-funded by QREN, FEDER.



Nanosomes: Novel Drug Delivery Vehicles to treat Glaucoma

F. de Cogan¹, L. Hill¹, P. Morgan-Warren¹, J. O'Neill¹, A. Peacock², R. Scott³ and A. Logan¹

¹School of Clinical and Experimental Medicine, University of Birmingham, Edgbaston, B15 2TT, UK

²School of Chemistry, University of Birmingham, Edgbaston, B15 2TT, UK

³Royal Centre for Defence Medicine, Queen Elizabeth Hospital, Birmingham, UK

f.decogan@bham.ac.uk

INTRODUCTION

Glaucoma is a blinding eye disease characterised by a high intraocular pressure with associated optic neuropathy.¹ It is estimated to affect 66 million people worldwide and is a leading cause of blindness.² The mainstay of treatment uses eye drops to deliver ocular antihypertensive drugs into the eye. These lower the intraocular pressure (IOP), but do not target the underlying pathology – that includes fibrosis of the main drainage portal, the trabecular meshwork (TM). The fibrogenic cytokine TGF β has been implicated in the aetiology of TM fibrosis.³ Decorin is a proteoglycan that attenuates fibrotic scarring by sequestering TGF β 1&2, directly binding to collagen and limiting fibrillogenesis and initiating fibrolysis by inducing matrix metalloproteinases against matrix molecules in both established and nascent scars.⁴ Decorin reduces TM scarring in a rat model of TGF β -induced raised IOP by reversing established fibrosis and therefore lowering the IOP. However, administration of Decorin involved bi-weekly intracameral injections that have poor translational potential. Synthetic short sequence peptide delivery vehicles easily penetrate the cornea and can be used as carriers to deliver proteins into the anterior chamber of the eye. These peptides are designed with multiple positive charges that modify the permeability of the peptide-protein complex to the corneal epithelium and the posterior corneal endothelium and are termed 'Nanosomes'. They allow active drugs attached to the peptides to access the anterior chamber of the eye.

The aim of this work is to utilise the cell penetrating ability of the Nanosomes to deliver Decorin into the anterior chamber of the eye to treat TM fibrosis in a rat model of glaucoma.

EXPERIMENTAL METHODS

Nanosomes were synthesised using standard solid phase peptide synthesis and Fmoc chemistry. The final product was purified by HPLC and characterised by mass spectrometry. Decorin was bound to the nanosomes by incubation in sterile PBS at room temperature.

In vivo experiments were carried out on male Sprague-Dawley (SD) rats weighing 175-250g under a 12 hour light and dark cycle with food and water *ad libitum*. Anaesthesia was induced under 5% isoflurane/1.5 L per minute of O₂ and maintained at 3% during surgery. Under anaesthesia, biweekly intracameral injections of TGF β 2 were given to 6 rats to induce fibrosis of the TM and raise IOP. IOP was measured every 3 days. After 3 weeks with maintained high IOP, Decorin-Nanosome drops were administered twice daily, topically to the cornea. After 5 weeks of treatment the animals were killed and perfused with 4% paraformaldehyde. The

ocular tissues were harvested for immunohistological analysis.

RESULTS AND DISCUSSION

The Nanosomes successfully entered the anterior chamber of the eye both alone and when complexed with Decorin. Each eye drop was able cross the cornea in 6 minutes (Figure 1) and delivered 17.9 \pm 3 ng/ml Decorin into the anterior chamber as measured by ELISA of aqueous humour; Decorin was also found in the posterior segment of the eye, SD rats with TGF β 2-induced raised IOP (16 mm/Hg) treated for 2 weeks with an eye drop formulation of the Decorin-Nanosome complexes had IOP lowered to normal levels (11mm/Hg).

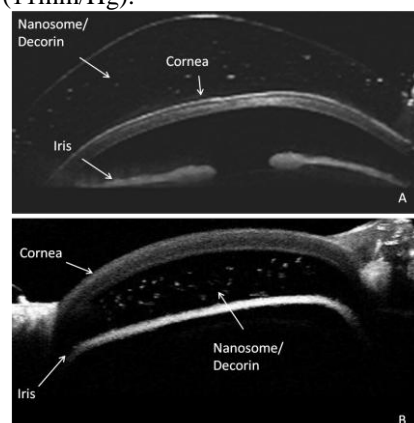


Figure 1 Optical Coherence Tomography images of Decorin-Nanosome complexes crossing the cornea of a SD rat A) at time 0 and B) after 6 minutes.

CONCLUSION

Nanosomes are simple biocompatible carriers, that allow the delivery of large therapeutic proteins across epithelial membranes. We have successfully used them to deliver anti-fibrotic proteoglycans into the eye and have shown their efficacy at treating raised IOP in a rat model of glaucoma. This work has translational potential to be brought forward as a novel ocular drug delivery vehicle.

REFERENCES

1. Junglas B, Kuespert S, Seleem AA, et al. *Am. J.Path.* 2012; 180:2386-2403
2. Weinreb R N, T KP. *Lancet.* 2004; 363:1711-1720
3. A. Leask, DJ. Abraham, *FASEB J.* 2004, 18,7,816
4. A.Logan, A. Baird, M. Berry, *Exp. Neuro.* 1999, 159,504

ACKNOWLEDGMENTS

The Authors would like to thank Ben Mead and Adam Thompson for their help with *in vivo* experiments. This work was funded by the EPSRC.



Emulation of Extracellular Matrix for the Development of Human Corneal Stromal Substitute

Pramod Kumar,¹ Abhigyan Satyam,¹ Xingliang Fan,¹ Brian Rodriguez,² Yuri Rochev,¹ Michael Raghunath,^{3,4,5} Abhay Pandit¹ and Dimitrios Zeugolis¹

¹Network of Excellence for Functional Biomaterials, National University of Ireland, Galway, Ireland, ²Conway Institute of Biomolecular & Biomedical Research, University College Dublin, Dublin, Ireland, ³Department of Bioengineering, Faculty of Engineering, ⁴Life Science Institute, ⁵Department of Biochemistry, Yong Loo Lin School of Medicine, National University of Singapore, Singapore, p.kumar1@nuigalway.ie

INTRODUCTION

Scaffold free cell-based therapies are potential approaches to avoid various deleterious effect of foreign material based scaffold. However, very few products have been reached to the clinics due to prolong culture time required¹. The keratocytes required 35-84 days culture to build a cohesive stromal substitute, which is poor in extracellular matrix (ECM) and thinner than the native tissue^{2,3}. The macromolecular crowding (MMC), the addition of inert macromolecules in culture media, can accelerate the cell specific ECM deposition within 2-6 days of culture, without change in cell phenotype⁴. Herein, the role of MMC on human corneal fibroblasts (HCFs) has been demonstrated, which were cultured on a NIPAAM based thermosensitive copolymer to generate ECM-rich HCFs cell sheets.

EXPERIMENTAL METHODS

HCFs cultured under MMC (100µg/ml dextran sulphate (DxS); and 50µg/ml Carrageenan (CR)). The ECM deposition was analysed by SDS-PAGE, immunocytochemistry (ICC) and proteomic analysis. Gene expression was assessed using the RT-PCR. Intact HCFs cell sheets were developed using NIPAAM/n-tert butyl acrylamide thermal responsive polymer.

RESULTS AND DISCUSSION

Densitometric analysis of SDS-PAGE and immunocytochemistry shows that MMC (DxS and CR) significantly increased collagen I deposition ($p < 0.05$) and more ordered ECM deposition. Immunofluorescence confirmed the enhanced ECM in the presence of MMC. Proteomic and genomics analysis confirmed the increase in stromal ECM/total proteins and phenotype maintenance respectively (results not shown). Successful detachment of HCFs cell sheet was demonstrated at low temperature after MMC, which showed the transparency similar to the control samples and high ECM deposition was confirmed using various techniques.

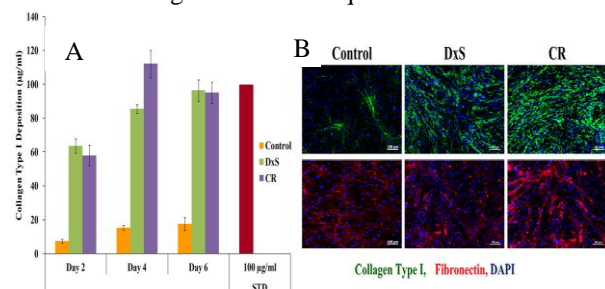


Fig. 1. (A) The densitometry for collagen type I at day

2, 4 and 6 (B) The immunofluorescence for collagen type I and fibronectin (C) at day 4 of MMC.

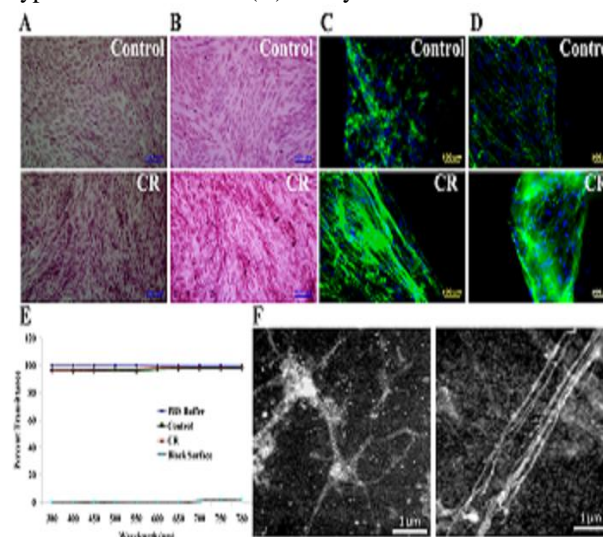


Fig. 2. The characterization of developed cell sheet using CR as a macromolecular crowding agents at day 4 (A) The trichrome staining for ECM (B) Picro-sirius red staining after MMC (C) Collagen type I immunofluorescence of cell sheet (D) Collagen type V immunofluorescence of cell sheet (E) Transmittance of the developed HCFs cell sheet demonstrated that there is no change in transmittance of cell layer after MMC (F) AFM analysis of HCFs confirmed the presence of collagen ECM in CR treated samples.

CONCLUSION

MMC of HCFs with DxS and CR significantly accelerates corneal specific ECM deposition without influencing the basic characteristic. The process also favours the development of ECM rich HCFs cell sheets using CR within 4 days. The thermal responsive copolymer allowed the detachment of intact, transparent and native ECM rich corneal stromal tissue substitute.

REFERENCES

1. Peck M. *et al.*, Materials Today. 15, 218, 2011.
2. Proulx S. *et al.*, Mol. Vision. 16, 2192, 2010.
3. Vrana N. *et al.*, IOVS. 49, 5325, 2008.
4. Lareu R. *et al.*, FEBS Letters. 581, 2709, 2007.

ACKNOWLEDGMENTS

The authors would like to thank, the College of Engineering and Informatics, NUI Galway, SFI (Grant-07/IN1/B031 & 09/ RFP/ENM2483) and SFI- ETS Walton award.

Nanostructured materials for tissue engineering: nanofibres, nanoparticles and nanofilms

Lucie Bacakova

Department of Biomaterials and Tissue Engineering, Institute of Physiology, Academy of Sciences of the Czech Republic, Videnska 1083, 142 20 Prague 4, Czech Republic; E-mail: lucy@biomed.cas.cz

INTRODUCTION

Bioartificial tissue replacements contain a cell component and a material component, which serves as a carrier for anchorage-dependent cells. The material component should actively promote the adhesion, growth, differentiation, phenotypic maturation and other cell functions in a controllable manner. The cell performance on the materials can be markedly improved by its nanostructure (i.e., nanoscale surface roughness or nanofibrous structure), which mimics the nanoarchitecture of the natural extracellular matrix.

EXPERIMENTAL METHODS

In the first part of this study, we have focused on fibrin nanofibrous layers prepared *in vitro* by a controlled simulation of a part of the physiological hemocoagulation process [1]. The layers were intended for inner coating of synthetic vascular grafts in order to improve their endothelialization.

In the second part, we have constructed (by electrospinning technique) synthetic nanofibrous scaffolds made of poly (L-lactide) (PLLA) or poly (lactide-co-glycolide) (PLGA) reinforced with hydroxyapatite or diamond nanoparticles for potential use in bone tissue engineering [2, 3].

Finally, we have created nanocrystalline diamond films for potential surface modification of metallic bone implants [4].

RESULTS AND DISCUSSION

The resulting fibrin layers were of various morphology, i.e. thin and thick, two- or three-dimensional, with short and sparse or long and dense fibrin nanofibers (Fig. 1A). Thick three-dimensional films supported cell-matrix and cell-cell adhesion of vascular endothelial cells, which was manifested by well-developed talin-containing focal-adhesion plaques (Fig. 1B), immunofluorescence of VE-cadherin at the cell edges (Fig. 1C) and formation of a confluent endothelial cell layer.

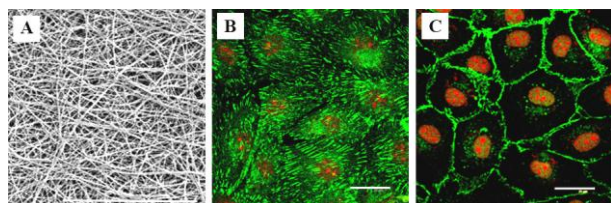


Fig. 1. A nanofibrous fibrin layer for inner modification of vascular prostheses (A), and immunofluorescence of talin (B) and VE cadherin (C) in endothelial CPAE cells in cultures on these layers. Bar 10 μm (A) or 25 μm (B, C).

Addition of diamond or hydroxyapatite nanoparticles to synthetic polymeric nanofibrous meshes improved some mechanical properties of the scaffolds (2, 3) and

supported the adhesion and growth of human bone-derived cells (Fig. 2). Scaffolds reinforced with 15 wt. % of hydroxyapatite increased the production of osteocalcin, i.e. an important marker of osteogenic cell differentiation, in these cells [3].

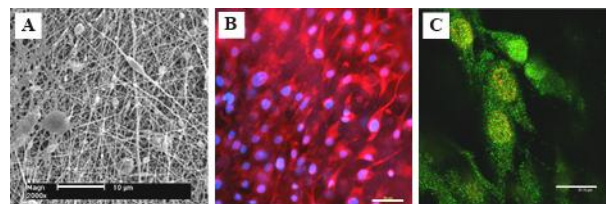


Fig. 2. Nanofibrous PLGA scaffolds reinforced with 23 wt% of nanodiamond (A), human osteoblast-like MG 63 cells in cultures on these scaffolds (B) and on PLLA scaffolds with 15 wt. % of hydroxyapatite nanoparticles (C). SEM microscopy (A), staining with Texas Red-C₂-Maleimide and Hoechst #33342 (B), immunofluorescence of osteocalcin (C). Bar 10 μm (A), 50 μm (B) or 20 μm (C).

Nanocrystalline diamond films also supported the adhesion, growth and osteogenic differentiation of human bone-derived cells, which was more apparent on more hydrophilic O-terminated films (Fig. 3) [4].

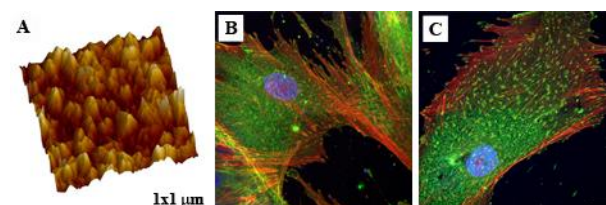


Fig. 3. Nanocrystalline diamond film (A) and human osteoblast-like Saos-2 cells in cultures on these films terminated with H (A) and O (B). AFM microscopy (A), immunofluorescence of talin combined with phalloidine staining of F-actin (B, C). Bar=20 μm .

CONCLUSION

All tested nanostructured materials, particularly thick nanofibrous fibrin films, nanofibrous PLLA scaffolds with 15 wt.% of hydroxyapatite and O-terminated nanocrystalline diamond films supported the adhesion, growth and phenotypic maturation of cells.

REFERENCES

1. Filova *et al.*: J Biomed Mater Res Part A 102A: 698-712, 2014
2. Parizek *et al.*: Int J Nanomed 7: 1931-1951, 2012
3. Novotna *et al.*: J Biomed Mater Res Part A, in press
4. Liskova *et al.*: Article in preparation

ACKNOWLEDGMENTS

Supported by the Grant Agency of the Czech Republic (grants No. P108/10/1106, P108/11/1857 and P108/12/1168).



Fabrication of Silk Fibroin and High Methoxyl Citrus Pectin(HMP) Based 3D Scaffolds for Bone Tissue Engineering

Sibel Ataol¹ Dilek Keskin^{1,2,3,5}, Akın Akdağ⁴, Ayşen Tezcaner^{*1,2,3,5}

Departments of ¹Biomedical Eng., ²Engineering Sciences, ³Biotechnology, ⁴Chemistry
Middle East Technical University, Ankara, Turkey

⁵BIOMATEN Center of Excellence in Biomaterials and Tissue Engineering, Middle East Technical University,
Ankara, Turkey email: sibel.ataol@metu.edu.tr

In bone tissue engineering approach, fabrication of scaffold and so the selection of materials have critical importance. Here, we describe two new biopolymers silk fibroin and citrus pectin based new functional scaffold fabrication.

INTRODUCTION

In construction of tissue engineered constructs, the scaffold plays a crucial role on regeneration of damaged tissue in body. Therefore the scaffold fabrication techniques and the selection of materials are critical decisions. In tissue engineering, both biologically and synthetic derived materials are studied. In general, biologically derived materials have an advantage because of their inherent properties like biocompatibility and adequate mechanical property¹. Silk fibroin and high methoxyl citrus pectin are natural derived structural biopolymers. Their biocompatibility, mechanical stability and properties as material are noteworthy. Both biopolymers were previously studied in bone tissue engineering individually^{2,3}. However fibroin and pectin have not been used together for scaffolding. In this study, silk fibroin and pectin are chemically crosslinked (carbodiimide crosslinking) and scaffold fabricated for the first time.

EXPERIMENTAL METHODS

Preparation of Silk fibroin and Citrus pectin solutions

Native *Bombyx mori* silk fibroin was degummed with 0.02 M NaHCO₃ solution at 100°C for 30 min. The degummed silk fibroin was dissolved LiBr solution at 60°C for 4 h. After dialysing for 2 days, the silk fibroin solution was filtered⁴. High methoxyl citrus pectin was dissolved in d H₂O and the reaction solvent was d H₂O

Preparation Silk fibroin/Pectin blend scaffolds

Silk fibroin and HMP was mixed with same amount of NaHCO₃ individually. For carboxylation of hydroxyl groups,, 5-fold excess of succinic anhydride was dissolved in DMF and added to fibroin and pectin solutions.

The reaction solutions were mixed in a flask and stirred for overnight. After blending of two modified fibroin and pectin, 4-fold molar excess of EDC to carboxyl groups was added. Ethylene diamine was then added drop wise under magnetic stirring, in ~10-fold molar excess to carboxyl group. The solution pH was adjusted to 6-7 and was monitored for 30 min. The solution was then poured into a petri plate for gelling and lyophilized after freezing at -80°C overnight for preparation of porous scaffolds. After crosslinking, the scaffolds were washed in distilled water to remove unreacted linker and crosslinker (Fig.1). FTIR and ¹H-NMR were done for confirmation..

RESULTS AND DISCUSSION

FTIR and ¹H-NMR analysis were performed to prove the carbodiimide facilitated amide bond formation between citrus pectin and silk fibroin.

CONCLUSION & FUTURE WORK

By this method, silk fibroin and high methoxylated citrus pectin were crosslinked and studied for the first time for biomedical study. The in vitro studies will be performed for these scaffolds. To enhance the crosslinking and cellular compatibility, new methods of crosslinking will be tried.

REFERENCES

- 1.Mano, J. F. *et al.* *J. R. Soc. Interface* **4**, 999–1030 (2007).
- 2.Ichibouji, T., Miyazaki, T., Ishida, E., Sugino, A. & Ohtsuki, C. *Mater. Sci. Eng. C* **29**, 1765–1769 (2009).
- 3.Kokkonen, H. *Aspects of Bone Sugar Biology*. (2009).
- 4.Mandal, B. B. & Kundu, S. C. *Biotechnol. Bioeng.* **99**, 1482–9 (2008).

ACKNOWLEDGEMENTS

I would like to thank the METU BAP-07-02-2013-001 for providing financial support to this project.

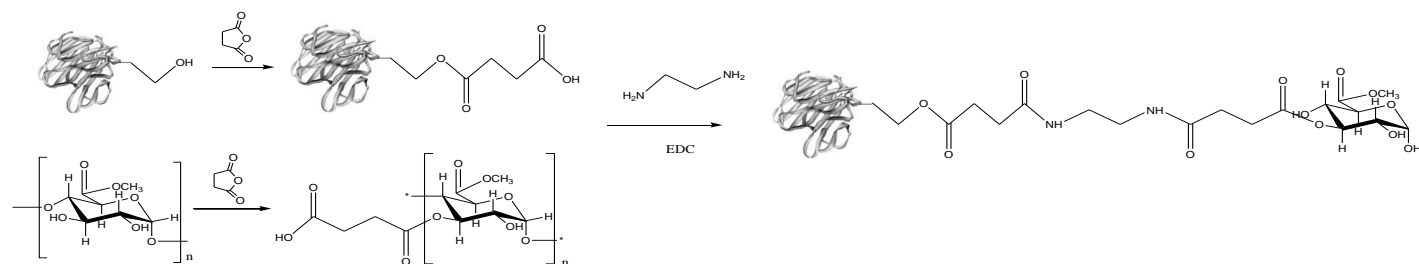


Figure 1. Crosslinking model of silk fibroin and pectin

Regulation of Chondrocyte Spheroid Size using Proline-containing Periodic Peptides

N. Takata¹, Y. Morita², Y. Hirano³, Y. Futaki³, and E. Nakamachi²

¹Graduate School of Life and Medical Sciences, Doshisha University, Japan

²Faculty of Life and Medical Sciences, Doshisha University, Japan

³Faculty of Chemistry, Materials and Bioengineering, Kansai University, Japan, ymorita@mail.doshisha.ac.jp

INTRODUCTION

It was reported that chondrocyte aggregation in spheroids prevented dedifferentiation of chondrocytes. However, if the diameter of the spheroids increased, necrosis may occur in the center of the spheroids due to lack of nutrient. Therefore, regulation of spheroid size is important to maintain nutrient supply into the center of the spheroid. Since we reported that mouse fibroblasts spheroids with uniform size were formed using proline-containing periodic peptides H-(Lys-Pro)₁₂-OH (KP24), it is considered that size of chondrocyte spheroids can be regulated using KP24. Therefore, the purpose of this study is to produce uniform chondrocyte spheroids using KP24 to prevent central necrosis in the spheroids.

EXPERIMENTAL METHODS

Preparation of chondrocyte spheroids: Chondrocytes were isolated from articular cartilage of femur of 6-month-old pig. Dulbecco's modified Eagle's medium supplemented with 10% bovine serum and ascorbic acid was prepared as culture medium. KP24 was added to the culture medium at concentrations of 0, 0.25, 0.5, and 1.0 mg/ml. Chondrocytes were seeded in 96-well plates at cell density of 1.5×10^5 cells/cm². Chondrocytes were cultured in the culture medium with KP24 for 3 days, and then chondrocytes were cultured in the culture medium with KP24 (KP24(+ +)) or without KP24 (KP24(+ -)) to investigate the effect of duration of KP24 supplementation on formation of spheroids for 4 more days. Morphology observation of spheroid, viability assay of chondrocytes in spheroid, and measurement of glycosaminoglycan (GAG) amount were performed after 3, 5 and 7 days of cultivation.

Evaluation of chondrocyte spheroids: Morphology of spheroid was observed using a phase contrast microscope. Equivalent circle diameter was calculated as the diameter of spheroid. In this study, cell aggregate with more than 30 μ m in diameter was defined as spheroid. The viability of chondrocytes was evaluated by observing spheroids stained with fluorescent reagents using a fluorescence microscope. GAG amount was measured using the DMMB method.

RESULTS AND DISCUSSION

Figure 1 shows microscopic images of spheroids for KP24(+ +) and KP24(+ -) at KP24 concentration of 0.5 mg/ml. Though fusion of spheroids was observed after 7 days of cultivation in the case of KP24(+ +) (Fig.1(c)), the spheroids grew larger with cultivation days in the both case. In the case of KP24(+ -), fusion of spheroids was prevented and uniform spheroids were formed after 7 days of cultivation (Fig.1(f)). Same tendency was observed in all KP24 concentration, but high KP24 concentration resulted in more rapid formation of

spheroids. The GAG amounts of the spheroids in one well increased with increasing KP24 concentration after 5 and 7 days of cultivation. According to fluorescent microscopy, number of dead cells remarkably increased in the spheroids when the diameter of spheroids was over 200 μ m. Figure 2 shows change in the diameter of the spheroids for KP24(+ -) with cultivation days. The average diameter of spheroids increased and the number of spheroids decreased with cultivation days. After 7 days of cultivation, the average diameter of spheroids for KP24(+ -) at concentration of 0, 0.25, 0.5, and 1.0 mg/ml were 232, 215, 308, and 261 μ m respectively, and the number of spheroids for KP24(+ -) at KP24 concentration of 0, 0.25, 0.5, and 1.0 mg/ml were 86, 100, 58, and 53 respectively. The number of spheroids with about 200 μ m in diameter became highest at KP24 concentration of 0.25 mg/ml. These results showed that uniform spheroids with about 200 μ m in diameter were obtained so as to prevent necrosis by changing duration of KP24 supplementation at KP24 concentration of 0.25 mg/ml.

CONCLUSION

Size of uniform spheroids was regulated to about 200 μ m in diameter in the case of KP24(+ -) at KP24 concentration of 0.25 mg/ml.

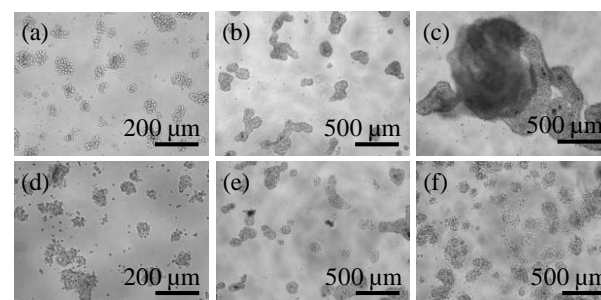


Fig. 1. Photos of chondrocyte spheroids (0.5 mg/ml). (a) KP24(+ +) at day 3. (b) KP24(+ +) at day 5. (c) KP24(+ +) at day 7. (d) KP24(+ -) at day 3. (e) KP24(+ -) at day 5. (f) KP24(+ -) at day 7.

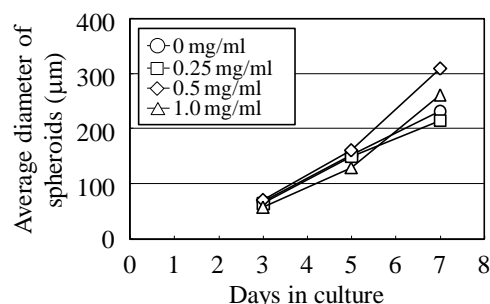


Fig. 2. Change in the average diameter of the spheroids for KP24(+ -).

Hyaluronic Acid Based-Hydrogels Attenuate Inflammatory Receptor and Neurotrophins in IL-1 β Induced Inflammation Model of Nucleus Pulposus Cell Cultures

Isma-Liza Mohd-Isa, David Tiernan, Akshay Srivastava, Peter Rooney and Abhay Pandit

Network of Excellent Functional Biomaterials, National University of Ireland, Galway, Ireland

I.MOHDISA1@nuigalway.ie

INTRODUCTION

Low back pain is associated with degeneration of Intervertebral Disc (IVD). Previous studies have shown that local production of neurotrophins stimulated innervation in degenerated IVD¹. High Molecular weight (HMw) Hyaluronic Acid (HA) is a potential therapeutic biomaterial for inflammatory pain of IVD as it exhibits anti-inflammatory effect and provides a better conducive microenvironment for IVD cells. The hypothesis of the study was that HA hydrogels alter inflammatory receptor and neurotrophins expression in IL-1 β induced inflammation model of NP cell culture. Specifically, to test this hypothesis an HA hydrogel system was developed and characterised for cytotoxicity and *in vitro* degradation. We further determined the effect of HA hydrogels in IL-1 β induced inflammation model in NP cell cultures by investigating activation of receptors IL-1R1, MyD88, CD44 and also examined protein and mRNA expression of neurotrophins {Nerve Growth Factor (NGF) and Brain Derived Neurotrophic Factor (BDNF)}.

EXPERIMENTAL METHODS

HA hydrogels were synthesized by using 7.5mg sodium HA Mw 1.2×10^6 Da (Lifecore Biomedical, USA) dissolved in 1mL distilled water and crosslinked with 150mg 4-arm PEG amine Mw 2000Da (Jenkem Tech, TX, USA). N-hydroxysuccinimide (NHS) (150mg) and 1-Ethyl-3-[3-(dimethylamino)propyl]carbodiimide (EDC) (100 μ L) were added to functionalise the carboxyl group of HA molecules². The sphere-shaped hydrogels were obtained through a pipetting a channel volume of 5 μ L onto a hydrophobic modified glass slide (TeflonTM, Fisher Scientific, Ireland) and incubated for three hour at 37°C to allow crosslinking reaction to complete. The gelation time of HA hydrogels was measured. The *in vitro* degradation of HA hydrogels with hyaluronidase and PBS was assessed at 1, 2, 3, 7, 14 and 21 days. The potential cytotoxicity was assessed against ADSCs by alamarBlue[®]. NP cells were isolated from disc T9-S1 of bovine tails and cultured for 10 to 20 days. The NP cell viability and distribution in 2D culture was examined for 24, 48 and 72 hours using Live/Dead[®] staining kit. The 5×10^3 cells were stimulated with IL-1 β (10ng/ml) to create an inflammatory milieu and treated with 100 μ L (5 μ L \times 20) hydrogels for day 1, 3 and 7. Activation of receptor IL-1R1, MyD88 and CD44 were determined by immunofluorescent imaging. Neurotrophins expression of NGF and BDNF were measured by ELISA and qPCR.

RESULTS AND DISCUSSION

The *in situ* gelation time for the formation of spherical shaped hydrogels were 5.5 minutes and the developed

hydrogels were stable at 4°C. Preliminary data of cytotoxicity study showed metabolic activity of ADSCs in presence of 100 μ L hydrogels ($94.75 \pm 1.18\%$, $94.02 \pm 14.10\%$, $97.95 \pm 4.69\%$) and over 73% ADSCs metabolic activity was observed in presence of 200 μ L hydrogels after 24, 48 and 72 hours in culture (Fig. 1.A). Inflammatory receptor IL-1R1 was down-regulated after treating with HA hydrogels in inflammation model of NP cell cultures (Fig. 1.C). The qPCR results showed NGF were up-regulated (fold change 3.2 and 8.1) in IL-1 β inflamed after 7 days.

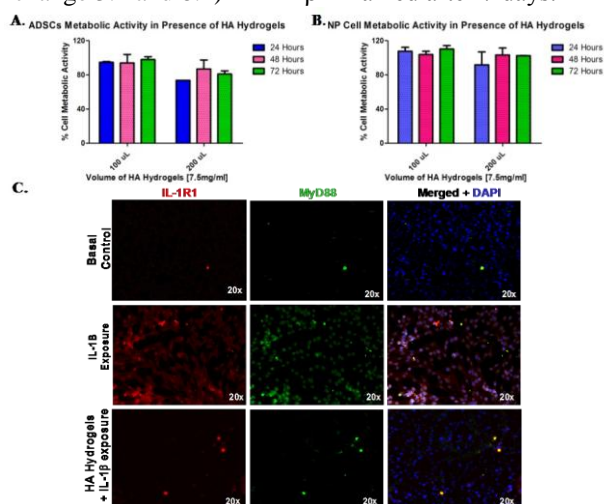


Fig. 1. **A.** Percentage ADSCs metabolic activity alamarBlue[®] test shows over 90% and 73% viability in presence of 100 μ L and 200 μ L hydrogels respectively, after 24, 48 and 72 hours in cultures. **B.** NP cells metabolic activity in presence of HA hydrogels shows 100% and 91% viability for 100 μ L and 200 μ L hydrogels. **C.** Immunoreactivity of inflammatory receptor IL1-R1 and MyD88 as observed by fluorescent microscopy for day 3. Inflammatory receptor IL-1R1 and complex MyD88 showed decrease fluorescent intensity after treating with 100 μ L HA hydrogels compared to IL-1 β control group.

CONCLUSION

Crosslinked-HA hydrogels show therapeutic effect by reducing inflammatory receptor and neurotrophins expression in an inflamed *in vitro* model of Nucleus Pulposus cells.

REFERENCES

1. Freemont *et al.*, J. Pathol. 197, 2002
2. Xian Xu *et al.*, J. Biomaterials. 33, 2012

ACKNOWLEDGMENTS

Majlis Amanah Rakyat (MARA) Malaysia (Grant no: ROG1112) for providing financial support to this project.



Osteogenic Activity of Adipose Derived Stem Cells on Micropatterned Collagen-Fibroin Blend Films

E. Sayin^{1,2,3}, E. T. Baran³, V. Hasirci^{1,2,3*}

Departments of ¹Biotechnology, ²Biological Sciences, METU, Turkey

³BIOMATEN, Center of Excellence in Biomaterials and Tissue Engineering, METU, Turkey, esayin@metu.edu.tr

INTRODUCTION

Scaffold microtopography and surface chemistry can help differentiate stem cells into a specific tissue type¹. Adipose derived stem cells (ADSCs) can be collected from patients easily with fast recovery after operation unlike bone marrow mesenchymal stem cell harvest². In this study, collagen-fibroin composite biomaterials were patterned with micropillars and grooves to investigate the level, osteogenic differentiation of ADSC for bone tissue engineering applications.

EXPERIMENTAL METHODS

Micropatterned films were produced by solvent casting collagen-fibroin solution on poly(dimethylsiloxane) (PDMS) templates. After carbodiimide and N-hydroxysuccinimide crosslinking, ADSCs were seeded on the films and cultured for 7 days without osteogenic medium (OM) and which was then changed to OM. Alamar blue assay (n=3-5) was used for cell proliferation and ALP assay (n=3-5) was carried out for osteogenic activity of ADSC. Statistical analysis was performed by using one way ANOVA with Tukey test ($p < 0.05$ shows statistically significant pairs).

RESULTS AND DISCUSSION

Cell proliferation results indicated that ADSC can proliferate on micropillars (MP) more vigorously than on unpatterned surfaces or TCPS control (Figure 1a). The lowest proliferation rate was detected on microchannel (MC) patterned film. After freeze drying films were brittle unlike their wet state (Figure b-c).

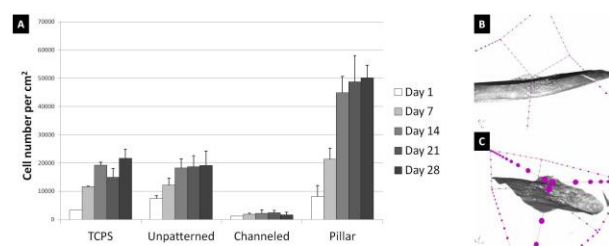


Fig. 1. ADSC proliferation level on Days (a) 1, 7, 14, 21 and 28. MicroCT images on Day 28: ADSC seeded (b) MC, and (c) MP patterned composite films (between points: 500 μ m, pixel size: 2 μ m).

However, slow cell proliferation and high ALP level, on MC films indicated higher osteogenic activity on this particular surface (Figure 2).

Detection of deposited collagen type I and calcium on the blend films were performed by collagen type I immunostaining (Figures 3a-c) and Alizarin red S (Figures 3d-f) staining, respectively, showed the osteogenic differentiation of ADSCs by osteogenic medium on both pattern types.

After staining of the cytoskeleton and image analysis of MC patterned composite films higher cell alignment and more elongated cell features were observed suggesting that the patterns which induce higher cell aspect ratio might also be responsible for the higher osteogenic activity of ADSCs.

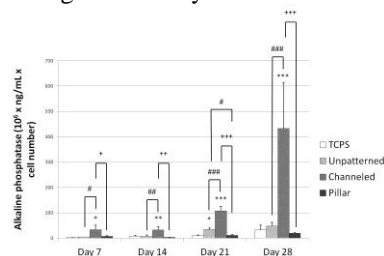


Fig. 2. ALP levels per cell were determined on Days 7, 14, 21 and 28. Statistical differences between TCPS and other groups were analyzed (* $p < 0.05$, ** $p < 0.01$, *** $p < 0.001$; *: TCPS vs unpatterned, MC and MP; #: unpatterned vs MC and MP; +: MC vs MP).

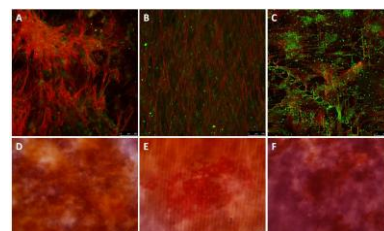


Fig. 3. Confocal laser scanning microscopy images of collagen type I immunostaining on Day 28 on (a) unpatterned, (b) MC, (c) MP patterned composite films (x10). Phase contrast microscopy images of Alizarin red S staining on (d) unpatterned, (e) MC, (f) MP patterned composite films (x20).

CONCLUSION

Collagen-fibroin composite films presented higher ADSC proliferation rates than TCPS and pillar patterns. Channel type patterns did not yield a high proliferation rate but they enhanced expression of the osteogenic differentiation marker. Secretion of collagen type I and deposition of calcium indicated ADSC osteogenic activity on all surface types. In conclusion, patterned collagen-fibroin blends appear to be suitable for ADSC growth and differentiation.

REFERENCES

- Li Z. *et al.*, Biomaterials. 34:7616-25, 2013
- Chai C. *et al.*, Mol. Ther. 15:467-80, 2007

ACKNOWLEDGMENTS

Authors acknowledge the financial support by METU through BAP-07.02.2013.101 project.



Regulation of mesenchymal stem cell differentiation by changing the molecular structure of supramolecular surfaces

Ji-Hun Seo^{1*}, Sachiro Kakinoki², Tetsuji Yamaoka², and Nobuhiko Yui¹

¹Institute of Biomaterials and Bioengineering, Tokyo Medical and Dental University, Japan, seo.org@tmd.ac.jp

²National Cerebral and Cardiovascular Center Research Institute, Japan

INTRODUCTION

Extensive research has been conducted on the regulation of mesenchymal stem cell (MSC) differentiation by altering physicochemical factors, including stiffness, microtopography, and three-dimensional mechanical strength. However, the importance of the surface mobility of polymer surfaces in a hydrated state, one of the characteristic properties of polymer surfaces, in controlling stem cell differentiation is not yet gaining much attention. A simple surface treatment capable of regulating stem cell lineages by changing the molecular mobility has great potential for many biomedical applications because it provides a simple and convenient method of directing stem cell lineage on various material surfaces without changing the bulk properties.

In the present study, we report the feasibility of directing stem cell differentiation on supramolecular surfaces that are prepared with a simple surface treatment. The underlying concept that we applied is modulating the morphology of adhering stem cells using a wide range of molecular mobility of polymer surfaces in a hydrated state. Because morphologies of adhering stem cells have been known as an important factor in determining stem cell differentiation, we hypothesized that a simply deposited supramolecular surfaces capable of changing the adhesion morphology of cells could induce different stem cell differentiation.

Polyrotaxane (PRX) is a supermolecule that contains molecularly movable host molecules [e.g., α -cyclodextrin (α -CD)] threaded on a linear guest molecule [e.g., poly(ethylene glycol) (PEG)]. By adopting this threaded macromolecular structure of polyrotaxanes, we developed polymer surfaces with a wide range of surface mobility by simple deposition method,^{1,2} and the effect of surface mobility on the differentiation of MSC was investigated.

EXPERIMENTAL METHODS

ABA-type triblock copolymers containing threaded PRX segment as B unit and surface anchoring group (A unit) were synthesized by reversible addition-fragmentation chain-transfer (RAFT) polymerization after synthesizing pseudo-PRX macro-chain-transfer agent (CTA). The surface anchoring group (A) is a random copolymer segment composed of 2-methacryloyloxyethyl phosphorylcholine (MPC) and n-butyl methacrylate (BMA) (PMB). PRX block copolymer with two different number of threaded α -CD was synthesized (PRX-A: 12threaded α -CD, PRX-B: 112 threaded α -CD) to modulate the surface mobility of polymer surface. As a non-PRX control sample, a methacrylate random copolymer containing similar chemical component with PRX block copolymer was further synthesized. The surface molecular mobility of the cast polymer was analyzed by means of quartz crystal microbalance-dissipation (QCM-D) equipment,

and MSC adhesion and differentiation was analyzed on each polymer surface.

RESULTS AND DISCUSSION

Surface molecular mobility of PRX-A, which has a smaller number of threaded α -CD, showed the highest value among the prepared polymer surfaces. In contrast, PRX-B surface, which has a larger number of threaded α -CD, showed the moderate value of surface molecular mobility. This is possibly due to the increased molecular rigidity or decreased mobility of the polymer surfaces induced by different number of threaded α -CD. The molecular mobility of the control random copolymer surface showed the lowest value among the polymer surfaces. This indicates that the PRX molecular platform is useful to prepare highly dynamic polymer surface, and the degree of molecular mobility could be easily modulated by simply changing the number of threaded α -CD.

MSCs adhering on the polymer surface with higher molecular mobility showed the narrow and protruded morphology. This resulted in the low expression value of Rho-related protein kinase (ROCK) activity, which is cytoskeletal signalling element related with the MSC differentiation, on the dynamic PRX surface (Fig.1). This indicates that the cytoskeletal signalling element is greatly affected by the surface mobility of the polymer surface. As a result, MSCs on the dynamic PRX surface were easily differentiated into adipogenic cells while those on the surface with lower molecular mobility were easily differentiated into osteogenic cells.

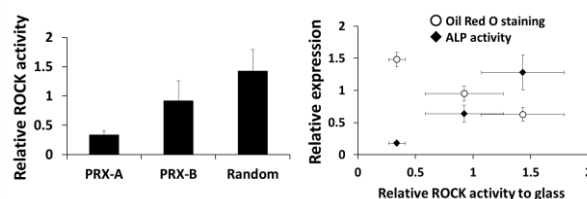


Fig.1 Relative ROCK activity of adhering MSC and the differentiation level of adhering MSCs

CONCLUSION

Different tendency of MSC differentiation was successfully induced by changing the surface mobility of simply deposited polymer surfaces. By adopting the threaded macromolecular platforms, we could demonstrate the importance of molecular mobility of polymer surface for regulating MSCs differentiation.

REFERENCES

- Seo J.-H. *et al.*, J. Am. Chem. Soc. 135:5513-5516, 2013.
- Seo J.-H. *et al.*, Biomaterials 34:55-63, 2013.

Cell Viability and Cell Attachment of Mesenchymal Stem Cells on Hydroxyapatite/Alginate *S.crassifolium* Composite Scaffolds

Decky J. Indrani^{1*}, Ismail Dologo², Yuyus Kusnadi³

¹Department of Dental Materials Science, Faculty of Dentistry, University of Indonesia, decky@ui.ac.id

²Department of Orthopaedic and Traumatology, Faculty of Medicine, University of Indonesia

³Stem Cell and Cancer Institute, Kalbe Farma, Jakarta, Indonesia

INTRODUCTION

Application of tissue engineering in site of bone defects has used scaffolds with respect to bone analogue concept, using inorganic and organic composites, and have shown cell growth^{1,2}. Preliminary studies have prepared hydroxyapatite and alginate *Sargassum crassifolium* (*S.crassifolium*) composite scaffolds with pore size up to 250 µm in diameter³. The hydroxyapatite powder was synthesized with low heat treatment temperature to obtain amorphous material^{4,5}. The alginate *S.crassifolium* powder were extracted from the macroalgae of Indonesia seas and has shown as typical alginates^{6,7}. The ability of cells to attach to the surface of the materials is important for further cellular process. The suitability for cell culture of the scaffold, however, has not been studied. The present study, therefore, aimed to observe cell viability and cell attachment in the hydroxyapatite/alginate *S.crassifolium* composite scaffolds after seeded with stem cells.

EXPERIMENTAL METHODS

Hydroxyapatite/alginate *S.crassifolium* composite scaffold samples were prepared following previous studies^{1,3}. For a control, scaffold samples from commercially available hydroxyapatite and alginate (Sigma-Aldrich, USA), were also prepared. Mesenchymal stem cells used in the present study was isolated from the medullary bone of human femur. Viability was initiated with cell culture for 24h in the presence of sterilized scaffold samples⁸. Cell viability test was conducted with extract medium concentrations ranging from 100% to 1%. The extract medium was removed and osteogenic medium with MTT assay was then added to the cultures. Incubation was conducted for 3h. Absorbance was measured in a spectrophotometer at a wavelength of 540nm. For cell attachment, sterilized scaffold samples were placed in a 24-well plate and suspended in osteogenic medium. Mesenchymal stem cells were then seeded over the whole upper surface of the sterilized scaffold samples. After 6 weeks of incubation, scaffold samples were sectioned in many planes and were then observed using a scanning electron microscope.

RESULTS AND DISCUSSION

Results of MTT assay test showed that the hydroxyapatite/alginate *S.crassifolium* scaffold samples with extract concentrations of 100% to 1% showed cell viability of 35.9% to 101.5%, in comparison to the control, i.e. 74.8% to 127%. After six weeks of cell seeding, majority of the cells were seen in the sterilized

scaffold samples, as well as, in the control. The cells were rounded morphology showing organelles appeared with extension to cell surfaces. Some cells appeared in cluster, while others were randomly solitary. Most cells were spread evenly and were well attached to the exterior and internal part of the interconnected pore walls of the scaffold samples. This cell attachment in the structure of the hydroxyapatite/alginate *S.crassifolium* composite scaffolds indicated that the materials used to prepare the scaffold did not have any negative effect on the cells.

CONCLUSION

The study showed that the hydroxyapatite/alginate *S.crassifolium* composite scaffolds have revealed with excellent cell viability to the mesenchymal stem cells used. The mesenchymal stem cells seeded onto the hydroxyapatite/alginate *S.crassifolium* composite scaffolds have presented the existence of cell attachment inside the scaffolds.

REFERENCES

1. Lin HR, Yeh YJ, J. Biomed Mater Res Part B: Biomater 71B:52-65, 2004
2. Turco G., et al, Biomacromolecules;10: 1575-83, 2009
3. Indrani DJ, Budianto E, Purwasasmita B, Proceeding 3rd International Conference on Instrumentation, Communications, Information Technology, and Biomedical Engineering, Bandung, Indonesia, November, 2013
4. Indrani DJ, Soegijono B, Indonesia Journal of Materials Science 12(2): 137-40, 2010
5. Nazarpak MH, Solati-Hashjin M, Moztafarzadeh, Journal of Ceramic processing Research 10(1):54-57, 2009
6. Indrani DJ, Budianto E, Dental Journal 46:22-25, 2013
7. Yabur R., et al, J Appl Phycol 19:43-53, 2007
8. Theiszova M., et al, Biomed Pap Med Fac Univ Palacky Olomouc Czech Repub 149:393-6, 2005

ACKNOWLEDGMENTS

This work was supported by research grant from the Indonesia government. The mesenchymal stem cells obtained from the research of Dr. Ismail, Sp.OT, and the technical assistance from Lakshmi Sandhow in the Regenic Lab, Stem Cell and Cancer Institute, Kalbe Farma, Jakarta, were greatly acknowledged.



Application of Bone Morphogenetic Protein-6 and Induced Pluripotent Stem Cells in Periodontal Tissue Regeneration

Kuang-Lin Tung¹, Yung-Hsin Cheng², Shih-Hwa Chiou³, Kuang-Dah Yeh^{4*}

¹Institute of Oral Biology, National Yang-Ming University, Taipei, Taiwan

²Department of Medical Research and Education, Taipei Veterans General Hospital, Taipei, Taiwan

³Department of Medical Research and Education, Taipei Veterans General Hospital, Taipei, Taiwan

^{4*}Tri-service General Hospital, Taipei, Taiwan, amytung16@gmail.com

INTRODUCTION

Periodontal disease can result in alveolar bone loss or even tooth loss, severely impacting on the aesthetics and masticatory ability of the affected patients. Bone morphogenetic proteins (BMPs) are powerful inducers of osteogenic activity during the embryologic bone formation phase. BMP-6 has been shown to have the ability to induce periodontal tissue regeneration, including the alveolar bone, periodontal ligament, and cementum.¹ Induced pluripotent stem cells (iPSCs) has been shown to create increased alveolar bone and cementum as well as periodontal ligament formation in a periodontal defect animal model. However, the effect of BMP-6 on the iPSCs ability to regenerate periodontal tissue has not been studied. The purpose of our research was to investigate the periodontal tissue (periodontal ligament cells, cementum, and alveolar bone) regeneration ability of iPSCs under the influence of BMP-6.

EXPERIMENTAL METHODS

In this study, a self-developed injectable thermosensitive chitosan/gelatin/glycerol phosphate (C/G/GP) hydrogel was used.² The cytotoxicity of the C/G/GP hydrogel was evaluated using crystal violet assay and lactate dehydrogenase assay. The *in vitro* release study of DEX-containing (2.5 mg/ml, 5 mg/ml, and 10 mg/ml) hydrogel was investigated using UV-spectroscopy. We added BMP-6 (0.1 ng/ml and 1 ng/ml) to the osteogenic medium in order to investigate the differentiation ability of iPSCs, then the mineralization ability was studied using Alizarin red S staining. For *in vivo* study, the BMP-6-containing hydrogel cultured with or without iPSCs was used as the periodontal defect substitute. The new bone formation at the periodontal defect region of rats was determined using micro-computed tomography (micro-CT); the histomorphology of defect region was investigated using the hematoxylin and eosin (H & E) staining.

RESULTS AND DISCUSSION

Compared with the control group (extract-free medium), the experimental group (extract of hydrogel) was non-

cytotoxic to iPSCs (Fig. 1 (a)), the cumulative releasing test shows that the DEX in hydrogel could sustain releasing (Fig. 1 (b)). The iPSCs-derived osteoblasts mineralization forming ability is shown in Fig. 1 (c), indicating that the 1 ng/ml BMP-6 group had the best mineralization ability among the test groups. The H & E staining analysis results shows that the periodontal ligament like-cells could be detected

CONCLUSION

The C/G/GP hydrogel has no cytotoxicity and is suitable for sustained delivery of DEX. The presence of BMP-6 enhances the mineralization forming ability of iPSCs. Compared with the control group (hydrogel only), the micro-CT and H & E staining analysis results indicate that the presence of BMP-6, cultured with or without iPSCs, enhances the new bone formation and the periodontal ligament-like cells formation at the periodontal defect region, respectively. We conclude that combining BMP-6 and iPSCs provides a potential method for periodontal tissue regeneration.

REFERENCES

1. Huang K.K. *et al.*, J. Periodontal Res. 40:1-10, 2005
2. Cheng Y.H. *et al.*, Biomaterials 32:6953-61, 2011

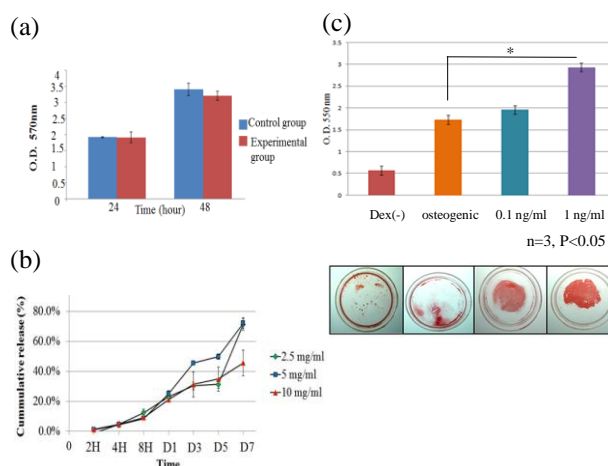


Fig 1. (a) Results of crystal violet assay for cytotoxicity (n=4, p>0.05); (b) release study of dexamethasone from hydrogel during 1 week; (c) iPSCs-derived osteoblasts mineralization forming ability

Dynamic Polysaccharide-based Carrier Systems for the Delivery of Biotherapeutics

Denise N. Bamberger¹ and Peter R. Wich^{1*}

¹ *Institut für Pharmazie und Biochemie, Johannes Gutenberg-Universität Mainz, Germany*
wich@uni-mainz.de

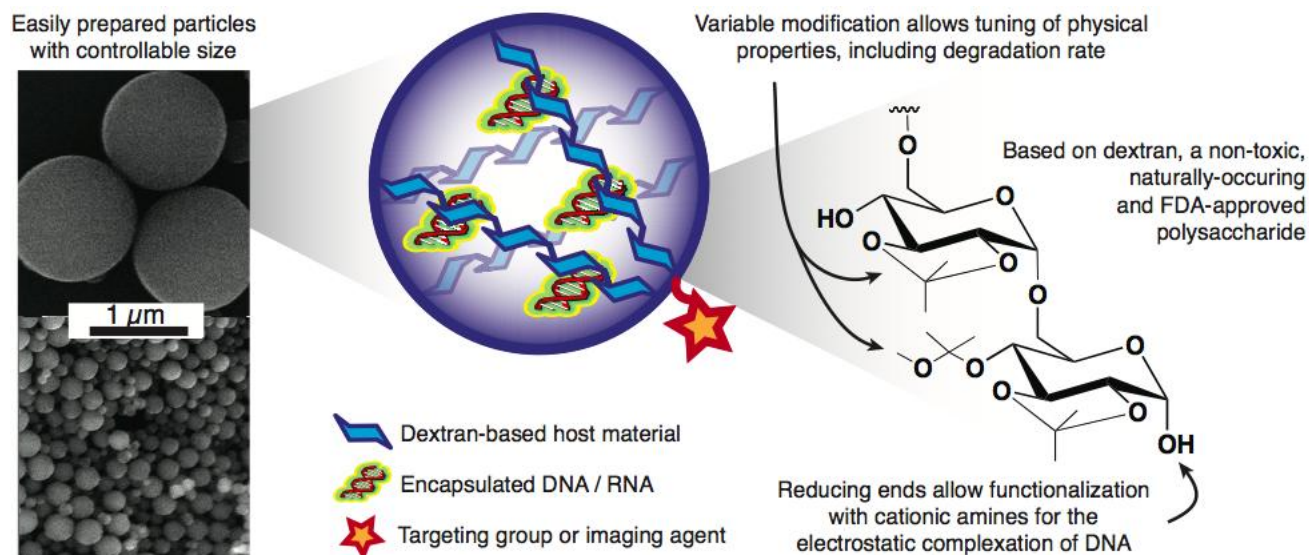
Polymer-based drug, vaccine and gene delivery systems can be easily modified and are particularly attractive because of their ability to perform several critical functions simultaneously. These include delivering therapeutic or other bioactive agents to a specific site via a targeting mechanism, increasing the circulation times of drugs in the body, protecting drugs from degradation, or increasing the bioavailability of poorly soluble drugs.

Recently, a new class of modular and acid-degradable, polymeric particles using acetal-modified dextran (Ac-DEX) was developed.¹ This biocompatible material can be formulated into particles using a variety of common emulsion-based techniques enabling control over both size and morphology. Due to their pH sensitivity, Ac-DEX particles can selectively and rapidly release their encapsulated payload under mildly acidic conditions including those found in sites of inflammation, tumor tissue, or endocytic vesicles. Upon hydrolytic degradation, Ac-DEX reverts back to FDA-approved dextran

without the generation of acidic by-products that could damage the encapsulated payload or lead to inflammation, as has been observed with some other commonly used polymer systems. In addition, Ac-DEX particle degradation rate can be easily tuned within the time scale of relevant cellular processes. This release tunability combined with their low-toxicity and payload versatility make Ac-DEX particles an ideal platform for a wide range of biotherapeutic delivery applications including immunotherapy² and gene delivery.³

REFERENCES

1. E.M. Bachelder, T.T. Beaudette, K.E. Broaders, J. Dashe, and J.M.J. Fréchet, *J. Am. Chem. Soc.*, 2008, **32**, 10494-10495
2. K.E. Broaders, J.A. Cohen, T.T. Beaudette, E.M. Bachelder, J.M.J. Fréchet, *Proc. Natl. Acad. Sci. USA*, **2009**, *106*, 5497–5502.
3. P. R. Wich, J. M. J. Fréchet, *Aust. J. Chem.* **2012**, *1*, 15–19.



Amphiphilic Graft Polyester-g-polysaccharide Copolymers for Sustained Drug Release

L. Martellotto¹, J. Buisson¹, H. Van Den Berghe^{1*}, J. Coudane¹

¹Artificial Biopolymers Department, Max Mousseron Institute of Biomolecules, University Montpellier 1, France, helene.van-den-berghe@univ-montp1.fr

INTRODUCTION

Biocompatible amphiphilic copolymers with well-defined architectures are one of the challenging areas in polymer science because they are able to form nanostructures in aqueous medium with potential as drug delivery systems^{1,2}. In this field, aliphatic polyesters, such as poly(ϵ -caprolactone) (PCL), are interesting hydrophobic candidates as a result of their biodegradability, biocompatibility and FDA approval. Moreover, polysaccharides, such as dextran, are hydrophilic polymers of choice because they are renewable, biocompatible and protein repellent that confer stealth to nano-objects³. However most of the graft copolymers described in the literature and prepared from these types of polymers was constituted of a hydrophilic backbone and hydrophobic side chains due to the lack of functionalities along the hydrophobic polyester chains. Few years ago, our team described a general synthetic route, *via* anionic activation, allowing functionalising polyesters along their backbone⁴. This new strategy gave access to numerous new functional polymeric structures such as propargylated PCL⁵. The purpose of this work is first to functionalise and make “clickable” dextran in order to covalently graft it onto propargylated PCL. Nanocarrier structures were built up with this graft architecture, to be used for drug encapsulation (anti-cancer agents, antibiotics, growth factors,...) and sustained release of these drugs.

EXPERIMENTAL METHODS

Synthesis. “clickable” dextran. Dextran was chemically modified to its reductive hemiacetal chain extremity by coupling bromopropylamine or cysteamine *via* reductive amination. Typically bromopropyl-dextran was then transformed in azidopropyl-dextran by reaction with sodium azide. *Amphiphilic PCL-g-dextran copolymer.* “Clickable” dextran was covalently grafted to propargylated PCL backbone by a “click” reaction.

Preparation of nano-objects. Nanoparticles or polymeric micelles were prepared by typical nanoprecipitation technique.

RESULTS AND DISCUSSION

The synthesis of “clickable” dextran was realised *via* a reductive amination pathway. Then the functionalized dextran was covalently grafted to propargylated PCL backbone (Figure 1) according to a click reaction, under mild conditions to preserve the copolymer from degradation.

The grafting and the resulting copolymer structure were demonstrated by DOSY analysis and Size Exclusion Chromatography measurements. The percentage of hydrophilic dextran chains grafted to a hydrophobic PCL backbone was determined by ¹H-Nuclear Magnetic Resonance.

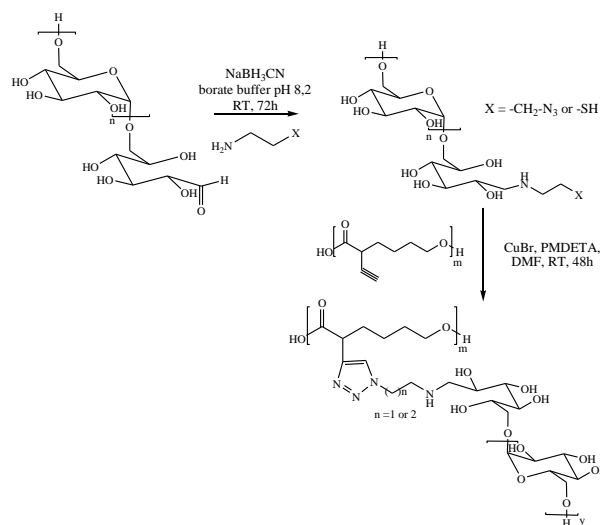


Figure 1: Synthesis of amphiphilic graft PLC-g-dextran copolymer

Nanoprecipitation route provided nano-objects (micelles or nanoparticles) in aqueous medium and characterised by quasi-elastic light scattering measurements. The resulting new nanostructures were compared to PCL nano-objects in terms of drug encapsulation load capacity and kinetic of *in vitro* drug delivery. These preliminary assays were realised with a hydrophobic drug model.

CONCLUSION

Well-defined functional PCL and “clickable” dextran were synthesised and used as building blocks for the synthesis of biocompatible amphiphilic PCL-g-dextran copolymers. Nanostructures of this new copolymer architecture were successfully prepared by nanoprecipitation and well-characterised. The versatility of the strategy developed herein paves the way for preparation of various nanocarriers, modulating the drug delivery kinetic according to the length of the native polymeric chains. Next step will consist in the covalent attachment of sugar residues (mannose, galactose) as targeting agents to the surface of micelles for site-specific drug delivery applications, for example the targeting of cancer cells.

REFERENCES

1. Gref R. *et al.*, Macromol. 35:9861-9867, 2002
2. Freichels H. *et al.*, Biomac. 13:760-768, 2012
3. Owens D.E *et al.*, Int. J. Pharm., 307:93-102, 2006
4. Ponsart S. *et al.*, Biomac. 1:275-281, 2000
5. El Habnoui S. *et al.*, Biomac. 14:3626-3634, 2013

ACKNOWLEDGMENTS

The authors are grateful to Sylvie Hunger and Aurélien Lebrun for their contribution in NMR spectroscopy.

Micro and Nano Systems in Medical Applications

Vasif Hasirci^{1,3,4} and Nesrin Hasirci^{2,3,4}

Middle East Technical University, Faculty of Arts and Sciences,¹ Biological Sciences Dept.,² Chemistry Dept.,
³ Biomedical Engineering Graduate Dept.,⁴ BIOMATEN, Center of Excellence in Biomaterials and Tissue Engineering,
06800, Ankara, Turkey
nhasirci@metu.edu.tr

INTRODUCTION

Micro and nano systems gained significant attractions in medical applications especially as diagnostic or therapy devices. One problem is the long term safety of these systems if they are not degradable or their degradation products are not biocompatible. One other problem is the laborious and expensive production of these systems (1-4). In this study some micro and nano systems prepared from various polymers or activated with certain polymers as drug carriers were examined. Some systems were converted to composite forms with addition of hydroxyapatite (HAp) or tricalcium phosphate (TCP) particles and added into scaffolds to use them for bone tissue engineering applications. Chemical structures, physical forms, mechanical and thermal properties and their effects on cells or tissue were examined.

EXPERIMENTAL METHODS

Various micro or nano particles were prepared from gelatin (G), chitosan (CH), polyvinylpyrrolidone (PVP), polyethyleneoxide (PEG), poly(lactic acid-co-glycolic acid) (PLGA) and poly(hydroxybutyrate-co-hydroxy valerate) (PHBV) as polymeric systems and some of them were blended with other polymers or inorganic apatite crystals. Chemotherapeutic agents as colchicine, methotrexate and 5-fluorouracil were loaded into G and CH micro particles; bone morphogenetic proteins were loaded into PLGA and PHBV nano capsules; gentamicin as an antibiotic and epidermal growth factor (EGF) as an bioactive agent were loaded in to gelatin or gelatin-TCP composite micro carriers. Release kinetics of each system was studied in vitro. Meanwhile, the effects of scaffolds containing these micro or nano systems on cells were examined in vitro and in vivo conditions implanting scaffolds in bone defects of rabbits (Figure 1).

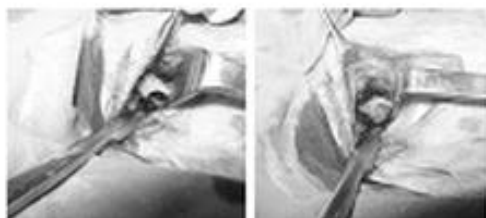


Figure 1. Surgical operation of scaffolds containing gentamicin loaded micro carriers

RESULTS AND DISCUSSION

Release of chemotherapeutic agents from gelatin microspheres were fast because of fast degradation of the particles. Chitosan micro particles were quite stable in buffer media and the release occurred only in the presence of enzyme lysozyme.

Microparticles containing colchicine, methotrexate and 5-fluorouracil all showed significant effect on breast cells. Microparticles containing antimicrobial agents were effective to *E.coli*; and nanoparticles having growth factors showed fast and proper tissue healing. Meanwhile, PCL scaffolds containing microspheres of β -TCP/G loaded with gentamicin caused an increase in bone regeneration without any adverse effect. The cells were able to attach and proliferate on these composite scaffolds. Histological analyses demonstrated enhanced tissue integration in the composite scaffolds.

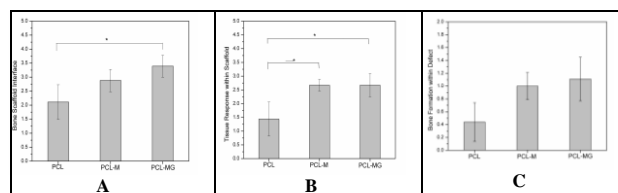


Figure 2. Results of histological scoring at 8 weeks post implantation: Scores for (A) the hard tissue response at the bone-scaffold interface; (B) the hard tissue response within scaffold; (C) bone formation within defect (Error bars represent SD for n=6; * p<0.05).

CONCLUSION

Micro nano carriers as well as scaffolds loaded with these carriers are effective tools for drug delivery and tissue engineering applications.

REFERENCES

1. N.Hasirci, Nanomaterials and Nanosystems for Biomedical Applications, Ed: M.R Mozafari, pp:1-26, Dordrecht, Netherlands, Springer, 2007.
2. Gunbas I.D, *et al.*, Ind. Eng. Chem. Res., 51, 11946–11954, 2012.
3. Sezer, U.A. *et al.* J Appl Polym Sci, 131:8, 2014.
4. Ozerkan, T. *et al.*, J Microencapsul, 30:8, 762-770, 2013

ACKNOWLEDGMENTS

Research was supported by TUBITAK and METU-BAP grants

Fibrin-based Microsphere Reservoirs for Delivery of Neurotrophic Factors

Juhi Samal¹, Eilis Dowd² and Abhay Pandit^{1*}

¹Network of Excellence for Functional Biomaterials,

²Pharmacology and Therapeutics, National University of Ireland, Galway, juhisamal@gmail.com

INTRODUCTION

Neurotrophic factors promote the differentiation, growth and phenotypic maintenance of neurons and act as a potential means of modifying neuronal dysfunction in neurodegenerative disorders like Parkinson's disease. However, their therapeutic application is limited by their short half life *in vivo*. This calls for a biomaterial based intervention which protects the neurotrophins until they are delivered to the desired site and allows a controlled release to achieve therapeutic effects. Fibrin as a biomaterial offers the advantage of being an autologous substrate where the rate of polymerization and degradation can be well controlled. The hypothesis of this study is to establish that template charge manipulation can lead to fabrication of hollow fibrin microspheres as a reservoir for controlled delivery of the neurotrophins. Specific objectives were to fabricate and characterize the fibrin based reservoir system, evaluate the loading and release profiles, investigate interaction with cells and impact of neurotrophin encapsulation on its bioactivity.

EXPERIMENTAL METHODS

Hollow fibrin microspheres were fabricated by template charge manipulation method¹. The hollow microspheres were characterized by Scanning Electron (SEM), Transmission Electron Microscopy (TEM) and zeta potential analysis. Protein loading and release from the microspheres was demonstrated using NGF as a model neurotrophin. Loading efficiency and release profiles under different conditions were determined using ELISA. Fluorescent labelling of NGF and microspheres was done to facilitate the detection of loading using fluorescence microscopy. Impact of different concentrations of fibrin microspheres on metabolic activity and viability of rat mesenchymal stem cells (rMSCs) and PC-12 cells was shown using alamar BlueTM and live/dead assay. Bioactivity of released NGF was demonstrated by neuronal outgrowth assay in PC-12 cells which was quantified using β III tubulin immunostaining. Statistical analysis was performed using two tailed Student t-test ($p < 0.05$, $n = 3$).

RESULTS AND DISCUSSION

Manipulation of template charge followed by core dissolution resulted in the formation of hollow fibrin microspheres which were stable across a wide range of working conditions. Also the microspheres showed high loading efficiency (>80%) for all sizes of microspheres used (Fig. 1A). NGF-microsphere interaction was also shown using fluorescent labelling of growth factor and microspheres (Fig. 2). The results from alamarBlueTM and live/dead assay showed that there was no adverse impact of fibrin microspheres on cell viability even at higher concentrations (Fig. 3A,B).

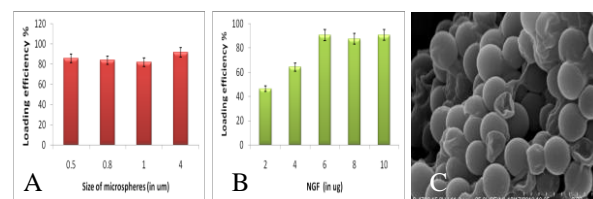


Fig.1. Loading efficiency of fibrin hollow microspheres for (A) different sizes of microspheres and (B) different doses of NGF (data represents mean \pm SD, $n = 3$) (C) Fibrin hollow microspheres after core dissolution using tetrahydrofuran (SEM)

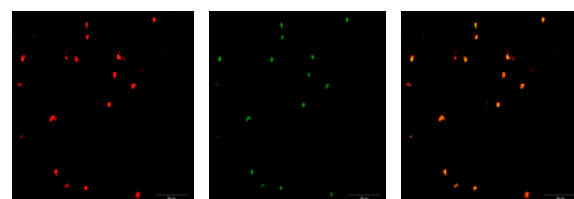


Fig.2. Fluorescence images for loading of NGF into the microspheres (green, fibrin spheres; red, NGF; yellow, colocalization of NGF and fibrin)

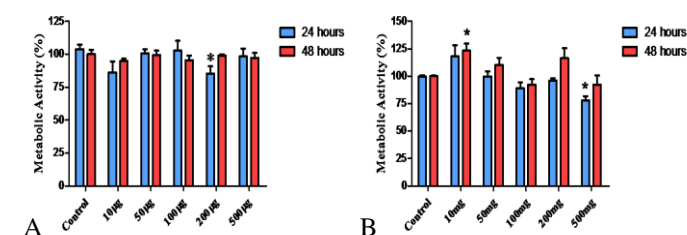


Fig.3 Cellular metabolic activity of (A) rMSCs and (B) PC-12 cells compared with PBS-treated cell (alamarBlueTM assay)

Neurite outgrowth assay and quantification using β III tubulin immunostaining showed that neurotrophin encapsulation into the microspheres did not alter its bioactivity.

CONCLUSION

Fibrin hollow microspheres act as a delivery platform for neurotrophic factors showing high loading efficiency, maintaining their bioactive form and no adverse interactions with cells. Also the absence of any chemical cross-linkers in this system offers an advantage over other biomaterial systems used in similar applications.

REFERENCES

1. Browne S., Fontana G., Rodriguez B.J., Pandit A. *Mol Pharm* (2012), 9:3099-3106.

ACKNOWLEDGMENTS

Hardiman Fellowship, National University of Ireland, Galway. Baxter healthcare, Vienna for Fibrin.

Synthesis and Evaluation of a Novel POSS-PEG-PLA Hydrogel for Periodontal Applications

David K. Wang,¹ Srinivas Varanasi,^{1,3} David J.T. Hill,²
Anne L. Symons,⁴ Andrew K. Whittaker,¹ and Firas A. Rasoul^{1,3*}

^{1*} Australian Institute for Bioengineering and Nanotechnology, ² School of Chemistry and Molecular Biosciences,
^{3*} School of Dentistry, University of Queensland, Brisbane, QLD 4072, **Australia**, f.rasoul@uq.edu.au

INTRODUCTION

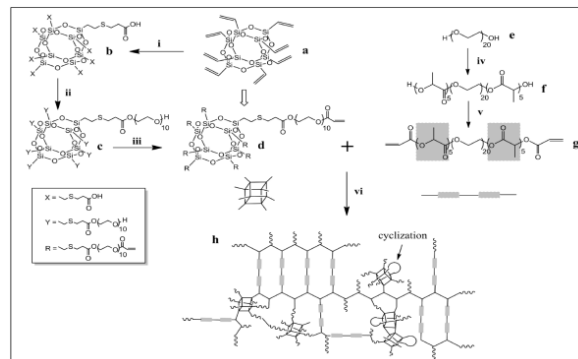
Repair of bone defects arising from disease or traumatic injury in the oral and maxillofacial complex is a major challenge for clinicians restoring form and function in this emotionally sensitive region. Therefore, therapeutic strategies are continually being developed to enhance bone regeneration and guide bone growth. Periodontitis is an inflammatory disease affecting tooth supporting structures and may result in loss of the supporting alveolar bone necessary to maintain teeth in the jaws. Periodontitis has been reported to affect 10-15% of the adult population and this may increase to affect 85% of adults over 70 years of age. Management of tooth loss may require the placement of a dental bridge and/or a dental implant. To further complicate clinical management of tooth loss, dental implants may be compromised by peri-implantitis, an inflammatory response resulting in bone loss around the implant. The clinical success for a dental implant is compromised by poor osseointegration with alveolar bone. However, osseointegration and management of peri-implantitis may be improved by optimising the regenerative potential of adjacent bone. Currently, regeneration of the periodontium is managed by a number of approaches. These include the use of autografts, allografts, cell occlusive barrier membranes, and biodegradable hydrogels. These materials are typically used in association with bioactive molecules to assist periodontal regeneration. In the current study, we have developed an injectable mixed macromonomer system able to be polymerized *in situ* and is biodegradable, to promote regeneration of the periodontium¹ and do not require a secondary surgical intervention.

EXPERIMENTAL METHODS

A water-soluble macromonomer based on octavinyl silsesquioxane has been synthesized with vinyl-terminated PEG-400 in each of the eight arms to promote water solubility (**POSSPEGA**). The methods for synthesis of this macromonomer and the copolymers prepared from it are outlined in Scheme 1 below. The equilibrium swelling ratios, degradation and hydrogel morphology as a function of the copolymer composition have been evaluated. Cytocompatibility for proliferation, viability, immunohistochemistry and attachment of periodontal fibroblasts was conducted using freshly prepared and degraded hydrogels.

RESULTS AND DISCUSSION

The **POSSPEGA** was characterized by NMR and ATR-FTIR analysis and its solution properties were examined.¹ In water it exhibits an LCST with a cloud point at 23 °C. TEM analysis showed that **POSSPEGA** forms spherical aggregates with a diameter of 22 ± 4 nm in water.¹



Scheme 1: Synthesis and polymerization of POSS based hydrogels

The **POSSPEGA** copolymers formed with diacrylated PLA-PEG-PLA, **PEGL₅DA**, show greater extents of swelling in water than in PBS at pH 7.4 because of salting out of the PEG chain segments. The hydrogels have a porous morphology with the size of the pores dependent on the comonomer composition.² In PBS, the hydrogels undergo extensive hydrolysis over time, and the rate of mass loss is strongly dependent on the initial amount of the incorporated lactide. A cytocompatibility study using periodontal fibroblasts, isolated from a female Lewis rats, showed no effect of the hydrogels on fibroblast proliferation, viability and immunoexpression of bFGF and vimentin, either initially and after one PLA hydrolysis half-life, but a minor inhibition of attachment was observed initially.

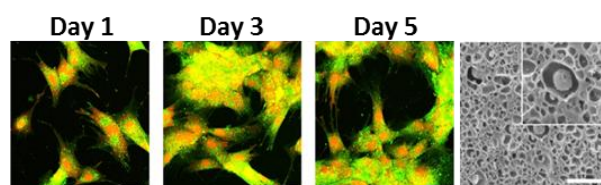


Fig 1: Confocal microscopy images of periodontal fibroblasts on **POSS** hydrogel (scale bar = 20 μm) and Cryogenic SEM micrographs of **POSS** hydrogel (scale bars = 10 μm).

CONCLUSION

The hydrogel was shown not to inhibit the fibroblast proliferation rate, or the fibroblast attachment after hydrolysis had proceeded to some extent (see Fig 1).¹ An *in vivo* study of the hydrogels has been successful in drug delivery during the repair of artificial defects in the mandibles of rats.

REFERENCES

1. Wang D.K *et al.*, Biomacromol. 15:666-679, 2014
2. Wang D.K. *et al.*, Polym. Degrad. Stabil., 96: 123-130, 2011

ACKNOWLEDGMENTS

The authors would like to thank The Queensland State Government Australia, NIRAP scheme for financial support.



Effects of Calcium Phosphate and an adhesion promoting monomer on Strength, Degree of Conversion and Adhesion of Dental Composites

Anas Aljabo¹ and Anne Young^{2*}

¹⁻² Biomaterials and Tissue Engineering/ Eastman Dental Institute, University College London, UK.
anas.aljabo.10@ucl.ac.uk

INTRODUCTION

Dental caries is one of the most common preventable diseases. It is associated with bacteria that, through acid formation, cause demineralisation of tooth structure, oral pain, and ultimately tooth loss. The acid is produced through bacterial fermentation of food. This disease is chronic but can be treated and potentially reversed at early stages (1, 2).

Once the disease has progressed through to the dentine treatment involves removal of diseased tissue and replacement with a filling. With the imminent worldwide ban on amalgam fillings arising from the Minamata agreement, alternative white dental composites and to a lesser extent resin modified glass ionomer cements will become the main tooth restorative materials. Composite failure rates, however, can be three times those of amalgam. Typically, 80% of composite restoration replacement is due to failure of the adhesive used to bond the composite to the tooth. The bond fails because during cure the composite shrinks. This then allows bacteria to penetrate (3).

The aim of this study is to develop a “smart” dental composite material that enables greater treatment rather than complete removal and filling of all caries affected tooth structure. Unlike current dental composite fillings, the new material should preferably bond to dentine without additional adhesive use. The following will assess if this can be achieved through addition of an adhesive monomer (4 Meta) and reactive mono and tri calcium phosphates (CaP).

This CaP mixture is known to promote water sorption induced swelling to compensate shrinkage and release of antibacterial chlorhexidine (CHX) (3). It can additionally promote hydroxyapatite precipitation from simulated dentinal fluid which should aid dentine repair. The aim of this study, however, is to assess what levels of CaP can be added without excessive loss of rapid controllable light activated setting or strength.

EXPERIMENTAL METHODS

Light curable dental monomers were prepared by mixing urethane dimethacrylate : triethylene glycol dimethacrylate : hydroxyethyl methacrylate : camphorquinone : dimethylparatoluidine : 4 Meta in the weight ratio 66:22:5:1:1:5. This was combined with silane – treated dental glass particles containing fibers (20wt%), CaP (0, 10, 20 or 40wt%) and CHX (10 wt%) at a powder to liquid ratio of 4.

The biaxial flexural strength of composite discs (10 mm diameter, 1 mm thick) was determined after 24 hours immersion in water. Monomer conversion (MC) (at 1 and 4 mm thickness) was checked via FTIR after 20s light cure. Depth of cure (DOC) was also obtained by condensing three specimens of each material type into metal molds (4mm diameter and 6mm deep), curing from one side for 20s and scraping away soft material

using a plastic spatula. The length of the remaining specimen (DOC) was measured. According to ISO 4049 this should be >3.0 mm. Shear bond strength (SBS) to ivory dentine was additionally determined. For comparison, a conventional commercial composite Z250 and two newer self-adhering composites (Vertise Flow (VF) and Fusio Liquid Dentine (FLD)) were utilized.

RESULTS AND DISCUSSION

Flexural strengths of experimental formulations without calcium phosphate reactive fillers were comparable with that of the commercial composite Z250. With raising CaP, strength declined but still remained higher than that of the commercial resin modified glass ionomer (RMGIC), Fuji II LC (84MPa). All composites except 40% CaP had a DOC above the required 3.0 mm minimum (Table 1). MC measurements, however, show significantly reduced monomer curing at 4 mm depth compared with 1 mm for all materials except the experimental control composite. These studies highlight that materials may appear hard with < 50% conversion. This could enable significant release of uncured monomer is possible and that additional studies to ISO tests are important. Higher levels of CaP enabled shear bond strengths comparable with self-adhering composites but below that of Z250 with ibond use.

CaP wt%	Strength (MPa)	DOC (mm)	MC (%)		SBS* (MPa)
			1 mm	4 mm	
0	175	4.2	70	68	13
10	160	3.6	71	50	15
20	149	3.0	70	40	26
40	137	2.6	70	37	33
Z250	180	5.0	50	35	40*
VF	148	4.6	65	39	32
FLD	150	5.0	66	38	35

Table 1. Comparison of experimental and commercial composite properties. * SBS was determined without use of adhesive except in the case of Z250

CONCLUSION

Monomer conversion at 4mm decreased with reactive filler addition due to decline in translucency. Although of reduced strength and monomer conversion the above composites with added CaP have improved bonding that could make placement easier, prevent bacterial microleakage and enhance restoration longevity.

REFERENCES

1. Aoba T. Solubility properties of human tooth mineral and pathogenesis of dental caries. Oral Diseases. 2004;10(5):249-57.
2. Mehdawi IM, Pratten J, Spratt DA, Knowles JC, Young AM. High strength re-mineralizing, antibacterial dental composites with reactive calcium phosphates. Dental Materials. 2013;29(4):473-84.
3. Bernardo M. Survival and reasons for failure of amalgam versus composite posterior restorations placed in a randomized clinical trial. The Journal of the American Dental Association. 2007;138(6):775.

ACKNOWLEDGMENTS

The research was funded by Libyan education ministry.



The bone-implant interface – Nano-osseointegration of functionally loaded, nano-textured, human dental implants

Furqan A. Shah^{1,2*}, Bengt Nilsson³, Rickard Brånemark⁴, Peter Thomsen^{1,2}, Anders Palmquist^{1,2}

¹Department of Biomaterials, Sahlgrenska Academy at University of Gothenburg, Sweden

²BIOMATCELL VINN Excellence Center of Biomaterials and Cell Therapy, Göteborg, Sweden

³Tandvårdshuset, Vetlanda, Sweden

⁴Centre of Orthopaedic Osseointegration, Sahlgrenska University Hospital, Göteborg, Sweden

furqan.ali.shah@biomaterials.gu.se

INTRODUCTION

Hierarchical surface treatments are often considered¹ for mimicking the different length scales of the constituent structures in bone, in order to improve biomechanical fixation of osseointegrated implants. Controlled micro- and nanoscale surface modification of cp-Ti surfaces by laser ablation has been shown to be favourable in this regard.² And indeed, nanoscale surface features modulate cellular behavior and differentiation.³ This study was aimed at resolving the fine structure of bone adjacent to osseointegrated, functionally loaded, nano-textured implants in human.

EXPERIMENTAL METHODS

Partly laser-modified (*Fig. 1a-c*) implants (BioHelix™; Brånemark Integration AB, Mölndal, Sweden) were retrieved after 47 months of functional loading, from the maxilla of a 66-year old Caucasian female, for reasons other than biological failure. Histomorphometry was performed by light microscopy (LM) and backscattered-scanning electron microscopy (BSE-SEM). Transmission electron microscopy (TEM) and high angle annular dark field-scanning TEM (HAADF-STEM) were used for ultrastructural analysis. Micro-computed tomography (μ CT) was employed to evaluate tissue architecture in 3D.

RESULTS AND DISCUSSION

On the histological level, well-organized osteonal lamellar bone was found within the implant threads. High amounts of mineralized bone (bone area >80%, bone-implant contact >80%) were observed within the threads by LM, BSE-SEM (*Fig. 1f*) and μ CT. HAADF-STEM showed a characteristic cross-striated pattern of collagen approximately perpendicular to and reaching up to 100 nm from the surface (*Fig. 1d*), closely following the surface micro-contour consistently up to 2 μ m away, suggesting topography-related organization of collagen. At greater distances, collagen fibrils organized into concentric bundles (ϕ =1–3 μ m). Selected area electron diffraction (SAED) revealed preferential orientation of apatite crystallographic *c*-axis, i.e. (002) or (004) reflections, aligned along the collagen fibril direction (*Fig. 1e*). Almost no (002) and (004) reflections were observed for transversally sectioned collagen fibrils (ϕ =50–70 nm). Individual fibrils were separated by multiple extrafibrillar mineral platelets 59.01 \pm 9.11 nm (length) and 5.05 \pm 0.61 nm (thickness). STEM-EDX showed at. % C/Ca=3.33 \pm 0.95 for these collagen fibrils. The mineral platelets showed at. % C/Ca=1.33 \pm 0.50 and at. % Ca/P=1.33 \pm 0.15 indicative of bone-apatite. These ultrastructural observations show that bone interfacing the implant surface is highly organized, exhibiting directional and size organization

similar to mature bone tissue.⁴ STEM-EDX also revealed an overlap of Ti, O, Ca and P signals at the interface zone, indicating gradual intermixing of bone-apatite with the TiO₂ layer. This overlapped zone has previously been resolved by electron tomography⁵ as bone ingrowth into nanoscale irregularities of the surface. Multi-scale analysis of retrieved, functionally loaded human implants is critical to extend pre-clinical understanding of osseointegration.

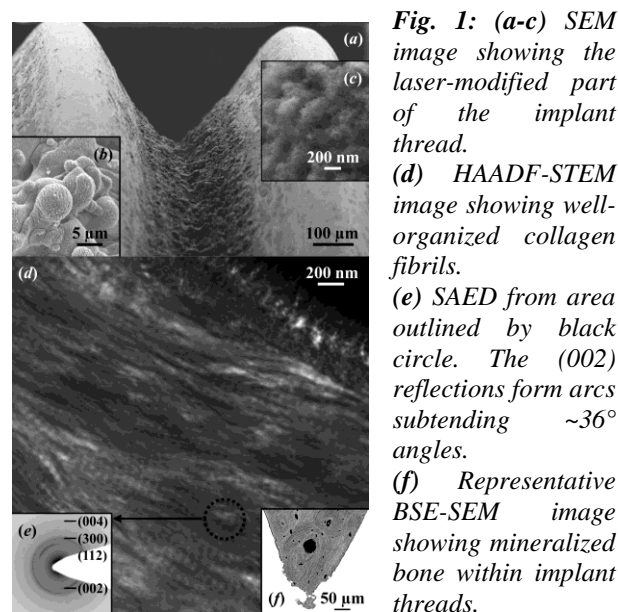


Fig. 1: (a-c) SEM image showing the laser-modified part of the implant thread. (d) HAADF-STEM image showing well-organized collagen fibrils. (e) SAED from area outlined by black circle. The (002) reflections form arcs subtending ~36° angles. (f) Representative BSE-SEM image showing mineralized bone within implant threads.

CONCLUSION

The present study demonstrates, for the first time in human, that nano-textured titanium implants promote hierarchical organization of bone, resulting in a functionally graded interface and direct bonding to the nanoscale surface TiO₂ layer.

REFERENCES

1. Davies JE. *et al.*, Biomaterials. 35:25-35, 2014
2. Brånemark R. *et al.*, Nanomedicine. 7:220-7, 2011
3. Dalby MJ. *et al.*, Nat Mater. 6:997-1003, 2007
4. McNally EA. *et al.*, PLoS One. 7:e29258, 2012
5. Grandfield K. *et al.*, Nanoscale. 5:4302-8, 2013

ACKNOWLEDGMENTS

The Swedish Research Council (grant K2012-52X-09495-25-3), BIOMATCELL VINN Excellence Center of Biomaterials and Cell Therapy, Region Västra Götaland, an ALF/LUA grant, the IngaBritt and Arne Lundberg Foundation, Dr Felix Neubergh Foundation, the Hjalmar Svensson Foundation, and Area of Advance: Materials Science at Chalmers and GU Biomaterials.

Morphology, surface chemistry and mechanical properties of commercial Guided Tissue Regeneration membranes

Pascal Borget^{1, 3*}, Paul G. Rouxhet¹, and Eric Rompen²

¹ Unité de Chimie des Interfaces – Université Catholique de Louvain, Croix du Sud 2/18 1348 Louvain-la-Neuve, Belgique

² Département de Chirurgie bucco-dentaire et de parodontologie – Centre Hospitalier Universitaire de Liège, avenue de l'Hôpital 13, 4000 Liège, Belgique

^{3*} Present address: Biomatlante S.A., 5 rue E. Belin, Z.A. Les Quatre Nations, 44360 Vigneux-de-Bretagne, France, pascalborget@biomatlante.com

INTRODUCTION

Nowadays the bone or tissue reconstruction is a clinical tool, particularly in dental surgery¹. The challenge is to promote the regeneration of specific cells and to prevent ingrowth of soft tissues. This goal can be achieved with non biodegradable² or degradable membranes made of polyester³ or collagen⁴. More than 20 products are available for this specific purpose. The evaluation of the clinical benefits of several commercial membranes is widely described in the literature. However no data are available concerning the physico-chemical and mechanical properties of this kind of biomedical material.

EXPERIMENTAL METHODS

In this study, seven commercially available membranes from different materials were analyzed on both faces: a synthetic non biodegradable membrane (PTFE), three synthetic biodegradable products (polyester) and three samples made of collagen.

The samples were first analyzed as received. Since most of the membranes are moistened before implantation, analyses were also performed with the samples soaked in an aqueous solution, except in the case of a contrary mention by the manufacturer.

Their morphology was investigated on both faces by scanning electron microscopy. The chemical composition and the hydrophilicity were evaluated before and after the water treatment and drying at room temperature, by X-ray Photoelectron Spectroscopy (XPS) and static angle contact measurements. The viscoelastic properties of the membranes were investigated by Dynamic Mechanical Analysis in the shear mode. The ease of handling the moist membranes was also evaluated and correlated with the dynamic mechanical analyses.

RESULTS AND DISCUSSION

Morphology

The biomaterials present various structures depending on the fabrication process: dense, fibrous or alveolar morphologies were found; an homogeneous or bilayer structure was also observed. Three membranes display asymmetrical faces (smooth and rough, respectively). It is well known that not only the chemical surface composition governs the interactions between biomaterial and cells, the surface topography is also a key factor to control the cell activity.

Hydrophilicity

Except for the PTFE membrane and one polyester membrane, the samples are either hydrophilic by nature (those made of collagen), or treated in surface or in bulk in order to improve the wettability and the water uptake.

Surface chemical composition

The elemental and functional composition of the surface layers was investigated by XPS. The detailed analysis of each peak shows the preferential segregation of specific blending components during the manufacturing process or the presence of surfactants, in the case of polyester membranes. Concerning collagen membranes, the drying stage leads to the migration of more hydrophobic species in the upper layers.

Mechanical properties

First, the hydrated samples were subjected to force-displacement experiences at 1 Hz in order to determine the range of the linear viscoelastic region. The relative position of each curve leads to a classification of commercial membranes, based on the rigidity and deformation properties. At small deformations, no dependence in frequency was observed between 0.1 and 100 Hz. The quantification of the pure elastic modulus and the loss factor leads to a better comprehension of the viscoelastic properties in the conditions of use by the periodontist.

CONCLUSION

This study devoted to the characterization of commercial membranes shows a wide variety of biomaterials for Guided Tissue Regeneration in dental surgery, regarding their morphology, surface chemistry or mechanical properties. The PTFE membrane is considered as a good barrier due to the inert nature of this biomaterial but the implant has to be removed. The membranes made of collagen display a good wettability for promotion of tissue integration but their handling strongly depends on the addition of a crosslinker. Although their morphology and wettability have been finely tuned for tissue regeneration, biodegradable polyester membranes are stiffer and less convenient to use, except by addition of a plasticizer.

REFERENCES

1. Nyman S, *et al.* J clin periodontol 9:290-296, 1982.
2. Gottlow J, *et al.* J clin periodontol 13:604-616, 1986.
3. Lundgren D, *et al.* Clin Oral Implants Res, 5:177-184, 1994.
4. Pitaru S, *et al.* J periodontol 59:380-386, 1988.

Dense fibrillated collagen transparent matrices as artificial corneas?

Aurelien Tidu¹, Djida Ghoubay², Barbara Lynch³, Céline⁴ De Sousa, Frank Wendel¹, Jean-Marc Allain³, Vincent Borderie², Gervaise Mosser^{1*},

¹ Sorbonne Universités, UPMC Univ Paris 06, CNRS, Collège de France, UMR 7574, Chimie de la Matière Condensée de Paris, F-75005, Paris, France. Gervaise.Mosser@upmc.fr

² Institut de la Vision, UPMC Univ Paris 06, UMR_S 968 / INSERM, U968 / CHNO des XV-XX / CNRS, UMR 7210, Paris, France.

³ Solids Mechanics Laboratory, Ecole Polytechnique, Centre National de la Recherche Scientifique, Palaiseau, France.

⁴ Banque de Cornées Saint Antoine, Etablissement de Transfusion Sanguine AP-HP, Hôpital Saint Antoine, Paris, France.

INTRODUCTION

Cornea, the outer layer of the eye, is the first lens of the eye. It is composed of several distinct layers, amongst which are the corneal epithelium and the corneal stroma. The stroma accounts for around 90 % of the total thickness. It is mainly composed collagen type I^{1,2}. Collagen fibrils are ≈ 20 nm in diameter, regularly spaced and form layers reminiscent of a plywood^{3,4}. In case of corneal diseases leading to a loss of vision, corneal allografting remains the standard procedure. Alternative treatments can make use of synthetic corneal implants. Several research groups across the world are developing collagen-based implants. Our approach makes use of the lyotropic liquid crystal properties of acidic collagen solutions to generate, after neutralization, dense organized and transparent matrices.

EXPERIMENTAL METHODS

3 mg/mL collagen solutions in 500 mM acetic acid were dialyzed to reach 70 mM acetic acid and 1.25 mM hydrochloric acid. Collagen solutions were subsequently concentrated by centrifugation-filtration up to 15, 30, 60, 90 mg/mL. The concentrated solutions were then pressed into cornea-like shape and submitted to ammonia vapour during 17 h hours to increase pH and induce fibrillogenesis of collagen. Transparent dense collagen matrices were collected and stored into water at 4°C until use. Human donor cornea explants were sewed on top of the scaffolds and immersed into cell culture buffer and cultured at 37° (95% air, 5% CO₂) for 15 days. The samples were analyzed for their ultra-structures, mechanical and optical properties and for epithelium development.

RESULTS AND DISCUSSION

Transmission electron microscopy revealed that fibril density and organization increased with concentration. At 90 mg/ml fibrils were organized in layers. Using a custom made device, mechanical tests revealed that the mechanical properties improved with increasing collagen density: the Young modulus was approximately 0.5 kPa for 15 and 30 mg/ml collagen matrices, while for 60 and 90 mg/ml, values reached respectively 1 and 2 kPa. The maximum stress and strain at rupture were similar for low concentrations (20 kPa and 90%) while for 60 and 90 mg/ml, maximum stresses respectively reached 45 kPa and 80 kPa for a similar elongation of 55%. After cell culture, ultra-fine sections of collagen matrices showed that cells had

formed epithelia on the scaffolds. Transparency was measured in the visible range with a spectrophotometer and calculated using the average optical densities measured. At 30 mg/mL the matrices were transparent (e.g. 84%). Transparency increased with time and was very little affected by the epithelium.

Last, experiments in glass microchambers⁵ revealed that liquid crystals organizations obtained with this collagen solution (70 mM acetic acid and 1.25 mM hydrochloric acid) generated cholesteric organization thus different from the plywood organization found in cornea. Therefore other physico-chemical conditions are currently checked for their plywood liquid crystal organizations⁶, their transparency and mechanical properties.

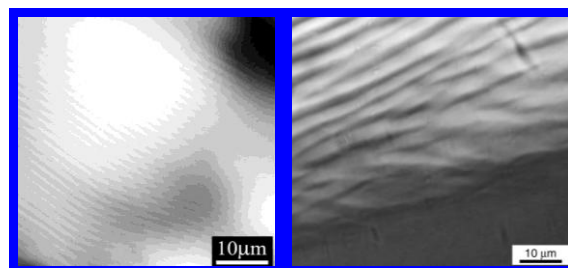


Figure 1 : Cholesteric (left) and plywood (right) organizations

CONCLUSION

Matrices made with collagen at 90 mg/mL (70 mM CH₃COOH and 1.25 mM HCl) present a stabilized cholesteric organization, a Young modulus of 2 kPa and $\approx 80\%$ transparency. They allow development of Human corneal epithelium *in vitro*. New ongoing developments are promising for *in vivo* applications.

REFERENCES

1. Hulmes D. New York, Springer. 15–74. 2008
2. Ihanamäki T. *et al.*, Prog. Retin. Eye Res. 23:403–434, 2004
3. Hassell J.R. *et al.* Exp. Eye Res., 91:326–335, 2010
4. Muller, L. J. Br. J. Ophthalmol., 85:437–443, 2001
5. De Sa Peixoto P. *et al.* Soft Matter, 7: 11203–. 2011,
6. Mosser G. *et al.* Matrix Biol., 25:3–13, 2006

ACKNOWLEDGMENTS

Authors acknowledge Corinne Illoul and Bernard Hayes for their technical support to the work. The authors would like to thank the Fondation pour la Recherche Medical (Grant DCM20121225759) for providing financial support to this project.



Cytotoxicity of Terbium-Crown Ether Complex Against *Acanthamoeba* sp. - A Causative Agent for Eye Keratitis

Eny Kusri^{1*}, Fatimah Hashim², Dewi Tristantini¹, Nurfatin Solehah Bustaman², Nakisah Mat Amin²

^{1*} Department of Chemical Engineering, Faculty of Engineering, Universitas Indonesia, Indonesia, ekusri@che.ui.ac.id

² School of Fundamental Science, Universiti Malaysia Terengganu, Malaysia

INTRODUCTION

Lanthanide ions exhibit unique spectroscopic and luminescent properties that can be applied for bioimaging and bioassay applications. The Ln^{3+} ions adapted easily to any chemical environment, thus it is ready to use as functional centers into a versatile applications. By complexation, we can increase the physico-chemical characteristics. Development of rare earths functionalization for antiamebic activity after exposed to lanthanide complex was investigated. In this study, we synthesized the $[\text{Tb}(\text{NO}_3)_3(\text{OH}_2)_3] \cdot (18\text{C}6)$ to observe biological activity of the Tb complex against *Acanthamoeba* sp. *Acanthamoeba* is a free living amoeba that can caused serious eye disease such as *Acanthamoeba* keratitis. Therefore, in this study the relationships between the dose concentrations of the Ln with the response of the test organisms, *Acanthamoeba* sp. was studied. The mode of *Acanthamoeba*'s cell death was also observed and results obtained indicated the potential of Tb complex as antiamebic agent.

EXPERIMENTAL METHODS

To 1.0 mmol $[\text{Tb}(\text{NO}_3)_3 \cdot 6\text{H}_2\text{O}]$ and 1 mmol 18C6 is dissolved in CH_3CN . The $[\text{Tb}(\text{NO}_3)_3(\text{OH}_2)_3] \cdot (18\text{C}6)$ complex was isolated after one day with yield 86%. For *Acanthamoeba* cytotoxicity studies, amoeba cells were first seeded in a 96-well microplate at 1×10^5 cells/well and were incubated at 30 °C. After 8 hrs, the medium was removed and replaced with medium containing the Tb complex over a range of doubling dilutions of 0 - 30 $\mu\text{g/mL}$. Triplicate cultures were established for each treatment and incubated for 48 hrs. The Tb's IC_{50} value determination was done by MTT assay. Morphological changes on *Acanthamoeba* cells after treatment with Tb complex at their IC_{50} value was observed under light microscopy followed by assessment for *Acanthamoeba* mode of cell death by application two cationic dyes, Acridine Orange and Propidium Iodide (AO/PI) dyes and viewed under fluorescent microscopy (Leica DMire Microscope, Germany).

RESULTS AND DISCUSSION

The elemental composition and structure properties of terbium trinitrate.trihydrate.18-crown ether-6 complex, $[\text{Tb}(\text{NO}_3)_3(\text{OH}_2)_3] \cdot (18\text{C}6)$, was successfully characterized. The Tb^{3+} ion was coordinated with three of nitrate anions by bidentate mode, three of water molecules, forming a nine-coordination number. The crystal system of terbium complex is orthorhombic with space group of Pnma. This structure is similar with the structure has been previously reported [1]. The IC_{50} value for Tb complex derive from the graph was 7 $\mu\text{g/mL}$. There were significant decreases ($p < 0.05$) in *Acanthamoeba* viability with increasing concentration of Tb complex used (Fig. 1).

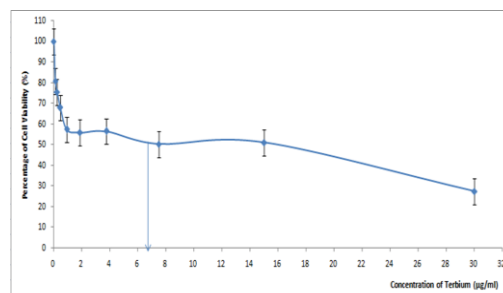


Fig 1: Cytotoxicity of $[\text{Tb}(\text{NO}_3)_3(\text{OH}_2)_3] \cdot (18\text{C}6)$ on *Acanthamoeba* sp. after 48 hours treatment, assessed based on percentage of cell viability by MTT assay. The data represent the mean (\pm S.E.M) of three separates experiments. The IC_{50} value obtained was 7 ($\mu\text{g/mL}$) derived from the graph.

Untreated and Tb-treated *Acanthamoeba* were observed under light and fluorescence microscopy demonstrated changes after treatment with Tb complex (Fig. 2).

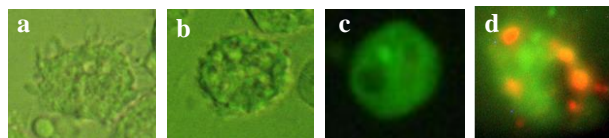


Fig.2: (a) untreated *Acanthamoeba* cells, (b) *Acanthamoeba* cells treated with Tb complex, (c) AO/PI stained of viable *Acanthamoeba* cells and (d) Tb-treated *Acanthamoeba*. Magnification was 400x.

Untreated *Acanthamoeba* can be seen as irregular shape of trophozoite with numerous acanthopodia on the surface (Fig. 2a). While *Acanthamoeba* exposed to Tb complex underwent encystment with rounded form of cell with loss of acanthopodia structure as shown in Fig.2b. The most important changes that were observed after AO/PI staining on *Acanthamoeba* were on membrane integrity, nuclear and lysosomal structure. Untreated *Acanthamoeba* was found to display healthy cells as indicated by green fluoresced cytoplasm and nucleus (Fig. 2c). Observation also indicated that the amoeba retain its membrane integrity after being exposed to Tb complex. However, organellar function was disrupted due to different colour emitted after viewed under fluorescence microscope as similar observation also observed in apoptosis event (Fig. 2d).

CONCLUSION

$[\text{Tb}(\text{NO}_3)_3(\text{OH}_2)_3] \cdot (18\text{C}6)$ complex was successfully synthesized and was characterized by single X-ray diffraction. Based on the cytotoxicity test, it was found that the terbium complex could trigger apoptosis in *Acanthamoeba* cells.

REFERENCES

1. Rogers, R.D., Rollins, A.N. Journal of Chemical Crystallography 24: 321 – 329, 1994.

ACKNOWLEDGMENTS

The authors would like to thank Universitas Indonesia and Universiti Malaysia Terengganu for providing facilities and financial support for this project.



Biodegradable Nanoneedles for Intracellular Sensing of Enzymatic Activity

Ciro Chiappini^{1,2}, Paola Campagnolo^{1,2}, Carina Almeida^{1,2}, Lesley Chow^{1,2}, Molly M. Stevens^{1,2*}

¹Department of Materials, Imperial College London, UK

²Department of Bioengineering and Institute of Biomedical Engineering, Imperial College London, UK
c.chiappini@imperial.ac.uk

INTRODUCTION

Access to the cytosol opens up the possibility for direct biochemical interaction within the cell, improving the efficiency of therapy, electrochemistry and biosensing. Unfortunately (or fortunately) the cell has evolved to prevent direct biochemical intracellular interaction with foreign agents, and the strategies developed so far to enable it present significant shortcomings. Mainly, most of the methods available lack versatility, as they are designed solely to deliver a specific cargo to the cell. Microinjection on the flipside provides a continuous interface with the cell granting greater versatility than the other strategy, but it is inherently low throughput and not amenable to *in vivo* conditions.

Translating microinjection to the nanoscale, using large arrays of nanoneedles, provides high throughput strategies to interface with cells, which also minimize toxicity, while retaining versatility and enabling patterning. Nanoneedles can probe excitable cells, deliver biomolecules and nanoparticles to the cytosol², and effectively probe the cell's biochemical activity³. Here we focus on the fabrication of a class of mesoporous, biodegradable silicon nanoneedles⁴ that can be used to build intracellular biosensors and translate nanoneedle-based diagnostics *in vivo* thanks to the biodegradability and elevated biocompatibility of porous silicon⁵⁻⁷.

EXPERIMENTAL METHODS

The nanoneedles were fabricated by combining conventional microfabrication with metal assisted chemical etch to obtain conical nanostructures with less than 100 nm diameter and 4 micron length. The nanoneedles were functionalised with a CFKK-TAMRA peptide, specifically cleavable by Cathepsin B, and with FITC as a pH sensitive fluorophore. Alexafluor 633 functionalisation provided a stable fluorescence reference for ratiometric measurements.

RESULTS AND DISCUSSION

The nanoneedles were tested for their ability to access the cell cytosol. A nanoneedle chip was placed over cells in culture with application of force. Confocal and scanning electron microscopy of focused ion beam milled sections confirmed that nanoneedles stably penetrated the cell cytosol (Figure 1).

The nanoneedle sensor was tested in physiologically relevant buffers in the range between pH 6 and pH 8. The fluorescence ratio between FITC and AF633 increased linearly in the range between pH 6 and pH 8, allowing for calibration of the sensing element.

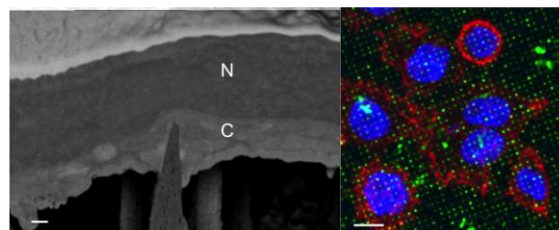


Figure 1 Nanoneedles penetrate the cell cytosol. (a) SEM of a cell penetrated by a nanoneedle. N indicates the cell nucleus, while C indicates the cell cytosol. Scale bar 200 nm (b) Confocal image of the cell membrane (red), nucleus (blue) and nanoneedles (green). Nanoneedles penetrate across the cell membrane. Scale bar 10 μm.

The efficiency of Cathepsin B at cleaving the substrate and releasing the fluorophore in solution was assessed in physiological buffer. Once successfully interfaced with cells in culture, the nanoneedles functionalized with FITC, AF633, and CFKK-TAMRA were able to discriminate cancer and healthy cells in co-culture by sensing their intracellular pH and Cathepsin B activity (Figure 2).

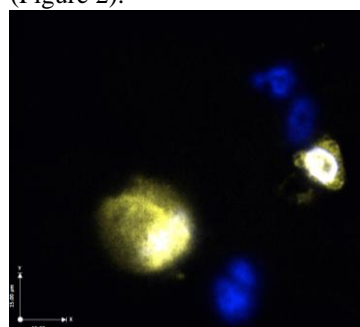


Figure 2 Confocal image of cancer cells in co-culture with healthy cells. The Cathepsin B sensing element releases TAMRA within cells with active Cathepsin B in the cytosol inducing the fluorescence of cancer cells (in yellow), while healthy cells do not fluoresce (nucleus in blue). Scale bar 15 μm.

CONCLUSION

Here we demonstrated the assembly of a porous silicon based nanoneedle platform capable of sensing the intracellular environment of cells in culture, with the ability to monitor protease activity and intracellular pH, and employ those measurements to detect cancer cells in co-culture.

REFERENCES

1. Robinson, J. T. *et al. Nat. Nanotechnol.* **7**, 180–184 (2012).
2. Shalek, A. K. *et al. Proc. Nat. Acad. Sci. USA* **107**, 1870–1875 (2010).
3. Na, Y.-R. *et al. Nano Letters* **13**, 153–158 (2013).
4. Chiappini, C., Liu, X., Fakhoury, J. R. & Ferrari, M. *Adv. Funct. Mater.* **20**, 2231–2239 (2010).
5. Anderson, S. H. C., Elliott, H., Wallis, D. J., Canham, L. T. & Powell, J. J. *phys. stat. sol. (a)* **197**, 331–335 (2003).
6. Goh, A. S.-W. *et al. Int. J. Radiation Oncol. Biol. Phys.* **67**, 786–792 (2007).
7. Park, J.-H. *et al. Nat. Mater.* **8**, 331–336 (2009).

Biosurface Induced Protein Manipulation for Measurement of Dynamic Platelet Function

D. Bishop¹, J. Cowman², E. Dunne², D. Kenny², A. Boyd¹ and B. Meenan¹

¹Nanotechnology and Integrated Bioengineering Centre, University of Ulster, UK

²Royal College of Surgeons in Ireland, Dublin, Ireland

bishop-d1@email.ulster.ac.uk

INTRODUCTION

Upon vascular injury the natural response of the body is to limit blood loss via thrombus formation on an exposed protein matrix. Platelet adhesion/activation in such conditions is directly dependent upon adherence of the blood protein von Willebrand Factor (VWF). VWF binds to the exposed sub-endothelial extra cellular matrix (ECM) which consists mostly of collagen fibres. Platelets tether and adhere to the bound VWF and initiate thrombus formation. However, an inability in certain patients to regulate this process results in conditions such as von Willebrand disease (VWD). The lack of a physiologically relevant diagnostic method to detect such conditions is a major concern¹. This work reports the development of a synthetic biomimetic surface with chemical and morphological properties designed to entrap VWF from blood. The interactions of platelets from the same patient with their bound VWF are then monitored within a representative assay platform allowing for patient specific treatments. A polymer demixing spin coating methodology has been shown to produce a topography representative of that encountered by VWF *in vivo*². By tailoring and optimizing this surface condition, the potential for diagnosis of conditions such as VWD and other platelet orientated cardiovascular diseases has been addressed.

EXPERIMENTAL METHODS

Polystyrene (PS) and PMMA (Sigma, UK) were dissolved at a 50:50 ratio at concentrations of 1%, 3% and 5% w/v in chloroform. The solutions were spin coated onto clean glass coverslips at 6000 rpm for 60s. Resultant morphology was characterised using atomic force microscopy (AFM) and scanning electron microscopy (SEM). Surface chemistry was evaluated by X-ray photoelectron spectroscopy (XPS) and water contact angle. To further mimic the *in vivo* conditions, plasma modification and protein printing of collagen were applied to the polymer demixed surfaces. Blood was perfused through a novel laser patterned fluidic device at a typical arterial shear rate of 1500s⁻¹. Platelet adhesion was observed via real time fluorescent microscopy. The response of platelets to the captured autologous VWF was compared to that on a pooled human purified VWF positive control. Inhibition of platelet binding, utilizing antibodies that block VWF binding sites was performed to ensure that the platelet activity was a result of interaction with captured VWF.

RESULTS AND DISCUSSION

Detailed characterisation of the demixed surfaces showed a relationship between polymer concentration and resultant surface feature size. AFM analysis showed that the 50:50 ratio results in a pitted morphology while the XPS results indicated a surface chemistry almost identical to that of pure PMMA. This would suggest

that the PMMA has formed a raised surface layer due to its dewetting from the PS particles. Platelets were seen to bind well to this surface when compared to the positive control signifying the entrapment of VWF from the circulating blood. This effect is strongly corroborated by the results of the inhibition study with complete absence of platelet adhesion observed after supplementation with any of the (VWF/platelet) blocking antibodies. This data confirms that the featured surface is capturing circulating VWF.

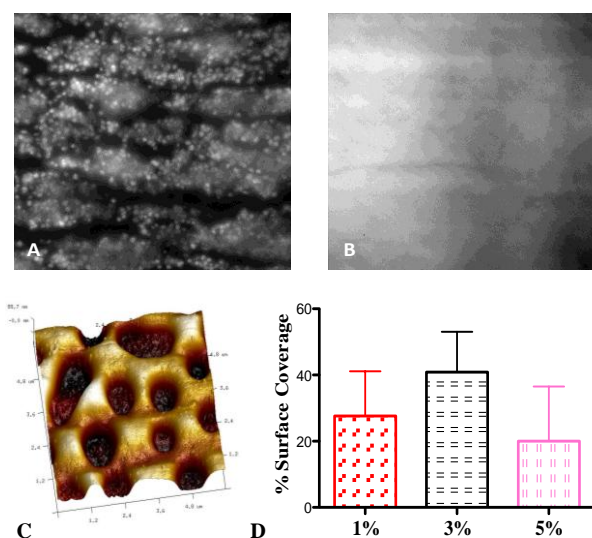


Fig 1: A) Platelet adhesion of non-supplemented and B) AK2 antibody supplemented blood C) AFM of the topography and D) Platelet surface coverage for 3 polymer concentrations.

Based on the rate and percentage of surface coverage the 3% PS/PMMA demixed solution was seen to produce the optimum topography for platelet adhesion.

CONCLUSION

Analysis of dynamic platelet behaviour indicates that a surface created by the PS/PMMA demixing process has the capacity to capture circulating VWF from blood. Furthermore, surfaces produced by spin coating a 3% polymer solution have a sub-micron to nanoscale topography capable of entrapping an individual's VWF and using this to measure their platelet interactions thereon. This is significant as, for the first time, a patient's own unique interactions can be observed under dynamic shear. This is a considerable milestone in the development of a diagnostic for platelet function and the transition towards personalised medicine.

REFERENCES

- 1: Lincoln B, Ricco AJ, et al. Anal Biochem 2010 10/15;405(2):174-183
- 2: Ton-That C, Shard AG, Bradley RH. Polymer 2002 8;43(18):4973-4977.

Targeted Gene Delivery into Peripheral Nervous System Mediated by Trimethyl Chitosan Nanoparticles

Carla Pereira Gomes^{1,2}, Aida Varela-Moreira^{1,3}, Maria Gomez-Lazaro¹, Michael Leitner⁴, Andreas Ebner⁵, Peter Hinterdorfer⁵, Ana Paula Pêgo^{1,2,6}

¹Instituto de Engenharia Biomédica, Universidade do Porto (U Porto), Portugal; ²Faculdade de Engenharia, U Porto, Portugal; ³Faculdade de Medicina, U Porto, Portugal; ⁴Center for Advanced Bioanalysis GmbH, Austria ⁵Institute of Biophysics, Johannes Kepler University, Austria; ⁶Instituto de Ciências Biomédica Abel Salazar, U Porto, Portugal; carla.gomes@ineb.up.pt

INTRODUCTION

In the present work the use of trimethyl chitosan (TMC), a partially quaternized chitosan (CH), is proposed for the development of a multi-component gene vector targeted to neurons of the peripheral nervous system. Contrary to CH, TMC has fixed positive charges and consequently it is soluble at wider pH range. This should allow the preparation of stable particles in physiological conditions, one of the major limitations of the use of CH as a gene delivery vector^{1,2}. Finally, we used molecular recognition force spectroscopy (MRFS)³ to find the optimal ligand density in the functionalized nanoparticles that mediate maximal neuron cell-specific interaction.

EXPERIMENTAL METHODS

TMC (Mn=43 kDa, DA=11% and quaternization degree of 30%) was used to prepare TMC:DNA complexes. Unmodified CH was used as control. The resulting particles were characterized in terms of size and zeta potential, complexation (SybrGold assay) and transfection (FACS) efficiency. The internalization and intracellular localization of the particles was assessed by imaging flow cytometry (ImageStream^X, Amnis, Millipore) at different time-points (0.5 to 24h). TMC was further modified with thiol groups to prepare neuron-targeted nanoparticles. The 50 kDa non-toxic fragment of tetanus toxin (HC) was grafted to the binary complex via a bi-functional poly(ethylene glycol) (PEG) linker reactive for the thiol moieties in the polymer. For the MRFS experiments either HC or nanoparticles with different densities of HC were tethered to an atomic force microscopy (AFM) tip via flexible PEG linkers. Measurements were carried out using a PicoPlus (Agilent) AFM instrument in both neuronal and non-neuronal cell lines (control).

RESULTS AND DISCUSSION

TMC complexes present higher stability under physiological conditions than CH complexes, resulting in decreased average sizes, lower polydispersion and higher DNA condensation ability. Accordingly, the transfection efficiency of the TMC particles was 15-fold higher, in comparison to CH polyplexes. When assessing the internalization process, TMC nanoparticles were found to be more abundant in the cell cytoplasm at all time-points tested (Fig.1), while CH complexes, especially at the earlier time-points, were predominantly associated to the cell membrane. In this way, at the longest time-point tested, the overall cellular uptake was 16-fold higher for TMC nanoparticles. The amount of vesicle-loaded nanoparticles per cell was also higher for TMC complexes. Moreover, after 2 h of incubation, DNA vectorized within TMC nanoparticles present higher co-

localization with cell nuclei. When taking into account the population of cells that internalized the nanoparticles, it seems at earlier time-points that for the nanoparticles based on CH a higher % of DNA in relation to the total internalized co-localizes with cell nuclei. This result is probably due to their instability in the physiological milieu (SybrGold assay). However, the total amount of DNA present in cells was always lower for CH nanoparticles, since they were less internalized (Table I).

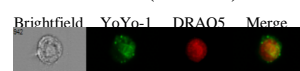


Fig. 1. Representative image acquired on ImageStream^X.

Table I. Percentage of YoYo⁺ cells at 2h. N/C (nucleus/cytoplasm).

	Cytoplasm	Nucleus	N/C (%)
CH	4.7 ± 1.3	0.3 ± 0.1	6.3 ± 0.2
TMC	77.0 ± 2.6	2.8 ± 0.6	3.6 ± 0.3

The uptake of the targeted nanoparticles significantly decreased in non-neuronal cell lines, indicating an increased specificity to neuronal cells. In order to maximize the targeting potential of the nanoparticles, MRFS studies are being conducted. The results obtained so far confirm the interaction between HC and its receptors on neuronal cells, with a binding probability (BP) of 16.5. Both the blocking of neuronal cells with free HC or the measurement in non-neuronal cells resulted in a significant drop of the BP, confirming the specificity of the interaction (Fig. 2).

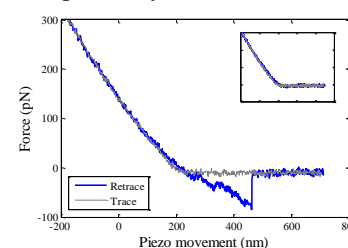


Fig. 2. AFM force-distance cycle curves. A single molecular unbinding event at 80 pN binding force between HC and ND7/23 cells. The inset shows a force-distance cycle measured after receptors blocking.

Similar experiments are now undergoing, using tips bearing nanoparticles with different densities of HC. One expects to extrapolate from the BP of the different formulations the nanoparticle gene-vectoring capacity.

CONCLUSION

The fixed positive charges on TMC facilitated their association with DNA in physiological conditions, yielding more stable particles. This resulted in higher internalization levels and DNA vectoring to the nucleus, resulting in a more efficient transfection of cells. Moreover, the functionalized particles presented an increased specificity towards the neuronal population.

REFERENCES

- Gomes CP *et al.*, MRS Bulletin. 39:60-70, 2014; 2. Zhao X, *et al.*, J Control Release (2010), 144: 46-54; 3. Oliveira H *et al.*, Small. 7:1236-1241, (2011)

ACKNOWLEDGMENTS FCT grants PTDC/CTM-NAN/115124/2009 and SFRH/BD/79930/2011.



Nanoscale neuroelectrode modification through self-assembly of block copolymers

Parvaneh Mokarian-Tabari^{1,2}, Catalina Vallejo-Giraldo³, Marc Fernandez-Yague³, Cian Cummins¹, Michael A. Morris^{1,2} and Manus J.P. Biggs³

¹ Department of Chemistry, University College Cork and Tyndall National Institute, Cork, Ireland.

² Centre for Research on Adaptive Nanostructures and Nanodevices (CRANN), Trinity College Dublin, Dublin, Ireland.

³ Network of Excellence for Functional Biomaterials (NFB), National University of Ireland, Galway, Ireland

manus.biggs@nuigalway.ie

INTRODUCTION

Neuroelectrodes are susceptible to deterioration via scar encapsulation following implantation. "Intelligent nanosurfaces" which mimic the biological length scale may prevent this deterioration via the modulation of protein adsorption and cell adhesion. Nanotopography may significantly enhance electrode performance via enhanced charge transfer.

Here we describe a self-assembly process for the production of aligned and dense arrays of silicon nanopillars using block copolymers. We discuss the effect of the surface modifications on cell-substrate interaction in vitro and how they may enhance electrode charge transfer and improve neuron/electrode integration.

EXPERIMENTAL METHODS

Polystyrene-*b*-ethylene oxide (PS-*b*-PEO) diblock copolymer was dissolved in 1 wt% toluene. The thin film was formed by spin cast and annealed at 50 °C exposed to toluene/water (1:1). The film was immersed at 40°C for 15h to obtain activated film. Different concentration iron (III) nitrate nonahydrate was dissolved and UV/Ozone treatment was used to oxidize the precursor and remove polymer. Surface morphologies were imaged by scanning probe microscopy in tapping mode and scanning electron microscopy. Electrochemical Impedance Spectroscopy was used to evaluate the charge transfer rate of the substrate. The effect of the surface modifications on cell-substrate interaction was carried by the culture of SH-5YSY neuroblastoma onto the surfaces and evaluating the metabolic activity (alamar blue®) for 1, 7 and 14 days.

RESULTS AND DISCUSSION



Figure 1. AFM topographic images of PS-*b*-PEO after annealing. The FFT image indicating a periodicity of 38 nm. b) After iron oxide inclusion to PEO (dark domains) to enhance the etch contrast. c) After UV/Ozone exposure to remove the matrix polymer (PS). The white domains are iron oxide arrays.

The resultant film is of regular thickness with no signs of de-wetting and is well-ordered across the entire substrate. The measured average centre-to-centre cylinder diameter is 47 ± 9 nm with a PEO cylinder height of 63 ± 20 nm and diameter of 23 ± 9 nm.

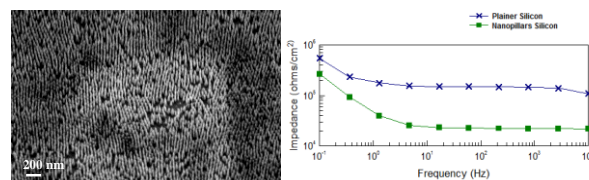


Figure 2. After pattern transfer to Si substrate following 10 s Si etch (C4F8/H2) + 90 s Si etch (C4F8/SF6) in ICP/RIE. b) Electrochemical impedance measurements. Si Nanopillar substrates were observed to reduce the electrical impedance relative to Plainer Silicon substrates ($n=3$).

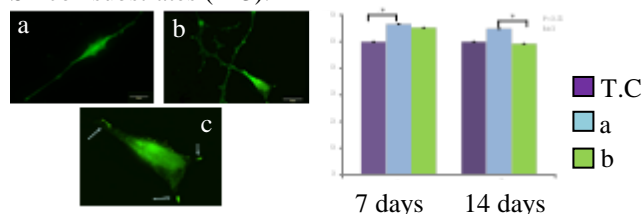


Figure 3. Neurospecific differentiation was achieved up to period of seven days in culture a) Plainer Silicon b) Nanopillars Silicon c) Magnified image showing focal adhesions (white arrows). Results of % of cell growth indicate SH-5YSY cells adhere and proliferate on Nanopillars Si Silicon Substrates (T.C: Tissue Culture)

CONCLUSION

We have fabricated sub-20 nm pillar features in silicon using a block copolymer mask technique. The impedance of the plainer and nanopillars silicon substrates was evaluated showing a remarkable reduction in the impedance magnitude when the nanopillars were present.

In addition, the adhesion and proliferation of SH-5YSY cells on the substrates was assessed resulting in a viable cell growth on the nanopillars silicon substrates as well as the plainer silicon. Furthermore, preliminary results indicate that neurospecific phenotype was maintained and focal adhesion formation induced on control and experimental substrates up to seven days in culture.

REFERENCES

1. Ghoshal. *et al.*, Adv.Mater. 24:2390-2397, 2012

ACKNOWLEDGMENTS

The authors would like to acknowledge CRANN and Science Foundation Ireland (SFI) for funding through SFI-CSET CRANN. Also Advance Microscopy Laboratory (AML) / CRANN for the collaborations. Bell Labs Ireland thanks the Industrial Development Agency (IDA) Ireland for their financial support. M.J. Biggs is an SFI SIRG fellow, grant no .11/SIRG/B2135".

Stimulation of angiogenesis by growth factor-free porous adhesive films made by hexanoyl group modified gelatin

Keiko Yoshizawa¹, Temmei Ito, Ryo Mizuta and Tetsushi Taguchi^{1,2}

¹ Graduate School of Pure and Applied Science, University of Tsukuba, Japan

² Biomaterials Unit, Nano-life field, International Center for Materials Nanoarchitectonics (MANA), National Institute for Materials Science (NIMS), Japan, TAGUCHI.Tetsushi@nims.go.jp

INTRODUCTION

To close the wound, some kinds of tissue adhesives have been developed to shorten surgical operation time. However, these adhesives still have some disadvantages on the bonding strength and biocompatibility. Especially for the bonding strength, adhesive bonded with soft tissues is exposed in quite adverse environment, because about 70 % of our body is made up with water, and body fluids spill out during surgery. To solve these obstacles, the molecular design of tissue adhesives which can bond moisture-containing tissues has been required. We developed hydrophobically modified gelatin (hm-Gltn)-based injectable adhesive and clarified that hm-Gltn adhesive with low modification ratio strongly bonded porcine arterial media compared with original Gltn-based ones¹⁻⁵. We also found that the flat films fabricated with hm-alkali treated-Gltn (hm-AlGltn) bonded strongly onto soft tissues. The results suggested that porous films composed by hm-Gltn will also bond soft tissues strongly. On the other hand, it is well-known that porous materials composed of naturally-derived polymers, synthetic polymers and their composites can work as scaffolds for tissue regeneration. Based on those backgrounds, porous films were fabricated with hexanoyl (Hx: C₆) group modified AlGltn (HxAlGltn) by salt leaching method, and the bonding ability, fibroblast viability, and biocompatibility of the porous films were compared.

EXPERIMENTAL METHODS

HxAlGltn was obtained by reaction between Hx chloride and amino group of AlGltn (Figure 1). The modification ratio of HxAlGltn was determined using 2,4,6-trinitrobenzoic acid (TNBS). For the preparation of porous films, HxAlGltn was dissolved in 10 % lactic acid/ dimethyl sulfoxide (DMSO) and mixed with various amount of NaCl. Trisuccinimidyl citrate (TSC) was then added to crosslink HxAlGltn followed by immersion in cold water to dissolve NaCl and to remove by-product such as N-hydroxysuccinimide and then freeze-dried to fabricate porous HxAlGltn films ((P)HxAlGltns). Porous AlGltn films ((P)AlGltns) were also fabricated by similar protocol. Porosity, bulk strength, bonding strength onto porcine intestine, L929 cell viability and biocompatibility of the porous films were evaluated.

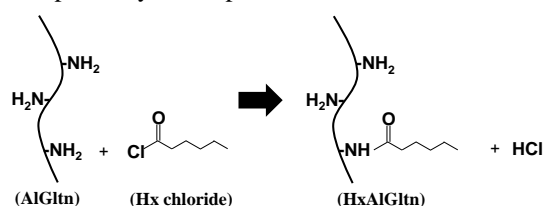


Figure 1. Reaction of Hx chloride to amino group on AlGltn molecule to obtain HxAlGltn.

RESULTS AND DISCUSSION

Amino groups of AlGltn were successfully modified with Hx groups. From the determination of residual amino groups in AlGltn by TNBS method, 27% of amino groups in AlGltn were reacted with Hx chloride (27HxAlGltn). Using 27HxAlGltn, (P)HxAlGltns those porosities were ranging from 1 to 65% were successfully obtained as shown in Figure 2. The porosities of (P)AlGltns and (P)HxAlGltns were proportional to the amounts of NaCl in those initial mixture solutions. Also, both (P)AlGltn and (P)HxAlGltn films with high porosity showed good water absorbency. From the mechanical/ adhesive strength measurement, it was clarified that (P)HxAlGltns were weak in bulk stiffness compared with (P)AlGltns, however, each (P)HxAlGltn film bonded with porcine intestine three times stronger compared with (P)AlGltn films. On the other hand, proliferation of L929 cells on (P)HxAlGltns was superior to (P)AlGltns with any porosities. Immunostaining after rat-subcutaneous implantation of porous films revealed that much CD34 marker and von Willebrand factor were expressed around the (P)HxAlGltn films indicating that (P)HxAlGltn film facilitated angiogenesis compared with (P)AlGltn.

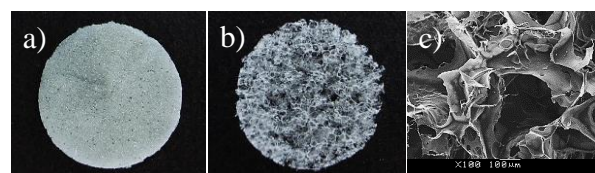


Figure 2. Macro/ micro images of (P)HxAlGltns fabricated without (a) or with (b, c) NaCl. The diameters of the discs were 1 cm.

CONCLUSION

(P)HxAlGltns were fabricated by salt leaching method. Compared with (P)AlGltns, (P)HxAlGltns were superior in bonding with porcine intestine, L929 cell viability and angiogenesis in rat subcutaneous tissue. These results suggested that (P)HxAlGltn can work as an adhesive material as well as a scaffold for tissue regeneration.

REFERENCES

1. Matsuda M. *et al.*, J. Bioact. Compat. Polym. 27:31-44, 2012
2. Matsuda M. *et al.*, Colloid Surf. B., 91:48-56 2012
3. Matsuda M. *et al.*, J. Bioact. Compat. Polym. 27:481-498, 2012
4. Matsuda M. *et al.*, Sci. Technol. Adv. Mater. 13:064212, 2012
5. Yoshizawa K. and Taguchi T., Int. J. Mol. Sci. 15:2142-2156, 2014

ACKNOWLEDGMENTS

The authors would like to thank the JSPS Programme (Grant no: 25·357) for providing financial support to this project.



Development of PLLA/BTO Nanofiber Sheet for Bone Tissue Engineering

A. Yamano¹, Y. Morita² and E. Nakamachi²

¹ Graduate School of Life and Medical Sciences, Doshisha University, Japan

² Faculty of Life and Medical Sciences, Doshisha University, Japan, ymorita@mail.doshisha.ac.jp

INTRODUCTION

Scaffold for bone regeneration requires suitable structure for cell adhesion, cell proliferation and early bone formation. In this study, we fabricated biocompatible and biodegradable poly-L-lactic acid (PLLA) nanofiber sheet that mimic nanostructure of natural bone to enhance cell adhesion and cell proliferation by an electrospinning method. Electrical properties of bone are closely related to activity of bone cells and bone formation. Therefore, it is expected that stimulation of surface potential generated on the nanofibers promote cell proliferation and bone formation by adding a piezoelectric material into the nanofibers. We used BaTiO₃ (BTO) nanoparticle which is a ferroelectric material and is a lead-free material. The purpose of this study was to develop PLLA/BTO nanofiber sheet for bone tissue engineering.

EXPERIMENTAL METHODS

Electrospinning condition optimization: Mixed solvent of 1,1,1,3,3,3-hexafluoroisopropanol and 1,3-dioxolane were used to PLLA into 10 and 12 w/v% solution at room temperature. The PLLA solution was electrospun on a copper plate target to fabricate nanofiber sheet. The flow rate is 32, 96 and 159 $\mu\text{L}/\text{min}$. The surface morphology of PLLA nanofiber sheet was observed by a scanning electron microscope (SEM).

Fabrication of PLLA/BTO nanofiber sheet: PLLA and BTO nanoparticles were dissolved in the mixed solvent. Concentration of solution were 10 and 12 w/v% and PLLA/BTO ratio were 1/0, 16/1 and 6/1. PLLA/BTO solution was electrospun on a copper plate target to fabricate nanofiber sheet at the optimum spinning condition. The surface morphology of PLLA/BTO nanofiber sheet was observed by SEM. Distribution of BTO nanoparticle in the nanofiber was observed by a transmission electron microscope (TEM). Osteoblast-like cell (MC3T3-E1) were seeded at density 1.0×10^4 cells/cm² on each nanofiber sheet and cultured for 15 days to investigate cytotoxic of BTO nanoparticles.

RESULTS AND DISCUSSION

Table.1 shows the fiber diameter of the PLLA fiber. The diameters of fiber obtained from 10 w/v% solution were lower than those obtained from 12 w/v% solution under all flow rates. Though the diameters of fibers obtained from 10 w/v% solution were less than 1 μm at all flow rates, beads were observed in nanofibers at the flow rates of 96 and 159 $\mu\text{L}/\text{min}$ as shown in Fig.1. Therefore, solution concentration of 10 w/v% and the flow rate of 32 $\mu\text{L}/\text{min}$ were obtained as optimum condition. Figure.2 shows the SEM images of PLLA/BTO nanofiber sheet fabricated under the optimum condition. The fiber diameter of PLLA/BTO

(1/0), PLLA/BTO(16/1) and PLLA/BTO(6/1) nanofiber sheets were 601 ± 180 , 617 ± 172 and 573 ± 141 nm respectively, and there were no significant differences among all PLLA/BTO nanofiber sheets. Addition of BTO nanoparticles did not affect to the fiber diameter. According to TEM observation, BTO nanoparticles were dispersed uniformly in both PLLA/BTO nanofibers, and the density of BTO nanoparticle in PLLA/BTO(6/1) nanofiber was higher than that in PLLA/BTO(16/1) nanofiber. Since DNA amount and ALP activity of MC3T3-E1 increased with cultivation days for all nanofiber sheets, and PLLA/BTO nanofiber sheet had no cytotoxicity.

CONCLUSION

PLLA nanofiber sheet with uniformly dispersed BTO nanoparticles was developed in this study. PLLA/BTO nanofiber sheet had biocompatibility for cell culture.

Table.1 The fiber diameter of the PLLA nanofiber.

	32 $\mu\text{L}/\text{min}$	96 $\mu\text{L}/\text{min}$	159 $\mu\text{L}/\text{min}$
10 w/v%	629 ± 211 nm	659 ± 302 nm	728 ± 306 nm
12 w/v%	1016 ± 241 nm	972 ± 265 nm	1360 ± 374 nm

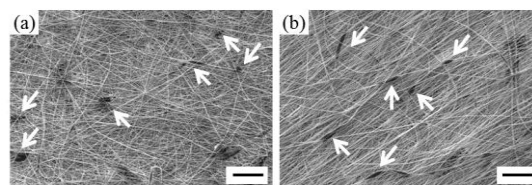


Fig. 1 SEM images of the PLLA nanofiber sheet at solution concentration of 10 w/v% (Bar: 50 μm , $\times 300$). (a) flow rate: 96 $\mu\text{L}/\text{min}$. (b) flow rate: 159 $\mu\text{L}/\text{min}$.

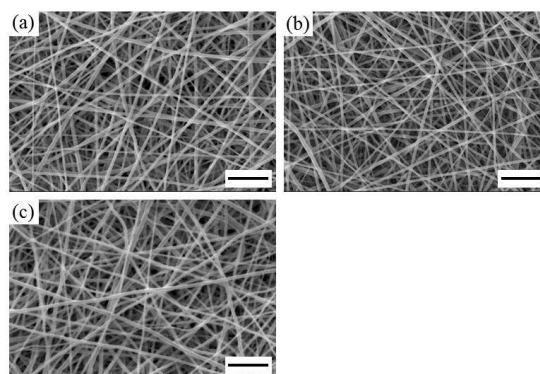


Fig. 2 SEM images of the nanofiber sheet (Bar: 10 μm , $\times 2000$). (a) PLLA/BTO(1/0). (b) PLLA/BTO(16/1). (c) PLLA/BTO(6/1).

ACKNOWLEDGMENTS

This work was supported by JSPS KAKENHI Grant Number 24560114. PLLA was gifted from TEIJIN. BTO was gifted from Murata manufacturing.



Preparation and Characterization of PHBV Porous Nanofibers

Lan-Xin Lyu^{1,2}, Ning-Ping Huang¹, and Ying Yang^{2*}

¹ State Key Laboratory of Bioelectronics, Southeast University, China

^{2*} Institute for Science and Technology in Medicine, School of Medicine, Keele University, UK, y.yang@keele.ac.uk

INTRODUCTION

Scaffolds with high surface area to volume ratio have attracted much attention when used for filtration industry, drug delivery system, sensor, and tissue engineering¹. Electrospun technology can generate nanofibrous scaffolds with high surface area to volume ratio. While, the surface of fibers fabricated via electrospinning is smooth, typically. Nanofibers with porous surfaces can make more advantages for their variety of applications. Phase separation and leaching method can generate porous fibers with high porosity². The aim of this research is to generate high porous poly(3-hydroxybutyrate-co-3-hydroxyvalerate) (PHBV) nanofibrous scaffolds through leaching hydro-soluble polyethylene oxide (PEO). The application of the porous scaffolds in bone regeneration has been explored.

EXPERIMENTAL METHODS

Electrospinning method was chosen to fabricate PHBV/PEO composite nanofibers. The procedures are as follows: 2% PHBV and PEO blend solution with different weight ratio (PHBV:PEO = 9:1, 8:2, 7:3, 6:4, 5:5) was made using 2, 2, 2-trifluoroethanol (TFE), which was fed into one syringe with 6# needle and continually driven by an advancing pump at a speed of 5 mL per hour. A 12 kV high DC voltage was applied between the metal needle and the collector at a distance of 30 cm. Films of the blends with the same ratio above were prepared by spin coating method.

Obtained five kinds of nanofibers and films were immersed in simulated body fluid (SBF) for 4 weeks and SBF was changed every 3 days. Four weeks later, SEM was used to observe the morphology of samples' surfaces and porosity of them was calculated using ImageJ software. Results are presented as mean \pm standard deviation from 10 counts for each kind of nanofibers. Weight loss of nanofibers samples was tested at the time points of 0, 2, and 4 weeks. Viability of bone marrow-derived mesenchymal stem cells (MSCs) cultured on nanofibrous surface was measured by Cell Counting Kit-8 (CCK-8, Dojindo, Japan) according to the manufacture's protocol. Six parallel repeats were tested for each sample. Morphology of MSCs on nanofibrous surface was observed by SEM.

RESULTS AND DISCUSSION

Porous PHBV nanofibers were obtained through immersing PHBV/PEO composite nanofibers into SBF for a certain period of time. From SEM images, it can be found that the morphology and diameters of fibers has changed rarely with the increasing of PEO. However, the surface of fibers became porous from smooth and the weight of fibers meshes lost sharply in

the first two weeks and then gradually in the second two weeks after immersed in SBF (Fig.1). The porous percentage of PHBV fibers with different PEO ratio (30%, 40%, and 50%) was 3.13 ± 0.51 , 7.36 ± 1.6 , 10.75 ± 0.56 , respectively. Cellular response cultured on PHBV nanofibrous meshes before and after immersed in SBF has been measured by CCK-8 and SEM. From Fig.2, it can be found that MSCs' proliferation was slowed down when PEO ratio reached up to 50%. Porous surface of PHBV nanofibers after immersed in SBF can enhance cell proliferation.

These results imply that leaching method can generate porous nanofibers conveniently and porosity of fibers can be enhanced by increasing the weight percentage of PEO. Porous property of scaffolds can enhance cell viability.

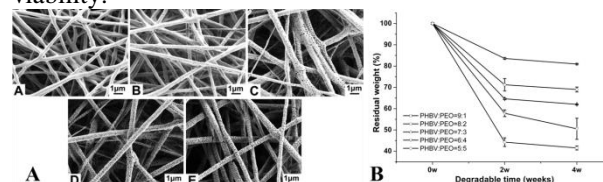


Figure 1 (A) SEM images of five kinds of PHBV fibers after immersed in SBF for 4 weeks. (A-E): PHBV:PEO = 9:1; 8:2; 7:3; 6:4; 5:5; (B) Residual weight of five kinds of PHBV fibers after immersed in SBF for 2 and 4 weeks

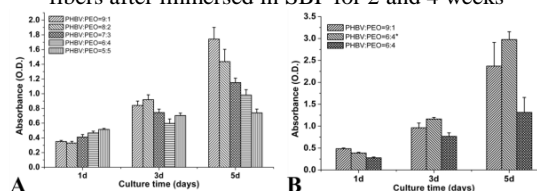


Figure 2 A: MSCs' viability on different PHBV scaffolds without SBF treatment after 1, 3 and 5 days of culture. B: MSCs' viability on different PHBV scaffolds in comparison to SBF treated scaffold denoted as *.

CONCLUSION

In this study, we have fabricated PHBV porous nanofibers through electrospun and leaching method. These obtained porous meshes can increase the adhesion and proliferation of MSCs and can be a good candidate for tissue engineering.

REFERENCES

1. Muhamad N. *et al.*, Polym. J. 39:1060-1064, 2007
2. Mehraban M. *et al.*, J. Appl. Polym. Sci. 1:12-13, 2013

ACKNOWLEDGMENTS

The authors would like to thank the National Science Foundation of China (Grant no: 30870626) and Marie Curie International Incoming Fellowship for providing financial support to this project.

Fabrication and Characterization of Carbon Nanotube Membranes for Neural Tissue Engineering

Sevde Altuntas¹, Buket Altınok², Belma Aslım², Fatih Büyükerin^{3*}

¹Micro and Nanotechnology Graduate Program, TOBB Univ. of Econ. & Technology, Ankara 06560, TR

²Department of Biology, Faculty of Science, Gazi University, Ankara 06500, TR

³Department of Biomedical Engineering, TOBB Univ. of Econ. & Technology, Ankara 06560, TR, fbuyukserin@etu.edu.tr

INTRODUCTION

Nanoporous anodized aluminum oxide (AAO) films are a unique class of biomaterials that can be synthesized by anodization of high purity aluminium.^{1,2} In addition to the native structure's topographic and chemical control advantages,¹ these membranes can also be coated with a conductive layer, and hence present electrical, topographic and chemical cues for the modulation of cell-material interactions. In this study we have utilized carbon (C) sputtering onto AAO films to create conductive C nanotube membranes (CNM) which were characterized by electrical, morphological and chemical characterization tools. Substantial neuron proliferation and adhesion was observed for bare AAO, collagen-coated AAO and collagen-coated CNM substrates compared with collagen-treated microplate controls. The CNM characterization studies and cellular data involving viability, adhesion and neurite growth on AAO and CNM will be presented.

EXPERIMENTAL METHODS

AAO films with 300 and 100 nm pores were produced by the two step anodization method² and coated with 10 nm C layer by a GATAN Precision Etching & Coating System. The fabricated CNMs were characterized by AFM, SEM, XPS, Ellipsometer and I-V measurements. PC 12 cell line (American Tissue Culture Collection) was used for cellular studies after they have been differentiated to the neuronal phenotype by the application of neuron growth factor (NGF 2,5S). A WST-1 kit was used to extract cell viability data of one week incubated PC-12 cells under appropriate cell culture conditions. Cell adhesion and neurite growth comparison was conducted by optical microscopy images after the cells were incubated on the AAO and CNM substrates, fixed and then stained with trypan blue.

RESULTS AND DISCUSSION

AAO and CNM substrates were characterized with SEM and AFM micrographs. Fig.1a illustrates AFM image of a CNM membrane showing nanoporous structure of the substrate. Fig. 1b is a depth profile obtained across a linear region on Fig 1a. It demonstrates that the pores are open after C deposition. The presence of this conductive C layer was further confirmed by ellipsometer, XPS, conductive AFM and I-V measurements and they will be presented.

Fig. 2a depicts cell viability data of PC 12 cells incubated on CNM membranes. It illustrates the enhanced cell proliferation obtained on the collagen-coated CNM. Similar results were also obtained from naked and collagen-coated AAO substrates.

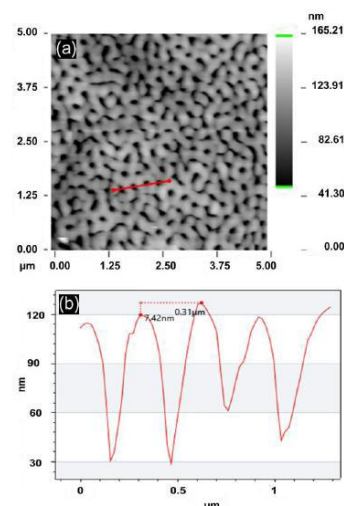


Fig. 1. AFM image of a CNM substrate (a), and depth profile (b) across a line in the AFM image.

Fig 2b. is a representative optical image of stained PC 12 cells displaying the neurites formed on the CNM substrates. Preliminary results dictate that the AAO and CNM substrates enhance cell adhesion compared to controls.

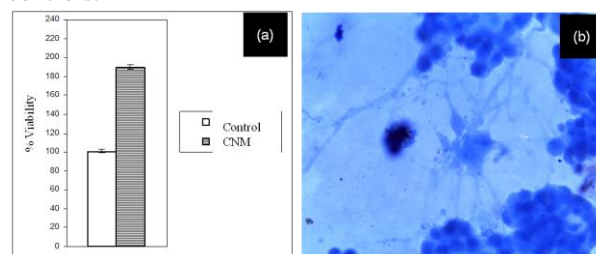


Fig 2. a) Cell viability for CNM, b) Micrographs of neurites on CNM (Pore diameter= 300 nm).

CONCLUSION

Conductive CNM substrates were prepared by using AAO templates. After extensive characterization, the neuronal behavior against both AAO and CNM were investigated which were quite promising with increased cellular proliferation and adhesion. Current efforts are comparison of neurite formation for different substrates and under the application of electric field to CNMs.

REFERENCES

1. Voelcker NH. *et al.*, Prog. Mater. Sci. 58:636, 2013
2. Fukuda K.. *et al.*, Science. 268:1466, 1995

ACKNOWLEDGMENTS

"This work was supported by The Scientific and Technological Research Council of Turkey, Grant No. MAG-111M686."

A Degradable Chitosan-graft-poly(ϵ -Caprolactone) Copolymeric Biomaterial Supports the Growth of Wharton's Jelly Mesenchymal Stem Cells for Soft Tissue Engineering

Amalia Skarmoutsou¹, Costas Charitidis¹, Maria Kaliva², Charalampos Pontikoglou⁴,
Maria Vamvakaki^{2,3}, Maria Chatzinikolaidou^{2,3}

¹ School of Chemical Engineering, National Technical University of Athens, Greece

² Dept. of Materials Science and Technology, University of Crete, Greece

³ Institute of Electronic Structure and Laser (IESL), Foundation for Research and Technology Hellas (FORTH), Greece

⁴ School of Medicine, Haematology Laboratory, University of Crete, Greece, mchatzin@materials.uoc.gr

INTRODUCTION

In tissue engineering the development of optimized scaffolds that promote cell growth and tissue development is crucial. The synthesized biomaterial-scaffolds should provide the appropriate mechanical and biochemical features to facilitate cell attachment, proliferation and differentiation. In the present study we investigated the physicochemical and nanomechanical properties of chitosan, poly(ϵ -caprolactone) and the chitosan-graft-poly(ϵ -caprolactone) copolymer as synthesized and after subjected in degradation process for three and four weeks. Furthermore, we investigated the growth of Wharton's jelly (WJ) mesenchymal stem cells (MSCs) onto these materials.

EXPERIMENTAL METHODS

We synthesized poly(ϵ -caprolactone) functionalized with a terminal carboxylic acid group and chemically grafted it to a chitosan backbone. The graft copolymer was analyzed by ATR-FTIR, ¹H NMR, SEM, and contact angle measurements [1]. For the in vitro study we used passages 1-4 of WJ-MSCs. We isolated Wharton's jelly mesenchymal stem cells from the inner lining of human umbilical cords of physiological labors from informed and consented women, immunophenotypically characterized them, and cultured them for different time periods on the grafted copolymer. We investigated cell morphology by confocal fluorescence microscopy and SEM. For the quantification of cell proliferation we used the PrestoBlue assay [2].

We fabricated two types of samples, thin films on glass substrates, and bulky discoid samples, both for the mechanical and biological testing.

RESULTS AND DISCUSSION

We measured hardness and Young's modulus values, as well as the time-dependent and viscous behavior of the as prepared samples. Furthermore, we introduced corrections on the measured modulus values in order to investigate the effect of viscoelasticity on the measured values calculated by the Oliver & Pharr model. We observed that the grafted copolymer has reduced nanomechanical properties compared to pure chitosan and poly(ϵ -caprolactone), with time-dependent and viscous behavior, attributed to the poly(ϵ -caprolactone) and the poor connectivity of the two compounds. Submersion of the poly(ϵ -caprolactone) and the grafted copolymer in α -MEM cell culture medium indicated

deterioration of the measured mechanical properties, as a result of the samples' degradation. However, after three weeks of degradation, resulting in a 35% weight loss, the grafted copolymer presented sufficient mechanical stability and elastic properties close to the ones reported for soft tissues. Additionally, we seeded Wharton's jelly mesenchymal stem cells onto the copolymeric discoids, and observed a cell proliferation increase after three and seven days in culture.

While the grafted copolymer degrades after 4 weeks in vitro, the developed WJ cell sheets support dense tissue formation as observed from the scanning electron microscopy images and the elevated values of ECM collagen production.

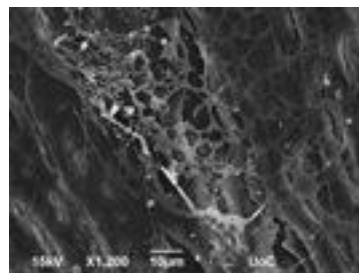


Figure 1 shows a strong tissue formation after four weeks, while the grafted copolymer degrades.

CONCLUSION

The present work shows the successful development of graft copolymeric discs, which demonstrate a strong cell adhesion and growth of WJ MSCs, together with mechanical properties similar to those of soft tissues. These results establish the basis for the potential use of this cell-material combination in soft tissue regeneration. Ongoing investigations on the differentiation of WJ MSCs may support this hypothesis.

REFERENCES

1. Chatzinikolaidou M. *et al.*, Current Pharm Design 20:000, 2014
2. Terzaki K. *et al.*, JBMR-A 101A(8):2283-2294, 2013

ACKNOWLEDGMENTS

The authors thank the General Secretariat for Research and Technology Grants Thales-MIS No. 380278 and Aristeia II No. 3438 for providing financial support to this project.

Application of Natural BMP Modulators on Bone Tissue Engineering

Guo-Chung Dong^{1,2,3*} and Chun-Hsu Yao⁴

^{1*}Institute of Biomedical Engineering and Nanomedicine, National Health Research Institutes, Taiwan,
gcdong@nhri.org.tw

²Ph.D. Program in Tissue Engineering and Regenerative Medicine, National Chung Hsing University, Taiwan

³Graduate Program of Biotechnology in Medicine, National Tsing Hua University, Taiwan

⁴Department of Biomedical Imaging and Radiological Science, China Medical University, Taiwan

Abstract

The purpose of this study is to search natural BMP modulators from TCM and applied it to control stem cell growth for bone formation. After screening from 60 of TCMs by using a surface plasmon resonance system, a potential TCM, *Gu-Sui-Bu*, was selected. *In-vitro* and *in-vivo* studies showed that GSB and *Naringin* could be good natural BMP regulators for bone tissue engineering.

INTRODUCTION

Bone morphogenetic protein (BMP) is a significant growth factor for bone regeneration. In stem cell studies, some research shows that BMP binding with different BMP receptor (BMPR-1A and BMPR-1B) will induce cell to different differentiation. Therefore, BMP is widely used in bone tissue engineering.^{1,2} Unfortunately, BMP binding is so hard to control that BMP still cannot be applied in clinical. Traditional Chinese medicine (TCM) is a high potential matter to regulate BMP signaling.^{3,4} The purpose of this study is to search natural BMP modulators from TCM and applied it to control stem cell growth for bone formation.

EXPERIMENTAL METHODS

In this study, natural BMP modulators were screening from TCMs by using immobilized BMPR and surface plasmon resonance (SPR). Selective TCMs were assessed in BMP signal pathway. Furthermore, TCM and potential compound, *Naringin* were incorporated respectively into gelatin composite (GHG) to form TCM-contained scaffolds. Physical and chemical properties of these scaffolds were analyzed by SEM and HPLC. Finally, these scaffolds were co-cultured with rabbit mesenchymal stem cells in vitro and were implanted into rabbit calvarial defect for bone repair assessment.

RESULTS AND DISCUSSION

Results show that some TCMs affect the binding of BMP and BMPR in SPR experiments. Among these, GSB is a subtle BMP modulator to inhibit the binding of BMP-2 with BMPR-1A and enhance the binding with BMPR-1B simultaneously. Otherwise, the marker compound in GSB, *Naringin*, was assessed by SPR and also showed the inhibition for BMPR-1A binding. More detail information about the mechanism of GSB in BMP signal pathway performed by monitoring phosphorylation of down-stream signals, SMAD proved

that GSB direct stem cell differentiation through inhibiting BMPR-1A signaling. As applying GSB on bone tissue engineering, GSB exhibit higher capacity to slow be released from scaffold and then promote bone formation via osteo-induction. Finally, GHG scaffold and *Naringin*-GHG scaffold were implanted into rabbit calvarial defects respectively. After 4 weeks, rabbits were sacrificed and bone regeneration in the defect were assessed. The defect containing *Naringin* scaffold showed better bone repair in X-ray image and more new bone generated in the histologic section by H&E stain. These results indicates that *Naringin* enhances bone regeneration in vivo. Combining with the results of SPR and Western blotting experiments, *Naringin* caused better bone regeneration results from BMPR-1A signaling block and BMPR-1B signaling directs cells to osteogenesis.

CONCLUSION

In this study, GSB and its marker compound (*Naringin*) can inhibit the binding of BMP-2 and BMPR-1A to control cell differentiation. Furthermore, this binding disturbance blocks BMPR-1A signaling and leads BMPR-1B signaling for osteogenesis. In order to prove this hypothesis, *Naringin* was incorporated into GHG composite to form TCM-contained scaffold for bone tissue engineering. In animal experiment, the bone defect implanted *Naringin* scaffold showed better bone repair and more new bone generated. According to these results, GSB and *Naringin* could be good natural BMP regulators for bone tissue engineering.

REFERENCES

1. Wong W.K. *et al.*, *Biomater.* 27:1824-1831, 2006
2. Chen K.Y. *et al.*, *J. Biomed. Mat. Res. A.* 101(4):954-962, 2012
3. Zhang P. *et al.*, *Eur. J. Pharmacol.* 607(1-3):1-5, 2009
4. Chen K.Y. *et al.*, *Evid. Based Complement Alternat Med.* 283941, 2013

ACKNOWLEDGMENTS

This project was supported by National Health Research Institutes, Taiwan (Grant no: 01A1-MEPP09-014). We would like to thank Dr. Ming-Chao Lin for providing C₂C₁₂ cell line and the Taiwan Mouse Clinic for X-ray image experiment.



Substrate-Mediated Nanoparticle/Gene Delivery to MSC Spheroids and the Applications in Peripheral Nerve Regeneration

Ting-Chen Tseng¹ and Shan-hui Hsu^{1, 2*}

¹Institute of Polymer Science and Engineering, National Taiwan University, Taipei, Taiwan

^{2*}Research Center for Developmental Biology and Regenerative Medicine, National Taiwan University, Taipei, Taiwan
d00549001@ntu.edu.tw

INTRODUCTION

Peripheral nerve injuries are often caused by trauma and may result in a partial or complete loss of motor and sensory functions. Cell transplantation with a nerve conduit is one of the therapeutic approaches. Recent studies revealed that a proper biomaterial substrate such as chitosan may drive the self-assembly of MSCs to form three-dimensional (3D) MSC spheroids¹. These substrate-derived MSC spheroids showed better self-renewal properties, differentiation capacity, and engrafting potential. Our previous study has also shown that nanoparticles (NPs) or genes can be delivered to MSCs during spheroid formation on chitosan-based substrates². The repairing capacities of these substrate-derived spheroids and advantages of simultaneous NP/gene delivery have not been verified *in vivo*. In this study, the effect of substrate-derived MSC spheroids vs. single cells on peripheral nerve regeneration was investigated.

EXPERIMENTAL METHODS

MSCs were labeled with superparamagnetic Fe₃O₄ NPs or transfected with brain-derived neurotrophic factor (BDNF) gene by the substrate-mediated NP/gene uptake. MSCs were combined with a polymeric nerve conduit to bridge a 10 mm transection gap of rat sciatic nerve. The transplantation of Fe₃O₄ NP-labeled MSC single cells or spheroids was tracked by high-resolution (7-Tesla) magnetic resonance imaging (MRI) *in vivo*. The regeneration capacity of MSC single cells, spheroids, or BDNF-transfected spheroids was assessed by functional recovery and histology after 31 days of implantation.

RESULTS AND DISCUSSION

Fe₃O₄ NP-labeled MSC single cells or spheroids in the conduits were successfully tracked by MRI *in vivo*, especially for MSC spheroids. Animals receiving BDNF-transfected MSC spheroids demonstrated the shortest gap bridging time (< 21 days) and the largest regenerated nerve at 31 days (Figure 1).

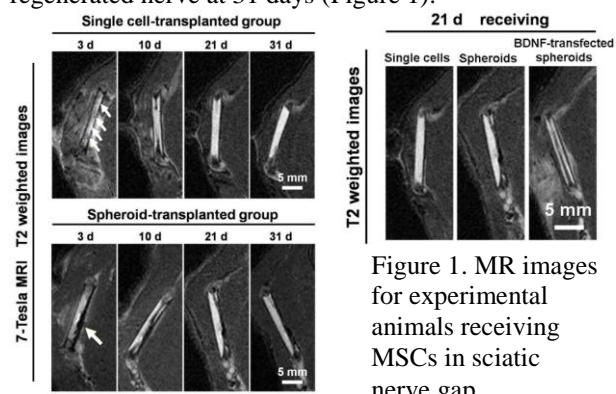


Figure 1. MR images for experimental animals receiving MSCs in sciatic nerve gap.

Compared to MSC single cells, the pristine or BDNF-transfected MSC spheroids significantly promoted the functional recovery of animals. The transplanted MSCs were incorporated in the regenerated nerve and differentiated into non-myelinating Schwann cells after 31 days.

Very early formation of fibrin cable (~ 10 days) and recruitment of MSCs along the cable were visualized for the sciatic nerve gap receiving MSC spheroids in a conduit. The gene modulation associated with neural development, neurotrophic factor, and chemokine receptor expressions may account for the observation and peripheral nerve regeneration. High-resolution MRI tracking of Fe₃O₄ NP-labeled cells offers useful information regarding how MSCs migrate during peripheral nerve regeneration.

CONCLUSION

When combined with a polymeric nerve conduit to bridge the transection gap of rat sciatic nerve, MSC spheroids (especially for BDNF-transfected MSC spheroids) were more conducive to nerve regeneration in comparison with MSC single cells. Animals receiving MSC spheroids or BDNF-transfected MSC spheroids showed significant functional recovery. The transplanted MSCs were differentiated into non-myelinating Schwann cells in the regenerated nerve after 31 days. The substrate-mediated Fe₃O₄ NP labeling for MSCs may be generally used as a bioimaging tool in animal studies. The substrate-mediated gene/NP delivery may equip MSC spheroids with extra values in carrying the therapeutic/diagnostic agents for cell-based therapy.

REFERENCES

1. Huang GS. *et al.*, Biomaterials 32:6929-45, 2011
2. Hsu SH. *et al.*, Biomaterials 33:3639-50, 2012

ACKNOWLEDGMENTS

This work was supported by the Program for Stem Cell and Regenerative Medicine Frontier Research (NSC102-2811-B-002-030) sponsored by the Ministry of Science and Technology, Taiwan, R.O.C. We are obliged to the Animal 7-Tesla MRI Core Lab of the Neurobiology and Cognitive Science Center, National Taiwan University, for technical and facility supports.



Influence of Inner Organization of Nerve Guide on Rat Bone Marrow Stem Cells (rBMSCs)

T.Dursun^{1,2}, D.Yücel^{1,4}, V.Hasırcı^{1,2,3}

¹BIOMATEN, METU Center of Excellence in Biomaterials and Tissue Engineering, Ankara, Turkey

METU, BIOMAT, Departments of ²Biotechnology, ³Biological Sciences, Ankara, Turkey

⁴Acıbadem University, School of Medicine, Department of Histology and Embryology, Istanbul, Turkey, tugbad@metu.edu.tr

INTRODUCTION

Age, diseases and trauma cause damages to the central nervous system which may even end up in the creation of gaps and inhibition of signal transfer [1]. Nerve guides are used to bridge these gaps in the treatment of spinal cord injury because the severed axons need to be reconnected during the healing process and the inner architecture of the nerve guides might be important in performing this function [2]. This study aimed to study the effect of organization of nanofibrous fillers on the growth and differentiation of rat bone marrow stem cells (rBMSCs) in vitro. For this purpose, two bilayer conduits, one consisting of aligned fibers and foam (AF-Fo), and the other, consisting of random fibers and foam (RF-Fo), were constructed and tested.

EXPERIMENTAL METHODS

The bilayer nerve guide model consisted of a fiber mat on a foam structure (Figure 1). The poly(3-hydroxybutyrate-co-3-hydroxyvalerate) (PHBV) foam was prepared by lyophilization. Aligned (AF) and randomly (RF) oriented PHBV/collagen (2:1) fiber mats were made by electrospinning directly on the PHBV foam. In situ biodegradation test was made in 10 mM PBS pH 7.4 at 37 °C. AF-Fo and RF-Fo nerve guides were seeded with rat bone marrow stromal cells (rBMSCs) and incubated with neural differentiation medium for 7 days. Cell behavior and differentiation to neural cells on these constructs was examined by SEM, fluorescence microscopy, flow cytometry, and neural specific enolase (NSE) ELISA kit.

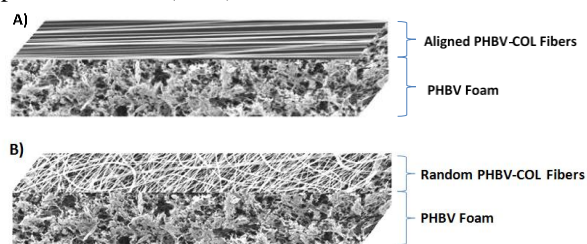


Figure 1. Bilayer constructs. (A) Aligned PHBV5/Collagen fibers on PHBV5 foam, and (B) random PHBV5/Collagen fibers on PHBV5 foam.

RESULTS AND DISCUSSION

Mercury porosimetry showed that porosity of the PHBV foam was 85%, and the pore sizes were in the range 5-200 nm. The porosity of random fibrous mat and the aligned fibrous mat were 59.7%, and 65%, respectively. These properties were quite suitable for cell growth. The fibers were without any beads and the fiber diameter was in the range of 200-650 nm. The average angle of deviation of the aligned fibers was 46.9 ± 7.3 . In situ biodegradation test revealed minimal weight loss in uncrosslinked guides in 28 days. Cell attachment and proliferation were found to be two times higher on the RF-Fo construct at the end of 7 days. On Day 2, the

cells on AF-Fo type of construct seem to have attached to the scaffolds in an aligned fashion, on Day 16, alignment of the cells became more apparent. While, the cells on the RF-Fo construct had no alignment on Days 2 and 16 as expected, they had grown on the construct in a random fashion (Figure 2).

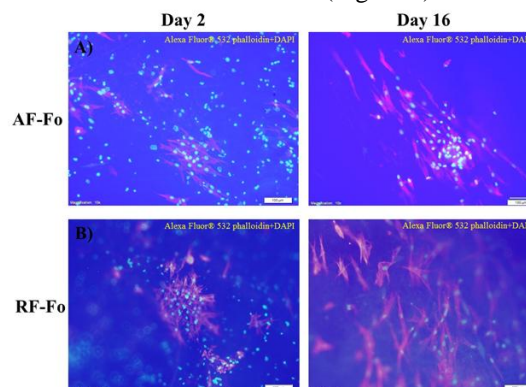


Figure 2. Fluorescence microscopy of (A) aligned fiber-foam (AF-Fo), and (B) random fiber-foam (RF-Fo) constructs of after Days 2 and 16 of cell culture.

Differentiation of BMSCs was studied with flow cytometry, NSE Elisa kit and immunostaining. It was seen that NSE levels increased in the rBMSC on both AF-Fo and RF-Fo type of scaffolds after 7 days of incubation in the neural differentiation medium. Flow cytometry showed that expression of neural markers, nestin and beta-III tubulin increased almost 2.5 fold after one week culture in the neural differentiation medium. Histological analysis also showed the increased expression of neural markers in the neural differentiation medium.

CONCLUSION

The effect of alignment of the inner architecture within the tubular nerve guides on bone marrow stem cell growth and differentiation showed that random fibers provided a better platform to have high cell numbers. Differentiation of rBMSCs to neurons was observed in both of the constructs when incubated with the differentiation medium. Therefore, both of these constructs have the potential for use as an implant at the nerve injury site.

REFERENCES

- Schmidt CE., and Leach JB. Annu. Rev. Biomed. Eng. 5: 293-347, 2003
- Stokols S. *et al.*, Tissue Eng, 12: 2777-2787, 2006.

ACKNOWLEDGMENTS

We gratefully acknowledge the support by METU through the project BAP 07.02.2012-101 and The Scientific and Technological Research Council of Turkey (TÜBİTAK) for the 2205 BİDEP-TÜBİTAK Fellowship.

Designing 3D cell niches exploiting peptide self-assembly

Victoria L. Workman¹ Aline F. Miller² and Alberto Saiani^{1*}

¹School of Material and Manchester Institute of Biotechnology (MIB), University of Manchester, UK ²School of CEAS and Manchester Institute of Biotechnology (MIB), University of Manchester, UK [*a.saiani@manchester.ac.uk](mailto:a.saiani@manchester.ac.uk)

INTRODUCTION

In the last two decades, significant efforts have been made to develop soft materials exploiting the self-assembly of short peptides for biomedical applications.¹ β -sheet forming peptides have been shown to allow the design of highly stable hydrogels with potential application in a range of fields.²⁻⁵ In particular, they offer a flexible platform for the design of 3D cell niches.

EXPERIMENTAL METHODS

We have developed a platform for the design of hydrogels with tailored properties and functionalities exploiting the self-assembly of short (4-10 amino acids) β -sheet forming peptides. The design of these peptides is based on the alternation of hydrophilic and hydrophobic residues. These novel materials have been characterized using a variety of techniques including small angle scattering and rheology.

RESULTS

The self-assembly process of these peptides was investigated and is schematically described in Figure 1. By altering the peptide primary structure, the formulation and the processing conditions the properties of these scaffolds (e.g.: modulus and functionality) can be easily controlled. We were able to design injectable, as well as sprayable, hydrogels that can be used for 3D cell culture as well as *in-vivo* cell delivery.

CONCLUSION AND DISCUSSION

We have developed a platform for the design of 3D scaffolds whose properties can be tailored to accommodate different cells' needs. We have used these novel materials for the culture of a variety of cells including chondrocytes⁵, osteoblasts, fibroblasts as well as embryonic stem cells. For the latter cell type we showed that their pluripotency is retained when embedded within the gels in 3D thus making these materials a potential ideal platform for the controlled differentiation of stem cells. Our results clearly demonstrate that our peptides offer great promise for the design of specific cell niches due to their low immunogenicity and the ability we have to control and tailor their properties.

REFERENCES

1. J. Collier *et al.* Chem. Soc. Rev., 39, 3413 (2010);
2. A. Saiani *et al.* Soft Mat., 5, 193 (2009);
3. S. Boothroyd *et al.* Faraday Discussions, 166, 195 (2013);
4. D. Roberts *et al.* Langmuir, 28, 16196 (2012);
5. A. Mujeeb *et al.* Acta Biomater, 9, 4609 (2013)

ACKNOWLEDGMENTS

The authors acknowledge an EPSRC Fellowship (EP/K016210/1) and EU-FP7 (BIOSCENT) for funding.

DISCLOSURES

Authors have no conflict of interest to disclose.

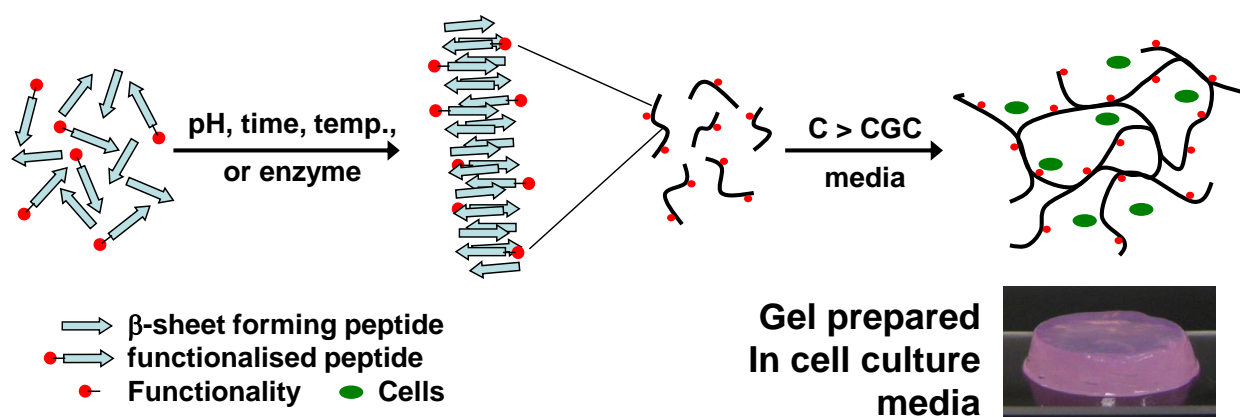


Figure 1: Schematic representation of the self-assembly process of our peptides.

Effect of Zinc-Containing Tricalciumphosphate (ZnTCP) on Growth and Osteogenic Differentiation of Mesenchymal Stem Cells

Joshua Chou^{1,3}, Jia Hao², Hirokazu Hatoyama¹, Besim Ben-Nissan³, Bruce Milthorpe³, Makoto Otsuka¹

¹Research Institute of Pharmaceutical Sciences, Faculty of Pharmacy, Musashino University

²Oral Implantology and Regenerative Dental Medicine, Tokyo Medical and Dental University

³Advanced Tissue Regeneration and Drug Delivery Group, Faculty of Science, University of Technology Sydney
(bruce.milthorpe@uts.edu.au)

INTRODUCTION

In a previous study, our results showed that zinc-containing tricalcium phosphate (ZnTCP) can be produced by hydrothermally converting calcium carbonate exoskeletons from foraminifera (Chou et al., 2013). The potential in the use of this material is that it naturally possesses an interconnected and uniform porous network throughout the material and this structure can be preserved during the conversion method (Chou et al., 2007). Furthermore, strontium and magnesium, which are also known metal dopants in bone cell regulations, are part of the material's natural composition (Chou et al., 2012).

In this study, as a first step to demonstrating the application of biomimetic material towards bone tissue engineering, zinc-containing tricalcium phosphate (ZnTCP) was investigated to determine its effect on the growth and osteogenic potential of MSCs.

EXPERIMENTAL METHODS

Material: Calcium carbonate foraminifera exoskeleton material was purchased commercially, cleaned in sodium hypochlorite, hydrothermally converted at 220°C for 48 hours with diammonium hydrogenphosphate adjusted to yield Ca/P molar ratios of 1.5 to produce tricalcium phosphate. Next, 30mg of zinc nitrate hexahydrate was added to the tricalcium phosphate and the samples were heated again to 220°C for 24 hours in a pressure vessel. The material was characterized by XRD and ICP-MS

Cell culture: Bone Marrow stem cells from 5 week-old Wistar rats were harvested and cultured by standard methods⁴. Cell proliferation was assessed by alamar blue staining and osteogenic differentiation by ALP expression on a per unit protein basis.

RESULTS AND DISCUSSION

The main results are shown in Figure 1 below.

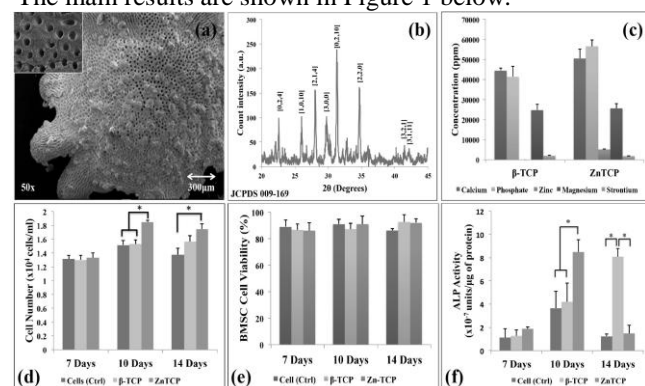


Figure 1. Scanning electron microscopy images showing (a) ZnTCP material with uniform pore distribution and (b) the corresponding XRD pattern matching JCPDS 009-169 for tricalcium phosphate. The chemical composition quantified by ICP-MS (c) shows the preservation of calcium and phosphate with the presence of magnesium and strontium. Zinc was only present after conversion. The growth of BMSCs (d) showing significantly higher cell number after day 10 and in day 14 and the complementing cell viability (e) showing >90% of BMSCs were viable after 14 days. The ALP activity level (f) showed ZnTCP to have significantly higher levels at day 10 suggesting earlier promotion of osteoblast differentiation.

CONCLUSION

In conclusion, this study was able to show that biomimetic ZnTCP can be easily produced at low temperature compared with high temperature sintering and possess the capability to induce and stimulate faster osteogenic differentiation of MSC to osteoblasts compared with β -TCP.

REFERENCES

- References must be numbered. Keep the same style.
1Chou J, et al. PLoS ONE 8(8) 2013: e71821. doi:10.1371/journal.pone.0071821
2Chou J, et al. J Aust Ceram Soc, 43: 44-48, 2007
3Chou J, et al. J Tissue Eng Regen Med. 2012. DOI: 10.1002/term.1544
4Maniopoulos C., et al, Cell Tissue Res, 254(2): 317–30, 1988

ACKNOWLEDGMENTS

The authors would like to acknowledge the financial support provided by UTS Chancellor's Postdoctoral Fellowship, the Japan Society for the Promotion of Science (JSPS) and the University of Technology Sydney Faculty of Science.

High-Throughput Quantitative Chondrogenic Assay for Stem Cell Differentiation

Amy Prosser¹, Colin Scotchford¹, Virginie Sottile², and David Grant¹

¹ Division of Materials Mechanics and Structures, Faculty of Engineering, University of Nottingham, UK

² Wolfson STEM Centre, School of Medicine, University of Nottingham, UK

expap3@nottingham.ac.uk

An improved cell differentiation assay for chondrogenesis has been developed integrating three robust quantitative measurements that can be used for high-throughput chondrogenic differentiation screening of stem cell populations.

INTRODUCTION

Three-dimensional (3D) cell micromass culture has been used to study *in vitro* chondrogenesis since the 1960s¹. In order to improve the throughput and reliability of this differentiation assay, we developed a cell culture protocol replacing the standard 15ml tube format with 96 well plates. In addition, three robust quantitative methods were developed and assessed to analyse chondrogenesis *in vitro*. Utilising established stains for glycosaminoglycans and proteoglycans, direct in-well methods have been developed. This method facilitates high throughput chondrogenic screening of stem cell and progenitor populations *in vitro*.

EXPERIMENTAL METHODS

Cell Culture – human bone marrow derived mesenchymal stem cells (MSCs)² were pelleted in V-shape plates by centrifugation. Standard culture conditions (Control) contained DMEM supplemented with 10% foetal calf serum, 1% L-Glutamine, 1% non-essential amino acids (NEAA) and 1 % penicillin/streptomycin (P/S) at 37°C and 5% CO₂. Chondrogenic culture conditions (CM) contained high glucose DMEM supplemented with: 1% L-Glutamine, 1% NEAA and 1% P/S, 0.1µM dexamethasone, 50µM ascorbic acid phosphate, 1mM sodium pyruvate, 40µg/ml L-proline, and Insulin-Transferrin-Selenium Supplement. TGF-β1 was used at 10ng/ml. Culture medium was manually replaced every day throughout the culture period of either 14 or 21 days.

DMMB – Pellets were washed and 100µl of water was added to each well, before plates were freeze thawed and papain digested. 50µl aliquots of each sample were transferred into a 96 well plate and combined with 50µl DMMB solution before being read at 540nm absorption.

Alcian Blue - Cultures were fixed in 4% paraformaldehyde before 100µl 1% Alcian solution was added to each well and incubated overnight. Wells were washed with PBS until all unbound dye had been removed. The stain was extracted using 6M guanidine HCl for 2 before quantifying at 650 nm absorbance.

Safranin-O – Cultures were fixed in 4% paraformaldehyde before 100µl Safranin-O in 50mM sodium acetate was added to each well and incubated at room temperature for 20 minutes. Wells were washed with PBS until all unbound dye had been removed before extraction using 10% cetylpyridinium chloride for 20 minutes. Quantification was achieved by reading the absorption of the extracted dye at 530 nm.

PicoGreen DNA Assay – was performed according to the manufacturer's instructions (Invitrogen) on plates that had been freeze thawed to lyse cells. All stain quantification results were normalised to DNA content.

Statistics – were performed in GraphPad Prism using a two way ANOVA analysis with a Tukey correction.

RESULTS AND DISCUSSION

Both Alcian Blue and DMMB stain GAGs and a comparative study was designed to test the sensitivity and reproducibility of the two assays. Figure 1 shows the level of stain per µg of DNA measured by PicoGreen analysis.

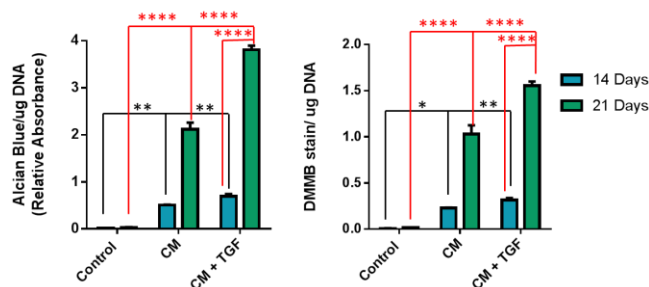


Figure 1 shows the level of Alcian Blue and DMMB stain per µg of DNA after 14 and 21 days of culture.

Parallel assays showed the same trend with significantly more stain after 21 days compared to 14 days (Fig. 1) and a significant difference between the control and chondrogenic conditions ($p < 0.01$). TGF-β1 was confirmed to significantly enhance differentiation in these assays, but only at 21 days. Interestingly, the error associated with each datapoint was low, highlighting the improved reliability of these assays.

CONCLUSION

This novel multi-parameter assay can efficiently analyse the kinetics of chondrogenic differentiation of MSCs, and can be used to assess the effects of growth factors, drugs and small molecules on the osteochondral differentiation potential of stem cell populations for regenerative medicine, which is currently under investigation as part of a larger research project.

REFERENCES

- Holtzer, H., et al., Proc Natl Acad Sci U S A, 1960. 46(12): 1533-42.
- Rashidi, H., et al., Cells Tissues Organs, 2012. 195(6): 484-94.

ACKNOWLEDGMENTS

The authors would like to thank the faculties of Engineering and Medicine (University of Nottingham) and "Innovabone" NMP3-LA-2011 for providing financial support.



Ioan Notingher

School of Physics and Astronomy, University of Nottingham, United Kingdom

ioan.notingher@nottingham.ac.uk

INTRODUCTION

A key challenge in tissue engineering and regenerative medicine is understanding the interaction between cells and biomaterials. The design of scaffold materials often aims to modulate the cellular activity and increase therapeutic effect. Therefore, it is important to detect molecular changes in cells that can be correlated with their phenotype and biological functions. Raman micro-spectroscopy (RMS) is a well-established analytical technique that allows label-free measurements on live cells cultured *in-vitro*; the Raman spectra can provide useful information regarding cell viability or differentiation¹. This presentation will report advances in RMS, focused on time- and spatially-resolved measurements of embryonic stem cells during osteogenic and cardiac phenotypes.

EXPERIMENTAL METHODS

Development of an optimised Raman microscope with an integrated environmental enclosure allowed the acquisition of time- and spatially-resolved Raman spectral maps of embryonic cells cultured in defined media to induce differentiation towards cardiac and osteogenic phenotype. The cells were maintained in purpose-built micro-bioreactors on the Raman microscope for 5 days (between days 5 and 9 of differentiation for cardiac differentiation) and 28 days (for osteogenic differentiation). Spatially-resolved spectra were recorded at 24 hours intervals.

RESULTS AND DISCUSSION

For osteogenic differentiation, the time-course Raman spectra of the stem cells detected the formation and mineralisation of bone nodules at days 15-20, as indicated by the increase in the intensity of the Raman band at $950\text{-}958\text{cm}^{-1}$ assigned to the PO43- symmetric stretching of hydroxyapatite (HA). The spatial and temporal analysis of the Raman spectra indicated that initially the bone nodules consist mainly of amorphous HA that transforms into crystalline HA. Amorphous HA is detected at the edges of the bone nodules even at the late stages of mineralisation, suggesting that during the development of the bone nodules, amorphous hydroxyapatite tends to form at the edges of the nodules, followed by a phase transformation.

In the case of cardiac differentiation of embryonic stem cells, the Raman spectra showed that the onset of spontaneous beating of embryoid bodies (EBs) at day 7 coincided with an increase in the intensity of the Raman bands associated to myofibrils and glycogen. The Raman spectral maps had a high positive correlation with the expression of the cardiac-specific α -actinin

obtained by immuno-fluorescence imaging of the same EBs.

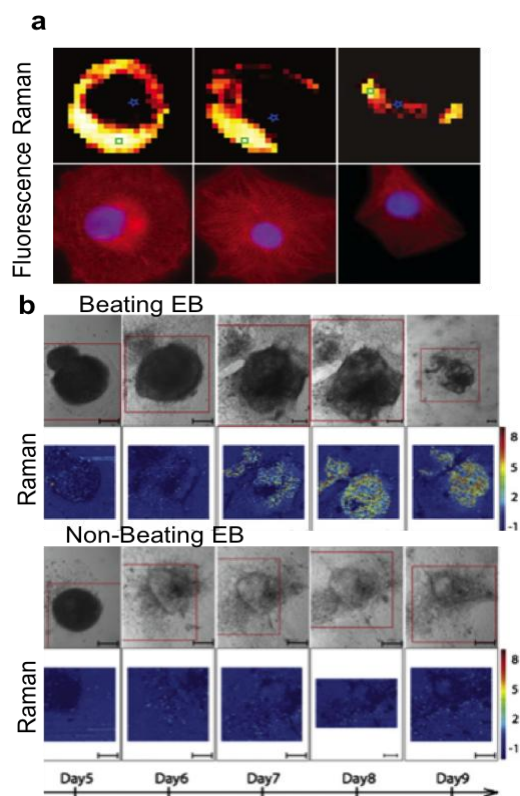


Figure 1. Time- and spatially-resolved Raman spectroscopy measurements of embryonic stem cells during cardiac differentiation. (a) Comparison between Raman and immuno-fluorescence imaging of α -actinin (cardiac marker); (b) The time-dependence of the Raman spectral markers for a beating (successful cardiac differentiation) and a non-beating EB.

CONCLUSION

These results demonstrate the potential of Raman spectroscopy for performing non-invasive time-course experiments on live stem cells over periods as long as four weeks and to measure molecular changes related to differentiation.

REFERENCES

1. Notingher I., Hench, LL, Exp. Rev. Med. Dev. 3:215-234, 2016

ACKNOWLEDGMENTS

The authors would like to thank the Biotechnology and Biological Sciences Research Council UK (BB/G010285/1) for providing financial support.

Substrate Mediated Enzyme Prodrug Therapy

A.N. Zelikin

Department of Chemistry and iNANO Interdisciplinary Nanoscience Centre, Aarhus University, Denmark
zelikin@chem.au.dk

INTRODUCTION: Site specific delivery of drugs is crucial to achieve a higher localized effect and a lower systemic distribution of the therapeutic. Specialized systems for controlled drug delivery are therefore in high demand. Herein, we present a novel paradigm termed Substrate Mediated Enzyme Prodrug Therapy (SMEPT), according to which the drugs are synthesised locally within the biomaterial bulk or the surface coatings. This is achieved using biocatalytic (i.e. enzyme-containing) biomaterials paired with corresponding prodrugs. This ensures localized synthesis of the drug for controlled drug delivery¹⁻⁶.

EXPERIMENTAL METHODS: Biocatalytic hydrogel biomaterials were assembled using poly(vinyl alcohol).¹⁻⁴ Enzyme immobilization was achieved via mixing the protein with the polymer and exerting physical gelation via a treatment with coagulating kosmotropic salt, sodium sulphate. For biocatalytic coatings,^{5,6} enzyme immobilization was achieved using the layer-by-layer polyelectrolyte deposition technique and adsorbing the protein at a nominated location within the multi-layered architecture. The two enzymes chosen for this study were β -galactosidase (β -Gal) or β -glucuronidase (β -Glu). Cell culture was performed using surface-adhered hydrogel biomaterials or polymer coatings using commercially available prodrugs for anticancer and anti-inflammatory agents as well as fluorogenic substrates. Images were obtained using DIC/fluorescence microscopy. Quantitative evaluation was performed via fluorescence readout and standard cell culture assays. Statistics were performed by one-way ANOVA using a Turkey test as means of comparison.

RESULTS AND DISCUSSION: The attractive feature of SMEPT lies in that the same biomaterial, be it a hydrogel or a surface coating, can generate multiple therapeutic agents with dissimilar structure and function. This is possible because e.g. β -Glu would convert any glucuronide into its parent therapeutic agent. The prodrugs can be administered at a nominated concentration (which translates into the concentration of the active agent generated within unit time), and be taken individually, sequentially, or in combination. Using these tools, we used biomaterials to synthesize the rationally designed quantities of drugs for their surface mediated delivery to adhering cells. Concentration of the drug generated by the biomaterial allows to fine-tune the therapeutic effects. Sequential administration of the prodrugs made it possible to use the same biomaterial to generate e.g. anti-inflammatory response in adhering cells today followed by cytotoxic (anti-proliferative) effect at a later time-point.¹ This scenario is relevant to the treatment of atherosclerosis. A highly efficacious mode of drug delivery is that of using combinations of drugs. This is highly important

for anti-cancer and anti-viral treatments as well as for pain management. Using drug eluting biomaterials, combination therapy is tremendously hard to engineer with few if any successes. SMEPT makes it easy and administration of the prodrugs with rationally chosen concentrations produced a combination of drugs resulting in their synergistic therapeutic effect.¹

Using fluidic perfusion chambers, we further demonstrated that SMEPT generates the drugs on demand, at the nominated time (Fig. 1,A). Using this set-up for cell culture revealed a site-specific nature of drug delivery: therapeutic response was higher at the site of drug synthesis than that registered “down-stream” from the biocatalytic coating.⁵

Taken together, our data present SMEPT as a powerful tool for localized drug delivery using biocatalytic biomaterials and coatings.

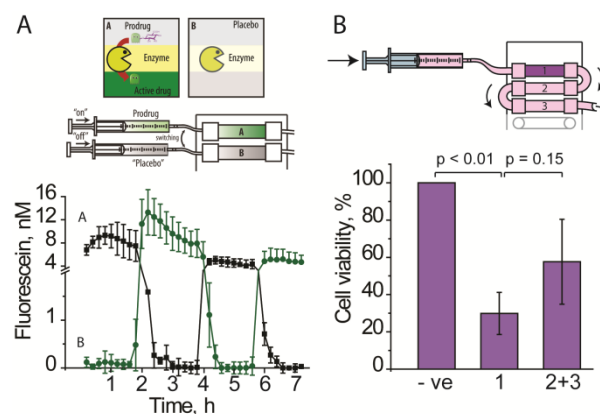


Fig. 1: (A) On-demand synthesis of a fluorescent agent from polymer matrices. (B) Localized delivery of a therapeutic agent under dynamic flow conditions to HepG2 hepatic cells. Reproduced with permission from Ref.⁵ Copyright 2013, Wiley-Interscience.

REFERENCES

1. Mendes, A. *et al.*, Adv. Funct. Mater. DOI: 10.1002/adfm.201304312.
2. Fejerskov, B. *et al.*, ACS Appl. Mater. Interfaces 4: 4981–90, 2012.
3. Fejerskov, B. *et al.*, PLoS ONE 7:e49619, 2012.
4. Fejerskov, B. *et al.*, Langmuir 29:344-54, 2013.
5. Fejerskov, B. *et al.*, Small 10:1314-24, 2014.
6. Andreasen, S.Ø. *et al.*, Nanoscale 6:4131-40, 2014.

ACKNOWLEDGMENTS: This work is supported by grants from the Lundbeck foundation, Novo Nordisk Foundation, and a Sapere Aude Starting Grant from the Danish Council for Independent Research, Technology and Production Sciences, Denmark.



Mesoporous SiO₂-ZnO-plex: Mechanistic approach, Complex of Nanoparticles of SiO₂-ZnO with DNA for Therapeutic Applications

Vijay Bhooshan Kumar^{1*}, Koushi Kumar¹, Yitzhak Mastai², Aharon Gedanken²,
Pradip Paik^{1*}

¹School of Engineering Sciences and Technology, University of Hyderabad, Hyderabad 500046, A.P., India,

²Institute for Nanotechnology and Advanced Materials, Department of Chemistry, Bar-Ilan University, Ramat Gan 52900, Israel, * E-mail: pradip.paik@gmail.com, ppse@uohyd.ernet.in

INTRODUCTION: The concept of using mesoporous nanocapsules as a carrier of nucleic acids, drugs/medicines and biomolecules such as DNA, siRNA for therapeutic applications is a promising approach in medical biotechnology. The wet chemical synthesis method is indeed a new era for designing new materials in the form of nanocapsules for various biomedical applications. The surface modification of nanocapsules is essential for using it in biomedical applications like targeted drug and gene delivery, cancer therapy etc. The drug/medicines molecules are usually loaded into the functionalized/non-functionalized capsules mechanically or with some external forces and delivered into the infected sites for killing/repairing the cells with in a time periods. However, none of the reported nanocapsules for delivery applications are ideal and individuals have their own limitations. Hence, there is a lot of scope to do in the same field.

EXPERIMENTAL METHODS: In this work, mesoporous SiO₂-ZnO nanocapsules have been synthesized using zinc acetate (ZnAc) and tetraethyl orthosilicate (TEOS) through a controlled wet chemical process and ultrasonication where the tiny ZnO nanocrystals are distributed throughout the SiO₂ matrix. We create the micelles first and then **drop wise** a mixture of ZnAc and TEOS was added (feeding rate 100µl/min) under ultrasonication condition. A network of precursors **is** formed, where the mesopores are formed after removal of the micelles through calcinations at higher temperature. Essential characterization were conducted with HRTEM, HRTEM, BET, UV-Vis-NIR, PL and for testing the biocompatibility MTT assay was performed. Finally small biomolecules and DNA molecules were loaded in mesoporous SiO₂-ZnO nanocapsules to form SiOZO-plex and tested the efficiency to kill the cancer cells with a time scale.

RESULTS AND DISCUSSION: This work represents a new materials mesoporous SiO₂-ZnO composite anocapsules of SiO₂ and ZnO with sizes of 40-60 nm and represents their potential applications in encapsulation of small biomolecules for possible uses in drug and gene delivery. The capsule size and morphology have been confirmed through the FESEM and HRTEM. The mesoporous structure of the novel materials has been confirmed through both BET and HRTEM and observed that pore diameter is c.a. 4-6 nm. The BET surface area of mesoporous SiO₂-ZnO was found to be ~ 650 m² g⁻¹. The chemical bonding and

structure have been analyzed through FT-IR spectroscopy and Energy dispersive X-ray spectroscopy (EDX). To demonstrate the biocompatibility, cell viability of the nanocapsules, normal and cancerous lymphocyte cells have been studied in a systematic way. Fluorescent dye (Rhodamin 6G), anticancer drug e.g., Doxorubicin (DOX) and EtBr-labelled DNA molecules were loaded efficiently into the nanocapsules to manifest the mesoporous nature of the nanocapsules and the efficiency to load the small molecules. The release kinetics of Rhodamin 6G, DOX and DNA were studied. The results highlight the potential of novel functional mesoporous SiO₂-ZnO nanoparticles for using as the carrier of drugs and formation of 'SiOZO-plex', a complex of mesoporous SiO₂-ZnO with DNA for gene delivery applications.

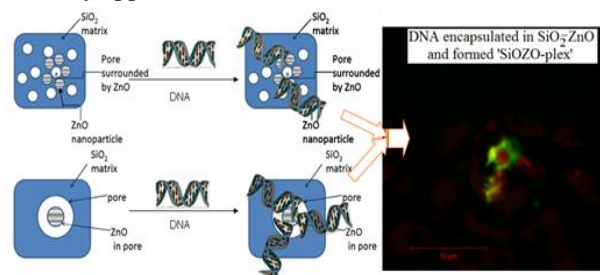


Fig. 1: Formation mechanism of SiOZO-plex (complex of mesoporous SiO₂-ZnO with DNA) useful for gene delivery

CONCLUSION: In conclusion, the important of the mesoporous nanocapsules in biomedical applications is growing significantly. Due to the increasing demands of suitable cargo nanocapsules for drug and gene delivery, herein, mesoporous SiO₂-ZnO nanocapsules were synthesized by newly adopted modified wet-chemical-sonochemical synthesis method. The critical advantages of the new nanocapsules are the biocompatibility and efficient ability to load small molecules and DNA inside the mesopores lead to the formation of 'SiOZO-plex', a SiO₂-ZnO and DNA complex. The resulted 'SiOZO-plex' is useful for gene delivery applications.

REFERENCES

1. P. Paik, Y. Zhang, *Nanoscale*, 3:, 2215-2219, 2011
2. P. Paik, A. Gedanken, Y. Mastai, *J. Mat. Chem.*, 20:4085-4093, 2010.

ACKNOWLEDGMENTS: Authors would like to acknowledge the financial support from DST Fast-Track Grant for Young Scientist (Ref: SR/FTP/ETA-0079/2011).



Estimation of Drug Loading Efficiency in Microspheres by “Shake Flask” Method

C.Y. Tham, Z. A Abdul Hamid¹, Z. Ahmad¹, H. Ismail¹

¹School of Materials and Mineral Resources Engineering, Universiti Sains Malaysia, Seri Ampangan 14300 Nibong Tebal Seberang Perai Selatan Pulau Pinang, Malaysia, szuratulain@eng.usm.my

INTRODUCTION

Drug loading efficiency (DLE) in polymeric microspheres (MS) has always been compared in different fabrication techniques, wherein high loading was desired with minimum drug lost in the system.¹ Thus, an estimation technique of DLE in MS prepared through emulsion and solvent evaporation (ESE) technique was discussed in this paper. The estimation technique applied was a “shake flask” (SF) method using in determining the drug’s partition coefficient.² ESE technique involved two immiscible liquid phases. It was hypothesized that higher drug retention in phase responsible for MS formation will leads to higher DLE in MS. This paper was aimed to investigate the potential of “shake flask” method in estimating the DLE in MS.

EXPERIMENTAL METHODS

Rhodamine B (RhB) and methyl orange (MO) dispersed in distilled water were used as model drugs. In ESE process, firstly, drug model solution dispersed in poly(lactic acid)/dichloromethane solution (PLA/DCM). Next, the mixture was emulsified in poly(vinyl alcohol)/water solution (PVA/water). The emulsion was continuously stirred for 24 hours for solvent evaporation.

In SF process, both immiscible DCM and water was vigorously shakes in flask until not distinct boundary observed. The mixtures were placed in rest for 24 hours for phase separation and stabilization. Phase being studies was extracted and diluted by using respective solvent.

RESULTS AND DISCUSSION

SF method gives promising results in estimating the DLE in PLA MS. The presence of MO in PLA MS was not detectable by UV-Vis spectrometer, while RhB was detected. This outcome was consistent with the SF observation obtained in Fig.1, where MO have limited tendency to dissolve in DCM as compared to RhB.

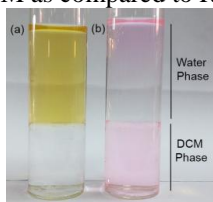


Fig. 1: Distribution of dye (a) MO and (b) RhB in both water and DCM phase in after SF

The effect of RhB concentration in both SF and PLA MS was studied. The changing trend of DLE for both SF (PLA/DCM phase) and PLA MS was consistent (Fig. 2). As RhB concentration increased, DLE in both SF PLA phase and PLA MS increased. The different in DLE between SF-PLA phase and PLA MS concentration shown in Fig. 2 was due to the presence of PVA in MS preparation. By using SF method in our studies, it was also proven that RhB content in water phase increased in the presence of PVA.

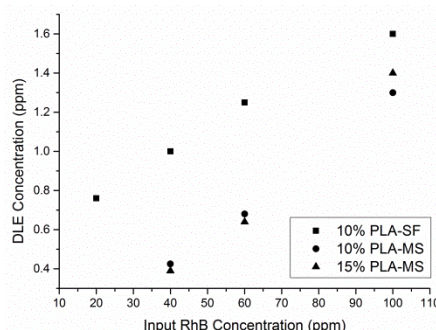


Fig. 2: DLE of SF-PLA phase and PLA MS in vary RhB concentration

CONCLUSION

“Shake flask” method was suitable to be used in estimating the drug loading efficiency in ESE technique. This method can be adjusted according to the materials (e.g. drugs, polymers, solvents and stabilizers) involved in each particular ESE processing. This estimation could use to evaluate the suitability of the fabrication system to encapsulate desired drug molecules.

REFERENCES

1. Jyothi N. V. N. *et al.*, J. Microencapsul. 27:3-187, 2010.
2. Scott D. C. & Clymer J. W, Pharmaceutical Technology North America. 26:11-30. 2002

ACKNOWLEDGEMENTS

Authors would like to thank Universiti Sains Malaysia for the financial support for this works through Research University Individual Grant (RUI) (1001/PBAHAN/814201).

Suzuki Coupling-Functionalized Boronic Acid Nanoparticles for Drug Delivery

André J. van der Vlies and Urara Hasegawa*

Graduate School of Engineering, Osaka University, JAPAN
andre.vandervlies@chem.eng.osaka-u.ac.jp

INTRODUCTION

We prepared cross-linked phenyl boronic acid (PBA)-containing nanoparticles (NPs) by a simple surfactant-free emulsion polymerization method. By adjustment of the feed ratio of monomers the particle size can be controlled in the range 50-200 nm, which is particularly suited for drug delivery application¹.

The presence of PBA groups on the NPs allow for further functionalization using the well-known Suzuki coupling reaction². Here we present the functionalization of the NPs using aqueous Suzuki reaction and couple the well-known drug Doxorubicin (Dox) via an acid-labile hydrazone linkage³. Upon endocytosis the decrease in pH leads to release of Dox intracellularly. We show that the Dox-NPs are bioactive in different cell lines.

EXPERIMENTAL METHODS

NPs were prepared in phosphate buffer pH 7 by free radical polymerization of PEG-acrylamide, a PBA-containing monomer and cross-linker. The NPs were characterized by dynamic light scattering (DLS) and transmission electron microscopy (TEM). Suzuki couplings were carried out with aryl iodides at 70°C using Na_2PdCl_2 and a water-soluble phosphine ligand as the catalyst and K_2CO_3 as the base. Conversion of the PBA groups was confirmed by the Alizarin Red fluorescence assay. In case of iodobenzoic acid as the coupling partner the carboxylic acid groups were reacted with hydrazine using standard EDC/sulfo-NHS coupling chemistry in MES buffer pH 5. Infrared spectroscopy (IR) was done with lyophilized samples. Dox was conjugated to the NPs in DMF in the presence of CF_3COOH as acid catalyst. Dox-NPs and free Dox were separated by size exclusion column chromatography using Sephadex LH20 and finally dialyzed in phosphate buffer pH 7.4. Dox-NPs were concentrated using an Amicon filter and sterile filtered before incubation with different cell lines. Cell viability was evaluated with the MTT assay.

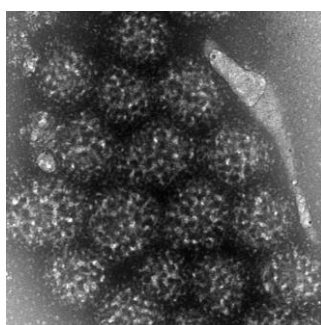


Figure 1 TEM picture of the PBA-NP (negative staining).

RESULTS AND DISCUSSION

DLS showed that the NPs were 190 nm in diameter and had a spherical shape as confirmed by TEM. Quantification of the number of PBA groups by the Alizarin Red Assay showed that 80-90% of the boronic acid monomer was incorporated into the NPs. Suzuki coupling between the NPs and iodobenzoic acid showed quantitative conversion and the presence of carboxylic acid groups was confirmed by IR. Functionalization with hydrazine and reacting the formed hydrazone with the ketone functionality of Dox afforded Dox-NPs. DLS showed that the size of the NPs was 200 nm. When incubated with RAW 264.7 macrophages and HT-29 colon cancer cell lines Dox-NPs showed a difference in cellular toxicity.

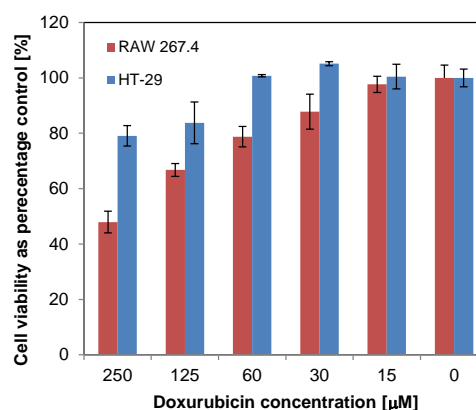


Figure 2 Dox-NP have increased cellular toxicity in RAW 264.7 compared to HT-29 cells.

CONCLUSION

We prepared PBA-containing NPs and showed successful modification using the Suzuki reaction. To show the potential of this NP platform for drug delivery application we conjugated Doxorubicin via a hydrazone linkage and showed cell-type dependent toxicity.

REFERENCES

1. Duncan R. Nat. Rev. Drug Delivery 2:347-360, 2003
2. Carin C. *et al.* Angew. Chem. 51:5062-5085, 2012.
3. Taskushi K. *et al.* Bioconjugate Chem. 2:131-141 1991.

ACKNOWLEDGMENTS

We thank Dr. E. Mochizuki (Osaka University, Japan) for TEM experiments. This work was supported by Grant-in-Aid for Young Scientists (B), No. 25750175, from the Japan Society for the Promotion of Science.

Polymeric Micelles for Hydrogen Sulfide-Based Therapy

Urara Hasegawa* and André J. van der Vlies

Graduate School of Engineering, Osaka University, Japan
urara.hasegawa@chem.eng.osaka-u.ac.jp

INTRODUCTION

With the discovery of important biological roles of endogenously-produced gases, their use as therapeutic agents has attracted growing attention. Among them, hydrogen sulfide (H_2S) has recently emerged as the third gaseous signaling molecule in mammals. H_2S has been shown to regulate inflammation, relax vascular smooth muscles, promote angiogenesis and mediate neurotransmission.¹ Recently, several organosulfur compounds, including dithiolethiones, have been reported as H_2S donors and used to explore the therapeutic potential of this gas.² However, poorly-controlled pharmacokinetic profiles of these donors often result in adverse effects and low therapeutic efficiency which limits their practical applications.

In the field of drug delivery, polymeric micelles as drug carriers have been extensively studied and shown to be powerful in overcoming many intrinsic problems of small drugs including rapid diffusion throughout the body, short circulation time in the blood stream and low bioavailability.

Here we report a novel H_2S delivery system based on polymeric micelles carrying anethole dithiolethione (ADT) moieties which is known to release H_2S in the body via metabolic digestion.

EXPERIMENTAL METHODS

Amphiphilic diblock copolymers containing ADT moieties (PEG-PADT, Figure 1(a)) were synthesized via reversible addition-fragmentation chain transfer (RAFT) polymerization followed by CTA end group removal, deprotection of *tert*-butyl ester group and conjugation with amino group-modified ADT derivatives (ADT- NH_2). ADT micelles were prepared by adding a PEG-PADT/DMF solution dropwise to milliQ water followed by dialysis. The micelles were characterized by dynamic light scattering (DLS) and transmission electron microscopy (TEM). H_2S release from the ADT micelles was detected using ISO-H2S100 hydrogen sulfide sensor. The effects on gardiquimod (GDQ)-induced nuclear factor- κB (NF- κB) activation and the cytokine production in RAW Blue cells were assessed by Quanti Blue and ELISA assays.

RESULTS AND DISCUSSION

PEG-PADT block copolymers were dispersed in water to form ADT micelles. DLS showed that the micelles were monodisperse with a diameter of 36 nm (Figure 1 (b)). Further characterization by TEM confirmed that the polymers formed spherical micelles (Figure 1 (c)).

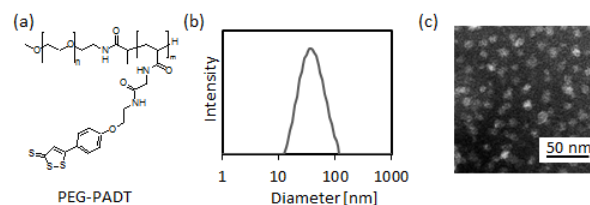


Figure 1. Characterization of ADT micelles. (a) Chemical structures of PEG-PADT. (b) Size distribution of ADT micelles by DLS. (c) TEM image of ADT micelles.

We investigated the H_2S release property of the ADT micelles. The ADT micelles released H_2S in cell lysate from murine RAW Blue macrophages, but not in PBS and 10% fetal bovine serum. This result indicated that the micelles release H_2S after cellular uptake.

The effect of the ADT micelles in inflammation was assessed using RAW Blue macrophages. Gardiquimod, a Toll-like receptor 7 ligand, was used to induce inflammation. ADT micelles exerted a synergistic effect with gardiquimod, and enhanced NF- κB activation and TNF- α production.

CONCLUSION

We developed a micellar H_2S delivery system. PEG-PADT block copolymers formed monodisperse spherical micelles. The ADT micelles were capable of releasing H_2S in the presence of cell lysate from murine macrophages. The ADT micelles exerted a synergistic effect with gardiquimod and enhanced proinflammatory responses. This H_2S releasing micelles may have potential in immunotherapy and vaccine development.

REFERENCES

1. Sezbo, C. *et al.*, Nat. Rev. Drug Discov. 6: 917, 2007
2. Caliendo, G. *et al.*, J. Med. Chem. 53:6275, 2010
3. van der Vlies, A. J. *et al.*, Nitric Oxide, 31: S581, 2013.

ACKNOWLEDGMENTS

We thank Dr. E. Mochizuki (Osaka University, Japan) for TEM experiments and Prof. M. Sadakane (Hiroshima University, Japan) for supplying Preyssler-type phosphotungstate staining agent. This work was supported by Grant-in-Aid for Young Scientists (B), No. 24700482, from the Japan Society for the Promotion of Science.

Amorphous Coordination Polymer Particles. From Basic Macromolecular Science to Theranostic Applications

F. Novio,^{1,2} F. Nador,² K. Wnuk,^{1,2} M. Borges^{1,2} and D. Ruiz-Molina^{1,2}

¹ Centro de Investigación en Nanociencia y Nanotecnología - Consejo Superior de Investigaciones Científicas, (CIN2-CSIC), Campus UAB, 08193 Bellaterra (Spain)

² Institut Català de Nanociència i Nanotecnologia (ICN2), Edifici ICN2, Campus UAB, 08193 Bellaterra (Spain)
fnovio@cin2.es

INTRODUCTION

Since the publication of the first nano-/microscale amorphous coordination polymer particles (CPPs) in 2005,¹ new and promising materials based on metal-ligand coordination assemblies (Figure 1) have emerged as novel platforms with application in biomedical fields.² The more recent studies showed the potential applications of this new class of materials for therapeutic and diagnostic uses. They are presented as alternative to other classical nanocarriers (liposome, polymer particle, dendrimer and inorganic particles) due to the nature of the coordination polymer that affords interesting optical, magnetic or catalytic properties. Thus the high tailorability and diversity of the CPPs can generate new multifunctional and biocompatible systems that exhibit high payload capacity to encapsulate different drugs and molecules,³ cell targeting⁴ and drug release in a controlled manner.⁵

EXPERIMENTAL METHODS

Recently in our research group we have been making progress on the control of thermal/chemical stability of the CPPs, the payload capacity for different species and the generation of stimuli-responsive nanoparticles (sensitive to pH changes, temperature or reducing environment). The design and synthesis of nanoparticles containing a specific drug integrated on the structure combined with a drug encapsulated is also reported as a dual nanocontainer with different drug release profiles. The combination of CPP with other nanomaterials such as iron oxide or gold nanoparticles allows applying these hybrid nanoplatforms for imaging or magnetic field/light-induced drug release. We have also performed in vitro cytotoxicity, surface functionalization and stability studies for different combinations to obtain an extensive knowledge about the characteristics of this type of materials.

RESULTS AND DISCUSSION

Although the research on the CPP for theranostic applications is still in an early stage, the recent results suggest the bright future for their application to biomedical field. With critical problems solved such as stability, targeting effect and controlled release profile and wide in vivo testing, CPPs will be the candidate of new generation of smart theranostic agents.

Our expertise, starting from macromolecular science, are developed to search new pharmaceutical strategies in nanomedicine based on rationally designed synthetic coordination polymers that can serve as novel antiviral medicines, detoxification agents, biosensors or drug

carriers. Our ultimate goal is to obtain a fundamental understanding of specific mechanisms of interaction of these nanoplatforms with the biological media to redirect their application to specific therapies/diagnosis. We attack this problem by synthesis of novel CPPs, the study of the physical-chemical properties in biological media and their ability to act as therapeutic or imaging agents.^{6,7}

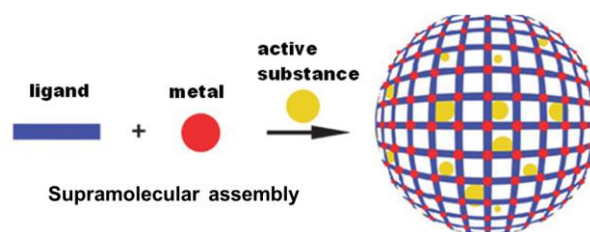


Figure 1

CONCLUSION

The advantage of the CPPs over the traditional nanoparticles is the unique properties associated to the metal-ligand units that confer novel and interesting properties with wider spectrum of application. We anticipate that results of our research will have a profound impact on the fields of general medicine, immunology and smart drug-delivery systems. Preliminary results indicate that these new nanosystems offer platforms with low toxicity, high cellular uptake, and smart responses to an external stimulus what open a new wide variety of possibilities to be used in therapy and diagnosis.

REFERENCES

1. Oh M. *et al.*, Nature 438:651, 2005.
2. Novio F. *et al.*, Coord. Chem. Rev., 257:2839, 2013.
3. Imaz I. *et al.*, Angew. Chem. Int. Ed., 48:2325, 2009
4. Taylor K.M.L. *et al.*, J. Am. Chem. Soc. 130:14358, 2008.
5. Imaz I. *et al.*, Chem. Commun., 46:4737, 2010.
6. L. Amorin *et al.*, Chem. Eur. J., 19, 17508 (2013)
7. F. Novio *et al.*, Adv. Healthcare Mat. Submitted

ACKNOWLEDGMENTS

The authors would like to thank the Ministerio de Economía y Competitividad for the financial support through project MAT2012-38318-C03-02. F.N. thanks the Ministerio de Economía y Competitividad (MINECO) for a JdC (JCI-2011-09239) post-doctoral grant.

Potential Use of 7-dehydrocholesterol coated Titanium Surfaces for Soft Tissue Integration of Dental Implants

Manuel Gómez-Florit[†], María Satué[†], Joana M. Ramis and Marta Monjo

Group of Cell Therapy and Tissue Engineering, Research Institute on Health Sciences (IUNICS), University of the Balearic Islands, Spain, m.gomez@uib.es. [†]Both authors contributed equally to the work.

INTRODUCTION

Vitamin D (VitD) plays an important role in the regulation of bone metabolism and immunological reactions. In humans, VitD is derived from dietary sources or made from 7-dehydrocholesterol (7-DHC) in the skin by exposure to ultraviolet (UV) rays. The function of VitD, via the active metabolite 1 α ,25-dihydroxyvitamin D3 (1,25D3), is to regulate the absorption of calcium and phosphorus in the intestine, and their mobilization in bone tissues. Recently, non-skeletal functions of VitD have gained notoriety [1].

Periodontal tissues consist of two hard tissues, bone and cementum, and two soft tissues, gingiva and periodontal ligament. It has been recently shown that gingival fibroblasts (HGF), the most abundant cells in the gingiva, can synthesize the active 1,25D3 [2]. In addition, there are evidences that link low VitD serum levels with increased periodontal inflammation and studies that show a positive effect of VitD on oral health [1].

Previous experiments of our group show that titanium (Ti) coating with UV-activated 7-DHC allow pre-osteoblasts to produce active VitD and to differentiate towards a mature state [3]. Furthermore, our current results prove that the addition of α -tocopherol (VitE) prevent 7-DHC oxidation whilst increase the biological potential of the coating.

The aim of the present study was to evaluate the response of HGF to 7-DHC:VitE coated titanium surfaces for improved soft tissue integration to dental implants.

EXPERIMENTAL METHODS

Machined Ti surfaces were coated with 7-DHC:VitE. Ti was also coated with ethanol (EtOH), 7-DHC or VitE, as controls. Surfaces were then exposed to UV light for 15 min and incubated at 23°C for 48 hours. Three different donors of HGF were cultured for 14 days on the different surfaces (n=6). Biocompatibility of surfaces was evaluated by a cytotoxicity assay and by cell morphology visualization (cytoskeleton and nuclei staining). Then, the expression of different genes was analysed by real-time RT-PCR.

RESULTS AND DISCUSSION

All surfaces were biocompatible although the 7-DHC control group showed increased cytotoxicity (less than 20%). HGF showed typical spindle-shaped morphology on all surfaces and were aligned to the machined texture.

After 14 days of cell culture, 7-DHC:VitE coated surfaces increased the expression of collagen III- α 1, a marker of fibroblastic maturation and scarless wound healing. Changes in the expression of matrix

metalloproteinase-1 (MMP1) and tissue inhibitor of metalloproteinases-1 (TIMP1) did not reach statistical significance. However, MMP1/TIMP1 mRNA ratio decreased on 7-DHC:VitE coated surfaces, suggesting that they may reduce MMP-related ECM destruction. Also, 7-DHC:VitE coated surfaces significantly decreased interleukin-8 mRNA levels, pointing to an anti-inflammatory effect.

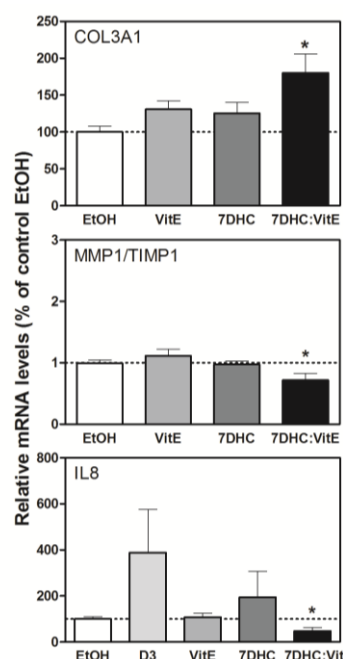


Figure 1. Gene expression levels of HGF cultured on coated surfaces. Data represent fold changes of target genes normalized to beta-actin and GAPDH (reference genes) expressed relative to cells grown on EtOH-coated Ti surfaces that were set at 100 %. Paired t-test was used to assess differences: * $P \leq 0.05$ versus EtOH.

CONCLUSION

These results suggest that UV-activated 7-DHC:VitE has a great potential to be used as a new coating for dental implant abutments to improve soft tissue integration to dental implants.

REFERENCES

1. Stein SH. *et al.*, J Periodontal Res. 2013
2. Liu K. *et al.*, PLoS One. 7:e52053, 2012
3. Satué M. *et al.*, Acta Biomater. 9:5759-70, 2013

ACKNOWLEDGMENTS

This work was supported by the Ministerio de Ciencia e Innovación del Gobierno de España (Torres Quevedo contract to MG, and Ramón y Cajal contract to MM).

Studying Interaction between Oral Mucosa and Titanium by SEM in Humans

Francesco Tassarolo^{1,2*}, Cristiano Tomasi³, Federico Piccoli⁴, Iole Caola⁴, Patrizio Caciagli⁴, and Giandomenico Nollo^{1,2}

^{1*}Healthcare Research and Innovation Program, Bruno Kessler Foundation, Trento, Italy tassarof@science.unitn.it

²Department of Industrial Engineering, University of Trento, Trento, Italy

³Department of Periodontology, The Sahlgrenska Academy at University of Gothenburg, Goteborg, Sweden

⁴Department of Medicine Laboratory, Azienda Provinciale per i Servizi Sanitari di Trento, Trento, Italy

INTRODUCTION

The installation of a titanium implant, put the severed mucosa in close contact with the implant surface. During healing, an attachment is formed between the mucosa and the titanium dioxide layer of the implant. Once properly matured, this attachment effectively separates the bone tissue from the oral cavity¹.

Experiments in the dog documented that several weeks are required to allow the establishment of an epithelial and connective tissue attachment to titanium implant¹. Corresponding data in humans are not available.

Recently, we proposed a human model to evaluate the morphogenesis of the mucosal attachment to implants². In this study we aimed at assessing the tissue at implant interface by scanning electron microscopy (SEM).

EXPERIMENTAL METHODS

Patient informed consent was obtained and after implant installation, a custom-designed experimental abutment was connected to the implant. A soft tissue biopsy and the titanium abutment were collected according to the method described by Tomasi et al.² after 12 weeks of tissue healing. The sample was fixed in 4% formalin for 48 h and stored in 70% ethanol solution. After fixation, four incisions, parallel with the long axis of the abutment, were made through the tissue to produce four portions. Each portion was separated from the experimental abutment using the previously described fracture technique¹. Samples were collected in a total six patients and one tissue unit (TU) with its experimental abutment (EA) were imaged in a XL30 FEI-Philips field-emission environmental scanning electron microscope (SEM).

TUs were re-hydrated by graded alcohol series to 100% water before analysis, and imaged in environmental mode at 10–15 keV and 60 to 95% relative humidity. The tissue surface in contact with the abutment was imaged from the apical margin to the marginal side of the biopsy collecting the signal of gaseous secondary electrons (GSE).

EAs were dehydrated, dried, gold sputtered and imaged at 15 keV in high-vacuum mode. Back scattered electron signal was acquired showing compositional contrast between titanium surface and biologic debris.

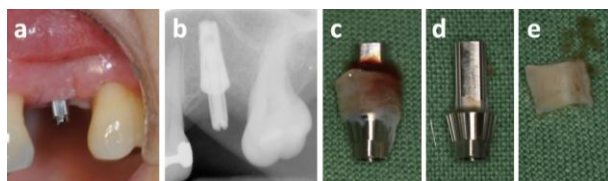


Figure 1: The experimental abutment at the end of the healing period (a, b). Samples obtained after fixation (c) and fracture technique (d, e)

RESULTS AND DISCUSSION

The sulcular epithelium showed exfoliating cells (Fig 2a). The analysis of the connective tissue interface revealed a surface topography that resembled that of the abutment. Collagen fibres induced a shirking of the sample during imaging (Fig. 2b). Results are in agreement with previous histological data² and were confirmed by the SEM observation of the tissue adhering to EA surface (Fig. 3a). From marginal to apical side, besides plaque on the emergent portion, we found a uncovered titanium band, an area with polygonal mono-layered cells (Fig. 3b) and a thicker tissue with fibrous appearance (Fig. 3c).

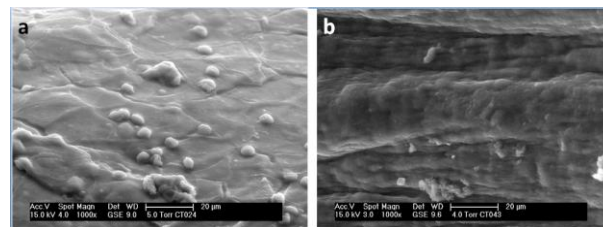


Figure 2: Surface of TU at marginal (a) and apical (b) side. Environmental SEM, GSE signal, 1000x.

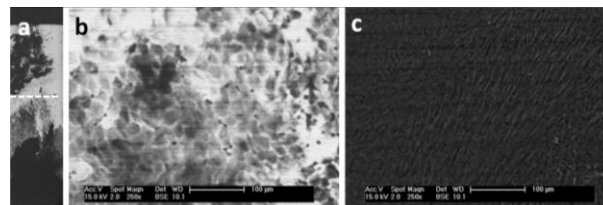


Figure 3: Surface of EA at marginal (a) and apical (b) side. Dashed line indicate mucosal margin. High vacuum SEM, BSE signal, 250x.

CONCLUSION

SEM characterization of tissue at implant interface showed two different tissue morphologies (epithelium-like and connective-like) on both biopsy and experimental abutment surface. This techniques associated to image analysis can provide quantitative data to complement the histological characterization of the oral mucosa in contact with titanium implants.

REFERENCES

1. Berglundh T. *et al.*, Clin Oral Implant Res. 2:81-90, 1991.
2. Tomasi C. *et al.*, Clin Oral Implants Res. 2013. Epub Jun 26.

ACKNOWLEDGMENTS

This study was supported by Dentsply Implants IH, Molndal, Sweden.

Synthesis and Characterisation of Novel Diopside Glass-Ceramics for Dentistry

J. Almuhamadi, N. Karpukhina and M. Cattell

Institute of Dentistry, Barts and The London School of Medicine and Dentistry, Queen Mary University of London, UK
j.m.a.almuhamadi@qmul.ac.uk

INTRODUCTION

Yttria Tetragonal Zirconia Polycrystalline ceramics (Y-TZP) have been stated as a successful all-ceramic system, regardless of the clinical indication¹. However, chipping of the veneering ceramic on zirconia restorations continues to be a problem² and is reported to be the most common clinical failure of these all-ceramic restorations. Rogers et al., 1970³ suggested that compositions which crystallise to form solid solutions are capable of controlling the thermal, chemical, physical and mechanical properties of the produced material. Diopside (Di, $\text{CaMgSi}_2\text{O}_6$) is an important member of *clinopyroxene* mineral family. It has a single chain silicate structure and is known to form a solid solution on cationic substitution for Ca^{2+} and Mg^{2+} . In particular, the solid solution forms as a result of coupled substitution of $\text{Ca}^{2+}/\text{Mg}^{2+}$ with $\text{Na}^+/\text{Al}^{3+}$ when $\text{CaMgSi}_2\text{O}_6$ is diluted with a stoichiometry of $\text{NaAlSi}_2\text{O}_6$. The aim of the study was to produce new diopside glass-ceramics based on this solid solution to prevent chipping of zirconia restorations.

Objectives were to:

Synthesise new glass/glass-ceramic formulations.

Characterise/optimize these materials.

Test the biaxial flexural strength.

EXPERIMENTAL METHODS

A series of glass compositions with varying amounts of sodium and aluminium oxides were synthesised using a melt-quench route, re-homogenised and processed into powders. Glass powders with a controlled particle size ($\text{PS} < 125\mu\text{m}$) were heat treated via two-step heat treatment cycles (nucleation and crystal growth) then held for 1 hour, quenched and ground to a powder. Glass-ceramic disc specimens ($15 \times 2\text{mm}$) were fabricated via sintering at variable sintering temperatures and holding times. Disc specimens ($n=30$) were tested using the Biaxial Flexural Strength (BFS, ball on ring) at a crosshead speed of 1mm/min . The BFS data were statistically analysed using (Dunn's multiple comparison tests, $p < 0.05$). Glass-ceramics were characterised using X-ray Diffraction (XRD), Dilatometry, Solid-State Nuclear Magnetic Resonance (NMR) and Scanning Electron Microscopy (SEM).

RESULTS AND DISCUSSION

XRD results of glass-ceramics revealed the diopside as the major crystalline phase. Platelet and dendritic diopside crystals with no signs of matrix micro-cracking were produced. Nano-scale fibres were also visible in the glassy matrix after sintering. Glass-ceramic (75Di-25Jd) and (50Di-50Jd) showed significantly higher BFS than all tested glass-ceramic groups ($p < 0.05$).

The mean (SD) and the median (Q1, Q3) BFS MPa results of the test groups are given in Table 1 where different superscript letters indicate significant differences between groups ($p < 0.05$). The measured thermal expansion coefficient of sintered specimens ($\text{TEC} \times 10^{-6} \text{K}^{-1}$, $100-400^\circ\text{C}$) was; 100Di-0Jd: 9.12, 85Di-15Jd: 9.22, 75Di-25Jd: 9.11, 50Di-50Jd: 8.65, 25Di-75Jd: 8.66. From the ^{27}Al NMR a sharp crystalline peak at -4ppm corresponding to Al(VI) species is present in all glass-ceramic formulations which was attributed to the formation of diopside solid solutions.

Glass-ceramic	Median BFS MPa (Q1, Q3)	Mean BFS MPa (SD)
100Di-0Jd	58.04 ^a (53.33, 61.22)	57.80 (7.26)
85Di-15Jd	125.14 ^b (105.17, 134.98)	119.62 (20.42)
75Di-25Jd	175.33 ^c (160.05, 204.33)	180.68 (28.62)
50Di-50Jd	164.45 ^c (145.22, 182.37)	168.11 (32.82)
25Di-75Jd	117.84 ^b (100.10, 143.38)	118.40 (29.44)

Table 1: BFS results of the experimental glass-ceramics

The results suggested that the formation of diopside solid solution led to remarkable increases in the BFS and TECs values in comparison to the 100Di-0Jd glass-ceramic which make the produced glass-ceramics suitable for all-ceramics diopside restorations.

CONCLUSION

New diopside glass-ceramic with acceptable mechanical strength and TECs compatible with Y-TZP ceramics were successfully produced. These glass-ceramics can be useful as a veneering material for Y-TZP ceramics and for all-ceramic diopside restorations. The produced glass-ceramics might also be a potential candidate for bone replacement materials.

REFERENCES

1. Della A. *et al.*, J.Amr. Dent.Ass. 139:8S-13S, 2008
2. Koenig V. *et al.*, J.Dent. 41:1164-1174, 2013
3. Rogers P. Miner Magaz. 37:741-758, 1970

ACKNOWLEDGMENTS

The authors would like to thank the Libyan Ministry of Higher Education for providing financial support to this project.



Functionally graded Guided tissue regenerative (GTR) membrane for periodontal lesions

S Qasim¹ R Delaine-Smith, A. Rawlinson, I. Rehman¹

¹Materials Science and Engineering Department, KROTO Research Institute, University of Sheffield, United Kingdom
sqasim@sheffield.ac.uk

INTRODUCTION

Chronic periodontal lesions largely heal by repair, with the formation of a long junctional epithelium and a limited amount of true regeneration of lost periodontal ligament, cementum and alveolar bone. Recently, a considerable amount of research has focused on increasing the regeneration of lost supporting tissues by the use of Guided Tissue Regeneration (GTR) membrane or the incorporation of biologically active molecules on the surface of membranes which will encourage regeneration. Both non-resorbable and resorbable GTR membranes are available, but with the limited success rate.¹ Consequently, there is a need for further research to develop bioactive functionalized GTR membranes (FGM) that may lead to improved regeneration of periodontal tissues lost due to the progression of disease.^{1,2}

The aim of this work is to design a biologically active, spatially designed, and functionally degradable occlusive membrane for periodontal lesions.

EXPERIMENTAL METHODS

Bioactive membranes, with controlled porosity and non-porous layers were developed using a combination of natural polymer Chitosan (CH) and Hydroxyapatite (HA). CH with two different molecular weights was used. Characterization was performed to analyze physiochemical and biological properties of the membrane. In-vitro tests (Alamar blue) assessed the viability and biocompatibility of the prepared specimens.

RESULTS AND DISCUSSION

The CH:HA membranes had a high degree of segregation of CH to HA. Other components of the FGM prepared were porous membranes and fibres obtained through freeze gelation and electrospinning. Scanning electron microscopy images showing prominent HA particles visible on one side of the membranes, freeze gelated membranes with a pore size of 150 to 200µm. (Figure 1). Highly oriented and random chitosan fibers were obtained by using ultrahigh molecular weight polyethylene oxide as a cross linker. Fourier transform infrared spectroscopy data (Figure 2) showed high degree of segregation in between the polymer and hydroxyapatite from the spectra collected on the top and bottom surfaces of various combinations used. Cell viability data (Figure 3) showed low molecular weight CH:HA 30:70 membranes had higher viability over a 7 day time period..

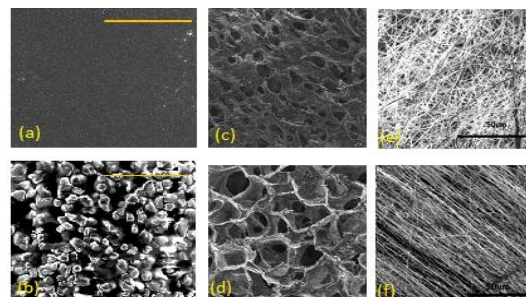


Figure1. (a, b) Top, bottom surface of CH:HA membranes, (c, d) Top, Cross section freeze gelated, (e, f) Random, aligned CH fibers

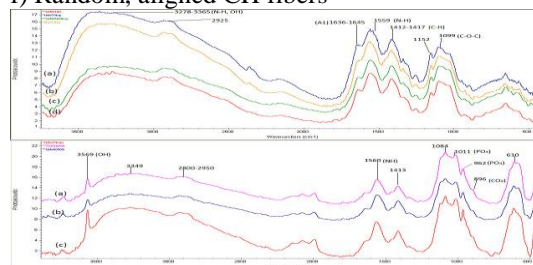


Figure 2 Top image of top surface of LMw CH:HA membranes, (a) 100:0 (b)70:30, (c) 50:50, (d) 30:70, Bottom image of bottom spectra (a)70:30, (b) 50:50, (c) 30:70).

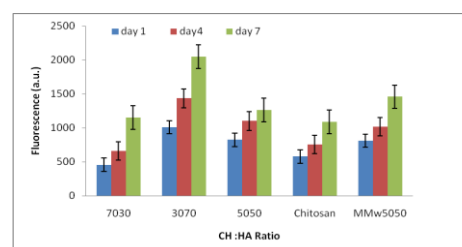


Figure 3 Alamar Blue on Day 1, 4 and 7

CONCLUSION

Functionally graded layers were successfully prepared. Membranes had bilayer surface, with CH dominating on top and HA on the bottom surface. Freeze gelated porous membranes and random and aligned CH fibers were prepared using nontoxic solvents. Bottom surface of membranes were biocompatible, which should be of value in periodontal regenerative procedures.

REFERENCES

1. Bottino MC, *et al.* Dent Mater.28:703-21. 2012
2. Dabra S, *et al.* Dent Res J.2012;9:671-80

ACKNOWLEDGMENTS

The authors acknowledge the support of ESPRC Delivery plan Pump Priming Grant.

Bioactivity Investigations with Calcia Magnesia Based composites

Emad Ewais^{*a}, Amira Moustafa^a, Karoline Pardun^b, Kuroschi Rezwan^b

^a Refractory & Ceramic Materials Division (RCMD), Advanced Materials Department, Central Metallurgical R&D Institute (CMRDI), P.O. Box 87, Helwan, 11421 Cairo, Egypt

^b Advanced Ceramics, University of Bremen, Am Biologischen Garten 2, 28359 Bremen, Germany

* Author to whom correspondence should be addressed (dr_ewais@hotmail.com)

Abstract

Different composite mixtures containing calcia-magnesia have been processed with addition of alumina, silica or zircon. These system powders were formed and fired at two different temperatures. Phase composition, microstructure, and physico-mechanical properties of these composites were determined. The in vitro bioactivity of these sintered composites were investigated by analysis of apatite-formation ability in the simulated body fluid (SBF) using SEM-EDS. The composite compositions termed “I”, “II” and “III” gave clear tendency toward the formation-ability of hydroxyapatite (HA). Composite “I” gave cubic and spindle HA crystallite, however, composites “II” and “III” fired at 1300 and 1400°C were formed typically “cauliflower” morphology and their evaluated physico-mechanical properties are similar to the properties of human cortical bone. Thus, composites “II”&”III” might be a promising bone implant materials. Besides the bioactivity of composite “I”, it contains highly cementing phase (CA) and bioinert (MA) phases, therefore, it might be nominated as a promised bioceramic material for different purposes such as scaffold, bone replacement, bone repair and coating.

Keywords: Calcia-magnesia, zircon, alumina, SBF, bending strength

Characterisation of Partially-Demineralised Dentine is a Prerequisite for Remineralisation Studies

Eleanor Ashworth*, Cheryl Miller, Christopher Deery and Nicolas Martin

School of Clinical Dentistry, University of Sheffield, UK

*mba07ema@sheffield.ac.uk

INTRODUCTION

There is a wide range of acids involved in the demineralisation of dentine but it is unknown how they differ in their effect on the remaining collagen matrix. There is increasing research interest in the development of a remineralisation technique for the management of partially demineralised dentine that enables the preservation and remineralisation of the affected collagen matrix¹. Understanding the effect of the different acids is key to the development of appropriate remineralisation strategies. Current remineralisation studies of acid-affected dentine are based on the presumption that all acids affect dentine in the same manner. In this way, research models of partially-demineralised dentine with formic acid, phosphoric acid or EDTA have become a ubiquitous standard used for remineralisation studies². The aim of this study is to fully characterise the partially-demineralised dentine matrix following exposure to a range of bacterial, dietary, gastric and laboratory acids.

EXPERIMENTAL METHODS

Dentine blocks were prepared from caries-free human premolars with a slow-speed precision saw. The dentine samples were divided into 8 groups: (1) water storage (control), (2) lactic acid (caries), (3) acetic acid (dietary), (4) phosphoric acid (dietary), (5) citric acid (dietary), (6) formic acid (laboratory), (7) EDTA (laboratory) and (8) hydrochloric acid (gastric). Each sample was immersed in 10 ml acidic solution for 14 days and refreshed every 24 hours. Demineralisation was terminated by alternating washes in 0.1 M cacodylate buffer and distilled water. Collagen integrity was analysed using scanning electron microscopy (SEM), surface micro-hardness (SMH) and hydroxyproline assay. Mineral content was measured using x-ray diffraction (XRD), energy dispersive spectroscopy (EDS) and micro computed-tomography (MCT).

RESULTS AND DISCUSSION

The characterisation techniques reveal a differential effect of the acids on the dentine structure and mineral content. Lactic acid causes the most demineralisation. Following lactic acid treatment, SEM images demonstrate that the collagen network becomes very exposed (Fig.1) and SMH results reveal the greatest decrease in hardness values. Additionally, EDS and MCT data reveal that the mineral content of dentine after treatment with lactic acid decreases the most (Fig.2).

Although lactic acid appears to demineralise the dentine samples the most, it does not appear to damage the

collagen network. EDS and XRD results show that citric acid has the least effect on mineral loss (Fig.4) but the hydroxyproline assay and SEM analysis (Fig.3) suggest that citric acid affects the collagen structure the most severely. Citric acid, in contrast to lactic acid, preserves mineral content but appears to degrade collagen the most.

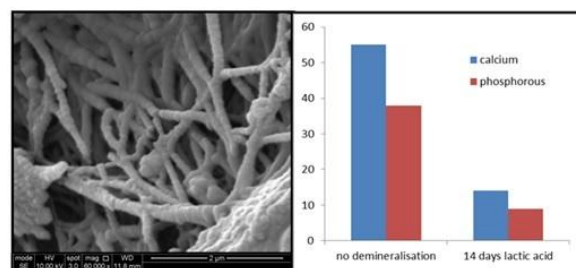


Figure 1: SEM of dentine after lactic acid treatment

Figure 2: Calcium and phosphorous levels after lactic acid treatment

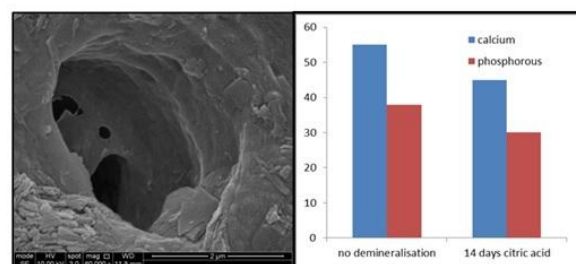


Figure 3: SEM of dentine after citric acid treatment

Figure 4: Calcium and phosphorous levels after citric acid treatment

CONCLUSION

Dentine demineralisation cannot be characterised by observing the collagen structure or measuring the mineral content alone. Complementary assays that analyse collagen integrity, surface hardness and mineral levels should be undertaken. The acids studied in this investigation have a markedly different effect on the dentine and this should be considered in the development of remineralisation strategies. This is especially relevant for studies that require a partially demineralised dentine model.

REFERENCES

1. Ten Cate JM. J. Dent. Res. 80:1407-1411, 2001
2. Zhang X. J. Mater. Sci. 23:733-742, 2012

ACKNOWLEDGMENTS

Thanks to BBSRC CASE studentship for financial support

Periodontal Regeneration by Combining Melt Electrospinning With Fused Deposition Modelling and Cell Sheet Technologies

Pedro Costa¹, Cédryck Vaquette², Qiyi Zhang³, Rui L. Reis^{4,5}, Saso Ivanovski⁶, Dietmar W. Hutmacher²

¹Institute for Medical Microbiology, Immunology and Hygiene, Technical University of Munich, Germany

²Institute of Health and Biomedical Innovation, Queensland University of Technology, Brisbane, Australia

³College of Chemical Engineering, Sichuan University, Chengdu, China

⁴3B's Research Group – Biomaterials, Biodegradables and Biomimetics, University of Minho, Guimarães, Portugal

⁵ICVS/3B's – PT Government Associate laboratory, Braga, Portugal

⁶Griffith Health Institute, School of Dentistry and Oral Health, Griffith University, Southport, Australia

pedro.costa@tum.de

INTRODUCTION

An inefficient or inexistent treatment of periodontal disease can ultimately result in tooth loss due to progressive destruction of surrounding soft and hard tissues¹. Despite not being totally predictable or surgically practical², Guided Tissue Regeneration (GTR)³ is the most widely used regenerative procedure for treating this disease. This study investigated the ability of an osteoconductive biphasic scaffold produced by combination of melt electrospinning and fused deposition modelling to simultaneously regenerate alveolar bone, periodontal ligament and cementum. The scaffold's design aimed at maximizing periodontal GTR treatment efficiency as well as the ease of handling by surgeons and commercial viability.

EXPERIMENTAL METHODS

An in-house melt electrospinning device (patent application in preparation) was utilized to produce medical grade polycaprolactone (PCL) (Lactel, USA) electrospun meshes. PCL was electrospun at 80°C, 20 µl/h feed rate, 7 kV voltage and 4 cm tip-to-collector distance. The obtained circular meshes reached 8 mm diameters after 4 min electrospinning periods onto aluminium foil covering the collector. The meshes were then attached to scaffolds produced by fused deposition modelling (FDM) through a quick melt and press-fitting process. The FDM component was composed of medical grade PCL and β -tricalcium phosphate (20% wt) (Osteopore Inc., Singapore), possessed 100% interconnectivity, 70% porosity and a 0/90 degrees lay-down pattern. Prior to attachment to the electrospun mesh and in order to increase osteoconductivity, the FDM scaffold was submitted to a calcium phosphate coating process by successive immersion into sodium hydroxide and simulated body fluid. Scaffold's morphology and coating composition were assessed by scanning electron microscopy (SEM) and X-ray diffraction (XRD) analysis, respectively. Biphasic scaffolds were seeded and cultured *in vitro* for 6 weeks with sheep primary osteoblasts on the FDM compartment and characterized by alkaline phosphatase activity/DNA content quantification, SEM and confocal laser microscopy. Micro computerized tomography (Micro-CT) analysis was also employed to assess the degree of mineralization. The cultured constructs were further tested in an ectopic *in vivo* study in rats. Briefly, the constructs were complemented with the placement

of several sheep primary periodontal cell sheets over the construct's electrospun mesh, attached to a dentin block and subcutaneously implanted into athymic rats for 8 weeks. The construct's *in vivo* performance was assessed by micro-CT and histological analysis.

RESULTS AND DISCUSSION

SEM and XRD analysis showed that the scaffold's bone compartment was homogeneously coated with a 600-800 nm calcium phosphate layer. The periodontal compartment was composed of randomly orientated PCL fibres with diameters of 100-400 µm. It was also visible that the fusion-press-fit scaffold assembly was not detrimental to the physical integrity of each individual component. The *in vitro* cell culture study showed that the coating of the scaffold's bone compartment resulted in significant increase in alkaline phosphatase activity and enhanced mineralization. Similar results were found *in vivo* where scaffold coating resulted in significantly greater bone formation. Histological analysis showed periodontal attachment at the dentin interface and that periodontal compartment's large pore size permitted vascularization of cell sheets. The developed scaffold technology is currently being commercially explored by the startup company Biofabrication Design Solutions Pty Ltd.

CONCLUSION

The studied biphasic scaffold displayed suitable properties for periodontal regeneration and promoted integration of tissues from both compartments. As well, high vascularization levels and tissue orientation were seen in the bone and periodontal compartments, which is of high significance for fibre attachment formation.

REFERENCES

1. Armitage G.C., Ann. Periodontol. 4, 1–6, 1999
2. Needleman I.G. *et al.*, Cochrane Db. Syst. Rev. 2, Art: CD001724, 2006)
3. Gottlow J. *et al.* J. Periodontol. 61, 680–685, 1990

ACKNOWLEDGMENTS

This work was supported by the Australian Research Council and National Health and Medical Research Council. Pedro Costa would like to thank the Portuguese Science foundation for his PhD fellowship and the TUM University Foundation for his current Postdoctoral fellowship.



Development of a pro-angiogenic cell-delivery vehicle based on RGD-alginate hydrogels

Sílvia J. Bidarra¹, Fátima R. Maia, Joana Gesta, Cristina C. Barrias¹

¹ INEB - Instituto de Engenharia Biomédica, Universidade do Porto, Portugal,
sbidarra@ineb.up.pt

INTRODUCTION

Neovascularization is a critical step towards recovery of injured and ischemic tissues. Cell-based approaches of endothelial cells (EC) transplantation are attractive, but clinical trials have not resulted in consistent benefit. The outcome might be improved by using biomaterial vehicles to protect cells from the harsh in vivo environment, enhancing their survival and engraftment. Alginate hydrogels are ideal candidates to mediate cell delivery and accommodate cells in a 3D microenvironment due to their ECM-like features¹. Embedded in this type of matrix, cells are expected to develop tissue-like order intercellular structures (cell-matrix and cell-cell interactions). This process is dependent on several matrix cues, such as cell-adhesion sites and matrix stiffness, which will in turn modulate cell-cell interactions. The potential of these hydrogels as vehicles for EC and mesenchymal stem cells (MSC)^{2,3} has been previously demonstrated. Considering the reciprocal regulation and functional relationship between both cell types and their role in the angiogenesis process, the aim of this work was to optimize 3D microenvironments for EC and MSC that could be further explored in the co-entrapment of both cell types as a pro-angiogenic therapeutic strategy.

EXPERIMENTAL METHODS

PRONOVA ultrapure sodium alginates LVG and VLVG (hereafter designated as high molecular weight, HMW (≈ 150 kDa) and low molecular weight, LMW (≈ 25 kDa); respectively) with a high guluronic acid content ($>67\%$) were purchased from FMC Biopolymers and further modified through grafting of RGD peptides to promote biofunctionality^{2,3}. Human umbilical vein endothelial cells (HUVEC, ScienCell) and MSC (Lonza) were entrapped within RGD-alginate combined with calcium carbonate, and gel formation was triggered by adding a fresh solution of gluconate delta-lactone. EC and MSC were entrapped alone or in co-culture within RGD-alginate under different conditions: 1 and 2 wt.% alginate with 100% HMW or 50%HMW/50%LMW (HLMW), with cell densities ranging from 5 to 30 million cells/mL and RGD densities from 50 to 250 μ M. Cell viability and metabolic activity were assessed by the trypan blue dyes exclusion assay and the resazurin assay, respectively. Cell morphology was analysed by CLSM (F-actin staining). To assess MSC migration through the hydrogels, cells were first seeded on PS beads that were then embedded in alginate. In some studies, cells were labelled CellTracker Blue (MSC) and Green (EC) and with Ac-Dil_LDL (EC). Fibronectin expression was analyzed by immunostaining.

RESULTS AND DISCUSSION

EC were only able to spread and form multicellular networks when entrapped in the softer matrices (1 wt.% alginate), containing RGD, at high cell densities (≥ 15 million cells/mL in HMW hydrogels, and ≥ 10 million cells/mL in HLMW hydrogels). Under these conditions cell viability remained high ($>70\%$). On the other hand, MSC were able to contract the matrix and form multicellular aggregates within 1 wt.% RGD-alginate (≥ 100 μ M RGD), but not within 2 wt.% RGD-alginate. Cell migration and matrix contraction were facilitated in HLMW as compared with HMW hydrogels (Fig. 1). In view of the previous results, MSC and EC co-cultures in 3D were established using 1 wt.% HLMW RGD-alginate hydrogels. Both cell types were able to rearrange inside the matrix, forming multicellular structures stabilized by a fibronectin mesh. Moreover, EC were able to align into tubular-like structures within these microtissues.

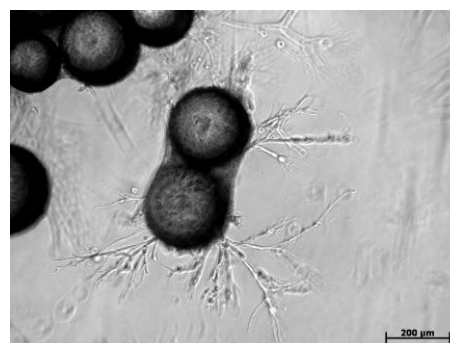


Figure 1. MSC sprouting from PS beads embedded within 1 wt.% HLMW RGD-alginate after 20 days in culture.

CONCLUSION

The combination of soft RGD-alginate matrices with co-entrapped MSC provides an adequate 3D microenvironment for EC, and might be a suitable strategy to create adequate vehicles for EC-based pro-angiogenic therapies.

REFERENCES

1. Bidarra SJ *et al.* Acta Biomater 10: 1646-62, 2014.
2. Bidarra SJ *et al.* Biomaterials 32: 7897-904, 2011
3. Maia FR *et al.* Acta Biomater, 10:3197-208, 2014.

ACKNOWLEDGMENTS

Portuguese Foundation for Science and Technology (FCT) for post-doctoral grant SFRH/BPD/80571/2011. FundoEuropeu de Desenvolvimento Regional, Programa Operacional Fatores de Competitividade-COMPETE, Quadro de Referência Estratégico Nacional, and Fundo Social Europeu [PEst-C/SAU/LA0002/201

The osteogenic potential of human mesenchymal stem cells - Connections to inflammation and infection

Cecilia Granéli¹, Xiaoqin Wang¹, Forugh Vazirisani¹, Margarita Trobos¹, Helena Brisby²,
Anders Lindahl³, Omar Omar¹, Karin Ekström¹, Peter Thomsen¹

¹Department of Biomaterials, Institute of Clinical Sciences, Sahlgrenska Academy at University of Gothenburg, Sweden.

cecilia.graneli@gu.se

²Department of Orthopaedics, Institute of Clinical Sciences, Sahlgrenska Academy at University of Gothenburg, Sweden

³Department of Clinical Chemistry and Transfusion Medicine, Institute of Biomedicine, Sahlgrenska Academy at University of Gothenburg, Sweden

INTRODUCTION

The inflammatory environment that arises from the immune response towards an infection, or in inflammatory diseases is believed to be detrimental for bone and exert negative effects on bone forming cells and their progenitors, the mesenchymal stem cells (MSCs). At the same time it has been demonstrated that MSCs act on the immune systems by for example suppressing the expression of pro-inflammatory cytokines.¹ Furthermore, monocytes of a pro-inflammatory phenotype, activated by inflammatory stimulus lipopolysaccharide (LPS), secrete both soluble factors and exosomes that have positive effects on the osteogenic response of human MSCs.^{2,3} However, the communication between immune cells and MSCs, especially in the context of regeneration in the presence of a pathogen or other molecules triggering inflammation, is a key process that is incompletely understood. The aim of the present study was therefore to investigate the effects of different immune-stimulatory molecules such as membrane vesicles (MVs), isolated from gram-positive bacteria *S. aureus* and *S. epidermidis* on the osteogenic differentiation and secretory response of hMSCs.

EXPERIMENTAL METHODS

- hMSCs were isolated from bone marrow aspirates taken from the *iliac crest*. The hMSCs were expanded *in vitro* and subsequently osteogenic differentiation was induced.
- MVs were isolated from *S. aureus* and *S. epidermidis*. MVs, and reference stimuli LPS and lipoteichoic acid (LTA) were added to osteogenic cultures of hMSCs.
- The secretion of cytokines by the hMSCs was determined by multiplex assay. Two time points were investigated, 72 hours and one week.
- The progression of the osteogenic differentiation, in the presence of inflammatory stimuli, was evaluated by measurement of ALP-activity and matrix mineralization quantification.
- The progression of the osteogenic differentiation, in the presence of inflammatory stimuli, was evaluated by measurement of ALP activity and quantification of matrix mineralization.

RESULTS AND DISCUSSION

All stimuli used in this study promoted osteogenic differentiation of hMSCs. This was demonstrated by significantly increased levels of ALP activity and matrix mineralization. ALP levels in the stimulated

cultures were up to three times higher compared to the control condition.

In response to stimulation with LPS, hMSCs significantly up-regulated the gene expression of TLR2 as well as the production of a majority of the cytokines analysed. Bacterial MVs had distinct effects on TLR gene expression and cytokine secretion. The levels of IL-17 and TNF- α were elevated in cultures treated with *S. epidermidis* MVs compared to unstimulated cultures. This stimulation also resulted in an up-regulated gene expression of TLR2 and TLR3 whereas this gene expression was unaffected by *S. aureus* MV-stimulation. However, *S. aureus* MV-stimulation of osteogenic hMSC cultures resulted in increased IL-4 secretion. Over time, a majority of the stimuli, including the osteogenic medium alone, resulted in an increase in IL-2, IL-4, IL-17 and TNF- α .

CONCLUSION

- Pro-inflammatory and immune-triggering molecules can promote the osteogenic differentiation and alter the cytokine secretion of hMSCs *in vitro*.
- Bacterial MVs released from gram-positive bacteria *S. aureus* and *S. epidermidis* promote osteogenic differentiation of hMSCs *in vitro*.
- Bacterial MVs affect the secretion of both pro-inflammatory and immunomodulatory cytokines by hMSCs, indicating that these cells may have a role in host defence processes.

REFERENCES

1. Maggini, J. *et al.* Mouse bone marrow-derived mesenchymal stromal cells turn activated macrophages into a regulatory-like profile. *PLoS ONE* **5**, e9252 (2010).
2. Omar, O. M. *et al.* The stimulation of an osteogenic response by classical monocyte activation. *Biomaterials* **32**, 8190–8204 (2011).
3. Ekström, K. *et al.* Monocyte exosomes stimulate the osteogenic gene expression of mesenchymal stem cells. *PLoS ONE* **8**, e75227 (2013).

ACKNOWLEDGMENTS

The authors would like to acknowledge the Swedish Research Council, BIOMATCELL VINN Excellence Center of Biomaterials and Cell Therapy, the IngaBritt and Arne Lundberg Foundation, the Vilhelm and Martina Lundgren Vetenskapsfond, and the Västra Götaland Region for providing financial support for this research.



Influence of Sintering Conditions on the Properties of Porous TiO₂ Bone Scaffolds

Katarzyna Reczyńska^{1,2}, Håvard J. Haugen² and Hanna Tiainen^{2*}

¹Department of Biomaterials, AGH University of Science and Technology, Poland

^{2*}Department of Biomaterials, University of Oslo, Norway, hanna.tiainen@odont.uio.no

INTRODUCTION

Microstructure typically has a strong influence on both the mechanical properties of bioceramics and the cell behaviour on their surface. Since the typical sintering process of previously developed TiO₂ scaffolds (20h at 1500°C) results in large and relatively inhomogeneous grain sizes,¹ the objective of this study was to evaluate the influence of different sintering conditions on the grain growth in highly porous TiO₂ bone scaffolds and the impact of the grain size on the material properties and cell behaviour on such scaffolds.

EXPERIMENTAL METHODS

Highly porous TiO₂ scaffolds were produced using polymer sponge replication as previously described.³ Sintering temperature, dwell time, and cooling rate were varied to examine the effect of these parameters on the grain growth and densification of the material. SEM imaging and micro-CT analysis were used to examine the microstructural features of the scaffolds, while the mechanical properties were assessed by compression test. An in vitro cell study using SaOs-2 cell line was performed to evaluate the impact of the altered grain size on the behaviour of osteoblast-like cells on the TiO₂ surface using fluorescent microscopy. Due to the complex 3D structure of the 3D scaffold, TiO₂ discs with three different average grain sizes (small: <5µm, medium: <10µm, and large: <50µm) were prepared using similar TiO₂ slurry and sintering conditions as for the porous scaffolds.

RESULTS AND DISCUSSION

In order to curb the grain growth in TiO₂ scaffolds, multistep sintering was applied in which the sintering is initiated at a temperature favouring after which the densification is completed at a lower temperature. The optimal temperature for initiating the sintering of the ceramic particles was found to be 1350°C, as higher temperatures resulted in exceedingly increased grain growth rate without significant increase in densification, while dwell time of 20h at 1250°C was required to achieve maximum densification of the TiO₂ material.

By multistep sintering the mean grain diameter was reduced tenfold from >50µm of the reference scaffolds sintered 20h at 1500°C to <5µm. Although finer and more uniform grain size generally improves the mechanical properties of ceramic materials, the refined microstructure did not increase the compressive strength of the TiO₂ scaffolds as the average strengths of all scaffold groups prepared by multistep sintering were less than 93% of that of the reference scaffolds. The high compressive strength of the scaffolds sintered for >20h at 1500°C can be attributed to folding of the

strut walls that partially eliminates the triangular void created by the polymer foam template,¹ which could not be achieved during any of the multistep sintering condition applied in this study (Fig 1). This was seen as a slight but not statistically significant increase in closed porosity in the scaffold structure.

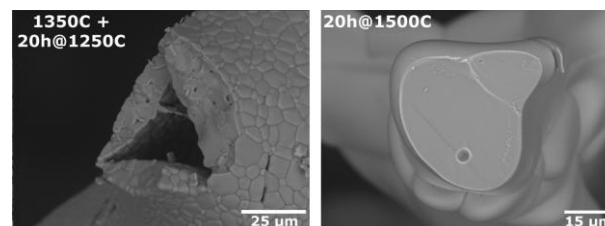


Fig.1: Cross-section of the scaffold struts after sintering.

The grain size of the TiO₂ material was also found to influence the cell behaviour of SaOs-2 cultured on TiO₂ discs. A considerably larger number of cells was present on the surface of the TiO₂ discs with large and medium grain sizes in comparison to the smallest tested average grain size at day 3. The cells on these surfaces were also more clustered, while the cells cultured on the small-grained samples tended to only cluster around superficial cracks in the material. In addition to having the highest number of cells at day 7, the cells on the large-grained TiO₂ discs were most clustered and spread on sample surface. This may be related to the distances between the grain boundaries as the cells are likely to use the grain boundaries as anchorage points onto the surface. No statistically significant differences were detected in ALP activity at any on the tested time points between the three different groups (1d, 3d, 7d; *n* = 3).

CONCLUSION

TiO₂ scaffolds with considerably refined microstructure were produced by optimising the sintering conditions. However, the folding and full densification of the strut structure could not be achieved during the multistep sintering, which limits reduction of closed internal porosity within the scaffold, thus reducing the mechanical strength of the scaffold struts. Furthermore, larger grain size appeared to favour the proliferation and spreading of SaOs-2 cells on TiO₂ surface.

REFERENCES

1. Tiainen H. *et al.*, J.Eur Ceram Soc, 33: 15-24, 2013
2. Tiainen H. *et al.*, J Mat Sci Mater Med, 21:2783-2792, 2010

ACKNOWLEDGMENTS

This study was supported by the Norwegian Research Council (NFR228415/070).

Biomaterials for 2D and 3D bio-hybrid robotic devices

Leonardo Ricotti* and Arianna Menciassi

The BioRobotics Institute, Scuola Superiore Sant'Anna, Italy

*Presenting author, e-mail: l.ricotti@sssup.it

INTRODUCTION

Robotics is nowadays facing emerging challenges, due to the need of designing and developing novel machines able to perform complex tasks in non-structured environments and to maintain their functionality for long periods (*e.g.* by self-repairing their structures).

Wet machines and bio-hybrid robotic components recently emerged, opening the way towards the integration of living cells and tissues within artificial devices¹. This approach allows to exploit the unique features of living elements (high efficiency, self-healing capability, glucose-based powering, etc.), although several technological challenges must be faced before achieving this objective^{2,3}.

This work aims at reporting the author's achievements in the field of bio-hybrid systems (mainly concerning bio-hybrid actuation) and at highlighting that 2D and 3D biomaterials are key components of any bio-hybrid machine.

2D BIO-HYBRID ACTUATORS

Actuation has been the most investigated function in the field of bio-hybrid systems, due to the current lack of suitable actuation technologies able to efficiently scale down in dimensions and to reproduce life-like movements in artificial devices⁴.

A possible strategy to build cell-actuated systems is to use 2D biomaterials, to be contracted by muscle activity⁵. Polylactic acid (PLA) ultra-thin films were developed by the authors to this purpose. Such structures were characterized by a high biocompatibility, easy tailorability and high stability (due to the long degradation time, typical of PLA). PLA nanofilms showing a 350 nm thickness were seeded with murine skeletal muscle cells (C2C12 cell line)⁶, achieving a good differentiation, and efficiently contracted by primary cardiomyocytes. Thinner films (down to 50 nm) were also developed by the authors, and coupled with rat cardiac precursors (H9c2 cell line)⁷.

The engineering of muscle cell behaviour on the biomaterial's surface is obviously of primary importance for achieving a functional bio-hybrid actuator. In order to tune surface electrical properties, the authors developed layer-by-layer nanofilms made of poly(sodium-4-sulfonate) (PSS) and poly(allylamine hydrochloride) (PAH). Surface charges were correlated to cell proliferation and differentiation levels⁸. Surface topography was also engineered. The authors fabricated electrospun polyhydroxybutyrate (PHB) scaffolds. The anisotropy of the produced biomaterial allowed an efficient cell alignment, which is a pre-requisite for achieving a bio-hybrid device able to exert a considerable force along one controlled direction⁹.

Recently, the authors demonstrated the synergic effects of a tuned elastic modulus (~ 14 kPa) of the substrate (made of polyacrylamide, PA), an anisotropic

topography and an intracellular stimulation mediated by active nanoparticles. C2C12 cells enhanced their electrical (and consequently their contractile) activity¹⁰.

3D BIO-HYBRID ACTUATORS

A shift towards 3D bio-hybrid actuators would allow to obtain easier-to-handle, usable and powerful machines. However, the need of a vasculature limits this ambitious objective. The recent literature reports some examples of 3D systems, but all of them are limited to small dimensions¹¹.

The authors recently reported the development of a large quasi-3D bio-hybrid system based on the self-assembly (by rolling) of a 2D polydimethylsiloxane membrane, previously seeded with muscle cells¹². The addition of a dedicated pseudo-vasculature to the biomaterials will allow to achieve really 3D functional and long-term stable bio-hybrid actuators.

BIO-HYBRID SENSORS

Bio-hybrid sensors can be fabricated by integrating living cells able to transduce signals and proper reading circuitries. Few examples of bio-hybrid sensors are described in the literature^{13,14}. Most of them do not focus on biomaterials with tuned properties, but only on the transduction mechanism assured by cells. The authors achieved preliminary results (not published) on a bio-hybrid tactile sensor. The use of a proper biomaterial as interface between the cells and the reading system can strongly modulate the signal output, thus opening new possibilities.

CONCLUSION

2D and 3D biomaterials constitute a key element for the development and maintenance of bio-hybrid systems. The combination of different material properties, able to drive cell behaviors towards the required performances, will enable a significant advancement of the bio-hybrid paradigm.

REFERENCES

1. Xi J. *et al.*, Nat. Mater. 4:180-184, 2005
2. Chan V. *et al.*, Lab Chip. 14:653-670, 2014
3. Kamm R.D. *et al.*, Ann. Biomed. Eng. 42:445-459, 2014
4. Ricotti L. *et al.*, Biomed. Microdev. 14:987-998, 2012
5. Feinberg A.W. *et al.* Science. 317:1366-1370, 2007
6. Ricotti L. *et al.*, Biomed. Microdev. 12:809-819, 2010
7. Fujie T. *et al.*, Langmuir. 27:13173-13182, 2011
8. Ricotti L. *et al.*, Biomed. Mater. 6:031001, 2011
9. Ricotti L. *et al.*, Biomed. Mater. 7:035010, 2012
10. Ricotti L. *et al.*, PLoS ONE. 8:e71707, 2013
11. Cvetkovic C. *et al.* Proc. Nat. Acad. Sci. 111:10125-10130, 2014
12. Ricotti L. *et al.*, Proc. Living Machines 2013. 8064:251-261, 2013
13. Yagi T. *et al.*, Int. J. Appl. Biomed. Eng. 2:1-5, 2009
14. Adamatzky A. *et al.* Sens. Act. B: Chem. 188:38-44, 2013



Self-healing Hybrid Nanocomposites based on Bisphosphonated hyaluronan and Calcium Phosphate Nanoparticles for bone regeneration

Reza Nejadnik¹, Xia Yang², Matilde Bongio¹, Hamdan S. Alghamdi¹, Jeroen J.J.P. van den Beucken¹, Marie C. Huysmans³, John A. Jansen¹, Jöns Hilborn², Dmitri Ossipov^{2,*}, and Sander C.G. Leeuwenburgh^{1,*}

¹*Department of Biomaterials, Radboud University Medical Centre, Netherlands, sander.leeuwenburgh@radboudumc.nl

²*Department of Chemistry-Ångström, Uppsala University, Sweden, dmitri.ossipov@kemi.uu.se

³Department of Preventive and restorative dentistry, Radboud University Medical Centre, Netherlands

INTRODUCTION

Nanocomposites formed via non-covalent interactions between acidic proteins and metallic ions or inorganic nanoparticles show outstanding structural properties in natural nanocomposite materials such as nacre and bone¹. Therefore, non-covalent interactions have been explored to construct complex, biomimetic materials that mimic the hybrid nanostructure of such natural materials². Herein, we present a novel method to develop an injectable, robust nanocomposite based on reversible bonds between calcium phosphate (CaP) nanoparticles and bisphosphonate-functionalized hyaluronan (HA). CaP nanoparticles and hyaluronan were selected as dispersed matrix composite components due to their biocompatibility and chemical tailorability. Bisphosphonates are known to exhibit an exceptionally strong affinity to the mineral CaP phase in bone. The covalent attachment of bisphosphonate groups to the hyaluronan backbone should facilitate the formation of a hybrid nanocomposite via reversible bonds between polymer-grafted bisphosphonate ligands and CaP nanoparticles.

EXPERIMENTAL METHODS

Materials: Bisphosphonated hyaluronan polymer was prepared via thiol-ene photopolymerization between acrylated pamidronate and thiol-modified hyaluronan. CaP nanoparticles were prepared using a wet-chemical neutralization reaction between calcium hydroxide and phosphoric acid at 60 °C. Physically cross-linked hybrid nanocomposites (HABP•CaP) were prepared by mixing bisphosphonate-modified hyaluronan with suspensions containing CaP nanoparticles. Three types of HA based hydrogels that were chemically cross-linked by means of covalent hydrazone cross-links (HA, HABP, HA+CaP) were prepared as controls.

In vitro characterization: Polymers were analysed by ¹H and ³¹P NMR and CaP nanoparticles were characterized by FTIR, XRD and TEM. HABP•CaP hybrid nanocomposites were investigated using SEM, rheology, and pull-off tests to evaluate mineral adhesion. In addition, swelling and mineralization were tested upon soaking in PBS and/or SBF. (n=3)

In vivo test: Samples were implanted for 4 weeks in bone (femoral condyle defects diameter of 2.85 mm and a depth of 3.0 mm) and subcutaneous tissue (200 µL cylindrical implants) of healthy, skeletally mature male Wistar rats (n=6). Sections were stained using methylene blue and basic fuchsin followed by a qualitative evaluation of the material appearance and tissue response. The new bone formation was quantitative evaluated.

RESULTS AND DISCUSSION

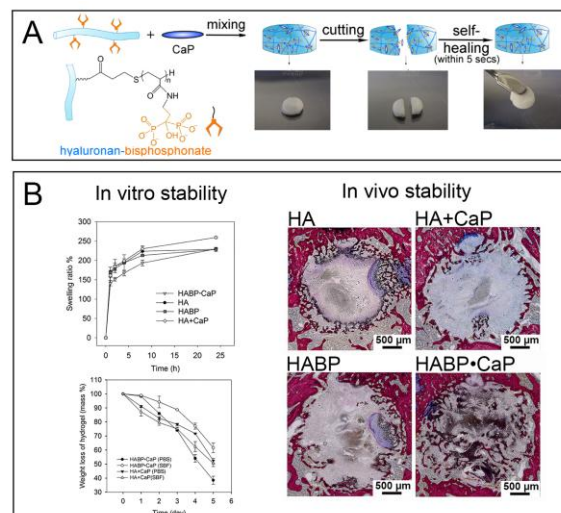


Figure 1A shows that the physically cross-linked hybrid nanocomposite formed by mixing hyaluronan-bisphosphonate with CaP nanoparticles. The hybrid materials displayed rapid (within 5 secs) and pronounced (98%) self-healing behavior. The reversible bonds between bisphosphonate groups and CaP nanoparticles were stronger than other non-covalent interactions. **Figure 1B** shows the stability of the chemically and physically cross-linked formulations in vitro and in vivo. Without the need for additional chemical -and potentially cytotoxic- cross-linking, HABP•CaP nanocomposites were as stable as chemically cross-linked HA hydrogels. Their stability increased under calcium-containing conditions (SBF and bone tissue). It indicated that the reversible bonds between bisphosphonate groups and CaP were sufficiently strong for bone regenerative applications.

CONCLUSION

We have presented a physically cross-linked hybrid nanocomposite, which outperforms conventional, chemically cross-linked analogues in terms of self-healing capacity and adhesiveness to mineral surfaces. Most importantly, these physically cross-linked composites were surprisingly robust yet biodegradable upon extensive in vitro and in vivo testing, thereby confirming that cohesive nanocomposites can be developed based on reversible bonds between polymer-grafted bisphosphonate ligands and calcium ions as present on the surface of nanoscale inorganic particles.

REFERENCES

1. Suzuki M. *et al.*, Science 325: 1388-1390, 2009
2. Dvir T. *et al.*, Nat. Nanotechnol. 6: 13-22, 2011

Development of novel LZ-8 protein-containing porous composite sponge scaffold for biomedical applications: biocompatibility evaluation and an animal study in rabbit

Chia-Yin Chen^{1,2,3}, His-Jen Chiang^{1,4}, Li-Hsiang Lin^{2,4}, Keng-Liang Ou^{1,2,3,5*}

¹Graduate Institute of Biomedical Materials and Tissue Engineering, College of Oral Medicine, Taipei Medical University, Taipei 110, Taiwan

²Research Center for Biomedical Devices and Prototyping Production, Taipei Medical University, Taipei 110, Taiwan

³Research Center for Biomedical Implants and Microsurgery Devices, Taipei Medical University, Taipei 110, Taiwan

⁴School of Dentistry, College of Oral Medicine, Taipei Medical University, Taipei 110, Taiwan

^{5*}Department of Dentistry, Taipei Medical University-Shuang Ho Hospital, New Taipei City 235, Taiwan, klou@tmu.edu.tw

INTRODUCTION

The success rate of dental implant in the maxilla is poorer because quality and quantity of bone in this area is often compromised due to resorption of alveolar crest or pneumatization of the maxillary sinus. Hence, the surgical technique is used to lifting the sinus membrane and creates extra-space for grafting materials to improve the insufficient bone quantity situation in the maxillary posterior area. Autogenous bone is considered the gold standard for grafting the elevated sinus space because of its excellent biocompatibility and bone regeneration potential. However, it still exists some disadvantages¹. Recently, incorporation of osteoinductive agents into the sinus graft materials was focused to accelerate de novo bone formation within the elevated sinus. Our latest research results found that the Ling Zhi-8 (LZ-8) protein can increase wound healing and osteogenic capability^{2,3}. Therefore, the purpose of this study was to develop and evaluate a novel LZ-8 protein-containing porous composite sponge (LZ-PCS) scaffold as the grafting material to elevate the sinus.

EXPERIMENTAL METHODS

The LZ-PCS scaffold was prepared by mixing with 1 mg/ml LZ-8 protein (Yeastern Biotech Co., Ltd., Taiwan), 5 mg/ml collagen, 10 mg/ml methyl cellulose and 15 mg/ml chitosan under -80°C cryogenic freeze drying. The MTT assay (osteoblast cell (MG-63) and fibroblast cell (NIH-3T3)) was employed to test the biocompatibility of the LZ-PCS scaffold. Twelve male New Zealand white rabbits (18–24 weeks, 3.3–3.8 kg) were included in the animal study (approved LAC-100-0053). The control group (TAI YEN Medifil, Taiwan) and LZ-PCS scaffold were inserted in the standardized bony defects (created by 2.5 mm trephine bur) of the nasal bones. The rabbits were sacrificed at 1, 2, 4 and 12 weeks postoperatively. Samples were subjected to histomorphometric examination for evaluating the quantity and quality of the regenerated bone.

RESULTS AND DISCUSSION

In MTT assay, the optical density (OD) values of the control sample increased with increasing the incubation periods when cultured with two different cells. High OD value indicates that the sample possesses a better cell adhesion behavior (i.e. well biocompatibility). As the LZ-PCS sample cultured with the two different cells for 72 h, it still exhibits a high OD value as compared with the control sample. This feature demonstrated that the LZ-PCS scaffold had no influence on the cell

adhesion and proliferation behaviors. The SEM observations of cell morphology of the LZ-PCS sample after culturing for 72 h also indicated that the cells exhibited good adhesion and differentiation. Histological results found that the control sample was largely resorbed at 4 weeks postoperatively (Fig. 1(a)). However, the LZ-PCS sample was filled with newly formed bones in the porous structure (Fig. 1(b)). The new bones of the LZ-PCS sample were found to have the greatest size and density compared with the control sample. The newly formed trabeculae were the smallest in the control group and had the least amount of structure. Flattening of osteoblasts and transformation to osteocytes in the lacunae were observed in the LZ-PCS sample. After 12 weeks surgery, the control sample was completely resorbed. In contrast, the new bone of the LZ-PCS sample cannot be distinguished from the surrounding bone histomorphometrically, which indicated completion of the bone remodeling.

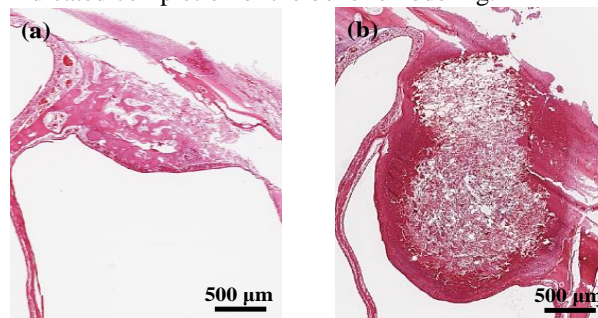


Fig. 1 Histomorphometric examination for the week 4 samples (H&E staining): (a) control group and (b) LZ-PCS group.

CONCLUSION

The LZ-PCS scaffold possesses good biocompatibility and well osteoinductive capability. Therefore, it can be developed as promising biomaterial for biomedical applications.

REFERENCES

1. Damien C.J. *et al.*, J. Appl. Biomater. 2:187, 1991
2. Lin H.J. *et al.*, Evid. Based Complement Alternat. Med. 2014:91531, 2014
3. Hsu H.A. *et al.*, J. Oral Maxillofac. Surg. 2014 (In press)

ACKNOWLEDGMENTS

This work was supported by the Department of Health, Executive Yuan, Taiwan (contract number MOHW103-TDU-N-211-133001).



Phase Constitution and Heat Treatment Behaviour of Ti-Mn-Sn Beta Type Alloys

Masahiko Ikeda^{1*}, Masato Ueda¹ and Mitsuo Niinomi²

^{1*}Department of Chemistry and Materials Engineering, Kansai University, Japan, hikoik@kansai-u.ac.jp

²Institute for Materials Research, Tohoku University, Japan

INTRODUCTION

Titanium and its alloys are suitable to biomaterials because of high specific strength, excellent corrosion resistance and good bio compatibility¹. Unfortunately, those alloys are constituted of rare metallic elements, e.g. molybdenum and niobium. Therefore, those alloys are costly. Users of biomaterials, e.g. medical doctors and patients, do not want to use higher cost biomaterials in all treating parts. Therefore, it is very important to develop reasonable cost metallic biomaterials, especially Ti alloys. To develop low cost Ti alloys as metallic biomaterials, Mn was adopted as beta stabilizing element. Mn is one of abundance metals in earth's crust and one of relatively easily available metals because of alloying materials used in steel making. Sn, which is no toxic for human body, was also adopted as alpha stabilizing element to suppress isothermal omega precipitation. As fundamental study to develop low cost beta type Ti alloy for medical application, phase constitution and heat treatment behaviour of Ti-9mass%Mn-Sn alloys were investigated through electrical resistivity and Vickers hardness measurements and X-ray diffraction.

EXPERIMENTAL METHODS

Ti-9mass%Mn-0, 1, 3 and 5mass%Sn alloys were prepared by laboratory scale arc furnace in high purity argon atmosphere. Obtained ingots were hot-forged and hot-rolled to about 4mm thickness at about 1120K. Specimens were prepared by cutting, grinding and polishing from hot-rolled flat bars. All specimens were solution treated at 1173K for 3.6ks and then quenched into iced water (STQ). Some STQed specimens were isothermally aged at 673K. In STQed and aged specimens, electrical resistivity was measured at room and liquid nitrogen temperatures. Vickers hardness was measured using 4.9N load at room temperature. Phase constitution was identified by X-ray diffraction at room temperature. In STQed specimens, microstructures were observed by optical microscope.

RESULTS AND DISCUSSION

In solution treated and quenched state (STQed state), beta phase was identified and equiaxed beta structures were observed in all specimens. Figure 1 shows changes in electrical resistivity at room and liquid nitrogen temperatures (ρ_{RT} and ρ_{LN}), resistivity ratio of ρ_{LN} to ρ_{RT} (ρ_{LN}/ρ_{RT}) and Vickers hardness (HV) with increase of tin content. Resistivities at both temperatures significantly increased at 1Sn and gradually increased up to 5mass%Sn.

Resistivity ratio significantly increases up to 3Sn and slightly increased at 5Sn. Vickers hardness (HV) decreased up to 3mass%Sn and then increased at 5Sn.

Increase of resistivity is due to dissolution of Sn in Ti. Decrease of HV is due to decrease of athermal omega with increase in Sn content².

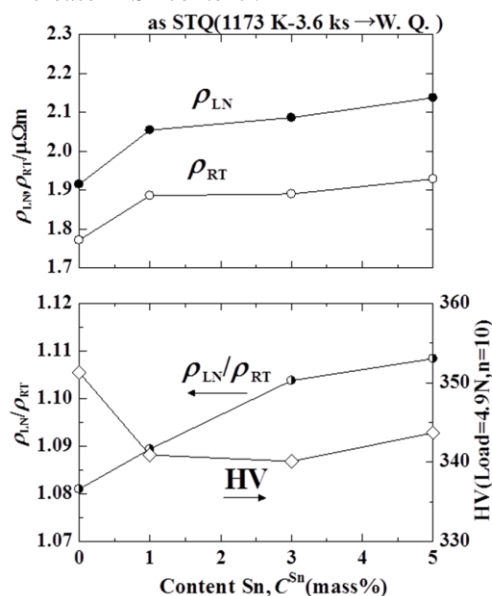


Fig. 1 Changes in ρ_{RT} , ρ_{LN} , ρ_{LN}/ρ_{RT} and HV with increase in Sn content.

In isothermal aging at 673K, isothermal omega was identified at aging time between 0.12 and 0.3ks in all alloys. On aging up to 300ks, alpha precipitates were identified in 0, 1 and 3Sn alloy. It is considered that isothermal omega precipitation was suppressed by tin addition. Therefore, aging time at which alpha precipitate was observed is late by tin addition.

CONCLUSION

Results obtained from investigation of phase constitution and aging behaviour of Ti-Mn-Sn alloy are shown as follows. In STQed state, only beta phase was identified in all alloys. Resistivity tends to increase and HV tends to decrease with increase in Sn content. On 673K aging, isothermal omega precipitated and then alpha precipitated.

REFERENCES

1. Niinomi M., Recent Biocompatible Metallic Materials, edited by N. Niinomi *et al*, Structural Biomaterials for the 21st Century, pp. 3, 2001.
2. Ikeda M. *et al.*, J. JILM, 622-626, 1992.

ACKNOWLEDGMENTS

One of authors thanks to the light Metal Educational Foundation, Inc. for providing financial support to this study.

Hyaluronic Acid Bound Bisphosphonates As A Novel Therapeutic Strategy For Osteoporosis

Sujit Kootala¹, Dmitri Ossipov¹, Xia Yang¹, Yu Zhang¹ and Jöns Hilborn^{1*}
¹Department of Chemistry/Polymer Chemistry, Uppsala University, Sweden
sujit.kootala@kemi.uu.se

INTRODUCTION

Osteoporosis affects nearly 30% of the female population and 20% of the male population worldwide. Clinically, bisphosphonates are commonly used as drugs for the treatment of osteoporosis. However, due to ineffective methods of targeting and delivery, it has been observed that administering the drug orally or intravenously leads to oesophageal cancer, osteonecrosis of the jaw and atypical stress fractures of the long bones. In this study, we demonstrate through an in vitro co-culture model that chemically linking bisphosphonates to biodegradable polymers like hyaluronic acid enhances the specificity of bisphosphonates by targeting osteoclasts and reduces off-target side effects thereby offering better delivery strategies at significantly lower dosages.

EXPERIMENTAL METHODS

Hyaluronic acid (HA) of 7.5 kDa and 150 kDa was purchased from Lifecore (U.S.A) and the fragments were linked to bisphosphonate (BP) groups as described previously (1). RAW 264.7 cells or Peripheral Blood Monocytes (PBMC's) were differentiated on one side of bone discs (Bone Slices, Denmark) according to published procedures for 21 days. MC3T3-E1 cells or Saos cells were cultured on the opposite side of the bone disc and differentiated using previously described procedures[2]. After 21 days of differentiation, the cells washed with 1X PBS and cultured for 24 hours with different doses of neutralized HA-BP in a concentration dependent manner. At 24 hrs, the cells were washed with 1X PBS, fixed with 4% PFA and cells were TRAcP stained for osteoclastic activity. Scanning Electron Microscopy (SEM) was performed post-processing the discs to observe resorption pits. [1].

RESULTS AND DISCUSSION

After the differentiation period of 21 days, the bone discs were processed to identify the extent of mineralization and resorption. Electron microscopy revealed large number of resorption pits with size range between 10µm to 100µm. TRAcP staining for osteoclast activity revealed numerous multinucleated cells. Cells with three or more nuclei were classified as osteoclasts using Image J for analysis. The HA-BP treatment on the 2-sided culture revealed a controlled reduction in the number of osteoclasts compared to discs with osteoclasts alone. The quality of mineralization by osteoblasts and the resorptive activity of the osteoclasts were unaffected in all the conditions, verified by electron microscopy and analysis of the metabolic activity of the cells.

Effects	Co-culture on same side	Co-culture on opposite side
Resorption pits	+++	++
Mineralized nodules	+++	++

Table 1 showing that the co-culture model performed equally or better than the same-sided culture with cells exerting control on each other.

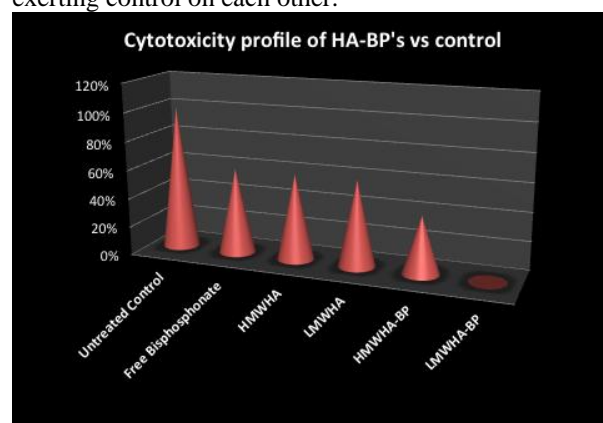


Figure 1. Low molecular weight HA-BP shows high potency towards human osteoclasts on the co-culture model normalized to untreated control and free drug.

Here we demonstrate the potency of etidronate linked to low molecular weight hyaluronic acid against murine and human osteoclasts both in single and two-sided cultures. Osteoblasts and osteoclasts together in two-sided culture result in fewer mature osteoclasts that could be attributed to cellular cross talk via soluble factors.

CONCLUSION

These results encourage the possibility of applying new delivery mechanisms as well as a novel in vitro method to test the effect of soluble drugs like bisphosphonates on bone related cells. This opens up the possibility of testing drugs at a lower dose and provides more useful information on the possible interaction of the drug with the behaviour of two different cell types, therefore moving a step closer to the in vivo scenario

REFERENCES

1. Hulsart-Billstrom, G., et al., *Biomacromolecules*, 2013. 3055-63.
2. Heinemann, C., et al., *Eur Cell Mater*, 2011. 80-93.

ACKNOWLEDGMENTS

"The authors would like to thank MutiTERM (Grant no: 238551) for providing financial support to this project".

Influence of Anchor Strand Related Parameters on Immobilized Amount and Hybridization Efficiency in a Nucleic Acid-based Immobilization System for Titanium Implants

Cornelia Wolf-Brandstetter¹, Jan Michael², René Beutner¹, Bernd Schwenzer², Henning Schliephake³,
Dieter Scharnweber¹

¹Institute of Materials Science, MBC, TU Dresden, Germany. Cornelia.Wolf-Brandstetter@tu-dresden.de

²Chair of General Biochemistry, TU Dresden, Germany,

³Dept. of Oral and Maxillofacial Surgery, George-Augusta-University, Göttingen, Germany

INTRODUCTION

For further improvement of titanium-based implants a nucleic acid-based immobilization system was developed [1]. The approach involves two steps. The first step is the immobilization of single-stranded nucleic acids (anchor strands = AS) on the implant surface via partial regioselective incorporation into an anodically grown oxide layer (Fig. 1 a,b). The second step, to be done prior to implantation, comprises the hybridization of the anchor strands with complementary strands conjugated with bioactive molecules, selected according to the needs of individual patients (Fig. 1c)¹. Standard γ -sterilization conditions can be applied after the first step. However, strand damages may occur, which are mainly attributed to the formation of reactive oxygen species during anodic polarization and sterilization as well as to the photocatalytic activity of the titanium oxide. Aim of this study was to correlate resistance against strand damage with the AS sequence. Instead of the formerly used AS consisting of 2 identical 30mer hybridization sequences (HS)¹ a newly designed AS (also a 60mer) containing the same HS (30mer) prolonged with a homomeric 30mer spacer based on either poly A, poly T, poly C or poly G was investigated. One of these AS was chosen for further studies referring to impact of anchor strand density to stability of the coating and hybridization efficiency.

EXPERIMENTAL METHODS

The immobilization of the AS was performed on sand-blasted and dual acid etched c.p.Ti discs (KLS Martin) by anodic polarization with 7 - 14 mA/cm² until a voltage of 7.5 V_{Ag/AgCl} was reached. For quantification either the AS or the complementary strand were labelled with ³²P. Hybridization experiments were performed with 3 different strands: a 25mer complementary strand (CS) or a 20mer CS.

RESULTS AND DISCUSSION

Depending on the used AS concentration a surface density of up to 40 pmol/cm² was observed with no significant effect of the strand design. Incubation for 24 h in phosphate buffered saline (PBS) resulted in a loss of ~ 30 - 50% of initially immobilized AS, most pronounced for AS rich in C. Hybridization experiments revealed significant differences depending on the AS's spacer sequence and on the treatment conditions between immobilization and hybridization. In general, higher amounts of CS could be hybridized to AS rich in A. The lowest degree of damage, on the other hand, was observed for AS rich in C especially under conditions with

increased damage by radicals due to prolonged anodization or photocatalytic effects.

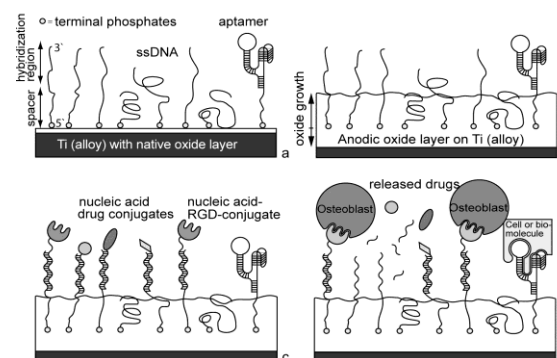


Fig. 1: Schematic figure of the immobilization system: a) adsorption of anchor strands on native oxide layer, b) regioselective fixation by anodic oxide growth, c) immobilization of bioactive molecules conjugated to complementary strands, d) release of bioactive molecules by degradation of DNA or direct interaction with target cells.

An increase in anchor strand density for pA resulted for the 25mer CS in increased hybridization efficiency, in particular if the samples were sterilized prior to hybridization. In contrast, hybridization with a 20mer CS resulted in overall higher hybridized amounts but reaching saturation at lower anchor strand density.

CONCLUSION

Our results show that the electrochemical fixation of AS differing only in the design of the spacer region leads to different hybridization behavior with the same complementary strand. The best performance was observed with poly A spacer and can probably be attributed to nucleotide staggering resulting in an elongated shape protruding from the surface and allowing for enhanced hybridization. Further hybridization experiments on immobilized pA imply that in case of the 25mer hybridization occurs via neighbored AS in close vicinity. Improved hybrid stability over several days could be achieved by use of the shorter 20mer CS.

REFERENCES

1. J. Michael *et al.*, J. Biomed. Mater Res 80:146-55, 2007

ACKNOWLEDGMENTS

The authors would like to thank the DFG (SCHA570/13-1) for providing financial support.

Functional octapeptide hydrogel to bone repair applications

Luis Castillo¹, Alberto Saiani², Julie Gough² and Aline Miller¹

¹Manchester Interdisciplinary Biocentre & The School of Chemical Engineering and Analytical Science

²The School of Materials, The University of Manchester, UK. luis.castillodiaz@prostadgrad.manchester.ac.uk

INTRODUCTION

Bone tissue is frequently damaged by diseases, which generally leads to its degradation, hence the regeneration of bone is currently attracting significant interest¹. The octa-peptide FEFEFKFK, where F is phenylalanine, E glutamic acid and K lysine is known to spontaneously self-assemble into β -sheet rich fibres that self-associate to form a rigid hydrogel when above a critical concentration². Here, the 3D culture of human osteoblasts (HOBs), the mechanical properties and the subsequently production of collagen type I inside FEFEFKFK, RDGFEFEFKFK, and RGDFEFEFKFK gels is explored.

EXPERIMENTAL METHODS

30 mg ml⁻¹ RGDFEFEFKFK, RDGFEFEFKFK (scrambled sequence), and FEFEFKFK hydrogels were prepared. Primary HOBs were grown in DMEM with 10% FBS, and 1% antibiotics, at 5% of CO₂/37°C. LIVE/DEAD, and Picogreen assays were carried out to determinate qualitatively cell viability proliferation respectively. The viscoelastic behaviour of FEFEFKFK gels, was determined using an ARG2 rheometer. ~150 μ L of gel was load onto the bottom plate. The elastic (G') and viscous (G'') moduli as function strain (0.01-100%) at 1 Hz and oscillatory frequency (0.01-100 Hz) at 1% strain. The expression of Collagen I was studied using a standard immunocytochemistry procedure³.

RESULTS AND DISCUSSION

HOBs viability (Figure 1) is similar for the three different gels, where living cells are predominant after 14 days of culture. It is also observed a clear cell spreading inside the RGDFEFEFKFK gel, which might have a positive impact on the attachment and subsequent cell proliferation rate.

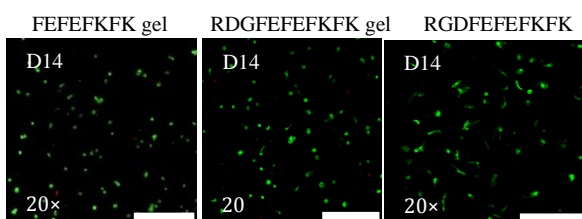


Figure 1. LIVE/DEAD assay. Green represents (alive cells), red (death cells). Scale bars = 250

The rate of cell proliferation is higher inside RGDFEFEFKFK gel (Figure 2). This might be favoured by the presence of attachment sites provided for the RGD sequence incorporated along the nanostructure of the gel.

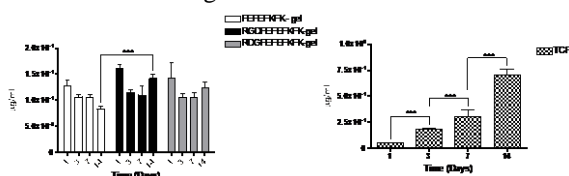


Figure 2. DNA content after two weeks of culture. *** Denotes $p < 0.001$ for comparison of DNA content between the different gels and time intervals.

When the mechanical properties of FEFEFKFK, RDGFEFEFKFK and RGDFEFEFKFK gels were explored, it is clear that G' modulus of the gels with cells, trend to increase the first 7 days under cell culture conditions, however after this time the strength of all gels decreased possibly due to the natural shrink that gels suffer due to the regular exchanges of media (Figure 3). The highest G' modulus values were observed for the FEFEFKFK gel.

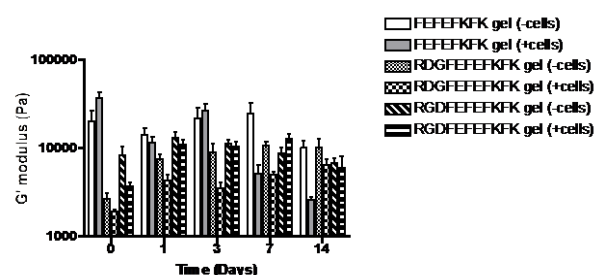


Figure 3. Mechanical properties of 3wt% FEFEFKFK, RDGFEFEFKFK, and RGDFEFEFKFK gels. The G' modulus is recorded with and without cells (control), over 14 days.

On the other hand, HOBs were able to produce and deposit collagen type I inside the three different type of gels in a similar rate. This is visually shown by immunocytochemistry images (Figure 4).

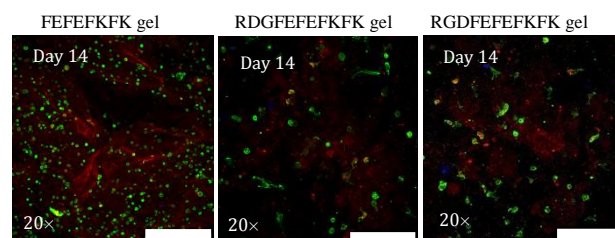


Figure 4. Immunocytochemistry representing the production of collagen I (red), and cell cytoskeleton (green) over 14 days of culture. Scale bars = 250 μ m.

CONCLUSIONS

The incorporation of the RGD motif to the FEFEFKFK peptide sequence, improved the cell spreading, attachment and proliferation of HOBs 3D cultured inside the gel during 14 days. The mechanical properties of the gel allowed to the cells not only proliferate even so, to maintain a sustained production of collagen I, which also was clearly deposited inside gels. Thus, the RGDFEFEFKFK system has potential to be used as 3D scaffold to culture HOBs with regenerative applications.

REFERENCES

1. Feng X. *et al.*, ARPM (2011),6:121-45.
2. Saiani A. *et al.*, SM (2009),5:193-202.
3. Mujeeb, A. *et al.*, AB (2012),9:4609-4617.

ACKNOWLEDGMENTS

"To CONACYT-Mex., Polymers & Peptides and tissue engineering research groups for financial support".

Pro-inflammatory Response to Novel Gelatin-based Biomaterials with Tailorable Mechanical Properties *in vitro*

Sandra Ullm^{1,2*}, Anne Krueger³, Tim P. Gebauer^{3,4}, Axel T. Neffe^{3,4}, Christoph Tondera^{1,2}, Andreas Lendlein^{3,4}, Friedrich Jung^{3,4}, Jens Pietzsch^{1,2}

^{1*} Helmholtz-Zentrum Dresden-Rossendorf, Institute of Radiopharmaceutical Cancer Research, Department of Radiopharmaceutical and Chemical Biology, Dresden, Germany, s.ullm@hzdr.de

² Technische Universität Dresden, Department of Chemistry and Food Chemistry, Dresden, Germany

³ Institute of Biomaterial Science and Berlin-Brandenburg Centre for Regenerative Therapies, Helmholtz-Zentrum Geesthacht, Teltow, Germany

⁴ Helmholtz Virtual Institute "Multifunctional Biomaterials for Medicine", Teltow and Berlin

INTRODUCTION

After implantation of polymer-based materials into the body, a cascade of inflammatory host reactions starts, initiating the regeneration of the injured tissue. Besides a myriad of cytokines and growth factors, various cell types play a major role during these different stages of tissue response, like macrophages and endothelial cells. Here, we studied gelatin-based polymer networks with tailorable elastic properties and degradation behavior due to different degrees of crosslinking with lysine diisocyanate ethyl ester. Preliminary experiments revealed good biocompatibility, appropriate cell adhesion and cell infiltration of these hydrogel films depending on their crosslinking degree. Now, investigations on their potential to activate human macrophages and endothelial cells in a pro-inflammatory manner will reveal further insights into biomaterial-cell interactions.

EXPERIMENTAL METHODS

Solutions of 10 wt.-% gelatin were crosslinked with 3- (G10_LNCO3) or 8-fold (G10_LNCO8) excess of isocyanate groups of lysine diisocyanate ethyl ester. Primary human aortic endothelial cells (HAEC) and human leukemia THP-1 cells, differentiated to macrophages (Mφ), were seeded either directly on biomaterial films or cultivated with material eluates in order to simulate hydrolytical or enzymatical degradation *in vivo*. Expression levels of the inducible inflammatory protein cyclooxygenase-2 (COX-2) and its constitutively expressed isoform COX-1, tight junction proteins occludin and claudin-5, and anticoagulant thrombomodulin (TM) were quantified via Western blotting. Additionally, profiles of secreted cytokines and matrix metalloproteases (MMP) were determined using magnetic bead- or color-coded microparticle-based multiplex assays.

RESULTS AND DISCUSSION

In both HAECs and Mφ no influence of hydrolytic or enzymatic eluates on COX-2 expression was observed. In contrast, direct contact to the materials enhanced COX-2 expression, indicating a possible pro-inflammatory reaction. The higher crosslinked material (G10_LNCO8) induced a higher COX-2 expression,

compared to G10_LNCO3. As expected, the expression of COX-1 remained constant (Figure 1).

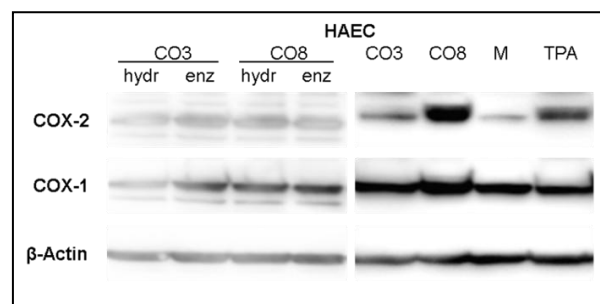


Figure 1: COX expression in HAEC after contact to hydrolytic (hydr) or enzymatic (enz) material eluates of G10_LNCO3 (CO3) or G10_LNCO8 (CO8), as well as after direct contact to the materials. M: medium control, TPA: inflammation control after treatment with 0.1 μM TPA for 48 h.

The expression of tight junction proteins and TM in HAEC, as well as their cytokine and MMP secretion, were not influenced by the materials, suggesting a maintained endothelial cell function.

In contrast, Mφ altered their cytokine secretion profile after material contact, depending on the crosslinking level of the material.

CONCLUSION

These results point out that direct contact between cells and the hydrogels investigated, but not contact to their hydrolytic or enzymatic degradation products, induced inflammatory reactions in the cells. This indicates an impact of the material surface structure. In general, the materials did not induce endothelial cell dysfunction, whereas macrophages showed inflammatory activation.

ACKNOWLEDGMENTS

The authors thank the Helmholtz Association for funding of this work through Helmholtz-Portfolio Topic "Technologie und Medizin – Multimodale Bildgebung zur Aufklärung des In-vivo-Verhaltens von polymeren Biomaterialien".

Sandra Ullm is recipient of a fellowship by Europäische Sozialfonds (ESF).

Dissecting the Regulating Cues of the Extracellular Matrix in Macrophage Plasticity

Katja Franke¹, Liv Kalbitzer¹, Jiranuwat Sapudom¹, Ulf Anderegg², Sandra Franz² and Tilo Pompe^{1*}

^{1*}Institute of Biochemistry, Faculty of Biosciences, Pharmacy and Psychology, Universität Leipzig, Germany, tilo.pompe@uni-leipzig.de

²Department of Dermatology, Venerology and Allergology, Universität Leipzig, Germany

INTRODUCTION

Extracellular matrix signals regulate in a complex manner cell behaviour *in vivo* and *in vitro*. We modulate important matrix parameters including 3D topology, mechanics as well as composition and presentation in respect to matrix proteins and glycosaminoglycans (GAG) to dissect their specific impact on macrophage phenotype. We apply defined collagen I-based matrices as well as long-term single cell tracking of the heterogeneous cell populations to reveal the dynamics and fate of macrophages in migration and differentiation. Based on these investigations we envision to reveal fundamental regulating parameters of macrophages function in wound healing.

EXPERIMENTAL METHODS

Immobilized layers (100 - 300 µm) of 3D fibrillar collagen I networks were reconstituted with defined topology and stiffness and functionalized with GAG (hyaluronan, sulfated hyaluronan, heparin). The new automated topological analysis provides quantitative measures (pore size distribution, fibril diameter).¹ Mechanical properties were determined by colloidal probe force spectroscopy. GAG content was quantified by fluorimetry and ELISA. CD14⁺ human monocytes were isolated from peripheral blood and differentiated into inflammatory macrophages by granulocyte macrophage colony-stimulation factor and lipopolysaccharide stimulation. Cell migration and differentiation was analysed within the 3D context of the biomimetic matrices using long-term time-lapse microscopy over 5 days. Our automated single cell tracking analysis revealed in-depth information on migration characteristics of the heterogeneous cell population on single cell level as well as population averages. Differentiation of macrophages was determined by IL10 and IL12 expression using ELISA and immunofluorescence supplemented by morphological analysis for single cell tracking.

RESULTS AND DISCUSSION

Biomimetic 3D collagen I networks could be engineered with a defined topology and mechanics. Pore sizes and Young's moduli were controlled in a

range of 0.5 µm to 5 µm and 10 Pa to 400 Pa. Covalent and non-covalent binding of hyaluronan, sulfated hyaluronan and heparin within the 3D networks provided various GAG presentation modes (immobilized vs. adsorbed) with up to 10% mass content of GAG per collagen I matrix.

Invasion and migration studies of monocyte-derived macrophages indicate distinct characteristics in dependence of matrix parameters. Enhanced invasion and modulated migration type was found for matrices with sulfated GAG. Single cell analysis of migration characteristics further indicated a strong spread of typical migration parameters, which was also reflected in the local expression of differentiation markers IL10 and IL12 determined by immunofluorescence as well as morphology features. These findings suggest a specific impact of matrix topology and GAG functionalization on macrophage characteristics.

CONCLUSION

Our studies demonstrated the advantage of analysing cell behaviour on a single cell level within defined biomimetic matrices *in vitro*. It allows to reveal the impact of topology, mechanics and GAG presentation on macrophage phenotype. Further, it can be concluded that the defined control of matrix parameters as well as single cell characteristics of heterogeneous cell populations is needed to correlate matrix parameters to cell characteristics.

REFERENCES

1. Franke K. *et al.*, Acta Biomater., 2014, in press

ACKNOWLEDGMENTS

L.K., U.A., S.F. and T.P. want to acknowledge financial support by the Deutsche Forschungsgemeinschaft (DFG, grant: SFB-TR67). K.F. and T.P. want to acknowledge financial support by ESF, EFRE and Free State of Saxony (grant: SAB 100140482, SAB 100144684). We gratefully acknowledge use of the imaging facility in the Magin lab, supported by DFG INST 268/230-1 to Thomas Magin.

Carbon Monoxide Releasing Nanoparticles

Ryosuke Inubushi, André J. van der Vlies, Hiroshi Uyama and Urara Hasegawa*

Graduate School of Engineering, Osaka University, Japan
r_inubushi@chem.eng.osaka-u.ac.jp

INTRODUCTION

Carbon monoxide (CO), one of the byproducts of heme catabolism via heme oxygenase-1 (HO-1), has recently been recognized as an important signaling mediator in mammals despite its bad reputation as an air pollutant. CO plays versatile roles in tissue protection via anti-inflammatory, anti-proliferative and anti-apoptotic effects. Toward therapeutic application of this gas, several transition metal carbonyls such as $\text{Mn}_2(\text{CO})_{10}$, $[\text{Ru}(\text{CO})_3\text{Cl}]_2$, and $\text{Ru}(\text{CO})_3\text{Cl}(\text{glycinate})$ have been reported as CO donor molecules that release CO under physiological condition.¹ Despite their beneficial effects *in vitro* and *in vivo*, the solubility and toxicity of these molecules remain issue in therapeutic application of this gas. In addition, this kind of small drugs in general has pharmacokinetic problems such as quick clearance from the body and lack of tissue specificity.

To overcome this disadvantage, we previously reported CO-releasing polymeric micelles prepared from triblock copolymers containing ruthenium carbonyl moieties.² The micelles successfully attenuated the inflammatory response in human monocytes and reduced toxicity of the ruthenium carbonyl complex. Although these micelles showed promise in immunotherapy, the complicated preparation limited their practical application.

Here we report novel CO-releasing nanoparticles (CONP). Catechol-bearing CO donors ($\text{Ru}(\text{CO})_3\text{Cl}(\text{L-DOPA})$) were conjugated to the phenylboronic acid-bearing nanoparticles (PBANP) via reversible covalent linkage. The anti-inflammatory effects of CONP were also assessed.

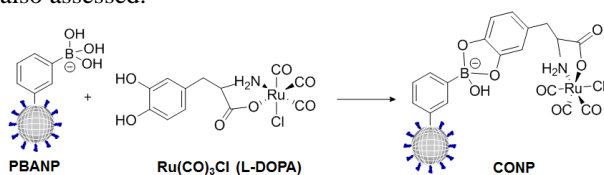


Figure 1. CO-releasing nanoparticles

EXPERIMENTAL METHODS

$\text{Ru}(\text{CO})_3\text{Cl}(\text{L-DOPA})$ was prepared by complexing tricarbonyl dichlororuthenium (II) dimer with L-3,4-dihydroxyphenylalanine (L-DOPA). PBANP were prepared by the surfactant-free emulsion polymerization method. The nanoparticles were mixed with $\text{Ru}(\text{CO})_3\text{Cl}(\text{L-DOPA})$ in buffer solution to yield the CONP. The nanoparticles were characterized by dynamic light scattering (DLS) and transmission electron microscopy (TEM). The amount of loaded $\text{Ru}(\text{CO})_3\text{Cl}(\text{L-DOPA})$ was determined by inductively coupled plasma atomic emission spectrometry (ICP-AES). The amount of released CO was determined by using the myoglobin (Mb) assay.³ The anti-

inflammatory effect of the CONP was assessed in murine macrophages RAW 264.7 cells.

RESULTS AND DISCUSSION

The PBANP of 85 nm diameter were loaded with a catechol-bearing CO-donor, $\text{Ru}(\text{CO})_3\text{Cl}(\text{L-DOPA})$, through the reversible covalent linkage between phenylboronic acid and the catechol moiety. Under physiological condition (pH 7.4), the particles showed high loading capacity (0.7 $\text{Ru}(\text{CO})_3\text{Cl}(\text{L-DOPA})$ per phenylboronic acid group). DLS showed that the particle size increased to 188 nm after loading of $\text{Ru}(\text{CO})_3\text{Cl}(\text{L-DOPA})$. The Mb assay revealed that the CONP were capable of releasing 0.8 mol of CO per mol of loaded $\text{Ru}(\text{CO})_3\text{Cl}(\text{L-DOPA})$.

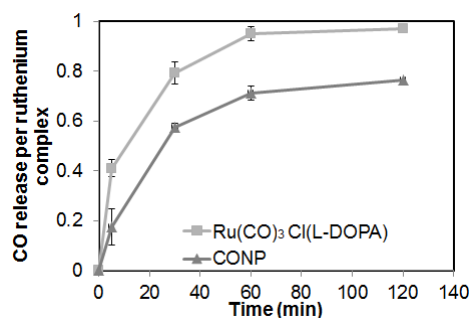


Figure 2. CO release from $\text{Ru}(\text{CO})_3\text{Cl}(\text{L-DOPA})$ and the CONP as a function of time (Mb assay).

Furthermore, the anti-inflammatory effect of the CONP was assessed in RAW264.7 macrophages. Upon the addition of the CONP, the production of inflammatory cytokines and nitric oxide was suppressed in lipopolysaccharide (LPS)-induced inflammation.

CONCLUSION

CONP (188 nm diameter) were successfully prepared. These particles exerted anti-inflammatory effects in murine macrophages. This novel CO-delivery system may show promise for therapeutic applications of CO.

REFERENCES

- 1 Mann B. E. *et al.*, Chem. Com., 4197-4208, 2007.
- 2 Hasegawa U. *et al.*, J. Am. Chem. Soc., 132: 18273-18280.
- 3 Motterlini R. *et al.*, Circ. Res. 90: E17-24, 2002.

ACKNOWLEDGMENTS

We thank Dr. E. Mochizuki (Osaka University, Japan) for TEM experiments and Prof. M. Sadakane (Hiroshima University, Japan) for supplying Preyessler type phosphotungstate staining agent. This work was supported by Grant-in-Aid for Young Scientists (B), No. 24700482, from the Japan Society for the Promotion of Science.

Effect of hydrophobic groups on the bonding strength of cod-derived gelatins-based tissue adhesives

Tetsushi Taguchi^{1,2}, Temmei Ito^{1,2}, Ryo Mizuta^{1,3}, Keiko Yoshizawa²

¹Biomaterials Unit, National Institute for Materials Science, Japan

²Graduate School of Pure and Applied Science, University of Tsukuba, Japan

³Graduate School of Life and Environmental Science, University of Tsukuba, Japan

TAGUCHI.Tetsushi@nims.go.jp

INTRODUCTION

Tissue adhesive is a biomedical material that can bond tissues together after surgical operations. It is also applied as a surgical sealant to prevent air or body fluid being released from organs and vascular tissue after the operation. There are three main types of tissue adhesive, however, commercial adhesives still have disadvantages on biocompatibility and bonding strength.

Recently, we have developed a tissue adhesive consisting of human serum albumin and an organic acid-based crosslinker, disuccinimidyl tartaric acid, and reported that this adhesive showed both high bonding strength and good biocompatibility¹. Furthermore, we have shown that tissue adhesives containing hydrophobically modified porcine-derived gelatins showed excellent bonding strength onto fresh vascular media compared with non-modified gelatin^{1,2}. However, porcine-derived gelatin solution with high concentration has low fluidity at room temperature because of its high contents of imino acids such as proline and hydroxyproline and is required to heat to use as a tissue adhesive^{2,3}.

Based on these backgrounds, we have chosen cod-derived gelatins (cGln) instead of porcine-derived gelatin as a base material for surgical adhesives because it has low transition temperature due to its low contents of imino acids including proline and hydroxyproline. We synthesized various hydrophobically modified cGlns (hm-cGln) with different hydrophobic groups and introduction ratios and evaluated their bonding effects on fresh arterial media by combining hm-cGlns with polyethylene glycol-based, four-armed crosslinker (4S-PEG)⁴.

EXPERIMENTAL METHODS

The modification of cGln with hydrophobic groups was carried out using a reaction of active ester of fatty acid chloride or cholesteryl chloroformate with the primary amine of cGln in the presence of triethyl amine. Modification ratio of cGlns with hydrophobic groups was calculated by determination of residual amino group using 2,4,6-trinitrobenzensulfonic acid. The measurement of bonding strength was performed using fresh arterial media as an adherend. The bonding strength was then measured using a Texture Analyzer (TA-XT2i, Stable Micro Systems, Godalming, UK). The hm-cGln concentration was fixed at 40 w/v% and fixed 4S-PEG concentration. After the bonding strength measurement, each sample was fixed with a 10% formalin neutral buffer solution followed by hematoxylin-eosin (HE) staining. Cross sections of the stained samples were observed with an optical microscope (BX51, Olympus, Tokyo, Japan).

RESULTS AND DISCUSSION

Hm-cGlns were successfully synthesized by the method as we reported previously^{2,3} (Figure 1). By changing initial concentrations of fatty acid chlorides or cholesteryl chloroformate, each hm-cGln with three different modification ratios of hydrophobic groups was obtained. The bonding strength of stearyl group modified cGln (Ste-cGln)-based adhesives against fresh arterial media increased with increasing modification ratio up to 9.6 mol% then decreased. This highest bonding strength of Ste-cGln based adhesive was 2-fold higher than that of original cGln (Org-cGln)-based adhesive and 10-fold higher than commercial adhesive. Bonding strength of hm-cGln increased with an increase of alkyl chain length under similar modification ratio. From the observation of HE staining sections after bonding strength measurement, dense adhesive layer was observed on the surface of arterial media, meaning that modified alkyl chains effectively work for the enhancement of interfacial strength between adhesive and arterial media. Also, we clarified that these hm-cGln based adhesives completely degraded within 8 weeks without causing any strong inflammation after the subcutaneous implantation in mice.

These results indicated that the introduction of hydrophobic groups effectively enhanced the interfacial strength between tissue and adhesive.

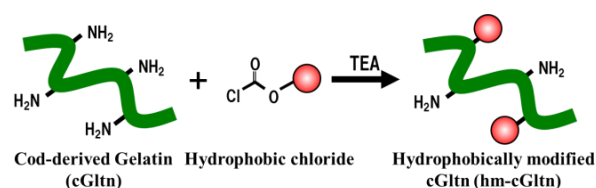


Fig. 1 Modification of cGln with various hydrophobic groups.

CONCLUSION

Tissue adhesive composed of hydrophobically modified cGln and 4S-PEG group-modified was developed. Resulting adhesive containing Ste-cGln had 10-fold high bonding strength compared with commercial adhesive. Ste-cGln based adhesive degraded within 8 weeks after subcutaneous implantation in mice without causing any inflammation.

REFERENCES

1. Taguchi T. et al., J. Bioact. Compat. Polym. 24:546-559, 2009
2. Matsuda M. et al., J. Bioact. Compat. Polym. 27:481-498, 2012
3. Matsuda M. et al., Colloids Surf. B. 91:48-56, 2012
4. Taguchi T. et al., Biomaterials 26:1247-1252, 2005

Examination of Local and Systemic Inflammatory and Immunological Reactions Following Implantation of Jellyfish Collagen Matrices in Rats

Uwe Walschus¹, Susanne Meyer², Silke Lucke¹, Andreas Hoene³, Udo Meyer², Michael Schlosser^{1*}

¹Department of Medical Biochemistry and Molecular Biology, University Medical Center Greifswald, Germany

²Bioserv Analytik und Medizinprodukte GmbH, Rostock, Germany

³Department of Surgery, University Medical Center Greifswald, Germany
*schlosse@uni-greifswald.de

INTRODUCTION

Collagen is the main component of the connective tissue extracellular matrix and frequently used for tissue engineering and different biomedical purposes. The main collagen sources are bovine and porcine skin and tendon. However, mammalian collagens potentially carry a risk of transmitting infectious diseases like BSE. Furthermore, bovine and porcine products are rejected in different cultural areas due to religious motives.

Marine animals provide an alternative collagen source without these problems. Jellyfish has a collagen amount of more than 60% of the solid content which is easy to extract. However, a prerequisite for using jellyfish collagen (JC) for biomedical purposes is an examination of its in vivo behaviour regarding biodegradation as well as induction of local and systemic inflammatory and immunological reactions. Therefore, this study aimed at investigating these aspects after implantation of JC matrices into rats.

EXPERIMENTAL METHODS

Preparation of matrices. Fibrillated jellyfish collagen from *Rhopilema spec.* was obtained from CRM GmbH, Kiel, Germany. Matrices were prepared by lyophilization from a 0.5% (w/v) solution and subsequent crosslinking with EDC/NHS. The matrices (JC content: 0.5mg, pore size: 20-200µm) were rigorously washed, stored in phosphate buffer and sterilized by gamma irradiation prior to implantation.

Examination of local tissue response. In a 1st series, one JC sample was implanted into the neck musculature of 24 male Lewis rats. After 7, 14 and 56 days, tissue samples were retrieved from 8 animals respectively. Cryosections were stained with antibodies for total macrophages/monocytes (ED1), tissue macrophages (ED2), total (R73) and activated (OX39) T lymphocytes, antigen-presenting cells (OX6), activated NK cells (ANK61) and nestin (rat-401) using the APAAP method. Cellular reactions were quantified by digital image analysis software ImageJ.

Investigation of systemic immune response. In a 2nd series, five rats received one JC sample implanted into the neck musculature. Additional implantations were performed after 14 and 28 days while the previous implants were removed. Blood was collected pre-OP and weekly post-OP until day 56. Detection of IgG and IgM antibodies against JC was performed using standard ELISA with the antigen (1% w/v) solid-phase coated in 96-well microplates, incubation of rat sera and detection of antigen-bound antibodies with Ig-class-specific anti-rat HRP conjugates.

Statistics. The non-parametric Mann-Whitney test was used for data analysis (GraphPad Prism 4.03).

RESULTS AND DISCUSSION

Biodegradation. In the 1st series, JC samples were still found in tissue of 7/8 animals after 7 days, 4/8 animals after 14 days but none of the 8 animals after 56 days, indicating complete biodegradation within 2 months. However, even in tissue sections with no detectable JC sample, the implant site was always identifiable.

Local tissue reactions. Within the matrices, more ED1-positive M1-type pro-inflammatory macrophages, T lymphocytes, antigen-presenting cells and NK cells were found on day 14 compared to day 7. This increase was probably associated with the biodegradation. On the other hand a concurrent increase of ED2-positive M2-type anti-inflammatory macrophages and nestin expression indicated ongoing tissue regeneration. Inflammatory reactions in the peri-implant tissue were generally not as strong as within the matrices and did not increase significantly from day 7 to day 56 for any cell type. While ED1-positive macrophages around the implants had a moderate non-significant increasing trend, a transient decrease on day 14 was found for T lymphocytes and ED2-positive macrophages.

Humoral response. A broad individual variability in humoral immune response against JC was observed. Regarding anti-JC IgG antibodies, 2/5 animals were positive after the 2nd implantation and 4/5 animals after the 3rd implantation, while 1 animal remained negative throughout the study. Occurrence of anti-JC IgM antibodies was usually short-lived and observed in 2/5 animals after the 1st implantation, in all 5 animals after the 2nd implantation and in 4/5 animals after the 3rd implantation. Anti-JC IgM levels generally increased after each implantation, and 3 animals had a longer-lasting response after the 3rd implantation. Taken together, the anti-JC IgG and IgM response clearly demonstrated a boost effect after repeated implantation.

CONCLUSION

The examined jellyfish collagen samples were completely biodegraded in vivo within 2 months. The local inflammatory response caused by their implantation was strictly confined to the implant site, particularly to the sample matrix, and accompanied by tissue regeneration. Examination of anti-JC IgG and IgM antibodies revealed that a pronounced humoral immune response was only observed after repeated implantation. These results demonstrate the potential of JC for tissue regenerative applications, with further work being required to optimize its in vivo behaviour.

ACKNOWLEDGMENTS

The study was supported by the German state Mecklenburg-Vorpommern (project SYNTERO).



Sulfated Hyaluronan Derivatives Interfere with TGF- β 1 Signalling

V. Hintze¹, A. van der Smissen², S. Samsonov³, L. Huebner¹, S. Rother¹, D. Scharnweber¹, S. Moeller⁴, M. Schnabelrauch⁴, M. T. Pisabarro³, U. Anderegg²

¹Max Bergmann Center of Biomaterials, Technische Universität Dresden, Germany, Vera.Hintze@tu-dresden.de

²Department of Dermatology, Venereology and Allergology, Leipzig University, Germany

³Structural Bioinformatics, BIOTEC, Technische Universität Dresden, Germany

⁴Biomaterials Department, INNOVENT e.V. Jena, Germany

INTRODUCTION

Sulfated hyaluronan (HA) derivatives are promising candidates for functional biomaterials since sulfate groups modulate the binding of growth factors and thereby influence their bioactivity. The interaction of differently sulfated HA derivatives (sHA) with TGF- β 1 in a sulfation dependent manner has previously been described¹. Collagen-based artificial extracellular matrices (aECM) containing sHA have been shown to have several effects on cells relevant in healing processes^{2,3}. In this study the influence of sHA on the binding of TGF- β 1 to its receptors TGF β receptor-I (TGF β R-I) and -II (TGF β R-II) and the resulting biological consequences on growth factor signalling were investigated by *in vitro* cell culture of human dermal fibroblasts (dFb), *in silico* molecular docking and surface plasmon resonance (SPR).

EXPERIMENTAL METHODS

Artificial ECM coatings were produced by *in vitro* fibrillogenesis of collagen-I in the presence of polymeric HA and sHA derivatives. Human dFb were cultured on aECM for 72 h either untreated or with recombinant human TGF- β 1 added to the cell culture medium after cell seeding or in the presence of aECM-adsorbed TGF- β 1 (10 ng ml⁻¹). TGF- β 1 was added to aECM for 2 h at 37°C to enable growth factor adsorption. The supernatant was removed and used for TGF- β 1 quantification by ELISA. After brief washing, wells were used for cell seeding. In an additional experiment dFb were exposed to TGF- β 1, solute non-sulfated HA or sHA as well as pre-incubated combinations of growth factor and HA derivatives. The synthesis of marker proteins for differentiated myofibroblasts (MFb) was analysed on mRNA (qRT-PCR) and protein level (immunofluorescence). The nuclear translocation of the second messengers Smad 2/3 was examined by immunofluorescence. Molecular docking experiments with non-sulfated HA and sHA tetrasaccharides to TGF- β 1 and to the complex TGF- β 1/TGF β R-II were done using Autodock 3 and spatial clustering with the DBSCAN algorithm. SPR analysis was performed with a BIACORE™ T100 instrument, using C1™ sensor chips. TGF- β 1 was pre-incubated with different concentrations of HA or sHA. The preformed complexes were injected over the immobilized TGF β R-I and TGF β R-II, respectively.

RESULTS AND DISCUSSION

Solute and aECM associated sHA prevented TGF- β 1-stimulated α SMA, collagen I (α 1) and ED-A fibronectin expression. Data suggest an impaired TGF- β 1 bioactivity and downstream signalling in the presence

of aECM containing sHA, shown by massively reduced Smad2/3 translocation to the nucleus. *In silico* docking experiments suggest the occupation of the TGF β R-I binding site by sHA, which is supported by SPR experiments. The latter demonstrate that pre-bound sHA prevents binding of TGF- β 1 to TGF β R-I. In addition SPR analysis proved that the binding of TGF- β 1 to TGF β R-II is also impaired by pre-bound sHA.

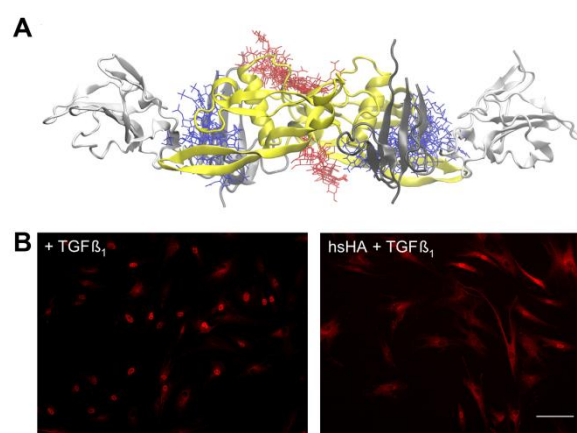


Fig. 1: Sulfated HA prevents TGF β 1-mediated signal transduction. (A) Molecular docking of non-sulfated HA (red) and sulfated HA (blue) tetrasaccharides on the surface of TGF β 1. The TGF β 1/TGF β R-I/TGF β R-II complex is shown (TGF β 1: yellow, TGF β R-I and -II: dark and light grey); (B) Immunofluorescence staining of dFb cultured with 5 ng ml⁻¹ TGF β 1 or growth factor pre-incubated with 50 μ g ml⁻¹ sHA to analyze nuclear translocation of Smad2/3 (red). Bar 100 μ m.⁴

CONCLUSION

The bioactivity of TGF- β 1 is significantly reduced by sHA. Data suggest that sHA prevents TGF- β 1 signalling by occupying the receptor binding sites and thereby reduces TGF- β 1 driven MFb differentiation.

REFERENCES

1. Hintze V et al. Acta Biomater. 8:2144-2152, 2012
2. Hempel U et al., Acta Biomater. 8:4064-4072, 2012
3. van der Smissen A et al., Biomaterials. 32:8938-8946, 2011
4. van der Smissen A et al., Acta Biomater. 9:7775-7786, 2013

ACKNOWLEDGMENTS

The authors would like to thank the Deutsche Forschungsgemeinschaft (TRR 67, A2, A3, A7, B4) for financial support.



Vascular network generation in hyaluronic acid by micromolding and photoimmobilization of fibronectin

A. Kömez^{1,4}, E. T. Baran⁴, N. Hasirci^{1,3,4}, V. Hasirci^{1,2,4*}

Departments of ¹Biotechnology, ²Biological Sciences, ³Chemistry, METU, Turkey

⁴BIOMATEN, Center of Excellence in Biomaterials and Tissue Engineering, METU, Turkey, komez.aylin@metu.edu.tr

INTRODUCTION

Microfabrication techniques are used to construct hydrogels with the desired architecture to control cell behavior and formation of tissue. Especially, micromolding and soft lithography are widely applied and easy to use methods.¹ Vascularization is very important for tissue constructs in terms of providing delivery of nutrients and elimination of waste products.² In this study, we aimed to construct microvascular network in methacrylated hyaluronic acid (MeHA) by using micromolding technique and the formed channels were modified with fibronectin by photoimmobilization for restricted area cell attachment.

EXPERIMENTAL METHODS

Micropatterned elastomer mold was obtained by casting and curing of silicone prepolymer on a photoresist (SU-8) coated glass which was developed by UV irradiation through a pattern printed photomask and wet etching. Then, MeHA solution was cast on the mold and crosslinked with UV. Fibronectin in benzoate solution was placed on the patterned gel and activated by exposure to UV through the mask with negative image for immobilization of the fibronectin only in the microchannels (Fig 1).

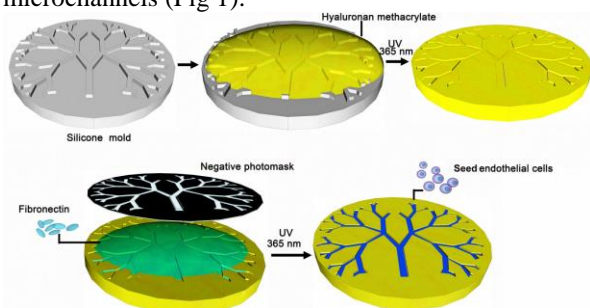


Figure 1. Micromolding of MeHA with microcapillary network and fibronectin photoimmobilization on the channels for cell attachment and vascularized tissue formation.

Human vascular endothelial cells (HUVEC) were seeded on fibronectin immobilized microchannels and incubated in DMEM medium after cell adhesion. At predetermined time points gels were analyzed under light and confocal microscope for analyzing cellular organization in the microchannel network.

RESULTS AND DISCUSSION

Microchannel network resembling a fractals tree pattern was successfully developed in MeHA gel (Fig 2A). Fibronectin was photo-immobilized on the pattern subsequently for guiding endothelial cells by physical and chemical cues, respectively. Light microscope images (Figs 2B and 2C) showed that cells could selectively adhere on the patterned area and organize on the capillary network.

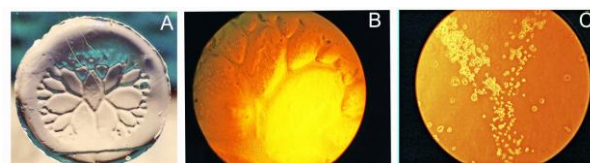


Figure 2. Image of MeHA hydrogel and HUVEC in microchannel network. (A) MeHA hydrogel, (B) Light microscope images of HUVEC in microchannel network at day 0 and (C) after 7 days of culture. Magnification: X50 (B); X100 (C).

Light reflection (Fig 3A) and confocal (Fig 3B) microscopy showed that cells can be both in elongated and aggregated state in the microchannel space. Confocal examination of the same region further showed that HUVEC adhered into the track of microchannel (Fig 3C) and filled concave space of microchannel (Fig 3D).

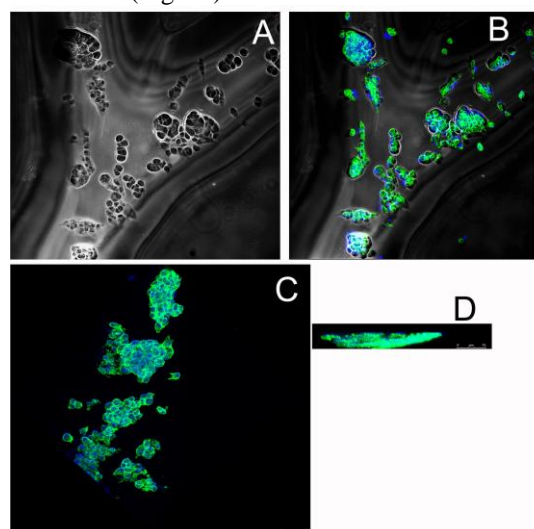


Figure 3. Light reflection and confocal images of cultured HUVEC. (A) Light reflection image, (B) and (C) confocal images showing HUVEC in the microchannel, (D) cross section of a channel with HUVEC. Blue and green luminescence show nucleus and actin staining by DAPI and Alexa Fluor-Phalloidin, respectively.

CONCLUSION

MeHA gel can be transformed into a vascular gel construct by microcapillary network patterning and photoimmobilization of fibronectin to study vascularization of tissue engineered constructs.

REFERENCES

1. Annabi N. *et. al*, Advanced Materials. 26:85–124, 2014.
2. Zorlutuna P. *et. al*, Advanced Materials. 24:1782–1804, 2012.

ACKNOWLEDGMENTS

Authors acknowledge the financial support from Project METU GATA OGEK-BAP-06-11-2013-039 and METU for supporting E.T. Baran as Project Expert.



Collagen(I)-Poly(Glycerol Sebacate)/Poly(Butylene Succinate-Dilinoleate) Fibrous Scaffolds for Cardiac Tissue Engineering

Marwa Tallawi^{1*}, David C. Zebrowski², Aga Kozłowska³, Mirka El Fray³, Felix B. Engel², Aldo R. Boccaccini¹

^{1*}Institute of Biomaterials, Department of Materials Science and Engineering, University of Erlangen-Nuremberg, 91058 Erlangen, Germany, Marwa.Tallawi@www.uni-erlangen.de

²Experimental Renal and Cardiovascular Research, Department of Nephropathology, Institute of Pathology, University of Erlangen-Nürnberg, 91054 Erlangen, Germany

³Polymer Institute, Division of Biomaterials and Microbiological Technologies, West Pomeranian University of Technology, Szczecin, Al. Piastów 45, Poland

INTRODUCTION

Myocardial infarction is the leading cause of death worldwide¹. A potential treatment is cardiac tissue engineering which requires a scaffold that would allow cell attachment, spreading, and maintains their differentiation status. In terms of biomaterials, novel materials have been designed. Mimicking the extracellular matrix (ECM) by fibrous structure enhances the cell attachment. In this study we investigated a novel electrospun collagen incorporated fibrous blend of poly(glycerol sebacate) (PGS) and poly(butylene succinate-co-butylene dilinoleate) (PBS-DLA) as a candidate for cardiac tissue engineering.

EXPERIMENTAL METHODS

All materials used in this study were purchased from Sigma-Aldrich if not mentioned elsewhere.

Electrospun Collagen(I)-PGS/PBS-DLA fiber mats were fabricated by dissolving the polymer blend (20 w/v %) in dichloromethane: Methanol (7:3). Electrospinning the polymer solution with the following parameters; working distance of 15 cm, flow rate of 1.6 ml/h and a voltage of 20 V.

Cardiomyocytes (CM) were isolated from 3-days old Sprague Dawley rats as previously described². CM were pre-plated for 2 h, then re-suspended in neonatal CM medium supplemented with 0.5 % horse serum and seeded in a 24-well plate for 5 days at a density of 0.5 million cells/well. Cells were cultured in 5 % CO₂, 95 % air humidified atmosphere at 37°C. Medium was changed every other day. Cell morphology and adhesion were studied via immunocytochemistry. Cells seeded on collagen-PGS/PBS-DLA matrices were fixed with 4 % PFA in PBS for 10 min at room temperature and were permeabilized with 0.1 % Triton x-100 in PBS for 15 min at room temperature. Protein expression of CM namely alpha-actinin (α -Act) was stained with specific antibodies.

RESULTS AND DISCUSSION

The obtained fiber mats had an average thickness of 100 μ m. and fiber diameter of 1.0 ± 0.2 μ m. FTIR analysis (fig. 1) showed the indicative transmission band of collagen type I, the triple-helical structure of amide I and II at 1645, and 2060 cm^{-1} respectively. Morphological studies (Fig. 2) revealed well-developed sarcomere structures in CM on collagen(I)-PGS/PBS fibres after 5 days of culture.

Collagen type I is a natural matrix protein, in order to mimic the myocardium ECM structure and biomolecules we developed a novel electrospun PGS/PBS-DLA blend incorporating collagen type I into the fibres without the need of using highly toxic solvents like 1,1,1,3,3,3-hexafluoro-2-propanol.

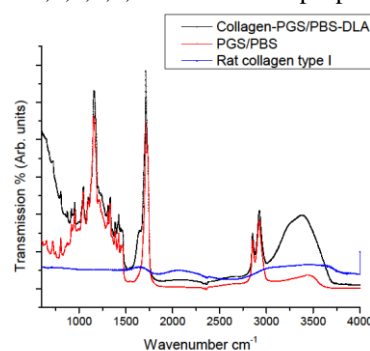


Figure 1: ATR-FTIR spectra spectra of collagen-PGS/PBS-DLA (black), neat PGS/PBS-DLA (red) and collagen (I) (blue).

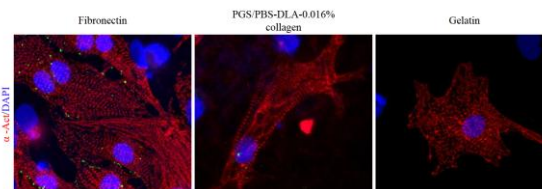


Figure 2: Evaluation of CM cell morphology after 5 days of culture on the indicated matrices, stained for sarcomeric α -Act (CM, red) and DAPI (nuclei, blue). Scale bars: 20 μ m.

CONCLUSION

Newly developed collagen(I)-PGS/PBS-DLA hybrid fibres were successfully fabricated by electrospinning. Immunostaining analyses showed that the hybrid fibres promoted CM adhesion, where CMs exhibited well developed sarcomeric structures comparable to those when grown on fibronectin, the natural matrix protein of CMs. Collagen(I)-PGS/PBS-DLA concludes to be a promising novel functional biomimetic nanofiber for cardiac tissue engineering.

REFERENCES

1. Roger VL. et al., *Circulation*. 125: e2-e220, 2012
2. Engel FB. *Circ. Res.* 85:294–301, 1999

ACKNOWLEDGMENTS

The authors would like to thanks Dr. Menti Goudouri for her technical help with the FTIR measurement.

Tri-Culture of Vascular Cells Promotes Vascular Tissue Remodeling

Caroline Loy¹; Lucie Levesque¹; Jayachandran Kizhakkedathu²; Diego Mantovani¹

¹Lab for Biomat and Bioeng, CRC-I, Dept of Min-Met-Materials Eng., Division of Regenerative Medicine, Research Center of CHU de Quebec, Laval University, Quebec, QC, Canada, caroline.loy.1@ulaval.ca

² Centre for Blood Research, Dept of Pathology and Lab Med, Dept of Chemistry, The University of British Columbia, Life Sciences Centre, Vancouver, BC, Canada

INTRODUCTION:

Scaffold-based vascular tissue engineering aims to regenerate vascular tissue for the replacement of diseased small-calibre blood vessels (diameter < 6mm). Collagen gel is a commonly used scaffold due to its biological properties including a high potential for supporting and guiding vascular cells in the regeneration process¹. The approach we privileged consists in first reproducing the media, which provide the high elastic properties of the vessel wall, thus making it an essential and effective component for blood and nutrients transportation. Starting from an original method, reported previously², for processing collagen and smooth muscle cells (SMCs), the overall goal of this project was to design and develop an endothelialised two layers collagen cell-based scaffold in a disc shape. The underlying layer is composed of fibroblasts (FBs) seeded within collagen. The upper layer is composed of SMCs seeded within collagen and endothelial cells (ECs) are seeded on this construct. This construct is finally expected to provide vascular tissue remodeling due to cells/cells and cells/matrix interactions and to produce an engineered tissue with properties close to that of blood vessel walls. It is also expected to provide a valid in vitro model for further studies of vascular patho-physiology.

MATERIALS AND METHODS:

ECs were isolated by trypsin treatment of human umbilical cords vein (HUVEC) and expanded in HyClone Media M199/EBSS (Fisher). SMCs were isolated from human umbilical cord artery (HUASMC). Initially, the Wharton's jelly that surrounds the arteries was carefully removed by cutting with scissors. The endothelial layer was removed by scraping the artery intima and afterwards, the arteries were cut to rectangle pieces using scissors and finally placed in a Petri dish with M199 medium. After two weeks, the pieces of the artery were removed and the cells were expanded. Aortic adventitial fibroblasts were purchase from LONZA (Walkersville, MD USA).

Type I collagen was extracted from rat-tail tendons and solubilized in acetic acid solution (0.02 N) at a concentration of 4 g/L according to a protocol previously describe³. The collagen solution (2 g/L) was mixed with DMEM and SMCs or FBs (10⁶cells/ml), NaOH (15 mM), and Hepes (20 mM) in deionized water. This mixture was then poured in a specific mold and then let jellify for 30 min at room temperature. Then ECs were seeded on the surface at 10⁵cells/cm² and the construct was incubated at 37°C for 1, 3 or 7 days.

RESULTS AND DISCUSSION

After 24 hrs of growth, the non-circular morphology of endothelial cells shown by immunofluorescence staining (Fig 1A) suggests that the cells are growing and proliferating to form a monolayer on top of the collagen gel layers. The presence of SMCs in the background, inside the gel was confirmed by the 3D confocal image (Fig 1B). Histological staining on transversal section of collagen gels shows the two layers of collagen, one containing SMCs and the others FBs, nested one within the other. After one week of culture, cells density in the gels increased because of gels compaction due to SMCs activities while the ECs layer was shown to remain intact. The alignment of cells due to the specific mold anchoring retaining the compaction in one direction was also observed.

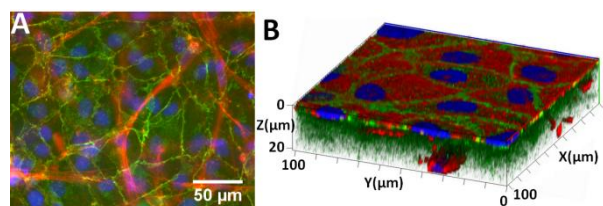


Figure 1: Immunofluorescence staining on (A) top view and (B) 3D confocal image, of cells organization right after 24h of static culture. HUVECs are stained for VE-Cadherin (green), f-actin of HUASMCs with Rhodamin Phalloidin (red) and nuclei with Dapi (blue).

CONCLUSION

Tri-culture of vascular cells were achieved on collagen scaffold without losing endothelial cells. Furthermore, the cells morphologies shown by immunofluorescence staining suggests that cells are making focal attachments. This ongoing experiment shows that it is possible to do vascular cells tri-culture using collagen gel scaffold. The interaction between cells will enhance the matrix remodeling and the properties of the arterial construct. This presentation will show the seeding parameters of all the cells on or in collagen gel. Characterization of cells localization in the collagen matrix will be also shown. Finally, hemocompatibility tests will be performed on this construct.

Acknowledgement: CL was awarded of a PhD Doctoral Scholarship from NSERC CREATE Program in Regenerative Medicine (<http://www.ncprm.ulaval.ca>)

References

1. Couet F. *et al.*, Med Eng & Phy. 2012, 34, 269-78.
2. Boccafroschi F, *et al.*, Macromol Biosci. 2007, 719-26.
3. Rajan N, *et al.*, Nat Protoc. 2006, 1, 2753-8.

Nanofibrous Vascular Grafts Releasing Nitric Oxide

Jana Horakova¹, Connor McCarthy², Megan Frost², Jeremy Goldman², David Lukas¹, Petr Mikes¹

¹Department of Nonwovens and Nanofibrous Materials/ Technical University of Liberec, Czech Republic

²Biomedical Engineering/Michigan Technological University, USA, jana.horakova@tul.cz

Small diameter vascular grafts incorporating long term nitric oxide (NO) release were prepared by electrospinning. Polycaprolactone (PCL) was modified by the addition of novel, NO-releasing compounds. An initial burst of NO was measured leading to long term release during 42 days at 37°C in PBS. This demonstrates the presence of NO-releasing groups entrapped within the fibers.

INTRODUCTION

Small diameter vascular grafts (< 6mm) demonstrate poor thrombogenicity and neointimal hyperplasia [1]. To overcome the main cause of failure for these grafts, nitric oxide (NO) release was incorporated in the grafts due to its ability to inhibit platelet activation and smooth muscle cell proliferation [2]. Small diameter vascular grafts were produced by electrospinning. Nanofibers promote cell adhesion and proliferation due to the similarity with the natural extracellular matrix [3]. The incorporation of novel NO-releasing compounds into the fibers brings new potential solutions to the problem of small diameter vascular graft failure. This incorporation of NO release will promote endothelial cell growth and proliferation to encourage the formation of a healthy vascular substitute by preventing thrombosis and neointimal hyperplasia as cells populate the graft.

EXPERIMENTAL METHODS

The custom designed electrospinning setup was used to produce small diameter vascular grafts by collecting fibers on a rotating mandrel. To incorporate NO release into the graft, S-Nitroso-N-acetylpenicillamine particles (SNAP particles) and SNAP-derivatized cyclam were added to the electrospinning polycaprolactone (PCL) solution. NO is released in the presence of catalytically active metals such as Cu^{1+} or reducing equivalents such as ascorbic acid. Therefore, double layered tubes with outer layer containing CuCl_2 were produced. Two single layered tubes (SNAP particles and SNAP-derivatized cyclam) and two double layered samples (SNAP particles- CuCl_2 , SNAP-derivatized cyclam- CuCl_2) were tested for NO release using a Siever's Nitric Oxide Analyzer. One centimeter samples were submerged in PBS to measure evolved NO from the grafts. After an initial burst of NO over 60 minutes, exogenous CuCl_2 and ascorbic acid were added to the PBS solution containing the sample and additional NO release was observed. Samples were immersed in PBS at 37°C and NO release was measured after 3, 10, 21 and 42 days in PBS for 5 minutes followed by the addition of CuCl_2 and ascorbic acid solutions (15 minutes). On the 42nd day, UV light (400 nm) was used to demonstrate continued control of NO release from

the material and determine if there was a further reservoir of NO available.

RESULTS AND DISCUSSION

Scaffolds were 5 cm in length with a 1.65 mm inner diameter. Tubes were cut at 1 cm and NO release was measured. Initially there was high NO flux after putting the tube into PBS solution. After 60 minutes, NO release decreased but when reducing agents were added, additional NO release was observed.

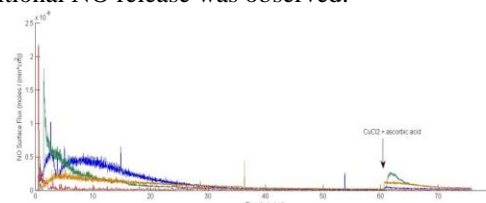


Fig. 1: NO release measured in PBS solution. After 60 minutes, CuCl_2 and ascorbic acid were added to the PBS solution. The blue line depicts NO release of PCL with incorporated SNAP particles, the red line depicts the double layered tube with SNAP particles- CuCl_2 , the green line PCL with SNAP-derivatized cyclam and the orange line the double layered graft with SNAP-derivatized cyclam - CuCl_2 .

After 3, 10, 21 and 42 days, measurement of NO release was carried out showing controlled NO release from the grafts after addition of CuCl_2 and ascorbic acid. After 42 days, the samples were illuminated using UV light to determine if the NO releasing reservoir was totally depleted. In all cases, NO was generated from the fibers upon exposure to UV light after 42 days.

CONCLUSION

Nanofibrous vascular grafts releasing NO were successfully fabricated using electrospinning. Addition of SNAP particles and SNAP-derivatized cyclam to the electrospun PCL fibers resulted in vascular grafts demonstrating long term NO release under physiological conditions. After an initial burst of NO (**Fig.1**), NO-releasing groups are present within the fibers, resulting in long term release. After the addition of physiologically present agents like copper ions and ascorbic acid, an increased NO release was observed after 3, 10, 21 and 42 days of incubation.

REFERENCES

1. Chlupac J. *et al.*, *Physiol. Res.* 58:119-139, 2009
2. Frost M.C. *et al.*, *Biomaterials* 26:1685-1693, 2005
3. Bhardwaj N. *et al.*, *Biotechnology Advances* 28:325-347, 2010

ACKNOWLEDGMENTS

JH acknowledges the Fulbright Program. The authors would like to thank the National Institutes of Health (NIH R15HL113954.) for providing financial support to this project.

Electrospun silk fibroin/gelatin composite tubular matrices as scaffolds for small diameter blood vessel regeneration

Chiara Marcolin¹, Valentina Catto^{1,2}, Federica D'Agostino¹, Serena Bertoldi^{1,2}, Silvia Farè^{1,2}, Maria Cristina Tanzi^{1,2}

¹Dip. Chimica, Materiali e Ingegneria Chimica "G. Natta", Politecnico di Milano, Milano, Italy

²Local Unit Politecnico di Milano, INSTM, Italy, chiara.marcolin@polimi.it

INTRODUCTION

Cardiovascular diseases are a leading cause of death. Currently available synthetic grafts are successful at the macrovascular level, but fail at smaller diameters ($\varnothing < 6$ mm) due to thrombogenicity of synthetic materials and compliance mismatches. The aim of this work was to develop an innovative small diameter vascular graft (SFt/gel) composed of an electrospun silk fibroin tubular (SFt) structure, coated by a crosslinked gelatin gel (gel)¹. SFt grafts demonstrated adequate properties as vascular grafts^{2,3}, also with a collagen coating⁴ which however can cause immune responses⁵. Gelatin may evade this problem, still promoting cell adhesion. In addition, our proprietary method for crosslinking gelatin occurs in mild conditions, giving cytocompatible gels with good stability at 37°C¹.

EXPERIMENTAL METHODS

SF tubular (SFt) structures (ID = 6 mm) were obtained by electrospinning on a rotating mandrel, as previously described². Gelatin A (from porcine skin, Sigma) was crosslinked via a Michael-type addition reaction with methylenebisacrylamide (MBA), in aqueous solution¹.

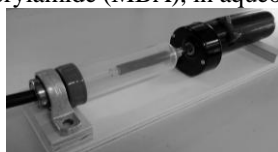


Figure 1: the home-made coating system.

For coating the SFt samples with the gelatin gel a home-made system was designed and fabricated (Fig. 1). SFt samples were mounted on a rotating glass mandrel, dipped in gelatin/MBA water solution and placed in the coating apparatus to complete the crosslinking reaction (50°C, 24h). SEM analyses were performed to investigate the coating homogeneity. Swelling and weight loss behavior were investigated at 37°C up to 25 days in water. Mechanical tensile properties of wet SFt/gel and SFt, used as control, were assessed at 37°C by circumferential, cyclic, creep/recovery, and stress relaxation/recovery tests. From the cyclic tests, compliance values (between 80 and 140 mmHg) of SFt and SFt/gel were obtained. *In vitro* tests were carried out with the L929 murine fibroblast cell line. Indirect cytotoxicity test was performed on the eluates of SFt/gel and SFt samples, by dipping them in DMEM for 1, 3 and 7 days. Direct cytocompatibility test was performed up to 7 days, by investigating cell viability with MTT assay.

RESULTS AND DISCUSSION

Electrospun matrices had a random fibrous structure with an almost uniform fiber size (755 ± 174 nm). SFt/gel structures were successfully obtained with a homogeneous coating of crosslinked gelatin (Fig.2),

which proved stability in water up to 25 days (37°C).

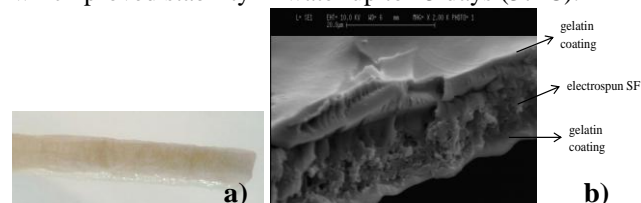


Figure 2: a) macro image of the SFt/gel tubular scaffold; b) SEM image of the cross-section of SFt/gel. Circumferential tensile tests showed higher stiffness (E values) for SFt (1.82 MPa) than SFt/gel (0.58 MPa) structures. Both SFt and SFt/gel proved compliance values similar to that of autografts, and higher than synthetic grafts commonly used (Fig. 3).

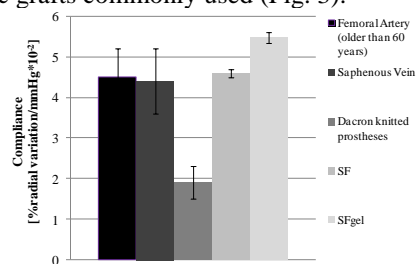


Figure 3: compliance values of autologous and synthetic grafts, SFt and SFt/gel structures.

Creep and stress relaxation tests evidenced a higher contribution of the viscous component for SFt/gel compared to SFt. *In vitro* cytotoxicity test revealed no release of cytotoxic substances, and cytocompatibility test showed, at 7 days, a cell viability significantly higher on SFt/gel ($p < 0.05$) than on SFt (Fig. 4).

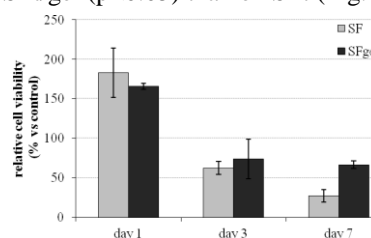


Figure 4: cytocompatibility test: MTT assay results

CONCLUSION

Novel 6 mm I.D. composite tubular structures were successfully obtained by coating electrospun SF tubes with a homogeneous layer of crosslinked gelatin. SFt/gel mechanical properties, in particular compliance, were similar to clinically used autografts. The gelatin coating was able to improve the biological characteristics of SF.

REFERENCES

1. Tanzi MC *et al.* 2011. Pat. num. WO2012164032 A1.
2. Marelli B *et al.* Acta Biomater 2010; 6:4019-26.
3. Cattaneo I *et al.* Int J Artif Organs 2013; 36:166-74.
4. Marelli B *et al.* Macromol Biosci 2012; 12:1566-74.
5. Jagur J *et al.* Polym Advan Technol 2010; 21:27-47

Design and synthesis of supramolecular biomaterials for *in-situ* cardiovascular tissue engineering

Olga JGM Goor^{1,2*}, Geert C van Almen^{1,2} and Patricia YW Dankers^{1,2}

¹Institute for Complex Molecular Systems and ²Laboratory of Chemical Biology, Department of Biomedical Engineering, Eindhoven University of Technology, P.O. Box 513, 5600 MB Eindhoven, The Netherlands

*o.j.g.m.goor@tue.nl

INTRODUCTION

Cardiovascular and valvular diseases are a major health burden worldwide¹. Although surgical interventions to replace heart valves or arteries provide a significant improve in quality of life, long-term failure of the implants often leads to a decreased life expectancy. To this extent, *in-situ* cardiovascular tissue engineering has evolved as a potential alternative to create instructive, biodegradable scaffolds that aim at using the natural regenerative potential of the human body to engineer a replacement tissue *in vivo*². We aim to synthesize and develop cell-free vascular graft materials, using supramolecular chemistry. These scaffolds are proposed to be indistinguishable from nature with respect to their mechanical and biochemical properties. Tailor-made materials are developed based on supramolecular polymers end-capped with ureido-pyrimidinone (UPy) moieties, able to dimerize upon quadruple hydrogen-bond formation³ providing a dynamic character, spaced with polycaprolactone (PCL) blocks to meet mechanical requirements⁴. Bioactive UPy-modified peptides are incorporated via a modular approach⁵ in order to provide necessary biological signals to attract and stimulate cells inside the scaffold.

METHODS

In the design presented here, we focus on the bioactivation of our materials to endogenously capture cells from the blood into the vascular grafts. More specifically, we aim to immobilize complicated growth factors and proteins onto the scaffold, in particular transforming growth factor beta (TGFβ), which is known to play an important role in the process of EndoMT (endothelial-to-mesenchymal transition)⁶. Via two different supramolecular methods we propose to complex TGFβ onto our surfaces. These approaches are all based on the expansion of our toolbox of UPy-polymers and UPy-peptides in order to gain temporal control at the surface of our biomaterials. Via our traditional approach we bioactivate our surfaces with TGFβ-derived peptides modified with UPy-units. As a new approach, we synthesized UPy-heparin binding peptides that can be incorporated into our UPy-scaffold materials. Upon immobilization of heparin onto the heparin binding peptides, we aim at complexation of TGFβ at the surface via its heparin binding domain.

RESULTS

UPy-functionalized peptides were synthesized using Fmoc protected solid phase peptide synthesis (SPPS). In the traditional approach we successfully synthesized and purified UPy-TGFβ derived peptides based on the LYIDFRKDLG sequence, yielding 72.2 mg (24%). Our heparin approach required the synthesis of UPy-heparin binding peptides, bearing the previously reported heparin binding GLRKKLGA motif⁷, which provided us 74 mg (20%) after purification. Heparin-FITC immobilization onto our supramolecular PCLdiUPy surfaces with 4 mol% incorporation of UPy-heparin binding peptides, showed a 6 fold increase in fluorescence in contrast to the PCLdiUPy control without peptide. In ongoing experiments we aim to immobilize complex proteins that contain a heparin binding domain (e.g. fibronectin) onto the heparin functionalized surfaces and moreover translate this towards *in vitro* cell studies.

CONCLUSION AND DISCUSSION

The two experimental approaches will allow for temporal control at the surface of biomaterials as a next step in the development of supramolecular biomaterials for cardiovascular tissue engineering purposes. Moreover, the strategy presented here to synthesize UPy-based biomaterials with UPy-modified peptides to immobilize full-length growth factor proteins onto these materials can easily be generalized and can also be applied in the field of for example renal regenerative medicine.

REFERENCES

1. B. Cannon, *Nature*, **2013**, 493, S2-S3.
2. C. Bouten et al., *Medicine, Chapter 8*, **2009**.
3. E.W. Meijer et al., *Science*, **1997**.
4. E.W. Meijer et al., *Adv. Mat.*, **2000**.
5. P.Y.W. Dankers et al., *Nature Materials*, **2005**.
6. A.M. Schor et al., *J. Cell. Sci.*, **1992**.
7. S.I. Stupp et al., *Nano Lett.*, **2006**.

ACKNOWLEDGMENTS

This research has received funding from the European Research Council (FP7/2007-2013) ERC Grant Agreement 308045.



Tissue Response and Degradation of Novel Gelatin-Based Biomaterials *in vivo*: Insights from Small Animal Multimodal Imaging

Christoph Tondera^{1,2*}, Sandra Ullm^{1,2}, Sebastian Meister¹, Tim P. Gebauer^{3,4}, Axel T. Neffe^{3,4}, Andreas Lendlein^{3,4}, Jens Pietzsch^{1,2}

^{1*} Helmholtz-Zentrum Dresden-Rossendorf, Institute of Radiopharmaceutical Cancer Research, Department of Radiopharmaceutical and Chemical Biology, Dresden, Germany, c.tondera@hzdr.de

² Technische Universität Dresden, Department of Chemistry and Food Chemistry, Dresden, Germany

³ Institute of Biomaterial Science and Berlin-Brandenburg Centre for Regenerative Therapies, Helmholtz-Zentrum Geesthacht, Teltow, Germany

⁴ Helmholtz Virtual Institute "Multifunctional Biomaterials for Medicine", Teltow and Berlin

INTRODUCTION

Biomaterials can be implanted in not self-healing, i.e. critical size defects, substituting temporarily for the extracellular matrix and assisting the healing process. The material of choice should be degraded in different time frames, depending on the tissue to be replaced, to allow for an optimal ingrowth of cells and support wound healing. Extracellular matrix (ECM) derived materials like gelatin-based hydrogels are degraded under biological conditions and, therefore, are particularly suitable for the regeneration of tissue. However, gelatin-based biomaterials are foreign matter to an organism, which can lead to adverse tissue responses. Using dedicated small animal multimodal imaging the rate of degradation as well as inflammatory responses to biomaterial implantation as important part of the biological evaluation of a biomaterial was studied *in vivo*.

EXPERIMENTAL METHODS

The hydrogels were synthesized by crosslinking a 10 wt.-% aq. gelatin solution using different amounts of ethyl lysine diisocyanate. Two gelatin-based hydrogels with different crosslinking levels (3-fold and 8-fold molar excess of isocyanate groups - G10_LNCO3 and G10_LNCO8) were implanted subcutaneously in immunocompetent SKH-1 mice and degradation was compared. The volume of implanted biomaterial was determined using dedicated 7 T small animal magnetic resonance imaging (MRI) with a specially designed T2 weighted TRARE measuring sequence. The used matrix was 256×128 pixel with a field of view of 4×2 cm. Slice thickness was 0.8 mm. After the measurement a voxel-based evaluation method was applied. Formation of reactive oxygen species (ROS) and induction of cyclooxygenase-2 (COX-2), two markers of pro-inflammatory reactions, were followed by dedicated small animal optical imaging. L-012, a luminol derivative, was used to detect ROS. To visualize the induction of COX-2, a rhodamine coupled indomethacin-based selective COX-2 inhibitor was used. The substances were injected intraperitoneally. Both tracers were preliminary evaluated in SKH-1 mice using a 12-O-tetradecanoylphorbol-13-acetate inflammation model.

RESULTS AND DISCUSSION

G10_LNCO3 and G10_LNCO8 showed different degradation properties. After an initial degradation

period the samples showed significant differences in degradation from day 14 onwards. G10_LNCO3 showed faster degradation compared to the material with the higher crosslinking degree (G10_LNCO8). The less crosslinked material was almost completely degraded ($V < 5\% V_{\text{day 1}}$) after 5 weeks while G10_LNCO8 still remained in the body for at least 8 weeks (Figure 1).

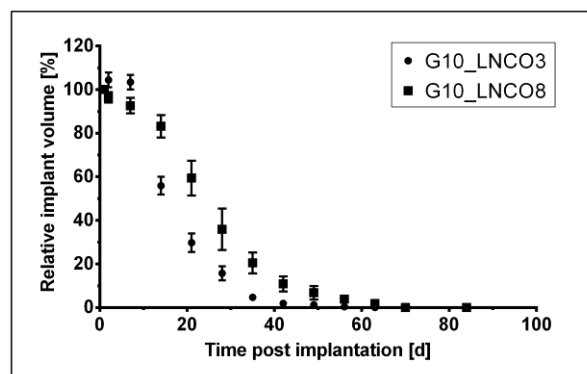


Figure 1: Degradation of gelatin-based hydrogels with different degrees of crosslinking in immunocompetent SKH-1 mice quantified by MRI.

Within the implantation *situs* production of ROS and induction of COX-2 could be observed up to 7 days post implantation around the surgical incision but not within the area of the implant. Onwards no further ROS production and COX-2 induction could be observed.

CONCLUSION

This multimodal imaging study revealed that the crosslinking level of gelatin-based biomaterials determines the degradation time of the material. This allows for targeted modification of the material according to the respective tissue that needs to be replaced. Furthermore, except for minor pro-inflammatory reactions at the incision site, no adverse tissue response could be observed during and after the degradation which is consistent with good biocompatibility of these novel materials.

ACKNOWLEDGMENTS

The authors thank the Helmholtz Association for funding of this work through Helmholtz-Portfolio Topic "Technologie und Medizin – Multimodale Bildgebung zur Aufklärung des In-vivo-Verhaltens von polymeren Biomaterialien".



Systemically Injected Gold-Silica Hybrid Nanovectors for Combined Cancer Therapy and Imaging

Coline Jumeaux^{1,2}, Ciro Chiappini^{1,2}, Rona Chandrawati^{1,2}, Matthew Hembury^{1,2}, Glenna L. Drisko⁴, Cédric Boissière⁴, Clément Sanchez^{4,5}, Alexandra Porter¹, Molly M. Stevens^{1,2,3}

¹Department of Materials, ²Institute of Biomedical Engineering, and ³Department of Bioengineering, Imperial College London, London, SW7 2AZ, UK; ⁴Sorbonne Université, UPMC Université Paris 06, UMR7574, LCMCP, France;

⁵Collège de France, UMR7574, LCMCP, France. E-mail : c.jumeaux12@imperial.ac.uk

INTRODUCTION

Nanomedicine is an emerging field of research partly driven by the pressing medical need for effective cancer therapy. Despite a significant level of development, conventional chemotherapy still fails to address the challenges of cancer treatment i.e., achieving high local concentration of the therapeutics at the vicinity of the tumour while minimizing adverse toxic effects on healthy tissues or cells. To overcome these drawbacks, we present a new class of carrier system, termed Quantum Rattles (QR), made of hollow mesoporous silica shells encapsulating two different populations of gold nanostructures - gold nanoclusters (AuNC) and gold nanoparticles (AuNP). AuNC, in particular, have generated a lot of attention thanks to their unique optical and magnetic properties.¹ Their strong photoluminescence, combined with good photostability, large Stokes shift and high emission rate make them good candidates for optical imaging. However, their instability, chemical reactivity and tendency for agglomeration prevent their widespread use since their properties critically depend on their stability.² The QR embodies a breakthrough for the use of AuNC in the biological setting. QR represents a simple, “one-pot” method for the synthesis of AuNC templated by mesoporous silica shells, conferring them stability in biological media. Moreover, the silica shell of the QRs can host a therapeutic payload. Overall, QR is a holistic platform for cancer theranostics, enabling multimodal imaging and combination therapy.

To further our aim in developing QR as injectable drug delivery system (DDS), we report the development of stimuli-responsive drug-delivery carriers based on QR by using the layer-by-layer (LbL) technique. Sequential deposition of thermoresponsive polymers is used to coat the QR. This facilitates effective encapsulation of therapeutics while allowing controlled release of the cargo only upon stimuli when the polymer layers undergo a conformational change caused by a local increase of the temperature, induced by gold nanoparticles-mediated hyperthermia.

EXPERIMENTAL METHODS

Properties of QR: Experimental techniques such as photoluminescence, UV-vis absorption, TEM imaging and size analysis by Dynamic Light Scattering were used to analyse the properties of QR. Cytotoxicity of QR against HeLa cells was evaluated by an MTS assay.

QR as Stimuli-Responsive Drug Delivery Carriers: The build-up of the polymer layers was demonstrated on planar substrates using Quartz Crystal Microbalance (QCM) and on QR using flow cytometry. Release of encapsulated therapeutics was monitored by fluorescence spectrophotometer.

RESULTS AND DISCUSSION

We describe the novel synthesis of QR and analyze QR properties (Figure 1), conferring QR great potential for *in vivo* imaging.

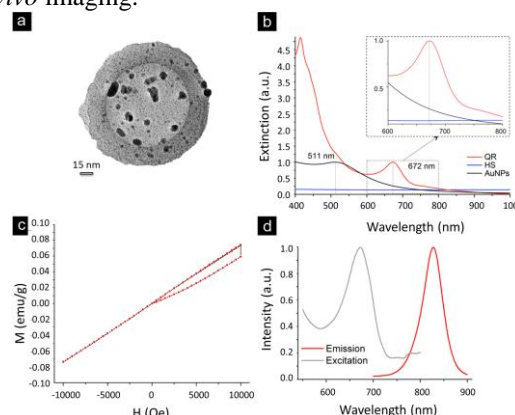


Figure 1: a) TEM image of QR (scale bar is 15 nm). b) UV-Vis absorption spectrum of QR. c) The M vs H magnetisation curves of QR at 2 K showing that QRs exhibit paramagnetic behaviour. d) Photoluminescence excitation (grey) and emission (red) spectra of QR.

We also show the potential of QR for combination therapy *via* both release of anticancer drug and photothermal therapy (PTT). When irradiated by a laser emitting in the NIR, QR generate gold nanoparticle-mediated hyperthermia, and we show the efficacy of QR PTT *in vitro* against HeLa cells.

We develop QR as injectable DDS by showing that coating QR with an optimized lipid bilayer³ promotes the stability of the dispersion at physiological conditions, which is crucial for ensuring a good biodistribution. We further emphasize the use of QR for triggered release of therapeutics, by demonstrating the build-up of thermoresponsive poly[tri(ethylene glycol) methacrylate] (pTEGMA) layers onto these colloidal substrates. The polymer multilayer films assembled on QR are stable at both assembly and physiological conditions as confirmed by flow cytometry. We then investigate the temperature-triggered release of doxorubicin.

CONCLUSION

Quantum Rattle, a novel smart drug delivery system, represents a promising multifunctional platform for cancer treatment, which combines thermally-triggered drug release and gold-mediated hyperthermia.

REFERENCES

- Samanta, A. *et al.*, J. Phys. Chem. C, 116:1748–1754, 2012
- Peer, D. *et al.*, Nature Nanotechnology. 2:751-760, 2007
- Ashley, C. E. *et al.*, Nature Materials. 10:389-397, 2011

ACKNOWLEDGMENTS

The authors would like to thank the Rosetrees Trust for providing financial support to this project.



Superparamagnetic Iron Oxide Nanoparticles Stabilized by Dextran Nanogel: New Nanomagnetogel as Contrast Agent for Magnetic Resonance Imaging. Biodistribution

Catarina Gonçalves¹, Yoann Lalatonne², Liliana Melro¹, Giorgio Badino¹, Miguel Ferreira¹, Laurence Motte², Carlos Geraldés⁴, José Alberto Martins³, F. M. Gama¹

¹Centre for Biological Engineering, Minho University, Campus de Gualtar 4710-057, Braga, Portugal; fmgama@deb.uminho.pt

²CSPBAT Laboratory, UMR 7244 CNRS, Université Paris 13, Sorbonne Paris Cité, Bobigny, France

³Departamento de Química, Universidade do Minho, Campus de Gualtar, 4710-057 Braga, Portugal

⁴Departamento de Ciências da Vida, Faculdade de Ciência e Tecnologia e Centro de Neurociências e Biologia Celular, Universidade de Coimbra, Portugal

INTRODUCTION

Superparamagnetic iron oxide nanoparticles (SPION) are of considerable interest as contrast agents due to their nanoscale dimensions, non-toxic nature and magnetic properties. Currently, two SPION are clinically approved, namely: ferumoxides (Feridex in the USA, Endorem in Europe) and ferucarbotran (Resovist). SPION effect is observed mainly on T_2^* relaxation and thus MRI is usually performed using T_2/T_2^* - weighted sequences in which the loss of tissue signal is due to the susceptibility effects of the SPION oxide core. In this study, we aim to develop a novel approach to prepare uniform polymeric particles, by stabilizing iron oxide nanoparticles within dextran nanogels - a class of nanocarriers well suited for numerous specific delivery applications [1]. Nanogels can be formulated by self-assembly of amphiphilic polymers. In such a typical self-assembled formulation, the hydrophobic nanodomains formed within nanogel can be loaded with a variety of therapeutic molecules or imaging agents.

EXPERIMENTAL METHODS

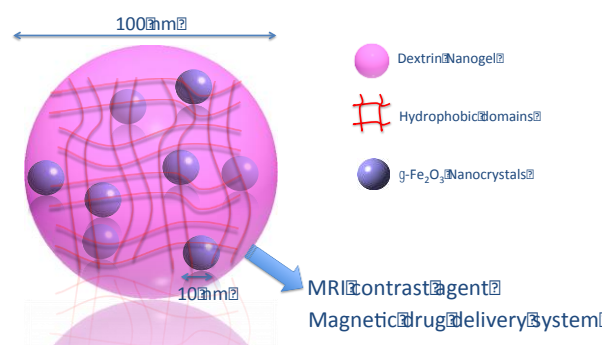
A nanomagnetogel (Figure) that consists on superparamagnetic iron oxide nanoparticles stabilized within hydrophobized-dextran nanogel was produced and characterized regarding physico-chemical (Transmission Electron Microscopy, Cryo-Scanning Electron Microscopy, Dynamic Light Scattering, Small Angle X-ray Scattering), magnetic (relaxometry, MIAplex) and biocompatibility (interaction with cells) properties.

RESULTS AND DISCUSSION

In this study, we have shown that the nanomagnetogel production is simple, reproducible, and exhibit long-term colloidal stability (in water dispersions), at least up to 8 weeks. Our first goal was to explore nanogel loading efficacy, using different nanogel/ γ -Fe₂O₃ ratios and nanogels with different degrees of substitution with alkyl chains (hydrophobic part). The inner structure of the nanomagnetogel was elucidated by combining dynamic light scattering, transmission electron microscopy and small-angle X-ray scattering analysis. The nanomagnetogel has a diameter of around 100 nm and comprises superparamagnetic nanoparticles randomly distributed within the polymer structure. The surrounding corona of dextran allows iron oxide

stabilization avoiding aggregation at physiological pH. The nanogel with the lowest degree of substitution with alkyl chains (NG1) 2.0 mg/mL and 10.0 mM of initial iron concentration was selected as the most interesting formulation, which corresponds to a nanomagnetogel with about 4.0 mM of iron content. Incorporation of iron oxide within the nanogel structure results in promising relaxometric properties, essentially as T_2 contrast agent for MRI [2].

The nanomagnetogel demonstrated non-toxicity for 3T3 fibroblast cultures and was efficiently internalized by bone marrow-derived macrophages, therefore bearing potential as contrast agent for MRI of the organs associated to the reticuloendothelial system (spleen, liver).



CONCLUSION

The nanomagnetogel exhibits r_2 values superior to those of commercially available formulations. The production is simple and easy to scale up, thus offering great technological potential.

REFERENCES

1. Fang, R. H. and Zhang, L. Journal of Nanoeng. Nanomanufact. 1, 106-112 2011
2. Gonçalves et al. J. Mat. Chem. B, 1:5853-5864, 2013

ACKNOWLEDGMENTS

The authors would like to thank the Euronanomed Programme and Fundação da Ciência e Tecnologia (Grant REBONE) for providing financial support to this project

A Non-Toxic Additive to Introduce X-Ray Contrast into Poly(lactic acid)s

Leo H. Koole*, Daniel G. Molin, and Yujing Wang

Departments of Biomedical Engineering/Biomaterials Science and Physiology, Faculty of Health, Medicine & Life Sciences, Maastricht University, PO Box 616, 6200 MD Maastricht, The Netherlands. l.koole@maastrichtuniversity.nl

INTRODUCTION

Drug-eluting bioresorbable vascular scaffolds are currently changing the landscape of percutaneous coronary intervention (1). The well-known *ABSORB* everolimus-eluting scaffold has struts from poly(L-lactic acid), and its drug-containing surface coating consists of poly(D,L-lactic acid). Bioresorbable vascular scaffolds are clinically successful. Recently, early (< 6 months), late (6-12 months), and very late (> 12 months) angiographic follow-up on 101 patients has shown 6 binary cases of in-segment restenosis, which are due to anatomical or procedural factors. Perhaps the only remaining drawback of these scaffolds is that they are radiolucent. Small platinum markers have to be introduced to visualize the scaffold fluoroscopically, during and after implantation.

We have developed a new contrast agent that can be blended into poly(lactic acid)s without inducing phase separation (2). The additive, (S)-2-hydroxy-3-(4-iodobenzoyloxy) propanoic acid, bears structural resemblance to lactic acid, and also contains covalently bound iodine. Toxicity of the new compound was studied, and found to be comparable with toxicity of L-lactic acid in numerous *in vitro* cell growth assays. We believe that the new contrast agent can be used to manufacture bioresorbable vascular scaffolds with whole-body X-ray visibility.

EXPERIMENTAL METHODS

The new contrast agent was synthesized in 3 steps from Boc-L-serine and 4-iodobenzyl bromide. Purity and identity of the crystalline compound were established by NMR spectroscopy and elemental analysis. Furthermore, the X-ray crystal structure was determined. In the crystal, the molecules are hydrogen bonded to form a one-dimensional chain along the crystallographic a-axis. The contrast agent was blended with a commercial poly(D,L-lactic acid): PURASORB PDL 20 in two ratios: 5 % and 10 % (by mass)., and circular specimens were prepared by hot-pressing. Comparisons were made (e.g., regarding cytotoxicity, hemocompatibility) with blends of PURASORB PDL 20 and Na-ditriazoate (a common X-ray contrast agent).

RESULTS AND DISCUSSION

The blends of the new contrast agent and poly(D,L-lactic acid) showed clear radiopacity (Figure 1). They were transparent materials, whereas the counterpart blends of Na-ditriazoate were white-opaque. This already provided evidence for structural compatibility in the first case, and phase separation in the control blends. This was confirmed by differential calorimetry and X-ray electron spectrometry, which showed homogenous distribution of iodine in the new materials, but not in the blends containing Na-ditriazoate.

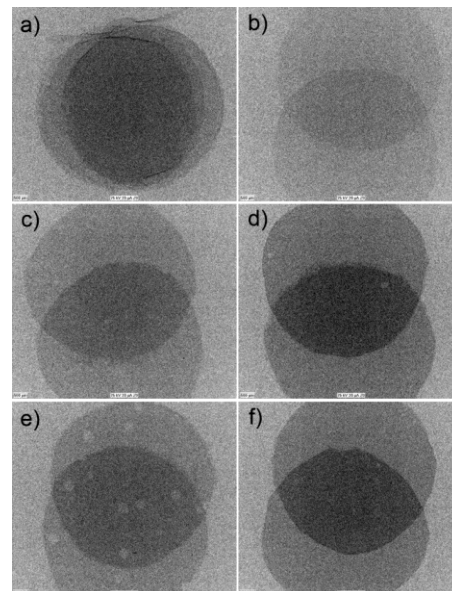


Figure 1. X-ray images of 10 stacked aluminium foils (a), two partially overlapping specimens of PURASORB PDL 20 (b), idem of blend 5 % Na-ditriazoate (c) idem of blend 10 % Na-ditriazoate (d), idem of blend 5 % new contrast agent (e), and idem of blend 10 % new contrast agent.

CONCLUSION

The new contrast agent from this study allows, by design, the manufacture of homogeneous radiopaque biodegradable blends of poly(lactic acid)s. Avoiding phase separation is mandatory to achieve control over the degradation kinetics. The concept may be used to manufacture bioresorbable implants with whole-body X-ray fluoroscopy. This is especially relevant for bioresorbable vascular scaffolds. Enhanced fluoroscopic visibility will help to improve accuracy and safety of coronary stenting.

REFERENCES

1. Nakatani S. et al., *EuroIntervention* 2014, 9 (online publish-ahead-of-print - February 2014)
2. Wang Y et al., *Adv. Healthcare Mat.* 2014, 3, 290-9.

ACKNOWLEDGMENTS

This study is part of the Interreg IV-A project "BioMiMedics" (www.biomimedics.org) in which the Universities of Maastricht, Aachen (G), Juelich (G), Liege (B) and Hasselt (B) cooperate. This particular study was financed through generous contributions from the Province of Dutch Limburg, The Dutch Ministry of Economic Affairs, Maastricht University, Limburg Innovation BANK (LIOF), and the company Interface BIOMaterials BV (Geleen, the Netherlands).

Novel Technique to Map the Biomechanical Properties of Entire Articular Surfaces Using Indentation to Identify Early Osteoarthritis-like Regions

Sotcheadt Sim^{1,2}, Anik Chevrier¹, Martin Garon², Eric Quenneville² and Michael D. Buschmann^{1*}

¹Biomedical & Chemical Engineering Department, Ecole Polytechnique de Montreal, Canada

^{2*}Biomomentum Inc., Canada. garon@biomomentum.com

INTRODUCTION

The identification and quantitative grading of early degenerated regions over an entire articular surface remains a challenging quest. However, mechanical testing has proved its efficiency for estimating early degeneration of articular cartilage¹. The objective of this study was to investigate the ability of a novel technique to automatically characterize mechanical properties of entire articular surfaces in indentation in order to rapidly and non-destructively discriminate between damaged and healthy articular cartilage regions.

EXPERIMENTAL METHODS

The distal femurs of eight human tissue donors were obtained and articular lesions were graded with a visual classification system². Mechanical properties were mapped ex vivo, using a novel technique allowing for automated alignment and indentation mapping of articular surfaces. Subsequently, the thickness was measured with an adapted version of the needle technique³. The instantaneous modulus at each position was obtained by fitting the load-displacement curve (with corresponding thickness) to an elastic model in indentation⁴. Osteochondral cores were harvested from visually healthy and osteoarthritis-like regions and tested in unconfined compression where mechanical properties were extracted from the stress relaxation curve⁵.

RESULTS AND DISCUSSION

OA-like regions were identified mechanically and were wider than the regions identified by visual assessment (Blue-green regions in Fig. 1). A strong correlation ($r=0.84$, $p<0.0001$) was observed between the mechanical properties measured in indentation and in unconfined compression (Fig. 2).

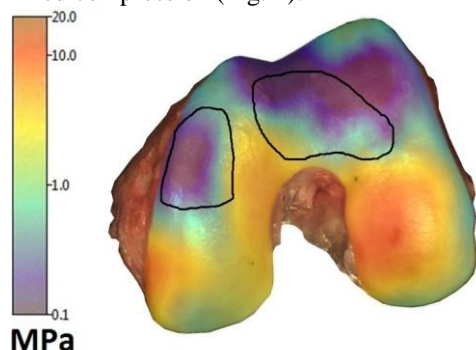


Figure 1: Mapping of the instantaneous modulus to identify early OA-like articular cartilage

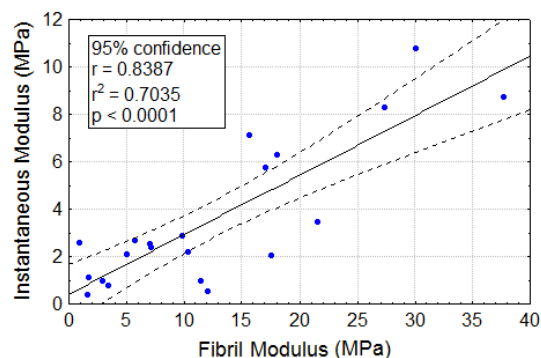


Figure 2: Significant correlation between the instantaneous modulus and fibril modulus

CONCLUSION

This indentation mapping technique provides fast, efficient and non-destructive measurements of the mechanical properties of the entire articular surface. We also successfully applied this novel technique to mice, rat, rabbit and sheep articular cartilage samples and would be of great use in the identification of wear patterns in osteoarthritis progression and for use in cartilage repair studies.

REFERENCES

1. Saarakkala S. *et al.*, Osteoarthritis Cartilage. 11:697-705, 2003
2. Mainil-Varlet P. *et al.*, J Bone Joint Surg Am 85-A Suppl 2:45-57, 2003
3. Jurvelin JS. *et al.*, J Biomech. 28:231-235, 1995
4. Hayes WC. *et al.*, J Biomech. 5:541-551, 1972
5. Soulhat J. *et al.*, J Biomech Eng. 121:340-347, 1999

ACKNOWLEDGMENTS

We acknowledge the technical contributions of Gabrielle Picard, Alexandre Torres, François Marcoux, Marie-Hélène Boulanger and Sylvain Gaufrès. Funding provided by the National Sciences and Engineering Research Council (NSERC), the Fonds de recherche du Québec - Nature et technologies (FRQNT) and Biomomentum Inc.

CONFLICT OF INTEREST

E. Quenneville and M. Garon are the owners of Biomomentum Inc.

Polymer Coating for *in vivo* MR Visualization of Tissue Reinforcement Prostheses

X. Garric^{*1}, S. Blanquer¹, O. Guillaume¹, V. Letouzey¹, L. Lemaire², F. Franconi³, R. DeTayrac⁴, J. Coudane¹.

1- IBMM, Artificial Biopolymers Group, UMR-CNRS 5247, UM1-UM2, 15 Av. C. Flahault, 34093 Montpellier, France.

2 - INSERM UMR-S 646, Angers University, 10 rue André Boquel, 49100 Angers, France.

3 - Plateforme d'Ingénierie et Analyses Moléculaires (PIAM), Angers University 2, Bd Lavoisier 49045 Angers, France.

4- Department of Obstetrics and Gynecology, Carémeau Hospital, 30 000 Nîmes, France

xavier.garric@univ-montp1.fr

Introduction: Since the late 90's, medical devices such as meshes are used for the soft tissue reinforcement in the surgical treatment of genital prolapse. One of the major drawbacks of these meshes is their erosion that occurs with time, and the lack of efficient imaging technique to follow erosion and/or motion of the device. As Magnetic Resonance Imaging (MRI) is the gold standard for abdomen and female pelvis imaging¹, we developed MRI visible meshes. The aim of this work was to synthesize a new MRI visible polymer by grafting a MRI contrast agent on the skeleton. The MRI visible polymer can be then coated or integrated into meshes allowing its *in vivo* MR visualization.

Materials and methods: Anionic activation of poly(methyl acrylate) (PMA) chain was performed by removing a proton from the methylene group in α -position of the ester carbonyl, using a non-nucleophilic base². The resulting macropolycarbanion can then react with the electrophile group of an activated DTPA (diethylene triamine pentaacetic acid) leading after hydrogenolysis to a polymer able to chelate Gd^{3+} ions. Grafted polymer was characterized by ¹H NMR and SEC. Coating was characterized by Environmental scanning electron microscope (ESEM). Influence of this MRI-visible polymer cytotoxicity was evaluated *in vitro* on fibroblast cells viability and pro-inflammatory response. MR signal enhancement of the new polymer was investigated on agarose gel using a 7 Teslas experimental MR apparatus compared to a clinical MRI, completed with first MRI visibility tests after prosthesis implantation using an *in vivo* model.

Results and discussion

MR contrast agent (DTPA-Gd) has been covalently grafted on poly (methyl acrylate). The grafted polymer was coated on commercial meshes by spray drying. The coated mesh is clearly detectable *in vitro* by MRI whereas the uncoated mesh remained undetectable. PMA-DTPA-Gd amount used in the coating provides sufficient signal to clearly define the margins of the mesh.

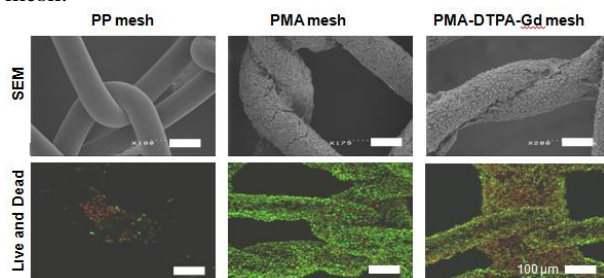


Figure 1 : SEM pictures and Confocal microscopy image of PP meshes compared to PMA and PMA-DTPA-Gd coated meshes after 8 day of incubation with L-929 cells and after live/dead staining. Scale bares represent 100 mm.

Cytocompatibility studies of the grafted polymer on L-929 fibroblasts showed that the DTPA-Gd-PMA coating does not significantly hamper cell adhesion, proliferation or vitality (Fig 1).

To assess the visualization of the coated mesh *in vivo*, two meshes were implanted in the rat's back (intramuscular and subcutaneous). The coated meshes were unambiguously detectable whatever the location (Fig. 2). The structure of the meshes and the limits were significantly detectable, suggesting that the hanging can be easily evaluated.



Figure 2: *In vivo* visualization of two meshes coated with poly(methyl acrylate)-DTPA-Gd implanted in a rat

Conclusion

MR-visible polymer was synthesized and coated on polypropylene-based medical devices. The T1-shortening effect of paramagnetic contrast agent (DTPA-Gd³⁺) grafted onto poly(methylacrylate) was used to visualize meshes for soft tissue reinforcement both *in vitro* and *in vivo*. New polymers covalently linked to contrast agents can easily be coated onto prosthesis (i.e. stent, mesh, suture...) to significantly enhance magnetic resonance signal, allowing a quick MR localization of the device.

References:

- 1- Functional MR imaging of the female pelvis. Koyama T, Togashi K. J Magn Reson Imaging. 2007 Jun;25(6):1101-12.
- 2- A novel route to poly(epsilon-caprolactone)-based copolymers via anionic derivatization. Ponsart S, Coudane J, Vert M. Biomacromolecules. 2000 Summer;1(2):275-81.

ACKNOWLEDGMENTS

The authors are grateful to Dr. Chantal Cazevieille (CRIC, University Montpellier I), Dr. Nicole Lautredou and Dr. Julien Cau (Rio Imaging, Montpellier) for their technical assistance and interpretation of ultrastructural data, to Sylvie Hunger for ¹H NMR analyses and to Dr. Olivier Bruguier (Geosciences, University Montpellier II) for his help in ICP-MS measurements. This work was partially supported by "Agence Nationale de la Recherche" grant no. ANR-08-TECS-020-01 and by the French Ministry of Education and Research.

S. Aureus Evades Leukocyte Antimicrobial and Mesenchymal Stromal/stem Cell Immunomodulatory Functions

David Antonio Cantu^{1,2}, Warren E. Rose¹, Peiman Hematti³, Weiyuan John Kao (PI, wjkao@wisc.edu)^{1,2,4}

¹School of Pharmacy, ²Department of Biomedical Engineering, ³Department of Medicine, ⁴Department of Surgery, University of Wisconsin-Madison, Madison, WI 53705, USA

Statement of Purpose: Mesenchymal stromal/stem cells (MSCs) intrinsic immunomodulatory activity has been utilized for the treatment of a number of inflammatory conditions and immune disorders¹. In mice cecal ligation models, MSC administration improved subject survival by attenuating excessive inflammation associated with septic shock/multi-organ dysfunction while enhancing phagocytic cell-mediated bacterial clearance in the blood stream^{2,3}. Previously, three-way interactions between encapsulated MSCs, adherent monocytes, and the biomaterial induced up-regulation of the M2 phenotype in monocytes, which was associated with attenuated inflammation and greater phagocytic activity^{4,5}. We hypothesize that MSCs can enhance neutrophil and/or monocyte/macrophage phagocytic function for the elimination of nascent *S. Aureus* biofilms.

Methods: The MBECTTM-HTP device was inoculated with *S. Aureus* (ATCC 29213, 3.0×10^8 CFU/mL) and incubated for either 6 or 24 hrs with continuous rocking (37°C, 10° inclination) to form biofilms. Pins removed from the MBECTTM-HTP device were placed in transwell co-culture containing either monocytes or neutrophils (top chamber) and encapsulated MSCs (bottom chamber) with RPMI 1640 supplemented with either 10% or 1% autologous human serum for 2, 6, or 12 hrs (depicted below) isolated from healthy, primary donors. Planktonic *S. Aureus* was also utilized. MSCs (passages 4 - 6) were encapsulated in either collagen hydrogels or gelatin/poly(ethylene) glycol (Gel-PEG) interpenetrating biomatrices⁶. The *S. Aureus* biofilms or planktonics were sonicated and plated on tryptic soy agar (24 hrs) before counting the observed colonies for Log CFU/mL determination. MSCs, monocytes, or neutrophils were imaged for viability using LIVE/DEAD®.

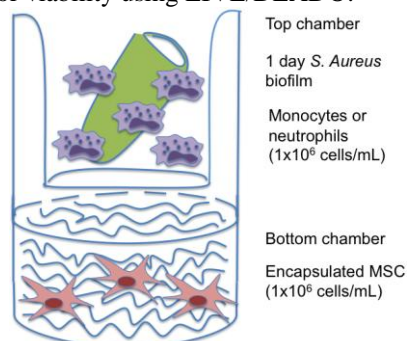


Figure 1. Transwell co-culture schematic.

Results: Biomatrix-encapsulated MSCs retained high viability for both materials (collagen and Gel-PEG) over various biofilm exposure times, whereas monocyte and neutrophil viability decreased with increasing biofilm

exposure time (2, 6, or 12 hr) or biofilm maturity (6 or 24 hr). A significant decrease in the observed Log CFU/mL was not observed for the various culture conditions with either immune cells (neutrophils or monocytes), co-culture times (2, 6, or 12 hrs), or biofilm maturity (6 or 24 hrs) when compared to the biofilm only condition (with the exception of the minocycline positive control). Similar trends were observed for planktonic *S. Aureus*.

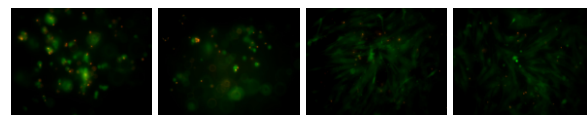


Figure 2. LIVE/DEAD® staining of encapsulated MSCs exposed to nascent biofilm (6 hr); left: [monoculture MSCs (Gel-PEG)]; middle left: [co-culture MSCs (Gel-PEG)]; middle right: [monoculture MSCs (collagen)]; right: [co-culture MSCs (collagen)].

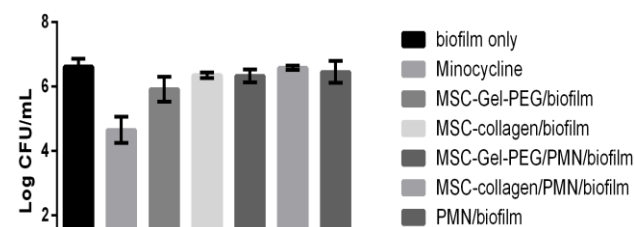


Figure 3. Log CFU/mL tryptic soy agar plating comparison of nascent *S. Aureus* (6 hr) biofilms in 2 hr monoculture or co-culture with neutrophils and/or encapsulated (Gel-PEG or collagen) MSCs (1:1, 1×10^6 cells/mL). Minocycline (2 mg/mL) was utilized as a positive control for bacteriostatic/bactericidal comparison.

Conclusions: Similar to implant-associated infection, *S. Aureus* biofilm and in planktonic form evades leukocyte antimicrobial activities and mesenchymal stromal/stem cell immunomodulatory functions. No direct bacteriocidal activity was observed for MSC.

Acknowledgements: NIH HL115482

References: **1** Annu Rev Biomed Eng 2010; 12:87-117. ; **2** Nature Med 2009; 15(1): 18-19. ; **3** Am J Respir Crit Care Med 2010; 182: 1047-1057. ; **4** Exp Hematol 2009; 37(12): 1445-1453. ; **5** Stem Cell Trans Med 2012; 1: 740-749.

Preparation and Characterisation of an Antibacterial Silver-doped Nanoscale Hydroxyapatite Paste

Caroline Wilcock¹, Monazza Fatima¹, Piergiorgio Gentile¹, Graham Stafford², Cheryl Miller¹, Yulia Ryabenkova³, Guenter Möbus³, Paul Hatton¹

¹Centre for Biomaterials and Tissue Engineering, University of Sheffield, UK

²Integrated Biosciences Group, University of Sheffield, UK

³Department of Materials Science and Engineering, University of Sheffield, UK
mta07cw@sheffield.ac.uk

INTRODUCTION

The management of bone infection remains a significant challenge in orthopaedics and dentistry. The introduction of a biomaterial into the body presents an opportunity for bacterial growth and colonisation which in turn can cause serious medical complications¹. Infections in bone are especially hard to treat due to the difficulty of achieving suitable antibiotic distribution in the infected skeletal tissue². Therefore, there is a great clinical need for bone augmentation materials that are able to encourage bone regeneration whilst possessing antibacterial properties. Nanoscale hydroxyapatite (nHA) pastes have recently been released on the market and early evidence suggests that the bone regeneration capacity of this new class of biomaterials is promising. The addition of silver ions to a nanoscale hydroxyapatite paste may present a novel injectable bone substitute material with antimicrobial activity. The aim of this study was therefore to produce a silver-doped nHA paste and investigate its antibacterial activity.

EXPERIMENTAL METHODS

A wet precipitation method based on Prakash *et al.*³ was used to synthesise a range of silver-doped nHA pastes (0, 2, 5 and 10 mol. %). The silver-doped nHA suspensions were dried in an oven at 60 °C until pastes of approximately 85 % water content were obtained. Complete dehydration of the silver-doped nHA suspensions was also carried out to form powder samples. These were then subjected to a high temperature sintering stage of 1000 °C for 2 h in order to investigate the thermal stability of the products. Characterisation techniques including x-ray diffraction (XRD), attenuated total reflectance-Fourier transform infrared spectroscopy (ATR-FTIR) and transmission electron microscopy (TEM) were used to investigate the materials produced. The antibacterial activities of the silver-doped nHA pastes were then tested against *Staphylococcus aureus* and *Pseudomonas aeruginosa* using agar diffusion and broth dilution methods (n=3).

RESULTS AND DISCUSSION

XRD and TEM results displayed the successful formation of nHA in all the samples produced. After heat treatment at 1000 °C, silver-doped nHA samples had an increased tendency to decompose into β -tricalcium phosphate. This suggested that the presence of the silver ions destabilised the nHA crystal lattice.

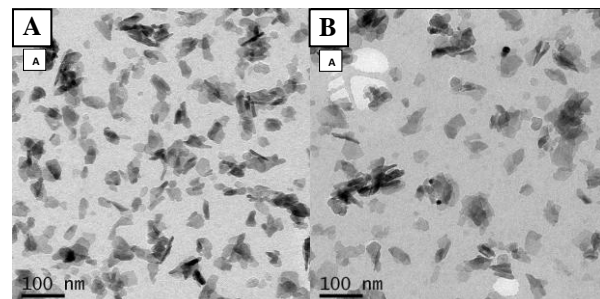


Fig. 1: Transmission electron microscopy images of 0 (A) and 10 (B) mol. % silver-doped nanoscale hydroxyapatite samples.

The silver-doped pastes had antibacterial activity against *Staphylococcus aureus* and *Pseudomonas aeruginosa*. Due to the inhibition of bacterial growth in the area surrounding the silver-doped pastes, it was suggested that the antibacterial action was due to the presence of diffusible silver ions. Furthermore the antibacterial effect of the silver-doped nHA pastes in a bacterial suspension culture varied in a dose dependent manner. Interestingly, the nHA paste with no silver doping also caused a reduction in bacterial growth when investigated in suspension culture, which may have been due to the adherence of bacteria to the nHA particles.

CONCLUSION

Silver-doped nHA paste with antibacterial properties was successfully produced using a wet precipitation method. It was concluded that silver-doped nHA paste is a promising material for preventing implant associated infection whilst promoting bone tissue regeneration.

REFERENCES

1. Darouiche R. O. *et al.* Clin Infect Dis, 36(10): 1284, 2003.
2. Di Silvio L. *et al.* J Mater Sci Mater Med, 10(10-11):653, 1999.
3. Prakash K. H. *et al.* Langmuir, 22:11002, 2006.

ACKNOWLEDGMENTS

The authors would like to thank Ceramisys Ltd. and the EPSRC for providing financial support to this project. Miller and Hatton are members of the EPSRC Centre MeDe Innovation.

Comparisons of the Properties of Linear and Highly-Branded Poly(N-isopropyl acrylamide) with Ligands that Bind Bacteria

P. Teratanatorn, R. Hoskins, J. Shepherd, K. Swindells, T. Swift, L. Swanson, S. MacNeil, I. Douglas, S. Rimmer*
University of Sheffield, UK, s.rimmer@sheffield.ac.uk

INTRODUCTION

Recently we introduced branched polymers that bind to bacteria and then pass through a coil-to-globule transition.¹ The switch from open coil to compact desolvated globule is accompanied by a change from a bacteria non-adhesive state to a bacteria adhesive state. Recent work, which we will describe here, points to a complex model in which the inner regions of the branched polymer are in a desolvated state but the outer regions are solvated in open-coil-like states. Figure 1 shows this model and illustrates the effect of binding, which involves the coil-to-globule transition occurring in the outer regions only.

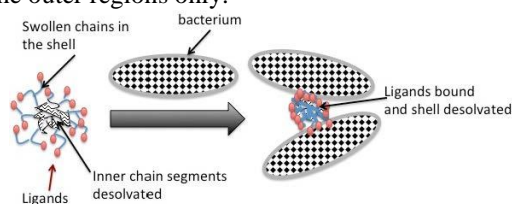


Figure 1 A Schematic diagramme of a highly branched polymer with ligands at the chain ends interacting with target bacteria. The inner regions of the polymer are desolvated but the outer (shell) segments are aquated a the charged end ligands increase shell swelling. Binding of the end groups by bacteria removes the effect of the end groups causing the desolvation of the shell.

The work presented will compares the performance of hyperbranched poly(N-isopropyl acrylamide) with vancomycin end groups (HB-PNIPAM+van) with different degrees of branching to linear copolymers of poly(N-isopropyl acrylamide) with pendant vancomycin groups (L-PNIPAM+van).

EXPERIMENTAL METHODS

Materials

HB-PNIPAM+van were prepared using our reported procedure.¹ L-PNIPAM+van were prepared by functionalising poly(N-isopropyl acrylamide-co-vinyl benzoic acid) with vancomycin.

RESULTS AND DISCUSSION

Comparisons were made on the performance of highly branched and linear polymers and as shown in figure 2 only highly branched polymers formed mats with *S. aureus*. The mats are formed as aggregates of polymers in the globule form with the bacteria. If the polymers do not form aggregates the bacteria precipitate and form a "button". Examination of polymers of varying degrees branching showed that critical degrees of branching were required to form polymer-bacteria aggregates. By labelling the polymers with fluorescent dyes we have been able to follow the binding of HB-PNIPAM+van and by examining the fluorescence anisotropy we confirmed that a coil-to globule transition does occur on binding.² The HB-PNIPAM+van polymers do not show a cloud point but a transition could be observed in microDSC analysis, which surprisingly was below the ambient temperature.

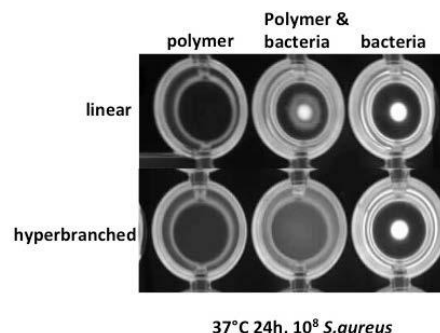


Figure 2 Images of L-PNIPAM and HB-PNIPAM in the presence and absence of *S.aureus*. The bacteria alone amass at the bottom of the well forming a button. However in the presence of the HB-PNIPAM the interactions between polymer and bacteria forms a mat. On the other hand a linear polymer with penadnt ligands fails to form a mat and the bacteria amass at the bottom of the well in a button.

Also, Nile Red is a dye, whose spectral characteristics are sensitive to the polarity of the environment. The wavelength of maximum absorbance shifts as the environment changes. Addition of this dye to the HB-PNIPAM+van showed that a transition occurred below the temperature of the bacteria binding experiments. Thus the data appeared to be contradictory in that microDSC and the use of Nile red as a probe indicated that the transition occurred below 37 °C but there was no increase in turbidity as would normally be expected in polymers displaying a lower critical solution temperature. On the other hand fluorescence anisotropy indicated that a transition occurred on binding at 37 °C and the mat-button experiments indicated a clear effect of branching.

The data indicated that the branched polymers that respond to binding are not in the fully open coil conformation before binding rather the inner regions of the polymer coil are desolvated but the outer regions are influenced by the chain ends and segments here are solvated in open coil conformation. Binding then causes these outer segments to desolvate producing a surface that bacteria adhere to. The use of Nile Red as a probe also allowed us to provide a quantitative signal of the amount of bacteria present because as the amount of bacteria increases the fluorescence emission intensity increased.

CONCLUSION

HB-PNIPAM+van responds to *S.aureus*. We propose that the performance of the polymers is associated with a coil-to globule transition in the shell of particles.

REFERENCES

1. Shepherd et al. J. Am. Chem. Soc., 132: 1736-1737, 2010
2. Sarker et al. Soft Matter, In press

ACKNOWLEDGMENTS

The authors would like to acknowledge TSB (UK), The Wellcome Trust and EPSRC for funding this work



Nanoscale Characterization of Cationic Polymeric Brushes and Bacterial Interactions Probed by Force Microscopy

Merve Gultekinoglu^{1,2}, Yoo Jin Oh³, Memed Duman⁴,
Peter Hinterdorfer³ and Kezban Ulubayram^{1,2*}

¹Faculty of Pharmacy, Basic Pharmaceutical Sciences Department, Hacettepe University, Turkey

²Institute of Science and Technology, Bioengineering Department, Hacettepe University, Turkey

³Institute for Biophysics, Johannes Kepler University Linz, Austria

⁴Institute of Science and Technology, Nanotechnology and Nanomedicine Department, Hacettepe University, Turkey
merve.g@hacettepe.edu.tr

INTRODUCTION

To conquest the fight against bacteria it is possible to endue a characteristic on biomaterial which has the ability to prevent surface adhesion of bacteria. Various surface coatings for biomaterials have been developed in an attempt to prevent infections; most of them work by incorporating and releasing such bactericidal agents as silver ions, quaternary ammonium salts, triclosan, antibiotics, enzymes or other drugs that leach into the environment¹. Recently, thin film coating based on antimicrobial polymer brushes have gained much popularity owing to the permanent antimicrobial activity. Especially; cationic compounds are promising candidate materials for antibacterial applications.

In this work, PEI molecules covalently grafted to polyurethane (PU) surfaces and then alkylated to increase surface charge². Nanoscale characterization such as topography, roughness, electrostatic potentials, stiffness and surface-bacterial interactions were investigated by force microscopy.

EXPERIMENTAL METHODS

PEI, was covalently grafted onto PU surface and *N*-alkylation was performed by bromohexane. Two different molecular weights of PEI were used to investigate the effect of chain length. The newly obtained surfaces were characterized by Attenuated Total Reflectance – Fourier Transform Infrared Spectroscopy (ATR-FTIR), X-Ray Photoelectron Spectroscopy (XPS) and Scanning Electron Microscopy (SEM). Antibacterial ability of the surface was also investigated by bacterial adherence test.

Topography images of surfaces were obtained by Agilent 5500 AFM (Agilent Technologies, Chandler, AZ) in contact mode under both air and liquid environments and roughness calculations were evaluated by using Gwyddion 2.34 software. Indentation measurements of sample groups were carried out at room temperature with Si₃N₄ AFM tip (Bruker) with 10 pN/nm spring constant. To investigate the electrostatic properties of brush surfaces in aqueous media, Kelvin Probe Force Microscopy (KPFM) technique was applied and contact potential difference (CPD) images were obtained. *E.coli* K-12 (wild type) strain was used to evaluate the single cell – surface interactions. A single cell was attached onto silicon nitride AFM tip. Approximately 60 different force curves were obtained for each sample groups.

RESULTS AND DISCUSSION

Antibacterial surfaces were obtained by PEI grafting onto PU surfaces with following *N*-alkylation. XPS and FTIR data confirmed that PEI grafting and alkylation steps were performed successfully.

Surface roughness in dry state dramatically increases from 65.8 nm to 277.7 nm and 145.2 nm for short and long chained brush-like grafting, respectively; whereas long chained brush-like surfaces exhibit more rough feature than short chained brushes in aqueous media (247.2 nm and 208.7 nm, respectively). AFM images also correlates with aforementioned situation. Since the calculated distances between two grafting points (*D*) were less than radius of gyration (*R_g*) for both long and short chains, it is assumed that the grafted surfaces have brush like characteristics.

The obtained force curves indicated that stiffness and Young's modulus values of the surfaces changes with brush-like layer.

Contact potential difference images obtained from KPFM analysis showed that surface potentials of sample groups exhibit various electrostatic characteristics in aqueous media and increases with *N*-alkylation. Single cell force spectroscopy study results indicate that bacteria-surface interactions are affected by the surface modifications as well.

CONCLUSION

Grafted PEI molecules on PU surface have brush-like conformation and these brush-like structures exhibit an anti-adhesive property against bacteria species via contact-active bactericidal polycationic feature and dynamic chain movement ability.

REFERENCES

1. Wong S.Y., Li Q. *et al.*, Biomaterials 31(14): 4079-4087, 2010.
2. Tiller JC. *et al.*, Adv. Polym. Sci. Bioact. Surf., 240:193–2173, 2011.

ACKNOWLEDGMENTS

“The authors would like to thank the TUBITAK, The Scientific and Technological Research Council of Turkey, (Grant no: 112M293) for providing financial support to this project”.



Effect of pH and biofilm formation on extracellular matrix synthesis in normal and chronic wound fibroblasts

Eleri M Jones¹, Steven Percival², Peter Clegg¹, John A Hunt¹ and Christine A Cochrane¹

¹Institute of Ageing of Chronic Disease, University of Liverpool

²Scapa Healthcare UK Ltd, Manchester, OL7 0ED, elerimj@liverpool.ac.uk

INTRODUCTION

Extracellular matrix (ECM) molecules are synthesised from fibroblast cells as they migrate into the wound space, they play a fundamental role in the process of wound healing and re-modelling. When the wound fails to heal it becomes chronic and the synthesis of ECM molecules becomes impaired. The wound environment changes often becoming infected with bacterial biofilms¹, most commonly *Staphylococcus aureus* and *Pseudomonas aeruginosa*, and the environmental pH becomes increasingly alkaline (pH7-9)².

The aim of this study was to determine any differences in the release of ECM molecules from fibroblasts derived from normal and chronic wound equine tissue when cultured in various environmental pH conditions and with bacterial conditioned media.

EXPERIMENTAL METHODS

Generating different media

The pH of DMEM was altered by addition of concentrated HCl or NaOH with a suitable buffer for that required pH (6 – MES hydrate, 7.5 – HEPES, 9 – CHES). *S. aureus* and *P. aeruginosa* bacteria were cultured in DMEM media overnight before diluting to equivalent of 10⁸ CFU/mL. Bacteria were removed and conditioned media kept for further experiments. *S. aureus* and *P. aeruginosa* biofilms were grown before then being cultured in DMEM media for 24 hours. Media was then collected and filtered and kept for further experiments as biofilm conditioned media.

**this work is on going*

Cell culture

Normal skin fibroblasts (NF, *n*=3) and chronic wound fibroblasts (CWF, *n*=3) were cultured for 24 hours in DMEM media, altered to either pH 6, 7.5 or 9 or in planktonic and biofilm DMEM conditioned media at pH7.5.

Analysing ECM synthesis

Conditioned media (CM) was collected after 24 hours and analysed for the presence of ECM molecules. These were collagen (hydroxyproline assay), fibronectin (FN; ELISA), glycosaminoglycans (GAGs; DMMB assay) and elastin (fastin assay).

RESULTS AND DISCUSSION

Table 1. Summary of the synthesis of ECM molecules analysed when cultured in each condition. Results are shown as an increase/decrease in synthesis compared to normal conditions at pH7.5.

Normal Fibroblasts			
	pH6	pH7.5	pH9
Collagen	↓	-	↑
Fibronectin	↓	-	↓
GAGs	↓	-	↑
Elastin	↓	-	↑
Chronic Wound Fibroblasts			
	pH6	pH7.5	pH9
Collagen	↑	-	↑
Fibronectin	↓	-	↓
GAGs	↑	-	↑
Elastin	↑	-	↓

Changing the environmental culture conditions of both normal and chronic wound fibroblasts affected the synthesis of ECM molecules vital for wound healing. Chronic wound fibroblasts (cultured in pH9 and the presence of biofilms) showed a decrease in the synthesis of collagen, fibronectin and elastin whereas GAGs synthesis significantly increased.

CONCLUSION

An alkaline pH environment, similar to that found in chronic wounds, has negative effects on the synthesis of ECM molecules from CWF cells. Shifting the pH of a chronic wound towards a more acidic environment and eliminating any bacteria present could improve wound healing.

REFERENCES

1. James et al., 2007, Wound Repair and Regeneration, 16:37-44
2. Schneider et al., 2007, Archives of Dermatological Research, 298:413-420

ACKNOWLEDGEMENTS

The authors would like to thank Scapa Healthcare UK for their financial funding and support.



Hybrid material (chitosan hydrogel/bioceramic) loaded with ciprofloxacin or simvastatin for bone reconstruction

Claudia Flores¹, Jean Christophe Hornez², Feng Chai¹, Gwenael Raoul¹, Juergen Siepmann¹, Joel Ferri¹, Bernard Martel³, H. Frederic Hildebrand¹, Nicolas Blanchemain¹

¹INSERM U1008, Biomaterials Research Group, University Lille 2, France. claudia.floresvilca@univ-lille2.fr

²EA2443, LMCPA, Université de Valenciennes Hainaut Cambrésis, France

³UMET, UMR-CNRS8207, Ingénierie des Systèmes Polymères, Université Lille 1, France

INTRODUCTION

Hydroxyapatite (HA), a calcium phosphate compound, is the major mineral component of bone and is widely used to repair and restrict small or average size bone defect caused by a cancer, a complicated fracture, a malformation, atrophy, or an osteite. It has excellent biocompatibility, bioactivity and osteoconduction properties¹. The HA is used as injectable, granules or macro-porous scaffolds. The risks of recidive associated to a risk of infections (1-2%) lead to dramatic consequences for the patient (new surgery, amputation, etc...). The objective of this work is to develop a chitosan based gel containing a bioactive molecule. This gel could be incorporated in the macro porosity of the scaffold, included with granules in a syringe as injectable material or lyophilised with granules to obtain a new absorbable material.

EXPERIMENTAL METHODS

The hydrogel were prepared by dissolving medium molecular weight chitosan (2%_{w/w}) in an acetic acid solution (1%_{w/w}) containing (2%_{w/w}) of Tween 80. The aqueous solution of genipin (0.5; 0.1; 0.05%) was then added to form a chemical gel. At the end of the process, the gel was freeze-dried (-62°C, 0.06mbar) and stored at room temperature.

The cross linking reaction between genipin and chitosan at 20; 30 and 40°C was followed by UV-spectrophotometry at 376 nm and 604nm. The swelling ratio was determined by placing 20 mg of dried gel in 10mL of water at room temperature. The hydrogel was removed from the water solution at predetermined time and the excess of water on the surface of the hydrogel was absorbed with a soft tissue. The swelling ratio (SR%) was calculated as follow:

$$SR(\%) = \frac{W_s - W_d}{W_d} * 100$$

Where W_s is the hydrogel in the Swollen state, W_d is the weight of the hydrogel in the Dry state.

The cytocompatibility of the hydrogel was evaluated with osteoblasts (MC3T3/E1) according to the ISO 10993-5 standards.

The bioactive molecules (ciprofloxacin/infections and simvastatin/osteogenic effect³) were incorporated in the hydrogel by dissolving in the aqueous genipin solution. The process of gel formation with or without bioactive molecule is the same. The *in vitro* drug release was performed in phosphate buffer saline (PBS) and analyzed by a spectrophotometric method for ciprofloxacin and high-performance liquid Chromatography (HPLC) for simvastatin.

RESULTS AND DISCUSSION

The kinetic of crosslinking reaction between chitosan and genipin showed that the time decreases when the temperature of reaction increases. In the same way, the time of reaction decreases when the concentration of genipin increases. Nevertheless, the evaluation of cell vitality by the method of the Alamar blue showed a low cytocompatibility of the hydrogel crosslinked with a concentration of genipin higher than 0.05%. The best conditions of crosslinking reaction to form a hydrogel of chitosan (2%_{w/w}) with genipin (0.05%_{w/w}) were 40°C during 24 hours. The swelling ability of the hydrogel is an important aspect to evaluate its property, used as scaffold material for tissue engineering or control drug release system. The Figure 1a shows the swelling behaviour of the CHT crosslinking by genipin in distilled water. The swelling rate of hydrogel increases rapidly to reach a plateau value. Indeed, a SR of 320% was obtained after 4 hours in distilled water.

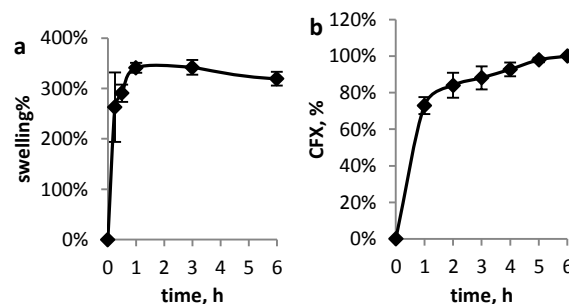


Fig. 1 Kinetic of swelling of hydrogel in distilled water (a); Kinetic of release of ciprofloxacin from hydrogel in PBS (pH 7.4; 80 rpm, 37°C)

The figure 1b shows that the CFX was quickly released from the CHT hydrogel in PBS during the first hour (80%). The prolonged release during the later hours is due to the diffusion process through the hydrogel. The same kinetic was observed with simvastatin. The hydrogel has successfully introduced in the macroporosity of HA (using the pressure of a syringe) or melted with HA granules without modification.

CONCLUSION

We demonstrated the possibility to prepare a cytocompatible chitosan based hydrogel crosslinking with genipin. The promising results could be applied to the prevention of infections or improvement of osteointegration.

REFERENCES

- Meurice *et al.*, JECS 32 :2673-2678, 2012
- Chen *et al.*, NR 30: 191 199, 2010

ACKNOWLEDGMENTS: The authors thanks OSEO (A1107030) and the region Nord-Pas-de-Calais for providing financial support to this project.



Development of Bisphosphonate-functionalized Gelatin Nanoparticles for Application in Colloidal Hydrogels for Bone Regeneration

K. Farbod, J.A. Jansen and S.C.G. Leeuwenburgh*

Department of Biomaterials, Radboud University Medical Center, The Netherlands, kambiz.farbod@radboudumc.nl

INTRODUCTION

An emerging concept in biomaterials research involves the development of colloidal hydrogels, which are cohesive materials made of nanoparticles as building blocks for macroscopic scaffolds¹. Colloidal gels offer several advantages compared to conventional monolithic scaffolds, including a favorable clinical handling behavior, ease of functionalization, cost-effectiveness and capacity to release multiple biomolecules at predetermined rates. Recently, a novel colloidal composite gel made of gelatin and calcium phosphate (CaP) nanoparticles was developed to improve the osteocompatibility of colloidal hydrogels¹. Since bisphosphonate (BP) groups bind strongly to CaP², we hypothesized that noncovalent bonds between CaP and BP-functionalized nanoparticles can be used to develop colloidal gels of improved cohesiveness. Therefore, the current study focused on conjugating BP molecules to gelatin nanoparticles in order to increase the affinity of these organic nanoparticles to CaP. Subsequently, these CaP-binding gelatin nanoparticles were mixed with CaP nanoparticles to investigate the effect of BP functionalization on the viscoelastic properties of the resulting composite colloidal gels.

EXPERIMENTAL METHODS

Using a two-step desolvation method, anionic type B gelatin nanoparticles were prepared as described previously^{1, 3}, which were subsequently functionalized with aminobisphosphonate alendronate (ALN) after glutaraldehyde (GA) crosslinking at various pH values and crosslinking densities. After this crosslinking step, residual aldehyde groups were available for crosslinking with the amine (NH₂) groups of ALN. Morphology and size of the gelatin nanoparticles were characterized in lyophilized and swollen state using Scanning Electron Microscopy (SEM) and cryo-Transmission Electron Microscopy (cryoTEM), respectively. Dynamic Light Scattering was used to characterize the hydrodynamic size and ζ -potential of the gelatin nanoparticles. Inductively Coupled Plasma-Optical Emission Spectrometry (ICP-OES) was used to quantify the degree of bisphosphonation as well as the retention of ALN to the gelatin nanoparticles. CaP nanoparticles were synthesized using a wet-chemical neutralization reaction between calcium hydroxide and phosphoric acid, and characterized using X-ray Diffraction (XRD), Fourier Transform Infrared spectroscopy (FTIR), TEM and cryoTEM. For all the prepared colloidal composite gels, the solid content was 20 w/v% and the gelatin:CaP ratio was 10:1. Storage and loss moduli as well as the extent of self-healing behavior (after destructive shearing at 1000% strain) of

the composite gels were analyzed using oscillatory rheometry.

RESULTS AND DISCUSSION

ICP-OES showed that the efficiency of the conjugation reaction increased with increasing the crosslinking density up to a molar ratio of [GA]:[NH₂]=[2]:[1]. The efficiency of the conjugation reaction was highest at pH 10 and lowest at pH 7, which was attributed to the lack of electrostatic repulsion between nanoparticles at neutral pH, resulting into a low yield. Retention tests showed that up to 70wt% of the initial amount of conjugated ALN was bound to the functionalized nanoparticles after one week of soaking in deionized water. CryoTEM micrographs of highly diluted mixtures of gelatin and CaP nanoparticles showed that interstitial spaces between gelatin nanoparticles were filled with smaller-sized CaP nanoparticles (Fig. 1).

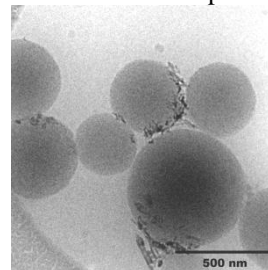


Fig. 1: Cryo-TEM micrographs of CaP and non-bisphosphonated gelatin nanoparticles.

Rheological measurements revealed that colloidal gels consisting of CaP and bisphosphonated gelatin nanoparticles exhibited a lower absolute storage modulus than composite gels consisting of CaP and unmodified gelatin nanoparticles, whereas the extent of self-healing behavior did not significantly change upon bisphosphonation of the gelatin nanoparticles.

CONCLUSION

ALN was successfully conjugated to gelatin nanoparticles through covalent bonding to residual aldehyde groups resulting from nanoparticle crosslinking. Colloidal composite gels consisting of CaP and bisphosphonated gelatin nanoparticles show approximately similar self-healing behavior compared to composite gels consisting of CaP and unmodified gelatin nanoparticles. Future studies will evaluate the self-healing behavior of colloidal composite gels as a function of gelatin:CaP ratio.

REFERENCES

1. Wang H. *et al.*, Adv. Mater. 23:119-124, 2011
2. Zhang S. *et al.*, Chem. Soc. Rev. 36: 507-531, 2007
3. Coester C.J. *et al.*, J. Microencapsul. 17:187-193, 2000

Tough Silica/PCL Hybrid Materials for Tissue Regeneration

F. Tallia¹, L. Russo², L. Gabrielli², L. Cipolla², J.R. Jones¹

¹Department of Materials, Imperial College London, South Kensington Campus, London, UK

²Department of Biotechnology and Biosciences, University of Milano-Bicocca, Milano, Italy

f.tallia@imperial.ac.uk

INTRODUCTION

Hybrid sol-gel materials have interpenetrating networks of inorganic-organic components that interact at the nanoscale and are indistinguishable above the nanoscale¹. Class II hybrids also contain covalent bonds between silica and polymeric chains and are preferred to Class I hybrids, characterised by weak linkages (e.g. hydrogen bonds). The aim is to achieve a new material where the two components act as a single phase, which has the advantage of enhancing the toughness of inherently brittle bioactive glass scaffolds used in bone tissue engineering. Polycaprolactone (PCL) is a synthetic polyester widely used for biomedical applications because of its total biocompatibility and biodegradability²; however, it lacks functional groups and has very low solubility. Therefore, to be covalently bonded to silica, functionalisation of PCL with a coupling agent before the introduction into the sol-gel process is required. Hybrids made with PCL functionalised with isocyanatopropyl triethoxysilane (ICPTS) were studied, but slow gelation and low mechanical properties limited their applications³. Herein the study of new Class II silica/PCL hybrids using glycidyloxypropyl trimethoxysilane (GPTMS) as coupling agent is described. Final objectives of the present work are: (i) functionalisation of PCL to enable coupling; (ii) optimising the composition for compromise between mechanical properties, biodegradation rate and bioactivity; (iii) tuning the viscosity of the sol to make it suitable for the 3D printing of scaffolds for tissue regeneration.

EXPERIMENTAL METHODS

Hybrid synthesis

SiO₂/PCL hybrids with different compositions were prepared by the introduction into the traditional SiO₂ sol-gel synthesis of PCL diol or triol, using tetraethyl orthosilicate (TEOS) as silica source and GTPMS as coupling agent. In a typical synthesis, PCL was initially functionalised with GPTMS through a two-step procedure: PCL hydroxyl terminal ends were firstly converted into carboxylic groups by oxidation; COOH groups were then covalently bonded to GPTMS epoxy ring ends. Sol-gel was subsequently made by the addition of hydrolysed TEOS into the polymer solution. The sol was then cast into Teflon moulds to obtain bulk cylindrical samples, whereas porous scaffolds were produced by 3D printing directly from the sol. All samples were finally aged at 40°C and dried at 60°C.

Characterisation

PCL functionalisation with GPTMS was assessed through Maldi-Tof, FTIR-ATR and solution-state NMR. Hybrid compositions were assessed through FTIR-ATR, XRD and TGA/DSC analyses. Hybrid

samples were characterised in terms of mechanical properties and *in vitro* biodegradation and bioactivity.

RESULTS AND DISCUSSION

FTIR, Maldi-Tof and ¹H-NMR spectra demonstrated that an almost complete end-capping of PCL OH groups with GPTMS was obtained.

FTIR and XRD analyses on resulting hybrids confirmed the presence of a homogeneous amorphous inorganic/organic hybrid network. Compared to the use of ICPTS as coupling agent, which leads to a gelation time of several days³, the covalent bonding with GPTMS caused faster network formation: gelation occurred within few hours, during which the viscosity of the forming gel can be tuned in order to make it suitable for the 3D printing of scaffolds (Fig.1).

Hybrids with different inorganic/organic ratio, verified from mass loss measured with TGA, were produced in order to evaluate the effect on mechanical properties: the interpenetration of PCL chains within silica network increased the toughness, the hybrids were flexible with elastomeric behaviour (Fig.2), which was more evident when higher polymer percentage was introduced.



Figure 1:
3D printing

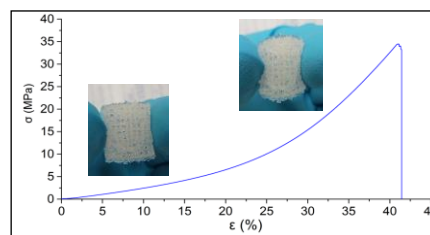


Figure 2: Stress-strain curve obtained from compressive test of a monolith.

CONCLUSION

A procedure to covalently couple PCL with GPTMS, exploiting OH groups exhibited by the polymer, was successfully developed. The functionalised PCL was then used for the sol-gel synthesis of innovative Class II SiO₂/PCL hybrids, characterised by an extremely high flexibility. By varying synthesis parameters different features can be achieved, leading to very promising materials for tissue regeneration.

REFERENCES

1. Novak B.M., Adv. Mater. 5:422-33, 1993
2. Sabir M. *et al.*, J. Mater. Sci. 44:5713-24, 2009
3. Rhee *et al.*, Biomaterials. 23:4915-21, 2002

ACKNOWLEDGMENTS

The authors would like to acknowledge the European Commission funding under the 7th Framework Programme (Marie Curie Initial Training Networks; grant number: 289958, Bioceramics for bone repair).

New Gelatine Functionalized Hybrid Sol-gel Coatings for Titanium Implants

I. Lara-Sáez¹, M. Martínez-Ibáñez², S. Barros³, A. Coso⁴, J. Franco⁴, M. Gurruchaga², J. Suay³, I. Goñi²

¹Biomaterials and Tissue Engineering Center, Universitat Politècnica de València, Spain.

²Polymer Science-Technology Department, San Sebastián University, Spain.

³Industrial Systems Engineering and Design Department, Castellón University, Spain.

⁴Ilerimplant S.L., Lleida, Spain, malase1@upvnet.upv.es

INTRODUCTION

Due to its properties, titanium is the election metal used in implant dental replacement treatment, although total osseointegration process do not finish until 4-6 months after implantation. With the aim to accelerate this process in patient benefit, we developed new formulations of hybrid sol-gel coatings that allow to anchor bioactive molecules to the implant surface and their controlled delivery, providing osteoinductive properties^{1,2}.

EXPERIMENTAL METHODS

Coatings were synthesized by the sol-gel method from specific mixtures of alkoxysilanes methyl trimethoxysilane (MTMOS), tetraethyl orthosilicate (TEOS) and glycidoxypopyl trimethoxysilane (GPTMS). Biocompatibility and osteoinductive capabilities of the coatings were *in vitro* studied with osteoblasts (MC3T3-E1) and *in vivo* through tibia rabbit model of implantation. Histological studies and Si release evaluation were done and light and electron microscopy images were obtained.

After the first *in vitro* and *in vivo* results, gelatine was added to functionalize coatings. *In vitro* and *in vivo* assays were done again with the gelatine containing formulations.

RESULTS AND DISCUSSION

Formulations without gelatine showed a similar cellular behaviour than titanium control, however gelatine containing coatings showed higher mineralization rate.

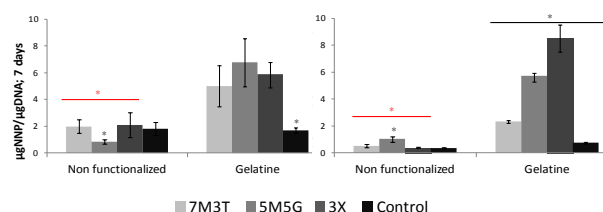


Figure 3 Gelatine functionalized coatings showed higher ALP activity than control (black) and than non functionalized coatings (red), at 7 (left) and at 14 days (right) of culture (T-Student, significance level 0,005 SPSS 17.0 software).

The histology of the non gelatine containing materials demonstrated that 70MTMOS:30TEOS formulation (7M3T) was totally resorbable at eight weeks, in contrast to the rest of materials in which the coating remained intact. A semiquantitative study showed a

higher biocompatibility behaviour at short times (1 and 2 weeks), than titanium control.

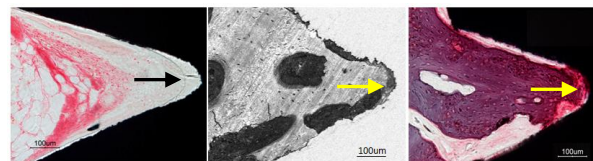


Figure 1 showed at 8 weeks after *in vivo* implantation 7M3T light and electron images, coating (black arrow) was resorbed in new bone contact zones (yellow arrows) and direct contact was observed between bone and implant.

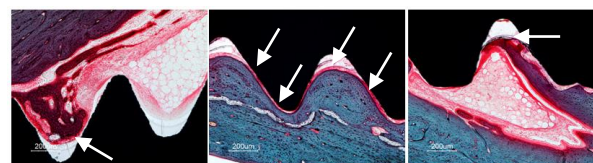


Figure 2 showed at 8 weeks after *in vivo* implantation of the rest of formulations samples, the coatings did not degraded, in contact with it a fibrous capsule was observed (white arrows) making impossible that a direct contact between bone and implant could exist.

No inflammation or infection signs were observed at gelatine coatings after *in vivo* implantation. Histomorphometric study is being carried out and early the statistical results will be available.

CONCLUSION

The *in vitro* and *in vitro* results carry out to expect that the histological results obtained for the last animal implantation of gelatine functionalized 70MTMOS:30TEOS coatings open a very interesting way to enhance osseointegration kinetics.

REFERENCES

- Hansson Toward S., CRC Press LLC: 39-52, 2000
- Reffitt D.M. *et al.*, Bone 32(2):127-135, 2003

ACKNOWLEDGMENTS

The authors would like to thank the Spanish Ministry of Economy and Competitiveness for providing financial support through INNPACTO (IPT-2012-0218-090000).

On the Applicability of Magnesium-containing Layered Double Hydroxides as Novel Implant Coating Materials

Marc D. K. Kieke¹, Andreas Weizbauer², Franziska Duda³, M. Imran Rahim⁴, Philip Dellinger⁵, Stefan Budde², Thilo Flörkemeier², Julia Diekmann², Nils K. Prenzler³, Muhammad Badar⁴, Peter P. Müller⁴, Hansjörg Hauser⁴, Sabine Behrens⁵, Kai Möhwald⁵, Friedrich-Wilhelm Bach⁵, Hans J. Maier⁵, Thomas Lenarz³, Henning Windhagen², Peter Behrens¹

¹Institute for Inorganic Chemistry, Leibniz University of Hannover, Germany

²Department of Orthopaedic Surgery, Hannover Medical School, Germany

³ENT Department, Hannover Medical School, Germany

⁴Helmholtz Centre for Infection Research, Braunschweig, Germany

⁵Institute of Materials Science, Leibniz Universität, Garbsen/Witten, Germany

Marc.Kieke@acb.uni-hannover.de

INTRODUCTION

In order to increase the period of use of implants such as orthopaedic prostheses, the application of coatings made from biocompatible, osteoproliferative materials could support implant incorporation. Also for local drug release purposes, as for middle ear implants, a controlled decomposition behaviour of the coatings is of interest.

In 2010 the osteoproliferative properties of Mg(OH)₂ were investigated by Janning *et al.*¹. The scope of possible applications is limited by the fixed composition of this single compound. Mg-containing Layered Double Hydroxides (Mg-LDHs) are a class of materials with adjustable compositions that can be derived from Mg(OH)₂ by replacing a certain amount of Mg²⁺ ions with trivalent cations such as Al³⁺ and Fe³⁺, leading to Mg-Al- and Mg-Fe-LDHs².

A variety of Mg-LDHs has been synthesized, processed and evaluated with respect to their applicability as implant coatings. Various *in vitro* and *in vivo* studies have been performed, including Mg-LDH based materials with and without drugs (e.g. ciprofloxacin). Different application sites like the middle ear or the condyle of New Zealand White rabbits were in the focus of the studies.

EXPERIMENTAL METHODS

Cell compatibility, osteoproliferative properties and applicability in local drug delivery systems had been in the focus of our earlier *in vitro* and *in vivo* studies.

In our recent *in vivo* study, the degradation behaviour of a Mg-Al-LDH coating in the middle ear of New Zealand White rabbits was investigated. Furthermore, the examination of the degradation rates of different Mg-LDH coatings is in the focus of our recent *in vitro* study.

RESULTS AND DISCUSSION

Mg-Al and Mg-Fe-LDHs were proved to be cell compatible with NIH3T3 and MG63 cells under standard conditions. Cylindrical pellets made from these LDHs (3x3 mm) were inserted into femur condyles of New Zealand White rabbits. According to CT and histological data gained in this *in vivo* study, the Mg-Al-LDH appeared to be the most promising Mg-LDH of our studies with respect to bone-healing purposes.

In another *in vivo* study, middle ear implants were coated with a ciprofloxacin/Mg-Al-LDH mixture and inserted into the middle ears of New Zealand White rabbits. The coatings could release sufficient amounts

of antibiotics to curb an infection that was triggered directly after surgery by *P. aeruginosa*, while the effect was attenuated when the infection was set one week after surgery¹. The controlled release could also be demonstrated in an *in vitro* infection model for over two weeks, employing similar ciprofloxacin/Mg-Al-LDH mixtures.

The *in vivo* stability of LDH coatings in the middle ear was investigated in a subsequent study. Over the time span investigated, the Mg-Al-LDH coatings turned out to be practically stable in the middle ear of New Zealand White rabbits, which opens possibilities for applications with extended functional life times.

In case of some LDHs, storable LDH nanosuspensions could be obtained. Also coating techniques for various substrates were established. For further applications, a spray coating chamber was customized and proved suitable for the semi-automatic spray coating of potential implant materials. This device was used to create samples for our latest *in vitro* study, which showed that different Mg²⁺ release rates can be realized by altering the coating conditions and, as expected, the Mg²⁺ contribution to the coating.

CONCLUSION

Mg-LDHs are a promising class of adjustable biomaterials with regard to the application as implant coatings. Under the experimental conditions the investigated LDHs showed good cell compatibility, osteoproliferative properties and were suitable for local drug delivery. The composition of the respective Mg-LDHs can be varied, i.e. the choice of ions and their ratios, making this class of materials adjustable for different purposes.

REFERENCES

1. Janning C. *et al.*, Acta Biomaterialia 6:1861-1868, 2010
2. Lv Z. *et al.*, Chem. Eng. Sci. 62:6069-6075, 2007
3. Hesse D. *et al.*, J Mater Sci: Mater Med. 24(1):129-136, 2013

ACKNOWLEDGMENTS

Financial support by the German Research Foundation (DFG) within the collaborative research centre SFB 599 is gratefully acknowledged by the authors. Also, this work profited from the collaboration in the Cluster of Excellence "Hearing4all".



Fatigue Characterization of Two Bone Cements Tested Using Various Methods over a Range of *In Vitro* Stress Amplitudes

E.M. Sheafi and K.E. Tanner

School of Engineering, University of Glasgow, Glasgow, UK, e.sheafi.1@research.gla.ac.uk

INTRODUCTION

Inconsistency in results of *in vitro* fatigue testing of bone cements has been reported. One possible reason for this variation is the use of a wide range of testing regimes, with limited consideration to the possible effects of the testing method and stress amplitude on the measured fatigue behaviour of various bone cement compositions. The effect of testing method (moulded or machined surfaces of rectangular or circular specimen shapes), but at only one stress level (± 20 MPa), has previously been examined¹ using two cements and significant variations in fatigue lives were found. An earlier study² considered only the effect of specimen cross sectional shape (produced by moulding), again at one stress level (± 15 MPa), showing longer fatigue lives for the circular specimens of the three cements tested. In terms of considering the effect of stress level, one study³ compared the fatigue behaviour of four bone cements. Fully reversed loading at five stress levels of circular machined specimens was compared to one level stress of tension-tension of rectangular moulded specimens. Significantly less range of differences was reported between the fatigue lives of the cements when the former method was used.

In the current study, the fatigue behaviour of two bone cements was compared over a range of *in vitro* fully reversed tension-compression stress levels. The process was comparably performed for different specimen types, followed by S-N analysis.

EXPERIMENTAL METHODS

Two different bone cement compositions were used: SmartSet GHV Gentamicin (including 2.9wt% ZrO₂ opacifier) and unmedicated DePuy CMW1 (including 6.2wt% BaSO₄ opacifier). Test specimens were manufactured by both direct moulding and machining as rectangular (ISO 527) or circular (ASTM F2118) cross sectional shapes. Four specimen types were produced: rectangular moulded (RDM), rectangular machined (RMM), circular moulded (CDM) and circular machined (CMM), providing four test specimen types. After a minimum of a week soaking in 37°C saline, at least 5 specimens from each category of both cements were tested to failure at each of four fully reversed tension-compression stress amplitudes: ± 12.5 , ± 15 , ± 20 and ± 30 MPa. Cycles to failure for each specimen was recorded and an S-N curve for each specimen testing method was established by plotting the maximum stress levels against the log of cycles to failure. S-N diagrams were produced which compare fatigue behaviour of the two cements in a specific specimen production and shape method.

RESULTS AND DISCUSSION

The S-N diagrams are shown in Figure 1. Each diagram compares the fatigue behaviour of the two cement

compositions for one type of specimen shape and surface finish. Generally, over the tested *in vitro* stress range, the results showed reverse fatigue performance of the two compositions such that SmartSet GHV, in comparison to DePuy CMW1, provided shorter fatigue lives at the highest stress levels and obviously longer lives as the stress amplitude decreased towards the *in vivo* levels. The results, meanwhile, showed differences in fatigue lives among the testing methods which also varied within the individual stress level.

This implies that the fatigue fracture of different cements can perhaps be dissimilarly and even contradictorily controlled by the adopted stress regime starting with the type of specimen used and ending with the stress amplitude allocated.

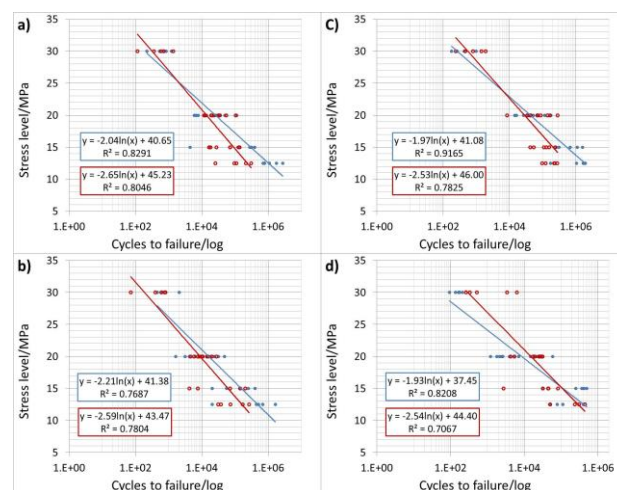


Figure 1 Comparison of S-N curves of SmartSet cement (blue) and DePuy CMW1 cement (red) using testing methods of a) RDM, b) RMM, c) CDM & d) CMM

CONCLUSIONS

Description of fatigue behaviour of bone cements can largely be driven by the selection of the specimen type along with the stress parameters. Thus, when measuring the fatigue life of bone cement, the effect of the stress regime is to be considered, unless an optimal criterion is agreed upon.

REFERENCES

1. E.M. Sheafi & K.E. Tanner, J Mech Behav Biomedical Materials, 29, 91-102, 2014.
2. G. Lewis & S. Janna, Biomaterials 24, 4315-4321, 2003.
3. K.E. Tanner *et al.*, Acta Biomaterialia, 6, 943-952, 2010.

ACKNOWLEDGMENTS

The authors thank DePuy CMW for the supply of the bone cements and mixing devices. The Libyan Government is thanked for providing ES with a scholarship.



Functionalization of Titanium Surfaces with $\alpha\text{v}\beta 3$ and $\alpha 5\beta 1$ Integrin Selective Peptidomimetics: Influence on Osteoblast-like Cell Behavior

Roberta Fraioli^{1,2}, Florian Rechenmacher³, Stefanie Neubauer³, José María Manero^{1,2}, Javier Gil^{1,2}, Horst Kessler³, Carlos Mas-Moruno^{1,2}

¹Biomaterials, Biomechanics and Tissue Engineering Group, Department of Materials Science and Metallurgical Engineering, Universitat Politècnica de Catalunya, Spain

²Research Networking Center in Bioengineering, Biomaterials and Nanomedicine (CIBER-BBN), Spain

³Institute for Advanced Study at the Department of Chemistry, Technische Universität München, Germany
roberta.fraioli@upc.edu

INTRODUCTION

Functionalization of the surface with cell adhesive molecules is a straightforward and versatile strategy to confer bioactivity to titanium implants and accelerate osteointegrative processes. Such approach has classically focused on the use of full-length proteins, protein fragments or synthetic oligopeptides derived from the extracellular matrix¹. However, defining which coating system guarantees the best cellular response has been a matter of discussion during the last decade. Peptidomimetics have emerged as a very promising alternative to amino acids based- ligands, due to their high and selective cell-binding activity, low immunogenicity and high stability in serum. In this study, an $\alpha\text{v}\beta 3$ and an $\alpha 5\beta 1$ integrin selective peptidomimetic² (fig. 1) have been covalently anchored to titanium surface, and their ability to promote osteointegration investigated by means of cell adhesion, proliferation and differentiation study of osteoblast-like cells.

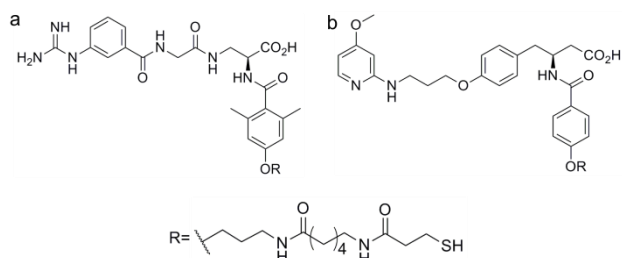


Fig 1. $\alpha 5\beta 1$ - (a) and $\alpha\text{v}\beta 3$ - (b) selective peptidomimetics.

EXPERIMENTAL METHODS

Commercially pure (CP) grade 2 titanium disks were polished to obtain mirror-like surfaces ($R_a \approx 40$ nm). Peptidomimetics were covalently immobilized on the surfaces via silanization with 3-(aminopropyl)-triethoxysilane (APTES). Vitronectin (VN) and fibronectin (FN) coated surfaces were selected as positive controls. Contact angle and surface energy measurements, white light interferometry, XPS and fluorescent labeling methods were used to characterize the physicochemical properties of the surface. Osteosarcoma cell line SaOS-2 was chosen to evaluate cell response, by means of adhesion, proliferation and differentiation studies.

RESULTS AND DISCUSSION

The coating strategy was proved effective to attach bioactive mimetics to Ti surface. Moreover, biological activity of the synthetic cues was retained after ultrasonication treatment, proving the mechanical

stability of the coating system. Both peptidomimetics significantly stimulated a positive cell response in terms of adhesion, proliferation and differentiation of SaOS-2 cells compared to uncoated Ti. Interestingly, cytoskeleton organization of cells was particularly enhanced on peptidomimetic functionalized surfaces, and projected area almost reached the one obtained on full-length proteins (fig. 2). Furthermore, peptidomimetics properly supported osteoblastic differentiation, which was assessed by alkaline phosphatase activity and calcified matrix deposition.

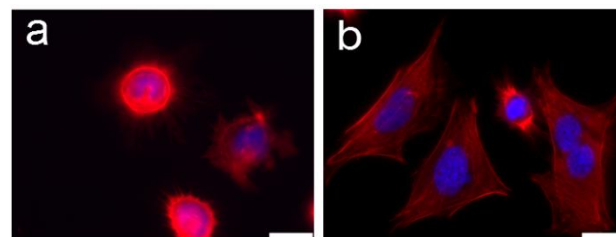


Fig 2. Immunofluorescence micrographs of SaOS-2 cells adhering on control Ti surface (a) and peptidomimetic functionalized Ti surface (b), after 4 h of incubation in serum-free medium. (bar = 20 μm)

CONCLUSIONS

The covalent immobilization of integrin-selective peptidomimetics on Ti surfaces was successfully achieved through a simple silanization protocol. The presence of integrin-selective cues significantly stimulated spreading and cytoskeleton organization of SaOS-2 cells. Proliferation and expression of both the early marker of osteoblastic differentiation and the early indicator of mineralized matrix deposition were also up-regulated.

Thus, the strategy reported in this study has proved effective for improving Ti bioactivity and holds great potential for stimulating osteointegration of implant materials *in vivo*.

REFERENCES

1. A. Shekaran, A. J. García, J. Biomed. Mater. Res. A, 96:261–272, 2011
2. F. Rechenmacher *et al.*, Angew. Chem., Int. Ed. 52:1572-1575, 2013

ACKNOWLEDGEMENT

RF and CMM thank the *Generalitat de Catalunya* for financial support (MAT2012-30706). CMM also thanks the European Commission (FP7-PEOPLE-2012-CIG) for funding.



Impact of Different Sterilization Methods on the Structure, Biodegradation and Cell Response of Collagen Scaffolds Designed for Peripheral Nerve Regeneration

Graziana Monaco^{1,2*}, Rahmat Cholas¹, Luca Salvatore¹, Marta Madaghie¹, Alessandro Sannino¹

¹ Department of Engineering for Innovation, University of Salento, Italy

^{2*} Dhitech Scarl – Distretto Tecnologico High Tech, Lecce, Italy, graziana.monaco@dhitech.it

INTRODUCTION

Cylindrical collagen scaffolds with longitudinal pore orientation have the potential to significantly improve the performance of tubular constructs for peripheral nerve regeneration which are used as alternatives to nerve grafts. The sterilization process is a fundamental step in the fabrication of implantable materials, and the selection of an appropriate sterilization method is critical since materials may undergo chemical and physical alterations that may compromise their structural integrity and functional characteristics¹. Moist heat cannot be used for sterilization of collagen products since autoclaving denatures protein² instead ethylene oxide gassing (EtO) and β irradiation are currently used for sterilising collagen scaffolds¹. As such, the objective of this study is to compare the impact of dry heat sterilization (DHS), EtO gassing and β irradiation on the microstructure, biodegradation and *in vitro* proliferation and infiltration of the rat Schwann cell line RSC96 within collagen scaffolds designed specifically for peripheral nerve regeneration. In this way we want to determine the ideal sterilization method for a novel class III implantable medical device.

EXPERIMENTAL METHODS

Synthesis and sterilization of collagen scaffolds.

Collagen scaffolds with axially oriented pores were fabricated by a freeze-drying procedure, starting from aqueous suspension of Type I collagen, and dehydrothermally and chemically crosslinked. Scaffolds were then sterilized by EtO, β -irradiation, or dry heat.

Scaffold characterization. Morphological evaluation was performed by scanning electron microscopy (SEM). Resistance to enzymatic degradation was evaluated by exposure to collagenase for different incubation times *in vitro*.

Cell response. Scaffolds were seeded with RSC96 and cultured for 6 days. Cytocompatibility and cell infiltration were identified by the MTT assay and histological staining, respectively.

Statistical significance was determined using one-way ANOVA and Fisher's PLSD test.

RESULTS AND DISCUSSION

Morphology. All the scaffolds showed a highly longitudinal oriented pore structure. No major differences in morphology were observed among scaffolds sterilized by the different methods.

Degradation. Preliminary analysis showed accelerated enzymatic degradation of β -sterilized scaffolds compared to EtO-sterilized and non-sterilized controls. This finding is consistent with the literature, which suggests that β sterilized collagen scaffolds may have

an altered biodegradation profile which could potentially affect the tissue regeneration process.

Cytocompatibility and cell infiltration. After 6 days of culture, cell proliferation measured by the MTT assay was not significantly influenced by β sterilisation; whereas, there was a 16% increase in cell proliferation compared to DHS ($p < 0.01$) when cells were seeded on scaffolds sterilized by EtO (Figure 1a). Thus, neither sterilization method resulted in reduced cell viability compared to the control. Cell infiltration, distribution, and morphology within the scaffolds, observed on H&E stained sections, were comparable among the different sterilization groups. In all cases cells were well dispersed throughout the entire scaffold and showed typical morphology (Figure 1b). Therefore, the ability to homogeneously seed the scaffolds with cells was not compromised by the three sterilization methods tested.

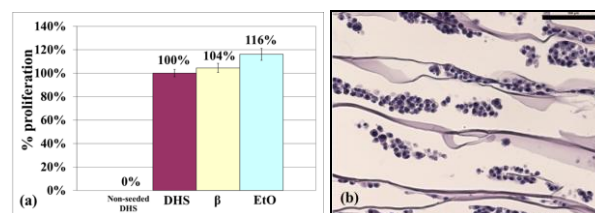


Figure 1. Cell proliferation by MTT assay within scaffolds after 6 days culture (a, mean \pm SD, $n=8$); Representative H&E stained section showing a cell-seeded scaffold (b, scale bar 100 μ m).

CONCLUSION

The clinical use of collagen scaffolds requires the selection of a suitable sterilization process, which causes minimal alteration of material properties and avoids the risk of cytotoxic residues. We found that EtO and β treatment did not induce morphological change of the collagen scaffolds, nor did they negatively affect cell proliferation within the scaffolds after 6 days of culture. However, preliminary results indicated an accelerated degradation of β -irradiated scaffolds which could have an effect on scaffold performance *in vivo*. Further characterization of the collagen scaffolds is ongoing in our laboratory to evaluate other parameters which could be affected by sterilization.

REFERENCES

1. Faraj K. *et al.*, Tissue Eng. Reg. Med 8:460-470, 2011
2. Friess W. *et al.*, Eur. J. Pharm. Biopharm. 45:113–136, 1998

ACKNOWLEDGMENTS

The authors acknowledge the Italian Ministry of Education, University and Research for providing financial support (Grant: PON RINOVATIS).



Artificial Immune Synapses; Nanoscale Control of Immune Cell Activation

D. Delcassian^{1*}, D. Depoil³, D. Rudnicka², M. Liu⁴, D. M. Davis^{2,5}, M. L. Dustin^{3,6} and I. E. Dunlop¹
 Contact: d.delcassian10@imperial.ac.uk

¹Department of Materials and ²Division of Cell and Molecular Biology, Imperial College London, United Kingdom

³Skirball Institute of Biomolecular Medicine and ⁴Department of Biostatistics, NYU School of Medicine, USA

⁵Manchester Collaborative Centre for Inflammation Research, University of Manchester, United Kingdom

⁶Kennedy Institute of Rheumatology, University of Oxford, United Kingdom

INTRODUCTION

The immune cell surface is self-organised into nano- and micro-scale domains of key signalling components that rearrange into more complex architectures on activation,¹ however it is not yet known whether this super-molecular organisation is a requirement, or by-product, of immune cell activation. Here, we fabricate an artificial immune synapse with controlled spatial distribution of key stimulatory ligands on the nanoscale, and use these materials to determine if the nano-scale organisation of stimulatory ligands can be used to control the activation of human immune cells.²

EXPERIMENTAL METHODS

Fabrication of Biofunctionalised Nanoparticle Arrays

Gold nanoparticle arrays were synthesised through Block Copolymer Micellar Lithography (BCML). Specifically, block copolymer PS-b-P2VP was used to generate reverse micelles in solution that were loaded with gold chloride, dip coated onto glass slides, and treated with a hydrogen plasma to generate hexagonally packed gold nanoparticles with uniform order and inter-particle spacing between 10-150nm. Gold nanoarrays were then functionalised with stimulatory ligands, antibodies or antibody fragments to present biomimetic surfaces with immune cell stimulatory ligands positioned precisely on the nanoscale.

Cellular Response to Nanoscale Arrays

Primary human T and NK immune cells were incubated on functionalised biomimetic nanoarrays. Cellular response to altering inter-ligand spacing across the nano-scale regime was measured by comparing the distribution of signalling molecules at the nanopattern-cellular interface region through optical and TIRF microscopy. Individual donor responses were normalised to internal controls. Results were analysed using non-parametric Mann-Whitney comparisons between spacing regimes.

RESULTS AND DISCUSSION

Human CD4⁺ T cells are sensitive to the nanoscale arrangement of stimulatory proteins. Early signalling events, such as phosphotyrosine signalling, decrease significantly as the spacing of stimulatory ligands moves from 25-104nm. Furthermore, when activatory ligands are positioned at 104nm spacing, immune cells fail to respond to biomaterials in an activatory manner (no greater response than adhesive background). The decrease in response between 25-104nm is seen in both adaptive (CD4⁺) and innate (NK) immune cell responses to these stimulatory biomaterials.

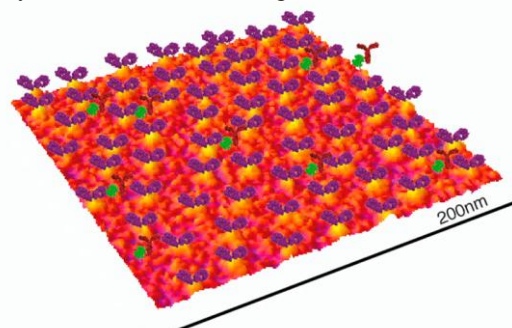


Figure 1: Model of nano-scale protein arrays formed by BCML. Image shows a 3D projected Scanning Electron Micrograph of the underlying nanopattern, superimposed with Anti-CD3 F(ab')₂ fragments.

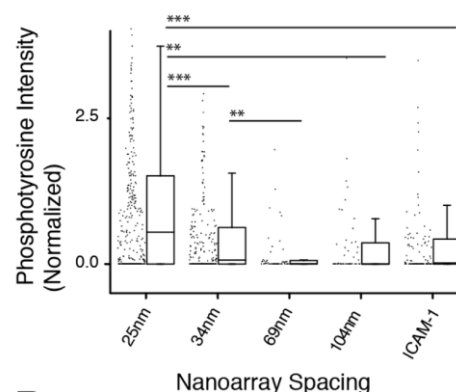


Figure 2: Human CD4⁺ cells were cultured on Anti-CD3 nanoarrays, where the anti-CD3 ligands were anchored at 25, 34, 69 or 104nm. TIRF microscopy was used to measure phosphotyrosine signalling at the nanopattern-cellular interface. p*** < 0.001 p** < 0.01

CONCLUSION

Here, we demonstrate that functionalised gold nanoparticle arrays can be used to form artificial immune synapses. Furthermore, we show that the stimulation of immune cells is sensitive to, and can be controlled by, the nano-scale arrangement of stimulatory ligands at the cellular-material interface, with a sub 110nm inter-ligand spacing being key to activation. This technology offers the potential to direct immunotherapy towards new biomaterials that can controllably activate immune cells.

REFERENCES

- (1) Lillemeier B.F *et al.*, Nat. Immunol., 11 (1) 2010
- (2) Delcassian D *et al.*, Nano Letters, 13 (11) 2014

ACKNOWLEDGMENTS

The authors would like to acknowledge the EPSRC (DTA Studentship) and the NIH (PN2 EY016586) for financial support throughout this project.



New Approaches to Control the Host Response to Gold-based Biomaterials

Guillaume Le Saux^{1*}, Annabelle Tanga², Laurent Plawinski¹, Sylvain Nlate¹, Jean Ripoche², and Marie-Christine Durrieu¹

^{1*} Institute of Chemistry & Biology of Membranes & Nanoobjects (UMR 5248), IECB, Université Bordeaux, 2 Rue Robert Escarpit, 33607 Pessac, France

²Bioingénierie Tissulaire U1026, Université de Bordeaux, 146 Rue Léo-Saignat, 33076 Bordeaux cedex, France
g.le-saux@iecb.u-bordeaux.fr

INTRODUCTION

Medical devices and biomaterial implants are clinically used in a variety of applications, and their performance is critical to a patient's overall health and quality of life. However, biocompatibility remains the key issue to be addressed for an optimal performance of such devices¹. Research is currently focusing on limiting the encapsulation of the device due to chronic inflammation and on increasing the sensitivity and longevity of the implant by enhancing neovascularization². Currently, the most commonly used method to overcome these obstacles is the use of drug releasing implants³. We believe that this paradigm should be reconsidered in view of their limited lifetime.

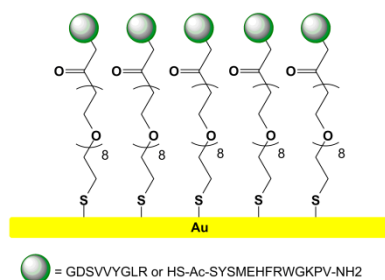
In the present work, we propose an innovative approach to overcome this pitfall: gold presenting covalently grafted anti-inflammatory or pro-angiogenic molecules. Gold is widely used in medical devices due to its excellent biocompatibility. Applications include wires for pacemakers and gold-plated stents used to inflate and support arteries in the treatment of heart disease, as well as gold-plated myringotomy tubes that are used for implantation in the tympanic membrane.

The objective of this study is to investigate the impact of the anti-inflammatory molecule α -Melanocyte Stimulating Hormone (HS-Ac-SYSMEHFRWGKPV-NH₂ or α -MSH)⁴, as well as the pro-angiogenic peptide sequence GDSVVYGLR⁵ on ameliorating the biocompatibility of gold surfaces.

EXPERIMENTAL METHODS

Biofunctionalization

Our model is based on self-assembled monolayers (SAMs) of thiol-bound carboxyl terminated oligo-ethylene glycol (EO₇-COOH) derivatives on gold. Following this, α -MSH is grafted using a thiol-maleimide bond, thus yielding EO₇-MSH surfaces, while SVVYGLR is coupled by peptide linkage to obtain EO₇-SVV surfaces. Peptide surface density was quantified using PM-IRRAS.



Schematic diagram of the bioactive modified gold surfaces used in this study.

Biological studies

Proliferation was investigated *in vitro* by seeding a small number of Human Umbilical Vein Endothelial Cells (HUVECs) onto our surfaces and by counting

adherent cells after 96h. To discriminate the effect of SVVYGLR from Vascular endothelial Growth Factor (VEGF), experiments were performed with three VEGF concentrations: 0.125%; 0.1% (normal) and 0% VEGF.

We assessed Foreign Body Reaction (FBR) *in vitro* by seeding macrophages onto our surfaces and quantifying their adhesion as well as the formation of multinucleated foreign body giant cells after two weeks.

RESULTS AND DISCUSSION

Surface characterisation

PM-IRRAS confirmed that the EO₇-COOH surfaces are well ordered; tightly packed and can be prepared in a reproducible manner. EO₇-MSH and EO₇-SVV were successfully produced with surface densities of SVVYGLR and α -MSH of 3 and 5 pmol per mm² respectively.

Proliferation

HUVECs proliferated more on the EO₇-SVV surfaces, regardless of VEGF concentration. Importantly, without VEGF stimulation, the surface grafted SVV was able to compensate the absence of stimulation and to still promote proliferation.

Foreign Body Reaction and inflammation

We observed a ten-fold decrease in macrophage adhesion to the EO₇-MSH surfaces when compared to bare gold and EO₇-COOH surfaces. In addition, macrophage fusion did not occur on the EO₇-MSH.

CONCLUSION

Bioactive gold surfaces with controlled surface density were produced and characterized. HUVECs respond to the presence of bioactive molecules by proliferating on surfaces presenting the SVVYGLR peptide. We plan to get a deeper insight into the phenotype of adherent cells by immuno-blotting for the MAP Kinase signaling pathway which is widely implicated in angiogenesis. Regarding FBR, surface bound α -MSH is beneficial in limiting macrophage adhesion. These results have motivated us to test for platelet adhesion and complement activation which are also involved in FBR. We also plan to probe for interleukin-6 expression in HUVECs to quantify their inflammatory response to our surfaces. Future work includes simultaneously modifying gold surfaces with both anti-inflammatory and pro-angiogenic molecules and to test their effect on cell behavior.

REFERENCES

1. Onuki, Y. *et al.*, J. Diabetes Sci. Technol. 2:1003-1015, 2008
2. Bridges, A.W. *et al.*, J. Diabetes Sci. Technol. 2:984-994, 2008
3. Norton, L.W. *et al.*, J. Control. Release 146:341-348, 2010
4. He, W. *et al.*, Adv. Mater. 19:3529-3533, 2007
5. Lei, Y. *et al.*, PLOS ONE. 7:e41163, 2012

ACKNOWLEDGMENTS

"The authors would like to thank the LabEx AMADEus providing financial support to this project."

Influence of hyaluronic acid molecular weight on the biocompatibility of chitosan/hyaluronic acid multilayer film

Jing Jing¹, Aurélie Moniot¹, Céline Mongaret¹, Saad Mechiche-Alami¹, Romain Reynaud², Frédéric Velard¹, Sophie C. Gangloff¹, Loïc Jerry³, Fouzia Boulmedais³ and Halima Kerdjoudj¹

1, EA 4691 "Biomatériaux et inflammation en site osseux", Pôle Santé, SFR CAP-Santé, Université de Reims Champagne-Ardenne, France, 2, Soliance, Pomacle, France. 3, Institut Charles Sadron, Centre National de la Recherche Scientifique, Université de Strasbourg, Unité Propre de Recherche 22, Strasbourg Cedex 2, France.

halima.kerdjoudj@univ-reims.fr.

INTRODUCTION

Layer by layer (L-b-L) deposition of polyelectrolytes is a versatile technique which has been explored as a smart coating for tissue engineering applications^{1,2}. The most studied film from synthetic polyelectrolytes, such as poly(styrene sulfonate) and poly(allylamine hydrochloride), are relatively stiff and thus favour cell behaviour. Their drawbacks for clinical use are due to the absence of approval by the European medicinal authorities and to potential inflammatory risks. Designing L-b-L using natural polyelectrolytes (polysaccharides or proteins) is then of great interest for medical applications. L-b-L made from Chitosan (CHI) and Hyaluronic Acid (HA) are highly hydrated and often behave as gel-like with a weak stiffness³. Yet, it is generally accepted that cells cannot be easily cultivated on those soft substrates. In this study, we aimed to investigate the effect of HA molecular weight on biocompatibility of CHI/HA multilayer coating.

EXPERIMENTAL METHODS

Hyaluronic acids (HA-1, HA-2 and HA-3 provided by Soliance, France), with 33 500 Da, 363 200 Da and 1.06 MDa molecular weight respectively, were dissolved in NaCl (0.15 M) and used as polyanion. Chitosan (CHI, from Sigma Aldrich) dissolved in HCl (4 mM) was used as polycation. On cleaned cover glasses, CHI was adsorbed for 5 min followed by HA adsorption (contact time of 5 min). Each polyelectrolyte adsorption followed by an extensive NaCl (0.15 M) rinsing step. This process was repeated until the buildup of 15 bilayers film, with an additional terminating layer of CHI.

Stem cells from Wharton's Jelly (WJ-SC) adhesion and proliferation of were highlighted through cytoskeleton visualization and MTS assay respectively.

RESULTS AND DISCUSSION

WJ-SC viability was assessed by MTS assay, following the mitochondrial activity, for 3, 6, and 8 days. CHI/HA films composed of HA-1 and HA-2, *i.e.* Mw < 400 kDa displayed significantly higher cell proliferation compared to corresponding films formed of HA with Mw > 1 MDa. Cells are able to sense their microenvironment and to respond by adjusting the organization of their cytoskeleton, so we highlighted CHI/HA biocompatibility by a complementary approach based on cell spreading *via*

cytoskeleton arrangement. After 15 days of culture, a confluent layer with typical fibroblastic cell shape and with polymerized F-actin fibers was observed on L-b-L made from HA-1 and HA-2 whereas WJ-SC cultivated on L-b-L made from HA-3 remained rounded (Figure 1).

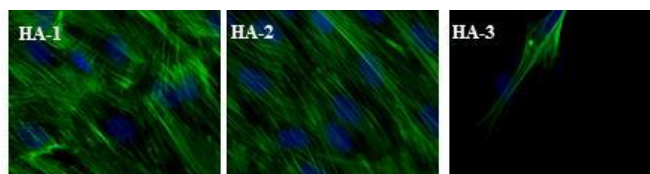


Figure 1: Visualization of cytoskeleton of WJ-SC after 15 days of culture on L-b-L made from CHI and HA named HA-1, HA-2 and HA-3 with 33 500 Da, 363 200 Da and 1.06 MDa respectively molecular weight. The cytoskeleton was visualized by actin filament staining with Phalloidin (green labeling) with Blue nucleus counterstaining of WJ-SC. Objective $\times 63$ Oil.

The Young modulus of the films is under investigation.

CONCLUSION

We demonstrated for the first time, that cell adhesion and proliferation on CHI/HA multilayer film could be improved using HA with MW<400 kDa. Our next step will be to determine the effect of Young modulus of these coatings on their osteogenic potentials.

REFERENCES

- 1- H. Kerdjoudj et al., *Soft Mater* (2010), 6: 3722–3734.
- 2- V. Gribova *et al.*, *Chemistry of Materials* (2011), 24: 854-869.
- 3- A. Schneider et al., *Langmuir*, (2007), 23: 2655-2662.

ACKNOWLEDGMENTS

The authors thank either PICT (URCA) and the Maison Blanche gynaecology service headed by Pr. O. Graesslin for providing umbilical cords

Cytotoxicity of functionalized graphene to osteoblast-like cells

Anke Bernstein^{1*}, Dirk Heinrich¹, Norbert P. Südkamp¹, Hermann O. Mayr¹, Michael Seidenstücker¹, Ralf Thoman², Markus Stürzel², Rolf Mülhaupt²

¹Department of Orthopedic and Trauma Surgery, Albert Ludwig University of Freiburg, ²Freiburg Materials Research Center (FMF) and Institute for Macromolecular Chemistry, Germany, anke.bernstein@uniklinik-freiburg.de

INTRODUCTION

Among carbon fillers, graphene-based carbon nanomaterials are expected to efficiently reduce wear, simultaneously improving the mechanical properties of UHMWPE composites in artificial joint applications. During the last decade, graphene development has become one of the hottest topics in the fields of material science, physics, chemistry, and nanotechnology. An important objective is to elucidate the interactions between graphene and bioorganism. The reinforcement of UHMWPE with graphene leads to a new family of artificial joints. However, graphene/UHMWPE composites are rarely reported.^{1, 2} Since wear of such graphene/UHMWPE composites can open an entry route of carbon nanoparticles into the body, it is imperative to learn more about the cytotoxicity of graphene. In this study we use aqueous emulsifier-free functionalized graphene (FG)- dispersions (FG-D), derived from thermally reduced graphite oxide (600 m²/g), as model system to examine the effect of FG on the in-vitro cytotoxicity.

EXPERIMENTAL METHODS

The cytocompatibility and the proliferation of different bone markers are assessed using MG 63 cells. Since FG rapidly aggregates when dispersed in the cell culture medium, suspensions of micro-sized FG assemblies (FG-S) are obtained for comparison, thus enabling to understand the role of size, shape and content of FG without changing the FG functionality. FG (0, 0.01, 0.1, 1, 10, and 100 µg/mL), prepared by thermal GO reduction, was diluted with serum free and phenol red free cell culture medium (FG-S) or in water (FG-D).³ WST-1 assay was used to examine cell status of two different dispersion of FG. We also estimated the number of live cells, the proliferations, the protein content, and the ALP- and LDH release. One focus of this study was the effect of FG in different suspensions on maturation of cultured osteoblast (immunohistological investigations: COLI, ON, and AP). To evaluate possible changes in cell morphology induced by graphene ESEM images were obtained. SPSS version 19 for Windows (SPSS Inc., Chicago, USA) was used for graphic presentation and statistical processing of the results.

RESULTS AND DISCUSSION

We report the synthesis, dispersion, and cytotoxicity of FG (600 m²/g), prepared by thermally reducing graphite oxide. As a function of the dispersion process and dispersion medium, it was possible to vary size and shape of FG without changing functionality. While suspension of FG in culture media afforded large

micron-sized FG-assemblies (FG-S), able FG nanosheet dispersions (FG-D) were obtained upon high pressure homogenization in water. It was possible to add FG-D to culture media without encountering FG agglomeration. Determination of cell viability, cell proliferation, cell shape analysis including detection of plasma membrane integrity and osteogenic cell differentiation show a good cytocompatibility of FG, independent of its size, shape, functionality, and surface area. The proliferation of different bone markers is also identical. There is no internalization of FG in osteoblast like cells up to 14 days. FG has a high adsorption capacity of proteins and cells, owing to the presence of functional groups. A high FG concentration of 100 µg/mL can lead to artefacts in biological assays and other investigation methods. To the best of our knowledge, this is the first study that examines the behaviour of osteoblast like cells over a prolonged period of exposure to FG.

CONCLUSION

Our studies have demonstrated that a high specific surface is resulting in a strong interactions of FG with the plasma membrane of cells. This process is not combined with cytotoxic effects up to 10 µg/mL. A concentration of 100 µg/mL can lead to artefacts in biological assays and other investigation methods concerning toxicity because of the very high surface area of TRGO. High protein adsorption followed by strong cell adsorption. This provides strong evidence that FG, independent of its size and shape, is highly cytocompatible below concentration of 100 µg/mL. In conclusion, FG incorporated in UHMWPE affords bearing materials for implants with a high cytocompatibility combined with improved mechanical properties, make them promising material for artificial joints.⁴

REFERENCES

- References must be numbered. Keep the same style.
1. Lahiri D et al. ACS Appl Mater Interfaces 4: 2234-41, 2012
 2. Ren PG et al. Macromolecular Materials and Engineering 29: 437-443, 2012
 3. Tolle, F J et al. Advanced Functional Materials 22: 1136-1144, 2012
 4. Sturzel, M et al. Macromolecules 45: 6878-6887, 2012



Subcutaneous Evaluation Of a Novel Pro-angiogenic Biomaterial For In Situ Bone Tissue Engineering Applications

Hugo Oliveira¹, Nadege Sachot^{2,3}, Sylvain Catros¹, Sylvie Rey¹, Oscar Castano^{2,3,4}, Joëlle Amedee¹, Elisabeth Engel^{2,3,4}

¹Inserm, U1026, Tissue Bioengineering, University Bordeaux Segalen, Bordeaux Cedex 33076, France,

²Institute for Bioengineering of Catalonia (IBEC), Barcelona, Spain,

³CIBER-BBN, Zaragoza, Spain, ⁴Dpt. Materials Science and Metallurgical Engineering, Universitat Politècnica de Catalunya, Barcelona, Spain; hugo.de-oliveira@inserm.fr

INTRODUCTION

In current bone tissue engineering strategies the obtention of sufficient angiogenesis during tissue regeneration is still a major limitation in order to attain construct integration and tissue functionality. This drawback is further relevant when considering large bone defects, where the amount of oxygen required for cell survival is limited to a diffusion distance between 150-200 μm from the supplying blood vessels. Several strategies have been described to tackle this problem, mainly by the use of angiogenic factors or endothelial progenitor cells. However, when facing a clinical scenario these approaches are inherently complex and present a high cost. As such, more cost effective approaches are awaited. We have recently demonstrated that the increased local concentration of calcium (Ca) ions could induce the migration, maturation and organization of endothelial progenitors¹. Moreover, a composite biomaterial of poly(lactic acid) (PLA) and Ca phosphate glass has shown to elicit proangiogenic and chemotactic properties on endothelial precursor cells *in vitro*². Here, we tested electrospun PLA fiber-based materials, containing different ratios of calcium phosphate glass nanoparticles, subcutaneously in mice. These distinct formulations allowing different Ca release kinetics to the vicinity of the matrix expect to improve vessel formation into the biomaterial.

EXPERIMENTAL METHODS

Aligned electrospun PLA nanofibers containing glass ceramic nanoparticles (CaP) at a mass ratio of 0, 10, 20 and 30% (i.e. PLA, NP10, NP20 and NP30, respectively) were prepared as previously described³. One cm diameter membrane disks were cut and sterilized by UV. The biomaterials were implanted subcutaneously in the dorsal pouch of swiss strain female mice (3 month, n=6 for each material). At 1 and 4 weeks post implantation animals were sacrificed and materials, together with the surrounding tissue, were recovered. Samples were fixed in 4% paraformaldehyde for 24 hrs at 4°C and then processed for cryosection. Sequential 8 μm sections were performed; samples were then processed for HE staining or immunohistochemistry for CD31. The same implantation procedure was equally performed for 3 weeks of implantation, samples were recovered, snap frozen and homogenized for total protein extraction. A dot blot array of angiogenic factors (Abcam) was used to assess the different composites. Using the Graphpad Prism 5.0 software, statistically significant differences between several groups were analyzed by the non-parametric Kruskal-Wallis test, followed by a Dunns post-test. A $p < 0.05$ was considered to be statistically significant.

RESULTS AND DISCUSSION

All constructs tested showed augmented cellular penetration with increased time of implantation. An increase on microvessel formation was observed in the case of the constructs containing glass ceramic nanoparticles, when compared with PLA alone, at both 1 and 3 weeks post implantation (see figure 1).

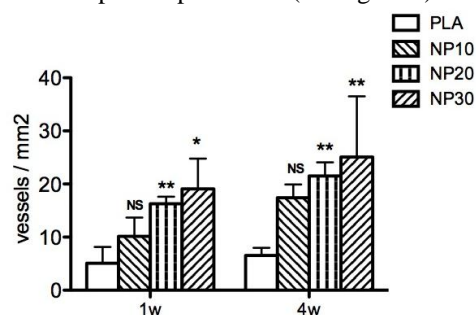


Figure 1- Evaluation of the number of vessels present inside the biomaterial (i.e. PLA, and PLA containing 10, 20 and 30% (w/w%) CaP nps) upon 1 and 4 weeks of subcutaneous implantation (Aver \pm SD, * and ** denote significant differences from PLA alone, with $p < 0.05$ and 0.025 , respectively, $n = 6$).

Additionally, this effect was shown to correlate with their mass ratio and their Ca release profile. Angiogenic factor array assessment, at 3 weeks post implantation, revealed an increased expression of key pro-angiogenic and chemotactic factors for the 20% composite materials in comparison with PLA alone or sham-operated animals. Further studies are being performed to clarify the *in vivo* mechanism for improved angiogenesis. Additionally, the evaluation of selected materials in a bone orthotopic site in a rat critical size defect model is underway and will shed light on the impact in bone regeneration strategies.

CONCLUSION

The developed composite materials have the ability, *in vivo*, to increase the vessel formation into the implanted structures. This approach, due to its simplicity, presents an attractive strategy for clinical musculoskeletal repair.

REFERENCES

1. Aguirre A. *et al.* Biochem Biophys Res Comm. 393(1): 156-61, 2010
2. Aguirre A. *et al.* Cells and Mater. 24: 90-106, 2012
3. Sachot N. *et al.* J R Soc Interface. 10: 88, 2013

ACKNOWLEDGMENTS

This work was supported by funding from the European Commission; PI11/03030, NANGIOFRAC, and the MINECO (Project MAT2011-29778-C02-01).

Gene Targeting Nanoparticles to Mediate Proliferation and Migration of Human Vascular Endothelial Cells

Yakai Feng^{1,2 *}, Juan Lv¹, Jing Yang¹ and Changcan Shi¹

^{1*}School of Chemical Engineering and Technology, Tianjin University, Tianjin 300072, China

² Key Laboratory of Systems Bioengineering of Ministry of Education, Tianjin University, Tianjin 300072, China, yakaifeng@tju.edu.cn

INTRODUCTION

Non-viral gene carrier plays an important role in gene delivery for gene therapy. Polyethyleneimine (PEI), which is regarded as the “golden” standard for gene delivery, is one of the most effective non-viral gene carriers *in vitro* and *in vivo* because of its unique combination of high charge density and enhanced “proton sponge effect” in endolysosome. High molecular weight PEI shows high transfection activity, but the high degree of toxicity of PEI to cells was caused by its membrane disruptive properties. Many approaches, such as acetylation of PEI and incorporation of nontoxic derivatives, have been explored to reduce the genotoxicity of PEI, the transfection efficiency of the modified PEI decreased generally with the amino modification of PEI.¹

Herein, we developed a novel biodegradable gene targeting nano-carrier for rapid endothelialization of endothelial cells (ECs) *in vitro*. We synthesized biodegradable amphiphilic copolymers having targeting peptides to form the nano-carriers with ZNF580 and VEGF genes by self-assembly.

EXPERIMENTAL METHODS

Three triblock amphiphilic copolymers, methoxy-poly(ethylene glycol)-block-poly(3(S)-methyl-2,5-morpholinedione-co-glycolide)-graft-polyethyleneimine (mPEG-b-P(MMD-co-GA)-g-PEI) with different 3(S)-methyl-2,5-morpholinedione and glycolide content were synthesized. Nanoparticles (NPs) were obtained via self-assembly of these copolymers.

The triblock copolymers were characterized by FT-IR, DSC, GPC and ¹H NMR. The morphology and properties of nanoparticles were evaluated by TEM, gel electrophoresis, zeta potential and particle size analysis. Cytotoxicity, cellular uptake and transfect efficiency were evaluated with EA. hy926 cells *in vitro*.

RESULTS AND DISCUSSION

mPEG was introduced as the initiator to form a hydrophilic corona due to its high hydrophilicity and flexibility of the backbone. As an effective cyclopeptide, 3(S)-methyl-2,5-morpholinedione (MMD) was copolymerized with glycolide (GA) to form the polydepsipeptide structure. The molecular weight of diblock copolymers and the content of mPEG, MMD

and GA in copolymers were estimated by ¹H NMR and/or GPC. The triblock mPEG-b-P(MMD-co-GA)-g-PEI copolymers were prepared by reaction with PEI through a reactive spacer, and also covalently linking with targeting peptides CAG or REDV.

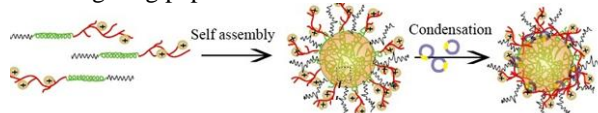


Fig. 1 NPs/gene complexes were prepared by self-assembly of three triblock amphiphilic copolymers and DNA condensation.

Nanoparticles (NPs) were obtained via self-assembly of these copolymers. The hydrophobic core composed of P(MMD-co-GA) segments provide crosslinking points for numbers of PEG and short PEI chains to form a high hydrophilic and positive charged corona/shell of NPs. Using these NPs, VEGF gene, ZNF580 gene for rapid endothelialization were efficiently transported into EA.hy926 cells. Because of hydrophilic PEG chains and low molecular weight PEI in the triblock copolymers, the cytotoxicity of these NPs and their complexes with pEGFP-ZNF580 was decreased significantly. The transfection efficacy of NPs/pEGFP-ZNF580 complexes was as high as LipofectamineTM 2000 reagent to EA.hy926 cells *in vitro*. The proliferation and migration of EA.hy926 cells were improved greatly by the expression of pEGFP-ZNF580 after 60 hours.

CONCLUSION

The mPEG-b-P(MMD-co-GA)-g-PEI based NPs could be a suitable non-viral gene carrier for ZNF580 gene to enhance rapid endothelialization.

REFERENCES

1. Shi C.C. et al., J. Mater. Chem. B, in press

ACKNOWLEDGMENTS

This project was supported by the National Natural Science Foundation of China (Grant No. 31370969), the International Cooperation from Ministry of Science and Technology of China (Grant No. 2013DFG52040, 2008DFA51170), and Ph.D. Programs Foundation of Ministry of Education of China (No. 20120032110073).

Developing Multi-layered Vascular Grafts from a Novel Collagen and Elastin Biomaterial

Alan J. Ryan^{1,2,3}, Fergal J. O'Brien^{1,2,3}

¹Tissue Engineering Research Group, Royal College of Surgeons in Ireland, Ireland.

²Trinity Centre for Bioengineering, Trinity College Dublin, Ireland. alanryan@rcsi.ie

³Advanced Materials and Bioengineering Research (AMBER) Centre, RCSI & TCD, Ireland.

INTRODUCTION

Cardiovascular disease is the leading cause of death worldwide, accounting for 29% of all global deaths and is set to rise to 23 million deaths a year by 2030¹. Arterial bypassing is generally performed with autologously harvested vessels or synthetic grafts. However, for small diameter vasculature (<6 mm), synthetic and autologous grafts suffer from poor patency rates due to thrombosis, aneurysm formation and compliance mismatch. Thus, the focus of this project is the development of a tissue engineered blood vessel (TEBV) for small diameter vessels.

In this context, the aim of this study was to develop a scaffold with optimised intrinsic physiochemical characteristics which displayed the capacity to support smooth muscle cells in vitro while subsequently displaying suitable viscoelastic properties capable of sustained biomechanical conditioning in a custom designed pulsatile bioreactor. In addition, in order to emulate the architecture of native vessels we investigated novel fabrication methods to develop a multi-layered tubular architecture.

EXPERIMENTAL METHODS

Elastin is a key component of native vasculature where it is responsible for the elastic recoil of vessels and has been shown to have a role in smooth muscle cell (SMC) behaviour². Thus, in this study, an elastin and collagen type I tubular composite scaffold was developed with the aim of providing a more natural viscoelastic response and to control SMC activity. An advanced biofabrication technique was developed which enabled the construction of a bilayered tubular construct via a combination of dehydration, freeze-drying and crosslinking.

Mechanical properties were analysed by uniaxial tensile testing, creep testing, and cyclical strain recovery to determine the viscoelastic response. Microstructure was analysed via porosity, pore size analysis and scanning electron microscopy. Subsequently, we evaluated the biological response by assessing the effect of elastin addition on SMC phenotypic modulation towards a synthetic or contractile phenotype, which was assessed via proliferation and gene expression analysis. Additionally, histology was carried out to determine the distribution of collagen and elastin as well as a qualitative assessment of the ability of smooth muscle cells to adhere to, migrate and proliferate within the scaffolds following 28 days culture.

RESULTS AND DISCUSSION

Elastin caused a more natural viscoelastic response via increased creep resistance and improved recoil ($p < 0.05$). Additionally, elastin addition resulted in earlier gene expression of mid/late stage contractile smooth muscle cell proteins which are necessary for a

vasoactive vessel. This biomimetic biomaterial was subsequently fabricated into an innovative architecture which partially emulates native architecture through its bilayered tubular structure. The outer porous layer was found to have a pore size ($\sim 90\mu\text{m}$) and porosity ($\sim 98\%$) in the ideal range to support cells while the dense inner layer was designed to support a confluent endothelium and increase the grafts mechanical properties. Following 28 days culture the SMC seeded tubular scaffold was remodelled into a dense organised tissue with a homogenous cell distribution.

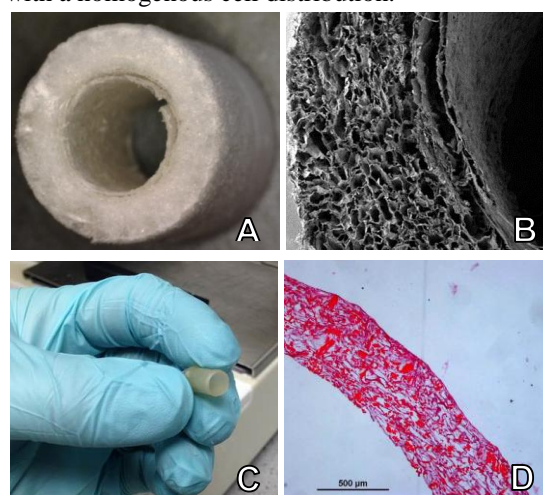


Figure 1 Macroscopic bilayered tubular collagen-elastin scaffolds (A), under SEM (B), following 28 day culture the construct was remodelled to a dense tissue (C) the organised matrix can be seen via H & E staining (D).

CONCLUSION

In this study, we have shown that elastin addition to collagen scaffolds can play a major role in the scaffolds biological and mechanical response. Collectively, this study has led to the development of a composite scaffold with optimised intrinsic physiochemical characteristics which displayed the capacity to support smooth muscle cells in vitro while subsequently displaying suitable viscoelastic properties. This multi-layered collagen-elastin scaffold represents an excellent scaffold choice for further culture in a biomimetic environment to produce a functional tissue engineered vascular graft. Consequently, ongoing research focuses on the application of dynamic biophysical stimulation within a custom-built vascular bioreactor to aid in the maturation of the engineered blood vessel.

REFERENCES

1. World Health Organization, Fact Sheet No 317, 2012.
2. Li D.Y. *et al*, Nature. 393: 276-280, 1998.

ACKNOWLEDGMENTS

Funding by European Research Council (ERC grant n° 239685). Integra Life Sciences, Inc. for collagen.



Elastomeric Biomaterials of Enhanced Microbiological and Mechanical Performance for Heart Assisting Devices

A. Piegat¹, M. Piatek-Hnat¹, Z. Staniszewski¹, R. Kustosz², M. Gonsior², M. El Fray¹

¹ West Pomeranian University of Technology, Szczecin, Division of Biomaterials and Microbiological Technologies, Al. Piastow 45, Szczecin, Poland

² Foundation for Heart Surgery Development, Zabrze, Poland
apiegat@zut.edu.pl

INTRODUCTION

Polyurethanes (PU) are the commonly used for cardiac valves, vascular prostheses, and heart assisting devices due to their acceptable blood compatibility and mechanical properties [1,2]. Nonetheless, polyurethanes are susceptible to hydrolytic degradation, encrustation and thrombosis [3]. Therefore, materials with improved biocompatibility and antimicrobial properties are still needed. Here, the basis for such materials are segmented copolymers with microphase separated structure (similar to segmented polyurethanes), but composed of hard segments as in poly(ethylene terephthalate) (PET). In this multiblock copolymer, the soft segments were composed of hydrophobic ethylene esters of dimerized fatty acid (DLA).

The present work will focus on the static mechanical properties and microbiological properties of new segmented polyester TPE containing dimerized fatty acid (PED), proposed as alternative material to PU.

EXPERIMENTAL METHODS

Static mechanical testing was performed with Instron 3366 according ISO 527-1:1998 at 22 and 37°C. TPU was used as reference material. *E. coli* cells were cultured on the surface of PED and reference PU polymers, respectively. The samples were incubated for 24 h in a medium containing *E. coli* cells (ATCC25922 strain) at 37°C under stationary conditions. After incubation, sample surfaces were extensively washed with deionised water and labelled by immersion in 1 ml PBS and 100µl MTT. The bacterial cells colonization was evaluated based on spectrophotometric measurements of absorbance at $\lambda=570$ nm.

RESULTS AND DISCUSSION

PED material containing 50wt% hard segments showed static mechanical properties comparable to medical grade PU (Table 1). The influence of temperature on mechanical stability of both PED and TPU materials is observed, modulus drops with increasing temperature, however for the polyester, decrease of the values is significantly lower than for polyurethanes.

The material susceptibility to *E. coli* colonization was assessed. PED showed distinctly reduced number of adhered bacteria ($0.026 @ \lambda=570\text{nm}$) as compared to medical grade polyurethane $0.033 @ \lambda=570\text{nm}$). The

reduced material susceptibility to microbial colonization is explained by the presence of fatty acids in PED-50, which have antimicrobial activity [4].

Table 1 Comparison of mechanical properties

Material	E @ 0,25-1% strain (MPa)	E @ 50 % strain (MPa)	E @ 100% strain (MPa)
PU @ 22°C	140,7±19,4	18,8±0,6	11,2±0,24
PED-50 @ 22°C	75,5±24,1	18,8±0,4	10,1±0,2
PU @ 37°C	66,6±10,2	10,2±0,5	5,7±0,3
PED-50 @ 37°C	48,6±3,6	16,1±0,5	8,6±0,3

Incorporating dimerized fatty acids into PED structure increases the number of carbonyl groups (hydrophilic) and methyl pendant groups (hydrophobic), resulting in a polymer with amphiphilic properties. We speculate that reduced number of adhered bacteria to PED surface can be attributed to such amphiphilic structure. Further it is possible, that these properties may also have a direct antimicrobial effect.

CONCLUSION

New segmented polyester TPE containing dimerized fatty acid (PED-50) shows markedly improved mechanical characteristics, compared to medical grade PU. PED-50 also showed diminished microbial colonization. This material offers great promise of higher safety and better performance in heart assisting devices.

REFERENCES

1. Lamba N.M.K., et al. (eds.), *Polyurethanes in biomedical applications*, CRC Press, Boca Raton Nowy Jork 1998
2. <https://www.dsm.com/>
3. Tatai L., et al., *Biomaterials*, 28:5407-17, 2007
4. Hurley CR, Leggett GJ., *ACS Appl Mater Inf.*, 1:1688–1697, 2009

ACKNOWLEDGMENTS

The authors would like to thank the National Center of Research and Development (Grant no: PBS1/A5/2/2012) for providing financial support to this project.



Supercritical Carbon Dioxide (sc-CO₂) Assisted Decellularisation of Aorta

Selcan Guler¹, Pezhman Hosseini², Esin Akbay³, Mehmet Ali Onur³, Halil Murat Aydin^{1,4}

¹Bioengineering Division, Institute of Science, Hacettepe University, Ankara, Turkey

²Nanotechnology and Nanomedicine Division, Institute of Science, Hacettepe University, Ankara, Turkey

³Biology Department, Faculty of Science, Hacettepe University, Ankara, Turkey

⁴Environmental Engineering Department, Faculty of Engineering, Hacettepe University, Ankara, Turkey
selcanguler@hacettepe.edu.tr

INTRODUCTION

Aorta tissue regeneration is quite important with consideration of the high prevalence of cardiovascular diseases. Cardio-vascular tissue engineering has produced a number of artificial vascular graft materials for the replacement of failed vessels¹. In addition to synthetic graft materials, decellularised tissue-engineered vascular grafts (TEVGs) have gained great attention due to their innate high immunological compatibility.

Most approaches to tissue decellularisation are based on chemical treatment methods where ionic, non-ionic detergents or enzymatic agents are applied. It was reported that the ionic detergent SDS (Sodium Dodecyl Sulfate) effectively removes cells and nuclear remnants whilst preserving ECM (Extra Cellular Matrix) structure². In this study, we have decellularised bovine aorta using a supercritical fluid extraction technique.

EXPERIMENTAL METHODS

Fresh bovine aorta samples obtained from a local farm (Kazan, Turkey) were dissected into 1 g annular pieces. These aorta samples were treated with supercritical carbon dioxide (sc-CO₂) in a supercritical fluid reactor (SFT, USA) at different pressures and for different time periods. In these experiments the temperature remained at 35 °C, the pressure was varied between 15 MPa and 20 MPa and treatment time was varied between 20 and 50 minutes. Ethanol was used as a co-solvent and, before treatment; the supercritical fluid reactor was filled with 20 ml ethanol (Sigma, Germany). Aorta samples were placed inside a porous metal carrier, which was then placed into the reactor. The degree of decellularisation was evaluated histologically by Haematoxylin-Eosin (H&E) staining and displayed microscopically (Olympus, Japan). In parallel with these treatments, chemical decellularisation was also performed using the ionic SDS detergent. Aorta samples were incubated in hypotonic 10 mM Tris Buffer (pH: 8.0) with 0.1% EDTA for 1 h. They were then exposed to continuous shaking in a solution of 0.1 % SDS with Tris buffer (10 mM Tris, pH 8.0) together with RNase A (20 µg/ml) and DNase (0.2 mg/ml) at 37°C for 48 h³. Subsequently, they were washed several times with PBS to remove excess chemical residues.

RESULTS AND DISCUSSION

Figure 1 shows that the aorta treated with sc-CO₂ (c) and 0.1% SDS (b) is quite different from native tissue (a). Both sc-CO₂ + ethanol and 0.1% SDS treatment completely removed cell nuclei from the ECM.

Additionally, the ECM structure of the sc-CO₂-treated aorta was preserved more than the SDS-treated aorta. The SDS-treated aorta showed a slightly loosened collagen waveform when compared to the sc-CO₂-decellularised aorta.

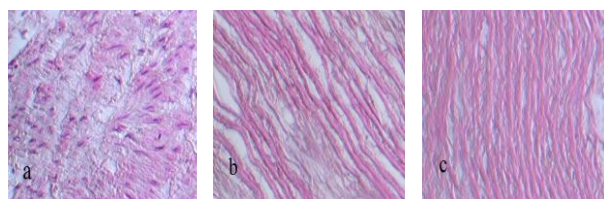


Figure 1 . Haematoxylin and Eosin staining of bovine aorta treated with supercritical carbon dioxide and SDS a) native aorta (40x). b) aorta treated with 0.1% SDS 48 h (40x). c) aorta treated with sc-CO₂ + ethanol (40x) (P=20 MPa, T=35°C, t=50 min).

As a result, the high transfer rate and high permeability of sc-CO₂ has established it as a successful decellularisation agent. Both characteristics allow the easy and complete penetration of the tissue at supercritical conditions (T:32 °C, P: 7.4 MPa).

CONCLUSION

Nearly all-chemical decellularisation protocols are based on excessive and time consuming procedures, which can take up to several weeks. Furthermore, detergents have a strong affinity to the ECM and even after several washing operations chemical residues cannot always be effectively removed. The decellularisation process disclosed in this abstract carries superiority to chemical decellularisation procedures as not only is the carbon dioxide removed completely from the tissue without leaving remnants after treatment but the method also takes a significantly shorter amount of time.

REFERENCES

1. Lynda V. Thomas. *et al.*, Internat. J. Cardiology. 4:1091-1100, 2013.
2. Gilbert T. Sellara T. *et al.*, Biomaterials. 27:3675-3683, 2006.
3. Zou Y. Zhang Y. *et al.*, J. Surgical Research. 175:359-368, 2012.

ACKNOWLEDGMENTS

The authors would like to thank BMT Calsis Co. for providing the chemicals and equipment.

Hemocompatibility Assessment of Uncoated and Heparin Coated Styrenic Block Copolymers for Cardiovascular Applications

Jacob Brubert^{1*}, Joanna Stasiak¹, Geoff Moggridge¹ and Hans Peter Wendel²

¹Department of Chemical Engineering and Biotechnology, University of Cambridge, UK jbb41@cam.ac.uk

²Department of Thoracic, Cardiac, and Vascular Surgery, University Hospital of Tuebingen, Tuebingen, Germany

INTRODUCTION

Owing to excellent mechanic properties, and easy processibility, styrenic thermoplastic elastomers (STE) have gained increasing interest in recent years as potential biomaterials. Furthermore, certain triblock copolymer STE may exhibit a cylindrical morphology with anisotropic mechanical properties, akin to those resulting from collagen orientation in some tissues, heart valve leaflets for example¹.

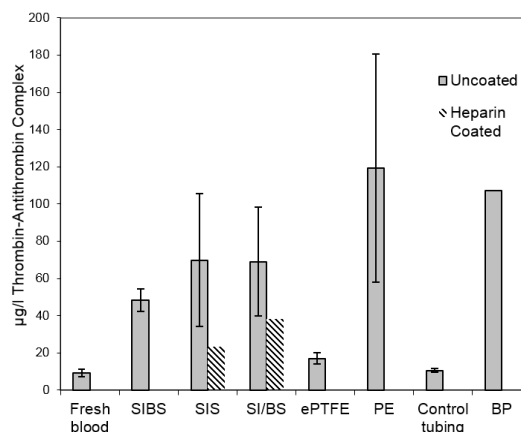
EXPERIMENTAL METHODS

4 compression moulded cylinder-forming block copolymers were examined: polystyrene-*block*-polyisoprene-*b*-polystyrene (SIS), containing 30wt% styrene from Kraton polystyrene-*b*-polyisoprene-*b*-polybutadiene-*b*-polystyrene (SI/BS), containing 19wt% styrene, and polystyrene-*b*-polyethylene-*b*-polypropylene-*b*-polystyrene (SEPS), containing 22wt% styrene, all from Kraton, and polystyrene-*b*-polyisobutylene-*b*-polystyrene having 30wt% styrene, manufactured by Innovia LLC., denoted as SIBS. SEPS was subsequently heparin coated (Corline) (SEPS-HEP). ePTFE, polyester (PE) and glutaraldehyde fixed bovine pericardium (BP) were used as reference materials.

Freshly drawn human whole blood was circulated for 90 mins in an in vitro closed loop model (modified Chandler-Loop)². Blood compatibility tests were performed according to ISO 10993-4, including measures of thrombogenicity, activation of coagulation, blood cell counts, platelet activation, and neutrophil inflammatory response. Biomaterial samples were also analysed with scanning electron microscopy.

RESULTS AND DISCUSSION

Polyester resulted in the greatest activation of the coagulation pathway as indicated by TAT complex formation, and uncoated STEs lead to moderate activation. ePTFE and heparin coated materials lead to minimal activation of the coagulation pathway.



Levels of PMN-Elastase indicated that STE biomaterials resulted in significantly less leukocyte activation than polyester, and comparable to ePTFE.

The full blood count showed no significant differences between biomaterials and ePTFE. However, STE biomaterials resulted in significantly greater levels of β -thromboglobulin release than in blood contacted with ePTFE.

No significant thrombus generation was seen on the biomaterials under SEM, and protein adsorption levels (Fibrinogen and CD41) were similar to ePTFE.

CONCLUSION

Uncoated STE biomaterials are superior to polyester, and bovine pericardium, but inferior to ePTFE, in measures of hemocompatibility.

Heparin coating of STE biomaterials results in hemocompatibility comparable to ePTFE.

STE biomaterials continue to show potential for cardiovascular implant applications.

REFERENCES

1. Stasiak J. *et al.*, *Func. Mater. Lett.*, 3,4:249-52, 2010
2. Sinn S. *et al.*, *J. Mater. Sci. -Mater. Med.* 22,6:1521-8, 2011

ACKNOWLEDGMENTS

The authors would like to thank the BHF New Horizons Grant no. NH/11/4/29059 for providing financial support to this project and the Armstrong Fund (Cambridge) for a studentship.

Capillary morphogenesis of primary endothelial mono- and co-cultures in starPEG-heparin hydrogels for controlled vascularization

Uwe Freudenberg, Karolina Chwalek, Mikhail V. Tsurkan, and Carsten Werner

Leibniz Institute of Polymer Research Dresden (IPF), Max Bergmann Center of Biomaterials Dresden (MBC) & Technische Universität Dresden, Center for Regenerative Therapies Dresden (CRTD), Dresden, Germany, freudenberg@ipfdd.de

INTRODUCTION

Angiogenesis, the outgrowth of blood vessels, is crucial in development, disease and regeneration. Studying angiogenesis *in vitro* remains challenging because the capillary morphogenesis of endothelial cells (ECs) is controlled by multiple exogenous signals. Therefore, a set of in situ-forming starPEG-heparin hydrogels was used to identify matrix parameters and cellular interactions that best support EC morphogenesis.

EXPERIMENTAL METHODS

Hydrogels were synthesized utilizing multifunctional starPEG-peptide-conjugates and maleimide pre-functionalized heparin.¹ Primary human vein endothelial cells (HUVECs) were cultured together with primary human aortic smooth muscle cells (SMCs), primary human dermal fibroblasts (HDFs) or human bone marrow mesenchymal stem cells (MSCs) applying cell-responsive starPEG-heparin hydrogels pre-functionalized with RGD-peptides, and pro-angiogenic factors (VEGF, FGF-2 and SDF-1)². The formation of tubular networks was analyzed utilizing time lapse microscopy, immunostaining combined with confocal laser scanning microscopy and transmission electron microscopy.

RESULTS AND DISCUSSION

First, the influence of mechanical matrix characteristics and the presentation of bioactive components to EC network assembly was investigated. We found, that a particular type of soft, matrix metalloproteinase-degradable hydrogel containing covalently bound integrin ligands (RGD) and reversibly conjugated pro-angiogenic growth factors (VEGF, FGF-2 (F) and SDF-1 (S)) could boost the development of highly branched, interconnected, and lumenized endothelial capillary networks.

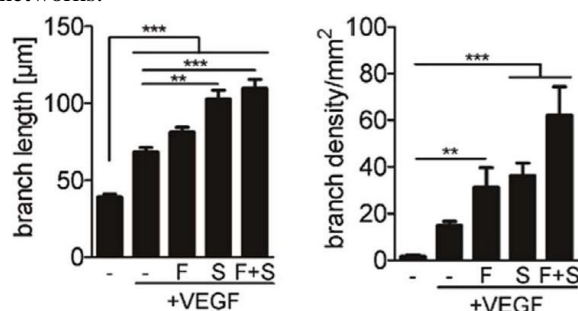


Figure 1: Capillary network formation is improved by the synergistic effect of VEGF165, FGF-2 (F) and SDF1-a (S): Mean branch length and branch density/mm² were quantified showing superior effect of soft hydrogels (200 Pa) containing VEGF165, FGF-2 and SDF-1a. *p , 0.05, **p , 0.01, ***p , 0.001, ANOVA.

Using these effective matrix conditions, 3D heterocellular interactions of ECs with different mural cells were demonstrated that enabled EC network modulation and maintenance of stable vascular capillaries over periods of about one month *in vitro*. Co-culture with MSCs resulted in the longest average branch length that contributed to the higher overall network density, while no significant differences were observed for the other co-cultures.

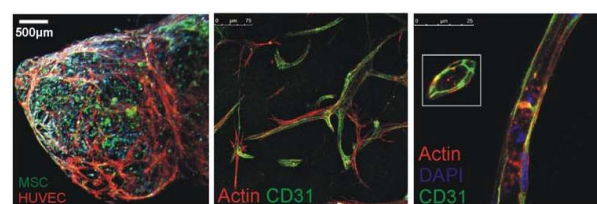


Figure 2: Left: Image of fluorescently labeled endothelial cells (red, CMFDA) co-cultured with 10% MSC (green, CMTMR) at 28 days showing capillary network in gross scale. Middle: Immunostaining of endothelial cells (green, CD31) and MSCs (red, F-actin) during the long-term culture showing cell co-localization. Right: Confocal longitudinal and cross-section image of a 28 day-old endothelial cell capillary (red-f-actin, green-CD31, blue-nucleus) showing its multicellular composition and internal lumen.

CONCLUSION

In summary, starPEG-heparin hydrogels enabled the long-term *in vitro* investigation of heterotypic cell-cell interactions during EC capillary formation, highlighting the important regulatory role of supporting mural cells in the angiogenic EC microenvironment. The combination of various different mural cells with the multifactor delivery in the hydrogel-based co-cultures of ECs facilitated the most versatile modulation of capillary EC networks, and could offer unprecedented options for generating tissue and disease-specific angiogenesis models.

REFERENCES

1. Tsurkan M. *et al.*, Adv. Mater. 25: 2606–2610, 2013.
2. Chwalek *et al.*, Sci. Rep. 4: 4414 DOI: 10.1038/srep04414, 2014.

ACKNOWLEDGMENTS

This work was supported by the Deutsche Forschungsgemeinschaft through grants SFB-TR 67, WE 2539-7 and FOR/EXC999, by the Leibniz Association (SAW-2011-IPF-2 68) and by the European Union through the Integrated Project ANGIOSCAFF (7th Framework Program).

The Zeta Potential as Indicator for Solid Surface Charge

Christine Körner^{1*} and Thomas Luxbacher¹

¹Anton Paar GmbH, Austria
christine.onitsch@anton-paar.com

INTRODUCTION

Surface characteristics play a vital role in the biocompatibility of any material. Studying surface properties is thus of paramount importance, as the outermost surface layer of a material has a tremendous effect on the success or failure of a biomaterial.

The present work deals with the role of zeta potential analysis as a surface sensitive technique for the characterization of biomaterial surfaces. The zeta potential is an interfacial parameter which describes the charge a surface assumes when it gets in contact with a liquid. Zeta potential analysis furthermore enables time-resolved adsorption studies of biological compounds on solid surfaces, thus contributing to the understanding of e.g. protein-biomaterial interaction.

Zeta potential analysis is applicable to all classes of materials used for biomaterial applications, i.e. metals, polymers and ceramics.

EXPERIMENTAL METHODS

Zeta potential analysis of various materials was performed with SurPASS Electrokinetic Analyzer.

The SurPASS method is based on the streaming potential or streaming current technique, respectively. If a surface is brought in contact with the electrolyte solution, charges are formed at the solid-liquid interface. Upon streaming the electrolyte solution across the solid surface, the charge distribution on the surface is shifted, giving rise to a – so called – streaming potential at the interface. The streaming potential is then used to calculate the zeta potential.¹

The zeta potential strongly depends on the pH value. The pH value where the zeta potential is 0 mV and a charge reversal takes place is called isoelectric point and describes the chemistry of a surface.

Being sensitive to the outermost surface layer of a material, the zeta potential is also used to assess adsorption processes².

RESULTS AND DISCUSSION

Figure 1 shows zeta potential vs. pH dependences of the inner surface of a poly(ethersulfone) (PES) hollow fiber membrane used for hemodialysis before applying surface treatment (1), after grafting with amino groups (2) and after final surface modification with heparin (3). The three curves allow for clear differentiation of the individual treatment steps: The isoelectric point of the

inert PES membrane is shown at pH 4, whereas it is shifted to alkaline pH (pH 8.2) after grafting with the amino groups, which behave basic. After subsequent treatment with heparin to increase the biocompatibility of the membrane, the surface charge was found to be negative due to the presence of sulfonic acid groups of heparin which dissociate when exposed to the electrolyte solution.

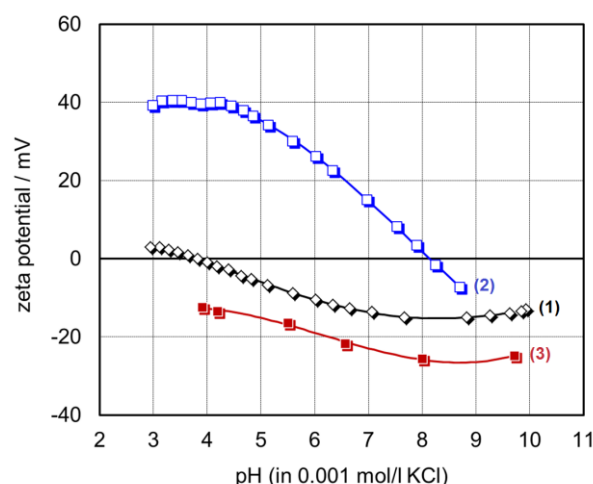


Figure 1: pH dependence of zeta potential for poly(ethersulfone) hollow fiber membrane with different surface treatment.

The results indicate the applicability of zeta potential analysis to study biocompatible surface coatings at real samples.

CONCLUSION

Zeta potential analysis is a valuable tool for the study of surface characteristics of biomaterials. A major benefit of the SurPASS method is its application to biomaterial samples of different shapes and geometries.

While the pH dependence of zeta potential provides information on the surface chemistry, the real-time study of adsorption kinetics furthermore enables the optimization of solid surface properties.

REFERENCES

1. Werner C. *et al.*, J. Biomater. Sci. Polymer Edn. 7:61-76, 1995
2. Norde W. *et al.*, J. Colloid Interface Sci. 139:169-176, 1990

Zeta Potential: a Useful Tool to Interpret the Hydrothermally Treated Titanium Behaviour as Biomaterial

Martina Lorenzetti^{1,2,*}, Thomas Luxbacher³, Spomenka Kobe^{1,2} and Saša Novak^{1,2}

^{1,*}Department of Nanostructured Materials, Jožef Stefan Institute, Ljubljana, Slovenia, martina.lorenzetti@ijs.si

²Jožef Stefan International Postgraduate School, Ljubljana, Slovenia

³Anton Paar GmbH, Graz, Austria

INTRODUCTION

Titanium is considered one of the most suitable materials for hard tissue replacement, due to its mechanical properties and bioinertness. It owes its properties mainly to the thin naturally-formed, amorphous TiO₂ film present on its surface. However, this unstable, thin film can be replaced by a firmly attached, hydrothermally-grown polycrystalline TiO₂-anatase coating, in order to enhance the surface properties of the bare titanium^{1,2}.

The study of the surface properties of a biomaterial is compulsory for interpreting their “bio” performances *in vivo*. The surface charge is one of the most relevant characteristics for understanding the events happening at the interface, when the biomaterial comes in contact with the human body. In particular, it is known that proteins from the blood stream are the first macromolecules which adsorb on the biomaterial surface³.

Thus, the purpose of this work was to study the surface properties of polycrystalline TiO₂-coatings, in connection with their nanostructure, by analysing the zeta potential and the protein adsorption on such surfaces.

EXPERIMENTAL METHODS

A series of polycrystalline, nanostructured TiO₂-coatings were prepared by hydrothermal treatment (HT) of titanium substrates, following the procedure previously described^{1,2}. In short, machined titanium discs were hydrothermally treated in aqueous suspensions of Ti(iOPr)₄ at 200 °C in different pH conditions and different times.

The surface nanostructure and crystal morphology were observed by scanning electron microscopy (SEM), while the surface wettability was examined by sessile drop contact angle (CA) measurements.

The zeta potential of bare (Ti NT) and HT titanium substrates was determined by the streaming current technique, using a SurPASS electrokinetic analyzer (Anton Paar GmbH, Graz, Austria). Potassium chloride (KCl) and phosphate buffer saline (PBS), with an ionic strength of 0.001 mol/l in both cases, were used as analytical solutions. Bovine serum albumin (BSA), dissolved in PBS, was used as model protein for the adsorption analysis.

RESULTS AND DISCUSSION

The SEM pictures revealed that the HT coatings varied in their nano-texture, since they were constituted of crystals of different morphologies and dimensions, depending on the synthesis route. Accordingly, diverse properties in terms of wettability and charge were expected.

The HT discs displayed a more hydrophilic character compared to the bare titanium, suggesting a higher presence of hydroxyl groups and higher surface energy. The streaming potential measurements revealed that all the surfaces were negatively charged at physiological pH (7.4). However, the surface charge of the HT samples was significantly different compared to the Ti NT. The zeta potential curves also showed a different behaviour among the substrates, which was even more highlighted when the analytical solutions were switched.

The different zeta potential affected the BSA adsorption, but not its adsorption kinetics.

All these differences were ascribed to the surface dissimilarities among the HT-Ti and Ti NT from the chemical point of view, especially due to the presence of hydroxyl groups and to the adsorption of ions from the solutions (e.g. phosphate ions contained in the PBS buffer).

CONCLUSION

Surface zeta potential analysis represents a valuable tool to estimate the behaviour of titanium and modified-titanium surfaces (namely, TiO₂-coated) under chosen conditions (e.g. physiological conditions).

This helped to make assumptions and a better interpretation for further *in vitro* experiments carried out on such substrates.

REFERENCES

1. Lorenzetti M. *et al.*, Materials. 7(1):180-194, 2014.
2. Lorenzetti M, *et al.*, Mat. Sci. Eng. C. 37(0):390-398, 2014.
3. Gristina AG., Science. 237(4822):1588-1595, 1987.

ACKNOWLEDGMENTS

The EU 7th Framework Programme FP7/2007-13 BioTiNet-ITN (Grant no: 264635) is acknowledged for providing financial support to this project.



The Role of Porosity on the Z-Potential of Calcium Phosphate Cements

Montserrat Espanol^{1,2,*}, Gemma Mestres³, Thomas Luxbacher⁴, and Maria-Pau Ginebra^{1,2}

¹Department of Materials Science and Metallurgical Engineering, Technical University of Catalonia, Spain

²Biomedical Research Networking Center in Bioengineering, Biomaterials, and Nanomedicine, Spain

³Department of Engineering Sciences, Uppsala University, Sweden

⁴Anton Paar GmbH, Graz, Austria

Montserrat.espanol @upc.edu

INTRODUCTION

Calcium Phosphate Cements (CPC) have long been recognized as excellent candidates in bone regeneration applications. Their great acceptance arises from their close similarity, both in composition and structure, to the mineral phase of bone. Another property that makes CPCs very unique is that they are injectable and by means of a simple dissolution-precipitation reaction are capable of hardening in the body. For cement formulations consisting of alpha-tricalcium phosphate (α -TCP), the set product results in an entangled network of nano- and sub-micron crystals of calcium deficient hydroxyapatite (CDHA). In spite of the many advantages that can be sought from such materials they are extremely challenging when it comes to interpretation of *in vitro* and *in vivo* data. One of the causes is the porous network created by the entangled crystals. Pores can concentrate and retain proteins as a function of their size altering the biological behaviour of the material¹. Along the same line it is reasonable to think that the presence of pores can alter the ionic species and ionic concentrations modifying in turn the surface potential of the material². The objective of the present work is thus to determine the zeta potential (ZP) of a series of CPC with various textures and porosities.

EXPERIMENTAL METHODS

CPCs were prepared by mixing a solid phase (98% α -TCP and 2% of precipitated hydroxyapatite) with a 2.5wt% of Na_2HPO_4 as liquid phase at two different liquid to powder ratios (L/P): 0.35 and 0.65ml/g. In addition, two α -TCP powders with different particle size were used: coarse (C) with a median size of 5.2 μm and fine (F) of 2.8 μm . Upon mixture of both phases the paste formed was mould in rectangles of 20mm (L) x 10mm (W) x 1mm (T) which were then allowed to set in water at 37°C for 4 days. The set cements were characterised by scanning electron microscopy (Jeol JSM-7001F), N_2 adsorption (ASAP2020) and mercury intrusion porosimetry (Autopore IV 9500 Micromeritics). A SurPASS electrokinetic analyzer (Anton Paar GmbH) was used to perform streaming current and cell conductance measurements by means of an adjustable-gap cell. The rectangular samples were fixed on sample holders with superglue and allowed to equilibrate overnight in 1mM KCl solution (500ml) before measurement. Measurements were performed at various cell gaps (80-120 μm) to separately determine the ZP of the cement and the conductance within pores.

RESULTS AND DISCUSSION

It is now well established that the porous structure of a material affects the surface ZP value owing to their

electrical conductance. Recent investigations have further proved that through streaming current and conductance analysis at different cell gaps it is possible to determine the ZP of both the external surface and the internal pore surfaces of a material². This has been implemented in the determination of the ZP of two CPC: C and F (Fig.1). Both cements share in common their identical chemistry and degree of porosity (55%), and they differ in their structure: F is built by the entanglement of needle-like crystals and C is composed of a mesh of larger plate-like crystals. The good fit obtained for the streaming current against gap cell allow to accurately determine the external ZP. Both textures resulted in very close external ZP values and in a negligible effective internal ZP. In spite of the fact that the conductance inside the pores in the F sample is very high as compared to the C sample, this does not necessarily imply it should contribute to the streaming current. The results in fact seem to support that the pores are too narrow to make any substantial contribution to the streaming current but further work is ongoing to fully confirm the results.

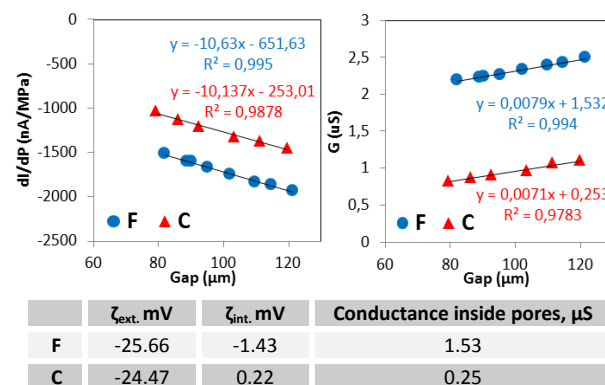


Figure 1. Streaming current and conductance analysis.

CONCLUSION

Although C and F cements had the same porosity, the different pore textures created by the entanglement of needles (F) or plates (C) were believed to be responsible for the differences in pore conductance. These differences did not affect the external ZP, which was found close to -25mV in both materials.

REFERENCES

1. Espanol M. *et al.*, Biointerphases 7:37, 2012
2. Yaroshchuck A. *et al.*, Langmuir 26:10882-889, 2013

ACKNOWLEDGMENTS

This study was supported by the Spanish Government through project MAT2012-38438-003-01.



The effect of surface oxygen functional groups on parylene C biocompatibility - comparison of MG-63 cells adhesion and bacteria strains attachment

M. Gołda-Cępa¹, M. Brzychczy-Włoch², K. Envall³, A. Kotarba¹

¹Faculty of Chemistry, Jagiellonian University, Krakow, Poland, golda@chemia.uj.edu.pl

²Department of Microbiology, Medical College, Jagiellonian University, Krakow, Poland

³Department of Chemical Engineering and Technology, KTH Royal Institute of Technology, Stockholm, Sweden.

mild oxygen plasma treatment of parylene C implant coating was evaluated as a tool for tuning of its surface morphology and biocompatibility (MG-63 cell line and *S. aureus*, *S. epidermidis*, *P. aeruginosa* from ATCC and clinical isolates). It was found that the surface of modified parylene C promotes MG-63 cells growth and at the same time does not influence bacteria strains adhesion. The results are discussed in terms of changes in chemical (oxygen insertion into the polymer matrix) and physical (surface nanotopography) properties.

INTRODUCTION

Internal biomaterial devices *in vivo* meet several challenges, among which the risk of material-associated infection and lack of tissue integration¹ belongs to the most important. Upon implantation, 'race for surface' takes place when process of tissue cell integration compete with bacterial adhesion to the medical device's surface. Microbial colonisation of the surface can cause serious infection which can lead to complications². For these reasons, biomaterial surface properties are currently vividly investigated and nanostructured materials are becoming promising in tailoring adequately the surface. A parylene C versatile polymer coating which limits the corrosion and heavy metal ions release from the metallic biomaterials can be adjusted to meet the current requirements. One of the methods of polymer surface modification that can be successfully applied is oxygen plasma. Treatment with oxygen can affect not only the composition of the surface functional groups, but also nanotopography of the polymer. As a result, an opposite behaviour of osteoblast cells and bacteria strains can be observed on the same surface - promotion of osteoblast function and reducing bacteria colonisation.

EXPERIMENTAL METHODS

Parylene C (8 µm of thickness) films were prepared by CVD technique (provided by ParaTech Coating Scandinavia AB). In order to modify the parylene C surface, the oxygen plasma treatment was carried out using a Diener electronic Femto plasma system. The etching parameters were selected in order to obtain a nanotopography within the range of 30–200 nm. For evaluation of cell adhesion, the MG-63 human osteosarcoma cell line was used. In the experiments, both kinds of samples, unmodified and treated with oxygen plasma, were used. Cells were grown for 24 h in 24-well tissue culture plates. For fluorescence confocal microscopy observations cells F-actin and nucleus were stained. The bacteria strains used in the study were

S. aureus, *S. epidermidis* and *P. aeruginosa*. The method applied to assess bacterial adhesion to the parylene C films was the static adhesion assay³. The experiments were performed in 24-well tissue culture plates and incubated for 4 h in 1 mL of a bacteria strain suspension (5×10^8 CFU/mL).

RESULTS AND DISCUSSION

The fresh and modified samples were thoroughly characterised by AFM, SEM, XPS, contact angle measurements (Fig. 1). The modified parylene C surface does promote the MG-63 cells attachment and does not promote higher bacteria stains attachment and biofilm formation. On the unmodified parylene C, only few cells/mm² could be observed (ca. 20 cells/mm²±3), while for the modified sample an increase in adhesion was observed (ca. 120 cells/mm²±5). The attachment of the bacteria strain *S. aureus* was 1.7×10^5 for the unmodified sample and 3.4×10^5 for the oxygen-plasma treated. No significant differences were observed for any of the investigated strains.

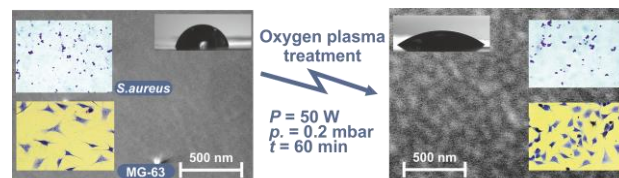


Fig. 1 The effect of oxygen plasma on parylene C biofunctionality (*S. aureus*, MG-63, contact angle and SEM topography background).

CONCLUSION

The results show that generated surface nano-irregularities together with oxygen-containing groups can stimulate the MG-63 cells growth on a parylene C surface. At the same time, the modification does not enhance bacteria growth, as was proven in parallel tests with 6 bacteria strains.

REFERENCES

1. Busscher H. *et al.*, Sci Transl Med. 4:153-163, 2012
2. Zimmerli W. *et al.*, Semin Immunol 33:295-306, 2011
3. Boeuf S. *et al.*, Acta Biomater. 8:1037–1047, 2012

ACKNOWLEDGMENTS

“The authors would like to thank the Foundation for Polish Science Ventures Programme, co-financed by the EU European Regional Development Fund, for providing financial support to this project”

Multilayer coating of a nonwoven polyester textile for antibacterial wound dressing

François Aubert-Viard^{1*}, Oumaira Rahmouni¹, Adeline Martin², Feng Chai¹, Nicolas Tabary², Christel Neut³, Bernard Martel² and Nicolas Blanchemain¹

^{1*} INSERM U1008, Biomaterial Research Group, University Lille 2, France, francois.aubert@univ-lille2.fr

² UMET, Ingénierie des Systèmes Polymères, University Lille 1, Lille

³ INSERM U995, Laboratoire de Bactériologie, University Lille 2, France

INTRODUCTION

Wound healing represents a public health problem with an increase in susceptible populations like geriatric or diabetic patients¹. The major complication is infection, associated to an increase of morbidity (amputation) or mortality (septicemia). In particular, the infection of the diabetic wounds delays the healing process and progresses to bone destruction². We recently develop a wound dressing functionalized by layer-by-layer system based on chitosan (positive polyelectrolyte, PE+) and cyclodextrin polymer (negative polyelectrolyte, PE-) for synergic bi-therapy with silver or iodide associated to chlorhexidine.

EXPERIMENTAL METHODS

In a first step, the non woven polyester (PET) is functionalized by chitosan (CHT) crosslinked by citric acid (CTR) to obtain a first charged layer (positive or negative in function of the CTR concentrations) or by genipin to obtain a first positively charged layer only. The textile is characterized by FTIR, SEM and the ionic charge density is evaluated by titration. Then the positively and negatively charged PET-CHT is impregnated in iodine or silver solutions to obtain the first bioactive coating. The drug loading is quantified by elementary analysis and titration. In a second step, the multilayer system is build up on the loaded PET-CHT according to the method develop in our lab³ using alternatively cyclodextrin polymer (PCD, PE-) and CHT (PE⁺). In a last step, the multilayer system is impregnated in a chlorhexidine (CHX) solution. The CHX loading and CHX release is measured by HPLC method in function of the number of bilayers. Finally, the kinetic of release of the final wound dressing (PET-CHT-Ag/CHX and PET-CHT-I/CHX) is studied in physiological medium (PBS, pH7.4, 37°C, 80 rpm). The antibacterial activity is evaluated on different bacterial strains (*S. aureus* CIP224; *E. coli* K12; MRSA 07001 and *P. aeruginosa* ATCC 27583) by kill-time method. At each step of the functionalization process, the cytocompatibility is evaluated with epithelial cells (ATCC-CCL5, L132) according to ISO 10993-5 standard.

RESULTS AND DISCUSSION

The evaluation of the charge density on the functionalized PET with CHT shows the ability of the system to be adapted with the CTR concentrations either with an anionic exchange functions ([CTR] >1%) either with a cationic exchange functions ([CTR] <1%). After impregnation of anionic and cationic PET-CHT in silver and iodine solution, the titration shows a silver loading of 3% and iodine loading of 1600 ppm. *In vitro*,

microbiology evaluation reports the efficiency of the loaded PET-CHT. Indeed, the silver loaded PET-CHT reduces significantly two bacterial population after 24 hours (*S. aureus* : 4 log; *E. coli* : 5 log reduction).

The multilayer system, applies on the loaded PET-CHT, has three functions thanks to the cyclodextrin polymer as previously described⁴ i) barrier effect to reduce the release of the cytotoxic silver into the wound ii) gel formation to drain exudates iii) complex-inclusion formation to adsorb other drug. Systems with 5.5, 7.5 and 10.5 bilayers are performed on the PET-CHT-Ag. As show in figure 1a, the presence of silver has no influence on the build-up of the multilayer. Additionally, the figure 1b shows the CHX loading and CHX release depends on the number of bilayers.

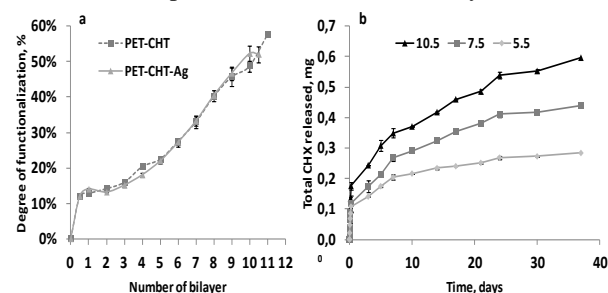


Fig 1. a. Evolution of weight gain of textiles during the construction of the system. b. Kinetic of release of CHX in function of the number of bilayer (PBS, 80rpm, 37°C) (b).

The evaluation of cell vitality by the method of the Alamar blue shows an excellent cytocompatibility of the functionalization of the dressings at each stage of the process (vitality rate >70%). Finally, microbiological evaluation confirms the CHX release studies with a prolonged antibacterial effect (>30 days) of the Ag/CHX loaded on wound dressing against *S. aureus* and *E. coli*.

CONCLUSION

We demonstrate the safety and the prolonged antibacterial effect of a multilayer wound dressing loaded with silver or iodide associated with CHX. The three main characteristics of multilayer system (drug sorption, gel formation, ionic exchange capacity) allow us to obtain a new generation of wound dressing for combined biotherapy.

REFERENCES

1. Ashcroft GS. *et al.*, Biogerontol. 3:337-345, 2002
2. Abbott CA. *et al.*, Diabet Med. 19:377-384, 2002
3. Martin A. *et al.*, Carbohydr Polym. 93:718-730, 2013
4. Martel B. *et al.*, J Appl Polym Sci, 2005

Keratinocyte and Fibroblast Adhesion on an Antibacterial Peptide Surface Coating

A. Leong^{*1,2}, M. Willcox¹

^{*}A.Leong@brienholdenvision.org; ¹School of Optometry and Vision Science, UNSW, Sydney, Australia.

²Brien Holden Vision Institute, Sydney, Australia.

INTRODUCTION

Infection of implanted medical devices was associated with an estimated cost of \$3.3 billion in the USA in 2004, occurring at a rate of 3–5% across a range of implant types [1]. Bacterial biofilms on infected implants often evade antibiotic treatment, necessitating replacement surgery [2]. An anti-infective surface coating for surgical implants is required. The ideal surface also supports integration with host tissue, promoting long-term success by allowing a robust immune response at the tissue-implant interface [3]. Our strategy in developing such a surface is based on a biocompatible cationic antimicrobial peptide (CAP).

EXPERIMENTAL METHODS

Surface Preparation

Fluorinated ethylene propylene (FEP) was coated with a plasma polymer of allylamine (ppAA). The CAP containing a single cysteine residue was covalently attached to ppAA *via* the amine-to-sulphydryl crosslinker, succinimidyl-4-[N-maleimidomethyl]-cyclohexane-1-carboxylate (SMCC).

Bacterial Adhesion to Surfaces

Staphylococcus aureus, *Staphylococcus epidermidis* or *Escherichia coli* clinical isolates were grown in broth medium, and diluted to 10^6 CFU/ml. Sample surfaces were incubated with bacteria at 37°C for 48 h. Surfaces were then rinsed, and adherent bacteria were stained to determine viability and imaged by fluorescence microscopy. The percentage area covered by bacteria was measured with ImageJ software.

Cell Adhesion to Surfaces

Human primary epidermal keratinocytes or dermal fibroblasts, maintained in serum-free conditions, were seeded at 5×10^3 cells/cm² on sample surfaces. After 48 h surfaces were rinsed, and adherent cells were stained, imaged by fluorescence microscopy, and counted. Counts per experiment were normalised such that cell numbers on ppAA are reported as 100%.

RESULTS AND DISCUSSION

Antibacterial Activity of Surfaces

Coverage by viable bacteria on the CAP surface, compared to FEP and ppAA surfaces, was significantly ($p < .05$) reduced for the three strains tested (Fig. 1).

Cell Adhesion to Surfaces

Numbers of keratinocytes and fibroblasts on CAP were approximately 80% of those on ppAA (Fig. 2). For each cell type, cell counts were significantly ($p < .05$) different on all surfaces except for keratinocytes on FEP vs CAP.

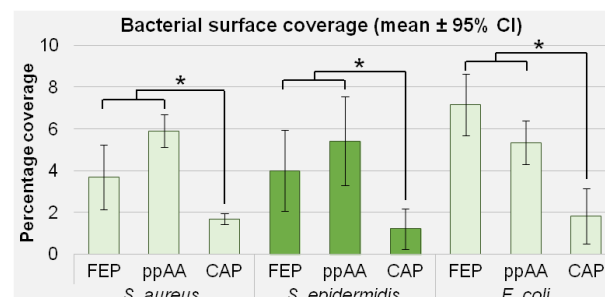


Figure 1. Percent viable bacterial surface coverage on CAP compared to FEP and ppAA at 48 h ($n=3$). $*p < .05$

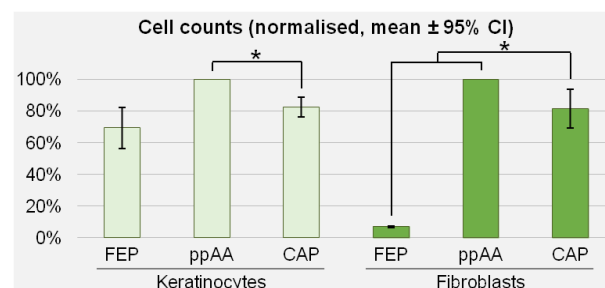


Figure 2. Human primary cell numbers on CAP compared to FEP and ppAA at 48 h ($n = 3$). $*p < .05$

Discussion

Relative to ppAA, our CAP surface reduces bacterial adhesion by 72% and 78%, respectively, for the *S. aureus* and *S. epidermidis* strains tested. These two Gram-positive species are responsible for two-thirds of all orthopaedic device infections [4]. Gram-negative *E. coli* is also susceptible to CAP, showing a 66% reduction. Our coating also allows mammalian cell adhesion and proliferation to about 80% of the level observed on the nonspecific, cell-compatible ppAA surface. Future experiments will examine the mechanism of adhesion to CAP, and test the biocompatibility and effectiveness of this surface *in vivo* in a rodent model.

CONCLUSION

Our *in vitro* results suggest our CAP is a good candidate for a surface coating for surgically implanted medical devices. Further investigation is warranted.

REFERENCES

1. Darouiche RO (2004) *N Engl J Med* **350**:1422-9
2. Schierholz M & Beuth J (2001) *J Hosp Infect* **49**:87-93
3. Gristina AG (1994) *Clin Orthop Relat Res* **298**:106-18
4. Montanaro L *et al.* (2011) *Future Microbiol* **6**:1329-49

ACKNOWLEDGMENTS

This research was funded by the Brien Holden Vision Institute. Plasma polymer coating was carried out at the Biointerface Engineering Lab, Swinburne University, a node of the Australian National Fabrication Facility.



Blood Compatible Antimicrobial Polymers with Degradable Backbone

K. Fukushima^{1*}, K. Kishi¹, Y. Inoue², C. Sato², A. Sasaki², and M. Tanaka²

^{1*}Department of Polymer Science and Engineering, Yamagata University, Japan, fukushima@yazyamagata-u.ac.jp

²Department of Biochemical Engineering, Yamagata University, Japan

INTRODUCTION

Current medical facilities use antibiotics to prevent immune compromised patients from various types of infections. In this decade, we have faced a threat of emerging drug-resistant bacteria. Thus, there is a pressing need for development of new types of drugs with a broad spectrum of antimicrobial activity and capability not to develop drug-resistance.

Amphiphilic polycations mimicking host defence peptides (HDPs) physically break down negatively charged bacterial cell membrane by static interaction, contributing to no generation of drug-resistance¹. Nederberg et al. have reported that biodegradable polycarbonates with quaternary ammonium (PC3QA) are effective against drug-resistant gram-positive bacteria methicillin-resistant *Staphylococcus aureus* (MRSA)². However, PC3QA needed more hydrophobicity to affect more pathogenic gram-negative bacteria, which also resulted in lysis of healthy red blood cells (RBCs)³. One challenge in synthetic antimicrobials is combining high antimicrobial and low hemolytic activities⁴.

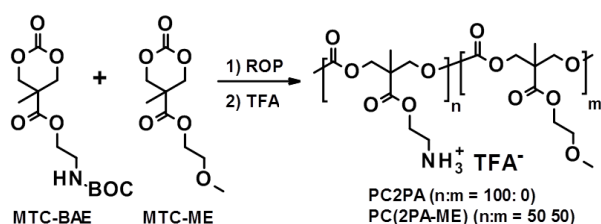


Figure 1. Synthesis of cationic polycarbonates

In this study, we synthesized similar aliphatic polycarbonates with primary ammonium (PC2PA) that can be partially deprotonated at neutral pH to form hydrophobic liberated amine. Some polymers with primary ammonium represent not only strong antimicrobial activity against gram-negative bacteria but also high hemolytic activity¹. Then we incorporate a blood compatible polycarbonate recently developed (PCME)⁶ into PC2PA to mitigate the potential hemolytic activity.

EXPERIMENTAL METHODS

Polymer Synthesis

Preparation and ring-opening polymerization (ROP) of MTC-BAE and MTC-ME (Fig. 1) have been already described elsewhere^{2,5}. The resultant polymers were then treated with trifluoroacetic acid (TFA) for deprotection of *tert*-butoxycarbonyl group (Boc) to generate primary ammonium salt.

Antimicrobial and hemolytic assays

Aqueous polymer solutions with different concentrations were incubated with human RBCs for 1 h and *E. coli* for 24 h at 37°C, respectively.

RESULTS AND DISCUSSION

Two polycarbonates were prepared in this study. PC2PA has all cationic residue and M_n 7,600. PC(2PA-ME) comprises 50% of cationic units and 50% of MTC-ME and has M_n 5,200 (PDI 1.38).

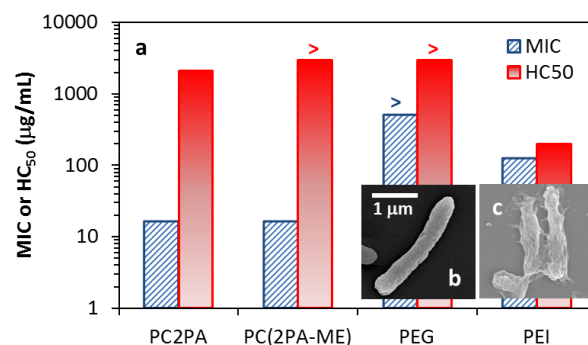


Figure 2. MIC against *E. coli* and HC₅₀ against human RBCs of each polymer (a). SEM images of *E. coli* before (b) and after (c) treatment with PC2PA

Both new cationic polycarbonates efficiently inhibited growth of *E. coli* with concentration (MIC) of 16 µg/mL. PC2PA induced 50% hemolysis at a concentration of 2000 µg/mL while PC(2PA-ME) remained hemolysis below 20% at a concentration over 3000 µg/mL. This implies that MTC-ME unit is beneficial to lowering hemolytic activity. In contrast, a typical cationic polymer PEI showed low antimicrobial and high hemolytic activities. (Fig. 2a). SEM observation revealed that PC2PA also disrupts bacterial cell membrane (Fig. 2b,c). Therefore, the PC2PA-based antimicrobials are expected to be effective against drug-resistant strains.

CONCLUSION

We successfully developed a blood compatible and antimicrobial polycarbonate potentially effective against drug-resistant bacteria.

REFERENCES

1. Parelmo E. F. *et al.*, Appl. Microbiol. Biotechnol. 87:1605-1615, 2010
2. Nederberg F. *et al.*, Nature Chem. 3:409-414, 2011
3. Englar A. C. *et al.*, Biomacromolecules 14:4331-4339, 2013
4. Fukushima K. *et al.*, Nat. Commun. 4: 2861, 2013
5. Fukushima K. *et al.*, PCT/JP2014/054948

ACKNOWLEDGMENTS

KF would like to thank the Izumi Science and Technology Foundation (Grant no: H24-J-129) and Japan Society for the Promotion of Science (Grant-in-Aid for Young Scientists (B), no: 25870078) for providing financial support to this project.

Combinatorial approach to composition-structure-property relationships in an antibacterial Ag-Ti thin film

Erik Unosson^{1*}, Daniel Rodriguez^{2,3}, Ken Welch¹, Håkan Engqvist¹

^{1*}Department of Engineering Sciences, Uppsala University, Sweden

²Department of Materials Science and Metallurgical Engineering, Technical University of Catalonia, Spain

³Biomedical Research Networking Centre in Bioengineering, Biomaterials and Nanomedicine (CIBER-BBN), Spain
erik.unosson@angstrom.uu.se

INTRODUCTION

Development of antibacterial surfaces is a necessity to reduce the number of implant-associated infections¹. A promising strategy is to incorporate silver (Ag) in biocompatible and bioactive structures such as hydroxyapatite (HA) or TiO₂ coatings, combining osseointegration with broad antibacterial properties. The appropriate composition, structure and subsequent Ag⁺ release from such coatings is still, however, much under development². This study presents a combinatorial approach to synthesizing and evaluating antibacterial and other properties of a binary Ag-Ti oxide gradient, elucidating composition-structure-property relationships.

EXPERIMENTAL METHODS

A single sample was evaluated in this study, created using a combinatorial physical vapour deposition (PVD) system. Opposing targets of Ag and Ti were used concurrently in a reactive (O₂) environment to deposit a binary compositional gradient coating across a 3-inch Si wafer. The gradient was then characterized and tested against *S. aureus* in a 2h adhesion test, and Ag⁺ release profiles were retrieved from opposing ends of the sample.

RESULTS AND DISCUSSION

In Fig. 1, the structural and compositional differences between the Ag-rich and Ti-rich ends are depicted. The Ag-contribution in the sample shifted from an integral part of a homogeneous, rough, nanofeatured structure, to coalesce as scattered nanoparticles on the Ti-rich end.

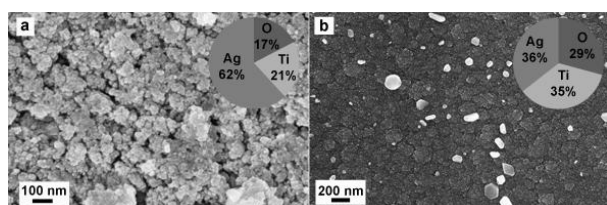


Fig. 1. SEM images of (a) Ag-rich and (b) Ti-rich ends of the coating. Composition in wt%.

Results of the bacterial assay are shown in Fig. 2, where a >99% reduction in viable *S. aureus* count was noted after contact with the Ag-rich end, compared to a negative control. The centre and Ti-rich end of the sample presented 60% and 25% reductions in CFUs, respectively.

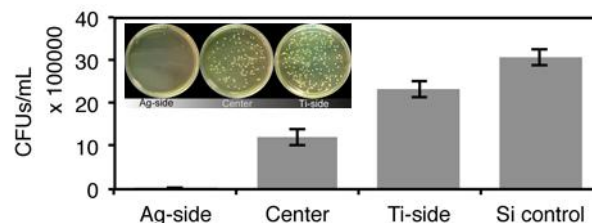


Fig. 2. CFU counts after 2h contact with three distinct parts of the sample, compared to a negative control.

The difference in Ag⁺ release from the two extremes of the sample is shown in Fig. 3, which explains the observed variety in antibacterial properties. This change in release properties is in turn explained by the structural variety of the Ag contribution along the gradient. Higher surface energy and surface area, along with smaller crystallite size and a larger degree of oxidized Ag served to increase the dissolution rate on the Ag-rich end.

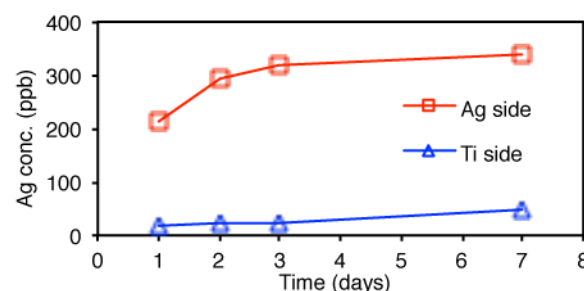


Fig. 3. Cumulative Ag⁺ release profiles (in PBS) from Ag-rich and Ti-rich ends of the combinatorial sample.

CONCLUSION

By applying a combinatorial approach, a continuous compositional and structural gradient between Ag and Ti was synthesized. The findings suggest that aspects of structure, rather than composition, dictates the release of Ag⁺, which could be utilized to better tailor implant coatings with antibacterial properties.

REFERENCES

1. Campoccia D. *et al.*, Biomater. 34:8018–29, 2013
2. Zhao L. *et al.*, J Biomed Mater Res 91B:470–80, 2009

ACKNOWLEDGMENTS

This research was funded by the Swedish Foundation for Strategic Research (SSF), through the ProViking program.

Biofilms Bioreactors: An Infection concern in Medical Devices and biomaterials

Steven L Percival^{1,2,3*}, Rebecca Booth³ and Sean Kelly³

¹Institute of Ageing and Chronic Disease, University of Liverpool, Liverpool, UK

²Surface Science Research Centre, University of Liverpool, Liverpool, UK

³Scapa Healthcare, Manchester, UK

*email: Steven.Percival@scapa.com

INTRODUCTION

There is mounting evidence that suggests many wounds are now becoming infected due to the possible recalcitrant nature of complex dynamic biofilms. Consequently we investigated whether biofilms, microorganisms, which attached onto a surface, generally within microcolonies, and encase themselves within a three-dimensional matrix of extracellular material, are able to proliferate in and on wound dressings. If biofilms are able to grow within and on a wound dressing they would, unless locked into the dressing, become a vehicle for seeding bacteria and endotoxins together with their extracellular material i.e enzymes and exotoxins into the wound bed. The dressing would behave like a bioreactor and continually disseminate biofilm phenotypic bacteria into the wound bed increasing the wounds microbial bioburden and heightening its propensity to infection and disease.

EXPERIMENTAL METHODS

Biofilm Development on gauze: A single colony from a purity plate (containing either *Staphylococcus aureus*, *Pseudomonas aeruginosa* or *Candida albicans*) was inoculated into 10 ml of sterile Tryptone Soya Broth (TSB) so that approximately 1×10^7 cfu/ml was achieved. To a sterile container, 9mls of Tryptone Soya Broth/Foetal Bovine Serum (TSB/FBS 50:50) was added. Each container was inoculated with 1ml of the previously prepared 1×10^7 cfu/ml suspension.

Dressings (foam, gauze, alginate, carboxymethylcellulose - $2 \times 2\text{cm}^2$ in size) were cut and aseptically transferred into each container and incubated for 24 hrs at 35°C (± 3) in a shaking incubator set at 100rpm.

Biofilm Confirmation: After 24 and 72 hrs incubation each dressing was removed and washed twice in 10 mls of 0.85% saline to remove planktonic bacteria. Each dressing was stained with 50 μl LIVE/DEAD BacLight (Life technologies) and analysed under scanning confocal laser microscopy to determine evidence of biofilms.

Total Viable Counts (TVC): After 24 hrs incubation each dressing was removed and washed in 10 mls of 0.85% saline twice. Each dressing was then placed into 10mls 0.85% Saline in a sterile container and left to

stand for up to 24hours. After 2, 4, 6 and 24 hrs samples of the resulting suspension were removed and diluted in maximum recovery diluent (MRD). Plate counts were performed on tryptone soya agar (TSA) (*S. aureus* and *P. aeruginosa*) or sabouraud dextrose agar (SDA) (*C. albicans*). Plates were incubated at 35°C (± 3) (*S. aureus* and *P. aeruginosa*) and $20-25^\circ\text{C}$ (*C. albicans*) for at least 24hrs. This was repeated in triplicate.

Plate Transfer Test: After 24 hrs incubation each dressing was removed and washed in 10 mls of 0.85% saline twice. Each dressing was then placed on to the surface of a TSA (*S. aureus* and *P. aeruginosa*) or SDA (*C. albicans*) plate and left in place for 2 mins. Each dressing was transferred to a fresh TSA/SDA plate and left for a further 2 mins. This was repeated 3 more times. Plates were incubated at 35°C ($\pm 3^\circ\text{C}$) (*S. aureus* and *P. aeruginosa*) and $20-25^\circ\text{C}$ (*C. albicans*) for at least 24hrs. This was repeated in triplicate.

RESULT

After 24 hours biofilms were evident on all the dressings. The biofilms contained the characteristic microcolony formation and also showed evidence of extracellular polymeric substance. The TVC showed that the level of microorganisms released from many of the dressings remained at a steady, but high level throughout the test period. This was confirmed by the growth present on the transfer plates.

CONCLUSION

In conclusion microorganisms from acute and chronic wounds will migrate and adhere to wound dressings. However, unlike dressings, which are known to lock in microorganisms and their intracellular components, many wound dressings are not able to do this. Consequently gauze, as an example, may act by disseminating sloughed biofilm, released from the biofilm within the gauze, back into the wound bed, together with their extracellular components, e.g. toxins and enzymes, and ultimately delay wound healing or initiate infection within that wound.

Formation of Multicellular Spheroids on Arrayed Microwells with Microstructure

Masahito Ban*, Yuuya Kogi

Systems Engineering Major, Graduate School, Nippon Institute of Technology, Japan

*ban@nit.ac.jp

INTRODUCTION

The application of biomaterials with the micro and nanostructure to cell scaffolds remains to be unknown, and it has been a significant subject to clarify the effects of the structure on cellular behaviors. Our group reported that a linear concavo-convex structure with a size of several μm was formed on Polydimethylsiloxane (PDMS) substrate by depositing diamond-like carbon (DLC) thin film¹, and mouse myoblast cells (C2C12) had a tendency to adhere to and grow along the linear structure². In this study, arrayed microwells with concavo-convex microstructure were fabricated by combination method of ink-jet and DLC deposition, and in which C2C12 cells were cultured to evaluate the cellular shape and configuration.

EXPERIMENTAL METHODS

Toluene was discharged arrangedly in a honeycomb geometry on polycarbonate (PC) substrates using an ink-jet spotting system. PDMS was transferred using the discharged PC substrates as the mold, and the DLC thin films were deposited on the obtained PDMS substrates using an inductively-coupled plasma (ICP) CVD system. Once again, PDMS was transferred with the mold of the DLC-coated PDMS. The culture tests having C2C12 cells were performed with the cell concentration varied using the PDMS substrates transferred DLC-coated PDMS.

RESULTS AND DISCUSSION

The confocal laser microscope observation results in Fig. 1 revealed that the fabricated PDMS substrate had the arrayed microwells of circular concave shapes (about 100 μm in diameter) with several μm concavo-convex structure formed on the surface.

C2C12 cells cultured using the prepared PDMS substrate as a scaffold showed a tendency to aggregate on the bottoms of the microwells, and formed spheroid-like configuration. Fig. 2 indicates the observation results, (a) F-actins (green) by phalloidin and (b) cell nuclei (blue) by DAPI, by a fluorescence microscope. Numerous cell nuclei aggregated into the spherical

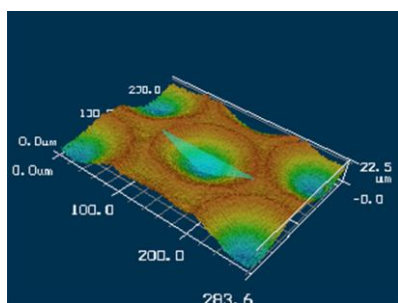


Fig. 1 Confocal laser microscope observation result of the fabricated PDMS substrate

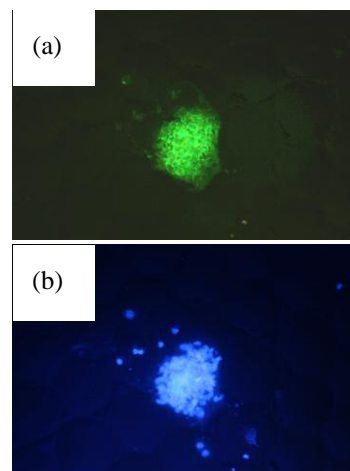


Fig. 2 Fluorescence microscope observation results

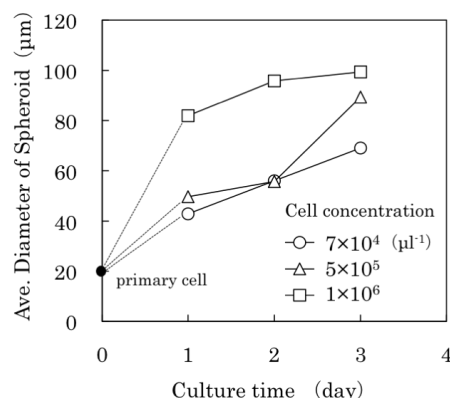


Fig. 3 Variations of spheroid diameters vs. culture time

shape consisting of F-actins, implying that a multicellular spheroid of C2C12 was formed.

The average diameters of the spheroids as functions of the culture time and the cell concentration are shown in Fig. 3. In the case of the cell concentration of 1×10^6 , it was found that the spheroid grew up to about 100 μm corresponding to the diameter of the microwell in three days of culture.

CONCLUSION

The 100 μm -diameter spheroid of C2C12 cells was formed using the arrayed microwells with several μm concavo-convex microstructure.

REFERENCES

1. M. Ban, T. Hagiwara, International Symposium on Microchemistry and Microsystems, Hong Kong, 2010, 136-137.
2. M. Ban, Y. Ueno, Y. Kogi, The 1st International Conference on Surface Engineering, Pusan, 2013, 72.

The role of CD68-positive macrophages in the biocompatibility of biomaterials a peritoneal adhesion prevention model

Christoph Brochhausen¹, Volker H. Schmitt¹, Andreas Mamilos¹, Constanze N. E. Planck², Bernhard Krämer²,
Taufiek K. Rajab³, Helmut Hierlemann⁴, Heinrich Planck⁴, C. James Kirkpatrick¹

¹REPAIR-lab, Institute of Pathology, University Medical Centre Mainz, Germany

²Department of Gynaecology and Obstetrics, University of Tuebingen, Germany

³Brigham and Women's Hospital, Harvard Medical School, Boston, USA

⁴Institute of Textile Technology and Process Engineering, Denkendorf, Germany

brochhausen@pathologie.klinik.uni-mainz.de

INTRODUCTION

Macrophages play a crucial role in the function and regulation of inflammation and biocompatibility. Today it is well known that macrophages represent a dynamic cell type with several phenotypic groups (fig. 1). We use a standardized adhesion prevention animal model to analyse the efficacy, biocompatibility and inflammatory reaction of different barrier materials. To determine if the CD68-positivity, which is required by the ISO norm in biocompatibility testing, represent sufficiently all the macrophage types and there different functions we analysed CD-68 macrophages and compared it with the extent of fibrosis and inflammation after use of 5 different adhesion barriers and an untreated control group.

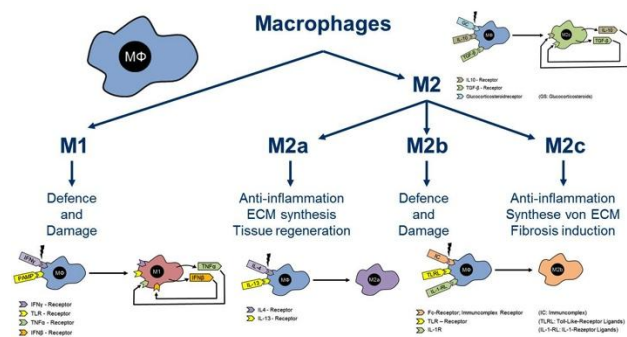


Fig. 1: Schematic depiction of the different macrophages and there characteristics

MATERIALS AND METHODS

Serosal wounding occurred by a standardised method in Wistar rats. The defects were left untreated (control) (n=14) or were treated with different clinically available barrier materials, namely Adept® (n=14) Intercoat® (n=33) Spraygel® (n=8), Seprafilm® (n= 29) and Suprathel® (n=14). After 14 days the animals were sacrificed and the treated tissue processed by standardised techniques for histological evaluation of fibrosis using Ladewig staining, haematoxylin & eosin and chloracetate esterase to estimate inflammation, as well as immunohistology using CD 68 staining to score macrophages. Histology was evaluated by two independent investigators.

RESULTS

No correlation was found between the number of CD68-positive macrophages and the amount of fibrosis or

inflammation. While some groups were associated with moderate infiltration of macrophages and no fibrosis (Intercoat[®] and Suprathel[®]), the Seprafilm[®] group revealed moderate inflammation with likewise moderate amounts of macrophages. On the other hand, a minimal number of macrophages was associated with minimal fibrosis in the control and Adept[®] group. Inflammation and macrophage infiltration were moderate in the Suprathel[®] group. In the Intercoat[®] and Seprafilm[®] treated animals moderate infiltration of macrophages was seen with minimal inflammation. Animals from the control and Adept[®] group revealed minimal inflammation and minimal macrophage infiltration. All in all, there was no correlation between the tissue response and the count of CD 68-positive macrophages (Table 1).

Table 1: Histochemical and immunohistological results

	Macrophages (CD68-positive)	Fibrosis	Inflammation
Control	minimal	minimal	minimal
Adept [®]	minimal	minimal	minimal
Spraygel [®]	mild	none	mild
Intercoat [®]	moderate	none	minimal
Seprafilm [®]	moderate	moderate	minimal
Surpathel [®]	moderate	none	moderate

DISCUSSION

The number of CD 68-positive macrophages does not predict tissue compatibility in adhesion prevention with respect to inflammation and fibrosis. Three different populations of macrophages have been described according to their activities in host defence, wound healing and regulation of immune response², and one subtype seems to participate in fibrosis during wound repair.^{3,4}

CONCLUSION

For biocompatibility studies the immunohistological subclassification of macrophages is required to clarify the role of macrophages during cellular reaction of biomaterials. This should be reflected regarding biocompatibility testing according to the ISO-norm.

REFERENCES

- 2) Mosser D and Justin PE (2008) Nat Rev Immunol 8:958-69
- 3) Hesse M *et al.* (2001) J Immunol 167:6533-6544
- 4) Munitz A *et al.* (2008) PNAS USA 105:7240-45

Swelling gradients of multilayers mediate directional cell migration

Lulu Han, Zhengwei Mao, Jindan Wu, Yang Guo, Tanchen Ren, Changyou Gao*

MOE Key Laboratory of Macromolecular Synthesis and Functionalization, Department of Polymer Science and Engineering, Zhejiang University, Hangzhou 310027, China. cygao@zju.edu.cn

INTRODUCTION

The cell migration plays a crucial role in a variety of physiological and pathological processes¹. The cell's compass is governed by various directional cues, such as soluble chemoattractants (chemotaxis), surface-attached molecules (haptotaxis), and mechanical cues (durotaxis)². So far the surfaces with chemical and physical gradients have been prepared and their influences on the cell migration have attracted increasing attention. Among the various surface engineering methods, the layer-by-layer (LBL) assembly can diversely tailor the substrate properties and is particularly suitable to modify the biomaterials surface³. It is found recently that the chitosan/heparin gradient multilayers pre-adsorbed with fibronectin are able to guide MG-63 osteoblast-like cells' movement⁴.

EXPERIMENTAL METHODS

To generate the gradient multilayers the substrate assembled with the poly(sodium 4-styrenesulfonate) (PSS)/poly(diallyldimethylammonium) chloride (PDADMAC) multilayers was vertically immersed into the 3-5 M NaCl gradient solution for 2 h, and was then washed with water and dried under a smooth stream of N₂. The smooth muscle cells (SMCs) were plated on the salt etched multilayers at low ($5 \times 10^3/\text{cm}^2$) and high ($1.5 \times 10^4/\text{cm}^2$) seeding densities, respectively. Approximately 12 h after the cell seeding, the cell migration was *in situ* recorded using a time-lapse phase-contrast microscope

RESULTS AND DISCUSSION

The gradient nature and physicochemical properties were characterized by X-ray photoelectron spectroscopy and ellipsometry. Compared to the random migration with a lower rate at a smaller cell-seeding density, the vascular smooth muscle cells migrated directionally to the low hydration side at an appropriate cell-seeding density ($1.5 \times 10^4/\text{cm}^2$) under the assistance of cell-cell interactions. The cell migration rates on the gradient surface were significantly larger than those on the corresponding uniform surfaces etched by salt solutions of the same concentrations (Figure 1). At the optimal condition, 95% of the cells moved toward the lower swelling region with a rate of $53 \pm 10 \mu\text{m/h}$, which are the best results achieved so far in this field. Relative cell adherent strength and focal adhesion formation were studied to unveil the intrinsic mechanism of the gradient

multilayers on the cell migration. It was found that both the gradient cues and cell-cell contact have major influences on the directional cell migration⁵.

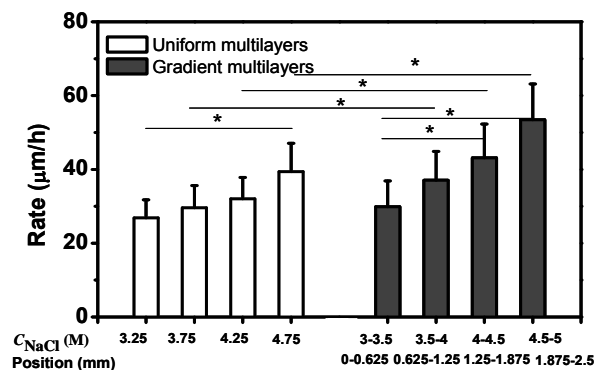


Figure 1. Cell migration rate on the uniform (left group) and gradient (right group) multilayers as a function of gradient position. Data were averaged from ≥ 15 cells. * indicates significant difference at $p < 0.05$.

CONCLUSION

The gradient PSS/PDADMAC PEMs with a gradually increasing swelling ratio were prepared. For the first time it was found that the directional migration of SMCs were guided by both the gradient physical cue and the cell-seeding density. The work establishes an effective method to prepare the gradient biomaterials with unique functions to guide the directional cell migration, providing the possibility to regenerate tissues and organs in a controlled time and spatial scale.

REFERENCES

1. Ridley A.J. et al, *Science* 2003, 302: 1704-1709.
2. Wu C.Y. et al, *Cell* 2012, 148: 973-987.
3. Tang Z.Y. et al, *Adv Mater* 2006, 18: 3203-3224.
4. Kirchhof K. et al, *Lab Chip* 2011, 11: 3326-3335.
5. Han L. et al, *Biomaterials* 2013, 34: 975-984.

ACKNOWLEDGMENTS

This study is financially supported by the National Basic Research Program of China (2011CB606203), and the Natural Science Foundation of China (21374097 and 51120135001).

Improvement of graphene nanoplatelet biocompatibility by surface oxidation

Artur Pinto¹, Carolina Gonçalves², Daniela Sousa², Agostinho Moreira², Inês Gonçalves², Fernão Magalhães¹

¹LEPABE, Faculdade de Engenharia, Universidade do Porto, Porto, Portugal

²INEB – Instituto de Engenharia Biomédica, Universidade do Porto, Porto, Portugal, icastr@ineb.up.pt

³IFIMUP and IN – Institute of Nanoscience and Nanotechnology, Universidade do Porto, Porto, Portugal

INTRODUCTION

In view of the growing interest in using graphene-based materials (GBMs) in medical applications, it is relevant to evaluate their biocompatibility, which depends on intrinsic physical-chemical properties (*e.g.* size, hydrophilicity). GBMs may induce cell death by generation of reactive oxygen species (ROS) or direct damage on cell membrane by a blade like action of GBMs sharp edges.¹ In this work, the biocompatibility of graphene nanoplatelets (GNP) with different dimensions and oxidation is studied. The work is focused in understanding mechanisms behind GBMs *in vitro* toxicity, and identifying how to minimize those effects, in order to allow uses in biomedical applications.

EXPERIMENTAL METHODS

Graphene nanoplatelets grades M-5 (GNP-M) and C-750 (GNP-C), were acquired from XG Sciences (Lansing, USA), with the following characteristics: GNP-M - thickness 6-8 nm, length 5 μm , surface area 120-150 m^2g^{-1} ; GNP-C - thickness <2 nm, length 1-2 μm , surface area 750 m^2g^{-1} . GNP-M was oxidized by modified Hummers method. The designations GNP-M-ox-1:3 and 1:6 represent the ratio GNP-M/KMnO₄ used. Scanning electron microscopy (SEM) was used to observe morphology. X-ray photoelectron spectroscopy (XPS) was used to determine chemical composition. Raman spectroscopy was used to evaluate the degree of oxidation. Thermogravimetric analysis (TGA) was employed for quantifying the mass loss by early degradation of oxidized materials. Live/Dead assay was performed by staining dead HFF-1 cells with propidium iodide (PI), live cells with calcein and the total number of cells with hoechst 33342. Cell death (%) was calculated as the number of cells stained with PI / number of cells stained with hoechst * 100. Transmission electron microscopy (TEM) images were obtained to evaluate GNP/cell interactions. Reactive oxygen species (ROS) were quantified using the indicator CM-H₂DCFH-DA which is converted indirectly by ROS to highly fluorescent DCF, detected in the fluorimeter.

RESULTS AND DISCUSSION

From SEM images (not shown) it was observed that GNP-C has lower diameter (1 μm) than GNP-M (5 μm). XPS and TGA results show that O at.% increases about 20% for both oxidized materials, comparing to GNP-M. Moreover, Raman spectroscopy reveals that oxidation of GNP-M-ox-1:6 is more homogeneous than for GNP-M-ox-1:3. Oxidized platelets present similar size, but less sharp edges (SEM). Hemolysis for all GBMs, was

below 3%, up to concentrations of 500 $\mu\text{g mL}^{-1}$ at 3h. Live/Dead assay shows that cell death is low (<13%) for all materials in concentrations between 1-100 $\mu\text{g mL}^{-1}$. GNP-M (cell death = 13%) is more toxic than GNP-C (6%), for a concentration of 100 $\mu\text{g mL}^{-1}$ at 72h. Also, GNP-M-ox-1:3 (9%) presents similar toxicity to GNP-M and GNP-M-ox-1:6 (1%) toxicity is significantly lower than GNP-M. The fact that GNP-M-ox-1:6 is homogeneously oxidized, presenting less sharp edges than GNP-M, suggests that less physical damages are induced, explaining lower number of dead cells. These results are in agreement with those obtained in resazurin assay (not shown). TEM images (not shown) show that GNP-M interacts with cell membrane and in few cases particles are found inside plasma membrane. GNP-C, which is smaller, is often spread in cytoplasm, interacting with organelles. Also, several vesicles are often found along cytoplasm and in some cases next to GNP-C particles. No damages are observed in cell membranes. GNP-C (50 $\mu\text{g mL}^{-1}$, 1h) increases ROS production by 4.4 fold comparing with negative control PBS 0.01M, while GNP-M only increases 1.5 fold. GNP-M-ox-1:3 present a slightly higher value of 2.1 and GNP-M-ox-1:6 of 1.6. These results indicate that size is the main factor leading to ROS formation, because smaller GNP-C penetrates cell membrane more easily than GNP-M and M-ox-1:3 and 1:6, inducing higher intracellular ROS formation.

CONCLUSION

GNP-C, due to presenting smaller size, enters cells and induces ROS production. This leads to 6% cell death, for a concentration of 100 $\mu\text{g mL}^{-1}$ at 72h. GNP-M, with bigger size and sharp edges, rarely enters cells but induces physical damages on cell membranes. The presence of GNP-M is more toxic (cell death = 13%) to cells. However, complete oxidation of this material (GNP-ox-1:6) prevents toxicity (cell death = 1%). It occurs because platelets present a more wrinkled shape, with smoother edges, which prevents physical damages. In most cases cell death increases with concentration. However, it is low for all materials and concentrations (1-100 $\mu\text{g mL}^{-1}$) until 72h. Hemolysis for all materials, was below 3%, up to concentrations of 500 $\mu\text{g mL}^{-1}$ at 3h.

REFERENCES

1. Pinto A. *et al.*, Coll Surf B. 11:188-202, 2011

ACKNOWLEDGMENTS

Artur Pinto wishes to thank FCT for PhD grant SFRH/BD/86974/2012 and funding through project PTDC/EME-PME/114808/2009.



Ibuprofen-loaded scaffolds for spinal cord injury regeneration – targeting RhoA at the lesion site

Liliana R Pires^{1,2}, Cátia DF Lopes^{1,3}, Daniela N Rocha^{1,2}, Luigi Ambrosio⁴, Mónica M Sousa⁵, Ana Paula Pêgo^{1,2,6}

¹ INEB – Instituto de Engenharia Biomédica, Universidade do Porto (U Porto), Portugal; ² Fac Engenharia, U Porto, Portugal; ³ Fac Medicina, U Porto, Portugal; ⁴ Institute of Composite and Biomedical Materials, National Research Council, Naples, Italy; ⁵ Nerve Regeneration Group, IBMC - Instituto de Biologia Molecular e Celular, Porto, Portugal; ⁶ Instituto de Ciências Biomédicas Abel Salazar, U Porto, Portugal.

lipires@ineb.up.pt

INTRODUCTION

Spinal cord injury (SCI) is characterized by the interruption of axonal pathways and the activation of inhibitory mechanisms that convert the lesion site into a non-permissive substrate for axonal re-growth [1]. It is well accepted that to promote regeneration in such an adverse environment, a multi-target strategy will be needed [2]. Ibuprofen is a non-steroidal anti-inflammatory drug that showed to support axonal growth in inhibitory substrates, being also able to induce an improved regeneration after SCI *in vivo* [3]. Its effect has been associated with the inhibition of RhoA activation [3]. In this study we describe the development of a scaffold based on poly(trimethylene carbonate-co-ε-caprolactone) [P(TMC-CL)] that provides physical guidance cues, via longitudinally aligned electrospun fibres, while serving as a platform for the delivery of ibuprofen.

EXPERIMENTAL METHODS

Bilayer scaffolds were prepared using P(TMC-CL) (11 mol% of TMC, Mn= 8.2x10⁴, Mw/Mn= 1.6). The outer layer was composed by a solvent cast film prepared from a 6% (w/v) P(TMC-CL) solution in CH₂Cl₂. Electrospun fibres were collected onto the solvent cast film fixed to a rotating drum (3000 rpm). A 10% (w/v) P(TMC-CL) solution in CH₂Cl₂ and DMF mixture (3:1) was applied. 5% (w/w of polymer) of ibuprofen was added in solutions to prepare ibuprofen-loaded scaffolds. To assess ibuprofen release (HPLC), scaffolds were incubated at 37°C (120 rpm) in phosphate buffered saline, refreshed at each evaluation time point.

ND7/23 cells were sub-cultured in supplemented DMEM and differentiated for 2 days. RhoA activation was induced by treating starved cells with lysophosphatidic acid (45 μM, 10 minutes). The effect of ibuprofen on RhoA activation was analysed by pre-treating ND7/23 cells with the drug (500 μM) in its soluble form or with extracts from P(TMC-CL) bilayer scaffolds. The activated form of RhoA assessed in a pull down assay.

Bilayer scaffolds (6x5 mm) were tested *in vivo* in a dorsal hemisection rat model of SCI. Three groups were included: (A) lesion, (B) P(TMC-CL) scaffolds and (C) ibuprofen-loaded P(TMC-CL) scaffold. Tissues were collected 5 days after injury and snap frozen for biochemical assays or fixed for histological analysis. Tissues were cryosectioned and immunolabelled for glial fibrillary acidic protein (GFAP).

RESULTS AND DISCUSSION

Bilayer P(TMC-CL) scaffolds were prepared. In the fibrous layer of the scaffolds, > 90% of the fibres were found to be oriented relative to the longitudinal axis. Fibre alignment was not significantly affected by the presence of ibuprofen. Fibre mean diameter was found to be 0.661 and 0.646 μm for non-loaded and ibuprofen-loaded fibres, respectively (Fig.1). Ibuprofen release in sink conditions was found to occur in the first 24hrs of incubation (Fig.1E).

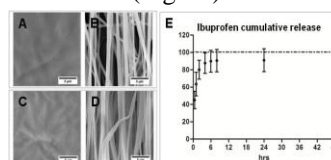


Fig.1. SEM micrographs of bilayer P(TMC-CL) (A,B) non-loaded and (C-D) ibuprofen loaded scaffolds. (E) Cumulative release of ibuprofen.

When ND7/23 cells were pre-treated with extracts obtained from ibuprofen loaded scaffolds, LPA-induced RhoA activation was significantly reduced indicating that the released drug retains its bioactivity as inhibitor of the RhoA pathway in a neuronal-like cell line.

The implantation of the P(TMC-CL) scaffolds did not compromise animal survival. A detailed histological characterization of the tissues is ongoing, but the preliminary analysis of the tissue cryosections suggests that the number of astrocytes at the lesion site is reduced when ibuprofen-loaded scaffolds were implanted.

CONCLUSION

Bilayer ibuprofen-loaded P(TMC-CL) scaffolds were successfully prepared. It was demonstrated that ibuprofen released from the scaffolds can have an active role limiting RhoA activation *in vitro*, in a neuronal-like cell line.

The assessment of the effect of ibuprofen release from the P(TMC-CL) scaffolds on reducing RhoA activation upon a spinal cord lesion is currently underway.

REFERENCES

1. Schwab JM, *et al.*, Prog Neurobiol. 78: 91-116, 2006.
2. McCreedy DA *et al.*, Neurosci Lett. 519: 115-121, 2012.
3. Fu Q *et al.*, J Neurosci. 27: 4154-4164, 2007.

ACKNOWLEDGMENTS

This work was financed by FEDER funds through the Programa Operacional Factores de Competitividade – COMPETE and by Portuguese funds through FCT (PEst-C/SAU/LA0002/2013; PTDC/CTM-NAN/115124/2009; SFRH/BD/46015/2008; SFRH/BD/64079/2009; SFRH/BD/77933/2011).

A role for platelet CD154 in the foreign body reaction to biomaterial

Annabelle Tanga^{1*}, Sébastien Lepreux¹, Julien Villeneuve², Nelly Bordeau³, Christian Combe¹, Alexis Desmoulière³, Shahram Ghanaati⁴, Jean Ripoche¹

^{1*}INSERM U1026, Bordeaux University, Bordeaux, France, annabelle.tanga@gmail.com

²Cell and Developmental Biology Program, Centre for Genomic Regulation, Barcelona, Spain

³Physiology Department, Faculty of Pharmacy, Limoges University, France

⁴Institute of Pathology, University Medical Center of the Johannes Gutenberg University Mainz, Germany

INTRODUCTION

The host response to foreign materials typically progresses under the form of foreign body reaction (FBR) associating macrophages and multinucleated giant cells (MGC)¹ and often results in the failure of implanted devices by several mechanisms, including fibrotic encapsulation. Understanding signals that control the FBR therefore represents an important issue. Platelets are activated on implanted biomaterials with subsequent release of a range of inflammatory mediators, among which CD154. Platelets are the main source of CD154 in the body and mononuclear phagocytes express CD40, the CD154 receptor, which signals macrophages mainly towards a pro-inflammatory phenotype². We asked the question whether CD154 plays a role in the FBR.

EXPERIMENTAL METHODS

To study the progression of the FBR, a model of absorbable suture graft was implemented in mice treated with the anti-platelet agent clopidogrel, which inhibits CD154 release by activated platelets, and in CD154KO mice. In these models, a FBR is triggered in response to the grafted biomaterial.

Male Balb/c CD154KO mice were generated as reported³. Bundles of absorbable polyglactin 910 suture threads were subcutaneously implanted in mouse backs. Macrophages were obtained by *in vitro* differentiation of peripheral blood monocytes; MGC were obtained through IL-4-mediated macrophage fusion. Phagocytosis assays and ELISA were performed using commercial kits. Immunofluorescence, histology/immunohistochemistry, real time RT-PCR, flow cytometry and biochemical measurements were performed according to standard protocols.

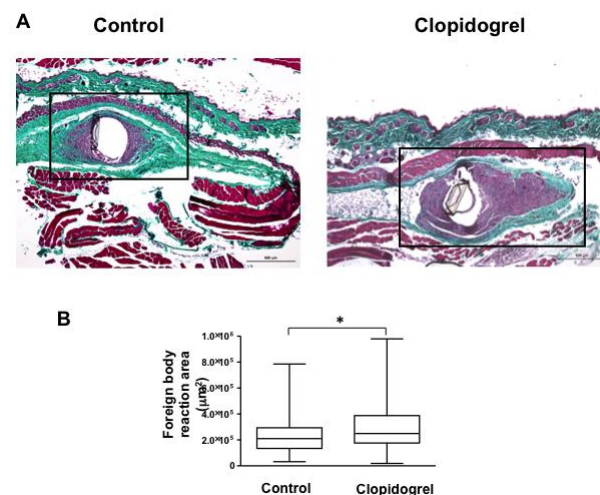
Data are presented as means \pm SD. Statistical comparisons between groups were performed using the Wilcoxon signed-rank test. $P < 0.05$ was taken to imply statistical significance.

RESULTS AND DISCUSSION

Suture bundle clearance occurred at 8 to 10 weeks post implantation. FBR areas were significantly larger at week 10 in WT mice treated with the platelet inhibitor clopidogrel, which inhibits CD154 release by activated platelets (average 30 versus 21 μm^2 , $p < 0.0001$, in treated and untreated mice, respectively) indicating delayed clearance.

We then studied CD154 role. In both WT and CD154KO mice, macrophages and MGCs expressing the F4/80 antigen were similarly organized as a FBR. Delayed clearance was also observed in CD154KO mice (average 31 versus 23 μm^2 , $p = 0.03$, in CD154KO and WT mice, respectively).

These results suggested that CD154 deficiency was associated with FBR impediment.



“Platelet activation inhibition leads to a delayed resolution of the FBR. (A): representative Masson's trichrome-stained tissue sections at week 10; squares highlight the foreign body reaction in subcutaneous tissues. (B): quantification of the granulomatous reaction area in control and clopidogrel-treated mice ((* $p < 0.0001$)).”

We studied potential mechanisms *in vitro*. CD154 may interfere with macrophage recruitment, adhesion to foreign material, activation and fusion. Macrophages and MGC expressed CD40. There were no differences in macrophage or MGC recruitment and CD154 had no effect on macrophage fusion. However, CD154 stimulated the phagocytosis of opsonized red cells by macrophages and drove macrophages polarization into a M1 phenotype.

CONCLUSION

Our studies suggest that platelets may play a role in the FBR to biomaterials through the release of CD154. The inhibition of CD40/CD154 interaction may represent a novel strategy to limit the FBR progression.

REFERENCES

- Anderson, J.M. *et al.*, Semin Immunol, 2008. **20**(2): p. 86-100.
- Suttles, J. *et al.*, Semin Immunol, 2009. **21**(5): p. 257-64.
- Villeneuve, J., *et al.*, Hepatology, 2010. **52**(6): p. 1968-79

ACKNOWLEDGMENTS

“The authors would like to thank the LabEx AMADEus and the Association pour la Recherche en Néphrologie providing financial support to this project”



The mechanical behavior and biocompatibility of polymer blends for Patent Ductus Arteriosus (PDA) occlusion device

Ying Ying Huang^{1*}, Yee Shan Wong¹, and Subbu S. Venkatraman¹

¹School of Materials Science and Engineering, Nanyang Technological University, Singapore
yingyinghuang@ntu.edu.sg

INTRODUCTION

Patent Ductus Arteriosus (PDA) is a cardiovascular defect that occurs in 1 out of every 2000 births¹, and if left untreated, may lead to severe cardiovascular problems. Although the incidence rates associated with current permanent PDA devices are low, the complication is usually serious enough to warrant immediate surgical retrieval^{2,3}. The purpose of this study was to develop a fully degradable occluder for the closure of PDA, that can be deployed percutaneously without open-heart surgery.

EXPERIMENTAL METHODS

For percutaneous deployment, both elasticity and sufficient mechanical strength are required of the device components. As this combination of properties is not achievable with currently-available homo- or copolymers, blends of biodegradable poly (ϵ -caprolactone) (PCL) and poly (L-lactide-co- ϵ -caprolactone) (PLC) with various compositions were studied as the potential material for the PDA occlusion device. Microstructures of this blend were characterized by differential scanning calorimetry (DSC) and tensile tests. Then, suitable blends were selected to fabricate a prototype of PDA occluder and its in vitro performance, in term of device recovery (from its sheathed configuration), biodegradation rate and blood compatibility, was evaluated. Finally, an artificial PDA conduit was created in a pig model, the feasibility and 1 month follow up study were carried out.

All data are presented as mean \pm standard deviation (SD). Statistical analysis was carried out using one way ANOVA and the values are considered significantly different when $p < 0.05$.

RESULTS AND DISCUSSION

DSC results demonstrated the immiscibility between PCL and its copolymer PLC. Furthermore, the mechanical properties, i.e. elastic modulus and strain recovery, of the blends could be largely tailored by changing the continuous phase component, as shown in Figure 1. Based on the mechanical tests, we selected PLC, PCL/PLC30 and PCL/B as the materials for the umbrella, the spoke & anchoring arm, and the stem of PDA occlusion device respectively. The in vitro recovery test based on the assembled PDA occlusion device showed that more than 70% recovery is obtained within 2 - 3 minutes, which is an acceptable closure time period in vivo. In terms of the biodegradation, the earliest mass loss was observed at month 2 and the PDA occlusion device started to disintegrate within 5 - 6 months. Furthermore, the leukocyte and platelet count results showed no adverse effect of the chosen materials in this study, and the inflammatory response and fibrosis capsule formation results showed comparable

performance to the HDPE control. Finally, the in vivo feasibility study demonstrated that the device was able to recover within 2-3 minutes in vivo for immediate closure of the artificial PDA conduit, and 1 month follow-up results confirmed that there was no leakage across the defect and that the device was completely covered by tissue, as shown in Figure 2.

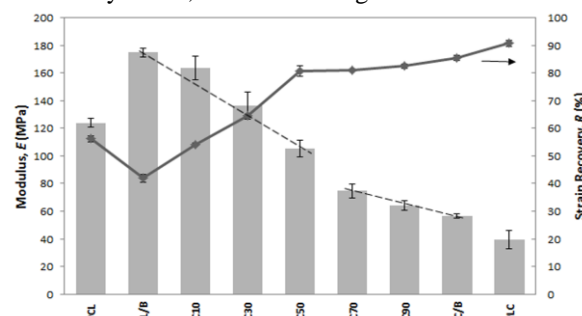


Fig. 1. Dependence of modulus (E) and strain recovery (R) on PLC content.

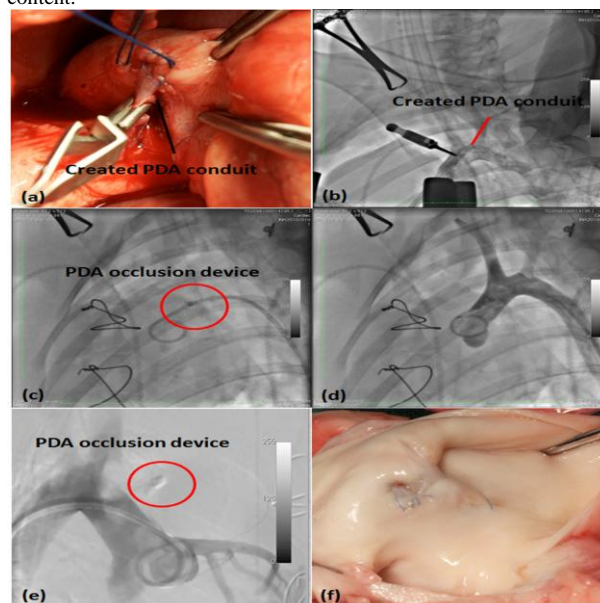


Fig. 2. (a) Photograph of the surgical created PDA conduit, (b) Angiogram of the created PDA conduit (red line), (c) Angiogram of post-implantation PDA occlusion device, (d) Angiogram of post-implantation PDA device, (e) Digital subtraction angiograms of 1 month post-implantation PDA device, and (f) Gross macroscopic examination of PDA device.

CONCLUSION

Thus, a novel prototype for PDA occlusion that is fully degradable has been developed to overcome the limitations of the currently used metal/fabric devices.

REFERENCES

1. Mitchell, S.C. et al., *Circulation* 43:323-332, 1971.
2. Cuaso, C. et al., *Pediatric Cardiology* 33:533-538, 2012.
3. Huang, Y. et al., *Acta Biomater* 10:1088-1101, 2014

Nanofiber-based biomaterials used to direct cellular responses associated with epithelial-mesenchymal transition

Raquel C. Barros^{1*}, Edith Gelens², Menno de Jong², Roel Kuijer¹, Theo G. van Kooten¹

^{1*}Department of Biomedical Engineering, University Medical Center Groningen (UMCG), University of Groningen, Hanzplein 1, 9713 GZ Groningen, The Netherlands, r.s.da.cruz.barros@umcg.nl

² Nano Fiber Matrices B.V. (Nano-FM), Zernikepark 6-8, 9747 AN, Groningen, The Netherlands

INTRODUCTION

Lens epithelial cells (LEC) change their phenotype to mesenchymal cells in a process called Epithelial Mesenchymal Transition (EMT)¹. This process is associated with fibrotic tissue formation, which is the basis of posterior capsule opacification (PCO) after cataract surgery². Cataracts are treated surgically by replacement of the lens nucleus with an intra-ocular lens (IOL). This EMT starts with the inflammatory response due to surgery and continue over a time due to the presence of IOL in the interior of the lens³. Different methods have been approached to avoid PCO, from the optimization of surgery to the use of drugs and new biomaterials for the intra-ocular lens (IOL). None of these approaches totally avoid total PCO. The purpose of this project is to study self-assembled nanofiber systems for their potential to avoid EMT and consequently avoid secondary PCO.

EXPERIMENTAL METHODS

Self-assemble nanofibers with different chemistry, hydrophobicity and morphology in the presence of LEC, human skin fibroblasts (HskF) and human mesenchymal stem cells (hMSC) were studied. Based on 2D and 3D analyses of cellular metabolic activity, real-time PCR and immunohistochemistry we extrapolate, by comparing LEC with HskF and hMSC, which nanofibers should be the best candidate to avoid and/or prevent EMT.

RESULTS AND DISCUSSION

Exceedingly different cell behavior in these different nanofibers was found. Conditions for cell proliferation and for cell repellency were created (Fig.1). Associated with these results nanofibers linked with peptides showed, in addition to different cell behavior, a high decrease in fibrotic markers.

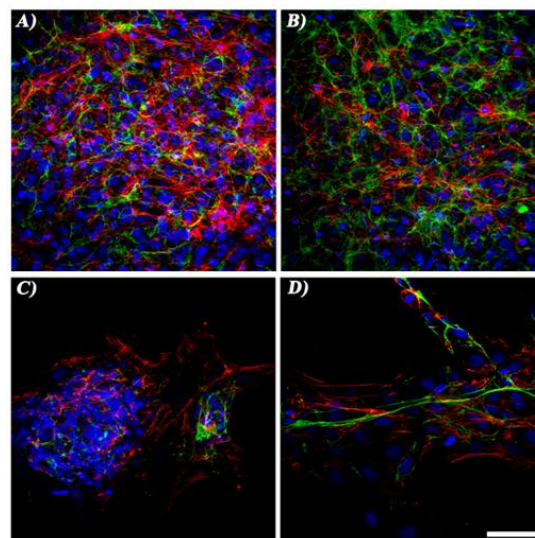


Figure 1: LEC in 2D contact with TCPS (A) and three different nanofibers (B, C and D). Large cellular proliferation on B); repellence of cells to the nanofiber with cell death (not showed) on C) and very low proliferation on D). Blue-DAPI; Red-Phalloidin (TRITC); Green- Fibronectin (FITC) Scale bar=75µm

CONCLUSION

In this study we found biologically active nanofibers to be able to reduce EMT markers. It shows a great potential of the use of these nanofibers in future clinical application.

REFERENCES

1. Kalluri R. *et al.*, The Journal of Clinical Investigation; 119:1420-8, 2009
2. Wormstone I.M. *et al.*, Experimental Eye Research; 88: 257-269, 2009
3. Heatley C.J. *et al.*, J. of Cataract and Refractive Surgery; 31:718-24, 2005

ACKNOWLEDGMENTS

The authors would like to thank the European Fund for Regional Development, and the Samenwerkingsverband Noord-Nederland for providing financial support to this project.

Incorporation of RANKL Promotes Osteoclast Formation and Osteoclast Activity on β -TCP Ceramics

J. Choy^{1,2}, C.E. Albers², K.A. Siebenrock², S. Dolder¹, W. Hofstetter¹, F.M. Klenke^{1,2}

¹Department of Clinical Research, University of Bern, Switzerland

²Department of Orthopaedic Surgery, Bern University Hospital, Switzerland, john.choy@dkf.unibe.ch

INTRODUCTION

β -tricalcium phosphate (β -TCP) ceramics are approved for the repair of osseous defects¹. In large defects, however, the substitution of the material by authentic bone is inadequate to provide sufficient long-term mechanical stability². We aimed to develop composites of β -TCP ceramics and receptor activator of nuclear factor κ -B ligand (RANKL) to enhance the formation of osteoclasts³ and promote cell mediated turnover of the β -TCP ceramics.

EXPERIMENTAL METHODS

RANKL (62.5 μ g in 2.5 ml coating solution) was immobilized on porous β -TCP ceramic cylinders (h: 2 mm, d: 14 mm, pore size 150-200 μ m, porosity 75 ± 5 %) by (i) superficial adsorption for passive short-term release and (ii) co-precipitation with calcium phosphate (CaP), resulting in incorporation of the protein into a crystalline layer of CaP and in a cell-mediated long-term release⁴. Immobilization of bovine serum albumin (BSA, 12.5 μ g in 2.5 ml) served as negative control.

Murine osteoclast precursors were seeded onto the ceramics in medium containing colony-stimulating factor 1 (CSF-1) at 30 ng/ml. Osteoprotegerin (OPG) was added in one group as RANKL inhibitor. After 15 days, osteoclasts were visualized by staining for tartrate-resistant acid phosphatase (TRAP) and TRAP activity was quantified in cell lysates. Levels of transcripts encoding the osteoclast products calcitonin receptor, cathepsin K and NHA2 were quantified by real-time PCR. The activity of newly formed osteoclasts was evaluated by means of a CaP resorption assay: murine osteoclasts were seeded onto a thin crystalline CaP layer with RANKL incorporated. After 48 hours, the resorbed area of the CaP was visualized by von Kossa staining and quantified using ImageJ 1.46r for Windows.

Data are presented as the mean \pm SD from one out of three individual experiments (n = 6). Data were analyzed by one-way ANOVA and Sidak post-hoc test using SPSS[®] V19.0 for Mac.

RESULTS AND DISCUSSION

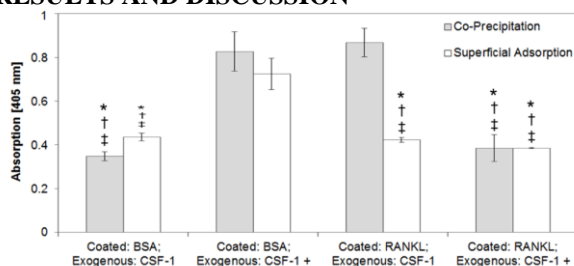


Figure 1. TRAP activity in cultures of osteoclast precursors seeded onto β -TCP ceramics after a culture period of 15 days. * $p < 0.001$ vs. co-precipitated RANKL and exogenous CSF-1; † $p < 0.001$ vs. coated BSA (co-precipitated) and exogenous CSF-1 + RANKL; ‡ $p < 0.001$ vs. coated BSA (superficially adsorbed) and exogenous CSF-1 + RANKL.

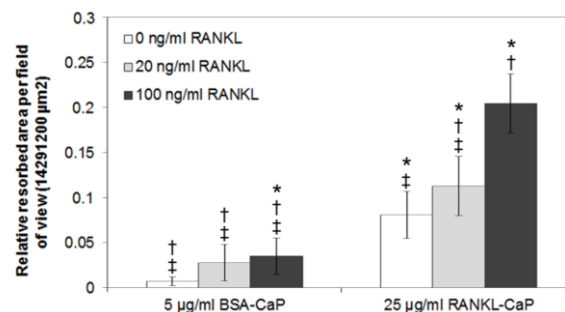


Figure 2. Resorptive activity of osteoclasts grown on crystalline CaP. 5 μ g/ml BSA or 25 μ g/ml RANKL respectively were incorporated into the crystalline CaP layer by protein co-precipitation (coating volume 0.5 ml). Additional treatment with 20 ng/ml and 100 ng/ml RANKL was performed in all groups. * $p < 0.05$ vs. 5 μ g/ml BSA-CaP, 0 ng/ml RANKL; † $p < 0.01$ vs. 25 μ g/ml RANKL-CaP, 0 ng/ml RANKL; ‡ $p < 0.001$ vs. 25 μ g/ml RANKL-CaP, 100 ng/ml RANKL.

Incorporation of RANKL (long-term release) induced the formation of TRAP⁺ (Fig.1) osteoclasts expressing the osteoclast markers calcitonin receptor, cathepsin K, and NHA2. Co-precipitated RANKL was effective in supporting the development of active, resorbing osteoclasts and promoted their resorptive activity. Additional exogenous RANKL enhanced osteoclast activity dose-dependently (Fig. 2). Adsorption of RANKL (short-term release) did not induce osteoclast formation showing that a long-term release system of RANKL is required to support osteoclast formation.

CONCLUSION

The technique by which RANKL is immobilized on the CaP ceramics plays a key role in the support of osteoclast development and activation. With the co-precipitation technique, the differentiation of osteoclasts is initiated due to a residual passive release of incorporated RANKL. Once formed, osteoclasts mediate the release of RANKL, thereby perpetuating their differentiation and activation, which results in a stimulation of cell-mediated CaP resorption.

REFERENCES

- Wiltfang J. *et al.*, J. Biomed. Mater. Res. 63:115-21, 2002
- Liu G. *et al.*, J. Mater. Sci. Mater. Med. 19:2367-76, 2008
- Kong Y.Y. *et al.*, Nature 402:304-9, 1999
- Wernike E. *et al.*, J. Biomed. Mater. Res. A. 92:463-74, 2010

ACKNOWLEDGMENTS

The study was supported by the Swiss National Science Foundation (FMK) and the ITI Foundation, Basel, Switzerland (FMK). RANKL and OPG were provided by Amgen Inc. (Thousand Oaks, CA, USA). β -TCP ceramics were provided by the Robert Mathys Foundation (RMS, Bettlach, Switzerland).



Calcium Phosphate Graft Substitute: When the Impact of Innovation is in the Form Rather Than Content

Francisco Braga¹, Antonio Carlos da Silva², Sérgio Allegrini³, Cyro Ottoni⁴

¹CCTM/IPEN, CNEN, Brasil

²CONSULMAT Prod. Técnicos Ind. e Com. Ltda., Brasil

³Coord. Pos-Grad./Universidade Ibirapuera, Brasil

⁴FMVZ/Universidade de São Paulo, Brasil

fjcbra@ipen.br

keywords: Synthesis, Biocompatibility, Interfaces

INTRODUCTION

The amorphous calcium phosphate is pointed in the literature as a precursor stage of the hydroxyapatite in bone tissue formation¹. Similar to a cotton swab, a set of micrometer fibers of amorphous calcium phosphate graft is obtained by Hager-Rosengarth process². The advantage of the shape as fiber makes possible the graft fits any configuration of defect, combining hemostatic function to its main characteristic, that is, be biocompatible, osseointegrated, resorbable and assisting in bone remodeling. The fibers presented high-purity composition, non-cytotoxicity, resorbable in months and osteo-conductive as any other graft of amorphous calcium phosphate³⁻⁵. It's rare to find scientific literature regarding ACP fibers.

EXPERIMENTAL METHODS

The starting material is obtained by hydrothermal reaction of CaO and P₂O₅ in a Ca/P > 1. The material is dried and ground and then heated to 1350 Celsius when flows into the rotational base of the Hager-Rosengarth machine forming the fibers with diameters ranging from 5 µm to 50 µm that can be seen in Figure1.

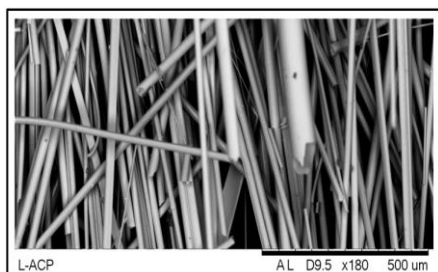


Figure1. ACP fibers.

RESULTS AND DISCUSSION

The non-crystalline condition of the obtained fibers is confirmed by X-ray diffraction as shown in Figure 2.

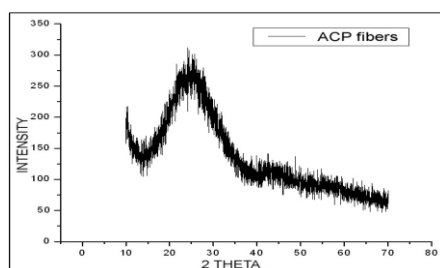


Figure 2. Fiber X-ray diffraction spectrum.

The ACP fibers show biocompatibility by means of the cellular viability curve above IC₅₀% line and are considered non-cytotoxic (Figure 3).

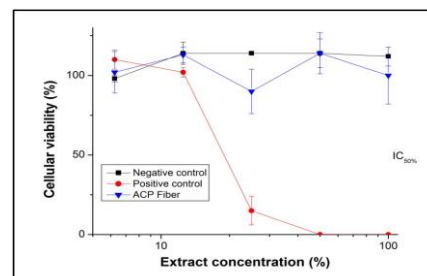


Figure 3. Cytotoxicity test of ACP fibers.

Two tests "in vivo" were performed: (a) in rat alveolus to check newly formed collagenous matrix, and (b) in human alveolus to prove the bone-conduction. Figures 4 and 5 show the images of these proofs respectively.

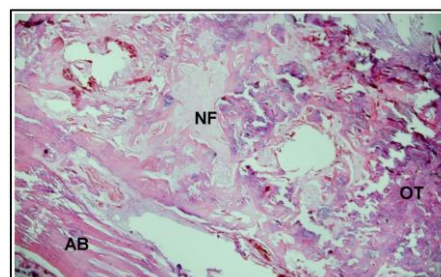


Figure 4. Alveolus bone (AB); newly formed bone (NF); osteoid tissue (OT).

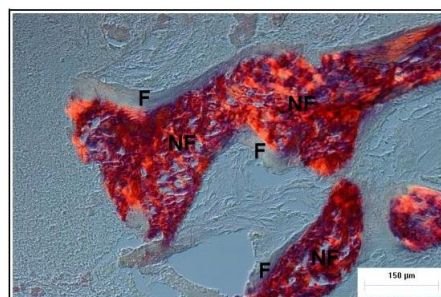


Figure 5. Newly formed bone (NF); fiber (F).

CONCLUSION

1. ACP fibers as a graft, result in good vascular infiltration, bone formation and consistent activities of deposit and remodeling. (Fig. 4).
2. Remaining fibers flanking the newly formed tissue, guide the deposition of bone matrix layers (Fig. 5).

REFERENCES

1. Weiner S., Bone. 39:431-433, 2006
2. Rosengarth F. *et al.*, U.S. Patent 2,234,087, 1941
3. Posner A. *et al.*, Acc. Chem. Res., 8: 273-281, 1975
4. LeGeros R., Clin Mater.14:65-88, 1993
5. Zhao J. *et al.*, Chem. Central J. 5:40, 2011.



EPA-Coated Implants Promote Osteoconduction in White New Zealand Rabbits

Ammar Mustafa^{1,2,3}, Christie Lung, Jukka Matinlinna³

¹ISF Consultancy Hospital (Lekhwiya)/Doha, Qatar

²Dental Materials Science/Faculty of dentistry, IIU-Malaysia

³Dental Materials Science/Faculty of dentistry, Hong University, China, drammar71@gmail.com

INTRODUCTION

The use of dental implant fixture coating based on an organic acid, such as eicosapentaenoic acid (EPA) with an ability of osteoconduction could be a promising treatment for some challenging cases of patients with a history of radiotherapy or patients with diabetes, osteoporosis, and other patients with poor wound healing. Biocompatibility and adequate biomechanical properties are the main requirements in determining the clinical success of any type of dental implant¹.

Eicosapentaenoic acid (EPA) is an omega-3 highly polyunsaturated fatty acid (n-3-PUFA) has been detected to provides advantageous effects on bone remodelling². Ultimately, n-3-PUFA, including EPA, has been verified to positively influence bone health and skeletal biology^{3,4}. Hypothesis was set that EPA-coated dental implants might 1) increase the osteoconduction process, verified by a significant difference between the test and control side of the same implant by testing the axial pull-out test of the implants. 2) increase the rate of new bone formation on the implant surface verified by Cone Beam Computed Tomography (CBCT) and X-ray findings.

EXPERIMENTAL METHODS

The current animal study was approved by the ethical committee of the University according to the regulations of (IACUC).

Twenty four planar titanium plates (5mmX5mmX1mm) were surgically fixed half way into the mandibular bone of twelve white New Zealand rabbits. The rabbits were randomly assigned into three study groups (n=4). The planar implants were coated with EPA on one side and were highly polished on the other side.

CBCT was used to inspect the bone-implant interface assessing the density and the new bone formation on the exposed part of the implant. The specimens were analysed by radiographs to the implants and the neighbouring bone structure to analyse osteoconductive bone formation at the coated side and to compare it with the bone at the control side. Axial pull-out tests were performed to the specimens to test osseointegration (Figure1).

Non-parametric Kruskal-Wallis test and multiple time series comparisons Friedman's test were employed. Both analyses were set at significance level of $p < 0.05$ to compare differences in the amount of implant covered by new bone formation between the coated and the not coated implant surfaces in different time intervals. Osseointegration was analysed by comparing the amount of force, as an action of axial pull-out test, after periods of 4, 8, and 12 weeks respectively.

RESULTS AND DISCUSSION

By using CBCT and radiographs, osteoconductive bone formation was estimated at the coated test side of Ti

compared to the polished non-coated side four weeks postoperatively (Figures 2-4). Statistical results showed significant difference after 8 weeks ($p=0.05$) on the EPA-coated side compared to the non-coated side. Also, statistical analyses revealed a significant difference ($p = 0.01$) between the amount of pull-out force after 8 and 12 weeks, compared to 4 weeks.

In the current experiments, the set up was designed to investigate the outcome of coating dental implants with omega-3 fatty acid on osteoconduction after fixation in the mandibles of rabbits. It has been found that osteoconduction was significantly obvious after 4 weeks of the surgery. Therefore EPA affects osteoconduction and functions as a growth factor in vivo. EPA coated titanium implants in rabbits were found to enhance osteoconduction at the bone-implant interface. This finding might be considered to point at an increased osseointegration capacity of EPA coated implants.

CONCLUSION

As titanium implant fixture coating, EPA coating seems to enhance the anchorage between bone and external fixation of the Ti prosthesis. EPA-based implant coating stimulates osteoconduction processes in rabbits. This coating might increase bone healing processes after implant surgery.

REFERENCES

1. Mallineni SK. *et al.*, J Investigat Clin Dent. 4: 9-19, 2013
2. Petzold C. *et al.*, J Mater Chem 18:5502-5510, 2008
3. Watkins BA. *et al.*, Exp Biol Med 226: 485-97, 2001
4. Murphy RA. *et al.*, Brit J Cancer 105:1496-73,2011

ACKNOWLEDGMENTS

"The authors would like to thank the Research Management Centre IIU-Malaysia (EDW B 12-370-0848) for providing financial support to this project".



Figure 1

Figure 2

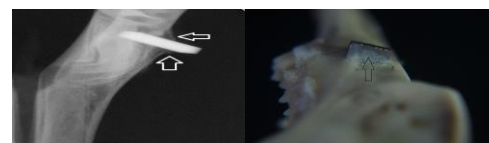


Figure 1

Figure 4

Tailored Ca^{2+} release in hybrid fibrous scaffolds for efficient osteo- and angiogenesis

Oscar Castaño^{1,2,3}, Nadège Sachot^{1,2}, Elena Xuriguera⁴, Elisabeth Engel^{1,2,3}, Josep A. Planell^{1,2,3}, Jeong-Hui Park^{5,6}, Guang-Zhen Jin^{5,6}, Tae-Hyun Kim^{5,6}, Joong-Hyun Kim^{5,6} and Hae-Won Kim^{5,6}.

¹ Biomaterials for Regenerative Therapies. Institute for Bioengineering of Catalonia (IBEC), Barcelona, Spain. ²CIBER-BBN, Zaragoza, Spain ³Dpt. Materials Science and Metallurgical Engineering, Universitat Politècnica de Catalunya, Barcelona, Spain ⁴Dpt. Materials Science and Metallurgical Engineering, Universitat de Barcelona, Barcelona, Spain ⁵Institute of Tissue Regeneration Engineering, Cheonan, South Korea ⁶Dpt. Nanobiomedical Science & BK21 Plus NBM Global Research Center for Regenerative Medicine, Cheonan, South Korea. ocastano@ibecbarcelona.eu

INTRODUCTION

In bone regeneration, Si-based calcium phosphate glasses (Bioglasses[®]) have been widely used since the 70s¹. However, they dissolve slowly because of their high amount of Si ($\text{SiO}_2 > 45\%$). Recently, our group has found that calcium ions released by the degradation of glasses in which the job of silicon is done by just 5% of TiO_2 are effective angiogenic promoters, because of their stimulation of a cell-membrane calcium sensing receptor (CaSR)². Based on this, other focused tests on angiogenesis have found that Bioglasses[®] also have the potential to be angiogenic promoters even with high contents of silicon (80%); however, their slow degradation is still a problem, as the levels of silicon cannot be decreased any lower than 45%³. In this work, we propose a new generation of hybrid organically modified glasses (ormoglasses) that permit a reduction of the Si content, therefore speeding up the degradation process. Using electrospinning as an accurate way of mimicking the extracellular matrix (ECM), we successfully produced hybrid fibrous mats with three different contents of Si (40% PCLS40, 52% PCLS52 and 70% PCLS70) – and thus three different calcium ion release rates – using an ormoglass-polycaprolactone blend.

EXPERIMENTAL METHODS

Sol-gel method was selected to develop the organometallic network by means of alkoxide precursors in an inert atmosphere through a partial hydrolysis and condensation process; ϵ -polycaprolactone (PCL) was the used biodegradable polymer. The aim was to join both domains at a nanometric level to obtain a tuned ion-agent release order to act as cell homing and enhance osteogenesis. Special attention was paid in the bulk, interface and degradation properties, evaluated by FE-SEM, EDS, DSC, TGA, tensile-strain assays, pH and Ca^{2+} release evaluation, contact angle measurements, AFM, ζ -potential. We also performed cell proliferation assays, ALP, western blotting analysis and PCR analysis. We performed *in vivo* subcutaneous tests to evaluate the osteogenic potential.

RESULTS AND DISCUSSION

The production of different blends of ORMOLASS/PCL with different Si contents was successful. Tensile-strain assays showed that the more Si content, the higher the Young's modulus. TGA analysis revealed that the inorganic content increase with the decrease of silicon. DSC analysis showed PCL-S40 fibers had the most crystalline structure (27.6%) compared with the rest of the blends. AFM showed that the lower the silicon content, the higher the stiffness, in contrast with tensile-strain assays. ζ -potential plots showed a significant increase of the surface charge for PCL-S40 com-

pared with the rest of the fibrous scaffolds. It was also the sample with a higher release rate of calcium and the most constant sustained decrease at higher time points. PCL-S40 showed the best cell-material interaction and the most enhanced MC3T3-E1 cells differentiation over the rest. No inflammatory signs and material related complications were observed. Surprisingly, numerous vessels were observed over the whole area of the mats. PCL-S40 showed the highest number of new blood vessels. Biological results not only confirm the osteogenic potential of the composition with less Si content, but also suggest a better angiogenic effect. The higher and sustained release of Ca^{2+} to the media plays a key role in the promotion of blood vessel formation.

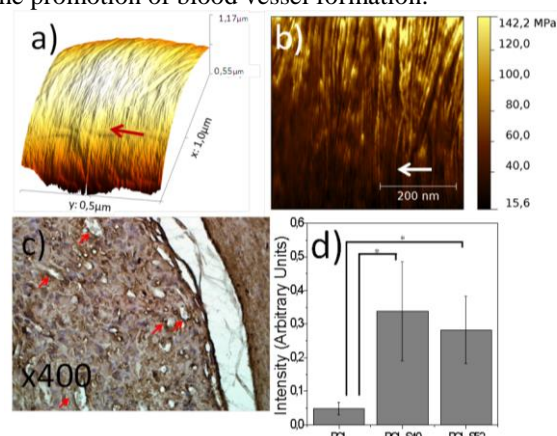


Figure 1. AFM plots showing the topography (a) and DMT modulus map (b). Staining optic microscopy images for vWF of PCL-S40 (c) and its quantification (d) at x200.

CONCLUSION

Material and biological characterization suggested that compositions of organic/inorganic hybrid materials with a Si content equivalent to 40%, which were also those that released more calcium, were osteogenic, with a greater ability to form blood vessels. These results suggest that Si-based ormoglasses can be considered an efficient tool for Ca^{2+} release modulation, which could play a key role in the osteo- and angiogenic promoting process.

REFERENCES

1. Hench, L. *et al.*, J. Mater. Sci.: Mater. Med., 17 (11): 967-978, 2006.
2. Aguirre, A. *et al.*, Eur. Cells Mater. 24:90-106 (2012)
3. Eldesogi, K. *et al.*, PLoS ONE 2013, 8,11: e79058.

ACKNOWLEDGMENTS

We thank the European Commission project PI11/03030, NANGIOFRAC, the MINECO (Project MAT2011-29778-C02-01) and grant from Priority Research Centers Program (2009-0093829), National research Foundation of Korea.

The Wear and Biological Activity of Antioxidant UHMWPEs in Total Hip Replacements

Nic Gowland¹, Sophie Williams¹, John Fisher¹, Joanne L Tipper¹

¹Institute of Medical & Biological Engineering, University of Leeds, Leeds, LS2 9JT
bs07n3g@leeds.ac.uk

INTRODUCTION

Oxidative degradation of highly irradiated UHMWPE has been shown to reduce the lifespan of UHMWPE in total hip replacements [1]. Antioxidant UHMWPE was developed to reduce oxidation in low-wearing highly irradiated UHMWPE, with vitamin E enhanced UHMWPE gaining FDA approval in 2007 and a hindered phenol antioxidant (AOX) in development.

This study investigated the wear of antioxidant UHMWPE (vitamin E, AOX) compared to virgin and highly crosslinked UHMWPE and also the biological response to antioxidant materials. Sterile wear particles were incubated with primary macrophages to determine the volume of particles required to stimulate a cytokine response. The cytokine response to vitamin E and non-vitamin E highly crosslinked UHMWPE is to be investigated.

Finally, the study investigated the effect of vitamin E enhanced UHMWPE on the production of reactive oxygen species (ROS), thought to be an important aspect of the role UHMWPE plays in stimulating a cytokine response from cells, and therefore vital to osteolysis.

EXPERIMENTAL METHODS

UHMWPE materials – 1050; 1050 virgin, Marathon (5MRad), HXL (10MRad), Vit E, Vit E 5MRad, Vit E 10MRad: 1020; 1020 virgin, AOX, AOX 8.5MRad. Wear testing was conducted using a 6 station pin-on-plate wear rig, with 10mm pins articulating against a smooth CoCr plates, using kinematics representative of the hip joint [2]. Wear was determined gravimetrically and converted into a wear factor.

For particle:cell culture, sterile particles were suspended in agarose gel and PBMCs isolated from human blood were seeded on to the gel. Cells/particles were incubated for 24 hours at 37°C, 5% CO₂. Cell viability was determined using ATP Lite assay; ELISA was performed to determine TNF-α production.

For ROS study, PBMCs were incubated directly with sterile particles for 48 hours, after which Image-IT Live staining was performed for ROS and Hoechst was used to stain the nucleus.

RESULTS AND DISCUSSION

Wear factors for UHMWPE materials are shown in fig 1. Vitamin E or AOX antioxidants had no significant effect on the wear factor. Increasing irradiation dose alone reduced the wear factor, with highly irradiated materials showing the lowest wear factors for each category.

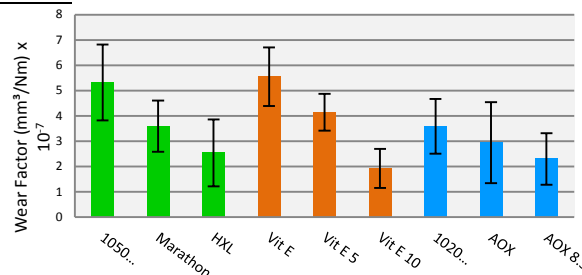


Figure 1 – Wear factor of different UHMWPE materials. Green shows non-antioxidant UHMWPE; orange shows vitamin E UHMWPE; blue shows GUR 1020 UHMWPE, including AOX enhanced. Error bars show 95% confidence level.

The cell: particle studies showed that PBMCs incubated with HXL particles at 100µm³ did not significantly stimulate TNF-α release in 24 hours. This assay was therefore optimised and it was found that incubation only at 600µm³ per cell stimulated a significant TNF-α release from PBMCs (fig 2). Particles containing vitamin E will therefore be seeded at 600 µm³ per cell.

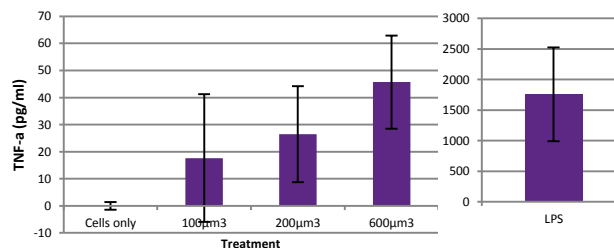


Figure 2 – TNF-α release from PBMCs incubated with 1050 HXL UHMWPE for 24 hours. Error bars show 95% confidence level.

Finally, an investigation into the production of ROS in PBMCs incubated with HXL and Vit E 10 particles was carried out. HXL particles stimulated the production of ROS in the cytoplasm of PBMCs. However, Vit E 10 particles did not stimulate the same intensity of ROS in cells, with results comparable to the cells only control.

CONCLUSION

The addition of an antioxidant to UHMWPE had no adverse effects on the wear factor of the material, where increased irradiation dose alone significantly improved the wear resistance of the material. However, the addition of vitamin E to highly crosslinked UHMWPE appears to reduce the production of ROS, suggesting vitamin E is available to cells and has the potential to reduce inflammation and osteolysis.

REFERENCES [1] Bracco & Oral.2011. Clin Orthop Relat Res, 469,8; [2] Galvin *et al.*2006. J Mater Sci Mater Med,17,3; [3] Ingham & Fisher, 2000. J Eng in Med.

ACKNOWLEDGEMENTS: Research funded by EPSRC and DePuy Synthes

Chitosan-hyaluronic acid based porous scaffold for bone regeneration

Jing Jing¹, Jérôme Josse¹, Céline Mongaret¹, Saad Mechiche-Alami¹, Romain Reynaud², Dominique Laurent-Maquin¹, Sophie C. Gangloff¹, Frédéric Velard¹ and Halima Kerdjoudj¹

¹ EA 4691 "Biomatériaux et inflammation en site osseux", Pôle Santé, SFR CAP-Santé, Université de Reims Champagne-Ardenne, France, ² Soliance, Pomacle, France.

jing.jing@univ-reims.fr

INTRODUCTION

Strategies for bone tissue engineering and regeneration rely on bioactive scaffolds to mimic the natural extracellular matrix and act as templates onto which cells attach, multiply, migrate and function.¹ The constituent and structure of bone repairing scaffolds need to be biocompatible, biodegradable during tissue regeneration process, structurally similar to bone, and with some degree of mechanical strength.²

In this work, we investigated a porous three-dimensional (3D) hybrid chitosan (CHI)/hyaluronic acid (HA) scaffold suitable for tissue engineering applications. Cell colonization was studied using Wharton's Jelly stem cells (WJ-SCs) which are considered as primitive stem cell much more proliferative, immunosuppressive, and even therapeutically active than adult stem cells.

EXPERIMENTAL METHODS

CHI (from Sigma, France) was dissolved in 0.1M acetic acid at 0.2 g/L. The solution was neutralized by the addition of β -glycerolphosphate (β -GP) at 4%. HA (from Soliance, France) was added with a concentration of 0.6 g/L. The two solutions were mixed at a ratio of 3:1 (v/v). Genipin solution was incorporated into the mixture to crosslink CHI/HA solution at 37°C for a night. Then, they were freeze-dried to make 3D scaffolds.

The porosity, pore size, water uptake ability, and structural compounds were investigated. Cellular compatibility and proliferation were highlighted through LDH and MTS assay respectively.

RESULTS AND DISCUSSION

Formation of 3D porous scaffold was demonstrated by scanning electron microscopy (SEM) (Figure 1) and confocal microscopy. Adding β -glycerolphosphate to the mixture was absolutely required for exhibiting interconnected pores. The porous interconnected network leads to enable rapid tissue ingrowth and unimpaired diffusion of nutrients, oxygen and wastes. Through the natural derived cross-linking reagents with low toxicity, genipin³, CHI/HA scaffold could keep its stable form even up to 21 days in culture media.

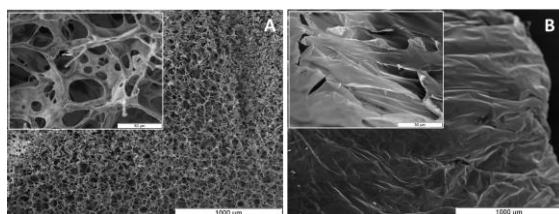


Figure 1: SEM images of CHI/HA scaffolds prepared with (A) and without (B) β -GP.

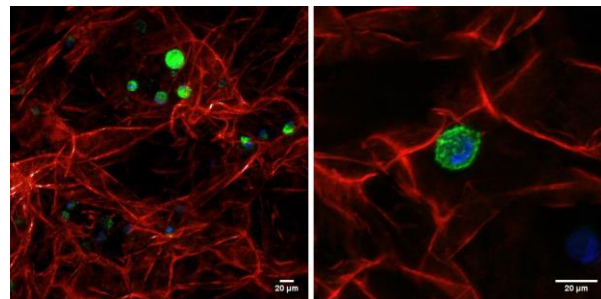


Figure 2: Confocal image of WJ-SCs cultivated in CHI/HA scaffold (red staining). The cytoskeleton was visualized by actin filament staining with phalloidin (green labeling) with blue nucleus counterstaining of WJ-SC. Scale bare = 20 μ m.

LDH assay showed that scaffold has no cytotoxicity effect on WJ-SCs survival. Confocal imaging demonstrated CHI/HA scaffold colonization by WJ-SCs (Figure 2). Opposed to the plastic cell culture, WJ-SCs kept a round morphology when grown on the developed scaffold. A possible reason is that the 3D scaffold provides a geometrical distribution of binding sites to cells rather than planer conventional substrate⁴.

CONCLUSION

In this work a novel cell-colonized scaffold which exhibit highly porous and possess highly interconnected pores was developed. The original and simple thermogelling then freeze-drying approach ensure an easy transfer to the orthobiological industries. Nevertheless, understanding the mechanism and process of cell colonization in these 3D porous scaffolds are necessary for further physiological tissue models application.

REFERENCES

1. Stevens M.M., *Materialstoday*, 11, 18-25, 2008
2. Giannoudis P.V. *et al.*, *Injury* 36, S20-S27, 2005
3. Sung H. *et al.*, *Biomaterials*, 21, 1353-1362, 2000
4. Lawrence B.J. *et al.*, *Cell Adhesion & Migration* 2 :1, 9-16, 2008

ACKNOWLEDGMENTS

The authors thank Dr. Canan OZCAN and Flora LEMAIRE for their technical support. We thank either PICT (URCA) and the Maison Blanche gynaecology service headed by Pr. O. GRAESSLIN for providing umbilical cords.

Superficial Zn-Doping into Biomaterials is Better than Bulk Doping

Yuqin Qiao and Xuanyong Liu*

State Key Laboratory of High Performance Ceramics and Superfine Microstructure, Shanghai Institute of Ceramics, China qiaoyq@mail.sic.ac.cn and xyliu@mail.sic.ac.cn

INTRODUCTION

Rapid development of zinc biology has broadened the applications of Zn-incorporated biomaterials to tissue engineering but also raised concerns about the long-term safety of released Zn^{2+} ions¹⁻². Hence, clinical success hinges on the amount of incorporated zinc and subsequent optimized release that is sufficient to stimulate osseointegration. In this study, zinc is incorporated into the superficial surface of TiO_2 coatings by plasma immersion ion implantation and deposition (PIII&D). The Zn-implanted coatings show significant improvement compared to the “bulk-doped” coatings prepared by plasma electrolyte oxidation in terms of osteogenesis *in vitro*.

EXPERIMENTAL METHODS

Preparation of Zn-incorporated TiO_2 coatings

Plasma electrolytic oxidation (PEO) was conducted in Ca-P containing mixed electrolytes without/with zinc acetate to prepare Zn-free (Z0) and bulk-doped coatings (PEO-Z1 and PEO-Z2)³. In cathodic arc PIII&D, Zn was implanted into the Z0 coating to obtain Z0-PIII-Zn. All these coatings were characterized by SEM, EDS and XPS to determine Zn amount and distribution.

In vitro biological activities

Rat bone mesenchymal stem cells were used in passage 3 and seeded on Ti, Z0 and Zn-incorporated TiO_2 coatings to investigate effects of different zinc incorporation strategies on osteogenic activities: ALP activities and mRNA expression of osteogenic-related genes.

RESULTS AND DISCUSSION

The cross-sectional EDS maps (Ti, Ca and Zn) illustrated that Zn is present throughout the entire PEO-Zn coating but only exists superficially on Z0-PIII-Zn coating (Fig. 1). The Zn release profiles are direct reflections of the zinc contents between coatings with the following order: Z0-PIII-Zn < PEO-Z1 < PEO-Z2. Despite smaller Zn release at all defined time points, molecular and cellular osteogenic activities demonstrate that rBMSCs cultured on the Zn-implanted coatings display enhanced ALP activity and up-regulated osteogenic-related gene expressions (OCN, Col-I, ALP, Runx2, Fig. 2) compared to the bulk-doped Zn coatings (PEO-Z1 and PEO-Z2) and controls. The degree of accelerated osteogenesis appears to be in contrast to the released Zn concentrations and it somewhat conflicts former belief that a larger Zn concentration within the safety limits generally results in better osteogenesis in a given system. Our results show clear differences between these two types of Zn-incorporated coatings.

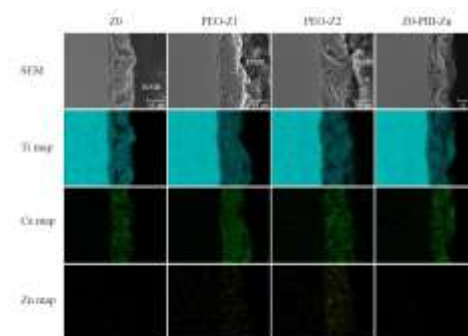


Fig. 1 Cross-sectional EDS mapping throughout the entire coating

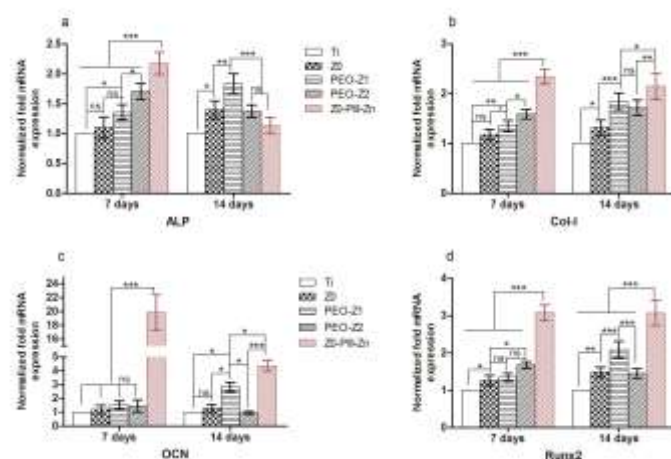


Fig. 2 mRNA expression of osteogenic-related genes

CONCLUSION

Given the great clinical need, an understanding of the zinc regulation for bone formation is of critical importance in the design and fabrication of biomaterials for tissue engineering. In the present study, a systematic investigation is performed on two different modes of Zn introduction, namely, PEO and PIII&D, and detailed *in vitro* osteogenesis studies are conducted. The Zn-implanted coating (Z0-PIII-Zn), which possesses the smallest total zinc concentration, shows the best osteogenic characteristics.

REFERENCES

1. Willis M. S. *et al.*, Am. J. Clin. Pathol. 123:125-131, 2005
2. Storrie H. *et al.*, Biomaterials 26: 5492-5499, 2005
3. H. Hu. *et al.*, Biomaterials 8:904-915, 2012

ACKNOWLEDGMENTS

The authors would like to thank the National Basic Research Program of China (973 Program, 2012CB933600) and National Natural Science Foundation of China (31200721) for providing financial support to this project.



Assessment of the biodegradability of ultrafine PCL fibers reinforced calcium phosphate cement

Yi Zuo^{1*}, Boyuan Yang¹, Fang Yang², Qin Zou¹, Jidong Li¹, Yubao Li¹ and J.A.Jansen²

^{1*}Research Center for nano Biomaterials, and Analytical & Testing Center, Sichuan Univ., China, zoe@scu.edu.cn

²Department of Biomaterials, Radboud University Nijmegen Medical Center, Nijmegen, The Netherlands

INTRODUCTION

Calcium phosphate cements (CPC) have gained clinical acceptance to repair the bone defect for their recognized bioactivity and moldability [1]. However, the inherent brittleness and slow resorption rate of CPC restrict its popular use [2]. In our previous study, electrospun fibers were added into CPC to fabricate a reinforced composite system [3], but the influence of the degradable fibers on CPC matrix degradation and tissue regeneration has not been addressed clearly. Herein, the effects of the incorporated ultrafine fibers on the composite CPC degradation and new bone formation were investigated by planimetric analysis as well as three-dimensional reconstruction method.

EXPERIMENTAL METHODS

Materials: The CPC cement powder (Biomet Merck, Germany) was mixed with 1wt% aqueous solution of Na_2HPO_4 . Ultrafine fibers ($\Phi 1.418 \pm 0.103 \mu\text{m}$) made of poly(ϵ -caprolactone) (PCL) (Mw 80,000, Sigma, USA) were prepared by electrospinning, then mixed with the CPC paste at fiber weight fractions of 0%, 3%, 7% to form the specimens (named UFRPC0, UFRPC3 and UFRPC7) with a dimension of $\Phi 5 \times 5 \text{ mm}$.

In vitro degradation: 5ml phosphate buffer solution (PBS) (pH=7.4) with 200 unit/ml lipoprotein lipase (Lipase-PS) was added in each vial. Electrospun fibers and UFRPC specimens were immersed in the lipase solution to study the enzymatic degradation for 1-7d at 37.8°C . The pH values of the residual solutions were measured at each time point. Then the specimens were fully washed and dried to a constant weight. A series of evaluations, such as mass loss, morphology observation, IR and XRD analyses, were carried out.

In vivo degradation: 36 New Zealand white rabbits were randomly divided into three experimental groups, and supracondyle defects ($\Phi 5 \text{ mm}$) were created in the femurs and filled with the UFRPC specimens. Macroscopic, histological and histomorphometric evaluations were performed at the time points of 4, 8 and 12 weeks post-operation. At 24 week, the remaining rabbits were sacrificed and the samples were harvested for micro-CT analysis.

RESULTS AND DISCUSSION

PCL has been used as a candidate polymer for long-term implantation due to its slow degradation ratio [4]. However, the ultrafine PCL fibrous structure could facilitate a faster degradation than its blocks; more than 50wt% fibers have been degraded in the enzyme solution on day 7. At the same time, the solution pH decreased with time until day 5 and then kept stable at a pH of 6.6. The mass loss data indicated that higher fiber content could accelerate the cement degradation. The SEM images showed that the ultrafine fibers on the cement surface degraded thoroughly after 3 days. The

IR and XRD analyses demonstrated a chemical transformation process that the α -tricalcium phosphate phase vanished by hydrolysis and formation of new hydroxyapatite crystals.

In vivo assessment suggested that the presence and degradation of ultrafine PCL fibers could promote the degradability of CPC matrix and new bone regeneration (Fig. 1). Comparing to pure CPC cement, the loaded ultrafine PCL fibers occupied more than 30vol% of the composite cement, and the degradation of fibers could afford abundant interconnective channels for CPC fast degradation and tissue regeneration. After 4 weeks, new bone has apparently grown into the UFRPC7 matrix. Afterwards, the cement matrix further degraded and the proportion of new bone reached 24% in volume at 24 weeks, higher than the ratio of others [5]. It can be seen from the blue colour of the 24-week longitudinal section (Fig.1b), the new bone tissue has formed an interconnective network structure in UFRPC7 composite cement, but the pure CPC cement maintained its dense structure without bone formation in its matrix.

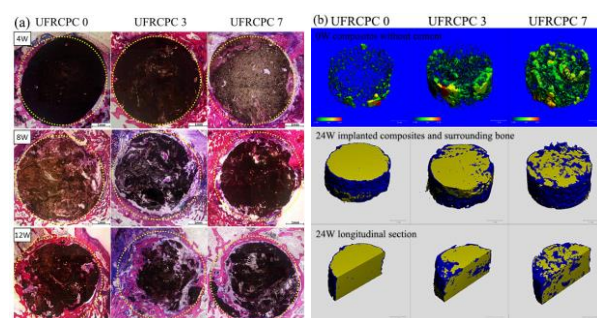


Figure 1 Histological sections (a) and 3D micro-CT reconstruction (b) of the implanted cement samples.

CONCLUSION

Loading of electrospun PCL ultrafine fibers could afford CPC cement faster degradation and more new bone formation. It provides a prospective method to use degradable ultrafine fibers in preparation of bone cements or bone tissue engineering scaffolds.

REFERENCES

1. Krüger R., *et al.*, *Biomaterials*. 33: 5887-5900, 2012
2. Sowmya S., *et al.*, *Prog. Polym. Sci.* 38(10-11): 1748-1772, 2013
3. Zuo Y., *et al.*, *Acta Biomater.* 6: 1238-1247, 2010
4. Okamoto M., *et al.*, *Prog. Polym. Sci.* 38: 1487-1503, 2013
5. Kim J., *et al.*, *J. Biomed. Mater. Res. B.* 100B: 1170-1178, 2012

ACKNOWLEDGMENTS

The authors would like to thank the supports of China NSFC fund (No.31370971) and Chengdu project (No.12DXYB145JH-005).

Biocomposites Containing Collagen, D-Amino Acids and Phytosome Nanoparticles as Drug Carriers and Tissue Engineering Scaffolds

Krishnamoorthy Ganesan^{1,2,*}, Thotappalli Parvathaleswara Sastry¹, Asit Baran Mandal¹ and Mukesh Doble²

¹ Bioproducts Laboratory,

CSIR-Central Leather Research Institute, Adyar, Chennai – 600 020, Tamil Nadu, India

² Bioengineering & Drug Design Laboratory, Department of Biotechnology,

Indian Institute of Technology (IIT) Madras, Chennai-600 036, Tamil Nadu, India

*Email Id: krishnamoorthyganesan@yahoo.com

INTRODUCTION

D-Amino acids (D-AAs) are non-genetically-coded amino acids (AAs) that either occur naturally or are chemically synthesized and becoming very important tools for modern drug discovery, chiral building block and also molecular scaffolds. D-AAs peptides are much more resistant to enzyme-catalyzed breakdown than L-residues. It is of profound interest to establish how the D-AAs exhibit better crosslinking of the collagen scaffolds in order to improve the thermomechanical properties and resistance to matrix metalloproteinase (MMPs) activities¹.

EXPERIMENTAL METHODS

This work was focused to design heterochiral collagen and improve the stability of collagen bioscaffolds by crosslinking them with D-AAAs and incorporation of phytosome nanoparticles (PNs) for their possible use in drug delivery and tissue engineering. In this study, D-AAAs assisted, 1-ethyl-3-(3-dimethylaminopropyl)-carbodiimide (EDC)/N-hydroxyl succinimide (NHS) initiated crosslinking of collagen matrix (Coll-D-AAAs) were prepared and characterized and also incorporated PNs on collagen-D-AAAs scaffolds. The molecular level understanding of interaction of collagen like peptide (CLP) with selected D-AAAs was studied by molecular docking method. The inhibitory effects of selected plant extracts on collagenase activity against the degradation of collagen were studied. The PNs composed of phospholipids (PLs) with phytochemicals with varying molar ratios were prepared by heating under the N₂ atmosphere. The biocomposites Coll-D-Lys-PNs were prepared by thermally triggered Coll-D-Lys with preformed PNs.¹⁻⁵

RESULTS AND DISCUSSION

The results from thermomechanical analysis (TMA), differential scanning calorimetric (DSC) analyses and thermo gravimetric analysis (TGA) of the Coll-D-AAAs matrices indicate a significant increase in the tensile strength, % Elongation (% E), elastic modulus, denaturation temperature and a significantly decreased decomposition rate. Scanning electron microscopic (SEM) and atomic force microscopic (AFM) analyses revealed a well-ordered, properly oriented and aligned structure of the matrix. The improved properties of matrices can be further manipulated into the functional matrix suitable for the designing of scaffolds. The docking study has provided clear evidence for stabilization of collagen. The enzyme inhibition

kinetics has provided convincing evidences that MMPs are inhibited by plant extracts against the collagen degradation. ZP measurement confirmed the particle sizes and charges, and the SEM analysis confirmed the spherical surface morphology of PNs. These PNs loaded in the Coll-D-Lys biocomposites showed significant binding affinity to the cell and prolonged the release of model drugs and DNA from the scaffolds.

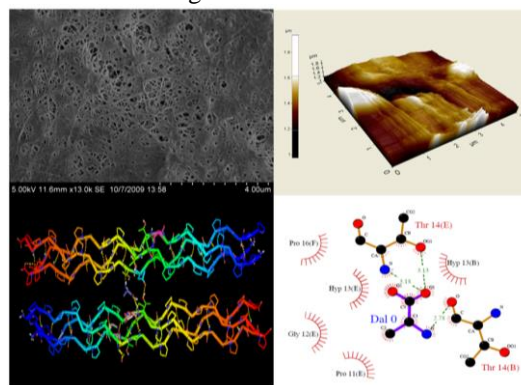


Fig. 1. SEM and AFM analyses and molecular modelling of Coll-D-Lys matrix.

CONCLUSIONS

These biocomposites could possibly be useful in bone and dental implants and in dura matter defects.

REFERENCES

1. Krishnamoorthy G. Biocomposites containing collagen, D-amino acids and Phytosome nanoparticles as drug carriers and tissue engineering scaffolds, PhD Thesis, Anna University Chennai, Tamil Nadu, India
2. Krishnamoorthy G. *et al.*, Biochem Engin J. 75:92-100, 2013
3. Krishnamoorthy G. *et al.*, J Biomed Materi Res Part-A, 101A:1173-1183, 2013
4. Krishnamoorthy G. *et al.*, J Biomater Sci: Polym Ed. 24:344-364, 2013
5. Krishnamoorthy G. *et al.*, Appl Biochem Biotechnol Part A: Enzy Eng Biotechnol. 165:1075-1091, 2011

ACKNOWLEDGMENTS

The first authors Dr. G Krishnamoorthy acknowledge the Council of Scientific & Industrial Research (CSIR), New Delhi, Government of India, for his CSIR-SRF fellowship.

Supramolecular Anticancer Nanostructures Formed via Self-Assembly of Curcumin Amphiphiles

Koji Nagahama*, Naho Oyama and Takayuki Kumano

Department of Nanobiochemistry, Konan University, Japan, nagahama@center.konan-u.ac.jp

INTRODUCTION

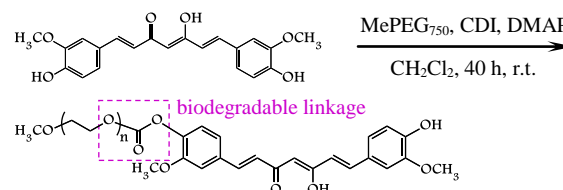
Curcumin (CCM) inhibits the proliferation of a wide variety of human cancer cell lines including multidrug resistant cancer cells and cancer stem cells¹. Thus, CCM is an important alternative candidate as cancer chemotherapeutic agent. However, its application is limited because of low aqueous solubility (< 29.9 nM in water), quick hydrolysis in neutral and alkaline conditions (half-life < 10 min in PBS at pH 7.2), and low cellular uptake². To overcome the problems, we herein propose a supramolecular strategy to directly assemble CCM into chemically- and physically stable anticancer nanostructures with high and quantitative CCM loading, high cellular uptake, and high anticancer effect through π - π associative and hydrophobic interactions of CCM amphiphiles.

EXPERIMENTAL METHODS

CCM amphiphiles were synthesized by coupling reactions of hydroxyl group of CCM with hydroxyl groups of poly(ethylene glycol) (PEG) using CDI as coupling agent (Scheme 1). These amphiphiles were dissolved in pure water and stirred vigorously at room temperature to prepare their self-assembled nanostructures. The size and the distribution of the CCM nanostructures were analysed by DLS. The CCM nanostructures were visualized by TEM observations. The amounts of CCM released from the nanostructures were quantified by measuring UV-Vis absorbance of CCM ($\lambda = 430$ nm) in supernatant. Cytotoxicity of the CCM nanostructures against human cancer cell lines (PC-3, HL-60, HepG2) were examined by MTT assay.

RESULTS AND DISCUSSION

Three types of CCM amphiphiles, PEG-CCM (**PC**), PEG-CCM-PEG (**PCP**), and CCM-PEG-CCM (**CPC**), with different hydrophilic/hydrophobic balance were synthesized and used following experiments. Purity of these amphiphiles was confirmed to be over 99% using gel permeation chromatography. TEM imaging reveals that all the CCM amphiphiles assembled into spherical nanostructures in water (Figure 1a and b). While **PC** and **PCP** formed micellar structures, **CPC** formed vesicular structures. Their ¹H-NMR spectra in D₂O reveals that CCM located interior of the nanostructures to form stable core and PEG chains located at the surfaces with well-extended structures to form water-soluble shell, suggesting that these nanostructures were formed through combination of π - π associative and hydrophobic interactions between CCM molecules. Diameters of the nanostructures were 228 ± 31 nm (**PC**), 180 ± 24 nm (**PCP**), and 155 ± 21 nm (**CPC**), respectively. Based on the geometry, these nanostructures were well-dispersed in water even at high concentrations. The maximum water solubility of CCM nanostructures were 15.6 mM (**PC**), 10.3 mM (**PCP**), and 14.1 mM (**CPC**), respectively. Although



Scheme 1. Synthesis of PEG-CCM conjugates (**PC**).

half-lives of CCM amphiphiles in water was shorter than 6 h at below their critical assembly concentrations which CCM amphiphiles can't form nanostructure, CCM nanostructures exhibited significant longer half-lives (**PC**: 42 h, **PCP**: > 168 h, **CPC**: 72 h). These results indicate that the supramolecular strategy is effective to improve water solubility and resistance to hydrolysis of CCM. The CCM contents (loading contents) of nanostructures were precisely controlled to be 32% (**PC**), 19% (**PCP**), 32% (**CPC**), respectively.

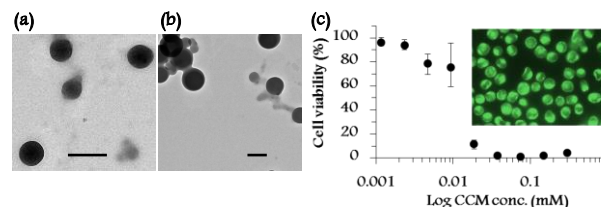


Figure 1. TEM images of **PC** (a) and **PCP** (b). Scale bar indicates 200 nm. (c) Anticancer effect of **PCP** against HL-60 cells. Inserted fluorescence microscopic image indicates HL-60 cells treated with **PCP** for 1 h.

CCM were gradually released from the nanostructures without initial burst and approximately 20% of loaded CCM were released after 14 days in cell culture medium at 37 °C. Almost 100% of CCM nanostructures entered both adhered (PC-3 and HepG2) and dispersed (HL-60) cancer cells after 2 h of incubation and mainly accumulated in the cytoplasm (Figure 1c). The CCM nanostructures inhibited cancer cell proliferation with 2-4 times lower IC₅₀ values than that of free CCM. Moreover, it was demonstrated that treatments of the CCM nanostructures induce apoptosis to cancer cells.

CONCLUSION

We have reported a novel strategy to construct CCM-based anticancer nanostructures with a high and fixed CCM content. We thought this strategy can be extended to fabricate nanostructures of other important anticancer drugs. Moreover, this strategy opens up new opportunity to develop "drug self-delivery systems".

REFERENCES

1. Esatbeyoglu T. et al., Angew. Chem. Int. Ed. 51:5308-5332, 2012
2. Naksuriya O. et al., Biomaterials 35:3365-3383, 2014

ACKNOWLEDGMENTS

The authors would like to thank JSPS foundation (KAKENHI 24700487) for financial support.

Silica/Collagen Nanocomposites for Local and Sustained Release of Therapeutic Biomolecules

Xiaolin Wang, Christophe Hélarly and Thibaud Coradin

Sorbonne Universités, UPMC Univ Paris 06 and CNRS, UMR 7574, Chimie de la Matière Condensée de Paris, France, wxlpharma@hotmail.com

INTRODUCTION

Local delivery of DNA and siRNA using a hydrogel scaffold extends the application of gene therapy for the treatment of tissue diseases such as chronic skin wounds. However, the inactivation and fast release of encapsulated DNA and siRNA strongly circumvent their efficacy¹. In this study, we propose to use nanocomposites consisting of polyethyleneimine (PEI)-DNA complexes associated with silica nanoparticles (SiNP) to modulate PEI toxicity², collagen hydrogel and 3T3 fibroblasts to build a local “cell factory” to achieve a sustained and programmed release of biomolecules.

EXPERIMENTAL METHODS

200 nm SiNP were prepared through the Stöber process and then subjected to surface modification with PEI of different molecular weights (1.8 kDa, 10 kDa and 25 kDa) in PBS pH 7.4. The SiNP-PEI particles were complexed with pCMV-GLuc plasmid and encapsulated³ within 1 mg.mL⁻¹ collagen hydrogels with 10⁵ cells.mL⁻¹ 3T3 mouse fibroblasts. The resulting 3D nanocomposites (Figure 1) were cultured over one week and samples collected at day 2, 5 and 7. Internalization of the SiNP-PEI in 3D system was checked by fluorescence microscopy. Cell transfection was assessed by measuring the luciferase activity (RLU) in the culture medium; cell viability was evaluated by the Alamar BlueTM Assay. PEI-DNA complexes were used as positive control.



Figure 1: Scheme of prepared nanocomposites

RESULTS AND DISCUSSION

Monodispersed SiNPs were obtained (Figure 2A) and internalization of SiNP-PEI-DNA into 3T3 fibroblasts was confirmed by fluorescence microscopy (Figure 2B). Successful cell transfection was detected by sustained release of luciferase over one week (Figure 2C). For the PEI-DNA complexes, an increase of cell transfection efficiency was observed with the increase of molecular weight. Regarding the SiNP-PEI-DNA complexes, 10kDa PEI allowed the highest expression of luciferase. This expression increased during the course of the experiment and was higher than that obtained with the 10 kDa PEI-DNA complexes. Interestingly, 1.8kDa PEI alone doesn't show any transfection capability while expression of luciferase was detectable when combined with SiNP. The enhancement of cell transfection for PEI 10 kD and 1.8 kD by SiNP suggests that SiNP offsets the positive charge of PEI while facilitating cell internalization of DNA complexes. The good cell viability through all group of DNA complexes

could be attributed to fast proliferation of the given cell line.

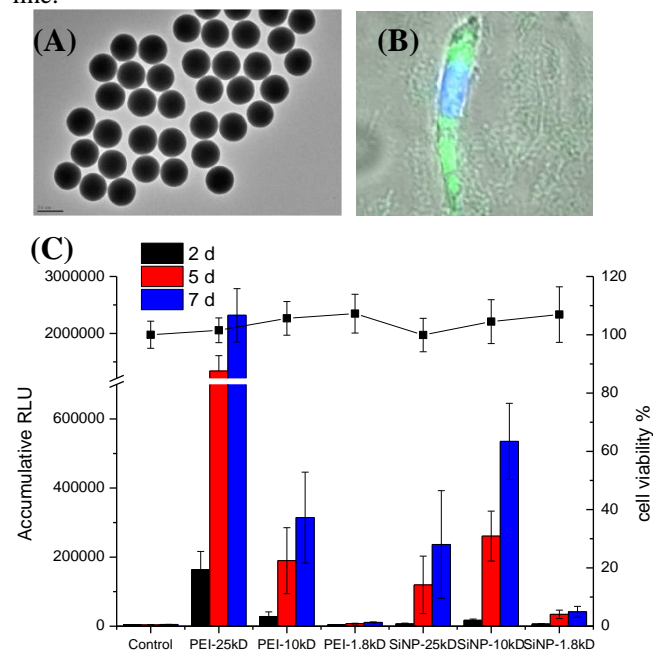


Figure 2: Transfection of 3T3 fibroblast by SiNP-PEI-DNA complexes in 3D. (A) TEM image of SiNP ($\times 11,000$). (B) Merged fluorescence microscopy image showing internalization of SiNP-PEI-DNA complexes within 3D system; complexes were labeled with FITC (green) and cell nucleus was labeled by DAPI (blue) ($\times 400$). (C) Accumulative RLU at 2d, 5d, 7d (histograms, $n=6$); cell viability was calculated in the percentage of control (dotted line, $n=6$).

CONCLUSION

These results show that nanocomposites obtained by entrapping SiNP-PEI-DNA together with cells inside collagen hydrogels can act as a reservoir for local and controlled gene delivery. By selection of PEI size, it is possible to lower toxicity while maintaining high transfection efficiency. Therefore, the as-constructed 3D system has promising applications for the controlled expression and release of therapeutic biomolecules for tissue engineering.

REFERENCES

1. Laura DL. *et al.*, Adv. Drug Deliv. Rev. 59:292-307, 2007.
2. Xia G. *et al.* Acc. Chem. Res. 45:971-979, 2011.
3. Desimone MF. *et al.*, Acta Biomater. 6:3998-4004, 2010.

ACKNOWLEDGMENTS

The authors would like to thank C. Illoul and B. Haye for technical assistance and the China Scholarship Council for providing financial support to this project.



Biomimetic thin films as reservoirs for BMP-2

Flora Gilde¹, Raphael Guillot¹, Laure Fourel², Ofelia Maniti¹, Thomas Boudou¹, Corinne Albigès-Rizo² and Catherine Picart¹

¹UMR 5628 (LMGP), Grenoble Institute of Technology and CNRS, France, flora.da-silva-gilde@grenoble-inp.fr

²Institut Albert Boniot, INSERM U823, CNRS ERL5284 Site Santé, France

INTRODUCTION

Bone Morphogenetic Proteins (BMPs) play an essential role in several developmental processes, especially in bone formation and regeneration. In the field of orthopedics and maxillo-facial surgery, localized delivery of BMPs from the surface of implantable materials may improve bone formation around the implant. Using the layer-by-layer technique, we have developed a biomimetic film made of biopolymers, which acts as a nanoreservoir to trap BMP-2 and to present it to cells in a "matrix-bound" manner^{1,2}. This presentation mode more closely mimics the natural environment *in vivo*. *In vitro* bioactivity of trapped BMP-2 was confirmed using alkaline phosphatase assay and SMAD signaling². *In vivo* osteoinductive potential was proved for films deposited on titanium scaffolds in a rat ectopic assay³.

Here, our aim was to analyse the implant/film interface and to understand how cells are sensing the BMP-2 presented in a "matrix-bound" manner by the film.

EXPERIMENTAL METHODS

Poly(L-Lysine/Hyaluronan (PLL/HA) films were built by the layer-by-layer technique using an automated dipping machine (DR3, Kierstein and Viegler) and subsequently cross-linked using carbodiimide chemistry. The loaded BMP-2 amount and its release over time were quantified using fluorescently labeled BMP-2 by means of a fluorescence spectrometer (TECAN Infinite 1000). The vertical diffusion of the fluorescein labeled BMP-2 inside the film (labeled with PLL-Alexa568) was studied using a confocal microscope (Zeiss LSM 700). Protein secondary structure in solution and in the films was assessed using FTIR spectroscopy (Bruker Vertex 70).

Uptake of BMP-2 by the cells was also studied by confocal microscopy. Several inhibitors of endocytosis were used to investigate the internalization route for BMP-2 as well as their effect on the BMP-2 signalling pathways. Knock-down of receptors using siRNA was applied to study the role of BMP receptors in the internalization process.

RESULTS AND DISCUSSION

The protein secondary structure was obtained by FTIR spectroscopy. Figure 1A shows the Amide I band spectrum of BMP-2 in solution (1 mM HCl, i.e. pH 3) and Figure 1B when loaded in a (PLL/HA) film. After isolating the protein spectrum from that of the film and decomposing the different bands, a very similar structure was observed for BMP-2 in solution or trapped inside the film matrix⁴. The structure of the film allowed BMP-2 to conserve its characteristic secondary structure: a large fraction of intramolecular β -sheets

(~ 50%) and to maintain its central α -helix⁴. The biopolymeric film plays the role of a stabilizer, or protective carrier for the protein⁴.

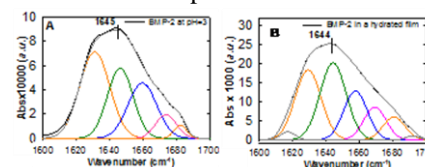


Figure 1: Secondary structure of BMP-2 (A) in solution and (B) inside a hydrated (PLL/HA) film. Structural elements: intramolecular β -sheets (orange), unordered structures (green), α -helix (blue), β -turns (purple) and intermolecular β -sheets (gray).

Furthermore, we evidenced that C2C12 cells internalize the fluorescently labeled BMP-2 as can be observed by the presence of green dots inside the cells, which are internalization vesicles (Figure 2). Several parameters related to endocytosis of BMP-2 were subsequently studied.

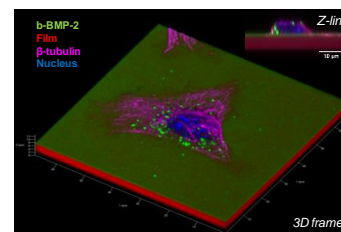


Figure 2: 3D reconstruction using confocal microscopy of a C2C12 myoblast on top of a biopolymeric film (red) loaded with BMP-2 (green) after internalization.

CONCLUSION

Understanding how cells can respond to bioactive proteins presented by a biomaterial is of importance for future clinical applications of this biomaterial. Here, we evidenced that matrix-bound BMP-2 can be internalized, which is related to BMP-2 signalling. The important role of BMP receptors in this process has also been shown.

REFERENCES

1. Crouzier T. *et al.*, Small 5:598–608, 2009
2. Crouzier T. *et al.*, Adv. Mater. 23:H111–H118, 2011
3. Guillot R. *et al.*, Biomaterials 23:5737–46, 2013
4. Gilde F. *et al.*, Biomacromolecules 11:3620–6, 2012

ACKNOWLEDGMENTS

This study has received funding from the ANR (Emergence Bio, ANR-09-EBIO-012-01) and from the European Research Council under the European Union's Seventh Framework Programme (FP7/2007-2013) / ERC GA259370 (BIOMIM).

Novel tool in nanomedicine: completely biocompatible and biodegradable superparamagnetic hydroxyapatite nanoparticles

S. Panseri¹, M. Montesi¹, M. Sandri¹, E. Savini¹, M. Iafisco¹, A. Adamiano¹, M. Ghetti², G. Cenacchi², A. Tampieri¹

¹Institute of Science and Technology for Ceramics, National Research Council, Faenza (RA), Italy.

²Department of Biomedical and Neuromotor Sciences, University of Bologna

silvia.panseri@istec.cnr.it

INTRODUCTION

Nanobiotechnology, the integration of nanotechnology with molecular biology and medicine, is an emerging research area that has experienced rapid growth over the past decade because it offers exciting opportunities for discovering new science, producing novel materials, and developing efficient processes.

Recently, the use of magnetic nanoparticles (MNPs) for biological and medical purposes has been increasing due to their unique reaction to applied magnetic forces (e.g., hyperthermia applications, as a contrast agent for magnetic resonance imaging and magnetic drug delivery). Recent interest has focused in their use for tissue engineering^{1,2}. Here novel biocompatible and bioresorbable superparamagnetic nanoparticles (NPs) fabricated by doping hydroxyapatite (HA) with Fe ions (FeHA), avoiding any coating and the presence of poorly tolerated magnetic secondary phases, were investigated in vitro. This study aimed to investigate the cellular response to FeHA NPs and to clarify the mechanism by which mouse mesenchymal stem cells internalized the FeHA NPs, in order to lay the basis for future approaches for biology and medicine applications.

EXPERIMENTAL METHODS

Magnetic biomimetic Fe-HA powder was prepared by a neutralization process using FeCl₂ and FeCl₃ as a source of Fe²⁺ and Fe³⁺ doping ions³.

HA nanopowder already employed in orthopaedic clinic applications was used as control. Mesenchymal stem cells were plated at a density of 1×10^4 cells/cm² and were incubated with two different concentrations of FeHA NPs: 200 µg/ml and 100 µg/ml for different time points.

Cell proliferation, cell viability and osteogenic differentiation were investigated (qPCR). Moreover, the cellular uptake was quantified by ICP-OES measure of iron [Fe] concentration in the cellular lysates. Immunofluorescence analyses and morphological analysis by transmission electron microscopy were assessed.

RESULTS AND DISCUSSION

Assays for cell proliferation, viability and morphology did not show any differences among FeHA NPs and HA NPs groups with different concentration at each time points. This indicated that the novel superparamagnetic FeHA NPs did not cause any cytotoxicity and were comparable to the HA NPs.

A very high ratio of live cells compared to the very few dead cells were seen in every FeHA NP group in quantities comparable to HA groups. Moreover these particles strongly enhanced MSCs osteogenic differentiation as demonstrated by gene expression analysis.

Cellular uptake shown that mesenchymal stem cells were able to quickly internalize the NPs and they became “magnetic cells”. In fact we were able to move and to align the cells when an external magnetic field was applied.

CONCLUSION

This study showed the great potential that novel MNPs may offer in biology and medicine applications.

The preliminary data obtained on the cellular uptake of FeHA NPs lay the basis to clarify the fate of the intracellular particles and open future prospective on the possibility to magnetize the cells with FeHA NPs. “Magnetized” cells could be injected and directed to a desired bone site to increase cell proliferation and enhance bone formation using an external magnetic field. Moreover FeHA NPs could be functionalized with several growth factors and/or drugs induce tissue regeneration and reducing the recovery time.

REFERENCES

1. Amirfazli A. *et al.*, Nature Nanotech 2(8), 467, 2007.
2. Arruebo M. *et al.*, Nano Today 2, 22, 2007.
3. Landi E. *et al.*, J Eur Ceram Soc 20, 2377, 2000.

ACKNOWLEDGMENTS

The authors would like to thank the European Project SMILEY (NMP4-SL-2012-310637) and Flagship Project NanoMAX (PNR-CNR 2011-2013) for providing financial support to this project.



Antioxidant Delivery for Inhibition of Angiogenesis

Masaki Moriyama¹, Stéphanie Metzger², Martin Ehrbar², André J. van der Vlies¹, Hiroshi Uyama¹ and Urara Hasegawa^{1*}

^{1*}Graduate School of Engineering, Osaka University, JAPAN, m-moriyama@chem.eng.osaka-u.ac.jp

²Department of Obstetrics, University Hospital Zurich, SWITZERLAND

INTRODUCTION

Reactive oxygen species (ROS) are closely linked with initiation and progression of cancer, arthritis and other inflammatory diseases.^[1] In addition, they are angiogenic mediators and promote angiogenesis which is essential for tumor growth and metastasis.^[2]

In the field of drug delivery, polymeric nanoparticles, generally in the range of 10-100 nm in dimension, are often used to deliver a wide variety of drugs including anti-cancer drugs and nucleic acids. They have been shown to prolong circulation time, improve biodistribution and minimize side effects of drugs.

The objective of this study is to develop antioxidant micelles which inhibit angiogenesis by scavenging ROS in tumor tissues. Here we report polymeric micelles bearing catechol moieties with antioxidative activity that have an inhibitory effect on angiogenesis.

EXPERIMENTAL METHODS

Poly(ethylene glycol)-poly(dopamine) (PEG-PDA) diblock copolymers (Figure 1A) were synthesized by reversible addition-fragmentation chain transfer (RAFT) polymerization. The antioxidant micelles were prepared by dispersing PEG-PDA diblock copolymers in acetate buffer (pH5.0). The micelles were characterized by dynamic light scattering (DLS) and transmission electron microscopy (TEM). To evaluate the oxidation stability of the catechol moieties under aerobic condition, dopamine (DA) and PEG-PDA micelles were kept in air-saturated phosphate buffered saline (pH7.4) at 37°C and tested for H₂O₂ scavenging activity using Amplex Red assay. To investigate whether DA and PEG-PDA micelles are able to exert an anti-angiogenic effect by scavenging endogenous ROS, we evaluated their effects on the tube formation of human umbilical vein endothelial cells (HUVECs) *in vitro*. Furthermore, the anti-angiogenic activity of PEG-PDA micelles was evaluated in the *ex ovo* chicken chorioallantoic membrane (CAM) assay.

RESULTS AND DISCUSSION

DLS showed that the PEG-PDA block copolymers formed micelles (50 nm in diameter) with narrow size distribution. The TEM image showed the spherical shape of the micelles.

Freshly prepared solutions of DA and PEG-PDA micelles scavenged 80-90% of the added H₂O₂. In the case of DA, the H₂O₂ scavenging activity was reduced under aerobic condition as function of incubation time. After 48 h, the amount of the scavenged H₂O₂ decreased to 50%. In addition, we observed a dark-brown precipitate. Contrary to DA, PEG-PDA micelles had similar H₂O₂ scavenging activity without formation of precipitate after 48 h.

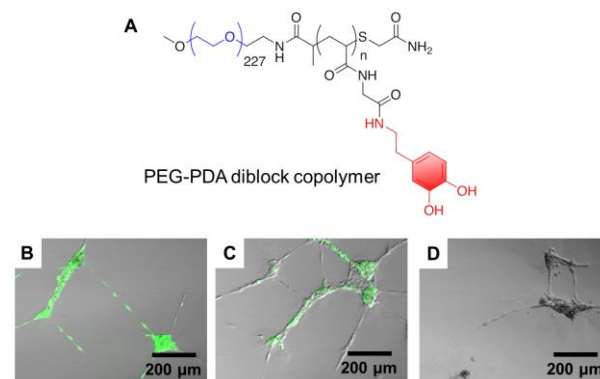


Figure 1. A) Chemical structure of PEG-PDA diblock copolymer. Fluorescence images of ROS in HUVECs treated with B) water (control), C) DA and D) PEG-PDA micelles.

The tube formation capacity in HUVECs was impaired upon the addition of PEG-PDA micelles while the treatment with DA did not show obvious effects. To confirm that the inhibitory effect was due to the ROS scavenging activity of the micelles, the intracellular ROS level in HUVECs treated with DA and PEG-PDA micelles was visualized using the ROS-detection dye, dichlorofluorescein-diacetate (Figure 1B-D). In the case of PEG-PDA micelles, the fluorescence due to the intracellular ROS was not observed while DA slightly diminished the intracellular ROS level. These results indicate that the long-lasting ROS-scavenging activity is critical to exert an anti-angiogenic effect.

We further evaluated the anti-angiogenic activity of the PEG-PDA micelles in the *ex ovo* chicken chorioallantoic membrane (CAM) assay. The micelles efficiently inhibited capillary formation on the CAM, while DA treatment showed only a weak inhibitory effect.

CONCLUSION

The PEG-PDA micelles showed high oxidation stability under aerobic condition. In the tube formation assay and the CAM assay, the micelles exerted anti-angiogenic activity. These results suggest that the antioxidant micelles may be useful in anti-angiogenic therapy to treat many diseases including cancer.

REFERENCES

1. Ushio-Fukai M., Cardiovasc. Res. 71:26–35, 2006
2. Folkman J. *et al.*, J. Med. 285:82–86, 1971

ACKNOWLEDGMENTS

We thank Dr. E. Mochizuki (Osaka University, Japan) for TEM experiments and Prof. M. Sadakane (Hiroshima University, Japan) for supplying Preysslertype phosphotungstate staining agent.

Design of Biodegradable pH-Responsive Microgels as Targeted Drug Delivery System

Miren K. Aiertza, Pablo Casuso, Adrián Pérez-San Vicente, Hans-Jurgen Grande, Germán Cabañero, Iraidia Loinaz and Damien Dupin

Biomaterials Unit, Materials Division, IK4-CIDETEC, Spain, maiertza@cidetec.es

INTRODUCTION

Efficient drug delivery is one of the most important challenges in cancer treatment¹. Considerable efforts focus on the preparation of targeted vehicle to transport drugs to tumour cells.² Such delivery system requires i) good encapsulation properties, ii) efficient drug targeting/release, iii) biocompatibility and, iv) facile elimination from the body.³

Stimuli-responsive microgels, which are submicrometer-sized particles that can be swollen by change of pH, have gained growing attractions as drug delivery systems. Herein, we report the design of folic acid-functionalised microgels that can transport hydrophobic compounds to the tumour cells and release their cargo during endocytosis at lysosomal pH.

EXPERIMENTAL METHODS

Microgel synthesis via aqueous emulsion polymerization. 2,2'-(diisopropylamino)ethyl methacrylate [DPA] was polymerized in water in the presence of *N*-(3-aminopropyl)-2-methylacrylamide hydrochloride (APMA) comonomer, 2-methylene-1,3,6-trioxocane (MTC), ethylene glycol diacrylate (EGDA) cross-linker, poly(ethylene glycol) ethyl ether methacrylate stabilizer (PEGMA) and ammonium persulfate (APS) initiator via aqueous emulsion polymerization at 70 °C to obtain PEGMA-PDPA particles. PDPA particles were decorated with folic acid.

Dynamic Light Scattering (DLS) and Zeta potential studies were carried out using Malvern Zetasizer Nano ZS on particles dispersion at 0.01 wt. % in PBS.

PDPA particles cytotoxicity was investigated via MTS and Live/Dead assays in the presence of HeLa cells.

RESULTS AND DISCUSSION

Lightly cross-linked PEGMA-PDPA particles of around 200 nm were obtained via aqueous emulsion polymerization.

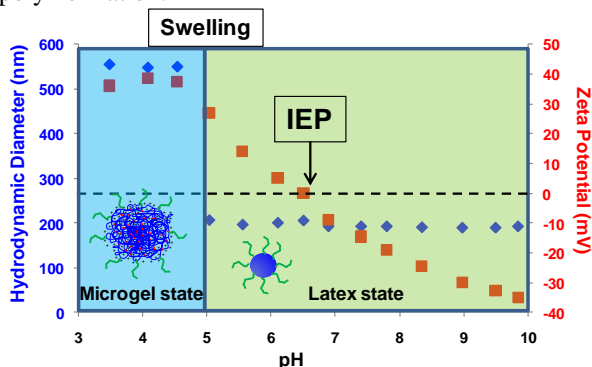


Figure 1. DLS (♦) and Zeta potential (■) of PEGMA-PDPA particles in function of the solution pH in PBS solution.

As judged by DLS, PEGMA-PDPA particles exhibited a latex-to-microgel transition at pH 6.5 due to the protonation of the tertiary amine of the DPA residues (**Figure 1**). This indicates that PEGMA-PDPA will swell up with water to 550 nm during the endocytosis process as originally targeted. It is worth mentioning that the presence of the PEGMA stabilizer is absolutely required to ensure colloidal stability in physiological conditions with high concentration of salt. Moreover, the copolymerization of MTC comonomer offered hydrolysable bonds into the particles facilitating its degradation. PEGMA-PDPA particles were efficiently degraded after 1 week in the presence of lipase at physiological conditions into shorter polymer chains easily eliminated by the kidney.

PEGMA-PDPA particles did not exhibit cytotoxicity in the presence of HeLa cells (**Figure 2**). Moreover, hydrophobic dye could be encapsulated into the particles. The presence of folic acid at the particle surface increased cellular uptake and the dye was released efficiently as judged by fluorescence microscopy.

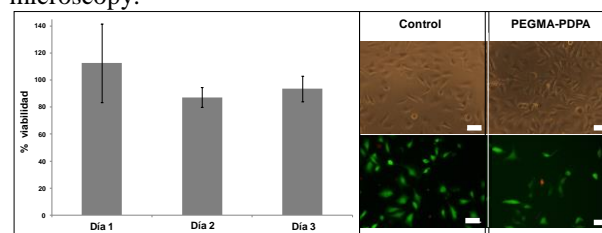


Figure 2. Viability (left) and Live/Dead assays (right) of HeLa cells in the presence of PEGMA-PDPA particles (50 µg L⁻¹) after 3 days (scale bar: 100 µm).

CONCLUSION

The judicious choice of stabilizer and comonomers allowed the preparation of stable, biodegradable and biocompatible pH-responsive microgels easily functionalised with targeting molecules. Hydrophobic compounds could be encapsulated at physiological conditions and efficiently released during endocytosis due to the swelling of the particles occurring at lysosomal pH.

REFERENCES

1. Branon-Peppas, L *et al.* Adv. Drug Deliver. Rev. 64:206-212, 2012.
2. Bae, Y H *et al.* J. Control. Release 153:198-205, 2011.
3. Kost, J *et al.* Adv. Drug Deliver. Rev. 64:327-341, 2012.

ACKNOWLEDGMENTS

The authors would like to thank the financial support from ETORTEK Program-BIOMAGUNE12(E12-332).

A Biotemplating Approach Using the Marine Diatom for Fabricating Drug Delivery Reservoirs

J. Chao¹, Y. Lang¹, A. Abdul-Rahman¹, M. Biggs¹, A. Pandit¹

¹Network of Excellence for Functional Biomaterials (NFB), National University of Ireland, Galway, Ireland
J.CHAOI@nuigalway.ie

INTRODUCTION

In the field of biomedical engineering, the use of natural systems as templates – termed “biotemplating” – has been argued to provide many biomimetic advantages over conventional biomaterials and drug delivery platforms¹. Diatoms are unicellular, eukaryotic algae surrounded by an outer “frustule” wall, which is highly differentiated and impregnated with amorphous silica². The hierarchical structure of the diatom is species-specific and composed of highly ordered pores, giving a large surface area for biomolecule conjugation; however, due to the cytotoxicity of the biogenic silica, there is a need to fabricate a polymeric replica of the diatom for drug delivery purposes. The authors have previously shown success in grafting a pDMAEMA-co-EGDMA polymer onto the diatom³ and, in this abstract, we present our findings on utilizing layer-by-layer (LbL) assembly of poly-L-lysine (PLL) and hyaluronic acid (HA) to form biodegradable polymeric bilayers on the marine diatom *Thalassiosira weissflogii*.

EXPERIMENTAL METHODS

Culturing of *Thalassiosira weissflogii*. Axenic cultures of *T. weissflogii* were grown in artificial seawater and enriched with Guillard’s f/2 marine enrichment media without silicates. Cultures were grown in polystyrene tissue culture flasks, with 14:10-hour light:dark cycle, 3000 lux light intensity, and temperature range of 16–22°C. Cultures were inoculated at a density of 1×10^4 cells/mL in 200 mL of ASW, and sodium metasilicate was added to flasks at a final concentration of 200 μ M.

Preparation & characterization of cleaned frustules. Cultures were collected 192 h post-inoculation and organic matter was removed by successive washes of H₂O (3x), 1:1 HCl:H₂O (3x), H₂O (3x), and methanol (6x), each rinse followed by centrifugation at 2500 rpm for 20 m. Cultures were treated with chitinase for 72 h to remove chitin extruded from the diatom.

Layer-by-layer assembly of polyelectrolytes. PLL and HA solutions were prepared in 0.05M MES buffer (pH 5.5) at 1 mg/mL. Polyelectrolytes were incubated with diatoms at 25°C for 15 m, and layers were confirmed using quartz crystal microbalance and zetasizer.

RESULTS AND DISCUSSION

Morphological and topographical characterization revealed a highly porous architecture (Fig. 1). Scanning electron microscopy was used to visualize the intricate hierarchical template, confirming clean and chitin-free diatom skeletons. Transmission electron microscopy revealed the porous architecture of the frustule with pore sizes measuring 40.4 ± 2.09 nm. Quartz crystal microbalance with dissipation monitoring (QCM-D) was used to quantify the layer thickness and mass deposited, and zetasizer indicated surface charge of the frustule to oscillate between 34.4 ± 1.90 mV and -22.6 ± 1.11 mV for PLL and HA layers respectively (Fig. 2).

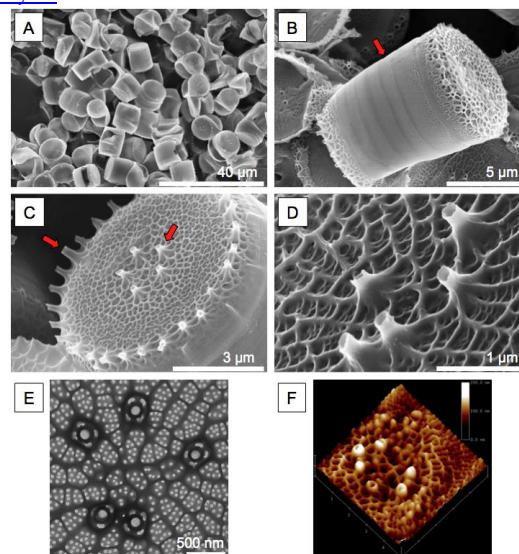


Figure 1. **Topography of *T. weissflogii*.** (A) Diatoms are abundant and amenable to scale-up. (B) Arrow highlights girdle bands alongside frustule. (C) External view of valve face with arrows highlighting fulcra. (D) Zoomed-in view of fulcra. (E) TEM shows porous architecture with rib-like structure. (F) AFM shows morphology of diatom valve face (scale = 200 nm, x-/y-axis div: 1 μ m, z-axis div: 200 nm).

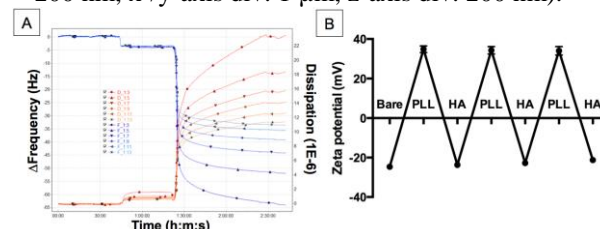


Figure 2. **Analytical methods confirm polyelectrolyte deposition.** (A) QCM-D shows polyelectrolyte binding. (B) Zeta potential of oppositely charged polyelectrolytes indicates binding of successive layers on diatom.

CONCLUSION

The authors have visualized and quantified the morphology of the diatom, as well as shown novel binding of PLL and HA bilayers onto a diatom template. Dissolution of biogenic silica will produce a free-standing biodegradable diatom replica. Model water-insoluble drugs with pDNA will be incorporated within the bilayers and release kinetics will be further investigated.

REFERENCES

1. Sarikaya M., PNAS **1999**;96:14183–5
2. Round FE. *et al.*, Cambridge: CUP **1990**
3. O’Connor J. *et al.*, Small **2014**;10:469–3

ACKNOWLEDGMENTS

The authors wish to acknowledge the financial support of Science Foundation Ireland (Grants 07/SRC/B1163, 11/SIRG/B2135) and the Atlantic Area Transnational Programme (Grant MARMED 2011-1/164).



Effect of mesoscale structure on the properties of composite scaffold: from micro to nano

Limei Li, Yi Zuo, Jidong Li, and Yubao Li*

*Research Center for Nano Biomaterials, and Analytical & Testing Center, Sichuan Univ., China, nic7504@scu.edu.cn

INTRODUCTION

Apatite/polymer composites have been developed to mimic the natural extracellular matrix of bone^[1]. The incorporation of apatite nanoparticles can significantly affect the properties of the polymeric matrix^[2]. And the nanoparticles tend to aggregate because of high surface energy^[3]. Moreover, mesoscale structure between the microscale and nanoscale, which formed a structure domain by the regular aggregation of organic molecules or inorganic crystals, has not been noticed for this class of composite. A more detailed understanding of the mesoscale domain formation in composite is associated with more stable and homogenous matrix for scaffold fabrication. This study tried to explore how the micro to nano mesoscale structure influences the properties of the composite scaffold.

EXPERIMENTAL METHODS

Polyurethane was chosen as the model polymer for its specific micro-structure formed by hard and soft chain segments. Here, castor oil (CO) and glycerin-esterified castor oil (GCO) copolymerized respectively in a three-necked flask with isophorone diisocyanate (IPDI) with addition of 40 wt% micro- or nano- hydroxyapatite (HA) particles. The weight ratio of IPDI to CO or GCO was 1:1 in all cases and the reaction was kept for a period of 3 h in an oil bath at 70 °C. Then HA/PU slurry was cured and foamed at 110 °C. Finally, we obtained four groups of porous scaffolds, i.e. n-HA/PU, n-HA/GPU, μ -HA/PU and μ -HA/GPU, in which PU was from CO, and GPU was from GCO.

Cryogenic ultramicrotome was used to prepare ultrathin samples and autheniumtetraoxide (RuO₄) was used as staining agent for TEM observation. NMR, XPS and FTIR were used to analyse the chemical composition and bonding. Thermal ability and dynamical mechanics performance were tested by DSC and DMA, respectively.

RESULTS AND DISCUSSION

Fig. 1 and Fig. 2 shows the TEM images of the four composites, in which the n-HA crystals are uniformly distributed in PU (1c, 1e) or GPU (1d, 1f) matrix with close interface integration (2c, 2d). However, there are clear interface gaps between the μ -HA particles and PU or GPU matrix, although the interface of μ -HA/GPU (1b) looks better than μ -HA/PU (1a). On the one hand, the GCO with more -OH groups can fully react with IPDI to increase the polymerization; on the other hand, the abundant functional groups of GCO will bond with the dangling P-O or -OH bonds of n-HA crystals to realize the close interface structure.

The peaks of NMR and XPS spectra in Fig. 3 (A-C) indicate that the chemical process enables n-HA crystals closely combine with PU or GPU matrix. It can be noted that the molar concentration of the peak at about 400.0 eV (CO-N-CO) increases in an order of μ -HA/PU,

μ -HA/GPU, n-HA/PU and n-HA/GPU, driven by the less reaction inhibition in n-HA/GPU (19.93%). The data coincide with the best miscibility of n-HA/GPU composite, characterized by either the close interface or the bonding domain of hard and soft segments (Fig. 2).

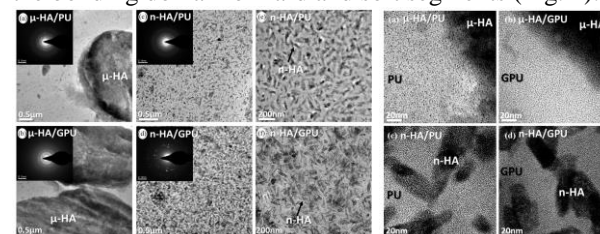


Fig. 1 TEM images and SAED patterns of composites

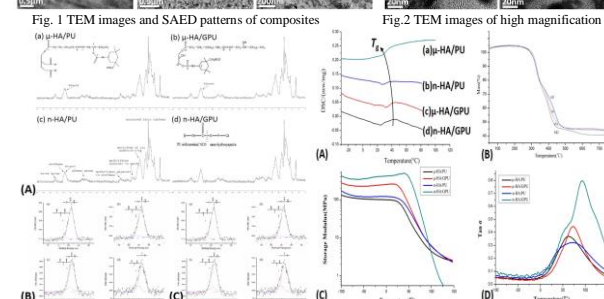


Fig.2 TEM images of high magnification

Fig. 3 (A) ¹³C NMR spectra, (B) C1s XPS spectra and (C) N1s XPS spectra of composites

Both the nanoscale of n-HA crystals and the esterified GCO, present a significant influence on the properties of the HA/PU composites. In the curves of DSC and DMA in Fig. 4, the value of T_g increases from 35 °C to 45 °C and storage modulus of composites increase largely with the hydroxyl value, from 159 mg KOH/g (CO) to 288 mg KOH/g (GCO). The homogenous nanoscale structure truly enhances the macro performance of the composites. The compressive strength is 2.23, 2.40, 2.44 and 4.27 for μ -HA/PU, μ -HA/GPU, n-HA/PU and n-HA/GPU, respectively.

CONCLUSION

This study testified that the mesoscale structures would affect the macro performance of HA/PU composites significantly and synergistically, not only by the nano size of the inorganic HA crystals but also by the bonding domain of soft and hard segments of polyurethane.

REFERENCES

- Okamoto M., *et al.*, Prog. Polym. Sci. 38: 1487-1503, 2013
- Johnson A., *et al.*, Acta Biomater. 7: 16-30, 2011
- Wang L., *et al.*, Biomed. Mater., 2: doi:10.1088/1748-6041/4/2/025003, 2009

ACKNOWLEDGMENTS

The authors would like to acknowledge the supports of China NSFC fund (No.31370971) and Sichuan project (No.2012FZ0125).

Factors influencing injectability of nano-hydroxyapatite paste: a rheological behaviour

Yulia Ryabenkova¹, Guenter Moebus¹, Paul V Hatton², Cheryl A Miller^{2*}

¹Department of Materials Science and Engineering, University of Sheffield, UK

^{2*}Bioengineering & Health Technologies Research Group, School of Clinical Dentistry, University of Sheffield, UK

y.ryabenkova@sheffield.ac.uk

INTRODUCTION

Biomaterials composed of hydroxyapatite (HA) are currently clinically employed for the treatment of bone defects resulting from trauma or surgery¹. Nanoscale hydroxyapatite supplied in the form of a paste is considered very attractive compared to calcium phosphate cements where powders and liquids need to be mixed immediately prior to surgery. In this study, we have tested nanoscale hydroxyapatite (nHA) pastes prepared using two types of nanoparticle with different morphologies (with particle-water load, macro-porosity and level of agglomeration being constant), and evaluated their properties at different temperatures. The aim of this research was to understand the structure-property relationships that underpin clinical success including handling.

EXPERIMENTAL METHODS

The nHA pastes were supplied by the IMCOSS project partners and characterized using X-ray diffraction (XRD) for phase analysis, and attenuated total reflectance-Fourier transform infrared spectroscopy (ATR-FTIR) for the determination of functional groups. Morphology studies were carried out using high resolution transmission electron microscopy (HR-TEM), whereas the rheological behaviour has been evaluated using a modular compact rheometer (MCR) in both rotational and oscillating modes.

RESULTS AND DISCUSSION

The HA particles of two types appeared to be rod shaped with the size ranging from 20 nm to 80 nm and differing from one another by aspect ratio and the level of roundness/sharpness (Fig. 1). They were shown to be made of a phase pure HA with low crystallinity, containing small inclusions of carbonates most likely due to the relatively high pH used during their preparation.

The rheological properties were investigated by performing steady and dynamic tests, and revealed that the nHA pastes were thixotropic shear-thinning non-Newtonian fluids. Differences in viscosity and yield stress were detected between the two pastes, with one of them having the highest viscosity and being harder to handle, thus suggesting poorer injectability properties. This was assumed to correlate with the morphology of the constituent particles. Interestingly, temperature modified the rheological behaviour, suggesting better

injectability may be obtained at lower temperatures (ca. 10°C).

In addition, the two materials with expected low and high viscosities were mixed at the stage of slurries forming the pastes, with the aim of producing homogeneity of mixing. Rheology tests of the resulting paste showed that the viscosity does not change linearly when mixing the two materials with different characteristics, thus giving the opportunity to prepare mixtures with the desired viscosity values.

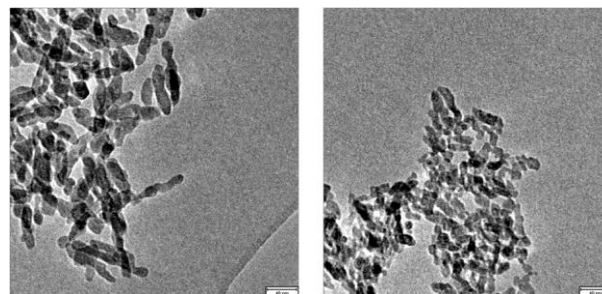


Figure 1. TEM micrographs of: (left) HA nanoparticles with higher aspect ratio, (right) HA nanoparticles with lower aspect ratio (scale 40 nm). The viscosity of the pastes changes drastically being significantly lower for the higher aspect ratio HA particles (on the left) thus leading to easier handling.

CONCLUSION

Injectability is a complex phenomenon with many determining factors. It was concluded that it was possible to influence injectability of the nHA pastes by combining particles with different morphologies. Temperature also appeared to be a critical factor that must be taken into account when handling these non-Newtonian bone graft materials, as it modified viscosity and therefore influenced the injectability.

REFERENCES

1. Yamamoto T. *et al.*, J Bone Joint Surg Br 82: 1117-1120

ACKNOWLEDGMENTS

The research leading to these results has received funding from the European Union's Seventh Framework Programme managed by REA - Research Executive Agency. <http://ec.europa.eu/research/rea> (FP7-SME-2012) under grant agreement n° 315679.

Designing biodegradable and biocompatible crosslinked film from polycarbonate urethane and zwitterionic polynorbornene as cell growth substrate

Yakai Feng^{1,2 *}, Musammir Khan, Juan Lv¹, Jing Yang¹ and Gregory Tew³

^{1*}School of Chemical Engineering and Technology, Tianjin University, Tianjin 300072, China

² Key Laboratory of Systems Bioengineering of Ministry of Education, Tianjin University, Tianjin 300072, China

³ Department of Polymer Science and Engineering, University of Massachusetts, Amherst, Massachusetts 01003, USA
yakaifeng@tju.edu.cn

INTRODUCTION

Biodegradable polyurethane elastomeric scaffolds have great interest in soft tissue repair and regeneration. But the proper design of these materials employed for tissue engineering application is still challenging because of the lack of tissue-material compatibility that are susceptible to provoke foreign body response and unwanted inflammatory reactions.

The presence of zwitterionic polynorbornene in the soft segment as chain extender with attached crosslinker in the polyurethane elastomer could provide with robust mechanical properties and faster degradation behavior. The present work is also continuations which address several important issues faced as well the approach employed thiol-ene click reaction, required mild experimental conditions, show high yields, require small concentrations of benign catalysts, have rapid reaction rates, require essentially no cleanup, and are insensitive to ambient oxygen and water. Moreover, the final materials exhibited some of the novel characteristics, such as mechanical, biodegradable and biocompatible properties, which have great demand for the current synthetic TE materials applications.

EXPERIMENTAL METHODS

The zwitterionic polymer, poly(NSulfoZI) was synthesized according to our previous method using the same designed principle of ring opening metathesis polymerization (ROMP).¹ Polyurethane (PCU) and zwitterionic polynorbornene based elastomeric crosslinked film as cell growth substrate was prepared using thiolene click-chemistry and crosslinking reaction.

They were characterized by FT-IR, water contact angle and mechanical test. Cytotoxicity, growth and proliferation of endothelial cells EA.hy926 were evaluated *in vitro*.

RESULTS AND DISCUSSION

The various cross-linked PCU films with different ratios (wt%) of zwitterion polynorbornene poly(NSulfoZI), acting as chain extender were prepared by a two steps method using a combination of click chemistry and crosslinking reaction (curing) at different temperature and time schedule. Firstly amine functionality was introduced into polynorbornene (poly(NSulfoZI) having functionalizable double bonds by treating with L-cysteine using photoinitiated thiolene click-reaction,

followed by controlled reaction with PCU-solution in the presence of diisocyanate cross-linker. The obtained films possessed improved tensile strength of (14-20 MPa) and initial modulus (8-14 MPa), in comparison to 12 ± 4 MPa and 3 ± 1 MPa respectively, for blank film. All of these films including blank one, showed high breaking strain (eb 740-900%), except with a highest zwitterion content of 28% (eb $470 \pm 80\%$). The biodegradability of these materials was enhanced, tested in PBS for 5 weeks as against blank PCU. The blank PCU-film surface could also be modified under the aforementioned condition using L-cysteine or β -marcaptoethanol as thiol-agents.

The cytocompatibility of all these materials investigated by MTT assay indicated that the designed materials were non-toxic and showed good cytocompatibility towards ECs, EA.hy926.

The adhesion and proliferation of EA.hy926 endothelial cells (ECs) on different films surfaces were morphologically evaluated by SEM for 1, 3 and 7 days. The modified films provided a good environment for the ECs growth. The blank PCU surface scarcely adhered ECs, and the adhered cells showed poor growth even after 3 and 7 days. So these finding indicated that these materials significantly improved support towards the growth of ECs when employed as growth substrate.

CONCLUSION

The elastomeric polycarbonate urethane and zwitterion crosslinked films were prepared through the convenient method using click chemistry and crosslinking reaction. These obtained films combined unique characteristics of both the parent materials such as improved biodegradability, reasonable mechanical and excellent biocompatible properties. Moreover, these designed materials showed enhanced growth and proliferation of endothelial cells.

REFERENCES

1. Colak S. and Tew G. N., Langmuir, 28: 666, 2012

ACKNOWLEDGMENTS

This project was supported by the National Natural Science Foundation of China (Grant No. 31370969), the International Cooperation from Ministry of Science and Technology of China (Grant No. 2013DFG52040, 2008DFA51170), and Ph.D. Programs Foundation of Ministry of Education of China (No. 20120032110073).



Periodic Mesoporous Organosilica (PMO) Coatings for Biomedical Applications

Natalja Wendt¹, Mandy Jahns¹, Nina Ehlert¹, Sabrina Schlie², Boris Chichkov², Peter Behrens¹

¹Institut für Anorganische Chemie, Leibniz Universität Hannover, Germany

²Laser Zentrum Hannover e.V., Hannover, Germany

natalja.wendt@acb.uni-hannover.de

INTRODUCTION

The interaction between the surface of an implant and the surrounding tissue is a crucial factor for its efficiency in the human body. If the surface is bioinert or bioincompatible, this property can be changed by establishing bioactive coatings. Our group has already successfully introduced mesoporous silica films as a novel type of coating which allows modification of and local drug delivery from implants¹⁻³. Periodic mesoporous organosilica (PMO) coatings⁴ could also offer a variety of useful characteristics for biomedical applications and are more versatile due to their hybrid construction. In PMOs, the siloxane bridges of silica are substituted by organic linkers. Correspondingly, the chemical, physical and mechanical properties of the PMO coatings can be adjusted by the chemistry of the organic bridging groups in the precursors. PMO films could be mechanically more flexible than pure silica films which is of interest for the coating of flexible implants. The pores of PMOs can exhibit more strongly hydrophobic properties which could be used for the delivery of unpolar, water-insoluble drugs. First studies with simple drug delivery processes from PMOs⁵ show promising results with regard to biomedical applications.

Here, we present comprehensive investigations on the properties of PMO coatings as a novel biomaterial. Apart from basic characterization, the focus is on mechanical properties, on biocompatibility studies as well as on the loading and release of the drug ciprofloxacin (CFX). The organic-inorganic silica precursor used for the synthesis of the PMO coatings is 1,4-bis(triethoxysilyl)benzene (BTEB). Here, the siloxane bridges of silica are substituted by phenylene units.

EXPERIMENTAL METHODS

PMOs coatings were generated on plain glass slides by sol-gel dip-coating. To obtain the coating solutions, the PMO precursor (here BTEB), structure-directing agents (SDAs, here Pluronic F127), ethanol, water and hydrochloric acid (HCl) were mixed. After dip-coating and drying at 60 °C, the coated slides were calcined at 350 °C in air to remove the SDA. The coatings were characterized by XRD, TEM, sorption measurements as well as mechanical testing by a nanoindenter. The cell viability properties were tested with human fibroblasts and human umbilical vein endothelial cells (HUVEC). The coatings were further functionalized with sulfonate groups by grafting and loaded with the drug ciprofloxacin. Drug release experiments in PBS were performed over two weeks, the released amount of the drug was measured by a photometer.

RESULTS AND DISCUSSION

We were able to establish novel coatings based on BTEB-PMO with uniform mesoporous structure (Fig. 1) in which the organic linkers are embedded in the walls of the silica network. These coatings are more flexible and less hydrophilic than their pure silica counterparts. The calcined, the sulfonate-modified as well as the drug-loaded PMO coatings show a good biocompatibility in cell culture experiments (Fig. 2). First drug release experiments with ciprofloxacin from PMO coatings show promising results in antibacterial activity tests. After the modification of the coatings with sulfonate groups, the loaded and the released amount of the drugs can be increased two-fold.

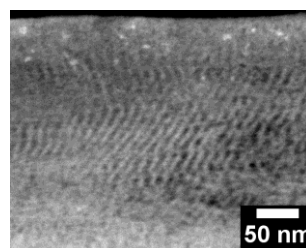


Fig. 1: TEM image of a PMO coating with 9 nm pores that are oriented perpendicular to the substrate surface.

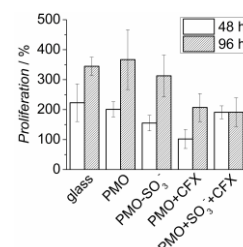


Fig. 2: Proliferation of human fibroblasts. The PMO coatings show good cytocompatibility.

CONCLUSION

PMOs coatings present a viable alternative to the well-characterized nanoporous silica bioactive films¹⁻³ and can – due to their good biocompatibility – be further developed as a novel biomaterial. Based on different PMOs precursors, it should be possible to adjust varying chemical properties, like pore size or hydrophobicity. In addition, the benzene units in the organic linkers offer interesting opportunities for further functionalizations, which can be useful for the binding of proteins or in drug release applications.

REFERENCES

1. Ehlert N. *et al.*, J. Mater. Chem. 21:752-760, 2011
2. Ehlert N. *et al.*, Acta Biomater. 7:1772-79, 2011
3. Ehlert N. *et al.*, Chem. Soc. Rev. 42:3847-61, 2013
4. Hoffmann F. *et al.*, Angew. Chem. Int. Ed. 45:3216-3251, 2006
5. Lin C.X. *et al.*, Microporous Mesoporous Mater. 117:213-219, 2009

ACKNOWLEDGMENTS

The authors would like to thank the DFG within the Collaborative Research Program SFB 599 (TP D1) for providing financial support to this project.

Polymer based scaffolds with microwave induced porosity

Antonella Giuri¹, Vincenzo Maria De Benedictis², Maria Grazia Raucci³, Christian Demitri¹, Alessandro Sannino¹

¹ Department of Engineering for Innovation, University of Salento, via per Monteroni, km 1,73100, Lecce, Italy
christian.demitri@unisalento.it

² High Tech District - DHITECH Scarl, via S. Trinchese, 61,73100, Lecce, Italy

³ Institute of Polymers, Composites and Biomaterials, National Research Council of Italy (IPCB-CNR), Italy

INTRODUCTION

In this work, interconnected porous materials was obtained by a new foaming method based on the combination of two steps. Initially, a stable physical foaming was induced using a surfactant (i.e. pluronic) as blowing agent of a homogeneous blend of polysaccharide and polyethylene glycol diacrylate solution [1]. Furthermore, the porous structure of the foam was chemically stabilized by radical polymerization induced by homogeneous heating of the sample in a microwave. Microwaving curing allow the foam formation, employing short reaction times [2]. This method is competitive if compared to any commercial process, and it is able to obtain natural polysaccharides-based foams.

EXPERIMENTAL METHODS

Different mixtures of a natural polysaccharides and polyethylene glycol diacrylate were cured in a laboratory microwave oven into silicone vessels. Azobis(2-methylpropionamidine)dihydrochloride was used as thermoinitiator (TI). Both sodium salt of carboxymethylcellulose (CMCNa) and polyethylene glycol diacrylate (PEG) and chitosan (CS) and PEG mixtures were prepared with different PEG/polysaccharide ratios in order to investigate the properties of final material. The rheological properties for each mixture before the curing process were evaluated by viscosity measurements (ARES Rheometric Scientific). The influence of different ratios of PEG/CMCNa and PEG/CS in the final product was evaluated by different techniques. Firstly, chemical properties of each sample have been evaluated by spectroscopy analysis FT-IR, before and after curing in order to maximize reaction yield, and optimize the kinetic parameters (i.e. time curing, microwave power). The mechanical properties of the final product were evaluated by the calculation of the elastic modulus. Porous structure and surface analysis were characterized by SEM. Water absorption capacity and stability of materials was evaluated by means of in-vitro degradation test in PBS media. Finally, preliminary biological characterization was carried out with the aim to prove the biocompatibility of the resulting material.

RESULTS AND DISCUSSION

During the foaming procedure, the solutions increased in volume at least by 100% of the initial volume after addition of Pluronic. All the foams with a lower PEG/polysaccharide ratio are homogeneous and stables. In contrary, the solutions with a higher polysaccharide concentration present increased viscosity, resulting in more stable foam. Based on spectroscopy analysis FT-IR, it is evident that the reaction is not complete. Therefore it was added a post-cure in oven at 45°C for

12 h that has improved reaction yield. Mechanical properties of the foam increase with the increased of the polysaccharide concentration. This is mainly due to the presence of physical entanglements resulting in a higher degree of cross-linking. PEG/CS foams have higher mechanical properties than PEG/cellulose foams. Fig. 1a shows the SEM image of foam 20P80CS2. It is evident a hierarchical structure with open pores of different size in all the composition. The results of the indirect contact assay (alamarBlue) after 24 h exposure of the cells to the supernatants from the leaching studies did not show a significant release of toxic compounds. In fact, the cells exposed for 24 h to eluents (3 days) reached values similar to the negative control. Moreover, the results of the direct tests are shown in figure 1b. There is a clear indication that the scaffold materials have no negative effect on the metabolic activity of the cells. Cell viability and proliferation increase in a statistically significant manner with culture time. Moreover, it is possible to observe that even if 20P80C2 material shows low values of alamarBlue at day 1, it becomes higher at 4 and 7 days, probably due to the presence of a greater amount of cellulose in the material that improves the cell proliferation

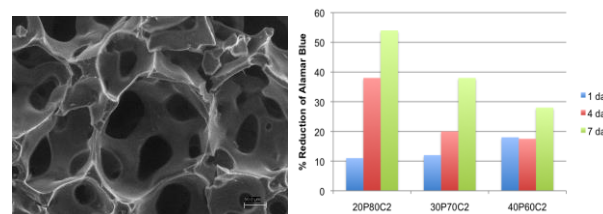


Figure 1. SEM micrography of 20P80CS2 sample (a). Cell proliferation short time 1,4 and 7 days for different blends of PEG/CMCNa(2%) (b).

CONCLUSION

This work demonstrated that physical foaming followed by thermo-polymerization induced by microwave is a quick and cheap foaming method to create structures with interconnected open porosity. The suitability to use two different polymer backbones has been successfully evaluated. Moreover, the preliminary biological analysis demonstrated the excellent biocompatibility profile.

REFERENCES

- [1] Eaves D. 2004 Handbook of polymeric foams, pp. 180 – 189. Shawbury UK: Rapra Technology limited.
- [2] Brent Tisserat 2012 Glycerol Citrate Polyesters Produced Through Heating Without Catalysis, Vol. 125, 3429–3437. Journal of Applied Polymer Science.

Fabrication of carbonate apatite coated calcite and its in vivo evaluation

Kunio Ishikawa^{1*}, Kanji Tsuru¹, Melvin L. Munar¹
Masako Fujioka-Kobayashi¹, Youji Miyamoto²

¹Department of Biomaterials/Faculty of Dental Science, Kyushu University, Japan

²Department of Oral Surgery/Institute of Health Biosciences, The University of Tokushima, Japan
ishikawa@dent.kyushu-u.ac.jp

INTRODUCTION

Carbonate apatite (CO₃Ap) block and granular prepared based on dissolution-precipitation reaction using calcite as precursors were found to be replaced to bone¹. However, the replacement to bone takes time. One of the methods to accelerate bone replacement may be to separate the role of surface and core materials of the bone substitute. In other words, the surface material is expected to show good osteoconductivity and should dissolve at weak acidic condition formed by the osteoblasts but should not dissolve at physiological condition. In contrast, the core materials should show higher dissolution than surface materials. In the present study, CO₃Ap coated calcite was fabricated and its behaviour at the bone defect was evaluated using rabbits

EXPERIMENTAL METHODS

Calcite block, one polymorph of CaCO₃ was prepared by exposing Ca(OH)₂ compacted uniaxially at 5MPa to CO₂ at room temperature for 7 days. Calcite granular, 600-1000µm, was immersed in 1 mol/L Na₂HPO₄ solution for prescribed period. Composition was evaluated by means of x-ray diffraction. Also, SEM and EDAX were used to observe the morphology and elemental analysis.

Cylindrical bone defects (φ5.0 mm×8.0 mm) formed at rabbit femur were reconstructed with 1) CaCO₃, 2) 10wt% CO₃Ap coated CaCO₃, 3) 30wt% CO₃Ap coated CaCO₃, 4) CO₃Ap. Also sham operation was made for comparison. Rabbits were sacrificed 4 weeks after surgery and analyzed by means of microcomputed tomography (microCT; Latheta LCT-200, ALOKA). Histological observation (MMA embedded; Villanueva-Goldner staining, Toluidine blue staining) was used to quantify volume of new bone at the defect site.

RESULTS AND DISCUSSION

Fig 1 summarizes the compositional transformation from calcite to CO₃Ap as a function of time at 40°C, 60°C and 80°C. As shown, calcite transforms to CO₃Ap and the rate of transformation was faster at higher temperature. 4 and 16 hours at 40°C were chosen to fabricate 10 and 30wt% CO₃Ap coated calcite. EDAX analysis confirmed that surface and core were CO₃Ap and calcite, respectively.

No inflammatory response was observed regardless of the composition of granular. Resorption was observed for all granules regardless of the composition of the granular. Resorption was remarkable in the case of calcite. 10wt% CO₃Ap coated CaCO₃ showed statistically higher resorption when compared to 30wt% CO₃Ap and CO₃Ap. Osteoclasts

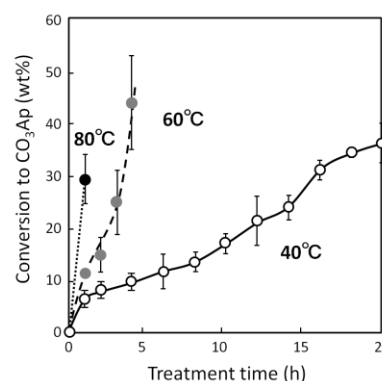


Fig 1 Compositional transformation from calcite to CO₃Ap as a function of time.

found on the surface of 10wt% CO₃Ap coated calcite was largest whereas those on the surface of CO₃Ap was smallest. Since resorption was largest in the case of calcite, most of the resorption of calcite is thought to be caused by physico-chemical dissolution rather than osteoclastic resorption.

New bone formation was observed on the surface of all granular including calcite. However, the amount of newly formed bone was limited in the case of calcite. Interestingly, approximately twice the amount of new bone was observed in the case of 10wt% CO₃Ap coated calcite and 30wt% CO₃Ap coated calcite when compared to CO₃Ap. Although the mechanism of the larger amount of bone observed for the CO₃Ap coated calcite has not been clarified in the present study, Ca²⁺ supplied by the dissolution of calcite may elicit the activation of osteoblastic cells.

CONCLUSION

CO₃Ap coated calcite was found to be fabricated based on the regulation of dissolution-precipitation reaction time of calcite granular in Na₂HPO₄ solution. CO₃Ap coated calcite seems to have good potential to be ideal bone substitutes since it has higher osteoconductivity and shows quicker replacement to bone when compared to CO₃Ap.

REFERENCES

1. Ishikawa K. *et al.*, Materials 3:76-83, 2009

ACKNOWLEDGMENTS

This study was supported in part by Grant for Strategic Promotion of Innovative Research and Development, Japan Science and Technology Agency, Japan and Grant-in-aid for Scientific Research from the Ministry of Education, Science, Sports and Culture, Japan.



Polysaccharide based nanocarriers for antioxidants

Ornella Bossio,¹ Laura G. Gómez-Mascaraque,^{1,2} Mar Fernández-Gutiérrez,^{1,2} Blanca Vázquez-Lasa,^{1,2}

Julio San Román^{1,2}

¹Institute of Polymer Science and Technology, CSIC. C/Juan de la Cierva, 3 28006 Madrid, Spain

²CIBER-BBN, Health Institute Carlos III. C/ Monforte de Lemos 3-5, 28029 Madrid, Spain, jsroman@ictp.csic.es

INTRODUCTION

The development of self-assembled nanoaggregate systems for antioxidants to improve their solubility and biocompatibility has received great attention in different fields such as biomaterials science.¹ Different hydrophilic and amphiphilic polysaccharides have been synthesized, chitosan (Ch) being one of the most used due to its genuine properties.² The aim of this work was the design and preparation of a nanocarrier for retinyl palmitate (RP) based on an amphiphilic chitosan (AmphCh) that can interact with the antioxidant. RP was selected due to its enhanced biological properties with respect to retinol and all-trans retinoic acid.

EXPERIMENTAL METHODS

Synthesis of the AmphCh was carried out by coupling reaction of palmitic acid (PA) mediated by 1-(3-dimethyl-aminopropyl)-3-ethylcarbodiimide (EDC) to get the Ch/P1 conjugate, and by the pair EDC/NHS (N-hydroxysuccinimide) to get the Ch/P2 conjugate. Nanoparticles (NP) of AmphCh either in presence or not of RP were prepared in distilled water at concentrations in the range 0.05 - 0.5 mg/mL. Physicochemical characterization was performed by FTIR and elemental analysis, and thermal characterization evaluated by TGA. Particle size distribution and zeta potential of NP were determined by dynamic light scattering (DLS) and morphology analysed by SEM, TEM and AFM techniques. Antioxidant behaviour was determined by the 1,1-diphenyl-2-picryl-hydrazyl (DPPH[•]) radical scavenging assay at 30 min. Biological studies were performed with fibroblasts of human embryonic skin.

RESULTS AND DISCUSSION

The coupling reaction of PA to chitosan proceeded successfully independent of reaction conditions, reaching yields of 89% and 95% for the synthesis of the Ch/P1 and Ch/P2 conjugates, respectively. Yield was only slightly higher for the synthesis using the pair EDC/NHS, but it allowed mild conditions. The amidation reaction was confirmed by analysis of FTIR spectra of amphiphiles, particularly in the regions 3000-2800 cm⁻¹ and 1650-1400 cm⁻¹. Substitution degree (DS) of chitosan calculated from elemental analysis gave values somewhat higher for Ch/P2 sample (10.3 %) compared with that of Ch/P1 sample (9.8 %). Free NH₂ groups of AmphCh determined by pH titration reduced from 68.5 % of initial Ch to 64.2 and 57.6 % for the Ch/P1 and Ch/P2 samples. The coupling reaction was also confirmed by thermal degradation analysis. Self-aggregated NP were formed by the association of the palmitoyl moieties (and RP in loaded NP) into

hydrophobic domains forming the cores and the chitosan backbones forming the hydrophilic outside shells. RP encapsulation was evident by FTIR spectroscopy. Loading efficiency (LE) values were 77.5 and 88.6 % and loading content (LC) values were 12.9 and 14.6 %, for the Ch/P1 and the Ch/P2 samples, respectively.

Values of apparent hydrodynamic diameter (D_h) were higher for Ch/P2 NP but they were similar for RP-loaded NP of both conjugates. Zeta potential (ζ) values reflected the positive charge of NP and stability in aqueous medium (Table 1).

Table 1. DLS results of NP. *2 mM NaCl solution.

NP	Conc. (mg/mL)	D _h (nm)	PDI	ζ (mV)
A	0.50	276±2	0.239±0.01	24.3±1.0
	0.10*	188±12	0.277 ±0.04	
B	0.50	437±8	0.213±0.04	26.1±0.8
	0.10*	466±11	0.259±0.05	
C	0.50	281±2	0.154±0.01	28.9±0.7
	0.10*	281±4	0.178±0.01	
D	0.50	274±19	0.310±0.01	28.9±0.3
	0.10*	328±3	0.304±0.02	

A: Ch/P1 NP. B: Ch/P2 NP. C: RP-loaded Ch/P1 NP.

D: RP-loaded Ch/P2 NP

Analysis of NP by SEM and AFM revealed an almost spherical morphology for all systems. NP examination by TEM confirmed the pseudo spherical morphology and the formation of the typical core-shell structure. DPPH[•] assay results gave a radical scavenging activity (RSA) of loaded NP of 33% for Ch/RP1 and 39% for Ch/RP2 samples. Unloaded NP had a RSA of 25%.

All NP were not cytotoxic, giving cellular viability values higher than 80 % in MTT tests. In addition, LDH assay results reflected no cytotoxicity via cellular membrane lysis. Uptake of RP-loaded NP was observed by endocytosis tests; however, blank NP did not enter the cells.

CONCLUSION

A palmitoyl chitosan conjugate is proposed as a suitable nanocarrier for RP with potential biomedical applications in areas such as skin diseases.

REFERENCES

1. Lim S.J. *et al.*, Int. J. Pharm. 243:135-146, 2002
2. Li Q. *et al.*, Eur. J. Pharm. Sci. 41:498-507, 2010

ACKNOWLEDGMENTS

The authors would like to thank the *Spanish Ministry of Economy and Competitiveness* (project MAT2010-18155) for financial support.



Effect of Kassinin and Collagen Fibrils on Cell Spreading and De-adhesion Dynamics

Edna George¹, Pradeep Kumar Singh¹, Samir Maji¹ and Shamik Sen^{1*}

¹Department of Bioscience & Bioengineering, Indian Institute of Technology (IITB), India ednasenlab@iitb.ac.in

INTRODUCTION

Amyloids are often associated with several diseases but studies have proved the importance of functional amyloids like curli proteins in *E.coli*, and Pmel17 in *H.sapiens* normal physiological functions of the host organisms. Additionally, amyloids have been proved to be non-toxic with high mechanical properties and tunable physio-chemical properties making them suitable candidate for tissue engineering application. Here, we studied the cell-amyloid interaction using Kassinin (Kas) which is a neuropeptide that belongs to tachykinin family¹. Lack of sufficient cell studies on Kas and the need for bio-friendly amyloids with desired mechanical properties to design suitable biomimetic matrices with natural topography led to the following study. We carried out cell studies using fibroblasts on kas coated substrates and compared the effects with collagen (Col) coated substrates to understand the cell spreading and contractile mechanics.

EXPERIMENTAL METHODS

Fibril preparation and Substrate coating: Kas fibrils were prepared as reported previously¹. For experiments, well-plates were incubated with Kas or Col (Sigma) at concentrations ranging from 0.5 to 7.5 μ M at 37°C for 2hrs. All the coated substrates were blocked with 2% F127 Pluronic (Plu) (Sigma) for 15min at room temperature and UV sterilized.

Cell Culture: NIH3T3 cells obtained from National Centre for Cell Science (NCCS, Pune) were maintained as instructed. Cells were harvested for experiments, seeded at a density of 4500cells/cm² and incubated for 24hrs at 37°C. For trypsin de-adhesion assay, cells were washed with 1x PBS, incubated with 0.25% trypsin-EDTA (HiMedia), and images were captured at 2s intervals at 10x magnification².

Image Analysis: All the images were analyzed using Image J software (NIH). ~100 cells for cell spread analysis and 30 cells for de-adhesion dynamics were pooled from two independent experiments for analyzing cell spread area, cell shape and retraction kinetics. For de-adhesion assay the cell spread area were traced as a function of time to obtain two time constants τ_1 and τ_2 . These values were normalized by fitting to a sigmoidal curve using Boltzmann equation².

RESULTS AND DISCUSSION

To exploit full potential of fibrils as a fully functional biomaterial, the extent of cell spreading were studied by analysing, phase contrast images acquired at 10x magnification (Fig 1A at $t=0$ sec). Fibroblasts showed a biphasic spreading response (Fig 1B) on Kas fibrils as well as on Col coated substrates across concentrations.

Additionally, the cell shape, which was measured as the circularity of the cell remained unchanged (data not shown). The negative control (only Plu coated substrates) showed a significant difference in cell spread area and cell morphology.

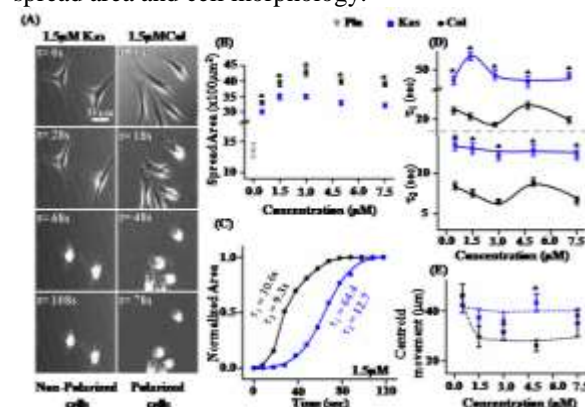


Fig1. Comparison of cell spreading ($t=0$ sec), retraction kinetics and polarity by NIH3T3 cells on Kas and Col of varying densities. (* $p<0.05$)

Significant difference in the spreading response between cells on Kas and Col suggested the probability of substrate dependent changes in biophysical properties of fibroblasts. Thus, we decided to probe the retraction kinetics of cells using trypsin de-adhesion assay. Here the changes in cell area were traced till the cells rounded up but remained attached to the substrate (Fig 1A). The de-adhesion dynamics showed that fibroblasts were more contractile (Fig 1C & D) and highly polarized on Col than on Kas fibrils (Fig 1E) irrespective of ligand density.

While blocking with Plu ruled out any possible effect of serum protein deposition that could enhance cell adhesion, unperturbed collagen deposition across all conditions (data not shown) eliminated the possible intervention of collagen secreted by fibroblasts. Hence, all the cellular and morphological changes were attributed to the effect of amyloid fibrils.

CONCLUSION

In conclusion, our studies demonstrate that kassinin can serve as a suitable biomaterial for tissue engineering applications. Long term studies on cells will help to understand the influence of kassinin on cellular processes like differentiation.

REFERENCES

1. Singh, P. K. & Maji, S. K.. *Cell Biochem. Biophys.* 64, 29–44 (2012).
2. Sen, S. & Kumar, S. *Cell. Mol. Bioeng.* 2, 218–230 (2009).



Fast Acting Antibacterial 45S5 Bioglass® Scaffolds Reinforced with Gelatin/Genipin for Bone Tissue Engineering

Wei Li^{1*}, Hui Wang², Seema Agarwal² and Aldo Boccaccini¹

^{1*}Institute of Biomaterials, University of Erlangen-Nuremberg, Erlangen, Germany, wei.li@ww.uni-erlangen.de

²Macromolecular Chemistry II, University of Bayreuth, Bayreuth, Germany

INTRODUCTION

45S5 Bioglass® is a promising material for bone tissue engineering scaffolds due to its excellent bioactivity, biocompatibility, osteogenic and angiogenic effects¹. However, uncoated 45S5 Bioglass® scaffolds exhibited insufficient mechanical properties². In addition, the risk of infection exists during scaffold implantation. Therefore, in order to improve the mechanical properties and incorporate antibacterial functionality, 45S5 Bioglass® scaffolds were coated with genipin crosslinked gelatin, and then loaded with antibacterial polyguanidine (poly(p-xylyleneguanidine)hydrochloride, PPXG)³.

EXPERIMENTAL METHODS

45S5 Bioglass® scaffolds were prepared by foam replication method². The obtained scaffolds were coated with 5% w/v gelatin-genipin (99:1) solution by dip coating method. PPXG loading was achieved by dripping the PPXG-methanol solution (40, 120 and 200 µg/mL) onto genipin crosslinked gelatin (GCG) coated scaffolds.

The morphology, structure and mechanical properties of scaffolds were characterized using SEM, FTIR and compression test. Simulated body fluid (SBF) was used to assess the bioactivity of scaffolds. Antibacterial activities to *E. coli* and *B. subtilis* were determined using Kirby-Bauer-Test and Time-dependent Test.

RESULTS AND DISCUSSION

Figure 1 shows that highly interconnected pore structure of scaffolds was maintained after coating. The strut was covered by a thin layer of gelatin. The porosity and pore size were 93% and 200-550 µm, respectively.

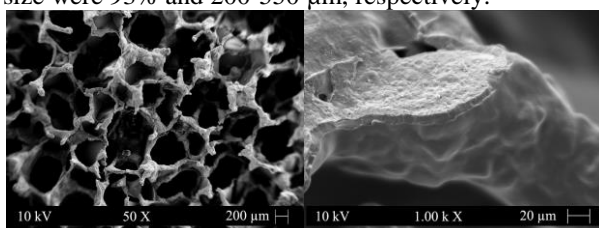


Figure 1: SEM images of GCG coated scaffolds.

The average compressive strength of uncoated and coated scaffolds was 0.04 MPa and 1.00 MPa, respectively. The area under the load-displacement curve of uncoated scaffolds was only 5 N·mm, whereas it was increased to 285 N·mm for coated scaffolds.

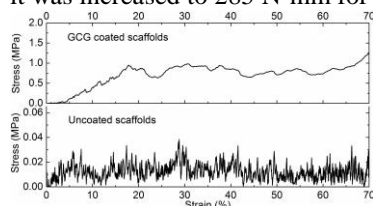


Figure 2: Typical stress-strain curves of uncoated and coated scaffolds.

The strengthening and toughening effects of GCG coating could be explained by micron-scale crack-bridging mechanism.

The FTIR spectra and SEM image of coated scaffolds show characteristic P-O and C-O bands of carbonated hydroxyapatite (HCA) and globular, cauliflower-like apatite crystals after 7 days immersion in SBF (Figure 3). The results indicate the retention of bioactivity of scaffolds after GCG coating.

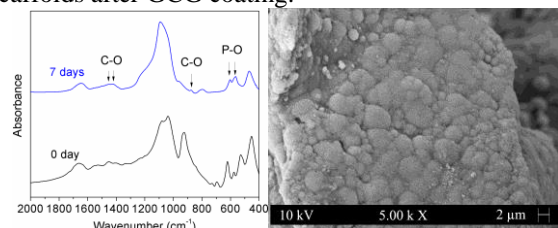


Figure 3: FTIR and SEM showing HCA formation.

As shown in Figure 4, PPXG provided antibacterial activity to the scaffolds against both Gram-positive and Gram-negative bacteria. The speed of antibacterial action varied on the amount of PPXG. Sample (3) and (5) killed 99.9% *B. subtilis* after 120 and 30 min, respectively.

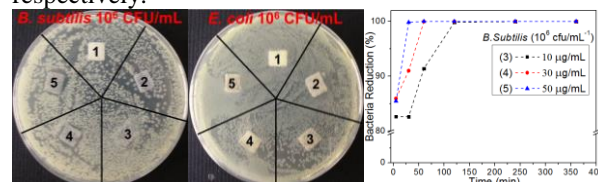


Figure 4: (1) uncoated scaffold, (2) coated scaffold, (3) coated scaffold + 10 µg/mL PPXG, (4) coated scaffold + 30 µg/mL PPXG and (5) coated scaffold + 50 µg/mL PPXG.

CONCLUSION

Improved mechanical properties were provided to 45S5 Bioglass®-based scaffolds by genipin crosslinked gelatin coating without sacrificing the *in vitro* bioactivity. Additionally, the scaffolds were made antibacterial against both Gram-positive and Gram-negative bacteria by using polyguanidine. The novel antibacterial bioactive 45S5 Bioglass®-based scaffolds with improved mechanical properties are promising candidates for bone tissue engineering.

REFERENCES

1. Hench L.L., J. Mater. Sci. - Mater. Med. 17:967-978, 2006
2. Chen Q.Z. *et al.*, Biomaterials 27:2414-2425, 2006
3. Mattheis C. *et al.*, Polym. Chem. 4:707-716, 2013

ACKNOWLEDGMENTS

Wei Li acknowledge the China Scholarship Council for financial support. The authors thank Ms. Yaping Ding and Dr. Menti Goudouri for experimental support.

Living biointerfaces based on non-pathogenic bacteria to direct cell function

Aleixandre Rodrigo-Navarro^{1,4}, Patricia Rico¹, Anas Saadeddin², Andres J. Garcia³, Manuel Salmeron-Sanchez⁴

¹Center for Biomaterials and Tissue Engineering, Universitat Politècnica de València, Spain

²Abengoa Research, Campus Palmas Altas, Sevilla, Spain

³Petit Institute for Bioengineering and Bioscience, Georgia Institute of Technology, USA

⁴Division of Biomedical Engineering, University of Glasgow, UK, Manuel.Salmeron-Sanchez@glasgow.ac.uk

INTRODUCTION

Understanding cell behaviour on synthetic surfaces is of foremost interest to engineer microenvironments that direct cell fate. As cells cannot interact directly with synthetic biomaterials, surfaces have been functionalized with a broad range of proteins, fragments, peptides and growth factors. However, these passive coatings can by no means provide the dynamic stimuli required to orchestrate cell responses and organise the formation of a new tissue at the material interface. Significant efforts have focused on engineering materials that recapitulate characteristics of ECM, such as the presentation of cell adhesive motifs or protease degradable cross-links, in order to direct cellular responses¹. However, the development of a cell/material interface able to provide biological stimuli upon demand has not been established yet. We hypothesised that non-pathogenic bacteria can provide such a role, as they can colonise the surface of a broad range of materials and can be genetically modified to express or secrete desired adhesive proteins or factors to a living cell population, upon demand. This work investigates the potential of a living interface based on *Lactococcus Lactis* expressing a FN fragment (FNIII₇₋₁₀) as a membrane protein to direct cell adhesion, signalling and differentiation². This system introduces engineered bacteria as a new tool to direct cell behaviour at the material interface.

EXPERIMENTAL METHODS

The GFP-containing pGFP-C2 plasmid was used to construct a vector with FNIII₇₋₁₀ downstream to GFP. FNIII₇₋₁₀ fragment was amplified from pET15b-FNIII₇₋₁₀ and cloned into the PT1NX plasmid. Transformed bacteria were cultured to establish a stable biofilm on glass surfaces. Biofilm viability was evaluated and observed using SEM and AFM. The surface density of FNIII₇₋₁₀ was quantified using ELISA with monoclonal HFN7.1 antibody and western-blot. C2C12 myoblasts were cultured on the living interface for up to 4 days. Cell adhesion and signalling was investigated by staining focal adhesions (vinculin) and FAK phosphorylation (western blot). Cell differentiation was quantified by staining sarcomeric myosin.

RESULTS AND DISCUSSION

Engineering microenvironments to provide cells with dynamic cues, as occurs in the natural extracellular matrix, is a field of intensive research seeking to direct the differentiation of stem cells and advance in strategies for tissue repair and regeneration. We engineered food-grade *Lactococcus* to present the FNIII₇₋₁₀ fibronectin fragment as a membrane protein,

containing RGD and PHSRN synergy sequences and promotes cell adhesion and differentiation (Fig. 1).

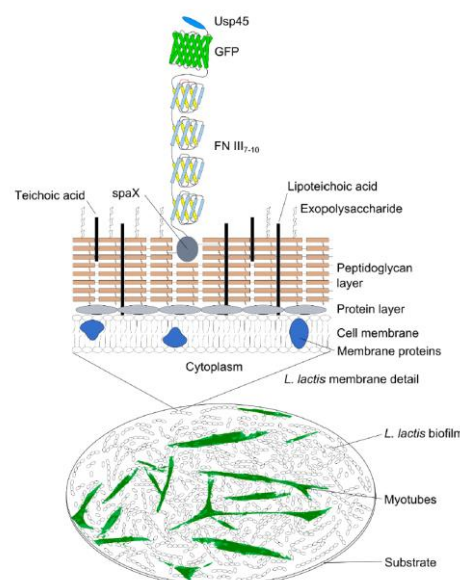


Figure 1. Schematic of the living biointerface. C2C12 myoblasts differentiated to myotubes on this system.

Cells adhere, spread, develop focal adhesions and promote the FAK phosphorylation on the FN-expressing *L. Lactis*, in a similar way as when seeded directly on a FN coating.. The myogenic differentiation triggered by *L. Lactis*-FNIII₇₋₁₀ strain was found higher compared to the non FN-expressing control strain and higher than on standard myogenic differentiation substrate (collagen I and native fibronectin coatings).

CONCLUSION

We have shown that non-pathogenic bacteria based on *L. Lactis* expressing the FNIII₇₋₁₀ fragment form a dynamic biointerface between synthetic materials and cells. Overall, this living interface enhances the myogenic differentiation process. Further genetic modification of this living interface is being done to engineer a dynamic system able to provide cells different temporal stimuli beyond cell adhesion, such as the delivery of growth factors and other molecules upon external demand, which can be then applied to several strategies to promote tissue repair and regeneration.

REFERENCES

1. Lutolf M. *et al.* Nature 462:433, 2009
2. Saadeddin A. *et al.* Adv Health Mater 2:1213, 2013

ACKNOWLEDGMENTS

ERC through HealInSynergy 3069



Self-Disinfecting Urinary Biomaterials: pH-Triggered Quinolone Release for Prevention of Catheter-Associated Urinary Tract Infections

Colin P. McCoy, Nicola J. Irwin, Christopher Brady, Louise Carson, David S. Jones, Sean P. Gorman
School of Pharmacy, Queen's University Belfast, 97 Lisburn Road, Belfast BT9 7BL, Northern Ireland, UK
n.irwin@qub.ac.uk

INTRODUCTION

The urinary tract, a common site of action of the quinolones, maintains a normal physiological pH range between pH 4.8 to pH 8¹. Elevations in urine pH to levels up to pH 9.1 are, however, reported during catheter-associated urinary tract infections (CAUTIs) as a result of urease-catalysed hydrolysis of urea into ammonia². In this study, we, firstly, examined the effect of pH on quinolone activity against the urease-producing pathogen *Proteus mirabilis*, and, secondly, exploited this bacterial-induced pH elevation in the development of infection-responsive candidate catheter coatings capable of releasing quinolone agents, specifically, and rapidly, at the onset of CAUTIs.

EXPERIMENTAL METHODS

Determination of antimicrobial susceptibility

Minimum inhibitory concentration (MIC), minimum bactericidal concentration (MBC) and minimum biofilm eradication concentrations (MBEC) of three quinolone agents: nalidixic acid, norfloxacin and ciprofloxacin, against *P. mirabilis* ATCC 35508 at pH 5, 7, 9 and 10 were determined according to Clinical and Laboratory Standards Institute methods.

Development of a chemically-triggered release system

A series of novel polymerisable ester nalidixic acid conjugates with varying vinyl chain lengths: 1-ethyl-7-methyl-4-oxo-1,4-dihydro-1,8-naphthyridine-3-carboxylic acid- (NAL-) 2-propen-1-ol ester, NAL-3-buten-1-ol ester and NAL-9-decen-1-ol ester, herein referred to as NAL2yl, NAL3yl and NAL9yl, respectively, were synthesised *via* a two-step procedure, involving preparation of a reactive anhydride intermediate, and subsequent esterification with a range of deprotonated vinyl alcohols: 2-propen-1-ol; 3-buten-1-ol; and 9-decen-1-ol. Drug conjugates (5% w/w) were copolymerised with 2-hydroxyethyl methacrylate before examination of release kinetics and resistance to adherence of *P. mirabilis* and *Staphylococcus aureus* in universal buffers of pH 7 and pH 10.

Statistical analysis

The effect of pH on antibacterial activity, drug release rates and bacterial resistance of the copolymers was statistically evaluated by a one-way analysis of variance, followed by Tukey's post-hoc test.

RESULTS AND DISCUSSION

All concentrations of nalidixic acid above the MBC displayed bactericidal activity selectively at alkaline pH, in contrast to the loss of cidal activity characteristic of high drug concentrations in pH 5 and pH 7 media. Elevation of media pH also caused an increase in both bacteriostatic and bactericidal activities of the two fluoroquinolones tested against both planktonic and

biofilm-associated *P. mirabilis*; MBC and MBEC values for ciprofloxacin decreased approximately 6000-fold and 10-fold respectively between pH 5 and pH 9.

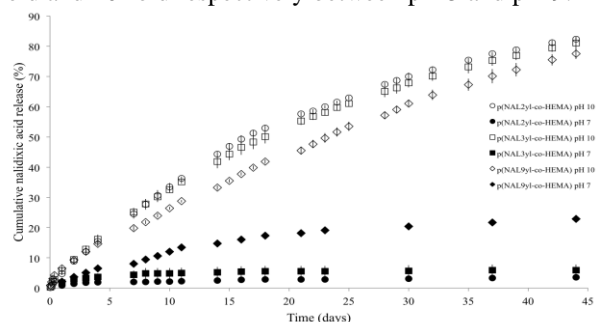


Fig. 1: The effect of pH on the mean (\pm S.D.) release of nalidixic acid from the conjugate copolymers at 37°C with shaking.

The *in vitro* pH-mediated kinetics of nalidixic acid release from the conjugate copolymers are shown in Fig. 1. A similar trend in release rate with respect to pH of the dissolution media was observed for all copolymers, irrespective of conjugate alkyl chain length. The ester bond mediating attachment of nalidixic acid to the alkyl spacer moiety was relatively stable at normal physiological urine pH - pH 7 - and therefore successfully delayed drug release from the copolymers, in contrast to the significantly more rapid rates of release demonstrated at the elevated pH typical of CAUTIs - pH 10. Adherence of *P. mirabilis* and *S. aureus* to p(NAL9yl-co-HEMA) was approximately 80% lower than to the p(HEMA) control after both 4 h and 24 h contact.

CONCLUSION

The observed increase in quinolone bactericidal activity in alkaline conditions provides rational for their use in the chemotherapy of urinary tract infections. Initial microbiological assessment suggests that the pH-responsive nalidixic acid conjugate copolymers developed herein hold significant promise for preventing CAUTIs when applied as urinary catheter coatings.

REFERENCES

1. Tallgren LG, von Bonsdorff CH. *Acta Med Scand.* 178:543-551, 2009
2. Stickler DJ, Morgan SD. *J Med Microbiol.* 55:489-494, 2006

ACKNOWLEDGMENTS

The authors thank the Department for Employment and Learning, Northern Ireland, for financial support.

Apatite Promoting, Low Modulus Composite Bone Cements with Low Heat Generation upon Set and High Subsequent Antibacterial Release

Muhammad Adnan Khan, Anne Young

UCL, Eastman Dental Institute, 256 Gray's Inn Road, London WC1X 8LD. Email: adnan.khan.11@ucl.ac.uk

INTRODUCTION

Vertebral compression fractures (VCF) can be stabilized by PMMA cement (Simplex-P®). Inherent drawbacks, however, include long setting time to enable hand mixing. Furthermore, high heat generation during set and monomer leaching upon incomplete cure can kill cells¹. Moreover, PMMA does not promote apatite formation to enhance bonding to living bone. This is combination with shrinkage during set, limits bone fixation. Antibiotic release from PMMA is also restricted (5-7%)¹.

Recent clinical studies have demonstrated significant advantages of using the composite cement (Cortoss®) instead of PMMA for VCF fixation². Dimethacrylates use in Cortoss, instead of less cell compatible methyl-methacrylate (in PMMA) is of particular benefit. Furthermore, composites can be mixed in seconds and dimethacrylate conversion need only be 50% rather than 100% to prevent monomer leaching. Cortoss also produces significantly less heat and shrinkage upon set and may promote low or negligible level apatite precipitation on surface. Cortoss, however, exhibits high modulus with lower strength and toughness³ than PMMA and is therefore less able to absorb energy before breaking. Cortoss has no antibacterial release or effect.

The aim of this study was therefore to compare curing and mechanical properties of experimental composites with those of Cortoss® and Simplex® and demonstrate their apatite-precipitation-enhancing and antibacterial-release features.

EXPERIMENTAL METHODS

UDMA, TEG-DMA dimethacrylate monomers were combined with initiator (BP) or activator (DMPT) to form two liquid phases. Two stable pastes were prepared by mixing with glass particles containing chlorhexidine (10%) (CHX), reactive mono and tri calcium phosphate (CaP – 10 or 20%) and a polymeric antimicrobial (PAM – 0 or 10%) (Table 1). FTIR was used to assess the time for half reaction and final conversion after mixing of the two pastes. The latter were used to calculate heat generation and shrinkage. Biaxial flexural strength (BFS) and modulus were measured. CHX and PAM

	CaP wt%	PAM wt%
F1	20	10
F2	10	10
F3	10	0
C	Cortoss®	
S	Simplex®	

Table 1: Formulations

release were assessed using UV and HPLC. Apatite precipitation on set material surfaces in simulated body fluid was quantified using mass change and confirmed using SEM, EDAX and Raman.

RESULTS AND DISCUSSION

The working time for all experimental material were comparable with Cortoss. Subsequent setting time (Half-life) of F1 and F2 was comparable with Cortoss but much lower as compared to Simplex. This reduces possibility of monomer leaking from the site of application in vivo. The final conversion was higher for all experimental formulations (74-80%) than for Cortoss (64%) (Table 2). This reduces subsequent potential monomer leaching. Heat generation and shrinkage of experimental material were beneficially lower than commercial. Although the strength of F1 and F2 were lower than Cortoss, their low modulus will improve toughness (Table 2) and potentially decrease the chance of brittle fracture in adjacent vertebra⁵. PAM release is 8-10 times faster than CHX and nearly 95% in 6 weeks (Fig-1). PAM also increases the release of other antibacterial component. Watersorption for all formulation is 1-3% of mass change. However, mass change for F1 and F2 is significantly increased due to hydroxyapatite formation on the material surfaces (Fig-2). SEM images shows

No.	Half life (t ₅₀) (s) 95%-CI	Final conversion (%) 95%-CI	Heat (cal/cc) 95%-CI	Shrinkage % (vol/vol) 95%-CI	Flexural strength (MPa) 95%-CI	Modulus (Gpa) 95%-CI
F1	265 ±5	79.6 ±0.6	26.4 ±0.3	4.3 ±0.02	60 ±2	1.1 ±0.1
F2	255 ±7	79.4 ±0.5	26.1 ±0.3	4.3 ±0.02	74 ±2	1.5 ±0.1
F3	300 ±5	74.1 ±0.6	25.1 ±0.3	4.2 ±0.02	115 ±4	2.3 ±0.2
C	310 ±5	64 ±0.5	30.1 ±0.3	5.0 ±0.02	99 ±4	3.3 ±0.3
S	402 ±17	81 ±0.2	46.8 ±0.3	7.6 ±0.02	128 ±4	1.7 ±0.3

Table 2: Half-life, final conversion, heat generation, mechanical properties of experimental and commercial materials.

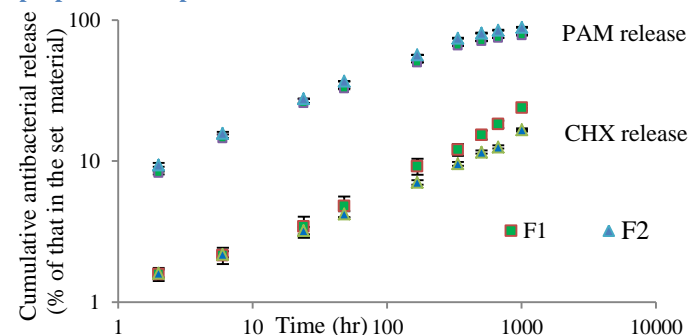


Figure 1: PAM and CHX release from F1 and F2.

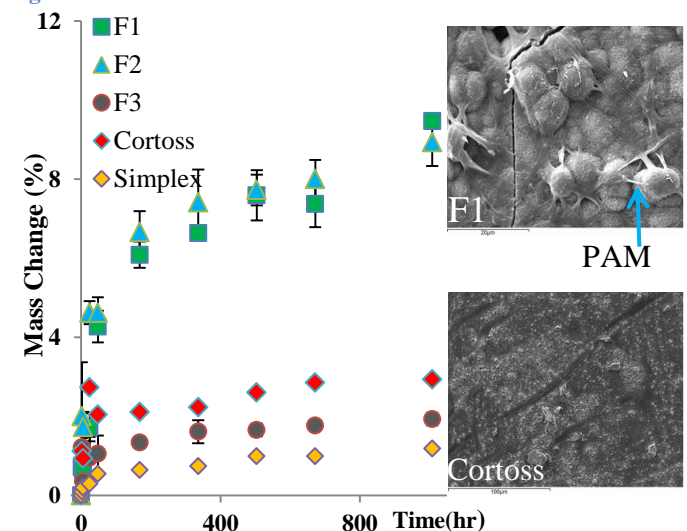


Figure 2: Mass change due to water sorption and apatite formation on the surface of specimen in simulated body fluid (SEM images).

hydroxyapatite potentially held together by PAM strands.

CONCLUSION

Experimental formulations F1 and F2 have high conversion in addition to low heat generation and shrinkage that should improve biocompatibility and bonding. Their low modulus could also prevent adjacent vertebral fracture. PAM is readily released to provide antibacterial action but in addition promotes rapid apatite layer formation.

REFERENCES

- 1-Santin M, JMC: MM. 2004;15(11):1175-80.
- 2- Muller SD, JBJS, 2003;85-B(SUPP I):13.
- 3-Boyd D, J. Mater. Sci. 2008;19(4):1745-52.
- 4-Baroud G ST, J Long Term Eff Med Implants. 2006;16(1):51-9
- 5-Heini PF, Eur Spine J 2000;9:445-450

ACKNOWLEDGMENTS

I would like to thank HEC Pakistan for sponsoring.

Toward potent antibiofilm degradable medical devices: generic methodologies for the surface modification of polylactide

Benjamin Nottelet^{1*}, Carla Sardo², Sarah El Habnoui¹, Xavier Garric¹, Vincent Darcos¹, Jean-Philippe Lavigne³, Gennara Cavallaro² and Jean Coudane¹

¹Institute of Biomolecules Max Mousseron (IBMM - CNRS UMR 5247), Artificial Biopolymers Department - Université Montpellier I, Université Montpellier 2, ENSCM - France

²Dipartimento di Scienze e Tecnologie Biologiche, Chimiche e Farmaceutiche, Sez. CTF - University of Palermo - Italy.

³Bacterial virulence and infectious disease, INSERM U1047- University of Montpellier 1 – France,
Benjamin.nottelet@univ-montp1.fr

Surface post-modification of polylactide is combined to CuAAC click chemistry or thiol-yne click photochemistry to yield antibiofilm surfaces.

INTRODUCTION

As a direct result of the life expectancy increase, implants are increasingly used for the restoration of human anatomy and functions. However, this is accompanied with the development of biomaterial-associated septic failures¹. To limit these risks, the modulation of the antibacterial surface properties of prosthetic materials appears therefore as a convenient and efficient strategy. In this frame, post-polymerization modification approaches, especially click chemistry, have attracted much attention in the last decade². In this communication, we wish to report on the recent post-modification strategies developed by our group to yield polylactide antibacterial surfaces.

EXPERIMENTAL METHODS

PLA surfaces were activated via anionic chemical modification to anchor alkyne moieties, according to a reaction previously described by our group³. This clickable PLA intermediate was then engaged in two distinct strategies. In a first approach, well-controlled quaternized PDMAEMA chains (5-10 kDa) with an azide chain-end were synthesized and covalently grafted to the PLA clickable surfaces by CuAAC 1,3-dipolar cycloaddition. In a second approach, cationic derivatives of α,β -poly(N-2-hydroxyethyl)-aspartamide (PHEA) were functionalized with lipoic acid (LA). Photoactivated thiol-yne reaction was done under UV by reacting PHEA-LA at the surface of the clickable PLA in the presence of TCEP. All polymers have been characterized by NMR and SEC analyses. After careful washes, surfaces were analysed by AFM and XPS. Antibacterial activity was tested against four bacterial strains. Adherence of bacteria and biofilm formation were tested. Cytocompatibility was evaluated with L929 fibroblasts. All data are expressed as means \pm SD and correspond to measurements in triplicate.

RESULTS AND DISCUSSION

Thanks to the use of optimized and mild activation conditions, alkyne functionalized PLA surfaces were obtained without degradation as already reported elsewhere⁶. CuAAC cycloaddition of QPDMAEMA chains was evaluated by XPS and showed an overall 10% coverage of the PLA surface by QPDMAEMA. No residual copper was detected. Activity was strong

against all bacterial strains, including *E. Coli* and *S. Aureus* with a clear dependence of the antibacterial activity over QPDMAEMA molecular weight and alkylating agent (Figure 1). Best results were obtained for Mn = 10 000 g/mol and heptyl group with adherence reduction factors > 99.999% (ASTM E 2149–01) and strong bactericidal activity.

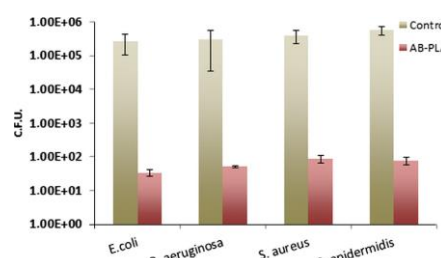


Fig. 1. Antibacterial activity of antibacterial PLA surface (red bars) against four bacterial strains. PLA plates are shown as control (brown bars).⁴

With short reaction times and no metals used, UV photoactivated thiol-yne grafting of PHEA-LA was studied as a green alternative to CuAAC. Advantageously, the heterogeneous surface reaction took place in aqueous media. Various solvent mixtures were tested and best results were obtained in slightly acidic water/ethanol (1:1) medium, in the presence of TCEP and with a 15 min irradiation time per PLA plate side. Under these conditions, XPS confirmed the covalent grafting of the cationic PHEA-LA derivative. As for CuAAC, antibacterial and antibiofilm activities were tested with again reduction factors > 99.999% and up to 80% biofilm decrease for all four bacterial strains. Interestingly, whatever the methodology used all surfaces showed a good cytocompatibility towards L929 fibroblasts cells with respect to TCPS control.

CONCLUSION

Antibacterial PLA surface modification was obtained in an efficient two steps approach by combining anionic and click chemistries. For the first time green thiol-yne strategy was applied to PLA surfaces, which paves the way to further developments in the biomedical field.

REFERENCES

1. Campoccia D. et al. Biomaterials 34:8018-8029, 2013
2. Theato P. & Klok H-A. Eds. Wiley-CH, 2013
3. El Habnoui S. et al. Adv. Funct. Mater. 21:3321-3330, 2011
4. El Habnoui S. et al. Acta Biomater. 9:7709-7718, 2013

ACKNOWLEDGMENTS

Authors thank the French MESR for PhD fundings.



Controlled release of gentamicin from gold nanocarriers

Stefano Perni^{1,3} and Prokopovich Polina^{1,2,3*}

¹School of Pharmacy and Pharmaceutical Sciences, Cardiff University, UK

^{2*}School of Engineering, Cardiff University, UK prokopovichp@cardiff.ac.uk

³Center for Biomedical Engineering, Massachusetts Institute of Technology, USA

INTRODUCTION

Antibiotics are still the most effective agents used to fight bacterial infections. Their administration to patients is generally through oral, topical or parenteral route; antibiotics are quickly metabolised or excreted from the human body, this leads to the need for frequent administration and their half-life is usually an important factor in the therapeutic choice. In order to render the administration less frequent, antibiotic release from a carrier can be employed. Gold nanoparticles have found numerous applications as drug delivery vehicle because of their stability and biological safety¹.

In this work, we synthesised gold nanoparticles capped with either glutathione or L-cysteine and covalently attached gentamicin to the capping agent.

EXPERIMENTAL METHODS

Conjugates preparation. Gold nanoparticles were synthesised from a HAuCl₄ water solution (17 mM) containing glutathione or L-cysteine (8 mM) as capping agent adding hydrazine. The nanoparticles were separated after 1 hour of mixing at room temperature adding methanol and centrifuging.

Conjugates were prepared dispersing the 100 mg of Au nanoparticles in 25 mM MES buffer (pH 6.5) in the presence of gentamicin (50 mg) along with NHS (25 mg) and EDC (45 mg). After 24 h at room temperature under vigorous mixing, the conjugates were separated through centrifugation and washing in methanol.

Gentamicin release quantification. Conjugates were dispersed in buffer pH=7 and incubated at 37 °C. At prefixed times samples were taken and the gentamicin in the buffer was quantified thorough fluorescence spectroscopy using o-Phthaldialdehyde.

Antimicrobial testing. *Staphylococcus aureus* (NCIMB 9518) and Methicillin resistant *S. aureus* - MRSA (NCTC 12493) were grown at 37 °C for 24h in Brain Heart Infusion (BHI) broth. Cells were diluted in fresh BHI broth to a concentration of 10⁴ CFU/ml prior to mixing with Au-gentamicin conjugates at various concentrations and then incubated at 37 °C. Cells were counted after 24 h through serial dilution and plating on BHI Agar.

RESULTS AND DISCUSSION

FTIR revealed that the hydrogen bond of the SH group present in both glutathione and L-cysteine disappeared after the synthesis of the gold nanoparticles demonstrating the stabilisation conferred to the nanoparticles by the strong affinity of gold for sulphur. Both capping agents exhibit carboxylic group that were employed for the conjugation of gentamicin that presents amino (NH₂) groups.

Gentamicin was released from the glutathione capped Au conjugates for two days, after 2 days no more bound

gentamicin was released. However when L-cysteine was used the released was completed after 24 hours. Furthermore, the over amount of antibiotic released was greater for glutathione capped conjugates than L-cysteine.

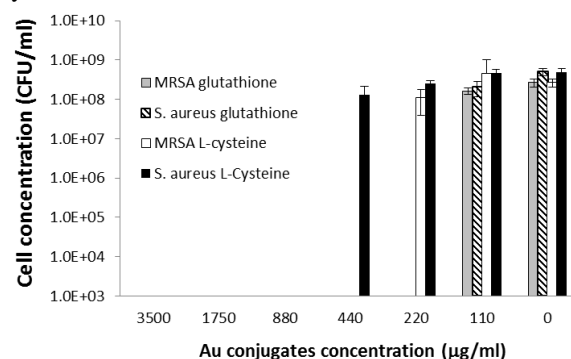


Figure 1. Bacterial cells survivors after 24h contact with gold conjugates at various concentrations.

No antimicrobial activity was exhibited by the unconjugated nanoparticles at concentrations as high as 3.5 mg/ml. The conjugates exhibited antimicrobial activity against *S. aureus* and MRSA (Fig 1). When glutathione was employed the MIC was 220 µg NP/ml irrespectively of the bacteria species tested. Whilst when cysteine was employed as capping agent the MIC was 440 µg NP/ml for MRSA and 880 µg NP/ml for *S. aureus*.

The MIC for pure gentamicin was 4 µg/ml for MRSA and less than 2 µg/ml for *S. aureus*, therefore, the higher resistance of *S. aureus* to the conjugates is not related to the antibiotic used but is connected to interference of cells growth with the antibiotic release from the carrier, possibly through pH changes of the media. Moreover, the higher activity of the glutathione capped conjugates is related to the higher amount of gentamicin released from these nanocarriers.

CONCLUSION

This work demonstrates that gold nanoparticles can be employed as antibiotic carriers providing a continuous release of antibiotic over few days. Glutathione appeared a better capping agent than cysteine allowing higher load of gentamicin resulting in lower minimum inhibitory concentrations of the conjugate against both MRSA and *S. aureus*.

REFERENCES

1. Pissuwan D. *et al.*, J. Control. Rel. 149:65-71, 2011

ACKNOWLEDGMENTS

The authors would like to thank Arthritis Research UK (ARUK:18461) for providing financial support to this project.



Plasma nanofilm as biocompatible and antibacterial coating for biomaterials

Michael Bergmann, Sebastian Lickert, Loic Ledernez, Gregory Dame and Gerald Urban

Department of Microsystems Engineering, Albert-Ludwigs-University of Freiburg, Georges-Köhler-Allee 103, 79110, Freiburg, Germany, michael.bergmann@imtek.de

INTRODUCTION

In the development of biocompatible materials for biomedical applications and biosensors the foreign body response is an important issue. [1] The healing of surrounding tissue often interferes with the function of an implanted biomaterial. Events like protein deposition, hemostasis, inflammation, tissue repair, infections and the encapsulation of the functional part of the implant are the main cause of failure of the implanted device. [2]

EXPERIMENTAL METHODS

In this study biocompatible nanofilms are produced by means of a plasma polymerization process using a low-pressure magnetron-enhanced 15 kHz glow discharge. [3] This process allows the precise control of the film nature and behaviour. The resulting hydrocarbon film has a thickness of a few nanometer and keeps therefore the inherent properties of the substrate material. X-ray photoelectron spectroscopy, dynamic contact angle, Fourier transformed spectroscopy and electrical impedance spectroscopy were used to investigate the chemical and physical properties of these nanofilms. Measurements on protein adsorption gave the possibility to tailor the thin films in the needed direction.

RESULTS AND DISCUSSION

The nanofilms were investigated using different surface analytical methods. Also the interaction in contact with different biological sample materials was tested in-vitro. The precise measurement of the adsorbed proteins indicated a native secondary structure of proteins on these surfaces.

Different in-vivo sensor dummies which are in contact with blood and soft-tissue were coated by these nanofilms. The explanted sensors were kept free of any encapsulation by this coating. This stands in good correlation with the measurement of adsorbed proteins. Additionally the nanofilms are equipped with an antibacterial property which minimizes the risk of post-operative infections.



Fig. 1: coated (lower) and uncoated (upper) PDMS-Stripes after 6 weeks of implantation

CONCLUSION

The first in-vitro results of the adsorption of blood proteins indicated already a very biocompatible character of these nanofilms. The explanted sensors were kept free of any encapsulation by this coating. These ground breaking coatings can open the door for many new applications in the field of in-vivo sensors but also other biomedical products.

REFERENCES

1. J Gray: The interaction of proteins with solid surfaces, Elsevier, 2004, 14:110–115
2. H. E. Koschwanetz and W. M. Reichert: In Vitro, In Vivo and Post Explantation Testing of Glucose-Detecting Biosensors: Current Methods and Recommendations, Biomaterials. 2007 ; 28(25):3687–3703.
3. M. Bergmann, et al. Nanofilms Produced by Magnetron Enhanced Plasma Polymerisation from methane and Oxygen for Coating of Rigid Contact Lenses, Plasma Processes and Polymers. 2013, 10 (11): 970-977

Fluoride-Containing Bioactive Glasses – from Structure to Cell Compatibility

D. S. Brauer^{1*}, E. Gentleman², R. G. Hill³ and N. Karpukhina³

^{1*}Otto Schott Institute of Materials Research, Friedrich Schiller University Jena, Germany, ²Craniofacial Development & Stem Cell Biology, King's College London, UK, ³Dental Physical Sciences, Queen Mary University of London, UK, delia.brauer@uni-jena.de

INTRODUCTION

Bioactive glasses (BG) bond with living tissue *via* formation of a surface apatite (Ap) layer and release therapeutically active ions. Fluoride (F) is known for its ability to prevent dental caries, and it also enhances bone formation [1], but owing to a narrow therapeutic window [2] its use in osteoporosis treatment had been dismissed. Recent meta analyses, however, have shown that F is efficacious at very low doses [3]. This opens the possibility of creating biomaterials that release F at appropriate levels to influence cell activity. We have incorporated F into BGs while keeping their silicate structure constant. This allowed us to examine the effects of low, controlled F release from BGs on osteoblasts without the complication of changes in glass structure.

EXPERIMENTAL METHODS

BG Preparation and Structural Analysis: BGs (SiO_2 – P_2O_5 – CaO – Na_2O – CaF_2 ; 0 to 18mol% CaF_2) were produced *via* a melt–quench route. CaF_2 was added while the ratio of all other components was kept constant. Glass structure was characterised using ^{29}Si , ^{31}P and ^{19}F MAS NMR spectroscopy.

Cell Culture: Prior to cell culture experiments, BG discs (1cm ϕ , 1mm height) were pre-conditioned in culture medium for 4 days. BG discs were seeded with human osteosarcoma cells (Saos-2) at 30,000 cells/cm² and cultured for up to 28 days. Cell viability was visualised by LIVE/DEAD[®] staining. Alkaline phosphatase (ALP) activity was measured using p-nitrophenyl phosphate. Statistical analyses were carried out using ANOVA with post-hoc Tukey test; $p < 0.05$ indicated statistical significance.

Ion Release and Apatite Formation: F released into the culture medium was analysed using a fluoride-selective electrode. Ap formation on the discs was analysed using X-ray diffraction (XRD) and scanning electron microscopy (SEM).

RESULTS AND DISCUSSION

Fluoride did not disrupt the silicate network (by forming Si–F bonds) but complexed Ca^{2+} and Na^+ instead. Therefore, by adding CaF_2 (rather than substituting for CaO), the silicate network structure was kept constant (Fig. 1). Phosphate in the glass was present as orthophosphate (no Si–O–P), allowing for phosphate release upon contact with fluids.

The CaF_2 -free BG formed Ap at later time points than CaF_2 -BGs (Fig. 2a), caused by formation of the less soluble fluorapatite (FAp) with F released from CaF_2 -BGs (Fig. 1) [4]. All CaF_2 -BGs formed Ap within less than a week according to XRD. Detectable F-release

occurred during the first few days of culture only, owing to the low-solubility FAp surface layer formed.

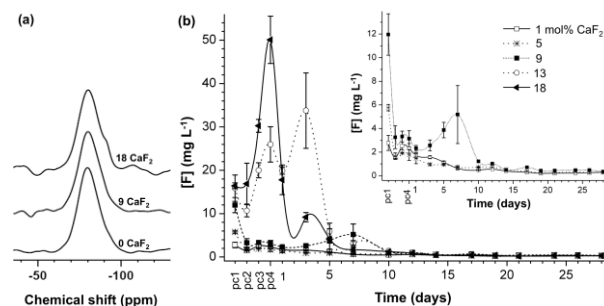


Figure 1: (a) ^{29}Si MAS NMR spectra of BG; (b) F release from BGs into culture medium.

Cells proliferated more extensively on low- CaF_2 BGs, while higher CaF_2 BGs promoted the formation of nodular structures (Fig. 2b). High- CaF_2 BGs also promoted significantly greater ALP activity per cell than low [5], suggesting that high- CaF_2 BGs stimulate osteoblast differentiation and mineralisation, likely through higher initial F-release.

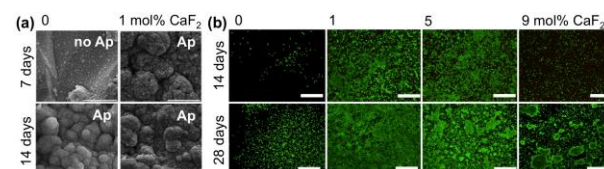


Figure 2: (a) SEM images of BG surface at 7 and 14 days and (b) LIVE/DEAD[®] staining of cells at 14 and 28 days. (Scale bars (a) 3 μm and (b) 500 μm)

CONCLUSION

By adding CaF_2 (rather than substituting for CaO) BG silicate structure and thus degradation and ion release are maintained, thereby enabling F-releasing BG to promote osteoblast activity. The combination of controlled F-release with the known benefits of BGs may make these materials of interest for a range of bone regeneration applications.

REFERENCES

1. Lundy MW, *et al.* Bone. 10:321-7, 1989
2. Aaseth J, J. Trace Elem. Exp. Med. 17:83-92, 2004
3. Vestergaard P, *et al.* Osteoporos Int. 19:257-68, 2008
4. Brauer DS, *et al.* Acta Biomater. 6:3275-82, 2010
5. Gentleman E, *et al.* Acta Biomater. 9:5771-9, 2013

ACKNOWLEDGMENTS

The authors would like to thank R.V. Law (Imperial College) for help with NMR measurements.

Atomic structure of Mg-based metallic glasses for biomedicine

Jamieson Christie*

*Department of Chemistry, University College London, U.K., jamieson.christie@ucl.ac.uk

INTRODUCTION

Mg-based alloys are often used for biomedical implantation, especially for orthopaedic applications, as they have similar density and Young's modulus to human bone. However, on implantation into the body, these alloys can corrode and release hydrogen gas, which is potentially harmful to the patient.

In 2009, certain compositions of Mg-Zn-Ca bulk metallic glasses were found to form a passivating layer on their surface, which prevented the release of hydrogen gas¹. This opened up the possibility to use these glasses as orthopaedic implants.

The atomic mechanism behind the formation of this layer is still unknown. To design and optimise these glasses for orthopaedic applications will require detailed knowledge of their atomic structure and mechanical properties, as well as an understanding of the processes which lead to the formation of the passivating layer. In this new project, we use computer simulations to understand the properties of these glasses and suggest directions for their optimisation.

EXPERIMENTAL METHODS

Molecular dynamics methods have been used to understand the structure and properties of many forms of glasses, including metallic glasses, and bioactive glasses. In particular, the bulk structure of bioactive silicate-based² and phosphate-based glasses³ is known to be very important in determining their behaviour on implantation into the body. We intend to use the same techniques that have elucidated the behaviour of these bioactive glasses to look at metallic glasses.

Models of Mg-Zn-Ca glass compositions which both do and do not form the passivating layer were prepared using first-principles Born-Oppenheimer molecular dynamics (MD) through the CP2K code⁴. The models are initially equilibrated at 1500 K, and then cooled down at a high cooling rate, before simulation at constant volume and temperature at ambient conditions. All data presented are averaged over this room-temperature run. The advantage of first-principles MD is that no empirical expression for the interatomic forces is required. The disadvantage is the high computational expense, which means that only small models (c.120 atoms) can be used.

RESULTS AND DISCUSSION

The local structure of the glass, in terms of bond lengths and coordination numbers, shows very little dependence on composition. Figure 1 presents the partial pair-correlation functions. As in other metallic glasses, icosahedra are present and identified based on their Voronoi signature⁵, but these are by no means the

dominant local structure. We infer that any structural differences occur at larger length scales, perhaps at the level of the packing of polyhedra, which are inaccessible to this level of simulations. Interatomic forces derived from these simulations will form the basis for the development of an accurate interatomic potential, using the “force-matching” method⁶, which will allow the simulation of larger systems.

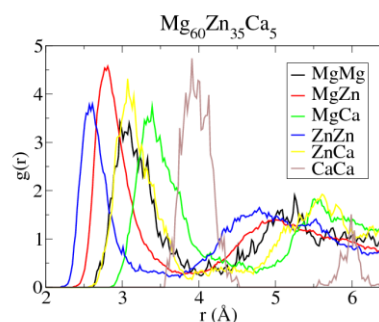


Figure 1: Partial pair-correlation functions for $\text{Mg}_{60}\text{Zn}_{35}\text{Ca}_5$.

During the talk, we will outline progress made toward the development of these potentials, as well as the possibility to obtain experimental diffraction data.

CONCLUSION

Differences between Mg-Zn-Ca glass compositions which form and do not form a passivating surface layer do not occur at the level of nearest-neighbour coordination spheres. We conclude that experimental data and larger simulations are required to understand these systems fully.

REFERENCES

1. Zberg B., Uggowitzer P. J., Löffler J. F., *Nature Mater.* 8:887-91, 2009
2. Tilocca A., *Proc. R. Soc. A* 465:1003-27, 2009
3. Christie J. K., Ainsworth R. I., Di Tommaso D., de Leeuw N. H., *J. Phys. Chem. B* 117:10652-57, 2013
4. see <http://www.cp2k.org>
5. see e.g. Peng H. L., Li M. Z., Wang H. W., *Phys. Rev. Lett.* 106:135503, 2011
6. Laio A. *et al.*, *Science* 287:1027-30, 2000

ACKNOWLEDGMENTS

We are grateful to University College London for the provision of an Excellence Fellowship, and to the UK's Engineering and Physical Sciences Research Council (EPSRC) for funding. Via our membership of the UK's EPSRC-funded HPC Materials Chemistry Consortium (grant EP/L000202), this work made use of the facilities of HECToR and ARCHER, the UK's national high-performance computing services. We are also grateful for UCL Research Computing Services for the provision of computer time.

Bioactive glass nanoparticles for therapeutic applications and incorporation into hybrids for bone regeneration

Sarah Greasley¹, Jesse V. Jokerst^{1,2}, Sanjiv S. Gambhir², Alexandra E. Porter¹, Julian R. Jones¹

¹Department of Materials, Imperial College London, UK, s.greasley12@imperial.ac.uk

²Department of Radiology, School of Medicine, Stanford University

INTRODUCTION

The aim of this work was to synthesise monodispersed bioactive glass nanoparticles, which will be used in three ways:

1. Incorporated into a degradable polymer matrix to form a scaffold for bone regeneration.
2. Intracellular delivery of active ions (e.g. Ca, Sr)
3. Biodegradable ultrasound contrast agents for cell therapy.

Bioactive glass scaffolds are bioactive, porous and biodegradable but are brittle. They can be toughened through hybrid synthesis^[1]. The degradable nature of the bioactive glass particles produced using this method is also desirable for therapeutic applications. Our previous studies show our bioactive glass particles can be uptaken by stem cells without affecting toxicity or stemness^[2]. Doping the particles with active ions can allow sustained intracellular delivery of these ions.

Silica nanoparticles are commonly produced by using the Stöber process^[2]. However, the introduction of calcium complicates the procedure^[3]. The aim was to revisit the Stöber process to understand monodispersed particle size control. Different methods of calcium incorporation and incorporation of additional elements were then investigated.

EXPERIMENTAL METHODS

Particle synthesis:

Using a modified version of the Stöber process^[2], ethanol, water and ammonium hydroxide were mixed in an ultrasonication bath. TEOS was then added. Once the particles reached their maximum size (determined by DLS) calcium nitrate was added. The solution was centrifuged to obtain the solid particles which were dried before being heated to 680 °C. The effect of reactant concentrations on particle size, shape and dispersity was investigated. The particles were then functionalized by leaving for 24h in a solution of APTES, ethanol and ammonium hydroxide to create NH₃ groups on the nanoparticle surface. Particles containing phosphorous and potassium were also obtained using diethyl phosphatoethyl triethoxysilane (DEPETES) and potassium nitrate.

Particle characterisation:

DLS and TEM were used to confirm the size and morphology of particles. ICP was used to determine the chemical composition of the particles and their degradation products in artificial lysosomal fluid (ALF). Zeta Potential measurements and FTIR were used to confirm the functionalization of particles.

RESULTS AND DISCUSSION

- Effect of reactants on particle size:

- Increased ammonia from 0.1 -2.5M resulted in an increase in particle size (Fig 1)
- Increasing water from 3 – 15M resulted in an initial increase and then a decrease in particle size.
- Varying TEOS over the range 0.17-0.28M had no effect on particle size.

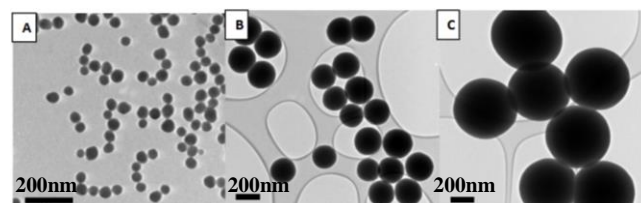


Figure 1 TEM images of silica particles produced using 0.28M TEOS, 6M H₂O and varying concentrations of ammonia A) 0.2M NH₃ B) 0.5M NH₃ C) 2M NH₃

- DLS results corresponded to TEM results for particles up to 300nm.
- Monodispersed particles from 20-500nm were synthesised containing 10mol% P₂O₅, 10mol% K₂O and up to 15mol% CaO.
- All particles were seen to degrade over time in ALF (Figure 2).
- Zeta potential of particles was seen to change from -20mV to +20mV due to functionalization.
- Functionalisation allows covalent coupling to a biodegradable polymer (e.g. gelatin) matrix.

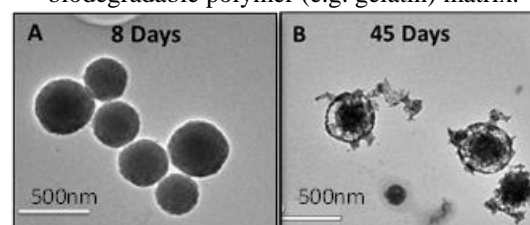


Figure 2. Silica particles doped with P and K before and after incubation for 45 days

CONCLUSION

By splitting the synthesis process into 3 steps (1. Synthesis of silica nanoparticles, 2. Incorporation of additional elements e.g. Ca, 3. Functionalisation) it enables functionalised, monodispersed nanoparticles of various compositions to be produced for a variety of applications.

REFERENCES

1. Jones, J.R., Acta Biomater, 2013. 9: 4457-86.
2. Tsigkou et al Adv Healthcare Mater 2014. 3: 115-125
3. Stöber, W et al, J Colloid Interf Sci, 1968. 26: 62-69.
4. Hong, Z et al, J Biomed Mater Res A, 2009 88:304-13.

ACKNOWLEDGMENTS

EPRSC for funding EP/I020861/

Antitumor Efficacy of Radioactive Holmium (^{166}Ho) Containing Silica Sol-gel Glass Granules on Osteosarcoma (MG-63) and Breast Cancer (MCF-7) Cells in Vitro

Riku Alaranta¹, Jessica J Alm^{1*}, Kaisa Lehtimäki¹, Heimo Ylänen², Tapio Ollonqvist³ and Hannu T Aro¹

^{1*}Orthopaedic Research Unit, Department of Orthopaedic Surgery and Traumatology, University of Turku, Finland

²Turku Biomaterials Centre, University of Turku, Finland

³Department of Oncology, Turku University Hospital, Finland, jessica.alm@utu.fi

INTRODUCTION

Metastatic bone disease is a frequent complication of treatment-resistant cancers causing significant pain and disability to the patients. Treatment of bone metastases is challenging and treatment decisions are especially difficult in patients with painful osteolytic metastatic lesions of the pelvis and spine, for which percutaneous osteoplasty has been introduced as a treatment¹. This minimally invasive surgical technique involves percutaneous chemical, thermal or cryoablation of the tumor cavity, followed by defect filling with bone cement. The radioisotope of holmium (^{166}Ho) has a half-life of 26.8h, with max and average tissue penetration depth of 10.2 mm and 2.1 mm, respectively. We hypothesize that an injectable biodegradable composite with transient radioactivity of spatial limitation could be a useful component for percutaneous osteoplasty in selected subgroups of patients. As a part of tumor ablation, it could kill the remaining cancer cells and ensure efficacy of local tumour control. The physical properties of ^{166}Ho could be optimal for targeted radiotherapy with minimal effect on surrounding healthy cells. In this study, we examined the *in vitro* tumor-killing efficacy of radioactive ^{166}Ho containing silica sol-gel glass granules.

EXPERIMENTAL METHODS

Holmium encapsulated silica (SiO_2) sol-gel granules were designed and manufactured as described previously². Granules with diameter of 315 – 500 μm contained 99 wt% SiO_2 and 1 wt% holmium. The incorporated holmium was activated by neutron bombardment (Map Medical Technologies Ltd, Finland). Non-radioactive holmium containing sol-gel granules were used as the control.

The effect of non-radioactive granules on cell viability of human osteosarcoma (MG-63) and breast cancer (MCF-7) cells was explored using the alamarBlue® assay. Cells were cultured alone (Ctrl) or with different concentrations (12.5, 25 and 50 mg/ml) of non-radioactive sol-gel granules. Seeded cells were allowed to adhere for 24h before adding the granules. Seeding density was adjusted so that ctrl cultures reached confluency in 7 days. Cell viability was monitored at day 3, 7 and 14.

AlamarBlue® assay, disk diffusion assay, and clonogenic assay were applied to define the antitumor efficacy of ^{166}Ho containing granules. Cells were seeded according to previous experiment, with the constant concentration (12.5 mg/ml) of radioactive or non-radioactive granules. Cultures without granules served as controls. The mean ^{166}Ho activity of activated

granules was 0.6 MBq/mg. AlamarBlue® and disk diffusion assays were performed at 3, 7, and 14 days and the clonogenic assay at 7 days. Results are presented as mean \pm SD (n=6 for all conditions of both cell lines in each assay). Differences between the groups were tested with one-way ANOVA or non-parametric test (Mann-Whitney test) depending on distribution and homogeneity of variances.

RESULTS AND DISCUSSION

The osteosarcoma (MG-63) and breast cancer (MCF-7) cells developed confluent cultures around non-radioactive granules. Although there was a significant inverse correlation between increasing amounts of non-radioactive granules and cell viability, cells treated with the lowest concentration (12.5 mg/ml) of non-radioactive granules had viability equivalent to control without granules. These results showed that non-radioactive holmium encapsulated sol-gel glass granules are non-toxic to malignant cells.

The three assays demonstrated that ^{166}Ho encapsulated radioactive granules efficiently kill malignant cells *in vitro*. Based on cell viability, breast cancer cells had a later response to radiation compared to osteosarcoma cells. At 14 days, significant growth inhibition areas were detected around the radioactive granules (p=0.018 for MG-63 and p<0.001 for MCF-7). Radioactivity also significantly reduced the clonogenic properties of cancer cells, i.e. ability of individual cells to produce multiple offspring in subcultures. Survival fractions after radioactive treated were 54 \pm 32% for MG-63 (p=0.003) and 60 \pm 29% for MCF-7 (p=0.008), compared with the non-radioactive group.

CONCLUSION

Based on these *in vitro* results, ^{166}Ho containing silica sol-gel glass granules have the expected tumor-killing efficacy. This injectable bioresorbable material could be a valuable addition to percutaneous osteoplasty of bone metastases. After decay of the radioactivity, the composite could act as an osteoconductive material for restoration of the bone stock.

REFERENCES

1. Papagelopoulos P.J. *et al.* Orthopaedics 29:315-323, 2006
2. Cacaïne D. *et al.* J. Mater. Sci. Mater. Med. 22:29-40, 2011

ACKNOWLEDGMENTS

The authors would like to thank the National Foundation for Technology and Innovation (TEKES) for providing financial support to this project. Professor Reidar Grenman is acknowledged for donating the cell lines.



Hybrid PLGA/Bioactive Glass Fiber Scaffolds for Bone Tissue Engineering

Anne-Marie Haaparanta^{1,2*}, Timo Lehtonen³, Ville Ellä^{1,2}, Peter Uppstu⁴, Markus Hannula^{1,2},
Ari Rosling⁴ and Minna Kellomäki^{1,2}

¹Biomaterials and Tissue Engineering Group, Department of Electronics and Communications Engineering,
Tampere University of Technology, Tampere, Finland

²BioMediTech, Institute of Biosciences and Medical Technology, Tampere, Finland

³PURAC Biochem bv, Gorinchem, The Netherlands

⁴Laboratory of Polymer Technology, Åbo Akademi University, Turku, Finland
anne-marie.haaparanta@tut.fi

INTRODUCTION

Bone tissue engineering requires highly porous scaffolds with good mechanical stability, and preferably osteoconductive properties¹. Synthetic bioabsorbable polymers, like polyesters, are often used for the application, but they lack the required bioactivity on their own, and their acidic degradation products provoke an adverse tissue response. By adding bioactive glass (BaG) into the scaffolds the mechanical stability and osteoconductive properties can be improved. The addition of glass is thought to buffer the acidic degradation products of polyesters².

In this study we prepared novel poly(lactide-co-glycolide) 70/30 (PLGA)/BaG hybrids by freeze-drying. In total, two different compositions of PLGA and bioactive glass were used and two different hybrid scaffolds with porous PLGA component together with bioactive glass fibers were studied *in vitro*.

EXPERIMENTAL METHODS

Two different PLGA polymers with lactide-to-glycolide ratio of 70:30 were synthesized by ring-opening polymerization: PLGA1 with M_w of 76 000 g/mol and PLGA2 with M_w of 48 000 g/mol. The bioactive glass fibers (BaG1 and BaG2) were cut to staple fibers, and carded into mesh.

The PLGA was dissolved in 1,4-dioxane at concentrations of 5 wt% and 3 wt% for plain and hybrid scaffolds, respectively. The PLGA solution was frozen at -30°C for 24 h and afterwards freeze-dried for 24 h. The hybrid scaffolds were produced by adding the BaG fiber mesh into the PLGA solutions prior to freezing. Table 1 shows the studied scaffold types and their compositions.

Table 1. Studied scaffold types and their compositions.

Polymer scaffolds		Hybrids
PLGA1	PLGA1 5 wt%	PLGA1/BaG1 PLGA1 3 wt% + BaG1 mesh
PLGA2	PLGA2 5 wt%	PLGA2/BaG2 PLGA2 3 wt% + BaG2 mesh

All the scaffolds were gamma sterilized at 25 kGy. *In vitro* degradation studies for 10 weeks were carried out for six parallel samples. The dimensional stability of the scaffolds, scaffold composition (TGA), pore size of the

scaffolds (SEM, MicroCT), the ability of BaG to buffer the acidic degradation products of PLGA, contact angle measurements, and degradation rates (GPC, DSC) of the scaffolds were studied.

RESULTS AND DISCUSSION

Freeze-drying of structures in which a BaG mesh was incorporated into a PLGA matrix was found to be an applicable method to produce highly porous hybrid scaffolds.

The interconnection of BaG fibres into PLGA matrix was good (SEM imaging and MicroCT studies). The pore structure in the scaffolds was more homogeneous in PLGA/BaG hybrids than in plain PLGA scaffolds. Furthermore, the plain PLGA scaffolds contained bigger macropores. All scaffolds had a highly porous structure, with a porosity of over 90% (MicroCT studies).

BaG buffered the acidic degradation products of PLGA in the hybrid scaffolds during the hydrolysis (measured by pH change of solution). Also, dimensional change was moderate for PLGA/BaG hybrid scaffolds while the plain PLGA scaffolds shrank and twisted during the hydrolysis.

CONCLUSION

The used method to combine these two three-dimensional porous structures, highly porous PLGA and BaG into a hybrid, showed preferable structure for bone tissue engineering. The dimensional stability of the studied hybrids was improved by BaG fibers, and also the buffering effect of BaG of the acidic degradation products of PLGA was confirmed.

REFERENCES

1. Karageorgiou V. and Kaplan D., Biomaterials, 26:5474-5491, 2005
2. Navarro M. *et al.*, Adv Polym Sci, 200:209-231, 2006

ACKNOWLEDGMENTS

Funding from the Finnish Funding Agency for Technology and Innovation (TEKES) is acknowledged (Grant no: 3110/31/08).

Development of Novel 45S5 Bioglass® Scaffolds with Fibrous Surface Morphology using Electroflocking Technology for Bone Tissue Engineering

Preethi Balasubramanian¹ and Aldo R Boccaccini¹

¹Institute of Biomaterials, Department of Materials Science & Engineering, University of Erlangen-Nuremberg, Germany
preethi.balasubramanian@ww.uni-erlangen.de

INTRODUCTION

Driven by increasing demand, new strategies for bone tissue engineering are fast developing. Electroflocking is a well-known technique in the textile industry. Walther et al¹ reported the application of flocking as a suitable technology for fabrication of scaffolds for cell culture and tissue engineering (TE). This method offers the possibility to produce scaffolds with fibrous morphology and anisotropic properties. In this study, we report, for the first time, the combination of polymer replication method and flock technology to produce 45S5 Bioglass® scaffolds with a fibrous surface morphology suitable for bone TE. After *in vitro* bioactivity study in simulated body fluid (SBF), complete mineralization of the flocked polyamide fibers in contact with the Bioglass® scaffold was observed.

EXPERIMENTAL METHODS

Polymer replication method: 45S5 Bioglass® scaffolds were produced as described by Chen et al².

Electroflocking: In this technique, short fibers are applied under an electrical field to a substrate covered with an adhesive. Figure 1 shows the experimental set-up for the flocking technique¹.

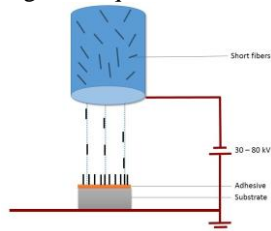


Figure 1: Schematic diagram of the electroflocking process

For our experiment, the Bioglass® scaffold was used as the substrate, gelatin is the adhesive and polyamide (PA) fibers of the length 0.5 mm and diameter 15 µm were used. Gelatin was dissolved in de-ionised water and applied on the top surface of the Bioglass® scaffolds. Short fibers were flocked over the gelatin layer to obtain a fibrous morphology on the surface of the Bioglass® scaffolds. Different flocking time periods (10s, 30s and 60s) were considered. The scaffolds were then taken for further characterisation and *in vitro* bioactivity studies.

RESULTS AND DISCUSSION

Three-dimensional porous scaffolds based on Bioglass® were produced from the polymer replica technique². The scaffolds were analysed by scanning electron microscopy (SEM). Other characterisation techniques were also used to investigate the scaffolds (not shown here). Figure 2(a) shows a SEM image of the Bioglass® scaffold after flocking with PA fibers for 60s. From Figure 2(b), the adhesion of the PA fibers on the gelatin layer can be seen.

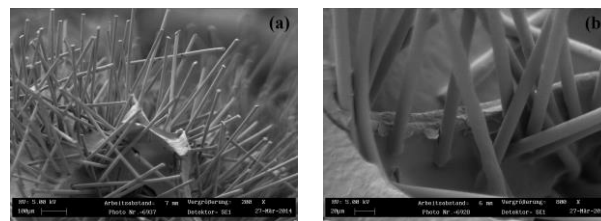


Figure 2: SEM micrographs of (a) and (b) PA fibers over the gelatin adhesive layer on Bioglass® scaffold after electroflocking for 60s

The Bioglass® scaffolds after flocking were immersed in SBF for a period of 28 days. Figure 3(a) and 3(b) show the formation of Hydroxyapatite (HA) on the Bioglass® as well as polyamide fibers after 28 days in SBF.

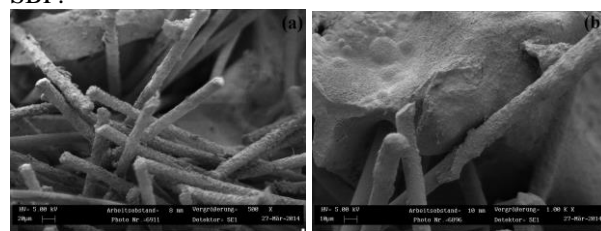


Figure 3: SEM micrographs of HA growth on (a) PA fibers (b) PA fibers and Bioglass® scaffold

Flocking after 10s produced surfaces with fibers of low packing density. Increasing the flocking time increased the packing density of fibers. Higher density of fibers on the surface prevented toppling of fibers as there is only limited space available. It was observed that after the SBF study, the orientation of the fibers had changed and not all the fibers were perpendicular to the substrate. Interestingly, the polyamide fibers were also completely covered with HA crystals. By choosing an appropriate flock density (i.e pore size), scaffolds with suitable properties for cell adhesion and growth can be created.

CONCLUSION

Novel scaffolds for TE combining the foam replica technique and electroflocking of PA fibers were fabricated. *In vitro* bioactivity studies indicated mineralization of both the Bioglass® scaffold and polyamide fibers. In the future, other types of fibers with encapsulated or surface functionalized proteins or biomolecules can be flocked over bioactive glass scaffolds for developing functional scaffolds for drug delivery applications for bone regeneration.

REFERENCES

- Walther A. *et al.*, Tex. Res. J.77:892-99, 2007
- Chen Q. *et al.*, Biomaterials 27:2414-25, 2006

ACKNOWLEDGMENTS

The authors would like to thank FP7 EU ITN BIOBONE project for providing financial support.



Translation of science to the clinic: Where preclinical research fits in the model

R. Geoff Richards

AO Research Institute Davos, AO Foundation, Clavadelerstrasse 8, 7270 Davos, Switzerland
geoff.richards@aofoundation.org

The AO Research Institute Davos (ARI) within the AO Foundation has many of the conditions desired to have success in translation of scientific results into surgical procedures, marketable substances or prototype concepts for medical devices¹. The ARI is a multidisciplinary highly motivated and focused research team in one location with a world-wide network of academic, clinical and industrial partners within specialised fields of trauma. All projects are initiated from specific clinical problems facing the trauma surgeon and funding is all project based (not department based) using full cost financial controlling. The ARI has accreditation of R&D processes, facility and animal care (ISO and AAALAC). Within the AO Foundation the ARI has access to the well respected and largest world-wide trauma surgeon network for clinical guidance. This network brings both international and regional based clinical problem experience and knowledge to help with analysis of clinical problems and development of research solutions. Within the AO Foundation also exists a central clinical trials team which works with the clinical network members. It can host multicenter trials and also can give accreditation to hospitals to participate. The AO Foundation also provides the ARI access to an experienced medical guided approval body for the devices and techniques with independent surgeons with regional and specialty representation. The AO Education Institute has a clinical education team which with its theme based on both faculty and curriculum development processes for the attendees and runs over 400 courses a year world-wide for surgeons and operating room personnel. Naturally this is the place to show new technology (techniques, devices, substances) which are either in development or already available clinically.

As the research part of the Foundation, bringing academic credibility to new substances, devices and techniques, one dilemma in would be whether to hold back publishing in order to submit a patent. This can delay academic recognition, yet helps to make the idea tradable after filing the patent and if given gives a strong legally enforceable protection of the invention (can take 5 or more years). First of all one should check that the idea is really novel through a patent search and knowing the literature and secondly if novel, it must also be inventive. Terminology here is critical as are the claims which must be solutions as opposed to problems.

Despite the great set up to nurture, approve and expose translation within the AO Foundation key areas of the translation cycle are missing in the more biological ideas. As the ARI has moved in the last 20 years slowly away from pure biomechanics to biology and tissue engineering and regenerative medicine it is evident the industrialisation steps are much more difficult. In the early 90's ARI performed early work with

biodegradable polymers for bone fillers (with and without cellular material), membranes for bone defects along with biological manipulation of surrounding tissues, such as periosteum transport and fillers between the periosteum and bone to encourage more bone repair. Unfortunately much of this work was never really translated to the clinics at that time and such areas have been "rediscovered" with newer materials and marketed as new ground breaking work.

There is an increasing clinical demand for the targeted and controlled delivery of active molecules (or even cells) to specific parts of the body which requires good well characterised biomaterial delivery platforms e.g. for localised delivery of antibiotics to infection sites or release of stimulants for local tissue regeneration. The biomaterials ideally should be biocompatible, biodegradable and allow temporal release of the active substances. It also makes things easier (and much cheaper) if the biomaterial platform's components are already used for other areas in the clinics. The translation of such a material to the clinics involves many more steps than is involved for a device made of steel or titanium. Should these missing areas of development for translation be brought into the translation circle internally by hiring specialists for technology transfer and licencing to industry, certification (e.g. CE), regulatory issues, GLP and GLM for tissue engineering or should these areas be outsourced to groups who specialise in these areas on a daily basis? This is difficult to answer.

This presentation will mention the generic development process and through examples show some of the pitfalls we have encountered in the last few years at the technology transfer stage. If you want industry to consider your idea you must have several patents covering the areas of interest and the patents must have passed the pre-examination stage. To make sure they do not buy your idea and shelve it, once you have your patent, which is also a commercial strategy, you must make an exploitation contract with financial penalties for inactivity and possible full loss of partnership (again with financial penalty) if no activity happens within a certain period.

There are thousands of great ideas, but to turn just one of these into a successful device, substance or procedure in surgery requires much more than a great idea. A well thought out plan with appropriate searches focussed initially on just one clinical problem is essential to get to an evidence based proof of concept to be able to present and licence or sell to industry.

REFERENCES

1. Richards RG. AO Research Institute Davos within the AO Foundation: A model for translation of science to the clinics. *Journal of Orthopaedic Translation*. (2013) 1, 11-18.



Innovation and Product Development in a Changing Regulatory and Socio-economical Environment

Andrea Montali¹

¹DePuy Synthes Biomaterials R&D, Oberdorf, Switzerland
montali.andrea@synthes.com

INTRODUCTION

Innovation and product development in orthopaedic medical device industry have largely been technology driven during the last decades. Advancements have been rapid and significant. Today's solutions have reached high standards and nowadays an individual suffering from a bone fracture in highly developed countries can count on receiving a state of the art treatment and regaining full mobility and quality of life in the vast majority of cases.

While in the past, technological advancements and new scientific insights have been driving innovation, today's product development occurs in a more complex environment, with multiple stakeholders involved. Each of these stakeholders can have different and sometimes conflicting requirements and expectations. While technological innovation may still be the driving force behind new product developments, in many cases it is not a sufficient justification.

FRAMEWORK OF PRODUCT DEVELOPMENT

Product development is nowadays always subject to the indirect or direct influence of three independent conditions:

- 1) Success rates of state of the art treatments are very high and any improvement is difficult to prove.
- 2) Regulatory authorities request proof of any improvement in performance.
- 3) The entire market is subject to significant cost and price pressure.

These frame conditions make any new product development and the implementation of any technological innovation an endeavour subject to continuous, in depth scrutiny questioning technological, regulatory and financial feasibility.

SHIFT OF PARADIGMS IN INNOVATION

To a certain extent these external factors are contradictory to the typical structure of a traditional R&D project, where an innovative technology is brought to maturity, made into a product and brought to the market.

Such a project can involve extensive pre-clinical testing to demonstrate safety and effectiveness; furthermore, in many cases significant investments in generating clinical proof of efficacy and safety may be required. This stands in stark contrast to the above stated requirements of profitability, as timelines and costs are significant.

Industry faces the need to expand and redefine its concept of innovation and product development in order

to offer added value to its customers and their patients, while still maintaining reasonable development timelines and project profitability.

This calls for taking a step back from the hitherto common definition of "product", which focuses on an implant and the related instruments and surgical technique necessary for implantation.

While optimal patient treatment with best possible outcomes remains the centre of the treatment around which everything else revolves, services addressing other aspects of the treatment continuum can bring benefits to different stakeholders, which in the end may justify a development even if minor technological improvements are not the driving force.

These can be services around simplifying logistics and warehousing in clinics, or support in pre-operative planning and post-operative patient support, which can lead to earlier release from the clinic and return to work. An industrial partner with a deep understanding of the processes needed to offer a successful and efficient treatment of patients, from the moment of injury to full reintegration into daily life, can offer new benefits and innovation in fields that were so far not considered to be in the scope of an orthopaedic company's development activities and product offerings.

CONCLUSION

In the coming years, new product developments in the field of orthopaedics will face more and more scrutiny with regards to the benefits they bring to patients and their overall profitability. More complex products involving bioengineered components, which typically require more extensive pre-clinical and clinical testing to demonstrate safety and efficacy, will face even more significant challenges than others.

However, treatments based on bioengineering technologies bear the potential to fully change the treatment of certain diseases and injuries, thereby offering real benefit, not just to the patient, but also to other stakeholders such as insurance companies or hospital administrations.

Assuring that a new product development is embedded in a more holistic consideration and takes into account all aspects of treatment, also those occurring outside the operating theatre, will open new possibilities to demonstrate efficacy and profitability. This is of utmost importance and will be the decisive factor determining the fate of a project and product idea.

ACKNOWLEDGMENTS

The author would like to thank Dr. Stefan Beck, DePuy Synthes Biomaterials, for proof reading the manuscript and fruitful discussions.



Development of dedicated tools for personalization of medical devices

Lara Vigneron¹, Daniel Daryaie², Sebastian De Boodt¹, Lars Neumann^{1*}

¹Biomedical Engineering Department, Materialise NV, Belgium, Lars.Neumann@materialise.be

²Biomedical Engineering Department, Materialise NV, UK

INTRODUCTION

Human beings are diverse in their physical makeup and there is a growing trend towards personalization of medical care. In the surgical field, it is translated by an increasing use of personalized or patient-specific anatomical models, surgical instruments and implants. Next and related to this trend of personalization, there is a push from public actors (government, regulatory entities, etc.) for evidence-based medicine, which leads to more thorough population analyses for improving design and evaluating surgical outcomes. In this paper, we describe the use of 3D medical image information of individual patients as well as selected patient populations, combined with computer aided engineering (CAE) tools and processes, in the rapid product development of personalized medical devices and the analysis of surgical outcomes.

EXPERIMENTAL METHODS

Medical imaging systems, like CT or MR scanners, typically generate stacks of gray scale images. To take full advantage of the 3D- and density information that is included in these image stacks, medical image and design software Mimics[®] Innovation Suite (Materialise NV, Leuven, Belgium) is used. It generates 3D models of the tissues of interest thanks to segmentation tools and advanced interpolation algorithms, allowing the user to create accurate 3D models. Personalized parts are then designed thanks to dedicated Computer Aided Design (CAD)-tools. Nowadays, most personalized medical devices are produced using 3D printing techniques, as they allow maximum flexibility to personalize production for each part to be built. 3D printing production requires dedicated tools and data format that are also included in the software.

Designs of standard implants are increasingly based on advanced population analyses that provide a better understanding and differentiation of the targeted population, including for example different ethnicities such as Caucasian or Asian, etc. or of healthy populations and populations showing specific disorders, e.g. osteoarthritis. We have thus developed dedicated software tools to build statistical shape models that allow the generation of virtual models representative of the population, i.e. average model and models presenting the main shape of variations. Conception and virtual testing of new designs can thus be performed using models that cover the target population in a better and more systematic way than using arbitrarily chosen datasets¹.

In order to evaluate surgical outcome, planning and postoperative results should be compared. The most accurate method is to acquire a new 3D image of the

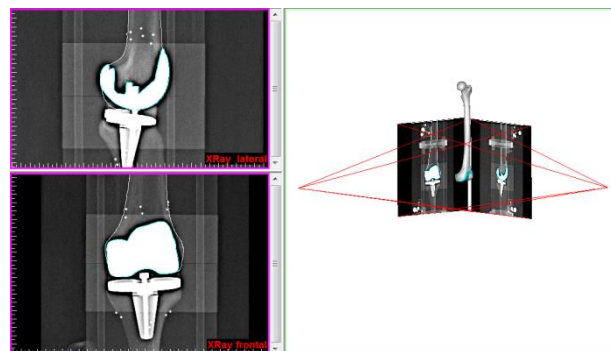
patient after the surgery that allows evaluating the exact position of the implant relative to the anatomy². However, this 3D postoperative image is often not included in the standard clinical protocol and it increases the level of radiation dose that the patient receives, which is to be avoided. We have thus developed a software tool for postoperative analysis based on a pair of X-ray images only, which reaches a level of accuracy that is comparable with the results obtained with a 3D postoperative image.

RESULTS AND DISCUSSION

Some of our results are presented below. The first figure presents (from left to right) a 3D model created from CT DICOM images and used to plan surgical cuts. An implant was then designed and produced that fits exactly onto the patient's bone anatomy. FEA analysis was performed to validate the stability of the implant under different loads.³



The second figure presents the method to perform a postoperative analysis using a pair of X-rays. These are used to define the relative position of bone and implant in 3D space. This position is subsequently compared to 3D surgical planning.



CONCLUSION

We have developed powerful tools to conduct the whole workflow going from design of patient-specific medical devices and planning of surgery to postoperative analysis.

REFERENCES

1. Plaster *et al.*, Am J Orthop. 39(6 suppl):9-12, 2010
2. Hirschmann *et al.*, J Bone Joint Surg [Br.].93(5):629-33, 2011
3. Jules Poukens *et al.* 2007, Case study done at Academic Hospital Maastricht, The Netherlands

Modulation of Cell Microenvironment Using Macromolecular Crowding: A Self Assembly Approach Towards *In Vitro* Organogenesis

Abhigyan Satyam¹, Pramod Kumar¹, Xingliang Fan¹, Yury Rochev¹, Lokesh Joshi², Héctor Peinado³, David Lyden³, Benjamin Thomas⁴, Brian Rodriguez⁵, Michael Raghunath⁶, Abhay Pandit¹ and Dimitrios Zeugolis¹

¹Network of Excellence for Functional Biomaterials (NFB), National University of Ireland Galway (NUI Galway), Galway, Ireland. ²Alimentary Glycoscience Research Cluster, NUI Galway, Galway, Ireland. ³Departments of Pediatrics, Cell and Developmental Biology, Weill Cornell Medical College, New York, USA. ⁴Central Proteomics Facility, Sir William Dunn Pathology School, Oxford University, Oxford, UK. ⁵Conway Institute of Biomolecular & Biomedical Research, University College Dublin, Dublin, Ireland. ⁶Faculty of Engineering and Department of Biochemistry, Yong Loo Lin School of Medicine, National University of Singapore, Singapore. abhigyanatomy@gmail.com

INTRODUCTION

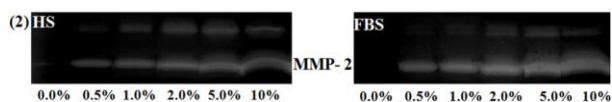
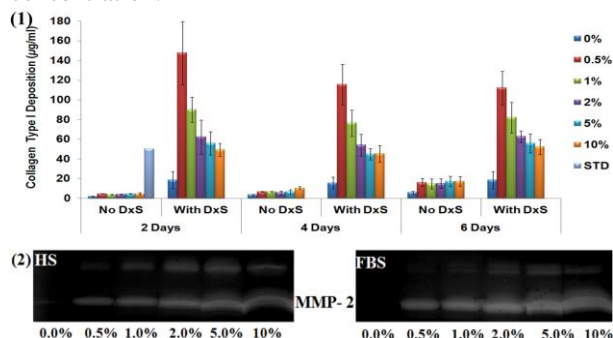
Advancements in tissue engineering and polymer chemistry have enabled development of scaffold-free substitutes; a technology termed as Tissue Engineering by Self-Assembly¹. Despite efficacious *in vitro* and *in vivo* results, very few products have been commercialized, primarily due to prolonged culture time^{2,3}. It has been demonstrated that macromolecular crowding (MMC) enhances deposition of extracellular matrix (ECM)^{4,5,6}. Here, we assessed the potential of combining MMC technology with a Tissue Engineering by Self-Assembly approach.

EXPERIMENTAL METHODS

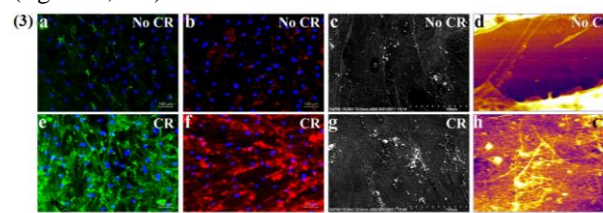
Human fibroblasts, tenocytes and osteoblasts were cultured under various MMC conditions [dextran sulphate (DxS); Ficoll™ & carrageenan (CR)] in a range of fetal bovine serum (FBS) and human serum (HS) concentrations (0.0-10%). ECM deposition was analysed by SDS-PAGE, immunocytochemistry (ICC), zymography, atomic force microscopy (AFM), scanning electron microscopy (SEM) and mass-spectrometry (MS). MMC molecules were characterized by dynamic light scattering (DLS) and nanoparticle tracking analysis (NTA). The influence of crowders on cell morphology, cell viability and metabolic activity were evaluated using phase-contrast microscopy, Live/Dead® and AlamarBlue® assays respectively. NIPAM based thermo-responsive polymers were developed to facilitate detachment of ECM-rich cell-sheets.

RESULTS AND DISCUSSION

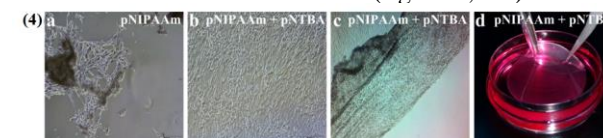
Densitometry of SDS-PAGE demonstrated that MMC significantly increase type-I collagen deposition ($p < 0.0001$) at all tested serum concentrations (maximum deposition was in 2 days & 0.5% FBS or HS). (figure-1). High matrix metalloproteinase-2 (MMP-2) content of FBS/HS was revealed by gelatin zymography (Figure 2), that attributed reduction in collagen content as a function of increased serum concentration.



ICC, AFM and SEM further confirmed enhanced deposition of fibrillar ECM in presence of MMC (figure-3, a-h).



DLS and NTA demonstrated that CR has highest polydispersity among all tested crowders. Phase-contrast microscopy, Live/Dead® and AlamarBlue® assays confirmed that cellular morphology, viability and metabolic activity respectively were not affected by MMC. Thermo-responsive coating with 65% NIPAM: 35% N-tert-butylacrylamide facilitated detachment of ECM rich cell-sheet from culture (figure-4, a-d).



Complementary ICC for MS validation confirmed the enhanced deposition of collagens (III, IV, V, VI) and other ECM molecules (laminin, fibronectin, hyaluronic acid, decorin, lysyl oxidase), without changing collagen-VII, elastin, fibrillin-1, transglutaminase-2, α -smooth muscle actin, epithelial keratin, tubulin, chondroitin sulphate, keratin sulphate, heparin sulphate, aggrecan, biglycan, CD248 and IL-10.

CONCLUSION

Modulation of *in vitro* microenvironment with polydispersed macromolecular crowders enhances ECM deposition even under low serum supplementation and facilitates production of intact ECM rich cell-sheets when combined with novel thermo-responsive polymer coating.

REFERENCES

1. Peck M. *et al.*, *Mat. Today*. 14:218-24, 2011
2. Vrana N. *et al.*, *IOVS*. 49:5325-31, 2008
3. L'Heureux N. *et al.*, *Nat. Medicine*. 12:361-5, 2006
4. Satyam A. *et al.*, *Adv. Mat.* 2014 (in press)
5. Cigognini D. *et al.*, *Drug Discov. Today*. 18:1099-108, 2013.
6. Zeugolis D. *et al.*, *European Patent*, EP 2532736 A1, 2011.

ACKNOWLEDGMENTS

The authors would like to thank the Science Foundation Ireland (Grant no: 09/RFP/ENM2483 & 07/IN1/B031) for financial support to this project.

Collagen Plasma Treatment of Poly-(ether-ether)-ketone for Improved Cell Attachment

Jessica S Hayes^{1*}, Declan M Devine, Mary Murphy¹

¹Orthobiologics, Regenerative Medicine Institute, NUI Galway IE

²Material Research Institute, Athlone Institute of Technology, IE, *jessica.hayes@nuigalway.ie

INTRODUCTION: Poly-(ether-ether)-ketone (PEEK) has proven successful in the stabilisation of non-load bearing areas of fracture healing¹. Given its desirable Young's modulus, mechanical strength and radiolucency for imaging^{2,3}, PEEK is now studied for more demanding load-bearing orthopaedic applications. A limitation of PEEK is its low surface energy which induces a peri-implant fibrous tissue capsule, thus preventing direct osseointegration⁴. Attempts have been made to 'activate' the surface of PEEK but have had limited success⁵. Our strategy involves the use of low energy plasma to molecularly re-engineer the first few nanometres of PEEK with Collagen to aid attachment. We hypothesise that biofunctionalisation of PEEK will produce a stable modification that improves human mesenchymal stem cell (hMSC) attachment compared to unmodified controls. The overall aim is to use this technology as a method for improving outcomes of osseointegration in orthopaedic applications.

EXPERIMENTAL METHODS

Surface Characterisation: PEEK and plasma treatment were supplied by EnBio Ltd, IE. Surface morphology post-treatment was assessed using Scanning Electron Microscopy (SEM). White light Interferometer was used to assess potential changes in surface roughness as a consequence of plasma treatment. X-ray photoelectron spectroscopy (XPS) was used to assess chemical compositional changes. Contact angle was performed at 0,1, 2, 3, 6 and 12 months to assess ongoing stability at room temperature. XPS was performed at 12 months and compared to time 0 results.

Biological Assessment: hMSC's (n=min 3 donors and min 3 biological replicates per experiment) were seeded at a density of 2×10^4 cells/cm² on 10mm 1) Unmodified PEEK (Unmod PEEK) and 2) Collagen plasma treated PEEK (PEEKCOL). Tissue culture plastic was included to control for donor variability. After 4 and 24hr cell attachment was assessed using Cell Titre Blue as was viability and proliferation up to 10d. Statistical analysis was performed using GraphPad Prism, $p < 0.05$ was deemed significant.

RESULTS AND DISCUSSION: Characterisation of surface morphology suggests that biological modification for the treatment time does not alter surface morphology (Fig1A) or microroughness compared to unmodified controls (Fig1A inset). PEEK was successfully modified with collagen, as indicated by XPS and contact angle. Interestingly, plasma treatment with collagen appears to remain stable for up to 12 months post-treatment (Fig1B). Initial cell attachment is significantly improved on modified surfaces compared to unmodified controls (Fig 1C). Furthermore, cell proliferation and viability are maintained (not shown).

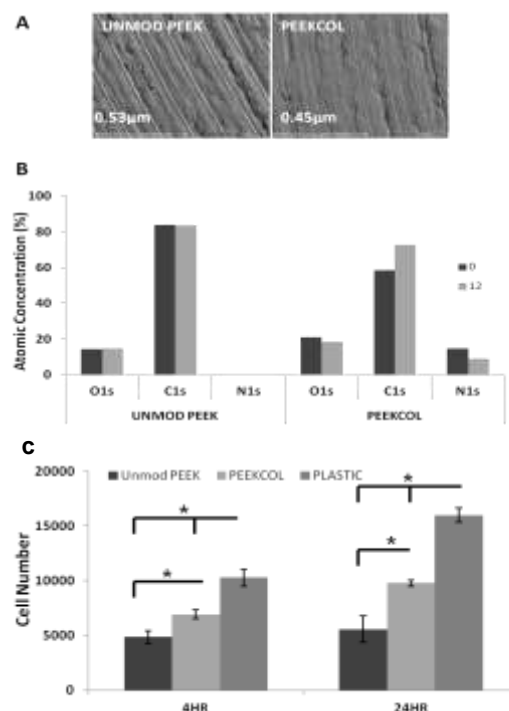


Fig.1.(A) Treatment does not alter surface morphology or roughness (B) XPS at 0 & 12 months indicating stability of modification (C) cell attachment is significantly ($p < 0.001$) improved on PEEKCOL samples compared to controls.

Bioactive PEEK holds great promise for load bearing orthopaedic applications. This approach also offers a commercially cost effective modification compared to current approaches. Given the modification is retained within the surface chemistry; this negates issues relating to internal cohesion rupture or delamination that have been observed for other coating modalities. Additional studies are focusing on the effect of modified PEEK for improving osteospecific differentiation, prior to testing in a relevant preclinical model.

CONCLUSION: Preliminary results suggest that plasma treatment of PEEK provides a clinically applicable method for enhancing cell attachment. A stable surface modification of PEEK can be achieved and in theory is not limited to PEEK or to the factors tested. This method may provide additional avenues to further improve outcomes of osseointegration.

REFERENCES

1. Kutrz & Devine, 2007 Biomaterials; 28, 4845-4869.
2. Converse et al., 2007 Biomaterials 28:927-935
3. Toth et al. 2006 Biomaterials 27: 324-334
4. Poulsson & Richards, 2012 PEEK Materials Handbook pp145-162
5. Garbassi et al., 1994 Polymer surfaces pp221-454

ACKNOWLEDGMENTS: Support provided by the Marie Curie Intra-European Fellowship Programme, SFI, Strategic Research Cluster and EU Regional Development Fund



PCL/HA functional gradient scaffold for Osteochondral Tissue Engineering applications

Alessandra Marrella and Silvia Scaglione*

National Research Council (CNR), IEIIT Institute, Italy, silvia.scaglione@ieiit.cnr.it

INTRODUCTION

Joints trauma and disease is one of the most prevalent disorders of the musculoskeletal system, involving structural damage to the articular tissue. It would be a major breakthrough to design and develop novel engineered grafts able to induce a specific cellular response addressed to the long-term in vivo tissue regeneration/integration besides properly interfacing with different host tissues^{1,2}.

We here propose novel morphologically and chemically graded 3D scaffold prototypes mimicking the physiological niche of the articular tissues to achieve continuous transition in both structural and functional tissue properties.

EXPERIMENTAL METHODS

Polycaprolactone (PCL) pellets and Hydroxyapatite (HA) powders were heated together (120°C) and poured into water with vigorous agitation (20.000 rpm) to obtain fibril-like PCL/HA-suspended solution (2/1 w/w ratio). Fibers were dried and re-suspended in water. The solution was centrifuged at different speeds and then freeze-dried; the final PCL/HA scaffold prototypes were mechanically reinforced heating nearby PCL melting temperature (59°, 1h). Morphological structure of scaffolds was observed by a scanning electron microscope (SEM). Functional tests have been also carried out in vitro with and without the use of a custom-made bioreactor able to apply a continuous perfusion and/or dynamic compression stimulation. Progenitor mesenchymal cells were cultured up to 2 weeks within scaffolds; cell survival, adhesion, differentiation and matrix deposition within 3D scaffolds have been evaluated at different time points.

RESULTS AND DISCUSSION

3D highly porous graded scaffolds were successfully realized via a fibril bonding process. The total porosity of prototypes resulted up to 80%±3% for all the scaffolds.



Fig.1: SEM images of the increasing porosity and decreasing gradient of HA (white spot) along the z-axis from left (bottom) to right (top).

Using 3000 rpm centrifuge speed for 5 minutes, SEM analysis confirmed a decreasing chemical gradient (provided by Ha powders) and an increasing pore size gradient along the z-axis (Figure 1). Both total porosity and pore size were statistically different ($p < 0,05$) comparing bottom and top side of the 3D scaffolds. These differences were maintained event introducing the chemical gradient (Figure 2).

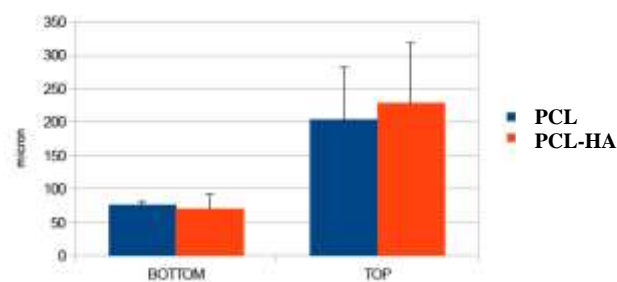


Fig.2: Morphological analysis of pore dimensions of graded scaffolds.

Preliminary biological experiments highlighted cells homogeneously colonizing the overall internal structure of graded scaffolds. Perfusing cell culture through the bioreactor increased the cell adhesion efficiency if compared with static culture.

CONCLUSION

This technique allowed realizing 3D functional graded grafts with different porosity ranges and chemical features, finally mimicking the physiological niche of the articular tissue and potentially guide a selective cellular differentiation and tissue regeneration.

These promising results open the possibility to validate in vivo such functionalized scaffolds, and produce novel bioactive replacement grafts for articular joint tissue engineering applications.

REFERENCES

1. Singht M. et al. Strategies and applications for incorporating physical and chemical signal gradients in tissue engineering. *Tissue Eng Part B Rev.* 2008 December;14(4): 341–366.
2. Se Heang Oha et al. In vitro and in vivo characteristics of PCL scaffolds with pore size gradient fabricated by a centrifugation method.

ACKNOWLEDGMENTS

The authors would like to thank the PRIN (Grant no: N. 2010L9SH3K 2013-2015) for providing financial support to this project.

Self-assembled Peptide Gels for Intervertebral Disc Tissue Engineering

Simon Wan¹ Alberto Saiani¹ Stephen Richardson² Julie Gough¹

¹School of Materials, the University of Manchester, UK

²Faculty of Medical & Life Sciences, the University of Manchester, UK

simon.wan@postgrad.manchester.ac.uk

INTRODUCTION

Low back pain (LBP) has reached epidemic proportions in the Western world and has been estimated to cost the UK economy £12 billion per annum¹. LBP aetiology is multi-factorial however intervertebral disc (IVD) degeneration is strongly associated with the condition². LBP prevalence is increasing whilst current treatments are ineffective, therefore a new strategy is required for LBP management. Cell-based therapies are regarded to hold particular promise as they have the potential to retard and even reverse IVD degeneration.

In this project, we investigated a self-assembling peptide hydrogel for its potential use as a cell-delivery tool and scaffold in nucleus pulposus (NP) tissue engineering. The hydrogel was chosen due to its biocompatibility, its injectability and the ease at which it can be modified to manipulate properties. The 3D culture of bovine NP cells (bNPCs) was first carried out as a model system then human bone marrow derived mesenchymal stem cells (h-BMMSCs) were investigated, as they have been identified as a promising cell source for NP tissue engineering, mainly due to their ability to differentiate into NP-like cells³.

EXPERIMENTAL METHODS

Cells were encapsulated in 30 mg ml⁻¹ gels. Atomic force microscopy (AFM) and rheology were used to characterise the gels. Bovine NPC and h-BMMSC morphology and viability was determined using fluorescence microscopy and LIVE/DEAD assay. Lactate dehydrogenase (LDH) assay was used to record changes in cell population. Dimethylmethylene blue (DMMB) assay was used to quantify glycosaminoglycan (GAG) production after bNPC encapsulation in the gel. Immunocytochemistry (ICC) was used to stain for extracellular matrix (ECM) components, specifically collagen, produced by bNPCs.

RESULTS AND DISCUSSION

AFM showed that the gel consisted of a dense nanofibrous network. Larger nanofibre assemblies were of similar size to type II collagen fibrils found in the native NP⁴. Rheology demonstrated that gels could be produced that were of comparable strength to the native NP which is crucial due to the mechanical roles of the tissue. Fluorescence microscopy showed that bNPC viability remained high throughout cell culture. Micrographs showed that cells displayed their characteristic rounded morphology when encapsulated. LDH assay showed no significant changes in cell population. Bovine NP cells were shown to produce ECM components associated with the NP. ICC demonstrated that type II collagen, which has a

mechanical role in the tissue, was being expressed inter- and extracellularly. Type I collagen wasn't produced by bNPCs; production of type I collagen is associated with IVD degeneration and NPC de-differentiation (**fig.1**). Bovine NPCs were shown to produce sulphated-GAGs with the amount produced per cell increasing with time point.

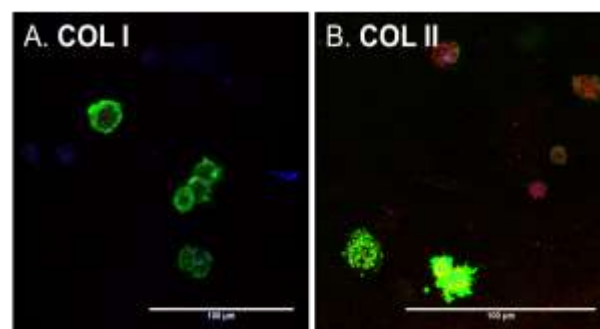


Figure 1. Collagen staining of 1×10^5 bNPCs encapsulated in peptide gel on day 7. [A] Negative staining for type I collagen [B] Positive staining for type II collagen. Collagen is stained red, F-actin is stained green and cell nuclei are stained blue.

Fluorescence microscopy showed that h-BMMSC viability was high for the duration of culture. LDH assay supported these findings with cell population remaining stable.

CONCLUSION

Results support the hypothesis that the peptide gel could act as an effective cell delivery tool and scaffold for NP tissue engineering. It is probable that the nanofibrous architecture of the gel biomimics the native NP tissue which is why bNPCs maintained a rounded morphology and produced the appropriate ECM components. Preliminary h-BMMSC results are promising but more investigation is required.

REFERENCES

- [1] Maniadas N *et al*, Pain **84**: 95-103 (2000) [2] Cheung K *et al*, Spine **34**: 934-940 (2009) [3] Minogue B *et al*, Arth & Rheu **62**: 3695-3705 (2010) [4] Aladin D *et al*, J Orthopaedic **28**: 497-502 (2010)

ACKNOWLEDGMENTS

The authors would like to thank the ESPRC for providing financial support for this project.

Utilizing Multifunctional Alginate Scaffolds for the Regeneration of Skeletal Muscle Defects in a Rat Crush Trauma Model

Taimoor Qazi^{1*}, Matthias Pumberger², Tobias Winkler², Sven Geißler¹, David Mooney³, Georg Duda¹

¹Julius Wolff Institute, Charité - Universitätsmedizin Berlin, Germany, taimoor.qazi@charite.de

²Center for Musculoskeletal Surgery, Charité-Universitätsmedizin, Berlin, Germany

³School of Engineering and Applied Sciences, Harvard University, USA

INTRODUCTION

Severe trauma to the skeletal muscle can not only result in fibrous scar tissue formation, but can also lead to loss in muscle functionality. The existence of such functional deficits due to insufficient regeneration is a serious issue in orthopaedic and trauma surgery. The potential of mesenchymal stem cells (MSCs) in regeneration of skeletal muscle following open crush trauma was shown previously by our group¹. Sustained delivery of pro-myogenic (IGF-1) and pro-angiogenic (VEGF₁₆₅) growth factors from an alginate scaffold has also been shown to result in functional improvement of skeletal muscle². We hypothesized that a combination of growth factors and MSCs delivered in a porous alginate scaffold would not only shield the cells from a harsh immune environment, but also act as a repository for the MSCs to exert their influence on muscle repair.

EXPERIMENTAL METHODS

Low and high molecular weight ultrapure alginates were oxidized and coupled with G₄RGDSP peptide sequences. The alginates were mixed in the ratio 1:1 and gelled using a calcium sulphate slurry. The growth factors (IGF-1 and VEGF₁₆₅) were mixed with the alginate at a concentration of 1 µg/µL before gelation. Samples of the hydrogel were stored at -80° C before being lyophilized to create a porous structure. MSCs were derived from bone marrow biopsies of female Sprague Dawley rats. Cell suspensions consisting of 1 million MSCs were seeded per scaffold. Preliminary assessment of scaffold structure, cell-matrix interactions, and growth factor release kinetics was carried out in vitro. The in vivo study design consisted of four test groups: (1) Blank Alginate, (2) Alginate + MSCs, (3) Alginate + Growth factors, (4) Alginate + MSCs + Growth factors. In each case, the transplantation was carried out following an open crush trauma to the soleus muscle. 1 and 4 weeks after transplantation, the rats were anaesthetised and muscle contraction forces (fast twitch and tetanic) were measured. The forces were normalized to those generated by the healthy leg. The soleus muscles were then explanted for histological evaluation.

RESULTS AND DISCUSSION

In vitro experiments showed a sustained release of growth factors (table 1) and good cell-matrix interactions (cell attachment and morphology, cell viability). Figure 1 depicts a scanning electron micrograph of the porous scaffold. No significant difference in muscle contraction forces could be observed in any group after 1 week of transplantation.

However, after 4 weeks, clear enhancements of fast twitch forces were seen for the groups Alginate + MSCs (74 ± 12 %), and Alginate + MSCs + Growth factors (83 ± 10 %), relative to the control (61 ± 9 %).

Table 1: Growth factor release kinetics from alginate scaffolds measured over a period of 28 days.

Day	IGF release (%)	VEGF release (%)
1	1.40 ± 0.1	9.0 ± 5.1
7	22.94 ± 8.5	78.90 ± 1.1
14	38.88 ± 2.4	83.17 ± 0.2
21	52.38 ± 3.3	85.44 ± 0.1
28	59.56 ± 9.1	87.59 ± 0

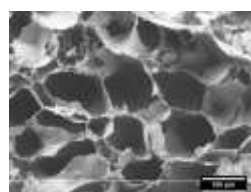


Figure 1: The porous structure of the alginate scaffolds was confirmed with Scanning electron microscopy (SEM).

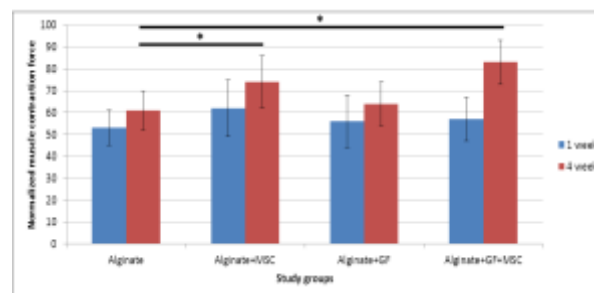


Figure 2: Fast-twitch muscle contraction forces of the control group (Alginate) and other study groups, 1 and 4 weeks after transplantation. * represents statistical significance (p < 0.05) compared to the control group.

CONCLUSION

These results show for the first time that transplantation of alginate scaffolds loaded with MSCs results in significant increase in muscle strength compared to blank scaffold transplantation. The effect is further enhanced upon incorporation of the growth factors IGF-1 and VEGF₁₆₅, indicating the utility of employing a combined approach for muscle regeneration.

REFERENCES

- Matziolis G. *et al.*, Tissue Eng. 12:361-367, 2006
- Borselli C. *et al.*, PNAS. 107:3287-3292, 2010

ACKNOWLEDGMENTS

The authors would like to thank the Einstein Foundation and the Friede Springer Stiftung for funding.



Engineering Hydrogel Polymer Networks for Cell Microencapsulation and Xenotransplantation

Françoise Borcard¹, Redouan Mahou¹, Virginia Crivelli¹, Elisa Montanari², Raphael P. H. Meier², Yannick Müller², Annalena Bollinger², Carmen Gonelle-Gispert², Jörg D. Seebach², Raphael Plüss³, Sandrine Gerber¹, Léo Bühler², Christine Wandrey^{1*}

^{1*}Institut d'Ingénierie Biologique et Institut des Sciences et Ingénierie Chimiques, Ecole Polytechnique Fédérale de Lausanne, Switzerland, christine.wandrey@epfl.ch

²Department of Surgery, Geneva University Hospital and University of Geneva, Switzerland

³Büchi Labortechnik AG, Switzerland

INTRODUCTION

The progress of medical therapies, which rely on the transplantation of microencapsulated cells, depends on the quality of the encapsulating material. Such material has to be biocompatible, its physical characteristics have to be adjustable, and the microencapsulation process must be simple and not harm the cells.

We produced biocompatible one- and two-component hydrogel microspheres (MS) by combining ionotropic gelation of sodium alginate (Na-alg) using calcium ions with covalent crosslinking of poly(ethylene glycol) derivatives (PEG)¹⁻⁴. Multi-arm PEG was either mixed with Na-alg^{1,3,4} or heterobifunctional PEG was grafted onto the carboxyl groups of Na-alg².

Differently to our previous materials, we present now hydrogels prepared by grafting either PEG onto the hydroxyl groups or cystamine dihydrochloride onto the carboxyl groups of Na-alg, and demonstrate their suitability for cell microencapsulation.

EXPERIMENTAL METHODS

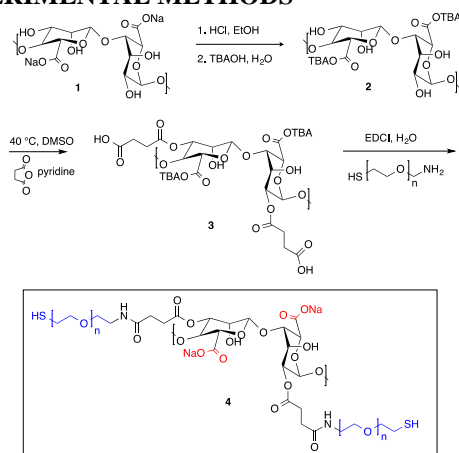


Fig. 1. Functionalization of Na-alg by grafting heterobifunctional PEG onto the hydroxyl groups (Na-alg-PEG).

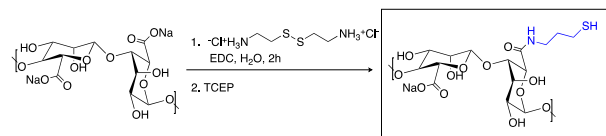


Fig. 2. Functionalization of Na-alg by grafting cystamine dihydrochloride onto the carboxyl groups (Na-alg-cys).

¹H-NMR, ¹³C-NMR and FTIR were used for polymer analyses. The polymer solutions were characterized by their viscosity and osmolality. An Encapsulator B-395 Pro was used to produce MS. The MS were characterized in terms of size/swelling (microscopy), mechanical resistance to compression (texture analyser TA-XT2), and permeability (ingress diffusion). Human

foreskin fibroblasts (EDX cells) and islets were used for *in vitro* and *in vivo* studies. Encapsulated rat and human islets have been transplanted into mice.

RESULTS AND DISCUSSION

The functionalized Na-alg-PEG and Na-alg-cys allow for cell microencapsulation by a one-step process. Upon extrusion into the gelation bath, the fast ionotropic gelation with calcium ions ensures the spherical shape of the hydrogel while the simultaneously but slowly occurring covalent crosslinking reinforces the hydrogel mechanically and adjusts its permeability. Both the mechanical properties and the permeability of the MS can be adjusted in a range considered favorably for cells by varying the degree of grafting and the polymer solution concentration.

Long-term survival and function of EDX cells *in vitro* confirmed the biocompatibility and durability of the two types of MS. Fig. 3 shows EDX cells in Na-alg-PEG.



Fig. 3. Left to right: Homogeneous distribution of EDX cells in Na-alg-PEG; single MS; FDA staining; PI staining; MS: 600 $\mu\text{m} \pm 10\%$.

Static incubation tests confirmed survival and function of microencapsulated rat and human islets. Upon xenotransplantation into diabetic mice, normoglycemia was achieved in the period of months. The long-term *in vivo* experiments continue.

CONCLUSION

Two novel types of alginate-based MS have been engineered. Their physical and biological properties as well as the production process are favourable for cell microencapsulation. *In vitro* and *in vivo* studies confirmed the suitability for the development of cell therapies.

REFERENCES

1. Mahou R. *et al.*, Macromolecules 43:1371-78, 2010
2. Mahou R. *et al.*, J. Mater. Sci: Mater. Med. 23:171-9, 2012
3. Mahou R. *et al.*, Macromol. Symp. 329:49-57, 2013
4. Mahou R. *et al.*, Materials 7:275-86, 2014

ACKNOWLEDGMENTS

The authors thank the FNS (205321-141286/1) and the CTI (13804.1 PFLS-LS) for financial support.



Development of Osteoconductive Organic-Inorganic Hybrid Materials Based on Calcium Silicates

Chikara Ohtsuki^{1*}, Toshiki Miyazaki² and Masakazu Kawashita³

^{1*}Graduate School of Engineering, Nagoya University, Japan, ohtsuki@apchem.nagoya-u.ac.jp

²Graduate School of Life Science and Systems Engineering, Kyushu Institute of Technology, Japan

³Graduate School of Biomedical Engineering, Tohoku University, Japan

INTRODUCTION

Bioactive glasses and glass-ceramics show direct bonding to living bone, i.e. osteoconduction, when implanted in bony defect. Their osteoconduction would be accomplished through formation of biologically active hydroxyapatite layer by chemical reaction of their surfaces with body fluid. This layer has similarity in its composition and crystalline characteristics to inorganic phase in natural bone, and is called bone-like apatite. Potential of the bone-like apatite formation can be evaluated *in vitro* using a simulated body fluid (SBF) reported by Kokubo and his colleagues¹. After the report on compositional dependence of the apatite formation on CaO-SiO₂-P₂O₅ glasses in SBF, CaO-SiO₂ binary glass has been regarded as important composition for the bone-like apatite formation. The CaO-SiO₂ glass show the bone-like apatite formation due to dissolution of Ca²⁺ to surrounding fluid, as well as heterogeneous apatite nucleation induced by Si-OH groups in silica hydrogel formed on the glass surface². However drawback of the bioactive glass is lower fracture toughness and higher Young's modulus than natural bone. This limits their applications to low loaded conditions. Organic-inorganic hybrids composed of organic polymers and inorganic species providing Si-OH groups and Ca²⁺ are expected to solve the above problems. In the present topic, design of organic-inorganic hybrids able to form the bone-like apatite is reviewed for development of novel osteoconductive materials.

EXPERIMENTAL METHODS

Sol-gel processing is a typical method for preparation of organic-inorganic hybrids through organic modification of calcium silicate. Polydimethylsiloxane (PDMS)-silicate hybrids with incorporation of calcium nitrate (Ca(NO₃)₂) were prepared by sol-gel processing³. Organically modified silicates with reduced amounts of siloxane networks were prepared from 2-hydroxyethyl methacrylate and methacryloxypropyltrimethoxysilane (HEMA-MPS) with addition of calcium chloride (CaCl₂)⁴. Polysaccharide-based hybrids were also prepared by appropriate modification with alkoxysilane and calcium salts. Alginate was chemically modified with aminopropyltriethoxysilane (APTES), followed by treatment with CaCl₂⁵. Starch-based hybrids modified with glycidoxypropyltrimethoxysilane (GPS) were prepared in different concentrations of GPS with incorporation of CaCl₂⁶.

SBF was prepared according to Kokubo's recipe¹. Apatite formation on the specimens was examined generally by X-ray diffraction, Fourier transform infrared spectroscopy and scanning electron microscopic observation. In some cases, changes in pH,

calcium and phosphorus concentrations of SBF were measured.

RESULTS AND DISCUSSION

Synthesis of organic-inorganic hybrid of PDMS-silicate with Ca(NO₃)₂ incorporation would give structure consisting of silica blocks with PDMS chains. Ca(NO₃)₂ incorporation may lead to the bone-like apatite formation in SBF³. HEMA-MPS hybrids showed improved flexibility that is expected by reduced amount of siloxane networks. Soft material could be obtained at starting composition of HEMA:MPS:CaCl₂ = 0.9:0.1:0.1 in molar ratio, and it deposited the bone-like apatite in SBF within 7 days⁴. Mechanical properties of the hybrids can be also well controlled by kind of the catalyst in sol-gel processing⁷.

Alginate modified with APTES and subsequently treated with CaCl₂ showed the bone-like apatite formation in SBF⁵. Starch-GPS hybrids modified with CaCl₂ also showed the bone-like apatite formation in SBF. The starch-based hybrids varied their mechanical characteristics by the amounts of GPS⁶. Thus modification of polysaccharide would facilitate development of osteoconductive hybrids with different biodegradation rate and mechanical properties.

CONCLUSION

Various types of organic-inorganic hybrids have been developed from the fundamental understandings on surface reaction of bioactive CaO-SiO₂ glass in SBF. The design of the osteoconductive materials may produce novel bioactive materials for bone repairing with various functions.

REFERENCES

1. Cho S.B. *et al.*, J. Am. Ceram. Soc. 78:1769-1774, 1995
2. Ohtsuki C. *et al.*, J. Non-Cryst. Solids 143:84-92, 1992
3. Tsuru K. *et al.*, J. Mater. Sci.: Mater. Med. 8:157-161, 1997
4. Ohtsuki C. *et al.*, Mater. Sci. Eng.: C 22:27-34, 2002
5. Hosoya K. *et al.*, J. Biomed. Mater. Res. 71A:596-601, 2004
6. Miyazaki T. *et al.*, Mater. Trans. 48:317-321, 2007
7. Uchino T. *et al.*, J. Biomater. Appl. 23:519-532, 2009

ACKNOWLEDGMENTS

This work was partially supported by Grant-in-Aid for Scientific Research (No. 22107007) on the Innovative Areas: "Fusion Materials" (Area no. 2206) from the Ministry of Education, Culture, Sports, Science and Technology (MEXT).



Formation of hybrid materials based on calcium phosphate deposit on carbon fiber scaffold

Q. Picard¹, S. Delpeux¹, J. Chancolon¹, N. Rochet², F. Fayon³, F. Warmont¹, S. Mikhalevski⁴, S. Bonnamy¹

¹ CRMD, CNRS / University of Orléans, 1B rue de la Férollerie, 45071 Orléans Cedex 2, France

² Institut de biologie Valrose INSERM/BIPOA, 06107 Nice Cedex 2, France

³ CEMHTI, CNRS, 1D Avenue de la Recherche Scientifique, 45071 Orléans Cedex 2, France

⁴ School of Pharmacy and Biomolecular Sciences, University of Brighton, UK

quentin.picard@cnrs-orleans.fr

INTRODUCTION

Due to their breathability, specific mechanical properties, i.e. high flexural and fatigue strength relative to their weight ratio and biocompatibility, activated carbon clothes (ACC) have previously been considered for hard and soft tissue implanting. However, their poor biological activity restricts their extensive use in medical applications and therefore needs to be enhanced^{1,2,3}. Thanks to their excellent biocompatibility, osteoconductivity and bioactivity, calcium phosphate (CaP) ceramics, especially hydroxyapatites (HA), have received much attention in the biomedical materials field and have been clinically applied in orthopaedics³. So, carbon fiber-reinforced HA composites, combining the highly biocompatible CaP matrix with the properties of carbon fiber, are promising bioceramic material, which could be particularly useful in the reconstruction of bone defects³.

EXPERIMENTAL METHODS

To get bioactive hybrid materials, CaP coatings are deposited on activated carbon scaffolds by sono-electrodeposition process. A mixture of $\text{Ca}(\text{NO}_3)_2$, $4\text{H}_2\text{O}$ and $\text{NH}_4\text{H}_2\text{PO}_4$ is used as an electrolyte. A three electrode system connected with a potentiostat-galvanostat is used to apply a cathodic polarization at the carbon electrode. The influence of electrochemical parameters is connected to the quantity, microtexture, structure and chemical composition of CaP phases. The materials biocompatibility was determined by culturing human osteoblast-cells (HOST) in contact with CaP/ACC hybrid materials.

RESULTS AND DISCUSSION

Data show that polarization duration influences the deposit thickness: from 500 nm to 5 μm . The mass uptake tends to a limit corresponding to the decrease of nucleation sites. The current density influences the CaP deposit quantity, morphology and chemical composition. Indeed, at low regime, the quantity of deposit is proportional to the applied current density. During CaP deposit, two phenomena occur due to water electrolysis: H_2 release at working electrode surface leads to a more or less homogeneous coating and the electrolyte pH decrease along polarization leads to CaP re-dissolution. SEM, TEM and FTIR characterizations show that the coating consists in a plate-like carbonated octacalcium phosphate for low current densities and needle-like carbonated calcium deficient HA (cdHA) for high current densities. ^1H and ^{31}P NMR MAS of

deposits confirm the presence of carbonated cdHA and underline the presence of minority disordered CaP phases.

In order to improve the coating adhesion, the ACC surface has been functionalized by sono-electrochemistry. Two paths are studied: on the one hand, ACC is oxidized by application of anodic current in Na_2SO_4 aqueous electrolyte. On the other hand, phosphates are grafted on ACC surface by electrochemical oxidation in phosphoric acid aqueous media. Mechanical tests are in progress to assess the adhesion properties between cloth and deposit. Concerning biological experiments, results have shown evidence of biocompatibility of hybrid materials and activity that has stimulated the HOST growth (Fig. 1).

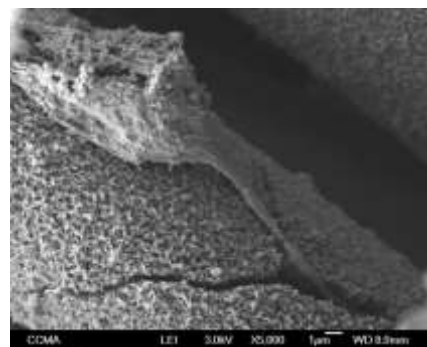


Figure 1: SEM images of human osteoblasts cultured for 7 days in the presence of CaP/ACC hybrid material obtained at low current density.

CONCLUSION

The sono-electrodeposition process consists in a co-precipitation of calcium and phosphate ions with hydroxides ions provided by water electrolysis. It is an efficient method to obtain a controlled thickness, morphology (platelets or needles) and chemical composition of CaP deposits. Preliminary *in vitro* studies of HOST interaction with CaP/ACC material show a good biocompatibility whatever CaP morphologies.

REFERENCES

1. Han HM. *et al.*, New Carbon Mat. 22:121-125, 2007
2. Stoch A. *et al.*, J. Mol. Struct. 651-3: 389-396, 2003
3. Kuo MC. *et al.*, Mat. Sci. Eng. C 20:153-160, 2002

ACKNOWLEDGMENTS

This work was supported by European People PF7-IRSES program: Advanced Biomaterials for Regenerative Medicine (ABREM) 2011-2014



Strontium Ion Release from Bioactive Ti Alloys with Ca enriched-Surface Layer

Seiji Yamaguchi^{1*}, Tomiharu Matsushita¹ and Tadashi Kokubo¹

¹Department of Biomedical Sciences, Chubu University, Japan

^{1*} Department of Biomedical Sciences, Chubu University, Japan, sy-esi@isc.chubu.ac.jp

INTRODUCTION

Titanium (Ti) metal and its alloy are widely used as orthopedic and dental implants because of their good biocompatibility and high mechanical strength. However, they do not bond to living bone. The present authors early showed that Ti metal and its alloys bond to living bone through an apatite layer formed on their surfaces in a living body, when a Ca-deficient calcium titanate layer was produced on the metals by NaOH, CaCl₂, heat and water treatments (Ca treatment) [1]. Recently, it was found that strontium (Sr) ions can be incorporated into the surface of Ti metal additionally to Ca ions by modifying the Ca treatment. Sr ion has been attempted to be used in bone healing therapy due to its effects of increasing new bone formation while reducing bone resorption. It is expected that the treated metal could bond to the bone in a shorter period of time because it releases Sr ions and form apatite on its surface.

In the present study, Sr ion incorporation was attempted on the surfaces of Ti alloys such as Ti-6Al-4V and Ti-15Zr-4Nb-4Ta by the modified Ca treatment. Apatite formation on the surface of the resultant product in a simulated body fluid (SBF) and release of Sr ions in a phosphate-buffered solution (PBS) were discussed in terms of the surface structure.

EXPERIMENTAL METHODS

Ti-6Al-4V and Ti-15Zr-4Nb-4Ta alloys with the size of 10 × 10 × 1 mm³ were soaked in 5 M NaOH aqueous solution at 60 °C for 24 h, then subsequently in a mixed solution of 50 mM CaCl₂ and 50 mM SrCl₂ at 40 °C for 24 h. They were heated at 600 or 700 °C for 1 h, and then soaked in 1M SrCl₂ solution at 80 °C for 24 h. The samples were washed with flowed ultra-pure water for 30 sec after each solution treatment.

Surfaces of the samples were examined by a field emission scanning electron microscope (FE-SEM) equipped with energy dispersive X-ray analyzer (EDX), thin-film X-ray diffractometer (TF-XRD), and laser Raman spectrometer (FT-Raman). Apatite formation on the samples were examined by soaking in SBF with ion concentrations (Na⁺ 142.0, K⁺ 5.0, Ca²⁺ 2.5, Mg²⁺ 1.5, Cl⁻ 147.8, HCO₃⁻ 4.2, HPO₄²⁻ 1.0, and SO₄²⁻ 0.5 mM) nearly equal to those of human blood plasma at 36.5 °C [2] for 3 days. The samples subjected to the chemical and heat treatments were soaked in 2 ml of PBS at 36.5 °C. After soaked in PBS for various periods up to 7 days, Ca and Sr ion concentrations in PBS were measured by inductively coupled plasma emission spectroscopy (ICP).

RESULTS AND DISCUSSION

FE-SEM observation showed that nano-scaled network structures were produced on both the surfaces of Ti-

6Al-4V and Ti-15Zr-4Nb-4Ta alloys by the chemical and heat treatments. EDX analysis revealed that former surface contains 1.3 % Sr and 1.8 % Ca, whereas the latter contains 1.1 % Sr and 1.1 % Ca. Thus the formed surface layers were found to be composed of Sr-containing calcium titanate, anatase and rutile by TF-XRD and FT-Raman analysis.

When the treated alloys were soaked in SBF, both of them formed apatite fully on their surfaces within 3 days. When they were soaked in PBS, Ti-6Al-4V gradually released 0.82 ppm of Sr ions in PBS within 7 days, whereas Ti-15Zr-4Nb-4Ta released Sr ions up to 0.38 ppm, as shown in Fig. 1. The lower release of Sr ions from Ti-15Zr-4Nb-4Ta alloy might be due to presence of alloying elements such as Zr, Nb, and Ta in the surface layer, since the Sr content in the surface of the alloy was comparable with that of Ti-6Al-4V alloy.

The released amounts of Sr ions in the present study fall into a range from 0.21 to 21.07 ppm, which is an effective range to increase ALP activity and the expression of a key osteoblast transcription factor gene in hMSCs [3].

It is expected that the treated alloys in the present study could enhance osteoblastic differentiation so as to promote bone formation by releasing Sr ions, and tightly bond to bone through an apatite formed on their surfaces.

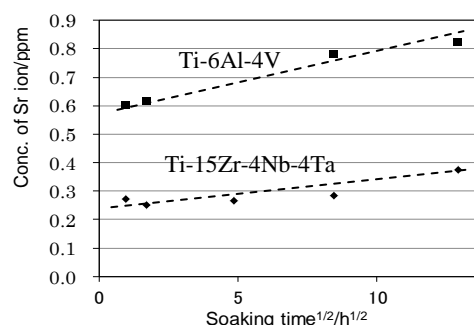


Fig.1 Released concentration of Sr ions from Ti alloys subjected chemical and heat treatments, as a square root of soaking time in PBS.

CONCLUSION

Ti-6Al-4V and Ti-15Zr-4Nb-4Ta alloys with Ca-enriched surface layers able to release Sr ions were prepared by the modified Ca treatments.

It is expected that the treated alloys might bond to living bone in a shorter period of time, since they release Sr ions in a living body to promote bone formation, and induces apatite formation on its surface.

REFERENCES

1. Fukuda A. *et al.*, Acta Biomater. 7:1379-1386, 2011
2. Kokubo T. *et al.*, Biomaterials 27:2907-2915, 2006
3. Sila-Asna M. *et al.*, Kobe. J. Med. Sci. 53:25-35, 2007

Cell-to-cell Communications of Osteocytes with Bone Marrow Cells on Ceramic Biomaterials

Miho Nakamura^{1*}, Teuvo Hentunen², Jukka Vääräniemi¹, Jukka Salonen², Naoko Hori¹ and Kimihiro Yamashita¹

^{1*}Institute of Biomaterials and Bioengineering, Tokyo Medical and Dental University, Japan

²Institute of Biomedicine/Cell Biology and Anatomy, University of Turku, Finland

*miho.bcr@tmd.ac.jp

INTRODUCTION

Ceramic biomaterials are used for clinical applications as bone grafts to reconstruct bone tissue in defects. Both bone-forming osteoblasts and bone-resorbing osteoclasts play prominent roles in bone formation surrounding the implanted ceramic biomaterials. Osteoclast formation are regulated by osteocytes embedded in bone matrix through the expression of receptor activator of nuclear factor- κ B ligand (RANKL)¹.

We designed the osteocyte-stimulating biomaterials without addition of any growth factors. Osteocytes are most abundant cells in bone, buried in the mineralized bone matrix. Although the osteocytes are used for the evidence for the osteoblast differentiation from the osteoblast progenitors, there are few studies on the interaction between the osteocytes and ceramic biomaterials. In the present study, the interactions of osteocytes with bone marrow cells through the cell-to-cell communications on various types of ceramic biomaterials, were investigated.

EXPERIMENTAL METHODS

Cell culture: Osteocyte-like cells² (MLO-Y4, kindly gifted from Prof. Bonewald) were cultured on the synthesized ceramic biomaterials such as hydroxyapatite (HA) and carbonate apatite (CA), β -tricalcium phosphate (β -TCP), and additionally on bone slices as a control. After 1d culture, bone marrow cells (BMC) isolated from mouse femurs (C57Bl/6J, male, 10-week-old) were added and co-cultured according to the procedure established by Zhao S³.

Staining: The cells adhered to the samples were washed with PBS and fixed with 4% paraformaldehyde. After the PBS washes, the cells were permeabilized with 0.1% Triton X-100 in PBS, stained with rhodamine-phalloidin and Hoechst. The fluorescence signals were observed using a fluorescence microscope.

The fixed cells were also stained for tartrate-resistant acid phosphatase (TRAP) to confirm the differentiation of BMC into osteoclasts.

Observation of resorption pits: After removing the cells, the resorption pits were observed using scanning electron microscope and quantified using laser microscope.

RESULTS AND DISCUSSION

The giant cells with multiple nuclei were formed both on the synthesized CA and bone slices after a co-culture of MLO-Y4 with BMC. These cells were positively stained for TRAP, which indicated that they were

differentiated from BMC into osteoclastic cells without any added differentiation factors. The number of TRAP-positive multinuclear cells was significantly higher on the CA compared to HA among the ceramic biomaterials.

Actin rings, which are specific markers for activated osteoclasts to resorb the substrata, were formed in osteoclasts on the CA and bone slices. The number of actin ring was significantly larger on CA compared to HA among the ceramic biomaterials. As a result, the resorption pits were formed on CA and bone slices.

The possible explanations of the enhanced differentiation and activation of osteoclastic cells on the CA are the cell-to-cell interactions and secretion of differentiation factors from MLO-Y4 cells. Osteoblasts and osteoclast precursor cells are known to interact with each other through the molecules, such as RANKL and macrophage colony-stimulating factor (M-CSF). Therefore, also osteocytes were considered to express the molecules for the differentiation of bone marrow cells into osteoclasts.

CONCLUSION

TRAP-positive and multinuclear cells with actin ring structures were formed by the interaction with osteocyte-like cells and BMC. The formation of mature and activated osteoclasts was enhanced on the CA compared to HA.

REFERENCES

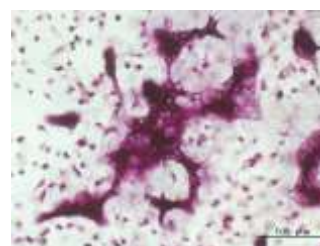


Fig. TRAP-positive cells were formed on the synthesized CA after co-culture of osteocyte-like cells with bone marrow cells without any differentiation factors.

1. Nakashima T, *et al.*, Nat Med (2011), 11: 1231-1234.
2. Kato Y. *et al.*, J Bone Miner Res (1997), 12: 2014-2023.
3. Zhao S, *et al.*, J Bone Miner Res (2002), 17: 2068-2079.

ACKNOWLEDGMENTS

The authors would like to thank the Shiseido Female Researcher Science Grant and the Murata Science Foundation for providing financial support to this project.



Critical Bone Defect Filling with Chitosan/Hydroxyapatite Hybrid Scaffolds in Rats

Valérie Brun¹, Christine Guillaume¹, Julien Braux¹, Richard Gouron², Romuald Mentaverri², Saad Mechiche Alami¹, Sylvie Bouthors¹, Dominique Laurent-Maquin¹, Sophie C. Gangloff¹, Halima Kerdjoudi¹, Frédéric Velard¹

¹ EA 4691 BIOS, University of Reims Champagne-Ardenne, Reims, France, frederic.velard@univ-reims.fr

² INSERM UMR-S1088, University Picardie Jules Verne, Amiens, France

INTRODUCTION

Masquelet technique also called induced-membrane procedure was developed to favor bone regeneration using autologous graft and biomaterials in large bone defects. On one hand, due to its osteoconductive properties, hydroxyapatite is a largely used biomaterial to fill bone defects but its tendency to fragment and generate debris with inflammatory potential remains a limitation¹. On the other hand, chitosan is a biocompatible, biodegradable and anti-inflammatory natural polymer². Thus we have combined chitosan and hydroxyapatite to synthesize hybrids and porous 3D scaffolds for bone regeneration³. This work aims to assess their long term biocompatibility *in vivo*.

EXPERIMENTAL METHODS

Scaffolds synthesis and characterization:

Scaffolds characterization included macroscopic and microscopic (Keyence VHX200 numeric microscope) observations, Equilibrium Swelling Ratio (ESR) measurement, EDXS and FTIR analyses and measurement of weight loss overtime.

In vitro biocompatibility study:

Using primary bone cells culture during 7, 14 and 21 days, we evaluated cells viability, proliferation and alkaline phosphatase (ALP) activity. Non parametric stratified permutation test was performed to assess significance of our results (n=6, p<0.05).

In vivo biocompatibility study:

Induced membrane technique was used in a murine model (12 Sprague-Dawley 12 week old male rats) following local animal ethic committee guidelines. After induced membrane generation (6 weeks), rats were treated with hybrid biomaterial or vertebral autologous bone grafts (used as control) for 4 or 12 weeks. Radiographs, echographs and microCT were performed on freshly isolated femurs whereas histological (HPS, Masson's trichrome and May Grünwald Giemsa stainings) studies were performed after decalcification.

RESULTS AND DISCUSSION

Freeze-dried scaffolds were hydrophilic, porous and biodegradable. Moreover detectable amount of β -GP used during hydrogel formation (EDXS and FTIR) was evidenced inside the cross-linked hybrid biomaterial. *In vitro*, cell response to the hybrid scaffolds in terms of cell death, proliferation or ALP activity followed with very few modifications, the measurements of the control patterns. *In vivo*, after four weeks, filling materials were found inside the defect but nor hybrid biomaterial neither autologous grafts allow new bone formation. Nevertheless, collagen neosynthesis could be observed with autologous bone graft. Using hybrid scaffolds, induced membrane appeared thickened more

vascularized and exhibited presence of inflammatory cells that were not present with autologous graft. After 12 weeks, microCT demonstrated that autologous bone was remodeled but failed to create clear union between the edges of the defect whereas osteolytic features seemed to be observed with hybrid scaffold (Figure 1). Histological studies are in progress to precisely assess the later observation, since induced membrane has been recently demonstrated to host many osteoclasts which can explain the strong scaffolds resorption observed³.

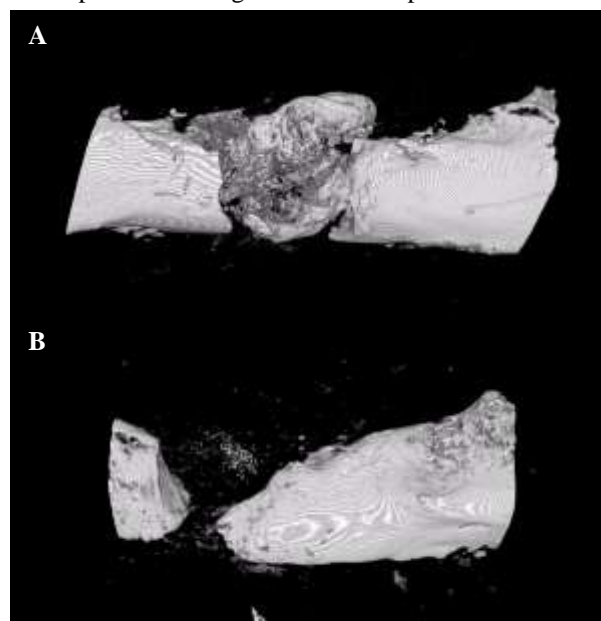


Figure 1: MicroCT photographs of critical defect filled with autologous vertebral bone graft (A) or hybrid scaffold (B) 12 weeks after implantation.

CONCLUSION

In this study, we have provided evidence that unexpectedly our hybrid scaffolds seemed not to be suitable for bone regeneration purpose. Future works will include selected biomacromolecules in the scaffolds to enhance osteoconductive and osteoinductive skills as well as immunomodulatory molecules to control peri-implant osteolysis.

REFERENCES

- 1 Velard F, *et al.* Acta Biomaterialia, 9:4956, 2013.
- 2 Di Martino A, *et al.* Biomaterials. 26:5983, 2005.
- 3 Gouron R, *et al.* Tissue Eng. Regen. Med. In press, 2014.

ACKNOWLEDGMENTS

Authors warmly thank URCA and Région Champagne-Ardenne for financial support and Dr Karim Madi from Orthopedic and Traumatology department of the University Hospital Center of Reims for bone samples.



Fibrinogen implants for bone regeneration: short- and long-term *in vivo* responses

Daniel M. Vasconcelos^{1,2}, Raquel M. Gonçalves¹, Susana G. Santos¹, Catarina R. Almeida¹, Inês Odila¹, Marta I. Oliveira¹, Nuno Neves^{1,3,4}, Andreia M. Silva^{1,2}, António C. Ribeiro¹, Elisabeth Seebach⁵, Katharina L. Kynast⁵, Thomas Niemietz⁵, Wiltrud Richter⁵, Meriem Lamghari^{1,2}, Mário A. Barbosa^{1,2}

¹INEB, University of Porto, Portugal; ²ICBAS, University of Porto, Portugal; ³Spine Group, Orthopedic Department, Centro Hospitalar de São João, Porto, Portugal; ⁴Faculty of Medicine, University of Porto, Portugal; ⁵Research Center for Experimental Orthopaedics, Department of Orthopaedics, Trauma Surgery and Paraplegiology, Heidelberg University Hospital, Germany

INTRODUCTION

Inflammatory response is a natural event following biomaterials implantation. The concept of “fighting inflammation” has been gradually shifting to “modulating inflammation”¹. Our team has previously shown that the incorporation of a pro-inflammatory and pro-healing molecule, fibrinogen (Fg), in chitosan scaffolds is able to modulate the systemic immune response while improve bone regeneration².

In this study we addressed the potential of Fg 3D scaffolds to promote bone regeneration. Also, we investigated the local and systemic response to these scaffolds at short- and long-term time-points after implantation.

EXPERIMENTAL METHODS

Fg scaffolds were prepared by freeze-drying method as previously described by our group for other materials². Animal work was approved by DGAV. Each Wistar rat (3 months) suffered a femoral critical size bone defect, which remained empty or received Fg scaffolds (n=12/group). Before implantation the scaffolds were neutralized and disinfected by an ethanol series gradient and kept in sterile PBS.

After 6 days (short-term) and 8 weeks (long-term) post-implantation, the animals were sacrificed. The blood (BL), lymph nodes (LN), spleen (SP) and femurs were collected. Some of the femurs (n=5) were processed for histology (H&E and Masson's trichrome staining) and were observed in a light microscope Olympus CX31. Gene expression analysis of inflammatory and bone-related markers was analysed at the defect site in the remaining femurs (n=7). Immune cell populations from BL, LN and SP were freshly isolated and analysed in a FACSCanto. The results were analyzed with FlowJo. Pro-inflammatory cytokines in plasma were also analysed by ELISA. Statistical analysis was performed using Prism software.

RESULTS

At 6 days post-implantation, local gene expression analysis at the bone defect revealed a significant increase in IL-6 and IL-8 levels for both, empty- and Fg-groups of animals when compared with non operated animals, while IL-1B remained constant. An increase of VEGF and TGF-B1 was also detected. At the same time-point post-implantation, TGF-B1 concentration in plasma was significantly increased in the “empty”-group of animals, while at 8 weeks post-

implantation no differences were observed between the groups of animals. The pro-inflammatory cytokines TNF-a, IL-6 and IL-17a were not detected in plasma, at either time point.

Also, Fg scaffold implantation correlated with changes on the proportions of immune cells at the systemic level. A reduction of myeloid cells (CD11b⁺) and B cells, with a concomitant increase on T cells, was particularly significant in SP at 6 days post-implantation. Fg also led to less NK and NKT cells in BL. Interestingly, BL, LN and SP Mac-1⁺ (CD18⁺/CD11b⁺) cells were significantly decreased in animals implanted with Fg scaffolds, while more TCR^{dim} T cells were found in LN of the animals with Fg implants. Moreover, BL myeloid cells (CD11b⁺) showed an activated phenotype (MHC^{high}) in Fg implanted animals.

Histological evaluation showed that Fg scaffolds eased cell migration. The increased infiltration of connective tissue at periphery of the defect in Fg-group correlated with a decreased defect size at day 6. By 8 weeks post-implantation Fg scaffolds were replaced by bone tissue.

CONCLUSION

Fg scaffolds promote bone formation after 8 weeks of implantation. A mild inflammatory response was observed 6 days after injury, either with or without Fg implants, when compared with non-operated animals. Moreover, alterations in immune cell proportions and their activation status, at an early time-point correlate with increased bone formation at a later stage.

REFERENCES

1. Mountziaris, P.M., *et al.*, TEPB (2011); 2. Santos SG, *Acta Biomaterialia* (2013);

ACKNOWLEDGMENTS

This work was financed by FEDER funds through *Programa Operacional Factores de Competitividade – COMPETE* and by Portuguese funds through FCT – *Fundação para a Ciência e a Tecnologia* in the framework of projects PEst-C/SAU/LA0002/2013 and PTDC/SAU-BEB/099954/2008, and North Region Operational Program (ON.2), in the framework of the “*Project on Biomedical Engineering for Regenerative Therapies and Cancer - NORTE-07-0124-FEDER-000005*”, through QREN. DV, MIO were supported by PhD and post-doc fellowships SFRH/BD/87516/2012, SFRH/BPD/37090/2007, respectively.



Nanoscale Control of Mesenchymal Stem Cells

Matthew J Dalby¹, P Monica Tsimbouri¹, Laura McNamara¹, Enateri Alakpa¹, Lesley-Anne Turner¹, Rebecca McMurray¹, Louisa CY Lee¹, Jingli Yang¹, Habib Nikukar¹, Gabriel Pemberton¹, Terje Sjostrom², Peter Childs³, Jugal Sahoo⁴, Vineetha Jayawarna⁴, Christopher West⁵, Karl Burgess⁶, Stuart Reid³, Bo Su², Maggie Cusack⁷, Nikolaj Gadegaard⁸, Rein V Ulijn⁴, RM Dominic Meek⁹, Bruno Peault⁵, Richard OC Oreffo¹⁰.

¹Centre for Cell Engineering, University of Glasgow, UK. ²Dental Materials, University of Bristol, UK. ³SUPA, University of the West of Scotland. ⁴Department of Pure and Applied Chemistry, University of Strathclyde, UK. CRM, University of Edinburgh, UK. ⁶Glasgow Polyomics, University of Glasgow, UK. ⁷Geographical and Earth Sciences, University of Glasgow, ⁸James Watt Nanofabrication Centre, University of Glasgow, UK. ⁹Department of Orthopaedics, Southern General Hospital, Glasgow, UK. ¹⁰Bone and Joint Research Group, University of Southampton, UK.

Matthew.dalby@glasgow.ac.uk

INTRODUCTION

Mesenchymal stem cells (MSCs) respond to nanoscale surface features through changes in growth and differentiation. In this talk we will discuss the contribution of nanoscale topography to MSC differentiation and self-renewal. MSCs in their niche undergo growth and differentiation in response to regenerative demand – this is at odds with static materials approaches where either growth or differentiation is influenced. Thus, dynamic surfaces that can be used to control stem cell growth and differentiation under user control will be presented.

Furthermore, the potential role of materials in stem cell discovery will be discussed. MSCs are adaptive to their environment and tune e.g. their metabolic response to different extracellular cues. Using tissue-matched hydrogels with control of elastic moduli coupled to analysis of metabolic adaptation and lineage specific depletion, data on selection of bioactive metabolites that drive MSC differentiation will be discussed. We will further extend some of this data to perivascular stem cells (pericytes).

RESULTS AND DISCUSSION

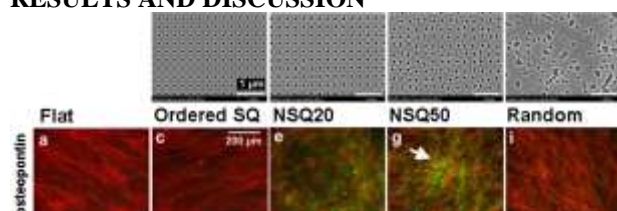


Figure 1. Nanoscale order is critical to MSC differentiation. Using electron beam lithography 120 nm diameter pits with 300 nm spacing were produced in PMMA. Where the pits were formed in an ordered square (SQ) lattice or with random placement little osteospecific differentiation was noted. If, however, small levels of disorder (near SQ, NSQ) were added (± 20 nm and ± 50 nm offset from centre position) then rapid osteogenesis was noted.

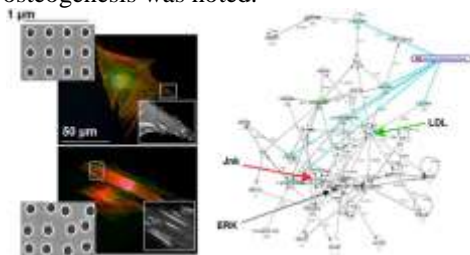


Figure 2. The way MSCs adhere to nanotopography alters depending if the surface controls growth or differentiation. These adhesion changes drive metabolomics changes that can be used to identify regulators of growth and differentiation.

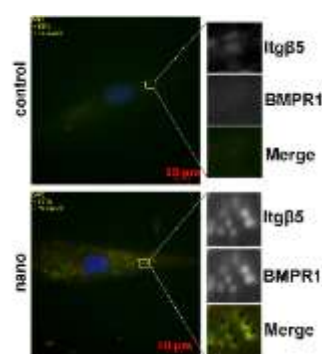


Figure 3. NSQ nanotopography promotes co-localisation of adhesions and the BMP receptor BMPR1a helping to enhance osteogenesis.

MSC adapt to their physical environment and this can be exploited for cell engineering purposes. We can use materials as tools to study MSC growth and differentiation. Furthermore, through following natural adaptive processes of the metabolome, we can identify signalling hubs involved in stem cell control and also identify bioactive metabolites that can be used as drugs to target the perivascular / MSC niches.

REFERENCES

1. Dalby *et al.* *Nature Materials* 6, 997-1003 (2007).
2. McMurray *et al.* *Nature Materials* 10, 637-644 (2011).
3. Tsimbouri *et al.* *ACS Nano* 6, 10239-10249 (2012).
4. McNamara *et al.* *Biomaterials* 32, 7403-7410 (2011).
5. Dalby *et al.* *Nature Materials* 13, 558-569 (2014).
6. Nikukar *et al.* *ACS Nano* 7, 2758-2767 (2013).

ACKNOWLEDGMENTS

We thank everyone at the Centre for Cell Engineering, especially Adam Curtis, Mathis Riehle, Catherine Berry and Chris Wilkinson. We also thank the GPF for genomic, proteomic and metabolomics analysis, Margaret Mullin and Peter Chung for SEM and all members of the Gadegaard, Ulijn, Su, Reid, Peault and Oreffo Groups. We thank BBSRC for grants BB/G008868/1, BB/J021083/1, BB/K006908/1, BB/K011235/1, BB/L008661/1 and BB/L023814/1, EPSRC for grants EP/G048703/1, EP/K034898/1 and MRC for grants MR/K011278/1, MR/L022710/1.

Photo-Crosslinkable Biopolymers Targeting Stem Cell Differentiation: the Candidature of Gelatin

Ine Van Nieuwenhove¹, Sandra Van Vlierberghe^{1*}, Winnok De Vos², Achim Salamon³,
Kirsten Peters³ and Peter Dubrue¹

¹ Polymer Chemistry and Biomaterials Group, Ghent University, Belgium, sandra.vanvlierberghe@ugent.be

² Cell Systems and Imaging, Antwerp University, Belgium

³ Junior Research Group Cell Biology, University of Rostock, Germany

INTRODUCTION

Organ or tissue transplantations are often crucial for patients suffering from untreatable diseases. Interestingly, regenerative medicine is an emerging research field which may offer novel treatments for patients suffering from failing organs or tissues¹⁻⁴. The present work is situated in the tissue engineering field as it focuses on the development of biomaterials to be applied as scaffolds to support the adhesion, the proliferation and the differentiation of adipose-tissue derived stem cells.

EXPERIMENTAL METHODS

Synthesis of photo-crosslinkable biopolymers

Photo-crosslinkable gelatin- and starch-based hydrogel precursors and their corresponding networks have been synthesized in combination with bio-active, extracellular matrix (ECM) compounds including fibronectin and aggrecan. Subsequently, the materials developed were characterized in depth via HR-MAS ¹H-NMR spectroscopy, IR mapping and rheology.

In vitro biocompatibility assays

Mesenchymal stem cells were derived from adipose tissue through liposuction followed by cell-seeding onto the scaffolds developed. In order to proof both the adipogenesis- as well as the osteogenesis-supporting potential of the materials, hydrogel films with a thickness of 1 mm were developed and compared regarding material characteristics and behaviour of stem cells *in vitro*. Moreover, fibronectin- and aggrecan-coatings were applied on the gelatin hydrogel films in order to evaluate their impact on the adipogenic as well as the osteogenic potential of the hydrogels developed.

Multi-parametric analysis of the cellular architecture

To monitor the cellular architecture, a number of characteristic cytoskeletal elements, such as actin filaments, intermediate filaments and tubulin, were (immuno-)labelled in order to acquire a profound understanding on how the composition and the accompanying mechanical properties of these substrates affect cell behaviour of adMSCs. The cell-matrix interactions were quantified through staining and by an automated counting procedure to assess the focal adhesion points.

RESULTS AND DISCUSSION

The mechanical strength and the cell-interactivity of the scaffolds were achieved by the self-structuring property of the biopolymer gelatin, while amylose/amylopectin (cfr. starch) and the ECM polymers influenced the cell

adhesion, proliferation and the migration processes. The presence of an additional starch phase in the gelatin matrix resulted in a decrease of the cell adhesion, with locally even cell detachment.

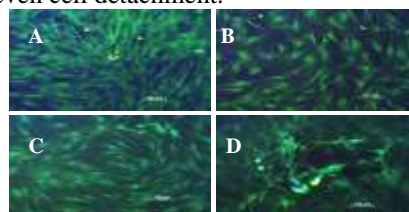


Figure 1 Vital cell staining on gelatin hydrogels revealing homogeneous cell coverage (A and B) and gelatin-starch hydrogels revealing C) a high density cell-region and D) a low density cell region with partial cell detachment (green = living cells, red = dead cells, blue = nuclei). Scale bars: 100 μ m.

Moreover, the hydrogels developed allowed *in vitro* adipogenic and osteogenic differentiation of the adMSC. The differentiation supporting potential increased upon increasing the crosslinking degree and thus the mechanical properties of the gelatin hydrogels for both adipogenic as well as osteogenic differentiation. The presence of a starch phase was observed to temper the differentiation supporting potential.

CONCLUSIONS

The hydrogels developed were shown to be biocompatible and supported cell adhesion of adipose-tissue derived mesenchymal stem cells. In addition, by varying the mechanical properties of the gelatin hydrogels developed, both adipogenic as well as osteogenic differentiation could be upregulated.

REFERENCES

1. G. Steinhoff, Springer, 2011.
2. A. Atala, Journal of Pediatric Surgery, 2012, 47, 17-28.
3. v. L. M. De Leij LFM, Harmsen MC, Kluwer Academic Publisher, 2003.
4. C. Liu, Z. Xia and J. T. Czernuszka, Chemical Engineering Research and Design, 2007, 85, 1051-1064.

ACKNOWLEDGEMENT

Ine Van Nieuwenhove would like to thank Ghent University for the financial support under the form of a doctoral fellowship. Sandra Van Vlierberghe would like to acknowledge the Research Foundation Flanders (FWO-Flanders) for financial support under the form of a post-doctoral fellowship and a research grant (Grant no: 1.5.194.12N). Finally, the authors would like to thank the ERA-NET EuroTransBio 7 programme for funding the ASCaffolds project.

Investigating the “Bone-shell divide”: Pearl oyster shell topography as a means of directing stem cell behaviour

Enateri V. Alakpa^{1,2}, Matthew J. Dalby¹ and Maggie Cusack²

¹Centre for Cell Engineering, University of Glasgow, UK

²Geological & Earth Sciences, University of Glasgow, UK. Enateri.Alakpa@glasgow.ac.uk

INTRODUCTION

Proteins such as perlustrin, typically found in the nacreous (mother of pearl) layer in molluscs, bear a 40% homology to insulin growth factor binding protein (IGF-BP). In addition, it also exhibits the ability to form complexes with insulin growth factor¹. This observation leads to the hypothesis that biomineralisation systems in molluscs and mammals may have common components in their phylogenetic lineage originating from a common ancestor. The juxtaposed use of calcium carbonate polymorphs (aragonite and calcite) in molluscs and calcium phosphate ($\text{Ca}_{10}(\text{PO}_4)_6(\text{OH})_2$) in mammals for biomineralisation processes is generally referred to as the “bone-shell divide”². Common physical and functional characteristics between bone and shells such as their strength and mechanical qualities provide an incentive to consider mimicry of aragonite and calcite properties for the subsequent design of synthetic biomaterials. This study explores the role that topographical detail of nacreous aragonite and prismatic calcite (referred to as ‘nacreous’ and ‘prismatic’ henceforth) has on the physical characteristics of human mesenchymal stem cells and whether these features in their own right contribute to instructing lineage commitment on differentiation.

EXPERIMENTAL METHODS

Physical and surface characteristics (roughness) of the pearl oyster shell (*Pinctada maxima*) were ascertained using atomic force & scanning electron microscopy. Nacreous and prismatic shell surface nanopatterns were embossed onto polydimethylsiloxane (PDMS) to form inverse patterned stamps used to imprint onto polycaprolactone (PCL) substrates. Mesenchymal stem cells acquired from human bone marrow were subsequently cultured on the patterned PCL substrates and the cells assessed for differentiation after 2 weeks by quantifying gene expression of known lineage biomarkers using RT-PCR.

RESULTS AND DISCUSSION

PCL replicas of nacreous and prismatic surfaces of *Pinctada maxima* were imaged using SEM (Figure 1A & B) and characteristic roughness determined using AFM. The prismatic surface had an average roughness of 102.8 nm compared to 26 nm for the nacreous surface rendering the latter surface as relatively smoother. Cells subsequently cultured on each of the surfaces showed slightly differing physical characteristics with cells cultured on the nacre topography observed as wider spread than the prismatic. These differences in morphological properties are likely to impact how the cells interpret their microenvironment and as such, phenotypic marker for

differentiation was assessed by RT-PCR. Cells on the nacre topography had shown significant up-regulation of the osteogenic marker osteopontin (OPN) suggesting that this topography favours osteoblasts formation. Cells cultured on the prismatic topography however had shown significant increase in the self-renewal marker ALCAM indicating that the prismatic topography is influential in retaining ‘stemness’ (Figure 1C).

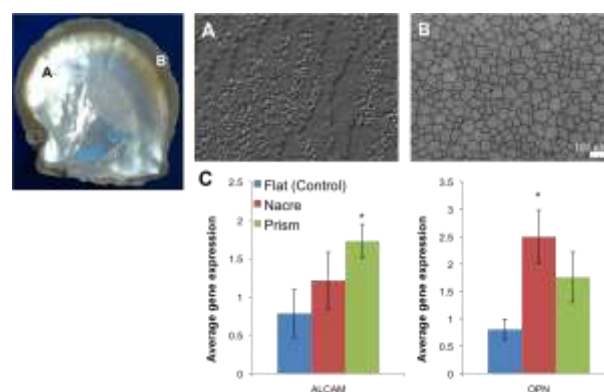


Figure 1: Scanning electron microscopy image of nacreous (A) and prismatic (B) surfaces of the pearl oyster shell. RT-PCR analysis of mesenchymal stem cells cultured on PCL topography replicas (C) showed increased expression of self-renewal marker ALCAM for cells on the prism surface while those cultured on the nacre surface undergo osteogenesis as shown through increased osteopontin (OPN) expression. Scale bar – 100 µm.

CONCLUSION

While the potential of nacre to drive osteogenesis in progenitor cells is known³, this study shows that it is also the case in MSCs and that this characteristic of nacre is, in part, due to the nanotopographical detail of nacre. However, the calcite or prismatic counterpart of the pearl oyster shell, although in itself does not support cell adhesion or growth, has shown that replicating its topography alone can be a potentially useful biomaterial design for maintaining self-renewal properties of stem cells.

REFERENCES

1. Weiss, I. M. *et al.*, Biochem. & Biophys. Res. Comm. 285:244 – 249, 2001.
2. Cusack, M. *et al.*, Chem. Rev. 108:4433 – 4454, 2008.
3. Duplat, D. *et al.*, Biomaterials. 28(12):2155 – 2162, 2007.

ACKNOWLEDGMENTS

This project is funded by the Medical Research Council (MRC).



Generation of 3D functional microvascular networks with mural cell-like human mesenchymal stem cells in microfluidic systems

S. Bersini^{1,2}, J. Jeon³, RD Kamm³ and M. Moretti¹

¹IRCCS Istituto Ortopedico Galeazzi, Milan, Italy

²Department of Electronics, Information and Bioengineering, Politecnico di Milano, Milan, Italy

³Department of Mechanical Engineering, Massachusetts Institute of Technology, Cambridge, USA
simone.bersini@grupposandonato.it

INTRODUCTION

The generation of physiological-like microvascular systems is required for the development of both *in vivo* long-lasting blood vessels and advanced *in vitro* models to replicate biological phenomena involving the interaction between capillaries and organ-specific tissues^{1,2,3}. However, the generation of a functional vasculature involves the recruitment of mural cells which provide mechanical stability and secrete factors affecting the endothelium homeostasis, e.g. angiopoietin (Ang)-1 and transforming growth factor (TGF)- β 1^{4,5}. The present study is focused on the generation of functional, perfusable 3D human microvascular networks, co-culturing endothelial cells (ECs) and bone marrow-derived human mesenchymal stem cells (BM-hMSCs) within a microfluidic device. Particularly, we analyze the role of Ang-1 and TGF- β 1 on mural cell-like recruitment and the resulting microvascular network structure.

EXPERIMENTAL METHODS

A microfluidic device consisting of two lateral media channels and a central gel channel was adopted. Primary human umbilical vein ECs were mixed with BM-hMSCs in a 2.5 mg/ml fibrin gel reaching 3×10^6 and 1.5×10^6 cells/ml densities, respectively. Selected microdevices were supplemented with 100 ng/ml Ang-1 or 1 ng/ml TGF- β 1 to analyze their effect on microvascular network and BM-hMSC mural cell commitment. Alpha smooth muscle actin (α -SMA), SM22 α , vascular endothelial-cadherin and zonula occludens-1 markers were assessed by immunofluorescence. The Fiji 2D skeletonize plugin was applied to quantify number of branches, average branch length and total network length (day6). Vessel permeability was quantified with 70 kDa dextran.

RESULTS AND DISCUSSION

The ability of BM-hMSCs to get a mural phenotype was increased in the presence of ECs. The α -SMA signal was 4.72 ± 0.99 fold higher with VEGF+Ang-1 whereas VEGF+TGF- β 1 devices showed values 5.06 ± 0.79 fold higher when normalized to VEGF only devices. However, addition of Ang-1/TGF- β 1 exerted a strong influence on BM-hMSC phenotypic transition only when BM-hMSCs were in direct contact with ECs. EC monoculture was compared to EC+BM-hMSC showing less branches (93.8 ± 9.4 vs.

142.2 ± 5.9), larger diameters (84.2 ± 2.7 vs $40.8 \pm 1.5 \mu\text{m}$) and shorter networks (10.13 ± 0.39 vs $12.86 \pm 0.35 \text{mm}$). While the addition of TGF- β 1 during culture enhanced BM-hMSCs phenotypic transition toward a mural cell lineage, systems with added TGF- β 1 generally resulted in shorter, fragmented networks. Conversely, co-cultures with VEGF+Ang-1 not only promoted formation of microvascular networks with even smaller vessel diameters (36.2 ± 1.6 vs $40.8 \pm 1.5 \mu\text{m}$) but also strongly induced BM-hMSCs mural cell commitment. Dextran perfusion confirmed the presence of patent lumens showing an *in vivo*-like diffusive permeability ($6.7 \times 10^{-7} \pm 2.74 \times 10^{-7} \text{cm/s}$).

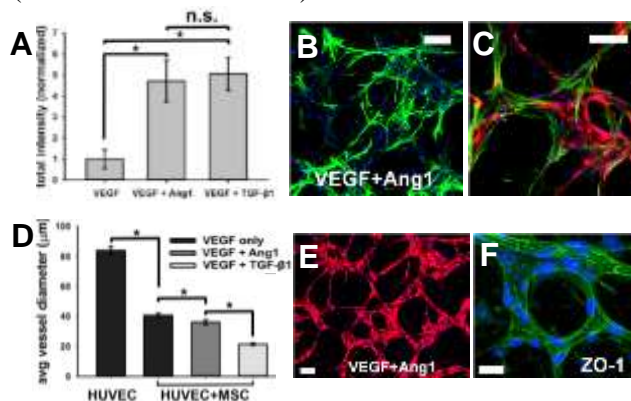


Fig 1. α -SMA intensity signal (A) and immunofluorescence (B, green), mural cell-endothelial cell co-localization (C, green: α -SMA), average vessel diameter (D), microvascular network structure (E) and zonula occludens-1 expression (F, green). Red: ECs, blue: nuclei. Bars: 100 μm (B,C,E) and 30 μm (F).

CONCLUSION

The addition of VEGF+Ang-1 was considered the optimal condition, leading to interconnected microvessels surrounded by co-localized α -SMA+ BM-hMSCs with promising applications for *in vitro* models requiring a functional microvasculature.

REFERENCES

1. Au P. *et al.*, Blood. 111:4551-58, 2008
2. Bischel L. *et al.*, Biomaterials. 34:1471-77, 2013
3. Bersini S. *et al.*, Biomaterials. 35:2454-61, 2014
4. Thurston G. *et al.*, Science. 286:2511-14, 1999
5. Gohongi T. *et al.*, Nature Medicine. 5:1203-8, 1999

ACKNOWLEDGMENTS

Support to S. Bersini provided by the Fondazione Fratelli Agostino and Enrico Rocca.

Atmospheric pressure plasma treatment increases the attachment and maturation of human pluripotent stem cell derived retinal pigment epithelial cells on biodegradable polymeric electrospun scaffolds

A. Sorkio¹, P. Porter², K. Juuti-Uusitalo¹, B. Meenan², H. Skottman¹ and G. Burke²

¹BioMediTech, University of Tampere, Tampere, Finland

² Nanotechnology and Integrated Bioengineering Centre (NIBEC), School of Engineering, University of Ulster, Northern Ireland

anni.sorkio@uta.fi

INTRODUCTION

Electrospun polymeric fibril meshes have been shown to replicate many of the cues and properties of the ECM, as well as having a porous network for the transportation of nutrients and metabolic waste¹. Such meshes have the potential to provide a biocompatible substrate suitable for a range of transplantation therapies including retinal implant applications. However, a most of the polymers used as synthetic tissue scaffolds or cell delivery systems are inherently hydrophobic, which can significantly hinder cell attachment and proliferation. In this work, a thin biodegradable electrospun polymer membrane, developed as a substrate for human embryonic stem cell derived retinal pigment epithelial (hESC-RPE) cells, has been modified via atmospheric pressure plasma processing. The effects that plasma induced changes to the polymer fibre surface properties have on hESC-RPE cell attachment, proliferation and maturation are investigated. Importantly, the conditions required to derive mature and functional RPE monolayer on biodegradable substrate were reported.

EXPERIMENTAL METHODS

Poly-L-Lactide/Caprolactone (PLCL) (PURASORB® PLCL 7015, 70/30 L-lactide/caprolactone) was used to produce the electrospun membrane. A 10% weight by volume (w/v) solution of PLCL, prepared in 9:1 v/v chloroform/dimethylformamide, was electrospun at an applied voltage of 18 kV with a polymer flow rate of 1ml/hour. Fibres were collected in a random orientation for 10 minutes for each membrane. The surface chemistry and topography of the membrane PLCL fibres were modified by exposure to an atmospheric pressure dielectric barrier discharge (DBD) treatment regime in air. Contact angle measurements, using glycerol as the test droplet, were obtained for DBD treated electrospun fibres and untreated fibres. Changes to the microstructure and surface chemistry were assessed by scanning electron microscopy (SEM), atomic force microscopy (AFM), X-ray photoelectron spectroscopy (XPS) and Fourier transform infrared spectroscopy (FTIR).

The propensity of hESC-RPE cells² to attach and proliferate on untreated and DBD treated electrospun PLCL membranes was examined by both cell counting and the AlamarBlue® cell proliferation assay. Cell adhesion and maturation were evaluated with light microscopy imaging, immunofluorescence staining and gene expression analysis. Development of epithelia barrier properties and the integrity of the RPE

cell monolayer on the PLCL membranes were examined with transepithelial electrical resistance (TER) measurements. The functionality of hESC-RPE cells on DBD-treated electrospun PLCL fibres was also assessed with an *in vitro* phagocytosis assay.

RESULTS AND DISCUSSION

All PLCL electrospun membranes had an unaligned fibre orientation with an extremely porous structure. DBD plasma treatment increased both the surface roughness and the oxygen to carbon ratio on the fibre surfaces. As a consequence, the surface treatment significantly reduced the surface wettability of PLCL electrospun membranes.

DBD plasma treatment of electrospun PLCL scaffolds had a beneficial effect on hESC-RPE cell attachment and proliferation. Cell count and proliferation assay data indicated that there were significantly higher numbers of hESC-RPE cells on the DBD plasma treated materials compared to the untreated membranes. Surface treatment of the membranes provided for the formation of confluent and uniform hESC-RPE monolayers; untreated films failed to support proper cell attachment and proliferation. Moreover, hESC-RPE cells on DBD plasma treated membranes showed the presence of a polarized mature epithelium and exhibited phagocytic activity.

CONCLUSION

Atmospheric pressure plasma treatment is an effective method to enhance the cellular attachment, proliferation and maturation of clinically relevant hESC-RPE cells on electrospun PLCL membranes. The work reported here has established for the first time that DBD plasma modified PLCL electrospun membranes in combination with hESC-RPE cells could potentially be used as a tissue engineered construct for retinal applications.

REFERENCES

1. Zhang Y. *et al.*, Int J Nanomedicine. 2(4): 623-638, 2007
2. Vaajasaari H. *et al.*, Molecular Vision. 17:558-575, 2011.

ACKNOWLEDGMENTS

The authors thank TEKES, the Finnish Funding Agency for Technology and Innovation, and the Academy of Finland (grant numbers 218050 and 137801). The award of a postgraduate studentship to PP by the Northern Ireland Department of Employment and Learning is also acknowledged.



Functionalising natural polymers with alkoxysilane coupling agents for tissue engineering applications

Louise S Connell¹, Frederik Romer², Oliver Mahony¹, Mark E Smith^{2,3}, John V Hanna², and Julian R Jones¹

¹ Department of Materials, Imperial College London, UK, l.connell10@imperial.ac.uk

² Department of Physics, University of Warwick, Gibbet Hill Rd, Coventry, CV4 7AL, UK

³ Vice-Chancellor's Office, University House, Lancaster University, LA1 4YW, UK

INTRODUCTION

Hybrids, with nanoscale interpenetrating organic and inorganic networks, show promise as tissue regeneration materials. The natural polymers gelatin, chitosan, and poly(γ -glutamic acid) (γ PGA) have been incorporated into the silica sol-gel process to produce bioactive hybrids that proliferate osteoblast-like cells¹, support mesenchymal stem cells², and improve nerve fibre regeneration³.

The success of hybrids in tissue regeneration depends upon their mechanical and degradation properties, which in turn rely upon covalent bonding between the networks². 3-glycidypropyl trimethoxysilane (GPTMS) is one of the most used coupling agents to introduce covalent bonding. It contains an epoxide ring, proposed to react with nucleophilic groups of natural polymers such as amines and carboxylic acids, and an alkoxysilane group which co-condenses with silica precursors to form an inorganic network.

There is dispute over whether or not the epoxide reacts with the nucleophilic groups as the reaction conditions are typically acidic and nucleophilic character will be reduced due to protonation^{4,5}.

The aim of this work was to use a range of NMR techniques to identify and quantify the extent of reaction of GPTMS with chitosan, γ PGA, and gelatin under typical functionalisation conditions.

EXPERIMENTAL METHODS

Solid state NMR samples were prepared by reacting chitosan with GPTMS for up to 24 h in deionised water at pH 2 and 4. The reaction was quenched in liquid nitrogen and freeze dried. ¹⁵N MAS NMR spectra were acquired to determine if a reaction occurs at the primary amine of chitosan and ²⁹Si MAS NMR was used to quantify the silica species present. Identification of side reactions and quantification of co-products under different pH conditions was carried out using solution state ¹³C, ¹H, quantitative ¹H-¹³C HSQC, and ¹H-¹³C HMBC NMR. Spectra were acquired for chitosan functionalised for 24 h at pH 2, 4 and 6, and for γ -PGA and gelatin functionalised for up to 48 h at pH 4.

RESULTS AND DISCUSSION

Splitting of the primary amine peak in ¹⁵N MAS NMR (Fig. 1) combined with solution state ¹H, ¹³C and HSQC NMR established that a reaction occurred between the epoxide ring of GPTMS and the primary amine in chitosan. A reaction also occurred between water and the epoxide, producing a diol. Low pH accelerated the reaction but only 20 mol% secondary amine was formed (relative to total products), irrespective of pH (Fig. 2). This is an important result that shows that acidic conditions do not inhibit the reaction as previously assumed, but that the efficiency is very low. Characterisation of the reaction between γ PGA and

GPTMS showed that the epoxide ring also reacted with carboxylic acid groups and it was confirmed with HMBC that the final product was an ester. Careful analysis of the complicated ¹H NMR spectra of gelatin before and after reaction identified specific amino acids that reacted with GPTMS and showed that amino acids containing carboxylic acid groups were favoured. The bonding within the inorganic network was also characterised and will be presented.

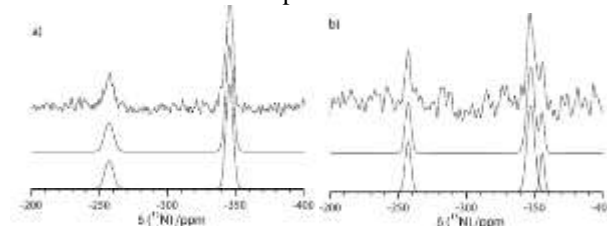


Fig. 1 – ¹⁵N MAS NMR of chitosan a) before, and b) after functionalisation for 24 h.

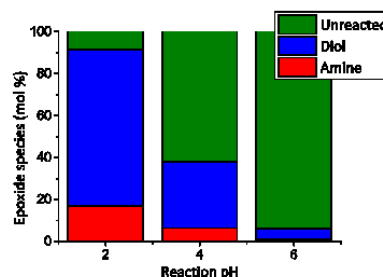


Fig. 2 – Effect of pH on amount of unopened epoxide, diol and secondary amine products after 24 h.

CONCLUSION

Solution state and solid state NMR techniques were used to show that even under acidic conditions the epoxide ring of GPTMS can react with a primary amine, such as in chitosan, to form a secondary amine or a carboxylic acid, as in γ PGA, to form an ester, albeit with low efficiency. To achieve controlled degradation and good mechanical properties, good covalent bonding is necessary. Polymers can be chosen or designed to contain appropriate functional groups for functionalisation and the reaction conditions optimised to achieve hybrid materials for tissue regeneration.

REFERENCES

1. Shirosaki Y *et al.*, Bioceram Dev Appl. doi: 10.4303/bda/D110112, 2011
2. Mahony O *et al.*, Adv Func Mater. 20:3835-3845, 2010
3. Amado S *et al.*, Biomaterials. 29:4409-4419, 2008
4. Connell L *et al.*, J Mater Chem B. 2:668-680, 2014
5. Gabrielli L *et al.*, RSC Adv. 4:1841-1848, 2014

ACKNOWLEDGMENTS

The authors would like to thank EPSRC (EP/I020861/1) for financial support and Mr Peter Haycock for assistance with the quantitative HSQC experiments.



Composition-Structure-Property Relationships for Strontium Borate Glasses for Biomedical Applications

Muhammad Sami Hasan and Daniel Boyd <mailto:sami.hasan@dal.ca>

Department of Applied Oral Sciences, School of Biomedical Engineering, Dalhousie University, Halifax, NS, Canada

INTRODUCTION

Borate glasses are attractive as medical materials based on bioactivity and degradability¹. Doping with various network formers (e.g. SiO₂, P₂O₅) may help to tailor their durability and bioactivity in terms of therapeutic effects or conversion into hydroxyapatite^{1,2}. However, correlation between structure and properties, especially the release kinetics its extremely difficult in a glass containing more than one network former. Vitreous borate glass is made of B₂O₃ rings that break into BO₃ and BO₄ units with the addition of network modifiers. Alkali and alkaline earth metal oxides have been incorporated in biodegradable glasses to control their degradation rate and to induce bioactivity². In this project, strontium for its therapeutic effect on bone cells, and titanium, for its antibacterial properties, alongside their effects on durability have been selected as modifiers of pure borate network. Investigations into chemical-structural changes, thermal properties variations, effect on durability, quantities of ions released and cytocompatibility per systematic compositional changes have been evaluated.

Table 1. Glass codes, actual compositions, thermal properties and density

Composition	Actual composition	T _g (°C)	T _c (°C)	T _m (°C)	ρ g/cm ³
B70Sr30	B67Sr33	631	764	918	3
B70Sr28Ti2	B66Sr31Ti3	625	765	882	2.93
B70Sr26Ti4	B67Sr28Ti5	611	784	888	2.89
B70Sr24Ti6	B66Sr27Ti7	603	795	890	2.83
B70Sr22Ti8	B65Sr26Ti9	565	805	890	2.79
B70Sr20Ti10	B64Sr24Ti12	541	809	902	2.72
B70Sr20Na10	B63Sr24Na13	546	685	897	2.74
B70Sr20Na8Ti2	B63Sr22.5Na12Ti2.5	534	698	885	2.76
B70Sr20Na6Ti4	B63Sr24Na8.2Ti4.8	555	744	893	2.77
B70Sr20Na4Ti6	B64Sr23Na6Ti7	564	763	913	2.76
B70Sr20Na2Ti8	B64Sr23.5Na3.2Ti9.3	571	780	920	2.75
B70Sr20Ti10	B64Sr24Ti12	541	809	902	2.72

EXPERIMENTAL METHODS

A melt-quenching technique was used to produce 11 glass compositions using: B₂O₃, SrCO₃, TiO₂ and Na₂CO₃. The glasses were ground using an automated grinder and sieved to 45-90µm. Glass rods were melt-casted in a graphite mold preheated at 5°C above T_g and cut into discs using a diamond saw. Digesting the glass in strong acid and detecting constituent oxides in an ICP-AES provided the actual compositions. The amorphicity of all the glass compositions was confirmed using X-ray diffraction spectra. ¹¹B magic-angle spinning nuclear magnetic resonance studies was carried out on a Bruker Avance NMR spectrometer. The thermal characteristic temperatures were characterized by a differential scanning calorimeter operated at a heating rate of 10°C/min from 25 to 1100°C. Density of glasses was measured using He-Pycnometer. Glass discs (9mm diameter, 4mm thick) were immersed into vials containing 30ml of phosphate buffered saline and incubated in an incubator at 37°C for 21 days. At specific time points, pH was measured, the discs were taken out of their respective containers and blot-dried and weighed. Glass extracts were prepared in tissue culture water at a ratio of 0.2g/ml incubated for up to 28 days at 37°C in a shaker incubator, agitated at 2Hz. The

elution-products were detected using ICP-AES. In vitro cytocompatibility of L929 mouse fibroblast was evaluated using the MTT assay with evaluations being on the basis of indirect exposure via the same extracts prepared for ICP-AES.

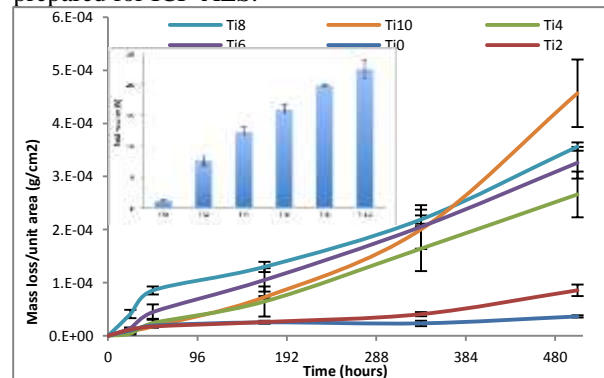


Figure 1. Degradation rates for glasses in series S1.

RESULTS AND DISCUSSION

Borate glasses in system (S1: 70B₂O₃-30-XSrO₂-XTiO₂ and S2: 70B₂O₃-20SrO₂-10-XNa₂O-XTiO₂, where X=2,4,6,8,10 in mol%) were prepared. The XRD traces confirmed the amorphicity of the glasses. Compositions of the glass were within 5-8% of theoretical compositions (Table 1). For glasses S1, a downward trend and for S2 no significant change in T_g was observed with increasing Ti content. Density appeared to have reduced in S1 and unchanged in S2. In S1, an increased solubility was observed with increased Ti content. However, no change in durability was observed for S2 (Fig 1). The pH was observed to change from 7.5 to 8.1-8.5 during the study. NMR investigations revealed structural changes in the glass series with increasing Ti content. The peak positions BO₃ (0.6ppm) and BO₄ (14ppm) did not change significantly. However, BO₃/BO₄ ratio increased suggesting the network-forming role of TiO₂, which explains the observed changes in the properties (thermal, density) in S1. Varying SrO content predominantly controlled the degradation rates, which in turn controlled the ion release kinetics. For both S1 and S2 a burst release up to 7th day and then a plateau due to saturation for all ions was observed which was directly related to the durability and the glass composition. Cytocompatibility assessments via MTT assay revealed no toxicity for S1 and significant toxicity for some compositions in S2.

CONCLUSION

Borate glass with controlled durability and continuous release of therapeutic levels of ions can be prepared. Alkaline earth metal is more effective in controlling the durability. Variation of modifiers/intermediates induced the structural changes in the glasses that lead to the change in characteristic properties.

REFERENCES

- Ouis et al. Pro & App of Cer 2012; 6: 141–9.
- Sinouh et al. Therm Anal Calorim. 2013; 111: 401-8.

ACKNOWLEDGEMENTS

The authors acknowledge the financial assistance of NSERC and CIHR, Canada for this research.



Unravelling the Structure of Bioglass® through the Application of Diffraction Techniques

Richard Martin

School of Engineering & Aston Research Centre for Healthy Ageing, Aston University, UK R.A.Martin@Aston.ac.uk

The atomic-scale structure of Bioglass® and its derivatives has been investigated using neutron and X-ray diffraction. Structural sites present in these glasses will be intimately related to their release properties in physiological fluids such as plasma and saliva, and hence the bioactivity of the material. Detailed structural knowledge is therefore a prerequisite for optimising material design.

INTRODUCTION

Melt-quenched silicate glasses containing calcium and phosphorous are of great importance due to their ability to bond chemically to bone and to stimulate new bone growth¹. Under physiological conditions the glass slowly dissolves, releasing calcium and phosphorous into solution. This forms an amorphous calcium phosphate layer which then crystallises into hydroxyapatite. The first key step in the bioactivity is therefore the dissolution of glass. Consequently, the atomic-scale structure of bioactive glasses and its effect on chemical durability and bioactivity has been the focus of much attention^{2,3}. However the addition of an alkali metal, an alkaline-earth metal as well as a second network former in the form of phosphorous means that the generation of a structural model of Bioglass and its derivatives is challenging.

In order to be able to model and predict the behaviour of these materials, and ultimately improve their design, it is necessary to understand the local structure of the glasses. The present work helps shed light on the atomic scale structure of Bioglass.

EXPERIMENTAL METHODS

Neutron diffraction spectra were collected using D4C diffractometer at the Institut Laue-Langvin, Grenoble and the GEM diffractometer at the ISIS spallation neutron source at the Rutherford Appleton Laboratory. Data corrections were undertaken to remove the background scattering, normalise the data, correct for absorption, inelastic and multiple scattering effects and subtraction of the self-scattering term. The individual pair-wise structure factors were then modelled to provide detailed information (interatomic distances, coordination numbers and the degree of disorder) on the atomic scale structure.

RESULTS AND DISCUSSION

The real space total diffraction patterns for Bioglass and strontium substituted Bioglass are shown in Figure 1. The total diffraction pattern was deconvolved and modelled to give the individual correlation functions. As a result the asymmetry of Na and Ca atoms, predicted by computer models has been experimentally confirmed^{4,5}. In addition the local environment of several modifying ions such as Sr, Ti⁶, Ni and Co⁷ has been examined. By understanding their structure and the role each of these

elements play in the glass formation (e.g. network / modifier) it is now possible to predict the effect these elements will have on the solubility and therefore bioactivity.

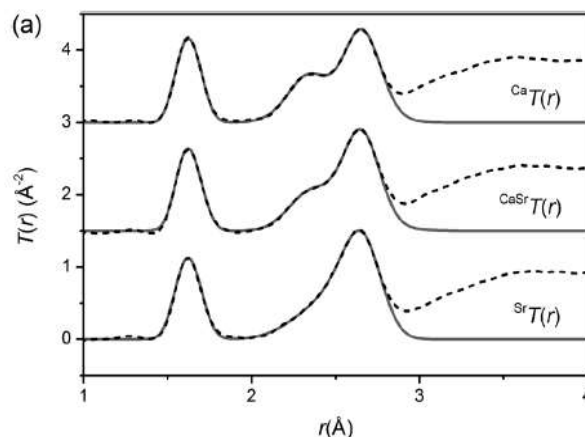


Figure 1. The real-space diffraction data for the total diffraction patterns, $T(r)$. The broken curves represent the experimental data and the solid curves are the resultant fits.

CONCLUSION

Neutron diffraction studies have provided direct experimental information on the atomic scale structure of bioactive glasses and their derivatives. Data provided indicates how particular modifiers should be incorporated into glasses to maintain the desired solubility

REFERENCES

1. Hench L.L., *J. Mat. Sci.:Mat. Med.* 17: 967-978, 2006.
2. FitzGerald V., *et al. Adv. Func. Mat.* 17: 3746-3753, 2007.
3. Tilocca A. & de Leeuw, N.H., *J Phys Chem B* 110: 25810-25816, 2006.
4. Martin R.A. *et al. Phys. Chem. Chem. Phys.* 14:12105-12113, 2012.
5. Martin R.A., *et al. J. Mat. Chem.* 22: 22212-22223, 2012.
6. Martin R.A., *et al. Phys. Chem. Chem. Phys.* 14: 15807, 2012.
7. Smith J.M., *et al, J. Mat. Chem. B* 1:1296-1303, 2013.

ACKNOWLEDGMENTS

I would like to acknowledge Professor Robert Newport for his significant contribution toward these studies. This work was funded by EPSRC grants EP/E050611/1 and EP/E051669/1 and the Royal Society Grant RG100147. The authors wish to thank STFC-ISIS for the allocation of neutron diffraction beam-time.



Surface functionalisation of sol-gel-based bioactive glass scaffolds for drug delivery

A. Philippart^{1*}, A. M. Beltrán², L. Pontiroli³, C. Vitale-Brovarone³, E. Spiecker² and A. R. Boccaccini¹

¹Institute of Biomaterials, University Erlangen-Nürnberg, Germany, anahi.philippart@fau.de

²Center for Nanoanalysis and Electron Microscopy (CENEM), University Erlangen-Nürnberg, Germany

³Institute of Materials Physics and Engineering, Applied Science and Technology Dept., Politecnico di Torino, Italy

INTRODUCTION

Bioactive glasses are widely used in bone tissue engineering (BTE) since they can develop strong bonds with bone through the formation of a hydroxyapatite (HA) layer¹. Within these materials, sol-gel-based bioactive glasses (SGBGs) are attractive due to their enhanced bioactivity and resorbability and their capacity of being functionalised with a large variety of moieties²⁻³.

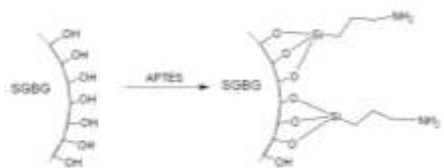
Surface functionalisation is an interesting approach to load drugs into the material and allow their release in a controlled manner³.

The aim of this study is the development of new SGBGs for 3D porous scaffolds and functionalisation of their surface by two different methods⁴⁻⁵ in order to enhance the drug delivery capability.

EXPERIMENTAL METHODS

Bioactive glass scaffolds with composition (in mol%) 60SiO₂ 30CaO 5Na₂O 5P₂O₅ were prepared by the sol gel method and the foam replica technique. Scaffolds were characterised by scanning electron microscopy (SEM) and μ -CT, in order to evaluate the macrostructure and porosity and by transmission electron microscopy (TEM) and N₂ adsorption porosimetry using the Brunauer-Emmett-Teller (BET) approach for mesoporosity characterisation. Bioactivity was revealed by Fourier transform infrared spectroscopy (FTIR) characterisation of the scaffolds after SFB immersion.

After heat treatment at 700°C, the scaffolds surface was functionalised by post-condensation of aminosilane, following the reaction shown below:



A second step was considered to avoid steric interference by adding a spacer and allowing an optimal loading of the model drug.

Both systems were loaded with a model drug, and the drug release capabilities were studied in two different media by UV-Vis spectroscopy.

RESULTS AND DISCUSSION

Scaffolds exhibited the required macropore size (~500 μ m) as well as high and interconnected porosity, of up to 90% as shown in Fig.1 (a-c). TEM (Fig.1 d) revealed the mesoporosity, confirmed by BET analysis (pore size: ~4nm; S_{BET} =150m²/g). Both porosities are features required by scaffolds for BTE and drug delivery applications¹⁻².

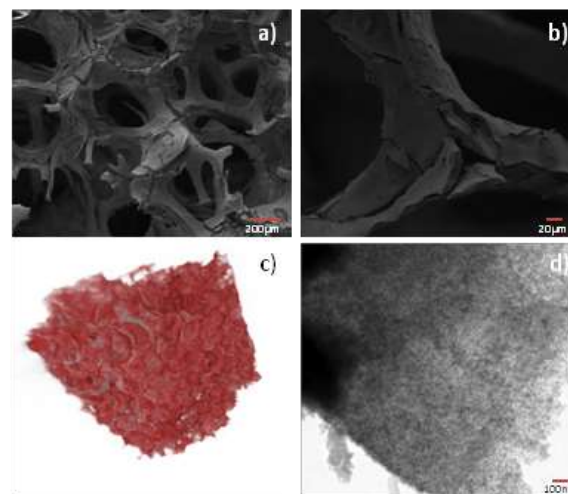


Figure 1. Images of scaffold a,b)SEM micrographs, c) μ -CT reconstruction, d)TEM micrograph

Amino-functionalisation of the surface was confirmed by zeta potential measurements, ninhydrine test as well as by element mapping in SEM.

The different drug release profiles showed that by surface functionalisation it was possible to achieve a reduced initial burst release of the drug in the tested media and a long-term sustained release.

CONCLUSION

According to SEM and μ -CT reconstructions, 3D porous scaffolds were successfully prepared, exhibiting macro- and mesoporosity. Furthermore, amino-functionalised surface allowed the system to exhibit a sustain release of the model drug compared to non-functionalised scaffolds.

REFERENCES

- Gerhardt L.C. *et al.*, Materials 3:3867-3910, 2010
- Jones J. R. *et al.*, Biomaterials 27:964-973, 2006
- Vallet Regi M.*et al.*, Phil. Trans. R. Soc. A 370:1400-1421, 2012
- Balas F. *et al.*, J. Am. Chem. Soc. 128:8116-8117, 2006
- Schneider M. *et al.*, Langmuir 29:6983-88, 2013

ACKNOWLEDGMENTS

The authors would like to thank ITN FP-7 project "GlaCERCo" for providing financial support; P. Rosner for the help provided in TEM; Prof. E. Verné and Dr. Sonia Fiorilli for the assistance in the material characterisation; Dr. A. Inayat for BET analysis.



In vitro assessment of 3D printed wollastonite – apatite-based glass ceramic biomaterials

M.A. Lopez-Heredia^{1,*}, A. Zocca^{2,3}, C. Gomes², J. Günster², R. Gildenhaar², P. Colombo³ and C. Knabe-Ducheyne¹

¹ Dept. of Experimental Orofacial Medicine, Philipps University, Marburg, Germany

² Federal Institute for Materials Research and Testing (BAM), Berlin, Germany

³ Department of Industrial Engineering, University of Padova, Padova, Italy

* Email: marco.lopezheredia@staff.uni-marburg.de

INTRODUCTION. Bioceramics are well-known materials used as bone substitutes¹. 3D printing techniques allow obtaining materials with one or several phases while giving more liberty on the confection of the structure^{2, 3}. Nevertheless, as these materials are intended to interact with the body, it is important to assess their interaction, at first instance, with cells⁴. The objective of this study was to assess the *in vitro* viability, cytotoxicity and apoptosis behaviour of two biomaterials made of wollastonite and an apatite-based glass ceramic (AP40) in interaction with MC3T3 cells.

MATERIALS AND METHODS. Materials were produced by a 3D printing polymer-derived ceramic material process. Briefly, green bodies of preceramic polymers, filled with active and passive ceramic fillers, were printed by a 3D printing process². Subsequently, green bodies were converted to fully ceramic bodies by a heat treatment. This process allowed obtaining materials composed of different contents of wollastonite and AP40 according to two different percentages of starting materials, *i.e.* 20%-80% (S1) and 60%-40% (S2). Materials were obtained on disc shape with 10 mm in diameter by 2 mm in height. Materials were characterized by Scanning Electron microscopy (SEM; Phenom, Germany) for morphology observation. Before any interaction with cells, discs were heat-sterilized at 300 °C for 3 h by using a furnace (HERATharm, Heraeus, Germany). MC3T3-E1, subclone 4, cells (ATCC, USA) were used for the *in vitro* assessment. Culture medium consisted of DMEM (PAA, Germany) with 10 % FBS (PAA, Germany), 50 µg/ml of ascorbic acid (SigmaAldrich, Germany), 5 mM of β-Glycerophosphate (Sigma Aldrich, Germany), 2 mM of L-Glutamine (Gibco, Germany) and 50 µg/ml of Penicillin-Streptomycin (Gibco, Germany). S1 and S2 discs were placed in 24-well plates for 24 h in contact with culture medium before seeding. Then, culture medium was removed, discs were placed in a new well plate and 50,000 cells were seeded on the materials. Cells were allowed to attach for 2 h and then the wells were filled with medium. Interaction was assessed at 3, 7 and 14 days. Three discs per condition, time point and material were assessed (*n* = 3). Cell viability (AlamarBlue®, Invitrogen, Germany), cytotoxicity (CellTox™ Green, Promega, Germany) and apoptosis (Caspase Glo® 3/7, Promega, Germany) behaviours were assessed by using a plate reader (GloMax®-Multi, Promega, Germany).

RESULTS AND DISCUSSION. SEM (Fig. 1) shown that S1 presented a mixture of “round” and “sand-like”

particles. After the 14 days of medium immersion S1 did not present any important changes on its morphology. S2 presented a double morphology aspect with a peripheral part presenting a morphology like S1 and at the center a mixture of this morphology and acicular crystals. These crystals created a discontinuous structure. Crystals seemed to grow thicker with the immersion time in medium. The different morphologies presented by S1 and S2 may be related to their compositions. Alamar Bleu® assay demonstrated a good cell growth over the 14 day period on both materials. S2 material presented a mean reduced value for the cell number at 3 days and 7 days but at 14 days it increased in a significant way. CellTox Green assay indicated, within the time period tested, the non-cytotoxicity of the materials for the cells. Caspase activity assay indicated a higher mean values for the S1 group at 3 days and 7 days. However, after 14 days S1 and S2 activities were similar.

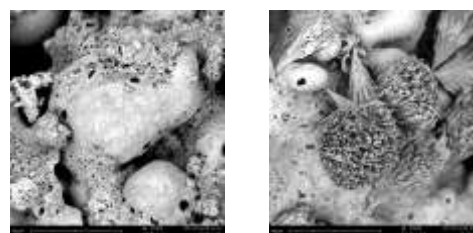


Fig 1. SEM images of S1 (left) and S2 (right).

CONCLUSION. Biomaterials produced by 3D printing techniques and made of wollastonite and AP40, *i.e.* S1 and S2, allowed cells to grow without creating a toxic environment to the cells. No apoptotic behaviour was observed. Further analysis need to be performed on these types of materials to assess their cellular signalling expression. However, these results prove the biocompatibility of these materials and open doors for their feasibility to be used as bone substitutes.

ACKNOWLEDGMENTS. Authors thank the DFG (Grant KN 377/8-1) for its financial support, the technical assistance of Mrs. A. Kopp and the invaluable help of Prof. Frankenberger and Prof. Roggendorf for the SEM imaging.

REFERENCES.

1. Bohner M. Injury; 31 Suppl 4:37-47 2000.
2. Bernardo E.. *et al.* Adv Eng Mater; 14:269-74 2012.
3. Habibovic P.. *et al.* Biomaterials; 29:944-53 2008.
4. Warnke P.H.. *et al.* J Biomed Mater Res B Appl Biomater; 93:212-7 2010.



Fabrication and Characterization of Electrospun PHB/PCL/Sol-gel Derived Glass Hybrid Scaffolds

Yaping Ding^{1*}, Teresa Müller¹, Judith A. Roether¹, Dirk W. Schubert¹, Aldo R. Boccaccini²

^{1*}Institute of Polymer Materials, University of Erlangen-Nuremberg, Germany, yaping.ding@fau.de

²Institute of Biomaterials, University of Erlangen-Nuremberg, Germany

INTRODUCTION

Polyhydroxybutyrate (PHB) and polycaprolactone (PCL) are both biocompatible and biodegradable biopolymers [1]. Silica containing biomaterials including bioactive glasses and biopolymers with Si ion releasing ability are favourable for bone and connective tissue restoration [2]. Unlike bulk blending of immiscible PHB and PCL which leads to phase separation and thus great loss of mechanical properties, in our preliminary study, electrospun PHB-PCL blend fibermats were produced which combine the high tensile strength and stiffness of PHB and the flexibility of PCL. PHB/PCL/sol-gel derived glass fibrous scaffolds were fabricated through electrospinning and sol-gel method in the present work. The study aims to develop an organic-inorganic hybrid scaffold, which is expected to attain the most crucial properties required for bone regeneration, namely suitability mechanical strength, hydrophilicity, bioactivity and osteoconductivity and to compensate the drawbacks and limitations of the single components [3].

EXPERIMENTAL METHODS

TEOS, TEP, EtOH, H₂O and CaCl₂·2H₂O with the molar ratio of 1: 0.133: 2: 2: 0.6 were used to prepare the 58S glass sol under an acid catalyst. PHB and PCL (w/w=7:3) were blended and dissolved in chloroform and dimethylformamide (v/v=8:2). Glass sol was added to the polymer solution and fed into the syringe for electrospinning. The operational parameters were 2 ml/h, 8 kV and 15 cm. All obtained samples were dried in a vacuum oven for further characterization. Properties including morphology, mechanical strength, thermal and chemical changes, bioactivity and biological properties were investigated. Samples were named by polymer and inorganic weight ratio, such as P1B0, P20B1 and P5B1.

RESULTS AND DISCUSSION

Hybrid scaffolds with an inorganic ratio from 0 to 20 wt%. were successfully fabricated. Figure 1 shows two typical morphologies of P5B1 produced with solution concentrations of 5% w/v (a) and 2.5% w/v (b), which represent normal non-woven and honeycomb like structures, respectively.

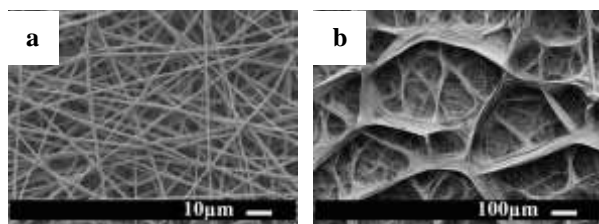


Figure 1. P5B1 fibermats obtained at solution concentrations of 5% w/v (a) and 2.5% w/v (b).

Table 1 shows the basic physical properties of the

fibermats. As the content of inorganic component increased, the fiber diameter and porosity increased, whereas the tensile strength decreased. The wettability switched from hydrophobic to hydrophilic with addition of the silicate component.

Table 1. Physical properties of hybrid fibermats fabricated using 2 ml/h, 8 kV, and 15 cm.

Sample	Diameter/ µm	Tensile strength/MPa	Porosity /%	Contact angle/ °
P1B0	0.7±0.2	2.8±0.3	82.9	129±1
P20B1	0.9±0.3	2.2±0.2	85.1	0
P5B1	1.2±0.2	1.9±0.2	88.8	0

The incorporation of bioactive glass in fibermats was confirmed using FTIR as shown in Figure 2. The broad band around 3400 cm⁻¹ indicates the formation of hydroxyl groups. The band observed between 500 cm⁻¹ and 800 cm⁻¹ (in P5B1) is due to the addition of sol-gel glass.

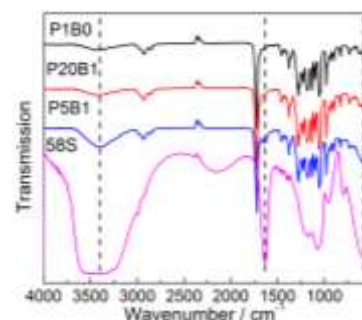


Figure 2. FTIR spectra of pure polymer fibermats and hybrid fibermats were presented.

The bioactivity and biological properties of the hybrid scaffolds are under investigation.

CONCLUSIONS

PHB/PCL/sol-gel derived glass hybrid scaffolds were fabricated by electrospinning. With varying solution concentration, normal non-woven fibermats and honeycomb-like structures were obtained which are attractive scaffold architectures. In addition, with varying silicate content, the mechanical properties, porosity and wettability of the scaffolds were altered.

REFERENCES

1. Kiekens P. *et al.*, Polym. Test. 21:433-442, 2002
2. Boccaccini A. R. *et al.*, Comp. Sci. Technol. 70:1764-1776, 2010
3. Lee E.J. *et al.*, Acta Biomater. 6:3557-3565, 2010

ACKNOWLEDGMENTS

Yaping Ding acknowledges the China Scholarship Council for financial support. The authors are grateful to A. Frey, H. Mahler, I. Herzer, M. Papp and J. Reiser for technical support and data analysis.

Development of a Competitive Calcium Phosphate Cement in a Crowded Marketplace

Philip Procter

Medical Device Industry Consultant, 01220 Divonne les Bains, France consultphilipprocter@gmail.com

INTRODUCTION

For many orthopaedic practitioners biomaterials are the hoped for bridge between the limit of the performance of metallic implants and the unmet needs in the patient treatment. Despite a huge number of biomaterials developments over the last 30 years very few biomaterials have made it from research bench to operating theatre outside of Calcium phosphate (CaP) and PMMA cements¹. Even fewer have clinical evidence of efficacy in a clinical indication². It is essential to have clearly defined unmet needs at the outset rather than to start from an existing technology and try to find applications. The present paper is a case study of the development of a commercially successful CaP Cement, the points of learning and thoughts for the future.

METHODS

The unmet needs for CMF, Trauma and Orthopaedic applications were obtained from customers already using a proprietary CaP, BonesourceTM. A business case was developed around unmet needs and value to clinical users. An external benchmark was defined, NorianTM. The CaP formulation goals were determined from the Voice of Customer (VOC). The primary focus was setting time and wet field properties whilst needs such as ease of mixing, strength, speed of remodelling were also considered. Studies were undertaken to determine acceptable mixing and working times, as well as the desired setting time in a representative range of clinical scenarios. As there are no established methods for some of the parameters eg wet field properties it was necessary to develop original tests to evaluate these. Preclinical studies were undertaken to provide data to support regulatory submissions as a non-load bearing void filler. As an additional goal the project aimed to establish screw augmentation as a new approved regulatory claim.

RESULTS AND DISCUSSION

Preclinical benchmarking in a lapine distal femoral defect model³ showed that the physicochemical and biological properties of the newly developed calcium phosphate cement were comparable with two other commercially available CaP's at 24 h, 6 weeks, 26 weeks, and 52 weeks. The intended clinical performance was assessed by clinicians in an animal test model. The setting time and wet field properties compared very favourably with the CaP benchmarks chosen. The data submitted both in EU and US confirmed approval as a non-load bearing void filler. The preclinical test data for the screw augmentation was accepted by the Notified body in Germany. However the FDA submission was achieved and augmentation of screws with CaP cements remains *off label* use in the

USA. Reimbursement for the combination of a screw and a CaP cement was established in Germany.

POINTS OF LEARNING

There were a number of learning points in the project. These included: formulation, sterilisation and delivery device issues and these will be reviewed.

For CaP cements in general there are still unmet needs: 1) Strength and load sharing potential in combination with screws and locked plates. 2) The long term remodelling remains a concern for most clinical users 3) the ability to combine with antiporotic and antibiotic agents are clinically desired. 4) The lack of specialty cannula eg for use with hip fracture devices, limits the clinical utility. 5) Easy mixing and handling in the operating room is still not generally available.

Biomaterials developers do not focus on these issues and Industry does not invest in the necessary research so progress toward better clinical outcomes is slow at best. In the author's opinion companies that invest in differentiating with clinical claims that produce measurably different clinical performance outcomes will ultimately win in the commercial marketplace. In the future biomaterials will have to be developed that have clinical indication specific properties for use in combination with indication specific devices; these will have to be approved indication by indication with an evidence based approach.

CONCLUSIONS

A case study of a commercially successful CaP cement, HydroSet is presented that has advantages in intraoperative handling. To further develop clinical applications of CaP's will require significant investment and is not without commercial and clinical risk high risk. However there are few signs that either biomaterials developers or the orthopaedic companies are prepared to invest the resources to achieve this.

REFERENCES

1. Larsson, S. and Procter, P. Optimising implant anchorage (augmentation) during fixation of osteoporotic fractures: Is there a role for bone-graft substitutes? *Injury*;42 Suppl 2:S72-6, 2011.
2. Namdari, S. *et al*, Absorbable and non-absorbable cement augmentation in fixation of intertrochanteric femur fractures: systematic review of the literature, *Arch Orthop Trauma Surg.*; 133:487–494, 2013.
3. Hannink, G. *et al* In Vivo Behavior of a Novel Injectable Calcium Phosphate Cement Compared With Two Other Commercially Available Calcium Phosphate Cements. *J Biomed Mat Res B Appl Bio.*; 85(2):478-88, 2008



The Commercial and Clinical Challenges and Opportunities for Advanced Materials in Regenerative Medicine

Kevin M Shakesheff

UK Regenerative Medicine Platform Hub in Acellular Technology, School of Pharmacy, University of Nottingham, NG7 2RD, UK kevin.shakesheff@nottingham.ac.uk

Regenerative medicine can transform many areas of clinical treatment in the future by restoring function tissues within patients. The field encompasses a broad range of product opportunities including drug therapies, biomaterials, cell therapies and engineered tissues. All of these product opportunities share a feature of being more complex in composition and function than the vast majority of pharmaceutical and healthcare products. This complexity allows considerable scope for innovation in the design, manufacture and administration of regenerative medicine products. However, complexity also introduces hurdles to commercial success that must be understood and planned for in research and development programmes.

Advanced materials offer a technology to enhance the efficacy and safety of cell therapies. The UK Regenerative Medicine Platform Hub in Acellular Technologies is a new collaboration to help clinical and industrial groups access materials to accelerate translation of promising candidates into products

This presentation will review the current and future use of materials in the following contexts:

1. Enhancing cell survival and function during and after administration.
2. Co-delivery of pharmaceutical agents and surface chemistry to promote regeneration
3. Creating complex architectures with materials to change cell behaviour
4. Improving manufacturing of cell products (led by the EPSRC Centre for Innovative Manufacturing in Regenerative Medicine).

ACKNOWLEDGMENTS

The research leading to these results has received funding from the European Research Council under the European Community's Seventh Framework Programme (FP7/2007-2013)/ERC grant agreement 227845.



Stratification and Personalisation of Biomaterials and Medical Devices in Musculoskeletal Disease

John Fisher

Institute of Medical and Biological Engineering, University of Leeds, UK
EPSRC UK Centre for Innovative Manufacturing in Medical Devices. J.Fisher@leeds.ac.uk

INTRODUCTION

Stratified and personalised medicine is becoming increasingly important in many areas of healthcare and has the potential to improve the effectiveness and cost effectiveness of many treatments. Stratified and personalised biomaterials and medical devices, is a major opportunity for researchers, manufacturers and clinicians. The recently funded UK EPSRC Centre for Innovative Manufacturing in Medical Devices is starting to address this opportunity, initially in the areas of musculoskeletal biomaterials and implants, with the aim of delivering “the right product, by the right process, to the right patient at the right time” to provide an enhanced standard of reliability, performance and cost effectiveness. This requires new approaches to the design, analysis, simulation, manufacture and pre-clinical testing of biomaterials and medical devices.

METHODS

In the treatment of musculoskeletal disease, the individual patients, the population and the treatments can be characterised, parameterised and stratified using anatomical imaging such as MRI and CT, through analysis and computational predictions of biomechanical function and through quantification of the surgical techniques. The EPSRC centre has identified two key research challenges “functionally stratified design and manufacture” and “personalised near patient manufacture” of biomaterials and implants. Both approaches can potentially deliver better function and patient outcomes. The current research is demonstrated through the description of some of the initial projects. Specifically current work and results will be described for the following research areas.

- Stratified analysis of hip and knee replacements
- Functional simulation of natural joints
- Biological scaffolds derived from natural tissues
- Additive methods for near patient manufacturing.

RESULTS AND DISCUSSION

Stratified analysis of hip and knee replacements:

The function, wear performance and longevity of hip and knee joint replacements are highly dependent on the surgical positioning and patient kinematics. Computational simulation methods have been developed, experimentally validated and parameterised predictions of the effect of surgical positioning and kinematics on wear performance have been defined.

Functional simulation of natural joints:

Novel biphasic computational models of the biphasic contact mechanics and tribology of the natural hip and knee joint have been developed and experimentally validated, and the effect of surgical interventions quantified.

Biological scaffolds derived from natural tissues:

Novel acellular biological scaffolds derived from animal and human tissue have been developed, with properties and function that match human tissue. Examples of the function of biological scaffolds for ligament, meniscus and bone repair are described

Additive methods for near patient manufacturing.

Additive manufacturing methods, which can be used to make patient specific implants close to the patient are being researched and are described.

CONCLUSIONS

New methods for the design, simulation, manufacturing and preclinical testing are needed to deliver stratified and personalised biomaterials and medical devices for musculoskeletal treatments.

ACKNOWLEDGMENTS

Research is supported by the EPSRC Centre for Innovative Manufacturing in Medical Devices at the Universities of Leeds, Bradford, Sheffield, Newcastle and Nottingham.



Layer-by-layer assembly of collagen and fibronectin for tissue engineering applications

Sara Mauquoy and Christine Dupont-Gillain

Bio and Soft Matter (BSMA), Institute of Condensed Matter and Nanosciences (IMCN), Université catholique de Louvain (UCL), Belgium, sara.mauquoy@uclouvain.be

INTRODUCTION

In vivo, cells are embedded in a complex extracellular matrix (ECM) which gives them signals for adhesion, proliferation and differentiation. Collagen (Col) is one of the major components of the ECM, giving to tissues their structural and mechanical properties. Fibronectin (Fn) is essential for the development of most cell types because it specifically binds integrins, which are transmembrane proteins of cells, to transmit signals from cells to the ECM and conversely. Tailoring biointerfaces with a complex architecture based on these two biomolecules will improve our control of cell-material interactions.

The layer-by-layer (LbL) method is an established approach to design structures with a good control of vertical heterogeneity. Developed by Decher in 1992¹, this method is based on the alternate dipping of a surface in a polycation and a polyanion solution, resulting in surface charge overcompensation at each step and hence in the build-up of multilayered films. Assembling proteins by LbL is however challenging in reason of the polyampholyte character of proteins and of their particular structure. The mechanism of assembly may moreover not only rely on electrostatic interactions, but also on specific interactions, as was reported for the assembly of Fn with gelatin², a compound obtained by Col hydrolysis. Here, we aim at combining Fn and Col in LbL assemblies, to create constructs with vertical heterogeneity and biosignaling properties.

EXPERIMENTAL METHODS

LbL assembly: LbL assembly with Fn and native Col (n-Col) or denatured Col (d-Col) was performed on a polystyrene substrate, in phosphate buffered saline (PBS; pH 7.4), HEPES buffer (pH 7.4) and acetate buffer (pH 5.4). These different buffers were compared to modulate the charge of the proteins and the nature of surrounding ions, thereby gaining a better understanding of the adsorption mechanisms. In some cases, poly(ethyleneimine) (PEI) adsorption was performed prior to the LbL assembly.

Characterization: Quartz crystal microbalance with dissipation monitoring (QCM-D) measures *in situ* the frequency (Δf) and dissipation (ΔD) shifts that can be related to the wet adsorbed mass. Ellipsometry is used to measure the dry thickness of the films, contact angle measurements to characterize their wettability and AFM to examine their morphology.

RESULTS AND DISCUSSION

Comparison of n-Col and d-Col assembly: QCM-D results show that the assembly works better with d-Col compared to n-Col. Fibrillation, which does not happen

with d-Col, could mask some interacting sites of n-Col with Fn and explain this observation.

Role of PEI as a primer: Thicker films were obtained when using PEI as an anchoring layer. AFM images show that such films are rougher.

PEI/(Fn/n-Col)_n films: QCM-D data are presented in Fig.1. Col, a 300 nm-long molecule, may extend in solution, and thus may lead to high shifts in frequency and dissipation. This is particularly the case in acetate buffer, in which Col is more positively charged (pH is further away from isoelectric point) and could be more hydrated. The next step of Fn adsorption likely induces a contraction of the film or a desorption of previously adsorbed matter. Since the thickness measured by ellipsometry for PEI/(Fn/n-Col)₂ is similar in all buffers (≈ 7.2 nm in HEPES and ≈ 6.6 nm acetate buffer; ≈ 5.5 nm in PBS), the differences recorded by QCM-D are mainly attributed to different amounts of water trapped in the films. The combination of results from all techniques indicates successful build-up of multilayers, with a growth which however does not seem sustainable. Further experiments are in progress to characterize the supramolecular organization of the obtained layers.

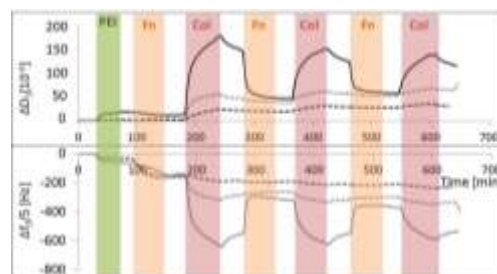


Figure 1: QCM-D monitoring of the construction of PEI/(Fn/n-Col)₃ films in HEPES buffer (dotted line), PBS (broken line) and acetate buffer (plain line). After each adsorption step of 1h, rinsing is performed during 30 min using the corresponding buffer.

CONCLUSION

By assembling Col and Fn in a variety of conditions, we now better understand their mode of assembly, and we have designed biointerfaces which will be further used to control the differentiation of mesenchymal stem cells.

REFERENCES

1. Decher, G., *et al.*, *Thin Solid Films* (1992) **210-211**, 831-835
2. Matsusaki, M., *et al.*, *Angewandte Chemie - International Edition* (2007) **46**, 4689-4692

ACKNOWLEDGMENTS

S. M. thanks the Belgian National Foundation for Scientific Research (FNRS) for her Research Fellow position and for the financial support.



Alginate-silica hybrid hydrogels through covalent coupling with APTES

Yuliya Vueva¹, Siwei Li¹, Frederik Romer^{2*}, John V. Hanna^{2*}, Julian R. Jones¹

¹ Department of Materials, Imperial College London, UK

^{2*} Department of Physics, University of Warwick, UK, y.vueva@imperial.ac.uk

INTRODUCTION

Bone and cartilage diseases are diminishing the quality of life in an ageing population. To date there is no fully successful surgical or pharmacological treatment which has led to considerable interest in tissue engineering strategies. Scaffolds based on natural polymers such as collagen, chitosan, gelatine, alginate etc. offer a good opportunity to generate functional cartilage and bone. Due to their good biocompatibility, biodegradability and close resemblance to extracellular matrix (ECM) they have been extensively studied for cartilage and bone regeneration applications¹. However, poor mechanical properties and uncontrolled degradation limit their use. Organic-inorganic hybrid materials composed of interpenetrating networks of polymers and silica show good promise in terms of tailored biodegradation and toughness². In this work we present organic-inorganic hybrids of alginate and silica produced by sol-gel method through covalent coupling with 3-aminopropyltriethoxysilane and study their potential for tissue engineering application.

EXPERIMENTAL METHODS

Silica-alginate hybrids were prepared in aqueous media by reacting alginate with 3-aminopropyltriethoxysilane (APTES) using N-ethyl-N'-(3-(dimethylamino) propyl) carbodiimide (EDC) and N-hydroxysuccinimide (NHS). Hybrids were made with different coupling (C=1-5) and some of the samples were cross-linked by calcium ions. Formation of amide covalent bonding between the components was monitored by ATR-FTIR, ¹³C CP NMR and ¹⁵N NMR analysis and ²⁹Si MAS NMR was used to study the formation of silica network. Scaffolds were produced by freezing at -20°C and their mechanical behaviour, degradation and swelling (in Tris buffer pH=7.3) were studied. Degradation was followed by ICP-OES (for Si release), FTIR and DSC/TG analysis. MC3T3 osteoblast pre-cursor cells were seeded on the 3-D scaffold. Cell attachment was analysed by scanning electron microscopy (SEM) following 3 days of culture.

RESULTS AND DISCUSSION

The alginate readily reacted with APTES forming amide bonding (evidenced by FTIR, ¹³C CPNMR and ¹⁵N CP NMR). As the pH of the media was basic the hydrolysed ethoxy groups of APTES co-condensed and gelled, resulting in silica-alginate hydrogels (confirmed by ²⁹Si MAS NMR). Along with the amide bond formation, a side reaction yielding N-acylurea also occurred, which was difficult to avoid as the reaction was performed in aqueous solution. Degradation study in Tris solution showed that the weight loss depended on coupling and when the sample was double cross-

linked (by silica and calcium) degradation in time was retarded. Si dissolution profile indicated that as the coupling increased, silica release reduced in time. However the sample with C=1 showed faster silicon dissolution which could be due to the higher amount of unreacted APTES molecules. Swelling was also dependent on the coupling: sample with lower coupling with APTES showed higher swelling. When the hybrid was double cross-linked by silica and calcium ions, the swelling was additionally reduced (Fig 1).

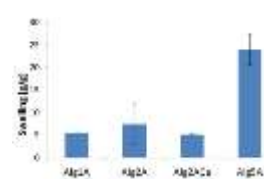


Fig 1. Swelling behaviour

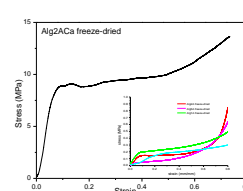


Fig 2. Stress/strain curves

The porous scaffolds had morphology typical for freeze-dried material with elongated pores having modal pore interconnect size ~ 150µm. All scaffolds regardless the coupling were elastic and flexible with stress/strain curves characteristic of a polymeric material (Fig. 2). Increasing the coupling degree slightly increased the stiffness however introduction of more silica (e.g. by co-condensation of APTES with TEOS) or additionally crosslinking with calcium increased the stiffness more substantially.

Cell attachment and distribution were evident. Individual and clusters of MC3T3 cells were seen and anchored to the scaffold surface by distinct filopodia.

CONCLUSION

Silica-alginate hybrids were produced with APTES using carbodiimide chemistry. Materials properties (degradation, swelling and compression strength) were influenced by the coupling with APTES and showed an improvement when hybrids were extra cross-linked with calcium ions. The porous scaffolds had elastic behaviour under compression indicating a potential for soft tissue application.

REFERENCES

1. Spiller L.K. *et al.* Tissue Eng. B 17: 281-288, 2011
2. Mahony O. *et al.* Adv. Funct. Mater. 20:3835-3845, 2010

ACKNOWLEDGMENTS

The authors would like to thank the FP7 program IEF-Marie Curie (Grant no: 299598)

The Effects of Current Density on the Morphology, Electrochemical and Biological Characteristics of Poly(3,4ethylenedioxythiophene): Poly(styrenesulfonate) (PEDOT-PSS) Conducting Films

Catalina Vallejo-Giraldo¹, Abhay Pandit¹, Manus Jonathan Paul Biggs¹

¹ Network of Excellence for Functional Biomaterials (NFB), National University of Ireland, Galway
c.vallejogiraldo@nuigalway.ie

INTRODUCTION

Following implantation of a recording or stimulating neural electrode, glial scar formation at the electrode-tissue interface accelerates neural loss and increases electrical signal impedance, compromising the efficiency of the stimulating system¹. Studies with conducting polymers (CPs) as functional electrode coatings have shown to enhance tissue/electrode integration and electrode performance in situ through reduced impedance and the presentation of neurotropic moieties². Electrodeposition is routinely employed for the formation of poly(3,4ethylenedioxythiophene): poly(styrenesulfonate) (PEDOT:PSS) conducting polymer electrode coatings. However, electrodeposition parameters and their influence on the electrical, morphological, chemical and cytocompatibility properties of electrode films needs to be addressed.

EXPERIMENTAL METHODS

PEDOT:PSS polymeric films were electrodeposited on ITO glass via a three-electrode electrocell system at 0.4 mA/cm², 4 mA/cm², 43mA/cm² current densities, and characterized by four point probe analysis and EIS (conductivity), AFM (roughness, durability), SEM (morphology), XPS (chemical composition) and optical profilometry (thickness). Finally the cytocompatibility of the PEDOT:PSS films was evaluated by culturing SH-5YSY cells on electrodeposited PEDOT:PSS films by alamar blue™, live and dead assay and fluorescent microscopy for adherent cell counting and cell neuritic outgrowth and elongation

RESULTS AND DISCUSSION

PEDOT:PSS polymeric films demonstrated altered roughness, thickness and conducting profiles by altering the current density of film deposition (Fig 1, 2). Furthermore, cellular studies show that SH-SY5Y cells, are associated with a greater viability and proliferation rate on the films formed at different current densities used. (Fig 3). In addition, neurospecific differentiation was achieved as cells began to show neuritic outgrowth and cell elongation up to period of fourteen days in culture.

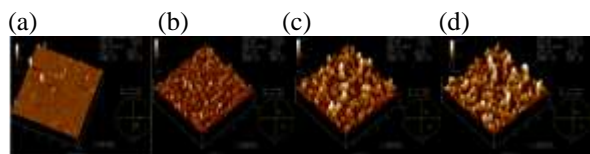


Fig 1. AFM roughness measurements of the PEDOT:PSS films over 10 μm². Film roughness varied with the different current density of

electrodeposition. (a) Control – Gold coated ITO Glass (b) 0.4 mA/cm² (c) 4 mA/cm² (d) 43mA/cm².

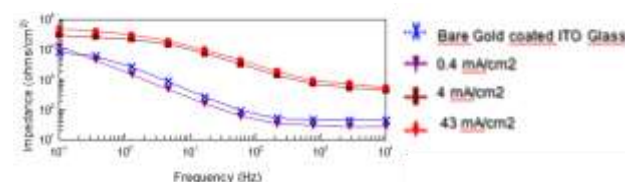


Fig 2. PEDOT:PSS films with different levels of conductivity were achieved by varying the current densities.

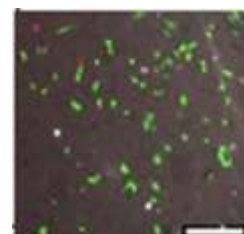


Fig.3. Fluorescent microscopy image of a film formed with the low current density (0.4 mA/cm²) showing a higher number of live cells present on the film. green= live cells, Red = dead

CONCLUSION

The topographical characterization showed that different levels of roughness can be obtained by varying the currents densities of film deposition. Furthermore, the films formed with current densities of 0.4 mA/cm² showed superior electrical performance compared to the higher currents densities evaluated in this work. The adhesion and proliferation of SH-5YSY cells on the surface of these films indicated the cytocompatibility of this material and no toxicity was detected. Thus, cell attachment was preferred on the PEDOT:PSS films formed using the low current density. Designing an optimized electrode coating material will require a trade-off between desired electrical, morphological, chemical and biological properties.

REFERENCES

- [1] Durand DM, Ghovanloo M, et al. J Neural Eng. 2014;11:020201.
- [2] Green RA, Lovell NH, et al. Biomaterials. 2008;29:3393-9.

ACKNOWLEDGMENTS

This work was funded through Science Foundation Ireland 11/SIRG/B2135. Thanks to Dr Donal Leech and the Biomolecular Electronics Research Laboratory, Ms Sarah Burke, Ms Caroline Tachet, and Dr Leo Quinlan.

Biomimetic scaffolds for annulus fibrosus regeneration

Sébastien B.G. Blanquer¹, Arjen W.H. Gebraad¹, Suvi P. Haimi^{1,2}, Susanna Miettinen², André A. Poot¹ and DirkW. Grijpma^{1,3}

¹ Dept. of Biomaterials Science and Technology, University of Twente, Enschede, The Netherlands;

² Institute of Biosciences and Medical Technology (BioMediTech), University of Tampere, Tampere, Finland

³ Dept. of Biomedical Engineering, University of Groningen, Groningen, The Netherlands;

s.b.g.blanquer@utwente.nl

INTRODUCTION

Nowadays, it is commonly accepted that the origin of chronic back pain is often assigned to the degenerative conditions of the intervertebral disc (IVD) tissue. More particularly, disc degeneration mainly leads to tearing of the annulus fibrosus (AF) and extrusion of the nucleus pulposus (NP). The current surgical strategies are suboptimal, and reconstruction of the AF tissue by a tissue engineering strategy seems to be a better alternative. However, regeneration of the AF is challenging due to its complex and non-homogeneous structure. AF tissue consists mainly of highly organized collagen fibers with a specific orientation¹. Therefore the challenge of tissue regeneration is to design and prepare scaffolds that should reproduce the specific collagen fiber distribution of the native AF tissue as well as recover the native mechanical properties.

As a rapid prototyping process, stereolithography (SL) can generate 3D objects with high a diversity of structures and specific predetermined geometries, porosities and morphologies. Thus, complex structures with oriented pore channel architectures can be generated by this method. Using poly(trimethylene carbonate) (PTMC) as a rubber-like surface-eroding polymer, that is well-suited for the repair of soft tissue, biomimetic scaffolds were prepared and seeded with primary and stem cells to evaluate the cell proliferation and the extra-cellular matrix (ECM) production and orientation.

EXPERIMENTAL METHODS

The synthesis of the PTMC macromer was carried out by ring opening polymerization of TMC following by end-functionalization with methacrylate groups. A PTMC resin with suitable viscosity to allow building by SL (Mw of 5 kg/mol), was formulated. The resin contained propylene carbonate diluent, with 5 % wt of initiator and 0.15 % wt of Orasol® Orange dye. The scaffold was designed with the use of computer-aided design file and a 3D software (Rhinoceros 3D), and built in the SL apparatus (EnvisionTec Perfactory). The porosity, pore size and pore distribution were determined by μ CT. Tissue culture was performed with human annulus fibrosus cells (hAFCs) and human adipose stem cells (hASCs) using commercial medium and differentiation medium with TGF- β 3 respectively. The cell culture was analyzed in terms of cell proliferation, GAG/collagen production and collagen orientation.

RESULTS AND DISCUSSION

PTMC scaffolds were prepared by SL with a design of pore channels that mimic the specific fiber orientation of the native AF ranging from 30° to 45°

in the horizontal plan. The scaffolds were made with 80% of porosity and 450 μ m of pore size channel. Mechanical properties (compression modulus) of PTMC scaffolds were measured to be close to those of the native AF tissue (\approx 0.4 to 0.7 MPa). Both investigated types of cells were seeded into the PTMC scaffolds.

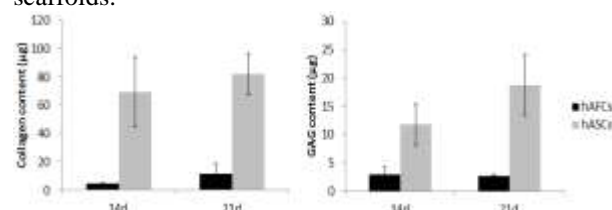


Figure 1: Collagen and GAG production of hAFCs and hASCs at 14 and 21 days of culture, A/Hydroxyproline assay; B/Sulphated GAG assay.

hASCs seeded in these PTMC scaffolds showed substantially higher production of collagen and GAG than hAFCs at both time points (Figure 1). In addition, the GAG:hydroxyproline production ratio of hASCs after 21 days was 1.7:1 similar to that of native AF tissue.

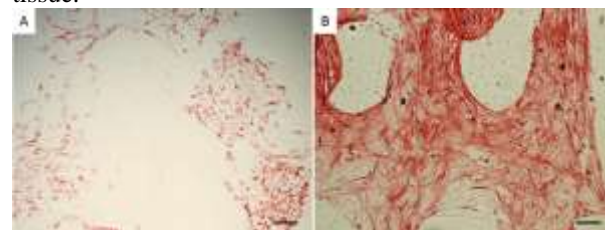


Figure 2: Visualization of collagen production in the PTMC scaffolds by picrosirius red staining, A/ hAFCs; B/ hASCs (scale bar 100 μ m).

The histological images after 21 days (Figure 2) showed that the scaffolds cultured with hASCs had pore channels filled with collagen fibers while the scaffolds cultured with hAFCs showed only limited collagen production. Polarised light imaging demonstrated that the produced collagen by hASCs formed remarkable fibers inside the pore channels.

CONCLUSION

Flexible and elastic scaffolds with oriented pore channel architectures were prepared by SL. hASCs produced collagen fibers in the biomimetic scaffolds that are comparable to those of the native AF tissue.

REFERENCES

1. Guterl C. *et al.* *eCM*. 25:1-21, 2013

ACKNOWLEDGMENTS

The authors would like to thank AO foundation for financial support.



Development of Bioamine Cross-linked Gellan Gum Hydrogels as Soft Scaffolds for Neural Tissue Engineering

J. Koivisto^{1,2,4*}, Sh. Teymouri^{1,4}, J.E. Parraga^{1,4}, T.O. Ihalainen^{3,4}, K. Aalto-Setälä^{2,4}, M. Kellomäki^{1,4}

¹ Laboratory for Biomaterials and Tissue Engineering Group, ELT, Tampere University of Technology, Finland,

² Heart Group, University of Tampere, Finland,

³ Stem Cells in Neurological Applications, University of Tampere, Finland,

⁴ BioMediTech - Institute of Biosciences and Medical Technology, Finland, janne.t.koivisto@tut.fi

INTRODUCTION

Gellan gum (GG) is a potential hydrogel for many tissue engineering applications due to transparency, tuneable mechanical characteristics, and easy processing.¹ However, conventionally the crosslink is done with Ca^{2+} and K^{+} ions, but a high ion content will interfere with cell functionality in case of neurons or myocytes. Photo crosslinking can be done with GG-methacrylate modification, but that method can cause cytotoxic effects.²

We have crosslinked GG with positively charged endogenous bioamine, spermine (SPM), to avoid the aforementioned problems. The effect of laminin immobilization in the gel was evaluated in cell culture. The mechanical properties of these hydrogels were determined by compression testing and diffusion profile was established by fluorescence recovery after photobleaching (FRAP) method.³

EXPERIMENTAL METHODS

GG and SPM stock solutions were made in 10 % sucrose water solutions and sterilized by filtration. The basic hydrogel samples were made by mixing the GG and SPM at +37 °C.

The compression test was done for cylindrical samples, Ø 20 mm and height 7 mm, with Bose Biodynamic Electroforce 5100 in uniaxial unconfined compression at 10 mm/min rate. For FRAP measurements³ confocal microscope Zeiss LSM780 was used. As a diffusion agent, four sizes of dextran-FITC (20 kDa, 150 kDa, 500 kDa, 2000 kDa) mixed with the gel during gelation were used. For cell culture, laminin-1 was immobilized by mixing into the base components and gel was cast in 48-well plate. One hour after gelation the cells were plated on top of the gel. Neurosphere cells, obtained with the method described by Pomp et al. 2008⁴, were used in this study. Neurosphere attachment was monitored by light microscopy. The final cell culture results were studied with Live/Dead-staining with calcein-AM for live and ethidium-HD for dead cells.

RESULTS AND DISCUSSION

Ionic bioamine crosslinking method is suitable for making transparent gels, which are strong enough to hold their own weight. The Young's modulus is close to the modulus of soft tissue. The crosslinking process continues strongly after exposure to salts of basic cell culture medium. The change in compressive Young's modulus with one week incubation in cell culture medium in +37 °C is shown in Table 1.

Table 1. Compressive modulus of GG-hydrogels.

Hydrogel composition	Modulus (kPa)
GG + 0.6 % SPM	7.8 ±1.7
GG + 0.6 % SPM (1wk DMEM)	116.8 ±13.2
GG + 1.1 % SPM	23.7 ±2.5
GG + 1.1 % SPM (1wk DMEM)	158.5 ±16.3

The SPM concentration of GG has little effect on diffusion, as shown in Figure 1. The fluorescent dextran molecules diffuse almost freely inside the hydrogel. The larger molecules diffuse slower than smaller ones.

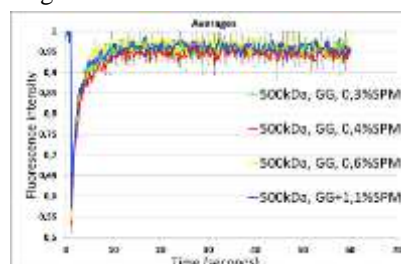


Figure 1. Diffusion profile by FRAP, fluorescence recovery is independent of cross-linker concentration.

Live/Dead-staining of neural cell cultures showed that the GG+laminin had significantly better cell survival than the non-laminin-GG, as shown in Figure 2. More and larger cell aggregates were attached than in non-laminin-GG. Future experiments are on the way to determine the effect of medium induced crosslinking.



Figure 2. Neurospheres on top of hydrogels, a) GG-1.1%SPM (no laminin), b) GG-1.1%SPM+laminin, c) GG-0.6%SPM+laminin.

CONCLUSION

The GG-SPM hydrogels are suitable for neural cell culture applications; however the cell culture medium affects the mechanical properties of the gel. The laminin-1 inside GG improved the attachment of cells.

REFERENCES

1. Smith, A., *et al*, J. Biomater. Appl. 22:241-254, 2007.
2. Fedorovich, N., *et al*, Biomaterials 30:344-353, 2009.
3. Kühn, T., *et al*, PLoS ONE 6:e22962, 2011.
4. Pomp, O., *et al*, Brain Res. 1230:50-60, 2008.

ACKNOWLEDGMENTS

The authors would like to thank the Human Spare Parts project of Tekes – Finnish Funding Agency for Innovation for financial support of this work.

Thermoresponsive self-setting calcium phosphate pastes for minimally invasive surgery and solid freeform fabrication

Yassine Maazouz^{1,2}, Edgar Montufar^{1,2}, Julien Malbert¹, Maria-Pau Ginebra^{1,2}

¹Dept. Materials Science and Metallurgical Engineering, Biomaterials, Biomechanics and Tissue Engineering Group
Technical University of Catalonia, Barcelona, Spain.

²Biomedical Research Networking Centre in Bioengineering, Biomaterials and Nanomedicine, Spain.
yassine.maazouz@upc.edu

INTRODUCTION

Rheology of ceramic pastes is of paramount relevance for both the development of injectable calcium phosphate cements for bone minimally invasive surgery and the fabrication of scaffolds by direct ink deposition or robocasting. This work assesses the thermoresponsive behaviour of self-setting calcium phosphate pastes prepared with a poloxamer hydrogel. Poloxamer hydrogels are known to have temperature-dependent rheological properties, i.e., their viscosity increases with temperature. The functionality of such pastes was evaluated, in terms of washout resistance in contact with liquids at physiological temperature, injectability and shape retention after injection. In addition, the hardening reaction of the pastes was studied either in simulated physiological conditions or in accelerated setting conditions by autoclaving.

EXPERIMENTAL METHODS

Coarse and fine alpha-tri-calcium phosphate (α -Ca₃(PO₄)₂, α -TCP) powders were obtained as described elsewhere¹. Solutions of poloxamer F127 (20 wt%) with and without accelerant (2.5 wt% Na₂HPO₄) were used as liquid phase. α -TCP was mixed with the liquid phase at liquid to powder (L/P) ratios of 0.35 and 0.5 mL/g. The extrusion behaviour was monitored at different paste temperatures (0, 7, 12, 15 or 20 °C) through injection tests¹. Paste cohesion was assessed injecting the pastes at different initial temperatures in Ringer's solution at 37 °C. Setting times were measured using Gilmore needles. Robocasted scaffolds were fabricated at room temperature using a customized robocasting device (Pastecaster, Fundacio CIM). The paste was dispensed with 250 μ m tapered tips following an orthogonal pattern to obtain cylinders of 6 mm \varnothing x 12 mm height with 45 % of theoretical macroporosity. Scaffolds were then set either by autoclaving (121 °C, 1 h) or by immersion in deionized water at 37 °C for 7 days. X-ray powder diffraction was performed after setting to quantify the crystalline phases present.

RESULTS AND DISCUSSION

The addition of poloxamer in the α -TCP paste avoided phase separation during injection and resulted in a temperature-dependent injectability: the injection force significantly decreased when the temperature of the paste decreased (Fig. 1a). The α -TCP/poloxamer extruded threads retained their shape when injected in Ringer's solution at 37 °C, irrespective to the initial temperature of the paste. The pastes with accelerant and L/P=0.35 mL/g were completely injectable through 1 mm cannula, and presented initial and final setting

times of 12 and 34 min respectively, and a compressive strength of 28.4 ± 5.1 MPa.

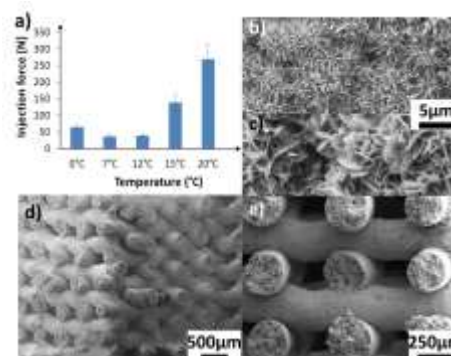


Fig. 1: a) Evolution of the injection force vs. paste temperature b) Needle shape crystals obtained with fine powder. c) Plate shape crystals obtained with coarse powder. d)&e) SEM micrographs showing the scaffolds architecture.

To fabricate robocasted scaffolds the L/P ratio was increased to 0.50 mL/g and no accelerant was used. Strand diameter matched the aperture size of the tip used for printing (250 μ m) and pore size was 200 μ m in the Z direction and 300 μ m in the X and Y directions (Fig. 1 d and e). α -TCP completely transformed into calcium deficient hydroxyapatite when the scaffolds were set in physiological conditions, whereas about 13 % of β -TCP was detected when they were autoclaved, due to the allotropic transformation of unreacted α -TCP. Different post-setting micro/nanostructures were obtained (i.e. needle- or plate-like crystals) depending on the initial particle size of the α -TCP powder used (Fig 1 b and c).

CONCLUSION

Totally injectable thermoresponsive self-setting calcium phosphate pastes presenting washout resistance, and clinically acceptable setting times and compressive strength were successfully produced. In addition to their potential application as injectable bone filler material, these pastes can be used for the fabrication of bone tissue engineering scaffolds by robocasting. Autoclaving is a fast processing route to consolidate the scaffolds. The combination of the self-setting α -TCP with thermoresponsive poloxamer hydrogel offers a versatile platform for bone regeneration, tissue engineering and drug delivery applications.

REFERENCES

1. Montufar E.B. *et al.* Acta Biomater 9:6188-98; 2013.

ACKNOWLEDGMENTS

To the Spanish Government for financial support through MAT2012-38438-C03-01 project and FPU scholarship of YM. MPG acknowledges ICREA Academia prize by the Generalitat de Catalunya.



Cholecalciferol synthesized after UV-activation of 7-dehydrocholesterol onto titanium implants inhibits osteoclastogenesis in vitro

María Satué, Joana M. Ramis and Marta Monjo

Group of Cell Therapy and Tissue Engineering, Research Institute on Health Sciences (IUNICS), University of the Balearic Islands, Spain, maria.satue@uib.es

INTRODUCTION

UV-activated 7-DHC is a biocompatible coating for titanium implants in osteoblastic cells producing active vitamin D with positive effect on osteoblast differentiation [1]. The successful osseointegration of an implant is achieved by bone remodeling around the implant site what requires a balance between osteoblast and osteoclast to form new bone tissue in the peri-implant region. Since Ti implants covered with UV-irradiated 7-DHC promote osteoblast differentiation in vitro, we aimed at determining the effect of this bioactive coating on osteoclastic cells (RAW 264.7 cells).

Moreover, 7-DHC and its metabolites are very labile. In particular, 7-DHC is the most reactive lipid known to maintain a peroxidative free radical chain reaction. Thus, we also aimed at improving the UV-activated 7-DHC coating in two ways. First, by the addition of an antioxidant agent, α -tocopherol (VitE), as some studies prove that VitE protects bone from damage and suppresses bone loss [2]. Second, by controlling time and temperature incubation of the coating in order to improve the synthesis of D₃, since some studies confirm that the thermal isomerization to D₃ is time and temperature dependent [3].

EXPERIMENTAL METHODS

Machined titanium (Ti) surfaces were coated with 7DHC:VitE. Controls (EtOH, 7-DHC or VitE) were also included in the study. Surfaces were exposed to UV for 15 min and incubated at -20, 4 and 23°C for increasing incubation times: 0, 24, 48 and 96 hours. HPLC analyses were performed to determine the coating composition. For in vitro analysis, RAW264.7 cells were cultured for 5 days with RANKL addition. The in vitro response of RAW264.7 cells to coated Ti implants was determined in terms of cytotoxicity, gene expression of specific markers and immunostaining of actin ring and TRAP protein.

RESULTS AND DISCUSSION

The composition of the UV-activated 7-DHC coatings depended on the time, temperature and antioxidant addition. Indeed, the higher D₃ production was found after 48 hours of incubation at 23°C. VitE reduced the oxidation of 7-DHC in a dose-dependent manner, synthesizing more D₃ with the higher antioxidant dose (7-DHC:VitE 1:1; m:m).

Therefore, this best performing coating was tested in RAW264.7 cells. Results showed no cytotoxic effect and a significant decrease in the gene expression of key osteoclastic markers. Moreover, the immunostaining

confirmed the inhibition of both, osteoclastogenesis and TRAP protein expression.

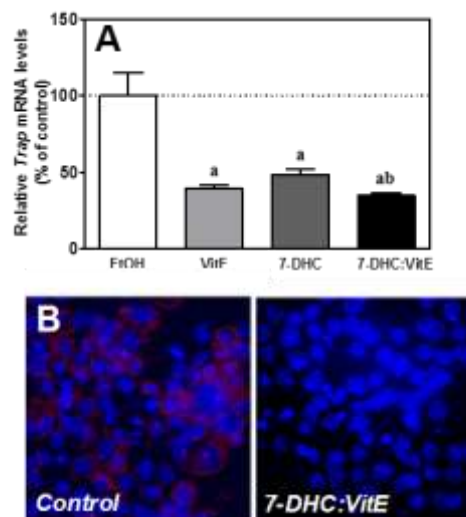


Figure 1. (A) Effect of the different treatments on mRNA expression levels of *Trap* in RAW 264.7 dosed with RANKL for 5 days. Data were normalized to reference genes (Gapdh and 18S rRNA). Values represent the mean \pm SEM (N=6). Differences between groups were assessed by Student's t test: ^a p < 0.05 treatment versus control and ^b treatment versus 7-DHC. (B) Representative images (63x) of confocal laser scanning of RAW264.7 cell cultured for 5 days. Cells were stained with DAPI (stains nucleous; blue) and anti-Trap labelled with Cy3 (red).

CONCLUSION

The addition of vitamin E to 7-DHC coating before its UV activation, together with the control of temperature and time of incubation of the coating improves the synthesis of D₃. These results in a potent inhibition of osteoclastogenesis, suggesting a reduction on bone resorption activity. All in all, 7-DHC:VitE coated implants promotes osteoblast differentiation whilst inhibits osteoclast formation, suggesting a positive bone remodeling balance. This bioactive coating is here proposed as a new approach for implant therapies in patients with compromised bone health.

REFERENCES

1. Satué M. *et al.*, Acta Biomater. 9:5759-70, 2013.
2. Nazrun A.S *et al.*, Adv Pharmacol Sci. 2012, ID 142702.
3. Holick M.F. *J Invest Dermatol.* 1:51-58, 1981.

ACKNOWLEDGMENTS

This work was supported by the MICINN (Ramón y Cajal contract to MM).



Mapping Phase Changes in Brushite Cements

A. Bannerman*, R.L. Williams and L.M. Grover

School of Chemical Engineering, University of Birmingham, UK

axb088@bham.ac.uk

INTRODUCTION

Brushite calcium phosphate cements have attracted interest as bone graft biomaterials due to their osteoconductive and resorbable properties¹. Degradation and bioactivity of the cement is highly dependent on the aqueous environment, and has been shown to vary significantly in the literature². Analysis of samples aged *in-vitro* and *in-situ* has largely used methods - such as scanning electron microscopy and x-ray diffraction - that give high resolution morphological, and/or overall bulk chemical information on the material at a given time point^{1,2}. These methods are often limited to the crystalline properties of the sample, and so can result in significant components or changes being unobserved.

In this study we aimed to fill the information gap of the current analytical methods, and provide further means to monitor cement degradation and help elucidate the bioactivity. Using confocal Raman microscopy (CRM) to map and quantify phase changes in brushite cement cylinders that were dynamically aged under physiological conditions in a range of media.

EXPERIMENTAL METHODS

Cylinder ageing: brushite cement cylinders (12x6mm) were produced from β -TCP and 3.5M orthophosphoric acid mixed at a ratio of 1.75g/ml and left to set overnight. Cylinders were sterilised under UV light then aged in 20ml of either phosphate buffered saline (PBS), Dulbecco's modified eagle medium, or fetal bovine serum, maintained at 37°C and changed every 24 hrs.

Image Mapping: cylinders were removed from media at staggered time points, dried, cut to expose the cross section and cryotomed to a smooth surface. Image mapping was performed using confocal Raman microscope with a 514nm 60mW laser. Observations were confirmed by XRD. **Computational analysis:** Data was exported to Matlab and baseline corrected. Clustering was performed to assign each pixel to the dominant phase of its' associated spectrum. Quantification was taken as a function of distance along the cylinder radius.

RESULTS AND DISCUSSION

Image mappings of PO_4 peaks associated with brushite and octacalcium phosphate (OCP) of cylinder cross sections showed evidence of a shell of OCP forming on samples aged in serum-free media. This study of the compositional evolution was taken further with a longer time series using PBS media that showed a clear development from an initially homogeneous distribution of brushite, to a three phase structure, as the outer layer of brushite underwent dissolution via hydrolysis, leaving a TCP scaffold that was subsequently seeded by OCP (Fig 1). Computational analysis to produce composite images of the dominant associated phase at each point is shown in Fig 2. Results support those in

Fig 1, showing a decrease in brushite leaving a β -TCP scaffold, with eventual seeding of OCP.

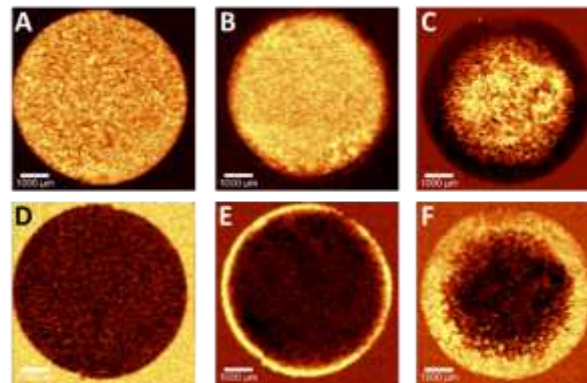


Figure 1: CRM mapping of brushite cylinder cross sections showing the PO_4 peak associated with brushite (A,B,C) and OCP (D,E,F) at 0 days (A,D), 10 days (B,E), and 30 days (C,F) ageing in PBS at 37°C. Scale bar 1000µm.

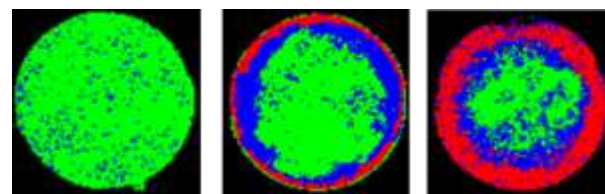


Figure 2: CRM mapping showing the dominant phase at each spatial location from Fig 1. (A) 0 days, (B) 10 days, and (C) 34 days. Colour key: Green - brushite, blue TCP, red OCP.

The results of this study have shown that phase changes inside the cement as a result of ageing in different media, are spatially detectable and quantifiable through CRM. This provides a complementary addition to the currently used imaging and analysis modalities, by providing spatial chemical information that is not dependent on the quantity of crystalline material in the sample. Such information may allow a significant insight into the degradation of implants, enabling improved material optimisation.

CONCLUSION

This study has shown that high resolution chemical mapping of calcium phosphate cements can be used to visualise and quantify chemical changes resulting from ageing under physiological conditions.

REFERENCES

1. Constantz B. *et al.*, J Biomed Mater Res. 43:451-461, 1998.
2. Grover LM *et al.*, Biomaterials. 24:4133-4141, 2003.

ACKNOWLEDGMENTS

The authors would like to thank the EPSRC for providing financial support via the PSIBS DTC for this project

Biomaterial induced bone nodules without medium supplements

S. Mechiche Alami^{1*}, J. Hemmerlé², F. Boulmedais³, J. Josse¹, P. Schaaf³, S.C. Gangloff¹, F. Velard¹, D. Laurent-Maquin¹, H. Kerdjoudj¹

¹ E.A. 4691 « Biomatériaux et Inflammation en site osseux », UFR Odontologie, SFR Cap Santé, URCA, France, ² INSERM UMR 1121, Faculté d'odontologie, Strasbourg, France, ³ Institut Charles Sadron, CNRS, UPR 22, Strasbourg, France.

* saad.mechiche-alami@etudiant.univ-reims.fr

INTRODUCTION

Future tissue engineering developments rely on cell-instructive scaffolds. Cell fate could be driven by physico-chemical information coded within the biomaterial. Calcium phosphate materials (CaP) are widely studied for bone regeneration because of their biocompatibility and their chemical structure close to bone mineral phase¹. Nevertheless, most studied CaP lack osteogenic potential that could induce stem cells differentiation into mature bone cell phenotype.

We report spraying technique of calcium and phosphate solutions to elaborate CaP that induce human umbilical cord Wharton's jelly stem cells (WJ-SCs) to form *in vitro* bone nodules without the use of osteoinducer supplements.

EXPERIMENTAL METHODS

An automated spraying device was used for deposition of calcium phosphate. 0.2 M $\text{NH}_4\text{H}_2\text{PO}_4$ solution at pH 10 and 0.3 M $\text{Ca}(\text{NO}_3)_2$ solution at pH 4 were sprayed simultaneously 50 times then rinsed with MilliQ water and dried. Physicochemical characterization of CaP was investigated by Scanning Electron Microscopy (SEM) and Fourier Transformed Infrared Spectroscopy (FTIR). Osteoblastic differentiation of WJ-SCs was investigated at genic and proteic levels after 7, 14 and 21 days of culture.

RESULTS AND DISCUSSION

Spraying calcium solution simultaneously with phosphate solution leads to creation of a white mineral phase. SEM observations revealed granular morphology with micro-sized particles. FTIR spectras showed peaks within $500\text{--}1100\text{ cm}^{-1}$ and $3400\text{--}3600\text{ cm}^{-1}$ regions revealing octacalcium phosphate phase.

With no use of osteoinducer supplements, WJ-SCs were seeded on the sprayed CaP. DNA quantification after 7, 14 and 21 days highlighted a cell proliferation on the sprayed substrate. SEM observation showed cuboidal cells which were organized into 3D structures after a week of culture whereas cells cultivated on glass kept their fibroblastic morphology (Figure 1).

Immunolabelling of the formed colonies revealed membranous localization of integrins $\beta 1$ and $\alpha 2$. These colonies, positive for alkaline phosphatase

activity, are heightened within time of culture (Figure 2)

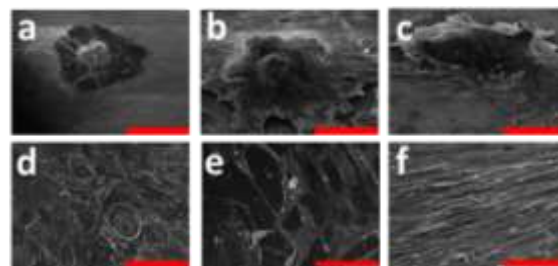


Figure 1: WJ-SC behaviour on sprayed CaP observed by SEM. **a:** Colony of cells with cuboidal morphology at day 7. **b:** Colonies are being heightened at day 14. **c:** Morphology of bone nodule at day 21. **d, e, f:** show cells seeded on untreated cover glasses at respectively 7, 14 and 21 days. (Scale bars = 100 μm).

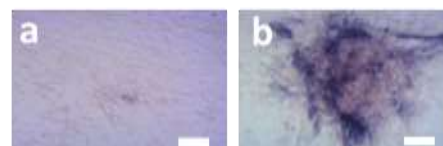


Figure 2: Alkaline phosphatase activity of WJ-SC at day 14 seeded on **a:** glass, **b:** CaP, note the presence of positive cells only at the nodule localization. (Scale bars = 50 μm).

CONCLUSION

Spraying calcium and phosphate solutions allows the buildup of osteoinductive CaP. Without the use of osteogenic medium, WJ-SCs cultivated on CaP form bone nodules, which are considered as a model of osteoblastic differentiation². Our aim is to study the extracellular matrix formed within these bone nodules.

REFERENCES

1. S. Samavedi *et al.*, Acta Biomaterialia (2013), 9: 8037-8045.
2. L. Malaval *et al.*, Journ. of Cellular Biochemistry (1999), 74: 616-627.

ACKNOWLEDGMENTS

The authors thank "Ville de Reims" for S. Mechiche Alami PhD financial support and the Maison Blanche gynaecology service headed by Pr. O. Graesslin for providing umbilical cords.

Fibronectin loaded hydroxyapatite for reduced healing time on osteoporotic rabbit bone

Javier Quintana-Plaza¹, Luis M. Rodríguez-Lorenzo^{2,3*},

¹Hospital Doce de Octubre, Madrid, Spain

²Polymeric nanomaterials and Biomaterials/ICTP-CSIC, Madrid, Spain

³GBP/CIBER-BBN, Spain

* luis.rodriguez-lorenzo@ictp.csic.es

INTRODUCTION

The gradual aging of the population results in an increased incidence of osteoporotic bone fractures. In a good quality bone, the success rate for fixation with consolidation screws is acceptable, but in osteoporotic bone fractures, in which consolidation delays and other complications are common, failure rates for fixation using screws raises up to 25%.

The aim of this project is to check the ability of fibronectin (Fn) adsorbed on hydroxyapatite (OHAp) to enhance the osseointegration of devices used in the reduction of osteoporotic fractures and thereby reduce the morbidity of them

EXPERIMENTAL METHODS

Hydroxyapatite (OHAp) have been prepared by reaction of $\text{Ca}(\text{OH})_2$ with H_3PO_4 at pH 9.4. Powders were washed, freeze dried, and ball milled for 24 hours. Fibronectin (FN) from Human plasma was purchased from Sigma. The ceramic powders was characterized by ATR-FTIR, X-Ray Diffraction (XRD), Thermogravimetric Analysis (TGA), Scanning and Transmission Electronic Microscopy (SEM), specific surface area (SSA), particle Size Analysis, Helium Picnometry, Contact Angle, Z potential and Nuclear Magnetic Resonance ($^1\text{H-NMR}$) techniques.

Adsorption of Fn on OHAp was assayed by mixing 10 mg of the apatite with 1.5 mL of Fn dissolved in PBS Buffer at pH 7[1]. Protein binding was studied with a UV/VIS Spectrometer Lambda 16, by Raman spectroscopy in a Renishaw spectrometer and a Quartz-Crystal Microbalance with dissipation (QCM-D) in a KSV Instruments QCM-z500.

The “in vivo” study was performed using cancellous bone screws (4mm x 14mm) implanted in an osteoporotic rabbit model. One group supplemented with Fn adsorbed on hydroxyapatite, a second group supplemented with hydroxyapatite and a control group free of supplementary material. 42 adult female rabbits (16-18 months) of 4-5kg (White New Zealand) were used. Trabecular bone morphometry was analyzed with a Micro- CT eXplore Locus SP provided by GE Healthcare. The following parameters were studied: BVF (Ratio of the segmented bone volume to the total volume of the region of interest (%) mg/mm^3), BMD (Bone mineral density, mg/cc), (TbTh, (trabecular thickness, mm), and TbSp (trabecular separation, mm). The Stevenel’s blue bone stain was used for histological analysis.

RESULTS AND DISCUSSION

Hydroxyapatite samples with a 97% crystallinity, 34 m^2/g specific surface area and 858 Å crystal size were selected to perform the Fn adsorption experiments. Fn is active only when the RGD domains of the N-terminal are accessible. From the dissipation energy analysis from the QCM-D experiments, it can be deduced that Fn have been adsorbed in the active form.

Obtained basal levels of BMD (336 mg/cc) are below normal bone values and it confirms the osteoporotic condition achieved for the specimens used in the vivo experiments.

Independent time analysis of samples, show no significant differences for BMD and BVF variables. However, the median is slightly higher for the variable BMD in the sample with Fn. Although no significant differences have been found, a trend is suggested for those variables that define the trabecular bone microarchitecture. TbTh median is greater (0.49/0.46/0.40) and TbSp median is lower (0.67/0.73/0.74) for specimens supplemented with Fn-OHAp than for the OHAp and the control groups.

Significant differences have been found in TbTh and TbTs analysis performed at different distances from the implanted osteosynthesis screw. p 0.012 has been obtained for a comparison between an area separated from the screw and an area adjacent to the screw for the TbTh in Fn-OHAp supplemented specimens and p 0.008 has been found for the TbSp parameter. A greater non inflammatory cellularity and connective tissue was observed after only 24 hours of implantation for the Fn-OHAp supplemented specimens in comparison with the OHAp supplemented and the control groups.

CONCLUSION

The conformation of Fn adsorbed on OHAp has been controlled to keep RGD domains available.

This combination of Fn and OHAp can be a route to reduce the healing time in osteoporotic fractures

REFERENCES

1. Fernandez-Montes Moraleda B. et al., J Biomed Mater Res 101A: 2332-9, 2013

ACKNOWLEDGMENTS

The authors would like to thank CICYT, Spain through project MAT2010-18155 for providing financial support to this project



Mineralization of phosphate prestructured gelatine – Bulk preparation and characterization as bone substitute

Benjamin Kruppke, Hartmut Worch and Thomas Hanke

Max Bergmann Center of Biomaterials, Institute of Materials Science, Technische Universität Dresden, Germany,
Benjamin.Kruppke@tu-dresden.de

INTRODUCTION

In vitro mimics of natural mineralization processes through integration of organic molecules with more or less strong template function has been a common subject of hard tissue research in recent years. Incorporation of non-collagenous proteins forming polymer induced liquid precursors into mineralization processes seems to be the most promising approach of biomineralization.¹ As against single ions and atoms used for crystal formation – organic molecules and mineral precursors use to restrict mineralization. Collagen in its denatured form (gelatine) is assumed to be able to restrict mineral formation itself. Therefore, prestructuring of gelatine with anions or cations and the following mineralization process initiated by adding counter ions was investigated regarding dental repair material by Kollmann *et al.*² Here, its transfer to bone substitutes as follows is presented.

EXPERIMENTAL METHODS

Preparation. Mineralization was performed as batch process. First, phosphate-prestructured (PPS) gelatine was produced. For this, a 0.6 % w/w gelatine suspension was mixed with 0.1 M Na₂HPO₄ solution in a volume ratio of 3:17. PPS-suspension was adjusted to pH 7.0. Aqueous cationic solutions (1 M) – CaCl₂·2H₂O or SrCl₂·6H₂O at pH 7.0 – were added to PPS-suspension at a rate of 2.5 mL/min. During the entire precipitation process, it has been stirred at 300 rpm. Thereafter, the milky suspension was centrifuged and lyophilized. Finally, the pellets were pulverized by a mixer mill. Precipitates were named PPGC and PPGS for phosphate-prestructured gelatine mineralized with calcium and strontium, respectively.

Characterization. Mineral precipitates were investigated using X-ray diffraction (XRD) and transmission as well as scanning electron microscopy (TEM/SEM). Amount of gelatine in the mineral precipitate was determined by loss-on-ignition (LOI). 200 mg mineral was heated to 1000 °C for 1 h. After cooling the differences to initial weights were determined and compared to precipitated mineral without gelatine. Biaxial strength was determined by ball-on-three-balls test.³ For that, 400 mg mineral was compressed (510 MPa) to a disk of 13 mm diameter and 1.5 mm height. Degradation was determined by static incubation of compacted mineral (100 mg, o. d. 5 mm, 510 MPa) in both 4 mL simulated body fluid (SBF) and 4 mL phosphate buffered saline (PBS). During degradation, pH, calcium and phosphate ion concentrations were determined after (1, 4, 8) h and (. Statistical analysis was performed using one-way ANOVA.

RESULTS AND DISCUSSION

Crystal structure and morphology of calcium and strontium precipitates differs substantially. XRD revealed

PPGC is mainly brushite and monetite. SEM showed typical platelet shaped crystals in a range of 10 µm to 80 µm width and submicrometer thickness. For strontium precipitates XRD revealed sharp peaks that could not be assigned. Morphology of PPGS can be described as foliated spherical particles according to SEM.

For both minerals TEM revealed a certain amount of gelatine within the particles as they started to melt during HRTEM investigations. It was determined by LOI to 5.7 % w/w for PPGC and 4.1% w/w for PPGS. Increasing the amount of gelatine in PPS-suspension by factor 5 leads to an increase of gelatine in PPGC to 22.7 % and in PPGS to 9.7 %. It suggests a saturation of gelatine inside the mineral. Gelatine bound within the mineral affected the mechanic stability as well. As the ball-on-three-balls test revealed, PPGC showed a biaxial strength of 150 % of the gelatine free samples. In contrast, density of 2.6 g/cm³ was almost identical.

Degradation of PPGC and PPGS was characterized by decrease of pH during incubation in PBS. The pH drop from 7.4 to 6.7 within 1 h was followed by an overall reduction to 6.2 during 7 days. Due to the higher buffer capacity of HEPES within SBF, here pH of 7.5 was constant during the mineral incubation. Release of phosphate ions was not detectable in PBS with a constant concentration of 3.5 mM. In SBF, concentration of phosphate ions was kept constant for PPGS (right below 1 mM) whereas PPGC caused a decrease of phosphate ions to 0.5 mM within 24 h of incubation followed by a release of phosphate passing 3.0 mM after 7 days. Calcium concentration in PBS drops from an initial release (1 h, 0.8 mM) within the first day to 0.4 mM, then increases to 0.7 mM during 7 days of incubation. In SBF, PPGC shows an initial release of calcium (5.3 mM) followed by constant decrease of calcium concentration to 1 mM after 7 days.

CONCLUSION

As hydroxyapatite (HAp) precipitates are well known for their high calcium binding capacity – inhibiting osteoblastic activity – PPGC and PPGS shows promising properties as mechanically loadable materials. Additionally in contrast to HAp, their time dependent degradation allows bone remodelling under release of physiological degradation products.

REFERENCES

1. Nudelman F. *et al.*, J. Struct Biol. 183(2), 2013
2. Kollmann T. *et al.*, Chem. Mater. 22, 2010
3. Börger A. *et al.*, J. Eur Ceram Soc 22, 2002

ACKNOWLEDGMENTS

We grateful acknowledge the Deutsche Forschungsgemeinschaft Grant TRR79-M03 for financial support.



Adhesion, Growth and Differentiation of Pre-osteoblasts on Novel Porous Magnesia- and Yttria-Stabilized Zirconia Ceramics

Chrystalleni Hadjicharalambous¹, Vladimir Promakhov³, Svetlana Buyakova³, Sergey Kulkov³ and Maria Chatzinikolaïdou^{1,2}

¹ University of Crete, Dept. of Materials Science and Technology, 71003 Heraklion, Greece

² IESL-FORTH, Vasilika Vouton, 71110 Heraklion, Greece

³ Tomsk State University and ISPMs RAS, 2/4 Akademicheskii ave. Tomsk, 634021, Russia, chad@materials.uoc.gr

INTRODUCTION

Zirconia (ZrO₂) bioceramics are frequently used in high-load bearing orthopaedic and dental applications due to their high mechanical strength and good biocompatibility. Among these, the most studied and widely used is yttrium-stabilized zirconia (YSZ) with excellent resistance to crack propagation¹. On the other hand, magnesia-stabilized zirconia (MgSZ) does not experience phase transformation and it has been shown to better resist degradation *in vivo*². Both of these materials are bioinert and thus lack osseointegration, which is important for implant fixation. Improving the initial attachment of osteoblast precursor cells to orthopaedic implant surfaces may lead to improved bone integration of the implant and long-term stability. We therefore investigated whether introduction of pores in these biomaterials could result in strong and bioactive scaffolds³. We fabricated sintered YSZ and MgSZ ceramics of medium 50-60% porosities and investigated the biological response of MC3T3-E1 pre-osteoblasts on these materials.

EXPERIMENTAL METHODS

Ceramic samples fabrication: The porous zirconia ceramics were produced by sintering powders obtained by plasma-spray pyrolysis⁴. The samples were characterized with respect to porosity, pore size distribution and mechanical properties.

Biological response: Cell viability and proliferation were assessed by the PrestoBlue™ assay, as well as by fluorescence microscopy. Cellular adherence and morphology were observed by SEM. Levels of ALP activity were measured to assess osteoblast differentiation whereas collagen production and Alizarine Red S staining were used for the evaluation of the extracellular matrix⁵.

RESULTS AND DISCUSSION

The ceramic substrates had similar porosities; 50% and 57% for the YSZ and MgSZ respectively. Pore size distributions were bimodal with two maxima at 0.7 µm and 167 µm for YSZ and 1 µm and 144 µm for MgSZ. Young modulus values were 10±3 GPa for YSZ and 6±2 GPa for MgSZ, whereas compressive strength values were 210±30 MPa and 120±30 MPa for YSZ and MgSZ respectively. Pre-osteoblasts were able to adhere, and spread on both substrates but cell morphology was different (figure 1). Cell viability and proliferation rates

were higher on YSZ than MgSZ. However, after 10 days, both substrate surfaces including interconnected pores were completely covered with cells. Abundant extracellular matrix formation was observed by SEM and quantified by collagen levels. ALP activity was detected as early as 7 days. Comparison of matrix mineralization showed higher levels on MgSZ. Apparently, surface chemical differences between porous YSZ and MgSZ exerted a significant influence over pre-osteoblastic cell attachment, morphology, and their capacity for proliferation and differentiation.

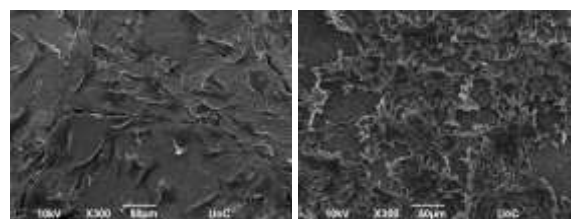


Figure 1. Cell adhesion of MC3T3 cells cultured on YSZ (left) or MgSZ (right) for 1 day. Pre-osteoblasts appeared more flattened on YSZ and more branched on MgSZ.

CONCLUSION

Despite differences in cell morphology and early proliferation patterns, both ceramics show mechanical properties similar to cortical bone and good biological properties, suggesting their potential as scaffolding materials for bone regeneration.

REFERENCES

1. Manicone P. *et al.*, J. Dent. 35:819–826, 2007
2. Hao L. *et al.*, J Biomater. Appl. 19:81, 2004
3. Lew K. *et al.*, J Biomater. Appl. 27(3):345, 2012
4. Kulkov S. *et al.*, Rus. Nanotech. 2:119-132, 2007
5. Terzaki K. *et al.*, Biofabrication, 5(4), 045002, 2013

ACKNOWLEDGMENTS

The authors would like to thank the GSRT Grant Thales-MIS 380278 and the Russian Grant No. 11.519.11.2020 for providing financial support to this project.

Mesenchymal Stem Cell Response to Covalent Functionalized Recombinant Fibronectin Fragments onto New Titanium-Niobium-Hafnium Alloy

C. Herranz-Díez^{1,2,3}, J. Guillem-Martí^{1,2,3}, F.J. Gil^{1,2,3}, J.M. Manero^{1,2,3}

¹Biomaterials, Biomechanics and Tissue Engineering Group, Department of Materials Science and Metallurgical Engineering, Technical University of Catalonia (UPC), Spain.

²Biomedical Research Networking Center in Bioengineering, Biomaterials and Nanomedicine (CIBER-BBN), Spain

³Center for Research in Nanoengineering (CRnE), Technical University of Catalonia (UPC), Spain

jordi.guillem.marti@upc.edu

INTRODUCTION

Titanium (Ti) is the most widely used material for bone substitution due to its biomechanical properties. However, in some cases the osseointegration is not achieved, ending with implant failure. Hence, modifications of Ti biomechanical properties are required. On one hand, the mechanical properties can be modified combining Ti with other ductile metals, generating Ti-based alloys¹. On the other hand, the use of several different extracellular matrix (ECM) proteins or ECM-derived peptides or protein fragments has demonstrated an improved cellular response².

The aim of this study was to compare the in vitro cellular response to different recombinant fibronectin fragments functionalized on a new Ti alloy based on the optimization of molecular orbital calculations of electronic structures³. Cell adhesion, proliferation and differentiation of rat mesenchymal stem cells were analyzed.

EXPERIMENTAL METHODS

The alloy was fabricated at Fort Wayne Metals Research Corp. (Fort Wayne, IN, USA). Bars of 10 mm diameter were obtained by vacuum arc melting and drop casting. The bar was vacuum-homogenized and annealed at 650°C. Characterization of the alloy was done analysing the microstructure, elastic modulus, corrosion resistance and superficial energy. Fibronectin Cell Attachment Site (CAS) and Heparin Binding II (HBII) domains were synthesized using recombinant protein methods. Linear and cyclic RGD were synthesized by solid phase synthesis. Plasma Fibronectin was used as control. Peptides, fragments and different fragments combinations were covalently bound to the alloy surface by APTES silanization. Adsorption was analysed by OWLS. Rat Mesenchymal Stems cells (rMSCs) were seeded on the functionalized alloy and adhesion (LDH quantification and immunofluorescence evaluation), proliferation (LDH quantification) and differentiation (ALP quantification) were evaluated after 4h and 7, 14 and 21 days.

RESULTS AND DISCUSSION

A Ti25Nb21Hf alloy mainly composed of β -phase grains was obtained. XRD and TEM results demonstrated a lower presence of martensite α' and martensite α'' phases. The alloy exhibited interesting material properties such as lower elastic modulus and higher corrosion resistance, higher surface free energy and higher zeta potential values compared to c.p. Ti and Ti6Al4V. Since the adsorption quantities of

recombinant fibronectin fragments were higher when they were covalently bounded with APTES, compared to physisorption, cellular analyses were done after silanization. Although there were no statistically significant differences in the number of adhered cells, cells were more spread when surfaces were functionalized with combinations of CAS and HB2, instead of CAS or HB2 alone. These combinations also exhibited higher proliferation rates. Noteworthy, the 70%CAS-30%HB2 showed highest amounts of ALP (Figure 1).

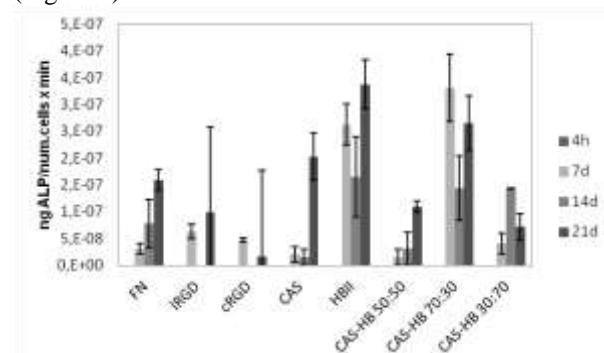


Figure 1. Differentiation of rMSCs on Ti25Nb21Hf functionalized with different fibronectin fragments (CAS, HB2 or combinations), adhesion peptides (linear or cyclic RGD) and whole fibronectin (FN).

CONCLUSION

The modification of Ti biomechanical properties using the combination of metal alloying and ECM recombinant fragments functionalization seems promising for bone substitution purposes. In vitro results suggested that combinations of CAS and HB2 recombinant fragments were better for cellular adhesion quality, proliferation and differentiation responses than single fragments, obtaining interesting results for 70%CAS-30%HB2 combination.

REFERENCES

1. Niinomi M. *et al.*, Metall. Mater. Trans. A 33:477-486, 2002.
2. Shekaran A. *et al.*, J. Biomed. Mater. Res. Part A 96A: 261-272, 2011.
3. Arciniegas M. *et al.*, Philos. Mag. 88: 2529-48, 2008.

ACKNOWLEDGMENTS

The authors would like to thank Fort Wayne Metals Corp. for material fabrication and the Spanish Government for financial support thorough MAT 2012-30706 project. CHD thanks to AGAUR for FI scholarship.



Combined Stimulation with Defined Extracellular Matrices and Pulsed Electrical Fields Enhance Osteogenic Differentiation of Human Mesenchymal Stem Cells

R. Hess¹, P. Lee¹, A. Jaeschke¹, H. Neubert², T. Henker², V. Hintze¹, S. Moeller³,
M. Schnabelrauch³, D. A. Hart⁴, H.-P. Wiesmann¹, D. Scharnweber¹

¹Institute of Materials Science / Max Bergmann Center of Biomaterials, TU Dresden, Germany

²Institute of Electromechanical and Electronic Design, TU Dresden, Germany

³Biomaterials Department, Innovent e.V. Jena, Germany

⁴McCaig Institute of Bone and Joint Health, University of Calgary, Canada, ricarda.hess@tu-dresden.de

INTRODUCTION

Bone formation is a complex, tightly regulated process, influenced by biochemical and physical factors. To develop a vital bone tissue engineering construct, all of these individual components have to be taken into consideration to gain an *in vivo*-like stimulation of target cells.

While previous studies in tissue engineering were mostly focusing on the influence of single factors, the purpose of the present study was to combine biochemical and physical stimulation using an artificial extracellular matrix (aECM) and electrical fields. Last ones have been induced by a new apparatus, applying electrical fields by transformer-like coupling (TC)¹.

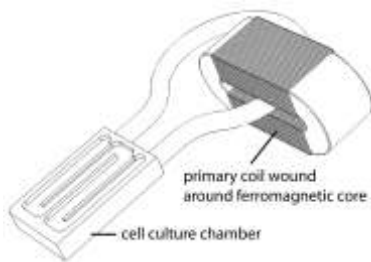


Fig. 1: Set-up for electrical stimulation of cells¹

This method allows a stimulation of cells with exclusive electrical fields, avoiding interfering side-effects which occur with previous systems [Figure 1].

EXPERIMENTAL METHODS

Human mesenchymal stem cells (MSCs) were seeded on non-coated or aECM-coated three-dimensional poly(caprolactone-co-lactide) scaffolds. The aECM are based on porcine skin collagen type I (coll) in combination with a mixture of chondroitinsulfate (CS) or chemically modified high-sulfated hyaluronan (sHya, average degree of sulfation ~3).

Cultivation was performed either in expansion medium or osteogenic differentiation medium (300 μ M ascorbic acid, 10 mM β -glycerophosphate and 10 nM dexamethasone) for up to 28 days. For electrical stimulation cells were exposed to rectangular pulses (7 ms, 0.36 V/m, 10 Hz) for a duration of 4 hours followed by a 4 hours break while controls were placed in identical chambers but with unpowered coils.

Proliferation of cells was determined by assessment of lactate dehydrogenase activity which has been correlated with cell number using a calibration curve of defined cell numbers. Osteogenic differentiation was evaluated by biochemical analysis (ALP-activity) and on gene-expression level (RUNX-2, ALP, OPN, OC).

Short term effects such as Ca^{2+} influx and cell orientation have been analyzed in a special designed microscope chamber allowing live cell imaging.

RESULTS AND DISCUSSION

Results showed that aECM containing sHya decrease proliferation and enhance osteogenic differentiation represented by increases in ALP activity and gene-expression of several bone-related proteins (RUNX-2, ALP, OPN). Stimulation with electrical fields alone does not influence cell proliferation, but enhances osteogenic differentiation if osteogenic supplements were provided, showing additive effects by the presence of sHya [Figure 2].

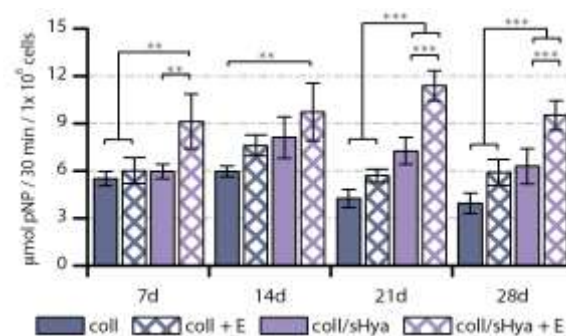


Fig. 2: Influence of selected coatings and electric fields on ALP activity of human MSCs

CONCLUSION

The results clearly show that microenvironment and physical environment in the form of electrical fields play a modulating role in human MSCs osteogenesis. Especially the combined treatment of cells exposed to coll/sHya coatings and electrical fields showed synergistic effects, so that this data provides fundamental information for a better understanding on bone regeneration, and thus support the future development of highly effective tissue engineered bone constructs.

REFERENCES

- Hess R. *et al.*, Cell Bioche Biophys. 64:223-32, 2012
- Hess R. *et al.*, Biomaterials. 33(35):8975-85, 2012

ACKNOWLEDGMENTS

The authors would like to thank Catgut GmbH for providing the scaffolds and the "BMBF" (03FPB00106) as well as the "TRR 67" for providing financial support to this project.



Influence of surface curvature on human mesenchymal stromal cell migration and differentiation

M. Werner^{1,2}, S. Blanquer¹, S. Haimi^{1,3}, D. Grijpma^{1,4}, A. Petersen^{2,5}

¹Dept. of Biomaterials Science and Technology, University of Twente, Netherlands

²Julius Wolff Institute, Charité—Universitätsmedizin Berlin, Germany

³Institute of Biosciences and Medical Technology (BioMediTech), University of Tampere, Finland

⁴Dept. of Biomedical Engineering, University Medical Centre Groningen, University of Groningen, Netherlands

⁵Berlin-Brandenburg Center for Regenerative Therapies, Germany

m.werner@student.utwente.nl

INTRODUCTION

The geometry of a microenvironment has demonstrated to impact cell behavior and potentially contribute to stem cell fate decision. It has been shown that 2D substrate geometries have an impact on cell traction forces and differentiation¹. Moreover, recent studies have indicated that substrate curvature influences tissue growth and cellular organization^{2,3}. However, a deeper insight into the role of geometrical cues is needed for the design of 3D biomaterial environments fostering tissue regeneration, e.g. in bone. In this study, we produced 3D substrates with specific curvatures by stereolithography (SL) and investigated the role of 3D surface curvature on the migratory and differentiation behavior of human mesenchymal stromal cells (hMSCs), hypothesizing geometry-induced alterations via changes in cytoskeleton organization.

EXPERIMENTAL METHODS

Cell culture substrates were designed containing convex and concave spherical, cylindrical and catenoid structures with principal curvatures of 1/125, 1/175, 1/250 and 1/375 μm^{-1} . The substrates were produced by SL using a poly(trimethylene carbonate) (PTMC)-based resin⁴. Substrates were homogeneously seeded with fluorescently stained bone-marrow derived hMSCs and cell migration in maintenance medium was observed up to 24 hours using time lapse multiphoton microscopy. The migration paths of $n > 13$ cells per structure were tracked and mean migration speed was determined. Groups were compared by two-way ANOVA with Tukey multiple comparison post-test ($p < 0.05$ for statistically significance). Furthermore, immunohistological stainings for osteocalcin, Runx2, and F-actin were performed after 10 and 3 days of culture in osteogenic medium (OM) respectively.

RESULTS AND DISCUSSION

hMSCs showed good attachment and migration behaviour on the PTMC substrate. Significantly faster migration was observed on concave spherical surfaces than on flat and convex surfaces. Migration speed on convex spheres showed a decreasing curvature trend towards the value on the flat surface (Fig 1).

Immunohistology revealed higher levels of Runx2 and osteocalcin for hMSCs on convex spherical surfaces compared to concave and flat surfaces (Fig 2).

Interestingly, higher signals for F-actin were found on concave compared to convex surfaces indicating higher cytoskeletal tension. This is in contrast to a previous study where a higher cytoskeletal tension was shown to promote osteogenic differentiation¹. Focal adhesion organization is currently under evaluation as it might help to explain our observations on stem cell

differentiation and migration due to its fundamental role in cell mechanics and cell-substrate interaction⁵.

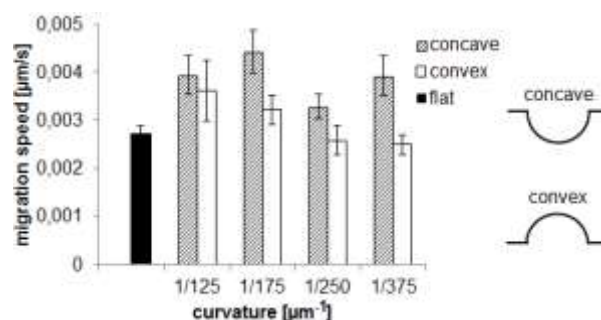


Fig 1. hMSC migration speed on a flat surface and on concave and convex spherical surfaces. Mean \pm standard error of the mean.

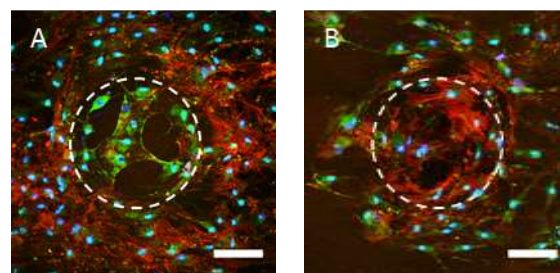


Fig 2. Immunohistological images of osteocalcin (green) in hMSCs on convex (A) and concave (B) spherical surface (1/175 μm^{-1}) after 10 days in OM (nuclei in blue, F-actin in red). Scale bar 100 μm . Dashed line highlights the spherical surface.

CONCLUSION

SL was proven to be suitable for the production of 3D substrates with specific geometrical features. Our results indicate that surface curvature is a relevant parameter in the control of hMSC migration and osteogenic differentiation. Further analysis of cells on cylindrical and catenoid structures will give insight on the influence of different curvatures in more complex geometries. Ultimately, the gained knowledge will help in the design of 3D scaffolds that promote specific cell behaviour (migration, differentiation) for improved tissue regeneration.

REFERENCES

1. Ruiz S. *et al.*, Stem Cells 26:2921–2927, 2008
2. Rumpler M. *et al.*, J. R. Soc. Interface 5:1173–1180, 2008
3. Joly P. *et al.*, PLoS ONE 8(9): e73545, 2013
4. Blanquer S. Macromol. Symp 334, 75–81, 2013
5. Huebsch N. *et al.*, Nature Materials 9:518–526, 2010

ACKNOWLEDGMENTS

We acknowledge financial support by the Berlin-Brandenburg Center for Regenerative Therapies.



Zinc Oxide Nanorod Interaction with Rat Mesenchymal Stem Cells

Giada Graziana Genchi^{1*}, Antonella Rocca¹, Virgilio Mattoli¹, Barbara Mazzolai¹, and Gianni Ciofani¹

¹Istituto Italiano di Tecnologia, Center for Micro-BioRobotics @SSSA, Viale Rinaldo Piaggio 34, 56025 Pontedera, Italy
giada.genchi@iit.it

Smart nanomaterials hold great promise in the manipulation of mesenchymal stem cells, due to their ability to promote peculiar cell behaviours by changing their properties upon physical stimulation. Here, we propose a toxicological investigation of piezoelectric ZnO nanorods on rat mesenchymal stem cells, first determining an optimal concentration for further future investigations.

INTRODUCTION

Zinc oxide nanostructures are receiving great interest in the scientific community thanks to their unique and tunable physical and chemical properties¹. Nonetheless, many contrasting results can be found in the literature about interactions between ZnO nanoparticles and cells², therefore the biocompatibility of ZnO nanostructures is still highly debated in nanomedicine.³ Here, we report on an investigation of the viability and proliferation of rat mesenchymal stem cells exposed to increasing concentrations of ZnO nanorods (NRs). Our findings show non-toxic effects up to 10 µg/ml of nanoparticles in the cell culture medium, encouraging further studies on the exploitation of ZnO NRs for the stimulation of stem cells.

EXPERIMENTAL METHODS

ZnO nanorods (773980 Sigma, 50 nm x 300 nm) were dispersed in 1 mg/ml gum Arabic (G9752 Sigma) at a concentration of 1 mg/ml with a short sonication (30 min, 20 W) in a 2510 Branson sonicator. This allowed NR stabilization in physiological solution through a non-covalent coating. The obtained NR dispersions were characterized by scanning electron microscopy in a FEI Helios 600 Dual-Beam system.

Rat mesenchymal stem cells (SCR027 Millipore) were cultured in low glucose Dulbecco's modified Eagle's medium with 10% fetal bovine serum, 100 IU/ml penicillin, 100 µg/ml streptomycin and 2 mM L-glutamine. Cells were maintained at 37°C in a saturated humidity atmosphere containing 95% air / 5% CO₂. Cells were seeded at a density of 6000 cell/cm² in 48-well plates, and incubated for 3 and 6 days with 0 (as control), 2, 5, 10, and 20 µg/ml of ZnO NRs. Cell proliferation was evaluated in terms of metabolic activity through the WST-1 assay (2-(4-iodophenyl)-3-(4-nitrophenyl)-5-(2,4-disulfophenyl)-2H-tetrazolium monosodium salt, BioVision). At each time point, cultures were treated with 200 µl of culture medium + 20 µl of the pre-mix solution for further 2 h and, thereafter, absorbance was read at 450 nm with a microplate reader (Victor3 Perkin Elmer).

Moreover, cellular adhesion and cytoskeletal conformation were evaluated following a 24 h incubation with 10 µg/ml ZnO NRs. Cytoskeleton/focal adhesion staining Kit (FAK100 Millipore) was used for the fluorescent staining of f-actin and vinculin,

following standard immunocytochemistry procedures that included incubation with an anti-vinculin primary antibody (1:200 diluted in 10% goat serum, GS) followed by incubation with a FITC-secondary antibody (AP124F Millipore, 1:400 diluted in 10% GS), 100 µM TRITC-phalloidin, and 1 µM DAPI for nucleus counterstaining. Samples were finally observed with a laser scanning confocal microscope (C2s Nikon).

RESULTS AND DISCUSSION

SEM investigation of ZnO NRs in gum Arabic denoted well dispersed nanostructures, with lengths in the range of 200-500 nm and diameter of 50-100 nm (Figure 1a). A qualitative study of cytoskeletal f-actin and vinculin (Figure 1b) revealed no significant changes in terms of cell morphology, cytoskeleton conformation, and nucleus shape in cells incubated for 24 h with 10 µg/ml NRs with respect to the control cultures (not shown). Finally, proliferation of MSCs evaluated in terms of metabolic activity by WST-1 assay did not result statistically different from the control cultures at concentrations up to 10 µg/ml within 6 days of treatment (Figure 1c). However, a significant decrement of cell proliferation was found for a dose of 20 µg/ml NRs ($p < 0.01$; ANOVA followed by Bonferroni's *post-hoc* test).

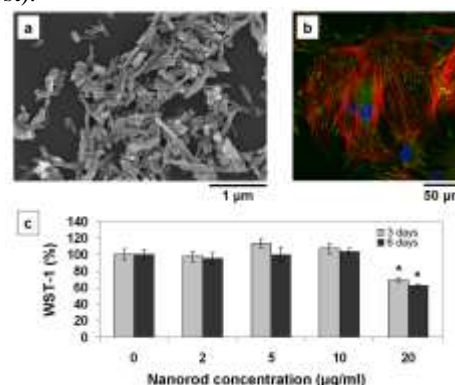


Figure 1: SEM imaging of ZnO NRs (a); confocal imaging of f-actin, vinculin and nuclei (respectively in red, green and blue, b); and WST-1 assay results at different NR concentrations and time points.

CONCLUSION

Although preliminary, our findings demonstrate no toxic effects of ZnO nanorods on rat mesenchymal stem cells, and encourage further investigations on the interaction of these nanostructures and MSCs. Future studies will be focused on the effects of ZnO NRs on the differentiation of MSCs, and on the exploitation of ZnO piezoelectric properties for cell stimulation.

REFERENCES

1. Ciofani G. *et al.*, Mat. Sci. Eng. C 32:341-347, 2012
2. Vandebriel R.J. *et al.*, Nanotechnol Sci Appl. 5:61-71, 2012
3. Xiong H.M., Adv. Mater. 25:5329-5335, 2013



Engineering Substrate Topography and Chemistry to Control Mesenchymal Stem Cell Function

Mohammed Khattak^{1,2}, John Hunt¹ and Raechelle A. D'Sa^{2*}

¹Clinical Engineering, Musculoskeletal Biology, Institute of Ageing and Chronic Disease, University of Liverpool, UK

^{2*}Centre for Materials and Structures, School of Engineering, University of Liverpool, UK, r.dsa@liverpool.ac.uk

INTRODUCTION

The ability to reliably control stem cell fate would have a significant impact for tissue engineering and regenerative medicine.¹ Various surface engineering strategies (chemical and topographic) have been exploited to direct stem cells differentiation into their various lineages. In general, mesenchymal stem cells (MSCs) can differentiate into adipogenic, chondrogenic, and osteogenic paths by varying the physical and topological features while keeping the chemistry constant. Topographically patterned surfaces have proven to be an important modality for controlling MSC function.² If the underlying topographically patterned surface had the same chemistry cell adaptation processes would play a major role and this would be independent on the differences in adsorbed proteins.³ Therefore, being able to control the underlying chemistry and topography would allow for the development of purpose specific cell regulating cues. We have compared differing nanotopographies and chemistries to ascertain configurations that have purposeful impacts on MSC growth and differentiation. Our aim was to explore the effects not only the size of the topographic features but also to see whether the underlying chemistry of the feature is an important parameter.

EXPERIMENTAL METHODS

Cell-substrata interactions were studied by using MSCs cultured on polymer-demixed nanotopographies. The nanofabrication system employed involves demixing of two immiscible polymers. Samples were fabricated using combination of three polymers (PMMA, PLA, and PCL) at different blend compositions, to produce polymer-demixed thin films with varying nanotopographies. The samples were analysed in terms of the surface topography, chemistry and wettability of each sample. Two representative sets of samples were chosen: one with similar topographies and differing chemistries and one with varying topographies and similar chemistries. Adult human MSCs, obtained from Lonza UK were used for the biological analysis. Following MSC culture and seeding onto each sample, analysis of cell proliferation, morphology and differentiation by immunostaining (using osteocalcin, collagen II and adiponectin markers) was performed at 7, 14 and 28 days.

RESULTS AND DISCUSSION

Polymer-demixing produces random topographic features, which is in contrast to uniform topographies produced by lithographic techniques. This technique advantageous as it is cost effective and able to produce features on large surface areas. Polymer demixed thin films from PMMA, PLA and PCL were used to fabricate differing nanoisland/nanopit topographies were. The feature size was controlled as a function of

the total polymer concentration in the spin-casting solution.

To the best of our knowledge, this is the first time that cell proliferation, morphology and differentiation has been investigated on these polymer-demixed samples. The results confirm that both physical and chemical characteristics can influence cell behaviour, specifically in terms of proliferation and differentiation. Cell proliferation was similar on the different samples studied at 7, 14 and 28 days. The morphology of the samples showed a shift from a fibroblast-like MSC morphology at 7 days, to a much more spindle-like morphology by 28 days. The images for the PCL/PLA sample are shown in Figure 1. The PCL/PLA sample had the highest levels of osteocalcin and collagen II compared with the PMMA/PLA and PCL/PLA samples. Furthermore, the PCL/PMMA sample showed the lowest production of adiponectin compared with the other blends. Representative images for staining of these proteins on the PCL/PLA surface are given in Figure 2.



Figure 1: Phase contrast images of MSCs on PCL/PLA sample at (a) 7 days (b) 14 days and (c) 28 days.



Figure 2: Immunofluorescence staining for (a) osteocalcin (b) collagen II and (c) adiponectin on PCL/PLA surfaces

CONCLUSION

Cells not only prefer nanotopographies, but the underlying chemistry also plays a significant role on differentiation. Modulation of the scale and pattern of chemically and topographically structures surfaces may allow for control of selective stem cell function regulation.

REFERENCES

1. Kulangara, K.; Leong, K. W. *Soft Matter*, 5 (21), 4072-4076, 2009.
2. Dalby, M. J.; et al. *Nat Mater*, 6 (12), 997-1003, 2007.
3. Lim, J. Y.; Donahue, H. J. *Tissue Eng*, 13 (8), 1879-189, 1, 2007.



Gel Aspiration-Ejection Fabricates Anisotropic Injectable Dense Collagen Gels with Controlled Microstructure for Regenerative Medicine

Showan N. Nazhat*, Neysan Kamranpour, Mark James-Bhasin, Amir K. Miri, Chiara E. Ghezzi and Benedetto Marelli

Department of Mining and Materials Engineering, McGill University, Canada. showan.nazhat@mcgill.ca

INTRODUCTION

Technological improvements in collagen gel fabrication are required to enable advances in the formation of physiologically relevant, cell seeded, injectable tissue-equivalent scaffolds for regenerative medicine. Strategies to modulate collagen gel fibrillar density (CFD) and meso-scale organization have been pursued to fabricate collagenous matrices with extracellular matrix-like features. Amongst others, the plastic compression (PC) technique fabricates dense collagen (DC) gels with CFDs ranging from 5 to 25 wt%; suitable in a range of tissues¹⁻⁴. However, PC does not allow for the formation of injectable anisotropic collagen gels. Indeed, the injection of collagen gels, and not of the soluble precursor solutions, is desired to effectively exert control over locally delivered cells.⁵ While cross-linking increases collagen gel mechanical properties and allows their extrusion through syringe needles, it compromises biocompatibility.

Herein, gel aspiration-ejection is presented to fabricate injectable dense collagen (I-DC) gels of anisotropically aligned nanofibrils, modulated CFDs, microstructure, and mechanical properties. I-DC maintained the viability and supported the accelerated osteoblastic differentiation seeded mice mesenchymal stem cells (m-MSCs).

EXPERIMENTAL METHODS

FDA approved tools were uniquely assembled to produce I-DC via gel aspiration-ejection (Fig. 1i). In brief, the core of the system is a manually operated pump (e.g., Angioplasty Inflation Device) used to generate a pressure differential and force the collagen gel into, and subsequently out of, densification needles of defined gauge sizes. Pre-fabricated highly-hydrated collagen gels were aspirated into the needles by applying negative pressure in the pump, resulting in gel fluid expulsion outside of the needle. Subsequent application of positive pressure in the pump, controllably ejected I-DC; aided by the introduction of a buffered solution within the pump chamber. I-DC CFD ranged from <5 to >30 wt% depending on needle gauge size.⁶

I-DC gels were characterised by scanning electron microscopy (SEM) (Fig. 1ii), non-linear laser scanning microscopy and tensile mechanical testing.



Fig. 1 I-DC production. (i) Left to right, interchangeable inflatable Vertebral Augmentation System needles, two luer-lock valves connected in series, a syringe and an Angioplasty Inflation Device. (ii) Image of I-DC gel (scale bar 4 cm). Inset, SEM micrograph showing collagen fibril alignment (scale bar 500 nm).

For m-MSC-seeded I-DC, murine MSCs (C57BL/6 mice, GIBCO) at 80% confluency were passaged and seeded at a density of 2×10^5 cells/mL pre gelling and densification. m-MSC seeded I-DC or DC (produced through PC⁽¹⁾) gels were cultured for up to 21 days. Osteogenic supplements consisted of 50 μ g/mL ascorbic acid, 50 mM β -glycerophosphate, and 1 μ M dexamethasone, with replenishment every 3 days. Seeded m-MSC viability, osteoblastic differentiation potential and mediated-mineralization of I-DC were investigated.

RESULTS AND DISCUSSION

There was an increase in I-DC CFD and corresponding extent of alignment with a decrease in needle gauge size. I-DC apparent modulus significantly increased with CFD ($p < 0.05$) (Fig. 2).

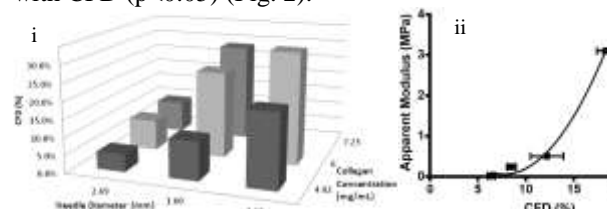


Fig. 2. I-DC CFD and apparent modulus. (i) CFD as a function of initial collagen concentration and gauge needle diameter. (ii) Apparent modulus (calculated from the linear phase of the tensile stress-strain curves) as a function of CFD.

m-MSC viability were maintained through gel aspiration-ejection, which induced preferential cell orientation (Fig. 3). Gene expression indicated that osteoblastic differentiation were accelerated in I-DC compared to DC (data not shown); increasing the extent of m-MDC-mediated-matrix mineralization.

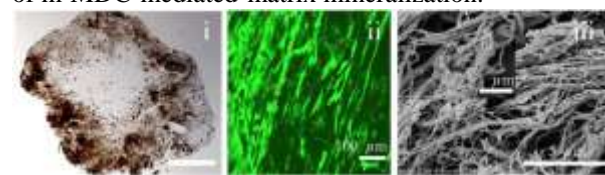


Fig. 3. m-MSC function in I-DC gels at day 21 in osteogenic medium. (i) Von Kossa stained histological sections indicating mineralization (scale bar 500 μ m). (ii) Confocal microscopy of viable m-MSCs (scale bar 100 μ m). (iii) SEM micrographs demonstrating mineralization (scale bar 5 μ m). Inset scale bar: 1 μ m.

CONCLUSION

Gel aspiration-ejection fabricates I-DC gels with controlled microstructure and creates unique opportunities in tissue engineering and regenerative medicine.

REFERENCES

1. Brown *et al.*, Adv Func. Mat. 2005, 15, 1762.
2. Ghezzi *et al.*, Biomaterials 2011, 32, 4761.
3. Marelli *et al.*, Biomaterials 2011, 32, 8915.
4. Ghezzi *et al.*, Biomaterials 2013, 34, 1954.
5. Macaya *et al.*, Adv Funct Mat 2011, 21, 4788.
6. PCT/CA2013/050615 (2013).

ACKNOWLEDGMENTS

NSERC, CIHR, CFI, Quebec MESRST, and McGill University Faculty of Engineering Gerald Hatch Faculty Fellowship are gratefully acknowledged.

Bone-like Apatite Deposition on Chemically Synthesized Collagen in Simulated Body Environment

Toshiki Miyazaki^{1*} Jin Furui¹ and Yuki Shirosaki²

^{1*}Graduate School of Life Science and Systems Engineering, Kyushu Institute of Technology, Japan,
tmiya@life.kyutech.ac.jp

²Frontier Research Academy for Young Researchers, Kyushu Institute of Technology, Japan

INTRODUCTION

Natural bone consists of organic collagen fiber and inorganic hydroxyapatite. Organic-inorganic hybrids are therefore expected to have high biological compatibility and similar mechanical performance to the natural bone. In addition, the hybrids are also expected for scaffolds supporting the regeneration of the bone tissue.

In order to construct such a hybrid, biomimetic process using simulated body fluid (SBF) or more concentrated solution has been proposed. Several researches have been reported concerning apatite formation on natural collagen through the biomimetic process¹. However, the animal-derived collagens still leave a risk for containing pathogens.

Recently, chemically synthesized collagen with triple helix structure similar to natural one has been developed as a safe biomaterial². Basic structure of the chemically synthesized collagen is amino acid sequence of proline (Pro) – hydroxyproline (Hyp) – glycine (Gly). Although apatite formation on the chemically synthesized collagen has been previously examined, highly supersaturated condition such as 1.5SBF with ion concentration 1.5 times those of SBF is needed to achieve apatite formation³. We recently revealed that immobilization with polyglutamic acid on the synthesized collagen is effective for inducing the apatite formation even in SBF. However process of the immobilization is still complicated.

In the present study, we attempted simple treatment of oxidation and Ca²⁺ incorporation for inducing the apatite formation in SBF.

EXPERIMENTAL METHODS

Films of chemically synthesized collagen were prepared by dropping the collagen solution on a glass plate and drying at room temperature. Then the films were subjected to the oxidation treatment in phosphate buffer solution containing TEMPO, sodium hypochlorite and sodium chlorite for 3 days. The films were then soaked in CaCl₂ solutions for 1 day and in SBF for 7 days. Surface structural changes were characterized by thin-film X-ray diffraction (TF-XRD) and scanning electron microscopic (SEM) observation.

RESULTS AND DISCUSSION

Figure 1 shows SEM photographs of the surfaces of synthetic collagen films without and with oxidation treatment, which were all treated with CaCl₂ and soaked in SBF for 7 days. Fine particles were observed for oxidized specimen, but not for non-oxidized one. The deposited particles were identified with low-crystalline apatite by TF-XRD.

The present results indicate that oxidation is effective for inducing the apatite formation. It is assumed that carbonyl groups are formed by oxidation of hydroxyl groups in hydroxyproline unit in the synthetic collagen. They would preferably attract Ca²⁺ and play a role in site for heterogeneous nucleation of the apatite.

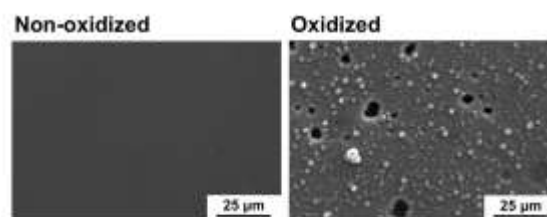


Figure 1 SEM photographs of the surfaces of synthetic collagen films without and with oxidation treatment, which were all treated with CaCl₂ and soaked in SBF for 7 days.

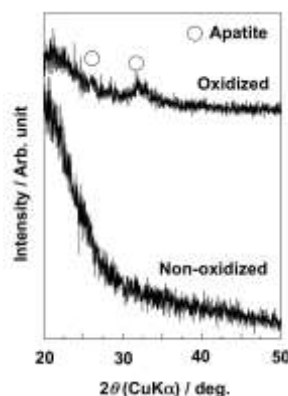


Figure 2 TF-XRD patterns of the surfaces of synthetic collagen films without and with oxidation treatment, which were all treated with CaCl₂ and soaked in SBF for 7 days.

CONCLUSION

It was found that oxidation treatment in an aqueous solution was effective for providing the chemically synthesized collagen with ability of the apatite formation in SBF. This process is expected for novel fabrication process of synthetic collagen-apatite hybrids.

REFERENCES

1. Girija E.K. *et al.*, Chem. Lett. 2002:702-703, 2002
2. Kishimoto T. *et al.*, Biopolymers 79:163-172, 2005
3. Kamitakahara M. *et al.*, Arch. BioCeramics Res. 5:210-213, 2005
4. Miyazaki T. *et al.*, Dent. Mater. J. 32:544-549, 2013



In Vivo Study of Resorbable Phosphate Glass fibre Reinforced Composite Bone Fracture Repair Plates

I. Ahmed^{1*}, A. Qureshi², A.J. Parsons¹, C.A. Scotchford¹, B.E. Scammell², C.D. Rudd¹

¹Division of Materials, Mechanics and Structures, Faculty of Engineering, University of Nottingham, Nottingham, UK

²Division of Orthopaedic and Accident Surgery, Queens Medical Centre, Nottingham, U.K

* Corresponding author (ifty.ahmed@nottingham.ac.uk)

INTRODUCTION

The main advantage of having a material that degrades is so that an implant would not necessitate a second surgical event for removal. In addition, biodegradation may offer other advantages. For example, a fractured bone fixated with a rigid metallic implant may refracture upon removal of the implant. This is because the bone does not carry sufficient load during the healing process. However, an implant prepared from biodegradable materials could be engineered to degrade at a rate that would slowly transfer load to the healing bone [1,2].

Recently, fully resorbable composite bone repair plates comprising a PLA matrix reinforced with phosphate glass fibres (PGF) were investigated. The aim of the study was to determine their in vivo degradation characteristics in an animal model and the adaptive bone response at the site of implantation.

EXPERIMENTAL METHODS

Poly lactic acid (PLA, PURASORB®PLDL 8038, PURAC, Netherlands) was reinforced with 38 ± 5 vol% phosphate based glass (PBG) fibres of formulation: $40\text{P}_2\text{O}_5 - 16\text{CaO} - 24\text{MgO} - 11\text{Na}_2\text{O} - 4\text{Fe}_2\text{O}_3$ (in mol%). Composites were produced by stacking PLA sheets sandwiched with unidirectional and random fibre mats, and pressed at 210°C for 15 minutes at 38 bar. Implant plates were produced according to the dimensions in Fig. 1. and gamma sterilised. Metal plates were used as controls made from surgical grade stainless steel of the same dimensions.

New Zealand White rabbits underwent surgical application of either the composite or metal plate to the anteromedial aspect of the intact right tibia using conventional stainless steel screws. The rabbits were divided into equal groups and the time points from surgery to sacrifice were 2, 6, 12, 26 and 52 weeks. Radiographs of both tibiae were taken immediately after surgery and at sacrifice. Retrieved tibiae from three of the five rabbits at each time point were subjected to flexural testing of the combined bone-plate construct with respect to the opposite unplated control tibia. Cortical thickness was analysed quantitatively using Nano CT imaging (composite only) and Scanning Electron Microscopy (SEM) of resin embedded axial slices of the bone-plate construct.

RESULTS AND DISCUSSION

No evidence of macroscopic inflammation at any time point of retrieval for the composite plates was observed. Bone formation was observed at the periphery of the plate and around the screws (Fig. 2.).

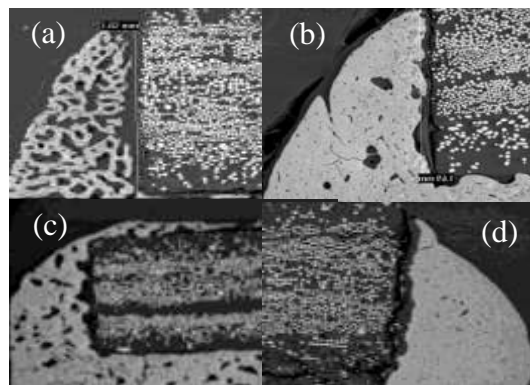


Fig. 2. Bone growth around the periphery of the plate at (a) 2, (b) 6, (c) 12 and (d) 26 weeks.

The mechanical properties showed a gradual decrease in properties of the composite plate itself at a rate at which the bone was able to adapt effectively. The metal plated bone properties showed a different trend; an increase to a peak followed by a decrease at later time points. SEM results revealed thinning of the cortex under the metal plate at later time points, which may be responsible for this decrease (Fig. 3). Despite the loss, the flexural biomechanical properties of the bone-plate construct remained higher than the control.

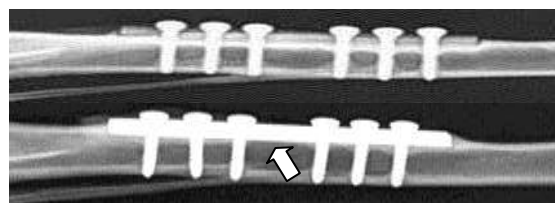


Fig. 3. 26 week X-rays revealed thinning of cortex under metal plate (bottom) but not for composite plate).

Nano CT analysis supported the X-ray and SEM findings in the composite plates.

Conclusions

The properties of the composite plate-bone construct were consistent for the period of the study, despite changes in bone density over the period. The metal-bone construct reached a peak before decreasing, with apparent loss of cortical thickness underneath the plate.

References

- [1] J.D. Bobyn et al, *Clin orthop relat r*, Vol. 274, pp 79-96, 1992.
- [2] R. Felfel et al, *J Mater Sci*, Vol. 47, pp 4884-4894, 2012.

Acknowledgements

This abstract presents research commissioned by the NIHR under the Health Technology Devices (HTD-432) program. The views expressed are those of the authors and not necessarily those of the NHS, the NIHR or the Department of Health.



Marine inspired biosilica-filled hydrogels for hard tissue repair

Pamela Walsh^{1,3}, Susan Clarke², Iossif Strehin³, Phillip Messersmith³

¹School of Chemistry & Chemical Engineering, Queen's University, Belfast, UK, pamela.walsh@qub.ac.uk

²School of Nursing & Midwifery, Queen's University, Belfast, UK

³Engineering Department, Northwestern University, Evanston, Illinois, USA

INTRODUCTION

There is currently a huge unmet need for suitable bone adhesives in trauma surgery¹. Emerging synthetic adhesive technologies using modified native chemical ligation (NCL) hydrogels offer an innovative biomimetic approach to repair soft tissue². This hydrogel system uses poly(ethylene glycol) (PEG) precursors that avail of both thioester and amide moieties to crosslink the polymer network with no cytotoxicity issues, as validated by the subcutaneous implantation of these gels in a mouse model. We have used these chemistries as a platform to develop a system that incorporates biosilica into the polymer network, to improve its mechanical and osteogenic properties for hard tissue repair. The therapeutic benefit of siliceous additives in bone cements (e.g. Apatech's Activase Shape™) and bone fillers (PerioGlas® 45S5) are gaining significant clinical interest in orthopaedics. The target application of this system in the first instance is fixation of bone fragments that are too small to be attached by conventional fasteners.

EXPERIMENTAL METHODS

PEG(NCL) hydrogels were prepared as per method described by Strehin *et al.*,². Biosilica was isolated from *Cyclotella meneghiniana* a unicellular microalgae that was sourced from the Mississippi River, USA. Silanisation chemistry was used to modify the surface of *C. meneghiniana* with amine (–NH₂) and thiol (–SH) terminated silanes. The biosilica was then incorporated into the PEG(NCL) hydrogel system. Outcome measures include surface analysis using XPS, compression testing to determine modulus of gels and cell viability using neutral red.

RESULTS AND DISCUSSION

XPS results (Table 1) confirm that functional groups (–SH and –NH₂) were successfully grafted onto the surface of *C. meneghiniana*.

Peak	Peak position binding energy (eV)	Atomic Concentration (%)		
		Unmodified	Modified AMINE	Modified THIOL
Si 2P	102.84	21.01 (±0.05)	11.40 (±0.65)	14.60 (±1.01)
O 1P	532.21	43.28 (±0.12)	30.24 (±0.74)	33.02 (±1.43)
N 1s	399.64	3.35 (±0.84)	11.01 (±0.34)	3.27 (±0.77)
S 2P	162.91	Nil	Nil	5.92 (±2.02)
C 1s	284.42	32.39 (±0.12)	47.58 (±0.44)	42.02 (±1.29)

Table 1: XPS Atomic Concentration data of *C. meneghiniana*

An increase in carbon concentration from 32.29 to 47.58 and 42.02% in functionalised *C. meneghiniana* is likely to be a result of the carbon chains in the silane linkers. The increase in the atomic concentration of sulphur from 0 to 5.92(±2.02)% in the –SH modified

sample and increase in nitrogen from 3.35(±.84) to 11.01(±.34)% –NH₂ modified sample indicates a successful silanisation reaction.

The addition of biosilica and biosilica modified with –SH and –NH₂ end groups showed improved mechanical properties. For example, the young's modulus increased from 132.7kPa (hydrogels only) to 189.7kPa (with unmodified Si) and 287.3kPa (Si modified –SH) after 24hrs. In addition, swell test data (Fig. 1) has shown hydrogels to swell to 16% their relative weight within the first 24hrs, before equilibrating to <3% of their original weight. Gelation times in these types of surgeries are important, as surgeons need to fix multiple fragments together. Our system was found to have a gelation time of <3 minutes when mixed at pH 7.4. No cytotoxicity was observed in either the bioSi-PEG(NCL) hydrogels, or biosilica fillers alone when tested *in vitro* in accordance's with ISO standards 10993-05

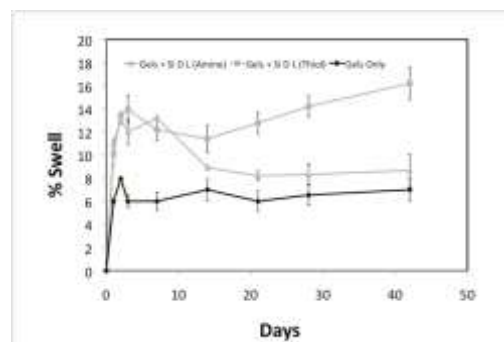


Fig 1: Swell Data of hydrogels with/without biosilica after 40 days in PBS at 37degC

CONCLUSION

Often the incorporation of an additional phase into hydrogels can disrupt the crosslinking network, causing excessive swelling and reduced strength. Our results have found no adverse effects to the addition of the biosilica phase. Preliminary cell results have found no toxicity with the use of natural biosilica. Work is ongoing to test the cytotoxicity and inflammatory response of the system *in vitro*.

REFERENCES

1. Farrar D.F., Int. J. Adhes Adhes 33:89-97, 2012
2. Messersmith, PB *et al.*, Biom Sc. 1: 2047-4830, 2013

ACKNOWLEDGMENTS

The authors would like to thank Marie Curie International Outgoing Fellowships from the EU for providing financial support to this project.



Elucidating the Biological Role of Soluble Silicon in Early Bone Mineralisation

Gurpreet Birdi^{1*}, Richard M. Shelton², James Bowen¹, Pola Goldberg Oppenheimer¹ and Liam M. Grover¹

¹School of Chemical Engineering, University of Birmingham, UK

²School of Dentistry, University of Birmingham, UK

g.birdi@bham.ac.uk

INTRODUCTION

The role of silicon in bone biology has been famously reported by Carlisle (1974)¹ and Schwarz et al (1973)². They demonstrated that when the levels of silica in an animal's diet were decreased to a critical level, bone and cartilage deformation resulted. Silicon at 0.5wt% *in vivo* has been shown to be present within the active mineralising osteoid regions, that is, the sites undergoing active calcification. This suggested that silicon may play a key role in the metabolism and stabilisation of the connective tissue present in bone and cartilage although its effect on calcification may arise indirectly through its interaction with matrix components. *In vitro* studies carried out by Reffitt et al (2003) demonstrated that type 1 collagen synthesis in human osteoblast-like cells was enhanced in the presence of 10-20µM orthosilicic acid³. Here we examine the evidence for a possible biological mechanism of orthosilicic acid (OSA), the soluble form of silicon influencing early bone mineralisation specifically focusing on its effect on mineral deposition and collagen fibril formation.

EXPERIMENTAL METHODS

MC-3T3s were cultured in Dulbecco's Modified Eagles Medium (DMEM) supplemented with 10% FBS, 2.5% HEPES, 1% penicillin/streptomycin and 2.5% L-glutamine. DMEM containing 0, 5 and 20µg/ml OSA was added after overnight attachment of the MC-3T3 cells. Cell mineralisation was determined using Alizarin red staining (Sigma Aldrich, UK) and Von Kossa assay. Collagen fibril formation was examined using atomic force microscopy (AFM), whereby collagen gels were prepared with a 2:1 ratio of DMEM and NaOH and various concentrations of sodium metasilicate were added to the gel solution and the pH adjusted to 8.0-8.5 with NaOH. TEM analysis was carried out to evaluate *in vitro* mineralisation within collagen fibres.

RESULTS AND DISCUSSION

The effect of OSA on cell mineralisation was carried out using Alizarin red staining and the Von Kossa assay, which indicate calcium and phosphate deposition respectively.

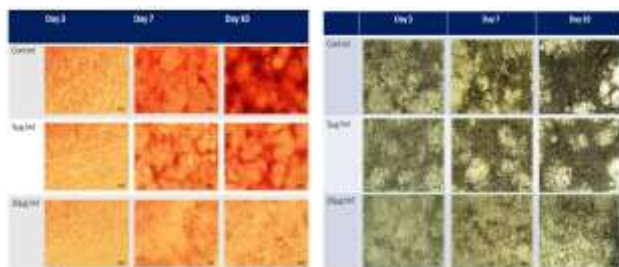


Figure 1: Calcium (Red) and phosphate (Black) deposition in MC-3T3s treated with or without OSA.

Cells without OSA and those exposed to 5µg/ml, showed an increase in the deposition of mineral. Cells treated with 20µg/ml OSA, however, showed to inhibit cell

mineralisation (Figure 1) suggesting that initial mineralisation is OSA concentration dependent.

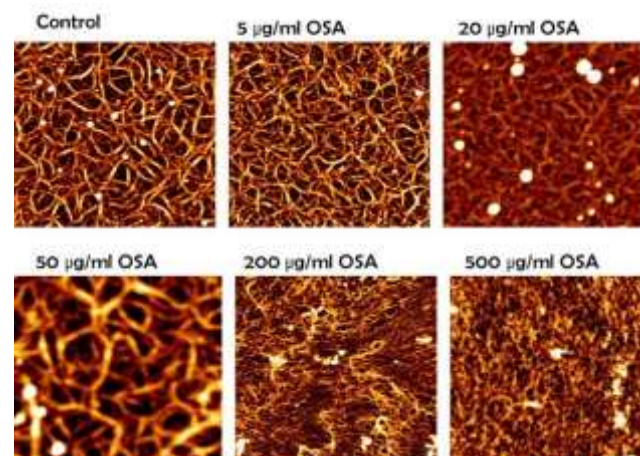


Figure 2: AFM images of collagen fibres produced in the presence of various concentrations of OSA.

The effect of collagen fibril formation *in vitro* was evaluated in the presence of various concentrations of OSA. Collagen gels made with 5-50µg/ml of OSA showed a more intricate network of fibers when compared to gels made without OSA (Figure 2). At higher concentration however, OSA led to the degradation of the gel, indicating that OSA in lower concentrations modifies the collagen fibril network, however, in supra-physiological concentrations fibril formation is inhibited. TEM demonstrated mineral deposition within the fibers when gels were incubated with 5µg/ml OSA for 21 days (Figure 3).

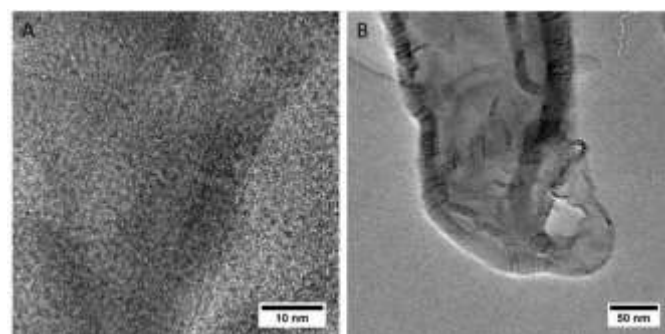


Figure 3: TEM images, illustrating *in vitro* mineralisation within collagen fibres in the presence of OSA (B). No mineralisation was seen in non-treated samples (A).

CONCLUSION

Here we have evaluated the effect of OSA on collagen fibril formation and *in vitro* mineralisation. Increasing OSA concentration results in the development of a complex collagen fibril network up to supraphysiological OSA concentrations when the fibril network becomes fragmented. TEM images demonstrate that 5µg/ml OSA aids in mineral deposition within collagen fibers.

REFERENCES

¹Carlisle, E.M., 1976. *The Journal of nutrition*, 106(4), pp.478-84. ²Schwarz, K., 1973. *Proceedings of the National Academy of Sciences of the United States of America*, 70(5), pp.1608-12. ³Reffitt, D., et al., 2003. *Bone*, 32(2), pp.127-135. ⁴Kadler, K.E., et al., 1996. *The Biochemical journal*, 316, pp.1-11.

Innovation and Product Development – Example of a leading medical device company

Yves Bayon, Michel Thérin

Covidien – Sofradim Production
michel.therin@covidien.com

Ideas and innovating concept proposals of medical devices are most often the starting point of any new product development projects. They may originate from any company employees or are submitted by external third parties. They are evaluated by a series of internal processes, more or less exclusive, but should fit a number of prerequisites as suggested by the following questions:

Do they align with the current priority of the company, in terms of new product development?

Do these proposals address specific unmet clinical needs which may improve the quality of life of patients and/or facilitate the treatment of patients by the medical staff?

What is the maturity and complexity level of the technology behind ideas / concepts? What are the overall project cost and the project timeline from the concept to the launch phase (time considerations beyond of the technical development of the new product: handoffs, funding, regulatory, clinical, marketing...)?

What would the adoption by clinical users – and/or patients be? Preliminary Voice of Customers (VOC) and Voice of Technology (VOT) should be carried out. Very early, ideas / concepts should be evaluated by clinical users such as surgeons (at least 5 from different countries), by submitting questionnaires and/or presenting prototypes.

What is the market potential? What is the net present value (NPV) and anticipated return on investment? The pricing strategy should more and more rely on health economics analysis for better acceptance of the products by users and/or better reimbursement.

What is the current status of the intellectual property (e.g. list of issued patents and patent applications; external vs internal intellectual property; freedom to operate)?

What is the regulatory environment, in Europe, the US, emerging countries such as China, India...?

What is the current product and under development project portfolio of the competition?

What are the company staff capabilities for the technical development of the ideas / concepts, but also for their clinical evaluation, manufacturing, marketing, sales...? The last point is extremely critical. The company may have at the end a great device, but will make no money from it since it does not have the appropriate sales channels.

What is the risk of executing the translation of ideas/concepts vs not executing it?

The first selection stages of ideas / concepts are generally quite informal with short circuits decision, at a Director / Vice-President level.

At the end of the first evaluation round, the idea or concept should not stay as simple abstract ideas. Preliminary technical and performance proofs of concept should be brought for selection as a New Product Development (NPD) project. This is commonly carried out during the pre-concept phase for any new internal initiatives with limited available budget. Additional funding may come from national (e.g. in France, ANR, FUI grants) and European subventions (e.g. H2020 grants). Any external third parties sharing proposals should reach a similar level of proof or even greater.

The transfer of ideas / new concepts into NPD projects is decided by the portfolio management team, composed of the leadership / senior leadership team members, representing the key functions of project development such as R&D, Medical Affairs, Marketing. The decision is not taken on the sole aspects of ideas / concepts, but essentially on its economic profitability for the company. Other criteria leverage the decision: mission, vision and culture, product mix strategy, fiscal “health” of the company, current portfolio and development progress of NPD.

Any selected NPD projects must then progress according to contracts and schedules, agreed with all stakeholders, with sufficient budget to bring the product to its commercialization, in the shortest possible time. Project reviews are planned after each phase, concept (proof of concept), feasibility (prototype selection), development (manufacturing process definition), qualification (safety and efficacy demonstration, process validation and regulatory filing) and launch (product branding and commercialization). Stop and go decisions are taken after the end of each phase. Intermediate reviews of projects can be planned according to the progress of projects.

Other innovation processes coexist in the company such as the funding of start-up / small companies for their innovation by corporate venture capital (VC).

The innovation and product development process will be illustrated by a couple of examples developed by the Trevoux site of Covidien (Sofradim Production), specialized in the development and manufacturing of commercial medical devices for hernia repair.

Launching and Building a Science-Based Business

Iain McDougall

Taragenyx, Caledonia House, Lawmoor Street, Glasgow, G5 0US, Scotland, iain@taragenyx.com

Despite the dire headlines, innovative new medtech businesses are still launching and venture capitalists are still investing in exciting new companies, even those at the early stage.

Iain McDougall CEO of 1-year old Orthopaedic biotech company Taragenyx explains what it's really like to be an early-stage entrepreneur in today's start-up world at the intersection of medicine and technology.

A fascinating and informative walk through launching and building science based business, Iain discusses:

- Getting started - some science, a patent, and a couple of crazy founders
- Getting invested - 24 hours and \$2million
- Getting hired - building an A+ team when you can't actually afford them
- Getting Customers - convincing people your technology might actually change the world

Getting through - life on the entrepreneurial roller coaster. It's not what you think..

Iain McDougall is a serial medicine and technology entrepreneur with demonstrated success of founding, developing and restructuring businesses through major value inflexion points. Currently founder and CEO of Taragenyx, a venture funded orthopaedic biotechnology company developing bio-regenerative implants for the orthopaedic, dental, and general surgery markets. Prior to his venture activities Iain was partner-track engagement manager with one of the world's top-tier global strategy consulting firms. Utilising his core strengths in execution strategy, market development and virtuoso team leadership, he specialised in building and leading high impact teams to accelerate complex technology ventures delivering high value opportunities.



Chitosan-silica hybrids for biomedical applications

Christos Pandis^{1,2*}, Estela Pérez Roman, Sara Trujillo, Christos Chatzimanolis-Moustakas, Sotiria Kriptou, Apostolos Kyritsis and José Luis Gómez Ribelles^{2,3}

¹Physics Department, National Technical University of Athens, Greece

²Centro de Biomateriales e Ingeniería Tisular, Universitat Politècnica de València, Spain

³Ciber en Bioingeniería, Biomateriales y Nanomedicina (CIBER-BBN), Spain

*pandis@mail.ntua.gr

INTRODUCTION

Chitosan (CHT) is a linear polysaccharide derived from the deacetylation of chitin. The biocompatibility, biodegradability, antibacterial activity, non-toxicity and cellular compatibility of chitosan have attracted the scientific research interest in the latest two decades for its use in biomedical applications¹. Nevertheless, the mechanical properties of chitosan in the hydrogel form can be insufficient for many applications. Thus, reinforcement with a stiff inorganic phase appears as an appealing strategy to prepare chitosan hybrids with enhanced mechanical properties. In this work, chitosan-silica hybrids were produced using sol-gel reactions for the synthesis of the inorganic network. Tetraethylorthosilicate (TEOS) and 3-glycidoxypopyl trimethoxysilane (GPTMS) were used as the silica precursors. GPTMS served also as the coupling agent between the free amino groups of chitosan and the silica network. The morphology, swelling ability and the thermal properties of the hybrids were studied using various techniques. The cytotoxicity of the hybrids was also assessed.

EXPERIMENTAL METHODS

Chitosan-silica hybrids were produced by employing sol-gel reactions using TEOS and GPTMS as the silica precursors. The GPTMS to TEOS percentage was kept constant and equal to three while varying the GPTMS/TEOS molar ratio with respect to chitosan. The primary CHT solution consisted of 1.5% chitosan dissolved in 1% acetic acid. Then GPTMS was added and left for stirring for 16h. TEOS was prehydrolyzed in aqueous solution using HCl as catalyst and added in the CHT/GPTMS solution. After 1h of stirring the solution was placed in petri dishes. The hybrid membranes were aged for 1 week at room temperature and then for 5 days at 50°C. Furthermore, pure CHT, pure GPTMS, CHT-GPTMS and GPTMS/TEOS films were prepared for comparison.

RESULTS AND DISCUSSION

The morphology of the hybrids was studied by a scanning electron microscope (SEM) equipped with energy-dispersive X-ray spectroscopy analysis. The results revealed the uniform distribution of the inorganic phase.

The influence of the incorporation of the inorganic phase was assessed by swelling measurements into water using gravimetric techniques providing also valuable information regarding the structure of the prepared hybrids. The swelling ability is suppressed by

the addition of GPTMS providing evidence of its crosslinking behaviour.

The thermal degradation of the hybrids was studied using thermogravimetric analysis (TGA) and the thermal transitions were followed by differential scanning calorimetry (DSC). A glass transition was observed below room temperature for the hybrids with higher GPTMS content and was attributed to the presence of a distinct GPTMS phase. The latter transition was further studied together with the dielectric relaxations of chitosan by employing dielectric relaxation spectroscopy (DRS) in a wide temperature and frequency range having characteristics of a primary dielectric mechanism.

Previous studies using nuclear magnetic resonance (NMR) have shown that the epoxy ring of GPTMS is opened and linked to the amino groups of chitosan at a yield of 20%². In this work the segmental motion of polymerized GPTMS phase in the prepared hybrids was probed and compared to pure GPTMS and GPTMS/TEOS samples showing that excess of GPTMS leads to the formation of a distinct GPTMS phase.

Finally, the cytotoxicity assay showed that the prepared hybrids are not cytotoxic irrespectively of the GPTMS content. The prepared materials could be used for the reinforcement of already prepared scaffolds using novel strategies proposed by our group that lead to porous structures with two co-continuous phases³.

CONCLUSION

Chitosan-silica hybrids were prepared using sol-gel reactions for the synthesis of the inorganic phase. GPTMS served as a crosslinker for the chitosan chains as well as the coupling agent between the inorganic and the organic phase. The physicochemical properties of the hybrids could be modified by varying the silica precursors content. The non-toxicity of the above hybrids makes them excellent candidates for their use for porous membranes fabrication or as a reinforcement of scaffolds for tissue engineering approaches.

REFERENCES

1. Dash M. *et al.*, Prog Polym Sci. 36:981-1014, 2011
2. Connell LS. *et al.*, J Mater Chem B. 2:668-680, 2014
3. Demirdögen B. *et al.*, J Biomed Mater Res A, 2013

ACKNOWLEDGMENTS

The research project is implemented within the framework of the Action «Supporting Postdoctoral Researchers» of the Operational Program "Education and Lifelong Learning" (Action's Beneficiary: General Secretariat for Research and Technology), and is co-financed by the European Social Fund (ESF) and the Greek State



Triphasic scaffolds for the regeneration of the bone-ligament interface

G. Criscenti^{1,2,3}, A. Di Luca¹, A. Longoni¹, P. S. B. de Sousa¹ and L. Moroni^{1,4}

¹Department of Tissue Regeneration, University of Twente, The Netherlands

²Research center "E. Piaggio", Faculty of Engineering, University of Pisa, Italy

³Istituto di Ricerca Traslazionale per l'Apparato Locomotore - Nicola Cerulli – LPMRI, Italy

⁴Department of Complex Tissue Regeneration, Maastricht University, The Netherlands.

g.criscenti@utwente.nl

INTRODUCTION

One of the main issues in tissue engineering (TE) is the fabrication of scaffolds that closely mimic the structural properties of the tissues to be regenerated. This is of pivotal importance in the case of graded tissues such as the bone-ligament interface. In this work, we propose the combination of electrospinning (ESP) [1] and 3D fiber deposition (3DF) techniques [2] to create triphasic scaffolds for the bone-ligament interface. By combining these techniques, poly-caprolactone (PCL) and poly lactic-co-glycolic acid (PLGA) based scaffolds with a graded variation of their physicochemical and mechanical properties were fabricated.

EXPERIMENTAL METHODS

Scaffolds were fabricated through a two-step process. Initially, PCL (average Mn ~45000) 3DF scaffolds were manufactured with a Bioscaffolder device (SysENG, Germany). The polymer was put in a stainless steel syringe and heated at $T = 100\text{ }^{\circ}\text{C}$. A nitrogen pressure of 5 Bars was applied to the syringe through a pressurized cap when the molten phase was achieved. The fiber diameter d_1 , the fiber spacing d_2 , the layer thickness d_3 and the number of deposited layers were set at 250 μm , 700 μm , 150 μm and 4, respectively. The scaffold architecture was determined by a 0-90 layer configuration where fibers were deposited with 90° orientation steps between successive layers. The plotting speed was changed within 275–325 mm/min. The PCL 3DF scaffolds were partially covered with a paper foil, fixed on a PDMS and positioned under an ESP jet. An aligned electrospun fibrous network was fabricated from a 4% (w/v) PLGA solution in 1,1,1,3,3,3-hexafluoro-2-propanol (HFIP). The voltage was 20 kV, the air gap was 20 cm, the flow rate was 1 ml/h, and the needle used had a diameter of 0.8 mm. The ESP fiber density was determined as the time frame used during fabrication, which was set to 90 minutes. The porosity of 3DF scaffolds was calculated following a theoretical approach [2]:

$$P = 1 - \frac{\rho}{4} \cdot \frac{d_1^2}{d_2 \cdot d_3}$$

The porosity of ESP and mixed regions was experimentally measured by measuring the ratio between the apparent density of the scaffold and the specific density of the bulk material. Human mesenchymal stem cells (hMSCs) were seeded on the triphasic scaffolds at a density of 1.4×10^5 cells/cm² and their metabolic activity assessed after 1, 5 and 7 days. After 7 days in proliferation medium and 7 days in mineralization one, metabolic activity and alkaline phosphatase (ALP) staining were measured.

RESULTS AND DISCUSSION

The scaffolds were characterized by three different regions: the 3DF, the ESP and the mixed parts (Fig. 1a).

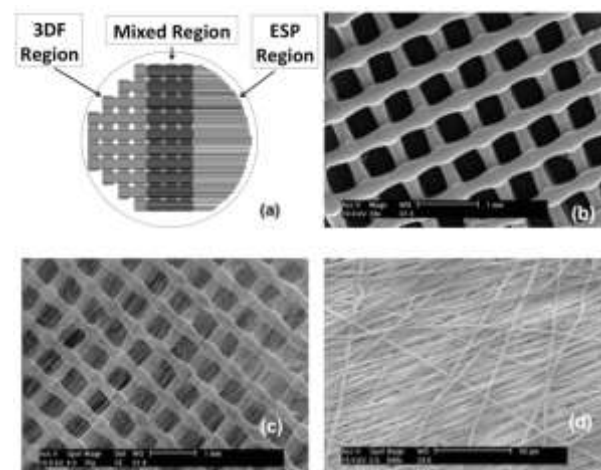


Fig. 1 – Triphasic scaffold structures

SEM analysis revealed a fiber diameter of $208 \pm 7.1\text{ }\mu\text{m}$, a fiber spacing of $734 \pm 15\text{ }\mu\text{m}$, and a layer thickness of $202 \pm 9\text{ }\mu\text{m}$ for the 3DF region (fig. 1b). The fiber diameter of the ESP network was $0.588 \pm 0.02\text{ }\mu\text{m}$ (fig.1c-d). This corresponded to a porosity of $77 \pm 1.7\%$ for the 3DF region, and to a porosity of $95.9 \pm 1.6\%$ for the ESP one. The porosity of the mixed region was measured as $68.9 \pm 3.1\%$. The scaffolds were interconnected porous structures and no layer delamination phenomenon occurred. An increase of the metabolic activity was measured within culturing time. A partitional analysis on the different areas of the triphasic scaffolds showed a similar trend after 7 days in differentiation medium. ALP staining showed a heterogeneous production of the protein in the scaffold, thus suggesting that our triphasic graded scaffold design may have potential for the regeneration of the bone-ligament interface.

CONCLUSION

The integration of ESP and 3DF represents a promising technique for the realization of scaffolds for interface TE applications, because it allows mimicking the structural biological environment through the combination of different biomaterials at different scales.

REFERENCES

1. Moroni L. *et al.*, Adv. Funct. Mater. 18:53–60, 2008
2. Woodfield *et al.*, Biomaterials 25: 4149–61, 2004

Cellular Responses to Elastin-Collagen Composite Scaffolds

D. Bax^{1*}, C. Grover¹, P. Lee², R. Farndale³, A. Weiss², S. Best¹, R. Cameron¹

¹Department of Materials Science and Metallurgy, University of Cambridge, UK

²School of Molecular Bioscience, University of Sydney, Australia

³Department of Biochemistry, University of Cambridge, UK

INTRODUCTION

Freeze-drying is a well-established technique for the fabrication of 3-dimensional (3D) porous collagen scaffolds [1]. Despite their excellent mechanical properties often these scaffolds do not recreate the elastic recoil of many tissues. Elastic fibers are key structural components of such tissues providing this recoil and resilience. We therefore explored the inclusion of elastin into porous 3D collagen scaffolds to impart flexibility to the resulting material. In addition to its mechanical properties elastin elicits biochemical responses such as cellular attachment, spreading, chemotaxis, proliferation and differentiation [2]. To elucidate the cellular cues that elastin could bestow on the resulting collagen-elastin composite scaffold we studied cell interactions with elastin.

EXPERIMENTAL METHODS

Scaffold preparation; Collagen +/- elastin (1%(w/v) total protein) was swollen in 0.05M acetic acid at 4°C overnight then homogenized. The suspensions were freeze-dried (VirTis adVantage benchtop (Biopharma Process Systems, UK)) at -0.9°C/min to a final temperature of -26°C for 4h. The ice phase was sublimed at 80mTorr, 0°C for 27h.

Scaffolds were chemically cross-linked with 1.150g EDC and 0.276g NHS per gram of scaffold in 75% v/v ethanol for 2h. The scaffolds were extensively washed with deionised water then freeze-dried.

Tensile testing; Rectangular sections with a cross sectional area of ~7x4mm were hydrated in deionised water for 1 h then extended at 6 mm min⁻¹ to failure. The Young's modulus (*E*), stress at 20% strain (σ), and failure strain were calculated from the stress-strain plot.

SEM; Cross-sections of scaffolds were mounted on stubs and sputtered with platinum then imaged with a JEOL-820 scanning electron microscope at 10 kV.

Tropoelastin constructs (fig. 2a) were expressed in the pET3d vector in *E. coli* BL21 (DE3) and purified by RP-HPLC.

Cell attachment analysis; Tissue culture wells were pre-coated with recombinant proteins then 2.5x10⁴ cells added for 45 min and the bound cells quantified.

RESULTS AND DISCUSSION

SEM showed that insoluble (IE) and soluble (SE) elastin were incorporated into the porous 3D structure of collagen based scaffolds (fig 1). Inclusion of IE and

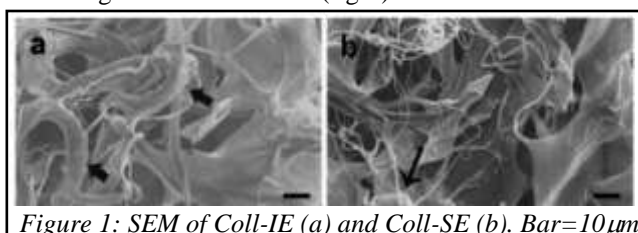


Figure 1: SEM of Coll-IE (a) and Coll-SE (b). Bar=10μm

SE reduced the stiffness of the collagen-based scaffolds showing decreased stress at 20% strain and decreased Youngs modulus (table 1). Therefore these composites possess mechanics that resemble native elastic tissues such as skin (Youngs modulus=5-12kPa).

	Strain at failure	Stress (kPa)	Youngs modulus (kPa)
Coll	0.32±0.01	7.8±0.9	81±8
Coll-IE	0.33±0.03	4.5±0.8	45±9
Coll-SE	0.41±0.02	2.6±0.2	27±2

Table 1: Elastin reduces the stress and Youngs modulus of collagen-based scaffolds

The mechanism of cell adhesion to elastin was studied to determine the biochemical properties that elastin incorporation imparts to collagen scaffolds. Cells adhered to recombinant tropoelastin constructs with the following affinity WT>N18>N10 (fig. 2b). This identified 2 binding sites on elastin; 1) a site beyond domain 18 which is accounted for by the reported C-terminal RKRK cell-binding motif; 2) A novel site between domains 10 and 18. Integrin $\alpha_v\beta_5$ inhibition prevented cell binding to N18, identifying this as a cellular receptor for this region (fig 2c). Therefore elastin incorporation can impart 2 cell-binding sites to collagen scaffolds and cell-adhesion via a distinct mechanism compared to a pure collagen scaffold.

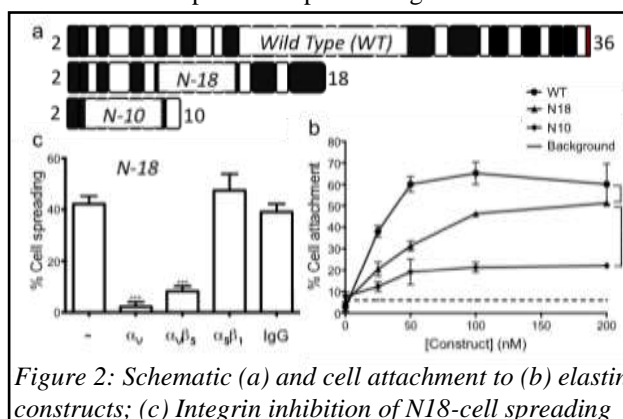


Figure 2: Schematic (a) and cell attachment to (b) elastin constructs; (c) Integrin inhibition of N18-cell spreading

CONCLUSION

Elastin reduces the stiffness of 3D collagen scaffolds and can bind to cells via integrin $\alpha_v\beta_5$.

REFERENCES

1. Davidenko N *et al.*, Acta Biomater. 6:3957-68, 2010
2. Almine J. *et al.*, Chem. Soc. Rev. 39:3371-79, 2010

ACKNOWLEDGMENTS

Funding was provided by the EPSRC, the European Research Council and the Australian Research Council



Chitosan-siloxane porous scaffold for nerve reconstruction

Yuki Shirosaki^{1*}, Satoshi Hayakawa², Akiyoshi Osaka², José D. Santos³, Ana C. Maurício^{4,5}, Stefano Geuna^{6,7}

^{1*}Frontier Research Academy for Young Researchers, Kyushu Institute of Technology, Japan, yukis@lsse.kyutech.ac.jp

²Graduate School of Natural Science and Technology, Okayama University, Japan

³CEMUC, Departamento de Engenharia Metalúrgica e Materiais, Universidade do Porto, Portugal

⁴Departamento de Clínicas Veterinárias, Instituto de Ciências Biomédicas de Abel Salazar and ⁵Centro de Estudos de Ciência Animal, Instituto de Ciências e Tecnologias Agrárias e Agro-Alimentares, Universidade do Porto, Portugal

⁶ Neuroscience Institute of the Cavalieri Ottolenghi Foundation and ⁷Department of Clinical and Biological Sciences, University of Turin, Italy

INTRODUCTION

Peripheral nerve injuries have a high incidence in today's society¹⁾. Despite recent progress in peripheral nerve trauma management, recovery of functional parameters is usually far from normal and thus much attention is being paid to nerve regeneration research. In a previous study^{2,3)}, flexible and biodegradable chitosan- γ -glycidopropyltrimethoxysilane (GPTMS) hybrid membranes exhibited better cytocompatibility in terms of osteoblastic cells than chitosan membrane. Porous chitosan hybrid membranes, derived by freeze-drying the hybrid gels, showed that the cells were attached and proliferated both on the surface and into pores. In this study, new biodegradable nerve guides from these chitosan hybrids were prepared and their biocompatibility was examined for the nerve regeneration by using animal model.

EXPERIMENTAL METHODS

A total of 25 adult male Sasco Sprague rats (Charles River Laboratories, Barcelona, Spain) weighing approximately 250 g at the start of the experiment were used. In Group 1, animals recovered from axonotmesis sciatic injury without any other intervention (Crush). In Group 2, axonotmesis sciatic nerve was infiltrated with a suspension of 1 250-1 500 MSCs (total volume of 50 μ L) (CrushCell). In Group 3, axonotmesis lesion of 3 mm was wrapped with a porous chitosan hybrid membrane covered with a monolayer of non-differentiated human MSCs (CrushChCell) and in Group 4, axonotmesis lesion of 3 mm was wrapped with a porous chitosan hybrid membrane (CrushCh). A standard crush injury was performed by a non-serrated clamp, exerting a constant force of 54 N for a period of 30 seconds, 10 mm above the bifurcation into tibial and common peroneal nerves, inducing a 3 mm axonotmesis lesion. All animals were tested preoperatively (week 0), and every week until week 8 and then every two weeks until the end of the 12-week follow-up time. Motor performance and nociceptive function were evaluated by measuring extensor postural thrust (EPT) and withdrawal reflex latency (WRL), respectively.

RESULTS AND DISCUSSION

The withdrawal reflex latency (WRL) test was used to assess nociception. In the first 2 weeks post sciatic crush injury, the WRL response was absent (i.e. lack of withdrawal within 12 seconds; the cutoff time to prevent thermal damage to the paw) in a large majority of animals. With time, the WRL improved in all animals and at week 12, the WRL values were

2.00 \pm 0.00, 1.29 \pm 0.18, 1.17 \pm 0.17, and 3.3 \pm 0.54 seconds, in Crush, CrushCell, CrushChCell, and CrushCh, respectively. A significant difference was observed between the groups in WRL data with delayed recovery in WRL performance in CrushCh compared to the other three groups. The sciatic nerve crush caused severe muscle force deficit in the affected limb immediately post-surgery. At week 1, the percentage of motor function deficit for the right hindlimb reached over 90% in all groups. A gradual recovery of the right hindlimb extensor postural thrust occurred during the 12-week survival time in all groups, so that at week 12, the EPT deficit in the affected side, although not fully reestablished, was reduced to only 4.16 \pm 5.60, 2.79 \pm 0.41, 3.24 \pm 0.42, and 7.43 \pm 3.58 in Crush, CrushCell, CrushChCell and, CrushCh, respectively. EPT performance was similar in all groups, although at the end of the 12 weeks of recovery, the EPT values were lower in CrushCell and CrushChCell groups. Fiber regeneration was good in all experimental groups, though the regenerated nerves presented smaller myelin fibers than the normal nerves without injury. Myelinated fiber density and total number were significantly higher than in controls in all nerve regeneration groups except for the CrushCh group. Axon and fiber diameter and myelin thickness were significantly lower in the 3 experimental groups compared to control group (normal sciatic nerve without injury). Analysis of the inter-group variability among regenerated groups, showed that CrushCh group had significantly lower fiber density and fiber total number and a higher myelin thickness while no statistically significant differences were detectable for the remaining histomorphometrical predictors of nerve regeneration (fiber diameter and axon diameter).

CONCLUSION

The porous chitosan hybrid membranes alone may represent a very promising clinical tool in peripheral nerve reconstructive surgery. Thus, human umbilical cord human MSCs can be expanded in culture and induced to form several different types of cells. They may therefore in future experiments, be tested as a new source of cells for cell therapy, including targets such as peripheral nerve in more serious lesions (neurotmesis with and without loss of nerve tissue) and muscle.

REFERENCES

- Schlosshauer *et al.*, *Neurosurg* **59**, 740-747 (2006).
- Shirosaki *et al.*, *Biomaterials* **26**, 485-493 (2005).
- Shirosaki *et al.*, *Chem Eng J*, **137**, 122-128 (2008).



Nano-spun Meshes as Scaffolds for Regeneration and Stiffness Remodelling of Pelvic Floor Soft Tissues

Mahshid Vashaghian¹, A. Ruiz Zapata², B. Zandie Doulabi³, T.H. Smit²

1. Obstetrics & Gynaecology, 2. Orthopedics, VU University Medical Center, Amsterdam, The Netherlands, 3. Oral cell biology, (ACTA), The Netherlands, M.vashaghian@vumc.nl

INTRODUCTION

In pelvic floor disorders, like pelvic organ prolapse, a mesh-like implant is used to restore the function of damaged tissues. Post-operational problems like erosion or adverse body response may happen which are directly a function of the mesh nature. Cell-based therapies are new disciplines for regeneration of the organs with the use of host cells and biomaterials as scaffolds for supporting cells in-growth. Electrospinning is a straightforward and inexpensive method for producing scaffolds with high surface area-to-volume ratio and ultra-thin fibrous structure. Owing to their architecture and isotropic orientation, non-woven meshes are well-known for their superior properties in resembling natural ECM, cellular adhesion and proliferation, therefore good candidates for regeneration of soft tissues as found in pelvic floor, for mesh-based surgical treatments.

AIM

To evaluate the potential of electrospun scaffolds for regeneration of soft pelvic tissues regarding biocompatibility, cell-scaffold interactions, matrix deposition, micro-structure, mechanical properties, and stiffness remodelling of the matrix.

EXPERIMENTAL METHODS

Polymeric solutions of PCL/gel 15% (70:30), PLGA/PCL 15% (75:25) and Nylon 20% were prepared in TFE, CHCl₃:MeOH and Formic Acid respectively. The solutions were electrospun horizontally into nanofibers and collected on aluminium foil (the processing conditions are not shown in the abstract version).

Meshes were vacuumed overnight, sterilized in 70% ethanol followed by another night incubation in 1% antibacterial medium. Human vaginal fibroblasts (Passage6) were seeded on sterile samples at a density of 150,000 cell/ cm² and cultured in DMEM supplemented with 10% FCS and 1% antibiotic. At days 1 and 3, 10 and 21 samples were collected for different characterizations. Live/dead staining of calcein AM and ethidium homodimer-1 was done for viability. Scanning electron microscopy (SEM) was used to characterize the micro-structure of the non-seeded meshes and cell-scaffold interactions. Histological analysis was performed on cryosectioned samples with H&E and PicoSirus Red staining. Meshes were evaluated for their isotropic micro-stiffness with indentation tests (Piuma, Optics11), with and without cells to monitor the changes of stiffness upon matrix deposition. De-ionized water drop was used to measure contact angel for hydrophilicity of the meshes.

RESULTS AND DISCUSSION

Live/Dead staining showed all the meshes are biocompatible (>95%, measured by number of live/total number of count), although viability was also dependent on hydrophilic creature of the meshes meaning that the more hydrophilic the mesh is like nylon, the more number of cells attach and therefore more viability is observed. Cells number increased from day 1 to day 3, stayed constant from day 3 to day 10 and increased again from day 10 to day 21.

This determines cells proliferated on all the meshes, and the most on Nylon, although the trend in cells increase was not constant all over the experiment.

SEM pictures, cells attach, elongate and spread all over the three meshes and grew into sheets from day 1 to day 21. Histological analysis confirmed the proliferation and matrix production on the meshes, although the infiltration of cells through the mesh thickness was low in all three (data not shown in here).

Material	PLGA/PCL	Nylon	PCL/gel
Fibers diameter	0.7-1.5 µm	100 nm	120-150 nm
Pore diameter µm	12-13	0.5-4	1-2.5
Porosity %	65	68	71.6
Thickness	60 µm	50-60 µm	70-80 µm
Indent stiffness (N/m)	24.9	20.3	16.75-19
Indent Y module (MPa)	2.3	0.86	1.1
Contact angel	120-130	45	70

Table1. Mesh characteristics

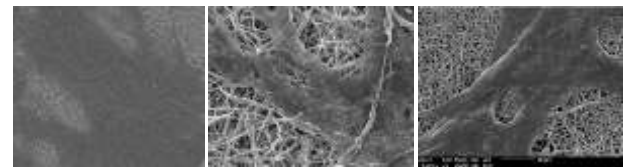


Figure1. Cell sheet on spun meshes at day 3 (rest of time points are not shown here) from left to right: Nylon, PCL/gel, PLGA/PCL.

Nano-indentation tests at different time points confirmed the deposition of matrix (soft areas as opposed to the cell-covered stiff areas) increasingly during 21 days of the experiment. This also confirmed the remodelling of the matrix by cells, replacing their surrounding from focal adhesions to prominent matrix proteins like collagen.



Figure2. PicoSirus red (staining for collagen) of meshes at day 3 (rest of time points are not shown here), from left to right: Nylon, PCL/gel, PLGA/PCL .

CONCLUSIONS AND FUTURE DIRECTIONS

Although non-woven electrospun scaffolds seem suitable for tissue engineering purposes, more of investigations are needed to have better insight into ECM deposition as well as mechano-biological responses on them.

REFERENCES

- 1-Pham Q.P. *et al*, Biomacromolecules 2006, 7.
- 2-Hiep N.T. *et al*, J Mater Sci Mater Med 2010,21(6).
- 3-Deprest J. *et al*, Int. Urog. J., 2006, 17.



Coating of polypropylene mesh with micro-structured gelatine as potential biomimetic composite for active hernia treatment

Selestina Gorgieva¹, Maja Kaisersberger Vincek¹ And Vanja Kokol^{1,2}

¹University of Maribor, Institute for Engineering Materials and Design, Smetanova ul. 17, SI-2000 Maribor, Slovenia
Presenting author: selestina.gorgieva@um.si

²Centre of Excellence NAMASTE, Institute for research and development of Advanced Materials and Technologies for the Future, Jamova 39, Ljubljana

INTRODUCTION. Polypropylene mesh (PP_{mesh}) implants used in abdominal hernia treatment frequently develops post-surgical complications such as infections, fistulas and viscera-to bowel adhesions, leading to pain, recurrence and even implant failure. Among many functionalization approaches which have been studied, not absolute disappearance of adhesions occurred, that, together with insufficient porosity and fluid permeability, represent the risk for post-operative seroma formations, in some cases restricting the cells' proliferations on damaged sites, thus suppressing their viability. In the contribution, innovative strategy for the fabrication of bio-active (PP_{mesh}) – micro-structurally generated gelatin (GEL_{scaffold}) composites, containing *in-situ* integrated, antimicrobially-active ε-poly-lysine (εPL), will be presented. The anti-adhesive potential, bio-stability, antibacterial and radical-scavenging activity, as well as *in vitro* cytotoxicity of fabricated composites will be discussed in means of preparation conditions.

EXPERIMENTAL METHODS. PP_{mesh}-GEL_{scaffold} composite was fabricated by temperature-controlled cryo-process and EDC/NHS cross-linking chemistry (Fig.1). For that purpose, oxygen plasma PP_{mesh} pre-activation was performed and analysed, related to carbonyl-type functionalities (XPS; FTIR) and its integration to GEL_{scaffold} was identified (FTIR; SEM). The micro-structuring (FM), biodegradation profile (gravimetrical measurement) and rheological properties (rheometry) of composites were examined in function of preparation parameters. Moreover, the integration of εPL within GEL_{scaffolds} was identified (DSC) and its releasing profile demonstrated (HPLC/GPC). Finally, the fibrin-related anti-adhesive potential (protein adsorption), antioxidative (ABTS radical scavenging capacity) and antibacterial properties, as well as cytotoxicity (toward human ASC cells) of composites were examined.

RESULTS AND DISCUSSION. Prolonged oxygen-plasma treatment generates higher amount of oxygen-containing functionalities on PP_{mesh} surface (preferably carboxyl type) resulting in better integration with GEL molecules than shorter treatment. Moreover, the μ-porosity gradient of GEL_{scaffold} within the composite (Fig. 2) may be modulated in 50-100 μm range at top-side to a loosely-porous on the bottom side by preparation parameters variation. The long-lasting GEL coating (> 2 months under incubation in collagenase-containing physiological media), provides ~60% reduction in fibrinogen adsorption. On the other hand, the εPL-releasing profile shows prominent dependence of cross-linking extent, affecting the antimicrobial activity against G+ *S. aureus* and the G- *E. coli*, which

positively correlates with pH and εPL concentration (causing up to 100% bacteria reduction), while negative correlation with EDC concentration was measured. Non cytotoxicity to human ASC cells after one week of incubation (excluding the sample with low εPL concentration) confirms composite biocompatibility, thus suitability for biomedical applications.

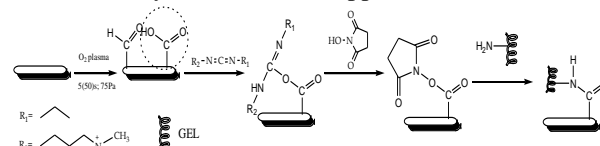


Figure 1 Immobilization of GEL to PP_{mesh} using oxygen-plasma pre-activation and EDC/NHS chemistry.

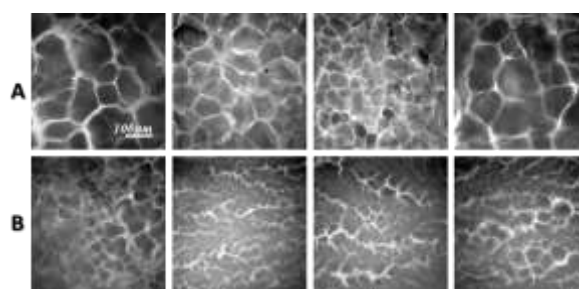


Figure 2 FM images presenting the top (A) and bottom (B) side of PP_{mesh}-GEL_{scaffold} composites.

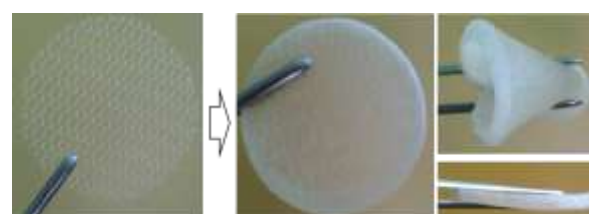


Figure 3 Photographic images of PP_{mesh} (left) and PP_{mesh}-GEL_{scaffold} composite (right).

CONCLUSION. Presented 3D and μ-structured PP_{mesh}-GEL_{scaffold} composites (Fig. 3) demonstrate high potential for active abdominal hernia repair treatments where intra-abdominal adhesions and bacterial-related infections are issues. Biomimetic nature and proved *in vitro* non-cytotoxicity is expected to provide appropriate environments for on-site cells, thus anatomically and physiologically appropriate tissue regeneration.

ACKNOWLEDGMENT. The authors acknowledge dr. Cristina Buemi (Company for production of prosthetic meshes DIPROMED, Turin, Italy) for providing the PP meshes, dr. Janez Štrancar and dr. Janez Kovač from Jožef Štefan Institute, Ljubljana Slovenia for performing the FMS and the XPS analysis, respectively.

Bioresorbable Polymer Based Novel Quick Vascular Closure Device (QVCD)

Carsten Linti¹, Michael Doser¹, Sven Oberhoffner¹, Erhard Müller², Monika Renardy², Bernd Neumann³, Hans-Peter Wendel³

¹Institut für Textil- und Verfahrenstechnik Denkendorf, Germany

²ITV Denkendorf Produktservice GmbH, Germany

³Klinik für Thorax-, Herz- und Gefäßchirurgie, Universitätsklinikum Tübingen, Germany

carsten.linti@itv-denkendorf.de

INTRODUCTION

Following arterial access procedures traditionally the hemostasis of the arteriotomy hole is achieved by manual compression. This is a labor and time consuming procedure followed by bed rest, extending the length of hospital stay. Still complications like fulminant bleeding and hematoma are common. Newer techniques try to reduce physician and nursing time by complicated, more or less automated suture devices, local application of hemostyptics or using metal clips and staples. These techniques have the disadvantage of being too time consuming, expensive or not efficient enough¹.

Our aim is to develop a self-expanding vascular closure device made from bioresorbable elastic polymer that can be applied through the placed introducer sheath. The advantages of the new VCD are cost efficient production by injection molding, quick application, easy instrumentation and early ambulation of the patients.

EXPERIMENTAL METHODS

Special bioresorbable block-co-polymers with soft-segments of glycolide, caprolacton and trimethylene carbonate have been synthesized. The chemical and mechanical degradation was determined in in vitro tests on injection molded plates in Sørensen's buffer solution.



Figure 1: First simplified molded VCD (left) and placement in the vessel wall with application system (right)

A simplified VCD was designed², a mold was build, and the molded parts were structured with CO₂-laser. The material with appropriate bending and degradation behavior was chosen for the injection molding of the first VCD specimen. A simplified application system was designed and used for first in vitro tests of the VCD (Figure 1) using porcine arterial vessels.

RESULTS AND DISCUSSION



Figure 2: VCDs placed in porcine vessel in vitro

The in vitro tests proved that the new VCD can be placed in the arteriotomy hole (Radiofocus Introducer II, Fr. 8) with minimal leakage. Degradation times could be adapted to vessel healing time of 7-14 days in in vitro test.

CONCLUSION

The in vitro testing of the new quick VCD shows the feasibility of the novel vascular closure technique. An improved design based on the in vitro results will be tested in an animal model in the next step.

REFERENCES

1. Hon L-Q. *et al.*, Curr Probl Diagn Radiol (2009),38(1):33-43
2. Wendel H-P, Neumann B: (2010) EP 1648 308 B1

ACKNOWLEDGMENTS

The authors would like to thank the German Federal Ministry of Education and Research (Grant no: 01KQ0902K) for providing financial support to this project.

Hydrophobically modified, cod-derived gelatins-based surgical sealants strongly adhere onto blood vessel under wet condition

Ryo Mizuta^{1,2}, Temmei Ito^{2,3}, Keiko Yoshizawa³, Mikio Kajiyama¹,
Toshimasa Akiyama⁴, Katsuhiko Kamiya⁴, Tetsushi Taguchi^{2*,3}

¹ Graduate School of life and Environmental Science, University of Tsukuba, Japan

^{2*} Biomaterials Unit, National Institute for Materials Science, Japan

³ Graduate School of Pure and Applied Science, University of Tsukuba, Japan

⁴ Senko Medical Instrument Manufacturing Co., Ltd., Japan

TAGUCHI.Tetsushi@nims.go.jp

INTRODUCTION

For the treatment of pulmonary air leaks and anastomotic sites between living tissues, surgical sealants have been widely used in clinical field. Fibrin sealant is a typical sealant which consists of human blood components, and its proportion is about 70 % in Japan. Fibrin sealant has excellent biocompatibility and versatile, however, it does not possess sufficient sealing effect because of its low interfacial bonding strength to tissues. Therefore, the molecular design of a tissue sealant which can adhere to a living tissue and organs under wet environment during surgery is required. In our previous study, we have shown that tissue adhesives containing hydrophobically modified porcine-derived gelatins showed excellent bonding strength onto fresh vascular media compared with non-modified gelatin^{1,2)}. However, porcine-derived gelatin solution with high concentration has low fluidity at room temperature because of its high contents of imino acids such as proline and hydroxyproline and is required to heat to use as a sealant.

In this study, we have chosen cod-derived gelatins (cGln) instead of porcine-derived gelatin as a base material for surgical sealants because it has low transition temperature due to its low contents of imino acids including proline and hydroxyproline. We synthesized various hydrophobically modified cGlns (hm-cGln) with different hydrophobic groups and introduction ratios and evaluated their sealing effects on fresh vascular tissue (blood vessel) by combining hm-cGlns with polyethylene glycol-based crosslinker (4S-PEG)³⁾.

EXPERIMENTAL METHODS

Modification of cGln with hydrophobic groups was carried out by nucleophilic substitution reaction of the amino group with fatty acid chlorides or cholesteryl chloroformate in dimethyl sulfoxide. Modification ratio of hydrophobic groups was calculated by determination of residual amino group using trinitrobenzenesulfonic acid. The measurement of burst strength for the porcine large intestine and blood vessel was performed according to the method reported as ASTM (F2392-04). As shown in Figure 1, the test sample with 15mm in diameter, 1mm in thickness was prepared. After opening pin hole with 3mm in the center of the sample, sealant composed of hm-cGlns and 4S-PEG was applied at fixed diameter and thickness. The burst strength was then measured by running a saline from the lower portion of the tissue at a flow rate of 2 ml/min at 37 °C.

RESULTS AND DISCUSSION

Hm-cGlns were successfully synthesized by the method as we reported previously^{1,2)}. By changing initial concentrations of fatty acid chlorides, each hm-cGln with three different modification ratios of hydrophobic groups was obtained. The burst strength of hexanoyl group modified cGln (Hx-cGln)-based sealants against fresh porcine blood vessel was 2-fold higher than that of original cGln (Org-cGln)-based sealant under fixed 4S-PEG concentration. Significant dependency of Hx content in cGln on burst strength was not observed. While, burst strength of cholesteryl group modified cGln (Chol-cGln)-based sealants increased up to the modification ratio of 8.3 mol%, then decreased. Highest burst strength of Chol-cGln-based sealant was 12-fold higher than that of fibrin sealant and 3-fold higher than that of Org-cGln-based sealant. Decrease in the burst strength at high Chol content of cGln is due to the increased inter/intra molecular aggregation of Chol-cGln and subsequent reduced penetration of Chol-cGln into vascular tissue. From the observation of fracture surface after burst strength measurement, the fracture area of Org-cGln-based sealant was more extensive than that of Chol-cGln-based sealant. And, Chol-cGln-based sealant still remained on the surface of vascular tissue. These results indicated that the introduction of hydrophobic groups effectively enhanced the tissue penetration of sealants and, increased the interfacial strength between tissue and sealant.

CONCLUSION

We developed surgical sealants which have high interfacial strength by combining hm-cGln with 4S-PEG. Highest burst strength against blood vessel was 3-fold higher than that of Org-cGln-based sealant by introducing hydrophobic groups. Therefore, our sealants can be applied in the field of cardiovascular surgery as well as thoracic surgery.

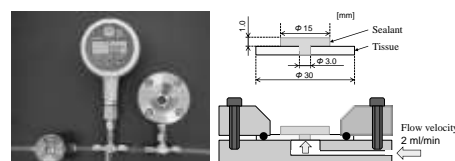


Figure1. Images of ASTM (F2392-04) burst strength test system

REFERENCES

1. Matsuda, M.; Inoue, M.; Taguchi, T., J. Bioact. Compat. Polym. 27, 481-498, 2012
2. Matsuda, M.; Ueno, M.; Endo, Y.; Inoue, M.; Sasaki, M.; Taguchi, T., Colloids Surf. B., 91, 48-56, 2012
3. Taguchi et al., Biomaterials, 26, 1247-1252, 2005



In situ-forming Pectin Hydrogels as Cell Delivery Systems

SC Neves^{1,2}, DB Gomes^{1,2}, A Sousa¹, SJ Bidarra¹, P Petrini³, L Moroni⁴, CC Barrias¹, PL Granja^{1,2,5}

¹INEB - Instituto de Engenharia Biomédica, Universidade do Porto, Porto, Portugal (sara.neves@ineb.up.pt)

²FEUP - Faculdade de Engenharia da Universidade do Porto, Porto, Portugal

³Laboratorio di Biomateriali, Politecnico di Milano, Milan, Italy

⁴MIRA - Institute for Biomedical Technology and Technical Medicine, University of Twente, The Netherlands

⁵ICBAS – Instituto de Ciências Biomédicas Abel Salazar, Universidade do Porto, Porto, Portugal

INTRODUCTION. Pectin is a complex natural polysaccharide present on the cell wall of higher plants. Despite the well-known use in the food industry as a gelling agent, only recently pectin started to be explored in the pharmaceutical and medical fields¹. Concerning regenerative medicine strategies, just a few studies are available²⁻⁴. The present work reports, for the first time, the ionotropic internal gelation of pectin as an *in situ* cell-delivery system using the CaCO₃/D-glucono-δ-lactone (GDL) gelation-triggering system. Since there is no medical grade or ultrapure pectin commercially available yet, pectin was purified before modification with an RGD-containing peptide to promote cell adhesion. The gelation kinetics of the hydrogels formed was evaluated by rheometry. Human mesenchymal stem cells (hMSCs) were embedded within the hydrogels and their behaviour evaluated. Finally, acellular pectin hydrogel discs were subcutaneously implanted in mice for the assessment of their *in vivo* degradation.

EXPERIMENTAL METHODS. Low-methoxyl citrus pectin (Classic CU 701) was a gift from Herbstreith & Fox (Germany) (RAWpec). RAWpec was purified (PURpec) using an adapted protocol⁵. Efficiency of purification was assessed by a Micro BCA Protein Assay (Pierce Biotechnology, USA), fluorescence spectrometry⁶, and Endosafe™-PTS system (Charles River, USA). PURpec was covalently grafted with the oligopeptidic sequence (Gly)₄-Arg-Gly-Asp-Ser-Pro (G₄RGDSP, Genscript, USA) by carbodiimide chemistry⁷ (RGDpec). Pectin was characterized by GPC/SEC and FTIR spectroscopy. Rheological properties of gel-precursor solutions and hydrogels were determined using a Kinexus Pro rheometer (Malvern, UK). hMSCs (8x10⁶ cells/mL) were mixed with the precursor solutions of RGDpec and non-modified pectin (BLKpec) at final concentrations of 1.5 and 2.5 wt% (14 days of culture). Metabolic activity was assessed by a resazurin-based assay, cell viability by a live/dead assay, and cell morphology and extracellular matrix (ECM) deposition were imaged using a confocal microscope (Leica SP2 AOBS). After implantation of acellular RGDpec hydrogel discs for 1 week in the dorsum of mice (C57BL/6), samples were harvested and stained with Safranin-O/Light-green (Sigma). Hematoxylin was used as counterstain.

RESULTS AND DISCUSSION. Purification lowered the content of protein on ca. 70%, polyphenols in 52%, and endotoxins levels in 96%. FTIR spectra indicated that the purification method did not affect pectin structure. SEC analysis showed that the M_w, the polydispersity index and intrinsic viscosity of RAWpec

and PURpec were similar. The UV spectrum of RGDpec confirmed that the RGD peptide was effectively grafted to the polymer. Rheometry studies allowed the optimization of pectin gelation towards cell embedding, with stabilization of hydrogels viscoelastic properties within 1h at 37°C (phase angle below 10°). Entrapped hMSCs were metabolically active and viable throughout the culture time within all pectin hydrogels. However, major differences were found in terms of cell morphology, as both the modifications in the pectin chemistry (RGD-grafting) and their physical properties (1.5 and 2.5 wt%) influenced hMSCs behaviour. Within RGDpec matrices hMSCs were able to spread and establish contacts with each other, leading to the establishment of an intercellular network. Cells were able to migrate outwards the matrix, populating the surface of the hydrogels and depositing endogenous ECM. The opposite could be observed for the non-functionalized matrices. After 7 days of culture, the stiffness of RGDpec was higher than BLKpec matrices. Also, the 1.5 wt% RGDpec hydrogels presented a higher stiffness than that of the 2.5 wt% ones, probably due to the softer nature of the former, offering less resistance for cells to deform the surrounding matrix, thus leading to the observed matrix contraction and establishment of a denser cellular network. The preliminary *in vivo* studies showed that a lower polymer content led to a higher degradation rate. The 1.5 wt% hydrogels presented a higher number of fragments, which were smaller and more spread throughout than the ones of the 2.5 wt% hydrogels.

CONCLUSION. Purified RGD-grafted pectin is a versatile biocompatible and biodegradable biomaterial, adequate for the preparation of *in situ* gelling cell delivery systems.

REFERENCES

1. Maxwell *et al.*, Trends Food Sci Technol. 24:64-73, 2012
2. Munarin *et al.*, Int J Biol Macromol. 51:681-9, 2012
3. Munarin *et al.*, Biomacromolecules 12:568-77, 2011
4. Takei *et al.* J Biomat Sci - Polym E 24:1333-42, 2013
5. Bender *et al.* WO 2009154440 A1, 2009
6. Skjåk-Bræk *et al.* Biotechnol Bioeng. 33:90-4, 1989
7. Rowley *et al.* Biomaterials 20:45-53, 1999

ACKNOWLEDGMENTS. This work was funded by the European Regional Development Fund through the Program COMPETE, and by Portuguese funds through FCT – Fundação para a Ciência e a Tecnologia in the framework of SC Neves doctoral grant, A Sousa and SJ Bidarra post-doctoral grants, the research position of CC Barrias, the research grant PEst-C/SAU/LA0002/2013, and co-financed by North Portugal Regional Operational Programme (ON.2).



Double Layer Nanofiber Sandwich System in Effective Delivery of Growth Factors for Osteogenic Differentiation

P. S. Gungor-Ozkerim¹, E. I. Bektas², A. S. Sarac³, G.T. Kose², F. N. Kok^{1*}

^{1*}Molecular Biology Genetics and Biotechnology Programme, Istanbul Technical University, Turkey

²Genetics and Bioengineering Department, Yeditepe University, Turkey

³Department of Chemistry & Polymer Science and Technology, Istanbul Technical University, Turkey
kokf@itu.edu.tr

INTRODUCTION

Poly-blend (mixtures of synthetic and natural polymers) nanofibers can mimic the tissue structure by providing surface features of native tissue that promote cell survival. In the current study, blends of poly- β -caprolactone, poly-L-lactic acid and gelatin polymers used to construct 3D scaffolds in a double-layer format. With the aid of a growth factor controlled release system, scaffolds were also made biologically active.

EXPERIMENTAL METHODS

Nanofibrous double-layer matrices were prepared by electrospinning technique with the bottom layer formed from PCL (poly- ϵ -caprolactone)/PLLA (poly-L-lactic acid) blend nanofibers and the upper layer from PCL/Gelatin blend nanofibers. Bottom layer was designed to give mechanical strength to the system, whereas upper layer, containing the natural polymer gelatin, was optimized to improve the cell adhesion. Gelatin microspheres were incorporated physically in the middle of these two layers for controlled growth factor delivery. This sandwich system prevented microsphere leakage from the scaffold. Whole procedure was described elsewhere¹.

Cell differentiation on the designed scaffold system was studied using adipose tissue derived stem cells (ADMSCs) and microspheres within the scaffolds were loaded with bone morphogenic protein-2 (BMP-2) which is a well established pro-osteogenic morphogen. Differentiation of ADMSCs towards osteogenic lineage was evaluated by alkaline phosphatase (ALP) assay and von Kossa staining for the detection of mineralization. Collagen type-I immunostaining was carried out to examine ECM formation by ADMSCs on electrospun fibrous mats.

RESULTS AND DISCUSSION

Experimental samples used were: (S1) PCL/PLLA – PCL/Gelatin double layer matrices with BMP-2 loaded microspheres, (S2) PCL/PLLA – PCL/Gelatin double layer matrices with unloaded microspheres and (S3) PCL/PLLA one layer matrices.

ALP activity assays showed that ADMSCs on the scaffolds undergoing osteogenic differentiation demonstrated higher ALP activity in the first week, as an early marker of osteogenesis, after which ALP activity decreases while mineralization increases.

Visualization of calcium deposits was done by von Kossa staining and results showed that ADMSCs cultured both on the scaffolds and TCPs produced a mineralized matrix. Mineral nodules (represented by the

brown/black deposits) were scattered in the samples (Figure 1). Since mineralization is a late osteogenic marker and the final phase of bone formation, staining of calcium deposits increased at the later periods of incubation (14 days vs 24 days). It was noticed that stained scaffolds containing BMP-2 (S1) showed darker staining indicating accelerated biomineralization after 14 and 24 days of incubation compared to the samples that do not contain BMP-2 (S2) and both exhibited higher mineralization when compared with S1.

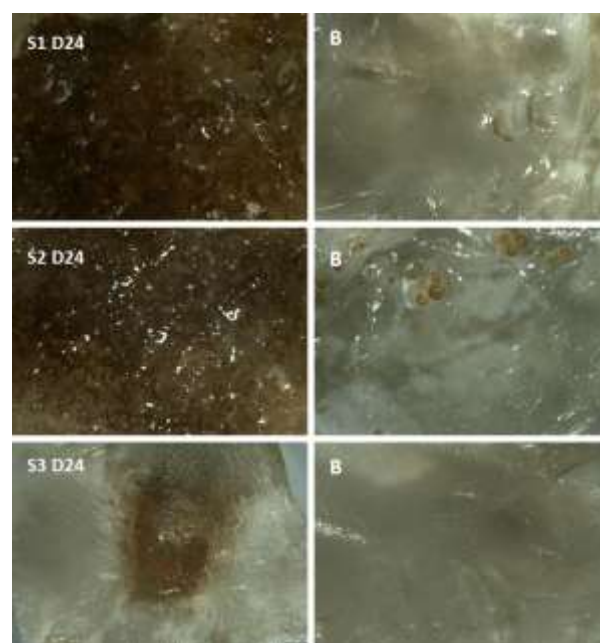


Figure 1 : von Kossa staining: Stereomicroscopy images of experimental groups (left column) with their blank samples (right column) on day 24

CONCLUSION

All samples supported the proliferation of ADMSCs. Both the sandwich-like architecture of the constructed scaffolds and presence of hydrophilic gelatin on the upper layer promoted improved migration and differentiation of ADMSCs.

REFERENCES

1. P.S. Gungor-Ozkerim et al, J. Biomedical Mat. Res.: Part A DOI: 10.1002/jbm.a.34857

ACKNOWLEDGMENTS

The authors would like to thank The Scientific and Technological Research Council of Turkey (Grant no: 111M787) for providing financial support to this project.



Patient-Customizable Scaffolds with Nano/Microenvironments Rich in Human Platelet's Lysate and Marine-Origin Polysaccharides for Bone Formation Induction

Sara M. Oliveira^{1,2,*}, Rui L. Reis^{1,2}, João F. Mano^{1,2}

¹3B's Research Group – Biomaterials, Biodegradables and Biomimetics, AvePark, Zona Industrial da Gandra S. Cláudio do Barco, 4806-909 Caldas das Taipas, Guimarães, Portugal.

²ICVS/3B's – PT Government Associate Laboratory, Braga/Guimarães, Portugal, sara.oliveira@dep.uminho.pt

INTRODUCTION

The design of bone tissue engineered constructs for future clinical application demands patient customizable 3D structures. These need to be able to sustain the mechanical solicitations, to support cellular functions and to induce bone formation. Our methodology is based on a combination of multiple techniques. This permits us to optimize and customize the final 3D structure at a multi-level scale by using human and marine-origin materials for the production of the primary nano/sub-micro environment that will dictate cell fate. 3D prototyped macro-porous scaffolds where subjected to layer-by-layer assembling and freeze-drying for hierarchical (hier) structuring with nanocoatings and micro-fibrillar structures. Those structures, rich in autologous growth factors (GFs) from human platelet's lysate (hPL), are stabilized throughout marine-origin polysaccharides functional groups and physical crosslinking. The potential of these nano/microenvironments for the conduction and induction of osteogenic differentiation of human adipose derived stem cells (hASCs) was assessed.

EXPERIMENTAL METHODS

Poly(ϵ -caprolactone)-PCL, ι -carrageenan and chitosan where obtained from Sigma-Aldrich. Human platelet's lysate was obtained as explained elsewhere.¹ The assembling of the polyelectrolytes (PEs) with hPL was studied by QCM-D. PCL scaffolds were prepared using a BioplotterTM rapid prototyping machine and modified by dipping LbL and freeze-drying.² hASCs were cultured in osteogenic (+dexamethasone, +Dex) and osteoconductive media (-Dex). After 28 days in culture, samples were harvested and characterized by several techniques for calcium by Alizarin Red S staining and SEM-EDS; for immuno-detection of osteocalcin (OC); for fat deposition by oil red O staining; and osteogenic-related gene expression by qPCR.

RESULTS AND DISCUSSION

Different types of microenvironments were assembled inside of the PCL scaffold pores: fibrilles and coatings obtained from 15 (PCL Hier hPL) and 30 (PCL Hier hPLx2) LbL dipping cycles, with and without hPL – see Fig.1.



Fig. 1. PCL scaffold before and after the modification (PCL Hier) with the fibrillar structures hydrated and contrasted in black.

The new structures supported hASCs osteogenesis both in the presence and absence of hPL in medium containing Dex –Fig.2. These structures conduced the deposition of CaP not only onto the surfaces (as in the case of PCL) but also in the void spaces of the pores. With the presence of these fibrillar structures the biomineralization occurs starting from the fibrilles in direction to the pores wall.

In the absence of Dex, the presence of hPL and the hierarchical structures synergistically induced the deposition of mineralized matrix and osteocalcin (Fig. 3).



Fig. 2. Alizarin Red S staining on several conditions after 28 days in culture.

PCL Hier hPL (15 cycles) was able to induce the hASCs deposition of OC and CaP in the absence of Dex – Fig.2, 3. Therefore, the environment created in PCL Hier hPL samples has triggered the differentiation of hASCs into the osteogenic lineage.



Fig. 3. Immuno-detection of osteocalcin (green) and nucleus (blue); Alizarin Red S staining (red).

PCL Hier hPLx2 has not shown mineralized matrix, nor has OC when cultured without Dex. This result reveals that contrarily to PCL Hier hPL, the nano and microenvironment of PCL Hier hPLx2 was not adequate for bone formation induction.

CONCLUSION

The developed methodology allows the preparation of 3D scaffolds with multi-level tunable nano- and micro-environments that highly affect cell fate. The structuring method has shown to be effective for the introduction and stabilization of osteoinductive factors derived from hPL. By playing with the structuring parameters, the density of the hPL presented to cells, the profile and even the spatial-temporal release, highly bioactive 3D tissue engineered bone constructs can be created.

REFERENCES

- 1-Santo V.E. *et al.*, J Control Release.162:19-27, 2012.
- 2- Oliveira SM, *et al.* Adv Health Mat. 2:422-27, 2013.

ACKNOWLEDGMENTS

FCT is gratefully acknowledged for the fellowship of S.M.O.(SFRH/BD/70107/2010).



Effect of Cyclic Compression on Osteogenesis of Self-Assembled Collagen-Cell Seeded Microspheres

Maryam Shariatzadeh, Cécile M. Perrault, Damien Lacroix

INSIGNEO Institute for in silico medicine, Department of Mechanical Engineering, University of Sheffield, UK
m.shariatzadeh@sheffield.ac.uk

INTRODUCTION

Mechanical forces such as shear stress, compression and 3D environment, can be used to control differentiation of Mesenchymal Stem Cells (MSCs)^{1, 2}. In this study, a novel microfluidic chamber is designed to apply mechanical stimulation on soft cellular microspheres. It is hypothesised that cell morphology and expression of osteogenic cell marker is different when cells are subjected to dynamic compressive strains.

EXPERIMENTAL METHODS

A microfluidic chamber was made of polydimethylsiloxane (PDMS) with a main channel of 1 mm width and constrictions of 0.5 mm (Fig. 1). Bovine collagen type I (Life Technologies) with concentrations of 2 mg/ml and 2450 heMSC/MG63 cells per 5 µl droplet was produced through gelation. The microspheres were passed through the constriction at a flow rate of 320 µl/min for 3 cycles/day for 3 days starting at day 3 post-encapsulation. Cell viability, proliferation and bone markers alteration were monitored and compared before and after compression with the same dynamic compression regime applied by a Bose biodynamic bioreactor.

RESULTS AND DISCUSSION

Cell viability and proliferation reduced after compression cycles compared to controls. Cell proliferation dropped gradually by 14% on day 7 post encapsulation and cells presented more rounded morphology immediately after and up to day 3 post compression compared to the initial cell seeding. (Fig. 2, & 3). Bovine Collagen demonstrated an efficient micro environment for cellular growth which supported cell proliferation and viability up to 35 days post encapsulation. Fluid flow rate above 320 µl/min caused damage to collagen microspheres and released the cells, while flow rate below 100 µl/min caused microspheres attachment to PDMS. Cell viability and proliferation of compressed cells increased steadily by 23% there compared to 30% growth in controls (Fig. 3).

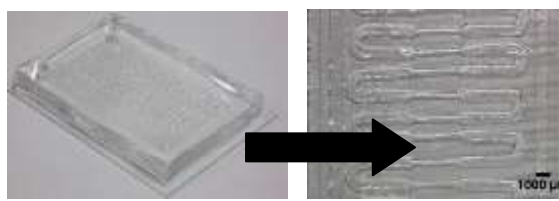


Fig. 1: Microfluidic chamber with constricted channel shown in the right.

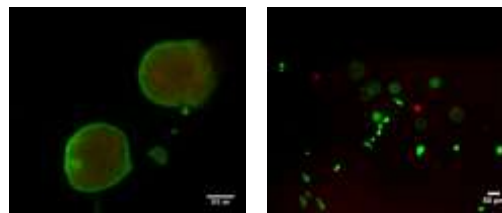


Fig. 2 : Collagen-MG63s microspheres day 7 post-encapsulation control (left), sample (right).

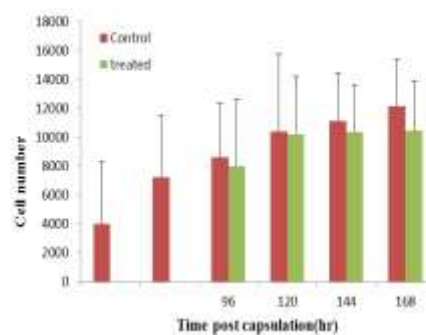


Fig. 3 : MG63 cell proliferation before and after compression. Error bars are standard deviation of four samples.

CONCLUSION

The microfluidic chamber enables chemical and mechanical stimulation of cells in a controlled environment, while reducing the overall volume of the systems. Such a system provides both reduction in cost and possibility of high throughput testing. The application of a compressive force on the cell-seeded microspheres supported cell viability and enhanced cell proliferation 24 h after ending the compressive cycles. However, extended period of cell monitoring is required to investigate the long term effects of compression. Application of compression cycles on MG63/heMSC cells could be used as a model to study the effect of mechanostimulation on osteogenesis.

REFERENCES

1. Chan, B. P. *et al.*, *Biomaterials* 2007, 28, 4652-66.
2. R. M. Delaine-smith *et al.*, *Vitam Horm* 2011, pp. 417-480.

ACKNOWLEDGMENTS

Financial support from the European Research Council (258321) is acknowledged

Ultra-thin Bioglass Fibres with Controlled Structures for Biomedical Applications

Yangyang Li¹, Ding Zhao^{1,2}, Binbin Li¹, Qihong Zhang¹, Yike Fu¹, Mingwei Chang², Xiang Li^{1*}

^{1*} Department of Materials Science and Engineering, Zhejiang University, P.R.China. xiang.li@zju.edu.cn

² College of Biomedical Engineering & Instrument Science, Zhejiang University, P.R. China.

INTRODUCTION

Sol-gel bioactive glass (SBG) has become one of the most important biomaterial groups since its discovery by Larry Hench in 90s due to its various advantages, such as strong bioactivity, microstructure control feasibility and large surface area [1]. Recently, ultra-thin SBG fibres with manipulated microstructures have been widely considered as a promising candidate for bone scaffold. The protein absorption and releasing behavior of a scaffold material plays a key role in tissue repairing progress [2]. Finding an efficient approach to manipulating the protein release kinetics can be rather important to improve the performance of SBG bone scaffold in clinic, but yet remains a challenge. In this study, a range of ultra-thin SBG fibres with well-controlled bovine serum albumin (BSA) releasing behaviors were synthesized using electrospinning. A feasible and effective protein absorption/release control method by only varying the sol-gel reaction condition was therefore established for SBG scaffold materials.

EXPERIMENTAL METHODS

TEOS, triethylphosphate (TEP) and calcium nitrate ($\text{Ca}(\text{NO}_3)_2$) were mixed in ethanol with a certain ratio. Water was added in the solution with four different ratios (Water/TEOS (X) = 2, 4, 6, 8 mol%) to control the hydrolysis process of SBG precursor. After stirring for 2h, PVP solution was added as electrospinning carrier. Four precursors prepared were transferred into a single nozzle electrospinning setup. The distance and voltage applied between the needle tips and the collector were set at 15 cm and 6–8kV, respectively. The as-spun BG fibres were then heat treated in air at 600°C to eliminate organic additives. The SBG fibres were characterized using SEM, TEM and FTIR. Subsequently, BSA protein was loaded on SBG fibres by immersing in two different solutions, BSA solution and BSA/SBF mixture, for 30 hours. The protein loaded fibres were then immersed in PBS solution, and the BSA release phenomena were studied using UV.

RESULTS AND DISCUSSION

In the bioglass sol-gel reaction, the hydrolysis process is important for its microstructural characteristics. In general, higher hydrolysis degree may induce more integrated Si-O-Si network. In our study, it was found that, under the same electrospinning condition, all four SBG fibres present uniform morphology. With the X ratio increased from 2 to 8, the fibre dimension increases from ~200nm to ~500nm, as shown in Fig 1a. This is due to the higher precursor viscosity induced by the enhanced hydrolysis degree. The FTIR study shows that the Si-O-Si asymmetric, stretching and symmetric bending modes, corresponding to the peaks at 1070 cm^{-1} , 800 cm^{-1} and 478 cm^{-1} , are remarkably enhanced with the increased X ratio. The increased water content induces the higher hydrolysis degree and the subsequent polycondensation reaction of silica network former. In

consequence, the Si-O-Si network integrity of the SBG fibre can be enhanced with higher X value.

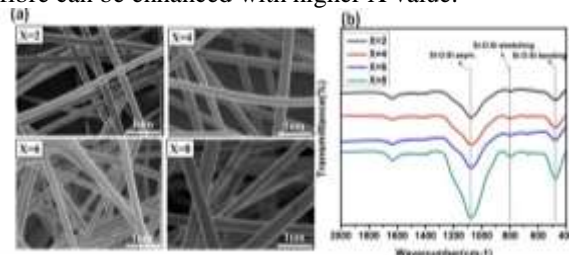


Fig.1. (a) SEM and (b) FTIR of SBG fibers with different X ratio.

When four types of SBG fibres were directly immersed in BSA solution. The releasing kinetics of all fibres presented similar characteristics. ~60% of BSA released within the initial ~5h. In contrast, when immersed in SBF/BSA mixed solution, only ~30% of BSA was released within initial ~5h for all fibres (Fig 2). This is due to the ‘anchoring’ effect of the porous apatite layer formed which prohibits the releasing of BSA molecules. More importantly, when X ratio decreased from 8 to 2, more sustained BSA releasing behaviour was observed. Higher X ratio induces more integrated Si-O-Si network, and thus weakens the bioactivity of SBG fibres. Consequently, less apatite contents with higher porosity is formed on the fibre surface when protein loading, which weakens its ‘anchoring’ effect to BSA molecules.

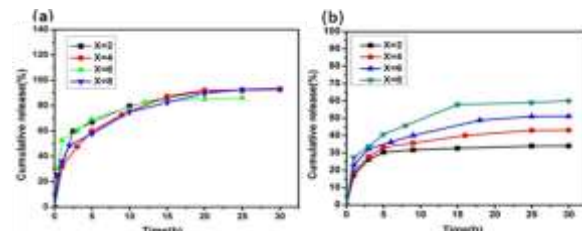


Fig.2. The protein release behavior of four SBG fibers loaded BSA in (a) BSA solution and (b) BSA/SBF solution.

CONCLUSION

A range of SBG fibres, ranging from ~200nm to ~500nm in thickness, with different Si-O-Si network structures were successfully synthesized using electrospinning. By loading BSA protein in SBF/BSA mixed solution, SBG fibres showed sustained and well-controlled BSA releasing kinetics, due to its controlled BG network integrity and bioactivity induced by the manipulated sol-gel hydrolysis degree. This study has therefore paved the way to the research of future functionalized SBG fibrous scaffold materials.

REFERENCES

- [1] Hench L.L. *et al.* J. Appl. Biomater. 4:231-139, 1991.
- [2] Wang C. H. *et al.* Biotechnol. Bioeng. 99:996–1006, 2008.

ACKNOWLEDGMENTS

Authors would like to thank National Natural Science Foundation of China (51103128), Education Ministry of China (20110101120014) and Science Technology Department of Zhejiang Province (2013R10037), for the financial support.



Serious adverse event of woven fabrics made of bioactive glass fibres of the Na₂O-K₂O-MgO-CaO-B₂O₃-P₂O₅-SiO₂ system in the rabbit spinal fusion model

Jane P. Frantzen,^{1,2} Jessica J. Alm,¹ Petteri Lankinen,¹ Niko Moritz,¹ Matias R  ytt  ,³ Hannu T. Aro^{1*}

¹Orthopaedic Research Unit, Department of Orthopaedic Surgery and Traumatology, University of Turku, Finland

²Neurosurgical Unit, Department of Surgery, Turku University Hospital, Finland

³Department of Pathology, Turku University Hospital, Finland, hannu.aro@utu.fi

INTRODUCTION

Bioactive glasses (BGs) of the system Na₂O-K₂O-MgO-CaO-B₂O₃-P₂O₅-SiO₂ were developed to provide BGs with larger working range¹. Of this system, BG 13-93, BG 1-98 and BG 3-98 have been found suitable for processing into fibres, microspheres and woven fabrics. We previously evaluated a woven fabric made of BG 1-98 and PLGA 80/20 (PLGA₈₀) fibres in a rabbit femur model, without any adverse effects². The current study aimed at evaluating the same fabric and a corresponding load-sharing 3D composite plate in a rabbit model of spinal fusion. Due to unexpected occurrence of serious adverse events the study had to be terminated before completion.

EXPERIMENTAL METHODS

Woven fabrics (25x45 mm) of plain weave canvas-type were made of BG 1-98 (SiO₂ 53%, Na₂O 6 %, CaO 22%, K₂O 11%, MgO 5%, P₂O₅ 2 %, B₂O₃ 1% by weight) fibers (20-30 µm) and PLGA₈₀ fibres (200 µm), or PLGA₈₀ fibres alone (control). BG fibres were multiplied to 70-140 filament threads for weaving. PLGA₈₀ monofilaments were used as warp threads². A load-sharing 3D composite plate (3x15x45mm) was made from hybrid knitwear of BG 1-98 fibres, PLA₉₆ and PLA₇₀ fibres.

The implants were tested in an established spinal fusion model of the rabbit. The animals were divided into four groups according to the used implants (Table 1). The implants served as the surgical beds for autogenous bone grafting. The control group (Group 1) had autogenous bone grating alone. Spinal fusions were evaluated at 6 weeks by X-ray, CT, biomechanical testing and histology. The original study plan contained 8 animals per group operated in a randomized order.

In vitro experiments using human bone marrow derived mesenchymal stromal cells (hMSCs) and methods previously established in our lab³ were conducted in an attempt to explore cellular responses to the implants. The analyses included pH monitoring, cell viability and osteogenic differentiation assays.

RESULTS AND DISCUSSION

Of the 28 operated animals, 21 completed the follow-up. After 7 animals out of 14 in the BG groups (Group 3 and 4) were lost due to unexpected postoperative death (n=4), or had to be euthanized, the experiment was terminated (Table 1). In the BG/PLGA₈₀ group, 2 animals were euthanized due to intractable pain and paraparesis. One animal in the 3D composite group was euthanized due to intractable pain and autophagia.

Infectious causes were ruled out by microbiological and histological samples of autopsies.

In the BG/PLGA₈₀ group, none of the completed animals had histological fusion. Tissue samples revealed severe local inflammation and necrosis. In the neuropathological examination, muscle samples showed necrosis, multinuclear macrophages, increased fibrosis capsule, increased endomysial fibrosis with accumulations of inflammatory cells. The sensory ganglia at level of fusion showed signs of edema. Neither necrotic muscle fibers nor inflammatory changes were observed above the fusion area.

Table 1. Summary of study outcome

Group #	Implants used with autogenous bone grafting	# Animals	Detected fusion at 6 weeks	Serious adverse events #
1	Control (autograft)	n = 8	81%	0
2	PLGA ₈₀	n = 6	25%	0
3	BG 1-98 /PLGA ₈₀	n = 11	0%	n = 6 (55%)
4	3D composite (BG 1-98/ PLA ₉₆ / PLA ₇₀)	n = 3	0%	n = 1

In vitro experiments with hMSCs showed growth inhibition next to BG fibers and radical pH changes, compromising cell survival and differentiation.

The current adverse events were unexpected. The underlying mechanisms remain unclear. It is possible that the high surface area of fibers with too high dissolution rate caused rapid increase of pH and toxic concentrations of ions.

CONCLUSION

The woven fabric made of BG 1-98 and polymer fibers resulted in serious adverse reactions, necessitating early termination of the study. *In vitro* testing of the fibres and fabrics with human MSCs supported the *in vivo* findings. We recommend a systematic safety evaluation of novel BG formulations before clinical use.

REFERENCES

1. Brink M. *et al.*, J Biomed Mater Res 37:114-21, 1997
2. Alm J. *et al.*, J Biomed Mater Res B 93:573-80, 2010
3. Alm J. *et al.*, Tissue Eng. 18:658-66, 2012

ACKNOWLEDGMENTS

The National Foundation for Technology and Innovation (TEKES) provided financial support to this project. Professor Minna Kellom  ki and M.Sc. Mikko Tukiainen from Tampere University of Technology, Finland, are acknowledged for production of the materials.



Towards Promoting Ability of Glass Ionomer Cements to Remineralise

R. Albeshti¹, A. Bushby² and N. Karpukhina¹

¹*Institute of Dentistry, Barts and The London School of Medicine and Dentistry, Queen Mary University of London, London E1 4NS, UK*

²*School of Engineering and Materials Sciences, Queen Mary University of London, London E1 4NS, UK*
r.m.a.albeshti@qmul.ac.uk

INTRODUCTION

Glass ionomer cements (GICs) are used extensively as restorative materials, due to their ability to release and uptake fluoride, to form strong chemical bonding to the tooth surfaces, as well as have good handling properties, no shrinkage on polymerization and minimal toxicity compared to other restorative materials¹. On the other hand, GICs are considered as a vital source of calcium, phosphorous and fluoride ions. These ions have an ability to form apatite similar to the tooth minerals (hydroxyapatite, HA) at favourable conditions. Furthermore, it is believed that GICs have a beneficial ability to form apatite with time at the interface between the filling and the oral environment. Therefore, GICs are at the essence of the atraumatic restorative treatment (ART), which is an alternative technique for dental caries management.

The remineralising ability of GICs has not been studied extensively and factors affecting this process are poorly understood. Consequently, this study was aimed to investigate the remineralisation of GICs and to establish how it could be promoted via incorporation of remineralising agents.

EXPERIMENTAL METHODS

Fluorine-free and fluorine containing ionomer glasses based on $4.5\text{SiO}_2\text{-}3\text{Al}_2\text{O}_3\text{-}1.5\text{P}_2\text{O}_5\text{-(}5\text{-x)CaO-xCaF}_2$, where $x=0,1,2,3,3.5,4$, were synthesised with varying calcium oxide (CaO) and calcium fluoride (CaF₂) proportions. The Ca:P ratio is 1.67 for all the glasses which is kept equal to Ca:P ratio of HA. The fine glass powders were mixed with the poly(acrylic acid) in powder form and then with water at a specific ratio P:L=5:1. Different percentages 0, 5, 10, 15% of HA and FA was substituted for the original ionomer powder in order to accelerate the remineralisation of GICs. Immediately, the cement discs were placed in artificial saliva (AS) at pH=6.5, and kept at 37°C for different time points for 7-180 days. After a certain time, the samples were collected via filtration, dried, ground into a powder and further characterised. The formation of apatite in GICs has been evaluated using Fourier Transform Infra-Red (FTIR) and Solid-State Nuclear Magnetic Resonance (NMR) Spectroscopies. Wilson's oscillating rheometer was used to measure the handling characteristic of GICs with and without addition of remineralising agents. The concentration of the ions, released from GICs after immersion in AS were measured by Inductively Coupled Plasma-Optical Emission (ICP-OES) Spectroscopy.

RESULTS AND DISCUSSION

The working and the setting times of GICs were decreased with increasing CaF₂ content while increased when increasing the substituted amount of HA. The ²⁷Al NMR spectra cement showed the conversion of Al(IV) to Al(VI) as the setting proceeds. The peaks around 50-53ppm and -4ppm are attributed to the presence of Al(IV) and Al(VI) respectively. This is in a good agreement with the previous study². Additionally, the ²⁷Al NMR showed that increase in fluoride amount in the base glass indirectly affects change of the coordination number of Al from four to six during the setting reaction. The formation of apatite in GICs on immersion in AS was probed with ³¹P NMR spectroscopy. The ability and the rate of apatite formation from GICs were highly depended on the composition of the ionomer glasses. Furthermore, the P:L ratio has found to have an important role in apatite formation. The apatite was partially consumed during the setting reaction. The deconvolution was done to quantify the amount of apatite consumption during the reaction. The phosphorous environment in the GICs before and after the immersion in AS compared to the original glasses will be discussed. A negligible quantity of Al was released from all GICs compositions. This confirms that Al was consumed during the setting reaction to form Al polysalts.

CONCLUSION

The potential ability of GICs to remineralise is a significant advantageous feature distinguishing the GICs from the other restorative filling materials. The concentration of calcium and phosphate ions is not the only factor promoting the remineralisation process; also it depends upon the composition of ionomer glasses as well as powder to liquid ratios.

REFERENCES

1. Nicholson J. Materials Technology: Advanced Performance Materials, 25:8-13, 2010
2. Stamboulis A. *et al.*, Journal of Dentistry. 34:574-581, 2006

ACKNOWLEDGMENTS

We thank Prof. Robert Hill for his advices and discussions. The funding of the Ministry of Higher Education of Libya is gratefully acknowledged.



The Retarding Effect of Zinc Oxide on Dissolution and Apatite Formation of a Fluoride Containing Bioactive Glass

Xiaohui Chen¹, Priyen Shah², Mohammed Mneimne², Robert G. Hill², and Natalia Karpukhina^{2*}

¹School of Dentistry, The University of Manchester, UK

^{2*}Barts and The London School of Medicine and Dentistry, Queen Mary University of London, UK,
n.karpukhina@qmul.ac.uk

INTRODUCTION

Fluoride containing bioactive glasses are attractive for incorporation into remineralising toothpastes for three reasons: (i) they form fluorapatite which is much more acid durable than hydroxycarbonated apatite; (ii) they release fluoride that is known to inhibit apatite dissolution and caries formation; and (iii) they have a more disrupted glass network with lower glass transition temperatures and should be softer and are therefore less abrasive towards enamel.

Fluoride containing bioactive glasses were originally studied by Spilman and Hench¹ in the 1970s but there has been increased interest in fluoride containing glasses in recent years including glasses with high phosphate².

Zinc Oxide has been incorporated into bioactive glasses³ and it is potentially attractive for use in toothpastes, since zinc salts are added to existing toothpastes where the zinc has a bacteriocidal action, an anti-caries action and an anti-gingivitis action.

This study examines the influence of ZnO incorporation on the dissolution and apatite forming ability of a high phosphate fluoride containing bioactive glass. Since ZnO is thought to act as an intermediate oxide it has been substituted for SiO₂ with additional CaO and Na₂O to charge balance the ZnO₄ tetrahedra and maintain a fixed network connectivity.

EXPERIMENTAL METHODS

Bioactive glasses with and without 2 mol% of ZnO were synthesised and studied. Glass degradation and apatite formation was followed by X-ray diffraction (XRD), Fourier transform infrared (FTIR) spectroscopy and magic angle spinning nuclear magnetic resonance (MAS-NMR). The ions in solution following immersion in Tris buffer were determined by inductively coupled plasma – optical emission spectroscopy (ICP-OES) and by a fluoride-ion selective electrode.

RESULTS AND DISCUSSION

The zinc free glass formed a fluorapatite (FAP) like phase in under two hours that was evident in the XRD patterns and FTIR spectra. The zinc containing glass did not show sharp XRD peaks of the apatite phase until 24 hours immersion and did not show the characteristic $\nu(\text{PO}_4)$ peaks of a crystalline orthophosphate in the FTIR spectra. The ³¹P and ¹⁹F MAS-NMR spectra showed that the zinc free glass formed FAP in under two hours and the dissolution of the glass was complete in less than 6 hours. The zinc containing glass also formed a FAP, but the apatite formed was in smaller amounts and the broader peaks indicate a more disordered apatite. The dissolution of the glass in terms of its fluoride and phosphate content was not complete in 24 hours.

CONCLUSION

Zinc oxide substitution in bioactive glass slows down rapid degradation of the bioactive glass and formation of the apatite phase. Thus, the studied composition of the zinc containing bioactive glass can be incorporated as a desensitiser into remineralising toothpaste. Sustained release of both fluoride and zinc ions from the bioactive glass can deliver therapeutic effect via toothpaste.

REFERENCES

1. Hench L.L. et al., US patent 4775646. 1988.
2. Mneimne M. et al., Acta Biomater. 7:1827-1834, 2011.
3. Linati L. et al., J Phys Chem B, 109:4989-4998, 2005.

ACKNOWLEDGMENTS

Authors would like to acknowledge Dr Rory Wilson for XRD measurements, Dr Andy Bushby, Dr David Gillam and Dr Jonathan Earl for useful discussions.

Hypoxia Mimicking Glasses For Use As Chronic Wound Dressings

AK Solanki¹, H Autefage¹, J Penide², F Quintero², J Pou², JR Jones¹, MM Stevens^{1,3}

¹Department of Materials, Imperial College London, United Kingdom, ²Applied Physics Department, University of Vigo, Spain, ³Department of Bioengineering, Imperial College London, United Kingdom, a.solanki@imperial.ac.uk

INTRODUCTION

Chronic wounds fail to heal within 6 weeks or reoccur frequently, and usually occur in patients already suffering from an underlying pathological condition. Patients with chronic wounds have a reduced quality of life, and treating chronic wounds has a significant economic burden to the healthcare system¹. Hypoxia can regulate many processes essential for tissue repair², such as angiogenesis and is therefore expected to promote chronic wound healing. Cobalt has been shown to mimic hypoxia and promote angiogenesis through the Hypoxia Inducible Factor-1 pathway³. Bioactive glasses have also been shown to promote angiogenesis in specific concentrations. This project aims to develop a dressing suitable for chronic wounds that promotes angiogenesis through incorporation of a cobalt containing glass. A glass composition has been developed that releases cobalt ions in a therapeutic range for at least 1 week. In parallel, formats suitable for clinical presentation have also been identified.

EXPERIMENTAL METHODS

Preparation of electrospun composite: A composite of glass particles and poly-ε-caprolactone (PCL) was produced by electrospinning. Glass particles were mixed with a solution of PCL in chloroform, and this was electrospun at a voltage of 16kV.

Preparation of glass fibres: Glass plates were produced by melting glass frit, and pouring into preheated graphite moulds. Glass fibres were then formed by laser spinning⁴.

Preparation and characterisation of glass particles: To form glass frit, carbonate precursors were melted at 1400°C and quenched into deionised water. The ion release from glass particles into TRIS buffer was measured over 1 week by Inductively Coupled Plasma – Optical Emission Spectroscopy (ICP-OES). The ability to form a hydroxy carbonate apatite layer on the glass surface was also investigated by incubating the glass in Simulated Body Fluid (SBF) for 28 days. Changes in glass structure were determined by Fourier Transform Infrared Spectroscopy (FTIR), X-Ray Diffraction (XRD) and Scanning Electron Microscopy (SEM).

RESULTS AND DISCUSSION

Glasses doped with 2 mol% cobalt oxide were produced⁵ and the dissolution behaviour of the particles in TRIS and SBF buffer was characterised. Over the period of 1 week, cobalt ions were released in a range that is expected to be therapeutic.

A composite mesh was successfully produced by electrospinning. Glass loadings up to 50 wt% have been achieved, with the particles appearing to be homogeneously distributed throughout the mesh and completely coated by PCL (Fig 1). At short timepoints,

the composite showed controlled release of all ions from the glass when compared to the glass particles alone (Fig 2). By the one week timepoint, there were minimal differences between the ion release from the powder and the electrospun composite.

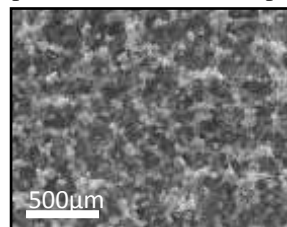


Fig 1: SEM image of the PCL-glass composite containing 50 wt% glass particles.

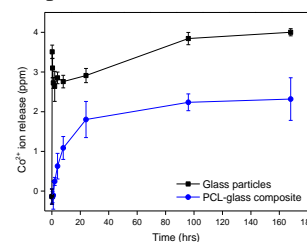


Fig 2: Cobalt ion release in TRIS buffer comparing glass particles and the PCL-glass composite.

Glass fibres produced by laser spinning had a wide range of fibre diameters, were interconnected and show favourable handling properties (Fig 3). During the laser spinning process, the glass fibres were rapidly cooled, which allowed the amorphous structure to be retained, and no crystal phases were observed in the glass fibres.

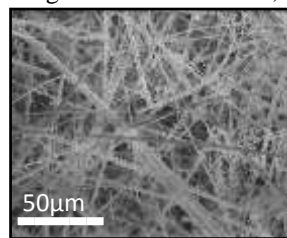


Fig 3: SEM image of the glass fibres.

CONCLUSION

PCL-glass composites and glass fibres were produced from glasses containing 2 mol% cobalt oxide, and characterised. The glass particles allowed release of ions in a range that is expected to upregulate the HIF-1 pathway. The PCL-glass composite and glass fibres both demonstrated controlled ion release at short timepoints, which is beneficial because by preventing a burst ion release, cell toxicity is expected to be reduced. They both have excellent handling properties, and are expected to be suitable for dressing different wound types. In vitro cell studies on a fibroblast cell line are ongoing, and the results obtained from this are expected to provide further insight on the therapeutic effects of the cobalt glass, and will indicate potential cytotoxicity.

REFERENCES

1. MeReC Bulletin, MeRec Publications, 21 (2010) 1-7
2. IR Botusan et al, Proc Natl Acad Sci USA, 105 (2008) 19426-31
3. Y Yuan et al, J Biol Chem, 278 (2003) 15911-161
4. F Quintero et al, Adv Func Mater, 19 (2009) 3084-90
5. M Azevedo et al, J Mat Chem, 20 (2010) 8854-64

ACKNOWLEDGMENTS

The authors would like to thank the NIHR (Project II-ES-1010-10094) for providing financial support to this project.



Bioactive glasses: Instructive biomaterials to Control Cell Microenvironment

Elisabeth Engel^{1,2,3}, Aitor Aguirre^{1,2}, Nadege Sachot^{1,2}, Oscar Castaño^{1,2,3}, Arlyng Gonzalez^{1,2}, Miguel A. Mateos-Timoneda^{1,2}, Soledad Pérez-Amodio^{1,2}, Josep A. Planell^{1,2}

¹Biomaterials for Regenerative Therapies Group /Institute for Bioengineering of Catalonia, Barcelona, Spain. ²CIBER-BBN, Zaragoza, Spain. ³Dept of Material Science and Metallurgical Engineering Technical University of Catalonia, Barcelona, Spain. eengel@ibecbarcelona.eu

INTRODUCTION

Instructive biomaterials play a key role promoting successful tissue repair by means of regenerative medicine approaches, and are expected to contain chemical, as well as mechanical cues that will guide the regenerative process. The use of these biomaterials are optimal for **in situ tissue regeneration**, that uses the body's own regenerating capacity by mobilizing host endogenous stem cells or tissue-specific progenitor cells to the site of the injury.

This approach relies on development of **target-specific biomaterial scaffolding system** that can effectively control the host microenvironment and mobilize host stem/progenitor cells to target tissues. Herein we report the biological properties of a bioactive, biodegradable calcium phosphate glass that can control degradation process and the release of the ions (which are becoming highly relevant enhancing several regenerative responses¹). The appropriate microenvironment provided by implanted scaffolds facilitates recruitment of host cells that can be guided to regenerate structural and functional tissues².

EXPERIMENTAL METHODS

Two types of composites were developed.

1) Scaffolds of Polylactic Acid and micro particles of Calcium phosphate glasses based on TiO_2 -CaO- P_2O_5 - Na_2O system, fabricated by means of solvent casting.

2) Hybrids ormoglasses. Based on the sol-gel method, calcium phosphate glass nanoparticles and/or silicon-based ormoglass polymers were blended with, polylactic acid electrospun nanofibers.

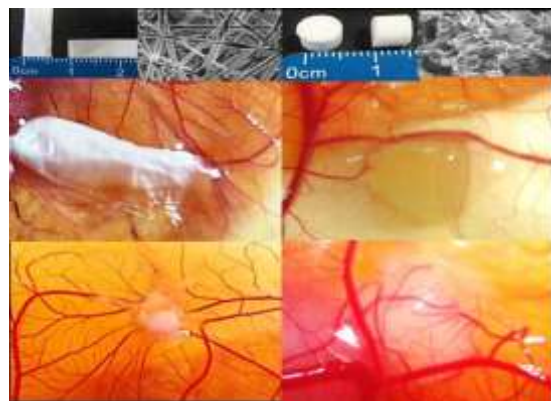
Characterization of the scaffolds in terms of degradation, ion release, surface wettability and topography, mechanical properties and biological performance in vitro and in vivo were conducted.

RESULTS AND DISCUSSION

The solvent casting scaffolds provided excellent mechanical properties to sustain endothelial progenitor cells proliferation and differentiation, as well as vessels formation. Mechanical properties and calcium release together promoted the expression of vascular endothelial growth factor (VEGF) as well as its receptor (VEGF-R).

The nanofibrous scaffold made of PLA afforded the flexible structural support while a sol-gel processed organic-inorganic bioactive glass supplies the chemical bioactive cues.

This method allows the fabrication of scaffolds with excellent hydrophilic properties, enhanced mechanical features, great cellular adhesion and tailored nanostructured topographies and stiffness by changing glass composition. Ca^{2+} release assay showed that nanofibers released more calcium than solvent casting scaffolds and this release was sustained a long time. In



Ex vivo test for vascularization potential of both scaffolds. Nanofibers of PLA and PLA/Glass (left up and down) and scaffolds of PLA and PLA/Glass (right up and down)

vivo, both scaffolds showed the capability to induce bone and vascular formation. Vascularization tests showed that nanofibers with glass exerted a higher potential for vascular growth and penetration.

These instructive biomaterials effectively combine two features that in our experience actively participate in the activation of the progenitor cells that respond and react to stimuli from its environment: bioactivity by means of the release of calcium, that acts as a cell homing and maturation of EPCs and MSCs; and mechanical properties that act synergistically with bioactivity.

CONCLUSION

In this decade, that a new generation of biomaterials have been postulated, the need of a versatile system that can be tuned to promote cell homing and differentiation is relevant for in situ regeneration processes. The fine control of surface properties leads to mobilize cells and support adhesion as well as differentiation. Calcium phosphate glasses display these properties and this study demonstrates the capability to regenerate bone tissue as well as vascularization.

REFERENCES

- Hoppe A, *et al.*, Biomaterials. 37:2757-2774. 2011.
- Sanzana ES, *et al.*; Acta Biomater 4: 1924-1933, 2008
- Aguirre A, *et al.*; eC&M 2 4: 90-106; 2012
- Castano O, *et al.* ACS Applied Materials & Interfaces (Under review).
- Gonzalez A, *et al.* Acta Biomater (In Press).

ACKNOWLEDGMENTS

The authors would like to thank the MINECO (MAT2012-38793) and the European Commission (European ERANET project PI11/03030, NANGIOFRAC) for providing financial support to this project, and O. Castaño also acknowledges the MINECO for the "Ramon y Cajal" contract.

Setting Kinetics and Micromechanical Properties of Flax Fibres Reinforced Restorative Glass Ionomers

Ensanya A. Abou Neel^{1,2,3*}, Wojciech Chrzanowski^{4,5}, Anne M. Young³

¹Division of Biomaterials, Conservative Dental Sciences Department, King Abdulaziz University, Jeddah, Saudi Arabia,

²Biomaterials Department, Faculty of Dentistry, Tanta University, Tanta, Egypt, ³Division of Biomaterials and Tissue Engineering, UCL Eastman Dental Institute, 256 Gray's Inn Road, London, WC1X 8LD, ⁴The University of Sydney, The Faculty of Pharmacy, NSW 2006, Sydney, ⁵Department of Nanobiomedical Science & BK21 PLUS NBM Global

Research Center for Regenerative Medicine, Dankook University, Cheonan 330-714, Republic of Korea,

eabouneel@kau.edu.sa; e.abouneel@ucl.ac.uk

INTRODUCTION

Due to their excellent adhesion and anticariogenicity, glass ionomer cements (GICs) have been widely in dentistry. Poor mechanical properties, long setting and high solubility, however, could limit their applications^(1,2). Addition of silver amalgam has been attempted to overcome these limitations. Regardless of the improvement achieved, the fluoride release was compromised. The use of natural fibres as reinforcing agents has been recently increased. The aim of this study was therefore to use flax fibres for reinforcement of GICs. The effect of flax fibres incorporation on the setting kinetics, surface topography and micro-scale mechanical properties of GICs were investigated.

EXPERIMENTAL METHODS

Sample preparation: Short flax fibres (~2 mm length) were included at 0, 1, 2.5, 5 and 25 wt% into GICs filling materials (KetacTM Fill Plus, 3M). The samples were coded: GIC, 1FFRGIC, 2.5FFRGIC, 5FFRGIC, 25FFRGIC respectively. The powder: liquid ratio was 3:1; the mixed paste was used for the reaction kinetic study. Discs of 5 mm diameter and 2 mm thickness were used for topography and mechanical characterisation.

Setting reaction kinetics: The setting reaction kinetics of each mixed cement has been studied using ART-FTIR spectrometer (Nicollet iS10). Spectra were obtained every 2 minutes during the first 60 minutes after mixing using OMNIC software. The spectra were obtained between 400 and 4000 cm⁻¹. To compare between different compositions, the relative reaction rate and reaction extent were used.

Surface topography and mechanical properties: Samples were scanned using atomic force microscope operating in amplitude modulated force microscopy mode (AMFM, MFP-3D-Bio, AsylumResearch) at frequency of 0.5 Hz and scan size was 20x20, 10x10 and 1x1 μm. Silicon tip with nominal spring constant 40 N/m was used. Topographical images, distribution of different phases in the material and maps of stiffness and energy dissipation which corresponded with phase separation and uniformity of the material were obtained from the collected data.

RESULTS AND DISCUSSION

The setting reaction of GIC followed three stages. Initially, no absorbance changes were observed; then polyacid neutralization was characteristic to intermediate changes-Fig.1a. Further loss of polyacid and concomitant formation of polyacrylate complexes were then seen. With incorporation of flax fibres, the setting reaction followed the same stages but with slightly slower initial rates while increasing the fibres weight%-Fig.1b.

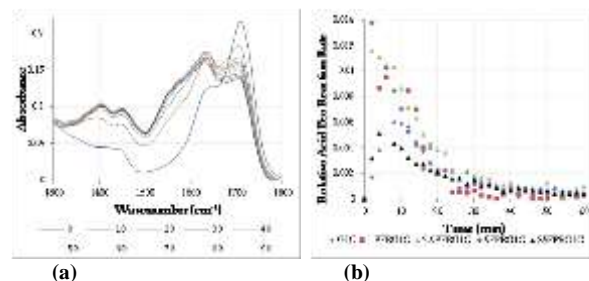


Fig.1: FTIR showing the reduction in 1707 cm⁻¹ peak indicating the progression of reaction (a) and the resultant reaction extent (b).

Qualitative imaging using AMFM showed the presence of a single phase in GIC, while biphasic structure was observed for FFRGIC-Fig. 2a&c. Both groups of material showed differences in topography (roughness); mean roughness for GIC samples was lower than for the samples with filler. Importantly, the incorporation of flax fibres was shown to increase Young's modulus with increasing about of filler content-Fig. 2b&d. The flax fibres were uniformly distributed for all tested samples and well integrated within the substrate, without visible interfacial separation.

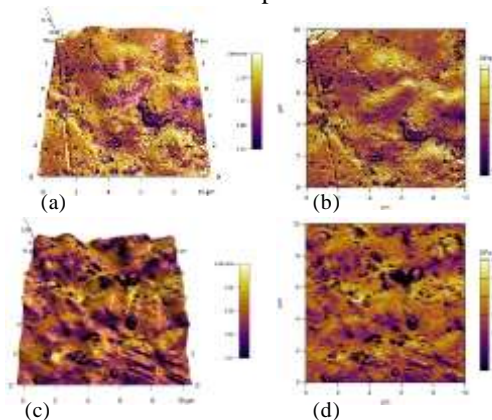


Fig. 2: Topography and stiffness map of GIC (a, b) and 1FFRGIC (c, d).

CONCLUSION

- Flax fibres slightly reduced the initial but not the final setting reaction rate.
- A slight increase in the mean roughness was observed with incorporation of flax fibres.
- Regardless of their physical incorporation, flax fibres were uniformly distributed and well integrated within GIC matrix.
- Flax fibres produced a significant improvement in Young's modulus of GIC.

REFERENCES

- (1) Hamouda IM. J Esthet Restor Dent 2011 23(5):315-22.
- (2) Elsaka SE et al., J. Dent 2011;39(9):589-98.

ACKNOWLEDGMENTS

This project was funded by the Deanship of Scientific Research (DSR), King Abdulaziz University, Jeddah, under grant no (440/254 /1434). The authors, therefore acknowledge with thanks DSR technical and financial support.



Hypoxia Mimicking Bioactive Glasses for Chronic Wound Healing

Maria Azevedo, Siwei Li, Wai Ho, Alex Burns, Luara Schoenewolf, Chris Nayar and **Gavin Jell**

Division of Surgery & Interventional Science, UCL, Royal Free Campus, London, UK, g.jell@ucl.ac.uk

INTRODUCTION

Novel methods to improve chronic wound regeneration are urgently needed. Hypoxia (low O_2 pressure) is the principle environmental cue that stimulates wound healing. The damaged vasculature of the wound causes a local drop in O_2 pressure which cells respond to via the HIF (hypoxia inducing factor) pathway. Stabilisation of HIF, following hypoxia, initiates a number of pathways important for wound healing including; α -microbial cell recruitment/activity, cell differentiation, ECM production, cell survival and the restoration of O_2 pressure through angiogenesis (Fig. 1). Furthermore in patients with chronic wounds (elderly patients and those with diabetes mellitus) there appears to be a diminished cellular ability to respond to hypoxia via HIF¹. Materials that regulate the HIF pathway could, therefore, be an attractive target in chronic wound management. Hypoxia Bioactive Glasses (HBG) containing the known hypoxia mimetic cobalt were developed to stabilise HIF-1 α and activate this wound regeneration pathway (Fig. 1).

a. Hypoxia Bioactive Glass b. Co^{2+} Stabilizing HIF-1 α c. Wound healing responses

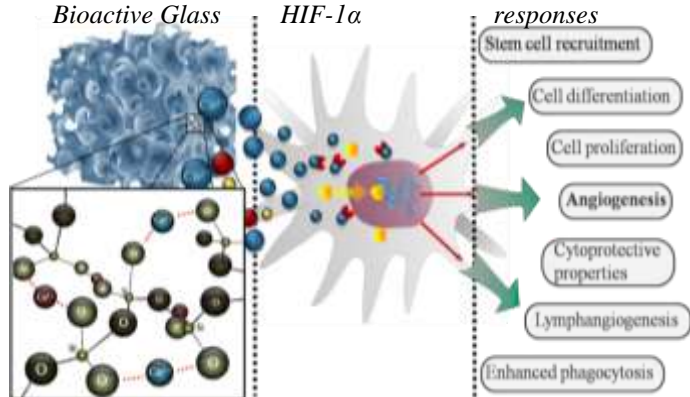


Figure 1. (a) Resorbable HBGs release physiologically active concentrations of Co^{2+} , (b) Co^{2+} inhibits the activity of the O_2 sensitive enzyme Phd thereby enabling the nuclear translocation of HIF-1 α and (c) causing the cell-type specific activation of hypoxia responsive elements associated with wound repair.

EXPERIMENTAL METHODS

Melt-derived HBGs (SiO_2 49.5%; P_2O_5 1%; CaO 19-23%; Na_2O 26.5%; CoO 0-4%) were manufactured and characterised as previously described². Endothelial cells (ECs), macrophages (M ϕ) and fibroblasts (FBs) were cultured in appropriate media which had been pre-incubated with HBGs (0%, 1%, 2% or 4 Mol % Co^{2+}). The ability of HBGs to stabilize HIF-1 α , promote pro-angiogenic factor production (FGF, VEGF) and promote cell migration was determined by immunofluorescence and the TransAMTM HIF-1 assay kit (Active Motif[®]), ELISA (R&D systems) and the Transwell[®] migration assay respectively. Anti-microbial activity was assessed by monocyte differentiation into M ϕ and phagocytic activity determined by pHrodoTM Bioparticles[®] uptake (Molecular Probes[®]). To mimic a

diabetic chronic wound these studies were also completed in high glucose (25mM) media with D-Mannitol (to balance osmolarity).

RESULTS AND DISCUSSION

Media conditioned with HBGs increased nuclear HIF-1 α expression ($P < 0.05$ as determined by the TransAMTM assay) and by immunofluorescence (Fig. 2), suggesting that HBG stabilise HIF1 α in normoxia.

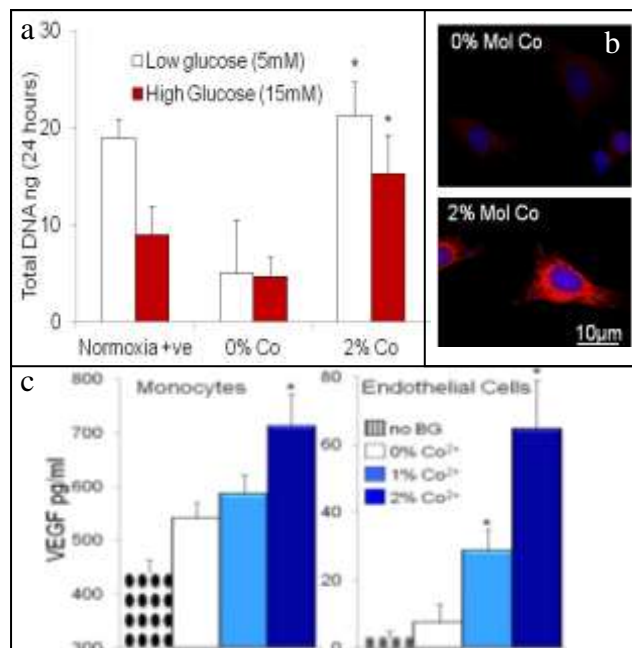


Figure 2. (a) HBG (2% Co^{2+}) increased EC migration in both low and high glucose environments (24hr) (b) HBG increased HIF1 α expression in both cytoplasm and nuclei. (c) HBG caused a concentration dependant increase in the expression of VEGF by M ϕ and ECs after 24 hr culture. * $P < 0.05$ compared to 0%BG

HBG conditioned media activated a number of regenerative process associated with wound repair including, increased cell migration, the increased of angiogenic factors (VEGF and FGF) and also promoting the differentiation of M ϕ and increasing phagocytic activity. Importantly some of these regenerative processes were observed in chronic wound-like conditions (high glucose).

CONCLUSION HBG offers a controllable ion release system that can stabilise HIF1 α and initiate upstream wound repair. Considerable further work is required to develop and translate these promising results into HBG-hydrogel wound healing constructs.

REFERENCES

1. Botusan IR, 2008. *PNAS* (105) 49, 19426
2. Azevedo MM, et. al. 2010, *J. Mat. Chem.*, (20) 8854

ACKNOWLEDGMENTS This work was possible due to the assistance of Prof. R .Hill (Queen Mary University), Prof. M. Stevens and Prof. J. Jones (Imperial College London).

Non-invasive and specific attachment of hernia mesh by click chemistry

R. Vestberg¹, M. Guerin¹, A. Radlovic¹, O. Lefranc¹, S. Ladet¹

¹Covidien Trévoux, France
robert.vestberg@covidien.com

INTRODUCTION

Hernia repair is frequently performed involving mechanical fixation of a surgical mesh that could be associated with chronic pain.

In this concept, a way to mimic the cellular adhesion mechanism in living tissue for fixation of surgical mesh was investigated. Leveraging the click chemistry technology, it would be possible to develop more precise fixation by targeting the specific areas to be attached while preserving sensitive anatomical structures. Moreover by spreading the fixation strength on the entire surface of the mesh, it is expected to reduce local constraints and associated pain. This innovative approach inspired by nature represents a precise and less invasive fixation mean to improve the clinical outcome of patient receiving hernia repair.

EXPERIMENTAL METHODS

Click chemistry¹ is a recent concept which is designed to replicate the physiological molecular interaction. In the click chemistry reaction two reactive entities are linked as a key and lock mechanism. In this work, cell and device surfaces have been activated with the two reactive entities (azide and alkyne) and the cells connected to the device surface using the copper mediated azide-alkyne cycloaddition click reaction (CuAAC).

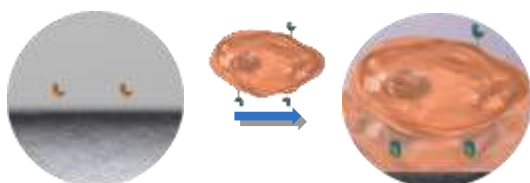


Figure 1. Schematic of non-invasive fixation of tissue to a medical device surface by click chemistry.

RESULTS AND DISCUSSION

To demonstrate the concept of interaction between living tissue and medical devices, cells with reactive Click entities need to be obtained. Cells were exposed to a manose containing the click reactive entity (azide), which was then expressed on the cell membrane². The expression of the click entity on the cell membrane was verified by attaching a fluorescent molecule (Alexa 488) containing the complementary click reactive entity (alkyne) to link the fluorescent molecule to the cell membrane. Flow cytometry results confirmed a successful functionalization of the cells with high cell viability

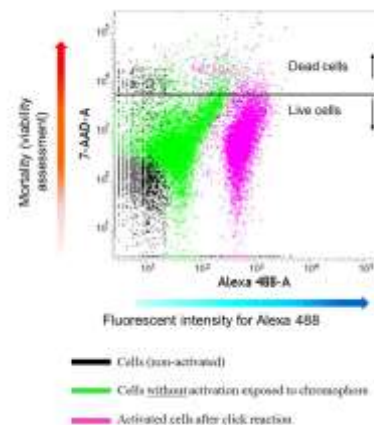


Figure 2. Results from flow cytometry.

To demonstrate the specificity of click fixation, activated cells were exposed to a patterned device surfaces. The patterned on the device surface was composed of alkyne substituted chitosan. To characterize the specific cell attachment to the surface, living cells were stained in green (Live/Dead staining).

It was demonstrated that cells could successfully attach only to the activated surface and that an activated devices could be precisely patterned to drive cell specific attachment (bracket area).

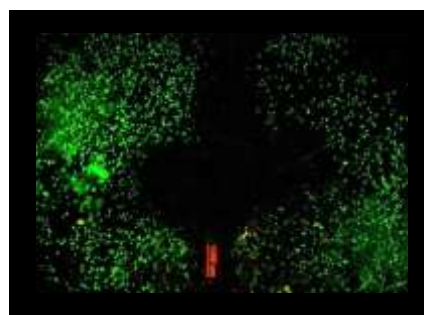


Figure 3. Fluorescent microscopy showing that cells can be driven to attach to a predefined part of a surface.

CONCLUSION

This work demonstrated that non-invasive and precise fixation of medical devices could be obtained by click chemistry activation. Click chemistry is a highly specific and versatile concept which can redefine the way we do surgery.

REFERENCES

1. K. B. Sharpless K. B. *et al.*, *Angew. Chem. Int. Ed.*, 40: 2004–2021, 2001
2. Wu, P. *et al.*, *JACS*, 132:16893-16899, 2010

Tubular compressed collagen scaffolds cultured in a novel flow-bioreactor system for ureter/urethra tissue engineering applications

Elif Vardar¹, Eva-Maria Balet¹, Hans Mattias Larsson¹, Jeffrey A. Hubbell¹, and Peter Frey¹

¹Institute of Bioengineering, École Polytechnique Fédérale de Lausanne, Switzerland, elif.vardar@epfl.ch

INTRODUCTION

Urological tissue engineering aims to overcome complications like secondary malignancies, intestinal adhesions, and chronic infections that are linked to classical surgical repair of urinary tract (1). The latest developments in urological tissue engineering have been intended to design novel scaffolds and cell culture techniques for urinary tract reconstruction. The use of bioreactors has brought many significant advantages, such as pre-determined culture conditions that are similar to physiological conditions, to the traditional tissue engineering approaches. In this study, plastically compressed (pc) tubular collagen scaffolds were evaluated under dynamic culture conditions inside a novel flow-bioreactor system imitating the dynamic environment of the ureter. After determining the flow conditions mimicking the best ureteral flow, biological performance of pc tubular collagen scaffolds was evaluated in the flow-bioreactor device.

EXPERIMENTAL METHODS

Scaffolds were prepared by casting a neutralized collagen solution (Rat tail collagen type I, First Link, 2.05 mg/ml) containing primary human bladder smooth muscle cells (hSMC) into tubular moulds. After polymerization, scaffolds were compressed by applying a compressive stress of 5 kPa for 2 min at room temperature. A ureteral flow cycle program was written by using ProgEdit software. Mean luminal pressure values along pc collagen tubes were determined by using a digital manometer, attached to the luminal outlet (Fig. 1). To induce flow, the chamber was connected to a sterile media reservoir via a peristaltic pump (Ismatec).

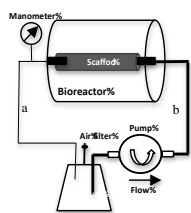


Figure 1. Schematic representation of the flow-bioreactor system. Inner diameter of silicon tubing “a” is smaller than that of “b” to create a flow resistance.

Burst pressure of pc collagen tubes was determined as connecting the tube to a water column and increasing gradually the hydrostatic pressure until the leak detection. The ultimate tensile strength (UTS), linear modulus (E) values were evaluated by Instron tensile machine. hSMC-seeded pc collagen scaffolds were assessed using AlamarBlue assay for cell proliferation, Live/Dead stain (Live/Dead® Viability/Cytotoxicity Kit for mammalian cells, Invitrogen) for cell viability, and Hematoxylin and Eosin (H&E) staining for cell distribution throughout the scaffolds. Change in gene expression of hSMCs was evaluated by RT-qPCR (Roche). Paraffin embedded sections of cell-seeded

scaffolds will be stained for alpha-smooth muscle actin (α -SMA), smoothelin (SMTN), and human collagen type I (COL1A1). Significant differences between datasets were determined by ANOVA tests.

RESULTS AND DISCUSSION

Around 23 cmH₂O pressure change, a value, which is in the range of ureteral pressure (2), was obtained within pc collagen scaffolds during a pump cycle at 20 rpm (Fig.2).

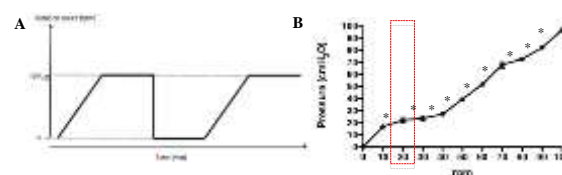


Figure 2. (A) The pump cycle scheme (B) The maximal pressure values within pc collagen tubes with increasing rpm values, *p < 0.001.

hSMC seeded within tubular pc collagen scaffolds showed a high cell viability up to day 7 and aligned parallel to the flow direction under dynamic conditions (Fig. 3).

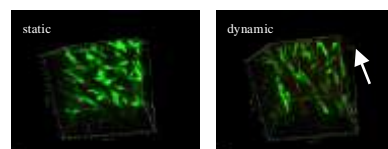


Figure 3. Live/Dead® Viability assay. Confocal z-stack images of hSMC seeded pc collagen tubes after 7 days of culture. Arrow shows flow direction.

Characterization of mechanical properties of pc collagen tubes, immunohistochemistry and gene expression studies are currently on-going.

CONCLUSION

Preliminary results show that our flow-bioreactor system provides dynamic conditions, which are similar to the physiological environment of the native ureter. Therefore pc collagen tubes, matured in this flow-bioreactor system, are a quite promising biomaterial for urological tissue engineering applications.

REFERENCES

- Atala A. *et al.*, British Medical Bulletin, 97: 81-104, 2011.
- Normand L. *et al.*, Annales d'Urologie, 39(1): 30-48, 2005.

ACKNOWLEDGMENTS

This study is supported by a Swiss National Grant (Grant number: 310030_13844).



Making medical stent in the way of laser spot welding of stainless steel wires L316

Delaram Mansourian¹ and Mahyar Fazeli^{2*}
And Jamshid Aghazadeh Mohandes³

¹Department of material science and metallurgy engineering , AmirKabir university of technology, Iran,
dmansurian@gmail.com

² Department of material science and metallurgy engineering , AmirKabir university of technology, Iran

³Department of material science and metallurgy engineering , AmirKabir university of technology, Iran

INTRODUCTION

Angioplasty is a technique in treatment for opening blockage in blood vessels. There are different techniques for the operation of opening blockage in vessels. Using angioplasty balloon is limited as 2-3 percent of patients need to open heart surgery and blockage in vessels would be backed in 30-50 percent of patients. At first, balloon was utilized only for opening coronary arteries, but while time passed problems like intimal dissection or recoil or being again blocked were appeared which sometimes made catastrophe. With the probability of early reclogging after some hours or days, scientist have invented stents to reduce the problem of reclogging coronary arteries after angioplasty. In 1987, Sigwart had reported that they implanted stent successfully. Stent is a small mesh tube that made from metal that open artery and would be remain inside it forever.

EXPERIMENTAL METHODS

Stainless steel thin wires 316 in 0.3 mm diameter has been employed in the research. Wire diameter is determining through exited stent from patient body. Polymer polexi sheets in 2 mm thickness were utilized to build a frame for shaping stent wire; the sheets had been cut with laser and five of them connected together for building a jaw frame. laser cutting was selected for constructing cardiovascular stent as it is commercial and have many advantages. with the country possibilities, it is impossible to build a cylinder with thickness about microns through extrusion; Stainless steel wire stent was selected which has lower cost price and better characteristics in this context. The stent was exited from one of the patient's coronary arteries that had been made from welded thin wires to each other. Thus, thin wire welding method which needs lower facilities, was selected in this project. For forming stainless steel wires in shape of stent, jaw like frames have been utilized that made from polymer polexi. Polymer sheets have cut by laser in model of stent and in 2 mm thickness. The machine conducts accurately the cuts through computer software. Design of stent was drawn by Corel Graphic Program exactly like the model and dimensions of the stent that was exited from the body. It was set to use laser spot welding like similar commercial samples for connecting each of the formed wires. Tensile test, metallographic testing of welding locations and SEM scanning electron microscopy have been done on laser welded stainless steel wires to consider laser welding. Another way has been considered to connect the formed wires. In the project,

stainless steel wires which formed with polymer frame were welded together through thermal soldering iron that is efficient in very fine electric board welding.

RESULTS AND DISCUSSION

Results of micro hardness testing on wires provided in dimensions of stent.

Mean of transverse micro hardness (Vickers)	Mean of longitudinal micro hardness (Vickers)
241/3	240/7

Results of micro hardness testing on stent wires which went away from the patient body

Mean of longitudinal micro hardness (Vickers)
169/3

Results of tensile testing have shown that strength of stent welding about 0.725 Mpa is more than strength of laser welding under test. A significant notice in tensile testing is that each of the connections were broken from welding point which explained welded point that is under test would not be weaker than stent laser welding that went away from the patient's body. Metallography images were taken from stent welding point and part of wire which did not weld, the structure of welding and not welding part is similar, as lower thickness of wires in stents laser welding has reduced welding time and laser temperature and then cannot make any changes in combination and structure. Wires laser welding is conducted through a programmed machine in constructing commercial stents which changes will not be created in the structure. Therefore, time and laser beam energy must be set to achieve appropriate strength in such cases and finally obtain the best condition for receiving the best strength.

CONCLUSION

SEM scanning electron microscopy presented a relative uniform welding with no crack. time and laser beam energy must be set to achieve appropriate strength in such cases and finally obtain the best condition for receiving the best strength. Results of micro hardness testing on wires provided in dimensions of stent and wires which went away from the patient body showed that these wires are appropriate for making stent in this project.

REFERENCES

1. Stent Coating or Brachytherapy, Their Future Role in Endovascular Therapy of Coronary Artery Disease- Progress in Biomedical Research- J. J. R. M. BONNIER- May 2000- pp. 229-231

Towards an Implantable Bioreactor: Synthesis and Surface Modification Strategy for a Soft Tissue Engineered Elastomer

D-E. Mogosanu^{1,2}, J. Vanfleteren², P. Dubruel¹

¹Polymer Chemistry and Biomaterials Research Group, Ghent University, Belgium

²Center for Microsystems Technology, Ghent University, Belgium, dianaelena.mogosanu@ugent.be

INTRODUCTION

For future construction of implantable tissue structures, the development of 3D biodegradable fluidic microsystems is necessary. In the last decade, poly (glycerol-sebacate) (PGS) has become one of the most studied elastomers for biomedical applications due to its biocompatibility and biodegradability. The first reported synthesis involved a 2 day reaction, followed by pre-polymer crosslinking¹. The goal of the current work is to overcome the common limitations of the conventional synthesis strategy that requires a long reaction time. We report a route that reduces by 30-fold the total synthesis time of PGS and a surface modification strategy that enhances the hydrophilicity as well as the cell-interactivity. Moreover, we are developing a unique technology for biodegradable 3D microsystems that can sustain cell co-cultures. This technology can be easily transferred to all poly(polyol sebacate)s present in literature.

EXPERIMENTAL METHODS

Synthesis and fabrication of PGS films

Equimolar quantities of reagents (Sigma-Aldrich) were mixed in a reactor at high temperatures for different reaction times. Films were fabricated by melting the pre-polymer on a polysaccharide coated mold and curing in a vacuum oven at 150°C.

Functionalization of PGS films

PGS films were functionalized via a graft polymerization procedure, followed by the attachment of gelatin to the surface. Both PGS and PGS-Gelatin films were analyzed via IR mapping, XPS, AFM, SCA and microscopy techniques.

Bioreactor development

Patterned silicon wafers were processed by standard lithographic processes. The micro-pattern (50-100 μm width and 100 μm height) was transferred to PGS. The patterned PGS layers were aligned and bonded. Porous membranes were inserted in between patterned layers in order to create proper conditions for cell co-culture.

RESULTS AND DISCUSSION

The polycondensation reaction performed via the strategy we report yielded a final yellowish elastomer. The reaction kinetics indicated an optimum synthesis

time of 1.5h, almost 30 times less than the time reported by the classical route¹. Surface modification of the native material is required due to its high hydrophobicity, similar to that of PDMS. Contact angle measurements showed a decrease from 92° for the PGS film to 35° for the gelatin modified PGS film. XPS analyses indicated that PGS-protein films have a similar N/C ratio to that of the pure gelatin. IR mapping showed a complete coverage, while AFM measurements indicated gelatin clusters present on the polymer surface.

Two- and three-layer microfluidic devices were developed in order to design a tissue-engineered organ. As vital organs contain multiple types of cells, we have integrated a porous membrane in the microfluidic device. This strategy would enable not only cell co-culture, but also distribution of nutrients and oxygen.

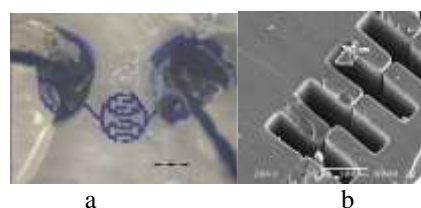


Figure 1a shows the perfusion test of a microfluidic device, while 1b presents the channels cross-section of a two-layer microfluidic device.

CONCLUSION

PGS was successfully synthesized via a rapid method. The usefulness of this approach has been demonstrated by the 30 times reduction of the conventional synthesis time. As synthetic biomaterials that mimic the ECM have a wide range of biomedical applications, we have also functionalized the polymer with a protein via a chemical immobilization technique. We are currently investigating the adhesion and proliferation of different cell types on the modified polymer surfaces, as well as the development of complex 3D microfluidic systems for cell culture and tissue engineering.

REFERENCES

1. Wang, Y.D. *et al.*, Nat Biotech, 20(6): p. 602-606, 2002.

ACKNOWLEDGMENT

Authors would like to thank FWO-Flanders for providing financial support to this project.



Development of an original model to investigate cell communication in bone tissue engineering

A. Grémare^{1,2}, A. Aussel^{1,2}, R. Bareille^{1,2}, J. Guerrero^{1,2}, J. Amedee^{1,2}, D. Le Nihouannen^{1,2}

¹Univ. Bordeaux, Bioingénierie Tissulaire, U1026, F-33000 Bordeaux, France

²INSERM, Bioingénierie Tissulaire, U1026, F-33000 Bordeaux, France, agathegremare@hotmail.fr

INTRODUCTION

Bone is a living tissue mainly populated with osteoblastic cells (OB), osteoclastic cells (OC) and endothelial cells (EC). Their crosstalk is essential for bone homeostasis and to optimize bone regeneration after biomaterial implantation. Whereas links between OB and OC as well as links between OB and EC are well established, the communication between OC and EC remains unknown¹. Moreover, no tri-culture system from human primary cells has been described in the literature³. In a previous work, a medium allowing the co-culture of OC and EC was established by our team (α MEM/EGM2*). In the present study, the capacity of this medium to be used in an original primary human tri-culture model was investigated. The osteoclastic resorption activity, the osteoblastic and endothelial phenotypes maintenance, and finally the set up of a tri-culture model, were assessed.

EXPERIMENTAL METHODS

Cell culture media: α MEM/EGM2* medium was made of equal volumes of α MEM (alpha Minimum Essential Medium) and EGM2* (Endothelial Growth Medium-2-MicroVascular (EGM2-MV) without ascorbic acid and hydrocortisone which inhibit OC differentiation).

Cell culture models: Mononuclear cells (MNC) were isolated from human umbilical cord blood. OC and EPC were obtained after MNC differentiation with specific cell culture conditions. Endothelial Progenitor Cells (EPC) were used as EC model.

Mesenchymal stem cells were isolated from human bone marrow and differentiated towards OB.

Cell differentiation assays: Osteoclastic resorption activity was assessed on calcium phosphate substrates using differentiated OC from MNC. Resorption lacunae were identified by scanning electron microscopy and quantified by image analysis.

Both in a single culture model and in a co-culture model, OB and EPC were characterized by Alkaline Phosphatase (ALP) staining and immunolabellings of von Willebrand Factor (vWF), CD-31 and VE-cadherin, respectively. Mineralization of extracellular matrix (ECM) was characterized by Von Kossa staining.

In the tri-culture model OB, OC and EPC were cultured both in direct and in indirect contact. In indirect contact conditions, OB and EPC were cultured in a transwell whereas MNC remained on the plastic. OB and OC differentiation was characterized by ALP and Tartrate Resistant Acid Phosphatase stainings, respectively.

Data are presented as means \pm standard error of the mean, with n indicating the number of independent experiments. Differences were assessed by paired Student's t-test and accepted as statistically significant when $p < 0.05$.

RESULTS AND DISCUSSION

In the presence of α MEM/EGM2* medium, osteoclastic resorption activity was not significantly changed with $5286 \mu\text{m}^2 \pm 1150 \mu\text{m}^2$ of resorbed area per substrate compared with $4335 \mu\text{m}^2 \pm 1104 \mu\text{m}^2$ of resorbed area per substrate in the presence of α MEM control medium ($n=6$, $p=0.24$).

Both in the single culture model and in the co-culture model, after 3 and 7 days, immunolabellings of vWF, CD-31 and VE-cadherin were similar for EPC cultured with α MEM/EGM2* compared with EPC cultured with α MEM/EGM2-MV medium (control condition). Similarly, comparable ALP expression as well as ECM mineralization after 10 days, were observed. These data showed that osteoblastic and endothelial phenotypes were preserved in α MEM/EGM2*.

The possibility of culturing the OB, OC and EPC together with the medium (α MEM/EGM2*) was then investigated. Aiming for osteoclast formation in this tri-culture model, OB and OC markers were assessed after 11 days of culture. Both TRAP positive cells and ALP positive cells were observed. However, as previously published³, EPC cannot be detected after more than 7 days of culture in a co-culture system. Interestingly, when the tri-culture was performed in indirect contact, a higher osteoclastogenesis was observed compared with the tri-culture in direct contact. These data suggested that osteoclast formation might be modulated by OB and/or EC direct contact in our model.

CONCLUSION

Results of this study validate the use of α MEM/EGM2* as a medium a) to obtain functional OC after MNC differentiation, b) to preserve osteoblastic and endothelial phenotypes both in mono- and co-cultured models and c) to set up a original tri-cultured model based on human primary OB, OC and EPC. This model is a promising tool both to study bone cell-material interaction and to optimize strategies in bone tissue engineering.

REFERENCES

1. Thebaud N. *et al.*, J. Tissue Eng Regen Med. 6:51-60, 2012.
2. Dohle E. *et al.*, European Cells and Materials. 27:149-165, 2014.
3. Stahl A. *et al.*, Biochem Biophys Res Commun 2004;322:684.

ACKNOWLEDGMENTS

The authors would like to thank Biomatlante for providing the calcium phosphate materials and the Marie Curie Carrier Integration Grant for their financial support.



Fabrication of porous titanium scaffolds by stack sintering of microporous titanium spheres produced with centrifugal granulation technology

Hongjie Chen, Xiangdong Zhu, Yujiang Fan, Xingdong Zhang

National Engineering Research Center for Biomaterials, Sichuan University, China, s_mitory@126.com

INTRODUCTION

Titanium (Ti) has been widely used for bone grafts in load-bearing sites. Nevertheless, stress shielding would lead to bone resorption and loosening of the implant. By controlling porosity and pore size distribution, the porous Ti scaffolds could be biomechanically compatible^{1, 2}. In the present study, a simple new approach to fabricating load-bearing porous Ti scaffolds with uniform porous structure, highly controllable pore size and excellent biocompatibility was developed. This scaffold was made by stack sintering of microporous Ti spheres produced with centrifuge granulation of commercial Ti powders. The porous structure, mechanical property and biocompatibility of the fabricated porous Ti scaffolds were investigated.

EXPERIMENTAL METHODS

By centrifuge granulation of commercial Ti powders (38-45 μm , 54-63 μm and 88-97 μm), microporous Ti spheres (500-600 μm , 800-900 μm and 1000-1250 μm) were fabricated. The Ti spheres were then filled into a cylindrical mold, compacted and sintered in a vacuum of 1×10^{-3} Pa at 1300 $^{\circ}\text{C}$ for 2 hours, forming the porous Ti scaffolds, as shown in Table 1. The morphology, pore size distribution and mechanical strength of the scaffolds were respectively assessed. To evaluate biocompatibility of the scaffolds, protein adsorption and cell culture experiments were performed.

RESULTS AND DISCUSSION

The macroscopic appearance and microstructure of the fabricated porous Ti scaffolds are shown in Fig. 1 (a) and (b). By this method, the macropores and micropores size distributions of the Ti scaffolds could be accurately regulated by choosing appropriate size ranges of the primary Ti powders and the secondary Ti spheres. With the increasing size of the primary Ti powders, the average micropores size increased from 6.8 to 14.0 μm . And with the increasing size of the secondary Ti spheres, the average macropores size of increased from 121.6 to 363.5 μm , as shown in Fig. 1 (c). With increasing size of the Ti spheres, the compressive strength of the scaffolds decreased from 108.9 to 83.4 MPa, as shown in Fig. 1 (d), but the Young's modulus had only a little decrease from 3.0 to 2.7 GPa. The results of serum proteins adsorption on the surface treated scaffolds was measured, and shown that there was more serum proteins adsorption on the scaffolds made from the microporous Ti spheres than that from the dense Ti beads. After 3 days of culture, a large number of MSCs were tightly attached to the rough and convex surface of the macropores, and part of them had polygonal or fibrous shape, meaning that the scaffolds could allow better growth and proliferation of the cells.

Table 1 Specification of porous Ti samples.

Designation	Ti powders/ μm	Ti spheres/ μm
Ti-600	-	600 (Ti beads)
Ti-600/54	54-63	500-600
Ti-900/38	38-45	800-900
Ti-900/54	54-63	800-900
Ti-900/88	88-97	800-900
Ti-1250/54	54-63	1000-1250

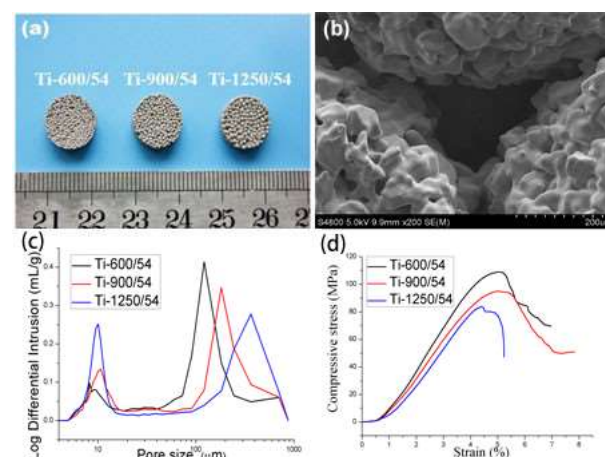


Fig. 1 (a) Digital photos of the scaffolds from different Ti spheres; (b) SEM images ($\times 200$) of the scaffold from the Ti spheres; (c) Pore size distribution of the porous Ti scaffolds influenced of the Ti spheres; (d) Typical compressive stress-strain curves of the Ti scaffolds.

CONCLUSION

This work developed a simple new method, i.e. stack sintering of microporous Ti spheres produced with centrifuge granulation technology, to fabricate porous Ti scaffolds with uniform porous structure. The micropores (6.8-14.0 μm) and macropores (121.6-363.5 μm) of the scaffolds could be accurately regulated by choosing appropriate size ranges of the Ti powders and the Ti spheres. The compressive strength (83.4-108.9 MPa) was high enough for use as load-bearing scaffolds. Besides, the scaffolds were favourable for adsorption of serum proteins, and the rough and convex surface promoted the attachment and growth of MSCs. In conclusion, the porous Ti scaffolds developed in the present study could have better potential to be used as bioactive scaffolds or coatings for the repair of bone defects in load-bearing sites.

REFERENCES

1. Karageorgiou V. *et al.*, Biomaterials. 26:5474-5491,2005
2. Olivares-Navarrete R. *et al.*, Biomaterials. 31:2728-2735,2010

Essential Model for Determining Biomaterial Attachment in Total Joint Replacement

R. Bloebaum^{1,2}, N. Abdo^{1,2}, R. Olsen^{1,4}, A. Hofmann³, J. Chalayan^{1,2}

¹George E. Wahlen Department of Veterans Affairs, Salt Lake City Health Care System, U.S.

²Department of Orthopaedics, University of Utah, U.S.

³Hofmann Arthritis Institute, Salt Lake City, UT

⁴imds, Logan, UT, Roy.bloebaum@hsc.utah.edu

INTRODUCTION

Extensive research began in the 1980s to develop biomaterials that would assure skeletal attachment in cementless total joint replacement (TJR)¹. Despite these efforts, early mechanical loosening, unrelated to wear, continues to be reported in clinical literature.

The acetabular component in the hip replacement and tibial and femoral components in the knee replacement are the most vulnerable to early mechanical loosening². One possible explanation is that the cancellous bone has less potential for osteointegration. Despite this knowledge, many investigators still use the transcortical model to screen new porous coatings. This study highlights the importance of using the appropriate and clinically predictive model to screen new biomaterials intended for cementless TJR.

The objective was to use the transcortical and intracondylar locations of the large animal model to determine the differences in bone responses to two different materials with two different shapes. The null hypothesis was that there would be no difference in the bone responses between the two materials and the two geometric dimensions.

EXPERIMENTAL METHODS

A weight-bearing ovine model was used because it has translated successful skeletal attachment clinically²⁻⁵. Porous-coated titanium (Ti) plugs (Thortex Inc., Portland, OR, TJO Inc., Salt Lake City, UT) were used as the investigative material (control) because they provide successful attachment in TJR. Coprolites, or dinosaur poop (DP), were used to establish a dramatic understanding that even this unique material (that would never be used in TJR) could demonstrate skeletal attachment at the transcortical location.

Figure 1:



Figure 1 displays the proud DP plug (left), proud Ti plug (middle), and inset Ti plug (right).

Ten sheep were used. Two 8 mm-diameter holes were drilled into the right lateral femoral condyle (intracondylar model) as well as into the diaphysis of the tibia (transcortical model). Four implants were placed within each sheep: one DP and one Ti in the condyle and one DP and one Ti in the tibia. Five sheep received inset plugs in both locations and five sheep received proud plugs in both locations.

The proud plugs were implanted in a “press-fit” fashion into the prepared hole. The inset plugs were inserted

leaving an inner 500-μm gap between the implant surfaces and the drill track. Literature has demonstrated that a distance greater than 100 μm results in fibrous encapsulation in cancellous bone¹¹. Sheep were euthanized at 12 weeks. Radiographic and histological assessment was performed.

RESULTS AND DISCUSSION

Histological data showed fibrous tissue around the DP plugs in all locations and dimensions. Bone traversed the 500-μm gap in the transcortical location but not in the intracondylar location. The Ti inset plugs showed fibrous tissue at the intracondylar site while the Ti proud plugs achieved bone attachment at both sites.

Table 1:

Material	Transcortical	Intracondylar	P-value
Ti	19.73%	62.51%	0.0001
DP	16.95%	46.22%	0.0013

Table 1 displays the average bone formation in the periprosthetic region of the inset plugs.

Table 2:

Material	Transcortical	Intracondylar	P-value
Ti	43.37%	3.10%	0.0094

Table 2 displays the average bone ingrowth into the inset Ti porous coating.

The results highlight the false positive nature of the transcortical model due to its native fracture healing response compared to the more limited healing capacity of cancellous bone. The data validated the intracondylar model for predicting cancellous bone ingrowth for acetabular and total knee components. The location of implantation, geometry, and material type affect skeletal attachment.

CONCLUSION

Intracondylar implantation is the reliable model to assure the performance of any biomaterial intended for cancellous bone attachment. There is no excuse for mechanical loosening of cementless TJR components if proper translational screening is performed.

REFERENCES

1. Khanuja H., JBJS. 93(5):500-509, 2011
2. Hofmann A., Acta Orthop Scand. 68(2):161-166, 1997
3. Hofmann A., CORR. 452:200-204, 2006
4. Willie B., JBMR. 69A(3):567-576, 2004
5. Bloebaum R., CORR. 470(7):1869-1878, 2012
6. Bloebaum R., JBMR 28:537-544, 1994

ACKNOWLEDGMENTS

The authors acknowledge imds, the Aaron A. Hofmann Foundation, DJO Surgical, and Thortex for providing financial support.



Incorporation of polyelectrolyte complexes into alginate hydrogels and their effect on the alginate matrix

R. Aston^{1*}, T. Klein², G. Lawrie¹ and L. Grøndahl¹

¹School of Chemistry and Molecular Biosciences, The University of Queensland, Australia, r.aston@uq.edu.au

²The Institute of Health and Biomedical Innovation, Queensland University of Technology, Australia

INTRODUCTION

Polyelectrolyte complexes (PECs) have attracted an increasing interest in biomaterials in recent years; mainly in the area of drug delivery.¹ PECs may also be useful as additives to biomaterial matrices to form composites and tune their mechanical properties. Key requirements for the use of PECs in this application include homogeneous distribution of the PECs throughout the matrix and interfacial interactions between the PEC and the alginate matrix. In this study, we investigated the effects of PECs on the structural and mechanical properties of two types of alginate (ALG) matrices.

EXPERIMENTAL METHODS

PECs prepared using a 1:1 ratio of ALG and chitosan (AC) or 40 % alginate dialdehyde and chitosan (ADC) at pH 4.2 and 7 were characterized using x-ray photoelectron spectroscopy (XPS) and elemental microanalysis. These PECs were then dispersed using 4 % (w/v) loading within ALG hydrogels prepared using both immersion (IM) and internal gelation (IG). Hydrogels were characterized using confocal microscopy, cryogenic scanning electron microscopy (cryo-SEM) and tensile and compressive testing.

RESULTS AND DISCUSSION

XPS analysis confirmed formation of the PECs by a change in the relative ratio of NH_2 to NH_3^+ peaks in the PECs compared to C, corresponding to electrostatic interactions between the NH_3^+ and COO^- . Elemental analysis confirmed 1:1 association between the anionic and cationic polymers within the PECs.

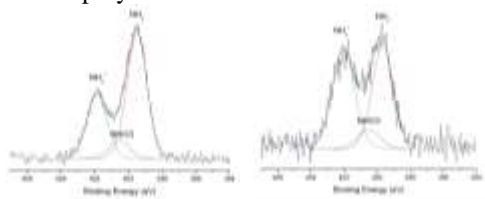


Figure 1. Left: XPS N 1s narrow scan of C. Right: ADC prepared at pH 4.2 Amine, protonated amine and amide peaks were required for the curve fit.

Data shows that no significant change was observed in mechanical properties for the ALG matrix with PEC incorporation.

Table 1. Tensile and compressive modulus (units MPa) of ALG and 4 % PEC loaded IM hydrogels.

Sample	Tensile modulus	Compressive Modulus
ALG	6.5 ± 0.6	5.6 ± 0.7
AC4.2	5.9 ± 0.2	5.3 ± 0.4
ADC4.2	6.4 ± 0.4	5.3 ± 0.5

Cryo-SEM images reveal a challenge in identification of the PECs in the hydrogel materials. Images show a more homogeneous porous structure in the high pressure frozen sample devoid of eutectics and hexagonal ice crystal artefacts present in slush frozen samples.

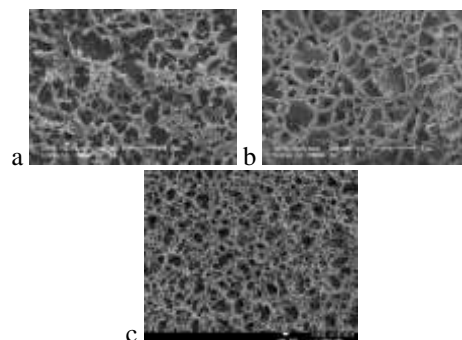


Figure 2. Cryo-SEM of (a) ADC prepared at pH 4.2, (b) ALG-IG with ADC loading using slush freezing, and (c) ALG-IG using high pressure freezing.

Confocal microscopy showed PEC dispersion.

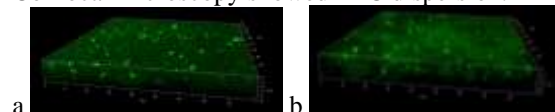


Figure 3. Confocal microscopy of ALG-IM with labelled (a) AC and (b) ADC.

PECs dispersed throughout the ALG matrix, with no effect on the mechanical properties of IM hydrogels. Investigation into the effects of higher loading is being investigated and will be presented. Investigation into cryo-SEM freezing regimes revealed the advantages of high pressure freezing over slush freezing. However, many imaging and sublimation challenges were encountered using cryo-SEM, and as such, this technique should be used with caution.

CONCLUSION

Dispersed PECs at low loading in ALG-IM hydrogels do not change the mechanical properties of ALG. IM and IG hydrogels have a porous structure identified using an appropriate cryo-SEM freezing and sublimation regime for the material.

REFERENCES

1. Lee, K. Y. And Mooney, D. J. Progress in Polymer Science. 37:106-126, 2012

ACKNOWLEDGMENTS

The authors thank The University of Queensland and The Queensland Government for financial support. We also acknowledge AMMRF at CMM, UQ.



Tissue Engineered Silk-fibroin Scaffolds for Meniscus Regeneration

Joana Silva-Correia^{1,2*}, Hélder Pereira^{1,2,3,4}, Le-Ping Yan^{1,2}, Ana Leite Oliveira⁵, João Espregueira-Mendes^{1,2,3}, Joaquim Miguel Oliveira^{1,2*} and Rui Luís Reis^{1,2}

¹3B's Research Group - Biomaterials, Biodegradables and Biomimetics, University of Minho, Headquarters of the European Institute of Excellence on Tissue Engineering and Regenerative Medicine, AvePark, Guimarães, Portugal;

²*ICVS/3B's - PT Government Associate Laboratory, Braga/Guimarães, Portugal, joana.correia@dep.uminho.pt;

³Saúde Atlântica Sports Center – F.C. Porto Stadium; Minho University and Porto University Research Center, Portugal;

⁴Orthopedic Department Centro Hospitalar Póvoa de Varzim – Vila do Conde, Portugal;

⁵CBQF–Center for Biotechnology and Fine Chemistry, Portuguese Catholic University, Porto, Portugal

INTRODUCTION

Tissue engineering (TE) of meniscus aims to restore the loss of meniscus tissue both anatomically and functionally, by transplanting a substitute that should be able to mimic the properties of native tissue¹. In this study, novel silk fibroin scaffolds² combined with human meniscus fibrochondrocytes were evaluated *in vitro* for their performance as meniscus substitutes.

EXPERIMENTAL METHODS

Silk-based scaffolds (10 and 12 wt%) were produced in the form of discs (4 mm in diameter and ~3 mm in height) by means of combining salt leaching and lyophilization methods. Human meniscus cells (HMC's) were isolated from macroscopically intact human fresh menisci using an enzymatic digestion-based technique and expanded using standard culture conditions. HMC's were then seeded at a cell density of 5×10^4 cells/scaffold and the cell-laden constructs were cultured in static conditions, up to 21d. Viability (Calcein-AM staining), metabolic activity (MTS assay) and proliferation (DNA quantification) were evaluated until 21d of culturing. HMC's adhesion was investigated by scanning electron microscopy (SEM). Expression of typical cell markers was observed by histology, immunocytochemistry and RT-PCR. Dynamic mechanical analyses (DMA) were also performed. Results are presented as mean \pm SEM, independently of the population used.

RESULTS AND DISCUSSION

Fibroblast-like (elongated form) and chondrocyte-like (rounded morphology) cells were observed in culture after HMC's isolation (Figure 1A). Calcein-AM staining showed that HMC's were viable up to 21d after culturing onto the silk-10% (Figure 1B for 7d) and silk-12% scaffolds. SEM analysis revealed that HMC's effectively adhered to scaffold's surface after 7d (Figure 1C). MTS assay (Figure 1D) and DNA quantification (Figure 1E) analysis showed that HMC's were metabolically active and proliferated throughout the period of culturing in both types of scaffolds.

Table 1 shows the influence of seeding HMC's on scaffolds' biomechanical properties studied by DMA analysis. It was observed that the E' value at 1 Hz of the cell-laden constructs increased with culturing time, reaching a maximum after 14d of culturing, *i.e.* $4.22 \pm 1.74 \times 10^5$ Pa and $11.67 \pm 1.10 \times 10^5$ Pa, for silk-10 and silk-12, respectively. Moreover, it was observed significantly higher values for the modulus of the cell-laden constructs when compared to the acellular scaffolds after 7 and 14d of culturing.

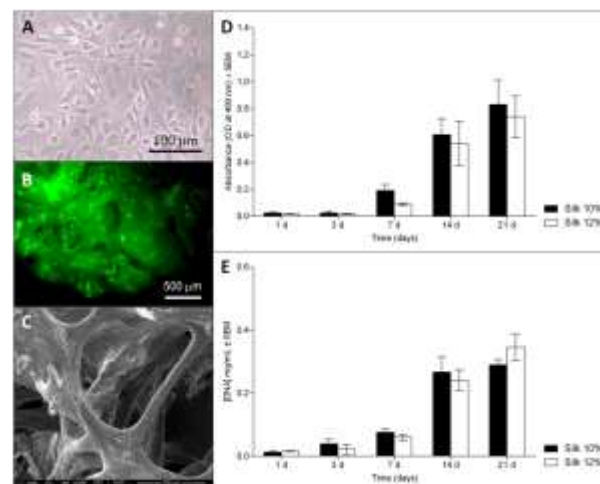


Figure 1. Performance of HMC's (A) loaded on silk fibroin scaffolds (10 and 12 wt%); (B) Calcein-AM staining and (C) SEM imaging of HMC's/silk-10% after 7d of culturing; (D) MTS assay ($n=9$); (E) DNA quantification ($n=9$).

Table 1. Storage modulus (E') of the silk scaffolds cultured with HMC's for different periods of culturing. Statistical analysis was performed based on the values obtained at 1 Hz and using a two-way ANOVA followed by Bonferroni's post test ($n=3$; *** $p < 0.001$).

E' ($\times 10^5$ Pa)	1d	3d	7d	14d	21d
Silk-10 + HMC's	1.89 ± 0.71	2.25 ± 1.57	3.32 ± 1.46	4.22 ± 1.74	2.23 ± 1.57
Silk-10 (Control)	2.06 ± 1.18	2.43 ± 0.31	1.75 ± 0.83	2.43 ± 0.71	2.20 ± 1.79
Silk-12 + HMC's	7.31 ± 1.55	7.98 ± 3.32	9.47 ± 1.27	$11.67 \pm 1.10^{***}$	6.94 ± 1.75
Silk-12 (Control)	6.45 ± 2.09	6.14 ± 0.78	5.35 ± 3.22	5.05 ± 1.69	6.31 ± 2.30

CONCLUSION

Silk scaffolds supported HMC's adhesion, proliferation and viability, while improving the biomechanical features of acellular scaffolds, and thus showed great promise for meniscus TE applications.

REFERENCES

- Pereira H. *et al.*, Arthroscopy 27:1706-1719, 2011
- Yan L.P., *et al.*, Acta Biomater. 8:289-301, 2012

ACKNOWLEDGMENTS

The research leading to these results has received funding from the EU FP7/2007-2013 under grant agreement n° REGPOT-CT2012-316331-POLARIS and from the Portuguese Foundation for Science and Technology (OsteoCart project - PTDC/CTM-BPC/115977/2009).



Design Functionalized Polyesters and Widen the Applicability in Porous Degradable 3D Scaffolds

Anna Finne-Wistrand¹, Jenny Undin¹ and Ann-Christine Albertsson¹

¹Department of Fibre and Polymer Technology, KTH Royal Institute of Technology, Sweden, annaf@kth.se

INTRODUCTION

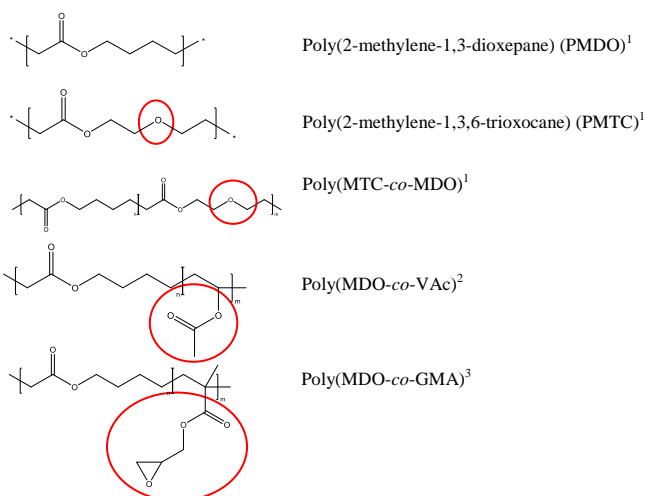
Synthetic biodegradable polymers are widely applied today as 3D scaffold materials in tissue engineering research because their chemical, physical and mechanical properties are predictable and extremely adjustable through variation of monomers, co-polymers, blends and architectures. However, a new generation of biocompatible and degradable synthetic polymers with various physicochemical, functional and biological properties is required to obtain scaffolds which facilitate advanced tissue engineering.

We have functionalized degradable aliphatic polyesters to extend their properties and the utility of this class of materials in biomedical applications. The mechanical and thermal properties of the polymers have been compared and also discussed in relation to their applicability in 3D porous and degradable scaffolds for tissue engineering.

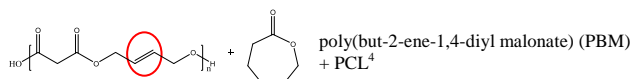
EXPERIMENTAL METHODS

The following polymers have been synthesized and compared:

- Functionalized polyesters from radical ring-opening polymerizations of ketene acetals:



- Functionalized prepolymers from step-growth polymerization, subsequently used in insertion-coordination ring-opening polymerization:



RESULTS AND DISCUSSION

The thermal property and the mechanical property are two crucial parameters to obtain successful scaffolds in for example 3D printing. Poly(ϵ -caprolactone) has successfully been used in 3D printing because of its relatively low melting temperature and its semicrystallinity. The thermal properties for our functionalized polyesters are summarized in Table 1.

Table 1. Thermal properties of functionalized polyesters.

Polymer	T _g ^a (°C)	T _m ^a (°C)
PCL	-54,9	61,8
PMDO	-57	
PCL-PBM	-58,1	60,2
PMTC	-48.3- (-51.2)	
Poly(MTC-co-MDO)	-49.9- (-55.1)	
Poly(MDO-co-GMA)	-14.6 - 23.9	
Poly(MDO-co-VAc)	-50.1 - 17.2	

The first three polymers in Table 1 have the same repeating unit, ϵ -caprolactone, (1) linear semicrystalline PCL (2) branched and amorphous “PCL” and (3) functionalized “PCL”. PCL-PBM has similar thermal characteristics as PCL and the double bonds in PBM enabled cross-linking, which resulted in porous scaffolds with an increased ability to recover after repeated loading.⁵

The three copolymers in the bottom of Table 1 were synthesized by radical ring-opening polymerization, an efficient pathway to vary the hydrophilicity (poly(MTC-co-MDO) and include functional groups (poly(MDO-co-VAc) and poly(MDO-co-GMA)). The acetate groups in poly(MDO-co-VAc) were successfully hydrolysed using an enzyme, forming a degradable polymer with vinyl alcohol repeating units. In comparison, heparin was attached to the epoxy group in GMA. These amorphous copolymers have some advantages during the scaffold forming procedure but there is a challenge to achieve stable 3D constructs.

CONCLUSION

We present ways to design a new generation of biocompatible and degradable synthetic polymers with various physicochemical, functional and biological properties. Doing this, we have the possibility to not only include functionality into the synthetic degradable polymers but also optimize the properties to increase their applicability.

REFERENCES

- Undin J. *et al.*, J. Polym. Sci., Part A: Polym. Chem. 48:4965-4973
- Undin J. *et al.*, Polym. Chem. 3:1260-1266, 2012
- Undin J. *et al.*, Biomacromolecules 14:2095-2102, 2013
- Målberg S. *et al.*, Chem.mat. 22:3009-3014, 2010
- Tyson T. *et al.*, Macromol. Biosci, 11:1432-1442, 2011

ACKNOWLEDGMENTS

The authors acknowledge ERC Advanced Grant, PARADIGM (grant number: 246776), the European Union 7th Frame Program, VascuBone (project number 242175) for providing financial support to this project.



Investigation of the role of shear stress and compression stimuli on cell seeded PCL scaffolds

M. Brunelli, C. M. Perrault, D. Lacroix

INSIGNEO Institute for in silico medicine, Department of Mechanical Engineering, University of Sheffield, UK
mep12mb@sheffield.ac.uk

Introduction

Cell commitment toward a defined phenotype can be regulated by the surrounding environment [1] and the sensed mechanical stimuli [2]. However, the effect on cellular differentiation of resting time applied between consecutive mechanical stimulation is still unclear. The objective of this study is to define a controlled environment able to provide uniform spatial distribution of the stimuli and able to bear and transmit compression load in order to investigate the effect of shear stress or compression stimuli both spaced out with resting periods over mesenchymal stem cells (MSCs) osteogenic differentiation. The focus is first on the mechanical properties of geometrically regular porous polycaprolactone (PCL) scaffolds; secondly on the effect of shear stress on cellular attachment on PCL by developing a microfluidic system and testing it with osteosarcoma cells (MG63); third on the injection of collagen gel embedding MSCs into scaffolds to transmit compression stimuli from the rigid PCL structure to cells and assess their viability in the collagen gel.

Materials and Methods

PCL mechanical properties. The scaffold (3D Biotek) is 5 mm in diameter, 1.5 mm thick and $40.4 \pm 0.3\%$ porous. The relaxation behaviour is tested applying and holding compression ramps at 80 and 110 μm for 6 h. Dynamic analysis are performed applying a 80 μm ramp followed by 30 μm amplitude sinewaves (1, 10, 100 cycles) at 0.5 Hz alternated with 4 h relaxation between each cyclic block.

Perfusion system. Polydimethylsiloxane (PDMS) is molded and cut to shape, drilling holes for scaffolds and tubing. After glass plasma bonding, the system is connected to pumps dispensing a suspension of MG63 cells (10^6 cells/ml) at different velocities (0.01, 0.1, 0.5 mm/s). After 24 h, fluorescence stain is added to assess cellular distribution.

Injection of collagen gel and collagen/MSCs into PCL. Bovine collagen type I (Gibco) solution (2 mg/ml) is injected in PCL applying vacuum for 20 min and samples undergo microCT scans (44 KV, 204 mA). MSCs are added to the collagen solution (125×10^3 cells/ml) and 50 μl of collagen suspension is injected in 7 samples. After 24 h, Presto Blue assay is performed.

Results

Calculating the gradient of the stress/strain curve on 7 PCL samples, the apparent Young Modulus is found to be 6.4 ± 3.0 MPa. PCL compression reached equilibrium after 3.5 and 4.5 h for 80 μm and 110 μm ramps

respectively. Dynamic stimulations showed that 1, 10 cycles or 100 cycles do not alter the equilibrium state as it is reached again immediately after the stimulation.

The perfusion system includes bubble traps and it simultaneously tests three samples (Fig.A). In vitro experiments showed a homogeneous cellular distribution through the scaffold confirming a constant flow for all velocities with the best attachment at 0.5 mm/s (Fig.1B).

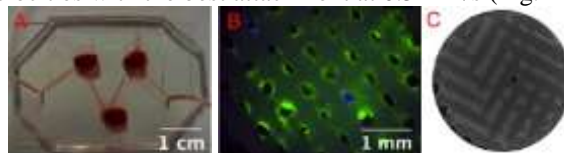


Fig. 1: (A) Perfusion chamber; (B) 0.5 mm/s seeding; (C) MicroCT cross-section of collagen injected PCL.

MicroCT scans showed penetration of collagen throughout the scaffold, leading to 96% of pores filled (Fig.2C). After 1 day seeding, MSCs seeded in 7 scaffolds embedded collagen have an average viability of 79% compared to control cells seeded in flask at the same density (3000 cells/cm²).

Discussion and Conclusions

Mechanical tests on PCL confirm its ability in bearing cyclic compression. Further investigation is necessary to ensure that plastic deformation is not occurring. The homogeneous cellular distribution obtained with the microfluidic system indicates a mechanically controlled environment. MicroCT scans and PrestoBlue show that collagen fills pores completely, enhancing cell growth. Future studies related to shear stress and compression stimuli involving the perfusion system and collagen embedded scaffolds will be carried out, focusing in particular on quantification of collagen and mineralized calcium content, and osteogenic genes expression through RT-PCR.

References

- [1] D. J. Kelly et al., *Birth Def. Res. C. Embryo Today* 85: 75–85, 2010.
- [2] D. Lacroix et al., *Philos. Trans. A. Math. Phys. Eng. Sci.* 367: 1993, 2009.

Acknowledgments

Funding from the European Research Council (FP7-258321) is acknowledged.

Disclosure

The author has nothing to disclose.



Engineered Dermal Micro-Tissues For Bottom-Up Tissue Engineering And TOC Applications

A. Garziano^{1,2} F. Urciuolo^{1,2} G. Imparato^{1,2} P. Netti^{1,2}

¹University of Naples Federico II, Naples, Italy

²Italian Institute of Technology (iit), Naples, Italy, alessandro.garziano@iit.it

INTRODUCTION

Tissue on chip (TOC) is emerging as the new frontier in high-throughput screening technology in drug assessment and development, nutraceuticals, cosmeceuticals and holds the potential to partially replace animal testing [1]. In this work we realized biological micro-modules that can be used as functional living units for TOC application as well as functional building block for the realization of 3D biological tissue in vitro. We demonstrate that μ TPs evolve over culture time resulting in micro-modules having different morphology, ECM organization, transport properties as well as different response to an external stimulus; in particular we evaluated the capability to respond to UVA exposition.

EXPERIMENTAL METHODS

To realize the μ TPs we loaded in a spinner flask human dermal fibroblast and biodegradable gelatine micro beads. The culture suspension was stirred intermittently at 30 rpm (5 min stirring and 30 min static incubation) for the first 6h post-inoculation for cell adhesion, and then continuously agitated at 30 rpm. The μ TPs were monitored along culture time, we focused our attention on the following parameters: oxygen consumption kinetics, diffusivity coefficient, collagen evolution, fusion rate and contraction of areas. Moreover in order to assess the response of the μ TPs to respond to external stimuli, UVA exposition was induced and cell apoptosis profile and mmp-1 expression were evaluated.

RESULTS AND DISCUSSION

The μ TPs realized are living micro-tissue that evolves with culture time (Fig. 1 e-h). The main feature is that they can partly recapitulate a native tissue because they consist of cells embedded in own ECM (Fig. 1 a-d) they well recapitulate the native tissue because are imbedded in own ECM (figures a-d). By monitoring μ TPs fusion capability by time lapse microscopy we found that the increasing of μ TPs fusion rate corresponds an increase in collagen content (Fig. 2 a) and decrease in oxygen consumption (Fig 2 b). This evidence demonstrates that the cells embedded in their own ECM decrease their oxygen need. In order to evaluate their response to an

external stimulus, we evaluated how they react to UVA irradiation by assessing the following reads out: apoptosis profile, mmp-synthesis (Fig 2 c), ECM organization. Interestingly we observe that also the response to UVA change related to the μ TPs age, highlighting a role of ECM in mediating the cellular response.

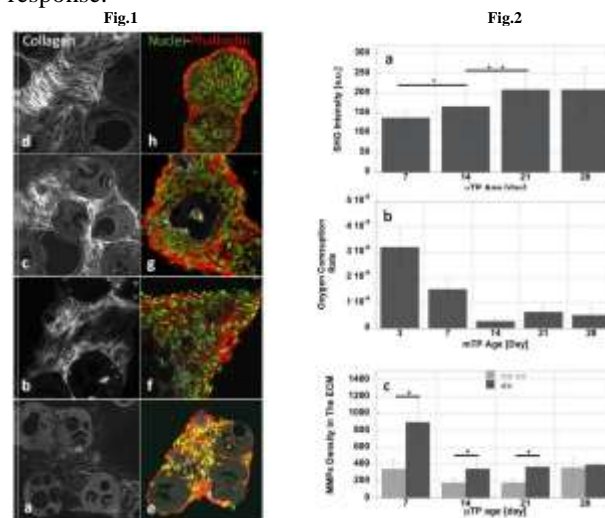


Fig.1 collagen evolution of the μ TPs by means of confocal multiphoton microscopy (green nuclei, red phalloidin, grey collagen, 7 days (a,e), 14 days (b,f), 21 days (c,g), 28 days (d,h))

Fig.2 collagen quantification (a), oxygen consumption kinetics (b), mmp-synthesis profile before and after UVA exposition

CONCLUSION

In conclusion, our results show that the μ TPs are living micro tissue elements that evolve their properties during culture time mimicking different status of a native tissue. Main peculiarity of our μ TPs appear to be the endogenous collagen, this feature makes them different from conventional in vitro tissue model and permits testing a large number of drugs and drug combinations in a well-replicate micro-scale human tissues equivalent.

REFERENCES

- 1 G. Imparato, F. Urciuolo, C. Casale, P. Netti Biomaterials Volume 34, Issue 32, October 2013, Pages 7851–7861
- 2 Du Y, Lo E, Ali S, Khademhosseini A. PNAS 2008;105:9522–7.3
- 3 C. Palmiero, G. Imparato, F. Urciuolo, P. Netti Acta Biomaterialia Volume 6, Issue 7, July 2010, Pages 2548–2553



Jet-Sprayed 3D Nanofibrillar Environment Decreases Myofibroblastic Activation

Halima Rabehi¹, Romain Debret¹, Pascal Sommer¹, Dominique Sigaudou-Roussel¹, Jérôme Sohier^{1*}

^{1*}Laboratory of Tissue Biology and Therapeutic Engineering (LBTI), UMR 5305, CNRS, Lyon, France, jerome.sohier@ibcp.fr

INTRODUCTION

Myofibroblastic activation of mesenchymal cells is essential to narrow margins and synthesize abundant extracellular matrix (ECM) during skin wound healing or to remodel heart valves ECM.

If recapitulation of natural repair mechanisms is crucial for functional regeneration of soft tissues, it must conversely be controlled to not resume a pathological behavior similar to fibrosis, which results in impaired functionality in skin repair and stenosis in tissue engineered heart valves¹.

Aside from control through physical (substrate rigidity) or chemical cues (TGF- β 1), we hypothesized here that the three-dimensional (3D) structure of nanofibrillar scaffolds can as well mediate myofibroblastic activation.

To investigate this hypothesis, polymer nanofibrillar scaffolds of very high porosities were seeded with skin fibroblasts and their ability to support cell colonization and growth evaluated. Myofibroblastic activation within the matrices was evaluated by immunofluorescence, western blot and quantitative gene expression over time, and compared to films of the same polymer to determine the role of the 3D environment.

EXPERIMENTAL METHODS

Nanofibrillar structures were obtained by jet-spraying² PCL (MW 80000 g/mol) while PCL films were solvent casted on lab-tek chamber slides. Porosity of cored nanofibrillar discs (1 cm x 0.6 mm) was calculated from polymer density and measured volume. Human primary fibroblasts (PCS 201-010, ATCC) were seeded in triplicates (5.105/disc, 1.104/cm² films) and cultured in Quantum 333 medium (PAA) for up to 20 days. Scanning electron microscopy, histology (DAPI staining), DNA quantification, immunofluorescence and western blot against α -SMA, and qPCR were used to characterize nanofibrillar structures and cell fate.

RESULTS AND DISCUSSION

Jet-spraying allowed the production of homogeneous matrices of high porosity (97%) and median pore sizes (55 μ m), composed of nanofibers in average 600 nm. This specific structure allowed an extensive cellular invasion and proliferation (7 fold increase) over time that bridged the matrices within 10 days (Fig. 1).

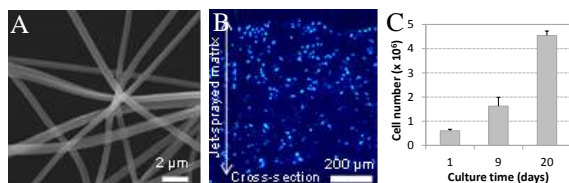


Fig. 1. Jet-sprayed PCL matrices (A), cell migration at 10 days (B) and proliferation within the matrices (C).

Interestingly, myofibroblastic activation acquired during cell expansion on 2D polystyrene (TCP) was reduced in PCL 3D matrices, as indicated by the extinction of α -SMA expression from 1 to 5 days. Conversely, fibroblasts on PCL films still showed α -SMA expression after 5 culture days (Fig. 2A). The increase of α -SMA expression on PCL films and the decrease in jet-sprayed matrices were confirmed by western blot while qPCR indicated a strong decrease of β -actin and α -SMA genes expressions after seeding (Fig. 2B).

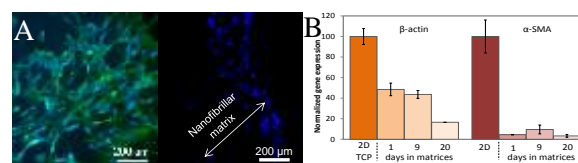


Fig. 2. α -SMA expression on PCL films and lack of expression in nanofibrillar matrices after 5 days (A); myofibroblastic gene expression over time (B).

Overall, these results show that 2D-activated myofibroblasts can be deactivated by a 3D nanofibrillar environment, through a mechanism not only linked to polymer rigidity as PCL films do not induce a similar phenomenon. Ongoing experiments at protein expression level and using stiffer polystyrene jet-sprayed matrices will further elucidate this mechanism.

CONCLUSION

The prospect to mediate myofibroblastic activation through nanofibrillar environments is important for soft tissue engineering, to prevent the formation of unorganized fibrotic tissues.

REFERENCES

- Schmidt D, Dijkman P, et al. J Am Coll Cardiol. 56,510-20, 2010.
- Sohier J, Corre P, et al. Tissue engineering. Part C, Methods. 2013.

ACKNOWLEDGMENTS

Rhône-Alpes ARC2 program is acknowledged for funding.

Fatty Tissue Equivalents – build up with mature adipocytes in a gelatin hydrogel

Birgit Huber¹, Eva Hoch¹, Günter Tovar^{1,2}, Kirsten Borchers², Petra J. Kluger^{1,2,3}

¹University of Stuttgart, Institute of Interfacial Process Engineering and Plasma Technology IGVP

²Fraunhofer Institute for Interfacial Engineering and Biotechnology IGB, Stuttgart, Germany

³University of Reutlingen, Process Analysis & Technology (PA&T), Reutlingen petra.kluger@igb.fraunhofer.de

INTRODUCTION

Large fatty tissue constructs are urgently needed for clinical applications. They are necessary if the subcutis is damaged or lacking due to high-graded burns, congenital deformities, tumor resection or trauma. To date, no suitable replacement is available; autologous fatty tissue transfer results in a high shrinkage of the tissue¹. Also the use of adipogen differentiated stem cells has not shown the requested long term functionality and differentiation². Our strategy is to build up a subcutis equivalent by using mature adipocytes in a chemically modified gelatin matrix, which allows an easy and fast tissue composition.

EXPERIMENTAL METHODS

For the generation of 3D constructs, bovine gelatin was methacrylated³. Cytotoxicity of methacrylated gelatin and the non-cured and cured photoinitiator lithium acylphosphinate (LAP) was determined. An isolation method for mature adipocytes from human fatty tissue was established. These mature adipocytes were characterized in a 2D culture by comparison to differentiated adipose-derived stem cells (ASCs) regarding cell morphology, size and lipid accumulation. Adipocytes were encapsulated into methacrylated gelatin and cultured for several weeks. The elasticity of the constructs was adapted to that of native fatty tissue which was evaluated performing rheological measurements. Viable cells were detected by staining of lipid droplets with Nile Red, nuclei with Hoechst 33342 and cytoplasm with fluorescein diacetate (FDA). Furthermore, H&E staining and the staining of perilipin A and collagen IV were performed on paraffin sections. Cell functionality was determined by glycerol and leptin release.

RESULTS AND DISCUSSION

Methacrylated gelatin as well as the non-cured and cured photoinitiator LAP showed no cytotoxicity tested with adipocytes. Isolated mature adipocytes showed a different morphology, cell size and lipid accumulation pattern compared to differentiated ASCs. A method for

the encapsulation of mature adipocytes into methacrylated gelatin was successfully established (Figure 1).

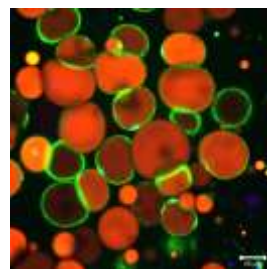


Figure 1: Mature adipocytes in a 3D gel. Lipid droplets were stained in red (Nile Red), cytoplasm in green (fluorescein diacetate) and nuclei in blue (Hoechst 33342).

The elasticity of the subcutis equivalents was comparable to that of native fatty tissue which was seen in rheological measurements. Cells stayed viable and functional for up to 14 days, which was shown by FDA staining, glycerol and leptin release as well as perilipin A and collagen IV stainings.

CONCLUSION

We were able to show that human adipocytes are a suitable cell type for buildup 3D subcutis equivalents. Methacrylated gelatin is an excellent matrix due to its biocompatibility and tunable properties. Our long-term goal is the composition of large subcutis constructs supplied by a vascular system.

REFERENCES

References must be numbered. Keep the same style.

1. Patrick, C., The Anatomical Record, 366, pp.361–366, 2001.
2. Bellas, E. *et al.*, Tissue Engineering Part C. 2013
3. Hoch, E. *et al.*, Journal of materials science. Materials in medicine, 23(11), pp.2607–17, 2012

ACKNOWLEDGMENTS

We thank the European Commission for funding the ArtiVasc 3D project under the Seventh Framework Program (grant agreement n°263416).

Development of Photocrosslinkable Hyaluronan Hydrogels with Platelets lysates for Tissue Regeneration

Ricardo Leandro Pires^{1,2}, Pedro S. Babo^{1,2}, Rui L. Reis^{1,2} and Manuela E. Gomes^{1,2}

¹3B's Research Group - Biomaterials, Biodegradables and Biomimetics, University of Minho, Portugal

²ICVS/3B's - PT Government Associate Laboratory, Portugal, pedro.babo@dep.uminho.pt

INTRODUCTION

The research on new biomaterials incorporating biochemical cues and well-defined architectures has opened horizons for the regeneration of complex tissues, such as the periodontium. The use of Platelet Lysates (PLs) have shown to have a great potential for tissue regeneration, as the growth factors (GFs) derived from platelets are involved in essential stages of wound healing and regenerative processes such as chemotaxis, cell proliferation and differentiation¹. Moreover, platelets release numerous cell adhesion molecules (fibrin, fibronectin and vitronectin) that are important for the formation of ECM and for the adhesion and migration of cells. Platelet derived GFs have been studied for tendon, bone, cartilage¹ and periodontium regeneration with promising outcomes². In this work we propose the development of multifunctional photocrosslinkable hyaluronic acid (HA) hydrogels by the incorporation of PL. HA is a glycosaminoglycan copolymer of d-glucuronic acid and N-acetyl-d-glucosamine that is present in connective tissues and plays a role in cellular processes including cell proliferation, morphogenesis, inflammation, and wound repair. The incorporation of PL in methacrylated HA is expected to produce a versatile material that could be crosslinked *in situ*, for the directed delivery of growth factors or cells to stimulate new tissue regeneration. Moreover, being photocrosslinkable, this hydrogel may adapt to diverse defect morphologies and/or be processed with defined topographies, using, for example photolithography technologies.

EXPERIMENTAL METHODS

Platelet concentrates with a cell count of 10^6 mL^{-1} were treated with repeated freezing and thaw cycles to generate PL. Methacrylated-HA (Met-HA) was obtained by reacting HA (1.5-1.8MDa) with methacrylic anhydride in basic conditions (pH 8.5). Photocrosslinkable membranes incorporating PL were produced by dissolving Met-HA in solutions of increasing concentration of PL (0, 50 and 100vol%), and using the photoinitiator Igacure 2959. The viscoelastic properties of the membranes were measured using dynamic mechanical analysis (DMA) equipped with the compressive mode in a hydrated environment, at 37°C. Swelling and degradability of the produced membranes incubated in PBS or hyaluronidase (Hase) was assessed up to 21 days. The release of PL proteins from membranes incubated in PBS was quantified by micro-BCA. Also, the viability and proliferation of human periodontal ligament fibroblasts (hPDLFs) either seeded or encapsulated into the developed membranes was evaluated *in vitro*, envisioning the future possible

application of such materials in the regeneration of periodontal ligament.

RESULTS AND DISCUSSION

It was possible to obtain transparent and flexible photocrosslinkable HA membranes (Fig1A) incorporating different amounts of PL, that can be tailored to different shapes/sizes, depending on the casting conditions used. The incorporation of PL improved the viscoelastic properties of the membranes. Moreover, the incorporation of PL enhances the resilience of the membranes to the degradation by Hases (Fig1B).

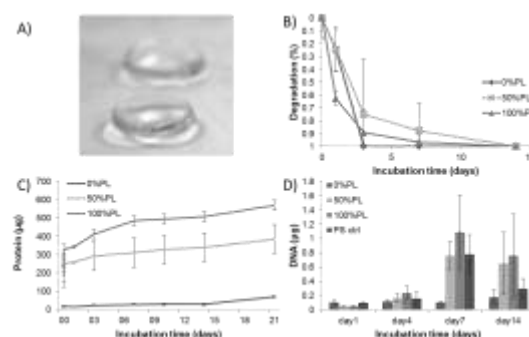


Figure 1. A- PL-based membranes. B- Degradability of met-HA membranes containing 0, 50 and 100% PL after incubation in Hase (100U/mL); C- Cumulative protein release from membranes containing 0, 50 and 100%; D- PL Proliferation of hPDLFs seeded in membranes incorporating 0, 50 and 100% PL.

The developed membranes were also able to release PL proteins in a sustained manner (Fig1C). hPDLFs either seeded or encapsulated in the photocrosslinkable membranes showed increased metabolic activity as well as cell proliferation over time in culture that was proportional with the incorporation of increasing amounts of PL (Fig1D).

CONCLUSION

This work demonstrates that is possible to obtain versatile photocrosslinkable HA-PLs membranes that provide adequate substrates for hPDLFs attachment and growth while enabling the sustained release of PLs. These results suggest the great potential of these materials as cell and/or autologous growth factors carriers for tissue engineering approaches targeting various tissues, namely the periodontal ligament. Ongoing experiments using micro-lithography techniques are being conducted to define the specific microarchitecture of these materials, as such features are important to direct organized tissue ingrowth for periodontium regeneration applications.

REFERENCES

1. Santo V.E. *et al.*, Tissue Eng B. 4:308-326, 2013
2. Chen F-M *et al.*, Tissue Eng B. 16: 219-255, 2010

Poly(vinyl alcohol) Physical Hydrogels as Functional, Biodegradable Matrices for Tissue Engineering

Bettina E. B. Jensen¹, Katrine Edlund¹, Anton A. A. Smith¹, Leticia Hosta-Rigau², Brigitte Städler², and Alexander N. Zelikin^{*1,2}

¹*Department of Chemistry, Aarhus University, Denmark

²iNANO Interdisciplinary Nanoscience Centre, Aarhus University, Denmark, bebj@chem.au.dk

INTRODUCTION

For regenerative medical applications, hydrogels have become increasingly attractive as biomaterials owing primarily to their resemblance of soft human tissue. The safety profile and versatility of the synthetic polymer, poly(vinyl alcohol), PVA, have laid the foundation for this material as an outstanding tool in the field of biomaterials science. Regrettably, the development of PVA hydrogels has partially stalled due to shortcomings such as limited opportunities in bioconjugation, poor retention of small molecular cargo, and lack of degradation mechanisms. Herein, we aim to revitalize PVA physical hydrogels by the redesign of PVA. Starting at the molecular level, amine functionality and controlled molecular weights are obtained allowing for optimization of drug loading and conjugation of protein cargo. This allows for the transformation of the hydrogel into a reservoir providing adhering cells with not only (bio)chemical but also physical cues and thus ultimately leading to improved cellular repair.

EXPERIMENTAL METHODS

End group modified PVA¹ was synthesized via RAFT polymerization². For hydrogel production, the microtransfer molding technique was utilized and physical crosslinks were induced via non-cryogenic routes³. Composite physical PVA hydrogels were prepared by incorporation of liposomal sub-compartments into the polymer matrix⁴. Differential interference contrast and fluorescence microscopy techniques were used for qualitative analyses. Flow cytometry was used for cell uptake studies. Cell viability assay was performed to evaluate therapeutic response. All results presented are average of triplicate experiments, reported as mean \pm SD. Student's t-test was used for statistical analysis of data.

RESULTS AND DISCUSSION

Anchoring of liposomal sub-compartments within PVA physical hydrogels was obtained through thiol-disulfide exchange between end group modified PVA and thiocholesterol embedded in the liposome bilayer. It was demonstrated that the amount of encapsulated cargo could be controlled by increasing the concentration of liposomes (Figure 1). Furthermore, liposome retention was evaluated as a function of polymer molecular weight of the matrix and liposome overhang. Lipogels were rendered cell adhesive using PLL or a polydopamine coating (Figure 2).

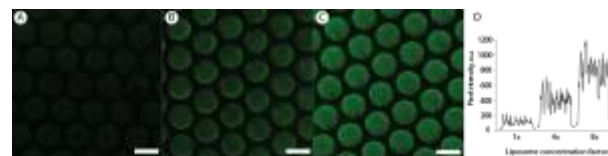


Figure 1: CLSM images of lipogels with different liposome content. Scale bars: 100 μ m.

The therapeutically active drug, Paclitaxel, was successfully delivered to adhering mammalian cells producing a cytotoxic effect over time.

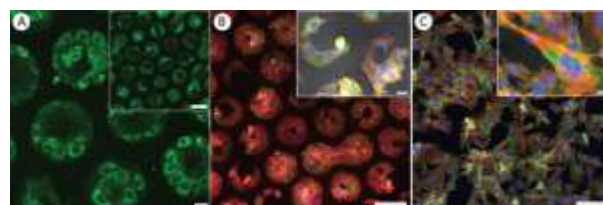


Figure 2: (A) Uptake of fluorescent cargo. Scale bars: 20 μ m and 100 μ m (inset). Myoblasts adhering to lipogels (B) blended with PLL and (C) PDA coated (red: actin filament; blue: DAPI; green: focal adhesion points). Scale bars: 100 μ m and 20 μ m (insets).

Lastly, conjugation of protein cargo under physiological conditions towards biofunctionalization of hydrogels afforded enzymatically active materials. This presents adhering cells with the localization of active, matrix bound proteins.

CONCLUSION

Cholesterol-assisted conjugation of liposomes to PVA allowed for hydrogel sub-compartments. Therapeutic response mediated by the lipogels illustrates the potential of PVA-based composite hydrogels as drug eluting interfaces suited for surface mediated drug delivery as well as protein immobilization for applications in tissue engineering.

REFERENCES

1. Chong S-F. *et al.*, *Small* 9:942-950, 2013
2. Smith A.A.A. *et al.*, *Polym. Chem* 3:85-88, 2012
3. Jensen B.E.B. *et al.*, *Soft Matter* 8:4625-4634, 2012
4. Jensen B.E.B. *et al.*, *Nanoscale* 5:6758-6766, 2013. Reproduced by permission of The Royal Society of Chemistry.

ACKNOWLEDGMENTS

Lundbeck Foundation and Sapere Aude Starting Grants from the Danish Council for Independent Research Technology, and Production Sciences, Denmark.

Calcium Concentrations for the Development of New Bioactive Dressings to Improve Skin Wound Healing

Claudia Navarro^{1,2}, Soledad Pérez-Amodio^{1,2}, Josep A. Planell^{1,2,3} and Elisabeth Engel^{1,2,3}

¹Institute for Bioengineering of Catalonia (IBEC), Barcelona, Spain. cnavarro@ibecbarcelona.eu

²CIBER de Bioingeniería, Biomateriales y Nanomedicina (CIBER-BBN), Barcelona, Spain

³Dpt. Materials Science and Metallurgical Engineering, Technical University of Catalonia (UPC), Barcelona, Spain

INTRODUCTION

Extracellular calcium has been proved to affect the healing process of skin injuries. Topical administration of this ion has been demonstrated to benefit the formation of granulation tissue (1). Moreover, usage of calcium-releasing dressings such as calcium alginates improves the healing process (2-3). However, it is still not well understood how Ca^{2+} affects cells *in situ*. The aim of this work is to analyze the effect of extracellular calcium on important aspects of the healing process carried out by dermal fibroblasts. The implication of the calcium-sensing receptor (CaSR) in the cellular events affected by calcium is also studied.

EXPERIMENTAL METHODS

Rat dermal fibroblasts were cultured in the presence of calcium concentrations, ranging from 0 to 7.5mM. Relevant features of the wound healing process were assessed by different *in vitro* assays, including proliferation, cell migration, collagen synthesis and matrix metalloproteinase (MMP) activity. Proliferation was measured by colorimetric immunoassay based on BrdU incorporation during DNA synthesis. Cell migration was quantified by the wound scratch assay. Total collagen synthesis was determined by means of the Sircol™ kit. Finally, MMP2 and MMP9 levels of activity were detected by gelatin zymography.

CaSR expression was assessed by immunofluorescence and Western blot. In order to understand the implication of this receptor in the studied cellular responses, the assays were repeated in the presence of the CaSR agonist gadolinium (Gd^{3+}) at concentrations between 0 and 50 μM .

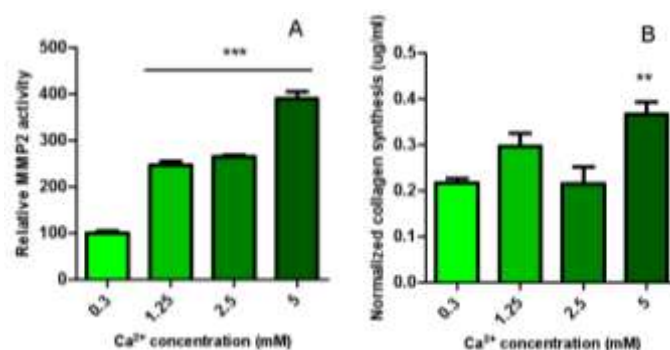
Each experiment was repeated three times with four replicates. Data were analyzed using ANOVA with Tukey's multiple comparison test.

RESULTS AND DISCUSSION

Proliferation was enhanced with 3.5 and 5mM Ca^{2+} . *In vitro* wound closure was increased using 2.5mM Ca^{2+} , indicating a faster migration of the cells at this concentration. In addition, 5mM of Ca^{2+} showed higher levels of MMP activity and collagen synthesis (Fig. A and B). CaSR was observed to be located in the plasma membrane. Two bands between 250 and 150kDa, corresponding to the dimmer and single form of the receptor, were observed by Western blot. Concentrations of Gd^{3+} between 25 and 50 μM induced proliferation, collagen synthesis and MMP activity in a

similar fashion as Ca^{2+} . Fibroblast migration seemed not to be affected by Gd^{3+} .

The finding that Gd^{3+} induces similar cellular responses as Ca^{2+} in proliferation, collagen synthesis and MMP activity suggests that the CaSR may mediate these calcium-induced cellular events.



CONCLUSION

This study demonstrates that extracellular calcium affects important aspects of the healing process. Assays with other calcimimetics (Mg^{2+} , Sr^{2+} , Zn^{2+} , Calindol, NPS R-568) and negative allosteric modulators of the CaSR (NPS 2143, Calhex 231) are currently in progress. These will provide insight into the implication of the CaSR upon calcium stimulation.

A better understanding of how dermal fibroblasts respond to calcium and the range of concentrations in which it affects may lead to a wiser design of novel bioactive dressings for skin wound healing.

REFERENCES

1. Mizumoto T. The Hokkaido journal of medical science. 622, 332, 1987.
2. Doyle JW *et al.* Journal of Biomedical Materials Research. 32, 561, 1996.
3. Belmin J. *et al.* Journal of the American Geriatrics Society. 50, 269, 2002.

ACKNOWLEDGMENTS

The authors would like to thank the Spanish MINECO (FPU grant ref. AP-2012-5310) and MAT2012-38793 for providing financial support to this project.



Swelling and Sealing Properties of a Novel Hemostatic Biomaterial

Daniel Spazierer^{1*}, Paul Slezak², and Heinz Gulle¹

¹Baxter Innovations GmbH, Industriestrasse 67, 1221 Vienna, Austria

²Ludwig Boltzmann Institute for Clinical and Experimental Traumatology in AUVA Research Center, Donaueschingenstrasse 13, 1200 Vienna, Austria

*Daniel_Spazierer@baxter.com

INTRODUCTION

Hemostatic agents are obtained from various biomaterials and sources, and have a long history in human use. Recent development trends in hemostatic agents are self-adhering pads¹⁻³. Those described in the literature usually are combinations of two or more materials of different functions. Here we present a novel “advanced” pad consisting of a NHS-PEG coated collagen pad (PCC). The PEG provides the means to rapidly affix PCC to a wound by crosslinking the collagen pad with blood and tissue proteins. Since blood is not the only fluid present during surgery the first aim of this study was to examine the impact different body fluids can have on the burst pressure of PCC. The second aim of the study was to examine the swelling properties of PCC since PEG-based materials are well known to swell⁴.

EXPERIMENTAL METHODS

Swell Profile:

PCC was placed into polystyrene plates filled with citrated human plasma. A weight of 227 g was placed on a section of each PCC to simulate application pressure by the surgeon. The rest of PCC was left uncompressed. The weight was removed after 1 min or 5 min and the samples were allowed to freely swell for up to 24 hours. The thickness, length, and width of the compressed and uncompressed areas were measured with a caliper at various time-points.

Burst Pressure Model

A burst pressure system similar to those previously described was used⁴. A 4 mm punch biopsy was made in the center of a sausage casing. The sausage casing was wetted with pure porcine blood or 33% and 67% mixtures of porcine blood with various other body fluids. PCC, or collagen pad without PEG coating (control), were placed over the punch biopsy hole and approximated for 2 min with dry gauze and a 200 g weight. After removing the gauze and weight, the treated sausage casing was mounted on a pressure chamber filled with citrated porcine blood. Pressure was applied at a constant rate and the maximum pressure until leakage recorded.

RESULTS AND DISCUSSION

Swelling basically was completed after 1 hour and no substantial swelling took place afterwards. Most of the swelling was observed in thickness due to the formation of a PEG hydrogel with plasma proteins. When compressed, swelling was greatly reduced—very likely—due to crosslinking of the collagen by NHS-PEG. Minor swelling in length and width was seen confirming that most of the swelling is due to the PEG

component. The calculated maximal total swelling for PCC was 65%. PEG-based biomaterials are known to swell >300% and this can lead to serious surgical complications⁴⁻⁶. While PCCs swelling properties are favourable, care must be taken to avoid placement in small spaces.

Addition of saline, urine, and cerebral spine fluid to blood up to a ratio of 2:1 did not significantly influence burst strength of PCC. Addition of lymph did not impact burst pressure at any concentration. In fact, very similar burst pressures were measured for blood and pure lymph fluid. Addition of bile to blood at all tested concentrations reduced burst pressure by approximately 1/3. Nevertheless, all measured values for any of the fluids were well above clinically relevant pressures⁷⁻⁹. In contrast, burst pressure values measured with the non-coated collagen pad were much lower with all tested fluids. This data indicates that as long as some blood is present PCC will adhere to tissue in the presence of the tested fluids.

CONCLUSION

In this study, we evaluated the swell and burst pressure properties of a PEG-coated collagen pad (PCC). PCC had a calculated maximum total swell volume of 65%, which is less than described for other PEG-based materials. PCC maintained burst pressures two times that of clinically relevant pressures. This makes PCC a promising material for various clinical applications.

REFERENCES

1. Maisano F. et al., Eur J Cardiothorac Surg. 36(4):708-714, 2009
2. Öllinger R. et al., HPB(Oxford) 15(7):548-558, 2013
3. Fischer C.P. et al., J Am Coll Surg. 217(3):385-393, 2013
4. Wallace D.G. et al., J Biomed Mater Res. 58(5):545-555
5. Pace Napoleone C. et al., Interact Cardiovasc Thorac Surg. 6(1):21-23, 2007
6. Neuman B.J. et al., Clin Orthop Relat Res. 470(6):1640-1645
7. Ghajar J. Lancet 356(9233):923-929, 2000
8. Malbrain M.L. et al., Crit Care 10(4):R98, 2006
9. Borly L. et al., Clin Physiol. 16(2):145-156, 1996

ACKNOWLEDGMENTS

The authors thank Dr. Heinz Redl and Stacy Hutchens for their critical review



A Pilot Renal Artery Embolization Study: Evaluation of “Imageable” Embolic Microspheres using Hybrid (Landrace Yorkshire) Farm Pigs

Sharon Kehoe¹, Robert Abraham^{1,2,3}, Charles Daly¹, Daniel Boyd^{1,2,3}

¹*ABK Biomedical Inc. 1344 Summer Street Suite 212 Halifax NS Canada, s.kehoe@abkbiomedical.com

²Department of Applied Oral Sciences, School of Biomedical Engineering, Dalhousie University, Halifax, NS, Canada

³Department of Diagnostic Imaging and Interventional Radiology, QE II Health Sciences Centre, Halifax NS, Canada

INTRODUCTION

Embolization using microspheres has emerged as a highly effective technique in the treatment of arteriovenous malformations and hypervascularized tumors. Radiopaque microspheres eliminate the need for contrast media and allows the interventional radiologist (IR) to directly monitor the spatial distribution and embolization effectiveness of the agents during the procedure¹. Using conventional imaging (*intraprocedural fluoroscopy and computed tomography, CT*) and histopathological techniques, imageable embolic microspheres were characterized in a pilot study for their *in vivo* spatial distribution and artifact potential during and after transcatheter embolization.

EXPERIMENTAL METHODS

Materials: Imageable embolic microspheres were synthesized from a multicomponent bioglass as per Kehoe et. al.² in particle size distributions of 40-150µm, 150-300µm and 300-500µm. The control article for implantation purposes was the commercial embolic agent ‘Embosphere’ (Merit Medical, Lot No. X415836-5) of particle size distribution 300-500µm.

Methods: Healthy hybrid farm pigs (*species sus scrofa*), mean weight 55.5kg, received unilateral or bilateral renal artery (RA) embolization with material allocation per Table 1. The pilot study received ethical approval from the Comité institutionnel de protection des animaux d’AccelLAB and was in full compliance with the Canadian Council on Animal Care regulations (CCAC).

Table 1: Test and Control Article Allocation.

Pig	Embolization	Pole	Left RA	Right RA
1	Bilateral	Main	300-500µm	300-500µm*
2	Bilateral	Cranial	150-300µm	300-500µm
		Caudal	150-300µm	300-500µm*
3	Unilateral	Cranial	-	40-150µm
		Caudal	-	40-150µm

where * denotes allocation of the Control Article.

An experienced IR performed all embolic procedures and post embolization angiography for each material. After embolization, all arteries in the observation region were qualitatively evaluated for perforation, rupture, non-target embolization and embolization effectiveness. All treated animals were subjected to necropsy. Kidney samples and selected organs were then stored in individually labeled containers filled with neutral buffered formalin. Analysis comprised high-resolution

kidney radiographs (Faxitron MX-20), and micro-CT of whole kidneys to identify (a) embolized areas for histology processing and (b) packing and embolization effectiveness for each material. Whole-body CT was utilized to assess the potential for artifacts arising from the imageable microspheres. Histology specimens were imbedded in MMA, ground to 60µm and H&E stained.

RESULTS AND DISCUSSION

Fig. 1 illustrates the high visibility and spatial distribution of the imageable microspheres within the renal vasculature. Conversely, the spatial distribution of the conventional embolic agent (caudal pole, right hand side) is impossible to assess. Micro-CT analysis indicates that the experimental materials provide for

Fig. 1. Whole body CT (left hand side) and micro-CT of



whole kidney (right hand side).

excellent distribution and packing throughout the renal vasculature for all particle size distributions examined. Histology (Fig. 2) generated in this pilot study indicated that both embolic microspheres were well tolerated, showing no evidence of any inflammatory cells.

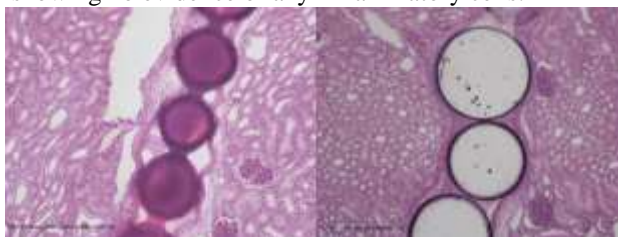


Fig. 2. Photomicrographs showing commercial (left hand side) and imageable microspheres (right hand side) through longitudinal tissue sections (H&E; 10X).

CONCLUSION

The imageable microspheres prepared in this study allowed immediate *in vivo* visual monitoring of their spatial distribution and embolization effectiveness inside target organs during the procedure. The safety and efficacy of these imageable microspheres were proven without the use of contrast media.

REFERENCES

- Sharma et al., J. Vasc. Interv. Radiol. 21:865-876, 2010.
- Kehoe et al., J. Func. Biomat. 4:89-113, 2013.



Optimizing properties of bioadhesive systems using fermentation derived human albumin

Assunta Borzacchiello^b, Luisa Russo^b, Birgitte M. Malle^a, Sara Poulsen^a, Luigi Ambrosio^{b,c}

^aNovozymes Biopharma DK A/S, Krogshoejvej 36; DK-2880 Bagsvaerd; Denmark,

^{b*}Institute of Polymers, Composites and Biomaterials, National Research Council, Naples, Italy.

^c Department of Chemical Science and Materials Technology DCSMT- CNR, Italy

Email: bassunta@unina.it

INTRODUCTION

Bioadhesive systems, i.e. surgical glues, are materials which polymerize rapidly joining tissues in an untraumatic manner. They offer significant advantages compared to traditional sealant techniques, such as sutures; in particular, they are easier to use, non-invasive, offer controllable mechanical resistance and elasticity and they can play an integral part in the healing mechanism of tissue [1]. Surgical glues have several applications such as tissue adhesion; in particular they strengthen and reinforce fragile tissues by tissue adherence, wound healing, sealing of body fluids in surgery, acute aortic dissection and surgery pulmonary parenchymal lesions.

The current surgical adhesive are generally based on fibrin, cyanoacrylates, polyethylene glycol (PEG) or albumin but they show some drawbacks such as the risks of transmission of viral diseases and toxicity of degradation products. The aim of this work was to propose a novel surgical glue based on a fermentation derived human albumin, that allows to overcome the problems related to the traditional glues, and of using 1-Ethyl-(3-dimethylaminopropyl) carbodiimide (EDC) as crosslinking agent in alternative to glutaraldehyde (GA). In particular we optimized the properties of the novel albumin based glue by studying how quick and how good the adhesion of crosslinked albumin (CL-albumin) is to different substrates (biological and no biological) as function of albumin concentration (AC), crosslinking degree (CD) and crosslinker type (CT).

To this aim mechanical, chemical, adhesive and biological properties of this novel glue were evaluated.

EXPERIMENTAL METHODS

The novel surgical glues were obtained by crosslinking recombinant human albumin (Novozymes Biopharma) with two different crosslinkers (EDC and GA), considering different CD and AC.

The rheological properties were evaluated by means of rotational rheometer (Gemini, Bohlin Instruments, UK). In particular the glues have been subjected to periodic oscillation in a dynamic experiment (Small amplitude frequency sweep tests) to evaluate the dependence of viscoelastic properties, i.e. the elastic and viscous moduli, G' and G'' , upon frequency.

To investigate how quick the adhesion of the albumin is on different substrates (pig skin, high density polyethylene, HDPE), it was necessary to find the crosslinking reaction rate of the CL-albumin. To do this the variation of G' , with the time, at a fixed frequency, was evaluated.

The crosslinked albumin samples (CL-albumin) were characterized in terms of their mechanical and adhesive properties, using an Instron Machine (mod.4204). A commercial glue was used as control.

Biological tests were performed on CL-albumin systems in order to determine the biocompatibility of these materials with natural tissues. Human fibroblast cell line were seeded on glues and tested with the Alamar Blue assay direct cytotoxicity evaluation, while PicoGreen assay was performed to evaluate cells proliferation.

RESULTS AND DISCUSSION

The results from rheological characterization of the albumin based glues show a predominant elastic behaviour, typical of a “strong gel”. The increase of AC and CD leads to an increase of elastic properties. Also from mechanical tests it was demonstrated that the maximum stress values increase by increasing AC and CD. Albumin based samples prepared using GA reach lower maximum stress values and lower deformation at break compared to EDC based gel.

From the variation of the elastic modulus upon the time it show that the maximum values of G' and G'' are achieved after 300 seconds and after 100 seconds the moduli are the 80% of the maximum value.

With regards to the adhesion tests on both biological and synthetic substrates, it was demonstrated that the increase of AC and CD has a positive effect on the adhesion strength of the glue.

Moreover the rheological, mechanical and adhesive properties of these novel glues seem to be as good or improved compared to the commercial products, even considering a lower AC and CD. Finally, the results of biological tests demonstrated that CL-albumin systems have no toxic effect on cell viability and proliferation.

CONCLUSION

Biocompatible surgical glues based on an animal-free recombinant human albumin, thereby reducing the risks of transmission of viral diseases were produced and their properties were optimized. Mechanical, rheological, chemical and biological characterization was performed and we demonstrated that these novel glues show improved properties and may have potential in bioadhesive applications.

REFERENCES

1. Berchane, N. S et al. J Mater Sci: Mater Med 19:1831–1838, 2008.



Nanoengineered biomaterials to fight gastric infection: exploring the glycan-adhesin specific interaction

Inês C. Gonçalves^{1,2,3,#,*}, Ana M. S. Costa^{1,2,#}, A. Magalhães³, Celso A. Reis³, M. Cristina L. Martins¹

¹INEB - Instituto de Engenharia Biomédica da Universidade do Porto, Portugal

²FEUP - Faculdade de Engenharia da Universidade do Porto, Portugal

³IPATIMUP - Instituto de Patologia e Imunologia Molecular da Universidade do Porto, Portugal

both authors contributed equally to this work

icastro@ineb.up.pt

INTRODUCTION

Helicobacter pylori (*H. pylori*) is a bacteria that infects half of the world population¹ and its persistent infection is associated with development of gastric carcinoma. Standard antibiotic treatment is fallible in ~20% of the cases², therefore alternative strategies urge. *H. pylori* blood group antigen binding adhesin (BabA) recognizes Lewis b (Leb) and H-type 1 and sialic acid binding adhesin (SabA) binds sialyl-Lewis a (sLea) and sialyl-Lewis x (sLex) expressed in gastric mucosa^{3,4}.

This work aims to develop a biomaterial which can be orally administrated, bind *H. pylori* in the stomach, removing them through the gastrointestinal tract.

It has been previously shown that 170 µm chitosan microspheres partially crosslinked with genipin are stable in acidic pH, have mucoadhesive properties, are not cytotoxic, are retained in the stomach of C56BL/6 mice for at least 2h and bind unspecifically different strains of *H. pylori*^{5,6}.

We herein evaluate the capacity of glycan-decorated chitosan microspheres (GlyR-Mic) to bind *H. pylori* through specific glycan-adhesin interactions and compete for bacterial adhesion with mice and human gastric mucosa. Efficacy studies were performed using a BabA+ *H. pylori* strain and Leb-positive gastric mucosa from mice and human gastric sections (in vitro) and from mice fresh stomachs (ex vivo).

EXPERIMENTAL METHODS

Chitosan microspheres (Ch-Mic; d=170µm) were produced and GlyR (Leb or sLex) immobilized by “click chemistry”. Immobilization of Leb and sLex was confirmed by transmission electron microscopy (TEM) after immunogold labeling with 1ary monoclonal Ab (BG6 or KM93) and 2ary immunogold conjugate Ab. Adhesion of FITC-*H. pylori* (17875/Leb strain; BabA+/SabA-) to microspheres (Ch-Mic, Leb-Mic, sLex-Mic and Al) (2h; 37°C; OD600i=0.04) was visualized by confocal microscopy. Competition assays for *H. pylori* adhesion between microspheres and gastric mucosa were performed using two in vitro models and one ex vivo model, all expressing Leb. Regarding in vitro studies, Mic were added before (to test their prevention capacity) or after (to evaluate their removal capacity) the FITC-*H. pylori* incubation with sections of paraffin embedded gastric mucosa from mice and humans. Bacterial adhesion levels were quantified using ImageJ software. An ex vivo model was designed to evaluate the ability of Mic to remove/prevent [³⁵S]-radiolabeled *H. pylori* adhesion to fresh mice gastric mucosa, quantified using a luminescence counter. Statistical analysis was performed using the Welch – ANOVA and T-test

(p<0.01) for results from in-vitro and ex-vivo studies, respectively.

RESULTS AND DISCUSSION

Glycan-adhesin specific *H. pylori* adhesion was confirmed since BabA+/SabA- *H. pylori* strain adhered to Leb-Mic but not to sLex-Mic.

Unlike sLex-Mic, Leb-Mic were able to compete with Leb carbohydrates expressed in all the gastric mucosa models tested using a BabA+ *H. pylori* strain. Moreover, Leb-Mic presented higher bacterial removal and prevention rates than Ch-Mic. Regarding the in vitro model of mice and human gastric mucosa, statistically significant differences were observed for bacteria removal rates of ≅60% and ≅43%, and prevention rates of ≅32% and ≅35% using Leb-Mic, respectively. The ex-vivo model using fresh mice gastric stomach also suggested Leb-Mic ability to both remove (≅65%) and prevent (≅78%) *H. pylori* adhesion from/to these gastric sections.

CONCLUSION

H. pylori adhesion to Leb-Mic is ligand specific, and efficiency studies revealed their increased capacity to compete with mice and human gastric mucosa for *H. pylori* adhesion comparing to chitosan microspheres without glycans. These results highlight the potential of glycan nanoengineered chitosan microspheres as alternative or complementary treatment to *H. pylori* gastric infection.

REFERENCES

1. Atherton, J.C. Annu Rev Pathol. 1:63-96, 2006.
2. Graham, D.Y. and E. Rimbara. J Clin Gastroenterol. 45(4): 309-13, 2011.
3. Ilver, D., et al. Science. 279(5349):373-377, 1998.
4. Mahdavi, J., et al. Science. 297(5581):573-578, 2002.
5. Fernandes, M., et al. Int. J. of Pharm. 454(1): 116-124.
6. Gonçalves, I.C., et al. Acta Biomaterialia. 9(12): 9370-9378.

ACKNOWLEDGMENTS

Authors would like to thank financial support from COMPETE and FCT for projects PEst-C/SAU/LA0002/2013, NORTE-07-0124-FEDER-000005, PTDC/CTM-BPC/121149/2010 and EXPL/CTM-BIO/0762/2013 and grant SFRH/BPD/75871/2011. Rui Fernandes from IBMC for the assistance in TEM studies and Prof. Fátima Carneiro from IPATIMUP for providing the human gastric mucosa



Highly selective nanoparticles based on Vitamin E derivatives for the treatment of cancer

Raquel Palao^{1,2}, Maria Rosa Aguilar^{1,2*}, Mar Fernandez^{1,2}, Juan Parra², Carolina Sánchez³, Ricardo Sanz³, Julio San Roman^{1,2}

^{1*}Group of Biomaterials, Department of Polymeric Nanomaterials and Biomaterials, Institute of Polymer Science and Technology, ICTP-CSIC, Madrid, SPAIN, mraguilar@ictp.csic.es

²Biomedical Research Networking Centre in Bioengineering, Biomaterials and Nanomedicine CIBER-BBN, SPAIN

³Fundación para la Investigación del Hospital Universitario de Getafe, Madrid, SPAIN

INTRODUCTION

Cancer is a leading cause of death worldwide closely related with genetics, environment and age. It encompasses more than 200 diseases in which abnormal cells divide without control and are able to invade other tissues. However, many cancers have something in common: their mitochondria are altered, and therefore, the energetic metabolism of cancer cells differs from that of normal cells. Consequently, mitochondria can be considered an interesting target for the development of new chemotherapeutics.

α -tocopheryl succinate (α -TOS) has been described as a mitochondrially targeted anti-cancer compound (mitocan) that selectively induces apoptosis of cancer cells and not of healthy cells in a narrow range of concentrations. However, this compound is highly hydrophobic and therefore, difficult to administrate.

We have patented and described in the last years the synthesis of new monomers based on vitamin E to prepare new microstructured amphiphilic copolymers with pseudo-blocks of *N*-vinyl pyrrolidone (VP, hydrophilic) and a methacrylic derivative of vitamin E (MVE or MTOS, hydrophobic). These copolymers were able to form active surfactant-free nanoparticles (NP) in aqueous solution. Moreover, NP were able encapsulate additional α -TOS maximizing the NP activity in a concentration-dependent manner.

The aims of this study are: (1) to study the mechanism of action of vitamin E-based NP. (2) to compare the activity of vitamin E-based NP on the different tumor cell lines and to correlate these data with the energetic footprint of these cells. A detailed study of the effect of the NP on the oxidative stress, nitrosative stress, apoptosis and expression of significant proteins was carried out for pharynx cancer cells.

EXPERIMENTAL METHODS

Monomers were synthesised as described elsewhere¹. Copolymers were obtained by free radical copolymerization of monomers with very different reactivity ratios and different hydrophilicity ($r_{VP} = 0.12$ and $r_{MTOS} = 1.20$ or $r_{VP} = 0.03$ and $r_{MVE} = 2.2$)¹. Loaded and un-loaded surfactant-free NP were obtained by nanoprecipitation. The copolymer (and α -TOS for loaded NP) was dissolved in dioxane and added dropwise to PBS under magnetic stirring and the resulting opalescent dispersion was dialysed against PBS for 72 hours (MW cut-off = 3500 Da).

Breast adenocarcinoma cells (MCF-7 and MDA-MB-231), colon adenocarcinoma cells (WirD), and pharynx cancer cells (Fadu) were cultured following the instructions of the manufacturer. Cell viability (MTT

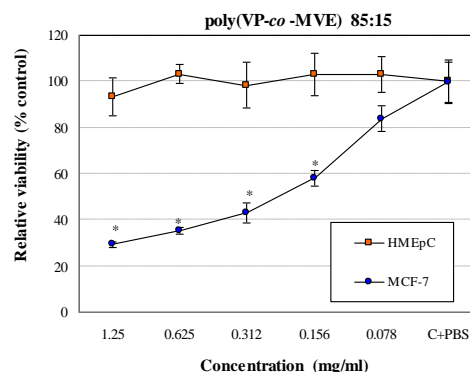
assay) in the presence of α -TOS-loaded or un-loaded NP was tested for all the cell lines and compared.

Oxidative stress (DHE), nitrosative stress (anti-nitrotyrosine), apoptosis (annexin-V and caspase 3), expression of EGFR and p53 and levels of EGF and VEGF were evaluated.

RESULTS AND DISCUSSION

Both MTOS and MVE based nanoparticles were active against breast cancer cells (MCF-7, MDA-MB-231), colon cancer cells (WirD) and pharynx cancer cells (Fadu) with little or no harm to epithelial healthy cells (HMEpC). As an example the selective action of Poly(VP-co-MTOS) (90:10) is shown in the Figure. Nanoparticles activity was higher in MCF-7 > MDA-MB-231 > WirD > Fadu, and this was related with the energetic footprint of the cells. The more glycolytic were the cells, the higher the activity of the nanoparticles.

Viability of proliferating endothelial cells (HUVEC) was significantly inhibited with no harm to quiescent endothelial cells.



CONCLUSION

The obtained results indicated that these NP present selective anti-cancer and anti-angiogenic activity. Moreover, their activity is related to the energetic footprint of the cancer cells. Therefore, vitamin-E-based NP can be considered excellent candidates for the treatment of highly glycolytic cancers.

REFERENCES

1. Palao-Suay, R., Parra-Ruiz, F. J., Aguilar, M. R., Fernández-Gutiérrez, M. M., San Román, J. & Parra, J. (2013), PCT/ES2013/070287

ACKNOWLEDGMENTS

The authors would like to thank the Fundación Eugenio Rodríguez Pascual, CIBER BBN-ECO program and MAT2010-14558 for providing financial support to this project



Enhancing *in vitro* and *in vivo* Viability and Functionality of Pancreatic Islets through a gelatine-based hydrogel

Serena Bertoldi^{1,2}, Simona Marzorati³, Rita Nano³, Lorenzo Piemonti³ and Silvia Farè^{1,2}

¹Dept. of Chemistry, Materials, and Chemical Engineering “G. Natta”, Politecnico di Milano, Milan, Italy

²Local Unit Politecnico di Milano, INSTM, Italy

³Diabetes Research Institute (OSR-DRI), San Raffaele Research Institute, Milan, Italy; silvia.fare@polimi.it

INTRODUCTION

The success of pancreatic islet transplantation for the treatment of Type 1 diabetes is hindered by the implant site, mechanical stress, exposure to high drug and toxin loads, strong inflammatory and immunological reactions occurring during the transplantation procedure of producing insulin cells (β -cells). Early islet loss, mainly due to the lack of engraftment, is a major limitation in this type of transplantation, together with the poor revascularization after cell transplant. To overcome this drawback, the use of biomaterials [1], in particular hydrogels based on natural polymers, to protect pancreatic islets and improve islet function has been increasingly proposed and investigated [2]. This work was aimed at assessing the use of an innovative crosslinked gelatin hydrogel to enhance pancreatic islet viability and functionality for islet transplantation.

EXPERIMENTAL METHODS

Type A gelatin (Sigma Aldrich) was crosslinked by Michael-type addition with methylene-bis-acrylamide (MBA, Sigma Aldrich), according to a patented process [3]. Gelatin hydrogels were then dehydrated or freeze-dried to obtain porous structures. Morphology was observed by Scanning Electron Microscopy (SEM). Swelling and weight loss were evaluated at 37°C in phosphate buffered saline (PBS, pH=7.4). Mechanical properties of the swollen samples were assessed using a dynamic mechanical analyzer in an unconfined cyclic frequency sweep test, evaluating storage (E') and loss (E'') modulus. Human and murine pancreatic islets, isolated as previously described [4], were seeded onto the freeze-dried and dehydrated hydrogels, and allowed to penetrate into the swollen hydrogels. Islet morphology, cell survival and insulin secretion were *in vitro* tested 48h post seeding by immunohistochemical analysis, MTT and glucose challenge test. Islets cultured in standard condition (i.e. TCP) were used as control. Dehydrated hydrogels were implanted in the intraperitoneal space (IP) of C57B1/6 mice up to 3 months to evaluate the *in vivo* tissue interaction. Furthermore, syngeneic islets (800 equivalent islets) encapsulated into the dehydrated hydrogel were implanted in IP of C57B1/6 mice (n=4) up to 2 months, using syngeneic islets cultured free floating as control.

RESULTS AND DISCUSSION

The hydrogels, both dehydrated and freeze-dried, were stable in PBS up to 50 days. The hydrogels exhibited storage modulus values in the range 15 – 60 kPa, observing, as expected, lower E' values for the freeze-dried samples, due to the presence of the pores. Immunohistochemical analysis demonstrated that human and murine islets maintained, into the hydrogel, their native 3D architecture, revealing islet retention

and demonstrating that islets seeded onto the scaffolds retained the architecture of native islets up to 6 days post seeding (Fig. 1). Either for human and murine islets, a higher islet survival was detected using dehydrated hydrogels compared to the freeze-dried ones. In particular, human islets reported also a stimulation index value higher than that obtained for islets seeded onto TCP, used as control.

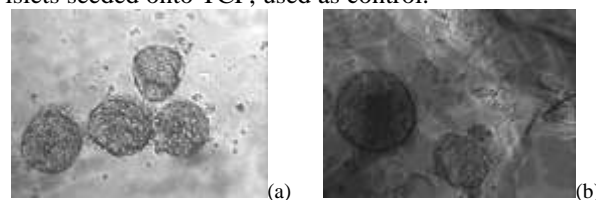


Fig. 1: Murine pancreatic islets cultured onto the dehydrated hydrogel for (a) 48 hours; (b) 6 days. 20 X magnification.

In vivo, no collagen capsule formation was observed after 3 months of implantation, and the hydrogel did not show any morphological change, demonstrating a good *in vivo* stability (Fig. 2a). Hyperglycemia was reversed in mice with islets seeded on hydrogel at day 48, whereas the control mice slightly reduced blood sugar without reversing the hyperglycemic state. After two months, a glucose tolerance test was performed to examine glucose responsiveness of the islet graft, showing a higher glucose responsiveness in islets transplanted with hydrogel than without (Fig. 2b).

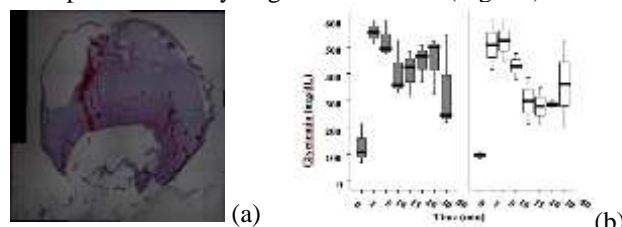


Fig. 2: (a) Dehydrated gelatin hydrogel implanted in IP of C57BL/6 mice after 1 month; (b) metabolic test performed 60 days after transplantation on mice receiving islet cultured onto the hydrogel (grey dot) and free floating (white dot).

CONCLUSION

The crosslinked gelatin hydrogels here proposed allow to maintain *in vitro* the 3D islet architecture. In addition, the hydrogel did not affect human and murine islet survival and functionality during short-term culture, ensuring *in vivo* a suitable microenvironment for pancreatic islet function and survival. This data provide a possible novel pre-clinical strategies for islet transplant, opening the way to a future potential clinical translation in humans.

REFERENCES

1. Borg DJ. *et al.*, Curr Diab Rep. 11:434, 2011
2. Kozlovskay, V *et al.*, Adv Funct Mat. 12: 3389, 2012
3. Tanzi MC. *et al.*, PCT/EP2012/060277, 2012
4. Nano R. *et al.*, Diabetologia. 48:906, 2005



Long-term Degradation of Electrospun Poly(ϵ -caprolactone) Fibre Yarns *In Vivo*: A 12-month Study

Lucy A Bosworth¹, Richard Wong¹, Marie A O'Brien¹, Jason K Wong², Duncan A McGrouther² and Sarah H Cartmell^{1*}

¹School of Materials, The University of Manchester, UK

²Institute of Inflammation and Repair, The University of Manchester, UK

*sarah.cartmell@manchester.ac.uk

INTRODUCTION

Poly(ϵ -caprolactone) (PCL) is a synthetic, biocompatible and biodegradable material commonly used in biomaterial and tissue engineering applications¹. Despite its slow degradation time (>12 months), there are few published studies that investigate this over the long-term in a biological environment^{2,3}. Electrospun PCL scaffolds are being investigated as a potential repair device for patients with damaged tendons⁴. It is therefore important to determine the degradation profile of these scaffolds *in vivo* and hence ascertain their longevity and performance. This study investigated the changes in molecular weight of electrospun PCL yarns implanted into the tendon of a mouse model over a 12-month period.

EXPERIMENTAL METHODS

PCL (Purac - Purasorb PC12) was dissolved in 1,1,1,3,3,3-hexafluoroisopropanol (HFIP; Sigma) at 10 % w/v and electrospun (20 kV, 1 ml/hr, 20 cm). Yarns were created from the collected electrospun fibres as described in Bosworth *et al*⁴. Sterilised in Ethanol (70-100 % v/v (in distilled H₂O) and washed in Phosphate Buffered Saline solution, yarns were cut to 2 mm lengths and individually implanted into a purpose-made defect in the flexor digitorum longus (FDL) tendons of mice. For degradation comparison, PCL yarns were also implanted into the soleus muscle. Scaffold molecular weight was measured using Gel Permeation Chromatography (GPC) and compared to the virgin PCL (yarns as-spun) for each time-point to provide percentage change. Time-points included, 0, 3, 6, 9 and 12 months. At each time-point, grafts were excised and surrounding tissues were enzymatically digested at 37 °C (Tendon: 0.37 mg/ml Collagenase Type II in Hanks Balanced Salt Solution, Muscle: 0.1 % Pronase in Dulbecco's Modified Eagle Medium), followed by their complete dissolution in Tetrahydrofuran (THF). Data sets were analysed using unpaired t-test ($p < 0.05$).

Visual comparison at these time-points was achieved by histological staining of the tissue (tendon only). Harvested samples were fixed in Zinc for 48 hours and paraffin embedded following processing. Serial sections of 5 μ m were cut and stained with haematoxylin and eosin (H&E).

RESULTS AND DISCUSSION

As expected the PCL grafts degraded within their biological environments over time (Fig.1). Both the number of chains and overall mass of the polymer demonstrated a gradual decrease over the time frame investigated with approximately 50 % loss after 12 months. There was no significant difference in

degradation behaviour between the two graft locations (i.e. tendon or muscle).

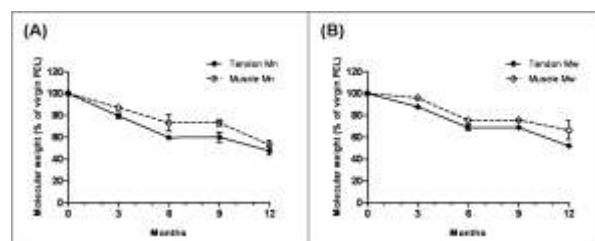


Figure 1 – Changes in molecular weight of PCL electrospun yarns implanted in tendon and muscle tissue, where (A) shows number average molecular weight (M_n) and (B) weight average molecular weight (M_w). Data presented as mean \pm SEM; T-test demonstrated no significant difference between tissue sites ($n=4$).

Corresponding histological sections for PCL yarns implanted in the FDL tendon demonstrated their close apposition following implantation (Fig.2). Cell infiltration into the yarn was observed from 3 months onwards and scaffold size appeared to visually decrease with time.



Figure 2 – H&E staining of tendon tissue highlighting PCL grafts *in situ* (indicated by arrows) after, (a) 3, (c) 6, (d) 9 and (e) 12 months (Scale-bar 500 μ m; mag x5).

CONCLUSION

This study demonstrates the long-term degradation of electrospun PCL yarns *in vivo*. Scaffold molecular mass decreased gradually over time and shrinkage was evident. Coupled with cell infiltration suggests these scaffolds could provide an appropriate physical structure and degradation rate to facilitate and support new tendon tissue ingrowth.

REFERENCES

1. Woodruff M.A. *et al.*, Prog Polym Sci. 35(10):1217-1256, 2010.
2. Sun H. *et al.*, Biomaterials. 27(9):1735-1740, 2006.
3. Lam C.X. *et al.*, J Biomed Mater Res A. 90(3):906-919, 2009.
4. Bosworth L.A. *et al.*, J Mater Sci - Mater Med. 24(6):1605-1614, 2013.

ACKNOWLEDGMENTS

The authors would like to thank the MRC DPFS (Grant no: G1000788-98812) for providing financial support to this project.

Design of biomimetic cell-interactive substrates using hyaluronic acid hydrogels with independently tunable stiffness and biochemical ligand density

Jing Jing¹, Marc R. Block² and Rachel Auzély-Velty^{1*}

¹Centre de Recherches sur les Macromolécules Végétales (CERMAV-CNRS), affiliated with Université Joseph Fourier, Grenoble, France

²Institut Albert Bonniot, CR INSERM U823, Université Joseph Fourier, Grenoble, France

*Rachel.auzely@cermav.cnrs.fr

Hyaluronic acid-based hydrogels with independently tunable stiffness and biochemical ligand density have been developed using thiol-ene photo-click chemistry and used to probe primary osteoblast cell responses to the varying biochemical signals.

INTRODUCTION

Engineering artificial scaffolds that enhance cell adhesion and growth in three dimensions is essential to successful bone tissue engineering. However, the fabrication of three-dimensional (3D) tissue scaffolds exhibiting controlled mechanical and biochemical properties as well as well-defined porosity still remains a challenge. Hyaluronic acid (HA) is a natural polysaccharide abundant in biological tissues with excellent potential for constructing synthetic extracellular matrix analogues. Although HA-based hydrogels have been used extensively for tissue engineering, there is still a need to develop HA-based scaffolds with customized functional properties that can provide greater control over the biological response. In this work, we synthesized HA-based hydrogels that offer independent control over biochemical functionality and mechanical rigidity. These biomimetic matrices formed by thiol-ene photo-click chemistry were then used to probe the dependence of pre-osteoblast spreading and proliferation as well as early stage osteogenic differentiation on the ligand functionalization and stiffness in 2D culture.

EXPERIMENTAL METHODS

The HA-based hydrogels were formed by thiol-ene photo-click reactions allowing to control both the density of grafted bioactive molecules (i.e. peptides) and the crosslinking density¹. For a given peptide, several HA derivatives were prepared by varying the density of grafted peptides while maintaining a sufficient amount of alkene groups in order to prepare hydrogels with controlled mechanical properties using poly(ethylene glycol) bis(thiol) (PEG-(SH)₂) as a cross-linker. Carboxymethylcellulose (CMC) was chemically modified according to similar reactions in order to compare the effect of the polysaccharide matrix on the biological response. The grafting of peptides was checked by ¹H NMR spectroscopy. Photorheometric measurements were used to characterize the mechanical properties of the hydrogels as a function of crosslinking density. Swelling experiments were also performed. MC3T3-E1 cells were subsequently seeded on the hydrogels and cultured for 21 days in DMEM supplemented with 10% fetal calf serum. Cell

spreading, proliferation and mineralization were analyzed at culture days 1, 10 and 21.

RESULTS AND DISCUSSION

Successful grafting of bioactive peptides on HA and CMC was confirmed by ¹H NMR spectroscopy which also allowed to determine the degree of substitution (DS, i.e. average number of mole of peptides per repeating unit). This was varied from 3 to 18, depending on the nature of the peptide ligand (GRGD and peptide derived from the bone sialoprotein containing RGD sequence (BSP(RGD))²). Then, using photorheometry for the real-time monitoring of HA crosslinking, we demonstrated the ability to finely control the mechanical properties of the HA hydrogels. For investigating the effect of peptide modification of HA/CMC matrices on the behaviour of primary osteoblasts, we prepared hydrogels having an elasticity modulus (storage modulus, G') of 10000 ± 1000 Pa. Studies of cellular responses to these gels demonstrated that pre-osteoblasts were able to adhere firmly on the HA hydrogels and spread to various degrees onto these substrates depending on the peptide density. HA and CMC gels at optimum peptide densities were then used to assess their ability to stimulate osteoblast proliferation and matrix mineralization. Our findings showed that HA hydrogels suitably modified with peptides BSP(RGD) may be used to favour bone formation.

CONCLUSION

In this work, we established a simple and dependable approach to prepare hyaluronic acid-based hydrogels with controlled stiffness and pre-osteoblast cell recognition properties. The results presented in this study provide a framework for the analysis of interactive biochemical and mechanical signaling on cells cultured in 2D as well as in 3D.

REFERENCES

1. Mergy J. *et al.*, J. Polym. Sci. Polym. Chem. 50: 4019-28, 2012
2. Harbers, G. M. *et al.*, J. Biomed. Mater. Res. A. 75:855-859, 2005.

ACKNOWLEDGMENTS

The authors would like to thank the "Agence Nationale pour la Recherche" (grant "ANR-TecSan 2009 program" : ANR-09-TECS-004) for providing financial support to this project.



Injectable Biocompatible and Biodegradable pH-Responsive Hollow Particle Gels Containing Poly(acrylic acid): The Effect of Copolymer Composition on Gel Properties

S. Halacheva^{1*}, D. Adlam², T. Freemont², J. Hoyland² and B. Saunders³

^{1*} University of Bolton, Institute for Materials Research and Innovation, Deane Road, Bolton, Greater Manchester, BL3 5AB, U.K., S.Halacheva@bolton.ac.uk

² Centre for Tissue Injury and Repair, Institute of Inflammation and Repair, Faculty of Medical and Human Sciences, University of Manchester, Oxford Road, Manchester, M13 9PT, U.K.

³ University of Manchester, School of Materials, Grosvenor Street, Manchester, M13 9PL, U.K.

INTRODUCTION

Injectable polymer/cell dispersions have emerged as a superior, non-surgical alternative for tissue regeneration.¹ We have previously explored novel types of pH and redox-responsive poly(methyl methacrylate-co-methacrylic acid)- (PMMA-MAA) and poly(ethyl acrylate-co-methacrylic acid) (PEA-MAA)-based hollow particle gels. The gels had micrometer-scale interconnected porosity, high elasticity and ductility values and are potentially suitable for future use in minimally-invasive tissue repair.² Herein we extend considerably our earlier studies with the aim of identifying a system which meets all necessary requirements for soft tissue repair – i.e., high porosity, biocompatibility, biodegradability and adequate mechanical strength. To investigate the effect of tuning hydrophobicity of the copolymer, the glass transition temperature and the pK_a of the particles upon the gel morphology, mechanical properties and performance, we studied the structurally related poly(*n*-butyl acrylate-co-methacrylic acid) (PBA-MAA), poly(methyl acrylate-co-methacrylic acid) (PMA-MAA) and poly(methyl methacrylate-co-acrylic acid) (PMMA-AA) copolymers for gel formation. These systems have been chosen to allow a wide range of structural variation for the constituent pH-responsive copolymers. We have established that MMA is the optimal hydrophobic monomer, whereas the use of various COOH-containing monomers, e.g. MAA and AA, will always induce a pH-triggered physical gelation.³

EXPERIMENTAL METHODS

All copolymers were characterised by ¹H NMR and GPC. Potentiometric titration was conducted using standardized NaOH solutions. Dispersions were deposited on SEM stubs by evaporation at room temperature. Rheology measurements were performed at 25 °C using a TA AR-G2 rheometer and a 250 μm gap with a 20 mm diameter steel plate at 25 °C. DLS measurements were performed on a Malvern Zetasizer Nano ZS90 autocorrelator, at pH values ranging from 6.0 – 10.0. The hydrodynamic diameter (D_h) of the particles was measured at 90°. The particle's volume swelling ratio, Q , was estimated using $Q = (D_h/D_{h(collapse)})^3$, where D_h and $D_{h(collapse)}$ are the hydrodynamic diameters of the particles at a given pH and in the collapsed non-swollen state, respectively.

RESULTS AND DISCUSSION

The physical gels were formed at physiological pH range only from concentrated dispersions of swollen,

hollow, polymer-based PMMA-AA particles crosslinked with either cystamine (CYS) or 3,3'-dithiodipropionic acid dihydrazide (DTP). A linear relationship between particle swelling ratios, gel elasticity and ductility was observed. The PMMA-AA gels with lower AA contents feature lower swelling ratios, mechanical strengths and ductilities. The mechanical properties and performance of the gels were tuneable upon varying the copolymers' compositions and the structure of the crosslinker. Compared to PMMA-AA/CYS, the PMMA-AA/DTP gels were more elastic and ductile. The SEM images of PMMA-AA/DTP gels show highly porous and interconnected structures (Figure 1). Biodegradability of the new gels was tested using glutathione. The rate of network disassembly was found to be strongly dependent upon the gel's structure. The responses of immortalised human chondrocyte cells to contact with the gels were measured by Live/Dead and MTT assay (Figure 1). The gels showed very good biocompatibility, with at least 80% cell viability after 48 hours. Increases in either the crosslinking density or AA content appear to decrease the cell viability.

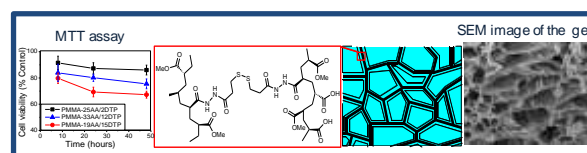


Figure 1. Redox- and pH-responsive hollow PMMA-AA/DTP particle gel scaffolds.

CONCLUSION

The new pH and redox-responsive PMMA-AA hollow particle gels show good biodegradability and biocompatibility, high interconnected porosity and adequate mechanical strength. Therefore, they constitute a promising prototype injectable gel for tissue repair.

REFERENCES

1. Richardson S. M. *et al.*, *Biomaterials* 27:4069-4078, 2006
2. Halacheva S. *et al.*, *J. Mater. Chem. B* 1:4065-4078, 2013
3. S. Halacheva *et al.*, *Biomacromolecules*, 2014, *accepted*

ACKNOWLEDGMENTS

The authors would like to thank the EPSRC for funding this study.



Dual Hydrogel System for Bioprinting of Strong Tissue Constructs

Ferry Melchels^{1*,2}, Wouter Dhert^{1,3}, Dietmar W. Hutmacher^{2,4} and Jos Malda^{1,2,3}

^{1*}Department of Orthopaedics, University Medical Center Utrecht, The Netherlands, f.p.w.melchels@umcutrecht.nl

²Institute of Health and Biomedical Innovation, Queensland University of Technology, Australia

³Faculty of Veterinary Medicine, Utrecht University, The Netherlands

⁴Institute for Advanced Sciences, Technical University Munich, Germany

INTRODUCTION

The objective of bioprinting is to assemble living cells or biological materials in 3D for the preparation of tissue constructs. Cell-laden hydrogels termed "bioinks" recapitulate several features of the natural extracellular matrix and allow cell encapsulation in a highly hydrated three-dimensional environment¹.

However, hydrogels used in 3D cell culture substrates are generally mechanically weak and unsuitable to build large volume constructs, specifically in the z-direction. Here, we explore the combination of a cell-laden bioink with a tailor-made cell-free reinforcing gel to fabricate constructs that allow tissue formation whilst providing sufficient mechanical stability.

EXPERIMENTAL METHODS

Hydrogel precursors L-LA-MA and L-CL-MA were prepared by ring opening polymerisation of either D,L-lactide or ϵ -caprolactone, using poly(ethylene glycol)₁₀₁-poly(propylene glycol)₅₆-poly(ethylene glycol)₁₀₁ (trade name Lutrol F127) as macro-initiator, and subsequently methacrylated using methacrylic anhydride in CH_2Cl_2 in the presence of triethylamine. For L-MA, Lutrol F127 was directly methacrylated. Gelatine-methacrylamide (gelMA) was synthesised as described earlier². Disc-shaped specimen (4x2 mm Dxh) were prepared at 10% w/v (gelMA) or 40% w/v (reinforcing gels) in PBS with 0.1% Irgacure 2959 photo-initiator, by exposing to 365 nm UV (2.6 mW/cm²) for 15 min (UVP CL-1000). Compression testing was performed at 0.2 N/min on a 2980 DMA (TA Instruments). Plotting was performed using a BioScaffolder bioprinter at 15°C.

RESULTS AND DISCUSSION

After photo-crosslinking, gelMA gels had a stiffness of 54 kPa. On the contrary, all reinforcing gels were 11x stiffer at 600 ± 67 kPa (Figure 1), and had a tough, rubber-like appearance.

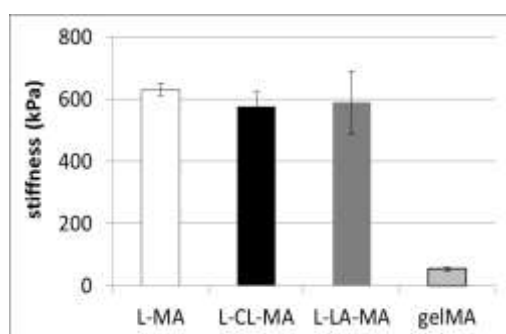


Figure 1: Compressive stiffness of Lutrol F127-based reinforcing gels (40 % w/v) and gelMA bioink (10 % w/v) after photo-initiated crosslinking.

The 3 reinforcing gels showed varying rates of degradation, from fast (L-LA-MA: 68% loss in stiffness over 2 weeks, via slow (L-CL-MA 20% loss in 10 weeks) to no significant loss in stiffness over 10 weeks for L-MA (Figure 2).

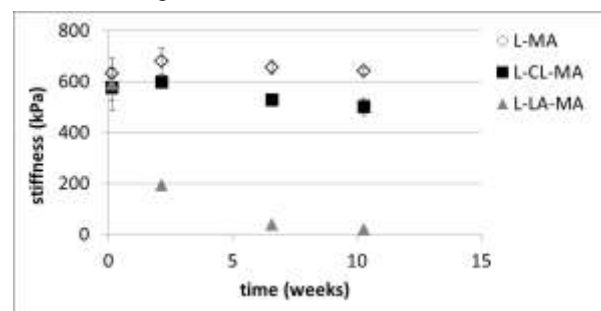


Figure 2: *In vitro* degradation of reinforcing gels in at 37°C PBS measured as decay in compressive stiffness over time.

Using the BioScaffolder bioprinter, all reinforcing gels were successfully plotted into porous constructs (L-CL-MA example in Figure 3).



Figure 3: Hydrogel construct plotted using L-CL-MA reinforcing gel (scale bar 5 mm).

Hydrogels that allow cells to develop new tissue are generally mechanically weak. The mechanical properties can be greatly improved by co-printing of a reinforcing scaffold, *e.g.* using thermoplastics³. Here, we present a platform of printable gels, which allows for the co-printing of a biodegradable reinforcing structure without the need for high temperatures.

CONCLUSION

Three printable hydrogels were developed that allow the biofabrication of mechanically favourable constructs, with tailored degradation kinetics.

REFERENCES

1. Malda J *et al.*, Adv Mater. 2013, 25, 5011
2. Melchels FPW *et al.*, J Mater Chem B. 2014, 2 2282
3. Schuurman *et al.*, Biofabrication 2011, 3, 021001

ACKNOWLEDGMENTS

We thank the EU for funding (Marie Curie Fellowship PIOF-GA-2010-27228)

Physical Hydrogels Based on Peptide Oligosaccharide Interaction

Robert Wieduwild¹, Mikhail Tsurkan², Carsten Werner², and Yixin Zhang^{1*}

¹* B CUBE Center for Molecular Bioengineering, Technische Universität Dresden, Arnoldstraße 18, 01307 Dresden, robert.wieduwild@bcube-dresden.de

²Leipzig-Institut für Polymerforschung Dresden e.V., Max Bergmann Center of Biomaterials and Technische Universität Dresden, Hohe Straße 6, 01069 Dresden,

INTRODUCTION

Non-covalent biopolymer structures that possess simple components with basic biochemical properties similar to the extracellular matrix (ECM) are considered highly promising for various biomedical applications, ranging from drug delivery to 3D cell culture¹. Tailor-made biomaterials with functional complexities can be produced through conjugating different bioactive molecules to simple scaffolds². In this study, we designed a non-covalent assembling system composed of peptide-four-arm-polyethylene glycol (starPEG) conjugates and oligosaccharide³. The hydrogel can be modified without losing its properties as a physical hydrogel or the chemical simplicity.

EXPERIMENTAL METHODS

Bead preparation: Syringes with 4.2 mM peptide-starPEG conjugate and 70 mM 5kDa dextran sulfate were separately prepared and injected in an in house microfluidics system. For cell embedding human neonatal dermal fibroblasts (HDFn) were premixed in KA7-starPEG mixture in full cell culture medium. After life/dead staining with 0.15 μ M fluorescein and 10 μ M propidium iodide images was taken using confocal laser scanning microscopy.

Bead coating: For coating of beads with cells KA7-RGDSP-starPEG conjugate was used and HeLa-actin-GFP cells were incubated with beads. For coating with functionalized peptide-starPEG conjugates, beads were incubated with 1 mg/ml functionalized RA7-starPEG conjugate and washed with PBS afterwards. Coating was imaged using confocal laser scanning microscopy.

RESULTS AND DISCUSSION

We designed and screened minimal peptide motifs whose conjugates with PEG interact with sulfated oligosaccharides (like heparin) to form non-covalent hydrogels (**Figure 1a**). Analysis of structure-function relationship revealed, that peptides containing both basic residues and heparin-induced α -helix formation are important for the assembly process (**Figure 1b**). Namely, the peptides contain repeats of a basic amino acid and alanine ((RA)_n and (KA)_n motifs)³.

Beads were formed by mixing KA7-starPEG conjugate and dextran sulfate in a microfluidic system. Dextran sulfate causes a short gelation time of 10 min. Cells can be embedded with high survival rate (98 \pm 1%, **Figure 2a/b**). Beads with KA7-RGDSP-starPEG can also be coated with cells. Freezing of beads with cells resulted also in high survival. Beads can be further non-covalently modified with proteins or fluorescent labels using RA7-starPEG conjugates (**Figure 2a/c**). Antibodies can be released quickly from the beads.

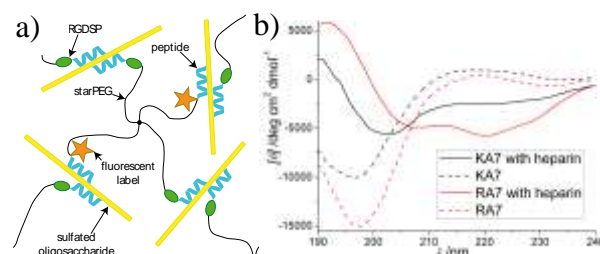


Figure 1: Structure of hydrogel. **a)** Scheme showing the structure of non-covalent matrix and modifications. **b)** Analysis of heparin-dependent structural changes of peptide by circular dichroism. KA7: (KA)₇, RA7: (RA)₇

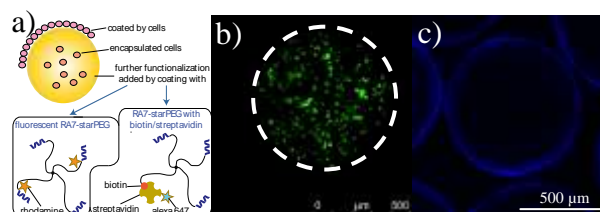


Figure 2: Non-covalent hydrogel beads. **a)** Scheme of beads used to embed or coat with cells and applying further non-covalent coatings. **b)** HDFn embedded in hydrogel beads after 7 days (green – alive, red – dead). **c)** Hydrogel beads coated with RA7-starPEG with biotin/streptavidin (Alexa 647 labelled).

Taking these results into account, this system could be used for analysing interaction between cells embedded in and coated around the beads (**Figure 2a**). Furthermore, this peptide-starPEG-oligosaccharide system can be used to **constantly release drugs** over months using the peptides as tags for drugs. Recently, the hydrogel is used to form **thin layers** with different structure and oligosaccharides for easy **surface functionalization**.

CONCLUSION

This novel physical hydrogel system is very versatile. The mildness to cells (as no chemical reaction is involved) and the ease of functionalization make it a biomaterial with many potential applications.

REFERENCES

1. Lutolf M.P. *et al.*, Nat. Biotechnol. 23:47-55, 2005
2. Cranford S.W. *et al.*, Adv. Mater. 25:802-824, 2013
3. Wieduwild R. *et al.*, J. Am. Chem. Soc. 135:2919-2922, 2013

ACKNOWLEDGMENTS

We thank Ulrike Hofmann, Peggy Berg, Andre Knapp, Iman El-Sayed and Sarah Duin for technical support and the BMBF for financial support (grant 03Z2EN12).



The physical properties of particles dominate cellular uptake and subsequent influences on cell functions

Zhengwei Mao*, Weijun Liu, Pengfei Jiang, Dahai Yu, Xiangyan Zhou, Changyou Gao*

MOE Key Laboratory of Macromolecular Synthesis and Functionalization, Department of Polymer Science and Engineering, Zhejiang University, Hangzhou 310027, China. zwmao@zju.edu.cn, cygao@mail.hz.zj.cn

INTRODUCTION

With the rapid development of nanotechnology, many kinds of nanoparticles have been and are being used in biological and medical fields of industry and scientific researches. Therefore, it would be of paramount importance to understand the influence of particles' physiochemical properties such as size, surface charge and stiffness on the interactions with cells, the smallest building blocks of tissues and organs, in terms of cellular uptake process and mechanism, localization inside cells, and the subsequent influences on cell viability, functions, and phenotypes. On one hand, this kind of study will provide design criteria of particles, which can have better functions in biological applications such as intracellular drug delivery. On the other hand, the impact of particles on cell toxicity and functions will be evaluated to address the safety issue. In this paper, we will give an example of the stiffness of particles that dominates the cell uptake and cell functions.

EXPERIMENTAL METHODS

Four types of poly(2-hydroxyethyl methacrylate) (HEMA) hydrogel particles with different amounts of crosslinking agent, N,N'-methylene-bis-acrylamide (BIS), and thereby compressive modulus were synthesized by an emulsion-precipitation polymerization. The physiochemical properties of the particles in different environment were characterized in terms of size, surface charge, morphology, stiffness and protein adsorption via dynamic light scattering (DLS), transmission electron microscopy (TEM), mechanical tester and bicinchoninic acid (BCA) protein assay. The cellular uptake process of the nanoparticles, including the internalization amount, uptake pathway and intracellular distribution were qualitatively and quantitatively studied. The cytotoxicity of the nanoparticles were studied in terms of cell viability, morphology and cytoskeleton organization, cell adhesion and migration.

RESULTS AND DISCUSSION

All of the particles had a diameter of 800nm in water. Adsorption of proteins (35 mg/g particles) occurred on all the particles, leading to a slightly increase of zeta potential from -20 mV (in water) to -5 mV (in serum containing medium). The softer particles were internalized by HepG2 cells at a faster rate and larger amount than the stiffer ones. Cellular uptake mechanisms were clarified by the addition of inhibitors to specific endocytosis pathways. All the hydrogel particles were internalized by an energy-dependent mechanism. However, uptake of the particles with different modulus follows different mechanisms: the softer particles are mainly internalized via macropinocytosis, whereas the stiffer ones are largely endocytosized via caveolae- and clathrin-mediated

endocytosis as well as macropinocytosis pathways. Uptake of all types of the particles did not cause an apparent decrease of cell viability and alteration of cell morphology, but changed the cytoskeleton organization to some extent. The cell adhesion and migration ability was significantly affected, especially after uptake of the stiffer particles.

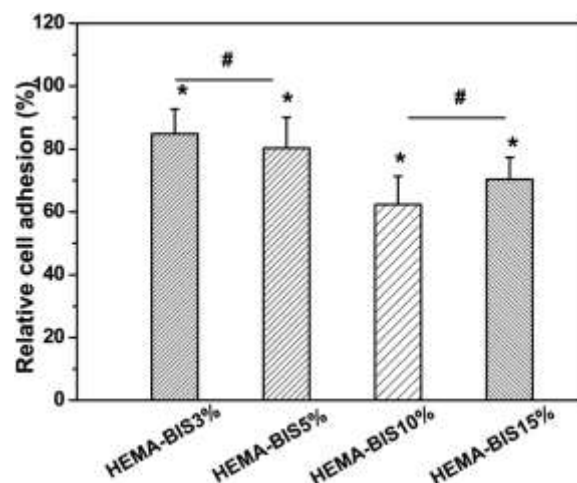


Figure 1. Cell adhesion percentage after the cells were pre-cultured with 50 μ g/mL hydrogel particles of different crosslinking degrees, respectively. The data were normalized to those of the particle-free controls. Asterisk indicates significant difference at $p < 0.05$ level, and # indicates insignificant difference at $p > 0.05$ level.

Conclusions: The present study discloses that the stiffness of hydrogel particles influences their cellular uptake amount, rate, and entry routes. Our results suggest that the mechanical properties of particles are an important factor that control cellular response, and should be carefully considered in designing versatile delivery vehicles and other carriers for biomedical applications.

REFERENCES

1. Mao ZW, et al. *Biomater Sci* 2013; 1; 896-911.
2. Yu DH, et al. *Macromol Biosci* 2013; 13: 1413-1421.
3. Liu WJ, et al. *Soft Matter* 2012; 8: 9235-9245.
4. Yu DH, et al. *Biomacromolecules* 2012; 13: 3272-3282.
5. Peng LH, et al. *Biomaterials* 2014; 35, in press.

ACKNOWLEDGMENTS

The authors would like to thank the financial support by the Natural Science Foundation of China (51120135001; 51003094), the Frame Work Program 7 of European Commission (HINAMOX, 228825; BRASINOEU, 318916).



The Size Effect of PLGA Microspheres on the Controlled-release of Fluorescein Isothiocyanate–Dextran as a Model for Targeting Synovial Macrophages *In Vitro*

Rui Chen^{#*}, Colette Redmond^{*}, John Innes^{*} and John A. Hunt^{**}

Clinical Engineering, UKCTE[#], The Institute of Ageing and Chronic Disease^{*}, University of Liverpool, UK
ruichen@liverpool.ac.uk

INTRODUCTION

SiRNA has already been widely used in basic science as a method to study the functions of genes and it may provide an alternative therapeutic promise to novel therapies in the future. However, before siRNA can achieve widespread clinical use, significant development must be made in the techniques of siRNA delivery that not only to improve efficiency of targeted delivery but also to protect siRNA from degradation by nuclease. The most studied carrier systems are virus-based, liposome-based and polymer-based delivery systems. Due to the safety concerns raised by virus-based systems and the relatively low transfection efficiency of liposome-based systems, polymer nanoparticles and microspheres have been developed. Polymer microspheres have the capacity to encapsulate large amounts of siRNA, allow co-delivery of multiple therapeutics, can be surface-modified to improve stability, and they also can offer the ability of controlled-release though the degradation of the polymers. The synthetic biodegradable polymers, polylactic acid (PLA) and polylactic-co-glycolic acid (PLGA), are versatile materials able to provide controlled-release and targeted delivery. Polymer microspheres can be applied to target synovial macrophages, utilising the host defence and the process of phagocytosis.

EXPERIMENTAL METHODS

Two fluorescein isothiocyanate-dextrans FD4 (Mw=3,000-5,000) and FD10s (Mw=10,000) were used as model molecules for siRNA. The FD4 and FD10s loaded PLGA microspheres were prepared using the water-in-oil-in-water (W1/O/W2) solvent-evaporation technique. The diameters of the microspheres were adjusted by the speed of stirring and the concentration of the PLGA solution. The degradation of PLGA microspheres and the model molecules release were determined up to 42 days by GPC, DSC, LSCM, spectrofluorimetry and SEM.

The delivery of substances to macrophages was investigated by co-culture of PLGA microspheres with DH82 cells *in vitro* up to 42 days. DH82 cells were seeded into the 6 well plates at 5×10^3 cells/cm². After one day, FD4 and FD10s loaded PLGA microspheres were added into the plates at a concentration of 1mg/ml.

RESULTS AND DISCUSSION

The different sizes PLGA microspheres loaded with FD4 and FD10s were prepared to study the degradation of the microspheres, the release rate of the model molecules and the phagocytosis of the microspheres. The results showed that the encapsulation efficiency was around 70%; the model molecules tended to aggregate and be distributed near the surface of

microspheres on the large microspheres ($\phi > 100\mu\text{m}$) but distributed more uniformly in the small microspheres ($\phi < 20\mu\text{m}$); from which there was controlled release, with 30 to 40% of the model molecules remaining in the microspheres after 6 weeks *in vitro* (Fig. 1). The morphology changes in the large microspheres were much greater than the smaller microspheres after 6 weeks. The small microspheres were effectively engulfed into DH82 cells, but most of the large ones were outside of the cells and easy to wash away after 1 week co-culture (Fig. 2).

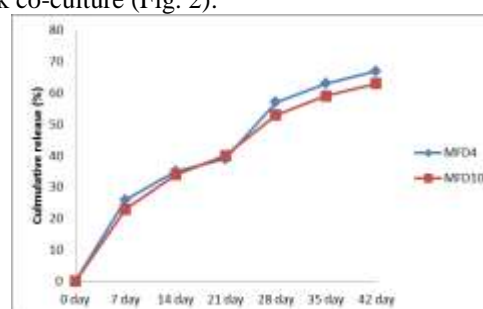


Fig.1 Cumulative release of FD4 and FD10s from PLGA microspheres

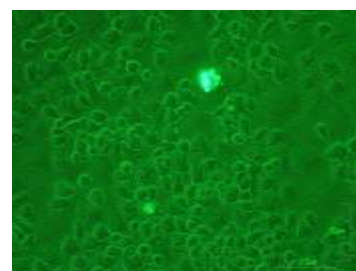
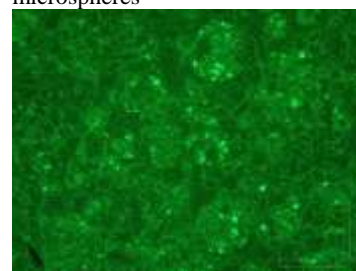


Fig.2 PLGA microspheres co-cultured with DH82 cells after 1 week. Top: small microspheres ($\phi < 20\mu\text{m}$); bottom: large microspheres ($\phi > 100\mu\text{m}$)

CONCLUSION

The results indicate that the small PLGA microspheres ($\phi < 20\mu\text{m}$) are better candidates than big PLGA microspheres ($\phi > 100\mu\text{m}$) for the controlled-release of siRNA for targeting synovial macrophages.

REFERENCES

1. Chen R. *et al.*, Biomaterials 2006; 27: 4453-4460
2. Curran S.J. *et al.*, Tissue engineering 2005, 11:1312-1322

ACKNOWLEDGMENTS

The authors would like to thank Pet Plan Charitable Trust (Grant no: 11-01) for providing financial support to this project.



Hybrid Hydrogel/Fiber Construct for Neural Engineering Applications

P.A. Wieringa^{1,2*}, R. Pinho¹, S. Micera², R. van Wezel¹, L. Moroni¹

¹MIRA, University of Twente, The Netherlands, p.a.wieringa@utwente.nl

²Biorobotics Institute, Scuola Superiore Sant'Anna, Pisa, Italy

INTRODUCTION

The extracellular matrix (ECM) of the peripheral nervous system (PNS) is comprised primarily of oriented collagen fibrils, arranged to delineate 2-20 μm diameter tube structures that act to guide neurites during regeneration¹. 3D environments have been proposed as more suitable to investigate and promote PNS repair, though these fail to replicate the structure of the native ECM. Electrospun scaffolds mimic the collagen fibril topography and are conducive to neurite growth, but fail to fully reproduce the tubular 3D organization². Hydrogels support neurites in a more 3D environment, but can also impede growth³. The objective of this work is to create a 3D culturing platform that is conducive to neurite growth and better captures the ordered heterogeneity of the PNS by emulating the scale, composition and structural organization of the ECM.

EXPERIMENTAL METHODS

Scaffold Fabrication. A hybrid hydrogel/fiber scaffold was realized by preparing a triple layered template of oriented fibers via electrospinning onto a gap electrode collector. Nanofibers comprised the upper and lower layers, prepared from a blended solution of 10% w/v 300PEOT55PBT45 and 4% w/v collagen in HFIP. Sacrificial microfibers prepared from a 50% w/v solution of PLA constituted the middle layer. The fiber template was heated to 65 °C for 1 hr to fuse the nanofibers to the periphery of the microfibers. Two sacrificial PCL plugs were fused to the fibers and placed approximately 7 mm apart. The template was embedded in a PEGDA precursor (+0.1% w/v Irigacure 2959) in a 15 mm diameter cylindrical mold. After crosslinking, the hybrid construct was placed in acetone at 50 °C to leach out the PCL plugs, forming 2 wells, and the PLA, forming channels to connect the wells.

Cell Culturing. Constructs were sterilized with EtOH and placed in 24 well plate. Dorsal root ganglions (DRGs) were extracted from Day 2 post-natal rat pups and placed in one well. Cultures were maintained for 8 days in Neural Basal medium with B27 supplement and 10 ng/ml NGF. Cells were fixed with 2% PFA, permeabilized with Triton-X, and stained for β 3-tubulin (neurite marker) and S100 (Schwann cell marker).

RESULTS AND DISCUSSION

The presence of interconnected microchannels between wells was verified by diffusion of fluorescent nanospheres between wells (Figure 1a). Channels were approximately 6.6 μm in diameter and SEM analysis revealed that the microchannels were lined with oriented nanofibers (Figure 1b). Seeded DRGs successfully innervated the hydrogel construct after 8 days (Figure 2), with a maximum length of 7 mm. Oriented microchannels with fibrous nanotopography lining the channel walls were successfully formed

within the compliant hydrogel matrix. These were shown to be of similar scale and structural organization to those observed in the PNS ECM. Constructs supported and guided neurite growth, validating the effectiveness of the 3D biomimetic platform.

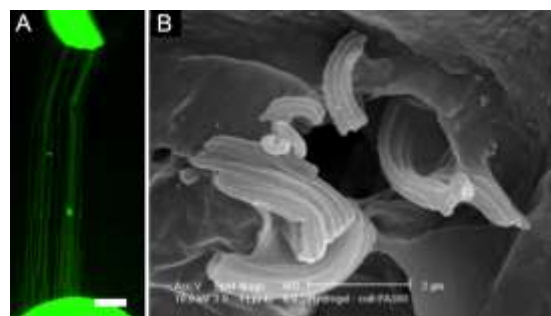


Figure 1. (A) Interconnected microchannels formed within hydrogel between wells (Scalebar: 500 μm). (B) Hydrogel cross section at high magnification showing a microchannel with aligned nanofibers on the periphery.

This opens the possibility of investigating neurite growth in a more representative 3D environment. The flexibility of this construct allows for different hydrogels, microchannel sizes and nanofibers to be used, allowing for the controlled exploration of neurite growth. Furthermore, the fabrication can be scaled to create larger scaffolds suitable for implantation.

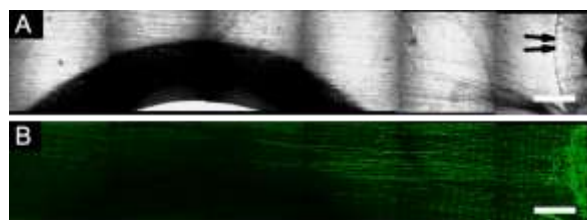


Figure 2. (A) Brightfield image of DRG outgrowth from well edge (double arrow) into hydrogel. (B) β 3-tubulin staining of neurite innervation of gel. (Scalebar 500 μm)

CONCLUSION

A 3D hybrid hydrogel/fiber construct was created with controlled, oriented anisotropic microchannel porosity and incorporated nanofiber topography to facilitate growth cone adhesion and guidance. Furthermore, this construct sustained directed growth of neurites.

REFERENCES

1. Ushiki, T. *et al.*, Cell Tissue Res **1990**, 260, 175–84.
2. Xie, J. *et al.* Nanoscale **2010**, 2, 35–44.
3. Labrador, R. *et al.*, Exp. Neurol. **1998**, 149, 243–52.

ACKNOWLEDGMENTS

The authors would like to thank the National Research Council of Canada the European Union's Seventh Framework Programme for research, technological development and demonstration under grant agreement no 280778-2 (MERIDIAN) for financial support.



Decellularized Matrix /Fibroin Injectable Hydrogels for Vascularized Adipose Tissue

Alisan Kayabolen¹, Dilek Keskin^{1,2,3}, Ferit Avcu⁵, Andac Aykan⁴, Fatih Zor⁴, and Aysen Tezcaner^{1,2,3}

¹Department of Biomedical Engineering, Middle East Technical University, Turkey

²Department of Engineering Sciences, Middle East Technical University, Turkey

³Center of Excellence in Biomaterials and Tissue Engineering, Middle East Technical University, Turkey

⁴Department of Plastic and Reconstructive Surgery, Gulhane Military Medical Academy, Turkey

⁵Department of Haematology, Gulhane Military Medical Academy, Turkey

alisan.kayabolen@metu.edu.tr

INTRODUCTION

Adipose tissue engineering is a promising field for regeneration of soft tissue defects. However, only very thin implants or avascular tissue implants can be used in vivo for which vascularization is critical in thick implants¹. Another problem is finding a biocompatible scaffold with good mechanical properties. In this study, the aim is to develop an injectable hydrogel of decellularized adipose tissue and fibroin, entrapping both endothelial cells and adipose derived stem cells and characterize in vitro and in vivo. The approach is to develop a vascularized implant that will integrate with the host.

EXPERIMENTAL METHODS

Decellularization & Solubilization of Adipose Tissue

Adipose tissue was decellularized based on the study of Young et al. (2011)² with some modifications. Briefly, human lipoaspirate was washed in PBS, and decellularized in 1% SDS for 2h. Then, it is delipidized in isopropanol until tissue color was turned from yellow to white. After washed in dH₂O, sample was frozen at -80 °C, and then, it was freeze-dried.

Lyophilized matrix was completely dissolved in pepsin/HCl solution and the solution was neutralized by raising pH to 7.4 with 1M NaOH. 10x PBS was then added as it is diluted to 1x PBS. After solubilization, composition analyses were performed.

Gelation and Cell Encapsulation

Decellularized adipose tissue (DAT) solution was mixed with fibroin solution with different ratios. Then, all samples were gelled by vigorously vortexing.

For cell culture experiments, adipose derived stem cells (ASCs) were isolated from rat adipose tissue. Then, endothelial and adipogenic differentiation of ASCs were induced separately. Both predifferentiated cell types were embedded in DAT:Fibroin gel just after gelation was triggered by vortexing.

Implantation of Cell Encapsulated Matrix for In Vivo Tests

In vivo biocompatibility experiments were performed by subcutaneous implantation to test host response of to hydrogels devoid of cells. Before implantation, fibroin solution was sterilized with autoclave and DAT samples were sterilized with EtO. Cell embedded matrices will be wrapped around a host vessel, to determine whether a vascularized adipose tissue will be formed.

RESULTS AND DISCUSSION

Decellularization and Composition Analyses

Decellularization was confirmed by fluorometer measuring after Hoechst staining. Average DNA

amount was found as 90 ng/ml in solubilized DAT. By BCA assay, total protein amount in solution was found as 3 mg/ml. Thus, DNA amount can be accepted as 30 ng/mg of DAT matrix which is lower than that in many decellularization studies^{2,3}. Delipidization was observed by color change (Figure 1) and Oil Red O staining. Also, total collagen and sGAG assays showed that ECM components were remained after these treatments.



Figure 1. Adipose tissue a) After SDS treatment b) After alcohol treatment

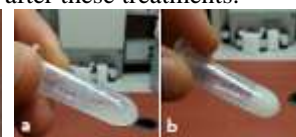


Figure 2. DAT-Fibroin mixture a) Before vortexing, b) After vortexing.

Gelation and Cell Encapsulation

Mixing DAT samples with fibroin allowed rapid gel formation by vortexing (Figure 2). It also provided to adjust mechanical strength by changing fibroin to DAT ratio. Based on compression tests, the one which has the most similar mechanical properties to adipose tissue was selected for cell experiments.

In vivo implantation

Subcutaneous implantation of hydrogels (Figure 3) resulted with no immunogenic reaction or infection. This shows that decellularization and sterilization steps were performed successfully. Localized implantation in which hydrogels wrapped around the host vessel are under study. It is expected that endothelial cells inside the hydrogel will form a capillary network and they will bind to the host vessel passing through hydrogel.



Figure 3. Subcutaneous implantation of DAT – Fibroin mixture

CONCLUSION

DAT-fibroin hydrogel has many natural ECM components and results showed that injectable DAT:Fibroin hydrogels hold promise for adipose tissue engineering, important outcome for esthetical reconstructive surgery

REFERENCES

1. Jain R.K. *et al.*, Nature Biotech. 23:821–3, 2005
2. Young D.A. *et al.*, Acta Biomater. 7:1040-9, 2011.
3. Uriel S. *et al.*, Tissue Eng Part C Methods. 15:309-21, 2009.

ACKNOWLEDGMENTS

We would like to thank Gulhane Military Medical Academy (GATA) for providing financial support to this project.



Reinforcement of Sol-Gel Processed Calcium Phosphate Cement using Functionalised CNTs

K. Natesan¹, H. R. Le², C. Tredwin³, R. Handy⁴

^{1,3}School of Dentistry, University of Plymouth, United Kingdom

²School of Marine Science and Engineering, University of Plymouth, United Kingdom

⁴School of Biological Sciences, University of Plymouth, United Kingdom

Kiruthika.natesan@plymouth.ac.uk

INTRODUCTION

Calcium phosphate is bioactive, biodegradable graft material with excellent biological properties. However, its low strength limits its use to only non-stress application¹. We hypothesized that a composite of calcium phosphate cement reinforced with multiwall carbon nanotubes (MWCNTs) could enhance the strength of the material and widen its applications. In this paper we have discussed a simplified process of fabricating calcium phosphate cement by sol-gel technique² along with the uniform dispersion and incorporation of MWCNTs. As the material can potentially be replaced with new bone after a period of time, it will satisfy the key requirements of an ideal bone graft.

EXPERIMENTAL METHODS

Calcium phosphate was prepared by the addition of dibasic ammonium phosphate $(\text{NH}_4)_2\text{HPO}_4$ solution over calcium acetate $\text{Ca}(\text{CH}_3\text{COO})_2$. The volumes of the solution were calculated for a ratio Ca/P = 1.5. Non-stoichiometric hydroxyapatite precipitates were annealed at 1000-1200°C to obtain β -tricalcium phosphate. XRD analysis was performed to study the crystal nature of material.

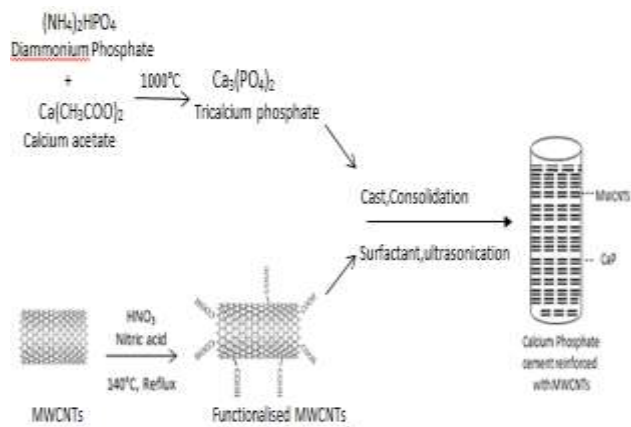


Fig 1. Simulative overview of process for reinforcement of CNTs in calcium phosphate matrix

Since as-received MWCNTs are hydrophobic they will be refluxed with 60% nitric acid to obtain carboxylated

MWCNTs (MWCNTs-COOH). Various surfactants were tried as dispersant to obtain uniform dispersion of MWCNTs in the solution containing calcium Phosphate particles. The final product will be cast and consolidated into cement blocks. The fundamental properties such as porosity, density and compressive strength of the final hardened body of the cement will be examined. The interaction of CNTs with the cement was examined using FT-IR, Raman spectroscopy and Scanning Electron Microscopy analysis. The implication of CNTs on the biocompatibility is being studied using osteoblast cell cultures.

RESULTS AND DISCUSSION

A uniform distribution of CNTs in calcium phosphate matrix (as depicted in the fig) was obtained. The functionalization and treatment of CNTs with surfactants increased their chemical compatibility with calcium phosphate. It is found that the efficacy of CNTs as reinforcement is dependent on the surface treatment, the plasticiser and the casting process. The addition of CNTs significantly improved the compressive strength of the cement. The implication of the CNTs on the biocompatibility is currently being studied using osteoblast cell cultures.

CONCLUSION

This paper presents an efficient method of synthesizing calcium phosphate cement reinforced with CNTs. The critical challenges in using CNTs are disaggregation and uniform dispersion. As the surface treatment of CNTs is vital to the biocompatibility of the resultant composites, an efficient method involving both mechanical method and chemical treatment to overcome this barrier is demonstrated. This would serve as a cost effective method of developing bone implant material.

REFERENCES

1. Xu H., Simon C., *Biomater.* 26:1337-1348, 2005
2. Stoia M. *et al.*, *Chem. Bull* 53:204-207, 2008

Dynamics of filopodium-like protrusion and endothelial cellular motility on 1-D extracellular matrix fibrils

Niannan Xue¹, Cristina Bertulli¹, Amine Sadok², Yan Yan Shery Huang^{3*}

¹Department of Physics, University of Cambridge CB3 0HE, UK

³The Institute of Cancer Research, 237 Fulham Road, London SW3 6JB, UK

^{2*} Department of Engineering, University of Cambridge CB2 1PZ, UK yysh2@cam.ac.uk

The dynamic interaction between endothelial cells (EA.hy926) and single fibrils of gelatin was studied. Particular focus was paid to the cellular motility and the characteristics of cytoplasmic protrusions. The effect of ROCK inhibition on these two aspects were also investigated. The results are hoped to further our understanding in the role of ECM fibrils in guiding angiogenesis.

INTRODUCTION

Extracellular matrices (ECM) fibrils provide specific adhesive features, together with topographical and mechanical cues, conduct cellular behaviors. *In vivo*, individual cells would interface with one or more ECM fibrils organized in a three-dimensional fashion. Cytoplasmic slender projections such as filopodia were suggested to function as antennae to sense the biochemical and biophysical cues given by the surrounding substratum such as ECM, in turn guiding cellular motility. Since fibril structures are the building blocks of an ECM, studying endothelial protrusion interaction with a single ECM fibril can be seen as a simple and physiologically relevant model system.

EXPERIMENTAL METHODS

We employ near-field electrospinning^{1,2} to create ordered patterns of collagenous fibrils of gelatin, based on an acetic acid and ethyl acetate aqueous co-solvent system. ROCK inhibition of EA.hy926 was induced by H1152. Live cell imaging was performed using a Leica confocal microscope.

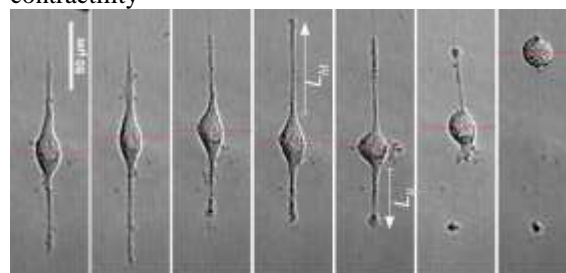
RESULTS AND DISCUSSION

The interaction between endothelial cells and extracellular matrix fibrils was recapitulated *in vitro*³. Live cell imaging shows that cellular migration along a gelatin fibril is accompanied by filopodial-like protrusion extension and retraction. When interfaced with a fibril, cells adopt a bipolar morphology with extended protrusions at both ends. Different modes of cell motility *vs.* temporal protrusion lengths are identified under normal culture and ROCK inhibition. Persistent migration was found to be one of the modes which permitted cell displacement for over 300µm at a speed of ~1µm/min. In particular, this migration speed is similar to fibroblast migration in a 3D collagen gel. However, it is to note that such a persistent migration is a rare event and majority of the time cells did not migrate further than their cell size.

Analyzing the patterns of protrusion length *vs.* cell displacement seems to indicate that short protrusions

better facilitate cell motility. ROCK inhibition, which significantly increased the temporal protrusion lengths, did not apparently alter the mean value of cell displacement; however, it had reduced the probability of long-ranged cell migration. Measuring the protrusion velocity indicates that the speeds of extension and retraction have very different distributions between the normal and the ROCK treated culture.

Occasional protrusion breakage is observed during cellular motility (see image below). Such protrusion breakage can occur on a variety of protrusion lengths (from 20µm to over a hundred microns). The associated characteristic lengths can act as indicators for cellular contractility



CONCLUSION

Near-field electrospinning of gelatin fibrils provides a simple and well-controlled model to recapitulate the ECM fibril topography. Future studies which involve comparison to *in vivo* systems are important to further validate the fibrils' physiological relevancy. Using this fibril system, we have defined the key morphological parameters of protrusion dynamics during cell motility. ROCK inhibition resulted in abnormally long protrusions, and diminished the persistent migration, but dramatically increased the speeds of protrusion extension and retraction. Finally, we also showed the breakage of protrusion during cell motility.

REFERENCES

1. Huang *et al.* *Nanotechnology* (2014) 23, 105305
2. Xue *et al.* *PLOS ONE* (2014, accepted)
3. Xue *et al.* *Interface Focus* (2014) 4, 20130060

ACKNOWLEDGMENTS

The authors thank M. Locard Paulet and C. Jorgensen for advising on cell staining and supplier of EA.hy926 cells; and E. Sahai, N. C. L. Gauthier, M. Oyen and A. Kabla for helpful discussions. This research was supported by an Oppenheimer Research Fellowship and a Homerton College Fellowship.



The Importance of Interconnectivity for Cell Invasion and Percolation through Collagen Scaffolds

J. Ashworth^{1*}, P. Buxton², T. Hart², S. Best¹ and R. Cameron¹

¹Cambridge Centre for Medical Materials, University of Cambridge, UK, *jca35@cam.ac.uk

²Geistlich Pharma AG, Wolhusen, Switzerland

INTRODUCTION

It is widely acknowledged that the efficacy of tissue engineering scaffolds is often limited by a lack of cell invasion into the porous structure. Such invasion is profoundly influenced by the pore size and interconnectivity of the scaffold. Whereas the effect of pore size is well-characterised in literature¹, interconnectivity is generally only studied qualitatively, with limited attempts at correlation with observed cell behaviour. Here a method based on percolation theory is implemented, to demonstrate that consideration of interconnectivity is vital for a thorough understanding of how cell invasion into tissue engineering scaffolds may be predictably controlled.

EXPERIMENTAL METHODS

Scaffolds were fabricated by freeze-drying a 1% w/v suspension of insoluble type I bovine collagen from Achilles tendon, hydrated in 0.05 M acetic acid. X-ray Micro-Computer Tomography (micro-CT) was used to produce a 3D representation of the scaffold structure. From this dataset, measurements of percolation diameter (d_c) were made. This parameter represents the diameter of a sphere able to pass through the pore space from one side of a scaffold to the other, and can be calculated using the expression²:

$$(d - d_c) \propto L^{-\frac{1}{\nu}}$$

Where d is the diameter of a sphere that can invade the pore space up to a distance L , and the constant ν is the standard value of 0.88 for percolation in 3D systems. Measurements of L and d were made using the software CTAn. The effect of pore size and percolation diameter on human primary fibroblast invasion was tested by surface seeding in triplicate, at 64,000 cells per 1 cm² scaffold. After 3 days of culture, Phalloidin-staining, cross-sectioning and confocal microscopy allowed measurement of mean invasion distances, displayed for each scaffold along with 95% confidence intervals.

RESULTS AND DISCUSSION

Independent variation of pore size and percolation diameter was found to be possible, as shown in figure 1.

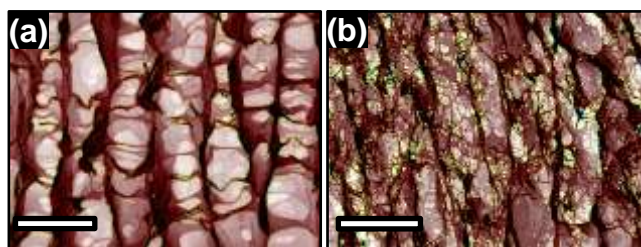


Figure 1: SEM images of scaffolds with varying percolation diameter: (a) 60 μm, (b) 40 μm. Pore size (70 μm) and orientation constant. Colour indicates strut density, increasing from red-blue. Scale bar is 100 μm.

Increasing freezing temperature increased the pore size, as has been documented previously in literature³, but was also observed to change percolation diameter. However, varying the cooling rate was found to be an effective way of altering pore size, while keeping percolation diameter constant. Furthermore, as shown in figure 1, the substitution of (a) 0.05M acetic acid for (b) 0.001M hydrochloric acid in the initial collagen suspension changes percolation diameter independently. Using this knowledge, 4 scaffolds were created for cell invasion studies, to examine the effect of independent pore size and percolation diameter variation (figure 2).

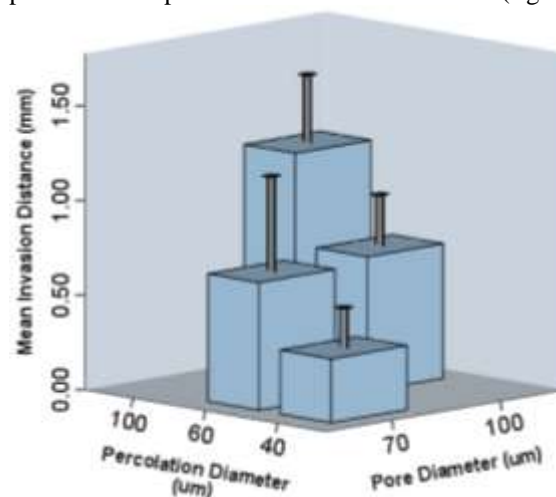


Figure 2: Effect of pore size and percolation diameter on fibroblast invasion distance after 3 days of culture.

It was found that a larger percolation diameter corresponded to enhanced cell invasion ability. In fact, it could be seen that a change in percolation diameter can cause substantial differences in cell invasion, even when pore size is kept constant. Therefore a description of scaffold architecture in terms of pore size alone is an incomplete approach to characterisation.

CONCLUSION

Pore size and percolation diameter both influence cell invasion ability. Architectural characterisation of collagen scaffolds should therefore combine pore size measurements with quantitative interconnectivity analysis in order to present a complete picture of the structural factors that will determine cell response.

REFERENCES

1. O'Brien, F. J. *et al.*, Biomaterials 25: 6, 2004
2. Saxton, M., Biophys. J. 99:5, 2010
3. Pawelec, K. M. *et al.*, J. R. Soc. Interface 11:92, 2014

ACKNOWLEDGMENTS

The authors acknowledge financial support of EPSRC, ERC Advanced Grant 3D-E and Geistlich Pharma AG.



Novel Continuous Plastic Flow Synthesis of Phase Pure Nano-Sized Hydroxyapatite

Aneela Anwar, Jawwad A. Darr*

Clean Materials Technology Group, Department of Chemistry, University College London, 20 Gordon Street, London WC1H 0AJ, a.anwar.11@ucl.ac.uk

INTRODUCTION

Calcium phosphates (CaP) are the most ubiquitous family of bioceramics well known for their use as bone graft substitutes, coatings on metallic implants, reinforcements in biomedical composites and in bone and dental cements.¹ Hydroxyapatite (HA), $[\text{Ca}_{10}(\text{PO}_4)_6(\text{OH})_2]$ is similar to biological apatite, the main mineral constituent of teeth and bone² because of its biocompatibility, bioactivity and low solubility in wet media. Such nano-bioceramics have been employed as a scaffold material to encourage new bone formation for osteoinductive coatings on metal implants and as a bulk bone filler.³⁻⁶

EXPERIMENTAL METHODS

Synthetic hydroxyapatite (HA) nanoparticles (~ 20 nm) were synthesised from aqueous solutions of calcium nitrate tetrahydrate and diammonium hydrogen phosphate mixed using a novel two pump continuous plastic flow synthesis (CPFS) system with a total reaction time of ca. 5 minutes performed under controlled temperature (60 °C) and pH 10. The product was obtained as a phase pure material with a stoichiometric Ca:P molar ratio of 1.67, without the need for a separate ageing step [Patent Filed UK Patent Application No. 1317747.2].

RESULTS AND DISCUSSION

The powders were then characterized by transmission electron microscopy (TEM), BET surface area analysis, X-ray powder diffraction, FTIR spectroscopy, Raman spectroscopy and X-ray photoelectron spectroscopy (XPS). Particles synthesized at 60 °C in 5 minutes residence time possessed remarkably high surface area of $264 \text{ m}^2 \text{ g}^{-1}$ and very small particle size of ~ 20 nm.

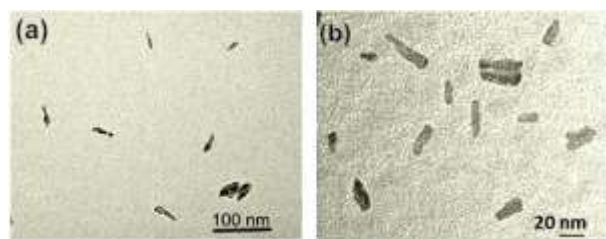


Figure 1. Transmission electron microscope images of hydroxyapatite nano-rods of sample HA60 synthesized by continuous plastic flow synthesis with scale bars, (a), (bar = 100 nm), (b), (bar = 20 nm),

Evaluation of *in-vitro* biocompatibility showed that HA disk-pressed powders supported osteoblast cell attachment and proliferation. The proposed synthesis strategy provides a facile and economical pathway to

rapidly obtain nano-sized hydroxyapatite with high purity, and ultra-high surface area.

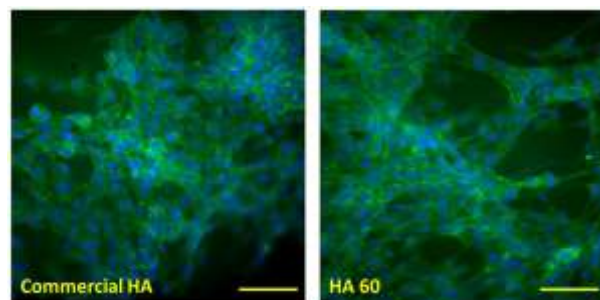


Figure 2. MG63 morphology on HA discs. Cells were visualised at day 7 for cell nucleus (DAPI in blue) and cytoskeleton (phalloidin-FITC in green) for MG63s cultured on HA 60, and commercial HA. Scale bar is 100 µm.

CONCLUSION

The conclusions have to be based on the facts in evidence and should be limited to minimal speculation about the significance of the work.

“Males and females students were critical criteria used to determine their emotions during...Consequently; if emotions can incarcerate us by hiding our complexity, at least their expression can liberate us by displaying our authenticity.”

REFERENCES

1. Elliot JC. Structure and chemistry of the apatites and other calcium orthophosphates. Amsterdam: Elsevier; 1994.
2. C. Liu, Y. Huang, W. Shen, J. Cui, Biomaterials 2001, 22, 301.
3. L. L. Hench, Biomaterials 1998, 19, 1419.
4. Hench, L. L., Bioceramics. J. Am. Ceram. Soc., 1998, 81, 1705–1728.
5. L. L. Hench, Current Orthopaedics 2000, 14, 7.
6. K. S. Katti, Colloids and Surfaces B-Biointerfaces 2004, 39, 133. M. Aitken, A. Chaudhry, M. Boxall, M. Hull, Occupational Medicine-Oxford, 2006, 56, 300.

ACKNOWLEDGMENTS

Islamic Development Bank and University of Engineering and Technology are acknowledged for granting scholarship and study leave, respectively. Dr. Robin M. Delaine-Smith is thanked for their help with biological testing at University of Sheffield.

The effects of ascending and descending strain rate on the mechanical properties of canine cranial cruciate ligaments

Rosti Hama Rashid^{1*}, Brendan Geraghty¹, Ahmed Elsheikh¹ and Eithne Comerford²

¹School of Engineering, University of Liverpool, Liverpool, L69 3GH, UK, *R.Hamarashid@liv.ac.uk

²Institute of Ageing and Chronic disease and School of Veterinary Science, Faculty of Health and Life Sciences, University of Liverpool, Neston, CH64 7TE

INTRODUCTION

Mechanical properties of knee ligaments, such as the anterior cruciate ligament (ACL), are of clinical importance, as they are critical to provide the structural stability of a given joint. There were over two million knee ligament injuries reported in one study during the period of 2000 to 2005¹. In the United States, approximately 250,000 people experience ACL rupture annually, costing over 2 billion dollars per year¹⁻⁴. Similarly the cost of ligament rupture in comparative species such as dogs remain high; in 2003 management of cranial cruciate ligament (CCL) rupture estimated as costing over \$1 billion⁵. CCL rupture is the most common cause of hindlimb lameness in the dog⁶. The aim of this study is to determine the viscoelastic properties of CCLs, leading to study tissue engineered ligaments, novel ligament prostheses and role of proteins in their composition. In this study, viscoelastic behaviour of CCL was investigated by studying strain rate sensitivity. Strain rate sensitivity is a time-dependent characteristic in which stress-strain behaviour changes based on the rate at which the strain applied. Strain rate sensitivity is one of the four main forms of viscoelastic behaviour. Knowledge of strain rate sensitivity can aid mathematical modelling of ligament's response to mechanical forces and therefore help with the development of finite element analysis models. The biomaterial properties of the ligament could then be included in the numerical model to carry out parametric studies.

EXPERIMENTAL METHODS

Sample preparation

Six skeletally mature breed and age-matched dogs with no evidence of stifle (knee) osteoarthritis euthanased with full ethical permission were used. Entire stifle joints were frozen at -20 °C for at least 24 hours, defrosted at room temperature and the CCLs were dissected when required. The CCLs removed from the knee joint, leaving 10mm of bony parts at each sides of the ligament resulting in a femur-CCL-tibia complex, Figure 1(b).

Testing

Uniaxial testing was carried out on the canine CCL samples using an Instron 3366 testing machine (Instron, Norwood, MA) equipped with a 10N load cell (Instron, Part No. 2530-428). The samples were secured using a custom-built clamp, Figure 1 (a). Before mechanical testing, specimen length and cross-sectional area were measured^{7,8}.

A small preload of 0.1 N was applied, followed by preconditioning the sample to ensure samples are in their steady state condition. The ligaments were preconditioned by applying 10 cycles of loading-unloading^{9,10} to a maximum load of 10 N at a strain rate of 10%/min. Subsequently, the clamped Femur-CCL-Tibia sample subjected to cyclic tensile tests, with a maximum applied load of 10 N at three different strain rates of 0.1, 1 and 10 %/min. During the test, the ligament load-elongation curve was recorded by the Instron load cell and stored in a personal computer.

To study the effect of strain rate, ascending (0.1, 1 and 10%/min) and descending (10, 1 and 0.1%/min) strain rate tests were carried out. Each loading-unloading cycle, including the preconditioning procedure were followed by 6 min recovery period. Study on descending strain rate was necessary to confirm that the increase of stiffness is not due to extension of the tissue but it is due to the rate of the strain.

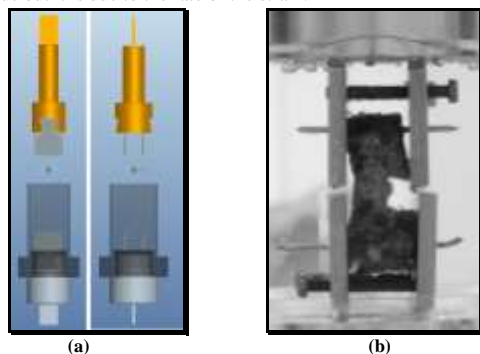


Figure 1: Custom designed clamps (a), and a clamped CCL complex mounted on the Instron testing machine.

Statistical analysis

The significance of associations between strain rate and mechanical stiffness (as measured by the tangent modulus), and the significance difference between ascending and descending regimes were assessed by ANOVA test. Analyses were performed in SPSS 20.0 (SPSS Inc., Illinois). $P < 0.01$ was considered an indication for statistical significance.

RESULTS AND DISCUSSION

In this study, two regimes (ascending and descending strain rate) were studied. The specimens exhibited non-linear stress-strain behaviour in both cases which can quantify the viscoelastic behaviour. The gradient of the stress-strain curve, the tangent modulus E , represents the stiffness of the ligament. Tangent modulus increased with increasing stress and strain rate, Figure 2. In agreement with previous studies¹⁷, it was also observed that the tissue showed statistically significant (p -value < 0.01) increase in stiffness when the strain rate increased. Statistical analysis ANOVA was carried out to see the difference between the two regimes and it was found that there is no significant difference between the two testing procedure with sig. value of $p = 0.109$ (p -value < 0.01).

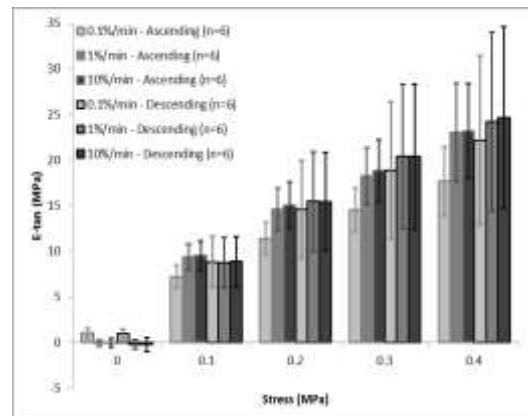


Figure 2: Change in tangent modulus (E -tan) with stress for ascending and descending test regimes

CONCLUSION

As predicted, the ligament illustrated non-linear stress-strain behaviour, and stiffness increased with increasing strain rate level. Further investigation on testing for ascending and descending strain rate showed that the tissue behaviour doesn't depend on the strain rate order but on the level of the strain rate.

REFERENCES

- Gianotti, S. M. *et al.*, *J. of Science & Medicine in Sport* 12, 622-627, 2009.
- Boden, B. P. *et al.*, *Orthopedics* 23, 573-578, 2000.
- Griffin, L. Y. *et al.*, *J Am Acad Orthop Surg* 8, 141-150, 2000.
- Novak, P. J. *et al.*, *Arthroscopy* 12, 160-164, 1996.
- Gottlob, C. A. *et al.*, *Clinical Orthopaedics and Related Research*, 272-282, 1999.
- Wilke, V. L. *et al.*, *J Am Vet Med Assoc* 227, 1604-1607, 2005.
- Griffon, D. J., *Veterinary Surgery* 39, 399-409, 2010.
- Vasseur, P. B. *et al.*, *Clinical Orthopaedics and Related Research*, 295-304, 1991.
- Goodship, A. E. *et al.*, *J. of Biomech* 38, 605-608, 2005.
- Woo, S. L. *et al.*, *J Orthop Res* 8, 712-721, 1990.
- Lujan, T. J. *et al.*, *J Appl Physiol* 106, 423-431, 2009.
- Savelberg, H. H. C. M. *et al.*, *J. of Biomech* 26, 1347-1351, 1993.
- Fung, Y. C., 2nd edn, 1993.
- Viidik, *Int Rev Connect Tissue Res* 6, 127-215, 1973.
- Butler, D. L. *et al.*, Vol. 1, 279-314 (West Palm Beach: CRC Press Inc., 1978., 1978).
- Lujan, T. J. *et al.*, *J Orthop Res* 25, 894-903, 2007.
- Woo, S. L. *et al.*, *J Orthop Res* 8, 712-721, 1990.

Larry's influences: from bioactive glasses to scaffolds for tissue engineering and nanoparticles for drug delivery

M. Vallet-Regí^{1,2,*}, A. Salinas^{1,2} and D. Arcos^{1,2}

¹ Dpt. Química Inorgánica y Bioinorgánica. Universidad Complutense de Madrid. Instituto de Investigación Sanitaria Hospital 12 de Octubre i+12. Spain.

^{2*} CIBER de Bioingeniería, Biomateriales y Nanomedicina (CIBER-BBN), Spain, vallet@ucm.es

Bioactive glasses bond to and integrate with living bone in the body without forming fibrous tissue around them or promoting inflammation or toxicity. This discovering was carried out by Prof. Larry Hench, and provided a new concept of bioceramics that opened new perspectives in the field of bone grafting materials. Bioactive glasses, especially the Hench's bioglass 45S5, exhibit many of the properties associated to an ideal material for bone grafting and regeneration. The high biocompatibility and the positive biological effects of their reaction products (both leached or formed at the surface) after implantation [1], have made bioglasses one of the most interesting bioceramics during the last 40 years. In 1991, the incorporation of sol-gel chemistry to the preparation of bioceramics resulted into a new generation of bioactive glasses, which exhibited a very high potential to develop better implants with osteogenic capabilities [2,3].

Inspired by the work of Prof. Hench, our research group has made efforts to contribute to the knowledge in the field of bioactive glasses. The preparation of organic-inorganic hybrids materials have resulted in materials with better mechanical properties, while keeping the bioactive behaviour of bioglasses [4,5]. We have also developed a new generation of mesoporous bioactive glasses (MBGs). MBGs results from the incorporation of structure directing agents to the sol-gel synthesis of bioglasses [6]. This strategy results in highly ordered mesoporous materials with surface and porosity five times higher than those obtained for the conventional sol-gel bioglasses. MBGs exhibits the fastest in vitro bioactivity observed up to date. The real clinical significance is still unknown, as the ordered mesoporous structure allows incorporating osteogenic agents, osteoclasts inhibitors, antitumoral drugs, etc. thus providing an excellent potential for the treatment of cancer and degenerative diseases in bone tissue [7,8]. Moreover, mesoporous materials can be also

manufactured as 3D macroporous scaffolds and nanoparticles [9,10].

This lecture deals with the main contributions of our research team during the last decade, regarding new compositions -both inorganic and organic-inorganic hybrid materials- intended for bone tissue repairing. The proofs of concept for all these topics have been already assessed, and now we ought to carry out the transition from the bench to the bedside

REFERENCES

1. Hench L. L. *et al.*, Science 295:1014-1017, 2002.
2. Li R. *et al.*, J. Appl Biomater 2:231-239, 1991.
3. Vallet-Regí M. *et al.*, Eur. J. Inorg. Chem. 1029-42, 2003.
4. Arcos D. *et al.*, Acta Biomaterialia, 6: 2874-88, 2010.
5. Vallet-Regí M. *et al.*, Chem. Soc Rev, 70:596-607, 2011.
6. López-Noriega A. *et al.*, Chem. Mater. 18: 3137-3144, 2006.
7. Vallet-Regí M. *et al.*, Angew Chem Int Ed. 46: 7548-7558, 2007.
8. Vallet-Regí M. *et al.*, Adv. Mater 23: 5177-5218, 2011.
9. Ruiz-Hernández E, *et al.*, ACSNano 5:1259-66, 2011.
10. Baeza A. *et al.*, Adv. Funct Mater 2014 (in press).

ACKNOWLEDGMENTS

The authors would like to thank Comunidad de Madrid for the project S2009/MAT-1472 and the Ministerio de Ciencia e Innovación (MICINN) for the projects MAT2012-35556 and CSO2010-11384-E (Ageing Network of Excellence).

Bioactive Glasses: from Hench to Hybrids

Julian R. Jones

Department of Materials, Imperial College London, UK julian.r.jones@imperial.ac.uk

INTRODUCTION

Larry Hench's Bioglass® has now been used in more than 1 million patients as a synthetic bone graft (e.g. NovaBone®, NovaBone Products LLC, FL) and is the active ingredient in Sensodyne Repair and Protect™ Toothpaste. Bioglass has outperformed other bioactive ceramics in comparative *in vivo* studies but its potential for bone regeneration is limited because it is only available as a particulate¹. A reason is that the original Bioglass 45S5 composition crystallises during sintering.

AMORPHOUS MELT-DERIVED SCAFFOLDS

New compositions now exist that can be sintered without crystallising and a new processing routes have been developed that can produce strong scaffolds, e.g. 3D printing and our foaming processes². *In vivo* studies of our foam scaffolds in an ovine model show 99% of the glass covered in new bone, including the internal pore structure. Laser spun glasses have potential in wound healing applications.

SOL-GEL SCAFFOLDS

Using the sol-gel foaming process also avoids the crystallisation issue and allows the use of more simple compositions, e.g. 70S30C; 70% SiO₂ and 30% CaO. *In vitro* data shows bone matrix production and active remodelling in osteoblast/osteoclast co-culture³. However *in vivo*, the results are more complex. The scaffolds only regenerated bone defects when preconditioned⁴ and then the bone ingrowth was similar to NovaBone and Si-HA (Actifuse®). Unlike the commercial products, pre-conditioned 70S30C scaffolds degraded and were replaced with new bone (Fig. 1).



Fig.1. Micro-CT of 70S30C foam in a rat tibia 3mm defect at 11wk

SOL-GEL HYBRIDS

All bioceramics scaffolds have the problem of being brittle. New developments in the synthesis of tough inorganic/ organic scaffolds with tailored degradation rates will be discussed. We have developed novel sol-gel hybrids with interpenetrating networks (IPNs) of degradable polymers and bioactive silica (Fig 2a). The aim is to create hybrid scaffolds with tailored degradation and mechanical properties that cells interact with as one material¹. However there are several challenges: The chemistry and processing is complex to create a successful bioactive hybrid. Challenges to overcome are: creating a porous structure while controlling degradation rate and mechanical properties. Critical to the success of the hybrids is achieving mechanical properties and controlled congruent degradation. This can only be achieved by synthesising hybrids that have covalent coupling between the IPNs.

HYBRIDS OF NATURAL POLYMERS

Natural polypeptides such as gelatin⁵ and poly-gamma-glutamic acid^{6,8} have been used. They are biodegradable and contain functional groups such as -COOH, which can be functionalised with a coupling agent for linking to the silica. Polysaccharides such as chitosan have also been used, but the presence of the -NH₂ group instead of -COOH changes the mechanism of coupling⁹.

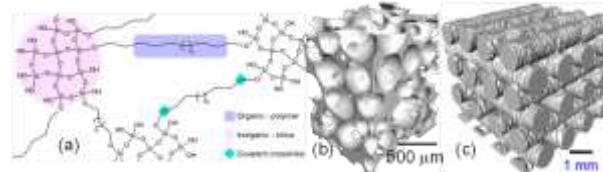


Fig. 2 (a) schematic of IPNs; micro-CT images of hybrid scaffolds made by (a) foam, (b) 3-D printing

HYBRIDS OF SYNTHETIC POLYMERS

Synthetic polymers can be synthesised with the coupling agents built in, e.g. acrylate based polymers containing links of TMSPMA, spacer monomers and biodegradable linkers. Degree of branching has a large effect on mechanical properties.

Conventional polymers such as polycaprolactone can also be functionalised to enable bonding via coupling molecules such as GPTMS.

SCAFFOLD PROCESSING ROUTES

Processing routes of sol-gel foaming (Fig. 2b), 3D printing (Fig. 2c), freeze casting and electrospinning will be compared.

CONCLUSION

Bioactive glass scaffolds can be produced by sol-gel processing and using new compositions of melt-derived glasses. Pore structure and ion release have to be controlled to ensure a good response *in vivo*. Hybrids have the potential to combine bioactivity with controlled degradation and mechanical properties.

REFERENCES

1. Jones JR Acta Biomaterialia, 2013;9:4457.
2. Wu ZY *et al*, Acta Biomaterialia 2011;7:1807.
3. Midha S, Adv Healthcare Mater, 2013;2:490.
4. Midha S *et al*, Acta Biomaterialia, 2013;9:9169.
5. Mahony O *et al*, Adv Func Mater 2010;20:3835
6. Poologasundarampillai G *et al*, J Mater Chem, 2010;40: 8952.
7. Valliant EM *et al*, Acta Biomaterialia 2013;9:7662.
8. Poologasundarampillai G *et al*, In Press DOI: 10.1002/chem.201304013.
9. Connell LS *et al*, J Mater Chem B 2014;2:668.

ACKNOWLEDGMENTS

Larry Hench for starting my career. My research group and collaborators. EPSRC for providing financial support. Research Campus at Harwell.



Clinical Use of S53P4 Bioactive Glass in Neurosurgery – Case Reports of Tumor Surgery, Infected Cervical Spine and Mucopyelocoe of the Frontal Sinuses

Janek Frantzen¹

¹Department of Neurosurgery, Turku University Hospital, Finland, janek.frantzen@tyks.fi

INTRODUCTION

Bioactive glasses (BAGs) are a group of synthetic surface-active composition-dependent silica-based biomaterials with osteoconductive, osteopromotive, and even angiogenic as well as antibacterial properties. The bone bonding properties of the two original BAGs (Bioglass® 45S5 and S53P4) were first delineated by Larry Hench in the early 1970's¹. BAG S53P4 has antibacterial properties, which have been suggested to be caused by the initial high pH and the subsequent osmotic effect caused by the dissolution of ions from the glass. Furthermore, BAG S53P4 has been shown in vitro to have effective bacterial-growth-inhibiting properties towards 17 anaerobic bacteria and 29 clinically important aerobic bacteria^{2,3}. BAG S53P4 has been successfully used as a bone substitute in the treatment of osteomyelitis of the spine and lower extremities⁴.

In general, it can be stated that in cases of infection in a surgical field all bone graft substitutes will be affected as if they were foreign objects, except for BAG, which has antibacterial properties and can potentially withstand bacteria to some extent.

METHODS

The following three clinical cases were operated by the author at the Turku University Hospital, Turku, Finland. Two of the patients were suffering from difficult to treat infections. The first patient got an iatrogenic cervical spondylodiscitis due to an perforation of the hypopharynx during revision surgery for malunion of level C3-C4. The second patient was treated for a mucopyelocoe in the left frontal region extending from a pansinusitis to the frontal bone and frontal lobe of the brain. Both were treated with a thorough debridement, broadspectrum antibiotic and the infection site was filled with S53P4 bioactive glass granules (Bonalive® Biomaterials Ltd, Turku, Finland). The third case was a patient with benign bone tumor of the skull where the surgical bone defect was filled with a recently developed bioactive glass putty (S53P4 granules with a water-soluble synthetic binder, Bonealive® putty, Bonalive Biomaterials Ltd, Turku, Finland).

RESULTS AND DISCUSSION

The patients have recovered initially well and the implanted material was well tolerated. No further reoperations were needed. For the infection cases, the follow-up is 3 months for the cervical spondylodiscitis and 10 months for the mucopyelocoe patient. Antibiotic treatment has ended and no recurrence of infection was observed. Thorough postoperative workup including plain X-rays, computed tomography (CT) and magnetic resonance imaging (MRI) has been performed in addition to the clinical follow up. For the tumor patient a 10-month follow up will be completed (5-months as writing). The healing of the wounds and no recurrence of the tumor has been noted on postoperative CT and MRI images.

The pre-clinical results in the literature concerning BAG's osteoconductive and osteopromotive properties are well translated into the clinical work in the field of surgery^{5,6}. These clinical infection cases describe a traditionally difficult to treat entity with a common need for concomitant revision surgery. The newly developed BAG putty has proven to be easy to use and has performed well in the filling of bone defects in the field of neurosurgery,

CONCLUSION

BAG S53P4 seems to be a well tolerated bone graft expander and bone void filler with broad anaerobic and aerobic antibacterial properties and as seen in these two difficult infection cases has performed well.

REFERENCES

1. Hench L, L.(I.) et al., US Army Medical R and D Command Contract DAMD 17-76-C-6033 with the University of Florida (1970–78), 1978.
2. Munukka, E et al., J.Mater.Sci.Mater.Med., vol. 19, no. 1, pp. 27–32. 2008
3. Leppäranta, O et al., J.Mater.Sci.Mater.Med., vol. 19, no. 2, pp. 547–551. 2008
4. Lindfors NC et al., Bone Aug;47(2):212-218. 2010
5. Frantzen J et al., J Spinal Disord Tech Oct;24(7):455-461. 2011
6. Rantakokko J et al., Scand J Surg 101(1):66-71. 2012



Bioactive glass S53P4 in the treatment of osteomyelitis – multicenter study

Nina Lindfors¹, Carlo Romano²

1. Helsinki University Central Hospital, Finland, nina.c.lindfors@hus.fi

2. Galeazzi Institute, Milano, Italy

INTRODUCTION

Bioactive glass (BAG) S53P4 is an osteostimulative bone substitute with proven antibacterial and bone bonding properties. In 2011 BAG-S53P4 received official indication for treatment of osteomyelitis.

This study shows that BAG-S53P4 can be used in treatment of osteomyelitis with excellent results. The best indication seems to be infected cavitory defects with or without fistular formation.

PATIENTS AND METHODS

In a retrospective multicenter study 67 patients (49 males, 18 females) with verified osteomyelitis were treated with BAG-S53P4 as a bone substitute. Several of the patients had previously undergone a number of procedures without success. The mean age of the patients was 50 years (16-87). According to the Cierny classification, most patients were of type 3. The location of the osteomyelitis was mainly in the tibia (N=33) followed by the femur (N=13) and calcaneus (N=7). In three patients the osteomyelitis was localized in the spine. The most common pathogens causing the osteomyelitis were *Staphylococcus aureus* or MRSA, followed by *Pseudomonas aeruginosa*. In 59 patients the procedure was performed as a one-stage procedure.

RESULTS

The mean follow-up was 27 months (3 months – 6 years and 8 months). Fifty-one patients had a total follow-up of more than one year. The total success rate was 90%. Six complications occurred in 6 months and they were either related to technical surgical problems or to lack of co-operation. Seroma leakage was observed only in one patient. In one patient an infection recurrence, related to incomplete debridement, occurred after a four-year follow-up.

CONCLUSION



In Vivo and In Situ Bioprinting of Cells and Biomaterials to Guide Tissue Repair

Virginie Keriquel¹, Sylvain Catros¹, Sophia Ziane¹, Reine Bareille¹, Murielle Rémy¹, Samantha Delmond², Benoit Rousseau³, Joëlle Amédée¹, Fabien Guillemot¹ and Jean-Christophe Fricain¹

¹ Inserm U1026, Université Bordeaux Segalen, Bordeaux Cedex 33076, France, ² CHU Bordeaux, CIC-IT, 33300 Pessac, France, ³ Univ. Bordeaux, Animalerie A2, 33000 Bordeaux, France, virginie.keriquel@orange.fr

INTRODUCTION

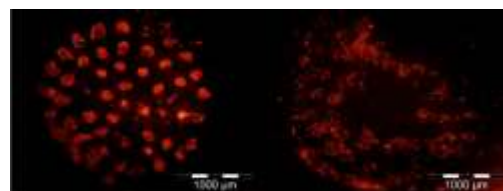
The development of Computer-Assisted Medical Interventions (CAMI) results from converging evolutions in medicine, physics, materials, electronics, informatics and robotics. CAMI aim at providing tools that allow the clinician to use multi-modal data in a rational and quantitative way in order to plan, simulate and execute mini-invasive medical interventions accurately and safely. In parallel, technological advances in the fields of automation, miniaturization and computer aided design and machining have also led to the development of bioprinting technologies which could be defined as the computer-aided, layer-by-layer deposition, transfer and patterning of biologically relevant materials.

EXPERIMENTAL METHODS

In this paper, we present the first demonstration of bioprinting 3D tissue constructs in situ and in vivo. These constructs were realized by depositing sequentially a collagen solution (type I) and mouse mesenchymal stem cells (from D1 cell line) that were realized using Laser- Assisted Bioprinting into critical size mouse calvaria defects. The MSC patterns were initially observed using intravital microscopy and D1 cells previously infected with lentivirus expressing the red fluorescent protein tdTomato. Cell proliferation was also followed-up till 8 weeks by measuring bioluminescence from D1 cells previously infected with a luciferase-expressing lentivirus using photon-imager (Biospace). Histological analysis of printed tissues was done at different time points using decalcified sections and X-ray microtomography.

RESULTS AND DISCUSSION

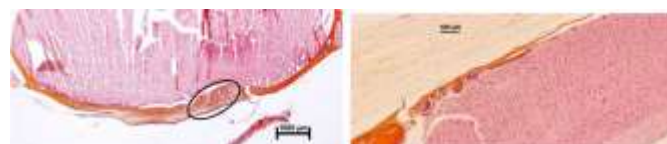
Laser-assisted Bioprinting allows to deposit patterns of cells in situ and in vivo (Fig.1) at a cell-level resolution. D1 cells printed in vivo survive, migrate and the results show a proliferation in vivo for 35 days. Moreover, histological analyses of the decalcified samples observed after 5 weeks of healing revealed presence of newly formed trabecular or woven bone (Fig.2).



a

b

Fig.1. Fluorescent image of D1-td-Tomato cells printed in situ (calvaria) with two patterns. (a) 2mm diameter-disk and (b) ring with 2.4/1.3mm external and internal diameters.



a

b

Fig.2. Histological pictures (HES staining) of materials implanted in the calvaria defects after 5 weeks. (a) Frontal section of the calvaria implanted with collagen and D1td- Tomato cells (disk) (x2). (b) High magnification of site implanted with collagen and D1Td-tomato cells (ring) (X10).

CONCLUSION

In conclusion, these results pave the way of using bioprinting technologies for Computer-Assisted Medical Interventions. More precisely, we show that 3D tissue constructs can be printed in vivo and in situ in relation with defect morphology. Interestingly, we demonstrate that printing cells in situ with a cell-level resolution tends to orientate tissue repair.

REFERENCES

1. Keriquel V and al. Biofabrication 2, 014101, 2010.

ACKNOWLEDGMENTS

The authors would like to thank the “Région Aquitaine”, “the Institut Français de la Recherche Médicale (IFRO)” and the “Agence Nationale de la Recherche (ANR)” for their financial support.

In Vivo Evaluation Of Bone Integration Of Poly(Vinyl-Alcohol) Hydrogel Fibers For Ligament Reconstruction

D. Moreau¹, A. Villain^{1,2}, M. Bachy², D.N. Ku³, D. Hannouche², H. Petite² and L. Corté¹

¹Centre des Matériaux Pierre-Marie Fourt, Mines Paristech, France. david.moreau@mines-paristech.fr

²Laboratoire de Bioingénierie et Bioimagerie Ostéo-Articulaire, Université Paris Diderot, France.

³George W. Woodruff School of Mechanical Engineering, Georgia Institute of Technology, USA.

INTRODUCTION

The design of an artificial device that successfully and durably replace torn ligaments is a long-standing challenge and demand in orthopedics. It could alleviate drawbacks and issues associated with autograft reconstruction, including donor site morbidity, graft availability and long recovery¹. Recently a new artificial system made of poly(vinyl alcohol) (PVA) hydrogel fibers has been shown to reproduce closely the tensile behavior of native ligaments². The potential of these systems as ligament substitutes is supported by the biocompatibility of PVA hydrogels, which has been found to be highly satisfactory in multiple applications³. Nevertheless, the *in vivo* response to these hydrogel fibers as ligament substitutes has not been explored hitherto. Here, we report the first *in vivo* evaluation of these implants in a rabbit model of tibial bone tunnel⁴. With this work, we explore whether these systems can be processed in agreement with sterile fabrication and implantation procedures.

EXPERIMENTAL METHODS

Implant fabrication

Implants were composed of cords of 15 twisted threads of 15 twisted PVA monofilaments, as presented in ref. 2. Gluing between fibers was produced by dip-coating in a 10wt% PVA aqueous solution and cross-linking of the PVA solution by applying three freeze-thaw cycles. Prior to surgery, implants were stored in physiological serum and sterilized by gamma irradiation.

Implantation protocol and follow-up

Six NZ white rabbits were implanted following a revised animal model by Li *et al.*⁴ (Fig 1a). PVA hydrogel implants were inserted in an extra-articular tibial bone tunnel of 2 mm of diameter and approximately 1 cm long. After implantation, animals were let free of any movement and fed *ad libitum*. Micro-CT scanners were performed at Day-0, 4 and 6 weeks. Histological study has been performed at 6 weeks. Samples surface was stained with Stevenel blue and Van Gieson picrofuchsin. The *in vivo* study was approved by the national ethical committee under the reference N09 (CEEALV/2011-02-01).

RESULTS AND DISCUSSION

Surgery was performed with no major difficulties. Implants were inserted into the bone tunnel without forcing and sutured to the periostum. Animals healed normally with no signs of inflammation nor weight loss. Micro-CT observations showed no bone osteolysis, as illustrated in Figure 1b at four weeks post-implantation. In several cases (N=4), new bone formation was noticed

growing from the internal surface of the cortical bone towards the middle axis of tibia (white arrows).

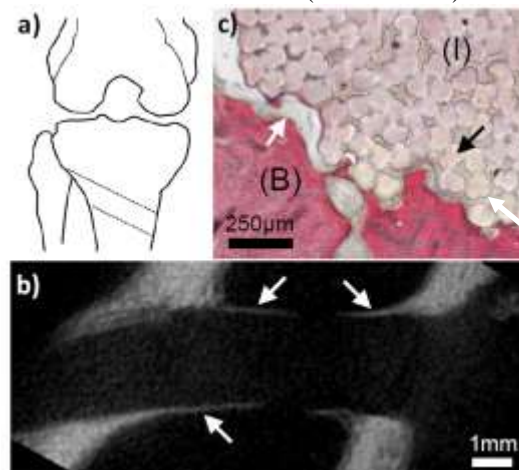


Figure 1: a) Implantation site (dashed lines); b) Micro-CT observation showing implant through the tibial tunnel at 6 weeks. c) Histological observation: (I) implant, (B) bone tissue, PVA fiber (black arrow), fibrous tissue layer (white arrow).

Histological analysis shows that the fiber assemblies remained intact after six weeks, as shown in Figure 1c. Fibers hold together and no fiber nor coating fragments were found in the surrounding tissues. A fibrous tissue layer was formed around the implant with a variable thickness and some direct contacts between bone and fibers. Remote bone formation around the implant was also noticed confirming the micro-CT observations.

CONCLUSION

This study reports the *in vivo* characterization of PVA hydrogel fibers in bone tunnels. Implants have been well tolerated. The biocompatibility observed for these systems in this animal model validates a manufacturing and bone implantation process that could serve as a basis for full ligament reconstruction in animal models.

REFERENCES

1. Mascarenhas *et al.*, McGill J. Med. 11:29–37, 2008.
2. Bach *et al.* J. Biomech. 46:1463–1470, 2013.
3. Baker *et al.*, J. Biomed. Mat. Res. B 100:1451–1457, 2012.
4. Li *et al.*, Appl. Surf. Sc. 257:9371–9376, 2011.

ACKNOWLEDGMENTS

The authors would like to thank Mines-ParisTech and Carnot Institute for financial support, as well as Y.Auriac (Mines-Paristech), M.Bensidhoum and F.Baudin (B2OA) for technical support.



Understanding nuclear deformation capacity of cancer cells thanks to micropillared surfaces

Florent Badique¹, Melanie Eichhorn², Jürgen Rühle², Oswald Prucker², Jean-Noël Freund³ and Karine Anselme^{1*}

^{1*} Mulhouse Materials Science Institute (IS2M), CNRS UMR7361, Université de Haute-Alsace, France,
karine.anselme@uha.fr

² Laboratory for Chemistry and Physics of Interfaces, IMTEK, University of Freiburg, Germany

³ INSERM U1113, University of Strasbourg, France

INTRODUCTION

Control of the cell behaviour onto artificial surfaces determines their usefulness in medical applications, such as medical implants or diagnosis tools. We have shown that a strong deformation of the nucleus occurs when cancer cells are brought into contact with polymer micropillars with a square morphology on top¹. On the contrary, healthy cells only deform during the initial stages of adhesion and immortalized cells show an intermediate deformation between the healthy and cancerous cells². These strong deformations of cells and of their organelles which don't affect viability and proliferation draw an analogy with the cell deformation occurring during metastatic process. These last years, we explored the role of materials properties as well as the biological mechanisms involved in this nuclear deformation in order to elucidate the mechanobiology of cancer cells on biomaterials³. Here, we propose to summarize the last results obtained in our group.

EXPERIMENTAL METHODS

Several cancer cells from different tumour origins (osteosarcoma, colon carcinoma) were cultured on polymer micropillared substrates. Cell adhesive [poly(l-lactic acid) PLLA, poly(n-butyl acrylate) PnBA] and cell repellent polymers [poly(dimethylacrylamide) PDMAA] were used in order to elucidate the role of surface chemistry in the adhesion and deformation of cells. Topography influence was explored by changing size, height and spacing between square micropillars but also pillar morphology (triangle, rectangle, rhombus...). Inhibitors of cytoskeleton and LINC complex molecules (cytochalasine D, nocodazole, blebbistatin, siRNA against lamin, nesprin 2, Sun1...) were used to determine the essential actors of nuclear deformation. Finally, movies of living cells deforming between pillars were acquired thank to an upright confocal microscope equipped with a cell culture chamber.

RESULTS AND DISCUSSION

Both osteosarcoma and carcinoma cells deform on micropillars. Osteosarcoma cells deform fast during adhesion (<6h) while carcinoma cells form cell-cell connections before to deform as a cell layer (~48h). The use of cytoskeleton inhibitors demonstrates that actin and intermediate filaments are the main actors of the deformation. Surprisingly, myosin is not essential to complete deformation. Some proteins of LINC complex (sun1 and nesprin2) are also needed. Changing shape of pillars does not modify the deformation of cells while increasing pillar height improves it. The capacity of cells to deform their nucleus when spacing between

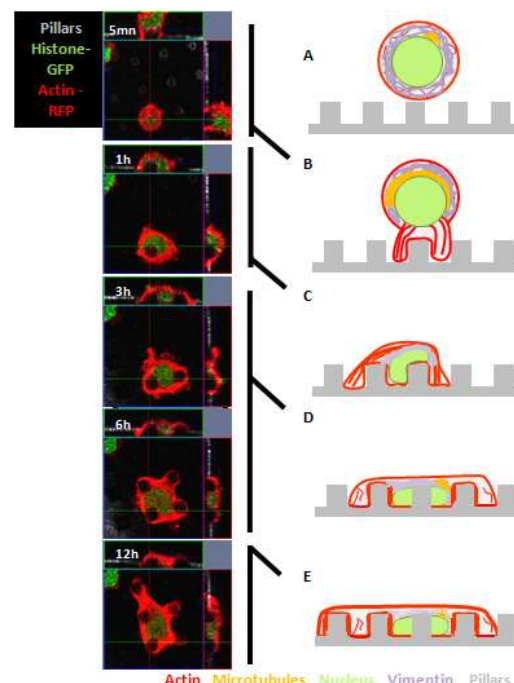


Fig. 1: Images of an osteosarcoma cell (SaOs-2) deforming on square pillars (size 7x7µm, height 6µm and spacing 7µm).

pillars is reduced is function of cell lines. When tops of pillars are cell repellent and walls of pillars cell adhesive, nuclear deformation increases. When the inverse is done, cells are also able to deform but less. Movies of living cells allowed us to elucidate the mechanism of deformation (Fig. 1). First, osteosarcoma cells adhere on pillars by focal adhesions. Secondly, an actin cap forms above the nucleus to push down and deform it between pillars. Further, the cell body spread over several pillars using actin and vimentin fibers to maintain the nucleus deformed during migration.

CONCLUSION

Micropillared substrates are useful tools for mechanobiology studies of cancer cells. Moreover, they are potential diagnosis tool to determine the cancerous potential of cells.

REFERENCES

1. Davidson P. *et al.*, Adv. Mater. (2009) 21:3586-90.
2. Davidson P. *et al.*, J. Mat. Sci.: Mat. Med.(2010) 31: 939-946.
3. Badique F. *et al.*, Biomaterials (2013) 34: 2991-3001.

ACKNOWLEDGMENTS

Financial support by Région Alsace, Ligue contre le Cancer Grand-Est and IRTG Softmatter Science GRK1642 is gratefully acknowledged.



Fatigue behaviour of selective-laser-melted nickel-titanium scaffolds

Therese Bormann^{1,2}, Bert Müller², Waldemar Hoffmann^{1,3}, David Wendt³ and Michael de Wild^{1*}

^{1*}Institute of Medical and Analytical Technologies, University of Applied Sciences Northwestern Switzerland, Muttenz, Switzerland, michael.dewild@fhnw.ch

²Biomaterials Science Center, University of Basel, Basel, Switzerland

³Department of Biomedicine, University Hospital Basel, Basel, Switzerland

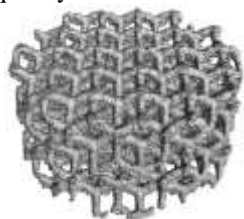
INTRODUCTION

The shape memory alloy nickel-titanium is a promising biomaterial for scaffolds and load-bearing implants. It exhibits pseudo-elastic or pseudo-plastic behaviour that allows mechanically stimulating the adherent cells and the adjacent tissue and, thus, can improve the osseointegration.¹ Its damping capacity allows for shock absorption.² For a metal, NiTi has a low elastic modulus, which facilitates the implant design to avoid stress-shielding.²

Selective laser melting (SLM) enabled us to fabricate NiTi scaffolds.^{1,3} Such SLM-scaffolds, however, are porous and reveal an irregularly shaped surface owing to partially integrated powder particles. These defects have a significant impact on the mechanical properties of the scaffolds and related future load-bearing implants. A detailed analysis of the fatigue behaviour is, therefore, highly desirable and the focus of this study.

EXPERIMENTAL METHODS

Fig. 1 represents a NiTi scaffold 4 mm high and 8 mm in diameter that we built by means of the SLM-Realizer 100 (SLM-Solutions, Lübeck, Germany) using NiTi powder (Memry GmbH, Weil am Rhein, Germany) with particle sizes between 35 and 75 µm. The scaffolds were designed to match the geometry of our compression bioreactor (CBR). The universal testing machine Zwick-Roell Z100, Ulm, Germany served for static compression loading with a speed of 0.5 mm/s. Uniaxial dynamic compression along the scaffold's cylinder axis was carried out by means of a servo-hydraulic testing machine (walter+bai AG, Löhningen, Switzerland) with a sinusoidal loading profile between 40 and 150 MPa mean stresses and a frequency of 10 Hz.



Ø 8 mm,
strut thickness ~300 µm

Fig. 1: The three-dimensional rendering of the SLM-NiTi scaffold shows the irregular surface topography.

RESULTS AND DISCUSSION

Static compression testing showed the pseudo-elastic response of the SLM-scaffolds, since they recovered up to 7 % of the applied deflection. The overall elastic modulus of the scaffolds was about (1.3 ± 0.3) GPa. The compressive strength referred to about 200 MPa. Cracks, however, were initiated already at deflections exceeding 5 % of the scaffold height, in particular at the hinge positions. From dynamic compression testing, a

stress-cycle diagram was derived by counting the number of load cycles until fracture at given loading amplitude, see fig. 2. The endurance limit of the NiTi scaffolds for reaching $5 \cdot 10^5$ cycles was about 50 MPa. Since the lattice-based scaffold geometry comprise of an inhomogeneous cross-section,⁴ the calculated stress is based on the minimal cross-sectional area of 7.9 mm². The fatigue performance suits the requirements of the CBR. Further, the formation of a well-defined Woehler-curve demonstrates that the SLM scaffolds exhibit reproducible fatigue behaviour even though the presence of small internal pores and a rough scaffold surface topography.

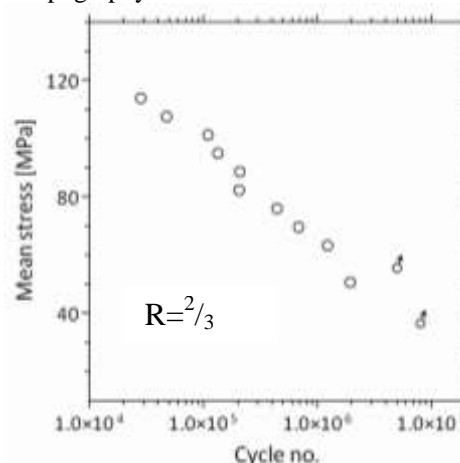


Fig. 2: The Woehler-diagram of the SLM-scaffolds. Run-outs achieving $5 \cdot 10^5$ loading cycles are marked with arrows.

CONCLUSION

The investigated static and dynamic mechanical properties confirm the performance of SLM NiTi scaffolds for load-bearing implants. Since the SLM fabrication process allows dedicated adjustment of the geometry, the mechanical properties such as the elastic modulus can be optimized to match the biomechanical characteristics of the implantation site.

REFERENCES

1. Bormann T. *et al.*, Acta Biomater 10(2):1024-34, 2014.
2. de Wild M. *et al.*, J Mater Eng Perform (in press), 2014.
3. Habijan T. *et al.*, Mater Sci Eng C 33(1):416-29, 2013.
4. Bormann T. *et al.*, Proc of SPIE 8689:868914, 2013.

ACKNOWLEDGMENTS

We sincerely thank MEMRY GmbH, Weil am Rhein, Germany, for powder and knowledge supply. The financial support of the Swiss National Science Foundation within the research program NRP 62 'Smart Materials' is gratefully acknowledged.



3D Printed Silica- Gelatin Hybrid Tissue Scaffolds

Maria Nelson¹, Siwei Li¹, Oliver Mahony¹, Molly M. Stevens¹, Gowsihan Poologasundarampillai¹, Kamel Madi², Peter D. Lee², Julian R. Jones¹

¹Department of Materials, Imperial College London, UK

^{2*} School of Materials, The University of Manchester, Oxford Rd, Manchester UK m.nelson12@imperial.ac.uk

INTRODUCTION

Tissue scaffolds provide a bioactive surface and porous structure to act as a temporary template to guide tissue repair. Using a 3D printing technique, the micro and macro structures can be tailored to different tissues and defect shapes. Sol-gel hybrids have nanoscale interpenetrating networks of inorganic and organic components. Use of a hybrid material allows tailoring of scaffolds as the composition can be adjusted during synthesis to alter degradation rate and mechanical properties¹. The aim was to directly print 3D structures from a gelatin– silica hybrid sol using (3-glycidioxypropyl) methyldiethoxysilane (GPTMS) as a coupling agent. Currently the work is focussed on bone and cartilage tissue regeneration.

EXPERIMENTAL METHODS

Gelatin was functionalized with GPTMS in dilute HCl and mixed with hydrolysed TEOS to create a sol. The sol was moved to a 40°C oven for 6 hours until the printing viscosity was achieved. The 3D printer was programmed to print the sol into 1cm cubes with 90° mesh structures. The scaffolds were sealed in a container and aged for 6 days followed by freezing at -20°C and freeze drying under vacuum at -111°C.

Hybrid scaffolds were characterized by FTIR, compression testing and imaging using SEM and X-ray microtomography. A study into the rheological characteristics of the gels at the point of printing was also carried out. The cytotoxic activity of the dissolution products were evaluated and cellular attachment of osteoblast and chondrocytes were analysed by immunohistochemical staining.

RESULTS AND DISCUSSION

To create a 3D structure the material must gel at the point of printing. Gelation is controlled by condensation of the silica-gelatin network. An as printed scaffold is shown in Fig. 1a. When designing a print file, the variables to consider are the spacing between individual struts, the height of each strut, the speed of printer head travel, printing nozzle diameter and rate of material deposition. Different scales and structures can be achieved during printing and retained by freeze drying (Fig. 1b and 1c).

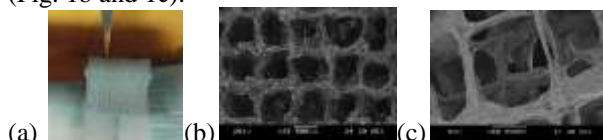


Figure 1. (a) 3D printing a scaffold; (b) and (c) SEM images of freeze dried scaffolds with a strut separation of 1mm and 0.5mm respectively.

X-ray imaging shows the structure of the scaffold to be porous in the x and z axis and dense across the XZ planes which imparts increased compressive strength; 1MPa +/- 0.2MPa parallel and 0.7MPa +/- 0.1MPa perpendicular to the dense planes. The scaffolds tested had strut separation of ~500µm, strut width of ~70 µm.

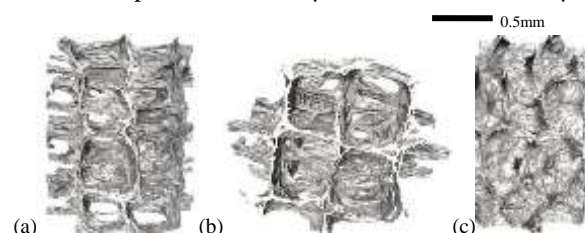


Figure 2. 3D reconstruction of a Silica-Gelatin scaffold (Diamond Light Source). (a) YZ view, (b) XY view, (c) XZ view

The metabolic activity assay demonstrated the material to have minimal cytotoxic activity and 3-D scaffolds were capable of facilitating cell attachment and spreading following a 3-day culture period (Fig. 3).

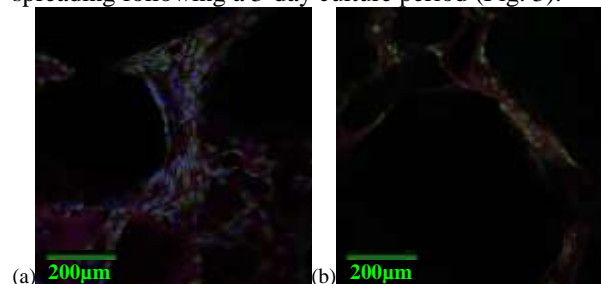


Figure 3. Confocal fluorescence images of (a) MC3T3 and (b) ATDC5 cells on the 3D printed scaffolds stained for cytoskeletal proteins actin (red), vimentin (green) and nuclei (blue).

CONCLUSION

3D printing silica– gelatin hybrids with covalent coupling directly from sol has been achieved and a variety of structures printed. This is a biomaterial suitable for bone regeneration and has potential for use in cartilage with a tailorable structure and composition. By imaging the structure, further developments to the design can be made.

REFERENCES

- (1) Mahony O *et al.*, Adv Func Mater. 20:3835-3845, 2010

ACKNOWLEDGMENTS

Research Campus at Harwell and EPSRC EP/IO21566/1; Diamond-Manchester beamline team; EPSRC Doctoral Student Prize and EP/IO20861/1 for providing financial support.

Tailoring Crimp Patterns of Electrospun Fibers by Using Thermal Shrinkage

H. Chen^{1,2*}, D. Baptista¹, J. Crispim¹, D. Saris¹, H. Fernandes¹, C.A. van Blitterswijk^{1,2}, R. Truckenmuller^{1,2}, L. Moroni^{1,2}

¹Department of Tissue Regeneration, University of Twente, The Netherlands. h.chen@utwente.nl

²Department of Complex Tissue Regeneration, Maastricht University, The Netherlands

INTRODUCTION

The periodic waviness of native collagen fibrils is observed in nearly all human tissue, such as tendon, blood vessels and valve leaflets¹. The features of crimp structures ensure that loads are sustained both by the surrounding extracellular matrix (ECM) and by the fiber network at low levels of tensile strain². A set of techniques has been developed to fabricate fibers with crimped, wrinkled and wavy structures for tissue engineering^{2,3}. For example, polyurethane buttressed rectangular membranes can be pre-extended and clamped over collagen fibers. The membranes are then relaxed to generate microcrimps, which are frozen at -80 °C and fixed in glutaraldehyde vapors. These microcrimped membranes can be used as templates to create ECM mimicking meshes although the fabrication procedures are multistep and complicated. Denver *et al.* found the aligned fibers from electrospinning (ESP) undergo crimping after removal from a mandrel used as a collector³. However, only limited control over the generated crimp patterns could be achieved. Here, we present a simple and versatile method to produce crimp-patterned electrospun fibers by using thermal shrinkage.

EXPERIMENTAL METHODS

A 20% (w/v) solution of Polyactive® (PA) (PolyVation, The Netherlands) was prepared in a 80/20 v/v mixture of chloroform and 1,1,1,3,3,3-hexafluoro-2-propanol, and stirred overnight at room temperature before ESP. The flow of the polymer solution was controlled by a pump at a feeding rate of 5 ml/h. The distance between the needle tip and the collector was set to 15 cm and the applied voltage was 16 kV. Fibers were deposited on a poly(lactic acid) (PLA) monoaxially oriented film. The thickness of the fiber meshes was controlled by the deposition time. Fiber-film constructs were then transferred to an oven pre-heated to 75 °C for 1 min to allow shrinkage of the PLA film and the formation of crimp patterns on the fibers. The morphology of the fibers was analyzed by scanning electron microscopy. Human mesenchymal stromal cells (hMSCs) were cultured on the wavy fibers to instigate the improvement of cell infiltration into the scaffold. Given the resemblance of the obtained fibers with the crimp patterns typical of tendons and ligaments we investigated if the wavy patterns could regulate a key signaling pathway involved in tendon and ligament maintenance TGF- β pathway. A TGF- β reporter cell line (T-MLEC) was seeded on flat and wavy fibers and the activation of the reporter was analyzed after 5 days of culture.

RESULTS AND DISCUSSION

Electrospun fibers were successfully fabricated with crimped structures. Crimp wavelengths varied between

0.7 to 10 μ m, depending on the processing conditions during ESP and the orientation of the electrospun fibers. The crimp pattern was dependent on the thickness of the fiber layer. For fiber layers with a thickness less than around 0.28 ± 0.10 mm, crimping occurred only on single fibers. Above this thickness threshold, crimping transferred to the whole electrospun sheet (**Figure 1**). The crimp pattern could be controlled by changing the orientation of depositing fibers. After 5 days of culture, an improvement on cell infiltration into the crimp scaffold was observed when compared to the flat scaffold alone. In addition, the crimp scaffold led to 1.7 times higher activation of the TGF- β reporter cell line when compared to the flat scaffold

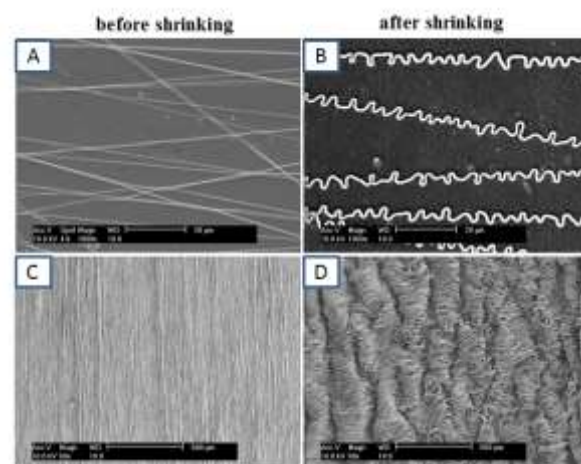


Figure 1. PA fibers before and after shrinking, showing crimp patterns at single fiber (A, B) and multiple fiber (C, D) levels.

CONCLUSION

PA fibers with crimp patterns were successfully fabricated in a very simple manner by controlled thermal shrinkage. The degree of crimp (amplitude and wavelength) was adjusted by the shrinkage extent of PLA films and the control of crimped patterns can be tailored by the thickness of the electrospun meshes. Furthermore, crimped structures improved hMSCs penetration into scaffolds and showed potential to be used in tendon and ligament engineering.

REFERENCES

1. Hiltner A. et al, Annu. Rev. Mater. Sci. 15:455-482, 1985
2. Jerry C. et al, Adv. Mater. 22:2041-2044, 2010
3. Denver S. et al, Biomacromolecules, 11:3624-3629, 2010

Acknowledgements

This work was supported by the Chinese Council Scholarship[2011]3005.



Real time analysis of the enzymatic digestion of chondroitin sulfate: role of the sulfation pattern

Carla Silva¹, Ramon Novoa-Carballal¹, Rui Reis¹ and Iva Pashkuleva^{*1}

¹*3B's Research Group – Biomaterials, Biodegradables and Biomimetics, University of Minho, Headquarters of the European Institute of Excellence on Tissue Engineering and Regenerative Medicine, AvePark, 4806-909 Taipas, Guimarães, Portugal; ICVS/3B's - PT Government Associate Laboratory, Braga/Guimarães, Portugal.

E-mail: carla.silva@dep.uminho.pt

INTRODUCTION

Chondroitin sulfate (CS) consists of repeating glucuronic acid (GlcA)/N-acetyl-galactosamine (GalNAc) disaccharide units joined by β 1,4 and 1,3 linkages respectively.¹ Multiple sulfotransferases involved in 4-O and 6-O sulfation of GalNAc units are responsible for the obtaining of CS with different degree of sulfation (0.1 – 1.3 per disaccharide unit) and patterns; CS may contain sulfate groups in both 4- and 6-positions the GalNAc unit (CS-E) but may also be exclusively 4-sulfated (CS-A) or 6-sulfated (CS-C).^{1,2} These different sulfation patterns influence the interactions between CS and proteins in the extracellular matrix or/and in the basement membrane and thus, can be critical in important physiological processes.² Herein, we demonstrate how the activity of two important enzymes, namely hyaluronidase and chondroitinase, are affected by the sulfation pattern of CS. We have established a protocol including GPC for the real time determination of the mechanism of enzyme action and ultrafiltration to obtain well defined oligosaccharides.

EXPERIMENTAL METHODS

The enzymatic digestion of CS-A, CS-C and CS-E by hyaluronidase and chondroitinase ABC was performed using 0.02Uenzyme/mg in phosphate buffer (0.1M, pH= 7.4) at 37°C for 48h. Aliquots of the reaction were taken at 1, 4, 8, 24 and 48 h. The enzyme was deactivated by heating and removed by centrifugation. The digested samples were then fractionated by ultrafiltration using 10kDa and 1kDa cut off membranes. All the products were lyophilized and analysed by gel permeation chromatography (GPC) and nuclear magnetic resonance (NMR).

RESULTS AND DISCUSSION

Digestion with Hyaluronidase

Hyaluronidase showed enhanced activity toward a 6-sulfation-rich substrate (CS-C, Table 1). In addition, the substantial distributions toward medium sized-polysaccharides support an endolytic mechanism of action (Fig. 1).

Table 1: Molecular weight and Infra-red (IR) area of digested species of CS by hyaluronidase for 24h

	CS-A (84kDa)	CS-C (54kDa)	CS-E(146kDa)
1h	42kDa (71.0%)	37kDa (73.6%)	72.6kDa (82.0%)
	1.2kDa (0.6%)	-	1.75kDa (1.1%)
	914Da (23.9%)	774Da (21.3%)	914Da (15.5%)
	558Da (4.6%)	495Da (5.0%)	690Da (1.0%)
24h	24.1kDa (72.4%)	11.4kDa (77.3%)	54.6kDa (76.4%)
	1.9kDa (1.6%)	-	1.9kDa (2.7%)
	940Da (22.0%)	369Da (17.7%)	936Da (18%)
	581Da (3.9%)	254Da (5.1%)	573Da (2.9%)

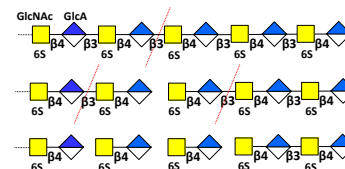


Figure 1: Schematic presentation of hyaluronidase endolytic action (red line) toward CS-C.

Digestion with Chondroitinase ABC

Similarly to the hyaluronidase, the CS-C was digested at higher degree (higher amount of low molecular weight species) as compared with CS-A and CS-E (Table 2). However, in this case low molecular weight species (disaccharides) were the major products of digestion, suggesting exolytic cleavage activity for chondroitinase (Fig. 2).

Table 2: Molecular weight and Infra-red (IR) area of digested species of CS by chondroitinase for 24h

	CS-A (84kDa)	CS-C (54kDa)	CS-E (146kDa)
1h	88kDa (83.0%)	-	130kDa (84.0%)
	1.8kDa (1.2%)	4.3kDa (14.4%)	2.2kDa (3.0%)
	948Da (13.1%)	1.7kDa (68.4%)	1.7kDa (68.4%)
	558Da (2.3%)	861Da (17.2%)	633Da (1.6%)
24h	78.7kDa (80.8%)	-	118kDa(82.0%)
	4.7kDa (1.3%)	5.5kDa (6.9%)	2.1kDa (3.9%)
	1.71kDa (1.0%)	1.9kDa (75.3%)	991Da (12.2%)
	934Da (14.3%)	990Da (17.7%)	-
	574Da (2.6%)	-	585Da (1.8%)

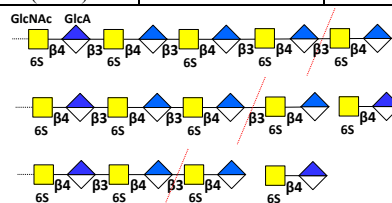


Figure 2: Schematic presentation of chondroitinase exolytic action (red line) toward CS-C.

CONCLUSION

The catalytic profiles of the studied enzymes were determined: hyaluronidase is mainly endolytic whereas chondroitinase acts via both endolytic and exolytic mechanisms. Both enzymes showed preference for CS-C, however in a different extent. Medium sized polysaccharides are obtained with hyaluronidase whereas higher amount of low molecular species are obtained with chondroitinase. This protocol can be also applied for obtaining of well defined oligosaccharides in a large scale.

REFERENCES

1. Yamada S. and Sugahara K., Curr Drug Discov Technol. 5: 289-301, 2008
2. Mikami, T. and Kitagawa H., Biochim. Biophys. Acta.: General subjects 1830(10): 4719-4733, 2013

ACKNOWLEDGMENTS

The FP7 project Polaris (316331) and the Programme NORTE-07-0124 FEDER-000016 are acknowledged.



Development and Characterisation of a Decellularised Bovine Osteochondral Biomaterial for Cartilage Repair

Hazel Fermor¹, Serena Russell², Sophie Williams², John Fisher² and Eileen Ingham¹

¹Faculty of Biological Sciences, iMBE, University of Leeds, UK

²School of Mechanical Engineering, iMBE, University of Leeds, UK, H.L.Fermor@leeds.ac.uk

INTRODUCTION

There is interest in the development of early intervention therapies for the repair of initial cartilage defects to prevent or delay the onset of osteoarthritis (OA). Current surgical treatments have variable success rates. The aim of this research is to produce an osteochondral graft from xenogeneic tissue with a similar extracellular matrix structure and composition to native human cartilage, retaining the natural biomechanical and biotribological properties, while removing the cells to ensure biocompatibility.

EXPERIMENTAL METHODS

Osteochondral pins (9 mm diameter, 12 mm deep, n=3) from the bovine medial femoral groove were decellularised using a process adapted from the work of Stapleton *et al.*¹. Tissue was analysed by histology using haematoxylin and eosin (H&E). DNA was extracted from tissues and isolated using Qiagen kits, then quantified using a nano spectrophotometer. Cartilage glycosaminoglycan (GAG) content was quantified following digestion with papain using the dimethylmethylene blue assay. Collagen content was assessed by quantification of hydroxyproline following acid hydrolysis using the p-dimethylamino benzaldehyde assay. Osteochondral pins were compressed using an indenter with a load of 0.8 N for 1 hour to determine cartilage deformation. Initial biocompatibility testing was performed to determine biomaterial cytotoxicity by culturing with BHK cells for 48 hours. For each set of numerical data the mean and 95 % confidence limits were calculated. Group means were compared using the T-test following one-way analysis of variance (ANOVA). A p-value <0.05 was accepted as significant. Percentage data were transformed using arcsin prior to statistical analysis and were then back-transformed for presentation

RESULTS AND DISCUSSION

Decellularisation of bovine osteochondral pins resulted in removal of cell nuclei as visualised by H&E staining (Figure 1).

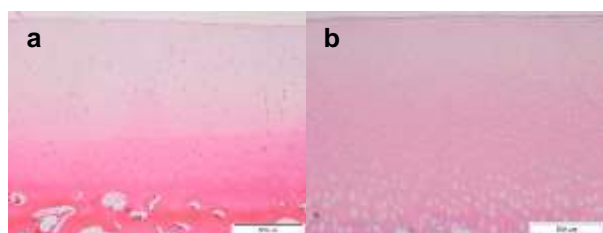


Figure 1: Native (a) & decellularised (b) bovine osteochondral tissues stained with H&E. Scale bar 500µm.

A 94 % reduction in DNA was achieved (native cartilage = $119.0 \pm 35.9 \text{ ng.mg}^{-1}$, decellularised = $7.0 \pm$

5.9 ng.mg^{-1} per cartilage wet weight, $p < 0.05$). The GAG content of the tissue was also significantly reduced (native = $261.1 \pm 29.3 \text{ µg.mg}^{-1}$, decellularised = $2.5 \pm 2.8 \text{ µg.mg}^{-1}$ per cartilage dry weight, Figure 2) and collagen content increased significantly as a proportion of tissue dry weight. Decellularised cartilage showed a significant increase in percent deformation (native = $30.4 \pm 7.6 / - 7.1 \%$, decellularised = $55.9 \pm 20.1 / - 21.2 \%$ deformation, $p < 0.05$, Figure 2). Decellularised bone was cytotoxic when cultured in contact with BHK cells. Increased wash cycles to improve scaffold biocompatibility lead to macro scale cartilage deterioration. Large osteochondral plates ($2 \times 4 \times 1 \text{ cm}$) decellularised using the same process showed reduced macro scale and histological cartilage damage compared to osteochondral pins.

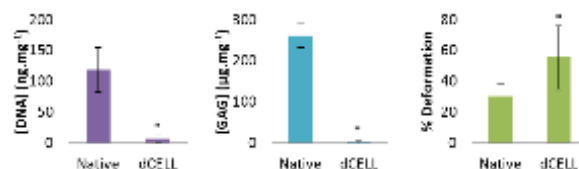


Figure 2: DNA and GAG content and percentage deformation of native (n=5) and decellularised (n=3) cartilage \pm 95 % CL. * significant, $p < 0.05$ (ANOVA).

Decellularisation of bovine osteochondral tissues was achieved, however the biological/ biochemical composition of the scaffold ECM significantly differed from that of native cartilage. These changes resulted in reduced biomechanical properties. Furthermore, the decellularised bone was shown to be cytotoxic. Alterations to the decellularisation process revealed cartilage matrix deterioration, which was found to be reduced by minimising the cut edge to cartilage ratio by processing larger cuts of osteochondral tissues. Further optimisation of the decellularisation process is required to produce a clinically relevant osteochondral graft.

CONCLUSION

This study has increased knowledge and understanding of the effects of decellularisation on osteochondral tissues which will form the basis for future development of a bioactive, acellular, natural tissue engineered repair material for osteochondral lesions to prevent or delay the onset of osteoarthritis

REFERENCES

1. Stapleton T.W. *et al.*, 2008, Tissue Eng. 14:505-518, 2008.

ACKNOWLEDGMENTS

This work was funded by EPSRC and partially through WELMEC, a Centre of Excellence in Medical Engineering funded by the Wellcome Trust and EPSRC, under grant number WT 088908/Z/09/Z.



An Injectable Silk-in-Silk system for Enhanced Proteoglycan Production

Sumit Murab^{1,2,3}, Akshay Shrivastava³, Juhi Samal³, Alok Ranjan Ray¹, Sourabh Ghosh², Abhay Pandit³

¹ Centre for Biomedical Engineering, IIT Delhi/AIIMS, New Delhi

² Department of Textile Technology, IIT Delhi, New Delhi

³ Network of Excellence for Functional Biomaterials, NUI Galway, murab.sumit@yahoo.com

INTRODUCTION- Hydrogels can be injected in situ in degenerated nucleus pulposus (NP) to mould precisely to the defect spaces, eliminating the need for invasive surgical procedures. N-acetylglucosamine (GlnAc) has been reported to increase GAG production by triggering the SMAD/MAPK pathway (1). This effect is seen up to a limited concentration after which the effect is reversed (2). The present study aimed to develop a regenerative medicine biomaterial platform consisting of silk hydrogel embedded with silk hollow microspheres loaded with GlnAc. The silk hydrogel will provide structural support to the degenerated tissue while the GlnAc released in a spatiotemporally controlled manner from the silk hollow microspheres will help increase GAG.

EXPERIMENTAL METHODS- Silk hollow microspheres were synthesized via template sacrificial technique by using polystyrene beads (3). The silk hydrogel was prepared by self assembly of 4% w/v solution at 37°C following ultrasonication. The rheological properties of the hydrogels were studied using a AR2000 instrument (TA instruments, USA). ADSCs were cultured in high glucose DMEM with 10% FBS & 1% PS. Bovine IVDs were isolated and digested by injecting 0.15 mL of collagenase type II (10 g/L) for 18 h at 37 °C. The discs were injected with silk hydrogel system and mechanically tested with a Zwick-Roell mechanical tester.

RESULTS AND DISCUSSION- The synthesized silk hollow microspheres through template sacrificial method had a low polydispersity index (0.2) and were significantly stable at varied pH and ionic strength range. The silk hollow microspheres showed no adverse effects on the cell viability of ADSCs as studied by alamarBlue®, CytoTox 96® and Live/Dead® cell assay.

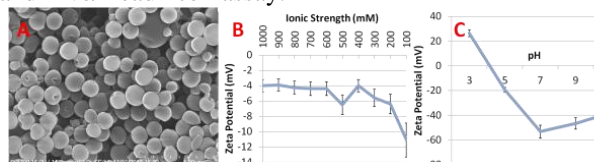


Fig. 1. a) Morphological analysis of silk hollow microspheres via SEM and b) & c) shows stability of the microspheres under varied ionic strengths & pH respectively.

The rheological properties of the silk hydrogel system demonstrated its injectability at RT withstanding the high ionic strength conditions inside the IVD (Fig. 2A).

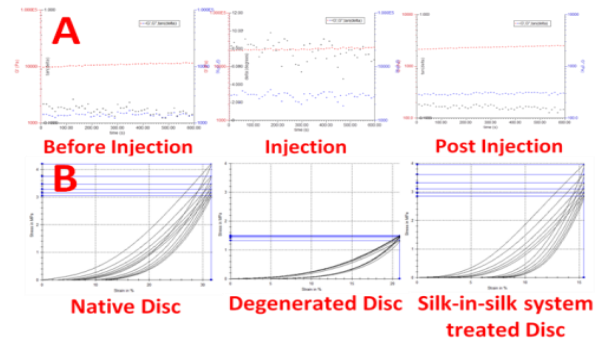


Fig.2. A) Rheological analysis showing the injectability of silk-in-silk hydrogel system. The system restores its native structure and rheological properties within 10 minutes of injection. B) Panels show average stress vs strain data for IVDs showing restoration of mechanical properties of the degenerated discs after injection with the silk-in-silk hydrogel system. Average data for IVDs containing PBS and also native IVDs are shown for comparison.

The loading efficiency of the silk hollow spheres with GlnAc was found to be >60% while a slow & steady release of the same was observed for 15 days. The static cyclic compressive testing showed a near complete restoration of the compressive properties of the IVDs (Fig. 2B). The seeded ADSCs showed a statistically significant increase in GAG and collagen production under a controlled release of GlnAc from the microspheres (Fig 3).

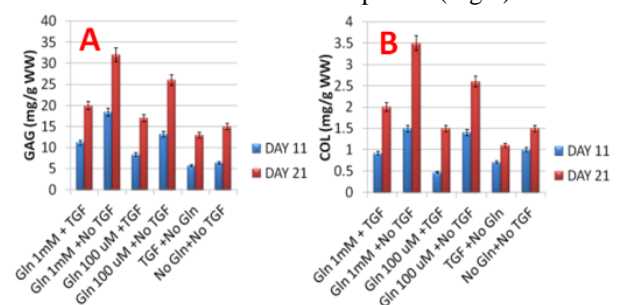


Fig. 3. GAG (A) and Collagen (B) estimation of silk hydrogels after 11 and 21 days. Values normalized to wet weight of the constructs.

CONCLUSION- The silk-in-silk hydrogel system through controlled release of GlnAc can help increase proteoglycan production while providing mechanical support.

REFERENCES

1. Lau KS *et al.*, Cell. 2007;129, 123–134.
2. Derfoul A. *et al.*, Osteoarthritis and Cartilage. 2007;15, 646–655.
3. Browne S. *et al.*, Mol Pharm. 2012;9(11):3099–3106.

ACKNOWLEDGMENTS

DST-SFI Indo-Ireland joint research project (RP02225)

Anatomically Shaped, Collagen-Fibre Reinforced Device for Meniscal Repair

Jennifer Shepherd¹, Daniel Howard², Siddhartha Ghose³, Simon Kew³, John Wardale², Ruth Cameron¹, Serena Best¹

¹Department of Materials Science and Metallurgy, University of Cambridge, UK

²Orthopaedic Research Unit, University of Cambridge, UK

³Tigenix Ltd, Byron House, Cambridge, UK

INTRODUCTION

Because of the greatly enhanced risks of osteoarthritis after meniscectomy, meniscus replacement has been advocated in cases of extensive meniscal damage or after total meniscectomy¹. Autogenous and allogeneous materials have been considered for this replacement as well as synthetic scaffolds. In the native meniscus, circumferentially oriented collagen fibre bundles allow load transfer through hoop stress and whilst a number of previous scaffold designs have included fibre reinforcement²⁻⁴ they have differed significantly from the native meniscus chemistry. The authors have previously considered the use of aligned collagen fibres in the reinforcement of collagen – chondroitin-6-sulphate (C6S) structures for load-bearing soft tissues such as tendon⁵ and a modified version may be used for meniscal replacement.

EXPERIMENTAL METHODS

Samples consisted of collagen-C6S porous structures reinforced with collagen fibre bundles produced through a semi-continuous extrusion process⁵. As previously⁵, collagen fibres were added to the collagen-C6S slurry before a lyophilisation process was applied to the composite sample. The nature of fibre reinforcement was investigated with number of fibre bundles and prior cross-linking of the fibre bundles both being considered. A custom designed anatomically shaped mould was used, with rectangular cross-section samples of equivalent volume also produced for mechanical analysis. SEM (JEOL 820) and X-ray Microtomography (skyscan1072) were used to characterise fibre integration and pore structure. Quasi-static tensile tests were carried out parallel to the fibre alignment and compression tests perpendicular to the fibre orientation (Instron 3343). As an initial indicator of cell response, scaffold sections were seeded with human meniscal cells previously cultured for 3 weeks (with ethical approval). After 7 days, samples were stained with Calcein AM.

RESULTS AND DISCUSSION

Meniscus shaped samples were produced successfully with circumferentially aligned fibre reinforcement. A combination of bundles with and without cross-linking prior to addition of the matrix slurry was found to optimise mechanics and pore structure. Cross-linked fibres retained their dense structure during freeze-drying and provided mechanical strength, whilst the significant porosity formed within and around the non-cross-linked fibres offered potential for aligned tissue regeneration as well as aiding compressive characteristics. As *Figure 2* demonstrates, a porous structure was formed around the reinforcing fibres.

Cells were shown to infiltrate and adhere in vitro (*Figure 3*). With 2 cross-linked and 1 non-cross-linked fibre bundle a compressive modulus of in excess of 80kPa and a load to failure of close to 120N was achieved. Although inferior to the mechanics of the native menisci, the scaffold is not designed to be a

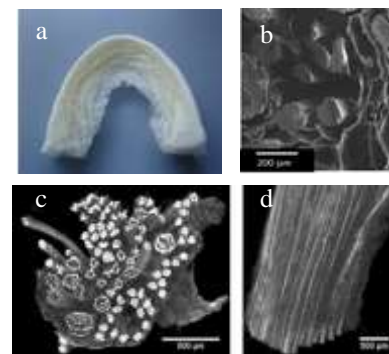


Figure 2: (a) photograph demonstrating anatomical shape, (b) SEM micrograph, and (c,d) 3D reconstruction of a small section of scaffold

permanent meniscal replacement; but a template for the regeneration of native tissue. The mechanical properties are sufficient to ensure a stable implant, and impart to at least some degree the biomechanical functions of the natural meniscus whilst cellular infiltration and tissue regeneration occurs. Additional work investigating the scaffolds in combination with Platelet rich plasma (PRP) also appears promising⁶



Figure 3: Calcein AM staining of cells adherent on the collagen fibre

CONCLUSION

Anatomically designed meniscal implants have been created with collagen fibres mimicking the circumferentially aligned fibres in the native meniscus. By combining collagen fibres with and without cross-linking, a pore structure has been produced suitable for cell infiltration and mechanical properties are sufficient to ensure implant stability and offer some of the biomechanical advantages of the native meniscus.

ACKNOWLEDGMENTS

The authors would like to acknowledge the funding of the EPSRC, and the NIHR (i4i grant)

REFERENCES

1. Messner, K. & Gao, J. *J. Anat* **193**, 161-178 (1998).
2. Wood, D. J., *et al. Biomaterials* **11**, 13-16 (1990)
3. Balint, E., *et al. J. Biomed Mat Res A* **100A**, 195-202, (2012)
4. Kon, E. *et al. Tissue Eng A* **18**, 1573-1582 (2012)
5. Shepherd, J. H. *et al. J. Biomed Mat Res A* **101A**, 176-184, (2013).
6. Howard, D. *et al. J. Orthop Res* **32**, 273-278, (2014).

"Nonswellable" hydrogel without mechanical hysteresis

Hiroyuki Kamata¹, Ung-il Chung^{1,2}, and Takamasa Sakai¹

¹Department of Bioengineering, School of Engineering, University of Tokyo, Japan, kamata@tetrapod.t.u-tokyo.ac.jp

²Center for Disease Biology and Integrative Medicine, University of Tokyo, Japan

INTRODUCTION

Hydrogels are three-dimensional polymer networks that contain a large amount of water inside. Certain hydrogels can be injected in solution and transformed into the gel state with the required shape. Despite their potential biomedical applications, the use of hydrogels has been severely limited because all the conventional hydrogels inevitably "swell" under physiological conditions, which drastically degrades their mechanical properties¹. Our strategy to achieve a robust hydrogel that can operate under physiological conditions is based on the control of swelling by the introduction of thermoresponsive segments—which collapse above a certain critical temperature because of predomination of hydrophobic interactions—into the polymer network. We designed and fabricated hydrogels composed of tetra-armed hydrophilic and thermoresponsive polymer units.

EXPERIMENTAL METHODS

Hydrogels comprising of thermoresponsive segments were prepared by mixing aqueous solutions of tetra-armed hydrophilic and thermoresponsive polymers that were synthesised via an anionic ring-opening polymerization (water content: ~ 95%) (Fig. 1), where the thermoresponsive segment ratio was defined as r_{th} . The hydrogels were immersed in Dulbecco's Phosphate Buffered Saline (D-PBS), and their equilibrium swelling ratio (Q) was measured. Elongation and compression tests were performed using the samples equilibrated under physiological conditions (i.e., in D-PBS at 37°C).

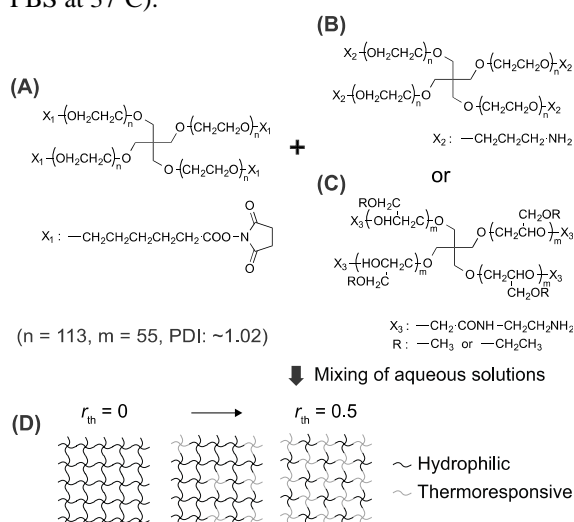


Fig. 1. Schematic of the thermoresponsive hydrogel system. (A) Hydrophilic tetra-armed poly(ethylene oxide) with active ester end-groups. (B) Hydrophilic tetra-armed poly(ethylene oxide) with amino end-groups. (C) Thermoresponsive tetra-armed poly(ethyl glycidyl ether-co-methyl glycidyl ether) with amino

end-groups. (D) Polymer networks composed of hydrophilic (black) and thermoresponsive (gray) polymer units where r_{th} represents the thermoresponsive segment ratio.

RESULTS AND DISCUSSION

The Q values under physiological conditions depended on r_{th} , while the hydrogel with $r_{th} = 0.4$ maintained its initial shape ($Q \sim 100\%$ = "nonswellable" hydrogel) (Fig. 2). The hydrogel composed only of hydrophilic polymers ($r_{th} = 0$, conventional hydrogels) endured 7-fold elongation in the as-prepared state. However, the swollen hydrogel failed at 2-fold elongation. In stark contrast, "nonswellable" hydrogel endured 7-fold elongation even in its equilibrium state under physiological conditions. Additionally, "nonswellable" hydrogel exhibited no mechanical hysteresis against a repetitive deformation and endured a compressive stress up to 60 MPa.

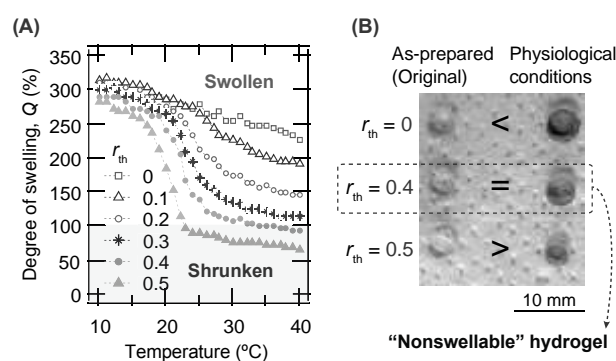


Fig. 2. Swelling behaviour of hydrogels in D-PBS. r_{th} represents the thermoresponsive segment ratio. (A) The swelling ratio (Q) as a function of temperature; $Q = V/V_0 \times 100$, where V is the volume of the samples in the equilibrium-swollen state at each temperature, and V_0 is the initial volume of the samples (i.e., before swelling). (B) Photos of the samples that exhibit different swelling degrees depending on r_{th} . The transparent hydrogels were coloured only for visibility.

CONCLUSION

Our results demonstrate that the swelling suppression of hydrogels helps maintain their initial shape and mechanical properties under physiological conditions². The hydrogel reported herein may constitute scaffolds for cartilage, which is exposed to a high mechanical overload.

REFERENCES

1. P. J. Flory, Principles of polymer chemistry, Cornell University Press (1953)
2. H. Kamata, et al., Science 343(6173):873-875, (2014)



A Collagen-Based Multimodal Delivery System Provides Therapeutic Factors as well as Physical Support for Treatment of Spinal Cord Injury in the Rat

R. Ronan^{1,2}, H. Kraskiewicz¹, B. Breen¹, T. Sargeant³, A. Pandit¹, S. McMahon²

¹Network of Excellence for Functional Biomaterials, ²Anatomy, National University of Ireland, Galway, Ireland;

³Covidien, 60 Middletown Avenue, North Haven, Connecticut 06473, United States; rachel08ronan@gmail.com

INTRODUCTION

Following injury to the spinal cord (SC) multiple biological responses occur, subsequently creating an environment which is inhibitory to axon growth, and which previous therapeutic attempts have failed to overcome. Biomaterial therapies are a promising option as they provide a 'bridge' through the inhibitory environment and can be functionalised, for example with therapeutic factors, which can then target specific aspects of the injury¹. Such therapeutic factors may target the inflammatory response e.g. interleukin-37 (IL-37) or provide support to neurons e.g. neurotrophin 3 (NT3). It was hypothesised that a dual delivery system² (Fig. 1A) could be used to both provide a 'bridge' and to deliver NT3 &/or IL-37 thus reducing the impact of the principle features of the injury, and promoting functional recovery after a hemisection SC injury in the rat. To examine this, lesion size, host response, glial scar and neuronal outgrowth across the lesioned area were quantified, and recovery of motor function was assessed.



Figure 1 Experimental design (A) A novel delivery system of injectable collagen hydrogel with IL-37 and NT3 loaded collagen hollow-spheres. (B) The cord was hemisectioned in the sagittal midline at T9 and hydrogel was applied immediately. (C) Summary of experimental groups. Sham group received laminectomy surgery only.

EXPERIMENTAL METHODS

Injury and application of treatment: 120 adult female Sprague-Dawley rats were anaesthetised and a T8 – T10 laminectomy performed to expose the cord. Injury condition and treatment were applied as shown in Fig. 1 B and C respectively.

Motor recovery analysis: Basso-Beattie-Bresnahan (BBB) locomotor rating scale was used to assess hind-limb motor function. Animals were assigned a score from 0-21 for each hind-limb at 1, 4 and 6 weeks post surgery, based on their movement in an open field.

Quantification of lesion size: Masson's trichrome histological stain was used to define the lesion area and to measure the change in lesion dimensions in response to treatment/over time.

Assessment of cellular responses: Anti-GFAP (glial fibrillary acid protein) and anti- β III tubulin were used to visualise glial scar and neuronal growth into the lesion. The host response was assessed by examining changes in the distribution and activity of macrophages. Both light and fluorescence images were obtained using the

Olympus Varioskan digital slide scanner. Statistical analysis involved one way ANOVA and Tukey's multiple comparison test.

RESULTS AND DISCUSSION

BBB analysis demonstrates an improvement in motor function across all treatment groups with hydrogel only, hydrogel + IL-37 and hydrogel + NT3 groups performing best. Improvement primarily occurs between weeks one and four. Histological assessment of SC sections shows a change in lesion size and shape over the 6 week study in all groups, with NT3 and/or IL-37 treatment showing greatest benefit (Fig.2).

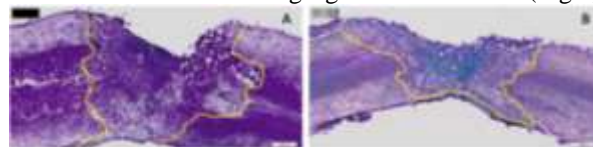


Fig.2. The size and shape of the lesion changes over time. Masson's trichrome stained images of cords from animals treated with hydrogel containing IL-37 at 1 week (A), and 6 weeks (B). Collagen is stained green while nuclei and cytoplasm are stained black and purple respectively. Scale bar = 500 μ m. Yellow line marks lesion borders. After six weeks neuronal growth into the gel and lesion area is evident from β III tubulin immunoreactivity (Fig. 3). A reduction in glial scar formation is to be seen in hydrogel treated animals in comparison to hemisection controls. The immune response to injury is also altered over time and in response to treatment.

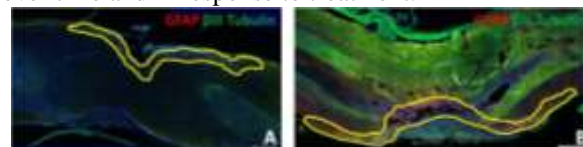


Fig. 3. Glial scar around the lesion border, highlighted within yellow outline, and neuronal ingrowth into the lesion. Images from hydrogel + NT3 treatment group at (A) 1 week (B) 6 week. Scale bar = 500 μ m.

CONCLUSION

Characteristics of SC injury including lesion size and shape, immune, glial and neuronal responses were quantified, and functional recovery was determined. Results suggest that collagen hydrogel is beneficial after hemisection injury to act as a platform both for drug delivery and on which axons can grow.

REFERENCES

- Madigan N. *et al.*, Respir Physiol Neurobiol. 169(2):183-99, 2009.
- Kraskiewicz H. *et al.*, ACS Chem. Neurosci. 4:1297–1304, 2013.

ACKNOWLEDGMENTS Funding support was provided thanks to Covidien LLC, IDA Ireland, European 7th Framework Programme, grant no. 304936



Enhanced Control of Stem Cell responses by Sub-Micron Material Parameters

John Hunt¹, Rui Chen¹, Sandra Fawcett¹, Judith Curran²

¹Clinical Engineering (UKCTE), The Institute of Ageing and Chronic Disease, University of Liverpool, UK

²Centre for Materials and Structures, School of Engineering University of Liverpool, UK
j.curran@liv.ac.uk

INTRODUCTION

Material induced biological responses are a fundamental research area that has implications in all technologies that require a cell/protein to come into contact with a synthetic substrate. Recent research has proven that cells can sense and respond to stimuli at the nanoscale. In addition to responding to stimulus introduced by changes in nanotopography, we have also proven that changes in the distribution of chemical groups at the nanoscale are a powerful tool for controlling protein and cell responses¹.

Here we present data relating to the sub-micron properties of a range of silane modified substrates, and how specific combinations of chemistry, energy and nanotopography can be used to effectively control stem cell responses. The data presented within this paper will emphasise how a combinatorial approach to substrate/interface design is a pre-requisite for effective control of protein/cell interactions. In addition we will present data relating to how control of protein adsorption and subsequent matrix formation on the highly defined synthetic substrates is a key factor in determining subsequent cellular responses.

EXPERIMENTAL METHODS

A range of $-NH_2$ and $-CH_3$ presenting chemistries were developed and characterised. Full disclosure of surface modification techniques is protected by IP. Resultant surfaces were characterised using X-ray Photoelectron Spectroscopy (XPS), Water Contact Angle (WCA), Atomic Force Microscopy (AFM) and Scanning Electron Microscopy (SEM). Test substrates were cultured in contact with varying concentrations of protein solutions, fibronectin (5-100 $\mu g/ml$) and vitronectin (2-200 $\mu g/ml$), protein adsorption profiles were visualised using immunohistochemistry and confocal microscopy. Commercially available human mesenchymal stem cells (hMSC, Lonza UK), were cultured in contact with test substrates in basal medium (Lonza UK) for time periods up to and including 28 days. Initial cell adhesion was characterised, fluorescent imaging of vinculin and actin and PCR arrays for cell adhesion (Qiagen), providing information regarding up regulation of selected integrins. In addition the phenotype of the adhering cell population was analysed using immunohistochemistry for the qualitative evaluation of proteins of interest i.e. STRO1, nucleostemin, fibronectin, collagen I and osteocalcin. The ability of cells to produce a calcified extra cellular matrix was also evaluated using von Kossa staining and light microscopy.

RESULTS AND DISCUSSION

Experimental evidence supported the hypothesis that combinations of optimised surface chemistry and

nanotopography increased the efficiency of previously reported material induced cell responses. $-CH_3$ modified substrates with a controlled nanotopography (peak-peak distance of $\sim 280nm$) was optimal for the formation of a cohesive fibronectin network and subsequent maintenance/enhancement of a stem cell phenotype.

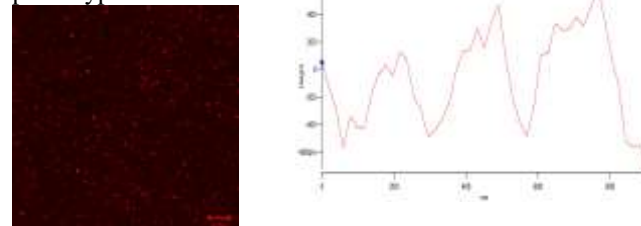


Figure 1: Fibronectin (5mg/ml) adsorption profile at 1 hour on a $-CH_3$ modified substrate. (B) Peak profile of $-CH_3$ modified substrate generated by AFM, showing a peak to peak separation distance of $\sim 280nm$.

In contrast optimised sub-micron properties on $-NH_2$ modified substrates (peak height greater than 100nm) resulted in substrates that had the ability to absorb phosphate from solutions directly onto the surface and resulted in a highly osteogenic substrate that had the capacity for matrix remodelling.

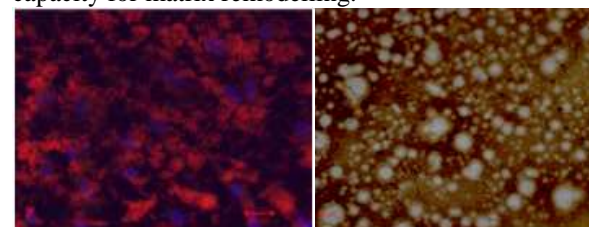


Figure 2: hMSC cultured in contact with $-NH_2$ modified substrates and stained for osteocalcin at 14 days (A) and (B) von Kossa at 28 days. There was extensive evidence of matrix remodelling on optimised substrates.

Changes in bulk surface chemistry can enhance the potential of specific proteins to adsorb to a surface, but subtle changes in the associated nanotopography of bulk chemistry can be used to direct matrix formation and subsequent cell adhesion on a much improved scale. Control of material parameters must be considered at the sub-micron scale to realise the potential of material induced biological responses.

REFERENCES

1. Curran J. *et al.*, J. Lab on a Chip. 10 (13):1662-70, 2010.

Synthesis, properties and *in vitro* toxicity of magnetic ferrite nanoparticles

Juan Sojo¹, Pier Bombilli², Karem Noris², Gema Gonzalez^{1*}

^{1*}Centro Ingeniería de Materiales y Nanotecnología /Instituto Venezolano de Investigaciones Científicas, Caracas, Vzla.

²Lab Ingeniería de Tejidos, Departamento de Biología Celular, Universidad Simón Bolívar, Caracas, Venezuela,

*gemagonz@ivic.gob.ve

INTRODUCTION

Magnetic nanoparticles have been intensively studied for different applications: electronic industry, biomedical devices, also as contrast agents in Magnetic Resonance (MR) and drug delivery agents, as a promising therapy for tumour treatment¹⁻². The latter called hyperthermia consists in the increase in temperature in the tumour induced by the magnetic nanoparticles upon application of an external magnetic field. Therefore it is desirable to obtain the highest heating power with the fewer amount of nanoparticles. Different ferrite nanoparticles (MFe_2O_4 , $M=Fe, Co, Ni, Zn$, etc) have been used for this purpose³⁻⁴. Their properties depend on nanoparticles size, structure and magnetic properties and on the magnetic field applied. On the other hand, there are limited reports on the toxicity of ferrite nanoparticles. In the present work the synthesis, characterization, magnetic properties, magnetothermic behaviour and *in vitro* cytotoxicity of zinc ferrite nanoparticles was studied.

EXPERIMENTAL METHODS

Synthesis of Zn-ferrite nanoparticles

The synthesis of magnetite (Fe_3O_4) was carried out by a precipitation method using $FeSO_4 \cdot 7H_2O$ and sodium hydroxide concentrations (0.074, 0.104, 0.134, 0.164, 0.194 M), and zinc ferrites ($Zn_xFe_{(3-x)}O_4$) were synthesized by a similar method but using 0.194 M of sodium hydroxide and potassium nitrate as oxidant agent. The particles were characterized by XRD, SEM, magnetization measurements and magnetothermic experiments using a magnetotherm system (NanoTherics, Ltd), at different frequencies from 108.7 kHz to 333.3 kHz and different magnetic fields from 2 to 10.7 kA/m, for nanoparticles concentrations between 2 to 20 mg/mL.

Cell Culture

VERO immortal cells were used as cell line, and the viability studied was carried out using CellTiter 96® Aqueous One Solution Cell Proliferation Assay (Promega®). 3000 cells/well were seeded in 96 well plates, for 48 h and exposed to two concentrations (10 and 100 µg/mL) of three different ferrite nanoparticles. Experiments were performed by triplicate. SEM analysis of the cell/nanoparticles culture was carried out.

RESULTS AND DISCUSSION

The structural characterization of the samples revealed that the magnetite and Zn-ferrite structure was obtained. Depending on the synthesis conditions different particle size and morphology was obtained. Nanoparticles size range from 50 nm to 90 nm was observed.

The magnetic measurements showed that all the samples present a superparamagnetic behaviour, and the saturation magnetization varied from 60 to 90 Am^2/kg , depending on Zn substitution on the ferrite (Fig. 1a)

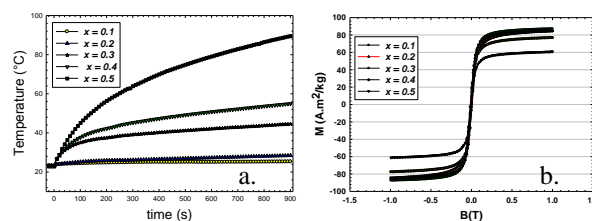


Fig 1 a. Magnetization curves for different Zn substitutions in ferrite samples. b. Temperature vs. time for different Zn content.

The magnetothermic experiments of magnetite samples and $Zn_xFe_{3-x}O_4$ tested at different frequencies (108.7-333.3 kHz) and different magnetic fields (2-10.7 kA/m) showed an increase temperature gradient with the increase in magnetic field, frequency and Zn content (figs. 1a,1b). It can be observed that a high magnetic field (10.67 kA/m) and low frequency (108.7 kHz) a temperature of 42°C can be reached in 80 s using a concentration of 20 mg/ml for the highest Zn substitution. The biological acceptable limit of frequency and magnetic field ($H \cdot f$) is 5×10^9 A/m.s⁵, therefore the parameters used in the present work are below this limit (1.16×10^9 A/m.s) within a safe range. The biocompatibility *in vitro* studies showed protrusion of filipodia interacting with the nanoparticles, no cytotoxicity effects of iron oxide nanoparticles with and without Zn substitution was obtained.

CONCLUSION

Ferrite nanoparticles has been synthesized with different Zn content, showing a high magnetization saturation and magnetothermic response, depending on the applied magnetic field and frequency used. No citotoxic effects were observed; therefore they can be considered as promising materials for magnetic hyperthermia therapy.

REFERENCES

1. Dormann J.L., Tronc E., and Fiorani D., Adv. Chem. Phys. 98: 283, 1997
2. Bärceña, C., Sra, A.K., Chaubey, G.S., Khemtong, C., Liu, J.P., Gao, J., Chem. Commun. 19:2224-26, 2008
3. R. Hergt, S. Dutz, R. Müller, M. Zeisberger, J. Phys. Condens. Matter 18: S2919-S2934, 2006
4. B. Jeyadevan, J. Ceram. Soc. Jpn. 118 (2010) 391-401
5. Hergt R. And Dutz S., J. Magn. Magn Mater. 311(2007) 187-192

ACKNOWLEDGMENTS

The authors would like to thank FONACIT PEI Programme (Grant no: 201200871) for providing financial support to this project.



Osteogenic Micro-Nanopatterned Titania for Orthopaedics

Laura E. McNamara^{1*}, T Sjöström², P Herzyk³, RMD Meek⁴, B Su², MJ Dalby¹

^{1*}Centre for Cell Engineering, University of Glasgow, UK, laura.mcnamara@glasgow.ac.uk

²School of Oral and Dental Science, University of Bristol, UK

³Polyomics Facility, University of Glasgow, UK

⁴Southern General Hospital, Glasgow, UK

INTRODUCTION

Suboptimal osseointegration can lead to failure of orthopaedic implants that would necessitate revision surgery. In order to maximise the biological fixation of orthopaedic implants, it would be advantageous to improve the bioactivity of bioinert load-bearing materials such as titanium. Topographical surface patterning offers the potential for this, and we have previously demonstrated the efficacy of 15 nm Ti high nanopillars for osteogenesis [1, 2]. In this study, these osteogenic pillar-like features were combined with micron-scale pits, to examine the response of human mesenchymal stem cells (MSCs) to these osteogenic cues.

EXPERIMENTAL METHODS

Nanopillar-like features were produced in Ti using a block copolymer masking approach [3], and micromachining was employed to produce the micropits. MSCs were cultured for 3 days on the surfaces and immunostained for focal adhesions (FAs), and FAs were quantified using image analysis. The bone marker osteocalcin was examined on these surfaces after 21 days of culture. Microarrays were used to assess the changes in relative transcript abundance between the cells on planar control and micronanopatterned Ti surfaces, including the assessment of small untranslated RNAs such as miRNAs. Ingenuity Pathways Analysis (IPA) was used to examine the functional networks of likely interactions between the gene products.

RESULTS AND DISCUSSION

The micro-nanopatterned substrates modulated FAs, and enhanced deposition of osteocalcin was also noted on the micro-nanopatterned Ti surfaces (Figure 1A). A number of osteogenic transcripts, including transcripts encoding bone morphogenic proteins (BMPs), miRNAs involved in the regulation of BMP signalling and differentiation, and 14 other small regulatory RNAs, involved in processes such as transcript editing, were up-regulated in MSCs cultured on the topographically modified Ti. A high-scoring network of likely interactions between some of the highlighted gene products, generated using IPA, is shown in Figure 1B. Importantly, the micro-nanopatterned topography could also be produced on the curved surface of Ti rods.

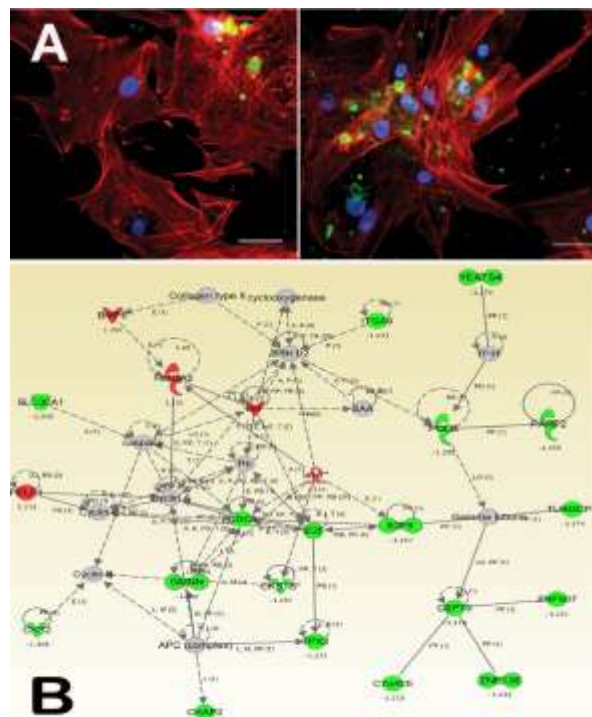


Figure 1A: Cells cultured on micronanopatterned Ti (right image) tended to form clusters around the micropits and express more osteocalcin than on planar controls (left image). Red – actin, green – osteocalcin, blue – DNA. Bar: 50 μ m. 1B: High-scoring IPA network illustrating some transcripts that were up-regulated (such as a BMP and a miRNA; red) or down-regulated (green).

CONCLUSION

The micro-nanopatterned surfaces were osteogenic, showing enhanced expression of osteogenic transcripts, small regulatory molecules associated with differentiation, and increased levels of bone markers. The micro-nanopatterned surfaces showed promise for use in orthopaedic implants.

REFERENCES

1. McNamara LE. *et al.*, Biomaterials, 2011
2. McNamara LE. *et al.*, J. R. Soc. Interface, 2012
3. Sjöström T. *et al.*, Adv. Healthcare Mater., 2013

ACKNOWLEDGMENTS

The authors thank Carol-Anne Smith and Dr. Jing Wang for assistance. This research was funded by the EPSRC.

Hydrogel-Based Injectable Systems for the Local Delivery of Sodium Alendronate - In Vitro Evaluation with Osteoblast- and Osteoclast-Like Cells

Urszula Posadowska^{1*}, Martin Parizek², Elena Filova², Krzysztof Pietryga¹, Lucie Bacakova², Elzbieta Pamula¹

^{1*}Faculty of Materials Science and Ceramics, AGH – University of Science and Technology, Krakow, Poland

²Department of Biomaterials and Tissue Engineering, Academy of Sciences of the Czech Republic, Prague
uposadow@agh.edu.pl

INTRODUCTION

Bisphosphonates, e.g. sodium alendronate (Aln), administered orally are considered as the first line treatment of osteoporosis¹. Aln amino side chain demonstrates strong inhibitory effect of osteoclast-mediated bone resorption and blocks hydroxyapatite loss². Unfortunately, the drug is characterized by low bioavailability (<1% when administered orally) and causes many side effects like fever or ulcers. Hence, it seems to be promising to replace systemic treatment by efficient local delivery of Aln³. Thus, in our study we propose injectable drug delivery system consisting of Aln-loaded nanoparticles suspended in a biocompatible hydrogel (gellan gum) and evaluate their biological performance *in vitro* in contact with osteoblast- and osteoclast-like cells.

EXPERIMENTAL METHODS

Aln (Polpharma SA) was encapsulated in poly(L-lactide-co-glycolide) (PLGA, 85:15, Mn=80 kDa) nanoparticles (NP-Aln) via a double-emulsification/solvent evaporation technique. NP-Aln were characterized with dynamic light scattering (DLS), laser electrophoresis, scanning electron microscopy (SEM), atomic force microscopy (AFM); UV-vis spectroscopy (OPA reagent, 332 nm) was used to assess loading and encapsulation efficiencies. In order to obtain injectable drug delivery system, NP-Aln were suspended in gellan gum (GelzanTM, Sigma-Aldrich) and cross-linked with Ca⁺² (GG-NP-Aln). The systems obtained were evaluated with respect to injectability, drug release and morphology (SEM). Then, they were studied *in vitro* via an indirect way. Extracts from the samples (in culture media prepared at 37°C for 72 h) were examined on osteoblast-like cells (MG-63) and osteoclast-like cells (RAW 264.7 differentiated by RANKL) (5x10³ cells/well, 96-well plate). Proliferation, viability (MTS assay), different staining (Live/Dead, Hoechst-Texas red, acid phosphatase - AP, tartrate-resistant acid phosphatase - TRAP) were conducted. Moreover impedance measurements on xCELLigence analyzer were performed to test cell proliferation in real-time.

RESULTS AND DISCUSSION

DLS studies showed that size of the carriers ranged from 200 nm to 400 nm, and AFM confirmed their spherical shape. Laser electrophoresis demonstrated negative zeta potential. Results of solubilization revealed encapsulation efficiency of 70.3±4.9% and drug loading of 5.14±0.60%. Injectability studies of the systems showed that extrusion force from the standard

18G needle was lower than 30 N, the force increased with NP-Aln addition. Drug release studies of GG-NP-Aln showed short burst release followed by sustained release phase. MTS and Live/Dead assays showed that the systems were not cytotoxic. Osteoblast-like cells adhered and proliferated well in medium with GG-NP-ALN extracts (Fig. 1 A1, A2); cell growth measured by xCELLigence system was also not altered (Fig. 1 A3). AP and TRAP staining confirmed differentiation of RAW 264.7 cells to osteoclasts (Fig 1 B1, B2). Osteoclast-like cells growth was reduced when they were cultured in medium supplemented with Aln or extracts from GG-NP-Aln as compared to control (Fig. 1 B3). It proves that manufacturing procedure of GG-NP-Aln systems does not diminish antiosteoclast potential of Aln.

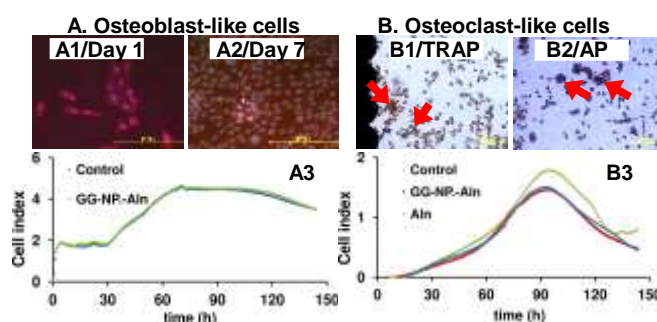


Fig. 1 Morphology of cells: osteoblast-like on day 1 (A1) and 7 (A2) (Hoechst-Texas red staining) and osteoclast-like after 7 days - TRAP staining (B1) and AP staining (B2) (red arrows show multinucleated giant cells - osteoclasts); Real-time dynamic monitoring of osteoblast-like cells (A3) and osteoclast-like cells (B3) proliferation using impedance xCELLigence analyzer in relation to control (pure media).

CONCLUSION

Our systems based on Aln-loaded PLGA nanoparticles suspended in gellan gum hydrogel matrix: i) were found to be injectable, ii) assured local sustained drug delivery, and iii) inhibited osteoclasts proliferation without affecting osteoblasts functions. The results show the promising potential of developed drug delivery systems for the local treatment of osteoporosis.

REFERENCES

1. Dolatabadi J. *et al.*, Colloids Surf B 117:21-28, 2014
2. Kimmel D. *et al.*, J Dent Res 86:1022-333, 2008
3. Lee J. *et al.*, Mater Lett 105:136-9, 2013

ACKNOWLEDGMENTS

The authors would like to thank the National Science Centre (Grant no: 2012/05/B/ST8/00129) for providing financial support to this project.

Bio-corrosion behaviour of chosen magnesium alloys from the Mg-Zn-Ca system

Katarzyna Kubok and Lidia Litynska-Dobrzynska

Department of Functional and Structural Materials,
Institute of Metallurgy and Materials Science Polish Academy of Sciences, Poland, k.kubok@imim.pl

INTRODUCTION

Magnesium alloys from the Mg-Zn-Ca system are attractive, because of their possible application as bioresorbable cardiovascular stents or orthopaedic implants. Magnesium alloys possess the density and Young's modulus close to that of cortical bone¹. The crucial issue is the precise control of corrosion rate, which is usually very rapid and connected with H₂ evolution. Alloying additions and their amount are among the most important factor influencing the corrosion behaviour. Therefore the wide range of Mg-3Zn-xCa wt.% alloys were examined in this study. The percentage addition of zinc was selected based on the literature review^{1,2}. Whereas calcium additions were selected due to our previous results³.

EXPERIMENTAL METHODS

Alloys of nominal composition presented in Table 1 have been prepared from Zn (99.999%), Ca (99.9%) and Mg (99.9%) under the argon atmosphere.

Tab. 1 Nominal compositions of investigated alloys

Alloy	Composition					
	wt.%			at.%		
	Mg	Zn	Ca	Mg	Zn	Ca
Pure Mg	99.9	-	-	99.96	-	-
Mg-3Ca	97	-	3	98.16	-	1.84
Mg-3Zn	97	3	-	98.86	1.14	-
Mg-3Zn-0.2Ca	96.8	3	0.2	98.74	1.14	0.12
Mg-3Zn-1Ca	96	3	1	98.24	1.14	0.62
Mg-3Zn-3Ca	94	3	3	96.97	1.15	1.88

Samples for immersion testing of 15 mm in diameter and 5 mm in thickness (total surface area = 3,14 cm²) were cut from cylindrical ingot. The specimens were polished and cleaned. The Hanks solution with calcium and magnesium was used as simulated body fluid in 37°C. The solution volume to surface area ratio was 28.6. pH was measured during the immersion test at different intervals. The corrosion products were removed using solution of 200g/l chromic acid with 10g/l silver nitrate in deionized water. The cleaned and dried specimens were weighted and the corrosion rate was calculated using formula:

$CR = \Delta W / (A \cdot t)$, where CR is the corrosion rate (mg/cm²/day); ΔW is the weight loss (mg); A is the original surface area exposed to the Hank's solution (cm²) and t is exposure time in hours. At least three samples for each alloys were assessed.

FEI ESEM XL30 with energy dispersive X-ray (EDX) has been used to observe the microstructure of all samples. The cross-sections (after 2 and 14 days of immersion) were observed in BSE mode and the surfaces without corrosion products in SE mode. Preliminary examination of phases in the as cast alloys has been done by XRD using Philips PW 1840 X-ray diffractometer. Different phases and their distributions

in the alloys were carefully investigated using transmission electron microscopy (Tecnai G2 F20 200 kV).

RESULTS AND DISCUSSION

Figure 1 shows cross-section of Mg-3Zn-0.2Ca and Mg-3Zn-1.0Ca after 48h of immersion in HBSS.

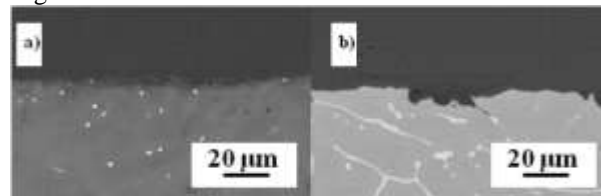


Fig. 1 SEM micrographs of a) Mg-3Zn-0.2Ca and Mg-3Zn-1.0Ca after 48 h of immersion

Mg-3Zn and Mg-3Zn-0.2Ca exhibit lower degradation rate than pure Mg. The corrosion rate of Mg-3Zn (~0.14 mg/cm²/day after 14 days) was similar to that reported by Kirkland *et al.* in MEM¹. Due to this fact results can be compared and considered even lower due to higher corrosion rate in HBSS than in MEM. The presence of high amount of Mg₂Ca phase in the Mg-3Ca and Mg-3Zn-3Ca alloy accelerates the corrosion rate up to ~7 mg/cm²/day after 14 days. On the other hand, the corrosion behaviour in Mg-3Ca and Mg-3Zn-3Ca alloys is inverse – in Mg-3Ca alloy the corrosion rate decreases with time while in Mg-3Zn-3Ca increases. The corrosion rate of alloy containing only ternary Ca₂Mg₆Zn₃ (Mg-3Zn-1Ca) is higher than that of pure Mg. In all cases, except for Mg-3Zn-0.2Ca pH after 7 days of immersion exceeds 10.0. For the Mg-3Zn-0.2Ca the pH value is ~ 9.0 after 7 days. The results connected to Mg-3Zn-0.2Ca and Mg-3Zn-1.0Ca alloys are very promising.

CONCLUSIONS

The corrosion rate can be tailored through precise control of alloying elements, type of phases and their distributions in the alloy. The further improvement of the corrosion rate may be obtained due to proper heat-treatment design.

REFERENCES

1. Kirkland N.T. *et al.*, Corros. Sci. 52:287-291, 2010
2. Pil-Ryung C. *et al.*, Sci. Rep. 3: 1-6, 2013
3. Kubok K. *et al.*, Arch. Metall. Mater. 52: 329-333, 2013

ACKNOWLEDGMENTS

The authors acknowledge gratefully the financial support from the project no. POKL. 04.01.00-00-004/10 co-financed by the European Union within the European Social Fund.



Biofunctionalization of CoCr Alloy for Bone Tissue RepARATION

Virginia Paredes^{1,2,3*}, Emiliano Salvagni^{2,3}, Enriquez Rodríguez⁴, José M. Manero^{2,3}

¹Antonio Nariño University.(UAN), Colombia

²Department of Science Materials, Technical University of Catalonia (UPC), Spain

³Nanoengineering Research Centre (CRnE), Spain

⁴Department of Inorganic Chemistry, University of Malaga, Spain
virgiparedes@gmail.com

INTRODUCTION

New developments in dental implantology are focused on bone-implant interaction to minimize complications or failure. One of the main drawbacks for metal implants is often due the inadequate interaction between materials and cells, leading to *in vivo* to foreign body reactions such as inflammation, infections, aseptic loosening, local tissue waste, implant encapsulation and thrombosis¹⁻³. The host response to a biomaterial is critical to determine the success of biomedical implants. A promising strategy is to anchor peptides to the metal surface due to their ability to stimulate cell bone response. The aim of this study was to generate and optimize the metal functionalization procedures and fully characterize each preparation step. Two activation methods were assessed by comparing contamination removal, hydroxyl groups (OH-act) formed on the surface, metal oxide ratio and changes in the chemical composition of the oxide layer. Then, three different organosilanes were employed as crosslinker for metal-peptide binding methods (CPTES, GPTES and APTES) and their metal coating capability was evaluated by measuring the amount of the metal bound Si and the stability of Si-O-Ti. Finally, covalent peptide immobilization of RGD, FRRRIKA and PHSRN and their mixtures was also investigated.

EXPERIMENTAL METHODS

Smooth CoCr alloys samples were bioactivated with either Oxygen Plasma (PO) or Nitric Acid (NA) and followed by silanization with CPTES, GPTES or APTES. These surfaces were then coated with different peptides as CGGRGDS, CGGPHSRN, CGGFHRRIKA, or mixtures of them (50/50): CGGRGDS + CGGPHSRN or CGGRGDS + CGGFHRRIKA). Non-treated CoCr alloys samples were used as control. Surfaces were characterized by contact angle measurements, X-ray Photoelectron Spectroscopy (XPS), Time-of-Flight Secondary Ion Mass Spectrometry (ToF-SIMS) and Zinc-complex Substitution Technique (ZT). The *in vitro* effect of modified surfaces was evaluated by cell adhesion assays, immunofluorescence and Scanning Electron Microscope (SEM). Mann-Whitney and Kruskal-Wallis statistical tests were used (p -value<0.05).

RESULTS AND DISCUSSION

The decrease in the CA values is associated with surface contamination removal as well as with the introduction of hydrophilic groups on the surface. XPS and ZT analysis showed that NA did not alter the $\text{Cr}^{n+}/\text{Co}^{n+}$ oxide ratios and a higher density of hydroxyl groups on the surface was observed. XPS analyses then confirmed that all strategies successfully immobilize peptides on the modified surfaces, showing a higher peptide density when APTES was used. Cell assays demonstrated an increase in density, morphology and area for mesenchymal cells when RGD motive (no- or combined) was covalently attached on the surface. (Figure 1).

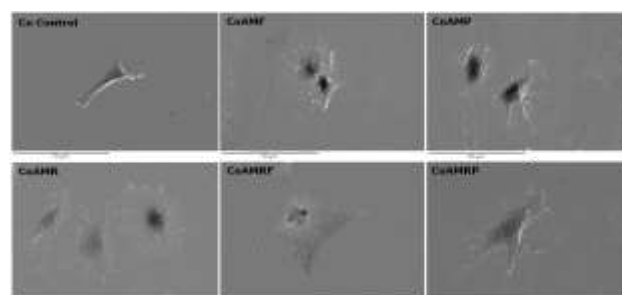


Figure 1. Effect of modified surfaces using APTES as silane on cells adhesion.

CONCLUSION

The metal functionalization strategy applied in this study allowed to successfully attach covalently peptides on CoCr alloy surfaces. These remarkable results demonstrated that covalent immobilization of different peptides moieties with APTES onto CoCr alloys surfaces induced an improved cell response.

REFERENCES

- 1.Kocijan, A., Milosev, I. & Pihlar, B. *Journal of materials science. Materials in medicine* **15**, 643–50 (2004).
- 2.Dunstan, E., Ladon, D., Whittingham-Jones, P., Carrington, R. & Briggs, T. W. R. *The Journal of bone and joint surgery. American volume* **90**, 517–22 (2008).
- 3.Malviya, A. & Holland, J. P. *Acta Orthopaedica Belgica* **75**, 477–483 (2009).

ACKNOWLEDGMENTS

This study was supported by Ministry of Science and Innovation (Project MAT2008-06887-C03-03) and Fundación Gran Mariscal de Ayacucho Venezuela.



Bioactive Glasses to Stimulate Angiogenesis

Alejandro Gorustovich¹, Aldo R. Boccaccini^{2*}

¹Interdisciplinary Materials Group-IESIING-UCASAL, INTECIN UBA-CONICET, Salta, Argentina

^{2*}Institute of Biomaterials, University of Erlangen-Nuremberg, Erlangen, Germany aldo.boccaccini@ww.uni-erlangen.de

INTRODUCTION

Enhancement of the angiogenic potential of implantable tissue scaffolds is the focus of considerable research efforts in tissue engineering (TE) strategies¹. New concepts to stimulate and control bone regeneration or to develop bone TE constructs based on biomaterials are needed that take into consideration angiogenesis. New blood vessels bring oxygen, nutrients and growth factors as well as serve as a route for inflammatory cells and bone precursor cells to reach to the highly metabolically active regenerating tissue. Indeed, enhancing angiogenesis could be a viable therapeutic approach for accelerated/improved bone regeneration clinically². Increasing number of investigations are being reported documenting that specific compositions of silicate bioactive glasses (BGs), used in bone regeneration approaches, not only stimulate new bone growth but also their ionic dissolution products (IDPs) may act as angiogenic factor and induce increased vascularization when incorporated in TE scaffolds³. In this overview presentation a series of experiments that prove the angiogenic potential of BGs, including both in vitro and in vivo studies, will be discussed in detail.

EXPERIMENTAL METHODS

The most investigated material in angiogenesis and bone vascularization studies has been the classic 45S5 Bioglass system of composition (in wt.%): 45% SiO₂, 24.5% Na₂O, 24.5% CaO and 6% P₂O₅. The material has been considered in particulate form and as filler and coating of biodegradable polymers to form composite scaffolds. More recently, 3D Bioglass-based scaffolds fabricated by the foam replica method^{4,5} and sol-gel derived foams⁶ have been considered in angiogenesis and vascularization studies. In addition, a series of novel bioactive glass compositions and ion-doped silicate systems have been investigated to assess angiogenic effects⁷. As it has been established that boron (B) may perform functions on angiogenesis and osteogenesis, the controlled and localized release of B ions from BG is expected to provide promising angiogenic effects.

RESULTS AND DISCUSSIONS

In vitro results showed that IDPs from 45S5 BG particles (< 5 µm) containing B₂O₃ (2 wt%) (labelled 45S5.2B) have a robust proangiogenic activity on human umbilical vein endothelial cells (HUVECs)⁸. Compared to controls, cell proliferation, migration, tubulogenesis and pro-angiogenic cytokines release of HUVECs were statistically significantly increased by conditioned media containing the IDPs of 45S5.2B BG. It has also been found that IDPs from 45S5.2B based scaffolds stimulated angiogenesis in the quail embryo

chorioallantoic membrane (CAM) bioassay (Fig. 1). Importantly, the angiogenic response reached the same extent as that obtained by bFGF. These findings are relevant to vascularized bone tissue engineering because IDPs from 45S5.2B BG are confirmed to act as an inorganic angiogenic agent serving as an alternative to expensive and potentially risky growth factors.

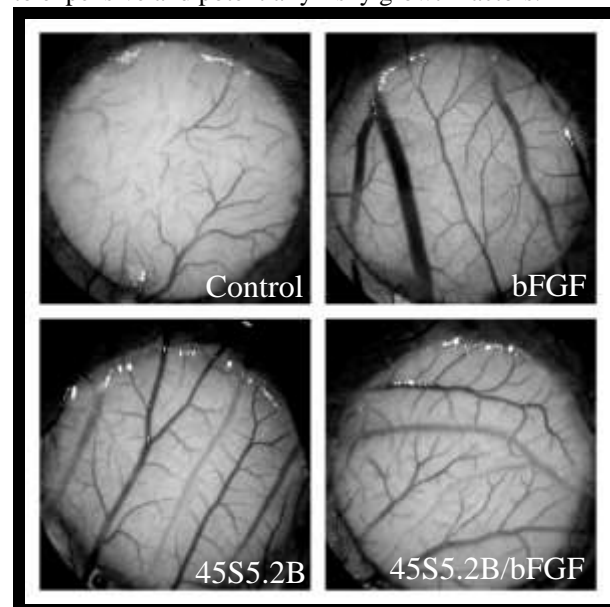


Fig. 1. Angiogenic CAM response at 5d after treatment. Orig. Mag. X35

CONCLUSIONS

The results indicate that 45S5.2B-based scaffolds are a promising candidate for bone TE due to their bioactivity and potential enhanced angiogenic effects provided by B. The results are in agreement with an increasing number of studies reporting the angiogenic properties of ion doped BGs for vascularized bone regeneration. The specific effects of different IDPs on vascularization are the subject of increasing research efforts and their understanding promises to have a significant impact on the application of BGs in bone tissue engineering.

REFERENCES

1. Nguyen L.H. *et al.*, Tissue Eng. B Rev. 18:363-382, 2012
2. Fassbender M. *et al.*, Eur. Cell Mater. 22:1-11, 2011
3. Gorustovich A. *et al.*, Tissue Eng. Part B Rev. 16:199-207, 2010
4. Arkudas A. *et al.*, Tissue Eng. C 19:479-486, 2013
5. Handel M *et al.*, Tissue Eng. A 19: 2703-2712, 2013
6. Midha S. *et al.*, Adv. Healthcare Mater. 2:490-499, 2013
7. Hoppe A. *et al.*, Biomaterials. 32:2757-2774, 2011
8. Haro Durand L. *et al.*, Regen. Med. 6:263, 2011

Porosity engineering in bioactive glasses: a sol-gel approach

J. Soulié^{1,2}, J. Lao¹, E. Jallot¹, J.M. Nedelec²

¹Clermont Université, Université Blaise Pascal, CNRS/IN2P3, Laboratoire de Physique Corpusculaire, BP 10448, F-63000 Clermont-Ferrand, France

²Clermont Université, ENSCCF, Laboratoire des Matériaux Inorganiques, BP 10448, F-63000 Clermont-Ferrand, France
j-marie.nedelec@univ-bpclermont.fr
j-marie.nedelec@ensccf.fr

INTRODUCTION

Among the various biomaterials used as bone substitutes or as prosthesis coatings in orthopedic surgery, bioactive glasses have attracted considerable interest^{1,2}. When in contact with living tissues, dissolution and precipitation take place at the material / biological medium interface, and this leads to the formation of a phosphocalcic layer. This apatite-like layer is used as a mineralization site for bone cells and finally allows an intimate chemical bond between the glass and the bone. A fine control of bioactivity can be achieved by using soft chemistry routes to tailor the morphology and the texture of such porous bioactive glasses. Pore size can span several orders of magnitude from the nanometer to the millimeter. Each level of porosity (meso, macro,...) could then have biological usefulness, like for drug delivery, vascularization of the implant, or cell adhesion for tissue engineering. With this respect, mesoporous, macroporous and glass foams have been prepared.

EXPERIMENTAL METHODS

Mesostructured glasses (Fig 1a) have been prepared by using surfactant as directing agent whereas polystyrene opals were used as template for the production of macroporous glasses with different pore size (Figure 1b). Finally using a surfactant and adapted dispersive equipment, a air/liquid foam has been used as template to obtain monolithical glass foams (Fig 1c).

All samples have been characterized using a various set of techniques including gas sorption, SAXS, thermoporosimetry, helium pycnometry and SEM/TEM microscopies.

RESULTS AND DISCUSSION

The control of the pore size and pores organization is demonstrated for meso and macro porous glasses. Glass foams exhibit a multiscale porosity with a high fraction of void making these materials attractive for tissue engineering applications.

Finally interactions between acellular biological medium and the different glasses have been studied for different delays. At each time period, quantitative chemical maps of samples were recorded with a micrometer resolution using Particle Induced X-ray Emission coupled to Rutherford Backscattering spectroscopy (PIXE-RBS)³. This technique allows monitoring spatial and chronological evolutions of elemental concentrations, thanks to measurements with an excellent sensitivity (10^{-6} g/g). The influence of porosity on the bioactivity has been determined. Comparison of mesoporous glasses exhibiting or not

spatial ordering is provided. Determining parameter for the biomineralization onto macroporous glasses is found to be the size of the interconnection window and a criterion is proposed for the homogeneous nucleation for HAp in glass foams.

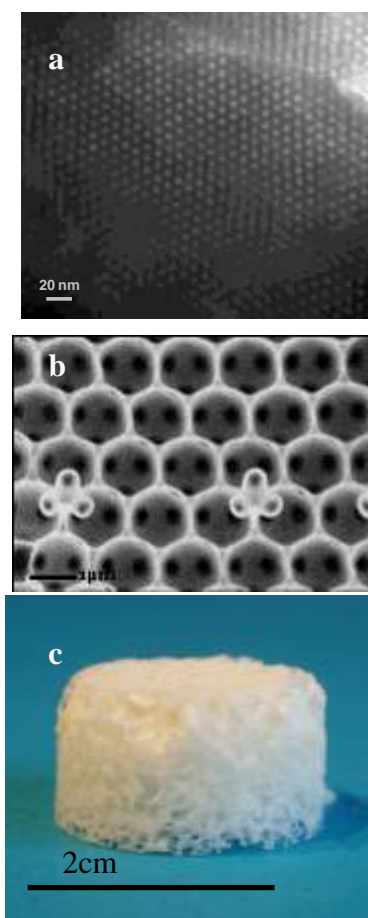


Figure 1: a) TEM image of a mesostructured bioactive glass (scale bar 20 nm), b) SEM image of a macroporous sample (scale bar 1 μ m) and c) picture of a monolithical glass foam (scale bar 2cm).

REFERENCES

1. Hench, L. J. Biomed. Mater. Res. 1998, 41, 511
2. J. Lao, E. Jallot and J.-M. Nedelec, Chem. Mat. 2008, 20(15) 4969-4973
3. E. Jallot, O. Raissle, J. Soulie, J. Lao, G. Guibert and J.M. Nedelec, Advanced Biomaterials, 2010, 12(7), B245-B255
4. E. Jallot, J. Lao, L. John, J. Soulié, Ph. Moretto, J.M. Nedelec, Applied Materials and Interfaces (ACS), 2010, 2(6), 1737-1742.

Bioactive Glass-Ionomer Cements for Bone Tissue Regeneration

Paul V. Hatton¹, Altair Contreras¹, Felora Mirvakily¹, Yulia Ryabenkova¹, Ian Brook¹, Aileen Crawford¹, Robert Moorehead¹, Andrew Rawlinson¹, Christine Freeman¹, Ian M. Reaney², and Cheryl Miller¹

¹Bioengineering & Health Technologies Research Group, School of Clinical Dentistry, and ²Department of Materials Science and Engineering, University of Sheffield, UK paul.hatton@sheffield.ac.uk

INTRODUCTION

Glass-ionomer bone cements have been used successfully in otological surgery for over 20 years. They have, however, been restricted to use in a relatively narrow range of surgical procedures due to the release of aluminium ions that interfere with the mineralisation of new bone tissue¹. There have therefore been numerous attempts to replace alumina in the parent glasses with other metal oxides (including iron, zinc and magnesium) to produce glass-ionomer cements that could be used in a wider range of clinical applications, but none of these have been sufficiently successful to justify clinical evaluation. The aim of this research was therefore to investigate whether classical bioactive glass compositions² could form the basis for usable cements that retained the osteoconductive properties of the parent glasses.

EXPERIMENTAL METHODS

Bioactive glass compositions were prepared by melting to obtain final molar compositions summarised below (Table 1). The amorphous nature of the glasses was investigated using X-ray diffraction (XRD), and the post-melt compositions were determined using X-ray fluorescence (XRF). Glasses were milled and sieved to obtain particles of <45 µm. Cements were prepared by mixing with poly(acrylic acid) with mean molecular weights of 45,000 (First Scientific GmbH) or 52,000 (Advanced Healthcare Ltd.) and distilled water or aqueous solutions of phosphoric acid. Working and setting times were measured using either a Gilmore needle or rheometer. Aqueous stability was determined by storage of cement discs (5 mm x 1 mm) in distilled water. The *in vitro* and *in vivo* biocompatibility of the novel cement based on 45S5 bioactive glass powder was further investigated using cultured rat mesenchymal stromal cells (MSCs) and a healing defect (1 mm) in the midshaft of the rat femur respectively.

Example number	Composition (mol%)				
	SiO ₂	Na ₂ O	CaO	P ₂ O ₅	SrO
1	46.1	24.4	26.9	2.6	0
2	50.9	22.1	25.6	1.3	0
3	50.3	21.9	25.3	2.6	0
4	46.1	24.35	24.2	2.6	2.7

Table 1. Pre-melt bioactive glass compositions used to prepare cements.

RESULTS AND DISCUSSION

All pre-melt compositions summarised in Table 1 formed glasses, with no crystalline phases detected by XRD. Glass powders were all capable of forming a setting cement system with poly(acrylic acid), and the substitution of water with phosphoric acid solution accelerated the setting reaction and appeared to improve

the stability of the cement in water. All cements reported here were stable in distilled water at 37 °C for a period of at least six months. Cell culture studies showed a reduction in the metabolic activity of MSCs cultured in the presence of cements based on 45S5 bioactive glass compared to Thermanox® reference materials, but it was also determined that MSCs could be cultured successfully for up to 21 days in the presence of this cement. *In vivo* investigation demonstrated the formation of a direct bone-implant interface after 4 weeks (Figure 1), suggesting rapid osseointegration with no evidence for the mineral defect reported previously for conventional glass-ionomer bone cements¹.

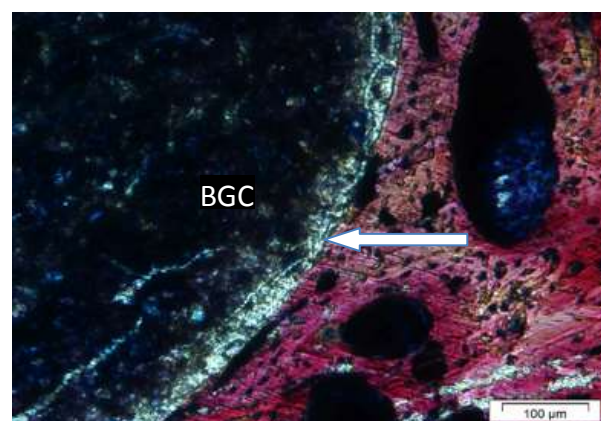


Figure 1. Formation of direct bone-implant interface (arrowed) after 4 weeks implantation of a bioactive glass-ionomer cement (BGC) prepared using 45S5 bioactive glass and poly (acrylic acid).

CONCLUSION

It was concluded that, despite the absence of alumina in the parent glass composition, it was possible to prepare a glass-ionomer cement using only bioactive glass compositions in combination with poly (acrylic acid), and cement formation was further improved through addition of phosphoric acid. The new cement based on 45S5 bioactive glass was biocompatible *in vitro*, and encouraged substantial bone tissue regeneration *in vivo*. These promising new materials have significant potential for use as cements, and also as pre-set graft substitutes or scaffolds for bone tissue regeneration³.

REFERENCES

1. Carter, D.H. *et al.*, 1997. *Biomaterials* 18: 459-466
2. Hench, L.L. 2006. *J Mater Sci:Mater Med* 17: 967-978
3. International Patent Application PCT/GB2013/053386

ACKNOWLEDGMENTS

The authors are grateful to Dr Robert Burton at Hallam University for XRF. Hatton, Crawford & Miller are members of MeDe Innovation. We acknowledge the EPSRC for funding through the local KTA account and the Regener8 IKC programme (POC020).



Well Ordered Mesoporous Bioactive Glasses for Bone Tissue Engineering and Drug Delivery

Chengtie Wu

State Key Laboratory of High Performance Ceramics and Superfine Microstructure, Shanghai
Institute of Ceramics, Chinese Academy of Sciences, Shanghai, China, chengtiewu@mail.sic.ac.cn

INTRODUCTION

As a new class of bioactive materials for bone regeneration, ordered mesoporous bioactive glasses (MBG) have attracted much attention in recent years. Compared with traditional bioactive glasses, the typical features of MBG are as follows: (1) They have highly ordered mesoporous channel structure (2-20nm), high surface area and pore volume; (2) Since the nanostructure is significantly improved, MBG have greatly enhanced apatite-mineralization ability and degradation; (3) MBG can be used to delivery drugs with its high specific surface area and pore volume [1-5]. The aim of this study is to explore the potential application of MBG for bone tissue engineering and drug delivery.

EXPERIMENTAL METHODS

MBG powders were prepared through chemical templating methods. MBG/polymer composites were prepared by using freeze drying methods. MBG scaffolds were prepared by polyurethane sponge template and 3D-printing technology. The functional effect of different elements and surface modification of MBG on the in vitro osteogenic differentiation of bone marrow stromal cells (BMSCs) and in vivo osteogenesis was systematically studied. The effect of drug delivery of MBG on the functional effect on the in vitro osteogenesis was investigated.

RESULTS AND DISCUSSION

MBG powders can improve the in vitro and in vivo osteogenic properties of polymer biomaterials such as PLA and silk protein. With the incorporation of functional elements into MBG scaffolds, the osteogenesis and potential angiogenesis were significantly enhanced. Moreover, with special component, we can obtain magnetic scaffolds, which may be used in hyperthermia to heal bone tumour. By using 3D-printing, the pore size of morphology of MBG scaffolds can be effectively controlled, which leads to improved mechanical strength. MBG scaffolds can be used for drug/growth factor carrier to load and release DEX, DMOG and VEGF. It is proved that the delivery of drug and growth factor significantly stimulated the osteogenesis and angiogenesis of BMSCs for bone tissue engineering.

CONCLUSION

MBG significantly improves the osteogenic differentiation of BMSCs and in vivo bone regeneration ability. MBG can be used as drug/growth factor carrier to accelerate the osteogenic differentiation of BMSCs. Therefore, MBG can provide an excellent platform for bone tissue engineering and drug delivery system.

REFERENCES

- [1] Wu C, Ramaswamy Y, Zhu Y, Zheng R, Appleyard R, Howard A and Zreikat H 2009 The effect of mesoporous bioactive glass on the physiochemical, biological and drug-release properties of poly(DL-lactide-co-glycolide) films *Biomaterials* **30** 2199-208.
- [2] Wu C, Zhang Y, Zhu Y, Friis T and Xiao Y 2010 Structure-property relationships of silk-modified mesoporous bioglass scaffolds *Biomaterials* **31** 3429-38.
- [3] Wu C, Miron R, Sculeaan A, Kaskel S, Doert T, Schulze R and Zhang Y 2011 Proliferation, differentiation and gene expression of osteoblasts in boron-containing associated with dexamethasone deliver from mesoporous bioactive glass scaffolds. *Biomaterials* **32** 7068-78.
- [4] Wu C, Zhou Y, Fan W, Han P, Chang J, Yuen J, Zhang M and Xiao Y 2012 Hypoxia-mimicking mesoporous bioactive glass scaffolds with controllable cobalt ion release for bone tissue engineering *Biomaterials* **33** 2076-85.
- [5] Wu C, Zhou Y, Xu M, Han P, Chen L, Chang J and Xiao Y 2013 Copper-containing mesoporous bioactive glass scaffolds with multifunctional properties of angiogenesis capacity, osteostimulation and antibacterial activity *Biomaterials* **34** 422-33.

ACKNOWLEDGMENTS

Funding for this study was provided by the Recruitment Program of Global Young Talent, China (Dr Wu), Shanghai Pujiang Talent Program (12PJ1409500), Natural Science Foundation of China (Grant 31370963, 81201202)



Glass Fiber-Reinforced Composite Cranial Implant with Bioactive Glass

Pekka K. Vallittu

Department of Biomaterials Science and Turku Clinical Biomaterials Centre – TCBC, Institute of Dentistry ,
University of Turku, Finland

Pekka.vallittu@utu.fi

INTRODUCTION

Large skull bone defects cause both functional and aesthetic problems to the patients. A bioactive fiber-reinforced composite (FRC) is presented to address some of the problems faced in current options for craniofacial bone reconstruction. Bioactive glass – glass fiber-reinforced composite (FRC) is potential new material for cranio-maxillo-facial reconstructions due to its non-metallic nature and bone like mechanical properties.^{1,2} Structure of the FRC implant couples osteoconductive and antimicrobial properties of bioactive glass (BG) with durable anatomically shaped FRC laminate. Osseointegration and biomineralization between FRC and bone has been demonstrated in preclinical and experimental studies.³ Synthetic, osteoconductive and antimicrobial, bioactive glass (BG) S53P4 with E-glass fibers in a new custom made composite implant for craniofacial reconstructions is presented.

EXPERIMENTAL METHODS

Retrospective series of 30 patients with craniofacial deformity, operated between 1/2007-5/2013. After the skull defect was characterized with three-dimensional computer tomography, a rapid prototype model of the skull was made from polyamide with a selective laser sintering method. This model was then used to manufacture a customized implant. The implant material consisted of a supporting fiber-reinforced framework, porous inner layers and bioactive glass filling. The composite structure of the implant allowed the biomechanical excellence of the fiber-reinforced structure to be coupled with the properties of bioactive glass. The bioactive component in the FRC implant was bioactive glass (S53P4). Static [18F]-fluoride Positron Emission Tomography (PET) fused with Computer Tomography (CT) was acquired 10-23 months post-operatively. PET-CT images were assessed for signs of new bone formation at the region of implants. Semiquantitative standardized uptake value (SUV) was obtained from [18F]-fluoride PET to evaluate metabolic activity of bone-implant interface, and mineralization was observed from CT. Histological samples were not obtained.

RESULTS AND DISCUSSION

The aesthetic and functional outcomes of all patients were good and patients were satisfactory for reconstructions. Normal progressive wound healing was observed in 28 cases out of 30. One late plate exposure and one periprosthetic infection led to implant removal, thus resulting in 6.7 % complication rate in this series of 30 patients. Both maximal and average SUV of the implant area (VOI 1) were higher compared to the reference area (VOI ref). Mineralized bone islands around the implant were observed at time-point of two years. Reconstruction of large skull defects with the novel bioactive FRC implant is a promising solution compared to conventional materials.⁴ As signs of new bone formation, bone formation activity and mineralization islets were observed two years after skull bone defect reconstruction with bioactive FRC implant.

CONCLUSION

With the limitations and the pilot nature of this study in mind, results of this study suggest that osteoconductive properties of bioactive glass can be combined with biostable fiber-reinforced composite implant even of large size, though bone bridging of such large defects is relatively slow.

REFERENCES

1. Ballo AM, *et al.* J Mater Sci Mater Med 2008;19:3169-77.
2. Zhao DS. *et al.* Med Eng Phys 2009;31:461-9.
3. Nganga S, *et al.* Dent Mater 2012; 28:1134-45.
4. Aitasalo K, *et al.*, G. *et al.*, Head and Neck 2013 DOI 10.1002/hed23370

ACKNOWLEDGMENTS

The authors would like to thank BioCity Turku Biomaterials Research Program (www.biomaterials.utu.fi) or providing support to this project.



Bioglass transformations by laser assisted techniques

F. Lusquinos¹, J. del Val¹, R. Comesaña², F. Quintero¹, A. Riveiro¹, M. Boutinguiza¹, J.R. Jones³, R.G. Hill⁴, J. Pou¹

¹Applied Physics Dpt., Universidade de Vigo, EEI, Lagoas-Marcosende, E-36310, Vigo, SPAIN

²Materials Engineering, Applied Mech. and Construction Dpt., Universidade de Vigo, EEI Vigo, SPAIN

³Department of Materials, Imperial College London, South Kensington Campus, London SW7 2AZ, UK

⁴Barts and the London, Unit of Dental and Physical Sciences, Mile End Road, London E1 4NS, UK
jpou@uvigo.es

INTRODUCTION

Bioglass and other silicate bioactive glasses are usually produced by casting, as bulk material with plate shapes or as powder. Applications such as middle ear prostheses or synthetic grafts are fulfilled with these material forms^{1,2}. However, extensive research has been accomplished during last years to increase the bioglass practical applications, using it as part of composites, or modifying the geometrical architecture. In this sense, a number of laser assisted techniques has been applied to face this challenge, also aiming the preservation of the bioactivity after the process and preferably being fast or economically feasible.

Bioglass-derived coatings into metallic implants were deposited by laser cladding to combine the metal mechanical properties with the bioglass superior osteoconductivity³. In addition, the three dimensional variant of the technique was employed to create free-form layered implants for low load craniofacial applications; neither moulds nor additional processing steps are required⁴. Moreover, rapid prototyping based on laser cladding allows to selectively introduce additional chemical species with antiresorptive, angiogenic or antibacterial capabilities.

On the other side, the nano-scale geometrical architecture plays an important role in the performance of scaffolds for tissue engineering. Nanofibrous structures with controlled architecture have excellent potential to mimic natural extracellular matrix and to be used as scaffolds for tissue growth. Another laser assisted process, the laser spinning technique, is the technique exclusively capable to produce nanofibers from 45S5@ BG^{5,6}

EXPERIMENTAL METHODS

Laser radiation with wavelengths in the near and mid-infrared spectra ($\lambda=1064$ nm; $\lambda=10600$ nm) is employed to irradiate bioglass microparticles. For the production of coatings on metallic surfaces, low absorbance near-infrared radiation can be used to heat up the interface layer over the transition temperature. Rapid prototyping based on laser cladding requires a high absorbance wavelength. The bioactive glass is melted within the molten pool, and the sequential substrate movement generates a layered three dimensional sample from a computer model, which resembles a specific geometry of the cranial bone.

Laser Spinning is a new technique for the production of very long amorphous bioceramic nanofibers. It employs a laser to melt a small plate of bulk bioglass while a high pressure gas jet drags it. Thus, the molten material forms glass fibers as result of its viscous elongation by

the drag force and rapid cooling by the convective heat transfer promoted by the gas jet.

RESULTS AND DISCUSSION

Laser cladding processing of bioglass produced full density coatings and three-dimensional samples (Fig.1). No species volatilization is produced and chemical composition of bioactive glass is maintained after the process. Processed samples show ion release profiles in Tris buffer equivalent to these produced by the precursor bioactive glasses; direct seeding of pre-osteoblastic cells reveal healthy morphologies.

SEM and TEM analysis show that the nanofibers obtained by laser spinning have a high length to diameter ratio. The electron diffraction patterns reveal the preservation of precursor glasses structure. EDS mapping performed by STEM shows that the elements are uniformly distributed along the fibers.

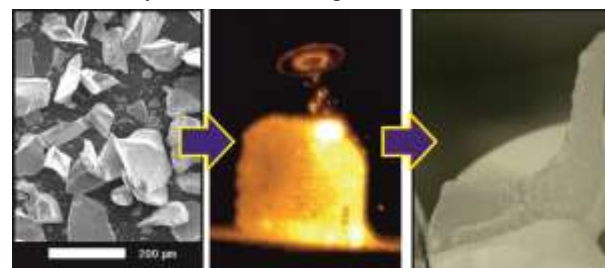


Fig.1 Implant made from BG particles by RP based on laser cladding.

CONCLUSION

The laser cladding based techniques allow to transform bioglass particles into sound coatings and 3D implants for low loading applications, without losing the bioactive behaviour. Laser Spinning allows to produce large quantities of nanofibers with lengths up to several centimetres, made with specific bioglass compositions. The precursor bioglass composition and structure was preserved after processing.

REFERENCES

1. Hench L.L. *et al.*, Science 226:630-6, 1984.
2. Jones J.R. Acta Biomaterialia 9:4457-86, 2013.
3. Comesaña R. *et al.*, Acta Biomaterialia 6:953, 2010.
4. Comesaña R. *et al.*, Acta Biomaterialia 7:3476, 2011.
5. Quintero F. *et al.*, Adv. Funct. Mater. 19:3084, 2009.
6. Cabal B. *et al.*, Nanoscale. 7:5(9):3948-53, 2013.

ACKNOWLEDGMENTS

This work was partially funded by the European Union Cross-border cooperation program 2007-2013 (Project 0330_IBEROMARE_1_P), the Spanish Government and FEDER (CICYT MAT2006-10481), FPU AP2006-03500 grant and by Xunta de Galicia (IN845B-2010/082).

Cell behaviour affected by properties of electrospun nanofibers

Yan Wei, Wentao liu, Xuehui Zhang, Xuliang Deng*

Department of Geriatric Dentistry, School and Hospital of Stomatology, Peking University, China,

kqdengxuliang@bjmu.edu.cn

INTRODUCTION

Cell–biomaterial interactions have been shown to exert a considerable influence on the function and differentiation of mesenchymal stem cells (MSCs).^{1,2} Nanofibers, universally accepted as niche-biomimetic scaffolds in bone regeneration, have also been found to enhance the proliferation and osteogenic differentiation of MSCs.^{3,4} Although many reports have described the phenotypic and genotypic phenomena that occur during the nanofibrous scaffold-mediated osteogenic differentiation of MSCs, the biological mechanisms underlying the osteogenic behavior of MSCs in response to nanotopography have not been clearly elucidated.

EXPERIMENTAL METHODS

Temporal changes in the osteogenic behavior and dynamic global gene expression patterns of hBMSCs were assessed during their culture on random and aligned electrospun poly-L-lactide (PLLA) nanofibers without an osteogenic supplement (OS). Osteogenic differentiation was examined by real-time quantitative PCR (RT-qPCR) and global microarray analysis at 4, 7, 14, and 21 days of culture. In-depth pathway analysis was employed to explore the possible mechanism triggered by nanofibrous topography.

RESULTS AND DISCUSSION

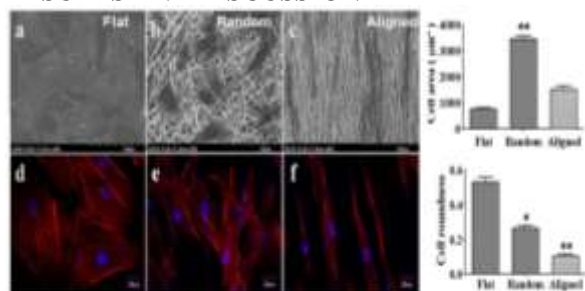


Figure 1: SEM images and Immunofluorescence staining of hBMSCs after 1 day of culture on (a,d) flat polymer films, (b,e) random nanofibers, and (c,f) aligned nanofibers. Cell area (g) and roundness (h) of hBMSCs.

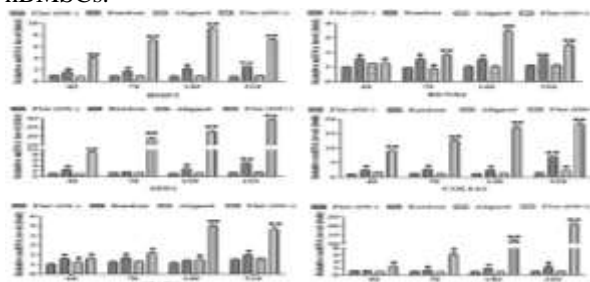


Figure 2: RT-qPCR analysis of gene expression in cells seeded on random and aligned nanofibers and flat polymer films with or without OS.

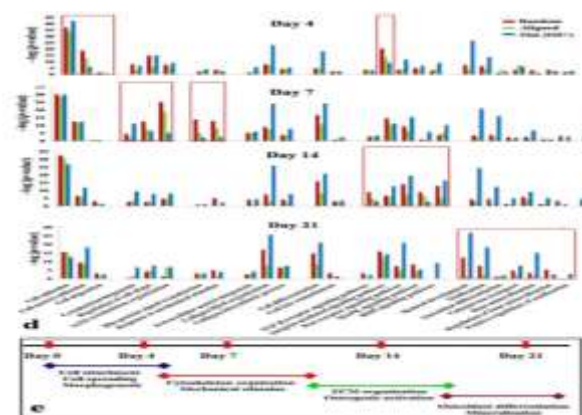


Figure 3: Gene ontology analysis and graphical summary of the osteogenic differentiation of hBMSCs triggered by random nanofibers.

The hBMSCs on random nanofibers exhibited a highly branched morphology with round nuclei, and those on aligned nanofibers displayed a polarized morphology with oval nuclei along the fiber directions. RT-PCR analysis of osteogenic marker genes and ALP activity assays demonstrated that hBMSCs cultured on random nanofibers showed enhanced osteogenic-specific fate compared with those on aligned nanofibers. Microarray analysis demonstrated a similar temporal change in gene expression patterns between hBMSCs cultured on random nanofibers and those induced with OS. However, the extent of osteogenic differentiation on the fibrous scaffold was much lower than that driven by chemical OS. In-depth pathway analysis revealed that focal adhesion kinase, TGF- β , Wnt and MAPK pathways were involved in the activation of osteogenic differentiation in hBMSCs on random nanofibers.

CONCLUSION

The findings suggested that a lower extent but similar rhythm of dynamic cellular behavior was induced on random nanofibers when compared with the OS condition, and that mechanotransduction could trigger nonspecific and multilevel responses in hBMSCs. This study provides insight into the regulation of osteogenesis directed by substratum surfaces.

REFERENCES

References must be numbered. Keep the same style.

- Engler AJ. *et al.*, Cell. 126: 677-689, 2006
- Wilson A. *et al.*, Nat. Rev. Immunol. 6: 93-106, 2006
- Zhu H. *et al.*, Biomaterials. 32: 4744-4752, 2011
- Dalby M J. *et al.*, Biomaterials. 29: 282-289, 2008

ACKNOWLEDGMENTS

The authors acknowledge the National Basic Research Program of China (2012CB933900), the National Natural Science Foundation of China (81171000), the National High Technology Research and Development Program of China (2012AA022501).



Two-photon polymerization as a high-resolution tool to control surface structure of polymeric biomaterials at micro- and nanoscale

David Barata¹, Paulo Dias¹, Clemens A. van Blitterswijk^{1,2}, and Pamela Habibovic^{1,2*}

¹Department of Tissue Regeneration, University of Twente, Enschede, the Netherlands

²MERLN Institute, Maastricht University, Maastricht, the Netherlands, *p.habibovic@utwente.nl

INTRODUCTION

Besides soluble factors, genetic background and cell-to-cell interactions, the physical cell culture environment has been shown to be determinant for cell fate and consequent tissue formation. For skeletal tissue regeneration, tridimensional macroscale scaffolds, often containing pores, provide essential functional compartments, allowing cell growth, differentiation and tissue infiltration¹. However, the surface topography features at micro- and nanoscale have also been shown to play an important role in cell proliferation and differentiation^{2,3}. Two-photon polymerization (2PP) is a unique technique for rapid prototyping of surface features at nano and microscale with high resolution. In this study, we have employed 2PP to design surface of a number of materials, exploring the effect of multi-scale physical cues on cell behaviour.

EXPERIMENTAL METHODS

A commercial setup for 2PP (Nanoscribe GmbH) was used for fabrication of master structures (Figure 1A). A polydimethylsiloxane negative mould was then created and replicas were manufactured in different polymeric materials by using thermal embossing (Figure 1B). In this manner, it was possible to create identical surface features, while varying chemistry of the biomaterial. MG-63 osteosarcoma cells were cultured on selected surfaces for 72h. Image analysis of cell morphology was performed after fluorescent staining for nuclei and actin. All experiments were performed in triplicate.

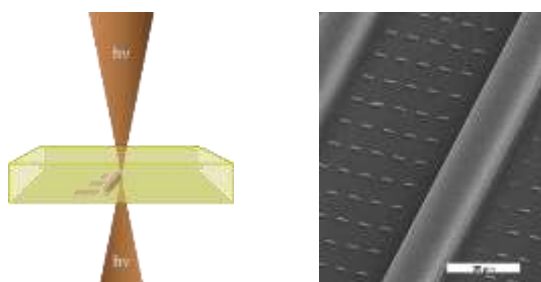


Figure 1 – Schematic showing structure fabrication by 2PP (A) and SEM image of replicated structures (B).

RESULTS AND DISCUSSION

Fluorescent staining for nuclei and cytoplasm allow the identification of cell morphology upon seeding and attachment on different surfaces. Initial analysis of the fluorescent microscopy images showed evident cell shape changes upon culture on surfaces with distinct micro- and nano features (Figure 2).

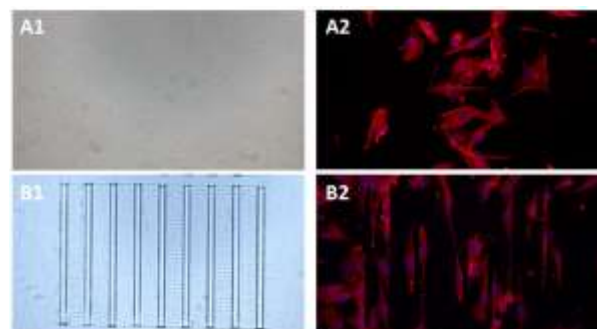


Figure 2 – Cell morphology on flat (A) and rails/dashed (B) surface. Fluorescent microscopy of nuclei (blue) and cytoskeleton (red) is shown.

On flat substrates, cells spread randomly, as opposed to substrates with micro and/or nanostructured features. For example, as is shown in Figure 2 – B2, cells tend to extend in the direction of larger, microscale features, whereas nanostructures in the opposite direction seem to be responsible for “bridging” the area between the microfeatures. Moreover, cell shape on flat surfaces presented lower eccentricity and apparent larger cell area.

We are currently performing a more systematic analysis to quantify critical parameters of cell shape, which have previously been shown to be predictive of cell fate².

CONCLUSION

Here we demonstrate the potential of two-photon polymerization as a versatile tool to provide surface of polymeric biomaterials with highly controlled topographical features at micro- and nanoscale. Since this technique is a relatively slow and thus expensive way for directly “write” the features on large area, we have used it to develop master moulds which can subsequently repeatedly be used for thermal embossing of various materials.

REFERENCES

1. Smith G. *et al.*, J. Biomech. 2: 5-11, 2011
2. Dalby M. *et al.* Nature Materials 6, 997 – 1003, 2007
3. Unadkat H. *et al.*, PNAS 108, 40:16565-16570, 2011

ACKNOWLEDGMENTS

The Netherlands Institute for Regenerative Medicine is acknowledged for financial support.

Facile Photochemistry Enables Protein and Cell Micropatterning in Open and Closed Polymer Systems

Esben Kjær Unmack Larsen, Morten Bo Mikkelsen and Niels B. Larsen*

¹Department of Micro- and Nanotechnology, DTU Nanotech, Technical University of Denmark, Denmark,
niels.b.larsen@nanotech.dtu.dk

INTRODUCTION

Micropatterning of proteins and cells on polymer surfaces are of great utility for cell analysis as well as advanced cell culture¹. The technology challenge is two-fold in creating a background coating exhibiting low adsorption of cell adhesive proteins to minimize non-specific cell adsorption and attachment of functional cell adhesive proteins with high positional accuracy at the intended surface areas. Photochemistry is an attractive base technology as patterning may be performed with sub-cellular resolution and the process can be performed in both open and closed transparent (micro-)systems.

EXPERIMENTAL METHODS

Base coatings resulted from covalent coupling and polymerization of poly(ethylene glycol)-diacrylate (PEGDA, 5 kDa) by UV-illumination (365 nm) of an aqueous solution of PEGDA (5 mg/mL) and the photoinitiator 4-benzoyl benzylamine hydrochloride (Bz, 1 mg/mL) applied to polystyrene or polyethylene polymer surfaces. Aqueous fibronectin (FN, 100 µg/mL) and Bz (1 mg/mL) or fluorescently labeled albumin (BSA, 100 µg/mL) and Bz (100 µg/mL) was applied to the resulting PEG-coated surfaces and coupling proceeded using patterned UV light (365 nm) on a home-built projection lithography system³. Surfaces with micropatterned fibronectin as well as uncoated (negative control) or fully coated (positive control) with fibronectin were employed for in vitro cell culture experiments using HT-29 adenocarcinoma cells in 1% human serum. Cells were cultured for 16 hours at 37 deg. C (5% CO₂) before washing off weakly attached cells by PBS and visualizing the remaining cells with phase contrast microscopy.

RESULTS AND DISCUSSION

Covalent attachment of an ultrathin (<5 nm) layer of the protein non-adhesive PEG coating was verified by x-ray photoelectron spectroscopy (data not shown). The spatial resolution of the method in closed microsystems was explored using fluorescently labeled albumin inside a 70 µm high polyethylene microchannel (Figure 1), showing defined lines-and-spaces of <10 µm width and very little non-specific adsorption on the PEG coating.

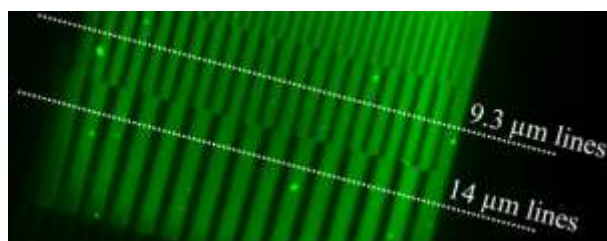


Figure 1. Micropatterned fluorescently labeled albumin on a low-binding coating of PEG.

Cell cultured on the surfaces with photopatterned fibronectin showed markedly higher adhesion on the fibronectin than on the surrounding PEG coating (Figure 2). This effect was most pronounced at low added serum concentrations, as culture in 10% added serum resulted in substantially higher non-specific cell adsorption for longer culture times (data not shown)

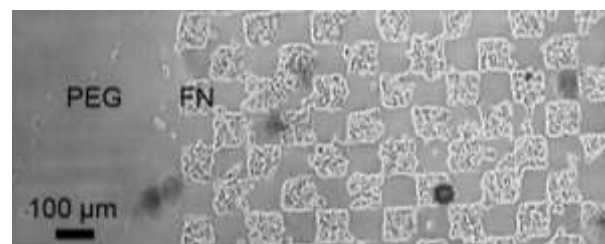


Figure 2. HT-29 cells templated on fibronectin (FN) photopatterned on a low-binding coating of PEG.

Our results shows that polymer surfaces can be functionalized with protein and cell adhesive or non-adhesive coatings using simple photochemical processing steps under chemically gentle conditions in aqueous medium. The method can be applied to a variety of protein types including antibodies and enzymes, as demonstrated in a previous publication³, with many possible applications in advanced cell culture and analysis in open or closed microsystems.

CONCLUSION

The presented facile method can introduce both low protein adsorbing base layers as well as the micropatterned bioactive protein coating using commercially available coupling chemistry in single process steps applicable to a multitude of polymer materials.

REFERENCES

1. Nilsson J. *et al.*, Anal. Chim. Acta 649:141-157, 2009
2. Larsen E.K.J. *et al.*, Biomacromolecules, 2014, doi: 10.1021/bm401745a
3. Larsen E.K.J. *et al.*, Lab Chip, 13:669-675, 2013, doi: 10.1021/bm401745a

ACKNOWLEDGMENTS

The authors thank Anne Henriksen for technical assistance in constructing the projection lithography setup.

We acknowledge financial support from the Danish Advanced Technology Foundation through the PILOC project (grant 064-2010-1) and the CELLGIGS project (grant 25-2011-5).



3D Plotting of biopolymer-based hollow and core/shell structures

Ashwini Rahul Akkineni¹, Yongxiang Luo¹, Tilman Ahlfeld¹, Anja Lode¹, Michael Gelinsky^{1*}

¹Centre for Translational Bone, Joint and Soft Tissue Research, Technische Universität Dresden, Dresden, Germany, michael.gelinsky@tu-dresden.de

INTRODUCTION

The application of rapid prototyping techniques for scaffold production provides potential solutions for repair and regeneration of defects associated with various tissues. Among other rapid prototyping techniques, 3D plotting (3DPI) is a fast, reliable and versatile method for processing of pasty materials into porous scaffolds using dispensing units. Using multiple dispensing channels, scaffolds consisting of more than one material can be processed. Scaffold preparation can be accomplished in principal at mild conditions allowing *in situ* colonisation with living cells during the fabrication process itself or plotting of delicate substances like growth factors. We have recently presented a method for 3DPI of hollow strands and 3D scaffolds thereof, consisting of highly concentrated alginate pastes¹. As advancement, we now have developed the processing of core/shell strands, consisting of two different biomaterials.

EXPERIMENTAL METHODS

3DPI was performed using a three channel BioScaffolder™ from GeSiM (Grosserkmannsdorf, Germany). As plotting pastes, several biopolymers and blends consisting of alginate, chitosan, gellan gum, collagen and gelatine as well as a pasty calcium phosphate bone cement² (InnoTERE, Radebeul, Germany) were applied. Conventional plotting of pure components or mixtures of the respective materials acts as control. For generation of hollow and core/shell strands, respectively, a self-made core/shell nozzle was used. Morphology of the strands and the respective 3D scaffolds were characterised microscopically and mechanical properties determined with a Zwick testing machine. Release experiments were carried out after loading of the respective scaffolds with BSA as a model protein during plotting.

RESULTS AND DISCUSSION

Manufacturing of hollow alginate strands and 3D scaffolds thereof could be realised with highly concentrated alginate pastes (16.7 wt.-%). After plotting in air, the alginate was cross-linked in an aqueous 0.5 M CaCl₂ solution, leading to stable structures with open lumina (Fig. 1). For plotting of hollow strands, the core-part of the core/shell nozzle was kept empty and only one of the three channels of the plotter was used.

By connecting the core-part of the nozzle with the second channel, the inner lumen of a hollow strand could be simultaneously filled with another pasty material; such core/shell strands could be used to manufacture 3D scaffolds (Fig. 2 shows an example, again consisting of alginate). 3D scaffolds consisting of core/shell strands have been manufactured from several material combinations (chitosan/alginate, gellan gum/alginate, gelatine/alginate and chitosan/CaP cement) and were char-

acterised concerning their structural and mechanical properties, as well as BSA release (used as model drug).

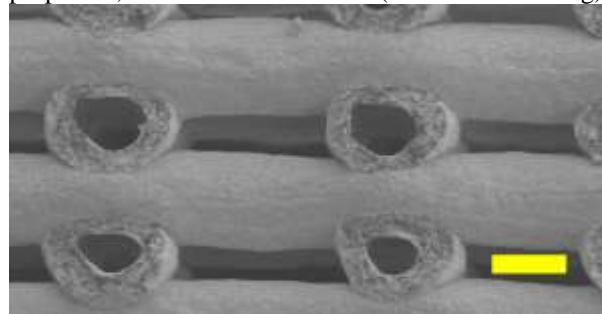


Fig. 1: SEM image of a 3D plotted scaffold, consisting of alginate hollow strands (scale bar: 200 µm)

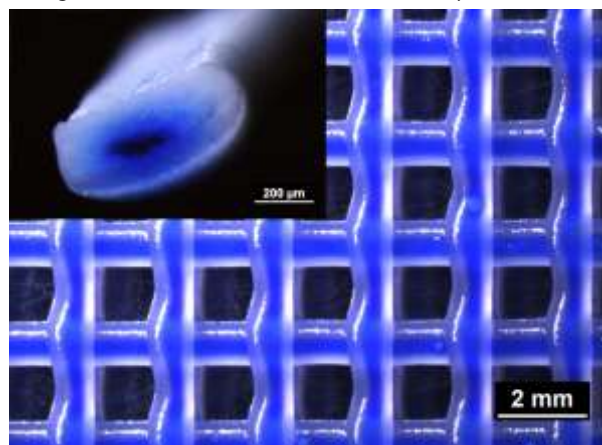


Fig. 2: 3D scaffold made of alginate-based core/shell strands; core part coloured with blue ink

Stiffness as well as porosity of novel core/shell scaffolds differed clearly from that of scaffolds, fabricated from both single components and homogeneous mixtures of the two materials. Loading of the core and shell part of these scaffolds with BSA leads to different release behaviour which facilitates the adjustment to the biological needs and opens up the possibility towards dual release of two different drugs from one scaffold.

CONCLUSION

3D plotting of hollow and core/shell strands provides a novel options to tailor the properties of 3D scaffolds and to create solutions for complex requirements. Mild processing conditions allow incorporation of sensitive substances like BSA during scaffold manufacturing.

REFERENCES

1. Luo Y. *et al.*, Adv. Healthcare Mater. 2:777-83, 2013
2. Lode A. *et al.*, J. Tissue Eng. Reg. Med. 2012 (in press; DOI: 10.1002/term.1563)

ACKNOWLEDGMENTS

The authors want to thank the Saxonian Ministry for Higher Education and Arts for financial support.



Magnetic PCL - based nanocomposites for soft/hard tissue regeneration

Ugo D'Amora^{1*}, Teresa. Russo¹, Roberto De Santis¹, Antonio Gloria¹, Monica Sandri², Anna Tampieri², L. Ambrosio¹

^{1*} Institute of Polymers, Composites and Biomaterials - National Research Council of Italy ugo.damora@unina.it

² Institute of Science and Technology for Ceramics - National Research Council of Italy

INTRODUCTION

Over the past years, great attention has been focused on polymer-based materials, as 3D scaffolds or injectable formulations, for the repair/regeneration of damaged tissue, benefiting from a multi-disciplinary approach.

The basic principles of magnetism and magnetic materials have been widely used in many modern medical applications (i.e. drug and gene delivery, hyperthermia treatment of tumors...). The possibility to extend these concepts to tissue engineering has opened an exciting wide research area of interest. In designing 3D magnetic scaffolds or injectable hydrogel-based nanocomposites with magnetic properties, the rationale should be summarized in the possibility to obtain structures that can be manipulated by means of magnetic force gradients in order to attract bioaggregates (i.e. vascular endothelial growth factors, VEGF) stimulating angiogenesis and bone regeneration. Furthermore, they can also be employed as hyperthermia agents able to deliver thermal energy to targeted bodies.¹

EXPERIMENTAL METHODS

In the field of hard tissue engineering, rapid prototyping technologies allow to obtain structures characterized by a precise control of its internal architecture (i.e. optimal size, geometry and spatial distribution of pores and interconnectivity).

Fully biodegradable and magnetic nanocomposite poly(ϵ -caprolactone)-based (PCL) scaffolds were designed layer-by-layer through "3D fiber deposition" technique, by alternatively plotting fibers along selected lay-down patterns. The performances of the designed scaffolds were assessed by means of experimental/theoretical *in vitro* investigations. In particular, morphological studies were performed through Micro-CT and SEM. Micro-, Macro- and Nano-mechanical analyses were carried out through compression, tensile and nanoindentation tests. Magnetic analysis was performed in order to assess the superparamagnetic behavior of these materials. Human mesenchymal stem cells were seeded onto the scaffolds in order to qualitatively study cell adhesion and spreading through confocal laser scanning microscopy. Cell viability/proliferation was assessed by using Alamar Blue assay, whilst cell differentiation was evaluated by the measurement of ALP activity.

In the field of soft tissue regeneration, different magnetic sodium alginate-based formulations were designed. Small amplitude oscillatory shear tests were carried out on the materials, in order to assess their viscoelastic properties. The dynamic moduli G' and G'' were evaluated in the investigated frequency range. The flow behaviour and functional injectability of the

proposed materials were also assessed through steady shear measurements and injectability tests.

RESULTS AND DISCUSSION

3D Magnetic scaffolds

Morphological analyses highlighted that 3D fiber deposition is a powerful tool to manufacture morphologically-controlled scaffolds.

Results from compression tests were consistent with FEM simulations highlighting a stress-strain curve which is similar to that of flexible foams, whilst results from tensile tests showed a ductile behaviour for both the polymeric and polymer-based fibers. In order to locally map mechanical properties, nanoindentation tests were performed showing interesting results in terms of hardness and reduced modulus. Confocal analyses have shown interesting results in terms of cell adhesion and spreading. An increase in adhered number and a more evident spreading of hMSCs have been evidenced, in comparison with results obtained from the neat PCL substrates. On the other hand, the Alamar Blue assay has provided a quantitative evaluation of cell proliferation and viability over the culture time. The results obtained in terms of percentage of Alamar Blue reduction were higher for nanocomposite scaffolds than for neat PCL.

Magnetic Hydrogels

Rheological measurements highlighted a shear thinning behaviour and mechanical spectra characterized by a crossover frequency. In particular, at low frequencies these materials show a predominant viscous character. Furthermore, injectability tests have provided load-displacement curves showing an initial linear region. After a maximum load occurred, load values sharply dropped, then fluctuating and reaching a plateau. At the end of the plateau-like region all the materials were completely injected.

CONCLUSION

3D Magnetic scaffolds should be considered as a potential alternative to bone graft substitute with attractive new performances. On the other hand, magnetic hydrogels should be employed in order to repair soft tissues.

REFERENCES

1. Gloria A. et al., J. R. Soc. Interface. 80 (10): 1, 2013.

ACKNOWLEDGMENTS

The authors would like to thank MAGISTER project (NMP3-LA-2008-214685), and FIRB MERIT (GAE: P0000570) for providing financial support to this project.



Artificial Ligaments From Poly(Vinyl Alcohol) Hydrogel Fibers

L. Corté¹, G. Zhang¹, F. Detrez¹, S. Cantournet¹, J.S. Bach² and D.N. Ku²

¹Centre des Matériaux Pierre-Marie Fourt, Mines-ParisTech, France, laurent.corte@mines-paristech.fr

²George W. Woodruff School of Mechanical Engineering, Georgia Institute of Technology, USA.

INTRODUCTION

Hydrogels can have unique biocompatibility and self-lubrication performances that are of outmost interest for tissue reconstruction¹. In particular, physically cross-linked networks of polyvinyl alcohol (PVA) form non-degradable biocompatible hydrogels, which have already shown a high potential in several soft-tissue replacement applications^{2,3}. For ligament or tendon repair, however, they are limited by insufficient tensile properties and their use is usually restricted to embedding or coating of a “dry” fibrous construct. Here, we explore the potential of spun PVA fibers that swell in water to form hydrogel fibers with a high degree of macromolecular orientation. By means of microscopic observations and mechanical experiments on both single fibers and fibrous constructs, we investigate how such anisotropic hydrogels provide new substitutes having a water content and a mechanical response close to those of native ligaments⁴.

EXPERIMENTAL METHODS

Materials

PVA monofilaments with water solubility above 90°C (Solvron®, Nitivy Ltd) were purchased in the form of 675-dtex threads composed of 15 twisted continuous fibers. Polyethylene fibers (Dyneema®, DSM) were purchased in the form of 1200-dtex threads composed of 4 braided bundles of 60 continuous fibers.

Tensile testing

Single fiber testing was performed on a Bose Electroforce apparatus immersed in water at 20°C. Local strain was measured by video extensometry. Swollen fibrous constructs were tested at 20°C in air with an Instron 5966 apparatus. Tests were repeated on at least 3 samples. Details are given in ref. 4.

RESULTS AND DISCUSSION

The studied fibers are made of PVA that is over 95% hydrolyzed, similar to other grades used for implant applications⁵. Below 90°C, these fibers swell in water to form stable insoluble hydrogel fibers containing about 40wt% of water, as illustrated by diameter measurements in Figure 1a. Microscopic observations under cross-polarized light and wide-angle X-ray scattering confirm that a strong macromolecular orientation is preserved after swelling.

Figure 1b shows the tensile response of one single hydrogel fiber after a couple of loading-unloading cycles to a maximum strain of 40%. The stiffness of these oriented fibers largely overcomes that of isotropic hydrogel films with a similar water content. Pure hydrogel constructs from those fibers exhibit a geometry, water content (~50wt%) and mechanical behavior close to those of native ligaments⁶. This is illustrated in Figure 1c for anterior cruciate ligament

(ACL) substitutes using twisted and braided constructs containing 3600 and 4500 PVA fibers, respectively.

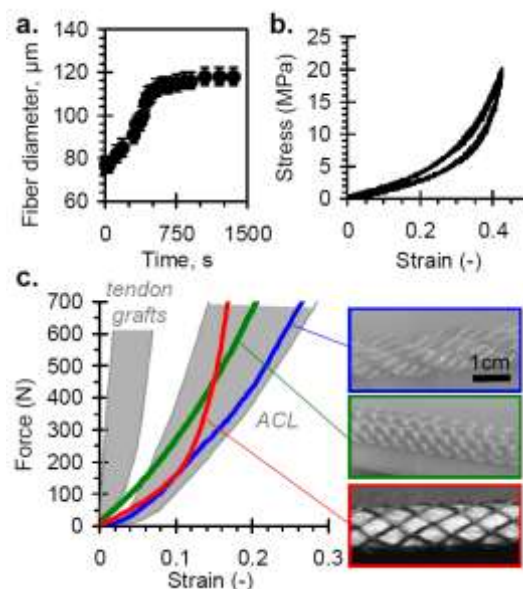


Figure 1: a. Swelling kinetics in water of a PVA fiber; b. Stabilized tensile behavior of one PVA hydrogel fiber; c. Tensile curves of PVA hydrogel fiber constructs (blue and green) and PVA hydrogel - UHMWPE constructs (red).

Smaller diameters and a safety factor in tensile strength are easily obtained when introducing polyethylene fibers. Using a hollow-braid design as shown in Figure 1c, the mechanics of these hybrid constructs can be modeled and adjusted to reproduce the non-linear tensile response with a toe region that is preferred for ligament reconstruction.

CONCLUSION

These results show that PVA hydrogel fibers with a 50wt% water content closely reproduce the large strain and non-linear elasticity of ligament tissues. This *in vitro* mechanical validation is a strong incentive to pursue more extensive *in-vivo* evaluations.

REFERENCES

1. Kopecek, *Biomater.* 28:5185-5192, 2007
2. Noguchi *et al.*, *J. Appl. Biomater.* 2:101-107, 1991
3. Sathe *et al.*, *J. Med. Devices* 1:105-112, 2007
4. Bach *et al.*, *J. Biomech.* 46:1463-1470, 2013
5. Baker *et al.*, *J. Biomed. Mat. Res. B* 100:1451-1457, 2012
6. Woo *et al.*, *Am. J. Sports Med.* 19:217-225, 1991

ACKNOWLEDGMENTS

The authors would like to thank CNRS, Mines-ParisTech, GeorgiaTech and the ANR EmergenceTec Programme (2008 LIGAGEL) for financial support.



Bioactivity of Medium Chain Length Polyhydroxyalkanoate Scaffold for Soft Tissue-Engineering Applications

Aitor Larrañaga^{1,*}, Jorge Fernández¹, Carmen Ronchel², José L. Adrio², Jose-Ramon Sarasua¹

¹Department of Mining-Metallurgy and Materials Science, Polymat, University of the Basque Country (UPV/EHU) Spain.

²NEOL BioSolutions S.A.
aitor.larranaga@ehu.es

INTRODUCTION

Polyhydroxyalkanoates (PHAs) are a group of biodegradable and biocompatible polyesters which are synthesized by several microorganisms as intracellular carbon and energy storage compounds¹. Medium chain length PHAs, that contain 6-14 carbon atoms in their backbone, have low crystallinity, low glass transition temperatures, low tensile strength and high elongation at break, making them elastomeric polymers². All these properties are highly appreciated for the regeneration of soft tissues, such as tendons or ligaments³. Incorporation of bioactive glasses to the aforementioned polymer matrices could improve their osteointegration with the bone tunnel⁴, avoiding the loosening of the graft and improving long-term survivability of the implant in tissue-engineering applications.

EXPERIMENTAL METHODS

In this work a poly(3-hydroxyoctanoate-co-3-hydroxyhexanoate) copolymer was employed as base material and fully characterized in terms of molecular weight, molecular organization, chemical structure and mechanical properties by means of gel permeation chromatography (GPC), nuclear magnetic resonance (NMR), Fourier transform infrared spectroscopy (FTIR) and tensile tests, respectively.

3-dimensional porous scaffolds were fabricated by solvent casting/particulate leaching. Bioglass 45S5 was incorporated to these scaffolds and a bioactivity study was performed by submerging the samples in simulated body fluid (SBF). The formation of a hydroxycarbonate apatite (HCA) layer was monitored by scanning electron microscopy (SEM), FTIR and X-ray diffractometry (XRD).

RESULTS AND DISCUSSION

Figure 1a shows the surface of an unloaded scaffold at the beginning of the bioactivity study. After 28 days submerged in SBF (Figure 1b) little changes were observed in the morphology of the surface and no deposits were discerned.

In Figure 1c a bioactive glass particle within the polymer matrix can be appreciated. Those samples containing 15 vol.% of bioactive glass developed a HCA layer on their surface after 7 days submerged in SBF (Figure 1d). These deposits became larger with immersion time and, at day 28 (Figure 1e and 1f) several deposits were observed, covering the surface of the scaffold.

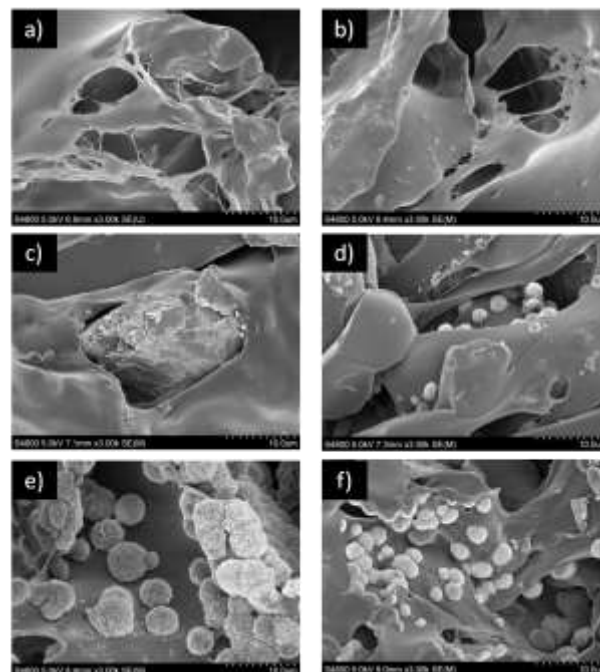


Figure 1.- SEM micrographs of unfilled scaffold at 0 (a) and 28 days (b) and scaffold filled with 15 vol.% of bioactive glass at 0 (c), 7 (d) and 28 (e and f) days.

The formation of a crystalline HCA layer on the surface of the samples was confirmed by means of FTIR and XRD (data not shown).

CONCLUSION

Scaffolds containing 15 vol.% of bioactive glass were able to develop a HCA layer on their surface only after 3 days submerged in SBF, whereas those scaffolds filled with 5 vol.% of bioactive glass needed 28 days. It can be concluded that addition of bioactive glass is a promising strategy to confer bioactivity to the employed scaffolds thus, improving the interaction with surrounding tissues.

REFERENCES

1. Lee SY. *Biotechnol.&Bioeng.* 49:1-14, 1996.
2. Rai R. et al., *Mater Sci Eng.* 72:29-47,2011.
3. Rathbone S. et al., *J Biomed Mater Res.* 93A:1391-1403, 2010.
4. Li H. et al., *Int Orthop.* 36:191-197, 2012.

ACKNOWLEDGMENTS

This project has been supported by Industrial Technological Center (CDTI) and IDEA agency. The authors also acknowledge the financial support from FEDER.



Biopolim-A



Bioinspired Composites: Link between Alignment Control, Platelets Content and Mechanical Properties

Laetitia Galea^{1,2*}, A. Studart³, Thomas Graule^{2,4} and Marc Bohner¹

¹*Skeletal Substitutes Group, RMS Foundation, Switzerland, ²Ceramic, TU Bergakademie Freiberg, Germany, ³Complex Materials, ETHZ, Switzerland ⁴Hochleistungskeramik, EMPA Dübendorf, Switzerland, laetitia.galea@rms-foundation.ch

INTRODUCTION

It is well known from composite technology that the higher the fraction of reinforcement phase, the stronger is the composite. This law is particularly well confirmed for long fiber composites. However, to obtain tough composites, short reinforcements are required. In this case, the strength also depends on the alignment and dispersion of the reinforcing elements. Indeed, if these parameters are insufficient, percolation occurs and the strength abruptly decreases. The strengthening effect is then limited to a given reinforcement fraction. Nature reaches very good alignment in ceramic-based composites, for example in nacre. In this case, 95vol% of ceramic does not weaken the tough structure thanks to its very high alignment. Natural materials are an inspiration source for engineers, because of outstanding combination of properties. However, we do not master nature's synthesis methods. That is why in this study, it was not attempted to mimic nature's route, but the natural structure was as much as possible imitated by the use of simple processing tools.

Solvent casting was used here to prepare composite films with aligned biodegradable ceramic platelets [1]. The fraction of reinforcement phase was increased until percolation was reached. This threshold was then increased by improving the alignment of the particles in a magnetic field [2].

THEORY

Based on the aspect ratio, s , of the reinforcing elements, the theoretical percolation limit, ϕ_p , can be calculated in function of the platelets mean angle, θ [3]:

$$\phi_p = \frac{1}{\theta \cdot s} \cdot p_c \quad (1)$$

Where p_c is a constant (0.718).

The theoretical reinforcement capacity, σ_{rel} , of a given fraction, ϕ , of a material can be estimated from its s [4]

$$\sigma_{rel} = \frac{\sigma_c}{\sigma_m} = \frac{s}{6} \cdot \phi + (1 - \phi) \quad (2)$$

with σ_{rel} the relative strength of the composite, σ_c , to the strength of the polymer matrix, σ_m .

Hence, the best performance of a composite obtained by a given method can be estimated based on the alignment degree achieved.

EXPERIMENTAL METHODS

Monetite (DCP, CaHPO₄) sub-micrometric platelets (with $s_{mean} = 15$) were produced according to [1]. Magnetization was obtained by nano iron oxide particles decoration [2]. The platelets were then mixed with a 2 wt-% chitosan solution and the slurries poured in Teflon molds. Drying was performed at 30 °C for non-magnetized samples. The magnetized samples were dried in ambient conditions in the vicinity of a magnet rotating around a vertical axis. All films were then

cured for 2h at 60 °C. Dog-bone samples were punched out of the films and tensile tested. Rocking curves were obtained by X-ray diffraction (XRD) to determine the mean platelet angle in the films, i.e. to measure the deviation from perfect alignment. Cross-sections were observed by scanning electron microscopy (SEM).

RESULTS AND DISCUSSION

As expected, the strength σ of the solvent casted (SC) composite films initially increased with increasing ceramic fraction ϕ . However, beyond a certain threshold value, σ decreased (Fig. 1, empty diamonds). In parallel, the alignment of the particles decreased (increase of mean platelet angle θ , Fig. 1, solid diamonds). Comparing θ of the different ϕ with the theoretical percolation limit θ_p confirmed that above this threshold, σ enhancement was impossible. Improving the alignment quality by the use of a magnetic field (M) (Fig. 1, solid squares) allowed increasing σ further with higher ϕ (Fig. 1, empty squares). However, percolation was still reached at much lower ϕ than in natural composites ($\phi_{nacre} = 95$ vol%, $\phi_{bone} = 50$ vol%). SEM observations bore out the differences measured by XRD.

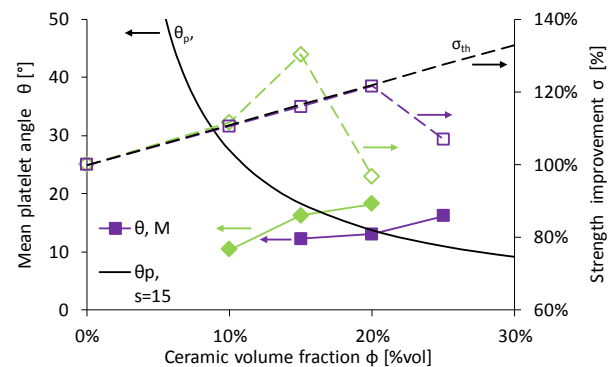


Figure 1: Mean platelet angle θ (left axis, solid lines) and relative tensile strength σ (right axis, dotted lines) as a function of ceramic fraction ϕ .

CONCLUSIONS

Classical composite synthesis methods do not reach nature's precision and scale, limiting the reinforcement possibilities in tough composites. In order to further improve strength and toughness of synthetic and biodegradable composite materials, new synthesis methods have to be developed to better control the architecture at the sub-micrometric level.

REFERENCES

1. Galea L. *et al.*, Biomaterials. 34:6388-401, 2013.
2. Erb R.M. *et al.*, Science. 335:199-204, 2012.
3. Lu C. and Mai Y.W., Phys. Rev. Lett., 95(8), 2005
4. Bonderer L. *et al.*, Science. 319:1069-73, 2008.



Development and Characterization of Bilayered Scaffolds Incorporated with Gold Nanoparticles as Potential Skin Substitutes

Ömer Aktürk¹ and Dilek Keskin^{1,2}

¹Department of Engineering Sciences, Middle East Technical University, Turkey

² Center of Excellence in Biomaterials and Tissue Engineering Research Center, Turkey, e129050@metu.edu.tr

INTRODUCTION

In this study, it was aimed to fabricate nanofibrous bilayered scaffolds incorporated with gold nanoparticles (AuNPs). AuNPs were utilized to understand the effect of nanoparticles on electrospinning of collagen fibers, their effect on fiber morphology and on other characteristics of the scaffolds as a potential skin substitute. It was reported that AuNPs have antibacterial and antioxidant properties; they increase cell and protein adhesion and cell proliferation on the scaffolds¹; enhance mechanical properties and resistance against degradation². Therefore, they were thought to be promising materials in skin tissue engineering.

EXPERIMENTAL METHODS

Sericin/collagen membranes³ were combined with collagen nanofibrous matrices produced by electrospinning method to obtain bilayered collagen matrices (BLCM) with AuNPs. Bilayered scaffolds cross-linked with glutaraldehyde (GTA) were characterized with the following tests: Equilibrium degree of swelling (EDS), water vapor transmission rate (WVTR), ultimate tensile strength (UTS), elongation at break (EAB), elastic modulus (E), hydrolytic and enzymatic degradation, morphological analysis (SEM), AuNPs size determination (TEM) and cytotoxicity (MTT assay) tests.

RESULTS AND DISCUSSION

AuNPs having a very homogenous size and shape distribution were synthesized at different average sizes (10-50 nm) and AuNPs having sizes greater than 20 nm were selected to be used in scaffolds regarding the preliminary cytotoxicity tests (data not shown). AuNPs could be entrapped inside the nanofibers successfully after blending with collagen/PEO (1:2.5) electrospinning solutions (Fig. 1).

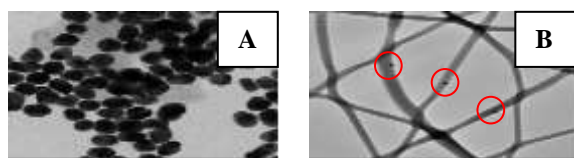


Figure 1. TEM micrographs showing AuNPs A) size (36.95 ± 4.05 nm) and shape (mostly spherical) and B) the distribution inside the collagen nanofibers. Red circles indicate the AuNPs.

Nanofibrous matrices with homogenous fiber diameter (262 ± 29 nm) and shape distribution (cylindrical) were obtained. Cross-linking treatment did not considerably change the porous structure of BLCM (Fig. 2), but increased the resistance of the scaffolds to both hydrolytic and enzymatic degradation.

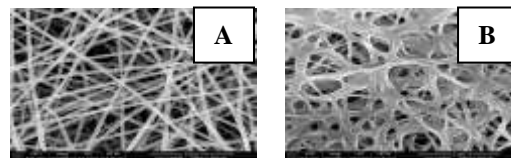


Figure 2. SEM micrographs showing collagen nanofibers A) untreated and B) GTA cross-linked

The main properties of the BLCM as a potential skin substitute were summarized in Table 1. Biocompatibility tests on 3T3 fibroblasts and keratinocytes showed that BLCM incorporated with AuNPs were not cytotoxic (Fig. 3). Antibacterial tests, in vitro cell adhesion and proliferation tests are still being carried out.

Table.1. Properties of BLCM

EDS (g/g)	WVTR (g/m ² /day)	UTS (MPa)	EAB (%)	E (MPa)
3.58 ± 0.58	1358.75 ± 82.62	3.36 ± 1.29	23.37 ± 8.35	40.82 ± 14.19

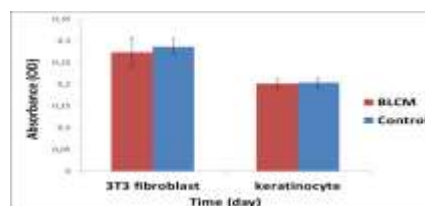


Figure 3. Cytotoxicity test (MTT assay) results on 3T3 fibroblasts and keratinocytes. BLCM: The extract medium of BLCM scaffold with AuNPs. Control: The group containing no AuNPs.

CONCLUSION

Selected AuNPs were successfully incorporated into collagen nanofibrous scaffolds. AuNPs enhanced the morphology of collagen nanofibers. BLCM incorporated with AuNPs were found to be biocompatible. According to characterization tests, BLCM incorporated with AuNPs could be a promising skin substitute.

REFERENCES

1. Chou C.W. *et al.*, J. Biomed. Mater. Res. A. 84:785-94, 2008.
2. Deeken C.R. *et al.*, J. Biomed. Mater. Res. B. Appl. Biomater. 96:1-9, 2011.
3. Akturk O. *et al.*, J. Biosci. Bioeng. 112: 279-288, 2011.

ACKNOWLEDGMENTS

We would like to thank TUBITAK (Project no: 111M 810) for providing financial support to this project.



Multi-scale geometric control of mechano-transduction and cell behaviour using polymer brushes

John Connelly¹, Jenny Malmström², Duncan Sutherland³ and J. E. Gautrot¹

¹*Institute of Bioengineering, Queen Mary University London, UK, j.gautrot@qmul.ac.uk

² School of Chemical Sciences, University of Auckland, New Zealand

³ Interdisciplinary Nanoscience Center, Aarhus University, Denmark

INTRODUCTION

The fate and behaviour of stem cells is determined by their microenvironment: a combination of biochemical (e.g. extra-cellular matrix, neighbouring cells, growth factors, cytokines), and physical cues (e.g. matrix mechanical properties, geometry and topography). Cell adhesion to extra-cellular matrix (ECM) is particularly important for regulating stem cell fate decision and tissue homeostasis in physiological as well pathological scenarios. In turn, this may have important implications for the design of biomaterials and engineered platforms in the field of regenerative medicine. Our work has focused on the role of micro- to nano-scale geometrical properties of the matrix on the control of the cell microenvironment and its impact on cell fate decision. To do so, we have designed well-defined engineered platforms using a combination of micro- to nano-patterning and polymer brush chemistry.

EXPERIMENTAL METHODS

Our work has focused on the design, preparation and characterisation of polymer brushes displaying ultra-low fouling properties (e.g. poly(oligo ethylene glycol methacrylate) or zwitterionic brushes), as well as novel strategies to bio-functionalise polymer brushes. In addition, we developed photo-activated chemical method to control such chemistry, thereby affording photo-dynamic platforms. Using a combination of micro- and nano-patterning approaches, we used the polymer brush systems we developed to control the behaviour of epidermal stem cells at different length scales, from multi-cellular cluster formation to individual nascent cell adhesions and studied the impact of such geometrical cues on stem cell fate decision.

RESULTS AND DISCUSSION

At the multi-cellular level, we observed that the adhesive geometrical landscape was responsible for the correct partitioning of epidermal stem cells and differentiated cells into distinct compartments, independently from the rate of differentiation¹. This phenomenon was mediated by the adhesive landscape

but controlled by adherens and desmosomal junctions. The micro-epidermis that we generated also mimicked correctly cell partitioning in squamous cell carcinoma, hence providing a novel strategy for cell assay design.

At the single cell level, we showed that epidermal stem cell spreading and shape were important determinants of fate decision^{2,3}. When cells were allowed to spread on large (50 µm diameter) or stretched adhesive islands (small 30 µm diameter with high shape aspect ratio), they differentiated less frequently. We found that this was a direct result of the rearrangement of the cell cytoskeleton and the redistribution of the pools of F- and G-actin, via the MAL/SRF pathway.

Finally, we found that controlling adhesive patterns with sizes in the 100-3000 nm range allowed the control of cell spreading and that this correlated with reduced differentiation. We found that such nano-scale effects were not mediated by the alteration of global protein sequestration to adhesion sites, but rather by the change in diffusion dynamics of the adapter protein vinculin.

CONCLUSION

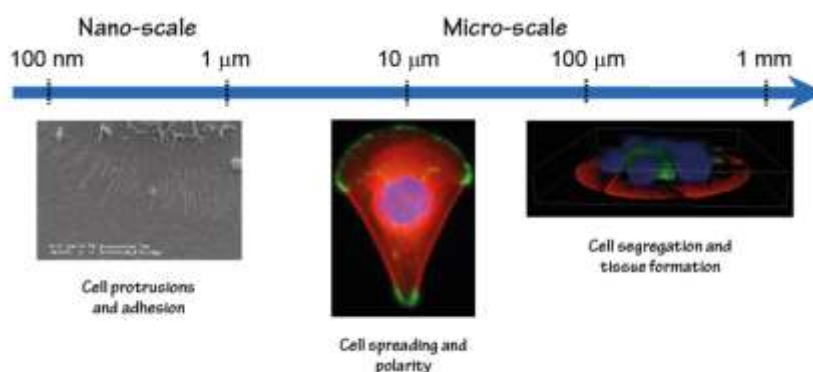
Our results show that simple geometrical control of the adhesive landscape at the micro- to nano-scale guides stem cell fate decision and we identified some of the key molecular players involved in these processes. These results are important as they can serve as a basis for the development of novel cell-based assays and tissue culture platforms for applications in regenerative medicine.

REFERENCES

1. Gautrot. *et al.*, Biomaterials. 33:5221-5229, 2012.
2. Connelly *et al.*, Nat. Cell Biol., 12:711-U177, 2010.
3. Tan *et al.*, Integ. Biol., 5:899-910, 2013.

ACKNOWLEDGMENTS

Funding from the Royal Society and the Engineering and Physical Sciences Research Council (EP/J501360/1) are acknowledged.



Is the presence of multinucleated giant cells within the implantation bed of natural-based biomaterials physiological? Assessment of *in vitro* and *in vivo* screening of three different porcine collagen membranes by means of multichamber three-dimensional systems

Shahram Ghanaati^{1,2}, Carlos Mota³, Mike Barbeck^{1,2}, Patrick Booms^{1,2}, Robert Sader², Clemens van Blitterswijk³, Lorenzo Moroni³, C James Kirkpatrick¹

1 Institute of Pathology, University Medical Center of the Johannes Gutenberg University Mainz, Langenbeckstraße 1, 55101 Mainz, Germany

2 Department for Oral, Cranio-Maxillofacial and Facial Plastic Surgery, Medical Center of the Goethe University Frankfurt, Theodor-Stein-Kai 7, 60596 Frankfurt/Main

3 University of Twente, Tissue Regeneration Department, Enschede, The Netherlands
E-Mail: shahram.ghanaati@kgu.de

INTRODUCTION

Currently porcine-based collagen membranes are frequently applied in oro-maxillofacial surgery. All of these membranes are claimed to be biocompatible and “ideal” for soft and bone tissue regeneration. However, little is known about the tissue response to these materials after their *in vivo* implantation. The present study was designed to analyze the tissue reaction of three different collagen materials within a multichamber three-dimensional (3D) system, which we already showed to be useful for discovering regenerative medicine therapies (1). This system allows the screening of different experimental conditions *in vivo* while reducing the animal number with comparable results to single material implantation (2,3).

EXPERIMENTAL METHODS

Rapid prototyping (1) was used to generate a 3D 3x3 multichamber (1,5 x 1,5 mm) made by 300PEOT55PBT45. Each device row was filled with one collagen material. Plain devices served as controls. In a parallel study, the same collagen membranes incubated with human monocytes were implanted into SCID-mice. Histological analysis and established histomorphometrical methodologies were applied after early and late points, i.e. from 10 to 60 days.

RESULTS AND DISCUSSION

In mice the devices were intact without any visible material breakdown. Three different cellular reactions to the materials were distinguished and differed in their inflammatory cell pattern, i.e.

mononuclear vs. multinucleated giant cell reaction and *in vivo* vascularization. *In vitro* cell-based experiments were performed within the device comparable to those in standard well-plates. Human monocytes were involved in material degradation and also enhanced implantation bed vascularization. The 3D multichamber system delivered comparable results to those observed with the same materials used as plain scaffolds. This system permits *in vitro* and *in vivo* investigations as well as characterization of material-specific inflammatory responses. This innovation could serve as a platform to help keep essential *in vivo* experiments to an ethically acceptable minimum.

CONCLUSION

It has to be questioned to what extent the observation of multinucleated giant cells within the implantation bed of natural based collagen membranes can be considered as a physiological reaction. Multinucleated giant cells are known to be key markers of the foreign body reaction.

REFERENCES

- 1) Higuera GA et al. Integrative Biology (2013)
- 2) Ghanaati et al. Biomed Materials (2010)
- 3) Ghanaati S. Acta Biomaterialia (2012)

ACKNOWLEDGMENTS

The authors would like to thank the Osteology Foundation as well as the University Frankfurt for providing financial support to this project”.



In vitro Bioactivity and Cell Differentiation Properties of Nanobioceramics with Different Nanostructure

Cristian Covarrubias^{1*}, Fabiola Arroyo¹, Consuelo Balanda¹, Isabel Celhay¹, Juan P. Rodríguez², Ana M. Pino², Carla Urra², Mario Díaz¹, Miguel Neira¹, Pablo Caviedes³

¹Laboratorio Nanobiomateriales, Instituto de Investigación en Ciencias Odontológicas, Facultad de Odontología, Universidad de Chile. ccovarru@u.uchile.cl

²Laboratorio de Biología Celular, INTA, Universidad de Chile.

³ICBM, Facultad de Medicina, Universidad de Chile.

INTRODUCTION

Bioactive glass and hydroxyapatite are ceramic materials well known for their osteogenic bioactive properties¹. Bone-repair commercial products use these bioceramics with micrometer particle size and completely amorphous structure. Nowadays advances in nanomaterial synthesis, offer the possibility of preparing bioceramics with controlled nanometric particle size and nanostructure. However, the effect of the different nano-scale properties on the bioactive response of the nanobioceramics has been less studied¹. In this work, hydroxyapatite (n-HA), bioactive glass (n-BG), nanoporous bioactive glass (MBG) and nanoporous bioactive glass nanoparticles (n-MBG) were synthesized and their bioactivity were evaluated in simulated body fluid (SBF) and by osteogenic differentiation of stem cells.

EXPERIMENTAL METHODS

n-HA, n-BG, MBG and n-MBG particles were synthesized by using sol-gel based methods^{1,2}. MBG was prepared by combining evaporation induced self-assembly (EISA) technique with sol-gel method. Nanostructure and particle size of bioceramics were characterized by X-ray diffraction (DRX), high-resolution transmission electron microscopy (HRTEM), and Attenuated Total Internal Reflectance Infrared Spectroscopy (ATR-FTIR). Total specific surface area of bioceramics was determined by nitrogen sorptometry.

The ability of the biomaterials to induce the formation of bone-like apatite was evaluated in SBF. Apatitic phase was analysed by scanning electron microscopy (SEM) coupled with X-ray energy dispersive analysis (EDX) and XRD. Osteogenic differentiation properties were studied by culturing the bioceramics with stem cells isolated from dental pulp (DPSCs). Osteogenic differentiation was assessed through early osteogenic marks such as alkaline phosphatase (ALP) enzymatic activity, and Runx2 and Osx gene expression.

RESULTS AND DISCUSSION

The particle size of the nanobioceramics were the following: n-HA~40 nm, n-BG~70 nm, MBG~20 μ m, n-MBG~100 nm. XRD and HRTEM analyses confirmed that MBG and n-MBG present an internal nanostructure constituted of highly ordered porous of 4 nm in diameter. The specific surface area of n-HA, n-BG, MBG, and n-MBG were 67 m²/g, 77 m²/g, 400 m²/g, and 440 m²/g, respectively.

Bioactive glass ceramics promotes a faster formation of apatite in SBF than n-HA, which is attributed to the more amorphous and reactive nature of the bioactive glasses. Particularly, n-BG and n-MBG particles accelerate the apatite mineralization process at short time of immersion in SBF (12 h). These nanosized particles also produce a higher activity of ALP (Fig. 1) as well as a high-level expression of osteogenic differentiation genes (Runx2) when cultured in presence of DPSCs.



Fig. 1 Qualitative ALP activity (staining) of DPSCs cultured in the presence of the nanobioceramics.

Although micro-sized MBG presented a high internal surface area due to its nanoporous structure, external surface area of the nanoparticles seem to be a more decisive factor on their bioactivity properties. Higher activity of n-BG and n-MBG particles can be attributed to their more rapid dissolution rate as consequence of its high external surface area exposed to the physiological medium, which is determined by the nanometric dimensions of the particle.

CONCLUSION

Nanoscale structure of bioceramics affects their bioactivity and osteogenic differentiation properties. It is concluded that nanometric particle size is a more decisive property than internal nanostructure on the bioactive response of the bioceramics with nanoscale dimensions.

REFERENCES

- Valenzuela F. *et al.*, J. Biomed. Mat. Res. B. Appl. Biomater. 100:1672-1682, 2012.
- Wu C. *et al.*, J. Mater. Chem. B, 1:2710-2718, 2013.

ACKNOWLEDGMENTS

The authors thank FONDECYT research project 1130342, U-Red NanoBiomat (U. Chile), and CONICYT/CONACYT Bilateral project for providing financial support to this investigation. C. Covarrubias also thank Dirección de Investigación, Facultad de Odontología, Universidad de Chile for the travel grant.

The Modelling of Self-Inflating Tissue Expanders

X. Min and J. T Czernuska

Department of Materials, University of Oxford, United Kingdom, xue.min@materials.ox.ac.uk

INTRODUCTION

Tissue expansion is a common clinical technique that generates tissue. It was first described by Neumann in a case of ear reconstruction from traumatic amputation in 1956.[1] Swan et al. developed a novel anisotropic self-inflating poly(NVP-co-MMA) hydrogel expander by hot-pressing[2]. This type of expander can absorb body fluid and swell in only one direction. This present study indicates the possibility of making a bilateral anisotropic expanding tissue expander, which expands in two directions. It is therefore essential to have a discussion on the necessity of bilateral expanders before the experimental research. In order to compare the discrepancy of tissue generating capacity given by different swelling pattern, a series of expander models in syndactyly has been designed and calculated.

EXPERIMENTAL METHODS

In the case of simple syndactyly, a section of fused fingers is selected and simplified into two cylinders bound with a layer of tissue. The expander models can therefore be placed between the tissue and phalanxes. The core idea in this study is to compute the final size of expander for generating the tissue required by a reconstructive surgery. The area of required tissue equals the area of tissue in the normal state minus the area of tissue in the syndactyly state. Therefore we obtain and compare the size of different swollen expanders.

RESULTS AND DISCUSSION

Three kinds of expanders have been studied: isotropic (Figure 2(a)), unidirectional (Figure 2(b)) and bilateral (Figure 2(c)). For the purposes of calculation, several conditions have been examined.

Firstly, for a certain expander, its insertion site can influence the final results. The expander can be placed in the middle, on the top or on both sides of phalanxes (shown in Figure 1).



Figure 1: Location of insertion

Second is the insertion pattern. The expanders can be placed as a single expander or a series of discrete expanders, as shown in Figure 1(b) and Figure 2(c) respectively. Discretely inserted expanders are designed to be spheres or cylinders, as shown in Figure 2.

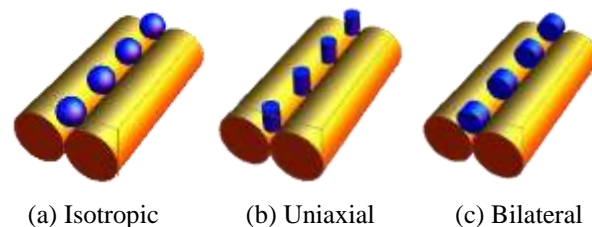


Figure 2: Discrete insertion of three types of expanders

Lastly, the coherence of tissue is considered. The area of tissue obtained by expansion can be affected due to the contact between tissue and expanders. For the sake of modelling, we take these two extreme cases into account: non-sticky tissue (Figure 3(a)) and complete adhesive tissue mode (Figure 3(b)). As a result, we have generated a possible range that should bound the real cases.

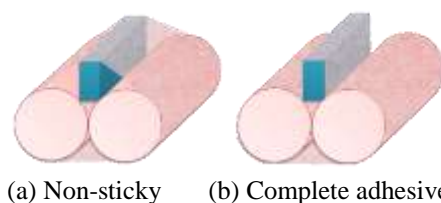


Figure 3: Contact modes between tissue and expander

According to the computational results of models that have included the above assumptions and situations, we obtained: (1) bilateral expander requires a smaller radius to generate the same amount of tissue as an isotropic expander; (2) uniaxial expander could have smaller sizes than bilateral expander, but only with a relatively high ratio of its height to radius. Such a sacrifice of connection area with tissue could result in tissue necrosis in practice; (3) insertion on both sides (top and bottom as in Figure 1(c)) is the most efficient way for a surgery.

CONCLUSION

These results should provide the surgeon a better insertion pattern for syndactyly. Bilateral self-inflating expanders could have advantages over other self-inflating expanders in syndactyly. Therefore, it is necessary to have a further study on the bilateral self-inflating tissue expanders.

REFERENCES

1. Neumann, C.G., Plastic and reconstructive surgery, 19:124-130, 1957
2. Swan, M.C. et al, University of Oxford, 2007

ACKNOWLEDGMENTS

The authors would like to thank China Scholarship Council for providing financial support for this project.

Protein nano-carriers from clicked glycosaminoglycan block copolymers

Ramon Novoa-Carballal^{a,b}, Carla Silva^a, Stephanie Möller^c, Matthias Schnabelrauch^c, Rui L. Reis^a and Iva Pashkuleva^a

^a 3B's Research Group – Biomaterials, Biodegradables and Biomimetics, University of Minho, Headquarters of the European Institute of Excellence on Tissue Engineering and Regenerative Medicine, AvePark, 4806-909 Taipas, Guimarães, Portugal; ICVS/3B's – PT Government Associate Laboratory, Braga/Guimarães, Portugal; e-mail: rnovoasc@yahoo.es

^b Department of Organic Chemistry and Center for Research in Biological Chemistry and Molecular Materials (CIQUS), University of Santiago de Compostela, Jenaro de la Fuente s/n, 15782 Santiago de Compostela, Spain.;

^c Biomaterials Department, INNOVENT e.V., Pruessingstrasse 27 B, 07745 Jena, Germany

INTRODUCTION

Nowadays, the treatment with conventional drugs is shifting towards therapeutic proteins that are exquisite specific and selective in executing diverse biofunctions. Glycosaminoglycans (GAGs) are natural partners of proteins in the extra cellular matrix: they stabilise and/or protect proteins from denaturation and enzymatic degradation; play a role in proteins storage or mediate their binding to specific receptors. Inspired by the native environment of proteins, we propose the use of sulfated (GAG) diblock PEG copolymers (GAG-*b*-PEG) for the encapsulation of proteins into nanosized interpolyelectrolyte complexes (IPECs).

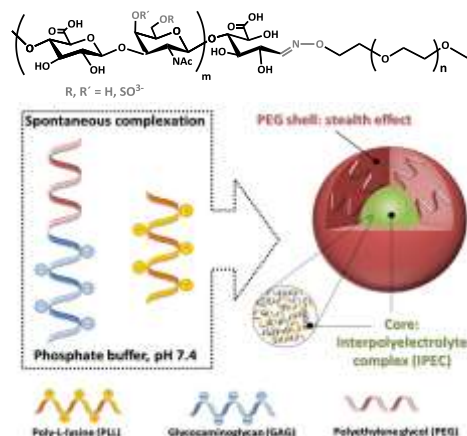


Figure 1. Complexation process between GAG-*b*-PEG and (PLL).

EXPERIMENTAL METHODS

The block copolymers were synthesised following previously described procedure for hyaluronan-*b*-PEG.¹ NMR and GPC were used to confirm the structure and molecular weight of the final products. IPECs were formed by adding a solution of poly-L-lysine (PLL) or FGF-2 in phosphate buffer pH 7.4 I=10 mM to the solution of GAG-*b*-PEG under vigorous stirring. IPECs were characterised by dynamic light scattering, nanoparticle tracking analysis and electron microscopy.

RESULTS AND DISCUSSION

Oxime click reaction was used for the synthesis of diblock copolymers of polyethylene glycol (PEG) and glycosaminoglycans (GAG) with different molecular weight (Mw) and degree of sulfation (DS) (Table 1). We have tested several ratios between the PLL and the obtained copolymers. The characteristic of the PLL/GAG-*b*-PEG complexes at minimal zeta potential and low PDI are included in Table 1. As can be seen, IPECs with tunable size at the nanometric scale and narrow distribution were obtained.

Table 1. Properties of GAG-*b*-PEG block and IPECs prepared from them with PLL

GAG _{nk} - <i>b</i> -PEG ^a	GAG 10 ⁻³ Mn, [g/mol] (Mw/Mn)	DS	R _h [nm]	PDI	ζ potential
CS _{2.7k} - <i>b</i> -PEG	2.7 (1.20)	0.7	208	0.49	0.4
CS _{14k} - <i>b</i> -PEG	14 (1.39)	0.9	40±1	0.05±0.04	-1.2
CS _{24k} - <i>b</i> -PEG	24 (1.33)	0.9	94±8	0.08±0.02	0.3
HAS _{12k} - <i>b</i> -PEG	12 (1.80)	1.7	22±1	0.09±0.02	-0.1
HAS _{36k} - <i>b</i> -PEG	36 (1.50)	3.0	25±1	0.16±0.05	0.4

^a subindex denotes the molecular weight of GAG block (kDa), PEG Mw is 5 kDa; CS- Chondroitin sulphate, HAS-sulphated hyaluronic acid.

Moreover, the size can be controlled by DS: highly sulfated GAGs form the smallest complexes that are stable to at least 500 mM ionic strength. Formation of IPECs was also achieved with a human protein FGF-2 with 98±7 nm radius and PDI 0.22±0.02 and CS_{12k}-*b*-PEG.

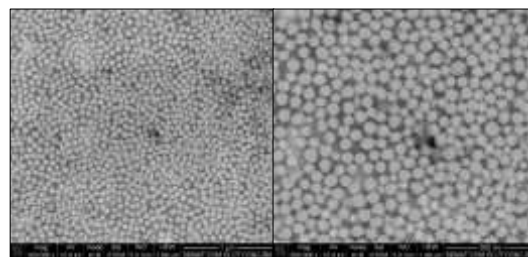


Figure 2. STEM images of the IPECs from PLL and CS_{12k}-*b*-PEG

CONCLUSION

The ability of sulphated GAG-*b*-PEG copolymers to carry positively charged proteins has been demonstrated by their assembly with poly-L-lysine as a model protein. The formed IPECs have neutral charge, nanometric size and stability at physiological ionic strength - properties that contribute to prolonged blood circulation times and thus, more effective delivery to the targeted site. Moreover, the complexation with basic fibroblast growth factor (FGF-2) demonstrates the feasibility of these copolymers for proteins encapsulation. These properties together with the possibility for tunable size emphasise the enormous potential of sulfated GAG-*b*-PEG copolymers for the engineering of delivery systems for positively charged proteins.

ACKNOWLEDGMENTS

The authors would like to acknowledge the European Union's Seventh Framework Programme POLARIS and NORTE-07-0124-FEDER-000016.

REFERENCES

1. Novoa-Carballal, R.; Müller, A. H. E. Chem Commun. 48, 3781-3, 2012.

Treatment of a degenerative/pro-inflammatory intervertebral disc organ culture with Chitosan/Poly- γ -glutamic acid nanoparticles carrying and anti-inflammatory drug

Graciosa Q. Teixeira^{1,2,3}, Catarina L. Pereira^{1,3}, Hans-Joachim Wilke², Anita Ignatius², Mário A. Barbosa^{1,3}, Cornelia Neidlinger-Wilke², Raquel Goncalves¹

¹Institute of Biomedical Engineering (INEB), Universidade do Porto, Portugal, ²Institute of Orthopaedic Research and Biomechanics, Center for Musculoskeletal Research, University of Ulm, Germany, ³Instituto de Ciências Biomédicas Abel Salazar (ICBAS), Universidade do Porto, Portugal, graciosa.teixeira@ineb.up.pt

INTRODUCTION

Low back pain related with intervertebral disc (IVD) degeneration is a major cause of lack to work in industrialized countries. Inflammation has been correlated with disc degeneration, although its role in discogenic pain remains controversial.¹ Here we purpose first to establish a pro-inflammatory disc organ culture model. Our goal is to evaluate a new anti-inflammatory therapy based on Chitosan (Ch)/Poly-(γ -glutamic acid) (γ -PGA) nanoparticles (NPs) with an anti-inflammatory drug (Diclofenac, Df) incorporated, previously developed by us.² Previous studies have shown that this delivery system was efficient in reducing macrophage activation in vitro.

EXPERIMENTAL METHODS

Bovine caudal disc punches cultures (DMEM with 5% FBS and 5 mM glucose, 400 mOsm and 6% CO₂ during 5 days) were needle-punctured and stimulated with: Lipopolysaccharide (LPS) 10 μ g/mL, or with Interleukin-1 β (IL-1 β), 10 and 100 ng/mL, for 48h. The effect of the pro-inflammatory stimulus was evaluated by gene expression of pro-inflammatory cytokines (IL-6, IL-8), metalloproteases (MMPs, MMP1 and MMP3), and extracellular matrix (ECM) proteins (collagen type II (Coll II), Aggrecan). Cell viability was analyzed by LIVE/DEAD assay while metabolic profile of the cultures was traced by Glucose/Lactic acid monitoring. As an anti-inflammatory therapy, Ch/Df/ γ -PGA NPs prepared by co-acervation method², were added to disc cultures 3h after pro-inflammatory stimulus. Untreated samples were used as controls. The effect of the anti-inflammatory therapy was evaluated by gene expression and by Prostaglandin E₂ (PGE₂) production.

RESULTS AND DISCUSSION

To establish a pro-inflammatory ex vivo model of IVD, LPS and IL-1 β treatments were compared. IL-1 β -treated discs showed a statistically significant up-regulation of the pro-inflammatory cytokines (IL-6 and IL-8), MMPs expression (MMP1 and MMP3), while ECM proteins (Coll II and Aggrecan) were significantly down-regulated (Fig.1). For all the conditions tested, cells remain viable and presented similar metabolic activity. IL-1 β stimulation was selected as the most adequate approach to study anti-inflammatory therapies for IVD. Regarding the effect of NPs as Df-delivery system in the IVD organ cultures, preliminary results showed that, IL-6 and MMP1 were down-regulated, when compared to IL-1 β stimulated groups, suggesting that this treatment not only reduces inflammation, but also can delay and/or decrease matrix proteins degradation.

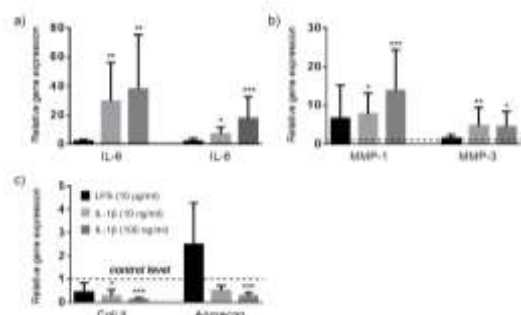


Fig.1. Quantitative analysis of pro-inflammatory markers of IVD organ cultures with pro-inflammatory stimulus (LPS and IL-1 β). mRNA expression of IL-6 and IL-8 (a), MMP-1 and MMP-3 (b) and Coll II and Aggrecan (c). Levels of mRNA were normalized to GAPDH and to the control group. Results are shown as Mean \pm StDev (n=4-10). * = p<0.05; ** = p<0.025; *** = p<0.001.

PGE₂ levels were reduced in the presence of Df-NPs for both IL-1 β concentrations, indicating that, in this range of concentrations, the effect of released Df is not IL-1 β concentration-dependent. We have compared the Df-NPs injection in IVD with Df-NPs in IVD culture medium. The results indicate that injection group induces a better response (Fig.2).

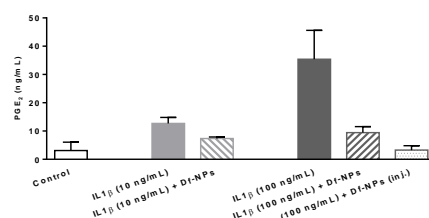


Fig.2. PGE₂ concentration detected at day 8, in culture medium supernatant, in the presence and absence of pro-inflammatory stimulus (IL1 β) and anti-inflammatory treatment with Ch/Df/PGA NPs. Results are presented as Mean \pm StDev (n=2-4).

CONCLUSION

An ex vivo model of degeneration/inflammation in IVD was here established, with increased levels of pro-inflammatory cytokines and MMPs and reduced ECM protein levels. This approach is suitable for in vitro testing of regenerative or anti-inflammatory strategies of disc degeneration. Ch/Df/ γ -PGA NPs revealed to be a promisor anti-inflammatory therapy to IVD.

REFERENCES

- Vadalà G. *et al.*, J Tissue Eng Regen Med. 2013.
- Pereira C.L. *et al.*, J Mater Sci Mater Med, 23: 1583-91, 2012.

ACKNOWLEDGMENTS

This work was financed by PEST funds, FCT, AO Foundation, Luso-German Integrated Actions 2012: CRUP/DAAD, and by the German Spine Foundation.



Detection of C-reactive protein using highly dispersible gold nanoparticles bearing phospholipid block copolymers

Yasuhiko Iwasaki^{1*}, Toshihiro Kimura¹, Masaki Orisaka¹, Hideya Kawasaki¹, Tatsuro Goda² and Shin-ichi Yusa³

¹Faculty of Chemistry, Materials and Bioengineering, Kansai University, Japan, E-mail: yasu.bmt@kansai-u.ac.jp

²Institute of Biomaterials and Bioengineering, Tokyo Medical and Dental University, Japan

³Department of Materials Science and Chemistry, Graduate School of Engineering, University of Hyogo, Japan

INTRODUCTION

Gold nanoparticles (AuNPs) are promising candidates as nanoscopically assembled materials for numerous applications due to the unique electronic and optical properties that result from their nanometer size and narrow size distribution.¹

In this study, the reducible biomimetic polymer-protected AuNPs were prepared by autoredution without the addition of any reducing agent, showing excellent colloidal stability at a high salt concentration and over a wide pH range. Label-free detection of an inflammation marker, C-reactive protein (CRP), was demonstrated by using the aggregation of the AuNPs.

EXPERIMENTAL METHODS

Poly(2-methacryloyloxyethyl phosphorylcholine)-*b*-poly(*N*-methacryloyl-(*L*)-tyrosine methylester) (PMPC-*b*-PMAT; Fig. 1) was prepared by reversible addition fragmentation chain transfer (RAFT) polymerization. For preparing AuNPs by autoredution, HAuCl₄/phosphate buffer saline (PBS) was added to the polymer aq. solution at different concentrations under vigorous stirring. NaOH aq. solution was introduced, and the reaction was allowed to proceed under vigorous stirring at 60 °C for 15 h. Characterization of AuNPs bearing PMPC-*b*-PMAT was performed by transmission electron microscopy (TEM), dynamic light scattering (DLS) analysis, thermogravimetric analysis (TGA) and UV-Vis absorption spectroscopy.

Detection of CRP with AuNPs bearing MPC block copolymers was demonstrated in pH 5.5. The AuNPs suspension was mixed with 500 µL of 2 mM CaCl₂ in 2-morpholinoethanesulfonic acid and monohydrate (MES) buffer or only MES buffer (Ca²⁺ free) in a plastic tube. Appropriate amounts of CRP/HEPES and MES buffer were then added to the tube. After all samples were mixed, the tubes were stored at room temperature and optical analyses for AuNPs were performed.

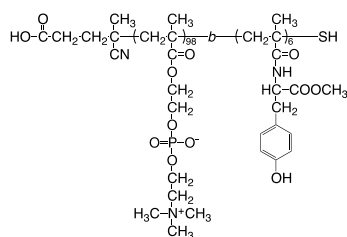


Fig. 1 Chemical structure of PMPC-*b*-PMAT

RESULTS AND DISCUSSION

To obtain PMPC-*b*-PMAT, PMPC was synthesized as a macro chain transfer agent (macro-CTA). The degree of polymerization (DP_n) of macro-CTA was adjusted to

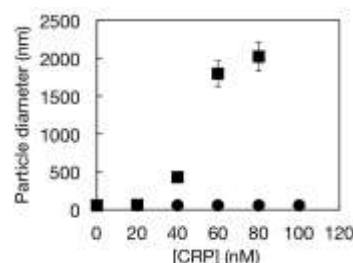


Fig. 2 Detection of CRP by PMPC-*b*-PMAT-protected AuNPs: (A) Change in the size of AuNPs in contact with CRP for 30 min. ■: [Ca²⁺] = 1 mM, ●: [Ca²⁺] = 0 mM

98. Block copolymerization of MAT proceeded at a [MAT]/[macro-CTA] ratio of 20. Under our experimental conditions, DP_n of MAT was 6, which was lower than that of the target DP_n.

The colloidal stability of the AuNPs bearing PMPC-*b*-PMAT was excellent. Both size and the absorption band (λ_{LSPR}) from the localized surface plasmon resonance (LSPR) of AuNPs did not change with additional increments of ion strength upto ~ 3.8 M NaCl in the aqueous medium.

Fig. 2 shows the CRP-concentration dependence on the aggregate sizes formed by the AuNPs and CRP. The pH of the medium was adjusted to 5.5 to facilitate CRP-PC interaction. When Ca²⁺ was not in the medium, the size of PMPC-*b*-PMAT-protected AuNPs did not change regardless of CRP concentration. In contrast, the AuNPs formed remarkable aggregates in the presence of 1.0 mM Ca²⁺ and the size of the aggregates increased with an increase in the concentration of CRP over the range of 0 to 80 nM. The acceptable detection levels were below 20 nM.

CONCLUSION

Autoredution of aurum ions with the reducible MPC block copolymers results in the generation of various, highly dispersible AuNPs, which can be used for biomedical applications. As proof of this concept, the label-free detection of CRP as an inflammation biomarker was successfully demonstrated by using the biomimetic block copolymer-protected AuNPs.

REFERENCES

1. Daniel M.-C. *et al.*, Chem. Rev. 104: 293, 2004.

ACKNOWLEDGMENTS

This study was supported by a Grant-in-Aid for Scientific Research on Innovative Areas "Nanomedicine Molecular Science" from MEXT, Japan (#24107524) and MEXT-supported Strategic Research Foundation Grant-aided Project for Private Universities, 2010-2014.



Antibody coated microparticles to fabricate functional 3D constructs in combination with cells

C. A. Custódio^{1,2}, V. E. Santo^{1,2}, M.B. Oliveira^{1,2}, M. E. Gomes^{1,2}, R. L. Reis^{1,2}, J. F. Mano^{1,2}

1-3B's Research Group – Biomaterials, Biodegradables and Biomimetics, University of Minho, AvePark, Zona Industrial da Gandra, S. Cláudio do Barco, 4806-909 Caldas das Taipas – Guimarães, Portugal.

2-ICVS/3B's, PT Government Associated Laboratory, Braga/Guimarães, Portugal. jmano@dep.uminho.pt

INTRODUCTION

The development of instructive substrates with application in tissue regeneration has become the focus of intense research in the last years¹. This work reports a new system that is simultaneously bioinstructive, due to the presence of immobilized growth factors (GFs) that control biological function, and bioresponsive as it promotes the assembly into microgels using cells as attachment points. It is well established that platelets are an important source of autologous and complex mixture of GFs that can modulate cell proliferation and differentiation². Herein we propose antibody-conjugated chitosan-based microparticles (μPs) as a method to select specific GFs from platelet lysates (PLs), which will then be used to modulate cell function.

EXPERIMENTAL METHODS

Microparticles (μPs) were fabricated by spraying a chitosan solution (1.5% w/v) through an aerodynamically assisted jetting equipment (Nisco Encapsulation Units VAR J30) into a solution of NaOH (1M). μPs were functionalized with anti-human Platelet Derived Growth Factor-BB (PDGF-BB) antibody through carbodiimide (EDC) chemistry. Briefly, EDC was used to activate the carboxylic groups of the antibodies. The activated samples were mixed with the μPs with gentle rotation for 3 hours at 4°C. PLs were obtained from different platelet collections performed at Instituto Português do Sangue (Porto, Portugal). Collected samples were subject to three repeated temperature cycles (– 196 °C; 37 °C). The selection of PDGF-BB, was obtained by mixing the μPs with the PLs at 4°C for 15min. μPs were washed and resuspended with human adipose stem cells (hASCs). Morphological analysis of the constructs was done by Scanning Electron Microscopy (SEM) and confocal microscopy. In vitro studies were performed for up to 7 days to analyze cell viability and proliferation.

RESULTS AND DISCUSSION

Cells present surface receptors that recognize and bind to PDGF-BB. Thus functionalized μPs with PDGF-BB will work as binding points for cells, leading to the formation of a 3D hydrogel-like structure while simultaneously promoting cell proliferation and differentiation within the construct (Fig. 1A).³ The capture of PDGF-BB from PLs was assessed by ELISA assay on the remaining lysates solution post-incubation with the μPs. Results show a decrease in the amount of this GF in solution when compared to TFG and VEGF. This results support our hypothesis that the functionalization of the μPs was effective and that they are selective for PDGF-BB. The assembly of the microgels was followed for up to 24 hours. Controls in absence of cells or by using non-modified μPs were

used. Results show (Fig.1B) that after 90min, a 3D structure is already formed on its own. On the other hand, controls were not able to form a stable structure. Biological activity of the obtained constructs was assessed up to 7 days by alamar blue assay and DNA quantification. Results show an increase in cell proliferation and activity up to 7 days. SEM and confocal images revealed a homogeneous 3D construct with hASCs entrapped within the μPs. (Fig. 1C)

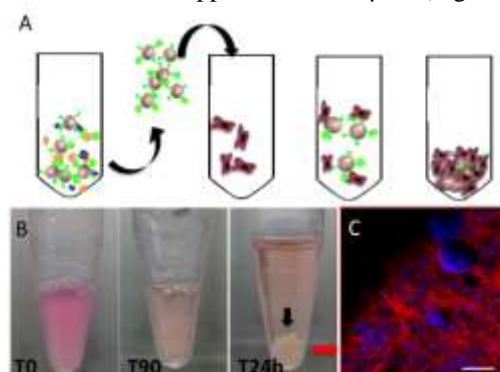


Figure 1. A) Schematic representation of the strategy. μPs modified with specific antibodies recruit GFs of interest from PLs. μPs are mixed with cells. A construct is formed through cell-particle interaction. B) Images of the assembly process at different time points. C) Confocal image of the construct after 3D in culture. Scale bar 100 μm

CONCLUSION

The present study addresses the hypothesis that the combination of μPs tailored with specific GFs and stem cells can generate bioactive microgels with tunable cell function through cell crosslinking. The obtained construct simultaneously provides support for stem cell proliferation, as well as localized and sustained presentation of factors to modulate cell function. Different formulations with a combination of GF can be used for a particular application based on the desired composition and intended cellular function. Furthermore, these instructive microgels may be used as an injectable system for non-invasive tissue engineering applications.

REFERENCES

1. Custódio, C.A. *et al.*, Adv. Healthcare Mater. doi: 10.1002/adhm.201300603, 2014.
2. Santo, V. E. *et al.*, J Tissue Eng Regen, 6:47-59, 2012
3. Custódio, C.A. *et al.*, Adv. Funct. Mater., 24:1391–1400, 2014

ACKNOWLEDGMENTS

FCT through the Doctoral grant with the reference SFRH/BD/61390/2009. European Union's Seventh Framework Programme (FP7/2007-2013) under grant agreement number REGPOT-CT2012-316331-POLARIS



Regulating Cellular Function Through Physicomechanical Engineering of the Nanobiointerface

Manus Biggs¹, Shalom Wind², Matthew Dalby³ & Abhay Pandit¹

¹ Network of Excellence for Functional Biomaterials, National University of Ireland, Galway, Ireland

² Department of Applied Physics and Applied Mathematics, Columbia University, NY, USA

³ Centre for Cell Engineering, Institute of Molecular, Cell and Systems Biology, University of Glasgow, UK
manus.biggs@nuigalway.ie

INTRODUCTION

The extra-cellular matrix represents a biological hierarchical nanocomposite and studies with mimetic nanomaterials have been shown these materials to have regulatory effects over stem-cell adhesion¹, migration², proliferation³, signalling⁴, genetic expression and stem cell fate⁵. Consequentially, biomaterial design has focused on the introduction of nanoscale elements that elicit directed cellular behaviour while imparting structural and mechanical advantages to induce the formation of functional tissues.

Adherent cells are complex, self-sustaining units that require extracellular matrix (ECM) anchorage to proliferate and undergo differential function. That nanoscale features can affect differential cellular behaviour through integrin-mediated cell adhesion is evident from studies with fabricated topographical features, however the mechanical properties of a cell's environment are also important factors in determining cell behaviour and ultimately, phenotype.

Thus far, many aspects of the cellular rigidity-sensing mechanism, particularly in reference to tactile cell sensing of discrete localised areas of increased or decreased rigidity are not understood. Here we discuss the roles of nanotopography and heterogeneous nanorigidity on stem-cell adhesion and differential function.

EXPERIMENTAL METHODS

Electron-beam lithography and di-block co-polymer self-assembly methods coupled with reactive ion etching were employed to fabricate nanomodified materials. Importantly, we describe a novel system driven by direct focused electron-beam patterning for the fabrication of soft (350 kPa) planar PDMS substrates, which present ordered submicron scale differential rigidity. Substrates were shown to undergo a linear increase in rigidity with E-beam dose, up to 3.5 MPa. We subsequently explored the response of human mesenchymal stem cells (MSC) isolated from bone marrow aspirates, to these materials.

RESULTS AND DISCUSSION

MSC's cultured on heterogeneous rigidity-patterned substrates were observed to colocalise focal adhesion formation to the stiffer regions, which correlated with spot stiffness (**Fig. 1**). However, focal adhesion colocalization was reduced by decreasing the spot diameter from 2 μm – 100 nm. Focal adhesions formed on regions of increased modulus were associated with an increase in paxillin recruitment, indicating a role in force-mediated focal adhesion reinforcement. Our studies suggest that cellular rigidity sensing and focal

adhesion reinforcement is initiated on discrete regions of modulated rigidity measuring $\sim 0.5 \mu\text{m}$, and that a 3x increase in elastic modulus is required to initiate differential focal adhesion on discrete regions of altered rigidity.

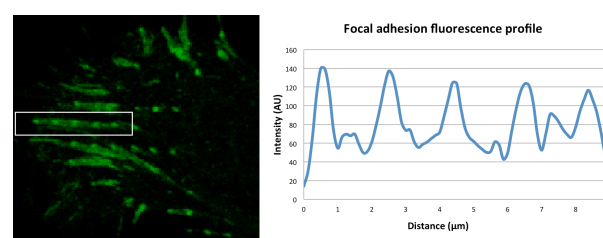


Fig. 1. (A) Trailing edge of an MSC cultured on patterned heterogeneous rigidity 2 μm spots. Green (paxillin). (B) Intensity profile of focal adhesion associated paxillin spanning five rigid spots.

CONCLUSION

MSC's respond to submicron scale topography and rigidity through differential focal adhesion formation. Furthermore, our studies indicate a submicron scale for a rigidity dependent contractile unit of the focal adhesion with which cells perceive discrete regions of altered rigidity. Future work will investigate the role of heterogeneous rigidity coupled with nanoscale topography in modulating the cellular phenotype and the translation of nanoscale topography to electrically conducting systems with aim to fabricating next-generation neuroelectrodes.

REFERENCES

- Biggs, M. J. P. et al. M. J. Journal of Orthopaedic Research. 2007: 25(2), 273-282.
- Lamers, E. et al. Eur Cell Mater. 2012: 13(23) 182 194.
- Hu, J. et al. BMC Musculoskelet Disord. 2014: 15(1), 114.
- Biggs, M. J. P., et al. Biomaterials. 2009: 30(28), 5094-5103.
- Ha, S. W. et al. Acs Nano. 2014 (in press).

ACKNOWLEDGMENTS

MB is a Science Foundation Ireland SIRG COFUND fellow (11/SIRG/B2135). The work was funded in part by the NIH Common Fund Nanomedicine Programme (PN2EY016586). He would like to acknowledge Ms. Catalina Vallejo-Giraldo and Dr. Parvaneh Mokarian.

The Response of Mesenchymal Stromal Cells to Strontium-Substituted Bioactive Glasses

M. Santocildes-Romero¹, P. Hatton¹, R. Goodchild¹, A. Crawford¹, I. Reaney² and C. Miller^{1*}

^{1*}School of Clinical Dentistry, The University of Sheffield, UK, c.a.miller@sheffield.ac.uk

²Department of Materials Science and Engineering, The University of Sheffield, UK

INTRODUCTION

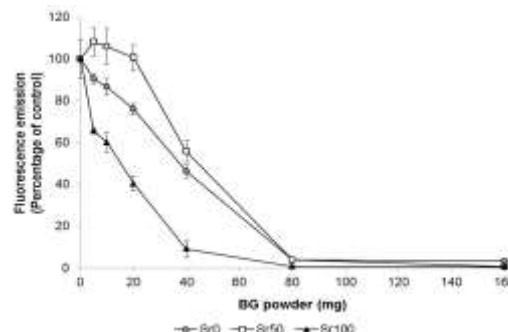
It has been reported that strontium-substituted bioactive glasses (Sr-BGs) may promote osteoblast proliferation and inhibit osteoclastic activity in bone cell line studies *in vitro*¹. These observations suggest that Sr-BGs may form the basis for the development of improved bone graft substitutes, an area of growing clinical need. To further explore their potential, the aim of this study was to investigate the effect of particulate Sr-BGs on bone marrow mesenchymal stromal cells (BM-MSCs) differentiation.

EXPERIMENTAL METHODS

Three Sr-BG compositions were fabricated by a melt-quench route based on 45S5 bioactive glass, in which calcium was substituted by Sr on molar proportions of 0 (Sr0), 50 (Sr50) and 100% (Sr100). Sr-BG powders (<45 µm, particle size) were produced through milling and sieving. The glasses were characterised using X-ray diffraction (XRD) analysis and differential thermal analysis (DTA). Glass solubility was measured using a method based on ISO6872, while density was calculated and then determined using the Archimedes method. Cytotoxicity of Sr-BG dissolution products was assessed using monolayer cultures of rat BM-MSCs (n=3) exposed to 5-160 mg of glass powders placed in tissue culture inserts for 72 h. A resazurin dye based assay was then used to determine metabolic activity by measuring fluorescence emission. Finally, the osteogenic effect of Sr-BGs was studied by measuring the levels of expression of 6 genes associated with the process of osteoblastic differentiation: *Bmp2*, *Runx2*, *Alpl*, *Col1a1*, *Bglap* and *Spp1* using real-time PCR (rt-PCR). The analyses were performed on monolayer cultures of BM-MSCs (n=3) exposed to 20 mg of Sr-BG powders placed in tissue culture inserts for 1, 3, 6 and 14 d and cultured using cell culture media with and without osteogenic factors.

RESULTS AND DISCUSSION

XRD spectra confirmed that the three Sr-BG compositions were amorphous and showed no significant crystalline phases. The diffraction maximum was observed to move to smaller values of angle 2θ with increasing strontium substitution. DTA showed a decrease of glass transition temperature with strontium substitution, from 525°C for Sr0 to 479°C for Sr100. Solubility and density were observed to increase linearly with strontium substitution. These results, in line with previously published work^{2,3}, suggested an expansion of the glass network in order to accommodate the larger Sr cation, increasing glass solubility and potentially affecting their cytotoxicity and bioactivity.



Metabolic activity of cultured BM-MSCs generally decreased in the presence of up to 80 mg of all Sr-BG powders used. Sr100 exhibited the greatest metabolic inhibition, suggesting a greater cytotoxic effect associated with the increased solubility. Sr50 was the most biocompatible composition evaluated in this part of the study.

Data from rt-PCR analyses showed that the presence of Sr-BG powders stimulated the up-regulation of all osteogenic genes studied. It may be that the presence of Sr in Sr50 and Sr100 BGs resulted in the enhanced up-regulation of genes *Alpl*, *Col1a1* and *Bglap* compared with Sr0.

CONCLUSION

The incorporation of Sr in the composition of BGs resulted in detectable changes in their physical properties, due most likely to the expansion of the glass network, potentially affecting their biological properties. Sr-BG dissolution products appeared to stimulate the up-regulation of several genes associated with the osteoblastic differentiation of BM-MSCs. In conclusion, these are highly promising biomaterials for use in bone regeneration applications, including as a component of a scaffold for bone tissue engineering.

REFERENCES

1. Gentleman E. *et al.*, Biomaterials. 31:3949-56, 2010.
2. O'Donnell M.D. *et al.*, Acta Biomater. 6:2382-5, 2010.
3. Fredholm Y.C. *et al.*, J. Non-Cryst. Solids. 356:2546-51, 2010.

ACKNOWLEDGMENTS

The authors would like to thank the EPSRC for providing financial support for this study through the Doctoral Training Grant. The presenting author is a member of MeDe Innovation.



Unsupervised techniques unexpectedly highlight steroid biosynthesis in the global response of human MSC to strontium-substituted bioactive glasses

H. Autefage¹, E. Gentleman^{1,2}, E. Littmann¹, M. Hedegaard¹, T. von Erlach¹, M. D. O'Donnell¹, M. Hedegaard¹, D. Winkler³, M. M. Stevens¹

¹Department of Materials, Imperial College London, UK; ²Craniofacial Development and Stem Cell Biology, King's College London, UK; ³Materials Science and Engineering, CSIRO, Clayton VIC, Australia
eileen.gentleman@kcl.ac.uk

INTRODUCTION

An important aim of regenerative medicine is to design smart biomaterials to trigger specific biological responses. Subsequent testing often focuses on assessing anticipated cell behaviour such as differentiation and/or tissue formation. Although this strategy allows for assessment of specific outcomes, the global cell response to and mechanism of action of many biomaterials remains unknown. Unsupervised techniques that allow for assessment of global response may highlight a biomaterial's mechanism of action and allow for prospective material design.

There is a need for smart biomaterials as alternatives to autogenic/allogenic bone grafts. Strontium ranelate reduces vertebral and non-vertebral fractures in osteoporotic women¹. The incorporation of strontium into bioactive glasses (SrBG) has been shown to upregulate bone formation *in vitro*^{2,3}. However, how biomaterials such as BG affect the global biological response and the means by which strontium influences bone formation are largely unknown.

EXPERIMENTAL METHODS

As a model for this alternative approach to examine cell response to biomaterials, we exposed human bone marrow-derived mesenchymal stem cells (hMSC – 3 donors) to cell culture medium conditioned with BG with and without strontium (0, 10, 100 mol%). hMSC were exposed for 30 minutes, 2 hours, 4 hours, 48 hours, 5 days or 10 days. Whole genome microarray analyses were carried out using an Affymetrix ST 1.0 gene array and data analysed using functional annotation clustering and other novel, unbiased approaches. Further investigations of cell response were performed using quantitative real-time PCR, In-Cell Western blotting, high resolution Raman spectroscopy mapping, and TIRF microscopy.

RESULTS AND DISCUSSION

Rather than directly upregulating hMSC osteoblast differentiation, which functional annotation clustering noted as only a secondary effect, SrBG strongly regulated the steroid biosynthesis and mavelonate pathways (Table 1). Moreover, a novel and unbiased sparse selection (expectation maximization) algorithm analysis revealed strong regulation of: *FDFT1*, encoding squalene synthase, a key protein of the isoprenoid pathway which controls the synthesis of sterol metabolites; *TMEM147*, a transmembrane protein found in the ER that binds to cholesterol; and *PMP22*, a glycoprotein associated with lipid rafts.

Functional annotation clusters	Enrichment Scores	p-values
Sterol/steroid biosynthesis and metabolic process	10.02	2.7E-13
Protein-DNA complex/nucleosome	3.55	1.9E-05
Histone H2A/citullination	3.06	1.6E-04
Fatty acid biosynthesis	2.76	1.7E-04
Cell cycle process	2.61	7.0E-04
Mitosis / cell division	2.38	6.0E-04
Steroid biosynthesis/endoplasmic reticulum membrane	2.27	1.6E-07
Sterol transport and homeostasis	1.75	1.5E-02
Bone development/osteoblast differentiation	1.74	2.7E-03
Fatty acid biosynthetic and metabolic process	1.48	4.8E-03
DNA repair metabolic process	1.40	1.8E-02
Condensed nuclear chromosome	1.37	2.8E-02

Table 1: Functional annotation clustering of differentially expressed gene clusters in Sr100- and control-treated hMSC.

Changes in gene expression (confirmed by RT-PCR and WB) were translated to modifications at the protein level. Sr100 treatment increased cellular and membranous cholesterol content and membrane lipid raft content (Figure 1).

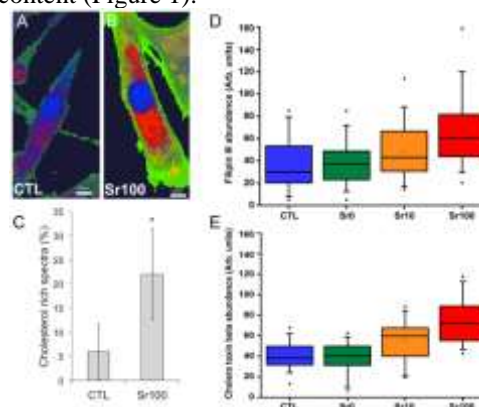


Figure 1: A) & B) False-colour Raman spectral maps of hMSC cultured in basal (CTL) and Sr100-conditioned medium. Areas with cholesterol-rich spectra appear red. C) Quantification of cholesterol-rich spectra. D) & E) Quantification of Filipin III (cholesterol) and cholera toxin β abundance (lipid raft content) from TIRF images.

CONCLUSION

These data highlight an unexpected potential mechanism of action for SrBG on osteoprogenitor cells via upregulation of the steroid biosynthesis and related pathways. They also show the potential for unsupervised approaches to transform materials design, particularly in bone regeneration.

REFERENCES

1. Meunier PJ, *et al.*, N. Engl. J. Med., 350(5):459-68, 2004.
2. Gentleman E, *et al.*, Biomaterials. 31(14):3949-56, 2010.
3. O'Donnell MD, *et al.*, J. Mater. Chem. 20(40):8934-41, 2010.

ACKNOWLEDGMENTS

The authors wish to thank the Technology Strategy Board for providing financial support for this project. E.G. acknowledges funding from the Wellcome Trust. M.M.S acknowledges the Medical Engineering Solutions in Osteoarthritis Centre of Excellence funded by the Wellcome Trust and the EPSRC for funding HA.

Application of FIBSEM and XRM to study the occlusion of dentine tubules from a calcium sodium phosphosilicate bioactive glass (NovaMin™)

Richard Langford^{*a}, Jonathan Earl^b, and Arno Merkle^c

^a*Cavendish Laboratory, University of Cambridge, UK., rml42@cam.ac.uk*

^b*Jonathan Earl, GlaxoSmithKline Consumer Healthcare, Weybridge, UK.*

^c*Carl Zeiss X-ray Microscopy, Pleasanton, USA.*

INTRODUCTION

Bioactive glasses are reported to bond to bone or dentine by forming a carbonated hydroxyapatite layer. Here we report on the study of a calcium sodium phosphosilicate bioactive glass of the 45S5 composition, trade name NovaMin™, and sold commercially as the active ingredient in toothpaste for the treatment of dentine hypersensitivity. Here we report on the use of various modern electron and x-ray microscopy (XRM) techniques used to study both the tubule occlusion and the remineralisation of demineralised dentine.

EXPERIMENTAL METHODS

Sound human molars were ethically acquired and were prepared into dentine discs in the standard way. These were then demineralised with 5% w/w citric acid for 30 seconds to open the dentine tubules before treatment by immersion in artificial saliva containing or not the calcium sodium phosphosilicate bioactive glass for up to 2 hours.

RESULTS AND DISCUSSION

Focussed Ion Beam Scanning Electron Microscopy (FIBSEM) was used to prepare site specific cross sections and to perform slice and view for 3D chemical and structural analysis. Figure 1 shows a secondary electron image of a FIB cross-section. The occluding of the tubule by the nucleated hydroxyapatite-like material can be seen. It was found to extend down to the depth of the cross-section (20 µm). The corresponding untreated demineralised samples showed a non mineralised band at the top of the sample that was 500 nm thick with no layer formed on the surface or occluding material.

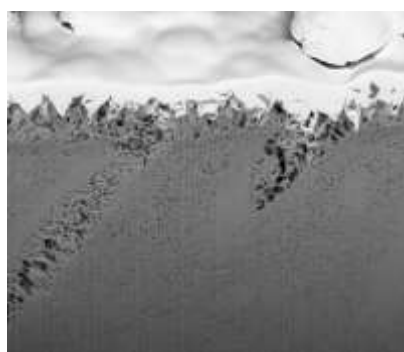


Fig. 1 – FIBSEM cross section through a NovaMin™ treated dentine sample

FIBSEM milling was also used to prepare a 30 µm square cube for x-ray tomography. The cube was cut out from the dentine substrate using the FIB and mounted onto a support pin by means of platinum

deposition within the FIBSEM. Figure 2 shows the 3D rendering of the non destructive x-ray tomography data. This data in conjunction with the FIB slice and view data has been used to quantify properties such as the volume filling of the tubules and the material mass density within the remineralised zone.

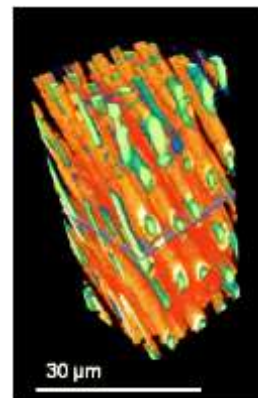


Fig. 2 – 3D rendering of nanoscale non-destructive XRM data

For high resolution analysis the FIB was used to prepare site specific TEM lamellae through the treated layers and the occluded material. High resolution nanoelectron diffraction and chemical analysis (EDS and EELS) showed that the material formed on the surface and in the tubules was hydroxyapatite-like. A detailed study of the remineralisation of the demineralised zone, the interface between the formed hydroxyapatite like material on the surface and the dentin matrix and the material nucleated onto and around the bioactive glass itself will be presented.

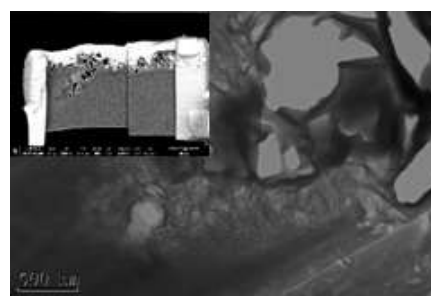


Fig. 3 – Bright field image of a FIB prepared lamella through a dentinal tubule showing the occluding material (insert shows a SE image of the whole lamella showing the material formed at the surface).

CONCLUSION

Various electron microscopy techniques have shown that the material of the layer occluding the tubules is hydroxyapatite-like and that it also results in remineralisation of demineralised dentine.

Acknowledgments: This study was funded by GlaxoSmithKline

Osteoblast-like cell reactions to soluble silicate ions released from bioactive glass and siloxane-containing vaterite

Akiko Obata^{1*}, Norihiko Iwanaga¹, Hiroataka Maeda¹, and Toshihiro Kasuga¹

¹Graduate School of Engineering, Nagoya Institute of Technology, Japan

obata.akiko@nitech.ac.jp

INTRODUCTION

Inorganic ions released from bioactive glasses have been reported to enhance several functions, such as proliferation, differentiation and mineralization, of osteogenic cells.¹ Soluble silica and calcium ions released from 45S5 type bioactive glass (BG) show the up-regulation effects on osteoblast activities. Many reports demonstrated that the two ions released from other bioceramics and glasses showed the similar effects on osteoblast activities. There are, however, differences in the Si ion concentration which is needed for the enhancement or inhibition of the cell functions between the reports. In addition, it was unclear whether the ions show the same stimulation effects on different types of osteoblast-like cells and the effects depend on ionic state of the ions.

Siloxane-containing vaterite (SiV) powders have been developed using aminopropyltriethoxysilane (APTES) as a siloxane source in our previous work.² SiV and poly(lactic acid) composites were prepared for the use in bone tissue regeneration. Mouse osteoblast-like cell (MC3T3-E1) showed a higher proliferation and differentiation abilities on the composite in comparison with a composite prepared with conventional vaterite.³ The soluble silica ions released from the composites were expected to stimulate the cell functions.

The aim of the present work is to estimate the effects of soluble silica ions released from BG or SiV on two different types of osteoblast-like cell functions.

EXPERIMENTAL METHODS

SiV powders were prepared with the carbonation method reported previously.² 150 g of calcium hydroxide, 60 ml of APTES and 2 L of methanol were mixed with the addition of CO₂ gas for 75 min at a rate of 120 L/h, and then dried at 110 °C, resulting in the formation of SiV powders (≈1.5 μm in diameter). The silicon concentration in the resulting powder was found to be 2 wt% by X-ray fluorescence analysis.

BG was prepared by a melt-quenching method. SiO₂, CaHPO₄·2H₂O, CaCO₃ and Na₂CO₃ powders were mixed and then melted at 1400 °C for 1 h. The obtained meltage was quenched on a stainless steel plate, and then pulverized (< 53 μm).

0.5 g of SiV or BG powders were soaked in 15 ml of a culture medium containing 10 wt% of foetal bovine serum and then incubated in a CO₂ incubator for 24 h. After the incubation, the sample was filtrated using a 0.2 μm PTFE filter. The obtained solution was diluted with the culture medium to set its Si concentration at 10 – 50 ppm.

Mouse osteoblast-like cells (MC3T3-E1) or human osteoblast-like cells (SaOS-2) were culture using each

Si-containing medium. The cell morphology was observed by staining actin in the cell with Alexa Fluor 488 Phalloidin. The cell proliferation was evaluated by colorimetry.

RESULTS AND DISCUSSION

The morphology of MC3T3-E1 and SaOS-2 cells was changed in both of the Si-containing medium, depending on the Si concentration. For example, in the case of 30 ppm, MC3T3-E1 cells exhibited a spindle shape in control (conventional medium) and SiV-medium, whereas they did a small radial shape in BG-medium. SaOS-2 cells showed a radial shape in control and BG-medium, whereas they did a spindle shape in SiV-medium. These changes in the cell morphology were found to depend on the Si concentration of each medium.

Results of the proliferation test for MC3T3-E1 cells demonstrated that the medium with 20 ppm of Si ions enhanced their proliferation in both cases of SiV and BG-medium. However, the dependence of the proliferation of SaOS-2 cells on the Si concentration was not the same as that of MC3T3-E1 cells. Thus, the stimulation effects of the soluble silica ions differed between different types of osteoblast-like cells.

The adhesion and proliferation of both cells were changed with the changes of not only Si concentration in the culture medium but also the silicate ion source materials. The silicate ion released from SiV contains amino groups in its structure and must form *T* groups. On the other hand, the silicate ion released from BG must form *Q* groups. These differences in ionic state of the silicate ions were supposed to relate to the effects on the osteoblast-like cell functions.

CONCLUSION

Two different types of osteoblast-like cells were cultured in the Si-containing media prepared using BG or SiV. Their adhesion and proliferation were influenced by the change of the Si concentration and the differences in materials (silicate ion source). This might be related to the ionic state of the silicate ions in the culture medium.

REFERENCES

1. Hoppe A. *et al.*, Biomaterials. 32:2757-2774, 2011
2. Obata A. *et al.*, Acta Biomater. 6:1248-1257, 2010
3. Obata A. *et al.*, Acta Biomater. 5:57-62, 2009

ACKNOWLEDGMENTS

This work was supported in part by Institute of Ceramics Research and Education (ICRE) of Nagoya Institute of Technology.



Atomic-scale Models of the Water-Bioactive Glass Interaction

Antonio Tilocca¹ and Alastair N Cormack²

¹Department of Chemistry, University College London, U.K.

²Inamori School of Engineering, Alfred University, USA

INTRODUCTION

The interaction with water is central for the biodegradation and the performance of bioactive glasses in a biological medium. This interaction eventually leads to release of key soluble species such as calcium, phosphate and silica, which play a role in both the bone-bonding and the activation of osteogenic cells.^{1, 2} Understanding the water-bioactive glass interaction at a fundamental level can support a thorough understanding of how these biomaterials work. Moreover, detailed data on the fate of water molecules absorbed in bioactive glasses can provide precious insight into the effects of sol-gel processing on the atomic-scale glass structure.³ We discuss atomistic simulations⁴ aimed to investigate the interaction of the glass surface with water monomers,⁵ in order to probe the activity of individual surface sites, as well as simulations of the extended interface between the glass and an aqueous contact medium.^{6, 7} This information allows us to build and analyse large models of the surface of glasses of different composition, thus revealing links between surface structure and bioactivity.⁸ These studies have allowed us to identify the role of specific surface sites in the key steps of the bioactive mechanism, namely ion release and dissolution of the silicate network

EXPERIMENTAL METHODS

Ab-initio Molecular Dynamics (AIMD) simulations of water on model 45S5® bioactive glass surfaces have involved probing the active surface sites based on their interaction with an adsorbed water molecule. The water probe was released next to a specific site, such as a ring, an unsaturated ion, or a siloxane bridge, and then left free to locate a stable adsorption minimum by AIMD. We also deposited a liquid film of water molecules on the surface and examined the dynamics and reactivity at the interface.⁷ Thereafter, based on the potential activity of specific sites revealed by AIMD, we have employed classical MD simulations⁹ to compare the surface features of bioactive and bio-inactive compositions.

RESULTS AND DISCUSSION

The models of the water monomer-45S5 surface highlighted that unsaturated Si atoms represent the strongest surface sites, able to induce spontaneous water dissociation at room temperature, provided that they are combined with a proton acceptor such as a non-bridging oxygen. Additional strong surface adsorption sites are located near to Na⁺ or Ca²⁺ cations, which appear to be directly involved in the glass dissolution mechanism, by providing favourable adsorption pathways that allow water to penetrate under the glass surface (Figure 1). Small (2- or 3-membered) silica rings are also common features of the 45S5 Bioglass® surface, not frequently found in the bulk. The accurate determination of

minimum energy paths⁵ and the direct AIMD simulation of the interface at room temperature⁷ shows that, despite a favourable energetic balance, opening of these rings upon water dissociation is hindered by a significant energy barrier.

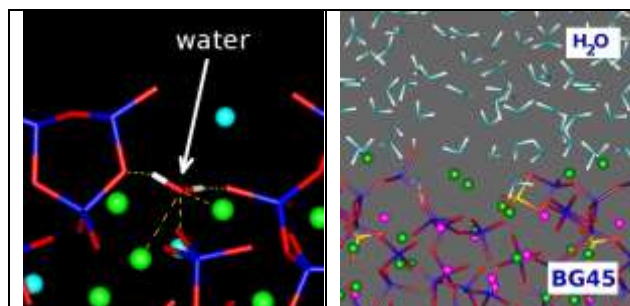


Figure 1: (left) Model highlighting penetration of a water monomer within the 45S5 surface. (right) Model of the 45S5-liquid water interface

CONCLUSIONS

The fragmented bulk structure of highly bioactive glasses⁹ is further reflected on the surface, which contains additional features that contribute to the favourable dissolution and biological properties. The presence of favourable alternative water adsorption sites, combined with kinetic effects, can stabilise some of the small rings exposed on the surface, protecting them from hydrolysis long enough for them to act as nucleation sites of dissolved Ca²⁺ and PO₄³⁻ ions in the initial stages of the bioactive fixation mechanism, as it has been proposed.⁹

REFERENCES

- ¹ ID Xynos, AJ. Edgar, LDK Buttery, LL Hench, and JM Polak, *J. Biomed. Mater. Res.* 55, 151 (2001).
- ² JR Jones, *Acta Biomater.* 9, 4457 (2013).
- ³ J Malik and A Tilocca, *J. Phys. Chem. B* 117, 14518 (2013).
- ⁴ A Tilocca, *J. Mater. Chem.* 20, 6848 (2010).
- ⁵ A Tilocca and AN Cormack, *J. Phys. Chem. C* 112, 11936 (2008).
- ⁶ A Tilocca and AN Cormack, *ACS App. Mater. Interfaces* 1, 1324 (2009).
- ⁷ A Tilocca and AN Cormack, *Proc. R. Soc. A* 467, 2102 (2011).
- ⁸ A Tilocca and AN Cormack, *Langmuir* 26, 545 (2010).
- ⁹ A Tilocca, *J. Mater. Chem.* 20, 6848 (2010).

ACKNOWLEDGMENTS

AT thanks the UK's Royal Society and EPSRC for financial support.



Applications of solid state NMR to the characterisation of bioactive glasses

Z. Lin¹, Julian R Jones², John V Hanna¹ and Mark E Smith^{1,3}

¹ Department of Physics, University of Warwick, Gibbet Hill Rd, Coventry, CV4 7AL, UK

² Department of Materials, Imperial College London, UK,

³ Vice-Chancellor's Office, University House, Lancaster University, LA1 4YW, UK, m.e.smith@lancaster.ac.uk

INTRODUCTION

Pioneering work by Hench showed that bioactive glasses based around calcium silicate compositions were exciting materials for tissue replacement and regeneration applications¹. The structures of these materials are important in conveying their properties. The potentially chemically complex and structurally disordered nature of these materials make their accurate characterisation somewhat problematic. Solid state NMR is an element specific probe technique with good sensitivity to the local atomic scale structural environment and has been applied to a wide range of materials². In bioactive sol-gel prepared calcium silicates ²⁹Si and ¹H have been the most studied nuclei³. However a multinuclear NMR approach opens up new insights including of the reaction with simulated body fluid (SBF) via ³¹P, direct probing network ordering and condensation via ¹⁷O and most challengingly of the siting of calcium via ⁴³Ca. ⁴³Ca has a very small magnetic moment (termed a low- γ nucleus) and also has a low natural abundance (0.14%) which lead to very low sensitivity. Nevertheless good quality NMR spectra at good signal-to-noise can be obtained, even at natural abundance, by using large samples. This contribution will review some of the solid state NMR applications to calcium silicate based sol-gel formed bioactive systems.

EXPERIMENTAL METHODS

Sample preparation has been previously described⁴. To overcome the sensitivity problems arising from the low natural abundance of ¹⁷O (0.037%) isotopically enriched H₂O was used in the preparation. NMR experiments were carried at 8.45 and/or 14.1 T at the Larmor frequencies of the observed nucleus. ¹⁷O MAS NMR spectra were collected using an echo sequence (θ - τ -2 θ)⁵ with a Bruker 4 mm probe spinning at 12 kHz. ¹H, ²⁹Si and ³¹P were all collected using a single pulse acquisition sequence. ⁴³Ca MAS NMR was performed using a 9.5 mm probe equipped with a low- γ box with spinning at 4 kHz and recycle delay 1 s using naturally abundant samples.

RESULTS AND DISCUSSION

¹⁷O has characteristic NMR parameters that are very sensitive to the local structural environment and can therefore directly probe the network ordering of sol-gel prepared silicate systems. ¹⁷O NMR can provide quantitative information about the bridging oxygen (BO):non-bridging oxygen (NBO) ratio of the silicate network. At a low heat treatment temperature (120°C), the network structure is dominated by bridging oxygen (Si-O-Si) with contributions from Si-OH at around 0 ppm. This indicates that Ca²⁺ ions are not yet intimately

part of the silicate network, probably remaining as a layer of the initial salt on the primary silica particles.

At higher temperatures ($\geq 500^\circ\text{C}$), NBOs become increasingly important, indicating that calcium now plays a central role and begins to dominate changes of the silicate network. The calcium species migrate into the silicate part of the materials, acting as a network modifier and gradually breaks down the silicate network by forming NBO. Changes in spectral parameters allow the oxygen sites to be clearly described and different species distinguished. An increase in the NBO resonance intensity is as a result of a modification of the silicate network and can be correlated to increases in the intensity of the ²⁹Si Q² and Q³ resonances.

The effects of increasing the heat treatment temperature on the direction of change of the chemical shifts is the same as increasing Ca/Si ratio, since both result in an increasing NBO resonance and decreasing polymerisation of the silicate network. The increasing chemical shifts can be understood as the consequences of deshielding effects when more calcium cations migrate into the silicate network forming large numbers of NBO with more deshielded oxygen sites, subsequently also influencing the surrounding BO resonances. ⁴³Ca can follow changes in the nature of the calcium site with increasing heat treatment.

Subsequent reaction of stabilised calcium silicate systems with SBF can also be followed by solid state NMR. ¹⁷O and ²⁹Si show changes in the network connectivity as the reaction progresses. On immersion with SBF there is rapid release of Ca²⁺ and decrease of NBO content. Also release of Ca²⁺ could open ways to surface hydration by ion exchange with H⁺ from the solution resulting in significant increase of Si-OH concentration on reaction. ³¹P NMR shows the formation of an apatite layer.

REFERENCES

1. Hench L.L., *Biomaterials* 74:1419-1423, 1998
2. MacKenzie K.J.D. and Smith M.E., *Multinuclear solid state NMR of Inorganic Materials* 2002
3. Martin R.A. *et al.*, *Phil. Trans. Roy. Soc. A* 370:1422-1443
4. Lin S. *et al.*, *J. Mater. Chem.* 19:1276-1282 2009
5. Kunwar A.C. *et al.*, *J. Magn. Reson.* 69:124-127 1986

ACKNOWLEDGMENTS

The authors would like EPSRC for funding the collaboration through various grants. The AWM Science City project and the University of Warwick are thanked for contributing funds for solid state NMR equipment. Various PhD students contributed to some of the work that will be reviewed in the talk and are thanked for their contributions.



Chloride Containing Bioactive Glasses

Robert Hill, Natalia Karpukhina and Xiaojing Chen

¹Dental Physical Sciences Dental Institute Barts and The London QMUL LONDON E1 4NS.

r.hill@qmul.ac.uk

INTRODUCTION

In our previous studies we investigated fluoride containing bioactive glasses¹⁻³. Fluoride ions form F-Ca(n) species in the glass. They result in reduced glass transition temperatures and bioactive glasses that form fluorapatite as opposed to hydroxycarbonated apatite. The chloride ion is substantially larger than the fluoride ion, which is similar in size to the oxygen anion. Chloride ions are naturally present in the body. The present study investigates the addition of calcium chloride to melt derived glasses. It is hypothesised that addition of calcium chloride will expand the glass forming range compared to calcium fluoride and will reduce the glass transition temperature and facility glass dissolution and apatite formation.

EXPERIMENTAL METHODS

The glass compositions were based on an initial glass with the composition in mole% of 38.1SiO₂6.3P₂O₅55.5CaO. To this glass was added increasing amounts of CaCl₂. The glasses were prepared by mixing the appropriate amounts of SiO₂, P₂O₅, CaCO₃ and CaCl₂ and melting in an electric furnace at temperatures between 100 and 1300°C depending on composition for 1Hr. The molten glass was fritted, dried, ground and sieved to give a particle size < 38 microns.

The glass powder produced was characterised by XRD high temperature DSC, ³¹P solid state NMR spectroscopy and FTIR spectroscopy. Selected glasses were heat treated to the observed crystallisation temperatures from the DSC experiments and XRD carried out.

The glass powder was immersed in Tris buffer pH 7.4 and their in vitro bioactivity assessed using Simulated Body Fluid. The solutions were analysed by ICP-OEM and apatite formation followed by XRD, FTIR and ³¹P ssNMR. The experimental techniques employed have been described fully for the related fluoride glasses³.

RESULTS AND DISCUSSION

All the glasses were optically transparent. The glasses exhibited weak diffraction lines corresponding to a mixed hydroxyl/chloroapatite upon XRD but were amorphous by ³¹P ssNMR. The presence of a mixed hydroxylchlorapatite arose from surface reaction with water during the XRD. The glass transition temperature reduced from 793 to 601°C on incorporating 20 mole% CaCl₂.

The glasses containing CaCl₂ crystallised to Calcium Chloroapatite, which is the first time this phase has been observed crystallising from a glass.

Incorporating CaCl₂ accelerated the dissolution of the glass and resulted in very rapid release of ions and rapid apatite like phase formation. Apatite like phases were detected in under three hours immersion by XRD, ³¹P ssNMR and FTIR (Figure 1). The apatite like phase formed was not chlorapatite, but is thought to be a phase with a composition between that of octacalcium phosphate and hydroxycarbonated apatite.

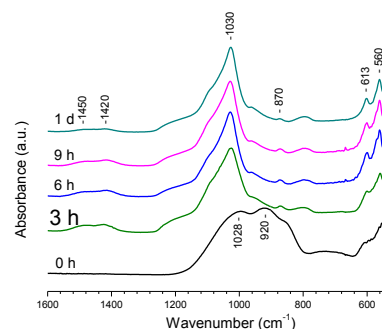


Figure 1 FTIR Spectra of a 4.5mole% CaCl₂ Glass after immersion in Tris buffer

The addition of CaCl₂ has a similar influence on glass properties as CaF₂. Bioactive glasses containing CaCl₂ overcome the disadvantages of high CaF₂ contents bioactive glasses, notably the formation of CaF₂ at the expense of apatite on dissolution and their tendency to crystallise during quenching. Furthermore unlike fluoride there are no restrictions on the amount of chloride that may be added to toothpastes.

The CaCl₂ glasses probably dissolve more rapidly compared to the equivalent CaF₂ glasses as a result of the larger ionic size of the chloride ion relative to fluoride that probably results in a more open glass structure that facilitates ion exchange and dissolution.

CONCLUSION

Calcium chloride containing bioactive glasses have been produced that show very rapid apatite like phase formation in Tris buffer and SBF on immersion.

REFERENCES

1. Brauer D *et al.*, J. Mater. Chem., 2009, 19, 5629–5636
2. Brauer D *et al.*, Acta Biomaterialia 6 (2010) 3275-82
3. Mneimne M *et al.*, Acta Biomater. 7 (2011) 1827-34.

ACKNOWLEDGMENTS

Authors would like to acknowledge useful discussion with Delia Brauer

Solid-State NMR Study on Strontium-Substituted 45S5 Bioglass®

Kie Fujikura^{1,2}, Natalia Karpukhina³, Akiko Obata¹, Toshi Kasuga¹, Delia S. Brauer², Robert G. Hill² and Robert V. Law^{3*}

¹Department/Research Institute, University, Country Nagoya Institute of Technology, Department of Frontier Materials, Graduate School of Engineering, Nagoya Institute of Technology, Gokiso-cho, Showa-ku, Nagoya 466-8555, Japan.

²Queen Mary University of London, Barts and The London School of Medicine and Dentistry, Institute of Dentistry, Dental Physical Sciences, Mile End Road, London E1 4NS, U.K.

³Imperial College London, Department of Chemistry, Exhibition Road, London SW7 2AZ, U.K., U.K., r.law@imperial.ac.uk

INTRODUCTION

The changes in the structure of 45S5 Bioglass and its heat-treated versions upon strontium substitution were investigated (1).

EXPERIMENTAL METHODS

The structures were investigated by solid-state multinuclear nuclear magnetic resonance, X-ray diffraction and differential scanning calorimetry. A series of the melt-derived glasses with strontium gradually substituted for calcium (0, 25, 50, 75 and 100%) on a molar basis was synthesised.

RESULTS AND DISCUSSION

T_g and crystallisation temperature decreased upon Sr substitution. Glasses with 75 and 100% of Sr substitution showed a minor crystalline phase. ³¹P MAS-NMR showed that phosphorus is present as orthophosphate in the entire glass series; ²⁹Si MAS-NMR data showed a predominantly Q² silicate network. A small step change in the position of the ³¹P and ²⁹Si MAS-NMR signals found between the glasses with 25 and 50% of Sr substitution is explained by an increase in the ring-type fraction of the Q² silicate glass over the mainly chain topology in the original 45S5 glass.

On heat treatment combeite silicate phases were identified. The polymerisation degree of phosphorus

increased and in addition to orthophosphate amorphous pyro- and meta-phosphate species were observed, the amount of which reduced with strontium substitution. Above 800°C, changes in ³¹P MAS-NMR spectra suggested that several phosphate containing phases, e.g. Na₃PO₄, crystallised and the fraction of the remaining glass became below the detection limit. In contrast to the Sr containing glasses, in the original 45S5 composition a significant fraction of phosphorus remained amorphous even after heat treatment at temperatures above 800°C.

CONCLUSION

The increasing substitution of Sr for Ca promoted crystallisation of a Sr-substituted combeite and the formation of ring structures in the glass.

REFERENCES

1. Fujikura K., et al. J. Mater. Chem. 22:7395-7402, 2012

ACKNOWLEDGMENTS

“The authors would like to thank JSPS International Training Program (ITP) “Young Scientist-Training Program for World Ceramics Network”.



Structural Evolution and Phase Formation During Synthesis of Phosphate-Containing Sol-Gel Derived Bioactive Calcium Silicate 58S Glasses

John V. Hanna^{1*}, B. Yu², Claudia Ionescu¹, Julian R. Jones² and Mark E. Smith^{1,3}

^{1*}Department of Physics, University of Warwick, Gibbet Hill Rd., Coventry, CV4 7AL, UK, j.v.hanna@warwick.ac.uk

²Department of Materials, Imperial College London, South Kensington, London, SW7 2BP, UK

³Vice-Chancellor's Office, University House, Lancaster University, LA1 4YW, UK

INTRODUCTION

Sol-gel bioactive glasses were first developed in the early 1990s, and the early work of Hench *et al.* demonstrated that their inherent nanoscale porosity increased apatite phase formation and bone bonding compared to melt-quenched glasses of similar composition¹⁻³. Bioactive glasses bond with host bone and their dissolution products can stimulate new bone growth¹; this bonding is thought to be facilitated by the reaction with body fluid which results in the formation of a hydroxycarbonate apatite (HCA) surface layer on the glass. Furthermore, the sol-gel process is widely thought to produce more homogeneous glass structure than melt-quench analogues since the silica network forms by a condensation reaction, usually of hydrolysed tetraethyl orthosilicate (TEOS), under constant stirring. However, Ca rich regions can occur in bulk sol-gel glasses⁴. Calcium nitrate and triethyl phosphate (TEP) are conventionally used as the precursors for introducing calcium and phosphate, respectively, although alternative calcium sources such as calcium chloride⁵, calcium acetate and calcium methoxyethoxide (CME) have been investigated⁶. The aim of this study is to investigate the evolution of the overall 58S structure, particularly focussing on the role of phosphate and the formation of an orthophosphate phase during the sol-gel synthesis. The development of the glass structure is compared with samples using different calcium precursor phases, and the effect of HF is investigated in the foaming process leading to porous scaffold production.

EXPERIMENTAL METHODS

Bioactive sol-gel glasses were made to the bioactive 58S (60 mol% SiO₂, 36 mol% CaO, 4 mol% P₂O₅) composition. Three calcium precursors CaCl₂, Ca(NO₃)₂•4H₂O, and calcium methoxyethoxide, Ca(OCH₂CH₂OCH₃)₂ (CME) were compared. Sol-gel solutions were gelled with and without hydrofluoric acid (HF) and different heat treatments were applied to the gelled samples. Each sample was characterised for elemental composition (ICP-OES), surface area (BET) and pore size (BJH), and further analysed using FTIR and XRD methods. Multinuclear ¹H, ¹³C, ¹⁹F and ³¹P solid state MAS NMR measurements were undertaken at 11.7 T using a Bruker Avance III spectrometer, while the accompanying ²⁹Si measurements were performed at 7.05 T on a Varian Infinity Plus spectrometer.

RESULTS AND DISCUSSION

Solid state MAS NMR and X-ray diffraction (XRD) studies show that phase separation was observed during conventional synthesis of 58S (60 mol% SiO₂, 36 mol%

CaO, 4 mol% P₂O₅) sol-gel glasses when triethyl phosphate (TEP) was used as the phosphate precursor and calcium nitrate tetrahydrate as the calcium source. The heat treatment of these samples to 400, 700 and 800 °C show the development of various phases, including the first reported observations of hydroxyapatite (HA) formation under these conditions. This observation is facilitated by the presence of phosphate anions which are charge balanced by calcium ions and clearly partitioned from the silica network (i.e. no Si-O-P bonds were established). The separation of the phosphate groups is attributed to the presence of water in the sol-gel process, the nature of TEP and calcium not being incorporated into the silica network until the gels were heated to at least 400 °C. Subsequent preparations using HF as a gelation catalyst induced the formation of a fluorapatite rather than HA. At all temperatures studied here samples synthesised with calcium methoxyethoxide (CME) as the calcium precursor phase were amorphous according to XRD, while the MAS NMR data showed some evidence of orthophosphate group and Si-O-P bond formation.

CONCLUSION

These studies demonstrate the first observations of HA formation during conventional sol-gel 58S synthesis using TEP as the phosphate precursor and calcium nitrate tetrahydrate as the calcium source. CME also performs as an excellent alternative to calcium salts for the incorporation of calcium into the silica network at processing temperatures below 60 °C, and for improved homogeneity of glasses stabilised at higher temperatures.

REFERENCES

1. Li, R. *et al.*, J. Appl. Biomater. 2:231-239, 1992
2. Hench, L. L. *et al.*, Science 295:1014-1017, 2002
3. Sepulveda, P. *et al.*, J. Biomed. Mater. Res. 58:734-740, 2001
4. Lin, S. *et al.*, J. Sol-Gel Sci. Technol. 53:255-262, 2010
5. Poologasundarampillai, G. *et al.*, J. Mater. Chem. 20:8952-8961, 2010
6. Poologasundarampillai, G. *et al.*, Soft Mater. 8:4822-4832, 2012

ACKNOWLEDGMENTS

JVH, MES and JRJ thank the EPSRC for funding this collaboration through various grants. JVH and MES thank the EPSRC, the University of Warwick and the AWM Science City project for contributions to the funding of the solid state NMR equipment in Millburn House at Warwick.



Nano/Micro Structured Bioglasses Synthesized via Sol-gel and Electrohydrodynamic (EHD) Approaches

Yangyang Li¹, Ding Zhao^{1,2}, Binbin Li¹, Qihong Zhang¹, Yike Fu¹, Juan Wang¹, Mingwei Chang², Zhaohui Ren¹, Xiang Li^{1*}

¹Department of Materials Science and Engineering, Zhejiang University, P.R.China.

²College of Biomedical Engineering & Instrument Science, Zhejiang University, P.R. China.

*Corresponding author: xiang.li@zju.edu.cn

In this paper we shall review our recent research on forming of bioglass architectures using simultaneous flow of precursors through a device which can contain several co-axial needles and operates in an electric field. In particular, research involving sol-gel and electrospinning technique combinations will be described. The co-flow in different situations can be made to jet and produce particles or tubes. In addition, silver ions can be accommodated in the glass precursor so that the Si-O-Si network forming process can be manually interfered at an atomic level, and the bioglass nanotube wall structure can be manipulated, from dense to a 'lace-like' structure (Fig 1a).

The synthesis of silica, a bioglass with pure SiO₂ contents in some extents, nanoparticles with a variety of mesoporous structures will be elucidated by demonstrating how nanoscale pores with different curvatures can lead to drug releasing kinetics being controlled. The process can also be used to form bioglass tissue engineering constructs and drug delivery vesicles, which can also be multifunctionalized by inducing different functional counterparts (i.e. up-conversion luminescent factors) due to its unique amorphous structural characteristics. In summary, the bioglass processing and forming described is useful to the interface of physical and life sciences, engineering and medicine, and examples of future prospects the process offers will be discussed.

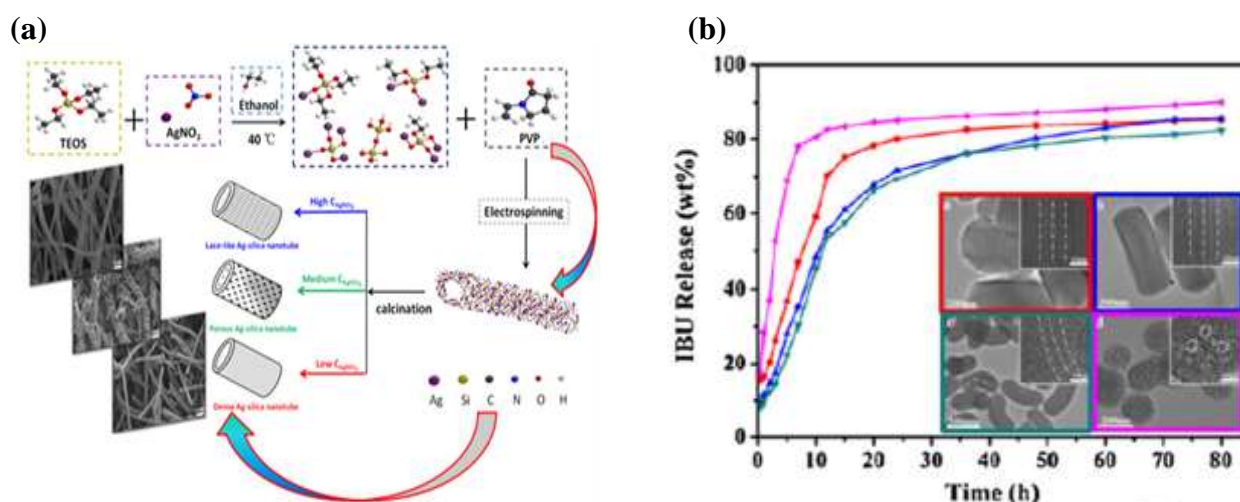


Figure 1 (a) The form procedures of bioglass nanotubes with well-controlled wall structures, and (b) silica particles with different drug releasing kinetics due to the mesoporous characteristics.

ACKNOWLEDGEMENT

Authors would like to thank National Natural Science Foundation of China (grant No. 51103128), Ph.D Program Foundation of Education Ministry of China (grant No. 20110101120014) and 'Qianjiang Talent' Program by Science Technology Department of Zhejiang Province (grant No. 2013R10037), for the financial support.

A unified *in vitro* evaluation for apatite-forming ability of bioactive glasses and their variants.

Anthony L. B. Maçon,^a Taek B. Kim,^a Esther Valliant,^a Katherine Goetschius,^b Richard Brow,^b Delbert Day,^b Alexander Hoppe,^c Aldo Boccaccini,^c Il-Yong Kim,^d Chikara Ohtsuki,^d Tadashi Kokubo,^e Akiyoshi Osaka,^f Maria Vallet-Regi,^g Daniel Arcos,^g Leandro Fraile,^g Antonio Salinas,^g Alexandra Teixeira,^h Yuliya Vueva,^{a,h} Rui Almeida,^h Marta Miola,ⁱ Chiara Vitale-Brovarone,ⁱ Enrica Verne,ⁱ and Julian Jones^{*a}

^aDepartment of Materials, Imperial College London, London, SW7 2AZ, E-mail: julian.r.jones@imperial.ac.uk

^bDepartment of Materials Science & Engineering, MS&T, Rolla, MO 65409, USA

^cDepartment of Materials Science, University of Erlangen-Nuremberg, Cauerstrasse 6, 91058 Erlangen, Germany

^dNagoya University, Furo-cho, Chikusa-ku, Nagoya, Japan; ^eChubu University, Matsumoto-cho, Kasugai-shi, Aichi, Japan

^fGraduate School of Natural Sciences and Technology, Okayama University, Tsushima, Okayama-shi 700-8530, Japan

^gDepartamento de Química Inorgánica y Bioinorgánica - Universidad Complutense de Madrid - 28040 Madrid - Spain and CIBER-BBN

^hDepartamento de Engenharia Química e Biológica / ICEMS Instituto Superior Técnico / TULisbon, 1049-001 Lisbon, Portugal

ⁱMaterials Science and Chemical Engineering, Politecnico di Torino, C.so Duca degli Abruzzi 24, 10129 Torino, Italy

INTRODUCTION

Bioactive glasses can bond to bone or dentin by forming a hydroxycarbonate apatite (HCA) layer on their surface. *In vitro*, simulated body fluid (SBF) is often used to quantify HCA nucleation [1] and has led to the development of a standardized test (ISO/FDIS 23317, "Implants for surgery – *In vitro* evaluation for apatite-forming ability of implant materials"). Unfortunately the standard is not appropriate for all bioactive glasses: it is based on a fixed surface area to SBF ratio, favouring monoliths and making the assessment of powder like or mesoporous (e.g. sol-gel) glasses difficult. It was also a static test. This study aims to compare a modified method, based on fixed mass to SBF ratio under agitation, to the existing ISO standard. A round robin study on the proposed method was carried out in 8 laboratories in 7 countries on several commercially available bioactive glasses of known composition. The method was also further modified to test toothpaste containing bioactive glasses, Sensodyne Repair & Protect (SRP) containing NovaMin®, GlaxoSmithKline, UK.

EXPERIMENTAL METHODS

A ratio of 75 mg of glass powder to 50 ml of media was used and agitated at 120 rpm in an incubating orbital shaker set at 37°C. The pH and temperature of the media was verified before use. The samples were immersed in media for 8 different time points at 0h, 4h, 8h, 24h, 72h, 1week, 2 weeks, 3 weeks and 4 weeks. At the end of each time period, the sample was removed from the incubator and the solids were collected by filtration. The powder was washed with acetone to terminate the reaction and dried at room temperature for 24 h and analysed by FTIR, XRD and SEM. The filtered solution was analysed by ICP. Each sample was tested in triplicate. For toothpaste, a similar method was used except that artificial saliva (AS) was used as a media and powders were collected by centrifugation and freeze-drying.

RESULTS AND DISCUSSION

Commercially available melt derived glasses (45S5, NovaBone, BonAlive, 13-93 and StronBone) and a sol-gel derived glass (TheraGlass) were immersed in SBF using the presented method where the concentration of glass in the media is fixed as opposed to the ISO where the surface area defined the amount of media used. A good agreement in the kinetics of nucleation of HCA among the different laboratories was found as shown in

Figure 1. Results were also compared with the standard. The proposed method exhibited higher dissolution of silica and calcium and a more defined decrease in phosphorus concentration (ICP) when HCA nucleated. The 13-93 composition is of particular interest as it has good results *in vivo*, but using the ISO standard HCA did not form on the surface until after 2 weeks in SBF. In the modified test apatite formed between 3 days to 1 week (XRD and FTIR). The effect of the morphology was also studied by looking at the dissolution behavior of 13-93 shaped into fibers and disks. Using the adapted method, analysis of the bioactivity of bioactive glass in toothpaste was proven to be possible. In this particular case, SRP, containing NovaMin®, was immersed in artificial saliva using the same glass to media ratio. HCA was found to nucleate on the bioactive glass after 2 hours of immersion in AS.

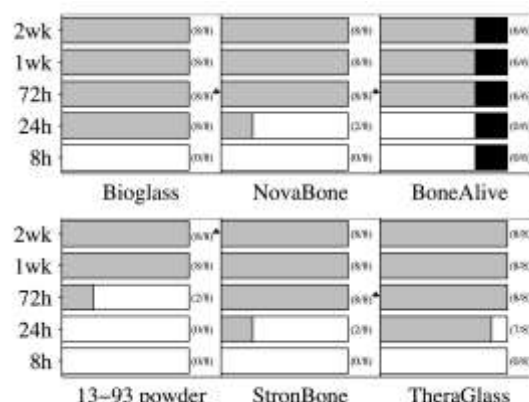


Fig. 1 – Summary of the different rate of HCA nucleation from the different laboratories for the different composition tested (* represents the rate obtained with the ISO methodology). Only 6 out of 8 laboratories tested BonAlive. Due to its high surface area (~80m².g⁻¹), TheraGlass was not tested using the ISO method as surface area was too high.

CONCLUSION

This proposed concentration-based method to assess the bioactivity *in vitro* of bioactive glasses seems to be more appropriate as high surface area and conditioned glasses are being developed as future biomaterials

REFERENCES

1. Kokubo, T., Takadama, H., *Biomaterials*, 2006, **27**

Acknowledgments: This study was conducted as a TC04 (Technical Committee 4) collaboration of the ICG (International Commission on Glass). GlaxoSmithKline (NovaMin) (UK), NovaBone (USA), BonAlive (Finland), RepRegen (UK), Mo-Sci (USA) and TheraGlass (UK) are thanked for sample provision. This research was part funded by GlaxoSmithKline.



Role of stromal vascular fraction from adipose tissue in association with a phosphocalcic scaffold to regenerate bone in irradiated area

Florent Espitalier,^{1,2} Audrey Théry,^{1,2} Pauline Bléry,¹ Jérôme Guicheux,¹ Paul Pilet,¹ Sophie Sourice,¹ Pierre Weiss,¹ Olivier Malard,^{1,2}

Corresponding Author: florent.espitalier@chu-nantes.fr

¹ INSERM U791, Center for Osteoarticular and Dental Tissue Engineering, University of Nantes, France

² Department of Otolaryngology-Head and Neck Surgery, University Hospital of Nantes, France

INTRODUCTION

We have previously demonstrated that the association of Total Bone Marrow (TBM) and Biphasic Calcium Phosphate (BCP) is the best combination to regenerate bone in irradiated area.¹ Recently, Stromal Vascular Fraction from adipose tissue (SVF) has been described as an alternative to TBM as a source of mesenchymal stem cells.² Studies showed that SVF could promote osteoformation in healthy bone.³ The subject of this study was to identify the capacity of the SVF to induce new bone formation in irradiated area.

EXPERIMENTAL METHODS

Four weeks after an external 20 Gy of irradiation on the hind limbs of 20 rats, 4 bone defects were created per animal and filled with SVF or TBM, associated or not with BCP. Three weeks after implantations, the bones were removed. Histological and scanning electron microscopy analyses were performed to obtain qualitative and quantitative analyses. The different conditions were compared using Mann & Whitney tests for unpaired comparisons after validation by an analysis of Kurskal & Wallis.

RESULTS AND DISCUSSION

The BCP-TBM mixture significantly improved bone ingrowth ($p < 0.05$). The BCP-SVF mixture did not provide new-bone formation over and above that induced by BCP alone (Figure 1).

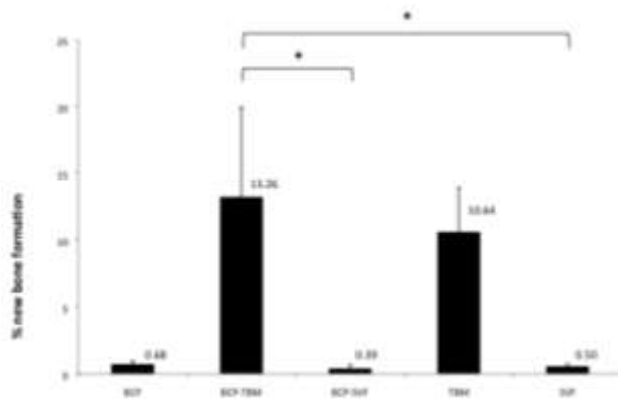


Fig. 1. Bone ingrowth in osseous defects (* $p=0.021$).

However, the histological staining of blood vessels showed that the BCP-SVF association induced more angiogenesis than BCP (Figure 2).

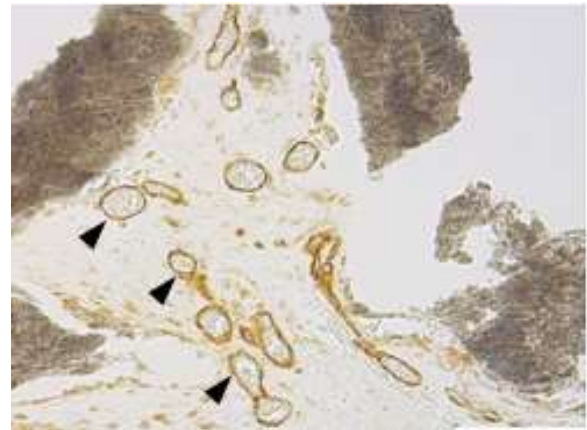


Fig. 2. BCP-SVF association: specific CD31 labeling of blood vessels (arrow heads).

Instead of the lack of vascularisation, our results suggest that the lack of cytokines and growth factors in the SVF could limit bone formation when compared to TBM in irradiated bone.

CONCLUSION

Despite the capacity of SVF to form blood vessels in irradiated bone defects, TBM associated to BCP appears to be the most efficient combination for bone reconstruction after radiotherapy today.

REFERENCES

1. Espitalier F. *et al.*, Biomaterials 30:763-9, 2009
2. Astori G. *et al.*, J Transl Med 5:55, 2007
3. Kim A *et al.*, Cytotherapy 14:296-305, 2012

ACKNOWLEDGMENTS

The authors would like to thank “la ligue contre le cancer, comités 22, 44 et 49” for providing financial support to this project.

Design of stimuli-responsive film through layer-by-layer assembly for the control of protein adsorption

A. Osypova^{a,b,c}, C.M. Pradier^{b,c}, C. Jérôme^d, J. Landoulsi^{b,c}, S. Demoustier-Champagne^a

^a Institute of Condensed Matter and Nanoscience (IMCN), Pôle Bio and Soft Matter (BSMA), Université Catholique de Louvain (UCL), Croix du Sud 1, Boite L7.04.01, B-1348 Louvain-La-Neuve, Belgium

^b Sorbonne Universités, UPMC Université Paris 06, F-75005, Paris, France

^c CNRS, UMR 7197, Laboratoire de Réactivité de Surface, F-75005, Paris, France

^d University of Liege, Center for Education and Research on Macromolecules (CERM) Bâtiment B6, allée de la Chimie 3 4000 Liège, Belgium
alina.osypova@uclouvain.be

The control of cell-material interactions is still challenging, as in vivo, cells evolve in a complex environment regarding both biochemical signals and structural organizations. Now it is well established that proteins play a pivotal role in this issue and that the control of their behavior at interfaces is crucial. In this context, the emergence of smart materials that “spontaneously” respond to environmental stimuli has opened new routes for the control of surface properties, particularly, the behavior of proteins at the solid-liquid interface.

In the present study, we report on the design of thin film, which is sensitive to physicochemical changes of the environment. For this purpose, we used the layer-by-layer (LbL) assembly technique to incorporate block copolymers of PAA and PNIPAM, with tunable and well-controlled block lengths of each segment. The combination of ellipsometry, quartz crystal microbalance (QCM-D) and infrared data revealed the possibility to build up (PAH/PAA-PNIPAM)_n multilayers. Furthermore, it appears that the presence of PNIPAM moieties did not affect the mechanism of multilayers growth.

The stimuli-responsive properties of the LbL films were examined by monitoring the adsorption of proteins by

means of QCM-D and fluorescence measurements, while varying (i) temperature, (ii) pH, (iii) ionic strength, or (iv) a combination of the above parameters. Results showed that the temperature strongly influences the amount of adsorbed proteins, in accordance with the expected behavior of PNIPAM. Interestingly, adsorption/desorption cycles revealed the ability of the films to switch from favorable to unfavorable configuration towards protein adsorption. In addition to the successful design of stimuli-responsive LbL films, the mechanism of protein adsorption is profoundly examined, as it seems to be more complex, compared to tests performed on “common” flat surfaces. This is due to the fact that physicochemical changes (stimuli) influence, at the same time, the properties of the LbL films, made with weak polyelectrolytes. Indeed, the protein adsorbed amount estimated by fluorescence measurements suggests that various processes may occur at the interface, such as protein aggregation and/or interdiffusion within the films, depending on the pH and the ionic strength of the solution, etc.

This research is conducted within the frame of the International Doctoral School in Functional Materials funded by the ERASMUS MUNDUS programme of the European Union.



Tissue engineering creates new basis for scientific research in cell-biomaterial interaction

Malgorzata Lewandowska-Szumiel^{1*}, Slawomir Ruminski¹, Katarzyna Walenko¹, Barbara Ostrowska², Wojciech Swieszkowski²

^{1*}Department of Histology and Embryology, Medical University of Warsaw, Poland, mszumiel@wum.edu.pl

²Department of Materials Science, Warsaw University of Technology, Poland

INTRODUCTION

"Scientists study the world as it is, engineers create the world that never was" says the well-known quotation by Theodore von Karman. Working on the new possibilities in tissue replacement and regeneration, tissue engineers create non-standard experimental systems based on the combination of cells and artificial materials. In the present study two selected examples of the influence of the materials on the differentiation of adipose derived stem cells (ADSC) are given. In the first one, more advanced differentiation of ADSC toward the osteogenic phenotype has been observed in 3D scaffolds as compared to the standard 2D culture surfaces. In the second one – materials of different stiffness were used as a support for cells in culture.

EXPERIMENTAL METHODS

Human ADSC obtained from liposuction were investigated. PCL/TCP composite scaffolds were used as the 3D system, while polyacrylamide and polydimethylsiloxane were used to obtain the support for cells - differing in stiffness. In the first system the observation was performed on day 21 and 42 and the markers of the advanced differentiation were detected, i.e. osteocalcin (Western blot) and mineralization (specific fluorescence staining). Observation of the role of the stiffness was performed on day 7 – so as to maintain a one-layer culture. Therefore, the early osteogenic markers were taken into account, i.e. RUNX2 (gene expression by real time PCR) and alkaline phosphatase (ALP) (gene expression by real time PCR and the enzyme activity).

RESULTS

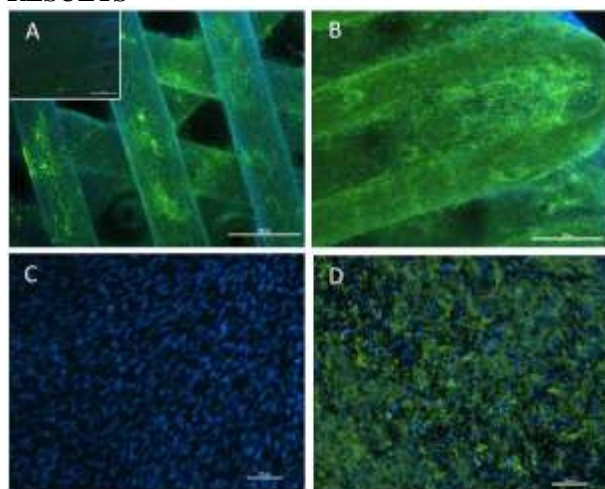


Fig. 1 shows abundant mineralization (green) on the 3D PCL/TCP scaffolds on day 21 (A) and day 42 (B); no mineralization on the 2D standard culture surface on

day 21(C) and modest (compare to B) mineralization in 2D on day 42 (D); scaffold without cells is shown in the upper left window.

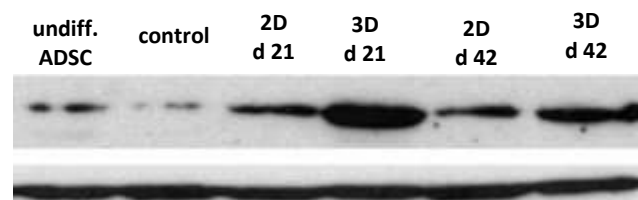


Fig. 2 shows Western blot – osteocalcin-up, and β -actin, as a reference-at the bottom; from the left: undifferentiated cells, control, i.e. ADSC cultured for 21 days in the medium enriched with vit. C, 2D or 3D culture in osteogenic medium on day 21 or 42.

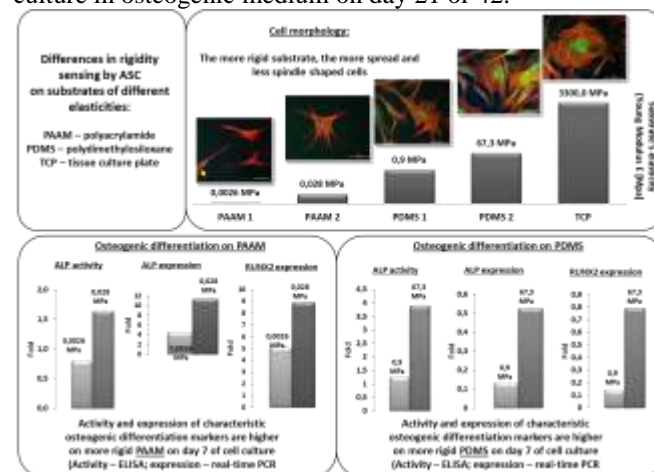


Fig. 3 stiffer material - better organized cell morphology (actin - red, vinculin – green), higher expression of RUNX2 and ALP genes and higher ALP activity.

DISCUSSION AND CONCLUSIONS

Both applied systems promoted ADSC osteogenic differentiation. The results were confirmed using the materials from several various (at least four) patients (informed consent was obtained). However, any definite statements from such observations are limited by the specific conditions of the particular experiments. The latter is a common weakness of the original reports in the field. It seems that tissue engineering is still rather at the stage of collecting data, while more general observations as well as the understanding of the particular mechanisms lying behind the observed phenomena are not yet achieved. In a way, tissue engineers, using new experimental systems have *"created the world that never was"*. It gives room for more specific *"scientific study"* in the field.

Wear and Friction of PEEK and CFR-PEEK Materials for Cervical Total Disc Replacement Bearings

Ksenija Vasiljeva¹, Phil Hyde¹, John Fisher¹, Richard Hall¹

¹ University of Leeds, Woodhouse Lane, Leeds, UK, k.vasiljeva@leeds.ac.uk

INTRODUCTION

PEEK (poly-ether-ether-ketone) and CFR-PEEK (carbon-fibre reinforced PEEK) polymers have been identified as a potential bearing material for use in cervical total disc replacement (c-TDR). However, there is limited knowledge concerning the wear and friction characteristics of PEEK bearing combinations. A recent study suggested that CFR-PEEK articulating against itself produces much less wear compared to conventional ultra-high molecular weight polyethylene (UHMWPE) on cobalt chromium (CoCr) [1]. The aim of this study was to investigate the wear and friction properties of medical grade PEEK and CFR-PEEK under cervical loading conditions and all bearing combinations, using conventional UHMWPE on CoCr as a baseline control.

EXPERIMENTAL METHODS

Wear and friction behaviour of PEEK and CFR-PEEK was studied using simple geometry pin-on-plate reciprocating wear test. Wear was studied using bearing combinations as follows: PEEK pin against PEEK plate (n=5), PEEK pin against CFR-PEEK plate (n=6), CFR-PEEK pin against PEEK pin (n=6), CFR-PEEK pins against CFR-PEEK plate (n=5). Contact pressure was 1.6MPa resulting from an 80N load and stroke length was 28mm at 1Hz with rotation applied to pin.

Friction was measured using all four possible combinations of PEEK and CFR-PEEK using n=6 except PEEK on PEEK experiment (n=16). Samples were tested at 4 mm/s sliding speed and 1MPa contact pressure. In both tests 25% diluted bovine serum was used as lubrication and a UHMWPE pin articulating against CoCr plate (n=6) was used as a reference control material.

RESULTS AND DISCUSSION

PEEK on PEEK and CFR-PEEK on CFR-PEEK had similar wear factors to the control bearing (Figure 1). Wear factors for CFR-PEEK on CFR-PEEK reduced with every 0.3 million cycles, suggesting bedding in wear was present. At the same time CFR-PEEK on PEEK and vice versa showed almost 10³ times higher wear than UHMWPE on CoCr.

The similarity in wear between PEEK on PEEK and UHMWPE on CoCr was also demonstrated by Grupp et al. [1] for a total disc replacement. However, in contrast to this study, Scholes et al [2] found CFR-PEEK on CFR-PEEK wear was lower than UHMWPE on CoCr. Friction coefficient for all material combinations was much higher than the control (Figure 2). Coefficient values ranged from minimum 0.4 for CFRP on PEEK to maximum value of 0.5 for PEEK on PEEK.

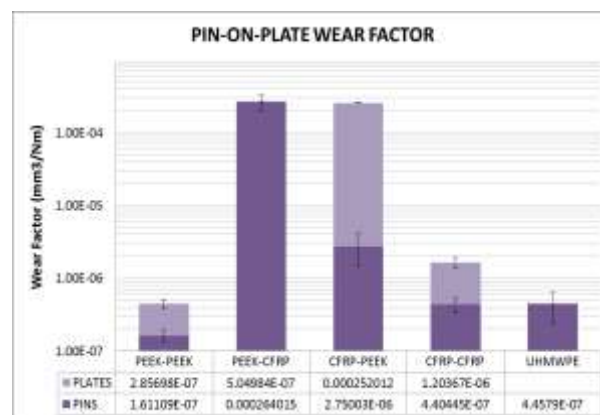


Figure 1 Pins and Plates wear factor (log scale) for PEEK and CFRP material combinations and UHMWPE pin on CoCr (control).

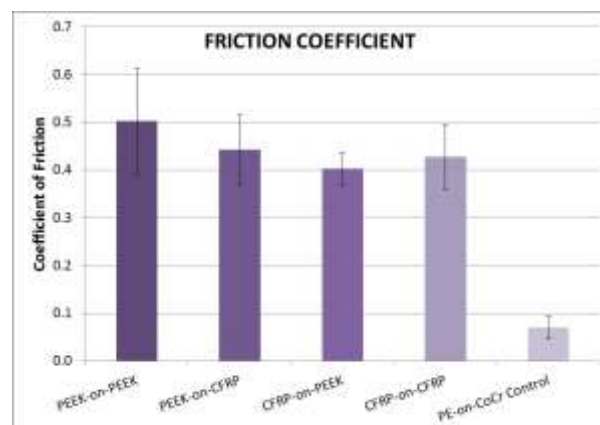


Figure 2 Friction coefficients for PEEK and CFR-PEEK combinations and UHMWPE on CoCr (control).

CONCLUSION

In comparison to the UHMWPE pin-on-plate control, both PEEK on CFR PEEK and CFR-PEEK on PEEK bearing combinations showed poor results in terms of wear. All PEEK and CFR PEEK bearing combinations demonstrated very high friction coefficients, approximately an order of magnitude higher than UHMWPE on CoCr.

REFERENCES

- Grupp T. *et al.*, J. Biomaterials. 31:523-531, 2010
- Scholes S. *et al.*, J. Wear. 268:380-387, 2010

ACKNOWLEDGMENTS

This work was funded through WELMEC, a Centre of Excellence in Medical Engineering funded by the Wellcome Trust and EPSRC, under grant number WT 088908/Z/09/Z. Materials were supplied by Invibio Ltd, Lancashire, UK

Hydrolytic and Oxidative Degradation of Electrospun Supramolecular Biomaterials: *In Vitro* Degradation Pathways

M. Brugmans^{1,2}, S. Sontjens³, M. Rubbens¹, A. Nandakumar¹, A. Bosman⁴, T. Mes⁴,
H. Janssen³, C. Bouten², F. Baaijens² and A. Driessen-Mol²

¹ Xeltis B.V., Eindhoven, The Netherlands, marieke.brugmans@xeltis.com

² Department of Biomedical Engineering, Eindhoven University of Technology, The Netherlands

³ SyMO-Chem B.V., The Netherlands, ⁴ SupraPolix B.V., The Netherlands

INTRODUCTION

Biodegradable polymers are widely used in the field of regenerative medicine to replace and regenerate damaged tissues^{1,2}. Electrospun scaffolds, produced from these polymers, should be able to provide mechanical stability immediately after implantation and stay mechanically reliable until sufficient tissue is formed. The degradation speed and mode of scaffolds depend on the chemical characteristics of the used polymers and need to be studied to determine clinical applicability of new materials. Mechanical performance and degradation behaviour of supramolecular materials are tuneable by combining polymers with the hydrogen bonding ureido-pyrimidinone (UPy) or bis-urea (BU) moieties³. This study shows how mechanical and chemical stability of novel supramolecular electrospun scaffolds are affected by different degradation pathways.

EXPERIMENTAL METHODS

Our model includes accelerated enzymatic hydrolysis and oxidative degradation pathways. Mechanical (n=3 per time point), chemical (n=1 per time point) and morphological (n=1 per time point) properties of polycaprolactone (PCL) based electrospun materials with UPy or BU moieties were investigated during degradation, while a conventional electrospun PCL scaffold served as a reference material. Time points were chosen up to 56, 96, and 400 hours for enzymatic lipase (100U/ml), cholesterol esterase (10U/ml), and oxidative degradation (0.1M CoCl₂+ 20% H₂O₂), respectively.

RESULTS AND DISCUSSION

The properties of the conventional PCL scaffold are significantly affected by enzymatic degradation (Fig. 1A and E), with severe mass loss (93%), decreased mechanical properties, and changes in fiber morphology compared to untreated scaffolds (Fig. 2A-B). As molecular weight (Fig. 1C) remained stable, surface erosion is assumed to be the mode of degradation. Supramolecular materials showed to be more stable against enzymatic degradation.

Degradation by oxidation demonstrated minimally affected conventional PCL scaffolds, while the supramolecular scaffolds showed broken fibers (Fig. 2C), moderate to severe mass loss, decreased mechanical properties and a decrease in molecular weight (Fig. 1B, D and F). These results suggest that supramolecular materials, as well as conventional PCL, will degrade after implantation, however by a different mode of degradation.

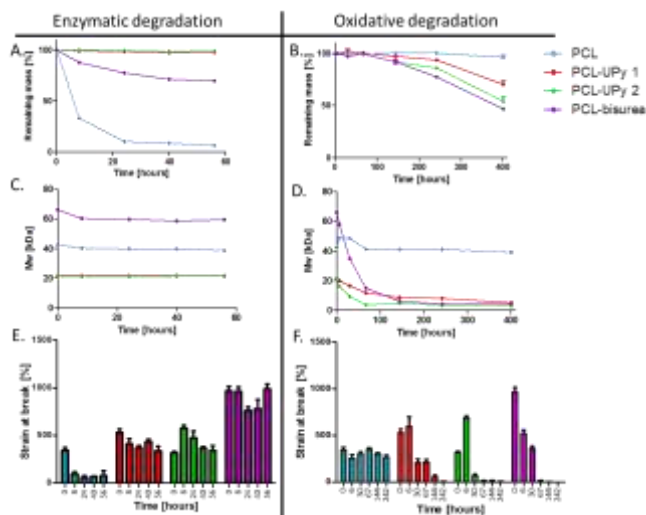


Figure 1. Characteristics of scaffolds during degradation.

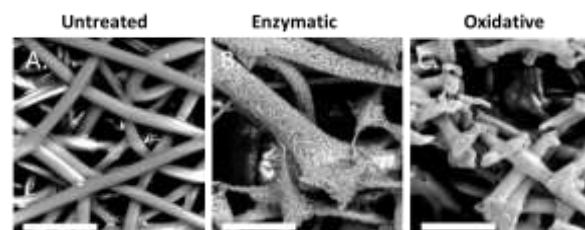


Figure 2. SEM images of scaffolds. White scale bars represent 20 μ m.

CONCLUSION

Developed *in vitro* tests show that the conventional PCL scaffold is more prone to enzymatic degradation, while the supramolecular scaffolds are more prone to oxidative degradation. The *in vitro* data obtained in this study will be correlated to *in vivo* data to obtain more insight into *in vivo* degradation pathways and used to predict degradation properties of new materials after implantation to assess clinical applicability of new materials.

REFERENCES

1. Ulery B. *et al.*, J Polym Sci B Polym Phys. 12:832–864, 2012
2. Tian H. *et al.*, Prog Polym Sci. 2:237-280, 2012
3. Dankers P. *et al.*, Biomaterials. 27:5490-5501, 2006

ACKNOWLEDGMENTS

This research forms part of the iValve program (P1.01) of the BioMedical Materials institute, co-funded by the Dutch Ministry of Economic Affairs. The Netherlands Institute for Regenerative Medicine (grant # FES0908) is also acknowledged for providing financial support.

Characterising the Effects of Different Sterilisation Techniques on Electrospun Fibre Scaffolds

Lucy A Bosworth and Sarah H Cartmell*

School of Materials, The University of Manchester, UK

*sarah.cartmell@manchester.ac.uk

INTRODUCTION

Scaffolds that are intended as future medical devices ultimately require sterilisation and validation of their sterility prior to being classed as safe for human use and implantation. The International Organisation for Standardisation (ISO) have developed (and maintain) several standards for sterilisation techniques that are recognised by regulatory bodies, such as the Medical Device Directive. Sterilisation is necessary for the elimination of bioburden (microorganisms) that may be present on the scaffold's surface or within the material bulk¹. Without this eradication, the success of the implant could be severely compromised due to infection. Accepted sterilisation processes can significantly affect the material properties of the scaffold and if not addressed early in the project timeline can lead to the research never translating from the bench to the clinic.

This study investigated the effects of different sterilisation methods on the material properties of electrospun fibre scaffolds.

EXPERIMENTAL METHODS

PCL (Purac - Purasorb PC12) was dissolved in 1,1,1,3,3,3-hexafluoroisopropanol (HFIP; Sigma) at 10 %w/v and electrospun (20 kV, 1 ml/hr, 20 cm). Aligned fibres were collected on a rotating mandrel (600 RPM). Fibres were cut into strips (20 mm* x 3 mm) with their alignment parallel to the long edge (*30 mm for tensile testing). Scaffolds were subjected to different types of sterilisation; gamma irradiation – 15 kGy (+10 % tolerance), 25 kGy (+10 %), 50 kGy (± 10 %); ethylene oxide (EO, double pass); submersion in ethanol (50, 70, 90 and 100 %v/v in distilled water); and surface radiation by ultraviolet light (UV) for 30 mins. Synergy Health were contracted to undertake gamma irradiation and EO sterilisation. Ethanol and UV treatments were performed in-house. Sterilised scaffolds were subjected to material characterisation and compared to non-sterilised scaffolds (virgin PCL), including molecular weight (Gel Permeation Chromatography (GPC), 0.2 %w/v in Tetrahydrofuran), and tensile testing (Instron 3344, 100 N load cell, 20 mm gauge length and 5 mm/min cross-head speed). Data were analysed using one-way ANOVA with Bonferroni post-tests where sample sets were compared to virgin PCL (Graphpad Prism v.5).

RESULTS AND DISCUSSION

Molecular mass distributions significantly decreased for all sterilisation processes compared to the virgin PCL scaffolds, suggesting substantial scissoring of the polymer chains had occurred (Fig.1).

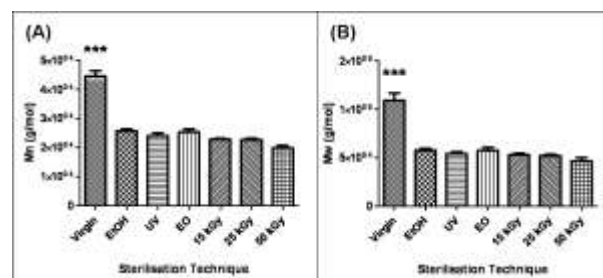


Fig.1 – Molecular mass distributions for PCL scaffolds, where (A) demonstrates number average molecular weight (Mn) and (B) weight average molecular weight (Mw). Data presented as mean \pm standard deviation (n=5); virgin PCL samples significantly different to all other scaffolds (** $p < 0.001$).

Despite the molecular weight decreasing by more than half its original mass, the tensile properties remained relatively unchanged, with no notable differences observed in stiffness or strength for sterilised scaffolds compared to virgin PCL samples (Fig.2).

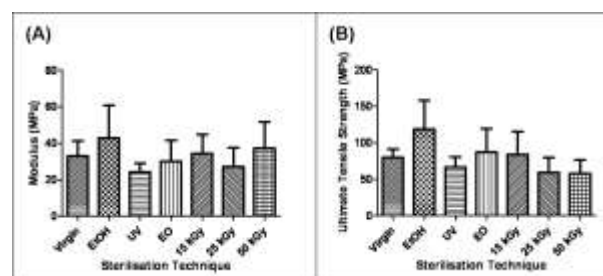


Fig.2 – Tensile properties of PCL scaffolds, where (A) indicates Young's Modulus and (B) Ultimate Tensile Strength. Data presented as mean \pm standard deviation (n=7); sterilised scaffolds demonstrated no significant difference compared to virgin PCL samples.

Being semi-crystalline in nature, scissoring of the amorphous regions of the PCL may have occurred preferentially, which could affect overall molecular mass whilst having minimal impact on mechanical strength¹.

CONCLUSION

Sterilisation can significantly impact the material properties of electrospun PCL scaffolds, in particular molecular weight, which in turn could markedly affect the degradation profile of this polymer. The effects of sterilisation should be considered early in the project in order to establish 'base-line' properties.

REFERENCES

- Gibb A. *et al.*, J Mater Sci: Mater Med. 24(3):701-711.

ACKNOWLEDGMENTS

This study was supported by the MRC DPFS (Grant no: G1000788-98812).



Novel Electric Discharge Assisted Mechanical Milling method as a mean of biomaterials synthesis in the Al-Zr-O system

M. Wyszomirska^{1*}, A. Calka², D. Wexler²

^{1*} Mechanical, Material & Mechatronic, University of Wollongong, Australia, mw966@uowmail.edu.au

² Mechanical, Material & Mechatronic, University of Wollongong, Australia.

Introduction:

Advanced materials manufacturing methods require clean non-pollution, high speed, precise process, and highly reliable final products. Many functional materials are traditionally synthesized by slow reaction processes that are energy and time consuming. In the present world there is strong demand on development of modern materials and materials processing methods that could offer rapid reaction rates, energy efficiency and be environmentally safe.

Electric discharge assisted mechanical milling (EDAMM)¹ is a new and exciting materials processing technique which combines the attributes of conventional mechanical milling with all effects generated by electric discharges. It is demonstrated that EDAMM can be used to synthesize a range of functional materials in a matter of minutes, rather than days. Possibilities of this method can be extended to biomaterials and lead to new, lower temperature and faster materials synthesis. In this work we are presenting the different aspects and results when processing pure Al and Zr metals and their oxides in different atmosphere and electrical conditions. Al-Zr phases are extremely difficult to obtain as they usually require high temperature, long and multistep processing², whereas studies on Al_xZr_yO_z properties will be first systematic investigation of this compound.

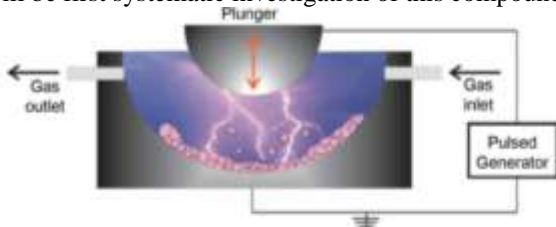


Figure 1 EDAMM processing chamber

Experimental methods

Al and Zr powders or their oxides were processed by a custom made EDAMM under different conditions. Their examination involved X-ray diffraction analysis for their chemical characterization, FESEM for the external shape and the cross-sectional, elemental analysis. In the later stage, the TEM examination will be also performed.

Results and discussion:

Two types of electrical conditions (AC,DC mode) as well as different atmospheres can be applied during EDAMM processing, determining the type of the chemical reaction. Pure metals processed in high purity Argon atmosphere enable fast and relatively low temperature synthesis of intermetallic phases such as

Al₂Zr, Al₃Zr, AlZr₃ etc. which are hard to obtain by conventional heat treatment². The same powders processed in the Ar/O₂ mixture enable to obtain Al and Zr oxides as well as ternary compounds of Zr-Al-O. Zirconium and Aluminium oxides, depending on the electric conditions, can form one or two phase material in which the main constituent of three element compound of Al-Zr-O with potential for biomedical applications. To our knowledge, there were no research focused on that ternary material, therefore its synthesis as well as properties may be of an interest of not only biomedical field. All the above mentioned synthesis can be performed in less than 5 min and much lower temperature than the conventional heat treatment, minimizing time consumption as well as the energy usage.

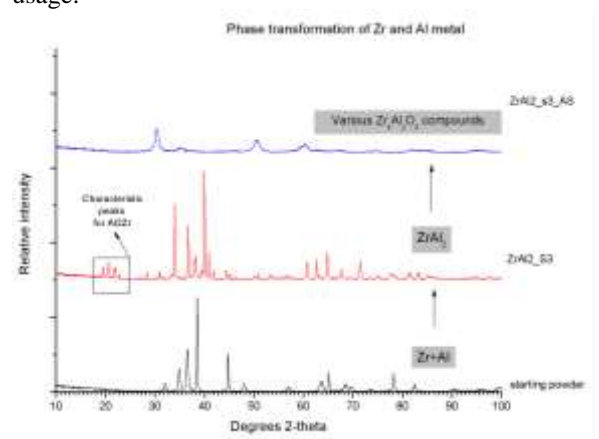


Figure 2 X-ray spectra of Al_xZr_yO_z compound processing route as an example of fast, 5-min compound synthesis

Conclusion

EDAMM is a novel method for materials processing in a powder form and allow fast and low temperature synthesis of materials. Optimization of the process includes the atmosphere of the process, mechanical impact and initial conditions of the powders, meaning the starting powders ratios and their mixing.

References:

1. A. Calka & D. Wexler, *Nature* 419, 147-151
2. R. A. Varin, *Metallurgical and Materials Transactions A*, 2002, Volume 33, Issue 1, pp 193-201

Acknowledgement

We are acknowledging David Wexler who helped with the sample preparation as well as SEM imaging. Investigation was supported by funding from the Australian Research Council (grant No. DP130101390).



Biofabrication of osteochondral grafts via 3D printing of cell-laden microcarriers in a gelatin methacrylamide/gellan gum bioink

Riccardo Levato,^{1,2} Jetze Visser,³ Josep A. Planell,¹ Elisabeth Engel,^{1,2,4}
Jos Malda,³ Miguel A. Mateos-Timoneda^{2,1}

¹Institute for Bioengineering of Catalonia, Barcelona, Spain

²CIBER en Bioingeniería, Biomateriales y Nanomedicina, Zaragoza, Spain

³Department of Orthopaedics, University Medical Center Utrecht, Utrecht, the Netherlands

⁴Department of Materials Science and Metallurgic Engineering, UPC, Barcelona, Spain
rlevato@ibecbarcelona.eu

INTRODUCTION

A major challenge in articular cartilage regeneration is to recapitulate the zonal organization of the tissue. Multimaterial structures that mimic it can be built with bioprinting, by 3D controlled deposition of strands of cell-laden hydrogels (bioinks)¹. Additional requirements to design functional osteochondral grafts are: 1) high cell content, which is hard to achieve with standard expansion methods and 2) inclusion of cues to guide cell differentiation in each specific gel layer.

A novel strategy to address these demands is to combine bioprinting with microcarrier technology, which allows for the extensive expansion of cells, while their phenotype can be controlled².

This work aims to fabricate novel living constructs via bioprinting of cell-laden microcarriers (MCs). Mesenchymal Stromal Cells (MSCs) cultured on polylactic acid (PLA) MCs were encapsulated in a gelatin methacrylamide bioink (GelMA), and cell homing on MCs was studied as promoter for bone differentiation and synthesis in 3D printed osteochondral grafts.

EXPERIMENTAL METHODS

PLA MCs (collagen I coated, mean diameter $\approx 120 \mu\text{m}$) were prepared via a green solvent-based method³. MCs were dispersed in GelMA/gellan gum solutions (10% w/v and 1% w/v, respectively) and the mixture was extruded and UV crosslinked. The compressive modulus was evaluated with a dynamic mechanical analyzer. MC-MSCs complexes in the hydrogel matrices were assessed for cell morphology (actin staining), viability (calcein AM/ethidium homodimer) and osteogenic differentiation (alkaline phosphatase activity, osteocalcin synthesis, and alizarin red staining of calcium deposits). Bioprinting was performed via layer-by-layer deposition of bioink strands with the Bioscaffolder system (SYS+ENG, Germany), combined with CAD/CAM software. The bioink included MC-MSCs precultured under static conditions or in a spinner flask bioreactor (BellCo, USA). Student's t-test was performed to assess statistical significance ($n=3$ or 5, $p<0.05$).

RESULTS AND DISCUSSION

GelMA/gellan gum loaded with up to 50 mg/mL MCs, was used as a printable, strand-forming bioink. MCs encapsulation increased the gel compressive modulus up to 2-fold. MSCs retained a spread morphology with well defined actin stress fibers and cell-cell contacts when expanded on the MCs surface and then suspended

in the hydrogel, (Fig.1A), whereas cells encapsulated in GelMA without MCs showed rounded morphology. Such control over cell shape and cytoskeletal organization in hydrogel matrices via addition of MCs has great potential in tuning cell bioactivity and extracellular matrix deposition⁴. In fact, MC-MSCs encapsulated in the gel supported osteogenic commitment of MSCs, inducing mineralized matrix deposition and improving osteocalcin secretion compared to MC-free controls. MC-MSCs complexes were viable after the gel printing and crosslinking. Bioinks loaded with MC-MSCs from spinner flask cultures permitted the fabrication of living constructs, with good shape fidelity, and with high concentration of cell-carrier complexes, which were homogeneously distributed (Fig.1B). Furthermore, a bilayered scaffold, representing an osteochondral graft, was printed with MC-laden gel as a subchondral bone layer, and a gel-only region recapitulating the cartilage zone (Fig. 1C).

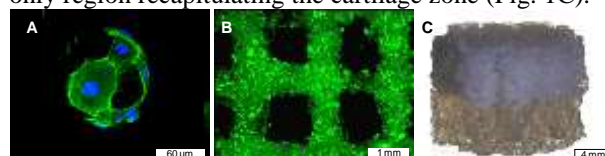


Figure 1: (A) MC-MSCs used for bioprinting, after 4 h culture, (B) MC-cell distribution in the biofabricated construct and (C) MC-laden GelMA-based osteochondral graft.

CONCLUSION

MCs-laden GelMA/gellan gum was proven to be a promising composite material for biofabrication. MCs acted as a mechanical reinforcement for the soft gel. Encapsulation of MC-MSCs complexes -with improved cell adhesion and cell-cell contacts- was effective to improve osteogenic differentiation and to support bone matrix deposition. MCs culture is of great interest for MSCs expansion and scaling-up of bone-like tissues bioprinting. These are key findings to build advanced constructs for bone and zonal osteochondral regeneration.

REFERENCES

1. Malda J. *et al.*, Adv Mat 25(36):5011-28, 2013
2. Sart S. *et al.*, Biotechnol Prog 29(6):1354-66, 2013
3. Levato R. *et al.*, Macromol Biosci 12(4):557-66, 2012
4. Wang C. *et al.*, Biomaterials 30:2259-69, 2009

ACKNOWLEDGMENTS

RL acknowledges the Spanish MECD (FPU grant ref. AP2010-4827). JV was supported by the Dutch NIRM (grant n°FES0908). JM was supported by the Dutch Arthritis Foundation.



Controlled and Reliable Carbonation of Low Temperature Calcium Phosphates

Anna Díez-Escudero^{1,2,*}, Montserrat Espanol^{1,2,3}, Yassine Maazouz^{1,2,3} and Maria-Pau Ginebra^{1,2,3}

¹Department of Materials Science and Metallurgical Engineering, Technical University of Catalonia, Spain

²Centre for Research in Nanoengineering, Technical University of Catalonia, Spain

³Biomedical Research Networking Centre in Bioengineering, Biomaterials and Nanomedicine, Spain

anna.diez-escudero@upc.edu

INTRODUCTION

Low temperature calcium phosphate materials like cements have long attracted the attention in the biomedical field for their close resemblance both, in structure and composition to the mineral phase of bone. Cements can also be easily processed as scaffolds which make them excellent candidates in tissue engineering applications. One aspect though that scientists seek is to incorporate carbonate groups in the apatite lattice of these materials to improve their biological performance^{1,2}. The most common approach used to accomplish this goal relies in the incorporation of calcium carbonate in the formulation of cements. Unfortunately this often leads to unreacted calcium carbonate as second phase masking interpretation of the results. In this work we have developed a very fast, clean and reliable way of introducing carbonate groups by autoclave treatment of the cements in the presence of sodium hydrogen carbonate.

EXPERIMENTAL METHODS

Cement foams (CF) were prepared by mixing a solid phase consisting of 98% α -TCP and a 2% precipitated hydroxyapatite with a liquid phase consisting of 1% Tween 80[®] which, as surfactant, helped to introduce macroporosity. The foams were prepared with a liquid to powder ratio of 0.55 ml/g, injected into moulds (5x10 mm) and immersed in distilled water at 37°C for 10 days to complete setting. Carbonation of the foams was investigated using different methodologies: 1) by addition of NaHCO₃ in the setting media and allowing setting for 17 days; 2) by immersing an already set cement in NaHCO₃ followed by autoclave treatment for 30 min at 120°C and 1bar; and 3) by immersing a non-set cement in NaHCO₃ followed by autoclave treatment to achieve simultaneously setting and carbonate incorporation. To preserve the cohesion of the cements they were maintained for 8-15h in a humid atmosphere prior to immersion in water or the carbonate containing solution. All final products were characterized by X-ray diffraction, scanning electron microscopy, elemental analysis for total carbon determination and infrared spectroscopy.

RESULTS AND DISCUSSION

α -TCP undergoes a hydrolytic reaction by which it transforms into nano- or submicrometric calcium deficient hydroxyapatite (HA) crystals during setting. One can take advantage of this reaction to incorporate foreign ions such as carbonate. Figure 1 evidences the various degrees of carbonation achieved by the three different carbonation methods. As expected, carbonation of the pre-set material yielded lower carbonate contents as compared to the other routes

owing to the slow diffusion of carbonate in the already formed crystals. However, when carbonation took place during setting, carbonate uptake markedly increased up to approximately 15 wt%. The major difference between carbonating during cement setting at 37°C or in the autoclave was the time taken for the conversion of the α -TCP to carbonate-HA: from over two weeks it was reduced to an autoclave cycle of 30min. Thus, autoclaving not only provides a way for incorporating carbonate, but it also speeds conversion of α -TCP to HA. Any of the methods allow a fine tuning of the carbonate content as it can be observed from Fig. 1.

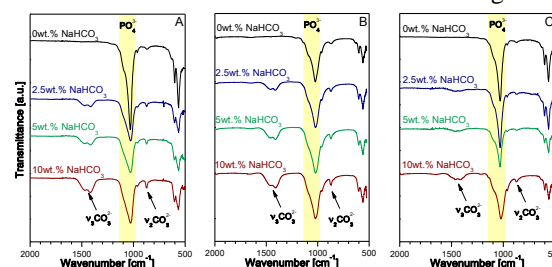


Figure1. IR spectra of CF in the various carbonation methods: during setting at 37°C (A); during setting in autoclave (B); carbonated after setting (C).

In terms of the nano/micro structure resulting from the various carbonation methods there are interesting differences as shown in Fig.2. The microstructure of the CF was preserved if carbonation was accomplished after cement setting (D) but it changed when carbonation and setting took place simultaneously (B, C). Smaller plate-like crystals were formed during carbonation at 37°C (B) as opposed to the larger crystals seen in the autoclave treatment (C).

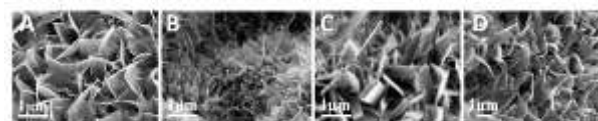


Figure2. SEM images of: A) CF; B) CO₃²⁻ during CF setting; C) CF autoclaved for setting; and D) set CF carbonated in autoclave.

CONCLUSION

This work proves that it is feasible to fine tune the carbonate content of low- temperature HA foams in a reliable manner at different stages of cement setting.

REFERENCES

1. Landi E. *et al.*, J. Eur. Ceramic S. 23:2931-37, 2003.
2. Sariibrahimoglu K. *et al.*, J. Biomed. Mat. Res. Part A 100A:712-19, 2012.

ACKNOWLEDGMENTS

This study was supported by the Spanish Government through project MAT2012-38438-003-01.



Characterization and Biocompatibility of a Collagen/Hydroxyapatite-Microsphere Composite Scaffold for Bone Regeneration

Rahmat Cholas*, Sanosh Kunjalukkal Padmanabhan, Francesca Gervaso, Gayatri Udayan, Graziana Monaco, Alessandro Sannino and Antonio Licciulli

Department of Engineering for Innovation, University of Salento, Italy, rahmat.cholas@unisalento.it

INTRODUCTION

Bone is a composite organic-inorganic material with a complex multi-scale structure. Biomaterial scaffolds which are designed with a structural and chemical composition similar to native bone tissue have been shown to be promising for use as bone implants¹. Specifically, collagen (Col)/hydroxyapatite (HA) composite materials which closely resemble natural bone tissue possess good osteoconductivity and osteoinductivity and may provide the appropriate cellular microenvironment to facilitate bone regeneration. Importantly, the scale of the structural features of the material is an important consideration when designing a scaffold for bone growth, and prior work suggests that multi-scale structures, with defined features at the nano-, micro-, and macro-scales, contribute to the mechanical and biological properties of the material². In this study we incorporated HA microspheres (mHA) with well-defined nano-pores into collagen scaffolds containing a well-ordered interconnected micro- and macro-pore structure and evaluate the cytocompatibility. Attractive properties of this composite scaffold include the ability to load the microspheres for drug delivery and the controllability of the pore structure at various length scales.

EXPERIMENTAL METHODS

HA microsphere synthesis and characterization.

Microspheres were synthesized using a spray drying method. The slurry for spray drying was obtained by precipitating HA nano particle using $\text{Ca}(\text{NO}_3)_2 \cdot 4\text{H}_2\text{O}$ and H_3PO_4 precursors and maintaining a Ca/P molar ratio of 1.67. Transmission electron microscopy (TEM) analysis was carried out to investigate the particle size of the HA used for spray drying. The phase analysis, morphology and size of HA microspheres were characterized by X-ray diffraction (XRD), scanning electron microscopy (SEM) and particle size analyzer, respectively. The specific surface area and pore size analysis of the microspheres were determined by BET and BJH methods.

Composite scaffold fabrication and characterization.

Porous scaffolds were fabricated by freeze-drying a suspension of type I collagen with and without HA microspheres, followed by dehydrothermal crosslinking. The morphology of the scaffolds was studied using SEM. In order to evaluate the mechanical strength of the composite scaffolds, mechanical compression tests in PBS were performed on scaffolds with and without HA microspheres.

Cell culture and cytocompatibility. Scaffolds were seeded with the human osteosarcoma cell line, MG-63, and cultured for 1, 3, 7, and 15 days. Cytocompatibility was identified by the MTT assay and histological

staining. Statistical significance was determined using one-way ANOVA and Fisher's PLSD test.

RESULTS AND DISCUSSION

The XRD analysis of the microspheres revealed a pure HA phase. SEM demonstrated the microspheres to be uniformly rounded (Figure 1a) and particle size analysis gave distribution values D_{10} , D_{50} and D_{90} of 1, 6 and 13 microns, respectively. BJH analysis showed the microspheres to be mesoporous with an average pore diameter of 16 nm. SEM observations of Col/mHA scaffolds revealed HA microspheres embedded within a porous collagen matrix with a pore size ranging from a few microns up to 200 microns (Figure 1b), which was also observed by histological staining (Figure 1c). The mechanical strength (σ - ϵ initial slope) of the composite scaffolds was significantly higher than pure collagen scaffolds, indicating mHA do not disrupt the collagen fibre structure (5.53 ± 0.82 vs 3.27 ± 0.81 KPa). Cell proliferation measured by the MTT assay showed more than a 3-fold increase in cell number within the scaffolds after 15 days of culture for both pure collagen scaffolds and collagen-mHA composite scaffolds (no statistical difference with and without mHA, Figure 1d), suggesting that the integration of the mHA microspheres is compatible with MG-63 cell growth.

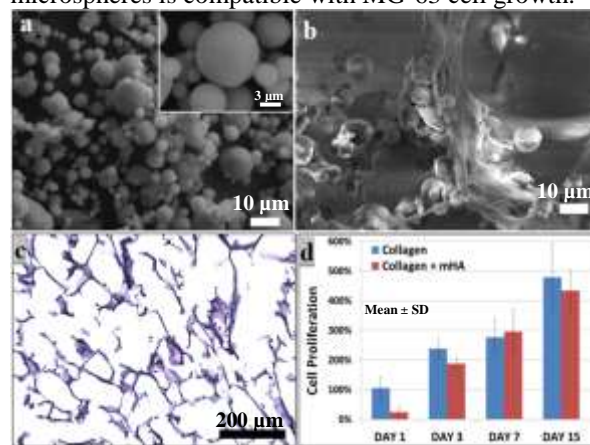


Figure 1.

CONCLUSION

A multi-scale collagen/HA-microsphere composite scaffold was fabricated with controllable structural features on the nano- micro- and macro-scale. The scaffold was found to support cell growth and may be a promising biomaterial for bone reconstruction as a non-load-bearing implant.

REFERENCES

1. Amini A. *et al.*, Crit. Rev. Biomed. 40:363-8, 2012
2. Jeon J. *et al.*, Anat. Rec. 297: 26-35, 2014

PEO Physicochemical Modification of Novel Low-modulus β -Ti Alloys Shows Comparable Cellular Behaviour to Commercial α - and $(\alpha+\beta)$ -Ti Alloys

Mehdi Golozar^{1*}, Constantin-Edi Tanase², Roger A. Brooks², and Serena M. Best¹

¹Cambridge Centre for Medical Materials, University of Cambridge, UK, mg628@cam.ac.uk

²Division of Trauma & Orthopaedic Surgery, Addenbrooke's Hospital, University of Cambridge, UK

INTRODUCTION

Surface modification of endosseous Ti implants at the nano-/micro-scale has been shown to enhance bone formation and encourage rapid osseointegration and biomechanical stability^{1,2,3}. Plasma Electrolytic Oxidation (PEO) creates a textured TiO₂ surface layer, suitable for orthopaedic applications. Among the three polymorphs of TiO₂ (anatase, rutile and brookite), anatase has been shown to enable rapid precipitation of HA in SBF⁴; hence, it is desirable to maximize the surface anatase content. Moreover, in comparison to α - and $(\alpha+\beta)$ -Ti alloys, β -Ti alloys have a modulus closer to that of natural bone, and thus potentially offer a lower stress shielding effect. This study explores the possibility of extending the application of PEO to novel low-modulus β -Ti alloys, while maintaining similar cellular activity as commercial α - and $(\alpha+\beta)$ -Ti alloys.

EXPERIMENTAL METHODS

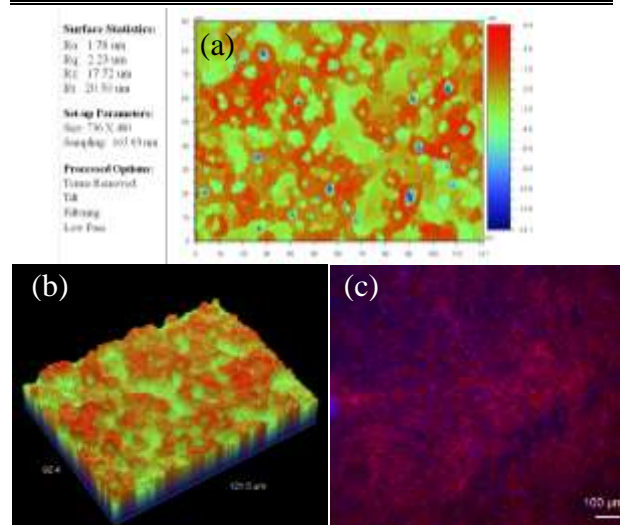
PEO was conducted in a 10 kW KeroniteTM rig using the initial current density of 20 A·dm⁻² and 0.05 M Na₃PO₄ electrolyte. The electrolyte temperature was kept at 20±2°C. Coatings were produced on α -Ti, $(\alpha+\beta)$ -Ti6Al4V, β -Ti13Nb13Zr and β -Ti45Nb discs after 2, 5, 10, and 30 minutes. The physicochemical variations of the PEO coatings were characterised using SEM, XRD-Rietveld Refinement, Optical Interferometry (R_a and R_z), and Drop Shape Analysis. The influence of coatings on metabolic activity, proliferation and differentiation of human foetal osteoblasts was studied using alamarBlue, CyQuant and ALP, respectively. The effects on human foetal osteoblast mineralization (OsteoImage kit), collagen release (immunoblotting), and surface distribution of cells (immunofluorescence) were also investigated.

RESULTS AND DISCUSSION

The development of surface physicochemical features during PEO was found to be time dependent and caused primarily by micro-plasma discharges. The micro-plasma discharges and the resulting surface roughness, anatase content and hydrophilicity seemed to depend on the initial formation of an electrically insulating oxide layer. At longer processing times, the anatase/rutile ratios dropped, while hydrophilicity and roughness increased, Table 1. Uniform pore size distribution was observed for all four alloys, Figure 1(a-b). *In vitro* biological evaluation of the coatings showed similar osteoblast metabolic activity, proliferation and differentiation on all four alloys. Osteoblasts were evenly distributed on coating surfaces, Figure 1(c). Osteoblast mineralization appeared to be enhanced after 30 min, which may be associated with increased coating thickness, surface roughness and/or hydrophilicity.

"Table 1: Properties of PEO-coated Ti alloys"

Titanium Alloys	Modulus (GPa) ^{1,5}	Roughness, R_a [μ m]			
		2min	5min	10min	30min
$(\alpha+\beta)$ -Ti6Al4V	110-112	0.774	0.993	1.032	4.253
α -Ti	100	0.851	0.978	1.137	1.344
β -Ti13Nb13Zr	77-84	1.319	1.753	1.751	1.949
β -Ti45Nb	~62	0.453	1.086	1.831	2.188



"Figure 1: Surface topography of 10 min PEO-coated Ti45Nb ($R_a=1.78 \mu$ m and $R_z=17.72 \mu$ m), a-b. Osteoblasts are evenly distributed over the surface (Pha+DAPI after 3 days of human foetal osteoblast culture on such surface), c."

CONCLUSION

PEO was shown capable of producing rough anatase-rich TiO₂ films on α -, $(\alpha+\beta)$ -, and β -Ti alloys. The surface physicochemical properties (roughness, phase content and hydrophilicity) were found to depend on PEO processing time and substrate material. Regardless of the contrast in bulk mechanical properties (stiffness), metabolic activity, proliferation and differentiation of osteoblasts remained consistent for all four alloys. This suggests that PEO application can be extended to low-modulus β -Ti alloys offering a lower stress shielding effect, without compromising the biological activity.

REFERENCES

- Geetha M. *et al.*, 54:397-425, 2009
- De Jonge L.T. *et al.*, 25:2357-2369, 2008
- Gittens R.A. *et al.*, 32:3395-3403, 2011
- Uchida M. *et al.*, 64:164-170, 2003
- Hanada S. *et al.*, 1284:239-247, 2005

ACKNOWLEDGMENTS

Authors would like to thank the Marie Curie Initial Training Network (Grant # 264635) for providing financial support. A special thanks to Dr. Curran and Dr. Dunleavy for their assistance concerning PEO.

Machining of Metallic Biomaterials: Comparison between Co-Cr-Mo and Ti-Al-Nb Alloys

Timotius Pasang^{1*}, Mamoru Takahashi², Daiki Shinohara², Patrick Conor¹, Kiyoshi Tanaka³ and Osamu Kamiya²

^{1*}Department of Mechanical Engineering, AUT University, 24 St Paul Street, Auckland, 1020, New Zealand Cooperative

²Cooperative Major in Life Cycle Design Engineering, Graduate School of Engineering and Resource Science, Akita University, 1-1 Tegatagakuen-machi, Akita, 010-8502, Japan

³Division of Dentistry and Oral Surgery, Akita University School of Medicine, 1-1-1 Hondo, Akita, 018-8543, Japan
tpasang@aut.ac.nz

INTRODUCTION

This paper presents a machining work performed on two biomaterials namely Cobalt-Chromium-Molybdenum (Co-Cr-Mo) and Titanium-Aluminium-Niobium (Ti-Al-Nb). These two alloys are known for applications on the dental area, and joint prostheses, respectively.

The objectives of this research are to study the milling performance of the above alloys, by measuring the forced required and by examining the milled surface as well as the chips produced.

EXPERIMENTAL METHODS

Lateral milling experiments¹, identical to milling on teeth, were conducted on two different alloys namely Cobaltan and TiAlNb (compositions in Table 1) using four types of drills made of tungsten carbide (WC). Three types of the drills were uncoated and the fourth type was coated with a diamond-like carbon (DLC) layer. The rotational speed used varied from 10,000 to 35,000 rpm with a feed rate fixed at 0.15 mm/second. Fig.1 shows the milling configuration and test mills.

Table 1. Nominal composition and hardness values

Alloy	Cr	Co	Mo	Ti	Al	Nb	Hv*
Co-Cr-Mo	65	29	6	-	-	-	365
Ti-Al-Nb	-	-	-	86	6	7	400

*Hv = Vicker's hardness

Cutting forces were measured and recorded during milling. The milling tests were carried out at room temperature without mill lubrication or cooling.

The surfaces of the drills, the workpieces and the chips were analyzed by scanning electron microscopy (SEM).



Figure 1. Schematic diagram showing lateral milling and the four types of mills used in this study,

RESULTS AND DISCUSSION

The cutting (milling) forces for Co-Cr-Mo alloy were generally higher at lower cutting speed than those required at higher cutting speed although the Type B (S21N) mill required approximately 60% lower force than the other three types of mills at 10,000 rpm

(Fig.2a). At cutting speeds above 15,000 rpm the forces were comparable, i.e. around 1N, with much less force required for one mill at 35,000 rpm. For Ti-Al-Nb, the cutting (milling) forces ranged from 0.5 to 2 N for all mills used (Fig. 2b).

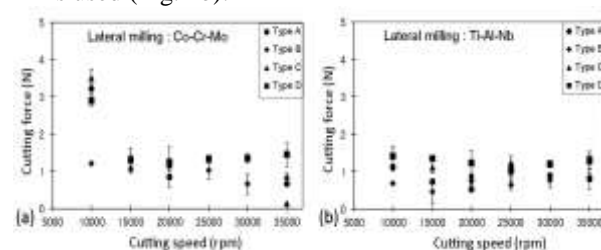


Figure 2. Cutting force required during lateral milling at constant feed rate and a range of mill rotation speeds.

The appearance of the machined surfaces showed significant variations related to the extent to which metal chips retained in the mill flutes had frictionally re-welded onto the surfaces behind the mill. This was considered to be partly due to the high temperature of the machining process resulting from the absence of liquid coolant but was also associated with tool wear.

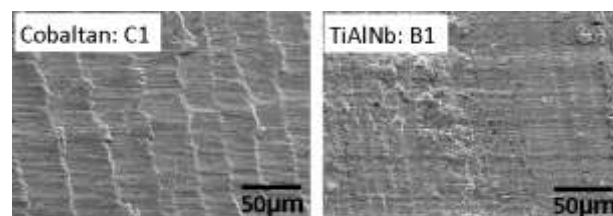


Figure 3. SEM images of machined surfaces.

CONCLUSIONS

The force required for high speed micro-milling of a cobalt alloy in the absence of coolant was relatively insensitive to speed and mill configuration at mill rotational speeds between 15,000 rpm and 25,000 rpm. For this alloy, relative cutting forces were affected by mill configuration at lower and higher rotational speeds. On a titanium alloy, cutting forces were relatively low at all speeds, with little influence of mill configuration at higher speeds. Metal chip re-welding affected the workpiece surface finish of both alloys.

REFERENCES

1. Takahashi M. *et al.*, to be published in Int. J. Soc. Mater. Eng. Resour., 2014

ACKNOWLEDGMENTS

The authors (TP and OK) would like to thank the Japan Society for the Promotion of Science (JSPS) for funding through JSPS Fellowship number L13711.



UKSB

ORAL PRESENTATIONS

The drive for simplicity in delivering cells to the clinic - clever cells and dumb scaffolds

Sheila MacNeil¹

¹Department of Materials Science & Engineering, Kroto Research Institute, University of Sheffield, UK
s.macneil@sheffield.ac.uk

INTRODUCTION

One of the challenges for the world of biomaterials and tissue engineering has been to what extent scaffolds need to be complex and mimic human physiology such as containing the collagenous extracellular matrix signalling motifs which promote cell binding and differentiation *in vivo*. Can synthetic scaffolds ever been good enough for tissue engineering purposes? How much complexity is necessary for clinical efficacy? Should we stick with natural decellularised scaffolds (for example for 3D tissue reconstruction for skin and oral mucosa) or can we make an altogether simpler synthetic alternative? There are pros and cons in working with natural tissues in that they can retain the native architecture, particularly basement membrane which helps give cells instructions. There are pluses in working with very simple synthetic scaffolds in terms of controllability, ease of sterilisation and regulatory issues. My group has been making tissue engineered materials for clinical use since early 1992 and has developed a good understanding of the pros and cons of both.

EXPERIMENTAL METHODS

We have delivered 3D tissue engineered skin to the clinic based on human donor skin which has been de-epithelialised and decellularised and then reconstituted with the patient's own keratinocytes and fibroblasts [1]. This methodology has also been used to deliver tissue engineered buccal mucosa to the clinic [2]. We have also developed simple 2D and 3D carriers for delivering keratinocytes to patients with extensive full thickness burns (developed as the product Myskin™) [3]. More recently this method has also been used to deliver other cells [4,5]. We have also developed 3D biodegradable scaffolds made of PLGA for delivering corneal limbal epithelial cells to the cornea in cases of limbal stem cell loss [6].

RESULTS AND DISCUSSION

Both natural materials and synthetic materials can deliver clinical benefit and our findings are that if one combines the right combination of cells in a very simple scaffold then the cells can achieve the appropriate phenotype *in vitro* for transplantation even with a "dumb" scaffold.

CONCLUSION

In developing cells and scaffolds to go to the clinic, it is always worth asking what is the least complex system that will work as the simpler the system, the less the problems in translating this to the clinic and in making it broadly applicable.

REFERENCES

1. MacNeil S.. Nature Insights. Nature 445, 874-880 (2007)
2. Bhargava S *et al.* European Urology 53(6):1263-1271. (2008)
3. Moustafa M *et al.* Regenerative Medicine 2(6):887-902. (2007)
4. Walker NG *et al.* Tissue Engineering. 18(2):143-55 (2012)
5. Jiang D *et al.* Biomaterials. 34(10):2501-15 (2013)
6. Deshpande P *et al.* Biomaterials. 34(21): 5088-5106 (2013)

ACKNOWLEDGMENTS.

We acknowledge funding from The Wellcome Trust – Affordable Healthcare for India - for the development of a carrier for corneal cell transplantation.

Fig. 1: The cell delivery carrier Myskin™ used to deliver autologous cultured keratinocytes to a patient with extensive burns injuries



Harnessing Scanning Probe Nanolithographies for Cell and Molecular Biology

Lu Shin Wong^{1,2*}

¹Manchester Institute of Biotechnology, University of Manchester, UK

²School of Chemistry, University of Manchester, UK

l.s.wong@manchester.ac.uk

INTRODUCTION

The ability to manipulate cell behaviour is a cornerstone of cell biology. Since its inception, the driving paradigm in this discipline has been to control cell physiology and phenotype through the application of a range of “drug-like” compounds such as small molecules, hormones and growth factors.

In contrast, there is now compelling evidence that cellular phenotype is dependent on the extracellular surface topography and the spatial location of chemical signals at the sub-micron scale.¹⁻⁴ The use of designer micro- and nanofabricated surfaces to control cell behaviour therefore offers an intriguing alternative to the conventional approaches in cell biology.

However, research in this area has until recently been hampered by the difficulty in fabricating such nanostructured surfaces suitable for exploratory cell biology. The vast majority of standard nanofabrication methods are derived from the microelectronics industry, and are poorly suited for the generation of nanoscale patterns of relatively fragile biomolecules in sufficiently large areas for routine cell culture.

As an alternative, we and others have started to apply scanning probe nanolithography methods derived from atomic force microscopy (AFM) such as dip-pen nanolithography (DPN) and polymer pen lithography (PPL) for the fabrication of micro- and nanoscale biomolecular arrays.^{2, 5, 6} These methods are compatible with biomolecules, operate under ambient conditions and enable nanopatterning over large areas (cm²).

Here, we describe some of our work related to the development of methods for the fabrication of large-area biomolecular arrays, down to the resolution of a single protein molecule; and the application of such arrays to manipulating mesenchymal stem cell (MSC) differentiation.

EXPERIMENTAL METHODS

For the control of MSC differentiation, full experimental procedures have been reported elsewhere.² Briefly, PPL was used to deposit features of 16-mercaptohexadecanoic acid on gold surfaces in a range of spot feature sizes from 300–1200 nm in diameter. These features acted as a template for the adsorption of fibronectin, upon which the MSCs were cultured. The cells were analysed by a combination of immunofluorescence microscopy, quantitative RT-PCR and Western blotting of the proteins of interest.

For the single molecule protein arrays, the arrays of gold nanoparticles were fabricated by scanning probe block copolymer lithography (SPBCL), where were then surface treated according to previously reported procedures.⁵ These nanoparticles served as the template for the attachment of individual protein molecules. The protein activity was analysed by a colorimetric assays, or through the selective binding of nanoparticle labels and subsequent transmission electron microscopy.

RESULTS AND DISCUSSION

Using the large arrays of fibronectin printed by PPL, it was found that the MSCs were cultured on fibronectin patterns with a feature size of 300 nm a pitch of 1200 nm demonstrated a statistically significant increase in the expression levels of the osteogenic markers even in the absence of the standard osteogenic culture media.

In the case of SPBCL templating of proteins, it was found that when the gold nanoparticles were similar in size to the target protein (~ 4 nm for streptavidin, ~ 10 nm for antibodies), on average only one protein molecule was attached to each individual nanoparticle on the array. Furthermore, activity assays and electron microscopy analysis of the labelled proteins showed that the attached protein retain their biological activity.

REFERENCES

1. J. M. Curran, R. Stokes, E. Irvine, D. Graham, N. A. Amro, R. G. Sanedrin, H. Jamil and J. A. Hunt, *Lab on a Chip* 10:1662-1670, 2010.
2. L. R. Giam, M. D. Massich, L. Hao, L. S. Wong, C. C. Mader and C. A. Mirkin, *Proc. Natl. Acad. Sci. USA* 109:4377-438, 2012.
3. C. P. Brown, *Nat. Rev. Rheumatol.* 9:614-623, 2013.
4. B. L. Ekerdt, R. A. Segalman and D. V. Schaffer, *Biotechnol. J.* 8:1411-1423, 2013.
5. J. Chai, L. S. Wong, L. R. Giam and C. A. Mirkin, *Proc. Natl. Acad. Sci. USA* 108:19521-19525, 2011.
6. L. S. Wong, C. V. Karthikeyan, D. J. Eichelsdoerfer, J. Micklefield and C. A. Mirkin, *RSC Nanoscale* 4:659-666, 2012.

ACKNOWLEDGMENTS

The author thanks the UK Engineering and Physical Sciences Research Council (EPSRC) for a Life Science Interface Fellowship, a Strategic Equipment Grant and for research funding under EP/F042590/1, EP/K024485/1 and EP/K011685/1, respectively.



Photochemical Functionalisation and Patterning of Diamond-Like-Carbon for Electronic Neural Interfaces

James Dugan and Frederik Claeysens

Department of Materials Science and Engineering, Kroto Research Institute, The University of Sheffield, UK.

J.Dugan@sheffield.ac.uk

INTRODUCTION

The development of electrodes for direct interface with the brain has the potential to greatly improve prostheses to aid victims of spinal injury or similar disablement. However, the development of such electrodes relies on careful engineering of the biological-electronic interface with control of scarring, cell phenotype and tissue organisation. Diamond-like-carbon (DLC) may be an ideal material for coating electrodes as it has flexible electrical properties, it is extremely stable *in vivo* and is already used as a coating for orthopaedic implants¹. Chemical modification is essential, however, to control and promote adhesion, differentiation and organisation of neurons and glia.

EXPERIMENTAL METHODS

DLC was coated on silicon by chemical vapour deposition. The surface chemistry of the DLC was modified by atom transfer radical polymerization (ATRP) in order to produce PEG-coated non-cell-adhesive surfaces. The surfaces were then further modified photochemically with charged monomers in order to promote cell adhesion and neuronal differentiation in a controlled fashion. Several techniques were also employed for surface patterning including the use of shadow masks, direct-write photopolymerisation of charged monomers and pulsed laser ablation of non-adhesive polymer coatings.

The modified DLC surfaces were characterised by AFM, XPS and Raman spectroscopy and for protein adsorption by immunofluorescence. The potential for use in neural-electronic interfaces was explored by culture and differentiation of primary neural progenitors.

RESULTS AND DISCUSSION

Freshly hydrogenated DLC and ATRP PEG-functionalized DLC were found to be non-adhesive to cells. By modification with surface initiated polyacrylic acid (PAA), hydrophilicity and cell adhesion were promoted. Neural progenitors adhered to the modified surfaces and a multipotent phenotype was maintained until withdrawal of growth factors. Spontaneous differentiation occurred on the modified surfaces with both neuronal and glial differentiation observed. Patterned tracks were prepared by masked polymerisation of charged monomers and promoted spatial organisation of neuronal cells. Spatial control of

cell adhesion was also achieved by pulsed laser ablation of ATRP PEG surfaces to reveal adhesive regions that supported protein adsorption and cell adhesion.

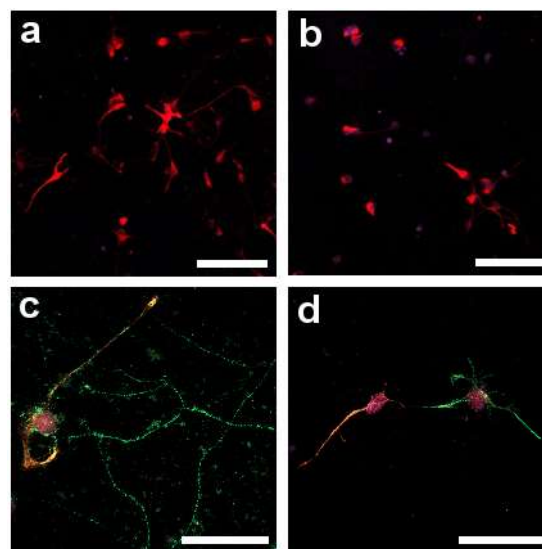


Fig. 1. Immunofluorescence micrographs of neuroprogenitors before (a, b) and after (c, d) spontaneous differentiation on glass (a) and polyacrylic acid coated surfaces (b, c, d). Cells were stained for nestin (red), β III-tubulin (green, c) and GFAP (green, d). Scale bars in a and b are 150 μ m. Scale bars in c and d are 80 μ m.

CONCLUSION

The surface chemistry of DLC was modified and patterned by facile photochemical methods. Such approaches allow for the tuning of biological properties and the rational design of the electrode-brain interface. Further studies on the differentiation of stem cells and the development of controlled patterning protocols will be carried out.

REFERENCES

1. Regan, EM *et al.* Biomaterials (2010), 31, 2, 207-215.

ACKNOWLEDGMENTS

Project funded by EPSRC. The authors are grateful to Dr O. Fox and Prof P. May at the University of Bristol for hydrogenation of DLC.

Impact Testing of Skin: Overcoming the Stratum Corneum Barrier for Microneedle Application

Kikelomo Moronkeji^{1*}, Simon Todd², Ahmed Elsheikh¹ and Riaz Akhtar¹

^{1*}School of Engineering, University of Liverpool, UK, K.Moronkeji@liverpool.ac.uk

²Renephra Ltd, Manchester, UK

INTRODUCTION

Due to limitations with conventional hypodermic needles, microneedles have been developed over a number of years to painlessly deliver drugs and vaccines through the skin¹. Microneedles are sub-millimetre arrays typically fabricated from polymers or metal which aim to penetrate the stratum corneum and directly access the underlying epidermis². However, it remains a major challenge to reproducibly penetrate the stratum corneum due to its inherent elasticity and other factors that affect the mechanical properties of the stratum corneum such as patient age. Previous studies have suggested that application speed and force influence penetration of stratum corneum with microneedles³, however there is little quantitative data in the literature. This study aimed to quantify the optimal insertion speed and force of Polyether ether ketone (PEEK) oblique microneedle arrays into skin.

EXPERIMENTAL METHODS

9 x 9 arrays of PEEK microneedles (Fig. 1) were utilised to penetrate neonatal porcine skin in vitro. Neonatal porcine skin has a comparable mechanical properties to human skin⁴. A dropped weight impact testing rig was developed to allow microneedle application to be varied as a function of velocities in excess of 2 m/s, with the total load of the drop mass measured by a force transducer being 0.4 N.

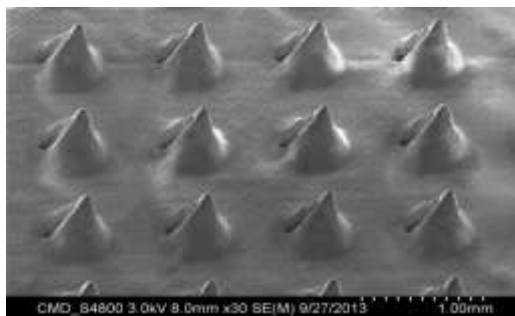


Fig. 1 SEM image of PEEK oblique microneedle arrays

RESULTS AND DISCUSSION

Impact speed significantly influenced the quality and consistency of microneedle penetration. Methylene blue and histological staining (H&E) were used to determine penetration. Successful penetration of the stratum corneum occurred at 3–5 m/s (Figs. 2 and 3), with no evidence of penetration at lower speeds – this is 1000 times⁵ the penetration speed required for hypodermic needles. The histology images at different regions on a single sample of skin show the breached profile follows the microneedle outline (Fig. 3) and the size of the tear in the epidermis was found to correlate with the size of the microneedle. Further, a series of gelatine gels (67%, 80%, 88% and 96% water content) were used to act as an underlying substrate for skin. The speed at

which successful penetration occurred significantly decreased at higher water contents.

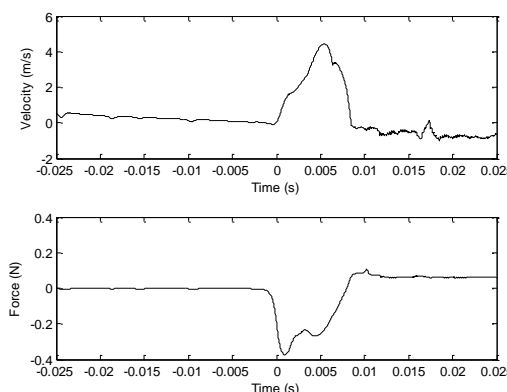


Fig. 2 Velocity-time plot of impact test on skin (back region) at 5 m/s and 0.4 N

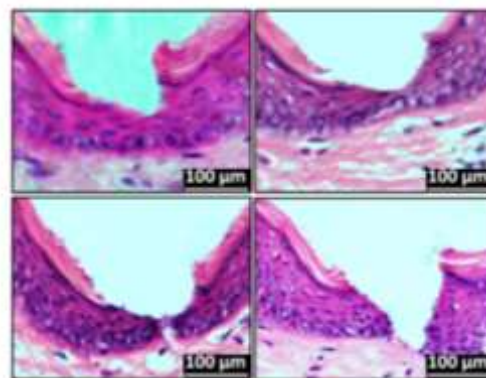


Fig. 3 Histology images of microneedle breach of the epidermis

CONCLUSIONS

Our findings suggests that for successful penetration of the stratum corneum far higher velocities are required than associated with conventional hypodermic needles and reduced penetration speed with increasing gel water content.

REFERENCES

1. Bhat S. C. *et al.*, Biomater., 3:e24717-(1-12), 2013
2. Prausnitz M. R., Adv. Drug Deliv., 56:581-587, 2006
3. Donnelly R. F. *et al.*, Pharm. Res., 28:41-57, 2011
4. Shergold O. A. *et al.*, Int. J. Impact Eng., 32:1384-1402, 2006
5. van Gerwen D. *et al.*, Med. Eng. & Phy., 34:665-680, 2012

ACKNOWLEDGMENTS

The authors would like to thank the European and Regional Development Fund and the Centre for Global Eco-Innovation for providing financial support for this project.

Exploring the Cell-Nanoneedle Interface

Ciro Chiappini^{1,3}, Jonathan O. Martinez², Enrica De Rosa², Paola Campagnolo¹, Ennio Tasciotti², Molly M. Stevens^{1,3*}

¹Department of Materials, Imperial College London, UK

²Department of Nanomedicine, Methodist Houston Research Institute, USA

³Department of Bioengineering and Institute of Biomedical Engineering, Imperial College London, UK
c.chiappini@imperial.ac.uk

INTRODUCTION

Nanoneedles are attracting increasing interest as a facile, high-throughput, minimally invasive strategy for intracellular investigation due to their low-cost, versatility and ease of use. Nanoneedles *in-vitro* have investigated the propagation of action potentials within excitable cells¹, as well as mediated the intracellular delivery of membrane-impermeant biomolecules such as peptides and nucleic acids². Despite these initial successes at probing the intracellular compartment, little is known of how nanoneedles interface with cells. Conflicting evidence exists as to whether the nanoneedles effectively cross the plasmalemma or they simply induce an increase in its permeability^{2,3}. In this study we aim to investigate the ability of porous silicon nanoneedles to cross the plasma membrane by observing their ability to deliver nanoparticles to the cytosol. At the same time we investigate the evolution of the cell-nanoneedle interface over time.

EXPERIMENTAL METHODS

Nanoneedles are fabricated combining photolithography, metal assisted chemical etching and reactive ion etching of a single crystal silicon substrate. The resulting nanoneedles are 55% porous with a pore size in the range of 15 nm. The nanoneedles are loaded with hydrophilic quantum dots from solution and interfaced with cells either by seeding HeLa cells over the nanoneedles or by pressing the nanoneedles over HeLa cells in culture. The samples are analysed by confocal microscopy and by dual beam focussed ion beam scanning electron microscopy.

RESULTS AND DISCUSSION

We have developed an array vertically aligned biodegradable nanoneedles that originate from our recent systematic investigation of metal assisted chemical etch. The nanoneedles were vertically supported over a silicon substrate, had a tip diameter smaller than 100 nm, 15 nm pores with 55% porosity, and a length of 3 microns (Figure 1). When seeding cells over the nanoneedles we observed that the needles had penetrated across the cell membrane within 1h (Figure 2). Up until 8h following seeding the cells descended along the nanoneedles, partly internalizing them. For the entire time, the needles localized within the cell cytosol but did not cross the nuclear envelope. The nanoneedles were able to deliver cell-impermeant quantum dots directly to the cytosol within 30 minutes from interfacing. The interfacing with nanoneedles did not induce any change in cell viability or proliferation, compared to controls grown on flat silicon substrates.

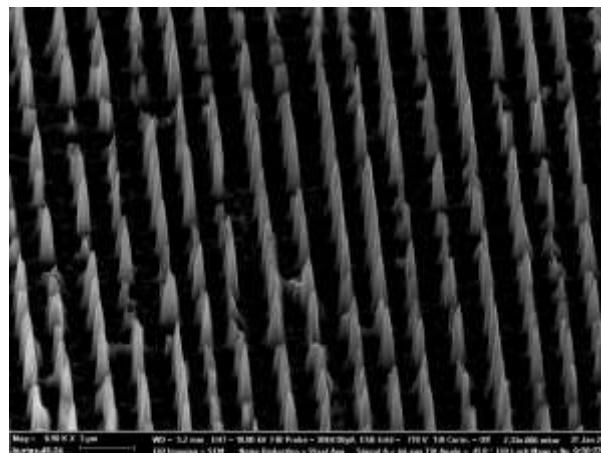


Figure 1 Scanning electron micrograph showing a vertical array of porous silicon nanoneedles with less than 100 nm tip and 3 μm length. Scale bar 2 μm.

The nanoneedles fully degraded both inside and outside the cell within a 27h timeframe, as supported by SEM and inductively coupled plasma – atomic emission spectroscopy.

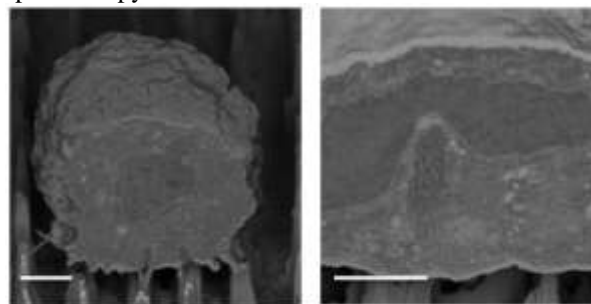


Figure 2 Nanoneedles penetrate the cell cytosol over time. Left FIB-SEM image showing nanoneedles penetrating within a cell 1h following seeding. Right, FIB-SEM imaging showing a nanoneedle penetrating within a cell 8h following seeding, inducing deformation of the cell nucleus. Scale bar 2 μm.

CONCLUSION

We demonstrated the fabrication of biodegradable nanoneedles that can rapidly cross the cell membrane to deliver cell-impermeant nanoparticles to the cytosol with minimal inherent toxicity for the cell. The nanoneedles degrade progressively over the course of 72 h.

REFERENCES

1. Robinson, J. T. *et al. Nat. Nanotechnol.* **7**, 180–184 (2012).
2. Shalek, A. K. *et al. Proc. Nat. Acad. Sci. USA* **107**, 1870–1875 (2010).
3. L. Hanson *et al. Nano Lett.* **12**, 5815–5820 (2012)

Strategies to Enhance the Cellular Response to Bioactive Surfaces

L. Rutledge¹, L. Randolph², I. Mutreja¹, B. Meenan,¹ A. Boyd¹

¹NIBEC, University of Ulster, United Kingdom, Rutledge-L1@email.ulster.ac.uk, ²Grenoble IPN, France.

INTRODUCTION

According to the National Joint Registry^[1], since 2011 there has been a rise of 7.4% in the number of hip and knee total joint replacements procedures carried out within the U.K. The current method of carrying out these procedures using hydroxyapatite (HA) are not ideal, as the HA coating is often prone to deficiency, resulting in unacceptably high revision rates for younger patients. In order to address this, and meet demand, this project seeks to renew impetus for the development of multifunctional, HA surfaces, e.g. Strontium or Silicon doped HA, which can augment the chemical and topographical surface properties of the orthopaedic biomaterial, making a more favourable physiological environment, which in turn will drive biological response and induce more rapid osteointegration. It is envisioned that this strategy will enhance the bone-biomaterial interface, improving the orthopaedic implant stability and long term survival, therefore enhancing the clinical outcome for the patient.

EXPERIMENTAL METHODS

A range of Calcium Phosphate (Ca-P) coatings were deposited onto medical grade titanium alloys (Ti-6Al-4V) using radio frequency (RF) Magnetron Sputtering. Coatings were produced from both pure HA and Sr doped HA (Sr-HA) starting powders (5-13% wt/wt). The starting target materials and the resultant coatings (as-received, thermally processed) were characterised using analytical techniques including X-ray diffraction (XRD), Fourier Transform Infrared (FTIR), Atomic Force Microscopy (AFM) and X-ray photoelectron spectroscopy (XPS). *In vitro* methods (PicoGreen® Assay) were used to look at the early osteoblast in response to the different coatings.

RESULTS AND DISCUSSION

The XRD and FTIR results show that the purity, crystallinity and stoichiometry of HA and Sr-HA (5% and 13%) starting powders were as expected, with the XRD data confirming that the HA materials conformed to the International Centre for Diffraction Data (ICDD) File (09-0432) for pure HA. FTIR and XRD results for the as-deposited HA and Sr-HA derived coatings indicate that they are amorphous and dehydroxylated. Upon annealing to 500°C, the FTIR data highlights that the HA coatings had all the expected OH⁻ and PO₄³⁻ bands, with a high degree of hydroxylation. In comparison, the Sr-HA coatings were dehydroxylated even after annealing, with dehydroxylation increasing with increasing Sr content. The XRD results for these materials indicated that after annealing all the coatings had well defined crystalline peaks, (Fig. 1.) However, the diffraction peaks shifted to lower 2θ values with increasing Sr content. XPS data (Fig.2) shows that when Sr is added to HA, Sr peaks appeared at 275eV (Sr3p) and 134eV (Sr3d).

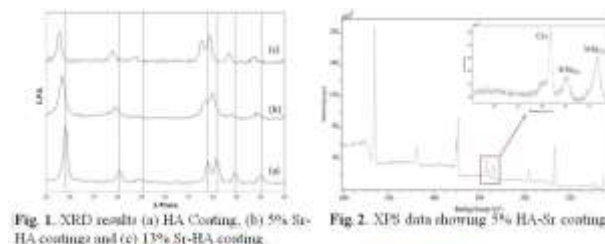


Fig. 1. XRD results (a) HA Coating, (b) 5% Sr-HA coating and (c) 13% Sr-HA coating

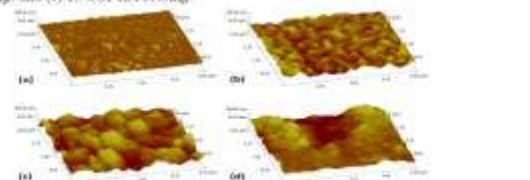


Fig. 2. XPS data showing 5% HA-Sr coating

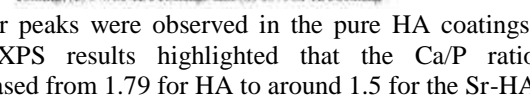


Fig. 3. AFM results for (a) titanium coated substrate, (b) HA coating, (c) 5% Sr-HA coating and (d) 13% Sr-HA coating

No Sr peaks were observed in the pure HA coatings. The XPS results highlighted that the Ca/P ratio decreased from 1.79 for HA to around 1.5 for the Sr-HA surfaces. Also, the Atomic Concentration (%) of Sr in the coatings increases from 1.21% to 3.47% for the 5% and 13% Sr-HA derived materials, respectively. The AFM data (Fig. 3) highlighted that the surface roughness (R_a) of the coatings increased with increasing Sr content. In particular, the R_a increases from 11.8 ± 1.6 nm to 16.2 ± 1.6 nm for the 5% and 13% derived Sr-HA coatings, respectively. All of these results indicate that increasing Sr content in the coatings was due to the Sr ions substituting for the Ca(II) ions causing significant disruption of the lattice. This is corroborated through the greater surface feature irregularity seen in the Sr-HA samples. *In vitro* studies show that the Sr-doped material show enhanced levels of cell attachment up to 72 hours.

CONCLUSION

RF Magnetron Sputtering provides a route to adding Sr to Ca-P coatings with process control. The results show that the coatings produced are similar to HA and are modified accordingly with the addition of different levels of Sr. The preliminary *in vitro* studies indicate that the Sr doped samples show enhanced levels of cell attachment at early time-points (24 and 72 hours), highlighting the potential benefit of adding Sr into such HA coatings. These results are preliminary and need to be expanded. In particular, understanding the potential of these surfaces to promote the differentiation of Mesenchymal Stem Cells, would be important as it would provide a route to developing enhanced surfaces, improving the clinical outcome for patients. Furthermore, it would be useful to study the effects of multi-ion doped coatings in this regard, as opposed to just single ion-doped materials, as further enhancements in surface properties may be possible.

REFERENCES

[1] National Joint Registry 10th Annual Report; 2013

The Effect of Extrinsic Tooth Bleaching Agents on Restorative Dental Materials: A Review

Paul Hatton

Bioengineering & Health Technologies Research Group, School of Clinical Dentistry, University of Sheffield, Claremont Crescent, Sheffield S10 1EX, UK. paul.hatton@sheffield.ac.uk

INTRODUCTION

Tooth bleaching has increased markedly in popularity in the past two decades, coupled to a rapid increase in the availability of both in-office and over-the-counter products that claim to improve the whiteness of teeth. The vast majority of bleaching systems are based on the delivery of hydrogen peroxide, a powerful oxidising agent that is known to be capable of causing tissue damage. Numerous studies of the potential effects of hydrogen peroxide on tissues have therefore been reported to date [1,2]. Effects on dental materials have not been investigated as thoroughly, despite the potential for hydrogen peroxide to cause damage. The aim of this paper was therefore to review data related to the interaction of hydrogen peroxide with restorative dental materials, and determine whether or not this interaction represents a risk to health. This paper will include consideration of experimental studies conducted in Sheffield.

EXPERIMENTAL METHODS

In experimental work, commercial spherical dental amalgams (Tytin® or Sybralloy®, Kerr, UK) were investigated in the form of discs (10 mm x 2 mm) that were exposed to either carbamide peroxide (a hydrogen peroxide generating system), hydrogen peroxide directly, or a range of control materials including distilled water, for 24 h at 37 °C. Ion release was determined using inductively coupled plasma-mass spectrometry (ICP-MS). Where reported, surface roughness was determined using a Talysurf (Mitutoyo Corporation, Japan), while specimen surfaces were investigated using scanning electron microscopy [3,4]. The data from these studies and other work conducted in Sheffield was reviewed alongside other relevant scientific publications.

RESULTS AND DISCUSSION

Several studies reported that hydrogen peroxide treatments were capable of increasing metal ion release from dental amalgam in a dose dependent manner. For example, Table 1 shows that mercury release from Tytin® was increased significantly by two different

[Hydrogen Peroxide] % (w/v)	Mean [Hg] (µg/l)	± Standard Deviation
0	3	1
3	316	75
30	1428	883

Table 1. Release of mercury (Hg) from Tytin® amalgam discs after 24 h exposure to different concentrations of hydrogen peroxide. Adapted from Al-Salehi *et al.* 2007 [3].

concentrations of hydrogen peroxide. No significant change in roughness was associated with these treatments [3]. The evidence that tooth bleaching systems interact with restorative materials is now compelling, and it is recommended here that clinicians protect restorations during these interventions in the same way that they protect soft tissues. With respect to over-the-counter products, there is clearly an even greater risk that consumers will not protect either soft tissues or materials. Despite these concerns, injuries or adverse health effects related to hydrogen peroxide have not been reported widely [5]. In comparison, clinical studies claimed that exposure to relatively high concentrations of carbamide peroxide (up to 16%, the equivalent of 5.3% hydrogen peroxide) was relatively safe and effective [6,7].

CONCLUSION

It was concluded that hydrogen peroxide, whether applied directly or generated by carbamide peroxide, interacted with restorative dental materials. These interactions were concentration dependent, they were potentially damaging to the biomaterial itself (primarily at the surface), and some of the events were potentially harmful to the health of the patient. Further research is undoubtedly needed to inform clinicians, regulators and the public so that informed decisions may be made related to the licensing and use of tooth bleaching systems. Given the increased availability of commercial systems, including chemicals of uncertain provenance than may be purchased easily via the Internet for home use, the need for further research is pressing.

REFERENCES

1. Joiner. *Journal of Dentistry* **34** 412-419. 2006.
2. Attin *et al.* *Dental Materials* **25** 143-157. 2009.
3. Al-Salehi *et al.* *Dental Materials* **22** 948-953. 2006.
4. Al-Salehi *et al.* *Journal of Dentistry* **35** 172-176. 2007
5. Tredwin *et al.* *British Dental Journal* **200** 371-376. 2006.
6. Meireles *et al.* *Operative Dentistry* **33** 606-612. 2008.
7. Meireles *et al.* *Journal of Dentistry* **42** 114-121. 2014.

ACKNOWLEDGMENTS

The author is grateful to local collaborators in Sheffield, especially Samira Al-Salehi, Cheryl Miller, and Cameron McLeod, who contributed to our published studies that was sponsored partly by Unilever plc. The presenter serves on the MeDe Innovation executive.



Synthetic Defensins: Novel Antibacterial Agents for Surface Attachment

Felicity de Cogan¹, Richard Williams², Anna Peacock³, Artemis Stamboulis⁴, Liam Grover², Robert Scott⁵ & Ann Logan¹

¹School of Clinical and Experimental Medicine, University of Birmingham, B15 2TT, UK & NIHR Surgical Reconstruction and Microbiology Research Centre, University Hospital Birmingham, Edgbaston, Birmingham

²School of Biochemical Engineering, University of Birmingham, B15 2TT, UK

³School of Chemistry, University of Birmingham, B15 2TT, UK

⁴School of Metallurgy and Materials, University of Birmingham, B15 2TT, UK

⁵Royal Centre for Defence Medicine, University Hospital Birmingham, Birmingham, B15 2TT, UK
f.decogan@bham.ac.uk

INTRODUCTION

The current management of microbial infection in injured tissues is by the systemic administration of antibiotic drugs. These are designed to eliminate pathogens while leaving the patient unharmed. This method is of limited efficacy as systemic antibiotics are not targeted to the site of infection and will often have poor penetration to areas around wounds and implants. The widespread use of prophylactic antibiotics has also led to increasing microbial resistance.

Naturally occurring defence proteins (Defensins) are found in all tissues and comprise a major part of the innate immune system.¹ These proteins are active against a wide range of microbes, fungi and viruses, are of great research interest as they have high antibacterial efficiency and are less likely to promote bacterial resistance. Unlike standard antibiotics, the Defensins target the microbial cell membrane, so, microbes must redesign their cell membrane to acquire resistance.

We are developing synthetic Defensin-related peptides as broad spectrum antibiotic surface coatings for a range of uses. The use of Defensins as equipment and device coatings will prevent infection of wound sites thereby protecting patients during their treatment pathway.

EXPERIMENTAL METHODS

Defensin-related peptides were synthesised using standard solid phase peptide synthesis and Fmoc chemistry. The final product was purified by HPLC and characterised by mass spectrometry. Peptides were attached to hydroxyapatite and titanium surfaces by electrostatic interaction by incubating the peptide with the material for 30 minutes at room temperature.

For covalent attachment hydroxyapatite surfaces were functionalised to incorporate thiol groups onto the surface of the titanium. Antimicrobial peptides were then functionalised onto the surface using maleimide crosslinkers. Titanium surfaces were functionalised by nitriding the titanium to give free amine groups on the surface. The antimicrobial peptides were then grafted to the surface using peptide coupling.

The antimicrobial activity of the synthetic Defensins was evaluated using the Antimicrobial Minimum Inhibitory Concentration (MIC) tests carried out using standard lab strains of *E. Coli*, *P. Aeruginosa* and *S. Aureaus*. The peptides were also tested against clinical isolates from eyes, general wounds, burn wounds and bone infections. The antimicrobial activity of the peptides while bound to the hydroxyapatite and titanium

surface by incubating Defensin coated blocks in bacteria cultures for 24 hours and monitoring solution phase bacteria growth plus biofilm and surface growth on the material.

RESULTS AND DISCUSSION

Two peptide sequences, RRIYGRGYIRR designed to mimic α defensins and RRRRRR-GALAG-RRRRRR-GALAG designed to mimic β defensins, were both shown to have broad spectrum antibacterial activity with MIC values of 3.9 μ g/mL – 1.25mg/mL. The peptides were similarly active when covalently and electrostatically bound to the titanium surface, prevented biofilm formation and sterilised the surrounding solution (Figure).

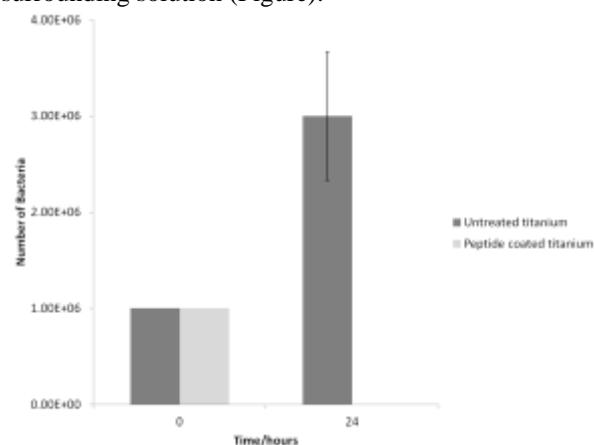


Figure Growth of MRSA on untreated and peptide treated surfaces.

CONCLUSION

We have designed and synthesised active antimicrobial peptides that can be electrostatically and covalently bound onto surfaces. We have shown that they are active in solution and when surface bound, preventing biofilm formation. This makes the peptide coatings a desirable surface modification for biomaterial and tissue engineered surfaces to prevent patient infections.

REFERENCES

1.JJ. Openheim, A. Biragyn, LW. Kwak, D. Yang, Ann. Rheum. Dis., 2003, 62, 17-21

ACKNOWLEDGMENTS

The authors would like to thank Mark Webber for his help with antimicrobial activity tests and Beryl Oppenheim for access to clinical isolates.



Development of decellularised conjunctiva for ocular surface reconstruction

Shivani Kasbekar¹, Rosalind Stewart¹, Stephen Kaye¹, Rachel Williams¹, and Paul Rooney²

¹Department of Eye and Vision Science, University of Liverpool, UK

^{2*}Research and Development, NHS Blood and Transplant, Liverpool, UK, s.kasbekar@liverpool.ac.uk

INTRODUCTION

A key advantage of decellularised tissue over allografts is that it is non-immunogenic and may provide an ideal scaffold for recellularisation with autologous cells. Conjunctival grafts are required to treat a range of ocular surface diseases and decellularised conjunctiva may prove to be a useful biomaterial in these applications. This study aimed developed a decellularisation process for conjunctival tissue and characterise its properties.

EXPERIMENTAL METHODS

Decellularisation was undertaken using a protocol described for dermis adapted by changing the detergent buffer in which varying concentrations of Sodium dodecyl sulfate (SDS) were used.^[1] DNA was quantified through isolation (DNAeasy, Invitrogen, UK) and fluorometric quantification using PicoGreen (Invitrogen, UK). In addition, a quantitative collagen denaturation assay was performed, histology with DAPI, H&E and Van Gieson's, and contact cytotoxicity by Giemsa staining using a conjunctival cell line (HCjE-Gi) and primary human fibroblasts. Bulbar conjunctiva from four human cadaveric donors was used for analysis in this study. SPSS was used to analyse data; ANOVA and student-t tests utilised where appropriate.

RESULTS AND DISCUSSION

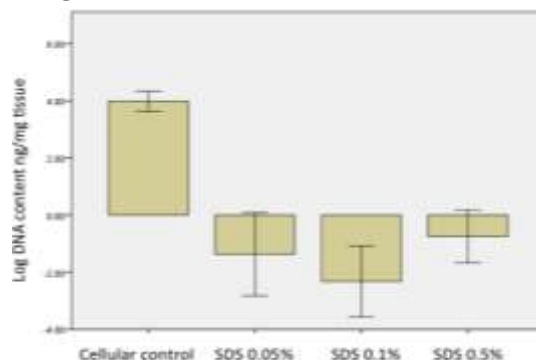
Decellularisation of conjunctiva was achieved using an adapted process for decellularisation of dermis and was successful at all SDS concentrations over 0.05%, $p < 0.0001$ (figure 1). This was reproducible in triplicates from three further donors ($p < 0.0001$). Conjunctival epithelial cells and human fibroblasts were found growing adjacent to and within the decellularised tissue on contact cytotoxicity testing (figure 2). There was no evidence of significant collagen denaturation as a result of decellularisation (student's t test $p = 0.14$, $p = 0.42$, $p = 0.84$ for quantified hydroxyproline in cellular compared with decellularised tissue using tissues from 3 donors in triplicate).

Table 1

Samples	Number of tissue samples	Mean DNA content ng/mg (+/- 2SD)
Cellular control	3	42.3 (7.4)
Donor 1 decellularised	3	0.47 (0.14)
Donor 2 decellularised	3	0.36 (0.08)
Donor 3 decellularised	3	0.33 (0.07)

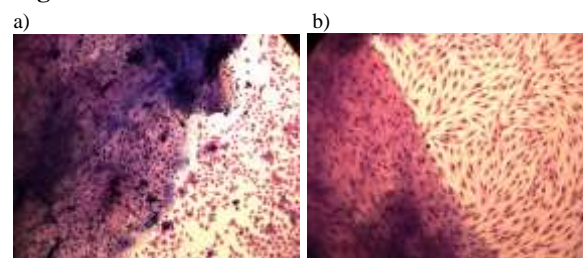
This table displays DNA ng/mg of conjunctival tissues from three separate donors, with triplicates analysed in each group. ANOVA $p < 0.0001$.

Figure 1



ANOVA $P < 0.0001$, DNA content $< 99\%$ decellularised versus cellular tissue (triplicate samples in each group); error bars display $\pm 2SD$

Figure 2



— 200µm Decellularised tissues are on the left hand side of both pictures a)HCjE-Gi cells b)primary human fibroblasts

The results of this study demonstrate that decellularisation of human conjunctiva can be effectively achieved using a modified protocol for dermis using an SDS concentration of 0.05% and is reproducible in several donors conjunctival tissue. The resulting tissues are not cytotoxic, the collagen is not significantly denatured and the tissue ultrastructure (examined by histology) is preserved whilst cellular material appears removed.

CONCLUSION

Decellularised human conjunctiva can be derived using our protocols in which the tissue architecture including collagen is preserved. This may prove to be an ideal tissue derived scaffold for the expansion of conjunctival epithelium to produce novel grafts for ocular surface reconstruction.

REFERENCES

1. Hogg, P., Cell Tissue Bank, 2013. 14(3): p. 465-74.

ACKNOWLEDGMENTS

The authors would like to thank the Medical Research Council, Royal College of Ophthalmologists and Novartis for providing financial support to this project



Highly swollen and compressible photo-activated collagen hydrogels

Giuseppe Tronci^{1,2}, Colin A. Grant³, Neil H. Thomson^{4,5}, Stephen J. Russell¹, David J. Wood²

¹Nonwovens Research Group, School of Design, University of Leeds, UK (g.tronci@leeds.ac.uk)

²Biomaterials and Tissue Engineering Research Group, School of Dentistry, University of Leeds, UK

³Advanced Materials Engineering RKT Centre, School of Engineering and Informatics, University of Bradford, UK

⁴Biomaterialisation Research Group, School of Dentistry, University of Leeds, UK

⁵Molecular and Nanoscale Physics, School of Physics and Astronomy, University of Leeds, UK

INTRODUCTION

Collagen is the most abundant building block of connective tissues¹ and has been widely applied for the design of biomimetic materials, *e.g.* for wound dressings and scaffolds for regenerative medicine. However, collagen materials often exhibit restricted material properties, *e.g.* high swelling and poor elasticity, in physiological conditions, resulting in challenging customisation of mechanical properties.² To address this challenge, an interdisciplinary approach was chosen in which crosslinking chemistry was used for the direct build-up of triple-helical collagen hydrogels.³ Together with molecular investigations on the network architecture and protein organisation, hydrated mechanical properties were closely characterised from the nano- up to the macro-scale.

EXPERIMENTAL METHODS

In-house isolated type I collagen was reacted with vinyl monomers of varied backbone rigidity and characterised via 2,4,6-Trinitrobenzene Sulfonic Acid (TNBS) colorimetric assay and ¹H-NMR. Full gel formation was accomplished following UV activation (Spectroline, 346 nm, 9 mW/cm²) of collagen precursors. Hydrogels were imaged and mechanically tested via AFM under ultrapure water (MFP-3D, Asylum Research Corp). A V-shaped silicon nitride cantilever (Hydra6V series, AppNano, Santa Clara, USA) was used with a spring constant ~0.3 N·m⁻¹ and tip radius of 15 nm. Elastic modulus was extracted from arrays of nanoindentation up to a load of 20 nN using Hertzian based theory, while imaging of the gels was performed using either contact or tapping mode. Together with AFM, bulk compression measurements were carried out on hydrogel discs (ø 0.8 cm) with a compression rate of 3 mm·min⁻¹ (Instron 5544 UTM).

RESULTS AND DISCUSSION

All hydrogels exhibited elastic moduli in the range of 10-400 kPa, whilst being highly swollen in the test conditions (water uptake > 700 wt.%). Variations in network architecture at the molecular level (Figure 1 A) dictated the mechanical behaviour of the hydrogels at both nano- and macroscopic scales, with the molecular stiffness of employed cross-linkers playing a major role. AFM elastic moduli correlated with the results obtained with bulk compression measurements. Hydrogels described nearly-elastic behaviour during the force-volume AFM measurements; minimal hysteresis (~attojoule) was observed between the approach and

retraction curves (Figure 1 B), likely due to the presence of the covalent network at the molecular level. AFM imaging elucidated the protein organisation of functionalised collagen molecules at the gel surface, depending on the cross-linker employed.

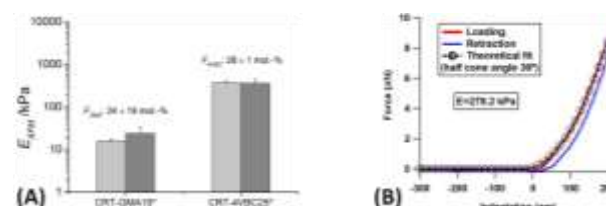


Figure 1. (A): Comparison of AFM elastic moduli in hydrogels functionalised with either glycidyl methacrylate (GMA) or 4-vinylbenzyl chloride (4VBC) with varied degree of collagen functionalisation (*F*). (B): Exemplary AFM force-indentation curve on collagen hydrogel.

CONCLUSION

Tunable collagen hydrogels were successfully synthesised from photo-active precursors and investigated from the molecular to the macroscopic scale. Remarkable swelling ratio and elastic modulus were observed in fully hydrated samples, depending on the collagen functionalisation introduced at the molecular level. AFM was successfully applied in hydrated conditions and yielded elastic moduli values comparable to the bulk values, whilst giving information on the fibril forming ability of functionalised collagen. In light of their remarkable swelling and mechanical properties, these collagen hydrogels are highly relevant to applications in cell biology and biotechnology as well as having great potential for clinical applications in wound care and regenerative medicine.

REFERENCES

- Grant C.A. *et al.*, Biophys. J. 97: 2985-2992, 2009
- Agostini de Moraes M *et al.*, Macromol. Biosci. 12: 1253-1264, 2012
- Tronci G. *et al.*, J. Mater. Chem. B, 1: 3705-3715, 2013

ACKNOWLEDGMENTS

This work was funded through WELMEC, a Centre of Excellence in Medical Engineering funded by the Wellcome Trust and EPSRC, under grant number WT 088908/Z/09/Z.



Mechanical and Cytotoxic Evaluation of a Novel Hydrogel with Potential Application as a Corneal Bandage

Andrew Gallagher^{1,2}, Don Wellings¹ and Rachel Williams²

¹Spheritech Ltd, Runcorn, UK.

²Department of Eye and Vision Science, University of Liverpool, UK. andy@liverpool.ac.uk

INTRODUCTION

A novel hydrogel biomaterial developed in-house at Spheritech Ltd (Proliferate™ Gel) was identified as having desirable properties associated with corneal bandages. These include; a high water content, excellent transparency and a modifiable surface chemistry. This study aimed to modify the mechanical properties of Proliferate™ Gel to achieve comparable properties to established contact lens materials. Some of these materials were used as a benchmark for four different Proliferate™ Gel polymers.

The cytocompatibility of Proliferate™ Gel towards a human corneal epithelium cell line (HCE-T) was also established. This study lays the framework for a more extensive investigation of Proliferate™ Gel as a corneal bandage.

EXPERIMENTAL METHODS

The hydrogel material used in this study was composed of poly-L-lysine and suberic acid using a carbodiimide-NHS cross-linking technique. Alterations in the level of cross-linking and the density of the polymer produced the different variants of Proliferate™ Gel. Percentage water content of Proliferate™ Gel was determined following ISO standard: 18369:4:2006. Mechanical properties of the variants were measured using a Linkam TST350 tensile tester. Stress, strain and Young's modulus were determined. The cytotoxicity of Proliferate Gel towards the HCE-T cell line was determined using a CCK-8 cytotoxicity kit following the manufacturer's protocol. Cellular morphology was imaged using a NIKON Eclipse TI-E inverted microscope.

RESULTS AND DISCUSSION

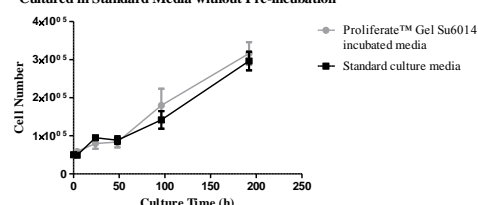
Material	% H ₂ O content	Young's Modulus (MPa)
HEMA/MAA	70%	0.77 (+/- 0.11)
Proliferate™ Gel Su6013 (60% cross-linked, 0.077g/ml polymer density)	67%	0.73 (+/- 0.12)
Proliferate™ Gel Su6014 (60% cross-linked, 0.071g/ml polymer density)	69%	0.50 (+/- 0.11)
VP/MMA	70%	0.49 (+/- 0.09)
Proliferate™ Gel Su6515 (65% cross-linked, 0.066g/ml polymer density)	71%	0.46 (+/- 0.08)
HEMA/VP	55%	0.36 (+/- 0.07)
Proliferate™ Gel Su6015 (60% cross-linked, 0.066g/ml polymer density)	70%	0.31 (+/- 0.04)

Table 1: Young's modulus data for common contact lens material compared to Proliferate™ Gel variants¹.

Proliferate™ Gel variants have the highest water content but still retain mechanical properties within the range of the commercial contact lens materials (table 1). In fact whilst the water content

of all the Proliferate™ Gel samples remain constant the Young's modulus values cover the range of those included in table 1.

Figure 1: Growth Curve for HCE-T Cells Cultured in Standard Media Pre-incubated with Proliferate™ Gel Su6014 in Comparison to Cells Cultured in Standard Media without Pre-incubation



The 8 day growth curve of HCE-T cells cultured in standard media compared to those cultured in media pre-incubated with Proliferate™ Gel Su6014 demonstrated there was no significant difference between the cell growth which suggests that Proliferate™ Gel Su6014 does not affect HCE-T cell survival and proliferation compared to the control (figure 1). This data suggests that any leachables from proliferate™ Gel Su6014 are non-cytotoxic towards the HCE-T cell line.

When the HCE-T cells were seeded in direct contact with the hydrogel very few cells attached to the surface and those that remained retained a



spherical morphology after 48 h (figure 2). Cells cultured on tissue culture plastic directly underneath Proliferate™ Gel Su6014 appear to have a typical cobblestone shape after 48 h as expected for this cell type (figure 3). These observations suggest that Proliferate™ Gel Su6014 is highly hydrophilic which inhibits cell attachment but is

non-cytotoxic to the corneal epithelium. Further evidence of this will be investigated in the near future.

CONCLUSION

This study has found that Proliferate™ Gel can be tailored to have mechanical properties similar to commercial contact lens materials. This coupled with the cytocompatibility of the material towards HCE-T cells merits further investigation of Proliferate™ Gel as a potential corneal bandage material.

REFERENCES

1. Tranoudis and Efron. Contact Lens & Anterior Eye. 27:177-191, 2004

Linking antimicrobial peptides with the surface of metallic implants

Zuzanna Trzcińska^{1*}, Anna Peacock² and Artemis Stamboulis¹

¹ Biomaterials Group, School of Metallurgy and Materials, University of Birmingham, United Kingdom,
zxt166@bham.ac.uk

² School of Chemistry, University of Birmingham, Edgbaston, Birmingham, United Kingdom

INTRODUCTION

Infections associated with bone replacement surgeries are one of the main causes of the early rejection of a prosthetic implant. The constant emergence of the antibiotic resistant bacteria strains calls for the use of different bactericidal solutions. Antimicrobial peptides (AMPs) have emerged as antibiotic substitute candidates.¹ AMPs are a part of innate immunity of all organisms and bacteria have not developed effective resistance towards them. Linking AMPs with the implant surface could lead to decrease of the infection related implant rejections.

Currently used implant materials do not allow for the stable conjugation of the antimicrobial biomolecules without use of harsh chemicals.² Peptide aptamers² or adhesive polymeric³ coatings formed by the dip-coating method could provide a surface chemistry functionalization which would link inorganic surfaces with AMPs.

EXPERIMENTAL METHODS

Ti6Al4V plates were grinded with SiC 400 grinding paper, followed by ultrasonic cleaning in acetone and deionised water.

AMPs and AMPs sequences conjugated with peptide aptamers (AMP-pas) were synthesized by Solid Phase Peptide Synthesis and were labelled with carboxyfluorescein dye (FAM). The purities and molecular weights of synthesized products were confirmed by High Pressure Liquid Chromatography (HPLC) and Mass Spectrometry (MS), respectively. AMP-pas were coated on the surface of Ti6Al4V via the dip-coating method and were used the same day.

The coating of Ti6Al4V plates with the adhesive polymer took place simultaneously with its polymerisation via dip-coating. AMPs were then conjugated with the polymeric thin layer.

Scanning Electron Microscopy (SEM) was used to image the surface of coated Ti6Al4V plates and Atomic Force Microscopy was used to compare the structure of the coatings.

Fluorescence Microscopy was performed at 495 nm to visualise and compare the amount of AMPs on the surface. The comparison was done based on the fluorescence intensities of the coated surface.

The stabilities of the AMPs on the surface were performed by immersion of the coated plates in simulated body fluid (SBF). Then they were analysed via fluorescence studies in terms of fluorescence intensity change, where the decrease in fluorescence is directly correlated to the amount of molecules being released.

RESULTS AND DISCUSSION

MS and HPLC have confirmed the molecular weight and the purity of the synthesised peptides which was >90%.

The SEM imaging of the adhesive polymer coating showed bead-like structures on the surface of Ti6Al4V (Figure 1), and the increase of roughness was confirmed by AFM. Fluorescence microscopy showed a uniform layer of AMP-pas (Figure 2a) and AMPs adhesive polymer coating on the surface of Ti6Al4V (Figure 2b).



Figure 1: SEM image showing polymeric coating (scale = 5 μ m)

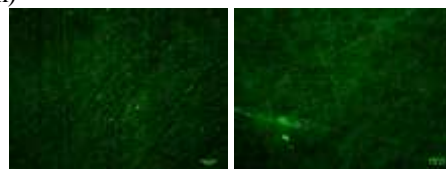


Figure 2: Fluorescence imaging of the coated surfaces a) AMP-pas (left), b) AMP-polymeric coating (right) (scale = 100 μ m).

The stability of peptides in SBF showed that 64% of the initial AMP-pas molecules are being released from the surface after the first hour while AMPs conjugated on the polymeric surface remain stable and attached for 720 hours or more (Table 1).

Table 1: Fraction of AMP bounded on the Ti6Al4V surface over time (n = 3)

	0.5 h	1 h	6 h	120 h	720 h
AMP-polymer	0.96 \pm 0.04	0.67 \pm 0.02	0.67 \pm 0.04	0.60 \pm 0.06	0.54 \pm 0.06
AMP-pas	0.47 \pm 0.03	0.36 \pm 0.05	0.11 \pm 0.02	0.05 \pm 0.05	0.01 \pm 0.02

CONCLUSIONS

Peptide aptamers and polymeric adhesives produce a linkage between the Ti6Al4V surface and the AMP molecule. The conjugation of the AMPs to the polymeric adhesive creates much more stable structure than the one made with the peptide aptamer and because of this this structure has a potential to have more efficient antibacterial property than the one where the peptide aptamers are being used.

REFERENCES

1. Pasupuleyi M. *et al.*, Critical Reviews in Biotechnology. 32:143-171, 2012
2. Seker U. *et al.*, Molecules. 16:1426-1451, 2011
3. Lee H. *et al.*, Nature. 448:338, 2007

Characterising the Micro- and Nano-mechanical Properties of Ageing and Diseased Soft Tissues

Riaz Akhtar

Centre for Materials and Structures, School of Engineering, University of Liverpool, UK, r.akhtar@liverpool.ac.uk

The mechanical properties of soft, elastic-fibre rich connective tissues such as skin and arteries are known to change with age and with disease states such as diabetes e.g. arteries become stiffer, a major risk factor for the subsequent development of strokes, aortic aneurysms, and heart failure. Normal function of these tissues is critically dependent on the biomechanical properties of two main microstructural components of the extracellular matrix; stiff, fibrillar collagens, and resilient elastic fibres. However, very little is known about the micromechanical properties of soft tissues. This is caused by the disparity between the length scale probed using traditional mechanical testing methods ($10^{-3} - 10^{-1}$ m) and that at which key biological tissue components are organized ($10^{-6} - 10^{-4}$ m). The variation in soft tissue stiffness as a function of length scale is shown in Figure 1.

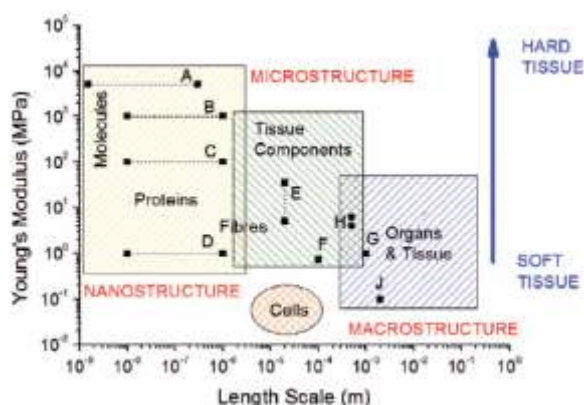


Figure 1 Length scale and elastic properties of soft tissues and their structural components. Superimposed

are measurements of the elastic moduli of aorta (from literature) and extracellular components at macroscopic, microscopic, and molecular length scales. A: single collagen fibrils, B: fibrillar collagen, C: fibrillin microfibrils, D: elastin, E: ferret aorta components²⁵, F: porcine aorta components, G: human radial artery, H: rat aorta, J: human aorta [1]

Most studies in the literature focus on macro-scale changes within these tissues. Knowledge of tissue properties at the micro- and nano- scale is of great importance to better understand the effects of ageing and disease on the properties of tissue¹, and to better understand the interactions of tissues with biomaterials at these length scales.

This talk will largely focus on changes with age and disease in large arteries which we have characterised with novel materials science techniques such as scanning acoustic microscopy (SAM) and nanoindentation that allow us to localise mechanical property changes at the microstructural scale. The talk will also touch upon nanomechanical measurements of soft tissues with atomic force microscopy (AFM). These data are compared with the in vivo and macroscopic response of the vessel.

REFERENCES

1. Akhtar. *et al.*, Materials Today. 2:5-11, 2011

Nanotubular Titania topography combined with amorphous calcium phosphate chemistry induces direct osteoblastic differentiation in mesenchymal stem cells

Robert McLister, Mura McCafferty, George Burke, Brian J. Meenan

Biomaterials and tissue Engineering Group, NIBEC, University of Ulster, Northern Ireland.

mc_lister-r@email.ulster.ac.uk

INTRODUCTION

Calcium phosphate (CaP) biomaterials, such as hydroxyapatite (HA), are recognised as an important class of bioactive compounds capable of inducing cellular attachment, proliferation and differentiation. Previous research has indicated that sputter deposited amorphous HA coatings have osteoconductive properties that can be advantageous in this regard (1). However, the non-crystalline form of CaP is highly soluble in aqueous cell culture media. Controlling the dissolution of the CaP surface layer is therefore necessary to ensure a bioactive response in long term culture. In this work, the response of mesenchymal stem cells (MSCs) to sputtered (amorphous) CaP coatings deposited onto titanium substrates with various nanoscale topographies has been determined. The role that the specific forms of nanotopography can play in controlling CaP dissolution has been determined. The *in vitro* response of MSCs to the amorphous CaP coatings over 21 days has compared to that for thermally annealed crystalline CaP coatings to further establish the role that solubilised CaP from the coating may have on MSC differentiation.

EXPERIMENTAL METHODS

RF magnetron sputtering from HA powder targets was used to deposit CaP coatings onto Titania Nanotube (TiNT) surfaces created by electrochemical anodisation of titanium coupons at 80V for 30 minutes in a solution of ethylene glycol with 0.3%wt NH₄F and 3%wt DI H₂O. Polycrystalline titania surfaces were prepared by sputtering from metal targets onto the titanium coupons. Batches of samples were annealed at 500°C to increase their relative crystallinity. Dissolution studies were undertaken by immersion in 2ml of DMEM at 37°C for 7 days. *In vitro* cell studies were carried out using mesenchymal stem cells at passage 5. Pico green and alkaline phosphatase (ALP) assays were applied at days 1, 3, 7 and 7, 14, 21 to determine cell viability and osteoblastic differentiation, respectively. Immunocytochemistry was used to identify the presence of bone related proteins at day 21 with bovine serum albumin (BSA) as a primary antibody and rabbit Polyclonal anti-Alkaline phosphatase as the corresponding secondary antibody. Samples were washed in PBS to remove any residual antibody present and then were counterstained with 4',6-diamidino-2-phenylindole (DAPI) for 2 minutes. Once mounting media was added samples were sealed with a glass cover slide and varnish. A Quanta 200 Dual Ion Beam SEM was used to image the different substrate topographies. Fluorescent images were acquired using an LSM 5 Pascal Confocal Laser Scanning Microscope (CLSM).

RESULTS AND DISCUSSION

Figure 1 indicates the topography of the TiNT surface with Figure 2 showing the surface after deposition of a CaP sputter coating. After 7 days exposure to aqueous culture media, FTIR and XPS analysis showed amorphous CaP was still present on the surface.

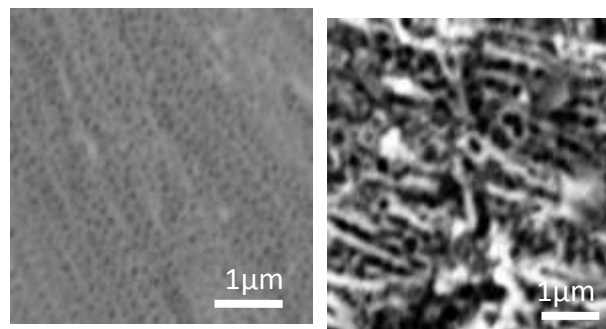


Figure 1. (Top left) TiNT 80V.

Figure 2. (Top right) TiNT 80V HA after 7 days dissolution.

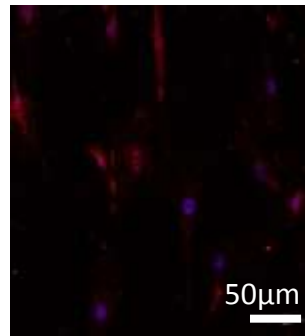


Figure 3. (Bottom Left). DAPI (blue) and ALP (red) staining of day 21 MSC study on TiNT amorphous CaP.

Pico green assay data showed significant cell viability on all surfaces. ALP protein expression indicated that differentiation to an osteoblastic lineage occurred for MSCs cultured for 21 days on the TiNT surface coated with CaP. As shown in Figure 3, confocal microscopy of stained MSCs provides evidence for the osteoblastic character of the cultured MSC cells.

CONCLUSIONS

This work indicates the potential to induce stem cell differentiation to an osteoblastic lineage using a combination of nanotubular topography and amorphous CaP. Importantly, the ability to control the dissolution of amorphous CaP thin film coatings via nanotubular substrate topography is confirmed.

REFERENCES

(1)Nagano M, Nakamura T, Kokubo T, Tanahashi M, Ogawa M. Differences of bone bonding ability and degradation behaviour in vivo between amorphous calcium phosphate and highly crystalline hydroxyapatite coating. *Biomaterials* 1996 9;17(18):1771-1777.

ACKNOWLEDGMENTS

The authors would like to thank the NI Department for Employment and Learning for providing financial support by way of a PhD studentship to RMcL



Microwave-assisted Synthesis of Calcium Phosphate Nanobiomaterials with Controlled Morphology

P.J.T Reardon^{1,2}, J. Huang¹, J. Tang^{2*}

¹ Department of Mechanical Engineering, UCL, London

^{2*} Department of Chemical Engineering, UCL, London Philip.reardon.09@ucl.ac.uk

INTRODUCTION

The performance of calcium phosphate (CaP) biomaterials depends greatly on morphology and size. For example, CaP nanoparticles can provide enhanced bioactivity.¹ Wire-like CaP can be used as biomaterial reinforcement due to excellent mechanical properties.² Recently porous CaP nanomaterials have shown high loading and favourable release properties for drug delivery.³ The use of microwave dielectric heating for chemical synthesis allows material production with altered morphologies, increased yields, narrow size distribution, and considerably reduced synthesis times. Therefore, this energy efficient 'green' process is used in the current study, to prepare biodegradable calcium phosphate nanomaterials with varied size, morphology and textural properties.

EXPERIMENTAL METHODS

Briefly, ethanol or ethanol/water solutions containing either $\text{Ca}(\text{NO}_3)_2 \cdot 4\text{H}_2\text{O}$ or H_3PO_4 were prepared and mixed at room temperature and pressure, then irradiated in a microwave solvothermal process (using a MARS, CEM). Material characterisation was performed using XRD, FESEM, TEM and N_2 adsorption analysis as previously reported.^{3,4}

RESULTS AND DISCUSSION

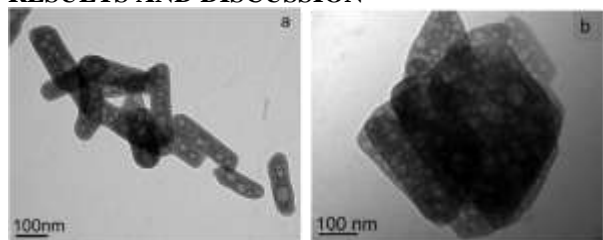


Figure 1 TEM micrographs of CaP (a) nanorods (60°C), (b) nanoplates (200°C).

CaP nanomaterials with controlled morphology have been synthesised using a microwave assisted process without the use of any toxic surfactants. The effect of solvent composition, mixing methodology, reagent stoichiometric ratio, synthesis temperature and synthesis time was systemically investigated. Single phase nanoplates and nanorods of monetite with controllable pores are produced by varying reaction temperature (Figure 1). Dimensionality (figure 2) and bicalcium phosphate composition (hydroxyapatite (HA)/monetite, Figure 3) were manipulated by changing the ratio of the $\text{H}_2\text{O}/\text{EtOH}$ solvent mixture. Three dimensional particles with minute amounts of HA were produced when a $\text{H}_2\text{O}/\text{EtOH}$ volumetric ratio of 20/80 was used (Figure 2a). Conversely, high aspect ratio (ca. 54) nanowires containing ca. 38 wt% HA were obtained with a 60/40 $\text{H}_2\text{O}/\text{EtOH}$ volumetric ratio (Figure 5b). Importantly, the quantity of HA in the high

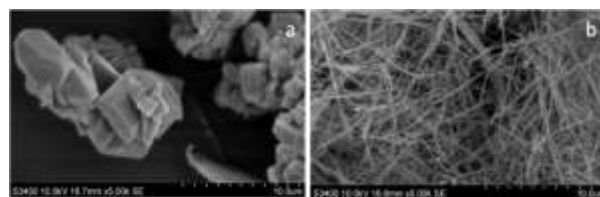


Figure 2 SEM micrographs of CaP: (a) microparticles ($\text{H}_2\text{O}/\text{EtOH} = 20/80$), (b) nanofibers ($\text{H}_2\text{O}/\text{EtOH} = 80/20$).

aspect ratio nanowires/needles was also controlled by varying the stoichiometric ratio of the reactants, demonstrating that 1D materials with close to 100% HA can be achieved when the Ca/P ratio is increased to 1.67.⁴ The influence of particle morphology on the loading efficiency of therapeutic agents was also studied. Interestingly, for all standard proteins the loading on CaP was found to be the highest for the nanoplate materials.

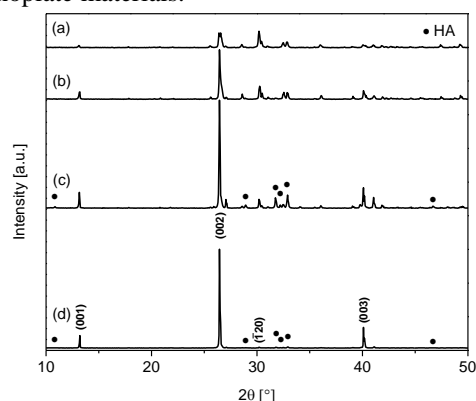


Figure 3 XRD patterns of materials synthesised using different $\text{H}_2\text{O}/\text{EtOH}$ volumetric ratios of: (a) 20/80, (b) 40/60, (c) 60/40, (d) 80/20.

CONCLUSION

The findings highlight that reaction parameters can be varied in tandem with microwave irradiation to tailor the morphology and composition of calcium phosphate materials, which are of very high importance in developing excellent materials suitable for bone tissue engineering and drug delivery.

REFERENCES

1. Kong, L. *et al.*, Eur. Polym J. 2006, 42, 3171-3179.
2. Costa, D. O. *et al.*, A. S., ACS Appl. Mater. Interfaces 2012, 4, 1490-1499.
3. Reardon, P. J. T. *et al.*, Adv. Healthcare Mater. 2013, 2, 682-686.
4. Reardon, P. J. T. *et al.*, J. Mater. Chem. B 2013, 1, 6170-6176.

ACKNOWLEDGMENTS

The authors would like to thank the ESPRC for providing financial support to this project.



A Dual Porosity Construct for Osteochondral Modelling and Repair

Alexander A. Popov^{1*}, George Roberts², David M. Grant², Colin A. Scotchford², and Virginie Sottile¹

¹ Wolfson Centre for Stem Cells Tissue Engineering & Modelling, CBS, University of Nottingham, UK

² Bioengineering Group, Faculty of Engineering, University of Nottingham, UK

* mzxaap@nottingham.ac.uk

INTRODUCTION

Regenerative therapeutic solutions are required to address the increasing prevalence of bone and cartilage diseases within the population. Limitations of existing treatments, such as bone graft reconstructions or biomaterial implants, suggest that osteochondral tissue constructs with the ability to support differentiation of mesenchymal stem cells (MSCs) into both osteoblast & chondrocyte lineages is desirable^{1,2}. The current project aims to overcome issues arising from the divergent differentiation requirements for each lineage by providing scaffolds with spatially resolved environments, each supportive of one of these cell lineages. The work reported here describes the porogen and cross-linker optimisation for the production of bi-layered chitosan scaffolds containing two distinct pore sizes. Scaffold characterisation was carried out before cell seeding and 3D culture in a perfusion bioreactor.

EXPERIMENTAL METHODS

Porous scaffolds were produced using a freeze-gelation method from a 4% chitosan solution mixed with polycaprolactone (PCL) porogen and cross-linked using either 0.5% glutaraldehyde or 0.3% genipin solutions. Porogen microspheres were produced by an emulsion method. Porogen particles and scaffold porosity were evaluated using scanning electron microscopy (SEM) and micro-computed tomography (MicroCT). Cytocompatibility was assessed after seeding of human mesenchymal stem cells (hMSC) onto fibronectin-treated scaffolds and culture in a perfusion bioreactor for up to 3 weeks.

RESULTS

Dual porosity scaffolds were produced and analysed by MicroCT, confirming different porosity and pore size distribution for bottom, middle and top sections of scaffolds made with PCL microspheres (Table 1).

	Bottom	Middle	Top
% Porosity	74	73	73
Pore size (μm) \pm SD	287 \pm 10.5	232 \pm 17.5	196 \pm 5.5

Large (300-425 μm) pores were designed to promote osteogenic differentiation of hMSCs and smaller, (180-300 μm) pores to support chondrogenesis. SEM analysis of the scaffolds illustrated the graded pore size distribution (Fig.1), and the absence of delamination between layers.

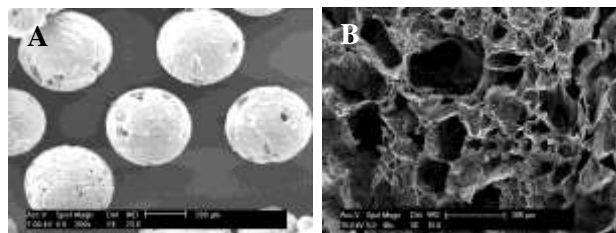


Figure 1 SEM images of PCL porogen microspheres (A) and resulting bi-layered chitosan scaffolds (B).

Scaffolds cross-linked with genipin displayed more uniform pore morphology than ones made with glutaraldehyde. Scaffolds were then seeded with hMSCs and cultured both in culture dishes and in a perfusion bioreactor for up to 21 days. Cell viability (Fig. 2) and differentiation were assessed at various time-points to measure osteochondral lineage maturation *in situ*.

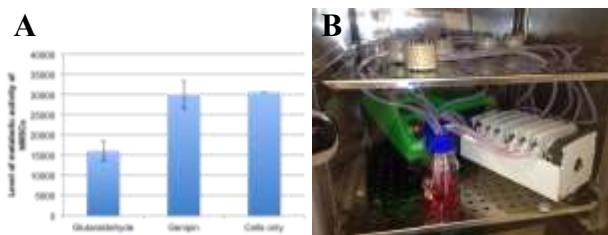


Figure 2 Metabolic activity of hMSC seeded on chitosan scaffolds (A). Perfusion bioreactor system used to culture cellularised scaffolds (B).

DISCUSSION AND CONCLUSION

A novel dual porosity chitosan scaffold was produced for osteochondral modelling. Results show that the emulsion-produced PCL microspheres permitted control over pore characteristics in the scaffolds. Subsequently, hMSC seeding methods were evaluated for optimal cell infiltration into the scaffold core to populate the construct. Scaffolds cross-linked with genipin allowed higher cell metabolic activity than glutaraldehyde, to a level comparable to tissue culture plastic. MSC differentiation analysed over 3 weeks highlighted the influence of scaffold structure on cell compatibility in 3D.

REFERENCES

1. Cengiz, Oliveira and Reis, *3D Multiscale Physiological Human*. 25-47, 2014.
2. France, et al., *Journal of Tissue Engineering and Regenerative Medicine*. doi:10.1002/term.1567, 2012.

Radiological assessment of bioengineered bone in a muscle flap for reconstruction of a critical-size mandibular defect

Randa Al-Fotawei¹, Edward Odell², Kurt Naudi¹, Matthew J. Dalby³, K. Elizabeth Tanner⁴, J McMahon⁵, Ashraf Ayoub¹

¹Glasgow Dental Hospital & School, University of Glasgow, Glasgow, UK, r.alfotawi.1@research.gla.ac.uk

²Department of oral pathology, Guy's Hospital, King's College London, UK.

³Institute of molecular, cell and system biology, University of Glasgow, Glasgow, UK.

⁴School of Engineering, University of Glasgow, Glasgow, UK

⁵Regional maxillofacial Unit, Southern General Hospital, Glasgow, UK

INTRODUCTION

Surgical reconstruction of functional and aesthetic defects, particularly following ablative cancer surgery, is often compromised by the limited and the associated donor site morbidity¹. A compromised vascular bed is a major obstacle for a successful uptake of a micro-vascular flap.

EXPERIMENTAL METHODS

This study presents a comprehensive radiological and histological analysis protocol to evaluate bone regeneration within a pedicled muscle flap for the reconstruction of a mandibular defect. A critical size defect (20 mm × 15 mm) was created in the mandible of ten experimental rabbits. The masseter muscle was adapted to fill the surgical defect, a combination of Calcium Sulphate/Hydroxyapatite cement (CERAMENTTM [SPINAL SUPPORT]), BMP-7 and rabbit mesenchymal stromal cells (rMSCs) were injected inside the muscle tissue². Plain Radiographic assessment was carried out on the day of surgery and at 4, 8, and 12 weeks postoperatively. At 12 weeks, the animals were sacrificed and cone beam computerized tomography (CBCT) scanning, micro-computed tomography (μ -CT), and histological assessment were performed.

RESULTS AND DISCUSSION

Clinically, a clear layer of bone tissue could be identified closely adherent to the border of the defected area. Sporadic radio-opaque areas within the defect were detected radiographically. In comparison with the opposite control side, the estimated quantitative scoring of the radio-opacity was $46.6\% \pm 15$, the mean value for the volumetric assessment of the radio-opaque areas was $63.4\% \pm 20$. The micro-CT analysis revealed a thinner trabecular pattern of the regenerated bone with more condensed trabeculae than the average number/mm³ of the surrounding bone. Histological assessment showed areas of bone formation and remnant of residual bone cement were observed throughout the muscle and connective tissue surrounding CeramentTM. Bone displayed a high degree of remodeling with an intricate network of woven bone within Cerament. Quantitative histomorphometry assessment reported percentage of area of bone regeneration, residual cement and soft tissue were $41.3\% \pm 14.9$, $27.9 \pm 8.3\%$ and $32.3 \pm 11.3\%$ respectively. The mineral apposition rate (MAR) was $1.29 \mu\text{m}/\text{day}$ which indicate higher rate of mineral deposition with respect to the non-operated side.

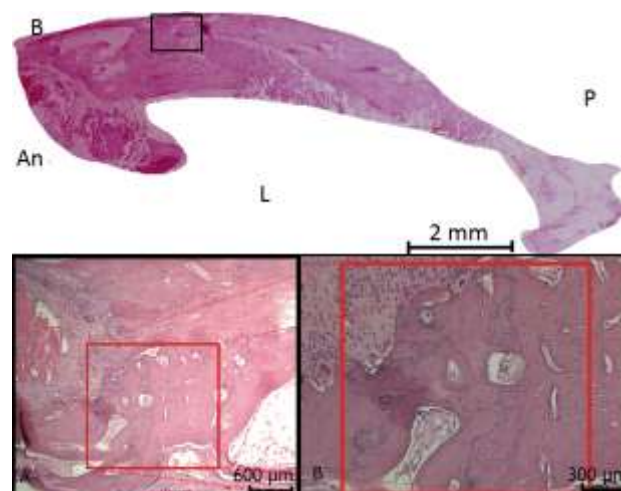


Figure 1: Decalcified histological section for area of the defect, showing the regenerated bone in top image, area of bone interface is filled with woven bone (boxes), scale bar=2 mm, A&B scale bar= 600 and 300 μm , P, L, B and An indicate proximal, lingual, buccal and Anterior wall of the defect.

Nevertheless, complete conversion of the muscle into bone and full reconstruction of the defect was not achieved. This is partially due to the physical nature of the injected cement that prevented the diffusion of the material at a micro level between the fibres of the muscle tissue.

CONCLUSION

The study provided the proof of the concept that bone formation could be induced within a pedicled facial muscle flap using an injectable biomimetic-scaffold which has clear potential applications. Further development and refinements of this approach are required before clinical use in maxillofacial bone reconstruction.

REFERENCES

1. Torroni A. Journal of Oral and Maxillofacial Surgery 67:1121-7, 2009
2. Alfortawi et al. Journal of Tissue Engineering, 4, <http://tej.sagepub.com/cgi/content/abstract/4/0/2041731413509645>

ACKNOWLEDGMENTS

Authors should acknowledge Bone support AB(Lund, Sweden) for provision of the CeramentTM bone cements, King Saud University, Ministry of higher education for supporting Randa Alfortawi.



The effect of a RF/DC magnetron sputtered coating on the dissolution behaviour and osteoblast response to an Mg-Y-RE alloy

Natasha A Bhuiyan¹, Robert Thornton², Joseph Robson¹, Julie E Gough¹

¹Material Science Centre, University of Manchester, UK

²Magnesium Elektron®, Manchester, UK

(email: natasha.bhuiyan@student.manchester.ac.uk)

INTRODUCTION

Magnesium alloys have shown promise as a new generation of biodegradable metals capable of supporting bone growth and regeneration. Whilst their mechanical properties are better suited to bone placement than Ti or Co-Cr alloys, the corrosion rate of Mg alloys is often too high, leading to a loss in mechanical integrity before the tissue has had sufficient time to heal¹. To overcome this limitation, we used a RF/DC (Radio Frequency/Direct Current) magnetron sputtering technique to fabricate a coating on a biomedical Mg-Y-RE (magnesium-yttrium-rare earth alloy) from the Elektron SynerMag® range, which has already demonstrated excellent corrosion resistance in simulated body fluid (SBF). In this study, we characterised the chemical and phase composition of the coating, as well as its effect on the dissolution behaviour and osteoblast response to SynerMag®.

EXPERIMENTAL METHODS

Material preparation: SynerMag® was manufactured by Magnesium Elektron® in accordance with Elektron SynerMag® technology. Ti, TCP (tissue culture plastic) and glass coverslips were used as controls. **SBF preparation:** A solution of SBF was prepared according to Kokobu's method². **Coating fabrication:** Magnetron sputtering was carried out by Eminite®, Nottingham, UK using a commercial vapour deposition system. In the system, a DC pulsed bias voltage of -25V was applied to the samples whilst RF power at a density of 3.8Wcm⁻² was simultaneously applied to a hydroxyapatite target. This was used to deposit a 300nm thick coating on the samples. **Heat treatment:** Samples were heated at a rate of 5°C/min in wet Ar for 12hrs at 570°C, then cooled to room temperature. **Coating characterisation:** FTIR (Fourier Transform Infra-Red) and XRD (X-Ray Diffraction). **Dissolution study:** Samples were immersed in SBF for 7 days at 37°C and analysed using SEM (Scanning Electron Microscopy), EDX (Energy Dispersive X-ray) and ICP-AES (Inductively Coupled Plasma- Atomic Emission Spectroscopy). **Cell culture:** Human osteoblasts (HOb, Promocell, Germany) were seeded at 50 000 cells/cm². **Proliferation and cell spreading:** PicoGreen®, Live-dead assay® (both Invitrogen, UK) and ImageJ. **Mineralisation:** BMP-2 ELISA (R&D systems, UK), alkaline phosphatase (ALP) (SigmaFast™ p-Nitrophenyl phosphate), Osteocalcin ELISA (OC) (Invitrogen, UK). **Statistical analysis:** Two-way ANOVA with Bonferroni post-test.

RESULTS AND DISCUSSION

Characterisation of the coating after heat treatment revealed hydroxyapatite phases that had undergone both carbonate substitution and dehydroxylation into β -tricalcium phosphate and β -dicalcium pyrophosphate.

XRD also detected a highly crystalline Mg₂Ca phase that may have formed as a result of Mg diffusion into the coating during heat treatment.

In the dissolution study, spherical crystals composed of interlocking plates were observed on the coated samples after 7 days immersion in SBF (Figure 1a/b). EDX analysis of these crystals showed these were composed of high levels of calcium, oxygen and phosphorus. Both the morphology and composition of these crystals are characteristic of octacalcium phosphate (OCP), which is considered a pre-cursor to apatite formation. ICP-AES analysis of Mg²⁺ release from bare and coated SynerMag® over 7 days, showed the coating improved the overall dissolution resistance of SynerMag®.

HOb proliferation studies conducted over 21 days, revealed significantly greater cell numbers and surface spreading on coated SynerMag® than bare SynerMag®. In addition, the coating appeared to stimulate mineralisation, as BMP-2 secretion, ALP activity and OC secretion were significantly higher on coated SynerMag® than bare SynerMag® and the Ti and TCP controls.

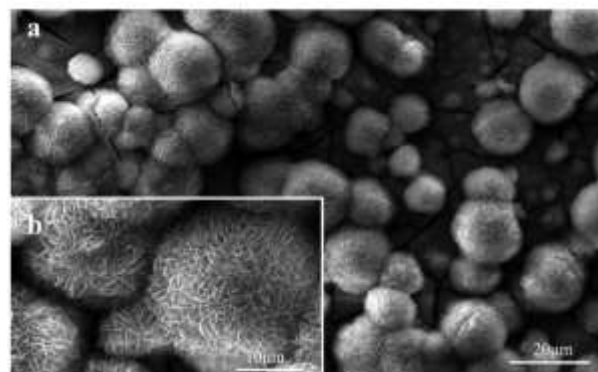


Figure 1 (a) OCP formation on coated SynerMag® after 7 days immersion in SBF (b) magnification of OCP crystals

CONCLUSION

Our findings demonstrate the RF/DC magnetron sputtered coating improves the initial dissolution rate of SynerMag® and also promotes the deposition and growth of the apatite pre-cursor, OCP, in SBF. When cultured with osteoblasts, the coating improved osteoblast adhesion and also, stimulated BMP-2 secretion, ALP activity and OC secretion during the first 7 days.

REFERENCES

1. Staiger. *et al.*, Biomaterials. 27:1728-1734, 2005.
2. Kokobu. *et al.*, Biomaterials. 27:2907-2915, 2006

ACKNOWLEDGMENTS

The authors would like to thank the EPSRC and Magnesium Elektron® for funding this project.

Novel Biomimetic Scaffolds for Osteochondral Repair

Amy Prosser¹, Leander Poocha², Gerhard Hildebrand², Klaus Liefeth², Colin Scotchford¹, Virginie Sottile³, and David Grant¹

¹ Division of Materials Mechanics and Structures, Faculty of Engineering, University of Nottingham, UK

² Institute for Bioprocessing and Analytical Measurement techniques (IBA) e.V. Heiligenstadt, Germany

³ Wolfson STEM Centre, School of Medicine, University of Nottingham, UK

epxap3@nottingham.ac.uk

The Innovabone project focuses on developing a novel biomimetic scaffold for bone repair applications¹. Using the 2PP process, a scaffold with a highly uniform structure and pore size has been developed. The proliferation and differentiation potential of MSCs on these scaffolds have been characterised as a part of the Innovabone project.

INTRODUCTION

The Innovabone project is a collaborative EU project that aims to develop a 2-step biomimetic product that consists of a bioactive scaffold and a bioactive self-setting gel, which will provide a microenvironment that promotes bone repair. Using a 2PP (two photon polymerisation) method, scaffolds consisting of different lactic acid (LA) and caprolactone (CL) ratios were produced. As a part of the wider study, the paper presents biocompatibility testing performed on identical scaffolds produced by 2PP but with different LA:CL ratios. Cell proliferation and osteogenic differentiation have been quantified to characterise the response of progenitor cells to this novel material.

EXPERIMENTAL METHODS

Scaffold Production – Scaffolds were provided by IBA based on a 2PP process². An ethyleneglycol based CL-LA degradable copolymer was end-capped with photo-reactive methacrylation groups by stannous catalysed ring-opening polymerisation. Three different LA:CL ratios were investigated as well as differences in molecular weight. Samples were coded LCM3, -4 & -6.

Cell Culture – human mesenchymal stem cells (MSCs)³ were seeded at a concentration of 1×10^6 cells per scaffold and cultured in DMEM supplemented with 10% foetal calf serum, 1% L-Glutamine, 1% non-essential amino acids, 1% penicillin/streptomycin, 0.1 μ M dexamethasone, 50 μ M ascorbic acid phosphate, and 10 mM β -glycerophosphate at 37°C and 5% CO₂.

Alkaline Phosphatase (ALP) (SigmaFAST) - was performed according to the manufacturer's instructions.

Alizarin Red – 1% alizarin red was added to samples and incubated for 20 minutes before wells were washed with PBS and stain was extracted using 100 μ l destain (20% methanol, 10% acetic acid, 70% distilled water). Quantification was at 405nm absorbance.

RESULTS AND DISCUSSION

The ALP activity and mineralisation of cells of the scaffolds is shown in figure 1. After 21 days there was no significant difference between the ALP activity on the different scaffolds ($p > 0.05$), but at earlier time points LCM3 had a significantly quicker increase in ALP activity than LCM6 ($p < 0.05$). This was also

demonstrated in the mineralisation of cells as the alizarin red staining on LCM6 scaffolds was only 69% of that on the LCM3 scaffolds. This may be due to the increased CL component in LCM3 compared to LCM6, which creates a more hydrophilic scaffold and promotes better cell attachment and colonisation of the scaffold.

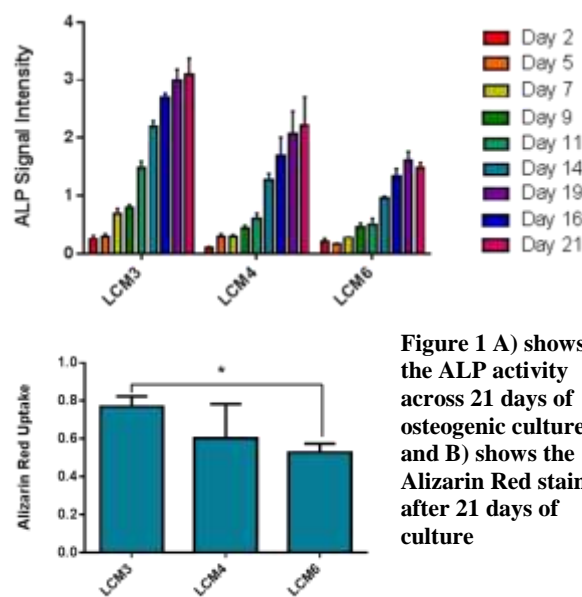


Figure 1 A) shows the ALP activity across 21 days of osteogenic culture and B) shows the Alizarin Red stain after 21 days of culture

PrestoBlue and Neutral Red assays were also performed at the same time intervals but no significant difference ($p > 0.05$) in the proliferation was observed between the scaffolds when seeded with the same starting concentration of cells.

Preliminary mechanical testing data has also shown these scaffolds to have desirable mechanical properties for bone repair applications.

CONCLUSION

All three types of scaffold were capable of supporting cell proliferation and osteogenic differentiation of MSCs over 21 days and are promising candidates for bone repair applications.

REFERENCES

1. www.innovabone.eu
2. Davis, K.A., J.A. Burdick, and K.S. Anseth, *Biomaterials*, 2003. 24(14): 2485-95.
3. Rashidi, H., et al., *Cells Tissues Organs*, 2012. 195(6): 484-94.

ACKNOWLEDGMENTS

The authors would like to thank the faculties of Engineering and Medicine (University of Nottingham) and "Innovabone" NMP3-LA-2011 for providing financial support.



Investigation into the Ability to Accurately Mimic Natural Extracellular Matrix Using Artificial Electrospun Scaffolds

Kirstie Andrews^{1*}

^{1*}School of Engineering, Manchester Metropolitan University, UK K.Andrews@mmu.ac.uk

INTRODUCTION

The field of tissue engineering is constantly seeking to create scaffolds that reproduce the structure, properties and functionality of the tissue they are replacing. Research has determined that the behaviour of cells within these tissue structures is induced by the nature of the extracellular matrix. This natural structure (nano-, micro- and macro-scale) significantly influences the cellular migration, growth and phenotype. This fibrous architecture, particularly the exact organisation of the collagen, also plays a significant role in the biomechanical functioning of the tissue¹.

Many research groups are investigating the ability to artificially replicate this matrix; electrospinning is one technique capable of producing such structures. It allows a high degree of control over the process, and ultimately the scaffold structures and properties, with these directly inducing predictable cellular behaviour for a range of cell types and long-term culture periods². There is much debate over the use of aligned or random electrospun fibres, and their optimum arrangement and structure for particular tissue applications.

It is well documented that electrospinning can reproduce the range and scale of extracellular matrix structure and properties; however, the exact mimicry or uniformity of the architecture itself has not been investigated. Therefore, the aim of this research was to compare a range of aligned and non-aligned electrospun scaffolds with natural extracellular matrix, and to assess the similarity with the 3-D architecture and structural organisation of the fibres.

EXPERIMENTAL METHODS

Artificial Scaffolds

A range of scaffolds was electrospun using both artificial and natural materials (including polyurethane, poly vinyl alcohol and gelatin). Fabrication parameters were altered to produce nano- and micro-scale, aligned and non-aligned structures.

Scaffolds were characterized, using SEM and image analysis, with respect to inter-fibre separation, fibre diameter, void fraction and fibre orientation. Surface and bulk properties, including stiffness, were assessed using mechanical testing and image analysis.

Additional data was collected from existing literature.

Natural Extracellular Matrix

L929 immortalised murine fibroblasts, human Schwann cells and bovine aortic endothelial cells were cultured separately on UV-Ozone sterilised TCP discs for 7 days (seeding density of 5×10^4 cells). The extracellular matrix of each cell type was characterized through the use of cryo-SEM (no fixation or dehydration). The matrix fibres were analysed as above; additional 2- and 3-D data was again obtained from literature.

Comparison of Structural Organisation

4 repeats of each of the artificial and natural structures were examined ($n=20$ for image analysis measurements per sample). Statistical analysis was then performed to obtain mean, standard deviation, and analysis of variance (ANOVA) with post hoc testing (Tukey) values (significance tested at $P<0.05$). Structures were compared across inter- and intra-sample groupings.

RESULTS AND DISCUSSION

Differences were determined in the organisation of the fibres across all natural and artificial samples. Aligned and non-aligned samples were shown to contain inherent non-uniformity in all parameters measured, with aligned fibres demonstrating higher values of variance (for both artificial and natural samples). The exact electrospinning methodology altered the structural arrangement of the laid-down fibres, as also did the location of the natural tissue extracellular matrix.

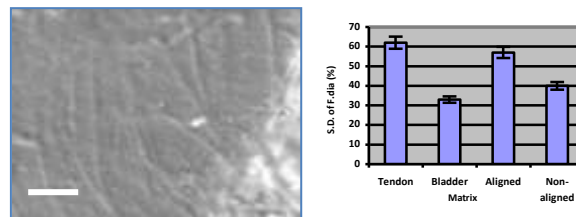


Figure 1 shows the inherent variance of natural extracellular matrix fibres (SEM image; scale bar 2µm). The graph shows that the deviation of fibre diameters in aligned natural and artificial matrix was comparable ($P>0.05$), as was natural and artificial non-aligned matrix ($P>0.05$). There were significant differences between the uniformity of the aligned and unaligned architectures ($P<0.05$).

CONCLUSION

Electrospinning offers the capability to reproduce the range of structures and properties encompassed within natural extracellular matrix; more significantly, these artificial structures can be fabricated with similar degrees of “non-uniformity” in their organisation and fibrous architecture to the natural structures. These inherent variances in the fibres produced through the use of this technique could prove significant in the development and functionality of scaffolds that accurately mimic natural tissue through artificially creating extracellular matrix.

REFERENCES

1. Badylak S.F. *et al.*, Acta Biomaterialia 5:1-13, 2009
2. Andrews K.D. *et al.*, Journal of Materials Science: Materials in Medicine 19:1601-1608, 2008

ACKNOWLEDGMENTS

The author would like to thank the MMU Early Career Research Accelerator Funding Scheme for providing financial support to this project.

Bioactive and Highly Porous Nanofibres via Solution Blow Spinning and their Formation into Macroporous Scaffolds

Eudes Leonnan¹, Ana Letícia Braz², Isaque Jerônimo¹, Aldo R. Boccaccini³, Showan N. Nazhat⁴, Eliton S. Medeiros^{*1}, Jonny J. Blaker^{5*}

¹Departamento de Engenharia de Materiais, Federal University of Paraíba (UFPB), Brazil

²Departamento de Ciências Farmacêuticas, Federal University of Paraíba (UFPB), Brazil

³Department of Materials Science and Engineering, University of Erlangen-Nuremberg, Germany

⁴Department of Mining and Materials Engineering, McGill University, Montreal, Quebec, Canada

^{5*}School of Materials, Materials Science Centre, Manchester University, UK, jonny.blaker@manchester.ac.uk

INTRODUCTION

We have developed a method to rapidly produce porous nanofibres by combining solution blow spinning¹ (SBS) and thermally induced phase separation² (TIPS). SBS can produce nanofibres, analogous to those electrospun from polymers dissolved in suitable solvents, yet with a production rate (per head) circa 100 times faster, and without the need for electric fields¹. In this work we freeze the nanofibres shortly after their formation, ahead of excessive solvent evaporation, causing phase separation within the nanofibres. Here we also address the challenge to produce interconnected macropores within 3-D nanofibre networks. Ice microspheres are used as *in situ* macroporosifiers, which become entangled during processing with the nanofibres. Subsequent compression of these ice/nanofibre entanglements, followed by freeze-drying, results in bioactive interconnected macroporous scaffolds, themselves formed of porous nanofibres.

EXPERIMENTAL METHODS

Amorphous polylactide (PLA) (used as a model polymer) was dissolved in dimethyl carbonate, at a polymer concentration of 15 m/v%. Up to 10 wt.% bioactive glass was added to the solution, which was then ultrasonicated to aid particle dispersion. Bioactive glass nanoparticles (20-30 nm diameter) were of the same composition as 45S5 Bioglass®. SBS was used to form nanofibres of this solution and conducted at air pressure 10-40 psi and polymer solution injection rates of 100-200 $\mu\text{L}\cdot\text{min}^{-1}$, delivered via a precision syringe driver to an inner co-axial surrounded by the higher pressure air sheath. The forming nanofibres were jetted directly into a liquid nitrogen bath, which resulted in TIPS within the nanofibres. Macroporous structures were generated by spraying water via a separate SBS head. The water formed ice microspheres proximal to the liquid nitrogen surface, measuring 300 μm – 2 mm in diameter. Different water injection rates allowed for the volume fraction of *in situ* macro-porosifiers to be controlled. The entangled ice sphere/nanofibre networks were compressed to form an interconnected network of ice. Subsequent lyophilisation resulted in macroporous scaffolds formed of bioactive porous nanofibres.

RESULTS AND DISCUSSION

Fibres of 15 m/v% had diameters 399 nm \pm 134, and exhibited a highly porous structure consisting of

elongated pores of ~50 nm by ~25 nm. Scaffolds were produced using ice microspheres at total volume fractions of between 0.4 to 0.8, resulting in interconnected macropores, themselves lined with nanofibres, as shown in Figure 1.

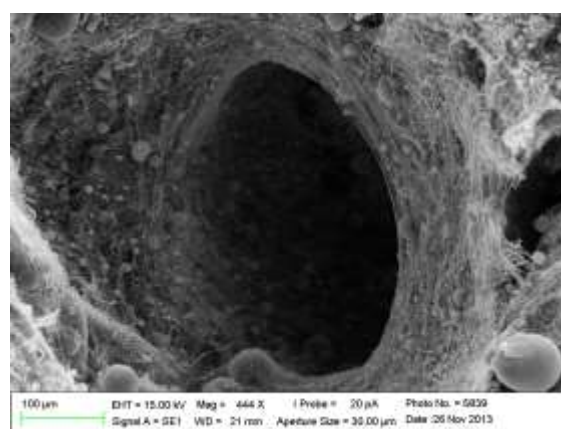


Figure 1. Porous bioactive nanofibres arranged into interconnected macroporous scaffolds

To the Authors' knowledge this is the first time that SBS has been used to produce porous nanofibres, as well as bioactive porous nanofibres, moreover, a method developed to form these into macroporous scaffolds via *in situ* porosifiers. These highly porous scaffolds have macroporosities of up to 76%, the nanofibres fibres themselves being up to 96% porous.

CONCLUSION

This technique provides a simple and rapid route to produce porous nanofibres, and macroporous scaffolds of controlled porosity, which can be rendered bioactive by bioactive nanoparticle inclusions.

REFERENCES

1. Medeiros E. S. *et al.*, J. Appl. Polym. Sci. 113:2322-2330, 2009;
2. Blaker J. J. *et al.*, Acta Biomateriala. 4:264-272, 2008

ACKNOWLEDGMENTS

JB acknowledges support from CAPES (Brazil), grant number PVE-18523129; JB, SNN and ESM acknowledge joint financial support from DFATD (CBJRP 2013-14 CA-1 McGill University) and CAPES.

ESB

POSTER PRESENTATIONS

Mechanical Properties of Zirconia 3-Unit Fixed Dental Prostheses Machined on a CAD/CAM System

Carlos Nelson Elias^{1*}, Heraldo Elias Salomão dos Santos¹ e Claudinei dos Santos²

¹Instituto Militar de Engenharia, Brazil, elias@ime.eb.br (presenting author)

²Universidade do Estado do Rio de Janeiro, Brazil

INTRODUCTION

Some works reported premature failure of femoral head alumina prostheses inside the human body¹. Biomedical zirconia was introduced to solve the problem of alumina brittleness and the potential failure of femoral ceramic prostheses², but its use in dental implants has not been thoroughly investigated.

Compared with alumina, zirconia-based ceramic used in fixed dental prostheses (FDPs) provide an adequate level of opacity, better esthetics, higher flexural strength, fracture toughness, and lower modulus of elasticity and hardness³. However, a limitation of zirconia application in FDP has been observed clinically: the degradation of zirconia when exposed to the oral environment, which may lead to a long-term decrease in strength and the possibility of failure⁴.

The manufacturing process of ceramics fixed dental prostheses (FDPs) is not the same as that of standardized samples for mechanical testing and, therefore, the surface finishing are not necessarily the same in both cases.

The purpose of this study was to compare the mechanical properties of standardized samples and FDPs before and after hydrothermal aging.

EXPERIMENTAL METHODS

Standardized samples with dimensions 43 x 3 x 4 mm were cut from commercial yttria stabilized tetragonal zirconia (3 Y₂O₃ mol%) blocks for CAD-CAM systems (ProtMat Advanced Materials, Brazil). After cut the blocks was submitted to subsequent grinding, surface polishing, and sintering in a furnace without atmosphere control (2 h at 1530°C). The flexural strength of standardized samples was measured using a 4-point bending test.

50 samples of 3-unit FDPs were machined with a CAD-CAM system from commercially ZrHP presintered blocks (Fig. 1). Samples were immersed in artificial saliva at a pressure of 2 bar for 30 h in an autoclave at 135°C. The mechanical bending tests of CAD-CAM FDPs were performed before (n=20) and after degradation (n=20).

The crystalline phases present in the presintered and sintered samples were identified by X-ray diffraction



Fig. 1. Dental prosthesis set up for 3-point bending testing.

RESULTS AND DISCUSSION

Table I shows the mean maximum force (N), flexural strength (MPa), and standard deviation for the 3-unit

FDP and standardized samples. Statistical analysis was performed.

Table I: Mechanical properties of 3-Unit FDP.

FDPs	F(N)	Stress (MPa)
Machined	740.90 ± 98.25	911.2 ± 184.1
Degraded	790.08 ± 150.18	871.9 ± 149.9
Polished	592.66 ± 101.36	573.8 ± 139.1
Standard sample		920 ± 108

The hypothesis that the CAD-CAM process changes the mechanical properties of zirconia is not confirmed. The mechanical properties of the standardized samples (920 MPa) are not statistically different from those of machined and sintered FDPs (911.2 MPa). Means comparison using Bonferroni Test, Scheffe' Test, and Tukey Test at the 0.05 level showed that the mechanical properties of the machined CAD-CAM FDPs and standard samples not significantly different (P = 0.96).

The standardized samples before sintering showed 5.8% of the tetragonal phase and 10.5% of the monoclinic phase. The content of 10.5% of the monoclinic phase is certainly related to the cutting process of the samples, which promoted phase transformation from tetragonal to monoclinic and induced residual stress.

After sintering, the standardized samples showed 98.2% of the tetragonal phase and 1.8% of the monoclinic phase. Polished FDPs have a higher percentage of monoclinic phase (14.5%) than standardized sintered samples.

CONCLUSION

1. CAD/CAM machining process introduces grooves in the surface of dental prostheses, but does not significantly change the flexural mechanical properties.
2. Hydrothermal aging does not significantly influence the mechanical properties of dental prostheses under bending, compression, and fatigue tests.

REFERENCES

1. D. F. G. Emery, DFG. *et al.*, J. Bone Joint Surg., 79:240–246, 1997.
2. Christel, P. *et al.*, Mat Characteristics Versus In Vivo Behavior," Ann. N. Y. Acad. Sci., 523:234-256, 1988
3. P. F. Manicone PF. *Et al.*, J. Dent. 35:819-826, 2007
4. A. Ortop A. *et al.*, J. Dent., 37:731-736, 2009
5. Yoshimura M. *et al.*, J. Mater. Sci. Lett, 6:465-67, 1987

ACKNOWLEDGMENTS

This work was carried out with financial support from the Brazilian Agencies CNPq (Process 472449/2004-4, 400603/2004-7 and 500126/2003-6) and FAPERJ (Process E-26/151.970/2004).

Nano-Crystallite TCP Synthesized by Mechanical Activation To Use Tissue Engineering

HASSAN GHEISARI DEHSHEIKH^{*a}, EBRAHIM KARAMIAN^b

^a Department of Material Engineering, Shahreza Branch, Islamic Azad University, Isfahan, Iran

^b Assistant Professor, Dept. of Materials Engineering, Najafabad Branch, Islamic Azad University, Isfahan, Iran

Email: *Hassan_Gheisary@yahoo.com

Abstract: Nowadays, TCP ($\text{Ca}_3(\text{PO}_4)_2$) that belongs to the group of calcium phosphate biomaterials as a hot topic of research for bone tissue repair applications and dentistry is studying. In this investigation, TCP powder was synthesized by mechanical activation method as a solid state process. The mixture was composed of a blend of pure calcite (CaCO_3) and silica amorphous (SiO_2) powder with 57 % wt. and 43 % wt, respectively. Then, the powder mixture milled by high energy ball mill with ball to powder ratio 10:1 and rotation speed 600 rpm for 10 h. After then, the materials milled heated at three temperatures 1100 °C, 1000 °C and 900 °C for 2 h in muffle furnace at the air atmosphere. X-ray diffraction (XRD), scanning electron microscopy (SEM) and BET technique performed on heated powders to characterize. According to XRD results, the patterns show that the phase TCP was just appeared in the mixture milled for 10 h. In addition, based on modified Scherrer calculator the TCP crystalline size was determined 37 nm. In fact, the present investigation indicated that TCP powder was composed of nano-crystallite structure, 30-40 nm, can be prepared by mechanical activation at 900 °C or 1000 °C to use as a new biomaterials for medical and dental purposes.

Keyword: Synthesis, TCP, Ball milling, Mechanical Activation, Nanostructure

Hyperbranched Poly(β -Amino Ester) for High Performance Gene Delivery

Dezhong Zhou, Wenxin Wang

Charles Institute of Dermatology, University College Dublin, Dublin, Ireland

wenxin.wang@ucd.ie

INTRODUCTION

Gene therapy holds great potential for the treatment of various diseases. Although linear poly(β -amino esters) have shown great potential in a variety of cell lines, the limited functional groups hinder further improvement of their potential^{1,2}. Herein, a novel poly(β -amino ester) (HPAE) with hyperbranched structure was synthesized and used as high performance gene delivery carrier.

EXPERIMENTAL METHODS

All the chemicals were purchased from Sigma-Aldrich and used as received. Molecular weight (Mw, Mn) and polydispersity index were tested on a Varian 920-LC GPC with DMF as elution solvent. Chemical structure was confirmed by a 300 MHz Bruker NMR with chloroform as solvent.

RESULTS AND DISCUSSION

HPAE (Figure 1a) was synthesized by two steps. First trimethylolpropane triacrylate (TMTPA), bisphenol A ethoxylate diacrylate (BE) and 4-amino-1-butanol (S4) were copolymerized by Michael addition to form base polymer. And then 3-morpholinopropylamine (MPA) was used to endcap the terminal groups. Chemical structure of the synthesised HPAE was confirmed by NMR (1b). Mw, Mn and PDI of the HPAE were 8918, 3426 and 2.60, respectively. NMR and GPC results indicated that HPAE was synthesised successfully.

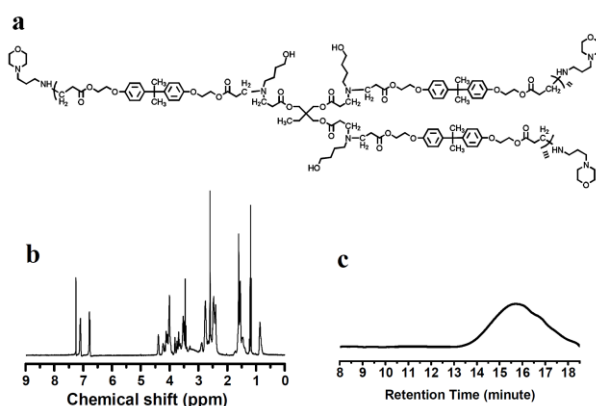


Figure 1 Chemical structure (a), NMR spectrum (b) and GPC curve (c) of HPAE

HPAE was used to carry out transfection in Hela, RDEBK and hADSC cell lines. As indicated by the GFP images, HPAE showed very high gene transfection efficiency in the presence of serum (Figure 2a). Gluciferase activity tests also indicated that the HPAE had much higher transfection efficiency compared to

the most widely used commercial transfection agents including superfect (SF), lipofectamine 2000 (LP), polyethylenimine (PEI) and xfect (Figure 2b), especially in RDEBK cells. Alamar Blue assay was used to test the metabolic activity of the transfected cells and the results showed that the HPAE was lowly toxic in all the three cell lines and over 80% of the transfected cells maintained good metabolic activity because of the biodegradability, which indicated that the synthesised HPAE was safe and biocompatible gene delivery carrier.

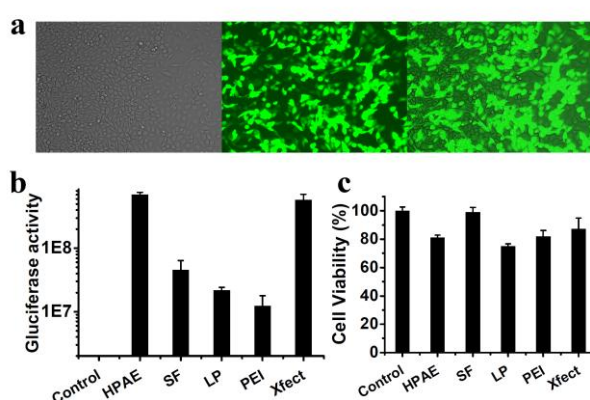


Figure 2 Fluorescence images of RDEBK cells transfected by HPAE (a), gluciferase activity (b) and cell viability (c) of cells transfected by HPAE, SF, LP, PEI and xfect after 48 hours.

CONCLUSION

Efficient and safe gene carrier is the prerequisite for successful gene therapy. In difference with the linear structured carriers, the unique hyperbranched structure of HPAE can overcome the limitation of linear counterparts by endowing multiple functional groups. HPAE was synthesised and characterized successfully. Transfection in Hela, RDEBK and hADSC cell lines indicated that the HPAE was a much more efficient and safer gene delivery carrier than all the most widely used commercial transfection agents.

REFERENCES

- Ledley F D., Hum Gene Ther. 6: 112-11249, 1995
- Green J J., Langer R., Anderson D G., Accounts Chem Res. 41: 749-759, 2008

ACKNOWLEDGMENTS

The authors are grateful to science foundation of Ireland (SFI) for financial support.

Optimisation of Macromolecular Crowding Conditions for Enhanced Extracellular Matrix Deposition *in vitro*

Diana Gaspar, Abhay Pandit, Dimitrios Zeugolis

Network of Excellence for Functional Biomaterials, National University of Ireland, Galway, Ireland

dimitrios.zeugolis@nuigalway.ie

INTRODUCTION

Cell-based tissue engineering strategies have limited clinical applicability due to delayed extracellular matrix deposition and consequent prolonged production time. Scaffold-free tissue production *in vitro* can be enhanced by macromolecular crowding (MMC)¹, a biophysical phenomenon that governs the intra- and extra-cellular milieu of multicellular organisms². Enhancement of tissue production *in vitro* can greatly contribute towards the development of cell-based therapies for a variety of clinical targets. Although a number of different conditions (crowding molecules, cocktails, concentrations) have been studied, an in depth understanding and optimisation have yet to be described.

EXPERIMENTAL METHODS

Human primary dermal fibroblasts were cultured for 14 days under different concentrations of FicollTM 400 (0, 10, 50 and 100 mg/ml) and constant concentrations of FicollTM 70 (37.5 mg/ml) and FicollTM 1000 (2.25 mg/ml). These were compared with non-crowded controls and a previously described FicollTM 70 (37.5 mg/ml) and 400 (25 mg/ml) cocktail¹.

Collagen I deposition was assessed by sodium dodecyl sulphate polyacrylamide gel electrophoresis (SDS-PAGE), $\alpha 1$ bands were quantified by densitometry using ImageJ software. Cell metabolic activity was quantified by alamarBlueTM as per manufacturer's protocol.

RESULTS AND DISCUSSION

Changes in FicollTM 400 concentration while maintaining constant FicollTM 70 and 1000 caused an increase when comparing to the non-crowded control (No MMC) and the well-established cocktail (Fc 70/400), when below 10 mg/ml. Above 10 mg/ml, increasing the concentration had a deleterious effect on the collagen I deposition (Figure 1A). The same tendency was observed by increasing the concentration of FicollTM 70. Despite the negative effect on collagen deposition, cell metabolic activity was not altered significantly (Figure 1B).

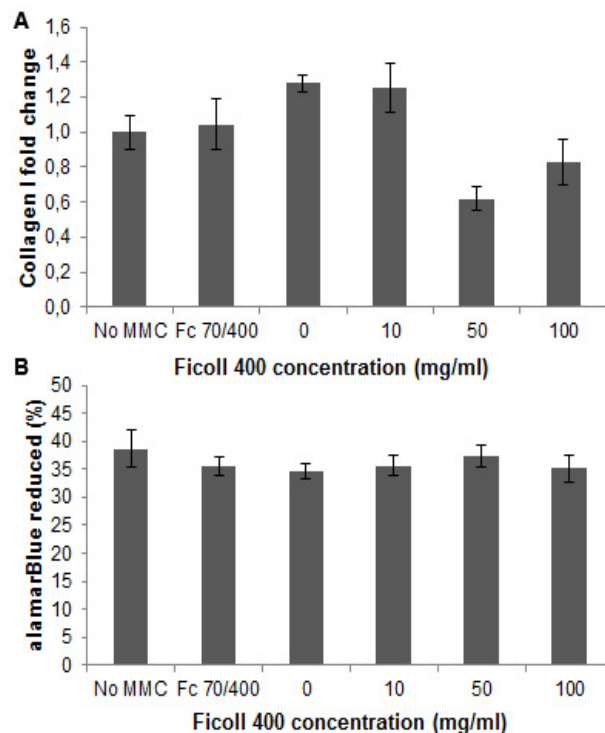


Fig. 1: Collagen I deposition (A) and metabolic activity (B) for varying concentrations of FicollTM 400 in a FicollTM 70, 400 and 1000 cocktail after 14 days in culture.

CONCLUSION

Although preliminary, these results pave the way for further understanding of macromolecular crowding and extracellular matrix deposition *in vitro*. Further characterization will be performed regarding extracellular matrix composition and concentration and excluded volume effect of these and other macromolecules.

REFERENCES

1. Satyam A. *et al*, Adv Mat, In Press
2. Chen C. *et al*, Adv Dr Del Rev 63: 277-290, 2011

ACKNOWLEDGMENTS

The authors would like to acknowledge the Irish Research Council for financial support.

Enhanced Extracellular Matrix Deposition and Maintenance of Mesenchymal Stem Cell Phenotype *In Vitro* using Macromolecular Crowding and Low Oxygen Tension

D. Cigognini¹, P. Kumar¹, A. Satyam¹, C. Sanz-Nogués², T. O'Brien², A. Pandit¹ and D. Zeugolis¹

¹Network of Excellence for Functional Biomaterials (NFB), NUI Galway, Ireland

²Regenerative Medicine Institute (REMEDI), NUI Galway, Ireland

Daniela.cigognini@nuigalway.ie

INTRODUCTION

Increasing evidence suggests that improving the accuracy of current *in vitro* microenvironment offers a better control over cell fate and subsequently can facilitate the development of clinically relevant tissue equivalents.^{1,3}

In this study we hypothesized that the synergistic application of macromolecular crowding² (MMC) and low oxygen tension,³ which represent two biologically relevant cell cues, would significantly enhance extracellular matrix (ECM) deposition in human mesenchymal stem cells (hMSC), while maintaining their undifferentiated phenotype and multipotency.

EXPERIMENTAL METHODS

First, optimal MMC conditions were identified by testing different concentrations of macromolecules (i.e. carrageenan² and a Ficoll mixture⁴) on cultured human bone marrow-derived MSCs. At four time points (2, 4, 7 and 14 days), ECM deposition, matrix metalloproteinase activity and cell viability were evaluated using SDS-PAGE and immunocytochemistry, gelatin zymography and alamarBlue® assay, respectively.

Then, the synergistic effect of low oxygen tension and MMC was investigated by culturing hMSCs under MMC at 20% O₂ or 2% O₂. ECM deposition and remodelling were assessed as described above, while hMSC phenotype and multipotency were investigated using flow cytometry, tri-lineage differentiation assays and gene expression analysis. Statistical analysis was performed using the one-way ANOVA –or the Kruskal-Wallis test for non-parametric analysis–, followed by *post hoc* tests.

RESULTS AND DISCUSSION

MMC significantly enhanced production of ECM, notably collagen I, by cultured hMSCs. MMC also increased the presence of activated metalloproteinases in the deposited ECM. Moreover, carrageenan seemed more effective than a previously published Ficoll mixture (Ficoll 70 + Ficoll 400) in inducing ECM deposition (Fig.1).

The addition of crowders on hMSCs cultured under 20% O₂ induced terminal differentiation. This MMC

effect was significantly reduced at 2% O₂, as shown by retention of hMSC surface markers and expression of stem cell transcriptional factors (e.g. Oct4). These data support previous finding and suggest that hypoxia can be used to maintain hMSC phenotype in a crowding environment.

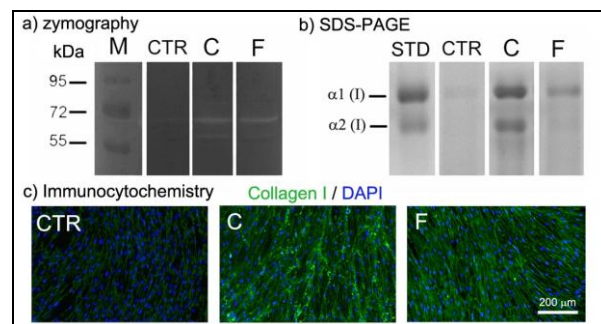


Fig. 1. MMC increased the presence of metalloproteinases in the ECM (a), and enhanced the deposition of collagen I (b-c). Legend: CTR: control, no MMC; C: carrageenan; F: Ficoll.

CONCLUSION

Here, we report that the introduction of both hypoxia and MMC helps hMSCs to build a more biologically relevant microenvironment *in vitro*. Although this strategy needs to be further investigated, a promising application is combining it with cell-sheet technology in order to enhance the formation of cell sheets rich in ECM and multipotent human MSCs.

REFERENCES

1. Cigognini D. *et al.*, Drug Discov.Today. 18:1099-1108, 2013
2. Satyam A. *et al.*, Adv. Mat. 2014, In Press
3. Grayson WL. *et al.*, Biochem Biophys Res Commun. 358:948-953, 2007
4. Zeiger AS. *et al.*, PLoS One. 7:e37904, 2012

ACKNOWLEDGMENTS

This work is supported by Health Research Board (HRA_POR/2011/84) and Science Foundation Ireland (09/RFP/ENM2483).

Synthesis and characterization of novel bioglass-ceramic $\text{CaO-Na}_2\text{O-SiO}_2\text{-P}_2\text{O}_5\text{-ZrO}_2\text{-TCP}$ by sol-gel processing

Parisa Eslami¹, Giovanni Baldi¹, Valentina Faso¹

¹Ce.Ri.Col Research Center of Colorobbia italia, Italy (FI), eslamip@colorobbia.it

INTRODUCTION

Bioactive glasses (BG) and glass ceramics (BGC) have been extensively studied for more than 30 years since Hench first invented bioglass. Because of the good bioactivity and biodegradability, BGs, as bone repair materials or fillers owing to their ability to form a bond to living bone, have been used in clinic for more than ten years¹.

Sol-gel processing, an alternative to traditional melt processing of glasses, involves the synthesis of a solution (sol), typically composed of metalorganic precursors followed by the formation of a gel by chemical reaction, and lastly thermal treatment for drying, organic removal, and sometimes crystallization. Compared with melt-processed BGs, sol-gel BGs are processed at lower temperature and have better compositional control, that leads to increase numbers of silanol groups and/or mesopores, both of which may act as nucleation sites for apatite formation². Not only silanol group provides proper sites for nucleation of hydroxyapatite (HA) but also zirconia in content of bioglass exhibits a bone bonding ability by forming an apatite layer on their surfaces in the living body when they are modified to have many Zr-OH groups on their surfaces³. In this study, we designed %23.5CaO,%4.2Na₂O,%48.6SiO₂,%12.2P₂O₅,%2.7ZrO₂,%8.8TCP BGC for the first time as a coating by sol-gel processing for Ti alloy for orthopedic disease.

EXPERIMENTAL METHODS

The glass-ceramic powders were synthesized by sol-gel process. First of all, tetraethoxysilane was mixed with 0.1M nitric acid in a breaker under vigorous stirring at r.t for 30 min. After the hydrolysis of the TEOS was completed the following reagents were added in sequence allowing 45 min for each reagent to react completely (C₂H₅)₃ PO₄, Mg(NO₃)₂, (Ca(NO₃)₂, NaNO₃, ZrO(NO₃)₂ and (Ca₃(PO₄)₂). After the reactants were stirred at r.t for 1 h, the transparent sol was formed. The sol was aged at r.t for 10 days transforming into gel and followed by being dried at 120°C for 48 h. The dried gel was ground and compacted into disk and then calcined at 750°C for 2 h to eliminate residual water and nitrates. In vitro bioactivity of the composites- as disk shaped specimens- was tested for various immersion time 1, 3, 7, 14, and 21 in Simulated Body Fluid (SBF) solution with pH=7.4 at 37 °C. The immersed materials were characterized by SEM, EDS and XRD.

RESULTS AND DISCUSSION

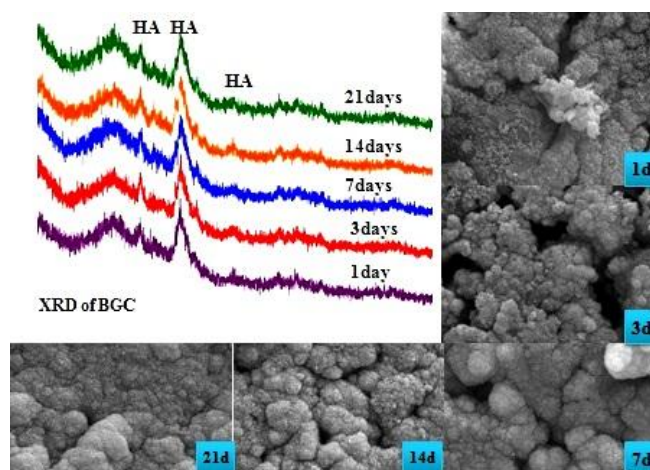
The in vitro bioactivity of BGC was studied by soaking BGC in SBF solution with PH=7.4 at 37 °C for 1, 3, 7, 14 and 21days. SEM and XRD (fig1) revealed the precipitation of HA on the surface of BGC after 1 day

and developing the growth of nanocrystalline HA on the surface during 3, 7, 14 and 21days. EDS analysis (table 1) clarified that a molar Ca/P ratio ranging 1.7-2.4 for BGC suggesting a thick and well-formed apatite layer on the surface of this BGC from 1 to 21 days. Therefore, the bioactivity response of the specimen BGC is rapid. Corresponding to table 1 pH variation with time increased up to 8 during first day until 21 days for BGC. As a result, more changes led to high bioactivity and this conclusion is corresponding to EDS results.

Table1

Ca/P	1 day	3 days	7 days	14 days	21 days
BG	2.03	1.73	2.42	1.81	1.81
pH=7.4	1 day	3 days	7 days	14 days	21 days
BG	7.71	7.72	8.00	8.01	8.20

Figure1



SEM of BGC

CONCLUSION

The novel bioglass-ceramic prepared by sol-gel processing showed high bioactivity. An apatite layer grew on its surface by immersion in SBF through a mechanism consisting on dissolution of ZrSiO₄, subsequent partial dissolution of ZrO₂ crystalline phases in glassy matrix and finally, nucleation and growth of a globular apatite layer on its porous surface.

REFERENCES

1. Kokubo T., Biomaterials. 12: 155-163, 1991.
2. Gupta R., Biomed. Mater. 3: 1-15, 2008.
3. Rabiee M., Int. J. Appl. Ceram. Technol. 10: 33-39, 2013.

ACKNOWLEDGMENTS

“The authors would like to thank the Marie Curie fellowship, GlaCERCo research team, and Colorobbia Italia for providing financial support to this project”



Interconnected porous calcium phosphate forming cement consisting of α -TCP foam granules and calcium phosphate acidic solution

Khairul Anuar Shariff, Kanji Tsuru, Kunio Ishikawa

Department of Biomaterials, Faculty of Dental Science, Kyushu University, Japan, mppusm@gmail.com

INTRODUCTION

Interconnected porous calcium phosphate forming cement is thought to be an ideal material as artificial bone substitute and scaffold for bone tissue regeneration, since its interconnected pores offer space that allows cells' growth and penetration. Trung Kien *et al.* successfully fabricated fully interconnected porous calcium phosphate cements based on the setting reaction of α -tricalcium phosphate (α -TCP) microspheres using calcium phosphate acidic solution at 37°C for 10 minutes¹. The mechanical strength of this cement was limited when compared with powder type cement. This is due to limited contact point at interface of α -TCP microspheres². In this study, the feasibility to fabricate interconnected porous calcium phosphate forming cement was evaluated based on the setting reaction of α -TCP foam granules with calcium phosphate acidic solution.

EXPERIMENTAL METHODS

α -TCP powder was prepared by a mixture of calcium carbonate (CaCO_3) and dicalcium phosphate dihydrate (DCPD) with Ca/P ratio of 1.5. α -TCP foam was prepared using polyurethane foam as a template³. Calcium phosphate coated polyurethane foam was heated in an electronic furnace at 1500°C for 5 hours. α -TCP foam granules size were regulated from 300 μm -1000 μm by crushing and sieving. 1.0 M monocalcium phosphate monohydrate (MCPM)-1.0 M phosphoric acid (H_3PO_4) was prepared as calcium phosphate acidic solution. This solution was saturated with respect to MCPM. α -TCP foam granules were placed into 6x3 mm split stainless steel mold and then treated with calcium phosphate acidic solution at 25°C for 1 minute with L/P ratio of 1ml/g. Specimens were washed with distilled water and then immersed in acetone for 10 minutes to arrest the setting reaction process¹.

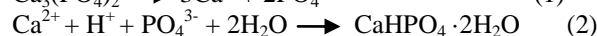
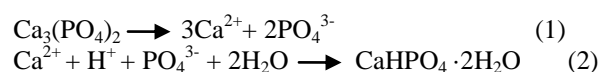
RESULTS AND DISCUSSION



Figure 1: Photographs of (a) α -TCP foam granules and (b) α -TCP foam granules after treated with 1.0 M MCPM-1.0 M H_3PO_4 solution at 25°C for 1 minute.

Figure 1 show α -TCP foam granules (a) before and (b) after being treated with 1.0 M MCPM-1.0 M H_3PO_4 solution for 1 minute at 25°C. As shown α -TCP foam granules set upon exposure to the calcium phosphate acidic solution.

The mechanism for setting reaction of interconnected porous calcium phosphate forming cement is thought to be similar with dicalcium phosphate dihydrate (DCPD) cements⁴. When α -TCP foam granules are exposed to MCPM- H_3PO_4 solution, specimens dissolve to supply Ca^{2+} and PO_4^{3-} ions as shown in equation 1⁵. This MCPM- H_3PO_4 solution would supersaturate regarding to DCPD phase. DCPD crystals would precipitate on the surface of α -TCP foam granules as shown in equation 2⁵. Precipitation of DCPD crystals from the liquid phase results in the decrease of its supersaturation and thus, α -TCP foam granules further dissolve to supply Ca^{2+} and PO_4^{3-} ions to the liquid phase. Based on this dissolution-precipitation reaction, DCPD crystals would precipitate on the surface of α -TCP foam granule with time and interlock each other to set and form interconnected porous cement.



CONCLUSION

It is concluded that this method might be useful to fabricate interconnected porous calcium phosphate for bone tissue regeneration.

REFERENCES

1. Trung Kien P. *et al.*, J. Aust. Ceram. 46:63-67, 2010
2. Ishikawa K. *et al.*, Key Eng. Mater, 493-494:832-835, 2012
3. Munar ML. *et al.*, Dent. Mater. J. 25:51-58, 2010
4. Mirtchi AA. *et al.*, Dent. Mater. J. 25:51-58, 2010
5. Han B. *et al.*, Acta Biomater. 5:3165-3177, 2009

ACKNOWLEDGMENTS

The authors would like to thank AUN-SEED/Net and JICA for their financial support. This study also supported by a Grant-in-Aid for Scientific Research from Japanese Society for Promotion of Science and Research

Antithrombogenic Surface on Poly(ether ether ketone) Prepared by Self-initiated Photoinduced Graft Polymerization of 2-Methacryloyloxyethyl Phosphorylcholine

Kazuhiko Ishihara¹, Masayuki Kyomoto,^{1,2} Tetsuji Yamaoka,³ Sachiyo Kakinoki³

¹Department of Materials Engineering, The University of Tokyo, Tokyo, Japan, ²KYOCERA Medical Co., Osaka, Japan,

³National Cerebral and Cardiovascular Center Research Institute, Osaka, Japan, ishihara@mpc.t.u-tokyo.ac.jp

INTRODUCTION

Poly(ether ether ketone) (PEEK) is a kind of superengineering plastic. PEEK exhibits high mechanical properties and heat-, chemical- and radiation-resistances. Therefore, PEEK has also employed as a biomaterials for trauma, orthopaedic and spinal implants. We thought to use PEEK in the cardiovascular devices, such as an artificial heart valve. The artificial heart valve requires high mechanical properties, antithrombogenicity and anti-infection. However, PEEK cannot satisfy those requirements. How to modify materials is changing bulk property and surface modification. In this study, we modified PEEK surface by “self-initiated photoinduced graft polymerization” for obtaining a super-functional PEEK [1]. The self-initiated photoinduced graft polymerization uses semi-benzopinacol radicals from benzophenone units in PEEK molecule structure under UV-irradiation. Advantages of this method are easy handling, well suited for application and graft polymer coating strongly binding the substrate. 2-Methacryloyloxyethyl phosphorylcholine (MPC) polymers exhibit excellent biocompatibility, that is, antithrombogenicity, anti-infection due to reduced protein adsorption. We controlled monomer concentration, polymerization temperature, UV intensity and solvent during the polymerization. Additionally, we evaluated the amount of adsorbed protein to predict antithrombogenicity.

EXPERIMENTAL METHODS

The surface of PEEK was ultrasonically cleaned in ethanol. The MPC was dissolved in degassed water and then adjusted to monomer concentration (0.25–1.0 mol/L) and temperature (25–60°C). PEEK was immersed in these solutions. Polymerization was carried out for 90 min on PEEK surface under UV (360 ± 50 nm) irradiation with intensity (2.5–9.0 mW/cm²). After polymerization, poly(MPC) (PMPC)-grafted PEEK surface was washed with clean solvent to remove monomers and free polymers. PMPC-grafted PEEK was analyzed by XPS, FT-IR/ATR, water contact angle measurement and protein adsorption by micro BCA method. Also, an artificial valve was prepared by PMPC-grafted PEEK and implanted it into pig for evaluating *in vivo* performance of the PMPC-grafted PEEK.

RESULTS AND DISCUSSION

Photoinduced graft polymerization of MPC on the PEEK proceeded well. In the XPS and FT-IR/ATR spectra and water contact angle measurement showed that the hydrophilic PMPC layer formed on the PEEK

substrate. With increasing the monomer concentration, IR intensity ratio increased. IR intensity ratio corresponds to the number of MPC units on PMPC-grafted PEEK. So the number of MPC units in the PMPC layer increased with increasing the monomer concentration. Generally, in the radical polymerization, the molecular weight of polymer increases with increasing the monomer concentration. It seemed that the PMPC layer thickness increased with increasing MPC concentration. The density of the PMPC layer increased with increasing UV intensity. The amount of adsorbed protein decreased with increasing MPC concentration in feed solution (Fig. 1). This is corresponding to the increase hydrophilic nature of the surface. The MPC polymers can inhibit blood cell adhesion and activation. Thus, we can consider that the PMPC-grafted PEEK will show both excellent antithrombogenicity and mechanical property. We have done implant experiment of artificial valve prepared with PMPC-grafted PEEK for a few weeks. It functioned well even it was *in vivo*. The fundamental results will be demonstrated.

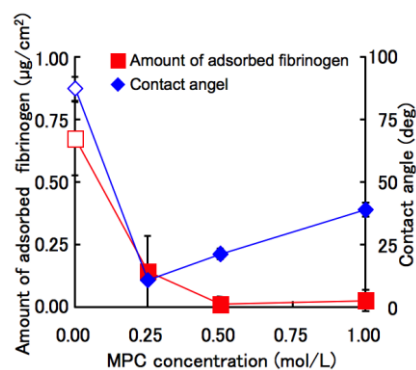


Fig. 1. Amount of adsorbed fibrinogen and water static contact angle of PMPC-grafted PEEK prepared in water. Open marks: Untreated PEEK.

Conclusions: It was successful to provide biocompatibility to PEEK surface by self-initiated photoinduced polymerization. The new materials will be useful for developing cardiovascular devices.

REFERENCE

1. Kyomoto M. *et al. Appl Mater Interfaces*. 2009;1;537-542.
2. Tateishi T. *et al. J Biomed Mater Res* 2014; published on WEB: DOI: 10.1002/jbm.a.34809

ACKNOWLEDGMENTS

This research was supported from Strategic Promotion of Innovative Research and Development (JST).

Development of bioengineered designer scaffolds for full thickness skin wound healing

Naveen Kumar*

Division of Surgery, Indian Veterinary Research Institute, Izatnagar-243122, Uttar Pradesh, India
naveen.ivri1961@gmail.com

INTRODUCTION

An ideal acellular matrix should be able to provide right biological and physiological environment to ensure homologous cell and extra cellular matrix (ECM) distribution. It should also provide the right size and morphology of neo-tissue required. Collagen ranks as the most widely used matrix material for the purpose of tissue engineering in the dermis. Due to their advantageous biological properties, collagen based scaffolds are under extensive investigations and used as matrices for tissue engineering. The advantages are that natural matrix materials mimic natural ECM structure and composition; emulate native stimulating effects of ECM on cells and allows incorporation of growth factors and other matrix proteins to further enhance cell functions. ECM has an important role in providing optimal chemical and structural environment for tissue growth and regeneration.

EXPERIMENTAL METHODS

Our group has been working in this area for last one decade and we have developed protocols for preparation of acellular matrix from different organs/tissues in our Biomaterial and Bioengineering Laboratory, Division of Surgery, IVRI, Izatnagar. Bioengineered designer scaffolds has been developed using abattoir waste materials, from tissues rich in collagen. The materials used are diaphragm, pericardium, blood vessels, skin, intestines and gall bladder. The techniques have been developed for making acellular matrix from these organs/tissues. Fibroblasts/mesenchymal stem cells were seeded on these collagenous matrices to prepare 3-D biengineered designer scaffolds. These designer scaffolds were evaluated for reconstruction of full thickness skin wound defects in laboratory animal

models as well as in clinical cases requiring reconstructive surgery. These matrixes were used either without crosslinking with chemicals or they were crosslinked with some crosslinking agents to delay the resorption of these matrices in the body so that reconstruction and repair of tissue takes place.

We have also developed some protocols for de-epithelization of skin in different species of animals, viz. rabbit, sheep, goat, buffalo and pig. In these protocols enzymes have been used for de-epithelization of the skin. We have also developed some patentable protocols for acellularity of de-epithelized skin. Acellular dermal matrix has been prepared using different combinations of enzymes, anionic and non-ionic biological detergents. These acellular dermal matrices will be used for further tissue engineering and for three dimensional culture configurations to promote 3-D tissue organization. Current major research programs of the division have been directed to develop novel, biodegradable and biomimetic "designer" scaffolds for regenerative surgery. An overview of different research methodologies and techniques optimized for developing designer scaffolds and their application in tissue engineering will be discussed in details during this presentation.

ACKNOWLEDGMENT

The author acknowledges the financial assistance received from the Department of Biotechnology, Ministry of Science and Technology, New Delhi, India to carry out this work.

Synthesis and *In Vitro* Biocompatibility of Carbonated Hydroxyapatite for Bone Tissue Engineering Application

Yanny M. Baba Ismail^{1,2,3}, Oana Bretcanu², Kenneth W. Dalgarno², Alicia J. El Haj¹

¹ Institute for Science and Technology in Medicine, Keele University, Stoke-on-Trent, ST47QB, UK

² School of Mechanical and Systems Engineering, Newcastle University, NE17RU, UK.

³ School of Materials and Mineral Resources Engineering, Universiti Sains Malaysia, Engineering Campus, 14300, Nibong Tebal, Penang, Malaysia.

Corresponding Author: a.j.el.haj@keele.ac.uk

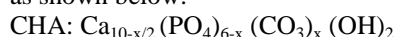
INTRODUCTION

Hydroxyapatite (HA) closely resembles the mineralised phase of bone and possesses good biocompatibility, bioactivity and osteoconductivity [1]. Thus, HA has become the most widely used bioceramic in the field of bone regeneration medicine. However, resorption of HA *in vivo* is too slow to induce massive formation of a new bone tissue and HA is known to be brittle in nature. Biological apatites differ chemically from stoichiometric HA in that they contain a number of trace elements (*e.g.* CO₃, Si, Zn, Sr, Na, and Mg). Carbonate is the major substituents among the trace elements which present typically about 2-8wt% which depends on the individual age.

Therefore, simulating the chemistry of mineralised tissue in bioceramic materials may be means of improving the level of biological response of the implant to the host *in vivo*. The aim of this study is to synthesise a range of carbonated HA (CHA) that mimic the levels of carbonate present in biological apatites, followed by *in vitro* cytotoxicity assessment of the as-synthesised powders in response to MG63 cells. It is intended that this novel formulation will improve both osteogenic behaviour and mechanical properties of the resulting scaffolds.

EXPERIMENTAL METHODS

Carbonated Hydroxyapatite (CHA) powders were synthesised at room temperature using Ca(NO₃)₂·4H₂O, (NH₄)₂HPO₄, and NH₄HCO₃ (Sigma-Aldrich, Gillingham, UK) by a nanoemulsion method [2]. The amounts of carbonate ($x = 0.5, 1.0, 2.0, 3.0$ and 4.0 molar content) substituted into the HA structure were calculated based on the stoichiometry empirical formula as shown below:



The physico-chemical properties of the as-synthesised powders were investigated through XRD, FTIR, CHN and ICP. The biocompatibility of the as-synthesised powders was then tested *in vitro* cell-culture with MG63 human osteosarcoma cell line via direct contact based on ISO10993-5.

RESULTS AND DISCUSSION

At low carbonate contents, only single phase CHA pattern was detected. However, as the amount of carbonate increased the calcite (CaCO₃) phase was also observed. This formation of secondary phase was caused by the higher amount of carbonate in the apatite structure. During synthesis the carbonate that could not substitute at phosphate sites in the apatite structure, due to limited substitution, would then react with calcium and thus form calcite, CaCO₃. The FTIR analysis of the

CHA powders clearly demonstrates typical peaks of B-type CHA with the bands originating from stretching vibrations of carbonate ions at 870-875, 1410-1430, and 1450-1470 cm⁻¹. The typical peaks of the A-type CHA, which usually appear at 877-880, 1500, and 1540-1550 cm⁻¹, were not visible in the spectra [3]. These confirmed that the as-synthesised powders were B-Type CHA. However, the CaCO₃ phase as detected in XRD was not detected in the FTIR spectra. No calcite band was observed at 712cm⁻¹ due to the small amount present [4]. The marker bands of aragonite around 713 and 700 cm⁻¹ and vaterite at 745cm⁻¹ were also not observed for all samples. From CHN analysis, it is considered that 2.0CHA is an ideal composition, as it possesses levels of carbonate (2-8wt%) which are typical of biological apatites.

In vitro biological assessment demonstrated that none of the powders are toxic to MG63 cells. The 2.0CHA formulation showed the highest level of DNA and total protein production, closely followed by 1.0 and 3.0CHA.

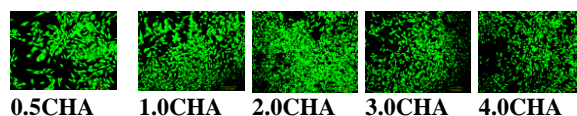


Fig.1. Live/dead images of the CHA powders after 14 days in culture

CONCLUSION

Carbonated Hydroxyapatite (CHA) with different degrees of carbonate substitutions has been successfully synthesised by a nanoemulsion method. Chemical analysis confirmed that carbonate has been successfully substituted the phosphate groups and formed B-type CHA. The data suggest that the optimum composition is $x=2.0$ (2.0CHA) as it retained single phase with purely B-type CHA and possesses an ideal amount of carbonate. Cell growth and proliferation were also found to be faster for this formulation.

REFERENCES

- [1] Sprio, S. *et al.*, Materials Science and Engineering C28: 179-187. 2008.
- [2] Zhou, W.Y. *et al.*, Journal Material Science: Material Medicine 19: 103-110. 2008.
- [3] Landi, E. *et al.*, Biomaterials 25: 1763-1770.
- [4] Krajewski, A. *et al.*, Journal of Molecular Structure 744-747: 221-228.

ACKNOWLEDGMENTS

The authors would like to thank Arthritis Research UK for providing financial support to this project.

Modification of Magnesium Coated Titanium Surfaces to Control Its Corrosion Rate

O. Mazmanoglu¹, S. Onder¹, F. N. Kok¹, K. Kazmanlı², M. Urgan²

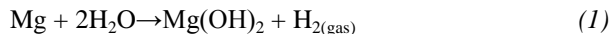
¹Molecular Biology Genetics and Biotechnology Programme, İstanbul Technical University, Turkey

² Department of Metallurgical and Materials Engineering, İstanbul Technical University, Turkey
okanmazman@yahoo.com

INTRODUCTION

Titanium (Ti) and its alloys are being used for production of metallic biomaterials currently because of their unique properties such as suitable mechanical properties and corrosion resistance¹. However, titanium has low wear resistance and limited osteointegration properties. Hence surface engineering studies focused on improvement of these insufficient properties of titanium alloys².

Magnesium is a biodegradable and biocompatible material with various other unique advantages. Mg²⁺ is the most abundant cation in human body and exists in natural bone structure. Furthermore, Mg²⁺ has been used to improve surface properties of Ti implant materials³. Nevertheless, usage of pure magnesium in biomaterial production or high proportional addition to alloys may cause degradation and corrosion issues³. According to a well-known phenomenon, hydrogen evolution related with magnesium biodegradation in physiological media, is one of the issues which is described as following overall stoichiometric equation⁴⁻⁷.



In this study we proposed a coating technique to obtain suitable magnesium proportions on titanium substrates via cathodic arc physical vapour deposition (PVD). It is considered that rapid corrosion of inner magnesium content from titanium substrates would be prevented by this surface modification technique.

EXPERIMENTAL METHODS

Pure Ti substrate specimens were cut in squares with ca. 1cm² surface area. The specimens were firstly chemically cleaned with acid mixture solution. Then cathodic arc PVD procedure was performed with different sputtering times and cathode current values (Table1). Etching, coating and final sputtering were carried out at bias voltages -800V, -50V and -600V respectively³.

Table 1: Process parameters of experimental coatings

Experiments	Current(A)		Coating Time(min)	Sputtering Time(min)
	Ti	Mg		
1	85	55	10	2
2	85	55	10	5
3	85	55	10	8
4	85	40	10	8
5	85	25	10	8

Surface characterization analysis were performed via electron dispersive spectroscopy (EDS), scanning

electron microscope (SEM) and X-ray diffraction (XRD).

RESULTS AND DISCUSSION

Sputtering time affected the Mg²⁺ amounts slightly after reaching a threshold (Table 2). In order to achieve lower Mg²⁺ amounts, different current values of Ti and Mg²⁺ cathodes were set under constant sputtering times.

Table 2: Approximate atomic Mg amounts of coatings by EDS analysis (kV=10kV, take-off angle 25.0°, line: Kα)

Experiments	Atomic Mg ²⁺ (%)
1	~25-28
2	~12
3	~11-12
4	~9-10
5	~3-4

Preliminary studies showed that Mg²⁺ amounts on Ti substrates could be controlled within 1 at. %. SEM micrographs, however, indicated nonuniform droplet formation on the surfaces (data not shown). Mg²⁺ corrosion mechanism and determination of different phases on modified surfaces are next steps for ongoing studies.

CONCLUSION

Sputtering process was selected to force the formation of a stable Mg²⁺ phase into Ti substrates. This approach could restrict the corrosion rate of Mg²⁺ and decrease the hydrogen evolution rate. The results are considered promising and could be a solution to lower the formation of subcutaneous hydrogen pockets after implantation operations by using magnesium based implants⁸.

REFERENCES

1. Staiger M. P. *et al.*, Biomaterials 27 :28-34, 2006
2. Cao P. *et al.*, Surf. Coat. Tech. <http://dx.doi.org/10.1016/j.surfcoat.2013.11.006> (Article in press), 2013
3. Onder S *et al.*, Mat. Sci. Eng C 33:7: 37-42, 2013
4. Witte F. *et al.*, Curr. Opin. Solid State Mater. Sci. 12:63-72, 2008
5. Kirkland N. T. *et al.*, Acta Biomater. 8 :25-36, 2009
6. Salunke P. *et al.*, Mater. Sci. Eng., B 176:11-17, 2011
7. Song G. *et al.*, Adv. Eng. Mater. 9 :98-02, 2007
8. Witte F. *et al.*, Biomaterials 26:57-63, 2005

ACKNOWLEDGMENTS

The authors would like to thank The Scientific and Technological Research Council of Turkey (Grant no: 112M339) for providing financial support to this project.



Dip TIPS as a Novel Process for Preparation of Anisotropic Channeled Porous Polymer Scaffolds for Guided Tissue Engineering Applications

Naresh Kasoju^{1*}, Dana Kubies^{1*}, Marta M. Kumorek¹, Lud'ka Machová¹, Jan Kříž², Daniel Jiráček², Eva Fabryová², František Rypáček¹

^{1*}Institute of Macromolecular Chemistry, Academy of Sciences of Czech Republic, v.v.i., Heyrovského Square 2, Prague 162 06, Czech Republic. kasoju@imc.cas.cz

²Institute for Clinical and Experimental Medicine, Videnska, Prague 140 21, Czech Republic.

INTRODUCTION

Much of research within the tissue engineering scaffold fabrication has been focused on the design of isotropic porous architectures. However, when using such scaffolds, the restriction on cell penetration and nutrient flow to the scaffold center due to rapid tissue formation on the outer edge of the scaffold generally leads to the formation of a necrotic core¹. Alternatively, scaffolds with anisotropic pore architecture improve the cell infiltration and nutrient flow thus avoiding any necrotic core formation². The unidirectional thermal induced phase separation (TIPS) process enables the fabrication of anisotropic channeled porous foams; however, the current setups are complex and limited^{3,4}. In contrast, here we demonstrate the proof-of-principle of a facile and versatile methodology based on the ideas of TIPS, termed as Dip TIPS, consisting of dipping of the template into the polymer solution followed by thermally induced phase separation to obtain anisotropic channeled porous polymer foams. The effects of polymer properties, processing conditions and template parameters on the pore architecture were investigated. The feasibility of scaffolds to provide cell infiltration and distribution within the foams in *in vivo* was tested.

EXPERIMENTAL METHODS

The setup consists of a thermally conductive template (*T*), which was fitted to the thermally conducting block (*C*). The block *C* was fitted to a non-metallic reservoir (*R*) for freezing mixtures (**Figure 1A**). The *T* bar was dipped into the polymer solution and the freezing mixture was poured into *R* to quench the polymer solution in the immediate vicinity of the *T* bar. After pre-set quenching times, the phase separated polymer was freeze-dried resulting in the 3D foam. The foam morphology was characterized by SEM and porosimetry analysis. The *in vivo* experiments were performed using male Norway brown rats (HE staining, trichrome staining, CD31 staining).

RESULTS AND DISCUSSION

The Dip TIPS follows the principles of the conventional TIPS. In contrast to the previous methods, Dip TIPS is *simple* - as it doesn't involve complex setups or procedures, *adaptable* - as it enables the preparation of tubular, open-capsular as well as flat 3D foams with variable sizes, and *scalable* - as many *T* bars can be fitted to *C* block. For example, the tubular/open-capsular foams prepared from poly(lactide-co-caprolactone) (PLA:PCL ratio of 93:7 mol/mol, $M_w = 300\,000$ g/mol, 5 % w/v in dioxane, quenched at $-80\text{ }^{\circ}\text{C}$ for 30 s) exhibit porosity of 86 %, thickness of 612 ± 22

μm , with $53 \pm 6\text{ }\mu\text{m}$ pores on the outer surface and $10 \pm 5\text{ }\mu\text{m}$ pores on the inner surface with the anisotropic and channeled structure of the pores (**Figure 1B**).

The detailed investigations revealed that (i) the pore size was inversely proportional to the applied quench depth and the polymer concentration and was directly proportional to the coarsening time (ii) the foam thickness was directly proportional to the quenching time, and (iii) the polymer type, polymer molecular weight and template dimensions also affected the pore architecture. The *in vivo* studies revealed that the foams supported the guided host cell/tissue infiltration and provided convenient conditions for the high density homogenous cell growth, without formation of fibrotic capsule or necrotic center (**Figure 1C**).

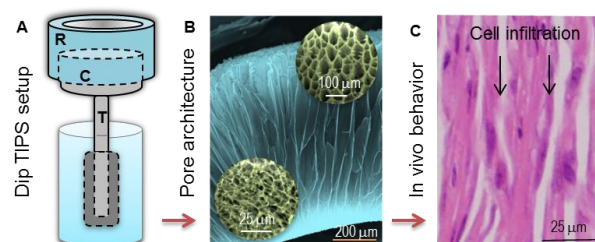


Figure 1. Schematic Dip TIPS setup (A); cross section (SEM) showing the anisotropic channeled pore architecture with a detail pore structure of outer and inner edges of the foam (B); Haematoxylin-eosin staining (pink) of 4-week old implant showing the guided host cell/tissue infiltration *in vivo* (C).

CONCLUSION

The Dip TIPS setup enabled the fabrication of anisotropic channeled porous foams in shapes such as tubular, open-capsular or flat with the foam thickness below 1 mm. The pore size was tuned by changing the polymer concentration and quenching temperature, while the thickness was regulated by altering the quenching time. The *in vivo* studies revealed the potential of these foams for guided tissue engineering applications.

REFERENCES

1. Mitchell G.R., *et al.*, *Procedia Eng.* 59:117–125, 2013;
2. Silva M.M.C.G., *et al.*, *Biomaterials* 27:5909–5917, 2006;
3. Ma P.X., *et al.*, *J. Biomed. Mater. Res.* 56:469–477, 2001;
4. Ma H., *et al.*, *Adv. Funct. Mater.* 20:2833–2841, 2010.

ACKNOWLEDGMENTS

The study was funded by the Ministry of Education, Youth and Sports, Czech Republic (project BIOPOL, EE2.3.30.0029), the Ministry of Health, Czech Republic (no. 00023001) and “European Regional Development Fund” (project BIOCEV, CZ.1.05/1.1.00/02.0109).

Different cryogel architectures as basis for 3D cell culture of prostate cancer cells

Anne Baecker¹, Bettina Goeppert, F.J. Gruhl

¹Karlsruher Institute of Technology (KIT),
Institute of Microstructure Technology (IMT)
anne.baecker@kit.edu

INTRODUCTION

Conventional 2D cell culture affords an unnatural microenvironment for growing cells that leads to the development of cells with altered properties. The flat and rigid plastic/-glass surface affects the cells by changing the form and shape (flat cell layer), decreasing their cell-cell communication as well as their proliferation rate. Consequently this method does not reflect the in-vivo 3D microenvironment where cells grow up and are surrounded by the extracellular matrix (ECM) which is a complex network of proteins and proteoglycans. Therefore it is very significant to construct a cell scaffold which mimics the required 3D *in vivo* situation and the corresponding adhesion molecules or functional groups for cell attachment. There are multiple applications based on the existing knowledge which promise the 3D cell culture within a tissue specific architecture. The aim of the project is the establishment of an optimal 3D cell culture model system for prostate cancer cells based on the high interconnected pore network of so-called cryogels. These, which are synthesized by different polymers synthetic and/or natural origin at subzero temperature, belong to the polymeric gels, hydrogels. The polymer structures used in this work consist of the monomers hydroxyethyl methacrylate-alginate-gelatin (HAG) and poly (ethylene glycol) diacrylate (PEGda) [1]. There are some properties (e.g. porosity, pore size and distribution, swelling behaviour and elasticity) which are mandatory in general for a cell scaffold in the 3D cell culture and play a crucial role for an effective cell attachment and other biological processes. The following abstract serves as an introduction to the methods using for the physical and chemical characterization of the cryogels and shows a part of the results.

EXPERIMENTAL METHODS

Scaffold fabrication

The cryogelation technique was used for the synthesis of a blend of hydroxyethyl methacrylate-alginate-gelatin (HAG) and poly (ethylene glycol) diacrylate (PEGda).

Microstructure analysis

By the use of scanning electron microscope (SEM) and the mercury porosimeter, it is possible to get significant results of the 3D morphology (e.g. pore size, pore distribution and pore volume, average porosity). In addition the environmental scanning electron microscope (ESEM) that allows the sample detection of "wet" or uncoated material. The X-ray CT scanner is used to scan the whole scaffold and its 3D porous structure.

Swelling kinetics and scaffold degradation

The Swelling kinetics of the cryogels was performed by conventional gravimetric procedure [2]. In this method, the solvent uptake capacity (e.g. culture medium RPMI 1640) and the equilibrium state of the porous cryogel materials with respect to time at 25°C were determined.

Estimation of visco-elastic behavior by unconfined compression test

Stress was given to the cylindrical-shaped (water saturated) cryogel samples using a Zwick/Roell machine with 50 N load cell under displacement control rate.

RESULTS AND DISCUSSION

The achieved results of the characterization of distinct pHAG-PEGda cryogel compositions (all data not shown) display the influence of every single monomer of the whole structure of the polymer. Nonetheless, one thing is conspicuous that the higher the concentration of monomers and cross-linker, the lower the swelling behaviour and porosity due to the reduction of the hydrophilic groups. Depending on whether you have changed the ratio of cross-linker or corresponding components, you received a new carrier structure. All of them show a high porosity and high swelling kinetics which is an excellent starting point for the three-dimensional cell culture.

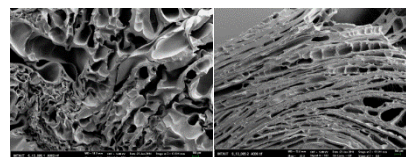


Figure 1 SEM images of two pHAG-PEGda cryogels with different initial concentration of Alginate and Gelatin (35x magnification) show obviously differences in pore size and shape as well as thickness of the pore walls. (A: 0.5% of Alginate and Gelatin; B: 2.25% of Alginate and Gelatin)

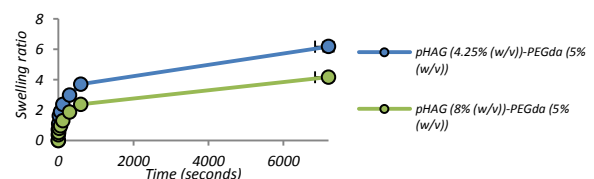


Figure 2 Swelling behaviour of the above cryogels with different initial concentration of Alginate and Gelatin. The scaffolds swollen up to six times of their initial weight and reaching equilibrium within 2 hours shows high solvent uptake capacity and interconnected morphology.

Cryogel	Average Porosity (%)	Elasticity (kPa)
pHAG(4.25%)-PEGda(5%)	31.90	41.45
pHAG(8%)-PEGda(5%)	29.40	40.16

Table 1 Comparison of the results of the porosity and elasticity of the two cryogels.

CONCLUSION

First and foremost, it was necessary to show that different pore structures of the synthesized scaffolds provide the optimal requirements for the cultured cell line. Our recent results show a stable and reproducible synthesis of the various cryogels and ideal prerequisites for future investigations.

REFERENCES

- [1] Singh et al., *Engineering three-dimensional macroporous hydroxyethylmethacrylate-alginate-gelatin cryogel for growth and proliferation of lung epithelia cells*, J. of Biomaterials Science, 24(11), (2013), 1343-1359.
- [2] Tripathi et al., *Multi-featured macroporous agarose-alginate cryogel: synthesis and characterization for bioengineering applications*, Macromol. Biosci., (11), (2011), 22-35.

ACKNOWLEDGMENTS

The authors would like to acknowledge the Ministry of Rural Affairs and Consumer Protection of Baden-Württemberg for the foundation of the project.

Rapid screening of potential biomedical zirconium alloys with 1 wt. % alloy additions

F.Y. Zhou¹, Y.F. Zheng^{1, 2*}

¹Center for Biomedical Materials and Engineering, Harbin Engineering University, China

^{2*}Department of Materials Science and Engineering, College of Engineering, Peking University, China,
yfzheng@pku.edu.cn

INTRODUCTION

Nowadays, magnetic resonance imaging (MRI) has wide applications in clinic diagnosis, such as dentistry, orthopedics and brain surgery, and its use is on the rise. However, MRI diagnosis is inhibited when there are some metallic implants in body. Because they can be magnetized in the intense magnetic field of the MRI instrument, which may produce image artifacts and therefore prevent exact diagnosis¹. To reduce the artifacts, medical devices with low magnetic susceptibility are required. Zirconium is biocompatible and it has lower magnetic susceptibility than stainless steel, Co–Cr alloys and titanium alloys². Therefore, developing novel Zr alloys with excellent biocompatibility and MRI compatibility are highly interesting. In this study, various Zr–1X (X=Ti, Nb, Mo, Cu, Au, Pd, Ru, Ag, Hf and Bi) alloys were designed and fabricated in order to screen the optimum alloy element(s) for novel biomedical Zr alloys with sufficient mechanical properties, improved corrosion resistance, excellent biocompatibility and low magnetic susceptibility. Besides, proper heat treatment was taken into consideration, for as-cast ingots, cold deformation and annealing were performed to obtain plate samples with high strength and good ductility.

EXPERIMENTAL METHODS

The binary Zr–1wt. % X alloys were prepared in a non-consumable arc melting furnace. The obtained ingots were hot-rolled to 3 mm thick sheets and then cold-rolled for a total reduction of 50%. The rolled samples were annealed at 600°C for 2 hours. The microstructure, mechanical properties, corrosion resistance and in vitro cytocompatibility of Zr–1X alloys were investigated by X-ray diffraction analysis, optical microscopy, uniaxial tensile test, microhardness test, electrochemical measurements, cytotoxicity test and ALP activity assay, respectively. The magnetic properties of Zr–1X alloys were investigated using a SQUID-VSM at room temperature. The magnetization (M) of sample against applied magnetic field (H) was measured and recorded, and its magnetic susceptibility, $\chi = M/H$, was obtained from the slope through linear fitting of the data.

RESULTS AND DISCUSSION

It was found that the annealed Zr–1X alloys consisted entirely or primarily of α phase. After annealing, a typical recrystallized structure was observed in pure Zr and Zr–1X alloys. All alloying elements significantly increased the strength and hardness of pure Zr. Among these Zr–1X alloys, Zr–1Ru alloy exhibited an optimum combination of strength and ductility, and both were the highest levels. The result of electrochemical corrosion measurements in Hank's indicated that adding various

elements into Zr improved its corrosion resistance and passivity, as indicated by the reduced corrosion current density and passive current density, respectively. Besides, the extracts of Zr–1X alloys did not produce any significant deleterious effect on inhibiting notably the proliferation and weakening differentiated function of osteoblast-like cells (MG 63), indicating good in vitro cytocompatibility. As shown in Fig. 1, all except for Zr–1Ag alloy showed decreased magnetic susceptibility compared to pure Zr and Zr–1Ru alloy had the lowest value. The magnetic susceptibility of Zr–1Ru alloy was comparable to those of α' -phase Zr–Mo alloys² and Zr–Nb alloys³, which was nearly one-seventh that of Co–Cr alloy and one-third that of Ti–6Al–4V alloy², indicating a better MRI compatibility.

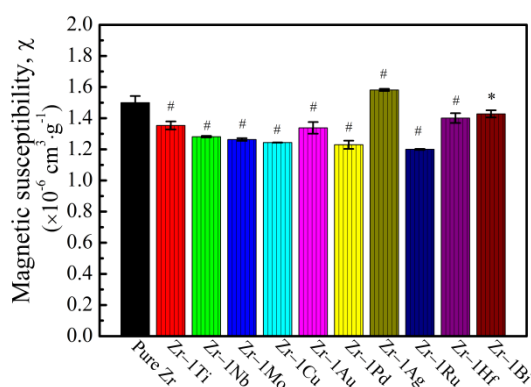


Fig. 1 The magnetic susceptibility of pure Zr and Zr–1X alloys. * indicates $p < 0.05$ when comparing with pure Zr while # indicates $p < 0.01$ when comparing with pure Zr.

CONCLUSION

Among these designed Zr–1X alloys, Zr–1Ru alloy had excellent mechanical properties, high corrosion resistance, good cytocompatibility and lowest magnetic susceptibility, and it may be a promising candidate for implant devices in an MRI environment, such as the encasing material of a pacemaker.

REFERENCES

1. Shafiei F. *et al.*, J. Dent. Res. 82:602-606, 2003.
2. Nomura S.N. *et al.*, Acta Biomater. 6:1033-1038, 2010.
3. Kondo R. *et al.*, Acta Biomater. 7:4278-4284, 2011.

ACKNOWLEDGMENTS

This work was supported by the National Basic Research Program of China (973 Program) (Grant No. 2012CB619102 and 2012CB619100), National Science Fund for Distinguished Young Scholars (Grant No. 51225101)

Iron Oxide Colloids as hyperthermia agents

Paula Soares^{1*}, Isabel Ferreira and João Paulo Borges¹

¹ Department of Materials Science, FCT-UNL, Campus de Caparica, 2829-516 Caparica, Portugal
*pi.soares@campus.fct.unl.pt

INTRODUCTION

Hyperthermia is an old technique which is recognized as a possible treatment option for cancer.¹ Cancer is a severe disease and currently is one of the leading causes of morbidity and mortality in the world, while chemo- and radiotherapy present several side effects due to their lack of specificity to the cancer type and the development of drug resistance.^{1,2}

Iron oxide nanoparticles are having been extensively investigated for several biomedical applications such as hyperthermia and magnetic resonance imaging for cancer treatment.^{3,4} In this context, a work was performed comparing the effect of surfactants on the stability and the heating ability of iron oxide colloids.

EXPERIMENTAL METHODS

Iron oxide nanoparticles were synthesized through chemical precipitation and stabilized using two surfactants: sodium citrate and oleic acid. The as-prepared nanoparticles were characterized by several techniques and their heating ability was evaluated using different sample concentrations and field intensities.

RESULTS AND DISCUSSION

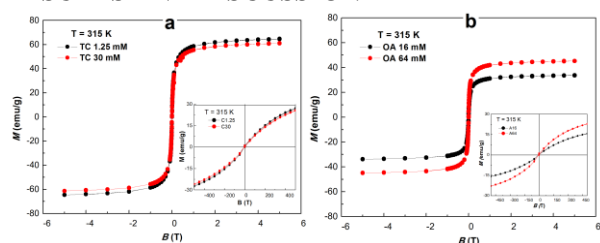


Figure 1 - Magnetization vs. applied magnetic field for Iron oxide nanoparticles coated with sodium citrate (a) and oleic acid (b).⁴

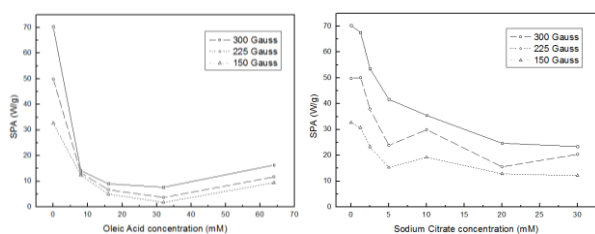


Figure 2 – Specific power absorption (SPA) vs. Surfactant concentration (left image – Oleic acid, Right image – Sodium

citrate) for three field intensities with a frequency of 418.5 kHz.

The hysteresis loops measured at temperatures 10 and 320 K for coated iron oxide nanoparticles are shown in Fig. 1. Comparing the effect of sodium citrate and oleic acid it is possible to observe that oleic acid is reducing the magnetic moments at the surface of the nanoparticles probably due to the diamagnetic contribution of the surfactant volume. For higher concentrations of oleic acid it seems to be an increase in the SPA values.

The hyperthermia results (Fig. 2) show a drastic reduction on the SPA value when oleic acid is added to the colloids, while for sodium citrate this reduction is not so pronounced.

CONCLUSION

These results show that oleic acid has a more severe effect on the magnetic properties and heating ability of the nanoparticles. This effect is probably due to the surfactant viscosity and the size of the molecule that is higher than sodium citrate.

REFERENCES

1. Soares P. *et al.*, Recent patents on anti-cancer drug discovery, 7(1): 64-73, 2012.
2. Soares P. *et al.*, Mini-Reviews in Medicinal Chemistry, 12:1239-1249, 2012.
3. Baptista A. *et al.*, A. Tiwari, A. Tiwari, Bioengineering Nanomaterials; CRC Press, Taylor & Francis Group, 2013, Chapter 4, p 93.
4. Soares P. *et al.*, Journal of colloids and Interface Science, 419:46-51, 2014.

ACKNOWLEDGMENTS

Financial support for this work was provided by FCT-MEC through Strategic PEST-C/CTM/LA0025/2013-2014 project. P. Soares acknowledge FCT for PhD grant SFRH/BD/81711/2011.

Biodegradable Shape Memory Polymer Composite for Endovascular Embolization

Yee Shan Wong^{1*}, Subbu S. Venkatraman¹, Kiang Hiong Tay², Wei Min Huang³ and William R. Birch⁴

¹School of Materials Science and Engineering, Nanyang Technological University, Singapore, yswong@ntu.edu.sg

²Department of Diagnostic Radiology, Singapore General Hospital, Singapore

³School of Mechanical and Aerospace Engineering, Nanyang Technological University, Singapore

⁴Institute of Materials Research and Engineering, A*STAR, Singapore

INTRODUCTION

One million people: the number of deaths worldwide caused each year by liver cancer, the 3rd leading cause of cancer death¹. Although surgical removal of liver tumors offers the best chance for a cure, more than 70% of the liver cancer patients are inoperable and are treated with palliative transarterial chemoembolization (TACE). In TACE, the hepatic artery is embolized following delivery of the chemotherapeutic agents into the artery. Usually, repeat procedures are common so patency of the hepatic arteries need to be restored before the next TACE can be performed. Currently, Gelfoam, a gelatin sponge, is typically used for embolization². However, it is required to cut into small pledgets and delivered as a particulate, resulting in an unpredictable occlusion level due to their variability in size and uncontrollable target embolization. While Gelfoam is degradable, its degradation period cannot be strictly controlled. Furthermore, it is also not visible under fluoroscopy. One solution to this is to develop a biodegradable shape memory embolic plug, which would address the shortcoming of the existing embolic agents.

Shape memory polymer represents promising candidate material for embolization, since it can be stored in a temporary compressed shape and deployed via a catheterization process until it is actuated on demand via external stimulus. In this work, we investigated the thermomechanical property of biomaterial, poly(D,L lactide-co-glycolide) (PLGA), and the effect of the incorporation of radio-opaque particles, barium sulphate (BaSO₄) on the thermal, mechanical and shape memory properties of PLGA composites.

EXPERIMENTAL METHODS

Material and Sample Preparations

PLGA (M_w = 9x10⁴) and BaSO₄ were purchased from Purac and Sigma Aldrich, respectively. Film samples were prepared by casting from a polymeric solution of PLGA in dichloromethane. For polymer composite samples, various fraction of BaSO₄ (10-50 wt%) was mixed into the PLGA solution. Solution was casted onto glass plates using an automatic film applicator and then dried in oven for 2 weeks at 60°C.

Material Characterisation

Glass transition temperature (T_g) was measured using TA Instruments MDSC 7 at a heating rate of 10°C/min under nitrogen medium from -20 to 150°C. Uniaxial tensile tests were performed with an Instron 5548 and the film samples were cut according to ASTM D638-V. Tensile experiments were conducted at temperature of

37°C with crosshead speed of 10mm/min. Shape recovery tests were performed in tensile mode. The specimen was stretched to 200% strain (ϵ_0) at 37°C and then cooled down to room temperature with the external force to maintain the deformation (ϵ_i). During the recovery process, the deformed specimen was immersed into 37°C water bath for 4 minutes and the change of specimen length (ϵ_r) was recorded. The recovery ratio R_r was defined as $(\epsilon_i - \epsilon_r)/\epsilon_i$. All tests were performed in triplicate and statistical analysis was performed using ANOVA, with significance level $p = 0.05$.

RESULTS AND DISCUSSION

Table 1 summarizes the thermal, mechanical and shape memory properties of PLGA and its composites.

	T _g (°C)	E Modulus (MPa)	Elongation to break (%)	R _r (%)
PLGA	44	736	901	94
PLGA/10%BaSO ₄	43	771	900	98
PLGA/30%BaSO ₄	43	1084	893	99
PLGA/50%BaSO ₄	45	1213	20	-

As shown in Table 1, PLGA is an amorphous polymer having a glass transition of 44°C and the addition of BaSO₄ into PLGA has very little effect on the T_g. On the contrary, the modulus is increased with addition of BaSO₄ when the BaSO₄ content is above 30 wt%. This is expected since rigid filler usually increases the modulus in a composite system. PLGA and its composites achieved high elongation to break of ~900%, except for PLGA/50%BaSO₄. The elongation to break for PLGA/50%BaSO₄ is 20%, which makes the composite too brittle for shape memory test and actual clinical application. In term of shape recovery, R_r is higher than 90%, indicating the PLGA and its composites exhibit good shape memory property. Interestingly, with the addition of BaSO₄, it enhances the shape memory effect of PLGA from R_r of 94% to 98% ($p < 0.05$).

CONCLUSION

PLGA/30%BaSO₄ composite exhibit enhanced mechanical and shape memory properties and it can be a promising candidate material for biodegradable shape memory embolic plug.

REFERENCES

- Clark H.P. *et al.*, RadioGraphics. 25:S3-S23, 2005
- Osuga K. *et al.*, Int. J. Clin. Oncol. 17:306-315, 2012

ACKNOWLEDGMENTS

The authors would like to thank the A*STAR Biomedical Engineering Programme for providing financial support to this project.



Analysis of PVA- hydrogels loaded with propolis for burn healing application

Renata N. Oliveira^{1*}, Regis Rouze³, Brid Quilty³, Gloria D.A. Soares¹, Rossana M.S.M. Thiré¹ and Garrett B. McGuinness²

^{1*}Department of Materials and Metallurgical Engineering, Federal University of Rio de Janeiro, Brazil, nunes@metalmat.ufrj.br

² Centre for Medical Engineering Research, Dublin City University, Ireland

³ School of Biotechnology, Dublin City University, Ireland

INTRODUCTION

PVA hydrogels are well established materials for dressings, since they have several characteristics of the ideal dressing, i.e. transparency and high swelling capacity in aqueous fluids^{1,2}. However, these gels do not have antimicrobial effects. Among the antimicrobial agents, bee propolis is a natural product used in folk medicine and it has been officially used in wounds healing since World War II³. The propolis properties vary with the propolis source⁴. Recently, gels loaded with propolis for wound healing application have been studied with promising results⁵⁻⁷. Since PVA gels loaded with propolis have not been reported, the goal of this work is to produce and characterize PVA-propolis gels intended for dressings.

EXPERIMENTAL METHODS

Aqueous solution of 10% w/v PVA was prepared (90°C, 4h, stirring) and different amounts of propolis were added (room temperature, stirring). Regular amounts of solution were poured in Petri dishes; they were freeze-thawed, dried and sterilized, resulting in samples with 0% ("PVA"), 0.075%, 0.15%, 0.45% and 0.90% propolis. Microstructural (XRD), thermal (DSC), and mechanical (tensile tests of the samples swollen in PBS) characterization as well as antimicrobial tests were performed.

RESULTS AND DISCUSSION

It could be observed that the propolis interferes with the polymer crystallization and that high amounts of propolis (> 0.15%) resulted in low crystallinity. The DSC results corroborated the XRD results, Table 1. The T_g decreased with propolis addition until 0.15%, then there is an increase in the T_g values with the propolis content. The X_c diminished for amounts of propolis > 0.15%. Higher amounts of propolis led to lower T_m values. The propolis interferes with the amorphous chains mobility, altering the T_g, and also with the PVA crystallization. Propolis could be located not only in the gels interstices, but also between the PVA crystal planes⁵. Propolis could lead to the formation of less and more imperfect crystals, lowering the T_m.

Table 1 – DSC results, crystallinity degree (X_c), melting temperature (T_m) and glass transition temperature (T_g)

	T _g (°C)	T _m (°C)	X _c (%)
PVA	71	222	36
0.075%	68	218	35
0.15%	62	215	37
0.45%	73	207	29
0.90%	118	201	0

The equilibrium of the swelling degree was established in 1 day of immersion, Figure 1 (a), where all the samples swelled at least ~300%. The tensile tests of the samples immersed in PBS for 1 day, Figure 1 (b), revealed that higher amounts of propolis led to higher secant modulus and failure strengths, an exception being the 0.90% propolis sample which presented the lowest values of the secant modulus and of the failure strength. Nonetheless, all samples presented adequate mechanical properties, failure strengths of > 0.13 MPa⁸.

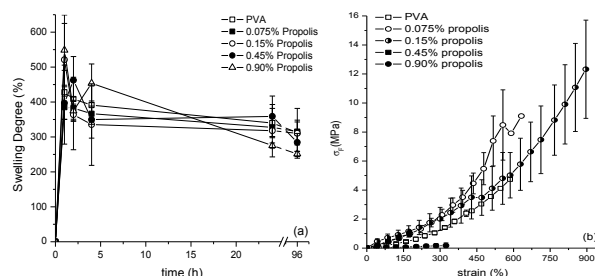


Figure 1 – (a) swelling degree of the samples and (b) tensile tests of the samples immersed in PBS.

The antimicrobial tests revealed the propolis was not active against *E. Coli* and *C. Albicans*. Nonetheless, the propolis used in this work was active against *S. aureus* for amounts of propolis ≥ 0.15% (inhibition zone of ~1000mm²), the most common bacteria in wounds⁹.

CONCLUSION

The presence of propolis interfered with the PVA crystallization and the highest amount of propolis used in this work had the poorest mechanical properties. Nonetheless, all samples presented adequate mechanical properties and high swelling degree. Propolis samples (propolis ≥ 0.15%) were active against *S. aureus*.

REFERENCES

- Hassan, C.M. *et al.* Macromol. 33:2472-2479, 2000.
- Kim, J.O. *et al.*, Int. J. Pharm. 359:79-86, 2008.
- Lotfy, M. Asian Pac. J. Cancer P. 7:22-31, 2006.
- Adewumi, A.A.; Ogunjinmi, A.A. Asian Pac. J. Trop. Biomed. S55-S57, 2011.
- Barud, H.S. *et al.* Evidence-Based Complem. Altern. Med. 1-10, 2013.
- Silva, A.J. *et al.* Mater. Lett. 116:235-238, 2014.
- Almeida, E.B. *et al.* J. Ethnopharmacol. 147:419-425, 2013.
- Singh, B. J. Mech. Behav. Biomed. Mater. 9:9-21, 2012.
- Zeighampour F. *et al.* Zahedan J. Res. Med. Sci. 16:25-30, 2014.

ACKNOWLEDGMENTS

Authors acknowledge CNPq, CAPES and FAPERJ.

Bone regeneration in human bone defect by octacalcium phosphate collagen composite

Tadashi Kawai¹, Shinji Kamakura², Keiko Matsui¹, Yuji Tanuma¹, Seishi Echigo¹, Osamu Suzuki³ and Tetsu Takahashi¹

¹Division of Oral and Maxillofacial Surgery, Tohoku University Graduate School of Dentistry

² Division of Bone Regenerative Engineering, Tohoku University Graduate School of Biomedical Engineering

³ Division of Craniofacial Function Engineering, Tohoku University Graduate School of Dentistry
ta-shi@dent.tohoku.ac.jp

INTRODUCTION

Synthetic octacalcium phosphate (OCP) has become recognized as a highly osteoconductive bone substitute material based on *in vitro* and *vivo* studies ^{1, 2}. OCP enhances osteoblastic cell differentiation *in vitro* in a dose-dependent manner ³. Furthermore, the dose-dependent stimulatory capacity of OCP was confirmed in *vivo* implantation with collagen matrix in rat critical sized calvaria defect ⁴. OCP has higher solubility than be-ta tricalcium phosphate (be-ta TCP) therefore more resorbable than be-ta TCP *in vivo* ⁵. It has been shown that OCP combined with collagen (OCP/Collagen) facilitates bone regeneration in comparison with OCP itself ⁶. The osteoconductivity of OCP/Collagen has been demonstrated also in critical-sized bone defect of dog ⁷. After that, we examined the effect of OCP/Collagen on alveolar bone regeneration in human small bone defect and confirmed the healing at the defect ⁸. In this study, we attempted to know about mandibular bone regeneration in larger bone defect of human by OCP/Collagen.

EXPERIMENTAL METHODS

OCP was prepared according to a method of synthesis by mixing calcium and phosphate solution ¹. Particle size of OCP was 300 – 500 µm in diameter. OCP/Collagen was prepared from pepsin-digested atelocollagen isolated from the porcine dermis and OCP. OCP/Collagen was molded in the shape of a disc, 9 mm diameter, and 1 mm thick. The protocol of the clinical trial was submitted and approved by the research ethics committee of the Tohoku University Graduate School of Dentistry. The patients were healthy men or women from 20 to 65 years old. The defect of longer axes was less than 50 mm. In this study, a 42 years old man, that diagnosis was a residual cyst at right mandibular the second premolar region and apical periodontitis at the first and second molars, consented to our investigation with enough explanation. We performed cystectomy or tooth extraction and implantation of OCP/Collagen in the bone defect that longer axes was 40 mm. We observed the healing at operative region and confirmed having infection or allergy, or not and radiographic examination or CT scan was performed until 1 year

after operation. Then, CT value was measured at bone defect.

RESULTS AND DISCUSSION

There was no abnormality for healing, no infection and no allergic reaction for the entire period. OCP or OCP/Collagen does not have radiopacity under normal X-ray condition. However, radiopacity of OCP/Collagen implanted in bone defect increased with time. CT scan showed radiopacities at 3 months after implantation. At 6 or 12 months, the radiopacity of bone defect was almost same as surrounding bone. CT value of bone defect increased significantly at 3 months, and at 6 months. CT value was almost same as surrounding bone of that in cancellous bone. In radiographic examination or CT scan, the radiopacities of implanted OCP/Collagen increased with time. The results suggest that OCP/Collagen itself may convert to hard tissue. At 6 months, CT value was almost same as surrounding bone. It is considered that OCP/Collagen enhances bone regeneration enough by 6 months.

CONCLUSION

This study revealed that OCP/Collagen may enhance bone regeneration in large bone defect of human. OCP/Collagen could be a good bone substitute material.

REFERENCES

1. Suzuki O. *et al.*, Tohoku J Exp Med 164: 37-50, 1991.
2. Suzuki O. *et al.*, Biomaterials 27: 2671-2681, 2006.
3. Anada T. *et al.*, Tissue Eng Part A 14: 965-978, 2008.
4. Kawai T. *et al.*, Tissue Eng Part A 15: 23-32, 2009.
5. Kamakura S. *et al.*, J Biomed Mater Res B 59: 29-34, 2002.
6. Kamakura S. *et al.*, J Biomed Mater Res B 79: 210-217, 2006
7. Kawai T. *et al.*, Clin Implant Dent Relat Res 13: 112-123, 2011.
8. Kawai T. *et al.*, Tissue Eng Part A in press, 2014.

Biological performance of injectable octacalcium phosphate-hyaluronic acid composites on bone augmentation

Kentaro Suzuki¹, Takahisa Anada², Tatsuya Miyazaki², Naohisa Miyatake³, Masami Hosaka⁴, Hideki Imaizumi⁵, Eiji Itoi⁴ and Osamu Suzuki^{2*}

¹Miyagai Cancer Center, Japan, ²Division of Craniofacial Function Engineering, Tohoku University Graduate School of Dentistry, Japan, ³Tohoku Orthopaedic Clinic, Japan, ⁴Department of Orthopaedic Surgery, Tohoku University School of Medicine, Japan, ⁵Osaki Citizen Hospital, Japan. *email: suzuki-o@m.tohoku.ac.jp

INTRODUCTION

We have found first that octacalcium phosphate (OCP), synthesized in a specified condition, enhances bone formation more than hydroxyapatite (HA) materials, including a Ca-deficient HA obtained from the original OCP through its hydrolysis reaction, if placed onto cortex or implanted in defect of murine calvaria, during its progressive physicochemical conversion from OCP to HA¹⁻³. OCP enhances osteoblastic cell differentiation of stromal cells^{2,4} and osteoclast formation from its precursor cells⁵ dose-dependently^{4,5}. However, OCP cannot be sintered with keeping its original crystal phase because OCP includes a large amount of water molecules in the structure. We have reported that if OCP is combined with hyaluronic acids (HyAs), having various molecular weights (MWs), then the composites of OCP/HyAs acquire not only a better handling property, including the moldability and injectability⁶, even in a granule form of OCP with several hundreds of micrometer, but also increase the osteoconductivity more than that of OCP alone^{6,7}. However, it is not clear that the addition of HyAs to OCP affects the biological performance in particular the osteoconductivity and the biodegradability of OCP with the prolonged implantation. The present study was designed to investigate about the long term performance of OCP/HyA composites if they were implanted in subperiosteal region of mouse calvaria with prolonged implantation (9 weeks) beyond the previous study (6 weeks)⁷.

EXPERIMENTAL METHODS

OCP was prepared by a direct precipitation under a supersaturated condition with respect to OCP and HA¹. Three sodium hyaluronic acids with different molecular weights, ranging from 90×10^4 , 190×10^4 and 600×10^4 (a chemically-modified sodium hyaluronate derivative), were used as source HyAs. OCP granules (300 to 500µm diameters) were obtained and mixed with HyAs at room temperature. The composites were hereafter referred to as OCP/HyA90, OCP/HyA190 and OCP/HyA600, respectively. These composites were implanted independently in polytetrafluoroethylene (PTFE) rings (OD 8 mm, ID 6 mm, 1 mm thickness) placed onto eight-week old ICR mice in comparison with OCP and HyA alone until 9 weeks. The rate of newly formed bone and the remaining implants was histomorphometrically estimated after the decalcification and the hematoxylin and eosin staining. The capability to form osteoclast-like cells was examined by inoculating macrophage RAW264 cells with RANKL, an osteoclast differentiation factor, in the presence or absence of HyAs. Number of tartrate-resistant acid phosphatase (TRAP)-positive

multinucleated giant cells was then evaluated to know the effect of the HyAs.

RESULTS AND DISCUSSION

The viscosity of OCP/HyA increased with increasing the MW of HyA used. However, all HyAs exhibited fluidity so that they were injectable the inside of PTFE ring at the surgical operation. Although the previous study⁷ showed that HyA90 and HyA600 worked as a stimulant for bone formation by OCP until 6 weeks, HyA190 also became increasing the positive role on new bone formation until 9 weeks as well as other two HyAs. The capacity to form new bone by OCP/HyAs finally became compatible to that by OCP alone, suggesting that HyAs in particular HyA190 and HyA600 have positive roles to activate new bone formation in the early stage of bone formation by OCP. OCP biodegradation progressively advanced until 9 weeks but the degradation rate at 9 weeks was similar between OCP/HyAs and OCP alone. In vitro study confirmed that TRAP-positive osteoclast-like cells from RAW264 cells with RANKL were formed more in the addition of HyA90 and HyA600 than that of HyA190. These results suggest that the observed early enhancement of bone formation by OCP/HyA90 and OCP/HyA600 may be stemmed from the stimulatory capacity of these HyAs on osteoclast formation, resulting in the enhancement of biodegradation of OCP followed by new bone formation.

CONCLUSION

The present study confirmed that the injectable OCP/HyAs provide a better handling property and that HyAs support the osteoconductivity of OCP most probably through modulating osteoclastic activity to biodegrade OCP in particular at the early stage of bone formation. Further study is underway to establish the molecular mechanism of HyAs on bone formation enhanced by OCP.

REFERENCES

1. Suzuki O *et al.*, Tohoku J Exp Med 164:37-50, 1991
2. Suzuki O *et al.*, Biomaterials 27:2671-2681, 2006
3. Suzuki O. Acta Biomater 6:3379-387, 2010
4. Anada T *et al.*, Tissue Eng Part A 14:965-978, 2008
5. Takami M *et al.*, Tissue Eng Part A 15: 3991-4000, 2009
6. Suzuki K *et al.*, Key Eng Mater 529-530:296-299, 2013
7. Suzuki K *et al.*, Acta Biomater 10:531-43, 2014

ACKNOWLEDGMENTS

This study was supported in part by Grants-in-aid (23106010) from the MEXT, Japan.



Mathematical Design and Experimental Evaluation of Borate Based Glass Ionomer Cements (GICs): Towards Predicting Antibacterial Efficacy and Ion Release

X.F. Zhang^{1,2*}, H. O'Shea³, D. Boyd^{1, 2*}

^{1*}Department of Applied Oral Sciences, Dalhousie University, Canada

^{2*}Department of Biomedical Engineering, Dalhousie University, Canada

³Department of Biology Science, Cork Institute of Technology, Ireland

Email: xf.zhang@dal.ca, d.boyd@dal.ca

INTRODUCTION: Boron (B) based glasses have variable degradation characteristics and are attractive for a diverse range of biomedical applications. B is associated with a variety of roles, from embryogenesis and bone growth, to enhanced immune functionality. It is also known as a potent antimicrobial agent against pseudomonas, enteric bacteria, and staphylococci, thus offering potential for engineered infection control properties in biomaterials [1]. Consequently, and based on nascent data in the literature, B-Ge based glasses may provide a suitable strategy for developing non-classical formulations of GICs [2], which consolidate a variety of fundamental design attributes (*i.e. suitable for multiple hard tissue applications*) into a single material formulation (*e.g. design attributes include intrinsic infection control bioactivity, and biodegradation characteristics*). The objective of this study was to utilize a combination of Mixture-Design (DOM) and experimental evaluations to permit composition-property modelling based on variable compositions of B-Ge based GICs based on infection control characteristics and degradation.

EXPERIMENTAL METHODS: A series of glasses (n=10) of formulation $x\text{ZnO}-y\text{B}_2\text{O}_3-(0.8-x-y)\text{GeO}_2-0.15\text{CaO}-0.05\text{ZrO}_2$ ($0.21 \leq x \leq 0.36$ mol. fraction) were designed via DOM, melt-quenched and ground to $\leq 45\mu\text{m}$. Each glass was utilized to form a contiguous GIC (n=10 GICs), with 55wt% polyacrylic acid ($M_w=37,700$) at a glass to acid ratio (P:L) of 3:2. Cement specimens $\varnothing 6\text{mm} \times 1\text{mm}$, (n=3 for each cement) were incubated at 37°C in 2mL tissue culture water for 24hrs. After incubation, cement specimens were placed in direct contact with *Lactobacillus casei* (L. casei) for a further 24h. In addition, filtered extracts were evaluated *via* indirect contact using L. casei. Tissue culture water and Fuji IX (GC Corp) were used as controls. B^{3+} , Ge^{4+} , Ca^{2+} , and Zn^{2+} levels were determined via inductively coupled plasma atomic emission spectroscopy. An optimized glass formulation for GIC synthesis (*based on maximum antibacterial efficacy*) was identified using Scheffe equation analysis.

RESULTS AND DISCUSSION:

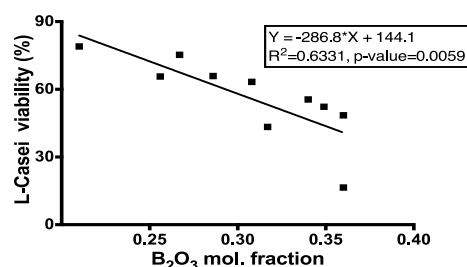


Figure 1: L-Casei viability (%) after 24h direct contact with cement specimens (based on B_2O_3 mol. fraction).

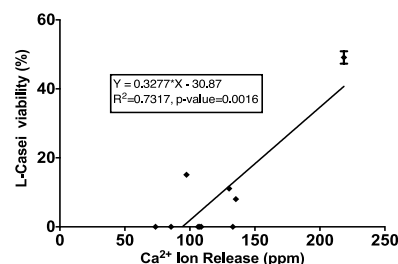


Figure 2: L-casei viability (%) after 24h indirect contact with filtered extract versus Ca^{2+} concentration.

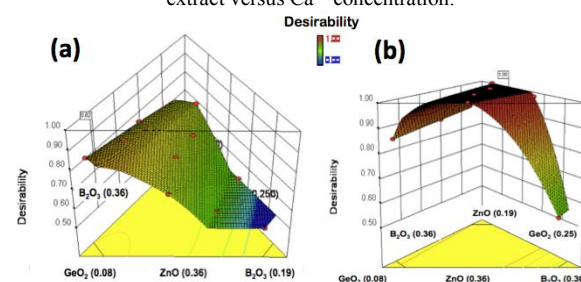


Figure 3: 3-D contour of optimal design formulations from: (a) direct contact, (b) indirect contact assays.

Of all compositional variables examined, the antibacterial efficacy of cements only *increased linearly with increased B_2O_3 content* in the glass (Fig 1). Total ion release ranged from 1142-2830ppm, 202-1243ppm, 75-222ppm, and 15-55ppm for B^{3+} , Ge^{4+} , Ca^{2+} , and Zn^{2+} , respectively; no direct mathematical relationship could be established for ion release *vs.* composition. Antibacterial efficacy appeared independent of the ions released, with the exception of Ca^{2+} ; where *increased Ca^{2+} release levels were directly related to increased bacterial viability* (Fig. 2) - an important finding given the inclusion of Ca in the formulation of many conventional bioglasses. Regression analysis relating to composition-property relationships (Fig. 3) indicates that *formulations comprising $0.275 \leq \text{B}_2\text{O}_3 \leq 0.33$ provide maximum antibacterial efficacy* for the GICs.

CONCLUSION: Mathematical design of biomaterial compositions, with a view to establishing composition-property relationships, is a valuable tool toward rational design and optimization of medical materials. Utilizing this approach, this data shows that the mol. fraction of boron directly increases the antibacterial efficacy of the novel GICs and that Ca, a common 'bioactive' additive in biomaterials promoted bacterial cell viability.

REFERENCES: [1] RD Houlby, M Ghajar, GO Chavez (1986) Antimicrobial agents and chemotherapy 29: 803. [2] UW-Z Xiaofang Zhang, Daniel Boyd (2014) Journal of Dentistry.

Acknowledgements: The authors would like to thank the Nova Scotia Health Research Foundation (NSHRF) Establishment Grant for providing financial support to this project.

Pre-osteoblast cell responses on phosphate and calcium co-immobilized titanium

Sunarso, Riki Toita, Kanji Tsuru, Kunio Ishikawa

Department of Biomaterials, Faculty of Dental Science, Kyushu University, Japan, sunarso_chemugm@yahoo.com

INTRODUCTION

Titanium (Ti) has been widely used for dental and orthopaedic implants due to its excellent biocompatibility and mechanical properties [1]. However, improve osteoconductivity is desired for strong clinical use. Surface modification is one of the most promising methods to increase the osteoconductivity of Ti.

Phosphate (P) and calcium (Ca) are known to play important roles in the osteoblast cell responses such as proliferation and differentiation (*e.g.*, increase of alkaline phosphatase (ALP) activity and mineral deposition) [2, 3]. Thus, the existence of P and Ca on the surface of Ti was expected to increase the cell response significantly.

In this present paper, we introduced a new technique to improve osteoconductivity of Ti implant by co-immobilizing phosphate and calcium on its surface. Both P and Ca can be easily immobilized on Ti surface by NaH_2PO_4 treatment and subsequent CaCl_2 treatment. Effect of P and Ca immobilization on cell responses was investigated using pre-osteoblast cells.

EXPERIMENTAL METHODS

Mirror polished pure Ti disks (14.5 mm $\phi \times 1$ mm) were used in this study. The Ti was washed with ultrapure water, ethanol and acetone, and then dried. The Ti specimen was treated with 30 mL of 100 mM NaH_2PO_4 aqueous solution at 80°C for 24h, followed by washing with ultrapure water, ethanol and acetone ultrasonically. The phosphate treated Ti specimen was then treated with 10 mM CaCl_2 aqueous solution at 80°C for 1h. The surface of the specimens was analyzed by X-ray photoelectron spectrometer (XPS). The non-treated and treated Ti were symbolized as Ti and Ca-P-Ti, respectively.

The MC3T3-E1 cell line (mouse pre-osteoblast cells) was used for *in vitro* study. The cells were differentiated in alpha minimal essential medium (α -MEM) containing 10% fetal bovine serum, 10 mM Na- β -glycerophosphate, 10 nM dexamethasone and 1% antibiotics under humidified atmosphere containing 5% CO_2 at 37°C. The cells were seeded at the initial density of 1×10^4 cell/cm² for cell proliferation, and 4×10^4 cell/cm² for ALP activity and Ca quantification on test substrates in 24-well culture plate. The medium was changed every 2 days.

RESULTS AND DISCUSSION

Figure 1 is the XPS spectra of the Ti surface after NaH_2PO_4 and CaCl_2 treatment. The original Ti showed Ti2p and O1s peaks, but did not show P2p and Ca2p peaks. In contrast, the P2p and Ca2p peaks were detected after NaH_2PO_4 and CaCl_2 treatment, indicating that both P and Ca were successfully immobilized on

the surface of Ti. Atomic percent of P and Ca were determined as 14.76% and 7.91%, respectively.

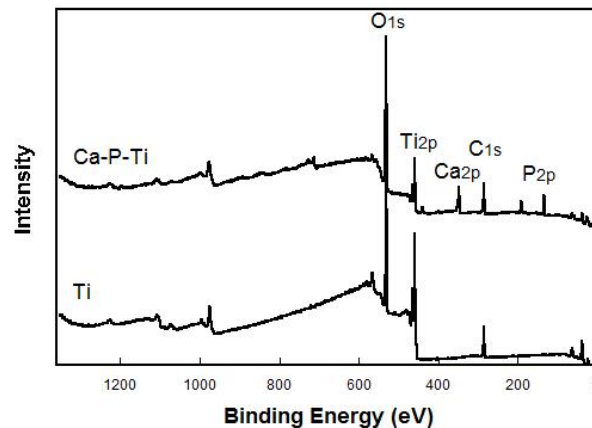


Figure 1. XPS spectra of Ti and Ca-P-Ti

The number of proliferated cells on Ca-P-Ti surface was higher when compared with that on the Ti. The ALP activities of cells on Ca-P-Ti were higher when compared with those on Ti at day 8, and tend to decrease after 16 days of culture. Meanwhile, the ALP activity on the Ti surface showed tendency to increase during 16 days of culture. The decrease of ALP activity at day 16 indicated that the cells were in the progress of maturation, which attributed with the production of mineralized matrix at the later. Mature osteoblast cells can form mineralized matrix consisted of apatite. The quantification of Ca amount thus can be used to indicate the mineralization process. Ca content of the cultures on Ca-P-Ti surface was two times higher than that on the Ti after 20 days, showing that more apatite deposition on Ca-P-Ti surface. These results clearly showed that co-immobilization of P and Ca facilitated proliferation and differentiation of pre-osteoblast cells.

CONCLUSION

The Ca-P-Ti surface showed higher proliferation, ALP activity and mineralization compared to the Ti surface. Co-immobilization of P and Ca on Ti could improve the osteoconductivity of Ti.

REFERENCES

1. Zhang L. *et al.*, J Biomed. Mater. Res. Part A 95A: 33–39, 2010
2. Feng B. *et al.*, Biomaterials 25: 3421–3428, 2004
3. Habibovic P. and Barralet J.E., Acta Biomaterialia 7: 3013–3026, 2011

ACKNOWLEDGMENTS

This study was supported in part by a grant-in-aid from JST, JSPS and AUN-SEED/Net JICA.

Nanohybrid Approach to Create Cell-Compatible Degradable Copolymer Thermogels as Cell Delivery Carriers

Naho Oyama and Koji Nagahama*

Department of Nanobiochemistry, Konan University, Japan, nagahama@center.konan-u.ac.jp

INTRODUCTION

In situ forming hydrogels have been attracted much attention as injectable cell delivery carriers for tissue engineering. Injectable gels currently studied are covalently cross-linked networks of synthetic- or biopolymers via click chemistry and enzymatic reactions¹. Although these methods allow forming ideal mechanically-stable hydrogels *in situ*, complicated chemistry are required for preparing gel precursors and harmful reagents/catalysts/substrates for preparing gels caused a decrease in cell viability¹. Thus there is a need to have alternative strategy for making cell-compatible injectable gels. Here we present a novel strategy to make physically cross-linked injectable gels having excellent cell-compatibility by means of nanohybrid technique using biodegradable poly(lactide-co-glycolide)-*b*-poly(ethylene glycol)-*b*-poly(lactide-co-glycolide) (PLGA-PEG-PLGA) and clay nanosheets.

EXPERIMENTAL METHODS

PLGA-PEG-PLGA copolymers were synthesized through ring-opening polymerization of DL-lactide and glycolide in the presence of PEG (M_w : 1.5k and 3.0k). Thermo-responsive behaviour of mixed aqueous solutions of PLGA-PEG-PLGA and clay nanosheets was examined by test tube inverting method. Degradation profiles of hybrid gels in PBS at 37°C and the molecular weight reduction was analyzed by GPC. Calcein-labelled L929 cells (1.0×10^5 cells) were dispersed in hybrid solutions and then incubated at 37°C to form cell loading hybrid gels. Live/Dead staining and confocal laser scanning microscopic observations of loaded cells were carried out to examine the cell viability and cell proliferation in the hydrogels.

RESULTS AND DISCUSSION

PLGA-PEG-PLGA copolymers, called as $P_{1.5k}$ and P_{3k} , were synthesized and the molecular compositions were determined by ¹H-NMR and gel permeation chromatography analyses. Although thermo-gelling property of PLGA-PEG-PLGA is useful for injectable cell delivery, these aqueous solutions indeed exhibit strong cytotoxicity against loaded cells, because PLGA segments are released from the destabilized micelle core by thermal stimulus and directly disrupt the cytomembranes of loaded cells. Here, in order to produce PLGA-PEG-PLGA based cell-compatible thermogels, we attempted to quench the cytotoxicity via preventing the release of PLGA segments by capping PEG loop located on the micelle surfaces using clay nanosheets (Laponite: LP) as nano-stabilizer. Peak intensity of PEG in ¹H-NMR spectrum of P_{3k} /LP hybrids measured in D₂O significantly lower than that of P_{3k} . Hydrodynamic diameter (averaged value) of P_{3k} /LP hybrid micelles and P_{3k} micelles was 44 nm and 33 nm, respectively. These results suggest that PEG loops located on the micelle surfaces are capped with

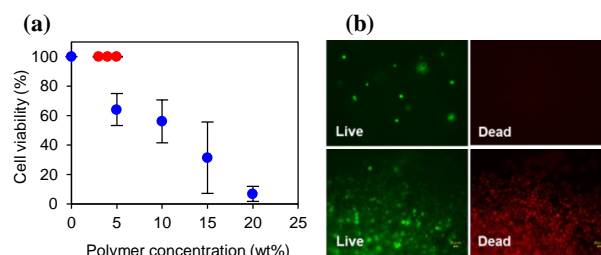


Figure 1 (a) Cell viability of L929 cells encapsulated in $P_{3k}5L1.1$ gels (●) and $P_{1.5k}$ gels (●) after 1 hour incubation. (b) Live/Dead staining of L929 cells encapsulated in $P_{3k}5L1.1$ gel (upper) and 15 wt% of $P_{1.5k}$ gel (lower) after 4 hours incubation.

LPs. We therefore investigated the influences of the capping micelle structures on their thermo-gelation. $P_{1.5k}$ aqueous solutions exhibited temperature-responsive gelation at above 5 wt% in reversible manner. P_{3k} /LP solutions with certain mixing ratios exhibited thermo-gelation at lower concentration (1 wt%) in irreversible manner, while P_{3k} solutions never exhibit thermo-gelation even at high concentration, suggesting that LPs located on micelle surfaces possess an ability to promote gel network formation.

Cell viability in $P_{1.5k}$ gels and P_{3k} /LP hybrid gels was examined by Live/Dead staining assay. L929 cells encapsulated in P_{3k} /LP gels (e.g., $P_{3k}5L1.1$ indicates hybrid of 5 wt% P_{3k} and 1.1 wt% LP) were completely alive (Figure 1a), whereas $P_{1.5k}$ gels exhibited cytotoxicity in dose dependent manner, moreover L929 cells encapsulated in $P_{1.5k}$ 15 wt% gels were completely dead after 4 hours (Figure 1b), meaning the excellent cell-compatibility of P_{3k} /LP thermogels and the compatibility should be owing to the capping micelle structures. Importantly, P_{3k} /LP hybrid gels achieved significantly high cell encapsulation ability by utilizing its thermo-gelling property (maximum cell number: 5×10^6 cells per 100 μ L of gel) because of their rich inner space derived from the low gelation concentrations. These results prove that this original nanohybrid strategy is useful to quench a cytotoxicity of PLGA-PEG-PLGA thermogels.

CONCLUSION

Since LP is known to absorb various kinds of proteins including growth factors, the nanohybrid thermogels could be applied as injectable cell delivery carries for various types of cells. In addition, the nanocomposite thermogels would have a potential as injectable scaffolds having sufficient space for cell migration, cell growth, and cell 3D organization in the hydrogels.

REFERENCES

1. Li. Y. *et al.*, Chem. Soc. Rev., 41:2193-2221, 2012

ACKNOWLEDGMENTS

The authors would like to thank JSPS foundation (KAKENHI 24700487) for financial support.

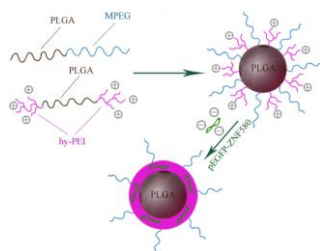
Self-assembly of PEI Modified Biodegradable Complex Micelles as Gene Transfer Vector for Proliferation of ECs

Juan Lv, Jing Yang, Xuefang Hao and Yakai Feng*

School of Chemical Engineering and Technology, Tianjin University, Weijin Road 92, Tianjin 300072, China
yakaifeng@tju.edu.cn

INTRODUCTION

Gene therapy is an attractive alternative to realize rapid endothelialization of artificial vascular grafts in current clinical treatments of coronary bypass surgery. Poly(ethylene imine) (PEI) has been widely used to deliver plasmid DNA¹. PEI with high molecular weight has perfect transfection efficiencies but high cytotoxicity². Low molecular weight PEI has been demonstrated a low toxicity³ but its transfection efficiency needs to improve. It is reported that PEI modified with other polymers showed high transfection efficiencies⁴, and grafting low molecular weight PEI onto biodegradable backbone is of intriguing interest. Herein, low molecular weight PEI ($M_w = 1800\text{Da}$) was used, and a complex micellar system with a biodegradable PLGA core and a mixed mPEG / PEI shell which was prepared by self-assembly of methoxy-poly(ethylene glycol)-*b*-poly(lactide-co-glycolide) (mPEG-*b*-PLGA) and poly(ethylene imine)-*b*-poly(lactide-co-glycolide) (PEI-*b*-PLGA) in aqueous solution. Then, a novel ZNF580 gene (plasmid fused to green fluorescence protein, pEGFP-ZNF580), which has the ability of enhancing the proliferation of vascular endothelial cells, was encapsulated onto the micelle core (Scheme 1). The aim of this work is to design a novel gene vector to adjust the cytotoxicity and the transfection efficiencies through easily changing the ratio of mPEG/PEI of the micelles.



Scheme 1 Schematic illustration of self-assembly mechanism of blank and gene-loaded micelles.

EXPERIMENTAL METHODS

PEI was grafted onto PLGA according to the literatures⁵. mPEG-*b*-PLGA and PEI-*b*-PLGA were dissolved in DMF. Then the solution was added dropwise into PBS (50 mL) under stirring to induce micellization. The mixture was dialyzed for 24 h to remove DMF. The ZNF580 gene was added into micelles solution, and the complexes were gently vortexed and incubated for 30 min at room temperature.

RESULTS AND DISCUSSION

The polymer micelles were prepared from the polymers with mass ratio of PEG/PEI = 3/1, 2/2, 1/3 and 0/4. The gene-loaded micelles were formed at N/P 5, 10, 15, and

20. The hydrodynamic diameter of the blank and gene-loaded micelles estimated by dynamic light scattering (DLS) was between 90 to 160 nm, which could be in favor with cellular uptake. When the ratio of PEG/PEI was 3/1 or 2/2, the gene-loaded micelles at different N/P ratios showed smaller size than the blank micelles, while the hydrodynamic size of micelles at PEG/PEI = 1/3 or 0/4 became larger after loading pEGFP-ZNF580. The decrease content of PEG in shell could lead to unstability of the gene-loaded micelles which may result in aggregation of these micelles. The zeta potential of gene-loaded micelles was reduced with decreasing N/P ratios.

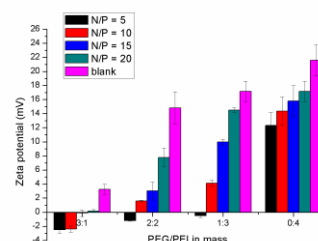


Figure 1 Zeta potential of blank and gene-loaded micelles at different PEG/PEI and N/P ratios.

CONCLUSION

A complex micellar gene delivery system with a biodegradable core and a mixed shell was prepared using grafting low molecular weight PEI onto biodegradable PLGA backbone. The hydrodynamic size and zeta potential of blank and gene-loaded micelles indicated that they were feasible to cellular uptake and gene transfection. These complex micelles could change the ratio of mPEG/PEI easily to adjust the cytotoxicity and the transfection efficiencies.

REFERENCES

- 1 Abdallah B. *et al.*, Hum. Gene Ther. 7:1947-1954, 1996
- 2 Fischer D. *et al.*, Biomaterials 24:1121-1131, 2003
- 3 Funhoff AM. *et al.*, Biomacromolecules 5:32-39, 2004
- 4 Lampela P. *et al.*, J. Controlled Release 88:173-183, 2003
- 5 Park JW. *et al.*, Biomacromolecules 12:457-465, 2011

ACKNOWLEDGMENTS

This project was supported by the National Natural Science Foundation of China (Grant No. 31370969), the International Cooperation from Ministry of Science and Technology of China (Grant No. 2013DFG52040).

Ultrasonic non-invasive monitoring of the mechanical properties of collagen vascular scaffolds in bioreactors

Bernard Drouin^{1,2}, Ramiro M. Irastorza³ and Diego Mantovani¹

¹ Laboratory for Biomaterials and Bioengineering, Department of Materials Engineering and Research Center of CHU de Québec, Laval University, Quebec City (Qc), (Canada), E-mail: Bernard.drouin@sympatico.ca

² Physics Dept., Cegep Garneau, Quebec City, Canada

³ Instituto de Física de Líquidos y Sistemas Biológicos (IFLYSIB), CONICET, La Plata, Argentina

INTRODUCTION

One of the main challenges that Tissue Engineering faces today is to have bioreactors that reliably and reproducibly allow cells to expand while forming tissues that can sustain physiological functions in vivo. One key factor in achieving this objective is to monitor the mechanical properties by non-invasive evaluation techniques¹. This will require substantial design features to be included into the bioreactor for constructs that have to provide an important mechanical function, such as blood vessels².

Ultrasonography imaging is widely used in medicine. In this application, the only direct measurement is the time delay between the emission and reception of a pulse. To assess distances, one must presume a mean speed of sound identical for all tissues. On the contrary, within a bioreactor, distances are known and the time delay between emission and reception of a pulse is determined with very high precision. This allows one to determine very accurate speed of sound (SOS) which is related to the ratio of Bulk Modulus to Density in the case of hydrogels.

$SOS^2 = K/\rho$; K = Bulk Modulus; ρ = density

EXPERIMENTAL METHODS

Mechanical behaviour of collagen gels has been investigated using unconfined compression. To assess SOS within disk-shaped gels made from Type-I collagen obtained from rat tail tendons, the upper moving plate attached to a 10 N Load Cell had an embedded ultrasonic probe. Newly formed collagen hydrogels have been submitted to relaxation, creep and cyclic tests similar to those encountered in bioreactors.

RESULTS AND DISCUSSION

This work is focused on the ongoing effort done in our lab to propose a global strategy to attain reliable and reproducible vascular tissue constructs. First part of this strategy is to gain an in-depth understanding of collagen hydrogels mechanical properties and in particular of the visco-elastic linear as well as non-linear models³ applicable in the various parts of the maturation process. Second part of the strategy is the necessity to rely on a non-invasive technique to assess the properties during the maturation process. Third part of the strategy is to develop an easy to use simulation tool in order to reproduce and predict the behaviour of these hydrogels in dynamic solicitation as encountered in bioreactors and, more generally, in experiments related to mechanobiology.

All relaxation tests indicate that a viscoelastic model based on two Maxwell bodies can satisfactorily reproduce relaxation load curves. Cyclic tests similar to the one reproduced in Figure 1, show steep variations whenever a change in the movement direction of the compression plate occurs. Moreover, the Load relaxation and the SOS relaxation do not exhibit the same behaviour. Load resume to the initial value while the SOS final value is much higher.

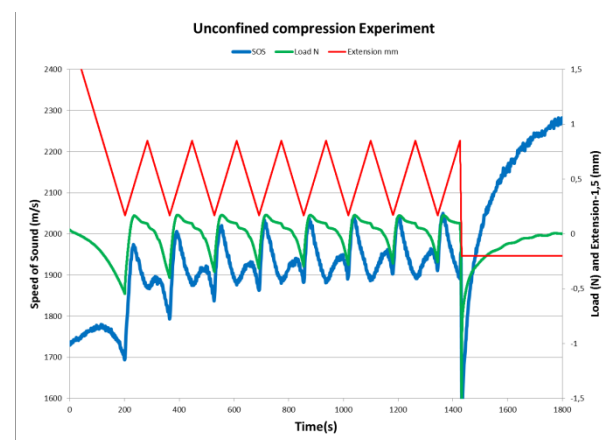


Fig.1. Load (Green), Speed of Sound (Blue) and extension (red) recorded during a compression test of a Collagen hydrogel sample.

This kind of tests has been made on a great number of samples. The results of these tests will be presented and discussed.

CONCLUSION

Results permit us to conclude that the overall objective of assessing mechanical properties of the construct with non-invasive ultrasonic techniques is feasible and attainable.

REFERENCES

1. Walker et al., Annals of Biomedical Engineering, 2011, 39, 10, 2521
2. Ratcliffe et al., Ann. N.Y. Acad. Sci. 961: 210-215 (2002)
3. Fung, Biomechanics: Mechanical properties of living tissues, 2nd ed. 1993

ACKNOWLEDGMENTS

NSERC-Canada, Canada Research Chair Program, and Research Center of CHU de Québec

Scaffold and tissue engineering by self-assembly therapies for tendon repair

Zeugolis, Dimitrios

Network of Excellence for Functional Biomaterials (NFB), National University of Ireland, Galway (NUI Galway), Galway, Ireland; dimitrios.zeugolis@nuigalway.ie

INTRODUCTION

Tendon and ligament injuries constitute an unmet clinical need with approximately 100,000 new cases annually in US alone [1]. Tissue grafts are considered the gold standard in clinical practice. However, allografts and xenografts can lead to disease transmission, whilst the limited supply of autografts restricts their use. To this end, scaffold and scaffold-free therapies are under development to address the tissue grafts shortage [2]. Herein, we describe biophysical, biochemical and biological methods to maintain tendon derived cell phenotype; development of tendon-equivalent facsimiles; and ultimately functional neotendon formation.

EXPERIMENTAL METHODS

Growth factor supplementation was assessed as means to maintain tendon derived stem cell phenotype. Biophysical and biochemical/biological features were assessed as means to maintain tendon derived cell phenotype and directional neotissue formation in rat patellar tendon model. Rich in tendon-specific extracellular matrix cell sheets were produced by appropriate modulation of the in vitro microenvironment [3].

RESULTS AND DISCUSSION

Fig. 1 indicates that after 28 days in culture, tendon stem cells (TSCs) treated with IGF-1 were positive for CD90 and CD44; negative for CD31 and CD34; and maintained similar expression level of extracellular matrix molecules, such as Tenascin C (TEN-C); Collagen I (Col I), Decorin (DCN) and Scleraxis (SCX), as TSCs at day 0 without IGF

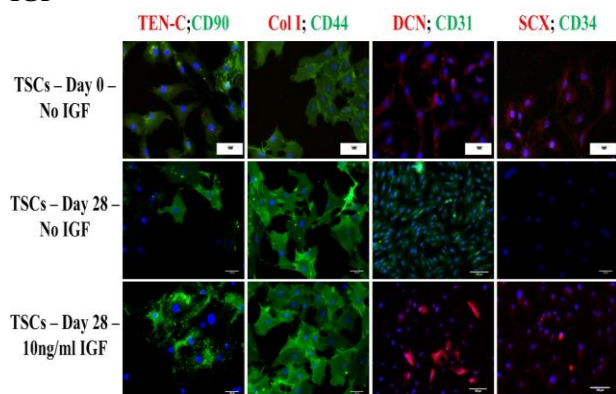
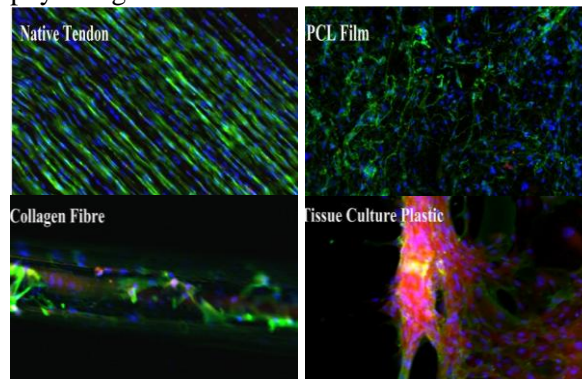


Fig. 2 shows that tenocytes seeded on low stiffness align electro-spun PCL films and hierarchically assembled collagen fibres were positive for CD90 (green) and negative for Tenascin C (red) similar to native tendon tissues, whilst on smooth rigid tissue culture plastic expressed far from physiological Tenascin C and CD90.



CONCLUSION

Treatment with IGF-1 preserved tendon stem cell multipotency for up to 28 days in culture and minimised changes in marker expression and extracellular matrix molecules production. Hierarchically assembled collagen scaffolds and anisotropically ordered polymeric substrates of rigidity similar to native tendons facilitate tenocyte phenotype maintenance in vitro. Modulation of the in vitro microenvironment of tenocytes with macromolecules enhances tendon specific extracellular matrix deposition within 6 days in culture, facilitating that way clinical translation of cell-sheets.

REFERENCES

1. Zeugolis, D.I., et al., In Tissue Engineering, N. Pallua and C.V. Suscheck, Editors. 2011, Springer. p. 537-572.
2. Bagnaninchi, P.O., et al., British J Sports Medicine, 2007. 41: p. 1-5.
3. Lareu, R.R., et al., Tissue Engineering, 2007. 13(2): p. 385-391.

ACKNOWLEDGMENTS

The authors would like to acknowledge: EU FP7 Marie Curie, IAPP; Irish Research Council; Enterprise Ireland; Collaborative Centres for Applied Nanotechnology; Irish Government under the National Development Plan 2007-2013; Science Foundation Ireland, Research Frontiers Programme.

Characterization of PCL based nano/micro fibrous scaffold for Bone Tissue Engineering

Izabella Rajzer^{1*}, Elżbieta Menaszek²

^{1*} Department of Mechanical Engineering Fundamentals, ATH - University of Bielsko-Biała, Poland
irajze@ath.bielsko.pl

² Department of Cytobiology, Collegium Medicum, UJ Jagiellonian University, Poland

INTRODUCTION

Nano/micro-fiber combined scaffold have an innovative structure, inspired by extracellular matrix that combines a nano-network, aimed to promote cell adhesion with a micro-fiber mesh that provides the mechanical support¹. The main objective of this work was to obtain new hybrid nano-/micro- fibrous materials which could be prospectively applied as a three-dimensional porous scaffold for bone tissue engineering purposes. In this study, it was found that the combined use of two techniques namely electrospinning and needle-punching processes, could be beneficial for the fabrication of 3D bioactive scaffolds with a desired pore size and a final nano-/micro- fibrous structure.

EXPERIMENTAL METHODS

Hybrid scaffolds were obtain by a combination of electrospinning method and the conventional needle-punching process. The properties of composite nano/micro fibrous scaffolds were investigated using the methods of: DSC, TGA, FTIR, SEM, EDX, WAXD and mechanical tests. Bioactivity was determined by assessing the formation of crystalline apatite on the surface of scaffolds upon immersion in Simulated Body Fluid (SBF). NHOst cells were seeded onto scaffolds to evaluate cell viability and morphology. Cell differentiation ability on the scaffolds was evaluated by measuring the activity of ALP. The mineralization was assessed by OsteoImage mineralization test (Lonza, USA).

RESULTS AND DISCUSSION

In this study, bioactive hybrid scaffolds were fabricated by direct spinning of nanofibers on micro-fibrous nonwovens. Both scaffold layers were modified with nano-hydroxyapatite in order to ensure the bioactive character of final hybrid scaffold. The presence of n-HAp was confirmed by FTIR and SEM studies. The macroscopic images of nano/micro fibrous scaffold are shown in Fig. 1. After immersion in SBF bone-like crystalline apatite layers completely covered the surface of samples, as shown in Fig. 2.

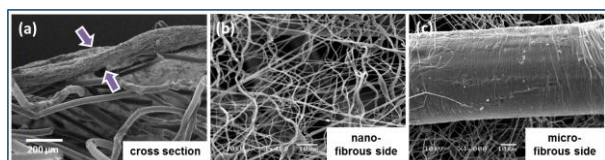


Fig. 1. SEM micrographs of hybrid scaffold (a) before and (b) after immersion in SBF.

The ability of cells differentiation was demonstrated in their morphology (Fig. 3), activity of the enzyme -

alkaline phosphatase, and the production of hydroxyapatites.

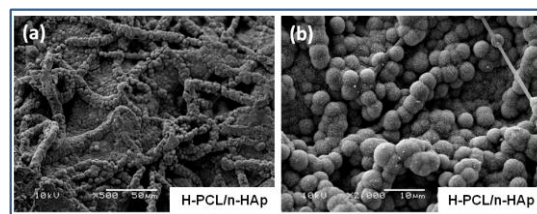


Fig. 2. SEM micrographs of hybrid scaffold after immersion in SBF.

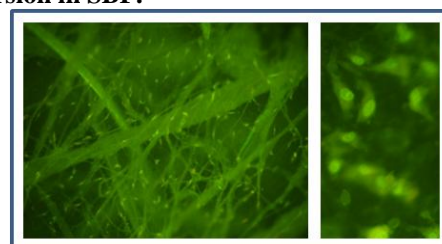


Fig. 3. Morphology of NHOst cells on hybrid scaffold.

The materials usually proposed for bone tissue engineering made of ECM-mimicking nanofibrous electrospun mats cannot be used as 3D scaffolds due to their very small pore size. It is well known that pore size distribution, porosity and pore interconnectivity are crucial parameters for tissue engineering scaffolds, as they provide the optimal spatial and nutritional conditions for the cells and determine the successful integration of the natural bone tissue and the material as well as enabling neovascularization and cell attachment.

CONCLUSION

By combining nano-fibers with micro-fibers, a new scaffold material with 3D structure and different pore size ranges was obtained. The bioactive character of these hybrid scaffolds was confirmed by an SBF mineralization study. Already after 7 days, the hybrid scaffold surface was totally covered by apatite deposits.

REFERENCES

1. Santos M.I. et al., *Biomaterials* (2008),29:4306-4313.

ACKNOWLEDGMENTS

The authors would like to thank the Polish Ministry of Science and Higher Education (project Iuventus Plus: IP2011044671) for providing financial support to this project.

Mechanism of Electrodeposition of Poly(Ethylene Glycol) to Titanium Surface

Takao Hanawa¹, Osamu Fukushima¹, Yusuke Tsutsumi¹, Hisashi Doi¹ and Maki Ashida¹

¹Institute of Biomaterials and Bioengineering, Tokyo Medical and Dental University, Japan
hanawa.met@tmd.ac.jp

INTRODUCTION

Immobilization of poly(ethylene glycol) (PEG) to titanium (Ti) surface has been attempted by electrodeposition technique. Both terminals of PEG are terminated with -NH_2 ($\text{NH}_2\text{-PEG-NH}_2$) and cathodic potential was charged to Ti. During charging, the $\text{NH}_2\text{-PEG-NH}_2$ electrically migrates to and is deposited on the Ti cathode^{1,2}. The amounts of the PEG layer immobilized onto the metals are governed by the concentrations of the active hydroxyl groups on each surface oxide in the case of electrodeposition³. The PEG-immobilized surface inhibits the adsorption of proteins and cells, as well as the adhesion of platelets⁴ and bacteria⁵, indicating that this electrodeposition technique is useful for the biofunctionalization of metal surfaces. However, the electrodeposition mechanism is still unclear. In this study, electrodeposition phenomena were investigated using a quartz crystal microbalance (QCM), an ellipsometer, and a potentiostat. This research will enhance to elucidate the mechanism of electrodeposition of other biofunctional molecules to metal surface.

EXPERIMENTAL METHODS

The following experiments were performed: (1) measurement of mass change to characterize the adsorption behaviour of $\text{NH}_2\text{-PEG-NH}_2$ to Ti (QCM), (2) injection of $\text{NH}_2\text{-PEG-NH}_2$ solution into NaCl solution where Ti was immersed and cathodic potential was charged, followed by measurement of mass change to characterize the electrodeposition behaviour of $\text{NH}_2\text{-PEG-NH}_2$ to Ti (QCM), (3) measurement of the thickness of immobilization layer of $\text{NH}_2\text{-PEG-NH}_2$ during cathodic polarization of Ti (ellipsometer), (4) measurement of mass change and current change of Ti during cyclic voltammetry (QCM and potentiostat).

RESULTS AND DISCUSSION

(1) $\text{NH}_2\text{-PEG-NH}_2$ adsorbed to Ti when Ti was immersed, while less unmodified PEG adsorbed to Ti, as shown in Fig. 1. Therefore, $\text{NH}_2\text{-PEG-NH}_2$ molecules immediately adsorbed to Ti by electrostatic force. (2) Injection of $\text{NH}_2\text{-PEG-NH}_2$ solution after immersion of Ti in NaCl solution increases the mass of Ti as shown in Fig. 2, indicating the electrostatic adsorption of $\text{NH}_2\text{-PEG-NH}_2$ occurred. When cathodic potential was charged to Ti, the frequency in QCM was disturbed by the evolution of H_2 and the mass increased. More $\text{NH}_2\text{-PEG-NH}_2$ molecules were immobilized by the charge of cathodic potential. The adsorbed $\text{NH}_2\text{-PEG-NH}_2$ attracted to Ti surface and the layer was condensed during cathodic charge. (3) When the potential charge was stopped, the thickness of $\text{NH}_2\text{-PEG-NH}_2$ layer increased again. Even anodic potential was charging, $\text{NH}_2\text{-PEG-NH}_2$ molecules did not desorb

from Ti and remained on Ti. (4) When cyclic voltammetry of Ti was performed, polarization curves showed difference between with and without $\text{NH}_2\text{-PEG-NH}_2$ molecules and the respond current showed hysteresis in the case of $\text{NH}_2\text{-PEG-NH}_2$ solution. This quantity of electricity was used for electrodeposition.

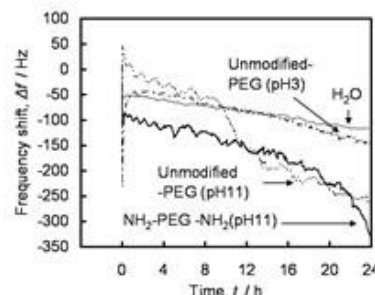


Fig. 1 Time transient of the frequency shift after the injection of each $\text{NH}_2\text{-PEG-NH}_2$ solution measured by QCM. The decreasing frequency shift indicates the increase of PEG molecules adsorbed on the Ti surface.

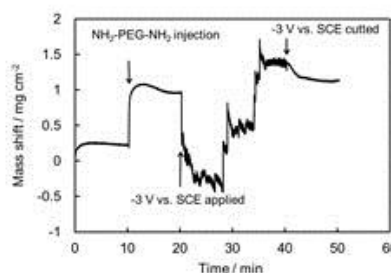


Fig. 2 Mass shift of the PEG layer on a Ti surface by QCM measurement. -3 V vs. SCE potential applied after $\text{NH}_2\text{-PEG-NH}_2$ injection.

CONCLUSION

$\text{NH}_2\text{-PEG-NH}_2$ immediately adsorbed to Ti surface by electrostatic force, but the bonding is weak and random. During cathodic charge of Ti, $\text{NH}_2\text{-PEG-NH}_2$ molecules rearranged and condensed to Ti surface with electrochemical reactions of the molecules and Ti surface.

REFERENCES

1. Tanaka Y. *et al.*, Mater. Sci. Eng. C27: 206-212, 2007
2. Tanaka Y. *et al.*, Mater. Trans. 48: 287-292, 2007
3. Tanaka Y. *et al.*, Mater. Trans. 49: 805-811, 2008
4. Tanaka Y. *et al.*, J. Biomed. Mater. Res. 92A: 350-358, 2010
5. Tanaka Y. *et al.*, J. Biomed. Mater. Res. 95A: 1105-1113, 2010

ACKNOWLEDGMENTS

This research is supported by Grant-in-Aid No. 2224059, JSPS, Japan.

Effects of Combination of Biomaterial and Stem cell Implants on the Hard and Soft Tissue of Experimental Animals

Mara Pilmane¹, Andrejs Skagers², Ilze Salma², Sandris Petronis³, Dagnija Loca⁴, Janis Locs⁴

¹Institute of Anatomy and Anthropology, Riga Stradins University, Latvia

²Institute of Stomatology, Riga Stradins University, Latvia, pilmane@latnet.lv

³Department of Surgery, Riga 2nd Hospital, Latvia

⁴Riga Biomaterials Innovation and Development Centre, Riga Technical University, Latvia

INTRODUCTION

Biphasic calcium phosphate (BCP) as bone grafting component confirmed bioactivity of synthetic hydroxyapatite (HAP) in activation of endogenous growth factors, remineralisation of atrophic host bone and integration in natural remodelling of bone¹. However, the results obtained by various researchers appear to differ² and to depend on different stimulatory factors. One of such factor is implantation of mesenchymal stem cells (MSC) that is known to increase biocompatibility and bioactivity of the implants and newly formed bones³. Objective of this study was to evaluate the tissue reactions after implantation of BCP ceramic granules with HAP/tricalcium phosphate (TCP) ratio of 90/10 in combination with injection of MSC in hard and soft tissues of experimental animal.

EXPERIMENTAL METHODS

We used 6 experimental New Zealand rabbits who underwent ovariectomy to develop experimental osteoporosis⁴, 1.5 months later the HAP/TCP and MSC was implanted into the hip bone and into the soft tissue, but animals were euthanized 5 months later. Blocks with implants were proceeded for BMP2/4, osteopontin (OP), osteocalcin (OC), tumour necrosis factor (TNF α) and IL1/IL10 immunohistochemically. Controls were developed by four animals with osteoporosis who received implants of bioceramic only in hard and soft tissue.

RESULTS AND DISCUSSION

Partially reabsorbed granuli enrolled by osteoclasts and distinct connective tissue capsule were detected in both – experimental and control animals. Bone with bioceramic and MSC demonstrated equal to the control side osteocalcin expression while osteopontin-containing cell number was moderate in comparison to the occasional cells found in control. These data suggest not only about active bone mineralization and/or growth, but also about possible ability of MSC to stimulate renovation of ground substance proteins. This our suggestion is proved by other authors observing the OP expression among those first factors which are secreted by differentiating into the osteoblasts MSC⁵. From other side, the increase of OP stimulates MSC migration⁶.

Soft tissue in control rabbits showed numerous IL1- and TNF α -containing cells, mainly they were fibroblasts and macrophages in the connective tissue capsule. Experimental animals demonstrated only occasional

TNF α positive connective tissue cells, but IL1 positivity was absent. Also there was a lack of IL10 immunoreactive cells in both – control and experimental animals. These data suggest about the presence of inflammatory and anti-inflammatory cytokines in tissue with implants which is diminished by MSC injections. Interestingly, proliferation marker Ki67 marked fibroblasts and macrophages in the connective tissue capsule, but selectively - only in control side. It is showed that rabbit dermal fibroblasts under the influence of MSC could show proliferation potential during chronic wound healing⁷. So, we speculate that this stimulation could persist also after biomaterial implants with following suppression of proliferation potential under the influence of MSC in our animals. This indirectly is proved also by other authors⁸ who revealed decrease of cellular proliferation via prostoglandin E2 depression in experimental osteoblast culture treated by MSC.

CONCLUSIONS

HAP/TCP and MSC implantation renovates stable expression of bone mineralization regulating protein osteocalcin and proves the combined influence of MSC and osteopontin in bone regeneration still 5 months after implantation.

The “hidden” inflammation characterizes soft tissue around biomaterial implants still 5 months after the implantation, but is notably decreased together with cellular proliferation under the combined treatment of tissue with bioceramic and MSC implants.

REFERENCES

1. Petronis S. et al., IFMBE Proceedings 38:174-177, 2012
2. Dorozhkin S.V. Acta Biomaterialia 8:963–977, 2012
3. Yu Z. et al., Int. Orthop. 36, 2163, 2012
4. Li Baofend et al., Acta Orthop. 81:396-401, 2010
5. Hu Y. et al., Genet. Mol. Res. 12: 6527-6524, 2013
6. Zou C. et al., Cell Biochem. Biophys. 65:455-462, 2013
7. Steinberg et al., Aesthet. Surg. J. 32:504-519, 2012
8. Tatara et al., Cytotherapy 13:686-694, 2011

ACKNOWLEDGMENTS

The authors would like to thank the The Era-Net Project (Grant no: BBM-2557) “Sonochemical technology for bioactive bone regeneration scaffold production” for providing financial support to this project.



Several drugs and model molecules controlled release studies from nanometric vesicles of polymer-lipid complexes

Virginia Saez-Martinez¹, Anisa Mahomed¹, Brian J. Tighe¹

¹ Biomaterials Research Unit, School of Engineering & Applied Science, Aston University, Birmingham B4 7ET, United Kingdom

v.saez@aston.ac.uk

INTRODUCTION

Delivering an effective dose to ocular tissues can be a challenge. The bioavailability of most topical ophthalmic medications is surprisingly limited. The major obstacle to targeting the eye with therapeutics in general, is the presence of various barriers which control the concentration and entry of solutes into the eye¹. Contact lenses used as drug delivery devices could minimize the drug loss and side effects^{2,3}. The duration of drug delivery and solubility of hydrophobic drugs can be increased if the drug is first entrapped in vesicles such as polymer-phospholipid complexes, which can be dispersed on very thin contact lens coatings to immobilize the drug on their surface. The properties of such vesicles would increase the bioavailability and therapeutic effects of the drugs on the eye. When hydrophobically associating polymers, such as poly(styrene-maleic acid) (PSMA) are combined with film-forming lipids, such as the phospholipid dimyristoylphosphatidylcholine (DMPC), they form lipid-polymer nanostructures analogous to lipoprotein micellar assemblies found in nature⁴. In this study, two types of complexes, stable at different pH values where synthesized and loaded with drugs of different hydrophilicities during their formation process. The controlled drug release was studied in vitro and compared to the release of the free drugs.

EXPERIMENTAL METHODS

Synthesis of drug-loaded PSMA-DMPC vesicles

Model molecules and drugs were encapsulated individually in the vesicles. Briefly, the phospholipid and the drug were homogenised in organic solvent that was subsequently evaporated. Then, 3 % (w/w) PSMA aqueous solution was homogenized with the lipid-drug mixture, in relative amount 3 to 1, for several minutes in a high speed homogenizer combined with a sonicating bath. When non-esterified PSMA was used, the vesicles were formed after decreasing the pH to their hypercoiling point (close to pH 5), the vesicles with esterified PSMA, however, were formed at neutral pH.

Physical characterisation of the vesicles

PSMA-DMPC vesicles were characterised by means of SEM, particle size distribution, polydispersity index, and Zeta potential (ZSizer).

RESULTS AND DISCUSSION

In Figure 1 a monodisperse particle size distribution characteristic of these nanometric vesicles can be observed; Table 2 shows the different sizes and surface charges of vesicles made from different PSMA samples.

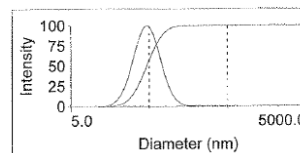


Figure 1. Particle size distribution of a vesicles sample.

Table 1. Particle size, PDI and Z potential of vesicles

Sample	size	PDI	Zpot.
AS(average of 7 samples)	48±11	0.23±0.03	-13.6±8.6
EAS (average of 3 samples)	434±8	0.37±0.01	-41.7±2.8

*AS=vesicles from PSMA 1600; EAS= from esterified PSMA 1600

Figure 2 shows how the free Rose Bengal kinetics profile is much higher than the Rose Bengal release from the vesicles.

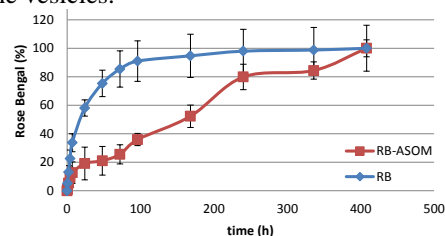


Figure 2. Cumulative percentage release profiles of free Rose Bengal (blue) and Rose Bengal from vesicles (red)

Depending on the PSMA used to form the vesicles, the pH stability, surface charge and average sizes can be tuned to encapsulate molecules of different natures and to achieve different drug loads and release profiles. The initial “burst” effect of the free drug can be avoided.

CONCLUSION

The nanoparticles synthesis can be tuned to achieve high encapsulation efficiency. This study is the starting point for the development of a more complex delivery system. An controlled delivery was observed in the release profile especially in the case of hydrophobic drugs, avoiding initial “burst” and with total drug released being moderated by the interaction of the drug with the phospholipid core.

REFERENCES

1. Urtti, A., Adv. Drug Deliv. Rev.; 58: 1131-1135. 2006
2. Schultz et al. Clin Exp Optom.; 92:343-8. 2009
3. Xu J, et al. Drug Deliv.; 18:150-8. 2011
4. S.R. Tonge, B.J. Tighe. US6436905 B1, 2002.

ACKNOWLEDGMENTS

This research was supported by a Marie Curie Intra European Fellowship within the 7th European Community Framework Programme FP7-PEOPLE-2012-IEF (Grant no: 328708).

Modification of PVC catheters with a binary graft of PEGMA and AAc to improve their biocompatibility

L. Islas, G. Burillo

Instituto de Ciencias Nucleares, Universidad Nacional Autonoma de México, leislas@gmail.com

INTRODUCTION

Healthcare associated infections (HCAs) continue to be a problem for healthcare facilities, costing both lives and money¹. In the US, urinary tract infections (UTIs) account for 70% of HCAs, with 95% of those due to urinary catheters². A catheter associated UTI (CAUTI) begins with contamination of the catheter's surface by bacteria, leading to the formation of a biofilm². One way of preventing CAUTIs is to modify the surface of the catheter to make it unfavourable for bacterial attachment. In this study, through the use of ionizing gamma radiation, we investigated the kinetics of the surface modification of poly(vinyl chloride) urinary catheters with a binary graft of poly(ethylene glycol) methacrylate, to prevent the formation of biofilm^{3,4}, and acrylic acid, a smart pH-sensitive polymer that will give the catheter the ability to retain and release biocides⁴.

EXPERIMENTAL METHODS

Materials Medical grade poly(vinyl chloride) (PVC) catheters were cut into 2 cm samples, washed with MeOH for 24 h, and dried for 8 h in a vacuum oven at 40°C. Acrylic acid (AAc) and poly(ethylene glycol) methacrylate (PEGMA) were distilled and washed before being used. The ionizing radiation comes from ⁶⁰Co (Gammabeam 650T). **Method** A PVC sample, in a glass ampoule, is pre-irradiated in the presence of oxygen to create active sites. Once irradiated, the sample is put in contact with a 5 mL solution of AAc or PEGMA. The ampoule is then bubbled with argon for 10 min and sealed. Afterwards, the ampoule is heated to initiate grafting. To graft the second monomer/polymer, the modified PVC catheter repeats the aforementioned cycle. Once grafted, the samples are removed from the ampoule and washed with distilled water. The samples are then dried and the grafted percent (%G) is calculated with the following formula,

$$\%G = \frac{W_g - W_o}{W_o} \times 100$$

where W_g is the final weight and W_o is the initial weight.

RESULTS AND DISCUSSION

Table 1 shows the amount of PEGMA grafted on PVC.

Sample	%G
1	14.63
2	13.69
3	14.27
4	14.58

Table 1: % PEGMA grafted on PVC at 60 kGy, 70°C, 8% (v/v) PEGMA in H₂O, and 5 h reaction time.

Figure 1 shows that in PVC-g-AAc more PEGMA is grafted than on PVC alone (table 1).

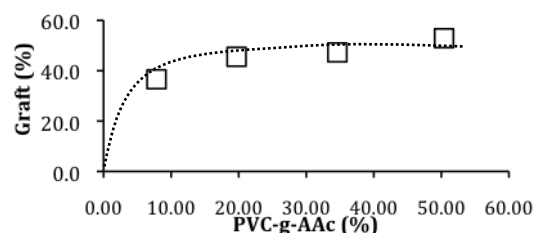


Figure 1: PEGMA graft on PVC-g-AAc at 60 kGy, 70°C, 8% (v/v) PEGMA in H₂O, and 5 h reaction time.

Figure 2 shows that more AAc is grafted on PVC-g-PEGMA than on PVC alone.

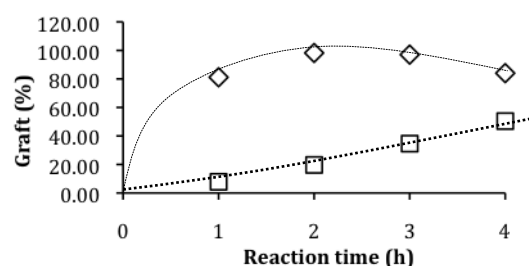


Figure 2: % AAc grafted on PVC (□) and PVC-g-PEGMA (◇) at 5 kGy, 80°C, 50% (v/v) AAc in H₂O

Figure 3 shows that grafted PVC catheters (AAc and AAc/PEGMA) present a critical pH response to changes in pH when swelling.

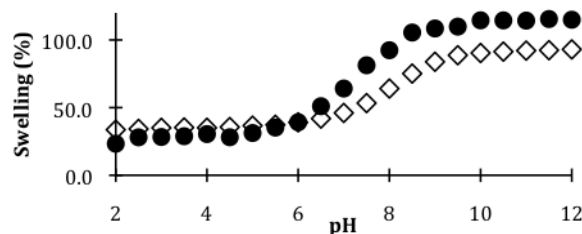


Figure 3: Maximum swelling as a function of pH for PVC-g-AAc(25%) (●) and [PVC-g-AAc(27%)]-g-PEGMA(28%) (◇)

CONCLUSION

The binary graft of PVC catheters is possible through the use of ionizing radiation, giving the catheter the ability to respond to changes in pH. The grafting of PVC is significantly higher when previously grafted with PEGMA or AAc.

REFERENCES

1. Allegranzi B. *et al.*, Report on the Burden of Endemic HCAI Worldwide. WHO 2011.
2. Spellberg B. *et al.*, Clin Infect Dis. 26:13-17, 2012
3. Park K. D. *et al.*, Biomaterials. 19:851-859, 1998
4. Kadajji V.G. *et al.*, Polymers 3:1972-2009, 2011

ACKNOWLEDGMENTS

The authors would like to thank F. García, M. Cruz and A. Ortega for their technical support, and the Mex-Brazil project supported by CONACyT-CNPq 174378.

Antibiotic-loaded silica nanoparticles/collagen composite hydrogels with prolonged antimicrobial activity for wound infection prevention

Christophe Hélar¹, Gisela S. Alvarez², Andrea M. Mebert², Xiaolin Wang¹, Thibaud Coradin¹ and Martin F. Desimone²

1. LCMCP - Materials and Biology Team - University Pierre and Curie - Paris – France
2. IQUIMEFA-CONICET- Facultad de Farmacia y Bioquímica - Buenos Aires – Argentina
christophe.helary@upmc.fr

INTRODUCTION

Cutaneous chronic wounds are characterized by an impaired wound healing after 6 weeks. In some cases, the absence of wound closure leads to infection and amputation. Current treatments are negative pressure therapy or application of wound dressings¹. To date, no ideal treatment is available. Nowadays, research orientation is towards medicated dressings for drug delivery of biomolecules. Collagen-based biomaterials are broadly used to treat chronic wounds as collagen is biocompatible, biodegradable and favors wound healing. Nevertheless, collagen hydrogels are poor drug delivery systems since the drug content is usually released within a few minutes². Hence, the combination of collagen with a drug delivery system is required to control and delay the release. In this study, silica nanoparticles/collagen nanocomposites have been evaluated as novel drug delivery systems for controlled release of antibiotics.

EXPERIMENTAL METHODS

Gentamycin, an antibiotic targeting gram positive and gram negative bacteria, has been encapsulated within plain silica nanoparticles (SiNPs) of various sizes (100, 300 and 500 nm) using a single step procedure. Particles presenting the best loading ability were selected. Subsequently, increasing doses of loaded SiNPs were immobilized within concentrated collagen hydrogels at 5 mg/mL. Structure was analyzed by scanning (SEM) and transmission electronic microscopy (TEM), mechanical properties of composites were assessed by rheological measurements. Biological activity of gentamycin, released from nanocomposites, was evaluated on *Pseudomonas Auriginosa*. Using a standard curve, antibiograms allowed for the quantification of released doses of gentamycin from materials. In parallel, cytotoxicity of nanocomposites was studied over 7 days using Alamar blue test.

RESULTS AND DISCUSSION

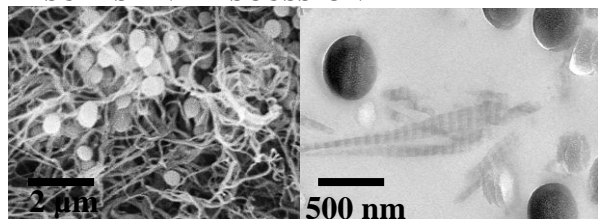


Fig1: Structure of SiNP/collagen nanocomposites with 250 mM SiNP observed in SEM (A) and TEM (B).

Silica nanoparticles of 500 nm in diameter presented the best loading capacity with 600 μg of gentamycin per SiNPs gram. Gentamycin-loaded 500 nm particles could be immobilized at high silica dose (from 250 mM to 1M) in concentrated collagen hydrogels without modifying their fibrillar structure (Figure 1) or impacting on their biomechanical behavior. Gentamycin release from the nanocomposites was sustained over 7 days, offering an unparalleled prolonged antibacterial activity on *Pseudomonas aeruginosa* (Figure 2). The drug release kinetic exhibited a linear profile without any initial burst. Particles immobilization within collagen hydrogels was not associated with any toxicity towards fibroblasts as cell viability was maximal despite the high SiNPs doses used. The drug release seemed to rely on the slow and low dissolution of SiNP, this avoids toxic effects.

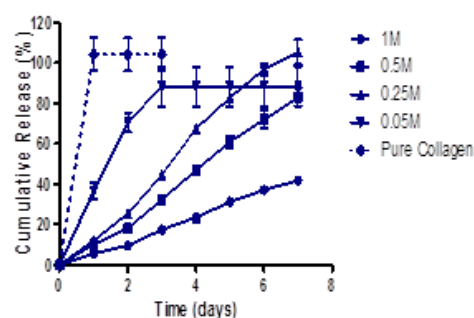


Fig2: Cumulative doses of gentamycin released from collagen/ silica nanocomposites at different SiNP concentrations.

CONCLUSION

Our study shows that collagen/SiNP nanocomposites allow for the sustained release of gentamycin over one week. Hence, these materials could be used as medicated wound dressing to prevent infection in the wound bed of chronic wounds. Nanocomposites associate a drug delivery system with a collagen bulk which has interesting properties in wound healing.

REFERENCES

1. Powers G. *et al.*, Dermatol Ther. 26:197-206, 2013.
2. Wallace DG. *et al.*, Adv Drug Deliv Rev, 55:1631-1649, 2003.

ACKNOWLEDGMENTS

Authors thank the Argentina- France MINCYT-ECOS-Sud (project A12S01) and CONICET-CNRS programs for financial support.

Fibroin reinforced calcium phosphate cement

Martha Geffers, Jürgen Groll, Uwe Gbureck

Department of Functional Materials in Medicine and Dentistry, University of Würzburg, Germany

martha.geffers@fmz-uni.wuerzburg.de

INTRODUCTION

The major advantage of brushite ($\text{CaHPO}_4 \cdot 2\text{H}_2\text{O}$) forming calcium phosphate cement is the high solubility under physiological conditions. This results in a rapid resorption and bone remodeling *in vivo*.¹ One disadvantage of this system is their brittle character. An opportunity to solve this problem is the combination of the CPC and a second material with better fracture behaviour properties such as polymers with a higher elasticity and fracture toughness. For example the work of fracture could be improved by more than one order of magnitude for a hydroxyapatite (HA)/2-hydroxyethylmethacrylate (HEMA) composite.² Since HEMA could not be resorbed *in vivo*, the reinforcement of brushite forming CPC was done in this study with the resorbable biopolymer fibroin, which is the main compound of the silk spun by the silk worm *Bombyx mori*.³

EXPERIMENTAL METHODS

Brushite cements were produced by mixing β -tricalcium phosphate (TCP) powder in an equimolar ratio with dicalcium phosphate anhydrous ($\text{Ca}(\text{H}_2\text{PO}_4)_2$, MCPM).¹ Fibroin was incorporated in the CPC/fibroin composite as non-woven or aqueous solution. First the silk cocoons were boiled in alkaline solution (0.02 M Na_2CO_3) to remove the sericin coating. For the non-woven the washed fibroin fibres were pulled in one direction to get an isotropic orientation. Subsequently the non-woven was embedded in the CPC paste. The aqueous solution was done by dissolving the washed fibres in 9 M lithium bromide and dialyzed against water. Afterwards the solution was added to the CPC powder as the liquid cement phase in a powder to liquid ratio of 1 g/ml. The fibroin concentration within the aqueous solution was analyzed by UV/Vis at 280 nm (approx. 4 w/v-%). The mechanical properties were measured by 4 point bending and compressive test. The morphology was analyzed by scanning electron microscopy (SEM). The phase composition was identified by Fourier transform infrared spectroscopy (FTIR) and X-ray diffraction (XRD).

RESULTS AND DISCUSSION

By the reinforcement of brushite cement with a non-woven fibroin fibre the bending strength could be doubled (Figure 1a). According to the test set up these composites could not load until their total fracture (Figure 1c) and the broken cement fractures were hold together by the fibres. These are promising results for *in vivo* studies since the cracks provide channels in the implant where angiogenesis and bone remodelling may take place.

The combination of the CPC raw powder and the aqueous fibroin solution results in a dual setting system

with both setting reactions running parallel and building up interconnective matrices (Figure 1f). The FT-IR and XRD measurements indicate that the water in the fibroin solution dissolves the CPC raw powder, meanwhile the released phosphates induce the β -sheet formation and gelation of the fibroin solution.

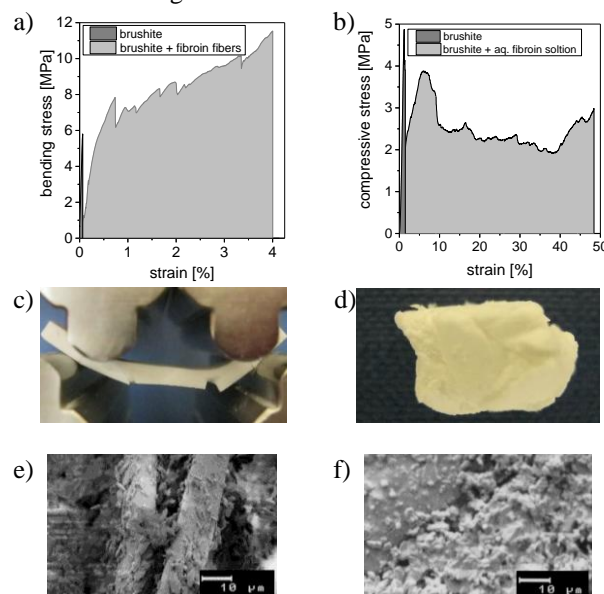


Figure 1: Stress-strain-diagram of exemplary brushite reference and fibroin fibre reinforced brushite (a) or brushite/aq. fibroin solution composites (b); image of these samples after their testing (c & d) and SEM images of their fracture surfaces (e & f).

During the mechanical test the composite samples are compressed until ~50 % without any cracking (Figure 1b & d).

CONCLUSION

The combination of two resorbable material show promising results for CPCs with improved fracture behaviour. For further enhancement the fibroin solution might be higher concentrated and a higher PLR could be used. Additionally other parameters are supposable for prospective new application fields: For example the encapsulation of biological agents or even cells in the fibroin solution to protect them during the acid setting reaction of brushite.

REFERENCES

1. Mirtchi A. A. *et al.*, *Biomaterials*, 10:475-480, 1989
2. Christel T. *et al.*, *J mater sci/ Mater medJMS: Mater med*, 24: 573-581, 2013
3. Vepari Ch. & Kaplan D. L., *Prog. Polym. Sci.*, 32: 991-1007, 2007

Influence of heat treatment and additives of alkali substituted calcium phosphate cements on their properties

Martha Geffers, Laura Straub, Jürgen Groll, Uwe Gbureck

Department of Functional Materials in Medicine and Dentistry, University of Würzburg, Germany

martha.geffers@fmz-uni.wuerzburg.de

INTRODUCTION

Alkali substituted calcium phosphate cements like calcium potassium sodium phosphate ($\text{Ca}_2\text{KNa}(\text{PO}_4)_2$) are of high interest as bone substitutes due to their higher solubility and hence resorption ability compared to normal apatites.¹ According to previous studies, they show better osteoconductivity² as well as antibacterial potency³. However, there are many differences published in the properties of these cement types like the phase composition after setting and the mechanical properties. Berger *et al.* observed no hydroxyapatite (HA) formation by cement setting⁴, whereby Gbureck *et al.* identified HA by X-ray diffraction (XRD) measurements³. One main difference of the cement manufacturing is the temperature treatment of the cement raw powders. Berger *et al.* processed molten powders above 1550 °C⁵. In contrast Gbureck *et al.* sintered it at 1050 °C³. Furthermore Berger *et al.* used additives like SiO_2 and MgO. In this study we analyzed in a systematically way the influence of the heat treatment and the additives on the cement properties of alkali substituted calcium phosphates.

EXPERIMENTAL METHODS

The $\text{Ca}_2\text{KNa}(\text{PO}_4)_2$ powders were synthesized by heating a mixture of monetite, potassium carbonate and sodium carbonate in a molar ratio of 4:1:1 with the addition of 3 – 12 wt.-% silicon dioxide or 3 – 6 wt.-% magnesium oxide for 24 h to 1050 °C or for 2 h above 1550 °C. The received powder cake was crushed and milled for 24 h. The particle size was measured by laser light scattering. The powders were mixed with water, 2.5 wt.-% Na_2HPO_4 solution or monocalcium phosphate (MCPA) and 0.1 M citric acid. Setting pH and time were studied. XRD-measurements were done with raw powders and set cements. The mechanical properties were analysed by compressive test. For visual observation SEM images were taken.

RESULTS AND DISCUSSION

The particle sizes for all raw powders were about $1.5 \pm 0.3 \mu\text{m}$ after mechanical activation by milling. $\text{Ca}_2\text{KNa}(\text{PO}_4)_2$ showed the typically XRD-pattern, which is known from literature⁵ (Figure 1: 0 % MgO). HA is formed with water or 2.5 wt.-% Na_2HPO_4 solution at low additive concentrations independent on the process temperature (Figure 1: 0 & 3 % MgO). This is in contrast to the observations of Berger *et al.*⁴. Interestingly all raw powders show a shift to β -tricalcium phosphate (β -TCP) with an increasing additive content (Figure 1: 3 & 6 % MgO). These cements set with 0.1 M citric acid and MCPA under acid conditions and transform into brushite. With an increasing additive content the setting time increased, whereas SiO_2 and MgO worked as a retarding agent in the setting reaction. Furthermore the conversion rate

decreased and the raw powders were still present in a high amount.

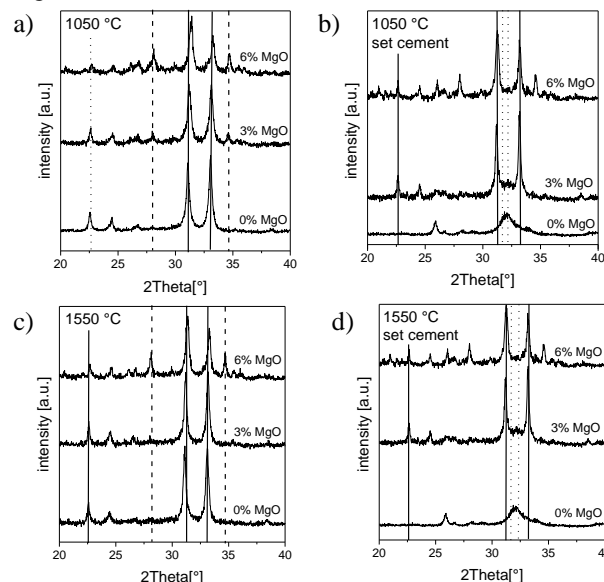


Figure 1: XRD-Pattern of $\text{Ca}_2\text{KNa}(\text{PO}_4)_2 + 0, 3, 6 \text{ wt.}\% \text{ MgO}$: sintered at 1050 °C (a) and set with 2.5 wt.-% Na_2HPO_4 solution (b) or melt at 1550 °C (c) and set with 2.5 wt.-% Na_2HPO_4 solution (d).

$\text{Ca}_2\text{KNa}(\text{PO}_4)_2$ set at an alkaline pH value, whereby the setting pH is highly influenced by the liquid cement phase. All cements showed low compressive strength values in a range between 0.3 and 3.7 MPa after 24 h setting, whereby the strength decreased with increasing additive concentration. This could be related to the decreasing conversion rate. There is no significant difference between the 1050 °C and the 1500 °C cements.

CONCLUSION

All measurements did not show significant differences between the results of the sintering at 1050 °C and melting at 1550 °C. This indicates that the discrepancy in the published results must be influenced by other parameters for example the sample preparation conditions. A promising observation is the phase composition change of the raw powders with an increasing content of SiO_2 or MgO. Here it would be very interesting to rise up the additive concentration for further experiments.

REFERENCES

1. Driessens F. C. M. *et al.*, Biomaterials 54:4011-4017, 2002
2. Knabe C. *et al.*, Clin oral implants res 16: 119-127, 2005
3. Gbureck *et al.*, Biomaterials 26: 6880-6886, 2005
4. Berger G. *et al.*, Key eng mater 284-286: 121-124, 2005
5. Berger *et al.*, Biomaterials, 16:1241-1248, 1995

Development of an in situ culture-free screening test for the rapid detection of *Staphylococcus aureus* within healthcare environments

Adam Le Gresley¹, Alex Sinclair¹, Lauren E. Mulcahy², Lynsey Geldeard¹, Samerah Malik¹ and Mark D. Fielder²

¹Pharmacy and Chemistry, SEC, Kingston University, UK a.legresley@kingston.ac.uk

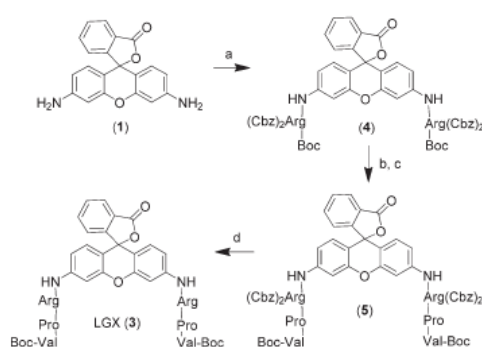
²Life Sciences, SEC, Kingston University, UK,

INTRODUCTION

Staphylococcus aureus (SA) infections are a significant problem within hospitals worldwide. In Europe alone, around 7% of all patients develop healthcare acquired infections and this is estimated to cost up to £11bn annually to diagnose and treat. Epidemiology suggests that up to 30% of the UK population are carriers of SA, currently UK hospitals only screen surgical patients.¹ It has been predicted that for an in-patient cohort of 70 000, cost savings of ~£600k could be achieved; along with the potential avoidance of 840 hospital acquired infections through the use of a routine pre-screen and treat strategy.² Current clinical detection methods for SA are limited by sensitivity. In all current detection methods, amplification of bacterial numbers via culturing or amplification of characteristic DNA via PCR are utilised for the detection of SA.²

EXPERIMENTAL METHODS

1. Synthesis of prototype fluorescent probe LGX (3)



Scheme 1 (a) HO-Arg(Cbz)₂NHBoc, EDCl, pyridine, DMF, 18%. (b) TFA, DCM, 94%. (c) HO-Pro-Val-NHBoc, COMU, NEt₃, DMF, 14%. (d) H₂, Pd/C, MeOH, DMF, 77%.

2. Biological Testing of LGX

Screening was carried out involving 15 clinical isolates of MRSA. These were cultured on nutrient agar overnight at 37 °C. Discrete colonies of each isolate were tested for coagulase activity using a staphylase test kit (Oxoid), and each MRSA isolate was shown to be coagulase positive. Following this, an inoculum of each respective sample was cultured overnight in nutrient broth under aerobic, shaking conditions at 37 °C. Each sample was washed in sterile 1 × phosphate buffered saline (PBS) and varying concentrations of bacterial suspension, ranging from 10⁰ to 10⁶ colony forming units per mL (CFU mL⁻¹) were generated by serial dilution in 1 × PBS. Solutions of 50 µM and 100 µM LGX were prepared aseptically. In order to detect the presence of staphylocoagulase and thus the efficacy of LGX, varying cell concentrations (10⁰–10⁶ CFU mL⁻¹) (50 µM LGX) and 10⁰–10⁴ CFU mL⁻¹ (100 µM LGX) were added to a microtitre plate (Nunc 96 well plates) in a 1 : 1 ratio with either 50 µM or 100 µM of LGX solution. This provided a final LGX concentration of 25 µM or 50 µM, respectively.

RESULTS AND DISCUSSION

Fig. 1 demonstrates the efficacy of LGX as both a selective and sensitive means of determining the presence of coagulase positive bacteria. As previously described, all bacterial strains were assessed for coagulase activity, and the coagulase status of each bacterium juxtaposed with the results demonstrated in this experiment

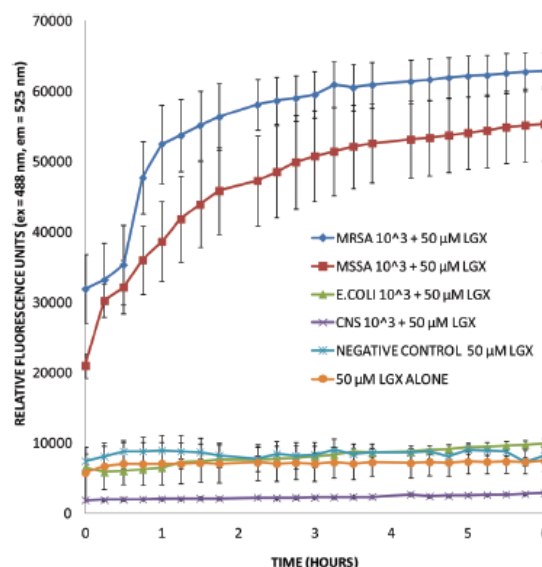


Figure 1. The efficacy of 50 µM LGX in demonstrating both selectivity and sensitivity in detecting coagulase positive MRSA and MSSA, compared to coagulase negative *S. epidermidis* and *E. coli* at concentrations of 10³ CFU mL⁻¹. Average of fifteen bacterial strains (n = 3). Error bars represent standard deviation.

CONCLUSION

We have developed a novel, selective fluorogenic assay, which obviates the need for time consuming culturing or genetic amplification, currently core to most hospital SA tests. Our test has proved itself to be rapid, presently giving a preliminary positive/ negative result within 30 minutes for bacterial concentrations commonly found on skin (>10² CFU mL⁻¹). The testing methodology described within this paper is currently undergoing further biological screening within our labs and work is ongoing towards the development of a rapid point-of-care testkit.³

REFERENCES

1. A. Voss, Br. Med. J., 2009, 339, b3721.
2. M. Scott, P. Panesar, A. Grosso, A. Urquhart, A. Jeanes and A. Wilson, J. Infect. Prev., 2011, 12(3), 119.1.
3. A. Sinclair, A. Le Gresley and M. Fielder, UK Pat. 1212853.4, Kingston University.

ACKNOWLEDGMENTS

The authors would like to thank Kingston University, Enterprise and PARC for funding and the EPSRC mass spectrometry service, Swansea, UK, for providing high resolution mass spectra.



New Technology Based on Combination of Cryogel and Nanoparticles for Wound Management

Timur Saliev ¹, Gulsim Kulsharova ², Alma Akhmetova ¹, Talgat Nurgozhin ¹, Ray D.L. Whitby ^{2,3} and Sergey Mikhailovsky ^{2,3*}

¹ Centre for Life Sciences, Nazarbayev University, Kazakhstan

^{2*} School of Engineering, Nazarbayev University, Kazakhstan, smikhailovsky@nu.edu.kz

³ School of Pharmacy and Biomedical Sciences, University of Brighton, United Kingdom

INTRODUCTION

The anti-microbial properties of noble metals have been known since ancient times. The new technology allows obtaining metal particles with programmed size and shape. Gold and silver nanoparticles have been employed for various bio-medical applications (1, 2, 3). In our study we developed the method of obtaining gold and silver nanoparticles with different shape. The nanoparticles are to be incorporated into the cryogel, which provides an ideal antimicrobial micro-environment for effective wound healing.

EXPERIMENTAL METHODS

Silver nanoparticles have been synthesized using sodium borohydride reduction of silver nitrate. The synthesis of gold nanoparticles for this method has been realized through Turkevich method (4). Turkevich method has been known as one of the oldest and most popular procedures for obtaining gold nanoparticles of 10-15 nm diameters in the water. Produced silver nanoparticles and gold nanoparticles were imaged by Tunnelling Electron Microscopy (TEM) and Scanning Electron Microscopy (SEM).

RESULTS AND DISCUSSION

Initially we have developed several methods for synthesizing gold and silver nanoparticles of varying shapes and sizes. We have achieved production of triangular and circular nanostructures made of noble metals. We do hypothesize that shape of the particle affects its anti-microbial properties.

As a second step, experiments for conjugating the metal nanoparticles to the surface of cryogel have been conducted. It has been achieved through formation of strong covalent bonding between gold nanoparticles and cysteamine. By following cysteamine functionalization to gold nanoparticles surface, we were able to form NH₂ bond sticking out of the surface. This was done in order to make sure that the nanoparticles are well attached and do not get detached from the surface.

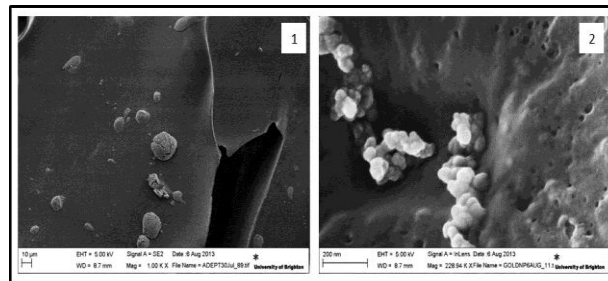


Figure 1. SEM image Attached gold nanoparticles on the surface of a cryogel.

Figure 2. SEM image Aggregated gold nanoparticles on the surface of a cryogel.

CONCLUSION

The manufacturing of several types of nanoparticles with programmed shape and size (made of noble metals) has been established. The form of particles has been confirmed by SEM and TEM imaging. Produced nanoparticles were attached to the surface of cryogel by forming bonds between cysteamine and noble metals. The obtained composition ‘metal-cryogel’ provides a perfect foundation for developing new type of wound dressings. The noble metals ensure an anti-microbial effect, whilst macro- and mesoporous structures of the cryogel provide an optimal environment for the process of wound healing by absorbing exudate and debriding the wound.

REFERENCES

1. Kim J.S. *et al.* Nanomed-Nanotechnol. 3(1):95-101, 2007
2. Rai A. *et al.* J. Mater Chem. 20(32):6789-98, 2010
3. Hernandez-Sierra J.F. *et al.* Nanomed-Nanotechnol. 4(3):237-40, 2008
4. Uppal M.A. *et al.* New J Chem. 34(12):2906-14, 2010

ACKNOWLEDGMENTS

The authors would like to thank the Ministry of Education and Science of the Republic of Kazakhstan (Grant No: 698) for providing financial support

Rapid Patterning of 1-D Collagenous Topography as an ECM Protein Fibril Platform for Image Cytometry

Niannan Xue¹, Xia Li¹, Cristina Bertulli¹, Zhaoying Li², Atipat Patharagulpong¹, Amine Sadok³,
Yan Yan Shery Huang^{2*}

¹Department of Physics, University of Cambridge CB3 0HE, UK

^{2*} Department of Engineering, University of Cambridge CB2 1PZ, UK yysh2@cam.ac.uk

³The Institute of Cancer Research, 237 Fulham Road, London, SW3 6JB, UK

Precision patterning of gelatin protein fibrils was achieved using near-field electrospinning (NFES). These fibrils were employed as an image cytometry assay testing the drug effectiveness against early stages of endothelial capillary formation.

INTRODUCTION

Cellular behavior is strongly influenced by the architecture and pattern of its interfacing extracellular matrix (ECM). For an artificial culture system which could eventually benefit the translation of scientific findings into therapeutic development, the system should capture the key characteristics of a physiological microenvironment. At the same time, it should also enable standardized, high throughput data acquisition. Since an ECM is composed of different fibrous proteins, studying cellular interaction with individual fibrils will be of physiological relevance.

EXPERIMENTAL METHODS

We employ near-field electrospinning^{1,2} to create ordered patterns of collagenous fibrils of gelatin, based on an acetic acid and ethyl acetate aqueous co-solvent system. Using these fibril constructs as cellular assays, we study EA.hy926 endothelial cells' response to ROCK inhibition (H1152)², because of ROCK's key role in the regulation of cell shape.

RESULTS AND DISCUSSION

Tunable conformations of micro-fibrils were directly deposited onto soft polymeric substrates in a single step. We observe that global topographical features of straight lines, beads-on-strings, and curls are dictated by solution conductivity (see Figure 1); whereas the finer details such as the fiber cross-sectional profile are tuned by solution viscosity.

The fibril array was shown to modulate the cellular morphology towards a pre-capillary cord-like phenotype, which was otherwise not observed on a flat 2-D substrate. Further facilitated by quantitative analysis of morphological parameters, the fibril platform also provides better dissection in the cells' response to a H1152 ROCK inhibitor.

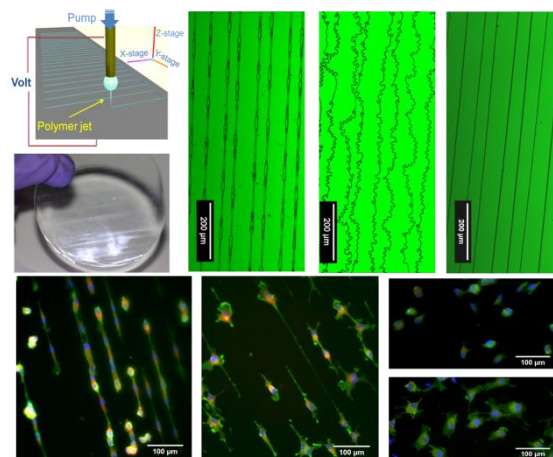


Figure1

CONCLUSION

In conclusion, the near-field electrospun fibril constructs provide a more physiologically-relevant platform compared to a featureless 2-D surface, and simultaneously permit statistical single-cell image cytometry using conventional microscopy systems. The patterning approach described here is also expected to form the basics for depositing other protein fibrils, seen among potential applications as culture platforms for drug screening.

REFERENCES

1. Huang *et al.* *Nanotechnology* (2014) 23, 105305
2. Xue *et al.* *PLOS ONE* (2014, accepted)

ACKNOWLEDGMENTS

The authors thank A. Buell and T. Knowles for *in-situ* AFM access and assistance in the AFM measurement; also helpful discussion from T. Mavrogordatos, and Y. Ji. Y.Y.S. Huang thanks financial supports from an Oppenheimer Research Fellowship and a Department of Engineering Starting Grant. We also thank the following sponsors for providing scholarships/studentships: X. Li (Chinese Scholarship Council), C. Bertulli (Fondazione Angelo Della Riccia), A. Patharagulpong (the Royal Thai Scholarship Council), and Z. Li (Engineering and Physical Sciences Research Council, UK).

Control of Bone Conduction on Pure Titanium by Surface Modification

Masato Ueda^{1*}, Masahiko Ikeda¹, Richard Langford², Jeremy Skepper³, Ruth E. Cameron⁴ and Serena M. Best⁴

^{1*} Faculty of Chemistry, Materials and Bioengineering, Kansai University, Japan, m-ueda@kansai-u.ac.jp

² Electron Microscopy Suite, The Cavendish Laboratory, University of Cambridge, UK

³ Department of Physiology, Development and Neuroscience, University of Cambridge, UK

⁴ Cambridge Centre for Medical Materials, Department of Materials Science & Metallurgy, University of Cambridge, UK

INTRODUCTION

Titanium and its alloys have been used widely as biomaterials for orthopaedic implants because of their excellent mechanical properties and biocompatibility. Despite the major research efforts in the field of osseointegrative materials, there are situations where this effect should be suppressed, for example when these alloys are employed in bone plates/screws which are removed after recovery. The purpose of the present study was to synthesise bioactive TiO₂ film and bioinert TiO₂-ZrO₂ film on pure Ti surfaces by a combined chemical-hydrothermal treatment¹. In addition, *in vivo* bone conduction in the tibiae of rats was also investigated.

EXPERIMENTAL METHODS

Commercial purity (CP-) Ti rods, 2 mm in diameter and 5 mm in height, were chemically treated with aqueous 5 M H₂O₂/0.1 M HNO₃ at 353 K for 20 min. The rods were hydrothermally treated with 1M NH₃ or 100 mM ZrOCl₂/5 M NH₃/400 mM C₆H₈O₇ (citric acid) aqueous solution in a Teflon-lined autoclave at 453 K for 12 h. The rods were implanted into tibiae of eight-week-old rats. After two weeks, the peripheral sections were extracted. Tissues embedded in polymer were cut and polished and the contact ratio between bone and implant was measured by using optical microscopy. The interfaces between the implants and cured bone were observed by transmission electron microscope (TEM).

RESULTS AND DISCUSSION

The Ti is uniformly covered by a film showing a sponge-like morphology after chemical treatment with aqueous H₂O₂/HNO₃¹. The film is anatase-type TiO₂ with very low crystallinity (TiO₂ gel)¹. The morphology of film changed dramatically as a result of the hydrothermal treatments. The surfaces of Ti were covered with cube crystals and the average sizes were measured to be 40 nm and 10 nm or less in the treatments with NH₃ and ZrOCl₂/NH₃/C₆H₈O₇ aqueous solution, respectively. Both films were anatase-type TiO₂ but the latter included a small amount of ZrO₂.

In the animal test, the bone-implant contact ratio, R_{B-I} , was calculated by following equation in order to evaluate bone conductivity.

$$R_{B-I}(\%) = \frac{\text{total length of hard tissue formation on implant}}{\text{total length of implant}} \times 100$$

Figure 1 shows contact ratios for cortical bone in the surface modified implants. Bone conduction was drastically improved on the TiO₂ film from that on the CP-Ti. In contrast, it was suppressed on the TiO₂-ZrO₂ film from the TiO₂. Apatite formation in simulated body

fluid was also reported to be promoted on TiO₂¹ but suppressed on TiO₂-ZrO₂². In addition, the TiO₂ film showed an adhesive interface to living bone (Fig. 2), but the TiO₂-ZrO₂ film always separated from it. Therefore, the present surface modifications have considerable potential for controlling direct bonding to living bone.

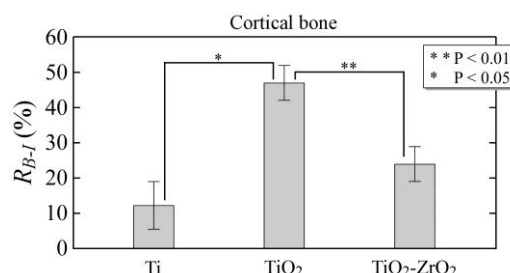


Fig.1 Contact ratios for cortical bone on the surface modified implants.

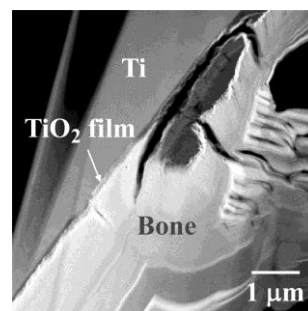


Fig. 2 TEM image of the interface between TiO₂ coated implant and living bone.

CONCLUSION

1. TiO₂ film or TiO₂-ZrO₂ composite film could be synthesised on CP-Ti surfaces by the hydrothermal treatment with NH₃ or ZrOCl₂/NH₃/C₆H₈O₇ (citric acid) aqueous solution, respectively.
2. Bone conduction was promoted on TiO₂ film but suppressed on TiO₂-ZrO₂ film. Therefore, this method has a potential for Ti alloys to control bone conduction and adherence to living bone.

REFERENCES

1. Ueda M. *et al.*, Mater. Trans. 49:1706-1709, 2008
2. Ueda M. *et al.*, Mater. Trans. 50:2104-2107, 2009

ACKNOWLEDGMENTS

The authors would like to thank the Ministry of Education, Culture, Sports, Science and Technology (MEXT), Grants-in-Aid for Scientific Research (Grant no: 22760546, 24656420) for providing financial support to this project.

Modification Of Electrospun Nanofibrous Scaffold By Ink-Jet Printing

Izabella Rajzer^{1*}, Monika Rom², Elżbieta Menaszek³

^{1*}Department of Mechanical Engineering Fundamentals, ATH - University of Bielsko-Biała, Poland
irajze@ath.bielsko.pl

²Institute of Textile Engineering and Polymer Materials, ATH-University of Bielsko-Biała, Poland

³Department of Cytobiology, Collegium Medicum, UJ Jagiellonian University, Poland

INTRODUCTION

Electrospinning as well as inkjet printing has emerged as a useful tools for creating spatially organized materials for tissue engineering¹. Electrospun nanofibrous scaffolds are aimed to mimic the architecture and biological functions of the extra-cellular matrix (ECM). By incorporating conductive material (PANi) and bioactive particles (HAp) into an electrospun scaffold we have formed a bioactive, hybrid scaffold system, which provides an electrically conductive environment. Combination of electrospun, biodegradable scaffolds with conductive polymers in the future would enable us (by the use of controlled electrochemical signals) to stimulate a multitude of cellular functions.

The aim of this work was to investigate the effect of inkjet printing on the properties of obtained scaffolds but also the effect of deposited conductive polymer on the attachment, proliferation, migration, and differentiation of bone cells.

EXPERIMENTAL METHODS

Electrospinning was carried out using custom-made apparatus consisting of a power supply, syringe and electrodes. The solution were placed in a 20 ml plastic syringe with a stainless-steel blunt needle of 0.7 mm in diameter. The solutions were spun at a working distance of 20 cm with a driving force of 30 kV. Conductive polymers were deposited on the surface of electrospun membranes using piezoelectric material printer DMP-2831. The complex structure of the scaffolds and their chemistry were characterized using SEM, FTIR, and WAXD. The nanocomposite scaffolds were also characterized in terms of their porosity, mechanical properties and bioactivity, and by in-vitro cellular tests using NHOst cells. Mineralization process and ALP activity were studied to estimate the cells differentiation.

RESULTS AND DISCUSSION

Ink-jet printing enables to obtain regular patterns on the fibrous support (Fig 1). We have noticed that due to the hydrophobic nature of electrospun material the printing was limited to the outer layer of nonwoven support.

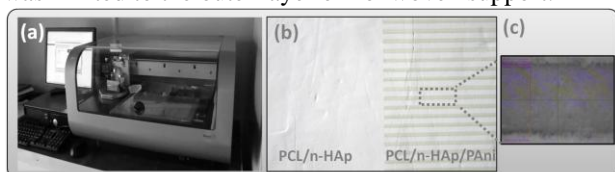


Fig. 1. (a) Piezoelectric material printer DMP-2831; (b-c) pattern printed on the electrospun material;

Our experimental data demonstrate that electrospun PCL/nHAp/PANi scaffolds are biocompatible, supporting attachment, migration, and proliferation of NHOst cells (Fig. 2 and 3).

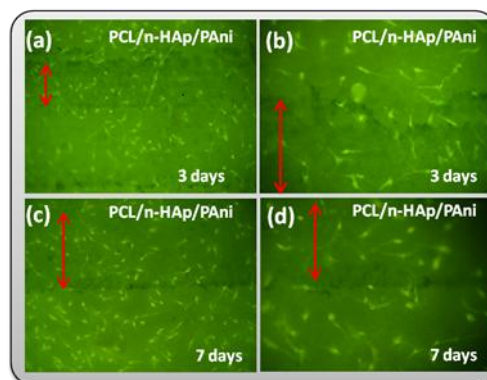


Fig. 2. Morphology of cells cultured on PCL/n-HAp/PANi scaffolds.

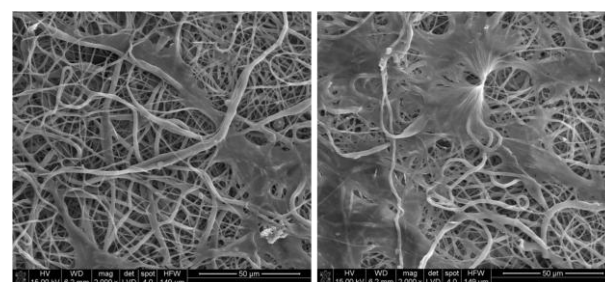


Fig. 3. SEM images of NHOst cells cultured on the PCL/n-HAp/PANi scaffolds.

CONCLUSION

PANi micropatterns were successfully inkjet printed on PCL/n-HAp membranes; Presence of PANi did not affect cell proliferation; Further studies will focus on cell stimulation by controlled electrochemical signals. The greater cell proliferation upon electrical stimulation is expected.

REFERENCES

1. Rajzer, I.; Rom, M.; Menaszek, E. J TISSUE ENG REGEN M 2012;6(supp 1):199-200.

ACKNOWLEDGMENTS

The authors would like to thank the Polish Ministry of Science and Higher Education (Iuventus Plus III Grant no. IP2012033372) for providing financial support to this project".

Chelate Bonding Mechanism of a Novel Magnesium Phosphate Bone Cement

Theresa Christel¹, Martha Geffers¹, Susanne Christ¹, Jürgen Groll¹ and Uwe Gbureck^{1*}

¹Department for Functional Materials in Medicine and Dentistry, University of Würzburg, Germany

*uwe.gbureck@fmz.uni-wuerzburg.de

INTRODUCTION

Magnesium phosphates have comparable characteristics to calcium phosphate bone substitutes, but degrade faster under physiological conditions. Farringtonite ($\text{Mg}_3(\text{PO})_4$), for example, is known to set with an aqueous $(\text{NH}_4)_2\text{HPO}_4$ solution to form struvite ($\text{MgNH}_4\text{HPO}_4 \cdot 6\text{H}_2\text{O}$) monolith which is naturally found in the calcifications of kidney stones¹. In the present study, an alternative setting mechanism of this magnesium phosphate cement was tested by replacing $(\text{NH}_4)_2\text{HPO}_4$ with phytic acid ($\text{C}_6\text{H}_{18}\text{O}_{24}\text{P}_6$). The latter is a strong chelating agent for Mg^{2+} and Ca^{2+} ions and is assumed to form stable complexes with the cement raw material.

EXPERIMENTAL METHODS

0.6 mol $\text{MgHPO}_4 \cdot 3\text{H}_2\text{O}$ and 0.3 mol $\text{Mg}(\text{OH})_2$ were sintered for 5 h at 1050 °C in a sintering furnace. The resulting $\text{Mg}_3(\text{PO})_4$ was sieved < 355 µm and milled in a planetary ball mill for 1 h at 200 rpm. $\text{Mg}_3(\text{PO})_4$ was mixed with 10, 20 or 30 % phytic acid in a powder-to-liquid-ratio (PLR) of 3.0 g/mL. The paste was transferred into silicon rubber molds (12x6x6 mm) and stored for 24 h at 100 % humidity and 37 °C. The compressive strength of these cuboids was measured by universal testing machine using a crosshead speed of 1 mm/min. The fractions were crushed and analyzed by X-ray diffractometry and infrared spectrometry. Furthermore, the development of the pH of the cement paste was analyzed during the first half hour of setting. Analysis of variance was examined by applying the Dunett's test by means of the excel sheet inerSTAT-a (M.H.Vargas, Instituto Nacional de Enfermedades, Mexico).

RESULTS AND DISCUSSION

The hardened cements had a compressive strength up to 64 ± 9 MPa (Fig. 1a). Infrared spectra showed a slight shift of the P=O valence vibration from 1635 to at least 1650 cm^{-1} (Fig. 1b) which implies a successful chelation. In addition, a little phase transformation took place from struvite to newberyite ($\text{MgHPO}_4 \cdot 3\text{H}_2\text{O}$) according to the recorded X-ray diffractometry spectra. The cement paste had a pH minimum of about 3.7 for 30 % phytic acid during the examined time period.

The performance of this chelating process by means of phytic acid was earlier approved on calcium containing phosphate formulations². The high compressive strength values in this study are comparable to those of the conventional magnesium phosphate cement setting reaction¹ and are not affected by the chelation mechanism. The novel cement system even combines the conventional cement setting with the novel

approach. The formation of newberyite out of farringtonite is already shown in literature and results from the acidic conditions, but those harden with worse mechanical properties³. As expected, the pH of the cement paste was low during setting reaction, but comparable to that of brushite cements ($\text{CaHPO}_4 \cdot 2\text{H}_2\text{O}$)⁴. However, the latter is already commercially available for bone substitution applications⁵.

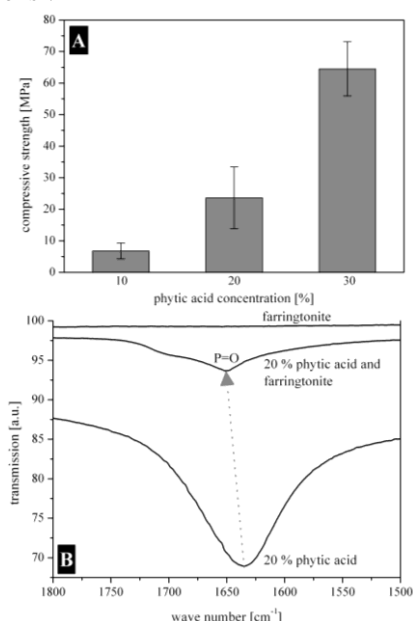


Fig. 1: Compressive strength of hardened samples with $\text{Mg}_3(\text{PO})_4$ and differently concentrated phytic acid solutions in a PLR of 3.0 g/mL after 24 h of setting. All the results differ significantly ($p < 0.01$) (a). Infrared spectra of $\text{Mg}_3(\text{PO})_4$, 20 % phytic acid and a mixture of both (b).

CONCLUSION

A novel approach to harden magnesium phosphate cements was successfully presented by combining chelation with a conventional setting reaction. Further characterization showed that this material composition development seems to be promising.

REFERENCES

1. Vorndran E. *et al.*, J. Mater. Sci.-Mater. Med. 22:429-436, 2011
2. Takahashi S. *et al.*, J. Ceram. Soc. Jpn. 19:35-42, 2011
3. Klammert U. *et al.*, Acta Biomater. 6:1529-1535, 2010
4. Ewald A. *et al.*, J. Biomed. Mater. Res. B. Appl. Biomater. 96B:326-332, 2011
5. Böhner M. *et al.*, Biomaterials. 26:6423-6429, 2005

Biocompatibility and Solubility of Calcium Doped Magnesium Phosphate Cement Granules

Theresa Christel¹, Martha Geffers¹, Susanne Christ¹, Uwe Klammert², Berthold Nies³, Andreas Höß³, Jürgen Groll¹ and Uwe Gbureck^{1*}

¹Department for Functional Materials in Medicine and Dentistry, University of Würzburg, Germany

²Department of Cranio-Maxillo-Facial Surgery, University of Würzburg, Germany

³InnoTERE GmbH, Radebeul, Germany

*uwe.gbureck@fmz.uni-wuerzburg.de

INTRODUCTION

Magnesium phosphate compounds, as for example struvite ($\text{MgNH}_4\text{HPO}_4 \cdot 6\text{H}_2\text{O}$), are comparable to calcium phosphate bone substitutes, but degrade faster under physiological conditions. In the present work, we used a calcium doped magnesium phosphate with the general formula $\text{Ca}_x\text{Mg}_{(3-x)}(\text{PO}_4)_2$ ($x=0.75, 1.0$ or 1.5) to set with $(\text{NH}_4)\text{HPO}_4$ solution and form struvite¹. The paste can be dispersed in a hydrophobic phase and stabilized as small droplets by surfactants until it hardens by cement setting. The resulting spherical granules (Fig. 1a) are suitable for applications in maxillofacial surgery (e.g. sinus floor augmentation). The problem with hydraulic cement pastes to form granules <1 mm by emulsification is their tendency to coalesce². The present study was aimed to fabricate small granules by the right choice of composition of the $(\text{NH}_4)\text{HPO}_4$ containing solution in the struvite forming cement paste and to show their biological properties.

EXPERIMENTAL METHODS

$\text{Ca}_x\text{Mg}_{(3-x)}(\text{PO}_4)_2$ was prepared by sintering $\text{MgHPO}_4 \cdot 3\text{H}_2\text{O}$, $\text{Mg}(\text{OH})_2$, CaHPO_4 and CaCO_3 for 5 h at 1100 °C in a furnace. The product (< 355 µm) was milled in a planetary ball mill for 4 h at 200 rpm. The powder was mixed with a 2.0 M $(\text{NH}_4)\text{HPO}_4/1.5$ M $\text{NH}_4\text{H}_2\text{PO}_4$ solution in a powder-to-liquid-ratio of 2.0 g/mL. This paste formed small granules < 1 mm via emulsification process. The paste was transferred into disc-shaped silicon rubber molds (15x2 mm) and stored for 24 h at 100 % humidity and 37 °C, washed in phosphate buffered solution for 14 d and disinfected in 70 % ethanol. Human fetal osteoblast cell line (hFOB) was seeded on the cement samples with a density of 100,000 cells/mL. After 4, 6 and 10 d, the cells were counted by means of Trypan blue and their activity was determined by the cell proliferation agent WST-1. Reference surfaces were both polystyrene (PS) and hydroxyapatite (HA). To analyze their passive solubility, the samples were also put in cell culture medium without hFOB and incubated for 10 d. The accumulated PO_4^{3-} , Mg^{2+} and Ca^{2+} content of the used media was measured by mass spectrometry.

RESULTS AND DISCUSSION

The cell activity of hFOB on the cement composition leading to an optimum granule size is exemplarily shown with the $\text{Ca}_{0.75}\text{Mg}_{2.25}(\text{PO}_4)_2$ formulation (Fig. 1b). The normalized activity per cell for the struvite samples remained constant during the culture period of 10 d. Cell activities were comparable to those on PS on day 4 and 6 and partially even higher than

those on HA. During the same period, a more than three times higher PO_4^{3-} content was detected in the medium released by struvite compared to HA. Simultaneously, no Mg^{2+} ions were released by HA, but more Ca^{2+} ions were detracted by the latter material.

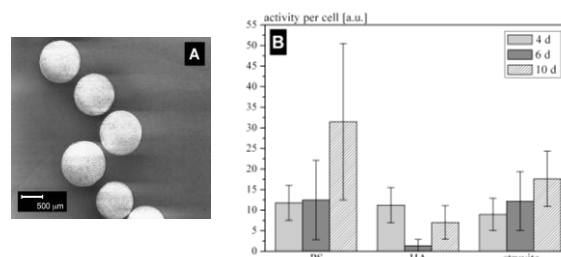


Fig. 1: Scanning electron micrograph of granules prepared by emulsification (a) and activity per cell on different surfaces for 4, 6 and 10 d. Struvite samples were made of $\text{Ca}_{0.75}\text{Mg}_{2.25}(\text{PO}_4)_2$ and 2.0 M $(\text{NH}_4)\text{HPO}_4/1.5$ M $\text{NH}_4\text{H}_2\text{PO}_4$ solution (b).

Both Mg^{2+} and Ca^{2+} promote proliferation and differentiation of osteoblasts and play an important role concerning bone deposition and mineralization³. The analyzed struvite samples favor the presence of both ion types in the cellular environment. The biocompatibility of struvite based mineral systems is already proved *in vitro*¹ and *in vivo*⁴, but the additional benefit of our system is its ability to be granulated via emulsification process and to build granules <1 mm.

CONCLUSION

We found an effective method to granulate a struvite based cement paste and verified the biocompatibility of the used formulation. Further experiments will focus on detailed bio(-chemical) studies concerning both the expression of genes and proteins and the active resorption of our surfaces by osteoclastic cells.

REFERENCES

1. Vorndran E. *et al.*, J. Mater. Sci.-Mater. Med. 22:429-436, 2011
2. Moseke C. *et al.*, J. Mater. Sci.-Mater. Med. 23:2631-2637, 2012
3. Wu F. *et al.*, Acta Biomater. 4:1873-1884, 2008
4. Klammert U. *et al.*, Acta Biomater. 7:3469-3475, 2011

ACKNOWLEDGMENTS

The authors would like to acknowledge financial support from the Federal Ministry of Education and Research (BMBF) under the grant number 13EZ1208B (NAKKRO).



Study and design of RGD-Self-assembling peptide hydrogels

Deidda Graziano,^{1,2} Mitraki Anna,^{1,2}
Graziano Deidda: grazianodeidda@gmail.com,

¹Materials Science Department, University of Crete, Heraklion, Crete, Greece,

²Institute of Electronic Structures and Lasers, Foundation for Research and Technology-Hellas (IESL-FORTH), Heraklion, Crete, Greece

INTRODUCTION

In the last decade, the development of peptide-derived 3D hydrogels and their use as scaffolds for cell attachment and proliferation has attracted lots of attention.³ In this work, we designed and characterized peptides comprising a natural self-assembling peptide building block together with a RGD integrin-binding motif. Moreover, we designed bifunctional building blocks carrying cysteine residues, a central self-assembling core, and an RGD motif. We have been evaluating the structure and self-assembly propensity of these peptides. These self assembling peptide materials will be targeted as scaffolds for angiogenesis in ischemic *in vitro* models.

EXPERIMENTAL METHODS

Six different RGD self-assembling peptides were tested for the ability to self-assemble in physiological solvents. Different microscopy techniques were utilized to monitor the kinetics of assembly and morphology of the assembled fibrils: Transmission Electron Microscopy (JEOL JEM-2100 TEM), Scanning Electron Microscopy (Field Emission JEOL JSM 7000F SEM) and Atomic Force Microscopy (AFM).

RESULTS AND DISCUSSION

The images collected from the aforementioned techniques (Fig. 1,2 and 3) demonstrated that all the designed RGD self-assembling peptides showed a distinct tendency to form porous networks of interconnected fibrils. Most of them form self-supporting hydrogels. The position of the RGD motif at the C-terminus or at the N-terminus and the presence or the absence of a cysteine residue seems to play an important role in self-assembly. Future experiments will focus on the identification of the most suitable candidate peptides for developing cell-recruiting fibrils.

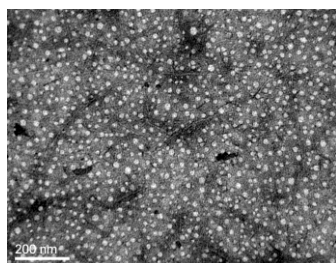


Figure 1: TEM analysis highlighted how thin fibers could form spontaneously after being suspended for 6 hours.

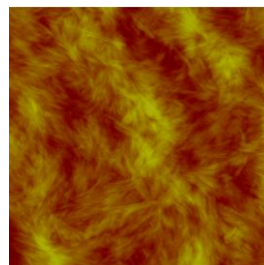


Figure 2: AFM analysis showed clearly fibril formation in most of the peptides.

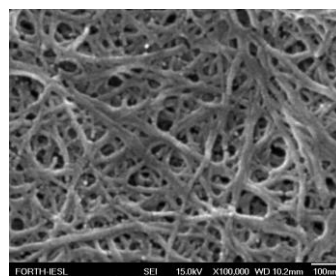


Figure 3: SEM images showed that most of the peptides could afford a dense, interconnected 3D web of fibers.

CONCLUSION

All the designed peptides are appropriate building blocks for the construction of higher order biological structures. Our long-term goal is to develop bifunctional scaffolds that will allow cell attachment and proliferation and could be simultaneously functionalized with angiogenesis signalling molecules through the cysteine residues. Such functionalized scaffolds will be tested for angiogenesis in ischemic *in vitro* models. The RGD-exposure geometry will also play a crucial role to guarantee these features.⁴

REFERENCES

- 3 - Hauser, A., E., Zhang, S. (2010), *Chem. Soc. Rev.*, **39**, 2780-2790.
- 4 - Haubner, R., Gratias, R., Diefenbach, B., Goodman, S. L., Jonczyk, A. and Kessler, H. (1996), *J. Am. Chem. Soc.*, **118**, 7461-7472.

ACKNOWLEDGMENTS

This research was supported by “AngioMatTrain” “Development of biomaterial-based delivery systems for ischemic conditions- An integrated Pan-European approach”, Marie Curie Industry –Initial Training Network (ITN), call FP7-PEOPLE-2012-ITN, www.angiomatrain.eu

Structure and Properties Study of Calcium Apatites

Y. Gao¹, R.V. Law^{1*}, N. Karpukhina², R.G. Hill²

¹Department of Chemistry, Imperial College London, UK

²Dental Physical Sciences/Institute of Dentistry, Queen Mary University of London, UK

yajie.gao11@imperial.ac.uk

INTRODUCTION

Calcium apatite is the basis for a multiplicity of inorganic solids important in geology and materials science[1]. As we know, hydroxyapatite (HA; $\text{Ca}_5(\text{PO}_4)_3\text{OH}$) is the main mineral component of human dental enamel and bone, and can react readily undergo fluoride substitution from solutions to form fluoride-substituted hydroxyapatite or hydroxyfluorapatite (HFA) $\text{Ca}_{10}(\text{PO}_4)_6\text{F}_{2x}(\text{OH})_{2-2x}$ ($0 < x < 1$). However, the different proportions of fluoride in fluoride-substituted hydroxyapatite may cause difference solubility and thermal stability. It is difficult to quantify fluoride substitution in hydroxyapatites using X-ray diffraction; this is because the patterns are very similar, as these apatites are isostructural [2]. High-resolution solid state nuclear magnetic resonance (NMR) is a sensitive local probe of atomic and molecular structure, which can be used to determine oxygen/fluorine ordering in the structure of calcium apatite. The quantitative and qualitative structural information of calcium apatites can be obtained by ^1H , ^{19}F and ^{31}P NMR spectra[3]. Lots of efforts and achievements have been made in apatite science[4]; however, the fine structural details are still not available.

EXPERIMENTAL METHODS

Various calcium apatites, HA and HFA, have been synthesised by both solution route and solid-state reaction methods[5] followed by heating in air at different temperatures. The various experimental techniques, like solid-state nuclear magnetic resonance (NMR), X-ray diffraction (XRD), differential scanning calorimetry (DSC), Fourier transform infrared spectroscopy (FTIR) and Scanning electron microscopy with energy dispersive X-ray spectroscopy (SEM/EDX), were used to characterise the synthesised powder samples

RESULTS AND DISCUSSION

FTIR spectra show PO_4 ν_4 , PO_4 ν_1 and PO_4 ν_3 bands in all of the samples; wet and dried samples contained a CO_3 ν_3 band, which disappeared after heat treatment. The XRD pattern indicates that two phases are formed

in HFA heat treatment samples. All of the samples have single ^{31}P resonance at 2.8ppm corresponding to phosphorus in an orthophosphate environment (PO_4^{3-}). From ^{19}F NMR spectra, the signals are observed in the range from -102ppm to -106ppm depending on degree of the fluoride substitution in HFA and water absorbed by the sample. The implications of these multiple ^{19}F NMR signals and how it can be related to the apatite structure will be discussed.

CONCLUSION

Experimental data suggest that synthetic apatite contains a small amount of carbonate which can be removed by heating samples above 873K in air. There are two phases in hydroxyfluorapatite heat treated at high temperature: tricalcium phosphate and apatite. The quantitative and qualitative structural information of calcium apatites were obtained by ^1H , ^{19}F and ^{31}P MAS NMR spectroscopy. The ^{19}F NMR results show two resonances at -104ppm and -102ppm, corresponding to the two F environments in the apatite structure after heat treatment at 1173K.

REFERENCES

- [1] M. Braun and C. Jana, *Chem. Phys. Letters* **1995**, 245, 4.
- [2] Manjubala and M. Sivakumar, *J. Mater. Sci.* **2001**, 36, 6.
- [3] a) K. Smith and D. P. Burrin, *J. Magn. Res.* **1989**, 84, 4; b) J. P. Yesinowske and M. Mobley, *J. Am. Chem. Soc.* **1983**, 105; c) G. Cho and J. P. Yesinowski, *Chem. Phys. Letters* **1993**, 105; d) L. B. Moran and J. P. Yesinowski, *Chem. Phys. Letters* **1994**, 222, 363
- [4] a) J. Wilson, T. Yamamuro and L. L. Hench, *Handbook of Bioactive Ceramics*, CRC Press, Florida, **1990**, b) S. Kalita, A. Bhardwaj and H. Bhatt, *Mater. Sci. Eng. C* **2007**, 27, 441-449, c) M. Mathew and S. Takagi, *J. Res. Natl. Inst. Standards Technol.* **2001**, 106, 10, d) T. Leventouri, *Biomaterials* **2006**, 27, 4, e) Manjubala and M. Sivakumar, *Journal of materials Science* **2001**, 36, 6, f) M. Aripova and Z. A. Babakhanova, *Glass Ceramics* **1998**, 10, 2, g) R. Murugan and S. Ramakrishna, *Biomaterials* **2004**, 25, 3829-3835, h) X. Chen, X. Liao, Z. Huang, P. You, C. Chen, Y. Kang and G. Yin, *J. Biomed. Mater. Res., Part B Appl. Biomater.* **2010**, 93, 194-202, i) J. C. Elliott, *Structure and Chemistry of the Apatites and Other Calcium Orthophosphates*, ELSEVIER, 2ed, **1994**, j) Rosenblum and Schulman, *J. Am. Dent Assoc.* **1997**, 128, k) S. A. Santander and A.P. Vagas, *J. Am. Dent Assoc.* **2010**, 163.
- [5] G. Penel, G. Leroys and C. Rey, *J. Mater. Sci. Mater. Med.* **1997**, 8, 7.

Development and study of poly(butylene succinate)/chitosan/hemp fiber fully biodegradable composites

Z. Terzopoulou¹, V. Nikolaidis¹, D. Bikiaris¹, E. Athanassiadou², E. Papadopoulou²

¹Department of Chemistry, Aristotle University of Thessaloniki, Greece

²CHIMAR HELLAS SA, Sofouli 88, 55131 Thessaloniki, Greece, terzoe@gmail.com

INTRODUCTION

The use of natural fibers to reinforce polymers is an established practice, and biocomposites have gained an increased interest in areas such as automotive, construction and agriculture¹. The purpose of the present work was the preparation and study of fully biodegradable ("green") composite materials using poly(butylene succinate) (PBSu) as polymeric matrix with hemp fibers (HF) and chitosan as fillers.

EXPERIMENTAL METHODS

Poly(butylene succinate) (PBSu)/Chitosan 90/10 and 80/20 w/w blends containing 10, 20, 35, 50 and 65wt% hemp fibers of 0.5cm length respectively were prepared by melt mixing in a Haake-Buchler Reomixer at 190°C and 35 rpm for 5 min. The polyester and the fillers were dried under vacuum prior to the melt mixing. Films of the samples were received using a hydraulic press, set at 190°C. Mechanical properties including tensile strength, elongation at break and impact strength were studied. Enzymatic degradation took place in aqueous solution in the presence of *R. Oryzae* and lysozyme in pH=7.2, at 50°C and soil degradation took place in conventional leaf soil, for 30 days. The effect of both enzymatic and soil degradation on the polymeric matrix was studied with SEM and weight loss measurements.

RESULTS AND DISCUSSION

SEM images of the composite materials revealed poor interfacial adhesion in general, though better coverage of the hemp fibers with chitosan for the PBSu/Chitosan 80/20 w/w composites. The addition of hemp fibers reduced the mechanical properties of the materials due to the fact that the natural fibers and chitosan are hydrophilic materials whereas the polyester has a hydrophobic character, which results in poor interaction between them². The better coverage of the hemp fibers in the materials with chitosan 20 wt%, as observed in Fig. 1, lead to better mechanical properties compared to the materials with chitosan 10 wt%, including tensile and impact strength.

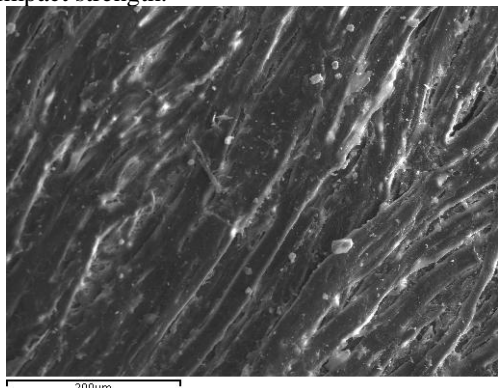


Figure 1: SEM micrograph of PBSu/Chitosan 80/20 w/w with hemp fiber 65 wt%.

The rate of both enzymatic and soil degradation was found to be greater for the composite materials compared to neat PBSu. While neat PBSu lost only the 1.5% of its initial mass after one month, the enzymes caused greater weight loss of up to 22% for the PBSu/Chitosan 90/10 w/w HF 65wt % composite. As the concentration of the hemp fibers increases, there is an increase in the biodegradation rate. The higher degradation in the composites, in comparison with neat PBSu, can be explained by the increase of the free surface of PBSu because of the gaps between the contact surfaces of the polymer and the fillers. The higher the concentration of the hydrophilic additive, the greater the moisture absorption and swelling, which results in increasing the rate of degradation of composites. SEM micrographs revealed that as the enzymatic degradation progresses, bigger parts of the fibers are revealed due to the biodegradation of PBSu and chitosan.

PBSu lost 5% of its weight while buried in soil for one month. The composite materials showed again greater degradation rates and mass losses (up to 27%) for the same reasons mentioned above for the enzymatic degradation, plus the rich population of microorganisms in the soil that can degrade our materials. In this case though, the final weight losses for all the composites was higher compared to the hydrolysed by enzymes materials. The water intake promoted the entrance of microorganisms present in soil due to the high hydrophilicity of the composites. SEM micrographs of the soil degraded samples confirmed the results from the weight loss.

CONCLUSION

Although the addition of both Hemp fibers and chitosan in PBSu resulted in decreased mechanical properties, they accelerated the degradation rate. Larger proportion of chitosan may have caused the creation of hydrogen bonds with the polymeric matrix and the fibres, resulting in a slight enhancement of the mechanical properties in comparison with the composites with 10 wt% chitosan.

REFERENCES

1. Summerscales J. *et al.*, Composites Part A 41:1329–1335, 2010
2. Mehan L. *et al.*, Compos Sci Technol. 60:1013-1026, 2000

ACKNOWLEDGMENTS

The authors would like to thank the EUREKA-EUROSTARS Programme E!6544 for providing financial support to this project.

Effect of Albumin Adsorption on MC3T3-E1 and RAW264.7 Cell Response to Hydroxyapatite and α -Alumina

Masakazu Kawashita^{1*}, Jumpei Hayashi¹, Tada-aki Kudo², Hiroyasu Kanetaka³, Zhixia Li⁴, Toshiki Miyazaki⁵, Masami Hashimoto⁶

¹ Graduate School of Biomedical Engineering, Tohoku University, Japan, m-kawa@ecei.tohoku.ac.jp

² Graduate School of Dentistry, Tohoku University, Sendai 980-8575, Japan

³ Liaison Center for Innovative Dentistry, Graduate School of Dentistry, Tohoku University, Japan

⁴ College of Chemistry and Chemical Engineering, Guangxi University, China

⁵ Graduate School of Life Science and Systems Engineering, Kyushu Institute of Technology, Japan

⁶ Japan Fine Ceramics Center, Nagoya 456-8587, Japan

INTRODUCTION

Osteoconductivity is the ability of biomaterials to support bone formation and chemically bond to bone. Hydroxyapatite (HAp) and alpha-type alumina (α -Al₂O₃) are typical osteoconductive and non-osteoconductive biomaterials, respectively. Post-implantation, the biomaterials are immediately coated with, and subsequently adsorb, layers of proteins from blood and tissue fluids¹. Importantly, all subsequent cellular responses are dependent on the implants' ability to adsorb protein at early time points. However, a detailed mechanism of the osteoconductive process is not yet clear.

In this study, we investigated adhesion, spreading, and proliferation in response to and bovine serum albumin (BSA)-adsorbed disc of HAp or α -Al₂O₃ using MC3T3-E1 osteoblastic cells and mouse RAW264.7 macrophages.

EXPERIMENTAL METHODS

Original discs were autoclaved at 121 °C for 20 min and adsorbed with BSA at 8.0 mg/mL in 2 mL of saline at 4 °C for 24 h. Following BSA adsorption, the samples were transferred to a 24-well culture plate. Each disc was seeded with 1x10⁴ MC3T3-E1 osteoblast-like cells or RAW264.7 monocytic cells in 1 mL of DMEM supplemented with 20% FBS and penicillin / streptomycin. For experiments, the cells were cultured for various periods of time ranging from 1 h to 14 days at 37 °C and 5% CO₂. For cell adhesion and spreading assays, cells adhered to discs were stained with fluorescein diacetate, and the number of adhered cells were counted and the maximum cell length was determined using an inverted fluorescent microscope. To determine cell proliferation, we isolated DNA from viable cells adhered to discs at 2, 7, and 14 days after incubation by using the AllPrep DNA/RNA/Protein Mini Kit and QIA Shredder columns, according to the manufacturer's protocol. Cell extraction was performed using cell scrapers and DNA was quantified by measuring absorbance at 260 nm by using a spectrophotometer.

RESULTS AND DISCUSSION

Effects of adsorbed BSA on MC3T3-E1 cell response are summarized in Table 1. Adsorbed BSA inhibited adhesion and spreading of MC3T3-E1 cells but it hardly affects MC3T3-E1 cell proliferation, no matter the substrate type. However, for HAp, we suggest that the inhibition effect of BSA is decreased because MC3T3-E1 cells adhered to HAp before sufficient adsorption of

BSA. This can be elucidated from the results regarding time-dependent adsorption of protein and MC3T3-E1 cell on HAp. These data suggest that the quick adherence of osteoblast cells might play an important role HA osteoconductivity.

Table 1 Effects of BSA adsorption on MC3T3-E1 cell response to HAp and α -Al₂O₃.

	Adhesion	Spreading	Proliferation
HAp	Inhibited	Inhibited	Not affected
α -Al ₂ O ₃	Inhibited	Inhibited	Not affected

The effects of adsorbed BSA on the RAW264.7 cell response are summarized in Table 2. Adsorbed BSA inhibits adhesion of RAW264.7 cells on α -Al₂O₃ but not on HA, whereas it hardly affected the spreading and proliferation of RAW264.7 cells on both HA and α -Al₂O₃ substrates. These results indicate that the initial adhesion of monocyte-macrophage lineage cells is inhibited by BSA adsorbed on α -Al₂O₃ but not by BSA adsorbed on HA. While a detail mechanism remains unclear, we speculate that the adsorption of BSA on HA plays some role in the cell response.

Table 2 Effects of BSA adsorption on RAW264.7 cell response to HAp and α -Al₂O₃.

	Adhesion	Spreading	Proliferation
HAp	Not affected	Not affected	Not affected
α -Al ₂ O ₃	Inhibited	Not affected	Not affected

SUMMARY

We investigated effect of adsorbed BSA on responses of osteoblast-like MC3T3-E1 cells and RAW264.7 macrophages. The adsorbed BSA inhibited adhesion and spreading of MC3T3-E1 cells, but it hardly affected the proliferation of MC3T3-E1 cells on both HAp and α -Al₂O₃. This suggests that MC3T3-E1 cells quickly adhered to original HAp before sufficient adsorption of BSA. The adsorbed BSA also inhibits adhesion of RAW264.7 cells on α -Al₂O₃ but not on HAp, whereas it does not affected the spreading and proliferation of RAW264.7 cells on both HAp and α -Al₂O₃ substrates. These results indicate that BSA adsorbed on HAp induces a different cell response than α -Al₂O₃. Moreover, the quick adherence of osteoblast cells and monocyte-macrophage lineage cell likely plays a role in HAp osteoconductivity.

REFERENCES

1. Puleo D.A. *et al.*, Biomaterials 20:2311-2321, 1999.



New Insights into the Control of 3D Architecture and Porosity in Collagen Scaffolds for Tissue Engineering

K. M. Pawelec¹, A. Husmann¹, S. Best¹, R. Cameron¹

¹Cambridge Centre for Medical Materials, University of Cambridge, UK, ah492@cam.ac.uk

INTRODUCTION

Ice-templated collagen scaffolds are a powerful tool of regenerative medicine. Scaffold structure is formed during freezing, when ice nucleates and grows, pushing collagen to the space between the ice crystals. Once removed via sublimation, the porous structure is a mirror image of the ice, and can influence the biological response of the scaffold¹. Many different factors have been used to control ice structure including collagen weight percentage, mould design, and freezing protocols²⁻³. Given the close relationship between ice crystallization and the final scaffold structure, we hypothesized that by understanding the physics of crystal growth, scaffold structure could be predicted, regardless of the processing.

EXPERIMENTAL METHODS

Collagen slurry (1 wt%) was frozen in a Perspex mould. The set freezing temperature ranged from -20 to -40 °C. A protocol with a thermal hold at -14 °C was also used. Thermal profiles were recorded with thermocouples at the slurry top and base; from these, the nucleation temperature, slurry cooling rate, freezing time and “time at equilibrium” were quantified, Figure 1. The time at equilibrium was defined, with differential scanning calorimetry, as the time the slurry spent above -1.5°C; within this range most active crystal growth and annealing occurs within the slurry. Pore size was determined using micro-computed tomography (25 kV, 132 µA). All data was analysed using a Mann-Whitney test, with a confidence interval of 95%.

RESULTS AND DISCUSSION

Changes to the set final freezing temperature significantly affected the entire freezing process, altering all thermal parameters. Adding a thermal hold only affected the freezing time and the time at equilibrium. The resulting pore size at the scaffold top changed significantly as the freezing protocol varied.

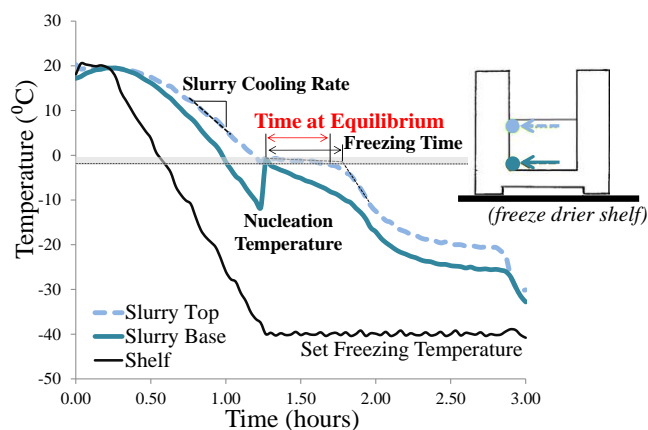


Figure 1. Description of thermal parameters quantified from a thermal profile recorded during freezing.

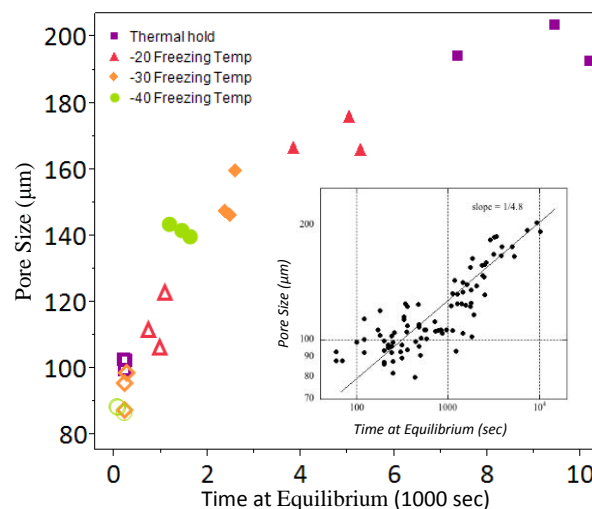


Figure 2. Relationship between time at equilibrium and pore size in collagen scaffolds (open marker: scaffold base, closed marker: top). *Inset: the slope of the curve was 1/4.8; fit with linear regression ($p < 0.05$, $R^2 = 0.8$)³.*

It was found that a strong relationship existed between the pore size and the time at equilibrium, Figure 2. The “time at equilibrium”, defined in the current study, is a measure of the efficiency of latent heat removal from the slurry, and is related to ice crystal growth. At the base of the slurry, which was close to the heat sink, heat removal occurred rapidly, despite changes to the freezing protocol, and the pore size remained constant. At the top of the mould, however, heat removal from the slurry was heavily dependent on the freezing protocol. With high set freezing temperatures or the addition of a thermal hold, the slurry at the scaffold top remained near equilibrium for longer periods, allowing the ice crystals to grow and anneal.

CONCLUSION

A fundamental relationship was revealed between the time at equilibrium and the final pore structure of tissue engineering scaffolds. By relating pore structure to the underlying physics of solidification, the curve should be robust regardless of processing changes. A predictive tool for tailoring scaffold architecture will be useful for future tissue engineering efforts.

REFERENCES

1. O'Brien *et al.* Biomaterials 26 (2005) 433–441
2. Pawelec *et al.* Mater. Sci. Eng. C 37 (2014) 141–147
3. Pawelec *et al.* J. R. Soc. Interface 11 (2014) 20130958

ACKNOWLEDGMENTS

The authors gratefully acknowledge the support of the Gates Cambridge Trust, the Newton Trust, and ERC Advanced Grant 320598 3D-E. A.H. holds a Daphne Jackson fellowship funded by Cambridge University.

Characterization and cytocompatibility of nanocellulose films

K.Hua, D.O.Carlsson, M.Strømme, A.Mihranyan, N.Ferraz

Nanotechnology and Functional Materials, Department of Engineering Sciences, Uppsala University, Sweden
kai.hua@angstrom.uu.se

INTRODUCTION

Characterized by exceptionally high degree of crystallinity, large surface area and broad chemical modifying capacity, nanocellulose deriving from the green algae *Cladophora sp.algae* has a great potential as a natural biomaterial for the development of medical devices and applications in healthcare ^[1]. In this study, we characterized pristine, cationic and anionic *Cladophora* nanocellulose in terms of surface charge, surface topography and specific surface area. The cytocompatibility of the nanomaterial was investigated by studying the behaviour of fibroblasts cultured on the *Cladophora* nanocellulose films.

EXPERIMENTAL METHODS

Cladophora nanocellulose (CC) was modified through glycidyltrimethylammonium chloride (EPTMAC) condensation and TEMPO mediated oxidation to obtain cationic and anionic CC respectively. Films of unmodified, anionic and cationic CC were prepared by vacuum filtration and characterized by measuring their ζ -potential and specific surface area. The surface topographies of the different CC films were observed under scanning electron microscopy (SEM).

In vitro cytocompatibility was investigated by assessing cell adhesion and proliferation on the nanocellulose films. Human dermal fibroblasts (hDF) were cultured on the surface of anionic, cationic and unmodified CC films for 24 h. Cell cultured on thermanox (TMX) served as positive control and cells cultured on TMX in the presence of 5 % DMSO were used as negative control. Cell viability was determined by the Alamar blue assay. Cell adhesion to the cellulose surfaces was studied in terms of cell number and morphology by SEM.

RESULTS AND DISCUSSION

The ζ -potential measurements at pH 7 showed that the surface charge of unmodified, anionic and cationic CC were -12, -41 and 31 mV, respectively. These results confirm that a significant number of negatively and positively charged groups have been introduced to the nanofibers by TEMPO oxidation and EPTMAC condensation respectively.

The specific surface areas of the different CC films were found to be 102 m²/g for unmodified CC (u-CC), 77 m²/g for anionic CC (a-CC) and 70 m²/g for cationic CC (c-CC), showing that the presence of charges resulted in a decrease in specific surface area. SEM micrographs of the CC films revealed that fibers of a-CC have aggregated, featuring co-axially aligned fibers rather than the randomly oriented fibers observed in u-CC and c-CC films (Fig. 1).

The Alamar blue assay showed that cell viability on the a-CC films was not significantly different from the

results of the positive control TMX. However, cells cultured on u-CC and c-CC showed poor cell viability, comparable to the values found for the negative control. SEM micrographs showed that a great number of fibroblasts adhered to the surface of a-CC films and showed typical fibroblast morphology. On the contrary, fewer and mainly round-shaped cells were observed on the c-CC and u-CC films (Fig. 2).

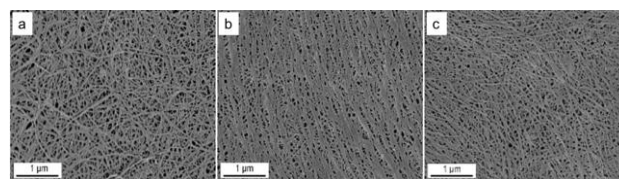


Fig. 1: SEM micrographs of a) unmodified, b) anionic, and c) cationic *Cladophora* nanocellulose films. Note the co-axial alignment of nanofibers in the anionic *Cladophora* nanocellulose film (panel b) compared with the random orientation of the fibers in the unmodified and cationic nanocellulose samples (panels a and c)

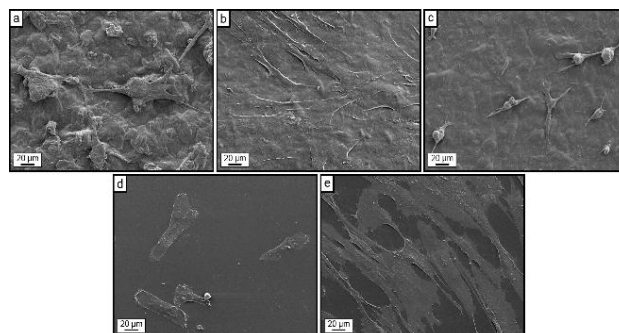


Fig. 2: SEM micrographs of hDF adhered on surfaces of a) unmodified, b), anionic, c) cationic *Cladophora* nanocellulose films, d) Thermanox in the presence of 5% DMSO and e) Thermanox, after 24 hours culture.

CONCLUSION

In this work, we found that a-CC promoted fibroblast adhesion and presented cell viability comparable to the results obtained with the tissue culture material thermanox. However, hDF cultured on u-CC and c-CC showed poor viability. We hypothesize that the distinct aligned nanofiber structure present in the a-CC films is responsible for the improved cell adhesion and viability. The results presented in this work suggest that TEMPO modified *Cladophora* nanocellulose (a-CC) is a good candidate to be further explored in tissue engineering. Other material properties like porosity and degree of crystallinity will be further investigated to relate such physicochemical properties with cell behaviour on the different cellulose materials.

REFERENCES

¹A. Mihranyan (2010) *J Appl Polym Sci* **119**:2449-60.



Bioactive hydrogels supporting angiogenesis produced by EB-irradiation

Bożena Rokita^{1,2}, Sławomir Kadlubowski^{1,2}, Piotr Komorowski^{3,4}, Bogdan Walkowiak^{2,3,4}, Janusz M. Rosiak^{1,2}

¹Technical University of Lodz, Institute of Applied Radiation Chemistry, Wroblewskiego 15. 90-924 Lodz, POLAND,

²Technical University of Lodz, European Centre of Bio and Nanotechnology, Zeromskiego 116. 90-924 Lodz, POLAND,

³Technical University of Lodz, Institute of Materials Science and Engineering, Stefanowskiego 1/15. 90-924 Lodz, POLAND,

⁴BioTechMed Advanced Technology Centre, Stefanowskiego 1/15. 90-924 Lodz, POLAND,
rokitab@mitr.p.lodz.pl

INTRODUCTION

Angiogenesis is the physiological process involving the growth of new blood vessels from pre-existing ones. It is a critical process not only during normal development, but also in pathologic situations, where inadequate vascular evolution contributes to health complications. Angiogenesis is predominantly regulated by local factors that promote or inhibit neovascularization like e.g. AcSDKP (N-acetyl-seryl-aspartyl-lysyl-proline, acetyl-N-Ser-Asp-Lys-Pro)¹ isolated originally from fetal calf bone marrow.

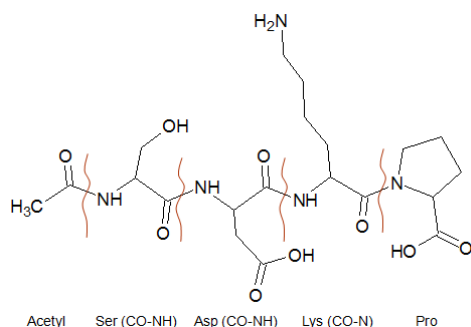


Figure 1. Structure of N-acetyl-Ser-Asp-Lys-Pro

It has been shown that AcSDKP acts as a mediator of angiogenesis which occurs both during embryonic development and in postnatal life. AcSDKP can be used as biologically active supplement in number of different biomaterials². That is why its support in angiogenesis process has been investigated. Because of using ionizing radiation as a method of choice for sterilization, its influence on tetrapeptide has been also studied.

EXPERIMENTAL METHODS

In this work hydrogel matrixes containing polyvinylpyrrolidone – PVP, poly(ethylene glycol) – PEG, agar and tetrapeptide were synthesized using EB-irradiation (25 kGy, 4μs, 50 Hz). Release kinetics of active substance from the hydrogel dressings by high performance liquid chromatography – HPLC and gel swelling kinetics by the gravimetric method were

investigated. The equilibrium swelling degree of hydrogels and gel fraction content were determined. Changes in gene expression of human endothelial cells EA.hy926 (CRL-2922™ ATCC) induced by hydrogel matrix containing AcSDKP were studied using Human Angiogenesis Oligo GEArray System (SABiosciences). Cells were grown, in the presence of hydrogel with AcSDKP, to 80% of confluence. Total RNA was then isolated from the cells. cRNA was obtained in PCR reaction, then it was amplified and labeled with biotin-16-dUTP. The synthesized molecular probe (biotined cRNA) was used for 12 hours of hybridization with oligonucleotide fragments immobilized on microarrays. Chemiluminescent reaction was triggered by an addition of CDP-Star (1,2-dioxetane). Gene expression was determined by the spot darkness analysis on X-ray film (Kodak) by using ImageQuant 300 and ImageQuant TL 8.0 software (GE Healthcare).

RESULTS AND DISCUSSION

It was observed that the amount of active substance released from hydrogel matrix into water at 25 °C reaches the level of 55 - 80% after 6 h. Furthermore, swelling degree of hydrogel matrix in water rises with the amount of active substance and achieves the equilibrium after 160 h swelling. Gel fraction of matrix decreases with increasing amount of AcSDKP. Contact of endothelial cells with hydrogel matrix containing AcSDKP results in a higher level of changes in expression of genes responsible for angiogenesis.

CONCLUSION

Hydrogel based matrix containing acetyl-N-Ser-Asp-Lys-Pro activating angiogenesis process can be synthesized using EB-irradiation technique.

REFERENCES

1. Wang D., *et al.*, AJP-Heart Circ Physiol 287:2099-2105, 2004
2. Fromes Y., *et al.*, Wound Rep Reg 14:306–312, 2006

Ionic liquid-doped and *p*-NIPAAm-based temperature responsive copolymer: Extraordinary entrapping and releasing behaviors of BSA at 38-42 °C

Jae-won Seo^{1,2}, Ueon Sang Shin^{1,2*}

¹Institute of Tissue Regeneration Engineering (ITREN), Dankook University, South Korea

²Department of Nanobiomedical Science & BK21 PIUS NBM Global Research Center for Regenerative Medicine, Dankook University, Cheonan, 330-714, Republic of Korea

*Corresponding author: e-mail) usshin12@dankook.ac.kr

INTRODUCTION

Environmentally sensitive materials have recently attracted considerable attention due to their biomedical application owing to the reversible responses to external stimuli, such as temperature, pH, ionic strength, electric field, magnetic field, light, etc. Poly (N-isopropylacrylamide) (*p*-NIPAAm) and their copolymers are the most well-known thermoresponsive polymers and have been extensively studied for biomedical applications owing to the reversible thermoresponsive phase transition from a hydrated random coil (or a swelled globule) to a deswelled compact globule at the lower critical solution temperature. However, they have limited applicability as a drug delivery system due to the too low LCST (below body temperature), a tedious drug-releasing profile in a wide temperature range (affected by encapsulated drugs and surrounding pH), or too low drug-carrying ability (about <0.35 mg drug per 1.0 mg polymer).

EXPERIMENTAL METHODS

Ionic Liquid (IL)-doping on the temperature responsive *p*-NIPAAm was achieved by radical copolymerization of N-isopropyl acryl amide (NIPAAm; 90 mol%) and 1-butyl-3-vinylimidazolium bromide ([BVIIm]Br; 10 mol%) to give a new temperature responsive copolymer (*p*-NIBIm).

RESULTS AND DISCUSSION

The as-prepared *p*-NIBIm copolymer showed the highly increased Zeta potential value and the optimal LCST (lower critical solution temperatures) value, respectively, +9.8 mV at pH=7 and 38.2 °C, compared to those (+0.3 mV at pH=7 and 32.1 °C) of *p*-NIPAAm. The temperature-dependent size change of the *p*-NIBIm micelles was determined in the range from 25 to 45 °C by SEM under dry condition and by Zeta Sizer under wet condition, showing a certain size contraction from 253±12.1 to 90.5±7.8 nm in diameter (about 95.4 % of volume contraction).

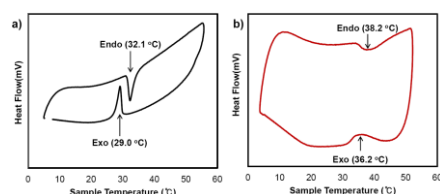


Figure 1. LCST determination of a) *p*-NIPAAm and b) IL-doped *p*-NIBIm using DSC scan.

The thermo-sensitive behaviors to entrap BSA protein at body temperature (37 °C) and to release the protein between 38-42 °C (near the LCST) also were tested by sizing of the complexes of *p*-NIBIm/BSA using Zeta Sizer and also by a colorimetric assay (Bio-Rad DC Protein Assay), resulting in a maximum entrapment of 1.02 mg BSA for 1.0 mg of the polymer at body temperature (37 °C) and in a maximum release of 0.73 mg BSA for 1.0 mg of the polymer (about 73% releasing of the entrapped amount) at the temperature range of 38-42 °C.

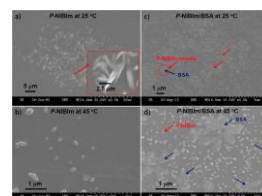


Figure 2. SEM microscopic images of the *p*-NIBIm copolymer and the *p*-NIBIm/BSA complex micelles.

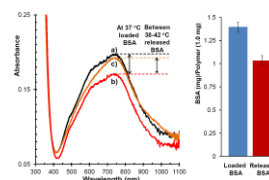


Figure 3. The BSA loading and releasing behavior of the *p*-NIBIm copolymer.

CONCLUSION

These results revealed the IL-doped and temperature responsive co-polymeric system has high applicability as a novel delivery system for negatively charged molecules as a natural (or synthetic) drug and DNA.

REFERENCES

- [1] Ramkissoon-Ganorkar C., Liu F., Baudys M., Kim S. W., J. Controlled Release 59: 287-298, 1999
- [2] Lou S. F., Wang L., Williams G. R., Nie H., Quan J., Zhu L., Colloids and Surfaces B: Biointerfaces, 113: 368-374, 2014
- [3] Luo Y. L., Huang R. J., Zhang L. L., Xu F., Chen Y. S., Colloids and Surfaces A: Physicochem. Eng. Aspects, 436: 1175-1185, 2013

ACKNOWLEDGMENTS

This study was supported by grants (2009-0093829 (Priority Research Centers Program) and 2012-003905) from the National Research Foundation of Korea.

Synthesis of a Bifunctional Silver-containing Biocomposite

Anna A. Ivanova¹, Roman A. Surmenev¹, Maria A. Surmeneva¹, Timur Mukhametkaliyev¹, Kateryna Loza², Oleg Prymak², Matthias Eppler²

¹Department of Theoretical and Experimental Physics, National Research Tomsk Polytechnic University, 634050 Tomsk, Russia

²Inorganic Chemistry and Center for Nanointegration Duisburg-Essen (CeNIDE), University of Duisburg-Essen, 45117 Essen, Germany, rsurmenev@mail.ru

INTRODUCTION

A long-term antibacterial ability of a biomaterial is desirable in order to prevent implant associated infection. Therefore, modification of implant surfaces is in the focus of many scientists worldwide [1]. The present study is directed towards the modification of metal implant properties to produce predictable clinical results of implant osseointegration by developing of a biocomposite ensuring both a higher bioactivity and prolonged antibacterial activity. Through the use of nanofabrication techniques a multifunctional biocomposite containing hydroxyapatite (HA) and silver nanoparticles (AgNPs) has been fabricated.

EXPERIMENTAL METHODS

PVP-coated silver nanoparticles were synthesized by a wet chemical reduction method of silver nitrate using glucose as a reductant and polyvinylpyrrolidone as a stabilizer [2]. AgNPs were deposited onto titanium substrate via dripping/drying technique and were further covered with CaP coating by means of RF-magnetron sputtering [3, 4]. A commercially available installation with a RF-magnetron source (COMDEL, 13.56 MHz) was used. The coating was deposited at an RF-power level of 500 W in Ar atmosphere at grounded substrate holder for 180 min. A target for sputtering was prepared from hydroxyapatite ($\text{Ca}_{10}(\text{PO}_4)_6\text{OH}_2$, HA). The morphology and composition of the samples on each preparation stage were estimated by SEM using an ESEM Quanta 400 FEG instrument equipped with EDX (Genesis 4000, SUTW-Si(Li) detector) operating in a high vacuum with gold/palladium-sputtered samples. To determine the internal structure and phase composition of studied thin films the Grazing-incidence small-angle X-ray scattering (GISAXS) was used.

RESULTS AND DISCUSSION

The negatively charged silver nanoparticles (zeta potential -21 mV) with a spherical shape and a diameter of the metallic core 50 ± 20 nm were coated with dense, nanocrystalline CaP film. X-ray diffraction studies showed that the synthesized HA film was nanocrystalline with hexagonal structure. The diffraction patterns of the formed coatings showed peaks corresponding to HA: 25.8° (002), 31.7° (211), 32.2° (112). Three peaks attributable to metallic silver low intensity at 46.3° (200), 64.5° (220) and 81.5° (222) are also observed. Meanwhile, the most intense Ag x-ray emission line at 38° (111) is overlapped by the line of Ti (002). SEM of the cross section in backscattering mode showed the layer of silver nanoparticles below the CaP layer (Fig.1). The release of Ag ions from the developed biocomposite in phosphate buffer was

evaluated via Atomic Adsorption Spectroscopy (AAS). The cumulative concentration of Ag^+ within 7 days of immersion was 0.27 ± 0.02 $\mu\text{g/mL}$, which is below the cytotoxic level of Ag ions found in the literature [5].

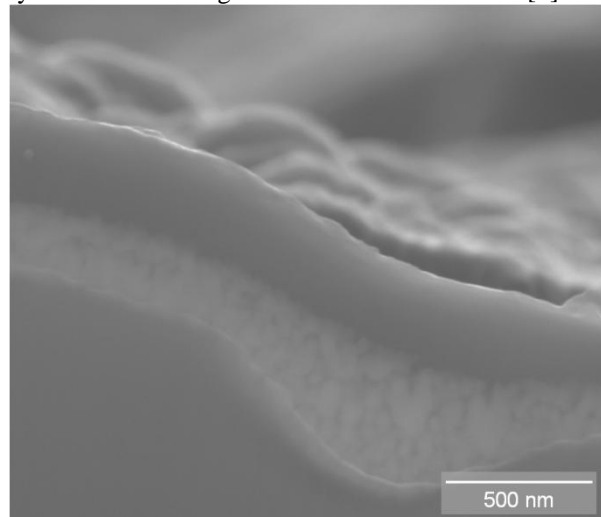


Fig. 1. SEM images of the composite cross-section representing the superposition of the images obtained in a second electron beam and backscattering reflections.

CONCLUSION

We suppose that the release behavior of Ag ions from the developed biocomposite could be adjusted by controlling the initial concentration of AgNPs on the substrate surface and HA coating structure. So, proposed approach seems to be promising to design a novel tunable antimicrobial biocomposite.

ACKNOWLEDGMENTS

This work was supported by the German-Russian Interdisciplinary Science Center (G-RISC) funded by the German Federal Foreign Office via the German Academic Exchange Service (DAAD), Eranet Mundus scholarship, President's Stipend SP-6664.2013.4, FP7 Marie Curie grant (327701), the Russian Fund for Basic Research (13-08-98082, 14-08-31027 mol-a) and MK-485.2014

REFERENCES

1. D.R. Monteiro, et al. Int. J. Antimicrob. Agents 34:103, 2009.
2. C. Greulich, et al, Acta Biomater. 7:347, 2011.
3. R.A. Surmenev, et al., Acta Biomaterialia. 10(2):557, 2014.
4. R.A. Surmenev, Surf. Coat. Technol. 206(8-9): 2035, 2012.
5. C. Greulich, et al., Rsc Advances. 2(17): 6981, 2012.



Osteoinduction and survival of human osteosarcoma MG-63 cells on nanoporous hydroxyapatite scaffolds

M. Beaufils-Hugot^{1*}, F. Burgio¹, S. Stevanovic¹, P. Chavanne¹, O. Braissant², P. Gruner³, R. Schumacher¹, U. Pieves¹

^{1*}FHNW, University of Applied Sciences and Arts of Northwestern Switzerland, Muttenz CH, marina.beaufils@fhnw.ch

²LOB2, Laboratory of Biomechanics & Biocalorimetry, University of Basel, Basel CH

³Medicoat AG, Mägenwil CH

INTRODUCTION

3-D printed hydroxyapatite (HA) scaffolds with defined macro porosity have emerged as attractive biomaterials in tissue engineering. In order to reinforce their compressive strength (CS) and change their properties, a combination of additives like biocompatible synthetic or natural (bio)polymers during the printing process, and extracellular matrix (ECM) generated by osteoblast-like cells, have been investigated. Osteoblasts are specialised fibroblasts that secrete and mineralise the bone matrix by regulating calcium deposition and mineralization. In our study, a human preosteoblast cell line (MG-63) was used as a model. Some preliminary experiments have been investigated *in vitro* to characterize the MG-63 differentiation on HA scaffolds by (a) cell proliferation, (b) matrix maturation and (c) matrix mineralisation studies.

EXPERIMENTAL METHODS

Scanning electron microscopy (SEM), MTT assay and Confocal Laser scanning microscopy (CLSM) were used to evaluate cell adhesion on HA scaffolds. Osteoblast differentiation was evaluated by determining alkaline phosphatase (ALP) activity at day 1, 3, 5, 14, 21. To quantify osteoblast differentiation, the mRNA expression of several osteoblast marker genes (ALP, OC, COL and Runx2) was assessed by a quantitative real-time polymerase chain reaction (qRT-PCR).

RESULTS AND DISCUSSION

When 10^5 cells per scaffold were seeded, cell number gradually increased with 7-fold higher after 14 days in comparison with day 1. After induction of ECM production with osteoblast stimulators (OS), qRT-PCR analysis showed a significant 9-fold increased for ALP expression (early differentiation marker) at day 3 in comparison with day 1. The matrix maturation was observed by SEM analysis (Fig 1) from day 5 to 21, and osteocalcin (mineralisation marker) was detected by immunofluorescence staining after 24 days (Fig 2B). Our preliminary studies demonstrated that MG-63 cells attached and proliferated as a monolayer over time on HA scaffolds (Fig. 2A). Our work proved also the ability of these cells to produce visible ECM after 14 days and, exhibit some mineralization indicator by the presence of osteocalcin after 24 days.

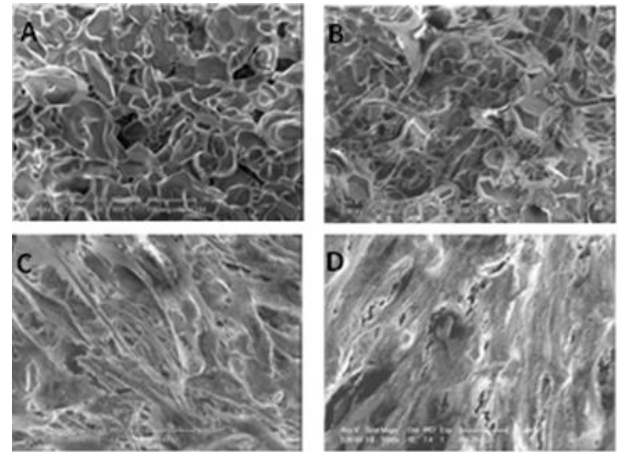


Fig. 1: SEM images of 3D-printed HA scaffolds without MG-63 cells A), and with MG-63 after 5 days B), after 14 days C), and after 21 days D) of differentiation.

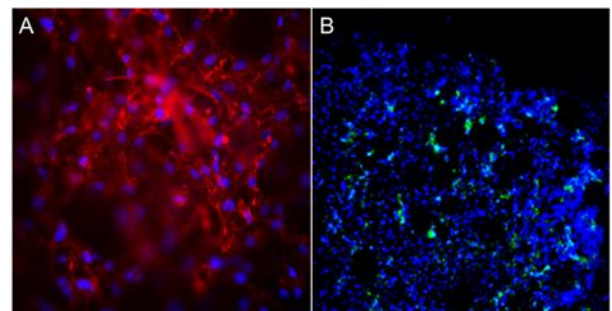


Fig 2: Immunofluorescence staining of MG-63 on HA scaffolds. Cytoskeleton (red) and nuclei (blue) showed the distribution of the cells after 10 days of differentiation A), and Osteocalcin (green) expression was observed after 24 days of differentiation B).

CONCLUSION

After these preliminary results with a cell model, long-term mineralization studies *in vitro* will be performed with stem cells under “dynamic” conditions (Perfusion Bioreactor) to get homogeneous cell distribution and higher level of mineralization.

REFERENCES

1. Chavanne P., Stevanovic S., Braissant O., Pieves U., Gruner P., Schumacher R., 3D printed chitosan/hydroxyapatite scaffolds for potential use in regenerative medicine, Biomed Tech (Berl)., Issue 58, 2013.

ACKNOWLEDGMENTS

This work is supported by a grant from the Schweizerischer Nationalfonds (SNF) (Grant number: 51NF40-144618).

Protein Adsorption onto Polymer-based Nanocarriers for Vaccine Delivery

Nitesh Kunda*, Gillian Hutcheon and Imran Saleem

School of Pharmacy and Biomolecular Sciences, Liverpool John Moores University, Liverpool, UK,
N.K.Kunda@2011.ljmu.ac.uk

INTRODUCTION

Progress in the vaccine technology has been to deliver the antigens by micro or nanoparticles (NPs). Particulate systems utilising polymers such as polylactic acid (PLA), polylactic-co-glycolic acid (PLGA), chitosan, alginate, polyanhydride, poly(glycerol adipate-co- ω -pentadecalactone) (PGA-co-PDL) etc. have been widely investigated^{1,2}. In addition, the biodegradable polymeric NPs offer numerous advantages such as controlled or sustained drug release, biocompatibility with the surrounding tissues and cells, lower toxicity compared to non-biodegradable polymers, are non-thrombogenic, act as adjuvants and are more stable in blood³.

The pulmonary route for vaccine delivery has gained significant attention due to an abundance of antigen presenting cells (such as macrophages, dendritic cells (DCs)) for targeting antigens⁴.

In this study, we adsorbed a model protein, bovine serum albumin (BSA), onto PGA-co-PDL NPs, and formulate into nanocomposite microparticles (NCMPs) for pulmonary vaccine delivery via dry powder inhalation.

EXPERIMENTAL METHODS

NPs were prepared by a modified oil-in-water (O/W) single emulsion solvent evaporation method. Particle size, polydispersity index (PDI) and zeta-potential were characterised using laser diffraction. The NPs were centrifuged and BSA was adsorbed onto NPs at different ratios from 100: 4 to 100: 20 (NPs: BSA) for 1 h. The effect of time on adsorption was evaluated using 100: 20 (NPs: BSA) for 30 min, 1, 2 and 24 h. The protein adsorbed was evaluated using micro BCA protein assay kit. The BSA adsorbed NPs were spray-dried using L-leucine (1: 1.5, NPs: L-leu) for pulmonary delivery. The resultant nanocomposite microparticles (NCMPs) were characterised for protein stability using SDS-PAGE and *in vitro* toxicity (MTT assay, A549 cell line).

RESULTS AND DISCUSSION

NPs of size 128.50 ± 6.57 nm, PDI 0.07 ± 0.03 and zeta-potential -24.56 ± 0.50 mV were produced indicating its suitability for targeting lung DCs.

The adsorption of BSA, μ g per mg of NPs, increased significantly from 100:4 (NP:BSA) loading concentration (4.75 ± 0.39) to 100: 20 (10.23 ± 1.87) (Fig 1). In addition, for 100: 20 (NP: BSA) loading concentration, the average adsorption increased significantly from 30 min (1.84 ± 0.82) to 1 h

(10.23 ± 1.87) with no significant difference beyond 1 h compared to that of 2 and 24 h indicating maximum adsorption at 1 h.

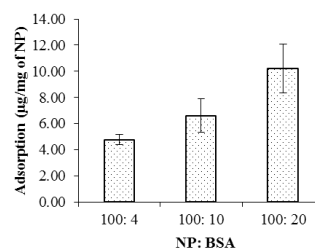


Fig 1: Amount of BSA adsorbed per mg of NPs at different concentrations (NP: BSA) (Mean \pm SD, n=3)

Langmuir (LM) and Freundlich (FM) models have been employed to study the relation between the amount of protein adsorbed effectively onto the NPs and the protein concentration in the solution at equilibrium. The regression coefficient (r^2 , LM ≥ 0.93 ; FM ≥ 0.98) was obtained for LM (C_e/Q_e vs C_e), FM ($\log C_e$ vs $\log Q_e$) where Q_e is the amount of protein adsorbed (μ g/mg) and C_e is the concentration in equilibrium (μ g/ml). The data fits the FM suggesting multilayer type of protein deposition onto PGA-co-PDL NPs surface, resulting from the competition of protein molecules to the particle surface. The LM does not consider the multiple sites available for adsorption nor the protein-protein interactions⁵.

The BSA adsorbed PGA-co-PDL NPs were spray-dried with L-leu resulting in NCMPs. The released BSA from NCMPs was analysed for stability using SDS-PAGE and the bands for released BSA were identical to the standard BSA indicating that the stability not affected by formulation processes. MTT assay showed cell-viability of $87.01 \pm 14.11\%$ at 1.25 mg/ml concentration after 24 h exposure indicating a good toxicity profile.

CONCLUSION

The results indicate effective BSA adsorption onto the surface of PGA-co-PDL NPs with BSA stable after spray-drying. In addition, the NCMPs displayed a good toxicity profile. This provides an indication about the feasibility of using PGA-co-PDL polymers as safe carriers for pulmonary vaccine delivery.

REFERENCES

- Alpar HO. *et al.*, Eur. J. Pharm. Biopharm. 40(4): 198-202
- Tawfeek HM. *et al.*, Int J Pharm. 441(1-2): 611-9
- Panyam J. *et al.*, Adv. Drug Delivery Rev. 55:329-347
- Scheuch G. *et al.*, Adv. Drug Delivery Rev. 58:996-1008
- Florindo HF. *et al.*, Int J Pharm. 390: 25-31

Surface functionalization of electro-spun Poly(L)Lactic Acid scaffolds with heparin to induce angiogenesis

Giulia Gigliobianco*, Sabiniano Roman, Chuh K. Chong and Sheila MacNeil

Kroto Research Institute, University of Sheffield, Sheffield, S3 7HQ, UK, email: dtp11gg@sheffield.ac.uk

INTRODUCTION

Delays in new blood vessel formation after implantation of a tissue-engineered construct within the host is a major limiting factor for the long survival of the constructs [1]. Smarter biomaterials are needed to be able to induce angiogenesis post-implantation and keep the newly formed tissue alive. Hence, biomaterials can be designed to be specifically functionalised for this purpose. The aim of this study is to develop a versatile approach to modifying scaffolds to induce angiogenesis once implanted.

EXPERIMENTAL METHODS

Electrospun PLA scaffolds were plasma polymerized with PolyAcrylic Acid (PAA) and coated with alternative layers of PolyEthyleneImine (PEI) and PAA or PEI and Heparin for a total of seven layers, in a layer-by-layer (LBL) coating approach. Coated scaffolds were then dipped in heparin solution, dried and immersed in Vascular Endothelial Growth Factor (VEGF) solution. Surface chemistry was verified by X-Ray Photon Electron Spectroscopy. An ELISA was used to quantify the amount of VEGF bound to the scaffolds. The Chick Chorionic Allantoic Membrane (CAM) assay was used to assess *in-vivo* the angiogenic potential of the scaffolds over a period of 7 days.

RESULTS AND DISCUSSION

XPS showed that plasma polymerization of the scaffolds with PAA was successful as the presence of S indicates Heparin is present. Heparin bound well to LBL-coated scaffolds, compared to non-functionalised scaffolds, and showed an increase in VEGF binding. The CAM assay showed that the functionalized scaffolds induced blood vessel formation compared to non-functionalised scaffolds.

Table 1. Atomic ratios of elements present on the surface of different scaffolds, normalized by the amount of carbon atoms present (C= carbon, N=Nitrogen, S=Sulphur, O=Oxygen).

Type of Scaffold	Atomic Ratios		
	O/C	N/C	S/C
Not-functionalized PLLA	0.375	0.011	0.000
1 layer functionalized PLLA	0.468	0.128	0.052
5 layers functionalized PLLA	0.542	0.155	0.076
7 layers functionalized PLLA	0.546	0.149	0.082

CONCLUSION

The LBL functionalization we describe allows heparin to be bound to the surface of the scaffold which can in turn bind VEGF. The CAM assay demonstrated that this bound VEGF is functional inducing directed neovascularisation. We conclude that this protocol (which can be applied to a range of scaffolds) offers a new approach to tackling the problems of delayed angiogenesis for tissue engineering. can liberate us by displaying our authenticity.”

REFERENCES

1. Lovett, M., et al., *Vascularization Strategies for Tissue Engineering*. Tissue Engineering Part B-Reviews, 2009. 15(3): p. 353-370.

ACKNOWLEDGMENTS

X-ray photoelectron spectra were obtained at the National EPSRC XPS User's Service (NEXUS) at Newcastle University, an EPSRC Mid-Range Facility.

Neuronal Growth on Nano-Pillar Substrates

Nahoko Kasai, Rick Lu, Touichiro Goto, Yoshiaki Kashimura, Azusa Oshima and Koji Sumitomo

NTT Basic Research Laboratories/NTT Corporation, Atsugi, Japan
kasai.nahoko@lab.ntt.co.jp

INTRODUCTION

An artificial synapse is a nano-micro-meter scale nano-biodevice that mimics neuronal synaptic functions (Figure 1). With the aim of realizing an artificial synapse, we have succeeded in forming a suspended lipid bilayer on a well [1] and examined the activity of an ion channel reconstituted in the lipid [2]. We have used scanning electron microscopy (SEM) to observe neurons and their interface with substrates to examine the optimal conditions for neuronal growth, and we have also observed the morphological changes in neurons induced by cell death [3].

In this study, we used the above SEM technique combined with nano-meter-scale fabrication technology to examine neuronal growth on a glass substrate consisting of nano-pillars. We employed this approach to investigate neuronal preferences, which determine the growing direction. This study will contribute to the control of neuronal growth when implementing artificial synapses.

EXPERIMENTAL METHODS

Amorphous silicon (a-Si) nano-pillars were fabricated on quartz substrates using electron-beam lithography. The pillar height was 500 nm, the pillar diameter was either 100 or 500 nm, and the distance was either twice or four times the pillar diameter. Rat cortical neurons were obtained from Wister rat cortex (embryonic 18 days), and cultivated on the nano-pillar substrate, without coatings, for 7 days in a neurobasal medium with L-glutamine, glutamate, gentamycin, and 2% B27 supplement, at 37 °C in 5% CO₂. After cultivation, the cells were fixed in two steps; the first was fixation with

paraformaldehyde (PFA) and glutaraldehyde (GA), and the second was fixation with osmium tetroxide (OsO₄). Then the cells were dehydrated using ethanol and freeze-dried in t-butanol.

RESULTS AND DISCUSSION

Figure 2 shows SEM images of tips of neurites, called growth cones and filopodia, cultivated on the nano-pillar substrates. Filopodia, which are thought to sense and to determine the growth direction, were successfully observed as they developed from growth cones attached to the nano-pillars (Fig. 2a,b). The widths of filopodia on different patterned substrates (Fig. 2c) indicated that the filopodia were wider with larger pillar diameters, and thinner on thin pillars. However their width was not greatly affected by the pillar distance.

These results suggested that the filopodia detected the pillars as an environment and that they changed their widths to enable them attach and to grow.

CONCLUSION

Although we must undertake a more detailed examination, this study demonstrated the possibility of controlling neuronal growing conditions using nano-pillar substrates. This will contribute to the development of artificial synapses, and also new nano-bio interfaces.

REFERENCES

1. Shinozaki Y. *et al.*, Appl. Phys. Express 3:027002, 2010.
2. Sumitomo K. *et al.*, Biosens. Bioelectron. 31:445, 2012.
3. Shinozaki Y. *et al.*, Appl. Phys. Express 4:107001, 2011.
3. Kasai N. *et al.*, e-J. Surf. Sci. Nanotechnol. in press.

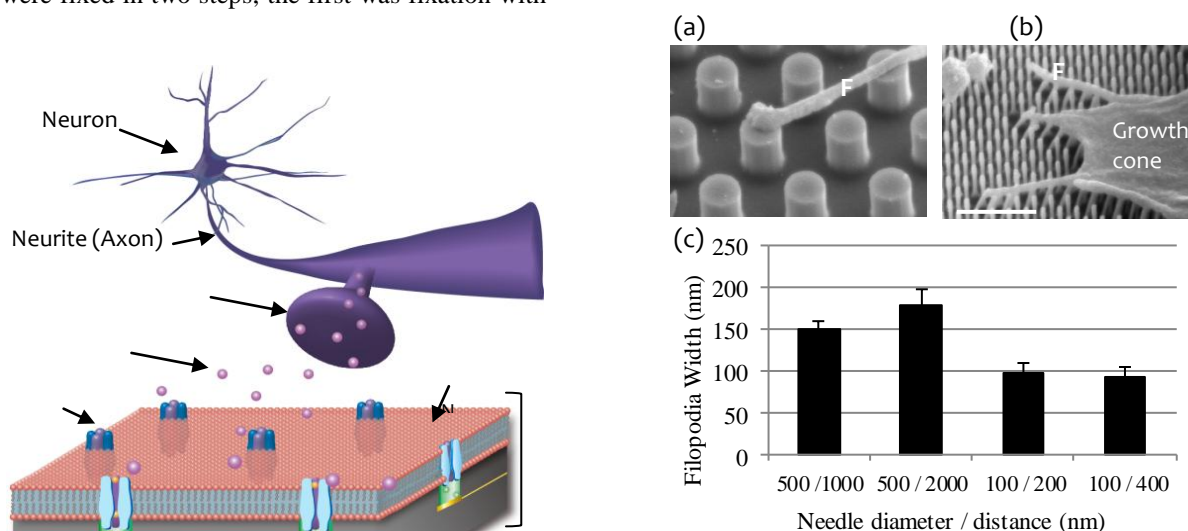


Figure 2 SEM images of tip of neuritis, growth cone and filopodia (a, b) and the filopodia widths (c) on nano-pillar substrates. Pillar diameters / distances were 500 / 1000 nm (a) and 100 / 200 nm (b). White bar: 1 μ m, F: filopodia. Error bar: standard error.

Biodegradable and Bioadhesive Hemostatics Comprising Polymer Complex Gel and Chitosan

Tomoko Ito, Masazumi Eriguchi and Yoshiyuki Koyama*

*Japan Anti-tuberculosis Association, Shin-Yamanote Hospital, Japan, ykoyama@shinyamanote.jp

INTRODUCTION

Local hemostasis is sometimes difficult especially in patients taking anticoagulant. When the patient taking anticoagulant underwent tooth extraction, dental surgery operation, or gastrointestinal endoscopy, they used to be indicated to quit taking the drug for several days prior to the surgery. However, serious adverse side effects such as formation of thrombosis were sometimes observed. They are, thus, now instructed not to stop taking the drug. Patient of this type should have periodic blood coagulation test, but blood sampling often caused prolonged and continuous bleeding. For such difficult-to-control bleeding, safe and efficient hemostatic device is desired.

We focused on a hydrogen bonding gel consisting of Poly(acrylic acid) (PAA) and poly(vinylpyrrolidone) (PVP), which are both highly safe synthetic polymers approved as pharmaceutical excipients. When PAA and PVP are directly mixed in water, soft hydrogel is immediately formed, but soon precipitated as a insoluble solid. Resulting rigid gel is not swelled, nor dissolved in water. Recently, we succeeded in preparation of a water-swellaable PAA/PVP spongy sheet by regulating the movement of polymer molecules. It formed a soft hydrogel on wet tissue, and strongly stick to it. Then, we applied it to patients taking anticoagulant medicines to control the bleeding after tooth extraction. Soon after putting on the bleeding site, the PAA/PVP sponge swelled to a hydrogel, tightly adhered to the tissue, and arrested the haemorrhage, effectively. However, it was sometimes difficult to achieve satisfactory hemostatsis in the patients with high PT-INR.

In this study, chitosan (CS), a blood-coagulating polysaccharide, was employed to improve the hemostatic effect of the gel. Here, we introduced CS into PAA/PVP spongy sheet, and application of the CS containing hemostatic device to patients with high PT-INR was attempted.

EXPERIMENTAL METHODS

Preparation of PAA/PVP/CS spongy sheet: PAA solution was dried up to a clear film. PVP aqueous solution containing CS was then poured upon the PAA film. It was then freeze dried, and spongy sheet was obtained.

Hemostatic effect on mice: Mice were injected with 50 IU of fragmin, a low molecular weight heparin. They were anesthetized by pentobarbital, and the skin over the femur was incised to expose the femoral vein. Soon after cutting the vein, PAA/PVP/CS sponge was put on the bleeding site, and hemostatic behavior was observed.

Clinical study: Clinical study was carried out on the patients taking the anticoagulant medicine after tooth

extraction. PAA/PVP/CS spongy sheet was placed on the bleeding socket, soon after the extraction, and hemostatic effect and recovery condition was observed.

RESULTS AND DISCUSSION

Mixing of the aqueous solutions of PAA and PVP results in formation of water-insoluble, and -inswellable precipitate. On the other hand, pouring PVP solution onto a dried PAA film, followed by lyophilization afforded a water-swellaable white spongy sheet. CS-containing sponge was similarly prepared by adding CS to the PVP solution, previously. PAA/PVP/CS spongy sheet immediately swelled on a wet tissue, and firmly stuck to it. Their adhesion strength was more than 50 g/cm².

Hemostatic effect of the spongy sheet was examined on the mouse treated with 50 IU of fragmin. The femoral vein was exposed and cut. The water-swellaable PAA/PVP or PAA/PVP/CS spongy sheet was placed on the bleeding site. When the thin PAA/PVP sheet without CS was put on the heavily bleeding site, spongy sheet sometimes got a hole in minutes being dissolved by the blood. Thick, or piled sheet was required for complete hemostasis. On the other hand, the treatment by the CS-containing PAA/PVP sheet effectively stopped the bleeding, and single thin spongy sheet could achieved immediate hemostasis.

Clinical study of the PAA/PVP/CS spongy sheet to control the bleeding after tooth extraction was performed on the patient taking anticoagulant medicine such as bayaspirin or warfarin. After tooth extraction, the PAA/PVP/CS spongy sheet was placed into the bleeding socket. The sponge absorbed the blood, and swelled to a hydrogel. It adhered to a bleeding site, and arrested the hemorrhage effectively, even in the anticoagulated patients.

CONCLUSION

Water-swellaable PAA/PVP/CS sponge could be obtained under certain particular conditions. It showed high hemostatic efficiency in mice treated with a large amount of heparin. Excellent efficacy of the sponge as a hemostatic device was also confirmed in the clinical studies, and no adverse side effect was as yet observed. Further clinical study is now ongoing.

ACKNOWLEDGMENTS

We Thank CBC Co., Ltd, and BASF Japan Ltd, for providing PAA and PVP, respectively. Kewpie Corp. and Shiseido Co., Ltd are also acknowledged for supplying HA. This work was partly supported by The MIKIYA Science And Technology Foundation, and Golden Orchid Brothers Inc..



The Effect of Water Saturation on the Compressive Properties of Calcium Sulphate Dihydrate

I Koh^{*1}, A López², B Helgason¹ and S Ferguson¹

¹Institute for Biomechanics, ETH-Zürich, Switzerland

²Division of Applied Material Science, Uppsala University, Sweden, ikoh@ethz.ch

INTRODUCTION

In the past years, ceramic cements started to gain popularity as biomaterials for musculoskeletal reconstruction due to their biological advantages. Characterisation of the biological and mechanical properties of newly developed ceramic cements is essential, and needs to be performed prior to clinical application. The mechanical properties of ceramic cements are often tested using an international testing standard developed for ductile acrylic cements and performed mostly in a dry condition. Given that ceramic cements are known to be brittle and degradable, the testing standard designed for ductile materials may not be suitable for ceramic cements. Therefore, the aim of the current study was to evaluate the suitability of the testing standard on dry and wet ceramic cements. The study was performed using calcium sulphate dihydrate (CSD).

EXPERIMENTAL METHODS

160 CSD cylinders (aspect ratio=2) were prepared by mixing β -CSH powder and water (L/P-ratio=0.67). Cylindrical Teflon molds were filled with slurries and vibrated on a vibration table for 5 minutes to remove entrapped air. The resulting CSD cylinders were removed from the mold and dried at room temperature for 21 days. The cylinders were randomly divided into four groups having different saturation levels (dry, wet) and end conditions (capped, non-capped). The cylinders in the wet groups were immersed in PBS for 24 hours prior to the test. Aluminium caps were glued to the end surfaces of the cylinders in the capped groups. Unconfined compression tests to failure were performed on all prepared cylinders. Specimen deformation was measured using two different methods (platen-to-platen, extensometer). Two effective moduli were derived, E_p and E_e (platen-derived and extensometer-derived, respectively). The moduli were compared between the groups to determine the effect of saturation level, end conditions and measurement methods. The testing standard developed for acrylic cement prescribes non-capped specimens and platen-derived displacement.

RESULTS AND DISCUSSION

The end condition in the wet group did not influence E_e . However, E_p of the wet capped group was higher than E_p of the wet non-capped group. This can be explained by the chemical and physical changes of CSD with water saturation. The formation of CSD is a reversible reaction. This means, reintroduction of water to CSD induces crystal dissociation, reducing the occurrence or weakening the crystal interlocks. As a result, the

mechanical strength of CSD decreases [1]. In addition, water molecules allocated within the CSD may act as a lubricant, reducing the frictional resistance, hence shear strength, at the crystal interlocks [1]. As a combined effect of reduced occurrence of crystal interlocks and frictional resistance, local shear deformation and damage at the platen-sample boundary (end effect) occur in wet non-capped specimens. Due to these local deformations and damage, the platen records a larger deformation than the extensometer, hence a lower E_p compared to E_e in non-capped samples.

On the other hand, the end condition in the dry group did not affect the moduli, when the same displacement measurement was used. This indicates that the end effect arises only in the presence of water.

The results indicate that the commonly adopted testing standard developed for ductile acrylic cement may not be suitable when wet ceramic cements are tested to determine effective modulus. It is suggested to use endcaps and/or an extensometer to measure displacements. These techniques remove and avoid the end effect respectively.

	Dry		Wet	
	Cap	NoCap	Cap	NoCap
E_p (GPa)	4.6±0.5	4.6±0.7	1.7±0.5	0.9±0.3
E_e (GPa)	6.3±1.5	5.7±1.3	1.9±0.3	1.7±0.5

Table 1 shows the summary of effective E-moduli derived using two different deformation measurement methods. Four groups having different saturation level and end-conditions were compared (Mean±SD).

CONCLUSION

It was found that water saturation substantially alters the mechanical properties of CSD. It is proposed that crystal dissociation and reduction in interstitial frictional resistance reduce the strength of the material. The reduction in the strength causes local shear deformation and damage at the platen-sample boundary (end effect). It is suggested to use endcaps and/or an extensometer to determine the effective elastic modulus of wet ceramic cements.

REFERENCES

1. Andrews H., J Chem Technol Biotechnol. 65:125-128, 1946

ACKNOWLEDGMENTS

Funding for this project was provided by the European Union through a Marie Curie action (FPT7-PITN-GA-2009-238690-SPINEFX).



Flexural Properties of Calcium Sulphate Dihydrate and Dicalcium Phosphate Dihydrate: Potential Role of Degradation with Water Saturation

I Koh*, B Helgason and S Ferguson

¹Institute for Biomechanics, ETH-Zürich, Switzerland, ikoh@ethz.ch

INTRODUCTION

Vertebroplasty is a common surgical procedure used to augment weakened vertebrae caused by osteoporosis or metastasis. In the recent years, studies were conducted to extend the usage of vertebroplasty for the treatment of young patients with complex vertebrae fractures [1]. The application of vertebroplasty in complex fractures is promising, when the biological advantages of ceramic cements are considered (osteoconductive, osteogenic). However, our own simulations indicate that the cement augmenting a complex fractured vertebra experiences tensile/flexural stresses under physiological, multi-axial loads, due to interfragmentary movement. Newly developed ceramic cements are commonly tested only under compression in dry conditions. To obtain complete tensile/flexural properties of ceramic cements, two common ceramic cements, calcium sulphate dihydrate (CSD) and dicalcium phosphate dihydrate (DCPD), were tested in 3-point bending in both dry and wet conditions. The results were used to identify the changes in the flexural properties of CSD and DCPD due to water saturation.

EXPERIMENTAL METHODS

67 CSD and 80 DCPD beams (90x8x6mm) were prepared for 3-point bending tests. CSD beams were prepared by mixing β -CSH and water (L/P ratio=0.67), while DCPD beams were prepared by mixing equimolar fractions of β -TCP and MCPM, and water (L/P ratio=0.5). Custom designed aluminium molds were filled with slurries of CSD and DCPD. The molds were placed on a vibrating table for 5 and 1 minute, respectively, to remove entrapped air. The beams were removed from the molds and air dried at room temperature for 21 days. 24 hours prior to the testing, 34 CSD and 40 DCPD beams were immersed in separate baths of PBS. This resulted in four different testing groups of: dry and wet CSD and dry and wet DCPD. 3-point bending tests were performed on an Instron at a crosshead speed of 1mm/min until failure. A custom made 3-point bending apparatus (designed according to ASTM standard [2]) was used to accommodate imprecise beam geometry. Effective flexural strength (strength) and modulus (modulus) as well as deflection at failure (deflection) were calculated.

RESULTS AND DISCUSSION

CSD had higher strengths than DCPD in both dry and wet groups (Table 1). Both CSD and DCPD showed lower strength in the wet groups. The observed strength reduction due to water saturation was higher in DCPD (74%) than CSD (58%). The reduction of compressive strength in water-saturated ceramic cements is commonly explained as a result of degradation.

However, given that the reduction in the strength of DCPD (with lower degradation rate) was higher than CSD (with higher degradation rate), the dissociation of crystals cannot fully explain the results observed in this study. Therefore, the existence of a different mechanism (other than crystal dissociation) that lowers the strength of DCPD or a factor that facilitates the degradation of DCPD is cautiously proposed.

The deflection of dry CSD at failure was equivalent to the deflection of wet CSD. However, wet DCPD showed a 56% lower deflection, compared to dry DCPD. This reflects the differences in the percentage reduction in strength and modulus. While the reduction of the CSD strength (58%) was matched by the reduction of the modulus (57%), the reduction of the DCPD strength (74%) was greater than the reduction of the modulus (46%) (Table 1). The larger reduction in the strength further supports the proposed differential degradation of DCPD.

Given that the degradation kinetics of DCPD is not fully understood, it is difficult to provide an accurate reasoning behind the results of the current study. Therefore, to better understand the dynamic mechanical properties of degradable ceramic cement, a series of carefully designed studies are required to determine the role of possible factors on the degradation of such cements.

	CSD		DCPD	
	Dry	Wet	Dry	Wet
Strength (MPa)	3.0	1.2	1.9	0.5
Modulus (GPa)	9.0	3.9	9.4	5.1
Deflection (mm)	0.14	0.14	0.09	0.04

Table 1 shows the summary of flexural test results (mean).

CONCLUSION

In conclusion, the influence of water saturation on is significantly different in CSD and DCPD cements. Further experiments examining the degradation kinetics of ceramic cements are required.

REFERENCES

1. Tarsuslugil S. *et al.*, Ann Biomed Eng, 42(4):751-761, 2014
2. ASTM, C1161, 2013

ACKNOWLEDGMENTS

Funding for this project was provided by the European Union through a Marie Curie action (FPT7-PITN-GA-2009-238690-SPINEFX). Informative discussions with Alejandro López on the potential medical applications of ceramic cements are gratefully acknowledged.



Osteoconductivity of Super Hydrophilic Valve Metals and Titanium Alloys

Kensuke Kuroda^{1*} and Masazumi Okido²

^{1*} EcoTopia Science Institute, Nagoya University, Japan, kkuroda@numse.nagoya-u.ac.jp

² EcoTopia Science Institute, Nagoya University, Japan

INTRODUCTION

Valve metals, such as titanium, niobium, tantalum, and zirconium, and also their alloys are widely attracted as bone-substitutional materials in dental and orthopaedic fields because they have high resistance to corrosion. It is important to modify the surface chemical characteristics to improve the osteoconductivity because of their poor bone-forming properties, for example, using hydroxyapatite¹ or oxide coatings².

Hydrophilicity of biomaterials surface is considered to be one of the most important properties to influence on the osteoconductivity. In this study, super hydrophilic surface was tried to attain on valve metals and their alloys using hydrothermal treatment, and their osteoconductivity was then evaluated in *in vivo* testing.

EXPERIMENTAL METHODS

Valve metals and their alloys (Ti, Nb, Ta, Zr, Ti6Al4V, Ti6Al7Nb, Ti29Nb13Ta4.6Zr) were polished with 0.05 mm Al₂O₃ powder and mirror finishing (Ra / μm < 0.15). Hydrothermal treatment of each sample was carried out in distilled water to obtain the hydrophilic surface at 180 °C for 3 h, and the hydrophilic samples were kept in the phosphate buffered saline solution (PBS) with 5 times concentration: 5PBS(-) in room temperature in order to maintain and improve the hydrophilicity. Surface characterizations of the samples were evaluated using SEM and XRD, XPS, water contact angle (WCA) measurement (2 mL), and the surface roughness. The surface roughness of the samples was measured using a laser microscope, and expressed with the average roughness, Ra (analysis area 150 × 112 μm). In *in vivo* testing, the rod samples ($\phi 2 \times 5$ mm) were implanted in male rat's tibiae for 14 days and the bone-implant contact ratio, BIC, was used to evaluate the osteoconductivity in the cortical and cancellous bone parts, respectively.

RESULTS AND DISCUSSION

The hydrothermal treated samples had thin oxide film, their surface roughness was equivalent to as-polished substrates. As-polished samples had WCA= ca. 70 deg. and hydrothermal treatment gave hydrophilic surface around WCA=15 deg. XPS analysis of the sample surface before and after hydrothermal treatment revealed that the amount of adsorbed -OH did not change and C-H reduced drastically. This is because the hydrothermal treatment at high temperature and high pressure removed adsorbed hydrocarbon on the surface. Therefore, this processing brought a clean surface and the hydrophilicity was improved. Furthermore, immersing hydrothermal treated substrates in 5PBS(-) gave super hydrophilic surface with WCA < 10 deg.

Various ions in 5PBS(-) were adsorbed on the clean surface, and they provided hydrophilicity.

Substrates immersed in 5PBS(-) after hydrothermal treatment were subjected to *in vivo* testing (Fig. 1). The surface treated samples had very high BIC value and which were higher than anodized TiO₂ films¹. We have already reported that the hydrophilic surface adsorbed much cell-adhesive protein in the body selectively, such as fibronectin and Type I collagen³. It is thought that this promoted the production of hard tissue on the implants.

CONCLUSION

Surfaces of Ti, Nb, Ta, Zr and Ti alloys became hydrophilic by applying hydrothermal treatment after polished without anodizing. Furthermore, immersing hydrothermal treated substrates in 5PBS(-) gave super hydrophilic surface with WCA < 10 deg. and shown high osteoconductivity.

REFERENCES

1. Kuroda K. *et al.*, Bioinorg. Chem. Appli. 2012: ID 730693, 2012
2. Yamamoto D. *et al.*, Mater. Trans., 53: 1956-1961, 2012
3. Omori M. *et al.*, 28th Annual Meeting, Academy of Osseointegration, 2013

ACKNOWLEDGMENTS

This work was partially supported by a Grant-in-Aid for Scientific Research (B) (No. 25289248).

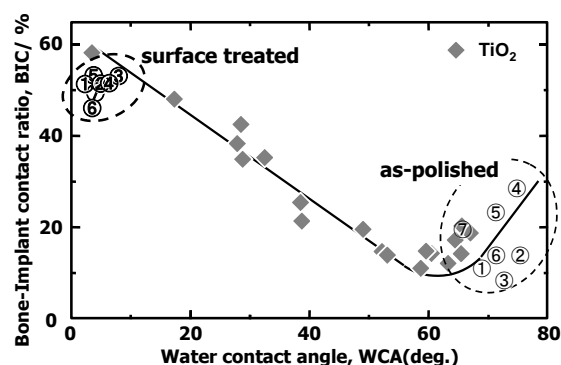


Fig. 1 Relationship between bone-implant contact ratio in the cortical bone part and water contact angle.

- 1: Ti, 2: Nb, 3: Ta, 4: Zr,
5: Ti29Nb13Ta4.6Zr, 6: Ti6Al4V,
7: Ti6Al7Nb, ◆: anodized TiO₂ films

Evaluation of Dense Collagen Matrices as Wound Dressing for the Treatment of Foot Diabetic Ulcers

Christophe Héлары¹, Gervaise Mosser¹, Aicha Abed², Didier Letourneur², Liliane Louedec², Thibaud Coradin¹, Marie Madeleine Giraud-Guille¹ and Anne Meddahi-Pellé².

¹. LCMCP - Materials and Biology Team - University Pierre and Curie - Paris – France

². INSERM, U698 - CHU Xavier Bichat ; BPC- Institut Galilée, University Paris 13- Paris - France
christophe.helary@upmc.fr

INTRODUCTION

Foot diabetic ulcers are characterized by an impaired wound healing. In some cases, the absence of wound closure leads to infection and amputation. Current treatments combine an antibiotherapy with the application of wound dressings¹. With the aim of improving the effect of antibiotics, research orientation is towards medicated dressings. Collagen-based biomaterials are broadly used to treat chronic wounds as collagen is biocompatible, biodegradable and favors wound healing. Nevertheless, drug content is rapidly released from current collagen materials because of their opened porosity. In this study, highly dense collagen matrices have been evaluated as novel medicated wound dressings for the treatment of foot diabetic ulcers.

EXPERIMENTAL METHODS

Collagen matrices were synthesized by gelation of collagen solutions concentrated at 5, 10, 20 or 40 mg/mL. Collagen matrices were called CM5, CM10, CM20 and CM40, respectively. Mechanical properties of matrices were assessed by rheological measurements. Their structure was analyzed by scanning (SEM) and transmission electronic microscopy (TEM). Dense collagen matrices were implanted in subcutaneous pockets in rat abdomen in order to study their biocompatibility. For this purpose, macrophages and neutrophils were detected on histological sections. Swelling abilities, resistance to collagenase digestion and water retention were evaluated over one week. Last, dense collagen matrices were loaded with ampicillin. Biological activity of ampicillin, released from collagen matrices, was evaluated on *Pseudomonas Auriginosa*. In parallel, cytotoxicity of matrices was studied on primary fibroblasts using Alamar blue test.

RESULTS AND DISCUSSION

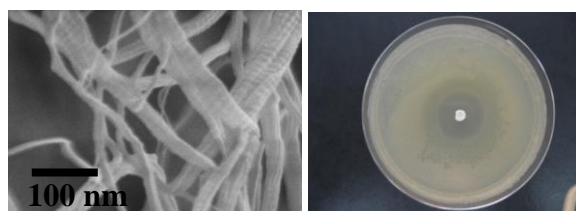


Fig 1: (A) Structure of CM40 (SEM). (B) Inhibition of bacterial growth by ampicillin-loaded CM40 after 4 days.

The stiffness of collagen matrices increased with the collagen concentration. Improved mechanical properties were associated with the high fibrillar density and the fibril thickness observed in CM40. In addition, fibrils bundles were observed (Fig 1A). After subcutaneous

implantation in rats, collagen matrices exhibited different behaviours. Macroscopic views revealed a good stability of CM20 and CM40. In contrast, CM5 and CM10 were partially degraded after 30 days. The absence of macrophages and neutrophils on histological sections revealed the absence of severe host response regardless of collagen concentration.

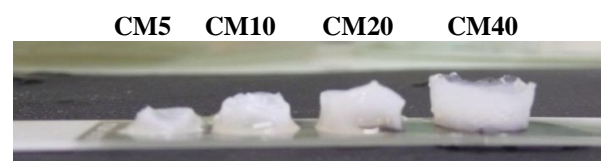


Fig 2: Swelling properties of dense collagen matrices.

CM40 exhibited the best swelling abilities as they could absorb 20 times their dry weight in water. Compared to CM5, swollen CM40 retained water for a longer period than the other matrices. Last, dense collagen matrices (CM40) had the highest resistance against accelerated digestion by collagenase (Fig 3). When loaded with 10 mg of ampicillin, CM40 released efficient doses of antibiotics which allowed the inhibition of *P. aeruginosa* over 4 days (Fig 1B). In parallel, no cytotoxicity was observed on human fibroblasts.

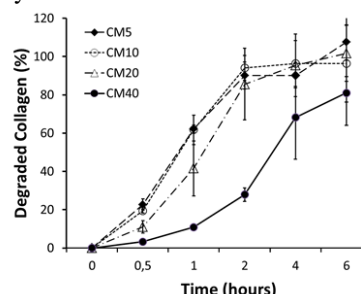


Fig 3: Degradation of collagen matrices by collagenase.

CONCLUSION

Our study shows that dense collagen matrices could be used as medicated wound dressing for the treatment of diabetic foot ulcers. They can absorb exudates as they have high swelling properties. In addition, they can prevent infection by the delivery of antibiotics; they are biocompatible, biodegradable and are stable.

REFERENCES

1. Powers G. *et al.*, Dermatol Ther. 26:197-206, 2013.

ACKNOWLEDGMENTS

The authors thank Corinne Illoul and Bernard Haye for their technical support.

Electrodeposition of Nanostructured Zinc Oxide on Zinc with Potential for Bioresorbable Medical Devices

M. Alves¹, C. Santos^{1,2}, M. J. Carmezim^{1,2} and F. Montemor¹

¹ICEMS/DEQ Instituto Superior Técnico, Universidade Técnica de Lisboa, Portugal, martammalves@tecnico.ulisboa.pt

²ESTSetubal, Instituto Politécnico de Setúbal, Portugal

INTRODUCTION

The demand for medical implants expanded during the past decades owing to increased life-expectancy and changing lifestyles. With it, an urgent need for a new generation of biomaterials has upsurge, in particular to assist several orthopaedic and cardiovascular disorders, two infirmities annually affecting millions of patients^{1,2}. Zinc seems to be a promising biomaterial with a corrosion rate apparently adequate for tissue healing³. In human physiology this micronutrient is emerging as ubiquitous element able to modulate several important processes, among them the regulation of skeletal development and cardiac remodelling⁴.

As the failure of medical implants is often associated to chronic inflammation and infections, zinc ability to modulate inflammatory responses in the human body together with an antibacterial coating, like zinc oxide, can potentially improve the success of implants. To produce a zinc oxide coating in a zinc substrate, an electrodeposition procedure was used and the resulting films characterized.

EXPERIMENTAL METHODS

The electrodeposition was performed in a conventional three-electrode electrochemical cell, using Pt as counter electrode, SCE as reference electrode, Zn (99%) as working electrode (2.5 cm²), and 50 mM Zn(NO₃)₂ and 50 mM H₃BO₃ at pH 6 as electrolyte. The process was carried at room temperature in a Voltalab PGZ 100 potentiostat (Radiometer). A square-wave potential (-0.6V and -1.9V with the same pulse duration of 1 s and a total of 20 cycles) was applied. The microstructure and chemical composition of the deposited film was analyzed by scanning electron microscopy (SEM, Hitachi S2400) and energy dispersive X-ray spectroscopy (EDS, Bruker), respectively. Static contact angles of water were measured through the sessile drop method. Drops generated with a micrometric syringe were deposited on the surface, inside a chamber saturated with water. The images were obtained with a microscope (Wild M3Z) coupled to a video camera (JAI CV-A50). The analyses were performed 30s after the droplet deposition using the ADSA-P software (Axisymmetric Drop Shape Analysis-Profile).

RESULTS AND DISCUSSION

The electrodeposition of the film with the square-wave potential, when the potential was switched from -1.9V to -0.6 V, the cathodic current density abruptly increased because of the reduction of nitrate. After having reached the maximum of 5 mA cm⁻², the cathodic current density decayed as a result of a declining slope of the nitrate concentration profile

(Fig.1A). The resulting electrodeposited structures, composed of small laminas intersected in one another as shown in Fig. 1B, have an average width of 200 nm.

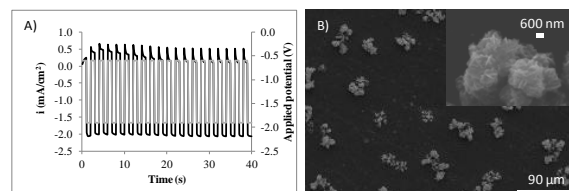


Fig.1. A) Applied potential (grey) and observed current density (black) during electrodeposition, B) SEM images of the resulting ZnO film.

The putative identification of zinc oxide was performed by EDS, where an increase in oxygen content was visible (Fig. 2). Further analyses are underway to confirm the presence of zinc oxide.

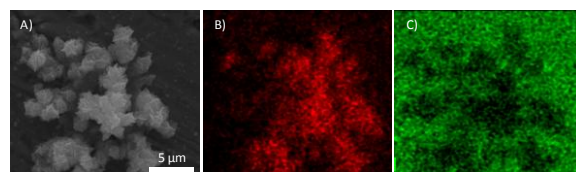


Fig.2. EDS mapping of ZnO film deposited on zinc, A) SEM image of ZnO crystal, B) EDS map of oxygen and C) EDS map of zinc.

Wettability, as an important property for cells adherence was evaluated. The resulting nanostructures did not change the water contact angle of pure zinc (92±4°).

CONCLUSION

The electrodeposition of nanostructured zinc oxide was successfully achieved in zinc. Further assays have to be performed to assess the immunoinflammatory modulation and antibacterial activity of the produced biomaterial.

The approach used in this work has good potential to improve bioresorbable materials for medical implants.

REFERENCES

1. Zethraeus N. *et al.*, Osteoporos. Int. 18:9-2, 2007
2. Leal J. *et al.*, Eur. Heart J. 27:1610-1619, 2006
3. Bowen PK. *et al.*, Adv. Mat. 25:2577-2582, 2013
4. Solomons N. Ann. Nutr. Metab. 62:8-17, 2013

ACKNOWLEDGMENTS

The author MA would like to thank FCT (SFRH/BPD/76646/2011) for providing financial support.



Mechanical Strength and Microstructure of Biomedical Beta-type Ti Alloy Subjected to Fine Particle Bombarding

Toshikazu Akahori¹, Yurie Oguchi², Tomokazu Hattori¹, Hisao Fukui³, and Mitsuo Niinomi⁴

¹Faculty of Science and Technology, Meijo University, Japan

²Graduate School of Science and Technology, Meijo University, Japan

³School of Dentistry, Aichi-Gakuin University, Japan

⁴IMR, Tohoku University, Japan, akahori@meijo-u.ac.jp

INTRODUCTION

Beta-type Ti-29Nb-13Ta-4.6Zr (TNTZ) was recently developed as a representative biomedical Ti alloy. As-solutionized TNTZ has a low elastic modulus of less than 60 GPa close to that of cortical bone along with very low cytotoxicity and good bone biocompatibility. Solution treatment and aging (STA) is a typical heat treatment for improving the mechanical properties of beta-type Ti alloys. However, STA also drastically increases the elastic modulus. Therefore, this study investigated the effects of fine particle bombarding, which is one of shot peening processes, on the mechanical properties of TNTZ subjected to more severe thermomechanical treatment in order to maintain a relatively low elastic modulus. The bone contact characteristics of TNTZ samples subjected to surface modification and cancellous bone were also compared.

EXPERIMENTAL METHODS

This study used cold-swaged TNTZ (working ratio: around 94%), which was designated as TNTZ_{SW}. TNTZ_{SW} was solutionized at 1063 K for 3.6 ks in a vacuum followed by water quenching (WQ); it was designated as TNTZ_{ST}. Some samples of TNTZ_{SW} were aged at 573 to 723 K in under aging conditions. Surface modification by a fine particle bombarding (FPB) machine was applied to some samples of TNTZ_{SW}, TNTZ_{ST} and aged TNTZ_{SW}; these specimens were designated as TNTZ_{SW}/FPB, TNTZ_{ST}/FPB and aged TNTZ_{SW}/FPB, respectively. Optical microscopy (OM), scanning electron microscopy (SEM), and X-ray diffraction (XRD) spectroscopy were carried out on each specimen to evaluate the microstructure. The Vickers hardness elastic modulus and the tensile and fatigue properties were investigated for each specimen to examine the mechanical properties. For the bone contact characteristics, some cylinder-type samples of TNTZ_{SW}/FPB and TNTZ_{SW} with mirror and as-machined surfaces were implanted into the femurs of Japanese white rabbits. All samples were extracted 12 weeks after implantation. The bone contacts were evaluated by image analysis.

RESULTS AND DISCUSSION

Figure 1 shows Vickers hardness profiles from very edge of samples of TNTZ_{SW} and TNTZ_{SW}/FPB to around 300 μm in depth on TNTZ_{SW}/FPB and TNTZ_{ST}/FPB. The Vickers hardness of the very edges for TNTZ_{SW}/FPB and TNTZ_{ST}/FPB showed the highest value, which is Hv 270 and Hv 235, respectively), and it tends to decrease

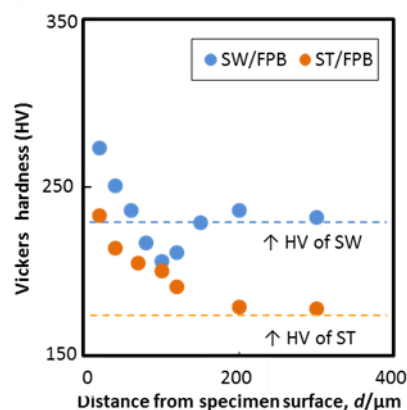


Fig. 1 Vickers hardness of ST/FPB and SW/FPB.

drastically as a function of distance from the surface to a depth of around 20 μm .

The fatigue strength of TNTZ_{SW}/FPB increased, especially in the high cycle fatigue life region. The fatigue limit of TNTZ_{SW}/FPB was around 400 MPa and around 100 MPa higher than that of TNTZ_{SW}. The Vickers hardness near the surface of the TNTZ_{SW}/m-SP specimen was around 200 Hv higher than that at the center of specimen, as noted above. As a result, the effect of residual compressive stress by FPB was marked in the high cycle fatigue life region.

In animal tests, TNTZ_{SW}/FPB had the highest bone contact ratio among the three kinds of sample, although the bone formation ratios of the three were almost the same.

CONCLUSIONS

- (1) The Vickers hardness of cold-swaged TNTZ subjected to fine particle bombarding was significantly increased within 20 μm from the very edge of the specimen surface.
- (2) The fatigue strength of TNTZ_{SW} subjected to fine particle bombarding increased in the high cycle fatigue life region only. The fatigue limit was around 400 MPa.
- (3) The bone contact ratio of TNTZ subjected to fine particle bombarding was better than that of TNTZ with the mirror surface.

REFERENCES

1. T. Akahori, M. Niinomi, H. Fukui, and A. Suzuki: Materials Transactions, Vol. 45, No. 5 (2004), 1540-1548.

Stoichiometric Control for Hydroxyapatite Thin Film Prepared by Pulsed Laser Deposition Technique

Hiroaki Nishikawa*, Ryota Yoshikawa

Fac. Bio.-Oriented Sci. and Technol., Kinki University, Japan, nishik32@waka.kindai.ac.jp

INTRODUCTION

Hydroxyapatite (HA), $\text{Ca}_{10}(\text{PO}_4)_6(\text{OH})_2$, is a typical bioceramics with excellent bone conduction ability. We have demonstrated that pulsed laser deposition (PLD) technique can be used to coat materials with very high quality HA thin films that have high adhesion strengths¹. One of the greatest advantages of PLD technique is that the target has a similar chemical composition to the thin film. However, the chemical composition of HA thin films we previously grew slightly deviated from the stoichiometry. Energy-dispersive x-ray (EDX) analysis revealed that our HA thin films had a Ca/P ratio of approximately 2.0. Therefore, in the present study, we investigate the optimal PLD conditions for growing high quality HA thin films with a Ca/P ratio close to 1.67 (10/6) of the stoichiometric ratio. The chemical composition of films grown by PLD technique depends on the energy density² (fluence) and the spot size³ of the laser beam that irradiates the target surface. The spot size can be controlled by varying the distance between the focal lens and the target. Because the total energy of the laser beam can be varied independently of the spot size, the fluence and the spot size can be changed independently of each other.

In this study, we have investigated the effect of each fluence and spot size for the stoichiometric control for the HA thin films independently.

EXPERIMENTAL METHODS

The HA thin films were prepared by PLD technique with KrF excimer laser (wavelength = 248 nm, pulse width = 14 ns) on Ti plates. The target used was commercially available HA pellet (PENTAX CELLYARD). The substrate was room temperature. During the thin film growth, O_2 gas through water bath was introduced with the partial pressure of 1.0×10^{-1} Pa. The thickness of the HA thin film was 250 ± 25 nm measured by a stylus surface profiler (ULVAC Dektak 150).

In order to change the fluence and the spot size independently, we employed following procedure. Since the fluence is energy density of laser pulse on the target, it can be calculated that the laser energy irradiating the target is divided by the spot size. So, when the fluence is changed independent of spot size, only the laser energy is changed. On the other hand, when the spot size is changed independent of fluence, the focal lens of the laser is moved as shown in Fig. 1. With the controlled spot size, the laser energy irradiating the target is changed to keep the constant fluence. The chemical composition of the prepared HA thin film was measured by an EDX.

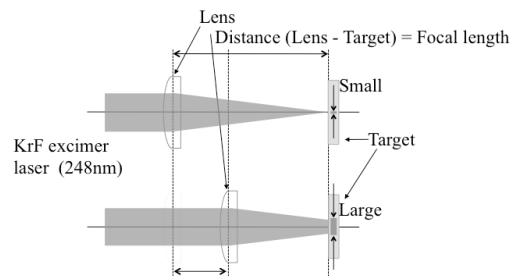


Fig. 1. Control of the spot size independent of the fluence.

Table I Measured Ca/P ratio of HA thin film with the various fluences and spot sizes.

Fluence [J/cm ²]	Spot size [mm ²]		
	0.77	1.6	3.8
2.0	2.1±0.2	2.0±0.1	1.9±0.2
2.7	2.0±0.1	1.9±0.1	1.7±0.1

RESULTS AND DISCUSSION

Four samples were prepared for each set of experimental conditions. Table I gives the average Ca/P ratio measured by EDX. The results show that increasing the spot size reduces the Ca/P ratio. Because the Ca/P ratio varies in a similar manner for both values of the fluence, the spot size was deemed to have a greater influence on the Ca/P ratio of HA thin films than fluence. Ohnishi *et al.* reported a change in the chemical composition²), but they simultaneously varied the spot size and the fluence. Thus, the present study is the first report of the independent effect of spot size on the chemical composition.

CONCLUSION

In order to prepare high quality HA thin film, we have noted to control the stoichiometry of the HA by the independent change of fluence and spot size. From the EDX measurement, it is found that the spot size can drastically control the Ca/P ratio as an important stoichiometry of the HA.

REFERENCES

1. Hontsu S. *et al.*, Thin Solid Films 295:214-217, 1997
2. Ohnishi T. *et al.*, Appl. Phys. Lett. 87:241919-1-241919-3, 2005
3. J. H. Song J. H. *et al.*, Adv. Mater. 20:2528-2532, 2008

The Influence of PBS and Lactic acid on vacuum-sintered bodies of a novel apatite for artificial bone and tooth

Kenichi Tamura¹ and Tomohiro Uchino¹

¹College of Engineering, Nihon University, Japan, tamura@mech.ce.nihon-u.ac.jp

INTRODUCTION

Titanium medical apatite (TMA[®]: $[\text{Ca}_{10}(\text{PO}_4)_6]\text{TiO}_3 \cdot n\text{H}_2\text{O}$) is a novel apatite for biomaterials. TMA bodies sintered at 1000–1500°C were converted to mixtures composed of three crystalline materials, namely α -TCP (tricalcium phosphate), β -TCP, and Perovskite- CaTiO_3 . After sintering temperature at 1300°C, the TMA vacuum-sintered bodies were white and the density was approximately 2.3g/cm³ (corresponding to that of a compact bone or a tooth). Further, it was possible to cut the TMA bodies into various forms with a cutting machine. On the other hand, the implants made from TMA vacuum sintered at 1300°C were inserted into a rabbit jaw bones. After one month, the TMA implants were well tolerated by the surrounding tissue, and no adverse tissue reactions were seen in any of the sections. The outer surface of TMA implants were covered by new bone formation because of the high biocompatibility of the TMA vacuum-sintered bodies [1-4]. An international patent on “Sintered body of titanium compound,” i.e., “TMA sintered body,” have in the United States, Canada, Australia, Japan, South Korea and China.

In this study, we have investigated the pH on TMA vacuum-sintered bodies using PBS and Lactic acid solutions by the in vitro.

EXPERIMENTAL METHODS

Materials are TMA vacuum-sintered bodies at 1300°C, $\times 10^{-3}\text{Pa}$ and HAp atmosphere-sintered bodies at 900°C using a resistance heating furnace. Test specimens are the disk (11mm in diameter \times 1.5mm in length). TMA bodies for the artificial bone are soaked PBS (-) solutions within 28 days. On the other hand, TMA bodies for the tooth are soaked Lactic acid solutions of pH2, pH3 and pH4 within 128 hours. The pH adjusts dilute the undiluted Lactic acid solution with pure water. So, pH2=500mM, pH3=6.40mM and pH4=0.21mM. Solution amount into the centrifuge tube has 30 ml per a specimen. Temperature of the centrifuge tube is kept 37°C using drying chamber. Tests carried out 3 times.

RESULTS AND DISCUSSION

Figure 1 show Relationships between pH and soaking time of TMA and HAp specimens into PBS solutions (pH7.4). The pH of TMA vacuum-sintered bodies and HAp atmosphere-sintered bodies were stable at pH7.4 solutions until 28 days. From this result, we think that TMA vacuum-sintered bodies were use as artificial bone materials to regenerate bone parts and produce bone reinforcement structures.

Figure 2 show Relationships between pH and soaking time of TMA specimens into Lactic acid solutions. The pH increase approximate 1.1 in the pH 2 solution, approximate 1.7 in the pH 3 solution and approximate

2.6 in the pH 4 solution. The change value is large as large pH because the molecular formula of Lactic acid: $\text{C}_3\text{H}_6\text{O}_3$. Lactic acid has both weak acidity of COOH and alkalinity of OH^- . So, the pH4 of diluted solution moved for alkalinity side. Test specimens are little melted the pH2 and pH3, but didn't melted the pH4.

REFERENCES

1. Kenichi Tamura, Tatsushi Fujita, Yuriko Morisaki; Central European Journal of Engineering, Vol.3-No.4: 700-706, 2013.

ACKNOWLEDGMENTS

This study was supported Tatsushi Fujita and Yuriko Morisaki of Immuno-Science Co. Ltd (Sapporo Japan). And “TMA” is trademark of Immuno-Science Co. Ltd.

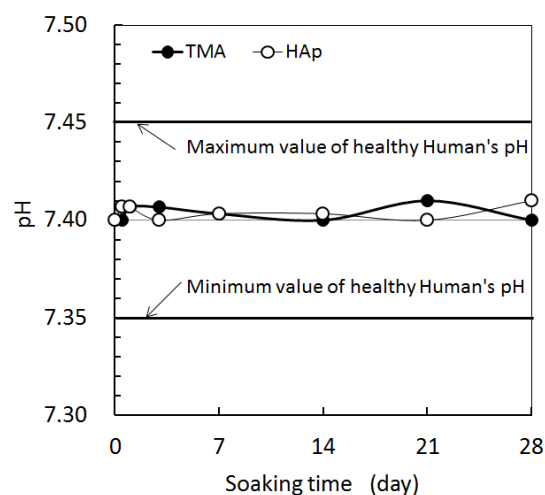


Figure 1 Relationships between pH and soaking time of TMA and HAp specimens into PBS solutions.

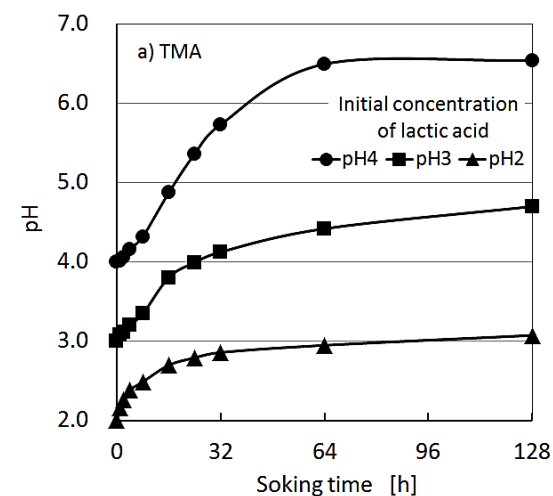


Figure 2 Relationships between pH and soaking time of TMA specimens into Lactic acid solutions.

Sol-gel assisted preparation of collagen hydrolysate scaffold: A Novel biomaterial for the treatment of chronic wounds

Satiesh kumar Ramadass[#], Sathiamurthi Perumal and Balaraman Madhan^{*}

¹CSIR- Central Leather Research Institute, Chennai-20, Tamil Nadu, India

[#] ramsatiesh@gmail.com

INTRODUCTION

Collagen based biomaterials remains as a treatment of choice for chronic wound therapy. Multi-step extraction procedure of collagen at cold condition indirectly increases cost of the collagen based biomaterial. In addition, low therapeutic loading of collagen due to its limited solubility, less porosity and ease collagenase degradation emphasize the need of developing a better therapeutic alternative and cost effective collagen based biomaterial. Collagen hydrolysate, an enzymatic hydrolyzed product of collagen contains peptides having beneficial properties such as stimulatory collagen synthesis, haemostatic property, tissue adhesiveness, maintaining moisture balance and antimicrobial property emphasize the need of developing collagen hydrolysate based wound dressing. The preparation of collagen hydrolysate would be simple, cost effective and it does not require multi-step extraction procedure. Therefore, the approach of using collagen hydrolysate as a main constituent in the scaffolding was proposed and composite material design adopted for sponge fabrication.

EXPERIMENTAL METHODS

Collagen Hydrolysate Composite Scaffold (CHCS) was fabricated through sol-gel transition methodology using tetraethoxysilane as silica precursor. The scaffold was characterized for morphology, porosity, water uptake capacity, enzymatic stability, biocompatibility and antimicrobial activity. *In vivo* study was experimented in rats using full thickness skin excision wound healing model.

RESULTS AND DISCUSSION

Rheology observation confirmed the increases in viscosity and sol-gel transition of CHCS composite solution. SEM morphology of CHCS scaffold revealed that the scaffold is porous with pore size ranging from 380 to 760 μm with an average pore size of 596 μm . CHCS showed controlled collagenase degradation and better water uptake capacity compared to the collagen scaffold. *In vitro* culturing with 3T3 Fibroblast cells showed that the CHCS could significantly promote the proliferation of cells compared to the collagen scaffold. Interestingly, CHCS exhibited inherent antimicrobial activity against tested wound pathogens. *In vivo* study demonstrated significant acceleration of wound healing treated with CHCS compared to the collagen sponge dressing.

CONCLUSION

The conclusions have to be based on the facts in CHCS scaffold exhibited better property compared to collagen scaffold in terms of porous morphology, biostability, water uptake capacity and biocompatibility. The antimicrobial activity of collagen hydrolysate is a great value addition for CHCS in treating infectious chronic wound. Against these findings, the CHCS sponge has a potential as a candidate for the treatment of chronic wound

REFERENCES

1. Ma L, Gao C, Mao Z, Zhou J, Shen J, Hu X, et al. Collagen/chitosan porous scaffolds with improved biostability for skin tissue engineering. *Biomaterials* 2003; 24:4833-41.

ACKNOWLEDGMENTS

The authors are grateful to CSIR, India for providing financial assistance under the M2D XII plan Project (CSC 0134).



Stress and Deformation in a Sutured Tendon Repair; an *in silico* Model

S D Rawson¹, L Margetts², J K F Wong³ and S H Cartmell¹

¹School of Materials, University of Manchester, UK, shelley.rawson@postgrad.manchester.ac.uk

²School of Earth, Atmospheric and Environmental Sciences, University of Manchester, UK

³Plastic Surgery Research, University of Manchester, UK

INTRODUCTION

Many suture repairs have been described to re-approximate severed tendons, yet no one repair is regarded as the gold standard. At present, 25% of hand tendon repairs do not obtain satisfactory mobility following healing, and over 7% of repairs re-rupture (1). Concluding the ideal suture repair would benefit over 800,000 people in the UK who suffer tendon injury per annum (2). Finite element (FE) modelling enables detailed stress analysis of implantable devices and materials for tissue regeneration. However, the *in silico* model is limited by the description of biological tissues. Past 2D (3) and 3D (4) isotropic descriptions of tendon are unsuitable for modelling complex suture repair geometry. As such, the aim of this work was to mathematically describe tendon tissue, informed by *ex vivo* tensile testing, to model and compare stress patterns arising due to various suture techniques.

EXPERIMENTAL METHODS

Porcine flexor digitorum profundus (FDP) tendons (n=12) were sliced 5mm wide and 2mm thick and loaded transverse to the long tendon axis in an instron 5569 load frame using Bose tissue grips placed 2.5mm apart. Strain was applied at 1%/s until failure. Stress and strain were calculated, followed by the transverse modulus and matrix modulus.

Fibril modulus (200-3000MPa; 5,6) was obtained from literature and the matrix modulus was calculated using the rule of mixtures for a continuous fibre composite. An idealised finite element model of tendon microstructure was developed (Fig. 1) and material properties were varied within the model, approaching those obtained experimentally. Homogenisation was performed to deduce the engineering constants which represent the microstructure model. This was then input into an FE model of a Kessler suture repair and suture loading was simulated. Results were validated against *ex vivo* tensile tests of sutured tendons (n=10).

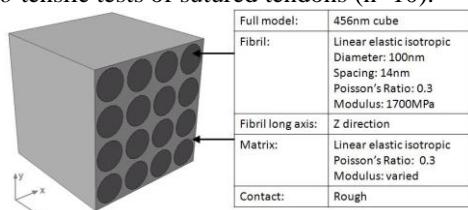


Fig. 1 FE tendon microstructure model, detailing model properties and dimensions.

RESULTS AND DISCUSSION

Tensile testing of the porcine FDP tendon yielded a transverse young's modulus ranging from 0.1035 ±0.0454MPa to 0.2551 ±0.0818MPa and a matrix modulus ranging from 0.0416MPa to 0.1021MPa.

As matrix modulus tends towards the experimentally determined values, FE results agree closer with laboratory data (Fig. 2.a). A higher matrix modulus results in a circular high stress region at the suture anchor point (See orange region in Fig. 2.b). As matrix modulus is reduced, and the material description approaches the highly orthotropic behaviour of tendon tissue, we see an elliptical high stress region (Fig 2.c). The elliptical high stress area agrees with areas of acellularity observed in a murine *in vivo* study (7) suggesting the acellular zone results from high stress.

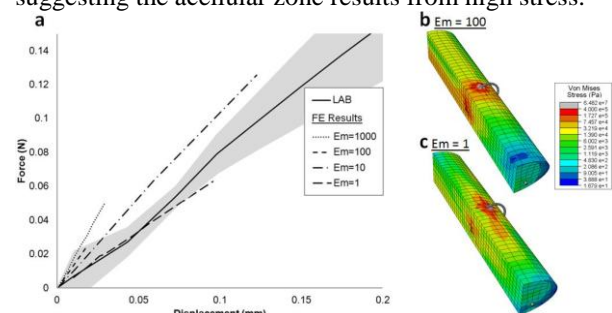


Fig. 2 (a) FE results with varying matrix properties compared with lab results. (b) Stress map when matrix modulus is 100MPa and 0.5mm gap between tendon ends is simulated. (c) Stress map when matrix modulus is 1MPa and 0.5mm gap between tendon ends is simulated.

CONCLUSION

We have developed an FE model of sutured tendon repair suited to identifying regions of augmented stress within the tendon that would adversely affect tissue health. High stress regions resulting in acellularity, and areas of stress shielding which affects tissue remodelling can be identified.

REFERENCES

1. Su B.W. *et al.*, J. Bone Joint Surg. Am, 87:923-38, 2005
2. Clayton R.A. and Court-Brown C.M., Injury, 39:1338-44, 2008
3. Funakoshi T. *et al.*, J Shoulder Elbow Surg., 17:986-92, 2008
4. Garcia-Gonzalez A. *et al.*, J. Biomech., 42:1697-704, 2009
5. Van Der Rijt J.A *et al.*, Macromol. Biosci., 6:697-702, 2006
6. Svensson. *et al.*, Biophys. J., 99:4020-7, 2010
7. Wong. *et al.*, Matrix Biol., 29:525-36, 2010

ACKNOWLEDGMENTS

The authors would like to thank the Engineering and Physical Sciences Research Council and the Medical Research Council for providing financial support.

Chemically cross-linked peptide-based hydrogels with potential biomedical applications

M.A. Elsayy^{1,3}, A. Smith^{1,3}, A.F. Miller^{2,3} and A. Saiani^{1,3,*}

¹School of Materials, University of Manchester, UK

²School of Chemical Engineering and Analytical Sciences, University of Manchester, UK

³Manchester Institute of Biotechnology, University of Manchester, UK

*Correspondence to a.saiani@manchester.ac.uk

INTRODUCTION

Peptide-based hydrogels are 3D fibrillar network, where fibres are formed by the self-assembly of short purposely designed peptides. One of the key challenges is the control of the mechanical properties and stability of these materials in order to expand their potential range of applications. In our group we have developed a platform for the design of such hydrogels through the exploitation of the self-assembly of so-called β -sheet forming peptide. In this project we will explore the possibility of using chemically cross-linked peptides to control of the mechanical properties and stability of these hydrogels (Fig 1).¹ Two cross-linking strategies based on the use of cysteine-containing peptides will be explored: disulphide bridging and Maleimide cross-linking.

EXPERIMENTAL METHODS

Solid Phase Peptide Synthesis: peptides, typically 8 amino acids long and based on the alternation of hydrophobic and hydrophilic residues, will be synthesized on a CEM LibertyTM automated microwave peptide synthesizer using standard solid phase synthesis protocols.

Peptide Cross-linking: The cross-linked peptides will be synthesised by treating the cys-containing peptide solutions with NaI and H₂O₂ (disulphide bridging) or dibromomaleimide/N-substituted dibromomaleimide pre-dissolved in the minimal volume of DMF (Maleimide cross-linking). The precipitated cross-linked products will be collected by filtration.

Hydrogels preparation and characterisation: Hydrogels will be prepared by dissolving the peptides (cross-linked and non-cross-linked) in water as described

previously^{2,3}. The hydrogels will be characterised using a range of techniques including rheology and microscopy.

RESULTS AND DISCUSSION

The gelation properties of the cross-linked peptides investigated as a function of peptide concentration allows us to understand the effect that cross-linking. In particular the effect of the position of the cross-link along the peptide chain, has on self-assembly and gelation properties of these peptides.

Characterisation of the effect of introducing cross-linked peptides in the hydrogel made from our usual peptides (FEFKFEFK)³ shows that the ratio between cross-linked and non-cross-linked peptides is important for the self-assembly process.

CONCLUSION

This project will allow us the possibility of using a simple peptide cross-linking approach to manipulate and control the properties of the peptide hydrogels expanding their potential uses, in particular in the biomedical field

REFERENCES

1. Boothroyd, A. *et al.*; Biopolymers. 106: 669-680, 2014
2. Mujeeb A. *et al.*, Acta Biomaterialia. 9:4609-46017, 2013
3. Saiani, A., *et al.*, Soft Matter. 5:193-202, 2009

ACKNOWLEDGMENTS

The authors would like to thank the Engineering and Physical Sciences Research Council (EPSRC Grant no: EP/K016210/1) for financial support

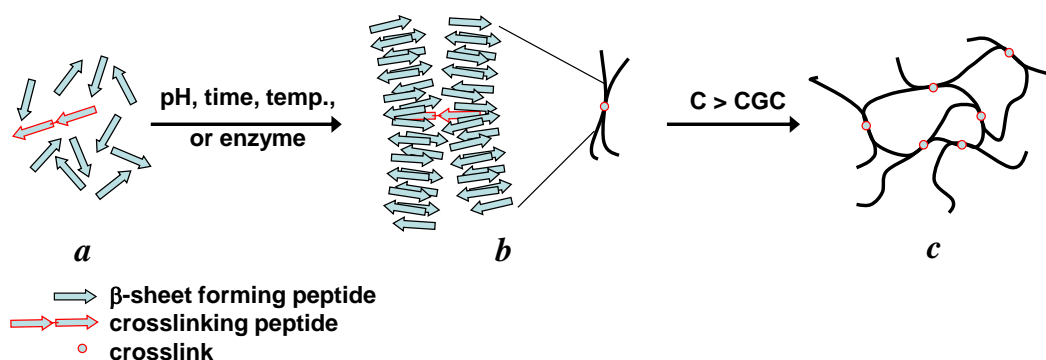


Figure 1: Schematic representation of the self-assembly and gelation process of cross-linked β -sheet forming peptides.

Calcium phosphate spheres incorporated into PMMA cement for enhanced antibacterial properties

Tao Qin, Alejandro López, Caroline Öhman, Håkan Engqvist, Cecilia Persson, Wei Xia

Department of Engineering Sciences, Uppsala University, Sweden
Tao.qin@angstrom.uu.se

INTRODUCTION

Infection at the site of an implant is a rare but potentially devastating complication, which could lead to painful disability, prolonged hospital stay and increased medical expenses. Antibiotic-loaded bone cement has been found to play a crucial role in the prevention and treatment of infection during and after arthroplasty^{1,2}. However, the present drug release from PMMA cements is not optimal. An increase in the release rate, after the initial burst release, would be beneficial. In this study calcium phosphate spheres were incorporated into PMMA cement in order to increase the rate of drug release. Mechanical properties, radiopacity and injectability were also investigated.

EXPERIMENTAL METHODS

Strontium doped calcium phosphate spheres (SCPS) were prepared in accordance with a previous study⁴. PMMA cements were prepared containing 2.5% of vancomycin, with and without 10% SCPS (wt% of powder). The release of vancomycin was carried out in PBS solution (pH 4 and pH 7.4) and samples were extracted at different time points (0.5 hour to 7 days). The antibiotic concentrations were measured at a wavelength of 280 nm, using UV-Vis spectrophotometer (Shimadzu UV1800, Kyoto, Japan). The mechanical properties were tested using AGS-H materials tester (Shimadzu, Kyoto, Japan). A displacement rate of 20mm/min was used. Injectability was investigated with an injection device which was placed in the materials tester and compressed at a displacement rate of 3 mm/min. Radiographs of the cements were taken of three specimens, 1mm in height and 5mm in diameter, per group at 80kv using MicroCT (Skyscan 1172, Bruker, Kontich, Belgium). The radiopacity was calculated using a standard curve (amount of light vs mm Al) created from an aluminum scale (0.5-4mm).

RESULTS AND DISCUSSION

Figure 1 shows that all groups gave an initial burst release during the first few hours, which was followed by a sustained release over the entire period investigated. When SCPS and vancomycin were mixed with PMMA, the modified cement showed a higher release rate of vancomycin. Incorporation of SCPS into cement may create more room for vancomycin to be easily released. In acidic environment, the release rate was higher since it facilitates the dissolution of SCPS. The incorporation of SCPS did not change the mechanical strength of the cement. The setting time was slightly increased for the PMMA/SCPS cement, but still in an acceptable range. The relative radiopacity of PMMA/SCPS was significantly higher than that of unmodified PMMA.

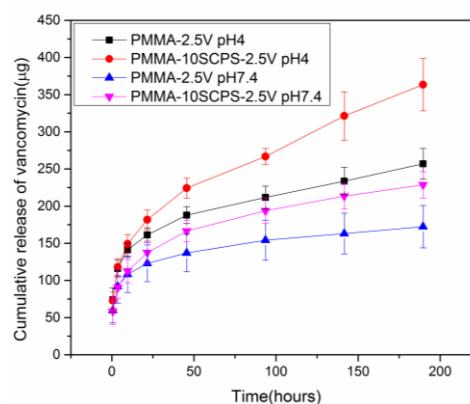


Figure 1 Cumulative releases of vancomycin in PBS

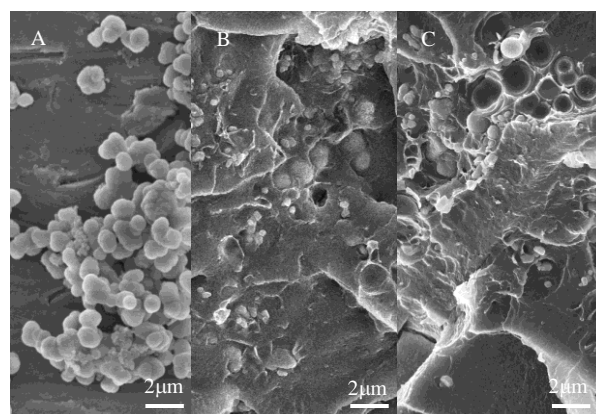


Figure 2 Morphology of SCPS (A) and Cross-section images of PMMA cement before (B) and after (C) drug release (pH 4).

CONCLUSION

After incorporation of SCPS, antibiotic-loaded PMMA cements showed enhanced antibiotic release while maintaining their mechanical properties, which suggests that this material could be advantageous in comparison to regular PMMA cement for the prevention and treatment of infections.

REFERENCES

1. Cui, Q. The Journal of bone and joint surgery. 89, 871–882 (2007).
2. KL, G. & AD, H. The Journal of bone and joint surgery. 77, 1576–1588 (1995).
3. E, J. Infect. Dis. 5, 1033–1048 (1983).
4. Xia, W. & Engqvist, H. Nanotechnology, 22, 1–10 (2011).

ACKNOWLEDGMENTS

The authors would like to thank the Swedish Research council (VR, Grant no: 2013-5419), VINNOVA (VINNMER 2010-02073) and China Scholarship Council for providing financial support to this project.

MP-SPR New characterization method for interactions and ultrathin films

Annika Jokinen, Niko Granqvist, Willem M. Albers and Janusz Sadowski

BioNavis Ltd., Finland
annika.jokinen@bionavis.com

Please download and read the instruction sheet to ensure all necessary formatting and abstract criteria are adhered to.

INTRODUCTION

Surface Plasmon Resonance (SPR) has been used already for a few decades for label-free detection and characterization of biochemical kinetics and affinities of many different types of analytes. The physical phenomenon is not limited to biochemistry, but is applicable to other nanoscale characterization of thin films¹.

EXPERIMENTAL METHODS

Aside of the traditional interactions, Multi Parametric Surface Plasmon Resonance (MP-SPR) can be utilized to determine unique refractive index (*RI*) and thickness (*d*) of ultrathin (*d* 0.5-100 nm) and slightly thicker films (*d* 300 nm- few μ m) without prior assumptions of the *RI* of the material. These are important properties not only for thin film coating industries and applications, but also for gaining important knowledge in biomaterials. Two methods utilizing MP-SPR to thickness and *RI* calculations have been introduced, either measuring in two different media (2M) with high *RI* difference, such as air and water¹⁻³, or at two or more different wavelengths (2W) of light^{2,3} in order to characterize properties of the thin films.

RESULTS AND DISCUSSION

MP-SPR is suitable for film deposition *in situ* or *ex situ*, which makes it compatible with several deposition methods and thereby makes it applicable to a wide range of polymers also. Polyelectrolyte multilayer deposition *in situ* was monitored in real-time with MP-SPR. Thickness of each deposited layers was determined utilizing two wavelength method (Fig.1).

Similarly layer thickness and *RI* was determined also for *ex situ* spin coated cellulose layer. MP-SPR was used not only to determine thickness and *RI* of the deposited layer but also for real time monitoring of other molecules interaction to the cellulose model surface^{4,5}.

Recently, MP-SPR was used also to monitor polymer layer structural changes in real time, such as polymer

swelling due to pH or electric potential change⁶. At pH = 9 poly (acrylic acid) (PAA) brushes were extended but the brushes collapsed at acidic pH (Fig.2).

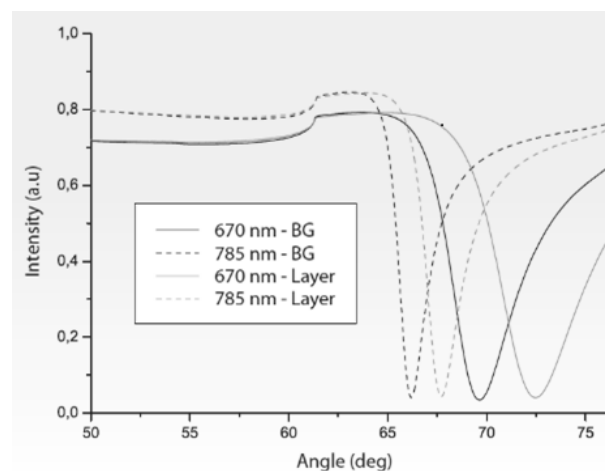


Fig1. Polyelectrolyte multilayer thickness and *RI* was determined with MP-SPR utilizing multiple wavelength method. Full angle range SPR curves before and after layer deposition.

CONCLUSION

With the ability to characterize both kinetics and nanoscale layer properties, MP-SPR proves to be a versatile tool for nanomaterial, biomaterial and biochemical interactions research, which makes MP-SPR invaluable for multidisciplinary research, where both physical and interaction properties of the materials need to be characterized.

REFERENCES

1. Albers, Vikholm-Lundin, Chapter4 in Nano-Bio-Sensing, Springer 2010
2. Liang, et al., Sens.Act.B, 149 (1), 2010, 212-220
3. Granqvist et al., Langmuir 29 (27), 2013, 8561-8571
4. Orelma et al., 12 (12), 2011, 4311-4318
5. Kontturi et al., J.Mater. Chem. A, 2013, (ASAP) DOI: 10.1039/C3TA12998E
6. Malmström et al., Macromolecules, 46 (12), 2013, 4955-4965

A Dimensionless Number for Electrospinning

William W. Sampson

School of Materials, University of Manchester, Manchester, UK
sampson@manchester.ac.uk

INTRODUCTION

Electrospinning of biocompatible polymers to yield heterogeneous fibre networks for application as scaffolds for tissue engineering is widely researched. Essentially the process of electrospinning is one of splitting a jet of dissolved polymer and extending the resultant filaments to produce very fine fibres in a disordered network on a collector. The process variables affecting fibre morphology and hence network structure include, but are not limited to: solution concentration, flow rate, voltage, surface charge, syringe needle diameter¹.

Typically, for electrospun scaffolds, we seek to optimise the pore dimensions and the specific surface of the resultant network. Theory describing the special case of *random* fibre networks, *i.e.* those where the location and orientation of any fibre is independent of all others, is well established and has been widely applied in many contexts².

Importantly, the dependence of pore size and specific surface on fibre dimensions and network densities are known and the primary variables of interest are the cross-sectional dimensions of fibres and the expected total fibre length per unit volume in the network³. As such, a useful descriptor of the efficiency of an electrospinning process would be a single number that quantifies the total fibre length generated by that process, relative to the volume of polymer solution delivered. Here we introduce a dimensionless number that provides this quantification.

THEORY

Consider a volume of polymer solution, V (cm³) with concentration, c (g cm⁻³) delivered via a syringe. If the diameter of the jet after the Taylor cone is d_j (μm), then total length of the solution delivered from the syringe is

$$L = \frac{4V}{\pi d_j^2}, \quad (1)$$

and the mass per unit length, or *linear density*, of the jet, on a dry basis, is

$$\delta = \frac{cV}{L} = \frac{\pi d_j^2 c}{4}. \quad (2)$$

Similarly, if the constituent fibres in the resulting network, have mean diameter, \bar{d}_f (μm), and the dry polymer has density, ρ_p (g cm⁻³), then their linear density is

$$\delta^* = \frac{\pi \bar{d}_f^2 \rho_p}{4}. \quad (3)$$

The ratio of the total fibre length in the mat, L^* , to that delivered from the jet provides our dimensionless number to characterize the electrospinning process; it is

easy to show that this is given by the ratio of the linear densities, *i.e.*:

$$\eta = \frac{L^*}{L} = \frac{\delta}{\delta^*} = \frac{\bar{d}_j^2 c}{d_f^2 \rho_p} \quad (4)$$

The dimensionless number, η provides a new variable against which measurable parameters of electrospinning processes can be compared. We know, for example, that the applied voltage and the distance from the syringe to the collector influence the dimensions of electrospun fibres and hence the properties of the network. If these result in different η , then we know that they have had a different net effect on the structure. The approach is illustrated by example in Figure 1 for the data of Wang *et al.*⁴; the gradients of the plots represent the number, η , with the steeper gradients representing the more efficient electrospinning process.

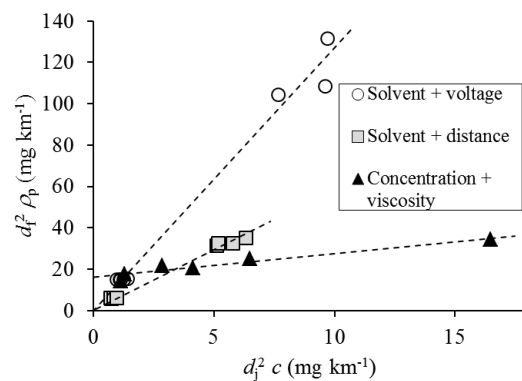


Figure 1. Data of Wang *et al.*⁴ for changes in solvent, collector distance and concentration for electrospun polystyrene.

CONCLUSION

A simple theoretical treatment has been presented to obtain a dimensionless number quantifying the efficiency of electrospinning processes. Preliminary comparison with experimental data from the literature suggests that this number may aid interpretation of the relative influence of the many variables affecting electrospinning, thus focussing experimental effort. Comparison of the theory with larger experimental data sets is ongoing.

REFERENCES

- Li, D. and Xia, Y. *Adv. Mater.* **16**(14):1151-1170, 2004
- Sampson, W.W. *Modelling Stochastic Fibrous Materials with Mathematica*, Springer, London, 2009.
- Eichhorn, S.J. and Sampson, W.W. *J. Roy. Soc. Interf.* **7**(45):641-649, 2010
- Wang, C., Hsu, C-H and Lin, J-H. *Macromolecules*, **39**(22):7662-7672, 2006

Acidic pH resistance of grafted chitosan on dental implant

Doris M. Campos^{1,2*}, B  reng  re Toury², M  lanie D'Almeida², Ghania N. Attik², Alice Ferrand², Pauline Renoud² and Brigitte Grosogeat^{1,2,3}

¹UFR d'Odontologie, Universit   Claude Bernard Lyon 1, Lyon, France.

²Laboratoire des Multimat  riaux et Interfaces (UMR CNRS 5615), Universit   Lyon 1, Villeurbanne, France.

³Centre de Soins, d'Enseignement et de Recherche Dentaires (Public Health department), Lyon, France.

doris.moura-campos@univ-lyon1.fr

INTRODUCTION

Chitosan (Chi) coating on titanium (Ti) implant surfaces have been proposed over the last decades to improve antimicrobial properties against peri-implantitis [1,2]. However, the attachment and stability of Chi coatings under drastic environments like the oral cavity have proven to be highly influenced by different factors such as pH value variations [3]. In this work, attention was mostly devoted to elaborating and evaluating a novel bioactive coating process to maintain greater Chi surface immobilization to withstand variations in the oral environment.

EXPERIMENTAL METHODS

Functionalization of Ti Surface. Ti foil samples were cleaned oxidized in fresh piranha solution and silanated by immersion in triethoxysilylpropyl succinic acid anhydride (TESPSA) in extra-dry toluene (v/v, 10/90) for 24 h. A biopolymer solution containing 4 wt.% Chi), 3% (v/v) acetic acid, and 97% (v/v) deionized water was grafted on the surface by dip coating. The Chi coated samples were then dried at 80  C for 24 h.

Titanium-coated Surface Chemical Properties. To evidence the Chi presence and resistance of coating on the substrate, infra-red (ATR-FTIR) and X-ray photoelectron (XPS) spectra were recorded at different pH levels (3 and 5) in saliva.

Adhesive Properties of Coating. The adhesion strength of the TESPSA/Chi coating on the Ti surface was observed by peel test. Standard adhesive tape was put on the pattern and pulled off at an angle of 180  . Results were compared with surfaces coated by simple dip deposition.

In vitro Analysis. Human gingival fibroblast-like (HGF-1) cells were seeded (1×10^4 cells/scaffold) onto Ti surfaces for 24 and 72 h. Actin microfilaments and cell nuclei were stained by immunostaining at room temperature. Image series were obtained with FV10i a confocal laser scanning biological inverted microscope.

RESULTS AND DISCUSSION

By XPS analysis, successful grafting of TESPSA on the Ti surface was indicated by the decrease in the Ti components and the arrival of Si components. Moreover, the presence of Chi is confirmed since the recorded spectrum presents at around 285.5, 399.3 and 532.5eV which are characteristic of the C1s, N1s and O1s Chi photoelectron peaks. After immersion in pH5 and pH3 solutions, the peak at 399.3eV which was assigned to N1s was still present for both immersions. The chitosan coating was also highlighted by ATR-

FTIR. The peaks at 1070, at 1011 and at 887 cm^{-1} are attributed to the saccharide structure of Chi [4]. Both of the added FTIR-ATR spectra showed equivalent signatures, meaning that Chi chains were still present on the sample surface even after acidic immersion. The peel-test revealed that at the samples coated by simple dip deposition, a large part of the coating has been removed, thus revealing the naked Ti substrate. By contrast, the TESPSA/Chi grafting is entirely stuck to the Ti surface. HGF-1 cell growth on uncoated and coated Ti implant surfaces respected their normal morphology following the 3 days of incubation (Fig. 1). The morphology of cells in contact with the TESPSA/Chi coated substrate was similar to that in contact with the uncoated titanium.

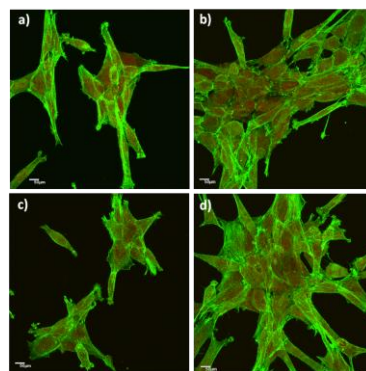


Fig.1. Confocal images of HGF-1 morphology: (a, c) and (b, d) cells cultured on uncoated and TESPSA/Chi Ti surfaces for 24 and 72 h, respectively. Scale bar = 50  m.

CONCLUSION

We have performed a biocompatible TESPSA/chitosan coated implant surfaces with chemical resistibility due to stable peptide bindings in a hostile environment such as in the oral cavity.

REFERENCES

1. Ikinci G. *et al.*, Int J Pharm. 235:121–7, 2002.
2. Hu X. *et al.*, Biomaterials. 31: 8854–63, 2010.
3. Kong M. *et al.*, Int J Food Microbiol. 144:51–63, 2010.
4. Sun T *et al.*, Eur Food Res Technol. 225(3,4):451–456, 2006.

ACKNOWLEDGMENTS

The authors wish to acknowledge Global D and Science et surface for analyses; the LST of the University of Lyon and the IFRO 2011 for their financial support.

Ex vivo osteo-chondral organ culture

Andrea Schwab, Jenny W Reboredo, Heike Walles

Tissue Engineering & Regenerative Medicine, University Hospital Wuerzburg, Germany

andrea.schwab@uni-wuerzburg.de

INTRODUCTION

Cartilage is an avascular and highly organized tissue that limits the regeneration capacity of (large) defects.

Intensive research has been performed in the development of functional cartilage implants that mimic the zonal tissue structure that is comprised of the following layers (Figure 1): superficial zone, middle zone, deep zone and calcified layer.

Up to now, successful tissue engineering (TE) strategies and clinical techniques in cartilage repair remain a major challenge as they only lead to insufficient tissue repair without maintaining the cartilage functionality and hierarchy.

Beside the cartilage tissue itself the sub-chondral bone and the synovial fluid may have an important role in cartilage regeneration. Pre-clinical testing of cartilage implants as well as new treatments in an osteo-chondral environment is needed to validate new healing approaches.

Therefore we want to establish a 3D osteo-chondral test system that incorporates TE scaffolds within an ex vivo environment. This more physiological in vitro cartilage defect model will allow predictive long term results on cartilage regeneration and repair therapies.

EXPERIMENTAL METHODS

Standardized and reproducible osteo-chondral explants (plugs) were isolated from porcine femoral condyles.

The explanted plugs were trimmed to a defined height, embedded in agarose and cultured in a 12-well plate under static conditions up to 4 weeks.

Cell vitality within the plugs was analyzed weekly over a period of 4 weeks via 3-(4,5-Dimethylthiazol-2-yl)-2,5-Diphenyltetrazoliumbromid (MTT). During static culture the supernatant of selected plugs was collected to measure LDH content. The plugs themselves were characterized immunohistologically with cartilage (collagen I, II, X, aggrecan (aggr), RUNX2, SOX9) and bone (bone sialo protein (BSP), osteopontin (OP), osteocalcin (OC)) specific antibodies as well as by histological stainings, such as Safranin-O and Alcian Blue. Biochemical analysis of the Glycosaminoglycan (GAG), DNA- and collagen content was performed of the cartilage layer at several time points during static culture.

Critical point drying of static cultured plugs was performed at several time points to analyze the characteristic structure of the plug by raster electron microscopy (REM).

RESULTS AND DISCUSSION

After cutting the plugs into half, the host cells of the explant reduced the MTT reagent to the blue formazan product for at least 4 weeks of static culture.

The histological stainings (Figure 1) clearly show the zonal architecture of articular cartilage. Within the different layers of the cartilage the chondrocyte density varies. Following, the GAG content of the superficial zone is diminished compared to the quantity in the deep zone.

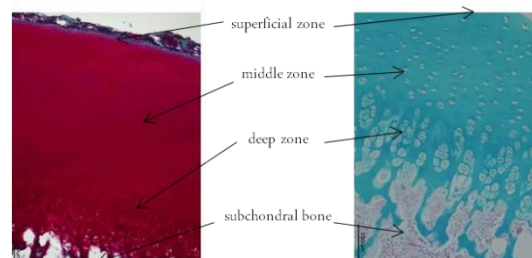


Figure 1: Safranin-O (left) and Alcian Blue (right) staining of a decalcified osteo-chondral plug at day 0; Scale bar 100µm

The normalized GAG content in cartilage part of the plug remained stable over more than 1 week. Histological analysis has shown positive expression of the bone markers BSP, OP, OC. Beside the SOX9 immune histological staining all other cartilage markers (collagen I, II and X, aggr, RUNX2) could be observed. During culture time the structural changes within the bone part of the plug were monitored.

CONCLUSION

Cutting edge bioreactor systems will improve the in vitro culture conditions and allow long term plug culture under more physiological cues up to 6 weeks. For this reason we need to give consideration to mechanotransduction.

Regarding the limited diffusion of the MTT reagent into the core of the plugs the diffusion of nutrients and removal of waste products will be characterized in more detail by µCT and MRI. Data obtained from REM, µCT, MRI and experimental results of plug culture will be used as input for the developing of a mathematical model. The in silico model will allow the simulation of biochemical and biophysical processes within the plug and contribute a better understanding of the different processes in the defect healing as well as in nutrition supply to keep the explant culture vital.

The establishment of the predictive 3D in vitro assay for (sub-) chondral implants requires the validation of the outcomes from our test system against in vivo models.

ACKNOWLEDGMENTS

The work leading to these results has received funding from the European Union Seventh Framework Programme (FP7/2007-2013) under grant agreement n° 309962.

3D powder printing of structured TCP/Alginate scaffolds for bone tissue engineering

Miguel Castilho^{1,4*}, Jorge Rodrigues¹, Inês Pires¹, Barbara Gouveia¹, Manuel Pereira², Claus Moseke³, Jürgen Groll³, Uwe Gbureck³, Elke Vorndran³

^{1*}IDMEC, Instituto Superior Técnico, Universidade de Lisboa, Lisbon, Portugal, miguel.castilho@ist.utl.pt

²CEPGIST/CERENA, Instituto Superior Técnico, Universidade de Lisboa, Lisbon, Portugal

³Department for Functional Materials in Medicine and Dentistry, University of Würzburg, D-97070 Würzburg, Germany; ⁴Altakit S.A., Loures, Portugal

INTRODUCTION

Calcium phosphate (CaP) bioceramics are widely used as pre-shaped bone graft for bone fracture treatment. However their brittleness, low reliability and toughness, limit their application¹. The main strategy to improve these limitations is to produce bone grafts with a core CaP phase, reinforced with a thin layer of a tough synthetic polymer, which was reported to have low degradation and reduce cell adhesion². Natural polymers, like alginate, are suitable for tissue engineering, thanks to their ease of gelation, excellent biodegradable and cell interaction properties³. Our approach was to develop directly a new structured biocomposite bone graft, composed of TCP/Alginate, by using a modified layer by layer low temperature 3D powder printing process (3DP)⁴.

EXPERIMENTAL METHODS

Four different powder mixtures were investigated, consisting of TCP (T) and different amounts of alginate (Alg), 2.5wt%, 5wt% and 7.5wt% (T2.5Alg, T5Alg, T7.5Alg). Sample manufacturing was performed with a 3DP system (Z510, Z-Corporation) using the powder mixtures and a phosphoric acid as binder. After printing, the samples were treated with binder solution. Different dense samples were prepared. Phase composition was evaluated by X-ray diffraction. Arquimedes porosity (ϕ), X-Ray microcomputed tomography (μ -CT) and SEM were used for sample characterization. Mechanical properties were evaluated under uniaxial compression (UC), three point flexure (3PF) and diametral compression (DC) tests, in dry conditions and in PBS buffer solution at 37°C, for 1, 7 and 14 days (wet14). Stress states were represented in Mohr's plane, and materials intrinsic strength determined (Fig 1). Weibull distribution parameters were estimated using the maximum likelihood method, and material toughness was evaluated by the strain energy density, U_0 , determination.

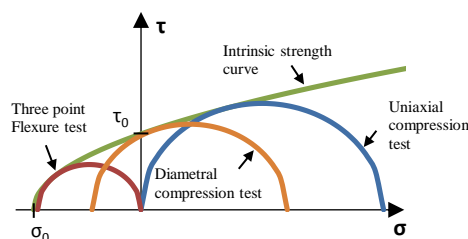


Figure 1: Schematic Mohr's plane, representing TAlg intrinsic strength curve and respective intrinsic strengths, σ_0 and τ_0 .

RESULTS AND DISCUSSION

3D structured TAlg samples were successfully printed. μ -CT (Fig 2), enabled us to access the microstructure differences of T and TAlg samples. Porosity decrease for T2.5Alg sample and increase with the content of Alg, being a function of Alg gelling efficiency. Intrinsic

strengths (Fig 3a) and toughness (~ 50 -70%) greatly improve for the T2.5Alg sample in dry tests. For immersed tests the intrinsic strengths are lower, but the verified improvement remains and keeps uniform over the 14 days of evaluation. Weibull analysis revealed that the sample reliability slightly lowered with Alg introduction (Fig 3b). Achieved mechanical properties for T2.5Alg are in the upper limit of the reported mechanical properties of the human trabecular bone.

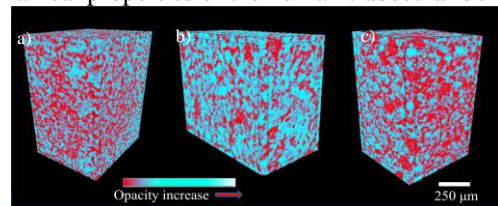


Figure 2: μ -CT reconstruction showing microstructure organization of a) T ($\phi=49\%$) b) T2.5Alg ($\phi=32\%$) c) T7.5Alg ($\phi=37\%$)

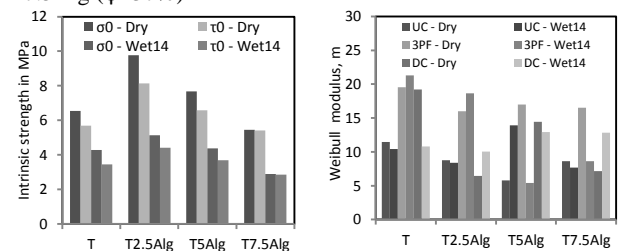


Figure 3: a) Intrinsic strengths as function of powder mixture and testing condition. b) Weibull modulus as a function of powder mixture, testing technique and condition.

CONCLUSION

As far as we know this is the first time report about the successful direct fabrication of structured 3D biocomposites of T and Alg, by 3DP. Alginate inclusion within the ceramic matrix, enhances the mechanical limitations addressed to the standard used ceramic bone grafts, and also preliminary biological tests evidence improvements in biological properties. These results suggest that 3DP powder printing of TCP/alginate biocomposites is a promising strategy for bone tissue regeneration.

REFERENCES

1. Bohner M. *et al.*, European Ceramic Society 32: 2663–2671, 2012.
2. Van der Elst M. *et al.*, Biomaterials 20:121-8, 1999.
3. Turco G. *et al.*, Biomacromolecules 10:1575–1583, 2009.
4. Gbureck U. *et al* Adv. Funct. Mater. 17: 3940–5, 2007

ACKNOWLEDGMENTS

The authors would like to thank the PhD scholarship financed by FCT within the company Altakit S.A., SFRH/BDE/51454/2011 (Miguel Castilho) and are very grateful to the Department for Functional Materials in Medicine and Dentistry, University of Würzburg.

Surface modification of Ti-6Al-4V alloy controlling OCP nucleation by electron cyclotron resonance plasma oxidation

Hiroshi Masumoto¹, Mayumi Oikawa², Yusuke Orii², Takahisa Anada², Osamu Suzuki² and Keiichi Sasaki²

Frontier Research Institute for Interdisciplinary Sciences (FRIS), Tohoku University, Japan¹

Graduate School of Dentistry, Tohoku University, Japan²

hiromasu@fris.tohoku.ac.jp

INTRODUCTION

Ti-6Al-4V alloy is used by dentistry and orthopedics as an implant material, since it is excellent in biocompatibility or mechanical property. It is known that the biocompatibility of Ti will change with the condition of the surface oxide (titania: TiO₂) film of implant Ti alloy. However, since the thermal expansion difference of Ti and TiO₂ is large, it is difficult to deposit the good TiO₂ film on Ti alloy at low temperature for a short time. Electron cyclotron resonance (ECR) plasma is high-active plasma, and high-quality crystalline films can be obtained at low temperature for short time. ECR plasma oxidation is effective surface modification of metal Ti for biocompatibilities, which became clearly in previous study^[1]. Our previous studies indicated that implantation of octacalcium phosphate [Ca₈H₂(PO₄)₆ · 5H₂O, OCP] was efficiently enhanced bone regeneration compared to HAp^[2]. In the present study, TiO₂ films were deposited on Ti-6Al-4V alloy by ECR plasma oxidation, and the effect of oxidation conditions on structure and precipitation behavior of OCP were investigated.

EXPERIMENTAL METHODS

ECR plasma apparatus was used for oxidation of Ti-6Al-4V alloy surface (10 x 10 x 1.0 mm³). A magnetic field (8.75x10⁻² T) was applied to the plasma chamber to satisfy the ECR condition. The microwave power was 900 W. The oxygen gas pressure during ECR oxidation was set to 0.003 -1.5 Pa and the oxidation time was set to 1.8ks. An infrared lamp was used for controlling the substrate temperature in the range from room temperature (RT) to 600 °C.

OCP was precipitated in phosphate-buffered solution on TiO₂ film deposited Ti substrate^[2]. The calcification ability was estimated by weighing the substrate before and after

the immersion. The structure and morphology of the films were characterized by X-ray diffraction analysis (XRD) and optical and scanning electron microscopy (SEM).

RESULTS AND DISCUSSION

Fig. 1 shows XRD patterns of the substrates that were oxidized by ECR plasma at various temperatures. Crystalline rutile-type TiO₂ films were obtained above 400 °C. The amount of rutile TiO₂ increased with increasing oxidation temperature. The ECR plasma was significantly effective to prepare crystallized TiO₂ films at low temperatures.

Fig. 2 shows macroscopic images of calcium phosphate deposits formed on the Ti-6Al-4V alloy substrate after ECR plasma oxidation at 400°C. Mixtures of OCP and dicalcium phosphate dihydrate (DCPD) peaks were observed after calcification. Whole surface was covered by Many flocculent precipitates of calcium phosphate. The amount of OCP and DCPD after calcification increased with increasing total pressure (P_T) from 3.3x10⁻³ - 1.5x10⁻² Pa, and showed the maximum at P_T = 1.5x10⁻² Pa.

Fig. 3 shows the effect of the oxidation temperature and time on calcium phosphate deposition onto the substrate surfaces. The amount of calcium phosphate deposition was maximized at 400°C.

It was suggested that ECR plasma oxidation method is effective surface modification for the Ti-6Al-4V alloy , because of their calcification ability.

Reference

1 Y. Orii, *et al. J Biomed Mat Res Part B, Appl. Biomater.*, (2010) **93**(2):476.

2 O. Suzuki, *et al. Biomaterials* (2006) **27**: 2671.

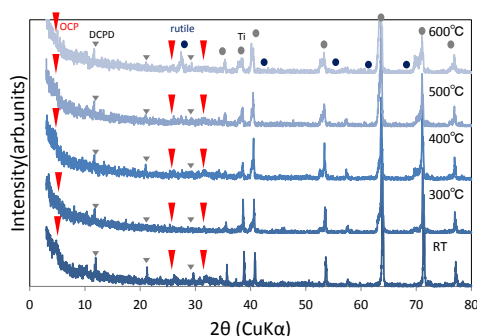


Figure 1. XRD patterns of the surfaces of Ti-6Al-4V alloys oxidized by ECR plasma and after calcification.



Figure 2. Macroscopic images of calcium phosphate deposits formed on the Ti-6Al-4V alloy substrate after ECR plasma oxidation at 400°C.

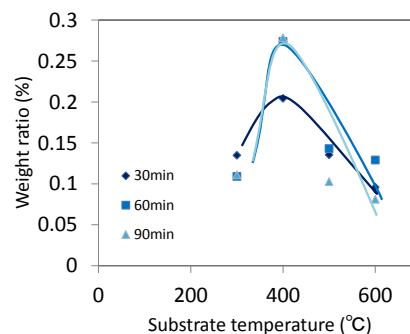


Figure 3. Amount of calcium phosphate deposits estimated by the weight ratio at different substrate temperatures.

Evaluation the Cellular Behavior on Poly Lactic-co-Glycolic Acid - Gelatin Scaffolds by Electrospinning Method

Farnaz Ghorbani¹, Haniyeh Nojehdehyan^{2*}, Ali Zamanian

- 1- Biomedical Engineering Department, Science and Research Branch, Islamic Azad University, Tehran, Iran.
- 2- Department of Dental Materials, Dental School, Shahid Beheshti University of Medical Science, Tehran, Iran.
- 3- Biomaterials Department, Materials and Energy Research Center, Karaj, Iran.

Farnaz_ghorbani.1991@yahoo.com

Introduction

The human being peripheral nerve has strong regeneration potentiality. The disrupted peripheral nerve could successfully regenerate if a proper environment were provided. There are certain limits for autografts, To overcome those disadvantages, artificial nerve scaffold has been developed [1]. Since the surface to volume ratio in electrospinning nanofibers is high, using them in neural tissue engineering [2]. In this research, 3D PLGA/Gelatin nanofibrous scaffolds were prepared by electrospinning method. We selected 2,2,2-trifluoroethanol as solvent to dissolve both synthetic and natural polymer with organic and aqueous basis, respectively.

Materials and methods

The experimental polymer composite solutions were prepared by dissolving PLGA and gelatin with the weight ratio 8:2 and concentration of 15% w/v in TFE. The mixture was stirred for 12 h room temperature to obtained homogeneous composite solution for electrospinning. The resulting biological and structural effects were evaluated using a range of methods including SEM images, porosity, cell culture, MTT assay.

Results and discussions

Fig. 1 shows the SEM images of electrospun nanofibrous PLGA/gelatin scaffolds. It illustrated nanofibers possessed smooth without bead defects with the average fiber diameters of 924nm and 777nm with injection rate 0.1 and 0.2 $\frac{ml}{hr}$, respectively. nanofibers diameter decreased with the addition of gelatin, because of increased the charge density of the solution which improved the stretching force and self repulsion of the jet, in addition decrease porosity of scaffolds. Increasing flow rate causes decreasing fiber diameter, so it can increase strength. The porosity of scaffolds was approximately 90%, indicating that they were beneficial for the adherence and proliferation of the cells. The cell proliferation (L929) of nanofibers with the injection rate of 0.2 $\frac{ml}{hr}$ after 2 and 7 days of cell culture are shown in Fig. 2. After 2 day, the cell adhered well randomly on the surface of all electrospun scaffolds. After 7 day, more cells were clustered around the nanofibers Initial cell adhesion could be affected by the surface hydrophilicity of scaffold. Figure 3 illustrate Cytotoxicity and biocompatibility of samples 2 and 7 days after cell culture. It shows increasing the number of cells in control samples (polystyrene plates) and test

samples. There was no significant difference between number of cells and rate of growth in samples.

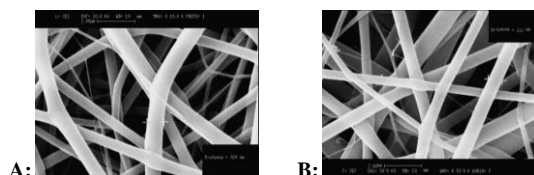


Fig. 1. Morphology of PLGA/gelatin scaffolds with injection rates 0.1 $\frac{ml}{hr}$ (A) and 0.2 $\frac{ml}{hr}$ (B)

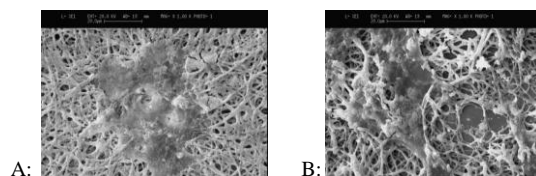


Fig. 2. Morphology of fibroblast on PLGA/Gelatin nanofibers after 3 (A) and 7 (B) days.

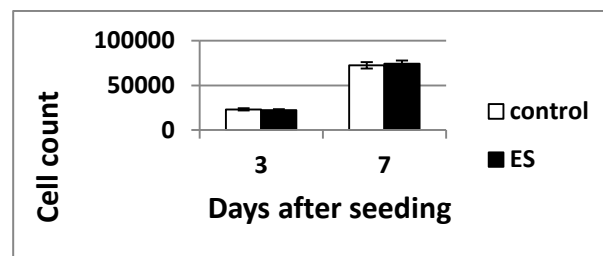


Fig. 3. Result of MTT assay

Conclusion

In this study, randomly PLGA/G scaffolds were fabricated through electrospinning. PLGA improve the mechanical properties. Gelatin causes hydrophilic structure and can improve the water absorption but decrease mechanical properties. The addition of gelatin enhanced the adhesion and proliferation of the cell. Scaffolds have about 90% porosity and Fiber diameter changes with changes in flow rate. In addition, morphology showed smooth and bead free surface feature of nanofibers.

References

- [1] R. V. Weber, S. E. Mackinnon, Clin. Plast. Surg. 32 (2005) 605.
- [2] Christiane B. Gumera, Georgia Institute of Technology, 2009.

Conducting Polymer Platform for Anti-Cancer Drug Delivery

K. Krukiewicz^{1*}, T. Jarosz¹, J.K. Zak¹, M. Łapkowski¹, P. Ruszkowski²,
T. Bobkiewicz-Kozłowska², B. Bednarczyk-Cwynar³

¹Department of Physical Chemistry and Technology of Polymers, Silesian University of Technology, Poland,

²Department of Pharmacology, Poznan University of Medical Sciences, Poland

³Department of Organic Chemistry, Poznan University of Medical Sciences, Poland

*katarzyna.krukiewicz@polsl.pl

INTRODUCTION

Chemotherapy is among radiotherapy and surgical resection, one of the most often applied ways of cancer treatment. The efficacy of chemotherapy is, however, limited by severe toxic side effects of anticancer drugs on healthy tissues [1]. This limitation could be overcome by employing local drug delivery systems (DDS) for anticancer agents [2]. Nowadays, intrinsically conducting polymers (CP) have been considered as promising materials for drug reservoirs in DDS because of their ion-exchangeable properties [3]. CPs are able to immobilise anionic drugs during oxidation and release them in the process of reduction. Triterpenoids are one of the most promising groups of anticancer compounds. These compounds are secreted by living tissues of numerous higher plants, granting them exceptionally good availability [4]. Oleanolic acid (HOL) has been found to be active in various stages of tumor development, including inhibition of tumor promotion, invasion and metastasis; its anticancer effects have been reported in several cancer cell lines, such as HeLa [5], L1210, K562 and HL-60 [6].

EXPERIMENTAL METHODS

Oleanolic acid (HOL) was isolated from waste-product obtained during production of mistletoe extract. Cyclic voltammetry (CV) was utilised for the fabrication and in situ analysis of PEDOT/OL⁻ composite layers *via* two different procedures: in-situ during the process of polymerisation (1-step procedure) and post-polymerisation modification (3-step procedure). The release of OL⁻ from the composite was followed by time-resolved UV-Vis spectroscopy. The biological activity of HOL solutions was determined using HeLa cancer cell lines.

RESULTS AND DISCUSSION

In the immobilization step, the positive potential was applied to entrap OL⁻ into the structure of PEDOT matrix.

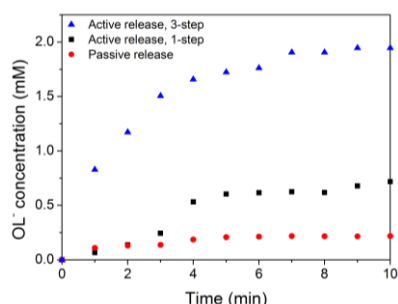


Fig.1. Release of OL⁻ from PEDOT/OL⁻ synthesised *via* 1- and 3-step procedures in passive and active modes.

The release of the immobilised OL⁻ was performed under spontaneous (passive) and electro-assisted (active) modes in PBS. The passive mode showed short term drug release followed by a plateau. When PEDOT/OL⁻ matrix was electrically stimulated, longer term sustained release was observed with higher OL⁻ concentration. PEDOT/OL⁻ matrix synthesized *via* 3-step procedure proved to be more effective drug carrier than matrix obtained *via* 1-step procedure.

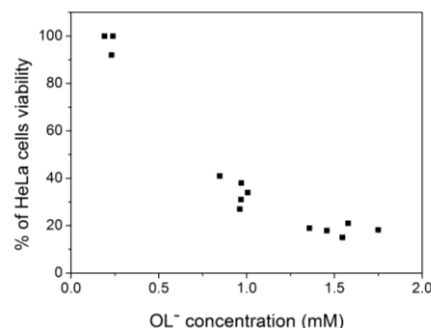


Fig.2. Cytotoxic activity against HeLa cells for OL⁻ immobilised and released from PEDOT/OL⁻ matrices.

It was crucial to determine whether immobilised and released OL⁻ maintains its anticancer properties. All OL⁻ solutions for which OL⁻ concentration was higher than 0.25 mM demonstrated anti-cancer activity. The highest anti-cancer activity showed OL⁻ solution obtained after active release from matrix synthesized *via* 3-step procedure.

CONCLUSION

PEDOT/OL⁻ composite was demonstrated to be a promising and robust material for drug delivery. The processes of immobilisation and release did not affect the anticancer properties of OL⁻.

REFERENCES

1. Ross R.W. *et al.*, J. Urol. 167: 1952-1956, 2002.
2. Matsusaki M. *et al.*, Expert Opin. Drug Deliv. 6:1207-1217, 2009.
3. Guimard N.K. *et al.*, Prog. Polym. Sci. 32:876-921, 2007.
4. Yeung M.F. *et al.*, Natura Proda Medica 2:77-290, 2009.
5. Srivastava P. *et al.*, Biotechnol. Bioproc. Eng. 15:1038-1046, 2010.
6. Ovesná Z. *et al.*, Mut. Res. 600:131-137, 2006.

ACKNOWLEDGMENTS

The authors would like to thank the Polish National Science Centre (Grant no: 2012/07/N/ST5/01878) for providing financial support to this project.

Stability of self-assembled hyaluronan polymeric micelle cores in aqueous solutions and whole human blood

Daniela Šmejkalová, Kristina Nešporová, Jana Šógorková, Pavlína Halamková, Jaroslav Novotný, Jakub Syrovátka, Gloria Huerta-Angeles

Contipro Pharma, Dolní Dobrouč, Czech Republic, daniela.smejkalova@contipro.com

INTRODUCTION

Hydrophobized polymers have gained popularity as vehicles for drug delivery. Among the widely studied vehicles are polymeric micelles formed from self-assembled amphiphilic polymers having core-shell architecture with diameters ranging from 20 to 200 nm. While the hydrophilic shell ensures aqueous dissolution of the polymeric micelle, the hydrophobic core may accommodate non polar drugs through non covalent bonding (encapsulation). Since such encapsulation of a hydrophobic molecule in aqueous media is only a result of thermodynamic equilibrium, the question which arises is how much the polymeric micelle integrity will be disturbed in time *in vivo*, after dispersion in blood.

To probe the drug encapsulation stability, a lipophilic donor – acceptor FRET (Fluorescence Resonance Energy Transfer) dye pair was loaded into polymeric micelle cores. When the micelle core is intact, distance between FRET pair dyes is short enough for energy transfer, resulting in FRET evolution. However, when the micelle core undergoes conformational changes or is disrupted, the distance between donor and acceptor dye becomes larger, and as a result FRET evolution is suppressed.

It was the aim to probe the stability of FRET loaded hyaluronan (HA) polymeric micelles in aqueous (pH 7.4 and 5.5) and saline media as well as in whole human blood.

EXPERIMENTAL METHODS

Caproyl (HAC6, Mw 5-42 kDa, DS = 60%) and Oleyl hyaluronan (HAC18:1, Mw 5-42 kDa and DS = 10%) were loaded with FRET pair dyes (DiIC18 and DiOC18) by solvent evaporation method.

Fluorescence emission spectra were collected after polymeric micelle dissolution in aqueous and saline solvents, human plasma and blood using Quanta Master 400 fluorescence spectrometer at excitation wavelength 484 nm and emission wavelength range from 490 to 600 nm. FRET ratio was calculated as $I_{DiI}/(I_{DiI}+I_{DiO})$.

RESULTS AND DISCUSSION

Since polymeric micelles are mostly prepared with the intention of intravenous applications, the micelle stability was tested at pH 7.4 (pH of blood), pH 5.5 (pH in some tumoral tissues) and in physiological solution (0.9% NaCl). Independently on hyaluronan Mw or length of hydrophobic acyl chain (C6 and C18:1), the FRET ratio of all samples remained constant during 24 hrs incubation of polymeric micelles in any of the media. The value of FRET ratio was close to 1.0, which suggested that the micelle cores remained intact and FRET dyes were not released from the core (i.e. their distance remained constant).

However, FRET ratio dropped to 0.8 (HAC18:1) and 0.7 (HAC6), when polymeric micelles were dispersed in serum. The micelle instability was attributed to the interaction of HA with plasma proteins. Among these proteins, albumin was found to be the prime factor disturbing the original integrity of micelle core and causing FRET dyes separation. As it is summarized in Table 1, showing half-life of HA micelles calculated from FRET ratio decrease, this interference was more evident (i) with decreasing concentration of polymeric micelles and (ii) for HA with shorter length of acyl chain. Similar tendency was then observed when polymeric micelles were incubated with human blood (Figure 1). The higher the polymeric micelle concentration, the smaller amount of interfered or disrupted micelles. Concentrations around 3.0 mg/mL of hyaluronan polymeric micelles in blood are reachable *in vivo*.

Table 1. Half-life ($\tau_{1/2}$) of polymeric micelles in the presence of albumin in 0.9% NaCl at 37°C.

Polymeric micelle	Mw (kDa)	$\tau_{1/2}$ (hod) c=0.5mg/mL	$\tau_{1/2}$ (hod) c=1.5mg/mL
HAC6	5	1.2	5.2
	15	0.8	2.5
	38	0.8	7.2
HAC18:1	5	2.8	>>24
	15	3.0	>>24
	38	Not soluble	

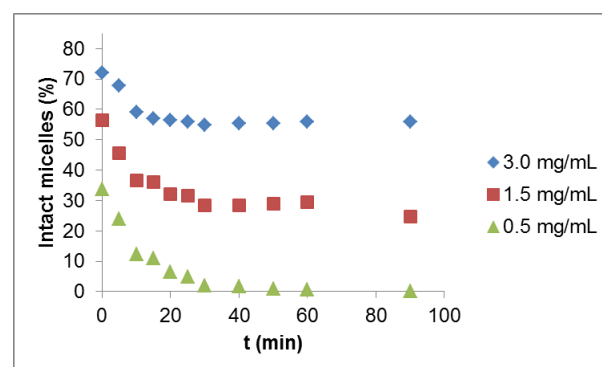


Figure 1. The amount of intact HAC18:1 polymeric micelles (15 kDa) after dispersion in full human blood.

CONCLUSION

The thermodynamic stability of hyaluronan polymeric micelles is mainly influenced by serum proteins, especially albumin. The stability is concentration dependent. Increased polymeric micelle concentration resulted in increased stability. For this reason, initial concentration of hyaluronan polymeric micelles *in vivo* in blood should be at least around 3.0 mg/mL so that drug bursting or adsorption to albumin is prevented right after intravenous injection.

Extracellular matrix proteins regulate Adipose Derived Mesenchymal Stem Cells and Amniotic Fluid Stem Cells attachment and proliferation: utility for tissue and organ regeneration

Anna Bajek^{1*}, Joanna Olkowska¹, Natalia Gurtowska¹, Tomasz Drewa^{1,2}

¹Department of Tissue Engineering, Chair of Medical Biology, Medical College, Nicolaus Copernicus University, Bydgoszcz, Poland; * a_bajek@wp.pl

² Department of Urology, Nicolaus Copernicus Hospital, Toruń, Poland

INTRODUCTION

Cells in tissues and organs are located in microenvironments which consist of Extracellular matrix (ECM) and neighboring cells. ECM affects different characteristics of cells including cell architecture, mechanics, polarity and function¹. Moreover, cell-matrix interactions are crucial for the successful repair and regeneration of damaged tissue and organ. The aim of this study was to check how different extracellular matrix (ECM) proteins affect proliferation and adhesion potential of human Adipose Derived Mesenchymal Stem Cells (hADSCs) and human Amniotic Fluid Stem Cells (hAFSCs).

EXPERIMENTAL METHODS

Human ADSCs and AFSCs were cultured on dishes coated with 4 types of ECM including collagen IV, fibronectin, laminin and poly-D-lysine for 7 days, and simultaneously cultured on a noncoated dish as a control. Proliferation potential was assessed by MTT assay while adhesion capacity by macroscopic observation.

RESULTS AND DISCUSSION

All of tested ECM proteins do not decrease the proliferation potential of hADSCs. However,

different trend was observed regarding hAFSCs. Laminin and poly-D-lysine caused the decrease in proliferation compared to the control. In both populations, the largest increase of proliferation was observed on collagen IV and fibronectin-coated dishes, which promote the spindle morphology of cultured cells as well. Additionally, we observed good adhesive properties of hADSCs and hAFSCs in 30 minutes after seeding on ECM-coated dishes.

CONCLUSION

These results suggest that the signal transduction of the cell-matrix interaction for the proliferation and adhesion of hADSCs and hAFSCs was activated when cultured on collagen IV and fibronectin-coated dishes. It indicates on ECM as an important component of the cellular niche in the tissue, supplying critical biochemical and physical signals to initiate or sustain cellular functions. It is also possible that ECM is required for the reconstitution of the niche of stem cells *in vitro*.

REFERENCES

1. Alamdari OG. Et al., Avicenna J Med. Biotech. 5:234-240, 2013.

Development of a new biomaterial based on Hyaluronan and oleic acid for drug delivery applications

Gloria Huerta-Angeles^{1*}, Martin Bobek¹, Daniela Šmejkalová², Kristina Nešporová² and Vladimír Velebný³

¹Department of scale up and optimization of processes-Contipro Pharma as, Dolní Dobrouč, 401, Czech Republic.

²Nanocarrier development group, Contipro Pharma as. ³Contipro group

huerta-angeles@contipro.com

INTRODUCTION

Hyaluronan (HA) is a lineal polysaccharide found in extracellular matrices of connective tissue and possesses a large number of biological functions. The use of HA in drug delivery is impeded by its high hydrophilicity and short self-life. In this study, we will present the design and synthesis of a novel derivative (SOH) based on Hyaluronic acid (HA) conjugated with oleic acid¹. The development of the reaction was transferred from laboratory scale to pilot plant with highly purity and chemical reproducibility. The aim of this work is to demonstrate the applicability of a new derivative of HA towards formulation in cosmetics or pharmaceutical fields.

EXPERIMENTAL METHODS

Amphiphilic derivatives were obtained by reaction of the hydroxyl groups of HA with mixed aliphatic aromatic anhydrides¹⁻². Mixed anhydrides obtained by the reaction of substituted-benzoyl chlorides (sBC) and oleic acid, were used as versatile reagents for the esterification of HA. The characterization of the derivatives was performed by SEC-MALLS, NMR, IR and Rheology. The effect of the degree of substitution on the critical micellar concentration (cmc) was determined by fluorescence spectroscopy. Cell viability assay was studied by interaction of the derivative with dermal fibroblasts.

RESULTS AND DISCUSSION

This novel protocol allows the modification of low (LMW-HA), medium (MMW-HA) and high molecular weight (HMW-HA) in a broad range of degrees of substitution (DS). As an example, it produces chemical modification from 2 up to 50% in (6,000-26,000 g/mol), up to 15% (MMW-HA) and 5% in (HMW-HA). The reproducibility of the reaction was tested in laboratory and semi-production scales. The covalent bond of the fatty acid and HA was demonstrated by DOSY (Figure 1). The structural characterization demonstrates that in aqueous solvents, the hydrophobic oleyl moieties of the SOH assembled themselves in hydrophobic cores, while these cores were surrounded by hydrophilic HA backbones (Figure 2). The encapsulation of different model drugs was tested. It was observed that (DS) may slightly change the value of critical micellar concentration from 1 to 0,5 $\mu\text{g}\cdot\text{mL}^{-1}$, which is around 1500 times lower than the concentrations needed to form micelles with low-molecular-weight surfactants such as SDS³.

The *in-vitro* results indicate that the tested compounds are non-cytotoxic (to a concentration of 1 mg/ml). Cell viability was not changed compared with unaffected control part up to 72 hours (Figure 3). We observe that after the chemical modification, the derivatives were more stable to enzymatic degradation

in compared to native HA and without losing biocompatibility. The hydrophilicity of the polysaccharide was decreased due to the covalent bonding of the fatty acid but the derivatives were still water soluble, which is a necessary condition for encapsulation.

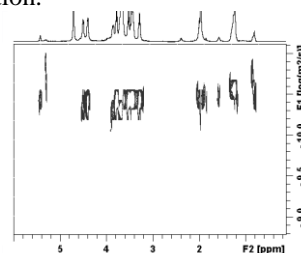


Figure 1. DOSY of sodium oleyl Hyaluronate

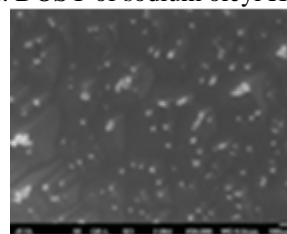


Figure 2. Formation of nano-aggregates of SOH loaded with α -Tocopherol

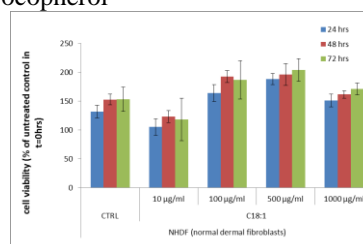


Figure 3. Cell viability of SOH derivative

CONCLUSION

The use of mixed anhydrides proved to be a good alternative for the chemical modification of Hyaluronic acid up to 50 %. The main advantages of the proposed reaction pathway are the mild conditions that allowed negligible degradation of the biopolymer after reaction. The chemical modification has not affected the biocompatibility of the polysaccharide.

REFERENCES

- Šmejkalová D., Huerta-Angeles G. *et al*, "patent pending application number PV2012-842"
- Šmejkalová D. *et al*, *International Journal of Pharmaceutics*, Vol. 466 (1–2), 147–155, 2014.
- Bian, F. *et al*, *Carbohydrate Polymers*, vol. 76, no. 3, pp. 454–459, 2009

ACKNOWLEDGMENTS

"The authors would like to thank the Ministry of Industry and Trade of the Czech Republic for providing financial support to this project".

Imaging of Biofilm Removal on Titanium and Glass by Dental Instruments

E. Pecheva^{1*}, N. Vyas^{1,2}, R.L. Sammons¹ and A.D. Walmsley¹

^{1*}School of Dentistry, University of Birmingham, UK, e.v.pecheva@bham.ac.uk

²Physical Sciences of Imaging for Biomedical Sciences (PSIBS), University of Birmingham, UK

INTRODUCTION

Bacterial biofilms, also known as plaque, form on teeth dental and implants, and may lead to dental caries, periodontal disease with tooth loss, serious infections or implant failure. Biofilms also mineralise, forming calculus that has to be removed mechanically.

Ultrasonic dental scalers are used in dentistry for plaque and calculus removal due to their efficiency and greater comfort for the patient than hand instruments. Another advantage is the generation of cavitation within the water flow over the dental tip, which increases the cleaning efficiency¹. Since ultrasonic scalers are not 100% efficient, in order to improve their ability to remove biofilm it is essential to study dental plaque growth, removal and structure, and non-destructive imaging techniques are integral to this work. This model can then be used to assess removal by the ultrasonic scaler. Each imaging technique has its own advantages and limitations. Therefore for detailed investigations, a selection of two or more complementary and non-destructive techniques is required to provide complete information on the components of the surface.

Our research aims to investigate the biofilm removal by a piezoelectric dental scaler.

EXPERIMENTAL METHODS

An in vitro biofilm model system using a non-pathogenic Gram-negative species of *Serratia* (NCIMB40259) was developed in a bioreactor² on titanium and glass surfaces. *Serratia* is capable of forming biofilm on various surfaces, as well as mineralising it to calcium deficient hydroxyapatite that chemically resembles calculus². A Satelec ultrasonic dental scaler (P5XS Newtron, France) with water irrigation of the tip was used to disrupt the biofilm for 30 seconds. The tips were applied with their front side parallel to the biofilm and tip end facing down. The removal was visualised by SEM, white light interferometry, optical microscopy, AFM and micro-CT, and quantified using image analysis.



Fig.1 Design of the tips chosen for the study: front of the tips. The free end of the tip is placed parallel to the biofilm during the disruption. The threaded end of the tip is attached to a handpiece.

RESULTS AND DISCUSSION

Tips with different shapes (fig.1) were operated at fixed power setting giving a tip displacement of 15µm. Two

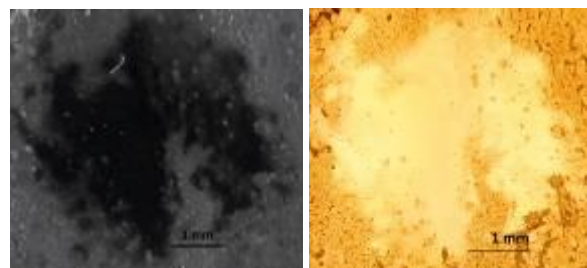


Fig.2 Images of the disrupted biofilm on glass, obtained by Nikon camera (left) and optical microscope (right). Tip 1 was used at 40 µm distance from the sample.

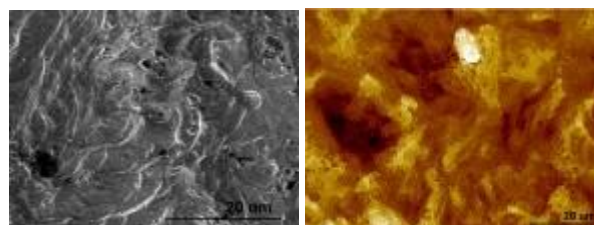


Fig.3 Disrupted biofilm on titanium imaged by SEM (left) and white light interferometry (right).

positions along the tip length were chosen to contact the biofilm – the tip end (A) and the tip curved side (B) where previous work has demonstrated higher cavitation in comparison to the tip end (unpublished data). An area of disruption on both glass and titanium occurred when the tip distance to the biofilm was set at 40 µm to avoid direct mechanical contact of the tip to the material surface (figs. 2 and 3). The most efficient removal was with the thinner tips 1 and 10P. The effect of the position along the tip (A or B) on the biofilm removal still has to be elucidated. It was more difficult to clean the titanium surface due to its higher surface roughness ($R_a = 415$ nm in comparison to the glass – 6 nm). SEM revealed bacteria still present in the cleaned area while there were no bacteria on the glass.

CONCLUSION

We have shown how to image biofilm removal. Both tip shape and material surface roughness were effective in biofilm removal when using an ultrasonic scaler.

REFERENCES

1. Walmsley AD. *et al.*, Clin. Oral. Invest. 17:1227–1234, 2013
2. Medina Ledo H. *et al.*, J. Mater. Sci. Mater. Med. 19:3419-3427, 2008

ACKNOWLEDGMENTS

We acknowledge the EPSRC (Grant № EP/J014060) for providing financial support to this project.

Poly (ϵ -lysine) dendrons as modulators of quorum sensing in *Pseudomonas aeruginosa*

Rahaf Issa, Steve Meikle, Stuart James, and Ian R. Cooper

School of Pharmacy and Biomolecular Sciences, University of Brighton, UK

r.issal@uni.brighton.ac.uk

INTRODUCTION

Quorum sensing (QS), an intercellular signalling system in *Pseudomonas aeruginosa*, regulates the expression of multiple extracellular virulence determinants via three main pathways (*las*, *rhl* and *PQS*). Given the rapidly expanding problem of antibiotic resistance, interrupting these pathways using synthetic molecules is being explored as a novel alternative to conventional antibiotics. We have previously shown the potential of hyperbranched poly (ϵ -lysine) dendrons, and their ability to enhance the efficacy of ciprofloxacin and reduce toxin production¹. In this study, we evaluate the effects of generation 3 poly (ϵ -lysine) dendrons, RG3K, on the production of QS-regulated virulence factors.

EXPERIMENTAL METHODS

Dendron Synthesis: RG3K, a hyperbranched macromolecule composed of 3 branching generations of lysine (K) and an arginine (R) root, was synthesised using solid-phase peptide synthesis. Dendrons were assembled from Fmoc-protected amino acids using a 4x molar excess of reagents, and characterised by analytical HPLC (Waters) and microTOF MS (Bruker).

Application: *P. aeruginosa* (PAO1) was exposed to increasing concentrations of RG3K (1 to 1000 μ M) after 0, 3 and 8h of growth. Cellular viability was determined at 18h. To ascertain the effects of RG3K on QS, a range of virulence factors was examined. LasA protease activity was determined by measuring the ability of PAO1 supernatants (20 μ L) to lyse boiled cells of *Staphylococcus aureus* NCTC 6571 (180 μ L) within 1h of exposure. The extent of PAO1 attachment and degree of biofilm biomass production was examined 2, 4, 6, 8, and 24h after treatment with RG3K in 96-well plates. Biofilms were stained with 0.1% (w/v) crystal violet, and quantified at OD₅₉₅. To further elucidate the effects of RG3K on biofilm structure, PAO1 was grown in the presence of RG3K (400 μ M) on borosilicate coverslips for 20h, stained with 0.01% (w/v) acridine orange, and the structure was analysed using CLSM. Data ($n = 4$ per assay) was analysed using ANOVA or t-test, where $P < 0.05$ was considered significant.

RESULTS AND DISCUSSION

Addition of RG3K after 3 and 8h of growth exhibited no significant inhibitory effects at $\leq 400\mu$ M, and the cell density at 18h was closely related to medium-only PAO1 ($P > 0.6$). Thus, any effects in subsequent assays at these concentrations are exhibited via a mechanism other than direct killing. RG3K did however cause a five-fold reduction in viability when added simultaneously with PAO1 at 1000 μ M ($P < 0.002$). LasA, a staphylolytic protease, is induced after ~6h of growth. At 400 μ M, RG3K reduced LasA activity when added after 0 and 3h ($P < 0.001$, respectively), but not

8h ($P > 0.68$), of growth (Table 1), suggesting that RG3K inhibits LasA production, but cannot reduce LasA levels post-production.

Table 1. LasA activity in response to RG3K, 400 μ M.

Conditions	LasA activity (at 18h)*
Medium-only	0.230 \pm 0.004
RG3K at 0h	0.004 \pm 0.003
RG3K at 3h	0.014 \pm 0.002
RG3K at 8h	0.262 \pm 0.010

*Expressed as reduction in OD₅₉₅ per hour ($n = 4 \pm$ SD).

The biofilm crystal violet assay, which stains extracellular matrix polymers, showed that exposure to RG3K caused a significant reduction in biofilm biomass in nutrient-rich and minimal media ($P < 0.005$). At concentrations between 100 and 400 μ M, RG3K caused a 10 to 40% biomass reduction in 2 to 8h-old biofilms, respectively. As QS is a cell-density dependent process², RG3K appeared to be more effective at preventing biofilm biomass production after 24h ($P < 0.001$), causing a dose-dependent activity. Thus, RG3K exerts its full effects with QS activation.

CLSM analysis revealed a reduction in microcolony formation (indicated using dashed lines) following exposure to RG3K (400 μ M), causing biofilms to appear notably thinner and more disperse (Figure 1).

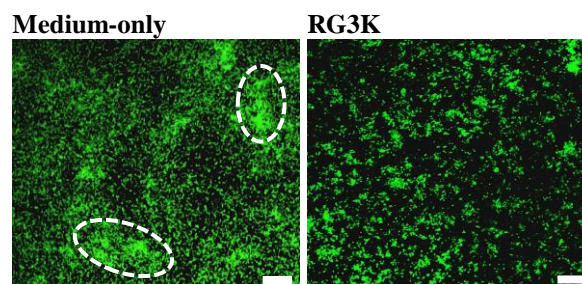


Figure 1. Biofilm structure in response to RG3K.

CONCLUSION

RG3K has the potential to intercept QS-regulated virulence factor production in *P. aeruginosa*, offering a promising novel and alternative strategy for eradicating antibiotic resistant bacterial infections.

REFERENCES

1. Issa R. *et al.*, *CPIS*. 572828:8, 2014.
2. Darch S.E. *et al.*, *PNAS*, 109(21):8259-63, 2012.

ACKNOWLEDGMENTS

This research is supported by a Pharmacy and Biomolecular Sciences funded PhD studentship from the University of Brighton.

Comparative Osteogenesis of Calcium Silicate Cement and Calcium Phosphate Cement

Shinn-Jyh Ding^{1*} and Shu-Ching Huang²

¹Institute of Oral Science, Chung Shan Medical University, Taichung 402, Taiwan, sjding@csmu.edu.tw

²School of Dentistry, Chung Shan Medical University, Taichung City 402, Taiwan

INTRODUCTION

Many artificial materials have been proposed as bone graft substitutes in replace of autografts, which are the gold standards. Calcium phosphate similar to the mineral components of bone tissue has been used to provide support, fill voids, and enhance the biological repair of skeletal defects. However, with the increasing popularity of minimally invasive techniques, the development of injectable systems that mould to the shape of the bone cavity and polymerise when injected in situ has attracted a great deal of attention. Thus, a variety of injectable cement systems have been widely developed. The self-setting calcium phosphate cement (CPC) has many favourable properties that support their clinical use in the repair of bone defects¹. Beside, calcium silicate cement (CSC) is shown to enhance the proliferation and differentiation of osteoblasts, suggesting that CSC could have potential as a material for orthopedic and dental surgical implants². This study aims to investigate comparatively the osteogenesis of the two calcium-based cements for clinical applications.

EXPERIMENTAL METHODS

Calcium silicate powder was prepared by the sol-gel method, as described elsewhere³. For the preparation of the cement the powders were hand-mixed at a liquid to powder ratio of 0.4 mL/g with distilled water. To prepare BoneSource® classic CPC (Stryker), the liquid phase was 0.25 M sodium phosphate and a liquid to powder ratio of 0.25 mL/g was used. The specimens were stored in an incubator at 100% relative humidity and 37 °C for 1 day to set. Prior to cell culture, the hardened cement discs were sterilized by soaking in a 75% ethanol solution and exposure to ultraviolet light for 2 h. The osteogenic properties of all the cement specimens were evaluated by incubation with human mesenchymal stem cells (hMSCs). To observe cell morphology on the specimen surface, specimens were washed three times with PBS and fixed in 2% glutaraldehyde after 3 h of seeding and then were dehydrated using a graded ethanol series. The dried specimens were viewed using a scanning electron microscopy. The reagent Alamar Blue was used for real-time and repeated monitoring of cell proliferation. The alkaline phosphatase (ALP) activity of hMSCs on the cement specimens was measured. The mineralized matrix synthesis was analysed using an Alizarin red S staining method. One-way ANOVA statistical analysis was used to evaluate the significance of the differences between the mean values. The results were considered statistically significant at a p value of less than 0.05.

RESULTS AND DISCUSSION

Scanning electron micrographs show that stem cells attached to the CSC surfaces are spread out, but the shape of cells attached to the CPC surfaces is round. This demonstrates that CSC could facilitate the cell attachment higher than CPC. Regarding cell proliferation, the results indicate that more cells significantly ($p < 0.05$) grow on CSC surface than on CPC surface at all culture times. Similarly, the ALP levels on CSC are significantly ($p < 0.05$) greater than those on CPC at most of culture times, indicating that the effect is material-dependent. It is generally accepted that an increase in the specific activity of ALP in bone cells reflects a shift to a more differentiated state. ALP enzyme activity is also associated with bone formation, and it is produced in high levels during the bone formation phase. Alizarin Red S staining is a common histochemical technique used to detect calcium deposits in mineralized tissues and cultures. The noticeable differences are observed after cell culture on the CSC and CPC surfaces. Clearly calcified tissue formation is seen in the cultures grown in the presence of the CSC on day 21 compared to CPC. The Si component of CSC plays important roles in the early stages of bone formation and the calcification process. According to the literature⁴, that silicate-substituted calcium phosphate supported attachment and proliferation of MSCs and induced osteogenesis to a greater extent than hydroxyapatite (HA).

CONCLUSION

Overall, these findings indicate that the CSC could enhance mesenchymal stem cell differentiation, making it suitable for bone repair applications. It also confirms that CSC may be more effective than CPC in such a way as to provide an osteoinductive microenvironment without addition of exogenous growth factor or pre-treatment with osteogenic medium.

REFERENCES

1. Sugawara A. *et al.*, J. Mater. Chem. B 1:1081-1089, 2013.
2. Ding S.J. *et al.*, J. Mater. Chem. 19:1183-1190, 2009.
3. Ding S.J. *et al.*, Tissue Eng. A 16:2343-2354, 2010.
4. Cameron K. *et al.*, J. Biomed. Mater. Res. 101A:13-22, 2013.

ACKNOWLEDGMENTS

The authors would like to thank the National Science Council of the Republic of China (Grant no: NSC 102-2221-E-040-001-MY3) for providing financial support to this project.



A study on PLLA/MWCNT nanocomposites compatibilized with pyrene-end-functionalized PLLA

I. Martínez de Arenaza¹, M. Obarzanek-Fojt⁴, J. R. Sarasua¹*, E. Meaurio¹, F. Meyer^{2,3}, J. M. Raquez², P. Dubois²*, and A. Bruinink⁴*

¹ Department of Mining-Metallurgy Engineering and Materials Science and POLYMAT/University of the Basque Country (UPV/EHU), Bilbao, Spain, jr.sarasua@ehu.es

² Laboratory of Polymeric and Composite Materials/University of Mons (UMons), Mons, Belgium

³ Laboratory of biopolymers and supramolecular nanomaterials/Université Libre de Bruxelles (ULB), Bruxelles, Belgium

⁴ Materials Biology Interactions/EMPA, St Gallen, Switzerland

INTRODUCTION

Biodegradable polymeric systems are potential candidates to replace metallic devices for fixation of small size bone fractures. Polylactide (PLA) presents remarkable physical properties in line with the requirement of high strength bone fixation materials. However, PLA implants will need nanofiller loading to form a composite material with improved properties. In this respect, a strategy consists in the formation of PLA-based nanocomposites including carbon nanotubes (CNTs) as nanofiller.^{1,2} One important pre-requisite to using CNTs as fillers, is to be able to improve the adhesion to and to disperse them into the polymer matrix. Purposely, the non-covalent functionalization will maintain the conjugated structure and therefore, the intrinsic properties of the CNTs within the nanocomposite.³

EXPERIMENTAL METHODS

PLLA and CNTs were provided by PURAC BIOCHEM and Arkema respectively; pyrene-end-functionalized PLLA (py-end-PLLA) was synthesized by Ring Opening Polymerization (ROP) of L-lactide.

Dispersion of the nanocomposites was examined by TEM. The mechanical properties were determined by tensile tests and the analysis of fracture surfaces was carried out by SEM. Biocompatibility was evaluated regarding cytotoxic effects cell adhesion and spreading of bone marrow derived mesenchymal stem cells (HBMC) on the composite surface and by assessing the multipotential to differentiate towards pre-osteoblastic phenotype taking the expression of osteogenic genes as an index.

RESULTS AND DISCUSSION

The ability of py-end-PLLA to interact with the surface of CNT through π - π interactions contributes to improve dispersion. In consequence, stillness and interphase adhesion of nanocomposites was enhanced. The tensile modulus and the elongation at break of nanocomposites containing py-end-PLLA increase regarding to PLLA (Fig.1). The morphology of the fracture surfaces observed by SEM show in PLLA/py-end-PLLA/CNT nanocomposites CNTs embedded in PLLA matrix, while in PLLA/CNTs nanocomposite the CNTs are agglomerated (Fig.2). Therefore, the incorporation of py-end-PLLA helps dispersion and increases the adhesion of interfaces leading to an improvement in

mechanical properties. Altogether, a good in vitro bioacceptance of the nanocomposites was shown with HBMC. The presence of CNT at the analyzed concentration range, indicate no adverse effects on cell adhesion or cell population size (Fig. 3).

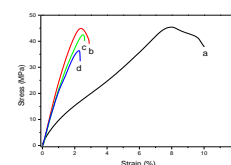


Fig 1. Tensile curves of PLLA/py-end-PLLA/CNT nanocomposites with a) 0, b) 0.1, c) 0.5 and d) 1.0 wt. % CNT.

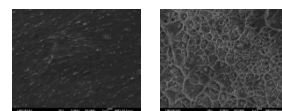


Fig 2. SEM images of a) PLLA/CNT, b) PLLA/py-end-PLLA/CNT nanocomposites.

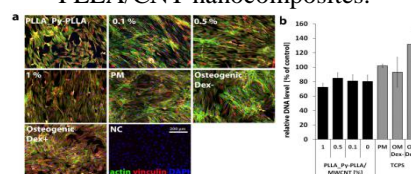


Fig 3. Cell adhesion, proliferation and spreading on PLLA/py-end-PLLA/CNTs nanocomposites.

CONCLUSION

In conclusion, the present study provides solid attestation that py-end-PLLA act as a good compatibilizer between PLLA and CNTs; and simultaneously those PLLA/py-end-PLLA/CNT nanocomposites exhibit excellent biocompatibility properties. Consequently, these new nanocomposite materials, from a bioacceptance point of view, can be interesting candidates for bone reconstruction applications.

REFERENCES

1. Martínez de Arenaza I. *et al.*, J. Appl. Polym. Sci. 130(6):4327-4337, 2013
2. Meyer F. *et al.*, Chem. Comm. 46:5527-9 2010
3. Obarzanek-Fojt M. *et al.*, Nanomed. (Online version)

ACKNOWLEDGMENTS

The authors are thankful to the European Community's 7th Framework Programme FP7/2007-2013 under grant agreement no. 213939. (POCO project)

Microgels Immobilizing Eudragit Nanoparticles for Indomethacin Release

Mihaela Nicoleta Holban*, Anca Niculina Cadinoiu, Elena Folescu and Vasile Burlui

*Acad. Ion Haulica" Research Institute; "Apollonia" University of Iasi, Romania, Faculty of Medical Dentistry
*holban_mihaela.nicoleta@yahoo.com

INTRODUCTION

The aim of this work was to develop complex systems of drug delivery, consisting of nanoparticles-containing microparticles. A major advantage is thought to be the retarded drug release and the higher protection of active principle from the environmental factors. Thus, new polymer systems were prepared by inclusion of cationic Eudragit RS100 or E100 nanoparticles into anionic polysaccharide microgels.

EXPERIMENTAL METHODS

Preparation of polymer nanoparticles. Eudragit RS100 or Eudragit E100 nanoparticles were prepared by nanoprecipitation, using a slightly modified version of a method described elsewhere¹. Indomethacin loaded nanoparticles were prepared by solving 0.05 g drug into organic phase prior to its addition to the aqueous phase. Fluorescent marked nanosuspensions were prepared by dissolving 1mg Nile Red at room temperature into the organic phase.

Preparation of pectin/HA microparticles. One part an aqueous solution containing low methyl pectin (LMP), hyaluronic acid sodium salt (HA) (LMP/HA=6/1 w/w) and polymer nanosuspension was emulsified into 4 parts silicone oil containing 2% (w/v) stearate sucroester for 30 min, at 1000 rpm. Then, 150 ml of calcium chloride (0.1 M) were added under stirring and then left for 30 min for particle curing. The formed microparticles were removed from the aqueous phase by paper filtration and washed twice with distilled water. Microparticles were stored at +4°C into HCl solution (pH 2).

Particles characterization. Size, size distribution and zeta potential of polymer nanosuspensions and nanoparticles-containing microparticles were measured. Nanoparticles morphology was observed by transmission electron microscopy (TEM). Microparticles morphology was visualized by optical microscopy and Nile Red-marked nano- and microparticles were observed by fluorescence microscopy. The entrapment efficiency (%) and *in vitro* release of Indomethacin were determined by UV-vis analysis.

RESULTS AND DISCUSSION

All nanoformulations were obtained as opalescent bluish liquids. The use of cationic polymers is reasoned by the aim of establishing electrostatic interactions between polymer nanoparticles and microgels composed of pectin and HA, the latter being a anionic natural polymer.

Microgels size was situated in the 40-110 µm range, a slight increase being registered when using Eudragit RS100. Zeta potential records were in accordance with

polymer charge; the presence of indomethacin into polymeric nanoformulations was shown by the decrease of zeta potential.

Nanoparticles are immobilized into microgels, as shown by fluorescence microscopy (Fig.1).

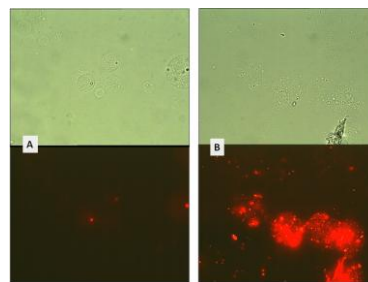


Figure 1. Superimposed photos of microgels containing Eudragit E nanosuspension (A) or Eudragit RS nanosuspension (B) in transmission and fluorescence mode (x 100)

Indomethacin was entrapped into nanoparticles in a rather satisfying percentage (~53%), considering the fact that a large portion was lost during microgels preparation.

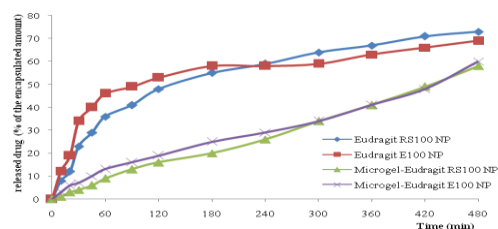


Figure 2. Release kinetics of indomethacin

The release of indomethacin from microgels in phosphate buffer pH 6.8 shows a delay compared with the release from nanoparticles.

CONCLUSION

New complex drug delivery systems have been prepared using Eudragit RS100/Eudragit E100 nanoparticles immobilized into pectin and hyaluronic acid based microgels. The systems showed ability to retard and control the release of indomethacin in simulated media.

REFERENCES

1. Mora-Huertas C. E. *et al.*, J. Nanopart. Res. 14:876, 2012.

Design of Biomimetic Fibronectin Fragment Used in Multi-layer Film Coating for Tissue Engineering

C. Dridi¹, B. Miladi¹, G. Bœuf¹, A. Elmarjou¹, S. Changotade², F. Poirier², D. Lutowski², A. Elm'selmi¹

¹Laboratoire de Biologie Moléculaire/EBInnov /Ecole de Biologie Industrielle, France

²CSPBAT/LBPS/ UMR CNRS 7244, Université Paris XIII, France, c.dridi@ebi-edu.com

INTRODUCTION

Biomimetic material development presents an important interest in biomedical and tissue engineering field and many engineered biomaterials are developed. The immobilization of bioactive molecules aimed specifically at improving rapid biointegration and promoting selective adhesion which has attracted considerable attention^{1, 2}. Cell adhesion is mediated by many biomolecules and one of the most important is a multifunctional glycoprotein: fibronectin (FN), used by many cells as adhesive substrate. FN contains a specific cell attachment site RGD exhibiting a strong affinity to integrin $\alpha_5\beta_1$ cell receptors³. Thus, FN is an interesting candidate for functional surface modification. The present study aims to produce a chimeric protein containing the cell adhesion domains III9-10 (rFN.9-10) of fibronectin and to immobilize this bioengineered protein on biomaterial surface in order to investigate its influence on cell attachment. A Colored Multi Affinity Tag (CMAT) (Fig. 1) containing a tracking marker (cytochrome b5) and two purification tags (HIS and SBP) was designed for expression and purification monitoring of rFN.9-10.

EXPERIMENTAL METHODS

Recombinant protein production and purification

DNA sequence encoding FNIII9-10 was amplified from pFN103 plasmid by standard PCR. The amplified sequence was cloned in phasis with CMAT (Fig. 1) into pET15b and sequenced. rFN.9-10 was generated in *Escherichia coli* BL21pLysS and purified by double affinity chromatography on Ni-NTA and streptactin columns then dialyzed.



Figure 1: rFN.9-10 cloning in phasis with CMAT

Protein Analysis

rFN.9-10 was analyzed by SDS-PAGE and identified by mass spectrometry (MS/MS).

Protein adsorption and cell adhesion assay

rFN.9-10 and full length FN were used for an overnight coating at 4°C. Cells were seeded (in the presence or absence of 1% BSA / serum) and allowed to adhere at 37°C and then quantified using an automated cell counter (Beckman coulter).

Experiments were run in triplicate. The variance and the significance (p value <0.05) were determined using ANOVA method.

RESULTS AND DISCUSSION

Protein analysis

SDS-PAGE analysis of the eluted fractions (Fig. 2) affirmed the expected molecular size (40 KDa) of the fused rFN.9-10 and revealed high purity purification.

The MS analysis of rFN.9-10 using Mascot software matrix generated peptides matching with a human FN and a murin cytochrome b5 precursors.

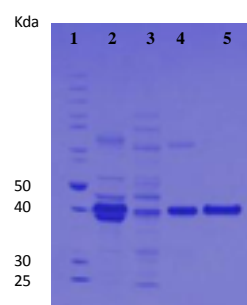


Figure 2: Expression and purification analysis of rFN.9-10. 1: molecular weight marker. 2 and 3: insoluble and soluble fractions respectively. 4 and 5: Ni NTA and Streptactin purified fractions respectively.

Protein adsorption and cell adhesion assay

Blocking with BSA in serum free condition reduces non-specific cell adhesion and material demonstrates the same cell attachment as the control. Surfaces coated with rFN.9-10 support cell attachment (Fig. 3a). Obviously, tethering efficiency of rFN.9-10 displays a comparable level to plasma FN (pFN) while no significant difference is observed relative to the control (Fig. 3b).

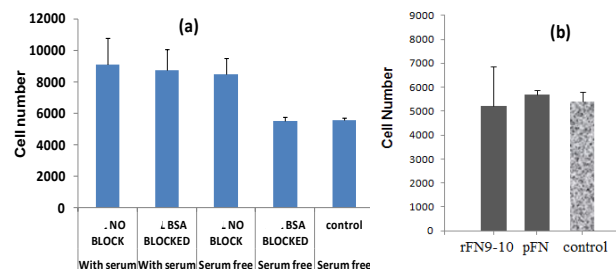


Figure 3: Cell adhesion (a) Effect of BSA and serum on cell adhesion. (b) Cell adhesion on surface coated with rFN.9-10 (R) and pFN. Reported values are the mean \pm sd (n=3)

In this work, we evaluated rFN.9-10 binding site as an adhesive ligand and we compared material adhesive property to a control. Thus, results demonstrated similar adhesive properties as the plasma FN.

CONCLUSION

This study provides active chimeric fragment implicated in cell adhesion process. The present experiment suggests that rFN.9-10 offers advantage for its novel oriented immobilization strategy on biomaterial. More results will be provided in the communication.

REFERENCES

1. Wang DA. *et al.*, Adv. funct. mater. 14:1152-1159, 2004
2. Zhang Y. *et al.*, Acta Biomater. 6: 776-785, 2010
3. Pankov R. *et al.*, J. Cell Sci. 115: 3861-3863, 2002



Effect of increasing alanine content in self-assembling FEK octapeptides

Andrew Smith¹, Stephen Boothroyd², Aline F. Miller² and Alberto Saiani^{1*}

¹School of Materials and Manchester Institute of Biotechnology, University of Manchester, United Kingdom

²School of Chemical Engineering and Analytical Science and Manchester Institute of Biotechnology, University of Manchester, United Kingdom
andrew.smith@manchester.ac.uk

INTRODUCTION

The ionic beta-sheet peptides that can self-assemble to form hydrogels is of interest for the development of materials that can be used in applications such as cell culture. Towards this end understanding the influence of the different residues in these peptides is important. It is already known that altering the length and the overall hydrophobicity of these types of peptide alters the self-assembly¹. However this has concentrated on replacing all of the hydrophobic residues in a peptide with an alternative amino acid. Here we have looked at variable amounts of differing amino acids for the hydrophobic content. The two peptide sequence extremes used in these studies are FEFKFKFK and AEAEAKAK with intermediates with different amounts of alanine and phenylalanine have been studied.

EXPERIMENTAL METHODS

Peptides were purchased from Biomatik and dissolved in ddH₂O at increasing concentrations to determine the critical concentration for hydrogel formation. Additionally, the pH of the solutions was varied to determine how this effected the hydrogel formation.

Rheology on a TA instruments Discovery Hybrid Rheometer using a plate/plate geometry.

The secondary structure of the peptides was determined using FTIR spectroscopy of peptides at a number of concentrations was used to confirm hydrogel formation

RESULTS AND DISCUSSION

The results from this study show that increasing numbers of alanine residues in the peptides increases the critical gelation concentration (CGC) for hydrogel formation. Additionally, the presence of more alanine residues results in a shift in the secondary structure of the peptides at low concentration, below the CGC,

towards an alpha-helical structure in comparison to a beta-sheet structure above the CGC.

These results support the concept that the amount of beta-sheet secondary structure is important for the formation of a hydrogel. Altering the hydrophobicity of the hydrophobic component of these peptides has a direct impact on the hydrogel formation. Also incorporation of amino acids that favour an alpha-helical secondary structure over a beta-sheet secondary structure also impacts on the CGC.

These results show that it may be possible to control hydrogel formation in these types of peptides by altering either the hydrophobicity or the secondary structure propensity of the peptides. This is an important factor in developing these peptide hydrogels towards applications.

CONCLUSION

Replacing the phenylalanine in FEK octapeptides with alanine, a less hydrophobic amino acid, results in an increase in the CGC and also a propensity to form alpha-helical structures

REFERENCES

1. Caplan M.R. *et al.*, Biomaterials 23:1, 219-227

ACKNOWLEDGMENTS

“The authors would like to thank the EPSRC Fellowship (Grant no: EP/K016210/1) for providing financial support to this project”.

Structural alterations in the dura mater after exposure to clinically relevant CoCr nanoparticles. An organ culture approach

Papageorgiou Iraklis^{1,2}, Abberton Thomas², Fuller Martin², Tipper Joanne L¹, Fisher John¹, Ingham Eileen^{1,2}

¹Institute of Medical & Biological Engineering, University of Leeds, Leeds LS2 9JT, UK

²Faculty of Biological Sciences, University of Leeds, Leeds LS2 9JT, UK,

I.Papageorgiou@leeds.ac.uk

INTRODUCTION

Total disc replacement is a surgical technique designed to reduce back pain and restore movement in the spine. Many artificial disc prostheses are manufactured using cobalt-chrome alloy popularized by the successful cobalt-chrome alloy artificial hip prostheses. The nanometre sized wear debris generated from such metal prostheses can however lead to adverse tissue reactions^(1,2). We have previously reported that clinically relevant CoCr nanoparticles can have significant biological effects upon cells isolated from the dura mater, a tissue in close proximity to spinal implants⁽³⁾. The aim of the current study was to investigate the biological effects of clinically relevant CoCr nanoparticles on the dura mater in an organ culture model.

EXPERIMENTAL METHODS

Dura-mater tissue organ-cultures were exposed to physiologically relevant doses of CoCr nanoparticles [5 and 50 $\mu\text{m}^3 \cdot \text{cell}^{-1}$] generated using a pin-on-plate tribometer. The resulting biological and structural effects were evaluated using a range of methods including tissue viability (MTT assay) pro-inflammatory cytokine production (ELISA) histology (H&E), immunohistochemistry, and TEM imaging of the CoCr-particle treated tissue compare to control tissue.

RESULTS AND DISCUSSION

There was no loss of tissue viability when the dura-mater was treated with either of the two doses of CoCr nanoparticles over 7 days. However, histological analysis and TEM imaging identified loosening of the epithelial layer of the dura-mater at both doses of nanoparticles (Fig.1).

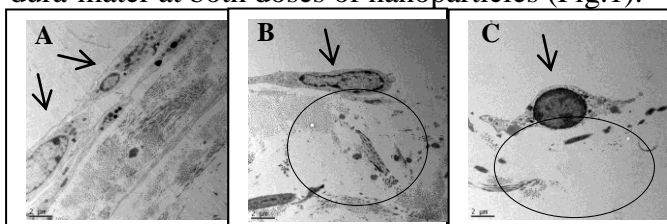


Figure 1. TEM images of the dura mater tissue after 7 days of incubation with (A) no particles, (B) 5 and (C) 50 $\mu\text{m}^3 \cdot \text{cell}^{-1}$ cobalt chrome nanoparticles. Single black lines arrows indicate the dural epithelial cells. Black circles indicated disruption of the collagen layer.

These structural alterations were associated with increased cell and tissue expression of MMP-1, -3, -9, -13 and TIMP-1 in response to both doses of CoCr nanoparticles but the expression varied between epithelial and fibroblast cells as well as the extracellular matrix as shown in Table (1)

Type of MMP	5 μm^3			50 μm^3		
	Epithelial cells	Fibroblasts cells	Extracellular matrix	Epithelial cells	Fibroblasts cells	Extracellular matrix
MMP-1	++	+	---	+	+	---
MMP-3	++	+	+	+	+/-	---
MMP-9	+++	++	++	+++	++	+++
MMP-13	+	+/-	+/-	++	++	++
TIMP-1	+++	+/-	---	+	+/-	---

Table 1. Expression pattern of different matrix metalloproteinases in dural epithelial and fibroblast cells as well as in the extracellular matrix. (Intensity of signal was assessed as: ---: no signal, +: light signal, ++: strong signal, +++: very strong signal)

Significantly increased levels of IL-8, TNF- α , IL-6, IL-33 and tenascin C were released after exposure of the dura mater to CoCr particles. Specifically, IL-8 levels for particle stimulated tissues were persistently higher than for the control tissue for the duration of the treatment (7 days) (Fig. 2).

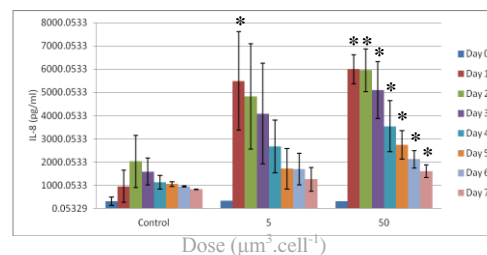


Figure 2. IL-8 release from the dura mater after exposure to CoCr nanoparticles for 7 days. Data is expressed as the mean (n=3) \pm 95% confidence limits. (*: $p < 0.05$)

CONCLUSION

The exposure of the dura-mater to CoCr-nanoparticle caused histologically detectable structural distortion after 7 days of treatment. This was possibly due to a local inflammatory response as well as the action of matrix metalloproteinases. The results generated from this study contributed to a greater understanding of the potential risks associated with the use of MOM total disc prostheses.

REFERENCES

- Berry M I *et al.*, JBJS - American Volume 2010;92(5):1242-45.
- Guyer RD *et al.*, Spine 2011;36(7):E492-97.
- Papageorgiou I *et al.* JBMR-B, 2014.

New Materials with Antibacterial Action of Functionalized Au Nanoparticles and Ga^{3+} Ions

Mario Kurtjak, Marija Vukomanović and Danilo Suvorov

Advanced Materials Department/Jožef Stefan Institute, Slovenia
mario.kurtjak@ijs.si

We designed a new kind of material with dual antimicrobial action: the release of Ga^{3+} ions and the contact-based action of Au nanoparticles, functionalized with amino acid. The material is a composite of Ga(III)-containing hydroxyapatite and Au nanoparticles with different amino acids on their surface.

INTRODUCTION

In our previous work¹ we prepared nanocomposite of Au nanoparticles functionalized with arginine and hydroxyapatite that possesses contact-based antibacterial activity. Here, we report on the further improvement of this material. We retained hydroxyapatite as the bioactive component and functionalized Au NPs as the selective antibacterial agent by mimicking the antibacterial peptides. However, we added another antibacterial component, the Ga(III) ions, which are known to prevent biofilm formation² and act mainly by substituting Fe(III) ions and thus hinder crucial redox reactions and enzymes for bacterial growth³. Moreover, some Ga(III) compounds are already in clinical use⁴. Hence, the nanocomposite should remain non-toxic to humans since all its components are non-toxic.

EXPERIMENTAL METHODS

Sonochemical method was used for the preparation of all the materials.

RESULTS AND DISCUSSION

For the development of Ga(III)-containing hydroxyapatite with functionalized Au nanoparticles, three different amino acids were used: glycine (Figure 1 (a), (b)), arginine (Figure 1 (c), (d)) and histidine (Figure 1 (e), (f)). This not only created different functionalization of the nanostructures, but also affected the size of the resulting Au nanoparticles. Their size increases in the order: Au/His, Au/Arg, Au/Gly. The presence of Ga in the material is confirmed by the EDS analysis (Figure 1 (g)). According to the literature, these ions are most probably present in the interstitions of hydroxyapatite structure⁵. The materials were tested for aging in medium with physiological acidity as well as in media with weak and strong acidic environments, which confirmed the release of Ga-ions. Antibacterial activity of materials is tested in *E. coli* (MG1655 strain). Observed action against bacteria is a consequence of coupling of antibacterial activity of functionalized Au nanoparticles and antibacterial activity of released Ga^{3+} ions.

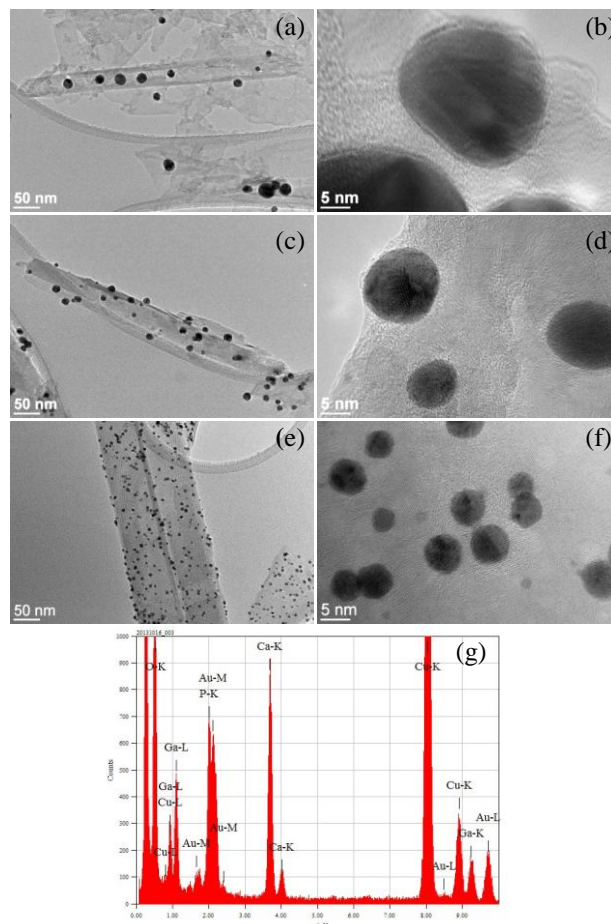


Figure 1: TEM images of Au/Gly@HAP(Ga) (a, b), Au/Arg@HAP(Ga) (c, d), Au/His@HAP(Ga) (e, f) and EDS analysis of Au/Arg@HAP(Ga) (g).

CONCLUSION

We developed nanocomposites with combined antimicrobial effect, which present an innovative way for prevention and cure of bacterial infections. Their different size and functionalization might provide different selectivity. Thus, they seem a promising human-friendly alternative for antibiotics and Ag-based antibacterial materials in treatments of infections by antibiotic resistant bacterial strains.

REFERENCES

1. Vukomanović M. *et al.*, J. Mater. Chem. B 2:1557-1564, 2014
2. Kaneko Y. and Thoendel M., J. Clin. Invest. 117:877-888, 2007
3. Bernstein L. R., Pharm. Rev. 50:665-682, 1998
4. Chitambar C. R., Int. J. Environ. Res. Publ. Health 7:2337-2361, 2010
5. Melnikova P *et al.*, Mater. Chem. Phys. 117:86-90, 2009

Biomimetic mineralization of early caries lesions with a self-assembling peptide

Sabrina Stevanovic¹, Lucy Kind¹, Iwona Dziadowiec², Bert Müller², Uwe Piesles¹

¹Institute of Chemistry and Bioanalytics, University of Applied Sciences and Arts Northwestern Switzerland (FHNW), Switzerland, sabrina.stevanovic@fhnw.ch

²BMC- Biomaterials Science Center, University Basel, Switzerland

INTRODUCTION

Enamel caries is the number one disease world-wide, presenting as progressive subsurface demineralization and ultimately resulting in mechanical failure and cavitation. Currently early dental caries is mainly treated by mechanical techniques, e.g. dental fillings or tooth extraction, or by applying protective barriers to the tooth surface, like fluoride containing varnishes¹. Therefore biomimetic mineralization is a very promising field to combine biocompatible materials with a non-invasive application. The present study is focused on a remineralization method to regenerate sub-surface carious lesions / early carious lesions in tooth enamel by means of a short self-assembling peptide, P11-4. This approach, based on the supramolecular fibrillar 3D network, is hypothesized to trigger the nucleation of hydroxyapatite (HA) nanocrystals along the fibrous network and consequently resulting in biomimetic mineralization^{2,3}.

EXPERIMENTAL METHODS

Artificial lesions in human teeth (Figure 1) were generated by incubation in acidic demineralization buffer (pH 4.4). P11-4 was directly applied on the lesion and then incubated in remineralization buffer (pH 7.4). For the detection of the monomeric and self-assembled P11-4 a specific primary antibody and Congo red was used. To detect the peptide P11-4 in treated lesions after a long term study (14 d) a matrix-assisted desorption/ionization-time of flight (MALDI-TOF) spectroscopy method was developed. The nucleation and growth of hydroxyapatite crystallites initiated by the self-assembled network of P11-4 was analysed by μ -computer tomography (μ -CT) measurements.

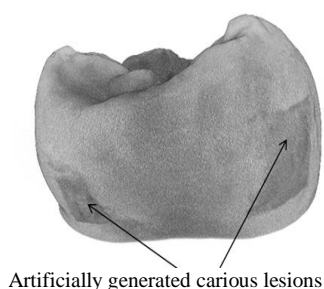


Fig. 1: Computer tomography (μ -CT) image of a natural human tooth crown with artificially generated carious lesions (arrows).

RESULTS AND DISCUSSION

A standardized procedure to demineralize natural human teeth in order to obtain sub-surface lesions (white spots - WS) has been successfully established. With the specific primary antibody and Congo red

staining we were able to selectively detect monomeric and self-assembled peptide P11-4. Remineralisation of the artificial lesion was observed with μ -CT. Increased density was clearly visible after two weeks (Figure 2). Moreover after incubating the tooth in remineralisation buffer for two weeks, P11-4 was still present in the lesions detected by MALDI-TOF.

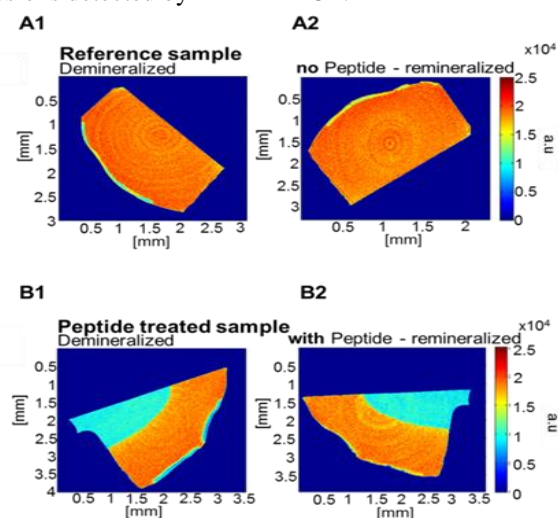


Fig. 2: μ -CT images of a transversal profile through a sub-surface lesion in a human tooth enamel. (A1 and B1) Tooth imaged after demineralization. (A2) Tooth treated without peptide (Reference sample). (B2) Tooth treated with peptide (P11-4), 14 days in remineralization buffer (Peptide treated sample).

CONCLUSION

The aim of the study was to analyse the remineralization process of artificial induced white spot lesions after treatment with the self-assembling peptide P11-4. MALDI and μ -CT were suitable methods to observe the presence of peptide P11-4 in the tooth and the biomimetic mineralization of the artificial induced white spot lesions.

Furthermore studies on restorative remineralization therapy by 3D-self-assembled peptide supramolecular networks, either in natural teeth or in artificial tooth model are in process.

REFERENCES

1. J. Kirham *et al.*, J. Dent. Res., 86:426, 2007
2. Rein V. Ulijn and Andrew M. Smith, Chem. Soc. Rev., 37: 664-675, 2008
3. Brunton, P. A. *et al.*, Br. Dent. J., 4: E6, 215, 2013

ACKNOWLEDGMENTS

Support by the Swiss-Nanoscience Institute (SNI) and Swiss National Science Foundation (SNSF) is gratefully acknowledged.



Bacterial Adhesion and Biofilm Formation Reduced by the Immobilization of hLf1-11 Peptide onto Titanium Surface: A Comparison Study between Direct and ATRP based Covalent Immobilization

Maria Godoy-Gallardo^{1,2*}, Carlos Mas-Moruno^{1,2}, Kai Yu³, Jose M. Manero^{1,2}, Javier Gil^{1,2}, Jayachandran N. Kizhakkedathu^{3,4}, Daniel Rodríguez^{1,2}.

¹Department of Material Science, Technical University of Catalonia, Spain

²Biomedical Research Networking Centre in Bioengineering, Biomaterial and Nanomedicine (CIBER-BBN), Spain

³Centre for Blood Research of Pathology and Laboratory Medicine, University of British Columbia, Canada

⁴Department of Chemistry, University of British Columbia, Canada

maria.godoy.gallardo@upc.edu

INTRODUCTION

Implant failure can be associated to infections which develop into peri-implantitis. In order to reduce biofilm formation, several strategies focusing on the use of antimicrobial peptides (AMP) have been studied^{1,2}. To covalently immobilize these molecules onto metallic substrates several techniques have been developed, including silanization³ and polymer brush prepared by surface-initiated atom transfer radical polymerization (ATRP).⁴

The aim of the present study was to compare the efficiency of these two methods to immobilize the hLf1-11 antibacterial peptide onto titanium, and evaluate their effect in the antibacterial activity *in vitro*.

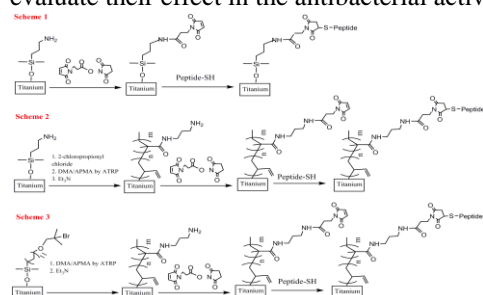


Figure 1. Synthetic route for silanization, copolymer brushes and peptide conjugation.

The aim of the present study was to compare the efficiency of these two methods to immobilize the hLf1-11 antibacterial peptide onto titanium, and evaluate the antibacterial activity *in vitro*.

EXPERIMENTAL METHODS

Smooth titanium (Ti) samples were coated under three different conditions: silanization with APTES, and polymer brush based (ATRP) coatings with two different initiators. These surfaces were conjugated with the hLf1-11 peptide. Surfaces were characterized by contact angle measurements, white-light interferometry, ellipsometry, and X-ray photoelectron spectroscopy (XPS). Moreover, the mechanical stability of the coatings under ultrasonication was studied. Cellular viability and proliferation were studied by LDH assay with human fibroblasts. The *in vitro* antibacterial properties of the modified surfaces were tested with two oral strains (*Streptococcus sanguinis* and *Lactobacillus salivarius*) by means of bacterial adhesion assay at 2 h and evolution of biofilm formation after 24 h.

RESULTS AND DISCUSSION

Compared to silanization, ATRP treatments formed polymer brushes on the titanium surface with an increased density of anchoring points for peptide

attachment, as estimated by GPC and ellipsometry. XPS analyses confirmed that the two strategies allowed a successful covalent attachment of the Lhf1-11 onto Ti. Surface roughness was not affected by these treatments. Cell viability and proliferation in the LDH assays were not affected by the presence of peptides. All surfaces biofunctionalized with the hLf1-11 peptide presented a significant antibacterial effect. The immobilization of the hLf1-11 peptide via polymer brush techniques showed a statistically significant higher reduction of bacterial adhesion than the use of silanization. However, both methods had a similar effect in the inhibition of biofilm formation. After 2h of sonication bacterial adhesion and biofilm formation slightly increased for all treatments, indicating some extent of mechanical instability for the coatings.

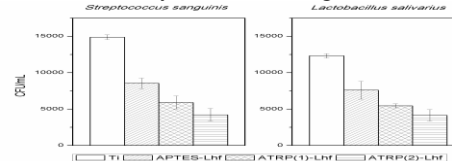


Figure 2. Effect of the surface modifications on bacterial adhesion.

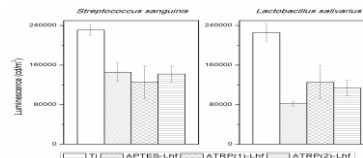


Figure 3. Effect of the surface modifications on biofilm formation for 24h.

CONCLUSION

A decrease in bacterial adhesion and biofilm formation was achieved once the peptide was immobilized onto titanium surfaces. A higher decrease in bacterial attachment was noticed when samples were modified by ATRP methods compared to silanization. This effect is likely due to the capacity to immobilize more peptide on the surfaces by using polymer brushes and hydrophilic nature of polymer brushes.

REFERENCES

- Costa F. *et al.*, Acta Biomater. 1:1431-1440, 2011.
- Zhao L. *et al.*, J. Biomed Mater Res B Appl Biomater. 91(B):470-480, 2009.
- Bauer S. *et al.*, Prog Mater Sci. 58:261-326, 2013.
- Gao G. *et al.*, Biomacromolecules. 12:3715-27, 2011.

ACKNOWLEDGMENTS

This study was supported by MICINN (Ministerio de Ciencia e Innovación) (Projects MAT2009-12547 and MAT2012-30706).



A Preliminary Examination of Composition-Property Relationships for Methotrexate-Loaded Germanium-Based Glass Ionomer Cements

Lauren Kiri^{1*}, Daniel Boyd^{1,2}

^{1*}School of Biomedical Engineering, Dalhousie University, Canada, lekiri@dal.ca

²Department of Applied Oral Science, School of Biomedical Engineering, Dalhousie University, Canada

INTRODUCTION

The addition of antineoplastic drugs to bone cement may prevent local cancer progression and failure of stabilization devices used to treat pathologic fractures. Germanium-based glass ionomer cements (Ge-GICs) have been recently identified as potential injectable bone cements, as they are (1) chemically adhesive to bone, (2) inherently radiopaque, (3) non-exothermic, (4) clinically practical in terms of handling and mechanical properties, and (5) aluminum-free and therefore circumvent the biocompatibility issues that have been identified with using conventional GICs for orthopaedic applications.¹ However, the effect of adding antineoplastic drugs to such GIC matrices is unknown. Consequently, the aim of this work was to investigate the ability of such materials to act as a drug vehicle for the anticancer agent, methotrexate (MTX).

EXPERIMENTAL METHODS

Glass powder (Mol. Fraction: 0.36ZnO/0.04SrO/0.215SiO₂/0.215GeO₂/0.025ZrO₂/0.025Na₂O/0.12CaO; particle size: $\leq 45\mu\text{m}$) was synthesized¹ and characterized using XRD and DSC. Cements were mixed at a constant powder/liquid ratio of 1.5/1.0 and poly(acrylic) acid (PAA) concentration of 50%. MTX was mixed into the cement at 0, 1, 5 and 10% w/w. Working time (t_w ; $n=3$), setting time (t_s ; $n=3$) and 1-day compressive strength (CS; $n=5$, incubated in PBS at 37°C) were measured for each drug loading condition, as per conventional methods.² For each drug loading condition, cement cylinders ($d=4\text{ mm} \times h=6\text{ mm}$) were synthesized ($n=5$) and incubated in PBS in a shaking mixer (2Hz) at 37°C. PBS was replaced after 1 h and each day for 10 days. MTX concentration was quantified using UV/VIS spectroscopy ($\lambda=303\text{nm}$). The release data was fitted to zero-order, first-order, Higuchi, Korsmeyer-Peppas, Weibull and Hopfenberg models, and statistically analysed to show model adequacies (Prism 6).

RESULTS AND DISCUSSION

The average t_w , t_s and 1-day CS are reported in Table 1. Curiously, the addition of MTX significantly decreased t_w ; however, there was no significant difference in t_w found among the different MTX loadings (1-way ANOVA). Furthermore, and also surprisingly, MTX addition did not significantly impact t_s or CS (1-way ANOVA).

Table 1: Handling and mechanical properties of MTX-loaded Ge-GIC.

Loading	t_w (sec)	t_s (sec)	1-day CS (MPa)
0	229	653	32
1	205	610	38
5	208	740	35
10	193	660	40

Figure 1 shows the MTX release profiles for each loading scenario. All profiles demonstrate the same general trend: a burst release followed by a slow sustained release over the 10 day period. Determination coefficients (R^2) for the resulting model linearizations are summarized in Table 2.

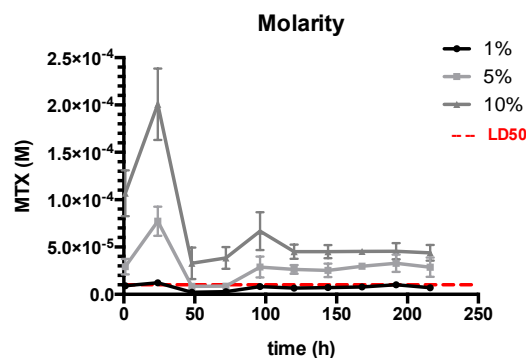


Figure 1: MTX release profiles (M) with respect to LD50 ($1 \times 10^{-5}\text{ M}$).

Table 2: R^2 values for modelled release profiles.

Model	R^2		
	1%	5%	10%
Zero-Order	0.5554	0.6314	0.5102
First-Order	0.8929	0.7303	0.6364
Higuchi	0.6119	0.7636	0.6667
Korsmeyer-Peppas	0.9066	0.9795	0.9912
Weibull	0.9194	0.9555	0.9741
Hopfenberg	0.7344	0.6868	0.6003

From Table 2, it is seen that the release profiles are best described by the Korsmeyer-Peppas and Weibull models. The resulting Korsmeyer-Peppas release exponents fell below 0.45 for all loading scenarios, which suggests Fickian diffusion is the primary mechanism of release. As shown in Figure 1, increased drug loading significantly increased the amount of drug released from the cement. However, increased drug loading did not significantly influence the percentage of MTX released; 1.3, 1.1 and 1.5% of the total MTX load was released at 240 hours for 1, 5 and 10% loading, respectively. At 24 h, the MTX concentration exceeded the LD50 for all loading scenarios. This was maintained for the 5% and 10% loading, while the 1% loading bordered the threshold for the elution period.

CONCLUSION

Ge-GICs are a potential vehicle for MTX. MTX loading imparts minimal effects to GIC handling properties with no effect to strength. The MTX-loaded Ge-GICs demonstrated sustained drug release at concentrations that imply cytotoxicity.

REFERENCES

1. Dickey, B.T. *et al.*, JMBBM 23:8-21, 2013

ACKNOWLEDGMENTS

The authors would like to acknowledge the financial assistance of NSERC and the Atlantic Canada Opportunities Agency.



PEI – Starch Nanospheres for siRNA based Gene Silencing Therapy for Cancer

Berke Bilgenur Kandemir^{1,3}, Bülent Özpolat⁵, Gamze Torun Köse^{3,4}, Vasıf Hasircı^{1,2,3}

Middle East Technical University (METU), Departments of ¹Biotechnology and ²Biological Sciences Ankara, Turkey

³BIOMATEN, METU, Center of Excellence in Biomaterials and Tissue Engineering, Ankara, Turkey,

bilgenur.kandemir@metu.edu.tr

⁴ Yeditepe University, Department of Genetics and Bioengineering, Istanbul, Turkey

⁵ University of Texas, Department of Experimental Therapeutics, MD Anderson Cancer Center, Houston TX, USA

INTRODUCTION

Conventional cancer treatment techniques like chemotherapy, radiation therapy and surgical operations are not sufficiently efficient and they even are harmful for healthy tissues. Recent studies suggest that small interfering RNA (siRNA) based gene silencing can be used as a highly effective targeted therapy¹. However, siRNA delivery into tumors and target tissues have proved to be difficult². This study aimed to develop an siRNA delivery system to cancer cells using positively charged nanospheres constructed of polyethyleneimine (PEI) and starch (S).

EXPERIMENTAL METHODS

PEI-starch nanospheres were prepared at different ratios by water-in-oil microemulsion method. PEI molecules were crosslinked using genipin. The PEI-starch nanospheres were characterized by measuring the zeta potential and the particle size, studying the topography with SEM, and measuring release rate of their content by spectrofluorometer. We also evaluated siRNA and nanoparticle uptake and target downmodulation by confocal laser scanning microscopy (CLSM) and western blot analysis, respectively.

RESULTS AND DISCUSSION

The mean diameter of PEI-starch incorporating siRNA was 84.6 nm. Zeta potential of PEI-starch nanospheres increased when the PEI /starch ratios were increased and was the highest (8.7 mV) at PEI:Starch, 9:1 (w/w) (Table 1).

Table 1: Surface potential of PEI: starch nanospheres and viability of MCF 7 cells treated with PEI – starch nanospheres constructed with PEI: starch (w/w) ratios of 1:9, 1:3, 1:1, 3:1 and 9:1.

PEI:starch (w:w)	Zeta potential (mV)	Cell viability (%)
1:9	-31	90.7
1:3	-26	86.6
1:1	-19	85.6
3:1	0	81.9
9:1	9	78.0

The nanospheres released 50 % of their siRNA content in the first 3 days and all of the content in a week. CLSM micrographs show the nanospheres and siRNA were taken up by MCF 7 breast cancer cells (Figure 1).

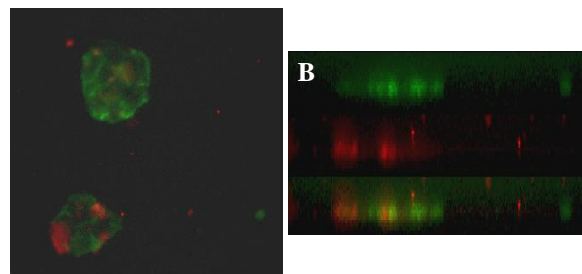


Figure 1: Confocal microscopy of MCF 7 cells treated with Alexa-555 labelled siRNA loaded PEI-starch nanospheres (A) fluorescence image of MCF 7 cells (green) treated with Alexa-555 labelled siRNA loaded PEI-starch nanospheres (red) (x 40), (B) Z-stack.

Western blot analysis demonstrated that EF2-Kinase siRNA loaded nanospheres significantly inhibited EF2K protein expression (90-100%) (Figure 2).

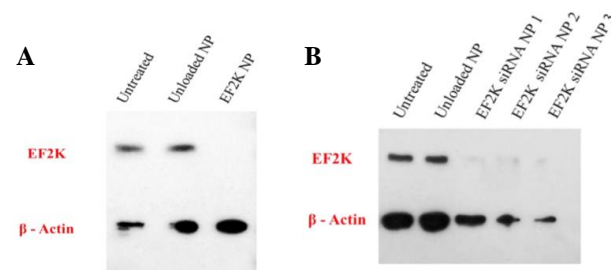


Figure 2: Western blot analysis of MCF 7 cells treated for 72 h (100 nM EF2K siRNA and 100 000 cells per well). (A) with EF2K siRNA loaded nanospheres (NP), (B) with various batches of EF2K siRNA loaded nanospheres (NP) (NP1, NP2, NP3).

CONCLUSION

In this study construction of a novel PEI-starch based siRNA carrier to initiate apoptosis in breast cancer cells was aimed. The PEI-starch nanospheres effectively penetrated into MCF 7 cells. Thus, we showed that the PEI-starch nanospheres are suitable in size, charge, release kinetics and as such they exhibit a potential to serve as an efficient vector for siRNA delivery to cancer cells.

REFERENCES

1. Ozpolat B. *et al.*, Adv. Drug Deliv. Rev. 66:110-116, 2013
2. Tekedereli I. *et al.*, Plos One. 7(7): e41171, 2012

Intracellular delivery system based on acylated hyaluronan

Kristina Nešporová^{1,2}, Jana Šógorková¹, Lucie Vištejnová^{1,2}, Daniela Šmejkalová¹, Hana Kolářová³, Vladimír Velebný¹

¹Contipro Biotech, Czech Republic Kristina.Nesporova@contipro.com

²Institute of Experimental Biology, Faculty of Science, Masaryk University, Czech Republic

³Institute of Biophysics AS CR, Czech Republic

INTRODUCTION

Various carrier systems, including polymeric micelles (PMs), are being developed for drug delivery or cell labelling purposes. Since hyaluronan and its derivatives represent biodegradable and biocompatible polymeric material, PMs based on acylated hyaluronan¹ have great potential for clinical use and applications.

The aim of this work was to probe the ability of acylated hyaluronan based PM to transport active compounds to the intracellular space and test if this transport is influenced by level of expression of the main receptor for hyaluronan, CD44.

EXPERIMENTAL METHODS

Nile red (NR) and 7-aminoactinomycin D (7-AAD) were loaded into hyaluronan PMs by solvent evaporation method. Human cancer cell lines MCF-7 and MDA-MB231 and primary human dermal fibroblasts (NHDF) were cultivated in DMEM supplemented with 10% FBS. Measurement of CD44 expression and quantification of intracellular transport of PM was performed on MACSQuant® flow cytometer (Miltenyi Biotec). Widefield fluorescence images were obtained using Ti-Eclipse inverted microscope (Nikon). Confocal images were obtained on confocal microscope TSC SP-5 X (Leica).

RESULTS AND DISCUSSION

For basic quantification and also to decipher if the PM uptake is influenced by CD44 presence on cell surface the three cell types with different CD44 expression were measured by flow cytometry after incubation with NR loaded PMs. Accumulation of fluorescent NR in cells didn't correlate with CD44 expression (Fig.1).

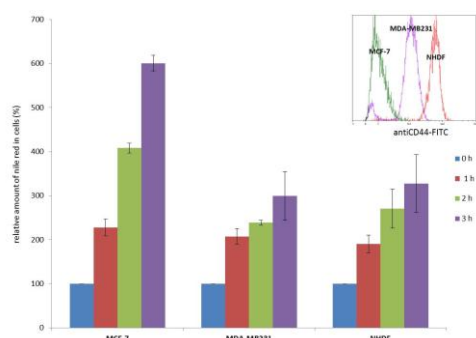


Fig.1: Accumulation of NR loaded in PMs during 3hrs incubation with cells. Graph shows the means from 4 independent experiments, error bars = SEM. Insert shows relative expression of CD44.

To confirm whether the NR is transported within the PM or is released from PM outside the cell and then transported alone the PMs were labelled with blue

pyrene. After incubation with MCF-7 cell the colocalization of NR and pyrene fluorescence was observed both on widefield and confocal microscopes (Fig.2). This suggests that PM is transported intact into cells and then the loaded compound is released.

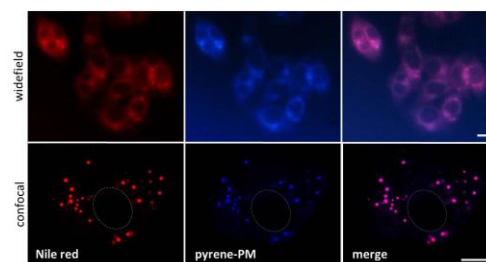


Fig.2: Colocalization of NR loaded in PM and pyrene labelled acylated hyaluronan in MCF-7 cells. Dotted circle indicates the position of nucleus. Scale bars = 10 μm

For further prove of role of PM as active transporter inside the cells NR in PMs was substituted for 7-AAD, compound normally impermeable for living cell plasma membrane. Viable cells (verified by calcein-AM staining) treated with 7-AAD in DMSO didn't show any red fluorescence while cells treated by 7-AAD loaded PMs has high red fluorescent signal from 7-AAD bound to DNA (Fig.3)

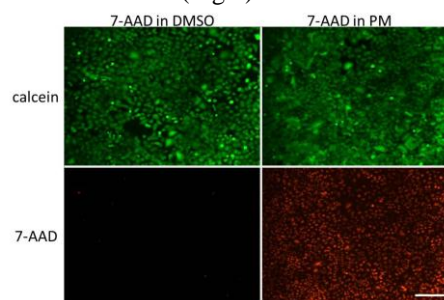


Fig.3: MCF-7 cell treated with 7-AAD in DMSO and 7-AAD loaded into PM. Green calcein marks viable cells. Scale bar = 100 μm

CONCLUSION

Results show that PMs based on acylated HA are able to transport active compound inside cell independently on the CD44 presence on cell surface. This transport is based on internalization of whole PM and not the release of active compound in the vicinity of plasma membrane. Thus PMs based on acylated hyaluronan are suitable for drug and other active compound delivery into cells.

REFERENCES

1. Smejkalova D. *et al.*, Carbohydr. Polym. 87(2): 1460-1466, 2012

***In vivo* Investigations of the Early Stages of Bone Healing with Microdialysis**

Yvonne Foerster¹, Claudia Rentsch¹, Stefan Kalkhof², Martin von Bergen², Stefan Rammelt¹

¹University Centre of Orthopaedics and Trauma Surgery and Centre for Translational Bone, Joint and Soft Tissue Research, University Hospital Carl Gustav Carus Dresden, Germany

²Helmholtz Centre for Environmental Research, Department Proteomics, Leipzig, Germany
Yvonne.Foerster@uniklinikum-dresden.de

INTRODUCTION

The treatment of critical-size bone defects represents a significant clinical problem. The bone healing itself is a complex process influenced by growth factors, cytokines, and other mediators, but the regulation of this process is not yet sufficiently understood. Because the early stages of bone healing are crucial for consolidation, it is important to characterise the active molecules and cellular mechanisms in the fracture hematoma directly after the injury. Therefore the authors developed microdialysis in bone defects as a method to identify mediators and growth factors in the early stages of the bone healing process.

EXPERIMENTAL METHODS

A 5 mm defect was created in the femur of male adult Wistar rats and stabilized with an internal fixator. The microdialysis catheter (cutoff 100 kDa, CMA microdialysis, Solna, Sweden) was placed within the defect, fixed to the skin and the dialysate was collected continuously under anaesthesia for 24 hours. The dialysates were analysed by ELISA (enzyme-linked immunosorbent assay) and Proteome Profiler™ array. The proteins attached at the membrane of the catheter were determined by HPLC/MS (high-performance liquid chromatography/mass spectroscopy). Rats with soft-tissue defects were used as controls.

RESULTS AND DISCUSSION

Determination of protein concentration showed that it was possible to collect protein continuously from the bone defect with the chosen experimental setting. The total protein concentration varied between 0.15 mg/ml and 0.44 mg/ml. We were able to determine interleukin-6 (IL-6) and transforming growth factor-β1 (TGF-β1) concentration over 24 hours. IL-6 was secreted within

the first 3 h and the highest concentration was measured between 12 and 15 h after the injury. The anti-inflammatory cytokine IL-10 could be detected in all samples with a slight increase toward the end of the detection period. By Proteome Profiler™ array and HPLC/MS analysis further chemokines that are potentially relevant to bone healing like chemokine (C-X-C motif) ligand 1 (CXCL1), CXCL4 and CXCL7 could be detected in the dialysate. Detailed studies of CXCL4 and CXCL7 by ELISA showed a rapid decrease of the concentration of these proteins immediately after injury suggesting the release of these proteins by activated platelets. The analysis of samples by HPLC/MS resulted in more than 1000 collected proteins that could be assigned to biological processes like immune system response, response to stimuli, cell adhesion and others. In addition, we were also able to assign the identified proteins to more than 100 different pathways which seem to be activated in the early stage of bone healing.

CONCLUSION

It can be concluded from these experiments that microdialysis appears to be a valuable method to characterise the humoral events during the early stages of bone healing. Further investigations are needed to show the influence of implant modifications on the composition of the fracture hematoma.

ACKNOWLEDGMENTS

The authors would like to acknowledge the German Research Council (DFG SFB-TR67) and the CRTD (Center for Regenerative Therapies Dresden) for support of these studies.

Characterization of Oxygen Plasma-treated Dental All-Ceramic Zirconia

Hsiang Kao, Chung-Kai Wei and Shinn-Jyh Ding*

Institute of Oral Science, Chung Shan Medical University, Taichung 402, Taiwan, kao52226@ms21.hinet.net

INTRODUCTION

Zirconia (ZrO_2) is applied as a base in clinical fixed prosthetic dentistry and femoral head of hip prostheses because of the merits of zirconia ceramics such as high strength, toughness, abrasion resistance, and chemical stability *in vivo*¹. However, this material has a limited applications range because it is a bioinert material that does not interact with bone tissue and thus does not easily integrate directly in the bone. To pursue the high bioactivity is still a concerned theme although commercial ZrO_2 systems are available today. Oxygen plasma treatment is relatively inexpensive and time efficient, as it is simple to transform the hydrophobic hydrocarbon surface of materials to the hydrophilic hydroxyl surfaces². This study was to create a hydrophilic layer on the commercially available ZrO_2 surface for improving the biocompatibility using oxygen plasma. Evaluation of this potential method included phase composition and contact angle analysis, particularly the protein adsorption and cell attachment and proliferation on oxygen plasma-treated ZrO_2 surfaces.

EXPERIMENTAL METHODS

The oxygen plasma treatment of Cercon ZrO_2 plates was carried out by using plasmochemical generator. Before treatment, the samples were mechanically polished to a roughness to #1200 grit level. The plasma was generated using a source power of 200 W.

High resolution X-ray diffractometry (XRD) was used to investigate the phase composition. Micro-Raman measurements were taken with a DXR instrument equipped with a laser at 780 nm. The static water contact angles were determined by the sessile drop method at room temperature. Bovine serum albumin (BSA) adsorption studies were done to investigate the effect of treated specimens on protein coverage.

Human mesenchymal stem cells (hMSCs) were used to assay the osteogenic properties of the plasma-treated samples. The cells were grown in Dulbecco's modified Eagle's medium supplemented with 10% fetal bovine serum and 1% penicillin/streptomycin solution. Cells seeded on the ZrO_2 samples without plasma treatment were used as a control. Actin cytoskeleton was analysed by fluorescence microscopy. Cell viability was examined using the MTT (3-(4,5-dimethylthiazol-2-yl)-2,5-diphenyltetrazolium bromide) assay. To evaluate early cell differentiation, the alkaline phosphatase (ALP)

activity of hMSCs on the various specimens was measured. One-way analysis of variance (ANOVA) was used to evaluate the significance of differences between means. In all cases, the results with a p-value of less than 0.05 were considered statistically significant.

RESULTS AND DISCUSSION

XRD and micro-Raman consistently indicated that the used oxygen plasma did not induce any significant phase evolution. The sample was composed of tetragonal zirconia phase with a tract of monoclinic zirconia. As expected, the water contact angle measured on the pristine substrate was significantly ($p < 0.05$) reduced from 65° to 18° after 1 min of plasma irradiation. The oxygen plasma can improve effectively the hydrophilicity of the ZrO_2 surfaces, possibly due to both the introduction of polar hydroxyl groups into the sample surfaces and elimination of hydrocarbon molecules. At 1 h of adsorption, greater amount of BSA protein was bound to the plasma-treated surface compared to the pristine ZrO_2 .

Early cell-cement interactions affect subsequent differentiation and mineralization. The fluorescence staining showed that at hour 3, hMSCs cultured on plasma-treated surfaces displayed highly tensioned actin stress fibres, whilst compared to the control, in agreement with the results of the contact angle and protein adsorption. Initial cell adhesion and spreading to the material surface is strongly dependent on the absorbed proteins³. The MTT assay was used to quantify cell number on the different samples. Cell attached to the plasma-treated surfaces at a rapid rate more than 100% binding at day 3 compared to the control. This demonstrated that during the culture periods, the number of viable cells on plasma-treated surface was significantly higher ($p < 0.05$) than on the pristine YZP. Regarding cell differentiation, the ALP level presented a higher value for the plasma group than the control after 10 days of incubation.

CONCLUSION

In summary, the present plasma method provides an effective method for improving the hydrophilicity and biocompatibility of dental all-ceramic ZrO_2 .

REFERENCES

1. Chevalier J., *Biomaterials* 27:535, 2006.
2. Wu C.C. *et al.*, *Surf. Coatings Tech.* 205:318, 2011.
3. Ding S.J. *et al.*, *Adv. Eng. Mater.* 13:B246, 2011.

High throughput screening of hMSC response to algorithm generated micro-topographies

^{1,2}Frits F.B. Hulshof, ¹Bernke J. Papenburg, ¹Roman K. Trückenmüller, ³M. Hulsman, ¹Natalie Fekete, ⁴Shantanu Sing, ¹Clemens A. van Blitterswijk, ⁴Anne E. Carpenter, ²Dimitrios Stamatialis, ¹Jan de Boer

¹Department of Tissue regeneration and ²Department of Biomaterials Science and Technology, MIRA Institute of Biomedical Technology and Technical Medicine; University of Twente, Enschede, The Netherlands; ³Delft Bioinformatics Lab, Delft University of Technology, Delft, The Netherlands; ⁴Imaging Platform, Broad Institute of MIT and Harvard, Cambridge, MA, USA. Email: G.F.B.Hulshof@utwente.nl

INTRODUCTION

Surface topography can have large effects on cellular parameters such as proliferation, orientation, morphology, gene expression and differentiation. Insight into the underlying mechanisms is valuable for the design for future biomaterials.

The TopoChip was developed for high throughput screening of thousands of topographies(1). An in-silico library of over 150 million unique topographies is generated using multi-parametric algorithms. From this library 2178 features are randomly selected and applied in duplo inside 300x300 μm^2 'TopoUnits' on a 2x2 cm^2 polymer surface, the 'TopoChip'.

Here we identified micro-topographies which are able to up-regulate tissue non-specific Alkaline Phosphatase (ALP). Moreover correlations of ALP expression changes with cell morphological parameters were explored.

EXPERIMENTAL METHODS

TopoChips are fabricated by hot embossing of a polymer using a silicon mould holding the inverse pattern that is fabricated by photolithography.

Human mesenchymal stromal cells (hMSC's) have been cultured on 8 poly(lactic acid) (PLA) TopoChips with a 200 nm titanium coating (n=16 for each unique surface topography).

ALP, filamentous actin and chromatin of hMSC's were fluorescently labelled for high content imaging. Images were analysed by Cellprolifer and custom Matlab® scripts.

RESULTS AND DISCUSSION

Analysis of the Topochip screen yielded a number of candidate hits that significantly up-regulated or down-regulated ALP compared to the mean of the data set. From these candidate hits several were verified by up-scaling the topographies from the 0.09 mm^2 TopoUnit size to 2.54 cm^2 discs and quantifying ALP expression by microscopy and flow cytometry (Fig 1). Positive Hits (PH1&PH2) almost doubled the amount of ALP positive cells in a similar range to the dexamethasone positive control.

Analysis of the actin cytoskeleton of the cells in the TopoChip screen showed a correlation between morphological parameters and ALP expression. This

suggests that changes in cytoskeletal properties induced by micro-topographies might be able to affect ALP expression, probably through a mechano-transduction pathway.

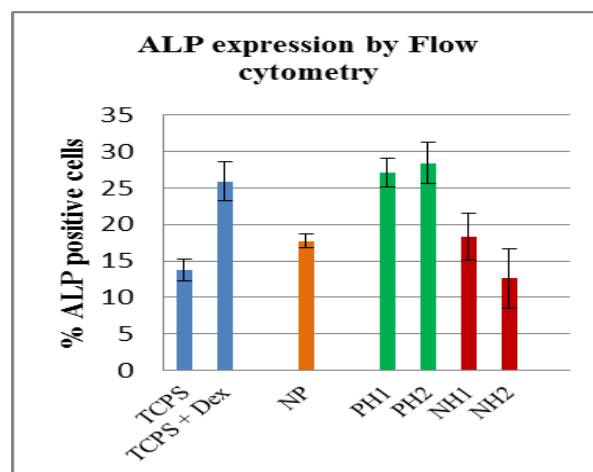


Fig1: ALP expression measured by Flow cytometry. Percentages of ALP positive cells cultured for 5 days on Tissue culture poly styrene(TCPS), non-patterned Ti coated PLA (NP) and positive (PH) and negative hit-topographies(NH) on Ti coated PLA.

CONCLUSION

Using the TopoChip we were able to identify several topographies which significantly up-regulated ALP expression of hMSC's. Cytoskeletal morphology showed a strong correlation with the changes in ALP expression.

REFERENCES

1.Unadkat HV, Hulsman M, Cornelissen K, Papenburg BJ, Trückenmüller RK, Carpenter AE, et al. An algorithm-based topographical biomaterials library to instruct cell fate. Proc Natl Acad Sci U S A. 2011;108(40):16565-70. Epub 2011/09/29.

ACKNOWLEDGEMENTS

The authors would like to thank the Nanonext NL Program for providing financial support to this project.

On the Biocompatibility of UV Pre-irradiated Hydrothermally Grown TiO₂-coatings

Martina Lorenzetti^{1,2,*}, Giulia Bernardini³, Katja Trinkaus⁴, Iztok Dogsa⁵, Thomas Luxbacher⁶, Katrin Susanne Lips⁴, Annalisa Santucci³, Reinhard Schnettler⁴, David Stopar⁵, Saša Novak^{1,2} and Spomenka Kobe^{1,2}

^{1,*}Department of Nanostructured Materials, Jožef Stefan Institute, Ljubljana, Slovenia, martina.lorenzetti@ijs.si

²Jožef Stefan International Postgraduate School, Ljubljana, Slovenia

³Department of Biotechnology, Chemistry and Pharmacy, University of Siena, Siena, Italy

⁴Laboratory for Experimental Trauma Surgery, University-Hospital of Giessen and Marburg, Giessen, Germany

⁵Biotechnical Faculty, Department of Food Technology, University of Ljubljana, Ljubljana, Slovenia

⁶Anton Paar GmbH, Graz, Austria

INTRODUCTION

Nowadays, titanium and its alloys are the most used metals for bone substitution in orthopaedics and dentistry due to their favourable mechanical properties and biocompatibility. Immediately after surgery, proteins coming from the blood circulation adsorb on the exterior of the inserted material, forming a pre-conditioning film which influences the “race” among cells and bacteria for colonizing that surface¹. Thus, the study of protein adsorption, cell differentiation, osteogenesis and bacterial adhesion, is fundamental to predict *a priori* the *in vivo* implant performances.

EXPERIMENTAL METHODS

Hydrothermal treatment (HT) is a well-known synthesis method for growing nanocrystalline TiO₂-anatase coatings on titanium substrates. Such coatings enhance the surface properties of Ti-based bone implants in favour of a higher biocompatibility after implantation. Moreover, photo-induced phenomena (e.g. super-hydrophilicity) can arise by UV irradiation of the anatase nanocrystals².

Coatings with different crystals morphology, wettability and surface charge were used in these studies in both non-irradiated and UV pre-irradiated state, in comparison with the non-treated titanium (Ti NT).

First of all, the study of the protein adsorption was accomplished by using the whole plasma; the quantification and identification of the species were performed on the gel maps obtained by 2D-PAGE, one of the most used proteomics techniques. Furthermore, ALP (alkaline phosphatase) production and Ca²⁺ uptake from the medium were used in order to evaluate *in vitro* the cell activity and the osteogenesis process of primary human mesenchymal cells. Fluorescence and scanning electron (SEM) microscopy were applied, as well, to observe cell morphology and spreading. Finally, the observation of the *E. coli* adhesion and the eventual biofilm formation on the TiO₂-coatings (with/without UV pre-irradiation) were estimated by fluorescence microscopy and CFU (colony forming units) counting.

RESULTS AND DISCUSSION

The different characteristics of the surfaces, together with the photo-induced effects, were taken into account for comparing the biocompatibility of the surfaces, under several points of view. The results suggested that the surface charge and the wetting grade of the coatings were the most influencing parameters for the plasma protein adsorption, while the UV photo-induced hydrophilicity generally decreased the amount of adsorbed proteins. In particular, the most favourable result was the significant reduction in the adsorption of inflammation-promoting proteins after UV pre-irradiation of the substrates. Photo-induced hydrophilicity was the fundamental parameter which enhanced the osteogenic ability of the HT coatings, leading to the cell differentiation and resulting in the formation of a well-developed mineral phase, even in the shape of bone-like nodules (Figure 1). Finally, the HT samples reduced the bacteria adhesion in comparison to the bare substrates and glass references.

CONCLUSION

Accordingly, the results suggested that the hydrothermally synthesized anatase coatings with an adequate morphology and surface properties can have a better osseointegration of the implant and that a large potential to be used in self-disinfection of medical devices may be expected, as a result of surface photo-activation before surgery.

REFERENCES

1. Gristina AG., Science. 237(4822):1588-1595, 1987.
2. Lorenzetti M. *et al.*, Mater. Sci. Eng., C. 37(0):390-398, 2014

ACKNOWLEDGMENTS

Funding from EU 7^o Framework Programme FP7/2007-13 BioTiNet-ITN (Grant no: 264635) is acknowledged. The authors would like to thank Mrs. Olga Dakischew and Ms. Špela Koželj for the provided support with cell cultures and bacteria experiments, respectively.

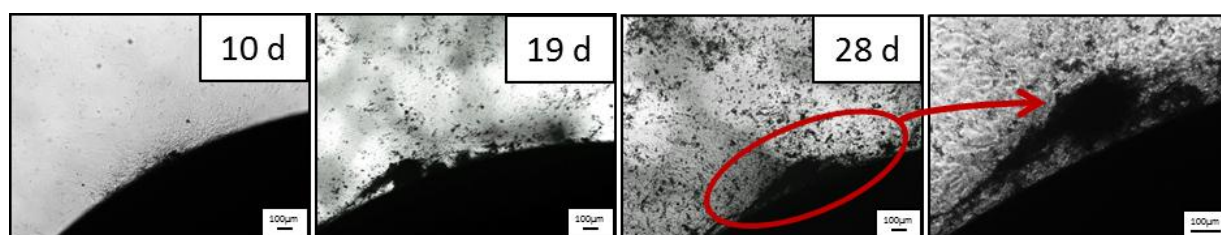


Figure 1. Formation of mineral phase and bone-like nodule during cell culture in osteogenic medium

Fabrication of Tissue Engineering Scaffolds from Poly(ester-anhydride) by Projection Stereolithography

Harri Korhonen¹, Pekka Lehtinen², Jouni Partanen², Jukka Seppälä¹

¹Laboratory of Polymer Technology, Aalto University, Finland

²Department of Mechanical Engineering, Aalto University, Finland, harri.korhonen@aalto.fi

INTRODUCTION

Additive manufacturing methods have been increasingly used in the preparation of 3D structures from bioresorbable polymers. We have previously fabricated tissue engineering scaffolds by stereolithography from photocurable poly(ϵ -caprolactone) macromers¹. The aim of the current study was to investigate if SLA can be used also for the fabrication of photocurable poly(ϵ -caprolactone) based poly(ester-anhydrides). The poly(ester-anhydrides) have been shown to exhibit a very fast surface erosion type degradation kinetics due to incorporation of labile anhydride linkages along the poly(ϵ -caprolactone) backbone. The poly(ester-anhydrides) have been used for zero-order drug release^{2,3} and for porogenization of scaffolds consisting of fast degrading poly(ester-anhydride) and a slower degrading polymer⁴.

EXPERIMENTAL METHODS

Photocurable poly(ester-anhydrides) were prepared in three steps. OH-terminated oligomers were synthesized by ring-opening polymerization of ϵ -caprolactone. Oligomers were further functionalized with succinic anhydride to carboxylic acid functionality. In the final step, COOH-terminated oligomers were methacrylated by reaction with methacrylic anhydride to obtain photocurable oligomers.

3D structures were fabricated by a self-made projection stereolithography (PSLA) system. The setup of PSLA is shown in Figure 1. The system was based on commercial video projector (Acer H6510BD, 1920*1080 pixels), collimating lens, and a narrow bandpass filter. In fabrications campherquinone (1 wt-%) and ethyl 4-dimethylaminobenzoate (1 wt-%) were used for photoinitiation, and Orasol Orange c (0.1 wt-%) as neutral absorber to control penetration depth of light into resin.

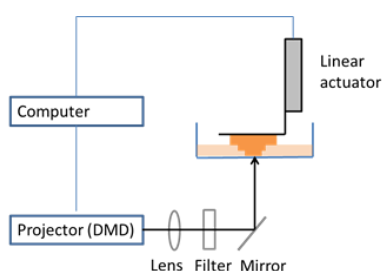


Figure 1. Illustration of projection stereolithography.

RESULTS AND DISCUSSION

Fabrication was carried out by using light intensity of 7000 $\mu\text{W}/\text{cm}^2$, layer thickness of 30 μm , and curing time

of 7s for each layer. Well-controlled 3D structures were obtained with the used fabrication parameters. The dimensions of the samples were 5*5*5 mm.

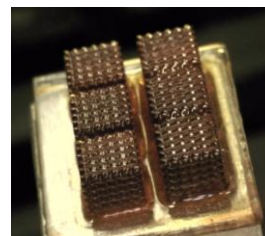


Figure 2. Fabricated samples before purification

The designed scaffold model had a gyroid-like pore architecture and porosity of 70 %. The prepared scaffolds closely followed the structure of the designed model.

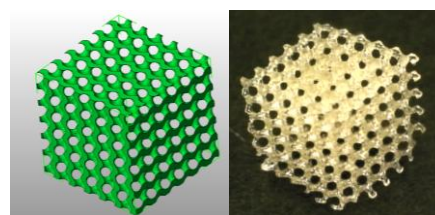


Figure 3. a) Designed model, b) fabricated sample

Poly(ester-anhydrides) are expected to find use in fast eroding tissue engineering scaffolds. In addition, they can be used as porogens for scaffolds prepared from slower eroding polymer. Since PCL-based poly(ester-anhydride) degrades by surface erosion, designed 3D structures obviously provide new possibilities for controlled release applications.

CONCLUSION

The results showed that poly(ϵ -caprolactone) based poly(ester-anhydride) is suitable material to be used in the fabrication by SLA.

REFERENCES

1. Elomaa L. *et al.*, Acta Biomaterialia 7:3850-3856, 2011
2. Mönkäre J. *et al.*, Eur J. Pharm. Biopharm. 80:33-38, 2012
3. Mönkäre J. *et al.*, J. Controlled Release, 148:49-50, 2010
1. Rich J. *et al.*, J. Macromol. Biosci., 9:654-660, 2009

ACKNOWLEDGMENTS

“The authors would like to thank the Academy of Finland (Grant no: 13141164) for providing financial support to this project”.



Novel sol-gel synthesis of $(P_2O_5)_{50}-(CaO)_{30}-(Na_2O)_{15}-(Fe_2O_3)_5$ glasses for biomedical application

Farzad Foroutan^{1,2}, Nora de Leeuw² and Jonathan Knowles¹

¹Division of Biomaterials and Tissue Engineering/Eastman Dental Institute, University College London, UK

²Department of Chemistry/Faculty of Math and Physical Science, University College London, UK

F.Foroutan.11@ucl.ac.uk

INTRODUCTION

Recently, interested in soft and hard tissue engineering to improve tissue regeneration has fuelled the need for novel biomaterials having specific bioactivity and controllable degradation rates^{1,2}. Bioresorbable materials can be resorbed in the body and replaced by bone and tissue cells. It is well accepted that phosphate-based glasses exhibit a great potential to act as a bioresorbable material for biomedical applications, since they show a controllable degradation rate with releasing bioactive and biocompatible ions^{3,4}. In addition, low synthesis temperature of the sol-gel method leads to the opportunity to incorporate drug molecules into the glass network for drug delivery applications, which can be homogeneously dispersed throughout the sol-gel derived glass during the synthesis procedure⁵.

Here we report the sol-gel preparation of a quaternary P_2O_5 -CaO- Na_2O - Fe_2O_3 (PCNF) glass system. The structure of the sample has been characterized using XRD, DTA, FTIR and elemental proportion measured by EDX analysis.

EXPERIMENTAL METHODS

The reaction was started by diluting n-butyl phosphate in MeO-EtOH (at the molar ratio of 1:3). Following that Ca-methoxyethoxide was added dropwise into the mixture (the whole reaction being carried out in a dried vessel). Then $Fe[OCH(CH_3)_2]$ solution was added to the mixture while it was magnetically stirring. After 1 h stirring NaOMe was poured into the vessel and in the last stage the vessel was cooled down in an ice-bath before n-DMF added to the mixture. The mixture turned to gel after about 10 min and aged at room temperature for 3 days. The sol-gel preparation is outlined by the flowchart in Fig. 1

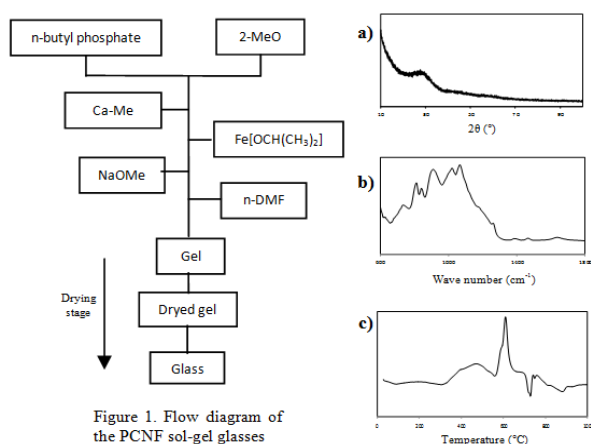


Figure 1. Flow diagram of the PCNF sol-gel glasses

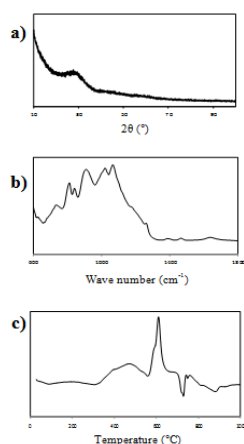


Figure 2. a) XRD, b) FT-IR, and c) DTA analysis trace of the stabilized PCNF sol-gel glass

In the drying stage the gel was kept at 60 and 120 °C for 3 and 2 days respectively before keeping at 150 °C for 1 h to remove any remained solvent and bulk, glassy-like sample was obtained.

RESULTS AND DISCUSSION

The XRD pattern was free from any detectable crystalline phase and a broad peak at 2θ values of around 20-35° confirmed the amorphous structure of the sample (Fig. 2a). The EDX result showed a reduction of around 5 mol% P_2O_5 with a concomitant increase in the percentage content of the other oxides to compensate. This loss was expected due to the relative volatility of phosphorus precursor. From the FTIR spectrum (Fig. 2b) of the glass sample three main regions can be distinguished⁶: the range between 1400-1150 cm^{-1} is characteristic of the vibration of non-bridging PO_2 groups, the region between 1150 and 900 cm^{-1} for terminal P-O- and PO_3 , and vibration of bridging P-O-P groups for the range between 900 and 700 cm^{-1} . And from the DTA graph (Fig. 2c) glass transition temperature (T_g) value of 435 °C was obtained. Also clear peaks were observed for the crystallization (T_c) and melting temperature (T_m), which are 609 and 728 °C respectively.

CONCLUSION

In this study for the first time a quaternary glass in the system P_2O_5 -CaO- Na_2O - Fe_2O_3 has been successfully synthesized via sol-gel method. The amorphous pattern and glassy nature were confirmed by XRD and EDX results revealed loss of phosphorus during the sol-gel process in relatively low. FTIR data show that while Fe_2O_3 slightly disrupts the glass network, however, its improved cross-linking of the phosphate units that can decrease the solubility of the glass for biomedical application. Future work will be undertaken on degradation study of these quaternary sol-gel glasses and production of nano/micro size glass beads for their potential drug delivery and imaging contrast agent applications.

REFERENCES

- [1] Hench LL, Polak JM. Science.295: 10-14, 2002
- [2] Knowles JC. J Mater Chem. 13: 395-401, 2003
- [3] Abou Neel EA *et al.* J Mater Chem.19: 690-701, 2009
- [4] Abou Neel E.A *et al.* Acta Bio. 1:553-563, 2005
- [5] Pickup DM. *et al.* J Biomater Appl. 26:13-22, 2012
- [6] Ilieva D. *et al.* J Non-Cryst Solids 293: 562-8, 2001

ACKNOWLEDGMENTS

This work was supported in part (JCK) by WCU Program through the National Research Foundation of Korea (NRF) funded by the Ministry of Education, Science and Technology (No. R31-10069).

Development of novel nanofunctionalised glass ionomer cements containing chlorhexidine-hexametaphosphate nanoparticles: mechanical properties and method of incorporation

Candice A Bellis^{1*}, James A Holder^{1,2}, Dominic J O'Sullivan¹, Michele E Barbour¹

¹Oral Nanoscience, School of Oral and Dental Sciences, UK ²Kemdent, UK; *candice.bellis@bristol.ac.uk

INTRODUCTION

Glass ionomer cements (GICs) are biomaterials used extensively in dentistry. Their applications include restorations, orthodontic adhesives, cavity liners and in atraumatic restorative treatment. GICs have many favourable properties, but a limitation to their use is their low strength, and it is important that any development in GIC science does not adversely affect strength. The main reason dental restoratives are replaced is due to bacteria-mediated decay adjacent to the biomaterial. A dental biomaterial with a sustained antimicrobial effect could have significant clinical impact. Chlorhexidine (CHX) is a cationic antiseptic which has broad spectrum antibacterial activity and is widely used in oral care products. CHX-releasing nanoparticles have recently been reported.^{1,2} The aim of this study was to incorporate CHX nanoparticles into a GIC using two different methods and to investigate how this affected mechanical properties.

EXPERIMENTAL METHODS

Nanoparticle synthesis-100 mL each of 10 mM CHX digluconate and sodium hexametaphosphate (HMP; both Sigma-Aldrich, Gillingham, UK) were combined under ambient laboratory conditions with vigorous stirring. 30 mL 1M KCl was added after 1 min and stored for 24 h without stirring. The supernatant was discarded and the remaining sediment centrifuged for 30 min at 5000 rpm. The supernatant was again discarded leaving a viscous white sediment paste.

Preparation of nanoparticles for GICs-Nanoparticles were added to GICs as either the viscous white paste described above, or as dry particles. To create the dry particles, the paste was dried under ambient laboratory conditions in a fume hood and then milled in a ball mill for 4 h on a rotating platform. Nanoparticles were then substituted at 1, 2, 5 or 10 % for the glass component with adjustment of acid concentration to correct for water in sediment specimens.

GIC specimens using nanoparticle paste-Powder and liquid were mixed in a 4:1 ratio according to the manufacturers' instructions. The nanoparticle sediment was added to the GIC liquid first and then this combined liquid was mixed with the powder.

Specimen preparation-For diametral tensile strength (DTS) testing, GIC specimens were created in cylindrical PTFE moulds of 4 mm (height) by 6 mm (diameter). For compressive strength (CS) testing a steel mould of 6 mm (height) by 4 mm (diameter) was used. After 5 min, specimens were removed from the moulds and stored in 100% humidity for 7 days.

Strength testing-DTS and CS were measured using an Instron universal testing machine.³ Data were analysed using Kruskal-Wallis tests. DTS n values: sediment

(n=15-20), ball milled (n=14-18). CS n values: sediment (n=16-21), ball milled (n=17-22).

RESULTS AND DISCUSSION

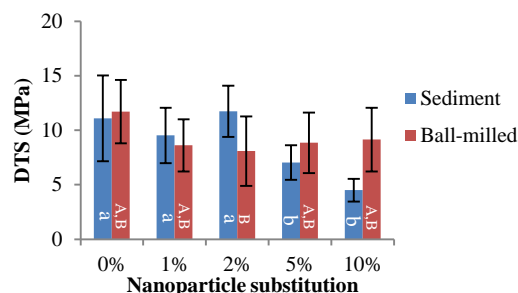


Figure 1. DTS of GIC specimens. Error bars are standard deviations. Letters indicate homogeneous groups (lower case: sediment; upper case: ball-milled).

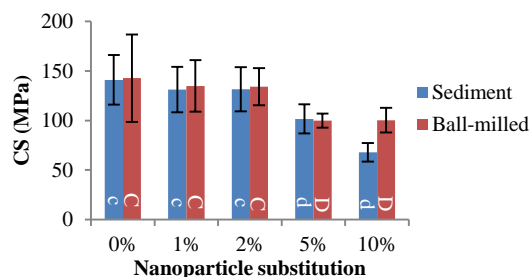


Figure 2. CS of GIC specimens. Error bars are standard deviations. Letters indicate homogeneous groups (lower case: sediment; upper case: ball-milled).

DTS decreased numerically as a function of % nanoparticle substitution; the effect was only statistically significant for the sediment-incorporated specimens. CS was statistically significantly reduced for 5 and 10 % substitutions using both methods but numerically lower for sediment specimens.

CONCLUSION

Experimental GICs containing CHX-HMP nanoparticles at a range of dopings were created. Reduction in both DTS and CS was observed for higher substitutions; the detrimental effect on strength was less pronounced for specimens made using dry, ball-milled nanoparticles than for wet, sedimented nanoparticles.

REFERENCES

1. Barbour et al, Int J Nanomedicine 2013, 8: 3507-19.
2. Hook et al, J Nanobiotech 2014, 12: 3.
3. Darvell, Materials Science for Dentistry, 9th edition, Woodhead Publishing 2009, 20-21.

ACKNOWLEDGEMENTS The authors are grateful to the Medical Research Council and Kemdent for funding CAB's PhD CASE studentship.

Evaluation of the effect of polymer content on drug release and mechanical strength of a Geopolymer ER Formulation for opioid drugs

Bing Cai, Håkan Engqvist, Susanne Bredenberg

Division for Applied Materials Science, Department of Engineering Sciences, Uppsala University, Sweden.
bing.cai@angstrom.uu.se

INTRODUCTION

Geopolymer is a porous ceramic material composed of a three-dimensional polysialate framework and has been suggested as a possible matrix material for ER formulation of opioid drugs¹. The diffusion process through the meso-pores is the main rate-limiting step for the drug release from the geopolymer-based delivery systems. However, in that study, the geopolymer formulation released drug faster in lower pH solutions, which in-vivo could cause dose dumping and serious side effects. Since the gastrointestinal absorption of most drugs usually takes place in small intestine, it is more safe and effective to have the major drug release at neutral pH in a controlled manner. In addition a high mechanical strength is of importance for a safe ER formulation².

This study aims to evaluate the impact of addition of one enteric coating polymer to the geopolymer formulation on drug release performance and tamper-resistance to physical milling. The geopolymer-based formulation was compared with ER formulation manufactured according to the reference regarding the drug release profiles and compressive strength³. Zolpidem tartrate was used as model drug.

EXPERIMENTAL METHODS

The geopolymer pellets were synthesized and moulded into cylindrical pellets (1.5 x 1.5mm diameter x height) and cured as the previous study². Eu x is noted for the geopolymer formulation with x g of the enteric coating polymer, Eudragit®, into 4g of metakaolin. The reference ER formulation was moulded into the same cylindrical shape with the composition published by Shailes³.

The drug releases from geopolymer and reference formulation were evaluated in triplicate by a standardized dissolution method in a USP 2 apparatus (Sotax AG, Switzerland) at two typical gastric conditions: pH 1 and pH 6.8. Aliquots (1 ml) were withdrawn and analyzed using a UV/VIS spectrophotometer (Shimadzu 1800, Japan). The compression strength was tested using Autograph AGS-H universal testing machine (Shimadzu corp., Japan) according to a standard testing method⁴.

RESULTS AND DISCUSSION

The drug release rate decreased with increasing amount of enteric coating polymer at pH 1 (Fig. 1). In contrast, the drug release rate increased with the polymer content at pH 6.8, probably due to the higher the dissolution of the polymer at neutral pH resulting in a higher surface area. The drug release profile for Eu 0.75 showed a lower drug release rate at pH1 and a higher rate at pH 6.8, which could improve the gastrointestinal absorption.

The drug release profiles of Eu 0.75 were compared with the comparison formulation. The release profiles

of geopolymer formulation at both pH conditions fitted well into the Higuchi model ($R_2 > 0.99$). It indicates that Eu 0.75 could maintain controlled release during the measured period and reduce the possibility of dose dumping. In contrast, the comparison formulation released the drug readily at both pH 1 and 6.8 and thus could not sustain the drug release for an elongated period.

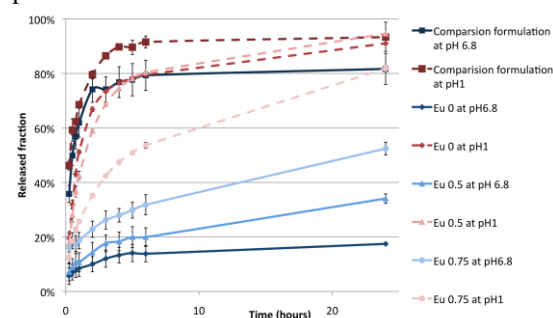


Fig. 1 The drug release from comparison ER formulation and geopolymer matrices with different amount of enteric coating polymer.

The compressive strength of Eu 0 was 83 MPa (SD: 7.5); of Eu 0.5 was 59 MPa (SD: 13.1) and of Eu 0.75 was 21 MPa (SD: 5.0). Even though the polymer content influenced the mechanical strength of geopolymer formulation, Eu 0.75 had the double mechanical strength of the comparison formulation (11 MPa, SD: 1.3). The higher compressive strength of geopolymer formulation could thwart the tampering formulation by physical manipulation.

CONCLUSION

The study showed that the enteric coating polymer reduced the drug release rate at pH 1 but increased release rate at pH condition similar to the small intestine. Although, the polymer content influenced the compressive strength of the geopolymer formulation, the strength was still higher than the reference ER formulation. The results indicate the enteric coating polymer has potential as an excipient in geopolymer formulation to improve the drug release performances.

REFERENCES

1. Jämstorp, E., et al., Journal of Controlled Release, 2010. 146(3): p. 370-377.
2. Bulter, S. F., et al., Harm Redct Journal, 2011. 8:p.29.
3. Shailes, T. P., et al., International Scholarly Research Network, ISRN Pharmaceutics, 2011.
4. ASTM F4512008, ASTM International.

ACKNOWLEDGMENTS

Orexo AB is acknowledged for supplying the materials and Vinnova and the Swedish Research Council are acknowledged for financial contribution.

Poly(butylene succinate) nanocomposites containing strontium hydroxyapatite nanorods for tissue engineering applications

M. Nerantzaki¹, Z. Terzopoulou¹, E. Roumeli¹, D. Papageorgiou¹, D. Bikiaris¹, J. Will², J. Hum², A. Hoppe², J.A. Roether², A.R. Boccaccini²

¹ Aristotle University of Thessaloniki, GR-541 24 Thessaloniki, Macedonia, Greece.

² Institute of Biomaterials, Department of Materials Science and Engineering, University of Erlangen-Nuremberg, Cauerstrasse 6, 91058 Erlangen, Germany, marinera002@gmail.com

INTRODUCTION

Poly(butylene succinate) (PBSu), a novel biodegradable aliphatic polyester with excellent processability is a promising substance for bone and cartilage repair. However, it typically suffers from insufficient bioactivity after implantation into the human body and low mechanical properties, which reduce its application possibilities¹. So, in order to overcome this problem, strontium hydroxyapatite nanorods $\text{Sr}_5(\text{PO}_4)_3\text{OH}$ (SrHNRs), were synthesized and introduced into the polyester via *in situ* polymerization. Concerning strontium it affects positively new bone growth inhibiting resorption and enhancing bone formation².

EXPERIMENTAL METHODS

In this work SrHNRs were synthesized by a chemical solution method. Afterwards, PBSu nanocomposites containing 0.5, 1 and 2.5wt% nanofillers were prepared by *in situ* polymerization technique for the first time and we examine the ability to be used as potential tissue engineering scaffolds. The prepared composites scaffolds were characterized using SEM, FTIR and XRD. Mechanical testing (Instron 3344) and contact angle measurements were also carried out. Additionally, the enzymatic degradation in aqueous solution containing mixture of *R. Oryzae* and *P. Cepacia* lipases, at 37°C and pH=7.2 and the *in vitro* biomineralization in simulated body fluid (SBF) were studied. Osteosarcoma cell line (MG-63) was applied in order to assess the biocompatibility of the composites.

RESULTS AND DISCUSSION

PBSu has a tensile strength at break of 27.4MPa and Young's Modulus 408. Its nanocomposite containing 0.5wt% SrHNRs, presented improved tensile strength and elasticity values of 30.7MPa and 415 respectively. However increasing the nanorods concentration the mechanical properties deteriorated. This small decrease could be attributed to the absence of any interaction between $\text{Sr}_5(\text{PO}_4)_3\text{OH}$ nanorods and the polyestheric matrix, as was verified from FTIR spectroscopy and thus the adhesion between the different materials is too low. From enzymatic hydrolysis, it was found that all nanocomposites have higher hydrolysis rates than neat PBSu and as the amount of nanofiller increases the hydrolysis rate becomes higher. The presence of hydroxyl groups in $\text{Sr}_5(\text{PO}_4)_3\text{OH}$ makes the nanocomposites more hydrophilic than neat PBSu and hence, absorb more water and subsequently degrade more rapidly. XRD study after biomineralization in SBF indicated the appearance of a crystalline phase of hydroxyapatite (Fig. 1).

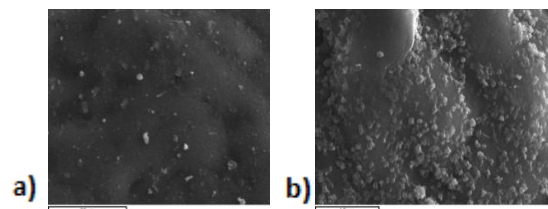


Fig. 1. SEM views of a) PBSu b) PBSu/ $\text{Sr}_5(\text{PO}_4)_3\text{OH}$ 0.5% after soaking in SBF for 28 days display that scattered and clustered particles are formed on the samples.

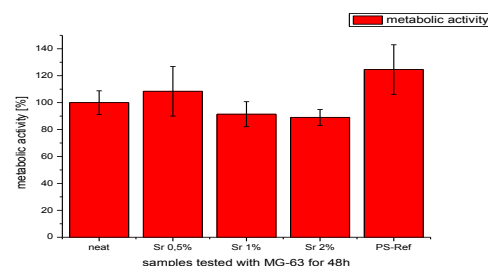


Fig. 2. Metabolic activity of MG-63 cells cultivated for 48h on plane composite samples.

SrHNRs can also induce osteoblast compatibility. Nanocomposites have rougher and more hydrophilic surfaces compared to pristine PBS, thereby causing more osteoblasts to adhere and proliferate on them¹.

CONCLUSION

PBSu nanocomposites containing $\text{Sr}_5(\text{PO}_4)_3\text{OH}$ nanorods at different concentrations were prepared and studied as potential materials for tissue engineering applications. The mechanical properties of PBSu improved only for the sample with 0.5% SrHNRs. The nanoadditives can accelerate the enzymatic hydrolysis of PBSu increase materials hydrophilicity. SrHNRs can transform the bioinert PBSu surface into a bioactive one, promoting hydroxyapatite formation in SBF solution, too. Cell biology studies showed that PBS/SrHNRs are biocompatible materials and metabolic activity was best at the cells on the PBSu/SrHNRs 0.5 wt% sample.

REFERENCES

1. Huaiyu W. *et al.*, Acta Biomater. 5:279-287, 2009
2. Bilström G. *et al.*, Injury, 44(S1): S28-S33, 2013

ACKNOWLEDGMENT The author wishes to acknowledge co-funding of this research by IKY (Greece) and DAAD (Germany), Action "IKYDA 2013

New N-(2-carboxybenzyl)chitosan hybrid biocomposites for scaffolds applications

M. Nerantzaki¹, Z. Terzopoulou¹, M. Mavidou¹, D.N. Bikiaris¹, M.D. Anastasopoulou², M.A. Karakassides², A.R. Boccaccini³

¹ Aristotle University of Thessaloniki, Chemistry Department, GR-541 24 Thessaloniki, Macedonia, Greece.

² Department of Materials Science and Engineering, University of Ioannina, Ioannina 45110, Greece

³ Institute of Biomaterials, Department of Materials Science and Engineering, University of Erlangen-Nuremberg, Cauerstrasse 6, 91058 Erlangen, Germany, marinera002@gmail.com

INTRODUCTION

Chitosan is a biocompatible substrate for cell propagation but is soluble only in acidic aqueous environment, characteristic that somewhat limits its applications in vivo. However, this hurdle can be easily overcome by carboxyalkylation of the amino group of chitosan¹. Reports also suggest that bioactive glass ceramics and nanophase ceramics such as titania, influence the cell adhesion, proliferation, differentiation and colonization on surface of implants². Therefore in this project, we address the preparation and characterization of CBCS/BG 45S5 and CBCS/TiO₂ composite scaffolds, relevant to tissue engineering applications.

EXPERIMENTAL METHODS

In this work N-(2-Carboxybenzyl)chitosan (CBCS) was synthesized via a Schiff reaction of chitosan with 2-carboxybenzaldehyde, followed by reduction of the imine derivative with sodium borohydride. Meanwhile, 0.5, 2.5 and 5% TiO₂ nanoparticles and 2.5% Bioglass 45S5 (BG45S5) were added during the carboxyalkylation reaction, in order to obtain different CBCS composites. The porous structure of scaffolds was obtained by freeze-drying technique. The carboxyalkylation was determined by UV and H¹NMR spectroscopies. The prepared biocomposites were characterized using SEM, FTIR and XRD. The swelling, degradation and in-vitro biomineralization of the composite scaffolds were also studied.

RESULTS AND DISCUSSION

The primary λ_{max} is visible in case of CBCS at 231 nm and corresponds to $\pi \rightarrow \pi^*$ transition indicating the incorporation of 2-carboxybenzaldehyde into chitosan backbone, in agreement with the H¹NMR spectra, where the characteristic multiple peak of aromatic protons (7.6–7.8 ppm) appeared. All the CBCS composite sponges revealed high compressive strength values, suggesting that both the benzoic rings and the inorganic fillers can attribute significant mechanical stiffness to the chitosan matrix. Interconnected pores (150–300 μ m) can be observed in all biocomposites by SEM (Fig. 1) appropriate for scaffolds applications.

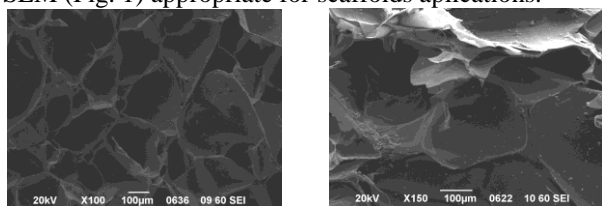


Fig. 1 SEM pictures of a) CBCS b) CBCS/BG 45S5 2.5%.

Both CBCS/TiO₂ and CBCS/BG composite scaffolds showed significant decline in the degradation rate after 1 and 2 weeks immersion in PBS compared to pristine CBCS scaffolds. Degradation of chitosan can result in acidic degradation products, which may be neutralized by alkali groups leaching out from Bioglass thus reducing the degradation rate. In addition, our results suggest that the composite scaffolds indicated increased swelling ratio, with increase of the concentration of the inorganic fillers. XRD study confirms the mineral deposition of minerals on the surface of both CBCS/BG 2.5% and CBCS/TiO₂ 2.5% composite scaffolds after 7 days incubation in SBF solution (Fig. 2).

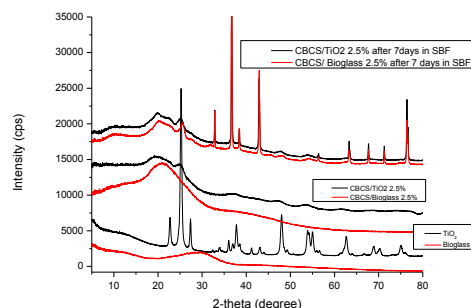


Fig. 2. XRD pattern showing characteristic peaks of HA at 36.7°, 38.3° and 43° (upper part)

CONCLUSION

CBCS was successfully synthesized and identified by UV and H¹NMR spectra. Composite materials were prepared by adding TiO₂ nanoparticles at different concentrations and Bioglass 45S5 during the modification reaction. Porous scaffolds were obtained using the lyophilization technique and they were characterized. They all showed interconnected pores and high mechanical properties. In addition, swelling, degradation and bioactivity studies of the composite scaffolds were performed. The developed composite scaffolds were bioactive and showed controlled swelling and degradation rate by the addition of inorganic fillers.

REFERENCES

1. Konstantinos K., *et al.*, Carbohydr. Polym. 82:181-188, 2010
2. Xuanyong L., *et al.*, Biomaterials 26:6143-6150, 2005

ACKNOWLEDGMENTS

The author wishes to acknowledge co-funding of this research by IKY (Greece) and DAAD (Germany), Action "IKYDA 2013.

Release of Propranolol hydrochloride from Polyethyleneglycol Modified Lactone Polymers

Sanja Asikainen, Minna Malin and Jukka Seppälä

Research Group of Polymer Technology, School of Chemical Technology, Aalto University, Finland,
sanja.asikainen@aalto.fi

INTRODUCTION

Biodegradable lactone polymers, especially poly(ϵ -caprolactone) (PCL), poly(lactic acid) (PLA) and their copolymers, have been widely studied for biomedical applications. Copolymerization can be used to tailor polymer properties and drug release from polymer matrix. Water soluble polyethylene glycol (PEG) block in lactone polymers increases the hydrophilicity of polymer.¹

The aim of this study was to investigate how copolymer composition and hydrophilic co-initiator affect the release of hydrophilic drug propranolol hydrochloride and the hydrolytic degradation of polymer.

EXPERIMENTAL METHODS

Materials Polymerization

Three different polymers were used in this study. PLCL (P(CL30-LLA70)) from Purac was used as reference polymer. Polymer of DL-lactide and copolymer of DL-lactide and ϵ -caprolactone were polymerized in bulk in a batch reactor by using 0.03 mol-% Sn(II) octoate as an initiator and 0.04 mol-% polyethylene glycol (PEG, 20 000 g/mol) as a co-initiator. The polymers were homopolymer PEG-PDLLA and copolymer PEG-P(CL30-DLLA70) having monomer ratio of 30 mol-% ϵ -caprolactone and 70 mol-% DL-lactide. The polymerization temperature was 160 °C and polymerization time was 4h. Polymers were used without further purification.

Preparation of samples

10 w-% of propranolol hydrochloride was blended into polymers in a corotating twin screw microextruder and melt pressed to receive cylinder-shaped devices having dimensions 5x2mm.

Thermal analysis

Glass transition temperatures were measured by differential scanning calorimetry (DSC). The analysis was performed on the temperature range of -90 °C to 200 °C at heating rate of 10 °C/min. The glass transition temperatures were determined from the second heating scan.

Molecular weight determination

Molecular weights were determined by room temperature size-exclusion chromatography. Chloroform was used as a solvent and eluent for polymers. Monodisperse polystyrene standards were used for primary calibration.

In vitro release experiments

Samples were weighted and immersed individually in 30 ml phosphate buffer solution (pH 7.4) at a temperature of 37 °C. The test specimens were removed from test tubes at different intervals and weighted after drying 24 h in vacuum at room temperature. The

amount of released propranolol HCl was determined from buffer solution using UV-spectrometer (Unicam Helios β v.1.30). The spectra were collected in the range of 200 to 350 nm. The maximum absorption was at 294 nm.

RESULTS AND DISCUSSION

No propranolol peak was seen in the DSC measurements of the drug blended with polymers. Therefore, it can be assumed that propranolol HCl was dissolved in the polymer matrices. Samples with propranolol HCl had slightly lower T_g compared to neat polymers (Table 1) which may be due to the effect of drug solubility to polymer. The effect was more significant with polymers containing PEG, which may indicate that hydrophilic PEG enhances solubility of hydrophilic propranolol HCl.

Table 1. Glass transition temperatures of polymers and drug blends.

	Neat polymer	Polymer + Drug
PEG-PDLLA	44 °C	40 °C
PEG-P(CL30-DLLA70)	10 °C	5 °C
P(CL30-LLA70)	22 °C	21 °C

Molecular weights of copolymers decreased slower compared to that of homopolymer during first month, which also affected the drug release rate. When molecular weight reached 40 % of its initial value the release rates became closer to each other.

For the first month, the release rate from P(CL30-LLA70) was faster compared to PEG-P(CL30-DLLA70). After 4 weeks PEG-P(CL30-DLLA70) started to swell remarkably and simultaneously the release rate increased. Homopolymer (PEG-PDLLA) showed faster release rate for the first month, but after that copolymer (PEG-P(CL30-DLLA70)) released drug faster.

CONCLUSION

Copolymerization and hydrophilic co-initiator can be used to tailor drug release properties of polymer. PEG enhanced the solubility of hydrophilic drug into the polymer matrix and affected drug release especially by increasing polymer swelling.

REFERENCES

1. Karjalainen T. et al., J. App. Pol. Sci. 81:2118-2126, 2001

ACKNOWLEDGMENTS

The authors would like to thank the Academy of Finland (Grant no: 13141164) for providing financial support to this project.



Titanium oxide coated cobalt-chromium-molybdenum; improving the osteogenic response of mesenchymal stem cells *in vitro*

N Logan^{1*}, A Cross³, S Collins², A Trayner², I Parkin³, L Bozec¹ and P Brett¹

¹ Biomaterials and Tissue Engineering, University College London, Eastman Dental Institute, UK.

² Corin Group, Cirencester, UK.

³ Department of Chemistry, University College London, UK
niall.logan.11@ucl.ac.uk

INTRODUCTION

Titanium (Ti) and its alloys are accepted as the current gold standard implant material for orthopaedic applications¹. Despite this, other materials, such as cobalt-chromium-molybdenum (CCM), are often used due to their superior mechanical properties. Whilst CCM provides additional mechanical strength, it does not have the biocompatibility of Ti². The objective of this study was to investigate if coating the surface of CCM in a layer of titanium oxide (TiO₂), could increase the bioactivity of the material, by masking the underlying bulk alloy with the same oxide layer as found on Ti.

EXPERIMENTAL METHODS

Human mesenchymal stem cells (MSCs) from 3 donors were used for the experiments. CCM discs of 15mm diameter, 1mm thickness, were ground and polished to achieve a smooth, featureless topography. Half of the CCM discs were then coated in anatase TiO₂ (CCMT) by way of atmospheric chemical vapour deposition (CVD). Discs of pure Ti were used as a positive control and uncoated CCM as a negative control. All discs underwent UV sterilisation before cell culture experiments. MSCs were cultured using DMEM supplemented with osteogenic additives, at standard culture conditions of 37°C/5%CO₂ in a humidified atmosphere. The osteogenic activity of the cells was assessed by monitoring proliferation (2x10³ cells per disc) and fluorescent microscopy analysis of both bone alkaline phosphatase (b-ALP) and hydroxyapatite, after 4 and 21 days, respectively (n=3) (12.5x10³ cells per disc). To ascertain the adhesion capabilities of the substrates, the expression of the focal adhesion protein, vinculin, was analysed by fluorescent microscopy after 3 and 24 hours in osteogenic culture (n=10) (5x10³ cells per disc). Images were quantified by a pixel based method using ImageJ software. Statistics were performed using the student's t test with p < 0.05 considered significant.

RESULTS AND DISCUSSION

MSC proliferation in OM was not inhibited and a minor rise in cell numbers through day 1 – 7 was observed on all substrates. By day 18, the amount of cells present had reduced on all three substrates, due to the creation of a mineralised tissue formed through MSC osteogenesis. Throughout the experiment, the CCMT substrate promoted osteogenic proliferation at a rate more comparable to that on the Ti substrate than the CCM.

The perceived intensity of b-ALP, an early stage marker of osteogenesis, was enhanced in MSCs on both CCMT and Ti surfaces after 4 days. b-ALP was observed in MSCs on the CCM substrate, but did not appear to exhibit the same level of expression as found on both CCMT and Ti.

Hydroxyapatite (HA) is one of the key components in the extra cellular matrix of bone tissue and is a late marker of osteogenesis. After 21 days in culture, HA was positively identified on all three substrates. Nodules of HA were observed on all three substrates, with the largest nodules found on the Ti substrate. The CCMT substrate stimulated the formation of bigger nodules of HA than CCM. This implies there was an enhanced level of osteogenic differentiation occurring on the CCMT substrate compared to CCM.

Vinculin is a focal adhesion protein involved in linking cell adhesion membranous molecules, and plays a role in the adhesion of the cell to the substrate. Fluorescent microscopy analysis showed an increase in the expression of vinculin on both CCMT and Ti surfaces compared to CCM, although this was only statistically significant for Ti vs CCM at 24 hours (p<0.05). Furthermore, MSCs on CCMT and Ti appeared to have a greater number of focal adhesions per cell. This analysis implies that the CCMT and Ti substrates may promote superior adhesion of MSCs, through heightened vinculin expression and greater numbers of focal adhesions per cell.

CONCLUSION

From the work in this study we have demonstrated that it is possible to improve the osteogenic behaviour of human MSCs on CCM by coating the substrate with a durable layer of TiO₂ by way of atmospheric CVD. This infers that TiO₂ coatings may be a promising method of improving other bio inert biomaterials.

REFERENCES

1. Geetha M, *et al.*, 2009.
2. Stiehler M, *et al.*, 2007.

ACKNOWLEDGMENTS

The authors would like to thank the ESRC, Molecular Modelling and Materials Science Engineering Doctorate centre UCL, and Corin Group.



Autophagy Modification by Intracellular Controlled Release of Rapamycin

Junpei Nagata, Makoto Matsui, and Yasuhiko Tabata

Department of Biomaterials, Fields of Tissue Engineering, Institute for Frontier Medical Sciences,
Kyoto University, Japan, yasuhiko@frontier.kyoto-u.ac.jp

INTRODUCTION

Autophagy plays an important role in maintaining the functional homeostasis of cells. Harmful intracellular harmful components, such as denaturalized protein aggregates and damaged mitochondria, are physiologically eliminated via autophagy. The intracellular accumulation of the components due to autophagy dysfunction causes neurodegenerative disorders¹ or tumorigenesis². If autophagy can be activated, the harmful accumulation will be suppressed to normalize the cell quality. To modify the autophagy activity, the mammalian target of rapamycin (mTOR) was inhibited by rapamycin. In this study, rapamycin was incorporated into nanospheres of poly(L-lactic acid) (PLA) for the controlled release. When cells were incubated with PLA nanospheres incorporating rapamycin or free rapamycin, the autophagy activity was compared. The cellular internalization of nanospheres and the controlled release of rapamycin from the nanospheres were examined.

EXPERIMENTAL METHODS

PLA with a weight-averaged molecular weight of 5,000 and rapamycin were dissolved in the mixed solution of acetone and ethanol (4/1 v/v). The mixed solution was emulsified in aqueous poly(vinyl alcohol) (PVA) solution, followed by the complete evaporation of organic solution to prepare PLA nanospheres incorporating rapamycin. The size of nanospheres was measured by a dynamic light scattering method, and the percentage of rapamycin incorporated was determined by high performance liquid chromatography (HPLC). *In vitro* rapamycin release was evaluated in phosphate-buffered solution (PBS), while the amount of rapamycin released was quantified by HPLC. Human hepatocellular carcinoma (HepG2) cells were cultured with PLA nanospheres incorporating coumarin-6, and then the nanospheres internalization was assessed by fluorescence microscopy. To evaluate autophagy activity and accumulation of ubiquitinated proteins, HepG2 cells were cultured with PLA nanospheres incorporating rapamycin or free rapamycin in the absence or presence of a proteasome inhibitor, MG-132 for 4 days, followed by lysing to extract cells proteins. The proteins extracted were evaluated by the antibodies of microtubule-associated protein 1 light chain 3 (LC3), and ubiquitin in western blotting assay for the evaluation of autophagy activity and ubiquitinated protein accumulation, respectively.

RESULTS AND DISCUSSION

The size of PLA nanospheres incorporating rapamycin ranged from 200 to 500 nm. The size increased with an increase in the concentration of PLA or PVA used in nanospheres preparation. The percentage of rapamycin incorporated into the nanospheres was about 100%. The

in vitro release test indicated that rapamycin was released over one week. PLA nanospheres were internalized into HepG2 cells within one hour and retained in the cells for 4 days. The western blotting assay revealed that autophagy was induced by incubation with free rapamycin or rapamycin-incorporated nanospheres for 1 day (**Figure 1**). However, after 4 days incubation, the induction of autophagy was observed only for the nanospheres incubation. On the other hands, the ubiquitinated protein accumulation was suppressed by incubation with free rapamycin or rapamycin-incorporated nanospheres for 1 day, whereas the accumulation suppression was observed only by 4 days incubation with the nanospheres. It is possible that rapamycin released from PLA nanospheres induced autophagy, resulting in the enhanced degradation of ubiquitinated proteins.

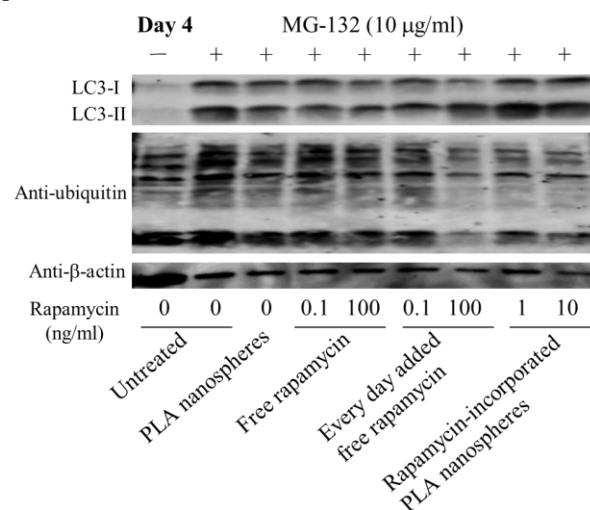


Figure 1. Western blotting of LC3 and ubiquitinated proteins in HepG2 cells incubated with PLA nanospheres incorporating rapamycin or free rapamycin in the presence of MG-132. The concentration of PLA nanospheres is 1, 10 μg/ml.

CONCLUSION

PLA nanospheres incorporating rapamycin with the size range from 200 to 500 nm released rapamycin over one week. The nanospheres were internalized in HepG2 cells to induce autophagy and allowed to intracellularly degrade ubiquitinated proteins for 4 days. Incorporating rapamycin into PLA nanospheres is promising to modify autophagy activity through rapamycin release.

REFERENCES

1. Marzena Ułamek-Kozioł *et al.*, *Neurochem Res.* 38:1769–1773, 2013
2. Alec C. Kimmelman, *Genes Dev.* 25:1999–2010, 2011

Bioactive orthopaedic devices for the local delivery of Gentamicin Sulfate preventing nosocomial infections

Loïc Pichavant^{1,2}, Hélène Carrié^{1,2}, Laurent Plawinski², Valérie Héroguez¹ and Marie-Christine Durrieu²

¹ CNRS UMR5629, Laboratoire de Chimie des Polymères Organiques, IPB-ENSCBP, Université de Bordeaux, Pessac, 16, av Pey Berland, France

² CNRS UMR 5248, CBMN, Université de Bordeaux, Pessac, 2, rue Robert Escarpit, France, lpichavant@enscbp.fr

INTRODUCTION

Since the beginning of the 1970s, controlled release technology has known great advancement, and motivated numerous researchers in materials science. These systems overcome the drawbacks of traditional drug dosage form, and offer more effective and favorable methods to optimize drug delivery in optimum dose to specific sites or to prolong delivery duration. Our research project deals with the synthesis of pH-controlled drug delivery systems for bone implant, allowing the local release of Gentamicin Sulphate (GS), an antibiotic communally used to prevent infections during orthopaedic surgeries. By systemic therapy, antibiotics may not be delivered efficiently and adequately without side effects. The goal of this project is to develop biomaterials allowing the controlled release, at the level of the site of implantation of these biomaterials (over an adjustable period of time), of an active molecule (GS) fixed covalently on the surface of the latter thanks to chemical anchoring of spherical particles (in particular of nanoparticles) functionalized by the active molecule. A cleavage reaction of the active particle-active molecule bond, activated by the contact of material with the physiological medium or by a modification of the pH, induces controlled release of the bioactive molecule in its native form.

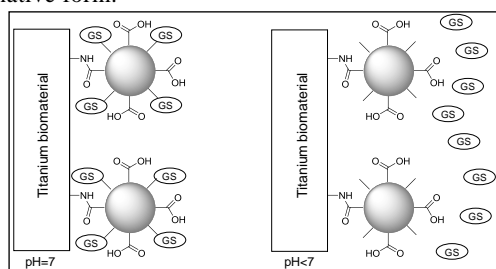


Fig. 1. Representation of the bioactive biomaterial

EXPERIMENTAL METHODS

α -norbornenyl poly(ethylene oxide) macromonomers were synthesized by anionic ring-opening polymerization of ethylene oxide and were ω -functionalized with a carboxylic acid (NB-POE-COOH) or the GS (NB-POE-GS). Macromonomers were characterized by ^1H NMR, Size Exclusion Chromatography (SEC) and MALDI TOF. Nanoparticles are obtained by Ring-Opening Metathesis CoPolymerization (ROMP) of norbornene with NB-POE-COOH and NB-POE-GS. Their colloidal stabilities were shown by Dynamic Light Scattering measurements. Titanium discs ($\varnothing = 5 \text{ mm}$; $h = 3 \text{ mm}$) were activated by functionalization with amine groups using aminosilane molecules (APTES). The NPs were covalently linked onto the titanium surface through the formation of an uncleavable amide bond between the carboxyl group of the NPs and the amide group of silane molecules available onto the surfaces of the disks activated by NHS and DCC. The grafting was characterized by Scanning Electron Microscopy (SEM) Fluorescence microscopy and μ -imagery. The *In vitro* evaluation was carried out by Minimum Inhibitory Concentration (MIC) measurements after GS release at acidic

pH. GS release kinetic profiles have been established by fluorescence spectroscopy.

RESULTS AND DISCUSSION

α -norbornenyl macromonomer was obtained with a size of about 4000 g.mol⁻¹ and a narrow distribution (PDI < 1.1). The ω -functionalization was carried out with high functionalization yields. Nanoparticles are synthesized with total conversions and diameters were about 350 nm.

Two controlled densities of NPs - corresponding to two densities of drug (0.15 and 1.0 $\mu\text{g}\cdot\text{cm}^{-2}$) - were anchored on the biomaterial surfaces and these densities were measured by three methods: scanning electron microscopy observations, μ -imagery using radio-labelled nanoparticles and fluorescence microscopy, using FITC-labelled nanoparticles. FITC-labelled biomaterials were also used to establish GS release kinetics as a function of pH (pH 4, 5, 6 and 7).

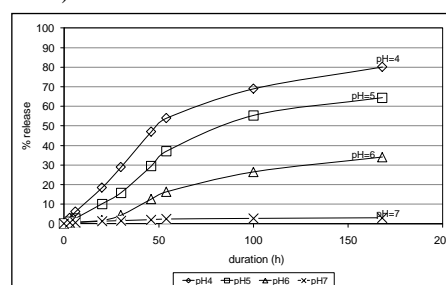


Fig. 2. GS release kinetic curves as a function of pH

The GS release efficiency was proved by *in vitro* bacterial inhibition tests using *staphylococcus epidermidis* as bacterial strain. GS was released from grafted titanium discs. A delivery only at acidic pH, (pH = 6, 5, 4) has been observed.

CONCLUSION

In this work was presented the synthesis of a bioactive biomaterial and their characterization. We also demonstrated the *in vitro* activity of such materials. *In vivo* experiments on rabbits have been done and produced so far encouraging results.

REFERENCES

- 1 Ouchi T. ACS Symp. Ser. 680:284-296, 1997
- 2 Pichavant L.; Bourget C.; Durrieu M.C.; Héroguez V. Macromol. 44:7879-87, 2011
- 3 Pichavant, L.; Amador, G.; Jacqueline, C.; Heroguez, V., Durrieu, M.C. J. Controlled release, 162:373-81, 2012

ACKNOWLEDGMENTS

The authors would like to thank the French “Agence Nationale de la Recherche” (ANR) and the “Société de Transfert de Technologie”, Aquitaine Science Transfert (SATT AST), for providing financial support to this project.

Design of a new composite structure based on resorbable synthetic and natural polymers for anterior cruciate ligament reconstruction

Coline PINESE¹, Xavier Garric¹ Benjamin Notellet¹ Jean Coudane¹ Christian Gagnieu²

¹ Artificial Biopolymers department/ Max Mousseron Institute of Biomolecules, Montpellier I University, France,

² National Institute of Applied Sciences, France, colinepinese@gmail.com

INTRODUCTION

Following accidents, anterior cruciate ligament (ACL) damages are increasingly, becoming a common public health problem. As ACL have poor regeneration ability^{1,2}, it can be removed and replaced by autologous grafts. However, current available solutions have several limitations encouraging research on degradable biomaterials alternatives³. To comply with the requirement of ligament regeneration, ligament reinforcement must be strong enough to support knee physiological strains, and must degrade while allowing the new ligament regeneration.

The aim of this study is to design a new composite composed of two parts:

- 1- A degradable and elastomeric scaffold to serve as temporary mechanical support
- 2- A collagen-GAG matrix to promote cell colonization and ligament tissue formation and maturation.

EXPERIMENTAL METHODS

Novel block copolymers PLA-Poloxamer based have been synthesized by ring opening polymerization. They were then spun for designing a tubular knitted fabric. In parallel, a collagen and glycosaminoglycans (GAGs) porous three-dimensional matrix has been developed to promote cell adhesion and proliferation. Knitted reinforcements associated with collagen-GAG matrix are designing as a composite structure. Subcutaneous implantation of composite structures was performed for 3 months in rats

RESULTS AND DISCUSSION

The main objective is to show the ability of a degradable and polymeric scaffold to provide a structural support with similar mechanical properties to those of ligament tissue.



Figure 1: Copolymere tubular fabric

Figure 1 shows the tubular fabric

	Copolymers tubular fabric	Ligaments
Young's Modulus (MPa)	67 MPa	50-150 MPa
Toe regions strain (%)	27,20%	7-16 %
Stress at failure (MPa)	22,5 MPa	16-36 MPa

Table 2: Copolymers tubular fabrics and ligament mechanical features

Table 1 show that main mechanical features of copolymers tubular fabric are similar to those of ligament tissue.

The second aim is to promote early neotissue formation.

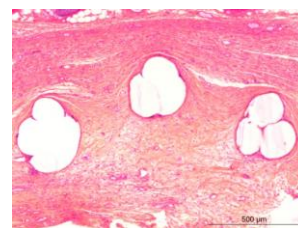


Figure 2: Composite structure subcutaneously implanted after one month

The figure 2 show that the inflammation is moderate after a month and composite structures are fully integrated allowing a new tissue formation composed of oriented collagen.

CONCLUSION

Fully integrated, the composite structure allows neotissue formation while gradually losing its mechanical properties after 3 months. The ability of composite structure to provide a structural support for ligament regeneration with mechanical properties similar to native tissues in dynamic environments, and their ability to support a new tissue formation make them of a particular interest.

REFERENCES

1. Nakanishi Y. *et al*, *Journal of Pediatric Surgery*, 38(12):1781-1784, 2003
2. Laurencin CT *et al*, *Biomaterials*, 26(36):7530-7536, 2005
3. De smedt M *et al*, *Acta Orthop. Belg*, 64(4) : 422-433,1998

ACKNOWLEDGEMENTS

We gratefully acknowledge Mrs Pagnon from the Novotech Institut for her help in the histologic study.

Impact of silver-coated wound dressings on bacteria biofilm viability for the prevention of skin infections

Federica Paladini[°], Cinzia Di Franco*, **Angelica Panico[#]**, Gaetano Scamarcio[^], Alessandro Sannino[°], Mauro Pollini[°]

[°] Department of Engineering for Innovation, University of Salento, Via per Monteroni, 73100 Lecce, Italy

*CNR-IFN Bari, via Amendola 173 Bari, Italy I-70126

[#] Dhitech Scarl, Via Salvatore Trinchese, 61, 73100 Lecce – Italy – angelica.panico@dhitech.it

[^] Dipartimento Interateneo di Fisica, CNR-IFN Bari, via Amendola 173 Bari, Italy I-70126

INTRODUCTION

The increasing antibiotic resistance of some bacteria strains and the risk of infections in acute and chronic wounds and burns have encouraged new approaches for the prevention of biofilm-associated infections, among them the use of silver. Unlike antibiotics, silver interferes with multiple components of bacterial cell structure and functions, so being less affected by specific micro-environmental variations. Recently, silver wound dressings have become widely accepted in wound healing centres and are commercially available. In this work, novel antibacterial wound dressings have been developed through a silver deposition technology based on the photochemical synthesis of silver nanoparticles.

MATERIAL AND METHODS

Conventional cotton gauzes were treated with 0.5 wt/v % of silver nitrate, according to a patented technique based on the *in situ* synthesis and deposition of silver nanoparticles¹. Plain gauzes and gauzes treated with 4 wt/v % Ag were adopted respectively as negative and positive control. Samples were analyzed by a field emission scanning electron microscope (FE-SEM) in order to verify the distribution of the silver coating on the cotton fibres. Thermogravimetric analysis (TGA) was adopted to measure the amount of silver deposited on the substrates. The antimicrobial capability of the silver-treated samples was determined by evaluating the efficacy of the silver coating in inhibiting the bacterial colonization of *Staphylococcus aureus* on the material, through agar diffusion tests and bacterial enumeration. Samples of untreated and silver-coated cotton gauzes were also characterized through SEM analysis of bacterial cells adhered onto the samples, after fixation of bacteria with glutaraldehyde and paraformaldehyde.

RESULTS AND DISCUSSION

The presence of silver on the substrates was verified through TGA analysis and resulted different between the treated samples. The result of the SEM showed a homogeneous silver coverage of the fibres, also with the lower silver concentration tested. No significant difference in the antibacterial properties was observed in the width of the bacterial inhibition growth areas induced by the silver treated samples between the different concentrations of silver tested. These data were confirmed by the results obtained by the bacterial enumeration and by SEM analysis of the bacterial adhesion on the cotton fibres, confirming a considerable reduction of the bacterial adhesion and proliferation.

Figure 1. SEM analysis of distribution of the silver coating on the cotton fibres: neat cotton fibres (a);

cotton fibres treated with 0.5 wt/v % silver (b); cotton fibres treated with 4 wt/v % silver (c); cotton fibres treated with 0.5 wt/v % silver at higher magnifications (11.74KX).

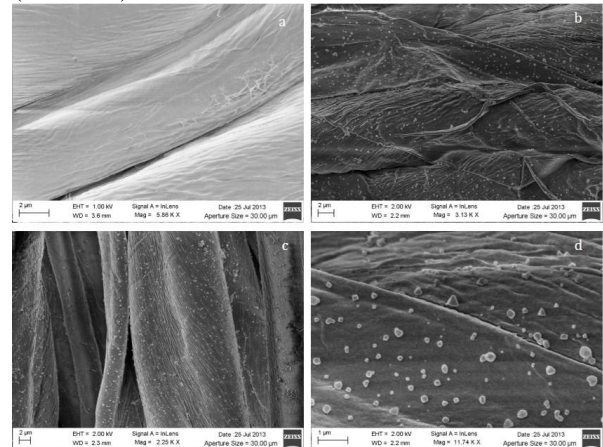


Figure 2. Agar diffusion tests on *S. aureus*: untreated sample (a); sample treated with 0.5 wt/v % silver (b); sample treated with 4 wt/v % silver (c).

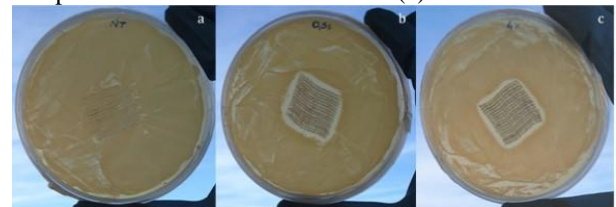
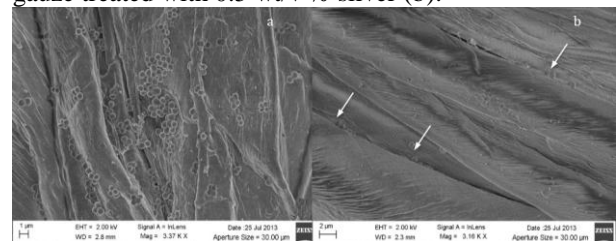


Figure 3. SEM analysis on bacterial cells adhered and proliferated on the cotton gauzes: untreated gauze (a); gauze treated with 0.5 wt/v % silver (b).



CONCLUSION

The results obtained demonstrated an impressive reduction in bacterial proliferation and adhesion. Thanks to the simplicity of the technology, the ease of preparation of the devices, the economic feature and the antibacterial effectiveness, these silver treated gauzes can represent an alternative to common medical treatments to contain the risk of wound contamination.

REFERENCES

1. Pollini M. *et al.*, European Patent No. EP1986499, 20081.



Characterization of Antibacterial Nano-Silver Coated Hydrogel Fibers for Biomedical Applications

Riccardo Raho^a, Fiorella Anna Lombardi^a, Federica Paladini^a, Sandro Boccarella^b, Alessandro Sannino^a, Mauro Pollini^a

^a Department of Engineering for Innovation, University of Salento, Via per Monteroni, 73100 Lecce, Italy

riccardo.raho@unisalento.it

^b Tecnofibre s.r.l., Via scalo zona industriale, 83040 Morra de Sanctis (AV), Italy

INTRODUCTION

Silver nanoparticles (AgNPs) have attracted intensive research interest because of their important bactericidal effect. AgNPs have been incorporated in fabrics, polymers, medical devices and burn dressings to eliminate microorganisms.

In this study a nano-silver antibacterial coating on hydrogel fibers was analyzed. Hydrogel blends obtained by different percentages of silver-treated and untreated fibers were compared to determine the best cost/antibacterial efficacy ratio in the final product.

EXPERIMENTAL METHODS

The substrates used were superabsorbent fibers based on crosslinking copolymers of acrylic acid (Oasis, Technical Absorbents Ltd, UK). Deposition on AgNPs was obtained through a well-known technique developed and optimized by University of Salento and based on the *in situ* photo-reduction of silver nitrate [1]. Three blends with different Treated/Untreated fibers ratios were prepared and named Blend A, B and C, with ratios of 1:1, 1:2 and 1:3 respectively. Untreated fiber (sample NT) was used as negative control and 100% treated fiber (sample T) was used as positive control.

The antimicrobial activity of the silver-treated substrates on *E. coli* and *S. aureus* was evaluated through agar diffusion tests and through optical density readings at 600 nm in Luria-Bertani Broth (LB). The swelling properties in phosphate buffered saline (PBS), simulated body fluid (SBF), chemical simulated wound fluid (cSWF), and deionized water (DI water) were investigated. Samples were analyzed by scanning electron (SEM) microscopy to study the morphology of silver coating and the distribution of AgNPs clusters.

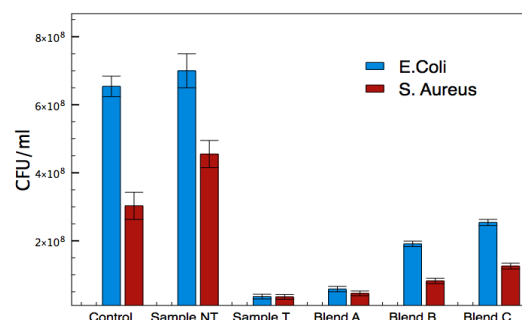
RESULTS AND DISCUSSION

Diffusion tests in agar were performed according to the Standard "SNV 195920-1992". The inhibition to bacteria growth was evaluated by measuring the width of the inhibition zone surrounding the sample. Results of this test are shown in Table 2.

	<i>S.Aureus</i>	<i>E.Coli</i>
Sample T	3.5 ± 0.3	4.8 ± 0.3
Blend A	3.2 ± 0.3	4.0 ± 0.3
Blend B	1.8 ± 0.3	2.0 ± 0.3
Blend C	1 ± 0.3	1.2 ± 0.3
Sample NT	0 ± 0	0 ± 0

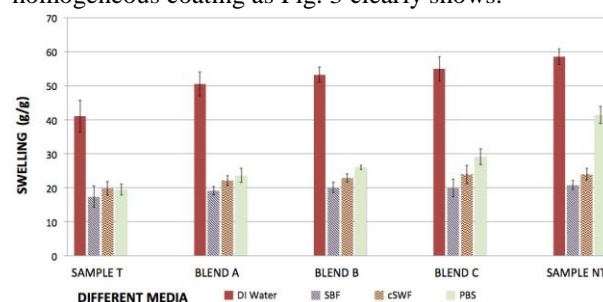
"Table 2: Inhibition zone (mean ± SD in mm)".

The results reported in Fig. 1 show the antibacterial effect of silver treated hydrogel fibers and its blends. The results obtained by the swelling tests are shown in Fig. 2.

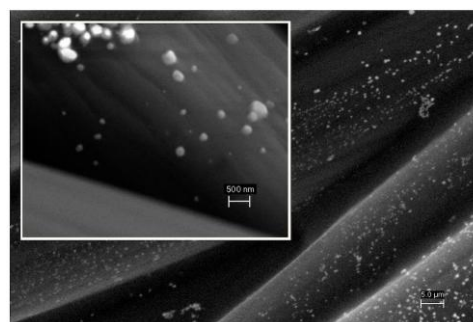


"Figure 1: Bacteria concentration (CFU)/mL ± SD"

The swelling degree significantly decreased with the increasing of the ionic strength of the swelling solution but can be considered good for applications such as exudate absorptive materials. SEM revealed a homogeneous coating as Fig. 3 clearly shows.



"Figure2: Swelling ratios in different fluids "



"Figure3: SEM images Sample T 3000x,inset 20000x"

CONCLUSION

The materials obtained demonstrated good swelling properties, uniform deposition and good antibacterial effects, even in the blends containing the lower percentage of silver treated fibers, thus indicating the effectiveness of the silver deposition technology and its potential use in the field of antimicrobial device for biomedical applications.

REFERENCES

- [1] Pollini M, Sannino A, Maffezzoli A, Licciulli A; Antibacterial surface treatments based on Silver clusters deposition 2008, EP20050850988.

Optimization of Silicone as Implant Material for the Application in the Middle Ear: Incorporation of Functionalized Nanoporous Silica Nanoparticles

Tanja Heemeier¹, Mandy Jahns¹, Songül Noyun¹, Laura Doniga-Crivat², Silke Besdo², Peter Behrens¹

¹Institute for Inorganic Chemistry, Leibniz University of Hannover, Germany

²Institute for Continuum Mechanics, Leibniz University of Hannover, Germany

Tanja.Heemeier@acb.uni-hannover.de

INTRODUCTION

Silicone as implant material is applied in many different medical applications because of its biocompatibility and biostability under the experimental conditions¹. The goal we pursue is to develop a silicone pad in order to optimize the contact between a middle ear prosthesis and the tympanic membrane. Such a prosthesis is applied when a patient lost the auditory ossicular chain due to infections. Up to now a small piece of cartilage is placed between the tympanic membrane and the headpiece of the prosthesis. The major disadvantage of this body's own material is that it degenerates gradually and its properties differ from patient to patient. However, the silicone pad, as a long-term stable material with steady properties, shall protect the tympanic membrane against forcing of the prosthesis. Additionally, an optimal sound transmission has to be ensured. For reinforcement and adjustment the silicone mixture is equipped with different fillers^{2,3} like functionalized hydrophobic nanoporous silica nanoparticles (NPSNP). If desired these NPSNP could be used as a local drug delivery systems as well.

EXPERIMENTAL METHODS

The silicones SILUPRAN[®] 2420 and 2445 served as base material and were mixed with functionalized hydrophobic NPSNP to adjust the mechanical properties for the desired application. The NPSNP with approx. 40 nm diameters were synthesized by using tetraethoxysilane, diethanolamine and cetyltrimethylammonium bromide in a water/ethanol mixture. The functionalization was carried out by the reaction with alkenyltrimethoxysilanes as well as different alkenyl- and alkylchlorosilanes. For optimization of the functionalization degree (FD) and the hydrophobicity the reaction conditions and concentrations were varied. Afterwards different amounts of functionalized hydrophobic NPSNP were mixed with the silicones in a SpeedMixer[™] DAC 150SP and cured at 120 °C.

RESULTS AND DISCUSSION

The synthesis of hydrophobic vinyl-functionalized NPSNP was successful. The FD of vinyl groups was determined with C/S analysis. With the variation of functionalization agents and their concentrations different FDs were obtained and tested in silicone mixtures. The comparison of SEM images of pure SILUPRAN[®] 2445 and SILUPRAN[®] 2445 with incorporated functionalized hydrophobic NPSNP shows no differences so that the nanoparticles added seem to be distributed homogeneously. Rheological measurements

(Fig. 1) of these samples show a slight increase of the storage modulus G' when functionalized NPSNP were incorporated compared to pure SILUPRAN[®] 2445. Thus, the incorporated nanoparticles have a positive reinforcing effect on the network.

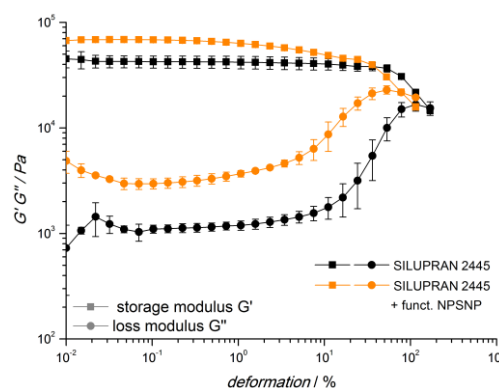


Fig. 1: Rheological measurements of SILUPRAN[®] 2445 with and without functionalized NPSNP.

These results and further investigations regarding more hydrophobic NPSNP and higher filler contents may help to find a silicone mixture with suitable mechanical properties for the silicone pad. Additionally, tensile testings for characterisation of the silicones are planned.

CONCLUSION

Nanoporous silica nanoparticles were vinyl-functionalized and hydrophobized with different functionalization degrees. Then, these nanoparticles were incorporated into silicone mixtures which showed slightly reinforcing behaviour. To find the optimal filler content for the application as silicone pad in the middle ear further investigations need to be done. The incorporated nanoparticles can also be used as local drug delivery systems to promote healing.

REFERENCES

1. Quinn K. J. *et al.*, Brit. Polym. J. 20:25-32, 1988
2. Boonstra B. B. *et al.*, Rubber Chem. Tech. 48:558-576, 1975
3. Floess J. K. *et al.*, J. Non-Cryst. Solids, 285:101-108, 2001

ACKNOWLEDGMENTS

This work was supported by the DFG within the Collaborative Research Program SFB 599 "Sustainable bioresorbable and permanent implants based on metallic and ceramic materials" (TP D1).

Temporary implant surfaces equipped with an anti-adhesive plasma fluorocarbon polymer film

Birgit Finke¹, Holger Testrich², Henrike Rebl³, J. Barbara Nebe³, Rainer Bader⁴, Uwe Walschus⁵, Michael Schlosser⁵, Klaus-Dieter Weltmann¹, Jürgen Meichsner²

¹Leibniz Institute for Plasma Science and Technology, Greifswald, Germany ²Institute for Physics, University Greifswald, Germany ³Dept. of Cell Biology and ⁴Dept. of Orthopedics, Rostock University Medical Center, Rostock, Germany ⁵Medical Biochemistry & Molecular Biology, University Greifswald, Germany; finke@inp-greifswald.de

INTRODUCTION

Metallic implants, especially made from titanium and its alloys, are state of the art in orthopedic and trauma surgery. Temporarily used implants such as intra-medullary nails, screws or external fixators for fractures support the mechanical stabilization of the bone consolidation but should not integrate into the bone because of their removal after fracture healing. An anti-adhesive coating could be very useful for these temporary implants to avoid protein and cell attachment as well as ingrowth into the surrounding tissue at last.

Gas-discharge plasma processes are successfully applied for the modification of titanium surfaces and could be very valuable for the improvement of implant performance [1]. A new surface functionalization strategy was developed in close collaboration with cell biologists. The plasma polymerization of octafluoropropane (C_3F_8) in a mixture with hydrogen (H_2) as precursor leads to the desired surface properties on Ti6Al4V.

Here, we present optimized plasma fluorocarbon polymer (PFP) films for both plasma discharges. Physico-chemical properties of the PFP-films were determined and the biological response *in vitro* and *in vivo* was tested.

EXPERIMENTAL METHODS

Discs (1 cm diameter) and platelets ($5 \times 5 \times 1 \text{ mm}^3$) from polished, chemically pure titanium alloy Ti6Al4V were used as substrates. They were coated with ~300 nm thin films applying continuous wave low-pressure microwave (MW) or radio frequency (RF) discharge plasmas. The PFP films were optimized by variation of the C_3F_8/H_2 ratio, power and pressure strongly correlated with cell culture investigations to guarantee minimal cell adhesion. Film properties were analyzed by XPS, FT-IR, water contact angle measurements, AFM, as well as mechanically testing, e.g. the determination of total wear debris with artificial bone per 1 million cycles. Film stability was checked by sonication (10°) in distilled water. Human osteoblasts (MG-63 cells) were cultured on the samples. Adhesion and cell cycle phases were calculated by flow cytometry. *In vivo* biocompatibility was studied after intramuscular implantation of untreated Ti6Al4V and PFP-coated platelets in male LEWIS rats. The inflammatory tissue response was analysed after 7, 14, and 56 days.

RESULTS AND DISCUSSION

A closed pinhole-free, strongly cross-linked (Fig.1), mechanical stable and very smooth PFP film could be obtained. Sonication of these films showed good resistance against hydrolysis and delamination. Using XPS, an F/C ratio >1 was found and Ti6Al4V could not be detected by XPS. An advantageous medium hydrophobicity exists with a water contact angle of about 110° . A C1s high resolution spectrum for a C_3F_8/H_2 mixture (70/30 ml) is shown in Fig. 1.

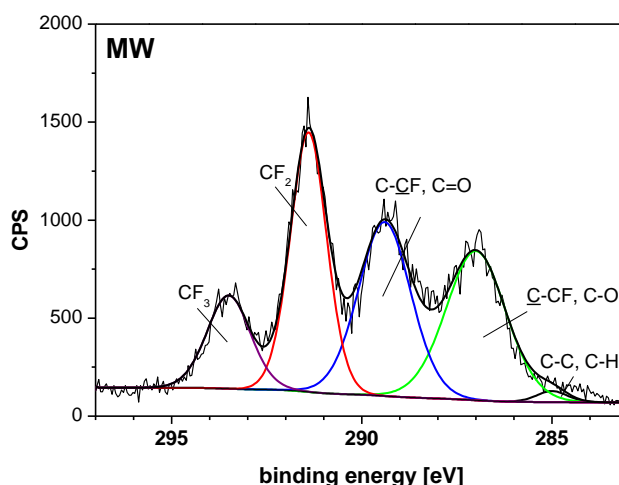


Fig. 1: C1s high resolution XPS spectrum of the PFP coating

Cell adhesion and cell spreading were drastically reduced on PFP coated Ti6Al4V *in vitro* in both discharges.

In vivo investigations revealed only a weak tissue reaction in comparison to untreated Ti6Al4V.

CONCLUSION

These optimized gas-discharge plasma-based PFP surface modification could be an option to improve the clinical handling of temporarily used Ti6Al4V implants.

REFERENCES

1. Quade A., *et al.*, Plasma Process. Polym. 8:1165-73, 2011.

ACKNOWLEDGMENTS

The authors thank U. Lindemann (INP), L. Middelborg for the excellent technical assistance. This study and BF, HT, HR, UW were supported by the BMBF (13N9779, 13N11188, Campus PlasmaMed).

Biocompatible Conductive Coatings based on Carbon Nanotubes

Niklas Burbli^{1*}, Katharina Kranz^{2*}, Athanasia Warnecke^{2*}, Peter Behrens^{1*}

^{*}Cluster of Excellence Hearing4all

¹Institute of Inorganic Chemistry, Leibniz Universität Hannover, Germany

²Department for Otolaryngology, Hannover Medical School, Germany

niklas.burbli@acb.uni-hannover.de

INTRODUCTION

Within the Cluster of Excellence Hearing4all a main requirement is the optimization of the long-term biointegration and functionality of the cochlear implant. Our approach is the chemical modification of the electrode surface to improve the contact of the cochlear electrodes to the nerve fibers on the one hand and to minimize the impedance of the electrical contact on the other hand¹. For this purpose, the platinum surface of these electrodes shall be equipped with a coating based on Carbon Nanotubes (CNTs).

Carbon Nanotubes represent a remarkable material with a chemically inert structure and a unique set of properties like high aspect ratio, high mechanical strength and excellent electrical conductivity. There are promising results for various biomedical applications of CNTs and especially CNT-based coatings of neural interface electrodes^{2,3}.

EXPERIMENTAL METHODS

As-received CNTs were purified via acid-treatment to remove residual catalyst and to get carboxylic acid-functionalized CNTs. Stable aqueous dispersions of the purified CNTs were obtained via ultrasonication.

Tailored gold- or platinum-coated silicon wafers (1.5x1.5 cm²) were coated with the aqueous CNT-dispersions via several methods, e.g. doctor blading method, spray or drop coating.

Characterization of the purified CNTs and CNT-coated films was carried out by SEM, Raman and IR spectroscopy. The purity and composition of the CNTs were additionally investigated by EDX and TG measurements. Thickness and topography of the films were determined with a confocal microscope.

Electrochemical characterization of the CNT-coated and non-coated substrates was performed via impedance spectroscopy scans by using a potentiostat/galvanostat (Versastat 4, Princeton Applied Research). A standard three-electrode electrochemical cell configuration with a Pt wire as counter electrode and an Ag/AgCl reference electrode was applied.

Cell culture experiments of the CNT-films were performed with NIH3T3 fibroblasts. The morphology and GFB expression were determined by transmission light and fluorescence microscopy.

RESULTS AND DISCUSSION

Long-time stable aqueous CNT-dispersions were successfully obtained via acid-treatment and following ultrasonication. A reduction of catalyst residue in the CNT-solid was determined with TG and EDX measurements. Raman and IR spectra show structural changes and the effective carboxylic acid-functionalization of the CNTs.

CNT-coatings have been prepared with a thickness below 100 nm via spray coating and a thickness of about half a micron via doctor blading method and drop coating. SEM images show a homogeneous covering of the substrate with CNTs (Fig. 1).

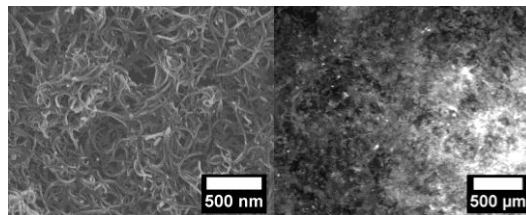


Fig. 1: SEM image of CNT-coating on Au substrate (left) and fluorescence microscopic image of NIH3T3 fibroblasts on CNT-coated glass substrates (right).

The cell culture experiments with NIH3T3 on CNT-coatings indicate a good biocompatibility (Fig.1).

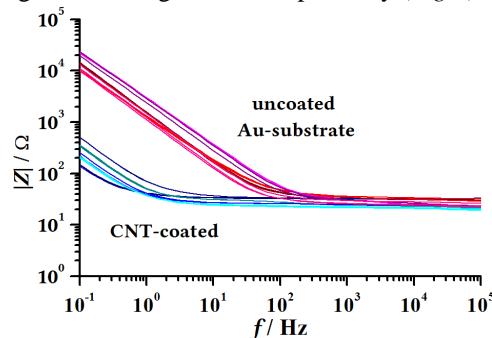


Fig. 2: Impedance spectroscopy measurements of CNT-coated and uncoated Au-substrates.

The impedance spectroscopy scan (Fig.2) shows the CNT-coating leads to decreased impedance at frequencies below 10² Hz.

CONCLUSION

Purification and functionalization of the CNTs lead to stable aqueous dispersions. These have been used to prepare CNT-films via variable coating methods. Cell culture experiments indicate good biocompatibility of the CNT-films. The electrochemical characterization of as-prepared electrodes shows a decrease of the impedance at frequencies below 10² Hz compared to a non-coated Au electrode.

REFERENCES

1. Stöver T., Lenarz T., GMS Curr Top Otorhinolaryngol Head Neck Surg 8:1-22, 2009
2. Kotov N. A. *et al.*, Adv. Mater. 21:3970-4004, 2009
3. Keefer E. *et al.*, Nature Nanotech. 3:434-439, 2008

ACKNOWLEDGMENTS

This work was supported by the DFG within the Cluster of Excellence Hearing4all in the sub-project "Improved biointegration of the electrode surface".

Installing multifunctionality on titanium with RGD-decorated polymeric nanocapsules: Towards new osteointegrative therapies

Pau Rocas-Alonso¹, Mireia Hoyos-Nogués^{3,4}, Josep Rocas², Fernando Albericio¹, José M. Manero^{3,4},
Javier Gil^{3,4}, Carlos Mas-Moruno^{3,4}

¹ Institute for Research in Biomedicine (IRB Barcelona), Spain

² Ecol Tech SL, Spain

³ Biomaterials, Biomechanics and Tissue Engineering Group, Department of Materials Science and Metallurgical Engineering, Technical University of Catalonia, Spain

⁴ Research Networking Center in Bioengineering, Biomaterials and Nanomedicine (CIBER-BBN), Spain

pau.rocas@irbbarcelona.org

INTRODUCTION

Installing multifunctionality on biomaterials is a powerful approach to increase their bioactivity. In particular, this strategy could be applied to metallic substrates to improve and accelerate osteointegrative processes¹. The aim of this work was to introduce an innovative methodology to synthesize polyurethane-polyurea nanocapsules (PUUa NCs) functionalized with cyclic RGD peptides (Fig. 1), which show great cell-binding activity and allow the encapsulation of hydrophobic drugs. Different PUUa NCs RGD-decorated were coated on Ti surfaces, and their effect on the adhesion of osteoblast like cells investigated. Moreover, the encapsulation of roxithromycin and its antibacterial effects were studied.

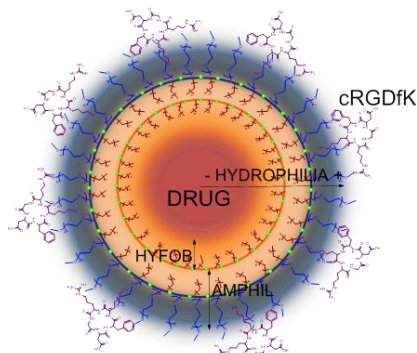


Figure 1: Schematic structure of PUUa NCs

EXPERIMENTAL METHODS

The NCs were covalently immobilized on Ti samples via a two-step protocol. First, PUUa NCs were synthesized by successive polycondensations between diisocyanate and diamino/diol monomers, followed by an aqueous emulsification². Subsequently, PUUa free isocyanate groups were reacted with Ti amino groups. To this end, Ti samples were previously activated with oxygen plasma and aminosilanized. The presence and distribution of the capsules was analyzed by SEM and fluorescence microscopy. The influence on cell behaviour was investigated using SAOS-2 cells by cell adhesion assays. The encapsulation of roxithromycin

was studied by HPLC, and evaluated in antimicrobial assays.

RESULTS AND DISCUSSION

The functionalization of Ti with the NCs was optimized by using distinct crosslinking units until an homogenous particle distribution was observed by SEM and fluorescence microscopy. RGD-nanocapsules significantly improved the adhesion of Saos-2 cells compared to controls (Fig. 2). Moreover, the presence of the PUUa-RGD capsules supported very good levels of spreading, with clear actin filaments and cytoskeletal organization, and the formation of focal adhesions. Encapsulation of roxithromycin (antibacterial, anti-inflammatory) was also explored.

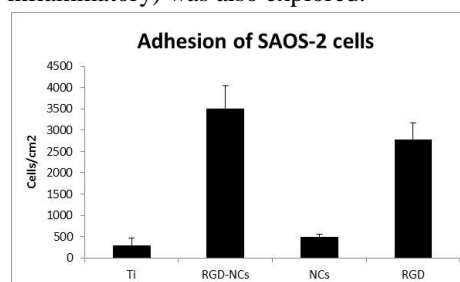


Figure 2: Cell adhesion on coated Ti after 4 h of incubation

CONCLUSION

The immobilization of PUUa NCs functionalized with RGD peptides onto Ti is a feasible and very promising strategy to increase the bioactivity of Ti and accelerate osteointegrative processes. Encapsulation of distinct drugs using these systems opens new prospects for applications in biomaterials and regenerative therapies.

REFERENCES

- [1] Chen X. *et al.* Colloid. Surf., B 107:189-97, 2013
- [2] Rocas Sorolla, J. *et al.* PCT/ES2014/070046, 2014.

ACKNOWLEDGMENTS

CMM thanks the Generalitat de Catalunya and the European Commission (FP7-PEOPLE-2012- CIG) for funding. PRA thanks MICINN for the INNPACTO project funding (IPT-090000-2010-1).

Improvement of Electrode Surfaces for Biomedical Applications by Nanoporous Platinum Coatings

Kim D. Kreisköther^{1*}, Nina Ehlert^{1*}, Natalja Wendt^{1*}, Hans-Christoph Schwarz^{1*}, Athanasia Warnecke^{2*}, Katharina Kranz^{2*}, Peter Behrens^{1*}

^{*}Cluster of Excellence Hearing4all

¹Institute of Inorganic Chemistry, Leibniz Universität Hannover, Germany,

²Department of Otolaryngology, Hannover Medical School, Germany

kim.kreiskoether@acb.uni-hannover.de

INTRODUCTION

The aim of our work is the optimization of the long-term biointegration and function of cochlear implants in the inner ear. By chemical modification of the electrode surface or by integrating delivery systems for active agents, the contact between the platinum sections of the cochlear electrode and nerve fibers can be improved. The loading and controlled release of drugs and neuronal growth factors is possible by introducing porous coatings on the substrate like nanoporous silica or porous platinum¹⁻³. Due to the porosity of the platinum coatings the impedance can also be reduced by the increased surface, what is favourable for the signal line of the cochlear implants⁴. We investigated the chemical and electrochemical preparation of nanoporous platinum films on metallic surfaces like gold- or platinum-coated silicon wafers. The focus of our investigations about porous platinum is lying on its biocompatibility as well as on the decrease of the impedance for applications in the inner ear.

EXPERIMENTAL METHODS

Porous platinum coatings were chemically deposited on gold- and platinum-coated silicon wafers by dip coating from surfactant-containing H_2PtCl_6 and PtCl_4 solutions. The surfactants used were Pluronic® F127 and C_{16}EO_8 , which were simultaneously removed during thermal reduction of the platinum.

For electrochemical platinum deposition from an aqueous surfactant-containing Pt^{4+} solution, a three electrode setup was used. Working electrodes were gold- or platinum-coated silicon wafers, as counter electrode a platinum wire was applied. The reference electrode was an Ag/AgCl system in saturated KCl-AgCl solution. Two different methods, direct and pulse potential electrodeposition were investigated at a constant potential of -0.5 V .

The coatings were characterized by SEM, EDX, confocal microscopy and impedance measurements. The cell culture tests of the chemical deposited platinum coatings were performed with NIH3T3 fibroblasts.

RESULTS AND DISCUSSION

The chemically deposited films consisted of a network of platinum nanoparticles which formed pores with diameters between 50 and 100 nm, shown in Fig. 1. Cell culture experiments of the chemically deposited platinum coatings with NIH3T3 fibroblasts indicated good cellcompatibility. As shown in Fig. 1, the fibroblasts exhibit a good cell proliferation on the stable platinum coating, thus a high cell density exists.

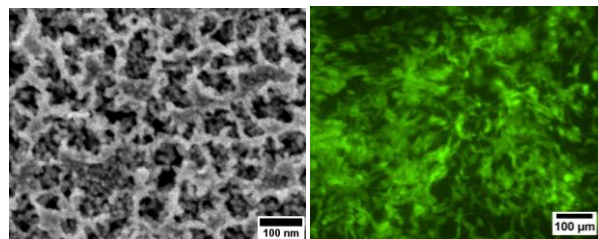


Fig. 1: SEM image (left) and image of NIH3T3 fibroblasts cell culture tests (right) of nanoporous platinum coatings by chemical deposition.

Impedance measurements of the chemically and electrochemically deposited platinum coatings showed a decrease of the impedance in comparison to the uncoated substrates, shown in Fig. 2.

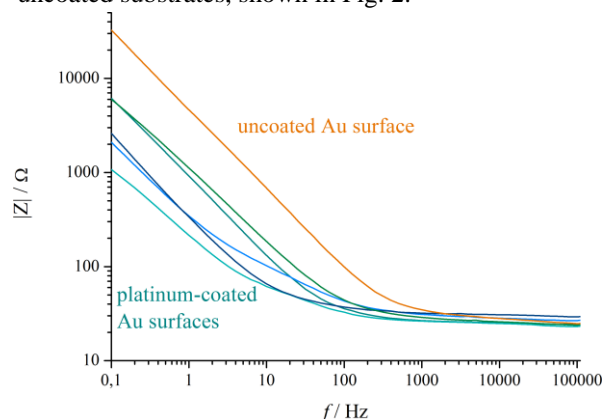


Fig. 2: Impedance measurements of uncoated and platinum-coated gold wafers.

CONCLUSION

We were able to deposit porous platinum coatings in two different ways. The chemical deposited porous platinum coatings by dip coating and subsequently calcinations showed good cellcompatibility in cell culture experiments. Both, chemically and electrochemically deposited porous platinum coatings exhibit decreased impedances.

REFERENCES

1. Ehlert, N. *et al.*, J. Mater. Chem. 21:752-760, 2011
2. Ehlert, N. *et al.*, Acta Biomater. 7:1772-1779, 2011
3. Ehlert, N. *et al.*, Chem. Soc. Rev. 42:3847-3861, 2013
4. Schlie-Wolter, S. *et al.*, ACS Appl. Mater. Interfaces 5:1070-1077, 2013

ACKNOWLEDGMENTS

This project is financially supported by the Cluster of Excellence Hearing4all.

Vancomycin loaded bioactive orthopaedic devices preventing infections

Hélène Carrie^{1,2}, Loïc Pichavant^{1,2}, Laurent Plawinski², Gilles Amador³, Valérie Héroguez¹ and Marie-Christine Durrieu²

¹ CNRS UMR 5629, Laboratoire de Chimie des Polymères Organiques, IPB-ENSCBP, Université de Bordeaux, Pessac, 16, av Pey Berland, France

² CNRS UMR 5248, CBMN, Université de Bordeaux, Pessac, 2, rue Robert Escarpit, France, Helene.Carrie@enscbp.fr

³ EA 3826, UFR d'odontologie, Faculté de Médecine, 1, rue Gaston Veil, F-44035 Nantes, France

INTRODUCTION

Bacterial infections are the most current complication which could occur during the fitting of a prosthesis in orthopaedic surgery. It can be the cause of morbidity and mortality and take place in 0.7 to 2.2% of the cases despite antibioprophyllaxis. Bacteria responsible for this kind of infections are *Staphylococcus Epidermidis* or *Staphylococcus Aureus* and mostly, it happens in per-operative conditions. Even if antibioprophyllaxis considerably decreases the rate of per-operative infection, it presents risks of allergy, side effects or bacteria resistance. Moreover, standard antibiotic protocols present little efficiency because of immuno-incompetent zone around implant, reduced sensitivities of bacteria growing in a biofilm and difficulties of achievement of the drug at the site of infection. That is why local antibiotic treatments are an excellent alternative to deal with these problems.

In a recent contribution to this field, we have presented a new biomaterial having applications as implant in orthopaedic surgery and allowing the release of an antibiotic (the Gentamicin Sulphate) only in case of infection [1, 2]. When methicillin-resistant bacteria are involved, glycopeptide antibiotics, as Vancomycin (VAN), are the drugs of choice to cure the infection. That is why we have explored a new route, with the use of this antibiotic. In this work, we propose to synthesize titanium alloy coated with vancomycin by covalently grafting drug functionalized polymeric NPs onto its surface.

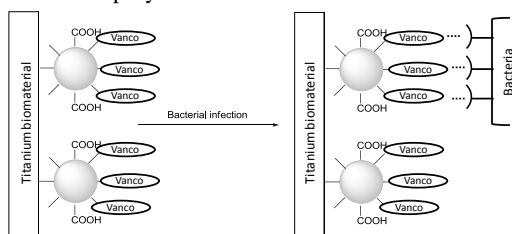


Fig. 1. Representation of the bioactive biomaterial

EXPERIMENTAL METHODS

α -norbornenyl poly(ethylene oxide) macromonomers were synthesized by anionic ring-opening polymerization of ethylene oxide and were ω -functionalized with a carboxylic acid (NB-POE-COOH) or the VAN (NB-POE-VAN). Macromonomers were characterized by ¹H NMR, Size Exclusion Chromatography (SEC) and MALDI TOF. Nanoparticles are obtained by Ring-Opening Metathesis CoPolymerization (ROMP) of norbornene with NB-POE-COOH and NB-POE-VAN. Their colloidal stabilities were shown by Dynamic Light Scattering measurements. Titanium discs ($\varnothing = 5$ mm ; h = 3 mm) were activated by functionalization with amine groups using aminosilane molecules (APTES). The NPs were covalently linked onto the titanium surface through the formation of an uncleavable amide bond between the carboxyl group of the NPs and the amide group of silane molecules available

onto the surfaces of the disks activated by NHS and DCC. The grafting was characterized by Scanning Electron Microscopy (SEM). The *In vitro* evaluation was carried out by Minimum Inhibitory Concentration (MIC) measurements on VAN functionalized macromonomers and particles. Antibacterial activity of the final materials was also characterized.

RESULTS AND DISCUSSION

α -norbornenyl macromonomers were obtained with a size of about 4000 g.mol⁻¹ and a narrow distribution (PDI < 1.1). The ω -functionalization was carried out with high functionalization yields. Nanoparticles are synthesized with total conversions and diameters were about 350 nm.

A controlled density of NPs was anchored on the biomaterial surfaces and this density was measured by scanning electron microscopy observations.

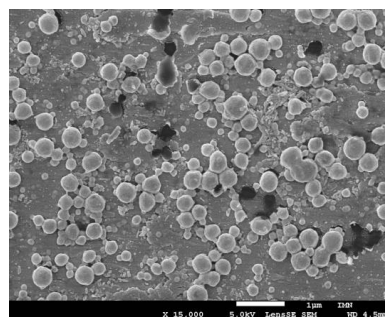


Fig. 2. SEM observation of the VAN functionalized biomaterial

The efficiency of the vancomycin functionalized biomaterials was proved by *in vitro* bacterial inhibition tests using *staphylococcus aureus* as bacterial strain.

CONCLUSION

In this work was presented the synthesis of bioactive biomaterials functionalized with Vancomycin and their characterization. We also demonstrated the *in vitro* activity of such materials. *In vivo* experiments on rabbits are now in progress.

REFERENCES

- 1 Pichavant L.; Bourget C.; Durrieu M.C.; Héroguez V. Macromol. 44:7879-87, 2011
- 2 Pichavant, L.; Amador, G.; Jacqueline, C.; Héroguez, V., Durrieu, M.C. J. Controlled release, 162:373-81, 2012

ACKNOWLEDGMENTS

The authors would like to thank the Société de Transfert de Technologie, Aquitaine Science Transfert (SATT AST), for providing financial support.

Amidation via DMTMM: A New and Efficient Method for Hyaluronan Biomaterials Preparation

Matteo D'Este^{1,2*}, Mauro Alini^{1,2}, David Eglin^{1,2}

¹AO Research Institute Davos, Clavadelerstrasse 8, 7270 Davos Platz Switzerland

²Collaborative Research Partner Acute Cartilage Injury Program of AO Foundation, Davos, Switzerland

*matteo.deste@aofoundation.org

INTRODUCTION

Hyaluronan (HA) is one of the most important biopolymers in the biomaterials field. Chemical modification can tailor HA towards specific uses as drug delivery system or in tissue engineering. Since its introduction¹ EDC/NHS has been the standard method for amidation of HA. Here we compare systematically ligation of amines to HA in water via EDC/NHS and DMTMM using an array of substrates including small, large and functional molecules: adipic acid dihydrazide (ADH); amino acetaldehyde dimethyl acetal (AADA); glycine ethyl ester hydrochloride (Gly); bovine serum albumine (BSA); doxorubicin (Dox) hydrochloride; poly(N-isopropylacrylamide) (pNIPAM)

EXPERIMENTAL METHODS

Syntheses were performed using DMTMM or EDC/NHS as condensing agent 1/1 to HA (4/1 for ADH, in order to compare with reference 1).

EDC/NHS Syntheses. After combining solutions of HA and the respective amine EDC+NHS in powder were added, and pH was corrected to 5.5. After 45 minutes pH was raised to 7.3 and the reaction let to proceed at room temperature for 5 days.

DMTMM Syntheses. After combining solutions of HA and the respective amine DMTMM in powder was added, pH was corrected to 6.5 and the reaction let to proceed at room temperature for 5 days.

For both methods products were precipitated and washed with ethanol, and characterized via FT-IR, ¹H-NMR, UV, rheology. Molar degree of substitution (DSmol) was calculated via NMR and when possible via UV.

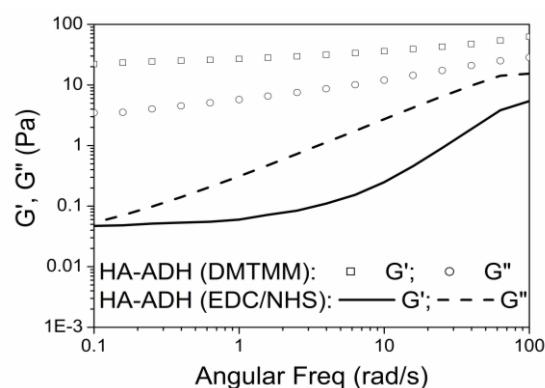
RESULTS AND DISCUSSION

The generation of the NHS ester of HA requires acidic pH, while the nucleophilic attack of the amine is only efficient at neutral or alkaline pH, where the NHS ester of HA is hydrolytically labile². The optimal conditions of coupling are therefore a non-trivial compromise. DMTMM conjugation was effective also in absence of pH control. For all the substrates tested DMTMM yields were superior at parity of feed ratio (table below).

Moiety	DSmol DMTMM	DSmol EDC/NHS
ADH	35%	18%
AADA	65%	49%
Gly	53%	22%
BSA	0.63%	0.16%
Dox	2.62%	2.24%
pNIPAM	4.5%	undetectable

Rheological features of pristine HA were modified upon functionalization, with the trend of the curves in good

agreement with DSmol and FT-IR³. The figure below compares the mechanical spectra of HA-ADH synthesized with both methods. For the EDC/NHS derivative loss modulus G'' is higher than storage modulus G' in the whole frequency range analysed, indicating a scarcely or non-crosslinked polymer. By contrast DMTMM derivative displays higher moduli and G' always over G'' all over the frequency range. Both features are signatures of a covalently crosslinked network, which is obtained owing to the higher ligation efficiency of DMTMM.



CONCLUSION

DMTMM is more efficient than EDC/NHS for ligation of amines to HA in water. Unlike EDC/NHS the reaction does not need accurate pH control to proceed. The advantages of DMTMM activation are particularly useful for the scale-up of preparations from the lab to the industrial scale, which is a critical step for the translation biomaterials in the clinical use³.

The materials synthesized display a wide range of physico-chemical and rheological properties, and are suitable for a plethora of different applications in the biomedical field. DMTMM-mediated ligation is a new promising chemical tool to synthesize HA-based biomaterials, controlled release systems and polymer therapeutics.

REFERENCES

1. Bulpitt, P. & Aeschlimann, D. Journal of Biomedical Materials Research, 47, 152-169, 1999.
2. Schantè, C. E., Zuber, G., Herlin, C., & Vandamme, T. F.. Carbohydrate Polymers, 85, 469-489, 2011.
3. D'Este M, Eglin D, Alini N, Carbohydrate Polymers, <http://dx.doi.org/10.1016/j.carbpol.2014.02.070>, 2014.

ACKNOWLEDGMENTS

Mrs. D. Sutter (ETH Zürich Switzerland) is sincerely acknowledged for performing NMR analysis. This work was financially supported by the "Collaborative Research Acute Cartilage Injury Program" of AO Foundation, Davos, Switzerland.

Silver nano-coatings on silk sutures for the prevention of surgical infections

De Simone Serena¹, Gallo Anna Lucia², Paladini Federica², Sannino Alessandro², Pollini Mauro²

¹Dhitech Scarl, Technological District Hi-Tech, via Salvatore Trinchese 61, 73100 Lecce, Italy

²Department of Engineering for Innovation, University of Salento, via Monteroni, 73100 Lecce, Italy.

serena.desimone@dhitech.it

INTRODUCTION

Surgical wounds are frequently complicated by infections of different severity, so giving rise to a range of clinical problems and prolonging hospitalization with increased healthcare costs¹. The definition of preventive strategies results essential for the management of 'Surgical Site Infections' associated to bacterial colonization and the onset of significant complications. In recent years, silver nanoparticles have been proposed as antimicrobial agent² in several commercial products for healthcare³. The aim of this work is the development of low-cost silver coatings on standard non-absorbable silk surgical sutures by adopting a patented⁴ technology based on the *in situ* photo-reduction of a silver precursor.

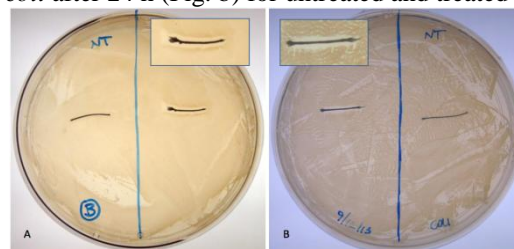
EXPERIMENTAL METHODS

The non-absorbable multifilament silk sutures (0.3 mm diameter) were dipped in a silver solution containing 0.5 wt/v % of silver nitrate and then exposed to UV lamp in order to induce the synthesis of silver clusters on the surface of the suture. After the treatment, the samples were washed in deionized water to remove the unreacted salt. The coated sutures were characterized in terms of antibacterial capability, quality of the coating, stability, durability and cytotoxicity. The morphology of the silver coating and the distribution of the silver clusters on the substrates were evaluated through scanning electron microscopy. The amount of silver deposited on the suture was quantified by energy dispersive X-ray spectroscopy. Tensile tests were carried out on silver treated and untreated samples to verify if the silver treatment affected the mechanical properties of substrate. The antibacterial activity of the treated sutures was measured by agar diffusion tests on *Escherichia coli* and *Staphylococcus aureus*, according to Standard 'SNV 195920-1992'. The percentage of antibacterial efficacy (ABE%) was calculated through bacterial enumeration and the bacterial adherence on the surgical suture surface was also quantified after 24 hours of incubation at 37°C for both the bacterial strains. Cytotoxicity tests were performed through MTT test on a selected cell population.

RESULTS AND DISCUSSION

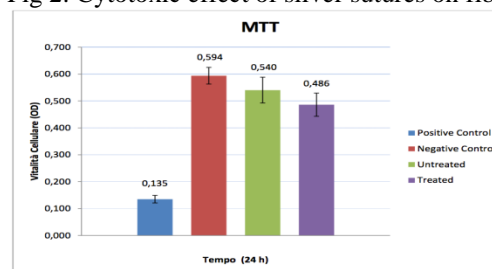
The microbiological characterization demonstrated the good efficacy of the silver deposition technology adopted in reducing the microbial colonization of medical device. An evident zone of inhibition to bacterial growth against Gram positive and Gram negative bacteria (Fig. 1). The evaluation of the ABE% of the Ag/silk resulted 81% and 78%, on *S. aureus* and *E. coli* respectively. The percentages in the reduction of bacteria adhered to the substrate were 34% and 35% for *E. coli* and *S. aureus* respectively.

Fig 1. Antibacterial test on *S. aureus* (Fig. a) and on *E. coli* after 24 h (Fig. b) for untreated and treated suture



The results of MTT test demonstrated that the presence of the silver particles did not affect the cell viability (Fig. 2).

Fig 2. Cytotoxic effect of silver sutures on fibroblasts.



CONCLUSION

The technology adopted for the deposition of silver is characterized by the excellent adhesion of the silver coating to the substrate. The antimicrobial capability of the silver treated materials was assessed on Gram positive and Gram negative bacteria in terms of reduction of bacterial viability and proliferation, and also of bacteria adhesion on the substrate. Moreover, the silver coating did not affect the mechanical properties of the materials and did not exhibit effect of cytotoxicity. The antibacterial-coated sutures developed may be considered as an interesting alternative in surgical practise for the prevention of the risk of infections with advantages also in terms of cost/effectiveness ratio.

REFERENCES

1. Suárez Grau JM *et al.*, Cir Esp 81:324–329, 2007
2. Sondi I *et al.*, J Colloid Interface Sci 275:177–182, 2004
3. Ip M *et al.*, J Med Microbiol 55:59–63, 2006
4. Pollini M *et al.*, European Patent NO.EP1986499, 2008.

Functionalisation of polyurethane films using YIGSR poly(ϵ -lysine) linked dendrons to manipulate the human mesenchymal cell response

Anna Guildford^{1*}, Nicola Contessi², Mariagemiliana Dessi¹, Steve Meikle¹, Serena Bertoldi^{2,3}, Silvia Fare^{2,3},
Maria Cristina Tanzi^{2,3} and Matteo Santin¹

¹ BrightSTAR, School of Pharmacy and Biomolecular Sciences, University of Brighton, UK

² BioMatLab, Dipartimento di Chimica, Materiali e Ingegneria Chimica "Giulio Natta", Politecnico di Milano, IT

³ Local Unit Politecnico di Milano, INSTM, Italy

A.l.guildford@brighton.ac.uk

INTRODUCTION

Adult mesenchymal stem cells (hMSCs) are being extensively investigated for their use in tissue regeneration. However, as they are found in very low numbers in adult tissue, expansion and quality testing *in vitro* is required to produce the desired MSC numbers for therapeutic delivery. The controlled differentiation and therapeutic uses of stem cells are dependent on providing the correct chemical cues and on mimicking their complex micro-environment or niche^[1]. Components of the niche such as the laminin glycoprotein play a crucial role in modulating stem cell behaviour via the activation of integrin pathways. These pathways influence the phenotypic fate of the cell by enhancing adhesion, and altering migration and differentiation.

In this study poly(ϵ -lysine) dendrons functionalised with the laminin mimicking peptide sequence YIGSR have been used to decorate the surface of polyurethane (PU) films. The aim is to control the *in vitro* morphology of hMSC preventing their uncontrolled differentiation into fibroblast-like cells and their consequent phenotypic change.

EXPERIMENTAL METHODS

Dendrons were synthesised from Fmoc-protected amino acids by solid-phase synthesis using a 4x molar excess of reagents. The dendron consisted of a root molecule of arginine, then 3 branching generations of poly(ϵ -lysine) and a final functionalisation of the uppermost branching generation with the YIGSR peptide. The dendrons were characterised by ATR/FT-IR and mass spectrometry.

PU films^[2] (1 cm discs) received from Milan University were plasma etched at 400 Pa pressure, 60 W air plasma for 5 minutes prior to treatment with NHS/EDC and dip-coating in a solution of the YIGSR-modified poly(ϵ -lysine) dendron (PLLYIGSR) and allowed to air dry. Contact angle goniometry and ATR/FT-IR were used to verify the dendron coating.

Human MSC (Lonza, UK) were seeded at a density of 4×10^4 onto each material and incubated in chemically defined media (CDM) (Lonza, UK) at 37 °C for 4 days. Prior to fixing in 3.7% paraformaldehyde and staining with DAPI, the cells were incubated for 1 h in CDM containing 5-Chloromethylfluorescein Diacetate

(CMFDA). Cell viability, adhesion and morphology were observed using confocal microscopy.

RESULTS AND DISCUSSION

Mass spectrometry of the unbound functionalised dendron confirmed the presence of the YIGSR peptide at a characteristic peak at 594.31247 m/z.

A reduced internal contact angle was recorded on the PU disc functionalised with PLLYIGSR (57°) when compared to the non-functionalised PU surface (83°) supporting the surface functionalization of the material. The material surface decoration was further confirmed by the observed cell morphology. hMSCs identified on all surfaces were viable prior to fixation as shown by the fluorescent green CMFDA staining in Fig 1. Cells seeded onto the functionalised surface formed spheroids (Fig 1(b)), in contrast to those seeded on to TCP, which presented a flat spindle-like morphology (Fig 1(a)), indicative of fibroblast like colonies associated with the de-differentiation of MSC.

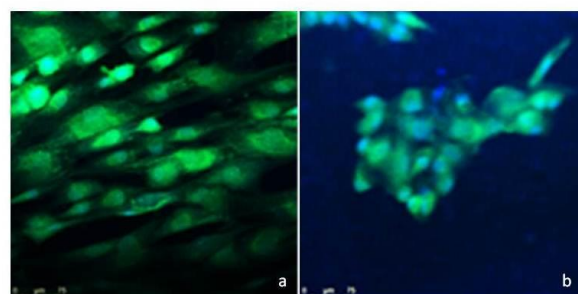


Figure 1. hMSC seeded onto TCP (a) and functionalised PU material (b).

CONCLUSION

Poly (ϵ -lysine) modified PU films were successfully functionalised to achieve increased stem cell binding with the ability to promote spheroid formation. These spheroid cultures have previously been shown to ensure continued stemness *in vitro* and offer the potential to expand hMSC in a controlled environment for tissue engineering applications.

REFERENCES

- ^[1] Shin H. *et al.*, B (2003), 24(24):4353-64.
- ^[2] Contessi N. *et al.*, submitted to 26th ESB conference, Liverpool, 31st August – 3rd September 2014.

Synthesis and Characterization of Chitosan/Hydroxyapatite Biocomposite Scaffolds for Potential Bone Repair Applications

Vitor César Dumont^{1*}, Nádia S. Vieira Capanema¹, Alexandra A. Piscitelli Mansur¹ and Herman Sander Mansur

^{1*}Center of Nanoscience, Nanotechnology and Innovation-CeNano²I, Department of Metallurgical and Materials Engineering, Federal University of Minas Gerais, Brazil, vitorcdumont@gmail.com

INTRODUCTION

Basically, the major goal of tissue engineering is to restore diseased or damaged tissue to its original state and function, reducing the need for transplants and joint replacements. Thus, one of the challenges faced by the research community in tissue engineering is related to the development of appropriate scaffold materials that can act as templates for cell adhesion, growth and proliferation¹⁻². In this sense, the scaffolds must present an adequate pore size and interconnectivity to promote cell in-growth, good biocompatibility, and controlled degradation kinetics to match the ratio of replacement by new tissue. Also, the scaffolds should provide an initial biomechanical support until cells generate the extracellular matrix¹⁻². In the last 2-3 decades a large number of biomaterials have been produced to behave as synthetic scaffolds that may guide and stimulate the tissue growth but no definitive solutions have been found yet for all kinds of bone tissue repair³. Among them, synthetic bioceramic materials based on calcium phosphates particularly tricalcium phosphate (TCP) and hydroxyapatite (HAp) have widely been studied and clinically used for bone tissue engineering due to their well-known osteoconductive and osteoinductive properties. However, when compared to cortical and cancellous bones, the synthesized calcium phosphates typically present unsatisfactory mechanical properties, especially in porous forms¹⁻⁴. One feasible solution is based on the combination of organic and inorganic components, forming hybrid materials, referred to as composites (or nano-composites). Thus, in this study it is reported the synthesis and characterization of the biocomposites based on polymer chitosan (Chi) and hydroxyapatite (HAp). It was investigated the effect of the relative concentration of the biopolymer (chitosan) to inorganic (HAp) components on the properties and structures of the scaffolds produced.

EXPERIMENTAL METHODS

Hydroxyapatite (HAp) was prepared by the precipitation method in alkaline aqueous media based on the procedure reported by our group⁴. Membranes were produced by cast method of chitosan (small, medium and high molecular mass) solutions prepared in water concentration at 1 % in acetic acid. The Chi/HAp biocomposites were synthesized by blending different proportions of the HAp to chitosan (ranging from 1 to 10 m/m%). Each component and the composites scaffolds were extensively characterized by Fourier Transform Infrared Spectroscopy (FTIR), Scanning and Transmission Electron Microscopy (SEM/TEM), Atomic Force Microscopy (AFM), X-ray diffraction (XRD), Thermogravimetry Analysis (TGA),

Differential Scanning Calorimetric (DSC) and swelling assays.

RESULTS AND DISCUSSION

Typical XRD results of the synthesized HAp bioceramic after drying at 110°C and thermal treatment at 900°C are shown in Fig.1 (curves a and b, respectively). It can be observed major peaks associated with the HAp crystalline pattern (ICDD - 96-900-3549) which is more evident after the sintering⁴ (Fig.1b). Similarly, FTIR spectra of HAp after drying at 110 °C and sintering at 900°C are shown in Fig.2 (curves a and b, respectively). It may be observed the major peaks related to HAp chemical groups (hydroxyls, phosphates), and also the presence of carbonates common to HAp produced by water precipitation methods. Chitosan FTIR spectra have indicated the presence of major chemical groups (amine, hydroxyls and acetyls). The morphological aspects, swelling and mechanical properties of Chi/HAp biocomposites were affected by the ratio of components.

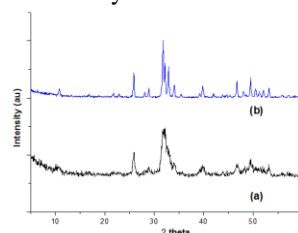


Fig.1. XRD patterns of the HAp after drying at 110°C (a) and thermal treatment at 900°C (b).

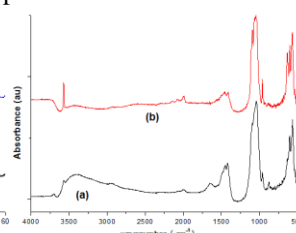


Fig.2. FTIR spectra of the HAp after drying at 110°C (a) and thermal treatment at 900°C (b).

CONCLUSION

Homogenous scaffolds of Chi/HAp biocomposites were produced and characterized. Their morphological aspects, swelling and mechanical properties were significantly affected by the ratio of components HAp/Chi. Thus, these Chi/HAp biocomposites may be considered as potential alternatives as biomaterials in the future for bone repair and substitutes.

REFERENCES

1. Ulrich A.S. *et al.*, *Annu. Rev. Med.* 2:443-451, 2001.
2. Blaker J.J. *et al.*, *Acta Biomater.* 7:829-840, 2011.
3. Li Z. *et al.*, *J. Mater. Sci. Mater. Med.* 16(3):213-219, 2005.
4. Santos M. *et al.*, *Mat. Res.* 7(4):625-630, 2004.

ACKNOWLEDGMENTS

The authors acknowledge financial support from CAPES, FAPEMIG, and CNPq. Also, the authors thank the Microscopy Center/UFMG staff for the TEM analysis.

Synthesis of morphology controlled calcium phosphate nanobiomaterials for biomedical applications

P.J.T Reardon^{1,2}, J. Huang¹, J. Tang^{2*}

¹ Department of Mechanical Engineering, UCL, London

^{2*} Department of Chemical Engineering, UCL, London Philip.reardon.09@ucl.ac.uk

INTRODUCTION

The performance of calcium phosphate (CaP) biomaterials depends greatly on morphology and size. For example, CaP nanoparticles can provide enhanced bioactivity.¹ Wire-like CaP can be used as biomaterial reinforcement due to excellent mechanical properties and recently porous CaP nanomaterials have shown high loading and favourable release properties for drug delivery.^{2,3} The use of microwave dielectric heating for chemical synthesis allows material production with altered morphologies, increased yields, narrow size distribution, and considerably reduced synthesis times. Therefore, this energy efficient 'green' process is used in the current study, to prepare biodegradable calcium phosphate nanomaterials with varied size, morphology and textural properties for biomedical applications.

EXPERIMENTAL METHODS

Briefly, ethanol or ethanol/water solutions containing either $\text{Ca}(\text{NO}_3)_2 \cdot 4\text{H}_2\text{O}$ or H_3PO_4 were prepared and mixed at room temperature and pressure, then irradiated in a microwave solvothermal process. In vitro protein loading and release measurements were carried out with Bovine serum albumin (BSA), Lysozyme, Fibrinogen and myoglobin using a UV-Vis spectrometer, the amount of loaded/delivered protein was calculated by the depletion method.¹ Material characterisation was performed using XRD, FESEM, TEM and nitrogen adsorption analysis as previously reported.^{4,5}

RESULTS AND DISCUSSION

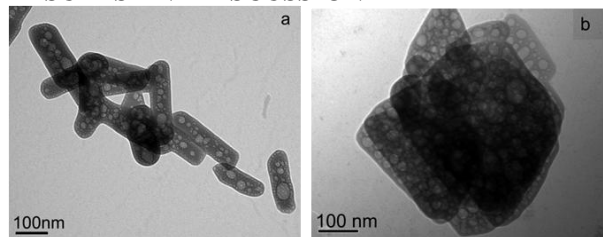


Figure 1 TEM micrographs of CaP (a) nanorods (60°C), (b) nanoplates (200°C).

Using a microwave assisted process, nanoplates and nanorods with controllable pores are synthesized without the use of any toxic surfactants by varying synthesis temperature (Figure 1). HA/monetite content and dimensionality were manipulated by changing the ratio of the $\text{H}_2\text{O}/\text{EtOH}$ solvent mixture. High aspect ratio (ca. 54) nanowires containing ca. 38 wt% HA were obtained with a 60/40 $\text{H}_2\text{O}/\text{EtOH}$ volumetric ratio (Figure 2a). Importantly, the quantity of HA in the high aspect ratio nanowires/needles was controlled by varying the stoichiometric ratio of the reactants, demonstrating that one dimensional materials with close to 100% HA can be achieved when the Ca/P ratio is increased to 1.67 (Figure 2b). Loading of proteins on CaP has been found to be the highest for the nanoplate

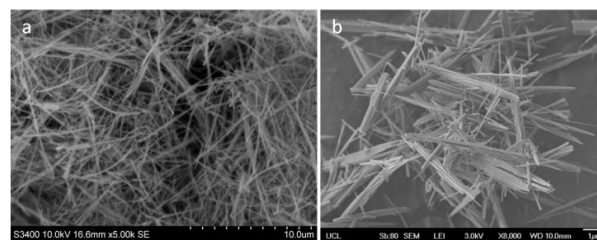


Figure 2 SEM micrographs of nanowires/needles obtained using Ca/P ratios of (a) 1.4 and (b) 1.67

samples. Interestingly, BSA loading was 2.5 times higher than a commercial hydroxyapatite nanomaterial even if the former has approximately half the surface area of the latter (Figure 3).⁴ Furthermore, the delivery period differed, lasting 8 times longer, indicating the morphology controlled nanostructured CaP could be a promising candidate for drug delivery with increased loading capacity and longer release period.

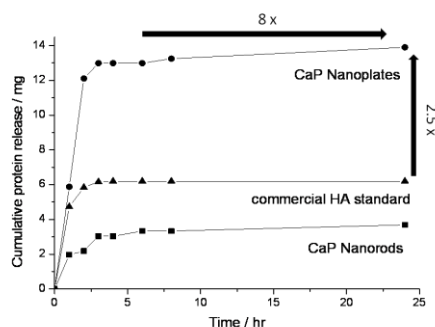


Figure 3 Protein delivery from nonomaterials of different morphology and a CaP standard.

CONCLUSION

The findings highlight that reaction parameters can be varied in tandem with microwave irradiation to tailor the morphology and composition of calcium phosphate materials, which are of very high importance in developing excellent materials suitable for bone tissue engineering and drug delivery.

REFERENCES

- Kong, L.; Gao, Y.; Lu, G.; Gong, Y.; Zhao, N.; Zhang, X., *Eur. Polym J.* 2006, 42 (12), 3171-3179.
- Costa, D. O.; Dixon, S. J.; Rizkalla, A. S., *ACS Appl. Mater. Interfaces* 2012, 4 (3), 1490-1499.
- Ng, S.; Guo, J.; Ma, J.; Loo, S. C. J., *Acta Biomater.* 2010, 6 (9), 3772-3781.
- Reardon, P. J. T.; Huang, J.; Tang, J., *Adv. Healthcare Mater.* 2013, 2 (5), 682-686.
- Reardon, P. J. T.; Handoko, A. D.; Li, L.; Huang, J.; Tang, J., *J. Mater. Chem. B* 2013, 1 (44), 6170-6176.

ACKNOWLEDGMENTS

The authors would like to thank the ESPRC for providing financial support to this project.



Dextran as a Versatile Scaffold for Hydrogel Formation with Hyaluronic Acid

Nick Dibbert¹, Bastian Dieter¹, Gerald Dräger¹ and Andreas Kirschning¹

¹Institute of Organic Chemistry, Leibniz University Hannover, Schneiderberg 1b, 30167 Hannover

Nick.Dibbert@oci.uni-hannover.de

INTRODUCTION

The major goal in the research of biopolymers is to generate a three-dimensional, biomimetic and biodegradable network. These networks are applied in artificial tissues for skin-transplantation, *in vivo* drug-release or as artificial muscle fibres.¹ In the case of myocardial infarction, a less-invasive injectable biopolymer serves as a favourable matrix for cell delivery and regeneration of damaged tissue.² There are two major strategies to construct a three-dimensional biopolymer network, either ionic interactions or covalent linkages, the latter approach is favoured in our case due to its stability. So as the condensation of hydrazide functionalized hyaluronic acid with oxidized dextran.

EXPERIMENTAL METHODS

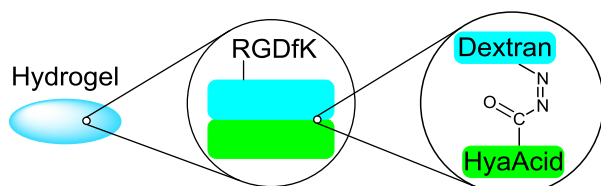
General procedure for oxidation³: To a 0.6M solution of dextran in dest. water, NaIO₄ was added in the dark and stirred for 12 h. The solution was ultrafiltrated for 3 d against water and lyophilized for 3 d. 100 mg oxidized dextran was dissolved in 5 mL dest. water and treated with 10 mL of a 0.25M solution of NH₂OH·HCl and 0.05% methyl orange. The mixture was stirred for 12 h and titrated with 0.09M NaOH solution till the end point⁴.

General procedure for decoration³: A 0.053M solution oxidized dextran (OxDex) was treated with a primary amine (Rutjes linker⁵, ethylene diamine, N-Boc-ethylene diamine, spermine, aniline) and stirred for 12 h.

General procedure for hydrogelation⁶: 25 µL of a 2 mg/100 µL solution of the hydrazide compound (hyaluronic acid hydrazide) were mixed in a silicon mask with 25 µL of a 3 mg/100 µL solution of the aldehyde compound (OxDex).

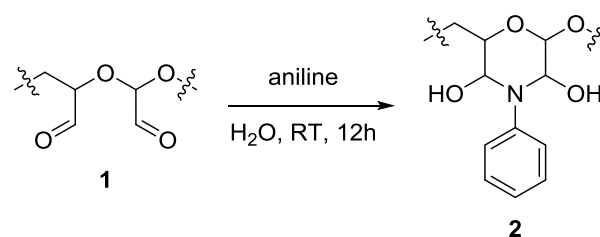
RESULTS AND DISCUSSION

To form a hydrogel that can be decorated with the RGDfK pentapeptide a preparation of the dextran was necessary. The idea was to oxidize dextran to a point where it can be modified with a linker molecule (**Scheme 1**) while having enough free aldehydes for hydrogelation.



Scheme 1. General strategy.

First of all we could define a range between 0.5 and 1.4 eq NaIO₄ where the chemical properties, in terms of solubility and forming stable hydrogels are ideal for our application. To get an idea of how the primary amine reacts with the polymer, experiments with various amounts of aniline were carried out as described and the remaining aldehydes were titrated.



Scheme 2. Suggested structure after decoration.

These titrations with aniline showed that for every equivalent of aniline two equivalents of aldehydes were consumed. This may suggest the structure as shown in **Scheme 2**.

Further titration experiments showed that there is a range between 0.01 eq and 0.3 eq of primary amine where enough aldehydes are present for a stable hydrogel formation. With greater than 0.3 eq of the primary amine, the polymer becomes insoluble in aqueous media.

Unfortunately, ultrafiltration of the decorated dextran leads to cleavage of the substrate and decomposition of the polymer. This may suggest that the reaction of the primary amine is reversible within the ultrafiltration.

CONCLUSION

We demonstrate a method to oxidize dextran reproducibly and determine the degree of oxidation. We also demonstrate a difference in the ability for hydrogelation between unfunctionalized and functionalized dextran

REFERENCES

1. Stamatialis D. F. *et al*, J. Membrane Sci. 1:308, 2008
2. Lee R. J. *et al*, Tissue Engineering 11:1860, 2005
3. Rist C. E. *et al*, J. Am. Chem. Soc. 76:4429, 1954
4. Heindel N. D. *et al*, Pharm. Res. 8:400, 1991
5. Kirschning *et al*, Macromol. Biosci. 10:1028, 2010
6. Kirschning *et al*, Biomaterials 34: 940, 2013

ACKNOWLEDGMENTS

The authors would like to thank the Deutsche Forschungsgemeinschaft (DFG, German Research Foundation) for the Cluster of Excellence REBIRTH (From Regenerative Biology to Reconstructive Therapy) for providing financial support to this project.

Adsorption of Col I on poly(NaSS) grafted Ti6Al4V surfaces improves MC3T3-E1 osteoblast-like cells mineralization

Helena Felgueiras^{1*} and Véronique Migonney¹

¹Laboratory of Biomaterials and Specialty Polymers, LBPS-CSPBAT CNRS UMR 7244, Institut Galilée, Université Paris XIII, 93430 Villetaneuse, France. felgueiras.helena@gmail.com

INTRODUCTION

Titanium (Ti) and its alloys are very common in the orthopedic field. These materials possess excellent corrosion resistance, low toxicity and “acceptable” compatibility with the living tissue, making them ideal bone substitutes. Nonetheless, their long term success remains a challenge (implant loosening). Based on the knowledge that the implant surface is the main responsible for the observed host response, our laboratory developed a strategy to overcome this problematic. It consists in the grafting of bioactive polymers bearing anionic sulfonate groups onto the metallic surfaces. Previous studies on model surfaces established the distribution of these groups instigates specific proteins’ adsorption (fibronectin, vitronectin...), which leads to favorable cell response including differentiation [1-5].

The purpose of the current investigation was to attest on the ability of the grafted poly(sodium styrene sulfonate) (poly(NaSS)) to induce osteoblastic differentiation on Ti6Al4V materials and, at the same time, to infer about the MC3T3-E1 maturation in the presence of proteins of interest such as albumin (BSA), fibronectin (Fn) and collagen type I (Col I), individually pre-adsorbed on Poly(NaSS) grafted and non grafted surfaces.

EXPERIMENTAL METHODS

13 mm diameter Ti6Al4V discs (CeraVer, France) poly(NaSS) grafted and non grafted [2,3] were used. The presence of sulfonate groups on the grafted surfaces was probed using X-ray photoelectron spectroscopy (XPS), Fourier Transformed Infrared (FTIR) and toluidine blue colorimetric method. Contact angle measurements were also conducted.

Prior to the cell culture experiments, 10% fetal bovine serum (FBS) in culture medium, 4000 µg/mL BSA in PBS, 20 µg/mL Fn in PBS and 10 µg/mL Col I in 0.1M acetate buffer (Sigma) were pre-adsorbed onto the surfaces for 1h. MC3T3-E1 osteoblastic cells (ATCC) were seeded at 5x10⁴ cells/mL and cultured from 5 min to 28 days. The cells viability, morphology, attachment strength, proliferation, differentiation and mineralization were followed.

RESULTS AND DISCUSSION

Poly(NaSS) grafting ($\approx 1.63 \times 10^{-5}$ g/cm²) led to an increase in the hydrophilicity of the surfaces which is due to the presence of the anionic sulfonate groups. Cell attachment was improved in the case of poly(NaSS) grafted surfaces and this was related to a better availability of the RGD domains of adsorbed Fn and Col I. Fluorescent images confirmed these observations. Significant cytoplasmatic expansion was observed on Fn pre-adsorbed substrates whereas Col I led to an increased attachment strength.

The presence of sulfonate groups augmented the osteoblastic maturation, both early differentiation and mineralization.

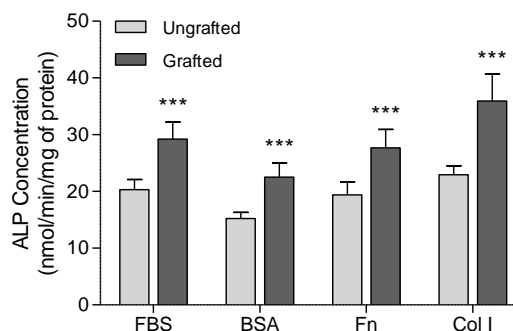


Fig.1. Production of alkaline phosphatase (ALP, early differentiation) by MC3T3-E1 cells.

Pre-adsorbed Col I onto grafted substrates enhanced significantly the alkaline phosphatase levels (Fig.1) as well as the calcium and phosphate production. BSA did not reveal any significant effect on the cells behavior.

CONCLUSION

In vitro tests using MC3T3-E1 osteoblastic cells confirmed the poly(NaSS) grafted Ti6Al4V potential for long term implantations by enhancing osteointegration. Col I pre-adsorbed on poly(NaSS) demonstrated a clear aptitude to induce osteoblastic maturation

REFERENCES

1. Felgueiras H, et al, IRBM, 34:371-375,2013.
2. Hélaré G, et al, Acta Biomater 5:124-33,2009.
3. Hélaré G, et al, J Mater Sci: Mater Med 21:655-63, 2010.
4. Khadali FE, et al, Biomacromolecules 3:51-6, 2002.
5. Long M, et al, Biomaterials 19:1621-1639, 1998.

Enhancement of integrin-mediated cell attachment by pre-adsorbed model proteins on poly(NaSS)-functionalized Ti6Al4V substrates: a QCM-D study

Helena Felgueiras^{1*}, Sven Sommerfeld², N. Sanjeeva Murthy², Joachim Kohn² and Véronique Migonney¹

¹Laboratory of Biomaterials and Specialty Polymers, LBPS-CSPBAT CNRS UMR 7244, Institut Galilée, Université Paris XIII, 93430 Villetaneuse, France and ²New Jersey Center for Biomaterials, Rutgers University, 145 Bevier Road, Piscataway, New Jersey 08854, USA felgueiras.helena@gmail.com

INTRODUCTION

The adsorption of proteins from blood and other body fluids onto a biomaterial surface is a complex phenomenon triggered seconds after the biomaterial exposure to the biological environment. Proteins that reach the surface provide an adhesion network of ligands for the attachment of cells *in vivo* and *in vitro*. Their orientation, conformation and packing density define the way bioactive sites are presented to specific receptors of the cellular membrane, the integrins, and characterize the observed host response [1-4].

The effect of albumin (BSA), fibronectin (Fn) and collagen type I (Col I) pre-adsorbed on poly(sodium styrene sulfonate) (poly(NaSS)) physisorbed Ti6Al4V substrates on the attachment of MC3T3-E1 cells was studied. Three other substrates, Ti6Al4V, gold and poly(DTE carbonate), were used for comparison. Antibodies against specific receptors on the cellular membrane were used to understand the role of protein conformation on protein-cell interactions.

EXPERIMENTAL METHODS

Protein adsorption and cell attachment were followed in real time using a quartz crystal microbalance with dissipation (QCM-D, QSense). The four substrates, Ti6Al4V, poly(NaSS) physisorbed on Ti6Al4V, poly(DTEc) and gold, as well as the proteins, BSA, Fn and Col I, used in this study were prepared as described in [5].

MC3T3-E1 osteoblastic cells were followed for 2h at static conditions on all sensors, both in the presence and absence of each protein (1h pre-adsorption). Anti-integrins $\alpha_5\beta_1$ and $\alpha_2\beta_1$ were selected to test the MC3T3-E1 attachment mechanisms on Fn and Col I pre-adsorbed sensors, respectively. Cytoskeleton organization and focal adhesions were observed by fluorescent microscopy (ZEISS AxioLab, Germany). On the Ti6Al4V sensors, antibodies against the RGD sequence and heparin binding domains were used to probe the Fn conformation. Base line was established with PBS. The results were analyzed using the Sauerbrey equation ($\Delta f = -C \cdot \Delta m$, Δf change in frequency, Δm change in mass, C constante = $17.7 \text{ ng/cm}^2 \cdot \text{s}$).

RESULTS AND DISCUSSION

Ti6Al4V substrates with physisorbed poly(NaSS) displayed the highest protein adsorption, and

provided the best conditions for cell attachment. Interestingly, although the protein deposition on the poly(DTEc) sensors was the lowest, a large amount of cells was detected. In addition, poly(NaSS) substrates were found to have a large influence on the protein conformation, particularly with respect to some important Fn binding domains, suggesting more active binding sites are exposed to cells in its presence.

On the same substrates, MC3T3-E1 cells attachment was found to be integrin dependent. Cells cultured for 2h in the absence of antibodies against α and β integrins exhibited abundant focal adhesions. By blocking important integrins ($\alpha_5\beta_1$ and $\alpha_2\beta_1$), the major transmembrane components of focal adhesions, inhibition of cell attachment was detected (Fig.1); this was accompanied by differences in cytoskeleton organization.

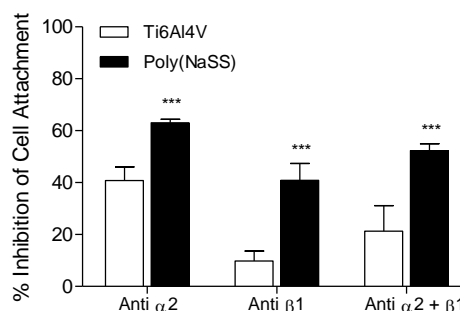


Fig.1. Inhibition of MC3T3-E1 cell attachment by the presence of $\alpha_2\beta_1$ anti-integrins on regular and poly(NaSS) coated Ti6Al4V sensors, pre-adsorbed with Col I.

CONCLUSION

Presence of sulfonate groups favored protein adsorption and cell attachment. On these altered surfaces, integrin-mediated attachment was predominant and played a major role in cell cytoskeleton organization. Poly(NaSS) was also found to have a large influence on Fn protein conformation, exposing more active binding sites.

REFERENCES

1. Puleo DA et al., Biomaterials 20:2311-21, 1999.
2. Wilson CJ et al., Tissue Eng 11:1-18, 2005.
3. Garcia AJ et al., Biomaterials 20:2427-33, 1999.
4. H  lari G et al., Acta Biomater 5:124-33, 2009.
5. Felgueiras H et al., IFMBE Proc 41:1597-1600, 2014.

Predicting Change in Constitutive Behaviour of Degrading Polymers

Hassan Samami, Jingzhe Pan

Department of Engineering, University of Leicester, UK, hs257@le.ac.uk

Introduction

Bioresorbable polymers such as Poly lactic acid (PLA) and poly glycolic acid (PGA) have been successfully used in many medical implant devices such as resorbable sutures. Hydrolysis degradation is a time dependent process which causes a significant change in the structural and mechanical property of bioresorbable polymers when they are implanted in a biological environment such as human body. This time dependent process occurs due to the attack of water molecules to the molecular chains of the polymer. Structurally, bioresorbable polymers are either amorphous or crystalline that could remain totally amorphous or undergo an increased crystallinity during the hydrolysis time. In the design of a bioresorbable device, it is important to predict the change in mechanical proprieties during degradation.

Micromechanical Model

This study shows that the constitutive law of a degrading polymer can be analytically obtained from the initial condition and the current average molecular weight of a polymer using only one empirical parameter. A chain scission is treated as an effective cavity as revealed by an atomistic study [1]. A degrading amorphous polymer is modelled by a continuum solid with increasing number of cavities that are randomly distributed.

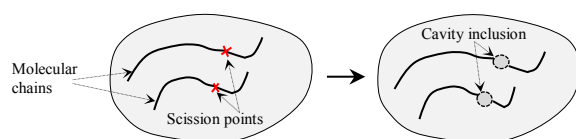


Fig 1: Formation of two inclusions within a degrading polymer

The cavities are inhomogeneities that are free from any stress field but can disturb the applied stress field [2]. Unlike the atomistic study [1], the cavities are assumed to be spherical and have a common radius. This radius is the only fitting parameter in the model that is unique to each polymer. The average molecular weight can either be taken from an experimental measurement or from the mathematical model developed by Pan and co-workers [3]. An analytical constitutive law predicting the Young modulus as well as the Poisson's ratio for the degrading polymer is then obtained using the Mori-Tanaka (MT) theory [4]. This theory takes into account of the elastic interactions between the cavities, which is important toward the later stage of the degradation.

Results and Discussion

The results of the Mori-Tanaka (MT) model are compared with the experimental data obtained by Tsuji [5] in Fig 2. It can be seen that the model can fit the data fairly well.

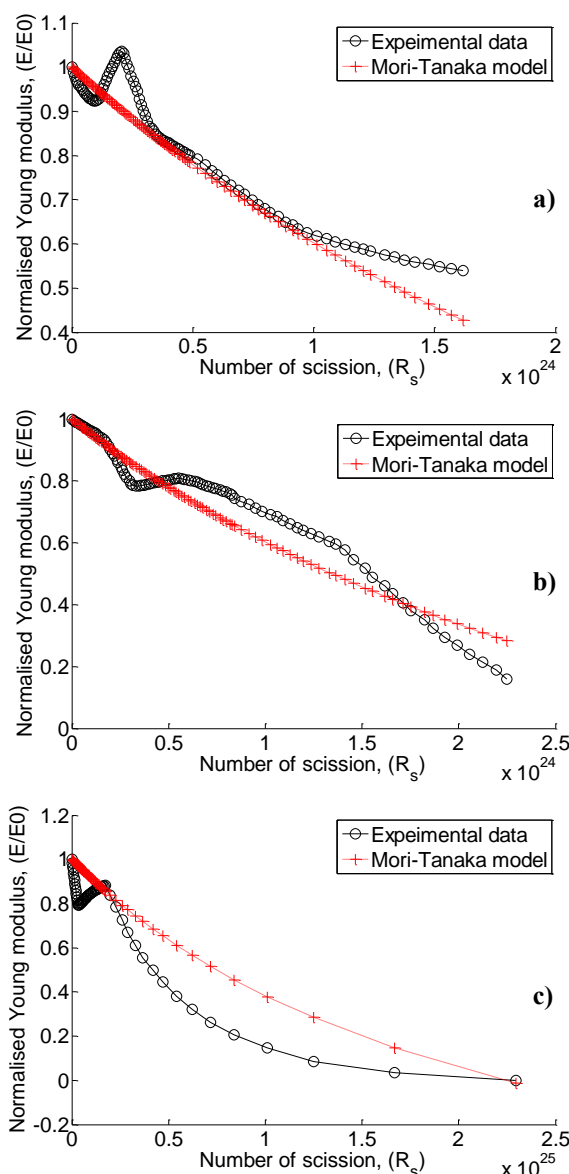


Fig 2: Change in Young modulus of amorphous non-blended films during 24 months of hydrolysis degradation

a) PLLA, b) PDLA, c) PDLLA

Conclusion

The Mori-Tanaka theory for solids with cavities are shown to be able to capture the trend of experimental data of Young's modulus of degrading amorphous polymers.

References

1. Gleadall, A. 2004. PhD thesis, University of Leicester.
2. Mura, T. 1987. Lancaster, Nijhoff.
3. Han, X. *et al.* 2010. Acta Biomaterialia, 6, 3882-3889.
4. Kachnov, M. 1993. J. Fracture, 59, R17-R21.
5. Tsuji, H. 2002. J. Applied Polymer Science, 43, 1789-1796.

Nitric oxide releasing polyester blends for topical skin vasodilation

Victor Baldim and Marcelo Ganzarolli de Oliveira*

Institute of Chemistry, University of Campinas, Brazil, mgo@iqm.unicamp.br

Keywords: Drug Delivery, Interfaces, Synthesis

INTRODUCTION

Nitric oxide (NO) is a signalling molecule involved in vasodilation, wound healing, immune response and neurotransmission. Reduced endogenous NO production plays a fundamental role in the pathogenesis of peripheral vascular diseases such as chronic leg ulcers and Reynaud's syndrome. Therapies with macromolecular NO donors have been used for the controlled release of NO in different quantities¹. We have already synthesized a polysulfhydrylated polyester (PSPE) and showed that its S-nitrosation leads to a polynitrosated polyester (PNPE)², capable of releasing NO spontaneously. In this work, we prepared a set of blends between PSPE and polycaprolactone (PCL), a well known polyester used for biomedical applications³. The S-nitrosothiol (S-NO) concentration of their nitrosated derivatives was measured by chemiluminescence and the topical skin vasodilation they promoted was evaluated by laser Doppler flowmetry.

EXPERIMENTAL METHODS

Synthesis of PSPE – PSPE was prepared by the acid-catalysed polycondensation reaction of thyoxyglycerol with mercaptosuccinic acid². The reaction proceeded under reflux, N₂ flow and magnetic stirring, at 120 °C for 14 h.

Polymer blend preparation - Solutions of PCL/PSPE in THF were prepared in the mass ratios: 100/0 (PCL), 85/15 (PSPE15), 75/25 (PSPE25) and films were prepared by solvent casting in Petri dishes. Films were characterized by DSC, TGA, XRD, SEM/EDS.

S-nitrosothiol quantification - Films of PSPE15 and PSPE25 were S-nitrosated by immersion in acidified NaNO₂ solution during 20 min at room temperature, protected from light leading to polynitrosated films (PNPE15 and PNPE25, respectively), whose NO charges were quantified by chemiluminescence (NOA, Sievers)⁴.

Skin blood flow measurement –Vasodilation promoted by the topical application of PNPE15 and PNPE25 films in forearm skin of a volunteer for 10 min was measured by Laser Doppler flowmetry (Transonic System Inc.)⁴.

RESULTS AND DISCUSSION

The PNPE films obtained are homogeneous and flexible. Their different S-nitrosothiol charges can be confirmed visually by the intensity of the orange colour developed (Fig. 1). This colour is due to the S-NO groups whose concentration is c.a. 0.14 $\mu\text{mol}/\text{cm}^2$ (Fig.1). Spontaneous homolytic cleavage of the S-NO bonds release free NO, which diffuses through the *stratum corneum*, reaching the dermal microcirculation.

The concentrations of S-NO groups achieved, proved to be sufficiently high for promoting a 6 to 10-fold dose response increase in blood flow, 10 min after the application of the films (Fig.2).

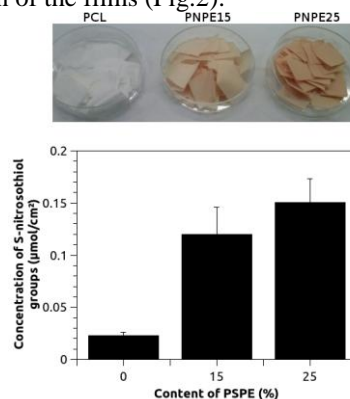


Figure 1. Solvent cast films of PCL, PNPE15 and PNPE25 (above) and their corresponding S-nitrosothiol groups concentrations measured by chemiluminescence (below).

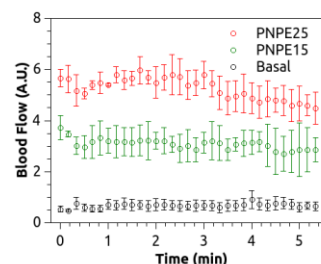


Figure 2. Skin blood flow measured by laser Doppler flowmetry in the forearm of a volunteer before (basal) and after topical application of PNPE15 and PNPE25 films.

CONCLUSION

PNPE films can be charged with different NO doses and lead to dose-dependent skin vasodilation in topical application. Therefore these materials may allow a new approach for the topical treatments of ischemic skin diseases.

REFERENCES

1. Jen, M. C. *et al.* Adv. Funct. Mater. 22, 239 (2012).
2. Seabra, A. *et al.* Biomacromolecules 6, 2512 (2005).
3. Woodruff, M. A. Prog. Polym. Sci. 35, 1217 (2010).
4. Marcilli, R. H. M. & de Oliveira, M. G. Colloids Surf. B. Biointerfaces (2013) – in press.

ACKNOWLEDGMENTS

The authors would like to thank CAPES for providing a Studentship for V.B. and CNPq (Grant no: 309390/2011-7) for financial support.

Structural Integrity Assessment of a Polymer-based Knee Implant

Y. Fong^{1*}, P. Reed², F. Pierron² and M. Browne¹

^{1*}Bioengineering Science Research Group, University of Southampton, United Kingdom, Y.K.K.Fong@soton.ac.uk

²Engineering Materials Research Group, University of Southampton, United Kingdom

INTRODUCTION

The state of the art total knee replacement (TKR) system employs a cobalt-chromium (CoCr) alloy femoral component¹. Although excellent success rates of above 94% at nine years across the main brands are associated with current systems, deficiencies, such as stress shielding and release of metal ions have been identified²⁻⁴. Recently, younger patients are being treated with TKR; with an increased life expectancy, these patients are likely to impose increased demands on the TKR. To address these issues, a novel TKR system has been proposed, which employs an injection moulded PEEK-OPTIMA[®] femoral component.

Before a new implant can be introduced and released into the market, it has to undergo preclinical testing to ensure it is safe for implantation. However, past experience has shown that a lack of rigorous preclinical testing could lead to extremely poor performance and early device recall. In the case of polymer based orthopaedic implants, there is an additional issue to consider in that standard testing tends to focus on high modulus, metallic implants, which do not exhibit the time and temperature dependent properties of polymer-based materials.

The aim of this study is to assess the effects of typical experimental variables on the performance of a PEEK-OPTIMA[®] based implant. As part of this work, multi-parameter tests will study the effects of test frequency, waveform, environment and temperature on the fatigue life of test coupons of PEEK-OPTIMA[®]. In the present work, the effect of frequency is examined.

EXPERIMENTAL METHODS

Tension-tension fatigue tests were carried out on a servohydraulic machine (Instron 8872) in ambient laboratory environment with sample dimensions specified in BS EN ISO 527-2:2012.

PEEK-OPTIMA[®] samples were tested at 2 Hz (n = 1), 5 Hz (n = 3) and 10 Hz (n = 20), with a R-ratio of 0.1, at 80 % yield. The number of cycles to failure was recorded in each case. Tests that did not fail were terminated at 5 million cycles.

An infrared camera (FLIR Cedip SC5000) was used to monitor the sample temperature from the beginning of each test until it either stabilised or failed. Samples were spray painted in matt black. An unloaded sample was placed next to the sample of interest as a control, such that temperature measurements could always be corrected against the room temperature.

For samples tested at 10 Hz, five different frequency ramping times were used – 0 s (n = 11), 30 s (n = 1), 60 s (n = 1), 90 s (n = 1) and 240 s (n = 6). As a result of the anomalous behavior observed from one of the samples, further tests (n = 3) were carried out at 10Hz to study the effect of cooling on the fatigue life of PEEK-OPTIMA[®].

RESULTS AND DISCUSSION

All samples tested at 2 Hz and 5 Hz ran out; whereas, nineteen out of twenty samples tested at 10 Hz without cooling survived a mean of $2,486 \pm 640$ cycles. One 10 Hz sample ran out. Where cooling was applied in the 10 Hz tests, the fatigue life was significantly enhanced (range: 64,918 to 4,018,741 cycles).

The rate of heating in the samples increased with increasing test frequency, as well as decreasing ramping time. The maximum temperature in the 2 Hz, 5 Hz and 10 Hz uncooled samples were found to be 8.0 °C, 17.7 °C and 67.0°C above ambient, respectively. The mean temperature of the 2 Hz and 5 Hz samples were seen to have stabilised at 2.3 °C and 6.0 °C above ambient, respectively.

In the absence of cooling, heat could not be dissipated from the 10 Hz samples quickly enough, causing the samples to soften, and exhibit a ductile fracture surface; whereas cooling tended to produce a smooth, flat fracture surface.

CONCLUSION

The fatigue life of PEEK-OPTIMA[®] was found to be frequency dependent and results to date suggest that the material fatigue behaviour is not compromised at 5 Hz and below. At 10 Hz, samples underwent softening and ductile failure. However, this effect was eliminated when cooling was applied. Further work will determine whether a frequency effect emerges between 2 and 5 Hz when variable amplitude loading is applied.

REFERENCES

1. Carr, B.C. *et al.*, Materials and Design, 30(2): 398-413, 2009.
2. National Joint Registry. 10th Annual Report 2013.
3. Bradley, G.W. *et al.*, The American Journal of Knee Surgery, 5(1): 3-8, 1992.
4. Moore, D.J. *et al.*, The Journal of Arthroplasty, 13(4): 388-395, 1998.

ACKNOWLEDGMENTS

The authors would like to thank Invibio[®] Biomaterial Solutions and the University of Southampton for providing financial support to this project.



Fabrication of hydroxyapatite thin film with entirely c-plane surface

Masanobu Kusunoki^{1*}, Yasuhiro Sakoishi¹, Katsuya Asano¹, Naoki Fujita¹, Takayuki Makino¹, Daisuke Okai²

^{1*}Faculty of Biology-Oriented Science and Technology, Kinki University, Japan, kusu@waka.kindai.ac.jp

²Department of Material Science & Chemistry, Graduate School of Engineering, University of Hyogo, Japan

INTRODUCTION

Hydroxyapatite [HA: $\text{Ca}_{10}(\text{PO}_4)_6(\text{OH})_2$] is useful in chromatography¹ because it adsorbs proteins via two types of interactions, with affinity for a calcium ion and ionic bonding for the phosphate group. The interactions based on electrical anisotropy correspond to the crystallographic anisotropy of HA. In chromatography, granular HA with surfaces of both a positively charged a-plane and a negatively charged c-plane is generally used. If we could obtain single surface with either the a- or c-planes, the separation efficiency could be improved and the apparatus size could be reduced. This also applies to bio-sensor such as quartz crystal micro balance² (QCM) and surface plasmon resonance³ (SPR), which monitor interactions between proteins as adsorption or decomposition. In this study, we investigated a method for fabricating HA films with entirely c-plane surfaces.

EXPERIMENTAL METHODS

The HA film was deposited by pulsed laser deposition. A KrF excimer laser with a wavelength of 248 nm and energy density of 2.5 mJ/mm² was used for HA abrasion. A sintered HA pellet was used as the abrasion target. Oxygen was supplied through a humidifier to a vacuuming chamber as atmospheric gas. The gas pressure was set to be 10 Pa. The film was deposited on a quartz substrate in a circular area of diameter 8 mm. The substrate was heated with a heater temperature of 700°C. The rate of film deposition under these conditions was 6.2 nm/min. The film was not annealed after the deposition. The crystal orientation of the HA film was controlled using a c-axis-oriented ZnO template layer, because ZnO has a hexagonal crystal structure. Since HA also has a hexagonal crystal structure, we expected hetero-epitaxial growth of the HA film on the ZnO template.

RESULTS AND DISCUSSION

Figure 1 shows a 2θ-X-ray diffraction pattern of the deposited HA film. The approximate thickness of the HA, ZnO, and Au films was 500, 200 and 10 nm, respectively. Only [002] and [004] peaks are observed for HA, indicating that a perfect c-axis HA film was obtained on the flat substrate surface. The ZnO film also showed c-axis orientation with the [002] peak. The c-axis-oriented ZnO film would be obtained regardless of the Au [111] film being placed under the ZnO template in this sample. For instance, the c-axis-oriented ZnO aligns directly on the quartz substrate. Au was placed here because we expected that the c-axis-

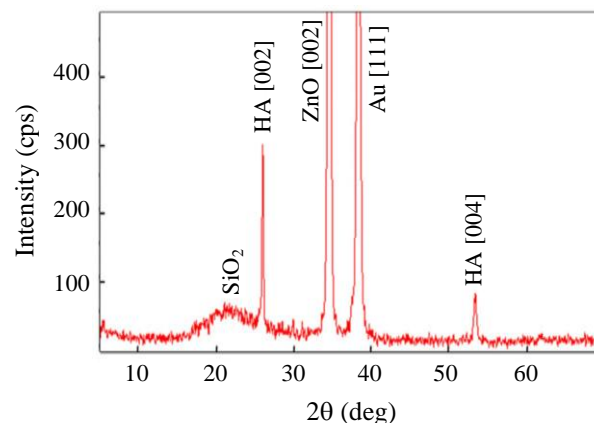


Fig. 1 X-ray diffraction of c-axis-oriented HA film deposited on ZnO template layer. Au [111] film placed under the ZnO template assuming that act as electrode of biosensor.

oriented HA would be applied to chromatography as well as bio-sensors such as QCM or SPR. The Au layer could act as the electrodes of the sensors. The HA film surface was fairly smooth as observed under an optical microscope.

CONCLUSION

A HA film having an entirely c-plane surface was fabricated with the aim of improving the performance of chromatography and bio-sensors. X-ray diffraction of 2θ-θ showed hetero-epitaxial c-axis orientation of the HA film on the ZnO template layer. The technique can be applied to new devices employing the crystallographic anisotropy of HA.

REFERENCES

1. Fountoulakis M. *et al.*, Electrophoresis 20:2181-2195, 1999.
2. Keller C. A. *et al.*, Biophysical Journal 75:1397-1402, 1998.
3. Hook F. *et al.*, Analytical Chemistry 73:5796-5804, 2001.

ACKNOWLEDGMENTS

The authors would like to thank JSPS KAKENHI (Grant No. 24560864) for providing financial support to this project.

A Parametric Study of a Mathematic Model for Degradation of Bioresorbable Polymers

X. Chen and J. Pan

Department of Engineering, University of Leicester, Leicester, UK, xc26@le.ac.uk

INTRODUCTION

Bioresorbable polymers have been used in human body as drug delivery stands, surgical sutures and bone fixation devices. To estimate the degradation rate and change in mechanical properties of these polymers a mathematical model has been established by Pan and his co-workers¹ based on the observed degradation pathway in experiments. The complexity of the degradation mechanism dictates that a large number of material parameters have to be used in the model. This work shows how the parameters affect the prediction of the model and therefore indicates a potential experimental method to measure these parameters.

MATHEMATICAL MODEL

The degradation model contains a list of material parameters. Among these χ_1 and χ_2 are used as partitioning parameters which take values between zero and one. χ_1 and χ_2 reflect the effect of carboxylic end groups on long and short chains working as catalysts for the hydrolysis reaction. k_1 and \bar{k}_2 represents reaction constants for non-catalytic and auto-catalytic hydrolysis reactions respectively. This work focuses on the effect of these parameters on the model prediction. Other parameters such as diffusion coefficient of oligomers were fixed in this study.

RESULTS AND DISCUSSION

Considering a sample of thickness 0.3mm, Fig 1 shows that two sets of these parameters predict almost identical molecular weight reduction as function of time. However when the sample thickness is increased to 2mm, as shown in Fig 2, the same sets of parameters predict very different molecular weight as functions of time. This suggests that the set of material parameters can only be determined uniquely using samples of different thicknesses.

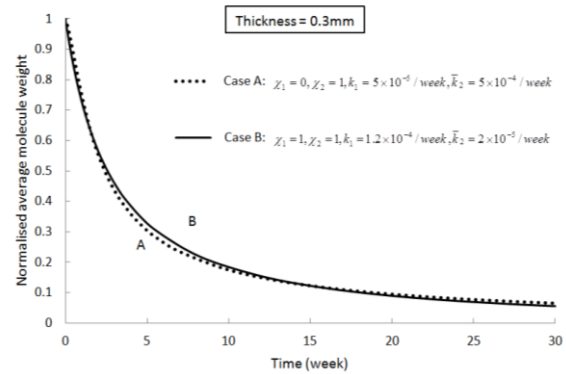


Figure 1 Calculated average molecular weight as functions of time for two different sets of parameters for sample thickness of 0.3mm.

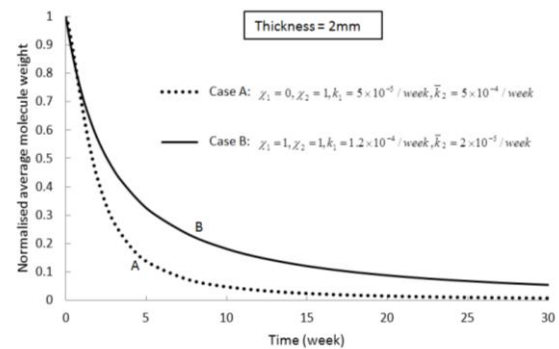


Figure 2 Calculated average molecular weight as functions of time for two different sets of parameters identical to those used in Fig 1 for sample thickness 2mm.

CONCLUSION

The mathematical model by Pan and his co-workers can be used for the design of bioresorbable devices. The model contains a large set of material parameters. This work shows that the set of parameters cannot be uniquely determined from degradation data that is obtained using samples of one thickness.

REFERENCES

1. Han, X. and Pan, J., Biomaterials. 30(3): p. 423, 2009



Patient Specific Implants Using a Novel Rapid Template Approach

A. Chan¹, P. Boughton¹, J. van Gelder², N. Young³ and A. Ruys¹

¹ Biomedical Engineering, Faculty of Engineering & IT, University of Sydney, Australia, acha3105@uni.sydney.edu.au

² Sydney Spine Institute, Neurosurgery Sydney Adventist Hospital, Australia

³ Department of Radiology, Centre for Biomedical Imaging Research and Development, University of Sydney, Australia

INTRODUCTION

Patient specific implants aim to provide improvements in functional outcomes by meeting anatomical constraints. Conventional modular implants can be inappropriate for patients with significant trauma or degeneration and can lead to risks of implant malpositioning and malfunction. While custom implants can result in shorter operative times and faster recovery, key remaining challenges include commercial viability, delivery timeframe and quality assurance of individually fabricated implants¹.

3D printing provides the accuracy and flexibility to fabricate anatomically specific implants however are accompanied with heavy regulatory loads. The exposure of print materials to oxidising temperatures results in the loss of optimal mechanical properties and limit implants to non-load bearing applications². 3D printed implants must also undergo sterilisation prior to surgery, leading to considerable delays.

The objective of this work is the development of a rapid-fabrication system for post-forming patient specific implants from terminally sterilised packaged precursors, whether bone cement or thermosensitive biomaterials or scaffolds. Forming implants from sterile packaged precursors using 3D printed templates eliminate delays associated with sterilisation and maintains superior biomaterial properties. Functional gradients can also be induced within the biomaterial to mimic the mechanical properties of the native tissue structure. This system has been investigated with bone cement for cranioplasty and soft tissue scaffolds as functionally graded meniscal replacements.

EXPERIMENTAL METHODS

Scaffold Design: A soft tissue aliphatic polyester scaffold was designed to suit the size and shape of the medial meniscus. Scaffold porosities and tensile moduli were used to determine the level of volumetric transformation required to acquire the circumferential tensile properties of the meniscus. Increased scaffold heights were defined for the outer meniscal rim.

Implant Fabrication: Anatomical geometries were derived from CT scans and processed using *ScanIP*. Implant models were developed into templates on Solidworks then rapid prototyped using fused deposition modelling. Implants were formed by packaging precursor materials in low density polyethylene (LDPE) envelopes then conformed within the template.

Model Analysis: Scaffold confinement within the meniscal template was simulated on Abaqus FEA using properties derived from previous work³. Porosity change was analysed using elemental volume.

RESULTS AND DISCUSSION

Implant Fabrication: Anatomical shapes were successfully translated onto implants and scaffolds using cranial and meniscal templates. Total lengths and widths differed by 3.74% and 0.19% for cranioplasty, and 2.5% and 1.96% for meniscal scaffolds respectively. Implant thicknesses were significantly thinner than model values for both applications. This was attributed to impeded material conformance within the template due to packaging constraints. Standard LDPE packaging imparted tension in the transverse direction, leaving a pleated texture on cranioplasty implants. LDPE films provided improved packaging conformance however removal from the template was significantly harder and packaging was prone to breakage. Future developments will improve packaging conformance through texturing and applying a stronger vacuum across the template.

Model Analysis: A macroscopic function gradation in porosity was observed across the meniscal scaffold. Excessive constraint led to the precursor partially conforming to the female template form. While thermal conditions were not included in the analysis, these values suggest a functional gradient can be induced during implant fabrication. This presents the possibility to fabricate meniscal implants that are anatomically specific to the patient with respect to geometrical and biomechanical properties of the native meniscus.

CONCLUSION

In this study, the development of a system to rapidly post-form patient specific implants has been applied in cranioplasty and meniscal applications. Anatomical geometries and functional gradients were successfully translated onto a range of materials. Optimisations in packaging and shaping techniques are recommended to account for buckling instability of packaging and introducing target scaffold functional gradations or heterogeneities. While this rapid fabrication system requires refinement, these developments have demonstrated promising potential in fabricating patient specific implants for a number of applications.

REFERENCES

1. Gerber, N. *et al.*, Conf. Proc. IEEE Eng. Med. Biol. Soc. 2010:3357–60, 2010
2. Gibson, I. *et al.*, Rapid Prototyp. J. 12:53-58, 2006
3. Chan, A., Hons. Thesis, University of Sydney, 2012

ACKNOWLEDGMENTS

The authors would like to thank Sydney Spine Institute, Maverick Biosciences Pty Ltd and Superscan for their support in this research.



Use of Ivory to Assess Composite Dentine Bonding

Saad Liaquat¹, Paul Ashley¹, Laurent Bozec¹, Anne Young¹

¹Eastman Dental Institute, UCL, London, UK, Saad.liaquat.11@ucl.ac.uk

INTRODUCTION

A current goal in dentistry is to develop a dental composite that can bond to human teeth without the need for the current complex acid etching procedures (e.g with phosphoric acid gel), and /or need for an adhesive (e.g Ibond). The aim of the study was to evaluate and compare the shear bond strength of two commercial (Z250, Gradia), and one experimental conventional composite (C-HEMA). In addition, a commercial (Vertise Flow), and experimental (C-4 META) potentially self- adhesive composite was studied.

Access to extracted human teeth for testing of composite bonding, however, is limited. Ivory was used as a substitute for human dentin in tensile adhesion measurements in 1979¹ and more recently to check the push out bonding of an adhesive system². In this study ivory is used (to access the shear bond of dental composites) in addition to human dentine to enable increased sample number, and thereby confidence in differences observed with dentine pre-treatment, and material type.

EXPERIMENTAL METHODS

Ivory Tusk & human teeth were cut to expose dentine surface. Cut sections were mounted using slow-setting viscous self-curing resin. Ivory dentine grinding & polishing was carried out using P120, & P500 paper until sound dentine was exposed. For Human dentine, grinding was stopped when superficial dentine was exposed.

All dentine surfaces were either treated with 37 % phosphoric acid gel etchant, or Ibond total etch for 0 or 20 s. Composite pastes were subsequently placed in a brass tube of 3 mm internal diameter, & 6 mm long placed on the dentine surfaces. Shear bond strength was determined using an Instron Universal testing machine with a "Flat-edge shear fixture", and 1 kN load cell at cross head speed of 1 mm/min (Table 1 & 2). Each test was performed in triplicate.

RESULTS AND DISCUSSION

From the combined results (Table 1 & 2) it can be seen that the biggest factor increasing bond strength is use of the adhesive Ibond (average of 28 vs 9 MPa). Acid etching can increase bonding both with (26 to 32 MPa) and without (7 to 12 MPa) use of adhesive. Addition of adhesion promoting monomers such as 4-META³ into the composites can improve bonding but only when no adhesive is employed (6 to 14 MPa increase). In comparison, differences in average bond strengths with ivory and human dentine were minimal demonstrating

that ivory is a good substitute for human dentine irrespective of treatment or material type (Table 1 & 2).

CONCLUSION

Ivory dentine can be used as a substitute for human dentine in adhesion tests. Additionally adhesive monomer 4-META in composites can increase bonding. Use of a separate adhesive, however, is more effective.

	No Ibond				Average
	No acid etching		Acid Etching		
	IVORY DENTINE	HUMAN DENTINE	IVORY DENTINE	HUMAN DENTINE	
GRADIA	4 (0.2)	4 (0.2)	9 (0.7)	5 (0.2)	6
Z250	4 (0.2)	4 (0.2)	10 (1.2)	7 (0.2)	7
C- HEMA	5 (0.3)	2 (0.1)	5 (0.2)	13 (1.2)	6
VERTISE	8 (0.4)	14 (1.1)	16 (1.2)	17 (1.4)	14
C-4 META	13 (0.8)	15 (1.2)	12 (0.9)	16 (1.5)	14
Average	6	7	10	13	9

Table 1: Comparison of shear stress (MPa) along with standard deviation SD of experimental (C-4 META, C-HEMA) and Commercial composites (Z250, GRADIA, VERTISE FLOW) using no Ibond, acid etch 0 or 20 s (Sample size n=3, Average error is 10+/-7%).

	Ibond				Average
	No Acid Etching		Acid Etching		
	IVORY DENTINE	HUMAN DENTINE	IVORY DENTINE	HUMAN DENTINE	
GRADIA	28 (2.2)	22 (2.1)	27 (2.3)	23 (0.7)	25
Z250	29 (3.4)	26 (2.9)	30 (3.5)	36 (3.2)	30
C- HEMA	25 (2.7)	26 (1.2)	37 (4.2)	35 (4.1)	31
VERTISE	25 (2.5)	25 (0.9)	28 (2.7)	28 (2.2)	26
C-4 META	27 (3.8)	24 (2.1)	29 (2.4)	28 (1.6)	27
Average	26	25	31	32	28

Table 2: Comparison of shear stress (MPa) along with standard deviation SD of experimental (C-4 META, C-HEMA) and Commercial composites (Z250, GRADIA, VERTISE FLOW) using Ibond, acid etch 0 or 20s (Sample size n=3, Average error is 10+/-7%).

REFERENCES

1. Fusayama T, Nakamura M, Kurosaki N, Masaaki I. Non-pressure adhesion of a new adhesive restorative resin. J Dent Res 1979; 58:1364-1370.
2. Thanjal, Narinderjeet Tina. Optimisation of interfacial bond strength of glass fibre endodontic post systems. Diss. 2011.
3. Nakabayashi N, Hiranuma K. Effect of etchant variation on wet and dry dentin bonding primed with 4-META/acetone. Dent Mater 2000; 16(4):274-9.

ACKNOWLEDGMENTS

This research is funded by Higher Education Commission, Government of Pakistan.



Preparation of Porous Titanium-Polyglycolide Composites

Nobuyuki Hayashi¹, Shun Kojima¹, Masato Ueda^{2*}, Masahiko Ikeda², Kenji Doi³, Kazuki Hanami³, Shigeo Mori³, Hisashi Kitagaki³, Shuntaro Terauchi³

¹ Graduate School of Science and Engineering, Kansai University, Japan

^{2*} Faculty of Chemistry, Materials and Bioengineering, Kansai University, Japan, m-ueda@kansai-u.ac.jp

³ Osaka Yakin Kogyo Co., Ltd., Japan

INTRODUCTION

Mechanical properties of metallic materials can be controlled by not only alloy design¹ but also constructing appropriate structure². A porous implant material with adequate pore structure and appropriate mechanical properties has long been sought as the ideal bone substitute³, because it exhibits low Young's modulus and bone ingrowth. The mechanical properties of porous materials change from day to day; the bone ingrowth into the pores makes the Young's modulus and the strength significantly increase after implantation. Therefore, it is necessary to implant the porous devices showing lower strength than that of living bone. In this case, the strength must be insufficient in the initial stage.

The purpose of the present study was to increase the strength of porous implants by heat-injection of biodegradable plastic into the pores. In addition, compressive strength was also investigated.

EXPERIMENTAL METHODS

Sodium chloroacetate ($\text{ClCH}_2\text{COONa}$, 98 % purity, Sigma Aldrich) was heated at 160 °C for 20 h under vacuum. NaCl was removed from the product polymer by stirring in distilled water for 5 h. The resultant powder of polyglycolide (PGA) was rinsed with ethanol twice and vacuum-dried at 80 °C. The compact of PGA powder and porous Ti (porosity: 60 %, $\phi 3 \times 5$ mm) were put in a die made of stainless steel and pressed up to 2 MPa at 210–240 °C by using a high frequency induction heating equipment.

Compression test was carried out at an initial strain rate of $1.66 \times 10^{-4} \text{ s}^{-1}$ for the porous Ti and the porous Ti-PGA composites.

RESULTS AND DISCUSSION

The resultant powder was determined as polyglycolide (PGA) by X-ray diffraction. Temperature scan between 30 and 250 °C was performed at a heating rate of $10 \text{ }^\circ\text{C min}^{-1}$ in differential scanning calorimetry. There is an endothermic peak, related to melting, with onset temperature of 167.8 °C, peak temperature of 205.4 °C and finish temperature of 215.0 °C.

Figure 1 shows (a) appearance and (b) cross-section of porous Ti-PGA composite prepared by heat-injection. All pores on the surface were filled by PGA. Furthermore, the PGA penetrated to the centre though few small cavities could be confirmed. The filling fraction was measured to be approximately 70 %.

The 0.2 % proof stresses were obtained from the stress-strain curves (Table 1). All stress-strain curves showed typical and smooth ones for ductile metals even in the composites. The porous Ti shows a proof stress of about 40 MPa. The compressive strength drastically

increased by filling the pores with PGA, it reached more than 90 MPa. This strength is comparable to that of cortical bone. In addition, the strength increased with increasing in injection temperature.

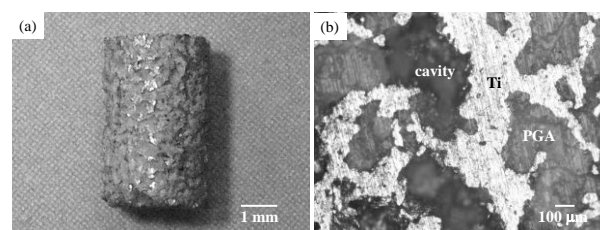


Fig. 1 Appearance (a) and cross-section (b) of porous Ti-PGA composite.

Table 1 Compressive strength in porous Ti and porous Ti-PGA composites.

	Injection temperature (°C)	0.2 % proof stress / MPa
Porous Ti	-	40
Ti-PGA	210	66
	225	93
	240	108

CONCLUSION

1. Porous Ti-polyglycolide (PGA) composites could be prepared by using a heat-injection method. The PGA penetrated to the centre of the porous Ti showing 60 % porosity.
2. Compressive strength was drastically improved by filling the pores with PGA. The strength increased with increasing in injection temperature.

REFERENCES

1. Niinomi M. *et al.*, Acta Biomaterialia 8:3888-3903, 2012
2. Nomura N. *et al.*, Mater. Sci. Eng. C 25:330-335, 2005
3. Takemoto M. *et al.*, Biomaterials 26:6014-6023, 2005

ACKNOWLEDGMENTS

This work was partly supported by Osaka Prefectural Government.

Mechanical Properties and Surface of Ultrafine Grained Titanium for Dental Implants

Carlos Nelson Elias^{1*}, Daniel J. Fernandes¹, Jochen Roestel²

¹Instituto Militar de Engenharia, Brazil, elias@ime.eb.br (presenting author)

²Conexão Sistemas de Prótese, jochen@conexao.com.br

INTRODUCTION

The area of human implants has undergone rapid and dramatic developments in the past years. This was greatly enabled by new materials with enhanced biocompatibility. Although implants have been used by humans since ancient times, there were many rejection problems and it is only recently that osseointegrated implants have become widely used. The corrosion resistance to body fluids as well as the mechanical strength, fatigue endurance, and impact toughness are important requirements of a biomaterial, especially for implant applications. Biomaterials are usually classified [1], in terms of their interaction with the body, into: biotolerant materials (e.g., stainless steel, CrCo alloy, and polymethyl-methacrylate) release substances in nontoxic concentrations, which may lead to the formation of a fibrous connective tissue capsule; bioinert materials (e.g., alumina and zirconia) exhibit minimal chemical interactions with adjacent tissue; and bioactive materials (e.g., hydroxyapatite, bioglass) stimulate a biological response from the body, such as bonding to either a soft tissue, like cartilage, or hard like bone.

The main application of unalloyed cp Ti (ASTM grade 1 to 4) is for dental implants. This metal is not, however, used for orthopedic application owing to its low mechanical properties. This work focuses on dental implants and in the introduction of ultrafine grained titanium (UFG Ti), obtained by severe plastic deformation (SPD) processing, for which properties were evaluated [2]. In particular, its strength was found to match that of Ti-6Al-4V alloy, commonly used in high strength structural implants.

EXPERIMENTAL METHODS

In this study samples for mechanical tests and implants were machined from bars of cp Ti G2, 4, 5 and cp Ti G4 cold hardening. The implants were subjected to surface treatments with double etching (HCl and H₂SO₄ solution) with the same concentration and for the same temperature and time interval.

Tensile test and surface morphology analysis was done.

RESULTS AND DISCUSSION

Figure 1 shows the surface morphology of dental implant surfaces after acid etching. It can be seen that the surface is homogeneous with uniformly distributed microcavities. Roughness in the nanometer scale is on Ti G4 cold hardening surface. Figure 1 does not show a significant micro morphology difference between Ti G4 and Ti G4 cold hardening after acid treatment. This result suggests that the use of dental implant made with Ti G4 cold hardening can be subjected to the same machining processes and surface chemical treatment as cp G4 without significant changes in biocompatibility.

Only at high magnification it is possible to observe that Ti G4 cold hardening has higher number of nanoscale surface features than Ti G4 and G5. It is expected that the interactions between the cells and the nanoscale surface are improved in the early stages after implantation. According to Meirelles et al [3], the nanoscale surface features improve the osseointegration mechanism.

The stress-strain curves are shown in Figure 2. It can be seen that the mechanical strength increases in the following order: Ti G2, Ti G4, Ti G5 and Ti G4 Hard.

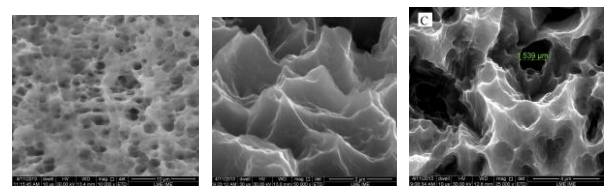


Figure 1: Surface morphology of dental implants after acid etching. (A) Ti alloy G5. (B) cp Ti G4. (C) cp Ti G4 cold hardening.

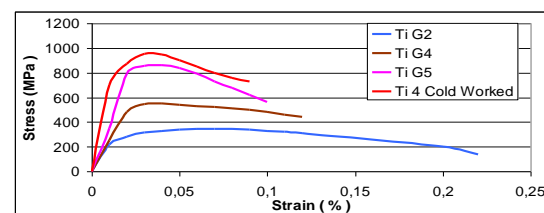


Figure 2: Tensile test of cp Ti and Ti alloy.

Figure 2 shows that all cp Ti and Ti 5 samples are ductile, i.e., have a high plastic deformation before fracture. The curves show that when the applied stress is higher than the yield strength, permanent deformation occurs and the ductility decreases. Ti 4 cold hardening is the strongest metal.

CONCLUSION

The results of the present work show that:

- The surface morphology of Ti G4 cold hardening has micro and nanoroughness, which can improve the dental implant osseointegration.
- The Ti G4 cold hardening is stronger than cp Ti and Ti G5.

REFERENCES

- [1] Elias CN, et al. JOM 2008; 60:46-9.
- [2] Valiev RZ. Nature Mater. 2004; 3:511-516.
- [3] Meirelles L, et al. Clin Implant Dent Related Res 2008; 10(4):245-54.

ACKNOWLEDGMENTS

This work was carried out with financial support from the Brazilian Agencies CNPq (Process 472449/2004-4, 400603/2004-7 and 500126/2003-6) and FAPERJ (Process E-26/151.970/2004).



Preparation and Characterization of Novel Composite Agarose Films for Wound Healing

Alma Akhmetova^{1*}, Matthew Illsley², Timur Saliev¹, Talgat Nurgozhin¹, Sergey Mikhlovsky¹, and Iain Allan²

¹Department of Translational Medicine, Longevity and Global Health/Center for Life Sciences, Nazarbayev University, Kazakhstan

²School of Pharmacy and Biomolecular Sciences, University of Brighton, UK, alma.akhmetova@nu.edu.kz

INTRODUCTION

Wound healing is a complex process that requires multipurpose approach. The common properties for desired products usually include absorption, stimulation of regeneration process, pain free removal, and no toxicity. In these terms agarose is a promising biomaterial for wound healing applications. It does not require additional crosslinking agents and forms a gel at room temperature. The transparent nature of this polysaccharide can allow monitoring of the wound state. Absence of toxicity and inertness of agarose may prevent unnecessary reactions at the wound site. Its slow degradation rate is beneficial for the end product properties such as longer shelf life.

To aid absorption of wound exudate, bacteria, and necrotic tissue, activated carbon (AC) was incorporated into agarose films. We developed and studied mechanical properties of agarose films of various concentrations. For the first time activated carbon particles were incorporated into agarose films and triple-layered films were developed.

EXPERIMENTAL METHODS

To prepare agarose films, agarose powder for general use was dissolved in distilled water which was brought to boiling. 0.5%, 1%, 1.5%, and 2% concentrations of agarose solutions were prepared. Each solution was poured into a plastic Petri dish (87x12 mm) and left to set for about 3-5 minutes. Then, 6-7 circles (27x3.3mm) were cut out and placed into plastic weighing boat. Samples were dried overnight in a vacuum oven at 60°C. Activated carbon particles were added to the agarose and distilled water and brought to boil. The above steps were repeated to prepare films.

The mechanical strength and elasticity of agarose films were assessed using texture analyser. Young's modulus of elasticity, tensile strength, and elongation at breaking point were measured and analysed. Solvent absorption capacity of the prepared films was tested following standard gravimetric procedure. Moisture content and swelling capacity of films were measured. All measurements were conducted in triplicates.

RESULTS AND DISCUSSION

The increase in concentration greatly affected mechanical properties of agarose films resulting in a curl of the edges and rigid structure. These films were prone to easy breakage. One-layered agarose films of

0.5% and 1% were elastic and straight. Activated carbon was added in 1:1 ratio to agarose. In the resulted films, incorporated AC particulates were found to detach from the agarose layer. To overcome this problem, the AC layer was sandwiched between two agarose layers with the inner AC layer having a lesser diameter than the surrounding agarose layers.

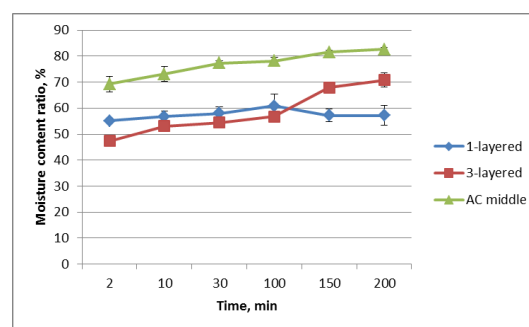


Figure 1 - Moisture content ratio of one-layered and three-layered agarose films, and three-layered agarose-activated carbon-agarose films.

Triple-layered, agarose-activated carbon-agarose, films almost immediately absorbed much higher volume of the solvent (Figure 1). The swelling ratio was twice larger in comparison to films containing only agarose. These results indicate that activated carbon particulates are freely available within agarose cascade. However, the equilibrium in both experiments was not reached for three-layered films. Therefore, the continuation of the experiments is required.

CONCLUSION

The prepared agarose films of low concentration were straight and elastic and suitable for easier application to the wound site. These films were non-adherent and, therefore, can be directly used to the wound enabling pain-free removal. Incorporation of activated carbon into agarose layer was successful only when the agarose-activated carbon layer was covered completely with two agarose layers. Inclusion of AC enabled much higher absorption capacity and swelling of the films.

ACKNOWLEDGMENTS

The authors would like to thank the Ministry of Education and Science of the Republic of Kazakhstan for providing financial support to this project.

New approaches for the local prevention and treatment of fragilized osseous sites using doped-calcium phosphate cements

C. Mellier³, V. Schnitzler³, E. Verron², F. Fayon⁴, C. Despas⁵, A. Walcarius⁵, N. Rochet⁶, J.-C. Scimeca⁶, O. Gauthier², J.-M. Bouler², B. Bujoli¹ and P. Janvier¹

PRES L'UNAM, CNRS UMR 6230, CEISAM¹, 2 rue de la Houssiniere, 44322, Nantes - FRANCE - Email: pascal.janvier@univ-nantes.fr

PRES L'UNAM, INSERM U791, LIOAD², 1, Place Alexis Ricordeau, 44042 Nantes - France

GRAFTYS SA³, 415 Rue Claude Nicolas Ledoux, 13290 Aix en provence - France

CEMHTI⁴, UPR CNRS 3079, 1D Avenue de la Recherche Scientifique - 45071 Orléans - France

University of Lorraine, CNRS UMR 7564 LCPME⁵, 405 Rue de Vandoeuvre, 54600, Nancy - France

University of Nice, FRE 3472 BIPOA⁶, 28 Avenue de Valrose, 06103, Nice - France

INTRODUCTION

Calcium phosphate based bone substitutes have the unique capacity to be resorbed *in vivo* according to bone remodeling kinetics and replaced by natural bone. Thus injectable calcium phosphate cements (CPCs) are under intense investigation since they offer additional advantages compared to ceramics and open up new applications in the field of drug delivery systems using minimally invasive surgery in pathological osseous sites. In this context, bisphosphonate (BP) antiresorptive drugs can be combined with CPCs¹, however, the way to introduce BP in a CPC has a critical influence on the setting kinetics. We have also explored the potential of gallium-doped calcium phosphate materials². It was shown that gallium (Ga) reduced the resorption activity, differentiation and formation of osteoclasts, in a dose-dependent manner without inducing any adverse effect on osteoblastic cells. For this reason, we are interested in investigating whether gallium can be combined with injectable CPCs for the development of a local delivery system of this ion in fragilized osseous sites. Meanwhile we are also interested in improving the bioactivity of these CPCs by the addition of autologous blood as a source of fibrinogen and growth factor in their liquid phase.

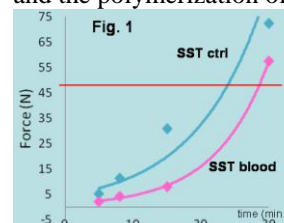
EXPERIMENTAL METHODS

The formulations were optimized from an apatitic-type CPC, with α -TCP as main component (78%), BP or Ga is introduced via (10%) calcium deficient apatite [BP-CDA or Ga-CDA]. The liquid phase consisted in a Na_2HPO_4 solution or blood. The BP used for our study was Alendronate. BP-CDA was obtained by suspending CDA in a solution of Alendronate, Ga-CDA was obtained by a pH controlled co-precipitation process between gallium nitrate, calcium nitrate and diammonium hydrogen phosphate. The products obtained were characterized by ³¹P MAS NMR, CPC setting by high frequency impedance and mechanical properties by texture analyser.

RESULTS AND DISCUSSION

Three approaches to incorporating Alendronate in the cement were investigated: BP (i) dissolved in the liquid phase (ii) added to the ground solid phase (iii) chemically combined with a component of the solid phase. As phosphonates are considered as retardant agents for the setting of Portland cements, the later approach has been shown to be the most promising particularly via the chemical association between CDA

and BP as previously demonstrated. In this study we have also compared the setting time obtained by using Gilmore needles method with high frequency impedance measurements³. ³¹P NMR has also been used to characterize the chemical transformation of α -TCP to CDA during the setting process. As for BP, the best approach to incorporating Ga in a CPC consists to combine it with a component of the solid phase. After changing the constitution of the solid phase of cement including incorporation of inhibitors of bone resorption, we also decided to change the liquid phase of the cement. For this, we replaced the aqueous liquid phase by blood. Our starting point is related to two commercial cements: a long setting time cement LST (initial setting time 15 min.) and a short setting time cement SST (initial setting time 8 min.). In the case of LST/blood cement, there is a competition between the precipitation of crystalline particles of CDA and the polymerization of fibrin during blood clotting.



In the case of SST/blood cement, the precipitation process can be achieved more easily and we obtain an injectable self-hardening cement which matches the control as shown Fig.1.

CONCLUSION

Here we demonstrate the feasibility of such medical device based on doped-calcium phosphate cement incorporating inhibitors of bone resorption in order to stimulate bone ingrowth. One can of course imagine to incorporate both gallium and bisphosphonate in the same cement which nevertheless raises the question of whether we are still dealing with a medical device. We also believe that the replacement of the aqueous liquid phase by blood is a promising way due to the presence of many circulating cells promoting bone healing. Preliminary "*in vivo*" experiments supports this assertion.

REFERENCES

- ¹Bujoli B. *et al.* Acta Biomaterialia 10:940-950, 2011
- ²Mellier C. *et al.* Inorg. Chem., 50:8252-8260, 2011
- ³Despas V. *et al.* Acta Biomaterialia 10:940-950, 2014

ACKNOWLEDGMENTS

This work was partially funded by ANR GaBIPHOCe (Biotecs Program), ANR BRB (Tecsant Program) and supported by Graftys SA.



Robotic Deposition of 3D Scaffolds Using β -tricalcium Phosphates Inks for Bone Regeneration

Raquel Costa Richard¹, Renata Nunes Oliveira^{1*}, Rossana Mara da Silva Moreira Thiré¹

^{1*} Department of Materials Engineering, Federal University of Rio de Janeiro, Brazil, nunes@metalmat.ufri.br

INTRODUCTION

Several approaches have attempted to replace extensive bone loss, but each of them has their limitation¹.

Even though health bone is able to self-regenerate, this regeneration is limited to a gap of a few millimeters. Therefore, filling the bone defect with a porous scaffold helps to enhance bone regeneration since the scaffold serves as a template for cell ingrowth as well as for extracellular bone matrix formation². It has been shown that three-dimensional (3D) scaffolds with interconnected macroporous, reproducing the shape of the patient's bone defect, help to improve the biocompatibility of the scaffolds after surgical procedure³.

The goal of the present study was to synthesize beta-tricalcium phosphate (β -TCP), beta-tricalcium phosphate substituted by magnesium (β -TCMP) and biphasic calcium phosphate substituted by magnesium (BCMP) via hydrolysis and to produce scaffolds for bone regeneration using robocasting technology.

EXPERIMENTAL METHODS

Calcium deficient apatites (CDA's) powders, with and without magnesium, were obtained by hydrolysis, calcined and physico-chemically characterized. Colorimetric cell viability assay, calcium nodule formation and the expression of alkaline phosphatase, osteocalcin, transforming growth factor beta-1 and collagen were assessed using a mouse osteoblastic cell line (MC3T3-E1).

Direct-write assembly of cylindrical periodic scaffolds ($\Phi = 8\text{mm} \times H = 5\text{mm}$) was done via robotic deposition with a robotic deposition device (Aerotech 3200, Stillwater, OK) using β -TCP, β -TCMP and BCMP colloidal inks. The sintered scaffolds were characterized by scanning electron microscopy and uniaxial compression test.

Statistical analysis of the mechanical compression data were performed by one-way ANOVA at 95% confidence interval using the software Origin 8.0[®] (OriginLab Corporation, USA). Multiple comparisons between groups were performed by the Tukey test.

RESULTS AND DISCUSSION

According to XRD spectra, β -TCP was obtained after calcining Mg-free CDA; β -TCMP or BCMP were obtained after calcining Mg-substituted CDAs, depending on the Mg/Ca molar ratio of the CDA. MTT assay showed that the β -TCP, β -TCMP and BCMP obtained promoted cell proliferation, indicating non-cytotoxicity. Calcium nodule formation results indicated that the degradation products of the β -TCP, β -TCMP and BCMP were conducive to bone formation. The amount of mineralized nodules was higher in the β -TCP, followed by β -TCMP and BCMP samples. The same behavior was observed for bone formation markers (ALP and osteocalcin) and for bone resorption

markers (TGF- β 1 and collagen) activity in MC3T3-E1 cell line. This behavior can be explained for the fact that the presence of Mg ions retards the dissolution of CaP^4 . The 3D structures obtained from the β -TCP, β -TCMP and BCMP inks were cylinders (8mm x 5mm) composed of 21 layers, with two perimeter rims surrounding a parallel array of rods (0.33mm) with an inter-rod spacing of, approximately, 460 μm . Figure 1 shows the macro and microstructure of a β -TCP sintered scaffold.

Studies with trabecular bone have been registered a wide variation of strength which is usually in the range of 4 to 12 MPa⁵. The mean compressive strength values of β -TCP, β -TCMP and BCMP scaffolds were 18.67 (± 4.14), 12.24 (± 2.67) and 7.63 (± 2.36) MPa, and the maximum compressive strength values were 26.58, 15.81 and 10.63 MPa, respectively.

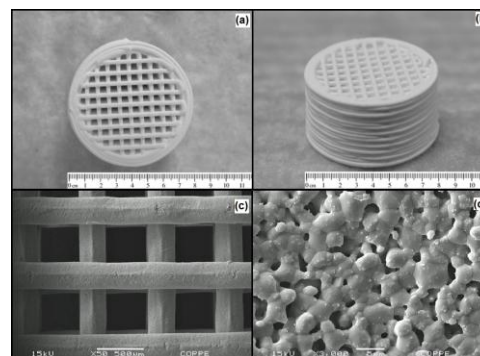


Figure 1- Macro (a,b,c) and microstructure (d) of β -TCP sintered scaffold.

CONCLUSION

According to the cell viability assay, the powders induced cell proliferation. Calcium nodule formation and bone markers activity suggested that the materials present potential value in bone tissue engineering. The scaffolds built by robocasting presented interconnected porous and exhibited mean compressive strength between 7.6 and 18.7 MPa, compatible with trabecular bone.

REFERENCES

- Scheller E.L. *et al.*, J of Oral Rehabilitation, 36: 368–389, 2009.
- Butscher A. *et al.*, Acta Biomaterialia, 7: 907–920, 2011.
- Uchida T. *et al.*, J. Biotechnol., 133: 213–218, 2008.
- Bose S. *et al.*, Bone 48:1282–1290, 2011.
- Houmard M. *et al.*, J Biomed Mater Res Part B, 101:1233–1242, 2013.

ACKNOWLEDGMENTS

The authors would like to thank Dr. Racquel LeGeros (*in memoriam*). Without her it would be impossible to achieve the synthesis results. This work was supported by CNPq, CAPES and FAPERJ.



Evaluation of Bone Replacement Materials in a Rabbit Cranial Defect Model using MicroCT and Hard Tissue Histology

Gerlind Schneider^{1*} and Dirk Linde¹

¹Department of Otorhinolaryngology / Friedrich Schiller University Hospital, Jena, Germany

^{*}gerlind.schneider@med.uni-jena.de

INTRODUCTION

For functional and structural restoration of bone deficiencies, various resorbable and nonresorbable alloplastic materials have been introduced, including metals, polymers and ceramics.

However, an optimal artificial replacement for craniofacial bone has not been found yet, and the search for improved reconstruction methods and alternative materials is going on. To assess and compare biocompatibility and osseointegration of these materials, adequate animal test models are indispensable.^{1,2}

EXPERIMENTAL METHODS

In a rabbit cranial defect model ("Jena skull model")¹, biocompatibility and osseointegration of polymeric and composite (3D printed tricalcium phosphate + polymer) bone replacement materials were evaluated at different time points after implantation. Calvaria including implants and surrounding tissue were explanted and embedded in methacrylate resin².

The samples were scanned with a nanotom® (phoenix|x-ray) microCT scanner and proceeded for histological examination by sawing-grinding technique³. Avizo® Fire (vsg) software was used for visualisation and processing of µCT data.

Qualitative and morphometric evaluation of osseointegration, fibrous encapsulation, and inflammation was performed on undecalcified histologic preparations of the explants, and on 3D reconstructions plus virtual slices derived from corresponding 3D microCT datasets.

RESULTS AND DISCUSSION

The obtained 3D microCT data enabled comprehensive qualitative and quantitative assessment of osseointegration and biodegradation of radioopaque composite implants.

Prerequisite for visualization and discrimination of materials by µCT is a significant difference of their Hounsfield values. Due to this limitation, radiolucent polymeric implant materials and soft tissue could not be distinguished from embedding resin (figure 1).

In contrast, histologic preparations of undecalcified hard tissue and implant materials enabled detailed visualization and examination of all tissues and implant materials (figure 1). The substantial disadvantage of hard tissue histology is the inevitable loss of information due to small number of slices and large gaps between specimens yielded by this method.

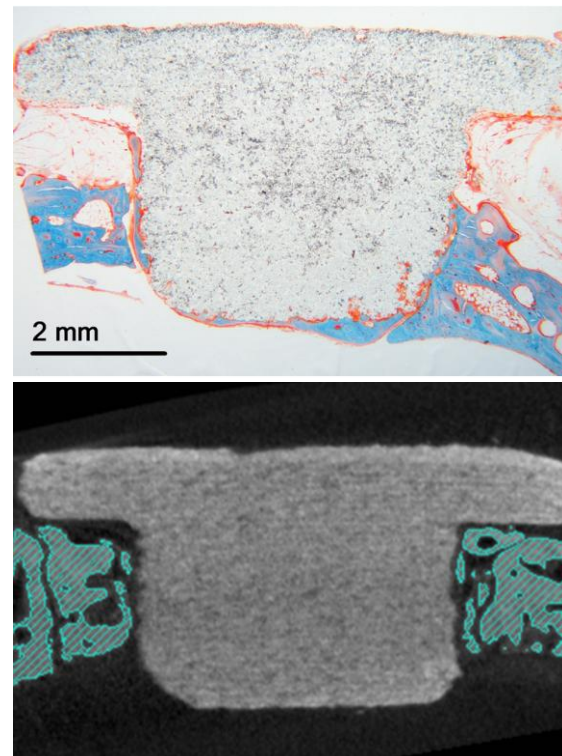


Figure 1: Explants from rabbit cranial defect model containing composite implant: histologic preparation (upper part) and virtual slice of µCT scan (lower part)

CONCLUSION

To obtain comprehensive and quantifiable information about biodegradation, biocompatibility and osseointegration of alloplastic bone replacement materials, microCT scans as well as histologic evaluation should be performed.

REFERENCES

1. Voigt S., Schneider G., *BIOMaterialien* 10(3/4): 151, 2009
2. Schneider G. *et al.*, *J. Mater. Sci. Mater. Med.* 21(10): 2853-2859, 2010
3. Donath K., Breuner G., *J. Oral. Pathol.* 11(4): 318-326, 1982

KEYWORDS

Imaging
In vivo Host Response
Ceramics and composites

A New Analytical Model of GAAS MESFET With Different Laws of Mobility

Y.Saidi , Z.Fares

Department of Physics, Faculty of Sciences, Mentouri University, Constantine, Algeria
e-mail: saidiyas09@yahoo.fr

1-Introduction

We present in this paper an analytical model of the current –voltage (I-V) characteristics for submicron range GaAs JFET and MESFET transistors. This model is take into account the two-dimensional analysis of the charge distribution in the active region and incorporates a field depended electron mobility, velocity saturation and charge build-up in the channel. In this framework an algorithm of simulation based on mathematical expressions obtained previously

2-Calculation of drain current in channel

To calculate the drain current expression as a function of the drain voltage, we must make some approximations [2,3]:

- voltage for various values of the gate voltage, we use some reasonable approximations (1):
- One neglects the current flow in the y-direction; this approximation is valid for the components with the length and short gate.
- An abrupt junction Schottky barrier.
- A channel of uniform doping N_d (x, y) = N_d , N_d is constant.
- Neglecting edge effects, the overflow area depopulated on the sides of the gate

3 - Effect of mobility variable

The characteristics current -voltage depend with the variations on the electron mobility according to the electric field. In area of weak electric fields, free carriers are in thermal equilibrium with the network and their average speed is proportional to the electric field:

$$V(E) = \mu_n E.$$

μ_n is the mobility of electrons at low electric field.

But, when the electric field is high, the electron transfer intervals induced in the GaAs, a decrease of

witch descript the variations of the mobility with the electric field in the submicron GaAs and several approximate analytical expressions have been proposed for this function. The mobilities law used in our I-V model are expressed by :

- For the weak electrical fields where $E < E_0$:
$$\mu = \mu_n \quad (4)$$
- For the high electric fields beyond E_0 ($E \geq E_0$) [3,4]

4) Results and discussions

The numerical calculation of the current of drain according to the biasing calls upon the expressions (8), (9), (10) established previously. The study was carried out on a submicronic gate GaAs MESFET.

In the linear regime, we notice a good coincidence between experiment values and theory and those that, for various acts of mobility, especially in the case of constant mobility, demonstrating the independence of the mobility of electrons in the field power, low drain voltages and also the close correlation between experience and the model proposed in the linear regime.

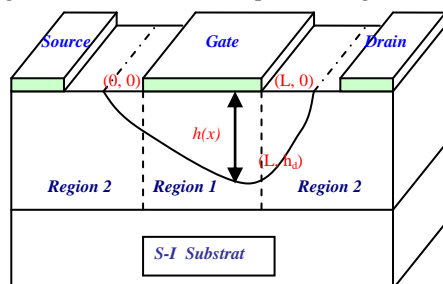
Conclusion:

In this study we have developed an analytical model to calculate the I-V characteristics of short gate length GaAs MESFET which takes into account the one-dimensional analysis of the charge distribution in the active region and incorporates a field depended electron mobility, velocity saturation and effect of these parameter to the current voltage expressions. The model compares favourably from a submicron GaAs MESFET . More ever, comparisons between the analytical models with different values of mobility proposed shown the effect of mobility it affects directly the output characteristics (I-V) of GaAs MESFET.

References :

- [1] S. Morarka, S. Mishra; newspaper off semiconductor technology and science, Vol 5, p 173-181, 2005.
- [2] C.S. Chang, D.Y. Day, IEEE Trans Elec Dev., Flight 36, N° 5, p 269, May 1989.
- [3] W.R. Frensley, IEEE Trans. on Electron Devices, vol. 28, n° 8, pp. 962-967, August 1991.
- [4] K. Shin, D.P. Klemer, J.I. Lion, Solid State Electronics, Vol 35, p 1639 - 1644, 1992.
- [5] S. Khemissi, NR Merabtine, Mr. Zaabat, C. Kenzai-Azizi, Y. Saidi, Semiconductor Physics Quantum Electronics and Optoelectronics, Vol 9 N°2 p 34 - 39, February 2006.
- [6] S.H lo, C.P.LE, IEEE Trans on electr Devices (1992).
- [7] Y.Saidi, Thesis of doctorate , Mentouri University, Constantine 2004.

Fig 1: Diagram MESFET with Depletion regions



the carrier velocity and leads to strong negative differential mobility. However, there is not a law

Tayloring the Interfacial Adhesion of Anodised TiO₂ Nanotubes on Ti-6Al-4V Alloy for Medical Implants

U. Danookdharree¹, H. R. Le¹, R. Handy² and C. Tredwin³

¹ School of Marine Science and Engineering, University of Plymouth, United Kingdom, ²School of Biological Sciences, University of Plymouth, United Kingdom, ³School of Dentistry, University of Plymouth, United Kingdom, urvashi.danookdharree@plymouth.ac.uk

INTRODUCTION

Self-assembled nano-structure on the surface of bone/dental implants has attracted significant interest in the last few decades. In this context, anodic TiO₂ nanotubes have been shown to have a beneficial effect on osteoblast differentiation and bone formation around implant [1-2]. However, there is uncertainty about the interfacial adhesion to substrate as a surface coating for medical implants [3]. In this study, the effects of anodising conditions on the morphology, composition and interfacial adhesion of the nanotubes grown on titanium alloy were investigated with various electrolytes, pH values and voltage sweep rate.

METHODOLOGY

Samples of Ti-6Al-4V alloy were polished using silicon carbide papers followed by an alkaline cleaning. The nanotubes were grown by anodisation under 0-20V, in 0.2-0.5 wt% ammonium fluoride (NH₄F) with 0.5-1M NH₄H₂PO₄ or 0.5-1M (NH₄)₂SO₄, for 60-120 minutes at room temperature. The experiments were performed at a range of pH and voltage sweep rate. The resulting samples were analysed using a field emission scanning electron microscope (JEOL JSM-7500F) combined with an Oxford Instruments system (AZtec) whereby an Energy-Dispersive X-Ray Spectroscopy (EDS) was also performed with the aim of quantifying the elements present in the surface coating. The adherence of the coating, prepared under various conditions, was tested using a pull-off test on a universal mechanical test machine. The interface failure mechanisms were examined afterwards using high resolution SEM.

RESULTS AND DISCUSSION

TiO₂ nanotubes of an average diameter of 30-100 nm were formed on the surface, with the aim of enhancing the attachment of human cells for its use as biomaterial. In the sulphate containing electrolyte, the nanotubes formed on the β -phase of the alloy were fully dissolved due to the high solubility of vanadium oxide (Fig. 1) while for the samples from the phosphate containing electrolyte, the β -phase had a thin layer of TNTs as shown in Fig. 2.

The pH played a crucial role in the growth of the nanotubes in terms of growth rate and wall thickness which in turn influenced the elements present on the nanotubes. The presence of fluoride and phosphorus ions in small amount (From EDS) is expected to have

antibacterial properties while helping in the initial attachment of bone cells [4]. The adherence of the nanotubes to the surface was obtained, highlighting the effects of coating thickness, residual stress and coating

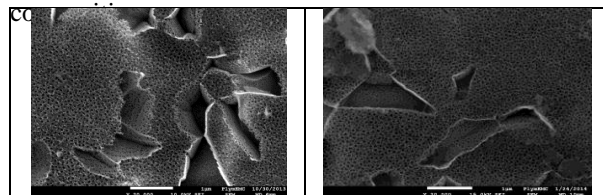


Fig. 1: TNTs obtained from sulphate containing electrolyte

Fig. 2: TNTs obtained from phosphate containing electrolyte

CONCLUSION

The presence of the micro and nanostructure on the surface at the same time was observed which will be beneficial in attachment and proliferation of human cells which can improve osseointegration. At the same time the appropriate thickness of the nanotubes layer, with a good adherence, was determined. It is envisaged that the nanotubular structure could act as a carrier for bactericidal or bone growth catalyst drugs to improve the anti-bacterial properties and bioactivity of an implant.

ACKNOWLEDGEMENTS

I would like to thank the University of Plymouth for sponsoring the project and all three supervisors who helped at every step in the study.

REFERENCES

- [1] N. Wang, H. Li, W. Lu, J. Li, J. Wang, Z. Zhang, and Y. Liu, "Effects of TiO₂ nanotubes with different diameters on gene expression and osseointegration of implants in minipigs," *Biomaterials*, vol. 32, no. 29, pp. 6900–6911, 2011.
- [2] J. Park, S. Bauer, K. von der Mark and P. Schmuki, *Nano. Lett.* 2007, 7, pp. 1686-1691.
- [3] C. R. Friedrich, M. Kolati, T. Moser, C. Sukotjo, T. Shokuhfar, "Survivability of TiO₂ nanotubes on the surface of bone screws", *Surface Innovations*, Vol. 2(1), 2013, pp. 60-68.
- [4] S. E. Kim, J. H. Lim, S. C. Lee, S.-C. Nam, H.-G. Kang, and J. Choi, "Anodically nanostructured titanium oxides for implant applications," *Electrochim. Acta*, vol. 53, no. 14, pp. 4846–4851, 2008.

Nano-sized α -tricalcium phosphate for bone cement

Linda Vecbiskena^{1*}, Karlis A Gross¹, Una Riekstina² and Thomas CK Yang³

¹Institute of Biomaterials and Biomechanics, Riga Technical University, Latvia, *linda.vecbiskena@rtu.lv

²Department of Pharmacology, University of Latvia, Latvia

³Department of Chemical Engineering and Biotechnology, National Taipei University of Technology, Taiwan

INTRODUCTION

In recent decades, calcium phosphate bone cement (CPC) research has focused on the improvement of injectability, mechanical strength and resorption¹ in an attempt to accelerate a good cell response at early implantation times. The preparation of α -tricalcium phosphate (α -TCP) has required heating to very high temperatures^{2,3} and time-consuming ball-milling to achieve the required reactivity^{4,5}. Therefore, the development of alternative synthesis pathways is eagerly awaited. A new bottom-up approach that makes pure α -TCP has the potential to improve the field of calcium phosphate bone cements. This research takes on the challenge, with attention to microstructural characteristics, to develop a nano-sized building block of resorbable bone cements – by heating amorphous calcium phosphate (ACP) precursor – that upon mixing with water transforms into calcium-deficient apatite.

EXPERIMENTAL METHODS

Amorphous calcium phosphate precursors (ACP) were synthesized from calcium nitrate tetrahydrate ($\text{Ca}(\text{NO}_3)_2 \cdot 4\text{H}_2\text{O}$), ammonium phosphate dibasic ($(\text{NH}_4)_2\text{HPO}_4$) and ammonium hydroxide solution (NH_4OH , 26% NH_3 basis). A 0.30 M calcium nitrate solution was formed by dissolving $\text{Ca}(\text{NO}_3)_2 \cdot 4\text{H}_2\text{O}$ in deionised water together with 30 ml ammonia solution and then combined with a 0.24 M ammonium phosphate solution. The resulting precipitate was immediately filtered and rinsed with water (then lyophilized), or treated with ethanol (then oven-dried). The powder was heated between 675 and 800 °C for 10 or 20 min in a cylindrical tube furnace. Particle size was measured in a scanning electron microscope and by Rietveld analysis. Phase composition and bonding in the crystallized powder was assessed by X-ray diffraction and Fourier-transform infrared spectroscopy. Biocompatibility of powders was investigated *in vitro* with a lactate dehydrogenase cytotoxicity assay on mesenchymal stem cells.

RESULTS AND DISCUSSION

All precipitated precursors showed the typical X-ray diffraction pattern for the amorphous phase⁶, a broad maximum at approximately 30°. The morphology of heated ACP powders is shown in Figure 1. The individual spherical particles (approximately 50 nm) have joined to form longer particles, and these connect to create a nano-sized pure α -TCP structure.

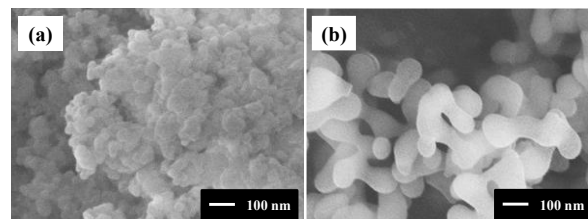


Figure 1. Morphology of (a) ACP and (b) processed at 775 °C.

Pure α -TCP, after hydrolysis to CDHA, demonstrated the highest biocompatibility (25% cytotoxicity) whereas the α -TCP with low amount of β -TCP (7–15%) showed an increased cytotoxicity (up to 40%).

CONCLUSION

Nano-sized pure α -TCP (50–100 nm) was obtained from an amorphous calcium phosphate precursor, treated with ethanol and heated above 700 °C. A lower purity α -TCP was obtained when ACP was rinsed in water and slowly cooled. Pure α -TCP showed the highest biocompatibility and this could be related to the 100% conversion to a calcium-deficient hydroxyapatite cement. A lower biocompatibility arose in the presence of β -TCP. Highlight: The first time a nano-sized pure α -TCP has been made and offers great promise for imparting greater functionality for use in regenerative medicine of hard tissues.

REFERENCES

1. Bohner M. Eur. Cell. Mater. 20:1-12, 2010
2. Bohner M. *et al.*, Acta Biomater. 5:3524-35, 2009
3. Cicek G. *et al.*, J. Mater. Sci. Mater. Med. 22:809-17, 2011
4. Espanol M. *et al.*, Acta Biomater. 5:2752-62, 2009
5. Lopez-Heredia M. A. *et al.*, J. Biomater. Mater. Res. Part B Appl. Biomater. 98:68-79, 2011
6. Sun L. *et al.*, J. Res. Natl. Inst. Stand. Technol. 115:243–55, 2010

ACKNOWLEDGMENTS

This work is partly supported by the European Social Fund within the project “Support for the implementation of doctoral studies at Riga Technical University” (No. 2009/0144/1DP/1.1.2.1.2/09/IPIA/VI AA/005), and the Taiwan-Latvian-Lithuanian Foundation for Scientific Co-operation within the project “Nanoscaled functional materials for biotechnological and optical applications” (No. IZM 11-13-130501/21).

Single Cell Tracking of Haematopoietic Stem Cells in 3D Biomimetic Gradients

Michael Ansorge¹, Jiranuwat Sapudom¹, Tilo Pompe¹

¹Institute of Biochemistry, Universität Leipzig, Germany
tilo.pompe@uni-leipzig.de

INTRODUCTION

The interaction of stem cells with their microenvironment determines cellular dynamics and cell fate decisions. This highly regulated entity is called 'stem cell niche'. The control mechanisms are based on cues of the extracellular matrix and neighbouring cells, such as biophysical factors, like matrix topology and stiffness, as well as biochemical factors, like matrix composition and growth factor presence.

We engineer defined biomimetic microenvironments for *in vitro* cell culture to dissect the specific signalling mechanisms in the stem cell niche. Reconstituted collagen matrices complemented with local gradients of signalling molecules are used to study cell fate in heterogeneous populations of primary haematopoietic stem and progenitor cells by label-free 3D single cell tracking.

EXPERIMENTAL METHODS

3D collagen I matrices were engineered with defined topological and mechanical properties as characterized using confocal laser scanning microscopy with a newly developed topology analysis and atomic force spectroscopy.¹

Gradients of signalling molecules (SDF-1, Dkk-1) were formed using biofunctionalized hydrogel microbeads to facilitate protein release over several days. Release characteristics were investigated with confocal laser scanning microscopy and fluorimetry in combination with fluorescence correlation spectroscopy to quantify local gradients around matrix-embedded microbeads.

Primary murine hematopoietic stem cells (CD150⁺ CD48⁻) were cultivated over several days inside the biomimetic scaffolds. Quantitative 3D single cell tracking was performed using brightfield microscopy and automated cell detection and tracking.

RESULTS AND DISCUSSION

The efficacy and accuracy of our new single cell tracking technology facilitate the *in vitro* long-term

study of label-free primary cells in 3D biomimetic matrices. By that we were able to quantify migration and proliferation characteristics of haematopoietic stem and progenitor cells within local gradients of SDF-1 and DKK-1, which mimic important regulating cues of the haematopoietic stem cell niche in the bone marrow. Change in directionality, positioning and dynamics of migratory behaviour could be correlated to the proliferative activity and local gradient fields of the signalling molecules. By comparing the heterogeneity of single cell behaviour and population-wide averages we could reveal the distinct impact of signalling molecule gradients on the behaviour of hematopoietic stem and progenitor cells.

CONCLUSION

Our label-free automated 3D single cell tracking tool allowed to analyse haematopoietic stem cell dynamics in biomimetic microenvironments of signalling gradients and to reveal regulating cues of the bone marrow niche. The combination of both technologies - biomimetic gradients and single cell tracking - provide an advantageous approach for in-depth *in vitro* studies of signalling mechanisms on a variety of biological and biomedical questions.

REFERENCES

1. Franke K. *et.al.*, Acta Biomaterialia. 2014 (in press)

ACKNOWLEDGMENTS

The authors want to acknowledge financial support by ESF, EFRE and Free State of Saxony (grant: SAB 100140482, SAB 100144684), Deutsche Forschungsgemeinschaft (grant: Graduate school BuildMoNa) and HFSP (grant RGP0051/2011).

We acknowledge further use of the imaging facility in the Magin lab, supported by DFG INST 268/230-1 to Thomas Magin.

Electrochemical dissolution of stainless steel endodontic files fractured in the middle and apical thirds of the root canal

Caroline Amaral¹, Fabiola Ormiga¹ and José Ponciano Gomes²

¹Department of Metallurgy and Materials and Department of Endodontics, Federal University of Rio de Janeiro, Brazil, caroline.chavadian@metalmat.ufrj.br

²Department of Metallurgy and Materials, Federal University of Rio de Janeiro, Brazil

INTRODUCTION

Under excessive stresses and tensions, the endodontic instruments may fracture in the middle or apical third of the root canal^{1,2}. Several methods have been described for removing fractured instruments from root canals^{3,4,5}, however these methods have some limitations, such as weakening and perforation of the root. In this context, a method to dissolve the fractured instruments was recently proposed⁶. The aim of this study was to investigate the process of active dissolution of stainless steel files in the middle and apical third of simulated root canals in solutions containing chloride and fluoride.

EXPERIMENTAL METHODS

Redox curves and anodic polarization curves were performed in [NaF 12g / L NaCl + 175.5 g / L] solution at pH 5.0 to evaluate the process of dissolution of the stainless steel alloy. The polarization of immersed files was performed to calculate the weight loss and length loss after the test. The tested files were observed using an optical microscope. The polarization of fragments a size 20 stainless steel K files was performed for 60 minutes in the middle and apical thirds of simulated root canals. Radiographic analysis of the simulated root canals was used to verify fragment dissolution. A size 10 file was used to verify the possibility to bypass the fragment before and after the tests.

RESULTS AND DISCUSSION

The stainless steel alloy suffered localized dissolution in [NaF 12g / L NaCl + 175.5 g / L] solution. The redox curve showed the stability of the solution to -0.2 V_{SCE}, but above this potential, the solution was unstable due to oxidation reactions. The progressive consumption of the files was observed in the total polarization time of 7 min (Figure 1). Ten fragments of size 20 files were partially dissolved in the middle and apical thirds of the simulated root canals (Figures 2 and 3). Radiographic analysis obtained before and after polarization tests showed loss of weight and thickness of the size 20 file (Figure 2 and 3 ab ab), allowing the bypassing of the fragment by a size 10 file (Figure 2 c and 3 c).

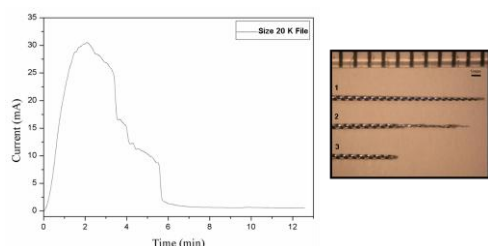


Figure1. Current values registered during the polarization of immersed a size 20 stainless steel K files

and optical microscope analysis (1) file as received, (2) file submitted to polarization for 3.5 minutes and 7 minutes.

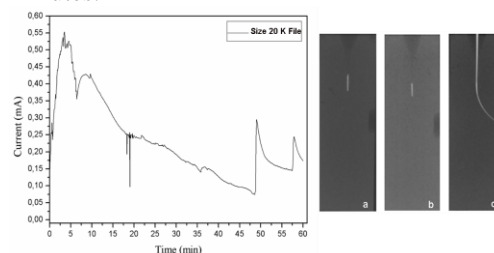


Figure2. Current values registered during the polarization of a size 20 K- file fragment in the middle third of simulated root canal and radiographic analysis (a) before polarization (b) after polarization and (c) fragment bypassed by a size 10 K file.

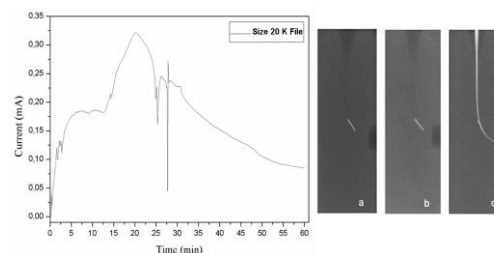


Figure3. Current values registered during the polarization of a size 20 K- file fragment in the apical third of simulated root canal and radiographic analysis (a) before polarization (b) after polarization and (c) fragment bypassed by a size 10 K file.

CONCLUSION

The method tested in the present study allowed a partial dissolution of fragments of stainless steel K- files in the middle and apical thirds of simulated root canals in a period clinically acceptable.

REFERENCES

1. Shneider S. *et al.*, O Surg. 32:271-275, 1971
2. Pruett J. *et al.*, J Endod. 23:77-85, 1997
3. Masserann J. J Br Endod Soc. 5:55-59, 1971
4. Feldman G. *et al.*, J Am Dent Assoc. 88:588-591, 1974
5. Ruddle CJ. *et al.*, Dent Clin North Am. 41:429-454, 1997
6. Ormiga F. *et al.*, J Endod. 36:717-720, 2010

ACKNOWLEDGMENTS

The authors would like to acknowledge the support of COPPE-TEC Foundation and CNPq.

Photochemical nitric oxide release from a Flutamin derivative incorporated in Pluronic F127 hydrogel

Patricia Taladriz-Blanco and Marcelo G. de Oliveira

Institute of Chemistry, University of Campinas, UNICAMP, SP, Brazil, patricia.taladriz@iqm.unicamp.br

Keywords: Hydrogels, responsive biomaterials, drug delivery

INTRODUCTION

Nitroaniline derivatives are known to release nitric oxide (NO) when irradiated with visible light.¹ This property offers the perspective of using these compounds for obtaining a controlled release of NO in medical applications. Pluronic F127, a triblock PEO-PPO-PEO copolymer with thermo-responsive behaviour, undergoes reversible micellization and gelation with heating. In the gel state, the hydrophobic nuclei of the micelles act as concentrating microenvironments for drugs with low solubility in water, including free NO. In this work, we have incorporated a Flutamin derivative, N-(3-aminopropyl-3-(trifluoromethyl)-4-nitrobenzenamine (ATN), in Pluronic F127 matrices. The resulting hydrogels were shown to be thermally stable and to release gaseous NO upon irradiation with visible light. These properties may allow the use of these hydrogels for delivering NO locally in topical applications.

EXPERIMENTAL METHODS

ATN was synthesized on the bases of procedures already described elsewhere.¹ Aqueous solutions of Pluronic F127 30wt% and 10wt% were prepared by the cold method.² ATN was dissolved in the F127 solutions to a final concentration of 0.19 mM. Solutions were kept in the dark until use. F127/ATN samples were irradiated at 15 °C and 37 °C using a 150 W Xenon Arc lamp through a 400 nm cut-off optical filter. The photochemical NO release from the F127/ATN solutions, below and above CMT, was characterized by chemiluminescence using an NO Analyser (NOA 280i, Sievers, Boulder, CO, USA).

RESULTS AND DISCUSSION

Fig. 1 shows the total amount of NO photochemically released from the F127/ATN formulations. It can be seen that at 10wt% and 5 °C, where F127 is below its critical micelle temperature (CMT), the total NO released in 10 min is 0.15 mmol (Fig 1, bar A) while at 37 °C, where F127 is above CMT, the amount of NO released in the same time is ca. 4-fold higher (Fig. 1, bar B). An enhanced NO release was also obtained at 30wt% at 15 °C, where F127 is above the critical micelle concentration (CMC). These results show that the enhanced NO release is associated with the presence of micelles. As the photochemical NO release from ATN implies the formation of a phenoxyl radical after NO ejection, this result can be assigned to the facilitated hydrogen abstraction from the methylene groups of the PPO blocks in the micelle nuclei, which blocks radical pair recombination, increasing the yield of the

photochemical NO release. This effect is absent below CMT or CMC. In addition, we have seen that above the gelation temperature, the amount of NO released is decreased (Fig. 1, bar D vs. bar B). This result suggests that viscosity constraints imposed on the diffusion of the phenoxyl radical in the gel state, favours radical pair recombination, decreasing the yield of photochemical NO release. Together, these two effects can be used as a tool to modulate the photochemical release of NO from these formulations in different applications. Although the inclusion of Flutamin in vesicles or β -CD, was already shown to increase the photodegradation of Flutamin relative to water³, the results presented in this work underscore a new effect of the F127 matrices, where the hydrophobic nuclei of micelles act as nanoreactors, increasing the yield of NO released in homolytic bond cleavages such as the photocleavage of the nitro group of ATN.

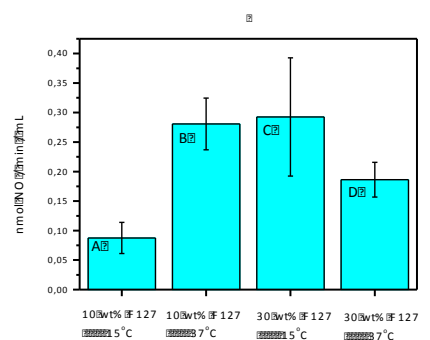


Figure 1. Bar graph showing the total amount of NO released from F127/ATN per min of irradiation with visible light.

CONCLUSION

F127/ATN comprise thermally stable formulations. F-127 micellization and gelation can be used as a tool for controlling the photochemical delivery of NO from the photodecomposition of ATN through the irradiation with visible light. The potential applications of such formulations may include the topical applications for increasing dermal vasodilation in ischemic tissues or for obtaining microbicidal actions on infected lesions.

REFERENCES

- Sortino, S. *Photochem Photobiol Sci.* 2008, 7, 911.
- Shishido SM et. al. *Biomaterials.* 2003, 24, 20, 3543.
- Sortino, S.; Marconi, G.; Condorelli, G. *Chem. Commun* 2001, 1226.

ACKNOWLEDGMENTS

The authors would like to thank FAPESP (Grant no: 2013/07173-8) and CNPq (Grant no: 309390/2011-7) for financial support.



Electrospun Human Hair Keratin Matrices Affect Human Fibroblast Behavior Through Topographical Cues

Wan Ting Sow¹ and Kee Woei Ng^{1*}

¹School of Materials Science and Engineering, Nanyang Technological University, Singapore,

*Email: kwng@ntu.edu.sg

INTRODUCTION

Natural polymers such as proteins and polysaccharides are potential materials as templates for tissue regeneration due to their natural bio-inductive abilities to improve cell-material interactions. However, most of these materials still present some shortcomings due to their animal origins¹.

From this perspective, hair keratin emerges as an attractive protein of human origin to be used as templates for tissue regeneration because it can be easily extracted from the unlimited supply of human hair².

In this work, we extracted keratin from human hair, fabricated it into fibrous matrices via a scalable technique, electrospinning and evaluated their potential as fibrous templates for supporting cell growth³. We prepared two types of keratin matrices, with random and aligned fibres, to study the effect of topography on cellular response.

EXPERIMENTAL METHODS

Keratin was extracted from human hair using 0.125M Na₂S solution. Subsequently, solutions of keratin were electrospun with 0.5 wt% of poly(ethylene) oxide added to improve processability³. Random and aligned fibres were generated via a flat collector platform and rotating drum, respectively. The resulting fibrous matrices were characterised using Scanning Electron Microscopy (SEM) to view their morphology and Fourier Transformed Infrared Spectroscopy (FTIR) to evaluate their chemical properties. Investigation of cell behaviour on keratin fibrous matrices was conducted using primary human dermal fibroblasts (HDFs). Cell viability was analyzed through evaluating cell metabolic activity using the AlamarBlue assay while cell proliferation was quantified using the Picogreen assay. These cell quantification results were evaluated statistically using the Student's t-test and the sample size was n=3. Live/Dead staining was also done to view the morphology and distribution of HDFs on keratin fibrous matrices.

RESULTS AND DISCUSSION

Our results showed that keratin fibrous matrices with beadless morphology were electrospun with a mean fiber diameter of $0.70 \pm 0.09 \mu\text{m}$ for random fibres and $0.74 \pm 0.10 \mu\text{m}$ for aligned fibres (Fig 1).

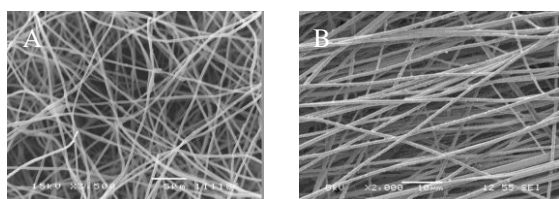


Fig. 1: SEM images of keratin fibrous matrices with A) random and B) aligned morphology.

FTIR analysis indicated that the chemical properties of fibrous matrices resembled those of extracted keratin, revealing that electrospinning did not significantly affect protein quality.

Results from cell studies showed that proliferation and metabolic activity of HDFs on keratin matrices were comparable to the positive control and significantly higher on aligned keratin fibres compared to random keratin fibres on day 3 after cell seeding (Fig 2). Besides, our live/dead staining revealed that HDFs cultured on the keratin matrices could form cellular networks according to the architecture of the matrices, implying that the cells were able to respond to the topographical cues rendered by keratin matrices (Fig 3).

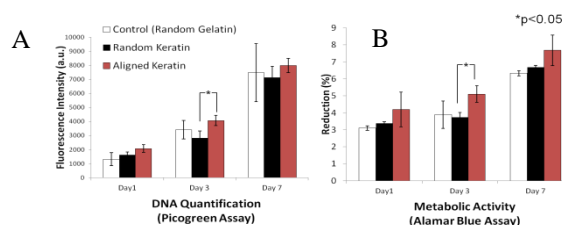


Fig. 2: Cell viability of HDF. A) Picogreen and B) Alamar Blue assays showed that proliferation and metabolic activity of HDFs on keratin matrices were comparable to the positive control (Gelatin).

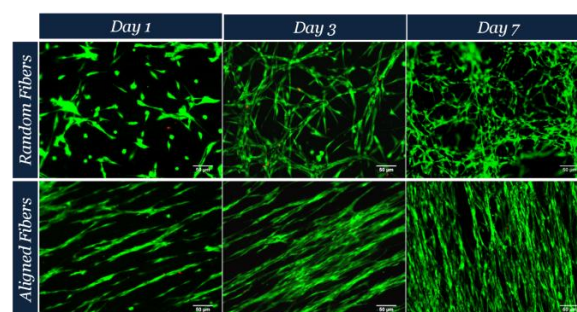


Fig. 3: Fluorescence microscopy images of HDF cultured on keratin matrices over 7 days showing that HDFs exhibited typical spindle morphology and could form cellular networks according to the architecture of the keratin matrices.

CONCLUSION

In this work, we showed that keratin fibrous matrices provide a conducive environment to facilitate the growth of primary HDFs and influence the cell network formation via topographical cues.

REFERENCES

1. Holmes TC. *et al.*, Trends Biotechnol. 20(1): 16-21, 2002
2. Rouse JG. *et al.*, Materials 3(2): 999-1014, 2010
3. Sow WT. *et al.*, Nanomedicine (London) 8(4): 531-541, 2013

ACKNOWLEDGMENTS

The authors would like to acknowledge the funding support from the Ministry of Education, Tier 1 grant RG42/13 and the Nanyang President's Graduate Scholarship programme.

Release Kinetics of Gentamicin, Moxifloxacin, Vancomycin, and Colistin from Gelatin Micro- and Nanospheres

J. Song¹, J. Odekerken², D. Löwik³, T. Welting², F. Yang¹, J. Jansen¹, and S. Leeuwenburgh^{1*}

^{1*}Department of Biomaterials, Radboud University Medical Centre, The Netherlands, jian kang.song@radboudumc.nl

²Laboratory for Experimental Orthopaedics, Department of Orthopaedic Surgery, CAPHRI School for Public Health and Primary Care, Maastricht University Medical Centre, The Netherlands

³Department of Bio-Organic Chemistry, Radboud University Nijmegen, The Netherlands

INTRODUCTION

A powerful strategy to reduce the complications and side-effects related to the systematic use of antibiotics involves local and sustained delivery of antibiotics at the site of infection. Gelatin micro- and nanospheres have been extensively used for controlled delivery of therapeutic proteins such as growth factors (GFs). These GFs were shown to bind to oppositely charged gelatin matrices through the formation of polyion complexes¹, thereby facilitating sustained delivery of large therapeutic biomolecules. The release kinetics of small biomolecules such as antibiotics from gelatin carriers has, however, not been studied before. We hypothesised that controlled and sustained release of charged antibiotics from oppositely charged gelatin carriers can also be achieved. Therefore, we have studied the release kinetics of various antibiotics of different molecular weight and charge from gelatin micro- and nanospheres, aiming at the development of an injectable delivery system for local and sustained delivery of antibiotics.

EXPERIMENTAL METHODS

Anionic gelatin B micro- and nanospheres of low and high cross-linking densities were prepared using water-in-oil emulsification and two-step desolvation methods², respectively. The morphology of the spheres was characterized by scanning electron microscopy, while their size, size distribution and ζ -potential were determined using dynamic light scattering. Four types of antibiotics of different molecular weight and charge were used in this study (Table 1). 25 μ g of each antibiotic was loaded onto gelatin spheres through diffusional post-loading. The release study was conducted at 37 °C in 1 ml PBS with or without 400 ng/ml collagenase. Release kinetics of moxifloxacin and vancomycin were monitored by high performance liquid chromatography, whereas release kinetics of colistin and gentamicin were determined by liquid chromatography-mass spectrometry and enzyme-linked immunosorbent assay, respectively. Moreover, in order to correlate the release rate of the antibiotics to the degradation rate of gelatin, the bicinchoninic acid assay was used to monitor the degradation rate of gelatin.

Table 1 Molecular mass and charge of gentamicin, moxifloxacin, vancomycin and colistin.

Name	Molecular mass (g/mol)	Charge
Gentamicin	477.6	+
Moxifloxacin	401.4	neutral
Vancomycin	1449.3	neutral
Colistin	1155.4	+

RESULTS AND DISCUSSION

Release kinetics of the antibiotics from gelatin micro- and nanospheres had similar trends. Vancomycin and colistin proceeded without any significant burst. The release of colistin was dependent on the degradation of gelatin, while the release rate of vancomycin did not correlate to the degradation rate of gelatin. Gentamicin and moxifloxacin, however, were released almost completely within 2 days, although charged gentamicin was released slightly slower than neutral moxifloxacin.

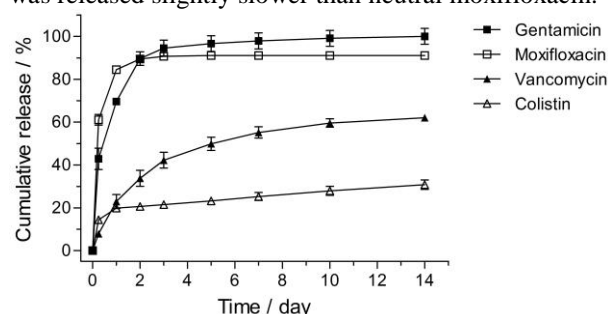


Fig. 1 Representative cumulative release of four antibiotics from gelatin B nanospheres with high cross-linking density under enzymatic conditions.

These results seem to indicate that the release of antibiotics from gelatin matrices is influenced most strongly by the molecular weight rather than the charge of antibiotics. Antibiotics of higher molecular mass (colistin and vancomycin) were released in a sustained manner. More specifically, the release rate of charged colistin was controlled by the degradation rate of gelatin, whereas the release kinetics of neutral vancomycin did not correlate with the degradation rate of gelatin, this is most likely due to a lack of electrostatic interactions between vancomycin and gelatin. Antibiotics of lower molecular mass (gentamicin and moxifloxacin) were both released in a burst manner irrespective of the charge of the antibiotics, but the release rate was higher for uncharged moxifloxacin vs. charged gentamicin during the first 2 days, which could be related to the electrostatic interaction between cationic gentamicin and anionic gelatin macromers.

CONCLUSION

Release kinetics of antibiotics from gelatin micro- and nanospheres are strongly dependent on the physicochemical characteristics of the antibiotics. Sustained release was observed for antibiotics of high molecular weight, while antibiotics of low molecular weight were released in a burst manner.

REFERENCES

1. Young S. *et al.*, J. Control. Release 109:256-274, 2005
2. Wang H. *et al.*, Biomaterials 33:8695-8703, 2012



Atmospheric Plasma Surface Modification of Electrospun Poly(L-Lactic Acid): Effect on Mat Properties and Cell Culturing

Laura Calzà¹, Vittorio Colombo^{2,3}, Luisa Stella Dolci¹, Andrea Fiorani⁴, Maria Letizia Focarete^{1,4}, Matteo Gherardi², Romolo Laurita², [Anna Liguori](mailto:anna.liguori@unibo.it)^{2*}, Santiago David Quiroga⁴, Paolo Sanibondi²

¹Health Sciences and Technologies - Interdepartmental Center for Industrial Research

^{2*}Department of Industrial Engineering, Alma Mater Studiorum – Università di Bologna, Italy

anna.liguori@unibo.it

³Advanced Mechanics and Materials - Interdepartmental Center for Industrial Research (AMM-ICIR)

⁴Department of Chemistry “G. Ciamician” University of Bologna, Italy

INTRODUCTION

Various studies in the field of tissue engineering prove plasma ability to modify polymeric scaffold surface without altering bulk properties [1-2]. Furthermore, it was demonstrated that cell cultures on plasma modified scaffolds display better proliferation and viability compared to pristine materials [3]. In this work we focus on the use of atmospheric pressure non-thermal plasma for surface modification of electrospun poly(L-lactic acid) (PLLA) non-woven mats [4].

EXPERIMENTAL METHODS

Electrospun mats (30-60 µm thick) have been fabricated by means of an electrospinning apparatus, made in house, composed by a high voltage power supply, a syringe pump, a glass syringe, a stainless-steel blunt-ended needle connected with the power supply electrode, and a rotating cylindrical collector. Modification of scaffold surface characteristics has been carried out exposing the substrate to the plasma region generated by three different non-thermal plasma sources operated at atmospheric pressure: a floating electrode dielectric barrier discharge (FE-DBD), a linear corona discharge (LC) using N₂ as working gas and a DBD roller (DBDR). A high voltage generator capable of producing pulses with a slew rate in the order of some kV/ns has been used. Effects of plasma-treatment on PLLA scaffolds have been evaluated through morphological evaluation, thermo-mechanical analysis and scaffold hydrophilicity measurement. In order to estimate the relative amount of carboxyl functional groups (-COOH) created during plasma treatment, a functionalization with fluorescein isothiocyanate (FITC) have been performed. Mouse embryonic fibroblast cells were cultured on untreated PLLA and treated PLLA surface to investigate the cell morphology.

RESULTS AND DISCUSSION

Morphological characterization attested a damage of the scaffold when treated with the FE-DBD, due to local heating of the substrate, while scaffolds treated with other plasma sources did not show any appreciable morphological alteration. Fluorescence intensity has been measured on both pristine and LC and DBDR treated scaffolds. The fluorescence signal measured for treated sample was 2 to 5 times higher than the value of

the pristine samples; the highest -COOH concentration was registered for the LC treated scaffolds. Moreover, no relevant variation of fluorescence intensity was observed after 48h from the plasma treatment and an hydrophilicity increase was preserved after 72h. Fibroblasts growth and shape-factor have been investigated both on treated and untreated electrospun PLLA scaffolds; while fibroblasts on PLLA resulted small and star-like, those grown on PLLA treated with LC assumed a very elongated shape.

Notably, plasma treatment further exacerbated elongated shape of fibroblast, thus confirming that a surface chemical modification could deeply affect cell biology. In fact, fibroblast shape is a complex phenomenon strictly regulated by transmembrane proteins (like integrins) linking binding domains of the extracellular matrix to the cell cytoskeleton [5], which is highly influenced by cell adhesion and mechanic forces [6]. The increase in carboxyl groups derived from plasma treatment, could be part in re-shaping of fibroblast.

CONCLUSION

Functionalization and biocompatibilization of PLLA electrospun scaffold can be achieved using low temperature atmospheric plasmas. A relevant increase of hydrophilicity and -COOH group concentration at the fiber surface is registered after LC and DBDR plasma treatment without alteration of bulk properties. Furthermore, cell proliferation is promoted on LC modified substrates. compared to pristine scaffolds.

REFERENCES

1. J.M. Goddard *et al.*, Prog. Polym. Sci. 2007, 32, 698.
2. G. Delaitre *et al.*, Soft Matter, 2012, 8, 7323.
3. P. K. Chu *et al.*, Mater. Sci. Eng. R Rep. 2002, 36, 143.
4. L.S. Dolci *et al.*, Plasma Process. Polym. 2014, 11, 203.
5. E. Zamir, B. Geiger, J Cell Sci. 2001, 20, 3583
6. B. Greig *et al.*, Net. Rev. Mol Cell Biol. 2009, 10, 21.

ACKNOWLEDGMENTS

This work has been supported by FP7 COST Action MP1101 “BioPlasma”.



Development and characterization of a tridimensional intestinal model to study protein drugs absorption

Carla Pereira^{1,2*}, Francisca Araújo^{1,3}, Pedro L. Granja¹, Bruno Sarmento^{1,4*}

¹INEB - Instituto de Engenharia Biomédica, University of Porto, Portugal

²FEUP – Faculdade de Engenharia, University of Porto, Portugal

³ICBAS – Instituto Ciências Biomédicas Abel Salazar, University of Porto, Portugal

⁴IINFACS – Instituto de Investigação e Formação Avançada em Ciências e Tecnologias da Saúde, Instituto Superior de Ciências da Saúde-Norte, Department of Pharmaceutical Sciences, CESPU, Gandra, Portugal

* clrc.pereira@ineb.up.pt; bruno.sarmiento@ineb.up.pt

INTRODUCTION

Changes in preclinical drug development are attributing significant importance to *in vitro* and *ex vivo* approaches, as result of financial and ethical considerations [1]. Although Caco-2 cell model represents the gold standard of intestinal drug permeability studies [2], this model do not cover the complexity of interactions between epithelial cells and the overlying lamina propria cells [3]. To reproduce these interactions, a physiologically improved tridimensional cell model seeded on the Transwell® filter was developed. This model comprises intestinal fibroblasts (CCD18-Co) embedded in Matrigel®, Caco-2 (enterocytes-like cells) and HT29-MTX cells (mucus-producing cells) on the apical side of the Transwell®. Raji B cells seeded on the basolateral side, protagonizing the conversion of Caco-2 in M-like cells.

EXPERIMENTAL METHODS

Tridimensional cell culture and TEER measurement

CDD18-Co cells were resuspended on Matrigel®. After gelation at 37°C, Caco-2 and HT29-MTX cell suspension (9:1) was added onto the overlying gel layer. After 14 days, Raji B cells were added on the basolateral side, maintained for 4-6 days. Transepithelial electrical resistance (TEER) was monitored every other day.

Histological sectioning

Samples were fixed with 4% paraformaldehyde and post-fixed with 1% glutaraldehyde. After a graded dehydration in ethanol, membranes were embedded in paraffin. Sections were performed between 5-10µm and stained with haematoxylin and eosin dyes.

Immunofluorescence staining

To identify the different cell in culture, membranes were fixed with 2% paraformaldehyde and permeabilized with 0.2% Triton X-100. Non-specific binding was blocked with PBST containing 10% of FBS. Samples were incubated with mouse anti-human vimentin (1:100, Santa Cruz Biotechnology) and with the secondary antibody goat anti-human AlexaFluor488 (1:1000, Life Technologies) and counterstained with DAPI (1µg/mL).

Permeability transport experiment

After 21 days in culture, permeability studies were carried out during 4h at 37°C with 100µg/mL insulin further quantified by HPLC.

RESULTS AND DISCUSSION

After 21 days, intestinal cells are disposed in a distinct layer supported by lamina propria mainly produced by fibroblasts. Moreover, permeability studies revealed the

efficient transport of insulin, resulting from reversible tight junctions opening.

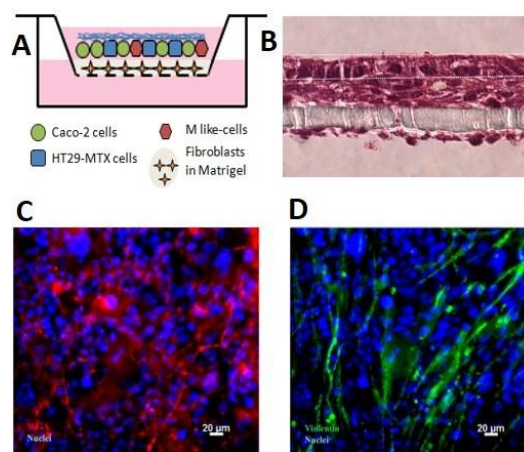


Figure 1A) Schematic diagram of a 3D coculture of intestinal epithelial cells with fibroblasts incorporated in Matrigel®. **B)** Histological staining showed epithelial cells on the top of fibroblasts embedded in Matrigel®. **C)** Identification of Caco-2 cells and intestinal fibroblasts in coculture labelled by WheatGermAgglutinin (WGA) (C1) and vimentin (C2).

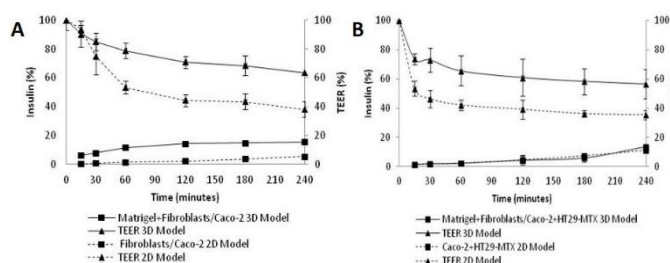


Figure 2A) Cumulative transport of insulin and TEER measurements of insulin across cocultures of Fibroblasts and Caco-2 cells and **B)** cocultures of Fibroblasts, Caco-2 and HT29-MTX cells.

CONCLUSION

Results support the functional character of the 3D model that closely resembles the structure of the native intestinal mucosa.

REFERENCES

1. Antunes F. *et al.*, Curr Drug Metab. 14:4-20, 2013
2. Araújo F. *et al.*, Int J Pharm. *in press*, 2014
3. Li N. *et al.*, Tissue Eng Pt C: Methods, 2013

ACKNOWLEDGMENTS

This work was financed by European Regional Development Fund through the Programa Operacional Factores de Competitividade – COMPETE, by Portuguese funds through FCT – Fundação para a Ciência e a Tecnologia (Project PEST-C/SAU/LA0002/2013, and co-financed by North Portugal Regional Operational Programme (ON.2) in the framework of project SAESCTN-PIIC&DT/2013, under the National Strategic Reference Framework (NSRF)

Antifouling coatings of poly(ethylene glycol) on titanium for dental implants

Judit Buxadera-Palomero^{1, 2, 3}, Sergi Torrent¹, Cristina Calvo¹, F. Javier Gil^{1, 2, 3}, Cristina Canal^{1, 2, 3}, Daniel Rodríguez^{1, 2, 3}

¹Biomaterials, Biomechanics and Tissue Engineering group, Escola Universitària d'Enginyeria Tècnica Industrial de Barcelona. Technical University of Catalonia (UPC)-Barcelona TECH

²Biomedical Research Networking Centre in Bioengineering, Biomaterials and Nanomedicine (CIBER-BBN), Spain

³Center for Research in nanoEngineering (CRnE), UPC, Spain

judit.buxadera@upc.edu

INTRODUCTION

Infection around dental implants is a relevant health issue since it is not detected until the bone loss induces an implant failure. To avoid this infection it is important to achieve a biological sealing of the implant before bacteria colonize the exposed implant surface¹. In this work, functionalized coatings with RGD peptide² were applied to titanium with either plasma polymerization or silanization³, and compared in terms of its antifouling effect and bacterial and cellular adhesion.

EXPERIMENTAL METHODS

Samples of polished titanium (Ti) grade 2, cleaned with ethanol, acetone and water were activated with argon plasma (0.40mbar, 100W, 5min). Later, they were treated with either: a) low pressure plasma poly(ethylene glycol) polymerization (PEG) from tetraglyme (0.40mbar, 100W, 60min with pulsed mode 20 μ s_{on}, 20ms_{off}), or b) grafting-to titanium of silanized-PEG by dip-coating of PEG-OSiCl₃ (adaptation of the Zhang et al. method³). RGD functionalization was performed by overnight immersion. Coatings were characterized by sessile drop contact angle, FTIR and XPS. Protein adsorption was tested with fluorophore-labelled BSA. Bacterial adhesion assays were done by immersion of the samples in culture medium with bacteria (*Lactobacillus salivarius* (LS) and *Streptococcus sanguinis* (SS)) for 2h followed by seeding and CFU counting. Cell adhesion LDH assays were done with human fibroblasts. For the characterization polished titanium samples were kept as controls.

RESULTS AND DISCUSSION

A more significant decrease was seen in BSA adsorption for the plasma polymerized coatings in contrast to silanized coatings.

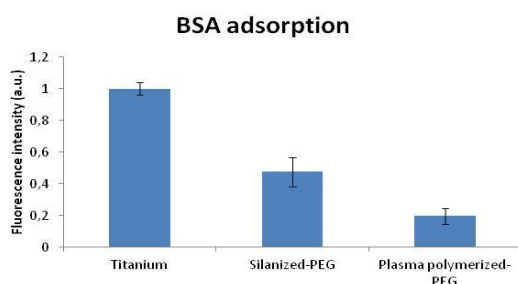


Figure 1. Albumin adsorption measured by fluorescence microscopy.

The coatings also present a significant decrease on bacterial adhesion compared to the titanium surfaces. The antifouling character of PEG that is seen in these results can be explained by the inertness of the polymer

backbone and also to its solvated configuration, which has steric repulsion to proteins⁴. The absence of proteins explains the decrease in bacterial adhesion.

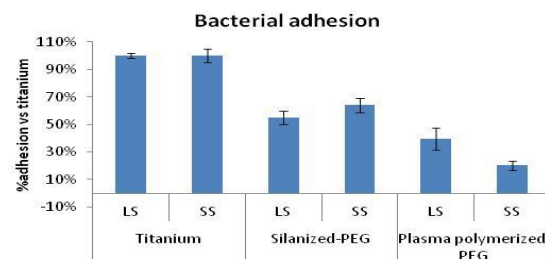


Figure 2. Bacterial adhesion to coated samples compared to the titanium control.

Fibroblast adhesion to the coatings is somewhat reduced, but it improves in the functionalized coatings.

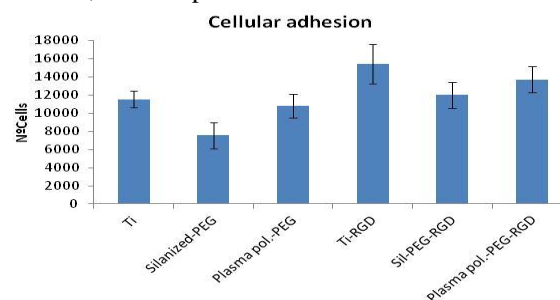


Figure 3. Cellular adhesion on the non-functionalized and RGD functionalized coatings.

CONCLUSION

PEG-coated titanium shows an antifouling character and a decreased bacterial adhesion. Cellular adhesion is lower in the coated samples, but it is improved by immobilization of RGD. While both silanized and plasma polymerized PEG show these characteristics, whereas plasma polymerized coatings result into a better antifouling performance and a lower decrease in the cellular adhesion.

REFERENCES

1. Bell BF. *et al.*, Clin Oral Impl Res, 22:865-872, 2011
2. Salwiczek M. *et al.*, Trends in Biotechnology, 32:82-90, 2014
3. Zhang M. *et al.*, Biomaterials, 19:953-960, 1998
4. Sharma S. *et al.*, Biosensors and bioelectronics, 15:227-239, 2004

ACKNOWLEDGMENTS

Authors acknowledge financial support of UPC and Fundación Ramon Areces through the fellowship of JB-P, of COST Action, and the project MAT2012-30706

Hierarchical Structure of Multicomponent Polysaccharide-Based ECM Mimetics

Ortal Levi¹, Guy Hochbaum¹ and Ronit Bitton^{1,2*}

¹ Department of Chemical Engineering, Ben-Gurion University of the Negev, Israel, rbitton@exchange.bgu.ac.il

^{2*} Ilse Katz Institute for Nanoscale Science & Technology, Ben-Gurion University of the Negev, Israel

INTRODUCTION

The challenge in the development of surrogate extracellular matrices (ECMs) is to design and prepare synthetic materials capable of influencing cell differentiation, proliferation, survival, and migration through both biochemical interactions and mechanical cues. Current efforts in the engineering of synthetic ECMs have focused on "installing" molecular features (peptides, proteins and bio-interactive polymers) within insoluble scaffolds, either by self-assembly or through covalent modifications of polymer or biopolymer networks¹⁻⁵.

Recent studies of engineered synthetic ECMs revealed that molecular features incorporated within insoluble scaffolds play a dual role in cell interaction. The functional moieties act directly on cells while also modifying the hierarchical structural organization and mechanical properties of the resulting material, thus affecting the cellular response indirectly⁶⁻⁸. While the former has been investigated extensively, studies of these structural effects induced by introducing bioactive molecular features are less conclusive. Elucidating the key factors involved in the structure-property relationships of these hydrogels will improve our ability to design and prepare tailor-made scaffolds for a variety of applications.

Here, we present a systematic exploration of the effect of bioactive molecules on the self-assembly of polysaccharide hydrogels and the resulting structures.

EXPERIMENTAL METHODS

Bioactive polysaccharide (hyaluronic acid, chitosan and alginate) hydrogels were prepared by covalently binding a peptide containing the cell adhesion ligand RGD to the polymer chain followed by addition of a gelling agent. In order to study the effect of peptide conjugation on their structural and mechanical properties, the synthesis was conducted with 1:1000 and 1:100 w/w peptide/polymer ratio.

Thorough characterization of the polysaccharides building blocks (both natural and modified) in aqueous solutions and as hydrogels were conducted using small angle X-ray scattering (SAXS), optical tensiometer, zeta potential, and rheology.

RESULTS AND DISCUSSION

The peptide G4RGDS was covalently attached (via EDC chemistry) to the polymer backbone of Hyaluronic acid, alginate and chitosan.

SAXS patterns obtain for all polymer (both natural and modifies in aqueous solution) show conjugation of RDG to HA, alginate and chitosan lead to small yet distinct changes in the scattering pattern i.e. structural differences at nano-scale. Fitting of these scattering curves to a model of a semi-flexible chain form factor combined with a structure factor based on PRISM where the intermolecular interaction is described by a gaussian function⁹ suggest peptide conjugation affects both the polymer chain conformation and the interaction between the chains, regardless of the polysaccharide used. Mechanical testing show peptide conjugation causes differences in the gel's moduli as well.

CONCLUSION

Conjugation of RDG to HA, alginate and chitosan lead to small yet distinct changes in both surface and bulk properties of their aqueous solutions. Preliminary mechanical testing suggests the conformational changes in the solutions are translated to changes in the polymer's young modulus.

REFERENCES

1. Collier, J. H.; Rudra, J. S.; Gasiorowski, J. Z.; Jung, J. P. *Chemical Society Reviews*, 39, 3413.
2. Jia, X. Q.; Kiick, K. L. *Macromolecular Bioscience* 2009, 9, 140.
3. Kopecek, J. *Biomaterials* 2007, 28, 5185.
4. Kopecek, J. *Journal of Polymer Science Part a-Polymer Chemistry* 2009, 47, 5929.
5. Place, E. S.; George, J. H.; Williams, C. K.; Stevens, M. M. *Chemical Society Reviews* 2009, 38, 113.
6. Berrier, A. L.; Yamada, K. M. *Journal of Cellular Physiology* 2007, 213, 565.
7. Cukierman, E.; Pankov, R.; Stevens, D. R.; Yamada, K. M. *Science* 2001, 294, 1708.
8. Gieni, R. S.; Hendzel, M. J. *Journal of Cellular Biochemistry* 2008, 104, 1964.
9. Josef, E.; Bianco-Peled, H. *Soft Matter* 2012, 8, 9156.

ACKNOWLEDGMENTS

The authors would like to thank the EC 7th Framework Programme (FP7 MC CIG) under grant agreement no PCIG10-GA-2011-303703) for providing financial support to this project.



Scavenging effect of Trolox released from brushite cements

Gemma Mestres¹, Carlos F Santos¹, Lars Engman², Cecilia Persson¹, Marjam Karlsson Ott¹

¹ Dpt. Engineering Sciences, Uppsala University, Sweden

² Department of Chemistry, BMC, Uppsala University, Sweden

gemma.mestres@angstrom.uu.se

INTRODUCTION

Implantation of a biomaterial in a living tissue causes post-surgical inflammation and may trigger reactions such as the release of pro-inflammatory cytokines, reactive oxygen species (ROS) and destructive enzymes. Antioxidants such as Trolox can be loaded into a biomaterial to cope with inflammation and protect the surrounding tissue during implantation. In this work, Trolox was loaded in calcium phosphate cements, which are commonly used as bone void fillers. The in vivo response to brushite cements has been found to depend on their composition¹. Limiting the initial inflammatory response may be beneficial for some cement formulations, especially when used in conjunction with other implant materials, such as metallic screws.

EXPERIMENTAL METHODS

Brushite cement powder was prepared by mixing 54 wt% β -tricalcium phosphate, 44 wt% monocalcium phosphate and 2 wt% sodium pyrophosphate. Trolox-loaded cement was prepared by adding 0.4 wt% of Trolox to cement powder. The cement paste was prepared by mixing the powder with distilled water at a liquid-to-powder ratio of 0.32 ml/g.

Setting time (Gillmore needles), mechanical properties (universal testing machine) crystalline phases (X-ray diffraction) and morphology (scanning electron microscopy, SEM) of the cements were evaluated. Trolox release was evaluated by immersing 1 cement disc ($\varnothing = 12$ mm, $h = 2$ mm) in 50 ml of phosphate buffered solution (PBS) for 5 days. At regular intervals, 1 ml-aliquots were removed and replaced by 1 ml of PBS. Aliquots were monitored by means of a UV-spectrophotometer. As controls, Trolox (0.08 mg/ml) and cement alone were included. Data were corrected for dilution caused by sampling and Trolox degradation, and finally modelled through Korsmeyer-Peppas equation².

The capacity of Trolox released by the cement to scavenge ROS produced by activated macrophages (Raw 264.7) was evaluated by a luminol amplified chemiluminescence assay³. Aliquots from the drug release study, including Trolox and cement alone, were added to a well plate in contact with a luminol solution. Luminescence was monitored for 60 min at 37°C.

RESULTS AND DISCUSSION

The initial and final setting times of the brushite cement were around 8.5 and 11 min, respectively. After 7 days in 100% humidity, set cements were mainly composed of brushite, constituted by rhomboedric crystals precipitated in random directions. The compressive strength was approximately 25 MPa. Trolox did not

significantly modify any of the previously described physical properties.

The drug release study showed a burst release from brushite cement for the first day, followed by a sustained release between 1 and 3 days after which the concentration of Trolox remained constant until day 5. Nearly 64% of Trolox was released from the cement, the release pattern fitting with a non-Fickian transport. While the extracts from the cement alone did not scavenge ROS, aliquots from Trolox-loaded cement were able to do so, in a similar manner as aliquots containing “pure” (non loaded) Trolox (Figure 1). Moreover, as time passed and more Trolox was released the scavenging effect became more pronounced.

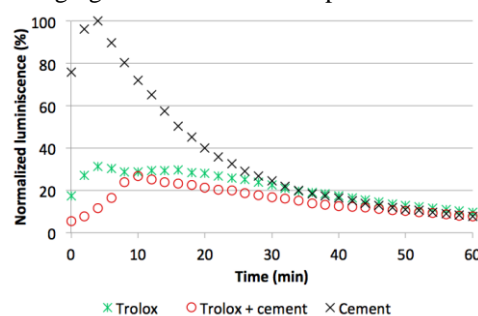


Figure 1. Luminescence measured over time for aliquots of Trolox (0.08 mg/ml), cement alone, and Trolox-loaded cement (22h-time point).

CONCLUSION

With the aim to create a calcium phosphate cement able to limit the acute inflammatory response, Trolox was added into a brushite cement. The presence of Trolox did not modify properties such as setting time, compressive strength or morphology of the cements. Trolox was released for 3 days through a non-Fickian transport. Trolox released from cement was able to scavenge reactive oxygen species produced by macrophages in a dose-dependent manner. The doped calcium phosphate cement is expected to partially protect the surrounding tissues from acute inflammation.

REFERENCES

1. Tamimi F, et al. Biomaterials 2009;30: 208-216.
2. Ritger PL, et al. J Control Release 1987;5:23-6.
3. Dahlgren C, et al. J Immunol Meth 1999;232:3-14.

ACKNOWLEDGMENTS

This work was funded by VINNMER grant (project n. 2013-01260), STINT grant (project n. IG2011-2047), Lars Hiertas Minne Foundation (project n. FO2013-0337) and Ollie & Elof Ericssons Stiftelse. Part of this work was performed at the BioMat facility /Science for Life Laboratory at Uppsala University.



Thermomechanical properties and bioactivity of silicone hybrids containing inorganic biomedical fillers

I.-G. Athanasoulia¹, S.P. Vasilakos¹, P.A. Tarantili¹, Tr. Papadopoulos^{2*}

¹Chemical Engin. School/Polymer Technology lab., National Technical Univ. of Athens, Greece

^{2*}Dental School/Biomaterials lab., University of Athens, Greece, trpapad@dent.uoa.gr

INTRODUCTION

Silicone rubbers (SR) present good biocompatibility, physiological inertness and easy handling, that make them recommended materials in prosthetic applications. However, in some cases, they do not organically unite with tissues, which leads to inflammation and foreign-body reaction after implantation. In order to improve the mechanical, physicochemical and biological properties of silicones, bioactive inorganic particles can be used as modifying additives. Hybrids with hydroxyapatite¹, β -Tricalcium phosphate (β -TCP)², CaO-SiO_2 ³, $\text{CaO-SiO}_2\text{-TiO}_2$ ⁴, were investigated for this purpose. In this work, silica nanoparticles in comparison with bioactive glass were studied for the modification of silanol terminated polydimethyl siloxane (PDMS).

EXPERIMENTAL METHODS

Silanol terminated PDMS, grade DMS-S31 (Gelest Inc.) of molecular weight 26,000 g/mol, was the silicone base elastomer used in this work. The vulcanization reaction system consisted of 10 phr tetrapropoxysilane as a cross-linker and 0.1 phr dibutyl tin dilaurate as catalyst (Sigma Aldrich). Composites were prepared by the sonication technique, using silica nanoparticles (Aerosil R972, Evonic Degussa GmbH) and bioactive glass (Bonalive) particles. The composites were characterized by differential scanning calorimetry (DSC), dynamic mechanical analysis (DMA). In addition, their tensile and tear properties were also tested. An “*in-vitro*” assay of bioactivity was carried out by soaking PDMS hybrids in Simulated Body Fluid⁵ (SBF) at pH 7.4 for 7, 21 and 40 days. The formation of hydroxyapatite was evaluated by FTIR-ATR spectroscopy and SEM/EDAX analysis.

RESULTS AND DISCUSSION

Silica nanoparticles decrease the temperatures of all the investigated transitions (T_g , T_c , T_m) as well as the enthalpies of “cold” crystallization and melting of the elastomer. The addition of bioactive glass into the PDMS matrix does not have any obvious effect on the T_g , T_c and T_m of the elastomer. However, significant decrease was observed in ΔH_c and ΔH_m of PDMS.

Regarding the investigated mechanical properties, from Table 1 it is obvious that the tensile and tear strength of polysiloxane is improved by the incorporation of the examined types of inorganic particles. However, the modulus of elasticity remains unaffected in the case of PDMS specimens reinforced with bioactive glass.

It has been reported that materials which form bonelike apatite on their surface in SBF can form the apatite even in the living body and bond to living bone through the apatite layer⁵.

Sample	Tensile strength (MPa)	Modulus (MPa)	Tear strength (Nt/mm)
PDMS	0.32	1.27	0.114
Aer R972/PDMS	0.63	1.48	0.122
BG/PDMS	0.70	1.27	0.147

Table 1 Tensile and tear test results of 5 phr loaded silica (Aerosil R972) and bioactive glass/PDMS composites.

The evaluation of hydroxyapatite formation on the surface of PDMS hybrid systems was performed by SEM and EDAX analysis. After 21 days and especially after 40 days of immersion in SBF, a large number of microparticles were detected on the surface of all the examined specimens. Using the EDAX technique, the percentage weight of Ca and P and then the molar ratio of Ca/P were calculated (Table 2). Ca and P are present at low percentage up to 21 days and their presence become significant after 40 days of immersion. These results are in agreement with those of FTIR analysis. Within this period of immersion, the Ca/P ratio is close to 1.67, which corresponds to hydroxyapatite. Deviations from this value were attributed to the formation of some defects during apatite growth.

	Ca	P	Ca/P	Ca	P	Ca/P
D	5 phr Aer R972/PDMS			5 phr BG/PDMS		
0	0.12	0.10	0.93	0.2	0.22	0.70
7	0.16	0.22	0.56	0.23	0.40	0.40
21	0.24	0.72	0.26	7.14	4.56	1.23
40	29.87	14.52	1.59	14.12	8.35	1.31

Table 2 The quantitative results using EDAX analysis on the examined PDMS composites versus immersion time in SBF.

CONCLUSION

Bioactive glass is a new alternative for the modification of biomedical prosthetic silicone elastomers, since it clearly enhances biocompatibility of polysiloxane matrix, despite the fact that it does not significantly improves its mechanical performance.

REFERENCES

1. Zhou C., Yi Z., Biomaterials 20:2093-2099, 1999
2. Zhang Y., Wang S.-l, Lei Z., Fan D., Aesth. Plast. Surg. 33:760-769, 2009
3. Tsuru K., Ohtsuki C., Osaka A., Iwamoto T. and Mackenzie J.D., J Mat Sci: Mat Med. 8:157-, 1997
4. Chen Q., Miyata N., Kokubo T., Nakamura T., J Mat Sci: Mat Med. 12:515-522, 2001
5. Kokubo T., Biomaterials 12:155-163, 1991

Kartogenin Conjugated Chitosan-Nano/Microparticles for the Intra-Articular Osteoarthritis Treatment

Mi Lan Kang, Ji Yun Ko, Ji Eun Kim, Gun Il Im*

*Department of Orthopedics, Dongguk University Ilsan Hospital, Korea, gunil@duih.org

INTRODUCTION

Recently, a study has been demonstrated that kartogenin (KGN) can induce chondrogenesis of mesenchymal stem cells (MSCs)¹. Intra-articular (IA) drug delivery is very useful in the treatment of osteoarthritis (OA), the most common chronic joint affliction. The conjugation of biodegradable polymers and small molecular weight drugs is an efficient approach to improve therapeutic properties. In this study, kartogenin conjugated chitosan (CS) nanoparticles (NPs) and microparticles (MPs), new polymer-drugs conjugates, were synthesized, characterized and investigated as IA drug delivery systems for regeneration of osteoarthritic joint.

EXPERIMENTAL METHODS

Bioconjugates of KGN and CS (low molecular weight CS (LMWCS) or medium molecular weight CS (MMWCS)) were synthesized by ethyl (dimethylaminopropyl) carbodiimide (EDC)/ N-Hydroxysuccinimide (NHS) catalysis. NPs and MPs were made by ionic gelation method with tripolyphosphate (TTP) using the conjugates of LMWCS-KGN or MMWCS-KGN, respectively. The conjugation of KGN and CS were confirmed by FT-IR and ¹H-NMR. The particles were characterized by DLS and FE-SEM. The amounts of KGN released from NPs or MPs in vitro were determined by HPLC. In vitro activities to induction of chondrogenesis by LMWCS-KGN NPs or MMWCS-MPs were evaluated in pellet culture of MSCs. The chondrogenesis was assessed by real-time PCR and Western blotting on markers such as collagenase type 2 (COL2) and aggrecan (AGC). The retention of fluorescent-labelled LMWCS-KGN NPs or MMWCS-KGN MPs in the joint of OA rats was carried out using the IVIS spectrum.

RESULTS AND DISCUSSION

Because CS has an amine group in its C2 position, it can be reacted with carboxylic group-containing KGN. The degree of KGN conjugated with CS estimated by ¹H-NMR was up to 80 mol%. Average sizes of LMWCS-KGN NPs and MMWCS-KGN MPs

measured by DLS were 150±39nm and 1800±547nm, respectively. The size of particles was not changed after two weeks due to the hydrophobic nature and small molecular weight of KGN. The release profiles showed sustained release of KGN from the particles. The amount of KGN released from LMWCS-KGN NPs was less than 30% of total conjugated KGN with CS for 6 weeks. The released KGN from the particles were induced more effective chondrogenesis than soluble KGN in MSCs. The LMWCS-KGN NPs and MMWCS-MPs were remained in the OA joint up to 3 weeks. Therefore, long-term drug exposure could achieve in the OA joint.

CONCLUSION

The conjugation of amine group of CS and carboxylic group of KGN was successfully carried out with EDC/NHS catalysis. The hydrophobic KGN could reside inside of the CS-KGN conjugated particles during ionic gelation with TPP. In vitro release studies demonstrated that the release of KGN from CS-KGN particles was delayed by the conjugation of KGN with CS. Due to the localized nature of the disease, IA drug injection is an attractive treatment approach for OA. However, the potential benefits of IA therapy for OA are not achieved using currently available medications and delivery vehicles due to the rapid clearance of therapeutic substances from the synovial space. In this study, the designed particles showed long retention time up to 3 weeks. In conclusion, CS-KGN conjugated particles have considerable potential for creating a sustained release KGN delivery system and providing long-term exposure of KGN in OA joint.

REFERENCES

1. Johnson K. *et al.*, Science. 336:717-21, 2012

ACKNOWLEDGMENTS

The authors would like to thank the National Research Foundation of Korea (Grant no: 2013R1A1A2062978) for providing financial support to this project.

Composition-Property Relationships for Lanthanum-Borate Glasses

K. O'Connell³, H. O'Shea³, Muhammad Hasan^{1,2}, D. Boyd^{1,2}

¹Department of Oral Sciences, Dalhousie University, Canada

²Department of Biomedical Engineering, Dalhousie University, Canada

³Department of Biological Sciences, Cork Institute of Technology, Ireland

Email: Kathleen.oconnell@mycit.ie, Helen.oshea@cit.ie, d.boyd@dal.ca, sami.hasan@dal.ca

INTRODUCTION: Boron (B) is an essential element utilized both in the natural environment and in the manufacturing of several commodities, including (but not limited to) glass & ceramics¹. The potential of B glasses as degradable systems in biomedical applications is of significant importance². B's popularity has grown due to its bioactivity, stimulating effects on bone formation, antimicrobial potentials for infection control & also, as a local drug delivery device³. Various B networks have shown promise, however if these materials are to be utilized to their full potential, greater control over the degradation rate is required. Previous reports have indicated that additions of up to 10mol% lanthanum (La) in a 70mol% B glass are expected to cause network stabilization⁴. Within this study the composition-property relationship of each La-B glass composition was evaluated.

EXPERIMENTAL METHODS: Six glass compositions (Table 1) were melt-quenched ground to a particle size of 45-150 μ m. Property analysis was then completed on each composition. Glass transition temperature (T_g) was determined by means of Differential Scanning Calorimetry (DSC). Volume and density measurements were obtained by a helium pycnometer. B³⁺, Sr²⁺, Na⁺ & La³⁺ ion release profiles associated with each composition was determined by ICP-OES for up to 30 day incubation periods.

Table 1: Mole fraction compositions of La-B glass compositions.

Glass Designation	B2O3	SrCO3	Na2CO3	La2O3
B100	0.7	0.2	0.1	0
LB100	0.7	0.2	0.8	0.2
LB101	0.7	0.2	0.6	0.4
LB102	0.7	0.2	0.4	0.6
LB103	0.7	0.2	0.2	0.8
LB104	0.7	0.2	0	1

RESULTS AND DISCUSSION

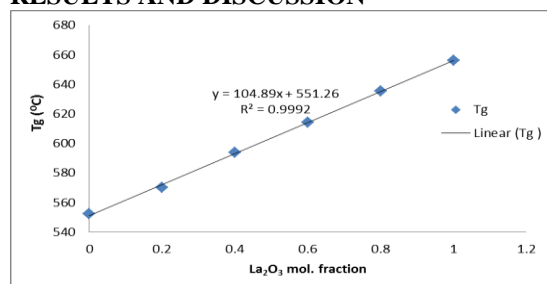


Figure 1: T_g for each glass composition (based on La₂O₃ mol. Fraction).

As illustrated in Fig 1 and 2, the 0-10mol% increase in La₂O₃ content had a direct effect on T_g and density, with linear increases from 553-656°C and 2.71-3.53g/cm³, respectively.

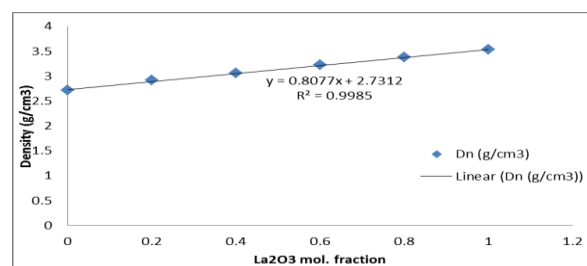


Figure 2: Density (g/cm³) for each composition (based on La₂O₃ mol. Fraction)

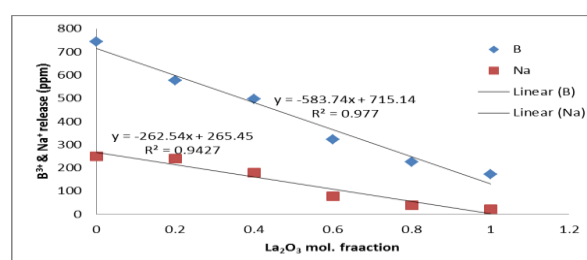


Figure 3: B³⁺ & Na⁺ ion release (30 day release) as a function of glass composition (La₂O₃ mol. Fraction).

B atoms can coordinate with both 3 and 4 oxygen (O₂) atoms forming triangular or tetrahedral structural units. These combine to form intermediate structural units which ultimately assist in stabilization. Fig. 3 indicated that, B³⁺ & Na⁺ ion release was directly affected by compositional variations. La³⁺ ion release remained constant at 200ppb irrespective of loading while Sr²⁺ release was affected but not in a linear fashion. These results are consistent with what was expected, that La₂O₃ incorporation would cause a modulation of network outputs and an increase in network connectivity and stabilization.

CONCLUSION: B containing glass networks are becoming increasingly important for a range of biomedical applications. Such networks have illustrated potential for bone regeneration & as *in situ* drug delivery devices, however in order to capitalize on the complete utility of these materials, stabilization & control over degradation is required. This data clearly illustrates the presence of a composition-property relationship, as up to 10mol% of La₂O₃ incorporation modulated all investigated glass properties in a linear fashion, thus indicating an increase in network connectivity of the B₂O₃ network.

REFERENCES: [1] Kabu, M., Akosman, M. S.R(2013) Rev. Environ. Contam. Toxicol 225, 57–76. [2] Saddeek, Y. B. & Gaafar, M. S.(2009) Mater. Chem. Phys. 115, 280–286. [3] Liu, X. et al.(2010) J. Mater. Sci. Mater. Med. 21, 575–82. [4] Chakraborty I.N., Shelby J. E.(1980) J. Am. Ceram. Soc. 67, 782–785.

ACKNOWLEDGMENTS: The authors acknowledge the financial assistance of CIT RÍSAM PhD Scholarship Programme (RDRP), NSERC (Discovery Award Program) and the Canadian Foundation for Innovation.

Osteogenic Differentiation of AdMSCs on 17 β -Estradiol Releasing Chitosan-Hydroxyapatite Scaffolds

Gülseren Irmak¹, T.Tolga Demirtaş¹, Damla Altındal², Mert Çalış³, Menemşe Gümüşderelioğlu^{1,2*}

¹Bioengineering Dept., Hacettepe University, Turkey

^{2*}Chemical Engineering Dept., ³Plastic Reconstructive & Aesthetic Surgery Dept., Hacettepe University, Turkey, gulseren.irmak@gmail.com

INTRODUCTION

Estrogen, substantially participates in the regulation of bone metabolism by inhibiting bone resorption and increasing bone formation¹. In this study, we decided to develop a novel effective 17 β -estradiol (E2) releasing system which consists of chitosan (CH)-hydroxyapatite (HA) scaffold and PLGA nanoparticles to promote osteogenic differentiation of adipose tissue derived rat mesenchymal stem cells (AdMSCs) for bone tissue regeneration.

EXPERIMENTAL METHODS

E2 loaded nanoparticles (Np) were prepared by using emulsion-diffusion-evaporation method. The encapsulation efficiency of E2 into the PLGA nanoparticles was determined by HPLC (Dionex Ultimate 3000, USA). CH-HA scaffolds were prepared according to the combined method of microwave irradiation and gas foaming, previously described by our group². Nanoparticles in aqueous phase were loaded into CH-HA scaffolds by two ways; i) stirring during scaffold manufacturing, ii) embedding after scaffold manufacturing. The morphology of scaffolds was investigated by SEM. Release kinetics of E2 was investigated from PLGA nanoparticle loaded scaffolds. *In-vitro* release studies were carried out in a shaking bath at 37°C and 70 rpm. E2 concentration in the release medium was determined using HPLC at 280 nm. Cell viability of AdMSCs on CH-HA scaffolds was analysed by using MTT assay. The morphology and attachment of AdMSCs onto the scaffolds were observed by SEM. Osteogenic differentiation of AdMSC's cultured on CH-HA scaffolds in the presence of E2 were determined by ALP analysis and RT-PCR. All data were expressed as mean \pm standard deviations of representative of three similar experiments carried out in triplicate.

RESULTS AND DISCUSSION

According to the SEM and TEM photographs of E2 loaded PLGA nanoparticles (approx. 240 nm), they have spherical morphology and narrow size distribution. Encapsulation efficiency for 65:35 PLGA copolymer was determined as 54 %. SEM photographs of PLGA loaded CH-HA showed that, nanoparticles consisting of E2 were successfully loaded and homogenously distributed through the scaffolds.

Release of E2 from CH-HA scaffolds that was containing PLGA nanoparticles loaded by embedding has continued in a controlled manner and 100% of the encapsulated E2 was released during 55 days. However, 92 % of E2 was released during 135 days from the scaffolds loaded with nanoparticles during scaffold fabrication.

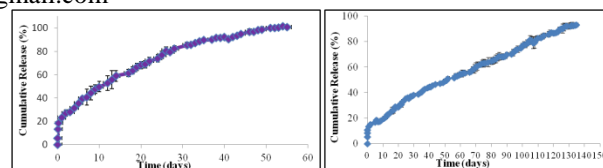


Figure 1: *In-vitro* release profiles of E2 from PLGA nanoparticles loaded scaffolds; a) loaded by embedding (CH-HA-Np), b) loaded during manufacturing by stirring (CH-HA+Np).

The results obtained from *in-vitro* culture of AdMSCs suggest that cells established good contacts with scaffolds and also with each other's, proliferated also changed their fusiform morphology to the cubical shape.

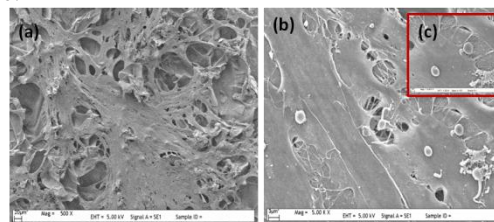


Figure 2: SEM photographs of AdMSC's growing on CH-HA scaffolds at the 14th day of culture: CH-HA-Np scaffold: a) 500X, b) 5,000X, c) 15,000X.

For all groups, ALP activities increased rapidly during 2 weeks, however, cells cultured on the CH-HA-Np scaffolds showed significantly highest ALP activity. According to RT-PCR result, OCN expression on that scaffolds that containing nanoparticles were observed at the 7th days of culture and on the 21st day were relatively higher value than that of CH-HA scaffolds, respectively.

We concluded that, scaffolds that containing nanoparticles were significantly enhanced matrix mineralization and osteogenic differentiation of AdMSCs by providing the controlled release of E2.

CONCLUSION

In conclusion, the 3D system carrying and releasing E2 is a novel and promising vehicle for bone tissue engineering *in vivo*.

REFERENCES

1. Nappi C. *et al.*, Contraception. 86:606-621, 2011
2. Beşkardeş I. *et al.*, Tissue Eng Regen Med DOI :10.1002/term.1677.

ACKNOWLEDGMENTS

The authors would like to acknowledge the support of Hacettepe University Scientific Research Foundation (Project No: 011D 10602001).

Understanding the Physiochemical Interactions between Denture Adhesives and the aqueous phase

S. Gill¹, B.J Tighe¹, N. Roohpour², C. Jeffrey²

¹Biomaterials Research Unit, School of Engineering and Applied Science, Aston University, UK

²GSK Consumer Healthcare, St Georges Ave, Weybridge, UK

gills10@aston.ac.uk

INTRODUCTION

Denture adhesives can provide many benefits to denture wearers, in particular enhancing comfort, retention, chewing ability and increasing confidence¹. Most formulation strategies aimed towards this application function to take advantage of the humid environment of the oral cavity, which effectively hydrates the adhesive, producing a mucilaginous layer with high tack and adherent properties. The primary objective of this study is to investigate the physiochemical interactions between different aqueous phases and the hydrophilic polymer groups within the adhesives in order to better understand the adhesion phenomenon involved. Two commonly used hydrophilic polymers in this application are carboxymethylcellulose (CMC) and mixed partial salts of methyl vinyl ether – maleic anhydride copolymer (MVE/MA).

EXPERIMENTAL METHODS

Most commercial denture adhesives involve the in vivo hydration of the polymer system. It was therefore important to investigate the effect of the nature of the aqueous phase on the adhesion mechanism. This was achieved by studying the addition of a range of aqueous phases at progressive ratios (10-50%) to a commercial product, Poligrip Ultra® (Stafford Miller, Ireland), A1. The aqueous phases exemplified here are DI water and electrolyte solutions based on CaCl₂ and NaCl. Adhesion strength (post-mixing) was studied using an adhesive lap joint shear test between Melinex (polyethylene terephthalate) strips. The data is augmented by water binding studies in which the freezable water content and primary water melting point corresponding to each sample was determined. Three adhesion replicates were taken at each point with a range of +/- 15% and six cycles performed in the DSC studies.

RESULTS AND DISCUSSION

Table 1 summarises the results of adhesion strength and water binding properties for A1 when mixed with 10, 30 and 50% aqueous phase. The quoted adhesion strength values were quoted at approximately 30 seconds post-mixing.

The presence of electrolytes and consequent interaction with the carboxyl groups in the adhesive system is found, as expected, to cause differences to the overall water binding properties of the adhesive. The electrolyte rich solutions showed a distinctly different effect on freezable water content than DI water and also lower primary melting points due to the colligative properties of the dissolved electrolytes.

Aqueous phase	Aqueous phase Content (%)	Adhesion strength (kPa)	Freezing water content (%)	Water Tm (°C)
DI water	10	3	0	-
	30	6.1	6.8	-3.8
	50	6.7	27.3	2.5
NaCl (0.9M)	10	7.2	0	-
	30	15.4	4.3	-8
	50	10.3	11.8	-2.9
CaCl ₂ (0.9M)	10	6.2	0	-
	30	9.8	3.4	-7.3
	50	10.3	15.6	-2.1

Table 1: Effect of aqueous phase on adhesion strength, water binding and primary water melting point.

These results show that the presence of electrolytes within the adhesive system has an effect on water structuring; a phenomenon that appears to be linked – although not in a simple and direct manner - to the adhesion capability of the product, A1.

Interestingly at 10% incorporation of all aqueous phases, no freezable water peaks are detected indicating that all the water is strongly associated with the polymer system. Increasing ratios of aqueous phase give increased levels of freezing water, higher Tm values, and also higher levels of adhesion than at the 10% level of aqueous phase. The standard deviations on the adhesion strength values show that the electrolyte-containing aqueous phases produce higher adhesion values at the same levels of aqueous phase incorporation.

CONCLUSION

The lap shear joint test method and DSC studies used provide useful initial insight into the effects of electrolytes within the adhesive system on adhesion strength at a moderate surface energy surface analogous to that of a conventional denture. The DSC results suggest that this is related to effects of aqueous phase constituents on the water binding properties of the system. This initial work forms the basis for more detailed studies of the components of saliva - a complex biological fluid - and adhesion behaviour at oral tissue interfaces.

REFERENCES

1. Panagiotouni E. *et al.*, J. Prosthet Dent. **73**:578-85, 1995

ACKNOWLEDGMENTS

SKG is grateful to BBSRC and GSK for financial support under the CASE scheme.



New approach of biomaterial design to enhance osteogenesis at the interface bone/implant

Ibrahim Bilem^{1,2,3}, Pascale Chevallier¹, Laurent Plawinski², Eli Sone³, Gaétan Laroche¹, Marie-Christine Durrieu^{2*}

¹Deprt of Min. Met. Mater, Lab of surface engineering/RC-CHUQ, Laval university, Canada. ibrahim.bilem.1@ulaval.ca

^{2*} CBMN-UMR 5248, Institut Européen de Chimie & Biologie (IECB), University of Bordeaux, France.

³Deprt of Mater.Sci.Eng, Institute of Biomaterials and Biomedical Engineering, University of Toronto, Canada.

INTRODUCTION

Orthopaedic biomaterials represent a crucial alternative to regenerate or replace bone tissue when it is severely damaged by diseases such as arthritis or by injury. However, failure of bone implant interface (lack of Osseointegration) leading to implants loosening remains the main drawback. Accordingly, the objective of this project is to enhance the osseointegration of orthopaedic implants since their long-term performance is restricted to 10-15 years with the currently available materials¹. The original approach of this project consists in the biochemical surface modification of biomaterials by grafting specific peptides while controlling their spatial distribution at the micrometer scale. Briefly, two mimetic peptides (RGD, BMP-2) were grafted on the surface of a model biomaterial. They induce respectively the adhesion and the differentiation of Mesenchymal Stem Cells (MSCs) into mature osteoblasts able to synthesize a mineralized extra cellular matrix (ECM)². Furthermore, our strategy is to graft these two mimetic peptides as micropatterns on the surface to create an appropriate distribution for osteoblastic differentiation³.

EXPERIMENTAL METHODS

Aminated borosilicate glass, used as biomaterial model, was used to conjugate RGD and BMP-2 mimetic peptides through SMPB crosslinker. These two peptides were grafted as micropatterns by using the maskless photolithography technique. The designed micropatterns corresponded to square, rectangle or triangle with a constant surface area of 50 μm^2 . The surface chemistry and topography of the material were assessed by using X-ray Photoelectron Spectroscopy (XPS) and Atomic Force Microscopy (AFM). Micropattern visualization was achieved using fluorescent peptides RGD-TAMRA and BMP-2-FITC visible under fluorescent microscopy.

RESULTS AND DISCUSSION

XPS analyses (Table 1) evidenced the grafting efficiency after each step of the peptide immobilization procedure. Even though the initial SMPB grafting is not evident, with only a slight decrease of the nitrogen surface concentration from 3.8 % on the aminated glass

to 3.2 % on the SMPB-grafted sample, surface immobilization of both peptides is confirmed by the increase in the nitrogen surface concentration coming from the peptide groups.

Table 1: Surface composition determined by XPS at grazing angle.

	% C	% O	% N	% Si
NH ₂ -glass	42.1	40.9	3.8	13.9
SMPB grafted	40.2	42.3	3.2	14.3
RGD grafted	46.8	34.5	5.9	12.7
BMP2 grafted	39.1	41.8	5.4	13.2

The peptides grafting were also confirmed by fluorescence microscopy as the use of fluorescent peptides allowed to visualize the different micropatterns (Fig. 1). Indeed, the spatial distribution of the two peptides designed as square, rectangular or triangular micropatterns was clearly evidenced and precisely defined (Fig. 1).

CONCLUSION

The strategy of designing specific peptides micropatterns onto orthopaedic material surfaces seems to be promising for osseointegration enhancement. Our preliminary surface characterization results evidenced efficient peptides grafting as well defined micropatterns. Future works will assess the effect of peptide micropatterning on the behaviour and fate of MSCs through cell proliferation, adhesion, and differentiation assays, as well as ECM mineralization experiments.

REFERENCES

1. Ducheyne D. *et al.*, J. Elsevier Sci. 109-123, 2011
2. Zouani O-F. *et al.*, J. Biol Open. 29, 872-81, 2013
3. Kilian K-A. *et al.*, J. PNAS. 11, 4872-4877, 2010

ACKNOWLEDGMENTS

The authors would like to thank *NSERC Create Program in Regenerative Medicine* for providing financial support to this project. <http://www.ncprm.ulaval.ca>

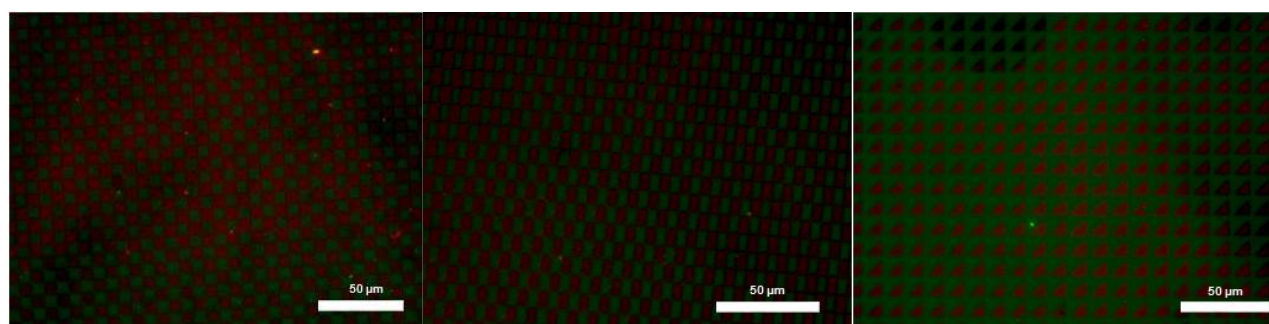


Figure1: Fluorescent images of peptides micropatterns grafted on borosilicate glass surfaces: RGD-TAMRA/BMP 2-FITC.



Development of nanostructured silicone copolymers to deliver antimicrobials to treat human infected wounds

S Finnegan¹, S Rimmer², S Macneil^{3*}, S Percival⁴

¹Department of Chemistry, University of Sheffield, United Kingdom, dtp11sf@shef.ac.uk

² Department of Chemistry, University of Sheffield, UK,

³Department of materials science and engineering, University of Sheffield

⁴Scapa Healthcare, Manchester, UK

INTRODUCTION

There are many types of cutaneous wounds with varying causes. They can be classified as acute or ^{1,2}. One of the major differences is that acute wounds proceed through an orderly and timely process of repair, whilst chronic wounds do not ¹. In the US alone it has been estimated that each year over 6 million people develop a wound that becomes chronic ⁵. It is estimated that caring for chronic wounds costs the US healthcare system tens of billions, while they cost the UK National Health Service about 1 billion pounds per year ⁶. The aim of this project is to enhance currently used silicone contact layers in wound dressings. Physical properties and permeability will be enhanced via integration of nanostructured silicone n-vinylpyrrolidone copolymer 'micelles' as well as the incorporation of antimicrobial agents that will be delivered through the same means.

EXPERIMENTAL METHODS

Preparation of PDMS macromonomer

Macro-monomers were prepared under a nitrogen atmosphere using living anionic polymerization. For example, a solution of hexamethylcyclotrisiloxane (0.03 mol, 7g) and lithium isopropoxide (3mol%, 0.4mL 2M solution in THF) in THF (10mL) was injected into a pre-sealed glass tube. The solution was stirred at room temperature for 3hrs and then allyl chloroformate (3mol%) was injected into the solution. The reaction mixture was ultrasonicated for 20 min and then stirred at room temperature for 24hrs. The solvent was evaporated by rotary evaporation and the liquid oligomer was dissolved in chloroform. The solution was washed with water and the organic layer collected. Chloroform was removed by rotary evaporation.

Preparation of PDMS - NVP copolymers

N-vinylpyrrolidone, PDMS functionalised macro-monomer, ACVA and tetrahydrofuran were mixed together in the desired ratio. The resulting solution was pipetted into a 100ml ampule and placed on a high vacuum line. The solution was frozen with liquid nitrogen and vacuum was applied (3×10^{-3} mBar) and then closed. The ampule was defrosted with tepid water, once thawed this process repeated until the ampule was completely degassed. The ampule was sealed using gas/oxygen blowtorch and placed in a water bath at 60°C for 24hrs. The ampule was opened by cracking and the product was removed via pipetting. The solvent was evaporated by rotary evaporation under reduced pressure and the product was precipitated and repeatedly washed with diethyl ether. This was removed by vacuum filtration obtaining a white powder.

Preparation of Silicone - Copolymer contact layer

The silicone matrix components were provided by Scappa healthcare™ and were prepared by adding

'component A' to 'component B' in an equal 1:1 ratio.

Copolymers were dissolved in the minimum volume of hexamethyldisiloxane before being combined with Rhodamine B or antimicrobial agent. This solution was then mixed with 'component A' before being mixed with an equal amount of 'component B'. The membrane were drawn down using 200µm K-bars onto release paper and set in an oven at 60°C for five minutes.

RESULTS AND DISCUSSION

Three membranes were chosen for SEM which where the 0, 0.1 and 10% copolymer, shown from left to right below in figure 1.

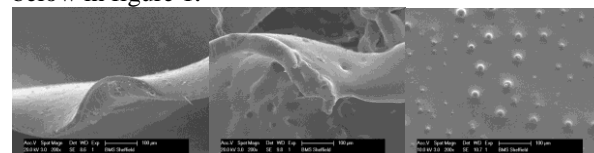
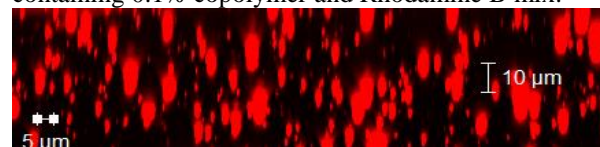


Figure 1 shows that as you increase the copolymer content from zero to 10% the surface morphology changes from being smooth to more rough with increasing populations of 'pimples' appearing. Z-stacked images using confocal microscopy were then taken to produce a projected image side on, shown below in figure 2 of a silicone matrix membrane containing 0.1% copolymer and Rhodamine B mix.



It is clear to see that Rhodamine B is encapsulated within the membrane suggesting that the hydrophilic molecule is being held within copolymer micelles.

CONCLUSION

A hydrophilic fluorescent agent (Rhodamine B) has successfully been incorporated into a hydrophobic cross linked silicone matrix and release has been monitored using UV-VIS spectroscopy over a two day period.

REFERENCES

1. Lazarus G.S. *et al. Wound Repair and Regeneration*, 3:165-170, 2002.
2. Monaco J.L. *et al. Clinics in plastic surgery*, 30: 1-12, 2003.
3. Kirketerp-Møller K. *et al. Journal of clinical microbiology*. 46: 2717-2722, 2008.
4. Rojas, A.I. *Dermatologic surgery*. 25:601-604, 2001
5. Singer, A.J. Cutaneous wound healing. *New England journal of medicine*, 341:738-746, 1999.
6. Rodrigues, I. *et al. Ostomy Wound Management*, 52:46, 2006.

ACKNOWLEDGMENTS

The authors would like to thank the ESPRC for providing financial support to this project and a thank you to colleagues who provided assistance with individual aspects.



Development of new approaches to fabricate scaffolds for deep zone engineered articular cartilage

Anne Canning¹, Paul Roach¹, Ying Yang¹, James Richardson²

¹Institute of Science and technology, University of Keele, United Kingdom

²The Robert Jones and Agnes Hunt Orthopaedic Hospital, Oswestry, United Kingdom

INTRODUCTION

Cartilage has defined zone architecture structure, changing through the thickness¹. The deep zone bridges cartilage and bone with unique vertical channels. Fabricating a scaffold which replicates the zonal architecture has an advantage to produce anatomically and functionally mimicking cartilage tissue². Here we aim to engineer deep zone cartilage by growing bone cells in a channelled polymer gel also presenting partly embedded biodegradable glass fibres³.

EXPERIMENTAL METHODS

The scaffold mould was designed on AutoCAD2012 software and printed on a 3D Makerbot printer. MG63 cells were seeded on 8 samples of poly (NIPAM) gels cast on the mould.

Cell attachment, migration and proliferation was monitored via H&E and TRITC-Phalloidin staining at 7, 14, 21 and 28 days.

The degradation and diffusion of minerals in the gel of Phosphate fibres was measured using Raman microscopy up to 2 weeks in vitro.

RESULTS AND DISCUSSION

An inverse template structure was produced using 3D printing and metal wires, allowing successful casting of a multi-channelled array in poly (NIPAM). Aligned vertical hollow channels of diameter 325 – 395 μm were produced within the gel, also presenting micro-porosity.

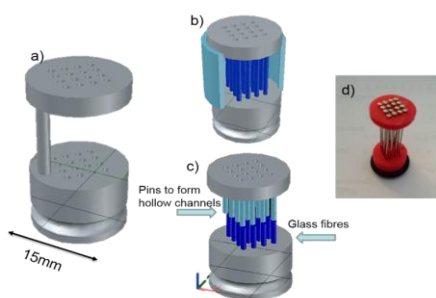


Figure 1) a-c AutoCAD design of engineered construct. b-blue cylinders represent pins threaded from top to base, c-dark blue cylinders represent embedded glass fibres, light blue represent removable pins. d-image of 3D printed mould threaded with metal pins.

(figure 1). MG63 cells were seeded on the gels and showed some adhesion and migration within the upper portion of the channels, moving toward the columnar distribution of cells found in deep zonal cartilage (figure 2).

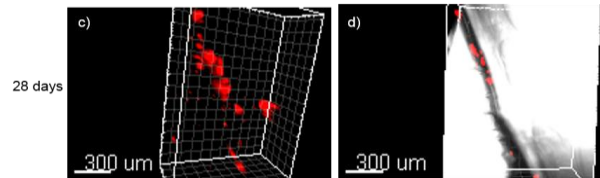


Figure 2) Confocal images of TRITC-Phalloidin stained cells at 28days (c-d). b,d image of fluorescence superimposed on bright field image of channels.

Phosphate glass fibres were thread into the mould and polymer cast to fabricate gels embedded with mineral rich glass fibres with a degradation rate of 28 days in vitro. The degradation and mineral diffusion was successfully measured using Raman microscopy (figure 3).

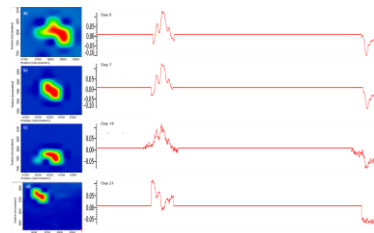


Figure 3): Principal component analysis at 2800-3100 and 1050-1150 cm^{-1} of embedded fibre in poly (NIPAM) incubated at 37 $^{\circ}\text{C}$ in buffer at PH7.4 at 0 days (a), 3 days (b), 7 days (c), 14 days (d).

CONCLUSION

These results show a promising prototype to be further investigated to form structures with an architecture that resembles that found in osteochondral defects.

REFERENCES

1. Barber, F.A., 2007. 1st edition. L. W. & Wilkins, ed., Practical Orthopaedic Sports Medicine & Arthroscopy.
2. Woodfield, T.B.F. et al., 2004. *Biomaterials*, 25(18), pp.4149–61.
3. Jones, J.R., 2013. *Acta biomaterialia*, 9(1), pp.4457–86

ACKNOWLEDGMENTS

The authors would like to thank Dr I Ahmed at The University of Nottingham for fabrication of the Phosphatefibres.

Adhesives and their role in the reduction of HCAI, skin and wound infections

Steven L Percival^{1,2,3}, Rebecca Booth³ and Sean Kelly³

¹Institute of Ageing and Chronic Disease, University of Liverpool, Liverpool, UK

²Surface Science Research Centre, University of Liverpool, Liverpool, UK

³Scapa Healthcare, Manchester, UK, email: Steven.Percival@scapa.com

INTRODUCTION

The increasing incidence of healthcare associated infections (HCAI) together with concerns surrounding the appropriate use of antibiotic agents means that there is a significant need for new approaches for both the prevention and treatment of wound infections¹. Acute wounds such as surgical wounds are susceptible to infection and therefore prevention of microbial colonisation and biofilm development is of paramount importance².

In this study we examined the use of a adhesives commonly used to attach biomaterials and medical devices to the body and investigated novel ways to deliver antimicrobial agents directly to the skin/wound interface.

EXPERIMENTAL METHODS

- Three antimicrobial agents (chlorhexidine, benzylkonium chloride and silver) were combined with medical grade adhesives at concentrations of 3-20% and coated on to a polyurethane (PU) backing film at different thicknesses.
- A customised zone of inhibition (ZOI) assay, log reduction assays, antimicrobial efficacy tests and anti-biofilm tests were performed using common clinical bacteria, *Staphylococcus aureus* and *Pseudomonas aeruginosa*.
- 3x3cm² pieces of sterilised adhesive films were placed on a surface inoculated agar plate and incubated for 24 hours. Areas beneath the material were observed for bacterial growth and then plates re-incubated to verify a bactericidal or bacteriostatic effect.
- 55mm diameter circles of sterilised PU film were incubated in 5mls of simulated wound fluid. 100µl of fluid was removed at 4, 24, 48, 72 and 96 hour time points and serially diluted provide log reduction data.
- Confocal laser microscopy was employed to evaluate real time killing of all antimicrobial adhesives.

RESULTS AND DISCUSSION

Overall, all 3 antimicrobial adhesives evaluated demonstrated an antimicrobial effect using the customised ZOI test when compared to the negative control. In the fluid log reduction test model, colony counts from all 3 adhesives also demonstrated a reduction in planktonic bacterial load throughout the time course indicating that the antimicrobials were eluted from the adhesive materials at sufficient levels to cause microbial death.

- Antimicrobial A caused the greatest log reduction over the complete 96 hour time course (8 log against *S. aureus*).
- Antimicrobial C caused the greatest log reduction in bacteria over the full time course. A 5 log reduction was seen with *S. aureus* and a 6 log reduction with *P. aeruginosa*.
- Antimicrobial B had the quickest action against *S. aureus* and demonstrated a 2 log reduction after 4 hours.

CONCLUSION

This proof of concept study provides evidence that adhesives can be used as a vehicle to deliver efficacious levels of actives and antimicrobials directly to the wound interface. These antimicrobial adhesives have potential applications throughout the field of healthcare including biomaterials, wound dressings, incision drapes, internal sealants and device fixation materials.

REFERENCES

1. Percival, S.L., Williams, D, Randle, J and Cooper, T (2014) Biofilms in Infection Prevention and Control: A Healthcare Handbook. 1st Edition, *Academic Press*. ISBN 0123970431.
2. Percival S.L., Hill, K, Williams, D., Thomas, D and Costerton J.W. (2012) Scientific Evidence of Biofilms in Wounds. *Wound Repair and Regeneration*, Sep-Oct;20(5):647-57.

The utilisation of poloxamer as a model to study the complexity of biofilms and antimicrobial efficacy in biomaterials

Steven L Percival^{1,2,3*}, Rebecca Booth³ and Sean Kelly³

¹Institute of Ageing and Chronic Disease, University of Liverpool, Liverpool, UK

²Surface Science Research Centre, University of Liverpool, Liverpool, UK

³Scapa Healthcare, Manchester, UK

*email: Steven.Percival@scapa.com

INTRODUCTION

Microorganisms found within and on the human body exist in two phenotypic states, the planktonic state, and the attached or sessile/biofilm state. The biofilm model has been highlighted, and widely acknowledged, as an explanation for the myriad of features observed in the non-healing of skin and chronic wounds. Consequently clinicians and researchers consider the biofilm state to be responsible for recalcitrance and the main reason that an infection occurs. Poloxamer is a non-toxic, di-block copolymer, which has previously been investigated for its potential to easily and reproducibly model the biofilm state *in vitro* (Gilbert *et al* 1998; Clutterbuck *et al* 2007; Percival *et al* 2007).

Here we investigate the growth and behaviour of common skin and wound bacteria, in a scaffold of Tryptone Soya Agar (TSA; 'quasi' biofilm) compared to 30% Poloxamer in Tryptone Soya Broth (Poloxamer; true biofilm). The aim of this investigation was to compare the architecture and biofilm development of these skin and wound isolates in order to gain greater knowledge for biofilm control and reduction in microbial dissemination into surrounding tissue.

EXPERIMENTAL METHODS

- 1 x 10⁸ cfu/ml of *S. aureus* or *P. aeruginosa* in Maximum Recovery Diluent (MRD) were inoculated into Poloxamer or molten TSA and 100µl pipetted onto the surface of glass microscope slides.
- Microscope slides were incubated in a moist environment at 35°C. At 24, 48 and 72 hours images were taken using a light and confocal microscope. Macroscopic images were also taken at 48 hours using a stereoscope microscope.
- Viable counts were performed on samples of inoculated agar and poloxamer. Images and counts of bacterial growth were obtained after 4, 24, 48 and 72 hours incubation at 35°C.

RESULTS AND DISCUSSION

- Macroscopic visualisation of *S. aureus* and *P. aeruginosa* grown in agar and poloxamer showed differences in microcolony formation that reflected the presence of high cell densities present in both substrates.
- Microscopic visualisation of inoculated poloxamer and agar demonstrated differences in bacterial microcolony formation after 24 hours incubation and continued throughout the time course.

- The inoculated agar samples showed closely packed spherical individual colonies of cells which increased in density over 72 hours.
- The poloxamer hydrogel samples demonstrated the formation of smaller, less tightly packed microcolonies that were more irregularly shaped. There was also evidence of microcolonies linking together. The growth of these colonies appeared to be slower when compared to agar.
- Overall, viable counts demonstrated that over time the number of *S. aureus* and *P. aeruginosa* organisms initially increased in both agar and poloxamer. Poloxamer biofilms demonstrated a 'steady state' of growth whereas numbers of viable organisms in agar showed a relatively quick increase followed by a decrease after 24 hours.

CONCLUSION

The use of poloxamer hydrogels to model biofilms was found to be a rapid and simple method to study biofilm development and architecture in relation to biomaterials and medical devices. Poloxamer recreates an environment, which mimics biofilm conditions. This investigation gathered qualitative and quantitative data to demonstrate the differences of microcolony formation and proliferation rates in 2 different bacteria, which are commonly isolated from skin, acute, and chronic, non-healing wounds. Future studies will look to examine the effects of various existing and novel antimicrobial and antibiofilm treatments that could be used to treat biomaterial related infections.

REFERENCES

1. Gilbert P, Jones MV, Allison DG, Heys S, Maira T, Wood P (1998) The use of poloxamer hydrogels for the assessment of biofilm susceptibility towards biocide treatments. *Journal of applied microbiology* 85: 985-990
2. Percival SL, Bowler PG, Dolman J (2007) Antimicrobial activity of silver-containing dressings on wound microorganisms using an *in vitro* biofilm model. *Int Wound J* 4(2): 86-91.
3. Clutterbuck AL, Cochrane CA, Dolman J, Percival SL (2007) Evaluating antibiotics for use in medicine using a poloxamer biofilm model. *Annals of clinical microbiology and antimicrobials* 6: 2.



The use of the MBEC assay for quantitative and qualitative investigation of biofilm forming isolates isolated from biomaterials

Rebecca Booth³, Sean Kelly³ and Steven L Percival^{1,2,3*}

¹Institute of Ageing and Chronic Disease, University of Liverpool, Liverpool, UK

²Surface Science Research Centre, University of Liverpool, Liverpool, UK

³Scapa Healthcare, Manchester, UK

*email: Steven.Percival@scapa.com

INTRODUCTION

Several *in vitro* methods have been developed to investigate biofilms however few of these lend themselves to high-throughput (HTP) assays. HTP protocols allow the rapid assessment of antimicrobial and anti-biofilm efficacy of novel actives and thus offer the ability to assess large numbers and concentrations of compounds efficiently. The ability to visualise surface biofilms and the effect that an active has on various stages of biofilm formation and maintenance is also desirable, therefore a model which can be used for both qualitative and quantitative assessment is advantageous. In this study we use the minimum biofilm eliminating concentration (MBEC™) assay (Ceri *et al*, 1999) to investigate the biofilm forming capacity of common bacteria that have been isolated from biomaterials, *Staphylococcus aureus* and *Pseudomonas aeruginosa*. The assay was used to generate both qualitative and quantitative data from biofilms formed on the pegs of MBEC™ plates.

EXPERIMENTAL METHODS

- 10⁵cfu/ml of *S. aureus* and *P. aeruginosa* in Tryptone Soya Broth (TSB) was inoculated into 96 well pegged lid plates and incubated on a shaking platform at 35°C for 48 hours to allow the growth of biofilms.
- Peg lids were rinsed in 0.85% saline to remove any planktonic bacteria.
- Pegs were removed, stained with Invitrogen LIVE/DEAD® BacLight™ stain and visualised using fluorescent and confocal laser microscopy.
- Pegs were removed placed in 10mls Maximum Recovery Diluent (MRD) and sonicated for 10 minutes to remove the attached biofilm. The MRD was serially diluted, plated on to Tryptone Soya Agar (TSA) plates and incubated at 35°C. After 48 hours the colonies were counted.
- The pegged lid was stained with 1% crystal violet for 10 minutes. After staining, the pegs were washed 3 times in 0.85% saline, before being placed in ethanol for a further 10 minutes. The resulting ethanol suspensions were measured at an absorbance of 595nm on a plate reader.

RESULTS AND DISCUSSION

- Visualisation of the pegs showed evidence of microcolony formation and the production of extracellular polymeric substance (EPS).
- Colony counts performed on bacteria isolated from MBEC™ pegs demonstrated that there were 10 times more *P. aeruginosa* cells adhered to the peg surface than *S. aureus*.
- Absorbance levels of crystal violet stain released from the biofilm-coated MBEC™ pegs indicated the presence of higher levels of adherent material in the *P. aeruginosa* biofilms in comparison to *S. aureus*. Stained material includes bacterial cells together with EPS. This study has demonstrated the biofilm forming capacity of bacterial strains, which are commonly found colonising biomaterials using a standard biofilm model. The MBEC model was developed to facilitate HTP screening of actives. The evidence gathered during this study indicates that this model can be used to investigate actives, which may be used to prevent, and/or treat biomaterial related biofilm infections. Furthermore, this study has gathered data to show that the MBEC™ model can be used for both quantification and visualisation of biofilms on the surface of the MBEC™ pegs. Using a fluorescent stain, adherent bacterial cells were visualised and the presence of EPS was also indicated. Cell counts revealed the differences in numbers of adherent cells between bacteria and showed very good reproducibility. A study of crystal violet dye retention demonstrated the differences in levels of total adherent material and was also shown to be highly reproducible across a plate.

CONCLUSION

The reproducibility and flexibility of the MBEC™ device supports the use of this model in HTP screening of biomaterial related biofilm infections.

REFERENCES

- 1.Ceri H, Olson ME, Stremick C, Morck D, Buret A. (1999) The Calgary Biofilm Device: New Technology for Rapid Determination of Antibiotic Susceptibilities of Bacterial Biofilms. *Journal of Clinical Microbiology* 37(6):1771-1776.

Physical and chemical characteristics of adhesives for application on the skin

Sean Kelly¹, Rebecca Booth¹ and Steven L Percival^{1,2,3*}

¹Scapa Healthcare, Manchester, UK

²Institute of Aging and Chronic Disease, University of Liverpool, Liverpool, UK

³Surface Science Research Centre, University of Liverpool, Liverpool, UK

*email: Steven.Percival@scapa.com

INTRODUCTION

Adhesives are used across a variety of healthcare applications including wound care dressings, medical device fixation such as ostomy fixation and transdermal delivery. The selection of the type of adhesive for these various applications is dependent on a number of factors including position on the body, wear time, contact with wounded skin and breathability requirements. Aggressive adhesives can damage the fragile skin of neonates and the elderly so choosing skin-friendly adhesives which cause minimal trauma to the skin is important. Dressings and other devices which require fixation to the skin for long periods of time (>48 hours) require adhesives to ensure a secure hold, be conformable so as not to restrict movement and ideally breathable to improve patient comfort and compliance. Few studies have been completed to fully understand and compare the various characteristics of skin adhesive materials. In this study we aim to compare the physical and chemical characteristics of 3 types of adhesive used in healthcare; acrylics, silicones and polyurethane (PU) gels.

EXPERIMENTAL METHODS

- Physical and chemical test methods were carried out following industry standard test protocols.
- Moisture vapour transfer rate (MVTR) was measured at 37°C equivalent to 24 hours using upright Paddington cups (BSEN 13726-2:2002).
- Peel adhesion was measured at a constant peel angle using a 25mm width of adhesive material.
- Trauma on removal was investigated using a porcine skin model. Adhesives were applied to the skin surface with constant pressure and then removed following 2 hours to understand the degree of skin trauma caused on removal of an adhesive.

- Effect of adhesive removal on the *in vitro* stratum corneum was visualised macroscopically and also quantified by measuring the absorbance of methylene blue dye released from tissue.

RESULTS AND DISCUSSION

- MVTR testing demonstrated that PU gel adhesive had the highest moisture vapour transfer rate, whilst silicone was proven to have a high level of occlusiveness.
- Peel adhesion testing highlighted that silicone gel adhesives had the lowest peel strength. However, the PU gel also showed low peel strength, particularly when compared to acrylic adhesives.
- Visual analysis of the stained porcine skin model indicated that the silicone and PU adhesive removed less stain when compared to an acrylic adhesive.
- Absorbance data verified this result with quantitative data and showed that silicone and PU removed the least dye from the surface and acrylic the most.

CONCLUSION

- The high MVTR level of PU gel adhesive proves that this adhesive is breathable and thus more comfortable when worn for extended periods of time.
- The acrylic adhesive had the greatest tack level however they also removed the highest amount of dye indicating that they caused the highest level of skin trauma on removal.
- Both the silicone and the PU gel adhesive indicated that they caused low trauma to skin on removal and were deemed to be more 'skin-friendly' than acrylic adhesive.

The role of adhesives in biofilm prevention

Steven L Percival^{1,2,3*}, Rebecca Booth³ and Sean Kelly³

¹Institute of Ageing and Chronic Disease, University of Liverpool, Liverpool, UK

²Surface Science Research Centre, University of Liverpool, Liverpool, UK

³Scapa Healthcare, Manchester, UK

*email: Steven.Percival@scapa.com

INTRODUCTION

Acrylics, polyurethanes and silicones are adhesives which are commonly used as biomaterials and used for adhering materials internally or externally on the human body. To date little work has been done to look at the affect these adhesives have on the prevention, formation and reattachment of biofilms. Biofilms are evident in all chronic wounds, with highly virulent biofilms relevant to the non-healing of chronic wounds. These wounds are frequently managed using wound dressings that use various adhesives to secure them to the skin. Adhesive wound contact layers ensure that dressing materials conform to the wound surface and thus may be in contact with wound biofilms. This study examined the influence of silicone, acrylic and polyurethane (PU) adhesives on the growth of *Staphylococcus aureus* and *Pseudomonas aeruginosa* biofilms using a novel poloxamer biofilm model.

EXPERIMENTAL METHODS

- 10⁸cfu/ml *S. aureus* and *P. aeruginosa* in Maximum Recovery Diluent (MRD) were inoculated into the poloxamer polymer.
- Samples (3 x 3cm) of silicone, acrylic and polyurethane adhesives were inoculated with 100µl of the Poloxamer bacterial suspension, and incubated at 35°C.
- At 24, 48 and 72 hours images of the bacteria, attached to the adhesives, growing in the poloxamer hydrogels were taken using a light and confocal laser microscope.
- Total viable counts were performed at 0, 4, 24, 48 and 72 hours. Samples of adhesives were placed in 10ml MRD and refrigerated to allow the poloxamer to liquify. When in solution, the MRD suspension was serially diluted, plated on to TSA plates and incubated 35°C. After 48 hours the colonies were counted. All adhesives were tested in triplicate.

RESULTS AND DISCUSSION

- Similar numbers of viable cells were isolated from *S. aureus* and *P.aeruginosa* poloxamer hydrogel biofilms grown in the presence silicone and acrylic adhesive.
- Visualisation of *S. aureus* and *P. aeruginosa* poloxamer biofilms demonstrated that biofilm development was similar in the silicone and acrylic exposed samples.
- Poloxamer biofilms of *S. aureus* demonstrated a fall in cell numbers after 24 hours when exposed to PU adhesive and images of these samples showed that biofilm formation was inhibited.

CONCLUSION

To date little work has been done to investigate the effects of adhesives on the formation of biofilms. The presence of biofilms in chronic wounds is generally clinically accepted, it is important to understand the effects that wound care adhesives may have on biofilms. Here we have used a simple and reproducible *in vitro* biofilm model to begin to understand these affects. We observed that the PU adhesive has an inhibitory effect on Gram positive *S. aureus* biofilms. *S. aureus* is often isolated from chronic and non-healing wounds and is known to form biofilms. PU gel adhesives have several characteristics that make them ideal for wound care applications including secure hold, breathability and low trauma upon removal. This study has indicated that the PU adhesive may have additional effects on biofilms, which could be beneficial if used as a wound contact layer. Further studies are required to fully understand the effects of adhesives on biofilm formation and maintenance, with particular focus on bacterial strains, which are isolated from chronic wounds.

Silicone adhesives and their use in skin and wound care

Sean Kelly¹, Rebecca Booth¹ and Steven L Percival^{1,2,3*}

¹Scapa Healthcare, Manchester, UK

²Institute of Ageing and Chronic Disease, University of Liverpool, Liverpool, UK

³Surface Science Research Centre, University of Liverpool, Liverpool, UK

*email: Steven.Percival@scapa.com

INTRODUCTION

Silicones have a number of qualities that make them ideal materials for use internally and externally as medical devices and biomaterials. They are inert, non-irritating, have low toxicity, low thermal conductivity and are water-repellent. A number of clinical studies have been performed which demonstrate how these properties confer specific advantages over other materials. Silicones are also used as a standard treatment for the prevention and treatment of hypertrophic and keloid scarring. Several studies have shown that long-term use of silicone gels and sheets can reduce itching and discomfort of scarred skin tissue, flatten and soften margins and reduce discolouration. Silicone can be made into adhesives and gels and are often described as a 'skin friendly adhesive' solution. Here we investigate the various characteristics of a new range of silicone materials designed specifically for use in skin and wound care.

EXPERIMENTAL METHODS

- Moisture vapour transfer rate (MVTR) testing was carried out on perforated and non-perforated silicone gel adhesives and measured at 37°C equivalent to 24 hours using upright Paddington cups (BSEN 13726-2:2002).
- Peel adhesion was measured at a constant peel angle using a 25mm width of adhesive material.
- Trauma on removal was investigated using porcine skin stained with methylene blue. Silicone gel and medical grade adhesive were applied to the skin surface with constant pressure and then removed following 2 hours to understand the degree of skin trauma caused on removal. Silicone gel adhesives were compared to medical grade acrylic adhesives.
- Effect of adhesive removal on the *in vitro* stratum corneum was visualised macroscopically and also quantified by measuring the absorbance of methylene blue dye released from tissue and adhesive samples in to 2mls of dimethyl sulfoxide (DMSO).

RESULTS AND DISCUSSION

- Both visualisation of the porcine skin and quantification of the methylene blue dye from the samples demonstrated that the silicone gel adhesive removed less of the stained skin surface cells than the medical grade acrylic adhesive.
- The silicone gel adhesive had a low MVTR value; however, perforation of the material permitted vapour transfer through the gel.
- Peel testing of the perforated and non-perforated material showed that the drop in adhesion was proportional to the amount of silicone adhesive removed and did not affect the overall adhesive performance of the material.

CONCLUSION

- As expected, the new silicone gel adhesive studied was shown to have a low MVTR level. This occlusive characteristic provides evidence that this material may help to reduce scarring on newly healed wounds.
- Perforation of the silicone gel adhesive allows for moisture permeability without significantly affecting the peel adhesion of the silicone gel, which allows this, adhesive to be used as a wound contact layer in combination with an absorbent layer such as a foam even in exuding wounds.
- Results of the *in vitro* skin trauma testing proved that the silicone gel had 'skin-friendly' characteristics since skin trauma was reduced significantly when compared to the acrylic adhesive.
- Skin-friendly silicone gel adhesives are ideal materials for use as skin and wound contact layers in applications ranging from advanced wound care to medical device fixation.

A Computer Model for Polymer Degradation in the Presence of Acidic Drug

K. Sevim and J. Pan

Department of Engineering, University of Leicester, Leicester, UK, ks377@le.ac.uk

INTRODUCTION

Poly(lactic acids) (PLAs), poly(glycolic acid) (PGA) and poly caprolactone (PCL)¹, are widely used to make bioresorbable devices such as drug delivery systems and tissue scaffolds². The basic degradation process for the polymers containing ester functional group in their main chain is hydrolysis. Water penetrates the polymers, breaking the long chains into oligomers. This process is known as chain scission. For PLA hydrolysis, acidity of the medium increases as more carboxylic acid dissociates that accelerates degradation of polymer. This process is known as autocatalysis³. The diffusion rate of drug in a polymer matrix is closely related to the level of polymer degradation. This paper presents a mathematical model for the interplay between an acidic drug (acetylsalicylic acid or aspirin) and polymer degradation.

MATHEMATICAL MODEL

The degradation behaviour of resorbable polymers is modelled considering three mechanisms: hydrolysis reaction between ester bonds and water molecules; acid disassociation of carboxylic ends and further catalytic effect arising from dissolution of acidic drug and its transport in the polymer matrix. Water concentration is not a limiting factor in the model and assumed to be abundant. The hydrolysis reaction takes place in the polymer matrix. As long ester bonds are broken into short chains, more and more carboxylic and alcoholic end groups are generated. Meanwhile, water dissolves the drug particles, leading to a further increase in acidity. The solubilised aspirin diffuses through the polymer matrix, further accelerates the degradation of polymer. In our model, the effect of aspirin diffusion on the degradation of polymer chains is considered. A numerical method is used to solve the differential equations.

RESULTS AND DISCUSSION

The model used here comprises a mathematical expression for polymer degradation by autocatalytic hydrolysis. Moreover, it considers drug particle dissolution, its diffusion through the polymer matrix and interaction with the hydrolysis of the polymer chains. Polymer degradation is modelled using a random chain scission model, while drug diffusion is governed by Fick's laws. The chain scission rate is given by a rate equation [1] developed by Pan and co-workers³:

$$\frac{dRs}{dt} = \left[Ce_0 \left(1 - \alpha \left(\frac{Rs}{Ce_0} \right)^\beta \right) \right] (k_1 + k_2' C_{H^+}) \quad [1]$$

in which dRs/dt is chain scission rate, Ce_0 is the initial concentration of ester bonds, C_{H^+} is the acid

concentration, and k_1 and k_2' are kinetic parameters of the ester bond. The effect of drug on degradation is reflected by C_{H^+} which is the sum of the acid disassociation of the carboxylic chain ends and the dissolved drugs in the polymer matrix.

Figure 1 shows the calculated distributions of drug concentration between two drug particles at different times. The left end of the curves is the interface between a drug particle and polymer matrix, while the right end is the mid-point between two drug particles. As time increases, drug concentration in the matrix changes from zero to a uniform distribution of its saturation value in the polymer. Because the drug concentration is not uniform in the polymer before the saturation, polymer degradation is also not uniform due to the different level of acidity, C_{H^+} , at different location. The differential degradation leads a huge difference in the diffusion coefficient of the drug at different locations because of its sensitivity to free volume. Consequently the model can handle a complex interaction between the polymer degradation and drug release.

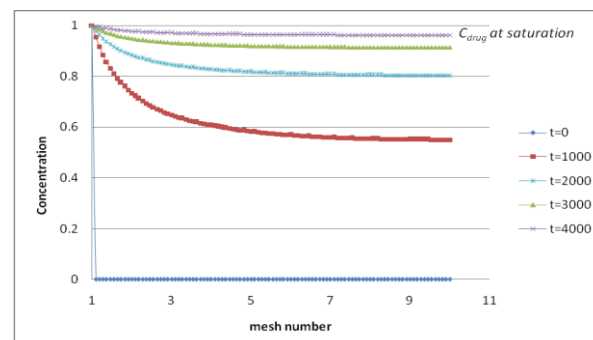


Figure 1 Computer simulated distribution of drug concentration at different times

CONCLUSION

The preliminary results of transport-reaction model is presented that takes into consideration of the autocatalytic effect of polymer chain ends and the transport of the dissolved drug on the degradation of the polymer matrix. The model is able to deal with a complex interplay between drug diffusion and polymer degradation.

REFERENCES

1. Gleadall A. *et al.*, J. Biotechnol Biomater. 3:154, 2013
2. Arosio P. *et al.*, Polym Int. 57:912-920, 2008
3. Wang Y. *et al.*, Biomaterials, 29(23): 3393-340, 2008

In vitro degradability, bioactivity and cell responses to mesoporous magnesium silicate for bone regeneration

Jie Wei^{1*}, Zhaoying Wu¹, Han Guo², Changsheng Liu^{1*}

^{1*}Key Laboratory for Ultrafine Materials of Ministry of Education, East China University of Science and Technology, P.R. China, jiewei7860@sina.com

²Shanghai Synchrotron Radiation Facility, Shanghai Institute of Applied Physics, Chinese Academy of Sciences, P.R. China

INTRODUCTION

Mesoporous magnesium silicate (m-MS) was firstly synthesized, and the in vitro degradability, bioactivity and primary cell responses to the m-MS were investigated. The results suggested that the m-MS with mesoporous channels of around 5 nm possessed the high specific surface area of 451.0 m²/g and pore volume of 0.41cm³/g as compared with magnesium silicate (MS) without mesopores of 75 m²/g and 0.21 cm³/g, respectively. The m-MS could absorb a large number of water with the water absorption of 74 % as compared with MS of 26 %. In addition, the m-MS could degrade in Tris-HCl solution with the weight loss ratio of 40 w% after immersion for 70 days. The m-MS had good in vitro bioactivity, which could induce apatite formation on its surfaces when soaked into

simulated body fluid (SBF), and the rate of apatite formation for m-MS was obviously faster than MS. The cell experiment results revealed that m-MS could obviously promote proliferation and differentiation of the MC3T3-E1 cells on its surfaces than MS with time, and exhibited normal cell morphology, indicating excellent cytocompatibility. This study suggested that the mesoporous magnesium silicate with high specific surface area and pore volume had suitable degradability, good bioactivity and biocompatibility, which might be an excellent candidate of a biomaterial for bone regeneration.

Macromolecular crowding maintains tenogenic phenotype *ex vivo*

Kyriakos Spanoudes, Abhigyan Satyam, Abhay Pandit, Dimitrios Zeugolis

¹Network of Excellence in Functional Biomaterials, National University of Ireland, Galway, Ireland.

kyriakos.spanoudes@nuigalway.ie

INTRODUCTION

Tendon tissue engineering is becoming increasingly important as the current surgical treatment modalities have numerous drawbacks. Cell-based therapies are aiming to create autologous treatments for patients. However, traditional culture conditions are associated with tenocyte phenotypic drift and incomplete tenogenic differentiation of stem cells. These difficulties have stemmed research towards creation of more functional *in vitro* micro-environments [1] that would resemble the native habitat of tenocytes *ex vivo*. Macromolecular crowding (MMC) has been postulated to imitate *in vitro* the *in vivo* dense extracellular milieu [2]. In this work, we hypothesise that MMC will maintain tenogenic phenotype *in vitro*.

EXPERIMENTAL METHODS

Human patellar tendon tenocytes were expanded up to passage 3 in DMEM media, supplemented with 10% foetal bovine serum and 1% penicillin / streptomycin. 50,000 / cm² tenocytes were subsequently cultured for a period up to 28 days, supplemented with ascorbic acid phosphate 100 µM/L and 75 mg/ml carrageenan (CR; MMC agent). The influence of CR on cell morphology, viability and metabolic activity was evaluated using phase-contrast microscopy, Live/Dead® and alamarBlue® assays respectively. Phenotype maintenance was verified using protein and gene assays based on the expression of positive markers (e.g. scleraxis, collagen I, tenascin C, tenomodulin) and trans-differentiation markers (e.g. osteopontin, osteocalcin, aggrecan).

RESULTS AND DISCUSSION

Preliminary results suggest that culture with CR does not compromise cell viability and metabolic activity, whilst maintains tenocyte phenotype. Further gene and protein analysis for longer time points are under way.

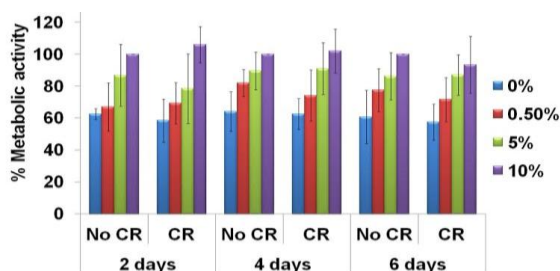


Fig. 1: Cell metabolic activity was maintained up to 6 days in culture.

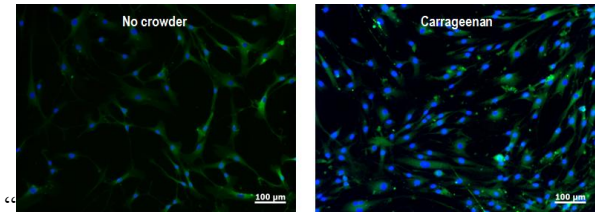


Fig 2: Tenomodulin expression was maintained up to 4 days in culture.

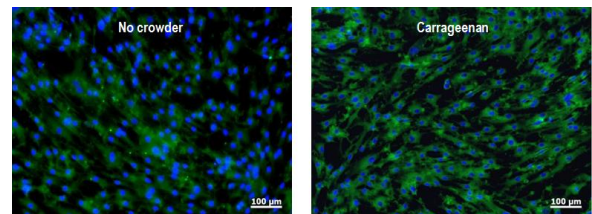


Fig 3: Collagen type V expression was maintained up to 4 days in culture.

CONCLUSION

Macromolecular crowding, is a valuable biophysical tool for a tenogenic phenotype maintenance regimen in the quest for tendon regeneration strategies.

REFERENCES

1. Cigognini D *et al.* Drug Discovery Today. 18, 1099, 2013.
2. Satyam A *et al.* Adv. Mater. DOI: 1.1002.adma.201304428

ACKNOWLEDGMENTS

Funding was generously provided by Science Foundation Ireland and College of Engineering and informatics, National University of Ireland, Galway.

Effect of cooling rates after casting and subsequent Solution Treatment on Microstructure and Mechanical Strength of Dental Silver Alloys with different Cu contents

Tomoya Yasuda¹, Toshikazu Akahori², Yushi Hoshiya¹, Tomokazu Hattori², Hisao Fukui³

¹Graduate School of Science and Technology, Meijo University, Japan

²Faculty of Science and Technology, Meijo University, Japan

³Dental School, Aichi-Gakuin University, Japan, 133434036@ccalummi.meijo-u.ac.jp

INTRODUCTION

The Ag–Pd–Cu–Au system was developed in Japan for applications in dentistry and is been widely used in inlays, crowns, etc. Recently, the mechanical strength of this alloy has been reported to be significantly enhanced when it is subjected to solution treatment (ST) at temperatures higher than 1073 K and subsequent water quenching without any aging⁽¹⁾. This unique hardening mechanism seems to be based on factors such as the ST temperature, cooling rate after ST, and initial microstructure before ST. Therefore, this study investigated the relationship between the mechanical strength and microstructure of samples with different constituent proportions of the Ag–Pd–Cu–Au alloy system. These were cast into plaster and Cu molds to control the various cooling rates followed by ST.

EXPERIMENTAL METHODS

Hot-rolled plates of Ag-20Pd-14Cu-12Au and Ag-20Pd-20Cu-12Au alloys were used and are designated as Ag-Cu_{low} and Ag-Cu_{high}, respectively. Samples were fabricated to have the same diameter and height, which is 2.0mm and 4.0mm, respectively, were fabricated by centrifugal casting. Plaster and Cu molds were used to control the cooling rate after casting. Some castings were subjected to ST at 1123 K for 3.6 ks in an argon gas atmosphere followed by water quenching. The castings and those subjected to ST were designated as As-cast and ST, respectively. Furthermore, they are distinguished by their diameters (e.g., As-cast/φ2.0 mm and ST/φ2.0 mm). A scanning electron microscope (SEM) equipped with a wavelength dispersive X-ray spectrometer (WDS) and X-ray diffraction (XRD) spectroscope were used to evaluate the microstructure of each specimen. The Vickers hardness (HV) test was performed to examine the mechanical strength.

RESULTS AND DISCUSSION

Figures 1 and 2 show BSE images of Ag-Cu_{low} and Ag-Cu_{high} cast in Cu and plaster molds and those after ST, respectively.

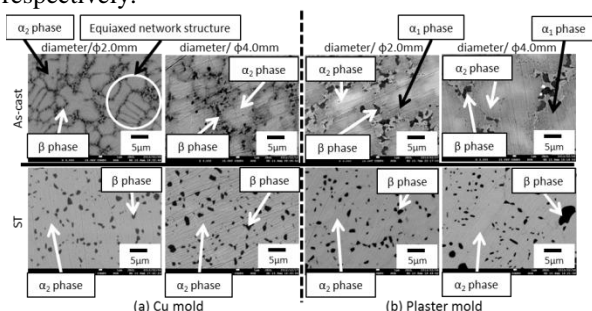


Fig.1 BSE images of Ag-Cu_{low} with Cu and plaster molds and those after ST.

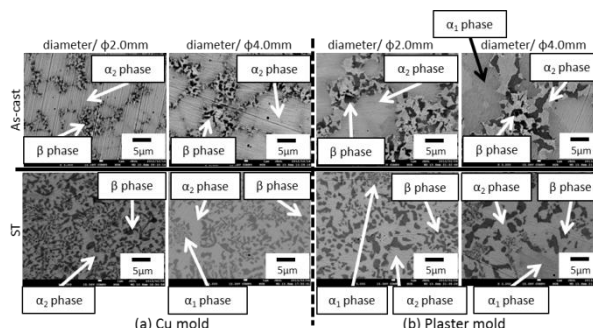


Fig.2 BSE images of Ag-Cu_{high} with Cu and plaster molds and those after ST.

The As-cast Ag-Cu_{low} samples demonstrated an equiaxed network structure, as shown in Fig. 1. The As-cast Ag-Cu_{low} sample with a φ2.0 mm diameter and cast into a Cu mold showed the smallest average diameter for the equiaxed network because it had the fastest cooling rate. Therefore, the average diameter tended to increase with the sample diameter and when the plaster mold was used. In contrast, the microstructure of The ST samples cast into Cu and plaster molds showed a large number of β-phases that precipitated at the boundaries of the equiaxed network structure. In this case, the coarsening of the β phase was significant for the sample with a diameter of φ4.0 mm and cast into a plaster mold as it had the slowest cooling rate.

The microstructure of the As-cast Ag-Cu_{high} sample cast into Cu and plaster molds also exhibited an equiaxed network structure similar to Ag-Cu_{low}, as shown in Fig. 2. However, the average diameter of the equiaxed β phase differed. The size and volume fraction of the β phase increased with the relatively high Cu/Ag ratio of 0.16. Furthermore, the microstructure after ST changed drastically: there was a large amount of β phase compound relative to As-cast.

CONCLUSIONS

- The diameters of the Ag-Cu_{low} and Ag-Cu_{high} equiaxed network structures decreased with increasing cooling rate after casting, which was controlled by the size of the casting and the material of the mold.
- The Ag-Cu_{low} and Ag-Cu_{high} microstructures after ST did not show an equiaxed network structure, but the sizes and volume fractions of the β phase were different from each other.

REFERENCES

- 1) T. Akahori, M. Niinomi, M. Nakai, H. Tsutsumi, T. Kanno, Y.H.Kim, H.Fukui, J. Japan Inst. Metals, 74(2010), pp. 337-344

Change in Microstructure and Mechanical Strength of Substitution Material for Dental Precious Alloys Fabricated by Solidification under Various Conditions

Yushi Hoshiya¹, Toshikazu Akahori², Tomoya Yasuda¹, Tomokazu Hattori², Hisao Fukui³

¹Graduate School of Science and Technology, Meijo University, ²Faculty of Science and Technology, Meijo University,

³Dental School, Aichi-Gakuin University

100434051@ccalumni.meijo-u.ac.jp

INTRODUCTION

In dentistry, Ag–20Pd–14Cu–12Au alloy (mass%) is widely used in inlays, crowns, etc. as a substitute material for precious metals. Recently, the mechanical strength of this alloy has been reported to be significantly enhanced when it is subjected to solution treatment at temperatures higher than 1073 K and subsequent water quenching without any aging. This unique hardening mechanism seems to influence the presence of the intermetallic compound (β phase) after solidification and the subsequent solution treatment. However, conditions that induce this unique hardening, such as the solidification temperature, have not yet been clarified. Therefore, this study investigated the relationship between the mechanical strength and microstructure of the Ag–20Pd–14Cu–12Au alloy after the solidification and subsequent solution treatment under various conditions.

EXPERIMENTAL METHODS

Hot-rolled plates of Ag–20Pd–14Cu–12Au alloy were used. Solidification was induced at temperatures of 1373, 1873, and 1973 K for 1.8 and 3.6 ks in an Ar gas atmosphere followed by water quenching (WQ). Some samples were fabricated with solution treatment (ST) at 1123 K for 3.6 ks in a vacuum followed by WQ. Hereafter, the samples with holding times of 1.8 and 3.6 ks for solidification were designated as As1.8ks and As3.6ks, respectively. The sample were further classified by the solidification temperature. As1.8ks and As3.6ks subjected to ST were designated as As1.8ks/ST and As3.6ks/ST, respectively.

Back-scattering electron (BSE) images from a scanning electron microscope (SEM) and elemental mapping by a wavelength dispersive X-rays spectrometer (WDS) were used to observe the microstructures and evaluate the phase constitutions. The Vickers hardness (HV) test was performed to evaluate the mechanical strength. The corrosion potential was measured in a 3 mass% NaCl solution to evaluate the corrosion resistance.

RESULTS AND DISCUSSION

Figure 1 shows the Vickers hardness of As1.8ks at solidification temperatures of 1373–1973 K and after ST.

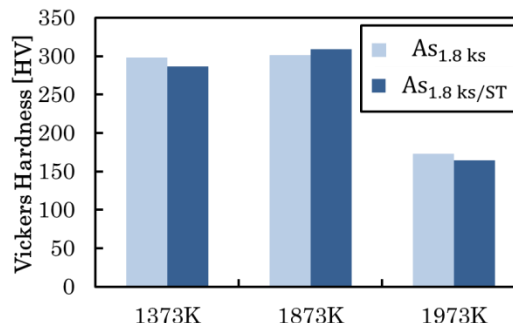


Fig. 1 Vickers hardness of As_{1.8ks} at solidification temperatures at 1373 K–1973 K and those after ST.

The Vickers hardness (HV) of As_{1.8ks}/1373K and As_{1.8ks}/1873K were almost the same at around 300 HV. However, the HV of As_{1.8ks}/1973K decreased remarkably. This decrease may be caused by the dissolution of almost all β phases by solidification at the highest temperature (1973 K) or the formation of oxide, which can restrict the formation of the β phase. The HV of the samples subjected to ST decreased slightly, although As_{1.8ks/ST}/1873K showed the reverse trend. This change in hardness may reflect the influence of the decreased solution hardening on the α_1 phase because of the presence of a large α_2 phase. As noted above, the remarkable decrease in HV may be due to the volume fraction and restriction of the β phase. Precipitation of the β phase, which is an ordered or disordered intermetallic compound, increased the strain on the microstructure. Therefore, the presence of the β phase was attributed to the change in HV. As_{3.6ks} and As_{3.6ks/ST} showed almost the same tendency as As_{1.8ks} and As_{1.8ks/ST}.

The corrosion potential of As_{1.8ks} and As_{3.6ks} increased with the solidification temperature, although the potential increased more through ST. The potential may have been increased by the decrease in the volume fraction of the α_1 phase with relatively high Cu content.

CONCLUSIONS

- (1) It was difficult to observe the β phase in As_{1.8ks} and As_{3.6ks} subjected to solidification at 1973 K because of the dissolution or formation of oxide.
- (2) The corrosion potential of As_{1.8ks} and As_{3.6ks} increased with the solidification temperature and subsequent ST.

REFERENCE

- 1) T. Akahori, M. Niinomi, M. Nakai, H. Tsutsumi, T. Kanno, Y.H. Kim, H. Fukui, J. Japan Inst. Metals, 74(2010), pp. 337-344

Morphological Control of Layered Double Hydroxide Crystals as Drug Carrier by Organic Molecules with Carboxyl Group

Taishi Yokoi*, Sota Terasaka and Masanobu Kamitakahara

Graduate School of Environmental Studies, Tohoku University, Japan, yokoi@mail.kankyo.tohoku.ac.jp

INTRODUCTION

Drug delivery is useful for enhancement of therapeutic effect by transporting pharmaceutical compounds to affected area. Layered double hydroxides (LDH) have been attracting interest as a drug carrier¹. LDHs are composed of positively charged metal hydroxide layers, which are composed of divalent and trivalent cations, and interlayer anions. Various anions can be incorporated into LDH crystal. The exchangeability of interlayer anions has been utilized to load, transport and deliver pharmaceutically active molecules.

LDH is synthesized through wet chemical processes, such as homogeneous precipitation². The obtained LDH crystals have generally hexagonal plate shape. LDH crystals grow the *a*- and *b*-axes directions and mainly expose the *c* face. If the crystal growth for the *a*- and *b*-axes directions is inhibited, unique and unusual-shaped LDH crystal will form. Morphological control of LDH crystals achieves development of novel drug carriers. However, the morphological control technique of LDH is still unclear. At the very beginning, to establish morphological control guideline of LDH crystals is important.

Isoelectric point of LDH containing Mg^{2+} and Al^{3+} as cationic components (MgAl-LDH) is around $pH=11^3$, hence MgAl-LDH has positively charge during the synthesis, namely homogeneous precipitation. Anionic molecules such as carboxylic acids should interact with LDH crystal and elicit morphological change. However, effects of carboxylic acids on morphology and crystal growth of LDH are not clarified. In the present study, we investigated effects of carboxylic acids addition for reaction systems on morphology of LDH crystals synthesized homogeneous precipitation method. We selected acetic acid and succinic acid as the additive, because these carboxylic acids do not make precipitates with Mg^{2+} and Al^{3+} .

EXPERIMENTAL METHODS

Solutions containing $100\text{ mol}\cdot\text{m}^{-3}$ magnesium nitrate, $50\text{ mol}\cdot\text{m}^{-3}$ aluminium nitrate, $300\text{ mol}\cdot\text{m}^{-3}$ urea and 0 or $100\text{ mol}\cdot\text{m}^{-3}$ morphological control agent, namely acetic acid or succinic acid, were prepared. The solution (50 cm^3) was maintained at 90°C for 5 days to form LDH. The precipitates formed were collected by vacuum filtration and dried at 90°C for over 24 hours.

Crystalline phases of the obtained samples were characterized by powder X-ray diffraction (XRD). Crystal morphology was observed under scanning electron microscopy (SEM) after thin Pt film coating.

RESULTS AND DISCUSSION

Crystalline phases of samples were characterized by XRD. Quintinite-3T ($Mg_4Al_2(OH)_{12}CO_3\cdot 3H_2O$), which is a kind of LDH, was detected in all the samples.

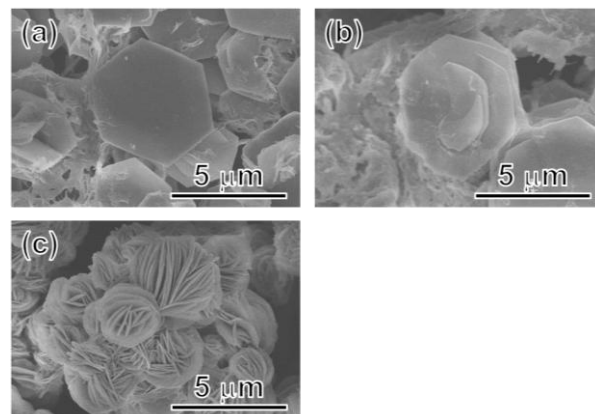


Figure 1 SEM images of samples: (a) LDH synthesized without morphological control agent, (b) LDH synthesized with acetic acid and (c) LDH synthesized with succinic acid.

Figure 1 shows SEM images of samples. Plate-shaped crystals were formed under the condition without morphological control agent. Stacked hexagonal plate-shaped crystals were formed in the condition with acetic acid. Aggregates constructing plate-shaped crystals were formed under the condition with succinic acid.

Spiral growth of LDH has been reported previously⁴. We considered that the adsorbed acetic acid molecules inhibited bonding between the substrate and newly formed LDH crystals thereby resulting in the formation of stacked disc-shaped LDH crystals. Assembled nuclei most likely grew to aggregates constructing plate-shaped crystals. Succinic acid should generate self-assembling of LDH nuclei.

CONCLUSION

We investigated effects of acetic acid and succinic acid addition on morphology of LDH synthesized by homogeneous precipitation. The morphology of LDH implied that acetic acid mainly affect crystal growth of LDH and succinic acid assist assembling of LDH nuclei. These findings can be applicable for development of novel drug carriers.

REFERENCES

1. Ladewig K. *et al.*, Expert Opin. Drug Deriv. 6:907-922, 2009
2. Yokoi T. *et al.*, Chem. Lett. 43:234-236, 2014
3. Li Y. *et al.*, Colloids Surf., B 303:166-172, 2007
4. Okamoto K. *et al.* Appl. Clay Sci. 37:23-31, 2007

ACKNOWLEDGMENTS

This work was supported financially by Kurita Water and Environment Foundation (Project No. 13A025)



Properties of β -TCP based Calcium Phosphate Cement using mechano-chemical process

J. Y. Bae¹, Y. Ida¹, K. Sekine¹, F. Kawano² and K. Hamada¹

¹ Department of Biomaterials and Bioengineering, ² Department of Comprehensive Dentistry, Institute of Health Biosciences, University of Tokushima, Japan, c301151014@tokushima-u.ac.jp

INTRODUCTION

Calcium phosphate cement (CPC) is widely utilized today for various clinical applications. CPC shows many advantages as a bone-substitution material. The objective of this research is to develop a new CPC indicating fine injectability, short setting-time and high strength, simultaneously, and to expand the application of CPC.

EXPERIMENTAL METHODS

β -tricalcium phosphate (control TCP; β -TCP) powder was modified mechano-chemically using ball-milling. The phase constitutions of calcium phosphate were investigated using X-ray diffractometry (XRD). The powder after milling (modified TCP; m- β -TCP) was mixed with 2.5 mass% CaCl_2 solution, and then 2.5 mass% NaH_2PO_4 solution at a powder/liquid ratio of 4:1:1. The paste after mixing was filled in a syringe and the time performing injectability was measured. The load pressurize to syringe was applied using universal testing machine (Autograph AGS-500A, Shimadzu, Japan). Cross head speed was 20 mm/min and the maximum load was 300N. The injectability was calculated according to the equation shown as follows,

$$\text{Injectability}(\%) = \frac{W_{\text{exp}}}{W} \times 100$$

where W_{exp} is the weight of paste expelled from syringe, and W is the total weight of paste before injection.

To investigate the initial setting time of the cement, we measured the strength through the compressive strength (CS) and diametral tensile test (DTS) each time from 1 h to 5 hrs. The paste after initial setting was kept for 1 w for complete setting. Mechanical properties were evaluated by CS and DTS according to milling time. The porosity of the set cement specimen was measured using a gas pycnometer (AccuPyc1330, Micromeritics, USA).

RESULTS AND DISCUSSION

XRD profiles indicated that the peaks of TCP powder after milling became broader with increasing milling time from 0 h to 24 hrs, and then the powder became partially amorphous.

β -TCP cement paste was set quickly within 5 min after mixing, while m- β -TCP cement paste did not lose a flowability for 7 hrs. Calculated injectability of β -TCP 5 min after setting and m- β -TCP 1 h after setting were 2.98% and 23.8%, respectively.

β -TCP compacts 1 h after mixing collapsed during removal from silicone mold. Compacts 2 and 3 hrs after mixing showed near zero for CS and DTS. CS and DTS 4 and 5 hrs after mixing were 1.07 MPa and 0.13 MPa, and 1.09 MPa and 0.14 MPa, respectively. m- β -TCP

compacts more than 1 h after mixing were durable for CS and DTS. CS and DTS increased with increasing time after mixing; CS and DTS 1 h and 5 hrs after mixing were 0.53 MPa and 0.08 MPa, and 8.02 MPa and 2.62 MPa, respectively. Reduction of initial setting time and acceleration of CS and DTS increase was supposed to increase the high dissolution rate of m- β -TCP powder due to the fine powder size and instability of amorphous powder after milling.

The dependence of CS, DTS and porosity of the compacts on the milling time are shown in Fig. 1. The CS and DTS of compacts 0 h to 24h hrs after mixing were 0.68 ± 0.15 MPa and 0.24 ± 0.05 MPa, and 26.47 ± 4.82 MPa and 3.89 ± 0.49 MPa, respectively. Those of porosity from 0 h to 24hrs were 53.15 ± 1.7 % and 41.9 ± 1.97 %, respectively. All the CS data and DTS data of m- β -TCP were significantly higher than those of β -TCP ($t < 0.01$). The porosity showed a slight decline according to the milling time. The reduction of porosity is supposed to affect the increase of CS and DTS of compacts after milling.

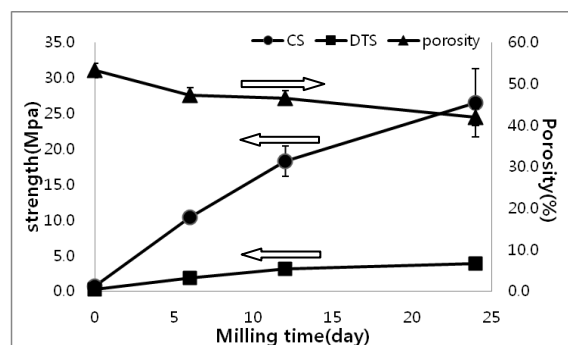


Fig.1 Dependence of CS, DTS and porosity according to the milling time.

CONCLUSION

These results suggested that the mechanochemically-modified calcium phosphate powder dissolved rapidly and accelerated hydroxyapatite precipitation, which successfully shortened the cement setting time and enhanced strength. The m- β -TCP in this study can be a candidate for injectable CPC under higher stress.

REFERENCES

1. U. Gbureck. *et al.*, *Biomater.* 24:4123-4131, 2003.
2. F. Granados-correa. *et al.*, *J.Chil.Chem.Soc.*3:252-255, 2009.
3. Kiyoko Sakamoto *et al.*, *Phosphorus Res Bulletin.* 25:64-67, 2011.

ACKNOWLEDGMENTS

This work was partially supported by the JSPS KAKENHI grant numbers 24592957.



Evaluation of osteoinductive properties of different combinations of macroporous biphasic ceramic (MBCP+™), simvastatin, total bone marrow cells and rhBMP-2 in a rat subcutaneous induced membranes model

Erwan de Monès^{1,2,3,*}, Silke Schlaubitz⁴, Reine Bareille^{1,2}, Chantal Bourget^{1,2}, Pascal Borget⁵, Guy Daculsi⁴, Marlène Durand^{1,2,4}, Jean-Christophe Fricain^{1,2}

¹ Université Bordeaux, Bioingénierie tissulaire, U1026, 146 rue Léo-Saignat, F-33076 Bordeaux cedex, France

² INSERM U1026, Bioingénierie tissulaire, 146 rue Léo-Saignat, F-33076 Bordeaux cedex, France

³ Chirurgie Cervico-Faciale et ORL, CHU de Bordeaux, Place Amélie Raba Léon, 33076 Bordeaux cedex, France

⁴ CIC-IT BioDiMI, CHU de Bordeaux / Inserm, PTIB, Hôpital Xavier Arnoz, Avenue du Haut Lévêque, 33600 Pessac, France

⁵ Biomatlante, 5 rue Edouard Belin, Z.A. Les Quatre Nations, 44360 Vigneux de Bretagne, France

erwan.de-mones-del-pujol@chu-bordeaux.fr

INTRODUCTION

Induced membrane technique has been proposed by Masquelet *et al.*¹ for wide segmental diaphysis bone reconstruction with autologous cancellous bone graft. To reduce donor site morbidity following bone harvest, some authors proposed to add synthetic bone substitutes in combination or not with bone morphogenetic protein 2 (BMP-2) to the graft. To avoid the expenses of the growth factor, the use of the cholesterol lowering statins was investigated in numerous studies showing an enhanced expression of BMP-2 mRNA and osteoblastic differentiation *in vitro* and *in vivo*. Therefore, statins were proposed as BMP-2 substitutes.

The aim of this study was to evaluate the osteoinductive capacity of simvastatin in comparison to BMP-2 in subcutaneous induced membranes filled with the bone substitute MBCP+™ (Biomatlante) in association with total bone marrow allografts in rats.

EXPERIMENTAL METHODS

In vitro studies evaluated simvastatin toxicity at 10^{-6} M and 10^{-8} M and early osteoblastic differentiation on rat Bone Marrow Stromal Cells (rBMSC) cultures in comparison to cells cultured in basal medium or differentiation medium, analysed by Alkaline Phosphatase Assay and quantitative RT-PCR.

Subcutaneous membranes were induced by silicon spacers during 5 weeks. After spacer removal, the volumes were filled with 10 different conditions of MBCP+™, associated or not with total bone marrow (BMr), simvastatin (7µg absorbed/ mg MBCP+™), and rhBMP-2 (Inductos®; 0.025 µg/ mm³ MBCP+™). Four groups of animals were injected with simvastatin at 30mg/ kg/ week. Samples were analysed by microCT and decalcified histology. Osteoid formation was quantified from sections stained with Masson's Trichrome.

RESULTS AND DISCUSSION

Simvastatin caused no cytotoxicity at 10^{-6} M and demonstrated early osteoblastic differentiation of rBMSCs by ALP assays and qRT-PCR for Osteocalcin and BMP2.

MicroCT analysis did not reveal significant differences. Histology demonstrated higher scaffold cellularity for conditions with bone marrow cells.

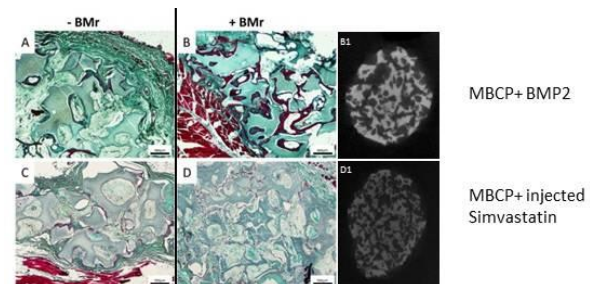


Figure 1: **Representative histological sections** of 4/10 conditions and **MicroCT images** of 2/10 conditions. Sections were stained with Masson's Trichrome (A-D). MicroCT images showing mineralization of the material. MBCP+™ granules were conditioned with rhBMP2 (A,B), or animals received Simvastatin injections (C,D), rat bone marrow (BMr) was associated to conditions in the two right panels (B,B1,D, D1).

All conditions with BMP-2 induced osteoid formation (Figure 1), more prominent in association with bone marrow. Simvastatin absorbed to the MBCP+™ scaffold did not improve osteoinductive properties, while Simvastatin injections had an effect in some of the samples, as evaluated by histomorphometric measurements.

CONCLUSION

Simvastatin affected osteoblastic differentiation, but didn't improve osteoinductive properties of the biomaterial in induced membranes. According to our experience, BMP-2 stays the gold standard in osteoinductive studies in induced membranes.

REFERENCES

1. Masquelet *et al.*, Langenbecks Arch Surg. 388(5):344-6, 2003

ACKNOWLEDGMENTS

The authors would like to thank the "Fondation de l'Avenir" (Grant no: ET1-632/ ET2-666) and the "Fondation des Gueules Cassées" (Grant no: FGC 27-2011) for providing financial support to this project.

Development and Characterization of Thermally Responsive PluronicF127-Chitosan-Kartogenin Conjugates Based Dual Drug Delivery System

Mi Lan Kang, Ji Yun Ko, Ji Eun Kim, Gun Il Im*

*Department of Orthopedics, Dongguk University Ilsan Hospital, Korea, gunil@duih.org

INTRODUCTION

PluronicF127 (F127) is a polymer possessing thermo-reversible and concentration-dependent gelation properties in aqueous solutions. Polymer-drug conjugates generally exhibit prolonged half-life, higher stability, water solubility, lower immunogenicity and antigenicity. The objective of this study was to develop and evaluate a novel drug delivery system which permits the thermally responsive drug release and dual drug delivery by polymer-drug conjugation and drug encapsulation.

Due to the localized nature of osteoarthritis (OA), a chronic joint disease, intraarticular (IA) drug injection is an attractive treatment approach. Recently, a study has been demonstrated that kartogenin (KGN) can induce chondrogenesis of mesenchymal stem cells (MSCs)¹. Therefore, KGN can be a useful regenerative medicine for OA treatment.

Here, we designed dual drug delivery system with thermo-responsiveness for OA treatment via IA injection which is composed of F127-chitosan oligosaccharide (COS)-KGN conjugated nanocapsules (NCs) encapsulating anti-inflammatory drug..

EXPERIMENTAL METHODS

Carboxylated F127 (F127COOH) can be obtained according to the reported work with maleic acid². ¹H-NMR spectrum confirmed the formation of chemical structure of F127COOH.

Bioconjugate of KGN and COS was synthesized by ethyl (dimethylaminopropyl) carbodiimide (EDC)/ N-Hydroxysuccinimide (NHS) catalysis. The F127-COS-KGN NCs were made by emulsification/solvent evaporation method. Conjugation of F127COOH and COS was carried out by adding EDC during the NCs synthesis process. The conjugation of COS with KGN or F127COOH was confirmed by FT-IR and ¹H-NMR. Diclofenac was encapsulated inside of the F127-COS-KGN NCs by change of wall-permeability according to temperature control. Size and morphology of the F127-COS-KGN NCs were characterized by DLS and FE-SEM, respectively. Especially, the size was investigated according to temperature control and molar ratio change of F127 and KGN.

Amounts of KGN and diclofenac released from NCs were determined by HPLC to confirm temperature controlled release. Toxicity of the NCs as a delivery vehicle was estimate by MTT assay.

RESULTS AND DISCUSSION

Pluronic F127 was activated by adding carboxyl groups from maleic acid to both ends of the polymer. The FT-IR spectrum of F127COOH showed a peak indicating the -COOH group. The ¹H-NMR spectrum of F127-COS-KGN NCs showed prominent resonance peaks corresponding to the methyl (-CH₃) and methylene proton at the C2 position of chitosan and benzene ring of KGN. Therefore, it can be supposed from these data that KGN and F127 was successfully conjugated with COS. Degree of KGN and F127 conjugated with COS estimated by ¹H-NMR was 3~5 and 40-50 mol%, respectively.

The F127-COS-KGN NCs are ~300 nm at 37 °C and expand to ~650 nm when cooled at 4 °C in aqueous solution. Temperature-controlled size variation was reduced according to increase of molar ratio of KGN. When the molar ratio of KGN was more than 0.5, size change of the NCs was not observed. Also, the more molar ratio of F127 was increased; the range of size change according to temperature control was grown. Therefore, the thermally responsive properties are dependent on the molar ratio of the F127COOH and KGN during synthesis.

While the encapsulated EB showed burst release for 6 hours, the conjugated KGN showed sustained release for 7 days. This is because higher structural stability of the conjugated system in the F127-COS-KGN NCs.

CONCLUSION

The F127-COS-KGN NCs were prepared dual drug delivery system having thermo-responsiveness for OA treatment via IA route. In conclusion, we can expect that rapid anti-inflammatory effect by burst released DCF and regeneration by sustained released KGN in OA joint. Further studies are ongoing in vitro and in vivo evaluation of anti-inflammatory activity and MSCs chondrogenesis.

REFERENCES

1. Johnson K. *et al.*, Science. 336:717-21, 2012
2. Hsu YC. *et al.*, Adv. Funct. Mater. 18:1799-1808, 2008

ACKNOWLEDGMENTS

The authors would like to thank the National Research Foundation of Korea (Grant no: 2013R1A1A2062978) for providing financial support to this project.

Transduction of Tissue-specific Transcription Factor Protein as a Tool for Tissue Engineering

Masayasu Mie, Shinya Hashimoto, Mami Kaneko and Eiry Kobatake

Department of Environmental Chemistry and Engineering, Tokyo Institute of Technology
mie.m.aa@m.titech.ac.jp

INTRODUCTION

Regulation of cellular differentiation is one of the important subjects for tissue engineering.

During developmental processes in animal, transcription factors play important roles in the regulation of cellular differentiation. Based on these facts, forced expression of tissue-specific transcription factors have been studied for induction of cellular differentiation^{1,2}. We therefore focused on tissue-specific transcription factors as signaling molecules for tissue engineering.

To introduce exogenous transcription factors, gene transfection was used as a conventional method in many studies. However, gene transfection is associated with problems such as genome integration. To overcome such problems, we paid attention to protein transduction methods. Generally, to introduce protein into cells, protein of interests are required to fuse with a short peptide called protein transduction domain (PTD) or cell penetrating peptide (CPP)³. In our previous study, we showed that basic helix-loop-helix (bHLH) type tissue-specific transcription factor proteins, NeuroD2 and MyoD, could be introduced into cells without addition of PTDs⁴⁻⁵.

In this study, we tried to regulate motor neuron and oligodendrocyte differentiation by transduction of Oligodendrocyte transcription factor (Olig2) protein. We showed that Olig2 could be introduced into cells without addition of PTDs and induce cellular differentiation.

EXPERIMENTAL METHODS

Expression and purification of Olig2 proteins

The mouse *Olig2* gene was cloned from Mouse Fetal Normal Tissue embryo Total RNA by reverse transcription-PCR. The cloned fragment was introduced into pET vectors to express proteins fused to His-tag. Other variants of Olig2 were constructed from this plasmid. Proteins were expressed in *E.coli* BL21(DE3). After induction of protein expression, cells were broken by sonication and proteins of interest were purified with nickel-charged affinity resin.

Evaluation of the cellular membrane transduction ability of Olig2 protein

Purified Olig2 and its variant proteins were modified with Oregon Green 488 carboxylic acid succinimidyl ester. Fluorescently labeled proteins were added to mouse embryonic carcinoma cell line P19 cells and incubated for 12 h. Then cells were trypsinized and inoculated on glass base dishes followed by observation using laser scanning confocal microscopy.

Induction of cellular differentiation by addition of Olig2 proteins

For induction of cellular differentiation, Olig2 proteins were added to P19 cells. Cellular differentiation was confirmed by immunostaining or RT-PCR.

RESULTS AND DISCUSSION

Olig2 and its variant proteins were expressed in *E.coli* and purified. To assess their transduction abilities, proteins were labeled with fluorescent molecules. Olig2 is a member of bHLH type transcription factors therefore we have been expected a highly basic domain in Olig2 could work as PTDs as same as NeuroD2 and MyoD. After addition of labeled proteins, cells were observed using laser scanning confocal microscopy. As expected, Olig2 protein was introduced into cells without addition of external PTDs.

After confirming internalizations, Olig2 protein without modification was added to cells to induce cellular differentiation. By addition of transcription factor protein, cells changed their morphology (Fig.1). These results showed that Olig2 protein could induce cellular differentiation.

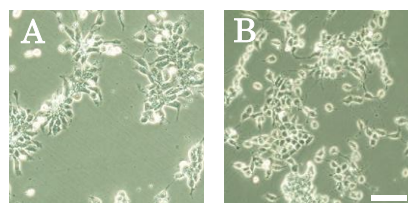


Fig. 1 Induction of neural differentiation by addition of Olig2 protein to P19 cells. Cells were cultured without Olig2 (A) and with Olig2 (B) protein. Scale bar represents 100 μ m.

CONCLUSION

Tissue-specific transcription factor protein, Olig2, has an ability to transduce into cells and induce cellular differentiation. These results suggested that tissue-specific transcription factor protein could be used as a signaling molecule for tissue engineering.

REFERENCES

1. Lassar AB. *et al.*, Cell 47:649-656, 1986
 2. Farah MH. *et al.*, Development 127:693-702, 2000
 3. Nagahara H. *et al.*, Proc. Natl. Acad. Sci. USA 96:14961-14966, 1999
 4. Noda T. *et al.*, J. Biotechnol. 126:230-236, 2006
 5. Noda T. *et al.*, Biochem. Biophys. Res. Commun. 382:473-477, 2009
- Mie M. *et al.*, Biochem. Biophys. Res. Commun. 427:531-536, 2012

ACKNOWLEDGMENTS

The authors would like to thank JSPS KAKENHI for providing financial support to this project.



Construction of Multifunctional Proteins by Integration of Scaffolds and Growth Factors

Eiry Kobatake and Masayasu Mie

Department of Environmental Chemistry and Engineering, Interdisciplinary Graduate School of Science and Engineering, Tokyo Institute of Technology, Japan, kobatake.e.aa@m.titech.ac.jp

INTRODUCTION

For tissue engineering, scaffolds with signalling molecules where cells can adhere, migrate, proliferate and differentiate efficiently are required. As signalling molecules, growth factors play essential roles for controlling such cellular functions. However, when the soluble growth factors are applied to cells, it is difficult to control their local concentrations due to diffusion, cell uptake, and degradation. These problems may be overcome if growth factors are immobilized in a non-diffusible form on an insoluble scaffold, allowing cell surface events involving signal transduction to occur.

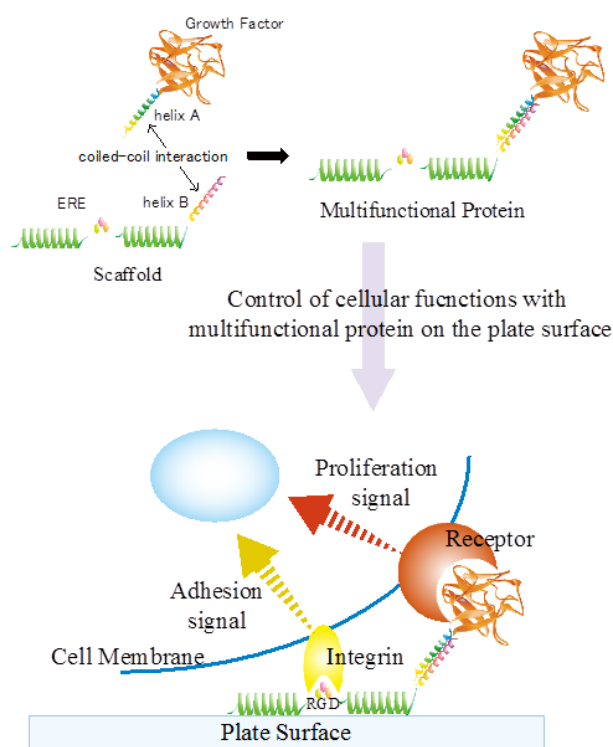


Fig.1 Schematic illustration for controlling cellular functions with multifunctional protein

Therefore we have constructed multifunctional proteins by integrating scaffolds and growth factors for tissue engineering. Here we present our strategy to construct multifunctional proteins. The method is based on formation of the complex between scaffold and growth factor by coiled-coil structure with hydrophobic and electrostatic interactions. Specifically, one peptide (Helix A; HA) capable of forming a coiled-coil structure was fused with a growth factor protein, and another peptide (Helix B; HB) with similar properties was fused with a scaffold protein. Growth factor fused with HA peptide was immobilized via coiled-coil helix formation on a cell-culture plate whose surface was coated with scaffold protein fused with HB peptide, and the cell behaviour on the surface was investigated.

EXPERIMENTAL METHODS

Promotion of cell growth: As the scaffold, we designed the protein (ERE-HB) which is consisting of elastin-derived structural unit, cell adhesive sequence (RGD), and HB. On the other hand, the fusion protein (HA-FGF) between basic fibroblast growth factor (bFGF) and HA was used as a signalling molecule. These proteins were expressed in *E. coli*, and purified. The surface of cell culture plate was coated with ERE-HB and modified with HA-FGF via coiled-coil structure. Cell adhesive activity and cell growth activity on the modified surface were investigated with human umbilical vein endothelial cells (HUVECs). Epidermal growth factor (EGF) with HA was also constructed and examined as another signalling molecule.

Induction of cell differentiation: For the induction of neural differentiation, the multifunctional scaffold protein (EAEC-HB) was constructed with elastin-derived structural unit, two functional peptide units that have the ability to enhance cell adhesive and neurite outgrowth, and HB unit for tethering growth factor. To induce more efficient neurite outgrowth, HA-FGF was utilized. Neurite outgrowth of PC12 cells was evaluated on the cell culture plate whose surface was modified with HA-FGF through coated EAEC-HB.

RESULTS AND DISCUSSION

Promotion of cell growth: On the ERE-HB-coated plate without HA-FGF as a negative control, clear cell growth was not observed. Contrary, significant cell growth was observed when HA-FGF was immobilized on the ERE-HB-coated surface. It is suggested that the bFGF moiety in the HA-FGF remained activity even after immobilization on the plate surface.

Induction of cell differentiation: PC 12 cells were well attached on the EAEC-coated plate. On the EAEC-coated plate without HA-FGF, little neurite outgrowth was observed. However, much higher rate of neurite outgrowth was observed in cells cultured on the bFGF-tethered scaffold protein.

CONCLUSION

A novel method for construction of biomaterials for tissue engineering was developed. One advantage of this technique is that the signalling molecule or a scaffold can be changed depending on the purpose. Such multifunctional proteins constructed by integration of growth factors and scaffold proteins could be a useful strategy for tissue engineering.

REFERENCES

1. E. Kobatake *et al.*, Bioconjugate Chem. **22**:2038-2042 (2011)
2. Y. Assal *et al.*, Biomaterials, **34**: 3315-3323 (2013)
3. M. Mie *et al.*, Biomed. Mater. **9** (2014)

Gel-in-Gel extrusion of cells for soft and hard tissue construction

Erkan Türker Baran^{1*} and Vasif Hasirci^{1, 2}

¹ BIOMATEN, METU Center of Excellence in Biomaterials and Tissue Engineering, Biotechnology Research Unit Bldg., Middle East Technical University, Turkey

² Department of Biological Sciences, Middle East Technical University, Turkey,

*erkanturkerbaran@gmail.com

INTRODUCTION

Additive manufacturing, also referred to as rapid prototyping (RP), provides new opportunities in manufacturing custom medical devices by using 3D data. RP is also being exploited in tissue engineering where the advantages of additive manufacture are being utilized to build highly complex scaffolds that can support the growth of living cells. In spite of increasing interest in using RP in tissue engineering, there are significant processing difficulties for hydrophilic biopolymers¹. Therefore, we propose RP microstructuring by gel-in-gel method, in which cell loaded alginate is extruded into a supporting gel matrix. Consequently, extruded polysaccharide incorporating cell is immobilized and solidified by Ca²⁺ crosslinking.

EXPERIMENTAL METHODS

Gel-in-gel injection method: To prepare a supporting gel, various concentrations of agar and CaCl₂ were tested for immobilizing extruded threads. The best formulation was detected in the 0.3-0.5 % agar (w/v) concentrations range with 3.6 mM internal CaCl₂ concentration and was used in the rest of the experiments. Extruded alginate was solidified by soaking in CaCl₂ and washed twice with isotonic saline. Suspending gel, alginate, carried silk fibroin at various compositions. The filter sterilized solution was then ultrasonicated for two minutes to induce self-assembly on fibroin². Into the fibroin-alginate solution SaOs-2 cells were added and this was extruded into agar manually or by the RP equipment (Bioscaffolder®, Germany).

In vitro studies: The cell laden gels in culture plates were incubated in DMEM or in osteogenic DMEM medium at 37°C and 5 % CO₂. For live/dead cell assay gels taken at predetermined time points were washed and treated with calcein and propidium iodide (Cal/PI) solution for 20 min and studied under a fluorescence microscope. Confocal images were also obtained after staining the cells with Nile red and then RP. Viability in the gels was determined with Alamar Blue® assay where absorbances were determined at 570 and 595 nm with a microplate reader.

RESULTS AND DISCUSSION

We saw that microstructuring of alginate carrying cells by Gel-in-Gel approach was feasible and microstructures could be built additively in an agar matrix. Confocal (CLSM) microscopy was used to further characterize the RP formed extruded gel rods and cell distribution. The orthogonally placed rods are seen to be partially fused and cells distributed homogeneously within solid alginate as the CLSM images show in Fig.1.

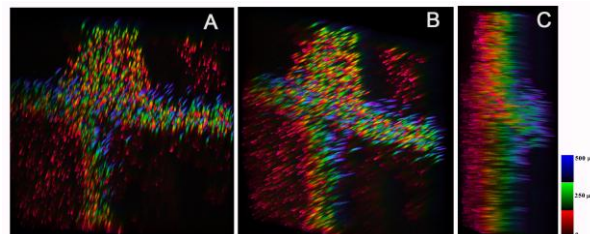


Figure 1. CLSM images of RP produced alginate-cell microstructures in agar: (A) top, (B) 45° angle, and (C) cross sectional views of the same cell loaded area.

Cal/PI staining and quantitative Alamar Blue® showed that blends especially with high fibroin (0.5-1 % w/v) and 1% alginate (v/w) composition had higher viability of SaOs-2 cells for up to four weeks with respect to the lowest fibroin (0.15 %) blend or pure alginate gel.

Upon incubation in osteogenic medium SaOs-2 cells showed intensive Alizarin Red (AR) staining in the manually extruded microstructures. With the high fibroin containing compositions the intensity was higher than the low fibroin sample (0.15 %), indicating increase of mineralization with increased fibroin. The AR staining of RP processed alginate microstructures showed that encapsulated cells deposit mineral in their vicinity (Fig. 2.)

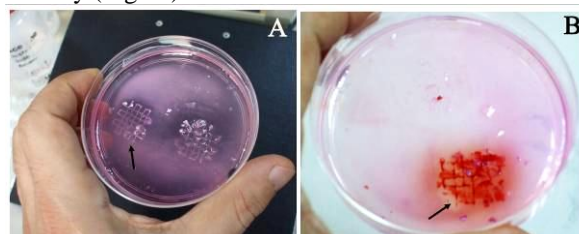


Figure 2. RP produced SaOs-2 microstructures in agar after 3 weeks of culture in the osteogenic medium (A). (B) Shows mineral deposition after AR staining.

CONCLUSION

Gel-in-Gel extrusion by manual and RP was applied successfully to hydrophilic biopolymer solutions. The cell viability in gel micropatterns was sustained for long periods in the presence of fibroin in the gel. SaOs-2 cells deposited the mineral in the microstructures depending on fibroin content.

REFERENCES

1. Billiet T *et al.*, Biomaterials 33:6020-6041, 2012.
2. Hwang CM *et al.*, Biomed. Mater. 8:1-9, 2013.

ACKNOWLEDGMENTS

The authors would like to thank the Postdoctoral Reintegration Fellowship (TÜBİTAK 2232 Program) and the Ministry of Development for the funding.

Real-time monitoring of chondrocyte activity by electrical impedance measurement

R. Mizota¹, Y. Morita² and E. Nakamachi²

¹ Graduate School of Life and Medical Sciences, Doshisha University, Japan

² Faculty of Life and Medical Sciences, Doshisha University, Japan, ymorita@mail.doshisha.ac.jp

INTRODUCTION

In cartilage regeneration, it is important to evaluate effects of mechanical and electrical stimuli in terms of cell activity, gene expression and extracellular matrix (ECM) synthesis. Histological observation and biochemical analysis were carried to estimate synthesis of ECM, but these analyses have problems such as long processing times for sample preparation and disruption of ECM including chondrocytes because of enzyme treatment and homogenization. Therefore, it is difficult to evaluate continuously cell activity and cell response against the stimulation. There is a need to develop new method to achieve real-time monitoring of cell response without damaging cells to investigate optimal stimulation condition. It is expected that activity of chondrocytes is estimated by measuring change in microelectrodes impedance caused by synthesized ECM with an electrical impedance method. The purpose of this study was to develop real-time evaluation method for activity of chondrocytes using an electrical impedance method.

EXPERIMENTAL METHODS

Fabrication of culture device: The culture device was prepared to measure electrical impedance during cultivation as shown in fig. 1. It consisted of an array of interdigitated electrodes on a glass substrate and a polycarbonate chamber. The interdigitated electrodes were fabricated on glass surface using a photolithographic procedure. The interdigitated electrodes were patterned and deposited by sputtering of platinum and the array had a total of 40 pairs of finger electrodes. The width of the electrodes and the distance between the electrodes were both 100 μm .

Cell culture: Chondrocytes were isolated from the distal femur of 6-month-old pigs. Chondrocytes were seeded into the culture device at a cell density of 1.0×10^6 cells/cm², and chondrocytes were cultured in a humidified atmosphere of 95% air with 5% CO₂ at 37 °C for 7 days. Dulbecco's modified Eagle's medium supplemented with 10% bovine serum and ascorbic acid was prepared as culture medium. Electrical impedance measurement was carried out every 24 hours. Measurement of glycosaminoglycan (GAG) amount and microscopic observation with safranin-O staining were carried out after 3 and 7 days of cultivation.

Electrical impedance measurement: Electrical impedance of the array at a frequency of 100 kHz was measured under voltage of 10 mVrms using a potentiostat. The measurement was started 2 hours after the culture devices were put into the incubator. In this study, the electrical impedance at each cultivation day was normalized by the initial electrical impedance at 0h.

RESULTS AND DISCUSSION

Figure 2 shows transition of the normalized impedance with cultivation days. The normalized impedance without chondrocytes was constant through cultivation. On the other hand, the normalized impedance with chondrocytes decreased with cultivation days, and it decreased by 3% after 7 days of cultivation. Morphology of chondrocytes did not change and the number of chondrocytes did not increase after 7 days of cultivation. According to microscopic observation with safranin-O staining, synthesized ECM around chondrocytes was observed after 3 and 7 days of cultivation, and the amount of GAG increased with cultivation days. Therefore, the normalized impedance depended not on morphology and the number of chondrocytes but on the amount of ECM, and it decreased with increasing the amount of GAG. These results showed that activity of chondrocytes can be estimated by measuring change in the electrical impedance caused by synthesized ECM.

CONCLUSION

The normalized impedance with chondrocytes decreased with increasing synthesized ECM. Our results showed that the activity of chondrocytes can be estimated using the electrical impedance measurement with the interdigitated electrodes.

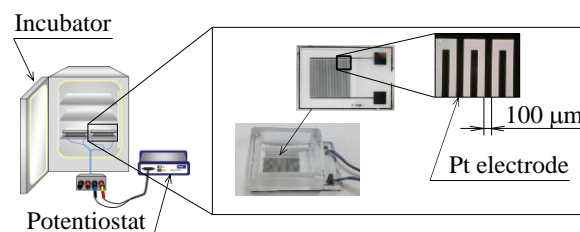


Fig. 1 Schematic drawing of the electrical impedance measurement system.

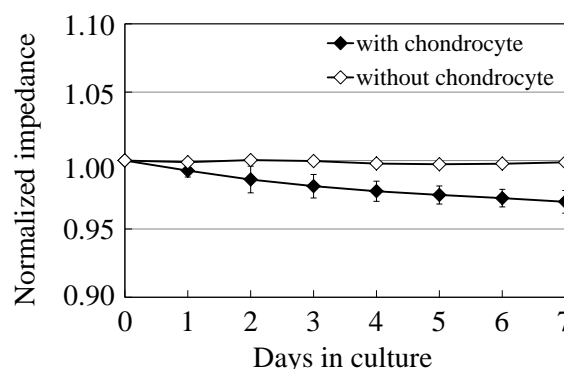


Fig. 2 Transition of the normalized impedance with cultivation days at frequency of 100 kHz.

Dynamic Hardness Evaluation of Two Phases of Au-xPt-8Nb Alloys for MRI-artifact-free Biomedical Devices

S. Inui, E. Uyama, E. Honda and K. Hamada

Institute of Health Biosciences, University of Tokushima, Tokushima, Japan, c301251012@tokushima-u.ac.jp

INTRODUCTION

A metal artifact due to volume magnetic susceptibility (χ_v) mismatch between metal devices in the human body and the human tissue is a major magnetic resonance imaging (MRI) artifact. The authors have developed Au-Pt-Nb alloys as candidates for MRI-artifact-free alloys with χ_v similar to that of the human tissue (approximately -9×10^{-6}) and with excellent mechanical properties¹.

Nb content for artifact-free alloy is fixed to 8 %, since the χ_v of the alloy depends only on Nb content. Hence only Pt content can control the mechanical properties of the alloy. Although the Vickers hardness (Hv) of Au-Pt binary alloy increases with Pt content increase², the Hv of Au-xPt-8Nb alloy decreases with Pt content increase. This reverse dependency makes it impossible to increase the Hv of the alloy by means of Pt content control, and Au-5Pt-8Nb alloy is selected as the candidate alloy for artifact-free biomedical devices.

In this study, the effects of alloy microstructure on the mechanical properties of Au-xPt-8Nb alloy were investigated to clarify the mechanism of the reverse tendency. The microstructure of Au-xPt-8Nb alloy consists of two phases that originated in phase separation of Au-Pt binary alloy from α phase to α_1 phase (Au rich phase) + α_2 phase (Pt-rich phase). The dynamic hardness (Hd) of each phase was examined individually using nano-indentation technique, and the correlation between the Hd of each phase and the Hv of the whole alloy was analysed.

EXPERIMENTAL METHODS

Au-xPt-8Nb ($x = 5-40$) alloy ingots (approximately 4 g) were fabricated by argon-arc-melting. The ingots were hot-rolled to approximately 1 mm in thickness at 973 K. The total rolling reduction was 60–70%. The hot-rolled plate was homogenized at 1273 K for 15 min and then aged at 973 K for 30 min. After hot-rolling and heat-treatment, the specimens were polished finally by

diamond paste with a grain size of 1 μm .

Nano-indentation test was carried out using ENT-1100a (Elionix Inc. Tokyo, Japan). The maximum load and the loading rate were 2000 mgf and 0.2 gf·s⁻¹, respectively. Hd was calculated from the indentation profile. The measurement was performed nine times for each sample and the maximum and minimum values were removed from the mean value calculation. All data were statistically analyzed using Student's t test ($p < 0.05$).

The microstructure of the alloy was investigated by SEM and optical microscope (OM).

RESULTS AND DISCUSSION

Fig. 1 shows Pt content effect on Hd of α_1 phase and α_2 phase of Au-xPt-8Nb alloy. Hd of α_1 phase of alloys above 15Pt were significantly smaller than that of 5Pt alloy. The linear regression of Hd-x for α_1 phase was;

$$\text{Hd} = -3.0 \times x + 198 \quad (R^2 = 0.93)$$

In contrast, Hd of α_2 phase did not indicate clear dependence on Pt content. However, that of 20Pt, 30Pt and 35Pt alloys was significantly larger than that of 5Pt alloy. The linear regression of Hd-x for α_2 phase was;

$$\text{Hd} = 5.2 \times x + 188 \quad (R^2 = 0.44)$$

The OM observation showed the color change of α_1 phase from light yellow to light gold with Pt content increase. It suggested the change of phase composition and also mechanical properties of the phase.

The XRD profiles¹ and microstructure observations indicated that the volume fraction of α_2 phase increased with Pt content increase. However, they suggested that the primary phase of all Au-xPt-8Nb alloys in this study was α_1 phase, and α_2 phase was the dispersed phase. The volume fraction and hardness of dispersed phase should affect the alloy hardness. However, the hardness of the matrix phase might be a dominant factor for Au-xPt-8Nb alloys in this study.

CONCLUSION

The dynamic hardness of α_1 phase of Au-xPt-8Nb alloy decreased with Pt content, which corresponded to the dependence of Vickers hardness of Au-xPt-8Nb alloy on Pt content.

REFERENCES

1. Uyama E. *et al.*, Acta Biomater. 9:8449-8453, 2013.
2. Darling AS., Platinum Met. Rev. 6:106-111, 1962.

ACKNOWLEDGMENTS

This work was partially supported by the JSPS KAKENHI grant numbers 21500427, 24500528 and 24800045, Japan Science and Technology Agency, and Tanaka Kikinzoku Research Fund.

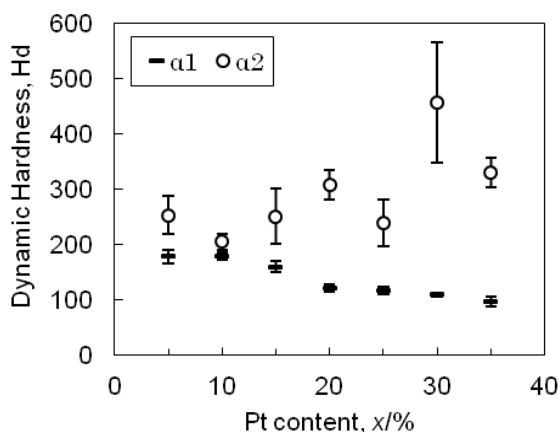


Fig. 1 Pt content effect on dynamic hardness of α_1 phase and α_2 phase of Au-xPt-8Nb alloy.



Electrospun fleeces fabricated from new biodegradable polyurethanes and evaluation of their use as tissue engineering scaffolds for adipose-derived stem cells

Thorsten Laube¹, Alfred Gugerell², Ralf Wyrwa¹, Johanna Kober², Torsten Walter¹, Sylvia Nürnberger³, Elke Grönniger⁴, Simone Brönneke⁴, Maike Keck², Matthias Schnabelrauch¹

¹Biomaterials Department, INNOVENT e. V., Prüssingstraße 27, 07745 Jena, Germany, ms@innovent-jena.de

²Division of Plastic and Reconstructive Surgery, Department of Surgery, Medical University of Vienna, Waehringer Guertel 18-20, 1090 Vienna, Austria

³Ludwig Boltzmann Institute for experimental and clinical traumatology, Donaueschingenstr. 13, 1200 Vienna, Austria

⁴Research Department Applied Skin Biology, Beiersdorf AG, Unnastr. 48, 20245 Hamburg, Germany

INTRODUCTION

An irreversible loss of subcutaneous adipose tissue in patients after tumor removal or deep dermal burns makes soft tissue engineering an important challenge in biomedical research. The development of a subcutaneous replacement (hypodermis) is still an unsolved problem. The ideal scaffold material should not only be stable for several weeks to serve as a framework for invading cells, but should also be fully biodegradable and hold a certain thickness and elasticity to provide plasticity as filler and shock protection. Certain characteristics such as tensibility or micro- and nano-structure are important to imitate the natural extracellular matrix.

We synthesized new polyurethane-based copolymers with different monomer ratios and different types of hydrolytically cleavable bonds to tune both the mechanical properties and the rate of biodegradation. The main goal of this study was to elucidate the adipose-derived stem cells (ASCs) viability, proliferation and differentiation on the two scaffolds evaluating their potential as a matrix in adipose tissue engineering

EXPERIMENTAL METHODS

A poly(ϵ -caprolactone-co-urethane-co-urea) (PEUU) and a poly[(L-lactide-co- ϵ -caprolactone)-co-(L-lysine ethyl ester)-block-oligo(ethylene glycol)-urethane] (PEU) have been synthesized as recently described.¹ Fleeces of this polymers have been prepared by solution electrospinning using a Spintronic apparatus (E. Huber, Gernlinden, Germany)¹. The material properties of the novel polymers were determined compared to a conventional poly(L-lactide-co-D,L-lactide (70/9, PL) using both polymer foils and fleeces. Polymer degradation was studied in Sörenson buffer at 37°C monitoring polymer weight loss and the released lactide amount over time.

Cell viability, adhesion, and morphology were examined cultivating ASCs on top of the polymers for 48 hours. Cell viability was analyzed by fluorescence staining (fluorescein diacetate/ethidium-homodimer-1), adhesion and morphology after staining the cytoskeleton with TRITC-phalloidin. Proliferation of ASCs grown on the materials was studied by MTT assay. The differentiation potential of ASCs grown on the polymers was determined after cell cultivation for 2 days followed by induction of adipogenesis for 3 days and further cultivation in nutrition medium. On day 21 lipids were stained with AdipoRed. Gene expression analysis of differentiating cells was performed as described.¹

RESULTS AND DISCUSSION

As hypothesized the new synthesized polymers strongly differ from the established biodegradable PL in their application relevant properties. Exemplarily, this is shown in Table 1 for the mechanical properties. Due to the presence of the ϵ -caprolactone soft segment, PEU and PEUU have much lower Young's modulus than PL and show a more elastic behaviour with a higher maximal elongation.

Polymer	Tens. strength [MPa]	Young's modulus [GPa]	max. elongation [%]
PEUU	37±5	0.18±0.01	1072±104
PEU	8 ± 1	0.13±0.08	15±0.7
PL	51 ± 4	1.4±0.3	6±0.6

Table 1: Mechanical properties of PEUU and PEU in comparison to PL.

The degradation of PEU was found to be only slightly diminished compared to PL (reference), whereas PEUU degrades much slower. Varying the type of linkage between the different polymer segments may therefore represent an effective tool to tune the degradation behaviour of scaffold materials.

ASCs were able to adhere, proliferate and differentiate on both PEU and PEUU fleeces. Morphology of the cells was slightly better on PEUU than on PEU showing a more physiological appearance. ASCs differentiated into the adipogenic lineage. Cells were forming lipid droplets showing a physiological phenotypical appearance after 21 days. Gene analysis of differentiated ASCs showed typical expression of adipogenic markers such as PPARgamma and FABP4.

CONCLUSION

Electrospun scaffold materials based on the newly synthesized polymers PEU and PEUU cover a broad range of properties due to their different chemical composition and structure. ASCs were able to adhere, proliferate and differentiate on both polymers. Overall, we can conclude that both PEU and PEUU fleeces are promising scaffold materials for adipose tissue engineering.

REFERENCES

1. Gugerell A. *et al.*, PLoS ONE. 9:e90676, 2014

ACKNOWLEDGMENTS

Funding from the European Union Seventh Framework Programme (FP7: ArtiVasc 3D project grant agreement n°263416) is greatly acknowledged.



Design, Synthesis and Development of a Self-Assembled Polymeric Nanoparticle System for Gene Delivery

Li-yen Wong¹, Ernst Wolvetang², Justin Cooper-White^{1*}

¹Tissue Engineering and Microfluidics Laboratory, Australian Institute for Bioengineering and Nanotechnology, The University of Queensland, St Lucia, Brisbane QLD 4072, Australia

²Stem Cell Engineering Group, Australian Institute for Bioengineering and Nanotechnology, The University of Queensland, St Lucia, Brisbane QLD 4072, Australia

*corresponding author: j.cooperwhite@uq.edu.au

Presenting author: l.wong5@uq.edu.au

INTRODUCTION

Gene delivery requires multifunctional vectors that are site-specific, carry and protect genetic material, and are safe for use in human gene therapy^{1, 2}. Targeted nanoparticle systems are emerging as promising gene delivery vectors², due to their ability to bind, condense and package plasmids, as well as release cargo upon changes in environmental stimuli while protecting the payload against nucleases³. In this study, we aim to construct nanoassemblies of cyclodextrin-based polymer systems involving the functionalization of targeting peptides, incorporation of stimuli-responsive features and multivalent interactions between specific moieties. This can then be utilized to engineer “smart” supramolecular nano-carriers that can efficiently deliver plasmids to a specific location, providing an effective alternative to viral vectors.

EXPERIMENTAL METHODS

Three self-assembling polymer components based on CD were synthesized to form a cationic, DNA condensing polymer (CDP), a pH-sensitive, membrane destabilising CD-loaded polyrotaxane (CDT), and a peptide-conjugated polymer (CD-pep). The conjugation efficiency of these polymers was determined by FTIR and ¹H-NMR. They were then self-assembled to form supramolecular nanoparticles (SNPs) and were assessed by dynamic light scattering (DLS). Picogreen assay was used to investigate the binding capacity of the SNPs to the plasmids, which was further determined by DNA retardation assay. Cytotoxicity of polymer components was evaluated by CCK8 assay. Targeted transfection of cardiac fibroblasts with SNPs displaying RGD and DDR2 ligands were investigated using fluorescent microscopy and FACs. All biochemical assays and biological studies were performed in triplicate and reported as mean ± standard deviation.

RESULTS AND DISCUSSION

Polymer conjugations were validated by FTIR and ¹H-NMR.

Samples	Size (D _h , nm)	Zeta potential (mV)	PDI
pDNA	103.1 ± 21.1		0.69 ± 0.06
pDNA-CDP	72.6 ± 26.2	42.8 ± 0.78	0.49 ± 0.09
pDNA-CDP/CDT	137.9 ± 3.5	36.4 ± 3.3	0.29 ± 0.01
pDNA/SNP-RGD	263.3 ± 10.8	10.6 ± 0.45	0.19 ± 0.01

Table 1. The Characterisation of the Self-Assembled Polymer. Results are reported as mean ± standard deviation.

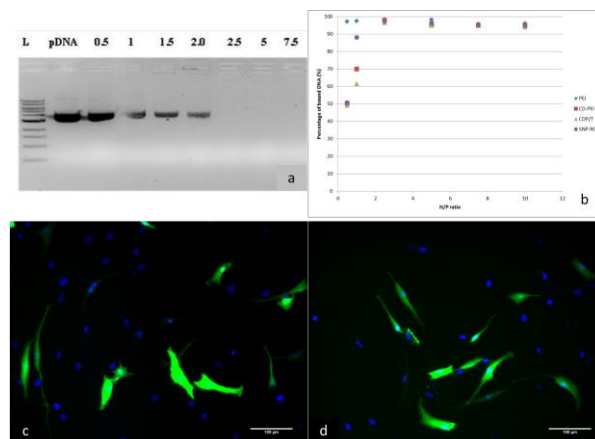


Figure 1. a) Gel electrophoresis of cationic polymer in different N:P ratios. b) Picogreen assay of binding capacity of particles to pDNA. Fluorescent images of transfected cardiac fibroblasts using c) RGD-targeted and d) DDR2-targeted nanoparticles. Scales bars represent 100µm.

These particles were shown to assemble in aqueous conditions as shown in Table 1, with a decreasing surface charge due to the addition of the polyrotaxane and targeting ligand. This indicates that the polymers interact to form a self-assembled structure. The CDP polyplexes were shown to fully bind to pDNA at N/P ratio of 2.5 as confirmed by gel electrophoresis and Picogreen assay (Fig. 1a, b). The polymer components were found to be non-toxic to cells. Figs. 1.c, d show that the particles can transfect primary cells in a targeted and specific manner with 5% efficiency. Future work is ongoing to enhance transfection outcomes.

CONCLUSION

In summary, we have developed a multifunctional, self-assembled supramolecular nanoparticle system which possesses pH-sensitive features and targeted specificity. This study has confirmed that this nanoparticle system can be loaded with plasmids, target and transfect specific cell types. This strategy has great potential for the design of future nanovectors for use in therapeutic treatments.

REFERENCES

1. Zhang, J. and Ma, P.X., Adv. Drug Deliv. Rev. 65(9): 1215-1233, 2013
2. Wang, H. *et al.*, Chem. Commun., 46: 1851–1853, 2010
3. Jackson, A.W. and Fulton, D.A., Polym. Chem., 4: 31-45, 2012

ACKNOWLEDGMENTS

This project was supported by Stem Cells Australia, an ARC Special Research Initiative, held by Prof Justin Cooper-White.



Biological Properties of an Acellular Xenogeneic Tendon Graft following Chemical and Irradiation Sterilisation

J H Edwards¹, J Fisher¹ and E Ingham¹

¹Institute of Medical and Biological Engineering, University of Leeds, Leeds, UK, j.h.edwards@leeds.ac.uk

INTRODUCTION

Damage to the anterior cruciate ligament (ACL) is increasingly common within a young and active population. In the case of ACL tears, replacement with autograft tendon is the gold standard treatment to maintain stability within the knee joint. Such grafting can cause donor site morbidity and associated problems for the patient¹ and a promising alternative is the use of acellular xenogeneic tissue. This study investigated the biological properties of an acellular porcine superflexor tendon (pSFT) graft following chemical and irradiation sterilisation methods.

EXPERIMENTAL METHODS

Acellular pSFT were produced following an established method involving peracetic acid (PAA) treatment for bioburden reduction and low concentration SDS for decellularisation. Grafts were packaged and stored at -80°C. Groups of tendons (n=6 in all cases) were sterilised using: PAA alone (standard method), 30 or 55 kGy gamma and 34 kGy electron beam (E-beam). Samples were analysed immediately after treatment and after 3 months storage at 4°C. The biological properties of the pSFTs were determined by histology (tissue structure), collagen (hydroxyproline assay) and denatured collagen (alpha chymotrypsin treatment) content, second harmonic generation (SHG) imaging (collagen structure) and *in vitro* biocompatibility assays. Biomechanical properties of grafts were assessed in a separate study. Two-way ANOVA was used to determine significance of differences between treatment groups (Tukey post-hoc analysis, p<0.05).

RESULTS AND DISCUSSION

Sterilisation using PAA or irradiation treatment did not cause any change in collagen content within the tendons immediately or three months after treatment. Denatured collagen content was increased significantly in irradiated samples at both timepoints (55 kGy > 30 kGy Gamma, 34 kGy E-beam > PAA only) (Figure 1).

Sterilisation and storage of grafts did not have any adverse effects on the *in vitro* biocompatibility of the tendon samples. Histological analysis showed some flattening of collagen crimp and separation of fibre bundles within the irradiated tissue samples (Figure 2). SHG imaging did not show any differences in collagen structure for any treatment group.

These results showed that irradiation sterilisation caused some disruption to the tendon structure, likely due to free radicals generated during the irradiation process. Although this had no effect on biocompatibility, it would be preferable to reduce these changes in order to ensure mechanical integrity of the grafts after implantation.

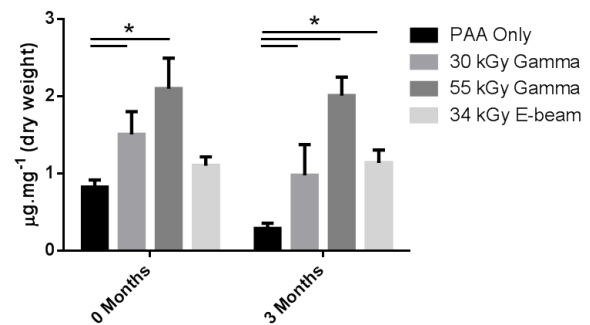


Figure 1: Denatured collagen content of pSFT samples following chemical and irradiation sterilisation. Results show mean ± 95% CI (n=6). * denotes significant differences compared to PAA only controls.

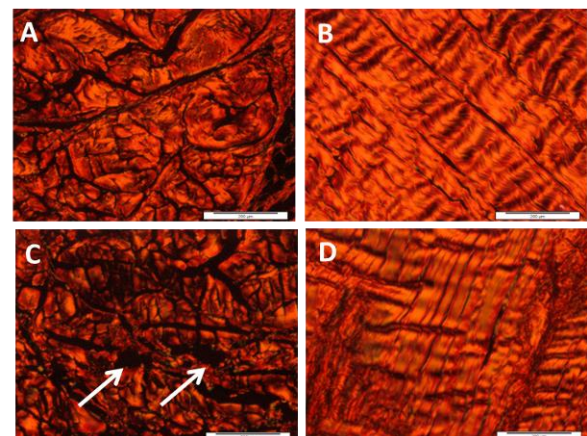


Figure 2: Sirius red staining in PAA (A,B) and 55 kGy Gamma (C,D) sterilised tendons after 3 months storage. Arrows indicate separation of bundles, scale bars show 200 µm.

CONCLUSION

Although irradiation sterilisation did not affect *in vitro* biocompatibility or collagen content of the tendon grafts, damage to the collagen structure was evident compared to PAA only controls. Fractionation or lower irradiation doses will be studied in the future in an attempt to reduce the adverse effects of the terminal sterilisation methods on this acellular pSFT graft. The effects of longer term storage of grafts will also be investigated to understand their suitability as an 'off the shelf' ACL repair solution.

REFERENCES

1. Macaulay A A. *et al.*, Sports Health 4(1):63-8, 2012

ACKNOWLEDGMENTS

The authors would like to thank the European Research Council (REGKNEE) for providing financial support to this project.

Improved early cell adhesion on bioinert ceramics by alkaline phosphatase immobilization

Aliieh Aminian*, Bahareh Shirzadi, Laura Treccani and Kurosch Rezwani

Advanced Ceramics, University of Bremen, Germany

* aminian@uni-bremen.de

INTRODUCTION

Early, firm adhesion and spreading of bone cells on biomaterials is considered a prerequisite to achieve fast implant integration and tissue healing. As these processes are protein-mediated, surface functionalization and activation with immobilized biomacromolecules are considered a highly promising strategy for the biomaterial interface improvement. The enzyme alkaline phosphatase (ALP) is known to play a central role in bone formation, osteoblast cell differentiation and mineralization. Different studies demonstrated in the presence of organic phosphates, immobilized ALP can trigger the formation of calcium phosphate on metal surfaces¹ and enhances bone cell mineralization². In this work ALP was specifically employed to biofunctionalize and bioactivate the surface of two highly bioinert ceramics, alumina (Al_2O_3) and yttria-stabilized zirconia (Y-TZP), which due to their remarkable mechanical, chemical properties and biocompatibility are widely applied for dental and load bearing orthopaedic implants. ALP was covalently immobilized on them and its effect on early cell attachment and spreading of mesenchymal stem cells (MSC), human osteoblasts (HOB) and human osteoblast-like MG-63 cells was investigated under serum-free conditions to prevent the effect of other adsorbed proteins³.

EXPERIMENTAL METHODS

Prior immobilization Al_2O_3 and Y-TZP substrates were silanized with aminopropyltriethoxysilane (APTES) according to Meder et al.⁴. ALP was covalently immobilized via carbodiimide-mediated chemoligation assisted by active esters using via the biocompatible zero-cross linking system N-(3-Dimethylaminopropyl)-N'-ethylcarbodiimidehydrochloride/N-Hydroxysuccinimid (EDC/NHS).

The attachment of MSCs, HOBs and MG-63 cells on ALP functionalized alumina and zirconia was monitored after 30 min, 2 h, 4 h and 6 h under serum free conditions according to³. Cell morphology, spreading and focal adhesion point was evaluated by immunofluorescent microscopy. Cell nuclei, cytoskeleton and focal adhesion points were stained with 4',6'-diamidino-2-phenylindol (DAPI), Alexa Fluor® 488 Phalloidin and anti vinculin, respectively⁵. Adherent cell number was also quantified with total amount of DNA using Quant-iT™ PicoGreen® dsDNA assay Kit. Cell activity was measured by the WST-1⁶.

RESULTS AND DISCUSSION

ALP immobilized on alumina and zirconia substrates was found to enhance cell adhesion and spreading and more pronounced stress fibers, filopodia and surface-contact area were observed. In figure 1 a representative

image of sHOBs onto ALP-functionalized substrates and non functionalized surfaces is given.

For all type of cells, a higher number of adherent cells was found on ALP functionalized samples in comparison to non-functionalized surfaces. Percentage of adherent human osteoblast cells during the first 6 hours are shown in figure 2.

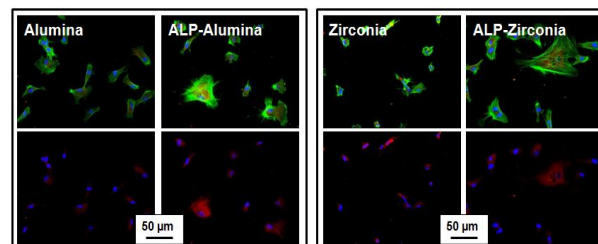


Fig 1. Immunofluorescence microscopy images of HOBs on non and ALP functionalized alumina and zirconia after 4 hours (Green: cytoskeleton, Blue: cell nucleus, Red: vinculin)

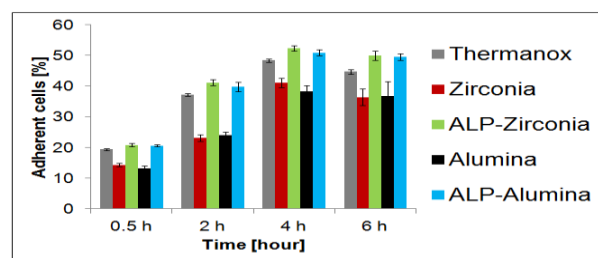


Fig 2. Percentage of adherent HOBs on non and ALP functionalized alumina and zirconia. Cell number was estimated by measuring total DNA amount.

CONCLUSION

Immobilization of ALP to the bioinert surfaces of alumina and zirconia was found to accelerate the initial adhesion of mesenchymal stem cells, human osteoblasts and human osteoblast-like MG-63 cells. These cells have more extended area on ALP functionalized samples than non-functionalized together with higher number of adherent cells. Our results demonstrate that biofunctionalization of inert ceramics with ALP can significantly improve initial steps of the cellular contact to the material surface and a considered highly feasible for designing bioactive materials for bone tissue engineering applications.

REFERENCES

1. de Jonge, L. T. et al., J. Acta Biomaterialia. 5: 2773-2782, 2009.
2. Douglas, T. E. L. et al., J. Macromolecular Bioscience. 12: 1077-1089, 2012.
3. Nebe, B. et al., J. Biomolecular Engineering. 24:447-454, 2007.
4. Meder, F. Et al., J. Acta Biomaterialia. 8:1221-1229, 2012.
5. große Holthaus, M., et al., J. Acta Biomaterialia. 8:394-403, 2012.
6. große Holthaus, M., et al., J. Biomaterials. 27:791-800, 2013.

ACKNOWLEDGMENTS

We thank Prof. Kathrin Mädler and Zahra Azizi (Canter for Biomolecular Interactions, University of Bremen) for providing mesenchymal stem cells for this project.



Thermoresponsive Hydrophobic Copolymer Brush for Cell Separation by Multi-Step Temperature Change

Kenichi Nagase^{1,*}, Yuri Hatakeyama², Tatsuya Shimizu¹, Katsuhisa Matsuura¹, Masayuki Yamato¹, Naoya Takeda², Teruo Okano¹

¹Tokyo Women's Medical University, Tokyo, Japan nagase.kenichi@twmu.ac.jp

²Waseda University, Tokyo, Japan

INTRODUCTION

In the fields of regenerative medicine, an effective cell separation method that can provide adequate purity, yield, and function after separation have been needed for fabricating transplantable tissues. In the present study, poly(*N*-isopropylacrylamide (IPAAm)-*co*-butylmethacrylate (BMA)), hydrophobized thermo-responsive copolymer, brush grafted surfaces with various BMA contents were prepared through surface-initiated atom transfer radical polymerization (ATRP). Temperature-dependent cells adhesion and detachment behaviour was observed for investigating the possibility of the surface as a cell separating materials.

EXPERIMENTAL METHODS

An ATRP initiator, 2-(*m/p*-chloromethylphenyl) ethyltrimethoxysilane, was modified on glass coverslips as shown in the first step in Fig. 1. Copolymerization of IPAAm and BMA was performed through surface initiated ATRP using CuCl/Me₆TREN as a catalyst and 2-propanol as reaction solvent. In the polymerization, α -chloro-*p*-xylene was added as free initiator and brush length was estimated using the prepared polymer in the reaction solution. BMA feed composition was varied from 0 to 5 mol%. Human umbilical vein endothelial cells (HUVEC), neonatal human dermal fibroblasts (NHDF), were used as model cells for observation of adhesion at 37 °C and detachment at 10 and 20 °C on the surfaces. GFP expressing HUVEC and NHDF were used for observation of cell separating behavior.

RESULTS AND DISCUSSION

Prepared P(IPAAm-*co*-BMA) brush grafted glass surfaces was characterized by ATR/FT-IR, ¹H NMR and GPC measurements. BMA composition increased with BMA feed molar ratio. Contact angle measurement and fibronectin adsorption measurement revealed that surface hydrophobicity increased with BMA composition of grafted copolymer. On observation of cells adhesion and detachment on the prepared copolymer brush, cells adhesion was enhanced with increasing BMA composition of copolymer, attributed to enhanced fibronectin adsorption. For investigating the effective temperature for cell recovery, cells detachment was observed at 10 and 20 °C (Fig. 2). HUVECs exhibited excellent cells detachment at 20 °C. On the contrary, NHDFs tend to detached at 10 °C. Using these cells' intrinsic thermo-sensitive properties for cell detachment, Mixture of HUVEC and NHDF was separated (Fig.3). A mixture of GFP-HUVEC and NHDF was seeded to thermoresponsive copolymer brush surface, and allowed to adhere on the surface at 37 °C. Subsequently, external temperature was reduced to 10 °C for recovering NHDFs. In this incubation

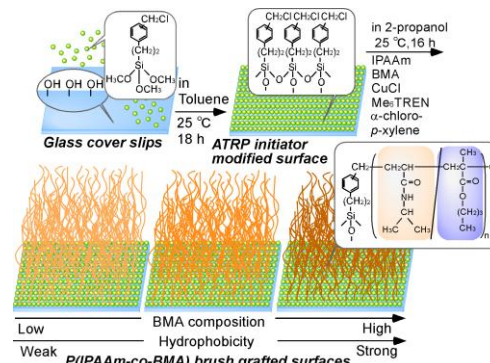


Fig.1 Scheme for preparation of hydrophobized thermo-responsive copolymer brush

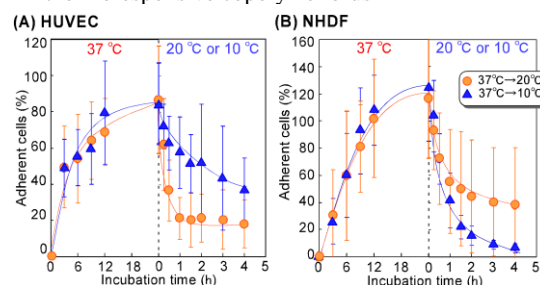


Fig.2 Cells adhesion and detachment profiles

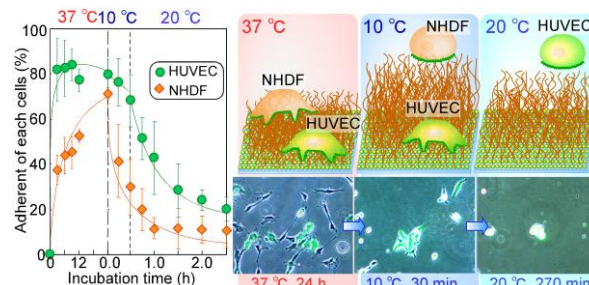


Fig.3 Cells separation using P(IPAAm-*co*-BMA) brush

period, NHDFs promptly detached while HUVECs adhered on copolymer brush surfaces. After 30 min incubation at 10 °C, the temperature was raised to 20 °C, and adhered HUVECs were recovered from the copolymer brush surface. The higher ratio of NHDFs and HUVECs was recovered in cell culture medium during the 10 °C and 20 °C incubation periods, respectively. Thus, hydrophobized thermoresponsive copolymer brush separated mixture of cells using cells' intrinsic detachment properties.

CONCLUSION

Hydrophobized thermoresponsive copolymer, P(IPAAm-*co*-BMA), brush can separate mixture of cells by using cells intrinsic thermo-sensitive properties for their detachment. Therefore, the prepared surfaces would be useful as cell separation materials without modification of cell surface.

A Novel Biological Polyester Based Wet Spun Scaffold for Bone Tissue Engineering

Ayşe Selcen Alagoz¹, Jose Carlos Rodriguez-Cabello⁵, Nesrin Hasirci^{2,3,4}, Vasif Hasirci^{1,2,4}

Depts. of ¹Biological Sciences, ²Biotechnology, ³Chemistry, METU, Turkey

⁴BIOMATEN- Center of Excellence in Biomaterials and Tissue Engineering, METU, Turkey, ⁵Department of Condensed Material, Universidad de Valladolid, Spain
selcen.alagoz@metu.edu.tr

INTRODUCTION

In this study, poly(3-hydroxybutyrate-co-3-hydroxyvalerate), PHBV, a biodegradable, natural polymer, was used as an alternative for the petroleum based polyesters to fabricate a wet spun scaffold for bone tissue engineering. VEGF and an elastin like recombinamers (ELR) with REDV sequences specific for endothelial cells¹ were introduced to the scaffold to make it attractive for endothelial cells so that it can be vascularized as needed in a thick implant which otherwise cannot maintain the viability of the cells that have penetrated deep into the scaffold.

EXPERIMENTAL METHODS

PHBV scaffolds prepared by wet spinning were characterized under compression, and fiber morphology and porosity were determined by SEM and micro CT. Surface of the fibers was coated with ELR by exposing PHBV film with oxygen plasma (50 W, 5 min) and then immersing into ELR solution. Toluidine Blue staining and FTIR-ATR analysis were used to show of protein on the surface. AFM was used to study the influence of the treatments used in the binding process. PHBV nanocapsules loaded with BSA were produced by the double emulsion. BSA was used as a model protein instead of VEGF. Size distribution of PHBV nanocapsules was determined by using the Zeta Potential and Mobility Measurement System. These PHBV nanocapsules were incorporated to scaffold fibers by adsorption from a solution. Scaffold was examined with fluorescence microscope and SEM to study final form ready for in vitro studies.

RESULTS AND DISCUSSION

The ultimate compressive strength of dry scaffolds under compression (5 mm/min) was 4.65 ± 0.69 MPa, which showed compressive strength adequate for substituting human cancellous bone (~ 2 -12 MPa) not the native human cortical bone (~ 100 -230 MPa)². The average fiber diameter was about 90 μm and porosity of scaffolds was measured as 75% by using both SEM micrographs processed with NIH Image J program and micro CT data (Figure 1). Blue spots on the surface of ELR attached PHBV films were observed after Toluidine Blue staining. FTIR-ATR showed that upon treatment with O_2 plasma new peaks at around 1530 cm^{-1} and 1650 cm^{-1} was observed due to stretching of carbonyl groups. After ELR attachment, these peaks became more intense. This was probably due to the amide I and amide II groups of ELR attached onto the PHBV film³. AFM micrographs showed that surface roughness decreased upon oxygen plasma treatment

from 343.4 nm to 160.0 nm and increased to 280.3 nm after ELR attachment.



Figure 1: SEM image of the PHBV scaffold

PHBV capsules were found to have an average diameter of 340 nm, with particle size in the range 190-530 nm. SEM images showed that PHBV nanocapsules were attached on PHBV fibers (Figure 2).

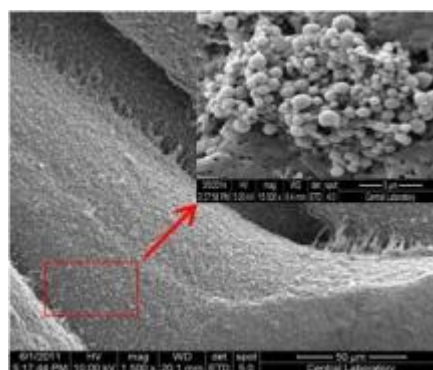


Figure2: SEM image of PHBV fibers and VEGF loaded PHBV nanocapsules

CONCLUSION

In this study a biological polyester PHBV, which is an alternative to petroleum based polyesters was used to design a novel cell carrier. It was treated with an endothelial cell attractive ELR and VEGF loaded nanocapsules were attached. Thus, a novel multifunctional scaffold with appropriate mechanical and physical properties could be prepared.

REFERENCES

1. Garcia et al., Tissue Engineering. 15(4): 887-899, 2009.
2. Sopyana et al., Science and Technology of Advanced Materials. 8: 116-123, 2007.
3. Serrano et al., Biophysical Journal. 93:2429-2435, 2007.

Development of novel hydroxyapatite-chitosan porous 3D scaffolds for biomedical applications

Dimitris Tsiourvas¹ and Triantafillos Papadopoulos²

¹ National Centre for Scientific Research “Demokritos”, IAMPPNM, Dept. of Physical Chemistry, Greece

^{2*} Department of Biomaterials, School of Dentistry, University of Athens, Greece, trpapad@dent.uoa.gr

INTRODUCTION

It is nowadays widely recognized that implantable scaffolds for bone grafting applications should possess materials characteristics close to those of natural bone in order to be successful in their application, and a controlled pore structure that allows cells to migrate and prosper. Consequently, a lot of research efforts are now directed towards the development of porous 3D scaffolds of hybrid inorganic-organic nature based on natural materials possessing osteoconductive properties and excellent biocompatibility and hemocompatibility. Hydroxyapatite (HAp) has been extensively used in biomaterials research because it has the above mentioned properties¹. On the other hand, chitosan (CS) - based materials gained particular attention in the field of medical tissue engineering. Interesting characteristics are its antibacterial nature, the minimal foreign body reaction, and the ability to produce porous structures, suitable for cell ingrowth and osteo-conduction². In this study were prepared and physicochemically characterized 3D porous hybrid scaffolds based on HAp and CS or *N*-acetylated CS and especially scaffolds with high HAp content (75 % w/w) for attaining increased mechanical strength.

EXPERIMENTAL METHODS

HAp nanoparticles having an average radius of ~ 20 nm were synthesized in the presence of poly(ethyleneimine) (MW=5000) following a synthetic procedure analogous to our previous work³. For comparison, HAp powder (Aldrich) was also used. CS (high molecular weight, Aldrich) was dissolved in acetic acid solution (1.5%) and the appropriate amount of HAp was added to obtain a final HAp:CS weight ratio of 75:25. The resulting thick solution was moulded in 6mm diameter tubes and frozen at -25°C. After lyophilisation the resulting cylindrical scaffolds (6mm diameter, 40 mm length) were extensively washed and kept for further characterization. *N*-acetylation of the chitosan scaffolds was attained by immersing the dried scaffolds in a dry methanol solution of acetic anhydride (20%) for 24 hours at 37°C. ATR-FTIR spectroscopy, X-ray diffraction, optical microscopy, scanning electron microscopy with SEI and BEI images in 300x and 600x resolutions, 3-D optical profilometry and μ CT-scan analysis were employed for the characterization of the scaffolds.

RESULTS AND DISCUSSION

ATR-FTIR spectroscopy of the scaffolds confirmed the presence of HAp, and CS or *N*-acetylated CS. X-ray diffractograms also reveal the presence of well crystalized nanohydroxyapatite nanoparticles and the basically amorphous nature of CS. Optical microscopy and μ CT-scan images (Fig. 1A and B respectively)

clearly reveal the open porous structure of the scaffolds. Pores were having dimensions ranging from about 10 μ m to 300 μ m.

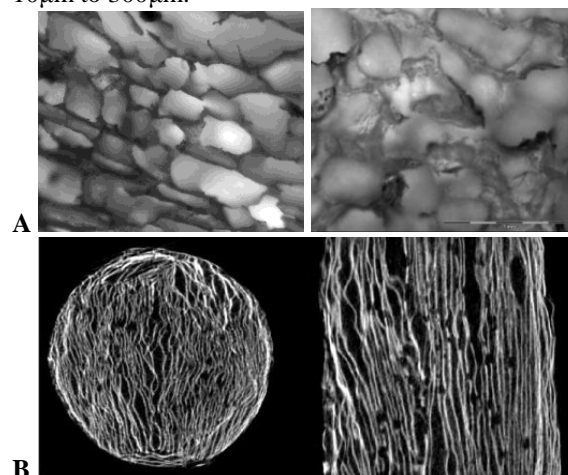


Fig 1. (A) Optical micrographs of scaffold sections (the bar represents 1mm); (B) μ CT-scan of a nanoHAp-CS scaffold.

Cross sections of μ CT-scan show a thick fiberlike structure of scaffold with dispersed HAp particles (black points) and irregular voids probably following randomly the setting after freezing of the fabricated liquid material. Vertical sections of μ CT-scan reveal an interlocking of the internal porosity throughout the mass of the scaffold. The optical microscopy and μ CT-scan results were in accordance with high resolution SEM images. The 3-D profilometry results show a bone like roughness of the experimental scaffolds presenting Sa values ranging between 10 and 30 μ m.

CONCLUSION

Based on the results of the present study promising porous scaffolds were developed covering the structural and biological demands for biomedical applications.

REFERENCES

1. E. Bonnucci, “Basic Composition and Structure of Bone” in “Mechanical Testing of Bone and the Bone Implant Interface”, Ed. by Y. H. An, R. A. Draughn. CRC Press, Boca Raton, FL, 2000.
2. Di Martino A. *et al.*, Biomaterials 26:5983–5990, 2005.
3. Tsiourvas D. *et al.*, J. Am. Ceram. Soc., 94:2023–2029, 2011.

This project was financially supported by the Action «Cooperation» EPAN-II 09SYN-41-757, GSRT, Programme.

Controlled release of drugs from innovative multi-layered biodegradable coating on polymeric orthopaedic implants

Nerea Argarate^{1,2}, Beatriz Olalde^{2,1*}, Garbiñe Atorrasagasti^{2,1}, Jesus Valero^{2,1}, Sandra Carolina Cifuentes³, Rosario Benavente⁴, Marcela Lieblich³, Jose Luis González-Carrasco^{3,1}

^{1*} Networking Research Centre on Bioengineering, Biomaterials and Nanomedicine (CIBER-BBN), Spain
Beatriz.olalde@tecnalia.com

² Biomaterials group, Health Division, Tecnalia Research & Innovation, Spain

³ Centro Nacional de Investigaciones Metalúrgicas, CENIM-CSIC, Spain

⁴ Instituto de Ciencia y Tecnología de Polímeros (ICTP-CSIC), Madrid, Spain

INTRODUCTION

Bone repair materials are widely applied in bone surgery, orthopaedics and dentistry¹. Polymeric materials based on polylactic acid (PLA), polyglycolic acid (PGA) and their copolymers are currently available for bone fracture repair applications with low load bearing². Given that bacterial-related complications can appear at early stages immediately after surgery, it is necessary to prevent/inhibit infections and inflammation processes. In this work, novel biodegradable multi-layered drug delivery coatings for polymeric implants are proposed as an strategy to reduce the risk of infections and inflammation simultaneously.

EXPERIMENTAL METHODS

Polymer implant processing: Polymer PLLDL (Purasorb PLLDL 7028, i.v. 2.91 dL/g, copolymer 70/30 L-lactide/DL-lactide, Purac) was used for discs preparation. Discs of 12 mm diameter and 4 mm height were prepared by compression moulding.

Polymer coating onto PLLDL implant: Medical grade poly(L-lactic acid,) PLLA (Purasorb PL 18, i.v.1.8dL/g, Purac) was used. A self-developed controller was used in the experiment for the dip coating process. Coated samples were prepared as follows:

Sample	Number of samples (n)	Coating polymer (Layer one)	Conc. Eugenol	Coating polymer (Layer two)	Conc. Dexamethasone
Control discs	3	8 % PLLA (w/v)	-	-	-
Bare discs	3	-	10% w/w	-	-
One layer discs	3	8 % PLLA (w/v)	10% w/w	-	-
Two layer discs (one drug)	3	8 % PLLA (w/v)	10% w/w	8 % PLLA (w/v)	-
Two layer discs (dual drug)	3	8 % PLLA (w/v)	10% w/w	8 % PLLA (w/v)	5% w/w

Characterization of the coating: Coating thickness (Profilometer), microstructure (SEM), and in vitro release kinetics of the drugs from the coated implants were studied. Eugenol and dexamethasone were quantified by RP-HPLC.

RESULTS AND DISCUSSION

Coatings thicknesses obtained after dip-coating of samples were evaluated by profilometer.

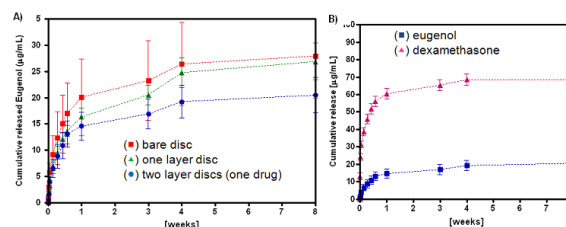
Table 1. Evaluation of obtained coating thickness [μm]:

Coating mode	Number of layers	Coating thickness [μm]
8 X PLLA	1	42.31 (± 2.21)
Eugenol (without polymer)	1	12.41 (± 0.10)
8 X PLLA with eugenol	1	36.36 (± 2.86)
8 X PLLA with eugenol / 8 X PLLA	2	78.85 (± 4.79)
8 X PLLA with eugenol / 8 X PLLA with dexamethasone	2	80.67 (± 2.20)

Table 1 shows that coating with 8% PLLA (w/v) resulted in approximately 10 mg/cm² and that two layer coating had an additive coating mass (20 mg/cm²).

These data were confirmed by the coating thicknesses with the same trend. Eugenol³, the main component of the essential oils of the clove with good local antiseptic and analgesic effect and dexamethasone a steroid used as anti-inflammatory drug and effects on cells⁴ were used. As shown in Figure 1A, polymeric coatings on implant discs have direct effect on the delivery profile of Eugenol. In Figure1B, the release kinetic of a two layer coating is shown in which the upper layer drug is released first and then the second layer drug in a sequential manner.

Figure 1. Evaluation of delivery rates of drugs: A) Eugenol delivery and B) Dual delivery of eugenol and dexamethasone.



This result implies that dip coating technique could be used for multi-layered coating of polymeric implants with sequential dual drug delivery.

CONCLUSION

It is possible to combine and control the sequential release of two different substances from a polymer coating of implants. Only one clinically approved polymer was used for the coating to entrap the substances. Dip-coating is an easy and simple technique for fast and sterile manufacturing process of polymeric bone implants.

REFERENCES

References must be numbered. Keep the same style.

1. Tan L. *et al.*, J. Mater. Sci. Technol. 29:503, 2013.
2. Maurus PB. *et al.* Oper Techn Sports Med. 12:158, 2004.
3. Walsh SE. *et al.* J Appl. Microbiol. 94:240, 2003.
4. Maniopoulos et al. Cell Tissue Res.254:317, 1988.

ACKNOWLEDGMENTS

The authors are thankful for financial support from MICINN, project MAT2012-37736-C05-01 and -02. CIBER-BBN is an initiative funded by the VI Spanish National R&D Plan 2008-2011, Iniciativa Ingenio 2010, Consolider Program, CIBER Actions and financed by the Instituto de Salud Carlos III with assistance from the European Regional development Fund.

Study on calcium silicate / zein scaffold implanted in vivo by synchrotron radiation-based X-ray Imaging

Han Guo^{1*}, Jie Wei², Changsheng Liu², Tiqiao Xiao¹

^{1*}Shanghai Institute of Applied Physics, CAS, P R China, guohan@sinap.ac.cn

²Engineering Research Center for Biomedical Materials of Ministry of Education, East China University of Science and Technology, P R China

INTRODUCTION

In order to quantitatively investigate the osteogenic effects on bone microstructure as well as to quantify the scaffold degradation within biopsy specimens sampled several months after implantation, histomorphometric quantification using synchrotron radiation (SR) X-ray imaging was performed. Compared with the conventional bone histological sections, 3D SR-micro-CT provides higher spatial resolution and contrast, and facilitates a more accurate distinction between newly formed bone and residual biomaterials. In the present study, we synthesized and characterized porous calcium silicate nanofiber / zein scaffolds, and investigated the bone regeneration in rabbit femur cavity defects by using SR-micro-CT.

EXPERIMENTAL METHODS

The calcium silicate nanofiber was synthesized by precipitation and hydrothermal treatment, and was uniformly dispersed into zein with different proportion to compose porous bioactive calcium silicate / zein (CSZ) scaffold for bone implant.

A long-term study in rabbit femur cavity defect model was carried out to investigate the efficacy of CSZ scaffolds in promoting bone repair and regeneration. 24 skeletal mature New Zealand white rabbits were used. Surgical intervention was performed under general anesthesia, afterwards lateral and medial approaches were performed in left shaved knees to exposure the distal femoral epiphysis and the cavitary defects were created with a medium speed burr (5 mm diameter and 5 mm depth). The CSZ scaffolds, as well as dense calcium phosphate cement (CPC) cylinders were implanted into the defects. The empty bony defects served as the control. Prophylactic antibiotic was given for 3 days. The animals were sacrificed for analysis at 4 and 12 weeks after surgery. In an attempt to explore the microstructure of scaffolds and to evaluate the repair process for the bone defects, SR-micro-CT measurements were performed at BL13W of SSRF (Shanghai, China). Bone radiomorphometric analysis was performed by using Image-Pro Plus and VGStudio 2.1. The amount of bone ingrowth into the scaffolds was quantified as the bone volume (BV) within the defined VOI (volume of interest) in each defect site. The bone mineral density (BMD) was also calculated for each region.

RESULTS AND DISCUSSION

The present study demonstrated that CSZ scaffolds exhibited noticeable weight loss in tris-HCl solution over time, indicating that CSZ scaffold was degradable. The in vitro cell culture results indicate that cells

adhered CSZ within the first 4 hours of culture. The superior ability of cells to attach to CSZ is probably associated with different surface features of biomaterials. The addition of silicate may give CSZ special surface properties – the silicon promoted cell attachment – and the hydrophilic surface of CSZ may be beneficial for cell adhesion.

The rabbits were scanned with SR X-ray imaging at 4 and 12 weeks to evaluate the in vivo osteoinductivity of CSZ scaffolds. At 4 weeks, the SR-micro-CT images revealed that obvious orthotopic bone formation in CSZ scaffold group occurred throughout the cross-section of the defect and the biodegradation of scaffolds was observed. Whereas, only a small amount of newly formed bone in dense CPC group appeared at the outer surface of cylinder.

At 12 weeks, the most extensive bone ingrowth was observed throughout the entire volume of the implants for CSZ scaffolds, and the formation of new bone cortex was observed as well. The dense CPC produced significantly less bone formation during the same period although the radiopaque areas enlarged with time. In control group, there was little radiopacity within the defects at both time points and an umbilicated cavity formed in the bone cortex at 12 weeks.

The regenerated bone volumes (BV) and bone mineral density (BMD) within the defect was also calculated to precisely evaluate the repair of bone defects. The results indicated that CSZ scaffold group contained higher bone volume than the dense CPC cylinder and control groups, respectively. A significant increase in BMD was observed for all groups from 4 to 12 weeks, which confirmed the results of the SR-micro-CT analysis. The CSZ scaffold group showed higher BMD values than dense CPC cylinder and control groups at 4 weeks, respectively. At 12 weeks, the BMD value of CZS scaffold was significantly higher than dense CPC cylinder and control groups, respectively.

CONCLUSION

By using SR X-ray imaging with high spatial resolution and density resolution, the cartilage, fibrous tissue and blood vessels around the defects could be clearly observed. Furthermore, three-dimensional and quantitative results of internal structure of the defect area provided a new analytical tools for investigating the mechanism of new bone formation and scaffold degradation.

ACKNOWLEDGMENTS

The authors would like to thank the National Natural Science Foundation of China (No. 31100680) for providing financial support to this project.



Fabrication and Characterization of Gelatin-based Polyurethane Vascular Graft for Tissue-engineering Applications

Paola Losi¹, Enrica Briganti¹, Luisa Mancuso^{2,4}, Alice Gualerzi⁴, Tamer Al Kayal¹, Simona Celi³, Silvia Volpi¹, Giacomo Cao², Giorgio Soldani¹

¹Laboratory of Biomaterials & Graft Technology, Institute of Clinical Physiology, CNR, Massa, Italy

²Dipartimento di Ingegneria Meccanica Chimica e dei Materiali, Università degli Studi di Cagliari, Cagliari, Italy

³Scuola Superiore S'Anna, Massa, Italy

⁴BT (Biomedical Tissues) Srl, Sestu (CA), Italy

INTRODUCTION

Peripheral artery disease and related revascularization procedures are increasing due to the aging population and growing incidence of diabetes mellitus. Up to now, autologous saphenous vein represents the conduit of choice for peripheral by-pass. Synthetic vascular graft in polyethylene terephthalate (Dacron®) and expanded polytetrafluoroethylene (ePTFE) are used when the vein is not available. However they have shown poor patency when used in small-diameter sizes (<6 mm) due to thrombosis and intimal hyperplasia. Attempts have been made to reduce the thrombogenicity of synthetic grafts by seeding the lumen with endothelial cells, therefore, the development of scaffolds that can support cell growth has become an important issue in the field of vascular tissue engineering.

The aim of this study was to prepare a composite vascular graft by spray, phase-inversion technique constituted by polyurethane and gelatin able to support cell growth.

EXPERIMENTAL METHODS

Gelatin-based polyurethane (PU-gel) grafts were fabricated co-spraying polyurethane (Estane®5714F1 2% in THF/DX) and gelatin aqueous solution (2%) to obtain a composite vascular graft. After materials deposition, grafts were placed in dH₂O at 4°C o.n. to allow solvents removal. Cross-linking of gelatin (PU-CLKgel) was obtained by exposition to glutaraldehyde vapour for 2 h at r. t. Then samples were immersed in 50 mmol/L glycine solution for 1 h to block residual aldehyde groups of glutaraldehyde. Polyurethane graft without gelatin (PU) was used as control. Graft microstructure was investigated by stereo-microscopical observation of Sudan Black stained samples and SEM. Uniaxial tensile tests were carried out to assess grafts mechanical properties. Static tests were performed until failure occurred on longitudinal and circumferential directions by a computer controlled tensile testing machine (100 N load cell) according to ASTM D412-06a protocol. Six test samples were evaluated for each graft materials and for both directions. For each samples stress-strain data, ultimate tensile strength (UTS), and ultimate elongation (UE) were calculated.

Human Mesenchymal Stem Cells (hMSCs) were obtained from bone marrow aspirate. Cells displaying a mesenchymal phenotype (CD34⁻, CD45⁻, CD44⁺, CD105⁺, CD90⁺ and CD73⁺) were used to evaluate the graft capability to support cell adhesion and growth.

PU-CLKgel and control grafts were punched to obtain round samples (2 cm² area). These samples were placed at the bottom of a 24-well plate and preconditioned in

culture medium for 30 min. hMSCs at passage 6 (six) were seeded onto the graft luminal surfaces (1.4x10⁴ cells/well). After 24, 48 and 72 h of incubation, cell viability was calculated by XTT assay and cells morphology was evaluated by Giemsa staining. Statistical analysis was performed using StatView™ by Student's t test.

RESULTS AND DISCUSSION

Microscopical observation of PU-CLKgel and control graft stained with Sudan Black did not show any difference at 40X magnification, however SEM analysis at higher magnification (500 and 2500X) evidenced differences between samples. The PU samples feature a microporous structure similar to that previously described relating to a polyurethane-polydimethylsiloxane graft obtained by spray, phase inversion technique [1]. The gelatin-based PU samples showed a fibrillar appearance typically to that owned by hydrogel. From the mechanical point of view, the presence of gelatin produced an increase of UTS (17.5% and 35.5%) and UE (9% and 20.6%) in both circumferential and longitudinal directions, respectively, compared to PU material. Similarly PU-CLKgel showed an increase of UTS and UE with respect to PU material.

Qualitative analysis of hMSC adhesion after 24, 48 and 72 h onto the grafts revealed remarkable differences between PU-CLKgel and control graft. hMSCs grown onto PU-CLKgel graft form a monolayer that reached confluence at 72 h and appeared to be similar to the physiological morphology of hMSCs grown on culture plastic. On the contrary cells seeded onto the control graft were not able to undergo appropriate spreading and proliferation, thus displaying a rounded morphology. hMSCs grown onto PU-CLKgel graft showed significantly higher O.D. value then cells seeded onto PU luminal surface at all time-points. Moreover hMSCs onto PU-CLKgel graft showed an increase of O.D. over the time indicating a proliferative activity.

CONCLUSION

A composite vascular graft was successfully produced by simultaneous spraying a synthetic polymer (Estane®5714F1) and a natural biopolymer (gelatin) in order to obtain a scaffold that combines the mechanical characteristics of polyurethanes with the favourable cell interaction features of the biopolymer fibers.

REFERENCES

1. Soldani G. *et al.*, Biomaterials 31:2592-605, 2010.



Controlling the Delivery of Vascular Endothelial Growth Factor and Platelet Derived Growth Factor

Laura Kelly¹, Laura Platt¹, Sheila MacNeil², Paul Genever³, Tim Chico⁴, Stephen Rimmer¹

¹*Department of Chemistry, University of Sheffield, UK. ²Kroto Research Institute, University of Sheffield, UK.

³Department of Biology, University of York, UK. ⁴Department of Biomedical Science, University of Sheffield, UK.

Email: dtp10lk@sheffield.ac.uk

INTRODUCTION

Angiogenesis is the formation of new blood vessels from a pre-existing vascular network. It plays a vital role in the repair of tissues by establishing a blood supply, however, in the case of acute injury the rate of angiogenesis can be slow. It has become a major aim of tissue engineering to be able to restore the blood supply quickly to tissue after injury or in tissue transplantation. Angiogenesis is stimulated by proteins called growth factors. Growth factors have been used to treat ischemic tissue for some time. Application of a single growth factor has had limited success. Therefore, there has been a move towards releasing two or more pro-angiogenic growth factors to induce blood vessel formation.

Two sets of materials have been used to successfully release either vascular endothelial growth factor (VEGF₁₆₅) or platelet derived growth factor (PDGF-BB)^{1,2}. These systems mimic heparin through electrostatically binding to the growth factor peptide sequences containing arginine and lysine amino acids. However, the aim is to produce more control over the availability of these growth factors than is possible with heparin functional materials.

EXPERIMENTAL METHODS

OPHP was synthesized from oleyl alcohol (Sigma Aldrich UK) and phenyl phosphodichloridate (Sigma Aldrich UK). PS-co-DVB core OPHP-co-EGDMA shell latexes were produced in an emulsion reactor heated at 70°C with stirring at 400rpm. The latexes containing glycerol methacrylate acetone (GMAC) were produced in the same manner. PBMA latexes were made via surfactant free emulsion polymerization with PAMPS was added as a stabilizer. This produced latexes with PAMPS incorporated. Particle size, zeta potential measurements and TEM were done on all latex samples. To study protein release and binding 0.5ml 100ng/ml VEGF or PDGF (PeproTech UK) solution containing 1% bovine serum albumin was added to each latex sample. The protein was left to bind for 12 hours at 4°C. The protein solution was changed for PBS and samples placed in a 37°C oven for varying time points. Protein release was analyzed using sandwich ELISA kits purchased from R&D systems (Minneapolis, MN 55413). *In vivo* work was done using

several zebrafish transgenic lines. VEGF was released *in vitro* for 7 days then particles and supernatant injected and imaged after a further 3 days.

RESULTS AND DISCUSSION

OPHP and PAMPS based systems showed controlled release of pro-angiogenic growth factors over the period of 31 days. The ratio of OPHP to EGDMA can be altered to give varying release profiles of VEGF₁₆₅ and PDGF BB. The addition of GMAC to the OPHP system produces a slower release profile, without the plateau seen with OPHP-co-EGDMA. The inclusion of GMAC gives a larger outer shell, allowing proteins to bind deeper within the shell of the latex. This gives the steadier release profile seen with OPHP after the inclusion of GMAC.

PAMPS functionalized latexes show steady growth factor release over 31 days, with no burst release. The branched PAMPS have a slower release profile compared to linear PAMPS. This is due to branched PAMPS producing a larger network structure, allowing growth factors to bind deeper within the outer shell of the particle. In contrast, linear PAMPS produced a more open structure which allows for easier diffusion.

In vivo work indicates that the released VEGF is still functional and can elicit a response in endothelial cells.

CONCLUSION

Two novel systems have been developed that can successfully bind and release biologically functional VEGF₁₆₅ and PDGF-BB by electrostatic binding of the growth factors on to or within the outer layer of polymer particles. The shell architecture has a size exclusion effect upon the proteins.

REFERENCES

1. Gilmore L. *et al.*, ChemBioChem. 10:2165-2170, 2009.
2. Platt L. *et al.*, J. Mater. Chem. B. 2:494- 501, 2014.

ACKNOWLEDGMENTS

The authors would like to thanks the doctoral training centre for tissue engineering and regenerative medicine and the EPSRC for funding.



Cell Behaviour on Self-assembled Nanohole Arrays on Type 316L Stainless Steel Formed by Anodic Process

Sayaka Miyabe*, Yushi Fujinaga, Hiroaki Tsuchiya and Shinji Fujimoto

Division of Materials and Manufacturing Science, Graduate School of Engineering, Osaka University, Japan

miyabe@mat.eng.osaka-u.ac.jp

INTRODUCTION

Various surface treatments have been examined to metals and alloys used as biomaterials in order to improve the biocompatibility. Recently, it has been reported that not just microscale but nanoscale environment has affects to cellular behaviour^{1,2}. Electrochemical approach to form highly defined porous alumina and TiO₂ nanotube layers has been reported^{3,4}. Under specific electrochemical conditions, self-organized nanohole arrays can be formed on stainless steel simply by anodization of stainless steel⁵. Cell behaviour of TiO₂ nanotube layers has been extensively examined⁶. But how cells behave on nanohole arrays on stainless steel surface is not clear yet. The present work reports how cells behave on nanohole arrays formed on type 316L stainless steel.

EXPERIMENTAL METHODS

Material examined was type 316L stainless steel, the composition is as follow: Cr: 17.35, Ni: 12.18, Mo: 2.07, Mn: 1.20, Si: 0.63, P: 0.030, C: 0.011, S: 0.001, Fe: Bal. (wt%). The material was cut into samples with a dimension of typically $\phi 15.5 \text{ mm}^2$ and 1 mm thickness. The samples were polished with SiC abrasive paper up to #2000 and finally mirror-finished with colloidal silica, then ultrasonically cleaned in acetone and ethanol, followed by rinsing with deionized water and dried at room temperature. Electrochemical treatments for the nanohole formation were carried out in ethylene glycol containing 2.01 M NaClO₄ using a two-electrode electrochemical cell with a platinum counter electrode. The electrochemical treatments consisted of sweeping the potential at 0.1 V/s from 0 V to a predetermined potential. Five types of specimens were prepared as follows; (a) nanohole anodized at 20 V, (b) nanohole anodized at 30 V, (c) nanohole anodized at 40 V, (d) polished with SiC #2000 and (e) mirror-finished. The diameter and depth of nanohole were measured by scanning electron microscopy (SEM) and atomic force microscopy (AFM). The specimens were sterilized in a steam using autoclave then provided for tests. Osteoblast-like cells (MC3T3-E1) were cultured on the specimens using cell culturing medium (α -MEM with 10 % FBS). The number of cell was counted during the cultivation. Cell activity was evaluated by measurement of ALP (alkaline phosphatase) activity.

RESULTS AND DISCUSSION

Figure 1 shows SEM images of highly ordered nanohole arrays on type 316L stainless steel. The diameter and depth increased in proportion to applied potential. Figure 2 shows the cell density on samples after cultivation of 3 days. The cell density on nanohole samples is significantly larger compared to that on mirror sample. Especially cell density on nanohole sample anodized at 20 V shows the highest. The ALP

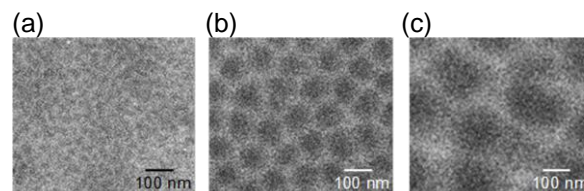


Fig. 1 SEM images of type 316L stainless steel surfaces formed at (a) 20 V, (b) 30 V and (c) 40 V for 300 s in ethylene glycol containing sodium perchlorate.

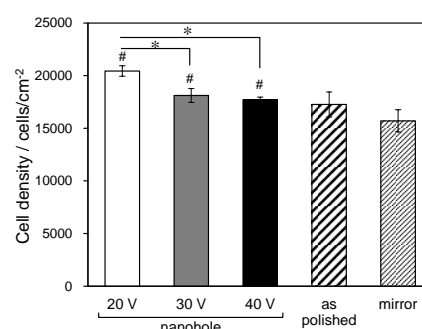


Fig. 2 Cell density of MC3T3-E1 cultured on different surfaces of type 316L stainless steel at day 3. Each value and bar represent the mean and SD ($n=3$). #: $p < 0.05$ vs. mirror. *: $p < 0.05$.

activity on the sample anodized at 20 V is significantly higher than that on other samples. These results indicate that the optimal geometry of nanohole arrays on stainless steel exists for cell compatibility.

CONCLUSIONS

The proliferation and activity of osteoblast-like cell on nanohole array produced on Type 316L stainless steel were examined and the following conclusions are made:

- 1 The cell density on nanohole array is significantly larger compared to that on mirror finished sample. Especially cell density on nanohole sample formed at 20 V shows the highest.
- 2 The ALP activity on nanohole sample formed at 20 V is significantly higher than that on other samples.

REFERENCES

1. Arnold M. *et al.*, ChemPhysChem. 5:383-388, 2004
2. Dalby M.J. *et al.*, Biomater. 27:2980-2987, 2006
3. Keller F. *et al.*, J. Electrochem. Soc. 100:411-419, 1953
4. Tsuchiya H. *et al.*, Electrochem. Comm. 7:576-580, 2005
5. Tsuchiya H. *et al.*, Electrochim. Acta 82:333-338, 2012
6. Park J. *et al.*, Nano Lett. 7:1686-1691, 2007

Strontium-substituted CaP bone cements for the treatment of osteoporotic bone defects

Matthias Schumacher^{1*}, Arne Helth², Anja Lode¹, Anne Bernhardt¹, Anja Henß³, Marcus Rohnke³, Seemun Ray⁴, Ulrich Thormann^{4,5}, Volker Alt^{4,5} and Michael Gelinsky¹

^{1*}Centre for Translational Bone, Joint and Soft Tissue Research, Technische Universität Dresden, Germany, matthias.schumacher@tu-dresden.de

²Leibniz Institute for Solid State and Materials Research (IFW), Dresden, Germany

³Institute of Physical Chemistry, Justus Liebig University Giessen, Germany

⁴Laboratory of Experimental Trauma Surgery, Justus-Liebig-University, Giessen, Germany

⁵Department of Trauma Surgery, University Hospital Giessen-Marburg GmbH, Campus Giessen, Germany

INTRODUCTION

Calcium phosphate (CaP) bone cements are frequently used in the reconstruction of bone defects. They possess excellent biocompatibility, are known to be resorbed *in vivo* and could be used to locally deliver therapeutic substances into a defect area. The incorporation of Sr²⁺-ions into such cements and their release into a bone defect upon implantation gives rise to cements that are adapted to the specific needs of osteoporotic bone healing. This concept is based on the dual effect of Sr²⁺-ions on bone cells: while the osteoblast-related new bone formation is stimulated by strontium, the cellular bone resorption by osteoclasts is reduced¹. However, such cements must neither suffer from poor mechanical properties nor show an excess release of Sr²⁺-ions to avoid possible cytotoxic effects.

Here, we investigated an easy-to-prepare, strontium-releasing CaP bone cement (SrCPC) that could support osteoporotic bone defect healing through stimulating new bone formation and inhibiting the osteoclast-mediated bone resorption specifically in the defect area (Fig. 1).

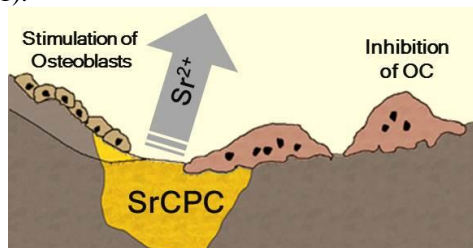


Fig. 1: Concept of Sr²⁺-release from a SrCPC and its action on bone cells.

EXPERIMENTAL METHODS

Sr-substituted CaP cements were obtained by simple substitution of SrCO₃ for CaCO₃ in the precursor of an α -TCP based cement as recently described². Cement paste and set samples were thoroughly characterised with a variety of methods, including XRD, ToF-SIMS, SEM and He-pycnometry. Release of Sr²⁺-ions from set cements was studied in salt buffer solutions and cell culture media w/o serum addition and quantified by ICP-MS. *In vitro* characterisation included experiments focussing on osteogenesis (employing primary human mesenchymal stem cells w/o osteogenic stimulation) and osteoclastogenesis (using osteoclastogenically induced primary human monocytes). Cements were implanted in critical-size metaphyseal defects in female

Sprague-Dawley rats with osteopenic bone status after bilateral ovariectomy and calcium-, phosphate- and vitamin D-deficient diet. Histology, histomorphometry as well as ToF-SIMS were used to analyse the defect area after 6 weeks.

RESULTS AND DISCUSSION

SrCPC set into Sr-substituted hydroxyapatite as demonstrated by XRD and were characterised by a homogeneous strontium distribution within the cement matrix (ToF-SIMS analysis). Substitution resulted in cements with suitable handling properties and enhanced compressive (but not biaxial bending) strength. Sr²⁺-ion release depended on the immersion medium and was hampered by the presence of proteins due to their adsorption. However, SrCPC was shown to release Sr²⁺-concentrations between 0.025 and 0.1 mM (depending on the degree of substitution) under cell culture conditions. Enhanced proliferation and osteogenic differentiation were found *in vitro* using osteogenically induced hMSC cultured on SrCPC compared to pure CaP cement. This could be attributed to the release of Sr²⁺-ions as well as a reduced ionic interaction of the SrCPC with the cell culture medium. Furthermore, osteoclast formation and their resorptive activity (determined by resorption pit formation) were reduced on SrCPC. *In vivo*, enhanced bone remodelling activity as well as higher content of osteogenesis-associated markers (ALP and OCN) and osteoid formation were observed (analysed by histomorphometry and immunohistochemistry).

CONCLUSION

In this study a promising, easy-to-prepare strontium-containing bone cement was developed that could fulfil the specific needs of osteoporotic bone defect healing, namely to enhance osteogenesis and reduce osteoclast-mediated bone resorption.

REFERENCES

1. Marie, P.J. *et al.*, Bone 40:S5-S8, 2007
2. Schumacher, M. *et al.*, Acta Biomater. 9:7536-44, 2013

ACKNOWLEDGMENTS

The authors would like to thank the German Research Foundation (Deutsche Forschungsgemeinschaft, DFG; grant SFB/Transregio 79) for providing financial support.

Mesoporous bioactive glass/CaP bone cement composites as drug delivery system

Matthias Schumacher^{1*} and Michael Gelinsky¹

^{1*}Centre for Translational Bone, Joint and Soft Tissue Research, Technische Universität Dresden, Germany, matthias.schumacher@tu-dresden.de

INTRODUCTION

Calcium phosphate (CaP) bone cements have been used for bone regeneration applications since the early 1980s. Besides their excellent biocompatibility and high bonding strength to natural bone tissue they are known to be resorbed *in vivo*. Furthermore, the mild setting conditions of most CaP cements, in particular, allow the integration of therapeutic substances into the cement. Such therapeutics shall be released upon implantation into the respective bone defect. Besides blending the therapeutics into the cement precursor or adding it into the cements liquid, e.g. polymeric microspheres have been employed to tailor the release kinetics or to protect sensitive therapeutics such as protein-based therapeutics as bone morphogenic proteins (BMP). Furthermore, such adsorption of the drug onto a special carrier or into the pores of secondary particles embedded in the cement matrix, often referred to as “entrapment”¹, might allow the incorporation of different therapeutics with specific release kinetics.

In this study we used mesoporous bioactive glass (MBG) particles to adsorb and sustainably release a model drug from an apatitic CaP bone cement (Fig. 1).

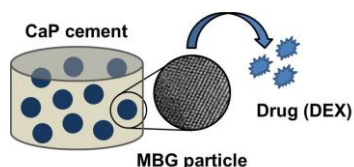


Fig. 1: Principle of drug release via MBG particles embedded in a CPC matrix.

EXPERIMENTAL METHODS

Mesoporous bioactive glass was prepared using a self-assembling method as described by Zhu *et al.*³: during solvent evaporation from a Ca- and phosphate-enriched orthosilicate gel formation of pores (approx. 5 nm in diameter) occurs. MBG was ground and sieved to obtain particles < 20 µm, of which 5 and 10 wt-% were added to an α -TCP based CaP cement (CPC) known to set into carbonated hydroxyapatite⁴.

The obtained cement pastes were characterised regarding their setting kinetics. Set cements were analysed by scanning electron microscopy (SEM, Phillips XL30), XRD (Bruker D8) and mechanical strength was tested in compression mode (Zwick Z1010).

For drug release studies, dexamethasone (DEX, used as a model drug) was adsorbed into the pores of MBG. Cements containing 5 and 10 wt-% of the drug-loaded MBG were prepared. Release of DEX was studied during immersion in phosphate-buffered saline (PBS). Cytocompatibility of CPC/MBG composites was studied using SaOS-2 osteoblasts cultured in McCoy 5A

medium (Biochrom) employing the WST-1 assay (Roche).

RESULTS AND DISCUSSION

Setting of the cement paste was only slightly increased by the addition of MBG and was within the range recommended for CaP cements. XRD analysis confirmed the formation of hydroxyapatite despite of glass addition to the cement, indicating the excess Ca- and phosphate-ions delivered by the highly soluble MBG did not alter the cement setting. Surprisingly, compressive strength increased significantly for MBG/CPC composites (Fig. 2).

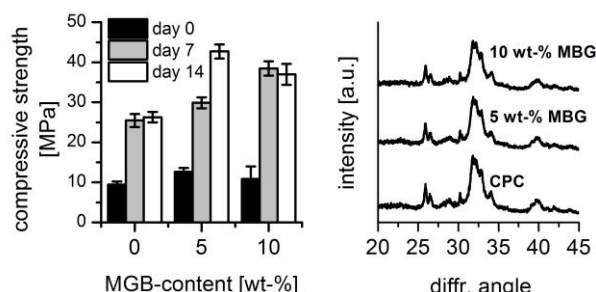


Fig. 2: Compressive strength evolution (left) and XRD-pattern (right) of CPC/MBG composites.

Metabolic cell activity on MBG/CPC composites well exceeded the level measured on CPC, which indicates an enhanced cell compatibility of the developed composites. Finally, release of the model drug dexamethasone was shown to be controlled by the presence of MBG particles.

CONCLUSION

We could demonstrate how mesoporous bioactive glass micro-particles can be used to adsorb and sustainably release drug molecules in CaP bone cements without chemical binding. Thus, MBG/CPC composites are a promising system to locally release delicate bone-specific drugs into a bone defect area.

REFERENCES

1. Ginebra M.-P. *et al.*, Adv. Drug Deliv. Rev. 64(12):1090-110, 2012
3. Zhu, Y. *et al.*, Micropor. Mesopor. Mat. 112:494-503, 2008
4. Schumacher, M. *et al.*, Acta Biomater. 9:7536-44, 2013

ACKNOWLEDGMENTS

The authors would like to thank the German Research Foundation (Deutsche Forschungsgemeinschaft, DFG; grant SFB/Transregio 79) for providing financial support.

The influence of PEG/PCL ratio on properties of PU/ β -TCP composites for orthopaedic applications

Piotr Szczepańczyk, Kinga Pielichowska, Jan Chłopek

AGH University of Science and Technology

Faculty of Materials Science and Ceramics

Department of Biomaterials

Al. Mickiewicza 30, 30-059 Kraków, Poland

pszczepa@agh.edu.pl

INTRODUCTION

Regenerative medicine and tissue engineering take advantage of biomaterials based on polyurethanes (PU) which exhibit wide range of properties suitable for regeneration of heart muscle, skin, bone, cartilage and nerve tissue. This can be achieved through variable contents of polyol and isocyanate and different ratios. Previous study disclosed multiple influence of β -tricalcium phosphate (β -TCP) on properties of composite materials with PU matrix. Their properties and microstructure could be improved using calcium stearate (CS) and red turkey oil (SCO) [1]. Physical and chemical properties of polyol also influence characteristics of the PU materials. PUs synthesized from poly(ϵ -caprolactone) diol (PCL) promoted cell growth and tissue repair [2]. Previous study showed the possibility of tailoring the hydrophilic properties through varying PEG/PCL ratios in synthesized PUs [3]. PCL contributed to better mechanical properties. Consequently this changed mechanical, thermal properties and degradation kinetics of PU materials [4]. Polyethylene glycol (PEG)/PCL based polyurethanes also exhibited regular microstructure and pore interconnectivity. Moreover, PEG/PCL based hydrogels effectively supported *in vivo* cranial osteoregeneration [6]. The aim of this study is to investigate the influence of varying PEG/PCL ratios on properties of polyurethane foams. The effect of β -TCP on microstructure was also studied. The essence of the present study was to understand relationships between different chemical structure of PU and properties.

EXPERIMENTAL METHODS

PU samples were synthesized via one-step procedure with varying PEG/PCL ratios and addition of β -TCP microparticles. Main substrates used for the reaction include 4,4'-methylene diphenyl diisocyanate (MDI), PEG, PCL, 1,4-butanediol (BDO), CS, SCO and β -TCP. Characterization included FTIR, DSC, TGA, DSA, mechanical and porosity measurements and SEM observations in order to evaluate the *in vitro* bioactivity.

RESULTS AND DISCUSSION

FTIR and DSC/TG measurements showed the relationships between phase separation and content of PEG and PCL. Contact angle values and mechanical properties also changed with varying PEG/PCL ratios. β -TCP affected formation of hydrogen bonds. Figure 1 presents photos of cross section taken with optical microscope.

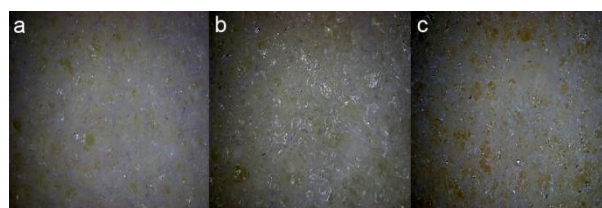


FIGURE 1 Cross section of PU samples synthesized from a) PEG b) PEG/PCL (50/50 wt/wt) c) PCL

CONCLUSION

Present study showed the possibility to modulate the properties of PU/ β -TCP foams via different PEG/PCL ratios. Exothermic effect of the polymerization also depended on the PEG/PCL ratios. The obtained polyurethane samples exhibited properties more suitable for bone tissue engineering.

REFERENCES

1. Szczepańczyk P. *et al.*, Eng. Biomat. 16:33-41, 2013
2. Asefnejad A. *et al.*, Int. J. Nanomed. 6:2375-2384, 2011
3. Gorna K. *et al.*, J. Biomed. Mater. Res. A. 67:813-827, 2003
4. Yeganeh H. *et al.*, Polym. Int. 56:41-49, 2007
5. Ni P. *et al.*, Biomat. 35:236-248, 2014

ACKNOWLEDGMENTS

This work was financed by statutory research 11.11.160.256 of Faculty of Materials Science and Ceramics AGH-UST.

Effect of fibre reinforcement on the crystallinity of PEEK for articular joint implants

Marco Regis^{1,2*}, Simonetta Fusi¹, Michele Pressacco¹, Marco Zanetti² and Pierangiola Bracco²

¹R&D Department, Limacorporate, Italy

^{2*}Chemistry Department, University of Torino, Italy, marco.regis@limacorporate.com

INTRODUCTION

In recent years, a lot of interest has grown on the use of PEEK and its composites in orthopaedic applications [1]. To date, the use of PEEK is limited to spine and trauma implants. In particular, concerns on wear resistance, as well as on body reaction to wear debris, and on material properties evolution during the in vivo use of PEEK were risen [2, 3], limiting its application in articular joints. As for every semi-crystalline polymer, PEEK properties largely depend upon its crystal structure. PEEK crystallinity has been extensively studied [4], but only little data is available on the effect of reinforcement addition on its crystallization behaviour, as well as on the resulting properties [5]. The aim of this study is therefore to investigate the effect of a carbon fibre reinforcement addition on PEEK crystallisation behaviour, to provide a material with controlled properties and enhanced mechanical performance to further extend the use of PEEK in orthopaedics.

EXPERIMENTAL METHODS

Non isothermal melt crystallization DSC studies were carried out to determine crystallization behaviour of unfilled PEEK (NI1) and two formulations of 30% wt. carbon fibre reinforced (CFR) PEEK, PAN and pitch based, named NI1CA30 and Motis, respectively (Invibio, UK). 6,5 to 8,5 mg samples were prepared from granules and tested in a TA Q20 DSC (TA inc, USA). Hermetic pans were chosen to encapsulate the samples. After a preliminary heating up stage at 400°C for 15 minutes, to eliminate the residual crystallinity and the small nuclei that might influence the crystal growth kinetics, samples were cooled down to 30°C at different cooling rates (2, 5, 10, 20 and 50°C/min). The tests have been repeated three times for each sample. DSC apparatus was calibrated with Indium samples for each of the cooling rates used in this test. n and Z_t were calculated from the Avrami equation derived from Arrhenius law:

$$\log[-\ln(1 - X_c(t))] = n \log t + \log Z_t$$

where $X_c(t)$ is the relative crystallinity degree at time t . n is the calculated slope of the linear portion of the $\log[-\ln(1-X_c(t))]$ vs. $\log t$ plot curve, and Z_t is the intercept of the same. Z_t has been then corrected taking into account the changes in crystal growth due to the different cooling rates [6]. The resulting samples crystallinity was evaluated as well, by heating up the samples to 400°C at 20°C/min in a subsequent DSC test.

RESULTS AND DISCUSSION

n and Z_c trends are reported in Figure 1. Despite some literature work indicates a decrease in n values with increased cooling rate [7], a clear opposite trend was observed for all materials.

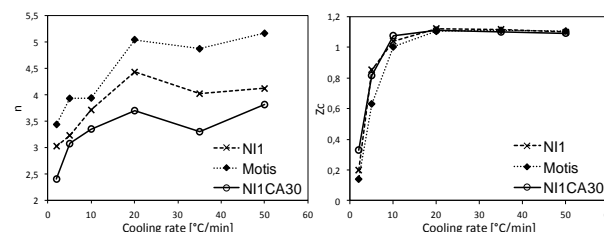


Figure 1. calculated n and Z_c trends at different cooling rates for NI1, Motis and NICA30

Moreover, n values for Motis CFR PEEK were higher than for NI1 unfilled PEEK, while NI1CA30 had lower n values compared to NI1. The $n > 3$ values suggests the growth of spherulite-shaped nuclei, while for $n < 3$, as for NICA30 at 2°C/min, crystals may form in different shapes [8]. The resulting crystallinity of CFR PEEK samples is illustrated in Figure 2 DSC thermograms.

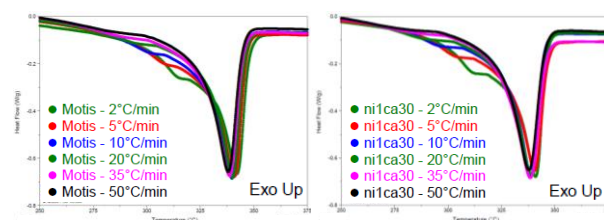


Figure 2. NI1CA30 (right) and Motis (left) crystallinity after the melt crystallisation study.

Peak appearance confirms the different crystal regions formed by varying cooling rates. At lower cooling rates, a second crystal order is formed, enhancing the overall crystallinity. The same trend was observed for each material tested.

CONCLUSION

The results suggest that different carbon fibres can play different roles in PEEK crystallization. Pitch fibres act as nucleation sites for a further crystal growth, while PAN fibres seem to be related to an entanglement obstacle for the chain organization. Also thermal history influences the resulting crystallinity, both in terms of overall amount and in terms of crystal type. This will have an impact on the final mechanical properties and on the in vivo behaviour of the material.

REFERENCES

1. Kurtz S.M., *et al.*, Biomaterials 28, 2007
2. Meyer M.R., *et al.*, JBMR 28, 1994
3. Chivers R.A., *et al.*, Polymer 35, 1994
4. Wei C.L., *et al.*, Polymer 44, 2003
5. Kuo M.C., *et al.*, Mater Chem and Phys 123, 2010
6. Kuo M.C., *et al.*, Mater Chem and Phys 99, 2006
7. Vasconcelos G., *et al.*, J Aerosp Tech Manag 2, 2010
8. Liu T., *et al.*, J Appl Poly Sci 67, 1998

Effect of surface roughness on the biocompatibility of $\text{Ti}_{40}\text{Zr}_{10}\text{Cu}_{38}\text{Pd}_{12}$ bulk metallic glass

Andreu Blanquer¹, Anna Hynowska², Carme Nogués¹, Elena Ibáñez¹,
Maria Dolors Baró², Jordi Sort³, Eva Pellicer², and Lleonard Barrios¹

¹Dept. Biologia Cel·lular, Fisiologia i Immunologia, Universitat Autònoma de Barcelona, Spain

²Dept. Física, Universitat Autònoma de Barcelona, Spain

³ICREA and Dept. Física, Universitat Autònoma de Barcelona, Spain

andreu.blanquer@uab.cat

INTRODUCTION

The importance of the use of biocompatible materials for tissue regeneration and transplantation is increasing. The good mechanical and corrosion properties of $\text{Ti}_{40}\text{Zr}_{10}\text{Cu}_{38}\text{Pd}_{12}$ bulk metallic glass (BMG) and its *in vitro* biocompatibility makes it a potential candidate for orthopaedic implants¹. Surface roughness has been identified as a key aspect to regulate cell adhesion, proliferation and spreading. Some authors have described that materials with nano-rough surfaces have improved biocompatibility², although some other studies have shown that the improvement depends on the range of surface roughness³. Here, we report on the effect of nano-mesh surface of $\text{Ti}_{40}\text{Zr}_{10}\text{Cu}_{38}\text{Pd}_{12}$ BMG compared to mirror-like surface and to commercial Ti6Al4V material. We analyse toxicity, adhesion, morphology and differentiation on a human osteoblast-like cell line.

EXPERIMENTAL METHODS

$\text{Ti}_{40}\text{Zr}_{10}\text{Cu}_{38}\text{Pd}_{12}$ disk surfaces were polished to mirror-like roughness and some of them were anodized at 25°C in 5M NaOH to achieve a nano-mesh surface.

Saos-2 cells were cultured in presence and absence of the alloy. Alloy disks were glued onto glass coverslips using silicone, and sterilized by UV light for 2h. Cytotoxicity was evaluated by detecting the activity of intracellular esterases, using live/dead viability/cytotoxicity kit (Invitrogen) according to the manufacturer's protocol. Cell adhesion was analysed by immunodetection of stress fibres (actin) and focal contacts (vinculin) with a confocal laser scanning microscope (CLSM). Cells were processed for scanning electron microscopy (SEM) to analyse their morphology. Differentiation was evaluated by detecting the alkaline phosphatase (ALP) activity after 14 days.

RESULTS AND DISCUSSION

Results indicated that $\text{Ti}_{40}\text{Zr}_{10}\text{Cu}_{38}\text{Pd}_{12}$ BMG had no effect on cell viability, because no significant differences were observed among the two different surface topographies and the commercial Ti6Al4V. The number of live cells was higher than 97% in all cases. These results are in agreement with a previous study of biocompatibility of mouse preosteoblasts grown on this BMG¹. In all cases, Saos-2 cells were able to adhere to

the alloy, showing focal contacts and a flattened polygonal morphology (Fig.1).

Osteoblast differentiation was analysed after 14 days in culture using ALP activity, which increases with osteoblast differentiation. ALP activity was higher on $\text{Ti}_{40}\text{Zr}_{10}\text{Cu}_{38}\text{Pd}_{12}$ alloy than on Ti6Al4V, indicating that the BMG alloy allows a better osteoblast differentiation than the commercial one. Moreover, ALP activities in mirror-like and nano-mesh surfaces indicated that nano-roughness does not affect Saos-2 differentiation.

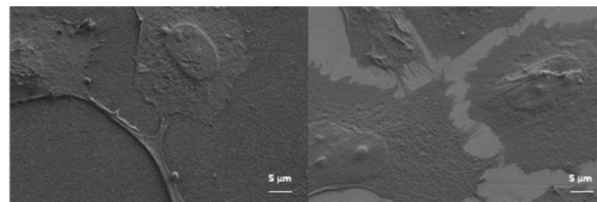


Fig. 1. SEM images of Saos-2 cells adhered to the nano-mesh surface (left) and to the mirror-like surface (right).

CONCLUSION

$\text{Ti}_{40}\text{Zr}_{10}\text{Cu}_{38}\text{Pd}_{12}$ BMG is biocompatible for human osteoblast-like cells in both surface structures, mirror-like and nano-mesh. Moreover this alloy seems to allow a better osteoblast differentiation than the commercial Ti6Al4V alloy.

REFERENCES

1. Blanquer A. et al., J Mater Sci: Mater Med. 25(1):163-72, 2014
2. Zuo J. et al., J Biomed Mater Res Part A. 101A:3278-84, 2013
3. Dowling D.P. et al., J Biomater Appl. 26(3):327-47, 2011

ACKNOWLEDGMENTS

This work has been partially financed by the TEC2011-29140-C03-03, 2009-SGR-282, 2009-SGR-1292, FP7-PEOPLE-2010-ITN-264635 (BioTiNet). A. Blanquer was supported by a predoctoral grant from UAB. M. D. Baró was partially supported by an ICREA ACADEMIA award. E. Pellicer acknowledges the Spanish MINECO for the Ramon y Cajal contract.

Plasma assisted production of residual solvent free PLLA electrospun scaffolds

V. Colombo^{1,2}, D. Fabiani³, M.L. Focarete⁴, M. Gherardi^{1*},
C. Gualandi⁴, R. Laurita¹, M. Zaccaria³

¹ Department of industrial engineering (DIN), Alma Mater Studiorum – Università di Bologna, Italy
matteo.gherardi4@unibo.it

² Industrial Research Centre for Advanced Mechanics and Materials (C.I.R.I.-M.A.M.), Bologna, Italy

³ Electrical, Electronic and Information Engineering Department, Alma Mater Studiorum – Università di Bologna, Italy

⁴ Department of Chemistry “G. Ciamician”, Alma Mater Studiorum – Università di Bologna, Italy

INTRODUCTION

Poly-L-lactic acid (PLLA) is a biocompatible and biodegradable polymer; PLLA nanofibrous scaffolds are suitable for tissue engineering, since they mimic the fibrillar arrangement of the extracellular matrix. Indeed topographical, morphological, and mechanical properties of nanofibrous scaffolds are very similar to the properties of different tissues and organs. Continuous polymeric or inorganic fibers having dimensions ranging from tens of nanometers to a few microns can be produced with the electrospinning technique¹: PLLA can be successfully processed into nanofibers through electrospinning starting from a polymeric solution containing the polymer dissolved in organic solvents, such as dichloromethane (DCM) and dimethylformamide (DMF). The latter is usually added to DCM in order to increase the dielectric constant of the solution, thus ensuring electrospinnability. However, the boiling temperature of DMF is around 153°C (higher than that of DCM which is about 40°C), and it is therefore difficult to completely avoid traces of residual DMF in the produced nanofibers, with the risk of unacceptably affecting cell proliferation. In this work, atmospheric pressure non equilibrium plasma is introduced to favour the electrospinning process through the treatment of the polymeric solution; defect-free fibers were produced from a plasma treated solution of PLLA dissolved in 100% DCM, without the addition of DMF. The same solution lead to the production of strongly defected fibers when plasma treatment was not performed.

EXPERIMENTAL METHODS

PLLA (Lacea H.100-E, Mw = 8.4×10^4 g/mol, PDI = 1.7) was supplied by Mitsui Fine Chemicals. DCM was purchased from Sigma–Aldrich. PLLA was dissolved in 100% DCM at 8, 10, and 13% w/v concentrations. Different plasma sources operated at atmospheric pressure were used: a direct liquid phase discharge reactor, a gas phase discharge reactor with liquid electrode and a single electrode argon plasma jet². The plasma sources were driven by different high voltage generators, either producing pulses with a slew rate of few kV/ns or producing waveforms (sinusoidal, triangular and square) with a slew rate of few kV/us. Polymeric solutions were plasma treated and kept at room temperature (RT) before being electrospun. The treatment was performed by randomly moving the source at constant stand-off.

The electrospinning apparatus, made in house, was composed of a high voltage power supply, a syringe pump, a glass syringe, a stainless steel blunt-ended

needle connected with the power supply electrode and a grounded aluminium plate-type collector.

RESULTS AND DISCUSSION

SEM images of fibers electrospun starting from a solution of PLLA dissolved in 100% DCM are presented in Fig.1. While the electrospinning of the pristine solution resulted in no fiber formation (left), plasma treatment was found to enable the production of nanometric defect-free fibers (right)³. The effects of treatment time, electrical parameters sustaining the plasma discharge (voltage, frequency and waveform), delay time between plasma treatment and electrospinning, as well as the type of plasma source, have been investigated in order to optimize the process. Among the tested conditions, the best results have been obtained using the plasma jet driven by nanosecond pulses, which resulted in the production of defect-free nanofibers. Moreover, the improved electrospinnability of the solution after plasma treatment was found to last for more than three hours.

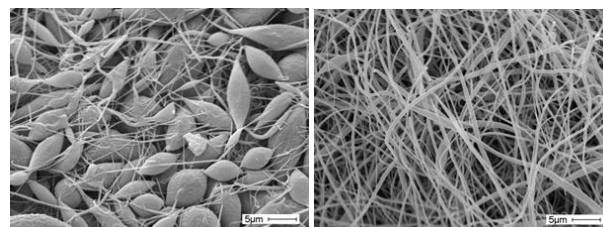


Fig.1 SEM images of PLLA fibers obtained from untreated solution (left) and solution treated with the plasma jet driven by nanosecond pulses (right).

CONCLUSION

The production of solvent- and defect-free PLLA nanofibrous scaffold suitable for tissue engineering and biomedical application was achieved through atmospheric pressure plasma treatment of the electrospinning polymeric solution.

REFERENCES

1. S. Ramakrishna *et al.*, World Scientific Publishing Co. Pte. Ltd, NJ, USA 2005.
2. M. Boselli *et al.*, Plasma Chemistry and Plasma Processing (2014) 1-17.
3. V. Colombo *et al.*, Plasma Processes and Polymers (2014), 11(3), 247-255.

ACKNOWLEDGMENTS

This work has been partially supported by FP7 COST Action MP1101 “BioPlasma”

Fabrication of Stable Biocatalytic Networks for the Cascadable Manufacture of Fine Chemicals

Christopher Hickling¹, Helen Toogood², Alberto Saiani³ Nigel Scrutton² and Aline Miller^{1*}

¹Chemical Engineering and Analytical Sciences, Manchester Institute of Biotechnology, University of Manchester, England

²Faculty of Life Sciences, Manchester Institute of Biotechnology, University of Manchester, England

³ Materials Science, Manchester Institute of Biotechnology, University of Manchester, England

christopher.hickling@postgrad.manchester.ac.uk

INTRODUCTION

Enzymes are finely tuned biological catalysts that perform chemical reactions, with high specificity, however, loss of activity is observed if denaturation under non-optimal conditions. By using the self-assembled, peptide, VKVKVEVK¹ hydrogels we have investigated whether we can create an enzyme functionalised biomaterial that is capable of performing the enzymatic biotransformations and whether the enzymatic activity can be maintained and/or 'superactivity' observed. To develop this material we have chemically and/or genetically conjugated the self-assembling VKVKVEVK tag to the enzymes; pentaerythritol tetranitrate reductase (PETNR)^{2,3} and carveol dehydrogenase (CDH)⁴ so that they can be incorporated within the hydrogel *via* the interaction of the octapeptide tag with the octapeptide fibres.

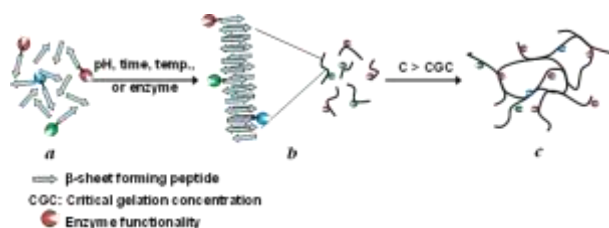


Figure 1. Cartoon of tagging, and interaction with fibre.

We hypothesise that by tagging the enzymes a reduction in leeching from the hydrogel will be obtained, thus increasing the longevity of the hydrogel bioreactors.

EXPERIMENTAL METHODS

Gas chromatography (GC) has been applied to determine the extent of biotransformations in solution and hydrogel enzyme experiments.

UV-Vis spectrometry is applied to monitor the leeching of the enzyme out of the hydrogel. A UV-Vis spectrophotometric method has been developed to assay gel enzyme activity.

Rheology, micro differential scanning calorimetry (μ DSC), atomic force microscopy (AFM) and small angle neutron scattering (SANS) have also been employed to obtain structural and morphological information.

RESULTS AND DISCUSSION

We have successfully tagged two enzymes; PETNR and CDH with VKVKVEVK tag, and been able to incorporate them into hydrogels whilst retaining activity. The tagging of PETNR has reduced the leeching from ~98 % release to ~7 %. The tagging of CDH allows hydrogel incorporation without the enzyme precipitating unlike non-tagged CDH. This shows that

the longevity of the catalytic biomaterial has been increased. PETNR functionalised hydrogels have been shown to be able perform biotransformations whilst retaining native enantio and stereo specificity.

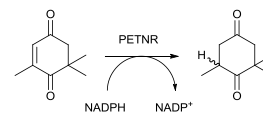


Figure 2. Transformation of ketoisophorone to levodione *via* PETNR.

The reusability of these hydrogels has been shown to be possible for up to 9 months, whereas PETNR in solution is inactive after 2 months. Thermal protection of the enzyme afforded by the hydrogel has been observed for elevated temperatures, and explained up by μ DSC data.

Activity studies have shown that by incorporating enzyme within VKVKVEVK hydrogels that denaturation through non-optimal conditions can be perturbed, thus maintaining activity.

CONCLUSION

The experiments undertaken show that incorporating enzymes within VKVKVEVK hydrogel biomaterial the reusability, longevity and operating conditions of PETNR can be expanded. This holds a lot of promise stabilising enzymes that are usually unstable, and may even up new reaction avenues. By bi-functionalising hydrogels enzymatic cascades are possible, thus allowing easy biphasic extraction, reducing time and solvent usage.

REFERENCES

- 1 D. Roberts, C. Rochas, A. Saiani and A. F. Miller, *Langmuir*, 2012, 28, 16196.
- 2 C. E. French, S. Nicklin and N. C. Bruce, *Journal of Bacteriology*, 1996, 178, 6623;
- 3 H. S. Toogood, A. Fryszkowska, V. Hare, K. Fisher, A. Roujeinikova, D. Leys, J. M. Gardiner, G. M. Stephens and N. S. Scrutton, *Advanced Synthesis & Catalysis*, 2008, 350, 2789.
- 4 M. J. van der Werf, C. van der Ven, F. Barbirato, M. H. M. Eppink, J. A. M. de Bont and W. J. H. van Berkel, *Journal of Biological Chemistry*, 1999, 274, 26296.

ACKNOWLEDGMENTS

The authors would like to acknowledge, David Roberts for discussion regarding the octapeptide VKVKVEVK. Finally, the authors would like to thank the past and present members of the 'Polymers & Peptides' research group. CRH would like to thank the BBSRC for funding for this project and his PhD studies.



Crosslinked albumin hydrogel as adhesion barrier to prevent postoperative fibrosis

Burkhard Schlosshauer¹, Dominic Stadel¹, Elke Rist¹, Helmut Wurst³, Jürgen Mollenhauer², Erich K. Odermatt⁴

¹ NMI Natural and Medical Sciences Institute, Reutlingen, Germany

² TETEC AG, Reutlingen, Germany

³ Cellendes GmbH, Reutlingen, Germany

⁴ Aesculap AG, Tuttlingen, Germany

schlosshauer.burkhard@nmi.de

INTRODUCTION

Postsurgical adhesions often lead to a pathological fibrosis which can cause severe dysfunctions of affected organs including heart, spine or gut. Therapeutic approaches focus on keeping lesioned tissue surfaces apart to prevent their fibrotic adhesion. This can be achieved e.g. by the implantation of a resorbable spacer such as a biocompatible membrane. In contrast, we use a cell-neutral hydrogel, that has previously been applied to support autologous chondrocyte transplantation for cartilage repair (1-3) to develop a novel *adhesion barrier*. The hydrogel concept includes albumin crosslinked via a thiolated polyethylene glycol crosslinker as bulk matrix and hyaluronate for enhanced viscosity during gel formation. Desired features of the implant material are: polymerisation *in situ*/adaptation of any tissue topography, rapid gel formation, minimally invasive and injectable, adhesive to organ surfaces, biocompatible, non-inflammatory, resorbable and ultimately, prevention of postsurgical adhesions.

EXPERIMENTAL METHODS

The modified hydrogel (technically termed "InGel") was produced by rapidly mixing two solutions: (1) purified maleimide-functionalized albumin and (2) bis-thio-polyethylene glycol. Gelation kinetics and viscoelastic properties were determined by rheology. Fluorescently labelled albumin and dextran beads were added to gel solutions to improve detectability of the gel matrix for subsequent experimentation and to analyse states of intermixing.

Fibroblasts were cultured on InGel for different intervals to determine cell adhesion and viability *in vitro* (microscopy and resazurin assay). Cell migration was monitored by time-lapse video recording. Cell infiltration and gel disintegration was monitored by immunocytochemistry of cryosections. Protease induction *in vitro* was analysed by gel zymography of conditioned media from cells cultured on InGel. Adhesion barrier function was histologically characterized after application of InGel into rats after lesioning of the abdominal peritoneum and the opposing cecum. Positive controls did not receive any implants. The postoperative periods were 4 weeks.

RESULTS AND DISCUSSION

Albumin and PEG-crosslinker solutions formed hydrogels macroscopically within a minute after mixing. Rheological analysis revealed that the storage modulus G' of InGel was significantly higher than the viscous modulus G'' , indicative of the hydrogel being able to resist structural changes under strain. Though fibroblasts attached to hydrogels, the cell permissiveness of the gel surfaces was clearly restricted as evident from decreasing cell numbers with ongoing time *in vitro*. Furtheron, time lapse video recording suggested that cell migration was impaired. Importantly, no significant cytotoxicity was evident *in vitro*. Longterm exposure of cells to gels did not induce the expression of specific secreted matrix metalloproteinases as shown by gel enzymography which was consistent with prolonged gel integrity after implantation into rodents. Distinct MMPs are possibly not instrumental in gel degradation. Simultaneously, hardly any infiltrating cells were observed in the gel matrix after culturing.

Because of the principle biocompatibility, the promising restricted cell permissiveness and the suitable degradation profile, we initiated *in vivo* experiments in the rat abrasion/incision model. Pilot experiments demonstrated that InGel reduced the formation of postsurgical adhesions which otherwise were evident in all positive controls. Histological analysis supported the notion that also collagen deposition was reduced in the presence of InGel in comparison to positive control animals.

CONCLUSION

InGel displayed proper gelation, viscoelastic properties, restricted cell attachment, resorption kinetics and prevented largely the formation of postsurgical adhesions. Thus, restriction of pathological fibrosis fostered recovery of lesioned tissues. Therefore, InGel could possibly be used for adhesion prevention in general surgery.

REFERENCES

1. Benz *et al.* BMC Musculoskeletal Disorders 13:54ff, 2012
2. Benz *et al.* Eur. Spine 21:1758-68, 2012
3. Scholz, B. *et al.* Europ. Cells and Materials. 20:24-37, 2010

ACKNOWLEDGMENTS

Supported by BMBF 13N12454 and BMBF 13N12455



Local Inflammatory Tissue Response After Implantation of Electrospun Polylactide Fiber Meshes With and Without Plasma-Polymerized Allylamine in Rats

Andreas Hoene¹, Matthias Schnabelrauch², Ralf Wyrwa², Birgit Finke³,
Silke Lucke⁴, Uwe Walschus⁴, Michael Schlosser^{4*}

¹ Department of Surgery, University Medical Center Greifswald, Germany

² Biomaterials Department, INNOVENT e.V., Jena, Germany

³ Leibniz Institute for Plasma Science and Technology, Greifswald, Germany

⁴ Department of Medical Biochemistry and Molecular Biology, University Medical Center Greifswald, Germany
*schlosse@uni-greifswald.de

INTRODUCTION

Electrospinning is a versatile method for production of matrices aimed at tissue engineering purposes including wound dressings, as these matrices are structurally similar to the extracellular matrix (ECM). Synthetic biodegradable polymers like Poly(L-lactide-co-D/L-lactide) (PLA) are suitable materials for these applications. However, one problem of PLA is its hydrophobicity which impairs initial protein adsorption and cell adhesion.

A plasma polymerized allylamine (PPAAm) film was shown to provide hydrophilic coverage with positive surface charge aimed at enhanced interactions with hyaluronan, a major component of the ECM. Furthermore, PPAAm-coatings have been demonstrated to promote adhesion of human osteoblasts (MG-63), gingiva epithelial cells (Ca9-22) and uroepithelial cells (SV40-HUC-1)^{1,2}. Furthermore, the *in vivo* inflammatory tissue response for PPAAm-coated titanium plates was comparable to uncoated plates shown in a previous study³. Therefore, the present study aimed at evaluating the influence of a PPAAm coating on the local inflammatory reactions against electrospun PLA fiber meshes.

EXPERIMENTAL METHODS

Implant samples. Pieces (5×5 mm) of electrospun PLA meshes were cleaned with O₂ plasma only (PLA), or cleaned and additionally coated with a PPAAm film (PLA-P).

***In vivo* study.** Each of 24 male Lewis rats received one PLA and one PLA-P sample simultaneously implanted into their neck musculature. After 7, 14 and 56 days, tissue samples containing the mesh matrices were retrieved from 8 animals per experimental day.

Histological examination. Cryosections (5µm) were prepared from explanted tissue samples and stained with primary antibodies for CD68-positive macrophages/monocytes (ED1), CD163-positive tissue macrophages (ED2), total T lymphocytes (R73), IL2R-positive cells (OX39), antigen-presenting cells (OX6), activated NK cells (ANK61) and the tissue regeneration marker nestin (rat-401) using the APAAP system. Additionally, mast cells were evaluated with toluidine blue staining. Morphometric evaluation of all histological images was performed by digital image analysis using the ImageJ software, and results were expressed as percentage of positively stained area.

Statistics. The non-parametric Mann-Whitney test was used for data analysis.

RESULTS AND DISCUSSION

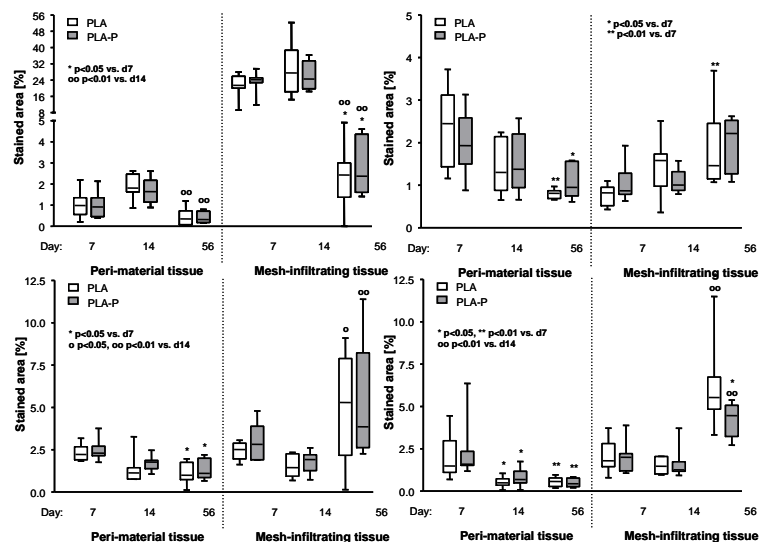


Figure 1: Response of CD68+ monocytes/macrophages (top left), CD163-positive tissue macrophages (top right), antigen-presenting cells (bottom left) and nestin expression (bottom right) in the peri-material and the mesh-infiltrating tissue. Boxes indicate median and interquartile range, whiskers highest and lowest individual value (n=8 animals/day).

CONCLUSION

All examined local inflammatory reactions were comparable for the PLA and PLA-P meshes, demonstrating that PPAAm did not negatively affect the tissue response. Compared to the peri-material tissue, the mesh-infiltrating tissue had a stronger response of pro-inflammatory CD68+ monocytes/macrophages, however declining until day 56. In contrast, anti-inflammatory CD163-positive tissue macrophages decreased in the peri-material tissue and increased in the mesh-infiltrating tissue, accompanied by increasing nestin expression indicating tissue regeneration. Additionally, no differences were found for all other cellular markers. Together with the cell-adhesive effects of PPAAm demonstrated earlier *in vitro*^{1,2} and recent data regarding PPAAm-coated titanium surfaces *in vivo*³, these results illustrate a general potential for PPAAm as a cell-adhesive biocompatible implant coating.

REFERENCES

1. Wyrwa R. *et al.*, Adv. Eng. Mater. 13:165–171, 2011
2. Finke B. *et al.*, Biomaterials 28:4521–4534, 2007
3. Hoene A. *et al.*, Acta Biomater 6:676–683, 2010

ACKNOWLEDGMENTS

The study was supported by the Federal Ministry of Education & Research (project Campus PlasmaMed).



Differentiation of Macrophage Involvement in Tissue Regeneration Following Implantation of Biodegradable Matrices in Rats

Silke Lucke¹, Uwe Walschus¹, Andreas Hoene², Jens-Wolfgang Pissarek³, Matthias Schnabelrauch⁴, Michael Schlosser^{1*}

¹Department of Medical Biochemistry and Molecular Biology, University Medical Center Greifswald, Germany

²Department of Surgery, University Medical Center Greifswald, Germany

³MBP - Medical Biomaterial Products GmbH, Neustadt-Glewe, Germany

⁴INNOVENT e. V., Biomaterials Department, Jena, Germany

*schlosse@uni-greifswald.de

INTRODUCTION

Implantation of biomaterials causes local inflammatory responses in the surrounding tissue which are characterized by the presence of different cell types including macrophages, T lymphocytes, NK cells and mast cells. While inflammatory reactions on the one hand can cause adverse effects like complications and implant failure, on the other hand they play also an important role in beneficial processes such as wound healing and tissue regeneration. Within these processes, macrophages are of central importance due to their ability to degrade and ingest foreign materials and their interactions with other involved cell types.

Recent research indicates that macrophages can be classified into different subsets, with pro-inflammatory M1-type and anti-inflammatory M2-type macrophages being the main phenotypes. To better understand the role of macrophages in tissue regeneration following implantation of biomaterials, the present work aimed at examining the association of different macrophage subtypes with the tissue expression of nestin, a marker of cell proliferation and migration, both characteristic for regenerative processes. For this purpose, two experimental series covering different biodegradable matrices were included in the analysis.

EXPERIMENTAL METHODS

In vivo experiments. In a 1st experimental study, 5×5 mm pieces of electrospun meshes made from poly(L-lactide-co-D/L-lactide) (PLA) were implanted intramuscularly into 24 male Lewis rats. After 7, 14 and 56 days, samples of the peri-implant tissue were prepared from 8 animals per experimental day. In a 2nd study, 12 rats received 5×5 mm pieces of a cross-linked acellular porcine dermis collagen matrix (NRX). Peri-implant tissue samples from these animals were examined after 56 and 112 days, with 6 animals for each day.

Immunohistochemical analysis. Cryosections were prepared from the frozen tissue samples and stained with primary antibodies for CD68-positive macrophages and monocytes (ED1; M1-type), CD163-positive macrophages (ED2; M2-type) and nestin (rat-401). Bound primary antibodies were detected using the APAAP system. Quantification of cellular reactions as positively stained area was performed by digital image analysis using the ImageJ software system.

Statistical analysis. For both series, a correlation analysis (Pearson correlation coefficient; GraphPad Prism 4.03) was performed between the three examined markers from all animals over the respective whole study period.

RESULTS AND DISCUSSION

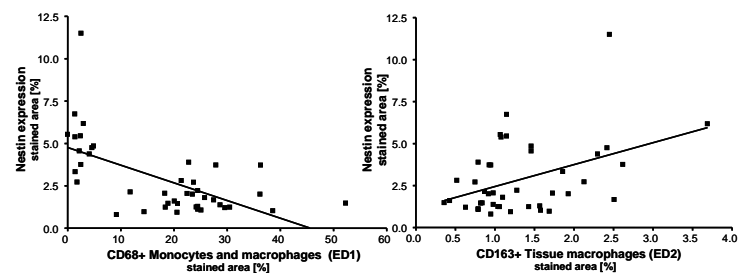


Figure 1: Scatter plots illustrating the relationship between reactions of CD68-positive macrophages/monocytes (ED1; M1-type) and nestin (left) as well as CD163-positive macrophages (ED2; M2-type) and nestin (right) over all experimental animals and days of the PLA series.

	PLA series		NRX series	
	r	p	r	p
ED1 vs. ED2	-0.4718	0.0016	-0.1810	0.5735
ED1 vs. Nestin	-0.6184	<0.0001	-0.3176	0.3412
ED2 vs. Nestin	0.4252	0.0050	0.2432	0.4711

Table 1: Correlation analysis between stained area of CD68-positive macrophages/monocytes (ED1; M1-type), CD163-positive macrophages (ED2; M2-type) and nestin. Data are given as Pearson's r and p values.

In the PLA series, a significant negative correlation between the amount of CD68-positive pro-inflammatory macrophages/monocytes (M1-type) and CD163-positive anti-inflammatory macrophages (M2-type) was found. Moreover, the CD68-positive macrophages demonstrated a significant negative correlation with nestin expression while the CD163-positive macrophages were significantly positive associated with this marker. Comparable trends without significance were found in the NRX series.

CONCLUSION

As demonstrated by the results obtained with two different implants, tissue regeneration of biodegradable matrices seems to be associated with anti-inflammatory M2-type macrophages. The fact that this correlation was stronger in the PLA series than the NRX series could be explained by the different time points and/or materials, possibly indicating a declining influence of M2 macrophages and/or finalized regeneration with longer implantation duration.

ACKNOWLEDGMENTS

The study was supported by the German state Mecklenburg-Vorpommern (project SYNTERO) and the Federal Ministry of Education & Research (project Campus PlasmaMed).



***In vitro* and *in vivo* osteoinductive potential of polycaprolactone-based bioactive composite scaffold fabricated via additive manufacturing technology**

Patrina S. P. Poh^{1*}, Dietmar W. Hutmacher¹, Boris M. Holzapfel¹, Molly M. Stevens² and Maria A. Woodruff¹

¹Institute of Health and Biomedical Innovation, Queensland University of Technology, Australia, *patrinapoh@qut.edu.au

²Department of Bioengineering, Imperial College London, London.

INTRODUCTION

Generally, bone tissue engineering (TE) involves the use a resorbable polymer-based scaffold which lacks osteoinductivity. Therefore, to achieve osteoinductive polymeric-based scaffolds, one can incorporate bioactive materials such as bioactive glass (BG) into the polymeric-based scaffolds. These BGs are bioactive, that is they are able to promote formation of strong bond with bone when in close proximity ^[1, 2]. It has been shown that different composition of BG can provide different effect on cell behaviour ^[3], of which, the incorporation of Sr²⁺ into the BG network has been reported to have beneficial effect on cells by promoting osteoblast activity while inhibiting osteoclast activity ^[4]. Therefore, in this project, we aimed to develop a fully synthetic and resorbable scaffold made of PCL and BG (45S5 or SrBG) intended for the treatment of bone defects by utilising melt extrusion (ME) technique, a form of additive manufacturing technology. The resultant composite scaffold can potentially be highly osteoinductive, thereby circumventing the use of biological factors to induce scaffold osteoinductivity.

EXPERIMENTAL METHODS

Scaffold fabrication and characterisation: composite scaffold made of PCL and 50 wt% of 45S5 Bioglass® (45S5) or strontium-substituted bioactive glass (SrBG) were fabricated using ME technique. Scaffolds' overall morphology, porosity and BG particles distribution were assessed using micro-computed tomography (μ-CT). **Scaffold *in vitro* degradation:** scaffold (PCL, PCL/50.45S5 and PCL/50.SrBG) were immersed in 5M sodium hydroxide (NaOH), at 37°C ^[5]. Percentage of mass loss was presented at time-points. **Scaffold *in vitro* bioactivity:** Scaffolds were immersed in serum-free culture media at 37°C for up to 10 weeks. At time-points, scaffold were retrieved and examined under SEM for surface precipitations, while media were retrieved and analysed for it Sr²⁺ and Si⁴⁺ concentration using inductively coupled plasma-optimal emission spectroscopy (ICP-OES). **Scaffold *in vitro* osteoinductivity:** each scaffold was seeded with 100,000 ovine bone marrow stromal cells and cultured with non-osteogenic or osteogenic media for up to 21 days. The gene expression of osteopontin (OPN) and osteocalcin (OCN) were quantified through reverse transcription-polymerase chain reaction (RT-PCR). **Scaffold *in vivo* osteoinductivity:** scaffold was implanted subcutaneously into the back of nude rats. After 8 and 16 week, scaffold were explanted, histologically processed and assessed for mineralised tissue formation using MacNeal's tetrachrome with von Kossa stain. **Data analysis:** all data were represented as mean ± SD

and were subjected to one-way ANOVA and Tukey's post-hoc test. Significance levels were set at $p < 0.05$.

RESULTS AND DISCUSSION

Structurally, composite scaffold (PCL/50.45S5 and PCL/50.SrBG) highly resembles that of PCL scaffold. In term of scaffold *in vitro* degradation, it was shown that the degradation rate of scaffold was in the order of PCL/50.SrBG > PCL/50.45S5 > PCL, and was similar to our previous findings ^[6]. As compared to our previous study ^[6], increased BG loading into the PCL matrix greatly enhanced the composite scaffold's *in vitro* bioactivity; whereby, calcium-phosphate (CaP)-based surface precipitation was observed after just 1 week. Furthermore, the increased level of Sr²⁺ and Si⁴⁺ ions in the immersion media over time indicated sustained dissolution of BG for up to 10 weeks. *In vitro* cell studies showed that when cultured in non-osteogenic media, OPN and OCN gene expression were upregulated in PCL/50.45S5 and PCL/50.SrBG groups. This phenomenon was not observed for PCL group indicating that the dissolution ions from the BGs have the potential to induce cells to differentiate into osteoblasts. When implanted subcutaneously into the back of nude rats, although it was shown that all scaffolds can support host tissue infiltration, no mineralised tissue formation was observed in any samples after 8 and 16 weeks. This indicated that when implanted subcutaneously into small animal model, the composite scaffolds are not osteoinductive after 8 and 16 weeks. To further evaluate if these scaffolds possess species specific osteoinductivity ^[7, 8], further animal studies using different animal species of soft tissue model is required.

CONCLUSION

Both PCL/50.45S5 and PCL/50.SrBG composite scaffolds show potential *in vitro* osteoinductivity. However, *in vivo*, the osteoinductivity capability was not observed after 8 and 16 weeks,

REFERENCES

1. Hench L.L., *J. American Ceramic Society*, 74, 1991
2. Jones J.R., *Acta Biomaterialia*, 9, 2013
3. Hoppe A. *et al.*, *Biomaterials*, 32, 2011
4. Gentleman *et al.*, *Biomaterials*, 31, 2010
5. Lam C.X.F. *et al.*, *Polymer Int.*, 56, 2007
6. Poh *et al.*, *Biofabrication*, 5, 2013
7. Yang *et al.*, *Biomaterials*, 17, 1996
8. Ripamonti U., *Biomaterials*, 17, 1996

ACKNOWLEDGMENTS

We would like to acknowledge support from the Australia Research Council funds LP110200082 and LP11020008.



PLA-Glass Composites For Bone Tissue Engineering

João S. Fernandes^{1,2}, Ricardo A. Pires^{1,2}, Rui L. Reis^{1,2}

¹ 3B's Research Group - Biomaterials, Biodegradables and Biomimetics, University of Minho, Headquarters of the European Institute of Excellence on Tissue Engineering and Regenerative Medicine, AvePark, 4806-909 Taipas, Guimarães, Portugal

² ICVS/3B's - PT Government Associate Laboratory, Braga/Guimarães, Portugal

INTRODUCTION

Poly(lactic acid) (PLA) polymers are eco-friendly, biocompatible and easily processed, which makes it highly attractive for biomedical applications [1, 2]. However, PLA is hydrophobic (results in low cells adhesion), presents an acidic medium when degrading, and lacks surface reactivity [2]. These limitations can be overcome by the incorporation of glass particles [3]. Glass particles can initiate the formation of apatite at the surface making its surface bioactive. This incorporation can be also used to control the degradation rate, and to improve cell adhesion. The basic environment generated by the leaching cations from the glass particles can contribute to a pH increase during PLA degradation, reducing the inflammatory response derived from the acidic pH.

The main objective of this work was to evaluate the suitability of silica-borate glass compositions as fillers of PLA-glass composite formulations targeting bone tissue-engineering applications.

EXPERIMENTAL METHODS

Glass compositions of general formula $0.20\text{B}_2\text{O}_3\cdot 0.40\text{SiO}_2\cdot x\text{MgO}\cdot y\text{CaO}\cdot (0.35-x-y)\text{SrO}\cdot 0.05\text{Na}_2\text{O}$ (molar ratio, where $x, y = 0.35$ or 0.00 , and $x \neq y$) were prepared ($<63\text{ }\mu\text{m}$), and composite fibres were formed by wet spinning of a PLA solution containing a suspension of the glass particles. Fibre meshes ($6\text{mm}\times 2\text{mm}$ discs) of the processed fibres were prepared and their cytotoxicity was evaluated by direct contact with human osteosarcoma cell line Saos-2, throughout 7 days of incubation ($37\text{ }^\circ\text{C}$ and $5\text{ }\%$ CO_2 atmosphere). Cell proliferation (DNA quantification) and metabolic activity (MTS) were monitored for 7 days. It was tested the water uptake and weight loss of the developed systems, as well as their capacity to form a calcium phosphate layer when immersed in simulated body fluid (SBF).

RESULTS AND DISCUSSION

PLA/Glass composite meshes were successfully obtained by Wet-Spinning and Fibre-bonding techniques.

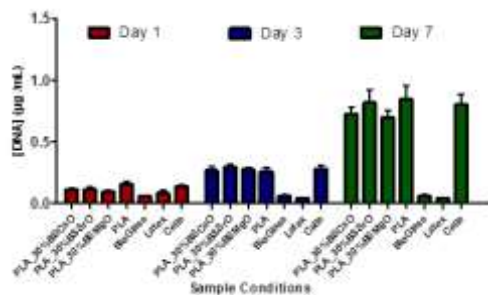


Fig.1 - Cells proliferation profile during 7 days culture of Saos-2.

Three different composites were successfully obtained with 30% (w/w) of each synthesized glass. The cytotoxicity assessment indicates that the cells remain viable during the 7 days of culture (Fig.1) and no cytotoxicity was detected.

An increase in the composite weight loss ($\approx 20\%$ in some cases) was observed when the synthesised glasses were compounded with PLA. For the PLA_BS0.35MgO sample there is an increase of $\approx 5\%$ in the water uptake (when compared with PLA) indicating that the glass particles increase the hydrophilic character of the composite. In addition, the degradation medium increases its pH with time, being consistent with the release of cations from the glass particles.



Fig.2 - SEM images of samples (PLA_BS0.35CaO, PLA_BS0.35SrO, PLA_BS0.35MgO and PLA) after 28 days immersion in SBF at 37°C.

Preliminary bioactivity tests (Fig.2) by immersion of samples in SBF for 28 days showed crystallites with a cauliflower morphology on the top of glass particles, suggesting their ability to induce the formation of hydroxyapatite in the surface of the composites.

CONCLUSION

PLA/glass composites meshes were successfully obtained by Wet-Spinning and Fibre-bonding techniques. Direct contact assay (MTS & DNA) allow us to state that cells remain viable during the 7 days of culture. A preliminary bioactivity screening by immersion of samples in SBF for 28 days suggested their ability to form hydroxyapatite on the surface domains that are closer to the glass particles. Preliminary degradation study indicates a limited degradation and pH increase during this period.

REFERENCES

1. Gupta, B., N. Revagade, and J. Hilborn, *Poly(lactic acid) fiber: An overview*. Progress in Polymer Science, 2007. 32(4): p. 455-482.
2. Rasal, R.M., A.V. Janorkar, and D.E. Hirt, *Poly(lactic acid) modifications*. Progress in Polymer Science, 2010. 35(3): p. 338-356.
3. Fu, H., et al., *In vitro evaluation of borate-based bioactive glass scaffolds prepared by a polymer foam replication method*. Materials Science and Engineering: C, 2009. 29(7): p. 2275-2281.

ACKNOWLEDGMENTS

Portuguese Foundation for Science and Technology (Ph.D. grant BD/73162/2010) and the European Union's Seventh Framework Programme (FP7/2007–2013) under Grant No. REGPOT-CT2012-31633-POLARIS.

Stability of Peptide Hydrogels in Cell Culture Conditions

I. Nawi¹, V. L. Workman¹, A. M. Smith¹, A. F. Miller² and A. Saiani^{1*}

¹ School of Materials & Manchester Institute of Biotechnology, The University of Manchester, Manchester, UK

² School of Chemical Engineering and Analytical Science & Manchester Institute of Biotechnology, University of Manchester, Manchester, UK

* a.saiani@manchester.ac.uk

INTRODUCTION

Three main components of tissue engineering are cells, matrix and signalling molecules. Currently, researchers use scaffolds as a temporary matrix that acts as a structural support for cells at the primitive stage of tissue development, both in terms of promoting desired phenotype and regeneration of tissues^{1,2}. Our main objective is to develop fully chemically and physically defined peptide-based hydrogels that can be used as three dimensional scaffolds for cell culture and tissue engineering applications. In this study, we will focus on how to control the stability of peptide hydrogels when used in cell culture conditions.

EXPERIMENTAL METHODS

Hydrogel preparation

Hydrogels were prepared using a series of β -sheet forming peptides (Figure 1) based on our previous work³⁻⁵. These peptides are based on the alternation of hydrophilic (lysine and glutamic acid) with hydrophobic amino acids (phenylalanine or valine).

Stability testing

Hydrogels stability was tested under cell culture conditions by investigating the physical degradation of the hydrogels at 37°C. Hydrogel weight loss, peptide dry content and the mechanical properties of the hydrogels were measured as a function of time.

Bovine chondrocytes were used as model cells to investigate the effect of the presence of cells on the stability of hydrogels. Viability tests and biochemical analysis to measure GAG and total collagen produced by the cells were carried out.

RESULTS AND DISCUSSION

Stability testing provides evidence on how the quality of hydrogels varies with time as a function of a variety of physiological factors. This work provides information on how to control the stability of these hydrogels. In future, this knowledge will allow development of new peptide formulations for increased cell culture duration.

Currently in cell culture application, the hydrogels persist for up to 21-30 days³. The study will also permit us to understand the relationship between peptide hydrogel formulation and stability, as well as the effect in the presence of cells.

CONCLUSION

We are one step forward in our objective to develop three dimensional scaffolds for *in vitro* and *in vivo* cell culture applications, with controlled physical properties and mechanical stability.

REFERENCES

1. Collier, J.H., et al., Chemical Society Reviews, 2010. **39**(9): p. 3413-3424.
2. Maude, S., E. Ingham, and A. Aggeli, Nanomedicine, 2013. **8**(5): p. 823-847.
3. Mujeeb, A., et al., Acta Biomaterialia, 2013. **9**(1): p. 4609-4617.
4. Saiani, A., et al., Soft Matter, 2009. **5**(1): p. 193-202.
5. Boothroyd, S., A.F. Miller, and A. Saiani, Faraday Discussions, 2013. **166**(0): p. 195-207.

ACKNOWLEDGEMENTS

The authors acknowledge an EPSRC Fellowship (EP/K016210/1) and Government of Malaysia for providing financial support to this project.

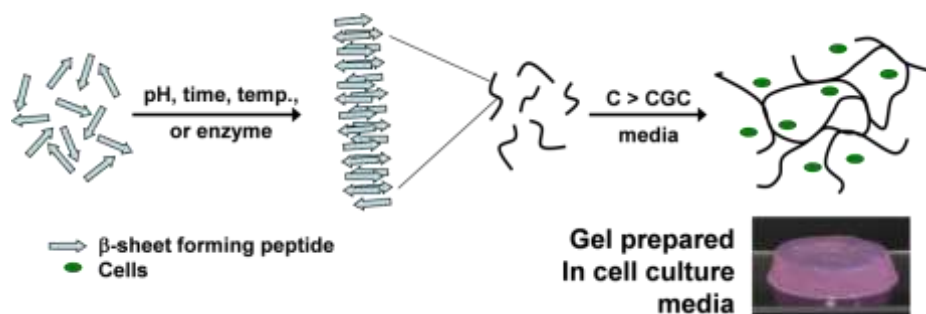


Figure 1: Schematic representation of the self-assembly and gelation process of β -sheet forming peptides.

Guiding bone cells with surface patterned nano-calcium phosphate

Gillian Munir¹, Mohan J. Edirisinghe, Lucy Di Silvio², Miriam Rafailovich³ and Jie Huang

¹Department of Mechanical Engineering, University College London, UK

²Department of Biomaterials, Tissue Engineering and Imaging, Kings College, UK

³Department of Materials Science and Engineering, Stony Brook, USA
g.heppe@ucl.ac.uk

INTRODUCTION

Template-assisted electrohydrodynamic atomisation (TAEA), a recently developed surface patterning technique, is able to pattern bioactive nanosized calcium phosphate on titanium to guide osteoblasts [1]. Cell modulus (stiffness) affects many cell functions, for example, its able to correspond with stem cell lineage, and used as a biomarker to distinguish normal and cancerous cells [2]. Studies showed that silicate-substitute hydroxyapatite (SiHA) is a highly attractive alternative to conventional HA in bone replacement [3]. In this study, nanoSiHA was incorporated in TAEA surface patterning to mimic the size and chemical composition of bone mineral. Thus the cellular responses of osteoblasts and dental pulp stem cells to nanoSiHA patterns on titanium (Ti), from cell attachment to cell elasticity, were systematically investigated.

EXPERIMENTAL METHODS

The TAEA process setup is shown in Figure 1a. Freshly prepared nanoSiHA suspension was syringed to the needle at a flow rate of 4 µl/min, and present a cone-jet patterning mode (Figure 1b) with the applied voltage between the needle and the ground electrode set at 4.5-5.5kV. Copper templates with different shape and dimensions were placed on the surface of Ti.

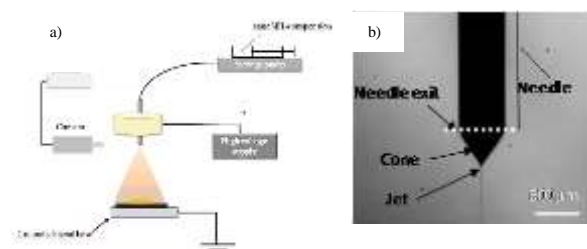


Fig.1 (a) Schematic diagram illustrating the TAEA patterning and (b) A stable cone-jet mode was obtained for patterning

The structure and morphology of nanoSiHA patterns were characterized firstly. The biological responses of human osteoblast (HOB) cells to linear track and pillar patterns of nanoSiHA on Ti were investigated. The proliferation, differentiation and gene expression of HOB cells on nanoSiHA coated Ti was measured by AlamarBlue™ assay, Alkaline phosphatase assay, and Rt-PCR; and the attachment, orientation and elongation length of HOB cells were examined using scanning electron microscopy (SEM) and confocal microscopy. In order to understand the influence of pattern topography on the mechanics of the cell, shear force modulation force microscopy (SMFM) was used to determine the elasticity of osteoblasts (MC3T3-E1) cell and dental pulp stem cell (DPSC).

RESULTS AND DISCUSSION

Well defined nanoSiHA patterns, pillars and tracks of 1 to 5 µm height, were obtained using TAEA. Confocal imaging revealed osteoblast alignment within the patterning (Fig 2a). AlamarBlue™ tests showed the proliferation rates of HOB cells increased when cultured on patterned substrates than those on nanoSiHA coating. An increase of alkaline phosphatase production, an osteoblast differentiation marker, was found on the HOB cells cultured on patterned surfaces, as well as on the pillar and track patterns when the thickness increased from 1 to 5 µm. The expression of ALP was higher for the HOB cells cultured on pillar patterns. Runx-2 expression and collagen production of HOB cells was also increased on track patterns when compared to pillar patterned and nanoSiHA coated Ti.

DPSCs on pillar thickness 1 µm exhibited similar moduli to the cells on the coated surface. The elasticity of DPSC was found to vary greatly depending on the location of the cell, on both track and pillar patterns of thickness 5 µm. Higher moduli were found on MC3T3-E1 cells in comparison with those on DPSCs, regardless of location on the substrate or thickness of the pattern (Fig. 2b). These preliminary findings indicate that the cell lineage can be controlled by patterned topography on the surface of an implant.

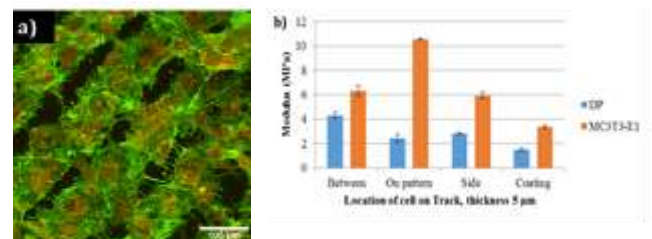


Fig. 2 (a) Confocal of MC3T3-E1 cells on nanoSiHA tracks (b) Comparison of modulus of dental pulp stem cells and MC3T3-E1 cells on track pattern, thickness 5 µm

CONCLUSION

Well defined 3-D surface topographies of nanoSiHA on Ti by TAEA patterning have been able to guide and support the growth and proliferation of human osteoblast cells. Interestingly, dental pulp stem cells alter the modulus depending on the surface location.

REFERENCES

1. Munir G. *et al*, 2011 *J. R. Soc. Interface*, 8, 678
2. Chiang, M.Y.M. *et al*, 2013, 34, 9754
3. Hing, K.A. *et al*, 2006 *Biomaterials*, 27, 5014

ACKNOWLEDGMENTS

The authors would like to thank ORUK for providing financial support to this project.

The Potential Role of Statins in the Regeneration of Osteoporotic Tissue and the Use of Star Degradable Polymers for Controlled Local Delivery

Jason Burke^{2*}, Sarah Cartmell¹, Nicola Tirelli¹

¹School of Materials, University of Manchester, England

^{2*}Institute of Inflammation & Repair, School of Medicine, University of Manchester, England

jason.burke@postgrad.manchester.ac.uk

INTRODUCTION

Statins have been shown to have anabolic effects in osseous tissues via their inhibition of the mevalonate pathway. Changes in the expression of key associated factors such as bone morphogenetic proteins (BMPs), core binding factor alpha 1 (CBF α 1/RUNX2) and vascular endothelial growth factors (VEGFs) have all been shown in a dose dependent response to various statin analogues. Furthermore, statins have also been considered to inhibit the resorption activity of osteoclasts via the same metabolic influences and are again thought to act respective of local statin concentrations.^{1,2}

To fully harness the potential of statins for inducing bone growth in a clinical setting, we believe that optimum local concentrations must be provided in vivo and therefore have sought to provide a reliable, controlled delivery system by utilising the influences of polymer architecture on the degradation, and thereby drug release, of degradable polymers. Degradable star poly(D,L lactic acid) (PDLLA) polymers were synthesised, characterized and then tested for their effectiveness in delivering statins efficiently and uniformly in an in vitro test environment.

EXPERIMENTAL METHODS

PDLLA star polymers were synthesized to form 4-arm and 6-arm samples of varying degree of polymerisation using pentaerythritol and dipentaerythritol polyol initiators respectively. Samples were then characterized (GPC, NMR, FT-IR) alongside linear samples of comparable molecular weights and evaluated in respect of their: degradation kinetics (GPC), erosion kinetics (mass loss, imaging), drug release behaviour (HPLC) and cytotoxicity (MTS, Griess – Raw264.7 cells). Furthermore, samples were also used as substrates for primary human osteoblast (pHOb) cultures, to evaluate the effects of the statin-loaded polymer system on osteoblast activity (ALP assay, RT-PCR (BMP-2, RUNX2, OPN)).

RESULTS AND DISCUSSION

Characterisation showed that reliable synthesis of linear, 4-Arm and 6-Arm PDLLA polymers of various molecular weights was achieved. Cytotoxicity results from Raw264.7 cultures showed all polymers exhibited good biocompatibility. Degradation and drug release studies showed significant differences in the behaviours of the star polymers relative to linear comparisons of equal molecular weight. Degradation was slower and

more uniform in the star polymers while linear polymers followed apparent 1st order behaviour, as can be seen from Fig.1. Drug release behaviour and material erosion followed similar patterns. Finally, osteoblasts exhibited normal levels of activity when cultured on PDLLA substrates and gene expression of key markers was increased in statin loaded samples relative to controls.

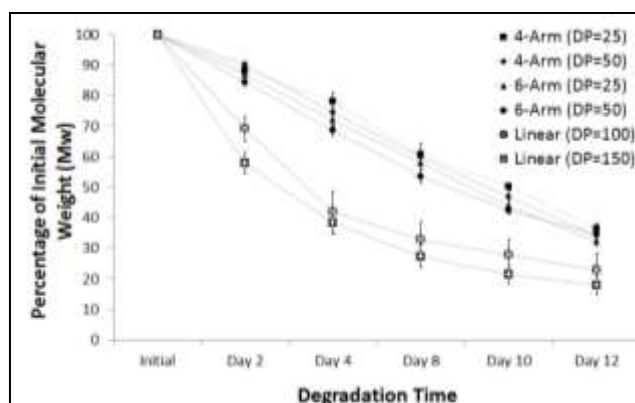


Fig.1 – Graph showing the percentage loss in molecular weight of varying star and linear PDLLA polymers during hydrolytic degradation.

CONCLUSION

In this work to date, we have demonstrated the significance of polymer architecture in the degradation of degradable polyesters. The uniform degradation behaviour seen in star PDLLA samples has shown potential for providing controlled drug delivery of statins to local environments in vivo, in attempts to provide anabolic influences in osseous tissues. We are continuing to evaluate these systems and further characterise their behaviour while assessing the response of osteoclasts to the presence of statins in osteoclast-only and in osteoblast-osteoclast co-cultures.

REFERENCES

1. Maeda et al, *Biochem Biophys Res Commun*. 2001 Jan 26;280(3):874-7.
2. Uzzan et al, *Bone*. 2007 Jun;40(6):1581-7.

ACKNOWLEDGMENTS

The Authors would like to thank the BBSRC for funding the project as part of the Doctoral Training Programme.



Effective Cellular Uptake of Exosomes Using Cationic Lipids and pH-sensitive Fusogenic Peptide

Ikuhiko Nakase^{1*}

^{1*} Nanoscience and Nanotechnology Research Center, Research Organization for the 21st Century, Osaka Prefecture University, Japan, i-nakase@21c.osakafu-u.ac.jp

INTRODUCTION

Exosomes are ~100 nm cup-shaped vesicles secreted by cells, and substantial attention has been paid to cell-to-cell communications. Genes (including microRNA) and bioactive proteins are encapsulated in exosomes, and they can regulate cellular functions of other marginal cells by cellular uptake of exosomes^{1,2}. In addition, exosomes are expected to represent next-generation biological tools for delivery of therapeutic molecules as nanomaterials, because they have advantages including 1) infinite secretion, 2) additional encapsulation of biofunctional molecules, 3) expression of functional proteins in membranes, 4) no cytotoxicity, 5) no immunogenicity. However, low cellular uptake efficacy of exosomes and insufficient cytosolic release inside cells are problems. Therefore, improvements should be further needed to achieve successful delivery using exosomes. In this presentation, we report our developed technique to attain enhanced cellular uptake of exosomes and cytosolic release with simple method using cationic lipids and pH-sensitive fusogenic peptide.

EXPERIMENTAL METHODS

GALA (pH-sensitive fusogenic peptide, sequence: WEAALAEALAEALAEHLAEALAEALAEALAA) was chemically synthesized by Fmoc-solid-phase peptide synthesis on a Rink amide resin. The structure of the synthesized peptide was confirmed by matrix-assisted laser desorption ionization time-of-flight mass spectrometry. Exosomes derived from CD63-GFP-expressing HeLa cells were purified using Total exosome isolation reagent (Invitrogen), and average size of exosomes was 45 nm analysed using scanning electron microscope. Cells were treated with complex of CD63-GFP-exosomes, cationic lipids (Lipofectamine LTX, Invitrogen), and GALA peptide, prior to confocal microscopic observation and FACS analysis. Encapsulation of Texas red-dextran (70 kDa, Molecular Probes) in exosomes was conducted using electroporation system (NEPA21 Super Electroporator, Nepa Gene).

RESULTS AND DISCUSSION

For improvement of cytosolic release efficiency, we studied effects of pH-sensitive fusogenic peptide, GALA³, to enhance disruption of endosomal and exosomal membranes in the process of intracellular traffic of exosomes via endocytosis. We have already reported that cationic lipids/GALA complex system is useful for efficient cytosolic delivery of proteins^{4,5}. In this research, we challenged to further apply this system

to enhanced cellular uptake and cytosolic release of exosomes.

We firstly examined effects of commercially available cationic lipids, Lipofectamine LTX, on cellular uptake of exosomes for enhancement of binding of exosomes to cell membranes and internalization into cells. Results showed that simple complex of cationic lipids (2% (v/v)) with exosomes (membrane potential of exosomes was changed from -11.6 mV to -1.2 mV by complex with cationic lipids) significantly enhanced (~10-fold) cellular uptake of the exosomes (average size: 80 nm) (20 µg/ml, 24 hr in the presence of 10% FBS) without cytotoxicity.

A 30-residue amphipathic peptide GALA was designed to mimic viral fusion protein sequences that mediate escape of virus gene from acidic endosomes to cytosol³. Cationic lipids were also employed as an “adhesive” to paste the GALA peptide, which has negative charges from glutamic acids^{4,5}, onto surface of exosomes. As a model macromolecule, Texas red-labeled dextran (TR-dex, 70 kDa) was encapsulated into exosomes using electroporation, and internalization efficiency of TR-dex were evaluated. When HeLa cells were treated with TR-dex-encapsulated exosomes complexed with cationic lipids increased its cellular uptake. Furthermore, addition of GALA to the complex successfully enhanced cytosolic release of TR-dex from the exosomes inside cells, suggesting that GALA contributes to disruption of endosomal and exosomal membranes.

CONCLUSION

By effective usage of cationic lipids and pH-sensitive fusogenic peptide, we attained establishment of the simple technique to enhance cellular uptake and cytosolic release of exosomes. This technique will contribute to not only drug delivery using exosomes but also studies of biological activities of exosomal contents derived from various types of disease-related cells including bioactive proteins and genes.

REFERENCES

1. Ohno S. *et al.*, Adv. Drug. Deliv. Rev. 65:398-401, 2013
2. Tan A. *et al.*, Adv. Drug. Deliv. Rev. 65:357-367, 2013
3. Subbarao N. K. *et al.*, Biochemistry 26:2964-2972, 1987
4. Nakase I. *et al.*, Methods Mol. Biol. 683:525-533, 2011
5. Kobayashi S. *et al.*, Bioconjug. Chem. 20:953-959, 2009



Borates-loaded Biomaterials to trigger Cell Differentiation

P. Rico^{1,2}, A. Rodrigo-Navarro¹, M. Salmerón-Sánchez³

¹Center for Biomaterials and Tissue Engineering, Universitat Politècnica de València, Spain

²CIBER, Spain, parico@upvnet.upv.es

³Division of Biomedical Engineering, School of Engineering, University of Glasgow, United Kingdom

INTRODUCTION

Poly(L-lactic acid) (PLLA) is a widely used bioabsorbable material, approved by the FDA for several biomedical applications, with remarkable properties for tissue engineering and orthopaedic applications such as excellent biocompatibility and biodegradability¹. Boron, a trace element found in the human body, plays an important role in bone growth and development². The aim of the present study was to engineer boron-containing materials and to evaluate the effect of boron on cell behavior. In this work we evaluate the ability of this novel material system to promote differentiation of C2C12 and MC3T3 cell lines into myoblastic and osteoblastic lineages respectively. Overall, the potential of boron-loaded materials to release boron and enhance cell commitment toward musculo-skeletal lineages was evaluated.

EXPERIMENTAL METHODS

PLLA films with 2% or 5% boron were obtained by solvent casting, where boron was loaded as borax decahydrate in constant stirring. Water contact angle (WCA) was measured for the different substrates by the sessile drop method. Surface morphology of materials was evaluated by SEM. Cells were seeded on substrates (C2C12 and MC3T3-E1 lines) in order to evaluate myoblast and osteoblast differentiation respectively. Cell morphology and myogenic/osteogenic commitment were quantified by sarcomeric myosin detection and qPCR amplification of specific genes.

RESULTS AND DISCUSSION

WCA results showed similar wettability between PLLA and boron-loaded PLLA systems (2% and 5% respectively, WCA 78.4 ± 3.3 degrees) suggesting that low quantities of boron used do not alter the chemical properties of system. The analysis of surfaces by SEM did not reveal any new topographical feature associated with the presence of boron, that cellular results can be correlated with boron content and release. Culture of C2C12 cells showed an increase in differentiated myotubes as the content on boron in biomaterial does (figure 1). To ensure that boron was the only factor implicated in cell differentiation, another experiment was performed using PLLA as a substrate and including equivalent percentages of borax decahydrate at culture medium. The obtained results showed that boron induces myoblast formation, suggesting that those surfaces had the potential as a release system.

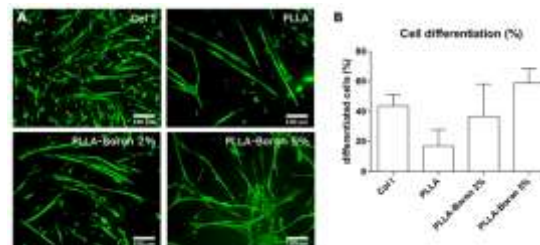


FIG 1: A) myotube formation detected by immunostaining of sarcomeric myosin protein. B) Quantification of C2C12 cells differentiation by image analysis.

Culture of MC3T3-E1 cells showed similar results after 15d of culture. We observed that differentiation markers increase with the content on boron does in the samples as obtained by the expression of specific osteoblastic proteins (Osteocalcin, Collagen I and Alkaline phosphatase). The gene expression of osteoblast markers (Runx2, IBSP) was also investigated obtaining major expression as a function of the boron content in substrates.

CONCLUSION

We observed that boron is able to direct cell differentiation in two different models: C2C12 cells to myotubes and MC3T3-E1 to osteoblasts.

Recent investigations have concluded that delivery of boron by degradation of borate glass is of special interest in biomedical applications but this is a toxic process due to the rapid release of boron. In this study, we found that the incorporation of boron into degradable materials produces a slow release of boron capable to promote cell differentiation. Furthermore, the study indicates that boron-loaded materials are excellent candidates to engineer cellular microenvironments aimed at the regeneration of musculo-skeletal systems.

REFERENCES

1. Burns, A.E. Varin, J. J Foot Ankle Surg 37: 37-41, 1998.
2. Wu, C. *et al.* Biomaterials 32:7068–78, 2011.

ACKNOWLEDGMENTS

The support of the project MAT2012-38359-C03-01 (including the FEDER financial support) as well as CIBER is acknowledged.



Animal Experiment on In-vivo Galvanic Corrosion of SUS316L and Ti-6Al-4V -Observation of tissue reaction at 52 weeks after implantation-

Y.Kato¹, A. Ito¹, T. Hattori^{1*}, T. Akahori¹, N.Kimata², K. Sato²

¹Dept. of Materials Science and Engineering, Meijo University, Nagoya, 468-8502, Japan.

²Dept. of Orthopedic Surgery, Aichi Medical University, Nagakute, 480-1195, Japan

*Corresponding Author: tomhat@meijo-u.ac.jp

INTRODUCTION

Because of the risk of galvanic corrosion, combined use of different metals such as SUS316L(SUS) and Ti-6Al-4V(Ti64) is supposed to be prohibited in in-vivo environment. However, there are unavoidable cases such as femoral shaft fracture after THA and internal fixation of complicated fracture. Although there are basic studies on the corrosion resistance with the standard electrode potential, there are few reports on in-vivo galvanic corrosion due to the combined use.

In this study, animal experiment was performed to investigate in-vivo galvanic corrosion in the combination use of SUS and Ti64. And tissue reaction and bone formation were investigated.

MATERIAL AND METHODS

Metal plates with 3 screw holes (15 x 5 x 1.2 mm) were made of SUS and Ti64 Mini DC plates. And cortex screws made of SUS and Ti64 (φ2.0 x 12 mm) were applied to fix the metal plates as the combined use and the control (Fig.1). These plates and screws were implanted into the medial aspect of proximal tibia in mature New Zealand white rabbits with 4 different combinations (Tab.1).

In order to investigate bone formation, X-ray pictures were taken at 0, 24 and 52 weeks after implantation. Then tibia bones were harvested with the implants. During harvesting, tissue reaction was carefully inspected every soft tissue layer.

The tibia bone was dehydrated and embedded in PMMA, and thin slices were made for Contact Micro Radiogram (CMR), cytological observation.

RESULTS AND DISCUSSION

(1).Successive X-ray observation

Bone formation around the implanted plates was observed. And cortical bone under the implanted plate became thin, and the plates were buried in cortical bone in all combinations at 52weeks. However osteolysis or abnormal bone formation was not observed (Fig.2).

(2).Visual observation of soft tissue and tibia bone

During harvesting, no discoloration and swelling were observed in soft tissue. The implants were mostly covered by newly formed bone tissue (Fig.3). It is considered that no influence of the galvanic corrosion was confirmed on surrounding soft tissue and tibia bone.

(3). CMR of cross section

The implanted plates were almost buried in cortical bone. And bone tissue became thin and porous under the implanted plates (Fig4). However, these changes were assumedly caused by the reduction of periosteal blood flow, and stress shielding due to the plate fixation.

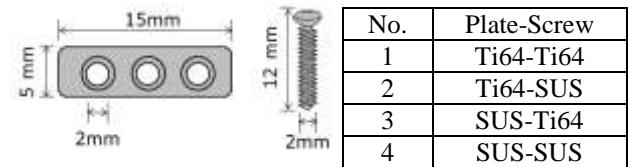
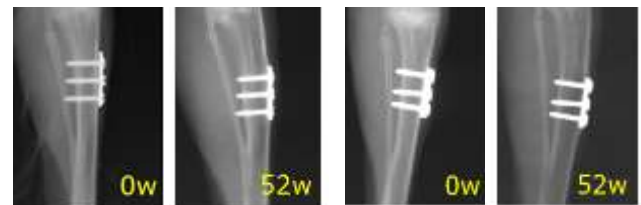


Fig.1 Plate and Screw Tab.1 Implant combinations

No.	Plate-Screw
1	Ti64-Ti64
2	Ti64-SUS
3	SUS-Ti64
4	SUS-SUS



(a) SUS-Ti64 (b) SUS-SUS
Fig.2 Bone formation around the implants



(a) SUS-Ti64 (b) SUS-SUS
Fig.3 Harvested tibia bone with the implants



(a) SUS-Ti64 (b) SUS-SUS
Fig.4 CMR of cross section



(a) Bone tissue (b) Soft tissue over the plate
Fig.5 Cytological observation (SUS-Ti64)

(4).Cytological observation

No inflammatory cells were observed, and quite normal findings were obtained in surrounding soft tissue and bone tissue (Fig.5).

CONCLUSIONS

At 52 weeks after implantation, no evidences of galvanic corrosion were observed in all investigation performed in this animal study. Further long term investigation is required to verify no galvanic corrosion.

The degradation relationship between mechanical and in vitro testing of a phosphate glass fibre composite

R. J. Colquhoun¹ and Prof K.E. Tanner¹

¹Department of Biomaterials, School of Engineering, University of Glasgow, Scotland
r.colquhoun.1@research.gla.ac.uk

INTRODUCTION

The degradation of phosphate glasses (PG) is regarded as being critical to the design of PG based biomaterials^[1]. Metaphosphate (50% mol P_2O_5) glasses represent a compositional group with structural networks highly suitable for fibrillation and have potential as reinforcing agents in degradable composites for tissue regenerative applications^[1,2]. However metaphosphate glass fibres (PGF) are susceptible to autocatalysis effects and accelerated dissolution rates (D_r) from their acidic degradation by-products^[1]. This effect can subsequently alter a PGF composite's mechanical property retention and cytotoxicity due to reductions in pH and the accelerated release of ions to cytotoxic levels.

With the D_r of PGF influenced by the ionic strength of experimental media^[1] it is important to consider how these degradation mechanisms translate across various testing techniques employing different ionic medias. The degradation properties of a PGF composite during mechanical testing and under conditions replicating those experienced *in vitro* were assessed.

EXPERIMENTAL METHODS

20mm, Ø20µm CorGlaes® Pure 107 metaphosphate glass fibres were degraded over 24 hours in distilled water (D.water), simulated body fluid (SBF), phosphate buffered saline (PBS) and Dulbecco's Modified Eagle Medium (DMEM) at 15 cm²/ml. Initial media ionic strength and mass loss recorded with D_r calculated.

CorGlaes® Pure 107/poly(lactic acid (PLA) composites were manufactured via a film stacking method at 0.2 fibre volume fraction (V_f). 60 x 15 x 2mm samples were degraded in D.water or DMEM at 37°C over 6 weeks (0.21 cm²/ml) with sample masses (wet and dry) and pH of the media and sample surface recorded periodically. Mechanical properties evaluated by three point bend technique following BS EN ISO 14125:1998+A1:2011.

RESULTS AND DISCUSSION

Table 1. Immersion media ionic strength/pH and D_r of CorGlaes® Pure 107 fibres

Media	Initial/ 24 hours pH	Ionic Conduc. (mS)	D_r (mg/cm ² /hour)
DMEM	7.40/6.56	11.47 ± 0.3	0.0072 ± 0.0004
SBF	7.40/2.01	19.53 ± 0.61	0.0139 ± 0.002
PBS	7.40/2.00	14.8 ± 1.14	0.0236 ± 0.002
D.Water	≈7.00/1.89	0.01 ± 0.0	0.028 ± 0.0003

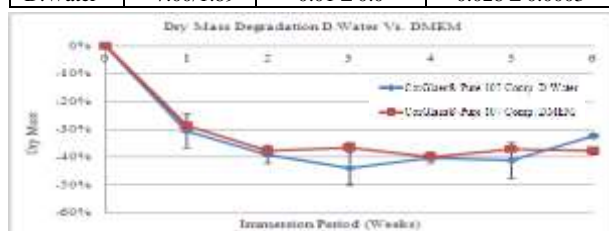


Figure 1. Composite dry mass, D.Water Vs. DMEM

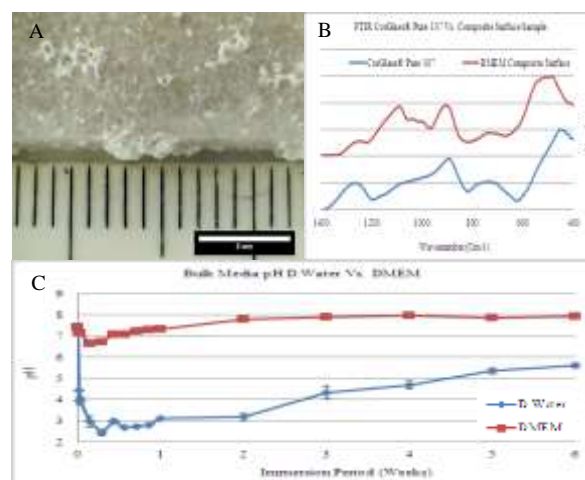


Figure 2.A) DMEM composite surface [1 week] B) FTIR of DMEM composite surface deposits vs CorGlaes Pure 107 C) Composite media pH

DISCUSSION

DMEM significantly retarded the PGF D_r and decrease in media pH compared to PBS and SBF (Table 1) but D_r failed to correlate with increasing ionic conductivity.

DMEM pH buffering was observed in bulk media during composite degradation (Fig 2C). However, comparable rates of mass loss (Fig 1) and mechanical properties attributed to fibre dissolution implied similar fibre D_r contrasting PGF dissolution data (Table 1). High surface area: volume ratio at fibre/matrix interface ($> 1 \times 10^4$ cm²/ml) was believed to counteract localised DMEM buffering. Precipitation of a surface layer during DMEM degradation appeared to be that of an amorphous calcium phosphate (ACP) incorporating elements of the PGF fibre composition (Fig 2A/B)^[3].

CONCLUSIONS

Degradation behaviour between D.water and DMEM media showed no alteration to the mass loss and mechanical retention mechanisms of the PGF composite despite the observed reduction in fibre D_r when assessed as a single element. This highlights the influence of the fibre/matrix interface on composite degradation and that mechanical degradation rates accurately represent those experienced during *in vitro* testing for a CorGlaes® Pure 107 fibre composite.

REFERENCES

1. Jones, J. and Clare, A. Bio-Glasses: An Introduction, Wiley Publishing (2012)
2. Ahmed, I. *et al.* Biomaterials, 25:501-507 (2004)
3. Clupper, D.C. *et al.* JBM R PA, 67A:285-294 (2003)

ACKNOWLEDGMENTS

The authors would like to thank Giltech® for their support and EPSRC for DTA financial support.



Animal Experiment on In-vivo Galvanic Corrosion of SUS316L and Ti-6Al-4V -Surface observation and EPMA element mapping analysis-

A. Ito¹, Y. Kato¹, T. Hattori^{1*}, T. Akahori¹, N. Kimata², K. Sato²

¹Dept. of Materials Science and Engineering, Meijo University, Nagoya, 468-8502, Japan.

²Dept. of Orthopedic Surgery, Aichi Medical University, Nagakute, 480-1195, Japan.

*Corresponding Author: tomhat@meijo-u.ac.jp

INTRODUCTION

According to the popularization of Ti-6Al-4V (Ti64) with good biocompatibility, the combination use with the conventional stainless steel of SUS316L (SUS) is increasing due to accidental misuse in emergency cases or necessary choice of stainless wire to tie up bone fragments in complicated fracture and femoral mid shaft fracture after Total Hip Arthroplasty.

Ideally, these high quality implant metals of SUS and Ti64 will avoid even galvanic corrosion due to the very stable oxide film. However, the combination use of different implant metal is prohibited by instruction manuals of the medical devices. And also there are few reports on in-vivo study of galvanic corrosion.

In this animal study, In-vivo galvanic corrosion of SUS and Ti64 was investigated by means of the surface observation and EPMA element mapping analysis.

EXPERIMENTAL METHODS

Mini DC plates (30 x 5 x 1.2 mm) and cortex screws (φ2 x 12 mm) made of SUS and Ti64 were subjected to this study, in which the plates were cut into the half length of 15mm with 3 screw holes. And Mature male New Zealand white rabbits were used as experimental animal. These specimens were implanted into the medial aspect of proximal tibia of the rabbits in 4 different combinations (Tab.1).

At 52 weeks after implantation, the tibia bones were harvested with the implants. Bone tissue formed on the implants was carefully detached, and the screws were removed. Then, the plates and the screws were observed by stereoscopic microscope. Furthermore, the tibia bones with the metal plates were cut into thick slice and dehydrated, then embedded in PMMA. And Element mapping analysis was performed, in which Chromium (Cr) was selected as a marker element of the anodic dissolution due to the galvanic corrosion because the standard electrode potential of SUS is lower than that of Ti64, SUS is accordingly supposed to be corroded.

Tab.1 Combinations of plate and screw

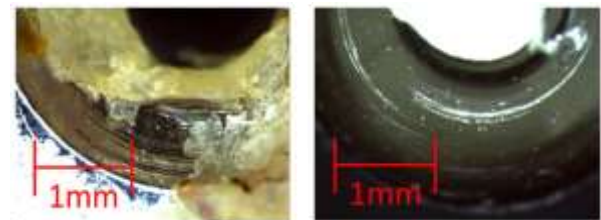
Specimen No.	Plate	screw
1	Ti-6Al-4V	Ti-6Al-4V
2	Ti-6Al-4V	SUS316L
3	SUS316L	Ti-6Al-4V
4	SUS316L	SUS316L

RESULTS AND DISCUSSION

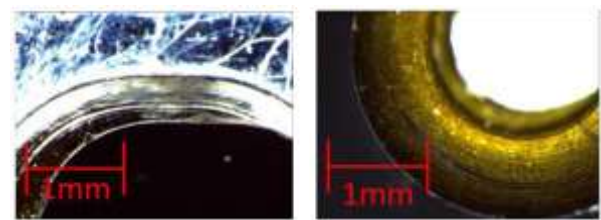
In microscopic observation, the concentric friction imprints were observed in the screw hole of the plates and the back surface of the screw head, which were supposedly caused by tightening the screws (Fig.1, Fig.2). However, no evidences of galvanic corrosion were observed in all specimens at 52 weeks.

Regarding the mapping analysis, Cr element was almost evenly detected at bone tissue because small amount of Cr is physiologically contained in bone tissue. In detail, Cr element detected with the concentration gradient around the SUS plates, which is suggested Cr element elution from the SUS plates (Fig.3).

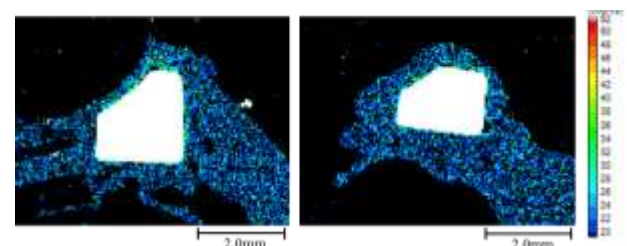
However, there is no difference between the combinations of SUS screw (identical metals) and Ti64 screw (different metals). Consequently, this Cr element elution is considered to be not due to the galvanic corrosion.



(a) Screw hole (b) Back of screw head
Fig.1 Combination of SUS plate - SUS screw



(a) Screw hole (b) Back of screw head
Fig.2 Combination of SUS plate - Ti64 screw



(a) with SUS screw (b) with Ti64 screw
Fig.3 Cr element mapping analysis on SUS plate.

CONCLUSIONS

In this animal study, it is demonstrated that galvanic corrosion was not generated in the combination of SUS and Ti64, or generated in very low level in 52 weeks after implantation.

Very small amount of Cr element elution is confirmed by EPMA element mapping analysis, which is considered as not due to the galvanic corrosion, but due to usual small electrolysis of SUS in the electrolyte solution of in-vivo environment.

Nanoscale Roughness Influences on Cell Proliferation

Prabhjeet Kaur Dhillon¹, Ajay Kumar², Shalmoli Bhattacharyya² and Subhendu Sarkar¹

¹ Department of Physics, Indian Institute of Technology Ropar, Nangal Road, Rupnagar, Punjab, 140001, India

²Department of Biophysics, Post Graduate Institute of Medical Education and Research, Sector 12, Chandigarh, 160012, India, prabhjeetd@iitrpr.ac.in

INTRODUCTION

Studies of cell proliferation on topographically different substrates are currently being explored for their potential applications in biomedical sciences¹. However, the results obtained so far have been often conflicting^{2, 3}. All these studies characterize a surface using its average roughness and try to correlate cell proliferation characteristics with the overall roughness. Recent research revealed that typical length scales for cell protrusions important for sensing the substrate are of the order of a few nanometers⁴. Therefore, correlating cell proliferation characteristics with the average roughness is an oversimplification since a typical rough surface exhibits a range of roughnesses over different length scales. Our study investigates this problem using universal scaling theories to understand the behaviour of cells on surfaces.

EXPERIMENTAL METHODS

The surfaces were prepared by isotropically etching Si (100) (1x1cm²) surfaces with HNA (HF, HNO₃, CH₃COOH) for different times (30s, 60, 120s, 240s, 360s, 480s & 600s). The resulting morphologies were investigated using atomic force microscopy (AFM). Dynamic scaling parameters were also evaluated from the AFM data^{5, 6}. Cell proliferation studies using Dental Pulp Stem Cells (DPSCs) were carried out on these surfaces by fluorescence microscopy.

RESULTS AND DISCUSSION

Observed proliferation of DPSCs over etched surfaces (Fig.1) was compared with roughness parameters of the surfaces for different length scales.

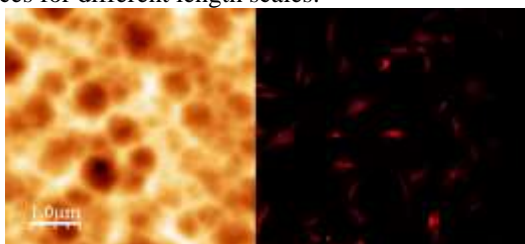


FIGURE 1. Isotropically etched Si(100)surface (360s) (Left) and fluorescence microscopy image of DPSC proliferation on it (Right).

According to Dynamic Scaling Theory (DST), root-mean-square (RMS) roughness, a measure of lateral correlations at the interface follows a power law w.r.t. length scale: $w_{\text{sat}} \sim L^{\alpha}$, where w_{sat} is the saturation value of interface width and α is the roughness exponent⁵. When α lies between 0 and 1, a smaller value of α corresponds to a rougher local surface, i.e., it signifies a more rapid change in surface heights⁷. It was found that cell proliferation was

influenced by the short length scale properties of the surfaces i.e. the local roughness at smaller length scales (~50–150 nm) instead of average roughness. For shorter length scale, local roughness increases ($\sim 1/\alpha$) till 240s (cell proliferation decreases). Thereafter local roughness decreases till 360s-480s and cell proliferation increases, further local roughness increases and cell proliferation decreases (Table 1).

Etching time (s)	30	60	120	240	360	480	600
Nano-roughness	Increases				Minimum		Increases
Average no. of cells in a single field	8	7	3	3	23	20	3

TABLE 1. Comparison of nano-roughness and cell proliferation

AFM imaging of DPSC (Fig.2) showed that the features on the cell surface were of the order of 100-200 nm thus indicating a correlation of proliferation, cell topography and small scale roughness.

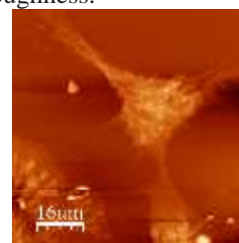


FIGURE 2. AFM image of single DPSC on cover plate.

CONCLUSION

DPSCs prefer to grow on locally smooth surfaces. Roughness at small length scales influences cell proliferation instead of average roughness of overall surface.

REFERENCES

1. Gentile F. *et al.*, Sci. Rep. 3:1461, 2013.
2. Chen W. *et al.*, ACS Nano 6:4094, 2012.
3. Webster T. *et al.*, Biomat. 25:4731, 2004.
4. Mogilner A. *et al.*, Biophys. J. 89:782, 2005.
5. Barabasi A.-L. and Stanley H.E., Fractal Concepts in Surface Growth. 1995, Cambridge University Press: NY.
6. Dhillon P. K. and Sarkar S., App. Surf. Sci. 284:569, 2013.
7. Pelliccione M. and Lu T.M., Evolution of Thin Film Morphology: Modeling and Simulations. 2008, Springer.

Role of Fibronectin assembly in Mesenchymal Stem Cell differentiation

P. Rico^{1,2}, H. Mnatsakanyan¹, M. Salmerón-Sánchez³

¹Center for Biomaterials and Tissue Engineering, Universitat Politècnica de València, Spain

²CIBER, Spain, parico@upvnet.upv.es

³Division of Biomedical Engineering, School of Engineering, University of Glasgow, United Kingdom

INTRODUCTION

Although significant progress in the last years has been made in the investigation of defined factors implicated in lineage commitment of stem cells, the effect of biomaterial properties on functional differentiation is poorly understood¹. Mesenchymal stem cell differentiation can be driven by the material/cell interface in absence of complex soluble chemistries or cellular reprogramming for example modifying the chemistry or topography². In this work we used materials with similar chemistry (PEA, poly(ethyl-acrylate) and PMA, poly(methyl-acrylate)) which results in different distribution and conformation of the protein at the cell-material interface. PEA induces FN fibrillogenesis network in the absence of cells while the protein conformation on PMA surface remain globular³. The aim of the present study is to evaluate the role of fibronectin distribution at the material interface – fibrillar vs globular – in promoting mesenchymal stem cell differentiation, by investigating cell commitment towards osteoblast and adipocyte lineages.

EXPERIMENTAL METHODS

Polymer sheets of PEA and PMA were obtained by radical polymerisation in UV. Thin films were prepared by spin-coating after dissolving the polymers in 2% toluene.

Protein adsorption was performed at a concentration of 20µg/ml and FN conformation was observed with AFM in tapping mode.

Mouse Mesenchymal Stem Cells (mMSC) were seeded on material surfaces in order to evaluate osteoblastic and adipogenic differentiation.

Cell adhesion was followed by immunofluorescence for focal adhesion proteins (vinculin, paxilin, talin). FAK and p-FAK expression were evaluated by western blot techniques. Cell contractility was evaluated by immunodetection of phosphorylated myosin light chain. For experiments including contractility inhibitors we used Y-27632 or blebbistatin.

Gene expression and adipogenic/osteogenic commitment were quantified by qPCR amplification and other immunostaining procedures of specific genes.

RESULTS AND DISCUSSION

Surface chemistries (PEA and PMA) showed similar wettability and total amount of adsorbed FN, but conformation and distribution of the protein were completely different. An interconnected FN network was found in PEA while on PMA FN conformation results in globular aggregates in AFM images.

Cell adhesion of mMSC, as followed by immunofluorescence, revealed the presence of well-

defined focal plaques formed on both, PEA and PMA substrates (Fig 1). Western blot analysis showed similar levels of FAK in both materials, while higher levels of pFAK were obtained on PMA substrates, which reveals higher signaling activity on globular FN.

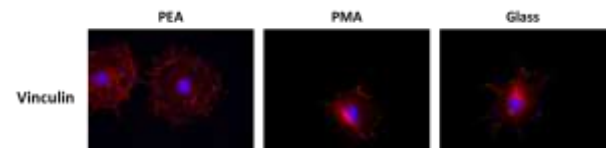


Fig. 1: Focal adhesion plaques detected by immunostaining of vinculin on different substrates.

Mesenchymal stem cells showed differences on gene expression between materials after 15d of culture, which were correlated to the different conformation of FN on material surfaces. qPCR results suggested that cell commitment to adipogenic or osteoblastic lineages are favoured on PEA compared to PMA and glass control (Fig 2) -in absence of differentiation factors. This is also correlated with cell contractility on both surfaces.

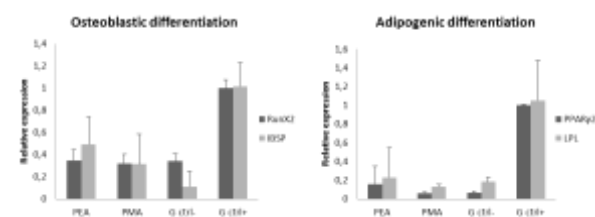


Fig. 2: qPCR expression levels of osteoblastic (RunX2 and IBSP) and adipogenic markers (PPAR and LPL).

CONCLUSION

We have shown that the conformation and distribution of FN –fibrillar vs globular – on different material surfaces influence mesenchymal stem cell commitment towards osteogenic and adipogenic lineages.

REFERENCES

1. Le Blanc K. *et al.*, Cytotherapy.7: 36-45, 2005
2. McBeath R. *et al.*, Dev. Cell. 6: 483-495, 2004
3. Rico P. *et al.*, Tissue Eng. 15: 3271-3281, 2009

ACKNOWLEDGMENTS

The support of the project MAT2012-38359-C03-01 (including the FEDER financial support) as well as CIBER is acknowledged.



Graphene oxide and 4-arm-PPO-PEO composite hydrogels for injectable biomedical applications

Yunki Lee, Jin Woo Bae, and Ki Dong Park*

Department of Molecular Science and Technology, Ajou University, Suwon, Republic of Korea, kdp@ajou.ac.kr

INTRODUCTION

Conventional polymeric hydrogels have been extensively used as a promising vehicle for tissue engineering and drug delivery applications. However, they appear to have some limitations for use as substitute materials of load-bearing tissues due to their insufficient mechanical properties. To improve mechanical properties of hydrogels, many strategies including double-network, topological cross-linking, and nanocomposite hydrogels, have been developed¹.

In this study, we report *in situ* forming graphene oxide (GO)-incorporated 4-arm-PPO-PEO-tyramine (Tet-TA) composite hydrogels with superior mechanical strength *via* chemical and physical cross-linking. Various properties of the composite hydrogels were characterized, and the effect of GO on mechanical strength of hydrogels was evaluated by varying the oxidation degree and feed amount of GO. Biocompatibility of Tet-GO hydrogels was investigated using MC3T3-E1 cells.

EXPERIMENTAL METHODS

4-arm-PPO-PEO block copolymer was modified by conjugating tyramine (TA) for horseradish peroxidase (HRP)-catalyzed cross-linking². Two kinds of GO varying in oxidation was prepared by a modified Hummers method and they were exfoliated using an ultrasonicator³. The chemical structures of GOs were characterized by X-ray photoelectron spectra (XPS) and fourier transform infrared spectroscopy (FT-IR). GO (0.1-0.4 wt%) was homogeneously suspended in Tet-TA (10 wt%) precursor solution prior to gel formation, and Tet-TA/GO hydrogels were subsequently formed in presence of HRP and H₂O₂ (Fig 1). The mechanical properties of hydrogels, including elastic, tensile, and compressive modulus, were evaluated by changing either oxidation level or feed concentration of GO. *In vitro* cyto-toxicity test was then investigated on the surface of hydrogels with MC3T3-E1 cells.

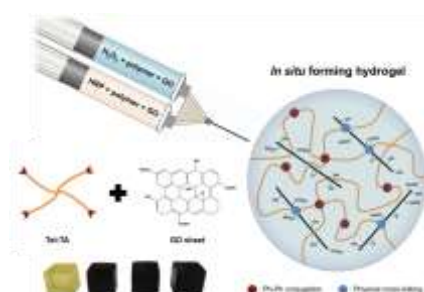


Fig 1. Schematic representation of injectable Tet-TA/GO composite hydrogels *via* enzymatic cross-linking.

RESULTS AND DISCUSSION

The various oxidation degree (O/C ratio; 0.09-0.59) of synthesized GO was identified by XPS and FT-IR

analysis. As additional cross-linkers, GO (0.1-0.4 wt%) was incorporated in Tet-TA hydrogels (10 wt%) formed *via in situ* oxidative cross-linking among the phenolic moieties catalyzed by HRP and H₂O₂. The gelation time of hydrogels was easily controlled by varying the HRP concentrations (8-58 sec) and oxidation level of GO affected cross-linking rate. Interestingly, the mechanical strength of Tet-TA hydrogels was effectively improved after incorporation of GO. Tet-TA/GO hydrogels exhibited 683 % increase in tensile strength and 983 % in compressive strength compared to pure Tet-TA hydrogels, indicating strong interaction between GO and Tet-TA polymer chain (Fig 2).

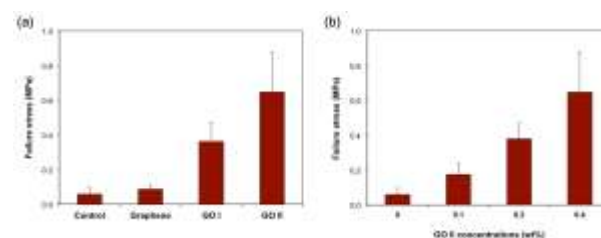


Fig 2. Compressive strength of Tet-TA/GO composite hydrogels with different oxidation degree (a) and feed amount of GO (b).

In vitro MC3T3-E1 cell culture for the evaluation of cyto-compatibility of hydrogels demonstrated that incorporation of GO within hydrogels had no effect on the toxicity of hydrogel matrix.

CONCLUSION

In situ Tet-TA/GO composite hydrogels have been developed as injectable replacements for load-bearing tissues. The obtained results demonstrated that physico-chemical properties of hydrogels could be controlled by adjusting oxidation degree and concentration of GO. Compared to pure Tet-TA hydrogels, optimized hydrogels showed 7.8 times and 10.8 times higher strength in tensile and compressive test. The incorporation of GO (0.4 wt%) into Tet-TA hydrogels did not affect the toxicity to MC3T3-E1 cells. As a result, *in situ* forming Tet-TA/GO composite hydrogels can be a promising candidate as an injectable scaffold for tissue replacement.

REFERENCES

1. Liu R. *et al.*, J. Mater. Chem. 22:14160-141671, 2012
2. Park K.M. *et al.*, Soft Matter. 7:986-992, 2011
3. Krishnamoorthy K. *et al.*, Carbon. 53:38-39, 2013

ACKNOWLEDGMENTS

This work was supported by Basic Science Research Program through the National Research Foundation of Korea (NRF) grant funded by the Ministry of Science, ICT & Future Planning (NRF-2012R1A2A2A06046 885)



pH-Mediated Surfactant Release in the Development of Self-Sterilising Urinary Biomaterials

C. P. McCoy, J. L. Trotter, N. J. Irwin, L. Carson, D. S. Jones

School of Pharmacy, Queen's University Belfast, 97 Lisburn Road, Belfast BT9 7BL, Northern Ireland, UK
n.irwin@qub.ac.uk

INTRODUCTION

To combat medical device-associated infection, previous research has focused on two main strategies: (i) modification of the device surface to create an inherently anti-adherent exterior; or (ii) incorporation of antimicrobial agents that will subsequently be released to target microbial cells¹⁻². Limited efficacy in preventing bacterial colonisation, particularly *in vivo*, in addition to concerns over potential toxicity of antimicrobial agents and the emergence of bacterial resistance with antibiotics, however, ultimately restrict their clinical potential. The microbial anti-adherent properties of surfactant-modified surfaces have been widely reported³⁻⁴. We propose that controlled release of surfactant can reduce adhesion of bacteria and subsequent biofilm formation, without the toxicity and resistance issue associated with antibiotic systems.

The aim of this study was to determine rates of release of a non-ionic surfactant, Triton X-100, from poly(hydroxyethyl methacrylate) (p(HEMA)) hydrogels at pH 7, representing normal physiological urine pH, and pH 10, representing the elevated pH reported at the onset of urinary catheter infections. Bacterial adherence studies were also performed to investigate the resistance of Triton-loaded p(HEMA) to colonisation of the urinary pathogen *Proteus mirabilis*.

EXPERIMENTAL METHODS

Triton-loaded p(HEMA) films, containing Triton X-100, were synthesized from mixtures of Triton X-100, 2-hydroxyethyl methacrylate, 2,2'-azobisisobutyronitrile and ethyleneglycol-dimethacrylate. The solution was injected into moulds and polymerised for 18 h at 60°C. Release studies were performed at pH 7 and pH 10 in universal buffer solutions having a constant ionic strength, prepared using the formulation of Koller *et al.*⁵. Released Triton X-100 was quantified by UV-visible spectroscopy in conjunction with calibration curves prepared using universal buffer solutions of relevant pH. Five replicates were performed at each pH. Microbiological assessments were performed to assess adherence of *P. mirabilis* to the surface of Triton-loaded p(HEMA) relative to the control p(HEMA). The effect of pH on the cumulative amount of Triton released at designated intervals, and the bacterial adherence after 4 h and 24 h were statistically analysed by a one-way analysis of variance, followed by Tukey's honestly significant difference test for post-hoc comparisons between means of singular groups. Differences were considered significant if $p < 0.05$ ⁶.

RESULTS AND DISCUSSION

The effect of pH on the release of Triton X-100 from Triton-loaded p(HEMA) at 37°C with shaking is shown in Figure 1. Release profiles for Triton-loaded p(HEMA) in pH 7 and pH 10 were statistically similar. For example, after 24 h, 22.2% and 26.8% of the loaded

Triton X-100 was released from the hydrogels at pH 7 and pH 10, respectively.

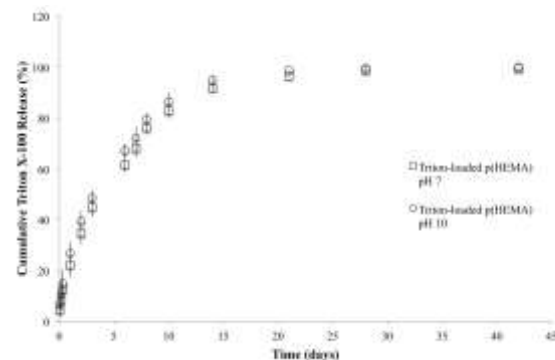


Fig. 1: The effect of pH on the mean (\pm S.D.) release of Triton X-100 from Triton-loaded p(HEMA) at 37°C with shaking. Sink conditions were maintained throughout the study. Open and closed symbols refer to release at pH 10 and pH 7 respectively.

The insignificant effect of pH on rates of release is explained by the absence of ionisable moieties in both Triton X-100 and p(HEMA), and the consequential absence of pH-dependent ionic interactions to promote or delay release. The high molecular weight of Triton X-100 ($\sim 647 \text{ g mol}^{-1}$) and possible entanglements of the long polyethylene oxide chains were responsible, however, for the prolonged release of Triton X-100 from the hydrogel over periods of up to three weeks. Furthermore, greater resistance to adherence of *P. mirabilis* was displayed by the Triton X-100-loaded hydrogels than the control p(HEMA).

CONCLUSION

Release of Triton X-100 from surfactant-loaded polymers proceeded in a pH-independent fashion. The prolonged release of Triton X-100, in addition to the encouraging resistance of the surfactant-loaded p(HEMA) matrices to adherence of *P. mirabilis*, are, however, promising for the use of surfactants in the development of infection-resistant catheter coatings.

REFERENCES

1. Munoz-Bonilla A, Fernandez-Garcia M. Prog Polym Sci. 37(2):281-339, 2012
2. Irwin N. Pharm Res. 30:857-865, 2013
3. Zeraik AE, Nitschke M. Curr Microbiol. 61:554-559, 2010
4. Mai-ngam K. Colloid Surface B. 49:117-125, 2006
5. Koller CN. *et al.*, J Med Chem. 184(2):692-699, 1992
6. Jones DS. Pharm Stats. Pharm Press. 2002

ACKNOWLEDGMENTS

The authors thank the Department for Employment and Learning, Northern Ireland, for financial support.

Silica Beads Grafted with Thermoresponsive Cationic Copolymer Brush Possessing Quaternary Amine Group for Effective Thermoresponsive Ion-exchange Chromatography

Kenichi Nagase^{1*}, Mike Geven², Saori Kimura³, Jun Kobayashi¹, Akihiko Kikuchi⁴, Yoshikatsu Akiyama¹, Dirk W. Grijpma^{2,5}, Hideko Kanazawa³, and Teruo Okano¹

^{1*}Institute of Advanced Biomedical Engineering and Science, Tokyo Women's Medical University, Japan nagase.kenichi@twmu.ac.jp ²University of Twente, The Netherlands University. ³Keio University, Japan. ⁴Tokyo University of Science, Japan. ⁵University of Groningen, The Netherlands

INTRODUCTION

Temperature-responsive chromatography using poly(*N*-isopropylacrylamide) (PIPAAm) grafted silica beads is highly useful to control function and properties of the stationary phase for high performance liquid chromatography (HPLC) by only change in column temperature.¹ Also, thermoresponsive cationic copolymer possessing tertiary amine group grafted silica beads was developed as thermoresponsive ion exchange chromatography matrices.² In the present study, we prepared silica beads grafted with thermoresponsive cationic copolymer brush possessing quaternary amine group as strong ion-exchange chromatography matrices. Characterization of the prepared beads was performed by observing elution profiles of adenosine nucleotides and acidic proteins.

EXPERIMENTAL METHODS

ATRP initiator, 2-(*m,p*-chloromethylphenyl)ethyl trimethoxysilane was immobilized onto silica beads (diameter of 5 μ m, pore diameter of 30 nm) (Fig.1). IPAAm, 3-acrylamidopropyl trimethylammonium chloride (APTAC), and *tert*-butylacrylamide (tBAAm) were copolymerized on silica beads surface using CuCl/Me₆TREN as ATRP catalyst and 2-propanol as ATRP reaction solvent. Prepared beads were packed into stainless steel column (50 \times 4.6 mm i.d.) and connected to HPLC system. Elution behaviour of adenosine nucleotide and acidic proteins was observed at various temperatures. For comparison, silica beads grafted with thermoresponsive copolymer possessing tertiary amine group (P(IPAAm-*co*-*N,N*-dimethyl aminopropylacrylamide)(DMAPAAm)-*co*-tBAAm) was also prepared for comparison of separation efficiency.

RESULTS AND DISCUSSION

Prepared beads were characterized by CHN elemental analysis and GPC measurements. Amount of grafted copolymer was 2.47-2.68 mg/m², and copolymer graft density was 0.11-0.15 chains/nm². The results indicated that dense cationic copolymer brush was successfully grafted on silica beads surface. The prepared beads packed column was connected to an HPLC system. Elution behaviours of adenosine nucleotides and human serum albumin (HSA) and fibrinogen were observed. Longer retention time of adenosine nucleotides was observed on quaternary amine column compared to that on tertiary amine column, attributed to strong cationic properties of quaternary amine group. Also, acidic protein HSA and fibrinogen was adsorbed high

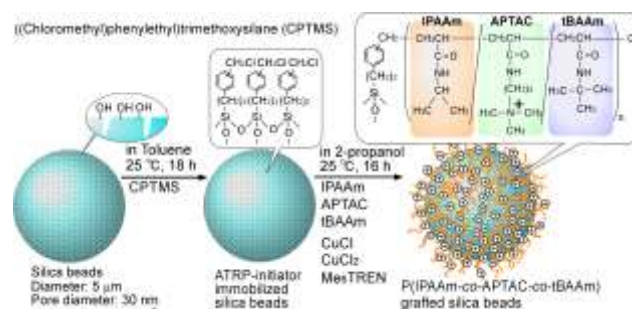


Fig.1 Scheme for preparation of silica beads grafted with thermoresponsive cationic copolymer brush

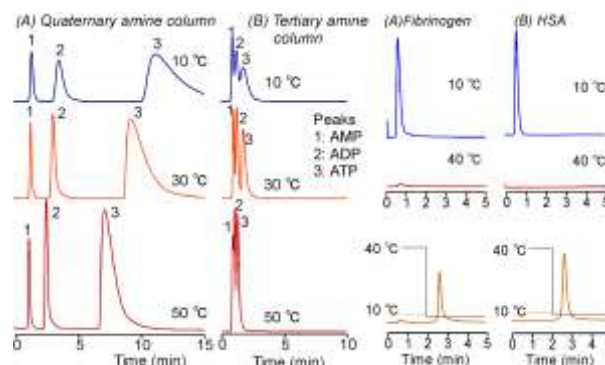


Fig.2 Chromatogram of adenosine nucleotides at various column temperatures

Fig.3 Acidic proteins elution from quaternary amine column

temperature and successfully recovered by reducing column temperature. This is because acidic proteins adsorbed to cationic copolymer brush through both electrostatic and hydrophobic properties at high temperatures. These results indicated that the silica beads grafted with thermoresponsive cationic copolymer possessing quaternary are effective thermoresponsive chromatography matrices for separation of acidic biomolecules proteins.

CONCLUSION

Silica beads grafted with thermoresponsive cationic copolymer brush possessing quaternary amine group was prepared through surface-initiated ATRP. The prepared beads would be useful for thermoresponsive strong ion-exchange chromatography matrices.

REFERENCES

1. Kikuchi A. *et al.*, Macromol. Symp. 207: 217-228, 2004
2. Nagase K *et al.*, Biomacromolecules 9: 1340-1347, 2008

Thermo-Responsive Nano-Structured Surface Modulates Cell Adhesion and Detachment

Yoshikazu Kumashiro^{1*}, Morito Sakuma^{1,2}, Masamichi Nakayama¹, Nobuyuki Tanaka¹, Kazuo Umemura², Masayuki Yamato¹, and Teruo Okano¹

^{1*}Institute of Advanced Biomedical Engineering and Science, Tokyo Women's Medical University (TWIns), Japan

²Department of Physics, Tokyo University of Science, Japan
kumashiro.yoshikazu@twmu.ac.jp

INTRODUCTION

Poly(*N*-isopropylacrylamide) (PIPAAm)s exhibit temperature-dependent behaviors above/below their lower critical solution temperature (LCST) at approximately 32 °C in aqueous solutions. As one of the most famous applications, cell adhesion and detachment control on PIPAAm-grafted surface has been investigated intensively¹. Cultured cells at 37 °C on the surface are spontaneously recovered by lowering temperature below the LCST. This study developed a Langmuir-Schaefer method for fabricating PIPAAm-deposited surfaces. The PIPAAm deposited surfaces with various area per molecule and chemical compositions were characterized and cell adhesion and detachment characters on the surfaces were also discussed.

EXPERIMENTAL METHODS

Block copolymer of polystyrene-*block*-PIPAAm (St-IP) with specific molecular weights were synthesized via reversible addition-fragmentation chain transfer radical (RAFT) polymerization. St-IP chloroform solution was carefully spread at an air-water interface. After forming the film with various densities, the film was horizontally transferred on a hydrophobic substrate (Fig. 1)². The St-IP surfaces were analyzed by various methods of surface analyses, and cell adhesion and detachment in response to temperature on the surface was also evaluated. Bovine carotid artery endothelial cells (BAECs) were cultured on a St-IP surface at a concentration of 1.0×10^4 cells/cm² at 37 °C for 24 h. Then, for investigating a temperature effect on cell detachment on St-IP surfaces, the cells were incubated at 20 °C for 120 min, and the number of adhering cells was counted.

RESULTS AND DISCUSSION

The chemical composition of obtained block copolymer was characterized by ¹H NMR. The number of St moieties was defined at 130 in the synthetic block copolymers and the number of IP moieties was modulated by a reaction condition. For example, Synthesized block copolymers were abbreviated to be St-IP110 that has 130 St moieties and 110 IPAAm moieties. The effects of density of St-IP and PIPAAm molecular weight toward temperature-dependent cell adhesion and detachment were investigated (Fig. 2). On the St-IP surfaces at 3 nm²/molecule, the numbers of adhering cells were below 0.6 cells/cm², which was much lower density compared with the control surface. At 40 nm²/molecule, the number of adhering cells was 0.8-0.9 cells/cm², which was almost the same as the control surface. Fig. 2 also shows the cell detachment

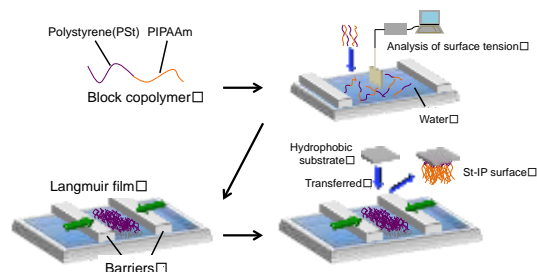


Fig. 1. Preparation of thermo-responsive surface transferred from Langmuir film.

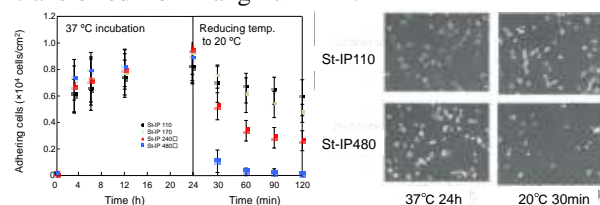


Fig. 2. Temperature-responsive cell adhesion and detachment on St-IP surfaces at 40 nm²/molecule.

on the St-IP surfaces after reducing temperature from 37 °C to 20 °C for 120 min. At 3 nm²/molecule, almost cells detached themselves from the LS surfaces by 30 min incubation. At 40 nm²/molecule, cells were gradually detached themselves from St-IP110, St-IP170 and St-IP240 surfaces, and perfectly detached from St-IP480 surfaces. These results indicated that (1) lower density was effective for increasing cell adhesion at 37 °C and (2) higher density and increasing PIPAAm molecular weight of St-IP molecule was dominant for acceleration cell detachment.

CONCLUSION

In this study, thermo-responsive block copolymer surface with various density was fabricated by a transference of Langmuir film and the cell adhesion and detachment properties were investigated. The precise control of density and composition of block copolymer was important factor for modulating cell attachment and detachment in response to temperature.

REFERENCES

1. Yamada, N. *et al.*, *Makromol. Rapid Commun.* 11:571-576, 1990
2. Sakuma, M. *et al.*, *J. Biomater. Sci. Polym. Ed.* 25:431-443, 2014.

ACKNOWLEDGMENTS

This study was supported by Creation of innovation centers for advanced interdisciplinary research areas Program in the Project for Developing Innovation Systems "Cell Sheet Tissue Engineering Center (CSTEC)" from the Ministry of Education, Culture, Sports, Science and Technology (MEXT), Japan.

Reciprocating Sliding Friction of Polyvinyl Alcohol Hydrogels as Articular Cartilage Substitutes

Takashi Hayami¹, Koji Morimoto¹, Yoshihiro Kimura², Noriyasu Hirokawa¹ and Tadashi Shibue¹

¹Faculty of Biology-Oriented Science and Technology, Kinki University, Japan

²Technical Development Dept., JAPAN VAM & POVAL CO., LTD, Japan, hayami@waka.kindai.ac.jp

INTRODUCTION

We studied the use of polyvinyl alcohol hydrogels (PVA-H) for the hemiarthroplasty of injured knee and hip joints¹. We prepared PVA-H in pure water (PVA-H/Water) and tested the basic tribological characteristics of PVA-H/Water artificial hemi-joints paired with hog articular cartilage in the end-face friction test². We compared the characteristics of reciprocating friction and end-face friction in PVA-H/Water paired with a hog articular cartilage joint.

EXPERIMENTAL METHODS

The PVA-H/Water solution prepared using 15 wt% PVA powder (DP: 1700) dissolved in pure water was stirred well and poured into a square mould and frozen at -20°C for 24 h. The resulting hydrogel was dried at room temperature, annealed for 5 h at 140°C in vacuum, and pressurized under 40 MPa at 140°C . The resulting specimen dimension and water content were $20\text{ mm} \times 50\text{ mm} \times 2.5\text{ mm}$ and $58 \pm 3\%$, respectively. Disciform articular cartilage specimens (7 mm in diameter) were harvested from the knee joints of hogs. The articular cartilages (thicknesses $1.5 - 2\text{ mm}$) were used in friction tests with intact synovial fluid and lamina splendens.

Fig.1 shows a schematic of the reciprocating friction test apparatus. The PVA-H/Water specimen was fixed to the bottom of the lubricant bath, and the cartilage specimen was fixed to a shaft with instant glue. The lubricant was a saline and bovine serum mixture. A normal contact pressure (P) of 1 MPa was assumed. The reciprocating frequency and stroke length were 0.4 Hz and 25 mm, respectively. The friction force (F) was detected using a strain gage load cell comprising two leaf springs. The friction coefficient (μ) was calculated from F and P . The friction distance (L) and root mean square speed was set to 144 m and 20 mm/s, respectively, under the same conditions as those employed in the previous end-face friction test. Further details about the synthesis of PVA-H/Water and the end-face friction test are provided elsewhere².

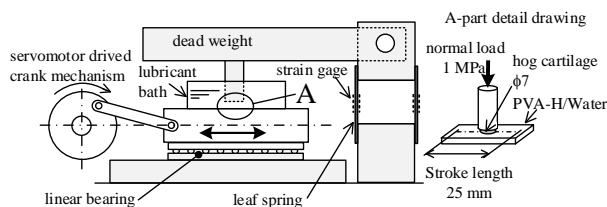
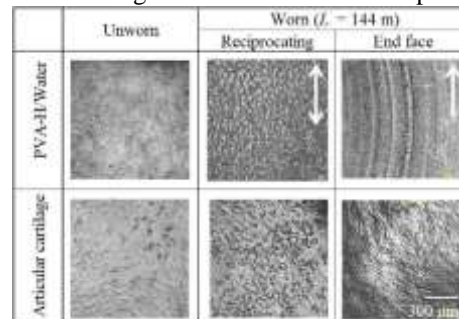


Fig.1 Reciprocating friction test apparatus.

RESULTS AND DISCUSSION

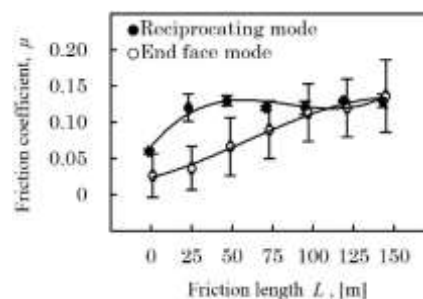
Fig.2 shows confocal laser microscopy (CLSM) images of the unworn and worn surfaces (at $L = 144\text{ m}$) of the PVA-H/Water and articular cartilage specimens for comparing the reciprocating and end-face friction modes. On the worn surface of PVA-H/Water, a linear

Fig.2 CLSM images of the surfaces of the specimens.



Arrows indicate friction direction.

Fig.3 Variation of Friction coefficient. $n=3, \pm\text{SD}$



abrasion mark with a surface roughness of $1.3\text{ }\mu\text{m Ra}$ was observed in the end-face mode, whereas a digging-up pattern with a number of irregularities ($3.8\text{ }\mu\text{m Ra}$) was observed in the reciprocating mode. On the cartilage surface, the fine bumpy pattern prior to friction remained on the worn surfaces of the end-face mode. In the reciprocating mode, however, the pattern was worn off, and larger irregularities formed along the friction direction. The roughness of the worn cartilage in both friction modes was $2.6 - 2.8\text{ }\mu\text{m Ra}$. As shown in Fig.3, in the end-face mode, μ increased from 0.025 to 0.14 as L was increased. However, in the reciprocating mode, μ rapidly increased from 0.06 to 0.12 at the start of friction. Even if L was increased to 144 m, μ remained nearly constant at 0.12 without obvious change.

The wear resistance of PVA-H/Water in the reciprocating mode was clearly lesser than that in the end-face mode. We concluded that the tribological characteristics of PVA-H/Water paired with the cartilage are altered by the friction modes. The loading of the alternate friction force enhances microvoids. A repeated loading can convert these voids into micro-cracks. Therefore, these results suggest the necessity for improving the fatigue and settling resistance of PVA-H/Water, particularly for decreased wear damage in reciprocating friction.

REFERENCES

1. Ushio K. *et al.*, J Biomed Mater Res. 68B: 325–329, 2004.
2. Morimoto K. *et al.*, IFMBE Proceedings 43: 714-717, 2014. : This work was supported by JSPS KAKENHI Grant Number 24500533.

Comparison of Inverse-opal and Salt-leached Silk Fibroin Scaffolds for Bone Tissue Engineering

Marianne Sommer^{1*}, Jolanda Vetsch², Jessica Leemann¹, Ralph Müller², Sandra Hofmann^{2,3,4} and André Studart¹

¹Complex Materials, Department of Materials, ETH Zurich, Switzerland, marianne.sommer@mat.ethz.ch

²Institute for Biomechanics, Department of Health Science and Technology, ETH Zurich, Switzerland

³Orthopaedic Biomechanics, Department of Biomedical Engineering, TU Eindhoven, Netherlands

⁴Institute for Complex Molecular Systems, TU Eindhoven, Netherlands

INTRODUCTION

Silk fibroin scaffolds for bone tissue engineering can be produced by porogen-leaching, lyophilisation or gas foaming^{1,2,3}. For the first approach, individually tunable pore and interconnection size can be achieved for scaffolds templated by porogens produced by microfluidics, known as inverse opals⁴. The homogeneous architecture of inverse opals has been shown to impact not only cell distribution and diffusion of macromolecules throughout the construct but also differentiation of preosteoblastic cells⁵. In this work, silk fibroin scaffolds exhibiting an inverse-opal structure were developed and compared to others fabricated by the conventional salt-leaching method in terms of performance in bone tissue engineering.

EXPERIMENTAL METHODS

Monodisperse polycaprolactone particles were produced in a microfluidic device by creating droplets of a polycaprolactone solution in water and subsequently slowly evaporating the solvent. After washing and assembling them into a close-packed lattice, a heat treatment was conducted to induce necking between the particles. The particle pack was then infiltrated with an aqueous silk fibroin solution. Upon complete evaporation of the water, the porogen particles were dissolved.

Salt-leached scaffolds were produced using table salt particles as porogens, as reported elsewhere¹.

The scaffolds were seeded with human mesenchymal stem cells and cultured in osteogenic and control medium as described elsewhere¹. Control groups of scaffolds cultured without cells were also investigated.

Scaffolds were characterized after 2, 4 and 6 weeks in culture. The amount of DNA was measured using a PicoGreen DNA assay (n=4). Alkaline phosphatase activity was quantified by measuring the conversion of p-nitrophenolphosphate to p-nitrophenol (n=4) and the degree of mineralization was measured using a calcium assay based on o-cresolphthalein (n=4). Statistical analysis was done by ANOVA, pairwise student's t-test, where applicable, with a posthoc Bonferroni correction.

RESULTS AND DISCUSSION

Increased calcium deposition per scaffold (1761 ± 390 vs. $3275 \pm 662 \mu\text{g}$; $p < 0.01$) was observed for the inverse-opal scaffolds (Figure 2), even though no statistical difference in cell number was observed (Figure 1). This increase might have arisen from differences in pore monodispersity, pore interconnectivity and/or pore wall stiffness.

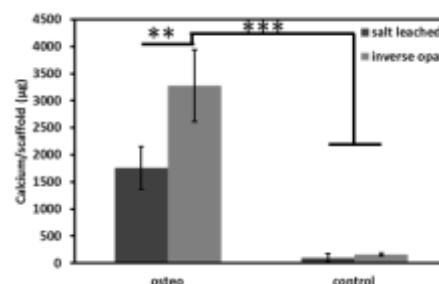


Figure 1: Calcium content measured per scaffold after 6 weeks in culture for salt-leached and inverse-opal scaffolds cultured in osteogenic or control medium.

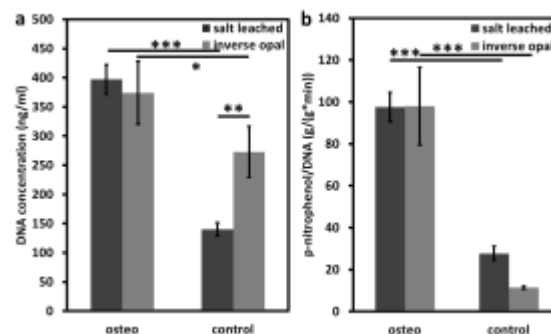


Figure 2: (a) DNA content measured on scaffolds after 2 weeks in culture in osteogenic and control medium. (b) Conversion of p-nitrophenolphosphate to p-nitrophenol by ALP after 6 weeks in culture in osteogenic or control medium for both scaffold types.

CONCLUSION

Similar cell number as well as ALP activity indicating osteogenic differentiation was measured on both scaffold types. Inverse opal scaffolds mineralize significantly more than salt-leached scaffolds.

REFERENCES

- Hofmann S. *et al.*, Biomater. 28:1152, 2007
- Hofmann S. *et al.*, J. Pharma Biopharma, 85:119, 2013
- Nazarov R. *et al.*, Biomacromol, 5:718, 2004
- Zhang YS *et al.*, Macromol. Rapid Commun, 34 :485, 2013
- Choi SW *et al.*, Langmuir, 26(24) :19001, 2010

ACKNOWLEDGMENTS

The authors would like to thank Trudel Inc for providing silk cocoons. The research leading to these results has received funding from the European Union's Seventh Framework Programme (FP/2007-2013) / EU Project No. FP7-NMP-2010-LARGE-4: 262948 and grant agreement No. PCIG13-GA-2013-618603.

Towards Biocompatible Medical Devices: Modification of Polymer and Metal Surfaces

J. Buchholz¹, C. Hess², A. Kirschning¹, L. Möller¹, M. Pflaum², S. Schmeckebeier², M. Stiesch³, B. Wiegmann², A. Winkel³, G. Dräger^{1*}

¹Institute of Organic Chemistry, Gottfried Wilhelm Leibniz Universität Hannover, Schneiderberg 1B, 30167 Hannover, Germany

²Leibniz Research Laboratories for Biotechnology and Artificial Organs (LEBAO), Hannover Medical School, Carl-Neuberg-Str. 1, 30625 Hannover, Germany

³Klinik für Zahnärztliche Prothetik und Biomedizinische Werkstoffkunde im Zentrum für Zahn-, Mund- und Kieferheilkunde, Hannover Medical School, Carl-Neuberg-Strasse 1, 30625 Hannover
jessica.buchholz@oci.uni-hannover.de

INTRODUCTION

One major problem with medical devices is the fact that surrounding tissue is not able to recognize the artificial surface as tissue like material. In case of blood oxygenators, this can induce blood coagulation which leads to blocking of the surface and inhibition of gas exchange.^[1] For metal implants such as pacemakers, incomplete tissue integration frequently promotes infection and additionally leads to implant migration.^[2]

RESULTS AND DISCUSSION

To prevent these problems, we are going to modify and humanize the surface. One approach is to covalently attach RGD-peptides to the implant surface promoting cellular adhesion and allowing the integration of the device in the tissue. The RGD-modified blood oxygenator can be seeded with lung endothelia cells which stealth the surface from the blood stream.

In a first step the activation of surfaces is performed with open-air plasma. This technology enables the chemical derivatization of surfaces in increasing wettability or introducing reactive groups.^[3] Linked to a PEG spacer it is possible to bind an oxanorbornadiene to the surface. With this system the ligation of azide-labelled RGD-peptides or other azide containing active component is performed in a copper-free "Click"-reaction.^[4]

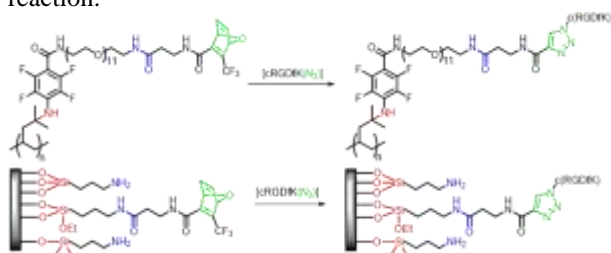


Figure 1: Attachment of RGD to polymer and metal surface

An alternative approach to bind specific proteins to the surface is followed using the high affinity of biotin to streptavidin. A biotinylated surface will allow the immobilization a variety of Strep-tagged proteins.^[5]

CONCLUSION

In order to prepare new materials for medical devices the plasma technology enables chemical reactions on biomedical surfaces, like polymers or metals. Functionalization with adhesion factors based on RGD it will be possible to seed cells on surfaces. Avoiding of a copper-mediated click reaction reduces the hazard of remaining toxic compounds on the surface.

The biological evaluation showed that this approach leads to a dense cell layer. New approaches are tested to varify the applications of this method.

REFERENCES

- [1] C. Hess, B. Wiegmann, A. N. Maurer, P. Fischer, L. Möller, U. Martin, A. Hilfiker, A. Haverich, S. Fischer Tissue Eng. Part A 2010, 16, 3043-3053.
- [2] H. A. Sabati, R. G. Menon, M. M. Maddali, J. Valliattu Journal of Medical Case Reports 2008, 2, 163-167.
- [3] L. Möller, Christian Hess, Jiří Paleček, Yi Su, Axel Haverich, Andreas Kirschning, Gerald Dräger Beilst. J. Org. Chem. 2013, 9, 270-277.
- [4] S. S. van Berkel, A. J. Dirks, M. F. Debets, F. L. van Delft, J. J. L. M. Cornelissen, R. J. M. Nolte, F. P. J. T. Rutjes, ChemBioChem 2007, 8, 1504-1508
- [5] (a) T. Schmidt, A. Skerra Nature Protocolls 2007, 1528-1535. (b) D.E.Hyre, I. Le Trong, E.A. Merritt, J.F. Eccleston, N.M. Green, R.E. Stenkamp, P.S. Stayton, Protein Sci.2006,459-467.

ACKNOWLEDGMENTS

The authors would like to thank the Deutsche Forschungsgemeinschaft (DFG, German Research Foundation) for funding the Cluster of Excellence REBIRTH (From Regenerative Biology to Reconstructive Therapy) and thus providing financial support to this project.

Evaluation of network and pore morphology of self-assembling peptides for biomimetic therapy

Franziska Koch¹ and Uwe Piesles¹

¹ICB/Nanotechnology, University of Applied Sciences, Muttensz (CH), franziska.koch@fhnw.ch

INTRODUCTION

Beside caries, periodontitis is nowadays a very common degenerative disease that affect adolescents and young adults. It is characterized by a microbial alteration which leads to a painful inflammation resulting in the degradation of alveolar bone, root cementum and periodontal ligament. If the progressive destruction of these three different tissues, named above, left untreated, it could lead to tooth lost.

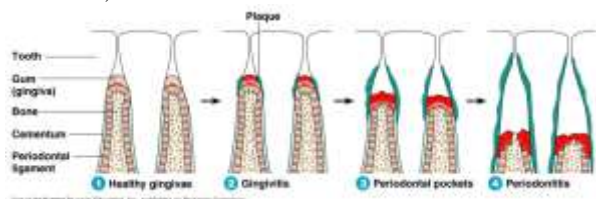


Figure 1: The development process of periodontitis.

Currently, there are a lot of different treatment options like conventional invasive open flap debridement, mechanical anti-infective therapies and bone replacement grafts¹. In the last years the idea came up to use self-repair mechanism in the patient and stimulate host's innate capacity². This treatment strategy uses different kinds of material which were placed in a periodontal defect where progenitor/stem cells from neighbouring tissues can be recruited for in situ regeneration. In the present study newly synthesized peptides were produced to form hydrogels which could be applied through an injection in a periodontal defect without a surgery. The peptides, called P11-4 and P11-8, consist of 11 amino acids which could be triggered via pH and salt concentration to form beta-sheet structures³. Furthermore these beta sheet structures could form higher ordered structures like fibrils and fibres leading to a 3D network that serve as extracellular matrix (ECM).

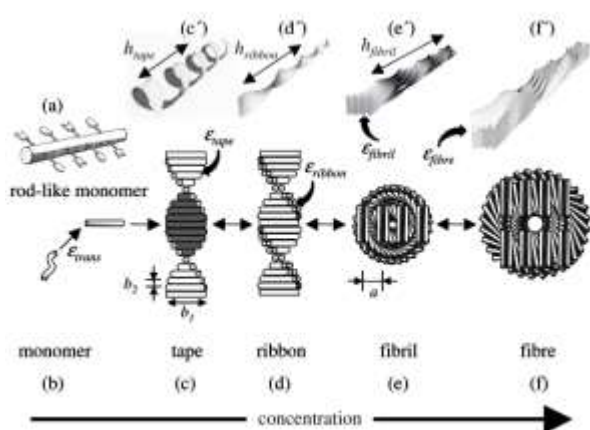


Figure 2: Model of hierarchical self-assembly of chiral rod-like units⁴

EXPERIMENTAL METHODS

The purpose of the present study was to investigate the morphology of different 3D networks and its pore sizes and distribution under physiological conditions. Therefore TEM, SEM and tensiometry was used to estimate the potential of the nematic gels to recruit neighbouring cells in a periodontal defect.

RESULTS AND DISCUSSION

The results showed first that P11-4 and P11-8 were able to form higher ordered structures like fibrils under physiological conditions which could be seen in Figure 3a and 3b. In general it was demonstrated that the pore size ranged from 95 μm to 400 μm and their distribution of the 3D networks in an aqueous environment varied depending on used peptide concentration.

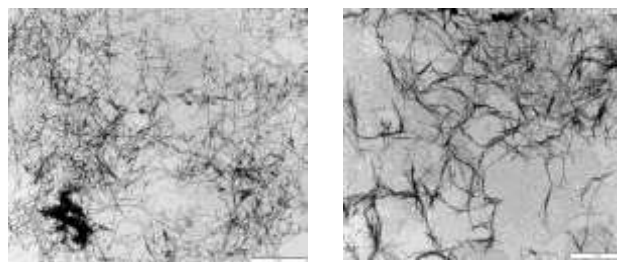


Figure 3: TEM image of a) P11-4 (20mg/ml) and b) P11-8 (20 mg/ml) Magnification 7000 x

It is known from Murphy & O'Brien 2010 that ultimately scaffolds should have a balanced distribution of pore sizes between 95 μm and 325 μm . The pore size is deciding if improved cell attachment is occurring, (optimal pore size range 95 μm to 150 μm), or cell migration (optimal pore size range 300 μm to 800 μm) or also to improve diffusion of nutrients in and waste products out of the scaffold⁴. Therefore the porous structure of self-assembled P11-4/8 peptides are beneficial candidates for tissue engineering as they show an optimal pore size distribution at concentration of 20 mg/ml for in vitro experiments.

CONCLUSION

The full potential of the peptides to act as a self-repair scaffold in the containment of periodontitis is still under investigation.

REFERENCES

- ¹ L. Shue et al. (2012) in *Biomatter* 2:4, 271 – 277
- ² F.M. Chen et al. (2010) in *Biomaterials* 31 (2010) 7892 e 7927
- ³ A. Aggeli et al. (2003) in *J. AM. CHEM. SOC.* 2003,125, 9619 – 9628
- ⁴ A. Aggeli et al. (2001) in *PNAS* vol.98 no.21, 11857–11862
- ⁵ C. Murphy & F.J. O'Brien (2010) in *Cell Adhesion & Migration* 4:3, 377-381

Morphological Gradients for Protein-Adsorption and Blood-Interaction Studies

Rebecca P. Huber^{1,2}, Katharina Maniura-Weber², Nicholas D. Spencer¹

¹Laboratory for Surface Science and Technology, Department of Materials, ETH Zurich, Switzerland

²Laboratory for Materials-Biology Interactions, Empa, St. Gallen, Switzerland, rebecca.huber@mat.ethz.ch

INTRODUCTION

To investigate the influence of a surface parameter on a given process, working with individual samples requires many repetitions with the challenge of maintaining the experimental conditions constant. This approach is laborious and cost-ineffective. Roughness gradients are a very promising tool to investigate the effect of surface topography on a biological system, as a wide range of parameters can be explored in a single experiment. Additionally, homogenous conditions are ensured during all measurements^{5,6}.

The success of a surgical implant is dependent on an appropriate biological response to the implant surface¹. Wound healing around implants is a complex process in which water molecules from the surrounding blood first come in contact with the surface. In the next step, ions and blood proteins adsorb and a fibrin network is formed, before osteoblastic cells respond to the protein-covered surface².

Blood protein adsorption and blood coagulation are greatly influenced by the topography of titanium surfaces^{3,4}, which may further impact the eventual adhesion, migration and differentiation of primary human osteogenic cells on a titanium implant. It is therefore of major importance for implantology to understand the early interaction between blood and the implant and how this further steers osseointegration.

EXPERIMENTAL METHODS

To study the effect of nano-roughness on protein adsorption and blood coagulation, nanoparticle density gradients were fabricated (see Fig. 1a)). A flat silicon wafer was first rendered positively charged with a coating of poly(ethylene imine), and then slowly immersed into a highly diluted silica-particle suspension, to generate a linear particle-density gradient on the surface. The gradient was subsequently heat-treated at 1050 °C to sinter the particles to the surface. In order to mimic the surface of implants, the samples were sputter coated with titanium. Finally, the gradients were exposed to fluorescently labelled albumin, fibrinogen or fibronectin. To achieve an easy and rapid data read-out, a fluorescence micro-array scanner was used to map all adsorbed proteins.

In a second step, the same gradients were used to study blood coagulation by incubation of the gradients for 2 to 10 min with partially heparinized (0.5 IU/ml) whole human blood from healthy volunteers. The formation of the blood clot was investigated by scanning electron microscopy and fluorescence microscopy.

RESULTS AND DISCUSSION

Particles of different sizes were tested, with diameters of 12, 39 and 72 nm. The protein-adsorption experiments showed no significant influence of nano-features on protein adsorption for all sizes of nanoparticle investigated.

In Figure 1 b) SEM images along a 39 nm nanoparticle density gradient following a 5 min blood-incubation experiment are presented. It is clearly visible that the appearance of the blood clot changes along the particle-density gradient. While coagulation was observed everywhere on the sample, a denser fibrin network could be detected towards the high-density end of the gradient. Such a fibrin network is of importance for further healing of the wound, as well as for cell adhesion and differentiation.



Fig. 1: SEM images taken every mm along the 39 nm nanoparticle density gradient. a) Gradient before blood incubation. b) Gradient after incubation for 5 min in whole human blood.

CONCLUSION

Nanostructures were shown to enhance blood coagulation, but appear to have no significant influence on protein adsorption from solutions.

This study suggests that implant surfaces with a high-density nanostructure show improved blood clot formation and should therefore enhance osseointegration.

REFERENCES

1. C.J. Wilson et al., Tissue engineering 11, Nr. 1/2 (2005): 1-18
2. B. Kasemo, Surface Science 500 (2002): 656-677
3. M.S. Lord et al, Nano Today 5, Nr.1 (2010): 66-78
4. Hong J et al, Biomaterials 20 (1999): 603-11.
5. S. Morgenthaler et al., Soft Matter 4 (2008): 419-434.
6. C. Zink et al, Biomaterials 33 (2012): 8055-8061

ACKNOWLEDGMENTS

We would like to thank the Scientific Center for Optical and Electron Microscopy of ETH Zurich (ScopeM) for their skillful SEM support The Swiss National Science Foundation (SNF, Grant no: CR31I3_146468) is gratefully acknowledged for funding.

An Innovative Intraocular Lens Surface Functionalization to Control Posterior Capsular Opacification

Yi-Shiang Huang^{1,2}, Virginie Bertrand¹, Dimitriya Bozukova³, Christophe Pagnoulle³, Edwin De Pauw¹, Marie-Claire De Pauw-Gillet¹, and Marie-Christine Durrieu²

¹Mass Spectrometry Laboratory, Department of Chemistry and Mammalian Cell Culture Laboratory, Department of Biomedical and Preclinical Sciences – GIGA R, University of Liège, Liège, Belgium

²CBMN UMR5248, Institut Européen de Chimie et Biologie, University of Bordeaux I, Pessac, France

³PhysIOL, Liège, Belgium

pokerface1031@gmail.com

INTRODUCTION

Posterior capsular opacification (PCO) is the fibrous capsule developed onto the implanted intraocular lens (IOL) by the transformed lens epithelial cells (LEC). Literature has shown that the incidence of PCO in hydrophilic acrylic IOL is much higher than hydrophobic IOL¹. Our previous study shows the adhesion of LEC is more favoured onto the hydrophobic than the hydrophilic materials². By combining these two facts, we propose a strategy of surface functionalization to promote LEC adhesion to control PCO.

EXPERIMENTAL METHODS

The RGD (Arg-Gly-Asp) peptide is grafted onto the conventional hydrophilic acrylic polymer, mainly composed by pHEMA (Poly(2-hydroxyethyl methacrylate)), using oxygen plasma followed by crosslinker coupling. After a cleaning procedure to remove the physical adsorbed peptides, the polymer samples were examined for the cytotoxicity, optical and mechanical properties as well as the ability to attract porcine LEC attachment.

RESULTS AND DISCUSSION

The surface functionalized surface exhibits enhanced biological properties in cell adhesion and cell morphology maintenance, which are similar to the hydrophobic material control (Fig. 1). In addition, there is no adverse feature observed in cytotoxicity (Fig. 2), optical (Fig. 3) and mechanical properties (Table 1).

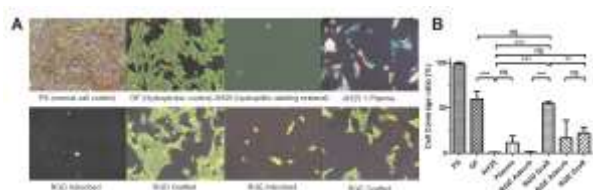


Figure 1 shows that LEC attachment enhanced by RGD peptide grafting to the level of hydrophobic material control. In addition, the spatial distribution and cell morphology are similar.

Figure 2 (next column, left) shows that the cell viabilities in the extracted medium from the surface functionalized materials are all above the 70%, the non-cytotoxicity definition by ISO 10993-5 (2009).

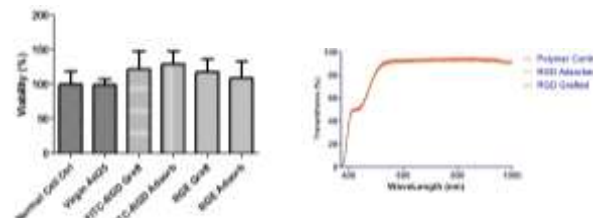


Figure 3 (upper right) shows that the light transmittances of the surface functionalized materials are unaltered. All the materials appear clear yellow for the “blue filtering” design from the manufacturer.

Sample	Diopter	Injector	Optic damage	Haptic damage	Injection force (N)
Virgin IOL	19.0-22.0	Accuject 2.2 – 1P	N	N	13,87
RGD Adorbed	19.0-22.0	Accuject 2.2 – 1P	N	N	14,41
RGD Grafted	19.0-22.0	Accuject 2.2 – 1P	N	N	13,64

Table 1 shows that the intraocular lens injection forces remain similar after the RGD peptide surface functionalization. No optic and haptic damage was observed.

CONCLUSION

With the enhanced attachment to the surface functionalized IOL material, the LEC could form a thin layer to reconstitute the physiological condition as it in nature lens. This is corresponding to the proposal of PCO development control³. In addition, the cells share similar spatial distribution and cell morphology to the hydrophobic material control, implying less chance to be transformed. On the other land, the surface functionalization keeps the original material properties for the ophthalmological implantation. Therefore, we conclude the surface functionalized IOL has the potential to control PCO.

REFERENCES

- Bozukova D. *et al.*, Mater. Sci. Eng. R-Rep. 69(6): 63-83, 2010
- Bertrand V. *et al.*, J Cataract Refract Surg. (In press, 2014)
- Linnola R. *et al.*, J Cataract Refract Surg., 10: 1539–42, 1997

ACKNOWLEDGMENTS

The authors would like to thank the Walloon region, Belgium (Project LINOLA, no: 1117465) for providing financial support to this research.

Optical Projection Tomography as a Tool for Visualizing Hydrogels Microstructures

A. M. Soto,^{1,4} J. Koivisto,^{2,3,4} J. E. Parraga,^{2,4} J. Silva-Correia,^{5,6} J. M. Oliveira,^{5,6}
R. L. Reis,^{5,6} M. Kellomäki,^{2,4} J. Hyttinen,^{1,4} E. Figueiras,^{1,4}

¹Computational Biophysics and Imaging Group, ELT Dept., Tampere University of Technology Finland,

²Laboratory for Biomaterials and Tissue Engineering Group, ELT Dept., Tampere University of Technology Finland,

³Heart Group, University of Tampere, Finland,

⁴BioMediTech - Institute of Biosciences and Medical Technology, Finland,

⁵3Bs- Research Group, Biomaterials, Biodegradables and Biomimetics, University of Minho, Guimarães, Portugal

⁶ICVS/3B's - PT Government Associate Laboratory, Braga/Guimarães, Portugal
ana.sotodelacruz@tut.fi

INTRODUCTION

Optical Projection Tomography (OPT), is a non-destructive 3D imaging technique, where a suspended specimen, immersed in an index-matching liquid, is rotated and an image is taken at each orientation. The 3D volume of the samples can be reconstructed using back projection algorithm [1].

Hydrogels are transparent biomaterials with a refractive index close to the refractive index of water. This reduces light reflection and scattering in hydrogels in a water solution, enabling OPT imaging without using optical clearing treatments. These optical characteristics enables the use of OPT to image the 3D microstructures of hydrogels and for *in vivo* OPT imaging of tissue engineered (TE) samples based on hydrogels. Here we present preliminary results of OPT imaging of different Gellan Gum (GG) hydrogels. Projections and 3D hydrogels reconstructions are shown and the statistical properties of the images are analysed.

EXPERIMENTAL METHODS

Four different hydrogels with physical crosslinking [*e.g.* monovalent cations or spermine (SPM)], different crosslinker quantities and chemical modifications with methacrylate (MA), and one hydrogel with combination of chemical and physical crosslinking, were imaged: (1) GG-MA 2% UV photocrosslinker, (2) GG-MA 2% ionic crosslinker, (3) GG 2% ionic crosslinker [2], (4) GG 1.1% ionic crosslinker (SPM) and (5) GG 0.6% ionic crosslinker (SPM). The hydrogels were inserted into fluorinated ethylene propylene tubes and submerged in water. Images were taken with a 5X objective, providing resolution of 3µm, around 360° at steps of 0.9 degree. 3D reconstructions were computed with back projection algorithm. Statistical information, as kurtosis (a measure of the shape of the probability distribution of the image histogram) and entropy (a measure of the randomness of the pixels intensities), were calculated from the projections and reconstructed slices in four samples of each hydrogel type.

RESULTS AND DISCUSSION

The projections and 3D reconstruction of hydrogels (1) and (5) are presented in Fig. 1 and 2. The microstructures of the hydrogels are visually different. These may be related with the properties of the hydrogels as density, viscosity and homogeneity.

Table 1 shows the mean values of the kurtosis and entropy, in the projections and 3D reconstructions, from each type of hydrogel. The hydrogels that present higher visual density of microstructures (hydrogels (1) and (2)) have lower values of kurtosis and higher values

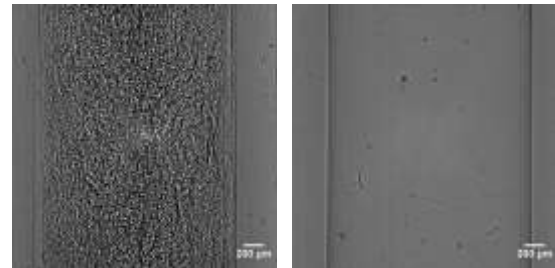


Figure 1: OPT projections of (a) GG-MA 2% UV photocrosslinker and (b) GG 0.6 % ionic crosslinker (SPM) hydrogels.

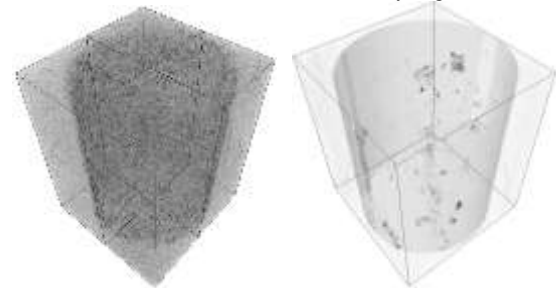


Figure 2: OPT 3D reconstructions of (a) GG-MA 2% UV photocrosslinker and (b) GG 0.6 % ionic crosslinker (SPM) hydrogels.

of entropy while the opposite happens for the transparent hydrogels (hydrogels (3), (4) and (5)). High kurtosis values are related with a more homogeneous pixels intensities distribution in transparent hydrogels while high entropy is related with a more random intensity distribution in high density hydrogels.

Table 1. Kurtosis and entropy values for the projections and reconstructions of (1) GG-MA 2% UV photocrosslinker, (2) GG-MA 2% ionic crosslinker, (3) GG 2% ionic crosslinker, (4) GG 1.1% ionic crosslinker (SPM), (5) GG 0.6 % ionic crosslinker (SPM) hydrogels. Mean Value \pm Standard Deviation

	Projections		Reconstruction	
	Kurtosis	Entropy	Kurtosis	Entropy
1	4.9 \pm 0.20	5.8 \pm 0.04	3.7 \pm 0.08	5.48 \pm 0.1
2	5.3 \pm 0.2	5.7 \pm 0.05	3.6 \pm 0.07	5.75 \pm 0.0
3	7.3 \pm 1.2	5.0 \pm 0.33	114.7 \pm 99.2	2.94 \pm 0.5
4	8.7 \pm 3.2	4.7 \pm 0.27	43.1 \pm 7.9	2.52 \pm 0.4
5	35.4 \pm 11.8	3.7 \pm 0.09	202.2 \pm 65.5	1.24 \pm 0.3

CONCLUSION

We have shown that OPT is a suitable tool for imaging hydrogel microstructure and that statistical data, such as kurtosis and entropy, could be used to characterize hydrogels according to their optical properties.

REFERENCES

- [1] Sharpe, J. *et al.*, Science. 296, 2002
- [2] Silva-Correia J, *et al.*, J Tissue Eng Regen Med 5, 2011

ACKNOWLEDGMENTS

We want to thank to Tekes and Finnish Cultural Foundation for supporting this work.



Adsorption Profiles of Inflammatory Cytokines by Activated Carbon Beads and Monoliths for Haemoperfusion

Alma Akhmetova¹, Sergey Mikhailovsky², Timur Saliev¹, Talgat Nurgozhin¹

¹*Department of Translational Medicine, Longevity and Global Health/Center for Life Sciences, Nazarbayev University, Kazakhstan

²School of Pharmacy and Biomolecular Sciences, University of Brighton, UK, alma.akhmetova@nu.edu.kz

INTRODUCTION

Kidney diseases affect millions of people worldwide. The incidence of kidney diseases is rising by almost 8% every year interdependently to its main causes: diabetes and high blood pressure. The chronic condition of the kidney illness eventually leads to the end stage renal disease (ESRD). The best treatment option in such a case is renal replacement. However, due to the high cost of the procedure the majority of the world population cannot afford it. Therefore, dialysis is considered as a cheaper alternative treatment. Dialysis is a life sustaining therapy for patients who progress to ESRD and do not receive a transplant. Despite the relatively high cost of dialysis patient survival remains poor. Current dialysis systems remove small, water soluble metabolites but fail to remove significant amounts of higher molecular weight and protein bound uraemic toxins whose retention is the most damaging. To address this problem, we are developing an alternative extracorporeal treatment using adsorption principle by activated carbon as the main clearing process.

EXPERIMENTAL METHODS

Activated carbon (AC) materials both beads and monolithic columns were assessed for their ability to adsorb inflammatory molecules from blood in a circulating system. The materials studied included AC granules from Norit (Netherlands) and MAST Carbon (UK) monoliths prepared from phenyl-formaldehyde resin precursors. These materials were assessed for their adsorptive capacity for a range of biological toxins in a recirculation system using fresh frozen human plasma to mimic the process of haemoperfusion in the clinic. An enzyme linked immunoadsorbent assay (ELISA) was used to determine the concentration of the proinflammatory cytokines, tumor necrosis factor (TNF), interleukin-6 (IL-6) and IL-8 (BD Biosciences) in the plasma samples.

RESULTS AND DISCUSSION

TNF, IL-6 and IL-8 cytokines were chosen because of a size range of molecules over which adsorption by the carbons can be assessed. All three cytokines were effectively removed from the solution and blood plasma. Figure 1 demonstrates results of adsorption of cytokine IL-8 over time. It is clearly seen that activated carbon particles from Norit with pore sizes between 4-100 μm effectively remove cytokines from the solution within 24 hours. Adsorption of cytokines was directly proportional to the time of incubation, where adsorption increases with increased time of incubation. IL-8 cytokine adsorption increases to 30 minutes of incubation and continues to fall after this time. In comparison to TNF, adsorption of IL-8 cytokines was

higher. This may be due to the difference in the molecular weight of cytokines, TNF is a larger molecule and thus may have a slower rate of adsorption and also may require larger pores within the carbon particle for its adsorption.

Monolith filtration/adsorption experiments to determine the adsorption capacity of the MAST carbon monoliths revealed the increasing adsorption of the cytokines TNF, IL-6 and IL-8 from blood over time up to 60 minutes of circulation. The greatest removal was measured for the smallest cytokine IL-8 with ~70% removal achieved at the 60 minute time point with ~65% removal of IL-6, whereas removal of the larger TNF molecule was less successful, reaching a maximum of 40% removal. These results followed the pattern of the adsorption by the Norit carbon particles, whereby the adsorption capacity for larger TNF molecule was lower than for the other two smaller cytokines.

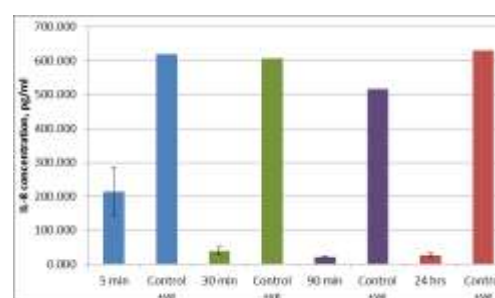


Figure 1. Levels of cytokine IL-8 remaining in the solution after incubation with activated carbon beads over time compared to the positive control (no adsorbent), (mean n=3, +/- sem).

CONCLUSION

The adsorption profile for the cytokines TNF, IL-6 and IL-8 revealed that the monoliths were able to remove clinically relevant levels from blood, although the removal of TNF was more challenging. These results suggest that using carbon monoliths as a haemoadsorption device could provide a potential therapy to treat patients with high levels of inflammatory cytokines in their systemic blood in conditions such as systemic inflammatory response syndrome and sepsis that possibly can lead to kidney dysfunction and renal failure.

ACKNOWLEDGMENTS

The project is led by the Institute for Combustion Problems, Almaty, PI Prof. Z.A. Mansurov, with participation of MAST Carbon International Ltd, Basingstoke, UK, and the University of Brighton, Dr. Carol Howell and Dr. Susi Sandeman.

Evaluation of short-term degradation of bicomponent electrospun fibres via AFM analysis

Marica Marrese, Vincenzo Guarino*, Valentina Cirillo, Luigi Ambrosio

Institute for Polymers, Composites and Biomaterials, National Research Council of Italy, Mostra D'Oltremare, Pad.20,
V.le J.F. Kennedy 54, 80125, Naples, Italy, vguarino@unina.it

INTRODUCTION

The use of atomic force microscopy (AFM) in biomaterials science and tissue engineering applications has increased quickly over the last few years. Beyond being a merely tool for characterising surface topography, AFM has made significant contributions in the understanding of the structure and properties of biomaterials surface and interfaces. Tip-sample interactions in AFM measurements provide complementary information about topography, chemical and elastic properties of any condensed matter. The aim of this study is to investigate on the chemical and morphological changes of Gelatin-rich Polycaprolactone (PCL) fibres during the degradation process in simulated culture medium by the use of Atomic Force Microscopy (AFM) in order to collect more information to better explain in vitro mechanisms of cell/fibre interaction.

EXPERIMENTAL METHODS

PCL/Gelatin fibres were successfully fabricated by using an automatic equipment (Nanon01, MECC, Japan) and then conditioned in simulated culture medium (SCM, i.e., Eagle's alpha minimum essential medium without protein serum) until 6 days. At the first stage, morphology of fibres was qualitatively investigated by Field Emission Scanning Electron Microscopy (FESEM) in low vacuum (LV). Then, morphological and structural properties were quantitatively estimated via Atomic Force Microscopy (AFM) as a function of process conditions and post-treatments in order to evaluate the effect of Gelatin degradation on the fibre architecture at different times. Tapping Mode (TM) was employed to scan electrospun fibres surface whereas AFM imaging was performed at room temperature by using a silicon cantilever probe, a resonant frequency of 320 kHz and a scan rate of 0.2 Hz. Mean fibre diameter was calculated averaging 10 measurements at different incubation times. The images of interest were first captured by AFM raster scanning and then processed using the NanoScope Analysis data processing software 1.40 (Bruker Corporation, USA).

RESULTS AND DISCUSSION

TM-AFM measurements reveal a random network of beadless fibres of untreated PCL/Gelatin electrospun membranes. Just after 1 day in SCM, changing in

topographical features can be detected onto the fibre surface due to the beginning of Gelatin loss along the fibre surface. As a consequence, a larger reduction of PCL/Gelatin fibres diameter respect to untreated ones is detected. Gelatin depletion directly affected the surface roughness (R_q), showing an increase of R_q value from (46.2 ± 5.3) nm up to (78.91 ± 15.94) nm, as the SCM treatment goes on. Recording AFM interactions between the tip and the surface, adhesion force and chemical surface changes during the treatment were detected. Since the scanned PCL/Gelatin fibres are a bicomponent polymer blend system, it has been possible to identify differences in material properties at different locations on the sample surface by AFM phase image. Phase contrast between PCL and Gelatin domains are ascribable to different sample characteristics such as sample hardness, adhesion and elasticity, with drastic changes at different times in SCM solution. Hence, these data suggest that Gelatin probably plays a complex role on the interaction with cells by modifying bioactivity and stiffness of fibres during in vitro culture.

CONCLUSION

In this study, AFM analysis has been properly set to estimate the Gelatin loss from fibre surface during SCM treatment. Results showed a progressive slowing of the hydrolytic degradation of protein which does not significantly alter fibrous structure. An increase of surface roughness as well as a decrease of fibre diameter have been detected. In this context, Gelatin release coupled with improved roughness of fibres surface should similarly occur in cell culture, positively influencing the basic mechanisms of cell adhesion and spreading, this better mimicking the real microenvironment of natural tissues.

REFERENCES

1. Guarino V. *et al.*, J. Bioactive and compatible Polymers. 26:144, 2011
2. Zhang Y. Z. *et al.*, J. Nanotechnology. 17:901-908, 2006

ACKNOWLEDGMENTS

This study was supported by MERIT, RBNE08HM7T and FIRB-NEWTON RBAP11BYNP.



Optimization of titanium foam scaffold with bioactive surface obtained by chemical treatment

Cristina Caparrós^{1,2,3}, Mónica Ortiz-Hernandez^{1,2,3}, Meritxell Molmeneu^{1,2,3}, Miquel Punset^{1,2,3},
Jose Antonio Calero⁴, F. Javier Gil^{1,2,3,*}

¹ Biomaterials, Biomechanics and Tissue Engineering Group (BIBITE), Department of Materials Science and Metallurgy, Technical University of Catalonia (UPC), Barcelona, Spain,

² Nanoengineering Research Centre (CRnE). Technical University of Catalonia (UPC), Barcelona, Spain

³ The Biomedical Research Networking Center in Bioengineering, Biomaterials and Nanomedicine (CIBER-BBN).

⁴ AMES S.A. Carretera Nacional 340, Pol. Ind. "Les Fallulles". 08620 Sant Vicenç dels Horts, Barcelona (Spain)

*francesc.xavier.gil@upc.edu

INTRODUCTION

Porous titanium had been proposed as implant materials in bone tissue engineering due to their low young modulus, their high biocompatibility and osteointegration properties. The study of the impact of different porous materials permits designing optimal porous implants due to the higher specific surface in contact with bone when compared with smooth surfaces.

Several methods had been proposed to ensure the formation of apatite in the titanium surface promoting an effective bone adhesion of an implanted titanium surface to living bone. Kokubo et al. (1) proposed a thermo-chemical method, which consist in a chemical and thermal treatment, to form a bone-like apatite layer on its surface in a simulated body fluid (SBF). For this, it is also important to evaluate how the surface composition and the porosity will influence in the cell-material interactions because of potential consequences for bone regeneration and vascularization.

The aim of this study was to investigate the effect of the bioactive treatment in novel sintered porous titanium materials for vertebrae stabilization implant. In this study, the surface of porous titanium scaffolds was compared with same material with different optimizations of typical bioactive treatments.

EXPERIMENTAL METHODS

A standard bioactive treatment consist in a chemical step of immersion of the porous samples in an aqueous NaOH solution at 60°C for 24 h, subsequent drying process at 60°C and in a thermal step by heating to 600°C for 1 h.(1).

The effect of the surface treatment was analyzed using scanning electron microscopy (SEM), TF-XRD, Optical Surface Profilometry (MI) and Raman dispersive spectrometer analysis. The apatite-forming ability of the samples was examined by soaking titanium samples in SBF and examining the homogeneity of the bioactive surface by SEM, focused ion beam (FIB) and TF-XRD.

RESULTS AND DISCUSSION

The bioactivity treatment was confirmed by the presence of titanates, over the surface and inside the pores, which will favour the apatite *in vivo* formation

(Fig.1) Different bioactive treatments were studied by TF-XRD and RAMAN techniques. Raman results suggested that the identified titanate structures will facilitate the *in vivo* apatite formation by promoting the ion interchange process for the apatite formation process, while other titanate structures are not able to induce ion interchange. The morphology and crystallinity of the obtained apatite may depend on this titanate structures.

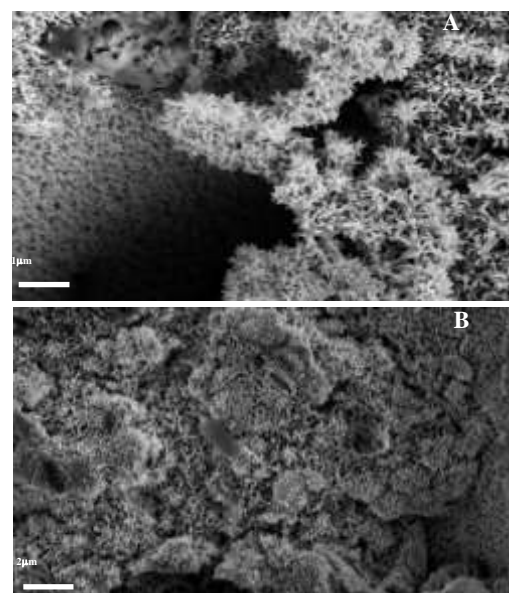


Figure. 1. SEM micrographs of the surfaces of some of the studied bioactive porous materials after immersion in SBF for 12 days. These samples were treated with different bioactive treatment conditions, A) NaOH 5M 1:1; B) NaOH 1:2.

CONCLUSION

The presented bioactive scaffolds show the beneficial effects for tissue ingrown for their use clinical use.

REFERENCES

1. T. Kokubo, S. Yamaguchi. Adv. Eng. Mat. 11 (2010) 12

ACKNOWLEDGMENTS

The authors would like to thank the UPC and CDTI project named – BioA+ for providing financial support to this project”.

Application of Central Composite Design to Evaluate the Effect of Dry-Spinning Parameters on Poly (ϵ -caprolactone) Fibers Properties

B. Azimi^{1*}, P. Nourpanah¹, M. Rabiee², M. G. Cascone³, A. Baldassare³, S. Arbab⁴, L. Lazzeri³

¹ Department of Textile Engineering, Amirkabir University of Technology, Tehran, Iran, azimiau@gmail.com

² Department of Biomedical Engineering, Amirkabir University of Technology, Tehran, Iran.

³ Department of Civil and Industrial Engineering, University of Pisa, Pisa, Italy.

⁴ ATMT Research Institute, Department of Textile Engineering, Amirkabir University of Technology, Tehran, Iran.

INTRODUCTION

Poly (ϵ -caprolactone), (PCL) has recently attracted considerable research attention notably in biomedical areas. It can be spun to fibers for subsequent fabrication of desirable textile structures. Due to excellent characteristics, such as biodegradability, biocompatibility and three-dimensional structures, PCL fibers whose diameter range from nanometer to millimeter, are broadly studied for biomedical applications such as bioresorbable constructs, drug delivery systems and tissue engineering scaffolds. Extrusion of the PCL into monofilament and multifilament may be achieved by melt spinning, solution spinning, and electrospinning. There are distinct features of each of these processes that are subsequently reflected in fiber properties. Many factors and variables can affect the ultimate properties of fibers obtained via solution spinning. In recent years, the mechanism of fiber formation and the influence of wet spinning parameters on PCL fiber properties have been studied through experimental observations [1, 2]. However knowledge on the influence of the dry - spinning parameters on the properties of PCL fibers through theoretical simulations is lacking. In this study, the effect of dry-spinning parameters including solution concentration, spinning speed and draw ratio on mechanical and morphological properties of fibers were systematically investigated using the response surface methodology (RSM).

EXPERIMENTAL METHODS

The effects of dry-spinning parameters on fiber properties were investigated applying a full-factorial Face Centered Central Composite Design (CCD) by using RSM (Design Expert 8.0.7.0, Stat-Ease, Inc., USA). The experimental range and coded levels of independent variables are presented in Table 1.

Table 1. Coded and actual levels of the design factors.

Variable	Code	Real values of the coded levels		
		-1	0	1
Concentration (wt %)	A	20	25	30
Spinning speed (cm/s)	B	3	5	7
Draw ratio	C	5	6	7

A three-factor CCD design with a total of 20 runs, including 8 factorial points, 6 axial points and 6 replicates at the center points, was used to fit a second-order response surface. Statistical significance of the model and the regression coefficients were estimated by analysis of variance (ANOVA) combined with the

application of Fisher's F-test as well as Student's T-test. The probability values (p-value) are utilized to consider the statistical significance of the determined model, with a threshold value of $p < 0.05$. The accuracy of the model was also checked by the coefficient of determination R-squared (R^2).

RESULTS AND DISCUSSION

The effect of dry-spinning parameters on mechanical and morphological properties of PCL fibers were systematically investigated using RSM. The ANOVA results indicated that the linear mass density ($\bar{\lambda}_m$) of fibers was most suitably described with a two factor interaction (2FI) model (Eq. 1).

$$\bar{\lambda}_m = +18.55 + 1.36A + 1.26B - 4.04C - 0.085AB \quad (1)$$

Statistical analysis shows that solution concentration (A) is the major factor affecting the linear density followed by draw ratio and spinning speed, respectively. Quadratic and linear models were fitted to the results of tensile strength (TS) and Young modulus (Y) respectively as following equations:

$$TS = -167.75 + 2.78A + 33.79B + 10.68C - 2.83B^2 \quad (2)$$

$$Y = -20.811 + 5.27A + 13.96B \quad (3)$$

The size and cross-sectional shape of fibers have direct effect on the surface properties of fibers. The size or diameter of fiber determines its total surface-to-volume ratio (L/A). In this study, the cross section of fibers were not completely circular therefore L/A ratio and the circularity (C) of fibers was calculated using image analysis of fiber cross section SEM images in Photoshop CS -5 software. The quadratic models were suggested to the results of L/A ratio and circularity of fibers respectively (Eq. 4, 5).

$$L/A = +0.128 - 8.23 \times 10^{-3}A + 3.35 \times 10^{-3}C + 1.37 \times 10^{-4}A^2 \quad (4)$$

$$C = -1.90 + 0.192A - 3.4 \times 10^{-3}A^2 \quad (5)$$

Statistical results show that the solution concentration (A) is the major factor affecting the L/A ratio and circularity of PCL fibers.

CONCLUSION

Response Surface Methodology (RSM) was performed to optimize the dry- spinning parameters for PCL fiber production. Different significant models obtained by Central Composite Design (CCD) are very useful for determining the optimal process parameter values for production of fibers with desirable properties.

REFERENCES

1. Puppi D. et al., Journal of tissue engineering and regenerative medicine. 5: 253–263, 2011.
2. Williamson R. et al., Biomaterials. 25: 459–465, 2004.



Gentamicin-Loaded Microparticles Immobilized on Porous Scaffolds for Prevention of Biomaterials-Related Bone Infections

Urszula Posadowska*, Malgorzata Krok-Borkowicz, Lucja Rumian, Elzbieta Pamula

*Faculty of Materials Science and Ceramics, AGH – University of Science and Technology, Krakow, Poland
uposadow@agh.edu.pl

INTRODUCTION

Surgical procedures performed on bone tissues are often accompanied by the risk of microbial infections¹. These infections frequently result in bone tissue damage, formation of treatment-resistant biofilm, or expansion of microbes to soft tissues². Microbes elimination requires application of antibiotics in high doses³. To avoid adverse effects recent studies have explored the usage of antibiotic-loaded implants⁴. Therefore, in our study we intended to produce poly(l-lactide-co-glycolide) (PLGA) micro-particles (MPs) containing gentamicin sulphate (GS) and immobilize them on PLGA scaffolds in order to produce a new type of local drug delivery system for prevention of biomaterials-related bone infections.

EXPERIMENTAL METHODS

Gentamicin sulphate (Galfarm) was encapsulated in PLGA (PLGA, 85:15, Mn=80 kDa) microspheres via double-emulsification technique. To optimize the size and solubilization properties of MPs emulsion formation in different conditions was tested. Parameters such as surfactant concentration (1%, 4% polyvinyl alcohol - PVA), amount of loaded gentamicin (2, 10, 20 mg/ 100 mg PLGA) as well as form of antibiotic (solid or dissolved) were adjusted. Solubilization properties (encapsulation efficiency and loading efficiency) and drug release from MPs were evaluated by derivatization with OPA reagent (UV-vis spectroscopy, $\lambda=332$ nm). PLGA porous scaffolds produced by solvent casting-particle leaching⁵ were pre-wetted either by UHQ-water or ethanol. MPs suspended in hydrogels (collagen type I or sodium alginate) were immobilized on the scaffolds. The effectiveness of MPs immobilization was analyzed by scanning electron microscopy (SEM).

RESULTS AND DISCUSSION

Physicochemical parameters of drug-loaded carriers highly affect drug release rate. For microparticles drug release and their presence in the extracellular space are advantageously longer than for nanoparticles⁶. Thus, our first aim was to produce micro-sized, homogenous particles characterised by good solubilization parameters. Performed studies showed that size of the MPs decreased with GS content - from 16 μ m to 3 μ m. The size did not depend on the form of drug, but loading and encapsulation efficiencies were significantly higher when GS was applied in a solid form (Fig 1, $p < 0.05$). Increase in PVA concentration resulted in improvement of MPs homogeneity. Drug release studies of MPs showed short burst release followed by prolonged release phase.

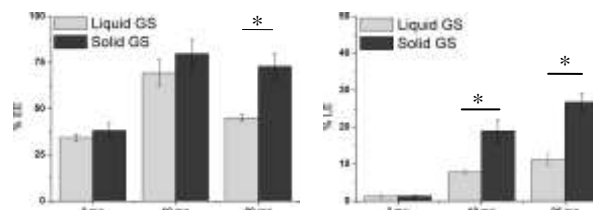


Fig 1. Encapsulation efficiency (%EE) and loading efficiency (%LE) of the microspheres with solid and liquid form of GS vs. initial drug amount (2, 10 or 20 mg / 100 mg PLGA).

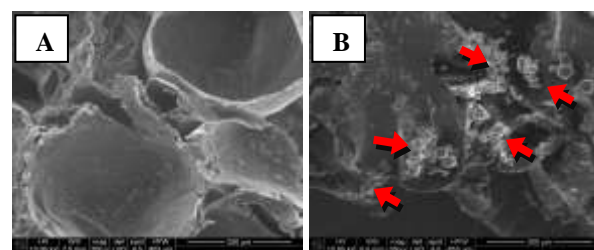


Fig 2. PLGA scaffolds microstructure (SEM) without modification (A) and with immobilized MPs in collagen type I hydrogel (B).

We detected positive effects of MPs immobilization when the scaffold were pre-wetted with ethanol, which improved PLGA hydrophilicity. Beneficial for immobilization effectiveness was when MPs were suspended in hydrogels – especially collagen (Fig 2). It can be attributed to collagen affinity to PLGA surface as already reported for PLGA scaffolds in our previous studies⁷.

CONCLUSION

We detected that immobilization of gentamicin-loaded MPs within the scaffolds was effective. Hence we may conclude that our biomaterials constitute a prospective solution in prevention of biomaterials-related bone infections.

REFERENCES

1. Clauss. M. *et al.*, Acta Biomater 6:3791-97, 2010
2. Bertazzoni E. *et al.*, Anaerobe 17(6):380-3, 2011
3. Duewelhenke N. *et al.*, Int J Surg 10:15-20, 2012
4. Diefenbeck M. *et al.*, Injury 37(2):95-104, 2006
5. Pamula E. *et al.*, J Mater Sci 19:425-435, 2008
6. Kohane D., Biotechnol Bioeng 96(2):203-9, 2007
7. Wojak-Cwik I. *et al.*, J Biomed Mater Res A 101:3109-22, 2013

ACKNOWLEDGMENTS

The authors would like to thank the National Science Centre (Grant no: 2012/05/B/ST/8/00129) for providing financial support to this project.



Investigating Mesenchymal Stem Cell Self-Renewal on Nanotopography

LCY. Lee¹, L-A. Turner¹, N. Gadegaard², S. Yarwood³, RMD. Meek⁴, MJ. Dalby¹

¹Centre for Cell Engineering, Institute of Molecular, Cell and Systems Biology, University of Glasgow, U.K.

² School of Engineering, University of Glasgow, U.K. ³Institute of Molecular, Cell and Systems Biology, University of Glasgow, U.K., ⁴ Southern General Hospital, Glasgow, U.K.

l.lee.1@research.gla.ac.uk; Lesley-Anne.Turner@glasgow.ac.uk

INTRODUCTION

Mesenchymal stem cells (MSCs) hold great potential in regenerative therapies, though low cell numbers in the body currently limits their use in clinical applications. We wish to greater understand stem cell renewal in order to promote expansion of MSCs and obtain an autologous population, which could be further differentiated into desired cell lineages. Previous work with nanoscale topographies demonstrated stimulated osteogenic differentiation of MSCs¹ or retention of multipotency² on two different nanopatterned surfaces, which provides a method to study MSC self-renewal and differentiation. We hope to determine the best conditions to promote MSC growth on nanotopography whilst retaining their multi-potentiality.

EXPERIMENTAL METHODS

MSCs were enriched from human bone marrow (adherent) mononuclear cells by magnetic activated cell sorting. MSCs were seeded onto flat (planar), a surface comprising a square lattice arrangement of pits (SQ) or a near-square arrangement incorporating an element of random distribution; $\pm 50\text{nm}$ (NSQ). Nanopits were 120nm diameter, with 300nm centre-centre spacing and 100nm depth. MSC responses to nanotopography were characterised using immunocytochemistry in conjunction with image analysis (CellProfiler) or coupled with in-cell western detection, Coomassie blue staining, scanning electron microscopy (SEM) and metabolomics. Statistical significance was assessed using paired students t-tests between two variables, with p values below 0.05 deemed significant.

RESULTS AND DISCUSSION

Optimisation of cell density was found to be important for effective use of these patterns with polycarbonate as a base material. Our optimised cell number allows for good coverage of the surface, retention of stem cell marker expression on SQ, whilst promoting a degree of clonal growth which may be important for promotion of self-renewal. Further investigation into the mechanism of self-renewal revealed changes in levels of cell cycle-related proteins between MSCs cultured on SQ and NSQ. SEM imaging showed that filopodial contact guidance was apparent on SQ in comparison to NSQ and flat (figure 1). Metabolomics identified a number of small molecules used and produced by MSCs in response to nanotopographies.

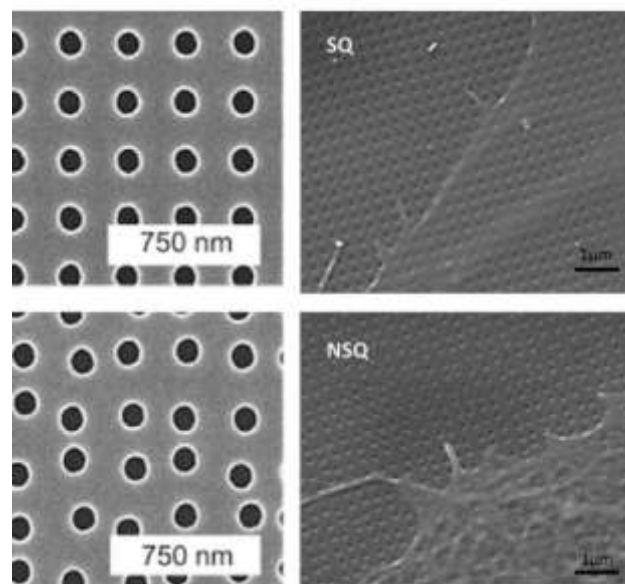


Figure 1. SEM imaging of the SQ and NSQ surfaces with representations of MSC filopodia distribution on SQ and NSQ after short-term culture (1hr). Scale bars: 750μm and 1μm as marked.

These results suggest that there is an association between physical interactions of MSCs with particular nanotopographies which parallel with differences in growth and eventual phenotype on the two surfaces.

CONCLUSION

Cell density was identified as being of key importance for effective retention of stem cell marker expression on SQ. We propose that morphological differences of MSCs on SQ in comparison to NSQ are linked to biochemical changes involved in cell cycle, and highlight a number of key metabolomic targets for maintenance of multipotency.

REFERENCES

- ¹ M. Dalby *et al.* Nature Materials. 6; 997-1003. 2007.
- ² RJ McMurray *et al.* Nature materials. 10; 637-644. 2011.

ACKNOWLEDGMENTS

LCYL is funded by an MVLS scholarship (University of Glasgow), financial provision is provided for LT by BBSRC, and MJD is funded by grants from BBSRC, EPSRC and MRC

Elastomeric Polycaprolatone scaffold for cardiovascular tissue engineering

Shraddha Thakkar¹, Anita Mol Driessen and Frank Baaijens

Soft Tissue Biomechanics & Tissue Engineering, Eindhoven University of Technology, the Netherlands
s.h.thakkar@tue.nl

INTRODUCTION

In situ tissue engineering of cardiovascular tissues is emerging as a promising approach to create living replacement by direct implantation of the scaffold *in vivo*. In this approach, the scaffolds must be able to withstand hemodynamic loads while enabling cell infiltration and tissue formation [1]. Scaffolds composed of synthetic materials have gained great attention due to ease in processing and characterization [2]. Polycaprolatone (PCL) is known for its biocompatibility, slow degradation rate and the ability to accommodate a wide variety of cells [3]. However, PCL has limited fatigue resistance and is relatively stiff, while fatigue resistance and flexibility are essential properties for cardiovascular scaffolds. We have developed multimaterial scaffolds using dual electrospinning. In this approach, a backbone polymer (BP) and fast degrading polymer (FDP) are spun simultaneously to form a multifiber scaffold. By elimination of the FDP, the void space in the scaffold is enhanced, facilitating cell infiltration [4]. Two biodegradable polymers have been investigated as BP: an elastomeric polycaprolatone (ePCL) and PCL, with polyethylene-oxide (PEO) as FDP. Scaffolds were subjected to biaxial tensile tests. Scaffold architecture (fiber diameter, porosity) before and after removal of PEO was analyzed using scanning electron microscope (SEM). ePCL results in higher porosity and fatigue resistance and less stiffness than PCL scaffolds. Further experiments to investigate cell recruitment, adhesion and differentiation should indicate which of these materials is best suitable for cardiovascular in situ tissue engineering.

EXPERIMENTAL METHODS

Scaffolds were produced by dual-electrospinning (Figure1). 14% w/w solution of PEO (Mw100,000) was prepared in chloroform was spun as FDP. 12.5% w/w ePCL or 20% w/w PCL was spun along with PEO. Biaxial tensile testing performed using 1.5N load cell. The scaffold morphology with and without PEO was analyzed using scanning electron microscope (SEM).

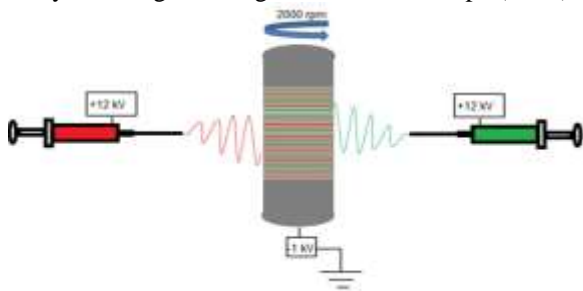


Figure 1: Dual electrospinning setup consisting of rotating target and two syringes attached to positive voltage

RESULTS AND DISCUSSION

Scaffolds were fabricated using the same spinning conditions. PCL scaffolds were thicker and stiffer in nature with fiber diameter of around 7-8.5 μm , while ePCL fiber diameter was 4-5 μm . Overnight degradation in water showed a significant decrease in weight of ePCL scaffold. Elimination of PEO enhances the void spaces, which in turn will improve cell infiltration. SEM images (Figure 2) after removal of PEO showed higher porosity in case of ePCL scaffolds compared to PCL scaffolds. Increase in porosity of the scaffold may lead to decrease in mechanical properties [5].

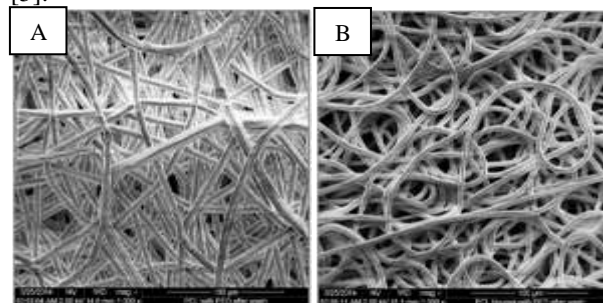


Figure 2: SEM images (1000X) of electrospun scaffolds without PEO A) PCL B) ePCL

PCL/PEO scaffolds were stiffer than ePCL/PEO scaffolds. After removal of PEO, PCL scaffolds showed a large decrease in mechanical properties, whereas ePCL scaffolds showed a minor decrease in mechanical properties and better fatigue resistance.

CONCLUSION

Scaffolds fabricated with ePCL are fatigue resistant and flexible, which are vital properties for the development of cardiovascular substitutes. Dissolution of PEO increases the porosity of the scaffold, while maintaining the overall scaffold morphology.

REFERENCES

1. Mitchell G, *procedia Engineering*, 59, 117-125, 2013
2. Filova E et al. *Physiol. Res*, 58, 141-158, 2009
3. Sohler J, et al, *Biomaterials*, 35, 1833-1844, 2014
4. Balguid et al, *TissueEng Part-A*, 15(2), 437-44, 2009
5. Tan Q. et al., *Int. J. Mol Sci.* 12, 890-904, 2011

ACKNOWLEDGMENTS

This work was supported by a grant from the Dutch government to the Netherlands Institute for Regenerative Medicine (NIRM, grant No. FES0908).

New Injectable Elastomeric Materials for Hernia Repair and their Biocompatibility *in vitro* and *in vivo*

J. Skrobot¹, L. Zair², W. Ignaczak¹, M. Ostrowski², M. El Fray^{*1}

¹ West Pomeranian University of Technology, Szczecin, Division of Biomaterials and Microbiological Technologies, Al. Piastów 45, Szczecin, Poland

²Clinic for General Surgery and Transplantology, Pomeranian Medical University, Szczecin, Poland
*mirfray@zut.edu.pl

INTRODUCTION

Polypropylene (PP) meshes are used since the 1970s, when Lichtenstein for the first time described utilizing polypropylene mesh for tension-free hernia repair [1]. Nonetheless, numerous experimental and clinical studies have revealed different problems: a typical foreign-body reaction at the interface of mesh devices, including inflammation, fibrosis, calcification, thrombosis or infection [2,3]. Recognizing the importance of the problem, we fabricated for the first time injectable polymers capable to turn into flexible materials in defected tissue cavity. These new materials are applicable in endoscopic procedures.

The present work will present the biological response *in vitro* and *in vivo* of flexible materials formed upon UV-curing of telechelic (meth)acrylic macromers comprising fatty acids [4]. In addition, we examined the potential of the injectable material for herniated tissue reinforcement and reconstruction in animal model.

EXPERIMENTAL METHODS

The basis for new injectable elastomeric materials for hernia repair were telechelic macromers end-capped with methacrylic functionalities which were synthesized according procedure described in [4] to provide UV curable systems (black light, $\lambda_{\text{peak}}=365$ nm, 2-5 min in air, 1-2% of photoinitiator IrgacureTM 819). Materials biocompatibility was assessed in *in vitro* and *in vivo* (rabbits) studies. Hydrolytic and enzymatic degradation was determined *in vitro*. Artificial hernia was created in rabbits by excision of 1 to 2 cm of muscular-fascia lobe and revealing the peritoneum. Viscous telechelic macromer was injected into hernia opening and irradiated with UV light for 5 min to create flexible film *in situ in vivo*.

RESULTS AND DISCUSSION

As we already demonstrated in earlier studies, new flexible networks fabricated from telechelic monomers are matching well the mechanical properties of the abdominal wall. The *in vitro* cytotoxicity test showed that polymer extracts caused a concentration-dependent decrease in viability of fibroblasts. The materials showed slow hydrolytic and enzymatic degradation with a mass loss of 8% after 49 days *in vitro*. The results of biocompatibility tests *in vivo* (28 days implantation) showed low level of inflammation with mostly fibroblasts, lymphocytes, and macrophages. Giant cells were not observed. Finally, hernia repair was performed by injecting the viscous macromer into

the area of the opening. After short UV-curing, the defect was closed with *in situ* polymerizing material. The visual inspection of healed tissue showed healthy tissue perfectly closing herniated tissue in a similar way as polypropylene mesh did (Fig. 1).

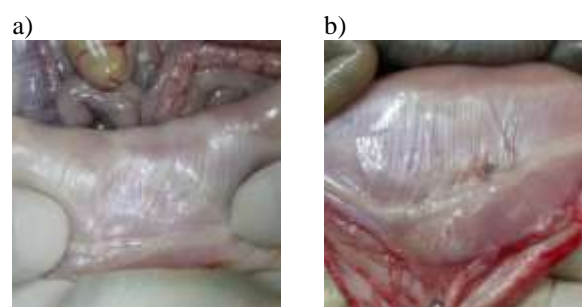


Fig. 1. Gross inspection of healed tissue after 28 days with a) injected new material, b) with PP mesh.

CONCLUSION

New injectable viscous biomaterials were fabricated. The results demonstrated that new injectable and photocurable systems can be used for minimally invasive surgical protocols in repair of small hernia defects.

REFERENCES

1. Lichtenstein IL, Shore JM. Am J Surg. 1976;132:121.
2. Klinge U, Klosterhalfen B, Muller M. Eur J Surg. 1999;165:665.
3. Falagas ME, Kasiakou SK. Clin Microbiol Infect. 2005;11:3.
4. El Fray M, Skrobot J, Bolikal D, Kohn J. React Funct Polym. 2012;72:781.

Corrosion resistance assessment of NiTi alloys in 0.9% NaCl solution

Camila Dias dos Reis Barros (Camila Barros)¹ and José Antônio da Cunha Ponciano Gomes (Ponciano Gomes)¹

¹Department of Metallurgy and Materials Engineering, Federal University of Rio de Janeiro, Brazil,
creis@metalmat.ufrj.br

INTRODUCTION

NiTi shape memory alloys are used as biomaterials because of their proprieties such as biocompatibility, good corrosion resistance and pseudoelasticity^{1,2}. The additions of ternary elements can improve the mechanical proprieties, however, changes in alloy composition can affect the corrosion resistance of these materials^{3,4,5,6,7}. This study aims to evaluate the corrosion resistance of NiTi, NiTiCo and NiTiCr alloys in 0.9% NaCl solution, and compare the results obtained.

EXPERIMENTAL METHODS

Electrochemical tests were performed such as impedance spectroscopy and anodic polarization. The corrosion potential were measured after 1h of immersion. The electrochemical impedance were performed in a frequency range within 10 kHz and 10 mHz. with 10 mV of amplitude. The anodic polarization were taken from the corrosion potential to 800mV above this in a range of 20 mv/min.

RESULTS AND DISCUSSION

The behavior of the alloys corrosion resistance were evaluated through the Nyquist diagram shown in Figure 1 and the anodic polarization curves shown in Figure 2. The results obtained though these electrochemical tests showed the good interconnection between the values of R_p (polarization resistance) and ΔE (passive range) through these curves.

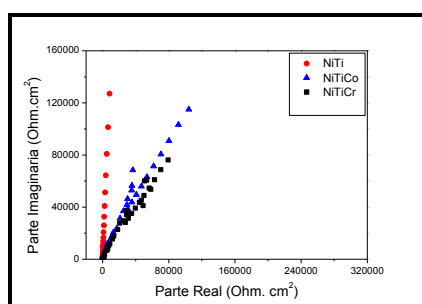


Figure 1: Impedance spectroscopy of NiTi alloys in 0.9%NaCl solution.

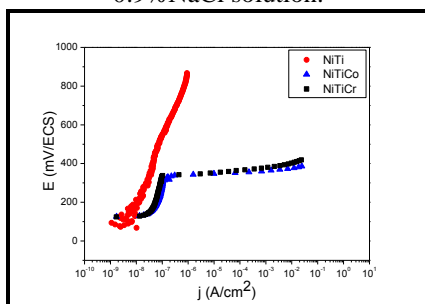


Figure 2: Anodic polarization of NiTi alloys in 0.9%NaCl solution.

The binary alloy presented the highest values of polarization resistance ternary alloys evaluated in impedance spectroscopy, while the ternary alloys showed low values of polarization resistance.

The binary alloy presented the highest values of corrosion resistance with greater passive range and without the presence of pitting, while the NiTiCo and NiTiCr alloys showed low values of pitting potential with a short passive range.

CONCLUSION

With the results obtained so far it was observed that the addition of ternary elements could implicate the corrosion resistance of the alloy, which were evidenced by the reduction of the passive range for ternary alloys compared to binary alloy that remained to be passive. Among the alloys studied, the corrosion resistance were observed in the following order: NiTi > NiTiCr > NiTiCo.

REFERENCES

1. Clarke B. *et al.*, J.Biomed. Mater.Res. A 79:61-70, 2006.
2. Shabalovskaya S. *et al.*, Acta Biomaterialia. 4: 447-467, 2008.
3. Es-Souni M. *et al.*, Biomaterials. 22:2153-2161, 2001.
4. Fasching A. *et al.*, J.Mater. Eng. and Perfomance 20: 641-645,2011.
5. Perssuad D. *et al.*, Trends Biomater. Artif. Organs. 26: 74-85, 2012.
6. Zarinejad M., Liu Y., Adv. Funct. Mater. 18:1-6, 2008.
7. Kassab E. *et al.*, Materials and Corrosion. 65: 18-22, 2014.

ACKNOWLEDGMENTS

The authors would like to thank the CNPq financial support to this project.



Supermacroporous Cryogels for Bioligand Binding

Ganesh Ingavle, Yishan Zheng, Carol Howell, Irina Savina and Susan Sandeman

Biomaterials and Medical Devices Research Group, School of Pharmacy and Biomolecular Sciences,
University of Brighton, United Kingdom, g.c.ingavle@brighton.ac.uk

INTRODUCTION

Polymeric cryogels are efficient carriers for the immobilisation of biomolecules because of their unique macroporous structure, mechanical stability and different surface chemical functionalities. Cryogels have been investigated for a number of bio-related applications, including bio-separations, bio-catalysis, chromatography, monolayer cell separation, and recently regenerative medicines [1-3]. Recently, a growing interest has been shown in using cryogels as adsorbents for diverse applications including protein purification and biomedical therapy [4-6]. The aim of the study was to demonstrate macroporous monolithic cryogel column potential in the field of biotoxin removal using covalent immobilisation of monoclonal antibodies.

EXPERIMENTAL METHODS

Cryogels with commonly used surface functional groups suitable for biomolecules immobilization such as hydroxyl and epoxy functionalities were synthesized using cryogelation technique (Fig. 1). The adsorptions of monoclonal IgG antibodies were evaluated on poly (vinyl alcohol), poly-hydroxyethyl methacrylate (HEMA-MBA), poly-hydroxyethyl methacrylate (HEMA-PEGDA) having hydroxyl functionalities and poly(acrylamide/allyl glycidyl/MBA) having epoxy functionality with immobilized protein A. The affinity ligand (protein A) was chemically coupled to the reactive hydroxyl and epoxy-derivatized monolithic cryogels and the binding efficiency of the IgG antibodies to the cryogel column were determined.



Fig. 1. Schematic showing the different steps involved in cryogel formation.

RESULTS AND DISCUSSION

The MTS and LDH assay results showed that the viability and membrane integrity of V79 cells after 24 hours of 100% and 50% cryogel extract treatments were very close to the control treatments, indicating that the cryogel extracts did not cause cytotoxic effect during

the 24 hours exposure time. Optimum binding capacities, 92.7 and 122.4 mg/g of adsorbent (cryogel), for protein A and IgG, respectively were observed in AAm/AGE/MBA cryogel as shown in Table 1. Our results show differences in the binding capacity of protein A as well as IgG to the cryogel adsorbents caused by ligand concentration, flow characteristics, physical properties and morphology of surface matrices (Table 1).

Table 1. Binding capacities of cryogel towards protein-A and IgG antibodies

	Protein-A mg/g of adsorbent	IgG mg/g of adsorbent
AAM-AGE	92.7	122.4
HEMA-MBA	40.5	60.5
HEMA-PEGDA	41.9	51.2
PVA-GA	86.8	97.4

CONCLUSION

This work demonstrated that it is possible to bind specific IgG monoclonal antibodies to the supermacroporous cryogels with different functionalities. The high binding capacity towards IgG antibodies, mechanical strength, biocompatibility, flow characteristics of the cryogel adsorbents indicated potential application of these materials for bio-toxins removals.

REFERENCES

1. Plieva F. M. et al., J. Sep. Sci. 30:1657-71. 2007
2. Kumar A. et al., J. Mol. Recogn. 18:84-93, 2005
3. Hwang Y. et al., Tissue Eng. Part A. 16:3033-41, 2010
4. Bereli N. et al., J. Chrom. A. 1190:18-26, 2008
5. Baydemir G. et al., Colloids Surf. B. 68:33-8, 2009
6. Sun H. et al., J. Sep. Sci. 31:1201-6. 2008

ACKNOWLEDGMENTS

The authors would like to thank Seventh Framework Programme the People Programme, Industry-Academia Partnerships and Pathways (IAPP), Adsorbent Carbons for the Removal of Biologically Active Toxins (ACROBAT) project.

Modification of nanofiber scaffold by biologically active substances and study of biocompatibility

Mária Hnáťová¹, Monika Michliková¹, Jana Dragúňová², Dušan Bakoš¹

¹ Faculty of Chemical and Food Technology, Slovak University of Technology, Bratislava, Slovakia

² Department of Burns and Reconstructive Surgery, Faculty of Medicine, Comenius University, Bratislava, Slovakia
maria.hnatova@stuba.sk, monika.michlikova@stuba.sk

INTRODUCTION

Nanofibres are currently one of the most intensively studied materials for applications in biomedical areas [1]. In order to apply nanofibres for biomedical use, it is convenient to modify their surface chemically and physically with bioactive molecules [2]. Therefore, potential toxic effects of modified biomaterials is necessary to determine as well. Developing new biomaterials based on nanofibres, any degree of toxicity are not suitable for further study.

EXPERIMENTAL METHODS

In this study the scaffold composed of nanofiber web – polyurethane (PUs) deposited on polypropylene textile substrate by electrospinning process was used.

In the first step, low-temperature plasma treatment in the atmosphere of air was applied to modify the surface of polyurethane nanofiber web. The scaffolds were subsequently modified with solution of berberine chloride (BRB) and solution of 0.5% chitosane containing β -cyclodextrine (CH/ β -CD). The modified scaffolds were prepared by dipping scaffolds, immediately after plasma treatment, to the solutions, drying them at room temperature and afterwards rinsing in distilled water.

Both human dermal fibroblasts and mouse fibroblasts (3T3 NIH) were used for “in vitro” biocompatibility tests - assay contact toxicity and MTT assay.

RESULTS AND DISCUSSION

The initial results indicated that after the process of modification the weight of scaffold increases to approx. 20%, although after rinsing in distilled water this increase was reduced to approx. 5%.

Results of ATR-IR spectroscopic determination of the modified scaffolds confirmed the presence of absorption bands related to the presence of modified ingredients (BRB, CH/ β -CD).

Toxic effect was evaluated visually by using microscopic observation and by counting the number of 3T3 and DF cells in corresponding parallel experiments.

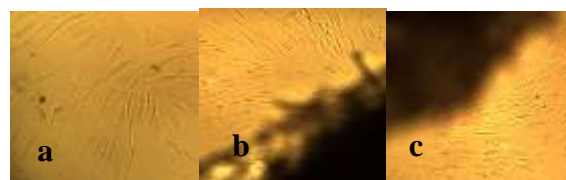


Fig. 1: Evaluation of toxic effects of scaffolds on DF cells by microscopic observation: **a**, DF cell control **b**, PUs-BRB **c**, PUs-CH/ β -CD



Fig. 2: Evaluation of toxic effects of scaffolds on 3T3 cells by microscopic observation: **d**, 3T3 cell control **e**, PUs-BRB **f**, PUs-CH/ β -CD

The microscopic observation did not show the toxicity of modified scaffolds. Cells in the contact with scaffolds PUs - BRB and PUs-CH/ β -CD (Fig. 1b-c, Fig. 2 e-f) were grown without visible changes comparable with the cell DF and 3T3 control (Fig. 1 a, Fig. 2 d).

Eluates of tested nanofiber webs were used for MTT test. Using MTT assay, we found that several day eluates prepared from modified scaffolds did not show toxic effects.

CONCLUSION

Experiments performed on both cell systems show that the modified scaffolds are not toxic. In the future it will be necessary to perform further analyses which clearly will demonstrate that the modified scaffolds are suitable for further use in the biomedical field.

REFERENCES

1. Širc, J. *et al.*, Journal of Nanomaterials, p.14, 2012
2. Yoo, H. S. *et al.*, Advanced Drug Delivery Reviews 61, p. 1033–1042, 2009

ACKNOWLEDGMENTS

This work was supported by the project grant of Slovak Ministry of Education Nr. 1/0584/10.

Pre-clinical Evaluation of Additive Manufactured Surfaces for Orthopaedic Applications

Grace Stevenson¹, John Haycock², Sarrawat Rehman¹, James Hunt³ and Edward Draper¹

¹JRI Orthopaedics Ltd, Sheffield, UK

²Centre for Biomaterials & Tissue Engineering, University of Sheffield, UK

³Mercury Centre, University of Sheffield, UK
grace.stevenson@jri-ltd.co.uk

INTRODUCTION

Cementless fixation of orthopaedic implants was introduced in the 1970s, and is the favoured method of fixation for younger, active patients¹. Cementless fixation can be achieved by bone ingrowth into porous metallic coatings prepared from sintered beads, bonded fibre metal mesh or plasma sprayed titanium². However, such surfaces are only available as coatings which can be prone to delamination and cracking which can lead to implant loosening¹. Additive manufacturing technologies, e.g. electron beam melting (EBM), are of great interest for orthopaedic applications, as they enable the manufacture of surfaces which mimic trabecular bone structure³. Such surfaces are impossible to produce via traditional manufacturing routes. Using EBM, parts are built up layer by layer from a CAD design, and solid implants with a porous surface can be created in one manufacturing step, therefore reducing the delamination issues associated with coatings³. Biological evaluation is a key step in assessing the suitability of surfaces prepared by new technologies for orthopaedic applications. The aim of this work was to carry out pre-clinical assessment of surfaces produced by EBM technology using primary human osteoblast culture, and cutting edge 3D confocal imaging to capture the shape and adhesion of the cells to the surfaces throughout the lattice structures.

EXPERIMENTAL METHODS

Titanium alloy (Ti6Al4V-ELI) discs (12 mm diameter x 9 mm depth) with a solid base and upper porous lattice structure were prepared by EBM (ARCAM S12 EBM machine). Lattices were prepared with two truss lengths (1.5 mm and 2.5 mm) to evaluate the effect of pore size. Scanning electron microscopy (SEM) and 3D profilometry were used to assess the morphology of the surfaces. *In vitro* bone cell response to the surfaces was investigated using commercially sourced primary human osteoblast (HOB) cells. Cell viability was examined using MTT absorbance, and cell shape, adhesion and calcium deposition on test surfaces were examined using 3D confocal microscopy and immunolabelling.

RESULTS AND DISCUSSION

SEM imaging showed clear differences in overall morphology between lattices with 1.5 mm and 2.5 mm truss lengths (Figure 1). Biological testing showed a significant difference (* $P < 0.05$ by Student's t-test) in cell viability between the 1.5 mm and 2.5 mm lattice structures, indicating that the lattice parameters had an effect on cell activity. 3D confocal microscopy enabled imaging of cells throughout the lattice structures, with

cells clearly observed along lattice trusses (Figure 2). Mineralised nodule formation was observed indicating that cells may subsequently lay down bone on these surfaces.

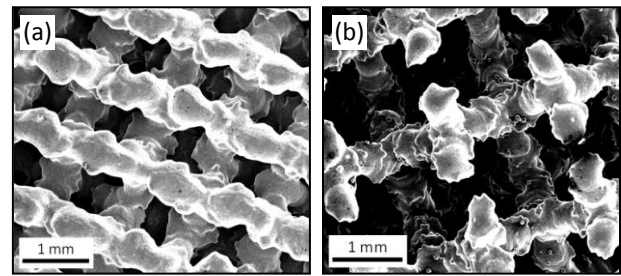


Figure 1 SEM micrographs of EBM lattice structures with truss length of a) 1.5 mm and b) 2.5 mm

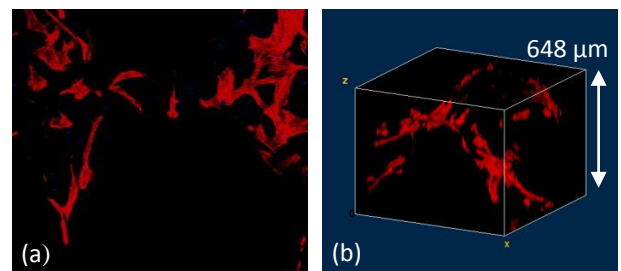


Figure 2 a) 2D and b) 3D confocal images of primary human osteoblast cells immunolabelled with phalloidin-TRITC to show actin filament distribution across an EBM lattice structure.

CONCLUSION

Additive manufacture technologies offer unique opportunities to create new surfaces for orthopaedic applications. This work demonstrates that human bone cells respond favourably to surfaces manufactured by EBM technology; however the lattice parameters used, e.g. truss length, can significantly affect cell response. It is essential that cells are able to penetrate through the lattice structures and adhere to the surfaces to enable bone ingrowth.

REFERENCES

1. Murr, L.E. *et al*; Int. J. Biomaterials; 2012; 245727
2. Levine, B.; Adv. Eng. Mater.; 2008; 10(9); 788-92
3. Biemond, J.E. *et al*; J. Mat. Sci. Mat. Med.; 2013; 24; 745-53

ACKNOWLEDGMENTS

The authors would like to acknowledge funding from the Technology Strategy Board, JRI Orthopaedics Ltd, EPSRC, BBSRC and Department of Health through the Knowledge Transfer Partnership scheme.

Central Venous Catheters Functionalised with Chlorhexidine-Hexametaphosphate Nanoparticles for Prolonged Anti-Biofilm Efficacy

Helena Grady^{1*,2}, Sarah Maddocks³, Rachel Dommett⁴, Rikke Meyer⁵, Mira Okshevsky⁵, Andrew Collins¹, Sameer Rahatekar⁶, Michele Barbour².

^{1*}Bristol Centre for Functional Nanomaterials, University of Bristol (UoB), UK, helena.grady@bristol.ac.uk

²Oral Nanoscience, UoB, UK, ³Cardiff School of Health Sciences, Cardiff Metropolitan University, UK,

⁴Clinical Sciences, UoB, UK, ⁵iNANO, Aarhus University, Denmark, ⁶Aerospace Engineering, UoB, UK

INTRODUCTION

Central Venous Catheters (CVCs) are essential in the treatment of critically ill and immunocompromised patients. However, they are associated with high rates of nosocomial bloodstream infection, with significantly higher incident rates among patients requiring long-term venous access.¹ Due to increasing concern regarding antibiotic resistance, there is a considerable drive to design and fabricate new antimicrobial CVC surfaces, to reduce initial colonisation by microorganisms and eventual biofilm formation without the need for conventional antibiotics.

Chlorhexidine (CHX) is well known for its broad-spectrum antimicrobial efficacy. Due to its mechanism of action, based on bacterial cell membrane disruption and subsequent intracellular leakage, CHX is thought less likely than antibiotics to promote the development of bacterial resistance. The purpose of this study is to investigate the antimicrobial efficacy of recently reported CHX-hexametaphosphate nanoparticles (CHX-NPs)² against methicillin-resistant *Staphylococcus aureus* (MRSA), *Pseudomonas aeruginosa* and *Escherichia coli*, for the development of an antimicrobial polyurethane (PU) CVC with long-lasting anti-biofilm efficacy.

EXPERIMENTAL METHODS

Nanoparticle synthesis: 5 and 50 mM CHX-NP suspensions were prepared by mixing a 1:1 ratio of aqueous CHX: aqueous HMP, at room temperature and pressure.²

Antimicrobial efficacy of CHX-NPs: Antimicrobial efficacy was investigated using total viable counts (TVC), time-kill kinetics, bacterial viability assays combined with Confocal Scanning Laser Microscopy (CSLM) and Scanning Electron Microscopy (SEM). For TVC and bacterial viability assays, CHX-NP functionalised specimens were inoculated with 1/100 dilution of a pre-culture of bacteria. CHX-NP solutions were inoculated with each microorganism for time-kill kinetic studies and subsequent TVCs were performed at 0, 30, 60, 90 and 120 min time points. MRSA, *P. aeruginosa* and *E. coli* were treated with 5 and 50 mM CHX-NPs for 0, 15 and 30 min for SEM.

RESULTS AND DISCUSSION

Live/Dead bacterial viability assays (Figure 1) indicated that 5 and 50 mM CHX-NPs prevented biofilm formation of MRSA, *P. aeruginosa* and *E. coli*. 5 mM CHX-NP time-kill kinetics demonstrated a pattern of bacteriostatic activity against MRSA and *P. aeruginosa*. *E. coli* showed a decrease in viable counts consistent

with bactericidal activity, defined as a reduction of $\geq 3 \log_{10}$ (99.9% killing) of the total count of CFU/ml.³

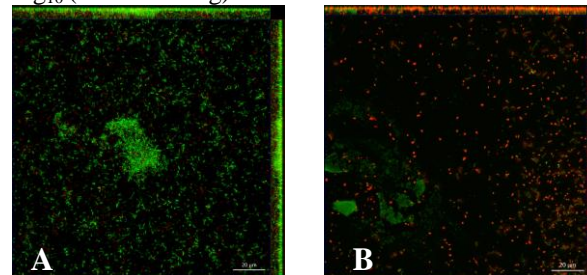


Figure 1. Maximum intensity projections of CSLM Live/Dead image stacks of untreated (A) and treated (B) *P. aeruginosa* with 5 mM CHX-NPs. Scale bars 20 µm ($Z = 7.815 \mu\text{m}$ (A) and $4.926 \mu\text{m}$ (B)).

After 15 min exposure to CHX-NPs, significant biofilm disruption was observed and cells showed surface irregularities, suggesting cell membrane disruption. After 30 min exposure, damaged bacterial cells were observed with cellular debris, thus suggesting cell lysis (Figure 2).

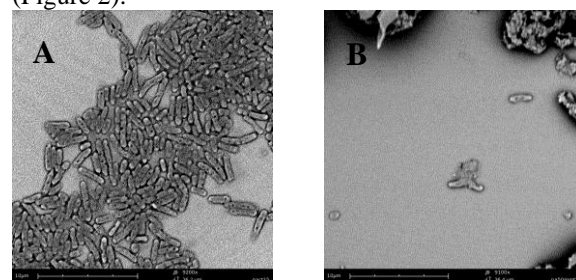


Figure 2. *P. aeruginosa* (A) untreated after 15 min and (B) treated with 50 mM CHX-NPs after 30 min. Scale bars 10 µm.

CONCLUSION

5 and 50 mM CHX-NPs prevented biofilm formation of MRSA, *P. aeruginosa* and *E. coli*. The bactericidal and bacteriostatic effects of CHX-NPs are thought to be mediated by cell membrane disruption. These findings suggest that the incorporation of novel antimicrobial CHX-NPs into a PU CVC may provide a promising new approach to the prevention of catheter-related infections.

REFERENCES

1. Fong, N. *et al.*, Acta Biomater. 6: 2554–2561, 2010.
2. Barbour, M. *et al.*, Int. J. Nanomedicine. 8: 3507–3519, 2013.
3. Petersen, P. J. *et al.*, Diagn. Microbiol. Infect. Dis. 59: 347–349, 2007.

ACKNOWLEDGMENTS

The authors would like to thank the BCFN and EPSRC for funding this project.

Preliminary data on sol-gel silicate glasses containing magnesium and zinc for dental tissue regeneration

G. Theodorou¹, E. Kontonasaki², L. Papadopoulou³, N. Kantiranis³, G. Zachariades⁴, O.M. Goudouri⁵, A. R. Boccaccini⁵, K.M. Paraskevopoulos¹, P. Koidis²

¹Department of Physics, ²Department of Fixed Prosthodontics, School of Dentistry, ³Department of Geology,

⁴Department of Chemistry,

Aristotle University of Thessaloniki, 54124 Thessaloniki, Greece

⁵Department of Materials Science and Engineering, Institute of Biomaterials, University of Erlangen-Nuremberg, Cauerstrasse 6, Erlangen 91058, Germany, gtheodo@physics.auth.gr

INTRODUCTION

As new three-dimensional materials for hard tissue replacement are needed in a variety of biomedical treatment approaches, artificial scaffolds are promising mainly due to their ability to support cell attachment, proliferation and differentiation¹. These 3D structures should exhibit biocompatibility, a high level of interconnected porous structure and pore size along with the necessary mechanical strength.

Several inorganic materials have been used for this purpose such as silicate bioactive glasses². Their ionic dissolution products can stimulate expression of several genes of osteoblastic cells³, stimulate angiogenesis⁴ and present antibacterial^{5, 6} effects, while ion release from Mg or Zn containing bioactive glasses can stimulate tissue formation⁷ and significantly enhance the proliferation and differentiation of mesenchymal cells. Therefore, tailoring bioactive glasses to meet the needs of dental tissue morphogenesis and regeneration could provide scaffolds containing elements like Mg and Zn.

EXPERIMENTAL METHODS

Two sol-gel derived glass-ceramic compositions were synthesized as shown in table 1, while a Zn-free Mg-based sol-gel bioactive glass was used as control⁸.

a/a	SiO ₂ (% wt)	CaO (% wt)	MgO (% wt)	ZnO (% wt)
60S10M	60	30	10	---
60S7M2Z	60	30	7.5	2.5
60S10M2Z	60	27.5	30	2.5

Sol-gel derived bioactive glasses were produced as described in literature⁹ and then the glasses were pulverized in a hydraulic press and sieved to particle size under 40µm. The sieved powders of the bioactive glasses were then soaked in SBF solution for various immersion times. The characterization of the samples before and after immersion in SBF was conducted using Fourier Transform Infrared (FTIR) Spectroscopy using a Perkin-Elmer Spectrometer Spectrum 1000 in MIR region, Scanning Electron microscopy with associated energy dispersive spectroscopic analysis (SEM-EDS) and X-Ray Diffractometry (XRD) using a Philips (PW1710) diffractometer with Ni-filtered CuKα wave radiation. Inductively Coupled Plasma Atomic Emission Spectroscopy (ICP-AES) was used for the measurement of the ionic concentration of the SBF solution before and after the soaking time.

RESULTS AND DISCUSSION

The synthesized bioactive glasses revealed the characteristic FTIR bands of silicate glasses¹⁰. The main characteristics of both spectrums are the broad band at ~1100 cm⁻¹ assigned to the Si-O stretching mode and a band at 490 cm⁻¹ assigned to the Si-O-Si bending one. The XRD patterns of all compositions reveal high amount of an amorphous glassy phase prior to SBF immersion.

After immersion, the identification of an amorphous Ca/P phase was revealed on the surface of the samples, by both FTIR spectra and XRD patterns after 3-10 days, depending on the composition. Zn-based bioactive glasses exhibited identical behavior. EDS analysis confirms this finding, whereas ICP-AES reveals the ionic variations during immersion time.

CONCLUSION

Sol-gel derived silicate glasses containing Mg and Zn were synthesized. Bioactivity evaluation revealed the formation of a Ca/P phase on the surface of the samples. Further work is needed to investigate their potential application in scaffolds synthesis for dental tissue regeneration.

REFERENCES

1. Bellucci D. *et al.*, Biocer. Devel. and App. 1, 2011.
2. Hoppe A. *et al.*, Biomat. 32: 2757-2774, 2011
3. Xynos ID. *et al.*, J. Biomed. Mater. Res. 55(2): 151-157, 2001.
4. Gorustovich AA. *et al.*, Tissue Eng. Part B Rev, 2009.
5. Jones J. *et al.*, J. Mater. Sci. Mater. Med. 17(11): 989-996, 2006.
6. Day RM. *et al.*, J. Biomed. Mater. Res. A. 73A (1):73-79, 2005.
7. Yamaguchi M. *et al.*, J. Trace Elem. Exp. Med. 11(2-3):119-135, 1998.
8. Goudouri OM, *et al.*, Key Engin. Mat. 493/494: 884-889, 2012.
9. Zhong J. *et al.*, J. Biomed. Mater. Res. 53: 694-701, 2000.
10. Kontonasaki E. *et al.*, Cryst. Res. Technol. 37: 1165 2002.

ACKNOWLEDGMENTS

This study was conducted under the action Excellence II (Project: 5105) and funded by the European Social Fund (ESF), the European Union (EU) and National Resource



Material-driven fibronectin networks: modulating the degree of fibrillogenesis

Hayk Mnatsakanyan¹, Aarón Maturana Candelas¹, Alexandre Rodrigo-Navarro¹, Patricia Rico^{1,2}, José Antonio Gómez Tejedor¹, Manuel Salmerón-Sánchez³, Roser Sabater i Serra^{1*}

^{1*}Center for Biomaterials and Tissue Engineering, Universitat Politècnica de València, Spain, rsabater@die.upv.es

²Biomedical Research Networking Centre (CIBER), Spain

³Division of Biomedical Engineering, School of Engineering, University of Glasgow, United Kingdom

INTRODUCTION

It has been recently shown that fibronectin (FN) is able to self-assemble into physiological-like (nano)networks in poly(ethyl acrylate) (PEA) in the absence of cells; i.e. as a consequence of the protein-material interaction, leading to the so-called material-driven FN fibrillogenesis¹. Interactions between chemical groups of PEA surface and FN molecules during the adsorption process might induce exposure of self-assembly sites of FN to drive fibril assembly. However, this phenomenon does not occur on poly(methyl acrylate) (PMA), on which FN is adsorbed keeping the globular conformation, even if the side chain differs only one in one single carbon².

A series of samples with different EA/MA ratio were synthesised seeking to modulate the degree of FN fibrillogenesis. We have studied FN adsorption and conformation of the protein at the material surface using AFM. Then, murine C2C12 myoblast adhesion and myogenic differentiation was investigated to address the relationship with the fibrillogenesis degree at the material interface.

EXPERIMENTAL METHODS

Samples were obtained by radical polymerization of a solution of both monomers PEA/PMA with ratio 100/0, 70/30, 50/50, 30/70 and 0/100, using 1wt% of benzoin as photoinitiator. DSC, DMA and water contact angle experiments were performed to characterise the properties of the copolymers. Conformation and amount of adsorbed FN were quantified by AFM and western blot respectively using two different concentrations of FN (5 and 20 µg/ml).

Focal adhesions formation (vinculin) and cell morphology were analysed after 3 h of culture on FN-coated samples by immunofluorescence (IF). For myogenic differentiation, C2C12 cells were cultured on FN coated samples for 4 days; cell differentiation was quantified by IF against sarcomeric myosin followed by image analysis.

RESULTS AND DISCUSSION

DSC and DMA characterisation show no phase-separation in the copolymers. When the amount of methyl acrylate (MA) increases, the glass transition shifts to higher temperature and the elastic modulus at 37 °C rises from 620 to 3000 kPa. Small differences in wettability have been found ($85 \pm 6^\circ\text{C}$)

The assembly of FN on the copolymers was modulated by the EA/MA ration. Fully interconnected FN fibrils were organised upon adsorption from a solution of concentration 20 µg/mL on PEA 100. The interconnection degree among fibrils decreased as the amount of MA increases (Figure 1).

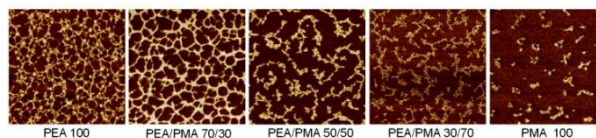


Figure 1. Material-driven FN fibrillogenesis on PEA/PMA copolymers. FN concentration 20 µg/ml and adsorption time 10 min. Phase AFM images (1µm x 1µm).

Both cell morphology and focal adhesions formation depend on the degree of fibrillogenesis attained on the different surfaces: Cell size decreases and circularity increases as the interconnection of FN is lost when the amount of MA in the system increases (Figure 2).

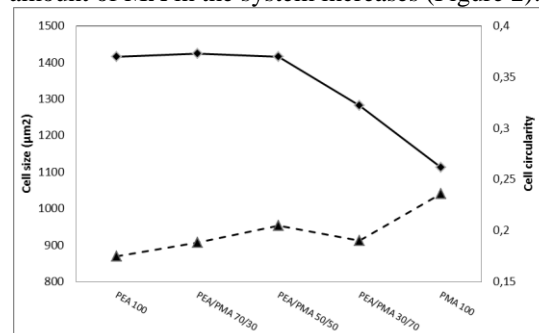


Figure 2. Cell size (♦) and circularity (▲) in C2C12 adhesion culture.

In cellular myogenic differentiation, FN-coated samples show significant differences compared to control (collagen I-coated glass) and differences between the copolymers were also found, with enhanced differentiation for samples with higher interconnected FN fibrils.

CONCLUSION

We demonstrated that the degree of fibrillogenesis can be modulated by controlling the percentage of PEA in PEA/PMA copolymers. When the amount of PEA decreases, fibrillogenesis degree decreases as well, which influences cell adhesion and differentiation.

REFERENCES

References must be numbered. Keep the same style.

1. Salmerón-Sánchez *et al.*, Biomaterials (2011), 32(8): 2099-2105
2. Brizuela Guerra N. *et al.*, Soft Matter (2010), 6:4748-4755.

ACKNOWLEDGMENTS

The support of the project MAT2012-38359-C03-01 (including the FEDER financial support) as well as CIBER is acknowledged.



Development of Biodegradable Virus and miRNA Eluting Stent Technology

Hannah Stepto^{1*}, Keith Oldroyd³, Lee Cronin², Andrew H Baker¹

^{1*}College of Medical Veterinary and Life Sciences/Institute of Cardiovascular and Medical Sciences, University of Glasgow, UK, h.steppto.1@research.gla.ac.uk.

^{2*}School of Chemistry/College of Science and Engineering, University of Glasgow, UK.

³Golden Jubilee Hospital, West of Scotland Regional Heart and Lung Centre, Glasgow, UK.

INTRODUCTION

Treatment of coronary artery disease often involves deployment of an intravascular stent to treat the culprit vessel. The main limitation of this treatment is in stent restenosis which is caused by neointimal proliferation following deployment of stents and subsequent vessel damage.¹ Stents represent a possible platform for localised delivery of therapeutic agents to target neointima formation. This has been exploited in the context of drug eluting stents (DES), although due to the lack of cell specificity of the drugs, DES have led to additional complications such as late stent thrombosis.² In this study we aimed to develop a system for coating stent materials, Stainless Steel (SS) and Poly Lactic Acid (PLA) in adenovirus 5 (Ad5) or miRNA in order to develop an effective delivery system for localised gene or miRNA based therapies.³ This will enable us to take advantage of the stents proximity to the target tissue and to explore the scope for gene/miRNA therapy for coronary heart disease.

EXPERIMENTAL METHODS

- PLA and SS used as model stent materials.
- Bovine Type I collagen (5 mg/mL) was diluted to (3mg/mL) with NaOH (1 M).
- Ad5 CMV *lacZ* (4.6×10^9 VP) or premiR 145 precursor (20 μ M, 1.5uL) incubated with SiPort Neo FX (3uL) was added to collagen and vortexed.
- Surfaces were coated with collagen solution (25 uL) and incubated at 37°C for 1 hour, RT for 1 hour.
- Surfaces were washed with PBS and placed on rat A10 smooth muscle cells and incubated for 72 hours.
- Surfaces were removed and cells were washed.
- Transduction of Ad5/miRNA from the surfaces was quantified by β -gal reporter assay/qRT-PCR.

RESULTS AND DISCUSSION

Adenovirus coated SS and PLA

After *in vitro* culture of the collagen-Ad5 coated PLA and SS discs, Ad5 was able to transduce A10 cells from both surfaces. PLA retained 71% of Ad5 administered to the gel whereas 37% was retained from the SS, this is likely to be because the collagen gel could not adhere as well to the SS surface.

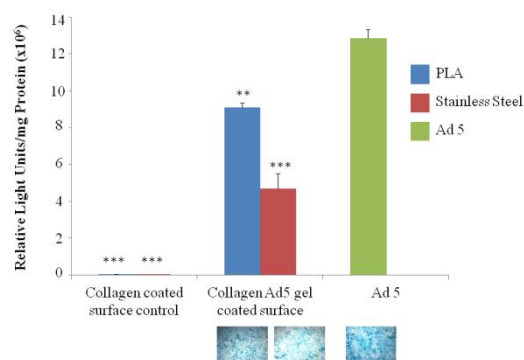


Figure 1. *In vitro* virus transduction of Ad5 from Ad5-collagen gel coated surfaces (n=3/group). β -gal activity of Ad5 transduction of A10 cells from a PLA, SS surfaces and control Ad5 in solution. A10 cells were seeded at 200,000 cells per well in a 12 well plate, and transduced at 21500 VP/cell. Error bars represent standard error of the mean of three individual samples. (**= $p < 0.01$, ***= $p < 0.001$ versus Ad5). Microscope images of the XGAL stained cultures are displayed underneath at 10x magnification.

miR145 mimic coated PLA

In vitro testing was also conducted from PLA surfaces by coating with a miR145 mimic collagen gel. After incubation of the PLA miRNA coated surfaces an upregulation by 14 fold of miR145 expression was observed. This indicates this method of coating the PLA with collagen gel is effective for encapsulation and release of miRNA in addition to Ad5.

CONCLUSION

It has been demonstrated that mixing Ad5 and miRNA with collagen prior to gel formation creates a coating which the virus and the miRNA can be eluted from into A10 cells. This method of coating is particularly suitable for PLA surfaces and therefore has scope to be applied to biodegradable PLA stents to provide localised delivery of genetic material to the vasculature.

REFERENCES

1. Dangas G. *et al.*, Circulation. **105**, p2586-2587, 2002
2. Simard T. *et al.*, Can J Cardiol. **1**, p35-45, 2014
3. Ghaderian S. *et al.*, Int J Mol Cell Med p50-57, 2013

ACKNOWLEDGMENTS

The authors would like to thank the University of Glasgow Kelvin Smith Scholarships and the British Heart Foundation for providing financial support.

Composite bone cement to improve the primary stability of orthodontic mini-screws

Alberto Lagazzo, Fabrizio Barberis, Elisabetta Finocchio, Cristian Restano, Marco Capurro
Department of Civil, Chemical and Environmental Engineering (DICCA), University of Genoa, Italy
alberto.lagazzo@unige.it

INTRODUCTION

Mini-screws are temporary anchorage devices used in orthodontic treatments¹, namely the practice of preventing and correcting irregularities of the teeth or skeletal structures. In comparison with the endosseous implants² used as fixing systems, the mini-screws do not require osseointegration and thus they can be immediately loaded, inserted and removed easily and, thank to their dimensions ($\varnothing 1.3\text{--}2.0\text{ mm}$), placed into the interradicular sites without patient compliance³. The mini-screws stability is yet strictly dependent on the cortical bone thickness and linked to the bone quality of the patient treated⁴. Others problems are the progressive decrease of their stability due to bone relaxation⁵ and a possible necrosis of the adjacent bone due to an excess of compression caused by the mini-screw⁶. In order to solving, at least partially, these inconveniences, in this work we have adopted a new method consisting in the inclusion of a composite bone cement inside a preliminary drilled hole made in the implant site.

EXPERIMENTAL METHODS

Amorphous glass fibres ($\varnothing 10\text{ }\mu\text{m}$, 5 mm in length) were introduced in a hole of 2 mm and depth 10 mm, preliminarily created with a drill in a thoracic pig rib, and then filled with a composite material prepared with powder of PMMA (20 %wt.) mixed with brushite before setting. The brushite was obtained from β -TCP, MCPM and water solution (0.5 M) of Na-citrate (s/l=2:1). The amount of glass fibres was about 10 %wt. Then two types of mini-screws (TomasTM and NovaxaTM) were manually introduced inside the hole without screwing and, after the cement setting, the samples were stored in physiological solution. The cement after the setting and the amount removed from the mini-screw surface after the pull out, at 1 week, from the hole were tested with FTIR in KBr. Primary stability was measured with a specific device used for dynamic mechanical analysis. The test, performed with an apparatus developed in the DICCA laboratory⁷, consisted in a transversal loading of the mini-screw head with a low frequency (2–5 Hz) oscillating force of 0.5 N of amplitude. By processing the time records of force and displacement via a Frequency Response Function (FRF), the complex compliance was obtained. The lower is the elastic compliance (real part) the higher is the stability of the screw.

For comparison, the same procedure was adopted to prepare and to test samples with self-tapping mini-screws directly inserted in the bone, without preliminary hole and without the use of bone cement.

RESULTS AND DISCUSSION

In Fig. 1 are represented the behaviour against the time (days) of the elastic compliance of mini-screws TomasTM and NovaxaTM, when they are directly screwed in the bone (DS) and when inserted in a pre-

hole filled with composite cement (CC). The choice of adding PMMA and glass fibres was done in order to confer more plasticity and tenacity to the brushite. FTIR spectra reveal the presence of brushite phase both at the setting and also inside the hole after 1-week storage of the sample in physiological solution.

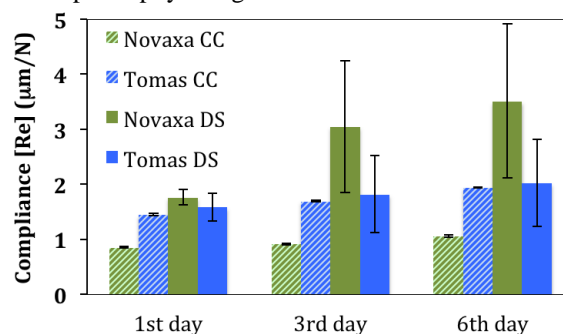


Fig. 1. Comparison of compliance of mini-screws inserted in bone with (CC) and without composite (DS).

It can be noted how, initially, the stability of the CC is very close to the one of the DS and how the CC samples maintain low values of the compliance also after one week. Moreover, a standard deviation of the stability values for CC, very lower than the one for DS, evidences a positive effect of the composite cement. As expected, the cement makes the support (bone) more homogeneous, reducing the influence of the cortical bone thickness in the stability of the mini-screws.

CONCLUSION

The use of composite cement coupled with orthodontic mini-screws to avoid inflammation and damage of the bone appeared to be encouraging. The compliance of the mini-screw are comparable with the one obtained for drilled mini-screws. Besides, no reduction of the stability after one week and a more homogeneous response of the inserting site (no effect of the cortical bone thickness) were observed.

REFERENCES

1. Mah J. *et al.* J. Clin. Orthod. 39:132–136, 2005
2. Ödman J. *et al.* Eur. J. Orthod. 10:98-105, 1988
3. Kuroda S. *et al.* Am. J. Orthod. Dentofacial Orthop. 131:9-15, 2007
4. Iijima M. *et al.* Eur. J. Orthod. 35(5):583-589, 2013
5. Tsui W. *et al.* J. Oral Maxillof. Surg. 41(11):1427-38, 2012
6. Shank S.B. *et al.* Am. J. Orthod. Dentofacial. Orthop. 141(4):412-18, 2012
7. Seminara L. *et al.* Sensor Actuat. A-Phys. 169:49-58, 2011.

ACKNOWLEDGMENTS

The authors wish to thank Marco Migliorati for the contribution given to this work during the preparation of its Ph.D. thesis.

Characteristics and Cytocompatibility of Novel Borophosphate Glasses

Chenkai Zhu¹, Ifty Ahmed¹, Xiaoling Liu¹, Andy Parsons¹, Jingsong Liu², Chris Rudd¹

¹ Division of Materials, Mechanics and Structures, Faculty of Engineering, University of Nottingham, UK,

² Sinoma Science & Technology Co., Ltd. Jiangning District, Nanjing, China,

eaxcz4@nottingham.ac.uk

INTRODUCTION

Bioresorbable phosphate-based glasses have been investigated for varying tissue engineering applications¹. The degradation rate of these glasses can be tailored by doping with varying metal ions such as Mg, Fe, Ti, and B². In this study, boron was added at varying quantities in place of phosphate. The effect of boron addition on the glass thermal properties, chemical durability and cytocompatibility was investigated.

EXPERIMENTAL METHODS

Glasses with three different compositions were produced, denoted as P48B12, P45B15 and P40B20. The thermal processing window T_{pw} (i.e. onset of crystallisation temperature T_{con} minus glass transition temperature T_g) of the glasses was investigated via Differential Thermal Analysis. The chemical durability was characterised in phosphate buffer saline at 37°C for 60 days. The cytocompatibility of the glasses was studied by culturing the human osteosarcoma cell line (MG63) directly onto the glass surface for 14 days.

RESULTS AND DISCUSSION

The thermal properties of the glasses in Table 1 revealed that T_{con} and T_c values decreased with the addition of B₂O₃, whilst only slight increases were observed for the T_g values. The thermal processing window (T_{pw}) was observed to decrease with increasing boron content, thus increased glass crystallisation tendency and reduced thermal stability³.

Table 1: thermal properties of glasses with B₂O₃ variation.

Glass code	$T_g/^\circ\text{C}$	$T_{con}/^\circ\text{C}$	$T_{pw}/^\circ\text{C}$	$T_c/^\circ\text{C}$
P48B12	545	800	255	860
P45B15	550	780	230	825
P40B20	555	750	195	770

The degradation study revealed the dissolution rate of P48B12 glass at $3.64 \times 10^{-5} \text{ kg cm}^{-2} \text{ hr}^{-1}$, which increased to $4.23 \times 10^{-5} \text{ kg cm}^{-2} \text{ hr}^{-1}$ for P45B15 and then have a further increase to $5.92 \times 10^{-5} \text{ kg cm}^{-2} \text{ hr}^{-1}$ for P40B20 (Figure 1). The decrease of chemical durability with boron addition was suggested to be due to the P₂O₅ content being replaced by B₂O₃, boron units BO₃ and BO₄ introduced into glass system while BO₃ units were not as resistance as BO₄ units⁴. For all three glasses, the metabolic activity of MG63 cell line (Figure 2) was seen to increase throughout the 14 days culture period. The metabolic activity of cells on P48B12 glasses and

P40B20 glasses were significantly close to tissue culture plastic (TCP).

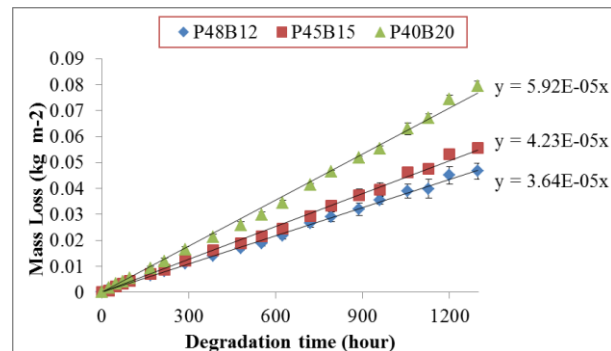


Figure 1: Weight loss vs time for glass compositions investigated.

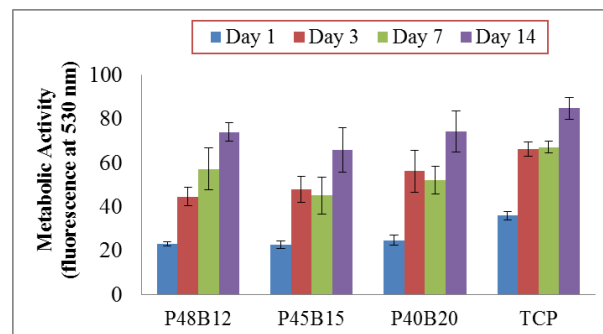


Figure 2: Metabolic activity of MG63 cells, (Alamar Blue assay).

CONCLUSIONS

Thermal stability and chemical durability of borophosphate glass decreased with the addition of boron in place of phosphate. Cell culture studies suggested all glasses produced had good cytocompatibility with the MG63 cell line.

REFERENCES

1. Ahmed I. *et al.*, JB, 25: 501-507,2004.
2. Sharmin N. *et al.*, Biomed Res Int, 2013: 1-2, 2013.
3. Massera, J., *et al.*, J Non Cryst Solids, 357: 3623–30, 2011.
4. ElBatal H. *et al.*, Mater. Chem. Phys, 110: 352-362, 2008.

ACKNOWLEDGMENTS

The author would like to thank University of Nottingham, providing Inter-Campus PhD Scholarship for this project, and Sinoma Science & Technology Co., Ltd. for technical formulation.

Gelatin/Chitosan Microspheres for a Modulated Drug Delivery System

Costantino Del Gaudio^{1*}, Valentina Crognale¹, Pierluca Galloni², Domenico Ribatti³, Alessandra Bianco¹

^{1*}Department of Enterprise Engineering, University of Rome "Tor Vergata", Italy, costantino.delgaudio@uniroma2.it

²Department of Chemical Science and Technology, University of Rome "Tor Vergata", Italy

³Department of Basic Biomedical Sciences, University of Bari, Italy

INTRODUCTION

The development of targeted drug delivery systems (DDSs) represents a valuable option to overcome the typical drawbacks associated to conventional systemic administration, which is not specifically directed to the organ or tissue to be treated. This means that the drug has to cross different biological barriers, often causing undesirable side-reactions or being partially inactivated¹. It is also well known that this approach implies fluctuating drug levels in the body, poor efficacy, and the administration of a high dose of drug to ensure that the required amount of agent eventually reaches the site of action². In addition, it is not possible to control the concentration, duration and bioavailability of bioactive substances, thus limiting the expected therapeutic outcome. On the other hand, DDSs can lead to a significant therapeutic efficacy, as the selected agent can be delivered to the target tissue in the optimal amount and in the right period of time, causing little toxicity and minimal side effects. An improved pharmacological strategy can be therefore planned, allowing a controlled and localised release of drugs, a reduction of the total amount required and a constant delivery over time. In this context, microspheres made of natural polymers, as here proposed, can be regarded as a valuable means to support this approach.

EXPERIMENTAL METHODS

Microspheres preparation

Microspheres were prepared by water-in-oil emulsion. Gelatin powder was added to distilled water, heated at 80 °C and gently stirred until complete dissolution, to produce a 10% w/v polymeric solution. In order to crosslink microspheres, genipin (1% w/v), was added to the solution that was then injected into the oil phase, preheated at 80 °C. The resultant emulsion was stirred, at the same temperature, for 1 h at 800 rpm. Microspheres were collected on a nylon filter in vacuum condition, and washed with acetone. Finally, the microspheres were air dried.

Chitosan microspheres were prepared using the same protocol with the difference that chitosan was dissolved in aqueous acetic acid solution (2% w/v). Blend microspheres were also prepared (chitosan/gelatin ratio: 1/5).

Finally, collected microspheres were loaded with methylene blue (MB).

Characterization

Morphological characterization of microspheres was performed by means of scanning electronic microscopy (SEM). The average diameter was determined from SEM micrographs (ImageJ, NIH).

In vitro MB release assays were performed by UV spectrophotometry.

CAM assay

Chicken embryo chorioallantoic membrane (CAM) assay was considered to evaluate the angiogenic properties of loaded microspheres. Microspheres were allowed to release MB in phosphate buffer saline (PBS) solution for three days at 37 °C. Treated PBS was then loaded into gelatin sponges to be placed on the CAM.

Statistics

Results are expressed as mean±standard deviation. Data analysis was performed with non-parametric tests (Kruskal-Wallis and Mann-Whitney U tests). *p* values less than 0.05 were considered significant.

RESULTS AND DISCUSSION

SEM analysis revealed homogeneous microspheres with a diameter distribution in the range 42-54 µm. Depending on the nature of the polymers here considered, the 100% MB release ranged from about 3 days (gelatin) to 30 days (chitosan) and can be correlated to the antiangiogenic properties of gelatin microspheres (CAM assay). Chitosan and blend samples were surrounded by allantoic vessels that developed radially towards the implant in a spoke-wheel pattern. This occurrence was not verified for gelatin and the control case (MB solution).

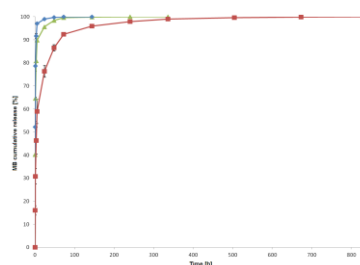


Fig. 1 –MB cumulative release from gelatin, chitosan and blend microspheres

CONCLUSION

The proposed microspheres can be a promising platform for drug delivery, allowing to modulate the expected outcome by properly selecting the polymers used for their preparation.

REFERENCES

1. Harsha S. *et al.*, Int J Pharm 380:127-32, 2009
2. Edlund U. *et al.*, Adv Polymer Sci 157:67-112, 2002

ACKNOWLEDGMENTS

This work was supported by European Project FP7-NMP-2011-SMALL-5: BIOTrachea, Biomaterials for Tracheal Replacement in Age-related Cancer via a Humanly Engineered Airway, (No. 280584-2).

Design of Multi-Component Artificial Extracellular Matrices and their Effects on Cells Relevant to Wound Healing

S. Rother¹, S. Thönes², J. Salbach-Hirsch³, S. Moeller⁴, M. Schnabelrauch⁴, U. Anderegg², L. C. Hofbauer³, V. Hintze¹, D. Scharnweber¹

¹Max Bergmann Center of Biomaterials, TU Dresden, Germany, Sandra.Rother@tu-dresden.de

²Department of Dermatology, Venereology and Allergology, Leipzig University, Germany

³Division of Endocrinology, Diabetes, and Bone Diseases, Medical Faculty, Department of Medicine III, TU Dresden, Germany

⁴Biomaterials Department, INNOVENT e.V. Jena, Germany

INTRODUCTION

The extracellular matrix (ECM) has a complex, tissue specific composition with collagen and glycosaminoglycans (GAGs) like hyaluronan (HA) being important components of skin and bone ECM. The modification of HA with sulfate groups (sHA) leads to an increased interaction with growth factors like TGF- β 1¹ and BMP-4². Collagen-based artificial ECMs (aECMs) containing high-sulfated HA support the growth of human dermal fibroblasts (dFb)³, enhance the osteogenic differentiation of human mesenchymal stromal cells⁴ and inhibit osteoclast differentiation and resorption⁵. Combining low- and high-sulfated HA derivatives and collagen type I to develop multi-component aECMs should lead to a better mimicry of the *in vivo* situation in comparison to aECMs with one GAG derivative. The purpose of this study was to engineer these aECMs and to reveal their effects on dFb and osteoclast-like cells.

EXPERIMENTAL METHODS

aECMs were prepared by *in vitro* fibrillogenesis of rat collagen type I alone or in the presence of low- (sHA1, degree of sulfation (D.S.) ~ 1, average number of sulfate groups per disaccharide repeating unit of HA) and high- (sHA4, D.S. ~ 4) sulfated HA derivatives as well as a combination of both to provide *in vivo* like ECM structures. DMMB assay, fluorescence measurement, Lowry assay and OPA assay were used to characterise the composition and release behaviour of the aECMs. Furthermore, the morphology was studied via AFM. The initial adhesion of dFb on aECMs after 60 min of incubation, their proliferation for 48 h and the viability of RAW264.7 cells after 24 h of cultivation was analysed.

RESULTS AND DISCUSSION

Design and characterisation of multi-component aECM
Using sHA1 and sHA4 with different fluorescence labels offers the possibility to distinguish between these GAGs while the DMMB assay can only determine the total GAG amount. Fig. 1 shows the composition and release behaviour of the multi-component aECMs after incubation in PBS at 37°C for up to eight days. The highest GAG release occurs during the first hour. Longer desorption in PBS results only in a slightly further decrease of GAG content. The results are in good agreement with the results of the DMMB assay. The AFM images of the aECMs reveal a decrease in fibril diameter with increased GAG concentration and sulfation as already shown for collagen type II⁶.

Effects on cells

GAG-containing aECMs show an increased adhesion and proliferation of dFb compared to the collagen reference. The proliferation of dFb and the viability of RAW264.7 cells are affected differently by the single- and multi-component-aECMs. Although previous studies revealed the ability to influence cellular behaviour by single-GAG-aECMs containing differently sulfated GAGs^{3,5}, these results show the potential of multi-component aECMs to modulate the cellular behaviour in a more defined manner allowing the precise adjustment of cellular actions.

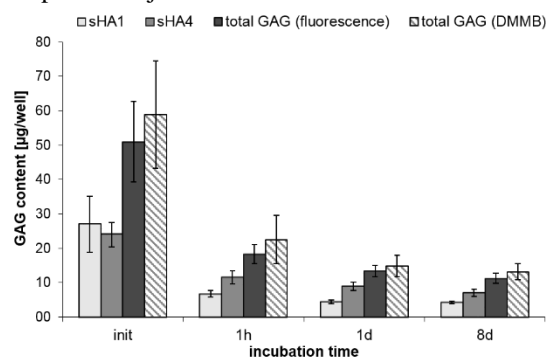


Fig. 1. Quantification of the sHA content in the multi-component aECM via fluorescence measurement and DMMB assay. Init: sHA content after two washing steps with deionized water.

CONCLUSION

GAG containing aECMs with defined physiological functions can be developed by varying their composition. These aECMs composed of collagen and sulfated HA derivatives are promising substrates for modulating the behaviour of cells relevant to wound healing.

REFERENCES

- Hintze V *et al.*, Acta Biomater. 8:2144-2152, 2012
- Hintze V *et al.*, Biomacromolecules. 10:3290-3297, 2009
- van der Smissen A *et al.*, Biomaterials. 32:8938-8946, 2011
- Hempel U *et al.*, Acta Biomater. 8:4064-4072, 2012
- Salbach J *et al.*, Biomaterials. 33:8418-8429, 2012
- Hintze V *et al.*, J. Tissue Eng. Regen. DOI: 10.1002/term.1528, 2012

ACKNOWLEDGMENTS

The authors would like to thank the German Research Foundation DFG (TRR 67; subprojects A2, A3, B2, B4) for financial support.



Nanowires on Ti-6Al-4V for Creation of Antimicrobial Orthopaedic Implant Surfaces

Terje Sjöström^{1*}, Angela Nobbs¹ and Bo Su¹

¹School of Oral & Dental Sciences, University of Bristol, UK terje.sjostrom@bristol.ac.uk

INTRODUCTION

Infection at the implant surface is one of the big challenges in biomaterial research. Reducing the risk of infection during and after surgery, without using antibiotics, would be of great benefit to both patients and the healthcare system. It has recently been suggested that nanotopographies found in nature, act as antimicrobial surfaces by physically damaging bacteria¹. By mimicking such topographies on relevant materials, it may be possible to create antimicrobial implant surfaces. In this work we have produced nanowire surfaces on Ti alloy substrates which are able to impair gram negative bacteria.

EXPERIMENTAL METHODS

Ti-6Al-4V (Ti64) samples were heated to 850°C in a tube furnace under Ar atmosphere. At the final temperature, acetone vapour was introduced at 500sccm for 45 minutes, and finally the furnace was allowed to cool under Ar. The substrates were then annealed in air at 600°C for 1h to remove carbon residue. *Pseudomonas aeruginosa* and *Staphylococcus aureus* were cultured on smooth and nanowire Ti64 surfaces at 37°C for 1h. The cells were then either stained for LIVE/DEAD and examined using fluorescence microscopy, or cultured with an alamar blue assay to examine cell viability.

RESULTS AND DISCUSSION

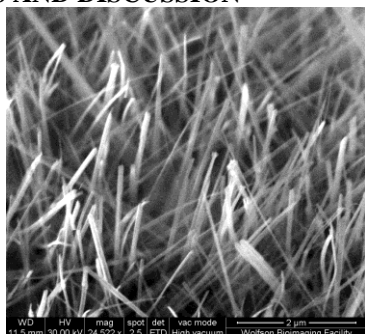


Figure 1. Side view SEM of nanowires grown on Ti64 substrate.

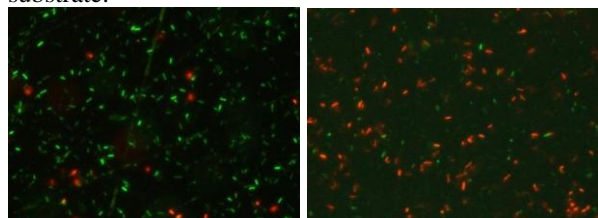


Figure 2. Microscopy images of LIVE/DEAD stained *P. aeruginosa* on smooth Ti64 (left) and nanowire Ti64 (right). Green = live cells. Red = dead cells.

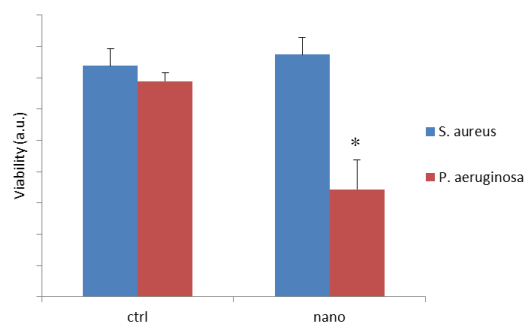


Figure 3. Cell viability measured with AlamarBlue, of *S. aureus* and *P. aeruginosa* on smooth Ti64 and nanowire Ti64. * $P < 0.05$.

Figure 1 shows the nanowires produced on the Ti64 substrates. The wires showed excellent surface coverage on both flat and 3D surfaces, were several micrometer long and terminated in sharp tips of approximately 20 nm.

Figure 2 shows that when *P. aeruginosa* were cultured on the nanowire surfaces, a large number of cells were killed, whereas on the smooth Ti64 surfaces most cells were still alive. These results were supported by the viability assay (Figure 3), displaying a 50% reduction of viable *P. aeruginosa* on the nanowire surfaces. On the other hand, *S. aureus* showed no reduction in viability on the nanowire surfaces. We presume that the same effect was not seen on the gram positive bacteria (*S. aureus*) because the thicker cell membrane of these bacteria makes them more difficult to physically rupture. This is in line with what was found for bacteria grown on nanotopographies on cicada wings¹.

CONCLUSION

Sharp nanowire features were produced on Ti64 alloys by a thermal oxidation technique. The nanowires were able to kill gram negative bacteria by physical means only. These surfaces have potential as use for antimicrobial surfaces for orthopaedic implants.

REFERENCES

- Ivanova, E.P. *et al.*, Small 8:2489-94, 2012

ACKNOWLEDGMENTS

The authors would like to acknowledge the EPSRC (Grant no: EP/K035142/1) for providing financial support to this project.

Evaluation of *In Vitro* Cytocompatibility of Alginate-Gelatin Crosslinked Hydrogels

Bapi Sarker^{1*}, Raminder Singh², Judith A. Roether³, Rainer Detsch¹, Iwona Cicha^{2,4}, and Aldo R. Boccaccini¹

¹Institute of Biomaterials, Department of Materials Science and Engineering, University of Erlangen-Nuremberg, 91058 Erlangen, Germany, *Email: bapi.sarker@ww.uni-erlangen.de

²Department of Cardiology and Angiology, University Hospital Erlangen, 91054 Erlangen, Germany

³Institute of Polymer Materials, Department of Materials Science and Engineering, University of Erlangen-Nuremberg, 91058 Erlangen, Germany

⁴Cardiovascular Nanomedicine Unit, Section of Experimental Oncology and Nanomedicine, ENT Department, University Hospital, 91054 Erlangen, Germany

INTRODUCTION

Alginate is considered an important biomaterial for regenerative medicine due to its rapid ionic gelation property with divalent cations¹. However, alginate does not promote cell adhesion and possesses slow and uncontrolled degradation kinetics². We hypothesized that these limitations of alginate could be overcome by using covalently crosslinked alginate-gelatin (ADA-GEL) hydrogel. In the current study, we seeded normal human dermal fibroblasts (NHDF) on ADA-GEL hydrogel to evaluate *in vitro* cytocompatibility.

EXPERIMENTAL METHODS

Synthesis of ADA-GEL and Preparation of Films

Alginate di-aldehyde (ADA) was synthesized by periodate oxidation of sodium alginate. ADA-GEL hydrogels of different compositions were synthesized by covalent crosslinking between ADA and gelatin, as described in detail elsewhere³. Hydrogel was cast into a Petri dish, ionically gelled by 0.1 M CaCl₂ solution and cut by punching.

Swelling and Degradation and Protein Release Study

In vitro swelling and degradation studies of ADA-GEL films were carried out in Dulbecco's modified Eagle's medium (DMEM) at 37 °C for 7 days. A protein release study of ADA-GEL films was conducted in serum free DMEM and protein concentration in the medium was determined by colorimetric protein assay.

Cell Study

NHDF were seeded on the films at a density of 85000 cells/film and incubated in a humidified atmosphere of 95% relative humidity and 5% CO₂, at 37 °C. Mitochondrial activity of NHDF grown on different hydrogel films was assessed by WST-8 assay. To assess the viability of cells, live staining was performed by Calcein AM and nuclei were visualized with DAPI. To assess the morphology of NHDF, F-actin of the cells were visualized with rhodamine phalloidin and nuclei were stained with SYTOX. Morphology of the cells was further analyzed by SEM.

RESULTS AND DISCUSSION

Swelling, Degradation and Protein Release

Initially alginate and ADA-GEL films of all compositions, except the one containing the highest amount of gelatin, exhibited similar swelling pattern. After 2 days of incubation, degradation of ADA-GEL films started and exhibited the degradation pattern corresponding to gelatin content. The result can be correlated to the release of gelatin, which remained uncrosslinked in the ADA-GEL. As expected, gelatin

release (wt%) from the ADA-GEL hydrogels was found to be very low during the incubation period of the hydrogel films in DMEM due to the covalent crosslinking of gelatin with ADA.

Cytocompatibility of ADA-GEL

As shown in Figure 1, clusters of NHDF were formed on alginate hydrogels after 7 days incubation. In contrast, a very good attachment and proliferation of cells was observed on ADA-GEL hydrogels. Moreover, mitochondrial activity of NHDF on ADA-GEL was significantly higher compared to alginate.

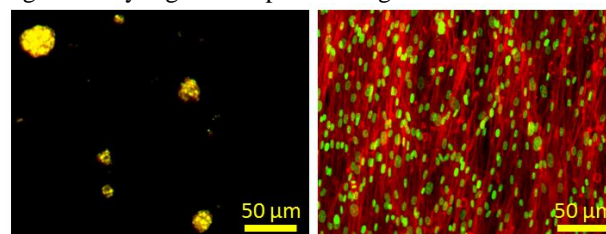


Figure 1. Fluorescent microscopy images of NHDF on alginate (left) and ADA-GEL (right) hydrogel films after 7 days of incubation. The cells were stained for actin (red) and nucleus (green).

Typical bipolar morphology of NHDF was observed on ADA-GEL. Moreover, cells arranged themselves parallel to each other on ADA-GEL, which is also a natural characteristic of NHDF.

CONCLUSION

The synthesized ADA-GEL hydrogels possess controlled degradation kinetics with minimal release of gelatin, and support stronger fibroblasts adhesion and proliferation. Therefore, it can be concluded that the major drawbacks of alginate-based hydrogels are successfully overcome with the covalently crosslinked ADA-GEL hydrogel.

REFERENCES

1. Boonthekul T. *et al.*, Biomaterials. 26: 2455-65, 2005.
2. Rowley J. *et al.*, Biomaterials 20: 45-53, 1999.
3. Sarker B *et al.*, J. Mater. Chem. B 2: 1470-82, 2014.

ACKNOWLEDGMENTS

The authors would like to thank the Emerging Fields Initiative (EFI) of the University of Erlangen-Nuremberg (project TOPbiomat) and the German Academic Exchange Service (DAAD) for providing financial support. The authors thank Prof. Dr. Michael Stürzl (Molecular and Experimental Surgery, University Hospital Erlangen) for providing NHDF cells.

Osteoblastic Differentiation Induced by Bioactive Glass-Ceramic Surfaces

E.P. Ferraz¹, P.T. de Oliveira¹, M.M. Beloti¹, M.C. Crovace², O. Peitl-Filho², A.L. Rosa¹

¹Cell Culture Laboratory, School of Dentistry of Ribeirão Preto, University of São Paulo, Brazil

²Vitreous Materials Laboratory (LAMAV), Federal University of São Carlos, Brazil

adalrosa@forp.usp.br

INTRODUCTION

The bioactive glass 45S5 favours osteoblast activities resulting in enhanced osteogenesis both in vitro and in vivo¹, but the relative poor mechanical properties restrict its use as bone substitute^{2,3}. In this context, novel full-crystallized bioactive glass-ceramics, Biosilicate[®] (Bio) and Biosilicate[®] for scaffold fabrication (Bio-sca), has been developed with better mechanical properties⁴. Considering the potential application of Bio-sca in bone tissue engineering procedures, the aim of this study was to compare the in vitro behaviour of osteoblasts at early stages of differentiation grown on 45S5, Bio and Bio-sca.

EXPERIMENTAL METHODS

Rat bone marrow cells were cultured in osteogenic medium for 5 days to obtain osteoblasts at early stages of differentiation. Then, these cells were cultured in non-osteogenic medium on 45S5, Bio and Bio-sca discs for periods of up to 17 days. Tissue culture polystyrene was used as control. Cell proliferation was evaluated by MTT assay at day 10. Osteoblastic differentiation was evaluated by colorimetric method to detect alkaline phosphatase (ALP) activity at day 10, real-time PCR to detect gene expression of runt-related transcription factor 2 (Runx2), special AT-rich sequence-binding protein 2 (SATB2), ALP, osteocalcin (OC), osteopontin (OPN) and bone sialoprotein (BSP) at day 10, and alizarin red to stain extracellular matrix mineralization at day 17. All evaluations were performed in quadruplicate (n=4) and data were compared by Kruskal-Wallis and Student-Newman-Keuls test, when appropriated. The significance level was set at p≤0.05.

RESULTS AND DISCUSSION

Cell proliferation on glass surfaces and polystyrene was similar without statistically significant differences, indicating that the glass-based biomaterials did not affect osteoblast proliferation. It was observed higher ALP activity in cells cultured on all glass surfaces compared with polystyrene without statistically significant

differences among them. Despite more mineralized matrix was observed on Bio and Bio-sca, the higher ALP activity did not result in more mineralization as noticed on 45S5. Gene expression was affected in a more complex way but all evaluated genes were more expressed in cells cultured on glass surfaces compared with polystyrene. Results are presented in Table 1.

Table 1. Cell proliferation, ALP activity and gene expression at day 10 and extracellular matrix mineralization at day 17 of cells cultured on distinct glass surfaces and polystyrene expressed as mean ± standard deviation (n=4).

Parameter	Polystyrene	45S5	Bio	Bio-sca
Proliferation	0.87±0.17 ^a	0.82±0.09 ^a	0.93±0.15 ^a	0.87±0.13 ^a
ALP activity	9.24±3.21 ^a	20.8±4.7 ^b	30.3±10.0 ^b	23.9±6.1 ^b
Runx2	1.04±0.18 ^a	5.93±1.00 ^b	4.01±1.53 ^b	3.18±1.08 ^b
SATB2	1.02±0.23 ^a	3.82±0.86 ^b	5.83±0.86 ^c	2.47±0.35 ^d
ALP	1.00±0.11 ^a	1.47±0.16 ^b	3.18±0.29 ^c	1.91±0.22 ^d
OC	1.00±0.14 ^a	93.2±14.3 ^b	68.4±15.5 ^c	20.7±4.6 ^d
OPN	1.00±0.12 ^a	13.6±0.8 ^b	7.06±0.39 ^c	4.42±0.22 ^d
BSP	1.01±0.04 ^a	26.0±2.1 ^b	63.5±4.6 ^c	16.9±0.2 ^d
Mineralization	0.05±0.01 ^a	0.01±0.01 ^b	0.11±0.08 ^c	0.18±0.18 ^c

Distinct letters indicate statistically significant differences

CONCLUSIONS

Results showed that glass-ceramic surfaces exhibit osteogenic potential. Considering that cells were cultured under non-osteogenic conditions, it is possible to suggest that these bioactive glasses are capable of inducing osteoblastic differentiation. Taken into account that Bio-sca can be fabricated as highly porous scaffolds, this glass-ceramic is a promising biomaterial for bone tissue engineering applications.

REFERENCES

1. Jones JR., Acta Biomater. 9:4457-4486, 2013.
2. Peitl-Filho O. *et al.*, Acta Biomater. 8:321-332, 2012.
3. Moura J. *et al.*, J. Biomed. Mater. Res. A. 82:545-557, 2007.
4. Kido HW. *et al.*, J. Biomed. Mater. Res. A. 101:667-673, 2013.

ACKNOWLEDGMENTS

Roger R. Fernandes and Fabiola S. Oliveira. Grants: FAPESP (# 2012/23879-5 and 2012/23525-9) and CNPq (# 305523/2013-9).

Effect of surfaces properties on bone differentiation in composite scaffolds

Vincenzo Guarino¹, Marica Marrese¹, Francesca Veronesi², Paola Torricelli^{2,3}, Monica Sandri⁴, Anna Tampieri⁴, Milena Fini^{2,3}, Luigi Ambrosio¹

¹ Institute of Polymers, Composites and Biomaterials, National Research Council of Italy, Mostra D'Oltremare, Pad.20, V.le Kennedy 54, 80125, Naples, Italy (vguarino@unina.it)

² Laboratory of Preclinical and Surgical Studies, Rizzoli Orthopaedic Institute, Via Di Barbiano 1/10, Bologna, Italy

³ Laboratory of Biocompatibility, Innovative Technologies and Advanced Therapies, Department Rizzoli RIT, Italy

⁴ CNR - Institute of Science and Technology for Ceramics (ISTEC), Via Granarolo, 64 48018 Faenza (RA) - Italy

INTRODUCTION

The osteo-inductive effects of three specific physical cues including substrate rigidity and nanotopography have been recently investigated in 2D cell culture or in 3D *in vitro* scaffolds [1]. Recent studies demonstrate that surface properties including hydrophobicity, surface charge, stiffness and roughness concur to influence specific cell materials interactions, so addressing specific features of local microenvironment in osteogenic way [2]. In this work, polycaprolactone (PCL) porous matrices processed by phase inversion/salt leaching were endowed with two types of calcium phosphates - Hydroxyapatite (HA) and Magnesium Carbonate Hydroxyapatite (MgCHA). According to recent studies [3], we suggest that inorganic phases effectively functionalize pore surfaces, promoting a better osseous tissue ingrowth towards a fully bone integration over long-term implantation. Here, we focus on correlation between *in vitro* behavior of MG63 (osteoblast-like cells) and surface properties mediated by the presence of MgCHA and HA bioactive fillers.

EXPERIMENTAL METHODS

Briefly, 0.50 g of PCL granules were dissolved in 10 ml of tetrahydrofuran (THF) and kept under magnetic stirring at room temperature for 24 h. HA and MgCHA particles were added to PCL solution before the solvent extraction to reach a volume ratio of about 3:1. To impart the required porosity to the scaffold, sodium chloride crystals - 300-500 micron sized - were also included. The size and shape of HA and MgCHA powders was analyzed by transmission electron microscopy (TEM, TECNAI120 - FEI) supported by 2D/3D image analyses. The morphological properties of the surface samples were qualitatively investigated by Scanning Electron Microscopy (FESEM, QUANTA200 - FEI) at 20kV after gold-Palladium sputter-coating and quantitatively estimated via Atomic Force Microscopy (AFM) in contact/tapping mode. MG63 cells were seeded onto HA and MgCHA cylinders (5 mm in diameter and 3 mm in width) for 3 and 7 days. At the end of experimental times, cell viability was evaluated with WST-1 test and the production of bone alkaline phosphatase (ALP), Osteocalcin (OC), Collagen type I (COL I), Transforming growth factor- β 1 (TGF- β 1) and Tumor necrosis factor- α (TNF- α) by ELISA tests.

RESULTS AND DISCUSSION

A preliminary investigation by TEM allows estimating HA and MgCHA embedded phase morphology, also calculating the elongation degree by image analysis in terms of particle aspect ratio (pAr) (e.g. width/length). pAr values equal to (0.44 ± 0.16) and (0.18 ± 0.06) for

HA and MgCHA reinforcement, indicate a higher elongation in the case of doped particles, related to the doping process conditions. Particle morphology influences the surface properties as confirmed by SEM images, in terms of roughness and surface charge, properly measured by AFM on different composite scaffolds. In particular, surfaces show a profile with a mean value of (51.7 ± 14.53) nm, (78.15 ± 32.71) nm and (136.13 ± 63.21) nm in the case of net PCL, HA and MgCHA loading samples, thus remarking the higher contribution of doped particles to roughness respect to un-doped ones. This may be ascribable to stronger constraints offered by more elongated particles to the polymer phase organization during the process. This is confirmed also by AFM phase image which allows detecting some microstructural differences in PCL matrix domains, related to different surface stiffness and elasticity which influence cell response. Despite cell viability did not present significant differences after 3 days, MG63 show higher viability after 7 days ($p < 0.005$) in the case of HA. From 3 to 7 days of culture, HAs stimulate a higher production of TGF- β 1 ($p < 0.05$) and OC ($p < 0.005$), which is also coupled to the production of the pro-inflammatory cytokine, TNF- α . Contrariwise, MgCHAs do not induce inflammatory response, but promote early osteogenic differentiation as remarked by higher ALP levels ($p < 0.005$).

CONCLUSION

Here we conclude that bioactive fillers with different chemistry and/or shape factors concur to particularize surface properties of composite scaffolds with effects on *in vitro* cell response. The set of morphological information - roughness, wettability and stiffness programmed into the scaffold surface corroborated by intrinsic bioactive cues of calcium phosphate fillers influence the osteogenic activity of MG63 as confirmed by differences in bone markers data. In comparison with HA loaded surfaces, MgCHA ones confirm a higher biomimeticity level due to the presence of Mg doped apatites which are better recognized by MG63 without production of cytokines, and promote higher ALP synthetic activity related to osteogenic differentiation.

REFERENCES

- [1] Ben P et al. 2013 Stem Cell Res & Ther 2013, 4:10
- [2] Jones J R et al, Acta Biomater. 9 4457-861. 2013
- [3] Guarino et al. J Tissue Eng Reg Med 2012 Jun 22. doi: 10.1002/term.1521

ACKNOWLEDGMENTS

TISSUENET (Grant No. RBPR05RSM2) and MERIT n. RBNE08HM7T.



Controlling Mechanical Properties of Electrospun Gelatin Scaffolds

Kaido Siimon¹, Paula Reemann², Uno Mäeorg³, Martin Järvekülg^{1,4}

¹Institute of Physics, University of Tartu, Estonia, kaido.siimon@ut.ee

²Institute of Biomedicine and Translational Medicine, University of Tartu, Estonia

³Institute of Chemistry, University of Tartu, Estonia

⁴Estonian Nanotechnology Competence Centre, Estonia

INTRODUCTION

Electrospun fibrous materials can be used in many applications including tissue engineering, wound dressing, drug delivery, filtration, protective clothing etc. Mechanical properties play a key role in most of these applications. Gelatin is biocompatible, biodegradable and could be useful in various applications. However, the mechanical properties of gelatin are not sufficient for most applications.

Cross-linking is an efficient way to increase mechanical strength of gelatin fibres and can be carried out by chemical, enzymatic and physical means. However, cross-linking agents are generally expensive and more or less toxic. Therefore, it is necessary to investigate the use of natural, non-toxic and cheap substances as cross-linking agents.

EXPERIMENTAL METHODS

Fibrous gelatin scaffolds were prepared by electrospinning from aqueous acetic acid solutions and cross-linked. Only natural, cheap substances and easy, cost-effective methods were used to manipulate the properties of the material. The scaffolds were analysed by scanning electron microscopy (SEM), Fourier transform infrared microscopy (FTIR), degradation test and tensile test. Cell culture experiments were carried out to demonstrate the suitability of the material for tissue engineering applications. A model was constructed to evaluate mechanical properties of the scaffolds using only tensile test results and easily (macroscopically) measurable values.

RESULTS AND DISCUSSION

Fibrous gelatin scaffolds were prepared by electrospinning. Fibrous structure of the scaffolds was confirmed by SEM (Figure 1). Cell culture experiments confirmed the suitability of the material for tissue engineering applications. Evaluation of mechanical properties revealed that Young's modulus of gelatin can

be increased up to a little over 1 GPa using only natural substances and simple methods.

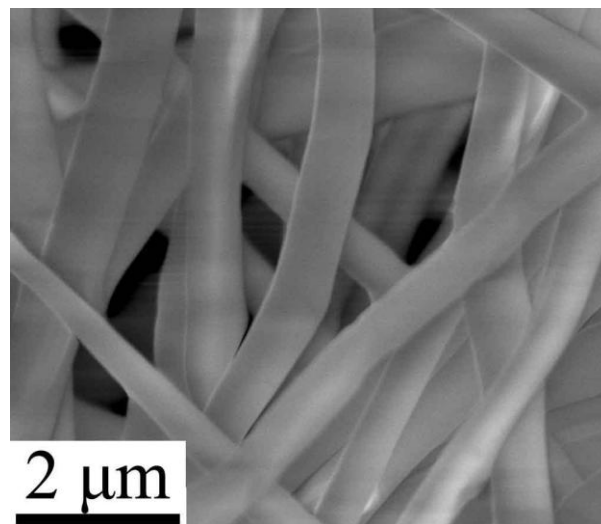


Figure 1. Gelatin fibres (SEM image)

CONCLUSION

A method has been developed for preparation of fibrous gelatin scaffolds using only natural, cheap, totally biocompatible substances and easy, cost-effective methods. Young's modulus of gelatin fibres can be increased to a little more than 1 GPa using this method.

ACKNOWLEDGMENTS

This study was financially supported by European Union through the European Regional Development Fund via projects "Carbon Nanotube Reinforced Electrospun Nano-fibres and Yarns" (3.2.1101.12-0018), "SmaCell" (3.2.1101.12-0017) and Centre of Excellence "Mesosystems: Theory and Applications" (3.2.0101.11-0029), the EMBO Installation Grant as well as Estonian Science Foundation grants IUT2-25, PUT4, PUT177, ETF8420, ETF9281 and ETF8932.

Nanoscale Imaging and Quantitative Nanomechanical Characterization of Biomaterials by Atomic Force Microscopy

Rob Field¹, Alex Winkel¹, Elmar Hartmann², Torsten Mueller², Florian Kumpfe², Joerg Barner²

¹JPK Instruments Ltd., Cambridge, United Kingdom, field@jpk.com

²JPK Instruments AG, Berlin, Germany

Topography, roughness, and mechanical properties of biomaterials are crucial parameters affecting cell adhesion/motility, morphology, and mechanics as well as the proliferation of stem/progenitor cells [1-4]. Nano-mechanical analysis of cells and tissue slices increasingly gains in importance in different fields of cell biology, like cancer research [5] and developmental biology [6]. Atomic force microscopy (AFM) is a powerful, multipurpose technology suitable not only for imaging a wide range of different samples with nanometer scale resolution under controlled environmental conditions, but also for mapping mechanical and adhesive properties of sample/cell systems and tissues.

To extend the versatility of AFM technology, we've been developing a new, distinct imaging mode called "Quantitative Imaging" (QITM) which is based on fast force-distance curves with intelligent control, to simultaneously obtaining topographic, nanomechanical, and adhesive sample properties. Next to this classical information, even more complex data like contact point images, Young's moduli images, or even recognition events can be achieved. In terms of biological applications, the QITM mode exhibits advantages compared to conventional AFM imaging techniques, particularly in liquid environments. Combining these remarkable capabilities with advanced optical microscopy (inverted as well as upright optical microscope techniques) allows for comprehensive characterization options of biomaterials and tissue slices.

To demonstrate the capability and flexibility of QITM, a variety of soft and hard samples have been investigated. Exemplarily, living cells as well as polymer surfaces and single biomolecules have quantitatively been analyzed. Furthermore, it is shown that challenging samples which are fragile or loosely attached, like viruses, bacteria or diatoms can reliably be measured using QITM [7]. Obviously, QITM offers new

perspectives in nanomechanical stiffness and high-resolution measurements in the field of interfaces, e.g., periosteal sheets [8]. A comparison between QITM, conventional force spectroscopy and traditional AFM imaging modes clearly reveals that supplementary information can be gained [9].

In conclusion, the traditional imaging modes demonstrated so far suffer from inherent drawbacks for challenging samples that have steep edges, as well as those that are soft, sticky, or loosely attached to surfaces. These drawbacks can impressively be overcome by using the QITM mode that is exclusively available for the JPK NanoWizard[®]3 AFM.

References

- [1] P. Elter, T. Weihe, R. Lange, J. Gimsa, U. Beck, *Eur. Biophys. J.* 40 (2011) 317-327.
- [2] D. Docheva, D. Padula, M. Schieker, H. Clausen-Schaumann, *Biochem. Biophys. Res. Commun.* 402 (2010) 361-6.
- [3] P. Tracqui, A. Broisat, J. Toczec, N. Mesnier, J. Ohayon, L. Riou, *J. Structural Biology* 174 (2011) 115-123.
- [4] R. Kirmse, H. Otto, T. Ludwig, *J. Cell Sci.* 124 (2011) 1857-66.
- [5] S.E. Cross, Y.S. Jin, J. Rao, J.K. Gimzewski, *Nat. Nanotechnol.* 2 (2007) 780-3.
- [6] M. Krieg, Y. Arboleda-Estudillo, P.-H. Puech, J. Käfer, F. Graner, D. J. Müller, C.-P. Heisenberg, *Nature Cell Biology* 10 (2008) 429-436.
- [7] S. Dhahri, M. Ramonda, C. Marlière, *PLoS ONE* 8 (2013): e61663. doi:10.1371/journal.pone.0061663
- [8] M. Horimizu, T. Kawase, T. Tanaka, K. Okuda, M. Nagata, D. M. Burns, H. Yoshie, *Micron* 48 (2013) 1-10.
- [9] L. Chopinet, C. Formosa, M.P. Rols, R.E. Duval, E. Dague, *Micron* 48 (2013) 26-33.

Transfer of CVD Graphene onto Polymer Substrates: Implications to Blood-Contacting Surfaces

Gordon Xiong¹, Antonio Castro Neto², Cleo Choong^{1,2}

¹ School of Materials Science and Engineering, Nanyang Technological University, Singapore, mxiong001@e.ntu.edu.sg

² Graphene Research Centre, National University of Singapore, Singapore

INTRODUCTION

Graphene is a single atomic layer nanosheet that has excellent electrical conductivity and mechanical strength¹. Recent advances in biology and tissue engineering have highlighted the roles of utilizing electrical stimuli to direct cellular phenotypes such as migration² and stem cell differentiation³. As such, the transfer of single-layer CVD graphene onto biocompatible polymeric substrates is an attractive proposition to create hybrid substrates that are conductive, but still retain bulk polymeric properties. We have previously modified polycaprolactone (PCL) and demonstrated their use as anti-thrombogenic surfaces⁴. In this work, we transferred CVD graphene onto polymer surfaces and performed characterization of the material's electrical properties and hemocompatibility.

EXPERIMENTAL METHODS

Raman spectroscopy was used to verify the G and 2D peaks of graphene transferred onto PCL and polyvinylidene difluoride (PVDF) substrates. Human umbilical endothelial cells (HUVECs) were seeded on graphene-PCL surfaces and graphene-PVDF surfaces (n=3 each). Cell proliferation assays over 5 days were conducted using the alamarBlue® reagent. The hemocompatibility of the substrates were assessed by 90 minutes incubation of platelet-rich plasma (PRP) on the surfaces before SEM imaging (n=2). The SEM preparation involved fixing in 2.5% glutaraldehyde (w/v) for 1 h at 4°C, followed by drying steps in an ethanol gradient and hexamethyldisilazane (HMDS). In order to ascertain that the transferred graphene layer was stable in cell culture medium, Raman spectroscopy was performed after incubation of graphene-PCL substrates after 1, 3 and 6 days in culture.

RESULTS AND DISCUSSION

Raman spectroscopy confirmed the successful transfer of CVD graphene onto the PCL surfaces (Fig. 1b). Retention of the graphene monolayer after 6 days of incubation in cell culture medium was confirmed by comparing the Raman spectra of both pure PCL with graphene-PCL substrates (Fig. 1a, b). Proliferation of HUVECs on graphene-PCL and graphene-PVDF was found to be significantly higher than that of PCL and PVDF substrates alone (Fig. 2). We postulate that it could be due to the better adsorption of growth factors in the culture media onto the graphene-polymer surfaces that led to increases in cell proliferation. Platelet incubation on native PCL surfaces resulted in an activated morphology, which could be observed under SEM, whilst those on the graphene-PCL remained inactivated.

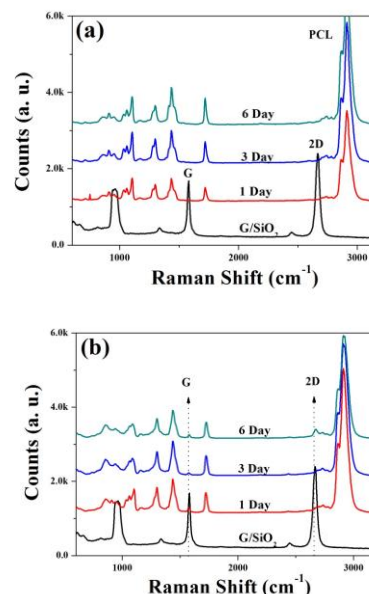


Fig. 1. Raman spectroscopy performed on (a) non-transferred PCL and (b) CVD graphene-PCL substrates at Day 1, 3 and 6 after incubation with cell culture medium. Graphene transferred on SiO₂ was used as a control to show distinct G and 2D peaks.

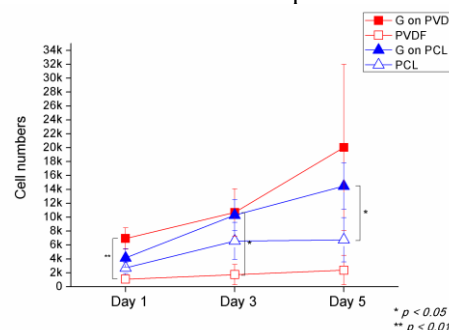


Fig. 2. Endothelial cell proliferation was significantly improved on graphene-PCL and graphene-PVDF over PCL and PVDF respectively.

CONCLUSION

We have successfully transferred CVD graphene onto biocompatible substrates relevant for blood-contacting devices. The graphene monolayer could be retained on the surface, and exhibited improved cytocompatibility, as well as inhibition of platelet activation. Further experiments would be performed with the electrical stimulation of the graphene-polymer surfaces to elucidate any effects on hemocompatibility.

REFERENCES

- Geim, Science 19: 1530-1534, 2009
- Pullar *et al.*, Mol. Biol. Cell 17: 4925-4935, 2006
- Creedy *et al.*, Tissue Eng. 19: 467-474, 2013
- Xiong *et al.*, J. Mater. Chem. B 2: 485-493, 2014

Contribution of new analgesic or antibacterial properties on an implant for parietal refection: an *in vitro* and *in vivo* evaluation

Nicolas Blanchemain^{1*}, Guillaume Vermet², Stephanie Degoutin², Feng Chai¹, Christel Rousseaux³, Christel Neut³, Bernard Martel², Frederic Hildebrand¹

^{1*} INSERM U1008, Biomaterial Research group, University Lille 2, France, nblanchemain@univ-lille2.fr

² UMET, Ingénierie des Systèmes Polymères, University Lille1, Lille

³ INSERM U995, University Lille 2, France

INTRODUCTION

The cure of hernia is the second second-most-practiced surgical act in France. The closure is carried out using a parietal reconstruction implant in the form of polyester mesh. This surgery causes pain after implantation at the abdominal level and the risk of infection is high (up to 9%)¹. Despite the IV administration of antibiotics and the use of an analgesic shoot deposited on the plate the day of the procedure, these complications remain. The solution we propose is to modify the mesh with a polymer of cyclodextrine to improve adsorption and prolonged release of the antibiotics and analgesics.

EXPERIMENTAL METHODS

Meshes (Polyethylene terephthalate, PET, Biomesh A1L[®]) were manufactured by Cousin Biotech (Wervicq Sud, France). The implants have been functionalized by a process developed and patented by Martel et al.² using hydroxypropyl-beta-cyclodextrine (Kleptose HPB, Roquette, France) and citric acid (Sigma Aldrich, France) as cross-linking agent. After functionalization, mechanical properties of implants were verified and the cytocompatibility according to ISO 10993-5 standard was evaluated with fibroblastic cells (NIH3T3). The kinetics of impregnation and release of ropivacaine (10 mg/ml, Kabi, France) and ciprofloxacin (200mg/100mL, Kabi, France) have been followed by HPLC (LC2010A, Shimadzu, France). Therapeutic activity of antibacterial and analgesic meshes was assessed *in vitro* and *in vivo* respectively. In the case of antibacterial activity, meshes were impregnated in ciprofloxacin. At regular time interval in PBS, the implants were removed and deposited onto agar seeded bacteria (*S. aureus* or *E. coli*). In the case of analgesic activity, meshes were impregnated in ropivacaine and implanted in rats at the level of the peritoneum. To assess pain, colorectal distension is practiced in rats every day³. In the same time, pharmacokinetic of ropivacaine was assessed and histological evaluation was performed.

RESULTS AND DISCUSSION

Studies of the functionalization of meshes allowed determining the optimal parameters to not change its mechanical properties and to ensure its safety. Indeed, the cytocompatibility tests showed that the NIH3T3 cell vitality was 70% with functionalized implants at 140°C for 1 hour. The functionalization rate of meshes after this process was 20%-wt.

The kinetics of adsorption of the two selected drug (ciprofloxacin and ropivacaine) were evaluated on the functionalized meshes. The resultants showed a quick

time of impregnation (< 15 minutes) to obtain the maximal amount of adsorbed drug: respectively XX mg/g of ciprofloxacin and XX mg/g of ropivacaine. The drug sorption was clearly increased compare to virgin sample, respectively an X and Y-fold improvement for ciprofloxacin and ropivacaine. Additionally, the kinetics of release carried out under SINK conditions in a paddle and flow-through cell system were prolonged with functionalized meshes (> 24 hours; virgin meshes <30 minutes).

In the case of antibacterial meshes, the *in vitro* antibacterial activity, measured by the presence of a radius of inhibition after 24 hours, is still more efficiency up to 3 days with functionalized implants against a few hours for virgin meshes. In the case of analgesic meshes, the *in vivo* evaluation (Figure 1) showed a significant reduction of pain at least for 7 days with functionalized meshes while no difference with virgin implants from the first day was observed.

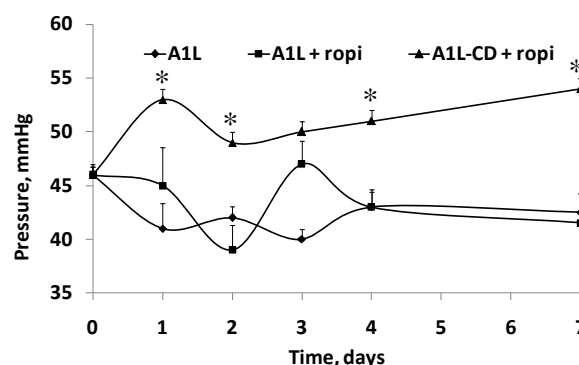


Figure 1: *in vivo* evaluation of the colorectal distension of rat after implantation of meshes. (* $p < 0.05$)

The pharmacokinetics showed that the highest level of ropivacaine in blood is 1 µg/ml and the histological evaluation revealed a slight increase of inflammatory response but with still acceptable results

CONCLUSION

This study shows the capacity of functionalised meshes with a polymer of cyclodextrine to quickly adsorb and prolong the release of analgesic or antibiotics but also significantly improve the *in vitro* and *in vivo* therapeutic activity of the medical device.

REFERENCES

1. Kehlet H et al. *The Lancet*. 367:1618-25, 2006
2. Martel et al. WO 2006/051227, 2006
3. Rousseaux et al. *Nature Medecine*. 13:35-37, 2007

ACKNOWLEDGMENTS : The authors would like to thank Cousin Biotech for providing financial support to this project and IBD (Lille) for animal assays..



Novel nano-particular calcium phosphate and carbonate phases made by electro-migration technique. A component of silica/collagen based bone replacement materials

Benjamin Kruppke, Christiane Heinemann, Sascha Heinemann, Anne Keroué, Maria Jäger, and Thomas Hanke*

Max-Bergmann-Centre of Biomaterials, Institute of Material Science, Faculty of Mechanical Engineering,
Technische Universität Dresden, Germany, thomas.hanke@tu-dresden.de

INTRODUCTION

Bone replacement materials for systemically altered (e.g. osteoporotic) bone has to meet various requirements. In case of post-menopausal high turnover osteoporosis the biomaterial should manipulate the osteoblast [Ob]/osteoclast [Oc]-ratio to the benefit of the bone forming Ob. Recently, the authors have shown that silica/collagen-biomaterials with or without added calcium phosphate phases¹ are able influence the Ob/Oc-ratio in a co-culture by controlling the extracellular calcium concentration². Furthermore, Oc-formation and activity are influenced by such composites with different calcium phosphate phases³. Here, novel calcium mineral phases (phosphate, carbonate), a newly developed electro-migration chamber as well as corresponding cell culture experiments are presented.

EXPERIMENTAL METHODS

The silica/collagen-biomaterials were prepared from bovine tropocollagen type I (GfN) and hydrolysed tetraethoxysilane (TEOS, 99%, Sigma)⁴. For the preparation of triphasic xerogels calcium phosphate or carbonate phases prepared by precipitation in a gelatin gel were used (cf. results and discussion).

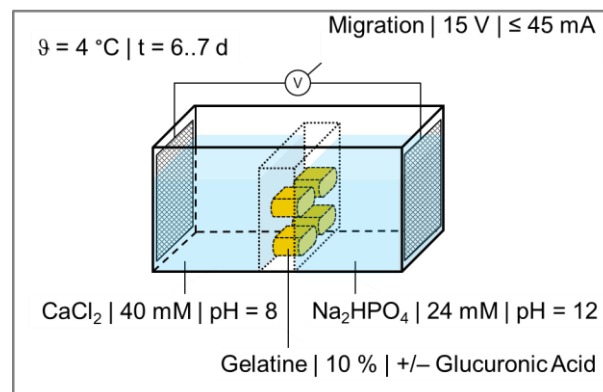
For cell culture experiments hydrogels were prepared by stirring silicic acid and collagen suspension to obtain a final composition of 70% silica and 30% collagen. Triphasic xerogels were prepared by previously adding gel precipitated calcium phosphate or carbonate phases to the collagen suspension². In these cases the final composition was 50% silica, 30% collagen, 20% calcium mineral phase. Mixtures were transferred to molds and dried in an Espec SH-221 climate chamber. Finally, disc-like composite xerogels (o.d. 5 mm, h. 3 mm) were obtained that fit in cell culture well plates.

Cell culture experiments were carried out using a Ob/Oc co-culture and monocultures of each cell type as previously described².

RESULTS AND DISCUSSION

In the electro migration chamber (cf. figure) a newly developed barrier is located between two reservoirs of CaCl_2 and Na_2HPO_4 solutions. Instead of Ca^{2+} and HPO_4^{2-} other cations (Sr^{2+}) and anions (HCO_3^-) or mixtures were used, too. The barrier consists of a plastic rack with gelatine gel (10% porcine) filled openings. Various numbers of openings with different shape and size in a rack were used, according to requirements, as gel composition, type of calcium mineral to be formed, further ingredients as well as the final size and shape of the biomaterial. An electric field was applied to accelerate the opposed migrations of cations and anions, respectively, into and within the gelatine gel. Over a number of days, the mineral was formed, then collected

by removing the gelatine using several alternating steps of heating and centrifugation.



The rack with the openings of defined geometry and size as a barrier in the electro migration chamber enables us to prepare particularly good defined mineral nano-particles. The influence of the mineral phases alone onto the extracellular calcium concentration was quantified. Cell culture experiments using monocultures of hMSC- derived Ob and monocyte-derived Oc and/or co-cultures thereof have shown that the triphasic xerogels - according to which mineral phases were used - can increase or decrease both populations of Ob and Oc, independently of each other or in a co-culture, then in opposite direction regarding the cell type.

CONCLUSION

Novel nano-particular calcium phosphate and carbonate phases were used as ingredients of triphasic silica/collagen based biomaterials. They are particularly suitable for control of calcium binding and release onto/from these xerogels. Consequently, the xerogels are supposed to act in a particular effective way as bone replacement materials manipulating the ratio between the bone-forming and bone-resorbing cells.

REFERENCES

1. Heinemann S. *et al.*, Biomater. Sci. 1:688-70, 2013
2. Heinemann S. *et al.*, Acta Biomater. 9: 4878-88, 2013
3. Glenske K. *et al.*, Biomaterials 35: 1478-95, 2014
4. Heinemann S. *et al.*, Compos. Science Technol. 71: 1873-80, 2011

ACKNOWLEDGMENTS

The authors would like to thank the *Deutsche Forschungsgemeinschaft* for providing financial support to this project (M03) in the framework of the Collaborative Research Centre (Transregio) TR79.

In-situ Synthesized Silver Nanoparticles in Silk Fibroin Nanofibers: Effect of Fibroin Morphology on Ag⁺ Release Kinetics

Semih Calamak^{1,2}, Eda Ayse Aksoy², Nusret Ertas⁴, Ceren Erdogdu³, Meral Ozalp³, Kezban Ulubayram^{1,2}

Hacettepe University, ¹Graduate Department of Nanotechnology and Nanomedicine, ²Faculty of Pharmacy, Department of Basic Pharmaceutical Sciences, ³Faculty of Pharmacy, Department of Pharmaceutical Microbiology, 06100 Ankara, Turkey. Gazi University, ⁴Faculty of Pharmacy, Department of Analytical Chemistry, 06330 Ankara Turkey.

ukezban@hacettepe.edu.tr

INTRODUCTION

Silver nanoparticles have versatile applications in many commercial products such as wound healing materials, antimicrobial coatings, fillers and medical biotextiles due to its well-known antimicrobial nature. An efficient silver ion release from these biomaterials is crucial for sustained antibacterial activity. Properties of polymer matrix such as polymer type, concentration, morphology, processing parameters and silver nanoparticle size, concentration of silver nanoparticles play a decisive role in silver ion release kinetics.

In silk based textiles and wound dressing materials, control of the silk morphology; random coil (Silk I) or β sheets (Silk II); is an important subject, which effects the release of silver ion and determines antibacterial efficiency of these biomaterials. Silk morphology can be changed and controlled by different post-treatment methods [1]. Even with the wide usage of Ag nanoparticles in medical textile materials, there are only few studies reported about silver ion release kinetics and cytotoxicity on cell lines.

In this work silver nanoparticles were *in situ* produced in electrospun fibroin nanofibers by UV reduction of silver nitrate. Composite nanofibers were treated using two post-treatment methods as follows; glutaraldehyde (GA) vapor and methanol treatment. The effect of silk morphology, random coil (Silk I) or β sheets (Silk II), on Ag⁺ release kinetics, antibacterial activity and indirect cytotoxicity were discussed elaborately.

EXPERIMENTAL METHODS

Native *Bombyx mori* silk fibers was degummed with NaHCO₃. Then rinsed with warm distilled water to extract the glue-like sericin proteins. The degummed silk fibroin was dissolved in the ternary solvent system of CaCl₂/CH₃CH₂OH/H₂O. Solution was dialyzed against distilled water using a dialysis membrane to remove the salts. After dialyzing, the silk fibroin solution was filtered and lyophilized [2]. Then different amounts of AgNO₃ (w/v 0.1%, 0.5% and 1%) was added to silk fibroin. Silver nanoparticles were synthesized by UV light (254 nm) exposure of composite nanofibers. Finally methanol and GA vapour treatments were applied.

RESULTS AND DISCUSSION

In order to obtain uniform Ag/Fibroin composite nanofibers the key processing parameters such as flow rate, applied voltage, and fibroin concentration were optimized. Ag/Fibroin composite nanofibers were in the

range between 200 to 600 nm with a smooth and uniform morphology. Presence of Ag in fibroin nanofibers was attested by EDX analysis (Fig 1).

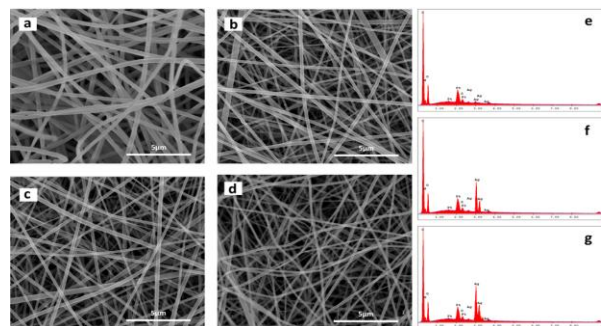


Fig 1. SEM micrographs of nanofibers (a) Fibroin, (b) Ag(0.1)/Fib, (c) Ag(0.5)/Fib, (d) Ag(1)/Fib, SEM-EDX of Ag/Fib composite nanofibers (e) Ag(0.1)/Fib, (f) Ag(0.5)/Fib and (g) Ag(1)/Fib.

Between the two post treated composite nanofibers, the cumulative amount of silver ions released from the Ag/Fib-G was greater than the amount released from the Ag/Fib-M ones due to its amorphous structure. Evaluation of antibacterial activities were studied against three microorganisms gram (+) *Staphylococcus aureus*, *Staphylococcus epidermidis* and gram (-) *Pseudomonas aeruginosa*. For Ag/Fib composite nanofibers, it was observed that zones of inhibition are clearer against *P. aeruginosa* than *S. aureus* and *S. epidermidis* (Table 1.).

Table 1. Inhibition zones of the composite nanofibers

Type of Samples	Inhibition Zone Diameter (cm) /Sample Diameter (cm)		
	<i>S. aureus</i>	<i>S. epidermidis</i>	<i>P. aeruginosa</i>
Ag(0.1)/Fib-M	0.50/0.50	0.50/0.50	0.83/0.50
Ag(0.1)/Fib-G	0.50/0.50	0.50/0.50	0.80/0.50
Ag(0.5)/Fib-M	0.50/0.50	0.50/0.50	0.73/0.50
Ag(0.5)/Fib-G	0.50/0.50	0.50/0.50	0.83/0.50
Ag(1)/Fib-M	0.60/0.50	0.57/0.50	0.87/0.50
Ag(1)/Fib-G	0.67/0.50	0.60/0.50	0.93/0.50

CONCLUSION

Smooth and uniform Ag/fibroin composite nanofibers having antibacterial properties were obtained and release studies demonstrated that the accumulative amount of silver ions depends on the silver content of nanofibers and polymer morphology.

REFERENCES

- Altman, G. et al., Biomaterials, 24(3):401-416, 2003.
- Min, B. et al., Biomaterials, 25(7-8):1289-1297,2004.



Sustained Release of Azithromycin from an Electrospun Polycaprolactone Membrane for Guided Tissue Regeneration

Asha Mathew¹, Cedryck Vaquette², Dietmar Hutmacher² and Saso Ivanovski¹

¹Tissue Engineering and Regenerative Medicine, Griffith University, Australia

²*Regenerative Medicine, Queensland University of Technology, Australia a.mathew@griffith.edu.au

INTRODUCTION

Periodontitis is an inflammatory disease affecting the periodontum resulting in the progressive loss of the alveolar bone around the teeth causing subsequent teeth loss [1]. For successful periodontal regeneration, the formation of periodontal ligament fibers and the insertion of these fibers into newly formed cementum on the root surface along with the adjacent resorbed alveolar bone are essential. Guided Tissue Regeneration (GTR) is a widely utilized surgical technique to promote periodontal regeneration. However, bacterial contamination on the sites undergoing GTR therapy reduces the efficiency of periodontal regeneration either by affecting the new connective tissue attachment or bone [2] or by affecting the attachment of periodontal ligament cells on the GTR membranes [3]. Therefore, this project aims at addressing a significant issue in periodontal regeneration: bacterial contamination on the sites of undergoing GTR. It is hypothesised that the local delivery and sustained release of azithromycin will significantly reduce any bacterial infection. For this purpose, the primary objective of the project is to engineer and assess a biocompatible and biodegradable polymeric matrix for the controlled delivery of azithromycin.

EXPERIMENTAL METHODS

PCL membranes are fabricated via solution electrospinning. The PCL membranes are then subjected to a calcium phosphate (CaP) coating process by successive immersion into specific reagents and solutions. Azithromycin encapsulation, release, antibacterial and cellular response when loaded onto PCL and PCL-CaP membranes are assessed on different doses of azithromycin. The statistical analysis are performed throughout the entire project using one-way ANOVA followed by a Tukey HSD post-hoc test in case of equal variance; otherwise a Games-Howell post-hoc test will be utilized.

RESULTS AND DISCUSSION

Azithromycin was successfully loaded onto PCL/PCL-CaP membranes using a novel ethanol evaporation technique. This method enables to reproducibly load azithromycin on to the electrospun membranes with a very high loading efficacy (around 75%) as depicted in Figure 1 A), which is unprecedented for such a poorly water soluble compound. PCL membrane surface topography has shown to have an effect on azithromycin encapsulation and efficiency. CaP coating on PCL membranes increased the roughness and surface area of the resulting material leading to higher loading efficacy and more uniform distribution of the antibiotic throughout the fibrous membrane. *In-vitro* release profile of azithromycin from the membrane demonstrated around 90% release from CaP coated and non-coated PCL membranes after 14 days of incubation

with PBS at 37°C (Figure 1B). This is of tremendous significance as a successful local drug delivery strategy must release the antibiotic over a defined period of time and avoid a burst release. Antibacterial activity of azithromycin loaded membranes on staphylococcus aureus suggest that the electrospun membranes loaded with azithromycin are capable to inhibit bacterial growth even after 14 days of release (Figure 2).

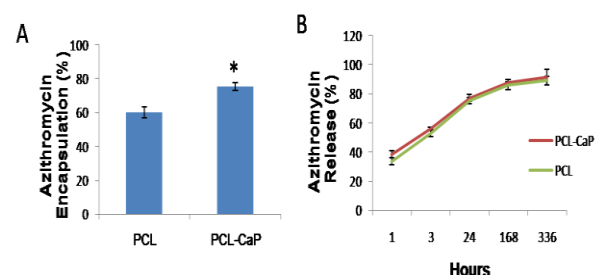


Figure 1: (A) Encapsulation efficiency of azithromycin loaded on to PCL and calcium phosphate coated PCL (PCL-CaP). n=4, p<0.05. (B) Cumulative release of azithromycin from PCL and calcium phosphate coated PCL (PCL-CaP) achieved as a continuous release over a period of 14days (n=3)

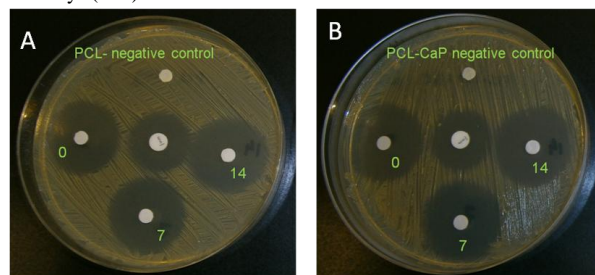


Figure 2: Growth inhibition of staphylococcus aureus after 20 hour incubation with 1mg azithromycin containing (A) PCL (B) PCL-CaP electrospun membranes after 0, 7 and 14 days release from PBS at 37°C.

CONCLUSION

In conclusion hydrophobic azithromycin was successfully encapsulated on to PCL/PCL-CaP membranes using ethanol evaporation technique. Our results have shown an excellent encapsulation efficiency of about 75% with a controlled release of 90% along with efficient antibacterial effect even after 14 days of release.

REFERENCES

- [1] Armitage GC. Annals of periodontology. 1999;4:1-6.
- [2] Rossa M, Lima L, Pustiglioni F, Hespanhol A, Kon S, Grigolli FJ, et al. Journal of the International Academy of Periodontology. 2006;8:115-24.
- [3] Hung S-L, Lin Y-W, Wang Y-H, Chen Y-T, Su C-Y, Ling L-J. Journal of periodontology. 2002;73:843-51.

ACKNOWLEDGMENTS

The authors also thank Dr Stephen Hamlet and Christina Theodoropoulos for their assistance in laboratory experiment.

Functional Characterisation of SDF-1 α GAG Binding Variants

Nydia Panitz^{1*}, Lars Baumann², Stephan Theisgen³, Daniel Huster³ and Annette G. Beck-Sickinger¹

^{1*}Institute of Biochemistry, University Leipzig, Germany, nydia.panitz@uni-leipzig.de

²Department of Chemistry, University of British Columbia, Canada

³Institute of Medical Physics and Biophysics, University Leipzig, Germany

INTRODUCTION

The stromal cell-derived factor 1 α (SDF-1) belongs to the CXC chemokines and interacts with its CXC-receptor 4 and 7. It plays an important role in immune system, angiogenesis and recruitment of tissue specific stem cells. Therefore the SDF-1 is an interesting target for the regeneration of damaged tissue e.g. after myocardial infarction. Recent studies focus on the development of hydrogels, which can be integrated in this type of damaged tissue. The aim of this study is to generate a stable, long-term chemotactic gradient by using immobilised SDF-1, which leads to the recruitment of stem cells and therefore to the regeneration of the affected tissue^{1,2}. The present work focusses on the influence and characterisation of SDF-1 variants with different GAG binding properties to recruit different cell types that express the CXCR4.

EXPERIMENTAL METHODS

For the investigation of specific amino acids of SDF-1 α for GAG binding different native and artificial GAGs were used for ¹H-¹⁵N-HSQC NMR spectroscopy. The activity of SDF-1 variants was studied by migration and Ca²⁺ release assays.

RESULTS AND DISCUSSION

¹H-¹⁵N-HSQC NMR with ¹⁵N-labeled SDF-1 was used to confirm previous studies by Ziarek *et al.*³. Similar results could be obtained for the binding of artificial GAG.

NMR results identified specific lysines and arginines for the subsequent migration experiments. The results showed only weak effects of the single mutants. Next the investigation of the signaling pathway was performed by using an Ca²⁺ release assay. Distinct mutations showed a quite similar EC₅₀ and E_{max} value in comparison to the SDF-1.

The presented NMR data provide an overview on the interaction of SDF-1 with different types of GAGs. This led to the hypothesis, that the sulfation of the GAG may play an important role for the interaction with the protein. This was shown earlier for related systems^{4,5}.

Based on the NMR-measurements single amino acids were exchanged by mutations. The migration assay demonstrated that the single mutation does not influence the ability of the SDF-1 to recruit specific cells. Accordingly, certain amino acids of the GAG binding site are not involved in the interaction of the SDF-1 with CXCR4, which is in agreement with previous modelling data⁶.

To identify the influence in signaling pathways, Ca²⁺ release assays were performed. For all receptor variants a similar effect in signaling strength could be detected compared to the native SDF-1 α . This indicates that the G-protein coupled signaling by the phospholipase C is not influenced.

CONCLUSION

Additional knowledge on the specific interaction of SDF-1 with different GAGs could be achieved and the influence of the GAG binding site of the interaction of the SDF-1 with its CXCR4 could be determined in more detail. Future experiments will give further information, which can be used to generate SDF-1 variants with better and poorer GAG binding properties for hydrogels to generate a long-term and stable chemotactic gradient.

REFERENCES

1. Prokoph S. *et al.*, Biomaterials. 33:4792-00, 2012
2. Baumann L. *et al.*, J Control Release. 162:68-75, 2012
3. Ziarek JJ. *et al.*, J Biol Chem. 288:737-46, 2013
4. Zhang S. *et al.*, J Biol Chem. 287:5542-53, 2012
5. Laguri C. *et al.*, J Am Chem Soc. 133:9642-45, 2011
6. Huang X. *et al.*, Biophys J. 84:171-84, 2003

ACKNOWLEDGMENTS

The authors thank Prof. J Rademann FU Berlin, for providing specific GAGs; Dr. C. Berger and M Keller for the support during fermentation and providing ¹⁵N labelled ammonium salts. The authors thank the DFG (TRR67, A4) and the European Union and the Free State of Saxony (ESF) for funding.

Polystyrene Sodium Sulfonate Grafted Electrospun Membrane for Applications in Guided Bone Regeneration

C. Vaquette^{1*}, V. Migonney², S. Ivanovski³, D. Hutmacher¹

¹Institute of Health and Biomedical Innovation, Queensland University of Technology, Australia,

²Laboratoire de Biomatériaux et Polymères de Spécialité (LBPS), Laboratoire Chimie, Structures, Propriétés de Biomatériaux et d'Agents Thérapeutiques (CSPBAT), UMR CNRS 7244, Université Paris 13 Sorbonne, France

³School of Dentistry and Oral Health, Griffith Health Institute, Griffith University, Australia

cedryck.vaquette@qut.edu.au

INTRODUCTION

Guided bone regeneration (GBR) is commonly utilized in dentistry for the treatment of insufficient bone or dehiscence defects. This strategy is aimed at enabling the regrowth of the damaged or compromised bone tissue in order to resume functional activity of the mandible or maxilla. GBR is based on 3 essential criteria: wound stabilization, space maintenance and selective cell repopulation for permitting bone ingrowth. This is traditionally achieved by the utilization of an occlusive membrane placed over the bony defect in order to prevent epithelial or fibrous tissue infiltration, hence fulfilling the principles of GBR [1]. To circumvent the limitations of the currently available GBR membranes (inappropriate degradation time, risk of exposure, poor handling properties), our group has developed an occlusive membrane made of a biocompatible and bioresorbable synthetic polymer (polycaprolactone, PCL) fabricated by electrospinning and subsequently bioactivated by polystyrene sodium sulfonate (PolyNaSS) grafting.

EXPERIMENTAL METHODS

Electrospinning: Biomedical grade PCL (80,000 g/mol) was used in this study to fabricate the electrospun membranes. The electrospinning conditions were 10kV, 2mL/hr, 20cm air gap, 10x10cm² aluminium collector using a 25% wt/vol PCL solution in chloroform/dimethylformamide (90/10)

PolyNaSS grafting: The grafting was carried out according to our in house protocol [2]

In vitro evaluation: The osteogenic performance of the grafted material was assessed by measuring the ALP expression, the cell adhesion and proliferation, the amount of mineralised matrix by alizarin Red S and micro-computed tomography (μ CT) over 8 weeks of in vitro culture using human mesenchymal stromal cells.

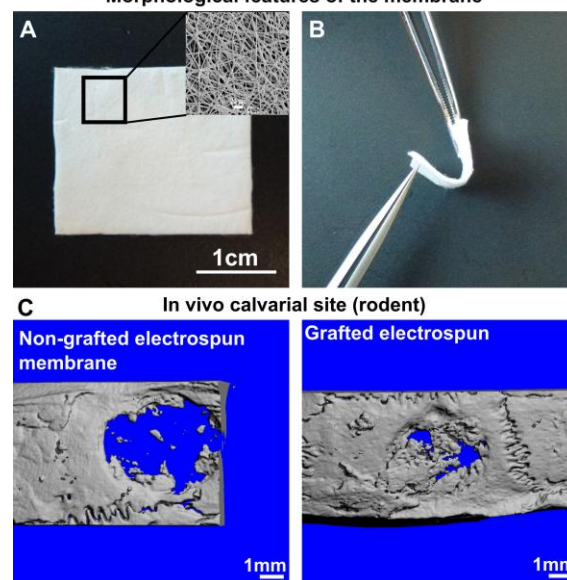
In vivo evaluation: the regenerative potential of the membranes was tested in a rat calvarial defect. Bone formation was assessed longitudinally at 2 and 4 weeks post-implantation by μ CT and by histology.

RESULTS AND DISCUSSION

Fig 1A shows the morphology of the PCL membrane and highlights the small pore size (in the micrometric range) obtained during the electrospinning process. These membranes are well suited for GBR as they can maintain the space while reaching a high degree of flexibility and resilience (Fig 1B) when bench marking against other commercial biodegradable products. The grafting resulted in up-regulation of ALP expression and higher volume of mineralisation in the case of the grafted membranes. This was further confirmed by the in vivo implantation as we demonstrated that the

PolyNaSS grafting significantly accelerated the healing response as shown in Fig 1C; full bridging of the calvarial defect was reached in the case of the grafted membrane as opposed to very little bone formation for the non-grafted membrane. The PCL electrospun membrane displayed a high porosity with a pore size small enough to prevent rapid infiltration of the fibrous tissue into the wound, hence fulfilling the principles of GBR. We observed that whilst the membrane maintained its occlusive properties in the initial stage of the healing process, the membrane was gradually colonised by the host cells permitting an appropriate tissue integration at a later stage.

Morphological features of the membrane



CONCLUSION

We demonstrated the superior performance of the PolyNaSS grafted membrane for bone formation. The grafted membrane can provide clinicians with a purely synthetic porous construct with excellent handling, biomechanical stability and fixation properties. These newly developed membranes possess significant advantages compared to existing commercially available products, such as no risk of disease transmission, controlled biodegradation, and lack of immunogenic response.

REFERENCES

- [1] Hockers T et al. Clin Oral Implant Res 1999;10:487. [2] Vaquette C et al. Biomaterials 2013;34:7048-63.

ACKNOWLEDGMENTS

The authors would like to acknowledge the Australian Research Council and the National Health and Medical Research Council for funding this research.



Chlorhexidine-based Antimicrobial Nanoparticles as a Coating for Dental Implants

Natalie Wood^{1*,2,3}, Howard Jenkinson², Dominic O'Sullivan², Sean Davis³ and Michele Barbour²

^{1*}Bristol Centre for Functional Nanomaterials, University of Bristol, UK, natalie.wood@bristol.ac.uk

²School of Oral and Dental Sciences, University of Bristol, UK

³School of Chemistry, University of Bristol, UK

INTRODUCTION

Titanium is the dominant component of many dental implant systems; this is due to its strength, corrosion resistance and biocompatibility.¹ Micro-roughened implant surfaces have shown a higher rate of osteoblast adhesion; however, this increased surface roughness means the implants become more susceptible to bacterial colonisation, which may increase the propensity of implant failure.²

Chlorhexidine (CHX) is a broad spectrum biocide used extensively in medicine and dentistry. It can be combined with hexametaphosphate (HMP) to yield a solid nanoparticle (NP).³ NPs are an attractive coating for dental implants due to their small size, meaning the majority of the titanium surface would be exposed and available for osseointegration. They also offer the possibility of tuneable surface coverage.

EXPERIMENTAL METHODS

Upon the addition of an aqueous chlorhexidine digluconate solution (10 mM) to an aqueous solution of sodium hexametaphosphate (10 mM), under constant stirring, CHX-HMP NPs were precipitated.

Commercially pure grade II titanium substrates were exposed to the rapidly stirred NP suspension for 30 s and rinsed for 10 s in deionised water, before being left to dry in air. Some samples were then soaked in stimulated, whole, human saliva for 2 hours to deposit a salivary pellicle (Ethics reference number: NJW161213; Saliva bank REC ref: 08/H0606/87+5).

NP size, charge and surface distribution were investigated using Dynamic Light Scattering (DLS), Atomic Force Microscopy (AFM) and Scanning Electron Microscopy. The release of CHX from the surfaces into water, with and without the addition of an acquired salivary pellicle, was monitored through the use of UV-spectrophotometry. The antimicrobial efficacy of the NP-coated surfaces against *Streptococcus gordonii*, with and without a salivary pellicle, was also investigated.

RESULTS AND DISCUSSION

The CHX-HMP NPs had an average size and charge of ~150 nm and ~ -50 mV, respectively (DLS). They readily adhered to titanium resulting in micron-sized porous plaques surrounded by titanium (AFM) (SEM), see Figure 1.

These NP-coated surfaces exhibited a steady release of CHX into water for over 50 days. The same was true when a salivary pellicle was applied; however, a lower final concentration was reached.

The adhesion and proliferation of *S. gordonii* were shown to be significantly reduced within 24 h due to the

NP coating; similar results were seen in the presence of a salivary pellicle, see Figure 2.

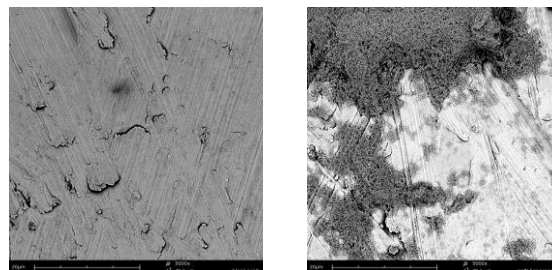


Figure 1. Scanning electron micrographs showing (L) uncoated titanium and (R) titanium post-NP deposition.

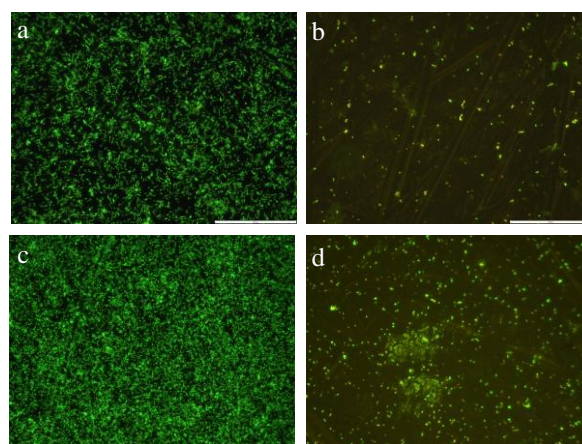


Figure 2. Optical micrographs of fluorescently labelled *S. gordonii*, live (green) and dead (red), on uncoated titanium (a) with a pellicle and (c) without a pellicle and on NP-coated titanium (b) with a pellicle and (d) without a pellicle, after 24 h. Scale bar is 100 µm.

CONCLUSION

CHX-HMP NPs have been synthesised and adhered to clinically relevant titanium substrates. These coated surfaces have shown a steady release of CHX from the surface for over a month, even in the presence of a salivary pellicle. All NP-coated surfaces, with and without a pellicle, exhibited a significant antimicrobial efficacy against the oral primary coloniser *S. gordonii*, within 24 h.

REFERENCES

1. Alla R. *et al.* Trends Biomater. Artif. Organs 25:112-8, 2011
2. Rimondini L *et al.*, J. Periodontol. 68:556-62, 1997
3. Barbour M.E. *et al.*, Int. J. Nanomedicine 8:3507-19, 2013

ACKNOWLEDGMENTS

The authors would like to thank the EPSRC for funding through the BCFN and the Oral Microbiology Group, University of Bristol for support.



PEGylation as a method of modification of collagen-elastin based scaffolds for tissue engineering

Joanna Skopinska-Wisniewska¹, Anna Bajek², Justyna Sitkowska¹, Alina Sionkowska¹

¹ Faculty of Chemistry, Nicolaus Copernicus University, Torun, Poland, joanna@chem.umk.pl

² Collegium Medicum, Nicolaus Copernicus University, Karłowicza 24, 85-092 Bydgoszcz, Poland

INTRODUCTION

Collagen and elastin are a main components of extracellular matrix most of the connective tissues. The mechanical properties of these proteins are complementary and provide a resilience to all kinds of tissues. In addition, the proteins ability to improve the cells adhesion and promote the production of extracellular matrix from proliferating cells causes that collagen and elastin have been the focus of biomaterials technology and tissue engineering for many years [1-3]. The mechanical properties, swelling and degradation ability of these proteins can be modified by cross-linking. Glutaraldehyde is one of the most efficient cross-linking agent. The stable bonds between aldehyde groups and amine rests of proteins can be created in the mild conditions, at physiological pH with a good efficiency. However, the free dialdehyde molecules which can stay in the scaffold are cytotoxic [4,5]. For this reason we decided to use poly(ethylene glycol)-dialdehyde molecules. On the one hand, it ensures the efficiency of cross-linking, but on the other hand the length of the molecules will prevent the release of the reagents into the tissues.

EXPERIMENTAL METHODS

The collagen type I was extracted in our laboratory from rat tail tendons and elastin from porcine aortas. The blends containing collagen and 5% and 10% of elastin were prepared. Both types of samples were cross-linked by the addition of 5% and 10% of two kinds of poly(ethylene glycol)-dialdehyde (PEG-dialdehyde) (MW 1000 and MW 3400) from Scholtz GMB (Germany). The mixtures of all reagents were incubated 30 min on magnetic stirrer and then dialysed against deionized water.

RESULTS AND DISCUSSION

The results of swelling degree measurements showed that the non-modified collagen-elastin materials exhibit the highest swelling ability. The cross-linking using PEG-dialdehyde 1000 causes only a small decrease of the swelling degree, while the use of PEG-dialdehyde 3400 results in significantly reduced swelling capacity. Mechanical test revealed that the cross-linking causes

increase of the samples stiffness. Although the compression modulus of the material containing 5% elastin is much higher than for the sample with bigger elastin content, but after cross-linking the both materials exhibit similar value of this parameter. It suggests that the effectiveness of cross-linking is higher for elastin than for collagen chains. Also the temperatures of thermal denaturation observed during DSC analysis are higher for cross-linked materials. However, the temperature differences for various samples are not significant.

CONCLUSION

The results demonstrate that the addition of the cross-linking agent improve the mechanical properties and thermal stability of the resulting materials. However, the cross-linking with PEG-dialdehyde 3400 causes significant decrease of swelling capacity, so the use of PEG-dialdehyde 1000 is more reasonable.

REFERENCES

1. A.J. Bailey, Mechanisms of Ageing and Development, 2001, 122, 735-755
2. W.F.Daamen, *et al*, Biomaterials 2003, 24, 4001-4009
3. D.G. Wallace, *et al*, Adv. Drug Deliv. Rev., 2003, 55, 1631-1649
4. R. Partenteau-Bareil, *et al*, Materials, 2010, 3, 1863-1887
5. M.T. Sheu, *et al*, Biomaterials, 2001, 22, 1713-1719

ACKNOWLEDGMENTS

“The authors would like to thank the National Science Centre (NCN, Poland, Grant no: UMO-2011/03/D/ST8/04600) for providing financial support to this project”.

Gelatin Biofunctionalization of Poly(L-Lactide-co-Glycolide) Surfaces by Post-Plasma Grafting of AEMA

Malgorzata Krok-Borkowicz¹, Olga Musial², Paulina Kruczala¹, Timothy Douglas², Sandra Van Vlierberghe²,
Peter Dubrue², Elzbieta Pamula¹

¹Department of Biomaterials, Faculty of Materials Science and Ceramics, AGH University of Science and Technology, Krakow, Poland, epamula@agh.edu.pl

²Polymer Chemistry and Biomaterials (PBM) Group, Department of Organic Chemistry, Ghent University, Belgium

INTRODUCTION

Several approaches to modify the surface of resorbable aliphatic polyesters (i.e. poly-L-lactide-co-glycolide, PLGA) in order to enhance their cell-interactive properties have been proposed in literature. These include: hydrolysis, UV-treatment, ozone and plasma treatments, etc. A very attractive and efficient method seems to be the introduction of primary amines on a polyester surface, which can subsequently be used for physisorption or the covalent immobilization of biomolecules. Such a multistep method, based on post-plasma grafting of 2-aminoethyl methacrylate (AEMA), has been recently developed for poly(ϵ -caprolactone) and it was found to positively impact rat osteosarcoma cell adhesion and viability¹. The aim of this study was to utilise a similar approach to functionalize PLGA by covalent bonding of gelatin and verify if such a treatment is beneficial for human osteoblast-like cell adhesion and growth.

EXPERIMENTAL METHODS

PLGA (85:15, $M_n=100$ kDa, $M_w=210$ kDa) foils prepared by solvent casting were submitted to a dielectric barrier discharge Ar plasma followed by air exposition and AEMA grafting under UV irradiation. Then gelatin (type B from bovine skin, obtained by alkaline process) was covalently immobilized with the use of EDC (Sigma) according to a method developed for poly(ϵ -caprolactone)¹. The surface of PLGA and PLGA-AEMA-GelB was characterized by XPS (FISONS S-PROBE), AFM (EXPLORER) and contact angle measurements (DSA10). MG-63 osteoblast-like cells were cultured on the samples for 1 to 8 days and both cell proliferation (MTT test) as well as cell morphology (after fluorescence staining by acridine orange) were assessed.

RESULTS AND DISCUSSION

The applied modification resulted in changes in PLGA surface chemistry (presence of nitrogen and decrease in carbon and oxygen), an increase in hydrophilicity and an increase in surface roughness (Tab. 1).

Tab. 1 Chemical composition, average roughness (R_a) and water contact angle of PLGA and PLGA-AEMA-GelB foils

	PLGA	PLGA-AEMA-GelB
C (at%)	68 \pm 6	64.6 \pm 0.3
O (at%)	29 \pm 5	27.8 \pm 0.8
N (at%)	bdl	7.6 \pm 0.6
N/C	0	0.118
Θ (°)	64 \pm 2	33 \pm 7
R_a (nm)	0.73 \pm 0.17	10.8 \pm 1.3

bdl - below detection limit

In vitro results show that MG-63 cell adhesion on PLGA-AEMA-GelB after 1 day was significantly higher than on PLGA. Cell proliferation was also significantly higher on day 8 (Fig.1), but still the cell proliferated better on TCPS. Microscopic observations show that the cells on PLGA-AEMA-GelB were more homogenously distributed and their flattened morphology was similar to that on TCPS. Contrarily, the cells cultured on PLGA tended to aggregate (Fig.2).

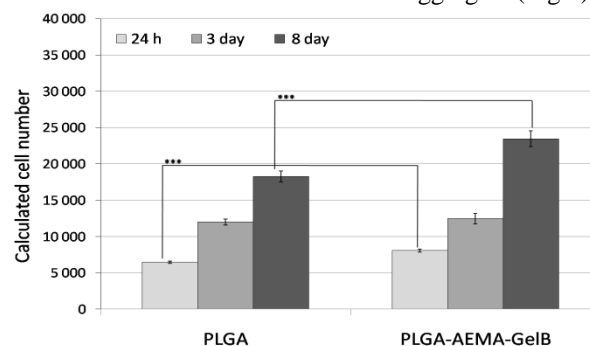


Fig. 1 Proliferation of MG-63 evaluated by MTT test after 24 h, 3 and 8 days. Asterisks indicate significant differences ($p^{***} < 0.001$) between PLGA and PLGA-AEMA-GelB.

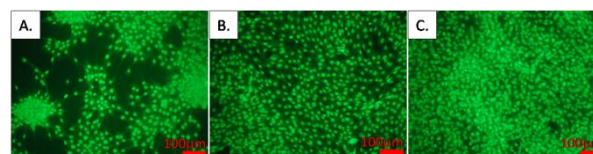


Fig. 2 Cell morphology on PLGA (A), PLGA-AEMA-GelB (B) and TCPS (C) after 8 days of culture.

CONCLUSIONS

Post-plasma AEMA grafting followed by gelatin B covalent immobilization had a significant influence on chemistry, topography and wettability of PLGA surfaces. The surfaces become rougher and more hydrophilic upon gelatin immobilization. As a result, MG-63 osteoblast-like cells, adhere and proliferate better than on non-modified PLGA.

REFERENCES

1. Desmet T. *et al.*, Macromol Biosci. 10(12):1484-94, 2010

ACKNOWLEDGMENT

The studies were financed from AGH statutory works (11.11.160.256)

Osteoinductive effects of simvastatin loading on mesoporous silica and titania nanoscaled thin films

Miriam López-Álvarez¹, Vanesa López-Puente², Jorge Pérez-Juste², Julia Serra¹, Isabel Pastoriza-Santos², Pío González¹

¹New Materials Group, Applied Physics Dpt, Institute of Biomedical Research of Vigo (IBIV), University of Vigo, Spain

²Colloid Chemistry Group, Chemistry-Physics Dpt, University of Vigo, Spain, pglez@uvigo.es

INTRODUCTION

Mesoporous materials with pore sizes in the range 2-50 nm and surface reactive functionalities have experienced an outstanding development during the last years due to their exciting prospects in bone tissue engineering^{1,2}. More in detail, titania and silica mesoporous thin films have been proven to promote *in vivo* an enhanced initial bone contact and better distribution of bone tissue due to their highly ordered arrays of monodisperse pores, high specific surface areas and bioactive properties³. On the other hand, it has already been demonstrated that pharmacological compounds can upregulate the intrinsic growth factors to stimulate bone growth. Thus, for instance, topically applied simvastatin, has been shown to stimulate BMP-2 and VEGF mRNA expression in osteoblasts and promote bone growth over mouse calvaria⁴. The main objective of the present work was to evaluate the MC3T3-E1 pre-osteoblasts response to mesoporous silica and titania nanoscaled thin films both loaded with different concentrations of simvastatin to determine the optimal range doses to ensure a pro-osteogenic activity.

EXPERIMENTAL METHODS

Silica and titania mesoporous thin films were produced by spin-coating using 125 µL of the precursor solution on top of a glass slide at a spinning rate of 4000rpm. The technique, previously reported², was based on the mesoporous-induced self-assembly (EISA) strategy using an inorganic precursor and a surfactant template in ethanol solution. Sterilized samples of 1x1cm² loaded with simvastatin dilutions in ethanol of 5mg/ml, 1mg/ml, 0.1mg/ml, 0.01mg/ml y 0mg/ml were seeded with 1.7x10⁵ cells/ml of MC3T3-E1 pre-osteoblasts in osteogenic medium. Cells morphology (SEM), cytoskeleton organization (CLSM), proliferation (MTT assay) and early differentiation (alkaline phosphatase, ALP) were evaluated up to 21 days of incubation. Tissue culture polystyrenes (TCP) were used as controls. Data are presented as mean ± standard deviation. Significant differences between groups were assessed with the Student's *t*-test, where ** corresponded to significant difference of *p*<0.01.

RESULTS AND DISCUSSION

Early differentiation of cells to osteoblasts on both mesoporous silica and titania films without simvastatin was quantified and, for instance, after 14 days of incubation (Fig.1a) the ALP activity was significantly higher on silica than on titania films and TCP controls. When differentiation was evaluated on simvastatin-loaded titania films results showed that again after 14 days (Fig.1b) statistically significant higher osteoblastic activity was obtained in the titania films with simvastatin doses of 0.01mg/ml. The dose of 0.1mg/ml

also promoted a higher ALP activity when compared with the 0mg/ml titania mesoporous films. These results proved the clear osteoinductor potential of silica films, which corresponded to previous results at literature related to the benefits in bone regeneration of certain silica based materials, as Bioglass®⁴.

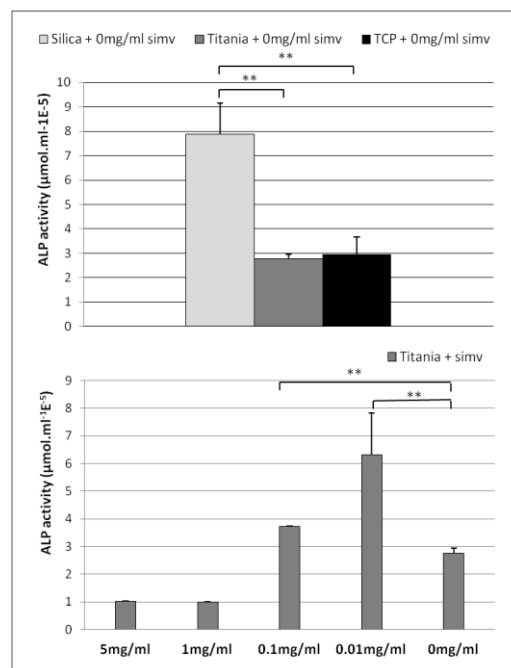


Figure 1. ALP activity for 0mg/ml silica, titania and TCP (a) and for all simvastatin doses on titania (b).

CONCLUSION

The biocompatibility of mesoporous silica and titania thin films has been proven, where, at the same time, silica thin films promoted higher ALP activity. Simvastatin loading in a controlled dose of 0.01mg/ml was demonstrated to improve the osteoblastic response. The threshold of cytotoxicity of simvastatin was established on ≥1mg/ml.

REFERENCES

1. Ravichandran R *et al.*, Micropor Mesopor Mat 187:53-62, 2014.
2. Angelomé PC *et al.*, Nanoscale 4:931-939, 2012.
3. Meretoja VV *et al.*, Tissue Eng 13(4):855-863, 2007.
4. Allon I *et al.*, J Oral Implantol, in press, 2012.

ACKNOWLEDGMENTS

M. López-Álvarez and V. López-Puente thank funding by FP7/REGPOT-2012–2013.1n.316265BIOCAPS and Spanish MINECO FPI scholarship, respectively. Xunta de Galicia (GRC2013-008) project is acknowledged.

Chitosan-catechol/graphene nanocomposite for biosensing applications

Peter Sobolewski^{1*}, Magdalena Pilarz¹, Małgorzata Aleksandrak², Ewa Mijowska², Jacek Podolski³, Mirosława El Fray¹

¹Division of Biomaterials and Microbiological Technologies, Polymer Institute

²Division of Nanotechnology, Institute of Chemical and Environment Engineering

West Pomeranian University of Technology, Szczecin, Al. Piastów 45, 71-311 Szczecin, Poland

³Meditest. Diagnostyka Medyczna. NZOZ, ul. Bronisławy 14d, 71-533 Szczecin, Poland

e-mail: psobolewski@zut.edu.pl

INTRODUCTION

The explosion of information provided by the “-omics,” (genomics, proteomics, etc.) has resulted in a pressing need to develop matching diagnostic technologies, so-called biosensors. Importantly, in addition to sensitivity and specificity, an ideal biosensor platform needs to be fast, affordable, and simple, in order to reduce the barrier of entry, especially in the developing world. Recent developments in polymer science, nanotechnology, and carbon-nanomaterials—graphene in particular—offer a great deal of promise in achieving these goals¹.

Here we present a chitosan-catechol/graphene nanocomposite suitable for use as an ink for ultrasonic, non-contact printing, for application as a matrix for the coupling of oligonucleotide molecular beacons for DNA biosensing.

EXPERIMENTAL METHODS

Chitosan/graphene dispersions utilizing 0.05% graphene oxide (GO) and chitosans of three different molecular weights (oligo, 5 kDa; low, 40 kDa; high, 890 kDa, Aldrich) were prepared in 1% acetic acid by a combination of sonication and mixing. The viscosity, conductivity, zeta potential, and stability of the dispersions was assessed, in order to determine ideal chitosan candidate for catechol modification. Catechol modification of chitosan was carried out with hydrocaffeic acid (HCA) by a carbodiimide coupling¹. Degree of modification was assessed via ¹H NMR.

RESULTS AND DISCUSSION

Oligo chitosan (5 kDa, 90% DD) solutions in acetic acid (2-4%) yielded GO dispersions of the highest conductivity (1-1,3 mS/cm), tunable viscosity in the required range for ink (up to 0,45 Pa s), high zeta potential (65 mV), and high stability over 21 days.

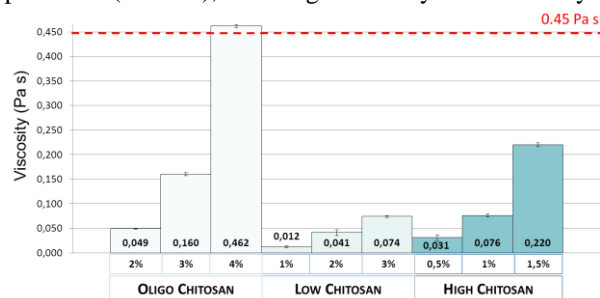


Fig. 1: Viscosity of chitosan/GO dispersions. Note: 0,45 Pa s is the maximum suitable for ultrasonic printing.

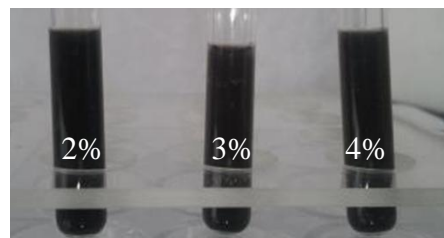


Fig. 2: Oligo chitosan/GO dispersions (2, 3, 4% oligo chitosan and 0,05% GO) remain stable after 21 days.

These parameters were deemed suitable for use as an ink for ultrasonic, non-contact printing, thus modification of oligo chitosan was carried out with HCA, to yield water soluble chitosan-HCA.

CONCLUSION

Novel nanocomposites consisting of water soluble, catechol modified chitosan and graphene oxide produced here will ultimately be combined with locked nucleic acid molecular beacons with the goal of producing printable DNA biosensors. The developed technology will allow fabrication of low cost, high sensitivity biosensors for point-of-care diagnosis.

REFERENCES

1. Shao, Y et al. *Electroanalysis* 22, 1027 (2010)
2. Kim, K et al. *Biomater. Sci.* 1, 783 (2013).

ACKNOWLEDGMENTS

The project is financially supported by NCBiR, under Graf Tech programme. The authors thank A. Piegat, PhD, J. Skrobot, and A. Niemczyk for useful discussions.

Fabrication of microparticles and patterned substrates for directing stem cell growth

Y. Yang^{1,2}, L. Glennon-Alty², A. Ahmed¹, L. Qian¹, P. Murray², D. Bradshaw³ and H. Zhang¹

¹ Department of Chemistry, University of Liverpool, UK, yonghong.yang@liv.ac.uk

² Institute of Translational Medicine, University of Liverpool, UK

³ Department of Chemistry, University of Southampton, UK

INTRODUCTION

Stem cells are able to self-renew and differentiate to produce specialized progeny, and thus have enormous potential for tissue engineering-based therapies¹. The use of suitable scaffolds is critical to grow cells for proper function and tissue engineering applications. 2D substrates with patterned surfaces can be readily used to investigate the interactions between the cells and the support scaffold. In this study, we have fabricated biocompatible micro-/nano-particles and 2D substrates to support and direct stem cell growth.

EXPERIMENTAL METHODS

Emulsion freeze-drying and emulsion evaporation were used to prepare poly(ϵ -caprolactone) (PCL) microparticles and poly(lactide-co-glycolide) (PLG) nanospheres. To fabricate the 2D substrates, the PLG nanospheres were suspended in aqueous chitosan solution. The suspension was dropped on a glass slide and spread evenly. A directional freezing process was then employed on a computer-controlled freezing stage.² The frozen sample on the glass slide was then freeze-dried to produce dry surface-patterned substrates.

Both the PLG microparticles and the substrates were used for the growth of mesenchymal stem cells (MSCs). The compatibility of the materials was firstly investigated based on the survival and growth of cells. The alignment of cell growth was particularly studied on the surface patterned substrates.

RESULTS AND DISCUSSION

For the emulsion freeze-drying approach, PCL was dissolved in dichloroethane which was then emulsified in aqueous poly(vinyl alcohol) solution with the aid of a surfactant. The emulsion was frozen and freeze-dried to produce a composite material. After dissolving the composite and collecting the microparticles by centrifuging, aligned porous PCL microparticles were produced. The cell culture study showed that PCL particles could support the growth of stem cells.

The study was then focused on the fabrication of surface-patterned substrates and directional growth of MSCs. A stable suspension was firstly formed by dispersing PLG nanospheres in chitosan solution. Chitosan was chosen because it is biocompatible and insoluble in neutral water. Aligned surface patterns on glass slides were produced with the ridges of the pattern composed of chitosan and PLG nanospheres. These patterns were stable in the culture. It was observed that the growth of MSCs was orientated (Fig. 1). The contact (hence interaction) between the cells and the PLG spheres could be observed by scanning electronic microscopy. It was possible to tune the width between the ridges on the surface pattern by changing the freezing condition. This, in turn, would be able to tune the MSC growth.

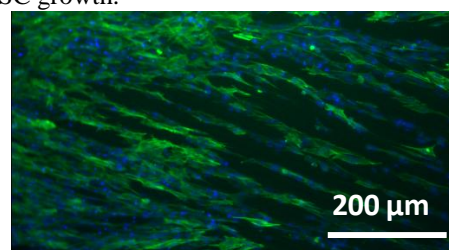


Fig. 1 The aligned growth of MSCs on surface patterned substrates.

CONCLUSION

A facile directional freezing and freeze-drying approach was employed to fabricate 2D substrates with aligned surface patterns. Such substrates could be used to guide stem cell growth

REFERENCES

1. Daley G.T. *et al.*, Cell 132: 544-548, 2008.
2. Zhang H. *et al.*, Nature Mater. 4: 787-793, 2005.

ACKNOWLEDGMENTS

The authors would like to thank the EPSRC and BBSRC for the PhD studentship funding.

Selenium-doped calcium phosphate coatings on titanium implants with inhibition properties on cancerous osteoblasts

Cosme Rodríguez-Valencia¹, Miriam López-Álvarez¹, Julia Serra¹, Pío González¹

¹ Department of Applied Physics, Institute of Biomedical Research of Vigo (IBIV), University of Vigo, 36310, Spain cosme@uvigo.es

INTRODUCTION

Nowadays, a common technique to treat bone cancer is the surgical removal and replacement of the affected tissue by an orthopaedic implant. However, cancer cells are not always completely removed and can return to the affected area after the surgery. Normally, titanium is the most used material for implants but these prostheses do not have any mechanism to prevent the reoccurrence of bone cancer. It is well known that hydroxyapatite (HA) as coatings on titanium prosthesis have osteo-inductive properties and at the same time selenium as nanoclusters² has been proven to inhibit the growth of certain types of bacteria¹ and the proliferation of certain cancerous cell lines. The objective of this study was to combine both properties, the osteoinductive of calcium phosphates and the anti-cancer of Se, in the same material as a coating (Se-CaP) to allow the prevention of the occurrence and reoccurrence of bone cancer and promote the healthy bone tissue growth.

EXPERIMENTAL METHODS

Following our previous work³, Ti6Al4V discs were coated with Se-CaP layers (0.6 and 2.5 at.% Se) by Pulsed Laser Deposition (PLD) technique and exposed to gamma radiation to their sterilization. In this study, healthy mouse pre-osteoblasts (MC3T3-E1) and human cancerous osteoblast (MG63) were cultured on coated titanium discs. To evaluate the behaviour of healthy osteoblast and cancerous osteoblast on the Se-CaP coatings, both cell types were stained with CFSE and Vybrant DIL fluorescent dyes, respectively. MC3T3-E1 and MG63 cells were seeded in the appropriated media (α -MEM and EMEM, respectively) at 5.000 cells/ml and then, were placed in an incubator under standard cell culture conditions. After the desired time period, media were exchanged and the cells were rinsed thrice with PBS. Both types of cells were observed under confocal laser microscopy (CLSM) at 1, 2 and 3 days. The number of the cells was counted in five random fields and averaged for each substrate. Uncoated and non doped HA coated substrates were used as controls.

RESULTS AND DISCUSSION

The MC3T3 culture assay showed an increasing cell proliferation along of time of culture, being more intense on coated titanium discs. After three days of culture, the MC3T3-E1 cell number was higher on Se-CaP coatings than on the controls, showing significantly difference ($p < 0.05$) on discs with 0.6at.% of selenium. On the other hand, there were more cancerous osteoblasts on controls than on the Se-CaP coatings. Also, on the non doped hydroxyapatite coatings was significantly higher ($p < 0.05$) than on the Se-CaP coatings with 2.5at.% of selenium.

The CLSM images showed normal healthy pre-osteoblasts (MC3T3-E1) proliferation and after 3 days of incubation, a greater number of cells were observed on Se-CaP coatings. In contrast, cancerous osteoblast densities were lower on Se-CaP coatings. In the case of SeCaP coatings with 2.5at.% of selenium, CLSM images showed that the cancer cell density decreased while healthy cell density increased, compared to the controls after 3 days of incubation.

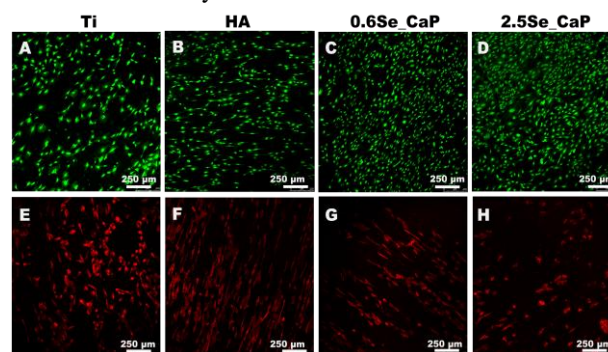


Fig.1. Cells stained in green, MC3T3-E1 on titanium (A), non doped HA (B), 0.6Se-CaP (C) and 2.5Se-CaP (D). Cells stained in red, MG63 cells on titanium (E), non doped HA (F), 0.6Se-CaP (G) and 2.5Se-CaP (H). Both cell types, after 3 days of incubation.

CONCLUSION

The biocompatibility of Se-CaP coatings with 0.6 and 2.5 at.% of Se was demonstrated. Particularly, those Se concentrations have been proven to promote the inhibition of cancerous osteoblastic cell line. At the same time, the healthy pre-osteoblasts proliferation was promoted, being in both cases statistically significant ($p < 0.05$). A new promising biomaterial based on selenium doped calcium phosphate coatings with interesting anti-bacterial and anti-cancer properties is proposed to improve the performance of the current commercial orthopaedic implants.

REFERENCES

1. Tran, P.L., *et al.* Appl. Environ. Microbiol. 75, 3586, 2009
2. Tran, P.A., Int. J. Nanomedicine. 5, 351, 2010.
3. Rodríguez-Valencia, C., *et al.* J. Biomed. Mater. Res. Part A. 101, 853, 2013

ACKNOWLEDGMENTS

UE-INTERREG2011-1/164MARMED, University of Vigo (CACTI), Xunta de Galicia GRC2013-008, FP7/REGPOT-2012-2013.1-316265 BIOCAPS are acknowledged.

Effects of stirring condition and fluid perfusion on the in-vitro degradation of calcium phosphate cement

Jie An, J.G.C.Wolke, S.C.G.Leeuwenburgh, J.A.Jansen

Department of Biomaterials, Radboud University Medical Center, The Netherlands
Jie.An@radboudumc.nl

INTRODUCTION

Calcium phosphate cements (CPCs) are the predominant type of bone substitute material used for reasons of injectability and hence perfect filling potential for bone defects. Recent studies have demonstrated that injectable CPCs combined with poly (lactic-co-glycolic) acid (PLGA) microspheres induced fast degradation¹. Many factors can affect PLGA degradation; molecular weight, chemical structure or geometric characteristics of the material or the characteristics of the surrounding medium. Currently, the in vitro degradation tests are performed in non-moving (static) soaking conditions, considering the extent flow in the physiological environment in vivo, dynamic soaking condition is probably more representative. Therefore, the aim of the present study is to investigate the in vitro degradable properties of PLGA/CPC composite tested under static and dynamic conditions in a bioreactor system and in a flow chambers.

EXPERIMENTAL METHODS

The CPC powder consisted of a mixture of 95% α -TCP, and 5% precipitated HA. PLGA (MW=17kDa, acid terminated, L:G=50:50) was used to prepare dense microspheres. PLGA/CPC formulations were prepared by adding 40%wt PLGA microspheres (mean particle size $94 \pm 29 \mu\text{m}$). PLGA/CPC composite was injected into teflon molds (cylinders $4.5 \times 9\text{mm}$).

For the degradation studies, the PLGA/CPC samples were placed in: (1) a bioreactor, static condition (BS), (2) a bioreactor, dynamic condition with a speed 200 rpm (BD) and (3) flow chambers, dynamic condition with a flow rate of 1.1 ml/min (FD). Phosphate buffered saline (PBS) was used as the soaking medium at 37°C. for 1, 2, 4 and 6 weeks (n=7). pH measurements of the PBS was performed directly after removal of the samples. The compressive strength was measured by using a testing bench with a crosshead speed of 0.5 mm/min (n=5). X-Ray diffraction (XRD) was used to determine the crystal structure. The morphology of the different formulation was determined by using scanning electron microscopy (SEM). Significant differences were determined using analysis of variance (Anova) and results considered significant if $p < 0.05$.

RESULTS AND DISCUSSION

The change of pH under each condition is shown in figure 1. After 6 weeks soaking the medium of the FD group shows a minimal pH decrease, this was higher than the bioreactor groups, where the pH decreased around 6.4. The compressive strength was given as a function of the degradation time (Fig 2). The FD group showed an increase in compressive strength upto 2 weeks soaking, while the BS and BD groups decreased already after 1 week soaking in PBS. It is clear that

during PLGA degradation lactic and glycolic acidic monomers are released and for the bioreactor groups the decrease in pH will accelerated cement degradation. XRD results showed after one week that the α -TCP phase was changed into an apatite phase, occasionally for all the groups upto 4 weeks an additional brushite phase was present. SEM examination demonstrated that after 4 weeks incubation for all the groups the microspheres were almost completely degraded.

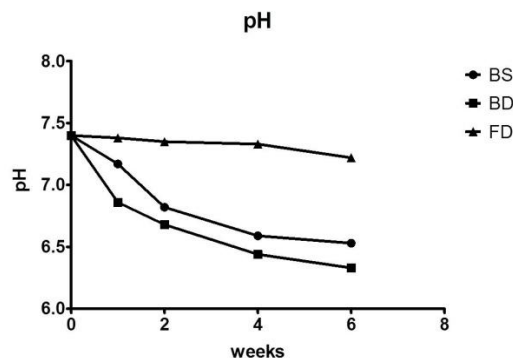


Fig 1: pH change of the PBS as a function of the degradation time in weeks.

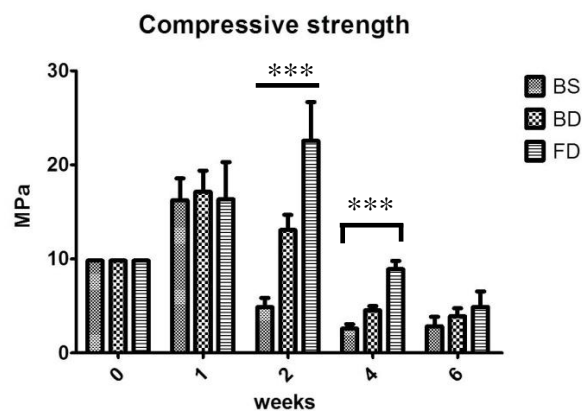


Fig 2: Compressive strength as a function of the degradation time in weeks.

CONCLUSION

The results indicated that the dynamic and static conditions influence the degradation of PLGA/CPC composite. The in vitro degradation of PLGA/CPC composite decreased in the order bioreactor static > bioreactor dynamic > flow chamber.

REFERENCES

- 1) Rosa P. *et al.*, J. Biomaterials. 32:8839-8847, 2011

ACKNOWLEDGMENTS

The authors would like to thank the China scholarship council (File No. 2011704027) for providing financial support to this project.

Ultrastructural features of mesenchymal stem cells in calcium alginate hydrogel during osteogenic differentiation by means of FIB-SEM

Jakub Grzesiak^{1*}, Krzysztof Marycz^{1,2}, Agnieszka Śmieszek^{1,2}, Anna Siudzińska¹

¹Electron Microscopy Laboratory, Wrocław University of Environmental and Life Sciences, Poland,

*grzesiak.kuba@gmail.com

² Wrocław Research Centre EIT+, Poland

INTRODUCTION

Three-dimensional hydrogel culture systems are more and more common in biomedical research. However, the evaluation of ultrastructural features of both cells and materials is remarkable challenge. In our work we present the huge potential of focused ion beam combined with scanning electron microscope for evaluation of ultrastructural features in cells and hydrogel during osteogenic differentiation. The FIB milling allows for observation the cellular interior with minimal invasiveness during sample preparation. Additionally, this device also allows for evaluation of changes in hydrogel's structure after osteogenic differentiation.

EXPERIMENTAL METHODS

Bone marrow- and adipose tissue-derived stem cells isolated from rat were encapsulated in 2% calcium alginate and put into the osteogenic culture conditions for 3 weeks. After culturing, samples were fixed in glutaraldehyde, dehydrated in acetone row, dried using critical point drying, and put for FIB milling and SEM observations, using Auriga 60 (Zeiss).

RESULTS AND DISCUSSION

Observations showed significant differences in both cellular and material's morphology between osteogenic-differentiated (OG) and non-differentiated (non-OG) specimens. In OG group, cells were arranged in groups and created cellular cavities within the calcium alginate. Cells showed high microvesicle release and were rich in lamellipodia (figure 1A). In non-OG group cells were arranged more individually, and did not create cavity, rather were embedded in alginate (figure 1B). Calcium alginate after osteogenic differentiation was rearranged, with decreased porosity and visible structures between fibres, probably the bone-like ECM synthesized by cells during osteogenic differentiation (figure 1C). In alginate from non-OG group, the alginate fibres were arranged regularly, with visible pores and no ECM-like features deposited by encapsulated cells (figure 1D).

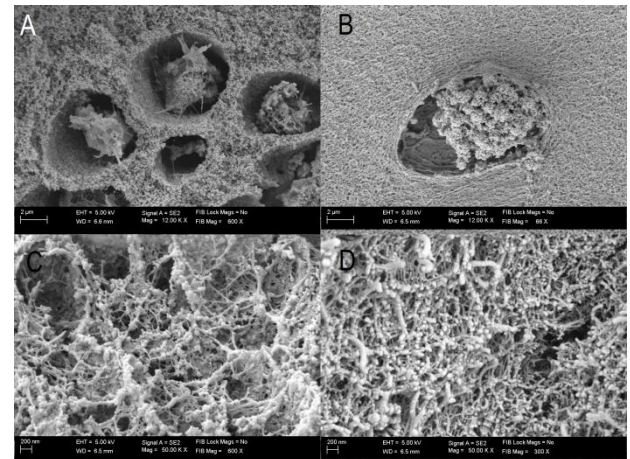


Figure 1. Morphology of cells in calcium alginate after osteogenic differentiation (A), and without osteogenic differentiation (B). The morphology of calcium alginate from osteogenic (C) and non-osteogenic (D) conditions.

CONCLUSION

We showed that focused ion beam combined with scanning electron microscope constitutes an excellent tool for evaluation of hydrogels with encapsulated cells during various bio-assays.

REFERENCES

1. Al-Abboodi A. *et al.*, Proceedings of Chemeca, 18-21 september, pp. 1-9, 2011.
2. Volkert C.A., *et al.*, MRS Bulletin 32:389-395, 2007.
3. Abbah S.A., *et al.*, J. Mater. Sci. Mater. Med. 19:2113-2119, 2008.

ACKNOWLEDGMENTS

We wish to thank the Wrocław Research Centre EIT+ staff for supporting us with hardware.

High Throughput Production and Analysis of Tissue Engineering Scaffolds prepared using Combinatorial Chemistry

Erwin Zant¹, Maarten M. Blokzijl¹, Dirk W. Grijpma^{1,2}

¹ Department of Biomaterials Science and Technology, University of Twente, The Netherlands, e.zant@utwente.nl

² Department of Biomedical Engineering, University Medical Centre Groningen, The Netherlands

INTRODUCTION

The current high throughput (HT) production of 3D scaffolds is limited to gradients of just two polymers at a time¹. A straightforward method involving thermally induced phase separation of polymer solutions inducing crystallization of the solvent allows the very fast production of porous structures². Mixing low molecular weight macromers and subsequent photo-crosslinking can produce huge libraries of different materials³. Furthermore, a newly developed HT mechanical screening (HTMS) device can assess the mechanical properties of multiple samples simultaneously⁴. Here a combination of a new HT scaffold production technique and HT screening method was evaluated. Poly(trimethylene carbonate-dimethacrylate), poly(D,L-lactide-dimethacrylate) and poly(ethylene glycol-dimethacrylate) macromers solutions in ethylene carbonate (EC) were combined to eventually fabricate 63 scaffolds with highly diverging mechanical properties. The compression moduli of wet scaffolds were measured in both a conventional and the novel HT fashion.

EXPERIMENTAL METHODS

Linear trimethylene carbonate (TMC) and D,L-lactide (DLA) based oligomers were synthesized by ring opening polymerization. These oligomers and polyethylene glycol (PEG) were functionalized using methacrylic anhydride to form methacrylate end-functionalized macromers. Six different macromers with molecular weights of 4 and 10 kg/mol were obtained. HT fabrication of scaffolds was performed by mixing the macromers (25 wt.%) in EC in 63 different combinations, solvent crystallization at 21°C, 20 minutes of photo-crosslinking at 365 nm and solvent extraction in water. Irgacure® 2959 was used as photoinitiator (1 wt.% to macromer). The samples were dried and swollen in distilled water for 48h. Compression tests were performed on a Zwick Z100 (single sample) and on the HTMS device. Compression modulus (E_{comp}) was recorded at 8% compression on the tensile tester and equilibrium modulus was measured on the HTMS device⁴.

RESULTS AND DISCUSSION

Mixing the macromers PTMC-dMA 4k, PTMC-dMA 10k, PDLLA-dMA 4k, PDLLA 10k, PEG-dMA 4k and PEG-dMA 10k in EC yielded 63 combinatorial scaffolds with comparable morphologies, an example is shown in figure 1. Overall, the obtained scaffolds were 50 vol.% porous and the pores were of hexagonal shape. Scaffolds with extremely varying water uptakes (1-1700 wt.%) and compression moduli (0,01-60MPa). The compression moduli were recorded using a (conventional) single sample test method and the

HTMS device. Results for the scaffolds ($E_{comp} < 1\text{MPa}$) are presented in figure 2.

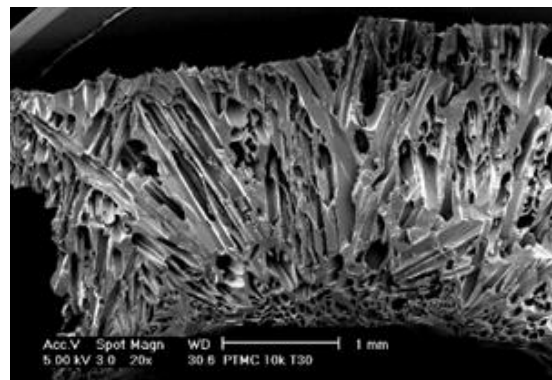


Figure 1: Scanning electron micrograph of a scaffold produced from PTMC-dMA 10k

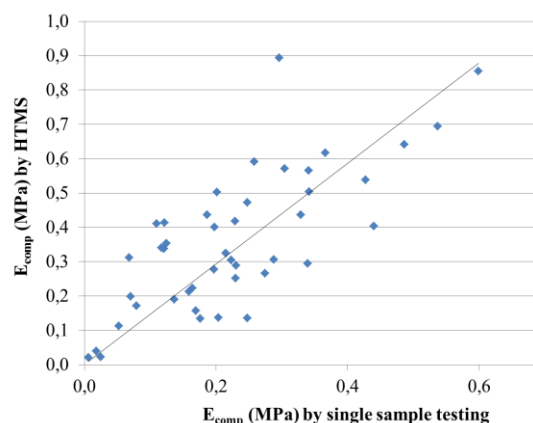


Figure 2: Comparison of E_{comp} between single sample testing and HTMS of wet scaffolds.

CONCLUSION

A new HT approach was successfully applied to produce numerous scaffolds hugely varying in hydrophilicity and mechanical properties. Furthermore, a new HT mechanical device was assessed showing a linear relation to conventional tests.

REFERENCES

1. Chatterjee K. *et al.*, Biomaterials 32:1361-1369, 2011
2. Aubert JH *et al.*, Polymer 26: 2047-2054, 1985
3. Anderson DG *et al.*, Nature Biotech. 22:863-866, 2004
4. Mohanraj B. *et al.*, Journal of Biomechanics, (0)

ACKNOWLEDGMENTS

We would like to acknowledge Bhavana Mohanraj and Robert Mauck (University of Pennsylvania, PA, USA) for the HTMS measurements. Furthermore the Netherlands Institute for Regenerative Medicine (NIRM) for funding.

Relationship between physical properties and biological response in tyrosine-derived polyarylates explored by association rules

Daniela C. Soto¹ and Loreto M. Valenzuela^{1,2*}

¹Department of Chemical and Bioprocess Engineering, Pontificia Universidad Católica de Chile, Chile

² Research Center for Nanotechnology and Advanced Materials “CIEN-UC”, Pontificia Universidad Católica de Chile, Santiago, Chile *lvalenzr@ing.puc.cl

INTRODUCTION

Polymers are widely used in several medical applications, from degradable scaffolds to drug delivery systems. Nowadays the focus is to design polymers with specific properties for each application¹. To achieve this goal, it is necessary to find relationships between polymer chemistry and properties (glass transition temperature (T_g) and air-water contact angle), polymer response in physiological environment (degradation, erosion and water uptake) and biological response of the host (protein adsorption and cell adhesion-proliferation).

Combinatorial chemistry has enabled the generation of polymer libraries¹. Several techniques have been used to build discrete² and numerical^{3,4} models for some of these polymer libraries. These studies only correlate the physical properties and chemical structure of polymers with protein adsorption or cell response separately. In this study, we used association rules to find relevant patterns between all of these properties on the L-tyrosine derived polyarylates library. Knowing these relationships would guide future experimental research, making easier to find polymers with desired properties.

EXPERIMENTAL METHODS

We used a polymer library of 112 polyarylates created by Kohn and coworkers⁵. The information available include T_g and water-air contact angle for all polymers of this library⁶, half degradation time for 23 of them, water uptake equilibrium (WU_{eq}) for 19⁷, fibrinogen adsorption for 45⁸, albumin adsorption for 41, normalized metabolic activity of rat lung fibroblast (RLF) for 69, and human normal foreskin fibroblast (NFF) for 94 of them². Only 5 polymers are fully characterized in terms of these properties.

Association rules were used to find patterns in the dataset, which was discretized using EM clustering⁹. This methodology recognizes when certain conditions occurred simultaneously. We set the minimum support as 10% or 8% (i.e., a rule must contain a pattern present at least in 10% or 8% of the polymers, respectively), and the confidence as 90% (i.e., the presence of certain condition(s) imply the presence of other condition(s) in at least 90% of the cases). The data-mining package WEKA (Waikato Environment for Knowledge Analysis) was used in this study¹⁰.

RESULTS AND DISCUSSION

The use of support of 10% corresponds to the most strict analysis, where for each rule at least 12 polymers must fulfill it. With this criterion, the value of T_g is

inverse to the one of contact angle, as observed previously⁶. Earlier, Abramson et al.² observed a strong relationship between T_g and RLF growth, which was observed in our study as well. They observed that higher values of T_g were correlated with higher values of NFF growth. However, our study suggests that with high T_g it is also required a high value of fibrinogen adsorption in order to have high NFF growth.

With a less restrictive analysis, considering a support of 8% (i.e., 10 polymers for each rule), we observed that higher values of NFF growth are related with lower values of half degradation time (i.e., faster degradation). This relationship is important because the growth of NFF was obtained after only few hours of incubation, while degradation was followed through time up to several months.

With our restrictions on the association rules, we did not find any relevant correlation between water uptake and other properties. We think that more data will be needed to build rules including this property.

CONCLUSION

There are relationships between different properties of a set of polymers, which can be explored through association analysis. Filtering relevant rules is the most challenging task in this methodology. Having the complete set of experimental values for all polymers, or a prediction of them, will allow more and better association rules that will in turn allow a better selection of polymers for different applications.

REFERENCES

1. Kohn, J. Nat. Mater. 3:745–747, 2004
2. Abramson, S. D. et al., J. Biomed. Mater. Res. A 73:116–24, 2005
3. Gubskaya, A. V. et al., Polymer. 48:5788–5801, 2007
4. Smith, J. R. et al., QSAR Comb. Sci. 24:99–113, 2005
5. Fiordeliso, J. et al., J. Biomater. Sci. 5:497–510, 1994
6. Smith, J. R. et al., Aerosp. Eng. 25:127–140, 2004
7. Valenzuela, L. M. et al., Polym. Degrad. Stab. 97:410–420, 2012
8. Weber, N. et al., J. Biomed. Mater. Res. A 68:496–503, 2004
9. Dempster, A. et al., J. R. Stat. Soc. B 39:1–38, 1977
10. Mark Hall et al., SIGKDD Explor. 11, 2009

ACKNOWLEDGMENTS

The authors thank Dr. Joachim Kohn and Dr. Sanjeeva Murthy from the New Jersey Center for Biomaterials for providing polymer data and useful discussions. This work was funded by Chilean agency FONDECYT (Project 1112-1392).



Generation of functional oxygen groups on parylene C for enhanced biocompatibility: LDI-MS investigations

M. Gołda-Cepa¹, N. Aminlashgari², M. Hakkarainen², K. Envall³, A. Kotarba¹

¹Faculty of Chemistry, Jagiellonian University, Krakow, Poland, golda@chemia.uj.edu.pl

²Department of Fibre and Polymer Technology, KTH Royal Institute of Technology, Stockholm, Sweden

³Department of Chemical Engineering and Technology, KTH Royal Institute of Technology, Stockholm, Sweden.

A novel application of LDI-MS (Laser Desorption/Ionisation-Mass Spectrometry) for the direct identification of functionalised compounds containing groups such as -COOH, -OH, and -C(O)H on the oxygen plasma treated parylene C surface is proposed. Such a modification is crucial from the medical point of view because it leads to higher hydrophilicity, and provides adhesion centres and further determines the bond strength between the cells and polymer surface. As a result, the polymer material is transformed into a highly valuable finished biomimetic interface.

INTRODUCTION

Parylene C is an excellent protective coating material for metal implants due to its *in vivo* compatibility, mechanical properties and stability in body fluids^{1,2,3}. It is not only corrosion resistant, but it substantially decreases the release of hazardous metal ions from metal implants into the body. However, for good attachment of cells and/or drug-loaded biodegradable polymers, their surface must be adjusted via introduction of functional groups, which are tangible adsorption sites. Taking that into consideration, there is a strong need for surface modification methods, which can transform popular materials into highly valuable final products. Low pressure plasmas are considered one of the universal options for such surface treatment, where the chemical structure of a top polymer layer can be tailored⁴. By adjustment of the plasma parameters the modification is confined to a shallow surface layer (~10 nm) of the polymer. The final polymeric material is uniformly modified over the whole surface. In this study, we investigated what kinds of oxygen containing groups are generated on the parylene C surface upon oxygen plasma treatment (Fig.1).

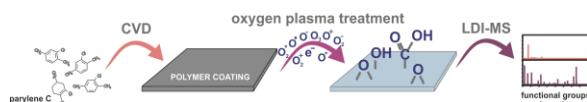


Fig. 1 The schematic representation of the experimental methodology.

EXPERIMENTAL METHODS

Parylene C (8 µm of thickness) films were prepared by CVD technique. The samples were provided by ParaTech Coating Scandinavia AB. In order to modify the parylene C surface, the oxygen plasma treatment

was carried out using a Diener electronic Femto plasma system (Diener Electronic GmbH, Nagold, Germany). The surface analysis of unmodified and oxygen plasma treated parylene C was performed on a Bruker UltraFlex time-of-flight (TOF) mass spectrometer with a SCOUT-MTP ion source (Bruker Daltonics, Bremen, Germany) in reflector mode and equipped with a 337 nm nitrogen laser.

RESULTS AND DISCUSSION

The LDI-MS analysis revealed that insertion of oxygen to the polymer backbone took place exclusively in the linker between the aromatic rings of the polymer chain. This is important for keeping the stable crystalline structure of parylene C, which prevents extensive penetration of the oxygen active species into the bulk during plasma treatment. Additional confirmation of stability of aromatic rings with chlorine substituent is provided by characteristic splitting of the main line of 2 m/z due to the presence of the natural abundance of ³⁵Cl and ³⁷Cl isotope. Moreover, the LDI-MS method allows for direct identification of the groups -COOH, -OH, and -C(O)H in functionalised polymer.

CONCLUSION

We demonstrate that the mild oxygen plasma technology provides a direct route for facile engineering of polymeric biointerface. The LDI-MS method provided a direct way to analyse the oxygen containing functional groups and their speciation formed on the parylene C surface, as well as their location in the polymer chain. Thus, LDI-MS was shown to be a versatile and powerful tool for direct characterisation of modified surfaces.

REFERENCES

1. Cieřlik M., *et al.*, Mater Sci Eng C, 32:31-35, 2012,
2. Cieřlik M., *et al.*, Mater Sci Eng C, 32:2431-2435, 2012.
3. Gołda M., *et al.*, Mater Sci Eng C, 33:4221-4227, 2013
4. *The Plasma Chemistry of Polymer Surfaces*, Friedrich J., 2012, Wiley-VCH

ACKNOWLEDGMENTS

“The authors would like to thank the Foundation for Polish Science Ventures Programme, co-financed by the EU European Regional Development Fund, for providing financial support to this project”.

Controlled Drug Delivery From Bioresorbable Magnesium Orthopaedic Implants

Jessica A. Lyndon¹ and Ben J. Boyd², Nick Birbilis¹

¹Department of Materials Engineering, Monash University, Australia

²Monash Institute of Pharmaceutical Sciences, Monash University, Australia, jess.lyndon@monash.edu

INTRODUCTION

Bioresorbable implants challenge the paradigm of permanent metallic implants where the implant can support and facilitate the remediation of dysfunction in bone trauma. Magnesium is a standout material for degradable implants as it is non-toxic, biocompatible, biodegradable and has mechanical properties similar to bone. Furthermore the degradation rate of magnesium can be fine-tuned by altering its composition¹. Degradable implants are advantageous over traditional permanent implants and present the possibility to utilise the implant as it corrodes as a local drug delivery system. If resorbable magnesium implants can be exploited to deliver pharmaceutical agents they can provide drug delivery to the implantation site with many benefits over systematic drug delivery. This paper outlines the proof of concept study in order to determine the drug release kinetics using a degradable magnesium drug/device system.

EXPERIMENTAL METHODS

Materials

Samples comprised of high purity magnesium, were wire cut to 20 mm in length, 5 mm in width and 5 mm in depth. 9 holes 1 mm in diameter were drilled 2 mm apart and filled with powdered ibuprofen sodium salt (Sigma Aldrich). One side of the sample was exposed by polishing to 1200 grit with ethanol.

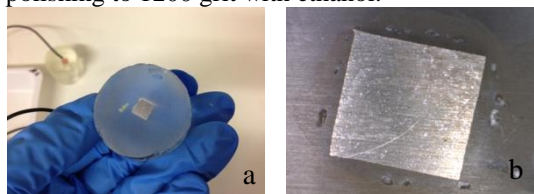


Figure 1: a) Epoxy mounted magnesium sample and b) magnesium surface before immersion in MEM.

Solutions

Experiments were carried out in Minimum Essential Media (MEM, Life Technologies) with 2.2 g/L sodium bicarbonate (Sigma Aldrich) buffer.

Ibuprofen Calibration Curve

1 mg/mL ibuprofen sodium salt was dissolved in MEM and characterised by UV-Vis spectroscopy (EnSpire Multimode Plate Reader, Perkin Elmer). When a typical absorption wavelength was found, known concentrations of ibuprofen were analysed at the typical wavelength and the intensity measured to generate a linear calibration curve.

Drug Release Study

Mass loss tests were conducted in 200 mL of MEM in a carbon dioxide atmosphere at 37 °C using a CO₂ Incubator (Sanyo MCO-15AC). Every 2 days 1.5 mL of the solution was frozen for UV-vis analysis, the depth

of degradation (as a measure of corrosion rate) and pH of solution were recorded and the solution replenished.

RESULTS AND DISCUSSION

Calibration Curve

The calibration curve generated in Figure 3 was used to determine the amount of ibuprofen present in the drug release study solutions.

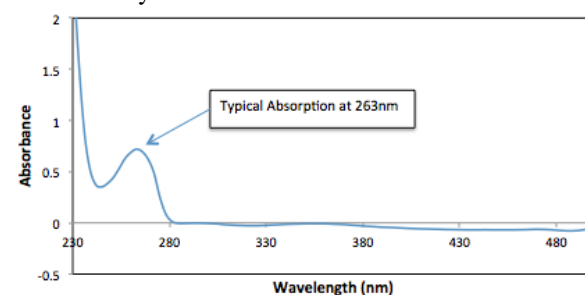


Figure 2: UV-Vis spectrum of 1 mg/mL ibuprofen sodium salt in MEM.

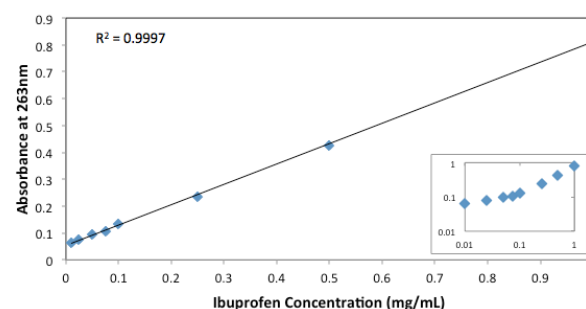


Figure 3: Calibration curve of ibuprofen sodium salt in MEM. Inset: data presented in log scale.

Drug Release Study

Initial results suggest that the ibuprofen is released when the degradation of the magnesium sample reaches the drug filled reservoir, as highlighted by the empty reservoir in Figure 4.



Figure 4: Surface of magnesium sample after 10 days in the incubator.

CONCLUSION

This pilot study indicates the promise of degradable magnesium orthopaedic implants as drug delivery devices.

REFERENCES

1. Kirkland, N.T. et al, Corrosion Science, 52 (2010) 287 – 291

Effect of Different Crosslinking Treatments on the Physical Properties of Collagen-based Scaffolds

Luca Salvatore¹, Deborah Pedone^{1,2*}, Emanuela Calò¹, Valentina Bonfrate¹, Marta Madaghiele¹

¹Department of Engineering for Innovation, University of Salento, Italy

^{2*}Dhitech Scarl – Distretto Tecnologico High Tech, Lecce, Italy, deborah.pedone@dhitech.it

INTRODUCTION

Collagen-based materials are widely used in the biomedical field due to their excellent biocompatibility and low antigenicity. In tissue engineering, collagen substrates are well known to modulate various aspects of cell behaviour like adhesion, proliferation and differentiation. However, major drawbacks such as rapid degradation and poor mechanical properties limit the number of possible applications¹. Collagen crosslinking and/or blending with other materials can be effective methods to overcome these constraints. The aim of this work was to investigate the influence of several crosslinking treatments on the physical properties of collagen-based scaffolds. Five different crosslinking agents (*i.e.* carbodiimide (EDC), glutaraldehyde (GTA), formaldehyde (FA), genipin (GP) and dimethyl suberimidate (DMS)) were selected to crosslink collagen following a standard dehydrothermal (DHT) treatment. The scaffolds were then assessed for swelling ratio, primary amine group content, denaturation temperature, dynamic mechanical properties and resistance against collagenase digestion. Preliminary cytotoxicity tests were also performed.

EXPERIMENTAL METHODS

Scaffold synthesis. An aqueous suspension of 3% w/v Type I collagen from bovine dermis was prepared by mixing for 5-6 hours at 10°C. Following casting and freeze-drying, porous collagen-based matrices were obtained. Several crosslinking treatments were performed (Table 1), according to established protocols¹⁻³. The matrices were then stored in phosphate buffered saline (PBS) at 4°C until further analyses.

Characterization experiments. Swelling ratio was determined through gravimetric measurements on dry and swollen matrices. The concentration of free primary amine groups (-NH₂) was determined using 2,4,6-trinitrobenzenesulfonic acid (TNBS) assay. Differential scanning calorimetry (DSC) was employed to measure the denaturation temperature (T_d) of the scaffolds. The shear modulus G of denatured samples was assessed by means of dynamic mechanical analysis (DMA) and used to estimate the elastically effective crosslink density (ρ_{xe}), according to the rubber elasticity theory⁴. The resistance to enzymatic degradation was evaluated *in vitro*, by incubating the scaffolds in bacterial collagenase solution at 37°C. The cytotoxicity of the matrices was assessed *in vitro* using a rat Schwann cell line (RSC96), by means of MTT assay. Statistical significance was determined using one-way ANOVA and Fisher's PLSD test (n=5).

RESULTS AND DISCUSSION

As expected, the crosslinking treatment was found to have a significant impact on the physical properties of

the collagen matrices. Higher values of the crosslink density, attained by the different treatments, were found to increase the shear modulus of the scaffolds (Table 1), while decreasing the *in vitro* degradation rate and the swelling capability. A good correlation between the elastically effective crosslink density and the inverse of free amine group content was detected. The thermal stability of collagen appeared to be more dependent on the specific crosslinking agent used, rather than the yielded crosslink density. Indeed, in spite of the large differences in ρ_{xe} , samples treated with GTA and DMS, which are crosslinking agents incorporated in the collagen network, showed a similar T_d value, while the highest T_d was attained by samples treated with EDC, which is conversely a 'zero-length' crosslinker. The preliminary MTT assay seemed to suggest that DMS was the least cytotoxic crosslinking agent among those tested. No significant difference in cell viability was detected between control cells and DHT samples.

Crosslink treatment	G (kPa)	ρ_{xe} (10 ⁻⁵ mol/cm ³)	NH ₂ (10 ⁵ mol/g)	T _d (°C)
None	/	/	5.6±0.7	36.9±0.9
DHT	10.0±0.4	1.2±0.0	5.4±0.1	37.4±0.5
DHT+GP	14.3±3.5	1.9±0.5	5.3±0.1	37.5±0.1
DHT+DMS	21.1±4.2	2.6±0.5	3.6±0.5	48.7±2.6
DHT+EDC	36.6±2.8	4.3±0.3	2.7±0.0	58.4±0.7
DHT+GTA	49.8±0.7	6.0±0.1	2.4±0.0	47.0±1.2
DHT+FA	52.7±0.9	5.9±0.1	2.3±0.1	50.4±0.6

Table 1. Summary of data obtained from DMA, TNBS assay and DSC (n=5).

CONCLUSION

The data obtained in this study provide further evidence that proper choice of the crosslinking agent and accurate control of the crosslinking treatment are fundamental for finely tuning the physical properties of collagen-based scaffolds, in order to tailor selected *in vitro* and/or *in vivo* applications.

REFERENCES

- Madaghiele M. *et al.*, J. Mater. Sci. Mater. Med. 20:1979-1989, 2009.
- Charulata V. and A. Rajaram. J. Biomed. Mater. Res. 36: 478-486, 1997.
- Liang H.C. *et al.*, J. Appl. Polym. Sci. 91:4017-4026, 2004.
- Flory J.P. Principles of polymer chemistry. Ithaca, NY: Cornell University Press; 1953.

ACKNOWLEDGMENTS

The authors acknowledge the Italian Ministry of Education, University and Research for providing financial support (Grants: PON RINOVATIS, FIRB MERIT).



Degradation and mechanical properties of biodegradable PLGA film

Reyhaneh Neghabat Shirazi^{1,2}, Yury Rochev², Peter McHugh¹

¹Mechanical and Biomedical Engineering, College of Engineering and Informatics, NUI Galway

²National Centre for Biomedical Engineering Science, NUI Galway, Ireland

r.neghabatshirazi1@nuigalway.ie

INTRODUCTION

Poly (lactic-co-glycolic) acid (PLGA) is a degradable polymer which is used for a variety of medical implant applications, including orthopaedic fracture fixation or as a coating for drug eluting stents¹. PLGA degradation is due to simple hydrolysis of the ester backbone in aqueous media. Depending on the application, the biodegradable implant can be subjected to different load and stress conditions, which may cause mechanical failure of the material. Hence the mechanical properties of the polymer during degradation are important to know to guide implant design. The specific aims of this work are to prepare a PLGA film and to characterise physical and mechanical properties of the film during the degradation.

EXPERIMENTAL METHODS

A 0.2 g mol⁻¹ solution of PLGA (50:50, $M_n=82$ kg mol⁻¹) in chloroform was prepared and casted onto a Petri dish. The samples were dried in vacuum desiccators for a week. All the films were of the same thickness (0.25 ± 0.04 mm). The specimens were placed in PBS (pH 7.4, 37°C) and characterized during degradation for water content, mass loss, average molecular weight (using GPC), crystallinity (using XRD), glycolic and lactic unit content (using FTIR) and were imaged using optical microscopy. Mechanical properties of the films were determined using nano-hardness testing with a Berkovich diamond tip over three different indentation loads. Values for Young's modulus and hardness determined based on Oliver and Pharr procedure².

RESULTS AND DISCUSSION

Figure 1 illustrates the indentation hardness and Young's modulus values of the films over three different indentation loads versus the molecular weight. As shown in Figure 1(a), the surface hardness reduced in the initial days of degradation suggesting that water acts as a plasticiser which results in reducing the yield strength of the film. Significant fluctuation in hardness value appeared during the degradation due to the high amount of surface roughness observed by optical microscopy. After a critical molecular weight (8 kg mol⁻¹), the value of hardness decreased significantly and reached less than 10 MPa.

As shown in Figure 1(b) a significant difference in Young's modulus value observed for different indentation loads due to the viscoelasticity of the film. Measurements of modulus using nanoindentation tended to increase with decreasing the applied load. The Young's modulus value from conventional tensile test (3.5 ± 0.2 GPa) for non-degraded film was found to be fairly close to the value obtained from nanoindentation

for 7 mN load. For the initial days of degradation the values of modulus remained constant. Following the degradation, it can be seen that the decrease in modulus showed down and it reduced to 0.3 GPa. All different loads showed nearly the same trend during the degradation.

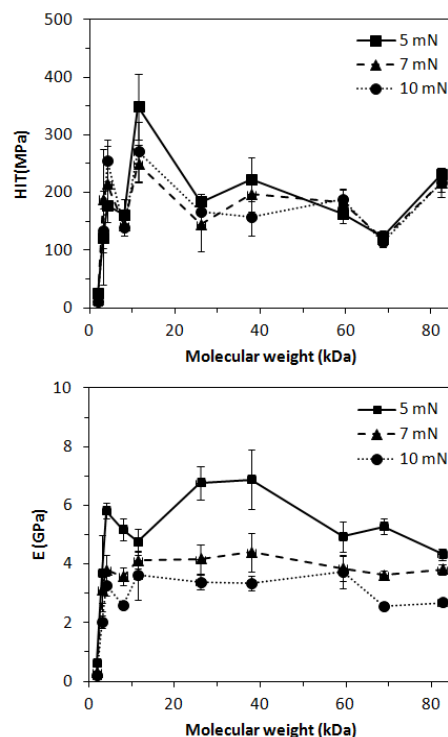


Figure 1: (a) Indentation hardness (b) Young's modulus of PLGA films over three different indentation loads versus the molecular weight (Mean \pm STDEV; n=10).

CONCLUSION

After a critical molecular weight, due to the significant degradation, the surface hardness and the Young's modulus of the films dramatically decreases and reduced to 16% and 10% of the initial values for non-degraded film, respectively. This information can be used to predict changes in the mechanical performance and degradation of PLGA film which is very useful to guide the design of biodegradable coatings.

REFERENCES

- Gulati, N. *et al.*, Acta Biomater. 8:449–456, 2012.
- Oliver, W. C., *et al.*, J Mater Res. 7: 1564-80, 1992.

ACKNOWLEDGMENTS

BMERM programme funded under PRTL and ERDF.

Temporal Analysis of Dissolution By-Products and Genotoxic Potential of Spherical Zn-Si Bioglass: “Imageable beads” for Transarterial Embolization

Muhammad Sami (Hasan)¹, Sharon (Kehoe)² and Daniel (Boyd)^{1,2}

¹. Department of Applied Oral Sciences, School of Biomedical Engineering, Dalhousie University, Halifax, NS, Canada

². ABK Biomedical Inc. 1344 Summer Street Suite 212 Halifax, NS B3H 0A8 Canada. <mailto:sami.hasan@dal.ca>

INTRODUCTION

Transarterial embolization of vascular tumors is frequently performed using particles as the principal embolic agent and regarded as an effective procedure, capable of eliminating the vascular supply to target tissues such as uterine leiomyomas and hepatocellular carcinomas. Radiopacity, durability and sphericity are three key parameters for an effective embolic agent [1]. Intrinsic radiopacity obviates the need of a contrast reagent and allows the radiologist to monitor spatial distribution of the particles. Sphericity allows a precise size classification and optimal and predictable vessel embolization. Yet, radiopaque spherical particles remain to be developed for clinical use. The current study produced radiopaque glass microspheres in a broad size range (45–500µm) and investigated the degradation by-products and their contingent genotoxic effect.

EXPERIMENTAL METHODS

Glass microspheres, comprising of three particle size ranges (45-150, 150-300, 300-500µm) with narrow size distributions were produced using a flame spherodization process. Digesting the glass microspheres in mineral acids and detecting the constituent ions using ICP-AES verified the composition of the glass post-synthesis. The authors confirmed the radiopacity of the glass microspheres previously, using X-ray and axial CT scans for microspheres suspended in either PBS or filled in a glass vial. The ion release (Si^{4+} , Na^+ , Ca^{2+} , Zn^{2+} , Ti^{4+} , La^{3+} , Sr^{2+} , Mg^{2+} and Zn^{2+}) from sterilized and non-sterilized glass microspheres were immersed and incubated in sterile tissue culture water and DMSO at 37°C, and quantified using ICP-AES over extended time periods (up to 30d). The effects of surface area as well as polar and non-polar media on the ion release profiles were explored. The effect of dissolution by-products on the bacterial gene expression was also investigated using the *in vitro* Ames assay, with extracts prepared at accelerated leaching conditions at 50°C over 72h. Quantities of the subsequent leachates were further investigated for the effect of various ions and their quantities on bacterial mutation. Finally, the results were correlated with previously reported ion release profiles from irregular shaped particles of the same glass formulation (up to 120h) [2].

RESULTS AND DISCUSSION

Radiopaque, non-degradable and non-deformable spherical glass particles were produced in various particle size ranges from 45 to 500µm (Fig 1). Ions released (Fig 2) from the microspheres were dependent upon surface area to volume ratio as well as the nature of elution media. Greater ions were released from the 45-150µm-particle size range owing to its largest surface area to volume ratio (*in polar medium*). For the genotoxic bacterial reverse mutation Ames-assay, the

concentrations of all the ions were well below their therapeutic concentration reported in the literature. No mutagenic effect was observed in the bacterial reverse mutation Ames test (Fig 2).

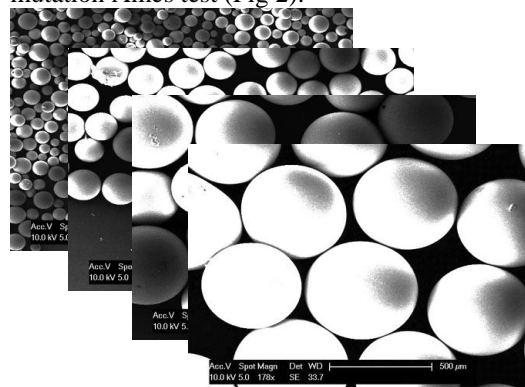


Fig 1. SEM micrographs of various sized glass microspheres.

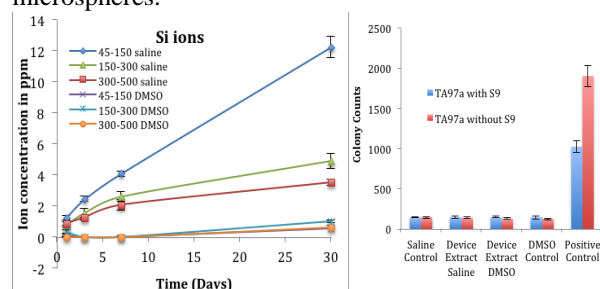


Fig 2. Representative graphs from Ion release (left) and genotoxicity (right) evaluations

CONCLUSION

Radiopaque glass microspheres (45-500µm) were successfully produced using the flame spherodization technique. However, larger particles were found difficult to spherodize using current setup. Approximately 80-95% of Gaussian distribution can be achieved by simple sieving. The ions released from the microspheres were dependent upon surface area to volume ratio as well as the nature of elution media. As expected, greater ions were released from the smaller particle size ranges in polar medium. However, concentrations for all ions were reported well below the therapeutic concentration reported in the literature. Most significantly, this is reflected in their benignity as observed in bacterial reverse mutation Ames test. Hence, it can be concluded that the glass microspheres produced in this study provide a non-mutagenic and safe choice for use as a potential embolic agent.

REFERENCES

1. Laurent, et al., Am J of Neu, 1996. 17(3): p. 533-540.
2. Kehoe et al., J of Func Biomat, 2013. 4(3): p. 89-113.

ACKNOWLEDGMENTS

The authors acknowledge the financial support of the Canadian Institutes of Health Research award # 276947 and the Canadian Foundation for Innovation (project # 2717).

A modular flow-chamber bioreactor as a tool for the analysis of degradable materials

Frank Feyerabend¹, Ralf Pörtner² and Regine Willumeit¹

¹Institute of Materials Research, Helmholtz-Zentrum Geesthacht, Germany, frank.feyerabend@hzg.de

²Institute for Bioprocess and Biosystems Engineering, Technical University Hamburg Harburg, Germany

INTRODUCTION

Bioreactors are widely used for 3D-tissue engineering purposes in different setups. Animal trials have to be replaced by cell culture assays, preferably by test systems with human material. This is especially true for biodegradable materials, in this case magnesium and its alloys. Here it is known that there is a discrepancy between observations *in vitro* compared to *in vivo*¹. Dealing with orthopaedic applications of the materials the next challenge is that there is not much known about the flow regime in bone, however it should be much lower than for e.g. vascular applications.

The aim of this feasibility study therefore was to develop a modular bioreactor system applicable for (I) material screening purposes and (II) implant prototype analysis. This system should be operated under cell culture conditions, cover a range of low flow conditions and it should be possible to vary the environmental conditions to approach the physiological conditions comparable to *in vivo*. Advantages of this reactor concept can be seen in removal of toxic reaction products, high cell densities, and improved metabolism². Specifically for degradation studies it should moreover reduce the local effects of high pH, osmolality and H₂-production.

EXPERIMENTAL METHODS

The environmental control was established by placing a custom made cell culture environment with highly precise CO₂ and O₂-regulation (C-Chamber system, Biospherix Ltd., US) in an incubator for temperature regulation (INE 600, Memmert, Germany).

Two designs are available (Fig.1): (I) A 24-well plate-based modular bioreactor (Medorex, Nörten-Hardenberg, Germany) for the analysis of 4 samples per row and (II) a modified version for the analysis of one prototype per row (maximum dimensions of prototypes: 8 cm length, 1 cm width). This bioreactor chamber has the option to install vessel-like structures by additional in- and outlets. Gas supply is granted via surface aeration directly in the chamber, medium supply is done by a circulation loop from reservoir bottles via peristaltic pumps.

RESULTS AND DISCUSSION

The whole system is fully autoclavable. The assembly can be performed under sterile conditions and the whole system afterwards be transferred to the cell culture environment. First experiments could demonstrate that the system could be kept sterile for more than 14 days. Due to the use of 4-channel peristaltic pumps it is possible to analyse two different flow rates at the same time with statistically relevant amount of samples

(n=8). Currently first degradation experiments of magnesium-silver alloys at flow rates up to 1 mL/min are performed. Additionally, a simulation of the flow conditions in this system is under way.

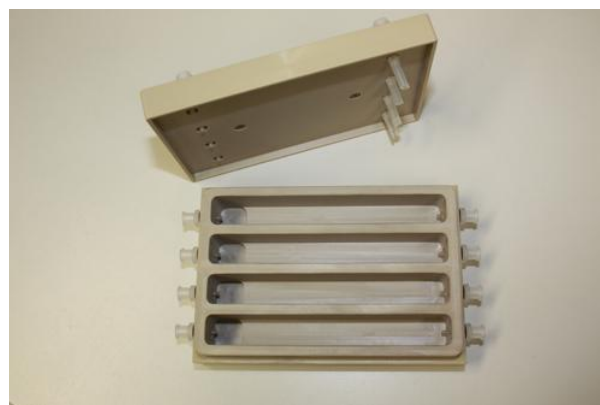


Fig. 1: The two designs of the modular flow chamber applied in this study

CONCLUSION

The introduction of flow should bring *in vitro* observations closer to *in vivo*. Due to the modularity of the system it is not only suitable for degradation studies, but also for the application of various cell models during degradation.

REFERENCES

1. Witte F. *et al.*, Biomaterials 27:1013-1018, 2006
2. Poertner et al., Adv Biochem Eng /Biotechnol 112: 145-182, 2009

ACKNOWLEDGMENTS

The authors would like to thank Bernhard Eltschig for the manufacturing of the design II chamber.

Use of a PTMC-PEG-PTMC coated PTMC film as a postoperative adhesion barrier

Vincent Verdoold^{1,2,*}, Ruben R.M. Vogels³, Kevin W.Y. van Barneveld³, Nicole D. Bouvy³ and Dirk W. Grijpma^{1,4}

¹MIRA Institute for Biomedical Technology and Technical Medicine, and Dept. of Biomaterials Science and Technology, University of Twente, The Netherlands, v.verdoold@utwente.nl ²Medisse BV, Ede, The Netherlands

³Department of General Surgery, Maastricht University Medical Centre, Maastricht, the Netherlands

⁴University of Groningen, University Medical Center, Groningen, Dept. of Biomedical Engineering, the Netherlands

INTRODUCTION In abdominal surgery, the incidence of postoperative adhesions is up to 95%. In these cases, the most severe complications are the result of small bowel obstructions 60-70% [1]. To prevent this, resorbable barrier membranes have been developed [2]. Such membranes are often fixed using sutures, staples and tackers. However, this can lead to additional postoperative adhesions of tissue [3].

Here we present a biocompatible poly(1,3-trimethylene carbonate) (PTMC) film [4], coated with a PTMC-PEG-PTMC tri-block copolymer as a tacky bonding agent for initial fixation of the PTMC film, as a novel postoperative adhesion barrier.

EXPERIMENTAL 1,3-Trimethylene carbonate (TMC, Foryou Medical), poly(ethylene glycol) (PEG) with Mn 3000 g/mol and stannous octoate (Sigma Aldrich) were used as received.

PTMC with an Mn of 250 kg/mol was prepared by ring opening polymerization of TMC using stannous octoate as catalyst at 150°C. The residual TMC content was less than 2 %, the stannous octoate content was less than 100ppm. PTMC films with an average thickness of 200µm were prepared by compression moulding at 160°C without additional purification of the polymer.

A PTMC-PEG-PTMC tri-block copolymer (Mn 1500-3000-1500 g/mol) was prepared by ring opening polymerization of TMC using stannous octoate as catalyst and PEG as initiator. A triblock copolymer film with an average thickness of 175µm was prepared by compression moulding 70°C.

The PTMC film was then coated with PTMC-PEG-PTMC by moulding the films onto each other at 70°C. The coating was applied to either one side or both sides of the PTMC films. The coated films were then sterilized in vacuum by 25 kGy gamma irradiation.

Table 1. Overview of the different experimental groups.

PTMC-PEG-PTMC-coated PTMC film	Orientation of the coating	Experimental group
Single side coated	Coated side faces organs	Organs
Single side coated	Coated side faces abdomen	Abdomen
Both sides coated	Coated sides face organs and abdomen	Double
No PTMC film		Control

The anti-adhesion performance of PTMC films coated with PTMC-PEG-PTMC was assessed in vivo using a validated peritoneal ischemic button model in the rat [5]. A midline incision of approximately 5-6 cm was made, and on each side 3 ischemic buttons were made (1 cm apart and 1 cm from the midline, 6 buttons per rat). To cover the visceral organs, a coated PTMC film

measuring 6x9 cm was implanted in each rat. The extent of adhesion is expressed as the relative number of ischemic buttons to which tissue has adhered.

An overview of the different PTMC-PEG-PTMC-coated PTMC films and the way they were implanted is given in Table 1. Eleven male Wistar rats per experimental group were used.

RESULTS AND DISCUSSION The formation of adhesions to the ischemic buttons was assessed upon termination of the animals after two weeks. The results are shown in Figure 1.

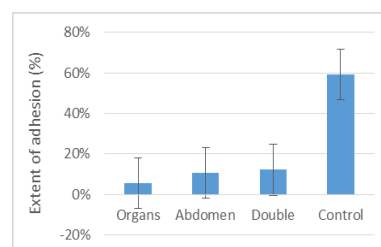


Figure 1. The extent of tissue adhesion after two weeks using PTMC-PEG-PTMC coated PTMC films for the different experimental groups.

All implanted PTMC films resulted in a significant reduction of the number of ischemic buttons to which tissue had adhered. The adhesions that had formed were either to ommental- or to scrotal fat. No adhesions between the buttons and the cecum nor between the cecum and the midline incision were observed.

Upon explantation, no remaining coating was visible on the PTMC films. The coating had transferred to the organs or to the peritoneum, likely contributing to the prevention of the formation of tissue adhesions. For all coated PTMC films, the adhesions formed to the ischemic buttons were approximately only 10%. The adhesions formed in the non-treated control group were significantly higher (approximately 62%). This indicates that use of these physical barriers is beneficial to prevent adhesions.

CONCLUSIONS Using an ischemic button rat model, use of PTMC films coated with PTMC-PEG-PTMC lead to significant decrease in adhesion formation. These novel anti-adhesion barriers could be highly beneficial in the clinic.

REFERENCES 1. M. Ditzel *et al.*, ESR 2012, 48(4):187-193; 2. R. Broek *et al.*, Lancet 2014 4;383(9911):48-59; 3. F. Ling *et al.*, IJGO 1989, 30(4):361-366; 4. K. Wójcik *et al.*, Macromol Symp 2011, 309-310:6; 5. T. Rajab *et al.* J Invest Surg. 2010, 23:35-39

Comparison of Sr-substituted Hydroxyapatite Obtained of Various Precursors through Neutralization Reaction: Characterisation at the Bulk and Particle Level

L. Stipniece*, K. Salma-Ancane and L. Berzina-Cimdina

*Institute of General Chemical Engineering, Riga Technical University, Latvia, liga.stipniece@rtu.lv

INTRODUCTION

Hydroxyapatite (HAp) are biocompatible and bioactive and thereby considered to be promising bone replacement material¹⁻⁴. It is known that Sr may replace Ca to form Sr-substituted HAp (Sr-HAp)¹. Sr ions with a radius greater than Ca ions significantly affects the morphology of a synthetic HAp, e.g. reduces the specific surface area (SSA)^{1,2}, low Sr concentrations (up to 25 %) results in the decrease of crystallite size, while higher amount of Sr substitution promotes the increase of HAp crystallite sizes³. Partial substitution of Ca ions with Sr ions greatly enhances the biological properties of HAp⁴. The most popular synthesis methods used to obtain Sr-HAp are wet chemical methods, which have been widely modified by changing the starting materials and technological parameters¹⁻⁴. As far as we know, there have not been published detailed studies cross-referencing the various precursor effects on Sr-HAp products. Thus, the main goal of this work was to synthesize Sr-HAp series through the neutralization reaction, and to evaluate the effect of various precursors on the synthesis product characterization in bulk and particle level.

EXPERIMENTAL METHODS

The HAp powders containing various amounts of Sr were synthesized through neutralization route. Two methods were used. The fundamental difference between these methods is variety in (Ca^{2+}) and (Sr^{2+}) sources. The solution of H_3PO_4 was used as a source of (PO_4^{3-}) in all synthesis. 2M H_3PO_4 was added at a slow addition rate (~ 0.75 ml/min). The stirring speed was 100 rpm, synthesis temperature – 45 °C.

Method A: Starting suspension were prepared by dissolving $\text{Ca}(\text{NO}_3)_2 \cdot 4\text{H}_2\text{O}$ and/or $\text{Sr}(\text{NO}_3)_2$ in deionised H_2O in various ratios. The pH of the synthesis mixture was kept around 9, using 25% ammonia solution.

Method B: Starting suspensions of $\text{Ca}(\text{OH})_2$ and/or $\text{Sr}(\text{OH})_2$ were prepared of CaO and/or SrO, and deionised H_2O by “lime slaking” process followed by homogenization in planetary ball mill. The pH of the synthesis mixture was adjusted to 9. The ammonia solution was used, if needed.

The precipitate was left overnight to mature, filtered, and washed with deionised H_2O three times if needed. Finally, the precipitate was dried at 105 °C for ~ 24 h and grounded. The obtained powders were uniaxially pressed (10 kN) in cylindrical tablets (\varnothing 10 mm) and sintered in air atmosphere at 1100 °C for 1 h.

Comprehensive characterization techniques were used to investigate the effect of Sr substitution on molecular, phase and chemical composition, crystallite size,

thermal stability, morphology and microstructure of as-synthesized powders and sintered bioceramics.

RESULTS AND DISCUSSION

XRD analysis confirmed the formation of pure apatite phase. In the case of *method A* changes in the crystallite sizes was observed with increasing the added amount of $\text{Sr}(\text{NO}_3)_2$ in the synthesis media, which coincide with the literature data indicating an initial crystallite size reduction followed by a rising with increasing the concentration of Sr in the samples³. However, in the case of *method B*, with the increase of SrO content in the synthesis media, the XRD peaks shift to smaller 2θ values were observed with no change in XRD peak intensities. Afterwards the reduction of crystallite sizes occurred, as indicated by the apatite phase characteristic XRD peaks shift to higher 2θ values, followed by an increase in the crystallite sizes. These results were confirmed by the SSA measurements. The morphology of synthesized powders was similar in the case of all synthesis products. With increasing Sr concentration in the samples, the particles became more elongated.

CONCLUSION

A series of Sr-HAp were successfully synthesized of various precursors by two routes. The results showed that high concentrations of Sr substitution promote destabilization of HAp structure, the disappearance of structural symmetry, and the changes of a phosphate surrounding environment. It is possible to conclude that the use of *method A* can lead to more efficient incorporation of Sr ions into the HAp structure, as the precursors used in the method have high solubility in H_2O that provide efficient interblending of them. The main disadvantage of the *method A* is the need for usage of ammonia solution to ensure alkaline pH. Thus, comparing the two methods, it can be concluded that the main advantage of *method B* is simplicity.

REFERENCES

1. Ten S.-H. *et al.*, J. Hazard. Mater. 179:559-563, 2010
2. Li Z.Y. *et al.*, Biomaterials 28:1452-1460, 2007
3. O'Donnell M.D. *et al.*, Acta Biomater. 4:1455-1464, 2008
4. Landi E. *et al.*, Acta Biomater. 3:961-969, 2007

ACKNOWLEDGMENTS

This work has been supported by European Social Fund within the project “Involvement of new scientist group for synergistic investigation to development of nanostructured composite materials for bone tissue regeneration”

No.2013/0007/1DP/1.1.1.2.0/13/APIA/VIAA/024

Hybrid Multi-layered Coatings for Surface Functionalization of Magnesium alloys for biomedical applications

Laura Córdoba^{1,2}, Christophe Hélar², Thibaud Coradin², Fátima Montemor¹

¹ICEMS/DEQ, Instituto Superior Técnico, Technical University of Lisbon, Av. Rovisco Pais, 1049-001 Lisboa, Portugal

²UPMC Univ Paris 06, CNRS, Chimie de la Matière Condensée de Paris, Collège de France, 11 place Marcelin Berthelot, F-75005 Paris, France, laura.cordoba_roman@etu.upmc.fr

INTRODUCTION

Magnesium alloys have attracted great attention as a new kind of temporary biodegradable implants¹. Their rapid corrosion rate can be taken as an advantage provided that an accurate control and knowledge of their degradation process can be achieved. In addition, the bioactivity of the implant surface is a major issue to be considered. An interesting strategy relies on the design of coatings that are able to slow down the corrosion rate while favoring cell adhesion and proliferation². In the present work a hybrid multi-layered coating was developed and applied to AZ31 and ZE41 commercial alloys, showing promising properties towards the safe application of Mg-based materials as biodegradable implants.

EXPERIMENTAL METHODS

AZ31 and ZE41 substrates (discs Ø25.4 mm x 3 mm thick) were prepared by mechanical polishing up to 1000 SiC grit paper and pre-treated with 12% HF solution for 15 min. A multi-layered coating was applied in two steps: (1) a bottom sol-gel layer composed of 3-glycidoxypyrrol-aminomethane (GPTMS) and titanium (IV) isopropoxide (TIP); (2) and a top layer of type I collagen deposited under acidic conditions. For the morphological characterization scanning electron microscope (SEM) and atomic force microscope (AFM) were used.

Electrochemical impedance spectroscopy (EIS) tests in simulated body fluid (SBF) were used to characterize the corrosion behaviour of the sol-gel coated alloys.

To evaluate the cell behaviour, fibroblasts in DMEM medium were seeded onto bare and coated samples. In particular, alloyS (alloy + sol-gel, e.g. AZ31S) and alloySC (alloy + sol-gel + collagen) were evaluated. The cells were cultured during 3 days at 37°C and 5% CO₂ and characterized for viability/proliferation by the alamarBlue® assay at 1 and 3 days.

RESULTS AND DISCUSSION

After optimization of the GPTMS:TIP ratio, an homogeneous crack-free sol-gel layer 3 µm-thick could be deposited on both alloys. After implementation of the collagen thin film deposition process³ an additional 1 µm-thick structured protein layer could be achieved. The sol-gel coating was found to efficiently protect the alloys against corrosion over two weeks, with a better resistive behavior towards ZE41 than AZ31 once the surface under the coating is exposed to the solution. Preliminary results suggest that fibroblasts can adhere on the sol-gel coated samples but exhibit low

proliferation rates afterwards. Moreover compared to the control, cell growth was confined on specific locations of the surface rather than homogeneously spread. This was independent on the composition of the alloy and was also observed for sol-gel coated glass substrates.

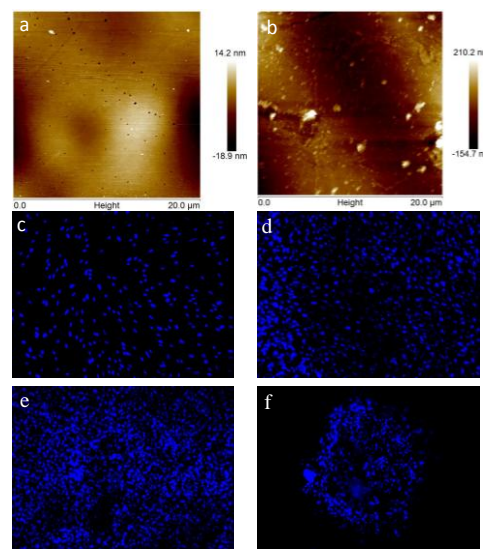


Fig. 1. AFM images of (a) ZE41S and (b) ZE41SC and microscopic images of fibroblasts attached on day 3 to (c) control, (d) sol-gel on glass substrate, (e) and (f) ZE41S (magnification 10X).

CONCLUSION

Our result show that coating Mg alloys with sol-gel formulations provide an efficient way to slow down their corrosion process without detrimental impact on fibroblast viability. However, cell proliferation is not favored. In this context, the successful subsequent coating by collagen should allow to overcome this issue and to extend our experiments to other relevant cells, such as osteoblasts.

REFERENCES

1. P.P. Staiger, A.M. Pietak, J. Huadmai, G. Dias, *Biomaterials*, 27:1728-1734 (2006)
2. G. Song, *Corrosion Sci.*, 49:1696-1701 (2007)
3. M.M. Giraud-Guille, C. Hélar, S. Vigier, N. Nassif, *Soft Matter*, 6:4963-4967 (2010)

ACKNOWLEDGMENTS

The authors would like to thank the 2012-EM05 project from the IDS-FunMat programme for providing financial support to this work.

Degradation in the Jar: Optimising the *in vitro* enzymatic degradation of collagen-based devices

Ayelén L. Helling¹, Eleni Tsekoura¹, Gerard Wall^{1,2}, Yves Bayon³, Abhay Pandit¹, Dimitrios Zeugolis¹

¹ Network of Excellence for Functional Biomaterials (NFB), National University of Ireland Galway (NUI Galway), Galway, Ireland; ²Department of Microbiology, NUI Galway, Galway, Ireland; ³Sofradim Production, Covidien, Trevoux Cedex, France, dimitrios.zeugolis@nuigalway.ie

INTRODUCTION

Collagen-based materials, used in soft tissue repair, are naturally degraded in the body by the complementary action of proteolytic enzymes¹, primarily MMP-1 and MMP-8, which are commonly encountered during physiological wound healing². However, customarily *in vitro* degradation assays, the composition of the device and the target host microenvironment are not taken into consideration, frequently resulting in overestimation of the device self-life. Herein, we aim to develop a collagen-based devices specific *in vitro* assay that would most closely imitate the *in vivo* degradation.

EXPERIMENTAL METHODS

Commercially available tissue grafts (fig.1) derived from porcine skin [PermacolTM (Covidien), non-cross-linked PermacolTM (Covidien) and StratticeTM (Life Cell)] were subjected to enzymatic degradation using MMP-1 (Sigma C0130) and MMP-8 (Invitrogen 17101015). The degradation assays were performed under three concentrations of each enzyme (50, 100 and 200 U/ml) and two pH values (5.5 and 7.4) at 3, 6, 9, 12 and 24 hours. The extent of degradation was assessed by visual inspection (fig 2); weight loss (table 1); hydroxyproline assay; and differential scanning calorimetry (DSC) (Table 3). Analysis are performed using statistical software MINITABTM, Minitab, Inc., State College PA.

RESULTS AND DISCUSSION



Fig 1. Environmental scanning electron microscope ESEM images of PermacolTM, non-cross-linked PermacolTM and StratticeTM surfaces before degradation.

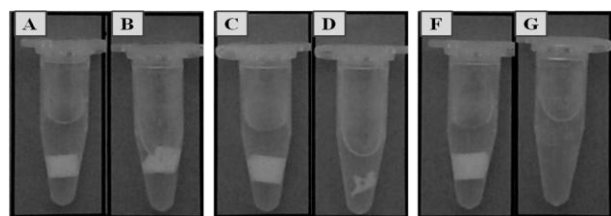


Fig 2. Images of PermacolTM (A: not degraded, B: 24h of degradation), non-cross-linked PermacolTM (C: not degraded, D: 24h) and StratticeTM (F: not degraded, G: 24h).

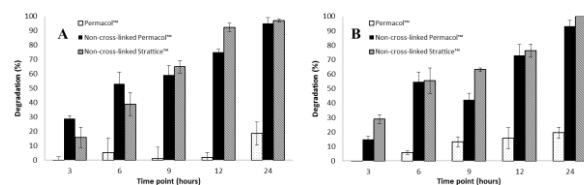


Table 1. Degradation with MMP-1(A) and MMP-8 (B) of the materials to different time points, 200 U/ml and pH 7.4 using weight loss assays.

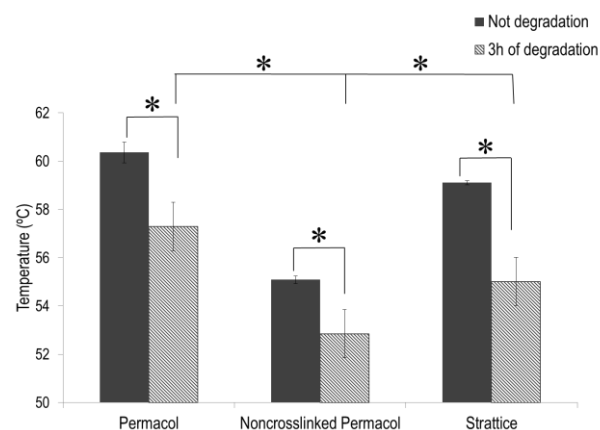


Table 2. Denaturation temperature measured with differential scanning calorimetry (DSC) of PermacolTM, non-cross-linked PermacolTM and StratticeTM before degradation and after 3 hours of degradation with MMP-8. (Anova: P<0.05)

The results showed a significant increase in the degradation with the time and with the concentration of the enzyme at pH 7.4. Also, the degradation of non-cross-linked materials is significantly higher than the cross-linked after 24 hours. The degradation temperature of the collagen-based meshes, measured with DSC, significantly decreases after enzymatic degradation.

CONCLUSION

The natural degradation of collagen-based meshes can be recreated *in vitro* in order to predict future results after implantation.

REFERENCES

1. Zeugolis, D. Compr. Biomater. 261–278, 2011.
2. Badylak, S. *et al.*, Acta Biomater. **5**, 1–13, 2009.

ACKNOWLEDGMENTS

The authors would like to acknowledge Covidien for providing financial support to this project.

Composite Collagen/Bioceramics Strips, Plugs for Bone Filling Defect Repair: A Comparative Study

Thomas Miramond^{1,2}, Thibaut Galtier², Guy Daculsi¹, Pascal Borget²

¹Inserm UMRS 791, Université de Nantes, France

²Biomatlante SA, Vigneux-de-Bretagne, France

thomas.miramond@univ-nantes.fr

INTRODUCTION

A focus on resorbable bone implants is growing, especially for malleable forms allowing surgeons easier and efficient handling to adjust to each type of defect. Spine fusion and general orthopaedic or maxillo-facial reconstruction need specific galenic shape whose strips, plugs and putties are the most innovative thanks to their handling and dissolution properties. Resorbable biopolymers by enzymatic digestion, such as Chitosan and Collagen, are from major interest¹. Combining these polymeric phases with osteoconductive crystallographic phases offers composite materials with relevant mechanical, resorption (ionic and osteoclastic) and osteoconductive properties². Granules of bioceramics can then be embedded into 3D polymeric matrix, which could be proposed either as a scaffold or as a membrane. In spite of same clinical indications, large differences in the micro-macrostructure of these composite can be observed. This study compares 6 composite samples (plugs, strips) approved in Asia or USA, in terms of physicochemical properties.

EXPERIMENTAL METHODS

Commercially available strips, plugs, 3 from Asia and 3 from US market, (Table 1) were quantitatively analysed in terms of spatial distribution homogeneity of bioceramics granules, bioceramics granules size and both intergranular and intragranular porosity by microtomography (μ -CT). Microstructures visualization was performed by scanning electron microscopy (SEM). Crystallographic phases of embedded bioceramics granules were identified by x-ray diffraction (XRD). Mechanical testing after immersion in physiological solution at 37°C of plugs and strips was performed.

Table 1: Samples analyzed

Sample	Size
Asia Strip1	15 x 50 x 3.5 mm
Asia Strip 2	20 x 20 x 3 mm
Asia Plug 3	Ø8 x 15 mm
USA Strip 1	115 x 75 x 3 mm
USA Strip 2	50 x 30 x 3 mm

RESULTS AND DISCUSSION

All samples were highly porous but only few of the samples have high intragranular macroporosity (Table 2). The smaller the bioceramics granules, the higher their spatial distribution in collagen matrix. But the less macroporous they are. Macropores are considered having a seminal role in bone remodelling as osteoconductive niche³. The association of microporous and macroporous structures is even considered as

potentially osteoinductive⁴. Moreover the total porosity is crucial for body fluids penetration, angiogenesis and cell colonization which provide a quality bone remodelling⁵.

Table 2: Micro-CT characterizations

Sample	Granules size (mm) / Homogeneity of spatial distribution (Coefficient of Variation)	Granules Volume ratio / Macropores presence
Asia Strip1	0.43 / 20%	22% / Medium
Asia Strip 2	0.42 / 35%	7% / Low
Asia Plug 3	0.34 / 38%	8% / Low
USA Strip 1	0.20 / 12%	26% / None
USA Strip 2	0.40 / 45%	27% / Medium
USA Strip 3	0.45 / 18%	25% / High

Although the finality of plugs and strips analysed is the same, that is to say, the bone filling, it is clear that the physicochemical and mechanical properties are various between the different commercial samples. The method of preparing the collagen with crosslinking or not, with prior dissolution (Atelocollagen) or not, leads to totally different properties of malleability, ductility and dissolution kinetics. Embedded synthetic bioceramic granules can be also differ in the volume ratio granules/collagen, nature, with or without macropores, with or without micropores, which will have high impact in terms of efficiency of bone regrowth⁶.

CONCLUSION

It is suitable for surgeons to be aware of these fundamental physicochemical differences necessarily involving different biological responses, bone remodelling efficacy and requiring clinical protocols adapted to each type of bone substitute.

REFERENCES

1. Teng S.H. *et al.*, J. Biomed. Mater. Res., Part B, 87:132-138, 2008
2. Daculsi G. *et al.*, J. Mater. Sci.: Mater. Med. 14:195-200, 2003
3. Pennesi G. *et al.*, Curr. Pharm. Biotechnol., 12:151-159, 2011
4. Ferretti C. *et al.*, Brit. J. Oral. Max. Surg., 48:536-539, 2010
5. Kanczler J. M. *et al.* Eur. Cell. Mater. 15:100-114, 2008
6. Hutmacher W. *et al.*, Biomaterials, 21:2529-2543, 2000

Development of Artificial Stem Cell Microenvironments for Tissue Engineering Applications

Ilida Ortega Asencio¹, Sheila MacNeil², Aileen Crawford¹, Paul Hatton¹, Frederik Claeyssens¹

¹The School of Clinical Dentistry and ²Kroto Research Institute, The University of Sheffield, South Yorkshire, UK,
i.ortega@sheffield.ac.uk

INTRODUCTION

Stem cell niches are well-defined and intricate microenvironments that play an important role in tissue regeneration¹. To date, research has focused on characterising the stem cell niche seeking to recreate both its biochemical environment and its complex morphology. Our aim is advance this work by manufacturing synthetic biomaterial devices containing artificial stem cell niches. These devices have potential for use in the regeneration of soft tissues (such as cornea reported here) and ultimately musculoskeletal tissues such as bone.

EXPERIMENTAL METHODS

Poly (lactide-co-glycolide) (PLGA) microfabricated scaffolds were made using a combination of additive manufacturing techniques (microstereolithography) and electrospinning² (fig.1). Biological evaluation was performed using rabbit limbal tissue and a 3D rabbit cornea model. Cells were characterized using CK3 (differentiation marker) and P63 (stem cell marker).

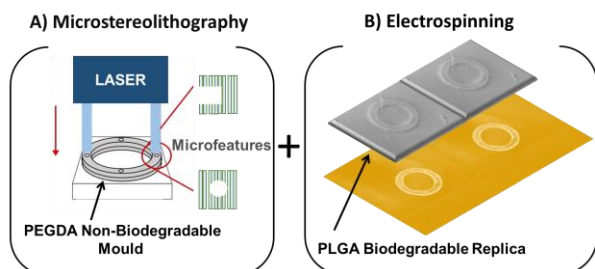


Figure 1. Schematic of the manufacturing process used for creating the corneal outer rings. The process is based on a combination of techniques. Firstly, additive manufacturing techniques are used for creating a non-degradable mould and, secondly, the underlying surface provided by the mould is replicated using electrospinning.

RESULTS AND DISCUSSION

The inclusion of microfeatures within the constructs affected both epithelial cell migration and morphology. The presence of a population of slow-cycling cells (positive for P63) was identified when tissue explants were cultured inside the pockets and placed on 3D

models (fig.2); this was not observed when using cultured limbal epithelial cells (RLE) suggesting that the enclosed microenvironments and the presence of native stromal cells within the explants play an important role in stem cell maintenance.

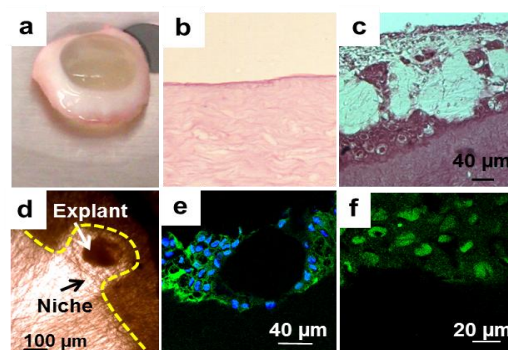


Figure 2. 3D Cornea model (a). Wounded cornea showing the absence of epithelium (b). Histology image of tissue engineered cornea using microfabricated scaffolds (c). Electrospun horseshoe-shaped niche containing a tissue explant (d). CK3 staining for cells growing out from a limbal explant (e). P63 staining for cells located in the proximity of a tissue explant (f).

CONCLUSION

This work focuses on the fabrication of novel biomaterial devices containing stem cell microenvironments. We have demonstrated that the presence of microfeatures has a direct effect on migration and directionality, as well as other parameters such as cell morphology and stemness³. The data shown here is based on a soft tissue model (corneal model), but the system is predicted to be adaptable to other tissues including bone.

REFERENCES

1. Fuchs E. *et al*, Cell. 116, 769, 2004
2. Ortega I. *et al*, Acta Biomaterialia. 9, 5511, 2013
3. Ortega I. *et al*, Biomater. Sci., 2014, (DOI: 10.1039/c3bm60268k)

ACKNOWLEDGMENTS

We thank the EPSRC Landscape Fellowship Scheme and the Wellcome Trust Foundation.

Fabrication of dispersible nanocrystals of bioceramics via a modified Pechini method under non-stoichiometric condition

Yuko Omori¹, Masahiro Okada^{2*}, Shoji Takeda², Naoyuki Matsumoto¹

¹Graduate School of Dentistry, Department of Orthodontics, Osaka Dental University, Japan

^{2*}Department of Biomaterials, Osaka Dental University, Japan, okada-m@cc.osaka-dent.ac.jp

INTRODUCTION

Hydroxyapatite (HAp; $\text{Ca}_{10}(\text{PO}_4)_6(\text{OH})_2$; stoichiometric Ca/P molar ratio of 1.67) is a kind of bioceramics and exhibits excellent cell adhesion because of favorable adsorption capacity of the HAp surface for bioactive substances. The nanoparticle form of HAp has attracted great interests for application as filler materials of cell scaffolds, drug/gene carriers, and coating agents for medical polymers. When low crystallinity HAp nanoparticles, which are generally obtained via a wet chemical process, are calcined to increase thermal and chemical stability, the particles sinter into large agglomerates consisting of polycrystals [1].

Here, we report a modified Pechini method with an initial Ca/P molar ratio greater than 1.67 for the fabrication of dispersible HAp nanocrystals. We hypothesized that the presence of Ca ions in a concentration that exceeded a Ca/P ratio of 1.67 leads to the formation of HAp nanocrystals embedded in CaO matrix and that the nanocrystals can be dispersed at the nanoscale after the CaO matrix is removed (Figure 1b).

EXPERIMENTAL METHODS

After $\text{CH}_3\text{COO})_2\text{Ca}$ and $(\text{NH}_4)_2\text{HPO}_4$ were dissolved in poly(acrylic acid) (PAA) solution in water (initial Ca/P molar ratio: 1.67–13.0), the volume of the solution was reduced on a hot plate at 80°C. The resulting yellowish resin was thermally treated at 1000°C (heating rate, 10°C/min) for 1 h, and then washed centrifugally with NH_4NO_3 aqueous solution until the pH of the aqueous medium decreased to almost 7.0, followed by washing with water three times. The particle morphology, the particle size in liquid media, and the crystal phase of the samples obtained were evaluated using scanning electron microscopy (SEM), laser-diffraction particle size analyzer, and X-ray diffraction (XRD), respectively.

RESULTS AND DISCUSSION

Before the samples were washed, the XRD patterns of each sample indicated the presence of a binary crystalline phase consisting of only HAp and CaO. The HAp wt.% of the product tended to be smaller than the theoretical value calculated from the initial Ca/P ratio,

suggesting that the rate of conversion into HAp decreased because of the lower PO_4^{3-} concentration. After the samples were washed with aqueous media, only a single HAp phase was observed, which indicates that the CaO matrix could be completely removed.

SEM observations revealed that most of the HAp nanocrystals sintered into micron-sized polycrystals in the case of the stoichiometric Ca/P value of 1.67 (Figure 1a). The content of micron-sized polycrystals decreased with increasing initial Ca/P ratio, and almost no polycrystals were observed in the cases where the initial Ca/P molar ratio was greater than 6.67. In higher-magnification images, each crystal exhibited a spherical or polygonal morphology (Figure 1b), and the crystal size decreased with increasing initial Ca/P molar ratio. The crystal size also varied with the thermal treatment temperature and time.

The particle size distribution in aqueous media was also evaluated. As expected, the particle size of powders dispersed in aqueous media decreased with increasing initial Ca/P molar ratio. The number-averaged size of the dispersed particles approximately corresponded to the crystal size measured from SEM images in cases where the initial Ca/P molar ratio was greater than 6.67, which indicates that most of the nanocrystals were dispersed as a single crystal.

CONCLUSION

We showed that the Pechini method under non-stoichiometric conditions led to the formation of binary crystal phases (*i.e.*, HAp and CaO), and high crystallinity bioceramic HAp nanoparticles that can be dispersed in liquid media mostly as single crystals are obtained by dissolving one crystal phase (*i.e.*, CaO). The modified Pechini method described here should be applicable to a wide range of the nanoceramic powders, and have significant benefits over existing technologies, because the methods is facile, inexpensive, and amenable to scale-up and processing.

REFERENCES

1. Okada M. and Furuzono T., Sci. Technol. Adv. Mater. 13:064103, 2012

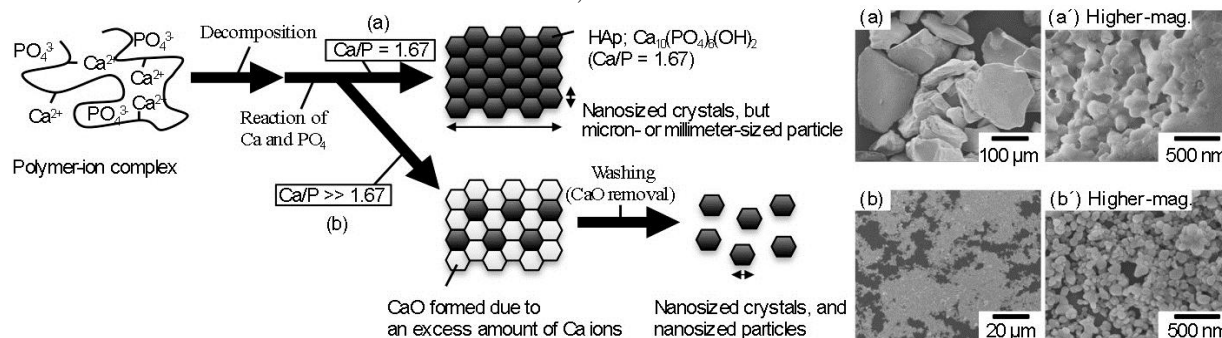


Figure 1. Formation of micron-sized polycrystals via sintering (a: initial Ca/P molar ratio = 1.67) and nanocrystals via a modified Pechini method (b: initial Ca/P molar ratio $\gg 1.67$) followed by washing.

Titanium with Nanotopography Drives Mesenchymal Stem Cells to Osteoblast Differentiation through miR-4448, -4708 and -4773 Downregulation

R.B. Kato¹, B. Roy², F.S. de Oliveira¹, E.P. Ferraz¹, P.T. de Oliveira¹, M.Q. Hassan², A.L. Rosa¹, M.M. Beloti¹

¹Cell Culture Laboratory, School of Dentistry of Ribeirão Preto, University of São Paulo, Brazil

²Department of Oral and Maxillofacial Surgery, School of Dentistry, University of Alabama at Birmingham, USA
mmbeloti@usp.br

INTRODUCTION

The nanotopography produced by H₂SO₄/H₂O₂ on titanium (Ti) surfaces enhances the osteoblast differentiation of cells grown under both osteogenic and non-osteogenic conditions¹. Considering the demand for novel implant surfaces that may favour the process of osseointegration, it is of relevance to investigate the intracellular mechanisms involved in the osteogenic potential of this nanotopography. As microRNAs (miRs) have recently risen as one of the most important post-transcriptional mechanisms involved in osteogenesis², here, we tested the hypothesis that Ti with nanotopography induces osteoblast differentiation by regulating the expression of miRs.

EXPERIMENTAL METHODS

Human mesenchymal stem cells (hMSCs) were cultured on both Ti with nanotopography and untreated (control) Ti discs under osteogenic conditions for periods of up to 21 days. Osteoblast differentiation was evaluated by real-time PCR to detect the gene expression of runt-related transcription factor 2 (Runx2), alkaline phosphatase (ALP), osteocalcin (OC) and osteopontin (OPN) at day 4, western blot to detect ALP protein at day 17, and alizarin red to stain extracellular matrix mineralization at day 21. At day 4, miR-sequencing analysis was performed and based on the results miR-4448, -4708 and -4773 were selected for further investigations. Gene expression of these miRs and their putative targets identified by bioinformatics, SMAD1 and SMAD4, key transducers of bone morphogenetic protein 2 (BMP-2) signalling, was evaluated by real-time PCR. To investigate the role of these miRs on the osteogenic potential of Ti with nanotopography, MC3T3-E1 cells were transfected with miR-4448, -4708 or -4773, or non-silencing (NS) miR and the gene and protein expression of SMAD1 and SMAD4 were evaluated, in addition to Runx2 and OC gene expression, at 48 hours. Also, MC3T3-E1 cells cultured on both Ti with nanotopography and control Ti discs were treated with either 100 ng of BMP-2 or vehicle and the gene expression of Runx2 and OC were evaluated at day 4. All experiments were carried out in triplicate (n=3). Data were analysed by Mann-Whitney U-test to compare hMSCs grown on Ti with nanotopography with control Ti, or each miR with NS miR in transfected MC3T3-E1 cells or MC3T3-E1 cells treated with either BMP-2 or vehicle. The level of significance was established at p≤0.05.

RESULTS AND DISCUSSION

It was noticed that Ti with nanotopography favours osteoblast differentiation of hMSCs compared with

control Ti as evidenced by higher Runx2, ALP, OC and OPN gene expression (p≤0.05), and ALP protein expression, in addition to a non-significant increase of extracellular matrix mineralization (p>0.05). The miR-sequencing analysis revealed that 20 miRs were upregulated (>2 fold) while 20 miRs were downregulated (>3 fold) in hMSCs grown on Ti with nanotopography compared with control Ti. Three miRs, miR-4448, -4708 and -4773 were significantly downregulated (>5 fold) by Ti with nanotopography and affected osteoblast differentiation of hMSCs. These miRs directly target SMAD1 and SMAD4, which were upregulated by Ti with nanotopography (p≤0.05). Overexpression of miR-4448, -4708 and 4773 in MC3T3-E1 cells noticeably inhibited gene and protein expression of SMAD1 and SMAD4 (p≤0.05) and by targeting them, these miRs repressed the gene expression of Runx2 and OC (p≤0.05). Treatment of MC3T3-E1 cells with BMP-2 upregulated the gene expression of Runx2 and OC on Ti with nanotopography and of OC on control Ti (p≤0.05). While BMP-2 treatment increased gene expression of Runx2 (1.1-fold) and OC (1.6-fold) on control Ti, the same treatment increased 1.4- and 2.3-fold, respectively, on Ti with nanotopography.

CONCLUSION

The results showed that the Ti with nanotopography directs hMSCs differentiation toward the osteoblast lineage. In addition, we have identified 3 miRs that target SMADs and play critical role in the osteoinductive effect of this nanotopography on hMSCs. By downregulating miR-4448, -4708, and 4773, Ti with nanotopography attenuates SMAD1 and SMAD4 degradation, intensifying BMP-2 signal transduction, which stimulates osteoblast differentiation. This novel mechanism involving a miR-SMAD-BMP-2 network in the nanotopography-mediated osteoblast differentiation is a major step for developing Ti surface modifications to modulate the osseointegration process.

REFERENCES

1. Rosa AL. *et al.*, J. Cell. Biochem. 115:540-548, 2014.
2. Lian JB. *et al.*, Nat. Rev. Endocrinol. 8:212-227, 2012.

ACKNOWLEDGMENTS

Roger R. Fernandes and Milla S. Tavares. Grants: FAPESP (# 2010/18395-3, 2010/19280-5) and CNPq (# 301023/2010-7).



Semi-interpenetrating polymer networks (SIPNs) incorporating polygalacturonic acid as biocompatible materials for implantable medical devices

A. O' Carroll, C. McCoy, and L. Carson

School of Pharmacy, Queen's University Belfast, United Kingdom, l.carson@qub.ac.uk

INTRODUCTION

Over 200 million people in the US are living with an implantable medical device¹, with similar figures anticipated for Europe. Complications associated with medical device implantation include the Foreign Body Response (FBR) and bacterial biofilm-mediated infection. The FBR is an inflammatory response to the implanted material and involves a complex sequence of events, including adsorption of host proteins and adherence of macrophages (MΦ) on the material surface. Both the FBR and device-associated infection can have detrimental consequences on the structural and functional integrity of the medical device^{2,3}, often necessitating removal. Materials are sought to mitigate both the FBR and device-related infection, leading to improved biocompatibility. The present work involves the synthesis of a polyelectrolyte hydrogel containing polygalacturonic acid (PGA), a biopolysaccharide similar in structure and charge to hyaluronic acid (a component of the extracellular matrix), with the aim of developing biomaterials with improved biocompatibility for medical devices.

EXPERIMENTAL METHODS

Synthesis and characterisation: SIPNs were formulated using 2-hydroxyethylmethacrylate (HEMA) and 2-methacryloxy ethyltrimethyl ammonium chloride (METAC) with aqueous PGA. AIBN (0.1%) was used as a thermal initiator. Control materials used the same volume of dH₂O in place of PGA solution. The resulting polymer films (final concentration 1% PGA) were characterised in terms of contact angle, swelling, and SEM analysis of surface topography.

Protein adsorption: PGA-incorporated polymers and controls were incubated in a solution of 10% BSA in PBS at 37°C for 2 hours after which adsorbed protein was sonicated into 1% SDS in PBS, and quantified by micro BCA Assay (Pierce).

MΦ adherence and cytotoxicity: Sterilised samples were seeded with 1x10⁴ RAW 264.7 murine MΦ. After 72h adhered MΦ were stained with DAPI/Rhodamine-phalloidin and examined by fluorescence microscopy. Direct contact and medium elution cytotoxicity studies were carried out against L929 murine fibroblasts, following ISO 10993-5 methodology.

Bacterial biofilm formation: Biofilm formation was assessed by incubation of samples with 1x10⁶ cfu/ml in Mueller Hinton Broth (MHB) of *Staphylococcus epidermidis* ATCC 35984 or *Escherichia coli* ATCC 11303 at 37°C for 24h, after which samples were stained with Live/Dead BacLight (Molecular Probes) for analysis by fluorescence microscopy, and quantification of biofilm by image analysis (Image J, NIH).

All experimentation described was performed in at least triplicate and data analysed using the statistical software package GraphPad Prism 5.

RESULTS AND DISCUSSION

Swelling studies revealed a high degree of water uptake (>100%), while a contact angle of 39.23° indicated a hydrophilic surface. Cryo-SEM of the hydrated materials showed a micro-textured PGA polymer surface, compared to the smooth appearance of the control material. While no significant difference in protein adsorption was observed compared to material control, MΦ adherence was significantly reduced on the PGA polymer, while maintaining no toxicity towards L929 fibroblasts. *S. epidermidis* biofilm formation was significantly increased on the PGA material when compared with control. PGA is composed of D-galacturonic acid residues that may potentiate *S. epidermidis* lectin-carbohydrate interactions. This promotion of biofilm formation was, however, not observed for *E. coli*.

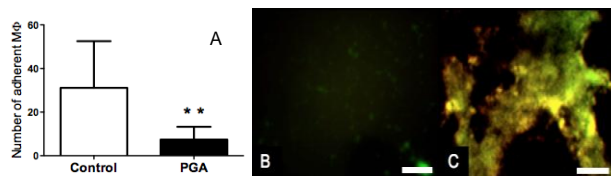


Figure 1 A. Number of adhered MΦ per 570 μm² field of vision (n=9, graph displays means ± SD), B. and C. *S. epidermidis* biofilm on control and PGA-incorporated polymer, respectively. Scale bars represent 5 μm.

CONCLUSION

This PGA-incorporated SIPN exhibits acceptable biocompatibility for future *in vivo* investigation, and shows a low level of MΦ adherence, holding promise for potential attenuation of the FBR. We are currently continuing to characterise the behaviour MΦ on these materials, particularly MΦ fusion towards foreign body giant cell (FBGC) formation. While promising results have been obtained for *in vitro* biocompatibility, the increased biofilm formation of *S. epidermidis* highlights a concern in terms of the potential for device-associated infection. Future work will focus on the improvement of an anti-infective surface whilst upholding biocompatibility.

REFERENCES

- Higgins D.M. *et al.* Am J Pathol. 175:161-170, 2009
- Anderson J.M. *et al.* Sem Immunol. 20:86-100, 2008
- Donlan R.M. & Costerton J.W. Clin. Microbiol. Rev. 15:167-193, 2008

***In Vivo* Assessment of Titanium Devices loaded with gentamicin in a methicillin-resistant *Staphylococcus aureus* Rabbit Osteomyelitis Experimental Model**

Gilles Amador¹, Loic Pichavant^{2,3}, Hélène Carrière^{2,3}, Laurent Plawinski³, Valérie Héroguez² Cédric Jacqueline¹ and Marie-Christine Durrieu³

¹ Université de Nantes, Faculté de Médecine, EA3826, 1, rue Gaston Veil, F-44035 Nantes, France

² CNRS UMR5629, Laboratoire de Chimie des Polymères Organiques, IPB-ENSCBP, Université de Bordeaux, Pessac, 16, av Pey Berland, France

³ Institute of Chemistry & Biology of Membranes & Nanoobjects (CBMN-UMR 5248), IECB, Université Bordeaux, 2 Rue Robert Escarpit, 33607 Pessac, France
Gilles.Amador@univ-nantes.fr

INTRODUCTION

Methicillin-resistant *Staphylococcus aureus* (MRSA) is an important nosocomial pathogen acting in a global endemioepidemic state. The options for treatment of bone infections due to methicillin-resistant *S. aureus* (MRSA) are limited by pharmacokinetic factors (such as penetration into bone tissues) and susceptibility pattern of the causal bacteria. For the treatment of prosthetic joint infections, continuous irrigation and antibiotic impregnated bone cement beads have become popular because of higher antibiotic concentration in soft tissue, bone, and/or joints.

In a recent contribution to this field, we have presented a new biomaterial having applications as implant in orthopaedic surgery and allowing the release of an antibiotic (the Gentamicin Sulphate ; GS) only in case of infection [1, 2]. A cleavage reaction of the active particle-active molecule bond, activated by the contact of material with the physiological medium or by a modification of the pH, induces controlled release of the bioactive molecule in its native form.

Release kinetic profiles and *in vitro* bacterial growth inhibition have been established and in this presentation, we prove the *in vivo* efficiency of these materials.

EXPERIMENTAL METHODS

Nanoparticles are obtained by Ring-Opening Metathesis CoPolymerization (ROMP) of norbornene with α -norbornenyl poly(ethylene oxide) macromonomers ω -functionalized with either carboxylic acid groups or GS through a pH-sensitive amine bond. Their colloidal stabilities were shown by Dynamic Light Scattering measurements. Titanium discs ($\varnothing = 4$ mm ; h = 20 mm) were activated by functionalization with amine groups using aminosilane molecules (APTES). The NPs were covalently linked onto the titanium surface through the formation of an uncleavable amide bond between the carboxyl group of the NPs and the amide group of silane molecules available onto the surfaces of the disks activated by NHS and DCC. The grafting was characterized by Scanning Electron Microscopy (SEM).

The aim of this study is to assess the *in vivo* efficacy of titanium devices coated with gentamicin in an experimental model of acute osteomyelitis in rabbit [3]. Femoral trepanation of rabbits was performed, followed by injection of 1 mL 10^9 CFU MRSA into the knee

cavity. A surgical debridement of the infected tissues was performed 3 days later and animals were randomly assigned to control group or titanium implantation. The strain studied is an MRSA strain (BCB8) obtained from blood cultures (gentamicin MIC < 0.5 μ g/mL).

RESULTS AND DISCUSSION

	Number of rabbits	Mean $\pm \sigma \log_{10}$ CFU/g of tissue	
		Bone Marrow	Spongy bone
Perop - Control	6	7.65 \pm 0.92	8.14 \pm 0.86
Per-operative induction	7	6.47 \pm 0.64 ^a	8.15 \pm 0.40

^aP < 0.05 vs preop-control

Significant difference was found between the bacterial counts of the control and the per-operative groups for bone marrow only. Titanium devices coated with gentamicin-nanoparticles showed no antimicrobial activity in spongy bone, compared to the control group.

CONCLUSION

The use of such devices appears not to be used alone in the treatment of acute bone infections, but in addition to systemic antibiotherapy. However, bacterial contamination during surgery uses smaller bacterial loads (10^2 to 10^4 CFU/ mL). It would be of a great interest to test these implants with these inocula.

REFERENCES

- 1 Pichavant L.; Bourget C.; Durrieu M.C.; Héroguez V. *Macromol.* 44:7879-87, 2011
- 2 Pichavant, L.; Amador, G.; Jacqueline, C.; Héroguez, V.; Durrieu, M.C. *J. Controlled release*, 162:373-81, 2012
- 3 Gaudin A.; Amador Del Valle G.; Hamel A.; Le Mabecque V.; Miegerville AF.; Potel G.; Caillon J.; Jacqueline C. *Lett Appl Microbiol*, 52:253-7, 2011

ACKNOWLEDGMENTS

The authors would like to thank the the French “Agence Nationale de la Recherche” (ANR) and the “Société de Transfert de Technologie”, Aquitaine Science Transfert (SATT AST), for providing financial support to this project.



Radially Aligned Collagen Scaffolds for Deterministic 3D Models of Cancer Migration

Anke Husmann¹, Jonathan Campbell¹, Samuel Troughton¹, Robert Hume², Christine J. Watson² and Ruth Cameron¹

CCMM, Department of Materials Science and Metallurgy, University of Cambridge, UK

^{2*} Department of Pathology, University of Cambridge, UK

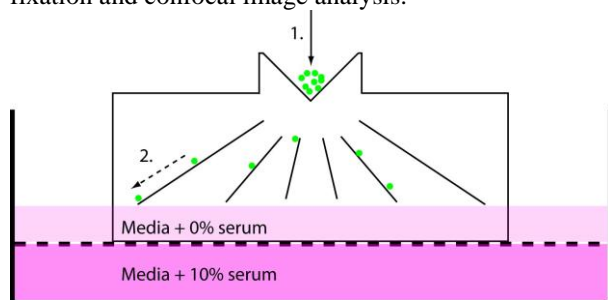
ah492@cam.ac.uk

INTRODUCTION

Freeze dried 3D collagen scaffolds have been used to develop complex analogues of tissue *in vitro*, for example mammary gland¹, and such models could provide important insights into cancer pathogenesis and spread. To increase model tractability the control of pore size and architecture is critical and Pawelec *et al.* have developed protocols to tailor such structures². We have extended this work by including metal nucleation sites to scaffold moulds, which has allowed us to create radially aligned collagen scaffolds. In the current study we investigate whether controlled pore architecture dictates 3D cancer cell migration.

EXPERIMENTAL METHODS

Low thermal conductive perspex and polycarbonate moulds of various geometries were designed to include metal nucleation sites. We used 1 wt% collagen slurry for our scaffolds. The freezing protocol was varied to control location and velocity of ice growth. We either used a cooling rate of 1°C/min down to -30°C or quenched the moulds by pre-cooling the freeze dryer to -40°C. Where possible, we monitored the temperature at various points on the moulds and in the slurry during cooling and freezing. The MCF-7 breast cancer cell-line was passaged under standard culture procedures. Scaffolds were sterilised in 70% ethanol and washed in PBS before loading 2x10⁶ cells in 5µl of PBS to the nucleation point. Seeded scaffolds were cultured on top of transwell chambers in a modified migration assay format (Fig 1). Cells were loaded with the live-cell marker 1µM Calcein AM for 1hr before overnight fixation and confocal image analysis.



1. Cells seeded at nucleation site

2. Ordered migration observed along directional collagen pores

Fig 1. Schematic of modified transwell migration assay.

RESULTS AND DISCUSSION

When moulds are cooled slowly and evenly to sub-zero temperatures with cooling occurring mainly through the base of the mould, ice crystallization results in isotropic pore formation. In contrast, if the metal tip is cooled faster than the thermally insulated moulds, nucleation occurs at the tip, which acts as a heat sink. This leads to a different thermal path during freezing and creates elongated and aligned pores.

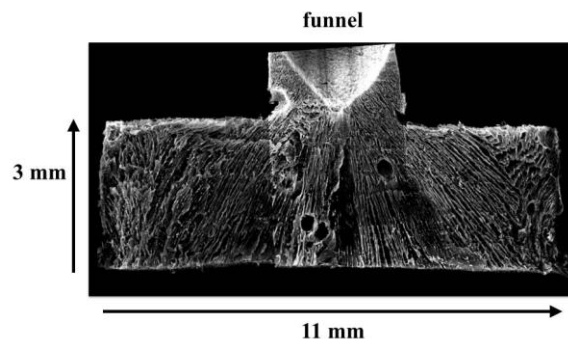


Figure 2 shows an SEM image of a scaffold where we have used a metal tip as a nucleation site, which in addition, generates a funnel for cell injection. This scaffold was formed by thermal quenching of the mould. We have also produced scaffolds with combined anisotropic and isotropic regions. Inoculation of scaffolds with MCF-7 cells resulted in a tight compaction of cells at the nucleation point at 24hrs, followed by their coordinated spread throughout the scaffold by 1 week along aligned collagen pores (Fig 3).

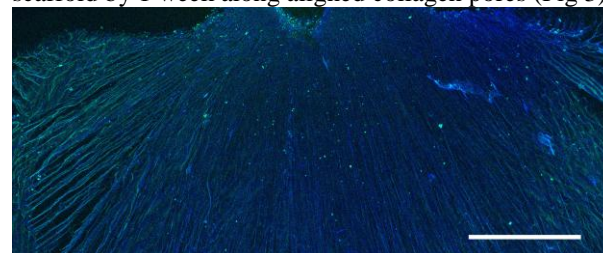


Fig3. Confocal projection of MCF-7 cells loaded with Calcein AM (green) 1 week following seeding. Bar = 2mm

CONCLUSION

We have extended our range of collagen scaffold designs from structures with isotropic pores to radially aligned pores that are suitable substrates for studying cancer cell migration rate and proliferation dynamics. We anticipate these models may eventually be adapted to better understand complex tissue interactions within the normal and tumour microenvironment, by incorporating multiple cell types to support stem cell niche regulation and studying homing of cancer phenotypes to target organs.

REFERENCES

1. Campbell, J.J. *et al.*, PloS ONE. 6(9): e25661, 2011.
2. Pawelec, K.M. *et al.*, J.R.Soc.Interface. 11(92):20130958, 2014.

ACKNOWLEDGMENTS

"The authors gratefully acknowledge the financial support of the Newton Trust, and ERC Advanced Grant 320598 3D-E. A.H. holds a Daphne Jackson Fellowship funded by the University of Cambridge.



Recombinant Production of Antimicrobial Spider Silk for Wound Dressing Materials

L. Nilebäck, R. Jansson and M. Hedhammar

Department of Anatomy, Physiology and Biochemistry, Swedish University of Agricultural Sciences, Sweden
linnea.nileback@slu.se

INTRODUCTION

In chronic wounds and implant sites, it is crucial to inhibit growth of pathogenic bacteria to avoid biofilm formation and extensive infections.^{1,2} Antimicrobial peptides (AMPs) from innate immune systems are less prone to induce resistance development in pathogens than conventional antibiotics and are therefore gaining interest.² In this work, we used recombinant technology to covalently link AMPs to a partial spider silk protein (spidroin). This protein assembles into silk-like materials that exhibit a unique combination of elasticity and strength. Recombinant production allows us to introduce new functions such as antimicrobial activity to the proteins already at DNA level, and to convert them into various 2D and 3D scaffolds.

EXPERIMENTAL METHODS

Fusion proteins of antimicrobial peptides and the partial spidroin 4RepCT were constructed using conventional cloning strategies and IPTG induced expression in *Escherichia coli* BL21(DE3). Target proteins, tagged with His₆ at the N-terminus, were purified using Zn²⁺ charged IMAC columns. Silk fibers and films were made according to previously reported methods.^{3,4} The number of Colony Forming Units (CFU) of *E. coli* Nova Blue before and after incubation on silk films (duplicates) was determined using the spread plate method on LB agar. Statistical significance was determined using SPSS Paired-Samples T test.

RESULTS AND DISCUSSION

Fusion proteins were constructed both with and without a solubility-enhancing domain N-terminally to AMP-4RepCT, and different expression conditions were compared to evaluate which strategy that is the most promising for recombinant production of antimicrobial spider silk. Highest yields were obtained from long-term expression at low temperatures for constructs containing the N-terminal solubility tag. Possibly, the tag at the N-terminus together with 4RepCT at the C-terminus blocks both sides of the AMP from interacting bactericidally with the membranes of the bacterial host during expression. This is in accordance with previous reports about the possibility to express AMPs recombinantly using various end-tagging systems.⁵ After expression, the N-terminal tag is removed from the product, leaving one side of the AMP free to interact with target bacteria.

Antimicrobial silk fusion proteins obtained with the described procedure could still assemble into stable films and fibers. An example of such a fiber, made from

a fusion of 4RepCT and Magainin I, an AMP from the African clawed frog *Xenopus laevis*, is shown in Figure 1.

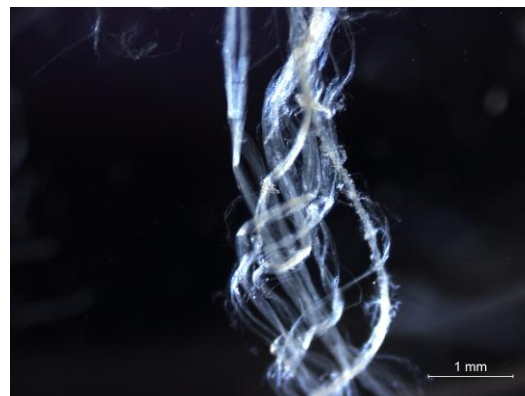


Figure 1. Silk fiber made of Magainin-4RepCT.

The antibacterial assays imply a bactericidal effect of AMP-functionalized spider silk compared to non-functionalized references in initial trials (n=2, p<0.1).

The possibility to express AMP-functionalized spider silk recombinantly leads the way to large-scale production of antimicrobial materials that can be processed into different silk formats adapted to the aimed applications, without risks for disease transmission or side effects from chemical compounds.

CONCLUSION

We present a method to recombinantly produce antimicrobial peptides fused to the partial spidroin 4RepCT in heterologous hosts. With this design, antimicrobial materials in suitable formats for wound healing applications can be produced.

REFERENCES

1. Percival S. and Cutting K., Microbiology of wounds. CRC Press, 2010
2. Costa F. *et al.*, Acta Biomater. **7**, 1431–1440, 2011
3. Stark M. *et al.*, Biomacromolecules **8**, 1695–1701, 2007
4. Widhe M. *et al.*, Biomaterials **34**(33), 8223–8234, 2013
5. Ingham A. *et al.*, Biotechnol. Appl. Biochem. **47**, 1–9, 2007

ACKNOWLEDGMENTS

The authors would like to thank The Swedish Research Council for providing financial support, and Spiber Technologies AB for providing silk proteins.

Sol-Gel Hybrids with RAFT-Polymerised Branched Methacrylate Copolymers as Organic component for Tissue Engineering

Justin Chung¹, Anthony Maçon¹, Theoni Georgiou¹, Julian R. Jones¹

¹ Department of Materials, Imperial College London, UK

Justin.chung11@imperial.ac.uk

INTRODUCTION

Sol-gel hybrids for tissue regeneration are of great interest because their nanoscale interpenetrating networks of silica and organic polymer can provide unique properties in terms of toughness and biodegradation rates.¹ Covalent coupling between the components is critical to attain these properties. Previously this was achieved using coupling agents such as glycidoxypyrpyl trimethoxysilane (GPTMS).¹ Here, polymers were synthesised that contain reactive silica groups for coupling to a silica network. Hybrids of branched co-polymer of methyl methacrylate (MMA) with 3-(trimethoxysilyl)propyl methacrylate (TMSPMA) for coupling and ethylene glycol dimethacrylate (EGDMA) as a branching agent were developed and tested.

EXPERIMENTAL METHODS

Prior to polymerisation, all monomers (MMA, TMSPMA, and EGDMA) were passed through basic alumina columns to remove inhibitors. Then they were dried over CaH₂. The branched co-polymers were synthesised by free-radical and reversible addition fragmentation chain transfer (RAFT) polymerisation using azobis-isobutyronitrile (AIBN) as an initiator. The molecular weight (MW) was regulated by introducing different ratios of thioglycerol (for free-radical polymerisation) and cumyl dithiobenzoate (for RAFT polymerisation) in the reaction chamber. The rate of branching was controlled by introducing different molar ratios of EGDMA. Tetraethyl orthosilicate (TEOS) was used as the inorganic precursor. The hybrid contained 40 wt% inorganic. Nuclear magnetic resonance (NMR) and gel permeation chromatography (GPC) were used to characterise the composition and MW, respectively, of the organic component. Fourier transform infrared spectroscopy (FTIR), compression tests and simulated body fluid (SBF) testing were performed.

RESULTS AND DISCUSSION

Both linear and branched TMSPMA homopolymer from previous studies did not improve the mechanical properties compared to conventional sol-gel derived bioactive glass. This was due to an excessive amount of covalent bonding to the silica network because TMSPMA contains alkoxysilane end groups. To solve this problem, TMSPMA units were spaced using branched pMMA (MMA-co-TMSPMA-co-EGDMA or branched pMCM). TMSPMA provided excellent coupling between the silica and the polymer. Figure 1 shows a stress-strain of the hybrids with different organic contents compared to that of bioglass 70S30C. Branched pMCM hybrids showed viscoelastic

mechanical property while sol-gel glass and TMSPMA homopolymer hybrids displayed brittle failure.

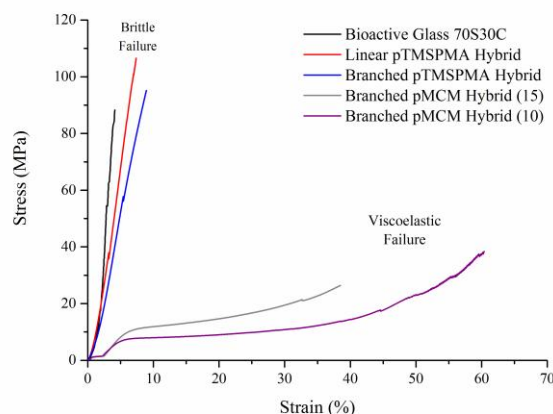


Figure 1: Stress-strain of 70S30C, linear, branched pTMSPMA, and branched pMCM hybrids.

Free-radical and RAFT polymerisation methods were used to synthesise the branched pMCM to compare the MW and branching rate. It is important to consider that polymer should be eliminated through kidney filtration of pores with a size comparable to 4 to 14 nm.² Also, the threshold of the filtration corresponds with the molecular weight ranging from 30 to 50 kDa, depending on the shape, molecular conformation, and flexibility of the polymer.³ RAFT polymerisation process gives more control of the MW and branching rate compared to that of free-radical polymerisation process.

CONCLUSION

Branched pMCM is a potential hybrid source for bone regeneration. It shows a viscoelastic mechanical behaviour and hydroxycarbonate apatite layer forms within two weeks of SBF immersion. RAFT polymerisation has demonstrated a higher control over regulating MW and branching. However, additional experiments and investigations are required to improve the mechanical property of the hybrids. In addition, replacing EGDMA with an enzymatically or hydrolytically degradable branching agent should be considered in the future.

REFERENCES

1. Jones J.R., *Acta Biomater* 9:4457-4486, 2013
2. Fox E. *et al.*, *Acc Chem Res* 42:1141-1151, 2009.
3. Duncan R. *et al.*, *Nat Rev Drug Discov* 2:347-360, 2003

ACKNOWLEDGMENTS

Imperial College London Rector's Scholarship Fund and EPSRC (EP/I020861) for financial support.

***In vitro* Evaluation of a Novel Injectable Thermo-Responsive Polymeric Hydrogel for the Delivery of Self-Assembly Peptide Nanoparticles Containing an Osteoconductive Agent**

S. Pentlavalli¹, P. Chambers¹, A. Massey¹, M. O'Doherty¹, H. McCarthy² and N. Dunne¹

¹School of Mechanical and Aerospace Engineering, Queen's University Belfast, Northern Ireland

²School of Pharmacy, Queen's University Belfast, Northern Ireland
s.pentlavalli@qub.ac.uk

INTRODUCTION

A major challenge in the repair of joint injuries is in the reattachment of the soft tissue to the bone¹. Knee injuries are common and associated with the development of osteoarthritis in later years¹. As such much investigation has taken place into the development of a scaffold with the ability to promote bone and soft tissue regeneration. Despite an understanding of the graded nature of the knee joint, only a few studies to date have focused on scaffolds that mimic this interface¹. For example, Li *et al* developed a graded calcium phosphate coating on the surface of electrospun nanofibres². However, these studies have resulted in limited success. In this study we propose a novel AAlg-g-PNIPAAm hydrogel, which has thermo-responsive properties for the delivery of self-assembly peptide (RALA) containing tricalcium phosphate (TCP) nanoparticles (NPs) with osteogenic activity.

EXPERIMENTAL METHODS

Preparation of hydrogel: Aminated alginate (AAlg) and carboxylic end capped PNIPAAm (PNIPAAm-COOH) was synthesised and coupled via amide bond linkages to form AAlg-g-PNIPAAm hydrogel with various ratios. ¹H NMR, FTIR and rheological was used to characterise the resultant hydrogels³.

Formulation of RALA/TCP NPs: NPs were prepared at a range of mass ratios, with particle size and zeta potential (ZP) measured using a Malvern Zetasizer Nano ZS to determine the optimal formulation, which was found to be a mass ratio of 10:1.

Analysis of the stability of the NPs: Longitudinal stability of the NPs prepared at a mass ratio of 10:1 across a temperature range of 4-40°C. Maintenance of particle size was the measure of stability.

Transmission electron microscopy (TEM): NPs were loaded onto a carbon coated formvar copper grid. Grids were subsequently stained using uranyl acetate for 5 min at room temperature and imaged using a Philips Tecnai TF20 D microscope.

Cell viability following treatment with TCP alone or RALA/TCP NPs: MG-63 osteosarcoma cancer cells were seeded at a density of 10,000 cells per 96-well plate and treated with different doses of TCP or transfected with RALA/TCP NPs at corresponding doses for 6h prior to replacement with complete medium. The doses used for drug only treatments were 0.75-5 µg and the doses of drug used for NP transfection were 0.75-2.5 µg.

RESULTS AND DISCUSSION

Preliminary studies demonstrate that the AAlg-g-PNIPAAm solutions exhibited increasing viscosity from 34-36°C as the aqueous solutions transformed to elastic hydrogels, which was indicative of their thermo-responsive properties. NPs prepared with a mass ratio of 10:1 were found to have a size of 51 nm ± 7.15 nm and a zeta potential of 36 mV ± 4.34 mV. The size of the

NPs was confirmed by TEM and the round shape elucidated. The NP particle size and ZP remained consistent for up to 14 days at room temperature demonstrating the physical stability of the NPs. The temperature study confirmed NP stability across a broad range (i.e. 4-40°C). Cell viability was unaffected by treatment with pure TCP at various concentrations, potentially due to TCP particle size at approximately 800 nm limiting their uptake into cells. However, encapsulation of the TCP with RALA resulted in a reduction in cell viability in the MG-63 osteosarcoma cell line, correlating with TCP dose.

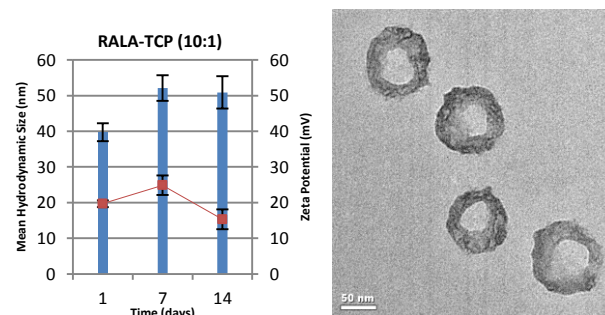
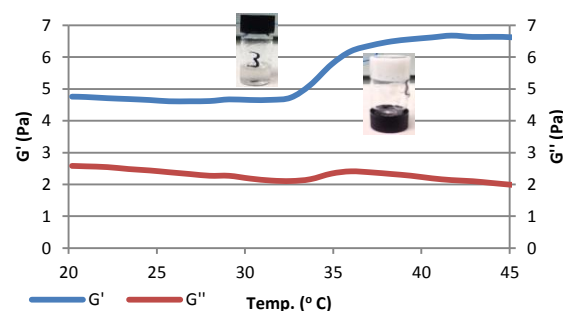


Figure 1. a) Storage modulus (G') and loss modulus (G'') of 3% AAlg-g-PNIPAAm solution (insert: the LCST behaviour of polymer solution). b) Size and ZP of RALA/TCP NPs (mean ± SEM, n=3). c) TEM image of RALA/TCP (10:1) NPs.

CONCLUSION

We have successfully produced a thermo-responsive polymer with the potential to behave as both a scaffold and delivery vehicle. Furthermore, RALA peptide was capable of forming NPs with TCP, which were stable across a range of temperatures and over an extended duration. Upon fine tuning of the hydrogel formulation, the degradation pattern and NP release from the hydrogel *in vitro* will be studied. The dual functionality of the hydrogel as a scaffold for bone regeneration and a delivery vehicle for osteoconductive NPs will finally be assessed *in vivo*.

REFERENCES

1. Yang P. *et al.*, Tissue Eng Part B Rev. 2:127-141, 2009
2. Li X. *et al.*, Nano. Lett. 7:2763-2768, 2009
3. Tan R. *et al.*, Carbohydr. Polym. 87:1515-1521, 2012

ACKNOWLEDGMENTS

We would like to thank the US-Ireland Grant (Grant no: 3568) and the Medical Research Council (Grant no: 1294) for providing financial support for this project.



Design of Drug-immobilized Polylactide-graft-Poly(ethylene glycol) as a Temperature-Responsive Injectable Polymer for Controlled Release of Low-molecular-weight Water Soluble Drugs

Yuichi Ohya^{1,2*}, Masay Umezaki¹, Yasuyuki Yoshida¹, Akihiro Takahashi², and Akinori Kuzuya^{1,2}

^{1*}Department of Chemistry and Materials Engineering, Kansai University, Japan, yohya@kansai-u.ac.jp

²Organization for Research and Development of Innovative Science and Technology(ORDIST), Kansai University, Japan

INTRODUCTION

Recently, great attention has been paid for biodegradable thermo-gelling polymers exhibiting sol-to-gel transitions as injectable polymers (IPs) in drug delivery system (DDS) or tissue engineering. The most typical molecular structures for IPs consisting of PEG and an aliphatic polyester are linear block-type architectures, but some other IPs having branched structures such as graft-type or star-shaped have also been reported¹⁻⁴. A graft-copolymer system had some advantages compared to block copolymer systems.⁴⁻⁵ Linear block copolymer-type IPs have limitations in PEG length and total molecular weight, which may be obstacles to achieve high physical properties in the gel state. Using graft-copolymer, the total molecular weight can be changed independently of the graft PEG length while retaining the sol-to-gel transition behavior.⁴⁻⁵

Although IP thermogel systems have been widely used for DDS, the release rates of water-soluble low-molecular-weight drugs are generally faster than hydrophobic and/or high-molecular-weight drugs. Recently, we synthesized a graft copolymer of poly(depsipeptide-co-DL-lactide) with PEG, poly[(glycolic acid-*alt*-L-aspartic acid)-co-DL-lactide]-g-PEG [P(GD-DL-LA)-g-PEG] exhibiting temperature-responsive sol-to-gel transitions.⁴ Using this system, the residual carboxylic acid groups can be used for further functionalization such as drug immobilization. In this study, we propose a new type of IP system, which can act as a macromolecular prodrug exhibiting sustained release of water-soluble low-molecular-weight drugs. Antibiotic levofloxacin (LEV) was chosen as a model of a hydrophilic low-molecular-weight drug. The LEV was attached to P(GD-DL-LA)-g-PEG to give a P(GD-DL-LA)-g-PEG/LEV conjugate. Temperature-responsive sol-to-gel transition behavior of the conjugate in aqueous solution and the release behavior of LEV from the hydrogel were investigated.

EXPERIMENTAL METHODS

P(GD-DL-LA) synthesized by the method reported previously⁴, LEV-ethyl-NH₃⁺Br⁻, DCC, NHS and DMAP were reacted in DMF at r.t. for 24 h. Then, MeO-PEG and DCC in DMF was added into the reaction mixture, and stirred at r.t. for 12 h. The unreacted MeO-PEG and LEV derivative were removed by reprecipitation using diethylether/methanol. The sol-to-gel transition behavior of the conjugate and P(GD-DL-LA)-g-PEG aqueous solution were investigated by the test tube inversion method.¹ The temperature-dependent rheological properties of the conjugate solution were measured by using a dynamic rheometer. The *in vitro* release of LEV from the conjugate hydrogel was investigated in PBS and compared with

P(GD-DL-LA)-g-PEG and PLGA-*b*-PEG-*b*-PLGA hydrogels physically entrapping LEV molecules. The opened vials containing the hydrogels were fully soaked in 80 mL of PBS, and incubated at 37 °C. After predetermined periods, 1 mL of supernatant was collected, and the absorbance at 287 nm was measured on a UV-vis spectrophotometer.

RESULTS AND DISCUSSION

Both P(GD-DL-LA)-g-PEG/LEV conjugate and P(GD-DL-LA)-g-PEG in PBS showed sol-to-gel transition between r.t. and 37 °C. These results indicate that the introduction of LEV into P(GD-DL-LA)-g-PEG had no significant influence on the gelation. P(GD-DL-LA)-g-PEG/LEV hydrogel showed gradual and continuous release of LEV derivatives for 11 weeks. On the other hand, the release rate of the LEV molecule from P(GD-DL-LA)-g-PEG and PLGA-*b*-PEG-*b*-PLGA hydrogel that physically entrapped LEV was significantly faster than that from the conjugate hydrogel. The release of LEV from P(GD-DL-LA)-g-PEG hydrogel was almost completed in 3 weeks. The release rate of LEV from PLGA-*b*-PEG-*b*-PLGA hydrogel was much faster. Thus, it was revealed that the release rate of a water-soluble model drug (LEV) from IP hydrogel could be sustained by using a graft-type thermo-gelling polymer [P(GD-DL-LA)-g-PEG], and further suppressed by covalent immobilization to the polymer backbone.

CONCLUSION

We developed a macromolecular prodrug-type IP system using a biodegradable graft-type thermo-gelling polymer, P(DG-DL-LA)-g-PEG. The obtained P(DG-DL-LA)-g-PEG/LEV conjugate exhibited temperature-responsive sol-to-gel transition behavior in PBS between r.t. and 37 °C. Sustained release of LEV derivative from the hydrogel was observed. The release rate of LEV from the conjugate hydrogel was much slower than that from control hydrogels physically entrapping LEV molecules. These results suggest that the covalent attachment strategy is effective for achieving sustained release of water-soluble low-molecular-weight drugs in IP systems, and can be applied to drug delivery devices for highly bioactive molecules.

REFERENCES

1. Nagahama, K. *et al.*, *Adv. Funct. Mater.* 18:1220-1231, 2008
2. Nagahama, K. *et al.*, *J. Polym. Sci. Part A Polym. Chem.* 46:6317-6332, 2008
3. Nagahama, K. *et al.*, *Polymer* 50:3547-3555, 2009
4. Takahashi, A. *et al.*, *J. Biomat. Sci. Polym. Edn.*, in press.

Localized Corrosion Behaviour of Stainless Steel and Titanium Based Hard Tissue Implants

Ilven Mutlu* and Enver Oktay

Metallurgical and Materials Engineering Department, Istanbul University, Turkey
imutlu@istanbul.edu.tr

INTRODUCTION

Pitting is a corrosion type that results in rapid penetration at small areas. Pitting can be evaluated by critical pitting potential, which is potential above there is increase in current. Crevice corrosion occurs within cracks where acidic solution is developed. Sensitisation occurs when metals are heated at intermediate temperatures. Depletion occurs at grain boundary due to precipitation. When sensitised metal is exposed to corrosive environment, depleted regions dissolve, leading to intergranular corrosion¹⁻³.

EXPERIMENTAL METHODS

Ti-Nb-Cu specimens were produced by powder metallurgy using Ti, Nb and Cu powders. 35 w.% Nb and 3, 5, 7, and 10 w. % Cu powder was added to Ti powder. Mixtures were compacted into cylindrical specimens. Sintering was carried out at 1100 °C for 45 minutes. AISI 316 austenitic stainless steel was investigated as wrought specimens. Stainless steel specimens were heated to develop sensitisation. Heat treatments were carried out at 825 °C for 1 hour. The specimens were then water quenched.

Electrochemical corrosion studies were carried out in simulated body fluid using a potentiostat (Interface 1000, Gamry, USA). A conventional three-electrode system was used. Cyclic polarization curves were analysed in terms of breakdown potential and repassivation potential values. Critical pitting potential test determines critical repassivation potential. Experiment starts with stimulation phase. Test compares the current to current limit. If current exceeds the limit, test goes to repassivation. If constraint is exceeded the test ends. Tsujikawa-Hisamatsu electrochemical (THE) test was used to assess susceptibility to localized corrosion. Potential scanned from -500 mV to 1500 mV. Mode was then switched from potentiodynamic to galvanostatic and 200 $\mu\text{A}/\text{cm}^2$ current density was applied. After galvanostatic step, potentiostatic steps were applied until crevice repassivation. Repassivation potential is determined as potential for which current density decreases with time. Electrochemical potentiokinetic reactivation (EPR) test can be used to evaluate degree of sensitization (DOS) to intergranular corrosion. Sample is potentiostated at activation E. Sample is then potentiostated. Finally, potential is swept back to OCP. Simple EPR command was used to calculate the DOS to IGC.

RESULTS AND DISCUSSION

Increasing Cu content of Ti-Nb-Cu was increased the peak current density according to EPR test. Decreasing pH of solution was increased the peak current density of stainless steel. EPR test is used to DOS but also can be

used in pitting and crevice measurements. Precipitates can results in excess charge during cathodic scan.

CONCLUSION

Increasing Cu content of Ti-Nb-Cu alloy was increased the peak current density according to EPR test. Decreasing pH of solution was increased the peak current density of stainless steel specimens. Increasing Cu content of the Ti-Nb-Cu alloy was decreased the critical pitting potential. Increasing pH of solution was increased the critical pitting potential. Crevice repassivation potential of Ti-Nb-Cu specimens was decreased with increasing Cu content according to THE tests. Increasing pH of the solution was increased the crevice repassivation potential of Ti-Nb-Cu alloy. Increased pH of solution was also increased the crevice repassivation potential of stainless steel.

REFERENCES

1. N.S. Zadorozne, *et al.* Electrochimica Acta 76 (2012) 94-101.
2. W.R. Osorio, *et al.* Electrochimica Acta 77 (2012) 189-197.
3. H.E. Buhler, L *et al.* Corrosion Science 45 (2003) 2325-2336.

ACKNOWLEDGMENTS

This work was supported by Scientific Research Projects Unit of Istanbul University, P.N: 23402.

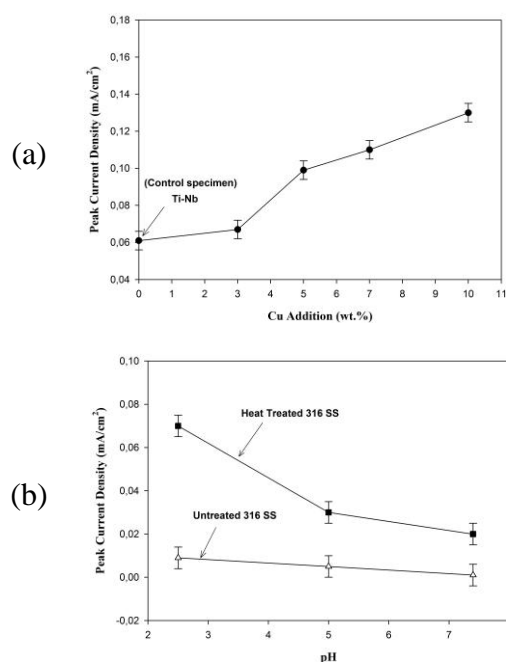


Figure 1. Variation of peak current density in the (a) Ti-Nb-Cu alloy and (b) AISI 316 stainless steel specimens

Degradation of Calcium-Phosphate Based Glasses Controlled by TiO₂ Addition

A. M. B. Silva^{1,2}, J. M. Oliveira^{2,3*}, M. H. V. Fernandes^{1,2}

¹ Department of Materials & Ceramics Engineering, University of Aveiro, 3810-193 Aveiro, Portugal

² Centre for Research in Ceramics and Composite Materials, CICECO, University of Aveiro, 3810-193 Aveiro, Portugal

^{3*} School of Design Management and Production Technologies, University of Aveiro, 3720-232 Oliveira de Azeméis, Portugal, martinho@ua.pt

INTRODUCTION

Calcium phosphate-based glasses and glass-ceramics have high potential for use as biomaterials due to their unique properties although a high solubility of these glasses is sometimes considered a serious handicap to their use in biomedical applications.

Almost all bioactive glass-based materials contain a large amount of silica, but development of new glass-ceramic biomaterials has recently concentrated on SiO₂-free glasses. It is well accepted that phosphate-based glasses without silica and with high CaO/P₂O₅ molar ratio (>1.5) exhibit a high potential for use as biomaterials¹⁻².

Titanium oxide does not form a glass alone, but it can be incorporated in significant amounts into other glass-forming oxide systems such as phosphates. The role of TiO₂ in bioactive glasses and glass ceramics is still under discussion but addition of this oxide to phosphate glasses usually contributes to improve glass-forming ability, chemical durability and glass structure stabilization. Moreover, TiO₂ addition to CaO-P₂O₅ based glasses does not compromise development of biocompatible and bioactive phases.³⁻⁵

Previous work has shown that incorporation of TiO₂ in calcium phosphate glasses can control their degradation rate.⁴

EXPERIMENTAL METHODS

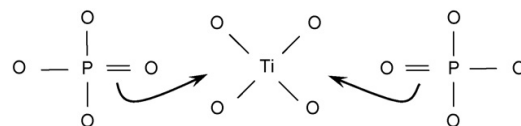
Glasses from TiO₂-P₂O₅-CaO system were prepared by conventional melting and pouring process⁴ and its amorphous state evaluated by powder X-Ray Diffraction. The glasses were studied by spectroscopic methods, Raman and ³¹P MAS-NMR (Magic Angle Spinning – Nuclear Magnetic Resonance), and immersed in synthetic plasma in order to evaluate the effect of structure on the surface reactivity of those glasses.

RESULTS AND DISCUSSION

Spectroscopic methods have revealed the features of the internal structure of glasses and showed that for TiO₂-free and TiO₂ lower contents chain phosphate units dominate the structure near the metaphosphate composition, Q², and for higher TiO₂ contents distorted Ti octahedral linked to pyrophosphate units, Q¹, dominate glass structure.

A progressive depolymerization of phosphate glass network occurs as TiO₂ content increases but the local cohesion of glass structure increases due to the

replacing of P-O-P bonds by stronger Ti-O-P bonds, figure 1.⁴



“Figure 1: Mechanism of P–O–Ti bonds formation from P=O bonds break.”

Degradation studies in synthetic physiological media showed that chemical stabilization increases with TiO₂ addition in accordance with indications of the spectroscopic structural results.

CONCLUSION

The results indicate that incorporation of TiO₂ in P₂O₅-CaO glasses may be used to control their dissolution in body fluids, thus providing a wide range of potential biomedical applications, namely in regeneration strategies or in drug delivery situations.

Studies in progress are showing that structural differences induced by TiO₂ content also influence the biological behavior of these glasses when contacting physiological fluids and cells.

REFERENCES

1. Saranti A. *et al.*, J. of Non-Cryst. Solids 352(5):390–398, 2006
2. Franks K. *et al.*, J. Mater. Sci: Mater. Med. 11:609-614, 2000
3. Abou-Neel E.A. *et al.*, Acta Biomaterialia 4:523-534, 2008
4. Silva A.M.B. *et al.*, J. of the Eur. Cer. Society 30(6):1253-1258, 2010
5. Lucacel R.C. *et al.*, J. of Non-Cryst. Solids 356:2869-2874, 2010

ACKNOWLEDGMENTS

“The authors would like to thank CICECO and financial support through SFRH/ BD/ 48657/ 2008 grant from FCT”.

Comparison of UV and EDC Cross-linking on Mechanical Properties of Collagen-based Scaffolds for Myocardial Tissue Engineering

Natalia Davidenko¹, Carlos Schuster¹, Ruth Cameron¹, Serena Best¹

¹Department of Materials Science and Metallurgy, University of Cambridge, United Kingdom, nd313@cam.ac.uk

INTRODUCTION

The concept of Tissue Engineering (TE) has led to the utilisation of 3D scaffolds as cell delivery vehicles. These biomaterials should mimic the function of ECM which not only provides mechanical support for cells, but also supplies signals that direct cell attachment, proliferation, differentiation and metabolism¹.

The objective of this work was the development of a series of collagen (Col) and gelatin (Gel)-based scaffolds with appropriate mechanical characteristics suitable for use in myocardial tissue regeneration and repair. Collagen was selected as main component as it comprises up to 80% of myocardial ECM providing the heart tissue its mechanical strength and stiffness. Gelatin, thermally denatured collagen, possesses more disorganised structure which should affect mechanical stability of resultant scaffolds. The addition of Gel to Col can tailor the mechanical properties of scaffolds and could be a design strategy for changing biochemical activity.

EXPERIMENTAL METHODS

Protein scaffolds (Col, Gel and Col/Gel= 50/50) were obtained by freeze-drying and cross-linked with EDC/succinimide (NHS) at different concentrations. EDC concentration of 11.5mg/ml (molar ratios to Col =5/2/1) was assumed as standard (100%) and was varied in the interval from 100 to 1%. UV irradiation ($\lambda=254\text{nm}$; $t=30\text{ min}$; at different light intensities) was also used for scaffold and film treatment. Compressive stress-strain analysis on scaffolds was carried out in the wet stage. The linear elastic (Young's) modulus was obtained via linear regression of the initial linear region of the stress-strain curve.

RESULTS AND DISCUSSION

The results of mechanical testing showed that EDC cross-linking and UV treatment mechanically stabilised all studied scaffolds to a different extent. Compressive modulus increases with the increase of EDC concentration for all the compositions. The reduction of standard EDC concentration (11.5mg/ml, 100%) to 10% still provides mechanical stability for all scaffolds compositions. Col matrices displayed the highest Young's Modulus. Low EDC concentrations (1%) stabilize only collagen scaffolds (Fig.1).

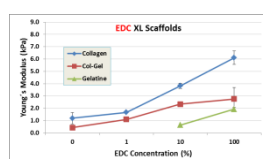


Fig.1 Influence of EDC concentration and composition on compressive modulus of scaffolds.

UV irradiation increases compressive properties of Col-based scaffolds while pure Gel matrices showed no differences in Young's modulus after UV exposure. The values of elastic modulus depend on the intensity of UV light and on the scaffold composition. Pure Col scaffolds showed the highest values in compressive modulus after UV treatment (Fig.2)

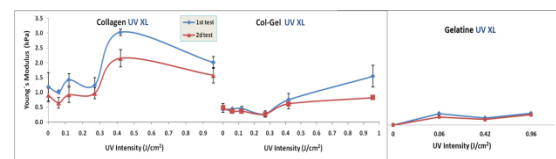


Fig. 2 Influence of UV intensity and composition on the Young's Modulus of scaffolds.

Relatively small increase in compressive properties of scaffolds after UV treatment (~2 times in the maximum comparing to ~4.5 times achieved with EDC XL for Col) may be related to the intrinsic limitation of UV light in forming high density network within polypeptide molecules (less than 2% of tyrosine and phenylalanine in Col molecules responsible for UV-mediated binding).

CONCLUSION

Mechanical properties may be tailored by changing composition and crosslink status of Col and Gel-based scaffolds. EDC cross-linking mechanically stabilised all the scaffold compositions while UV irradiation increased only Col-based scaffold compressive properties and to relatively small extent. Varying scaffold composition and XL method provide a simple but effective way to modulate the mechanical parameters of these scaffolds to better suit their use in specific soft tissue engineering applications.

REFERENCES

1. Chen O. *et al.*, Mat Sci Eng R. 59:1-37, 2008)

ACKNOWLEDGMENTS

The authors would like to thank the British Heart Foundation (Grant NH/11/1/28922) for providing financial support for this project.

Electrochemical Corrosion Behaviour of Highly Porous Beta-Type Ti-Nb-Cu Alloy

Ilven Mutlu^{1*}

¹Metallurgical and Materials Engineering Department, Istanbul University, Turkey
imutlu@istanbul.edu.tr

INTRODUCTION

Metal foams exhibit structure similar to bone and provide anchorage for surrounding tissue. Implants suffer from mismatch of Young's modulus with bone^{1, 2}. Ti alloys are used for high strength to density ratio, biocompatibility and corrosion resistance. However, there are disadvantages such as high Young's modulus. Ti has hexagonal close-packed (α -phase) structure that transforms to body-centered cubic structure (β -phase) at 883 °C, which can be increased by α -phase stabilizers (Al, O, N) or lowered by beta (β)-phase stabilizers (Mo, Nb, V). β -Ti alloys have low Young's modulus (close to bone) and biocompatibility. Beta-Ti stabilizer Nb is biocompatible. Cu addition enhances sinterability³⁻⁵.

EXPERIMENTAL METHODS

Foams were produced by space holder method using Ti, Nb and Cu powders. 35 wt.% Nb and 3, 7, and 10 wt. % Cu powder was added to Ti powder. As a space holder, carbamide was used. Mixtures were compacted at 200 MPa. Specimens were immersed in water and then carbamide was leached out. Sintering was carried out at temperatures between 1000 and 1250 °C for 45 minutes. Amounts of reagents for preparation artificial saliva are 0.4 g/l NaCl, 0.79 g/l CaCl₂·H₂O, 0.4 g/l KCl, 0.005 g/l Na₂S 9H₂O, 0.78 g/l NaH₂PO₄·H₂O, 0.35 g/l Urea.

Electrochemical corrosion studies were carried out in artificial saliva using a potentiostat (Interface 1000, Gamry, USA). A conventional three-electrode system was used. Open circuit potential was measured before carrying out experiments. Potentiodynamic polarization was carried out from -500 mV to +1500 mV. Tafel curves were obtained by polarizing the specimens from -250 mV to +250 mV. Corrosion density, Tafel slopes, corrosion rate and corrosion potentials were obtained from Tafel analyses. In linear polarization resistance test, specimens were polarized from -20 to +20 mV, in order to measure polarization resistance. Cyclic polarization experiments were carried out from -500 mV to apex potential and to final potential. Electrochemical impedance spectroscopy (EIS) measurements were carried out in potentiostatic mode. EIS studies were conducted in frequency range from 100 kHz to 0,001 Hz, with 5 points per frequency decade. Impedance spectra were fitted by an equivalent circuit model using Gamry, EIS100 software.

RESULTS AND DISCUSSION

Pore size and morphology of foams replicated initial size and morphology of space holder particles and mean pore sizes of foams was about 450-500 μ m, which is suitable for implant applications. Microstructure of Ti-Nb-Cu specimens (at the cell walls) was consisted of beta-Ti phase and Ti₂Cu at grain boundaries.

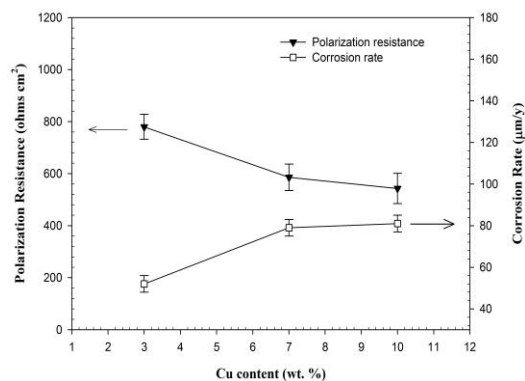


Figure 1. Effect of Cu content on corrosion behaviour

EIS measurements were showed capacitive semicircle, whose size was decreased as F increased and as pH decreased. At low F level, a capacitive semicircle is shown. Diameters of capacitive semi-arcs decreased with increasing Cu content of alloy. Impedance spectra of foams are presented as Nyquist and Bode plots. Nyquist plot is characterized by incomplete semicircle, indicating capacitive response of passive film. Diameter was increased with decreasing porosity. Bode magnitude plots are characterized by two regions.

CONCLUSION

Increased F concentration of artificial saliva was reduced the corrosion protection behaviour of alloy. F ions attack the alloys and severity of attack depends on the pH of saliva. OCP measurements show active behaviour in F⁻ added saliva due to presence of F⁻ that dissolve the passive film. Stability of the specimens was decreased at high concentrations of F⁻ and at low pH. Increasing Cu content of alloy was increased the corrosion rate and current density and decreased the corrosion potential. Although Cu addition was slightly reduce the corrosion properties, Cu addition to alloys was increased the mechanical properties. Cu addition was also enhanced the sinterability.

REFERENCES

1. I. Mutlu, *et al.* Materials Science and Engineering C 33 (2013) 1125-1131.
2. L.J. Gibson. Biomechanics of cellular solids. J. Biomech. 38 (2005) 377-399.
3. J. Huang, *et al.* Scripta Materialia 66 (2012) 682-685.
4. E.S.N. Lopes, *et al.* Materials Characterization 62 (2011) 673-680.
5. Z.C. Zhou, *et al.* Journal of Alloys and Compounds 509 (2011) 7356-7360.

ACKNOWLEDGMENTS

This work was supported by Scientific Research Projects Unit of Istanbul University, P.N: 23402.

Recombinant Affinity Silk for Presentation of Active Protein Domains

R. Jansson¹, N. Thatikonda¹, P.-Å. Nygren², M. Hedhammar¹

¹Department of Anatomy, Physiology and Biochemistry, SLU, Sweden, ronnie.jansson@slu.se

²Division of Protein Technology, School of Biotechnology, KTH Royal Institute of Technology, Sweden

INTRODUCTION

Functionalization of silk fibers via chemical or genetic incorporation of peptides or proteins with binding or enzymatic functionalities has been recognized as a promising route forward to generate novel materials for both biotechnological and medical applications. The recombinant partial spider silk protein, 4RepCT, self-assembles into macroscopic fibers under physiological-like conditions¹. Recently, cell binding peptides were genetically incorporated to 4RepCT resulting in functionalized spider silk of potential use as cell growth supports in regenerative medicine². Incorporation of larger proteins with a folding-dependent activity into chimeric 4RepCT proteins, retaining an ability to form fibers, would pave the way for additional types of functionalized silk-like materials. Thus, we have herein investigated the possibility to use recombinant DNA technology to develop functionalized silk materials that present whole functionally folded protein domains. In the present study, 4RepCT was genetically fused to the IgG binding domains Z³ and C2⁴, and to the albumin binding domain ABD⁵.

EXPERIMENTAL METHODS

The gene for 4RepCT was genetically fused to DNA encoding Z, C2 and ABD. Corresponding fusion proteins were expressed in *Escherichia coli*, purified using IMAC and silk-like fibers and films formed. Selective binding of target molecules (IgG to Z and C2, albumin to ABD) after incubation with serum or plasma were analyzed by gel electrophoresis. Distribution of target binding to functionalized silk films was analyzed by fluorescence microscopy after binding of directly or indirectly fluorophore-labeled target molecules. Selective binding of dual-functionalized Z/ABD-4RepCT silk after incubation with plasma was analyzed by gel electrophoresis. For presentation of human vascular endothelial growth factor (hVEGF) on Z-4RepCT, anti-hVEGF antibodies were first bound to Z-4RepCT films, followed by capture of hVEGF and detection by fluorescence microscopy.

RESULTS AND DISCUSSION

Three affinity domains of different origin and structure, the IgG-binding domains Z and C2, and the albumin-binding domain ABD, were all successfully produced as soluble silk fusion proteins under non-denaturing purification conditions, and able to form silk-like materials. Gel electrophoresis revealed selective binding of IgG to Z-4RepCT and C2-4RepCT silk from serum, and of albumin to ABD-4RepCT silk from plasma, implying folded and accessible affinity domains in the functionalized silk materials. Fluorescence microscopy revealed that target binding to functionalized silk films was distributed all over the

film surface (Figure 1a). Moreover, silk materials from a mixture of functionalized silk proteins showed combined binding properties, showing upon the possibility of tailor-making silk with multiple binding functionalities with defined stoichiometry.

By using a two-step approach it was possible to capture a growth factor (hVEGF) on Z-4RepCT films, by first decorating the film with antibodies against hVEGF, followed by capture of hVEGF (Figure 1b). By choosing a suitable antibody, this two-step approach could be used for decoration of Z-4RepCT silk with almost any target of interest, even complex multi-domain mammalian proteins, such as growth factors.

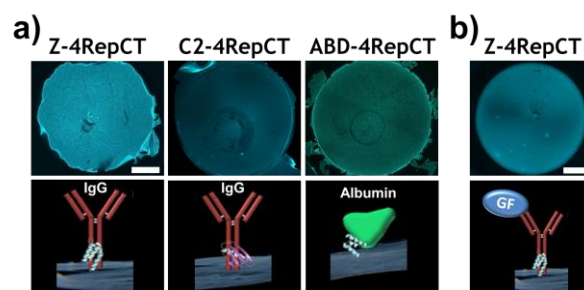


Figure 1. (a) Binding of fluorophore-labeled target molecules to functionalized silk films. (b) A two-step approach for presentation of growth factors to IgG decorated Z-4RepCT silk. Scale bars indicate 1 mm.

CONCLUSION

Herein we describe a novel strategy for immobilization of functional protein domains to recombinant spider silk. The chimeric spider silk proteins maintained both the ability to form silk-like materials and a folding-dependent affinity. By decoration of Z-4RepCT silk with suitable antibodies, an almost unlimited repertoire of targets can be presented, *e.g.*, growth factors. Production of silk with multiple functionalities further broadens the area of application.

REFERENCES

1. Stark M. *et al.*, *Biomacromolecules*. 8:1695-1701, 2007.
2. Widhe M. *et al.*, *Biomaterials*. 34:8223-8234, 2013.
3. Nilsson B. *et al.*, *Protein Eng.* 1:107-113, 1987.
4. Sauer-Eriksson A.E. *et al.*, *Structure*. 3:265-278, 1995.
5. Kraulis P.J. *et al.*, *FEBS Lett.* 378:190-194, 1996.

ACKNOWLEDGMENTS

Spiber Technologies AB is acknowledged for providing 4RepCT protein and The Swedish Research Council, Vinnova and Magnus Bergvall's foundation for financial support.

One-pot synthesis of hybrid biocompatible hydrogels based on methacrylamide gelatin and polyacrylamide

**A. Serafim^{1*}, C. Tucureanu², D. Petre¹, D.M. Dragusin³, A. Salageanu², S. Van Vlierberghe³,
P. Dubruel³, I.C. Stancu¹**

^{1*} University Politehnica of Bucharest, Romania, andrada.serafim@gmail.com

² Cantacuzino National Research and Development Institute for Microbiology and Immunology, Romania

³ Polymer Chemistry and Biomaterials Group, Ghent University, Belgium.

INTRODUCTION

Biocompatible hydrogels based on methacrylamide-modified gelatin (GELMA) have recently attracted increasing attention due to their wide range of possible applications. While GELMA is an appealing polymerizable collagenous derivative, with all biocompatibility-related attributes, acryl synthetic monomers remain a critical component of many biomedical products. The aim of the present work is to develop a one-pot synthesis method in order to synergistically combine the well-known innate biological properties of gelatin with the practical advantages of a synthetic hydrophilic biocompatible polymer, polyacrylamide (PAA). PAA is a conventional inert synthetic hydrogel, considered appealing for the development of multicomponent superabsorbent scaffolds for various tissue regeneration uses.

EXPERIMENTAL METHODS

GELMA-PAA hydrogels were obtained through free radical network-forming polymerization of acrylamide (with/out) synthetic crosslinking agent - MBA) and GELMA [1]. GELMA acts as crosslinking agent and also as a co-monomer in the polymerization of acrylamide. Properties such as water affinity, elasticity and biocompatibility were investigated.

RESULTS AND DISCUSSION

Bicomponent hydrogels were obtained through a one step network-forming polymerization reaction of C=C bonds from AA and GELMA. The obtained GELMA-PAA hydrogels were denoted P1-P4, according to an increasing AA concentration going from 50/1 to 1000/1. A second series of GELMA-PAA hydrogels (T1-T4) was synthesized using the same procedure, after supplementing the reaction medium with a synthetic crosslinking agent. Control GELMA and PAA hydrogels (T0 and T0') were prepared using similar methods.

The swelling behaviour of the bicomponent hydrogels was found to be strongly depended on the chemical composition. Accordingly, the values of the maximum swelling degree (MSD) increased from P1 to P4; the use of synthetic crosslinker significantly increased the network density, thus decreasing the swelling ability of the resulting T1-T4 hydrogels when compared to samples P1-P4 (fig. 1a). The mechanical behaviour of the hydrogels swollen at equilibrium indicated that increasing PAA in the polymerization mixture decreased the compression modulus; accordingly the elasticity of the bicomponent hydrogels was increased. Additional crosslinking with MBA generates stronger gels, with higher compression modulus and lower

elasticity when compared to P1-P4 (fig. 1b). These data are in agreement with the swelling behaviour of GELMA-PAA in water, the elasticity of the materials being justified by the corresponding equilibrium values.

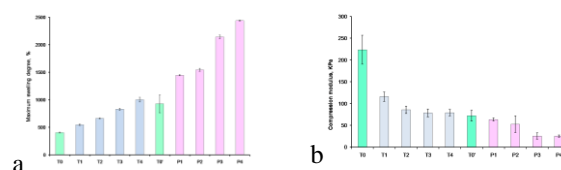


Fig. 1. MSD (a) and compression modulus (b) for the synthesized hydrogels

The biocompatibility of the synthesized hydrogels was investigated through seeding of L-929 cells on the hydrogels' surface (fig. 2).

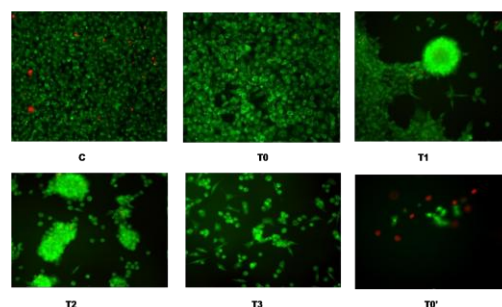


Fig.2. Cellular response at 7 days post-seeding.

Cell adhesion was enhanced by the increase of natural polymer, confirming the cell adhesion potential of GELMA-PAA bicomponent hydrogels.

CONCLUSION

GELMA and AA were successfully covalently bound using a one-pot polymerization reaction, to obtain inexpensive hybrid hydrogels with controlled properties. The composition-properties correlation allows control over the material characteristics. It was demonstrated that the addition of PAA sequences improved the water affinity and elasticity while the presence of GELMA sequences improved the cellular response of the bicomponent hydrogels.

REFERENCES

1. A. Serafim *et al.*, New J. Chem, 2014, DOI: 10.1039/C4NJ00161C

ACKNOWLEDGMENTS

"The authors would like to thank the National Research Council (Grant no: PNII 183/2012) for providing financial support to this project".

Bactericidal and cell compatible titanium surfaces with TiO₂ nanowires

T. Dui¹, M. Ryadnov², N. Faruqi², B. Lamarre², H. Jenkinson¹ and B. Su¹

¹School of Oral and Dental Sciences, University of Bristol, UK

²National Physical Laboratory, UK, omxhd@bristol.ac.uk

INTRODUCTION

When an implant is inserted into the body, a race between bacteria and host mammalian cells occurs in a bid to habituate the implant surface¹. For orthopaedic and dental implants, successful osseointegration occurs when host osteoblasts adhere and proliferate on the material but if it is infected with the growth of a bacterial biofilm, it will lead to a higher risk of implant removal. Implant materials with controllable cellular and bacterial activity will no doubt result in high success rates of surgical implants and surface topography has been recognised as one of the possible means. Titanium as a biomaterial substrate is a popular material of choice for dental and orthopaedic implants due to its biocompatibility and resistance to corrosion. Titanium discs that underwent a simple hydrothermal process produced TiO₂ nanowires where its dimensions can be adjusted by changing experimental parameters and were found to be compatible with mesenchymal stem cells². Physical rupture of gram negative *P. aeruginosa* cells have been observed on the nanopillars found on the wings of psaltoda claripennis³, due to the thin peptidoglycan layer on the outer membrane of *P. aeruginosa*. In this study, the TiO₂ samples were incubated with various gram positive and gram negative bacteria to test for mechanical rupture with the different morphologies of the nanowires, as well as its compatibility with MG-63 osteoblast-like cells.

EXPERIMENTAL METHODS

Fabrication of TiO₂ nanowires: Ti discs were cut from a sheet of Ti (Titanium metals Ltd) and mechanically polished. The plates were placed in 10mL of acetone and sonicated for 10 minutes and rinsed with distilled water. These were then dried in air before being placed inside a PTFE lined vessel and filled with 60mL of 1M NaOH (Sigma-Aldrich). The vessel was placed in an oven for 3 and 8hrs at 240°C, to create surfaces with sharp nanowires (3 hHT) and nanowires that formed pockets and ridges (8 hHT) respectively.

Preparation of bacteria: *P. aeruginosa*, *S. aureus*, *E. coli*, *B. subtilis*, *E. faecalis* and *K. pneumoniae* were refreshed into their appropriate media and incubated to exponential growth. The growth was centrifuged at 5000rpm and harvested twice with 10mM tris HCl buffer (Sigma). The pellet was resuspended to OD=0.30 and incubated with Control Ti, 3 hHT and 8 hHT for 1hr. Surfaces were stained with LIVE/DEAD BacLight (Invitrogen) for imaging on the confocal microscope to count the ratio of live and dead cells. Tests were done in duplicates.

Cell Culture: MG-63 human osteosarcomas were maintained in Eagle's minimum essential medium with supplements. 20k cells were seeded onto each surface sample in triplicates before incubating for 1, 4, 7 and 14 days at 37°C with 5% CO₂. PrestoBlue reagent

(Invitrogen) was used to monitor the viability of the cells by incubating PrestoBlue with the cells for 1hr before aliquotting into a 96-well plate for reading.

RESULTS AND DISCUSSION

LIVE/DEAD assays show higher kill rates for motile bacteria rather than non-motile bacteria regardless of their gram identity (Figure 1). Viability assays on MG-63 seeded on the discs indicated that both hydrothermal surfaces can support cell life for at least 14 days albeit the proliferation rate is not as fast as cells on Control.

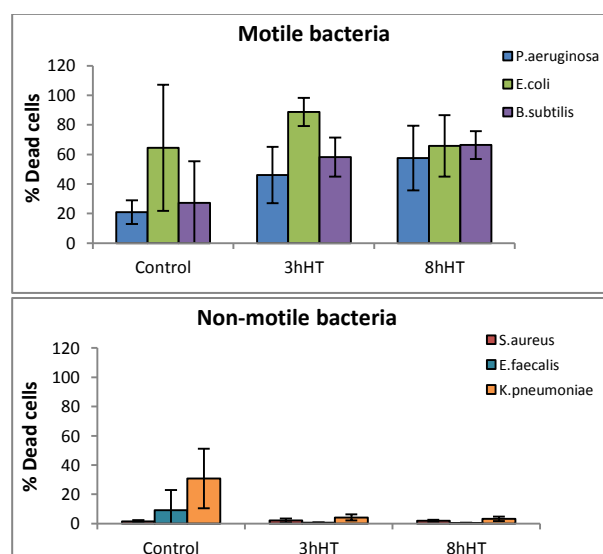


Figure 1: Higher kill rates seen on both 3 hHT and 8 hHT for motile bacteria but low percentage of dead cells found for non-motile bacteria after 1hr incubation.

CONCLUSION

TiO₂ nanowires created by hydrothermal technique have shown to be quite effective in the killing of motile bacteria due to physical means but do not affect non-motile strains. Despite this, MG-63 cells seeded on both 3 hHT and 8 hHT were found to proliferate well for at least 14 days. This is the preliminary step toward creating a surface that can simultaneously deter biofilm formation and be biocompatible with mammalian cells.

REFERENCES

1. Gristina, A. G. et al., *Medical Progress Through Technology* 1988, 14, 205-224.
2. Dong, W. et al., *Chemistry of Materials* 2007, 19, 4454-4459.
3. Ivanova, E. P. et al., *Small* 2012, 8, 2489-2494.

ACKNOWLEDGMENTS

This work was funded by EPSRC and National Physical Laboratory with imaging support from the Wolfson Bioimaging Facility and the Electron Microscope Unit from the University of Bristol.

Precise Hyaluronan-tyramine synthesis for tailored cellular microenvironments

Claudia Loebel^{1,2}, Matteo D'Este¹, Mauro Alini¹, Marcy Zenobi-Wong² and David Eglin¹

¹AO Research Institute Davos, Davos Platz, Switzerland

² ETH Zurich, Cartilage Engineering and Regeneration Laboratory, Department of Health, Science and Technology, Zürich, Switzerland, claudia.loebel@aofoundation.org

INTRODUCTION

Due to its good biocompatibility, biodegradability and excellent gel-forming properties, tyramine-based hyaluronan hydrogels (HA-tyr) have great potential in regenerative medicine (1). So far, HA-tyr conjugate has been synthesized using conventional carbodiimide chemistry. The mechanical properties and gelation rate of the hydrogels have been tuned by varying the hydrogen peroxide (H_2O_2) and horseradish peroxidase (HRP) (2). However, the well-accepted HA-tyramine synthesis has the tendency for formation of byproducts and hydrogel tuning via controlled tyramine substitution has not been achieved (1). Here we demonstrate the applicability of 4-(4,6-dimethoxy-1,3,5-triazin-2-yl)-4-methylmorpholinium chloride (DMTMM) as an effective agent for the controlled synthesis of HA-tyr conjugates. Further, we hypothesised that DMTMM mediated HA-tyr conjugates enable predictive viscoelastic properties, swelling and hyaluronidase mediated degradation of HA-tyr hydrogels.

EXPERIMENTAL METHODS

HA-tyr conjugates were prepared in a one-step reaction by adding different molar ratios of tyramine, hyaluronan and DMTMM coupling agent. Degree of substitution (DS) was measured by ultraviolet visible spectrophotometry ($n=3$) and proton nuclear magnetic resonance (1H NMR). HA-tyr conjugates (2.5 w/v %) in PBS were cross-linked with H_2O_2 (0.34 mM) and HRP (1 Unit/ml) and hydrogel properties were investigated using rheology, mechanical testing, swelling and enzymatic degradation assays ($n=3$).

RESULTS AND DISCUSSION

The efficiency of DMTMM could be demonstrated and an optimized ratio of HA, DMTMM and tyramine (1-1-1 molar ratio) resulted in low amounts of byproducts as seen by 1H NMR. Various DS's were achieved depending on the reaction time and temperature.

At constant HA-tyramine concentration and increasing DS, the storage modulus (G') was linearly increased from 100 to 900 Pa with an excellent correlation ($R^2=0.729$), while maintaining constant HRP and H_2O_2 concentrations (Figure 1a). Thus, G' values can reliably be predicted by the DS of HA-tyramine conjugates ($G'=176.56 \cdot (DS, \%) - 12.72$) (Figure 1a).

A linear correlation could further be demonstrated for swelling ($R^2=0.896$) and degradation properties. Interestingly, concentrations of H_2O_2 from 0.17 mM to 0.78 mM, suitable for cell encapsulation, enable additional tuning of the hydrogel mechanical properties (Figure 1b).

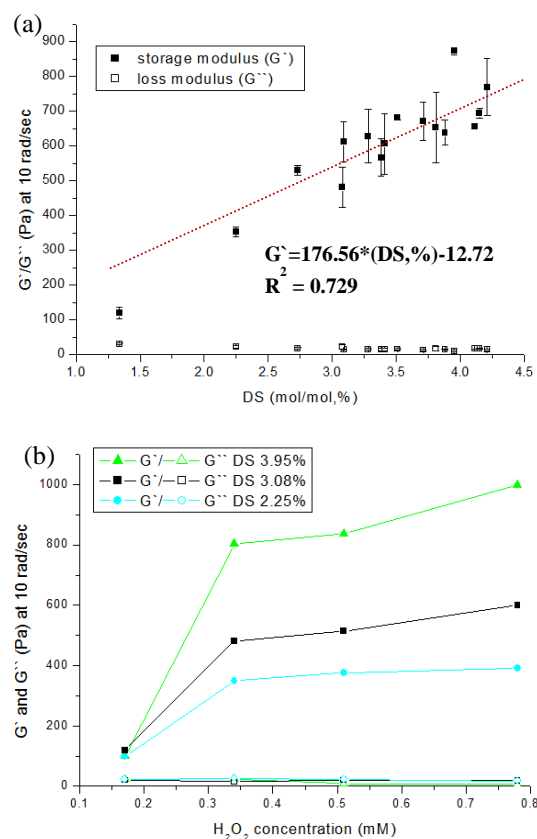


Figure 1 shows the frequency sweep of cross-linked hydrogels (2.5 % w/v) at 10 rad/sec (a) in relation to the DS in mol% ($n=3$; 0.34 mM H_2O_2) and (b) in relation to increasing H_2O_2 concentrations with storage modulus G' (filled shapes) and loss modulus G'' (empty shapes).

CONCLUSION

DMTMM conjugation is an efficient preparation method for HA-tyr derivative synthesis. The unprecedented control over DS allows for predictive hydrogel properties. HA-tyr hydrogels present excellent cell compatibility. This will be useful for the tuning of 3D microenvironment for stem cells encapsulation.

REFERENCES

- (1) Darr & Calabro, 2009; Kim et al., 2011
- (2) Lee, Chung & Kurisawa, 2008

ACKNOWLEDGMENTS

The authors are grateful to Mrs. D. Sutter from ETH Zurich (Switzerland) for permitting and performing NMR analysis. The authors gratefully acknowledge the financial support from the SNF and the European Science Foundation, COST Action 1005 NAMABIO.

Hyaluronic Acid-Coated Chitosan Nanoparticles: the Influence of Hyaluronic Acid Presentation

Arianna Gennari¹, Erwin Hohn¹, Abdulaziz Almalik³, Nicola Tirelli^{1,2}

¹Institute of Inflammation and Repair, School of Medicine, University of Manchester, UK

²School of Materials, University of Manchester, UK

³King Abdulaziz City for Science and Technology, Saudi Arabia

Arianna.gennari@manchester.ac.uk

INTRODUCTION

Hyaluronic acid (HA) is not only a natural component of the extracellular matrix, but it is also heavily involved in cellular signalling. Due to the overexpression of its main receptor, CD44, in pathological phenomena such as inflammatory reactions and several types of tumours, in the past few years HA has also been seen as a potential means to target the action of an active principle. Two points are discussed here:

- The affinity of HA (in solution or on a substrate) to CD44 depends on its chain length and on its spatial arrangement, therefore the way HA is presented on a carrier structure may have profound effects on the way a carrier would bind to a receptor.
- After binding CD44 is internalized, and then it is represented only very slowly; therefore CD44-mediated endocytosis easily reaches saturation. Therefore, the amount of internalisable material depends on the interplay between limited number of available receptors and their affinity to the material, with the paradoxical result that increased affinity, i.e. higher number of receptor clustered around a carrier structure, may lead to lower internalisation.

EXPERIMENTAL METHODS

Nanoparticles were prepared by polyelectrolyte complexation of chitosan (CS) of variable molecular weight with triphosphate (TPP), and the successive coating by HA. The size and ζ -potential of the nanoparticles were measured by Dynamic Light Scattering (DLS) and their morphology was studied via Atomic Force Spectroscopy (AFM) and Transmission Electron Microscopy (TEM).

The *in-vitro* effect of the nanoparticles (cytotoxicity, uptake and uptake mechanism, induction of the production of inflammatory cytokines) was assessed on different cell lines (RAW 264.7 macrophages, XS106 Langerhans cells).

Nanoparticles were also loaded with functional plasmids or RNAs and their ability of acting as transfecting agent was compared to the one of lipofectamine.

RESULTS AND DISCUSSION

CS molecular weight (MW) influences the nanoparticle structure (higher cross-link density with lower CS MW) and thus the complexation with HA. Low MW (25 kDa) chitosan yielding nanoparticles coated by a rather extended HA *corona*. On the contrary, the more porous

core obtained with high MW CS (684 kDa), leads to a higher entanglement between the two polymers. and high MW chitosan producing nanoparticles with more tightly bound HA.¹

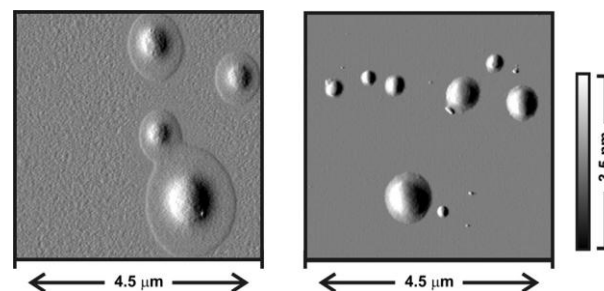


Fig. 1. Deflection images of CS(25)/HA (left) and CS(684)/HA (right) nanoparticles obtained via contact mode AFM. (Figure from ref. 2)

The internalization of both particles in macrophages is CD44 mediated, and better presentation (low MW chitosan) corresponded to both higher affinity and lower capacity/uptake rate.²

Using nucleic acid payloads, we observed a positive correlation between transfection efficiency and CD44 expression in different cell lines. Interestingly, despite a lower internalization, low molecular weight CS/HA particles provided higher transfection, likely due to a more efficient cytoplasmic delivery.³

CONCLUSION

HA presentation heavily influences the efficiency of CD44 targeting, but intracellular events may be more important in the overall picture of the delivery action.

REFERENCES

1. A. Almalik *et. al.*, J Control Release 172:1142-1150, 2013
2. A. Almalik *et. al.*, Biomaterials 34:5369-5380, 2013
3. A. Almalik *et. al.*, Macromol Biosci 13:1671-80, 2013

ACKNOWLEDGMENTS

Financial support from the Marie Curie Industry-Academia Partnerships and Pathways (IAPP) "Replixcel" project (No. 251420) and from a King Abdulaziz City for Science and Technology (KACST) is acknowledged.

Real-time Monitoring of DNA Plasmid Interactions with Poly (ϵ -lysine) Dendrons using Optical Waveguide Lightmode Spectroscopy (OWLS)

Steve Meikle¹, Valeria Perugini¹, Mariagemiliana Dessi¹, Wanda Lattanzi², Enrico Pola³, Giandomenico Loggoscino³, Gary Phillips¹, Matteo Santin¹

¹BrightSTAR Group, School of Pharmacy and Biomolecular Sciences, University of Brighton, Brighton, UK

²Istituto di Anatomia e Biologia Cellulare, Università Cattolica del Sacro Cuore, Rome, Italy;
Banca del Tessuto Muscolo Scheletrico – Regione Lazio, Rome, Italy

³Istituto di Clinica Ortopedica e Traumatologica, Università Cattolica del Sacro Cuore, Rome, Italy

s.meikle@brighton.ac.uk

INTRODUCTION

Non-viral delivery systems have become popular over the past decades, given the concerns over the long term effects of using viral systems¹. One such commonly used delivery system is dendrimers². These are hyperbranched molecules which may be synthesised from saccharides, organic molecules or amino acids. However the use of larger generations of dendrimers is associated with a higher level of cytotoxicity. To overcome this problem the use of lower generation three dendrons can be used. In this study, generation three poly (ϵ -lysine) dendrons were tested for their ability to bind DNA plasmid for potential as gene delivery carriers for *in situ* gene therapy.

To allow real-time monitoring of the binding of the DNA plasmid and dendron Optical waveguide lightmode spectroscopy (OWLS) will be used. OWLS allows for the real-time monitoring of biomolecular interactions at the nanoscale³, utilising changes in the refractive index above the surface of the waveguide region (upto 200 nm).

EXPERIMENTAL METHODS

Dendron Synthesis

Synthesis of generation three poly (ϵ -lysine) dendron (CG3K) was performed using Fmoc solid phase peptide synthesis at x4 molar. Dendrons with different root molecules (Cys) were synthesised from Fmoc-protected amino acids by solid-phase synthesis using a 4x molar excess of reagents. The dendron consisted of a root molecule (Cys), then 3 branching generations of ϵ -lysine to produce CG3K. The dendron was characterised by analytical HPLC (Waters) and microTOF mass spectrometry (Bruker).

OWLS

Using OWLS (Microvacuum), refractive index measurements (RIM) were performed to monitor the real-time binding of a DNA plasmid construct (MW 4377 kDa) containing a gene (LMP3FL-eGFP) and vector plasmid (pcDNA3.1/V5-His-TOPO, Invitrogen) to CG3K dendron.

Initially, the temperature of the system was set to 25 °C. Deionised water was pumped through the OWLS biosensor at a flow rate of 0.5 ml/minute until a stable baseline ($<10^{-8} \text{ s}^{-1}$) was achieved. Next 10 mM Tris HCl (pH 7.4) was flowed through the system at 0.5 ml/minute until a stable baseline was achieved. To activate the surface of the waveguide two injections of 2.5 % glutaraldehyde (aq) (50 and 100 μL respectively) were performed. The temperature of the system was

then increased from 25 to 37°C and once the baseline stabilised, 50 μL CG3K dendron (2 mg/ml) was then injected, the baseline then stabilised. Next an injection of 20 μL DNA plasmid (450.17 ng/ μL) was performed.

RESULTS AND DISCUSSION

CG3K (MW 2043.7) was successfully synthesised from results of analytical HPLC single peak at 10.5 minutes and mTOF MS ($[\text{CG3K}]^{4+}$ 511.4 m/z). The yield was 130 mg at <90% purity. From the OWLS experiments (Figure 1), it was found that 38.5 ng/ cm^2 of CG3K dendron was bound to the surface this was able to bind 39.4 ng/ cm^2 DNA plasmid. These surface coverage (ng/ cm^2) values equate to 1.55 ng (0.76 pmoles) CG3K dendron and 1.587 ng (3.63×10^{-4} pmol) DNA plasmid. Which equates to a molar ratio of 2093:1.

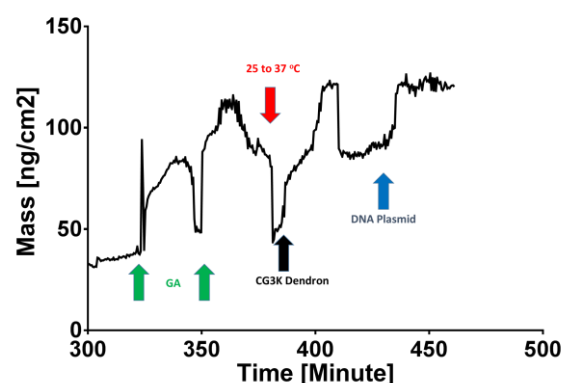


Figure 1 OWLS binding of DNA plasmid to CG3K dendron attached to surface of waveguide.

(GA = 2.5 % glutaraldehyde)

CONCLUSION

Optical Waveguide Lightmode Spectroscopy was shown to be effective in following, in real-time, the binding between the CG3K dendron and the DNA plasmid. This shows that lower generation poly (ϵ -lysine) dendrons may be utilised for the effective binding of DNA plasmids as non-viral delivery systems.

REFERENCES

- Behr, J.-P. Acc. Chem. Res. 26, 274-278, 1993
- Tang, M. X *et al.* Bioconjugate Chem. 7, 703-714, 1996
- Voros, J *et al.* Biomaterials 23, 3699, 2002

ACKNOWLEDGMENTS

This work has been supported by the EC FP7 Project OPHIS, contract n. FP7-NMP-2009-SMALL-3-246373.

The Atomic-Scale Structure of Bio-Resorbable Glasses: $\text{Na}_2\text{O}:\text{P}_2\text{O}_5$

David Pickup^{1*}, Robert Moss¹, Jenni Vibert¹ and Robert Newport¹

¹School of Physical Sciences, University of Kent, UK

*d.m.pickup@kent.ac.uk

INTRODUCTION

Diffraction has become an important tool for determining the atomic-scale structure of materials and advanced instrumentation has made the collection of high quality data possible. However, analysis and interpretation of that data can be difficult, particularly where the material has a complicated structure. Bioactive glasses fall into this category: they are necessary amorphous and usually comprise several elements. Thus, a single experimental method is not sufficient for an understanding of their structure. Moreover, the results from such structural probe methods are intrinsically one-dimensional: models of the 3D arrangement of atoms may only be inferred.

Neutron diffraction, ND, provides a quantitative insight into the overall structure of such materials and offers some distinct advantages as a structural probe. Use of a pulsed source, for example, offers a particularly wide dynamic range to the resultant interference function and therefore unparalleled resolution to real-space pair distribution functions; neutron scattering cross sections usefully do not vary monotonically across the Periodic Table (*c.f.* X-ray diffraction, XRD) and they are, moreover, isotope-dependant.¹

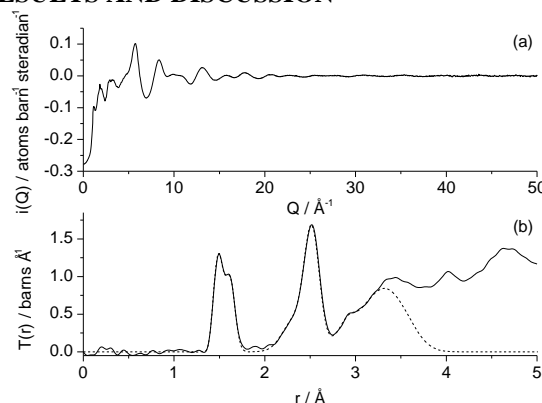
Phosphate based glasses have many unique properties, the most interesting of which, from a biomedical standpoint, is their ability to dissolve completely in aqueous media; this behaviour may be controlled via the chemistry of the glasses. We present here a study of the atomic-scale structure of a $(\text{Na}_2\text{O})_{0.5}(\text{P}_2\text{O}_5)_{0.5}$ bio-resorbable and bio-compatible glass using the complementarity of ND and XRD data. The data is used within the Reverse Monte Carlo, RMC, computer modelling approach whereby the simultaneous fitting of both data sets provides a more robust 3D model structure than would be attainable with one data set alone.² Experimental data from glasses of composition $(\text{CaO})_{0.5-x}(\text{Na}_2\text{O})_x(\text{P}_2\text{O}_5)_{0.5}$, where ($x = 0, 0.1$ and 0.5), will be used to provide additional insight.³

EXPERIMENTAL METHODS

The phosphate glasses were prepared using NaH_2PO_4 , CaCO_3 and P_2O_5 . The precursors were placed in a Pt/10%Rh crucible and loaded into a pre-heated furnace at 300°C ; it was melted at 1100°C for 1 h. The molten glass was then poured into a pre-heated (370°C) graphite mould, and left to cool to room temperature. Elemental analysis (ICP-AES and gravimetric) and macroscopic density (He pycnometry) characterization was undertaken. ND data were collected on the GEM diffractometer on the ISIS spallation neutron source at the Rutherford Appleton Laboratory, UK. The samples were in the form of 8 mm diameter rods; time-of-flight

data were collected over a wide range of Q (up to 60 \AA^{-1} , where $Q = 4\pi \sin \theta/\lambda$; note: $\Delta r \sim 2\pi/Q_{\text{max}}$).

RESULTS AND DISCUSSION



“Figure 1. ND data from $(\text{Na}_2\text{O})_{0.5}(\text{P}_2\text{O}_5)_{0.5}$ glass: (a) interference function, $i(Q)$, and (b) pair distribution function, $T(r)$, (solid) together with fit (dashed)”

The results illustrated in Fig. 1 have been used within RMC modelling; they suggest that the glass has a structure based on chains of Q^2 phosphate groups. The P–O bonds to bridging and non-bridging oxygens are better resolved than in ND data from samples containing CaO, indicating a change in the nature of the bonding as the field strength of the cation increases decreases. The NaO_x polyhedra evidently share edges, leading to a well-defined $\text{Na}\cdots\text{Na}$ correlation. This model is consistent with the theory proposed by Hoppe *et al* for cation inclusion into phosphates.⁴

CONCLUSION

RMC modelling provides direct evidence of edge-sharing by the NaO_x polyhedra leading to a well-defined Na - Na correlation, as predicted by the established structural model of Hoppe.

REFERENCES

1. Skipper L.J. *et al.*, J. Mater. Chem. 15:2369-2374, 2005
2. McGreevy R.L., J. Phys.: Condens. Matter 13:R877-913, 2001.
3. Pickup D.M. *et al.*, J. Phys.: Condens. Matter 19:415116, 2007
4. Hoppe U. *et al.*, J. Non-Cryst. Solids 263&264:29-47, 2000

ACKNOWLEDGMENTS

The authors gratefully acknowledge the financial and facilities-based support of UK Research Councils (EPSRC, STFC) via a series of grants, and the University of Kent.

Preparation and characterization of Sr, Zn, Si and Fe-doped hydroxyapatite nanoparticles

Zhitong Zhao^{1,2}, Montserrat Espanol^{1,2}, Maria-Pau Ginebra^{1,2}

¹Department Materials Science and Metallurgy/Biomaterials, Biomechanics and Tissue Engineering Group, Technical University of Catalonia, Spain

²Biomedical Research Networking Centre in Bioengineering, Biomaterials and Nanomedicine, CIBER-BBN, Spain.
zhao.zhitong@upc.edu

INTRODUCTION

Hydroxyapatite (HA) being the mineral phase of bone has been widely used as synthetic material in orthopaedic and dental applications. Recently, more and more efforts have been made to explore the potential of using hydroxyapatite nanoparticles (NPs) as the carrier for drug and genes due to its good affinity to DNA and various drug molecules¹. Since gene and drug delivery are dependent on cellular uptake, understanding the interaction of HA nanoparticles with cells is crucial for such applications². Although there have been various groups that have focused their attention to studying the effect of nanoparticle size, morphology and surface charge on cells, very few works have been devoted to investigating how the composition of HA nanoparticles affect the cellular behaviour. In the present work, strontium (Sr), zinc (Zn), silicon (Si) and iron (Fe)-doped HA nanoparticles were synthesized by wet chemical precipitation, and fully characterized. The same synthesis route was applied to allow comparison of the NPs. The interaction of the various NPs with cells will be further investigated to assess their cytotoxicity and potential as delivery vehicle.

EXPERIMENTAL METHODS

To synthesize hydroxyapatite, 2.475g $\text{Ca}(\text{OH})_2$ was magnetically stirred in 100ml water to obtain a homogenous suspension. H_3PO_4 (0.2mol/L) was added dropwise (1mL/min) to the $\text{Ca}(\text{OH})_2$ suspension until the pH value was 7.9. The solution was stirred for a further 20 min and left overnight for maturation. The precipitate was then washed with milliQ water until constant conductivity and freeze dried.

For the preparation of the cation substituted HA, the salt of interest ($\text{SrCl}_2 \cdot 6\text{H}_2\text{O}$, ZnCl_2 or $\text{FeCl}_3 \cdot 6\text{H}_2\text{O}$) was first mixed with the $\text{Ca}(\text{OH})_2$ and for the synthesis of Si-doped hydroxyapatite, tetraethyl orthosilicate (TEOS) was mixed with H_3PO_4 . Various salt concentrations ranging from 1-30wt% were explored. Characterization of the NPs comprised X-ray diffraction (XRD), Fourier infrared spectroscopy, He pycnometry, N_2 adsorption and transmission electron microscopy (TEM).

RESULTS AND DISCUSSION

Analysis by XRD of all NPs showed that indeed the NPs were phase pure as only peaks corresponding to HA could be identified (Fig.1). A careful look at the peak corresponding to the (002) reflection (26° 2θ angle) showed a gradual shift depending on the concentration of the doping ion and a change in shift direction depending on the type of ion (Fig.1). These shifts were interpreted as the efficient incorporation of the doping ion in the crystal lattice of HA. The different

dimension of the doping ions is in fact responsible for the differences in shift direction. Along with the shifting of the peaks, the incorporation of the doping ions was also found to alter the crystallinity of the NPs. This was observed from a change in the width of the peaks. The morphological evaluation of the NPs as observed by TEM (Fig.2) suggested that the doping ion had little influence on the morphology of NPs as in all cases they kept their needle like structure. The specific surface area (SSA) of Zn-doped HA ($135 \text{ m}^2/\text{g}$) and Fe-doped HA ($150 \text{ m}^2/\text{g}$) were greater than the values obtained for the rest of NPs ($100 \text{ m}^2/\text{g}$). This was explained by a reduction in size of the needle-like NPs as can be seen from the TEM micrographs.

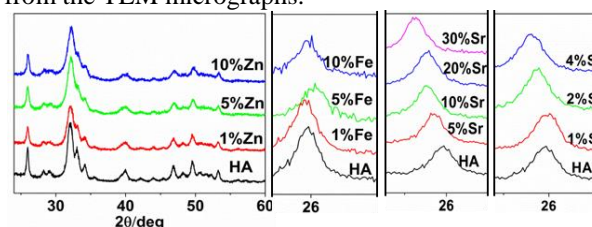


Fig. 1. XRD of the various ion-doped NPs.

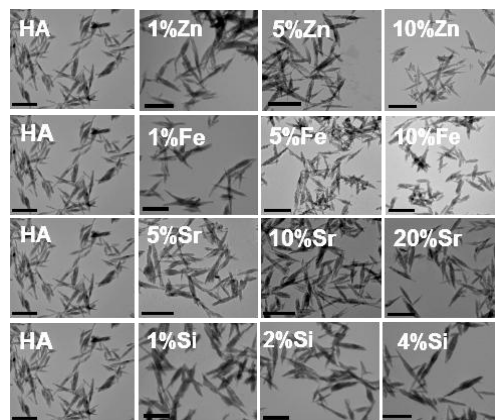


Fig. 2. TEM micrographs of the NPs. Scale bar 200 nm.

CONCLUSION

Doping of HA with different contents of Zn, Fe, Sr, and Si was successfully accomplished by wet precipitation synthesis. The various NPs with different contents of doping ion show similar morphologies. These NPs will be tested for cytotoxicity to evaluate their adequacy in drug and gene delivery applications.

REFERENCES

1. C.J. Loo. *et al.*, Curr. Pharm. Biotechnol.11:333, 2010
2. L. Chen. *et al.*, Nanotechnology 22 :105708, 2011
3. A. Albanese. *et al.*, Annu. Rev. Biomed. Eng.14:1,2012

ACKNOWLEDGMENTS This study was supported by the Spanish Government through the project MAT2012-38438-003-01.



Endothelization and thrombogenicity response of CoCr alloy nano depth patterns for cardiovascular stents

R. Schieber^{1,2,3,4}, M. Fernández-Yagüe^{1,2}, M. Hans⁴, M. Díaz-Ricart⁵, G. Escolar⁵, F. Javier Gil^{1,2}, F. Mücklich⁴, M. Pegueroles^{1,2}

¹Biomaterials, Biomechanics and Tissue Engineering Group, Materials Science Dept., Universitat Politècnica de Catalunya, Spain

²Biomedical Research Networking Centre on Bioengineering, Biomaterials and Nanomedicine (Ciber-BBN), Spain

³Centre for Research in NanoEngineering (CRnE), Spain

⁴Chair of Functional Materials, Faculty of Natural Sciences and Technology, Saarland University, Germany

⁵Univ. Barcelona, Hosp Clin, Dept Hemotherapy Hemostasis, IDIBAPS, Spain, marta.pegueroles@upc.edu

INTRODUCTION

Cardiovascular bare-metal stents (BMS) main drawbacks are restenosis and in-stent thrombogenicity diseases after 6 months implantation. Nano and microscale modification of implant surfaces is a strategy to recover the functionality of the artery by stimulating and guiding molecular and biological processes at the implant/tissue interface^{1,2}. However, the optimal topographical conditions that aim to induce an active and healthy endothelium without generating platelet agglomeration remain to be elucidated. Few techniques are available to create metallic surface patterns with low depths compatible with a low platelet adhesion rate, - inferior to 300 nm³. In this study, CoCr alloy surfaces are modified via laser interference surface structuring, L.I.S.S., in order to regenerate the damaged endothelium and to modulate platelet response.

EXPERIMENTAL METHODS

Polished CoCr alloy (ASTM F90) discs were topographically modified by L.I.S.S. based on a Nd:YAG laser (Spectra Physics Quanta-Ray PRO210) used at $\lambda = 355$ nm, $f = 10$ Hz and $t_{\text{pulse}} = 10$ ns. Surfaces were structured with multiple, adjacent one pulse spots of 1×1 mm² each. Laser fluencies from 0,8 up to 5,0 J/cm² were applied to obtain different pattern depths. SEM, interferometry, AFM, contact angle and XPS were used to determine surface patterns physico-chemical characteristics. Fibronectin adsorption, 40 µg/ml 4h, and HUVEC adhesion, 24 h, were visualized by classical fluorescence and SEM. Thrombogenicity was evaluated through platelet adhesion and aggregation, by circulating human blood onto patterned surfaces using a flat chamber perfusion at 75 ml/min during 5 min and 37°C to then, stain by immunofluorescence. Polished surfaces were used as control.

RESULTS AND DISCUSSION

CoCr alloy surfaces were polished ($R_a = 6.8 \pm 2.0$ nm) and successfully nanopatterned by L.I.S.S., with different periodicities P ($\approx 3, 10, 20$ and 32 µm) and depths D (Low, $L \approx 20$ nm and High, $H \approx 800$ nm). The 8 obtained patterns were named: 3/L; 3/H; 10/L; 10/H; 20/L; 20/H; 32/L and 32/H. SEM and interferometry

PSD analysis confirmed the periodicity and the homogeneity for all the obtained patterns except 3/H which showed some totally melted areas due to the application of high fluency. High depth structures, present a thicker oxide layer overall the topography, as determined by XPS. Whereas, low series show a chemical pattern with topography: valleys have a thicker oxide layer compared to control. XPS analysis indicated an increase of hydroxyl groups on patterned surfaces, which could influence surface energy and wettability. Anisotropic wetting character, due to chemical and topographical pattern, was identified. No changes of the material corrosion resistance were detected by electrochemical testing.

HUVEC cell adhesion and morphology is affected by surface topography periodicity and depth. In particular, low depth patterns stimulated cell adhesion by a higher spreading and number compared to control. Moreover, 10 and 20 µm periodicities surfaces present cell alignment morphology following pattern's lines. HUVEC cells adhered preferentially to pattern peaks on high depth structures, probably due to a higher fibronectin adsorption while at low series the protein adsorption is homogeneous, as detected by fluorescence. Platelet adhesion and aggregation was affected by topography periodicities and depths.

CONCLUSION

L.I.S.S. technique allows obtaining a CoCr surface microscale patterns with nanodepth grooves. Laser patternings affect physico-chemical surface properties according to the applied fluency. HUVEC cell adhesion and thrombogenicity can be controlled by surface nanopatterning.

REFERENCES

1. Nazneen F. *et al.*, J Biomed Mater Res B Appl Biomater. 100, 7: 1989-2014, 2012
2. de Mel A. *et al.*, Int J Biomater, 2012.
3. Park J.Y. *et al.*, Biomaterials. 22:2671-2682, 2001

ACKNOWLEDGMENTS

Authors acknowledge the financial support in the MAT2012-30706 project. RS acknowledges the European Commission for funding through an Erasmus Mundus Scholarship.



Cell Spraying Approach *in vitro* for Coating of Respiratory Tissue Engineered Constructs

A. L. Thiebes¹, S. Albers¹, S. Jockenhoevel¹ and C. G. Cornelissen^{1,2}

¹Tissue Engineering and Textile Implants, AME, Helmholtz-Institute, RWTH Aachen University, Germany

²Internal Medicine I – Section Pneumology, University Hospital Aachen, Aachen, Germany, thiebes@hia.rwth-aachen.de

INTRODUCTION

Spray coating of cells was first proposed by Bahoric et al. in 1997 for application of epidermal cells to burn wounds¹. Since then, research continued with a focus on application of dermal cells in wound models. Some groups also investigated spray application of cells for tissue engineering. Kaminski et al. proposed endothelial cell spraying for coating of tissue engineered heart valves².

Here, we present an *in vitro* study on survival rates and differentiation of ovine vascular smooth muscle cells (vSMCs) and respiratory epithelial cells (RECs) after spraying with a spray system clinically used for spray application of fibrin gel. The influence of air pressure on vSMC survival was studied and the differentiation of vSMCs and survival and differentiation of RECs assessed with the best spraying pressure.

EXPERIMENTAL METHODS

For our experiments, we used the Tisseel EASYSpray Set (Baxter, USA). In the first experiment, the pressure was changed to find out the influence on vSMC survival. For all following experiments the pressure was set to 0.4 bar. For all experiments, an amount of 200 µl cell suspension was sprayed in one well of a 12-well plate with a concentration of $9.8 \cdot 10^5$ and $1.6 \cdot 10^6$ cells/mL for ovine vSMCs and RECs, respectively which corresponds to a seeding density of $5 \cdot 10^4$ and $8 \cdot 10^4$ cells/cm². As a negative control, air pressure was set to 0 bar. Living cells were stained with Calcein AM for 30-60 minutes at 37°C prior to the experiment. Afterwards, propidium iodide solution was added to stain dead cells. A sample number of 5 was used for all experiments. For automatized analysis, images were processed with a macro for counting particles in ImageJ. Statistical significance was tested with an unpaired, two-tailed student's t-test. A p-value below 0.05 was considered significant. Differentiation of the cells was shown with immunohistological stainings with antibodies against α -smooth muscle actin (α -SMA) and pan-cytokeratin.

RESULTS AND DISCUSSION

Figure 1 shows the different survival rates of varying air pressures for spraying vSMCs. In contrast to pressures between 1.2 and 2.0 bar where survival rates were 57.9-87.9 %, pressures of 0.4 and 0.8 bar have shown no significant difference on the survival compared to the control with survival rates of 99-100 %. Thus, the following experiments were accomplished with air pressures of 0.4 bar.

For RECs the survival rate with 0.4 bar was 88.5 % of the control.

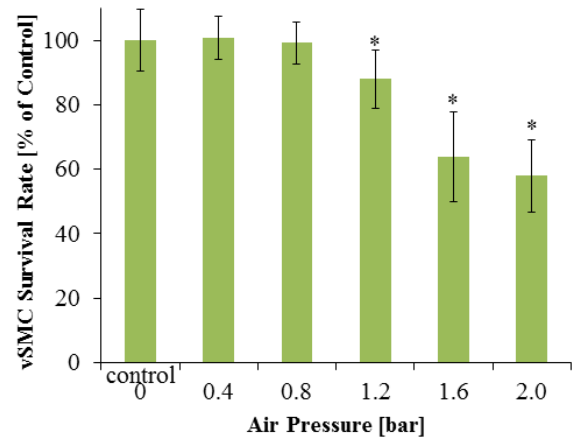


Figure 1: Survival of vSMCs depending on the air pressure when spraying.

In further experiments sprayed and non-sprayed vSMCs and RECs were cultured 3-5 days and stained for α -SMA and pan-cytokeratin, respectively. Sprayed and non-sprayed vSMCs showed uniform expression of α -SMA which indicates differentiation. Same applies for RECs with pan-cytokeratin.

These results imply that spray application is highly suitable for respiratory tissue engineering. With a simple spraying system which is approved for clinical use cells could be easily sprayed. As shown by Cornelissen et al. fibrin gel proves as a good scaffold for tissue engineering of respiratory epithelial cells³. Thus, experiments will be continued by combined spraying of cells with fibrin gel to allow proper attachment of the cells to tissue engineered constructs.

CONCLUSION

This study provides the evidence that spray application of cells is suitable for respiratory tissue engineering with ovine epithelial cells. We have shown the influence of varying air pressures on survival and differentiation potential of cells after spray processing with survival rates of up to 100 % and 88.5 % compared to the controls for vSMCs and RECs, respectively.

REFERENCES

1. Bahoric A. *et al.*, Plastic surgery. 5:153-6, 1997
2. Kaminski A. *et al.*, Tissue Eng Part C. 17:299-309, 2011
3. Cornelissen *et al.*, Ann Biomed Eng. 40:679-87, 2012

ACKNOWLEDGMENTS

The authors would like to thank the European Union's Seventh Framework Programme (FP7/2007-2013 under grant agreement n° NMP3-SL-2012-280915) for providing financial support to this project.

Biodegradable hyper-branched tissue adhesives for meniscus tears

Agnieszka I. Bochynska^{1,2}, Tony G. van Tienen¹, Gerjon Hannink¹, Pieter Buma¹, Dirk W. Grijpma^{2,3}

¹Orthopaedic Research Laboratory, Dept. of Orthopaedics, Radboud Centre for Molecular Life Sciences, Radboud University Nijmegen Medical Centre, Nijmegen, The Netherlands;

²Dept. of Biomaterials Science and Technology, University of Twente, Enschede, The Netherlands;

³Dept. of Biomedical Engineering, University of Groningen, Groningen, The Netherlands;

a.i.bochynska@utwente.nl

INTRODUCTION

Meniscus tears are one of the most common knee injuries. They result in pain, swelling and locking of the knee joint, and eventually may lead to osteoarthritis. Currently, the gold standard technique to repair a torn meniscus is suturing. However, the procedure is complicated, time consuming and expensive. Furthermore, the success rate of suturing in the avascular inner zone of the meniscus is low. Therefore, there is an urgent need for a new method to repair a torn meniscus. Tissue adhesives are considered to be a promising solution, since they are easy to apply and cause minimal tissue trauma. It has been previously reported that isocyanate-terminated copolymers based on poly(ethylene glycol) (PEG) and biodegradable trimethylene carbonate (TMC) can be successfully used as such tissue adhesives¹. In this study we designed and evaluated novel hyper-branched isocyanate-terminated copolymers. The mechanical and adhesive properties of the formed networks were tuned by varying the composition and the degree of branching of the structures.

EXPERIMENTAL METHODS

Oligomers were synthesized by ring opening polymerization of TMC using PEG as initiator. Subsequently, these oligomers were reacted with different amounts of citric acid (CA) to introduce diverse degrees of branching. The hydrophilicity was adjusted by varying both the molecular weight of the PEG (200 or 600 g/mol) and the amount of TMC coupled to it (one or two units per arm of PEG). Reactive copolymers were synthesized by functionalizing the terminal groups of the oligomers with hexamethylene diisocyanate (HDI). The resulting networks were evaluated in a tensile tests and their potential as tissue adhesives was assessed in a lap shear adhesion test using bovine meniscus tissue. *In vitro* degradation both in PBS and cholesterol esterase (CE) solutions over a period of 4 weeks was evaluated. The effect of adding reactive oligomers on cell viability was assessed using bovine meniscus cells with an Alamar Blue[®] reduction assay in a trans-well system.

RESULTS AND DISCUSSION

The experimental results showed that the shear adhesive strength of the networks to bovine meniscus tissue was between 20 to 100 kPa. This shows a strong influence of the design of the network precursors on the adhesive strength of the glue. The elastic modulus of the obtained polyurethane networks varied from 1.5 to 45 MPa, which is in the same range of values as that of soft tissues. Degradation of the networks both in PBS and in CE solutions showed higher degradation rates for the networks based on PEG₆₀₀ (mass loss up to 30%) than PEG₂₀₀ (9%), indicating the effect of the different network compositions. The cell viability study after 1, 3 and 7 days showed that cell viability is dependent on the amount of reactive oligomer administered to medium with cells. At lower quantities (up to 3mg of reactive oligomer/mL of medium) cell viability was not affected, but decreased to 60% when a higher amount of 12 mg/mL was added.

CONCLUSION

We showed that the proposed isocyanate based networks are favorable candidates to be used as resorbable and biocompatible tissue adhesives for meniscus repair. They have satisfactory adhesive and mechanical properties after curing. These properties can be adjusted by varying the composition and architectural design of the copolymer precursors. In the future experiments we will focus on the biomechanical evaluation in a joint environment in cadaveric knees and *in vivo* in a relevant animal model.

REFERENCES

1. Blanquer S.B.G. *et al.*, J Appl Biomater Function Mater, 10 (3), 177-184, 2013

ACKNOWLEDGMENTS

The authors would like to thank Reumafonds, the Dutch Arthritis Foundation for providing financial support to this project.

Impact of Surface Treatment on the Properties of Dental Implant Materials

M. Murphy¹, R. Lindsay¹, A. Thomas² and N. Silikas³

¹School of Materials, University of Manchester, UK,

²School of Physics, University of Manchester, UK,

³School of Dentistry, University of Manchester, UK
matthew.murphy-2@postgrad.manchester.ac.uk

INTRODUCTION

Dental implant materials are being constantly developed to meet the demands of dentists and patients alike. One area of significant activity is the engineering of their surface properties to improve the reliability and rate of healing.

In this work two different commercial implants (developed by Straumann) have been studied, namely SLA and SLActive. The implants are fabricated from either CP-Ti or Ti/Zr-alloy. Both types have similar longer-term stability, but differ considerably in terms of initial osseointegration rates, i.e. SLActive achieves a much higher degree of bone-implant contact after 2-4 weeks compared to SLA¹.

Concerning surface engineering, initially both implant types are sandblasted and acid etched. The procedure only diverges in the final step, where SLActive is cleaned under N₂ and stored in saline, whilst SLA is cleaned and stored in air. Subsequent to such processing, SLActive is found to be hydrophilic, and SLA hydrophobic. It has been suggested that this difference is a result of saline immersion preventing the deposition of atmospheric carbon onto the SLActive implant, which may underpin improved osseointegration kinetics². However, further substrate characterisation is required to fully understand the performance of these implants, including the impact of nanometre-sized features previously observed on SLActive³. On this basis, the aim of this work is to further characterise these surfaces in order to understand the effect of storage in saline solution on surface structure and chemistry.

EXPERIMENTAL METHODS

Various Ti and Ti/Zr samples (~ 5 mm diameter discs) were prepared by Institut Straumann AG to facilitate studying the impact of different stages of surface engineering. Surface topography was studied using white light interferometric microscopy and SEM. XRD was used to understand the effect of the surface treatment on the bulk material, and Raman spectroscopy was employed to reveal surface phases.

RESULTS AND DISCUSSION

Clear differences were observed between samples with different surface treatments. Three tiers of structures were observed on SLActive samples: 10-20 µm pits created by sand blasting; 1-5 µm sized pits were

obtained through acid etching; 20 nm particles formed during storage in saline. The diameter of the pits and nano-size features was observed to be different on the CP-Ti and Ti/Zr-alloy samples, resulting in a difference in roughness, CP-Ti SLActive S_a=3.23 µm and Ti/Zr-alloy SLActive S_a=1.99 µm. SLA surfaces lacked the presence of the nano-size features.

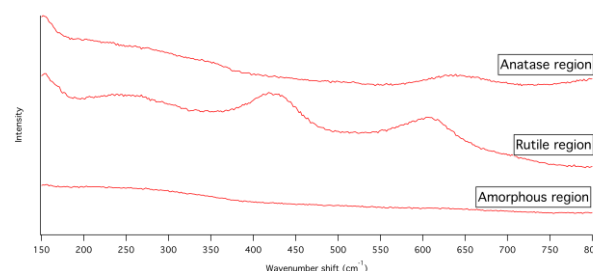


Figure 1: Example of Raman spectra obtained from various areas on CP-Ti SLActive

No crystalline oxide phases were observed on CP-Ti SLA substrates, whereas all other samples exhibited a mixture of amorphous/rutile/anatase TiO₂ (see figure 1). XRD demonstrated that acid etching introduced hydrogen into the matrix, which resulted in partial conversion of α -Ti grains into δ -TiH₂.

CONCLUSION

As may be expected, both sandblasting and acid etching increase surface roughness. Non-uniform surface crystallinity was observed on all the samples except CP-Ti SLA. The SLActive treatment creates a hydrophilic surface on both CP-Ti and Ti/Zr-alloy. This treatment also creates additional nanosized features, compared to SLA. The presence of these features on SLActive surfaces and differences to surface oxide phases suggest that rather than acting as merely a protective environment, storage in saline modifies the surfaces.

REFERENCES

1. Buser D. *et al.*, J. Dent. Res. 83(7):529-533, 2004
2. Rupp. F *et al.*, J. Biomed. Mater. Res. A, 76(2):323-334, 2006
3. Wennerberg A. *et al.*, Clin. Oral Impl. Res. 0:1-7, 2012

ACKNOWLEDGMENTS

MM thanks EPSRC for financial support through the Advance Metallic Systems CDT. Straumann are thanked for supplying samples.



Monodisperse microspheres loaded with gentamicin dioctyl sodium sulfosuccinate for the treatment of orthopaedic infections

Gert-Jan A. ter Boo^{1,2}, Dirk W. Grijpma², Geoff Richards¹, Fintan T. Moriarty¹ and David Eglin¹

¹AO Research Institute Davos, AO Foundation, Davos, Switzerland

²Department of Biomaterials Science and Technology, University of Twente, Enschede, The Netherlands
gertjan.terboo@aofoundation.org

INTRODUCTION

Infection limits the success of orthopaedic implants in a small but significant percentage of patients. Treatment of implant related bone infection requires high local concentrations of antibiotic over an extended period. The ability of certain strains of bacteria (e.g. *Staphylococcus aureus*) to invade and survive within osteoblasts [1] further complicates treatment, as many antibiotic agents do not penetrate the eukaryotic cell membrane. We hypothesised that by hydrophobic modification of a commonly used antibiotic, gentamicin-sulphate (GEN-SULPH), its release can be extended and intracellular targeting achieved. Here we present the preparation of monodisperse microspheres loaded with hydrophobic modified gentamicin (GEN-AOT) as a potential delivery system in the treatment of orthopaedic infections.

EXPERIMENTAL METHODS

Preparation of GEN-AOT

Hydrophobic ion-pairing of GEN with dioctyl sodium sulfosuccinate (AOT) was performed by adding equal volumes of a GEN-SULPH solution in buffer (10mM sodium acetate, KCl and CaCl₂ (pH 5)) (0.40 w/v %) to AOT in DCM (1.25 w/v %). This solution was stirred vigorously for 3h and left for 0.5h for the two phases to separate. GEN-AOT was isolated from the DCM layer.

Toxicity towards human fibroblast cell line

The effect of GEN-AOT on cell-viability was assessed by an assay with cell titer blue. Viability of hTERT BJ-1 fibroblasts was assessed after 24h and 72h culture by measuring the fluorescence intensity (FI).

Antimicrobial susceptibility testing

S. aureus NCTC 12973 (SA), *Escherichia coli* NCTC 12241 (EC) and *S. epidermidis* 103.1 (SE) were selected for testing. Antibiotic solutions were prepared in Cation adjusted Mueller Hinton broth, in a concentration range of 0.06 – 256 µg/ml for GEN-SULPH. AOT and GEN-AOT solutions were prepared in an equimolar range with GEN-SULPH. Minimum inhibitory (MIC) and minimum bactericidal (MBC) concentration were determined according to NCCLS M7-A5 guidelines for bacteria that grow aerobically.

Preparation of antibiotic loaded microspheres

For the preparation of monodisperse antibiotic loaded Poly(trimethylene carbonate) (PTMC) and Poly(D,L-lactide) (PDLLA) microspheres (MSs) a microsievetm emulsification technology of Nanomi(The Netherlands) was used. 1% PTMC and PDLLA solutions were used, to which 20% GEN-AOT was added for the preparation of GEN-AOT loaded MSs. These solutions were given into the feed for the microsievetm emulsification device.

RESULTS AND DISCUSSION

The antibiotic GEN-SULPH showed low toxicity towards fibroblasts even at high concentration. On the contrary, hydrophobic GEN-AOT, showed reduced viability at lower concentrations, at 11×10^{-6} M cell viability was reduced with ~50% (figure 1).

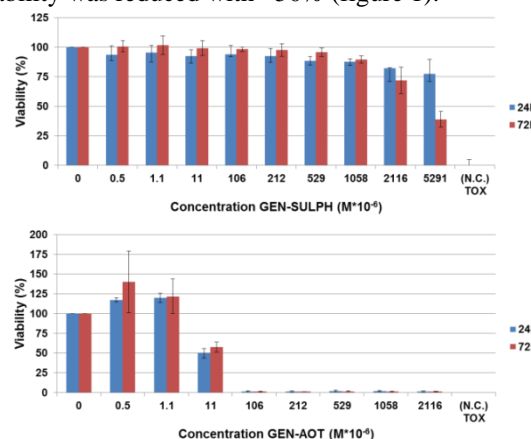


Figure 1. hTERT BJ-1 fibroblast viability

An explanation could be found in the location of action, as GEN-AOT should be able to act intracellularly.

Table 1. Susceptibilities for GEN-AOT

	S.aureus NCTC 12973		S.epidermidis 103.1		E.coli NCTC 12241	
	MIC (µg/ml)	MBC (µg/ml)	MIC (µg/ml)	MBC (µg/ml)	MIC (µg/ml)	MBC (µg/ml)
GEN-SULPH	2	8	0.5	4	8	8
GEN-AOT	5.7	22.7	1.4	1.4	11.4	22.7
AOT	242	242	242	>242	>242	>242

Both GEN-SULPH and GEN-AOT were able to inhibit SA and SE at equal molar concentration (Table 1) (2.1×10^{-6} M (SA) and 0.5×10^{-6} M (SE)). However, GEN-AOT seems to be more bactericidal for SE at lower molar concentration than GEN-SULPH.

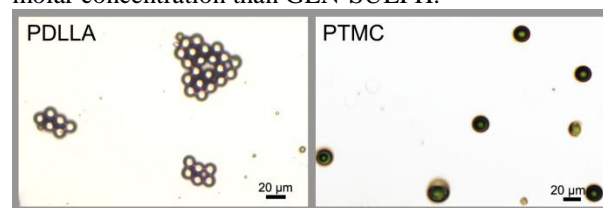


Figure 3. Monodisperse PDLLA and PTMC MSs loaded with GEN-AOT

Highly monodisperse GEN-SULPH and GEN-AOT loaded PDLLA and PTMC MSs were produced (fig 3).

CONCLUSION

Studies are ongoing to investigate the release and bactericidal efficacy of the GEN-AOT loaded MSs. Also an intracellular infection model will be used to test the intracellular activity of GEN-AOT.

REFERENCES

1. Ellington J.K. *et al* J Orthop Res. 24(1):87-93,2006

Retention of Myoblast Differentiation Capacity in 3D Culture on TIPS Microspheres

Nina Parmar, Richard Day

Applied Biomedical Engineering Group, Division of Medicine, University College London, UK
nina.parmar@ucl.ac.uk

INTRODUCTION

Faecal incontinence (FI) is often attributed to injury of anal sphincter muscles and regenerative medicine treatments are sought. Cell therapy is an emerging option but to date has been unsuccessful.

Highly porous microspheres produced using Thermally Induced Phase Separation (TIPS) have features ideally suited for cell delivery^{1, 2}. We report our findings on the study of attaching primary cultures of human skeletal muscle myoblasts (HSMM) to TIPS microspheres and the ability to retain control of cell proliferation and differentiation *in vitro*.

EXPERIMENTAL METHODS

Poly-DL(lactide-co-glycolide) (75:25) dissolved in dimethylcarbonate (1:24) (w/v) was used to fabricate TIPS microspheres measuring 250-425 μM . Static-dynamic incubation conditions were used to attach primary cultures of HSMM followed by static-dynamic incubation for 7 days in culture medium to induce either cell proliferative or differentiation.

The proliferative/differentiation status of HSMM cells was investigated using PCR and in-cell Western analysis of specific myogenic proliferation and differentiation markers (Ki67, Pax7, MyoD, myogenin, desmin, myosin and myosin heavy chain). The profile of these markers was assessed in HSMM attached to TIPS microspheres at days 1 and 7 incubation in proliferation medium compared with those incubated in differentiation medium for 7 days.

A bromodeoxyuridine (BrdU) cell proliferation assay was performed on HSMM-TIPS microspheres attached for 1-7 days.

RESULTS AND DISCUSSION

Quantitative analysis of the gene and protein profiles of myoblasts attached to TIPS microspheres incubated under proliferation conditions for either 1 or 7 days resulted in the consistent expression of myogenic proliferation markers Ki67, Pax7, MyoD, myogenin. This result was verified by data from the BrdU assay over 1-7 days. These data demonstrate the use of TIPS microspheres to retain the proliferative capacity of myoblasts *in vitro*.

HSMM-attached to TIPS microspheres and incubated in differentiation medium for 7 days resulted in the increased expression of Ki67, Pax7, MyoD, myogenin, desmin and myosin heavy chain compared with control cells incubated on tissue culture plastic.

CONCLUSION

This study demonstrates the ability to attach primary human myoblast cells to TIPS microspheres. Once attached, myoblasts retain their capacity to either proliferate or differentiate under controlled conditions. These data are important for future use in cell therapy applications.

REFERENCES

1. Blaker J *et al.*, Acta Biomaterialia (2008), 4: 264-272
2. Ahmadi R *et al.*, Acta Biomaterialia (2010) 7: 1542-1549

ACKNOWLEDGMENTS

The authors wish to thank Miss Veronika Kallo and Professor Surjit K. Srai for their assistance with PCR.



Corrosion behaviour of beta titanium alloys containing zirconium for dentistry

J. Fojt*, L. Joska, A. Bernatikova and J. Malek

Department of Metals and Corrosion Engineering, Institute of Chemical Technology in Prague,
Czech Republic, fojtj@vscht.cz

¹UJP Prague, Czech Republic

INTRODUCTION

To increase an implant lifetime, researchers are now concerned on the development of new titanium alloys with suitable mechanical properties (low elastic modulus, high fatigue strength), corrosion resistance and good workability. Titanium exhibits an excellent corrosion resistance in human body environment due to the formation of a stable oxide film on the surface. However, despite this fact and good tissue acceptance, high Young modulus of titanium is not comparable with bone. While the elastic modulus of cortical bone is close to 20 GPa, the modulus of titanium is 116 GPa. To increase implants lifetime new titanium alloys with lower Young modulus, good workability and high corrosion resistance are now developed. Corrosion resistance of these alloys should be comparable with that of pure titanium.

The aim of this project was to study microstructure, mechanical properties and corrosion behaviour of two beta titanium alloys Ti-35Nb-2Zr and Ti-35Nb-2Zr-0.4O.

EXPERIMENTAL METHODS

Metallographic study and mechanical properties measurement were based on standard procedures. Corrosion behaviour was measured in physiological saline solution and, with respect to possible use of these materials in dentistry, in the same solution with decreased pH and fluoride ions added. Electrochemical measurements consist of the open circuit potential, electrochemical impedance (60 kHz – 1 mHz, 10 mV amplitude) and potentiodynamic curves measurement. Surface chemistry was evaluated by X-ray photoelectron spectroscopy (XPS).

RESULTS AND DISCUSSION

The structure of Ti-35Nb-2Zr-0.4O (TNZO) and Ti-35Nb-2Zr (TNZ) is beta and deformed martensitic structure respectively. Tensile strength was 807 MPa for TNZ and 1227 MPa for TNZO. More important were Young modulus values. They were over twice lower in comparison with pure titanium or Ti-6Al-4V alloy - 47 GPa and 61 GPa for TNZ and TNZO respectively. It is evident that presence of oxygen has significant impact on both structure of material and its mechanical properties.

Corrosion resistance was compared with that of commercially pure titanium. Passive layer of non exposed specimens was slightly enriched, in comparison with bulk material, by niobium (XPS). Open circuit potential level of both alloys and titanium indicates passive state of all materials during exposure in physiological solution. It was also confirmed by XPS analysis - all alloys components were present in the

highest oxidation state. Addition of 5000 ppm of fluoride ions caused general decrease of corrosion resistance. This change was the most significant in the case of titanium, corrosion resistance of beta alloys was significantly higher. This behaviour is probably caused by presence of niobium and zirconium in passive layer detected by XPS.

Analysis of electrochemical impedance spectroscopy data from pure saline solution showed that surface of alloys consists of compact inner layer overlaid by porous layer. Situation was more complicated in the case of electrolytes with decreased pH and fluorides added. There was thick porous layer of precipitated corrosion products on titanium surface which negatively affected corrosion resistance of samples. Precipitation of corrosion products was detected on alloys too; however, in this case the corrosion resistance was significantly higher. There were detected increased concentrations of niobium in passive layer; therefore one can assume preferential dissolution of titanium.

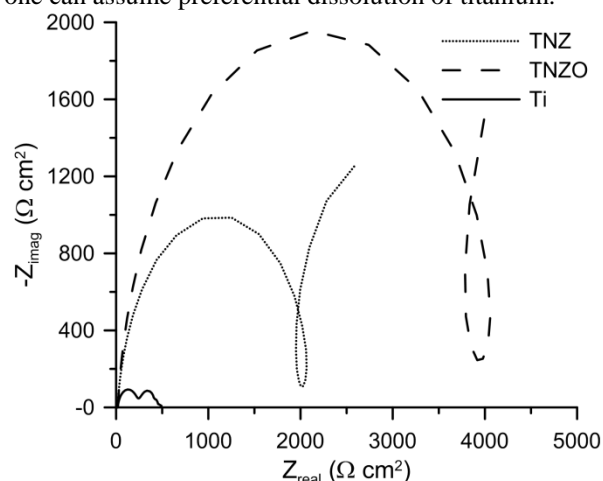


Fig. 1. Impedance spectra of studied materials in physiological solution at pH 4.2 with 200 ppm of fluorides ions.

CONCLUSION

New titanium alloys with suitable mechanical properties containing niobium and zirconium were prepared. Corrosion properties were in physiological saline solution comparable with titanium. Corrosion resistance of zirconium containing alloys was significantly better than that of titanium in the presence of fluoride ions.

ACKNOWLEDGMENTS

The works were carried out as a part of the TA 020 10409 project, which is financially supported by Technology Agency of the Czech Republic.

Surface modification of Ti-surfaces by alginate polyelectrolyte layers

Dana Kubies¹, Ognen Pop-Georgievski¹, Eliška Mázl-Chánová¹, Josef Zemek², Neda Neykova², Roman Deminachuk¹, Milan Houska¹, Elena Filová³, Lucie Bačáková³, František Rypáček¹

¹ Institute of Macromolecular Chemistry, Academy of Sciences of the Czech Republic, v. v. i. Czech Republic, [email: kubies@imc.cas.cz](mailto:kubies@imc.cas.cz)

² Institute of Physics, Academy of Sciences of the Czech Republic, v. v. i., Czech Republic

³ Institute of Physiology, Academy of Sciences of the Czech Republic, v.v.i., Czech Republic

INTRODUCTION

Currently, the biological fixation of the bone embedded cementless implants is often improved by the application of bioactive coatings (calcium phosphates such as Hap and TCP) on the implant surface (1). However, the thin calcium phosphate layers could exhibit nonhomogeneous porosity, weak adherence to metal substrates, and/or degradation and delamination during a long-term functioning (2). Our aim is to develop a degradable thin layer on titanium (Ti) surfaces based on an alginate carrier containing nanosized bioactive inorganic components (Hap, TCP) and bifunctional bisphosphonates (BF) as a coupling interface. Bioactive components would be available for cells continuously during the coating degradation. Herein we present the results obtained for the first step of the coating process, i.e., the activation of Ti surfaces introducing active groups required for the coupling of stable BF layers following by the coating with a thin alginate layer.

EXPERIMENTAL METHODS

Commercially available Ti or model Ti surfaces were subjected to different physical (solvents) and chemical treatments (chemicals and oxygen plasma) following by a coating with 6-aminohexylidenedihydroxybisphosphonate (BP). Surface properties were analyzed using contact angle analysis, profilometry, SEM, X-ray photoelectron spectroscopy (XPS), spectroscopic ellipsometry (SE) and infrared spectroscopy. The morphology and homogeneity of the layers were revealed by SEM, profilometry and atomic force microscopy (AFM). The *in vitro* studies using human osteoblastic cell line Saos-2 are in progress.

RESULTS AND DISCUSSION

The Ti layers were exposed to two acidic and two alkaline surface treatments. Based on XPS analysis, the highest content of Ti in the form of Ti^{4+} as well as the highest content of OH groups was formed by $NH_4OH/H_2O_2/H_2O$ treatment following by exposition to oxygen plasma. The thickness of the upper TiO_2 film on the Ti surface was 21.5 ± 4.6 and the thickness of the bound BP layer was 1.7 ± 0.5 nm. The presence of BP on the Ti surface was proved by XPS (Tab.1) and the BP layer was stable in water conditions for 28 days.

The alginate film was then attached to the Ti surfaces by physisorption in the form of the polyelectrolyte complex or by covalent coupling using EDC/NHS chemistry with a coupling BP layer. The alginate immobilization led to the homogeneous hydrophilic surfaces with randomly distributed agglomerates (Fig.1).

Table 1 XPS analysis of the Ti surface modified by bisphosphonate

Modification of Ti surface	Surface composition % at. (XPS)				
	C	O	Ti	N	P
$NH_4OH/H_2O_2/H_2O$	23.0	59.0	18.0	-	-
NH_4OH treat. + BP	25.5	54.8	13.6	1.7	3.0
Ti model-BP	33.8	46.6	12.7	2.8	2.8

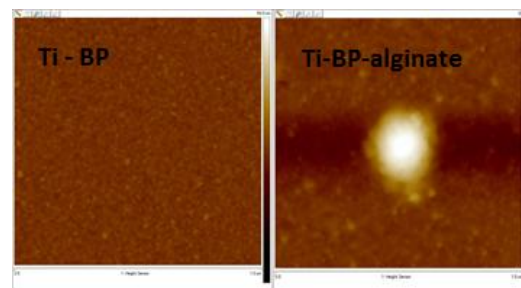


Figure 1 The surface topography of Ti surfaces with covalently bound bisphosphonate layer and after the alginate coating (AFM analysis, $1 \times 1 \mu m$, z-scale 50nm)

The preliminary *in vitro* experiments following the feasibility of the prepared surfaces to support adhesion and proliferation of human osteoblastic cell line Saos-2 are under study.

CONCLUSION

We have developed activation and BP-binding procedures on ‘real life’ and model Ti surfaces. Such activated surfaces were coated with alginate layers via physisorption and/or a covalent immobilization. All modification steps have been carefully investigated by surface-sensitive techniques, such as XPS, SE, IR or AFM. The successful deposition of the alginate coating opens the gate for further modifications of surfaces with biologically active compounds.

REFERENCES

1. Franchi M *et al.* Micron 36, 2005: 665 -671.
2. Lusquinos F *et al.* J Biomed Mat Res -Part A 2003, 64, 630-637; Yang YC *et al.* Thin Solid Films 2003, 444, 260-275.

ACKNOWLEDGMENT. The authors acknowledge the support of the Grant Agency of the Ministry of Health of the Czech Republic (No. NT/13297-4), the Ministry of Education, Youth and Sports of the Czech Republic. (grant No. EE2.3.30.0029) and European Regional Development Fund (the project “BIOCEV” grant No. CZ.1.05/1.1.00/02.0109)

Hydrophobic quaternized chitosan for efficient nanoparticle formation and transfection of therapeutic oligonucleotides

Pedro M.D. Moreno¹, Joyce C. Santos^{1,2}, Carla P. Gomes^{1,3}, Aida Varela-Moreira^{1,4}
Artur Costa¹, Francisco Mendonça¹, Ana P. Pêgo^{1,3,5}

¹INEB-Instituto de Engenharia Biomédica, Universidade do Porto (U Porto), Portugal, ²CeNano²I, Department of Metallurgical and Materials Engineering, UFMG, Brazil, ³Faculdade de Engenharia, U Porto, Portugal, ⁴Faculdade de Medicina, U Porto, Portugal, ⁵Instituto de Ciências Biomédicas Abel Salazar, U Porto, Portugal
pedro.moreno@ineb.up.pt

INTRODUCTION

Antisense gene therapy with the use of single-stranded oligonucleotides (ONs) holds great therapeutic potential. Especially, splice-correcting oligonucleotides (SCOs) have been recognized as capable of tackling many genetic diseases arising from mutations that produce aberrant alternative splice patterns¹. Although the use of “naked” ONs for cell delivery *in vivo* is possible, development of delivery vectors for this specific class of molecules could further improve their efficiency, attaining a controlled delivery and decreasing toxicity levels. To this end, chitosan, a biodegradable biomaterial based vector, associated with negligible toxicity effects, holds great potential as a nucleic acid carrier, although its efficiency needs further improvements. Furthermore, its potential for delivery of ONs has not been duly investigated². In this work we explored the use of a hydrophobic quaternized chitosan for ON complexation and condensation, as well as mediation of delivery of a SCO *in vitro* in a luciferase splice-correction model cell line, seen as a more reliable method for accessing delivery efficiencies of ONs by different vector types³.

EXPERIMENTAL METHODS

A trimethylchitosan (TMC₄₃, Kitozyme) (Mn 43.3 kDa, 11% DA, 30% quaternization (DQ)) was reacted with succinimidyl-modified stearate (NHS-SA) attaining a modification degree of 2±0.8% (mol%). TMC/ON complexes were prepared at different N/P ratios by a coacervation method aided by SO₄²⁻ crosslinking. Strength of interaction between TMC and ON was determined by gel electrophoresis assay. Size and zeta potential were determined by DLS. DLS was also used to verify the stability of formed complexes in serum containing medium. The extent of cellular association of TMC/ON complexes was analysed by flow cytometry. Transfection efficiency was evaluated by adding complexes to HeLa/Luc705 cells and analysing splice-correction of the mutated Luciferase gene in terms of increased luciferase activity³. All values represent means of at least 3 experiments ± SD.

RESULTS AND DISCUSSION

TMC-SA showed slightly higher interaction strength with ONs in comparison with TMC₄₃ when analysed by gel retention assay. Nevertheless, both TMCs were able to retain the ON with >90% efficiency for N/P >2. The average hydrodynamic diameter of both TMC₄₃/ON and TMC-SA/ON ranged from 100-150 nm with particles at the highest range of size given by higher N/P ratios (N/P >120). Stability of TMC/ON particles after

incubation in serum containing cell medium showed a striking difference between both TMCs. While TMC₄₃/ON particles showed an increase in average size and decreased peak intensity, TMC-SA/ON particles retained almost completely the DLS profile when comparing to non-treated control samples (Fig. 1).

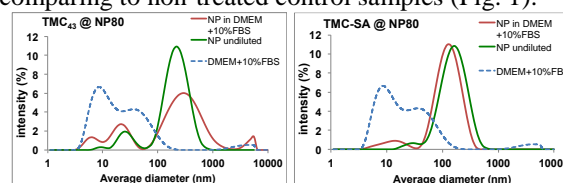


Fig.1: Stability of complexes in serum containing medium analysed by DLS. TMC/ON complexes at N/P 80 were incubated at 37°C for 1h with serum containing cell culture medium.

Transfections with TMC/SCO complexes showed close to 10-fold increase in efficiency of TMC-SA in relation to TMC₄₃, and around half the efficacy when comparing to LipofectamineTM 2000 (Fig. 2)..

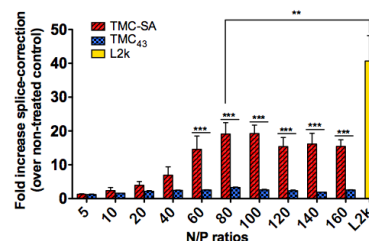


Fig. 2: Splice correction activity of TMCs/SCO complexes in HeLa/Luc705 cell line. SCO was used at 0.3 µM final concentration. (n=3, **P=0.019; ***P<0.001)

Flow cytometry showed similar extent of cellular interaction for TMC-SA/ON complexes and Lipofectamine pointing to other mechanisms playing a role in the transfection efficacy differences seen between both vectors.

CONCLUSION

Hydrophobic modification of TMC was found crucial for preparation of stable TMC/ON nanoparticles and produced splice-correction efficient complexes when high N/P ratios (≥80) are used. This is the first report showing the successful use of a chitosan-based biomaterial for improved delivery of a SCO in a splice correction model.

REFERENCES

1. Spitali, P., *et al.* Cell, 148(6): 1085-8, 2012.
2. Gomes, C.P., *et al.* MRS Bulletin, 39(01): 60-70, 2014.
3. Kang, S.H., *et al.* Biochemistry, 37(18): 6235-9, 1998.

ACKNOWLEDGMENTS

Marie Curie Actions (PIEF-GA-2011-300485), FCT grants SFRH/BD/79930/2011, PTDC/CTM-NAN/NAN/115124/2009 and HMSP-ICT/0020/2010.

***In Vitro* Response of Human Osteoprogenitor Cells to Cross-Linked Poly(Lactide-co-Caprolactone) Dimethacrylate for Bone Repair**

Laura Brown¹, Jessica Gwynne¹, David Shepherd¹, Leander Poocha², Gerhard Hildebrand², Klaus Liefeth², Roger Brooks³, Serena Best²

¹CCMM, Department of Materials Science & Metallurgy, University of Cambridge, United Kingdom

²Institute for Bioprocessing and Analytical Measurement Techniques e.V., Heilbad Heiligenstadt, Germany

³Orthopaedic Research, Addenbrooke's Hospital, University of Cambridge, United Kingdom

lvb26@cam.ac.uk

INTRODUCTION

Autologous bone grafts remain the gold standard for treatment of critical size bone defects¹. However, this approach has significant drawbacks; limited supply, a second injury site, increased infection risk. Various materials have been investigated as synthetic bone substitutes. Resorbable α -hydroxyacids are an attractive choice for controlled implant degradation. Copolymers of lactide and glycolide have been widely studied for applications such as resorbable sutures. Copolymers containing the longer chain caprolactone monomer have a longer degradation time, which is tunable with composition². Such materials may be a good choice for a bone substitute material, which should ideally resorb at a rate to match the ingrowth of new bone.

EXPERIMENTAL METHODS

Poly(lactide-co-caprolactone) dimethacrylate (LCM) materials were synthesised by stannous catalyzed ring-opening polymerisation of cyclic caprolactone and the D,L-lactide dimer, using diethylene glycol as the initiator. LCM is a tapered copolymer consisting of crosslinked oligomers of 10 (LCM6.1) or 20 (LCM3,4) monomer units. LCM4 and LCM6.1 materials have a nominal lactide content of 80wt%, LCM3 contains 70wt% lactide. After methacrylation, crosslinking was performed by two methods to give different microstructures. Disc samples were UV-crosslinked. Scaffolds samples were produced by spatially selective two-photon polymerisation, an additive manufacturing technique, to create a well-defined structure from a CAD model. Our chosen structure is a Schwartz P unit cell with cell parameter 500 μ m. Pore interconnectivity gives this structure high permeability - the scale chosen reflects optimum pore size for bone cell migration³.

Primary human osteoprogenitor cells isolated from bone tissue of patients undergoing total knee replacement were cultured for two weeks on gamma-sterilised disc and scaffold samples in 24-well microplates. Cell proliferation was monitored by alamarBlue assay throughout and cell differentiation by ALP staining at Day 7. For disc samples, tissue culture plastic discs of similar size were used as a positive control for good cell response; for scaffolds, a clinically successful bone substitute scaffold, Vitoss, was used as positive control.

RESULTS AND DISCUSSION

For disc samples (Fig 1a), cell proliferation was comparable to the control material for LCM3 and LCM4 materials, suggesting little effect of copolymer composition over the range studied. Cell proliferation

was lower for the LCM6.1 material, perhaps due to lower methacrylation efficiency resulting in an acidic oligomer component. This might be improved by increasing the methacrylate:oligomer ratio.

For scaffold samples (Fig 1b), cell adhesion was lower for the LCM materials than the control, but subsequent proliferation was significantly higher than the Vitoss control, despite its status as a clinically approved bone substitute material. There were no significant differences in attachment or proliferation between the three LCM materials tested, suggesting two-photon polymerisation improves the gel content of the LCM6.1 material compared with 'bulk' UV crosslinking.

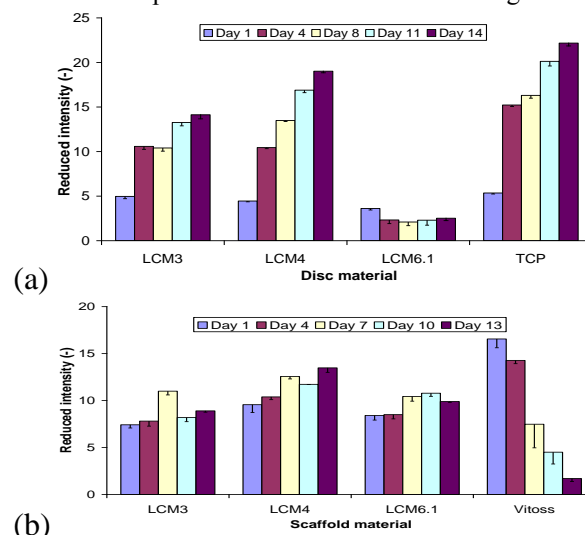


Figure 1: alamarBlue intensity, normalised to no cell control, for disc (a) and scaffold (b) samples

Osteoprogenitor cells on all LCM materials showed ALP staining at day 7, indicating support of a more differentiated cell phenotype.

CONCLUSION

Osteoprogenitor cells showed good attachment and proliferation when cultured on the LCM materials in both disc and scaffold form. This is a promising result for the *in vivo* biocompatibility of the LCM materials.

REFERENCES

1. Langer R. *et al.* Science, 1993, 260: 920-926
2. Agrawal C. *et al.* J.Biomed. Mater. Res., 2001, 55: 141-150
3. Rajagopalan S. *et al.* Med. Imag. Anal., 2006, 10: 693-712

ACKNOWLEDGMENTS

The authors wish to thank EU FP7 (Grant 263363 - InnovaBone) for funding this work, the EPSRC for funding for LB, and the NIHR for funding for RB.



Drug delivery carriers based on two functionalized spider silk proteins: a novel approach for cancer therapy

Anna Florczak^{1,3}, Katarzyna Jastrzebska^{1,3}, Andrzej Mackiewicz^{2,3}, Hanna Dams-Kozłowska^{2,3}

¹NanoBioMedical Centre, Adam Mickiewicz University, Poznan, Poland

²Department of Diagnostics and Cancer Immunology, Greater Poland Cancer Centre, Poznan, Poland

³Chair of Medical Biotechnology, Poznan University of Medical Sciences, Poland

annaflorczak84@gmail.com

INTRODUCTION

Current strategies for cancer treatment are to design a nanosystem for a delivery of therapeutic agents specifically to the site of tumor, therefore avoiding potential side effects. A silk biomaterial combines superb mechanical properties, biocompatibility and biodegradability [1], thus it can be used as a drug carrier. Moreover, the bioengineered silk protein may be functionalized by fusion of tumor homing peptides [2]. The aim of present study was to obtain novel drug delivery carriers based on functionalized spider silk proteins. The specific aim was the evaluation of physical as well as biological properties of bioengineered spider silk-based particles made of two different silk proteins and their blends.

EXPERIMENTAL METHODS

The bioengineered silk proteins (MS1 and MS2 based on the proteins from *N. clavipes*) and theirs Her2-directing hybrid variants were designed. Obtained proteins were processed into spheres by salting out process [3]. The MS1/MS2 blends were produced in different weight ratios. Spheres were characterized in terms of morphology, size (scanning electron microscopy), secondary structure (FTIR), Zeta potential (ZP), stability (spectrophotometry). The binding (flow cytometry and confocal microscopy) and drug delivery potential of silk particles to cancer cells were investigated. Next, the anticancer therapeutic doxorubicin was incorporated into silk spheres and the cytotoxicity of drug loaded spheres was examined by using MTT assay.

RESULTS AND DISCUSSION

Particles based on MS1 and MS2 proteins demonstrated differences in morphology, stability, zeta potential and binding to targeted cells. The increasing MS2 concentration into MS1/MS2 blend improved physical properties of spheres, however lowered their cell binding efficiency. For 80/20% blends (functionalized MS1/MS2), the binding efficiency was maintained with greatly improved sphere stability.

The spheres made of functionalized spider silk indicated significantly higher binding to the Her2-overexpressing cells (SKOV3, SKBR3) comparing with Her2-negative

cells (MSU1.1) and comparing to control spheres without the targeting domains.

	SKOV3	SKBR3	MSU1.1
MS1/MS2	14.97 (± 7.62)	13.93 (± 2.11)	3.8 (± 2.16)
H2.1MS1/H2.1MS2	64.22 (± 14.14)	74.43 (± 7.16)	14.83 (± 8.18)
H2.2MS1/H2.2MS2	78.63 (± 12.99)	74.53 (± 1.10)	7.63 (± 5.41)

Table 1: Flow cytometry analysis of cell binding assay with functionalized silk spheres indicated as % of binding ± SD.

The functionalized silk spheres loaded with doxorubicin significantly higher reduced the cell viability of Her2-overexpressing cells comparing with Her2-negative cells and comparing to control spheres without the targeting domains.

CONCLUSION

Two different bioengineered silk proteins were examined in terms of sphere formation. We showed that blending process can be used as a controlling factor of particle properties.

Moreover, spheres made of functionalized MS1/MS2 blend were loaded with the model drug and efficiently killed targeted cells.

The obtained results indicated the potential for the delivery of a therapeutic agent confined in silk spheres to the specific tumor microenvironment.

REFERENCES

1. Tokareva O. *et al.*, Acta Biomater. 10(4):1612-1626, 2014
2. Numata K. *et al.*, Macromol Biosci. 12:75-82, 2012
3. Lammel A. *et al.*, ChemSusChem. 1:413-6, 2008

ACKNOWLEDGMENTS

The study was supported by the International PhD Projects Programme of Foundation for Polish Science operated within the Innovative Economy Operational Programme (IE OP) 2007-2013 within European Regional Development Fund.

Controlling Intramembranous Bone Mineralisation using a Bone Tissue Engineering Approach

Anthony J. Deegan¹, Halil M. Aydin^{1,2}, Bin Hu¹, Sandeep Konduru^{1,3}, Jan H. Kuiper¹, Ying Yang¹

¹Institute of Science and Technology in Medicine, School of Medicine, Keele University, UK

²Bioengineering Division, Institute of Science, Hacettepe University, Turkey

³University Hospital of Staffordshire, Orthopedics Department, UK

INTRODUCTION

The requirement for rapid high quality bone fusion and the difficulties associated with harvesting autologous bone represent an ever present challenge to orthopaedic surgery. Without intervention at the defect sites, automatic bone formation in such areas may not occur¹. Gold standard interventions include the addition of bone grafts, the administration of growth factors or applying low-intensity pulsed ultrasound¹⁻³. However, even these gold standard interventions are not without problems. Tissue engineering offers an avenue by which the required results can be obtained and surgical disadvantages avoided. Given that bone formation involves stepwise cell-cell and cell-ECM interactions, the regulation of the osteoblast culture microenvironments can tailor osteoblast proliferation and mineralization rates and thus the quality and/or quantity of final calcified tissue. Using substrate chemistry modifications to induce bone aggregate formation in large quantities and with variable sizes, the aim of this study is to identify the variables that control the mineralization process and the quality and spatial distribution of minerals formed in *in vitro* 3D aggregates.

EXPERIMENTAL METHODS

Aggregate Formation

An osteoblast cell line, MLO-A5, was used for aggregate formation. Aggregates of two sizes were formed by adjusting the wettability of polystyrene and creating suspension culture environments of differing hydrophilicities.

Aggregate Analysis

The aggregates were assessed on gene, protein and mineral levels using various analytical techniques. Synchrotron-sourced FTIR analysis was carried out at Diamond Synchrotron, Oxfordshire. Groups were compared using independent T-tests or one-way analysis of variance (ANOVA). A p-value below p=0.05 was denoted to indicate statistical significance.

RESULTS AND DISCUSSION

We show that the development of bone aggregates and the control of aggregate size are two important factors for rapid bone formation. The modification of culture substrate properties that force cells to aggregate can lead to the production of a high quantity of cellular aggregates in a short period of time (24 hours). The degree of substrate modification determines aggregate size (ø79-745µm). Our data demonstrate that cells in an aggregate culture, particularly in larger aggregates, can generate visible and quantifiable mineralized matrix within just 24 hours. The cells in monolayer failed to do so. Synchrotron-sourced FTIR analysis quantitatively measured mineralization levels comparing culture duration and aggregate size effects.

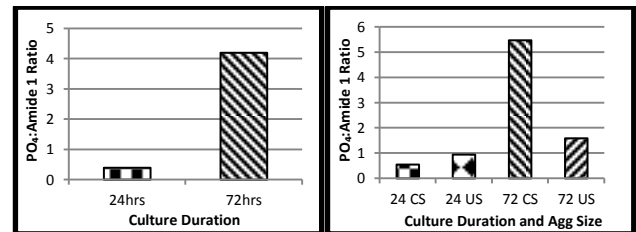


Figure 1: PO₄:Amide 1 ratios displaying differing calcification levels over duration and suspension culture type. CS denotes large aggregates, US denotes small aggregates.

This analysis also offered an insight into the spatial distribution of developing calcification and how it differs between aggregate size and culture duration. SEM-EDX analysis corroborated these data.

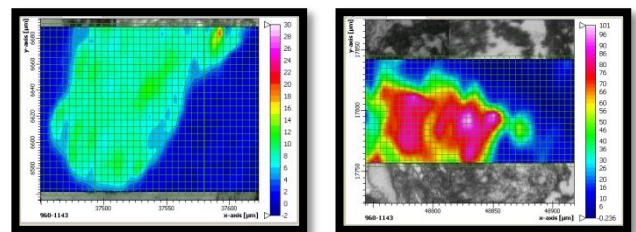


Figure 2: FTIR mapping images highlighting the PO₄ regions of 24 hour (left) and 72 hour (right) coated suspension aggregates (large aggregates).

CONCLUSION

This study confirms that aggregate culture is sufficient to induce rapid mineralization and that aggregate size determines the rate of mineralization. In addition, the spatial distribution of mineralisation can be visually identified and quantitatively measured. This bone tissue engineering approach may establish a good model to study regulation factors at different development phases of the osteoblastic lineage.

REFERENCES

1. Hannouche D. *et al.*, The Journal of Bone and Joint Surgery. British Volume, 83(2):157–164, 2001
2. Bostrom M.P.G. *et al.*, The Orthopedic Clinics of North America, 30(4):647–658, 2013
3. Duarte L.R. Archives of Orthopaedic and Traumatic Surgery, 101(3):153–159, 1983

ACKNOWLEDGEMENTS

The authors are grateful for the financial support from European Union FP7 IEF Marie Curie Actions (PIEF-GA-2009-237762) and NHS Orthopaedic Charity funding (001502). We thank Dr David Bolton for the technical support on the application and data processing of Cell IQ system. We would also like to thank the senior scientist, Dr Gianfelice Cinque, and support scientist, Dr Paul Donaldson, of beamline 22, Diamond Synchrotron, Oxfordshire, for their support during FTIR data collection and analysis.

Generation of Electrospun Yarns for Use as Tissue Engineered Blood Vessel Scaffolds

Richard O'Connor* and Garrett B. McGuinness

Centre for Medical Engineering Research, Dublin City University, Ireland, richard.oconnor2@mail.dcu.ie

INTRODUCTION

Electrospinning is a polymer processing technique capable of producing continuous submicron diameter fibres¹. In a typical electrospinning process a capillary with a metallic spinneret acts as a reservoir for a polymer solution. A high voltage potential is generated between the spinneret and a grounded metallic target. A jet of polymer in turn erupts from the spinneret tip and subsequently deposits on the target². The nanofibre structures produced have been identified as potential scaffolds for tissue engineering applications due to their high surface area-to-volume ratio and high porosity levels^{2,3}. A significant trade-off however is the decrease in a scaffolds mechanical strength when porosity is increased to allow for cellular infiltration³. Studies have shown the capability of producing electrospun nanoyarn structures using dynamic liquid collection techniques⁴⁻⁶. These nanoyarns exhibit an increased porosity and fibre alignment compared to traditional electrospun structures enhancing cell infiltration rates while maintaining mechanical strength⁶. The aim of this study was to produce three-dimensional electrospun nanoyarn constructs for vascular reconstruction applications using poly(ϵ -caprolactone) (PCL) a biodegradable polyester.

EXPERIMENTAL METHODS

14wt% solutions of PCL dissolved in chloroform and ethanol (7:3; v:v) were prepared by stirring overnight at room temperature. A custom built dynamic liquid collection apparatus (Figure 1) based upon Teo *et al.*⁴ was used to produce the electrospun yarn scaffolds.

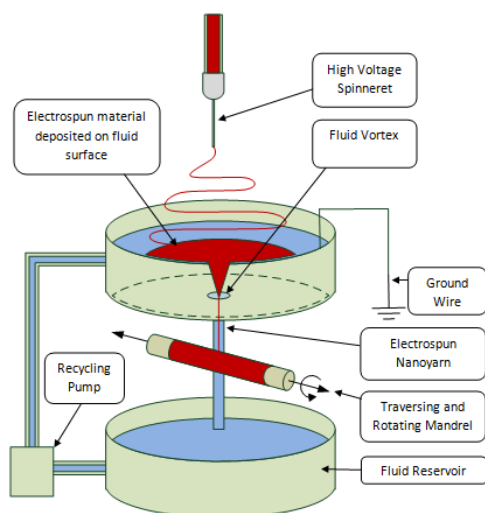


Figure 1- Dynamic liquid collector apparatus.

Briefly the dynamic liquid collector apparatus consists of a circular tank with an outlet located on the bottom surface. A reservoir tank and pump positioned below the outlet re-circulates water to the upper tank to maintain a constant fluid level. A grounded wire is

inserted into the water to remove residual charge. Electrospun material deposited on the water's surface is drawn downwards by a vortex generated by the draining fluid. This vortex aids in the bundling and alignment of the electrospun material to form a yarn structure. A traversing and rotating mandrel positioned below the outlet is used to collect the yarn material. SEM imaging was performed on samples and fibre diameter measurements ($n=30$) were taken for each scaffold.

RESULTS AND DISCUSSION

Images of an electrospun yarn scaffold and a conventional flat membrane can be observed in Figures 2(a) and 2(b), respectively. Both were produced using 14wt% PCL solutions. The yarn scaffolds exhibited a fibre diameter range of $(2.55 \pm 0.74 \mu\text{m})$ while the flat membranes showed a range of $(2.39 \pm 1.22 \mu\text{m})$. Visible differences in fibre orientation and porosity can be seen with the flat membrane showing a dense random fibre structure compared to the yarn, which exhibits a highly aligned structure with large pores between fibres.

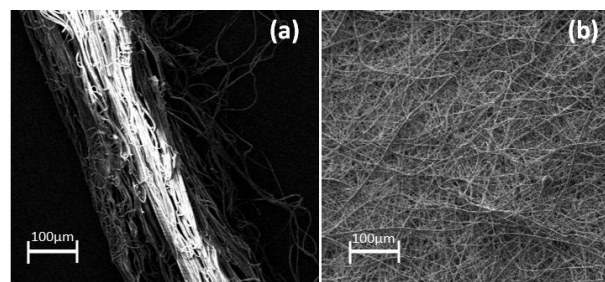


Figure 2- Electrospun structures produced in study (a) Nanoyarn scaffold using dynamic liquid collector (b) Flat membrane using metallic plate target.

CONCLUSION

Electrospun PCL yarns containing micron scale diameter fibres and multi-scale porosity were successfully produced. Further optimisation of the scaffold morphology along with mechanical characterisation is currently being completed with the end goal being the development of a cell seeded scaffold.

REFERENCES

1. Huang Z-M. *et al.*, Compos Sci Technol. 63:2223-2253, 2003
2. Li D., Xia Y., Adv Mater. 16:1151-1170, 2004
3. Zhong S. *et al.*, Tissue Eng Pt B-Rev. 18:77-87, 2012
4. Teo W.E. *et al.*, Polym Commun. 48:3400-3405, 2007
5. Wu J. *et al.*, Mater Lett. 89:146-149, 2012
6. Xu Y. *et al.*, Tissue Eng Pt C-Meth. 19:925-936, 2013

ACKNOWLEDGMENTS

The authors thank the IRC for providing financial support under the Embark Initiative (RS/2012/52).

Injectable Thermo-responsive Hyaluronan Hydrogel in a Rabbit Osteochondral Defect Model

D. Eglin, M. D'Este, I. Dresing and M. Alini

AO Research Institute Davos, Switzerland and Collaborative Research Partner Acute Cartilage Injury Program of AO Foundation, Switzerland. david.eglin@aofoundation.org

INTRODUCTION

Regeneration of cartilage and osteochondral defects after a trauma is still highly limited². Our main objective is to address the issue by developing a minimally invasive tissue engineered approach. For this we developed a bioresorbable thermo-responsive hyaluronan hydrogel (HApN) which allow for cells encapsulation and *in situ* application, and gelation at 30°C. In this study we assessed the safety and effect of the HApN on the defect repair.

EXPERIMENTAL METHODS

HapN was prepared as previously reported, sterilized and reconstituted at 10 w:v % in PBS¹. The *in vivo* study was approved by the Veterinary Commission of the Canton of Grisons, CH. Skeletally mature female New Zealand White animals [32± 4 weeks, Charles River, Germany] were included in this study and divided randomly into an empty group and a material group (2 x n=6). An osteochondral defect (2,7 mm diameter x 4 mm depth) was created in the central area of the medial trochlear ridge. 100µl of HApN solution was injected through a 19G needle into the defect. After 12 weeks, the rabbits were euthanized, soft tissues collected to assess biocompatibility and the defects evaluated macroscopically. Histology sections of soft tissues were stained with H&E, defects stained with H&E and Safranin-O/Fast green were prepared and scored. Aggrecan, collagen type I and II immunostaining were prepared and analysed. For statistical evaluation (SPSS) Mann Whitney U non-parametric test was performed (p 0.05).

RESULTS AND DISCUSSION

The gelation of the HapN *in vivo* occurred in less than 2 min. Temperature at the joint surface was 33±2°C before and 34±2°C after injection. After 12 weeks, observation of the kidney, liver, spleen, *inn* popliteal and joint capsule histological sections showed no difference between groups. Macroscopic ICRS Cartilage Repair Assessment System score (/12) values were 9.7± 1.0 and 11.1± 1.5 for Empty and HapN group respectively. Both groups were graded as nearly normal. HapN group had a significantly higher macroscopic score than the empty group (p=0.015). Histomorphometrical score values assessed using O'Driscoll's score (/23) were 16.3±1.3 and 18.8±2.1 for Empty and HapN group respectively. HapN group had a significantly higher microscopic score than the empty group (p=0.041). Qualitative analysis of immunostains suggested that the distribution of aggrecan, collagen type I and collagen type II was slightly improved in the HApN compared to empty group. However, collagen type I was present in the whole cartilage repair region.

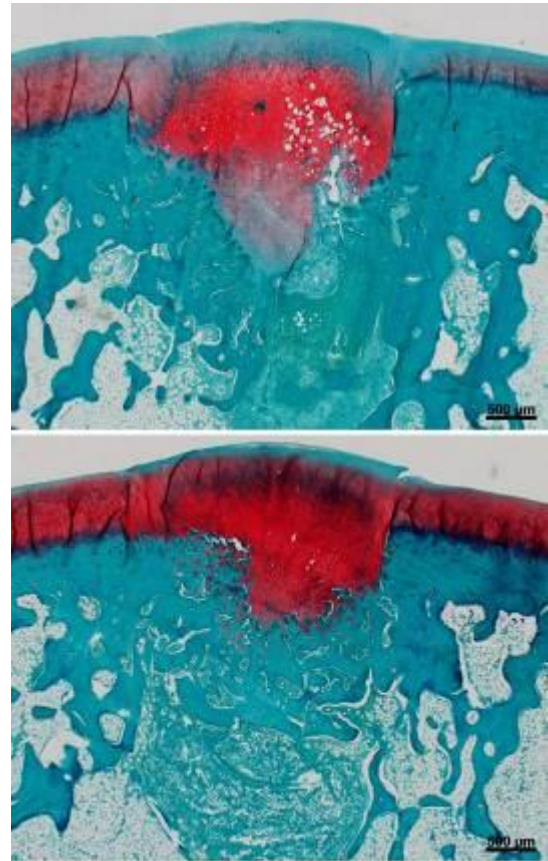


Figure 1. Representative Safranin-O/Fast green stained histological images of the osteochondral defect at 12 weeks after surgery: Empty (top); HapN (bottom). Scale bar 500µm.

These results indicate the safety of the injectable HApN after 12 weeks. The injectable hyaluronan hydrogel has a potential beneficial effect on the rabbit osteochondral defect repair at 12 weeks.

CONCLUSION

HapN was injected and gelled *in vivo* in an osteochondral defect. The hydrogel was biocompatible. A significant improvement of the architecture and composition of new tissue formed was found compare to empty defect as shown by the results. This matrix could be used for the delivery of potent biologics.

REFERENCES

1. Johnstone B, *et al.*, Eur Cell Mater. 25:248-67, 2013.
2. D'Este M, *et al.*, Carbohydr Polym. 90:1378-85, 2012.

ACKNOWLEDGMENTS

This work was supported by the Collaborative Research Centre, AO Foundation, Davos, Switzerland.

Modification of Porcine Pericardium with Low-Energy Non-thermal Electron Beam

Jessy Schönfelder¹, Eberhard Spörl², Richard Funk³, Christiane Wetzel¹

¹Fraunhofer Institute for Electron Beam and Plasma Technology, Germany, jessy.schoenfelder@fep.fraunhofer.de

²Department of Ophthalmology, University Hospital Dresden, Germany

³Institute of Anatomy, Faculty of Medicine, TU Dresden, Germany

INTRODUCTION

Bovine and porcine pericardium is widely used as implant material, e.g. for heart valves, for patch closure in blood vessel reconstructions or soft tissue repair as it is highly biocompatible¹. Xenogenic biological materials are commonly chemically treated, mostly with glutaraldehyde, to induce crosslinks for enhanced stability, to decrease immunogenicity and to sterilize^{1,2}. In the past concerns arose because of the toxicity and calcification-enhancing properties of glutaraldehyde, especially in biological heart valve prosthesis, which leads to premature deterioration and failure^{2,3}. As an alternative to chemical treatment ionizing irradiation with UV, gamma and electron beam were discussed in the literature⁴. A special method of treatment is irradiation with low-energy (< 300 keV) non-thermal electron beam. The penetration depth of electron beam as well as dose and dose rate can be closely regulated. By randomly inducing radicals the electron beam is able to crosslink and sterilize the material.

The aim of this study was to investigate material alterations after low-energy non-thermal electron beam treatment of porcine pericardium.

EXPERIMENTAL METHODS

Porcine pericardia obtained from a local abattoir from 6 months old pigs were stored in cooled PBS (4...10 °C). Attached fat, blood vessels and pleura pericardiaca were removed. Samples were washed in PBS twice and stored in fresh PBS at 4 °C overnight.

The following day moist samples were irradiated with electron beam of 150 keV in nitrogen atmosphere at 1 bar with varying doses (10...500 kGy). Untreated and glutaraldehyde treated (0.2% for 30 min at RT) samples served as references.

Swelling ratio was determined by dividing the difference between sample moist mass and dry mass by the dry mass. Sample size was 10x10 mm².

Stress-strain curves were determined with a Miniature Materials Tester (Polymer Lab.) on moist 13x10 mm² samples (size between clamps ~8x10 mm²) after pre-stretching to 0.02 N with a speed of 4 mm/s.

SEM was performed on a DSM 962 (Zeiss) after dehydrating with ascending ethanol series and critical point drying with CO₂ in an EM CDP300 (Leica).

At least 6 independent experiments were performed. Mean and SD were calculated.

RESULTS AND DISCUSSION

There was a change in swelling ratio (see fig.). Samples irradiated with doses up to 150 kGy had a lower water uptake compared with untreated samples with a minimum at samples with 100 kGy. The water uptake of these 100 kGy-samples was comparable with glutaraldehyde treated samples. After irradiation with

higher doses swelling ratio was comparable (200, 500 kGy) or even higher (350 kGy) than untreated samples. Crosslinking results in a lower water uptake because of steric hindrances as observed at samples irradiated with doses up to 150 kGy.

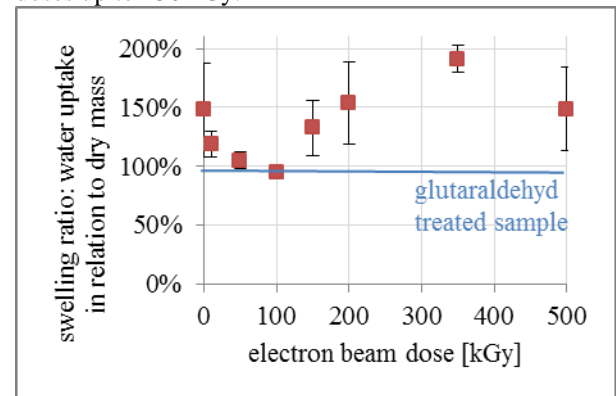


Fig.: swelling ratio (see text for explanation)

Stress-strain curves of 100 kGy-irradiated samples were similar to those of glutaraldehyde treated samples. In general, stress-strain curves showed an elongated toe region and a decreasing slope with rising irradiation dose compared to untreated samples. This indicates that especially after irradiation with higher doses (500 kGy) there is an increasing degradation of collagen molecules. This is also supported by SEM images.

SEM revealed that after irradiation with 500 kGy the crimp structure of collagen is nearly completely vanished, whereas after irradiation with 200 kGy the crimp structure appears more aligned compared to untreated samples.

During electron beam irradiation crosslinking as well as degradation of collagen molecules occurs at the same time³. The obtained results indicate that at lower doses up to 100 kGy crosslinking is the major process and at higher doses (500 kGy) it is degradation.

CONCLUSION

Treatment with low-energy non-thermal electron beam is able to alter characteristics of porcine pericardium in a dose-dependent manner.

REFERENCES

1. Li X. *et al.*, Ann Vasc Surg. 25(4):561, 2011
2. Simionescu D., Expert Opin Biol Ther 4(12):1971, 2004
3. Gallyamov M. *et al.*, Mater Sci Eng C 37:127, 2014
4. Jiang B. *et al.*, Biomaterials 27:15, 2006

ACKNOWLEDGMENTS

The authors would like to thank Mrs. L. Kenner for performing SEM images and the local abattoir (Wurschtelpeter, Eschdorf) for providing the pericardia.

Developing a Method for Tracking and Quantifying Metallic Particle Internalisation

Hayley (Floyd)^{1*}, Janet (Lord)², Edward (Davies)³, Owen (Addison)⁴, Hamid (Dehghani)⁵, Liam (Grover)¹

^{1*}School of Chemical Engineering, University of Birmingham, UK, HXF750@bham.ac.uk

²Centre for Translational Inflammation Research, University of Birmingham, UK

³Royal Orthopaedic Hospital, Birmingham, UK

⁴School of Dentistry, University of Birmingham, UK

⁵School of Computer Science, University of Birmingham, UK

INTRODUCTION

Metal alloys are used extensively in implants today and there is great interest in the effect of particulate wear debris on the local tissue environment. For example, one area of great concern is the use of metal-on-metal bearings in hip implants, which is associated with significant rise in both the local and systemic levels of particulate wear debris [1,2] and increased risk of aseptic loosening. Literature highlights particles of size ~10µm as the most immunologically relevant, however few studies attempt to track and quantify interactions with the debris at the cellular level. The difficulty encountered is a consequence of the fact that debris can be visually similar to structures within the native cell itself. The focus of this work is to study the cellular uptake of metallic particles in cells, and develop a method for tracking and quantifying particle internalisation.

EXPERIMENTAL METHODS

Wear particle generation: CoCr wear particles were generated by subjecting a CoCr femoral head to 250,000 cycles in a wear simulator using fetal calf albumin as a lubricant. To assess metallic debris as a whole, manufactured metallic powders are used initially to provide a model for various appropriate size ranges.

Cell culture/imaging: MC3T3 cells were cultured, using standard techniques, in live cell imaging dishes. The particles, isolated through centrifugation and re-suspended in phosphate buffered saline with penicillin streptomycin, are then introduced. Imaging is performed through transmission and reflection mode using a Zeiss LSM 710 confocal microscope.

Image analysis: Image analysis consists of two steps, segmentation and tracking. To separate a cell from the background and also the particles close to membrane a contrast enhanced gradient field applied to a bright-field image followed by k-means clustering is used. In order to discriminate the particles from organelles within the cell this is used in conjunction with the reflectance channel. Once particles are isolated, tracking methods such as cross-correlation [3] and direct Gaussian fit [4] can be applied.

RESULTS AND DISCUSSION

Figure 1 shows preliminary segmentation of particles, however the cellular granulation saturates the bright-field image and hence no useful information is gained about particle positions. Nevertheless, the ability to discriminate particles from cells as shown is the first step leading to particle tracking through the cell. However, in order to answer the question posed, co-labelling of various organelles and inhibitory strategies

will be used thus enabling particle fate and cellular entry mechanisms to be determined.

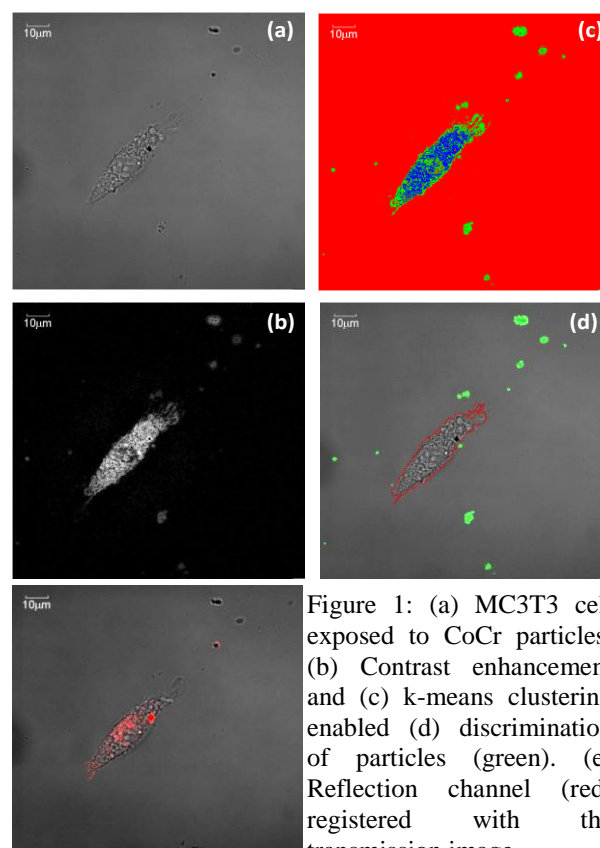


Figure 1: (a) MC3T3 cell exposed to CoCr particles. (b) Contrast enhancement and (c) k-means clustering enabled (d) discrimination of particles (green). (e) Reflection channel (red) registered with the transmission image.

CONCLUSION

A method of metal wear debris tracking from live cell confocal reflectance and fluorescence images has been developed. The method was used as a tool for quantifying debris internalisation at the cellular level and complement immunological assay data (Queen Elizabeth Hospital, Birmingham) to explain the reported effects of metal implants at the tissue level.

REFERENCES

1. Vendittoli PA. *et al.*, J. Bone Joint Surg. 92B:1:12-19, 2010
2. Lee PTH. *et al.*, J Bone and Joint Surg. 87-B:III:232, 2005
3. Geller J. *et al.*, Nature. 331:450-453, 1988
4. Anderson CM. *et al.*, J. Cell Sci. 101:415-425, 1992

ACKNOWLEDGMENTS

Thanks to EPSRC for financial support (EPSRC ref: EP/F50053X/1), and Jeremy Pike for preparing and taking the images presented above.

Endothelialization of gas exchange membranes to provide antithrombogenicity

A. Wenz¹, K. Linke², M. Schandar², F. Metzger³, E. Novosel³, J. Schneider³, P. Kluger^{2,4}

¹ University of Stuttgart, Institute of Interfacial Process Engineering and Plasma Technology IGVP, Stuttgart, Germany

² Fraunhofer Institute for Interfacial Engineering and Biotechnology, Stuttgart, Germany

³ Novalung, Heilbronn, Germany

⁴ Reutlingen University, Process Analysis & Technology, Reutlingen, Germany

annika.wenz@igvp.uni-stuttgart.de

INTRODUCTION

For patients with lung failure, the availability of systems for oxygenation and decarboxylation of the blood is mandatory. Currently, oxygenators containing membranes made of polymeric fibres (e.g. polymethylpentene, PMP) are used. Due to the lack of anti-thrombogenic properties of the fibre materials, the occurrence of thrombus formation is likely and decreases the gas exchange rate and the durability of the membrane. Therefore, the endothelialization of the fibre surface is pursued to obtain an anti-thrombogenic surface¹.

EXPERIMENTAL METHODS

Human dermal microvascular cells (HDMECs) isolated from skin biopsies were seeded on both sides of a unmodified PMP fibre mat. After adhesion of the cells under culture conditions, the fibre mat was put into a flow perfusion bioreactor and the cells were cultured for 2 to 7 days under dynamic conditions. Another seeded fibre mat was cultured under static conditions in parallel as a control.

Afterwards, the fibres were assessed for cell coverage and the cells were analysed in terms of viability, proliferation, metabolic activity, monolayer integrity and expression of HDMEC-specific markers. This was done via live-dead staining with fluorescamindiacetat propidium-iodide (FDA/PI), staining of antigen Ki-67, the metabolism of 3-(4,5-dimethylthiazol-2-yl)-2,5-diphenyltetrazolium bromide (MTT), immunofluorescence staining of vascular endothelial cadherin (VE-Cadherin), and staining of PECAM-1 and vWF, respectively. Overall cell coverage of the fibres was evaluated by determining the surface area stained with FDA/PI via ImageJ.

RESULTS AND DISCUSSION

Cell seeding resulted in the coverage of an extended part of the fibres' surface with viable cells, as shown by FDA/PI staining and quantification by ImageJ directly after the adhesion period. After dynamic culture, the cell density on the whole fibre mat was reduced due to the fact that cells were washed away by the media flow. Still, when looking at the FDA/PI staining of the individual sides of the fibre mat, it became obvious that the

cells mainly detached from the fibres' media inflow side. Looking at the opposing side of the fibres, the cells remained on the PMP and even seemed to have proliferated during the culture period. After static, as well as after dynamic culture, the cells on both sides of the fibres showed expression of PECAM-1 and VE-Cadherin. Those proteins, which are found at the intercellular junctions between endothelial cells, are important markers for the integrity of the endothelial monolayer, what is seen as a prerequisite for antithrombogenicity.

CONCLUSION

In contrast to other studies^{2,4}, the experiments showed successful seeding and static culture of endothelial cells on PMP fibres without previous surface modification. Additionally, even after culture under dynamic conditions, viable cells expressing important proteins for monolayer integrity were found on the unmodified fibres. Nevertheless, dynamic culture of the cells significantly reduced the cell number on the fibres in comparison to static culture conditions, what necessitates modification of the fibre surface for improvement of cell adhesion, even under dynamic conditions, to obtain an anti-thrombogenic endothelial cell monolayer.

REFERENCES

1. McGuigan A. *et al.*, Biomaterials, 28(16):2547-2571, 2008
2. Hess C. *et al.*, Tissue Eng. Part A 16:3043-3053, 2010
3. Möller L. *et al.*, Beilstein J. Org. Chem. 9:270-277, 2013
4. Cornelissen C. *et al.*, Biomed. Eng. Online 12:7, 2013

ACKNOWLEDGMENTS

The authors want to thank the European Commission for funding the AmbuLung project under the Seventh Framework Programme (grant no 304932).

Influence of TCP Content on Chitosan Agglomerated Scaffold Properties

Martyna Kucharska^{1*}, Katarzyna Walenko², Małgorzata Lewandowska-Szumiel², Tomasz Brynk³, Tomasz Ciach¹

¹Biomedical Engineering Laboratory, Faculty of Chemical and Process Engineering, Warsaw University of Technology,

²Institute of Fundamental Technological Research, Polish Academy of Science

Poland, *martyna.kucharska@gmail.com,

³Department of Biophysics and Human Physiology, Medical University of Warsaw, Poland

⁴Faculty of Materials Science and Engineering, Warsaw University of Technology, Poland

INTRODUCTION

In hereby presented work a novel technique for bone scaffold preparation is described. This technique is based on the agglomeration of chitosan /composite microspheres. Previously the method was presented [1], however in this work it was modified and simplified. The improvement relied on the reduction of steps in the fabrication process and there was ceramics employed for material improvement. The next modification that was applied was the use of higher DD (deacetylation degree) chitosan, which was found to be more suitable for cell attachment and proliferation [2]. Authors present the method for scaffold fabrication, essential properties of the materials and the influence of various TCP concentrations on material morphology, mechanical properties and preliminary study on the interaction between the materials and HBDCs cultured.

EXPERIMENTAL METHODS

In the first step microspheres (CH, CH_5%TCP and CH_10%TCP) were extruded in the drop forming rate from chitosan solution into precipitation bath. When completely dried they were subjected to agglomeration in presence of acetic acid, then subsequently neutralized, washed and finally dried. In order to evaluate the influence of TCP content on materials morphology and topography they were studied by microscopic techniques. There was also porosity, pore interconnectivity investigated and an effect of ceramics content on the granules size distribution. Mechanical properties were studied by compression tests and were conducted for the materials with the same dimensions. Universal electromechanical testing stand MTS Q / test 10 was employed for the purpose. Cytocompatibility of chitosan scaffolds with three different contents of TCP (0%, 5%, 10%) was investigated in preliminary observation. Human bone derived cells (HBDCs) were cultured in vitro within the scaffolds and cell viability (XTT) was determined after 48h.

RESULTS AND DISCUSSION

The presented technique allows generating porous materials with controllable shape, pore size distribution and their interconnectivity. Volumetric porosity of fabricated materials equals about 40% . Ceramics content significantly affected material microstructure and it was confirmed that increasing TCP concentration significantly influenced the material roughness. Microspheres' size was strongly determined by TCP concentration and it was found that those extruded from pure polymer solution

were much smaller than those made of chitosan and TCP. The diameters of granules from pure chitosan reached 600 – 1000µm. On the other hand, considering CH/TCP material it was established that the diameters were mostly over 1000µm (1000-1450). It was also confirmed that CH_10%TCP material revealed higher percentage contribution (~60%) of diameters reaching out 1450 µm. The influence of ceramics was also studied during mechanical properties evaluation. Young modulus established on the basis of stress-strain curves was similar for all of the materials and reached out 250 MPa. On the other hand we found that compression strength decreased with increasing TCP concentration. Our preliminary study concerning HBDC culture did not show any clear influence of TCP concentration on the viability of the cells, but XTT measured after 48 h revealed values enclosing in the range of 60 and 85% when compared with control sample.

CONCLUSION

In contrast to other methods for porous materials fabrication that were described so far, the presented technique allows manufacturing scaffolds with well-developed surface for cell attachment and well defined architecture. Mechanical properties were found to be similar to natural bones. Satisfactory viability results of HBDCs culture in direct contact with the investigated material were obtained. For the purpose detailed studies on the interaction between the chitosan scaffolds and cells are planned .

REFERENCES

1. Martyna Kucharska et al, Materials Letters, 64:1059-1062, 2010
2. Seda Tıǧlı R et al, Journal of Materials Science: Materials in Medicine 18: 1665-1674, 2007

ACKNOWLEDGMENTS

This work was financially supported by the European Union in the framework of European Social Fund through the Warsaw University of Technology Development Programme.



HUMAN CAPITAL
NATIONAL COHESION STRATEGY



In-situ Charge Formation on Hydroxylapatite Coatings

L. Pluduma¹, K. A. Gross¹, H. Koivuluoto², P. Vuoristo², M. Kylmälahti², A. Bystrova³, Yu. Dekhtyar³

¹Institute of Biomaterials and Biomechanics, Riga Technical University, Latvia, liene.pluduma@rtu.lv

²Department of Materials Science, Tampere University of Technology, Finland

³Institute of Biomedical Engineering, Riga Technical University, Latvia

INTRODUCTION

The body response to hydroxyapatite (HAp) coatings solely depends on the phase purity, crystallinity, topography and surface characteristics. Besides surface chemical groups, surface charge plays an important role and has shown preferential attachment of osteoblast cells to negatively charged surfaces. Negatively charged polarized HAp has increased the bone growth and implant coverage [1]. These surfaces have not been tested for surface charge and chemical groups, and it has been assumed that the charge is the governing factor in determining the greater bone growth and attachment. This work will use a new approach to introduce aligned hydroxyl groups in the surface.

The aim of this work is to investigate in-situ charge generation of HAp coatings. If HAp dehydroxylates during spraying, then perhaps rehydroxylation can occur after coating, with an additional alignment of hydroxyl groups. Rehydroxylation can be easier by orienting the grains so that hydroxyl ions will directly interface with the biological environment. This double orientation, within the microstructure and the crystal structure of the grains and hydroxyl groups, respectively, will be investigated for advanced coatings. Introducing a textured coating with a controlled hydroxyl orientation offers a new capability for enhancing the properties of HAp.

EXPERIMENTAL METHODS

The HAp powder (particle size of 44 – 55 µm) was delivered from the powder feeder (Metco 4MP-Dual, Perkin Elmer) into a flame spray torch (Casto DynDS 800) operated using acetylene and oxygen, with air as carrier gas. Commercially pure titanium substrates (grit blasted) were positioned 12 cm from the torch and preheated to 250 °C to produce round splats and ensure crystal alignment [2].

Three kinds of experiments were carried out: (1) conventional coating procedure; (2) an electric field was applied during spraying and maintained during steam generation for 10 min after spraying; (3) spraying was performed without an electrical field, but as-sprayed coatings were treated with water vapour for 10 min.

An 8 kV/cm electric field was generated using a high voltage power supply (Series 230, Bertan Associates Inc.). Steam was produced from a boiler (SC 1,050, Kärcher).

The crystal alignment and phase composition of the coated samples were analysed by X-ray diffraction (XRD). Fourier transform infrared spectroscopy (FTIR) and Raman spectroscopy allowed the detection of

functional groups and quantify the [OH] concentration. The microstructure of the samples was examined using scanning electron microscope (SEM). The surface charge was determined from the photoelectron work function measurements.

RESULTS AND DISCUSSION

XRD results showed that all coatings are hydroxyapatite with good crystal alignment and a small amount (~5%) of tricalcium phosphate.

Post treatment with water vapour to restore [OH] in the HAp structure, depleted during the high temperature spraying, was observed with FTIR spectroscopy. FTIR results showed that samples subjected to water vapour contain more [OH] groups in the structure compared to the conventional procedure for coating.

The electric field during the spraying procedure was applied to promote the polarization of the HAp particles which leads to enhanced surface charge, however the conductivity within the flame lowered the effective electric field. Analysis of the electron work function revealed the highest level for the coatings sprayed through the electrical field followed by water vapour treatment also in the electrical field. Based on previous work that shows rehydroxylation on the very surface [3], it is believed that the retention of the electric field assists the orientation of [OH] despite the absence of the higher water vapour level during the initial period of generating steam.

The combination of the oriented grains together with a [OH] guidance mechanism and higher water vapour content is important to optimize the charge on the coating surface. This will further improve the remodeling capability found with oriented coatings [2].

CONCLUSION

In-situ charge generation of thermal spray hydroxyapatite technique was developed. The retention of [OH] in the lattice requires the presence of steam after coating. A higher [OH] content in the structure and electrical field favours polarization in the HAp splats.

REFERENCES

1. Nakamura S. et al. J. Biomed. Mater. Res. 61: 593–99, 2002.
2. Gross K.A. et al. Acta Biomater. 8: 1948-56, 2012.
3. Gross K.A. et al. J. Mater. Sci. 33: 3985-3991, 1998.

ACKNOWLEDGMENTS

KAG was supported by a Marie Curie reintegration grant (#PIRG05-GA-2009-249306).



Preparation and Characterization of Porous Hydroxyapatite Based Microcarriers for Cell and Drug Delivery

Merve Guldiken¹, Caner Durucan^{3,4}, Can Özen¹, Dilek Keskin^{1,2} and Ayşen Tezcaner^{1,2}

¹ Department of Biotechnology, Middle East Technical University, Turkey,

² Department of Engineering Sciences, Middle East Technical University, Turkey,

³ Biomaterials and Tissue Engineering Center of Excellence, Middle East Technical University, Turkey,

⁴ Department of Metallurgical and Materials Engineering, Middle East Technical University, Turkey,

e177435@metu.edu.tr

INTRODUCTION

Microcarrier systems have been widely used because of their practical and commercial value in the production and delivery of biological substances including vaccines, antibodies, enzymes, hormones and nucleic acids. In recent years, the microcarriers have often been preferred for cell culture studies in tissue engineering applications. Spherical particles provide large surface to volume ratio, consequently, the microcarriers reduce the required space with respect to monolayer cell culture. Suspension culture requires less cell density and culture media [2].

The aim of this study is to prepare and characterize porous hydroxyapatite (HAP) microcarrier system that will serve as both statin and cell delivery system for bone tissue engineering applications.

EXPERIMENTAL METHODS

Preparation of Microcarriers

Microcarriers were prepared by modified W/O emulsion method (1). Briefly, HAP powders were mixed with camphene (Sigma, USA) in a ratio of 1:0.9 (w/w) and stirred with a magnetic stirrer at 60°C. After that, the slurry was mixed with 10% w/v gelatin (Sigma, USA) solution in 2% PVA (Sigma, USA) aqueous solution in the ratio of 1 g HAP powder per 2 ml gelatin solution. After surfactants were added, the whole slurry was dispersed into oil phase and was stirred at 350 rpm overnight. Prepared microcarriers were rapidly solidified in ice cooled bath at 4°C for 5 min. Microcarriers were then filtered and rinsed with ethanol (Sigma, USA). Filtered products were stored at -80°C for 10 minute and camphene was sublimated in freeze dryer overnight. Dried products were sintered at 1250°C for 3 h and left to cool at room temperature.

Drug Encapsulation

Simvastatin (SIM) at a concentration of 1, 0.5, 0.1, 0.01 mg/mL (n=4) in methanol were used for drug loading. 20 mg microcarriers were soaked in a glass tube containing 1 ml of each concentration for 2 hours. Drug loading efficiency was studied by UV-HPLC (High Performance Liquid Chromatography). In vitro release studies are being conducted.

Cell culture Studies

In vitro cell culture studies using unloaded HA microcarriers were conducted with Saos-2 cells. 24 hours after cell seeding, the cells were investigated by SEM (Scanning Electron Microscopy) and CLSM (confocal laser scanning microscopy, Zeiss LSM 510). For confocal imaging, the nuclei and F-actins intermediate filaments of cells were stained with Propidium iodide (PI, red) and fluorescent phalloidin (phalloidin-FITC, green), respectively.

RESULTS AND DISCUSSION

Sintered microcarriers were examined by CLSM. Non-specific FITC staining of microcarriers was also observed. Only nuclei of attached cells were stained. After 24 hour of cell seeding, it was found that the cells were attached and spread on microcarriers surface (Figure 1). Strong signals were observed up to 63 µm from stained cells with PI (as seen in Figure 1) and the intensity of those signals diminished starting from 120 µm. The cell penetration into microcarriers suggests that the interconnectivity is high in porous carriers. Cell growth into the pores was observed in Z-stack analyses with CLSM. Drug loading efficiency decreased when 100µg/mL or lower drug concentration was used for loading.

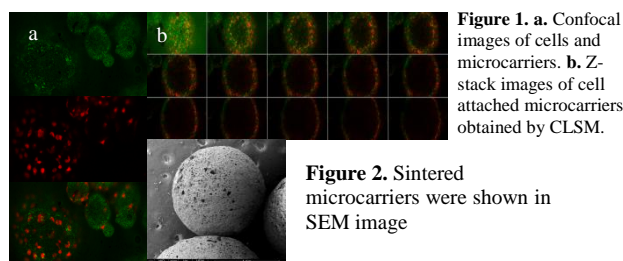


Figure 1. a. Confocal images of cells and microcarriers. b. Z-stack images of cell attached microcarriers obtained by CLSM.

Figure 2. Sintered microcarriers were shown in SEM image

Table 1. Drug loading amounts

Stock Solution (n=4)	Loading (µg/mg microcarriers)	Drug Encapsulation efficiency
1000µg/mL(1mg/ml)	48 ± 2 µg/mg	96.1 %
500 µg/mL	23.60 ± 2 µg/mg	94.42 %
100 µg/mL	3.23± 2 µg/mg	64.63 %
10 µg/mL	0.4± 2 µg/mg	87.7 %

CONCLUSION

Microcarriers are promising options for drug and cell delivery in bone tissue engineering. Porous microcarriers and their cell compatibility were proved. According to these results, release properties of drug loaded microcarriers and their osteogenic activity on cells will be examined.

REFERENCES

1. Yang, J.-H. et al., J.Biomed Mater. Res B, *App. Biomater*, (2011), 99(1) :150–7
2. Goh et al., BioResearch Open Access, 2:2, 84-97, 2013

ACKNOWLEDGMENTS

The authors would like to thank Middle East Technical University (project no: BAP-03-10-2012-001) for providing financial support to this project. The authors also thank Gözde Alkan for her assistance in SEM analyses.

***In Vitro* studies to measure the inflammatory response of crosslinked poly(lactide-co-caprolactone) dimethacrylate scaffolds**

David Shepherd¹, Laura Brown¹, Leander Poozca², Gerhard Hildebrand², Klaus Liefeth², Roger Brooks³, Serena Best¹

¹CCMM, Department of Materials Science and Metallurgy, University of Cambridge, United Kingdom

²Institute for Bioprocessing and Analytical Measurement Techniques e.V., Heilbad Heiligenstadt, Germany

³Orthopaedic Research, Addenbrooke's Hospital, University of Cambridge, United Kingdom

dvs23@cam.ac.uk

INTRODUCTION

Current implant materials may limit bone healing as a result of inflammation, poor vascularisation and improper mechanical strength and durability. Therefore there is a need for a novel material to overcome these limitations. It is hoped a new smart bioactive 3D scaffold containing a biogel with growth factors and calcium phosphate particles will address these concerns. The work presented here shows investigations carried out using monocytes to measure the inflammatory response to poly(lactide-co-caprolactone) dimethacrylate (LCM) that form the scaffolds. Where the amount of caprolactone (CL) and lactide (LA) was varied to compare the osteoconductive material characteristics of slow, acid-free degradation (CL) and a high stiffness (LA) against the disadvantages like softening of the material (CL) and fast degradation with problems of local acidification (LA). Initial work was carried out on solid discs of the material before the polymeric scaffolds were produced and also characterised using primary human monocytes.

EXPERIMENTAL METHODS

LCM was produced consisting of 10 (LCM 6.1) or 20 (LCM 3, 4) monomer units with varying ratios of lactide and caprolactone synthesized by stannous catalyzed ring-opening polymerization of cyclic caprolactone and the D,L-lactide dimer, where diethylene glycol is the starting alcohol. The materials were then either made into discs through UV cross linking or a scaffold with microstructure of 500µm Schwarz P unit cell with pore sizes of around 300µm and a total porosity of 0.66% which was generated by the two-photon polymerization with a Ti:Sapphire femtosecond laser, followed by development in acetone. Prior to use the scaffolds and discs were sterilized using gamma sterilization.

Monocytes were derived from a leukocyte cone (National Blood Service) through density centrifugation with a gradient and then labeling for CD14⁺ monocytes through CD14 antibody coated magnetic bead selection (Miltenyi Biotec). These were then seeded onto the materials (initially discs and later scaffolds) and cultured for up to 7 days, with media removed and replaced at regular intervals to measure the production of TNF- α , IL-6 and LDH. Controls were used including a positive control, lipopolysaccharide (LPS); negative control, cells seeded on tissue culture plastic (TCP); and commercial material Vitoss for scaffolds.

RESULTS AND DISCUSSION

The levels of LDH are shown in *Figure 1*. Levels were similar for each of the polymers.

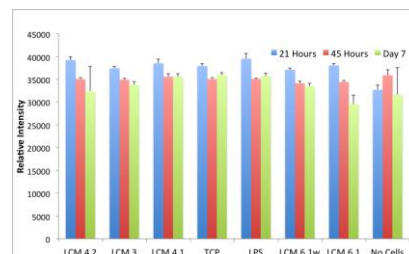


Figure 1: Levels of LDH present with various samples of LCM (6.1_w indicates samples were pre-wetted, 4₁ and 4₂ indicate differing photo-initiators) and controls

When TNF- α was measured (*Figure 2*) levels were also found to be similar. The levels of IL-6 present were negligible for all samples apart from the LPS positive control (*Figure 3*). Work on scaffolds showed that there were similar responses for small samples ($\approx 8\text{mm}^3$).

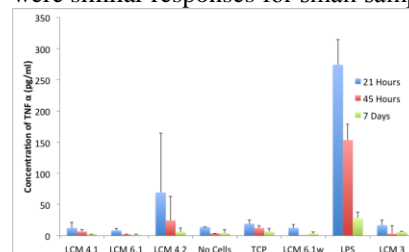


Figure 2: Levels of TNF- α present with various samples of LCM (6.1_w indicates samples were pre-wetted, 4₁ and 4₂ indicate differing photo-initiators) and controls.

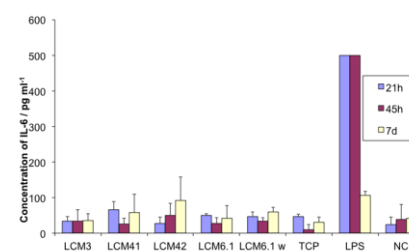


Figure 3: Levels of IL-6 present with various samples of LCM (6.1_w indicates samples were pre-wetted, 4₁ and 4₂ indicate differing photo-initiators) and controls.

CONCLUSION

The inflammatory response of materials made of LCM with varying monomer composition was investigated using monocytes and found to produce neither an inflammatory nor a cytotoxic response.

ACKNOWLEDGMENTS

The authors would like to acknowledge EU FP7 Grant Agreement No. 263363 INNOVABONE and funding from EPSRC for LB and NIHR for RB.

A comparison of two approaches to the formation of antibacterial surfaces: doping with bactericidal element vs drug loading

I.V. Batenina¹, D.V. Shtansky¹, Ph.V. Kiryukhantsev-Korneev¹,
A.N. Sheveyko¹, N.Yu. Anisimova² and N.A. Gloushankova²

¹ National University of Science and Technology "MISIS", Russia, irina_btnn@mail.ru

² N.N. Blokhin Russian Cancer Research Centre of RAMS, Russia

INTRODUCTION

During the past decade, various advanced materials with bactericidal properties have been developed [1]. Implant-related microbial infection can be reduced by using materials with antimicrobial properties. Comparative investigation of different approaches to surface fictionalization by giving antibacterial characteristics is presented. The surface modification was fulfilled either by Ag-doped TiCaPCON film deposition or by development of a surface roughness following by drug loading. Antibacterial effects against pathogenic bacteria *S.aureus*, *S.epidermis*, and *K.pneum ozanae* were studied.

EXPERIMENTAL METHODS

The substrates intended for drug loading were produced by selective laser sintering. The Ti substrate with pre-coated Ti powder layers was scanned by laser beam in two orthogonal directions two form a network structure with square-shaped blind pores. 3 mg of lyophilized Augmentin (SmithKline Beecham PLS, United Kingdom) with ratio Amoxicillin/clavulanic acid=5:1 was dissolved in 10 ml and 1 ml of sterile Hanks solution (PanEko, Russia). Augmentin concentration was 0.3 mg/ml and 3 mg/ml, respectively. Samples were covered by 100 µl of the solution. After water evaporation, the formed precipitate was embeded into the sample relief using disposable spreader (SPL Life Science). TiCaPCON films with 0.7-4% of Ag were deposited by simultaneous sputtering of TiC-Ca₃(PO₄)₂ and Ag targets.

To evaluate chondrocytes adhesion to the TiCaPCON-Ag films, DiOC6 staining was used. The biocompatibility of films was investigated by means of MTS and Picogreen tests. The bioactivity of the TiCaPCON-Ag films and SLS/Augmentin samples was evaluated using ALP activity test.

RESULTS AND DISCUSSION

The results obtained show that the Ag-doped films did not inhibit the growth of all tested bacteria, but were able to change the bacterial colony morphology. In general, *K.pneum. ozanae* form circular mucous grayish white colonies, but in the presence of 0.7% Ag *K.pneum. ozanae* colonies take an irregular shape. In the case of materials loaded with *Augmentin*, pronounced inhibition zones were observed. When an amount of *Augmentin* was increased from 2.4 mg to 4 mg, the size of inhibition zone after 48 hours raised from 11.3 mm to 18.7 mm against *S. aureus*, from 15.7

mm to 16.4 mm against *S.epidermidis*, and from 8.1 mm to 9.7 mm against *K. pneum. ozanae*.

In vitro test showed no toxic effect of all used concentrations of *Augmentin* for MC3T3-E1 cells. The cells underwent osteogenic differentiation and exhibited a high level alkaline phosphatase activity. We did not find statistically significant differences in the ALP activity of cells cultivated on *Augmentin*-doped Ti samples.

To assess whether the drug can easily be washed away from the rough surface, the SLS samples were preliminary held in Hanks solution for 1, 2 and 3 days. The subsequent antibacterial tests showed that after 1 day immersion in Hanks solution, the bacteria growth was suppressed for 1 day compared to untreated samples which demonstrated longer effect for 4 days.

The best chondrocytes adhesion was observed on the surface of Ag-free TiCaPCON films. Doping with Ag slightly decreased the chondrocytes adhesion, but the results were not statistically different from the control (glass). According to MTS test, the presence of Ag resulted in the slowing of metabolism leaving the cells life unaffected. After 4 days of cultivation, all films had the same level of cells proliferation. It is known that Ag ions can replace the ions of microelements in the enzymes responsible for the metabolism and reproduction. This leads to disruption of cell function and its death. In the case of Ag-doped TiCaPCON films, bactericide element had a tendency to suppress the cells metabolism but did not cause the cells death.

CONCLUSION

This study evaluates antibacterial performance of two types of samples: Ag-doped TiCaPCON films and Ti materials with high surface roughness loaded with *Augmentin*. The sample with medicine can provide a strong antibacterial action at the beginning of implantation without compromise with material bioactivity. Due to the fast drug release, the antibacterial effect was limited to 24 hours. In contrast, the Ag-doped films demonstrated less effective, but longer bactericidal effect (up to 5 days).

REFERENCES

[1] Adv Drug Deliv Rev. 2013 65(1):104-20. Advanced materials and processing for drug delivery: the past and the future. Zhang Y, Chan HF, Leong KW.

ACKNOWLEDGMENTS

The authors would like to thank the Russian Foundation for Basic Research (Grant no: №13-03-12081) for providing financial support to this project



Investigation of Factors Influencing Deposition of Nanocomposite Coating onto Open Cell Foams using Layer-by-Layer Assembly: Design of Experiment Approach

Monika Ziminska¹, Helen McCarthy², Nicholas Dunne¹ and Andrew Hamilton¹

¹School of Mechanical & Aerospace Engineering, Queen's University Belfast, Northern Ireland, mziminska01@qub.ac.uk

²School of Pharmacy, Queen's University Belfast, Northern Ireland

INTRODUCTION

Sufficient structural integrity and a porous architecture that supports tissue cell in-growth are crucial characteristics for functional bone tissue scaffold designs. Scaffolds have a load-bearing function and are often exposed to high levels of mechanical stress; hence an adequate level of strength and stiffness is a fundamental requirement. A high level of interconnected porosity is also required to stimulate bone growth into the scaffold, however high porosity reduces the mechanical properties. (1) This on-going challenge can potentially be addressed by deposition of a stiff and strong polymer-nanocomposite coating assembled onto a porous template using Layer-by-Layer (LbL) deposition. LbL assembly involves the adsorption of oppositely charged polyelectrolytes onto a substrate resulting in multilayer films, and has been established as one of the most versatile means to control film properties and molecular architecture at the nanoscale level. (3).

The aim of this study was to quantify the influence of fabrication parameters on the mechanical properties of porous substrates coated with polymer nanocomposites assembled via LbL deposition. A Design of Experiments (DoE) approach was used to correlate a range of processing parameters with the compressive modulus of nanocomposite-coated foams.

EXPERIMENTAL METHODS

The processing parameters investigated include: pH of Polyacrylic Acid (PAA) and Polyethyleneamine (PEI), number of multilayer deposited between samples drying, adsorption time, and salt concentration. The ranges of interest given in Table 1 were selected based on a review of relevant literature (4), and Design-Expert Version 5.0.8 (State-Ease) (DoE) software was used to determine the parameter space for experimental investigation.

Table 1: DoE Factors

	Factor	Unit	Low	High
A	PAA pH	[H+]	4	9
B	PEI pH	[H+]	7	10
C	Drying	no. of m-layers	5	15
D	Deposition time	sec	30	45
E	Salt concentration	M	0	2

LbL deposition was conducted using aqueous solutions of 50 wt.% PEI, MW 750,000, 35 wt.% PAA, MW 100,000, and hydrophilic bentonite nanoclay, MW 180.1 (Sigma Aldrich). Solutions were prepared as previously described (5). The open-cell polyurethane (PU) foam substrates (45 PPI) were purchased from EasyFoam Ltd.

Prior to LbL deposition, the foam substrates were cut into cylinders (dia. 12.7 mm height 10 mm), rinsed with de-ionised (DI) H₂O and dried with compressed air. Substrates were then alternately subjected to cationic (PEI), and anionic (PAA and nanoclay) solutions using a custom-built apparatus that controls fluid flow through the substrates. Each solution rinse was followed by rinsing with DI H₂O to prevent intermingling of oppositely charged mixtures.

The full PEI/PAA/PEI/bentonite deposition cycle was repeated in intervals of 5 multilayers to obtain the total desired number of multilayers. The coated samples were dried for 24 h in a desiccator after each interval and the total mass of the coating was determined before subsequent deposition of additional multilayers. Mechanical properties of coated foams were determined by quasi-static mechanical testing in compression using a Texture Analyser (Manson Technology TA-XT2i) and following ASTM D1621-10 with non-standard specimen sizes.

RESULTS AND DISCUSSION

The initial set of coated samples were fabricated under the following fabrication conditions: PAA pH 9, PEI pH 10, 5 m-layers deposited between drying, salt concentration 0, deposition time 30 sec. Gravimetric results reveal a consistent increase in mass as a function of the number of multilayers deposited.

The results of mechanical tests on uncoated foams, and foams coated with 60 multilayers of nanocomposite coating indicate an increase in stiffness (166%) compared to the uncoated foams (Table 2).

Table 2: Elastic Modulus \pm SD for $n \geq 3$

	Uncoated	60 m-layers
Modulus (kPa)	70.81	188.75
Standard Dev.	18.76	54.84

Representative stress-strain curves for uncoated and nanocomposite-coated specimens (Fig. 1) illustrate this increase in stiffness derived from the coating.

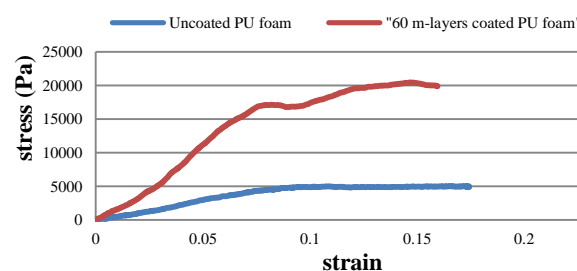


Figure 1: Stress-strain curves for uncoated and nanocomposite coated PU foams.

Extending this experimental investigation over the range of processing parameters will determine the fabrication conditions for obtaining materials with suitable mechanical properties and pore structure for bone tissue scaffold applications.

REFERENCES

- Hutmacher, D. (*et al*), J Tissue Eng Regen M, 1: 245-60, 2007.
- Decher, G. (*et al*), Multilayer Thin Films – Seq. Assem. of Nanocomp. Mat. Wiley-VCH, 2012.
- Yoo, D (*et al*), Macromolecules, 31: 4309 – 18, 1998.
- Podsiadlo, P. (*et al*), Nano Lett, 8: 1762-70, 2008.
- Ziminska, M. (*et al*), Proceedings of the 20th BinI Conference, Limerick, Ireland, 2014.

In-vivo response of a novel Ti-Ta-Zr-Nb alloy for medical implants

Patrik Stenlund^{1,2*}, Omar Omar^{1,5}, Ulrika Brohede^{1,3}, Susanne Norgren^{1,2,3}, Lena Emanuelsson^{1,5}, Jukka Lausmaa^{1,2}, Peter Thomsen^{1,5} and Anders Palmquist^{1,5}

¹BIOMATCELL VINN Excellence Center of Biomaterials and Cell Therapy, Sweden

²Dept. of Chemistry, Materials and Surfaces, SP Technical Research Institute of Sweden, patrik.stenlund@sp.se

³Sandvik Coromant R&D, Stockholm, Sweden

⁴Dept. of Engineering Sciences, Appl. Mat. Sci., Ångström Laboratory, Uppsala University, Sweden

⁵Dept. of Biomaterials, Sahlgrenska Academy at University of Gothenburg, Sweden,

INTRODUCTION

Today, the need for medical devices is higher than ever and there is an increasing demand for stronger materials allowing reduced dimensions with sustained mechanical properties. The material needs to be biocompatible in order for the long-term osseointegration to be successful. The Ti-6Al-4V alloy has long been favoured as implant material for high load applications, such as hip arthroplasty and small diameter dental implants. However, concerns have been raised about the potential harmful effect of Al and V motivating research towards the development of new materials¹.

The present work evaluates a novel Ti-Ta-Zr-Nb alloy, i.e. only consisting of elements considered non-toxic and biocompatible *in-vivo*², using a well-established rat model with an early and a late time point of 7 and 28 days, respectively.

EXPERIMENTAL METHODS

Screw-shaped implants, total length of 2.3 mm, Ø 2 mm and discs with Ø 9 mm were manufactured from cp-Ti grade IV (denoted TiGr4) and Ti-10.1Ta-1.7Zr-1.6Nb (denoted TiAlloy). All implant surfaces were modified by acid etching. The physicochemical properties of the implant surfaces were characterized by SEM (stereo), XPS and contact angle measurements. Screw-shaped implants were implanted in the rat tibia (4 implants per animal) for 7 or 28 days. Half of the implants underwent biomechanical evaluation. Thereafter all implants were retrieved en bloc and processed for histology, histomorphometry and electron microscopy.

RESULTS AND DISCUSSION

The two materials showed similar surface morphology, topography (3D-SEM) and wettability (contact angle). The surface chemistry analysis (XPS) indicates a thin (<10nm) TiO₂ oxide layer for both materials, but with enrichment of Ta and Nb at the TiAlloy surface.

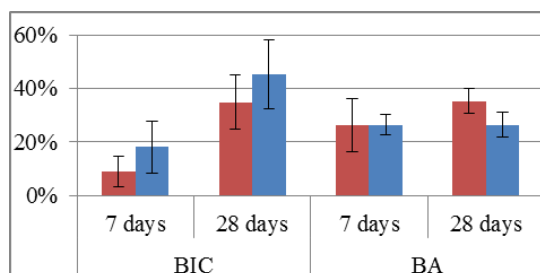


Fig. 1. The histomorphometry presented as the mean bone implant contact (BIC) and the mean bone area (BA) within all threads of each implant. (Red: TiGr4, Blue: TiAlloy, standard deviations are indicated).

The quantitative histomorphometry showed significantly higher bone-implant contact (BIC) for the TiAlloy surface compared to the TiGr4 surface at 7 days, with a similar trend at 28 days (Fig. 1). The amount of bone around the implants, as judged by the bone area (BA) within the threads, showed significantly higher values for the TiGr4 implant compared to the TiAlloy at 28 days, while no difference was observed at 7 days.

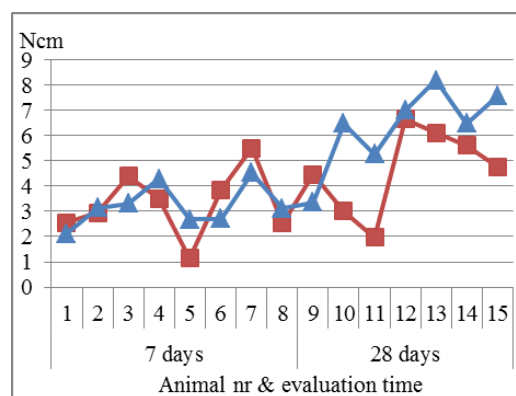


Fig. 2. Maximal removal torque of individual animal retrieved implants at 7 and 28 days, respectively. (Red: TiGr4, Blue: TiAlloy).

The implant stability evaluation revealed equally high removal torque for both materials at either time point, even though the TiAlloy material showed a tendency ($p=0.0614$) towards higher stability at the later time point (Fig. 2).

CONCLUSION

The Ti alloy has proven as biocompatible as Ti grade 4 and showing good osseointegration levels. The Ti alloy displays significantly higher bone implant contact and a trend towards higher mechanical implant stability after 4 weeks *in-vivo* compared to the Ti grade 4.

REFERENCES

- Haynes, D.R. *et al.*, Journal of Bone and Joint Surgery-American Volume 1993;75A:825-34.
- Matsuno, H. *et al.*, Biomaterials 2001;22:1253-62.

ACKNOWLEDGMENTS

BIOMATCELL VINN Excellence Center of Biomaterials and Cell Therapy, the Region Västra Götaland, the Swedish Research Council, and the Hjalmar Svensson Foundation are gratefully acknowledged for providing financial support to this project.



Adipose derived stem cells cultured in 2D and 3D settings for the use in bone tissue engineering

Claudia Kleinhans^{1,2}, Inga Satler², Lena Schmohl², Jakob Barz², Thomas Schiestel², Günter Tovar^{1,2}, Petra J. Kluger^{2,3}

¹Institute for Interfacial Process Engineering and Plasma Technology IGVP, University of Stuttgart, Nobelstr. 12, 70569 Stuttgart, Germany, claudia.kleinhans@igb.fraunhofer.de

²Fraunhofer Institute for Interfacial Engineering and Biotechnology IGB, Stuttgart, Germany

³Hochschule Reutlingen, Process Analysis & Technology (PA&T), Reutlingen

INTRODUCTION

Adipose tissue is an abundant source of mesenchymal stem cells (MSCs). Two major advantages are displayed by using adipose derived stem cells (ASCs) in contrast to MSCs from bone marrow: the isolation is more comfortable for the patient and adipose tissue is supposed to have a higher frequency of stem cells (1). It would be a benefit if ASCs could be used for bone-tissue engineering.

In this study we evaluated the potential of human ASCs as an alternative cell source in 2D and 3D environments. Therefore, we characterized the cells and seeded them on planar polystyrene samples but also on porous, ammonia-plasma treated polylactid-hydroxyapatite (PLA-HA) scaffolds to analyze their osteogenic differentiation in comparison to hMSCs.

EXPERIMENTAL METHODS

Human ASCs were isolated of lipoaspirate and were characterized by FACS analysis, histochemical stainings and qRT-PCR studies.

3D-scaffolds were treated by low pressure ammonia-plasma and examined concerning cell distribution and differentiation within the scaffolds. Several time points (day 1, 7, 14 and 21) were selected to perform histological staining as well as to analyze the gene expression by qRT-PCR experiments.

RESULTS AND DISCUSSION

ASCs were successfully isolated of human lipoaspirate and characterized. MSCs isolated from bone marrow showed a higher osteogenic differentiation potential in the 2D setting, however, a similar osteogenic related marker expression was observed in the 3D environment. A nearly homogenous cell distribution within the PLA-HA-composites could be achieved and the expression of Alkaline Phosphatase (ALP), Collagen Type I and Osteopontin as well as a calcificated extracellular matrix were detected in hASCs and hMSCs seeded scaffolds (see figure 1).

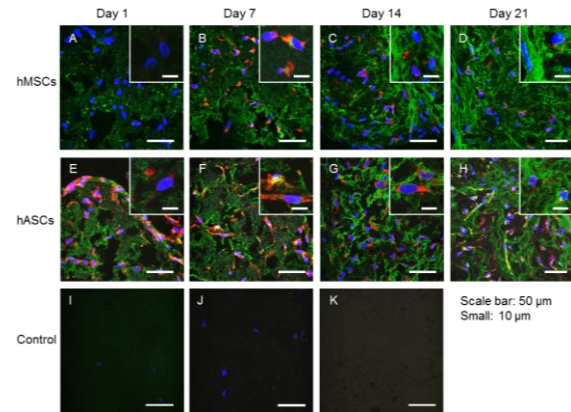


Figure 1: Confocal microscopic analysis of hMSCs and hASCs cultured in NH₃-plasma treated porous PLA-HA scaffolds for 21 days in osteogenic media. Cross sectioning of the scaffold was performed on day 1 (A, E), 7 (B, F), 14 (C, G) and 21 (D, H) and immunofluorescence staining against Col Type I and Alp was conducted. Cell nuclei are stained by DAPI (blue).

DISCUSSION

Essential factors that must be considered in tissue engineering are the availability of a suitable matrix, a sufficient amount of cells and culture conditions that allow a three-dimensional (3D) culture to produce artificial tissue equivalents. The results of this study indicate the importance of a 3D setting that approaches the in vivo situation and should be further extended by e.g. mechanical stimulation or the co-culture with relevant other cells.

CONCLUSION

HASCs are able to differentiate into different tissue cells. For the use in bone tissues engineering the cells are a promising alternative to hMSCs from bone marrow. Osteogenesis related marker expression occurs in a 3D environment and is comparable to the expression of hMSCs.

REFERENCES

1. Fraser *et al.*, Trends Biotechnol Apr;24(4):150-4, 2006

ACKNOWLEDGMENTS

The authors would like to thank the Fraunhofer-Gesellschaft for financial support.

Bioengineered spider silk spheres as anti-cancer drug carriers

Katarzyna Jastrzebska^{1,2}, Anna Florczak^{1,2}, Yinnan Lin³, Rosalyn Abbott³, Andrzej Mackiewicz^{2,4}, David L. Kaplan³, Hanna Dams-Kozłowska^{2,4}

¹ NanoBioMedical Centre, Faculty of Physics, Adam Mickiewicz University, Poznan, Poland

² Department of Cancer Immunology, Chair of Medical Biotechnology, Poznan University of Medical Sciences Poznan, Poland

³ Department of Biomedical Engineering, Tufts University, Medford, MA, USA

⁴ Department of Diagnostics and Cancer Immunology, Greater Poland Cancer Centre, Poznan, Poland
kasia.kz@amu.edu.pl

INTRODUCTION

A drug carrier should fulfill requirements of biocompatibility, biodegradability, nanoscale size as well as ability to bind and release the bioactive compound. The biomaterial used to form a drug delivery vehicle should also be durable enough to transport the active compounds within an organism.

Spider silk proteins have an ability to self-assemble into spherical particles that can be utilized for drug delivery⁽¹⁾. Moreover, the bioengineered proteins can be modified by adding a new functional domain (responsible for binding drug or a cell receptor). The objective of the study was to generate the bioengineered spider silk biomaterial by expression in bacterial culture with efficient purification techniques⁽²⁾, followed by studies of drug loading and release.

EXPERIMENTAL METHODS

The bioengineered spider silk proteins: MS1 and MS2 were derived from the *N. clavipes* spidroins: MaSp1 and MaSp2, respectively. Recombinant proteins were produced in *E. coli* and purified by thermal extraction⁽³⁾. The spherical particles were produced by mixing a soluble silk protein with potassium phosphate at different conditions. Physical properties of the particles were characterized using scanning electron microscopy, infrared spectrometry and zeta potential measurements. Cytotoxicity of the spheres was investigated using a MTT assay. The binding of anti-cancer drugs to the spheres was investigated. The levels of drug incorporation and release profiles of doxorubicin, mitoxantrone and etoposide were studied spectrophotometrically.

RESULTS AND DISCUSSION

The MS1 and MS2 proteins formed spheres of different morphology and size. The size of the particles was controlled by the concentration of the silk protein mixed with phosphate, while the phosphate concentration influenced stability of the silk spheres. The MS1-spheres presented a positive, while MS2 spheres a negative zeta potential. Both particle types were non-toxic towards eukaryotic cells (fibroblasts 3T3) *in vitro*. MS1 particles showed stronger affinity to the anti-cancer drugs doxorubicin and mitoxantrone than MS2

spheres. Doxorubicin showed a pH-dependent release profile from the particles. Both types of drug carriers maintained their spherical structure after 14 days of drug release at physiological conditions *in vitro*.

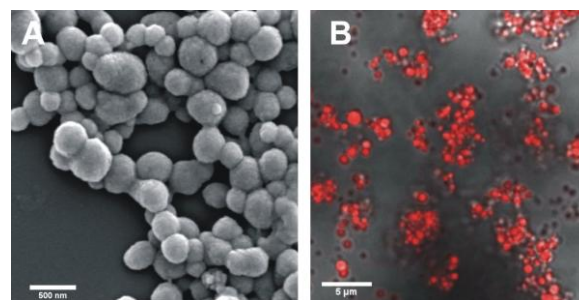


Figure 1: (A) Scanning electron image of the MS2 spheres; (B) Doxorubicin-loaded MS1 spheres under a confocal microscope

CONCLUSIONS

The bioengineered spider silk proteins formed stable spherical particles. Spheres made of the MS1 and MS2 protein showed different properties and different affinity to anti-cancer drugs. The bioengineered silk spheres could target the cancer cells by using a functional domain. Moreover, they are non-toxic and biodegradable. These features, combined with the affinity to anti-cancer drugs will determine the potential of bioengineered spider silk spheres as the drug carriers for cancer therapy.

REFERENCES

1. Lammel A. *et al.*, Biomaterials; 32 (8) 2233–40, 2011
2. Tokareva O. *et al.*, Acta Biomater. 10(4):1612–1626, 2014
3. Dams-Kozłowska H. *et al.* J Biomed Mater Res A. 101A (2) 456–64. 2013

ACKNOWLEDGMENTS

Studies were supported by the International PhD Projects Programme of Foundation for Polish Science operated within the Innovative Economy Operational Programme (IE OP) 2007–2013 within European Regional Development Fund.

Aligned electrospun PLGA fibres reinforcing tubular small intestine submucosa

Omaer Syed¹, Richard Day² Jonathan Knowles¹

¹ Division of Biomaterials and Tissue Engineering, Eastman Dental Institute, UCL, UK

²Centre for Gastroenterology and Nutrition, UCL, UK

omaer.syed.10@ucl.ac.uk

INTRODUCTION

An artificial oesophageal replacement would provide the ability to repair damaged oesophageal tissue as a result of trauma or disease or to replace absent tissue in congenital conditions such as atresia. Tissue engineering has been applied to this problem with limited success though a better understanding of the requirements of such a construct has emerged. It was hypothesized that small intestine submucosa (SIS) would represent a suitable base material from which to form such a construct though it suffers from poor mechanical properties due to early remodeling¹. SIS was produced in a tubular form this was then reinforced with electrospun microfibers of poly(lactic-co-glycolic acid) (PLGA) on a rotating mandrel to reinforce the mechanical properties. This work would form the basis of further work into the construction of a multifaceted scaffold system.

EXPERIMENTAL METHODS

Tubular SIS samples were prepared by well-documented methods² and then decellularised using a detergent-perfusion method. Samples were then freeze dried and mounted on a rotating mandrel. Electrospinning was carried out using a 15%(w/v) solution of PLGA (in 8:2 dichloromethane: dimethylformamide). Samples were coated at the rotational speeds: 10, 500, 1000, 2000, 3000, 4000rpm.

Analysis was carried out by mechanical uniaxial tensile testing carried out in both longitudinal and circumferential directions (n=8) and extensive SEM imaging. The SEM images were analysed to determine the thickness of the electrospun layer, the fibre diameter and the alignment of the fibres. Biocompatibility studies were carried out, with human (o)esophageal smooth muscle cells (HESMC) cultured onto the scaffold samples using a MTS cell viability assay.

RESULTS AND DISCUSSION

SEM imaging showed that the fibre layer thickness and the diameter of the fibres remained largely unaffected by the variations in rotational speeds. Fibre alignment (perpendicular to the long axis of the mandrel) was found to significantly increase in the samples which were electrospun at 2000rpm and higher (the highest percentage of fibres in the 60-90° grouping of alignment

relative to the long axis of the mandrel) which has also been observed in related studies³.

The results indicate that the addition of the fibre layer produced an increase in certain mechanical testing criteria including the elastic modulus, the yield stress and the failure strain for all spun samples when compared to the control. The alignment of the fibres was found altered the properties of the samples. It was found that the failure strain and the elastic modulus of the samples increased as a result of increasing fibre alignment when tested in the direction of the alignment. This was also accompanied by a decrease in the sample properties in the perpendicular direction. A balance of improved properties was found along both testing directions at 2000rpm. The cell viability work showed that the fibre alignment did not alter the biocompatibility of the scaffolds.

CONCLUSION

It was concluded that the addition of an electrospun fibre layer resulted in an increase in the elastic modulus, yield strength and the failure strain of SIS when compared to the control. It was also shown that with rotation of the mandrel at speeds of 2000rpm or higher that the fibres became more highly aligned. The alignment of the fibres resulted in changes in the mechanical properties and it was concluded that the SIS with the layer of fibres spun at 2000rpm had the best balance of elastic modulus, yield stress and failure strain when tested longitudinally and circumferentially. It was speculated that the lower degree of entanglement when the fibres were highly aligned resulted in less mechanical reinforcement when the scaffold was stressed perpendicularly to the alignment of the fibres.

Further work in this will involve more complex characterisation of the scaffolds and a more time-extended cell culture study.

REFERENCES

1. Badylak S. et al., JSR (2001), 99(2): 282-287.
2. Lantz G. et al., ASR (1990), 3(3): 217-227.
3. Subramanian A. et al. Biomedical Materials (2011):6.

ACKNOWLEDGMENTS

The authors would like to thank UCL Grand Challenge for providing financial support to this project.

Hyaluronic Acid Regulation of Cytokine Secretion, GAG Production and Permeability in Urothelial Cells

Peadar Rooney¹ Akshay Srivastava¹, Leo Quinlain², Abhay Pandit^{1*}

¹Network of Excellence for Functional Biomaterials, ²Department of Physiology, National University of Ireland Galway, Ireland, *abhay.pandit@nuigalway.ie

Introduction: Hyaluronic acid has been used in the clinic as an injectable biomaterial treatment for interstitial cystitis (IC). IC is a chronic debilitating disease, with a significant impact on the quality of life for patients. In IC alterations in the proteoglycan composition on the luminal wall of the bladder has been proposed as the primary pathology of IC(1). Previous studies have shown that inflammatory cytokines and glycosaminoglycan levels are drastically altered in urine(2). In order to ultimately create a comprehensive tissue engineering strategy, the mechanistic effects of HA must be investigated. In this study the role of hyaluronic acid (HA) to alter inflammatory cytokines, glycosaminoglycan pathways and permeability of urothelial cells was investigated.

Experimental Methods: Urothelial cells were grown on 0.4µm transwell inserts. The effect of HA on biomolecule migration by measuring the migration of fluorescence labeled dextran, sampling at 2 hr time points. IL-6 and IL-8 ELISA (eBioscience) was performed. DMMB assay was performed for sGAG levels(3). RNA was isolated using RNeasy kit and RNA reverse transcribed using Superscript VILO (Invitrogen), RT-PCR performed using Taqman primers for CSGALNACT1/2 (Hs00218054_m1/ Hs00603821_m1) and HAS2 (Hs00193435_m1) on Lightcycler 480 system (Roche Diagnostics). Relative gene expression was determined using $\Delta\Delta C_T$ method.

Results and Discussion: HA significantly decreases the TNF α induced cytokine expression in urothelial cells (Figure 1A, 1C). Sulphated glycosaminoglycan (sGAG) expression is measured by DMMB assay shows HA significantly increases secreted sGAG (Figure 1B). RT-PCR demonstrated that HA increases the expression of key enzymes involved in the expression of chondroitin sulphate. In order to examine the effect of HA on permeability the expression of tight junction proteins by FACS analysis and permeability using transwell migration assay was performed. The results demonstrate decreased permeability when HA is present on the cells for large molecules (Figure 1D), with no increase in tight junction expression (Figure 1E), suggesting a physiochemical surface interaction, rather than a change in the cellular tight junction expression that alters permeability.

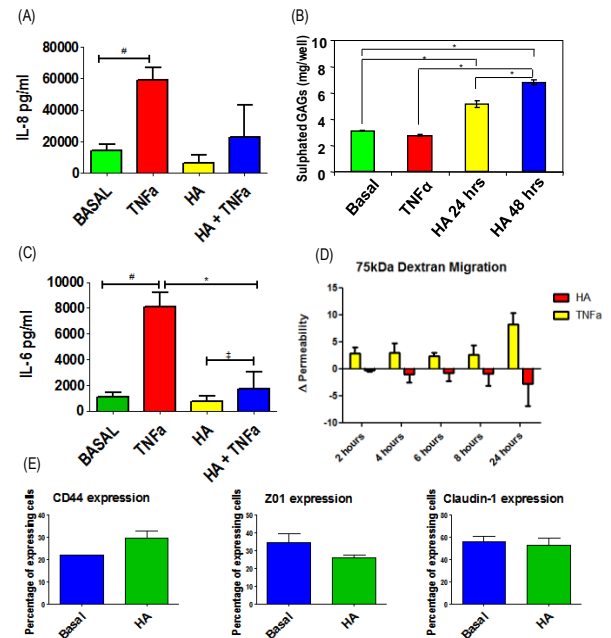


Figure: Urothelial cells secreted significantly higher levels of IL-8 and IL-6 after exposure to TNF α (10ng/ml) compared to basal. HA significantly decreased the effect of TNF α on the secretion of IL-6 (A), and dramatically decreased IL-8 secretion (C). Sulphated GAG secretion significantly increased over 24 and 48 hours when treated with HA (B). HA significantly decreased the permeability of urothelial cells to 150kDa Dextran (D). FACS used to examine the effect of HA on the expression of tight junction expression (E).

Conclusions: These results demonstrate that hyaluronic acid has an anti-inflammatory effect, increases expression of sGAG and increases permeability without altering cell surface proteins closely associated with permeability. Taken together these results show that HA has a significant effect on inflammation and GAG synthesis.

References

1. Erickson DR *et al.* J. Urol. **160**, 1282, 1998;
2. Erickson DR *et al.* J. Urol. **179**, 1850, 2008;
3. Mort JS. Methods Mol. Med. **135**, 201, 2007;

Disclosures: Authors have nothing to disclose.

Acknowledgments: Mylan has provided clinical grade hyaluronic acid (Cystitat). Enterprise Ireland Grant (IP/2011/0096)

Nanohelical Shape and Periodicity dictate Stem Cell Fate

R. K. Das¹, O. F. Zouani¹, G. Kemper¹, L. Plawinski¹, C. Labrugère², R. Oda¹ and M-C. Durrieu¹

¹ Institute of Chemistry & Biology of Membranes & Nanoobjects (CBMN-UMR 5248), IECB, Université Bordeaux, 2 Rue Robert Escarpit, 33607 Pessac, France

² CNRS-Université de Bordeaux, Plateforme Aquitaine de Caractérisation des Matériaux, UMS 3626, 87, avenue du Dr. Schweitzer, 33608 Pessac Cédex, France
r.das@science.ru.nl

INTRODUCTION

Growing tissue from stem cells is a promising approach in tissue engineering because of their pluripotency and long-time proliferation^[1], but their use in regenerative medicine requires understanding and controlling of stem cell actions. Stem cells can be cultivated in designer scaffolds with programmed chemical and physical cues mimicking the extracellular matrix^[2]. Bioactive functionalization and mechanical properties of such scaffolds are known to impact stem cell behaviour^[3]. In this work, we demonstrate how hMSCs adhesion and commitment are influenced by periodicity and shape of a 2D synthetic nanofibrillar matrix^[4].

EXPERIMENTAL METHODS

Chiral structures with different nanometric periodicities (periodicity ~100 nm and 65 nm, respectively) and shapes (twisted vs helical) were synthesized by silica transcription of organic precursors made by self-assembly of enantiomerically pure gemini surfactant tartrates^[5], functionalized with GRGDS and covalently grafted to a glass substrate. Human mesenchymal stem cells were cultured on these substrates and their adhesion (after 24 h) and commitment (after 96 h) were investigated using SEM and immunostaining.

RESULTS AND DISCUSSION

Successful grafting of peptide-functionalized twisted and helical nanoribbons was confirmed by fluorescence microscopy and SEM. Immunostaining revealed more and stronger focal adhesions on helical nanoribbons, compared to samples with twisted nanoribbons. hMSCs on helical ribbons exhibited a lower occurrence of the stem cell marker STRO-1 and significantly stronger expression of osteogenic markers Osterix (Osx) and Osteopontin (OPN) than on the other surfaces, including twisted ribbons and control glass substrates functionalized with RGD.

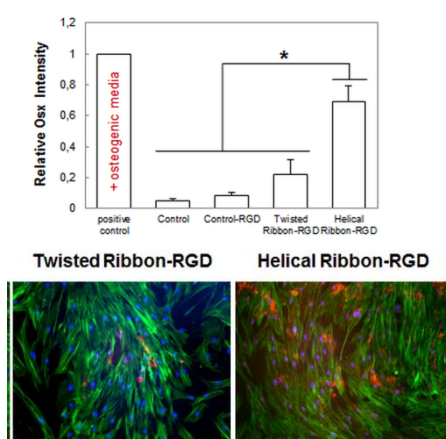


Fig. 1. *Osx* detection in hMSCs on helical ribbons, twisted ribbons, peptide functionalized and unfunctionalized glass substrates (graph, top). OPN detection from fluorescence microscopy (red emission).

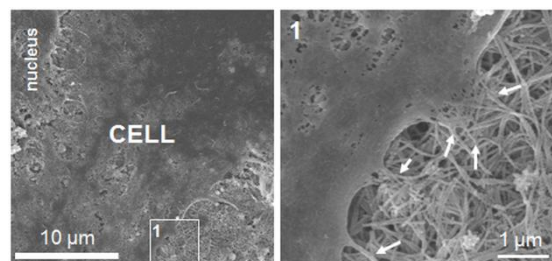


Fig. 2. SEM image of hMSC interaction with helical nanoribbons grafted on functionalized glass substrate

These results imply an enhanced osteogenesis on helical ribbons compared to twisted ribbons. Osteogenic commitment was not observed when blebbistatin was added to block non-muscle myosin II, which suggests that the described effect is probably myosin II-dependent, like the cellular reaction to substrate stiffness.

CONCLUSION

Silica helical nanoribbons with the periodicity of 65 nm promote fibrillar focal adhesion and enhance osteogenic commitment of hMSCs through a non-muscular myosin II dependent pathway, whereas twisted nanoribbons with the periodicity of 100 nm had much less effect on the differentiation. It was clearly demonstrated that significant osteogenesis can be induced simply by choosing adequate nanoperiodicity and shape of our synthetic nano-fibrillar matrix. These results provide promising insight for designing scaffolds for stem cell based bone tissue engineering.

REFERENCES

- [1]. Huebsch N. and Mooney D. J., Nature 462: 426-432 2009
- [2]. Huebsch N. *et al.*, Nat. Mater. 9: 518-526, 2010
- [3]. Engler A. J. *et al.*, Cell 126: 677-689, 2006
- [4] Das R. K. *et al.*, ACS Nano 7: 3351-3361, 2013
- [5]. Oda R. *et al.*, Nature 399: 566-569, 1999.

ACKNOWLEDGMENTS

The authors thank “Région Aquitaine”, the GIS “Advanced Materials in Aquitaine”, the “Agence Nationale pour la Recherche” (ANR) and Erasmus Mundus programme for financial support.

Controlling the Modulus of Gellan Gum Hydrogels for Inkjet Printing Cell Culture Substrates

Sam Moxon & Alan M Smith

Department of Pharmacy, School of Applied Sciences, University of Huddersfield, UK

INTRODUCTION

Successful culturing of tissues within polysaccharide hydrogels is reliant upon specific mechanical properties. Namely the stiffness of the gel has been shown to have a profound effect on cell viability in 3D cell cultures¹. The usual way of tuning the mechanical properties of a hydrogel to suit tissue engineering applications is to change the concentration of polymer used. In this study we have investigated using probe sonication applied at various amplitudes to control the viscosity gellan gum solutions and the viscoelasticity of gellan gum hydrogels cross-linked with DMEM. These modifications could be beneficial when applying gellan gum to bio-ink applications².

EXPERIMENTAL METHODS

Gellan solutions were prepared by dissolving low acyl gellan gum in deionised water at 85°C at a concentration of 1% w/v. Test specific concentrations of gellan were made by diluting this 1% solution accordingly (0.06% to 0.02% w/w for $[\eta]$ measurements and 0.4% w/w was used for steady shear viscosity measurements). Samples were sonicated using an ultrasonic probe at various amplitudes and rheological studies were then conducted using a Bohlin Gemini rheometer. Cooling scans to determine gelation temperature were conducted at a frequency of 10 Rad/s and a constant strain of 0.5%. Solutions were mixed 1:1 with unsupplemented DMEM and cooled at a rate of 2 °C/min and G' and G'' were measured as ions in the DMEM caused gelation of the gellan. Viscosity tests were also conducted. Intrinsic viscosity was calculated using a Rheotek u-tube viscometer and shear thinning behaviour was measured over a shear rates ranging from 0.1 s⁻¹ 1000 s⁻¹ using a Bohlin Gemini rheometer. Following the shear thinning measurements the samples were cross-linked with DMEM and frequency sweeps were conducted to determine the mechanical spectra of the gels.

RESULTS AND DISCUSSION

Table 1 – The impact of sonication amplitude on intrinsic viscosity and dynamic viscosity of gellan gum

Sonication Amplitude (%)	Intrinsic Viscosity (dL/g)	Shear rate s ⁻¹ at which Viscosity is below 0.02 Pas
0	12.927	730
20	7.875	670
40	6.021	570
100	4.991	390

Table 1 highlights that increasing sonication amplitude applied to gellan gum solutions decreased both the

intrinsic viscosity of the samples and the dynamic viscosity. For use as a bio-ink, it has been reported that the polymer solution should have a dynamic viscosity of less than 0.02 Pas³. We have showed that sonication of the samples results in a lower required shear rate to achieve such viscosities. Furthermore, the modulus of gellan gum hydrogels produced following sonication reduced in an exponential fashion as a function of sonication amplitude. Interestingly this did not alter the gelation temperature. This could enable the prediction of a DMEM cross-linked gellan gum construct by a simply determination of the intrinsic viscosity of the sample. Such effects on the gel are thought to be a result of a reduction in the molecular weight of the gellan gum as a direct result of the sonication process. The reduction in molecular weight however was not sufficient to prevent the transition from disordered polymer chains to the ordered conformation which is required for gelation. As a result, the polymer can still form gels but with reduced mechanical strength.

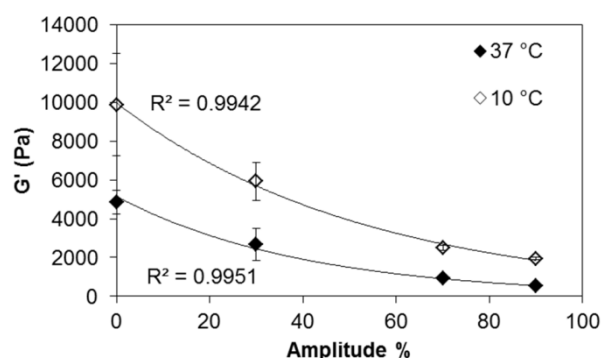


Figure 1 - The reduction of G' in gellan gum hydrogels as a result of sonication

CONCLUSION

In summary, we have showed that it is possible to control both the viscosity and modulus of gellan gum without changing the polymer concentration. This simple approach could be applied to predict gel stiffness in gellan gum cell culture substrates and improve the performance of gellan gum as a bio-ink for ink jet printing of cellular constructs.

REFERENCES

- Engler, A.J. *et al.*, Cell 126:677–689, 2006
- Ferris, C.J. *et al.*, Biomater Sci. 1:224-230 2012
- Sandler, N. *et al.*, J Pharm Sci 100:3386-3395, 2011

ACKNOWLEDGMENTS

Authors would like to acknowledge Professor Liam Grover University of Birmingham for his helpful discussions and the University of Huddersfield for the financial support to this project.



Nano-Micro Architectural Hybrid Composite Scaffold for Bone Tissue Engineering

Prabhash Dadhich¹ and Bodhisatwa Das¹, Pavan Kr. Srivas¹, Pallabi Pal¹, Sabyasachi Ray^{2*} Santanu Dhara¹

^{1*}Biomaterial and Tissue Engineering Laboratory, School of Medical Science and Technology, Indian Institute of Technology Kharagpur, India.

^{2*}Midnapore Medical College and Hospital, India. prabhashd11@gmail.com

INTRODUCTION

Healing of complicated bone fractures, fibrous non-unions and severe trauma require additional support material as scaffolds to aid the healing process¹. Selection of such scaffolds depends on organization behaviour and physico-mechanical properties of bone². Calcium phosphate (CaP) and functionalized biopolymer (FP) based hybrid composite scaffolds have become a promising approach for bone graft replacement. Therefore, development of three dimensional CaP based microstructures intermingled with functionalized polymer has been proposed as an attractive approach for rejuvenation of native tissues towards self-repairing and regeneration.

This hybrid composite mimicking the design from natural bone, as inorganic phase will provide toughness, strength and organic matrix will provide elasticity and resistance to stress, bending and fracture.

EXPERIMENTAL METHODS

Here we represent a method for fabrication of multiphasic highly interconnected multi-scalar porous CaP aligned fibres from natural sources (egg shell). Further, aligned CaP fibres coated with natural origin (chitosan) nano- fibrous patterned FP and intermingled with FP. Scaffolds were characterized for physico-chemical properties using SEM, TEM, EDS, XRD, FTIR, TG-DTA and stereo-zoom microscope. Cells metabolic, attachment, migration, proliferation, differentiation studies were carried out to evaluate its suitability for intended application.

In vivo studies at heterotopic site were conducted in rabbit animal model to assay the osteoinductivity³.

RESULTS AND DISCUSSION

Natural sources were successfully used for synthesis of multiphasic highly interconnected multi-scalar porous, fibrous CaP aligned fibres. Highly porous interconnected microstructure appeared on CaP fibrous scaffolds. CaP provide high mechanical support and interphase for bone tissue growth. Intermingled and integument FP enhance cell attachment and act as non-collagenase proteins during osteogenesis. Not only combination of two different phases, but also their

organization can also be varied with analogues to the bone in terms of microstructure and mechanical properties. CaP based composite scaffold with polymers have pH buffering effect which can control degradation and resorption rate of scaffold.

Preliminary cytotoxicity assay, hemocompatibility assay shown promising results. Mesenchymal stem cells survival percentage, growth rates and differentiation has been found enhanced with scaffolds. During ectopic site implantation, hybrid composite scaffold displayed increased RNA expression of collagen I and osteocalcin.

CONCLUSION

Micro fibrous CaP based hybrid scaffolds can be used as a bone graft replacement. Both the Calcium phosphate phase and functionalized polymer phase are originated from biological waste material, transformed in to biological active material in a cost effective way.

REFERENCES

1. Place, E. S., Evans, N. D., & Stevens, M. M. (2009). Complexity in biomaterials for tissue engineering. *Nature Materials*, 8(6), 457–70. doi:10.1038/nmat2441
2. Bose, S., Roy, M., & Bandyopadhyay, A. (2012). Recent advances in bone tissue engineering scaffolds. *Trends in Biotechnology*, 30(10), 546–54.
3. Barradas, A. M. C., Yuan, H., Blitterswijk, C. A. Van, Habibovic, P., & Medicine, T. (2011). Osteoinductive biomaterials : current knowledge of properties, 21, 407–429.

ACKNOWLEDGMENTS

Authors would like to acknowledge IIT Kharagpur for providing infrastructural facility. Finally, all lab members of Tissue Engineering laboratory at SMST, IIT Kharagpur are acknowledged for support.

Bioactive and Highly Porous Nanofibres via Solution Blow Spinning

Jonny J. Blaker^{1*}, Eudes Leouann², Ana Letícia Braz³, Isaquê Jerônimo², Aldo R. Boccaccini⁴, Juliano E. Oliveira², Eliton S. Medeiros², Showan N. Nazhat⁵

^{1*}School of Materials, Materials Science Centre, Manchester University, UK, jonny.blaker@manchester.ac.uk

²Departamento de Engenharia de Materiais, Federal University of Paraíba (UFPB), Brazil

³Departamento de Ciências Farmacêuticas, Federal University of Paraíba (UFPB), Brazil

⁴Department of Materials Science and Engineering, University of Erlangen-Nuremberg, Germany

⁵McGill University, Materials Engineering, Montreal, Quebec, Canada

INTRODUCTION

We have developed a new combinational technique to rapidly produce porous nanofibres, as well as porous microspheres via solution blow spinning¹ (SBS) and thermally induced phase separation² (TIPS). SBS can produce nanofibres, analogous to those electrospun from polymers dissolved in suitable solvents, yet with a production rate (per head) circa 100 times faster, and without the need for electric fields¹. In this work we freeze the nanofibres shortly after their formation and ahead of excessive solvent evaporation, causing the solvent to freeze and hence phase separation. Subsequent freeze-drying of the fibres removes the solvent, yielding the highly porous nanofibres, and depending on polymer solution concentration, porous microspheres.

EXPERIMENTAL METHODS

Preparation of porous nanofibres and spheres via solution blow spinning

Amorphous polylactide (PLA) (used as a model polymer) was dissolved in dimethyl carbonate, at polymer concentrations (m/v%): 1, 2, 4, 6, 8, 10, 12, 15 and 20%, with respect to the solvent volume, providing a range of viscosities. SBS was conducted using pressures of 10-60 psi, and polymer solution injection rates of 100-200 $\mu\text{L}\cdot\text{min}^{-1}$ via a precision syringe driver. Polymer solutions were jetted directly into a cryogenic bath, which immediately resulted in TIPS of the polymer and solvent within the nanofibres/microspheres. Samples were then lyophilised to yield both porous nanofibres and microspheres, which were characterised by scanning electron microscopy and their diameters and pore dimensions assessed using image J. Nanofibres were rendered bioactive by inclusion of 5 and 10 wt.% bioactive glass nanoparticles (of the same composition as Bioglass45S5@; 20-30 nm in diameter), relative to the polymer, with ultrasonication ahead of SBS.

RESULTS AND DISCUSSION

Polymer solutions of > 6 m/v% formed nanofibres analogous to those spun via electrospinning. However, below concentration of 10 m/v% the presence of porous microspheres become increasingly prevalent, as well as the nanofibres becoming increasingly thinner ($< \sim 200$ nm). Fibres of 15 m/v% had diameters $399 \text{ nm} \pm 134$, and exhibited a highly porous structure consisting of elongated pores of ~ 50 nm by ~ 25 nm, as shown in Figure 1. Thermogravimetric analysis revealed the

bioactive glass content to be within $\pm 2\%$ of the intended filler volumes, indicating successful incorporation.

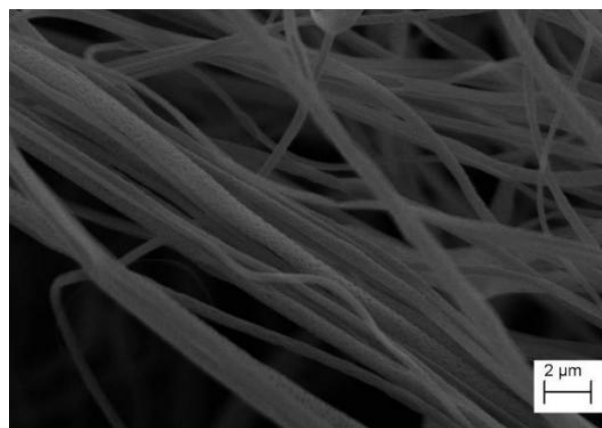


Figure 1. Porous bioactive nanofibres

To the Authors' knowledge this is the first time that SBS has been used to produce porous nanofibres, as well as bioactive porous nanofibres. Porous fibres have been produced using electrospinning yet with substantially lower rates³, our technique allows for the rapid production of open porous cotton-wool like structures.

CONCLUSION

This technique provides a simple and rapid route to produce nanofibres, as well as porous nanofibres, which can be rendered bioactive by bioactive nanoparticle inclusions. Using polymer concentrations lower than 6 m/v% it is also possible to produce highly porous microspheres, with dimensions as small as 500 nm.

REFERENCES

1. Medeiros E. S. *et al.*, J. Appl. Polym. Sci. 113:2322-2330, 2009
2. Blaker J. J. *et al.*, Acta Biomateriala. 4:264-272, 2008
3. McCann J. T. *et al.*, J. Am. Chem. Soc. 128: 1436-1437, 2006

ACKNOWLEDGMENTS

JB acknowledges financial support from CAPES (Brazil), grant number PVE-18523129; JB, SNN and ESM acknowledge joint financial support from DFATD (CBJRP 2013-14 CA-1 McGill University) and CAPES.

The Reciprocal Relationship between Pore Size and Crosslinking, and Their Impact on Porous Scaffold Strength

S. Ali Poursamar¹, Alexander N. Lehner², A.P.M. Antunes^{1*}

¹Institute for Creative Leather Technology, Park Campus, The University of Northampton, UK.

²School of Health, Park Campus, The University of Northampton, UK.

*paula.antunes@northampton.ac.uk

INTRODUCTION

Gas foaming has been frequently used to prepare porous scaffolds. It includes 3 simple steps: Foaming, Casting, and Freezing¹. It was observed that in this method, decision about placing foaming before or after casting can be used to manipulate the scaffold pore size. Using such a feature, in this study two sets of scaffold pore sizes were prepared. Each set were crosslinked with a range of concentrations of glutaraldehyde (GTA) to investigate the reciprocal relationship that exists between pore size and GTA concentration and the effect that they collectively have on the scaffold tensile strength. It was shown that larger pore sizes cause lower tensile strength. However, this effect is more noticeable when the GTA concentration was increased.

EXPERIMENTAL METHODS

20% w/v gelatin aqueous solution was prepared by dissolving gelatin in 60°C de-ionised water. Two varieties of gas foaming method were performed:

- **Foaming BEFORE casting**
0.3g Sodium hydrogen carbonate and 360µl acetic acid were added to gelatin solution to initiate foaming. The foam was then cast in the mold.
- **Foaming AFTER casting**
The gelatin solution was cast in a mold. 0.8g Sodium hydrogen carbonate and 360µl acetic acid were added to the gelatin solution.

Each of these 2 groups of scaffolds were separately crosslinked using 5 different concentrations of GTA (0.00, 0.25, 0.50, 0.75, 1.00% v/v). Tensile tests were performed on each sample using a texture analyser (SMS, Surrey, UK). The obtained results formed triplet data points consisting of: pore size, GTA concentration, and tensile strength. The data points were plotted into a curve fitting software (Lab Fit, V.7.2., www.labfit.net) to find the best fitting binominal function.

RESULTS AND DISCUSSION

As a first result of this study, it was shown that undertaking foaming before casting led to smaller pores. This is due to release of the emitted gas before casting which led to smaller pores. This was independent of GTA concentrations. Fig. 1 shows side by side view of 2 separate SEM images taken from two sets of samples crosslinked at 1.00% GTA. It shows the effect of casting after foaming on the pore size.

Furthermore, the obtained results showed that the scaffolds with smaller pores had a higher tensile strength. This is due to function of pores as crack

initiation sites². Larger pores produce larger longitudinal cracks that lead to weaker scaffolds.

Finally obtained results showed that the effect of pore size on tensile strength is more noticeable when the concentration of GTA is higher. Higher concentration of GTA causes the structure to become more brittle. A more fragile construct is more susceptible to crack growth and fails at lower force³.

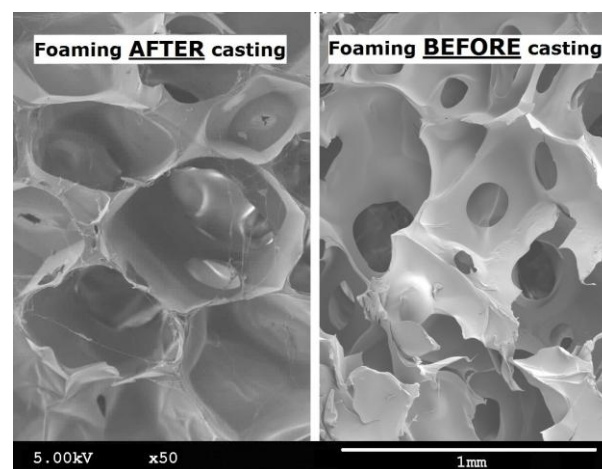


Figure 1: Side by side view of 2 SEM images taken from 2 separate scaffolds crosslinked at 1.00% GTA solution. Foaming after gelatin casting causes larger pores. This effect was independent of GTA concentration.

CONCLUSION

the Equation 1 can be proposed to show the relationship between the pore size, GTA concentration, and how they affect tensile strength. Equation 1 shows that value of GTA concentration exponentially raises the negative impact of pore size on the tensile strength.

$$\text{Tensile Strength} \propto \frac{1}{\text{Pore Size}^{\left(\frac{\text{GTA \%}}{0.03}\right)}} \quad (\text{Equation 1})$$

This study can help highlight the complexity that exists in the mechanical behaviour of porous structure. It illustrates the function of highly reactive crosslinkers like GTA as an element with dual effect. Whilst crosslinking using higher GTA concentration normally causes the mechanical strength to increase, in the case of a porous structure it can have a negative impact on the strength by turning the structure more brittle and enhancing the detrimental effect of pore size.

REFERENCES

1. Dehghani F., Curr. Opin. Biotech., 22:661-6, 2011
2. Liu X. Biomaterials, 27:3980-7, 2006
3. Price, C.A., J. Dent Res, 65:987-92, 1986

Tuning the 3D Architecture of Gelatin Hydrogel-PLLA Combination Scaffolds

Jasper Van Hoorick¹, Marica Markovic², Aleksandr Ovsianikov², Tristan Fowler³, Oskar Hoffmann³, Peter Dubrue¹ and Sandra Van Vlierberghe^{1*}

^{1*}Polymer Chemistry & Biomaterials Research Group, Ghent University, Belgium, sandra.vanvlierberghe@ugent.be

²Institute of Materials Science and Technology, Vienna University of Technology (TU Wien), Austria

³Dept. of Pharmacology and Toxicology, University of Vienna, Austria

INTRODUCTION

The present work aims at the development of 3D scaffolds using both fused deposition modelling as well as a cryogenic treatment to create a fully interconnected pore network. Two material classes will be applied as starting compounds including polyesters (for their mechanical properties) and crosslinkable gelatin precursors (for their cell-interactive properties).

EXPERIMENTAL METHODS

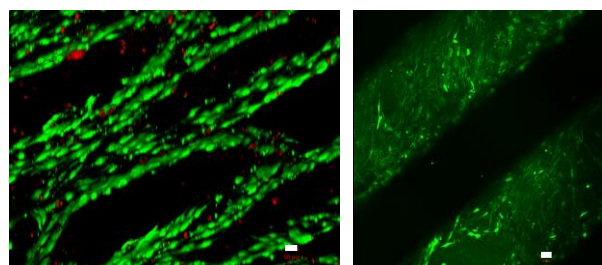
In a first part, poly-L-lactic acid (PLA) was processed using fused deposition modelling (Ultimaker). Next, the porous PLA scaffolds were incubated in aqueous methacrylamide-modified gelatin (gel-MOD) solutions of varying concentrations (i.e. 2 – 10 w/v%) containing 2 mol% Irgacure 2959. The gelatin applied had a modification degree of 80%. Next, after vacuum application, the scaffolds were exposed to UV-light (365 nm) for 2 hours, placed in a cryo-unit and cooled from room temperature to -30°C during 5.5 hours while applying a temperature gradient of 30°C between top and bottom of the scaffolds. In a final step, the frozen hydrogel-PLA combination scaffolds were transferred to a freeze-dryer to remove the ice crystals. The scaffolds were characterized using micro-computed tomography (μ CT) and scanning electron microscopy (SEM). In addition, we assessed the *in vitro* swelling behaviour, the mechanical properties and the degradation behaviour. Furthermore, MC3T3 cells were seeded onto the scaffolds to determine cell interaction, attachment and proliferation.

In parallel, similar hydrogel precursor solutions containing MC3T3 cells were introduced into the 3D printed PLA scaffolds, followed by hydrogel crosslinking through UV irradiation. The scaffolds containing encapsulated cells were characterized using confocal laser scanning microscopy and Presto blue to determine cellular metabolic activity.

RESULTS AND DISCUSSION

First, the efficiency of the UV crosslinking of gel-MOD was assessed after its introduction in the porous PLA. Interestingly, the results indicated that relatively high gel fractions were obtained varying according to the polymer concentration applied which were comparable to the ones obtained in the absence of PLA. *In vitro* degradation tests indicated that the crosslinked gelatin was still prone to degradation in an enzyme containing solution, despite the presence of the surrounding PLA scaffold. Preliminary cell tests showed that upon exceeding a critical gelatin concentration (i.e. 10

w/v%), the presence of cryogels diminished cell migration throughout the PLA scaffolds. Currently, additional cell work is ongoing to optimize the balance between cryogel architecture and stability on the one hand and sufficient cellular infiltration on the other hand. However, the reference samples consisting of crosslinked hydrogel precursors encapsulating MC3T3 cells present in the PLA scaffolds were very promising as indicated in the figures below (scale bars equal 50 μ m). After 7 days, an increase in metabolic activity was observed, indicating the occurrence of cell proliferation in the scaffolds. In addition, live-dead stains only showed a limited number of dead cells due to UV crosslinking (see figure below). Moreover, positive ALP staining indicates the potential for these scaffolds to support osteogenesis.



CONCLUSIONS

The UV crosslinking of cell-interactive hydrogel precursors in the presence of suspended cells is a very valuable route to introduce cells throughout 3D PLA scaffolds. Alternatively, the combination of a gelatin cryogel and a PLA scaffold is a potential candidate for cell seeding purposes in the tissue engineering field. Taken together, these results indicate that the applied polymer-related and cryogenic parameters are crucial to determine the optimal cell seeding efficiency and the ultimate cellular infiltration in 3D PLA scaffolds.

REFERENCES

1. Van Vlierberghe S. *et al.*, Biomacromolecules 8: 331-337, 2007

ACKNOWLEDGMENT

The authors would like to acknowledge the Research Foundation Flanders (FWO-Flanders) for financial support under the form of a post-doctoral fellowship and a Research Grant ('Development of the ideal tissue engineering scaffold by merging state-of-the-art processing techniques', FWO Krediet aan Navorsers).

Fine-Tuning Self-Assembling Peptide Hydrogels for Cell Culture Applications

Laura Szkolar^{1,2}, Alberto Saiani^{1,2}, Aline F Miller², Julie E Gough¹.

¹School of Materials, The University of Manchester, UK

²Manchester Institute of Biotechnology, The University of Manchester, UK Laura.Szkolar@Manchester.ac.uk

INTRODUCTION:

Degenerative diseases of cartilage affect a high proportion of the population. One of the main focuses of current research is to produce replacement cartilage *in-vitro* [1]. For this purpose the design of a suitable 3D scaffold for chondrocyte culture is essential.

Self-assembly has emerged as a powerful tool for the fabrication of novel functional biomaterials [2,3]. A variety of molecular building blocks can be used for this purpose. One such block that has attracted considerable attention in the last 20 years is *de-novo* designed peptides [4]. We have recently developed, in our group, a family of hydrogels that exploit the self-assembling properties of short peptides, typically 8 amino acids long [5,6]. The properties of these hydrogels can be tailored for use in a variety of biomedical application ranging of tissue engineering [7] to drug delivery [8].

In the present work we investigated the effect of peptide charge on the culture of primary bovine chondrocytes. The octapeptide FEFKFEFK (F-8) which is stable at pH 7.5 was shown in a recent work to be suitable for the culture of bovine chondrocytes [7]. The natural ECM exhibits a net positive charge due to the attraction of sodium ions by proteoglycans. For this reason a nonapeptide analog to F-8 comprising an additional positive charge (F-9) was chosen for comparison.

METHODS:

Cells were extracted [9] and cultured in 5 % CO₂ at 37 °C. BC's were maintained in DMEM supplemented with 10 % FBS 1 % antibiotic and 50µg/mL of ascorbic acid. Peptide solutions were prepared at concentrations of 10-30 mg mL⁻¹ and adjusted to pH 7.5 with 1M NaOH. Cells were suspended in media at 5x10⁵ cells per 300µL and cultured in 3D. Cell counting was performed using a haemocytometer by dissolving the gel in excess media.

RESULTS AND DISCUSSION

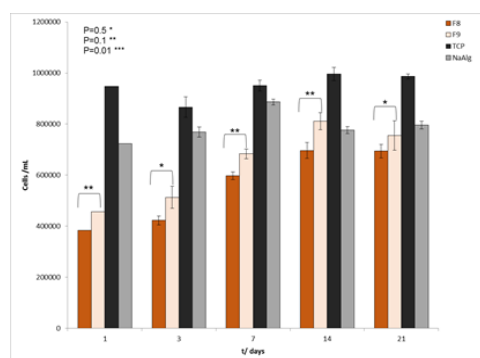


Fig.1) Cell numbers, 21 days on F-8[red] and F-9[pink]. Hydrogels had a G' of 10,000 Pa, 30mgmL⁻¹

Two peptide hydrogels with different net charges at pH 7.5 were produced: F-8 hydrogel neutral and F-9 hydrogel positively charged. The two hydrogel moduli were kept constant by changing the concentration of peptide used to ensure that the differences observed are due to overall hydrogel charge and not differing mechanical properties.

Primary Bovine chondrocytes were cultured in 3D for 21 days. It was observed cell numbers on F-9 showed a statistically significant increase over the 21 day culture period, when compared with F-8. This suggests that the net-positive charged gel provides a suitable scaffold for bovine chondrocyte proliferation. Between days 14 and 21 it is seen that cell numbers appear to be stable, suggesting the chondrocytes have adapted their non-proliferative state, seen in natural cartilage. Rheological data and antibody staining also supported this idea, with ECM production present.

CONCLUSIONS:

We have shown that the introduction of charge may allow a route by which the proliferation and growth of bovine chondrocytes may be influenced, without the use of growth factors. These primary bovine chondrocytes grown on hydrogels carrying a +1 charge allowed for higher cell numbers than those grown on the neutral charge peptide.

REFERENCES: ¹ Benjamin D. Elder et al (2010) *Neurosurgery* 12:722-727, 201. ² Nicholas Stephanopoulos et al, *Acta Materialia* 61 (2013) 912–930 ³ J.E. Gough, A. Saiani, A.F. Miller; [Bioinspired, Biomimetic and Nanobiomaterials](#), 1, 4-12 (2012) ⁴ Hiroshi Tsutsumi and Hisakazu Mihara, *Mol. Biosyst.*, 2013, 9, 609 ⁵ J.-B. Guilbaud, E. Vey, S. Boothroyd, A.M. Smith, R.V. Ulijn. A. Saiani and A.F. Miller [Langmuir](#), 26, 11297-11303 (2010) ⁶ A. Maslovskis, N. Tirelli, A. Saiani, and A.F. Miller [Soft Matter](#), 7, 6025-6033 (2011) ⁷ A. Mujeib, *Acta Biomater.* 2013 Jan;9(1):4609-17 ⁸ D. Roberts, C. Rochas, A. Saiani, A.F. Miller; [Langmuir](#), 28, 16196–16206 (2012) ⁹ JJABarry (2004) *Biomater* 25:3559-3568

ACKNOWLEDGEMENTS:

Peptisyntha (a member of the Solvay Group), Belgium (<http://www.peptisyntha.com>)

Sol-Gel Dip-Coating for Immobilization of Poly (ϵ -lysine) Dendrons on Biomaterials Surfaces for Regenerative Medicine Applications

Maria Elena Verdenelli¹, Steve Meikle², Matteo Santin², Roberto Chiesa¹

¹Department of Chemistry, Materials and Chemical Engineering, Politecnico di Milano, Milan, Italy

²BrightSTAR Group, School of Pharmacy and Biomolecular Sciences, University of Brighton, UK

verdenelli@hotmail.it

INTRODUCTION

Protein adsorption and the ensuing cell adhesion, events that regulate host responses to materials, occur at the biomaterial-tissue interface, and the physicochemical properties of the material surface modulate these biological events¹. Therefore, in order to improve the biological, chemical and mechanical properties, surface modification is required in many cases². In this research surface modification by sol-gel techniques, one of the most promising solutions for attaching biomolecules onto biomaterial surfaces will be performed, using hyperbranched molecules called dendrons. These dendrons will be modified to promote the adhesion, proliferation and differentiation of specific cell types³ for the regeneration of new tissue i.e. in orthopedic applications for better integration of implants or vascular tissue as a treatment of ischemic injury.

EXPERIMENTAL METHODS

Different sols have been produced and sol-gel coating have been applied to titanium surfaces using a dip coater and samples have been immersed at different speeds. Dendrons branched up to three generations (G3) have been synthesized using solid-phase peptide synthesis. This synthesis process has been used to functionalize the generation 3 dendrons with three specific peptide sequences: -KRSR, to inhibit fibroblast adhesion, -FHRRIKA to facilitate osteoblast migration and -YIGSR to promote osteoblast adhesion. Dendron spray-coating has been applied to the sol-gel coating. Cytotoxicity and cell morphology were assessed *in vitro*, using two cell lines, primary mouse embryonic fibroblast derived cells (3T3) and primary human osteosarcoma derived cells (SAOS-2).

Sol-gel coating has been characterized by stereomicroscopy and scanning electron microscopy (SEM) to analyze the coating structure. Mass spectrometry (MS) has been used to characterize the produced dendrons. To determine if the dendron coating has been effectively applied, ninhydrin test, SEM analysis and preliminary *in vitro* cell studies have been performed.

RESULTS AND DISCUSSION

Macroscopic and SEM analyses have shown that samples immersed at low speeds (40 mm/min) led to a more stable and homogeneous sol-gel coating. SEM images (Fig.1) of the sol-gel coating and the dendron spray coated sol-gel also have shown topographical differences between the samples surfaces. *In vitro* results, in particular from the morphologic analyses, have proven that functionalized dendrimers induce different cellular responses depending. Indeed, -KRSR does not allow fibroblast attachment; -FHRRIKA

supports osteoblast migration and finally -YIGSR induces osteoblast adhesion (Fig.2).

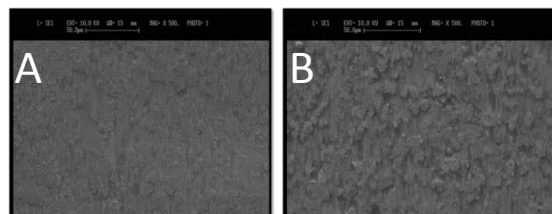


Figure 1. Scanning electron micrographs of Sol-Gel 40% coating (A) and Dendron coating (B)

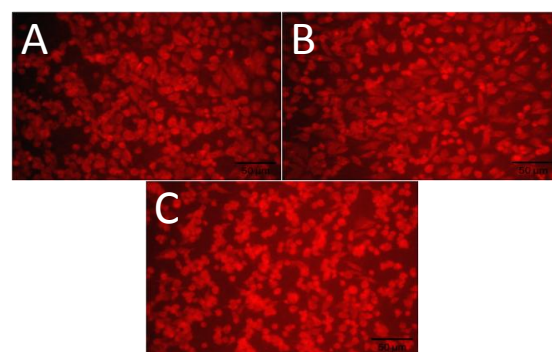


Figure 2. SAOS-2 morphology with Phalloidin staining after 48h. (A) sol+D+YIGSR; (B) sol+D+FHRRIKA; (C) sol+D+KRSR

CONCLUSION

The aim of this research was to produce and characterize a new method to modify biomaterial surfaces that included sol-gel technique and dendron synthesis. The principle was to match features of sol-gel coating with those of the dendrons, to obtain a functionalized biocompatible coating. The research has highlighted that this aim could be easily achieved: dendrons can be functionalized with any sort of moiety and can increase the surface to functionalize due to their hyperbranched structure. In addition, sol-gel was proven to provide a stable coating exhibiting functional groups on the surface. In this study it has been demonstrated that the different peptide sequences used truly induce a different cell response. Therefore this approach could be suitable for many regenerative medicine approaches e.g. regeneration of bone for better implant integration or for regeneration of tissue for the treatment of ischemic injury.

REFERENCES

1. Atala A. *et al.*, Foundations of Regenerative Medicine, Academic Press, 2009
2. Liu X. *et al.*, Materials Science and Engineering, R 47:49–121, 2004
3. Meikle S. *et al.*, J. R. Soc. Interface 10; 79, 20120765, 2013

Characterization of Silicone-polycarbonate-urethane/PDMS based Material for Polymeric Heart Valves

Marianna Asaro¹, Tamer Al Kayal¹, Silvia Volpi¹, Paola Losi¹, Simona Celi², Mattia Glauber¹, Giorgio Soldani¹

¹National Council of Research, Institute of Clinical Physiology, Massa, Italy masaro@ifc.cnr.it

²Scuola Superiore S'Anna, Massa, Italy

INTRODUCTION

Worldwide the increasing number of deaths per year caused by heart valve diseases, made valve replacement the most common surgical therapy. The research for polymeric heart valves (PHV) has been proposed to overcome problems such as no physiological flow conditions, calcification and limited durability of the currently available heart valves prostheses (mechanical or biological). Segmented polyurethanes have been utilized in medical devices since years due to their established biocompatibility and excellent mechanical properties, but their tendency to degradation hampered their use in long-term implantation.

The aim of this work was to study a thermoplastic copolymer chain of polycarbonate-polyurethane and silicone [polydimethylsiloxane (PDMS)] modified with increasing percentages of extra-chain PDMS, for the development of a novel single-body polymeric tri-leaflet PHV made by a spray, phase-inversion technique.

EXPERIMENTAL METHODS

CarboSil® (CS) in grain form was dissolved in THF/DMAc 1:1 (v/v) to obtain a 2% (w/v) solution. CarboSil® solutions containing 10% (CS10) and 30% of PDMS (CS30) were obtained by a reaction under stirring and nitrogen flow for 6 h at 82 °C. For each materials planar patches were obtained by a spray, phase-inversion technique on a rotating cylindrical mandrel [1]. After materials deposition the patches were placed for 1 h in dH₂O to allow solvents removal, and then pressed (50 g/cm²) during an heat treatment at 100°C for 90 min.

In vitro tests were carried out to evaluate the biocompatibility, hemocompatibility, calcification [2], hydrolytic degradation (ISO 13781: Sorensen buffer, pH = 7.4), oxidative degradation [3], environmental stress cracking (ESC) degradation [4] and mechanical properties (ASTM D1708-02).

The material cytotoxicity was studied through extraction method according to ISO-10993-5 on L929 fibroblasts; the hemocompatibility was assessed after 2 h of static blood contact to evaluate platelet adhesion, activation and coagulation parameters.

After calcification and degradation tests, samples were investigated by infrared analysis and SEM.

Uniaxial static tensile tests were performed until failure on both longitudinal and transverse directions on a computer controlled tensile testing machine (100 N load cell). Ten samples were analysed for each materials. For each samples stress-strain data, ultimate tensile strength (UTS) and ultimate elongation (UE) were calculated.

A prototype of a tri-leaflet PHV, whose leaflets had the same thickness (300 µm) and characteristics of the tested patches, was obtained by the spray technique. A 3D mould housing a stent, made by rapid-prototyping

technique, was used to reproduce the morphology of a commercially available biological aortic valve and a 3D counter-mould was used to press/cure the valve prototype.

RESULTS AND DISCUSSION

All material extracts are devoid of any cytotoxic effects on mouse fibroblasts, since no decrease in cell viability (MTT test) and growth (BrdU proliferation test) was observed in comparison with untreated cells.

CS30 material induced a lower in vitro platelets adhesion than the CS one, while the coagulation times were similar for all the tested materials.

SEM analysis demonstrated that CS10 and CS30 presented significantly less formation of spots of calcification compared to CS. Infrared analysis demonstrated no significant differences among CS, CS10 e CS30 samples after the hydrolytic degradation test. CS30 samples exhibited less susceptibility to oxidative degradation and to ESC. Uniaxial tensile tests show a decrease of the UTS for the CS10 and CS30 with respect to the CS material of about 32%. No significant differences were found between all materials as far as the UE value.

A single-body PHV prototype (Fig.1), with a stent incorporated and kept in place without sutures along the peak of the crown, was successfully obtained by spray, phase-inversion technique with CS30.

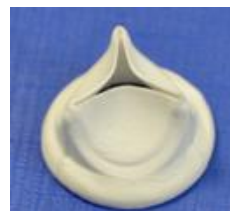


Fig. 1. Example of CS30 valve.

CONCLUSION

This study demonstrated that the combination of the properties of the CarboSil®-PDMS with those of a controlled valve fabrication technique, such as the spray material deposition on a 3D mould, allowed the feasibility of a new low-cost and potentially long-term performing PHV.

REFERENCES

1. Briganti E. et al., J Control Release 25:14-21, 2010
2. Bernacca G.M. et al., J Mater Sci: Mater Med 3:293-298, 1992
3. Dempsey D.K. et al., J Biomed Mater Res Part A doi: 10.1002/jbm.a.35037. 2013
4. Faré S. et al., J Biomed Mater Res 45:62-74, 1999

ACKNOWLEDGMENTS

Authors wish to thank DSM Biomedical (Berkeley, CA, U.S.A.) for providing the CarboSil® and Scienza Machinale (Navacchio, Pisa, Italy) for providing the 3D valve mould.

Study of the effect of SLS manufacturing parameters on the porosity of PHB scaffolds for tissue engineering

Tatiana F. Pereira¹, Bruna N. Teixeira^{1*}, Sara C Marques¹, Marcelo F. Oliveira², Izaque A. Maia², Jorge V. L. Silva², Gutemberg G. Alves³, Marysilvia F. Costa¹, Rossana M. S. M. Thiré¹

¹Programa de Engenharia Metalúrgica e de Materiais, PEMM-COPPE-UFRJ, [*bnarj86@gmail.com](mailto:bnarj86@gmail.com)

²Centro de Tecnologia da Informação Renato Archer, Campinas, SP

³Unidade de Pesquisa Clínica, Hospital Universitário Antônio Pedro - UFF

INTRODUCTION

The Selective Laser Sintering (SLS) is an additive manufacturing process which reproduces, layer by layer, physical models using powder material and a laser beam [1]. This technique has been widely used in aerospace and automotive industry and also to develop scaffolds for tissue engineering. [2]. The visual quality and the mechanical properties of devices manufactured by SLS process are determined by the correct choice of manufacturing parameters and of materials' properties [3]. The poly (3-hydroxybutyrate) (PHB) is a natural polymer and has been widely studied as raw material for the production of scaffolds for tissue engineering. PHB is biocompatible and has no toxicity to several cells lines [4].

The goal of this study was to evaluate the effect of experimental parameter PLT of the SLS process on the morphology and mechanical properties of PHB scaffolds and to evaluate the behavior of cells growth on them.

EXPERIMENTAL METHODS

PHB scaffolds were produced by SLS 3D printer (Sinterstation® 2000, maker: 3D Systems), using digital model in a tetragonal shape (13 mm x 13 mm x 26 mm) with 3D orthogonal periodic porous architecture formed by a square (1mm x 1mm x 1mm) and struts of 1 mm. Three groups of samples were produced by variation of the layer thickness – PLT - (0.08, 0.18, 0.28mm). The laser power, scan spacing, part bed temperature, laser beam speed and part build orientation were kept in 15 W, 0.15 mm, 100 °C, 2000 mm/s and 45°, respectively. The images of the scaffolds external surfaces were analysed using a scanner (HP Deskjet F4580) and the Image-Pro Plus 6.0 software for pores dimensions measurement. Length, width and height were obtained using Matlab R2007b software. To determine the porosity of scaffolds of PHB, it follows the standard ASTM F250-10.

Mechanical characterization of the samples was carried out using a universal testing machine (compression mode, Instron 5567), 2 kN load, cross-head speed of 1.3 mm/min.

The cytotoxicity in vitro was assessed using neutral red incorporation in cells cultured for 24 hours in the materials extracts.

RESULTS AND DISCUSSION

The physical models showed dimensional deviations in the geometries of the external surfaces and in the pores compared to the digital model. All scaffolds showed reduction in the size of pores with respect to that established in the digital model. Printed scaffolds

showed pores area values of 0.34 mm², 0.50 mm², 0.58 mm² for PLT of 0.08mm, 0.18mm and 0.28mm, respectively, the increase of PLT reduced the size deviation. The porosity of samples increased with the increase of the PLT. These results can be attributed to the decrease in the amount of energy supplied each layer's volume with the increase of the PLT, as indicated by the volume energy density, that affects the degree of sintering.

The results of compression tests showed that, with the increase in PLT there was a decrease in the modulus values. The mechanical properties the scaffolds, as well as the morphology, were significantly influenced by the PLT. The scaffolds were considered non-cytotoxic.

"Table 1 shows the values of the mechanical tests"

(PLT) mm	Volume Energy Density (J/mm ³)	Compressive Modulus	Compressive Strength
0.08 mm	0.625 J/mm ³	(65.98 ± 13.33) MPa	(3.02 ± 0.17) MPa
0.18 mm	0.277 J/mm ³	(12.70 ± 0.82) MPa	(0.66 ± 0.02) MPa
0.28 mm	0.178 J/mm ³	(3.59 ± 0.19) MPa	(0.26 ± 0.01) MPa

CONCLUSION

Regarding layers thickness, increasing PLT led to an increase in the porosity, since for thicker layers, less energy laser beam is donated, interfering with the sintering process and leaving more voids. The scaffolds with thinner layer had high modulus, which can also be attributed to the better sintering. In addition, the framework with a thickness of 0.08mm presented modulus similar to that of human trabecular bone [5]. More tests are being conducted to evaluate the behavior of cells on scaffolds.

REFERENCES

- Pereira, T.F. et al., Virtual and Physical Prototyping. 7:275-285, 2012
- Cooper, K.G. Rapid prototyping technology selection and application. New York: Marcel Dekke, 2001.
- Ho, H.C.H. et al. Industrial & Engineering Chemistry Research. 42: 1850-1862, 2003.
- Chen, G-Q. and Wu, Q. Biomaterials. 26: 6565-6578, 2005.
- Kramschuster, A. and Turng, L.-S. Journal of Biomedical Materials Research Part B: Applied Biomaterials, 92B: 66-376, 2010.

ACKNOWLEDGMENTS

The authors thanks CNPq, CAPES and CTI.



Assessment of the Corrosion Behaviour and Cytocompatibility of a Nano-fluorided Coating Obtained by Simple Chemical Conversion on AZ31 Biodegradable Mg Alloy

Emerson Alves Martins^{1,2}, Dorota Artymowicz¹, Kwangchul Shin², Andrey I. Shukalyuk², Roger C. Newman¹

¹ Department of Chemical Engineering and Applied Chemistry, University of Toronto, Canada

² IBBME – Institute of Biomaterials and Biomedical Engineering, University of Toronto, Canada
emerson.alvesmartins@utoronto.ca

INTRODUCTION

Magnesium based alloys have attracted great attention in recent years for possessing a natural ability to biodegrade due to corrosion when placed within aqueous substances. This is promising for orthopaedic and cardiovascular device applications. The natural tendency of this material to degrade is attributed to the high oxidative corrosion rates of Mg, however, this can limit the use for biomedical application^{1,2,3}. In order to improve corrosion resistance, a two-step treatment was prepared on AZ31 magnesium alloy by simple chemical conversion method. *In vitro* cytotoxicity tests were performed in order to evaluate if the metal ions released from the AZ31 alloy may cause biological responses.

EXPERIMENTAL METHODS

Preparation of the coating

Specimens with dimensions of 8 mm x 2 mm x 2 mm were cut from a rolled sheet of AZ31 Mg alloy. Each sample was abraded up to 2000 grid, cleaned in deionized water and ethanol, then dried. The surface treatment consisted of a two-step treatment process with immersion in 0.05 M $\text{Ca}(\text{NO}_3)_2 \cdot 4\text{H}_2\text{O}$ and 0.03 M $\text{NaH}_2\text{PO}_4 \cdot 2\text{H}_2\text{O}$ for 48 h at room temperature followed by immersion in 4g NaOH L⁻¹ and 5 g NaF L⁻¹ for 24 h. The morphology of the coating was observed by optical microscopy.

Electrochemical tests

The corrosion resistance was evaluated by electrochemical tests using simulated body fluid phosphate buffer solution (PBS). The PBS composition was NaCl 8.77g/L⁻¹, NaH_2PO_4 2.68 g/L⁻¹ and KH_2PO_4 2.72 g/L⁻¹, pH 7.4. A three-electrode cell was used with Ag/Ag/Cl as reference, a platinum electrode as the counter, and the sample as the work electrode. The electrochemical impedance spectroscopy (EIS) tests were performed at the open circuit potential with AC amplitude of 10 mV over the frequency range from 10⁵ Hz to 10⁻² Hz and potentiodynamic tests were carried out from -2.2 V to -1 V at a scan rate of 10 mV s⁻¹.

Cytotoxicity tests

Standard cell culture tests according to ISO 1993 using L929 fibroblast cells grown in Eagle's minimum essential medium (MEM) at 37° C for 10 days were used for obtaining a 100% test solution concentration. Extracts were prepared with the concentrations 100%, 50%, 25%, 12.5%, 0% and colorimetric analysis were used for assessing the cellular viability in these different concentrations. Negative and positive controls were used to establish an appropriate response.

RESULTS AND DISCUSSION

The two-step treatment resulted in a formation of a layer with needle-like morphology uniformly covering the specimen surface. The improvement of corrosion

resistance was confirmed by the electrochemical tests which showed that E_{corr} moved towards the active direction and that i_{corr} decreased due to the coating. EIS plots showed charge transfer resistance for the coated AZ31 Mg alloy compared with the uncoated one. The cytotoxicity tests indicated good cytocompatibility of L-929 cells with the first step treatment in the AZ31 alloy when cells were incubated 2 hours or 12 hours. However, the final step treatment had a positive trend after short-term cell exposure (2hrs) but was inconclusive after 12-hour exposure (see Figure 1).

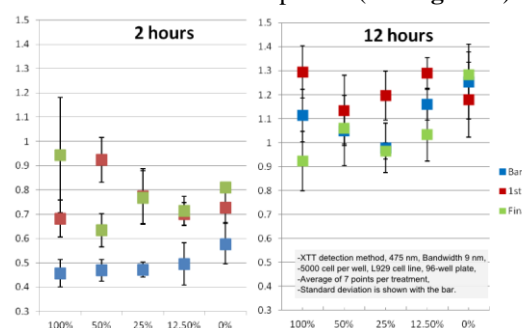


Figure 1 L-929 cell viability in the different concentrations and exposure times.

CONCLUSION

The polarization curves and EIS plots indicated that the coating formed by simple chemical conversion on AZ31 improved the corrosion potential and polarization resistance. The cytotoxicity tests indicated good cytocompatibility of L-929 cells with the layer formed in the first step of the treatment. However, the cytotoxicity result of the second step of the treatment was inconclusive after 12-hour exposure suggesting that a series of optimizations need to be performed.

REFERENCES

1. Peuster, M., et al., *A novel approach to temporary stenting: degradable cardiovascular stents produced from corrodible metal - results 6-18 months after implantation into New Zealand white rabbits*. Heart, 2001. **86**(5): p. 563-569.
2. Witte, F., *The history of biodegradable magnesium implants: A review*. Acta Biomaterialia, 2010. **6**(5): p. 1680-1692.
3. Heublein, B., et al., *Biocorrosion of magnesium alloys: a new principle in cardiovascular implant technology?* Heart, 2003. **89**(6): p. 651-656.

ACKNOWLEDGMENTS

"The authors would like to thank Capes/Brazil - Science without borders Programme (238013-7) and UofT Faculty of Chemical Engineering and Applied Chemistry for providing financial support to this project".

Mechanical Response of Calcium Phosphate Biocements

D.E. Mouzakis¹, S.P. Zaoutsos¹, S. Rokidi², N.Bouropoulos²

¹*Laboratory of Advanced Materials and Constructions, Department of Mechanical Engineering, Technological Educational Institute of Thessaly, GR 41110-Larissa, Hellas, mouzakis@teilar.gr

² Department of Materials Science, University of Patras, Rion 26500, Patras, Greece

INTRODUCTION

Calcium phosphate (CaP) cements are potential implanted materials for biomedical use due to the fact that they can be easily in-situ prepared by mixing a liquid with a powder phase composed of calcium phosphate salts. In spite the good biological properties of CaP based biocements they are usually plagued by low inherent mechanical properties [1]. The main objective of the current study as part of an overall project for the development of new CaP bone cements is the study of calcium phosphate cements with enhanced mechanical properties.

EXPERIMENTAL METHODS

For the preparation of α -TCP powder, equimolar quantities of calcium carbonate and calcium pyrophosphate ball milled and next the mixture was placed in alumina crucible, dried at 80 °C, placed in a furnace at 1300 °C for 12 hours and rapidly quenched on a metallic surface. The resulted material was crushed in the ball mill. The cement powder was mixed with 4 % w/v Na_2HPO_4 solution in an agate mortar at a powder/liquid ratio of 0.32 and the product in form of a paste, was moulded in 90 mm x 12.8 mm x 2.2 mm moulds. The specimens were remained in 100 % humidity for 12 hours and were then removed from the mould and placed at 37 °C in a polyethylene vial containing 60 ml of Ringer solution for 14 days for hardening [2]. Flexural properties of the materials were determined in three point bending mode. Moreover, DMA testing was conducted at three point bending loading for the CaP based biocements, in order to determine the dynamic properties of the material @ 25-200°C.

RESULTS AND DISCUSSION

It can be seen from the flexural properties presented in Table 1 below of the α -TCP based bone cements that their mechanical properties are comparable to those of the human bones (e.g. cortical bone), making them candidates for implants in bone deficiencies.

Property	E-modulus [MPa]	Flex. Strength [MPa]	Ultimate strain [%]
Mean	4879.8±972	3.39±0.28	0.07±0.01

Table 1. Typical Flexural properties of the bone cements studied.

Representative SEM images showing the morphological characteristics of the hardened cements are shown below in Figure 1. In the top-left is the α -TCP prior to the maturing procedure

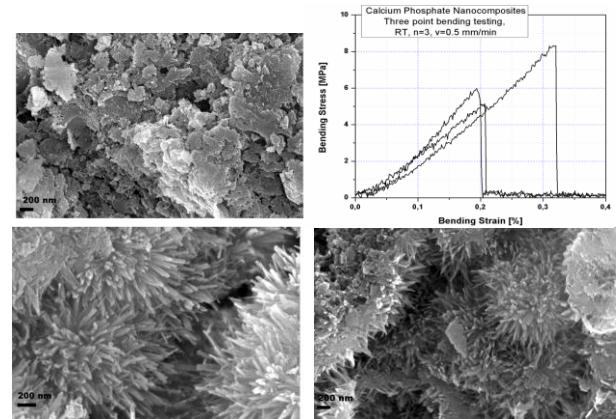


Figure 1. Flexural response and representative SEM pictures from the specimens tested.

An entangled network of nanoneedles is observed (bottom pics). These structures are composed of calcium deficient hydroxyapatite which is the result of the hydrolysis of α -TCP. Also, As seen in Figure 2, dynamic moduli of the CaP cements showed sensitivity to testing temperatures.

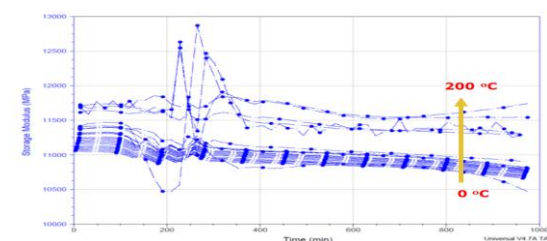


Figure 2. DMA scans, Storage moduli of Cap cements

CONCLUSION

Based on the analysis performed, it was shown that it is feasible to produce bone cements based on α -TCP, with an evolving nano-structure during the maturing-hardening phase with satisfactory biomechanical properties and dynamic behaviour.

REFERENCES

- Hockin H. *et al.*, Biomed Mater Res, 52:107–114, 2000
- Andriotis O., *et al.*, Cryst Res Technol. 1–5:2010

ACKNOWLEDGMENTS

The authors would like to thank the European Union and Greek national funds through the Operational Program "Education and Lifelong Learning" of the National Strategic Reference Framework (NSRF) - Research Funding Program: THALES. (Grant no: MIS 379380) for providing financial support to this project.

Bacterial Cellulose Based Electrospun Scaffolds for Bone Tissue Engineering

Deniz Atila¹, Ayten Karataş², Dilek Keskin^{1,3}, Ayşen Tezcaner^{1,3}

¹Department of Engineering Sciences, Middle East Technical University, Turkey

²Department of Molecular Biology and Genetics, Istanbul Technical University, İstanbul, Turkey

³Center of Excellence in Biomaterials and Tissue Engineering, Turkey, atila.deniz@metu.edu.tr

INTRODUCTION

Success in tissue engineering studies highly depends on properties of materials used and parameters of the chosen method¹. Materials used specifically in bone tissue engineering, require high resistance to mechanical stress and biodegradability^{1,2}. We aim to prepare a nanofibrous three dimensional and porous electrospun scaffold for regeneration of bone tissue with modified bacterial cellulose (BC), produced by species of bacteria *Acetobacter xylinum* since BC is a crystalline biopolymer with good mechanical properties^{2,3}.

EXPERIMENTAL METHODS

BC was produced by culturing ATCC 10245 *Glucanoacetobacter xylinum* species and purified (Fig.1). After a sulphuric acid treatment⁴, BC was electrospun with another natural polymer pullulan (PULL) in order to make electrospinning easier⁵.

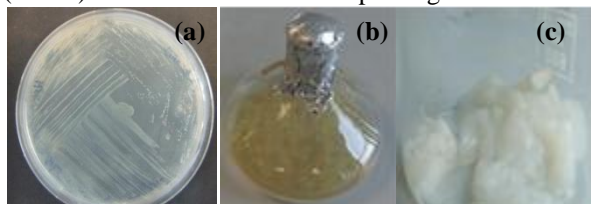


Fig 1. *G. xylinum* species seeded (a), BC produced on the culture (b), and BC purified (c).

Mixed BC/PULL (50/50 w/w %) dissolved in DMAc/DMSO/NMMO (Sigma-Aldrich) (1/1/2) were electrospun with 10-14 % of polymer concentrations. Wet electrospinning method was used with a collector bath filled with ethanol absolute (Merck). The applied voltage, tip-to-collector distance, and flow rate were fixed as 20 kV, 12 cm, and 1 ml/hr. Produced scaffolds were freeze-dried and analyzed.

RESULTS AND DISCUSSION

Macro-scale interpretations of the 3D carriers showed that the scaffolds become more compact after freeze-drying (Fig.2).

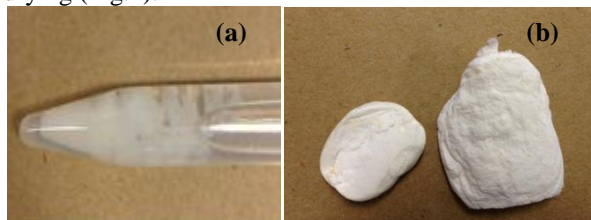


Fig 2. Electrospun BC/PULL carriers in ethanol before (a) and after freeze-drying step (b).

Dimensions of the carriers (either diameter or height) could be adjusted by changing the electrospinning time (i.e. the amount of electrospun meshes) according to intended application area.

SEM analysis was conducted to examine the morphological structure of 3D nanofibrous mesh (Fig.3). As the polymer concentration increases, fibre diameter decreases. In addition, huge beads within fibrous structures were scaled down.

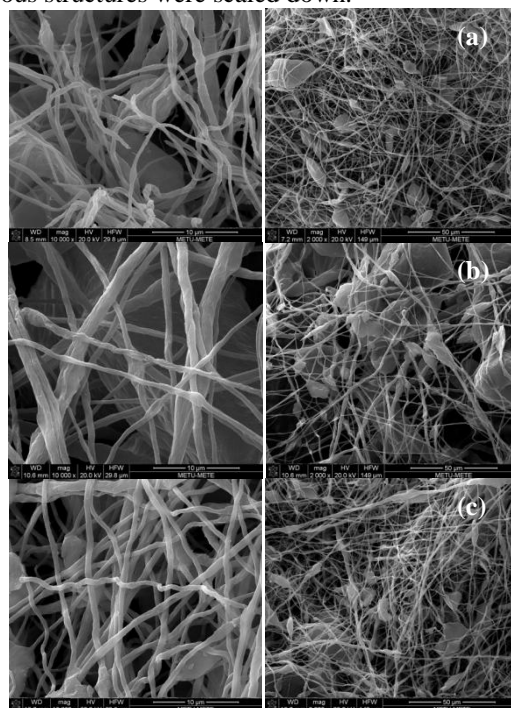


Fig 3. SEM images of electrospun BC/PULL scaffolds with polymer concentrations 10 (a), 12 (b), and 14 % (c).

CONCLUSION

BC/PULL electrospun scaffolds were prepared for the first time. These scaffolds hold promise for bone tissue engineering applications.

REFERENCES

1. Swetha M. *et al.*, Int. J. Biol Macromol, 47:1-4, 2010.
2. Mano J. F. *et al.*, J. R. Soc. Interface, 4:999-1030, 2007.
3. Svensson A. *et al.*, Biomaterials, 26:419-31, 2005.
4. Park W.-I. *et al.*, Macromol Symp, 249-250:289-294, 2007.
5. Stijnman A. C. *et al.*, Food hydrocolloid, 25:1393-1398, 2011.

ACKNOWLEDGMENTS

We would like to thank the Scientific and Technical Research Council of Turkey, (Project no: TUBITAK-112T749) for providing financial support to this project and Kale Kimya Grubu for providing PULL for our studies.

The Influence of Porosity and Pore Shape of PCL Electro-spun Nano-fibrous Meshes on Macrophage Activation

Kieran P. Fuller^{1,2}, Colm O'Dowd², Abhay Pandit¹, and Dimitrios Zeugolis¹
dimitrios.zeugolis@nuigalway.ie

¹Network of Excellence for Functional Biomaterials, National University of Ireland Galway, Ireland

²Vornia Biomaterials, Galway, Ireland

INTRODUCTION

Clinical data in wound healing models indicate that current non-absorbable products are characterised by chronic inflammation, as a result of persistent foreign body reactions¹. It has been postulated that identification of modulatory effects of macrophage M1 and M2 activation will create clinically relevant meshes, which will minimise patient complications and improve recovery rates². Indeed, recent data indicate that topographical features preferentially modulate macrophage response³. Herein, it is hypothesised that macro-porous nano-fibrous constructs not only will have adequate mechanical properties, but will also minimise inflammatory response.

EXPERIMENTAL METHODS

Electro-spun meshes of 30, 50 and 70% porosity were created in rhomboid, circles, and square pore shape. Randomly orientated electro-spun fibres and solvent cast films acted as control. Morphological features were assessed with a stereo microscope and SEM. Mechanical properties were measured using uniaxial tensile testing. Human skin fibroblasts were used to assess cytotoxicity. Murine macrophages (Raw 264.7) were used to assess immunogenic response.

RESULTS

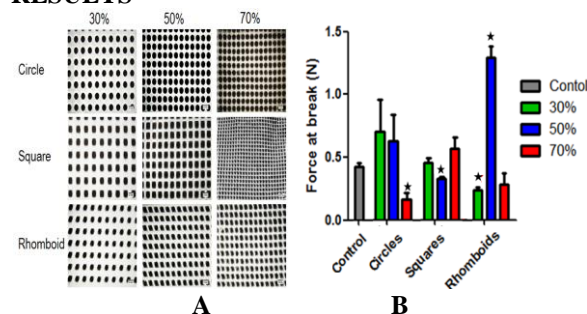


Figure 1: **A:** Optical analysis indicates that the produced meshes have clearly defined porosity. **B:** Uniaxial tensile testing analysis indicates that while the % porosity has a significant effect, the pore shape affects the mechanical properties to a higher degree as can be seen by the variation between samples, N=5.

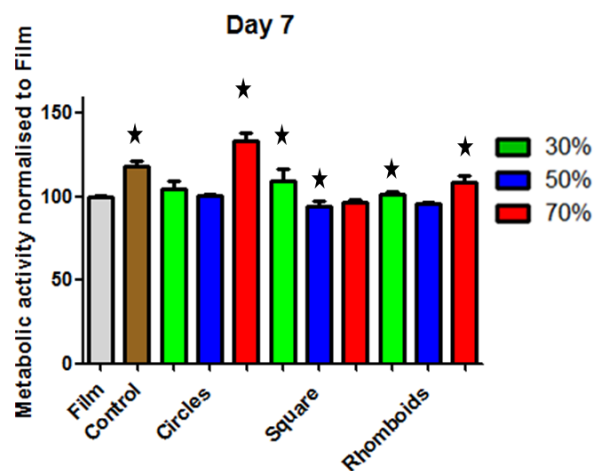


Figure 3: The metabolic activity is equivalent or higher on the nanofibrous material compared to the film.

DISCUSSION AND CONCLUSION

The introduction of pores with a well-defined shape might improve mechanical properties over a random control but this is dependent on the porosity. The metabolic activity is not affected by any pore shape or porosity when compared to a film. Further analysis with macrophage response is in progress.

REFERENCES

1. Berrevoet F *et al*, Surgery. 148, 5, 2010.
2. Brown B *et al*, Acta Biomaterialia. 8, 3, 2012.
3. Saino E *et al*, Biomacromolecules. 12, 5, 2012.

ACKNOWLEDGMENTS

The research has received funding from the Irish Research Council and the EU FP7 Programme under n° 263289 (Green Nano Mesh).

Production and Characterization of a Chitosan Coating on Titanium with Silver Nanoparticles

Daniel Rodríguez^{1,2,3}, María Godoy-Gallardo^{1,2,3}, Marc Avilès¹, Montserrat Español^{1,2,3}, F.Javier Gil^{1,2,3}

¹Biomaterials, Biomechanics and Tissue Engineering group, Escola Universitària d'Enginyeria Tècnica Industrial de Barcelona. Technical University of Catalonia (UPC)-Barcelona TECH

²Biomedical Research Networking Centre in Bioengineering, Biomaterials and Nanomedicine (CIBER-BBN), Spain

³Center for Research in nanoEngineering (CRnE), UPC, Spain, daniel.rodriguez.rius@upc.edu

INTRODUCTION

Formation of bacteria biofilms on implanted titanium surfaces is a growing health issue. Biofilms are linked to infection of medical devices, jeopardizing their long-term service.

A chitosan coating of titanium doped with silver nanoparticles has been evaluated for conferring antibacterial properties to medical device surfaces [1]. A dip-coating method of deposition was chosen for its versatility and ease of application [2]. Both chitosan coating formation and silver nanoparticle incorporation in the coating have been evaluated to achieve an improved antibacterial response.

EXPERIMENTAL METHODS

Silver nanoparticles were created by a chemical precipitation reaction of silver nitrate in sodium citrate, with a concentration, temperature and time controlled process. The nanoparticles were characterized by SEM and TEM, and particle sizes were established by dynamic laser light scattering.

Chitosan films were manufactured from an acidic solution containing 1% chitosan of medium molecular weight. Grade 2 titanium polished surfaces were used as substrate. Chitosan coatings with and without silver nanoparticles were prepared by dip-coating titanium samples at 1mm/min. Samples were characterized by contact angle, surface roughness, mechanical resistance and chemical composition measurements.

Bacterial adhesion and proliferation assays were made *in vitro* with two strains present in oral biofilms, *Streptococcus sanguinis* and *Lactobacillus salivarius*. Cytotoxicity was evaluated with an LDH assay.

RESULTS AND DISCUSSION

Silver nanoparticles were produced with rounded geometry and diameter from 20 to 50nm, depending on processing conditions.

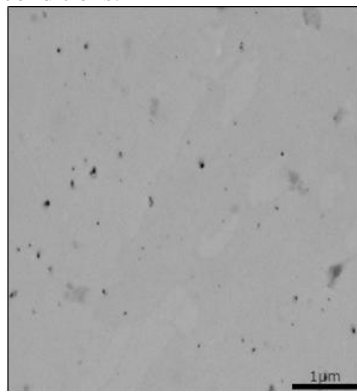


Figure 1. TEM image of silver nanoparticles dispersion in a chitosan coating.

A good dispersion of nanoparticles within the chitosan coating was achieved (Figure 1).

The layers formed on titanium chitosan showed a good adhesive strength, with detachment stresses over 3.8MPa.

The chitosan-nanoparticles combination showed an antibacterial effect in cell adhesion assays, producing the best results layers with smaller nanoparticles (figure 2).

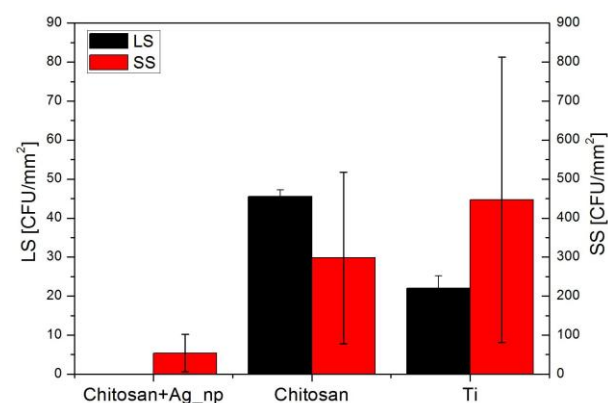


Figure 2. In vitro antibacterial effect of chitosan (with and without silver nanoparticles) and titanium, used as a control.

The chitosan coatings, with and without silver nanoparticles, did not exhibit cytotoxicity *in vitro*.

CONCLUSION

A practical process for creating chitosan coatings doped with silver nanoparticles on titanium surfaces has been developed and characterized. The chitosan coatings doped with silver nanoparticles have a reasonable adhesive strength to the substrate and they present a noteworthy *in vitro* antibacterial activity.

REFERENCES

1. Pelgrift R. *et al.*, Adv. Drug Deliv. 65:1803-15, 2013.
2. Li L. *et al.*, Small 20:487-503, 2012.

ACKNOWLEDGMENTS

Authors acknowledge financial support of Fundació Ramón Areces and Spanish Ministry of Economy and Competitiveness, through project MAT2012-30706.

Photo-crosslinkable and biopolymer-based inks for inkjet-bioprinting of artificial cartilage

Eva Hoch^{1*}, Achim Weber², Günter E.M. Tovar^{1,2} and Kirsten Borchers²

^{1*}Institute for Interfacial Process Engineering IGVP, University of Stuttgart, Germany, eva.hoch@igvp.uni-stuttgart.de

²Fraunhofer Institute for Interfacial Engineering and Biotechnology IGB, Stuttgart, Germany

INTRODUCTION

The future vision of implants comprises individually tailored prosthesis and the generation of artificial tissues and organs with sophisticated, biomimetic structure prepared from the patient's own cells. This challenging intention needs fabrication processes that do not set any limitations to the generation of various shapes. Thus, current research activities focus on the application of freeform fabrication methods, e.g. inkjet printing, for the deposition of cells and biomaterials into spatial orientations and geometries to reproduce the complexity of native tissues in a controllable and automated manner. This so called bioprinting requires biomaterials that are printable and, at the same time, hold appropriate physical, chemical, and biological properties. Thereby, biomolecules from the extracellular matrix of native tissues constitute very promising materials as they hold natural signaling motifs for the stimulation of cell adhesion, migration and function.

EXPERIMENTAL METHODS

For additive assembly of bioartificial tissue, photo-crosslinkable gelatin was prepared by derivatization with methacrylic anhydride.¹ In view of constituting bioartificial cartilage, chondroitin sulphate (CS) was also modified. Hydrogels were gained by photo-induced radical crosslinking in the presence of the water-soluble photoinitiator Irgacure 2959. The viscoelastic properties and long-term stability of the gels have been analyzed by swelling experiments and rheological measurements. Gels were investigated as encapsulation matrices for porcine articular chondrocytes to evaluate their applicability in respect to the generation of artificial cartilage. Processability by piezoelectric printing of the precursor solution was analyzed and printing of viable chondrocytes was performed (Nanoplotter NP2.1, GeSiM mbH, Germany).² Finally, cell-laden hydrogels were prepared by alternate printing and UV-induced crosslinking.

RESULTS AND DISCUSSION

We provide ECM-based hydrogels with tunable physico-chemical properties for use as biomimetic extracellular matrix for three-dimensional tissue substitutes. The developed precursor solutions hold low viscosities and show no gelling effects. Hence, the hydrogel system is suitable for processing in additive manufacturing, e.g. piezoelectric inkjet bioprinting. We

proved that the addition of CS to the bioartificial ECM substitute could promote the re-constitution of the chondrocyte-specific phenotyp after expansion in 2D cultivation.

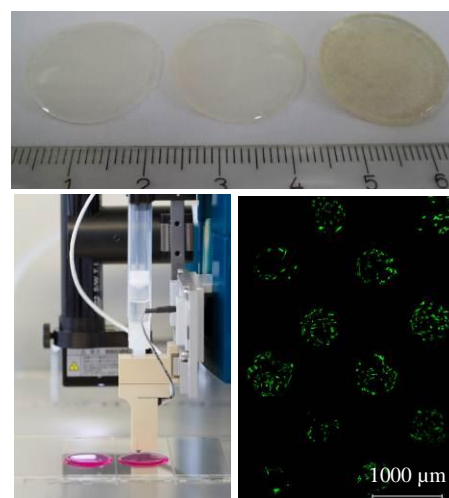


Figure 1 shows photocrosslinked gelatin-based hydrogels with different mechanical properties (top), inkjet bioprinting of gelatin-based ink (bottom left) and viable printed chondrocytes (bottom right).

CONCLUSION

The developed biobased hydrogel system is suitable for processing by printing techniques and constitutes a biofunctional ECM substitute. Thus, it will contribute to the development of biological implants in the near future.

REFERENCES

1. Hoch E. *et al.*, J. Mater. Sci. Mater. Med. 23:2607-2617, 2012.
2. Hoch E. *et al.*, J. Mater. Chem. B 1:5675-5685, 2013.

ACKNOWLEDGMENTS

The authors thank the Fraunhofer-Gesellschaft, the European Commission (Artivasc3D, GA 263416), and the Peter und Traudl Engelhorn Stiftung for financial support.

A Bioreactor-based 3D Culture System for skeletal Muscle Engineering in Fibrin Scaffolds

Philipp Heher^{1,2,3}, Christiane Fuchs^{3,4,5}, Johanna Prüller⁴, Babette Maleiner⁴, Josef Kollmitzer⁴, Dominik Rünzler^{3,4}, Andreas Teuschl^{3,4,5}, Susanne Wolbank^{1,2,3} and Heinz Redl^{1,2,3}

¹ Trauma Care Consult, Vienna, Austria

² Ludwig Boltzmann Institute for experimental and clinical Traumatology/AUVA Research Center, Vienna, Austria

³ Austrian Cluster for Tissue Regeneration, Vienna, Austria

⁴ Department of biochemical Engineering, UAS Technikum Wien, Vienna, Austria

⁵ City of Vienna Competence Team Bioreactors, UAS Technikum Wien, Vienna, Austria

Presenting Author: heherp@technikum-wien.at

INTRODUCTION

Fibrin is a versatile biomaterial that has been used extensively in a variety of tissue engineering applications. We have developed a 3D *in vitro* culture system using a bioreactor (MagneTissue) which allows mechanical stimulation of myoblasts embedded in a ring shaped fibrin scaffold by application of strain. Using this system we sought to analyze the effects of mechanical strain on cell alignment and distribution, viability and expression of muscle markers.

EXPERIMENTAL METHODS

Fibrin rings were prepared by injection molding (TISSUCOL DUO 500 Fibrin Sealant Kit, Baxter) with following final concentrations: 4×10^6 C2C12 myoblasts embedded per ring, 20 mg/ml fibrinogen and 0.625 U/ml thrombin. The rings in the strain group were applied to the bioreactor system. At day 3, growth medium was changed to differentiation medium (both supplemented with 100 KIU/ml Aprotinin) for strain and control groups and 10% static strain was applied to the strain group daily for 1 hour for the rest of the culture period (until d9). All data are presented as mean \pm SD of at least three independent experiments. Statistical analysis was performed using the student's t-test and values of $p < 0.05$ were considered significant.

RESULTS AND DISCUSSION

We demonstrate that over a culture period of at least 9 days the cells remain viable and differentiate into myotubes. Application of static mechanical strain leads to parallel cell alignment (Fig.1A) and also seems to facilitate nutrient diffusion within the scaffold, demonstrated by improved cell distribution (Fig.1B).

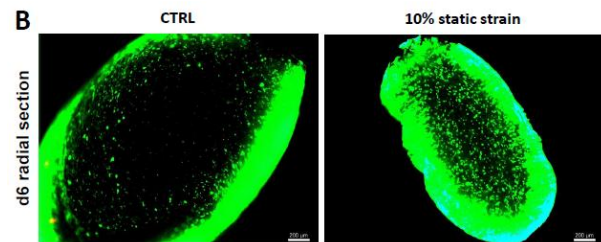
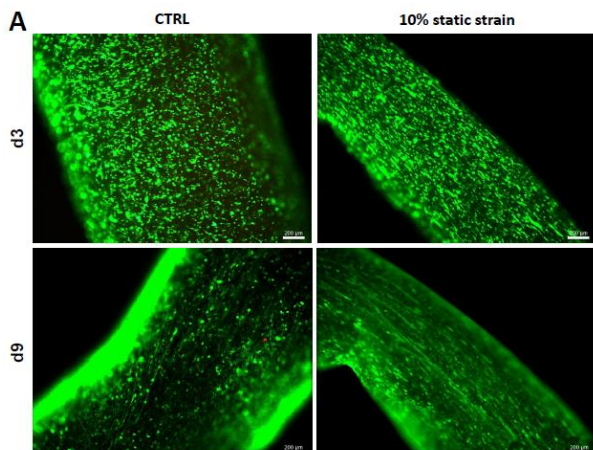


Fig.1: Calcein-AM/PI co-stainings of cells embedded in a fibrin ring: (A) ring surface, (B) radial section.

Furthermore, RT-qPCR results reveal that expression of mid- and late-stage specific myogenic markers is significantly increased when static strain is applied, demonstrating the subtle involvement of mechanotransduction in myogenic differentiation (Fig.2).

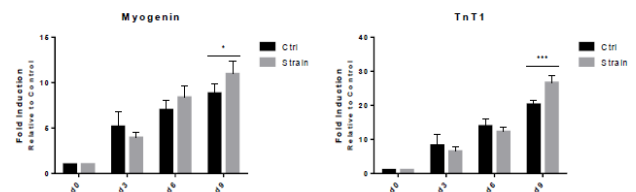


Fig.2: Relative expression levels of Myogenin and TnT1 at indicated timepoints over the course of the culture period (* $p < 0.05$, *** $p < 0.001$).

Our findings demonstrate that static mechanical strain has the ability to not just improve cellular alignment, a prerequisite for myotube formation, but to also increase myogenic differentiation by upregulation of myogenic marker expression. More importantly, variation of strain application can serve as a way to provide differential developmental cues and therefore allows for partial guidance of cellular fate decisions.

CONCLUSION

The use of this 3D culture system may provide a powerful tool to study myogenic differentiation, mechanotransduction and muscle physiology or disease. In this respect, further optimization of different strain application patterns might increase the degree of myogenic differentiation and functionality, with the long-term goal of providing patients with fully functional engineered skeletal muscle transplants.

ACKNOWLEDGMENTS

This work was funded by the EU 7th Framework Programme (BIODESIGN).

Functionalization of Polyurethane Substrates with Dendrons for Stem Cell Culture

Nicola Contessi¹, Serena Bertoldi^{1,2}, Steven Meikle³, Anna Guildford³, Silvia Farè^{1,2}, Matteo Santin³ and Maria Cristina Tanzi^{1,2}

¹Dept. of Chemistry, Materials, and Chemical Engineering "G. Natta", Politecnico di Milano, Italy

²Local Unit Politecnico di Milano, INSTM, Italy

³Centre for Biomedical and Health Science Research, School of Pharmacy and Biomolecular Sciences, University of Brighton, Brighton, United Kingdom; serena.bertoldi@polimi.it

INTRODUCTION

The *in vitro* study of stem cell expansion and stemness maintenance has received growing attention in the last years, to possibly exploit the stem cell therapeutic use [1]. Finding a functional and transparent substrate for *in vitro* culture of stem cells, while preserving their stemness, is one of the challenging goals to be attained. Since not only the substrate type, but also its biofunctionalization represent a possible way to acquire the specific features during stem cell culture, the aim of our work was to prepare transparent 2D polyurethane (PU) substrates and functionalize them with bio-competent dendrons, so to provide the adequate surface for stem cells culture.

EXPERIMENTAL METHODS

The PU films were prepared using similar reagents as already set up for cytocompatible PU foams (MDI prepolymer, a polyether-polyol mixture with 1-1.5% water, and Fe AcetylAcetonate as catalyst) [2], but spreading a proper quantity of the reaction mixture on a glass plate (6, 4 or 3.5 g) and setting up the procedure. PU films (PU6, PU4 and PU3.5, according to the amount of reaction mixture spread) were characterized for morphology (optical and SEM observations), wettability (static contact angle), ATR-FTIR spectroscopy and mechanical tensile tests. Dendrons composed by an arginine root with a generation-three branched structure of lysine (RG3K) were synthesized and functionalized with betaine (RG3K(CB)₁₆) or with the amino acidic sequence YIGSR (RG3K(YIGSR)₁₆), as already described [3]. The surface of the most transparent and homogenous PU film (i.e. PU3.5) was activated by air plasma and NHS/EDC chemistry and subsequently biofunctionalized with dendrons or dip-coated with dendron-modified poly-L-Lysine (PLL). The effective PU film functionalization was assessed by contact angle and ATR-FTIR. Human Mesenchymal Stem Cells (hMSCs) were seeded (7000 cells/cm²) and cultured for 7 days on PU3.5 film ($\Phi=10$ mm) functionalized with dendrons or dip-coated with dendron-modified PLL, using not modified film and the culture plastic (TCP) as control. Cell morphology, in particular cell aggregates, was evaluated by SEM, CellTracker and DAPI staining [4].

RESULTS AND DISCUSSION

PU films produced by spreading 6g or 4g of the reaction mixture on the glass substrate proved to be thick, not homogenous and not completely transparent, mostly due to the presence of air bubbles. Instead, PU3.5 films were transparent and homogeneous (Fig. 1a), with lower thickness (~ 80 μ m, $p<0.05$) compared to PU6 and

PU4. No significant differences in elastic modulus ($p>0.05$) were observed for all the produced PU films.

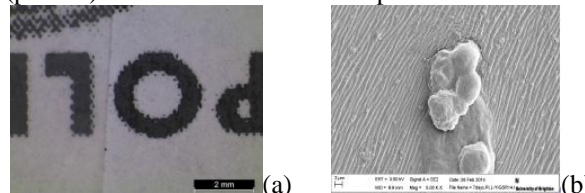


Fig. 1: (a) Stereo image of PU3.5 film on a written paper (scale bar=2 mm); (b) hMSCs cultured on PU3.5 film dip-coated with RG3K(YIGSR)₁₆-modified PLL (scale bar=2 μ m). The synthesis and functionalization of the dendrons was demonstrated by mass spectrometry and ATR-FTIR. Surface wettability of the PU films functionalized with dendrons or dendron-modified PLL increased ($p<0.05$) compared to not modified films (Fig. 2), validating the efficacy of air plasma and NHS/EDC chemistry in activating the PU surface and of functionalization with dendrons and dendron-modified PLL.

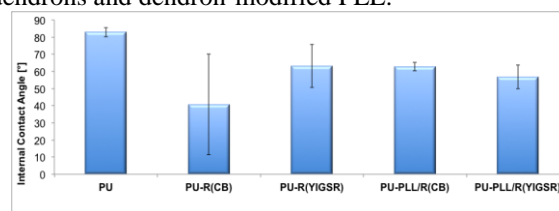


Fig. 2: Contact angle of PU3.5 before and after the functionalization with dendron and dendron-modified PLL.

hMSCs cultured on dendron-modified PU films showed spherical morphology, in particular when in contact with RG3K(YIGSR)₁₆ dendron and RG3K(YIGSR)₁₆-modified PLL. On these modified substrates, a first formation of 3D cell aggregates, indicating cell viability and stemness maintenance, was noticed (Fig. 1b).

CONCLUSION

The possibility to produce transparent, homogeneous and reproducible PU 2D substrates, and then to surface modify and functionalize them was demonstrated. The encouraging results obtained with the hMSCs culture preliminarily indicate the suitability of the described biofunctionalized PU films as substrates for *in vitro* stem cell culture, not affecting their stem phenotype.

REFERENCES

1. Meirelles LS. *et al.*, Cyt Gr Factor Rev 20:419, 2009
2. Bertoldi S., J. Mat. Sci., Mat. in Medicine 21: 1005, 2010
3. Meikle S. *et al.*, Macromol Biosci 11:1761, 2011
4. Guildford A. *et al.*, submitted to 26th ESB conference

ACKNOWLEDGMENTS

The authors thank NAMABIO Cost Action for providing financial support for the STSM (COST-STSM-MP1005-15696).



Quantification of Volume and Size Distribution of Internalised Calcium Phosphate Particles and Their Influence on Cell Fate

Richard Williams¹, Midhat Salimi¹, Gary Leeke¹, Paula Mendes¹, Liam Grover¹
¹ School of Chemical Engineering, University of Birmingham, Birmingham, UK.
rxw946@bham.ac.uk

INTRODUCTION

Calcium phosphates (CaPs) have been used extensively as bone replacement materials, substrates for drug release and transfection agents because of their non-cytotoxic nature and chemical similarity to the mineral component of human bone [1]. However, the fate of CaPs upon cellular internalisation is not fully understood, which has implications as a consequence of the effects of CaP wear debris from bone implants on surrounding tissues. Through surface modification and fluorescent tagging of CaPs, we were able to track particle internalisation within cells. We report observations from cell studies showing that the size distribution of internalised material – not just total volume – affects cell fate.

EXPERIMENTAL METHODS

Surface modification and fluorescent tagging of Silicon-substituted hydroxyapatite (SiHA) was based on a previously developed [2]. Briefly, 230mg of SiHA was added to a 3%(v/v) solution of 3-mercaptopropyltrimethoxysilane and 3%(v/v) DI water in methanol (10mL total volume, pH 5, left for 3 hours). pH then adjusted to 10, left overnight and washed. **Live cell imaging:** As described in [2]. Briefly, SiHA was mixed with a 1mL 100µM solution of Fluorescein-5-Maleimide in PBS. MC3T3 cells plated into live cell imaging dishes were exposed to the labeled SiHA for 24 hours with 50 µM LysoTracker Red added 30mins prior to confocal imaging. **Image analysis:** fluorescent SiHA and lysosomes were segmented by grey-level thresholding. Particle size and volume was estimated by computing the area of a bounding box, computing major/minor axis values and calibrating the voxel scale from the data file.

RESULTS AND DISCUSSION

Structures up to 1µm were most prevalent within the cells, but sizes up to 3-4µm were also observed. Lysosomes were generally found to contain structures up to 2-3µm (Figure 1), leaving any larger structures within the overall cell. No clear relationship was found between the volume of material transferred to lysosomes and the total material internalised by the cell as a whole. All particles ranging from 0.2-3µm in lysosomes correlated to cell morphology change from elongated to round shape. When particles larger than 2µm were not encapsulated within lysosomes, a dramatic increase in number of lysosomes and their convergence around the structures was observed. Cells appeared to detach from the plate when structures larger than 1µm were left exposed within the cell. This suggests that cell fate may not be dictated by the volume of material internalised alone. The location of any particulates >1µm within the cell (regardless of the total

volume of material) appears to have a strong influence on cell response.

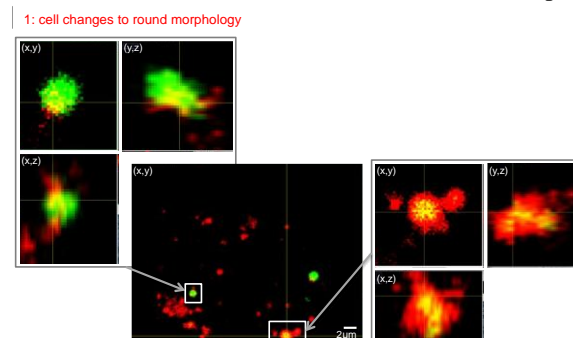


Figure 1: Confocal images of labelled SiHA structures (green), partially (left) and fully (right) encapsulated by lysosomes (red).

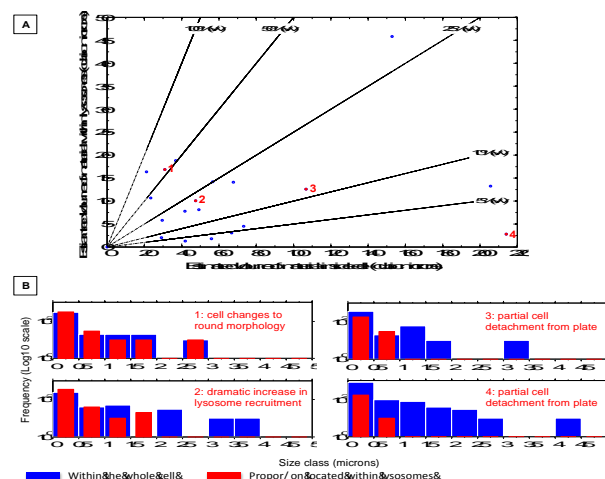


Figure 2: Volume of material in lysosomes (A) and size distribution of material in 4 example cases of changes of cell behaviour (B).

CONCLUSION

This study has revealed that CaP particles of >1µm in size can enter MC3T3 cells, but cannot be internalised in lysosomes. The results presented here demonstrate a correlation between the presence of particles of this size range and cell death. This result may have wider implications for the understanding of how particles eroded from the surface of implants may influence biological response.

REFERENCES

1. Kalita, S.J. *et al.*, *Mat. Sci. Eng. C*, 27(3):441–449, 2007.
2. Williams R.L *et al.* *J. Mater. Chem. B*, 1, 4370–4378, 2013.

ACKNOWLEDGMENTS

EPSRC ref: EP/F50053X/1

Functional PEPM-A-HA cryogels for drug conjugation and cartilage integration

Joana Magalhaes^{1,2*}, Luis Rojo del Olmo^{1,3,4}, Lara M. Nieto Couce^{1,2}, Julio San Roman^{1,3} and Francisco J. Blanco²

^{1*}CIBER in Bioengineering, Biomaterials and Nanomedicine, Spain

²Rheumatology Division. Tissue Engineering and Cellular Therapy Group (GBTTC-CHUAC). INIBIC. Sergas, Spain

³Department of Biomaterials, Institute of Polymer Science & Technology. CSIC, Spain

⁴ King's College London GKT Dental Institute, United Kingdom

joana.cristina.silva.magalhaes@sergas.es

INTRODUCTION

The high incidence of lesions in articular cartilage, associated to the soaring rise of life expectancy of the western population, has stressed the urgent need for medical solutions for osteoarthritis. Current clinical treatment of diseased or injured cartilage does not sufficiently restore long-term function and relieve joint pain.¹ This brings new opportunities for scalable regenerative solutions that involve the combination of biomaterials and chondrogenic inductive agents that can reliably induce the formation of functionally acceptable neocartilage and resolve challenges such as neo-tissue integration at the donor site.² In this work we synthesize cryogels of poly [2-ethyl-(2-pyrrolidone) methacrylate] (PEPM) and functionalized hyaluronic acid with aldehyde groups (A-HA), incorporating transforming growth factor- β_3 (TGF- β_3) and study their properties and potential for cartilage repair strategies.

EXPERIMENTAL METHODS

Porous semi-interpenetrating networks (sIPN) were prepared by the cryopolymerization of EPM (0.725M) using triethyleneglycol dimethacrylate (1.7% molar fraction) as crosslinker and potassium persulfate (2×10^{-2} M), as radical initiator activated with TEMED (0.27% v/v), in the presence of aqueous solutions of pure A-HA (5% w/v) or A-HA previously functionalized with TGF- β_3 . Reacting mixtures were first cooled to 0°C, deoxygenated during 30 minutes and progressively reduced to -15°C, at a cooling rate of 0.5 °C/min, within a cryostat. After 12 hours of reaction, both PEPM-A-HA cryogels were demolded, cut into discs (6 x 2.5 mm) and freeze-dried, until constant weight. Physicochemical characterization of the cryogels was performed (nuclear magnetic resonance - NMR, morphology and swelling). TGF- β_3 in vitro release profile was followed during 21 days and quantified using an ELISA kit. The chondrogenic differentiation of human bone marrow-derived MSCs on PEPM-A-HA cryogels with or without TGF β_3 was studied over 4 weeks. Thereafter the expression of cartilage interest genes and the quality of the synthesized extracellular matrix were analyzed, respectively, by using real-time PCR and histological staining.

RESULTS AND DISCUSSION

HA polysaccharide backbone was oxidized with sodium periodate to form aldehyde groups with an efficiency of 39% as confirmed by NMR. The aldehyde functionality of the A-HA conjugates with amines present at TGF- β_3 via Schiff-base reaction (confirmed by ELISA). The

morphology of PEPM-A-HA cryogels was characterized by scanning electron microscopy (SEM) micrographs that revealed an interconnected and highly porous network structure, uniformly distributed, with a pore size in the range of 15-50 μ m. Cryogels were able to swell up to 600% of their initial dry weight. PEPM-TGF- β_3 -A-HA cryogels presented a total cumulative amount of nearly 70% (ELISA). BM-MSCs were metabolically active when seeded in the synthesized cryogels and the pore configuration allowed cell penetration. Moreover from the alamar blue assay (Figure 1) it is clear a significant positive influence of the release of TGF- β_3 in cell's proliferation over 14 days ($p < 0.05$, using one-way ANOVA) regarding both TCPS control as well as PEPM-A-HA. MSCs were able to undergo chondrogenic differentiation in the presence of both produced systems.

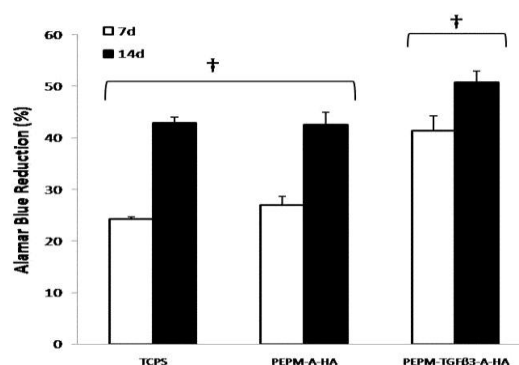


Fig 1. Alamar blue dye reduction assay after 7 and 14 days for tissue culture plastic polystyrene (TCPS) as positive control, PEPM-A-HA and PEPM-TGF- β_3 -A-HA cryogels (n=5).

CONCLUSION

The incorporation of TGF- β_3 into PEPM-A-HA cryogels enhanced BM-MSC proliferation and chondrogenic differentiation presenting potential use in cartilage repair.

REFERENCES

1. Blanco F.J. *et al.*, Ann Rheum Dis. 5:631-4, 2013.
2. Wang D.A. *et al.*, Nature Materials. 5:385-92, 2007.

ACKNOWLEDGMENTS

The authors would like to thank CIBER-BBN and Marie Curie Actions, for providing financial support and BIOIBERICA for the supply of hyaluronic acid.

Biaxial stretching of poly(L-lactide) tubes for improvement of mechanical properties

A. Løvda¹, J. Wenzel Andreassen², L. Pilgaard Mikkelsen³, K. Agersted², K. Almdal¹

¹Department of Micro- and Nanotechnology, Technical University of Denmark, Denmark

²Department of Energy Conversion and Storage, Technical University of Denmark, Denmark,

³Department of Wind Energy, Technical University of Denmark, Denmark

alvlo@nanotech.dtu.dk

INTRODUCTION

Poly(L-lactide) (PLLA) is a semi-crystalline bioabsorbable polymer, which has been widely investigated for medical devices despite its inferior stiffness and strength compared with conventional materials such as metal alloys¹. Due to the semi-crystallinity behaviour of the polymer, strain-induced crystallinity is expected to improve such mechanical properties by orientation of the crystals as seen in biaxial films^{2,3}. The objective was to investigate improvement of mechanical properties and the changes in crystallinity, crystal size and orientation in simultaneous biaxial strained PLLA tubes.

EXPERIMENTAL METHODS

PLLA (2003D) was extruded into tubes (OD 3.4mm). The tubes were heated to 74°C and longitudinally strained while applying internal pressure, initiating a tube expansion in the heated zone, resulting in a simultaneous biaxial strain.

The degree of strain in each direction is noted as the ratio between the longitudinal and radial strain (LxR). Mechanical testing was conducted to evaluate material properties and the effect of orientation. Orientation and crystal size was determined by X-ray diffraction (XRD), while total crystallinity (X_c) was determined by differential scanning calorimetry (DSC).

RESULTS AND DISCUSSION

Tensile testing of specimens in the circumferential direction show the typical strain hardening behaviour of

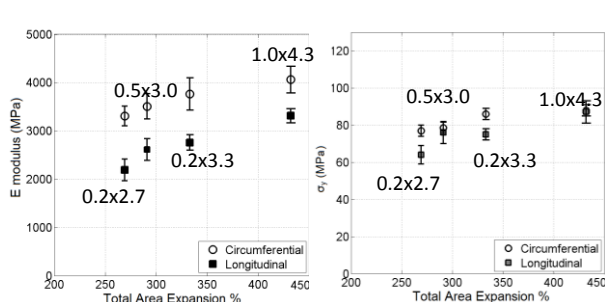


Fig1: Elastic modulus and yield stress for PLLA tubes with different LxR ratio obtained from tensile testing in the circumferential and longitudinal direction.

a semi crystalline polymer, but this is not seen for specimens tested in the longitudinal direction.

The elastic moduli (Fig.1) in the circumferential direction were superior to the modulus in the longitudinal direction at all times, due to the higher degree of strain in the given direction. Also the modulus is improved with degree of total area expansion, whereas the LxR ratio does not determine the

properties. The yield stress is less affected by the total area expansion (T_{area}).

XRD images in Fig 2 show that crystal orientation is predominant longitudinal when only strained in the longitudinal direction (LxR =1.0x0). The intensity plot in Fig. 2 show that once the tube is expanded, the peak in the 110/200 plane is no longer at perpendicular orientation to the longitudinal direction, but parallel. Despite a larger degree of T_{area} or LxR ratio, the orientation did not change.

X_c does not increase with the degree of T_{area} or LxR ratio, and the improved stiffness of the tubes is therefore not explained by neither crystal orientation nor an increase in strain-induced crystal formation.

XRD measurement also showed that crystals initially formed during uniaxial strain have a large crystal size circumferentially (183Å) and smaller axially (62Å), but this relation is flipped if radial expansion occurs simultaneously with 65Å radially and 134Å axially. The crystal size does not change significantly in the circumferential direction (65-70Å) with expansion or as function of LxR ratio, whereas the crystal size in the longitudinal direction decrease from 160Å to 137Å.

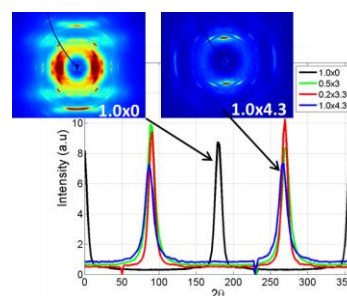


Fig 2: Intensity plot obtained from XRD of tubes with a different L/R ratio.

CONCLUSION

By biaxial stretching PLLA tubes improvement of stiffness and strength was obtained in both directions. Longitudinal stretching leads to crystal orientation in that given direction. Crystal orientation gained from this strain is reduced by degree of radial strain and altering the crystal alignment longitudinally. X_c does not increase with degree of radial strain and the improved properties are therefore not related to the crystal orientation nor a higher degree of crystallinity, but possibly stretching of the amorphous regions.

REFERENCES

1. Ambrose C. and Clanton T., Ann. Biomed Eng 32: 171-177, 2004
2. Stoclet G. *et al.*, Polymer 53:519-528, 2012
3. Ou X. and Cakmak M., Polymer 51:783-792, 2010

Controlled IL-2 Delivery from Novel Photocured Biodegradable Poly (decane-co-tricarballylate) Elastomers

Husam M. Younes* and Mohammad Shaker

Pharmaceutics and Polymeric Drug Delivery Research laboratory, College of Pharmacy, Qatar University, PO Box 2713, Doha, Qatar. husamy@qu.edu.qa

INTRODUCTION

One of the main challenges in interleukin-2 (IL-2) cancer immunotherapy is achieving localized and efficient delivery over a sustained period of time with proper maintenance of its stability and bioactivity¹. New biodegradable elastomeric poly (decane-co-tricarballylate) [PDET] matrices which utilize the osmotic-driven controlled release mechanism were designed in an attempt to overcome stability and bioactivity challenges facing IL-2 delivery²⁻⁴.

EXPERIMENTAL METHODS

Elastomer synthesis was achieved by polycondensation reaction between tricarballylic acid and alkylene diols, followed by acrylation and photocuring. IL-2 loaded matrices were prepared by intimately mixing lyophilized IL-2 powder with the acrylated prepolymer prior to crosslinking. Protein release was analyzed using ELISA and the in vitro bioactivity of released IL-2 was assessed using C57BL/6 mouse cytotoxic T lymphocytes. The influence of various parameters such as the elastomers' crosslinking density, the volumetric loading percentage and the incorporation of osmotic excipients on the release kinetics of the drug was also studied.

RESULTS AND DISCUSSION

Disk-shaped loaded matrices showed faster controlled IL-2 release patterns than microcylinders, with drug release proceeding via typical zero-order release kinetics. The increase in the device's surface area and the incorporation of trehalose in the loaded lyophilized mix increased the IL-2 release rate. As well, it was shown that the decrease in the degree of prepolymer acrylation of the prepared devices increased the IL-2 release rate. The cell based bioactivity assay for IL-2 over a release period of 28 days showed that the released IL-2 retained more than 94% of its initial activity.

CONCLUSION

A new protein delivery matrices composed of biodegradable PDET elastomers demonstrated to be promising and effective for linear, constant and sustained osmotic-driven release of IL-2 and other similar cytokines.

REFERENCES

- 1- Shaker M and Younes HM. Interleukin-2: Evaluation of Routes of Administration and Current Delivery Systems in Cancer Therapy. *J Pharm Sci* 2009; 98: 2268-2298
- 2- Shaker M, Doré J and Younes HM. Synthesis, Characterization & Cytocompatibility of Poly (diol-tricarballylate) Visible Light Photocrosslinked Biodegradable Elastomer. *J Biomat Sci* 2010; 21: 507-528.
- 3- Shaker MA, Daneshtalab N, Doré JJ, Younes HM. Biocompatibility and biodegradability of implantable drug delivery matrices based on novel poly (decane-co-tricarballylate) photocured elastomers. *J Bioact Compat Pol* 2012; 27: 78-94.
- 4- Shaker M and Younes HM. Osmotic-Driven Release of Papaverine Hydrochloride from Novel Biodegradable Poly (Decane-co-Tricarballylate) Elastomeric Matrices. *Therap Deliv* 2010; 1: 37-50.

ACKNOWLEDGMENTS

This work has been financially supported by a grant to HM Younes provided by Qatar National Research Foundation through the National Priorities Research Program grant # 09 - 969 - 3 - 251. M Shaker is a postdoctoral fellow financially supported by the same grant.



Incorporation of Elastin Enhancement Agents on Nano-scale Fibers

F.Damanik¹, C. van Blitterswijk¹, J. Rotmans², and L. Moroni^{1*}

¹ Department of Tissue Regeneration, MIRA Institute for Biomedical Technology and Technical Medicine, University of Twente, The Netherlands; E-mail: f.damanik@utwente.nl

²Department of Nephrology, Eindhoven Laboratory, LUMC, The Netherlands

INTRODUCTION

Over the past years, electrospinning has been the preferred technique for fabrication of nano-scale fibres due to its simplicity, tunability and versatility to spin a wide range of polymers. Owing to its adaptability on porosity, broad selection of material and architecture, electrospun fibres have been developed as biocompatible scaffolds or drug delivery systems for tissue engineering¹. Elastin has been the missing link in vascular tissue engineering². Therapeutic agents such as minoxidil, retinoic acid and aldosterone have been studied to enhance elastin synthesis. However, side effects may develop if the release of these agents is not localised and controlled. In this study, we developed a drug delivery system by incorporating these elastin enhancement agents into electrospun scaffolds to provide a local and controlled release.

EXPERIMENTAL METHODS

Electrospinning. Poly (ϵ -caprolactone) (PCL) solutions (15, 20, and 30% w/v) were prepared by dissolving the polymer in a 8:2 chloroform:methanol mixture under gentle stirring overnight. A stock solution of 3mg/ml in methanol for each elastin enhancing agent was added to the PCL solution to obtain different concentrations (0.01-0.5%) and stirred overnight. Solutions were electrospun by tuning flow rate (0.5-2ml/hr), working distance (15-20cm) and voltage applied (15-30kV) to modulate the controlled release of agents and minimize burst release. SEM was done to analyse the structure of loaded electrospun scaffold.

In vitro release and loading efficacy. Electrospun scaffolds were incubated at 37°C in PBS and supernatant collected at day 1, 4, 7, 10, and 14 for release measurements. For loading efficacy, loaded scaffolds were dissolved in chloroform:methanol mixture and vortexed. The absorbance of the samples and standard were read at each respective wavelength of the agent by a spectrometer.

In vitro cell culture. Human dermal fibroblast and mesenchymal stem cells were seeded onto loaded electrospun scaffolds with a cell density of 50,000 cells/scaffold. Analysis of cell metabolic activity, proliferation and morphology was done with presto blue, DNA assay and immunostaining.

RESULTS AND DISCUSSION

SEM analysis shows capability to obtain nano-scale fibers of $128 \text{ nm} \pm 62 \text{ nm}$ through electrospinning and maintenance of fibre morphology with loaded agents.

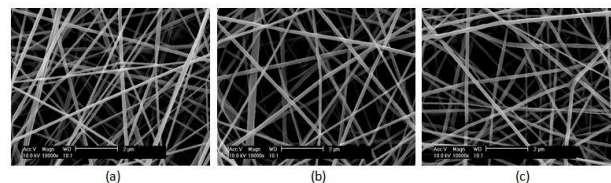


Figure 1. SEM images of (a) PCL, (b) PCL-retinoic acid and (c) PCL-minoxidil electrospun sheets. Scale bar: 2µm

By modulating the parameters, loading efficacy increased from 30% to 75%. Preliminary study on release showed minimized burst release in comparison to dip-coated samples. Metabolic activity of cells seeded on loaded PCL scaffold increased compared to unloaded PCL scaffolds. Immunostaining showed strong cell attachment and formation of multiple focal adhesion on the loaded scaffolds.

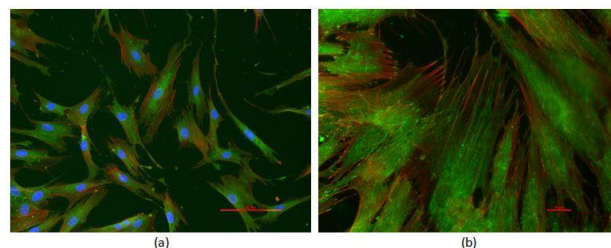


Figure 2. Immunostaining of vinculin-FITC and phalloidin-Texas red on PCL loaded scaffolds. Scale bar: (a) 50µm, (b) 10µm.

By tuning different parameters, one could electrospin PCL loaded fibers to obtain similar fibre morphology of PCL unloaded scaffold, and deliver the targeted agents in a controlled manner. Loaded scaffolds did not show any adverse reaction, but instead increase metabolic activity of cells, possibly enhancing elastin synthesis. Further quantification of elastin will be performed to confirm this.

CONCLUSION

In conclusion, elastin therapeutic agents were successfully incorporated into electrospun scaffolds while maintaining desired nano-scale fibre architecture, and were delivered in a controlled manner.

REFERENCES

1. Zamani M. *et al.*, Int. J. Nanomed. 8:2997-17 2013
2. Patel A. *et al.*, Cardiovasc. Res. 71(1):40-9 2006

ACKNOWLEDGMENTS

This research forms part of the Project P3.03 DialysisXS of the research program of the BioMedical Materials institute, co-funded by the Dutch Ministry of Economic Affairs, Agriculture and Innovation. The financial contribution of the Nierstichting Nederland is gratefully acknowledged.

Mineralized Porous Pullulan Microcarriers for Bone Tissue Engineering

Hazal Aydoğdu¹, Dilek Keskin^{1,2,3}, Ayşen Tezcaner^{1,2,3}, Erkan Türker Baran³

¹ Biomedical Engineering, Middle East Technical University, Turkey, e-mail: ahazal@metu.edu.tr

² Engineering Sciences, Middle East Technical University, Turkey

³ METU BIOMATEN Center of Excellence in Biomaterials and Tissue Engineering, Turkey

INTRODUCTION

Because of ageing population there is increased clinical need for tissue engineered bone substitutes that incorporate autologous bone cells and osteogenic materials. Previously apatite precipitations on polymeric scaffolds showed a suitable microenvironment for osteogenic cells¹. Therefore, we developed a three-dimensional pullulan hydrogel based microcarrier by using porogen leaching and *in vitro* apatite formation for efficient osteogenesis. We aim to create mineralized macroscopic tissue constructs carrying osteoblasts that can be injected into the defect site for bone tissue regeneration.

EXPERIMENTAL METHODS

Porous pullulan microspheres were prepared through water-in-oil emulsion crosslinking of stirred micro droplets of polymer with sodium trimetaphosphate and calcium carbonate granules (about 20 µm in size). Calcium carbonate was then removed by hydrochloric acid leaching leaving pores behind. Morphologies and average diameters of cross-linked microspheres were assessed with microscopic techniques. Microspheres were incubated in simulated body fluid (SBF) to create bonelike apatite by biomimetic mineralization. For cell culture the mineralized microspheres are seeded with Saos-2 cells and incubated in growth medium. Saos-2 cells were seeded onto SBF incubated (7 day) pullulan microspheres for 1 day and were analysed by fluorescence microscopy to see the effect of mineralization on cell-material interactions.

RESULTS AND DISCUSSION

Pullulan microspheres, fabricated by emulsion at 500 rpm, had spherical shape and porous structure with an average diameter of 115 µm with 30% porogen calcium carbonate. The porogens were found to be homogeneously distributed (Fig 1). The incubation of the microcarriers in SBF led to the nucleation and growth of apatite improving the osteoconductive character of the microspheres.

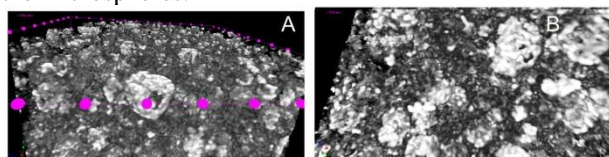


Figure 1. µCT of upper (A) and frontal section view of CaCO₃ incorporating packed pullulan microspheres.

The cell culture study showed that SBF incubated microspheres had better surface properties cell attachment (Fig. 2). The cells had more tendency to interact with the SBF incubated and biomimetically mineralized microspheres than untreated microspheres with SBF.

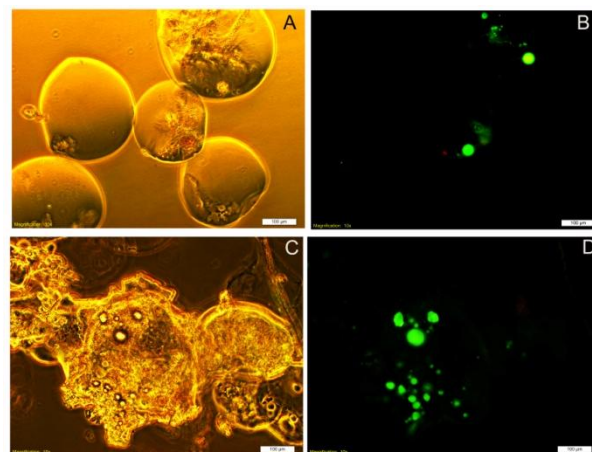


Figure 2. Phase contrast and fluorescence microscope images of SaOs-2 seeded on native (A, B) and SBF incubated pullulan microspheres (B, C), respectively. Green illuminance shows Nile red stained SaOs-2 cells.

CONCLUSION

We introduce data to demonstrate that biomimetically mineralized porous pullulan microspheres serve as a suitable cell carrier system. The apatite obtained through biomimetic process can be similar to the natural bone mineral and thus may provide a more preferential environment for bone formation. Thus mineralization of the cell-seeded microspheres can enhance cell adhesion and generates an injectable system that can be applied to bone defect sites for an improved response by accelerating regeneration of the bone.

REFERENCES

1. Kim, S.-S., et al. (2006). "Accelerated bonelike apatite growth on porous polymer/ceramic composite scaffolds in vitro." *Tissue engineering* 12(10): 2997-3006.

ACKNOWLEDGMENTS

This study was supported by the METU BAP-07-02-2014-007-059.

Interaction Study between Functionalised Si-Nanoparticles and Colon Carcinoma Cells for Theranostic Applications

Helena Montón^{1,2}, Colin Moore³, Antonio Aranda-Ramos¹, Vladimir Gubala³, Arben Merkoçi^{2,4}, Carme Nogués^{1*}

^{1*}Dep. Biologia Cel·lular, Fisiologia i Immunologia, Universitat Autònoma de Barcelona, Spain;

²Nanobioelectronics & Biosensors Group, Institut Català de Nanociència i Nanotecnologia (ICN2), Spain;

³Medway School of Pharmacy, University of Kent, UK;

⁴ICREA - Institució Catalana de Recerca i Estudis Avançats, Barcelona, Spain.

helena.monton@campus.uab.cat, helena.monton@icn.cat

INTRODUCTION

The use of biofunctionalised nanoparticles, in which the specificity for recognising and the capacity for releasing effective drugs to targeted cells are combined, has become a promising tool in theranostics. In this context, Silica nanoparticles (SiNPs) turned out to be a good approach for *in vivo* applications [1]. However, available data on basic interaction studies between biofunctionalised SiNPs and their target cells are limited.

The present study was aimed at investigation of fluorescent anti-EpCAM-modified SiNPs (70 nm) fabricated to specifically detect malignant Colon Carcinoma cells (Caco2) so as to be used, in the future, as a drug-delivery carrier. Cytotoxicity, association and internalisation of plain-, dendrimer- and EpCAM-SiNPs were assessed on Caco2 cells using different techniques such as MTT assay (dehydrogenase enzymes activity), Flow Cytometry (FC), Confocal Laser Scanning Microscopy (CLSM) and Scanning Electron Microscopy (SEM). HeLa cells were used as non-targeted control cells.

EXPERIMENTAL METHODS

Association study by FC and SEM

Caco2 and HeLa cells (1×10^5) cultured in a 6-well plate were incubated with 50 $\mu\text{g/mL}$ SiNPs during different times (20 min and 24 h) then cells were either trypsinised or fixed with 2% glutaraldehyde to carry out FC or SEM analysis, respectively.

Internalisation evaluation by CLSM

Internalisation rates were evaluated using the same concentration of SiNPs and the same incubation times as for association studies. After removing SiNPs, cell plasma membranes and nuclei were further labelled with Cell Mask and Hoechst respectively. Analysis by CLSM was carried out acquiring xyz stacks of images in order to have a 3D reconstruction of the cells.

Cytotoxicity assessment by MTT assay

Cells were incubated with SiNPs for 1 h and a standard MTT assay was performed at different post-incubation times (0h, 6h, 24h, 72h, 7 days).

RESULTS AND DISCUSSION

Cell-NP association was detected by FC 20 min after SiNPs incubation (Fig. 1a). The percentage of cells associated to fluorescent SiNPs reached its maximum at 24 h (Fig. 1b). FC charts show the increment of cell population with green fluorescence over time (Fig 1a, b). SEM analysis showed that SiNPs could still be seen adhered to the plasma membrane of Caco2 cells at 20

min. However, the number of SiNPs decreased over time disappearing completely at 24 h.

Data obtained by CLSM analysis (Fig 1c) are in agreement with that obtained by FC and SEM. SiNPs seem to be entrapped in endosome or lysosome compartments at 24 h (Fig 1c).

Finally, MTT assays demonstrate that SiNPs are not toxic for Caco2 cells in the concentration used (50 $\mu\text{g/mL}$ SiNPs). Cells have been cultured in presence of this SiNPs up to 7 days (data not shown). The production of insoluble formazan indicates that cells are metabolically active and that SiNPs do not hamper cell proliferation.

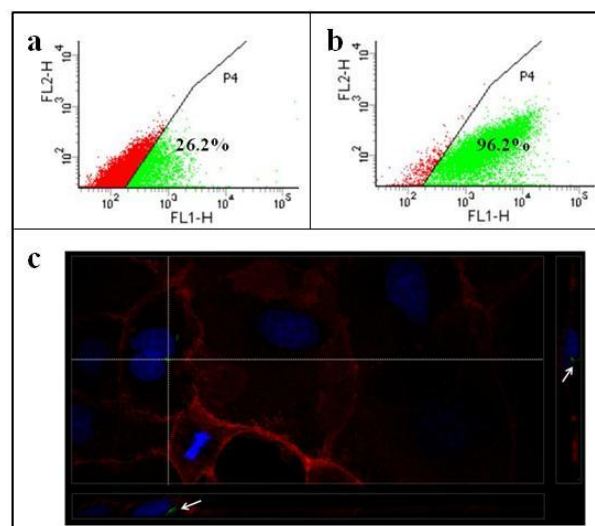


Fig.1. Caco2 cells incubated with NPs (plain, dendrimer- or EpCAM-SiNPs). In the analysis by FC performed at 20 min (a) and 24 h (b) an increase of the percentage of positive association over time can be seen. CLSM image shows SiNPs internalization.

CONCLUSION

SiNPs designed and fabricated to be used as drug delivery platforms demonstrated to be non-toxic for Caco2 cells. NPs can be internalized and probably they are entrapped in endosomes or lisosomes.

REFERENCES

1. Tivnan A. et al., *PlosONE* 7:5, e38129, 2012

ACKNOWLEDGMENTS

"This work has been partially financed by the MINECO (TEC2011-29140-C03-03 & MAT2011-25870 projects) and 2009- SGR-282".

Expression of Bone Markers in Pre-Osteoblastic Cells Grown on Titanium Surface with Nanotopography

L. M. S. de Castro-Raucci¹, L. N. Teixeira², P.T. de Oliveira¹, A. L. Rosa¹, M.M. Beloti¹

¹Cell Culture Laboratory, School of Dentistry of Ribeirão Preto, University of São Paulo, Brazil

²Department of Oral Pathology, School of Dentistry of Piracicaba, State University of Campinas, Brazil
larissa_spinola@yahoo.com.br

INTRODUCTION

The biocompatibility of dental and orthopaedic metal implants is strongly associated with osteoblastic responses to the surface of the biomaterial. Nanostructured titanium (Ti) surfaces can be obtained by a simple method, based on deoxidation and reoxidation controlled by means of chemical etching with solution H_2SO_4/H_2O_2 ¹. Previous studies have shown that the nanotopography accelerates and/or increases the extracellular matrix mineralization compared with untreated surface in cell cultures derived from newborn rat calvaria², indicating an enhanced osteoblast differentiation. The mechanisms by which nanotopography surfaces act on cells promoting osteoblastic differentiation and mineralization of the extracellular matrix are not fully understood. Considering that BMPs, including BMP-2/4, regulate osteoblastic differentiation and bone formation, the aim of this study was to evaluate the effect of Ti with nanotopography on the expression of key osteoblastic markers and BMP-2/4.

EXPERIMENTAL METHODS

Commercially pure Ti discs were polished with silicon carbide abrasive papers (320 and 600 grit) and treated with a mixture of H_2SO_4/H_2O_2 during four hours to generate nanotopography (Nano). Polished Ti discs were used as Control. Murine pre-osteoblastic cell line MC3T3-E1 (subclone 14) were plated on both Ti surfaces, i.e. Nano and Control, at 20,000 cells/well and cultured under osteogenic conditions for 3 days. Osteoblastic differentiation was evaluated by real-time PCR to detect the gene expression of runt-related transcription factor 2 (Runx2), alkaline phosphatase (ALP) and osteocalcin (OC). Quantitative gene expression data were normalized to the expression of the housekeeping gene GAPDH and calibrated by the expression of Control group. At the same time point, ELISA was performed to detect protein content of BMP-2 and -4. The quantitative data were submitted to Mann-Whitney test ($p < 0.05$).

RESULTS AND DISCUSSION

Gene expression assay revealed that Ti with nanotopography increased mRNA levels of Runx-2,

ALP and OC in MC3T3-E1 cell line (Table 1). On the other hand, protein content of BMP-2 and -4 was not altered by the treatment of Ti surface (Table 2). However, the role of BMP-2 and 4 on the osteogenic potential of Ti with nanotopography should not be neglected since other proteins related to BMP signalling pathway, as SMADs, may be affected by nanotopography.

Table 1. Gene expression of Runx-2, ALP and OC in MC3T3-E1 cells grown on Control and Ti with nanotopography surfaces.

Experimental groups	Gene expression		
	Runx-2	ALP	OC
Control	1.1±0.16	1.0±0.04	1.0±0.09
Nano	3.5±0.59	5.8±0.32	5.29±1.17
<i>p</i> value	0.029	0.029	0.029

Table 2. Protein syntheses of BMP-2 and -4 in MC3T3-E1 cells grown on Control and Ti with nanotopography surfaces.

Experimental groups	Protein content	
	BMP-2	BMP-4
Control	441.5±15.67	119.4±37.61
Nano	168.1±18.40	132.7±7.35
<i>p</i> value	0.7	0.1

CONCLUSION

The results showed that the nanotopography generated by treatment of Ti surfaces with mixture of H_2SO_4/H_2O_2 increases gene expression of bone markers without interfering with BMP-2 and -4 protein syntheses.

REFERENCES

1. Nanci A. *et al.*, Biomed. Mater. Res. 40:324-335, 1998.
2. De Oliveira PT. *et al.*, J. Biomed. Mater. Res. A. 80:554-564, 2007.

ACKNOWLEDGMENTS

Roger R. Fernandes, Fabíola S. de Oliveira and Milla S. Tavares. Grants: (FAPESP # 2013/00147-1, 2012/01291-6).

A novel method to measure the primary stability of dental implants and orthodontic screws

Fabrizio Barberis¹, Alberto Lagazzo¹, Stefano Benedicenti², Marco Migliorati², Marco Capurro¹

¹Department of Civil, Chemical and Environmental Engineering (DICC), University of Genoa, Italy

²Department of Integrated Surgical and Diagnostic Sciences (DiSC), University of Genoa, Italy

alberto.lagazzo@unige.it

INTRODUCTION

In dentistry and orthodontics there is an increasing tendency towards short-term loading of respectively implants and temporally anchorage devices (TADs)¹. This means that only the so-called primary stability (PS), namely the mechanically locking of prosthetic tools inside bone, previous to osseointegration, is called into play². Many indirect methods have been applied to evaluate PS in ex-vivo tests in view of a comparison of different devices and application techniques^{3,4}, but none of them is based on the measurement of the response of the implants to forces transversal to their axis. This way of loading is an important fraction of the load experienced by the implant in service.

In the present work we describe a specific apparatus developed to measure PS of dental implants or TADs through their compliance to a dynamically applied transversal point force. Some results obtained on different types of orthodontic mini-screws implanting on porcine bone samples are discussed. The same apparatus could be also employed in long-term experiments or fatigue tests.

EXPERIMENTAL METHODS

An instrumentation currently adopted for Dynamic Mechanical Analysis (DMA) of materials has been used to measure the dynamic compliance to transversal load. The implant is inserted following a related clinical protocol in a segment of medio-thoracic porcine rib encased in a plaster block. This block is bolted to the fixed head of the testing machine. The implant abutment is fixed to the moving head by means of an adjustable grip. The grip is designed as a hinge, preventing any displacement relative to the abutment, but allowing for rotation. The load line was vertical and perpendicular to the implant axis with a fixed lever arm with respect to the bone surface. The displacement of the abutment in the load direction was measured by a laser vibrometer with a resolution of 0.1 μm , which focused on the grip head. A piezoelectric force sensor is also assembled on the moving head of the apparatus.

The test consists in loading cyclically the sample at frequencies which can be automatically swept in any selected range between 0.5–1000 Hz. The amplitude of the applied oscillating force can be varied in the range between 0.1–1 N. The DMA device processed the time records of force and displacement via a Frequency Response Function (FRF), which provided a complex compliance spectrum of the sample. The real part of the spectrum corresponds to the elastic compliance, while the ratio of imaginary to real part (loss factor) provides an estimate of the energy dissipated in a cycle. The execution of tests is completely automatic being controlled by a dedicated software.

The apparatus was used to test the complex compliance of 12 samples prepared with 4 different types of mini-

screws for orthodontic applications. In this case a very narrow frequency interval was scanned (2–2.5 Hz), so the spectrum practically is reduced to a single value of compliance and a single value of loss factor for each test. The applied transversal forces were about 0.35 N. These tests were repeated in 5 consecutive days after the implantation. The specimens were stored during tests in physiological saline solution (NaCl 0.9%, pH 5.5), with the addition of antibiotic powder.

RESULTS AND DISCUSSION

In Fig. 1 complex compliance measurements (real part) of four types of mini-screw implants, measured with the method described above, are reported in their time evolution within 5 days from the insertion.

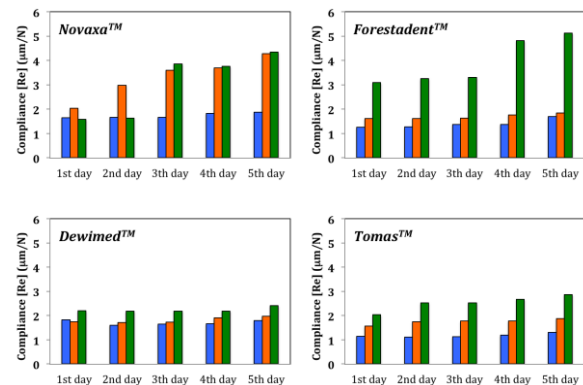


Fig. 1. Comparison of compliance of different types of mini-screws inserted in porcine bone.

Three types of behaviour can be easily observed: stable through all tests, gradually increasing or abruptly increasing.

The same apparatus can be also controlled for fatigue tests.

CONCLUSION

In this work a novel method of investigating the PS of dental implants or orthodontics mini-screws, based on the dynamic compliance with respect to a transversal point force, is illustrated. This method applied to a set of orthodontic mini-screws permitted to discriminate the performance allowing for clinical decisions.

REFERENCES

- Costa A. *et al.* Int. J. Adult Orthod. Orthognath. Surg. 13(3):201–209, 1998
- Raghavendra S. *et al.* Int. J. Oral Maxillof. Implant. 20:425–431, 2005
- Veltri M. *et al.* Am. J. Orthod. Dentofacial Orthop. 135:642–648, 2009
- Baker D. *et al.* Int. J. Oral Maxillof. Impl. 14:722–8, 1999

Development of novel tamponades to treat retinal detachments

Victoria Kearns^{1*}, Robert Poole², Albert Caramoy³ and Rachel Williams¹

¹Department of Eye and Vision Science, University of Liverpool, UK

² Centre for Engineering Dynamics, University of Liverpool, UK

³Department of Ophthalmology, University of Cologne, Germany, *vkearns@liv.ac.uk

INTRODUCTION

Silicone oils are frequently used as long-term ocular tamponades in the treatment of complex retinal detachments. Although they have some properties that are advantageous for this application, such as the ability to exclude aqueous from the wound site and provide long term physical support, there are several aspects that could be improved:

1. Standard silicone oil is lighter than water, meaning that it can only support the superior retina. Oils heavier than water are required to treat tears in the inferior retina¹.
2. In clinical practice, lower viscosity oils are easier to inject into the eye, but are also less emulsification resistant. Emulsification is known to cause complications such as secondary glaucoma, macrophage activation, and pigment epithelium proliferation.
3. Formation of scar tissue within the retina or vitreous can occur. The tamponade agent could be used to deliver a pharmacological adjunct to treat this.

Modifications to address any of these may change other properties of the oil, so a detailed characterisation of the rheological, emulsification and biocompatibility behaviour must be conducted. In this study we exploited the ability of very high molecular weight polymers to increase viscoelasticity and potentially resist emulsification. Results of the rheological examination of these novel heavy tamponade formulations are presented.

EXPERIMENTAL METHODS

Polydimethylsiloxane (PDMS) oils with shear viscosity of 1000 mPa.s or 5000 mPa.s, a high molecular weight additive and perfluorohexyloctane (F6H8) (Fluoron GmbH, Germany) were blended in various ratios. Densiron 68 (Fluoron), a commercially-available heavy tamponade, was used as a control.

Rheological measurements were carried out using a TA Instruments Rheolyst AR 1000 N controlled-stress rheometer (TA Instruments, Elstree, United Kingdom) using a 60 mm diameter, 2° acrylic cone geometry. Measurements of the shear viscosity (μ) in steady shear and of the storage (G') and loss moduli (G'') in small amplitude oscillatory shear (SAOS) were conducted.

RESULTS AND DISCUSSION

The shear viscosity of the blends increased with the addition of the high molecular weight polymer (HMW) (data not shown). Further investigation suggested that there was a power-law relationship between the amount of additive and the increase in shear viscosity above that of the base solvent (μ_s) (Figure 1). This empirical

relationship allows prediction of the shear viscosity for any amount of HMW additive falling within the tested range. For every blend of oil through the frequency range, G'' was significantly greater than G' , confirming that these fluids are only weakly elastic. As the amount of HMW additive increased, the relaxation time increased, demonstrating that the addition of the HMW polymer increased the viscoelasticity of the oil blends. For blends based on 1000 mPa.s oil, relaxation times were 1.5-10.0 ms. For blends based on 5000 mPa.s oil, relaxation times were 1.5-4.4 ms. Using these data it is possible to choose a particular blend to achieve the desired shear and viscoelastic properties.

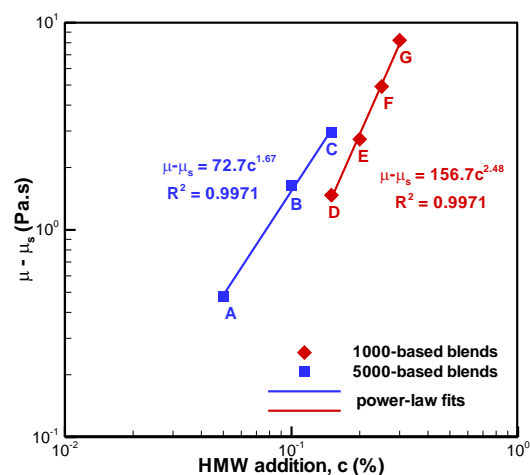


Figure 1: Difference in shear viscosity of blend (μ) compared to base solvent (μ_s) for different concentrations of high molecular weight polymer addition for both 1000 mPa.s and 5000 mPa.s based oils including power-law fits to the data.

CONCLUSION

Modifications to standard silicone oil tamponade formulations can be made to improve various aspects of the tamponade performance, including the ability to support the inferior retina while maintaining clinically useful injection properties. A full characterisation of physical properties and the biological response to novel tamponades must be conducted before using these oils clinically.

REFERENCES

1. Heimann H, Stappler T, Wong D. *Eye (Lond)*. 22(10), 2008

ACKNOWLEDGMENTS

The authors would like to thank Fluoron GmbH for providing materials for this project and Fight for Sight for financial support for VK

Ambient Temperature Patterning of Bioactive Deposits on Curved Metallic Substrates For Orthopaedic Implants

A. Nithyanandan* and M. Edirisinghe

UCL Mechanical Engineering, University College London, United Kingdom *anouska.nithyanandan.11@ucl.ac.uk

INTRODUCTION

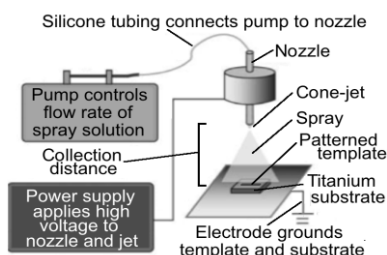
Modifying the surface of load-bearing orthopaedic implants with patterned deposits of bioactive materials, can support cell proliferation and orientation, improving direct biological fixation. Practically this results in increased functional service life of implants, and fewer revisions surgeries for patients. Template assisted electrohydrodynamic atomisation (TAEA) spraying is novel ambient temperature process that can be employed to apply deposits in a wide range of materials, including biopolymers¹ and potentially biological agents and drugs during manufacture. The topography can be controlled via template choice, and the biological benefit of such patterns over continuous coatings has been established². The development of TAEA for application on curved substrates is a natural progression of research, which has been exclusively on flat surfaces to-date³, and is a key milestone towards commercial viability. This work aims to further develop TAEA for the applications of bioceramic patterns onto curved titanium substrates for the first time. The resultant pattern microstructure and topographical geometry were analysed to establish whether the process could be controlled to create patterns closely resembling the initial template.

EXPERIMENTAL METHODS

Appropriate quantities of TiO₂ (titanium dioxide) were mixed in ethanol. The weight ratios of TiO₂ to ethanol were as follows: (TiO₂:ethanol) 2:98, 4:96, 6:94 i.e. 2, 4 and 6wt% TiO₂ in ethanol respectively. Copper templates with parallel patterned mesh with a strut thickness of 50µm and spacing of 100µm were used in all experiments. The controlled flow rate was varied (5, 10, 15, 20 and 25µlmin⁻¹), and TAEA spraying was carried out to fully coat the titanium substrate and copper template (schematic of TAEA process shown in Figure 1), then it was left for the solvent to evaporate away before removing the template, leaving the bioactive pattern in the shape of the inverted template.

All experiments were carried out at ambient temperature (~20°C), and collection distance was kept at 60mm, collection time at 300s. The morphology and structure of the coatings were determined using optical and scanning electron microscopy. The width of deposits were measured via image analysis with n=50.

Figure 1: Schematic diagram of the TAEA process



RESULTS AND DISCUSSION

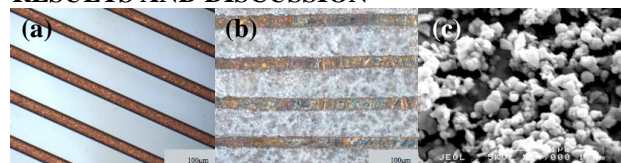


Figure 2: (a) optical micrographs of copper template, strut thickness 50µm, spacing of 100µm (b) TiO₂ pattern on curved substrate (c) scanning electron micrograph of TiO₂ pattern microstructure on curved substrate. Coating is 4wt% TiO₂ with flow rate, applied voltage and collection time, 20µl.min⁻¹, 10kV and 300s respectively. Substrate is 25.4mm diameter convex Ti surface.

Figure 2 shows that TiO₂ patterns have been applied onto curved titanium substrates with uniform and ordered topography, and there was a clear correlation between the template shape and size and the achieved pattern was established. Results for the parallel template (with strut thickness 50µm, spacing of 100µm) show that the mean distance between patterned lines is 54µm and the mean strut thickness is 97µm (standard deviation 6µm and 12µm respectively). This was achieved for the samples shown above. Figure 2(c) shows that the coatings exhibit a microporous surface, with pore less than 1µm in diameter. This is beneficial for cell attachment and enhances bioactivity²².

CONCLUSION

For the first time, ambient temperature TAEA has produced bioceramic TiO₂ patterns on curved titanium substrates (d=25.4mm) with a high degree of control over the pattern geometry. TiO₂ patterns with parallel line microstructures (mean strut thickness is 97µm, standard deviation 12µm) have been successfully produced. A clear correlation between the template shape and size and the achieved pattern was established, therefore the template can chosen to reflect the specific clinical needs of the coating. This work is ongoing, but results to-date show that the TAEA process is highly controllable and compatible on a range of substrate geometries, including flat and curved substrates. Due to the versatile nature of the process, TAEA could provide increased capabilities regarding the coating of orthopaedic implants.

REFERENCES

1. Nithyanandan A *et al.*, Mat Sci Eng C. 33:4608-15, 2013
2. Munir G *et al.*, J R Soc Interface. 8(58):678-88, 2011
3. Li X *et al.*, Bio-Med Mat & Eng. 17(6):335-46, 2007

ACKNOWLEDGMENTS

The authors would like to thank University College London and JRI Orthopaedics Ltd for financially supporting this work.

Effect of Substrate Geometry on Mineralization and Cell Proliferation of Calcium Phosphate Ceramics

E.R. Urquia Edreira¹, Astghik.Hayrapetyan¹, J.G.C. Wolke¹, J.A. Jansen¹, J.J.J.P. van den Beucken¹

¹Department of Biomaterials, Radboud University Nijmegen Medical Center, The Netherlands,
EvaRaquel.UrquiaEdreira@radboudumc.nl

INTRODUCTION

Calcium phosphate ceramics in combination with implant surface geometry have been shown to influence biological performance. Ripamonti et al. have extensively investigated the osteogenic effect of repetitive surface concavities on bulk ceramics and calcium phosphate coated titanium implants¹⁻³. These studies have shown that the presence of concavities affects osteoinductive capacity without application of osteogenic soluble factors.

In our previous study we tried to rationalize the mineralization process through an *in vitro* test in SBF⁴. Bianchi et al. showed that the mineralization process started preferentially within the concavities in hydroxyapatite (HA) disks sintered at 1200 °C and concavity size controlled the extent of mineralization.

It is also known that micro- and nano-scale morphology of the calcium phosphate surface can strongly influence osteoblast and stem cell adhesion, proliferation, and differentiation⁵⁻⁷. In our current study we aimed to investigate how cells populate concavities and to what extent concavity size influences mineralization when cells are present. We hypothesized that surface concavities facilitate cell proliferation and mineralization and that these effects are increased in the smaller concavity.

EXPERIMENTAL METHODS

Cavity sizes of 400, 800 and 1600 µm were created on the surface of HA disks sintered at 1200°C and cultured with adipose tissue mesenchymal stem cells (AT-MSCs) in osteogenic medium for up to 28 days at 37°C. At selected time points (3, 7, 14, 21, and 28 days), samples were removed and after fixation cells were fluorescently labelled with phalloidin-Alexa 568 (1:250; molecular probes) for filamentous (F-) actin and DAPI (1:2500) for nuclear staining. Cells were imaged and examined with a confocal laser scanning microscopy (CLSM) Olympus FV1000.

RESULTS AND DISCUSSION

Immunofluorescence three-dimensional (3D) image analysis showed differences in cell number between concavities at early culture time points (3 days). The highest number of cell nuclei was found in the 400 µm cavity (Figure 1) and the lowest number in the 1600 µm. Firstly, cells were able to migrate towards the concavities and adhere to their edges and walls. Preferential mineralization was observed inside the concavities. Cells spread over and to the bottom of

concavities covering all their volume and creating multilayers on their surfaces.

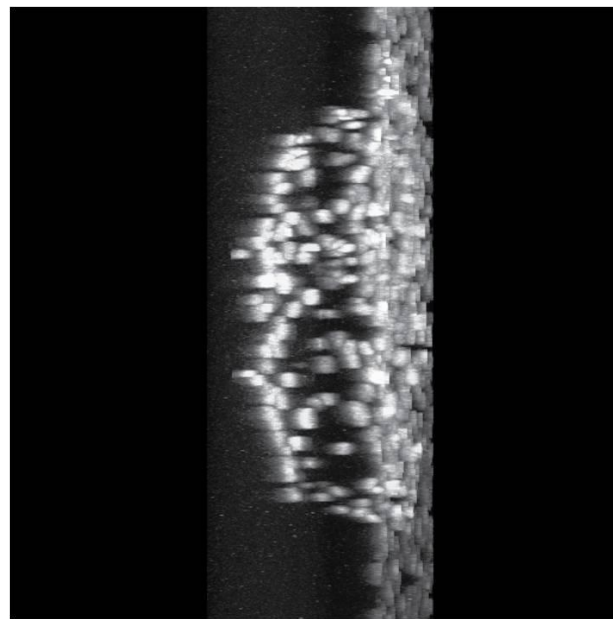


Figure 1. Immunofluorescence images at three days showing nuclei of cells on the 400 µm concavity.

CONCLUSION

High resolution 3D images gave qualitative and quantitative data on concavity volumes. CaP ceramics with surface concavities induced cell (AT-MSCs) adhesion and migration towards the concavities and were able to create multilayers. Results from this study suggest a correlation between mineralization and cell proliferation within concavities.

REFERENCES

1. Ripamonti U. *et al.*, J. Cell. Mol. Med. 13, 2953, 2009
2. Scarano A., *et al.*, Clin. Implant Dent. Rel. Res, 2009
3. Ripamonti U. *et al.*, Biomaterials, 3813, 2012
4. Bianchi M. *et al.*, Acta Biomaterialia, 10, 2012
5. Li B. *et al.*, Acta Biomaterialia, 8, 2012
6. Prodanov L. *et al.*, Biomaterials, 34, 2013
7. Graziano A. *et al.*, PloS One, 2, 2007

ACKNOWLEDGMENTS

The authors would like to thank the Research Program of the BioMedical Materials Institute (Project P2.04 BONE-IP), co-funded by the Dutch Ministry of Economic Affairs, Agriculture and Innovation for providing financial support.

Bone mineralization in Zebrafish embryos treated with Silicon ions

M.Montazerolghaem¹, L.Nyström¹, H.Engqvist¹ and M. Karlsson Ott¹

¹Materials in Medicine, Division of Applied Materials Science, Department of Engineering Sciences, Uppsala University, Sweden, maryam.montazerolghaem@angstrom.uu.se

INTRODUCTION

Silicon (Si) is a mineral that has an important role in bone formation. Studies have shown that Si supplementation accelerates the rate of bone mineralization¹. Because of this Si has been incorporated into different biomaterials to improve their osteogenic properties.

Zebrafish are used as a model system for investigating bone development and bone formation².

In this study our aim was to assess whether zebrafish could be used to evaluate the effect of Si ions on bone formation. For this purpose we supplemented fish media with Si ions and investigated the effect of bone mineralization. We also studied mineralization *in vitro* by using the murine osteoblastic cell line, MC3T3-E1.

EXPERIMENTAL METHODS

Mineralization in zebrafish

Zebrafish embryos were reared in embryonic medium E1. 3 days post fertilization the medium was supplemented with sodium metasilicate (625 μ M or 125 μ M). The embryos were kept in the supplemented medium for an additional 6 days and then stained with alizarin red. The embryos were then anesthetized and pictures were taken. The amount of mineralized bone was measured using the image analysis software Image J and statistical analysis was made using students t-test.

Mineralization in cell culture

MC3T3-E1 (subclone 14) was cultured in α -MEM medium, supplemented with sodium metasilicate (625 μ M and 125 μ M). After three days in culture, ascorbic acid and β -glycerophosphate was added. After an additional 10 days the mineralization was visualized with alizarin red stain.

RESULTS AND DISCUSSION

The results showed a dose dependent response to the Si ion concentration for both the zebrafish embryos (fig. 1) and MC3T3 cells (fig. 2). The mineralized area in the zebrafish embryos supplemented with 625 μ M Si was significantly higher as compared to the control and the lower concentration of Si. Interestingly the results show that the same concentration range increased the mineralization for both zebrafish and osteoblasts. Moreover these results indicate that zebrafish embryos can be used as a model system for evaluating osteogenic effects of Si ions.

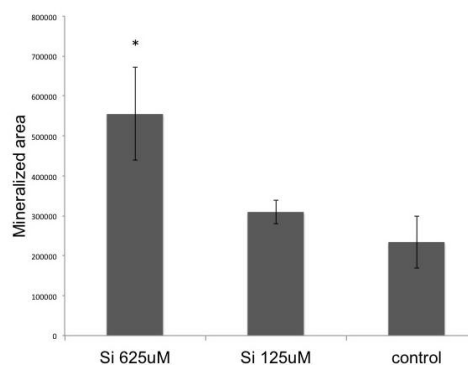


Figure 1. The amount of mineralized bone area in zebrafish embryos treated with sodium metasilicate, after 9 days post fertilization. * indicate statistical significant difference from control group, (n = 5).

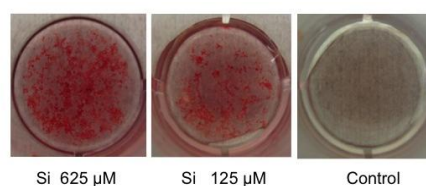


Figure 2. A dose dependent increase in mineralization of MC3T3 cells supplemented with sodium metasilicate.

CONCLUSION

In this study we have proven that mineralization in zebrafish embryos show a dose dependent response to Si ion supplementation. Since zebrafish have the complete bone remodelling system it could potentially be a useful *in vivo* model for evaluating Si doped biomaterials, in contrast to using only osteoblastic cells or osteoblastic cell lines.

REFERENCES

- References must be numbered. Keep the same style.
1. Prince C. T. *et al.* J Endocrinology 2013:1-6, 2013
 2. Du S. J. *et al.* Dev. Biol 238:239-246, 2001

ACKNOWLEDGMENTS

Part of this work was performed at the Zebrafish facility /Science for Life Laboratory at Uppsala University.

PolyHIPE-based porous microparticles for bone tissue engineering
T. Paterson¹, C. Sherborne¹, R. Owen¹, S. Puwunun¹, G. Reilly¹, F. Claeysens¹

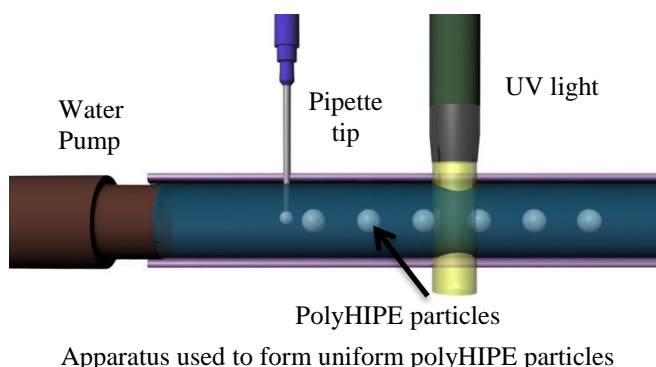
¹Kroto Research Institute, Department of Materials Science and Engineering, University of Sheffield, Sheffield, S Yorkshire, United Kingdom, mta08tp@sheffield.ac.uk

INTRODUCTION

Particle-based systems have great potential as scaffolds for tissue engineering, since they are injectable, avoiding the need for open surgery. In this study we are investigating how the osteogenic human cell line (hESMP) responds to monodisperse microporous particles. Particles with different size averages and Young's Moduli (YM) will be investigated. The microporous material is constructed from a HIPE (High Internal Phase Emulsion[1]) via photocuring. The YM of the polyHIPE can be controlled by varying the ratios of its monomers. It has been demonstrated that the YM of the surface affects the behavior of hESMP cells. We have used microfluidics for production of microparticles with highly controlled size and shapes. Engineering the shape of these particles allows tuning of the overall porosity to enhance angiogenesis within these scaffolds, as well as the ability to incorporate regions of specific functionality such as stem cell niches.

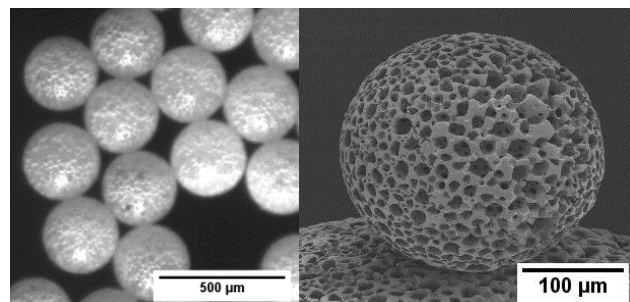
EXPERIMENTAL METHODS

Porous polyHIPE particles were created by a T-junction set-up in which a small internal diameter (100 μm) syringe needle injects the photocurable polyHIPE into a 6 mm diameter silicone tube containing a continuous stream of H_2O (sustained via a peristaltic pump) and subsequently curing the spherical particles with a UV lamp. By changing the flow of the liquids and the size of the needle tip dispensing the polyHIPE, it is possible to finely control the size of the resulting particles. Particles were produced in three different size ranges: 100, 200, and 300 μm . The polyHIPE was formed in three formulations* to produce particles of 200 μm in size with three different YM. To improve cell adhesion, particles are coated with acrylic acid in a plasma deposition chamber. hESMP cells are cultured under both continuous and static conditions to simulate the future processes required to produce injectable bone tissue engineering scaffolds. Cell growth was investigated using MTT and cell number per particle for proliferation data. Sectioning, confocal imaging and SEM were used to gather information on hESMP cell behaviour.



RESULTS AND DISCUSSION

Spherical particles have been produced with the microfluidic method at 80, 200, and 320 μm in size. All particles have a size variance of less than 30 μm . Bulk material of the different polyHIPE formulations was also formed into testing specimens and tested on a Bose mechanical testing machine (ELF3200) to determine the YM. MTT data on primary human fibroblast growth on thin films of the polyHIPE material will be presented. This data reveals that the porosity of the HIPEs increases cell proliferation as compared to a non-porous equivalent of the material. The data also showed that acrylic acid coating increases cell growth on both porous and non-porous material, as is reported in literature.[2] Exploiting both surface chemistry and porosity of the scaffolds greatly increases the cell adhesion and proliferation on these surfaces. Cell proliferation on the porous particles will also be reported upon.



PolyHIPE particles. Left: optical microscope image of 320 μm particles. Right: SEM image of 200 μm particle

CONCLUSION

Microporous particles have been produced in sizes between 100 μm and 1 mm with a controlled and narrow size distribution. Different polyHIPE materials have been formulated with a spread of YM as determined by mechanically testing. Human fibroblasts have been successfully cultured on the polyHIPE materials and these experiments demonstrated that both porosity and acrylic acid coating increases cell survivability. Work is ongoing to determine hESMP response to both particle size and YM.

REFERENCES

1. Johnson, D.W., et al., *Advanced Materials*, 2013. 25(23): p. 3178-3181.
2. Mattioli-Belmonte, M., et al., *Journal of Bioactive and Compatible Polymers*, 2005. 20(4): p. 343-360.

ACKNOWLEDGMENTS

We acknowledge the EPSRC for funding, Chris Hill for aiding with the SEM imaging, and Nicola Green for helping with confocal imaging.

Retrieval Analysis of Titanium – Nitride Coated Femoral Heads Articulating Against Polyethylene

Łukasz Łapaj¹, Justyna Wendland², Adrian Mróz², Jacek Markuszewski², Tomasz Wiśniewski²

¹Department of General Orthopaedics, Musculoskeletal Oncology and Trauma Surgery, Poznan University of Medical Sciences, Poland, esperal@tlen.pl

^{2*}Metal Forming Institute, Poznan, Poland

INTRODUCTION

Titanium nitride (TiN) coatings are used in total hip arthroplasty to reduce friction of bearing couples or to decrease the allergic potential of orthopaedic alloys. Little is known about performance of these implants, since only few retrieval studies were performed, furthermore they included a small number of implants manufactured over 15 years ago [1,2].

That is why we decided to perform a retrieval analysis of modern TiN coated femoral heads articulating against ultra-high molecular weight polyethylene (UHMWPE)

EXPERIMENTAL METHODS

This study included six 28 mm femoral heads with a made of TiAl6V4 alloy and coated with TiN using Physical Vapour Deposition (PVD). All heads were retrieved after at least 12 months of use (mean 31,2 range 14-52). The reason for revision was aseptic loosening in 5 cases and recurrent dislocations of one uncemented hip replacement (five episodes).

All implants were evaluated with light microscopy, Scanning Electron Microscopy (SEM) with Energy-Dispersive X-ray Spectroscopy (EDS). 30 SEM images from each implant were digitally analysed using ImageJ software to compare surface topography in loaded and non weight-bearing parts of the heads.

RESULTS AND DISCUSSION

Studies with light microscopy revealed severe damage to the dislocated femoral head, with multiple metallic scratches. Slight discoloration of the bearing surfaces were observed in other implants.

SEM studies indicated presence of multiple scratches as well as pinholes with a diameter of 1-10 µm. (Fig. 1a) Their number and surface area evaluated using digital image analysis differed between implants, however we found no statistical difference between weight-bearing part of the head and other segments within each head.

In all implants we found irregular areas (diam. 20-50 µm) where the coating was delaminated from the substrate metal (Fig. 1b). Some of these debonded fragments were embedded into the PVD layer in weight-bearing parts of all heads (Fig. 1c). In one head, (which was dislocated) we observed deposits of titanium alloy from the acetabular shell. The deposits were accompanied by large patches of delaminated coating as well as multiple cracks (Fig. 1 d). Small fragments of the acetabular titanium alloy damaged the coating in third body mechanism.

Residue from the manufacturing process was present in all implants in form of pure Ti droplets found

in round voids (Fig 1e). Surprisingly in three implants we EDS analysis revealed similar structures containing Niobium (Nb) particles (bright spots, Fig 1f)

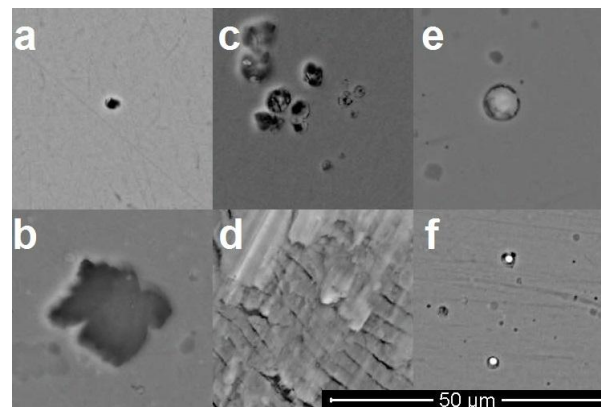


Fig. 1 SEM findings in retrieved TiN coated femoral heads

Similarly as in previous reports [1,2] our findings indicate that TiN coating degrades during in vivo use predominantly due to delamination. Contrary to previous papers we also observed wear in third body mechanism, especially in the dislocated head. Microscopic findings suggest, that mechanical failure of the coating results from its high stiffness, compared to the substrate material, similarly as observed in laboratory studies [3]. Another previously unreported finding is the presence of Nb residues in some implants, which, as we believe were formed during the manufacturing process. We hypothesize that different types of coatings were applied in the same vacuum chamber and residues from some batches could have contaminated other implants.

CONCLUSION

Our study indicates, that the TiN coating degrades during in vivo use, and underline the need for further development of the manufacturing process in order to avoid contamination of the coating.

REFERENCES

References must be numbered. Keep the same style.

1. Raimondi. *et al.*, Biomaterials. 21 (2000), 907-913
2. Harman *et al.*, J. Arthroplasty 12 (1997) 938-945
3. Chen *et al.*, Surface & Coating Technology 206, (2011) 1977-1982

ACKNOWLEDGMENTS

This research was funded by a grant from the National Science Centre nr 012/05/D/NZ5/01840.

Investigation of Ion Exchange between Silicate-substituted Bone Graft Substitutes and Cell Culture Media and the effect on Osteoblast-like Cell Response

N. K. Chana^{1*}, S. C.F. Rawlinson² and K. A. Hing¹

¹ School of Engineering and Materials Science, Queen Mary University of London, UK

² Queen Marys School of Medicine & Dentistry, Barts & The London, Queen Mary University of London, UK
n.k.chana@qmul.ac.uk

INTRODUCTION

Ionic dissolution from bone graft substitutes (BGS) to the surrounding medium has an effect on the cell response around implants due to the changes in ionic concentrations¹⁻². The aim of this study was to investigate the effect of varying reservoir volumes of media (PCM) circulating through silicate substituted hydroxyapatite (SA) granules on ion exchange and the subsequent impact this had on cell response under static conditions.

EXPERIMENTAL METHODS

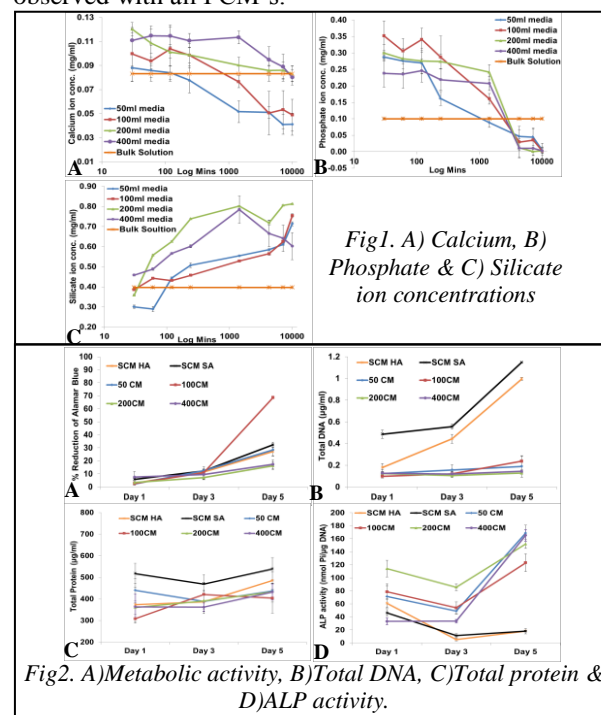
PCM was obtained by circulating known volumes of media (50ml, 100ml, 200ml and 400ml) at a flow rate of 0.7ml/min through 0.45g of 0.8wt% SA granules (20% strut porosity), packed in an 8 mm diameter tube. The media comprised Dulbecco's Modified Eagle Medium containing 1% Penicillin-Streptomycin (DMEM). 5ml of solution was extracted at time intervals of 0.5, 1, 2, 4, 24, 72, 120 and 168 hours and replaced with 5ml fresh DMEM. Calcium, phosphate and silicate ion concentrations of the extracted solutions were analysed using colorimetric assays¹. At 168 hours (7 days) the four volumes of DMEM were collected, individually sterile filtered and supplemented with 10% Fetal Bovine Serum (FBS) and stored as PCM.

MG63 osteoblast-like cells (passage 4) were seeded on 0.45g of stoichiometric hydroxyapatite granules in 24 well plates at a density of 4×10^4 cells/ml in serum containing media (SCM) composed of DMEM supplemented with 10% FBS and allowed to attach at 37°C and 5% CO₂. After 2 hours the SCM was replaced with either one of the four PCM or fresh SCM as a control. SA granules with SCM were also used as a second control. The cells were incubated for periods of 1, 3 and 5 days. The media was refreshed at 24 hours then 48 hours thereafter. DNA quantification, ALP specific activity and total protein release was monitored at each time point. Cell metabolism was also monitored using the Alamar Blue assay.

RESULTS

From Fig 1 it can be seen that a variation in ion concentration occurred throughout the entire length of the conditioning experiment. At 24 hours a depletion of Ca from the media in the two low volume media (50, 100ml) was observed in contrast to an initial elevation in for the two higher volumes of media (200, 400ml), Fig 1A. All media demonstrated a depletion in Ca from 0.5-168 hours, however the level of depletion was reduced for the two higher volumes of media in comparison to the lower volumes. All media volumes showed an initial increase in PO₄ ion concentration over the first 24 hours, Fig 1B, after which there was a depletion of PO₄ ions from all media to levels nearing

zero. SiO₄ ion release was observed in all media volumes however, sustained release was only observed for the two lower media volumes. Cell response to incubation on HA granules in conditioned media clearly demonstrated sensitivity to ion levels, Fig2. Cell metabolic activity was elevated with 100PCM but proliferation was suppressed with all PCM in comparison to the controls. At day 5 lower protein productions but significantly elevated ALP activity was observed with all PCM's.



DISCUSSIONS AND CONCLUSIONS

The circulating study demonstrated that there is a fluctuation in ion concentration with not only time but also volume of circulating media. The cell study demonstrated that variation in Ca, PO₄ and SiO₄ ion concentrations has a clear impact on osteoblast-like cell response. After 7 days circulation 100PCM provided the most supportive environment for cell proliferation on HA granules as compared to the other PCM despite the significantly depleted levels of Ca and PO₄ ions to SCM and a similar level of SiO₄ ion enrichment to 50PCM. The depletion of PO₄ ions from all PCM seemed to affect cell proliferation. To overcome this we can suggest that the 3D perfusion experiments should be partially or continuously refreshed in order to reflect more closely the *in vivo* environment if the mechanisms behind osteoinductivity are to be investigated *in vitro*.

REFERENCES

- Guth, K et al, (2011), J Mater Sci: Mater Med 22:2155-2164
- Guth, K et al (2006), Key Eng Mater, 309-311 (1-2):117-12

Highly Reinforced Bioactive Glass – Gellan Gum Composite Hydrogels For Biomedical Applications

Ana Gantar^{1,2}, Rok Kocen^{1,2} and Saša Novak^{1,2}

¹Department for Nanostructured materials, Jožef Stefan Institute, Slovenia

²Jozef Stefan International Postgraduate School, Slovenia, ana.gantar@ijs.si

INTRODUCTION

Combining man-made three-dimensional (3D) construct with cells to regenerate damaged tissue is considered as promising approach to replace the current techniques in use. However, effective regeneration of a bone tissue requires scaffolds mimicking natural conditions. In this case, replacing bone tissue, which is a complex structure of more than one material, with polymer-glass/ceramic composite, is an obvious choice. Recently, a novel gellan gum (GG) hydrogel reinforced with bioactive glass (BAG) nanoparticles was proposed as a promising material for biomedical bone applications¹. Although the addition of BAG particles improved the mechanical properties of the GG, the properties were still far from those characteristic for the natural bone. Therefore, to further improve the properties of the composites, another set of experiments was performed with a high fraction of BAG particles embedded in GG. In addition, to better understand the effect of the BAG on gelation of GG, in situ rheology studies were performed. As the BAG-GG composite is proposed as a temporary scaffold for tissue regeneration, mechanical properties of the hydrogels during immersion in simulated body fluid were also investigated.

EXPERIMENTAL METHODS

Particulate nano-sized BAG², in composition of 70 mol. % SiO₂ and 30 mol. % CaO, was obtained by modified sol-gel process. The bioactive particles were afterwards added to GG as reinforcement (0 to 90 wt. % of BAG) to obtain composite hydrogels. GG hydrogels were formed by ionic cross-linker and change of temperature. Exploiting phase separation process, porous scaffold were obtained by lyophilisation of the as prepared hydrogels for 72 h. In scaffold with higher percentage of reinforcement the porosity was introduced by addition of reactive chemical, which forms oxygen - forming connected porosity when heated. Mechanical properties of lyophilized hydrogels were studied by compression test. To understand the temperature dependent gelation process and the effect of the BAG concentration on the GG material, rheology studies were performed. The microstructure of highly reinforced GG lyophilized scaffolds was examined by scanning electron microscopy (SEM) and ability to form hydroxyapatite (HA) by immersion in simulated body fluid (SBF). Compression properties of samples during the SBF immersion were evaluated at different time points.

RESULTS AND DISCUSSION

With increasing percentage of the BAG particles, the porosity of the lyophilized hydrogels decreased as well as the average pore size. Mean pore size decreased from over 500 µm for GG to 100 µm for the composite with 50 wt. % BAG and to even much lower pores, down to 10 µm, for the highly reinforced composites. Accordingly, the mechanical properties of the material increased from 0.5 MPa for GG to ~2 MPa for moderately reinforced composites, however, obtained mechanical properties were still insufficient to apply the material for the load bearing regeneration.

Due to the insufficient porosity of the BAG-GG composites with high BAG content, hydrogen peroxide was implemented into the system to obtain pores in range of 100 µm. Incorporation of the hydrogen peroxide and adjustment of the process reaction resulted in anisotropic porosity.

One of the important contributions of the incorporated BAG is formation of hydroxyapatite in body fluid that gives the material a potential to retain the mechanical properties during the degradation. This was verified by measuring mechanical properties after the materials were soaked into a simulated body fluid. As it was expected, the presence of BAG, which promoted rather fast HA formation resulted in less pronounced decrease in the mechanical properties of the scaffold.

CONCLUSION

With the focus on material processing, 3-dimensional BAG-GG composites with high porosity were prepared. Highly reinforced composites containing up to 90 wt. % BAG exhibited properties that promise the use in bone tissue engineering. During dissolution of both components in simulated body fluid, hydroxyapatite induced by BAG dissolution products is formed within the 3D structure that enables the material to partly retain its mechanical properties.

REFERENCES

1. A. Gantar, et. al., Nanoparticulate Bioactive Glass - Reinforced Gellan Gum Hydrogels for Bone Tissue Engineering. - Under revision
2. Novak, S.; Drnovšek, N. Implant having a multilayered coating and a process for preparing thereof: patent application PCT/SI2011/000020. 2011.

ACKNOWLEDGMENTS

The presenting author would like to thank Slovenian Research Agency for providing financial support for this project (PR-03770).



***In vitro* testing of osteoinductivity and osteoconductivity of titanium alloys with nanostructured surface for orthopaedic applications**

E. Jablonská^{1*}, J. Lipov¹, J. Fojt², L. Joska², T. Ruml¹

¹Department of Biochemistry and Microbiology, Institute of Chemical Technology, Prague, Czech Republic, eva.jablonska@vscht.cz

²Department of Metallic materials and Corrosion Engineering, Institute of Chemical Technology, Prague, Czech Republic

INTRODUCTION

Titanium and its alloys have been considered as a gold standard among biomaterials for permanent implants. Moreover, their mechanical properties (especially elastic modulus) and also biocompatibility can be improved. Osteoinductivity and osteoconductivity of the material are achieved by creating nanostructured surface via anodic oxidation in appropriate electrolytes¹. These nanotubes formed *in situ* enhance preferential adhesion of osteoblasts, and thus support osteointegration and prevent development of fibrous layer on the material-bone interface². Specific parameters of the nanotubes and their influence on the cell growth have been extensively studied recently. Here, we present data on titanium alloys with different nanotube diameter and their ability to enhance adhesion and growth of osteoblast-like cell line.

EXPERIMENTAL METHODS

U-2 OS cells were seeded onto the surface of the tested metal discs placed in 12-well plate in the density of 7,000 cells·cm⁻². After 1, 2 and 5 days, the cells were fixed with 4% formaldehyde, permeabilized (0.1% Tween-20) and stained with TRITC-phalloidin (1 µg·ml⁻¹) and DAPI (0.5 µg·ml⁻¹). From each sample, 20 fields of view were recorded using wide-field fluorescence microscope (100-fold magnification). Morphology of the cells was evaluated and the cell number (via number of nuclei) was determined using ImageJ 1.43.

RESULTS AND DISCUSSION

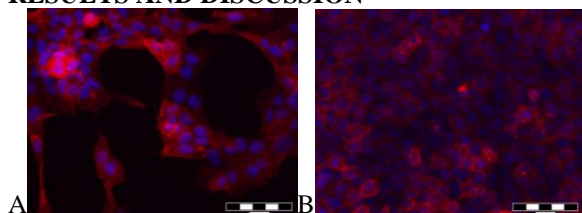


Fig. 1 U-2 OS cells grown on Ti-alloy samples with nanotubes (A – 50 nm, B - 100 nm in diameter) after 5 days of inoculation. Scale bar equals to 100 µm.

After 5 days of cultivation, the cells showed improved proliferation on nanotubes with larger diameter (100 nm) compared to smaller diameter (50 nm). On the contrary, Park *et al.*³ reported enhanced cell growth on nanotubes with smaller diameter (15 nm) when using different cell model. Interestingly, cells grown on 50nm nanotubes were strongly elongated in comparison to the control cells grown on glass coverslips. Similar phenomenon was also observed by Brammer *et al.*⁴.

CONCLUSION

These preliminary results indicate that the nanotubes with greater diameter possess better osteoinductive and osteoconductive properties. Nevertheless, for further studies, we would like to use more appropriate model (MC3T3-E1 or SaOs cells) and also evaluate parameters such as ability of extracellular matrix formation and mineralisation, which can be studied via monitoring of type I collagen and osteocalcin expression using qPCR. In the next step, newly developed beta-titanium alloys with elastic modulus closer to bone will be studied.

REFERENCES

1. Regonini D. *et al.* Mater. Sci. Eng., R. 74:377-406, 2013
2. Minagar, S. *et al.* J. Biomed. Mater. Res. A 101:2726-2739, 2013
3. Park J. *et al.* Nano Lett. 7:1686-1691, 2007
4. Brammer K. S. *et al.* Acta Biomater 5:3215-23, 2009

ACKNOWLEDGMENTS

Financial support from specific university research (MSMT No 20/2014) and the Technology Agency of the CR (project no. TE01020390).

Influence of collagen cross-linking on fibroblast and macrophage response

Luis M. Delgado¹, Abhay Pandit¹, Dimitrios I. Zeugolis^{1*}

^{1*}Network of Excellence for Functional Biomaterials, National University of Ireland, Galway, Ireland, dimitrios.zeugolis@nuigalway.ie

INTRODUCTION

Given that the native lysyl-oxidase cross-linking of collagen does not occur *in vitro*, exogenous cross-linking methods are under investigation to increase the mechanical and enzymatic stability of collagen-based devices¹. However, chemical methods based on aldehydes, epoxides and carbodiimide are often associated with cytotoxicity, macrophage activation and foreign body reaction². Alternative cross-linking methods, based on plant extracts and polyethylene glycol (PEG) have attracted great scientific attention the recent years, due to their low cytotoxicity^{3,4}. Herein, it is hypothesised that collagen films can be optimally cross-linked with PEG and plant extracts to induce adequate stability, whilst avoiding toxicity and macrophage activation. The specific objective is to optimise collagen films stability modulating macrophage response without compromising cell toxicity.

EXPERIMENTAL METHODS

Collagen films were cross-linked with 0.625% glutaraldehyde (GTA), 50 mM 1-Ethyl-3-(3-dimethylaminopropyl) carbodiimide (EDC), 1 mM 4-arm PEG succinimidyl glutarate MW 10,000 (4SP), 0.625% Genipin (GEN) or 0.1% Oleuropein (OLE). As control, non-cross-linked films (NCL) were used. Films were assessed by SEM, mechanical testing, DSC, swelling and collagenase assay. Cytotoxicity was assessed using WS1 fibroblast, and subsequent cell morphology, metabolic activity (alamarBlue™) and cell proliferation (PicoGreen®) analysis. *In vitro* response was assessed using human monocyte-derived THP-1 macrophages and subsequently by morphology, alamarBlue™, PicoGreen and multiplex assay for the main inflammatory cytokines. As control, macrophages seeded on TCPS were activated by lipopolysaccharide (LPS). Statistical significance was set at $p < 0.05$.

RESULTS AND DISCUSSION

Fibroblast seeded on all cross-linked films showed over 90% cell metabolic activity and similar proliferation rate at day 3; only GEN increased fibroblast proliferation (Fig. 1).

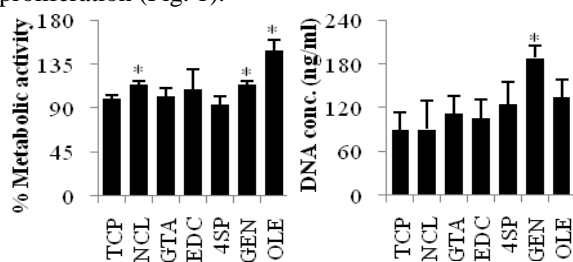


Fig. 1. Fibroblast metabolic activity and proliferation for cross-linked collagen films after 3 days in culture. * indicates statistical significance compared to TCP.

Moreover, GEN increased macrophages metabolic activity as LPS treated macrophages. Other cross-linked films maintained similar activity as non-treated macrophages (Fig. 2). Also, some preliminary data showed that cross-linking can affect macrophage morphology (Fig. 3).

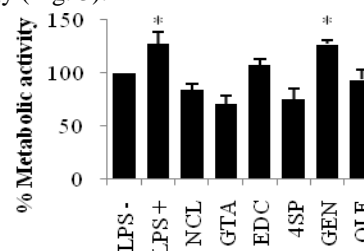


Fig. 2. Macrophage metabolic activity for different cross-linked collagen films after 1 day in culture. * indicates statistical significance compared to LPS-.

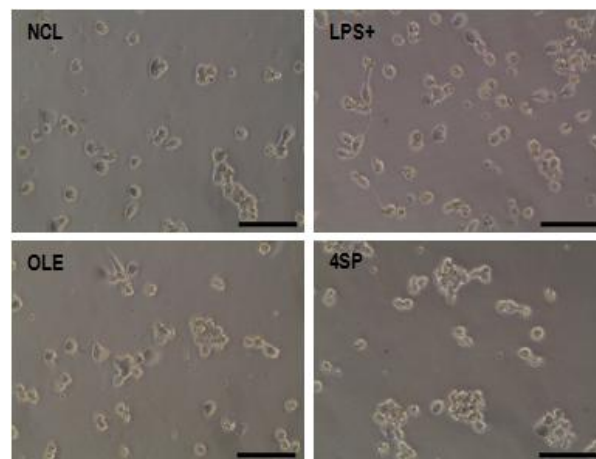


Fig. 3. Macrophage morphology for different cross-linked collagen films after 1 day in culture. OLE maintained morphology while 4SP induced macrophage aggregation.

CONCLUSION

PEG and plant extract cross-linkers have shown to increase stability and none of them had an effect on fibroblast viability and metabolic activity. Although preliminary macrophage culture shows that some of these cross-linking methods may activate macrophages as the positive LPS control.

REFERENCES

1. Zeugolis D. J Biomed Mat Res. 89, 895-908.
2. Brown B. Acta Biomater. 9,4948-55, 2013.
3. Collin E. Biomaterials. 32, 2862-70, 2011.
4. Rowland C. Biomaterials. 34, 5802-12, 2013.

ACKNOWLEDGMENTS

European Union Seventh Framework Programme (Grant n°263289 - Green Nano Mesh).

Preparation of chitosan nanowires and their application to hemostasis

Ying-Chiang Ho¹ and Yi-Chang Chung^{2*}

¹ Institute of Biotechnology, National University of Kaohsiung, Taiwan R.O.C.

^{2*} Department of Chemical and Materials Engineering, National University of Kaohsiung, Taiwan R.O.C.

ycchung@nuk.edu.tw

INTRODUCTION

Sudden heavy bleeding in a surgery or from a wound always leads to severe damage or life-threatening effect for a patient. Commercial products mainly including powders and sponges are made of cellulose, alginate, collagen, chitosan, zeolite, and so on. Frequently-used sponge-like patches supply fast hemostatic effect on covered wound; however, do not cover the whole area of a wound with irregular shape. Powdered hemostatic materials provide large contact area with wounds and high exudate adsorption. However, difficult quantity control for sprinkling a powder on a wound surface and possible overdose of powder are frequently happened in hemostasis process. Hemostatic spray might be a better design which could display excellent thrombogenicity using a small amount and form a thin film to cover irregular-shape wound. Furthermore, chitosan with positive abundance ammonium pendent groups in its structure when it is dissolved in a weak acid solution, the positive charges can absorb and activate negatively-charged platelets. These activated platelets aggregate to form a platelet plug, release agonists which recruit more platelets to the growing thrombus, and form a clot mass to stop bleeding in a short time. In order to rapidly induce thrombus and fibrin formation, chitosan nanowire suspensions were synthesized to constitute network-like structure to improve particle-like powder to provide a potential hemostatic spray material.

EXPERIMENTAL METHODS

1. Preparation of chitosan nanowires. Chitosan (MW= 35000) was dissolved in 90 wt.% acetic acid to prepare a 10 wt.% chitosan solution after heating at 50 °C for an hour with gentle stir and then constantly stirring for 24 hr. The chitosan solution was then poured into a 5 ml syringe fitted with a 23G needle (inside diameter 0.34 mm) and connected to a microsyringe pump. The high-voltage power supply was then connected to the needle tip and the other electrode, stainless steel mesh with a 0.6 x 0.6 mm² grid, was grounded with a 7 cm distance to the needle. The metal mesh was supported with a beaker containing 1 wt.% NaOH aqueous solution to solidify and collect those forming chitosan nanowires. The injection rate was controlled at 0.1 ml/hr. The schematic of apparatus is shown in Fig. 1. The other composition, chitosan mixed with polyvinyl alcohol (PVA) in a ratio of 2:1 was used to prepare CS-PVA nanowires for a reference. The dried nanowires were then crosslinked using 2 ml 0.25 wt.% alginate solution (or 1 mg/ml triphosphate solution) to react for one hr.

2. Characterization and physical property measurement. The dimension analysis of nanowires was carried out using SEM and STEM.

3. Clotting test and blood cell adherence measurement. Replace collection liquid to an aluminium disc to prepare a chitosan nanowire-coated surface with electro-spraying for 5 min. Then the sample discs were used to contact whole blood sample for 3 min. The cells adhered on the discs were rinsed, fixed, and observed for their surface morphologies via SEM. As for the clotting time measurement, the 20 mg nanowires were located into a glass tube and 2 ml blood sample was then poured into in a 37 °C water bath. The other portion 200 µl 0.2 M calcium chloride solution was added into the vertically-standing test tube which was then turn to horizontally-lying every 30 sec to check the blood flow until it stop flowing.

RESULTS AND DISCUSSION

We improved the traditional electro-spinning process to fabricate short nanowires using high-boiling-pointed acetic acid and low-molecular-weighted chitosan. Due to low evaporating property of the solution and less entanglement between polymer chains, the shortened chitosan nanowires could be obtained via collecting nanowires passing through a grounded metal mesh in a basic alcoholic solution. The diameters of nanowires could be controlled via some parameters: precipitating agents, operation voltages, and working distances, and so on. Higher operation voltage generated relatively narrow nanowires. the precipitating agents using different NaOH/ethanol ratios could dominate the morphology of nanowires, affect the precipitation, and change diameters of nanowires. In blood coagulation tests, TPP could enhance fibrin formation but take more time; while alginate-crosslinked chitosan might exhibit high water adsorption to intercept more blood and cells. However, surface-crosslinked chitosan might be neutralized on those positive ammonium groups, decreasing the positive charges on surfaces and also the adsorption and activation of platelets.

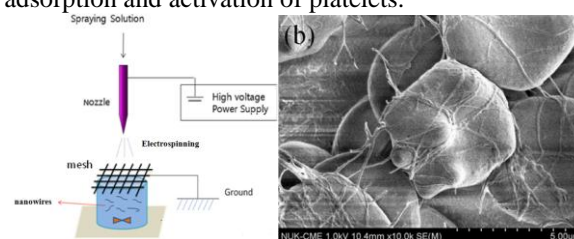


Fig.1. Schematic of electrospray apparatus and SEM image of RBS tied with nanowire networks.

CONCLUSION

We used chitosan nanowires as hemostatic materials in this research according to the hemostasis property of chitosan, which can also absorb and activate platelets and enhance the formation of fibrin.

Mobilization of Mesenchymal Progenitor Cells to Improve Bone Healing

P.S. Lienemann¹, A.S. Kivelioe¹, S. Metzger¹, S. Höhnel², A. Roch², O. Naveiras², A. Sala¹, V. Milleret¹, F. E. Weber³, W. Weber⁴, M.P. Lütolf², M. Ehrbar¹

¹ Department of Obstetrics University Hospital, Zürich, Switzerland, Martin.Ehrbar@usz.ch

² Laboratory of Stem Cell Bioengineering, EPF Lausanne, Switzerland

³ Craniofacial Surgery, University Hospital Zürich, Switzerland

⁴ Faculty of Biology and BIOS Centre for Biological Signalling Studies, University of Freiburg, Germany

INTRODUCTION

Bone morphogenic proteins have shown unexpectedly low bone healing capacity in clinical situations and thus are need in doses, exceeding the physiological ones by several orders of magnitude. By use of adequate delivery systems which provide a continuous low level of osteogenic growth factors and the appropriate co-signaling with integrins bone formation could be enhanced, while adverse off-site effects are kept minimal. On the on the hand, optimizing early stages of bone healing could likely provide improve the mobilization of mesenchymal progenitor cell (MPC) ¹. As MPCs have both a great proliferation potential and the capacity to form bone they could have a major impact on bone healing efficiency.

Materials and Methods

Transglutaminase factor XIII cross-linked PEG-based hydrogels (TG-PEG) ^{2,3} of 5mm diameter and 1mm thickness were formed at low cross-link density (1.7%) and placed in 5mm critical sized calvarial defects of GFP-mice. After 1, 2, and 3 week of implantation hydrogels were harvested and mobilized cells and tissues were characterized by FACS or immunohistochemistry. Prospectively isolated non-endothelial (CD31⁻) and non-hematopoietic (CD45⁻/Ter119⁻) cells were selected based on their expression of the cell surface markers Sca1 and Alcam ⁴. The obtained cell fractions were tested for their ability to form colony forming units fibroblast (CFU-F) at a seeding density of 10³ cells per cm². Additionally they were allowed to form microtissues (over night, as a hanging drop) which were embedded in a TG-PEG hydrogel (1.5%) and cultured in presence of a series of 20 factors known to be involved in mesenchymal cell migration at concentrations of 50ng per mL of culture medium. Best growth factor candidates were admixed to forming hydrogels and implanted in critical sized murine calvarial defects. The healing of defects is characterized by longitudinal evaluation of bone formation using micro computed tomography as well as

by histological (haematoxylin & eosin) and immunohistochemical (CD31, Sca1, CD45) stains.

Results and Discussion

Trapped cells could be readily obtained from the healing bone defect by digestion of the provisional TG-PEG hydrogels using collagenase. By prospective isolation of non-hematopoietic and non-endothelial cells, three mesenchymal populations of ca. 10⁴ cells per defect were obtained which were Alcam⁺/Sca1⁻, Alcam⁻/Sca1⁻ or Alcam⁻/Sca1⁺. Although all three mesenchymal cell populations could be expanded in vitro most of the CFU-Fs were formed by Alcam⁻/Sca1⁺ fraction. Additionally this cell fraction could be differentiated towards the osteogenic, chondrogenic and adipogenic lineages, indicating that it contains cells with characteristics compatible with the definition of MPCs. When entrapped in TG-PEG hydrogels, microtissues consisting of Alcam⁻/Sca1⁺ cells, they were promoted to migrate out of the microtissue by a number of factors described to be involved in mesenchymal cell recruitment. Currently, selected growth factors are being tested for their ability to promote the recruitment of mesenchymal progenitor cells and the formation of novel bone in the murine critical size defect.

Conclusion

Cells trapped at the site of bone defect healing contain MPCs, which can be prospectively isolated and are promising candidates for the screening of factors involved at different stages of bone regeneration.

REFERENCES

1. Lienemann P.S. ADDR 64, 1078-1089 (2012).
2. Ehrbar M. Biomacromolecules 8, 3000-3007 (2007)
3. Ehrbar M. Biomaterials 28, 3856-3866 (2007).
4. Nakamura Y. Blood 116, 1422-1432 (2010)

ACKNOWLEDGMENTS

We thank F. Nicholls and E. Kleiner (University Hospital Zurich) for help with animal experiments and histology.

Modification of polylactide surfaces with PLA-b-PEO nano-colloids

Eliska Mazl Chanova, Ognen Pop-Georgievski, Marta Maria Kumorek, Ludka Machova and Frantisek Rypacek

Institute of Macromolecular Chemistry of the Academy of Sciences of the Czech Republic, v.v.i., Czech Republic
chanova@imc.cas.cz

INTRODUCTION

Formation of surface brush layers based on deposition of amphiphilic block copolymers composed of polylactide (PLA) and poly(ethylene oxide) (PEO) from selective solvents is studied as a method of surface modification of PLA-based biomaterials for tissue engineering.¹ Nano-colloid printing of functional PLA-*b*-PEO is under investigation for preparation of specific surface pattern of biomimetic groups that would influence cell adhesion, growth and differentiation.² The crucial factor of this approach, i.e. to provide specific cues for cells through the synthetic oligopeptides present on the biomaterial surface, is the resistance of such surface to nonspecific protein adsorption, otherwise the proteins from the cell culture medium or body fluids will cover present bioactive groups. In this study, we investigate the effect of the deposition of PLA-*b*-PEO copolymer nano-colloids on PLA surface and the efficiency of resistance of such surfaces to proteins, e.g. albumin and fibrinogen, with respect to the molecular parameters of used copolymers.

EXPERIMENTAL METHODS

PLA-*b*-PEO block copolymers with matching PLA block (7 kDa) and different PEO block length (5, 10 and 15 kDa) were synthesized by ring opening polymerization of L-lactide in toluene using α -hydroxy- ω -methoxy-PEO as a macroinitiator and Sn(Oct)₂ as a co-initiator. PLA-*b*-PEO copolymers were deposited on PLA surface on poly(dopamine) (PDA) coated Au SPR chips and characterized by spectroscopic ellipsometry, infrared reflection adsorption spectroscopy (IRRAS), contact angle measurement (CA), atomic force microscopy (AFM) and surface plasmon resonance measurement (SPR) to determine the optical thickness of polymer films, composition of top layer, wettability, topography and protein resistivity of prepared surfaces.

RESULTS AND DISCUSSION

Amphiphilic block copolymers such as PLA-*b*-PEO in selective solvents can associate to self-assemblies and/or with surface compatible with PLA block.

Three PLA-*b*-PEO copolymers with increasing PEO block length were spin coated from the selective solvent (acetone/methanol 1/9 v/v) on the top of PLA film providing layers with optical thickness about 20 nm without any significant difference with respect to PEO block length. The presence of PLA-*b*-PEO top layer was confirmed by IRRAS where the spectral contributions of PEO rise with increasing molecular weight of PEO block. Further, the length of PEO block, and the PLA/PEO ration in copolymer affected the surface topography (Figure 1). The lamellar structure of PLA/PEO-15kDa top layer can be attributed to the ability of PEO to crystallize (Figure 1A).

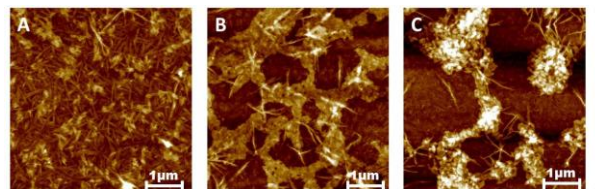


Figure 1: AFM topography images of PLA/PEO-15kDa (A), PLA/PEO-10kDa (B) and PLA/PEO-5kDa (C) layer deposited on PLA surface. Scan size: 5x5 μ m, Z-scale: 50 nm.

The deposition of PLA-*b*-PEO nano-colloids resulted in surfaces with highly hydrophilic character (PLA/PEO-15kDa and PLA/PEO-10kDa) and moderately hydrophilic character (PLA/PEO-5kDa) compared to pure hydrophobic PLA. The wettability corresponds well with the fouling properties where the adsorption of albumin and fibrinogen decreases with increasing hydrophilicity of the surface. For example, the adsorption of fibrinogen to PLA-*b*-PEO-5kDa was determined to be more than ten times lower compared to pure PLA, and furthermore, the adsorption to PLA-*b*-PEO-15kDa was lower about 200 times.

The results demonstrate that the character of deposited copolymer layer, and hence, the formation of PEO brush were affected by the molecular parameters of used copolymer. The copolymer with longer PEO block provide hydrophilic layer with PEO exposed on the surface when the surface is in contact with water. The PEO chains can be hydrated and expanded, thus providing an efficient shield against protein adsorption.

CONCLUSION

Poly lactide biomaterials can be effectively modified by deposition of amphiphilic PLA-*b*-PEO copolymers. The efficiency of modification and the non-fouling character depends on molecular parameters of used copolymers. The most efficient surface modification was achieved with PLA-*b*-PEO copolymer with longer PEO block, particularly 15kDa, providing hydrophilic surface with significantly suppressed adsorption of albumin and fibrinogen in comparison to pure PLA.

REFERENCES

1. Tresohlava E. *et al.*, Biomacromolecules 11:68-75, 2010
2. Knotek P. *et al.*, Mat. Sci. Eng. C 33:1963-1968, 2013

ACKNOWLEDGMENTS

The financial support from Czech Science Foundation (GACR, Grant No.: P108/12/P624) and from the Ministry of Education, Youth and Sports of the Czech Republic (Grant No. EE2.3.30.0029) is acknowledged.



Local Delivery of Alendronate and Bone Remodelling in Rat Models

Necati Harmankaya^{1,2*}, Johan Karlsson³, Anders Palmquist^{1,2}, Mats Halvarsson⁴,
Martin Andersson³ and Pentti Tengvall^{1,2}

¹Dept. Biomaterials, Sahlgrenska Academy at University of Gothenburg, Sweden, ²BIOMATCELL VINN Excellence Center of Biomaterials and Cell Therapy, ³Dept. Chemical and Biological Engineering, Applied Chemistry, Chalmers University of Technology, Sweden, and ⁴Dept. Applied Physics, Microscopy and Microanalysis, Chalmers University of Technology, Sweden, *neco@biomaterials.gu.se

INTRODUCTION

Patients suffering from osteoporosis or other osteopenic conditions are in higher risk of revision surgeries of skeletal devices. An improved primary implant fixation is possible if implant surface is employed as a drug reservoir from which drugs can be delivered site of healing. This also brings about higher drug efficacy and mitigation of side effects. In the present work, Ti implants were coated with 200 nm thick mesoporous (MP) TiO₂ [1-3] loaded with alendronate (ALN), a N-bisphosphonate, and evaluated *in vivo* in terms drug efficacy, distribution and bone anchorage in healthy or osteoporotic rat models.

METHODS

Mesoporous TiO₂ coatings were synthesized on machined Ti implants by Evaporation Induced Self-Assembly (EISA), achieving an ordered structure and a narrow pore size distribution ($\Phi=6$ nm). Approx 500 ng/cm² of ALN was deposited from solution (0.8 mg/ml) into the coatings, and the implants inserted in the tibia of mature male- or ovariectomized female rats. As reference, ALN was given systemically. Bone anchorage in terms of bone area (BA), bone-implant-contact (BIC) and removal torque (RTQ) were determined after 4 weeks of healing. In addition, expression of bone remodelling markers were analysed in qPCR and the distribution of locally given ALN was assessed after 8 weeks by ¹⁴C-ALN analysis in autoradiography and Liquid Scintillation Counting (LSC).

RESULTS AND DISCUSSION

MP coatings were proven successful for local delivery of ALN in healthy and osteoporotic bone. Significantly higher BIC and RTQ values were observed for locally delivered ALN than systemically delivered ditto (see Table 1). BIC was 48% higher and RTQ 45% higher (local vs. systemic, $p<0.05$, $n=8$). BA showed a similar same trend, but not with a significant difference between the groups. The implant close distribution of ALN declined slowly thru 8 weeks, confirming its long residence time and high affinity to bone. Autoradiographic data were analysed with respect to imaginary profiles cross the implant, which revealed the release of ALN in relation to distance from tibial cortex vs. intermedullary space. When overlapped with backscattered SEM, the high affinity of ALN to apatite was clearly depicted (see Fig.1). LSC revealed a release of ALN in the range of 3-500 ng in peri-implant tissue when using MP TiO₂ thin films as a drug reservoir.

Table 1 Summary of μ CT data showing BIC and RTQ data showing bone-anchorage after local or systemic ALN delivery. Implantation time 4 weeks in rat tibia. (* $p<0.05$, $n=8$)

	BIC (% \pm SD)	RTQ (Ncm \pm SD)
Implant w/ALN	41.8 \pm 4.6*	5.06 \pm 0.71*
No drug	34.3 \pm 6.8	3.59 \pm 0.86
Systemic ALN	31.8 \pm 4.3	3.48 \pm 0.78
Saline	32.2 \pm 4.4	3.35 \pm 0.81

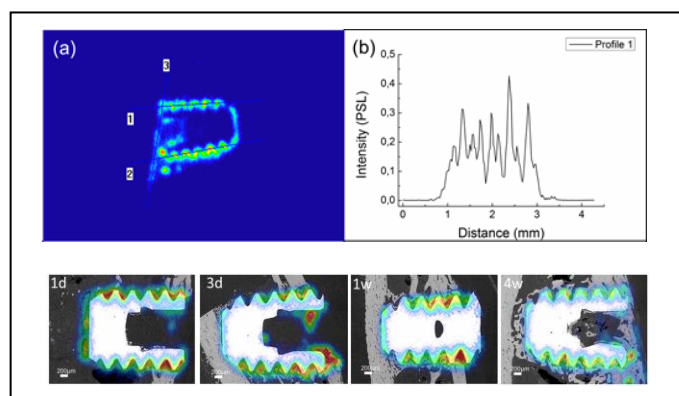


Fig. 1: (upper) Profile analysis in autoradiography after 4 weeks of healing. (lower) Overlap of the autoradiographic and backscattered SEM images thru 4 weeks of implantation in rat tibia.

CONCLUSION

When early implant fixation is impaired in compromised patient groups, ALN can be delivered locally from implant surfaces. With high affinity to bone, the high drug efficacy improves bone-anchorage and mitigate systemic effects that may be otherwise related to systemic administration of bisphosphonates.

REFERENCES

1. Andersson M. *et al.*, Chem. Mater. 17:1409-1415, 2005.
2. Karlsson J. *et al.*, Acta Biomater. 8:4438-4446, 2012.
3. Harmankaya N. *et al.*, Acta Biomater. 9:7064-7073, 2013.

ACKNOWLEDGEMENTS

The authors gratefully thank the Materials Area of Advance at Chalmers University of Technology and BIOMATCELL VINN Excellence Center for Biomaterials and Cell Therapy for providing the financial support.

Localized cell differentiation with BMP-2 in a PEG scaffold using a streptavidin linker

S. Metzger¹, P. S. Lienemann¹, C. Ghayor², M. Karlsson^{3,4}, F. E. Weber², W. Weber^{3,4}, M. Ehrbar¹

¹ Department of Obstetrics, University Hospital Zurich, Switzerland, ² Department of Cranio Maxillofacial Surgery, University Hospital Zurich, Switzerland, ³ Department of Biosystems Science and Engineering, ETH Zurich, Switzerland,

⁴ Faculty of Biology and BIOS Centre for Biological Signalling Studies, University of Freiburg, Germany
stephanie.metzger@usz.ch

INTRODUCTION

Mimicking the extracellular matrix (ECM) by binding growth factors (GFs) and cell-instructive cues inside naturally occurring or synthetic scaffolds in vitro allows the study of biological processes taking place between cells and the ECM in living tissue. This work presents a strategy for the local immobilization of GFs inside polyethylene glycol (PEG) hydrogels [1] using a streptavidin linker that is enzymatically cross-linked to PEG hydrogels by the transglutaminase FXIII. We hereby demonstrate a way to efficiently immobilize and display recombinant human bone morphogenetic protein-2 (rhBMP2). Scaffolds with spatially defined rhBMP-2 areas were generated and promoted the localized differentiation of a myoblastic cell line and of mesenchymal stem cells (MSCs) towards the osteogenic lineage, characterized by the expression of alkaline phosphatase (ALP).

EXPERIMENTAL METHODS

A peptide linker composed of the streptavidin sequence and the substrate sequence of FXIII was produced. Its functionality was assessed by Western blotting to show its incorporation into PEG hydrogels. Its ability to capture biotinylated ALP (ALP-biotin) was showed using the SEAP assay. Biotinylation of rhBMP-2 was carried with NHS-PEG₄-biotin and detected by Western blotting. The functionality of biotinylated rhBMP-2 (rhBMP-2-biotin) was assessed with the ALP activity assay on C2C12 cells. Binding of rhBMP-2-biotin to PEG hydrogels with the linker was determined by incubating the hydrogels in a solution of rhBMP-2-biotin and measuring the rhBMP-2-biotin left in the solution via ELISA. The release of immobilized rhBMP-2-biotin from the hydrogels was also determined by ELISA by incubating the hydrogels in cell culture medium for 5 days and quantifying the amount of rhBMP-2-biotin released into the buffer at day 1, 2 and 5. Localized differentiation of C2C12 cells and bone marrow-derived MSCs (BM-MSCs) in PEG hydrogels was demonstrated by colorimetric staining of ALP and immunostaining against bone ALP.

RESULTS AND DISCUSSION

The streptavidin linker was reacted with PEG components and FXIII and incorporation was shown by the increased molecular weight of the linker due to cross-linking. Hydrogels containing the linker were incubated in a solution of ALP-biotin and the amount of ALP-biotin left in the solution was measured with the SEAP assay. Hydrogels containing 50 μ M and 125 μ M of linker were able to bind almost 50% and 80% of the ALP-biotin in solution after 24 hrs respectively.

Following experiments were carried with 100 μ M of streptavidin linker. After biotinylation, the biological activity of rhBMP-2-biotin was compared to rhBMP-2. The ALP activity assay showed that almost 98% of the biological activity was retained. The binding study showed that over 80% of rhBMP-2-biotin was captured by the hydrogels after 16 hrs incubation, out of which approximately 25% were slowly released after 2 days of incubation in cell culture medium (compared to 90% release without linker), showing improved retention of the GF. Finally PEG hydrogel constructs with locally immobilized rhBMP-2-biotin and seeded with C2C12 cells (Fig. 1A) or BM-MSCs (Fig. 1B) were prepared. After 9 days in culture, the cells growing in the rhBMP-2-biotin area expressed ALP, whereas the cells surrounding this area did not.

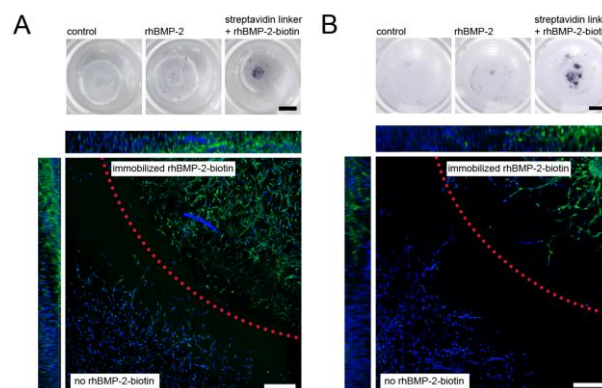


Figure 1. PEG constructs with locally immobilized rhBMP-2-biotin or soluble rhBMP-2 and seeded with C2C12 cells (A) or BM-MSCs (B) showing localized ALP expression (top: colorimetric staining, scale bar = 2mm; bottom: immunostaining, scale bar = 200 μ m).

CONCLUSION

The streptavidin linker was successfully used to immobilize rhBMP-2-biotin into PEG hydrogels and to obtain local differentiation of cells. This linker could be potentially used in conjunction with other types of linker compatible with the enzymatically cross-linked PEG hydrogel system [2] in order to achieve controlled immobilization of GFs in precise patterns.

REFERENCES

1. Ehrbar M. *et al.*, Biomaterials. 28:3856-66, 2007
2. Lienemann P. S. *et al.*, Adv. Healthc. Mater. 2:292-6, 2013

ACKNOWLEDGMENTS

We would like to thank Aida Kurmanaviciene for the production and purification of the linker and her help in establishing the PEG hydrogel constructs.

Plasma Spraying of Zinc Substituted Hydroxyapatite

David Shepherd¹, Roger Brooks² and Serena Best¹

¹CCMM, Department of Materials Science and Metallurgy, University of Cambridge, United Kingdom

²Orthopaedic Research, Addenbrooke's Hospital, University of Cambridge, United Kingdom
dvs23@cam.ac.uk

INTRODUCTION

With an ageing population there is an ever-increasing demand for implants. Current implants have a finite life that could be extended by improving the implant-bone interface. This could be achieved by improved coatings; reducing the amount of resorption taking place at the bone implant interface but also increasing bone apposition around the implant.

Zinc has a proven effect on bone cells, by increasing the activity of osteoblasts but also inhibiting the activity of osteoclasts, and may thus lead to an overall increase in bone deposition.

Work previously carried out by the authors showed that it is possible to substitute zinc into hydroxyapatite and that it has an inhibitory effect on osteoclast number and subsequent activity^{1,2}.

The aim of this work was to investigate if it is possible to plasma spray zinc substituted hydroxyapatite and examine the coatings.

EXPERIMENTAL METHODS

Zinc substituted hydroxyapatite (ZnHA) of 0.65wt% and pure HA (0wt% zinc) were produced using a method described previously¹. These powders were then prepared for plasma spraying according to a previously described procedure². From previous studies applying hydroxyapatite coatings by plasma spraying it was decided to investigate the coatings produced from operating voltages of 25, 30 and 35 kV.

The coatings were physically characterised by XRD, to identify the phases present and SEM to study the morphology of the coatings and splats produced through the plasma spraying technique

RESULTS AND DISCUSSION

Through XRD analysis of the coatings (Figure 1) it could be observed that there were other phases present. These included calcium oxide (CaO) and tri-calcium phosphate (TCP). These phases are formed through the decomposition of HA. As these are not normally observed using plasma spraying of hydroxyapatite it can be hypothesised that the zinc substituted into the HA lattice leads to a lowering of the thermal stability of the apatite. The reduction of the CaO phase with lower operating voltages and thus lower plasma temperature tends to agree with this hypothesis.

SEM images (Figure 2) shows that there were splats produced at all operating voltages. The best coating was unsurprisingly produced with the highest operating voltage. The coatings produced at 30 kV and 25 kV were similar in appearance. Any further reduction in

operating voltage would have led to incomplete melting of the particles and hence, a poor coating.

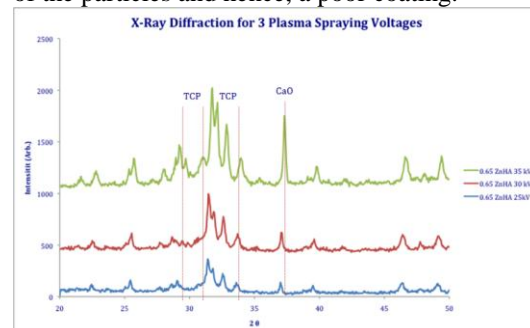


Figure 1: XRD Patterns for Plasma Sprayed 0.65 wt% ZnHA at the three operating voltages 35 kV, 30 kV and 25 kV

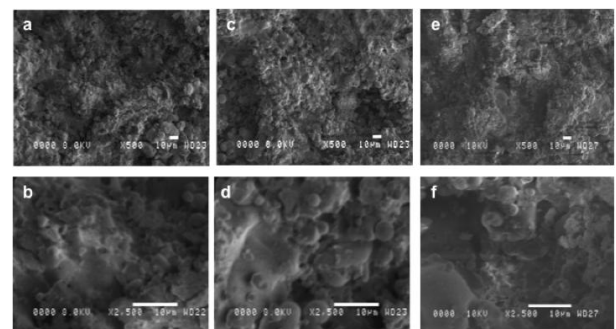


Figure 2: SEM images of the plasma coatings; a + b 35 kV; c + d 30 kV and e + f 25 kV

Results from the 2 physical characterisation techniques showed that the coating produced at 35 kV, whilst producing the optimum splat morphology, has high levels of CaO and so has to be discounted. The morphology of the splats for the operating voltages of 30 and 25 kV were very similar but XRD analysis of the coating at 30 kV also has a high level of CaO and so also has to be ruled out as a coating parameter.

CONCLUSION

The work found that it is possible to produce a plasma sprayed coating of ZnHA and the optimum operating voltage is 25 kV. Further studies are required to determine if this coating is suitable for consideration for use on orthopaedic implants.

REFERENCES

1. Shepherd, D. *et al*, Biomed. Mater. 8:02003, 2013
2. Shepherd D. *et al*, J Biomed Mater Res A, 2014
3. Tang Q. *et al*, J Mater Sci-Mater M, 10:173, 2010

ACKNOWLEDGMENTS

The support of Orthopaedic Research UK is gratefully acknowledged. The support of NIHR is also gratefully acknowledged for Roger Brooks.

***Candida glabrata* in mouthwash -coated endotracheal tubes: antibiofilm activity by electronically scanning microscopy**

Danielle Bezerra Cabral¹, Evandro Watanabe² and Denise de Andrade¹

¹Fundamental Nursing/ University of São Paulo at Ribeirão Preto/ College of Nursing, Brazil

²Restorative Dentistry/ Faculty of Dentistry/University of São Paulo at Ribeirão Preto, Brazil
dannyebezerra@usp.br

INTRODUCTION

Candida glabrata has emerged as a notable pathogen oral mucosa and may promote concomitant infection with *C. albicans*. It is known for its pathogenicity in the oropharynx with difficult treatment and relevance in global casuists¹. The oral microbiome is major factors to health and disease process and its rupture indicate or influence the course of oral diseases². Furthermore, the fungi can colonize substrates polymeric compounds, ceramics, wood and glass, and this is due to not having antimicrobial activity³. This study aimed to evaluate antibiofilm activity of endotracheal tubes (ETT) coated alcohol-free mouthwash containing 0.12% chlorhexidine gluconate, 0.075% cetylpyridinium chloride (CPC) and Listerine® as well as tea tree oil (TTO) by quantification of colony forming units (CFU/ml) and visualization of biofilm by scanning electron microscopy.

EXPERIMENTAL METHODS

Of the total 20 oral clinical isolates of *C. glabrata* available in the database ambulatory of dentistry from the University of Sao Paulo, we used 4 strains to form biofilm, in triplicate and *in vitro*. Each mouthwash was injected 10 ml inside segments (2cm) of TETs at 45° and homogenized for 10sec in orbital shaker solutions AP -59 (Phoenix Luferco®, Brazil). There was masking by the principal investigator to use the technique of coating ETT with mouthwash. The cuts were kept in the wells plates for 24 hours at room temperature. For the formation of biofilm was transferred 100 µl standard microbial inoculum for the test-tube containing Sabourand dextrose broth, 2g glucose and 4g sucrose (V=10 ml) and then homogenized for 1 min. 50µl each culture was serially diluted and transferred to petri plates, generating five replicated plates for each isolate and then incubated at 37°C and visualized after 48 h. Following incubation, these plates were assessed for counting colony forming units per millilitre (CFU/ml) and also by scanning electron microscopy (SEM, JSM 6610LV, JEOL, Tokyo, Japan). The statistical analysis of biofilm formation will be performed using the software R version 3.0.2⁴, applying the likelihood ratio test, considering a significance level of $\alpha = 0.05$. To investigate the efficacy of mouthwashes on biofilms formation will be analyzed data by the distribution free Kolmogorov-Smirnov test.

RESULTS AND DISCUSSION

Preliminaries data showed the mean counts of total viable *Candida glabrata* had a range from 10^2 to 10^5 CFU/mL. The media and standard desviation of each mouthwash tested were: A= $4,8 \times 10^5$ (MD) \pm $2,2 \times 10^5$ CFU/ ETT (SD); B = $4,6 \times 10^5$ (MD) \pm $2,6 \times 10^5$

CFU/ ETT (SD); C = $3,1 \times 10^5$ (MD) \pm $2,6 \times 10^5$ CFU/ ETT (SD); D = $5,8 \times 10^5$ (MD) \pm $2,9 \times 10^5$ CFU/ETT (SD); E = $2,3 \times 10^5$ (MD) \pm $2,7 \times 10^5$ CFU/ ETT. The PC (Fig. 1a) showed inhibition of colony formation, in duplicate, but a clinical isolate (2 strains) had microbial count of 7.7×10^4 CFU/ETT. An important virulence factor of *Candida* species is their ability to form biofilms and these can be formed on abiotic surfaces such as medical devices⁵. *Candida glabrata* has ability to form oral biofilms and present a high tolerance to antifungal agents used in fungal infection treatment. Thus, biofilms this study were visualized in other mouthwashes (Fig 1b).

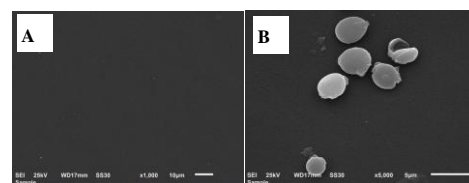


Fig. 1 Representative scanning electron microscope images of clinical isolates of *C. glabrata*. **A** - Antibiofilm activity of 0.075% CPC against clinical isolate of *C. glabrata* at 1,000 \times magnification, 25kV. **B** - *C. glabrata* biofilm growth in ETT coated tea tree oil at 5,000 \times magnification, 25kV.

Our findings also show that the planktonic isolates of *C. glabrata* tested were susceptible to TTO with average of 8.3×10^5 CFU/ETT and all other mouthwashes tested showed relatively poor activity biofilm against the isolates tested.

CONCLUSION

It is speculated that the 0.075% cetylpyridinium chloride had antibiofilm activity against clinical isolates of *Candida glabrata* on the preliminary results.

REFERENCES

1. Dignani MC. et al., In: Anaisse, McGinnis, Pfaller, editors. Chapter 8. 1st ed. Philadelphia: Churchill Livingstone; 2003.
2. Mager DL. et al., J Clin Periodontol. 30(7):644-54, 2003.
3. Coad BR et al. Biotechnol Adv., 7: S0734-9750, 2013.
4. R CORE TEAM. R: A language and environment for statistical computing. R Foundation for Statistical Computing, Vienna, Austria. 2013.
5. Donlan RM. Emerg Infect Dis. 7:277-81, 2001.

ACKNOWLEDGMENTS

The authors would like to thank the Coordination for the Improvement of Higher Education Personnel (CAPES) for providing financial support to this thesis.

Simple Silver Deposition Strategy for Antibacterial Titanium Implants

Kennedy Omoniala, David Armitage, Susannah Walsh
Leicester School of Pharmacy, De Montfort University, Leicester, England
kennedy.omoniala@email.dmu.ac.uk

INTRODUCTION

Support tissue replacement has become a mainstay of modern medical practice. With this evolution has emerged titanium as the replacement material of choice because of its numerous advantages over other materials hitherto in use. Two of the common factors influencing in situ longevity of implants are the strength of the bond between the implant material and the surrounding mechanical (bone) tissue, and bacterial colonisation of the now poorly vascularised tissue-implant interface¹. In this study, a simple strategy for modifying the titanium implant surface to improve osteo-integration and also confer anti-bacterial properties is evaluated.

EXPERIMENTAL METHODS

Surface Modification: Titanium discs were water-jet cut from 1mm sheet (Goodfellow, Cambridge). Polishing was carried out by grinding with silicon carbide paper followed by final polishing with colloidal silica and hydrogen peroxide. The mirror finished surfaces were then sonically cleaned with acetone. Polished surfaces were then subjected to a thermo-chemical treatment involving a pre-treatment with 10M NaOH for 24hrs, brief washing in deionised water and treated with 1M AgNO₃ for 24hrs. All treatments were performed in a shaker water-bath maintained at 80°C and 60rpm. All treated surfaces were characterised for surface energy, composition, and morphology by means of goniometry, SEM/EDX, and AFM².

Biofilm Formation: 18 Ti discs in groups of 6 unpolished, mirror-finished and Ag-treated, together with 6 polycarbonate discs were exposed to biofilm formation on their surfaces, in a CDC-Biofilm reactor, using *Staphylococcus aureus*. Biofilms formed on the surfaces were aseptically removed, suspended in sterile distilled water and serially plated on 90cm nutrient agar using a spiral plater. The plates were incubated at 37°C for 24hrs and bacteria colony forming units counted. The procedure was repeated for 3 more batches of 18 Ti disc and 6 polycarbonate discs, making a total of 24 discs in each group. Inhibition zones for the different surfaces were also determined. The normality of distribution of data and the significance in variations between the various groups were tested using SPSS.

RESULTS AND DISCUSSION

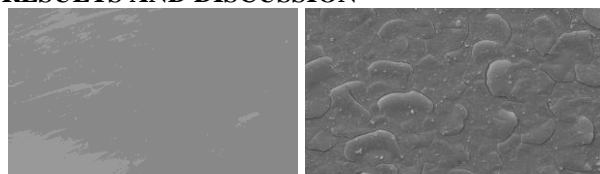


Figure 1: SEM of polished/ mirror-finished and Ag treated Ti surfaces

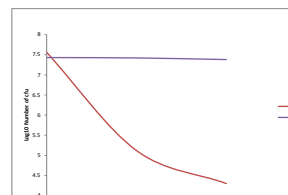


Figure 2: Log reduction of bacteria over time for Ag treated and polished surfaces

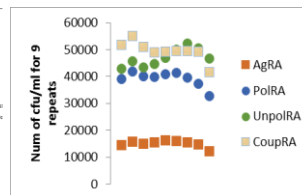


Figure 3: number of cfu from biofilms on Ag and control surfaces for 9 repeats

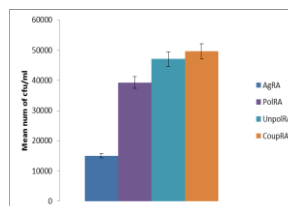


Figure 4: Mean number of bacteria cfu from biofilms on Ag and control surfaces in 24hrs

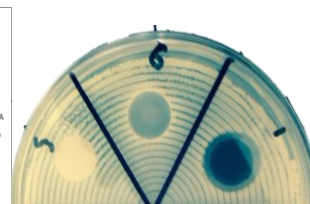


Fig 5: Inhibition zones around various from surface after 24hrs: 1-Ag,5-Polished,6-Coupon

The experimental data indicated the surface modification technique used here, involving polishing the commercially pure titanium (cpTi) surface to a mirror finish allowed for a significantly higher amounts of ionic Ag to be deposited on the modified surface ($7.51.3\% \pm 2.08$), than on the unmodified surface ($2.48\% \pm 0.19$), with a paired sample test sig. <0.05 . The incorporation of Ag⁺ onto the Ti surface as opposed to simple drying out of AgNO₃ on the surface is evident in the negligible amount (nil in some cases), of nitrogen on the SEM/EDX. A *staph. aureus* suspension assay indicated a steady stationary phase over 60min for the mirror finished surface. For the same period, the silver treated surface showed a 32% reduction in bacteria cfu after 30min, and 43% reduction after 60min. Bacteria biofilm formation assays appear to indicate that the deposited Ag significantly inhibits the survival and growth of the bacterial, (sig. <0.05 , 95%). This was 3.3, 2.93 and 2.7 folds respective reduction in biofilm formed for the Ag treated surface compares to the control coupon, unpolished and polished surfaces.

CONCLUSION

The chemical surface modification strategy described above, applied to pure titanium surfaces, can lead to the deposition of significant amounts of Ag⁺ on a titanium implant surface. The deposited Ag⁺ is available in sufficient amounts to provide a significant reduction in bacterial biofilm load. This has the potential to reduce the incidence of peri- and post-surgery related incidence of implanted associated infections.

REFERENCE

1. Zimmerli, W. et al., *Prosthetic-joint infections*. New England Journal of Medicine, 2004. **351**(16): p. 1645-1654
2. Armitage, D., *Therapeutic ion release from modified-titanium surfaces*. Journal of Pharmacy 2009.**61**: A15-A16

Assessment of the bioactivity of gold doped hydroxyapatite-polyvinyl alcohol nanocomposites

Amany Mostafa^{1*}, Hassane Oudadesse² and Mayyada El Sayed^{3*}

^{1*}Biomaterials Department/National Research Centre (NRC), Cairo, Egypt,

²Biomaterials Department/UMR CNRS, University of Rennes1, France

^{3*}Chemical Engineering Department, National Research Centre, Cairo, Egypt

¹amany.mostafa@univ-rennes1.fr, amani.mostafa@gmail.com, ³ Mayyada@aucegypt.edu

INTRODUCTION

Generation of safe, multifunctional and biocompatible materials is an enormous challenge in nano-chemistry. Metals nanoparticles especially gold (Au) can be used as efficient materials for protein immobilization and have already been widely used in biosensor fabrication. Gold and silver nanoparticles were used as a template for the growth of HA crystals when immersed in simulated body fluid^{1,2}. The uptake kinetics of Ca and P onto hydroxyapatite/polyvinyl alcohol (HAV) doped with silver NPs were experimentally investigated and theoretically modelled and high uptake capacities were obtained in the presence of silver NPs³. This work investigates the effect of adding gold NPs in ppm on the bioactivity of nanocomposites prepared from HAV using a kinetic approach.

EXPERIMENTAL METHODS

HAV prepared by an in situ biomimetic approach was doped with different concentrations of gold NPs (HAV-Au) named U1.5, U5 and U16, and the formed powder samples were characterized by different physicochemical techniques such as ICP-OES and DTA. Bioactivity was evaluated in simulated body fluid (SBF) through studying the kinetics of Ca and P uptake onto the different nanocomposite samples.

RESULTS AND DISCUSSION

Table 1 shows the concentrations in (ppm) of Ca, P and Au elements in the composite powders of HAV and the different compositions doped with Au composites along with the corresponding Ca/P molar ratios.

Sample	Ca	P	Au	Molar
symbol	(ppm)	(ppm)	(ppm)	Ca/P
HAV	29.51	12.80	—	1.78
U1.5	36.57	15.41	ND	1.83
U5	29.26	11.83	0.045	1.90
U16	25.09	9.80	0.144	1.97

Figure 1 shows the TGA and DTA of the prepared samples where the total weight loss was apparently increased by the addition of the gold nanoparticles from -20% up to -70% after heating up to 1200 °C. A peak around 450 °C appears as shoulder in U1.5 and is transformed to a significant peak by increasing the amount of gold NPs. Uptake kinetics for Ca and P onto the different composite samples was well described by a pseudo-second-order model (Eq 1) that correlates

uptake (q) to time (t), parameters thereof are compiled in Table 2.

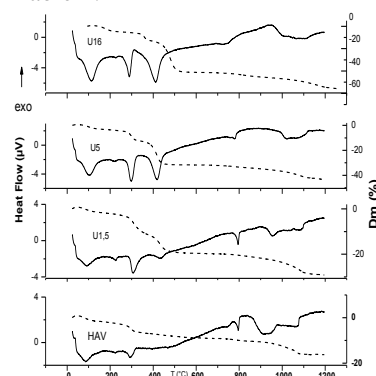


Figure 1. DTA results for HAV and HAV-Au samples.

$$\frac{t}{q} = \frac{1}{k_2 q_e^2} + \frac{t}{q_e} \quad (1)$$

Table 2. Values of the pseudo second-order (k_2) kinetic rate constants and maximum uptake (q_e) for Ca onto HAV and different HAV-Au composites.

	k_2	q_e	R^2	χ^2
	(g/mg.h)*10 ⁸	(mg/g)		
HAV	193.88	12.89	0.987	0.32
U1.5	2.10	87.72	0.939	0.11
U5	7.97	47.17	0.959	0.60
U16	10.60	29.50	0.956	0.40

It can be deduced that adding Au NPs to HAV enhances the uptake of both Ca and P (not shown). The lowest added concentration of Au NPs (U1.5) gave the highest uptake for both Ca and P. Even though increasing the concentration of Au NPs in the HAV-Au samples decreases the uptake amount, it however substantially increases the rate of uptake as clear from the k_2 values.

CONCLUSION

Gold NPs significantly enhanced the bioactivity of HAV nanocomposites where high uptake capacities of Ca and P were obtained. The developed nanocomposites promise to be excellent biomaterials for bone and reconstructive surgery applications.

REFERENCES

1. Lee I. *et al.*, Adv. Mater. 13:1617, 2001
2. Lee I. *et al.*, Adv. Mater. 14:1640–3, 2002
3. Mostafa A. *et al.*, J. Biomed. Mater. Res. A: 2014, DOI: 10.1002/jbm.a.35144

ACKNOWLEDGMENTS

Authors would like to thank Campus France for providing financial support to this project”

Haemocompatibility of Citrate Stabilised Gold Nanoparticles

Brian G. Cousins^{1*}, Niloofar Ajdari² & Alexander M. Seifalian^{1,3}

^{1*}Centre for Nanotechnology & Regenerative Medicine, University College London, NW3 2PF, brian.cousins@ucl.ac.uk,

²Department of Mechanical Engineering, Imperial College London, SW7 2AZ.

³Royal Free London NHS Foundation Trust, NW3 2QG, United Kingdom.

INTRODUCTION

Gold nanoparticles (AuNPs) have received global attention in applications ranging from therapeutics to diagnostics and use in advanced imaging systems.¹⁻² Their unique physicochemical properties such as adsorption of near infrared light to release thermal energy offers new opportunities in the treatment of disease. Their size range similar to many important biomolecules gives rise to unique reactivity, and strategies tailored towards chemical modification offers enhanced bioactivity and targeted delivery. The aim of this study was to evaluate the effects of size using citrate stabilised AuNPs as a simple model system to study their interactions in whole blood and influence on blood coagulation.

EXPERIMENTAL METHODS

Citrate stabilised AuNPs were produced through chemical reduction of Au (III) chloride (HAuCl₄) following the method of Frens.³ Each Au dispersion was standardised by calculating the mean number of Au atoms per particle to determine the molar concentration. Transmission electron microscopy (TEM) evaluated the size of AuNPs via random sampling of multiple fields of view (n=20). Differential centrifugal sedimentation (DCS, Analytik Ltd, UK) was used to determine particle size and distribution. Fresh whole blood was collected from healthy consenting volunteers using collection tubes containing 0.5ml buffered sodium citrate. 255µl of whole blood was added to 85µl of AuNPs (0.66nM). The solution was transferred in to polystyrene TEG[®] cups, and 20µl CaCl₂ (0.2M) was added to initiate blood coagulation, and measured immediately using a TEG[®] 5000 haemostasis analyser (Medicell Ltd, UK).

RESULTS AND DISCUSSION

A range of stable Au dispersions was obtained using the citrate reduction method to yield different sized NPs identifiable by their unique colour (Figure 1, A-B).

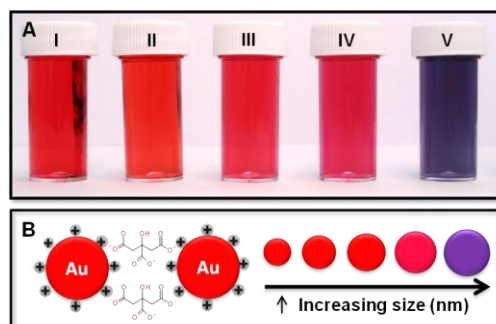


Figure 1. Digital image of Au dispersions (A), and a schematic image (B) highlighting charge stabilisation via negatively charged citrate ions (C₃H₅O(COO₃³⁻)).

TEM and DCS confirmed the particle size/distribution, which revealed spherical NPs ranging from 15, 21, 35, 50, and 60 nm in diameter (samples I-V). Elemental analysis using energy dispersive X-ray (EDX) confirmed the composition of AuNPs. TEG[®] was used as a simple laboratory screening tool to monitor the effects of citrate stabilised AuNPs on blood coagulation. TEG[®] analysis of whole blood found that 35 nm particles (sample III) were the most prothrombogenic with the highest clot rate and stability (Figure 2, A-D).

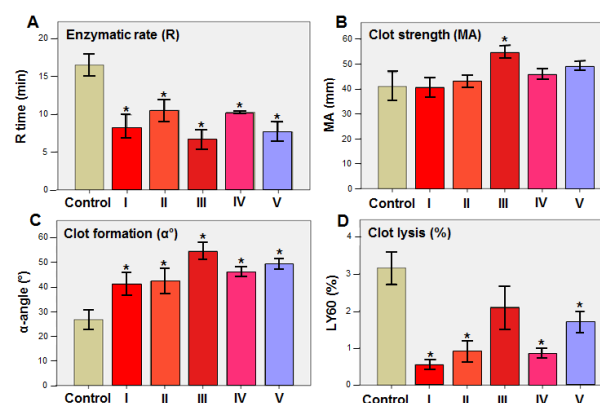


Figure 2. TEG[®] analysis of Au dispersions in (A) highlighting the contribution of enzymes (R time), (B) fibrinogen and platelets (MA), (C) clot formation (α-angle°), and (D) clot lysis (LY60). * = P < 0.05 when compared with citrated whole blood (n = 4).

CONCLUSION

It can be seen that TEG[®] is well suited to evaluate blood compatibility of AuNPs, and offers a better selection of test candidates for *in vitro* and *in vivo* testing based on size, shape and chemistry. Much effort is needed to determine the role of serum proteins, enzymes, platelets and cells with AuNPs in the blood for site specificity and targeted delivery. However, before such tools become available, in-depth studies in the basic science of NP interactions are essential steps in their evolution.

REFERENCES

1. Alkilany AM. *et al.*, J. Nano. Res. 12: 2313, 2010.
2. Soenen SJ. *et al.*, Nano Today. 6: 446, 2011.
3. Frens G. Nature. 241: 20, 1973.

ACKNOWLEDGMENTS

The authors would like to thank Miss Maria Menikou for technical assistance, and Mr Innes Clatworthy from the Royal Free EM Unit for TEM analysis.

Vitronectin Tunes The Biological Activity Of Material-Driven Fibronectin Matrices

M. Cantini^{1,*}, K. Gomide¹, C. González-García^{1,2}, and M. Salmerón-Sánchez¹

¹Biomedical Engineering Research Division, University of Glasgow, Glasgow, UK

²Parker H. Petit Institute for Bioengineering & Bioscience, Georgia Institute of Technology, Atlanta, US

*marco.cantini@glasgow.ac.uk

INTRODUCTION

The challenge for creating new synthetic materials able to serve as biologically active scaffolds that support key aspects of tissue regeneration has driven multidisciplinary efforts for the identification of cell-free routes able to recapitulate the properties of extracellular matrices. Cells within tissues are in fact surrounded by fibrillar matrices that support and regulate cell adhesion, migration, proliferation and differentiation. Within this perspective, the development of artificial biologically active fibronectin (FN) networks through cell-free routes gains a distinct bioengineering interest, because it is a way to enhance the biocompatibility of materials. In our group, we have identified specific surface chemistries that promote the cell-free formation of biologically active physiological-like fibronectin fibrils.¹ In this work, we address the role of another multi-functional adhesive glycoprotein, vitronectin (VN), in the regulation of the biological activity of the material-driven fibrillogenesis of FN, following previous indications that VN confers higher mobility to the protein matrix.²

EXPERIMENTAL METHODS

Polymer sheets were obtained by radical polymerization of ethyl acrylate. Thin films of polymer (PEA) were prepared by spin coating a 2.5% polymer solution in toluene on 12 mm glass coverslips at 2000 rpm for 30 s. FN and VN from human plasma were adsorbed onto the surfaces at a total concentration of 10 µg/ml in different weight ratios (100/0, 70/30, 50/50, 30/70, 0/100). Protein distribution and conformation were evaluated by AFM in tapping mode, while the amount of FN adsorbed onto the substrates was quantified by western blot.

Murine C2C12 myoblasts cells were cultured on protein-coated materials at a density of 20000 cells/cm² for 4 days under differentiation conditions, immunostained for sarcomeric myosin, and differentiation levels were quantified through image analysis. For protein blocking experiments, the RGD domain on FN and on VN were blocked using HFN7.1 and Mab1945 monoclonal antibodies, respectively. To follow the evolution of cell differentiation over time, cells were fixed at 5 time points (3h, 24h, 48h, 72h and 4 days) and the actin cytoskeleton was stained.

RESULTS AND DISCUSSION

AFM shows that FN adsorbed on PEA assembles into a fibrillar network that resembles its physiological cell-mediated assembly. The presence of VN during the adsorption results in the incorporation of VN molecules into the protein network, facilitating the mobility of the protein at the material interface and resulting in higher

adsorption of FN and faster dynamics of network formation at certain FN/VN ratios (70/30, 50/50).

When C2C12 cells are cultured on these surfaces, the presence of VN non-monotonically tunes myogenic differentiation, as the degree of differentiation reaches a minimum for a 50/50 protein ratio, whilst cell density is increased (Figure 1). Moreover, the presence of VN triggers higher levels of cell fusion with the formation of bigger multi-nucleated myotubes compared to sole FN (Figure 1).

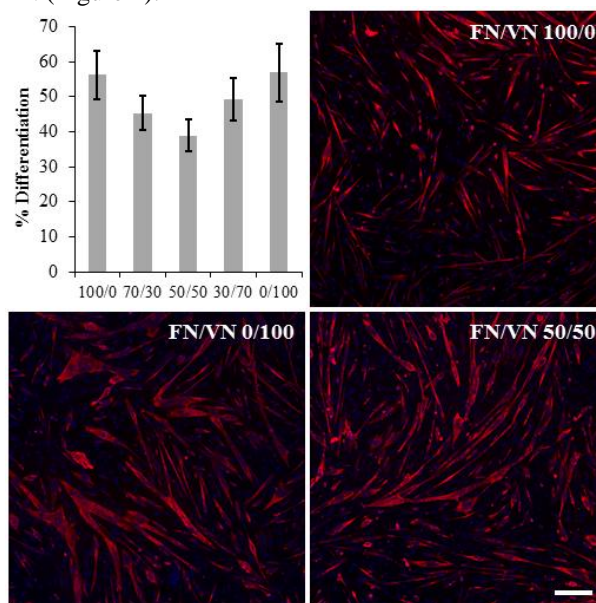


Figure 1. Myogenic differentiation as determined by the percentage of sarcomeric myosin-positive cells and fluorescence staining images. Bar is 200 µm.

Myotube formation was followed over time to better elucidate the dynamics of cell fusion in the presence of VN. The role of the mobility conferred by VN to the protein layer was also addressed by blocking cell adhesion to VN via monoclonal antibodies.

CONCLUSION

VN tunes material-driven FN fibrillogenesis and modulates myogenic differentiation, both in terms of differentiation levels and dynamics of cell fusion.

REFERENCES

1. Salmerón-Sánchez M. *et al.*, Biomaterials 32:2099-2105, 2011.
2. González-García C. *et al.*, Colloids Surf B Biointerfaces 111:618-625, 2013.

ACKNOWLEDGMENTS

The authors would like to thank the European Research Council for providing financial support to this project through HealInSynergy 306990.

Investigation on Mechanical Loading of Hydrogels for Cartilage Tissue Engineering

Stefanie Biechler^{1*}, Sandy Williams¹, and Ruochong Fei¹

¹Bose Corporation, ElectroForce Systems Group, Eden Prairie, MN, USA, stefanie_biechler@bose.com

INTRODUCTION

Degeneration of joint cartilage can result from primary osteoarthritis, injury or disease. Unfortunately, adult cartilage has very limited tendency to self-heal, and it possibly leading to further degeneration, increased pain, and reduced quality of life. Currently, donor site morbidity and limited availability of autologous osteochondral plugs hinder the possibility of mosaicplasty and autologous chondrocyte implantation. Therefore, there is a pervasive need for effective clinical treatments to repair cartilage injuries. In recent years, regenerative medicine has been looked at to replace damaged cartilage with tissue-engineered cartilage constructs. Specifically, hydrogels have been used in many of these efforts because they not only provide a boundary for retention of cells, but also act as a substrate to which anchorage-dependent chondrocytes can adhere.

It is known that mechanical stimulation has a significant impact on cell differentiation and proliferation during three-dimensional cell culture. Sinusoidal waveforms are typically used when studying the relationships between cell growth and dynamic mechanical stimulation. However, it would be more relevant to study these relationships under physiological mechanical loading because such “in vivo”-like loading protocols are directly applicable to cell stimulation during culture. Thus, applying accurate and efficient mechanical stimuli is crucial in quality control of the final tissue engineered construct. In this study, the mechanical response of polyethylene glycol (PEG) hydrogels was observed in response to physiologically relevant loading conditions and an irregular waveform to mimic the dynamic compressive strain on knee cartilage during a walking gait cycle was applied to stacks of hydrogel sheets.

EXPERIMENTAL METHODS

A waveform model (Figure 1) of strain vs. gait cycle based on simulation of human walking was used in this study [1]. This waveform was extracted using Matlab. According to normal human walking speed of 5 km/h, a one gait cycle time of 1.1 sec was used. An ASCII file was constructed and the percent strain was scaled according to specimen thickness. The final point-by-point file was directly imported into the control software for application to the hydrogels.

Polyethylene glycol (PEG) hydrogel sheets (4" × 4") were purchased from Medline Industries and specimens were punched from the hydrogel sheet (12 mm in diameter and 6 mm in height). The samples were soaked in 37C saline for two hours prior to placement on the mechanical loading frame. A preloading force of 0.1 N was applied initially to ensure that the entire

scaffold surface was in contact with the compression platens prior to application of the walking gait waveform. In addition to individual sample loading, simultaneous loading of 24 hydrogel samples was performed in a multi-specimen compression bioreactor to assess the loading accuracy when stimulating multiple samples with the same actuator.

RESULTS AND DISCUSSION

Initially, three specimens were tested with the custom waveform to record the corresponding loads and determine the statistical repeatability of the loading waveform (Figure 1). Similar testing results of three specimens were achieved, and reliable repeatability of this testing method was demonstrated (displacement difference between samples: < 2.5%; load difference between samples: < 13.9%). Compared to the original extracted waveform in the ASCII file, the majority of the waveform details were retained accurately, including micron-level changes in strain. Similarly, when applying the load to 24 samples simultaneously, the sample stage was found to synchronously and evenly distribute the load to all 24 specimens.

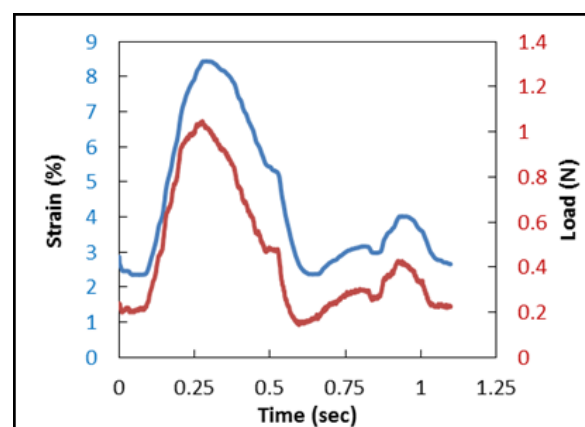


Figure 1: Representative walking gait waveform and load response on a single hydrogel sample.

CONCLUSION

In this study, a physiologically relevant walking gait waveform was used to dynamically compress hydrogels for the application of cartilage tissue engineering. The load response of the hydrogels was observed and the waveform was determined to be applicable to future cell culture studies. The next steps will be to repeat the loading protocol for an extended period of time on a cell-seeded construct to investigate the biological response of chondrocytes to mechanical loading.

REFERENCES

1. Halonen KS. *et al.*, J. Biomech. 46(6): 1184-92, 2013

ACKNOWLEDGMENTS

None applicable



Biological Performance of Cell-Laden Methacrylated Gellan Gum Hydrogels

Joana Silva-Correia^{1,2*}, Mariana B. Oliveira^{1,2}, João F. Mano^{1,2}, Joaquim M. Oliveira^{1,2} and Rui L. Reis^{1,2}

¹3B's Research Group - Biomaterials, Biodegradables and Biomimetics, University of Minho, Headquarters of the European Institute of Excellence on Tissue Engineering and Regenerative Medicine, AvePark, Guimarães, Portugal;

²ICVS/3B's - PT Government Associate Laboratory, Braga/Guimarães, Portugal, joana.correia@dep.uminho.pt

INTRODUCTION

Tissue-engineered hydrogels hold great potential as nucleus pulposus substitutes (NP) since it can mimic the native 3D environment¹. Methacrylated gellan gum (GG-MA) hydrogels have been reported as suitable matrices for NP regeneration², due to their remarkable biological and biomechanical properties. In this study, the biological performance and mechanical properties of cell-laden GG-MA hydrogels were evaluated *in vitro*.

EXPERIMENTAL METHODS

Human intervertebral disc (hIVD) cells were isolated from herniated patients submitted to surgery, following an enzymatic digestion-based method and expanded using standard culture conditions. Prior to cell encapsulation, hIVD cells were characterized by flow cytometry regarding the expression of markers specific for: NP (CD24 and HIF-1), adipose-derived stem cells or mesenchymal stem cells (CD29, CD73, CD90, CD105) and hematopoietic and endothelial lineages (CD34, CD45). The hIVD cells were then encapsulated at a cell density of 2×10^6 cells/mL and cultured within ionic- (iGG-MA) and photo-crosslinked (phGG-MA) hydrogel discs, up to 21 d. Cell behaviour was studied in terms of viability (Live/dead assay) and morphology (DAPI/Texas red-Phalloidin staining), production of a cartilage-like tissue by histological staining and expression of typical chondrogenic markers and specific NP-markers through immunocytochemistry from 2 h until 21 d of culturing. The cell-laden constructs were also analyzed by dynamic mechanical analysis (DMA) after each culturing time.

RESULTS AND DISCUSSION

Different populations of hIVD cells, which were isolated from male/female patients (25-57 years) at different passages, were characterized by flow cytometry. Generally, hIVD cell populations were positive for CD29, CD73, CD90 and CD105 and negative for hematopoietic markers such as CD45 and CD34. Differences were found in the expression of NP-specific markers between the populations/passages analyzed. A population obtained from a 51-year old female patient, with an expression of 13% and 0.5% for CD24 or HIF-1alpha respectively, was selected for the subsequent assays.

Cell viability was evaluated in both cell-laden iGG-MA and phGG-MA constructs (Figure 1). It is possible to conclude from the microscopy images that both hydrogels enable cellular encapsulation, allowing for a good distribution of cells and support cell viability until 21 d of culturing. The effect of encapsulating hIVD cells on the mechanical performance of the hydrogels was evaluated by DMA. The incorporation of cells seems to have an immediate negative effect (not statistically significant) on the mechanical properties of

the hydrogels, which is recovered after 1 d of culturing (data not shown). An increase in E' value (in relation to acellular hydrogels) was observed only after longer culturing times (*i.e.*, 21 d; Figure 2), which is consistent with the viability and production of extracellular matrix by hIVD cells, as demonstrated by the evaluation of biological performance.

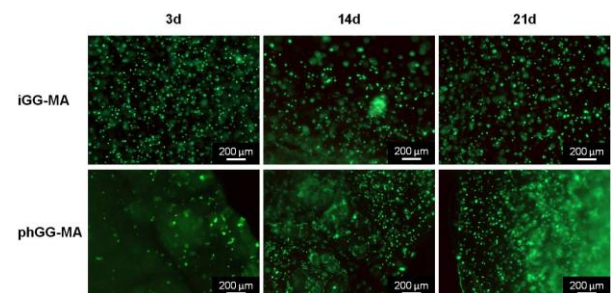


Figure 1. Fluorescence microscopy images of hIVD cells encapsulated within iGG-MA and phGG-MA hydrogels, after 3, 14 and 21 d of culturing (green color – Calcein AM – corresponds to live cells and red color – PI – to dead cells).

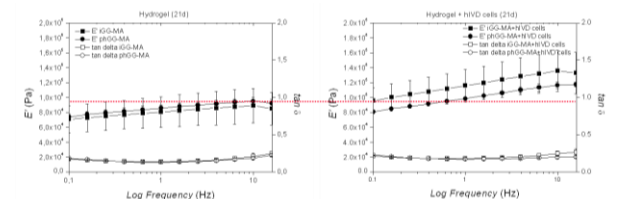


Figure 2. Dynamic mechanical analysis of acellular and cell-laden iGG-MA and phGG-MA hydrogel discs after culturing for 21 d, showing the storage (E') modulus and loss factor ($\tan \delta$) measured in PBS at 37°C. Statistical analysis was performed based on the values at 1 Hz and using a two-way ANOVA followed by Bonferroni's post test ($n=6$; * $p < 0.05$).

CONCLUSION

This study showed that the iGG-MA and phGG-MA hydrogels are stable and non-cytotoxic *in vitro* and present adequate mechanical properties. The hydrogels supported hIVD cells encapsulation and viability, thus possessing promising properties for being tested in cellular-based tissue engineering strategies aimed to restore the functionality of NP.

REFERENCES

- Silva-Correia J., *et al.*, Biotechnol. Adv. 31:1514-1531, 2013
- Silva-Correia J., *et al.*, J. Tissue Eng. Regen. Med. 5:e97-e107, 2011

ACKNOWLEDGMENTS

The research leading to these results has received funding from the EU FP7/2007-2013 under grant agreement n° REGPOT-CT2012-316331-POLARIS and grant agreement n° NMP3-LA-2008-213904-DISC REGENERATION.



Melt Electrospinning Of PCL/Bioactive Glass Composites In Direct Writing For Highly Ordered Scaffolds For Non-Load Bearing Defects

Keith A. Blackwood¹, Nikola Ristovski¹, Sam Liao, Nathalie Bock¹, Jionguy Ren, Giles T.S. Kirby¹, Roland Steck¹, Molly M. Stevens², Maria A. Woodruff¹.

¹ Institute of Health & Biomedical Innovation, Queensland University of Technology, Brisbane, Queensland 4059, Australia.

² Department of Materials, Imperial College, London, SW7 2AZ, United Kingdom. Keith.Blackwood@qut.edu.au

INTRODUCTION

Melt electrospinning has been recently utilised to control fibre deposition in a manner in-line with conventional 3D printing technologies, producing fibres in the range of 1 to 30 microns with a high degree of order, a size range which has been deemed highly suitable for biofabrication^{1,2}. Recently our lab has produced melt electrospun fibres with a high degree of order up to 2 mm in thickness, 10× greater than previously presented data.

Many polymers can be melt spun, however the most commonly used one is Polycaprolactone (PCL). PCL has many features which makes it suitable for electrospinning and biofabrication, including good viscoelastic properties for fabrication and low melting point (~65°C)³. While PCL is bioresorbable, by itself it is not bioactive. This functionality can be added to PCL scaffolds by combining them with bioactive molecules, such as the osteogenic bioactive glasses (BGs)^{4,5}. Previous work has shown that BG particles can be intergrated into molten PCL and melt spun, although aligned fibres were not achieved⁴.

The combination of PCL and bioactive glasses with melt electrospinning present the possibility to develop pro-osteogenic scaffolds whose structures have a high degree of order and thinner fibers than conventional 3D printing technology.

EXPERIMENTAL METHODS

45S5 Bioglass® and Strontium substituted bioactive glass (supplied by Prof Molly Stevens' Group, Imperial College London) were used for this experiment. Particle size distribution was determined by a Master Sorter 3000 (Marlvern). BGs were then ground via a Micronizing mill (McCrone) for 2 hours 30 min, and size distribution resampled.

PCL (*Capa 6400*; Perstorp UK Limited) was mixed with the BG (ground or unground) particles (10% wt) chloroform (10 ml per gram of PCL) at room temperature, followed by ethanol precipitation and air drying, prior to loading into a syringe for melt electrospinning.

A bespoke melt electrospinning device with dual voltage control and an X-Y-Z stage was used for the scaffold manufacture. Electrospinning conditions were: +7.5 kV tip charge, -3.5 kV collector charge, feed rate 40 µl hour, G19 needle, 90°C melt temperature and 10 mm tip to collector distance.

Fibre size, alignment and particle distribution were assessed by light microscopy (Zeiss Axio Imager M2).

Scaffolds were etched NaOH for 1 hour before being cultured with MC3T3 preosteoblastic cell line (~5000 cells per 30 mm²). Confocal microscopy of DAPI/Alexa Fluor® 488 phalloidin + Alizarin red staining of BG particles was used to assess cell attachment.

RESULTS AND DISCUSSION

PCL/BG (unground 13 – 110 µm) composite scaffolds could be spun with average fibre size higher than PCL alone. Obtaining alignment was impossible due to instability in the jet causing random deposition of fibres (Fig 1A). PCL/BG (ground 1 – 7 µm) composite scaffolds exhibited superior jet stability, and they were successfully spun in straight lines (Fig 1B). MC3T3s preferentially attached to areas of scaffold where BG particles were exposed (Fig 1C).

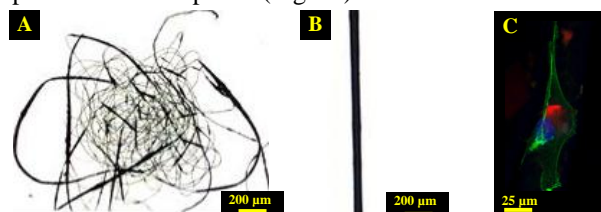


Fig. 1. Light microscopy of unground (A) and ground (B) PCL/BG composite scaffolds, and MC3T3 cellular attachment to the composite (C). Scale bars as shown.

CONCLUSION

By reducing the particle size of the BGs, superior spinning characteristics were achieved, and melt spun composites were able to be directly written as a straight line. These results further the potential for using melt electrospinning as an effective 3D additive manufacturing technique for biomaterial fabrication.

REFERENCES

1. Dalton, P. D. *et al. Biomater. Sci.* **1**, 171 (2013).
2. Teo, W.-E., Inai, R. & Ramakrishna, S. *Sci. Technol. Adv. Mater.* **12**, 013002 (2011).
3. Woodruff, M. A. & Hutmacher, D. W. *Prog. Polym. Sci.* **35**, 1217–1256 (2010).
4. Ren, J. *et al. J. Biomed. Mater. Res. Part A* (2013). doi:10.1002/jbm.a.34985
5. Poh, P. S. P., *et al. Biofabrication* **5**, 045005 (2013).

ACKNOWLEDGMENTS

The authors acknowledge the support from the Australian Research Council Linkage Grants LP110200082 and LP100200084 for providing financial support to this project.



Material-driven fibronectin fibrillogenesis promotes growth factor binding and stem cell differentiation

V. Llopis-Hernández¹, M. Cantini¹, P. Rico², M. Tsimbouri³, A. García⁴, M. Dalby³, M. Salmerón-Sánchez¹

¹Division of Biomedical Engineering, School of Engineering, University of Glasgow, UK

²Center for Biomaterials and Tissue Engineering, Universitat Politècnica de València, Spain (virlllohe@upv.es)

³Institute of Molecular, Cell and Systems Biology, University of Glasgow, UK

⁴Woodruff School of Mechanical Engineering & Petit Institute for Bioengineering and Bioscience, Georgia Institute of Technology, Atlanta, GA, USA

INTRODUCTION

Fibronectin (FN) is a ubiquitous extracellular matrix (ECM) protein that is organised into fibrillar networks by cells through an integrin-mediated process that involves contractile forces. This assembly allows for the unfolding of the FN molecule, exposing cryptic domains that are not available in the native globular FN structure and activating intracellular signalling complexes. We have demonstrated cell-free, material-induced FN fibrillogenesis into a biological matrix with enhanced cellular activities upon simple FN adsorption onto poly(ethyl acrylate) (PEA) surfaces (material-driven fibronectin fibrillogenesis).¹ Engineering cellular environments to promote tissue healing involves the design of complex systems that combine materials, ECM proteins and growth factors (GFs). We have engineered biomimetic fibronectin fibrillar networks to enhance the presentation and activity of growth factors (using the promiscuity of the FNIII₁₂₋₁₄ domain present in FN to bind GF) during tissue healing making use of the material-driven fibronectin fibrillogenesis.

EXPERIMENTAL METHODS

Glass coverslips were coated with PEA, poly(methyl acrylate) (PMA) or P(EA-co-MA) (50/50) in toluene. FN from human plasma was used to coat the samples at 20 µg/ml, followed by 1% BSA coating and BMP-2 (25 ng/ml) when required. AFM (tapping mode) experiments were performed using a NanoScope IIIa instrument on samples coated with FN (3 µg/ml), BMP-2 (1 µg/ml) and FN followed by BMP-2 (20 µg/ml and 25 ng/ml respectively); also, in this last condition immunogold was used to label BMP-2 adsorbed on FN-coated samples. BMP-2 adsorption was quantified by sandwich ELISA. The availability of FNIII₁₂₋₁₄ domain was measured by ELISA. Early signalling in human mesenchymal stem cells was studied after 40 min by sandwich ELISA for ERK1/2 phosphorylation. SMADs signalling was studied after 40 min (pSMAD1, 1/5, and 1/5/8 using western blot). Osteogenic differentiation was studied after 14 days using immunofluorescence and qRT-PCR for osteocalcin (OCN) and osteonectin (ON).

RESULTS AND DISCUSSION

FN adsorption from a solution of concentration 20 µg/ml on material substrates, as shown by AFM, results in globular aggregates on PMA, organisation into (nano)network on PEA and a less interconnected network on P(EA-co-MA). FNIII₁₂₋₁₄ domain (heparin II domain) was more exposed on PEA than on PMA (Figure 1a). AFM images of FN and BMP-2 showed that BMP-2 interacts with FNIII₁₂₋₁₄, the promiscuous

GF binding domain in FN, as confirmed by immunogold (Figure 1b). Presentation of BMP-2 to MSCs via FN networks enhanced phosphorylation of ERK1/2. Osteogenic differentiation by qRT-PCR for OCN and ON was higher on PEA coated with BMP-2 after FN adsorption compared with PEA where the BMP-2 was only present in the medium (Figure 1c).

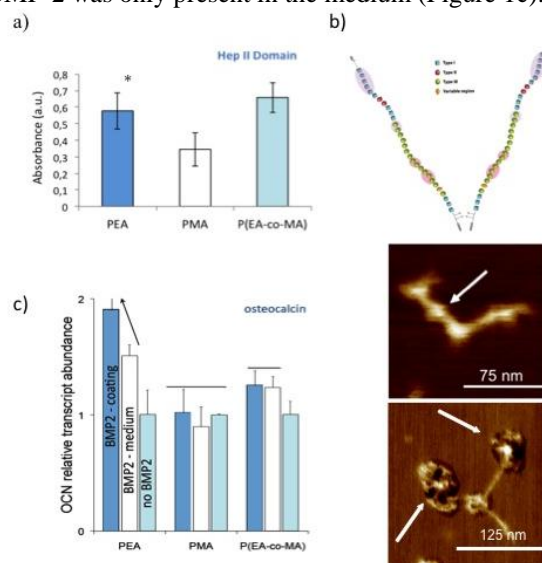


Figure 1. a) ELISA for Hep II domain availability on the different materials. b) FN molecule with indication of the different domains and two AFM images of a single FN molecule on PEA. Arrows show the BMP-2 on the Hep II region. In the second image BMP-2 is detected using immunogold labelling. c) OCN mRNA abundance on the different materials after 14 days.

CONCLUSION

We made use of the ability of some material surfaces to direct the physiological organization of FN into fibrillar networks in absence of cells (material-driven fibronectin fibrillogenesis) to engineer advanced micro-environments for cell culture. These surfaces trigger the organization of FN upon simple adsorption from solution and provide a functional biomimetic interface with the ability to bind growth factors. BMP-2, presented to MSCs through synergistic interaction between integrins and GF receptors, enhanced their osteogenic differentiation.

REFERENCES

1. Llopis-Hernández, V *et al* BioResearch 2013, 2(5): 364-373

ACKNOWLEDGMENTS

Support from the European Research Council through the ERC-StG_20111012 and 306990 (HealInSynergy) is acknowledged.



Design, Development and Characterization of Novel Polyacrylates to direct Kidney Progenitor / Stem Cell Differentiation

Isabel Hopp¹, Rachel Williams², Simon Dixon³, Patricia Murray¹

¹ Institute of Translational Medicine, University of Liverpool, Liverpool L69 3GE, UK, isahopp@liverpool.ac.uk

² Institute of Ageing and Chronic Disease, University of Liverpool, Liverpool, L69 3GA, UK

³ Biomer Technology Ltd., Seymour Court, Tudor Road, Manor Park, Runcorn, Cheshire, WA7 1SY, UK

INTRODUCTION

The importance of the extracellular matrix (ECM) in regulating stem cell differentiation is now well-recognized¹. Apart from influencing cell behaviour through specific cell-matrix interactions, the physico-chemical properties of the ECM are also important (e.g., hydrophobicity, elasticity and nanoscale topography²). We have previously shown that biomaterials that mimic aspects of ECM proteins can regulate the differentiation of mesenchymal stem cells³. This study aims to design biomaterials that are able to control the differentiation of mouse kidney-derived stem cells (mKSCs) into either proximal tubule cells (PTCs) or podocytes, two cell types that are commonly involved in kidney disease. We have developed polyacrylate polymers (ESP03, ESP04, ESP07, BTL15) with various functional groups, such as amine, hydroxyl and carboxylic acid groups, as well as integrated hydrophobic spacer chains, to mimic aspects of key ECM proteins normally found in the kidney. Using various types of physicochemical analyses, we have investigated the effects of the chemical modifications on the physical properties of the substrates, including surface wettability and topography. So far we found that two of our polymers, referred to as ESP07 and BTL15, were able to direct the differentiation of mouse KSCs into PTCs. These two polyacrylates differ in topography and wettability, but, interestingly, show very similar surface chemistry.

EXPERIMENTAL METHODS

Glass cover slips (Fisher Scientific) were coated with a solution of 3% polymer in DMF; 22mm² discs for Dynamic Contact Angle (DCA) analyses and 13mm discs for all other analyses. Atomic Force Microscopy (AFM) was conducted using a Multimode 8 system (Bruker) equipped with silicon nitride probes and operated in Peak Force Tapping mode. X-ray Photoelectron Spectroscopy (XPS) analyses were performed using an NCESS ESCA300 XPS spectrometer (VG Scienta). Survey, C1s, O1s and N1s spectra were analysed at 150 eV, 0.8 mm slit, 1.8 kW. DCA was recorded using the Willhelmy method with a Cahn DCA322 microbalance. Advancing and receding contact angles were calculated for each sample in distilled water (72.6 dyne cm⁻¹). Samples were sterilized under UV light prior to cell culture. mKSCs⁴ were cultured on tissue culture dishes (Corning) and fed every other day. Cells were passaged once per week. For differentiation studies, 1000 cells were seeded on polymer coated coverslips, left for 4 days and subsequently analysed.

RESULTS AND DISCUSSION

Surface analyses showed that the polymers show only small differences in surface elemental composition (carbon, nitrogen, oxygen). However, there were relative differences in the COOH, OH and NH₂ content between the polyacrylates (Table 1).

Table 1: Functional groups within polyacrylates.

Functional group	Trend within range of polymers
C-COOH	ESP04<ESP7<BTL15<ESP03
C-NH ₂	ESP04<BTL15<ESP03=ESP07
C-OH	ESP07<BTL15

Surface wettability confirms the XPS results showing higher contact angles for polymers with higher carbon content and vice versa. The trend for advancing/receding contact angle is as follows:

BTL15=ESP03<ESP07<ESP04. Surface topography analyses showed that the polymers appear to have very different characteristics with hill-like features differing strongly in height between polymers. ESP07 was the smoothest with maximum peak to trough height of 100 nm, for ESP03 and ESP04 this varied between 300 and 600 nm and for BTL15 it was in the order of 1µm. Preliminary results have shown that, following a 4 day culture period of mKSCs on polyacrylates ESP07 and BTL15 (the substrates with hydroxyl and amine functionality) the cells differentiate towards PTCs as these cells express higher amounts of megalin and alkaline phosphatase.

CONCLUSION

Polyacrylate substrates ESP07 and BTL15 have high potential to direct the differentiation of mKSPCs into specialized renal cells. These findings could provide a significant contribution to stem cell research by providing materials with specific surface properties that promote directed cell differentiation.

REFERENCES

- Engler *et al.*, J. Biomech. 43 (1), 2010
- Wang *et al.*, Reg. Med. & Tis. Eng., InTech: (2011)
- Glennon-Alty *et al.*, Acta Biomaterialia, 2012
- Fuente Mora *et al.*, SC & Development, 21.2, 2011

ACKNOWLEDGMENTS

The authors would like to thank the Marie Curie FP7 ITN 'NephroTools' for funding this work.



Antibacterial Polyurethane Surfaces: Modification with Chitosan by Covalent Immobilization

Filiz Kara¹, Eda Ayse Aksoy², Serpil Aksoy¹ and Nesrin Hasirci^{3,4,5}

¹Faculty of Sciences, Department of Chemistry, Gazi University, Turkey

²Faculty of Pharmacy, Department of Basic Pharmaceutical Sciences, Hacettepe University, Turkey

³BIOMATEN, Center of Excellence in Biomaterials and Tissue Engineering, Middle East Technical University, Turkey

⁴Middle East Technical University, Department of Chemistry, ⁵Biomedical Engineering Graduate Dept. Turkey
nhasirci@metu.edu.tr

INTRODUCTION

In the cases where medical devices contact with physiological media such as blood, saliva or living tissue, the first biological reactions occur on the surface interface. Therefore, surface of medical materials are extremely important for biocompatibility of the device. If the surface has some affinity for bacteria adhesion, the presence of bacteria can cause pathogenic biofilm formation and subsequent infectious complications. There are some techniques used to modify the surfaces and chemical modification with antibacterial agents is still the most preferable and reliable strategy for the prevention of biofilm formation. In this study, it was aimed to prepare surface functionalized medical grade polyurethane (PU) having stable antibacterial activity. For this purpose, PU films were synthesized in medical purity and surfaces were covalently modified by chitosan (CH) which is a multifunctional natural biopolymer since it has high biocompatibility, biodegradability and antibacterial activity. Surface properties of the modified films, such as chemistry, functionality, topography, hydrophilicity, surface free energy and antibacterial efficiencies against *P. aeruginosa* and *S. aureus* were investigated.

EXPERIMENTAL METHODS

Polyurethane films (PUh) were synthesized in medical purity by using hexamethylene diisocyanate and polypropylene ethylene glycol without addition of any other ingredients such as catalyst, chain extender, solvent¹. PUh surfaces were activated by oxygen plasma (100W, 10 min) and modified by CH via covalent immobilization in two different concentrations (0.5 mg/mL and 2.0 mg/mL) (Figure 1).

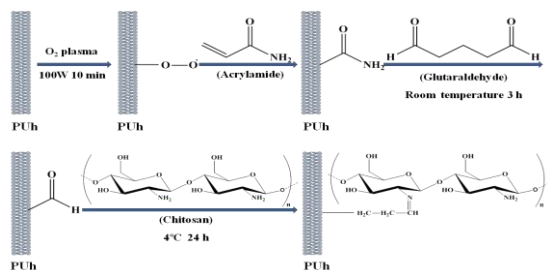


Figure 1. Surface modification steps of PUh films with CH.

PUh and CH immobilized PUh surfaces (PUh-CH-0.5 and PUh-CH-2.0) were characterized by FTIR-ATR, ESCA and goniometer. Surface topographies were examined by AFM. Antibacterial activity and bacterial anti-adhesion properties were examined by viable count method and SEM against Gram negative *P. aeruginosa* and Gram positive *S. aureus*.

RESULTS AND DISCUSSION

ESCA results showed variations in the composition after CH immobilization on film surfaces. Presence of CH caused an increase in nitrogen content from 0.4% (PUh) to 4.4% and 4.5% for PUh-CH-0.5 and PUh-CH-2.0 samples, respectively (Table1). PUh-CH films had an extra peak due to O-C-O of saccharide units of CH.

Table 1. ESCA C-1s binding energy and relative contents (%)

Samples	C-C/C-H 285 eV	C-O/C-N 286.6 eV	O-C-O 288.1 eV	N-C=O 289.2 eV
PUh	38.2	58.7	-	3.1
PUh-CH-0.5	41.6	48.1	8.1	2.2
PUh-CH-2.0	41.9	47.0	8.9	2.2

Modified films were more hydrophilic than PU ones and water contact angles of pristine films decreased from 86° to 78° and 76° for PUh-CH-0.5 and PUh-CH-2.0, respectively. Plasma application caused some roughness on the surface but this roughness decreased by immobilization of CH. Bacterial adhesion of *P. aeruginosa* and *S. aureus* on both modified surfaces decreased compared to PUh films. Figure 2 show that both PUh-CH-0.5 and PUh-CH-2.0 demonstrated strong antibacterial activity for both bacteria types.

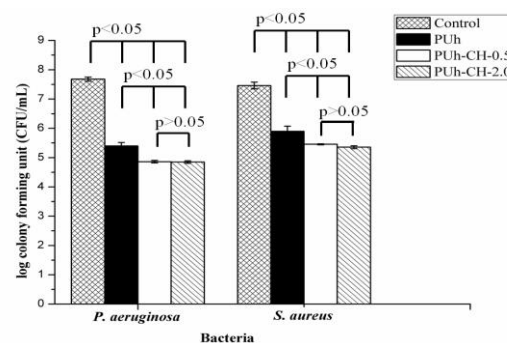


Figure 2. Antibacterial activities of control and modified films.

CONCLUSION

The surface chemistry and topography of the film samples changed after CH immobilization and modified films demonstrated strong antibacterial activities. The results shows surface modification with CH is an effective technique to control the antibacterial or anti-adhesive properties of biomaterials.

REFERENCES

1. Aksoy E.A. et al., *J Biomat. Tissue Eng.* 2:345-354, 2012

ACKNOWLEDGMENTS

The authors thank to Assoc. Prof. Zehranur Yuksekdağ for guidance in antibacterial tests

Catechol-Chitosan/Genipin Hydrogel as Mucoadhesive Buccal Drug Delivery System

J. Xu¹, S. Strandman², J. Zhu², J. Barralet³ and M. Cerruti^{*1,3}

¹Department of Mining and Materials Engineering, McGill University, Montreal, Quebec, H3A 0C5, Canada; ²Department of Chemistry, Université de Montréal, Montreal, Quebec, H3C 3J7, Canada; ³Faculty of Dentistry, McGill University, Montreal, Quebec, H3A 07C, Canada. marta.cerruti@mcgill.ca

We developed a hydrogel made in catechol-modified chitosan (Cat-CS) crosslinked by genipin (GP) as a mucoadhesive drug delivery system through buccal mucosa. We show enhanced mucoadhesion and controlled release of a model drug, lidocaine (LD) both in-vitro and in-vivo in rabbit models. This hydrogel is especially promising for the delivery of sensitive proteins and nutraceuticals that cannot be delivered using dry pellets currently used in buccal delivery.

INTRODUCTION

Oral transmucosal delivery is a non-invasive way of drug administration that prevents presystemic clearance at gastrointestinal tract and avoids the first-pass elimination in the liver during systemic circulation¹. To sustain drug release, materials for buccal delivery should adhere tightly to the buccal mucosa. Currently dry tablets are used for this purpose. The drawback of this approach is that bioactive compounds needing to stay hydrated cannot be delivered. Chitosan (CS) is a mildly mucoadhesive, biocompatible natural polysaccharide. A catechol-containing compound is responsible for the outstanding underwater adhesion of marine mussels². We previously showed that adding catechol-containing compounds to CS gels can increase their adhesion to intestinal membranes³. Here, we covalently bond catechol groups to CS (i.e. Cat-CS), and crosslink the resulting polymers using a non-toxic natural compound, genipin (GP), to form Cat-CS/GP hydrogels. We test the hydrogel mucoadhesion in-vitro to porcine buccal tissue, and both in-vitro and in-vivo in rabbit models for the delivery of LD, a local anesthetic commonly used in dental procedures.

EXPERIMENTAL METHODS

Catechol functional groups were covalently bonded to chitosan by EDC coupling, preparing Cat-CS with catechol contents of 9% and 19%. Hydrogels were prepared by crosslinking Cat-CS with GP. Rheological behavior was tested by both time and stress sweeps using cone/plate steel geometry (Φ 40 mm, 2°). Lidocaine (LD) as model drug was loaded into the hydrogels. Drug release was quantified in vitro by liquid chromatography. Mucoadhesion was evaluated by measuring detachment time from pig buccal mucosa surface in PBS (pH6.8), at 300 rpm continuous stirring. Drug-loaded hydrogel patches were attached to the buccal mucosa of rabbits for the in-vivo tests. Blood samples were collected, followed by HPLC quantification of drug concentration in the serum. CS crosslinked by GP hydrogels (CS/GP) were used as controls. Histology was performed on the tissue in contact with the hydrogel patches.

RESULTS AND DISCUSSION

Both NMR and FTIR confirmed the successful synthesis of Cat9-CS and Cat19-CS. Cat-CS hydrogels were denser than control CS hydrogels. The gelation of both CS/GP and Cat-CS/GP hydrogels reached equilibrium after 12 h at 37 °C. Cat-CS/GP showed higher ultimate shear strength than CS/GP, indicating Cat-CS/GP hydrogels are stronger than CS/GP. Cat-CS/GP significantly enhanced the adhesion time at pig buccal mucosa in PBS (Fig.1A). Sustained release of LD was achieved in both Cat-CS and CS hydrogels in-vitro, and a slower release was observed for the Cat-CS hydrogels. In-vivo tests in rabbits showed that LD could be detected in the rabbit serum after 3 hours only if it was released from Cat-CS/GP hydrogel patches. Only very low LD values were measured after release from CS/GP hydrogels (Figure 1B). Histology showed that Cat-CS/GP hydrogels did not cause any adverse reaction on the tissue in contact.

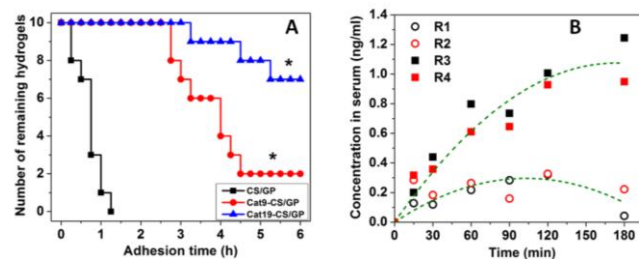


Figure 1. (A) Adhesion of CS/GP and Cat-CS/GP hydrogels on porcine buccal mucosa in PBS. (B) LD concentration measured in the serum of rabbits R1-R4 after application of drug-loaded Cat19-CS/GP (R3 and R4) and control CS/GP hydrogels (R1 and R2) on the buccal mucosa

CONCLUSION

Cat-CS/GP hydrogels are promising candidates as buccal drug delivery systems, showing excellent mucoadhesion in-vitro and sustained LD delivery both in-vitro and in-vivo. The improved in-vivo behavior is to be related to the intimate contact between the Cat-CS hydrogels and buccal mucosa due to their strong mucoadhesion.

REFERENCES

1. Patel VF et al. *J Control Release*. 161:746-756, 2012
2. Catron N et al. *Biointerphases*.1:134-141, 2006
3. Xu J et al. *Langmuir*. 28:14010-14017, 2012

ACKNOWLEDGMENTS

We acknowledge support from the Canada Research Chair foundation, the Natural Sciences and Engineering Research Council of Canada, and the Advanced Foods & Materials Network.

Inflammatory Response to Magnesium Based Biodegradable Implant Materials

Maria Costantino¹, Bérengère Luthringer¹, Regine Willumeit^{1*}

¹ Helmholtz-Zentrum Geesthacht, Zentrum für Material- und Küstenforschung, Germany

^{1*} Helmholtz-Zentrum Geesthacht, Zentrum für Material- und Küstenforschung, Germany, regine.willumeit@hzg.de

INTRODUCTION

The biodegradability and the mechanical properties of magnesium alloys make them a suitable material for orthopaedic implant applications. Several papers are studying the interaction of bone cells with these materials [1, 2]. Still during implantation a variety of cells is interacting. Among them are cells of the immune system which are responsible for the inflammatory reaction of the organisms. Macrophages play a central role in the inflammatory process and their interaction with the degrading material is consequently the target of this study.

EXPERIMENTAL METHODS

In order to evaluate the influence of ion release, pH changes and hydrogen evolution produced by degrading magnesium alloys on the inflammatory process, undifferentiated (monocytes) and PMA stimulated (macrophages) U937 cells were cultured with three different magnesium alloys: WE43, Mg10Gd and Mg2Ag. Two different culture methods were employed: either the cells were exposed to an extract of the degrading material or they grew directly on the material. For the extract assay the three materials were incubated under cell culture conditions for 72h in cell culture media. During this time the materials degraded and extracts with defined Mg concentrations (measured by Xylidyl Blue Assay) were obtained. Then the cells (5×10^5 cells / mL) were subsequently cultivated with these extracts (diluted 1 to 10 to decrease the osmolality) for 1 and 10 days. For the direct assay the cells (5×10^5 cells / mL) were cultured on the surface of discs (1mm x 10mm) for 1 and 6 days. Cells without material contact were used as control.

inflammatory cytokines in the cell culture supernatant. The expression of specific genes such as CD36, TLR4, ICAM, IL-1 β and OPN were obtained by real time Polymerase Chain Reaction (RT-PCR). Every sample was tested in triplicates.

RESULTS AND DISCUSSION

Undifferentiated U937:

The analyses revealed that when cells are growing directly on the Mg alloys, the material can stimulate undifferentiated U937 cells (monocytes) to release chemotactic factors such as IL-8 (Interleukin-8) and MCP1 (Monocyte Chemotactic Protein-1) and anti-inflammatory cytokines such as IL-4 (Interleukin-4) and IL-10 (Interleukin-10).

PMA stimulated U937:

For PMA stimulated U937 – which we consider here to be differentiated U937 = macrophages – PCR analysis showed a decreased expression of inflammatory genes.

CONCLUSION

Our results indicate that at least for the three Mg alloys tested two mechanisms depending on the maturation of cells (monocytes / macrophages) play a role: (1) a recruitment of monocytes towards the damaged tissue is possible and (2) when differentiated into macrophages the material can induce the down regulation of the inflammatory reaction.

REFERENCES

1. Fischer J. *et al.*, Mat Sci Eng B 176: 830–834, 2011
2. Wu L. *et al.*, Acta Biomater (2014) DOI information: 10.1016/j.actbio.2014.02.010

ACKNOWLEDGMENTS

The research leading to these results has received funding from the People Programme (Marie Curie Actions) of the European Union's Seventh Framework Programme FP7/2007-2013/ under REA grant agreement n° 289163.

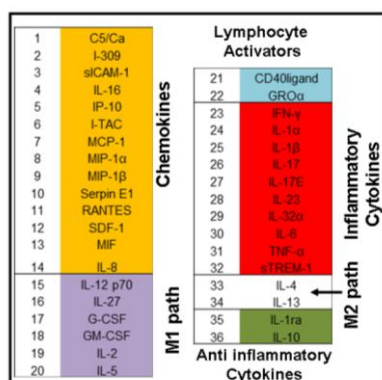


Fig. 1: Overview of cytokines analysed in this work.

The inflammatory activity of the cells was assessed by a Human Cytokine Array Panel (Fig. 1) which is a qualitative method for the simultaneous analysis of 36 cytokines. In addition standard and multiplex ELISA (Qplex) measurements were performed to detect

Surface modification of poly(D,L-lactic acid) scaffolds for orthopedic applications: a biocompatible, non-destructive route via diazonium chemistry

H. Mahjoubi¹, J. Kinsella², M. Murshed³ and M. Cerruti*¹

Materials Engineering, McGill University, Canada, marta.cerruti@mcgill.ca

Department of Bioengineering, McGill University, Canada

Faculties of Medicine and Dentistry, McGill University, Canada

We show that diazonium chemistry can be used to modify the 3D structure of poly(D,L-lactic acid) (PDLLA) scaffolds with phosphonate groups, using a simple 2-step method. This modification does not degrade PDLLA, and allows for the formation of a thick layer of hydroxyapatite (HA) upon immersion in simulated body fluid (SBF). MC3T3-E1 preosteoblasts seeded on PDLLA films treated in the same conditions as the scaffolds show greater spreading and growth than those seeded on bare PDLLA films. This work introduces diazonium chemistry as a simple and biocompatible technique to modify scaffold surfaces, allowing to covalently and homogeneously bind a number of functional groups without degrading the scaffold polymeric matrix.

INTRODUCTION

Scaffolds made with synthetic polymers such as polyesters are commonly used in bone tissue engineering due to their biocompatibility, biodegradability, and adequate mechanical properties¹. However, polyesters do not have specific biological cues and their surface is not ideal for cell adhesion and growth. Surface modification of these materials is thus crucial for enhancing the scaffold integration in the body. Most techniques used to modify biomaterial surfaces either provide weak bonds (physisorption) or are destructive (hydrolysis) or cannot fully coat the inner structure of 3D scaffolds (plasma). Here we test if diazonium chemistry can overcome these weaknesses. Diazonium chemistry was developed to modify a number of surfaces². Here we use it for the first time on PDLLA to first bind an amino terminated layer, and then transform this into a phosphonate layer. Phosphonate groups are known to enhance nucleation and growth of HA by attracting calcium cations³. An HA layer coating is ideal for biomaterials for orthopaedic applications. We test HA deposition on modified scaffolds by immersing them in SBF. Finally, we grow MC3T3 preosteoblasts on films modified with a similar procedure used for the scaffolds.

EXPERIMENTAL METHODS

We prepared PDLLA scaffolds by salt leaching, and modified their surfaces by diazonium chemistry. After generating an amino-rich layer using dianiline, we introduced phosphonate groups by adding 2-aminoethylphosphonic acid. We perform X-ray Photoelectron Spectroscopy (XPS) to confirm functionalization, and gel permeation chromatography (GPC) to check for PDLLA degradation. We then immerse all scaffolds in SBF and characterize them after 2 and 4 weeks with XPS, Raman and FT-IR

spectroscopy. We seed MC3T3 preosteoblasts on PDLLA films modified similarly to the scaffolds and test their viability and mineralization using standard bioassays.

RESULTS AND DISCUSSION

XPS shows that treated scaffolds contain both N and P on their surface, and that the amount grafted is controllable by simply changing the functionalization time. Both outer surface and inner pores of the scaffolds can be modified by evacuating the scaffolds prior to immersing them in the diazonium-containing solutions. GPC shows that despite the acidity of the diazonium reaction solution, PDLLA is not degraded.

After immersion in SBF, larger and more abundant agglomerates are observed on the treated scaffolds (Figure 1A). XPS shows that these aggregates are composed of Ca and P, and more Ca and P are present on the surface of the treated scaffolds compared to non treated scaffolds. Raman and FT-IR spectroscopy reveal that the Ca/P precipitates are HA. Cytocompatibility tests show that MC3T3 cells are alive on all films, and they proliferate and spread better on phosphonate-modified films than on unmodified PDLLA (Figure 1B). More mineralization is observed on modified than on bare films, too.

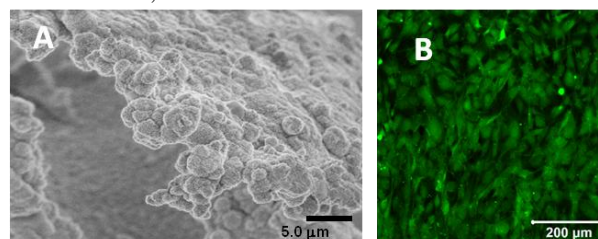


Figure 1. (A) SEM image of 2 h vacuum treated scaffold immersed in SBF for two 4 weeks; (B) live/dead assay showing only live cells (green) on phosphonated PDLLA membrane

CONCLUSION

PDLLA scaffolds can be easily and effectively modified with diazonium chemistry. The simplicity of this method, its biocompatibility and the fact that PDLLA is not degraded during the treatment makes it an ideal candidate to modify scaffolds for a variety of biomedical applications.

REFERENCES

1. Liu XH et al. *Ann. Biomed. Eng.* 32: 477-479, 2004
2. Combellas C et al *Chem. Mater.* 17: 3968-3970, 2005
3. Zhang RY et al *Macromol. Biosci.* 4: 100-102, 2004

ACKNOWLEDGMENTS

We acknowledge the Canada Research Chair foundation and the Natural Sciences and Engineering Research Council of Canada for financial support.



Bioactive glass for treatment of tooth hypersensitivity during or after treatment with bleaching agent

Nataša Drnovšek¹, Kaja Križman¹, Sebastjan Perko², Saša Novak^{1,3}

¹ Department for Nanostructured Materials/Jožef Stefan Institute, Slovenia

²Ustna Medicina d.o.o., Slovenia

³Jožef Stefan International Postgraduate School, Slovenia

natasa.drnovsek@ijs.si

INTRODUCTION

Dentin hypersensitivity is one of the most commonly occurred dental conditions and is also the biggest problem of the tooth bleaching. In the most bleaching agent the active ingredient is hydroxyperoxide or peroxide releasing agent, which is due to formation of free radicals a strong oxidizing agent. Free radicals released from the hydroxyperoxide chemically brake down the organic molecules of the stained tooth and also modify the enamel and dentin structure that results in tooth hypersensitivity, especially when peroxide penetrates into the pulp chamber. Due to the pain produced, hypersensitivity demands for treatment.

A possible solution is to use bioactive glass to occlude and to remineralize dentin tubules by formation of hydroxyapatite from bioactive glass dissolution products. Hydroxyapatite fills or reduces the size of open dentin tubules, which are the cause for making the teeth sensitive to outside stimuli, thermal, chemical, mechanical or osmotic, because the nerve receptors are stimulated by movement of the fluids through the dentin tubule. To prevent development of hypersensitivity, treatment with bioactive glass could be performed at the time of bleaching or right after it and thus avoid long lasting and repeating procedure².

In this study 3 different methods of bioactive glass treatments were compared: bioactive glasses added in a form of nanosized powder directly into a bleaching gel to prevent tubule opening during the treatment, bioactive glass in a form of a gel applied right after bleaching procedure for a rapid remineralization after the treatment and for comparison only bioactive glass powder in artificial saliva.

EXPERIMENTAL METHODS

Bioactive glass (BAG) was prepared by particulate sol-gel method by a dropwise addition of reagents and under controled pH maintained by Titrand 835. BAG powder was characterized by SEM, TEM and FTIR. Dissolution of ions from BAG in artificial saliva was analyzed by ICP-MS and by measuring the pH change. For bleaching test BAG powder was mixed with bleaching gel followed by the overnight bleaching treatment, BAG powder mixed with cellulose or glicerol, to form a gel was applied on a bleached teeth or teeth were soaked and brushed in a mixture of BAG powder and artificial saliva. Formation of hydroxyapatite in dentin tubules opened by a bleaching agent or by etching was then analysed by SEM and FTIR.

RESULTS AND DISCUSSION

Particulate sol-gel method resulted in formation of porous particles (Fig.1) for which the ion leaching test revealed fast formation of Ca-phosphate as the concentration of Ca and P ions in saliva started to decrease after an hour, whereas concentrations of Si and Na ions were increasing.

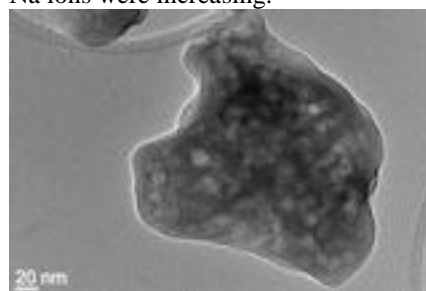


Figure 1: TEM image of porous BAG particle with a composition 70 SiO₂- 30 CaO (mol%)

Brushing the samples with particulate BAG powder in artificial saliva resulted in formation of Ca-phosphate layer on dentin and in dentin tubules. Interestingly, BAG in a form of gel stimulated growth of HAP in a form of rods. BAG applied to the teeth in the time of bleaching procedure resulted in less opened dentine tubules compared to the treatment with bleaching agent alone (Fig.2).

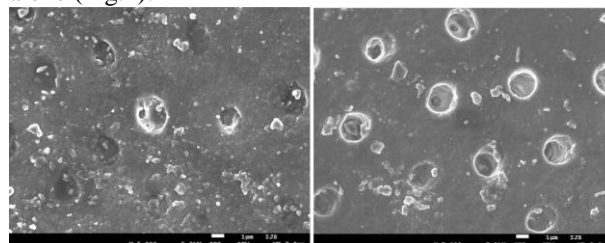


Figure 2: Dentin tubules after the treatment with a) composite BAG/bleaching agent and b) only bleaching agent.

CONCLUSION

Bioactive glass prepared by particulate sol-gel-method showed promising results for occluding dentin tubules and thus reducing dentin hypersensitivity caused by bleaching.

However, the method of BAG application is important as BAG applied directly into a bleaching agent was less effective than other two methods, where BAG was introduced after the bleaching procedure.

REFERENCES

References must be numbered. Keep the same style.

1. Lynch, E., *et al.*, Dent. Mat. 28:168-178, 2012
2. Trushkowsky, R. D., *et al.*, Dent. Clin. North. Am. 3: 599-608, 2011.

Selenium-containing hydroxyapatites – spectroscopic studies

J. Kolmas, E. Oledzka and M. Sobczak

Department of Inorganic and Analytical Chemistry/Faculty of Pharmacy, Medical University of Warsaw, Poland
joanna.kolmas@wum.edu.pl

INTRODUCTION

Hydroxyapatite (HA) is commonly used in bioceramics for reconstructive surgery applications [1]. An exceptional feature of apatite is the ability of various ionic substitutions determining its physicochemical and biological properties.

It is well known that selenium plays a significant role in diverse metabolic process [2]. Moreover, selenium may prevent carcinogenesis and inhibits the growth of tumor cells [2]. Recent articles shows that selenium deficiency is disadvantageous for the growth of human bone [3]. Thus, it seems reasonable to prepare Se-containing HA for a bioactive scaffold for the new bone.

EXPERIMENTAL METHODS

“Pure” hydroxyapatite and SeO_3^{2-} -containing hydroxyapatite (with various selenites content) were synthesized by the wet method. Precipitates were aged, decanted, washed and dried at 100°C . For physicochemical studies, the following methods were applied: powder X-ray diffractometry, scanning electron microscopy (SEM), atomic absorption spectrometry (AAS). Solid-state NMR techniques (standard Bloch-decay ^1H , ^{31}P , ^{77}Se and $^1\text{H} \rightarrow ^{31}\text{P}$ cross polarization kinetics), Raman and FTIR spectroscopies were used for structural analysis.

RESULTS AND DISCUSSION

The obtained materials are nanocrystalline hydroxyapatites; PXRD method shows that the materials do not contain any additional crystalline phases. The incorporation of selenite ions causes elongation of a axis of the unit cell. Crystallinity of substituted samples slightly decreases with increased value of selenium content. FTIR and Raman spectra shows the bands from selenites incorporated into the HA crystals.

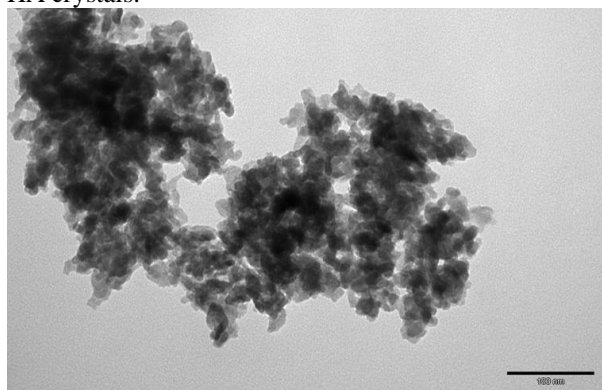


Fig. 1. TEM image of selenium-doped HA.

The ^{31}P and ^1H solid-state NMR spectra confirm hydroxyapatite structure of the samples. The ^{77}Se NMR

experiments show that in the samples with lower concentration of selenium, selenite ions are located into the crystal interior, whereas in the samples with high selenium content, the selenites are present both in the crystal lattice and on the crystal surface.

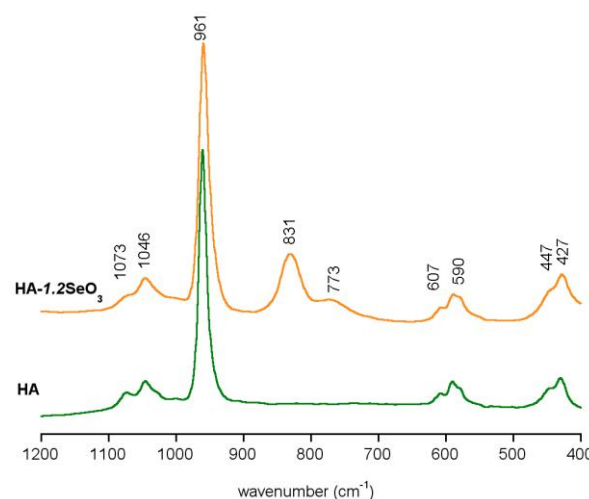


Fig. 2. Raman spectra of “pure” and substituted HA.

CONCLUSION

Nanocrystalline selenium-doped hydroxyapatite were successfully synthesized by the wet method. Future studies will focus on evaluation the *in vitro* biocompatibility assays.

REFERENCES

1. Dorozhkin S.V. and Epple M., *Angew. Chem. Int. Ed.* 41:3130-3146, 2002.
2. Rayman M.P., *Lancet* 356:233-241 2000.
3. Moreno-Reyes R. et al., *J. Bone Miner. Res.* 16: 1556-1563, 2001.
4. Kolmas J. et al., *Mater. Sci. Eng.* 39 C:134-142, 2014

ACKNOWLEDGMENTS

This work was supported by the research program (Project MNiSzW-2011/03/D/ST5/05793) of the Polish Ministry of Science and Higher Education.

The TEM studies were performed in the Laboratory of Electron Microscopy, Nencki Institute of Experimental Biology, Warsaw, Poland (the equipment was installed within the project sponsored by the EU Structural Funds: Centre of Advanced Technology BIM – Equipment purchased for the Laboratory of Biological and Medical Imaging.

Determination of metallic biomaterials susceptibility to crevice corrosion

L. Joska*, J. Fojt, A. Bernatikova

*Department of Metals and Corrosion Engineering, Institute of Chemical Technology in Prague, Czech Republic, joskal@vscht.cz

INTRODUCTION

Implants are generally produced from stainless steels, alloys based on cobalt and nowadays the most frequently from titanium. Titanium alloys based on beta structure with low modulus of elasticity and excellent mechanical properties are studied at present. Corrosion resistance of all materials used for implantation into the human body has to be very high; corrosion rate should be lower than 0.25 $\mu\text{m}/\text{year}$. The most of metallic materials used in human medicine is not noble; their high resistance is generally based on passivity. Passive metals are susceptible to non-uniform forms of corrosion. Initiation of e.g. crevice corrosion leads to local increase of corrosion rate resulting in local body burden by corrosion products and/or as the worst result to malfunction of the implant. Whilst general corrosion behaviour of biomaterials is widely studied not too many publications are dedicated to non-uniform corrosion. Several methods, in principle exposure and electrochemical (potentiodynamic, potentiostatic) tests, are used for passivity breakdown studies. Two standards dealing with crevice corrosion are dedicated to biomaterials - ASTM F746 and ASTM F2129. Both methods are accelerated electrochemical tests.

The objective of this study was to assess resistance to crevice corrosion of titanium-zirconium-tantalum alloys and to compare results of the tests realised according to ASTM standards and exposure test.

EXPERIMENTAL METHODS

Measurements were done with experimental Ti-35Nb-2Zr, Ti-35Nb-2Zr-0.4O, Ti-35Nb-6Ta beta alloys and common Ti-6Al-4V material for comparison.

Samples were in all cases exposed at 37°C in physiological saline solution, pH was adjusted to several levels. With respect to application of these materials in dentistry fluoride ions were added. Exposure environment chosen was more aggressive than phosphate buffered solution required in ASTM standards.

Experimental procedure according to ASTM F746 – 1 h stabilisation of open circuit potential (OCP), potentiostatic polarisation to +850 mV/silver-chloride electrode (SCE) for 15 min, return polarization to pre-selected potential.

Experimental procedure according to ASTM F2129 – 1 h stabilisation of OCP, potentiodynamic sweep to +850 mV/(SSCE) and back to OCP.

Exposure setup - 24 h exposure in selected environment, specimens were adjusted in crevice former (fig. 1-c).

Artificial crevices were created in all cases (O-rings ASTM F746 and F2129, crevice former according to ASTM G-78 in exposure test).

RESULTS AND DISCUSSION

According to results of all used methods studied materials were resistant in physiological saline solution. This fact was not surprising, titanium and its alloys general corrosion resistance and resistance to non-uniform corrosion in chloride media is good known. Different were results acquired in environments containing addition of fluoride ions. This model is focused on application of these materials in dentistry. Fluorides in high concentrations and often at pH in acidic region are applied in this area. Results of both electrochemical methods were not-typical. Potentiodynamic curves were relatively smooth in the whole range of potentials without common sharp current increase after passive layer breakdown (Fig. 1a). Response of samples exposed potentiostatically at +850 mV/SSCE was always the same (Fig. 1b) – exponential current decrease. Samples exposed for 24h with crevice former were frequently attacked by crevice corrosion. The main reason for differences seems to be in dynamic character of short term electrochemical measurements in comparison with “static” exposure test.

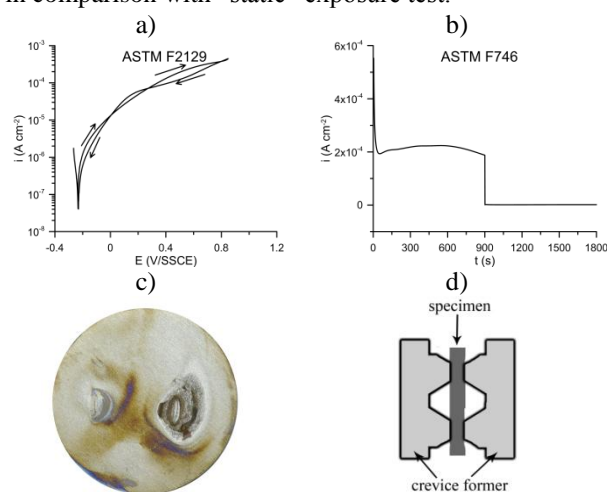


Fig. 1. Results of a) F2129, b) F746, c) exposure tests, d) sample prepared for exposure test.

CONCLUSION

Crevice corrosion is probably the most dangerous form of non-uniform corrosion. Both electrochemical methods are in principle able to detect breakdown of passivity. These measurements are helpful as screening tool. Detailed study must be based on combination of both short term electrochemical and exposure tests.

ACKNOWLEDGMENTS

The works were carried out as a part of the TA 020 10 409 project, which is financially supported by Technology Agency of the Czech Republic.

Characterization of Poly (Lactic-co-Glycolic Acid) / Poly (Isoprene) Blend for Application in Tissue Engineering

Douglas Ramos Marques¹, Luis Alberto dos Santos¹, Sarah Harriet Cartmell², [Julie Elizabeth Gough](mailto:Julie.Elizabeth.Gough@man.ac.uk)²

¹Biomaterial Laboratory / School of Engineering, Federal University of Rio Grande do Sul - UFRGS, Brazil

²Materials Science Centre / School of Materials, University of Manchester, United Kingdom, email@presenting.author

INTRODUCTION

Tissue engineering can be easily described as the in vitro seeding and attachment of human cells onto a scaffold in order to develop new tissue/organ substitutes to facilitate the restoration and maintenance of biological functions. The application of polymers as scaffolds brings desirable properties to this procedure, such as bioresorbability, biocompatibility and mechanical behavior similar to that presented by the original tissue.^{1,2}

Poly (Lactic-co-Glycolic Acid) (PLGA) is one of the most common biodegradable polymers used in the medical field since the 70's. The blend with Poly (Isoprene) (PI) generates a material with higher plastic deformation, that may be ideal for restoration of soft tissues. However, to apply the blend as a biomaterial, viability cell tests must be performed to detect the occurrence of toxic effects and the biological behavior of the material at the cellular level.

EXPERIMENTAL METHODS

PLGA ($M_n=250,000$) and PI ($M_n=295,000$) were dissolved in Chloroform (99.8%) in a 60% ww PLGA to 40% ww PI proportion, followed by homogenization and drying. FTIR spectra were obtained using a Perkin Elmer model Spectrum 1000 FTIR at room temperature (25°C). In order to investigate the polymers miscibility, differential scanning calorimetry (DSC) was carried on TA Instruments QS, between -80°C and 150°C.

For in vitro analysis, fibrous substrates were prepared by the dripping method.³ After dripping process, the fibers formed were left to dry in lyophilizer Terroni Enterprise II for 24h, vacuum, at -40°C. The dried fibers were then mounted onto coverlips, in cylindrical shape of Ø10mm #10µm. Human dermal fibroblasts were cultured in DMEM containing 2mM D-glucose and 10% Fetal Bovine Serum, at a density of 15×10^4 cell/well. Population density over the blend disks (treated group) and glass disks (control group) were observed after 1, 3, 7 and 14 days. Both groups had surface washed with phosphate buffered saline, cells fixed with paraformaldehyde 4%, and cells dyed in Toluidine Blue 1% for 1 minute. Observations were carried out using a Leica DMBR optical microscope, with cell counting procedure and statistical analysis using ANOVA ($\alpha=0,05$).

RESULTS AND DISCUSSION

FTIR analysis showed infrared spectrum bands relative to PLGA in the C=O and C-O bonds. Due to the structure of the PI, there was variation of intensity of the bands relative to the vibrations C=C and =CH. Pandey

et al (2008) reported that the use of chloroform in PLLA (Polylactic acid) blends and PGA (Polyglycolic acid) showed significant variation in polymer structure, in relation to materials used.⁴ This variation also indicated the formation of mixtures in the molecules, turning the material similar to a copolymer and no longer a blend. When several chlorine atoms are bonded to the same carbon atom, as is the case with chloroform (trichloromethane), the bands are more intense at 850cm^{-1} . For the blend, bands were observed at 756cm^{-1} , but it can also be deduced that the signals with low intensity are relative to the -C-H vibrations, given that this grouping is found in both polymer chains.

Through DSC analysis is possible to see that the glass transition temperatures (T_g) relative to raw PLGA and PI are 58,88°C and -65,74°C, respectively. For the blend, the T_g related with PI shows an expressive deviation to approximately 25°C. Deviation also observed for the PLGA T_g , to 48,95°C. This approximation of glass transition temperatures indicates a partial miscibility between the polymers.

The cell counting showed that the population over the material is significantly smaller than the population presented in the control group for all the periods. However, while the control group showed a population peak at 7 days, the treated group showed a bigger population after 14 days, with significant growth when compared to day 1. Therefore it can be assumed that the material is tolerable for further investigations around its application as biomaterial.

CONCLUSION

Both blending and dripping techniques have no major influence over the material's chemical structures, with no residual solvents presented. For the blend in this proportion, PLGA and PI showed a partial miscibility. In the biological analysis, the material seemed to present a biotolerable behavior, being viable for further investigations for biomedical applications.

REFERENCES

1. McCullen, S. D. *et al.*, 2011. Current Opinion in Biotech. 22:715–720, 2011
2. Xhang, Y. *et al.*, Biomaterials 31:8651-8658, 2010
3. dos Santos, L. A. *et al.*, Patent: 0000221109247952, 2011
4. . Pandey, A. *et al.*, J. Mech. Behav. Biomed. Mat. 1:227-233, 2008

ACKNOWLEDGMENTS

The authors would like to acknowledge the funding and support from CNPq & CAPES - Brazil.



Calcium phosphate nanoparticles carrying BMP-7 plasmid DNA induce osteogenic differentiation in MC3T3-E1 pre-osteoblasts

Chrystalleni Hadjicharalambous^{1,2}, Viktoriya Sokolova³, Diana Kozlova³, Matthias Epple³ and Maria Chatzinikolaïdou^{1,2}

¹ University of Crete, Dept. of Materials Science and Technology, 71003 Heraklion, Greece, ² IESL-FORTH, Vasilika Vouton, 71110 Heraklion, Greece and ³ Inorganic Chemistry and Center for Nanointegration Duisburg-Essen (CeNIDE), University of Duisburg-Essen, 45117 Essen, Germany, chad@materials.uoc.gr

INTRODUCTION

Calcium phosphate (CaP) nanoparticles (NPs) have gained increasing interest in medicine as bone substitution materials owing to their chemical similarity to human bone and teeth¹. These biodegradable materials can also be used as vehicles for transferring genetic information (plasmid-DNA) into living cells thus directing protein expression to enhance bone tissue regeneration locally. Such DNA-carrying systems have been previously used for the transfection of different cell lines and showed promising results².

In this study, we used CaP/PEI/DNA/SiO₂-SH (NPs-DNA) nanoparticles functionalized with plasmid DNA encoding for bone morphogenetic protein 7 (BMP-7), aiming to transfect MC3T3-E1 pre-osteoblasts. We investigated the transfection efficiency, cellular viability, as well as the production of hBMP-7 by transfected pre-osteoblasts. The subsequent induction of an osteogenic response triggered by hBMP-7 was examined.

EXPERIMENTAL METHODS

Synthesis of nanoparticles: Calcium phosphate nanoparticles were precipitated from aqueous solutions of calcium lactate and diammonium hydrogen phosphate, stabilized by polyethyleneimine (PEI) and loaded with DNA (plasmid BMP-7). In order to synthesize CaP/PEI/DNA/SiO₂-SH nanoparticles, a layer of silica was added followed by covalent functionalization of silanol groups, leading to a thiol-terminated surface³.

Transfection of MC3T3-E1 pre-osteoblasts: Transfection efficiency was determined by fluorescence microscopy, using CaP/PEI/Plasmid-EGFP/SiO₂-SH nanoparticles. Also, the concentrations of hBMP-7 in the cell culture medium following transfection with CaP/PEI/Plasmid-BMP7/SiO₂-SH (NPs-DNA) were measured using an ELISA kit (Abcam, UK). Cell viability and proliferation were assessed by the PrestoBlue™ assay (Invitrogen).

Osteogenic differentiation: We investigated the potential of the functionalized nanoparticles to induce differentiation by measuring alkaline phosphatase (ALP) activity, as well as calcium biomineralization by staining with the Alizarin Red S reagent (Sigma)⁴. Nanoparticles without DNA (NPs) were used as control. We performed at least three independent experiments in triplicates.

RESULTS AND DISCUSSION

The NPs-DNA did not affect the viability of MC3T3-E1 up to 7 days of culture. The transfection efficiency was measured at 25% and hBMP-7 was detected in cells

three days after transfection with NPs-DNA (figure 1). After 3 days of culture, NPs-DNA transfected cells showed higher levels of ALP activity, an early marker of osteogenic differentiation, compared to non-transfected control cells. In addition, the nanoparticles had a positive effect on matrix biomineralization as observed by the increase of calcium production detected after alizarin red staining at 14 days of culture (figure 2). Ongoing experiments aim to measure gene expression of specific osteogenic markers induced following transfection with NPs-DNA.

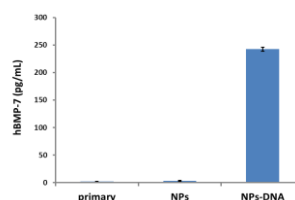


Figure 1: Expression of hBMP-7 in pre-osteoblasts transfected with NPs-DNA. Controls: untreated cells in primary medium and cells transfected with NPs.

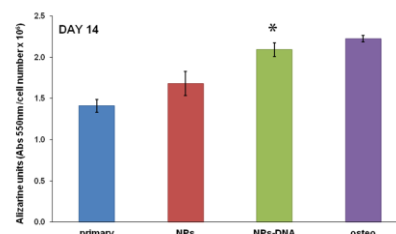


Figure 2: Enhanced calcium mineralization in pre-osteoblasts transfected with NPs-DNA. *p<0.001 vs NPs and primary control.

CONCLUSION

Successful transfection of MC3T3 cells with CaP NPs functionalised with BMP-7-encoding DNA, led to expression of hBMP-7 and an enhanced osteogenic response. This indicates the potential of the NPs to be used as DNA carrier materials to enhance bone formation.

REFERENCES

1. Epple M. *et al.*, J. Mater. Chem., 20, 18-23, 2010
2. Chernousova S. *et al.*, RSC Adv., 3,11155-61, 2013
3. Sokolova V. *et al.*, J. Mater. Sci., 45, 4952-57, 2010
4. Terzaki K. *et al.*, Biofabrication, 5(4), 045002, 2013

ACKNOWLEDGMENTS

The authors would like to thank the General Secretariat for Research and Technology Grant Thales-MIS 380278 for financial support.

Synthesis and *in vitro* Bioactivity of Cu and Zn doped sol-gel- silicate bioactive glasses

J. Bejarano^{1*}, H. Palza¹, P. Caviedes²

¹Department of Chemical Engineering and Biotechnology, University of Chile, Chile, ^{*}jbejarano@ing.uchile.cl

²Center for Clinical Research and Pharmacological Studies, University of Chile, Chile

INTRODUCTION

Bioactive glasses are widely studied for replacement, repair and regeneration of bone tissue. These materials have the ability to form a biologically active apatite layer when exposed to body fluid allowing a strong bond to bone¹. The sol-gel process permits synthesis of bioactive glasses with different addition of inorganic metal ions that can be used as therapeutic agents in bone regeneration. Cu and Zn are essential trace elements of the body and act as enzyme cofactors. Controlled release of these ions from biomaterials improves its interaction with osteoblast cells increasing the bioactivity related with osteogenesis, angiogenesis and bacterial control². Despite the good properties of these metal ions, a comparative relationship between its presences and the glass microstructure and bioactivity has not been reported. The goal of the present contribution is to analyze the effect of adding Cu and/or Zn ions on the *in vitro* bioactivity and cytotoxicity of a bioactive glass.

EXPERIMENTAL METHODS

Bioactive glass microparticles based on 60SiO₂-25CaO-11Na₂O-4P₂O₅,% mol system (NaBG) doped with 1mol% of Cu (1Cu-NaBG) and Zn (1Zn-NaBG) (and co-doped, 1Cu1Zn-NaBG) were synthesized using a sol-gel process. The effect of incorporating Cu and Zn on the *in vitro* formation of calcium phosphate (CaP) layer during immersion in simulated body fluid (SBF) was evaluated by XRD and SEM techniques. The cytocompatibility (MTT cytotoxicity assay) was evaluated with osteoblast-like cells (SaOS-2). The Cu and Zn ion release was further measured in culture medium (DMEM/F12).

RESULTS AND DISCUSSION

NaBG glass crystallized from synthesis and showed apatite and Na₂SiO₄ phases. Cu²⁺ ions were present in the glass structure as CuO crystals while Zn²⁺ remained within the glass network. Cristobalite also was present in Cu and Zn doped glasses. Results from *in vitro* bioactivity showed that Cu allowed the formation of a CaP layer while Zn inhibited it. When Cu and Zn ions were together (1Cu1Zn-NaBG), CaP formation was observed. Figure 1 shows the glass surface of the soaked samples in SBF after 7 days. SEM images confirm the CaP formation (spherical particles) on NaBG, 1Cu-NaBG and 1Cu1Zn-NaBG, while on 1Zn-NaBG not was observed crystals of CaP.

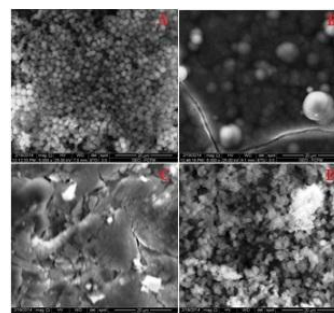


Figure 1. SEM images of glasses after 7 days in SBF. A)NaBG, B)1Cu-NaBG, C)1Zn-NaBG and D)1Cu1Zn-NaBG.

Figure 2 (left-side) confirms that the doped bioactive glasses were able to release metal ions although the time evolution depends on the kind of metal.

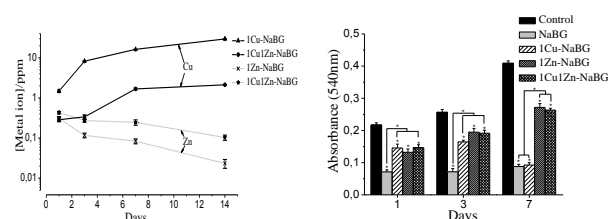


Figure 2. (left side) Release of Cu²⁺ and Zn²⁺ ions in DMEM. (right side) MTT test of glasses with SaOS-2.

Figure 2 (Right-side) shows that NaBG glass was cytotoxic to the osteoblasts. However, Cu and/or Zn doped glasses were less cytotoxic than NaBG glass during the firsts 3 days. After 7 days Cu doped glass was more cytotoxic than Zn and Cu/Zn co-doped glasses because of the higher metal ion concentrations.

CONCLUSIONS

The presence of metal ions modified the microstructure and bioactivity of glasses. In particular, Cu allowed CaP crystallization while Zn inhibited the CaP formation on the bioactive glass. The cytotoxicity depended on the amount and kind of metal added to the glass.

REFERENCES

1. Hoppe, A. et al.. *Biomaterials* **32**, 2757–74 (2011).
2. Hoppe, A. et al. *Biomater Science* **1**, 254 (2013).

ACKNOWLEDGMENTS

The authors would like to thank to The National Commission for Scientific and Technological Research (CONICYT) for the doctoral scholarship and research grant 1110078 from FONDECYT.



A pH-responsive polymer-based drug-delivery platform demonstrating intracellular siRNA target-gene knockdown

D Roebuck^{1,2*} and R Chen¹

¹Department of Chemical Engineering, Imperial College London, UK

²MedImmune, Cambridge, UK, *droebuck13@imperial.ac.uk

INTRODUCTION

The successful delivery of siRNA therapeutics to the cell interior is often limited by their instability and poor cell penetration¹. These challenges prevent the effective use of siRNA in treating diseases, including cancers. PP-75, a novel, anionic and amphiphilic, pH-responsive polymer, demonstrates promise as an effective intracellular drug-delivery platform². Following endocytotic cell uptake, PP-75 undergoes a coil-to-globule conformational transition with the acidification of the endo-lysosomal pathway. This structural change facilitates endosomal membrane destabilisation, and subsequent delivery of payloads to the cell interior^{3,4}. Acidic tumour microenvironments can be similarly exploited by PP-75, enhancing the delivery of cancer therapeutics. Synthetic siRNA therapeutic payloads therefore present as ideal candidates for PP-75 intracellular delivery. The results presented here report the cellular applications of PP-75 for cytoplasmic siRNA delivery. Human breast cancer cell lines, MDA-MB-231 and SK-BR3, have been used to develop a model Dual-Luciferase[®] Reporter (DLRTM) cell system. Following intracellular siRNA delivery, the model system can distinguish between target-specific gene knockdown and non-specific cytotoxicity. Here we will demonstrate that PP-75 displays enhanced delivery efficiency and lower cytotoxicity, when compared against commercially available delivery systems.

EXPERIMENTAL METHODS

Model Reporter Cell System: Luciferase expressing reporter cells were developed by MedImmune (Cambridge, UK) following the stable transfection of wild-type MDA-MB-231 and SK-BR3 human breast cancer cell lines with firefly (Fluc) and Renilla (Rluc) luciferase gene constructs. Target gene inhibition was studied, discriminating between targeted knockdown (Fluc) and off-target cytotoxicity (Rluc). **Synthesis of PP-75 and PP-75-siRNA Conjugates:** PP-75 was synthesised according to the method of Chen *et al*⁵. Sulfhydryl cross-linkers were grafted onto PP-75 allowing conjugation with thiol containing siRNA payloads. **Cellular Uptake and Cytotoxicity of PP-75:** Confocal microscopy and flow cytometry were used to confirm cellular uptake of fluorescently labelled PP-75 (PP-75 FITC). The concentration dependent cytotoxicity of PP-75 was assessed by measuring viable, metabolically active, cells over 72 h via the CellTiter-Glo[®] Assay (Promega). **Intracellular siRNA Delivery and Target-Gene Knockdown:** MDA-MB-231 Fluc/Rluc and SK-BR3 Fluc/Rluc cells were treated with siRNA loaded delivery systems at various concentrations. Cells were harvested at 24 h intervals to assess relative levels of Fluc and Rluc. mRNA

knockdown was quantified using RT-qPCR, following extraction of total RNA. Protein knockdown was determined, measuring relative luminescence in the DLRTM assay (Promega). Results were plotted relative to control cells and compared to Lipofectamine[®], a cationic, liposomal delivery agent.

RESULTS AND DISCUSSION

The delivery of fluorescently labelled PP-75 to the cell interior was observed using confocal microscopy and confirmed by flow cytometry; FITC acting as a model delivery payload. PP-75 cytotoxicity was negligible in both MDA-MB-231 Fluc/Rluc and SK-BR3 Fluc/Rluc cell lines; viability remaining close to 100% following treatment with PP-75 up to 2.5 mg ml⁻¹ over 72 h, assessed using the CellTiter-Glo[®] viability assay. Fluc gene knockdown was observed in MDA-MB-231 Fluc/Rluc and SK-BR3 Fluc/Rluc breast cancer reporter cell lines following intracellular siRNA delivery. The results demonstrated concentration and time dependent intracellular knockdown, following treatment with 5-25 nM siRNA concentrations, over 72 h. RT-qPCR confirmed Fluc knockdown at the mRNA level relative to endogenous control genes (including Rluc) over 72 h and the DLRTM assay demonstrated parallel knockdown at the protein level, maintained with extended treatment times. Expression of endogenous mRNA and Rluc protein levels indicate high levels of Lipofectamine[®] associated cytotoxicity compared to untreated cells and siRNA only treated cells.

CONCLUSION

These results begin to validate PP-75 as an effective drug-delivery platform, promoting intracellular target-site delivery, of functional siRNA payloads.

REFERENCES

1. Gavrilov K. and Saltzman W. M. *Yale Journal of Biology and Medicine* 2012; 187-200.
2. Chen R. et al. *Biomaterials* 2009; 30:1954-1961.
3. Liechty W. B. et al. *Advanced Materials* 2009; 21: 3910-3914.
4. Khormaei S. et al. *Advanced Functional Materials* 2013; 23: 565-574.
5. Chen R. et al. *Journal of Materials Chemistry* 2009; 19: 4217-4224.

ACKNOWLEDGMENTS

Thank you to Dr Ralph Minter and Dr Sandrine Guillard, for support and supervision at MedImmune, Cambridge. Also thanks to Dr Jefferson Revell, MedImmune, for guidance with chemical synthesis. Thank you to the BBSRC (Grant no: BB/I016058/1, BB/I016058/2) and MedImmune for providing financial support to the project.



Using Simulation to Predict the Thermomechanical behaviour Of the Hydrogel Matrix Applied in Drug Delivery System

Nirina Santatriniaina¹, Dominique Pioletti^{2*}, Lalaonirina Rakotomanana¹, Mohandrea Nassanjan^{2*} and Arne Vogel^{2*}

¹Mathematics/ Mathematical Research Institute, University of Rennes, France

^{2*} Laboratory of Biomechanics Orthopaedics, Federal Polytechnics School of Lausanne, Switzerland.

[email: nirina.santatriniaina@univ-rennes1.fr](mailto:nirina.santatriniaina@univ-rennes1.fr)

INTRODUCTION

In the context of drug delivery, controlling the release of the drug in a specific target tissue becomes a crucial issue [1]-[2]. Numerous methods to deal and to optimize the delivery techniques were established by using diffusion model [3]. The Hydrogel matrix has dissipation properties inducing temperature change under cyclic load [4]. First this phenomenon may be used to optimize drug delivery device actioned by the temperature change, as in cartilage joint that is always under cyclic load [5]. Second temperature change may induce defect in the material and may influence the formation of transfer film and contact at the interface between biological tissues and implants [6]. Then, we need to develop a predictive model to qualify and to quantify the temperature effect in this material and to determine the maximum allowable temperature under various conditions. The mechanical loading is accompanied by a production of entropy and heat, which can influence the temperature and the behaviour of the material. Generally the behaviour is viscoelastic. Then, some part of the energy is converted into heat as dissipation, thus resulting into an irreversible temperature and entropy augmentation. The goal of this study is to investigate this evolution law by using models and numerical methods to analyse the response under a cyclic load.

EXPERIMENTAL METHODS

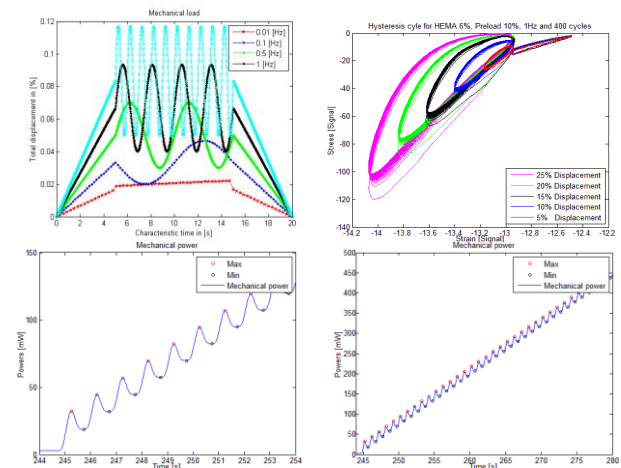
For measuring temperature change in sample under cyclic load, deformation micro-calorimetric test was used. It consists to apply in a cylindrical sample of hydrogel matrix (4 [mm] and 6 [mm] of HEMA-EGDMA hydrogels) a cyclic load. Experimentally, various frequencies are applied to observe the variations of entropy and temperature by using micro-calorimetric test. We assume that system is adiabatic.

MATHEMATICAL MODEL

Theoretical models include heat conduction, wave propagation, and constitutive laws of the hydrogels matrix. Transient analysis is investigated in the present study. A numerical approach based on finite element formulation is introduced to solve the problem. Numerous types of boundary conditions are treated. The model is designed to predict reversible and irreversible entropy and heat production. Numerical results vs. experimental measurements are presented in this work.

RESULTS AND DISCUSSION

Two cyclic mechanical loads were studied. For each test, we change the frequency of the load.



Figures report entropy production during cyclic loading: (a) 1st row: mechanical load vs. time (left); hysteresis curves of the material (right); (b) 2nd row: mechanical power (left); temperature change vs. time (right).

CONCLUSION

Theoretical model was successfully established in the present work to perform the thermomechanical behaviour of HEMA-EGDMA hydrogel. New constitutive equation was developed, by assuming an adiabatic system. Original numerical approach to solve the coupled partial differential equation by using finite element method has been developed. Reciprocal interaction between mechanical and thermal energy has been highlighted. This approach revealed detailed information to qualify and to characterize the entropy production under cyclic thermomechanical loads. It can be applied for biological tissues as tendon, ligament and cartilage. Results show that the heat effects to the dissipation energy are significant and may be exploited to control the drug delivery device driven by temperature change.

REFERENCES

- Philippe Abdel-Sayed *et al*, J. Mech. Behaviour of Biomedicine Materials, 30: 123-130, 2014.
- Mohandrea Nassanjan *et al*, Biomaterials 2013.
- N.S. Landinez-Parra *et al*, Comp Meth and Prog in Biomedicine 104 (3): 58-74, 2011.
- Mahaman-Habidou *et al*, J. Math Appl, 84: 407-470, 2005.
- Chi-Chung Hu *et al*, Mat Sci Eng, 17: 11-18, 2001.

ACKNOWLEDGMENTS

This work is financially supported by Cooperation between the Laboratory of Biomechanics Orthopaedics of EPFL Lausanne Switzerland and Mathematical Research Institute of Rennes, Univ of Rennes, France.

Using Bioactive Scaffolds to synthesise an *in vitro* 3D Bone Model for Implant Testing

G. Tetteh^{1,2}, I. U. Rehman¹, and G. C. Reilly^{1,2}

¹ Kroto Research Institute, University of Sheffield, Sheffield, UK S3 7HQ

² INSIGNEO Institute for in silico Medicine, University of Sheffield, Sheffield, UK S1 3JD,
gift.tetteh@sheffield.ac.uk

INTRODUCTION

Bone tissue engineering (TE) aims at improving musculoskeletal health, by providing a living bone graft substitute to fill and aid in the repair of bone defects caused by trauma, disease, or congenital malformations, or to augment bone stock around an implant site. Bone TE also has the potential to provide 3D experimental systems which can be used to test orthopaedic pharmaceuticals and materials.

Particulate leaching is an established fabrication technique which allows close control over pore size and interconnectivity, and has advantages for creating scaffolds for bone regeneration.

Our aim is to develop a tissue engineered bone construct that could be used for studying *in vitro* bone formation around implant materials. The scaffold therefore needs to have good mechanical strength and resilience with high porosity, low degradation rate and be osteoconductive.

EXPERIMENTAL METHODS

Polyurethane (PU) and Polyurethane-Hydroxyapatite (PU_HA) composite scaffolds were fabricated with the particulate leaching technique. 15%wt PU dissolved in 70/30 DMF/THF solvent was combined with NaCl particles (~250 µm) for PU scaffolds.

To create composite scaffolds, PU solutions were doped with either micro or nano-sized HA particles in a ratio of 3 PU: 1 HA. Micro-CT analysis and Scanning Electron Microscopy were used to analyse scaffold morphology, whilst FTIR and Raman spectroscopy were used for chemical and structural characterisation of the scaffolds.

Compression mechanical testing (Bose Electroforce-3200) was used to assess the mechanical properties of the fabricated scaffolds. Scaffolds were sterilised with an autoclave prior to cell culture and seeded with human Embryonic Mesenchymal Progenitor (hE-SMP's) cells. Assays for cell viability and matrix production were conducted over a 28 Day period.

RESULTS AND DISCUSSION

PU scaffolds had the highest pore size but the lowest Young's Modulus and yield strength. However, with an average pore size of $190 \pm 75 \mu\text{m}$, composites with nHA particles had the highest Young's Modulus and yield strength of $0.671 \pm 0.080 \text{ MPa}$ and $0.040 \pm 0.014 \text{ MPa}$, respectively.

Micro – CT analysis showed good pore interconnectivity in all scaffolds whilst FTIR and

Raman spectroscopy confirmed the presence of HA in all composite scaffolds before and after autoclaving. Alamar Blue cell viability assay showed that cells were viable on all scaffolds whilst Alazir red and Sirius red staining confirmed mineral deposition and collagenous extracellular matrix formation, respectively.

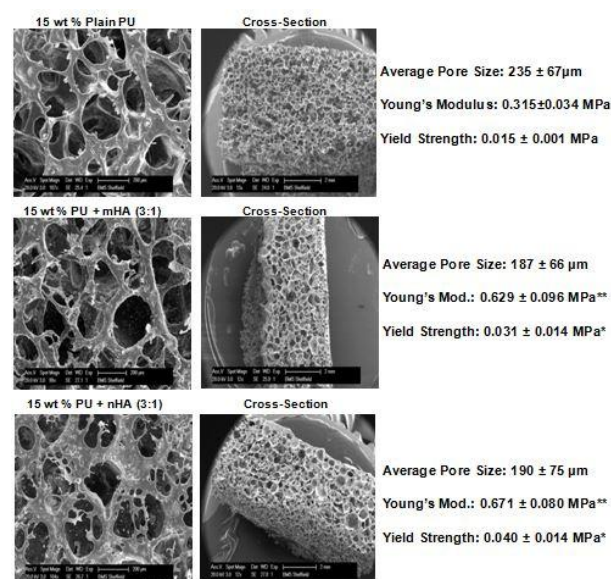


Figure 1: SEM images of particulate leached scaffolds; left: top view (scale bar=200µm) and right: cross-sectional view (scale bar=2mm) Text: Mean \pm standard deviation; (n=6) one way Anova **= $p < 0.001$ and *= $p < 0.05$

These particulate leached scaffolds composed of highly interconnected macro and micro porous network (>60% porosity) with pore sizes previously described as optimum for bone regeneration (>180µm)^[1,2], support bone matrix formation and have good mechanical properties in relation to their good porosity.

CONCLUSION

We therefore propose the use of these autoclavable scaffolds as a support for tissue engineered constructs, and for in-vitro studies of bone formation including testing of implant materials.

REFERENCES

- [1] KLAUITTER, J., HULBERT, S. 1971 *Journal of Biomedical Materials Research* 5, 161-229.
- [2] GOGOLEWSKI, S. & GORNA, K. 2007. *Journal of Biomedical Materials Research Part A*, 80, 94-101.

ACKNOWLEDGMENTS

The authors would like to thank the Ghana Education Trust Fund for providing financial support to the project.



Bis-urea based supramolecular materials for tissue engineering

Samaneh Kheyrrooz^{1,3}, Patricia Y.W. Dankers^{2,3}, Rint P. Sijbesma^{1,3}

1. Laboratory for Macromolecular and Organic Chemistry,
2. Laboratory of Chemical Biology, 3. Institute for Complex Molecular Systems.
Eindhoven University of Technology, Eindhoven, The Netherlands

S.Kheyrrooz@tue.nl

INTRODUCTION

Monomeric units in supramolecular polymers are held together via non-covalent interactions. Due to these reversible non-covalent interactions, supramolecular materials are dynamic in nature. The combination of order and dynamic behaviour makes supramolecular polymers promising materials for biomedical applications.

Urea groups are known to form strong bifurcated hydrogen bonds. Self-assembly of bisurea based bolaamphiphiles, UnU, led to formation of rod-like micelles in water (Figure 1).² Introduction of new functionalities to this supramolecular system can be readily done by mixing guest molecules with bisurea moieties, such as fluorophores. Self-sorting of bisurea based bolaamphiphiles has been studied by fluorescence spectroscopy using pyrene and dimethylaniline probes which form exciplex when in molecular contact with each other.^{2,3}

Inspired by the bisurea based bolaamphiphiles, we have designed segmented polymers with bisurea units in hydrophobic alkyl segments, and poly(ethylene glycol) (PEG) as hydrophilic segments (Figure 1). These bisurea-PEG polymers (PUnU) form hydrogels in aqueous environment.⁴

The bisurea supramolecular motif was also incorporated into biodegradable polycaprolactone (Figure 1).⁴ Supramolecular incorporation of bioactive guest molecules shows promising cell adhesion.⁵

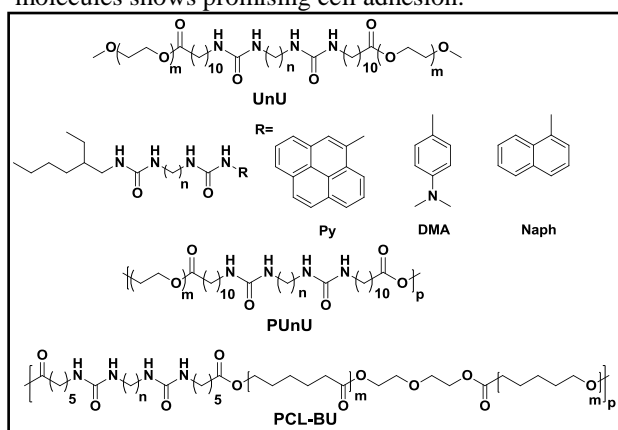


Figure 1: Molecular structure of bisurea based bolaamphiphiles (top), fluorescent probe molecules (middle), Segmented PEG based bisurea polymer (PUnU), PCL-BU polymer (bottom).

The main goal of the current study is to use dynamic supramolecular interactions in a modular approach to bring together different properties of various bisurea based molecules. Prior to that, fundamental characterization of the system is required to understand potential use of our supramolecular materials as a scaffold for tissue engineering. Next, the biocompatibility of several bisurea-molecules were

investigated. At a later stage, molecules of different properties will be mixed to obtain a 'smart' biomaterial.

EXPERIMENTAL METHODS

Fluorescence spectroscopy was utilized to monitor dynamics and mechanism of the UnU exchange in an aqueous solution. Biocompatibility of UnUs was checked by resazurin assay.

RESULTS AND DISCUSSION

In figure 2, rate constants of exchange of UnUs were summarized from four different methods. These results show that the system is dynamic, and it takes approximately 20 min to reach equilibrium.

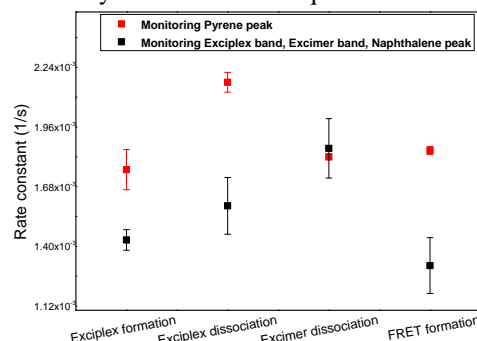


Figure 2: Rate constants of monomer exchange of U4U. Cell viability testing of different types of bisurea containing molecules showed no toxicity (Figure 3).

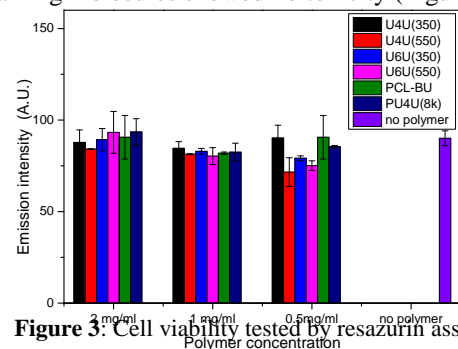


Figure 3: Cell viability tested by resazurin assay.

CONCLUSION

Bisurea based supramolecular systems were used to design a suitable platform to obtain smart biomaterials. Taking advantages of various molecules by just mixing is the key feature of our system.

REFERENCES

1. Boekhoven J. *et al.*, Adv. Mater. **2014**, 26, 1642–1659.
2. Pal A. *et al.*, J. Am. Chem. Soc. **2010**, 132, 7842–7843.
3. Pal A. *et al.*, J. Am. Chem. Soc. **2011**, 133, 12987–12989.
4. Pawar G.M., *et al.*, Biomacromolecules. **2012**, 13, 3966–3976.
5. Wisse E. *et al.*, Biomacromolecules. **2006**, 7, 3385–3395.

Acknowledgment. The authors would like to thank NWO for financial support of the project.

Biomaterialized hydroxyapatite nanocrystals/graphene oxide as filler for bone tissue engineering

¹Maria Grazia Raucchi, ¹Daniela Giugliano, ¹Angela Longo, ¹Stefania Zeppetelli, ¹Gianfranco Carotenuto and ^{1,2}Luigi Ambrosio

¹Institute of Polymers, Composites and Biomaterials – National Research Council of Italy. Mostra d'Oltremare Pad.20 - Viale Kennedy 54, 80125- Naples, Italy.

²Department of Chemicals Science and Materials Technology, National Research Council of Italy (DSCTM-CNR), P.le Aldo Moro 7, 00185 – Rome, Italy. mariagrazia.raucchi@cnr.it

INTRODUCTION

Biomaterialization is the process that gives rise to small and large inorganic-based structures in biological systems, and it often results in sophisticated materials having elaborate morphologies, excellent mechanical and vital biological functions. Thus, the convergence of the study of graphene with biomaterialization is expected to widen the horizons of material science. To date only few studies have analyzed the possibility to synthesize new and functional hybrid materials for tissue engineering combining Hydroxyapatite [$(\text{Ca}_{10}(\text{PO}_4)_6(\text{OH})_2$, HA] with carbon based materials such as graphene and its derivative, for example graphene oxide (GO). The presence of abundant epoxide, hydroxyl and carboxylic groups on the GO basal plane could provide enormous reactive sites for chemical interactions. Herein, we report a dual approach to prepare hydroxyapatite nanocrystals (HA)/graphene oxide (GO) in order to develop a new class of multi-functional biocomposite materials with excellent biological properties, and make them highly promising materials for biomedicine.

EXPERIMENTAL METHODS

HA/GO gel materials were prepared by a dual approach as sol-gel technology and biomimetic method. Sol-gel approach allows to obtain HA/GO hybrid materials in aqueous solution at room temperature where the gelation take place after 2hrs of magnetic stirring at room temperature. A second approach concerns the preparation of HA/GO biocomposite by a biomimetic method based on a simulated body fluid solution (SBF). The SBF having ion concentrations analogous to those of human extracellular fluid is often used for biomimetic process to precipitate hydroxyapatite. In order to accelerate the hydroxyapatite deposition, 5xSBF with ion concentrations 5 times those of SBF is also used. Physico-chemical characterization was carried out to evaluate the chemical interaction between two phases. The morphology of the biocomposites was characterized by using SEM and TEM microscopy. Furthermore, biological tests were performed to estimate the effect of biocomposites on cellular behavior by using human mesenchymal stem cells.

RESULTS AND DISCUSSION

Sol-gel technology allows to synthesize HA/GO hybrid materials at room temperature. Biomimetic mineralization was induced by incubating GO sheet in a supersaturated 5xSBF solution. The presence of anionic functional

groups in GO facilitates, in the first step of treatment, the nucleation of biomaterials by attracting more Ca^{2+} cations to deposit onto film surface and subsequently forming biomaterials with PO_4^{3-} . Moreover, TEM images demonstrated a hybridization of HA nanoparticles in GO sheet for materials obtained by sol-gel approach (Fig.1). In fact, spindle-like HA nanoparticles with a diameter of about 5 nm and a length around 70 nm, were intercalated uniformly and strongly with the GO sheets. The interaction between HA nanoparticles and GO improves the bioactivity of materials. In fact a layer of apatite on GO sheet was obtained after biomimetic treatment. Biological studies performed by using hMSC demonstrated that the presence of GO induces an osteogenic differentiation evaluated by using a media without osteogenic factors.

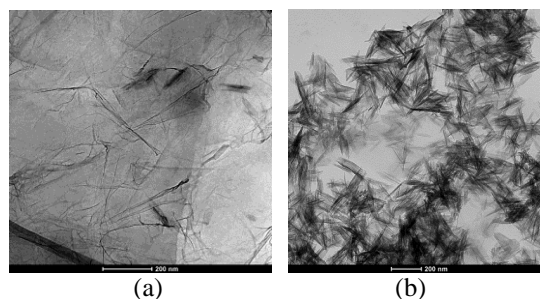


Fig. 1: TEM analysis of GO sheet (a), and HA/GO materials (b).

CONCLUSION

In this work, we have demonstrated that the combination of HA with GO leads to the further development of a broad new class of multi-functional biomaterials. *In vitro* bioactivity and biocompatibility results of biomaterialized graphene materials present the new prospect of utilizing graphene-based materials in clinical and biomedical applications. The combination of HA with GO leads to the further development of a broad new class of multi-functional biomaterials.

ACKNOWLEDGMENTS

This study was supported through funds provided by the PNR-CNR Aging Program 2012-2014. The authors also thank Mrs. Cristina Del Barone for TEM investigations.

Effects on growth and osteogenic differentiation of mesenchymal stem cells by the strontium-added sol-gel hydroxyapatite gel materials

¹Maria Grazia Raucci, ¹Daniela Giugliano, ²M.A. Alvarez-Perez, ³C. Demitri and ^{1,4}Luigi Ambrosio

¹Institute of Polymers, Composites and Biomaterials – National Research Council of Italy. Mostra d'Oltremare Pad.20 - Viale Kennedy 54, 80125- Naples, Italy.

²Tissue Bioengineering Laboratory; DEPeI, Faculty of Dentistry, National Autonomous University of Mexico; 04510, Mexico DF, Mexico.

³Department of Engineering for Innovation, University of Salento, Via Monteroni, 73100 Lecce, Italy.

⁴Department of Chemicals Science and Materials Technology, National Research Council of Italy (DSCTM-CNR), P.le Aldo Moro 7, 00185 – Rome, Italy. mariagrazia.raucci@cnr.it

INTRODUCTION

Osteoporosis is a systemic disease "characterized by low bone mass and microarchitectural deterioration of bone tissue, leading to enhanced bone fragility and a consequent increase in fracture risk", which results from an impaired balance of bone resorption and formation by osteoclasts and osteoblasts, respectively. Various therapies have been developed for the clinical treatment of osteoporosis based on either the inhibition of bone resorption or the anabolic stimulation of bone formation. Strontium(II) ions have been demonstrated to both increase the bone formation by osteoblasts as well as to decrease the osteoclast-mediated resorption of the bone matrix. Here, we propose Strontium - modified CaP gels obtained at room temperature by using sol-gel method. In fact, sol-gel synthesis approach appears to be among the most suitable route towards performing injectable CPC. The effect of these modified gel materials on the proliferation and differentiation of mesenchymal stem cells have been studied in the light of the biomaterial compositional changes.

EXPERIMENTAL METHODS

Sr-HA gels containing 5 - 10 - 15 and 20 mol % Ca^{2+} replaced by Sr^{2+} were synthesized at room temperature by using calcium nitrate tetrahydrated $\text{Ca}(\text{NO}_3)_2 \cdot 4\text{H}_2\text{O}$ and di-ammonium hydrogen phosphate $(\text{NH}_4)_2\text{HPO}_4$ as precursors and using water as solvent. Strontium nitrate $\text{Sr}(\text{NO}_3)_2$ was dissolved in water and used to replace Ca^{2+} ions. The chemical composition of Sr-HA and the effect of strontium on viscosity properties have been evaluated by physico-chemical and rheological analysis. The morphology of the materials was characterized by using SEM and TEM microscopy. Furthermore, biological tests were performed to estimate the effect of strontium on cellular behavior by using human mesenchymal stem cells.

RESULTS AND DISCUSSION

A preliminary investigation showed a difference in the gelification time (from 1hr to 3hrs) of the biomaterials prepared at different Sr concentration. However, all gels synthesised at room temperature could be successfully equilibrated at pH 7.4 without any significant dissolution thus ensuring their compatibility with biological systems. From the TEM evaluation in Fig. 1, it is shown that the

HA particles show a length about 70-80nm and a diameter of 4-5nm. In 10 and 20mol% Sr-doped HA an agglomerate structure was observed; the particles were changed in size, in fact a length of 40 nm and diameter of 10nm were observed. An increasing in the amount of Sr ions doped into HA made the agglomerated particles smaller. The substitution of large Sr^{2+} into small Ca^{2+} lead to denser atomic packing of the system causing retardation of crystals growth. Biological results performed also by gene expression analysis show that HA-10Sr, HA-15Sr and HA-20Sr promote the expression of ALP; in contrast HA-10 and 20Sr promote the expression of OPN on lesser degree as compared with the expression of OPN promoted by HA-15Sr. Moreover, OCN expression was significantly enhanced on HA-15 and 20Sr meanwhile faint signal was detected on HA-10Sr.

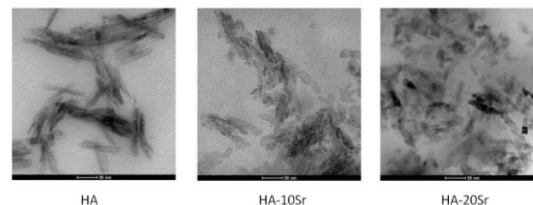


Fig. 1: TEM analysis on HA gel and strontium-doped hydroxyapatite at 10 and 20 mol%.

CONCLUSION

In this study, strontium-substituted hydroxyapatite with different Sr content has been synthesized at room temperature by using a sol-gel approach. The strontium incorporated in the hydroxyapatite structure decrease slightly the size of HA nanoparticles as demonstrated by morphological analyses. Moreover, biological results demonstrated that strontium-doped hydroxyapatite gels up 20mol% show good biocompatibility without significative cytotoxic effect. This work confirms the ability of the hydroxyapatite modified Sr materials to induce hMSC differentiation towards the osteoblast-like phenotype

ACKNOWLEDGMENTS

This study was supported through funds provided by the PNR-CNR Aging Program 2012-2014. The authors also thank Mrs. S. Zeppetelli for facilitating biological analysis and Cristina Del Barone for TEM analysis.

Development of Nerve Guide Scaffold with a Microstructured Intraluminal

Atefeh Mobasseri^{1,2}, Alessandro Faroni², Julie Gough¹, Giorgio Terenghi² and Adam Reid²

¹School of Materials, The University of Manchester, Manchester, UK

²Centre for Tissue Injury and Repair, The University of Manchester, Manchester, UK

Atefeh.mobasseri@manchester.ac.uk

INTRODUCTION

The management of peripheral nerve injuries is still a major clinical need. End-to-end neuroorrhaphy is only feasible when there is no nerve gap. Autologous nerve grafting is the current approach to repair the nerve injuries in presence of nerve loss. In order to minimise the complications associated with autografting, a bioengineered solution using a nerve guide scaffold has been sought. In the present study, we examined and evaluated a nerve guide scaffold with the micro-grooved inner surface made of a biodegradable polymer *in vivo*.

EXPERIMENTAL METHODS

Solvent casting of polymer solution (polycaprolactone (PCL)/ poly lactic acid (PLA) blend) on the patterned silicon substrate was used to make the ultra thin grooved films (1). The films were rolled around a cannula (gauge 16) and heat sealed to form a conduit with 1.6mm inner diameter and 12mm length. A rat sciatic nerve model with 10mm gap was used to assess the conduits *in vivo* for 3 and 16 weeks. The experimental groups were grooved conduit (C), differentiated adipose-derived stem cell (dASC)-primed conduit (C+C) and autografts (Ag) (n=5 each group/timepoint). Experimental outcomes analysed were axonal regeneration, myelination and end-organ re-innervation.

RESULTS AND DISCUSSION

At the time of harvesting, the conduits structure was maintained with no major deformation or degradation. Analysing the inner surface of conduit with SEM, it was shown that grooved structure was kept after 3 and 16 weeks of implantation, although several cracks were formed on the surface following 16 weeks experiment (Fig. 1). At 3 weeks nerve transection, the regenerated nerve bridged the gap in all experimental groups. At 16 weeks, the measured features of regenerating axons including axon size, myelination area and axonal density were comparable between C and Ag groups (Fig. 2). However, including dASCs inside the conduits did not improve the quality of nerve regeneration. Muscle atrophy measured by wet muscle weight ratio of injured/operated side was significantly lower in C+C group (44 ± 6.35) when comparing to C (63 ± 7.13) and Ag (58 ± 7.01). The skin re-innervation density at the footpad skin showed no significant difference across the groups.

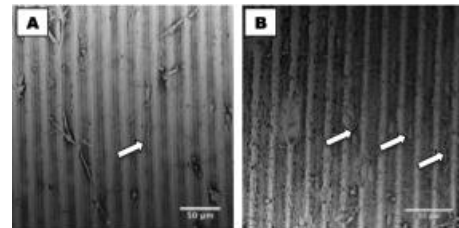
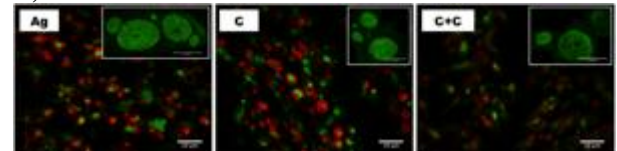


Figure 1: SEM images of the grooved intraluminal structure of a conduit after A) 3 weeks and B) 16 weeks of implantation

A)



B)

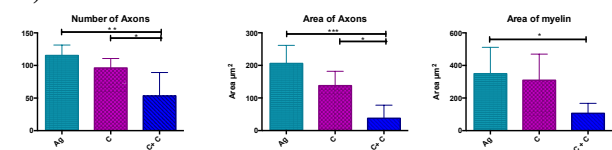


Figure 2: A) Immunostaining images of regenerated nerves following 16 weeks of nerve transection at 3mm distally, B) Quantitative measurements of features of axonal regeneration

CONCLUSION

This investigation addressed the application of the biodegradable polymer conduits with the intraluminal structure to be used in peripheral nerve repair. The PCL/PLA conduit demonstrated a promising nerve regeneration length in 3 weeks study by bridging a 10mm gap. The features of axonal regeneration as well as end-organ re-innervation and muscle mass were similar to autograft group. The promising outcomes suggested the grooved PCL/PLA conduits could be a potential alternative to nerve grafting. Further experimental investigation needs to be conducted to develop the cell-primed conduits and improve their performance for peripheral nerve repair.

REFERENCES

1. S A Mobasseri, G Terenghi, S Downes, J Mater Sci Mater Med. 1–9, 2013.

ACKNOWLEDGMENTS

The Authors would like to thank NIHR i4i program for their financial support.

From Bench to bedside: realization of a bioartificial, wearable lung assist device

Esther Novosel¹, Annika Wenz², Kirsten Borchers³, Markus Schandar³, Jörg Schneider¹, Georg Matheis¹, Petra Kluger^{3,4}

¹Novalung GmbH, Heilbronn, Germany, ²Interfacial Engineering, University of Stuttgart, Germany, ³Cell and Tissue Engineering, Fraunhofer IGB Stuttgart, Germany, ⁴Applied Chemistry, University of Reutlingen, Germany

Corresponding Author: esther.novosel@novalung.com

INTRODUCTION

Chronic obstructive pulmonary disease is the 4th leading cause of death worldwide. Extracorporeal lung assist devices that promotes oxygenation/decarboxylation of the patients' blood like the Novalung interventional lung assist device (iLA®) can improve lung protection and increase quality of life [1]. Those systems limit patients mobility. Due to that and to inappropriate material characteristics till nowadays there is no long term solution available. Therefore we aim to develop the first wearable miniaturized lung assist device [2].

EXPERIMENTAL METHODS

3D models and prototypes of new miniaturized hard- and software components as well as a suitable carrying system were developed. We designed a new gasexchange disposable with a optimized geometry to minimize blood damage and blood clotting events. Hemolysis tests were performed.

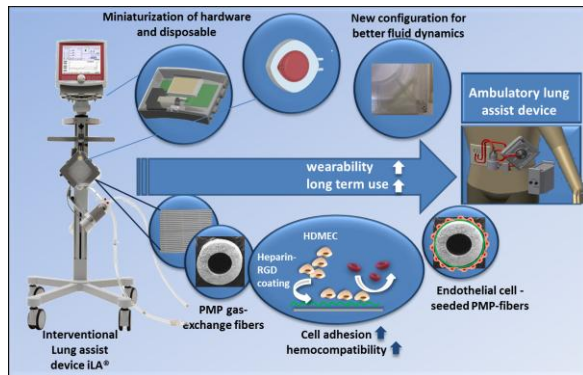


Fig1: necessary steps to transform the iLA to a longterm ambulatory lung assist device.

To improve the hemo- and biocompatibility of the gasexchange material Polymethylpentene (PMP), we managed to seed the fibers with human endothelial cells. Therefore a cell adhesion promoting biochemical surface with benzophenone modified heparin and suitable chemical side chains to perform both, peptide-coupling and covalent conjugation to PMP- membranes was developed. In order to provide cell adhesion sites RGD-peptides were coupled.

Human dermal endothelial cells (HDMEC) were seeded to the surface and analyzed with FDA/PI.

RESULTS AND DISCUSSION

We succeeded in miniaturization of all hardware components as well as in a new design of the gasexchanger to improve blood distribution (Fig.2a). Fig. 2b shows FDA stained vital endothelial cells after 48 h on the PMP fibers under static cell culture conditions condition (37°C, 5% CO₂).



Fig.2: a) lateral inflow and square shape design of the gasexchanger was successfully modified into a new central inflow with modified lid. B) HDMEC on PMP fibers stained with FDA/PI (vital cells are shown in green).

CONCLUSION

We developed the first miniaturized wearable lung assist device. In the future, cell seeding experiments will be performed under dynamic conditions in a bioreactor system. In a next step the whole device will be seeded with cells. Animal tests will be performed.

REFERENCES

1. "Protective and ultra-protective ventilation: using pumpless interventional lung assist (iLA)", Quintel et al. *Minerva Anesthesiol.* 77(5):537-44. 2011
2. "Artificial lung: progress and prototypes.", Zwischenberger et al. *Expert Rev Med Devices.* (4):485-97.2006

ACKNOWLEDGMENTS

We like to thank our consortium partners from Imperial College London and the University of Florence as well as the EU for the financial support under the 7th framework program through the key action "medical technology for transplantation and bioartificial organs".

Gelatin/hydroxyapatite multicomponent system with a modulate biological signals

Daniela Giugliano¹, Maria Grazia Raucci¹ and Luigi Ambrosio^{1,2}

¹Institute of Polymers, Composites and Biomaterials – National Research Council of Italy. Mostra d'Oltremare Pad.20 - Viale Kennedy 54, 80125- Naples, Italy.

²Department of Chemicals Science and Materials Technology, National Research Council of Italy (DSCTM-CNR), P.le Aldo Moro 7, 00185 – Rome, Italy. E-mail: daniela.giugliano@unina.it

INTRODUCTION

Tissue engineering strategies rely on the use of cells, bioactive factors, and scaffolds or combinations thereof. The scaffold serves the purpose of a delivery vehicle, a space-filling and structurally supportive agent, and can be designed to be biointeractive, i.e. to guide tissue regeneration. The coordinated regeneration of multiple tissues in the complex osteocondral environment requires a deep understanding of their physiology and remodeling characteristics. Desirable osteochondral tissue engineering constructs are osteoconductive and osteoinductive. HA has excellent biocompatibility with hard tissues, and high osteoconductivity and bioactivity despite its low degradation rate and osteoinductive potential. Gelatin (GEL) is compositionally virtually identical to the collagen from which they are derived, and shows to be biocompatible and resorbable. A composite scaffold of HA and GEL is therefore expected to show increased osteoconductivity and biodegradation. In this context, chemically inspired approaches based on the sol-gel transition and colloidal precipitation of calcium phosphates may efficiently improve the particles dispersion by a direct control of precipitated grain sizes through the interaction between calcium and phosphate precursors under controlled temperature and pH conditions [1]. Proposed approach enables to efficiently exploit the peculiar features of composite material bulk and surfaces by modulating the spatial distribution of bioactive signals. The aim is create an HA gradient into the scaffold section, in order to modulate biological signals.

EXPERIMENTAL METHODS

The GEL-HA nanocomposite scaffolds were fabricated by sol-gel synthesis of HA within a gelatin sol and further freeze-drying. Two types of viscous sols, gelatin, type B (pH= 5) and gelatin type A (pH=4.5) solutions were prepared in distilled water at 40°C. The gelatin solutions were mixed progressively with calcium and phosphate solution and pH at alkaline values was adjusted to allow the sol-gel transition. The Ca/P ratio was fixed at 1.67 and the HA contents with respect to gelatin-HA were considered at 20 and 30 wt%. The gelatin amount respect the total water content is fixed at 10% w/v. The dried scaffolds were crosslinked for several hrs by using a specific amount of EDC as crosslinker agent. Chemico-physical characterization (XRD-FTIR), thermal (TGA) and morphological analyses (SEM-TEM) were performed to evaluate composition, chemical interaction among the phases and hydroxyapatite gradient into longitudinal section of scaffold. Furthermore, the effect of the organic and inorganic phases () on human mesenchymal stem cell (hMSC) was studied at 7, 14 and 21 days of

culture by evaluation both cell proliferation, osteogenic and chondrogenic differentiation.

RESULTS AND DISCUSSION

By sol-gel transition in gelatin solution combined with freeze-drying, is possible to obtain a tridimensional gelatin structure interconnected with hydroxyapatite crystals, internally and externally. As shown by SEM (figure 1A), and confirmed by TEM, the crystal shape and degree depend on HA/GEL ratio. The experimental data, reported by TGA analysis (figure 1B), confirm HA gradient in the sample with HA content of 30%w. Moreover, HA residual% calculate are very close to the original amounts of calcium phosphate used to prepare the scaffolds. As demonstrated by FTIR results, the Ca^{2+} ions will make a covalent bond with R-COO^- ions of GEL molecules.

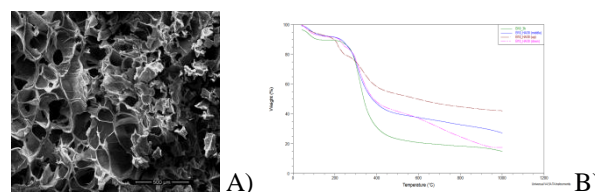


Fig. 1: A) SEM image: cross-section of GEL/HA scaffold; B) TGA analysis of three different section of the same scaffold, and gelatin powder

Mechanical properties show crosslinking efficiency. In accordance with biological tests, material are nontoxic, not affecting the cell proliferation and support osteogenic and chondrogenic differentiation of hMSC.

CONCLUSION

This work demonstrated that, by an opportune GEL/HA ratio, is possible to create an HA gradient into the scaffold section, as confirmed by morphological, thermal and chemo-physical investigations. Thermal and mechanical analyses show that in GEL/HA scaffold, success of crosslinking by EDC depend on number of carboxyl group, content in polymer typology, and inorganic phase amount. Biological test performed by hMSC demonstrates that the materials have a good biocompatibility and support osteogenic/chondrogenic differentiation.

ACKNOWLEDGEMENTS

This study was supported by MERIT n.RBNE08HM7T from the Ministero dell'Università e della Ricerca. The authors also thank Mrs S. Zeppetelli for facilitating biological analysis.

REFERENCES

- [1] M.G. Raucci et al. *Compos Sci Technol* 2010;70:1861-1868.

Osteogenic differentiation induced by biomineralized gelatin scaffold

Daniela Giugliano¹, Maria Grazia Raucci¹ and Luigi Ambrosio^{1,2}

¹Institute of Polymers, Composites and Biomaterials – National Research Council of Italy. Mostra d'Oltremare Pad.20 - Viale Kennedy 54, 80125- Naples, Italy.

²Department of Chemicals Science and Materials Technology, National Research Council of Italy (DSCTM-CNR), P.le Aldo Moro 7, 00185 – Rome, Italy. E-mail: daniela.giugliano@unina.it

INTRODUCTION

The coordinated regeneration of multiple tissues in the complex bone environment requires a deep understanding of their physiology and remodeling characteristics. The extracellular matrix of bone has been described as a composite material constituted by collagen type I fibrils mineralized with nanocrystals of hydroxyapatite. Approximately 70% of bone by weight is composed of calcium salts, with hydroxyapatite $\text{Ca}_{10}(\text{PO}_4)_6(\text{OH})_2$ as the primary mineral constituent. Bone formation occurs in two phases: matrix synthesis followed by extracellular mineralization. Combining the literature with the target of mimic natural structure, we propose a strategy employs the use of a scaffolds (natural polymer such as gelatin) and a modulating bioactive factors (hydroxyapatite crystalline), where hydroxyapatite should improve the osteogenic differentiation meanwhile gelatin increases the chondrocyte proliferation. Here, we present three-dimensional (3D) porous gelatin scaffolds, firstly fabricated by freeze-drying followed by biomimetic method in order to obtain a superficial mineralization. Cross-linking treatments to produce the formation of molecular structures have been suggested to avoid a rapid gelatin degradation.

EXPERIMENTAL METHODS

Biomineralized gelatin scaffolds were obtained by a combination of two simple methods as freeze-drying and biomimetic approach. The contributes of gelatin type/amount (Type A and B at 5 and 10 % w/v) and crosslinking time (1, 3, and 6 hrs) were evaluated, in order to study crosslinking treatment, biomimetic approach and MG-63 cells response. Suitably choosing the time and freezing temperature, it is possible to obtain a 3D structure with interconnected pores. Accelerated Kokubo treatment is able to create an hydroxyapatite coating on the surface and into the porous wall. Swelling and degradation tests, chemico-physical (FTIR), thermal (DSC-TGA) analyses were performed to study the effect of the crosslinking time on the hydrogel materials properties. By compressive tests is evaluated the enormous EDC contribute: Young modulus increased from 0.179 KPa (non-crosslinked scaffold) to 180 and 150 KPa (without and with

biomineralized treatment). To evaluate the influence of material surface on the cellular behavior, it is compared biological study on crosslinked gelatin, before and after biomimetic treatment. For this purpose the adhesion, proliferation and differentiation studies using pre-osteoblast (MG-63 cell line) were done. Moreover, osteogenic and chondrogenic differentiation of hMSC in a basal medium was evaluated.

RESULTS AND DISCUSSION

Mineralized porous gelatin (A and B type) hydrogels were obtained by using a combined freeze-dried and biomimetic approach. The swelling and degradation tests show that the crosslinked samples maintains the original shape, and are able to reduce the water absorption since to 28 days. SEM images show a bi-dimensional microporosity and the regular deposition of hydroxyapatite into the hydrogel structure. Mechanical properties, FTIR-DSC-TGA analyses show the effectiveness of the crosslinking treatment and the difference between three crosslinking time (1, 3, 6 hrs). Cytotoxicity assay performed by using MG-63 cells demonstrated that the percentage of EDC cross-linker has not toxic effect on cell viability. Moreover, a promising viability of hMSC cells and increase of osteogenic proliferation and differentiation has been observed in gelatin scaffold crosslinked by EDC solution and biomineralized by modified Kokubo treatment.

CONCLUSIONS

Biomineralized gelatin scaffold was obtained by freeze-drying and biomimetic approach. Chemo-physical, thermal and mechanical analysis demonstrated the crosslinking efficiency by EDC and the compression modulus (E) improvement. Moreover HA crystalline phase is sufficient to obtain an increasing of osteogenic proliferation and differentiation.

ACKNOWLEDGEMENTS

This study was supported by MERIT n.RBNE08HM7T from the Ministero dell'Università e della Ricerca. The authors also thank Mrs S. Zeppetelli for facilitating biological analyses.

REFERENCES

[1] M.G. Raucci *et al.* Compos Sci Technol 2010;70:1861-1868

Implantable biocomposite based radical oxygen species scavengers as a therapeutic strategy to manage age related macular degeneration

Marta O. Freitas¹, Ana S. Neto^{1,2}, B. Moreno³, E. Chinarro³, and Ana P. Pêgo^{1,2,4}

¹INEB – Instituto de Engenharia Biomédica, Universidade do Porto, Porto, Portugal, ²FEUP - Faculdade de Engenharia da Universidade do Porto, Porto, Portugal, ³Instituto de Cerámica y Vidrio, CSIC, Madrid, Spain, ⁴ICBAS – Instituto de Ciências Biomédicas Abel Salazar, Universidade do Porto, Porto, Portugal, mfreitas@ineb.up.pt

INTRODUCTION

Age related macular degeneration (AMD) is the leading cause of blindness in the elderly worldwide. Although AMD does not cause total blindness, there is a progressive loss of central vision attributable to degenerative and neovascular changes in the macula.¹ One of the key phenomena known to contribute to extra-cellular senescence is the shift in the reactive oxygen species (ROS) synthesis/degradation balance.²⁻⁴ The ultimate objective of this project is to develop a novel class of hybrid biomaterials based on TiO₂ with integrated bioactivity in terms of ROS scavenging. It is hypothesised that by modulating the ROS synthesis/degradation balance one counteract the processes, which contribute to systemic and tissue ageing of the eye and so the progression of AMD. Here we describe the effect of different TiO₂ powders in scavenging radical species generated chemically or biologically by means of inflammatory cells. Also, the non-toxic effect of these materials was assessed either with inflammatory cells or cells present in the blood-retinal barrier (BRB).

EXPERIMENTAL METHODS

TiO₂ nanopowders were synthesized by the precipitation route and then calcined in air at 200°C and 600°C for 12 hours. Mixtures of these powders were also prepared. Three commercially available powders with different ratios of anatase and rutile phases were obtained from Sigma-Aldrich. The ROS scavenging capacity of the different TiO₂ powders was addressed by generating chemically ROS using two methods: 1,1-diphenyl-2-picryl-hydrazyl (DPPH) and 3-morpholinonylhydronitrimine hydrochloride (SIN-1). A human monocytic cell line (THP-1) was cultured and further differentiated in macrophages. Non-activated and activated macrophages (lipopolysaccharide, LPS) were cultured in the presence of a range of concentrations of the different powders to address their scavenging capacity. RPE cells (ARPE-19 cell line) were cultured in the presence of different concentrations of the TiO₂ powders and the cell metabolic activity assessed (rezasurin assay).

RESULTS AND DISCUSSION

Characterization of the TiO₂ powders prepared showed higher agglomerate size for the 600°C calcined powder (0,5-50µm), comparing with the powders calcined at 200°C (0,2-30 µm). XRD patterns have shown that the powders have different crystal structure in relation to the calcination temperature and comparing with the commercial ones. In this study, we addressed the ROS scavenging capacity of different TiO₂ powders with chemical assays using artificial ROS. The results show that the 200°C and 600°C calcined TiO₂ powders promote the best reduction of ROS concentration. Next,

we assessed the bioactivity of these powders in the presence of macrophages. A viability assay showed that the powders have no toxic effect in macrophages at concentrations of 1mg/ml or below. Furthermore, at these concentrations TiO₂ powders do not promote macrophage activation. Also, we observed that, among the tested materials, the powder with the best scavenging capacity was the 600°C calcined TiO₂ powder, despite having the lowest specific surface, leading 30% reduction in the ROS detected inside macrophages when at 1 mg/ml (see Fig. 1).

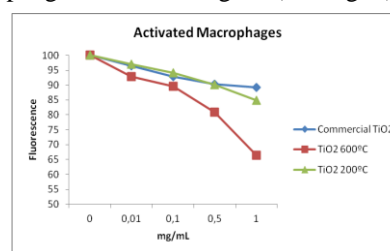


Figure 1: ROS scavenging by different TiO₂ powders. Activated macrophages were incubated with a range of concentrations of different TiO₂ powders.

At present we are extending the work to RPE cells, components of the BRB. We performed a viability assay and observed that the powders have no toxic effect on RPE cells at concentrations of 0,1mg/ml or below. The effect of the powders is being assessed on RPE cells kept under oxidative stress conditions caused by the presence of ROS, induced by two different oxidants – tertbutylhydroperoxide (tBH) and 4-hydroxynonenal (HNE).

CONCLUSION

Taken together, these results suggest that the TiO₂ powders with the best ROS scavenging capacity are the 200°C and 600°C calcined powders, showing no toxic effect on cells at lower concentrations. The produced TiO₂ powders, being materials capable of ROS scavenging either of artificial ROS or ROS generated by inflammatory cells, present themselves as valuable tools in the design of new strategies for application in the treatment of AMD.

REFERENCES

1. Rando TA. *Nature*. 2006; Jun 29;441(7097):1080-6.
2. Swanson MW, McGwin G Jr. *Optom Vis Sci*. 2008; 5(10):947-50.
3. Lu L, Hackett SF, Mincey A, Lai H, Campochiaro PA. *J. Cell. Physiol*. 2006; 206:119-125.
4. Rabin DM, Rabin RL, Blenkinsop TA, Temple S, Stern JH. *Aging*. 2013; Jan Vol. 5 No 1.

ACKNOWLEDGMENTS

The authors would like to thank the Fundación General CSIC and Obra Social “La Caixa” (Project BIOAMD) for providing financial support to this work



Soft Matrices vs. Hard Minerals: Biomimetic Morphogenesis of Calcium Phosphate in Lyotropic Liquid Crystals

Wenxiao He* and Martin Andersson

Department of Chemical and Biological Engineering, Chalmers University of Technology, Sweden

*wenxiao@chalmers.se

INTRODUCTION

Biomaterials are diversified in morphologies, the organic/inorganic organisation, etc. For example: bone, nacre, coccolith. The common feature is that: Biomaterialization occurs in viscous gel like matrix, which provide spatial delineation and diffusion limited conditions.

The organics: molecular self-assembly, collagen matrix, Liquid crystalline phases are of great interests, and relevance.

Organisms use “soft” organic compartments to control morphology of the embedded “hard” minerals. Here we present a simple method using liquid crystal (LC) phases as “soft” and “inert” templates to prepare nanostructured calcium phosphates (CaP), which are inorganics of known bioefficacy. Specifically, 6 nm-thick CaP nanowires and CaP sheets that precisely replicate a reverse hexagonal (H_2) and lamellar (L_a) LCs have been successfully synthesized and we attribute this to the sufficient spatial regulation offered by the negative (H_2) or flat curvature (L_a) of the aqueous domain. Normal hexagonal (H_1) phase possesses a positive curvature of the aqueous domain, therefore limited spatial restriction. For this reason, precise replication of H_1 phase by CaP has not been possible. Interestingly, the dynamic nature of the template allowed the construction of micron-sized brushite objects with a laminated structure decorating a specific facet, possibly as a result of epitaxial overgrowth of nano-sized brushite subunits.

Skeletal biomaterials possess distinctive morphological, compositional, crystallographic features and organizational order, and thereby exhibit superior material properties. An eminent example is the mineral phase in mammalian bone. Bone apatite nanoplatelets (a highly substituted polymorph of calcium phosphate, CaP) uniaxially align within collagen matrix, which provide mammals optimal protection, support and other specialized functions.¹ The synthesis of these biomaterials mostly proceeds within micro- to nanoscopic compartments, i.e. structural matrix assembled by insoluble biomacromolecules.¹⁻⁴ In addition to the spatial confinement, soluble components including ions and nonstructural biomacromolecules synergistically modulate the mineralization process.¹⁻⁴ To elucidate the geometric effects in tuning the morphology and polymorphism of biomaterials, herein, we report the “softly” confined morphogenesis of CaPs into well-aligned nanowires, nanosheets, ordered laminated structures in “inert” liquid crystal (LC) phases, as well as a site-specific-decoration strategy to construct CaP

superstructures with ordered nano-features. The precise control of CaP nanostructures by gentle spatial confinement and the possibility to add-on the structure onto pre-existed architectures offers new opportunities for rational design of nano-inorganics and hybrid materials for advanced applications including artificial bone, biocompatible sensing and nanophotonic devices.

Molecular self-assembly in nature is a key process for constructing a variety of hierarchical biological structures and materials. An elegant example is mammalian bone, where bone mineral (apatitic CaP) forms within the nanometric spaces in collagen matrix. The dimension of the compartments here regulates the size of grown mineral, while the intrinsic order in collagen matrix orients mineral along collagen fibrils, which ensure the optimal mechanical strength of bone.[1] To truly mimic bone, a well-organized organic matrix is a prerequisite. Polymer networks having LC structure are ideal for this purpose, since collagen matrix, in essence is polymerized LC.

Earlier we found that LCs are capable to provide spatial restriction of the growth of ACPs as c.a. 10 nm nanospheres are formed and stabilized in LC.

In this study, we would like to explore ... use a simple inert system-lyotropic liquid crystal phases to explore the role of organic matrices on constructing hierarchical CaP superstructures,...

EXPERIMENTAL METHODS

For synthesis using LC, $\text{Ca}(\text{NO}_3)_2 \cdot 4\text{H}_2\text{O}$, 85% H_3PO_4 ($\text{Ca}/\text{P}=1.67$) were dissolved in Milli-Q H_2O . Then by mixing the salt solution with the surfactant (Pluronic L64 or F127) and oil (p-xylene or butanol), a reverse hexagonal (H_2) LC phase, a lamellar (L_a) phase and a normal hexagonal (H_1) LC were formed. The LC phases were placed in an ammonia atmosphere to start the reaction.

REFERENCES

1. He W. *et al.*, Chem. Mater. 24:892-902, 2012
2. He W. *et al.*, J. Mater. Chem. B accepted, 2014

ACKNOWLEDGMENTS

We acknowledge the Swedish Research Council (VR) and NanoSphere centre for funding.



Development of titanium alloy-based scaffold by 3D printing for bone tissue engineering

Pavan Kumar Srivas,¹ Kausik Kapat,¹ Prabhsh Dadhich¹,

¹Indian Institute of Technology Kharagpur, Kharagpur, West Bengal, India
email: pavanks@smst.iitkgp.ernet.in

INTRODUCTION

Additive Rapid Prototyping technique is an advanced technique to develop 3D physical model by computer controlled sequential transfer of energy and/or material to identified points in space. This technique has been extensively studied to develop customized implants through manipulation of geometrical distribution, modification of mechanical properties and creating porous structures for tissue in-growth as well as better fixation. Amongst all other biomaterials, metals have great potential for long-term load-bearing applications due to its excellent resilience and mechanical strength. Titanium and its alloys exhibit better performance in this aspect.

EXPERIMENTAL METHODS

A 3D model was created in SolidWorks software that was used to develop the 3D physical model. Ti6Al4V loose powder (Good Fellow, U.K.) was mixed with 4 wt% chitosan solution in 2% acetic acid into a homogeneous dispersion suitable for printing. The slurry was printed to a 3D scaffold by a 3D printer machine and finally sintered at 1450°C in inert atmosphere.

RESULTS AND DISCUSSION

The scaffolds showed good compressive strength which is close to natural bone. It also showed promising results in *in vitro* study for 3 days, 5 days and 7 days and bio-compatibility *in vivo*.

CONCLUSION

The scaffolds showed good compressive strength which is close to natural bone. It also showed promising results in *in vitro* study for 3 days, 5 days and 7 days and bio-compatibility *in vivo*.

REFERENCES

1. K.-H. Shin, Y.-M. Soon, Y.-H. Koh, J.-H. Lee, W. Y. Choi, and H.-E. Kim, "Fabrication of highly porous titanium (Ti) scaffolds with two interlaced periodic pores," *Mater. Lett.*, vol. 63, no. 15, pp. 1341–1343, Jun. 2009.
2. S. Maleksaeedi, J. K. Wang, A. El-Hajje, L. Harb, V. Guneta, Z. He, F. E. Wiria, C. Choong, and A. J. Ruys, "Toward 3D Printed Bioactive Titanium Scaffolds with Bimodal Pore Size Distribution for Bone Ingrowth," *Procedia CIRP*, vol. 5, pp. 158–163, Jan. 2013.
3. D.-T. Chou, D. Wells, D. Hong, B. Lee, H. Kuhn, and P. N. Kumta, "Novel processing of iron-manganese alloy-based biomaterials by inkjet 3-D printing," *Acta Biomater.*, vol. 9, no. 10, pp. 8593–603, Dec. 2013.

ACKNOWLEDGMENTS

The authors acknowledge the Defence Research and Development Organisation for the Funding from Ministry of Defence, India.

Mechanical-stress-assisted rapid cell sheets recovery from poly(*N*-isopropylacrylamide) grafted PDMS surfaces

Yoshikatsu Akiyama^{1*}, Miki Matsuyama², Naoya Takeda², Masayuki Yamato¹ and Teruo Okano¹

¹ Institute of Advanced Biomedical Engineering and Science, Tokyo Women's Medical University, TWIns, Japan. E-mail. akiyama.yoshikatsu@twmu.ac.jp

² Graduate School of Advanced Science and Engineering, Waseda University, Japan.

INTRODUCTION

Temperature-responsive cell culture surface (TRCS) has been used for fabrication of cell sheets from various tissues and organs. Conventionally, EB irradiation method has been used for the preparation of TRCS, grafting nano-scaled PIPAAm gel in tissue culture polystyrene (TCPS) (PIPAAm-TCPS). It was reported that the temperature-induced cell attachment and detachment character of PIPAAm-TCPS depended on the graft polymeric gel thickness. In the case of the fabrication of bovine carotid artery endothelial cell sheets (BAECs), 20-nm thickness PIPAAm layer was optimal to express the character.¹ In contrast, cell adhesion character depends on the cell species to be cultured. The graft polymer thickness was modulated, depending on the target cell species for the fabrication of their cell sheets. Based on the concept that graft PIPAAm thickness would be modulated by stretching the basal substrate, we developed PIPAAm-grafted PDMS (PIPAAm-PDMS) surfaces as a new TRCS and characterized the PIPAAm-PDMS surfaces at stretched and shrunk states. As a result, it was found that PIPAAm-PDMS at a stretched state showed more hydrophobic property than that at a shrunk state.²

In this presentation, based on the concept that the mechanical-stretching affects the cell detachment character as well as the surface properties, we applied the PIPAAm-PDMS surface to rapid cell sheet recovery by using the mechanical-stretching method. After culturing BAEC to reach confluent on stretched PIPAAm-PDMS surfaces, cell detachment behaviors from shrunk and stretched PIPAAm-PDMS were investigated at 20°C. For comparison, cell detachment behavior from shrunk PIPAAm-PDMS at 37°C was also investigated for comparison.

EXPERIMENTAL METHODS

PIPAAm-PDMS was prepared according to a previous report.² In brief, IPAAm monomer dissolved in 2-propanol (10 wt% - 50 wt% monomer in 2-propanol) was spread onto PDMS surfaces (4-well PDMS chamber purchased from STREX, Inc.) followed by O₂ plasma and (3-aminopropyl)trimethoxysilane (APTMS) treatments. And then, the surface was subjected to EB irradiation treatment to graft PIPAAm on the PDMS surface. PIPAAm-PDMS was characterized by FT-IR / ATR, XPS analysis, contact angle measurement and cell detachment / attachment assay. For the evaluation of rapid cell sheet recovery from PIPAAm-PDMS, PIPAAm-PDMS with 14.1 µg/cm² of PIPAAm graft density was used.

RESULTS AND DISCUSSION

PIPAAm-PDMS surfaces were characterized by various method. Through the characterization, PIPAAm was successfully grafted onto PDMS surfaces. In addition, contact angle measurement of shrunk and

stretched PIPAAm-PDMS surfaces revealed that shrunk PIPAAm-PDMS surface was more hydrophilic, probably because the graft polymer density increased and the PIPAAm-PDMS become more hydrophilic by shrinking the PIPAAm-PDMS.

BAECs were seeded and cultured on the stretched PIPAAm-PDMS surface. BAECs were adhered and proliferated to reach confluency at 37°C in 4 days. After confluency, cell sheets detachment behaviors were evaluated by using three different approaches as shown in Fig. 1 (a)-(c). Time required for complete cell detachment from stretched PIPAAm-PDMS surface was 126 min by decreasing temperature at 20°C (Fig. 1 (a)). Stretched PIPAAm-PDMS surfaces showed characteristic of TRCS. By shrinking PIPAAm-PDMS to an upstretched state after the confluency, cell sheets were not recovered (Fig. 1 (b)). In contrast, cell sheets were more quickly recovered by decreasing temperature to 20°C followed by shrinking PIPAAm-PDMS to an unstretched state (Fig. 1 (c)). These results suggested that the mechanical-stimuli increased the PIPAAm graft density as well as the surface hydrophilic property, resulting in the rapid cell sheets recovery.

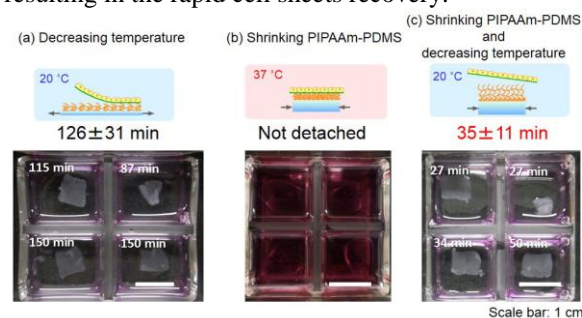


Fig. 1. Cell sheets detachment behaviors from the stretched PIPAAm-PDMS surfaces (20% stretching). Times required for the complete cell sheets recovery from the surface were shown in the photographs.

CONCLUSION

By applying mechanical-stress to PIPAAm-PDMS surface, the surface property as well as cell attachment and detachment behavior on the surface are modulated. The PIPAAm-PDMS was expected to be a new type of TRCS, which possessed a stretchable property.

REFERENCES

1. Akiyama Y. *et al.*, Langmuir. 20, 5506-11, 2004.
2. Akiyama Y. *et al.*, Journal of Robotics and Mechatronics. 25, 631-6, 2013

ACKNOWLEDGMENTS

Part of this work was financially supported by the Global COE Program, MERCREM from MEXT of Japan and a Grant-in-Aid for Scientific Research (Grant No. 23106009) on Innovative Areas "Bio Assembler" (Area No. 2305) from the MEXT of Japan.

The Oceans as a Source and as an Inspiration for Biomaterials Development: Some key examples

Tiago H. Silva^{1,2*}, Alexandre A. Barros^{1,2}, Ana L.P. Marques^{1,2}, Ana Rita C. Duarte^{1,2}, Gabriela S. Diogo^{1,2}, Joana Moreira-Silva^{1,2}, Lara L. Reys^{1,2}, Simone S. Silva^{1,2}, Rui L. Reis^{1,2}

¹ 3B's Research Group – Biomaterials, Biodegradables and Biomimetics, AvePark, Zona Industrial da Gandra S. Cláudio do Barco, 4806-909 Caldas das Taipas - Guimarães, Portugal.

² ICVS/3B's - PT Government Associate Laboratory, Braga/Guimarães; Portugal.

tiago.silva@dep.uminho.pt

INTRODUCTION

Since ever scientists and engineers have been looking into Nature as inspiration for the development of new materials, architectures, design, functions, devices, etc. Marine environment in particular has been the source of a myriad of natural products with diverse chemistries and biological activities, which are being explored as pharmaceuticals, including some examples on the market. Besides, several marine biopolymers have been produced and are used in fields from food and biotechnology to cosmetics, pharma and medicine. In the latter case, marine biopolymers can be found as wound dressings, membranes, drug delivery devices and biomaterials¹. In this presentation, the authors will address the advances that are being made in our research group concerning the development of marine inspired biomaterials towards tissue regeneration, from biopolymer extraction and processing, to biomaterials development and applicability assessment, including nature-made scaffolds.

EXPERIMENTAL METHODS

Biopolymer extraction

Collagen has been extracted from fish skins with acid aqueous solutions, complemented by enzymatic treatment by using pepsin. In parallel, it has been also extracted from marine sponges with acid or basic aqueous solutions, including with chaotropic agents.

Chitin has been extracted from squid pens by NaHO treatment and further converted into chitosan with concentrated NaHO solution.

Sulfated polysaccharides have been extracted from algae with hot water and precipitated with organic solvents. Additional steps can be added for matters of purity improvement.

Development of biomaterials

Solutions of the extracted biopolymers with different concentrations (1 to 4%) have been prepared and further used to produce porous structures. Different processing techniques have been used, in particular, freeze-drying (chitosan and collagen), agglomeration of previously prepared particles (chitosan and composites with nanohydroxyapatite, coagulated in NaHO solutions) and rapid prototyping (carrageenans, following ionic gelation) and will be presented. Crosslinking with different chemical agents, namely genipin (chitosan and collagen), EDC/NHS (collagen) and HDMI (collagen), has also been explored to tune mechanical stability of the developed constructs. Their morphological properties were assessed by SEM and micro-computed tomography (μ CT) and mechanical properties evaluated by compression tests.

Moreover, natural collagenous structures were produced from marine sponges after supercritical fluid processing to both decellularize and extract toxic compounds from the samples.

Applicability assessment

Biological performance of the developed constructs has been tested with chondrocyte-like cell line ATDC5 (chitosan and collagen scaffolds), osteoblast-like cell line SaOS2 (collagen structures) or adipose derived stem cells, ASCs (chitosan scaffolds).

RESULTS AND DISCUSSION

Marine collagen has been crosslinked with genipin for the production of hydrogels. Alternatively, freeze-drying of collagen solutions rendered membranes, which were successfully crosslinked with EDC/NHS. Crosslinking of freeze-dried collagen structures was also achieved with genipin, under dense CO₂, which supported the culture of ATDC5 cells.

The porous structure of marine sponges and its collagenous composition has inspired the development of nature made scaffolds by decellularization and removal of toxic compounds, in which osteoblast-like cells have been successfully cultured.

Carrageenan-based scaffolds were produced by 3D plotting and ionic gelation with K⁺ solutions, revealing to be non cytotoxic to a fibroblast cell line.

Chitosan scaffolds were produced by freeze-drying, with different pore sizes. ATDC5 cells adhered and proliferated to the interior of the scaffold when squid chitosan was used. Porous scaffolds made by agglomeration of squid chitosan particles or composites with nanohydroxyapatite supported the culture of ASCs for up to 7 days.

CONCLUSION

Several polymeric constructs have been produced with marine origin polymers and assessed as 3D support for culture of different cell types. The development of marine inspired biomaterials is being taken to the next level, envisaging the promotion of their use on tissue regeneration therapeutic approaches.

REFERENCES

1. TH Silva, ..., RL Reis, Int Mater Rev 57: 276-306, 2012.

ACKNOWLEDGMENTS

Funding is acknowledged from projects IBEROMARE (POCTEP), MARMED (Atlantic Area), NOVOMAR (POCTEP), POLARIS (FP7) and SPECIAL (FP7).



Development and Characterization of Lithium-Releasing Silicate Bioactive Glasses for Bone Repair

Valentina Miguez-Pacheco¹, A. Malchere², J. Chevalier² and Aldo Boccaccini¹

¹ Institute of Biomaterials, University of Erlangen-Nuremberg, 91058, Erlangen, Germany. E-mail: valentina.p.miguez@ww.uni-erlangen.de; Tel: +4991318520807, Fax: +4991318528602

² MATEIS Bât. B. Pascal, 5^e étage - 7, avenue Jean Capelle, 69621 Villeurbanne, France. E-mail: jerome.chevalier@insa-lyon.fr; Tel: +33472436125

INTRODUCTION

Bioactive glasses (BGs) are biocompatible materials developed to aid bone repair and regeneration, which are based on amorphous silicate compositions [1]. 45S5 Bioglass® is a well-known BG formulation that has been demonstrated to be bioactive and osteoconductive and is already in clinical use [2], [3]. In the search for improving the biochemical properties of Bioglass® for bone tissue engineering applications, different metallic ions are being incorporated into the glass compositions to stimulate healthy bone formation [4]. In this study, different amounts of Li₂O were substituted for Na₂O in the original Bioglass® formulation to obtain lithium-containing bioactive glasses (Li-BGs) at 2.5, 5 and 10 wt% Li₂O. Lithium (Li) was chosen because it has been reported to increase bone mineral density and enhance osteogenic gene expression [5], [6].

EXPERIMENTAL METHODS

High purity SiO₂, CaCO₃, CaPO₄, NaCO₃ and LiCO₃ powders were weighed and mixed. The homogenized powders were melted in Pt crucibles at 1400 °C for 1 hour. The melt was then quenched rapidly in water and then milled into fine powders. 45S5 Bioglass® powder was used to as a base material to compare the properties of the Li-BGs.

The sintering behaviour of the Li-BGs was investigated by heating glass samples at a constant rate. It was monitored by environmental scanning electron microscopy (E-SEM) to observe the morphological changes in the glass particles as a function of temperature. The bioactivity of the Li-BGs was investigated by immersing sintered pellets in SBF for up to 30 days and examining the deposition of hydroxyapatite (HA) on their surface.

X-Ray diffraction (XRD) was carried out in powdered samples at characteristic temperatures to examine the crystallization behavior of the Li-BGs. Fourier-transform infrared (FTIR) spectroscopy was performed on samples treated in SBF to confirm the formation of HA. Scanning electron microscopy (SEM) images of the samples treated with SBF were obtained to investigate the deposition of HA on the surface of the samples.

RESULTS AND DISCUSSION

In the E-SEM images, changes in morphology of the BG granules were evident as temperature increased. A softening of the granule edges and viscous flow of the glass was achieved, leading to fusion of particles in close proximity (Fig. 1).

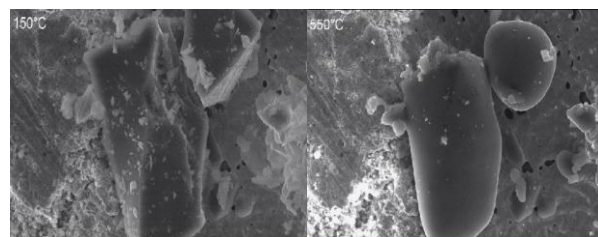


Fig. 1: Morphological changes of 10% Li-BG particles during sintering observed by E-SEM

The XRD spectra for the unsintered Li-BG samples exhibited broad peaks, thus confirming the amorphous nature of the materials. After sintering, the diffraction patterns of the samples showed that there was partial crystallization, as expected. Characteristic peaks for the formation of HA were observed in the FTIR spectra of samples soaked in SBF solution, and SEM micrographs showed that there was formation of HA crystals on the surface of the Li-containing samples.

CONCLUSION

From these experiments it can be speculated that the addition of Li to the glasses causes a decrease in their glass transition, as evidenced by the softening of the BG particles at lower temperatures and an earlier densification with an increasing proportion of Li in the glass increases. Furthermore, the addition of Li did not impair the bioactivity of the Li-BGs as evidenced by the deposition of a layer of HA on the surface of samples immersed in SBF, however further studies are necessary to fully ascertain the effect of Li ions on the bioactivity of Li-BGs and to monitor Li release kinetics in suitable media.

REFERENCES

- [1] Boccaccini, A. R. et al., *Faraday Discussions*, 136, 27, 2007
- [2] Chen, Q. Z., et al., *Biomaterials*, 27(11), 2414–25, 2006
- [3] Hench LL, *J. Am. Ceram. Soc.*, 81, 1705–1728, 1998
- [4] Hoppe, A. et al., *Biomaterials Science*, 1(3), 254, 2013
- [5] Khorami, M. et al., *Materials Science and Engineering :C*, 31(7), 1584–1592, 2011
- [6] Han, P., et al., *Biomaterials*, 33(27), 6370–9, 2012

ACKNOWLEDGMENTS

The authors would like to thank funding from the EU BioBone Initial Training Network. The E-SEM experiments were conducted in the Consortium Lyonnais de Microscopie (CLYM).

Effect of magnesium extract on osteoblastic progenitor cells differentiation

Bérengère J.C. Luthringer¹, Lili Wu¹, Frank Feyerabend¹, Arndt F. Schilling², Regine Willumeit¹

¹Structural Research on Macromolecules, Materials Physics, Helmholtz-Centre Geesthacht, Germany

²Department of Plastic Surgery and Hand Surgery, Klinikum Rechts der Isar, Technical University Munich, Munich, Germany
berengere.luthringer@hzg.de

INTRODUCTION

Even if already investigated during the first half of the last century, the interest of using magnesium-based implant material declined until recently. The unique properties of Mg and its alloys to combine metal related mechanical properties, biocompatibility, and biodegradability (up-to now restricted mainly to polymers and calcium-phosphates) justify this renewal of attention¹. Magnesium-based implants have been shown to influence the surrounding bone structure². In an attempt to partially reveal the cellular mechanisms involved in the remodelling of magnesium-based implants, the influence of increased extracellular magnesium content on human osteoclasts was studied.

EXPERIMENTAL METHODS

Peripheral blood mononuclear cells were driven towards an osteoclastogenesis pathway *via* stimulation with receptor activator of nuclear factor kappa-B ligand (RANKL) and macrophage colony-stimulating factor (M-CSF) for 28 days. Concomitantly, the cultures were exposed to variable magnesium concentrations (from either magnesium chloride or magnesium extracts). Osteoclast proliferation and differentiation were evaluated based on cell metabolic activity, total protein content, tartrate-resistant acid phosphatase activity, cathepsin K and calcitonin receptor immunocytochemistry, and cellular ability to form resorption pits.

RESULTS AND DISCUSSION

While magnesium chloride first enhanced and then opposed cell proliferation and differentiation in a concentration dependent manner (peaking between 10 and 15 mM magnesium chloride), magnesium extracts (with lower magnesium contents) appeared to decrease cell metabolic activity (50% decrease at day 28) while increasing osteoclast activity at a lower concentration (twofold higher).

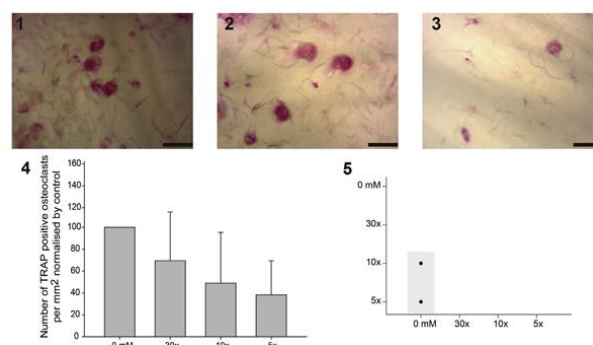
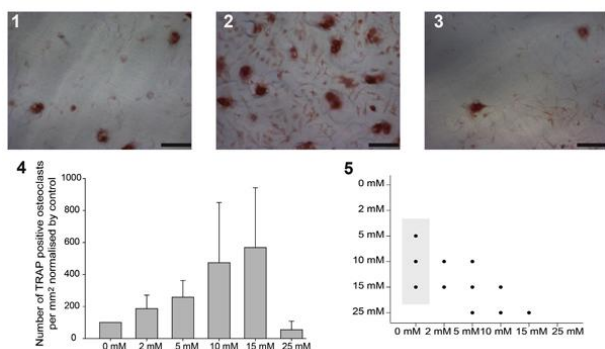


Fig. 1. TRAP staining at day 28: (A) MgCl₂ and (B) Mg extract assays. (1–3) Micrographs of TRAP staining for dentine (A: 0, 15 and 25 mM, respectively; B: 0 mM, 30x and 5x, respectively; scale bar 100 µm). (4) The number of TRAP-positive cells recorded for the 0 mM treatment was set as the control (100%), to which the numbers of TRAP-positive cells under the other concentrations (A) or dilutions (B) were normalised. (5) The respective statistical analyses are presented in multiple comparison graphs.

CONCLUSION

Together, the results indicated that (i) variations in the *in vitro* extracellular magnesium concentration affect osteoclast metabolism and (ii) magnesium extracts should be used preferentially *in vitro* to more closely mimic the *in vivo* environment.

REFERENCES

1. Staiger MP *et al.*, Biomaterials. 27:1728-1734, 2006.
2. Witte F. *et al.*, Biomaterials. 26:3557-3563, 2005.

ACKNOWLEDGMENTS

The authors wish to sincerely thank colleagues from the Department of Plastic Surgery and Hand Surgery (TUM) and the Department for Structural Research on Macromolecules (HZG) for their generous help in the laboratory and for providing useful guidance. Financial support from the CSC council and the Helmholtz association are acknowledged.

Fabrication of bilayer nano/microfibrous scaffold for skin tissue engineering

Pallabi Pal ,Pavan Kumar Srivas, Prabhash Dadhich, Bodhisatwa Das, Santanu Dhara

School of Medical Science & Technology, Indian Institute of Technology Kharagpur, West Bengal, 721301, India,
pallabipal@smst.iitkgp.ernet.in

INTRODUCTION

Layered architecture of human skin with epidermis and dermis is separated as compartments by specialized extracellular matrix, basement membrane, with nano/micro fibrillar arrangement allowing formation of a highly interconnected porous network with adequate structural resilience essential for cellular function. For successful development of skin graft, it is important to reciprocate the nano/microscalar architecture of tissue matrix as well as its biological cell recognition character. Biodegradable and biocompatible polymer, polycaprolactone has been fabricated into 3D printed scaffold onto which electrospun chitosan nanofibers were attached. Collagen molecules were further attached to increase its hydrophilicity, biodegradability and cell recognition cues finally giving rise to a nano/microscalar structure in an attempt to mimic extracellular matrix.

EXPERIMENTAL METHODS

PCL in glacial acetic acid was used for fabricating 3-D printed scaffold. Chitosan in acetic acid and PCL in chloroform/methanol were used for electrospinning while the collagenous layer was freeze dried on the 3-D printed layer. The microstructures of samples were evaluated by scanning electron microscopy (SEM). FTIR spectroscopy, porosity percentage, mechanical properties, rheological properties, contact angle, swelling behavior, biodegradation kinetics of matrices was studied for their suitability as tissue engineering scaffold. MTT assay, Rhodamine-DAPI staining, live/dead assay, SEM analysis were carried out to evaluate matrix cytocompatibility, cell attachment and proliferation using keratinocytes and fibroblasts cells.

RESULTS AND DISCUSSION

SEM results showed 3-D printed PCL layer attached to the nanofiber layer. The matrices showed moderate swelling of upto 60% , slower degradation rate, high mechanical strength and contact angle of nanofiber is 90° $p < 0.05$. FTIR data of PCL and chitosan blends showed characteristic peaks of both PCL and chitosan. SEM results showed good cell attachment on 3-D printed PCL layer as well as on nanofiber layer. MTT assay Rhodamine-DAPI staining, live/dead assay indicated cytocompatibility of the scaffold

CONCLUSION

Incorporation of chitosan and collagen increased hydrophilic as well as well degradation rate of the scaffold. Results using primary keratinocyte and fibroblast showed, non-toxic and cytocompatible nature of the matrix. Material characterization yielded definite results proving the scaffolds potential for tissue engineering application.

REFERENCES

1. Synergistic effect of surface modification and scaffold design of bioploted 3-D poly-ε caprolactone scaffolds in osteogenic tissue engineering, H.A. Declercq et al., *Acta Biomater.* 2013, 8:7699-708.
2. Fabrication and biocompatibility of novel bilayer scaffold for skin tissue engineering applications. R.A. Franco, et al, *J Biomater Appl*, 2013, 27(5):605-615

ACKNOWLEDGMENTS

Authors would like to thank Council for Scientific and Industrial Research and IIT Kharagpur for financial assistance.

Chemical Guiding of Magnetic Nanoparticles in Dispersed Media Containing Poly(methylmethacrylate-co-vinylpyrrolidone)

Myriam G. Tardajos^{1,3}, Inmaculada Aranaz³, Carlos Elvira³, Helmut Reinecke³, Erhan Piskin², Alberto Gallardo^{3*}

¹Polymer Chemistry and Biomaterials Group, Ghent University, Belgium

²Department of Chemical Engineering, Hacettepe University, Turkey

^{3*}Institute of Polymer Science and Technology, Consejo Superior de Investigaciones Científicas, Spain,
miriam.gomezardajos@ugent.be

INTRODUCTION

The conventional free radical copolymerization of methyl methacrylate (MMA) and N-vinylpyrrolidone (VP) in methanol under stirring yields, at high conversion, a high compositional heterogeneity which displays unusual phase separation behavior; the dispersed phase is rich in copolymers with a high content of hydrophobic MMA while the continuous phase is rich in copolymers with a high content of hydrophilic VP.¹ The hypothesis of this work is that the dispersed and the continuous phase of the parent emulsion may be functionalized quite selectively just by adding a third methacrylic or vinyl comonomer to the copolymerization. This differentiated functionalization may be translated to the different components of the solid microspheres in water (partial functionalization of VP or MMA may respectively imply a functionalization of the surface or core).

In this work, this has been tested by incorporating methacrylic comonomers bearing sulfonate and carboxylic acid, and a sulfonate VP derivative. The selective functionalization has been shown by adding and guiding magnetic nanoparticles (mNPs).

EXPERIMENTAL METHODS

Copolymerizations were carried out in methanol at 60°C for 48 h using AIBN as the initiator.

The details of production and characterization of the (Fe₃O₄) mNPs were given elsewhere.²

Emulsion droplets were hardened under stirring in a shaker by slowly dropping water into the emulsion giving rise to the formation of solid particles.

RESULTS AND DISCUSSION

Interactions of several dispersed systems based on poly(MMA-co-VP) copolymers with mNPs stabilized with tetramethylammonium hydroxide have been studied. The mNPs have a cationic surface that may interact with complementary anionic groups such as sulfonate units. Therefore, the influence of the incorporation of a very small amount (0.5% molar fraction) of the sulfonate functionality by using sodium sulfopropyl methacrylate (Met-Sulf) and sulfopropyl-vinylpyrrolidone³ (VP-Sulf) has been studied. Methacrylic acid (Met-Carb) was also studied for comparison reasons.

When mNPs are incorporated into the control emulsion, they are located, partially agglomerated, in the continuous phase. If the sulfonate functionality is introduced via the VP derivative (VP-Sulf), the mNPs are located preferentially in both the interface and in the continuous medium. Also, the location of mNPs at the

interface indicates that the VP-rich chains are effectively interacting and stabilizing the MMA-rich droplets. The use of Met-Sulf causes all of the mNPs to be located in the inside of the dispersed phase while the use of Met-Carb gives rise to a very peculiar result: most of the mNPs were located at the interface. These results confirm the initial hypothesis: both phases can be functionalized selectively.

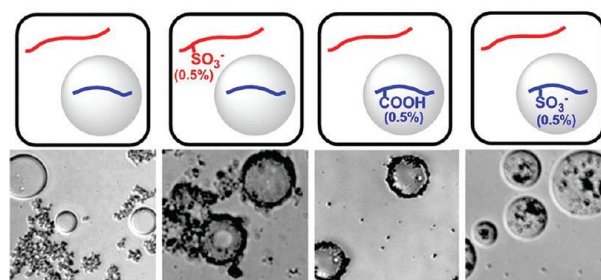


Figure 1: Scheme of the location of the functionality in the emulsions and optical images showing the location of the mNPs in each type of emulsion.

The emulsions can be easily hardened by adding water dropwise at room temperature rendering solid microspheres. EDAX measurements proved that the selectivity moves to the microspheres incorporating the mNPs either at the surface or in the core.

CONCLUSION

Methanolic emulsified systems containing heterogeneous poly(MMA-co-VP) can be selectively functionalized in a simple one pot procedure by using small amounts of homologous functionalized monomers. This selectivity has been confirmed by monitoring the location of mNPs with cationic surfaces. This allows preparing composite microspheres selectively locating the mNPs for different purposes. Particles covered with magnetic materials may be of interest as active beads in different fields. Also mNPs have been proposed as nanoheaters so their encapsulation in polymer beads may be used in medicine to combine this hyperthermia effect with other complementary purposes in the drug delivery field.⁴ Tardajos, M. G. *et al.*, Langmuir 2012, 28, 5555-5561.

REFERENCES

1. Aranaz, I. *et al.*, Polymer 2011, 52, 2991.
2. Utkan, G. *et al.*, J. Col. Interface Sci. 2011, 353, 372.
3. Perez, M. *et al.*, Eur. Polym. J. 2010, 46, 1557.
4. Brule, S. *et al.*, Adv. Mater. 2011, 23, 787.

ACKNOWLEDGMENTS

The authors gratefully acknowledge support from Grants MAT-2010-20001 and MAT2008-2174.



Influence of Surface Roughness Parameters on MG63 Cell Viability: Studies on Laser Microtextured Ti6Al4V Surfaces

Sumanta Mukherjee^{1*}, Partha Saha¹, Santanu Dhara²

^{1*}Mechanical Engineering Department, Indian Institute of Technology Kharagpur, India

²School of Medical Science and Technology, Indian Institute of Technology Kharagpur, India, talk2sumanta@gmail.com

INTRODUCTION

Surface roughness has long been considered an important aspect of orthopaedic implants. Researchers have suggested that in some average roughness ranges, the surface shows improved biocompatibility both in-vitro and in-vivo. But, the average roughness does not reveal the exact nature of roughness on the surface. Moreover, the mechanism through which the surface roughness can influence the cell behaviour is yet to be fully understood.

In this study, attempt has been made to correlate the surface roughness parameters with cell viability on the surface. For this, laser microtexturing has been performed on Ti6Al4V surfaces, and the viability of human osteoblast-like MG63 cells has been studied on them.

EXPERIMENTAL METHODS

Using a 2 kw Ytterbium fibre laser, grooves of depth ~20 µm and width ~200 µm were created on Ti6Al4V samples by operating the laser with different power, scan speed, duty cycle and frequency settings. MG63 cells were cultured on three types of surfaces that were similar in terms of average roughness but different in terms of other roughness parameters. The parameters that were used to create the three types of samples are presented in Table 1. The experimental details have been reported elsewhere [1].

Sample ID	Laser Power (w)	Scan Speed (mm/min)	Duty cycle (%)	Frequency (%)
2381	200	3,000	80	100
3561	300	5,000	60	100
2366	200	3,000	60	60

Table 1

The cell counts after 3 and 5 days of culture were estimated from MTT assay. The average spread area and the fractal dimension of the cells were calculated using ImageJ software by taking fluorescence micrographs of Rhodamine/Dapi stained cells. Anselme et al [2] earlier proposed a detachment index and a proliferation index to draw relationship between the 2d surface roughness parameters and cell behaviours. In this study, we used their model, and after fitting the curve, the residual values for different 3d surface roughness parameters were compared.

RESULTS AND DISCUSSION

Anselme's work suggested that new surface roughness parameters may be required to reveal the relationship between surface features and cell behaviour. But, according to our findings, 3d surface parameters like

surface kurtosis and surface skewness are strongly correlated with the cell viability on the surface.

The cell spread, i.e., average surface area of the cells was also found to be higher on the surface that had higher surface kurtosis value.

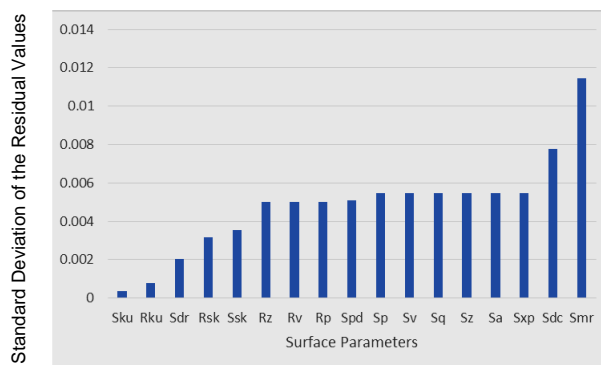


Fig. 1: Standard deviation of residual values for the different surface parameters, after fitting the cell count to the Anselme's equation. The lower the standard deviation of the residuals, the higher the correlation with cell viability.

CONCLUSION

Surface kurtosis is the measure of sharpness of the peaks present on the surface. Higher value of kurtosis means sharper peaks. The surface of Ti6Al4V is negatively charged in an aqueous environment because of the presence of TiOH⁻ ions. On a surface with sharp peaks, the charge density on the peaks is high. The positive ends of the quadrupolar protein molecules get clustered around those sharp peaks. The MG63 cells also have negative charges on their surface. As a result, the cells get attached to those preferred adherence points. This may be the reason for higher cell attachment and cell spread on the surface with higher kurtosis value.

REFERENCES

1. Mukherjee S. *et al.*, Int J Adv Manuf Technol, DOI 10.1007/s00170-013-5277-2
2. Anselme K. *et al.*, J Biomed Mater Res. 49(2):155-66, 2000

Extended Release Drug Layer for POSS-PCU Cardiac Stents

Megan Livingston¹ and Alexander Seifalian¹

¹Division of Surgical and Interventional Sciences, University College London, United Kingdom;
megan.livingston.13@ucl.ac.uk

INTRODUCTION

Coronary Artery Disease (CAD) is the most common type of heart disease and is the leading cause of death for both men and women in the United States¹. Coronary angioplasty is used to treat CAD by expanding a cardiac stent at the site of the vascular occlusion in order to restore blood flow. The most common types of stents used are Bare Metal Stents (BMS) and Drug Eluting Stents (DES) but each of these come with long-term health risks like restenosis and late stent thrombosis due to the stents inability to keep the vessel wall clear.

DES incorporate a drug release system, most commonly utilizing an anti-proliferative drug such as paclitaxel or sirolimus. It has been suggested that rates of success with DES could be increased if the drug release occurred over a much longer time than observed with currently approved DES². The research presented here works to create an extended release drug layer for POSS-PCU coated cardiac stents by utilizing organic-inorganic hybrid liposomes, called cerasomes, loaded with paclitaxel, developed by Katagiri, et al³.

EXPERIMENTAL METHODS

Cerasome-Forming Lipid Synthesis

Synthesis protocol to create cerasome-forming lipids was adapted from the work published by Katagiri, et al³.

Drug Release Profile

Paclitaxel-loaded cerasomes (PTX-CS) were formed using protocol published by Cao, et al⁴. Release profiles were established over 8 weeks in both a PBS (pH ~ 7.4) with tween 80 solution and serum. PTX-CS were held in dialysis tubing spinning in the release medium. At each time point, samples from the release medium were analysed with UV/Visible Spectroscopy in order to measure paclitaxel concentration.

Smooth Muscle Cell Proliferation

PTX-CS attached to a POSS-PCU polymer sample was incubated *in vitro* with human vascular smooth muscle cells (hVSMCs) for 4 weeks in order to determine the long-term anti-proliferative ability of the drug layer. Proliferation of hVSMCs was determined with a total DNA assay at each time point. Controls included a polymer control (only POSS-PCU) and non-loaded cerasomes bound to POSS-PCU.

RESULTS AND DISCUSSION

Illustration of the PTX-CS fabrication with drug loading can be seen in Figure 1. The surface of the lipid bilayer of the cerasomes incorporates silicon oxide groups which degrade slower than organic groups, allowing for extended drug release.

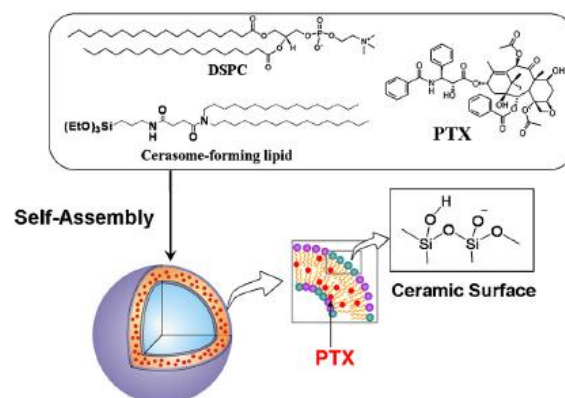


Figure 1: Paclitaxel-loaded cerasome fabrication⁴

Release profiles and cell studies have not yet been performed but will be collected prior to and presented at the conference.

CONCLUSION

The extended drug release layer for POSS-PCU cardiac stents composed of paclitaxel-loaded cerasomes presents significant potential for cardiac technologies because of the variability available. Cerasomes can be loaded with any drug, whether hydrophilic or hydrophobic, and functionalised for attachment to any amine-expressing polymer surface. The results should support the potential for this application of extended release technology.

REFERENCES

1. National Heart, Lung, and Blood Institute. 2014.
2. Venkatraman S & Boey F, J Control Release. 120(3):149–60, 2007
3. Katagiri K. *et al.*, J. Chemistry.13(18):5272–81, 2007
4. Cao Z, *et al.*, Colloids Surf B Biointerfaces.98:97–104, 2012

ACKNOWLEDGMENTS

Many thanks go to Dr. Yasmin Rafiei and Arnold Darbyshire for their guidance and research assistance. This research has been funded by Dr. Seifalian and the Whitaker International Program.

Practical Application of Whole Slide Imaging in Biomaterial Science

C. Brochhausen¹, H. B. Winther¹ and C. J. Kirkpatrick¹

¹REPAIR-lab, Institute of Pathology, University Medical Centre, Mainz, brochhausen@pathologie.klinik.uni-mainz.de

INTRODUCTION

Whole slide imaging (WSI), also known as virtual microscopy, has gained relevance in teaching, routine diagnostic activity and scientific research. We created a new WSI application called Pate (<http://pate.um-mainz.de>). This application was originally developed with an emphasis on student teaching for histopathological courses.

Many WSI applications are based on proprietary technologies, such as Adobe Flash and Microsoft Silverlight. These technologies require the installation of a specialized browser plug-in.

EXPERIMENTAL METHODS

We created a client application based on modern internet technologies, such as the Hypertext Markup Language 5 (HTML5), Cascading Style Sheets (CSS) and JavaScript. The server is powered by Python, utilizing the TurboGears 2 framework. The Apache 2 is employed as application server. So far, two glass-slides with tissue-biomaterial-interactions have been digitized and uploaded to Pate.

RESULTS AND DISCUSSION

Although initially an emphasis was placed on medical-student teaching, the tools implemented are also highly instructive for students in the field of biomaterials. The tools for training histomorphological skills enable an effective illustration of complex tissue reactions in the

context of biomaterial applications *in vivo*. Furthermore, Pate is suited for displaying any kind of high resolution images, thus offering the potential for various applications such as evaluation of new vessel formation. We published the slides “[Full thickness cartilage defect](#)” and “[Punch-Biopsy Skin-wound](#)” to demonstrate the potential benefits of WSI applications in biomaterial research. These slides are enriched using non-destructive annotations as well as points of interest. Each slide in Pate can be shared by distributing the Uniform Resource Locator (URL). This allows easy sharing of large images as soon as the slides are digitized. Utilizing modern internet technologies, such as HTML5, CSS and JavaScript, enables the user to view the image material with a modern web browser. No proprietary plug-in is required.

CONCLUSION

Whole slide imaging offers huge potential benefits in the field of biomaterial sciences. The technology enables quick and easy sharing of large images as well as non-destructive annotations and points of interest. This opens up new perspectives in teaching of biomaterial-tissue interactions and various evaluation skills in biocompatibility and tissue regeneration.

ACKNOWLEDGMENTS

We thank “Grüne Kommunikationsdesign” for assistance in creating a comprehensive user interface.

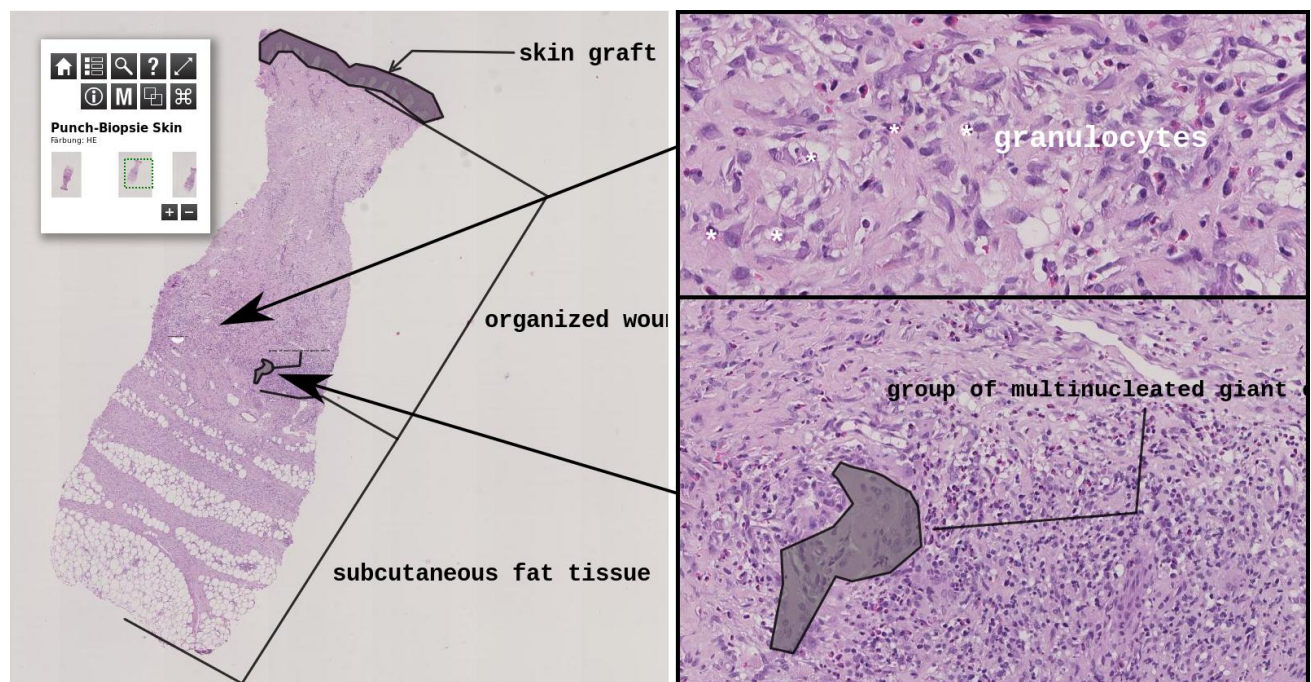


Figure 1: Screenshot of Pate, demonstrating the features of non-destructive annotations, points of interest and latitude in the slide. Different magnifications of the slide “[Punch-Biopsy Skin-wound](#)” can be seen.

Cryostructured hierarchical scaffolds with zonal biochemistry and anisotropic porosity for biomimetic in situ cartilage tissue engineering

Kai Stuckensen¹, Jenny Reboredo², Andrea Schwab², Uwe Gbureck¹, Heike Walles² and Jürgen Groll¹

¹Department for Functional Materials in Medicine and Dentistry, University of Würzburg, Germany

²Department for Tissue Engineering and Regenerative Medicine, University of Würzburg, Germany

kai.stuckensen@fmz.uni-wuerzburg.de

We present the fabrication of cartilage mimetic scaffolds by an oriented cryostructuring process. The resulting collagen-based scaffolds feature distinct biochemically different zones with oriented continuous pores and show evidence for inducing zonal specific differentiation of human mesenchymal stem cells in culture.

INTRODUCTION

Articular cartilage and meniscus are specialized collagenous tissues with spatial varying compositions and aligned structure of the extracellular matrix.^{1,2} The local cells, so called chondrocytes, maintain the structural and functional integrity of the matrix. Characteristic zones, each with distinct physicochemical and biological properties and functions, work together to impart shock absorbing and wear resistant behaviour to these kinds of cartilage.

Like in native tissues, the respective composition of different areas in our osteochondral and meniscus scaffolds is mimicked by the presence of collagen I, collagen II, glycosaminoglycans (GAG) and calcium phosphates. An integral cell ingrowth is facilitated by a continuous pore system which in turn approaches the pathway of the collagen fibers in the native tissues. The fabrication of these monolithic tissue mimetic scaffolds is enabled by a novel cryostructuring based processing route.

EXPERIMENTAL METHODS

Collagen I and collagen II was isolated from murine and bovine sources, respectively. Together with chondroitin sulphate (GAG), brushite ($\text{CaHPO}_4 \cdot 2\text{H}_2\text{O}$) and acidic acid multiple solutions with tissue zone mimetic composition were prepared. These aqueous precursors were arranged inside a custom build cryostructuring device. Being subjected to a directional temperature gradient, anisotropic ice crystals grew continuously through the precursors. After ice crystal removal by lyophilisation, the porous structures were covalently cross linked by using carbodiimide (EDC). On the surface of osteochondral scaffolds electrospinning of polyester-based fibers was additionally applied.

The scaffolds were seeded with human mesenchymal stem cells and cultured under static and perfusion conditions. Additionally endothelial cell seeded decellularized porcine jejunal segments (BioVaSc) were co-cultured together with the meniscus scaffolds.

RESULTS AND DISCUSSION

Osteochondral and meniscus scaffolds with tissue mimetic structure and composition were fabricated and cell cultured. (Figure 1) Human mesenchymal stem cells established chondrogenic differentiation. The first

evidences of still ongoing studies suggest, that the tissue mimetic zonal composition (collagen I, II and varying GAG content) is causing zonal stem cell differentiation.

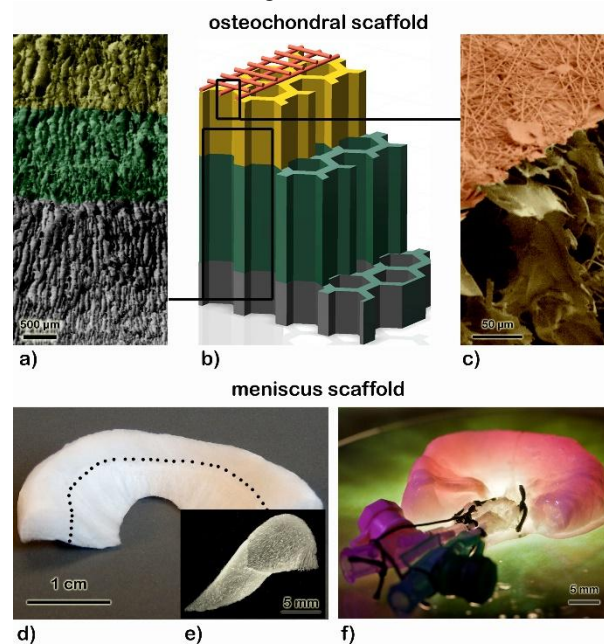


Figure 1: Schematic scaffold design (b) and colored SEM images of osteochondral scaffolds (a, c). Consecutive pores run perpendicular to the joint surface through subchondral (collagen I & brushite), deep and middle chondral zone (collagen I, II & GAG) (a), while electrospun polyester-based fibers of the superficial chondral zone run parallel to the joint surface (c). Meniscus scaffolds (Photographs d, e) consist of an inner (collagen I, II & GAG) and an outer meniscus section (collagen I & GAG) which are penetrated by shape following pores. Co-culture of meniscus scaffold inside a vascularized porcine jejunal segment (Photograph f).

CONCLUSION

Our scaffolds represent promising candidates for biomimetic in situ tissue engineering of osteochondral and meniscus tissue. In ongoing cell culture studies we want to prove that biochemical stimuli together with the imitation of the structure of native tissue is inducing zonal specific stem cell differentiation and thus might facilitate biomimetic cartilage tissue engineering and eventually the formation of functional tissue.

REFERENCES

1. Klein T. J. *et al.*, *Macromol. Biosci.* 9:1049–1058, 2009
2. Fox A. J. *et al.*, *Sports Health* 4:340–351, 2012

Additive Manufactured 3D Scaffolds with Tailorable Surface Topography by a Single-Step Method

SC Neves^{1,2,3}, C Mota³, CC Barrias¹, PL Granja^{1,2,4}, L Moroni³

¹INEB - Instituto de Engenharia Biomédica, Universidade do Porto, Porto, Portugal (sara.neves@ineb.up.pt)

²FEUP – Faculdade de Engenharia da Universidade do Porto, Porto, Portugal

³MIRA - Institute for Biomedical Technology and Technical Medicine, University of Twente, The Netherlands

⁴ICBAS – Instituto de Ciências Biomédicas Abel Salazar, Universidade do Porto, Porto, Portugal

INTRODUCTION

The gold standard approach in tissue engineering (TE) strategies involves the use of a three-dimensional (3D) artificial extracellular matrix (ECM), commonly referred to as scaffold¹. In addition to supporting the growth of neo-tissue, the properties of these structures must be tailored to enhance tissue regeneration. It is well established that surface topography, from the micro- to the nanoscale, can influence stem cell behaviour². However, most of the current studies have been carried out on 2D polymeric substrates³, with just a few reports in 3D³, mainly due to the challenge to transfer in a controlled manner the tailored surface topographies onto 3D scaffolds. In this study, we aimed at combining wet-spinning, a non-solvent induced phase separation technique that has been used to produce polymeric fibres with different characteristics, with additive manufacturing (AM), which allows the processing of scaffolds with a defined architecture, based on layer-by-layer fabrication from 3D model data⁴. A library of scaffolds with controlled surface roughness can be then obtained to study their effect on human mesenchymal stem cells (hMSCs) behaviour.

EXPERIMENTAL METHODS

A PEOT/PBT copolymer (PolyVation, The Netherlands) with a 300/55/45 composition was used. Following an *a*PEOT*b*PBT*c* nomenclature, *a* is the molecular weight in g/mol of the starting PEG blocks used in the copolymerization, while *b* and *c* are the weight fractions of the PEOT and PBT blocks, respectively. 300/55/45 was dissolved in chloroform (20 wt%) overnight at room temperature to obtain a homogeneous solution. The prepared solution was placed into a glass syringe fitted with a stainless steel needle. A syringe pump (NE-1000, New Era Pump Systems Inc., USA) was used to control the extrusion flow rate of the polymer solution. A container with two different PEOT/PBT non-solvent solutions (isopropanol and 90% v/v ethanol in water) was fixed to the fabrication platform and used as coagulation bath. Scaffolds were fabricated using a Bioplotter (Envisiontec GmbH, Germany), which is basically an XYZ plotting machine as previously described⁵. Scaffolds geometry and architecture were characterized by scanning electron microscopy (SEM). hMSCs were seeded (125000 cells/scaffold) and cell activity, morphology, and tissue growth were assessed by SEM and fluorescence microscopy.

RESULTS AND DISCUSSION

From the different 300/55/45 solvent/non-solvent combinations studied, the use of chloroform as solvent and isopropanol and 90% v/v ethanol (in water) as non-solvents allowed the most reproducible plotting of 3D scaffolds with defined geometry (Fig.1). These different non-solvents allowed the tuning of fibre-surface topography without the need to treat the scaffolds after plotting. hMSCs attached and proliferated on the scaffolds during 15 days of culture (Fig.2).

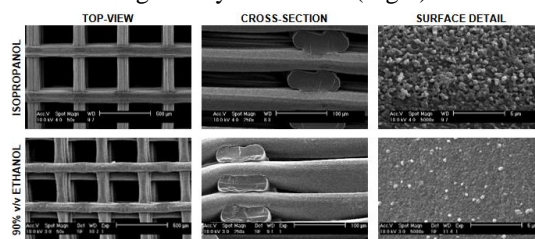


Figure 1

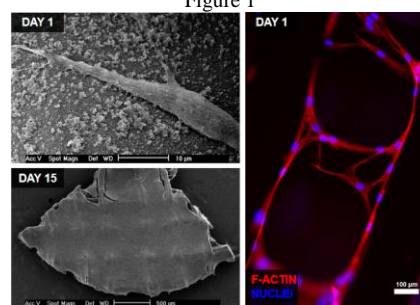


Figure 2

CONCLUSION

The combination of an AM with wet-spinning allowed the processing of PEOT/PBT scaffolds with a defined structure and, more interestingly, with different fibre-surface topographies by varying the non-solvent. The preliminary *in vitro* studies indicate that these scaffolds support hMSCs culture. Therefore, further studies will be performed to better understand the hMSCs fate-instructive character of these scaffolds.

REFERENCES

1. Melchels *et al.*, Progr Pol Sci. 37:1079-104, 2012
2. Bettinger *et al.*, Angew Chem Int Ed. 48:5406-15, 2009
3. Kumar *et al.*, Biomaterials. 33:4022-30, 2012
4. Mota *et al.*, J Bioact Compat Polym. 28:320-40, 2013
5. Moroni *et al.*, Biomaterials. 27:974-85, 2006

ACKNOWLEDGMENTS

This work was funded by the European Regional Development Fund through the Program COMPETE, and by Portuguese funds through FCT – Fundação para a Ciência e a Tecnologia in the framework of SC Neves doctoral grant, the research position of CC Barrias, the research grant PEST-C/SAU/LA0002/2013, and co-financed by North Portugal Regional Operational Programme (ON.2).

Biodegradable Biopolymer and Calcium Phosphate Composites Manufactured via Impregnation Method

Marina Sokolova¹, Janis Locs¹

¹Rudolfs Cimdins Riga Biomaterials Innovations and Development Centre,
Riga Technical University, Riga, Latvia; marina.sokolova@rtu.lv

INTRODUCTION

Bioresorbable materials are promising candidates in the field of bone regeneration. Hydroxyapatite (HAp) and tricalcium phosphate (TCP) are one of the most used implant materials in the reconstructive surgery to repair damaged hard tissues¹. Calcium phosphates (CaP) have excellent biomaterial properties due to their similarity to the inorganic component of the bone matrix. However, their clinical applications are restricted because of inherent brittleness and poor shape ability². To capitalize the advantages and overcome drawbacks of CaP, it is combined with polylactic acid (PLA) to generate biocomposite material. Polylactic acid is a thermoplastic, biodegradable, biocompatible, synthetic polymer with high strength and modulus³. It can be easily processed into shapes such as screws, pins and plates for orthopedic applications, and fabricated into scaffolds for replacement and regeneration of tissues. Calcium phosphate and polylactic acid composites have received a great deal of interest in orthopedic and dental applications, which is attributed to their good osteoconductivity, biodegradability and high mechanical strengths⁴.

EXPERIMENTAL METHODS

CaP slurry was prepared by wet chemical precipitation synthesis method from calcium oxide and orthophosphoric acid solution. The method is characterized by low cost and easy application in industrial production, and that the only by-product is water. Synthesized calcium phosphates phase composition is found to be highly depended on the changes in synthesis technological parameters. Synthesized precipitates were filtered, homogenized and pressed into cylinders using a PTFE mold, and dried using three-stage drying procedure to avoid formation of cracks.

CaP/PLA composites were prepared using vacuum impregnation technique. First, CaP cylinders were placed into a vacuum vessel and held in 400 mbar vacuum for 15 minutes, then immersed into 5 – 20 wt% PLA solution for 15 minutes until pressure normalization. This procedure was repeated for three times. Another batch of the cylinders were processed with subsequential pressure impregnation, also for three times. The samples were pressed isostatically in PLA solution at 300 MPa for 3 minutes. All samples were dried and weighted after each processing step to determine PLA uptake. To improve composite mechanical strength, after impregnation all samples were pressed isostatically at 0.15 GPa and 0.20 GPa. Compressive strength of fabricated CaP/PLA composites was measured at ambient temperature. The crosshead was run at 0.05 mm/min.

Fourier-transform infrared spectroscopy (FT-IR) was used to determine the various functional groups in the nanocomposite samples. X-ray diffractometry (XRD) was used to analyze phase composition of obtained calcium phosphate samples. Scanning electron microscopy (SEM) is used to characterize the morphology of the obtained samples.

RESULTS AND DISCUSSION

Highest PLA uptake was achieved using 10 wt% PLA solution and three cycles of vacuum impregnation – 7 wt%. PLA mass fraction after three impregnation cycles increased for only 0.3 wt% (Fig. 1). Impregnation efficiency for samples treated with 10 wt% PLA solution in first processing cycle is 87 ± 3 %. Isostatic pressing didn't significantly increase PLA uptake into CaP matrix.

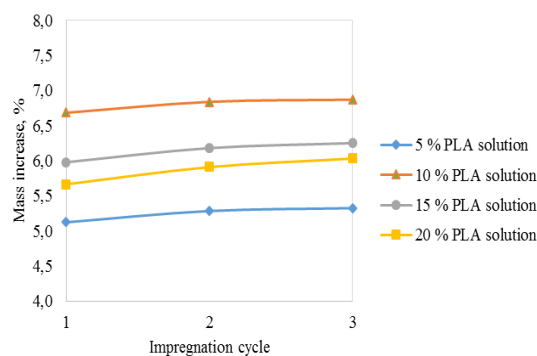


Fig. 1 Composite mass increase vs impregnation cycles of used PLA solutions in vacuum impregnation

CaP/PLA composites with 5 – 7 wt% PLA have porosity of 48 – 47 %, and compressive strength 20 – 30 MPa, which is similar to trabecular bone.

CONCLUSION

CaP/PLA composite strength can be adjusted by varying PLA amount in the composite. Highest compressive strength of 20 – 30 MPa is achieved for composites with 7 wt% PLA. FTIR studies indicated, that there is a concentration gradient of PLA in the prepared CaP/PLA cylinders.

REFERENCES

1. Rezwan K. et al., *Biomaterials*. 27:3413-3431, 2006
2. Felfel R.M. et al., *J. Mech. Behav. Biomed.* 18:108-122, 2013
3. Wagoner Johnson A.J. et al., *Acta Biomater.* 7:16-30, 2011
4. Rakovsky A. et al., *J. Mater. Sci.* 45:6339-6344, 2009

ACKNOWLEDGMENTS

This work has been supported by the M-ERA.NET within the project “Tough, Strong and Resorbable Orthopaedic Implants” (GoIMPLANT).

Collagen IV and Fibroblasts as Supportive Factors in Angiogenesis Performed in a Perfusion Bioreactor Setup

Franziska Kreimendahl¹, Stefan Weinandy¹, Julia Frese¹, Michael Vogt² and Stefan Jockenhoevel¹

¹Tissue Engineering and Textile Implants, AME, Helmholtz-Institute, RWTH Aachen University, Germany

²Interdisciplinary Centre for Clinical Research (IZKF Aachen), RWTH Aachen University, Germany,
kreimendahl@hia.rwth-aachen.de

INTRODUCTION

Due to a limited oxygen diffusion depth of 100-200 µm the field of Tissue Engineering is restricted in manufacturing transplants with a certain thickness and complexity¹. An approach in Tissue Engineering is the generation of blood vessels to supply complex tissues with oxygen and nutrients. In angiogenesis blood vessels, which are generated by sprouting processes, are supported by smooth muscle cells attaching to the endothelial cells². Furthermore the vessels are strengthened by endothelial cell mediated collagen expression in the basement membrane³. Here we show the generation of blood vessel-like structures within a 3-D fibrin gel under dynamic flow conditions with subsequent analysis of collagen IV production and fibroblast attachment by Two-Photon Laser Scanning Microscopy (TPLSM).

EXPERIMENTAL METHODS

Following experiments (n=3) were performed with venous endothelial cells isolated from umbilical cord (HUVECs) and human foreskin fibroblasts (HFFs). The fibrin gel scaffold consisted of fibrinogen (5 mg/mL), thrombin (3 U/mL), CaCl₂ (4.75 mM). Additionally HFFs were added with a concentration of 4.5x10⁵/mL and HUVECs with 9x10⁵/mL. The total volume of the fibrin gel scaffold was 150 µL. The scaffolds were cultivated under dynamic (perfusion bioreactor) and static (well) conditions for 14 days and stained afterwards with CD31/Alexa Fluor 594 and anti-collagen IV/Alexa Fluor 488. The analysis was done by TPLSM with an Olympus FluoView 1000MPE two-photon microscope equipped with a 25X NA1.05 water dipping objective for imaging. For excitation of Alexa Fluor 594 and 488 the laser was tuned to a wavelength of 800 nm. The emission of Alexa Fluor 594 and 488 was collected at 590-650 nm and 495-540 nm, respectively. Fibroblast attachment was imaged additionally by using autofluorescence at an emission of 419-465 nm. The supportive software was Imaris 7.6 (Biplane).

RESULTS AND DISCUSSION

Figure 1 represents the generation of blood vessel-like structures under static (A) and dynamic conditions (B) stained with CD31 as endothelial specific marker (red). Additionally we imaged the collagen IV expression in both conditions (C, D) under performance of anti-collagen IV staining (green). The static controls showed increasing formation of blood vessels compared to scaffolds cultivated under perfusion conditions. Furthermore the collagen IV expression and fibroblast attachment was dependent on the level of angiogenesis.

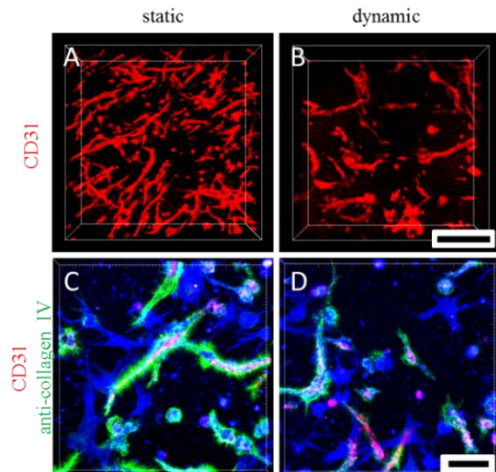


Figure 1: TPLSM images of static (A, C) and dynamic (B, D) cultivated scaffolds, stained for CD31 (A, B) and anti-collagen IV (autofluorescence in blue) (C, D); scale: 300 µm (A, B) and 50 µm (C, D).

The results imply an inhibitory effect of dynamic cultivation conditions on the level of angiogenesis. This is probably caused by high shear stress and dilution of growth factors. These parameters also have a negative effect on the attachment of fibroblasts, causing a lacking support for blood vessels⁴. Furthermore there is less expression of collagen IV which leads to a reduced formation of extracellular matrix surrounding and supporting the blood vessel-like structures.

CONCLUSION

The results of the present study demonstrate a highly significant effect of cultivation conditions on the amount of vessel-like structures in *in vitro* 3-D angiogenesis models. Dynamic cultivation by perfusion of the scaffolds leads to a reduced number of blood vessel-like structures, less attachment of fibroblasts, decreasing collagen IV expression in endothelial cells and a depressed basement membrane formation. However in the static culture vessel-like structures developed well and a distinct network was generated.

REFERENCES

1. Carmeliet P. *et al.*, Nature. 407: 249-257, 2000.
2. Carmeliet P. *et al.*, Nat. Med. 6: 389-395, 2000.
3. Rest, v.d. M. *et al.*, FASEB J. 5: 2814-2823, 1991.
4. Song S. *et al.*, Lab Chip. :1602-1611, 2013.

ACKNOWLEDGMENTS

This work was supported by the Core Facility "Two-Photon Imaging", a Core Facility of the Interdisciplinary Center for Clinical Research (IZKF) Aachen within the Faculty of Medicine at RWTH Aachen University.

Asymmetric Biodegradable Scaffolds for Vascular Tissue Engineering

Patrycja Domalik-Pyzik^{1*}, Anna Morawska-Chochół¹, Jan Chłopek¹, Elżbieta Menaszek², Izabella Rajzer³

¹ AGH University of Science and Technology, Faculty of Materials Science and Ceramics, Department of Biomaterials, al. A. Mickiewicza 30, 30-059 Krakow, Poland

² UJ Jagiellonian University, Collegium Medicum, Faculty of Pharmacy, Department of Cytobiology, ul. Medyczna 9, 30-068 Krakow, Poland

³ ATH University of Bielsko-Biala, Department of Mechanical Engineering Fundamentals, Division of Materials Engineering, Willowa 2, 43-309 Bielsko-Biala, Poland

*pdomalik@agh.edu.pl

INTRODUCTION

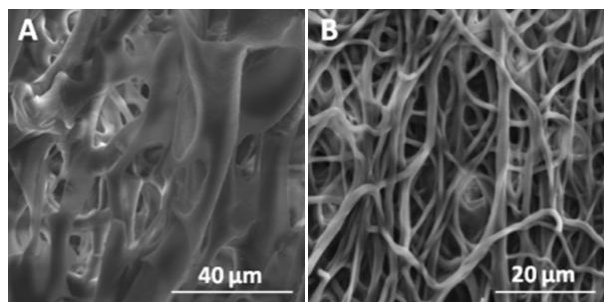
Since cardiovascular diseases are nowadays considered one of the main causes of death in western world, searching for new treatment solutions and improving existing ones seems crucial¹. This applies particularly to the wide field of biomaterials and tissue engineering. Vascular tissue engineering focuses especially on developing new solutions for replacement of diseased small-calibre (inner diameter < 6 mm) blood vessels as biomaterial solutions currently available on the market are unsatisfying. Synthetic vascular prostheses cannot be applied when it comes to the small blood vessels because they often fail due to early thrombosis. Therefore, small cylindrical biodegradable constructs with appropriate properties are intensively investigated^{2,3}. This work focuses on designing and manufacturing tube-shaped biodegradable scaffolds with different microstructures of outer and inner layers destined for use in tissue engineering of small blood vessels.

EXPERIMENTAL METHODS

Scaffolds with inner diameters of 5 mm were fabricated with the use of two methods, that is electrospinning and freeze-drying. Pure polylactide (PLA) nonwoven tubes were coated with polycaprolactone (PCL) solution (1g/40ml of glacial acetic acid). Then, samples were frozen in -20°C for 0,5h and freeze-dried for 24h. Microstructural observations were performed with NOVA NANO SEM 200 (FEI EUROPE COMPANY). Mechanical (tensile test, Zwick 1435) and wettability (water contact angle, Kruss 10 DSA) tests, and also cell culture assays (HAoEC) and spectroscopy (ATR) analysis were performed too.

RESULTS AND DISCUSSION

Figure 1 shows different microstructures of outer (A) and inner (B) surfaces of the scaffold.



Scaffold were asymmetric. Inner surface comprised of polylactide nanofibres, outer of porous polycaprolactone, and there was also an intermediate layer between them. Such construction was created to distinguish growth conditions of vascular endothelial cells (inner surface) and smooth muscle cells (outer surface).

Covering of PLA nonwoven with PCL solution enhances tensile strength (R_m) and Young's modulus (E) of the scaffold⁴ as it is shown in table 1.

Material	R_m [MPa]	E [MPa]
PLAes	$0,83 \pm 0,04$	$2,27 \pm 0,05$
PCL40	$0,76 \pm 0,23$	$13,11 \pm 1,94$
PLAes/PCL40	$1,98 \pm 0,24$	$150,43 \pm 4,58$

Cell tests confirmed biocompatibility of designed scaffolds. HAoEC adhered well to the surface and began to organize in chain-like structures.

CONCLUSION

Designed scaffolds can potentially be used in vascular tissue engineering. Their asymmetric construction reflects structure of natural blood vessel and creates different conditions for growth and proliferation of EC and SMC. Utilisation of such simple manufacturing methods like electrospinning and freeze-drying as well as use of medically verified biodegradable polymers (PLA and PCL) for creating vascular scaffolds opens possibilities for many different modifications, e.g. addition of DNA encoding growth factors.

REFERENCES

1. World Health Organization, Cardiovascular diseases, Fact sheet N°317, 2013.
2. Peck M, *et al.* Cells Tissues Organs. 195(1-2):144–58, 2011.
3. L'Heureux N, *et al.* Nature Clinical Practice Cardiovascular Medicine. 4(7): 389–95, 2007.
4. Domalik-Pyzik P, *et al.* Engineering of Biomaterials. 120:2-7, 2013.

ACKNOWLEDGMENTS

This research was financed by the statutory research No 11.11.160.256 of Faculty of Materials Science and Ceramics, AGH University of Science and Technology, Krakow, Poland.

Biodegradation studies on some magnesium alloys without Al for biomedical application

Julian Antoniac, Florin Miculescu, Aurora Antoniac and Ana-Iulia Blajan

Department Materials Science and Engineering, University Politehnica of Bucharest, Romania
antoniac.iulian@gmail.com

INTRODUCTION

Studies regarding biodegradable materials have shown that magnesium alloys are potential biomaterials for orthopedic application due to its major advantage to biodegrade in biological medium¹. One of the most used alloying elements for magnesium in order to obtain biodegradable magnesium alloys for biomedical application is calcium, considering that the degradation products are expected to be non-toxic^{2,3}. In this study, we evaluate the biodegradation of magnesium alloys from Mg-Ca, comparatively with the alloys from Mg-Zn-Zr systems, in different simulated biological medium.

EXPERIMENTAL METHODS

Different binary Mg-Ca alloy with 1% and 2% calcium content obtained in our laboratory and an commercial alloy type ZK60 (from Mg-Zn-Zr system) was chosen as experimental material. For experimentally obtained alloys, ingots of commercial available high purity magnesium (99.96 %) and calcium (99.8%) particles were used as starting materials. Experimental samples of circular shape and 2mm x10mm size were polished on metallographic papers and washed with ethanol. For immersion tests were used three different mediums: Phosphate buffer solution (PBS), Hanks' Balanced Salt Solution (HBSS) and Dulbecco Modified Eagle Medium supplemented with fetal bovine serum (DMEM + 10% FBS). Mg-1Ca alloys were immersed in 50 ml solution each (total surface area to volume of solution =314mm²:50mL) at 37 °C for 3, 7, 14, 21 and 30 days. The samples were weighted before and after the immersion. For microstructural characterization of the experimental samples was used an Olympus BX51 optical microscope and a Philips XL30-ESEM scanning electron microscope. Also, the chemical composition determination was performed using EDS.

RESULTS AND DISCUSSION

The degradation process of experimental Mg alloy was evaluated during the immersion period on the basis of loss/gain weight. Also, the surface macro-morphologies of investigated alloys were analyzed using SEM. Immersed samples show different patterns of degradation depending on the type of medium and an accelerated corrosion process with increasing immersion time. In the case of phosphate buffered solution (PBS) it can be noticed a fine crystals deposit on the surface. Chloride ions from saline solution exhibit a reduced action on the alloy due to formation of a partially protective Mg (OH)₂ layer. For the samples tested in Hanks' Balanced Salt Solution (HBSS) we observed a different pattern of degradation with rapid accumulation of corrosion products and loss of integrity up to the end of the test. Corrosion products formed are

adherent to the surface and EDS results showed that these products are mainly formed of magnesium hydroxides, phosphates and carbonates. An relevant example for Mg-1Ca alloy related to the SEM micrographs and EDS result of the samples after immersion in PBS (A), HBSS (B) and DMEM + 10% FBS (C) for 21 days are shown in figure 1. When we used Dulbecco Modified Eagle Medium supplemented with fetal bovine serum (DMEM + 10% FBS) we observed that the proteins seems to form a passivation layer on top.

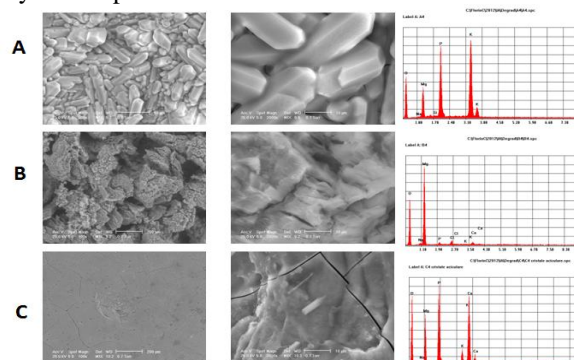


Fig. 1. SEM micrographs and EDS result of Mg-1Ca alloy samples after immersion in PBS (A), HBSS (B) and DMEM + 10% FBS (C) after 21 days

CONCLUSION

The aim of this study was to evaluate the effects of different mediums on magnesium alloys and to determine the optimal degradation medium. Regarding this issue it have been used both phosphate-based and cell culture medium to observe the influence of amino acids and vitamins and also proteins present in the added amount of fetal bovine serum. Best results were obtained in case of Dulbecco Modified Eagle Medium supplemented with fetal bovine serum (DMEM + 10% FBS). Hanks' Balanced Salt Solution (HBSS) proved to be the most aggressive medium given the highly porous surface morphology and the fact that experimental sample almost desintegrated after 30 days. Considering the immersion test results the experimental Mg-1Ca alloy appear to be suitable for medical applications.

REFERENCES

1. M. Salahshoor *et al.*, Materials 5:135-155, 2012.
2. Xuenan Gu *et al.*, Biomaterials 30:484-498, 2009
3. F. Witte *et al.*, Biomaterials 26(17):3557-63, 2005

Glucose sensitive gelation of hydrogel based on hyaluronan-tyramine conjugate

Lenka Kohutová, Martin Pravda, Julie Bystroňová, Lucie Wolfová, Vladimír Velebný

¹ Contipro Biotech s.r.o., Dolní Dobrouč, Czech Republic
Lenka.Kohutova@contipro.com

INTRODUCTION

Hyaluronan-tyramine conjugates (HA-TA) are promising materials for application in biomedicine. HA-TA is capable to form covalently crosslinked hydrogel by horseradish peroxidase (HRP) mediated reaction.¹ Crosslink reaction is initiated by addition of highly diluted H₂O₂. Our group developed new type of HA-TA conjugate where tyramine moiety is attached to the polymer backbone via suitable aliphatic linker (HA-LIN-TA). Presence of the aliphatic linker increases flexibility of HA polymer segments and variability of polymer microconformations. This effect leads to enhancement of mechanical properties of formed hydrogels and rapid gel formation.² Recently Sakai et al. described generation of H₂O₂ by glucose oxidase (GOx)-catalysed glucose oxidation for triggering of HRP mediated hydrogelation of alginate-tyramine conjugate. Aim of this study was to optimize an amount of used enzymes (HRP and GOx) to gain a system capable of rapid hydrogelation of HA-LIN-TA solution at concentration of glucose close to glycaemia.

EXPERIMENTAL METHODS

HA-LIN-Ta derivative was prepared according previously published procedure.² Briefly polyaldehydic derivative of hyaluronan was prepared by TEMPO mediated reaction. This was further conjugate with 6-amino-*N*-[2-(4-hydroxyphenyl)ethyl]hexanamide via reductive amination. Gained HA-LIN-TA derivative was characterized by NMR (degree of substitution 1.5%) and SEC-MALLS (*M_w* = 360 kDa). Precursor gel solutions containing HA-LIN-TA 2% (w/w), HRP (0.25 – 2.91 U/ml) and GOx (2.5 – 50 U/ml) were prepared. Hydrogelation was initiated by addition of glucose. Final concentration of glucose in the solution was 5 mM. Influence of concentration both HRP and GOx on gelation time and mechanical properties was studied. To determine the gel point the complex moduli was measured as a function of time. The critical gel point (GP) was detected as cross-over point where the elastic and viscous moduli were equal ($G' = G''$). Time of gelation was determined at 37 °C. Young's modulus (Y), compressive stress at breaking point (S) and toughness (T) were chosen as parameters for hydrogel mechanical properties evaluation. Measuring of mechanical properties was 3 times repeated with variability $\pm 10\%$.

RESULTS AND DISCUSSION

In situ forming hydrogel are valuable system for cell and drug delivery in the field of regenerative medicine.

Rapid gel formation prevents undesirable leakage of delivered material out of site of implantation. Sufficient mechanical strength of hydrogels is necessary proper cell proliferation. HRP mediated crosslink of HA-LIN-TA derivatives leads to hydrogels which fulfil these criteria. To prepare a glucose sensitive crosslinking system we used GOx as source of H₂O₂ for incitation of hydrogelation. Gelation time of system was clearly dependent on the concentration of HRP. Chosen concentration of GOx were able at level of glucose close to glycaemia supply H₂O₂ to system at rate which did not influence rate of gel formation.

Experiment	1	2	3	4	5	6	7
H ₂ O ₂ [mM]	1	-	-	-	-	-	-
HRP [U/ml]	0,36	0,42	0,42	0,42	2,91	2,91	2,91
GOx [U/ml]	-	5	10	25	5	10	25
GP (s)	15	11	10	10	<6	<6	<6

Table 1: Influence of enzymes concentration on time of gelation

Evaluation of mechanical properties showed that both glucose and peroxide triggered systems produce hydrogels with comparable mechanical properties.

Experiment	1	2	3	4	5	6	7
H ₂ O ₂ [mM]	1	-	-	-	-	-	-
HRP [U/ml]	0,36	0,25	0,42	0,97	2,91	2,91	2,91
GOx [U/ml]	-	5	5	25	25	2,5	10
Y[kPa]	6	6	6	6	5	7	6
S [Pa]	266	174	324	309	236	393	314
T [kJ/m ³]	18	13	24	21	12	25	23

Table 1: Evaluation of mechanical properties prepared hydrogel

CONCLUSION

Glucose sensitive hydrogelation of HA-LIN-TA derivative is promising approach for exploitation in situ crosslinkable hydrogels suitable for cell and drug delivery. For practical use it will be necessary to properly investigate biocompatibility of whole system.

REFERENCES

1. Kurisawa *et al.*, J. Mater. Chem. 20: 5371-5375, 2010.
2. Wolfova L *et al.*, WO/2013/127374, 2013.
3. Sakai, S., *et al.*, Rsc Advances 2: 1502-1507, 2012.



Surface modification of injectable microspheres for cell therapy applications

Abdulrahman Baki¹, Omar Qutachi¹, Toby Gould², Emily Overton¹, Kevin Shakesheff¹ and Cheryl Rahman¹

¹Drug Delivery and Tissue Engineering Department, School of Pharmacy, University of Nottingham, UK

²Centre for Children's Brain Tumour Research, School of Medicine, University of Nottingham

Paxab12@nottingham.ac.uk

INTRODUCTION

Injectable microspheres offer a minimally invasive approach to deliver cells for tissue repair. As substrate elasticity has been shown to direct stem cell fate¹, this study aims to harness this effect by developing a method to alter the surface elasticity of PLGA microspheres. To achieve this, methacrylated gelatin (gelMA) was immobilised on PLGA microspheres using surface entrapment. Cross-linked gelMA is known to support cell growth², and its elasticity can be controlled by altering the methacrylate content and cross-linking time³. The technique of surface entrapment was selected as it is used to immobilise molecules on a polymer surface without changing its chemical composition⁴. Developing a method to modify the surface of injectable microspheres with gelMA presents the opportunity to tune the microsphere surface elasticity and thus influence cell fate for regenerative medicine applications.

EXPERIMENTAL METHODS

Gel-MA Hydrogel characterization: Gel-MA was prepared by methacrylating porcine and fish gelatin. GelMA hydrogels were formed by UV crosslinking gelMA with photo-initiator (Ergacure 2959). Hydrogel elasticity was assessed with aTA.HD+ texture analyser.

Surface modification of PLGA microspheres: PLGA microspheres ($32 \pm 12 \mu\text{m}$) were surface modified using a modifying mixture of TFE/GelMA solution. Immobilised GelMA was UV cross-linked.

Surface Analysis: Microspheres were visualised using fluorescent microscopy and scanning electron microscopy (SEM). The bicinchoninic acid (BCA) protein assay was used to quantify immobilised gelMA.

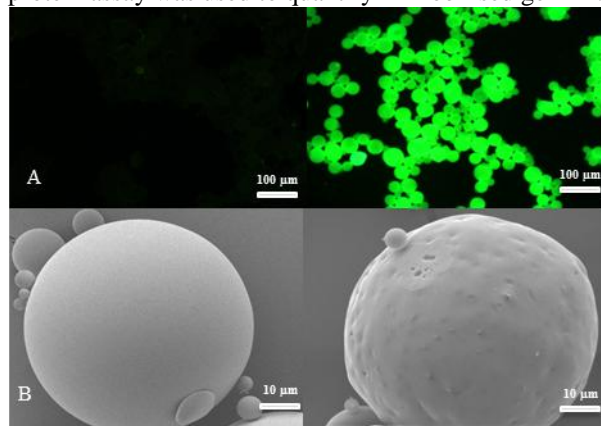


Figure 1 Images of blank PLGA microspheres (Left) and gelMA modified microspheres (Right) as shown in (A) fluorescent microscope, and (B) scanning electron microscope SEM.

RESULTS AND DISCUSSION

The presence of FitC-labelled gelMA was observed on the surface of modified microspheres using fluorescent microscopy (Figure 1A).

Differences in surface morphology between non-modified (blank) and surface modified microspheres were visualised by SEM (Figure 1B).

The BCA assay results demonstrated the presence of a

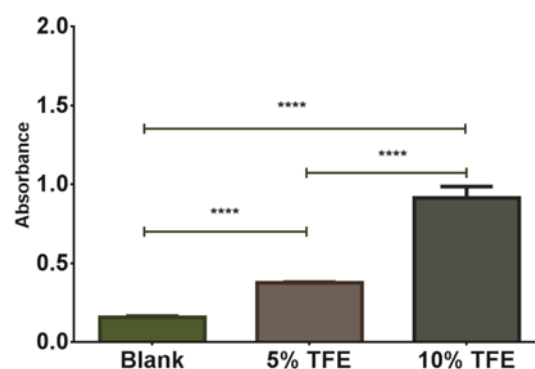


Figure 2 BCA assay results showing the change in gelMA concentration on modified PLGA microspheres.

protein (gelMA) on modified microspheres (Figure 2). A significant increase in the detection of gelMA was observed between blank and modified microspheres, and between different concentrations of solvent (TFE) used in the entrapment process.

CONCLUSION

A promising approach for modifying the surface of PLGA microspheres with gelMA hydrogel was developed in this study. Solvent concentration was also found to affect the level of gelMA entrapment. Future work will focus on altering the thickness and elasticity of the gelMA layer to create a tuneable cell delivery system for regenerative medicine applications.

REFERENCES

- Engler, A.J., et al., Cell, 126(4): 677-689, 2006.
- Nichol, J.W., et al., Biomaterials, 31(21): 5536-5544, 2010.
- Van Den Bulcke, A.I., et al., Biomacromolecules, 1(1): 31-38, 2000.
- Quirk, R.A., et al., Macromolecules, 33(2): 258-260, 2000.

ACKNOWLEDGMENTS

Authors would like to thank the UK Regenerative Medicine Platform Hub for the support in this research.

Photocrosslinkable divinyl-fumarate poly-ε-caprolactone for stereolithography application

A. Ronca¹, S. Ronca², G. Forte², A. Gloria¹, R. De Santis¹, L. Ambrosio^{1,3}

¹ Institute for Polymers, Composites and Biomaterials - National Research Council of Italy, Mostra d'Oltremare Pad.20, Viale J.F. Kennedy 54, 80125 Napoli, Italy; alfredo.ronca@cnr.it

² Department of Materials, Holywell Park Loughborough University, Leicestershire, UK, LE11 3TU

³ Department of Chemical Science and Materials Technology – National Research Council of Italy, P.le Aldo Moro, 7 - 00185 Roma, Italy

INTRODUCTION

The functionalization of resorbable oligomers such as those based on polyester with unsaturated groups and subsequent radical polymerization and crosslinking has been extensively studied¹. Typically, photocrosslinkable resins are composed of mixtures of two or more monomers that combine a relatively viscous dimethacrylate base monomer². The diffusion of unpolymerized methacrylates is one of the most important factors causing irritation in tissues³. Another anticipated risk of acrylates is a higher level of skin sensitization as compared to most vinyl ethers. Stannous Octoate Sn(Oct)₂ has been widely used as the initiator for ROP⁴ of Caprolactone (CL) and, although very efficient, its cytotoxicity has recently caused deep concern about biosafety of the materials synthesized from it and used for implantation purpose⁵. In this work, a Sn-free catalyst has been used for the ROP of CL, achieving more than 95% monomers conversion at room temperature, with hydroxyethyl vinyl ether (HEVE) as both initiator and photo-curable functional group. Fumarate functional group has been added to this precursor, to improve the degrees of reticulation in order to investigate the feasibility to photo-polymerize oligomers with hybrid functionalities.

EXPERIMENTAL METHODS

A Sn-free catalyst based on Al⁶ has been used in the polymerisation of CL at room temperature, coupled with HEVE as photocurable initiator⁷, according to the scheme below. The initiator/CL ratio has been varied to achieve a range of M_w comprised between 2000 and 5000 g/mol, as determined via rheological experiments and NMR. Following the synthesis of the vinyl-terminated PCL, its reaction with fumaryl chloride results in chains containing photocrosslinkable vinyl units at both ends and in the middle of the chain.

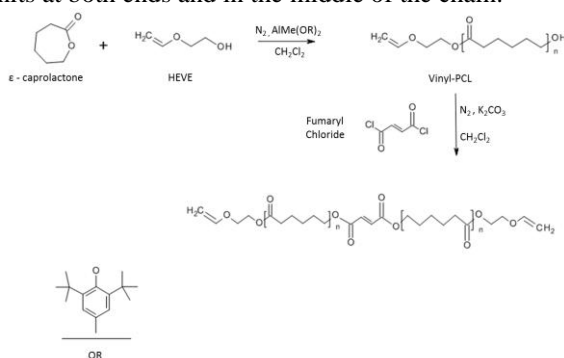


Figure 1: Synthetic procedure of the divinyl-fumarate PCL

Differential scanning calorimetry (DSC) has been used to evaluate the dependence of glass transition

temperature (T_g) and melting temperature (T_m) from polymer molecular weight.

RESULTS AND DISCUSSION

In the preliminary experiments, we polymerized CL by using HEVE in the presence of AlMe(OR)₂. Vinyl-PCL was reacted with Fumaryl Chloride to obtain a divinyl-fumarate-PCL. The resulting polymer was characterized by its molar weights, functional end groups and transition temperatures, using several techniques including Rheometry, Nuclear Magnetic Resonance (NMR), Fourier Transformed Infrared Spectroscopy (FTIR), Differential Scanning PhotoCalorimetry (DPC) and Differential Scanning Calorimetry (DSC). NMR and FTIR confirm the presence of functional groups linked to the PCL oligomers. Moreover vinyl double bond conversion is confirmed by the DPC exothermic peak.

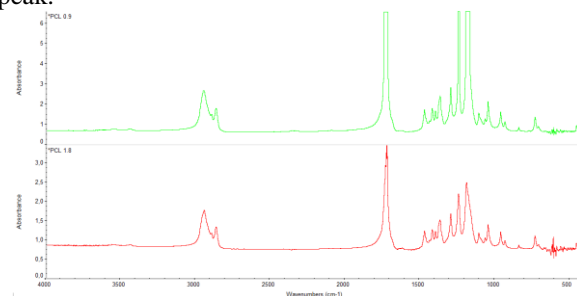


Figure 2: FTIR spectra of functionalized PCL

CONCLUSION

PCL network was successfully produced from UV curing of V/F hybrid oligo-caprolactone. This is an attractive alternative to diacrylated-PCL in reducing the potential immune effect related to acrylates.

REFERENCES

1. Ronca A et al., Acta Biomater. 9, 5989-5996, 2013.
2. De Santis R et al., J Appl Biomater Biom. 7: 132-140, 2009.
3. De Santis R et al., Dent Mater. 26: 891-900, 2010.
4. Penczek S et al., Macromo Symp. 157: 39-46, 2000.
5. Kricheldorf HR et al., Macromol Symp. 159: 247-258, 2000.
6. Akatsuka M et al., Macromolecules. 28: 1320-1322, 1995.
7. Liow SS et al., J Polym Res. 19:9748-9757, 2012.

ACKNOWLEDGMENTS

"The authors would like to thank the MAGISTER Research Project (NMP3-LA-2008-214685) co-funded by the European Community's under the FP7-Cooperation Programme for providing financial support to this project.

Novel radiopaque UHMWPE sublaminar wires in a growth-guidance system for the treatment of early onset scoliosis: feasibility in a large animal model

Alex Roth, Rob Bogie, Paul Willems, Lodewijk van Rhijn, Jacobus Arts

¹Department Orthopaedic Surgery, Researchschool Caphri, Maastricht University Medical Centre, Maastricht, the Netherlands j.arts@mumc.nl

INTRODUCTION

Growth-guidance or self-lengthening rod systems are an alternative to subcutaneous growing rods for the surgical treatment of early onset scoliosis (EOS). The main advantage in comparison to growing rods is the marked decrease in subsequent operative procedures. Ultra high molecular weight polyethylene (UHMWPE) or other polymeric sublaminar cables have already been introduced for spinal deformity surgery; the soft and flexible structure of woven UHMWPE wires decreases the risk of neurological injury, while the broad shape distributes contact forces over a greater area, thus allowing for higher correction forces. Radiolucency of UHMWPE wires has limited the possibility for postoperative radiological assessment and subsequent clinical use. The goal of this study consists of two parts: (1) to test the stability and biocompatibility of novel radiopaque UHMWPE wires as sublaminar wire, and (2) to assess the potential of using UHMWPE sublaminar wires in a growth guidance system for EOS

EXPERIMENTAL METHODS

In 12 immature sheep, thoracolumbar spines were instrumented with radiopaque (Bismuth Oxide additive) UHMWPE sublaminar wires. Wires were placed at 5 levels (T11-L3), while pedicle screws at L5 held dual CoCr rods in place. A control group consisted of 4 age-matched animals. Radiographic control was performed at 4 week intervals. After a follow-up period of 24 weeks, the animals were sacrificed and the spines were harvested. Harvested spines and vertebrae were embedded in PMMA for histological evaluation.

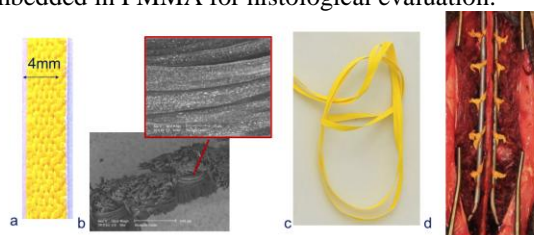


Fig 1. (a) 4mm wide, woven radiopaque UHMWPE sublaminar wire (b) SEM close-up image of radiopaque UHMWPE wire showing homogenous bismuthoxide particle distribution (c) double-loop sliding knot (d) intra-operative view of UHMWPE sublaminar wires looped around the laminae and after tensioning the knots

RESULTS AND DISCUSSION

No neurological deficits occurred during the postoperative period. One animal died during follow-up (7 weeks postoperatively) due to unknown cause. At sacrifice, none of the cables had loosened and all instrumentation remained stable. Substantial growth occurred in the instrumented segments (L5-T11) in the intervention group (2.67 ± 0.16 cm). Spinal growth was slightly higher in the control group, (2.96 ± 0.35 cm),

but this difference was not statistically significant ($p=0.42$).

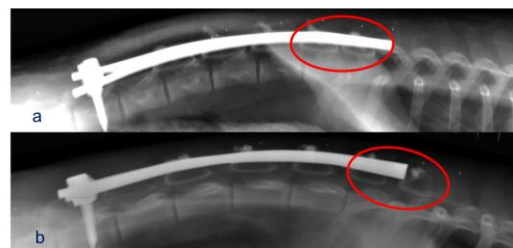


Fig 2. Lateral radiograph of the instrumented spine (a) directly post-operative and (b) after 24 weeks. The red circle clearly illustrates growth by sliding of the cable along the rod.

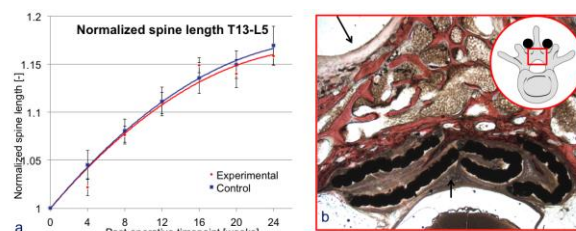


Fig 3. Quantification of spinal length shows no significant difference between the operated and control groups. (b) Histological slice of PMMA-embedded vertebrae (Hematoxylin & Eosin stained) showing fibrous encapsulation of the wire, which is a typical physiological reaction to foreign materials (also seen around rods, arrows)

Histological analysis revealed fibrous encapsulation of the novel radiopaque UHMWPE sublaminar wires in the epidural space, with no evidence of chronic inflammation or wear debris. HR-pQCT analysis showed interlaminar ossification, possibly a result of periosteal stripping during opening of the flaval ligament. Typical bone formation encircling the posterior rods coupled with degenerative facet joint changes were also seen.

CONCLUSION

Despite the occurrence of spontaneous ossification, UHMWPE sublaminar cables allowed for almost normal continued growth of the instrumented spinal segments during follow-up. Fibrous encapsulation of the cable and preservation of instrumentation stability during the course of this study show that the application of these novel radiopaque UHMWPE sublaminar cables in spinal deformity correction surgery is safe. Further research into the fate of bismuth-oxide particles however is ongoing.

ACKNOWLEDGMENTS

This research forms part of the Project P2.05 Spineguide of the research program of the BioMedical Materials institute, co-funded by the Dutch Ministry of Economic Affairs.

3D Plotting of hydrogels based on fibrillar collagen to create scaffolds with defined inner and outer architecture

Anja Lode¹, Kristin Faulwasser¹, Sophie Brüggemeier¹, Birgit Hoyer¹, Hagen Baltzer², Michael Meyer², Claudia Winkelmann³, Frank Sonntag³, Michael Gelinsky^{1*}

¹Centre for Translational Bone, Joint and Soft Tissue Research, Technische Universität Dresden, Dresden, Germany, michael.gelinsky@tu-dresden.de

²Research Institute of Leather and Plastic Sheetting (FILK) Freiberg, Germany

³Fraunhofer IWS Dresden, Germany

INTRODUCTION

The rapid prototyping technique of 3D plotting (3DPI) allows the processing of a variety of synthetic and natural materials in form of slurries, highly viscous solutions, suspensions, blends and melts. The mild process conditions enable the application of biopolymers such as collagen and even the integration of sensitive components like growth factors or living cells.

We have investigated the conditions for 3DPI of pure, fibrillar collagen as well as of mineralised collagen, a nanocomposite artificial extracellular bone matrix.

EXPERIMENTAL METHODS

3DPI was performed using a BioScaffolder™ from GeSiM (Grosserkmannsdorf, Germany). As plotting materials, highly concentrated fibrillar collagen type I pastes, derived from porcine skin (FILK, Freiberg, Germany), as well as bovine tendon collagen (Syntacoll, Saal/Donau, Germany), mineralised with nanocrystalline hydroxyapatite ("mineralised collagen¹") were used. If necessary, blending with carboxymethyl cellulose or gelatine was done to prevent liquid segregation. The porous, cubic 3D scaffolds were freeze-dried and crosslinked chemically after plotting in air with an EDC solution and characterised concerning their structural and mechanical properties.

The suitability of the plotted 3D scaffolds for soft (pure collagen) as well as bone tissue engineering (mineralised collagen) was evaluated in cell culture experiments with human mesenchymal stem cells (hMSC). The cell-matrix constructs were cultivated in the presence of adipogenic and osteogenic supplements, respectively, and adhesion, proliferation and differentiation of the cells was investigated.

RESULTS AND DISCUSSION

At low pH values, the native collagen type I paste was plottable without additives to generate pure collagen scaffolds which were subsequently stabilised by chemical crosslinking with the carbodiimide derivative EDC. At neutral pH, the collagen suspension was processible by 3DPI only if blended with other biopolymers like carboxymethyl cellulose which were able to counter the liquid segregation (phase separation) during the plotting process. The same strategy was used to manufacture plotted scaffolds from mineralised collagen but here the blending with gelatine was successful for preventing phase separation (Fig. 1).

EDC crosslinking led to sufficiently stable constructs for all investigated scaffold compositions which could be stored under cell culture conditions for several weeks

without disintegration. Beside the macroporosity, originated by 3DPI according to the predesigned geometry, the freeze-drying process generated an additional microporosity within the strands.

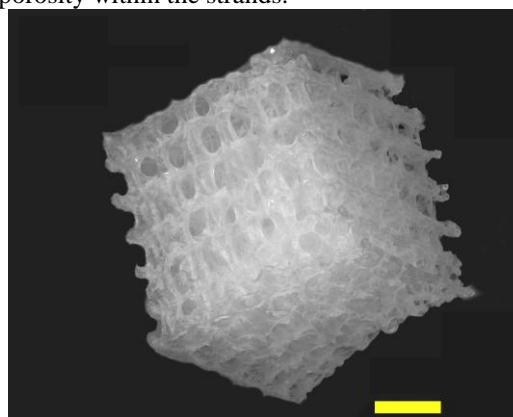


Fig. 1: 3D plotted scaffold, consisting of mineralised fibrillar bovine collagen type I (scale bar = 2 mm)

Human MSC could adhere, proliferate and differentiate towards the adipogenic (non-mineralised collagen scaffolds) or osteogenic (mineralised collagen) lineage in presence of the established supplements. Adipogenic differentiation was proven by measurement of GPDH enzyme activity and expression of perilipin, PPAR γ , FABP4 and LP lipase on RNA level, osteogenic differentiation by observation of a strong increase of specific alkaline phosphatase (ALP) activity over time.

By combining pure and mineralised collagen pastes (or other suitable biomaterials like calcium phosphate bone cement (CPC) or biopolymer hydrogels like alginate or gellan gum) in a multi-channel 3D plotting process, complex scaffolds suitable for the treatment of defects at tissue interfaces (soft tissue/bone or cartilage/bone) can easily be fabricated – as recently demonstrated by combining a CPC paste with alginate hydrogel².

CONCLUSION

Rapid prototyping of scaffolds and tissue engineering constructs is a fast growing research field and provides new options for individualised therapies. We have demonstrated that collagen as well as mineralised collagen pastes can be used for 3D plotting of porous scaffolds of defined architecture and that those matrices are suitable for hMSC culture and differentiation towards the adipogenic and osteogenic lineage, respectively.

REFERENCES

1. Gelinsky M. *et al.*, Chem. Eng. J. 137:84-96, 2008
2. Luo Y. *et al.*, J. Mater. Chem. B 1:4088-98, 2013

Porous bioactive glass foam scaffolds: Comparison of 3 compositions

Amy Nommeots-Nom¹, Aine Delvin², Naomi Todd², Robert Law,³ Hua Geng⁴, Christopher Mitchell,² Peter D. Lee,⁴ Julian R. Jones¹

¹Department of Materials, Imperial College, London, UK

²Centre for Molecular Biosciences, University of Ulster at Coleraine, Coleraine UK

³Department of Chemistry, Imperial College, London, UK

⁴School of Materials, The University of Manchester, Oxford Rd, Manchester UK
an108@ic.ac.uk

INTRODUCTION

Larry Hench's original Bioglass® 45S5 composition [1] cannot be made into porous scaffolds while maintaining an amorphous glass structure due to its susceptibility to crystallise during sintering. Melt-derived glasses have recently been developed which avoid this crystallisation, enabling bioactive glasses to be manufactured into porous constructs. The aim was to use a new modified gel-cast foaming technique to create porous glass scaffolds using three different glass compositions. The new process switched *in situ* polymerisation [2] for thermal gelation of a polymer binder. The effect of composition on the glass structure, processing and *in vitro* and *in vivo* behaviour was investigated.

EXPERIMENTAL METHODS

Glasses: ICIE16 (49.46 SiO₂, 36.27 CaO, 6.6 Na₂O, 1.07 P₂O₅ and 6.6 K₂O, in mol.%), 13-93 (6.0 Na₂O, 7.9 K₂O, 7.7 MgO, 22.1 CaO, 1.7 P₂O₅, 54.6 SiO₂ in mol.%) and SBP-3 (4.0 Na₂O, 4.0 K₂O, 7.5 MgO, 17.80 CaO, 17.80 SrO, 4.5 P₂O₅, 44.50 SiO₂ in mol.%) were manufactured via melt quenching. Frit was formed and ground into particle size less than 32 µm. A new gel cast foaming technique with a polymeric gelling agent was used to produce porous glass scaffolds, which were then freeze dried and sintered. Sintering effectiveness was optimised for each glass composition. Scaffolds were characterized via XRD, SEM, FTIR, porosimetry, solid state phosphorous NMR, ICP and SBF testing. *In vivo* comparison, using a rat tibia model (3 mm defect), between SBP-3 and ICIE16 scaffolds was completed. Sample sizes were 3.06 ± 0.20 mm diameter, 2.02 ± 0.07 mm thick.

RESULTS AND DISCUSSION

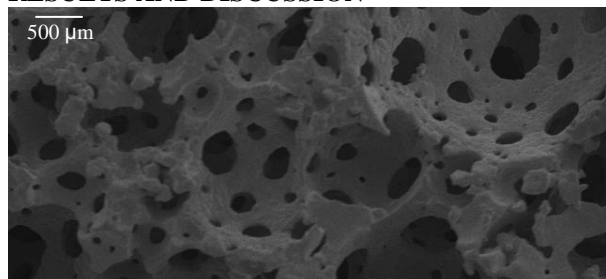


Fig. 1: SEM of sintered ICIE16

Surfactant concentration and sintering profile was optimised to create scaffolds (e.g. Fig. 1) with modal interconnects (mercury porosimetry) of 100-200 µm and 85% porosity. Each glass had different network connectivity (NC^{*}): 2.13, 2.84 and 3.01 respectively,

suggesting that ICIE16 should be the most bioactive and 13-93 the least, however SBF data showed SBP-3 reacted the slowest (Fig. 3), implying the cations in SBP-3 are acting as network intermediates, slowing dissolution.

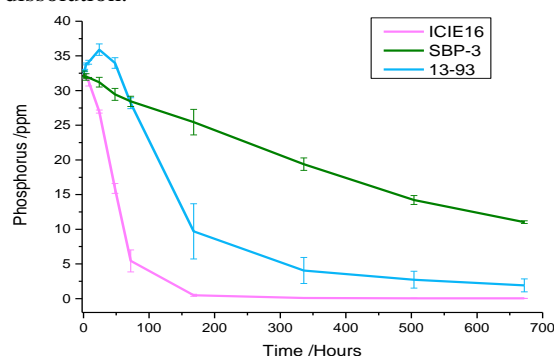


Fig. 3: ICP data of P content of SBF.

In vivo results: scaffolds implanted had equivalent modal pore diameter. Defects containing the scaffolds showed bone integration at 12 weeks although the composition of the glass affected rate of regeneration (Fig. 4). More bone seemed to fill the ICIE16 scaffolds, which was in agreement with ICIE16 forming an apatite layer more rapidly *in vitro*. Quantification of bone ingrowth will be presented.

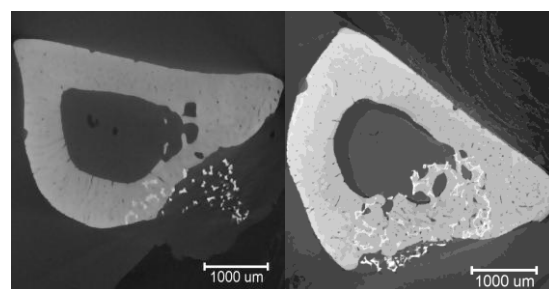


Fig. 4. X-ray tomography images of a rat tibia at 12 weeks of (a) SBP-3; (b) ICIE16.

CONCLUSION

In a rat model, bone ingrowth through a bioactive glass scaffold with lower network connectivity, and faster rate of HCA formation in SBF, was greater than for a scaffold with higher network connectivity, even though the latter contained Sr.

REFERENCES

1. Hench, LL, *J Mater Sci – Mater Med*, 17 (2006):967-978
2. Wu, Z, et al, *Acta Biomaterialia* 7 (2011): 1807-1816

ACKNOWLEDGMENTS

EPSRC (EP/I020861/1, EP/I021566/1) for funding.

Biodegradable nanoparticles coated with hyaluronic acid for targeted and sustained drug delivery to tumors

Laura Mayol¹, Marco Biondi¹, Luisa Russo², Carla Serri¹, Assunta Borzacchiello^{2*}, Luigi Ambrosio^{2,3}.

¹Department of Pharmacy, University of Naples Federico II, Italy

^{2*}Institute of Polymers, Composites and Biomaterials, National Research Council, Naples, Italy.

³ Department of Chemical Science and Materials Technology DCSMT- CNR, Italy

*bassunta@unina.it

INTRODUCTION

Nanoparticles (NP) can passively accumulate into tumors, taking advantage of enhanced permeation and retention (EPR) effect.

Major criticisms for the therapeutic effect of anticancer drugs loaded in NP are a limited NP cell internalization and/or the release of the loaded drugs before NP uptake.

Furthermore, the chemotherapeutic drugs suffer from the lack of specificity toward tumors, thus causing severe systemic effects. In this context, hyaluronic acid (HA) is attractive for tumor-targeted delivery since it can specifically bind to cancer cells, which overexpress CD44 receptor.

For this reason, several HA-based drug carriers have been studied for tumor targeting. A major challenge of this task is the development of the drug-carrier not altering the HA binding affinity to the receptors¹.

In this context, the aim of this work was to formulate HA-coated biodegradable NPs for the intracellular targeting of chemotherapeutic(s). In particular, NPs made of poloxamers and poly(lactic-co-glycolic acid) (PLGA) blends were coated with HA by a modified emulsion technique. NPs were characterized for their size, morphology and zeta potential (ZP).

Irinotecan (IRI) and Doxorubicin (DOX), two widely employed chemotherapeutic drugs, were loaded into NPs, and their *in vitro* release kinetics assessed.

EXPERIMENTAL METHODS

NPs were produced by a single emulsion/solvent evaporation technique. Briefly, solutions of PLGA (Boehringer Ingelheim, Germany), and poloxamers (F127 and F68 1:1 w/w; Lutrol, Basf, Germany) in acetone, at different weight ratios, were prepared. The organic phase was emulsified by sonication with an aqueous phase containing different HA (Novozymes Biopharma, 850 KDa) and poloxamers amounts.

The obtained NPs were characterized in terms of size and zeta potential by means of Photon Correlation Spectroscopy (PCS; N5 Submicron Particle Size Analyzer, Beckman-Coulter, Malvern, USA). Morphology was studied by transmission electron microscopy (TEM, FEI Tecnai G12 Spirit Twin).

In vitro drug release studies were carried out by placing NPs in dialysis membranes in phosphate buffer solutions (PBS) and quantifying the drug by spectrophotometric

assay. NP stability was evaluated by measuring their size over time.

RESULTS AND DISCUSSION

The obtained HA-coated NPs were spherical and with a mean size of approximately 110- 290 nm depending on HA/PLGA/poloxamer weight ratio. In figure 1 a selected TEM micrograph of NPs was reported.

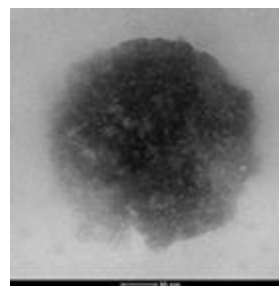


Figure 1: Selected TEM micrograph of nanoparticles

ZP was negative for all formulations, and decreased from approximately -27 mV to -40 mV when HA was added. Morphological, ZP and size analyses confirmed an effective HA coating on NP surface.

The presence of HA on NP surface promoted device stability for at least 10 days compared to NPs made up of PLGA alone, which immediately aggregate in PBS.

Both IRI and DOX were efficiently loaded, and these studies demonstrated NP ability to sustain their delivery for at least 14 days.

CONCLUSIONS

Biodegradable and biocompatible NPs, exposing superficial tumor targeting HA, were produced. NPs possessed a negative ZP, were stable in suspension over 10 days and could provide a sustained drug delivery.

REFERENCES

1. Choi KY *et al.*, Colloids Surf B Biointerfaces (2012), 99:82-94.

ACKNOWLEDGMENTS

The authors acknowledge the Italian Ministry of University and Research for providing financial support (Project: MIUR-PON Diateme).

Human bone marrow as a unique source of both microvascular endothelial cells and mesenchymal stem cells for vascularised bone tissue engineering

Julien Guerrero^{1*}, Hugo de Oliveira¹, Sylvain Catros¹, Robin Siadous¹, Reine Bareille¹, Mohammed Derkaoui², Didier Letourneur², Joelle Amédée¹

^{1*}Inserm, U1026 Tissue Bioengineering, University of Bordeaux, France, julien.guerrero@inserm.fr

²Inserm, U698 Cardiovascular Bioengineering, University Paris Sorbonne, France

INTRODUCTION

In the field of bone tissue engineering, one of the main clinical limitations resides in the repair of large bone defects. In this sense, biomaterials may offer alternatives to autografts but most do not promote sufficient vascularization as to support the process of tissue regeneration. One approach to tackle this limitation is the pre culture of vascular endothelial cells and mesenchymal cells in the tissue-engineering construct. Nonetheless, this approach presents some drawbacks, as it comprises the use of different cell sources and at distinct stages of differentiation. The identification of a sole source of reparative cells represents a major challenge for the development of bone tissue engineering products applicable in a clinical scenario. Stem cells from bone marrow are an important reservoir of reparative cells. In this context, our aim was to develop a simplified approach for bone tissue engineering by using a total human bone marrow cell fraction (hWBMCs) without the need for a step of selection and amplification.

EXPERIMENTAL METHODS

Our strategy involved the identification and characterization of two specific populations of cells (microvascular cells¹ and mesenchymal stem cells) among all the cells of the human bone marrow. As such hWBMCs, obtained from hip placement procedures (66 years \pm 11 years), were characterized for endothelial and mesenchymal markers by flow cytometry. For the *in vitro* studies, hWBMCs were seeded in pullulan/dextran matrices² and cultured in standard conditions. The formed aggregates were characterized in terms of osteoblastic and endothelial phenotype at 1, 6 and 12 days. The colonized materials were equally subcutaneously implanted in NOG female mice for 3 and 8 weeks (n=10). The animals were then sacrificed, the matrices recovered, fixed and processed for histology. Immunohistochemistry for CD31 and HLA-I, and Masson trichrome staining were performed as to characterize material endothelialisation, the fate of the human implanted cells and the formation of an osteoid tissue, respectively.

RESULTS AND DISCUSSION

The flow cytometry analysis reveals that we have 13,3 % \pm 5,0 % of mesenchymal stem cells and 7,0 % \pm 2,2 % of endothelial cells into the total human bone marrow cells. *In vitro*, when in a three-dimensional microenvironment, cells spontaneously form cell aggregates and show the establishment of communicating junctions. Additionally, we observed the augmentation of osteoblastic markers and the formation of a pseudo vascular network within the

aggregates. We also evidenced the promotion of cell to cell junctions, as observed by the expression of Connexin43, known to play a major role in the differentiation of mesenchymal stem cells to osteoblastic cells². Ectopic implantation of the matrices, loaded with hWBMCs, validated the suitability of the spheroidal structures to support bone and vessel formation *in vivo*. Indeed, osteoid formation significantly increased by two fold with time of implantation from 3 to 8 weeks. Importantly, we also demonstrated that hWBMCs spheroid-seeded scaffolds supported an increased vascularization in the periphery of the scaffold and inside the matrix, with time of implantation (Figure 1).

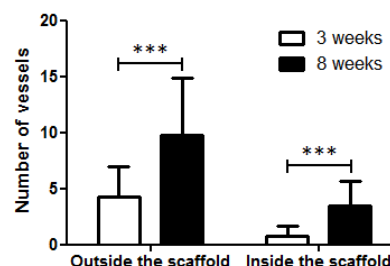


Figure 1 : Number of vessels during the time, outside the scaffold and inside the scaffold.

The role of the human cells loaded within the matrix and their impact in the neovascularization process was assessed by HLA-I immunolabelling (marker for human cells). Human cells were detected in the aggregates inside the scaffold up to 8 weeks of implantation, suggesting their contribution to the bone formation and/or the vascularization of the tissue. In addition, human cells were also observed associated with host vessels in the periphery of the implants. However, the exact mechanism involved in the communication and the cell interactions formed between human and murine cells remains unknown.

CONCLUSION

Here we demonstrate the potential of the total human bone marrow cell population, without preliminary isolation or expansion, for the development of a bone regeneration and vascularization strategy, once seeded in an appropriate bioactive matrix.

REFERENCES

1. Rafii S. *et al.*, Blood. 84 :10-9, 1996
2. Guerrero J. *et al.*, Acta Biomater. 9 :8200-13, 2013

ACKNOWLEDGMENTS

This work was supported by grants from INSERM (National Institute for Health and Medical Research), from University of Bordeaux and by grants from the French Research National Agency (ANR-10-EMMA-009-01 MATRI+; ANR-12-TecSan-0011 INEOV).



Effect of Calcium Phosphate Ceramics Substrate Geometry on Mineralization and Cell Organization and Differentiation

E.R. Urquia Edreira¹, A. Hayrapetyan¹, J.G.C. Wolke¹, J.A. Jansen¹, J.J.J.P. van den Beucken¹

¹*Department of Biomaterials, Radboud UMC, The Netherlands, EvaRaquel.UrquiaEdreira@radboudumc.nl

INTRODUCTION

Calcium phosphate ceramics in combination with implant surface geometry have been shown to influence biological performance. Ripamonti et al. have extensively investigated the osteoinductive effect of repetitive surface concavities on bulk ceramics and calcium phosphate coated titanium implants¹⁻³. These studies have shown that the presence of concavities allows for osteoinductive capacity without loading the ceramic scaffold osteogenic soluble factors or osteogenic cells.

In our previous study, we tried to rationalize the mineralization process through an *in vitro* test in SBF⁴. Bianchi et al. showed that the mineralization process started preferentially within the concavities in hydroxyapatite (HA) disks sintered at 1200 °C and concavity size controlled the extent of mineralization.

It is also known that micro- and nano-scale morphology of the calcium phosphate surface can strongly influence osteoblast and stem cell adhesion, proliferation, and differentiation⁵⁻⁷. In our current study, we aimed to investigate how cells populate concavities and to what extent concavity size influences cellular mineralization. We hypothesized that surface concavities facilitate cell proliferation and mineralization and that these effects are increased in the smaller concavity due to increased 3D cellular organization.

EXPERIMENTAL METHODS

Cavity sizes of 400, 800 and 1600 µm were created on the surface of HA disks sintered at 1200°C and cultured with adipose tissue mesenchymal stem cells (AT-MSCs) in osteogenic medium for up to 28 days at 37°C. At selected time points (3, 7, 14, 21, and 28 days), samples were removed and after fixation cells were fluorescently labelled with phalloidin-Alexa 568 (1:250; molecular probes) for filamentous (F-) actin and DAPI (1:2500) for nuclear staining. Cells were imaged and examined with a confocal laser scanning microscopy (CLSM) Olympus FV1000.

RESULTS AND DISCUSSION

Immunofluorescence-based three-dimensional (3D) image analysis showed differences in cell number between concavities at early culture time points (3 days). The highest number of cell nuclei was found in the 400 µm cavity (Figure 1) and the lowest number in

the 1600 µm. Additionally, cells were able to migrate towards the concavities and adhere to their edges and walls. Preferential mineralization was observed inside the concavities. Cells spread over and to the bottom of concavities covering all their volume and creating multilayers on their surfaces.

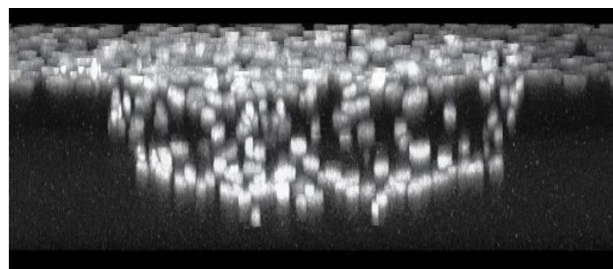


Figure 1. Immunofluorescence images at three days showing cell nuclei within the 400 µm concavity.

CONCLUSION

High resolution 3D images gave qualitative and quantitative data on concavity volumes. CaP ceramics with surface concavities induced cell (AT-MSCs) organization within the concavities and were able to create cell multilayers. Results from this study suggest a correlation between concavity size, cellular organization, mineralization and concavity induced osteoinductive properties.

REFERENCES

1. Ripamonti U. *et al.*, J. Cell. Mol. Med. 13, 2953, 2009
2. Scarano A., *et al.*, Clin. Implant Dent. Rel. Res, 2009
3. Ripamonti U. *et al.*, Biomaterials, 3813, 2012
4. Bianchi M. *et al.*, Acta Biomaterialia, 10, 2012
5. Li B. *et al.*, Acta Biomaterialia, 8, 2012
6. Prodanov L. *et al.*, Biomaterials, 34, 2013
7. Graziano A. *et al.*, PloS One, 2, 2007

ACKNOWLEDGMENTS

The authors would like to thank the Research Program of the BioMedical Materials Institute (Project P2.04 BONE-IP), co-funded by the Dutch Ministry of Economic Affairs, Agriculture and Innovation for providing financial support.

Biomechanical & morphological analysis of blend polymeric electrospun scaffolds for Cardiovascular Tissue Engineering

Alexandros Repanas¹, Birgit Glasmacher¹ and Dimosthenis Mavrilas^{2*}

¹Institute for Multiphase Processes, Leibniz University Hannover, Germany

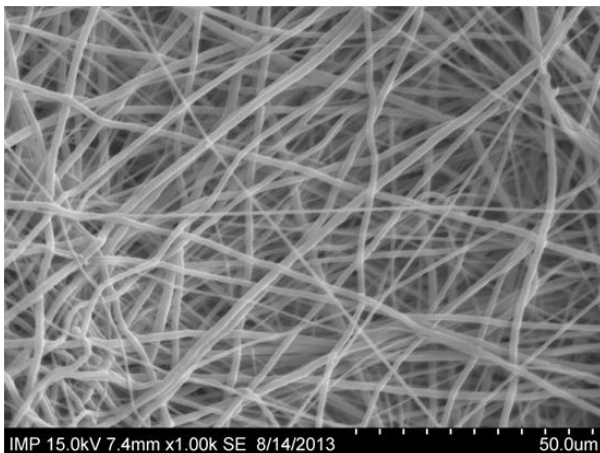
^{2*}Laboratory for Biomechanics & Biomedical Engineering, Mechanical Engineering & Aeronautics, University of Patras, Greece, mauril@mech.upatras.gr

INTRODUCTION

Polycaprolactone (PCL) and chitosan (CS) are polymers with attractive properties (excellent biocompatibility & degradation time, resp. cytocompatibility)^{1,2}. However their mechanical properties separately do not satisfy the needs for cardiovascular tissue engineering. In the present work we aimed to optimize electrospinning parameters to obtain a flexible PCL/CS polymeric scaffold, with combined nano- and micro-fiber architecture and appropriate mechanical properties for cardiovascular tissue engineering in regenerative medicine.

EXPERIMENTAL METHODS

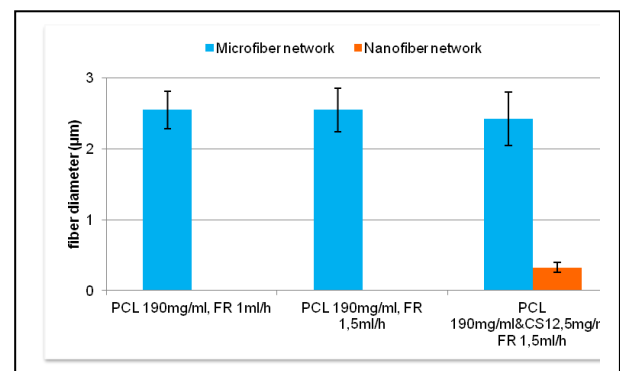
PCL and CS were dissolved in acetic acid (AAC) and 2,2,2-trifluoroethanol (TFE) using different concentrations. Electrospinning was performed at a custom made apparatus, at room temperature. Morphology of the fibrous membranes was examined by SEM. Cyclic sinusoidal uniaxial mechanical tests were performed with a Bose electroforce dynamic tensile testing system. Rectangular, 15x10 mm strips were cut and tested at 0-30% strain, 1 cycle/sec, RT, dry conditions, room temperature. The applied force and the local principal strain were monitored and stress/strain data was computed. Mechanical properties like Young's modulus (the elastic modulus at high slope - post transition phase - linear portion of stress/strain curve) were evaluated³. For biophysical characterization FTIR spectroscopy and contact-angle studies were performed. Statistical differences (One-way ANOVA) considered significant if $p < 0,05$.



“An example of the combined nano/micro-fiber network form the combination CS and PCL”

RESULTS AND DISCUSSION

SEM observations showed a micro fibrous (2 μm) structure in PCL scaffolds and a combined nano/micro- (0.25-2 μm) arrangement in PCL/CS blend scaffolds. For a 0-30% strain range, Young's modulus showed a significant drop from $18,48 \pm 2,04$, $n=8$ MPa (PCL in TFE) to $4,80 \pm 1,84$ or $5,06 \pm 1,69$ ($n=8$) MPa (flow rates 1 & 1,5 ml/hr resp., PCL in AAC). For blended PCL+CS the modulus was lowered to $11,85 \pm 2,85$, $n=8$ MPa for TFE and $2,89 \pm 1,02$, $n=8$ MPa (1 ml/hr) for AAC, changed with increasing CS concentration. Hydrophilicity of the scaffolds was significantly higher with the addition of CS in the polymeric blend as the contact angle experiments showed.



“Difference in fiber diameter (mean \pm SDEV, $n=8$) between different process conditions during the PCL electrospinning process without and with the addition of CS. (FR: flow rate).”

CONCLUSION

From the obtained results it seems that the concentration of CS plays an important role in structural appearance of electrospun PCL fibers. A combination of small porous nanofibers with a greater porous microfibers arrangement was obtained in polymer blends, suitable for potential cell seeding. Elastic modulus of polymer blends, especially in higher CS concentration, was close to properties measured in soft cardiovascular tissues.

REFERENCES

1. Woodruff M.A. *et al.*, Progress in Polymer Science 35:1217-1256, 2010
2. Rinaudo M., Progress in Polymer Science 31:603-632, 2006
3. Mavrilas D. *et al.*, Journal of Biomechanics, 38:761-768, 2005

Biological interaction between a novel Sr-substituted bone cement and mesenchymal stem cells

M. Montesi¹, M. Dapporto¹, S. Panseri¹, S. Sprio¹, A. Tampieri¹

¹Institute of Science and Technology for Ceramics, National Research Council, Faenza (RA), Italy.
via Granarolo 64, 48018 Faenza (RA) Italy, phone: +39 0546699771
monica.montesi@istec.cnr.it

INTRODUCTION

Osteoporosis is a global public health problem currently affecting more than 200 million people worldwide. It is characterized by an imbalance in bone remodelling process, leads to progressive loss of bone mass and microarchitecture that increased fracture risk¹. Various therapies have been developed for the treatment of osteoporosis. Biphosphonates therapies and methyl methacrylate cements, used in advanced osteoporosis fractures, show several side effects and confine the problem without resolving it^{2,3}. A promising solution may be represented by the use of new strontium-substituted apatitic bone cements (Sr-BCs), endowed with ability to induce new bone formation, to be progressively resorbed and with sufficient mechanical strength for early physical stabilization of the defect. Such injectable devices can be integrated into the surrounding bone, due to its biomimetic and biodegradability characteristics, and can act as a local release system of Sr into the bone defect. Sr²⁺ has been shown to enhance the proliferation and differentiation of mesenchymal stem cell and pre-osteoblast into bone-forming osteoblast, with a mechanism probably involving membrane-bound calcium sensing receptor (CaSR)⁴.

The aims of this works were to investigate the biological interaction occurring between mouse mesenchymal stem cells (MSCs) and BCs substituted with two different concentration of Sr²⁺.

EXPERIMENTAL METHODS

Strontium (Sr)-substituted BCs powders with different strontium content (2% and 5% mol) were synthesized by solid state reaction of stoichiometric amounts of calcium carbonate, dicalcium phosphate dibasic anhydrous and strontium carbonate. The pure BC without Sr, was used as a control; the samples and control names are indicated in Table 1.

The powders were dry-mixed, thermally treated at 1400 °C for 1 hour and then rapidly quenched. The product was then milled and mixed with an appropriate amount of aqueous solution containing a natural polymer. Milling times and liquid-on-powder ratio (L/P) were optimized to obtain a final product in accordance with clinical needs.

Mouse mesenchymal stem cells (MSCs) were seeded at 1.5×10^4 cells/cm² on the top of the each cements and cultured for 24, 48, 72 hours, 7 and 14 days in osteogenic culture media. pH measurement of the culture media, cell viability and proliferation (MTT assay), cell morphology (Actin staining), and the expression of osteogenic related gene (qPCR) were investigate (Runx2, ALP and Col 15).

Name	Sr ²⁺ % mol
BC	0
Sr2%-BC	2
Sr5%-BC	5

Table 1 shows the name and composition of the samples tested,

RESULTS AND DISCUSSION

MSCs viability and proliferative potential were increased in the cells grown in direct contact with both Sr2%-BC and Sr5%-BC, compared to BC. These results were confirmed by the morphological evaluation indicating that, after 72 hours, cells were spread with good morphology and firmly attached to the BCs surface, without any differences among the samples.

Moreover, the evaluation of osteogenic related genes, after 7 days of culture, showed that Sr2%-BC increased significantly expression of Runx2 and ALP mRNA compared to the inductive effect exert by Sr5%-BC; both Sr2% and Sr5%-BCs strongly increased also Col15 mRNA respect to BC, after 7 days of culture (fold-change 3.1 and 2.4, respectively). These differences in mRNA levels disappear after 14 days.

CONCLUSION

The results obtained in this *in vitro* study, showed the positive influence of Sr²⁺ modification of bone cement on proliferation and osteogenic differentiation of MSCs. The combination of biomimetic characteristics of the bone cements with the inductive effect of Sr²⁺ open brilliant prospective for the *in vivo* use of this biomaterial as innovative strategy for the osteoporosis therapy.

REFERENCES

1. Gelinsky M. *et al.*, *Acta Biomaterialia* 9:9547-9557, 2013.
2. Rizzoli R. *et al.*, *Osteoporos Int.* 22(2):373-90, 2011
3. Stolz A. *et al.* *Mechanisms of Ageing and Development* 129:3,163–173, 2008
4. Bonnely E. *et al.*, *Bone* 42: 129-38, 2008.

ACKNOWLEDGMENTS

The research leading to these results has received funding from the European Union's Seventh Framework Programme ([FP7/2007-2013]) under grant agreement n° 246373, OPHIS.

In vitro study of the combined effect of hydroxyapatite nanoparticles and lactoferrin in bone homeostasis

Monica Montesi¹, Silvia Panseri¹, Michele Iafisco¹, Alessio Adamiano¹, Anna Tampieri¹

¹*Institute of Science and Technology for Ceramics, National Research Council, Faenza (RA), Italy.

* via Granarolo 64, 48018 Faenza (RA) Italy, phone: +39 0546699771

e-mail: monica.montesi@istec.cnr.it

INTRODUCTION

Lactoferrin (LF) is a bioactive glycoprotein that becomes recently interesting in field of bone biology for its modulatory effect on cells regulation to bone remodeling, that results compromised in some pathological conditions, as osteoporosis^{1,2}. We have already showed that the coupling of LF and HA leads to a combined effect in the induction of osteogenic differentiation of mesenchymal stem cells³.

On the basis of these evidences this study aims to combine LF with biomimetic hydroxyapatite (HA) nanocrystals, a bioactive material well known for its osteoconductive proprieties⁴, to study their combined effect as anabolic complex (HA-LF) on bone cells, and its modulatory effect on bone homeostasis.

EXPERIMENTAL METHODS

HA were functionalized by mixing (37°C, 24h) 50 mg with 7.5 ml of cow's milk LF solution at 0.5 mg/ml concentrations (HEPES buffer, pH 7.4). Murine pre-osteoblast cells line (MC3T3-E1) an murine osteoclast cells line (Raw 264.7) were cultured in presence of two concentration of HA with 6.6 wt% amounts of surface loaded LF (10 and 100 µg/ml); HA only, LF only at the same concentrations, and cells grown without material, were used as a controls. Histological analysis were done to evaluated cellular morphology and interaction with the conjugate HA-LF. Osteogenic differentiation of MC3T3-E1 was evaluated by mRNA analysis (qPCR). Cell viability and anti-apoptotic effect of HA-LF on MC3T3-E1 were evaluated by Live&Dead assay and nuclear fragmentation analysis. TRAP staining was used to detect the inhibitory effect of the conjugate on the osteoclastogenesis.

RESULTS AND DISCUSSION

No differences in cellular morphology and spreading were detected among all the samples tested. Gene expression analysis showed that HA-LF exerts its inductive effect in pre-osteoblast differentiation, as indicated by the increasing in OSTERIX and IBSP mRNA. The pre-osteoblast viability seems to be not compromised by the presence of HA-LF in the osteoblast culture; besides, the nuclear fragmentation analysis showed an inhibition of apoptosis induced by HA-LF conjugate. Preliminary results on the

inhibition of osteoclastogenesis, detected by TRAP staining, showed also a weak effect exert by HA-LF conjugate.

CONCLUSION

The promising *in vitro* results obtained in this work showed that the coupling of LF and HA leads to a combined effect in the modulation of bone cells. The possibility to combine the unique features of HA and LF in a complex, that not only maintains their individual stimuli, but enhances the anabolic bone activity, opens future prospects in the use of this functionalized material in bone tissue engineering and regenerative medicine.

REFERENCES

1. Amini AA. *et al.*, Tissue Eng Part A. 19(9-10):1047-55, 2013.
2. Goncalves MJ *et al.*, Acta Med Port. 26(4):445-455, 2013.
3. Montesi M. *et al.*, J Biomed Mater Res A. doi: 10.1002/jbm.a.35170, 2014.
4. Iafisco M. *et al.*, Dalton Trans 40(4):820-7, 2011.

ACKNOWLEDGMENTS

The authors would like to thank PNR-CNR Aging Program 2012-2014 for providing financial support to this project.

DISCLOSURES

The authors declare no conflict of interest.



Fabrication of De-epithelialized Amniotic Membrane/Silk Nanofibre Scaffolds for Skin Tissue Engineering

Shaghayegh Arasteh¹, Somaieh Kazemnejad¹, Mohammad Mehdi Akhondi¹, Hamed Heidari-Vala¹, Afsaneh Mohammadzadeh², **Sahba Mobini***¹

¹Reproductive Biotechnology Research Centre, Avicenna Research Institute, ACECR, Iran

²Reproductive Immunology Research Centre, Avicenna Research Institute, ACECR, Iran

*sahba.mobini@gmail.com

INTRODUCTION

Irreversible or extensive damages to skin impair skin functions which might even lead to death¹. Human amniotic membrane (AM) has been widely used as wound dressing. In spite of all attributes, AM suffers from inferior mechanical strength² and enzymatic digestion²⁻³. Electrospun silk fibroin nanofibres⁴ have the potential to biomimic the microstructure of natural extracellular matrix (ECM) of skin. Surface modification through plasma treatment has been attempted to enhance cell adhesion⁵. In this study we have introduced a novel scaffold aiming to regenerate ECM of skin tissue which has been fabricated through coating de-epithelialised AM (DA) with electrospun silk fibroin nanofibres (DAF) followed by surface plasma treatment (DAFP). Subsequently, scaffolds were fully characterized.

EXPERIMENTAL METHODS

Scaffold Fabrication: After procurement of AM, the spongy layer was removed avoiding inconsistencies in clinical outcomes⁶ and de-epithelisation was carried out⁷ through optimised method. Next, AMs were freeze-dried for convenient use. Fibroin extracted from silkworm cocoons⁸ was dissolved in formic acid (20% wt.v⁻¹). The solution was electrospun at a rate of 0.2 ml·min⁻¹ in an electric field generated by 20 kV. At a tip-to-collector distance of 80mm, nanofibres were collected on the basement membrane side of de-epithelialized AMs (1500 rpm). For plasma treatment, specimens were put on the electrode within reactor chamber. After chamber evacuation, the pressure was stabilised at 70 mTorr and by controlling the electrical power of 30 W at 13.56 MHz radio frequency, specimens were exposed to oxygen plasma for 2 min.

Characterisation: To assess cell denudation, AM and DA were stained histologically with H&E. Tissue continuity was evaluated by fibronectin immunofluorescent staining. The microstructure of electrospun fibres was visualised using Scanning Electron Microscope (SEM). Mechanical strength of HAMs before and after cell denudation and coating with nanofibres was investigated using a Santa Mechanical Testing Device. Water contact angle on surface of specimen was measured using Sessile Droplet Method. Proliferation of mouse embryonic fibroblast (MEF) on DA was studied for 14 days *in vitro*.

RESULTS AND DISCUSSION

Histological characterisation and immunohistochemical localisation of fibronectin is demonstrated in Figure 1. Bead-free silk fibroin nanofibres were obtained (Figure 2) with the mean diameter of 249±116 nm.

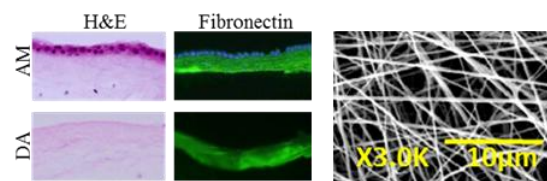


Figure 1 Amnion Characterisation

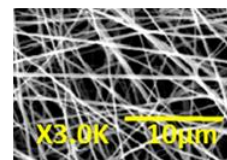


Figure 2 Electrospun fibres

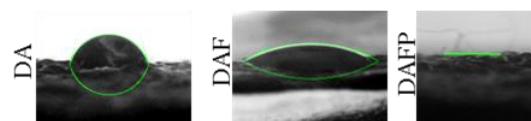


Figure 3 Water contact angle measurements

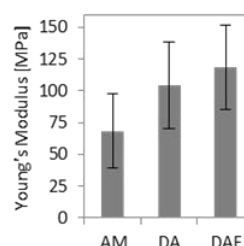


Figure 4 Mechanical Evaluation

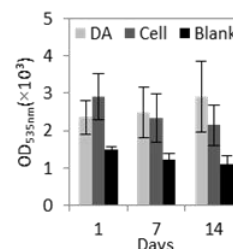


Figure 5 In vitro studies

Contact angle decreased from 68.5±5.8 to 26.3±6.4 after coating with nanofibres and reached zero value after oxygen plasma treatment (Figure 3), representing a rise in hydrophilicity of scaffolds. Mechanical evaluation of DAF showed significant enhancement in terms of Young's Modulus (Figure 4). *In vitro* study of MEF cells cultivation on DA revealed that processed amniotic membrane remarkably supported the cell proliferation (Figure 5).

CONCLUSION

The de-epithelialised AM/silk nanofibres scaffold exhibited promising mechanical properties and water permeability. Ongoing studies focus now on the evaluation of these novel scaffolds in an *in vivo* model as wound dressing.

REFERENCES

1. Zhong S.P. *et al.* Wiley Interdiscip Rev Nanomed Nanobiotechnol 2:510-525, 2010
2. Ma D.H.-K. *et al.* Biomaterials 31:6647-6658, 2010
3. Koizumi N. *et al.*, Invest. Ophthalmol. Vis. Sci. 41:2506-2513, 2000
4. Reddy J. *et al.* Wound Repair Regen 21:1-16, 2013
5. Jeong L. *et al.*, Int. J. Biol. Macromol. 44:222-228, 2009
6. Dua H. son. Google Patents 2006
7. Hopkinson A. *et al.*, Tissue Eng Part C Methods. 14:371-381, 2008
8. Mobini S. *et al.*, J. Biomed. Mater. Res. A. 101:2392-2404, 2013

Bioprinting of vasculature at cell-compatible conditions

Jing Yang¹(jing.yang@nottingham.ac.uk), Kevin Shakesheff¹

¹ Division of Drug Delivery and Tissue Engineering, School of Pharmacy, The University of Nottingham, UK

INTRODUCTION: Metabolically active tissues must reside within 200 μm of a capillary lumen to gain sufficient oxygen and nutrients for survival. Incorporation of a perfusing blood supply in tissue engineering design is vital for the scalability, survival and integration of almost all tissues with the exception of a few poorly vascularised tissues such as skin epidermis and cartilage. Delivery of angiogenic growth factors, genes and regenerative cell types as well as combination therapies have been employed to promote vascularisation. However, the integration of these engineered tissues with the host remains a monumental challenge. To meet this challenge, the establishment of functional vasculature in engineered tissue constructs is likely to be required before transplantation. To this end, a recent research highlight has been the use of a sacrificial lattice of carbohydrate fibres to fabricate vascular-like tubule networks.¹ Here, we demonstrate a novel method for engineering vascularised tissues using 3D printing. A construct with an embedded tubule network in a hydrogel matrix has been successfully printed at cell-compatible conditions. The tubule network was then perfused with endothelial cells to form vasculatures.

METHODS: A Fab@HomeTM printer was used to print the tubule network and the hydrogels. To form tubule network, a thermo-responsive material and alginate were printed into a pre-designed structure. The printed network was then dissolved away at physiological conditions to form tubes which were later perfused with endothelial cells. In addition, human umbilical vein endothelial cells (HUVECs) were mixed in Matrigel, and printed into a network within alginate. Cells were labelled by live/dead fluorescent stains or labelled by a red cell tracker, and imaged using a fluorescent microscope.

RESULTS: HUVECs after 8-days culture were labelled with live/dead fluorescent stains (Figure 1). A tubule network facilitating the perfusion of HUVECs was printed within alginate (Figure 2).

CONCLUSIONS: The method reported here allows the fabrication of a vascular network at physiological

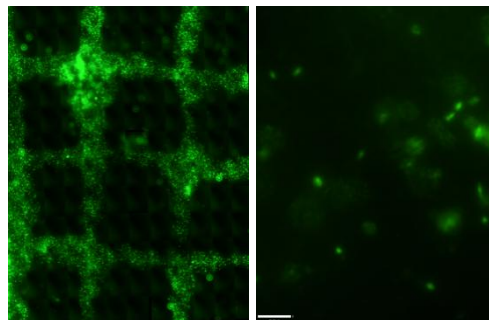


Figure 1 A stitched image of a printed network with HUVECs embedded in Matrigel (Left). An image of encapsulated HUVECs showing spreading of some cells (Right).

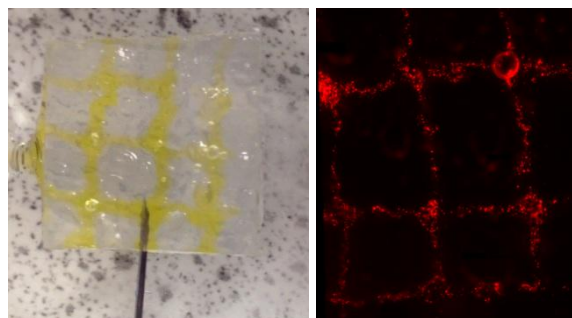


Figure 2 Images of tubule networks embedded in a hydrogel perfused with a protein solution (Left) and HUVECs (Right)

conditions, which is an advance compared to methods in which materials are printed at elevated temperatures unsuitable for cells and biomolecules. The cell-compatible printing environment permits the patterning of the tubule networks which mimic blood vessels, biomolecules and multiple cell types in a single printing process. Future work will look to improve, measure and validate the architecture and function of the engineered vasculature.

ACKNOWLEDGEMENTS: The authors would like to thank the Nottingham Research Fellowship scheme and the ERC Advanced Grant (227845) for supporting this work.

REFERENCES: ¹ Miller, et al (2012) *Nat Mater* 11:768-774.

Creating albumin-binding nanostructured surfaces using a thrombin-inhibiting peptide

Sidónio C. Freitas^{1,2,3}, Sílvia Maia⁴, Ana C. Figueiredo⁵, Paula Gomes⁴, Pedro J.B. Pereira⁵, Mário A. Barbosa^{1,6},
M. Cristina L. Martins^{1,6}

¹INEB-Instituto de Engenharia Biomédica, Universidade do Porto, Portugal

²Universidade do Porto, Faculdade de Engenharia, Portugal;

³Universidad Cooperativa de Colombia, Facultad de Odontología, Medellín, Colombia.

⁴CIQ-UP – Departamento de Química e Bioquímica, Faculdade de Ciências, Universidade do Porto, Portugal

⁵IBMC – Instituto de Biologia Molecular e Celular, Universidade do Porto, Portugal;

⁶Universidade do Porto, Instituto de Ciências Biomédicas Abel Salazar, Portugal; cmartins@ineb.up.pt

INTRODUCTION

Failure of some blood-contacting medical devices has been associated with thrombus formation initiated by the adsorption of certain blood proteins onto the biomaterial surface. This protein layer can induce complex and interlinked processes, such as activation of the intrinsic coagulation system and adhesion and activation of platelets¹. Biomaterial haemocompatibility can be improved by coating its surface with antithrombotic agents² or with compounds that can adsorb albumin from blood plasma in a selective and reversible way, since this protein is not involved in the coagulation cascade and in platelet adhesion/activation³. This work reports that the immobilization of the thrombin inhibitor D-Phe-Pro-D-Arg-D-Thr-CONH₂ (fPrt)⁴ onto nanostructured surfaces (self-assembled monolayers - SAM) induces selective and reversible adsorption of albumin, delaying the clotting time when compared to peptide-free surfaces.

EXPERIMENTAL METHODS

Peptide: fPrt was synthesized with two glycine residues attached to the *N*-terminus (GGfPrt) to improve its exposure from the surface.

SAMs: Pure solutions of (1-Mercapto-11-undecyl) tri(ethylene glycol) (EG3) and (1-Mercapto-11-undecyl) hexa(ethylene glycol) carboxylic acid (EG6-COOH) were prepared at a concentration of 2 mM in absolute ethanol. Mixtures of EG3 and EG6-COOH-thiols were obtained by mixing the pure solutions in different ratios at final concentrations of 1 mM.

GGfPrt immobilization: SAMs were immersed in a freshly prepared solution of NHS (*N*-hydroxysuccinimide) and EDC (1-(3-dimethylamino-propyl)-*N*-ethylcarbodiimide hydrochloride) at a final concentration of 0.05 and 0.20 M, respectively. NHS-activated SAM were immersed in GGfPrt solution (1 mM) prepared in sodium phosphate buffer (25 mM, pH 8.0) for 24 h at RT and 100 rpm. As control, the same reaction was performed without the peptide. SAM were washed with Milli-Q water and preserved under Argon.

SAMs were characterized by ellipsometry, infrared reflection absorption spectroscopy (IRRAS) and X-ray photoelectron spectroscopy (XPS). Protein adsorption was followed using ¹²⁵I-labelled proteins. The effect of GGfPrt on thrombin proteolytic activity was evaluated by assessing the protease ability to cleave *N*-p-tosyl-Gly Pro-Arg-p-nitranilide and fibrinogen in solution. The anticlotting capacity of the surfaces was evaluated using the recalcified plasma clotting assay.

RESULTS AND DISCUSSION

In solution, GGfPrt was able to inactivate the enzymatic activity of thrombin and to delay plasma clotting time in a concentration-dependent way. After surface immobilization, and independently of its concentration, GGfPrt lost its selectivity to thrombin and its capacity to inhibit thrombin enzymatic activity against the chromogenic substrate. In contrast, immobilized GGfPrt was able to adsorb albumin from plasma in a selective and reversible way (Fig.1).

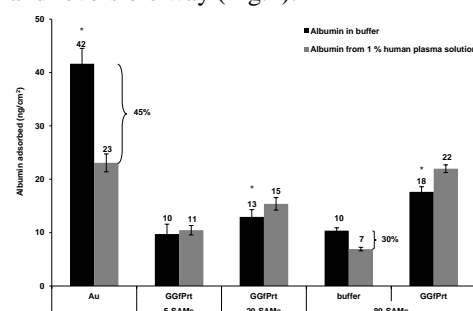


Fig.1. ¹²⁵I-Labelled human albumin adsorption on different surfaces from pure albumin solution and from 1% human plasma. The percentages designate the reduction of adsorbed albumin due to the presence of plasma proteins.

Surfaces with low concentrations of GGfPrt could delay the capacity of adsorbed thrombin to cleave fibrinogen, but high GGfPrt concentrations induced the procoagulant activity of the adsorbed enzyme. However, all GGfPrt-coated surfaces had a plasma clotting time similar to the negative control (empty polystyrene wells), showing resistance to coagulation, which is explained by their capacity to adsorb albumin in a selective and reversible way.

CONCLUSION

Immobilized GGfPrt avoided the coagulation activation induced by GGfPrt-free SAMs, due to the adsorption of albumin in a selective and reversible way. This work opens new outlooks to improve the haemocompatibility of biomaterials.

REFERENCES

1. Gorbet MB et al., Biomaterials. 25:5681-703,2004.
2. Freitas SC et al., Biomaterials. 31:3772-80, 2010
3. Gonçalves IC, et al., Biomaterials, 30:5541-51,2009.
4. Figueiredo AC et al. PLoS One 7:e34354,2012

ACKNOWLEDGMENTS:

PEst-C/SAU/LA0002/2013, PEst-C/QUI/UI0081/2011 and SFRH/BD/40537/2007



Electrochemical deposition of calcium phosphate coatings on Ti6Al4V substrate

Richard Drevet, Nader Ben Jaber, Ahmed Tara, Joël Faure And Hicham Benhayoune

LISM EA 4695, Université de Reims Champagne-Ardenne, France, richard.drevet@univ-reims.fr

INTRODUCTION

Titanium and its alloys are widely used as implant materials in orthopaedic surgery because of their good biocompatibility with bone. However, a way to make them bioactive is to coat them with calcium phosphate ceramics which are able to form a real bond with the surrounding bone tissue *in vivo*. In our laboratory, we are developing an innovative process to produce prosthetic calcium phosphate coatings: electrodeposition¹⁻³.

EXPERIMENTAL METHODS

Electrodeposition is carried out by using a three-electrodes system (the cathode (Ti6Al4V substrate), the counter electrode and the reference electrode, immersed in an electrolyte prepared by dissolving 0.042 M $\text{Ca}(\text{NO}_3)_2 \cdot 4\text{H}_2\text{O}$ and 0.025 M $\text{NH}_4(\text{H}_2\text{PO}_4)$). We are also developing an original electrodeposition protocol which combines pulsed current mode and the incorporation of hydrogen peroxide (H_2O_2) into the electrolytic solution.

The morphology of the coatings is observed with a LaB6 electron microscope (SEM JEOL JSM-5400LV) operating at 0-30 kV associated to an ultrathin window Si(Li) detector for X-ray measurements (GENESIS, Eloïse SARL, France) and by a standardized method based on XRD (Bruker D8 Advance using a $\text{Cu}_{K\alpha}$ radiation), determining the characteristic Ca/P atomic ratio of these coatings. Moreover, the thermal treatment of the material is optimized under controlled atmosphere to improve the mechanic properties of the coatings and to obtain an appropriate value of their adhesion to the metallic substrate.

On the other hand, the bioactivity of the elaborated coatings is evaluated in a physiological environment by studying firstly their corrosion behaviour (polarization curves and impedance spectroscopy) and secondly by studying the dissolution-precipitation reactions that occur during a prolonged immersion.

Finally, the flexibility of the electrodeposition process is used to uniformly incorporate strontium (an active agent) in the calcium phosphate coating.

RESULTS AND DISCUSSION

The original electrodeposition protocol developed leads to homogeneous and compact calcium phosphate coatings whose chemical composition is controlled. They may consist of a calcium-deficient hydroxyapatite with a variable deficit or of a stoichiometric hydroxyapatite.

After prolonged immersion in physiological solution, we observed the formation of a “bone-like” apatite layer on the surface of the electrodeposited coating.

In the case of calcium phosphate coatings electrodeposited with strontium, we have observed that the incorporation of this element in the coating modifies the proportion of the phases that compose the coating after a suitable thermal treatment.

The elaboration protocol developed allows the modulation of the different behaviours in physiological medium (kinetic of the bone-like layer formation, strontium release in the physiological environment).

CONCLUSION

In this work, we succeeded the synthesis of calcium phosphate coatings by pulsed electrodeposition. The effects of hydrogen peroxide on the stoichiometry of the coating have been demonstrated. The behaviour of the coating in physiological medium has been studied by corrosion tests and by observing the formation of a bone-like layer on the implant surface.

Finally, the original protocol has been used to produce coatings that contain a doping element (strontium) whose release in physiological environment is controlled by the parameters used during the electrodeposition protocol.

REFERENCES

1. Drevet R. *et al.*, Mater. Charact. 61:786-795, 2010
2. Drevet R. *et al.*, J. Mater. Sci.: Mater. in Med. 22(4):753-761, 2011.
3. Drevet R. *et al.*, Mater. Sci. and Eng. C 33:4260-4265, 2013.

Soft-matrices based on keratin/alginate for regenerative medicine

Raquel Silva¹, Raminder Singh^{2,3}, Bapi Sarker¹, Judith A. Roether⁴, Iwona Cicha^{2,3}, Joachim Kaschta⁴, Dirk W. Schubert⁴, Rainer Detsch¹, and Aldo R. Boccaccini^{1*}

^{1*}Department Materials Science and Engineering/Institute of Biomaterials, University of Erlangen-Nuremberg, Germany, aldo.boccaccini@ww.uni-erlangen.de

²Laboratory of Molecular Cardiology/Medical Clinic 2, University Hospital Erlangen, Germany

³Cardiovascular Nanomedicine Unit/ Experimental Oncology and Nanomedicine University Hospital Erlangen, Germany

⁴Department of Materials Science and Engineering/Institute for Polymer Materials, University of Erlangen-Nuremberg, Germany

INTRODUCTION

Hydrogels from naturally occurring polymers are widely used due to their unique properties, especially regarding the cell environment and morphology similar to the extracellular matrix (ECM) of native tissues.¹ Our aim was to blend alginate (Alg) with keratin (K) extracted from wool. The self-assembly properties of K, and its ability to mimic the ECM were combined with the excellent chemical and mechanical stability and biocompatibility of Alg to produce hybrid hydrogels. The synergistic effects of each blend component were analysed using different techniques. Furthermore, the cell-material interaction was assessed by primary human umbilical vein endothelial cells (HUVECs).

EXPERIMENTAL METHODS

Preparation of hybrid hydrogels

K was previously extracted from merino wool using a reductive treatment. To obtain the hybrid hydrogels, Alg (2%, w/v) was mixed with K (1%, w/v) to prepare blends of 50/50. The hydrogels were obtained by ultrasound treatment under specific conditions.²

Physico-chemical characterization

To study the water uptake (WA), the weight loss (WL), as well as protein release (PR), the blends were immersed in HBSS and DMEM, over 21 days (d). The mechanical properties were performed over time using the dynamical mechanical thermal analysis (DMTA). Measurements were recorded in triplicate.

Cell-material interaction

HUVECs were isolated from freshly collected umbilical cords. 3×10^5 cells/film were seeded onto hydrogels. The culture medium was changed on the day after seeding, and then every 3d. Mitochondrial activity was assessed using the WST-8 assay kit. The viability of cells was determined by live staining with Calcein, AM and the nuclei were visualized by DAPI after 10d.

RESULTS AND DISCUSSION

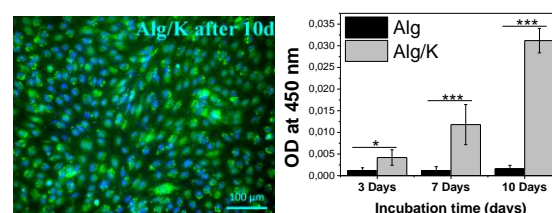
The physico-chemical characterization of hybrid hydrogels was performed in HBSS or DMEM medium. The addition of K protein leads to a decrease of the amount of WA in the presence of either HBSS or DMEM. This fact can be attributed to the diffusion of water inside the network, which decreases due to the electrostatic and hydrophobic interactions that occur between the K chains and also with Alg molecules. The WL of hybrid hydrogels was lower as compared with Alg. This fact can be related to the sonication treatment: The ultrasound induces the degradation of polysaccharides producing fragments with lower

molecular weight that lead to a decreased stability of the hydrogels.

Table1: Physico-chemical characterization

Material		WA after 3d (%)	WL after 21d (%)	PR after 21d (%)
Alg	HBSS	3372±70	53±9	---
	DMEM	3554±80	57±5	---
Alg/K	HBSS	2269±23	28±6	8±0.9
	DMEM	2288±31	35±2	12±1

Regarding the PR, the amount of protein released over time is low, indicating that a significant quantity of K remained in the material that could enhance cell-material interactions. The DMTA analysis demonstrated a small increase in storage modulus (E') with the increase of frequency and revealed that the blend with K promotes an increase of E' from ≈ 100 to ≈ 400 kPa (evaluated to 10 Hz), indicating that the addition of K increases material stiffness. To investigate the cell-material interactions, the attachment and growth, as well as cell morphology and mitochondrial activity of HUVECs were analysed. The results demonstrated that the cells seeded on the surface of Alg/K hydrogels have a significant increase in mitochondrial activity, and form monolayer, demonstrating the typical cobblestone-like endothelial morphology after 10d of culture.



CONCLUSION

The hydrogels were successfully produced and an extensive physico-chemical characterization was carried out. The cell-material interaction demonstrated that the Alg/K supported cell attachment, spreading and proliferation. Thus, the developed hybrid hydrogels represent a promising candidate biomaterial for tissue engineering and regenerative medicine.

REFERENCES

1. Peppas NA. *et al.*, Adv. Mater. 18: 1345-1360, 2006
2. Silva R. *et al.*, Ultrason. Sonochem. 17: 628-32, 2010

ACKNOWLEDGMENTS

The authors thank the “Emerging fields Initiative” (TOPbiomat) of the University of Erlangen, for financial support.

***In Vitro* Evaluation of Nanohydroxyapatite Biocompatibility in 2D vs 3D Cell Culture Systems**

Aileen Crawford¹, Abigail Pinnock¹, Veronika Hruschka², Heinz Redl², Paul V Hatton¹, Cheryl A Miller¹

¹Bioengineering & Health Technologies Research Group, School of Clinical Dentistry, University of Sheffield, UK

²Ludwig Boltzmann Institute for Experimental and Clinical Traumatology, AUVA Research Centre/Austrian Cluster for Tissue Regeneration, Austria

a.crawford@sheffield.ac.uk

INTRODUCTION

Classical monolayer culture systems are regularly used to determine *in vitro* biocompatibility and mechanism of action of biomaterials and pharmacological agents. However, it is well known that in 2-dimensional (2D) cell culture, primary cells may not fully retain or express the same cell phenotype and biological responses observed in the native tissues. Hence, 2D systems may not truly reflect the *in vivo* activity of a test compound. In contrast, in 3-dimensional (3D) culture systems usually promote retention or permit re-differentiation of the cultured cells and should therefore be more reflective of the native tissue. Nanohydroxyapatite (nHA) pastes have promise as agents for bone augmentation *in vivo*^{1,2}. Therefore, the aim of this study was to compare the biocompatibility of nHA pastes using human bone-derived cells (osteoblastic cell lines, primary osteoblasts) and bone marrow-derived mesenchymal stem cells (MSCs) in 2D and 3D cell culture systems.

EXPERIMENTAL METHODS

Cells: human MSCs and human primary osteoblasts (HOBs) were purchased from Promocell Ltd. The human osteoblastic cell lines Saso2 and MG63 were obtained from Sigma Aldrich.

Cell cultures: 2D cultures: 5×10^4 cells/well were added to 24-well plates and incubated for 48h with nHA pastes [BP1, BP2, OP2a, OP2b (particle sizes 60-70nm) and an injectable, commercially available nHA bone graft material]. For 3D cultures, 2×10^6 MSCs or osteoblastic cells were seeded onto polyglycolic acid (PGA) discs 5mm x 2mm for 72h before incubation with the nHA pastes for 48h.

Assays: Viability of the cell cultures was assessed by measuring reduction of resazurin dye to resorufin using PrestoBlue (Invitrogen). Cellstain (Sigma Aldrich) was used to visualise live and dead cells. Potential cellular uptake of nHA was investigated by transmission electron microscopy (TEM) after exposure of cells to nHA.

RESULTS AND DISCUSSION

Exposure of all cell types to all the nHA pastes (including the commercial nHA graft material) caused a reduction in cell viability which was particularly marked in the 2D cell cultures [For example, cell activity in the presence of BP1 was $29.2 \pm 6.3\%$ (HOB) $16.1 \pm 5.8\%$ (MSCs) $72.9 \pm 29.3\%$ (MG63) and $23.0 \pm 7.0\%$ (Saso-2) of the control values]. The nHAs did not cause any changes in pH or osmolarity of the culture media. Prewashing the nHA pastes did reduce

this apparent toxicity. 3D cultures showed a lower impact of nHA on the cell viability of the cells (For example: MG63 and MSCs exposed to BP1 showed 70-90% cellular activity compared to controls). TEM showed numerous nanoparticles in the cytoplasm of the cultured cells (Figure 1)

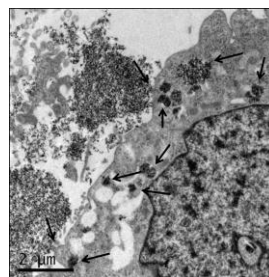


Figure 1: TEM image showing hydroxyapatite nanoparticles in the cell after exposure of MG63 cells to BP1. Arrows indicate location of the nanoparticles.

2D cultures exhibited greater toxic effects of the nHA pastes than 3D cell cultures. This may be because of the greater numbers of cells used in 3D models compared to 2D and their phenotype is more reflective of the *in vivo* environment. Interestingly, MSCs and the more mature osteoblastic phenotype (HOB, Saos-2) were more sensitive to the nHA than cells with a more immature osteoblastic phenotype (MG63). The mechanism of the apparent toxicity of the nHAs is unknown but is likely to be a result of the cellular uptake of nanoparticles released by the nHA pastes.

CONCLUSION

We conclude that 3D culture systems may be preferable for the study of *in vitro* biocompatibility of nanoscale materials as they may be more reflective of the reported *in vivo* activities of nHAs^{1,2}.

REFERENCES

¹. Canuto RA *et al* Clin Oral Impl Res 24: (suppl A100), 442-48. 2013. ²Brandt J *et al*. J Mater Sci:Mater Med 21:283-294. 2010.

ACKNOWLEDGMENTS

We are grateful to other consortium members, Ceramisys Ltd, Fluidinova SA and Primequal SA. The research leading to these results has received funding from the European Union's Seventh Framework Programme managed by REA-Research Executive Agency. <http://ec.europa.eu/research/rea> (FP7-SME-2012) under grant agreement n°3156.



Engineering of Staple Electrospun Fibres for Biodegradable Nanocomposites by Particle Enhanced Ultrasonication

E. Mulky^{1,2}, G. Yazgan^{2,3}, K. Maniura-Weber², R. Luginbuehl¹, G. Fortunato³, A. M. Buehlmann-Popa³

¹ Chemistry & Biology, RMS Foundation, Switzerland, elias.mulky@rms-foundation.ch

² Laboratory for Materials-Biology Interactions, Empa, Swiss Federal Laboratories for Materials Science and Technology, Switzerland

³ Laboratory for Protection and Physiology, Empa, Swiss Federal Laboratories for Materials Science and Technology, Switzerland

INTRODUCTION

Staple fibres are added to polymeric materials and cement-based matrices to engineer fibre reinforced composites (FRC) that have superior mechanical properties as compared to pure matrix materials. In the sub-micro- and nano-meter regime, To obtain fibres in the micron- to nanoscale range E-spinning is the method of choice a process that typically yields continuous, oriented or randomly aligned, fibre non-wovens. Therefore, subsequent processing steps are required to cut¹ and unbundle aggregates into free-standing staple fibres of desired length, which can be further dispersed into relevant polymer or inorganic matrices. The goal of the present work was to demonstrate the potential of particle-assisted ultrasonication² to engineer submicron- to nano-metre diameter staple fibres from biopolymers such as PLLA, without any additional chemical pre- or post-treatments. The staple fibres/nanoparticle dispersions were then used to fabricate calcium phosphate-based cements that can be used as bone substitute material.

EXPERIMENTAL METHODS

Bioabsorbable Poly-L-Lactic Acid (PLLA) was electrospun from a solution of 5% (w/w) PLLA in chloroform : DMF : formic acid (8:1:1 w/w). The obtained fibres were further ultrasonicated at low temperatures in the presence of Hydroxyapatite nanoparticles in order to obtain fibres with small aspect ratios. The influence of the dispersion medium, the sonication bath temperature and time on the respective length distribution of the obtained nanofibres was investigated. To manufacture the cement, one part of the resulting particle/fiber precursor was mixed with two parts (w/w) 2.6 M aqueous solution of monocalciumphosphate monohydrate and allowed to react in a cement reaction and allowed to set and harden for 72h.

RESULTS AND DISCUSSION

Electrospinning yielded continuous fibres with diameters in the range of 244 ± 78 nm. The sonication resulted in separation of the fibres and a homogeneous dispersion within the HA particle matrix (Fig. 1a). The resulting staple lengths were in the range between 60 μ m and 39 μ m depending on the bath temperature. With lower bath temperatures shorter fibres were obtained with narrower distributions (Fig. 1b). The resulting set bone void filler composed of Brushite and 5% (v/v) PLLA fibres exhibited an approximately 90% increase

in compressive strength when compared to non-reinforced control cement.

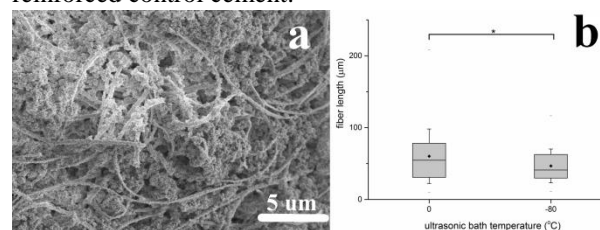


Figure 1: a) SEM micrograph showing staple PLLA fibres sonicated together with HA nanoparticle agglomerates. b) Box plot showing lower temperatures yielding shorter staples fibres with narrower length distributions.

CONCLUSION

Staple PLLA nanofibres were produced by electrospinning and subsequent sonication at low temperatures. Lower temperatures resulted in shorter fibres and narrower length distributions. Increased sonication time resulted in an asymptotic decrease of fibre length and a narrowing of fibre length distribution. The addition of nanoparticles reduced the efficiency of the fragmentation process and fibres with higher average lengths were obtained. Particle-assisted sonication allowed a good distribution of the particles between the nanofibres. This effect further allowed the homogeneous dispersion of the fibre-particle precursor within a HA-based matrix, making the technique suitable for the fabrication of fibre-reinforced cements, demonstrated in this work by successful production of a PLLA-Brushite composite cement with high compression fracture strength. The method presented is thus a promising technique for the fabrication of FRCs with very good mechanical properties, which can be further integrated in biomedical products.

REFERENCES

1. Sawawi, M., et al., Polymer, 4237-4252, 16, 2013
2. Perelshtein, I., et al., ACS, 1999-2004, 7, 2010

ACKNOWLEDGMENTS

This work was funded by the Swiss National Research Programme "Opportunities and Risks of Nanomaterials" NRP 64, grant no. 406440_131273. The authors would like to thank Jeannine Krieg and Philippe Däster from RMS Foundation for conducting the particle size and fracture test measurements.

Electrochemically grown mesoporous titania layers

Sureeporn Uttiya¹, Daniele Contarino¹, Sonja Prandi², Maria Maddalena Carmasciali³, Ranieri Rolandi¹, Maurizio Canepa¹, Ornella Cavalleri¹

¹Department of Physics, University of Genova, Italy

^{2*} ARPAL, Department of Genova, Italy

³ Department of Chemistry and Industrial Chemistry, University of Genova, Italy
cavalleri@fisica.unige.it

INTRODUCTION

Titanium is a key material for biomaterial applications. Its resistance to corrosion due to the presence of a stable oxide layer and its good mechanical properties make titanium an ideal material for the development of dental and orthopaedic implants as well as for the design of drug delivery devices^{1,2}. With the aim of developing implantable devices an accurate control of the surface device is needed since the surface structural properties modulate the bio-integration process. Recently, large attention has indeed been focussed on the growth and characterization of titanium dioxide layers^{3,4}. In this study we investigate the structural properties of titania mesoporous layers grown by anodic oxidation in order to correlate the growth conditions with the resulting surface layer structure.

EXPERIMENTAL METHODS

Mechanically polished titanium sheets were electrochemical oxidized by: i) anodic spark deposition (ASD) in 1M H₂SO₄ or 1.5 M H₃PO₄ for 1 min at voltages ranging from 70 V to 150 V; ii) anodization in 1M H₂SO₄/0.5%wt HF for 20 min at 20V. Oxidized samples were thoroughly rinsed with Milli-Q water and dried.

Titania surfaces were analysed by Tapping Mode Atomic Force Microscopy (TM-AFM), Scanning Electron Microscopy (SEM) and Raman Spectroscopy (RS).

RESULTS AND DISCUSSION

Titania layers grown by ASD in both H₂SO₄ or H₃PO₄ solutions are characterized by a mesoporous structure. Typical SEM and AFM images of this typology of samples are reported in Fig. 1a and b.

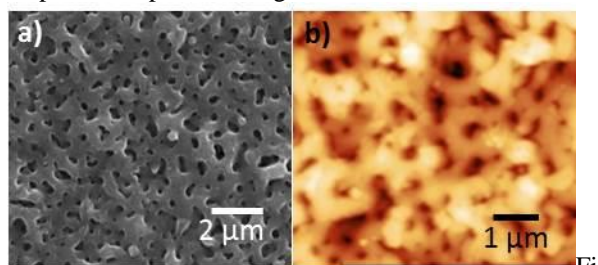


Fig. 1. a) SEM image and b) AFM image of a TiO₂ surface prepared by ASD in 1M H₂SO₄.

The typical pore diameter varies from 100 nm up to 400 nm when the anodization potential is increased from 70 V to 150 V.

Titania layers grown by anodic oxidation in H₂SO₄/HF solution are characterized by a nanotubular structure as shown in Fig. 2.

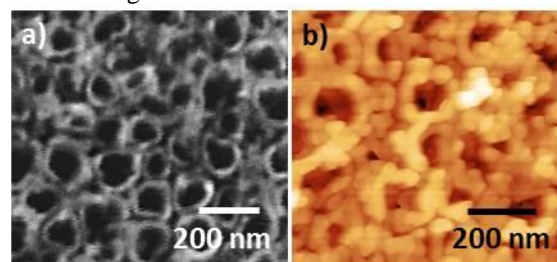


Fig. 2. a) SEM image and b) AFM image of a TiO₂ surface prepared by anodic oxidation in H₂SO₄/HF solution.

Nanotubes are found to have an average inner diameter of about 80 nm and an average wall thickness of about 30 nm.

Raman spectroscopy measurements on the TiO₂ surface indicate the ASD grown oxide layers are characterised by the anatase phase.

CONCLUSION

We investigated the influence of the anodic oxidation conditions on the structural properties of the resulting TiO₂ layers. The possibility of tailoring the TiO₂ surface structure makes this system interesting for biomaterial development.

REFERENCES

1. D.M. Brunette *et al.* Eds, Titanium in Medicine, Springer-Verlag, Berlin Heidelberg GmbH, 2001
2. M.S. Aw *et al.*, Chem. Commun., 48:3348–3350, 2012
3. R. Zhang *et al.*, NanoToday, 7:344-366, 2012
4. S. Tanaka *et al.*, ACS Appl. Mater. Interf., 5:3340-3347

ACKNOWLEDGMENTS

The authors would like to thank Dr. M. Salerno (IIT, Genova) and Dr. A. Barbucci (DICCA, Genoa University) for helpful discussions.

Characterisation of DNA Interactions with Cationic Polymer Brush

Mahentha Krishnamoorthy* and Julien Gautrot

School of Engineering & Materials Science, Queen Mary, University of London, UK

*m.krishnamoorthy@qmul.ac.uk

INTRODUCTION

Polymeric nanoparticles adsorb or encapsulate oligonucleotides/gene and act as sustained release matrices for genetic drugs. Poly (2-(dimethylamino) ethyl methacrylate), PDMAEMA, is a cationic polymer known for its efficiency in gene transfection as a non-viral gene delivery vector¹. It has the ability to condense DNA and form complexes to allow efficient uptake via endocytosis. However, the homopolymer's high cytotoxicity prevents it from being used in gene therapy. The physicochemical properties of the vector is crucial for controlling gene delivery as is indicated by several independent reports however there isn't one system that allows the control of all these parameters hence the focus of this work is to develop such a system.

EXPERIMENTAL METHODS

We developed a cationic system, using surface-initiated polymerisation, to understand and control the physicochemical properties (chemistry, charge, architecture, size & shape) and biopharmaceutical behaviour of the gene delivery agent, and its interaction with cells.

DNA interaction studies were performed to characterise the particle-DNA complexes formed at various N/P ratios via dynamic light scattering, zeta potential measurement and surface plasmon resonance. This also allowed us to probe the strength and reversibility of polymer brush/DNA binding².

RESULTS AND DISCUSSION

Characterisation of DNA interactions showed that a change in the N/P ratio affected the charge and size of the complexed system, with DNA being condensed well at equal ratio, causing aggregation at an intermediate N/P ratio or having very little effect at a higher N/P ratio.

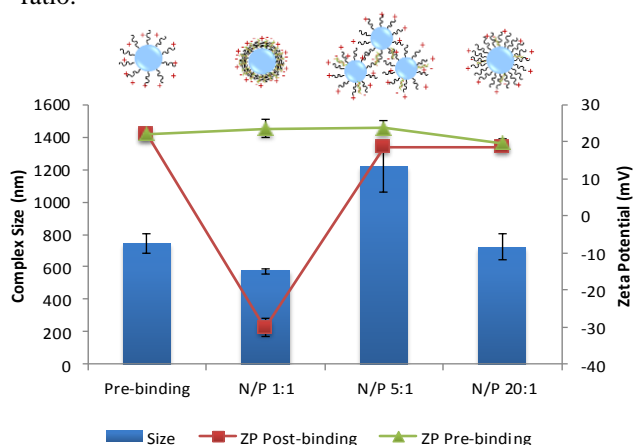


Figure 1 shows changes in complex size and zeta potential (ZP) before and after DNA binding with

PDMAEMA-grafted silica nanoparticles at varying N/P ratios.

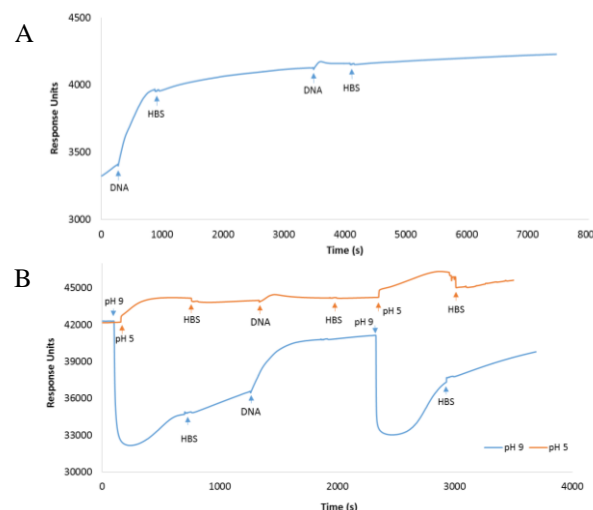


Figure 2A is an SPR sensorgram trace which shows DNA binding following a 2-step injection, washed with HBS, B) shows changes in the association and dissociation phase of DNA to PDMAEMA brush when injected with pH 9 (blue) and pH 5 (red) HBS buffer.

The SPR results confirmed that there was indeed binding of DNA to PDMAEMA brush and the interaction is relatively strong as DNA remained following the washing step. Increase in pH significantly affected the interaction and it was also observed that the DNA could recurrently interact with the brush.

CONCLUSION

Our results show that there are very strong and stable interactions between PDMAEMA and DNA which raises the question of whether the polymer brush could be a good candidate for releasing DNA once the complexes enter the cell. In this respect, we have been investigating complex-cell interactions, gene delivery and expression efficiency as well as the origin of PDMAEMA cytotoxicity and the influence of N/P ratios on cells. Lower cytotoxicity, reduced immunogenicity and better gene delivery can lead to the cationic vector's use in clinical applications.

REFERENCES

1. Pack D. *et al.*, Nature Rev. Drug Discov. 2:581-593, 2005
2. Wink, T. *et al.*, Anal. Chem. 71:801-805, 1999

ACKNOWLEDGMENTS

The authors would like to thank EPSRC (Grant no: EP/J501360/1) for providing financial support to this project.



Physicochemical Characterization and *In Vitro* Hemolysis Evaluation of UV Poly(ethylene glycol) Hydrogels

M. Flores-Reyes¹, J. Flores-Estrada², M.V. Dominguez-Garcia³, M.S. Camarillo-Romero³, M.V. Flores-Merino^{3*}

¹Faculty of Medicine, Autonomous University of the State of Mexico (UAEM), Mexico

²Faculty of Chemistry, UAEM, Mexico

^{3*}Research Center in Biomedical Science, UAEM, Mexico, mvfloresm@uaemex.mx

INTRODUCTION

Hydrogels are polymeric tridimensional networks attractive for numerous biomedical applications^{1,2}. A commonly used method for hydrogel synthesis is photopolymerization, which is employed in regenerative medicine applications (i.e. cell encapsulation, blood contact devices, etc...). Irigacure 2959, the most frequently used photoinitiator, displays different toxicity depending on cell type³. Therefore, efforts are focused on studying novel hydrogel systems and photoinitiators to improve performance of biomaterials. Here, a facile synthesis of poly(ethylene glycol) (PEG) hydrogels using a photoinitiator scarcely reported for polymers and not described for polymer network formation was studied. Physicochemical properties and *in vitro* hemolysis, most common method to determine the hemocompatibility properties of biomaterials⁴, was evaluated.

EXPERIMENTAL METHODS

Hydrogel preparation. Poly(ethylene glycol) dimethacrylate (PEGDM) was obtained by microwave synthesis (700 watts, 6 minutes; Daewoo) of linear PEG (MW = 4000 g.mol⁻¹; Polioles, MX) and methacrylic anhydride (Sigma-Aldrich, USA). Hydrogel was prepared by long wavelength UV light photoinitiated free radical polymerization of aqueous solutions of PEGDM and α , α' -azodiisobutyramidine dihydrochloride (Sigma-Aldrich, USA).

Physicochemical characterization. Chemical structure and bulk reaction kinetics of PEGDM and PEG hydrogel were analyzed by FTIR, the test was done by triplicate. Swelling behavior was studied by gravimetry of previously dried cylindrical samples of hydrogels (n = 9) until equilibrium was reached in a phosphate buffer saline solution (PBS; pH = 7.4).

Biological characterization. Direct *in vitro* hemolysis assay was performed based on ISO 10993-4 (1992). Briefly, sterile PEG hydrogel samples were incubated in a solution of human red blood cells (RBC; 5 %) obtained from blood samples of healthy volunteers. UV spectrophotometry was used to measure the percentage of hemolysis. All incubations were performed twice with different donors and triplicate sets of samples in parallel (n = 6). The authors certify that all research involving human subjects was done under full compliance with all government policies and the Helsinki Declaration (2013).

RESULTS AND DISCUSSION

A PEG hydrogel was obtained by photopolymerization (Fig. 1A). Quantitative hemolysis by UV

spectrophotometry (data not shown) and qualitative (Fig. 1B) analysis showed that samples are compatible (<5% hemolysis). Hydrogel reached equilibrium at 12h with a maximum swelling ratio of 4.55 ± 0.7 (Fig. 1C).

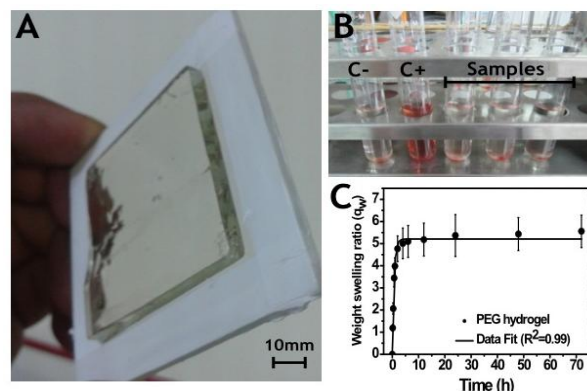


Figure 1. PEG hydrogel. A) Photograph after 10 min photopolymerization of solutions of PEGDM and photoinitiator, B) qualitative hemolysis assay (5% human RBC, 60 min incubation, 37 ± 1 °C) C+ and C- = positive and negative control and C. weight swelling behavior in PBS of dried cylindrical samples at room temperature (n=9).

CONCLUSION

A PEG hydrogel was prepared using a single molecule system for the photoactivation and initiation of the crosslinking reaction. The synthesis reported in this work is a simple but useful method to obtain polymer networks. *In vitro* hemolysis study as initial biocompatibility assay, showed that PEG hydrogel is hemocompatible. This hydrogel is a promising biomaterial for blood contact or tissue engineering applications.

REFERENCES

1. Fichman G. and Gazit E. Acta Biomaterialia. 10: 671–1682, 2014
2. Nicodemus G.D. and Bryant S.J., Tissue Eng Part B Rev. 14: 149–165, 2008
3. Williams C.G. *et al.*, Biomaterials. 26: 1211-1218, 2005
4. Henkelman S. *et al.*, Materials Science and Engineering: C. 29:1650-1654, 2009

ACKNOWLEDGMENTS

The authors would like to thank PROMEP (Grant no: 103.51/13/6535) for providing financial support to this project and support from the Autonomous University of the State of Mexico

Gold-Containing PMMA Microspheres. A Route to New Highly Radiopaque Cements for Vertebroplasty

Leo H. Koole^{1,*}, Keti Saralidze¹, Eva Jacobs², Alex Roth², and Paul Willems²

¹Department of Biomedical Engineering/Biomaterials Science, Faculty of Health, Medicine & Life Sciences, Maastricht University, PO Box 616, 6200 MD Maastricht, The Netherlands. ²Department of Orthopedic Surgery, Maastricht University Medical Centre Plus, Maastricht, The Netherlands. l.koole@maastrichtuniversity.nl

INTRODUCTION

Vertebroplasty is a minimally invasive procedure to treat or to prevent vertebral compression fractures. There are two major indications: (i) age-related osteoporosis, and (ii), after minimally invasive removal of an osteolytic tumor, which had grown inside the vertebra. In essence, vertebroplasty is the injection of a cement, either into the osteoporotic voids, or into the cavity that is left after tumour removal. During injection, the cement is a soft dough, which is formed by mixing poly(methyl methacrylate) (poly(MMA)) microspheres and MMA. The material hardens *in situ*, and then augments the vertebra. Vertebroplasty cements bear a clear resemblance with bone cements for hip and knee arthroplasty. A major difference, however, is that cements for vertebroplasty must exhibit a much higher level of X-ray contrast. Hence, they contain a large portion of the contrast agent BaSO₄ (up to 30 % by mass, vs. 8 % for hip/ knee bone cements). This affects the physical-mechanical properties of the vertebroplasty cements. The contrast agent influences the flow characteristics of the cement in the dough phase (i.e. between 5 – 12 min after cement mixing). The high content of BaSO₄ may also lead to increased risk for leaching of Ba²⁺ ions *in situ*, which can cause local osteolysis.

Here, we describe a new highly radiopaque bone cement that does not contain BaSO₄. The X-ray contrast is introduced by gold (Au) microparticles; these are incorporated into the PMMA microspheres of the powder phase. The embedded Au particles produce excellent X-ray contrast and favourable rheological characteristics of the cement dough.

EXPERIMENTAL METHODS

PMMA microspheres incorporating Au microparticles were prepared in a suspension polymerization reaction. Inclusion of the Au particles was not trivial; details of the process will be outlined. The PMMA/Au particles are isolated, purified, size-sorted, and mixed with dibenzoyl peroxide. The powder was mixed with MMA; the resulting dough, as well as the hardened cement during were evaluated in several respects.

RESULTS AND DISCUSSION

Figure 1 shows a polished sample of the hardened new cement, observed with backscattered scanning electron microscopy. Poly(MMA) appears black, the gold particles are seen as white spots. Note that the gold particles are located in dispersed circles; these are the microspheres that first formed the powder part of the cement. The dark material around the microspheres is the *in situ* polymerized poly(MMA).

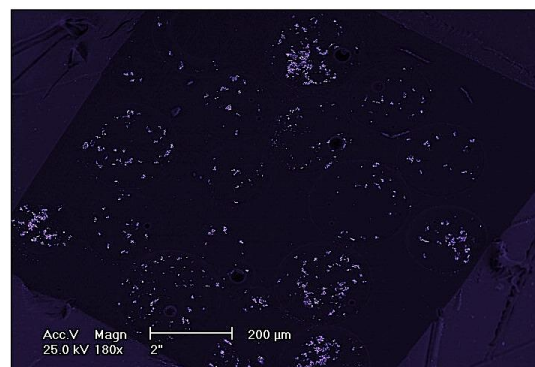


Figure 1. Scanning electron micrograph (backscattered mode) of the gold-containing cement after hardening. The gold particles are seen as white dots in dispersed circles. Bar = 200 micrometer.

Injectability of the doughs of the new cement, and of a commercial counterpart cement (BaSO₄) was studied. A comparison with a commercial cement was made, using fresh frozen human osteoporotic vertebrae. The experiments confirmed that the new cement flows easier through the needle, and penetrates deeper into the pores within the vertebrae. This can be explained by the fact the gold particles are *in* the microspheres, whereas the BaSO₄ crystals are grouped *around* the microspheres.

CONCLUSION

The new gold-containing bone cement exhibits promising properties due to the fact that X-ray contrast agent is incorporated in PMMA microspheres. This leads to improved rheology of the cement dough, and avoidance of contrast leakage. Further studies on this new biomaterial are warranted.

REFERENCES

1. Jay B, Ahn SH. Semin. Intervent. Radiol. 2013; 30: 297-306.
2. Dodwad SM, Khan SN. Orthop. Clin. North Am. 2013; 44: 243-9.

ACKNOWLEDGMENTS

This study is part of the Interreg IV-A project “BioMiMedics” (www.biomimedics.org) in which the Universities of Maastricht, Aachen (G), Juelich (G), Liege (B) and Hasselt (B) cooperate. This particular study was financed through generous contributions from the Province of Dutch Limburg, The Dutch Ministry of Economic Affairs, Maastricht University, Limburg Innovation BANK (LIOF), and the company Interface BIOMaterials BV (Geleen, the Netherlands).

3D Direct Laser Writing of Biomimetic Structures for Osteogenesis Enhancement

Attilio Marino^{1,2*}, Carlo Filippeschi¹, Barbara Mazzolai¹, Virgilio Mattoli¹, Gianni Ciofani^{1*}

^{1*}Istituto Italiano di Tecnologia, Center for Micro-BioRobotics @SSSA, Viale Rinaldo Piaggio 34, 56025 Pontedera, Italy; attilio.marino@iit.it, gianni.ciofani@iit.it

²Scuola Superiore Sant'Anna, The Biorobotics Institute, Viale Rinaldo Piaggio 34, 56025 Pontedera, Italy

A biomimetic micro-environment, resembling the natural trabecula, is obtained thanks to the Direct laser Writing approach. This structure has been evaluated *in vitro* in terms of bone-like cells differentiation, demonstrating an enhancement of the osteogenesis on the proposed scaffolds.

INTRODUCTION

Several cell behaviors, such as adhesion, survival, proliferation and differentiation depend on the physical and chemical extracellular micro-environment. Different bioinspired approaches have been proposed to artificially recapitulate this microenvironment, in order to regulate cell fate and to foster the appropriate functions *in vitro*.

In the latest years, increasing interest towards the Two-Photon Polymerization (2pp) technique is arising among the scientific community. Particularly, 2pp was found to be an intriguing tool for the fabrication of 3D structures aimed at fostering cell behaviours,¹ and at the investigation of cell-substrate interactions.²

In this work, we propose to recreate *in vitro* the 3D micro-environment of the bone, taking inspiration from the X-ray μ -CT scans of human trabecular bone, in order to improve the osteogenic differentiation of bone progenitor-like cells.

EXPERIMENTAL METHODS

Fabrication of 3D trabecular-like structures through slice-by-slice 2pp technique.

The biocompatible ceramic-like resistOrmocomp was used for the photo-polymerization of the biomimetic structures, by using a Direct Laser Writing (DLW) system (Photonic Professional, Nanoscribe GmbH).

Cell culture and differentiation on the 3D structures and on flat control substrates.

SaOS-2 human osteosarcoma-derived cell line (ATCC HTB-85) was adopted as bone-cell progenitor model. The differentiation protocol consisted in a 4-days treatment with osteogenic factors (10 mM β -glycerophosphate, 100 nM dexamethasone, 50 μ M ascorbic acid). Immunostaining toward Ki-67 (Millipore) was performed to label nuclei of proliferating cells, and OsteoimageTM bone mineralization assay (Lonza) was used to detect the amount of the hydroxyapatite deposits secreted by SaOS-2 cells during the osteogenesis progression. Cells were imaged through an inverted fluorescence microscope (Nikon).

Statistical analysis

Data were analyzed through the non-parametric Kruskal-Wallis test in order to compare the different distributions; p -values < 0.05 were considered significant.

RESULTS AND DISCUSSION

After 4 days since the osteogenesis induction, we observed a decrement of the Ki-67⁺ nuclei of cells differentiating on the artificial trabeculae ($50.0 \pm 6.6\%$) with respect to cells on flat control substrates ($64.5 \pm 4.8\%$, $p < 0.05$), so indicating a promotion of the exit from the cell-cycle when SaOS-2 are differentiated on the trabeculae-like structures.

Furthermore, we detected a remarkable increment of the hydroxyapatite deposits secreted by the SaOS-2 cells differentiated on the trabecular-like structures (84 ± 29 HA deposits, which covered $16 \pm 9.0\%$ of the surface area) compared to control substrates (3.0 ± 1.7 HA deposits, which covered $0.94 \pm 0.34\%$ of an analogous surface area; Figure 1).

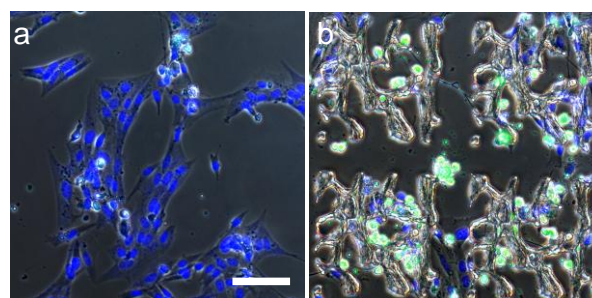


Figure 1: nodules of hydroxyapatite deposited during the osteogenic differentiation of SaOS-2 cells grown on flat control substrate (a) and on the 3D artificial trabeculae (b). In green, HA deposits; in blue, nuclei. Scale bar: 100 μ m.

All these results indicate as the presence of the physical micro-environment represented by the 3D bioinspired trabecular-like structures is able enhance the *in vitro* osteogenic differentiation. The observed phenomenon could be triggered by several different factors, such as the 3-dimensionality of the micro-environment, the biomimetic shape of the artificial trabeculae, the high stiffness of the ceramic material and/or by a combination of all of these mechanical cues.

CONCLUSION

Our findings open new perspectives in the exploitation of 2pp as an innovative tool for the design and the fabrication of biomimetic 3D micro-environments able to control cell behavior, with important outcomes in tissue engineering, regenerative medicine, and, more generally, in the study of bio/non-bio interactions.

REFERENCES

References must be numbered. Keep the same style.

1. M.T. Raimondi *et al.*, Acta Biomater. 2013, 9, 4579.
2. A. Marino *et al.*, ACS Appl. Mater. Interfaces 2013, 5, 13012.

Understanding material properties of 3D poly(ϵ -caprolactone)-based ternary composite scaffolds responsible for highly improved colonization by Human Bone Marrow Mesenchymal Stem Cells

J. Idaszek^{1*}; A. Bruinink²; J. Rębiś¹; V. Zell²; W. Świąszkowski¹

¹ Faculty of Materials Science and Engineering, Warsaw University of Technology, Poland

joanna.idaszek@inmat.pw.edu.pl

² Materials-Biology Interactions Laboratory, Empa, Swiss Federal Laboratories for Materials Science and Technology, St. Gallen, Switzerland

INTRODUCTION

Fused deposition modeling (FDM) is one of the most popular techniques among the Rapid Prototyping family. FDM is based on extrusion of molten polymer fibres in a layer-by-layer fashion and enables fabrication of scaffolds with precisely controlled architectures. Poly(ϵ -caprolactone), PCL, is a FDA-approved bioresorbable polyester, which due to excellent processability exhibits great compatibility with the FDM technique¹. However, PCL suffers from low stiffness and relatively long degradation rate². In order to overcome those drawbacks we fabricated in our laboratory a series of PCL-based ternary composite scaffolds. Our approach resulted not only in increased mechanical properties and accelerated degradation, but also in highly improved cellular response measured by means of a novel 3D cellular test set-up, namely multicellular spheroids³. The aim of this study was to investigate surface wettability, roughness and energy of the PCL-based composite scaffolds in order to understand relationship between those properties and the improved colonization by cells migrating out of multicellular spheroids.

EXPERIMENTAL METHODS

Porous scaffolds with compositions given in Table 1 were fabricated by means of FDM device (Syseng). Surface roughness (R_a) was measured using optical profilometer (Veeco Wyko 9300). The scans were performed at magnification of 40.5x in a Vertical Scanning Interferometry (VSI) mode. Water contact angle (WCA) was determined using a sessile drop method by means of a goniometer (Contact Angle System OCA, Dataphysics). The surface wettability was measured on solvent cast films. Multicellular spheroids were formed of vitally labelled primary human bone marrow mesenchymal stromal stem cells (HBMC) according to Idaszek *et al.*³. Images of the cultures were taken after 7 days of incubation using a fluorescent microscope (Axio Imager M1, Zeiss).

Table 1. Composition of the prepared materials. TCP- Tricalcium Phosphate; PLGA- Poly(lactide-co-glycolide)

Name	PCL (wt %)	TCP (wt %)	PLGA (wt %)
PCL	100	0	0
PCL-TCP	95	5	0
Ter_25	70	5	25

RESULTS AND DISCUSSION

Both, surface wettability and roughness were strongly influenced by addition of PLGA. The R_a of ternary composite Ter_25 increased by 90% and WCA was reduced by 10°, if compared to neat PCL. Figure 1 depicts WCA plotted against surface area colonized by HBMC. We found a linear relationship between wettability and outgrowth of cells out of multicellular spheroids ($R^2 = 0.9777$). However, the surface colonization was not proportional to the R_a and surface energy. The improved bioacceptance could be a result of increased adsorption of cell adhesion-mediating proteins, which is maximal at surfaces with WCA around 70°⁴.

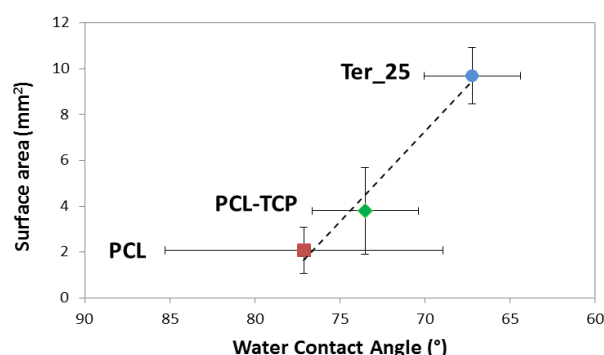


Figure 1. Surface area colonized by HBMC after 7 days in culture as a function of water contact angle.

CONCLUSION

Surface wettability can be modified by addition of PLGA and has a strong effect on cytocompatibility of PCL-based composites.

REFERENCES

1. Zein I. *et al.*, Biomaterials 23:1169-1185, 2002
2. Lam C. *et al.*, Biomed. Mater. 3: 034108, 2008
3. Idaszek *et al.*, Mater. Sci. Eng. C Mater. Biol. Appl. 33:4352-60, 2013
4. Tamada Y. *et al.*, J. Coll. Interf. Sci. 155: 334–339, 1993

ACKNOWLEDGMENTS

This work was supported by the project BIO-IMPLANT (Grant No. POIG.01.01.02-00-022/09) and Polish-Norwegian Research Programme (Contract No. Pol-Nor/202132/68/2013). The stay of Joanna Idaszek at Empa has been supported by the European Union in the framework of European Social Fund through the Warsaw University of Technology Development Programme, realized by Center for Advanced Studies.

The vascularization of porous calcium phosphate ceramics: an in vitro and in vivo study

Ying Chen¹, Xiangdong Zhu¹, Yujiang Fan¹, Xingdong Zhang¹

¹National Engineering Research Center for Biomaterials, Sichuan University, People's Republic of China
constanceyin@sina.com

INTRODUCTION

Bone defect is one of the major diseases threatening human health, and treat for large volume of bone defects is still a challenging clinical problem. Recent studies had confirmed that osteoinductive porous CaP ceramics without addition of any growth factors or cells could have the equivalent repair effect on healing the large bone defects of animals with autologous bone grafts. Angiogenesis is considered essential to fracture healing.

In the present study, we chose the CCD-18Co human fibroblasts (HFs) and human umbilical vein endothelial cells (HUVECs) as cell models, and investigated the effect of various porous CaP ceramics with similar porous structure and different phase composition on proliferation and angiogenic factors secretion of the two types of cells by in vitro cell culture. Also, the role of the conditioned media collected from these cells in enhancing HUVECs proliferation and tubule formation was evaluated. In addition, we selected an intramuscular implantation model in mice, which was used to evaluate ectopic bone formation of porous CaP ceramics in our previous study, to investigate the neovascularization of the ceramics. Meanwhile, temporal gene expressions of the key angiogenic factors of the cells ingrowth into the inner pores of the ceramics were analyzed.

EXPERIMENTAL METHODS

In vitro experiments: Cell lading and culturing, MTT assay, CLSM, in vitro angiogenesis assay, NO staining assay, Quantitative real-time polymerase chain reaction (qRT-PCR).

In vivo experiments: Implantation of the porous ceramics in mouse muscle pouch, SEM, HE, Immunohistochemical Staining Analysis (IHC), Microvessel Density (MVD), Quantitative real-time polymerase chain reaction (qRT-PCR).

RESULTS AND DISCUSSION

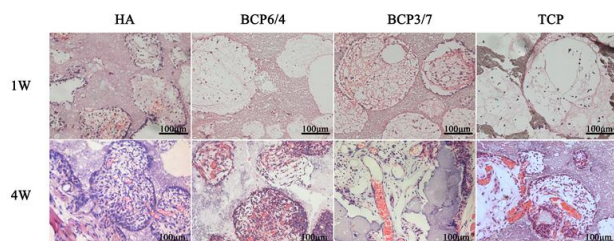


Fig. 1 Photomicrographs of HE staining for the decalcified sections of porous CaP ceramics implanted into the thigh muscles of mice. At the 4th week, completely mature blood vessel networks had formed within the ceramics

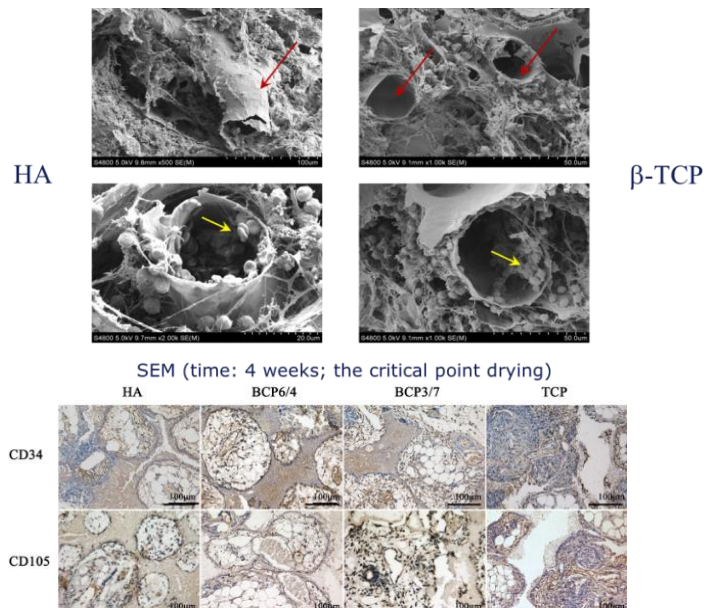


Table Comparison of MVD determined using monoclonal antibodies against CD34 or CD105 in porous CaP ceramics implanted into the thigh muscles of mice

Groups	No. of cases	Microvessel counts (mean \pm SD) using antibodies to	
		CD34	CD105
HA	12	7.58 \pm 2.87	5.67 \pm 3.58
BCP6/4	12	11.67 \pm 3.89	8.91 \pm 3.77
BCP3/7	12	19.58 \pm 4.10*	14.75 \pm 5.37*
TCP	12	15.17 \pm 4.17*	13.83 \pm 4.59*

CONCLUSION

The vascularization of CaPs was related to the factor secretion of HFs and HUVECs. Different chemical compositions of CaPs could lead vascularization to varying levels, among which β -TCP phase was more conducive to the generation of new blood vessels.

REFERENCES

1. Nkenke E. et al., International journal of oral and maxillofacial surgery. 2004;33:157-63.
2. Kessler P. et al., The British journal of oral & maxillofacial surgery. 2005;43:51-6.
3. Rojban H. et al., Journal of biomedical materials research Part A. 2011;98:488-98.
4. Hak DJ. et al., Journal of the American Academy of Orthopaedic Surgeons. 2007;15:525-36.

ACKNOWLEDGMENTS

This work was financially supported by the National Basic Research Program (973 Program) of the People's Republic of China (Contract Grant No. 2011CB606201) and the Natural Science Foundation of China (Contract Grant No. 81190131).

Thermal Ageing Effect on the Micromechanical Properties of Fiber-Reinforced Composites for Orthopaedic Applications

Radek Sedláček^{1*}, Tomáš Suchý^{1,2}, Karel Balík², Zbyněk Sucharda², Zdeněk Padovec¹

^{1*}Laboratory of Biomechanics, Dept. of Mechanics, Biomechanics and Mechatronics, Fac. of Mechanical Engineering/CTU in Prague, Czech Republic, radek.sedlacek@fs.cvut.cz

²Dept. of Composites and Carbon Materials/Institute of Rock Structure and Mechanics, Academy of Sciences of the Czech Republic, v.v.i., Czech Republic

INTRODUCTION

A great number of devices are applied in orthopaedics, including surgical intra-operative guides and instrumentations, screening equipment accessories, ranging from hand tables and head supports to cantilevered angiography and full body CT cradles. In this study we present an investigation of the influence of steam sterilization on micromechanical properties. The effect of widely-used steam sterilization multiple processes on the micromechanical properties of the composite, particularly in the interphase region between the polymer matrix and the reinforcing fibers, was studied by nanoindentation.

EXPERIMENTAL METHODS

A composite material was prepared on the basis of ARAMID balanced fabric reinforcement and polydimethylsiloxane (PDMS) matrix. The mechanical properties were measured before sterilization and after 100 sterilization process periods. An autoclave for steam sterilization (134°C, 304 kPa, 10 min) was used for this purpose. After sterilization, a cross-section area of the specimens was polished according to the polishing protocol by Godara et al.¹. The assessment of the influence of multiple sterilization cycles on the mechanical properties of the composites (reduced elastic modulus E_r [GPa]) was studied using the Hysitron TriboIndenter™ TI 950 nanomechanical instrument. For each tested composite sample, indents were applied on three 25x25 µm areas where the fibers were perpendicular to the polished surface as a matrix of 5x5 indents.

RESULTS AND DISCUSSION

Representative reduced elastic modulus–contact depth relationship obtained from the indentation tests (no sterilization treatment) is illustrated in Figure 1.

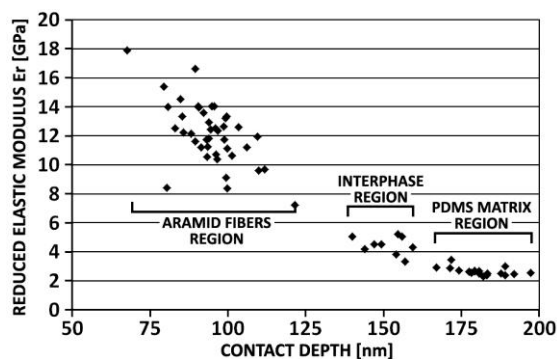


Figure 1 Some representative indentation responses showing the reduced elastic modulus (E_r) of the composite sample

In this figure, the three different regions (fiber, interphase zone, and bulk matrix) are schematically indicated according to the indentation depth values. The matrix/fiber interphase region was investigated (Figure 2). The zones identified as interphase regions show different mechanical property values after application of the sterilization cycles. The 100 times steam-treated specimens show a trend toward a reduced elastic modulus value, indicating a modification in the properties of the PDMS matrix in this region. This decrease can be estimated to be equal to approx. 30% in comparison with the untreated samples. Nanoindentation analyses verified the findings of an assessment of the impact of multiple sterilization processes on the inner structure of composites carried out by Suchý et al.² at flexural tests.

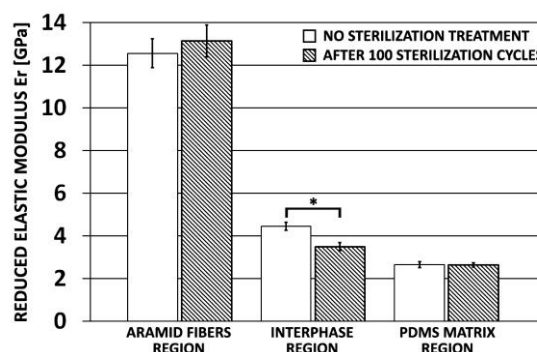


Figure 2 Mean values of reduced elastic modulus with confidence intervals ($p=0.05$) of investigated regions. * denotes statistically significant differences in the case of comparison of each region before and after sterilization treatment (Mann-Whitney test, $p=0.05$)

CONCLUSION

The results of nanoindentation analysis of an ARAMID/PDMS composite provided an assessment of the influence of multiple sterilization processes on the inner structure of the studied composite. The steam-treated specimens show a trend toward a reduced elastic modulus value in the fiber/matrix interphase region, indicating weakening of the bond between fibers and matrix after application of multiple sterilization cycles.

REFERENCES

- Godara A. et al., Acta Biomater. 3:209-30, 2007
- Suchý T. et al., Ceramics-Silikáty, 55:401-09, 2011

ACKNOWLEDGMENTS

This research was supported by the Technology Agency of the Czech Republic (project No. 03010209).

Fabrication of a Bone Graft Substitute based on a Pre-set Bioactive Glass-Ionomer Cement

Altair Contreras¹, Paul V. Hatton¹, Ian Brook¹, Abigail Pinnock¹ and Cheryl A Miller¹

¹Bioengineering & Health Technologies Research Group, School of Clinical Dentistry, University of Sheffield, UK

INTRODUCTION

Bioactive glasses based on 45S5 have been used as bone graft substitutes with some success¹. However calcium phosphates, dominate the medical market due to their excellent biocompatibility, but they have a complex setting chemistry and are difficult to handle clinically. On the other hand, glass ionomer cement systems are widely known, and a recent patent describes the fabrication of glass ionomer cements (GICs) where the glass component is based on Hench's 45S5 bioactive glass². Therefore, the aim of this research was to fabricate and characterise a granule prototype prepared from the aforementioned bioactive glass ionomer cement (BGIC). If successful, the resulting medical device could potentially combine the excellent biocompatibility of set GICs with the advantages of bioactive glasses, addressing current clinical needs.

EXPERIMENTAL METHODS

Glass based on 45S5 composition was prepared by a melt-quench route. X-ray diffraction (XRD) was used to assess glass formation, and post-melt composition was investigated using X-ray fluorescence (XRF). Scanning Electron Microscopy (SEM) was used to characterise the granules morphology and presence of a porous structure by Micro Computed Tomography (μ CT). Glass frit was processed to obtain particles of $< 45 \mu\text{m}$. Cement granules were prepared by mixing glass, calcium carbonate powder (5% weight), 45k Mw poly(acrylic) acid (Advanced Healthcare Ltd) and an aqueous solution of phosphoric acid (50% w/v). The resultant material was left to age at 37°C . Granules were obtained by grinding and sieving to achieve particle sizes ranging from 0.5 to 1.0 mm, which is commonly used in commercial bone grafting products. The *in vitro* response of MG63 cells cultured on the granules (50 mg and 100 mg) and Tissue Culture Polystyrene was investigated using Presto blue assay.

RESULTS AND DISCUSSION

The amorphous nature of the glasses was confirmed by XRD. It was possible to produce stable granules in media at 37°C under the conditions described above.

XRF showed good correlation between the theoretical and experimental composition values. SEM showed that the obtained granules have irregular shapes and surfaces while μ CT indicated the presence of a porous internal structure. *In vitro* studies showed a reduction in the metabolic activity of cultured cells in the presence of the granules compared to Tissue Culture Polystyrene, possibly due to the rapid release of alkaline ions from the glass.

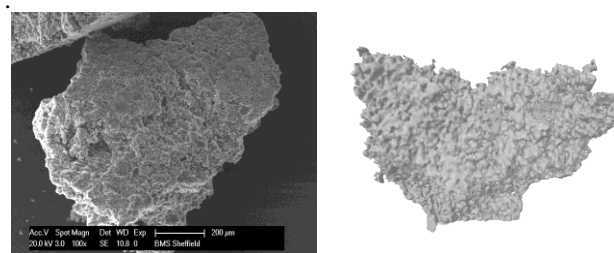


Figure 1. (a) SEM micrograph and (b) μ CT image of the prototype granules produced from the preset BGIC.

CONCLUSION

It was concluded that it was possible to prepare novel bone graft substitutes based on bioactive glass-ionomer cement technology i.e. using only 45S5 based glass composition in combination with poly(acrylic acid) and a phosphoric acid solution. Future work includes testing with other bioactive glass compositions and application of alternatives fabrication methods to improve granule morphology.

REFERENCES

1. Hench, L.L. 2006. *J Mater Sci: Mater Med* **17**:967-978
2. International Patent Application PCT/GB2013/053386

ACKNOWLEDGMENTS

The authors are grateful to Robert Burton at Hallam University for XRF, Advanced Healthcare for providing the PAA. Hatton and Miller are members of MeDe Innovation. We acknowledge the EPSRC for funding through the Regener8 IKC programme.

***In vivo* Response of Biodegradable Biphasic 3D Printed Scaffolds for Bone Tissue Engineering**

S. Ghanaati^{1,2}, M Barbeck^{1,2}, T. Serra^{3,4}, P. Booms^{1,2}, R. Sader^{1,2}, J. A. Planell^{3,4}, M. Navarro^{3,4}, C. J. Kirkpatrick¹

¹ Institute of Pathology, University Medical Center of the Johannes Gutenberg University Mainz, Langenbeckstraße 1, 55101 Mainz, Germany

² Department for Oral, Cranio-Maxillofacial and Facial Plastic Surgery, Medical Center of the Goethe University Frankfurt, Theodor-Stein-Kai 7, 60596 Frankfurt/Main

³ Institute for Bioengineering of Catalonia, Barcelona, Spain

⁴ CIBER in Bioengineering, Biomaterials and Nanomedicine (CIBER-BBN), Spain
E-Mail: shahram.ghanaati@kgu.de

INTRODUCTION

Development of 3D scaffolds for guided tissue regeneration (GTR) is still a major goal in tissue engineering. Rapid prototyping (RP) allows precise fabrication and customization of 3D scaffolds for tissue regeneration.

EXPERIMENTAL METHODS

In this work, novel biphasic scaffolds combining polylactic acid (PLA) and biodegradable CaP glass were made by additive manufacturing, giving 3D structures with pores of $165 \pm 5 \mu\text{m}$, struts of $70 \pm 5 \mu\text{m}$ and having 70% porosity. The aim of the present study was to evaluate the *in vivo* behaviour of these scaffolds in the subcutaneous tissue of mice. Explanted tissue was evaluated by histological analysis and established histomorphometrical methods, focusing on early and late inflammatory responses for up to 30 days of implantation. Polylactic acid (PLA) and biodegradable (PLA/CaP glass) were used as controls.

RESULTS AND DISCUSSION

The results of the study revealed that all materials underwent marked tissue integration. PLA mainly induced mononuclear cells and remained stable over the study period, while the tissue reaction to PLA/CaP glass was predominantly characterized by the presence of TRAP-positive multinucleated giant cells and was associated with a faster material degradation over time. The biphasic group induced a combination of both

above-mentioned tissue reactions. Its PLA-side remained as a stable matrix, while the PLA-CaP glass aspect underwent a comparably faster biodegradation. The present study revealed that biphasic materials could play a key role in GTR, as they combine both stability and biodegradative characteristics.

Emotions	women	Men
----------	-------	-----

CONCLUSION

Materials based on combination of polylactic acid (PLA) and biodegradable CaP could find application particularly in the regeneration of maxillofacial defects, as in these locations materials should prevent soft tissue ingrowth, while acting as osteoconductive matrices for bone regeneration.

REFERENCES

Ghanaati et al. 2011, Biomaterials
Serra et al. 2014, Mater Sci Eng C Mater Biol Appl.

ACKNOWLEDGMENTS

“The authors would like to thank the Research Fund of the Goethe University Frankfurt for providing financial support to this project”.

Cobalt alloy specific regulation of bone remodelling via HIF: a cause of aseptic orthopaedic implant failure?

Yutong Li, Johannes Staufenberg, Jay Mashari, Divyahline Logitharajah and Gavin Jell

Division of Surgery & Interventional Science, UCL, Royal Free Campus, London, UK, rmhklif@ucl.ac.uk

INTRODUCTION

The biological response to orthopaedic implant wear debris is the principle cause of peri-prosthetic osteolysis and aseptic loosening¹. Cobalt ion (Co^{2+}) containing orthopaedic implants have higher aseptic failure rates (~14% in 7 years) compared to other implant materials such as titanium (~4.1% over 7 years)². We hypothesise that this higher aseptic failure rate is partly due to Co^{2+} causing inflammation and altering bone remodelling dynamics via the hypoxia inducible factor (HIF) pathway. Co^{2+} has been previously reported to stabilise HIF at concentrations present in the peri-prosthetic tissue of failed implants (1-500 μM)³. Here we investigate the effects of the median reported Co^{2+} concentrations present in the peri-prosthetic on osteoclast formation, osteoblast proliferation and macrophage activity.

EXPERIMENTAL METHODS

Clinically relevant concentrations of Co^{2+} , Ti^{4+} , Cr^{3+} and CoCr ions were used in culture over 6 days. Osteoclast (RAW264.7) formation was determined using Tartrate-Resistant Acid Phosphatase (TRAP) assay and Phalloidin fluorescence microscopy. Osteoblast (SaOs-2) proliferation (total DNA) was determined over the same period. Macrophage (RAW264.7) phagocytic activity was determined using fluorescent particles (pHrodoTM Bioparticles[®], Molecular Probes[®]).

RESULTS AND DISCUSSION

Co^{2+} increased ($P<0.001$) osteoclast formation in the absence of osteoclast differentiation factor RANKL (Fig.1), whilst decreasing osteoblast proliferation (Fig.2)

(Fig.1) whilst decreasing osteoblast proliferation (Fig.2) and increasing the phagocytic activity of macrophages ($P<0.001$). Co^{2+} in the presence of RANKL further augmented osteoclast formation compared to RANKL alone (a 300% increase). The decrease in osteoblast proliferation at Co^{2+} 12.5 μM was similar to that observed to osteoblast cultured in 1% O_2 conditions (hypoxia). As Co^{2+} increased there was a further reduction of osteoblast proliferation (25 and 50 μM).

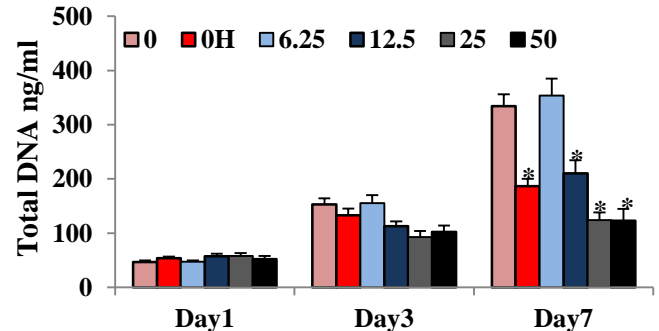


Figure 2. Co^{2+} [above 6.25 μM] and hypoxia (H) reduces osteoblast proliferation in a concentration dependent manner. *= $p<0.05$.

The increased osteoclastogenesis and decreased osteoblast proliferation may contribute to bone resorption leading to aseptic loosening of the implant. Our results showed that Co^{2+} acts via hypoxia pathway corresponding with previous studies⁴. Furthermore, the increase in the phagocytic activity of macrophages in the presence of Co^{2+} may be important in wear particle uptake *in vivo* and the perpetuation of the inflammatory environment present in the peri-prosthetic tissue. Previous studies have shown that Co^{2+} wear debris stabilises HIF-1 α and increases the expression of pro-inflammatory factors *in vitro*⁵ and *in vivo*^{5,6} but this is the first study demonstrating a direct role on bone remodelling. Further studies are currently being completed on confirming the role of HIF in this process using siRNA and HIF-1 α inhibitory chemicals.

CONCLUSION

Co^{2+} ions present in the peri-prosthetic tissue may play an important role in aseptic loosening of CoCr orthopaedic implants by increasing osteoclast formation whilst inhibiting osteoblast via hypoxia pathway. Increased osteolysis promotes aseptic orthopaedic implant failure. These results raise important questions about the use of cobalt in orthopaedic implant manufacturing.

REFERENCES

- Revell P.A. *et al.*, Proc Inst Mech Eng H. 211; 187-197, 1997.
- NJR 10th Annual Report 2013.
- Li, Begley & Jell *in prep*, 2014.
- Jell G. *et al.*, Mat. Chem. 20; 790-797, 2010.
- Samelko L. *et al.*, PloS one, 8(6): e67127. 2013.
- Jell G M R. *et al.*, J. Mat. Sci. 12(10-12): 1069-1073. 2001,

ACKNOWLEDGMENTS I would like to acknowledge the support of Dr Eileen Gentleman (KCL)

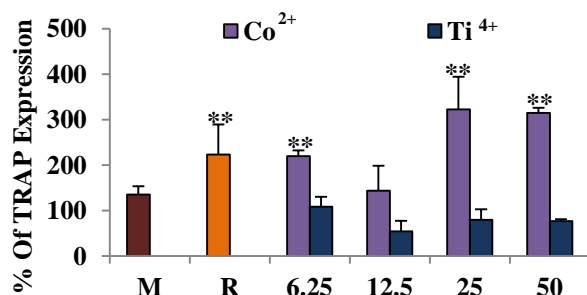
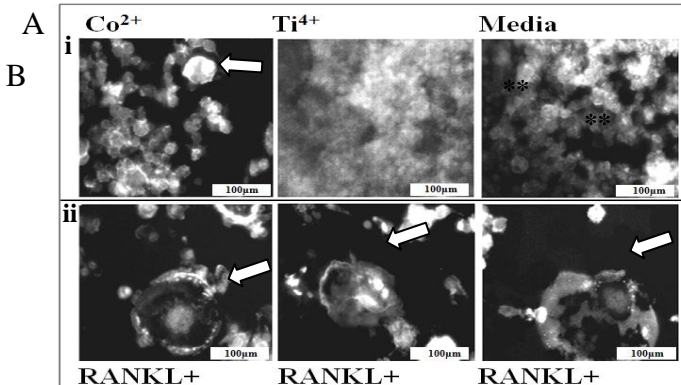


Figure 1. A. Fluorescent Phalloidin images of osteoclasts (arrow) with 50 μM Co^{2+} and 1000 μM Ti^{4+} . B. % of TRAP expression by macrophages cultured with Co^{2+} and Ti^{4+} [μM] compared with media, M= Media, R= RANKL+, **= $p<0.001$



Trimethyl Chitosan-Based Nanoparticles Intracellular Trafficking and Transfection: a Bioimaging Study

Aida Varela-Moreira^{1,2}, Carla Pereira Gomes^{1,3}, Maria Gomez-Lázaro¹, Pedro Miguel Moreno¹, Ana Paula Pêgo^{1,3,4}

¹INEB - Instituto de Engenharia Biomédica, Universidade do Porto, Portugal; ²Faculdade de Medicina, Universidade do Porto, Portugal; ³Faculdade de Engenharia, Universidade do Porto, Portugal; ⁴Instituto de Ciências Biomédicas Abel Salazar, Universidade do Porto, Portugal. aida.moreira@ineb.up.pt

INTRODUCTION

Trimethyl chitosan (TMC) recently emerged as a promising gene delivery vector for biomedical applications. Due to the quaternization of the primary amines, chitosan (CH) acquires a permanent positive charge, thus solubility under physiological conditions (pH 7.4)¹, overcoming its low transfection efficiency. One key issue when using materials for biomedical applications is the biodegradation and the fate of the resulting by-products. CH enzymatic biodegradation occurs between acetylated monomers being the degree of acetylation (DA) the main parameter affecting biodegradation². In this work, we explored the impact of the DA on the enzymatic degradation and biological properties of TMC-based nanoparticles, mainly stability, internalization and transfection efficiency.

EXPERIMENTAL METHODS

TMC with a Mn 43.3 kDa, 11% DA and 30% DQ (degree of quaternization) (TMC₁₁) was used to prepare TMC/DNA complexes with different N/P ratios (moles of quaternized amines/moles of phosphate groups) (1 to 15), in 20 mM HEPES buffer with 5% (w/v) glucose at pH 7.4. CH with similar Mn and DA was used as control. In order to vary the DA, the original TMC was deacetylated and subsequently re-acetylated. To evaluate TMC nanoparticles enzymatic degradation with different DA's, a competition assay previously setup in our team was used³. The influence of the DA on TMC-nanoparticles internalization and intracellular localization was evaluated by Imaging Flow Cytometry (ImageStream^X Amnis, Millipore) at different time-points (0.5h to 24h) on ND7/23 cells. Finally, the impact of nanoparticle biodegradation on transfection efficiency was assessed 72 h post-transfection, using GFP as a reporter gene.

RESULTS AND DISCUSSION

The original TMC₁₁ was successfully deacetylated (DA 2%, TMC₂) and subsequently acetylated (DA 17%, TMC₁₇), with no significant alteration of the polymer molecular weight. TMC-DNA complexes were efficiently prepared, with an average diameter between 160 nm and 200 nm irrespectively of the N/P ratio and polymer DA. The enzymatic degradation profile of the TMC-nanoparticles was found to be in accordance to what is described in the literature for TMC solutions: a higher DA leads to a higher degradation rate of the polymer. Moreover, comparing the degradation profile of TMC₁₁ with CH₁₁, we observed a higher degradation rate of TMC₁₁ nanoparticles despite having the same DA. The internalization efficiency of the prepared nanoparticles was evaluated by imaging flow cytometry. Using this novel technique, we are able to not only determine the % of cells with nanoparticles but also discriminate to which cell compartment the

nanoparticles are associated to, which represents an advantage over the classical flow cytometry-based internalization studies. Over a period of 24 hrs, CH-based nanoparticles are internalized in a steadily fashion. For TMC nanoparticles, 80% of the cells had already internalized nanoparticles after 4h of contact. Although between different TMC's the overall internalization was equal, the % of membrane bound nanoparticles was higher in the TMC₂ nanoparticles, comparing to TMC₁₁ and TMC₁₇. By staining the nuclear DNA with DRAQ5, we were able to evaluate when pDNA (YOYO-1+) co-localized with the cell nucleus. At 0.5h of contact, already 4% of cells were showing co-localization, irrespectively of the DA. A significant difference is seen between TMC's from the 4h time point on, where TMC₁₁ mediated the delivery of a higher quantity of pDNA to the cell nucleus. It was also for this polymer that the highest levels of transfection (% of cells expressing the delivered reporter gene) were observed.

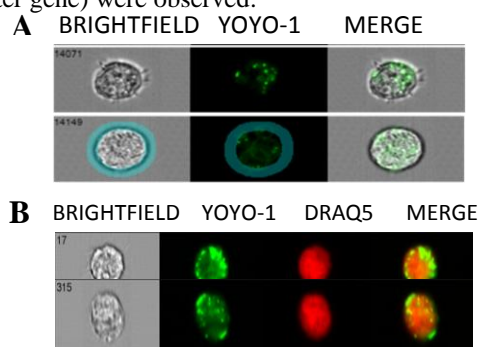


Figure 1- Illustrative images of ND7/23 cells with TMC₁₁ based nanoparticles internalized (N/P 15), after 4h of contact.

A. In blue is defined the mask for the cellular membrane. Plasmid DNA in green (YOYO-1); **B.** Co localization of pDNA (in green) with the nuclear DNA (DRAQ5), in red.

CONCLUSIONS

TMC nanoparticles biodegradation can be positively correlated with the TMC DA. While the % of cells that internalized the nanoparticles is very high for all tested TMC formulations, transfection was found to be significantly affected by the DA of the polymer. The 24 h study of nanoparticle internalization presented herein discloses important data about the process of intracellular trafficking, indicating that biodegradation, hence associated DNA unpacking, is key for the overall transfection process.

REFERENCES

1. Gomes, CP. *et al.*, MRS Bulletin 39 (01): 60-70, 2014;
2. Varum KM *et al.*, Carbohydr Res. 26: 99-101, 1997 ;
3. Pires LR. *et al.*, Nanomedicine 6: 1499-512, 2011.

ACKNOWLEDGMENTS FCT grants (SFRH/BD/79930/2011, PTDC/CTM-NAN/115124/2009) and Marie Curie Action of the European Community's Seventh Framework Program (PIEF-GA-2011-300485).



Electrospun Polyvinylpyrrolidone Nanocomposites Mesh with Silica-coated Magnetic Nanoparticles

Rebecca Zhiyu Yuan, Jian Ping Fan and Jie Huang*

Department of Mechanical Engineering, University College London, United Kingdom, rebecca.yuan.10@ucl.ac.uk

INTRODUCTION

The use of magnetic nanoparticles (MNPs) for biomedical applications has increased exponentially over the past decade. Iron oxide nanoparticles (IONPs) can be injected intravenously and endocytosed by tumour cells. However, the majority of the NPs are rapidly cleared from the bloodstream by the reticuloendothelial system although surface modifications have been done to improve tumour targeting. IONPs have been encapsulated in a gel matrix; there are concerns of toxic side-effects of organic solvents. Encapsulated electrospun nanofibre web has offered an attractive alternative¹. In this study, a core-shell structure of maghemite ($\gamma\text{-Fe}_2\text{O}_3$) and silica (SiO_2) nanoparticles were synthesised and water soluble polyvinylpyrrolidone (PVP) was used to produce an electrospun nanocomposite mesh.

EXPERIMENTAL METHODS

The maghemite ($\gamma\text{-Fe}_2\text{O}_3$) nanoparticle (NP) core was made by precipitation of iron (III) chloride hexahydrate and, Iron (II) chloride tetrahydrate and ammonium hydroxide and then oxidised with sodium hypochlorite². A sol-gel silica glass from tetraethylorthosilicate (TEOS) was used to coat maghemite NP to obtain a biocompatible protective silica shell, in order to reduce the agglomeration and improve colloidal stability. The microstructure of NPs was examined by transmission electron microscopy (TEM).

MNPs were added into a series of PVP/ethanol solutions (20 to 50 wt. %) to make suspensions for electrospinning (ES). Under ES set up, suspension was infused by a programmable syringe pump (Harvard Apparatus) and subjected to an electrical field by a high voltage generator (Glassman High Voltage Inc.). The flow rates of suspensions (0.2 - 5 $\mu\text{L}/\text{min}$), nozzle diameters (0.68 mm, 0.86 mm and 1.08 mm) and applied voltages (0 - 15 kV) were varied to optimise the formation of nanofibres mesh. The distance between the needle and the collector was set at 10 mm. The microstructure of the nanofibre mesh was examined by scanning electron microscopy (SEM).

RESULTS AND DISCUSSION

Figure 1 shows the microstructure of the $\gamma\text{-Fe}_2\text{O}_3\text{-SiO}_2$ core-shell NPs examined under TEM. The average size of the MNPs was 50 ± 10 nm, coated with silica.

All the PVP solutions were able to produce electrospun nanofibres successfully, where 30 wt. % PVP was found to with minimum beads formation. Processing parameters were then varied to build a nanofibre formation map. As summarised in Table 1, the minimum suitable applied voltage was 8 kV and

suspension flow rate was $2 \mu\text{L}/\text{min}$.

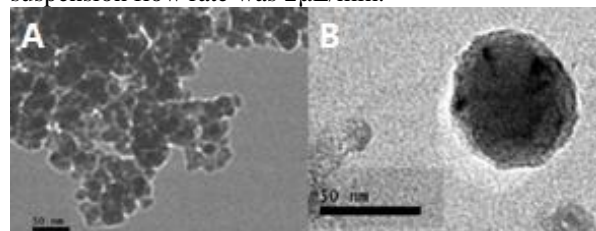


Figure 1. TEM micrographs of the $\gamma\text{-Fe}_2\text{O}_3\text{-SiO}_2$ NPs

	0-7kV	7-8kV	8-15kV
Applied Voltage	No Fibre	Fibre with beads	Fibre with average size 200-500nm
	0.68mm	0.86mm	1.08mm
Needle Sizes	No Fibre	Fibre with average size 200-500nm	Fibre with average size $\geq 500\text{nm}$
	0.2-2 $\mu\text{L}/\text{min}$	2-3 $\mu\text{L}/\text{min}$	3-5 $\mu\text{L}/\text{min}$
Feed Rates	Fibre with beads	Uniform fibre	Unstable jetting

Table 1. Summary of the effects of processing parameters on electrospun PVP fibres

Figure 2 shows the microstructure of the PVP nanofibre mesh incorporated with MNPs. The diameter of the electrospun nanofibres was in the range of 200-500 nm.

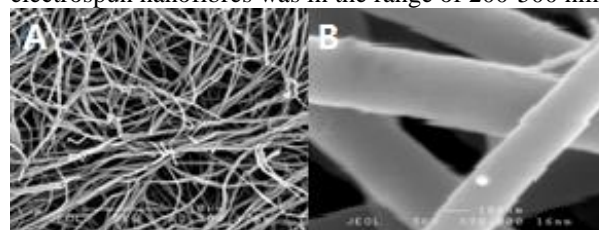


Figure 2. SEM micrographs of the surface morphology of the PVP nanofibres (A) and incorporated with MNPs (B)

CONCLUSION

Core-shell MNPs- SiO_2 nanoparticles were successfully prepared and incorporated into electrospun PVP nanofibre mesh. The size and morphology of the nanofibres can be controlled by varying polymer concentrations and electrospinning processing parameters. The nanocomposite mesh developed offers great potential in drug delivery and magnetic hyperthermia applications.

REFERENCES

- Huang C *et al*, Adv Funct Mater, 22, 2479, 2012
- Chekina N, *et al*. J. Mater. Chem., 21, 7630, 2011

Laser Surface Modification of Anodically Grown Oxide of Titanium for Biomedical Applications

Diego Pedreira de Oliveira¹ Laís Tereza Duarte¹ Adriano Otuka² Claudemiro Bolfarini¹

¹ Departamento de Engenharia de Materiais, Federal University of São Carlos, Brazil

² Instituto de Física de São Carlos, Universidade de São Paulo, 13560-970, São Carlos, SP, Brazil
dpedreira@ufscar.br

INTRODUCTION

Surface modifications of titanium alloys can be successful techniques to control cells behaviour after implantation surgery¹.

Laser structuring of surface is gaining importance for this application due to avoid contamination and impart micro and nanoscale modifications²⁻⁴. However, the laser irradiation can be detrimental to fatigue properties. To overcome this drawback this study aims to modify the surface of an oxide anodically grown on the surface of Ti-6Al-4V.

Some results of fatigue behaviour will be presented and correlated to the surface modification problems. The expectation is that the laser modification be restricted to the oxide layer to keep fatigue properties of the sample of Fig.1.

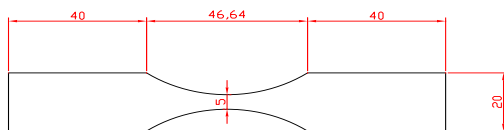


Figure1: Sample dimension for fatigue tests.

EXPERIMENTAL METHODS

The process of growth of the oxide can be performed by anodization in phosphate buffer solution and then the oxide can be modified with laser with pulse duration on the order of 500 femtoseconds (ultrafast laser).

The structure obtained will be analyzed by scanning electron microscopy (SEM/EDS) to examine surface morphology, surface characteristics of interest will be underwent by evaluation of fatigue property.

RESULTS AND DISCUSSION

The results will include the oxide thickness before and after surface modification with SEM analysis. Figure 2

shows the morphology of one surface containing some micro to nano features that can favour bone apposition.

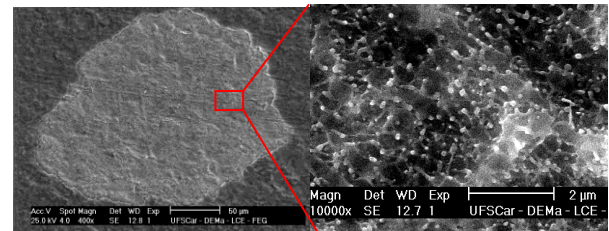


Figure 2: surface morphology of an oxide modified by laser irradiation.

CONCLUSION

Fatigue experiments are being carried out. Expectations are based in obtaining fatigue properties not lower than polished surfaces. This can be interesting for this field of biomaterials to control cells activities with surface modification ensuring good fatigue properties.

REFERENCES

- 1.Oliveira, D. P., Palmieri, A., Carinci, F. & Bolfarini, C. Osteoblasts behavior on chemically treated commercially pure titanium surfaces. *J. Biomed. Mater. Res. Part A* **00A**, 000–000 (no prelo) (2013).
- 2.Vorobyev, A. Y. & Guo, C. Femtosecond laser structuring of titanium implants. **253**, 7272–7280 (2007).
- 3.Oliveira, V., Ausset, S. & Vilar, R. Surface micro / nanostructuring of titanium under stationary and non-stationary femtosecond laser irradiation. *Appl. Surf. Sci.* **255**, 7556–7560 (2009).
- 4.Brånemark, R., Emanuelsson, L., Palmquist, A. & Thomsen, P. Bone response to laser-induced micro- and nano-size titanium surface features. *Nanomedicine* **7**, 220–7 (2011).

ACKNOWLEDGMENTS

The authors would like to thank the financial support from FAPESP, CAPES and CNPQ from Brazil.

Fibrin-Hyaluronic Acid Interpenetrating Network Hydrogel with Improved Fibrin Stability

Yu Zhang¹, Philipp Heher², Sujit. Kootala¹, Heinz Redl², Jöns Hilborn¹ and Dmitri Ossipov^{1*}

¹Science for Life Laboratory, Department of Chemistry-Ångström, Uppsala University, Uppsala, Sweden

²Ludwig Boltzmann Institute for Experimental and Clinical Traumatology, Vienna, Austria,
yu.zhang@kemi.uu.se

Introduction

Fibrin hydrogels have been widely used in a variety of tissue engineering (TE) applications because they support cell adhesion, proliferation and stem cell differentiation¹. However, its low mechanical stiffness and rapid degradation before the proper formation of tissue engineered structure are two major disadvantages that limit practical use of fibrin hydrogel as a promising scaffold in TE applications². In this work we constructed fibrin-hyaluronic acid (fibrin-HA) interpenetrating network (IPN) to overcome this problem, in which fibrin hydrogel was combined with an in situ formed disulfide cross-linked hyaluronic acid (HA) hydrogel.

EXPERIMENTAL METHODS

HA-thiol (HA-SH) and HA-pyridinyldithio (HA-SSPy) derivatives were synthesized according to our previously published protocol³. Fibrinogen and thrombin (Tissucol Kit, 1.0 mL, two-component fibrin sealant) were from Baxter AG, Vienna, Austria.

Preparation of 2%Fibrin-1%HA IPN hydrogel: 75 μ L of 8% (w/v) fibrinogen was mixed with 75 μ L of 2% (w/v) HA-SSPy solution; 75 μ L of thrombin (4U/L) was mixed with 2% (w/v) HA-SH solution; mixture of fibrinogen/HA-SSPy was mixed with solution of thrombin/HA-SH and then transferred into a syringe module to form a hydrogel.

RESULTS AND DISCUSSION

In this study, we have reported preparation of an IPN hydrogel composed of fibrin and orthogonally reactive formed hyaluronic acid network which improved fibrin stability (Figure 1). Fibrin-HA IPN was formed as a result of thiol-disulfide cross-linking reaction between HA-SH and HA-SSPy chains as well as simultaneous and orthogonal thrombin-induced conversion of fibrinogen.

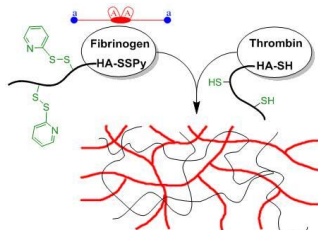


Fig. 1. Fibrin-HA IPN by simultaneous and orthogonal enzymatic and disulfide networking

Electron microscopy studies showed fibrillar structure of formed IPN (Figure 2a), indicating formation of fibrin. In comparison, when thrombin was omitted from the gel preparation, the resulting structure (Figure 2b)

showed similar structure of pure HA hydrogel, indicating that fibrinogenesis did not compromise disulfide cross linking between HA-SH and HA-SSPy. During the degradation study, fibrin hydrogels got dissolved during incubation in PBS for a week while fibrin-HA IPN hydrogels kept shape, revealing the support of interpenetrating HA network to fibrin hydrogel.

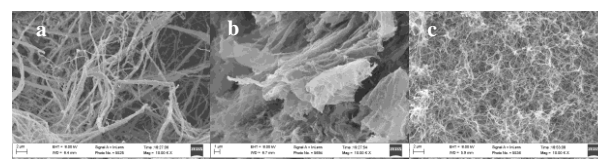


Fig. 2. SEM images of (a) 2%Fibrin-1%HA IPN (b) 1%Fibrinogen-1%HA (c) Fibrin hydrogels

Pure HA hydrogel was poor at cell adhesion. Here we confirmed that fibrin-HA IPN hydrogels supported proliferation of encapsulated osteoblasts analogously to fibrin hydrogels (Figure 3).

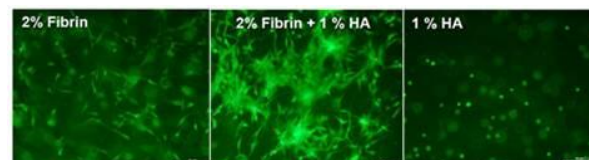


Fig. 3. Morphology of osteoblasts encapsulated for 8 days in fibrin, fibrin-HA IPN, and HA hydrogels (live cells stained green).

CONCLUSION

Fibrin-HA IPN hydrogels were formed through thrombin-induced polymerization of fibrin monomers and disulfide cross-linked hyaluronic acid and showed improved stability over analogous fibrin hydrogel while retaining the ability to support proliferation of encapsulated osteoblasts as pure fibrin hydrogel did. The result suggests that fibrin-HA IPN hydrogel is a potential scaffold in tissue engineering application.

REFERENCES

1. Weisel J W., Adv. Protein Chem. 70:248-299
2. Hincke M., *et al.*, Tissue Eng.: Part B, 14: 199-215, 2008
3. Ossipov D. *et al.*, J. Macromolecules. 46, 4105-4113, 2013

ACKNOWLEDGMENTS

This work was supported by the European Communitie's FP7 (Biodesign)



Effect of Preconditioning on 70S30C Bioactive Glass Foam Structure and Protein Adsorption

Gowsihan Poologasundarampillai^{1*}, Peter D Lee², Dave Clark³, Julian R Jones^{1*}

^{1*}Department of Materials, Imperial College, UK, gowshp@gmail.com

²School of Materials, University of Manchester, UK

³STFC Rutherford Appleton Laboratory, Harwell Science and Innovation Campus, UK

INTRODUCTION

Bioactive glasses have great potential as template scaffolds for bone regeneration¹. They bond to bone, degrade in the body and release ions which stimulate bone regeneration. Sol-gel derived porous bioactive glass scaffolds with 70 mol% SiO₂ and 30 mol% CaO (70S30C) have an interconnected macroporous network achieving compressive strengths similar to human trabecular bone². *In vivo* studies have shown that a preconditioning (PC) treatment (3 days in cell culture media) is required for bone regeneration in a rat tibial defect models³. Also, poor bone ingrowth and inflammation was found for non-preconditioned (dry) sol-gel foams³. The aims of this investigation are to understand the effect of PC on the scaffold chemistry and structure and link it to protein adsorption and bone formation.

EXPERIMENTAL METHODS – Determination of Structural changes

Bioactive glass foams were produced by air foaming a sol-gel solution containing H₂O, HNO₃, tetraethyl orthosilicate and Ca(NO₃)₂. The foams were aged, dried and stabilised to 700 °C. These were then cut to thin slices of 5x5x0.8 mm³ and some were PC in cell culture media α -MEM for 3 days. The samples were then analysed using synchrotron x-ray tomography (S μ CT on the Diamond I13), SEM, XRD and FTIR. To dynamically study the influence of PC on the bioactive glass serum containing α -MEM was perfused through both dry and PC samples. The pH and ion concentration of the media was measured as a function of time for up to 4 hours. Following perfusion with media the foams were imaged on S μ CT and SEM. XRD and FTIR were also performed.

Protein adsorption was studied using a bioreactor to flow protein containing phosphate buffered solution (PBS) through the dry and PC bioactive glass foams. Fluorescently labelled sera proteins albumin, fibrinogen and globulin at a concentration of 0.1 mg ml⁻¹ were flowed through at 0.3 ml min⁻¹ for 30 minutes to investigate the kinetics of protein adsorption on the bioactive glass surface and their relative intensities. Multiphoton confocal imaging was performed at the Harwell Octopus facility.

RESULTS AND DISCUSSION

Preconditioning of the bioactive foams produced a calcium rich precipitate within the pores and walls of the porous bioactive glass foams (Figure 1). The precipitates were identified to be either calcite or amorphous calcium carbonate (ACC) depending on the location of the precipitate in relation to the pore network. Calcite was found to precipitate within the larger pores while ACC was often found within smaller and closed pores.

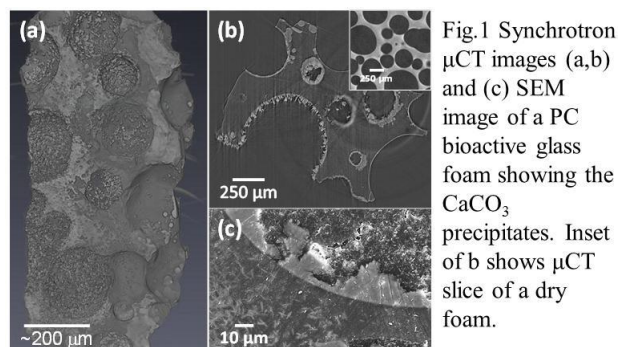


Fig.1 Synchrotron μ CT images (a,b) and (c) SEM image of a PC bioactive glass foam showing the CaCO₃ precipitates. Inset of b shows μ CT slice of a dry foam.

Preferential protein adsorption was observed (Fig. 2). Adsorption plateau was attained for the dry foams within 5 minutes of flow indicating monolayer adsorption. On the dry foams fibrinogen was found to adsorb on the surface regions of the pores while albumin was found to adsorb throughout the bioactive glass foams (Fig. 2a). After PC (Fig. 2b), even after 30 minutes of flow the adsorption intensity of fibrinogen and globulin continued to increase, indicating multilayer adsorption. Additionally, fibrinogen was found to preferentially adsorb on the calcium carbonate precipitates.

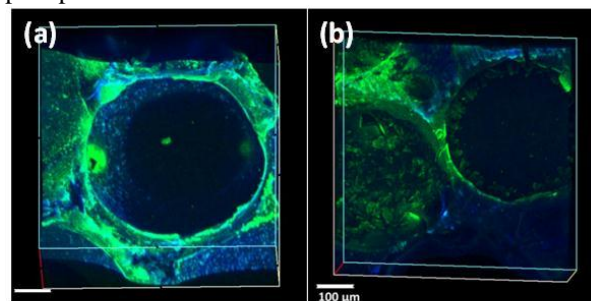


Fig.2 Fluorescence images of (a) dry and (b) PC bioactive foams after flowing sera proteins through for 30 minutes. Scale bar 100 μ m.

The results indicate that the preconditioning treatment has a significant influence on the structure, composition and properties of the bioactive glasses foams hence they both behave differently *in vivo*.

CONCLUSION

Sol-gel bioactive glass 70S30C when preconditioned in α -MEM forms a CaCO₃ precipitate which has significant influence on the *in vivo* performance of the material.

REFERENCES

1. Hench L.L. *et al.*, Science 295:1014-17, 2002.
2. Jones R.J. *et al.*, Biomaterials 27:964-73, 2006.
3. Midha S. *et al.*, Acta Biomater. 9: 9169-82, 2013.

ACKNOWLEDGMENTS

EPSRC funding (EP/E057098, EP/E051669 and EP/I020861/1) and Colleagues at Research Complex at Harwell, especially Dr Kamal Madi for help with μ CT.

Synthesis and Characterization of Silicate Glasses with the Sol-Gel Process Containing ZnO or SrO

G. Theodorou^{1*}, E. Kontonasi², K. Chrissafis¹, L. Papadopoulou³, N. Kantiranis³, T. Zorba¹, K.M. Paraskevopoulos¹, P. Koidis²

¹Department of Physics, ²Department of Fixed Prosthesis and Implant Prosthodontics, School of Dentistry, ³Department of Geology,

Aristotle University of Thessaloniki, 54124 Thessaloniki, Greece, *gtheodo@physics.auth.gr

INTRODUCTION

Bioactive glasses with the ability to bond to both soft and hard tissue and to promote bone growth have been well documented^{1,2}, since several studies have reported these properties for a number of sol-gel produced materials in vitro as well as in vivo^{2,3}. New studies over the introduction of various metallic ions when synthesizing bioactive glasses report that in small amounts, when used, could prove beneficiary⁴. Specifically, the addition of Sr has been proposed to show beneficial effects on bone cells and bone formation in vivo^{5,6} whereas the addition of Zn ion shows anti-inflammatory effects and stimulates bone formation in vitro by activating protein synthesis in osteoblasts⁷. The aim of this work was to successfully synthesize and characterize two sol-gel systems, 60S10Zn (SiO₂ 60, CaO 30, ZnO 10 in wt %) and 60S10Sr (SiO₂ 60, CaO 30, SrO 10 in wt %) in order to evaluate their bioactive behaviour.

EXPERIMENTAL METHODS

Sol-gel derived bioactive glasses (Table 1) were produced as described in literature⁸, pulverized in a hydraulic press and sieved to particle size under 40µm.

a/a	SiO ₂ (%wt)	CaO (%wt)	SrO (%wt)	ZnO (%wt)
60S10Sr	60	30	10	---
60S10Zn	60	30	---	10

"Table 1 show the composition of the synthesized materials".

The sieved powders of the bioactive glasses were then soaked in SBF solution for various immersion times with renewal conditions, as proposed by Zhong and Greenspan⁹. The amount of powder immersed in SBF solution was determined by the ratio 1ml:1.5mg as indicated by Kokubo *et al*¹⁰. The characterization of the samples before and after immersion in SBF was conducted using Fourier Transform Infrared (FTIR) Spectroscopy using a Perkin-Elmer Spectrometer Spectrum 1000 in MIR region, Scanning Electron microscopy with associated energy dispersive spectroscopic analysis (SEM-EDS) and X-Ray Diffractometry (XRD) using a Philips (PW1710) diffractometer with Ni-filtered CuKα wave radiation. Differential thermal and thermogravimetric analysis were performed with a Setaram thermogravimetric-differential thermal analyzer SETSYS 16/18-TG-DTA (1400 °C rod), with heating and cooling rates 10 °C/min - in nitrogen atmosphere - and furnace cooling, respectively.

RESULTS AND DISCUSSION

Both synthesized materials presented the characteristic FTIR bands of silicate glasses which are; a broad band at 900-1100 cm⁻¹ assigned to the Si-O stretching mode and a band at 490 cm⁻¹ assigned to the Si-O-Si bending one¹¹. After immersion, the identification of an amorphous Ca-P phase was revealed on the surface of the Zn-containing samples and apatite formation on the surface of the Sr-containing samples, by both FTIR spectra and XRD patterns after 5 days. EDS analysis confirms these findings.

CONCLUSION

Strontium and Zinc containing bioactive glasses have been successfully synthesized via the sol-gel method. It was possible to acquire the stabilization temperature through Differential thermal and thermogravimetric analysis. In vitro bioactivity tests showed that apatite formation was possible on the surface of Strontium-containing bioactive glass while only a Ca-P phase was developed on the surface of the Zinc-containing bioactive glass. Future work is planned in order to evaluate the behavior of the bioactive glasses when in contact with cells and the investigation of their possible application for dental tissue regeneration in scaffolds fabrication.

REFERENCES

1. W. Cao and L. L. Hench, *Ceramics International* 1996;22: 493-507,
2. J. R. Jones, P. Sepulveda, L. L. Hench, *J Biomed Mater Res* 2001;58: 720-726.
3. J. Zhong, D. C. Greenspan, *J Biomed Mater Res* 2000;53: 694-701.
4. Hoppe, N. S. Guldal, A. R. Boccaccini *Biomaterials* 2011;32: 2757-2774
5. Marie PJ, Ammann P, Boivin G, Rey C. *Calcif Tissue Int* 2001;69(3):121-9.
6. Marie PJ. *Bone* 2006;38(2, Suppl. 1):10-4.
7. Yamaguchi M. *J Trace Elem Exp Med* 1998;11(2-3):119-35.
8. Zhong J. *et al.*, *J. Biomed. Mater. Res* 2000;53: 694-701.
9. J. Zhong and D. C. Greenspan, *J Biomed Mater Res A* 2000;53: 694-701.
10. T. Kokubo *et al.*, *J Biomed Mater Res* 1990;24:721-734.
11. Kontonasi E. *et al.*, *Cryst. Res. Technol* 2002;37: 1165

ACKNOWLEDGEMENTS

This study was conducted under the action Excellence II (Project: 5105) and funded by the European Union (EU) and National Resources.



Mechanical Stabilisation of Non-Toxic Collagen Fibres for Tendon Repair

Anna Soroushanova, India Sweeny, Abhay Pandit, Dimitrios Zeugolis

Network of Excellence for Functional Biomaterials (NFB), National University of Ireland, Galway, Ireland,
a.soroushanova1@nuigalway.ie

Introduction

Tissue grafts are commonly used for tendon repair, however they lack mechanical stability and often associated with donor morbidity. Therefore, development of novel scaffolds with increased stability is required. Crosslinking the collagen fibres could potentially increase the mechanical properties and strength of the scaffolds. However, based on previous studies, cross-linkers such as GTA are cytotoxic for tenocytes and therefore alternative cross-linkers are required². We hypothesise that StarPEG crosslinking of collagen fibres will optimally stabilise collagen tendon scaffold, providing sufficient mechanical stability and maintain tenocyte function, and promote tendon regeneration *in vivo*.

Experimental Methods

Collagen fibres were extruded using an established protocol¹. Fibres were cross-linked with 4 arm StarPEG. GTA and EDC/NHS cross-linked fibres were used as negative control and non-cross-linked fibres were used as a baseline control. Hydrothermal stability was tested by differential scanning calorimetry (DSC). Mechanical properties were assessed by tensile testing. Enzymatic degradation was assessed by collagenase assay and levels of free amines assessed by ninhydrin. Fibres were arranged into bundles and subsequently pre-incubated in complete media for 24 hours. Human tenocytes (passage 2-3) were seeded onto collagen fibre bundles at concentration of 10×10^3 cells/cm². Media changes were performed every other day. At 3, 7, 14, 21, 28 day time points *in vitro*, Rhodamine Phalloidin and DAPI staining were used to assess the alignment, elongation and morphology of cells on fibre bundles and alamarBlue was used to assess metabolic activity. Tenocyte markers including decorin, scleraxis, tenomodulin and tenascin-C were assessed using immunocytochemistry and gene analysis. SEM was used to examine the structure of the fibres.

Results

Tensile testing and DSC showed an increase in mechanical and thermal properties compared to the non-cross-linked collagen fibres. Over time the collagen fibre bundles degraded into small fragments as assessed by collagenase assay. Over time the collagen fibre bundles degraded into small fragments as assessed by collagenase assay. Ninhydrin showed a low level of free amines in the

StarPEG cross-linked fibred compared to the controls. Collagen fibre structure was seen with SEM. Elongation of tenocytes on collagen fibre bundles was observed, with a steady increase until the 28th day time point. Tenocytes aligned in parallel orientation along on the StarPEG collagen fibre bundles as seen in figure 1. Immunocytochemistry and gene analysis showed the expression of tenogenic markers specific to tenocytes.

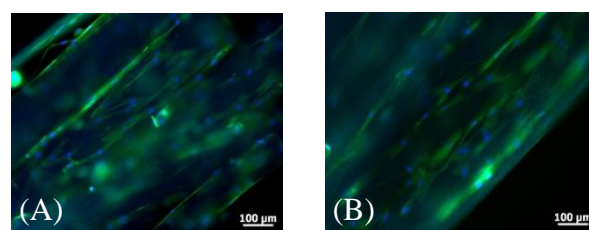


Fig.1 (A) (B) Human tenocytes stained with DAPI and Rhodamine Phalloidin demonstrating cellular alignment along fibre direction

Discussion and Conclusion

StarPEG crosslinking provided collagen fibres with sufficient mechanical properties and stability for use as a tendon graft substitute compared to non-cross-linked tendon fibres. *In vitro* assessment of tenocytes showed proliferation and alignment on StarPEG collagen fibres, indicating tenocyte function was not compromised compared to GTA and EDAC-HCL. PCR results showed expression of tenogenic markers specific to tendon. Ongoing and future *in vivo* work is a sheep Achilles tendon model.

Reference

1. Zeugolis, Dimitrios I., Gordon R. Paul, and Geoffrey Attenburrow. Journal of Biomedical Materials Research Part A 89.4:895-908, 2009
2. Gough, J. E., Scotchford, CA., Downes, S. J Biomed Mater Res 61(1): 121-130, 2002

Acknowledgments

The author would like to thank Teagasc, Irish Agriculture and Food Development Authority (ROG1088), for providing financial support for this project.

Disclosures

The author has nothing to disclose.

Cell Osteogenic Function Enhancement and Selective Apoptosis by Hydroxyapatite Nanoparticles

Fangzhu Qing, Zhe Wang, Yanfei Tan and Xingdong Zhang*

National Engineering Research Center for Biomaterials, Sichuan University, P. R. China, prww@qq.com

INTRODUCTION

Because of the similarity in composition to bone minerals, calcium phosphates, notably hydroxyapatite [$\text{Ca}_{10}(\text{PO}_4)_6(\text{OH})_2$, HA], were widely used as bioactive materials for bone repair. Specially, HA was demonstrated to present the biological function of broad anti-cancer activity^{1, 2}. And studies revealed that HA nanoparticles (HA-NPs) could induce apoptosis to many kinds of tumor cells. Meanwhile, some researches reported that HA-NPs could promote the proliferations of normal cells³. Considering the broad application of osteogenic function, HA-NPs functions of both promotion on osteogenic function and selective apoptosis to tumor cells had newly potential of nano materials. But up to now, little researches referred to thus selective biofunction. Hence, in the present work, the biological effects of the HA-NPs to both osteosarcoma cells MG63 and normal osteoblasts were examined in details. Especially, emphasis was laid on observations of the genes expressions not only related to apoptotic process, but also to the osteogenic function.

EXPERIMENTAL METHODS

The dispersive HA-NPs with ~50 nm were prepared via hydrothermal process. Phase composition of the prepared HA-NPs was assessed by X-ray diffraction (XRD) and morphology of HA-NPs was observed by field emission scanning electron microscopy (FE-SEM) (Fig. 1A, B). Osteosarcoma cells MG63 were employed as tumor cells and osteoblasts isolated from small specimens of trabecular bone as normal cells. The MG63 cells and osteoblasts were cultured with the HA-NPs solutions at the concentration of 0, 25, 100, 250, and 500 $\mu\text{g/mL}$, respectively. The cell viability of those two kinds of cells was tested by MTT (3-(4, 5-dimethylthiazol-2-yl)-2, 5-diphenyl tetrazolium bromide) assay and fluorescent staining assay. Ultrastructure changes of the cells were observed under transmission electron microscopy (TEM). Gene expressions of markers in cell apoptosis and osteogenic function were monitored via Quantitative Real-Time Polymerase Chain Reaction (qRT-PCR).

RESULTS AND DISCUSSION

According to the MTT assay and fluorescent staining assay, HA-NPs inhibited the growth of MG63 cells in a time and concentration dependent manner, but supported proliferation of the osteoblasts. The entrance of HA-NPs to both two kinds of cells was confirmed by TEM observations. The particles could enter the nucleus and distributed in the nucleus of the MG63 cells, while no particles were observed in the nucleus of osteoblasts. The deformation of nucleus and whole cell of MG63 indicated apoptosis emerged when treated with HA-NPs (Fig. 1C, D). HA-NPs exhibited no toxicity and induced apoptosis to osteoblasts. As

markers of cell apoptosis, Caspase-8, Caspase-9 and Caspase-3 of MG63 cells in all treated groups were high expressed in different concentration of HA-NPs, indicating that the apoptosis of MG63 cells developed from both intrinsic and extrinsic signal pathway. As markers of cell osteogenic function, gene expressions of ALP, Collagen type I (Col I), osteocalcin (OCN), BMP-2, osterix and Runx2 were analyzed. In both two kinds of cells, HA-NPs did not inhibit the gene expressions of ALP, Col I and OCN; BMP-2 and osterix in both cells were upregulated after treatment for 24 hours; Runx2 was significantly stimulated to a greater extent in MG63 and maintained a relatively high level in osteoblasts. These results proved that HA-NPs could upregulate the osteogenic function relative genes expressions of both MG63 and osteoblasts.

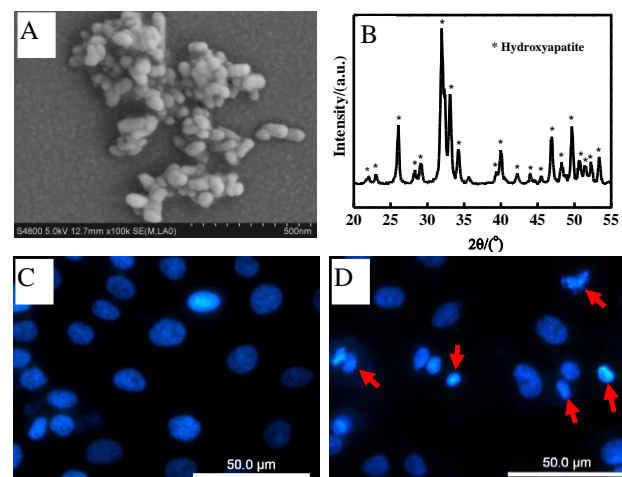


Figure 1. (A) XRD patterns and (B) SEM of HA-NPs; Fluorescent images of MG63 cells (C) untreated and (D) treated with 100 $\mu\text{g/mL}$ HA-NPs after 1 day's exposure which was stained with DAPI.

CONCLUSION

The results proved that HA-NPs have selective affections to cells, with promotion to MG63 apoptosis and osteoblasts proliferation. Furthermore, HA-NPs can enhance osteogenic function in both cells.

REFERENCES

1. H. Aoki. *et al.*, Rep. Inst. Med. Dent. Engineer. 27:39-44, 1993.
2. Y. Hong. *et al.*, Mater. Sci. Engineer. R. 70:225-242, 2010.
3. Y. Cai. *et al.*, J. Mater. Chem. 17:3780-3787, 2007.

ACKNOWLEDGMENTS

The authors would like to thank the National 973 Program (Grant no: 2011CB606201) for providing financial support to this project.

Low Temperature Aqueous Precipitation of Nanocrystalline Hydroxyapatite Containing Strontium and Magnesium for Biomedical Application

Kristine Salma-Ancane^{1*}, Liga Stipniece¹, and Liga Berzina-Cimdina²

^{1*}Rudolfs Cimdins Riga Biomaterials Innovation and Development Centre, Riga Technical University, Latvia,

²Institute of General Chemical Engineering, Riga Technical University, Latvia, kristine.salma-ancane@rtu.lv

INTRODUCTION

Over the last decade, hydroxyapatite (HAp) has been of special interest to dentistry, the orthopedic industry and nanomedicine because of their excellent performance¹. It is established that nanosized and nanocrystalline HAp can mimic the dimensions of mineral component of calcified tissues^{1,2}. The major inorganic component of bone mineral is a biological apatite, which can be defined as a non-stoichiometric, carbonated, ion-substituted and calcium deficient HAp (CDHAp)^{1,3}. The non-stoichiometry of biological apatites arises from the incorporation of foreign ions, either into the crystal lattice or adsorbed onto the surface^{3,4}. Substituting ions present in native hard tissues such as Sr, Mg, and Zn into HAp structure can lead to advantageous effects on biomaterial physic-chemical properties which directly influence bioactivity on living system⁴. In order to investigate the influence of Sr and Mg incorporation on the physico-chemical properties of nanocrystalline HAp we have prepared compositions of pure, Sr- and Mg-substituted HA by a low temperature aqueous precipitation.

EXPERIMENTAL METHODS

A series of Sr-substituted, Mg-substituted and pure HAp were synthesized using an aqueous precipitation method under identical experimental conditions. The synthesis was carried out on a 10 g scale. In this synthesis, CaO, H₃PO₄, MgO and SrO (all of analytical grade) were applied as sources of Ca, P, Mg and Sr, respectively. The added amounts of Mg and Sr sources were 0.0, 1.0, 2.0 and 3.0 wt.% in respect to Ca source, respectively. The baker with Ca(OH)₂ or Sr(OH)₂/Ca(OH)₂ or Mg(OH)₂/Ca(OH)₂ suspension was placed in an ice-salt bath and intensively stirred at 400 rpm. The 2M H₃PO₄ solution was rapidly added to the beaker in drop-wise. The temperature of the synthesis media was kept at 0°C and the pH adjusted to 10. The final synthesis solution was stirred for 10 min. The filtered precipitate was centrifuged, stored in a freezer at -24°C for 24 h and finally dried at 40°C for 24 h. The phase, molecular and chemical composition, crystallite size and morphology, specific surface area (SSA) of synthesized powders were assessed by X-ray diffraction (XRD), Fourier transform infrared spectroscopy (FT-IR), scanning electron microscopy - energy dispersive spectroscopy (SEM-EDS) and Brunauer-Emmett-Teller (BET) method with N₂ adsorption.

RESULTS AND DISCUSSION

XRD patterns of as-synthesized powders show the formation of single poorly crystalline hydroxyapatite phase. The major peaks indicate the nanocrystalline form. No other secondary phases were identified. The

peaks in the XRD patterns of Sr- and Mg-substituted HAp are identical to the XRD pattern of pure HAp. As Sr and Mg concentration increases, the XRD peaks of the samples become broader, indicating lower crystallinity and crystallite size. These results were confirmed by the SSA measurements. Evaluation by BET shows that SSA values of as-synthesized powders increased with increasing of Sr and Mg content in samples. Respectively, as-synthesized pure and Mg-substituted HAp reach SSA between 164 and 185 m²/g. The levels of Sr and Mg substitution in HAp structure were measured by SEM-EDS and all expected elemental peaks were identified including Sr and Mg suggesting that substitution elements were incorporated into the synthesized HAp. The amount of Sr and Mg increases with increase in the amount of Sr and Mg added in the synthesis media. Consequently, Mg-substituted samples contain 0.30, 0.50, 1.14. wt% of Mg. The major functional groups including [PO₄] and [CO₃] were identified by FT-IR. The broad band of adsorbed water was observed for all samples. A major characteristic of nanocrystalline carbonated HAp is the presence of the ν₃ bands of [CO₃] groups observed between 1460 cm⁻¹ and 1470 cm⁻¹ and ν₂ band at 871 cm⁻¹. This is due to the substitution of [PO₄] groups by [CO₃] species.

CONCLUSION

A series of nanocrystalline carbonated Sr-, Mg-substituted and pure hydroxyapatite powders were synthesized by low temperature aqueous precipitation method. Experimental results show that the addition of small amounts of Sr and Mg (from 1 to 3 wt%) can induce a remarkable effect on the physico-chemical properties such as crystallinity, crystallite size, specific surface area of nanocrystalline hydroxyapatite.

REFERENCES

1. Dorozhkin S.V. et al., Acta Biomater. 6:715–734, 2010
2. Bose S. et al., Acta Biomater. 8:1401–1421, 2012
3. Cox S.C. et al., Mater. Sci. Eng., C 35:106–114, 2014
4. Boanini E. et al., Acta Biomater. 6:1882–1894, 2010

ACKNOWLEDGMENTS

This work has been supported by European Social Fund within the project “Involvement of new scientist group for synergistic investigation to development of nanostructured composite materials for bone tissue regeneration”

No.2013/0007/1DP/1.1.1.2.0/13/APIA/VIAA/024



Controlled release of nucleic acid to enhance bone regeneration

Bita Sedaghati¹, Alexander Ewe², Achim Aigner², Michael C. Hacker¹, Michaela Schulz-Siegmund¹

¹Pharmaceutical Technology, University of Leipzig, Germany, bita.sedaghati@uni-leipzig.de

²Rudolf-Boehm-Institute of Pharmacology and Toxicology, Clinical Pharmacology, Faculty of Medicine, University of Leipzig

INTRODUCTION

Bone morphogenic protein (BMP-2) is a registered drug for the treatment of certain defined bone defects (1). These therapeutic approaches are cost intensive and require high dosages of the protein. We could recently show that osteogenic effects of BMP-2 on the osteogenic differentiation of human adipose tissue stromal cells (hASC) could be improved when the BMP-2 antagonist chordin is silenced by a single treatment with siRNA against chordin in a non-viral approach (2). However, improvement regarding late osteogenic markers, such as mineral accumulation, showed donor dependencies and depended on rapidly differentiating cells. We therefore hypothesize that sustained silencing of BMP-2 antagonists such as chordin by controlled release of siRNA improves osteogenic differentiation and eventually bone formation. In this study, we set up a controlled release system for nucleotides involving poly(caprolactone) (PCL) and gelatine with the aim to eventually generate a scaffold system as an implant for controlled release of siRNA. Here, we show the effects of siRNA content and gelatine amount as well as ratios between nucleotide and gelatine to engineer promising controlled release profiles. To this end, PCL, gelatine and pDNA were processed to film-like discs. Nucleic acid was encapsulated in a gelatine matrix and coated in a freeze drying step on the PCL microparticles in order to stabilize the nucleotide and allow for homogeneous distribution in such discs.

EXPERIMENTAL METHODS

ASCs silencing and differentiation: ASCs had been isolated from liposuction aspirates of different donors. Cells were transfected with siRNA against chordin and noggin using liposomal or poly(ethyleneimin) strategies. Next day, the transfection medium was replaced by osteogenic medium with and w/o 100 ng/ml BMP-2 (BOM and OM). Gene expression of chordin was determined by qPCR. ALP activity and matrix mineralization as early and late osteogenic markers, respectively, were quantified.

Biomaterials: PCL particles were generated from PCL pellets by precipitation. Prior to lyophilization up to 7.5% of gelatin (type A, 140 bloom) along with up to 5 µg plasmid DNA were added to obtain drug loaded particles. Disc were formed by hydraulic compression of weighted aliquots as a model for scaffold based drug delivery system.

Release study: The discs were placed in 24 well plates and 0.5 ml of PBS were added. The released DNA was quantified with the Pico green assay over a period of one month and normalized to samples from discs

containing the same amount of gelatin without nucleotide.

RESULTS AND DISCUSSION

Gene expression assay on ASCs treated with siRNA against noggin and chordin showed significant silencing of noggin and chordin on day 4, whereas no significant effect on BMP-2 gene expression were observed. ASCs that were silenced for either chordin or noggin, showed enhanced noggin expression when treated with 100 ng/ml BMP-2 after two weeks of differentiation. This may explain why late osteogenic markers showed stronger variability in response to siRNA treatment than earlier markers.

The release of pDNA from PCL discs was prolonged for up to one month. pDNA release between 5 and 100 % was found depending on the gelatin content and the pDNA loading of the discs. In general, we found a positive correlation of the released amount with gelatin content of the disc. 5-7.5% of gelatin effectively suppressed burst release effects and modulated the release efficacy. Beside the gelatin content, the amount of nucleic acid per disc does also influenced the release. With 5 µg pDNA we found significantly lower release than with 1 and 2.5 µg. We hypothesize that a certain ratio of pDNA and gelatin is required for reasonable pDNA release. Further investigations on optimal composition are ongoing. For the envisioned scaffold based siRNA delivery strategy, a controlled release of siRNA over one month is assumed to improve osteogenic differentiation of ASCs and bone formation to a greater extent than BMP-2 alone.

CONCLUSION

Suppression of BMP-2 antagonists in BMP-2 treated ASCs is able to induce osteogenic differentiation. A single treatment with siRNA against these antagonists may not suffice for longer term stimulation of osteogenic differentiation. We show a promising system for siRNA release that may allow to overcome the problem of silencing BMP-2 antagonists over a longer period of time with the aim to stably induce bone formation for a reasonable time.

REFERENCES

1. INFUSE® Bone Graft Summary of Safety & Effectiveness Data. P000058, 2002.
2. Schneider H. *et al.*, Tissue Engineering Part A 20 (1-2), 335-45, 2014.

ACKNOWLEDGMENTS

The authors would like to thank SMWK (Saxonian Ministry of Science and Art) and DAAD (German Academic Exchange Service) for providing financial support to this project.



Determination of Anti-Cancer and Anti-Bacterial Efficacy of Selenium Doped Hydroxyapatite Coating on Titanium Alloy

Bengi Yılmaz¹, Zafer Evis^{1,2}, Aysen Tezcaner^{1,2} and Sreeparna Banerjee^{2,3}

^{1*}Department of Biomedical Engineering, Middle East Technical University, Turkey

²Department of Engineering Sciences, Middle East Technical University, Turkey

³Department of Biological Sciences, Middle East Technical University, Turkey

ybeni@metu.edu.tr

INTRODUCTION

Ti6Al4V alloy is one of the most commonly used metallic materials in the manufacture of orthopedic implants, due to its optimal mechanical properties and excellent biocompatibility. However, it fails to show bioactivity, which is very important for the bone tissue integration of the implants. Therefore, the Ti6Al4V implant surfaces are typically coated with hydroxyapatite.

On the other hand, pure hydroxyapatite coatings on metallic biomaterials are lack of features, such as preventing the formation and recurrence of cancer and reducing the risk of infection at the implant site unless they are functionalized with some ions. In this sense, selenium ions are attractive candidates because the functions of the selenium in the body include regulating metabolism, improving immunity, enhancing reproductive performance and preventing cancer¹. The main aim of this study is to obtain a selenium doped hydroxyapatite coating on Ti6Al4V plates.

EXPERIMENTAL METHODS

Ti6Al4V plates with the dimensions of 20×20×2 mm³ were abraded and pretreated with 5M NaOH at 80°C for 3 days and exposed to a temperature of 600°C for 1 hour. The plates were coated in conventional² and 0.15 mM selenate ion added 1.5×SBF at 37°C for 14 days. Pure and selenium doped coatings was observed by field-emission scanning electron microscopy (FE-SEM, Quanta 400F). The coatings were also examined by Fourier-transform infrared spectroscopy (FTIR, Bruker IFS 66/S) in the range 4000–400 cm⁻¹. X-ray diffraction (XRD, Rigaku Ultima-IV) was performed with Cu-K α radiation at 40 kV and 30 mA. Cell viability tests were performed by using normal human osteoblasts (hFOB 1.19) and osteosarcoma cells (Saos-2). Anti-bacterial efficacy of the coated plates was determined by seeding *Staphylococcus epidermidis* bacteria onto the plates. After 3 days of incubation period, the bacteria attached on the plates were collected by vortexing and the numbers were determined by using a spectrophotometry (Thermo Scientific, Multiscan GO).

RESULTS AND DISCUSSION

From SEM micrographs, it was observed that the entire surface was successfully coated with a calcium phosphate layer after 14 days in both solutions. The coating obtained from the selenate ion added 1.5×SBF exhibited the standard hydroxyapatite XRD peaks, as the coatings obtained from the normal 1.5×SBF. There

were also no significant differences observed in the FTIR spectra.

From the results of the cell viability tests, it was shown that by adding 5×10⁻⁸g selenium into 1.1ml of the cell culture media it is possible to inhibit the growth of Saos-2 cells while promoting the growth of hFOB 1.19 cells. However, from Figure 1, it can be said that the Saos-2 cells attached firmly and spread on the the both types of coatings following the surface topography.

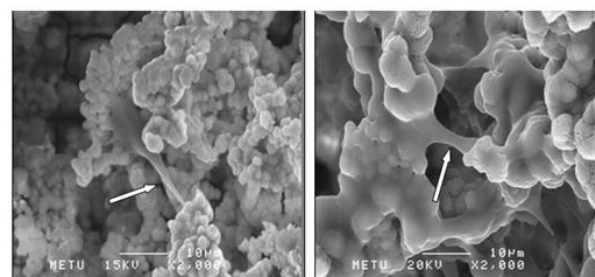


Figure 1. The SEM images (2000×) of the Saos-2 cells incubated for 7 days on the coating in normal 1.5×SBF for 14 days (left) and the coating in selenate added 1.5×SBF for 14 days (right). Arrows indicate cell extensions.

From, bacterial attachment and proliferation tests, it was seen that the number of *S. epidermidis* bacteria that were attached on coatings obtained from the selenate added 1.5×SBF and normal 1.5×SBF was very low.

CONCLUSION

Based on the results obtained in this study, it can be concluded that selenium can inhibit the growth of osteosarcoma cells and offers a promising solution for eliminating bacterial attachment but further studies are needed to determine the structural changes of hydroxyapatite after selenium doping.

REFERENCES

1. Yang J., *et al.*, Dig. Dis. Sci., (2009), 54: 246–254.
2. Bigi A., *et al.*, Biomacromolecules, (2000),1:752–756.

ACKNOWLEDGMENTS

The authors would like to thank the Scientific and Technological Research Council of Turkey (Grant no: 111M262) for providing financial support to this project and Prof. Nezahat Gürler and Bahar Akgün Karapınar, MD from Istanbul Faculty of Medicine, Istanbul University for providing bacterial isolates and their invaluable contributions.

Microfluidic Neuronal Circuitry – Towards Therapies for Huntington's Disease

Munyaradzi Kamudzandu^{1,2}, Paul Roach² and Rosemary A. Fricker¹

Institute for Science and Technology in Medicine, Keele University, ¹Huxley Building, Keele, Staffordshire, UK, ²Guy Hilton Research Centre, Stoke on Trent, UK

INTRODUCTION

Huntington's disease (HD) damages a circuitry of neurons in the brain resulting in involuntary movements and cognitive impairment¹. Microfluidic devices can be used to replicate the circuitry *in vitro*, to model the disease process and provide a high throughput system for testing neuroprotective therapies².

EXPERIMENTAL METHODS

A 5-compartment microfluidic device template was designed using AutoCAD. A master was then fabricated using the template via a process of photolithography. Microfluidic devices were fabricated via soft-lithography; polydimethylsiloxane (PDMS) polymer was cast onto a master and allowed to cure for approximately 1 h at 60°C. Devices were pre-coated with poly-D-lysine (PDL) and laminin prior to cell culture. Different types of dissociated rat central nervous system (CNS) cells were cultured for 14 - 21 days. Cells were examined for electrophysiology properties using patch clamp and calcium imaging.

RESULTS AND DISCUSSION

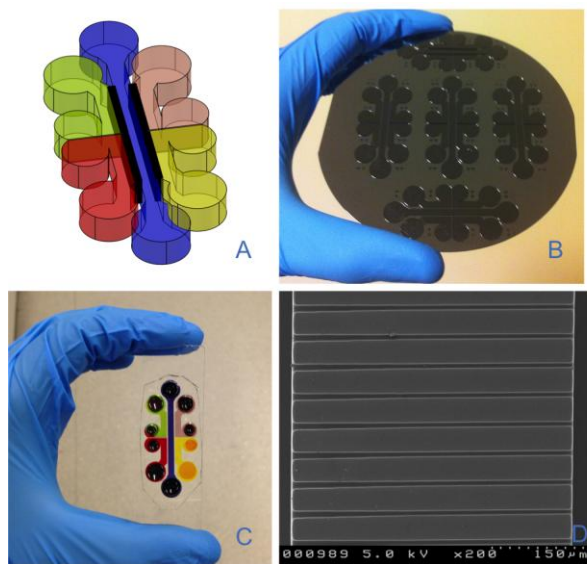


Fig 1: AutoCAD template design for microfluidic device, A. Compartments in different colors are separated by tapered microgrooves (black). 5-compartment device silicon master, B. PDMS microfluidic device with 5 compartments in different colors, C and PDMS, soft-lithography fabricated grooves, tapered (left to right) D.

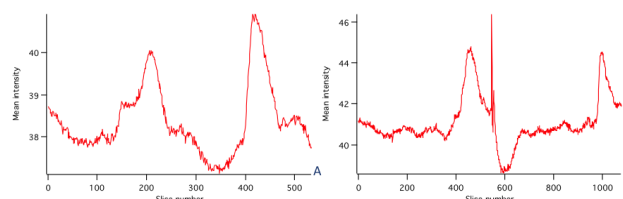


Fig 2: Calcium oscillations. A and B show Z-axis profile of mean intensity through a stack (ImageJ) for a cortical and LGE neuron, respectively. Rise and fall of intensity equals neuron depolarization.

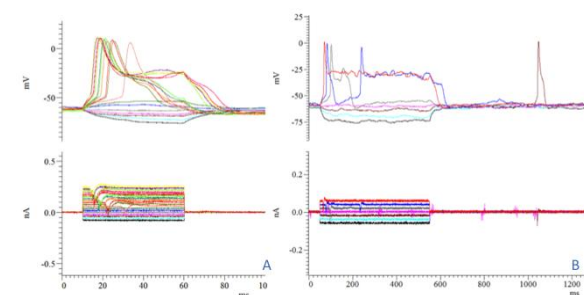


Fig 3: Patch clamp performed on cortical neuron. Depolarization and hyper-polarization spikes after current injection, A. Spontaneous firing observed after 1000ms, since no current injection was applied when spike was observed, B.

A compartmentalized microfluidic device (Fig 1) was fabricated and provides a platform for developing cultured neuronal networks. Different types of neurons can be cultured and connectivity is established via tapered microgrooves (Fig 1D). Calcium oscillations, using Fluo4 dye, were observed for unconnected cortical and lateral ganglionic eminence (LGE) neurons (Fig 2). Spontaneous firing was observed for cortical neurons using patch clamp (Fig 3).

CONCLUSION

Calcium imaging and patch clamp provide ways of measuring connectivity within a cultured neuronal network. Continuing work will involve more calcium imaging, viral transfection for tracing/imaging generation of action potentials across compartments as well as use of microelectrode arrays (MEAs) for studying extracellular electrical activity of networks.

REFERENCES

1. Handley, O.J, Dunnett, S.B, and Rosser, A.E., *Clinical science* (2006), 110(1): pp.73-88.
2. Chan, A, Orme, R.P, Fricker, R.A, and Roach, P., *Advanced drug delivery reviews* (2012)

ACKNOWLEDGMENTS

This work was carried out through funding from EPSRC DTC in Regenerative Medicine.

Nanoscale Analyses of *Parawixia bistrata* Synthetic Spider Silk Fibres

Valquíria A Michalczechen-Lacerda^{1,2*}, Giovanni R Vianna², André M Murad², Luciano P Silva², Elíbio L Rech²

¹Department of Cell Biology/ Institute of Biology, University of Brasília, Brazil, * kira21bio@gmail.com

^{2*}Synthetic Biology and Nanobiotechnology Group/Embrapa Genetic Resources and Biotechnology, Brazil,

INTRODUCTION

Spider silks are remarkable natural polymers and, with advances in genetic engineering, it is possible to produce synthetic silks based on recombinant proteins obtained from heterologous hosts even at large-scale. The core repetitive domain is a block copolymer-like arrangement, where amino acids sequence can result in a protein with unique biomechanical properties. Different protein sequences may result in new types of spider silks-based biomaterials. They also display biocompatibility and a slow rate of degradation, making synthetic spider silks promising candidates as biomaterials for tissue engineering, guided tissue repair, cosmetic products and industrial materials. The aim of the present study was to characterize synthetic *P. bistrata* MaSp2 fibres, for surface topography, viscoelasticity, roughness, Young's Modulus, separation and interacting forces using atomic force microscopy (AFM) image analyses and force spectroscopy experiments.

EXPERIMENTAL METHODS

A silk monomer gene from *P. bistrata* major ampullate 2 (MaSp2) was designed (DNA2.0). The 16 mer plasmid was constructed using a "head to tail" cloning strategy¹. All plasmids were confirmed by DNA sequencing. The 54 kDa protein containing a histag was induced at *Escherichia coli* BL21(DE03) with 1 mM isopropyl- β -D-thiogalactopyranoside (IPTG) for 4 hours, at 37°C, 200 rpm, in LB medium. After immobilized metal affinity chromatography (IMAC) purification, protein was dialyzed against distilled water, lyophilized and dissolved into 95% hexafluoroisopropanol (HFIP) + 5% formic acid. The fibers were wet spun by a pump syringe and extruded in 100% isopropanol coagulation bath. A total of 20 fibers with 1 cm length were separated in two groups: control (10 fibres) and isopropanol 80% treatment with 1 \times stretch (10 fibres). Surface and force spectroscopy analyses were performed by AFM under ambient conditions on a SFM-9600 instrument (Shimadzu, Kyoto, Japan) as previously described². Statistical significance was determined by student t test using the software Assistat 7.7 Beta (Assistat, Campina Grande, Brazil).

RESULTS AND DISCUSSION

The fibres presented inhomogeneous topographical characteristics. At least 2-4 different areas of each fibre were analysed. All groups presented a similar general pattern for Rz (maximum height), Rzjs (10 points mean roughness based on the five highest peaks and lowest valleys in the entire sampling length), Rp (maximum peaks and lowest valleys) presenting no difference between control and isopropanol groups. However, Ra

(arithmetic average roughness), Rq (root-mean-square roughness), Rv (maximum valley depth) analysis showed a decreased for isopropanol treatment compared to control group ($P < 0.05$).

For the fibre force spectroscopy measurements there were no difference between control group and isopropanol treatment for detachment force (comprised adhesive forces), Young's Modulus (local elasticity), maximum load force and energy dissipated during the analyses. Only the snap-in, which illustrate the attractive force resulting from the primary surface interactions of the fibre with the tip, showed an increase for the isopropanol treatment group ($P < 0.01$).

The isopropanol-treated group did not differ significantly from the control group as expected. It is known that alcohols might be responsible for induction β -sheet formation. In a previous work², isopropanol seems to result in a better fibre formation than using methanol for post-spinning treatments, and they also found a decrease for Rv parameter². Other studies have shown inferior mechanical properties for synthetic fibres from recombinant protein with low molecular mass compared to natural fibres. However, synthetic fibres can increase its mechanical quality as a natural fibres as long as the monomers and protein molecular mass are increased³. Synthetic spider silk fibre with high molecular mass as native one (300 kDa) needs to be measured with this technology.

CONCLUSION

The synthetic fibres presented irregular surface, elasticity and strength. This biomaterial depends on their molecular organizations which are not completed even after extrusion. Different bath coagulation and a treatment post-spinning still needs to be optimized for the production of synthetic fibres with quality similar to natural dragline silk fibre. Analyses by AFM are a reliable method to qualitatively describe the mechanical properties of silk fibres.

REFERENCES

1. Teulé F *et al.*, Nature Protocols. 4:341-355, 2009
2. Menezes GM *et al.*, Polymer Journal. 45:997-1006, 2013
3. Xia XX *et al.*, PNAS. 107:14059-14063, 2010

ACKNOWLEDGMENTS

The authors would like to thank National Council for Scientific and Technological Development (CNPq), Coordination for the Improvement of Higher Education Personnel (CAPES), Fundação de Apoio a Pesquisa (FAP-DF), Embrapa Genetic Resources and Biotechnology and University of Brasília (UnB) for providing financial support to this project.



Characterization and *In Vitro* Testing of Calcium Phosphate Coatings on Dense and Porous Substrates

Alexandre Antunes Ribeiro^{1*}, Roseli Marins Balestra¹, Mônica Calixto de Andrade², Emanuela Prado Ferraz³, Adalberto Luiz Rosa³, Paulo Tambasco de Oliveira³, Marize Varella de Oliveira¹

^{1*}Powder Technology Laboratory, National Institute of Technology, Brazil, alexandre.antunes@int.gov.br.

²Polytechnic Institute of Rio de Janeiro, Rio de Janeiro State University, Brazil.

³Department of Oral Surgery, Ribeirão Preto Dental School, University of São Paulo, Brazil.

INTRODUCTION

New developments have shown that titanium (Ti) implants with interconnected porous structure improves osseointegration because it provides space for anchoring bone cells and for vascular and bone tissue ingrowth¹. As Ti does not exhibit osteoinduction, calcium phosphate (CaP) bioactive coatings on Ti surfaces have been studied².

In this work, a biomimetic methodology consisted in a simplified solution (SS) with calcium (Ca) and phosphorus (P) ions, was used in order to deposit CaP coatings on Ti substrates by a simple and fast technique³. The main objective of the work was to assess the composition and biocompatibility by *in vitro* testing of CaP coatings on Ti substrates precipitated from SS solution.

EXPERIMENTAL METHODS

Porous Ti samples produced by powder metallurgy (C-PTi) and dense commercially pure Ti sheets (C-DTi), both ASTM F67-grade 2, were used as control substrates. The samples were chemically treated with 5 mol/L NaOH solution in ultrasonic bath, for 2 hours at room temperature and heat treated at 200°C/2h in a chamber furnace in air, for enhancing surface bioactivity. Then they were immersed for 10 days in the SS solution, prepared with pH 7.0, resulting in the following ionic concentration (10^{-3} mol/L): 2.0 (Na^+), 2.5 (Ca^{2+}), 5.0 (Cl^-), 1.0 (HPO_4^{2-}). Coated samples were named as PTi and DTi. Fourier Transform Infrared Spectroscopy (FTIR), Scanning Electron Microscopy (SEM/EDS) and X-Ray Photoelectron Spectroscopy (XPS) were used for characterization. The rapidly mineralizing UMR-106 cell line was used to assess matrix mineralization by alizarin red-S staining and extraction at days 7, 10 and 14.

RESULTS AND DISCUSSION

Figure 1a shows the SEM topographic view of C-PTi substrate without CaP coating, with $61.38 \pm 0.04\%$ average porosity and large interconnected macropores. Figure 1b displays a CaP coating with network microstructure on PTi substrate, as confirmed by FTIR and XPS analyses.

Figure 2 depicts the results of UMR-106 cultures. All Ti substrates supported the development of the osteoblastic phenotype. However, the porous substrates showed the highest alizarin red-S values, especially for those coated with CaP.

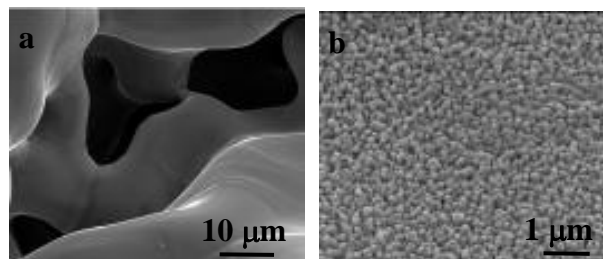


Figure 1: SEM images of C-PTi sample without CaP coating (a) and PTi with CaP coating (b).

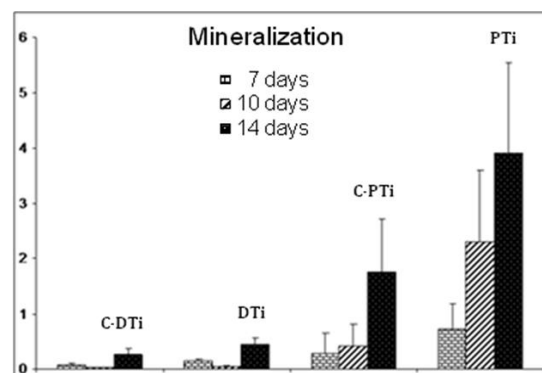


Figure 2: Alizarin red-S extraction of UMR-106 cell cultures grown on C-DTi, DTi, C-PTi and PTi substrates for 7, 10 and 14 days.

CONCLUSION

CaP coatings were deposited on porous and dense Ti substrates, as indicated by SEM/EDS, FTIR and XPS analyses. *In vitro* testing revealed that all Ti substrates were able to support the development of the osteoblastic phenotype, but the porous Ti exhibited the greater osteogenic potential. In addition, the effect of CaP coating was more pronounced for the porous group.

REFERENCES

1. B. Dabrowski *et al.*, J. Biomed. Mater. Res. Part B: Appl. Biomater. 95B:53-61, 2010.
2. B. León and J.A. Jansen, Thin calcium phosphate coatings for medical implants, Springer Science, 2009.
3. A. A. Ribeiro *et al.*, Appl. Surf. Sci. 265:250-256, 2013.

ACKNOWLEDGMENTS

The authors thank to National Council for Scientific and Technological Development (CNPq/Brazil) and Carlos Chagas Filho Research Foundation of the State of Rio de Janeiro (FAPERJ/Brazil) for financial support.

Synthesis and Characterization of Novel Chitosan Hydrogels for Biomedical Applications

Krzysztof Pazdan*, Kinga Pielichowska*, Jan Chłopek,

AGH University of Science and Technology,
Faculty of Materials Science and Ceramics,
Department of Biomaterials,
Al. Mickiewicza 30, 30-059 Kraków, Poland
*e-mail: kpazdan@agh.edu.pl, kingapie@agh.edu.pl

INTRODUCTION

Biodegradable materials for drug delivery and bone tissue engineering have recently been intensively investigated, but there are still a lot of problems concerning their bioactivity, biocompatibility, drug release profile etc.

The most promising materials are composites based on natural polysaccharides such as chitosan. Its properties like bioactivity, biodegradability, non-toxicity etc. make them one of the most promising material for biomedical application. Referring to some studies, chitosan hydrogels could promote the proliferation and osteogenesis, but only with moderate swelling ratio of material. However, the most common organic cross-linker for chitosan is glutar aldehyde which causes adverse effect on living organisms. In this work, Laponite® was used to cross-link hydrogel and to improve bioactivity of the composite.

EXPERIMENTAL METHODS

Selected type of Laponite® and two chitosan types with different molecular weight - 100,000-300,000 and 600,000-800,000 purchased by Acros Organics were used. Synthesis was performed at room temperature or at 50°C and under mechanical stirring or using sonication. In synthesis process chitosan was dissolved in 2% aqua solution of acetic acid. All samples had the same content - 3% of chitosan and 7.5% of Laponite®. They were also precipitated as a beads to 5% solution of tripolyphosphate ions to achieve ionic gelation chitosan phase. Preliminary bioactivity assessment was performed using Kokubo method and surfaces of the samples were analyzed by SEM. The obtained samples were also investigated by means of XRD, FTIR and DSC methods.

RESULTS AND DISCUSSION

Results of DSC investigations of all chitosan/Laponite composites are presented in Fig. 1. The obtained results suggest that the reaction conditions significantly influenced on material properties. DSC results show that increase temperature of reaction up to 50°C (samples with 'c' index in sample name) or sonication ('u' index) leads to changes in thermal properties of the samples in comparison to samples obtained at room temperature ('z' index).

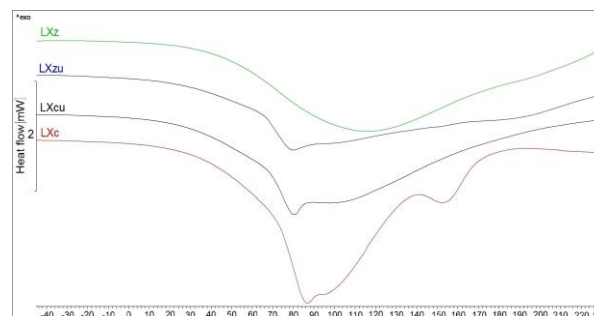


Fig. 1. DSC curves of low molecular weight chitosan/Laponite composites.

CONCLUSION

Using Laponite as a cross-linker, glutar aldehyde was eliminated. Obtained samples showed different thermal properties, depending on the reaction conditions. However, results for samples obtained using sonication treatment were similar to thermal characteristics of samples obtained at higher temperature. Moreover results of *in vitro* investigations show potential bioactivity of the chitosan/Laponite composites - the formation of an apatite layer on the samples surface during incubation in SBF was observed.

REFERENCES

1. Pielichowska K., Błażewicz S., Bioactive polymer/hydroxyapatite (nano)composites for bone tissue regeneration. *Advances in Polymer Science* 2010, 232, 97–207.
2. Kokubo T., Takadama H.: How useful is SBF in predicting *in vivo* bone bioactivity. *Biomaterials* 27 (2006) 2907–2915
3. Giri T.K., Thakur A., Alexander A., Ajazuddin, Badwaik H., Tripathi D.K.: Modified chitosan hydrogels as drug delivery and tissue engineering systems: present status and applications. *Acta Pharmaceutica Sinica B* 2/5 (2012) 439-449
4. <http://www.laponite.com> (10.07.2013)

ACKNOWLEDGMENTS

This work was financed by statutory research 11.11.160.256 of Faculty of Materials Science and Ceramics.

Silver Nanoparticles Modified Titanium for Medical Implants

Barbara Szaraniec¹, Magdalena Oćwieja², Marta Kujda² and Bartosz Piec¹

¹ Department of Biomaterials, Faculty of Materials Science and Ceramics,
AGH – University of Science and Technology, Poland szaran@agh.edu.pl

² Jerzy Haber Institute of Catalysis and Surface Chemistry,
Polish Academy of Sciences, Poland

INTRODUCTION

Titanium and its alloys are the most widely used engineering materials for implants in dental and bone surgery due to their good mechanical properties and biocompatibility. In literature there are reports of serious infections - both acute and delayed ones - caused by titanium. These cases must be treated with care, as bone infections can be very dangerous to health and difficult to treat. One approach is to design implants to be bactericidal. Introduction of silver nanoparticles into materials can provide them with antibacterial and antiviral functions, thanks to silver's antimicrobial properties [1,2] and long period of activity [3].

EXPERIMENTAL METHODS

Bulk and porous cylinder-shaped titanium specimens (11 mm in diameter and 4 mm tall) were manufactured by powder metallurgy. Titanium powder (Atlantic Equipment Engineers, USA) was mixed with porogen (ammonium bicarbonate, Chempur) at 70/30 and 50/50 weight ratio. The amount of porogen determined the final porosity: $30 \pm 5\%$ and $53 \pm 4\%$ [4,5]. Isostatically pressed cylindrical die stampings were thermally treated at 1200°C under vacuum conditions.

Using the defined silver particle suspension (15nm), studies of adsorption on titanium modified by poly(allylamine hydrochloride) (PAH) were carried out [6]. The coverage of adsorbed particles was directly determined by AFM (atomic force microscopy) and SEM (scanning electron microscopy) imaging. Antibacterial activities of silver nanoparticles modified titanium against *Escherichia coli* (K12) were tested. Zones of inhibition of *E. coli* around titanium disks were determined by a disk-diffusion method in Mueller Hinton broth + 1,5% agar. Inhibition zones were observed after 12h lawn growth of *E. coli* cells at 37°C . As a reference sample untreated titanium sinters were used.

RESULTS AND DISCUSSION

AFM and SEM analysis (fig.1) indicate that the surface coverage of silver particles was about $38 \pm 5\%$ and they formed uniform monolayer.

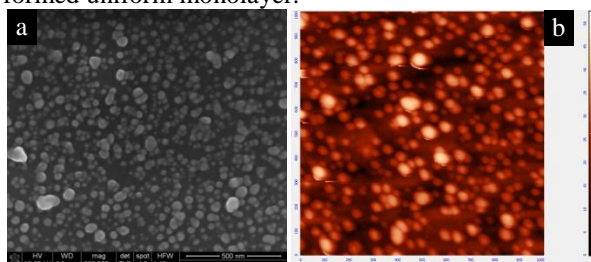


Figure 1 SEM (a) and AFM (b) images of titanium surface with silver nanoparticles.

Modified sinters exhibit different antibacterial activity, dependantly on their porosity (tab.1.). Greater porosity is connected with greater surface area and larger number of silver nanoparticles. Therefore, antibacterial effect is the most noticeable for sinters with 50% porosity.

Table 1 Zone and area inhibition for initial and modified titanium

material	zone of inhibition [mm]	area of inhibition [mm ²]
Ti	0	0
Ti/PAH/nAg	3	132
Ti30/PAH/nAg	4	189
Ti50/PAH/nAg	7	396

(Ti-untreated bulk titanium, Ti/PAH/nAg – modified bulk titanium, Ti30/PAH/nAg and Ti50/PAH/nAg – modified porous titanium with porosity 30% and 50%, respectively)

CONCLUSION

The measurements suggest that it is feasible to produce uniform silver particle monolayers of desired coverage in the self-assembly process of particles.

Both bulk and porous titanium modified by silver nanoparticles using that method, exhibit bactericidal effect. They are promising materials for medical implants. Using such materials like can make medical procedures more successful and safer even among high-risk patients.

REFERENCES

1. Kang H.Y. *et al.*, J Biotechnol Bioeng 15 2000 521
2. Kawashita M. *et al.* Biomaterials 21 (2000) 393
3. Toshikazu T. Inorg Mater 6 (1999) 505
4. Szaraniec, B. *et al.*, Eng Biomat 81-84:49-52, 2008
5. Ścisłowska-Czarnecka A. *et al.*, Tissue & Cell 44: 391–400, 2012
6. Oćwieja M., Z. Adamczyk, *Langmuir*, 29:3546-3555, 2013.

ACKNOWLEDGMENTS

The authors acknowledge financial support from AGH-UST project no 11.11.160.937

Synergistic Reinforcement of Poly(ϵ -caprolactone)/Gelatin Nerve Tissue Engineering Scaffolds by Graphene Oxide Nanosheets

S. Soltanian-Zadeh¹, Z. S. Ghazali¹, M. Rabiee¹, F. Moztarzadeh¹, M. Mozafari²

¹ Biomedical Engineering Department, Amirkabir University of Technology, Tehran, Iran, sepeedah@aut.ac.ir

² Nanotechnology and Advanced Materials Department, Materials and Energy Research Center (MERC), Iran

INTRODUCTION

Damage to the nervous system is devastating to patients and although methods such as nerve autografts and allografts have been developed, they have limitations such as shortage of donor nerves or rejection by the body's immune system¹. In recent years, engineered materials for the regeneration of the nerve tissue have been proposed. These engineered materials must possess balanced characteristics in terms of biocompatibility, biodegradability, mechanical properties, surface properties, and permeability². To this end, composites of natural and synthetic polymers are designed. It is also desirable to mimic the structure of the extracellular matrix (ECM) which has a fibrous structure. One common method for the synthesis of nanometer fibers is electrispinning³. Ghasemi et al.⁴ electrospan poly(ϵ - caprolactone) or PCL and gelatin and showed that although the 50:50 ratio of PCL/gelatin has good wettability, it lacks mechanical integrity compared to the PCL/gelatin 70:30 nanofibers.

Recently carbon nanomaterials such as graphene have gained much attention due to their unique properties. Graphene is a 2-D sheet of sp^2 bonded carbons with high Young's modulus and good electrical conductivity⁵. Graphene oxide (GO) is the oxidized form of graphene which has carboxyl and carbonyl groups on the edges, and epoxide and hydroxyl functional groups on its basal plane. Due to these functional groups, GO is hydrophilic. In this work we utilize GO as nanofiller for 70:30 PCL/gelatin electrospun scaffolds and report the morphology and biocompatibility of these structures towards neural cells.

EXPERIMENTAL METHODS

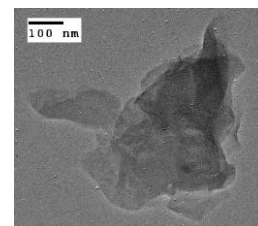
Graphene oxide was prepared through a modified Hummer's method⁶. In a typical procedure, graphite powder (0.5 g) and $NaNO_3$ (0.5 g) were added to H_2SO_4 (23 mL). Mixture was stirred at 0°C and $KMnO_4$ (3 g) was gradually added. The temperature was raised to 35°C and stirred for 24 hours. Afterwards DI water (140 mL) and H_2O_2 (3 mL) were added until gas evolution ceased. The mixture was allowed to rest for 1 day. The supernatant was removed and the remaining particles were washed and centrifuged with HCl (1M) and water to remove remaining salts and acids. The aqueous solution of graphite oxide was ultrasonicated for 1 hour to achieve GO dispersion. This solution was dried at 40°C to yield the solid form of graphene oxide. Two dispersions of 0.5 wt% and 1 wt% of GO were prepared in dimethylformamide (DMF) solvent via ultrasonication. PCL and gelatin were added to these solutions with a weight ratio of 70:30, and a

total concentration of 5 wt%. A control solution containing only PCL and gelatin was also prepared. These solutions were electrospun with mass flow rate of 0.6 mL/h with an applied voltage of 12 kV.

The chemical properties of the synthesized GO nanosheets were characterized by FT-IR. XRD was used to show interlayer spacing of the sheets. AFM and TEM analyses were performed to determine sheet thickness and morphology respectively. Morphology, fiber diameter, and porosity of the scaffolds were determined by SEM images. Mechanical properties of the scaffolds were also determined. In order to observe neural biocompatibility of the samples, PC 12 cells were proliferated for 2 days. Cell viability was determined by MTT assay.

RESULTS AND DISCUSSION

FTIR and XRD analyses confirmed successful formation of GO nanosheets. Also, TEM images (shown on the right) showed the sheet like structure of these nanoparticles.



SEM images of the scaffolds exhibited the desirable morphology for nerve regeneration. Moreover, mechanical properties of the scaffold was enhanced using GO as a nanofiller. Biocompatibility of these scaffolds was confirmed by the viability of neural cells.

The enhanced mechanical properties can be attributed to the addition of GO nanoparticles and their ability to bond with PCL and gelatin through functional groups such as the hydroxyl and carboxyl groups.

CONCLUSION

Addition of GO as a nanofiller not only enhances the mechanical properties of the scaffolds, but also can make the scaffolds less hydrophobic due to its hydrophilic nature; hence making the scaffold suitable for nerve regeneration applications.

REFERENCES

1. Fraczek-Szycpta A. *et al.*, J. Mat. Sci. Eng.:C. 34: 35-49, 2014
2. Gu X. *et al.*, J. Prog. Neuro. 93: 204-230, 2011
3. Cao H. *et al.*, J. Adv. Drug. Del. Rev. 61: 1055-1064, 2009
4. Ghasemi *et al.*, J. Biomat. 29: 4532-4539, 2008
5. Zhu Y. *et al.*, J. Adv. Mat. 22: 3906-3924, 2010
6. Hummers W. *et al.*, J. Amer. Chem. Soc. 80: 1339-1339, 1958

Mechanical reinforcement of chitosan-poly(lactic-co-glycolic) acid scaffolds by 58S bioactive glass

Katayoun Nazemi¹, Fathollah Moztarzadeh¹, Masoud Mozafari²

¹ Biomedical Engineering Department, Amirkabir University of Technology, Iran

² Nanotechnology and Advanced Materials Department, Materials and Energy Research Center (MERC), Iran,
katy.nazemi@yahoo.com

INTRODUCTION

In the recent years, so much attention has been paid to nanocomposites for using in tissue engineering. Many of composites are currently has been used as scaffolds for biomedical applications¹. In bone tissue engineering, scaffolds served as the matrices of tissue formation plays a pivotal role and should be highly porous, required surface property that promotes cell adhesion, proliferation and differentiation, desirable mechanical properties, non-cytotoxicity and osteoconductivity. Currently, composites of polymers and ceramics are being developed with the aim to increase the mechanical scaffold stability and to improve tissue interaction².

In this study, we synthesized a bioactive glass 58S using sol-gel method. Then, investigate the mechanical behavior of the samples by using mechanical compressive test.

EXPERIMENTAL METHODS

The bioactive glass 58S powder (60% SiO₂, 4% P₂O₅, and 36% CaO) (mol%) has been synthesized via sol-gel method. For the preparation of each scaffold samples, 250 mg chitosan dissolved in 1% acetic acid solution. Different percentages of bioactive glass 58S were added into the chitosan solutions and stirred for 12 h. Next, 62.5 mg of PLGA has been dissolved in 3 mL of dichloromethane, and then added into the dispersing phases [0% (S1), 0.5% (S2), 1% (S3), 1.5% (S4), 2% (S5) of bioactive glass 58S] under moderate magnetic stirring³.

RESULTS AND DISCUSSION

The microstructures of the cross-section of the typical prepared scaffolds have been observed with SEM, shown in Fig. 1.

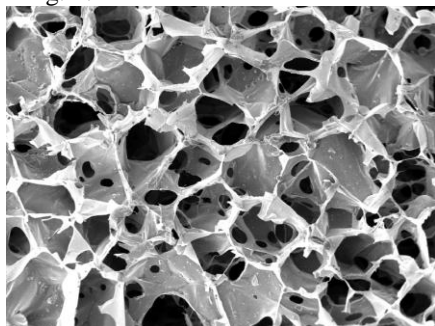


Fig.1. Low magnification SEM micrograph of the prepared scaffold, sample S3

The prepared scaffolds have been tested to determine the effects of increasing bioactive glass 58S on the mechanical properties. Fig. 2. shows the data obtained

from mechanical compressive tests of the samples, and compares them with natural cancellous bone. In our study, the results represented that E and σ both increased progressively by further addition of bioactive glass 58S. It is worth mentioning that σ and E of the samples containing higher amounts of bioactive glass 58S have been in the range of cancellous bone.

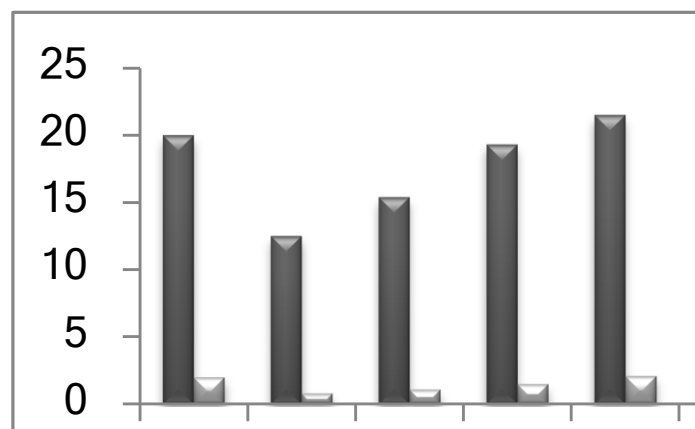


Fig.2. the mechanical properties of the scaffolds from compression tests compared with cancellous bone

CONCLUSION

In conclusion, the elastic modulus of the scaffolds was comparative to the natural cancellous bone and also by increasing weight percentage of bioactive glass 58S the mechanical strength increased.

REFERENCES

1. D.W. Huttmacher, Scaffolds in tissue engineering bone and cartilage, *Biomaterials* 21 (2000) 2529–2531.
2. L.D. Shea, D. Wang, R.T. Franceschi, D.J. Mooney, Engineered bone development from a pre-osteoblast cell line on three-dimensional scaffolds, *Tissue Eng.* 6 (2000) 605–617.
3. K. Nazemi, F. Moztarzadeh, N. Jalali, S. Asgari, M. Mozafari, Synthesis and characterization of poly(lactic-co-glycolic) acid nanoparticles-loaded chitosan/bioactive glass scaffolds as a localized delivery system in the bone defects, *Biomed Research International*. (2014) (In Press)

ACKNOWLEDGMENTS

The authors would like to thank many colleagues, PhD students and collaborators who have made a vast contribution to this area of research.

Co-culture of human monocytes and mesenchymal stem cells in order to simulate the bone remodelling processes

Claudia Kleinhans^{1,2}, Freia Schmid², Franziska Schmid², Petra J. Kluger^{2,3}

¹Institute for Interfacial Process Engineering and Plasma Technology IGVP, University of Stuttgart, Nobelstr. 12, 70569 Stuttgart, Germany, claudia.kleinhans@igb.fraunhofer.de

²Fraunhofer Institute for Interfacial Engineering and Biotechnology IGB, Stuttgart, Germany

³Hochschule Reutlingen, Process Analysis & Technology (PA&T), Reutlingen

INTRODUCTION

In the field of orthopedics and traumatology, the improvement of implant materials plays a crucial role for the patient's quality of life. Newly developed biodegradable materials have the potential to provide enhanced mechanical properties and reduce the need for implant removal surgery. The initial evaluation of newly designed materials in vitro to predict the outcome in vivo is strongly desired. Therefore, to approach the in vivo situation we established co-culture conditions for primary human mesenchymal stem cells (hMSCs) and monocytes (MCs) to address the bone remodelling process. Our aim of this study was the evaluation of the osteoclastogenesis of monocytes in consequence to the interaction and cross talk with hMSCs without any differentiation factors by media supplementation.

EXPERIMENTAL METHODS

Human monocytes were isolated of buffy coats and were characterized by FACS analysis, histochemical staining and differentiation studies.

For co-culture experiments, hMSCs were seeded either on tissue culture plates (TCPS) or on bovine cortical bone slices. Two set ups were considered: proliferative media and the induction of the osteogenic differentiation for 14 days. Subsequently, monocytes were seeded on top of the pre-cultured hMSCs and were evaluated after another 14 days for an osteoclastic phenotype by immunofluorescence staining and REM analysis.

RESULTS & DISCUSSION

MCs were successfully differentiated to osteoclasts by media supplementation including RANKL and M-CSF (Fig. 1 D). Co-culture of hMSCs and MCs led to the expression of an osteoclastic phenotype after 14 days (Fig. 1 B). Cathepsin K, VNR and Actin/Vinculin were

expressed and analyzed by immunofluorescence staining revealing multinucleated cells within the co-culture set up.

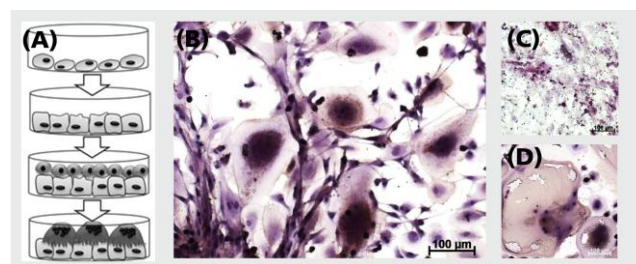


Fig. 1 Development of culture conditions for a successful co-culture of osteoblasts and osteoclasts. (A) VNR staining of co-cultured hMSCs and monocytes (B) osteogenic differentiated hMSCs (C) and differentiated monocytes (D).

The co-culture of hMSCs and hMCs leads to an osteoclastic phenotype after 14 days. The interaction of both cell types is therefore sufficient to generate osteoclast like cells.

CONCLUSION

The bone remodelling process can be simulated in vitro by using monocytes and mesenchymal stem cells. However, the activity of the osteoclasts must be further investigated e.g. by the detection of resorption pits in order to test efficiently the degradation potential of newly designed materials. The co-culture could further be transferred into a three-dimensional setting to consider the influence of a multilayer culture.

ACKNOWLEDGMENTS

The authors would like to thank the Fraunhofer-Gesellschaft for funding the “DegraLast” project.

Electrospun Poly(ϵ -caprolactone)/Gelatin Scaffold Electrophoretically Coated with Graphene Oxide for Nerve Tissue Engineering

Z.S. Ghazali¹, S. Soltanian-Zadeh¹, F. Moztarzadeh¹, M. Mozafari²

¹ Biomedical Engineering Department, Amirkabir University of Technology, Iran, mahya.ghazali@yahoo.com

² Nanotechnology and Advanced Materials Department, Materials and Energy Research Center (MERC), Iran

INTRODUCTION

The peripheral nervous system in small injuries has an intrinsic ability to regenerate itself under the appropriate conditions. In human, axon regeneration occurs in a very low rate, approximately about 2-5 mm/day. Surgical techniques like autograft, allograft and xenograft have been used for treating transection injuries in peripheral nerves and autologous nerve grafting became a golden standard technique compared to other methods. However, it has disadvantages such as limited availability of donor sites¹. Therefore, developing artificial nerve grafts has become a great challenge in tissue engineering. It has been widely recognized that advanced materials including carbon-based nanomaterials could be considered as promising candidates for applications in regenerative medicine due to their unique physical, chemical and biological properties. Graphene is a two-dimensional carbon nanostructure arranged in a hexagonal network. Due to its unique properties like flexibility, electrical conductivity, high strength, stiffness, and biocompatibility, it has become a very attractive biomaterial in recent years. Graphene oxide (GO) is a nanomaterial containing epoxide, carboxyl and hydroxyl functional groups. The presence of functional groups on the surfaces of scaffolds play a key role in cell adhesion, proliferation, migration and has particular effect for aligning neural cells². Electrophoretic deposition (EPD) is an electrochemical method which is based on two stages. First an electric field is applied between two electrodes, then in the second stage the particles deposit to form a relatively compact film³. The intrinsic negative charge of GO make it suitable for this purpose.

Poly(ϵ -caprolactone) (PCL) has been widely used for the reconstruction of various tissues, but it lacks functional groups on its surface which results in poor cells adhesion. In addition electrospun nanofibers are known to be suitable scaffolds for neural tissue engineering applications and modification of the substrates often provides better environments for neurite outgrowth⁴. Our study is aimed at coating GO on a PCL/gelatin scaffold for nerve tissue engineering and investigating the effect of this coating on the mechanical properties and bioactivity of the scaffolds.

EXPERIMENTAL METHODS

1. Synthesis of GO

Natural graphite powder (particle diameter of ≤ 20 μm , Sigma Aldrich) was utilized to produce graphite oxide suspension by modified Hummer's method⁵. Graphene oxide nanosheets were obtained by ultrasonication of the graphite oxide suspension at frequency of 40 KHz and power of 150 watt for 1 h.

2. Preparation of electrospun scaffold

PCL/DMF and gelatin/DMF solutions were prepared separately under continuous stirring for 2 h. Then they were mixed to obtain a solution with 70:30 PCL/gelatin ratio. A voltage of $1\text{kV}\cdot\text{cm}^{-1}$ and a flow rate of 0.5 ml h^{-1} were applied for 6 h to prepare the scaffold.

3. Coating the scaffold via EPD

EPD was done by using two electrodes which were connected to a DC voltage source with the scaffold situated at the center of the EPD cell.

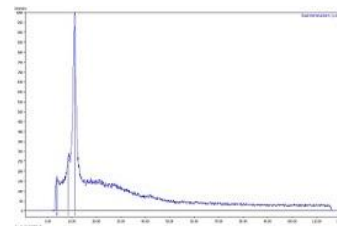
4. Neural cell culture on the scaffold

In order to investigate the effect of the prepared scaffold on nerve cell viability, PC 12 cells were seeded onto the coated PCL/gelatin nanofiber scaffold and MTT assay was executed.

RESULTS AND DISCUSSION

Water solubility of GO

and the presence of functional groups on its surface caused a homogeneous coating on the PCL/gelatin scaffold and made it more hydrophilic; which in turn provides a significantly better substrate for protein absorption. The results indicate that GO was successfully synthesized as it is shown in the XRD test below. The results are also confirmed by TEM, FT-IR and SEM analyses. Presence of the GO layer on the PCL/gelatin scaffold provides a biocompatible and nanostructured surface topography that improves cell viability.



CONCLUSION

An improvement in the bioactivity of the PCL/gelatin nanofibrous scaffold is observed in the presence of GO coating. This method can be used for other tissue engineering scaffolds to functionally customise the final characteristics.

REFERENCES

1. Cao H. *et al.*, J. Adv. Drug. Del. Rev. 61: 1055-1064, 2009
2. Aniruddh S. *et al.*, J. Adv. Mater. 25:5477-5482, 2013
3. Chavez-Valdez A. *et al.*, J. Phys. Chem. 117:1502-1515, 2012
4. Alvarez-Perez M A. *et al.*, J. Biomacromolecules. 11:2238-2246, 2010
5. Hummers W. *et al.*, J. Amer. Chem. Soc. 80: 1339-1339, 1958

Morphometry of bone tissue around endossal implantation of Hap/TCP granules and autologous mesenchymal cells in rabbits with experimental osteoporosis

Aleksandrs Grishulonoks¹, Vita Zalite², Inese Cakstina³, Arvids Jakovlevs⁴, Andrejs Skagers¹

¹Department of Oral and maxillofacial surgery, Riga Stradins University, Latvia, ²Rudolfs Cimdins Centre for innovations and development of Biomaterials, Riga Technical University, ³Laboratory of Biodosimetry and bioanalytical methods, Faculty of Biology, University of Latvia, ⁴Department of Pathology Riga Stradins University, or_aleksandrs.gr@gmail.com

INTRODUCTION

The current trend is the biologisation of non-organic bioceramic material to be close to natural living bone and the replacement of bone grafting by bioceramics saturated with growth factors or/and potential cells^{1,2,3}. As scaffold biphasic calcium phosphate bioceramics is evident⁴.

EXPERIMENTAL METHODS

Synthetic porous HAP ceramics Hap/TCP 90/10 with open porosity 61 % produced in Rudolfs Cimdins Biomaterials Innovations and Development Centre were used. Granules have macroporous structure with pore size 50 – 450 µm. All samples were sintered at 1150°C for 2 hours. Purity of hydroxyapatite phase was investigated using X-ray diffractometry and Fourier transform infrared spectroscopy. With permission of Latvian Food and Veterinary Administration on 10 Californian rabbits under general anesthesia with Dormicum and Ketamine experimental osteoporosis by ovariectomy and 8 weeks intramusculary metilprednisolone 1 mg/kg was developed. During the same surgery fat tissue from *omentum majus* were collected in tubes (Sarstedt) with physiological solution and heparin. Samples were then washed with PBS and treated with Collagenase type XI for 2 - 5 h in at 37°C. Cell pellet was seeded in tissue culture flasks in DMEM/20%FBS, soaked in 100%FBS for 2 h. lets and DMEM/10%FBS was added. Samples were incubated at 37°C, 5% CO₂ for one day. Before implantation samples were washed with PBS twice. Under local anesthesia with 1% Lidocaine and 1 mg Dormicum intramusculary implants loaded with cells on one side and pure Hap/TCP on other side in rabbit lower jaw hole were inserted. Samples were taken out after three and six months, histologic specimens stained with Hem/eoz and Masson trichrome in light microscope were evaluated. Image Pro+ morphometry was performed.

RESULTS AND DISCUSSION

Essential osseointegration of Hap/TCP granules in jaw bone was estimated. No signs of inflammation were detected.

Morphometric evaluation obtained average osseointegrated trabecular bone width only with Hap/TCP (90/10) granules - 271 mkm, trabecular bone width with granules and mesenchymal autologous cells 236mkm (p=0,107); cortical bone width only with Hap/TCP (90/10) granules 739 mkm, cortical bone

width with granules and mesenchymal autologous cells 753 mkm (p=0,341).

CONCLUSION

Morphometric measurement of osteoporotic bone osseointegrated with Hap / TCP (90/10) granules implanted in rabbit lower jaw with and without autologous mesenchymal cells after six month observation period was without statistically significant morphological differences.

REFERENCES

1. Ripamonti U, Crooks J, Khoali L, Roden L. The induction of bone formation by coral-derived calcium carbonate / hydroxyapatite constructs. *Biomaterials*.30:1428-39,2009
2. Scarano A, Degidi M, Iezzi G, Pecora G, Piattelli M, Orsini G, Caputi S, Perrotti V, Mangano C, Piattelli A. Maxillary sinus augmentation with different biomaterials: a comparative histologic and histomorphometric study in man. *Implant Dent*. 15(2):197-207,2006
3. Best SM, Porter AE, Thian ES, Huang J. Bioceramics: Past, present and for the future. *Journal of the European Ceramic Society*.(28):1319–1327,2008
4. A.Skagers, I.Salma, M.Pilmane, G.Salms, L.Feldmane, L.Neimane, L.Berzina-Cimdina/Trippl confirmation for bioactivity of synthetic hydroxyapatite (Hap) in bony environment // Termis EU 2011 Annual Meeting Tissue Engineering&Regenerative Medicine International Society, Granada, June 7-10,2011.

ACKNOWLEDGMENTS

The presented work was supported by Latvian State Research program's activity 4.5 "New materials and technologies for evaluation and substitution of biological tissue".

A Study On 45S5 Bioglass® Foam Dissolution

V. Melli¹, L.-P. Lefebvre², L. Altomare¹, L. De Nardo¹

¹Dipartimento di Chimica, Materiali e Ingegneria Chimica G. Natta, Politecnico di Milano, Italia

²National Research Council Canada, Boucherville, Canada, virginia.melli@mail.polimi.it

INTRODUCTION

The production of 45S5 Bioglass®-resorbable scaffolds for bone substitution has been strongly limited by the effects of thermal treatment on microstructure. [1] Several studies demonstrated that despite a glass ceramic structure, obtained scaffolds still maintain bioactivity, and ability to dissolve; however, a reduction in the kinetic of formation of HA in SBF solutions is in general reported. [2] Moreover questions related to the ability of crystalline phase to dissolve remained unanswered; ion release analysis displayed a plateau suggesting a stop in dissolution. [3] The presence of insoluble phases, that might provoke an inflammatory reaction if released in the form of particulate, cannot be excluded. [4]

The aim of the work is to understand behavior of glass ceramic scaffolds, made of 45S5 Bioglass® through a powder metallurgy process, in water.

EXPERIMENTAL METHOD

6 samples were immersed, in DI H₂O pH 4.5 at 80°C, 40°C and 20°C. H₂O was replaced every day ("D") in the three temperature conditions, kept static ("S") or stirring ("St") at 20 °C. For the first 28 days other samples were soaked in SBF+TRIS pH 7.4, replaced every 3 days, at 37 °C. Weight reduction was measured every 4 days after drying. In "epoxy test" a sample was embedded in epoxy resin and a polished surface was exposed to H₂O replaced every day at 80 °C. Scaffolds have been analyzed via SEM, XRD and micro-CT in order to elucidate the dissolution kinetic of the obtained glass ceramic scaffold.

RESULTS AND DISCUSSION

XRD pattern showed that the scaffold contains crystalline phases [5], with main crystalline phase Na₂Ca₂Si₃O₉ and a smaller amount of CaNaPO₄.

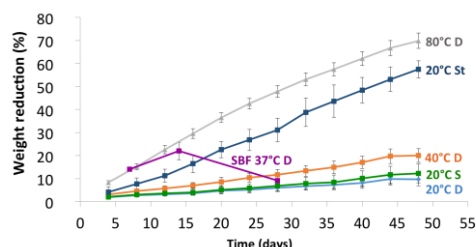


Fig.1: Weight reduction of bioglass foam sample in water and SBF solution.

As shown in fig.1, the weight reduction of sample immersed in water is linear with time in all the studied conditions. Raising temperature the slope of dissolution lines is increased. "D" condition at 20 °C has no effect on the dissolution rate probably because the process is still far from equilibrium after 24 h of dissolution. Otherwise, stirring solution provides a very fast

dissolution kinetic being all the surface area involved in the reaction. All this results are in contrast to the behavior in SBF solution, where the dissolution appears fast in the first 14 days but after the weight is again increased with the growth of the bioactive CaP layer thickness.

The linear dissolution trend suggests the absence of insoluble phases. On the contrary, CaP coating has a passive effect lowering dramatically the dissolution kinetic. The fast initial dissolution of bioglass in SBF could be ascribed to the effect of a higher solution pH, that can increase the dissolution product of the silica network. [3,6]

After dissolution in water the microstructural changing (e.g. the crystallites decomposition) observed in the case of SBF soaked samples [7], is no more evident and the scaffold maintained the same crystalline phase content after 16 days of dissolution.

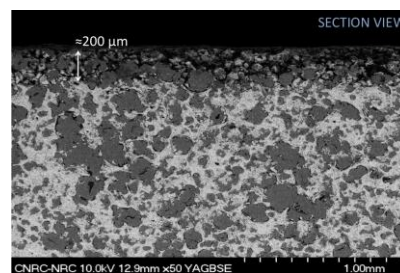


Fig.2: Section view of the dissolved polished surface of an epoxy embedded bioglass foam sample after 28 days.

The epoxy tests showed that different part of the foam can follow different dissolution kinetics resulting eventually in an homogeneous reduction of the bioglass foam height with respect to the epoxy surface. (fig.2) These observations suggested a heterogeneous dissolution due to the different dissolution kinetics.

CONCLUSIONS

Crystalline bioglass foam showed the ability to completely dissolve in water although with different kinetics. The macro dissolution behavior is homogeneous. Ongoing test are aiming to assess if insoluble micrometric crystallites are released or not in the bulk solution.

REFERENCES

- [1] Jones J.R., *Acta Biomater.* 9:4457-4486, 2013.
- [2] Chen Q.Z. *et al.*, *Biomaterials* 27(11):2414-2425, 2006.
- [3] Cerruti M. *et al.*, *Biomaterials* 26(14):1665-1674, 2005.
- [4] Hallab N.J. and Jacobs J.J., *Bull. NYU Hosp. Jt. Dis.* 67(2):182-188, 2009.
- [5] Aguilar-Reyes E.A. *et al.*, *J Am. Ceram. Soc.* 95(12):3776-3780, 2012
- [6] Alexander G.B. *et al.*, *J Phys. Chem.* 58(6):453-455, 1954.
- [7] Boccacini A.R. *et al.*, *Faraday Discuss.* 136(0):27-44, 2007.

Biocompatibility of Poly High Internal Phase Emulsion Scaffolds prepared using Stereolithography

Atra Malayeri^{*1,2}, Ilida Ortega¹, Frederik Claeysens², Colin Sherborne², Neil R Cameron³, Paul V. Hatton¹

¹School of Clinical Dentistry and ²Kroto Research Institute, University of Sheffield, UK and ³Department of Chemistry and Biophysical Science Institute, Durham University, UK. dtpl1am@sheffield.ac.uk

INTRODUCTION

Complex bone defects in the head and face would benefit significantly from the use of custom-shaped devices or scaffolds that stimulated tissue regeneration after implantation. Despite some promising data, resorbable polymeric biomaterials have not yet been optimised for preparation of custom structures using contemporary advanced manufacturing methods. Poly high internal phase emulsions (PolyHIPEs) have been reported to provide structures with interconnected micropores that have the potential to enhance biocompatibility. Despite their promise, only a limited volume of work has been reported on the biocompatibility of PolyHIPEs prepared using 2-ethylhexyl acrylate and isoboronyl acrylate, and only recently the fabrication of simple 3D structures via stereolithography has been reported¹. The aim of this study was therefore to evaluate the biocompatibility of this polyHIPE system using cultured bone cells, and to manufacture more complex “woodpile” three-dimensional scaffolds using stereolithography.

EXPERIMENTAL METHODS

Simple polyHIPE disks (approximately 1 cm diameter) based on 2-ethylhexyl acrylate and isoboronyl acrylate were fabricated. Some disks were further modified by plasma polymerization using acrylic acid to form a poly (acrylic acid) surface. The microporosity of these was studied using scanning electron microscopy (SEM). The *in vitro* response of MG63 osteosarcoma cells to both untreated and plasma treated scaffolds was investigated using SEM and MTT assay for up to 7 days culture. More complex 3D “woodpile” structures were prepared using the same polyHIPE materials and stereolithography. The structure of these was also investigated using SEM.

RESULTS AND DISCUSSION

Simple polyHIPE disks were shown to have a high degree of microporosity using SEM (Figure 1a). Cultured MG63 cells actively colonised the surface of these materials and remained viable for up to 7 days, as demonstrated by SEM (Figure 1b) and MTT assay. In all micrographs the open-cellular porous morphology was very evident. MTT assay further suggested that although cells were viable on all PolyHIPE disks, respiratory activity appeared to be greatest on acrylic acid plasma coated materials at all time points (1, 3 and 7 days). More complex “woodpile” PolyHIPE scaffolds were then fabricated via stereolithography (Figure 2).

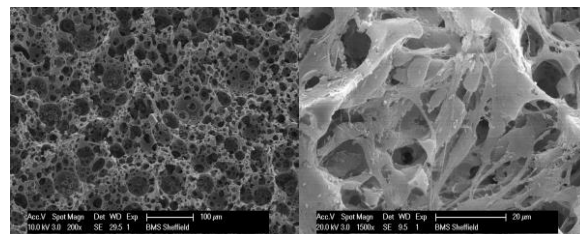


Figure 1. Scanning electron photomicrographs of the surfaces of a simple polyHIPE disc prepared by UV polymerisation (a) prior to tissue culture and (b) after 7 days of culture of MG63 bone cells.

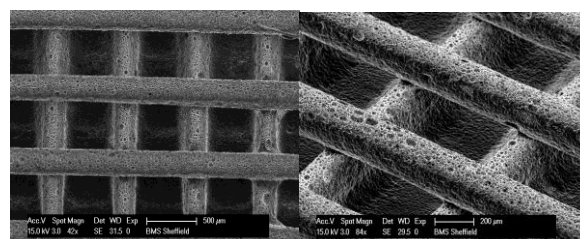


Figure 2. Scanning electron photomicrographs of basic “woodpile” structures formed from polyHIPE using stereolithography at (a) low and (b) higher magnification.

This data showed that the polyHIPE biomaterial reported here were both biocompatible in a bone cell culture model, and it was possible to manufacture more complex 3D structures to provide both macro- and microporous architecture in the same scaffold or device. Further work is continuing on these materials and other promising polyHIPEs including novel materials based on poly (ϵ -caprolactone) polyHIPEs.

CONCLUSION

It was concluded the acrylate-based PolyHIPEs described here supported the growth of bone cells *in vitro*, and that plasma polymerisation appeared to further improve cell response. Using stereolithography, it was possible to prepare even more complex 3D scaffolds or devices that have great potential for tissue engineered craniofacial surgery.

REFERENCES

1. Johnson D. *et al.*, Advanced Materials. 3178:81-25, 2013.

ACKNOWLEDGMENTS

The authors are grateful to Thomas Patterson for assistance in the laboratory, and also to the EPSRC for funding through the White Rose DTCTERM. Hatton, Claeysens and Ortega Asencio are members of the EPSRC Centre for Innovative Manufacturing of Medical Devices (MeDe Innovation).

Implantable hybrid composite for reducing inflammation in age related macular degeneration

E. Chinarro¹, L. Pires², Ana P. Pêgo^{2,3,4} and B. Moreno¹

¹Instituto de Cerámica y Vidrio, CSIC, Madrid, Spain, ²INEB – Instituto de Engenharia Biomédica, Universidade do Porto, Porto, Portugal, ³FEUP - Faculdade de Engenharia da Universidade do Porto, Porto, Portugal, ⁴ICBAS – Instituto de Ciências Biomédicas Abel Salazar, Universidade do Porto, Porto, Portugal, martin@icv.csic.es

INTRODUCTION

Age-related macular degeneration (AMD) advances causing a gradual loss of central vision and the deterioration of the macula. From all the phenomena that contribute to extra cellular ageing, the imbalance between the synthesis and the elimination of reactive oxygen species (ROS) is one of the most relevant. In addition, the innate immune system, particularly the phagocytes and the complement system, are involved in the progression of the disease. The insertion of an implant with potential anti-inflammatory activity is a reliable therapy, however the materials choice is a key parameter for its success. Our aim is to develop a new class of hybrid biomaterials based on the union of polymethyl methacrylate (PMMA) and a ceramic material, titanium dioxide (TiO₂). The hybrid design should present a built-in bioactivity able to modulate the extracellular microenvironment and connective tissue of the eye in order to prevent and control those inflammatory processes that occur during the progression of the disease. To reach this goal, the synthesis and characterization of hybrids based on PMMA-TiO₂ is described evaluating its ROS scavenging activity by two different methods SIN-1 and DPPH.

EXPERIMENTAL METHODS

TiO₂ nanopowders were used after its calcination at 600 °C in air. These processed powders were mixed with previously purified commercial PMMA. With this aim purified PMMA was dissolved in THF and then mixed with a TiO₂ suspended in THF as well. Membranes were processed through two different techniques: casting and spin-coating. With the aim of having the TiO₂ powders exposed in the surface of the membrane, the films obtained were treated with acetone. Moreover, the films have been prepared by deposition of TiO₂ powders (with xerography) onto the PMMA membrane. Morphological characterization of the membranes has been done. The ROS scavenging capacity of the different membranes was addressed by generating chemically ROS using two methods: 1,1-diphenyl-2-picryl-hydrazyl (DPPH) and 3-morpholinocarbonylhydrazine hydrochloride (SIN-1).

RESULTS AND DISCUSSION

Characterization of the casted membranes showed that TiO₂ powders sediment during the processing, creating a TiO₂ concentration gradient but avoiding the exposure of the powders (Figure 1, B). After the etching with acetone it was clearly observed how the TiO₂ agglomerates are present in the surface of the membrane, but remained anchored to the polymer phase (Figure 1, C). The membrane prepared by spreading TiO₂ powders on the surface of a just-casted PMMA film shows TiO₂ clearly exposed in the surface,

although the dispersion of the powder was less homogeneous than in the previous case.

In this study, we addressed the ROS scavenging capacity of different membranes with chemical assays using artificial ROS. The results show that although PMMA itself reduces the ROS created, its mixture with TiO₂ calcined at 600°C enhances the concentration of ROS depleted.

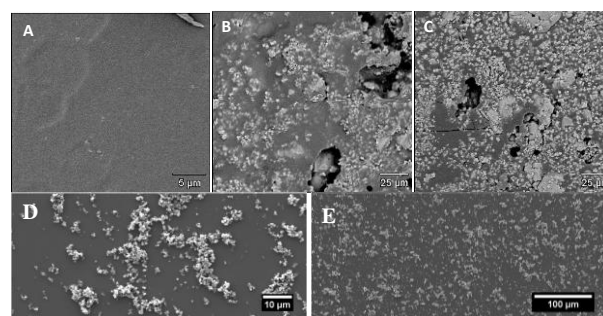


Figure 1: SEM of the membranes obtained. A) PMMA membrane prepared by casting, B) PMMA/TiO₂ membrane prepared by casting, C) PMMA/TiO₂ membrane prepared by casting after etching with acetone; and D) and E) Spin coating films prepared from PMMA solutions (5% (w/v), dimethylformamide) containing TiO₂ particles (5% (w/v)).

At present we are extending the work to spin coating films. We were able to prepare thin PMMA films over coverglass where TiO₂ is deposited afterwards. We have to test the supported films with the chemical assays described above to evaluate the ROS scavenging activity of this material and to relate it with the degree of TiO₂ exposure.

CONCLUSION

Taken together, these results suggest that the synthesis and processing of PMMA/TiO₂ hybrids has been successfully approached. Moreover, the surface treatment of the membranes with acetone allowed enhancing the degree of TiO₂ exposed and able to react in the chemical assays carried out. It was found that PMMA itself showed a mild ROS scavenging activity that was improved in the hybrids prepared with the TiO₂ powder calcined at 600°C.

REFERENCES

- 1 Suzuki R et al., Clinical orthopaedics and related research, 2000, 372: 280-289.
2. Chen X et al, Free radical Research, 2010; 44(6): 587-604.

ACKNOWLEDGMENTS

The authors would like to thank the Fundación General CSIC and Obra Social “La Caixa” (Project BIOAMD) for providing financial support to this work.

Hypoxia inducible factor-1 α (HIF-1 α) stabilization for enhanced cell and tissue construct survival

Wai Ho, Barry Fuller and Gavin Jell

Division of Surgery and Interventional Science, University College London, Royal Free Hampstead Hospital, wai.ho.12@ucl.ac.uk

INTRODUCTION

Cell and tissue construct survival following implantation is low due to stresses association with storage and when implanted, low oxygen and nutrient supply. Strategies to increase cell survival following implantation would enhance cell therapy efficacy and promote tissue construct integration. Cell or tissue construct survival may be artificially increased by stabilising HIF-1 α through the use of HIF stabilising mimetics, in normoxic conditions prior to implantation or storage. Stabilising HIF in normoxia may activate a number of pro-survival factors whilst preventing the oxidative stress associated with hypoxia-reoxygenation reperfusion injury¹.

EXPERIMENTAL METHODS

Osteoblast (SaOS-2), Keratinocytes (HaCaT) and Fibroblast cells (HDFa) were preconditioned in either untreated media (control group), or media treated with a range of hypoxia mimicking agents (Co²⁺, DFX (1mM), DMOG (1mM) and Hypoxia Bioactive Glass in conditioned media² (which has 2 Mol % Cobalt incorporated in the glass network)) in normoxia or hypoxia incubator for 24 hours. Following cryopreservation cell survival was determined using haemocytometer and Trypan Blue assay prior to cell recovery being determined by cell proliferation (day 1, 3 and 7) in a hypoxia incubator (1%O₂, 95%N and 5%CO₂), with a total DNA assay (Hoechst staining).

Abbreviations: DFX = Deferoxamine mesylate; DMOG = Dimethylxalylglycine;

RESULTS AND DISCUSSION

Cells preconditioned with hypoxia mimetics showed higher proliferation rates when cultured in hypoxia incubator for 7 days following resuscitation (Fig. 1). Furthermore, cells preconditioned with hypoxia mimetics or in low oxygen level appeared have higher metabolic activity on resuscitation, which may due to hypoxia adaption to oxygen independent metabolism during preconditioning (Fig. 2).

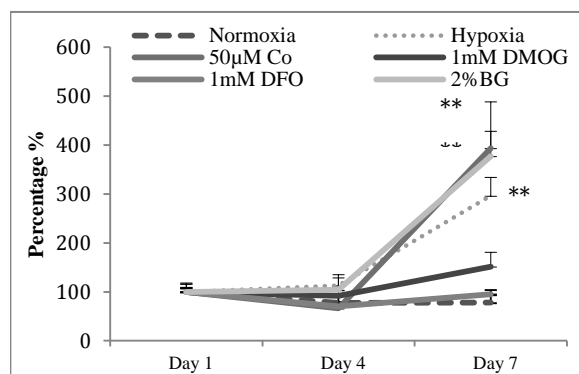


Figure 1. Cell Proliferation and Survival. Preconditioned cell with cobalt ion and 2% Cobalt ion in BG have higher cell recovery. **P<0.01 vs. normoxia.

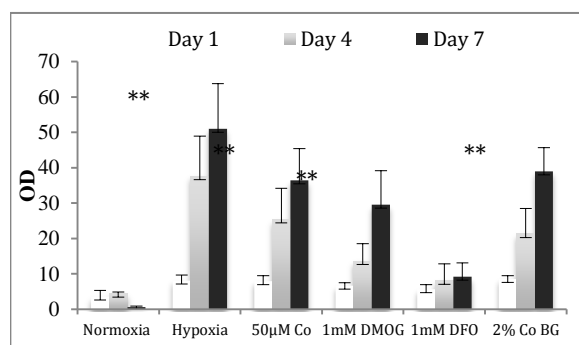


Figure 2. Metabolic Activity. Cells preconditioned with hypoxia mimetics and low oxygen level has higher metabolic activity following resuscitation. **P<0.01 vs. normoxia)

These results have demonstrated that preconditioned cells in hypoxia mimetic agents may increase the survival of cells in adverse conditions (e.g. low nutrient and nutrient). Current Studies are underway to understand the pro-survival factors expressed in HIF stabilised cells.

CONCLUSION

Preconditioning cells with HIF mimetics can increase cell proliferation and viability in adverse environments. The incorporation of HIF mimetics into tissue scaffolds may provide a means to increase cell survival following implantation.

REFERENCES

1. Chacko.S.M. et al., Am. J. of Phy. C1562-70, 2010
2. Jell G. et al., J. of Mat. Chem. 20(40): 8854, 2010

Practical fixation issues of multifunctional bioresorbable miniplates for osteotomies

Karol Gryń¹, Anna Morawska-Chochół¹, Barbara Szaraniec¹, Magdalena Ziabka², Jan Chłopek¹

¹*Department of Biomaterials, Faculty of Materials Science and Ceramics, AGH University of Science and Technology, Krakow, Poland. Corresponding author: kgryn@agh.edu.pl*

²*Department of Ceramics and Refractories, Faculty of Materials Science and Ceramics, AGH UST*

INTRODUCTION

In literature there are many biomaterial concepts describing a range of biodegradable polymers and composites used for trauma surgeries [1]. Apart from the benefits of rigid fixation and the advantage of biodegradation [2], the general conclusion shows the main drawbacks as well. Miniplates made of biodegradable polymers or composites are characterised by relatively low mechanical properties, when compared to e.g. titanium or stainless steel [3]. Moreover, as their degradation process continues, mechanical parameters of the implant decrease [4]. Thus, the application of such devices is limited only for osseosynthesis in non-loaded areas of bones or in hybrid systems. In a hybrid system the internal plate is fixed to the pieces of the broken bone to keep them in position, whilst a combined metal stabilizer (usually an external one) bears higher loads [5].

In our research we wanted to find out which factors downgrade the mechanical properties of implants during the degradation process.

To verify this query we prepared different types of materials and various shapes of miniplates. Their mechanical properties were determined. Complimentary mechanical tests concerning simulated work conditions (including proper fixation, biological fluids presence and higher temperature of the environment (37°C)) were assessed.

EXPERIMENTAL METHODS

The present study uses bioresorbable polylactide acid (PLA) (Ingeo 3051D by NatureWorks) and composites of PLA with bioceramic additives: hydroxyapatite (HAP) (nGimat) and tricalcium-phosphate (TCP) (SigmaAldrich). For the sake of this research, three different materials were used to manufacture miniplates: pure PLA, PLA/7% wtTCP, PLA/7% wtTCP/0,3wt%HAP. Injection moulding was applied to fabricate different shapes of miniplates (*I,H,T,Y*) (165-175°C). The samples were mechanically tested (Zwick 1435). Static and dynamic research was carried out along with fatigue (cyclic uniaxial tensile strain and creep). The maximum torque that can be applied to the fixation screw was measured (PolTorque PRO) and the maximum load a miniplate can bear was determined. Two types of screws were used: with countersunk head and pan head. This test revealed also information about stability and durability of the fixation. To verify the influence of degradation processes on mechanical stability additional mechanical testing in simulated work conditions was conducted. The samples were tested in two manners of proceedings: a) after 2 and 6 weeks incubation in

simulated body fluids and Ringer's solution at 37°C; b) implants were placed in the chamber filled with Ringer's solution at 37°C and tested "in situ". The material's microstructure was observed using SEM.

RESULTS AND DISCUSSION

Bioceramic additives (TCP and HAP) not only modified bioactivity and the implants osseointegration (proved in our previous research) but also changed their mechanical behaviour from rigid to more plastic. Hence, the composite miniplates didn't crack/snap instantly when a force or a torque was applied (fixation). Moreover, they displayed higher creep and fatigue resistance than the miniplates made of pure PLA. It can be stated that composite miniplates are more reliable then. On the other hand, bioactive additives increase the rate of degradation and - as a consequence - the mechanical properties decrease. Another factor that negatively influenced durability of the implant was the shape of a fixing screw head (and matching hole in the miniplates). When countersunk head screws were used adverse circumferential tensile stress appeared around miniplate holes.

CONCLUSION

The results of this study show that not only material, geometry of the implant and the testing conditions are crucial but also the way the implant is fixed. As we know more about the subtle factors changing implants' mechanical behaviour during their degradation, we are one step closer to tailoring mechanical characteristics of bioresorbable implants to the actual need of a healing bone tissue referring to Wolff's law. Hence what at the beginning was seen as a drawback does not necessarily need to be one.

REFERENCES

1. Eligin D., Alini M. *Eur. Cells and Mat.* Vol. 16 2008
2. Laughlin R.M. *et al.* *J.Oral Maxillofac Surg* 65:89-96, 2007
3. Gomez M.E., Reis R.L. *Int. Material Reviews* Vol.49 No.5 2004
4. Moser R.C. *et al.* Wiley Interscience DOI 10.1002/jbm.b.30238 2004
5. Wittwer G. *et al.* *Oral and Maxillofacial Surgery* Vol. 100 No.6 Dec.2005

ACKNOWLEDGMENTS

This research was financially supported by the research project No 5.23.160.254 financed by the Ministry of Science and Higher Education with cooperation with MEDGAL Company.



Dynamic Surfaces for Stem Cell Differentiation and Retention of Stem Cell Phenotype

Laura E. McNamara^{1*}, Jemma N. Roberts^{1,2}, Jugal Sahoo², Karl V. Burgess³, Jake Hay¹, Hilary Anderson¹, Richard O.C. Oreffo⁴, Rein Ulijn² and Matthew J. Dalby¹

^{1*}Centre for Cell Engineering, University of Glasgow, UK, laura.mcnamara@glasgow.ac.uk

²Department of Chemistry, University of Strathclyde, UK

³Polyomics Facility, University of Glasgow, UK

⁴Department of Bone and Joint Research, University of Southampton, UK

INTRODUCTION

The ability to have ‘on demand’ control over the fate of stem cells would have great benefit for the supply of both stem cells and mature cell types for research and clinical applications. Although some topographical and chemically patterned surfaces have been fabricated that are capable of enhancing the retention of stem cell character or promoting differentiation [1], the ability to trigger a change from stem cell retention to maturation on the same substrate would be highly advantageous to facilitate the expansion of stem cells prior to differentiation. In this study, an enzyme-cleavable surface chemistry was utilised to modulate stem cell fate by concealing or exposing adhesive –RGD groups.

EXPERIMENTAL METHODS

Surface chemistry synthesis: Peptide-modified glass surfaces were produced on glass coverslips, which either presented a cell adhesive –RGD sequence, or had the –RGD sequence masked with an adjacent –Fmoc or –PEG blocking group attached to an elastase-cleavable linker. Glass controls and –RGE, –RGD, and –PEG presenting surfaces were used as controls. At least 3 surfaces were examined per experiment.

Cell culture: Mesenchymal stem cells (MSCs; Stro-1+ selected) were cultured on the peptide surfaces in the presence (‘switched’) or absence (‘unswitched’) of elastase (which could cleave off the –Fmoc or –PEG blocking groups).

Immunostaining/focal adhesion (FA) quantification: Cells were stained for the stem cell marker Stro-1+, and markers of differentiation such as osteopontin and osteocalcin. FAs were also immunostained, imaged using a fluorescence microscope and quantified using ImageJ.

Metabolomic analysis: Solvent-extracted metabolites were analysed using an Orbitrap Exactive mass spectrometer. Metabolite analysis was performed using in-house software and Ingenuity Pathways Analysis to assess the likely functional significance of the differentially abundant metabolites and analyse potential interactions between metabolites.

RESULTS AND DISCUSSION

Stem cells cultured on the lower adhesion ‘unswitched’ surfaces had greater retention of the stem cell marker Stro-1+ than cells cultured on glass controls after 2 and 4 weeks of culture. On the ‘switched’ surfaces, and control –RGD substrates, where the –RGD sites were exposed and higher cytoskeletal tension was promoted, there were quantitative distinctions in the size of focal adhesions, and bone differentiation was stimulated. The

bone markers osteocalcin and osteopontin were enriched on the switched substrates.

Most interestingly, the metabolic profile of stem cells cultured on the ‘unswitched’ –Fmoc terminated surfaces was distinct from that of the cells on the ‘switched’ substrates. MSCs cultured on the unswitched substrate were enriched for unsaturated lipids, which were depleted on the switched surfaces (Figure 1).

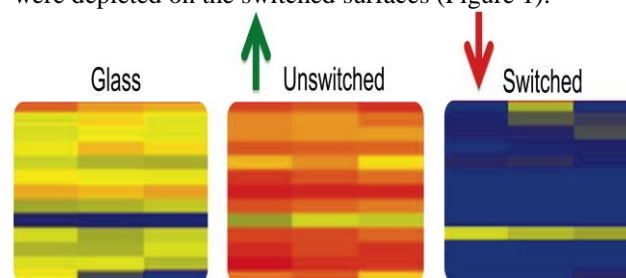


Figure 1: Relative abundance of lipid metabolites on unswitched (–RGD concealed), enzymatically switched (–RGD exposed) and glass control surfaces. Red indicates highest abundance and blue indicates lowest abundance. Note the relative enrichment of unsaturated lipid metabolites on the unswitched surface relative to the glass control, versus depletion on the switched surfaces.

Enrichment of unsaturated metabolites has previously been associated with stem cell plasticity [2]. Cells cultured on the switched surfaces had depleted levels of these metabolites, consistent with a more metabolically active, differentiating phenotype.

CONCLUSION

The ‘unswitched’ –RGD surfaces were more effective at retaining stem cell character, and MSCs cultured on these surfaces were metabolically distinct from those on the ‘switched’ surfaces. The switched surfaces were effective at modulating FAs and promoting osteogenic differentiation. This system offers great potential for the retention of stem cell characteristics prior to the controlled induction of differentiation.

REFERENCES

- Curran *et al.* Biomaterials. 25; 7057-67, 2005.
- Yanes *et al.* Nat. Chem. Biol. 6:7; 411-7, 2010.

ACKNOWLEDGMENTS

The authors thank Julia Wells (University of Southampton) for assistance in stem cell isolation and selection, and the BBSRC for funding this project.

Cytotoxicity control of SiC nanoparticles introduced into polyelectrolyte multilayer films

Aldona Mzyk¹, Roman Major¹, Bogusław Major¹

¹Institute of Metallurgy and Materials Science, Polish Academy of Sciences, Poland
aldonamzyk@gmail.com

INTRODUCTION

Nowadays, biosensors technology development is directed toward improvement of sensing devices biocompatibility. Polyelectrolyte multilayer film (PEM) seems to be appropriate for electrode coverage and semiconducting nanoparticles localization in order to create controllable polymer – nanoparticles tridimensional network. However, control of nanoparticles release from films and in a consequence their cytotoxicity is still a challenge. In this study we demonstrated that cytotoxicity of silicon carbide (SiC) nanoparticles introduced by physical vapour deposition (PVD) method into poly-L-lysine/hyaluronic acid (PLL/HA) or poly-L-lysine/alginate acid (PLL/ALG) films could be controlled by chemical cross-linking of coating.

EXPERIMENTAL METHODS

Multilayer (48 bilayers) polyelectrolyte films were prepared by “layer by layer” method on the silicon substrate. Coatings were cross-linked by mixture of 100 mM N-hydrosulfosuccinimide (NHS) and 260 mM, 400 mM or 800 mM 1-ethyl-3-(3-dimethylamino-propyl)carbodiimide (EDC) respectively. For the comparison various concentrations of the second cross-linker, genipin (1 mM, 10 mM or 50 mM) were tested. Nanoparticles were introduced to films by PVD, in 5-10s ongoing process. At first topography observations were done using Scanning Electron Microscopy technique (SEM) on Quanta 200 3D. Microstructure characterization was performed using Transmission Electron Microscopy technique (TEM), on cross-section by the Tecnai G² F20 (200kV) FEG. Potential cytotoxic effect of coatings was determined according to the ISO 10993-5 2009 standards.

RESULTS AND DISCUSSION

Analysis of nanoparticles distribution has shown aggregate-like structure formation in each type of investigated polyelectrolyte films. Nanoparticles have penetrated polymer coating and have formed a phase directly on the substrate (Fig. 1). Only a small number was anchored in the polymer multilayer. Nanoparticles phase composition revealed silicon carbide presence. We supposed that such charged molecules interact with polymer films in varying degrees depend on multilayer cross-linking state. The biological verification considered cytotoxicity of coatings modified by SiC nanoparticles has shown changes dependent on type of applied polyelectrolytes, cross-linker type and cross-linking rate. It was noticed that PLL/HA affected cells viability much more than PLL/ALG polyelectrolytes.

It has placed probably due to higher rate of swelling and release of polymer chains from PLL/HA. Multilayers cross-linked by NHS/EDC were more cytotoxic than the same non-cross-linked films. Moreover it was found that genipin cross-linker had lower necrotic effect than NHS/EDC. This might be a result of specificity and differences in cross-linking action mechanism of applied reagents. Cytotoxicity of NHS/EDC cross-linker was mentioned by Va'zquez et al. as a result of toxic unreacted amounts of applied reagents or reaction side products¹. The most important observation comes from this studies is that SiC nanoparticles could cause cytotoxic effect. Contrary, in literature silicon carbide was considered as a highly biocompatible material. However, up to date only a few toxicological data were available^{2,3}.

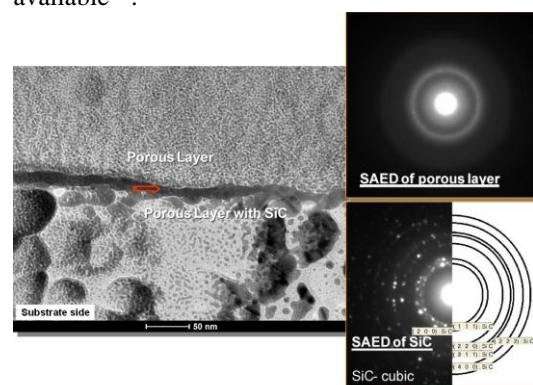


Fig. 1. Cross section TEM analysis of the SiC nanoparticles introduced into porous polymer coatings.

CONCLUSION

This studies present that SiC cubic nanoparticles could affect cellular viability. Among tested cross-linkers, genipin seems to be more suitable for nanocomposite properties control due to lower cytotoxicity and more effective stabilization of polymer – nanoparticle interaction.

REFERENCES

1. Va'zquez C.P. *et al.*, Langmuir 25:3556-3563, 2009.
2. Pourchez J. *et al.*, Journal of Nanoparticle Research 14(10):1143, 2012.
3. Barillet S. *et al.*, Toxicol Lett. 198(3):324-30, 2010.

ACKNOWLEDGMENTS

The research was financially supported by the EU under the European Social Found within Project No. POKL.04.01.00-00-004/10.

Effects of Plasma Electrolytic Oxidation Treatment of Titanium and Titanium-Niobium-Zirconium alloys on Leucocyte Inflammatory Response and Human Osteoblast Mineralization

Constantin-Edi Tanase^{1*}, Mehdi Golozar², Kim Hoenderdos³, Serena M. Best², Roger A Brooks¹

¹Division of Trauma & Orthopaedic Surgery, Addenbrooke's Hospital, University of Cambridge-UK, cet48@cam.ac.uk

²Cambridge Centre for Medical Materials, Department of Materials Science & Metallurgy, University of Cambridge-UK

³Department of Medicine, Addenbrooke's Hospital, University of Cambridge-UK

INTRODUCTION

Titanium and titanium alloys are widely used in orthopaedic and dental implants. Early osseointegration is affected by surface characteristics and modification of the surface via plasma electrolytic oxidation (PEO), which is considered to be more conducive to cell attachment, spreading and proliferation of osteoblast-like cells [1]. A recent study using transcriptional profiling of cells during osseointegration revealed that several mechanisms, including inflammatory responses, play a significant role in the wound healing process related to osseointegration [2]. Therefore, the inflammatory process is an important factor which should be taking into consideration when evaluating implant materials. The aim of this study was to determine the effect of PEO surface modification of titanium and titanium alloy, on the inflammatory response and osteoblast growth and mineralisation.

EXPERIMENTAL METHODS

Ti13Nb13Zr and commercially pure titanium (cpTi) discs were selected for this study. PEO was conducted in a 10 kW KeroniteTM rig using the initial current density of 20 A·dm⁻² and using 0.05 M Na₃PO₄ electrolyte. The chemistry and surface morphology of the coatings were studied using XRD and SEM. Inflammatory responses were evaluated using human neutrophils and monocytes, purified by dextran sedimentation and discontinuous plasma-Percoll gradients, for up to 6 and 48 hours, respectively. Human foetal osteoblast cells ((Public Health England Culture Collections) were cultured on the materials for 29 days. To investigate inflammatory responses, pro-inflammatory tumour necrosis factor-alpha (TNF-α) a multifunctional cytokine with pro-apoptotic properties and anti-inflammatory interleukin-10 (IL-10) a potent deactivator of monocyte pro-inflammatory cytokine synthesis, were measured using paired antibody ELISA kits (R&D Systems). The metabolic activity of the foetal osteoblasts was monitored using alamarBlue (AbDSerotec); collagen release was determined by immunoblotting and mineralization using the OsteoImage kit (Lonza).

RESULTS AND DISCUSSION

Porous TiO₂ coatings with varying anatase-to-rutile phase proportions were produced on the surfaces of Ti13Nb13Zr and cpTi discs (Figure 1 A & B). In this study the cytokine production wasn't surface related. However all surfaces induced higher TNF-α at early time points and lower at later time points for both

neutrophils and monocytes studies. Furthermore there was no surface related difference in early release of IL-10 and the low released levels of IL-10 and TNF-α with no significant differences when exposed to PEO-treated and untreated titanium alloy or cpTi discs were evaluated. The change in metabolic activity with time was not significantly different between cell cultures on the different surfaces. However, mineral nodule formation was more apparent on the PEO-treated surfaces after 29 days (Figure 1 C & D).

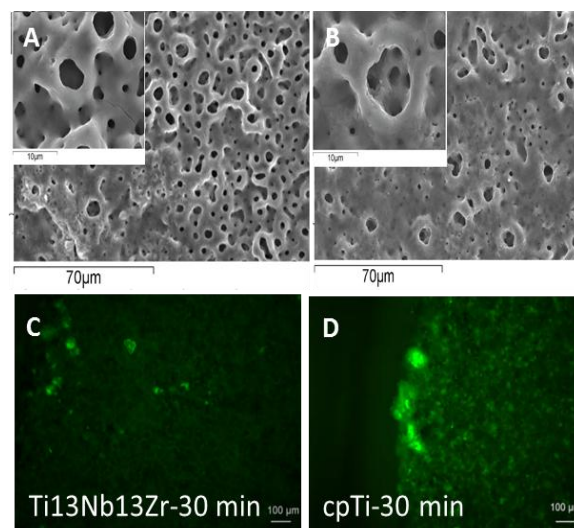


Figure 1. SEM surface morphology of Ti13Nb13Zr (A) and cpTi (B) discs after 30 minutes of PEO coating and mineral nodule formation (C and D) (green fluorescence) after 29 days of human foetal osteoblast culture on Ti13Nb13Zr and cpTi discs.

CONCLUSION

Modification of Ti-alloy materials using PEO increased mineral formation with no adverse effects on the metabolic activity of human foetal osteoblasts. There was a low level release of TNF-α from both neutrophils and monocytes, which *in vivo* may contribute to wound healing; however, no difference was seen between PEO treated and untreated titanium surfaces.

REFERENCES

1. Ueno T et al. Biomaterials, 32, 7297-7308, 2011.
2. Ivanovski S et al. Clin Oral Implants Res, 22(4), 373-381, 2011.

ACKNOWLEDGMENTS

Funding by the European Commission - BioTiNet (FP7-PEOPLE-2010-ITN-264635) and National Institute for Health Research for RAB.

Development of new bioactive phosphate-based glasses and study of the particle size effects on osteoblasts response for bone implant applications

Martin Stefanic, Xiang Zhang

Lucideon Ltd., Stoke-on-Trent, United Kindom

martin.stefanic@lucideon.com

INTRODUCTION

Phosphate based glasses (P-glasses) have many attractive properties for biomedical applications, such as an ability to completely dissolve in the body and the fact that their composition can be tailored across a wide range to give glasses with versatile properties [1]. P-glasses studied so far as bone implants were mainly too soluble for clinical applications. Therefore our aim was to develop and characterize more stable P-glasses with the composition (in mol.%): $40\text{P}_2\text{O}_5\text{-}25\text{-CaO-}5\text{Na}_2\text{O-(}30\text{-x)MgO-xSrO}$ ($x=0, 1, 5, 10$) and to study the influence of strontium content on the physico-chemical and biological properties of glasses.

Furthermore, we will report on the effects of glass particle size ($<1\text{ }\mu\text{m}$ vs $25\text{-}38\text{ }\mu\text{m}$) on the response of osteoblasts.

EXPERIMENTAL METHODS

Four P-glasses at compositions shown in Table 1 were prepared via melt-quenching route using $\text{NH}_4\text{H}_2\text{PO}_4$, Ca(OH)_2 , MgOH_2 , Na_2CO_3 and SrCO_3 as starting materials. The composition and structure of the prepared glasses was studied using XRD, XRF and FTIR.

Table 1. Composition of the studied P-glasses (mol.%).

Abbreviation	P_2O_5	CaO	Na_2O	MgO	SrO
P-glass_0Sr	40	25	5	30	0
P-glass_1Sr	40	25	5	29	1
P-glass_5Sr	40	25	5	25	5
P-glass_10Sr	40	25	5	20	10

Dissolution test. Dissolution of prepared glasses was tested in distilled water and in PBS with pH 7.4.

In vitro bioactivity in a simulated body (SBF). The in vitro bioactivity of phosphate glasses was evaluated by immersing 0.3 g of glass granules ($250\text{-}500\text{ }\mu\text{m}$) in 30 ml of SBF solution for various periods of time.

Effects of glass particle size on the cell response. For this study, dense P-glass/alginate hybrid membranes were prepared. In the composites P-glass particles were exposed on the surface of membranes and were not covered with a polymer. Two different size ranges of P-glass were investigated and compared, i.e. a) $<1\text{ }\mu\text{m}$ and b) $25\text{-}38\text{ }\mu\text{m}$. Sub-micron glass particles were obtained by milling the glass frit using a high-energy planetary ball mill (Retsch, Germany). An amount of P-glass particles in the composite membranes was optimized using an image analysis programme (SPIPTM, Image Metrology A/S, Denmark), such that the total surface

area of the glass in a membrane exposed to the cell medium was in the same range for both the sub-micron and micron-size glass particles.

RESULTS AND DISCUSSION

XRD analyses of the prepared glasses showed that all the glasses were amorphous. Figure 1 (left) shows degradation profiles obtained for the investigated P-glass formulations. Test of bioactivity in a simulated body fluid showed that a bone-like apatite layer precipitated on all the studied P-glasses after 7 days of immersion, indicating that investigated P-glasses have a bone-forming capacity (Figure 1(right)). Figure 2 shows SEM images of P-glass/Alginate membranes with submicron- and micron-sized P-glass particles.

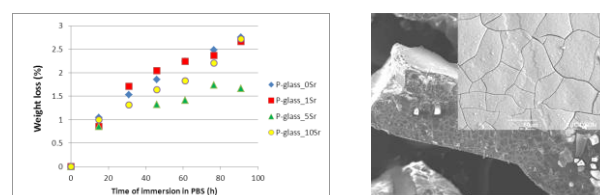


Figure 1. Left) degradation profiles of studied P-glasses in PBS. Right) SEM image of the P-glass_0Sr granule after 7 days of immersion in SBF.

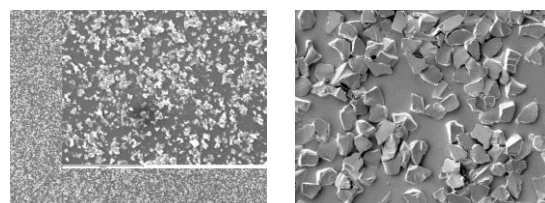


Figure 2. SEM images of the P-glass/alginate hybrid membranes with (left) $<1\text{ }\mu\text{m}$ and (right) $25\text{-}38\text{ }\mu\text{m}$ size particles.

CONCLUSION

Amorphous P-glasses in the system $40\text{P}_2\text{O}_5\text{-}25\text{-CaO-}5\text{Na}_2\text{O-(}30\text{-x)MgO-xSrO}$ were successfully prepared via the melt-quenching route. P-glass with 5 mol.% of SrO showed the highest stability in PBS. According to the SBF test, all the P-glasses studied are bioactive and possess bone-forming capacity.

REFERENCES

[1] Knowles, J.C.(2003). *J Mat Chem*, 13 (10), 2003.

ACKNOWLEDGMENTS

The authors would like to thank EU project BioBone ITN for providing financial support to this project.

Backside wear in fixed-bearing total knee arthroplasty : the effect of liner locking mechanism and surface roughness of tibial tray

Łukasz Łapaj¹, Jacek Markuszewski¹, Justyna Wendland², Adrian Mróz², Jacek Kruczyński¹

¹Department of General Orthopaedics, Musculoskeletal Oncology and Trauma Surgery, Poznan University of Medical Sciences, Poland, esperal@tlen.pl

^{2*}Metal Forming Institute, Poznan, Poland

INTRODUCTION

Backside wear of polyethylene (PE) inlays in fixed-bearing total knee replacement (TKR) generates high number of wear debris, but is poorly studied in modern plants with improved locking mechanisms [1]. That is why we decided to perform a retrieval studies of contemporary TKRs

EXPERIMENTAL METHODS

This study included five types of implants, retrieved after a minimum of 12 months (14-71) : three models with a peripheral locking rim and two models with a dove-tail locking mechanism occupying part of the circumference (Table 1)

Implant model (group name)	Alloy, mean Ra ¹	Locking mech. type	Nr. of inlays
Stryker Triathlon (Triath)	CoCrMo 5,61 µm	Periph. rim	15
Aesculap Search (Srch)	CoCrMo 0,81 µm	Periph. rim	9
DePuy PFC Sigma (PFC)	TiAlV 0,61 µm	Periprh. rim	13
Zimmer Nex-Gen (NGen)	TiAlV 0,34 µm	dovetail	11
S&N ² Genesis II (Gen2)	TiAlV 0,11 µm	dovetail	9

Table 1. Implants included in the study, (1) mean Ra – mean surface roughness (2) Smith & Nephew

Wear of bearing surface and back side of retrieved inlays was examined in 10 sectors under a light microscope. Seven modes of wear were analysed and quantified according to the Hood scale [2]: surface deformation, pitting, embedded third bodies, pitting, scratching, burnishing (polishing), abrasion and delamination. Damage of inlays caused by backside wear was also evaluated using scanning electron microscopy (SEM). Roughness of tibial tray was evaluated using a contact profilometer.

RESULTS AND DISCUSSION

We found no differences between wear scores on the articulating surface in all group, they did not correlate with backside wear scores in all groups as well. Backside wear scores the NGen group was significantly higher compared to other implants ($P < 0,001$ Wilcoxon test; Fig. 1). Lowest wear rates were found in implants from both Ti and CoCr alloys and peripheral locking rim.

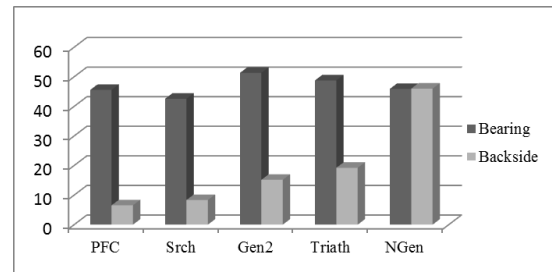


Fig. 1 – Hood wear scores of bearing surface and backside of retrieved implants

SEM analysis demonstrated different wear modes in implants with dovetail mechanism and peripheral rim. The first group demonstrated signs of gross rotational instability, with severe abrasion with an arch-shaped pattern and delaminated PE (Fig 2a). In one design we observed severe extrusion of PE into screw holes of the tibial tray (Fig 2b). Inlays from trays with peripheral rim presented two types of wear : flattening of machining marks (Fig 2c) or protrusion of the material caused by the rough surface (Fig 2d).

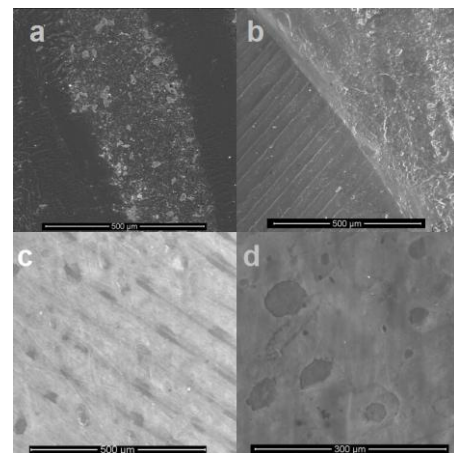


Fig. 1 SEM analysis of retrieved inlays (bars indicate 500 µm – a,b,c and 300µm –d)

CONCLUSION

This study demonstrates that backside wear is still a problem in modern TKR. Our findings suggest that it is predominantly affected by type of locking mechanism (with peripheral rim performing better), to a lesser extent by surface roughness of the tibial component, while material type does not seem to play an important role.

REFERENCES

1. Azzam. *et al.*, J Arthroplasty 011, 26, 523-530.
2. Hood *et al.*, J. Biomed. Mat Res. 1983,175, 829-42.

ACKNOWLEDGMENTS

This research was funded by a grant from the National Science Centre nr 012/05/D/NZ5/01840.

Paraffin versus frozen sectioning in the histologic evaluation of biomaterial implants – a pilot study

Volker H. Schmitt^{1,2}, Christoph Brochhausen^{1*}, Dominic Schwarz¹, Christine Tapprich¹,
Andreas Mamilos¹, Helmut Hierlemann³, Heinrich Planck³, C. James Kirkpatrick¹

¹REPAIR-lab, Institute of Pathology, University Medical Centre, Johannes Gutenberg-University Mainz, Germany

²Department of Medicine 2, University Medical Centre, Johannes Gutenberg-University Mainz, Germany,

³Institute of Textile Technology and Process Engineering, Denkendorf, Germany

* Correspondence: brochhausen@pathologie.klinik.uni-mainz.de

INTRODUCTION

In the histologic assessment of biomaterials and their tissue response frozen sections are used in common practice. It is believed to best preserve the material by this method. In tissue preparation for paraffin sectioning alcohol series and xylol are used for dehydration. The chemicals could cause the disappearance of the material out of the section. On the other hand, the effect of rapid freezing on tissues and materials is not well investigated the applicability of frozen sections is greatly restricted for immunohistological staining – an important method to evaluate various tissue reactions like inflammation. For this reason, in the present pilot study, frozen and paraffin sections of dermal wound dressing materials were compared.

EXPERIMENTAL METHODS

In house pigs dermal lesions were performed and treated with natural degradable collagen-based wound dressing materials. Five punch biopsies were taken and of each one frozen and one paraffin section was performed. The samples were then compared regarding specimen quality, the preservation of the material, the preservation of the section and the quality of margins.

RESULTS AND DISCUSSION

In both paraffin and frozen sections material or residuals of material were present. In frozen sections the material appeared more densely whereas in the paraffin samples the material remnants were fluffy in most parts. However, in the frozen sections the material including surrounding tissue was often broke out of the sample, implying a loss of a part of the sample. These findings could be explained by the different processing methods. While in frozen sections the freezing causes stiffness of the material and tissue leading to preservation without greater chemical alteration. The cutting process then may lead to an avulsion of the material and the surrounding connected tissue including the loss of a part of the sample. Within histological processing in paraffin

sectioning the sample is exposed to several chemicals which lead to a dissolving of the material which can explain the fluffy structure of the material in the present study. The dissolving leads to a soft liberation without avulsion and loss of surrounding tissue or parts of the sample. Therefore, the material-tissue-interaction is better preserved in paraffin than in frozen sections. In preserved material-tissue areas gaps were present between the material and the tissue in the frozen sections. In contrast, in the paraffin samples the material-tissue-junction was well-preserved. Also, with both methods a loss of tissue was present, but the samples of paraffin sections contained more undamaged tissue and less tissue loss compared to frozen sections. Margins were sharp in paraffin sections, whereas the margins in the frozen sections were rather blurry.

CONCLUSION

Paraffin sections are not inferior to frozen sections to histologically evaluate material implants. If it is regardless whether paraffin or frozen sections are taken regarding the possibility of histological evaluation, clearly paraffin sections should be performed. The reason is the enlarged methodical possibility by e.g. producing histological stains which play a major role to help evaluate various tissue reactions like inflammation. A further important aspect is the far more easy way of storage of material for paraffin sections compared to frozen sections. To store frozen material is expansive, sophisticated and bears the risk of material loss if e.g. the fridge breaks or power failure occurs. Tissue treated with paraffin, by contrast, is easy and cheap to store and sections are easy to reproduce since the slice is always cut from the same surface.

Altogether, paraffin sections are as good as frozen sections and should then be the preferred method since tissue is easier to store and the diagnostic spectrum is broadened e. g. by the possibility of immunohistological staining.

Composition-Property Relationships for Gallium-Borate Glasses

K. O'Connell³, H. O'Shea³, Muhammad Hasan^{1,2}, D. Boyd^{1,2}

¹. Department of Oral Sciences, Dalhousie University, Canada

². Department of Biomedical Engineering, Dalhousie University, Canada

³. Department of Biological Science, Cork Institute of Technology, Ireland

Email: Kathleen.oconnell@mycit.ie, Helen.oshea@cit.ie, d.boyd@dal.ca, sami.hasan@dal.ca

INTRODUCTION: Various glass systems have become increasingly attractive and have been used in areas, such as oncology (localized radiotherapy) and bone regeneration¹. These glasses may be compositionally engineered to provide for an appropriate host response in a number of applications². Boron based glasses in particular have displayed variable degradation rates which can be subject to intermediate ion additions³. The loading of these systems with therapeutically relevant ions is increasingly considered in the literature and as demonstrated promising early results. Within this study, gallium (Ga) was incorporated (0-10mol%) into 70mol% B₂O₃ glasses and the composition-property relationship of each was evaluated. Ga was chosen as it possess certain characteristics which may enable it to interact with cellular processes and important proteins, specifically those related to the cellular uptake of iron. Ga has shown promising results in the areas of metabolic bone disease, cancer & infectious disease⁴.

EXPERIMENTAL METHODS: Six glass compositions (Table 1) were melt-quenched, ground, then sieved to a particle size distribution of 45-150µm. The glass transition temperature (T_g) of each glass was determined by means of Differential Scanning Calorimetry (DSC). Volume & density measurements were obtained by a helium pycnometer. B³⁺, Sr²⁺, Na⁺ & Ga³⁺ release dissolution characteristics were determined for each composition via ICP-OES for specimens incubated under simulated physiological conditions for up to 30 days.

Table 1: Mole fraction compositions of Ga-B glass compositions.

Glass Designation	B2O3	SrCO3	Na2CO3	Ga2O3
B100	0.7	0.2	0.1	0
GB200	0.7	0.2	0.8	0.2
GB201	0.7	0.2	0.6	0.4
GB202	0.7	0.2	0.4	0.6
GB203	0.7	0.2	0.2	0.8
GB204	0.7	0.2	0	1

RESULTS AND DISCUSSION

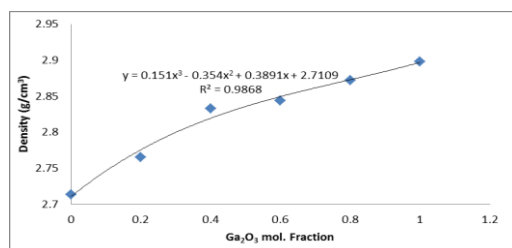


Figure 1: Density (g/cm³) for each composition (based on Ga₂O₃ mol. Fraction)

Fig. 1 and 2 illustrate that the compositional alterations (0-10mol% Ga₂O₃)

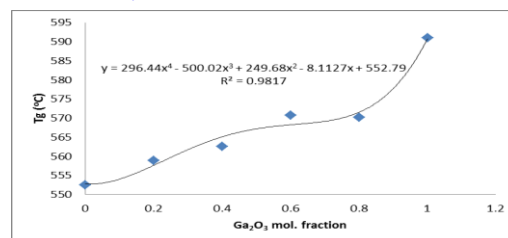


Figure 2: T_g for each glass composition (based on La₂O₃ mol. Fraction)

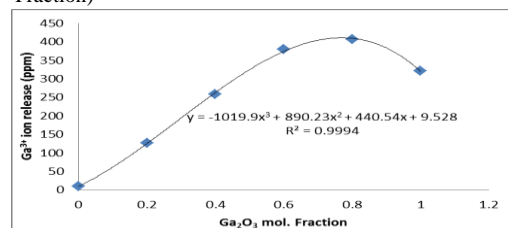


Figure 3: Ga³⁺ release (30 day) as a function of glass composition (Ga₂O₃ mol. Fraction).

had a pronounced effect on density and T_g, with a sharp increase occurring at 10mol% Ga₂O₃. Fig. 3 illustrates Ga³⁺ ion release after 30 days; ion release increased with increasing Ga₂O₃ content, however a maximum was reached at 8mol% Ga₂O₃, after which a decline in ion release was observed. Na⁺ showed a direct linear relationship with compositional alterations (decreasing additions of Na₂O). B⁺ & Sr²⁺ release appeared consistently high, increasing at 4 & 6mol% Ga₂O₃. B atoms can coordinate with both 3 and 4 oxygen (O₂) atoms forming triangular or tetrahedral structural units. The presence of additional O₂ atoms may instigate a conversion in the coordination number which can ultimately stabilize the B network.

CONCLUSION: The ability to compositionally engineer glass networks has resulted in their growth in popularity, specifically in the field of biomedical engineering. Ga₂O₃ was successfully incorporated into the 70mol% B₂O₃ network at varying additions (0-10mol%) and consequently the composition-property relationships of each was evaluated. The data obtained demonstrates increases in density and T_g along with distinct decreases in the release levels of each component ion (at 10mol% Ga₂O₃), indicating stabilization of the B₂O₃ network. These results support the proposal to further optimize these networks and Ga³⁺ release.

REFERENCES: [1] Saddeek, Y.B., Gaafar, M. S. (2009) Mater. Chem. Phys. 115, 280–286. [2] Kehoe, S. et al. (2013) *J. Biomater. Appl.* **28**, 416–33. [3] Halimah M. K., et al. (2007) *Am. J. Appl. Sci.* **4**, 323–327. [4] Bernstein, L. R. (1998) *Pharmacol. Rev.* **50**, 665–82.

ACKNOWLEDGMENTS: The authors would like to thank the CIT RÍSAM PhD Scholarship Programme (RDRP), the NSERC (Discovery Award Program) and the Canadian Foundation for providing financial support for this project.

RF-Magnetron Sputter Deposited Cap-Based Coatings on the Surface of Titanium

Maria A. Surmeneva¹, Roman A. Surmenev¹, Oleg Prymak², Matthias Eppe², Irina I. Selezneva³

¹Department of Theoretical and Experimental Physics, National Research Tomsk Polytechnic University, 634050 Tomsk, Russia

²Inorganic Chemistry and Center for Nanointegration Duisburg-Essen (CeNIDE), University of Duisburg-Essen, 45117 Essen, Germany

³Institute of Theoretical and Experimental Biophysics, Russian Academy of Sciences, Pushchino, 142292, Russia, rsurmenev@gmail.com

INTRODUCTION

This study reports on hydroxyapatite (HA) coatings and HA-based coatings doped with silicate ions [1-3].

EXPERIMENTAL METHODS

Plates of Ti grade 4 were used as substrates. The targets consisted of a powder of stoichiometric HA and silicate-containing HA (Si-HA) $\text{Ca}_{10}(\text{PO}_4)_6 \cdot x(\text{SiO}_4)_x(\text{OH})_{2-x}$ ($x=0.5$ and 1.72) were used. Thin nanostructured calcium phosphate (CaP)-based coatings were deposited by RF-magnetron sputtering with a power of 30-290 W, a negative substrate bias up to 100 V, and a pressure of 0.1 Pa [1]. As-deposited thin CaP coatings (up to 1 μm thick) were characterized by EDX, ESEM, XRD, IR spectroscopy, and pull off test. The primary dental pulp stem cells (DPSCs) and NCTC murine fibroblasts (clone L929, ATCC CCL1) were used to study the biocompatibility of the uncoated Ti substrates and deposited CaP-based thin films.

RESULTS AND DISCUSSION

As-deposited CaP-based coatings were dense and pore-free, and their composition was close to that of the precursor target composition. The chemical and phase composition as well as thickness and structure can be varied by adjusting the deposition control parameters. A low RF-power density ($0.1\text{--}0.5 \text{ W cm}^{-2}$) resulted in amorphous or low crystalline CaP-coating structure, and an increase in RF-power level ($>0.5 \text{ W cm}^{-2}$) induced the crystallization of the coating. The mineral in the coatings consisted of HA; all observed X-ray diffraction peaks matched the ICCD 9-432 card (HA). The four strongest peaks assigned to HA were observed at 25.8° (002), 31.7° (211), 32.2° (112), and 32.9° (300) (Cu K α radiation; 1.54 \AA). The (002) peak dominated the diffraction pattern, indicating a preferred c-axis crystallographic orientation. Its intensity increased with deposition time, i.e. film thickness. With an increase in the substrate bias voltage from 0 to -100 V , the intensity of the (002) peak gradually decreased. The XRD peak width of the coatings deposited at a negative bias voltage was broader than that deposited at zero bias, which indicates the presence of smaller crystals or smaller grain size. These differences in grain size were in good agreement with the data obtained by scanning electron microscopy. The XRD pattern of the coating at

different negative bias revealed a halo located at 32° typical for a nanostructured material. The negative substrate bias allowed us to vary the Ca/P ratio from 1.53 to 4. The adhesion strength of the coatings was higher than 40 MPa. Based on the biological assays it was concluded that low-crystalline HA coatings with the thicknesses 170, 250 and 440 nm stimulated cells to attach, proliferate and form mineralized nodules on the surface compared to uncoated Ti substrates. The absence of cytotoxicity of CaP coatings was shown *in vitro* assays using primary dental pulp stem cells and mouse fibroblast NCTC clone L929 cells. No suppression of metabolic activity of cells was observed. No significant effect of CaP coating thickness on cells behavior was found.

CONCLUSION

The results presented in this study showed that RF-magnetron sputtering allowed us to prepare CaP-based coatings with different structure and stoichiometry. These characteristics can be controlled by the deposition parameters. Based on the obtained results we suggest that RF-magnetron sputter-deposited HA-based coatings are prospective for clinical application, e.g. in stomatology or craniofacial medicine, where the initial material surface porosity for a further bone in growth should be preserved. It is suggested that the actual geometric and physical properties of the CaP coating must be important regulators in attachment and migration of the cells.

ACKNOWLEDGMENTS

This work was supported by the German Academic Exchange Service (DAAD), President's Stipend SP-6664.2013.4 and MK-485.2014, FP7 Marie Curie grant (327701), the Russian Fund for Basic Research (13-08-98082, 14-08-31027 mol-a).

REFERENCES

1. R.A. Surmenev, M.A. Surmeneva, K.E. Evdokimov, V.F. Pichugin, T. Peitsch, M. Eppe. *Surf. Coat. Technol.*, 205(12), 3600, 2011.
2. R.A. Surmenev, M.A. Surmeneva, A.A. Ivanova, *Acta Biomater.*, 10(2), 557, 2014.
3. R.A. Surmenev, *Surf. Coat. Technol.*, 206(8-9), 2035, 2012.



Electrochemical Surface Treatment for Making Antibacterial Porous Oxide Layer on Ti

Yusuke Tsutsumi^{1*}, Naofumi Niizeki², Peng Chen¹, Maki Ashida¹, Hisashi Doi¹, Kazuhiko Noda³ and Takao Hanawa¹

^{1*}Institute of Biomaterials and Bioengineering/Tokyo Medical and Dental University, Japan, tsutsumi.met@tmd.ac.jp

²Graduate School of Engineering, Shibaura Institute of Technology, Japan

³Department of Materials Science and Engineering, Shibaura Institute of Technology, Japan

INTRODUCTION

Titanium (Ti) is widely used in both orthopaedic and dental fields due to their good mechanical properties, high corrosion resistance, and biocompatibility. Micro-arc oxidation (MAO) is a useful surface treatment based on electrochemical reactions under high voltage in a specific electrolyte. MAO treatment can easily alter the surface properties of metals and is also effective to improve the bioactivity of Ti. Our previous study revealed that certain amounts of extra elements presented in the electrolyte are incorporated in the porous oxide layer during the MAO process. Therefore, in this study, MAO treatment was performed on Ti in silver (Ag)-containing solution. The incorporation of Ag in the porous oxide layer can lead the slight release of Ag ions and the improvement of antibacterial property after implantation in a living body. The surface layer of MAO-treated Ti was characterized by surface analyses. The behavior of the Ag-ion release from the oxide layer was also evaluated by immersing in a simulated body fluid. ICP-AES was performed to determine the concentration of Ag ions in the fluid.

EXPERIMENTAL METHODS

A commercially pure Ti rod was sliced to make disk-shaped specimens with 8 mm in diameter and 1.5 mm in thickness. The surfaces of the disks were grinded with up to #800 grid SiC abrasive papers followed by ultrasonic cleaning in acetone and ethanol. The specimen was fixed in a polytetrafluoroethylene holder that allows exposing to an electrolyte only the specimen surface (7.0 mm in diameter). A Type-304 stainless steel plate was used as a counter electrode. The electrolyte for MAO treatment was 0.1-mol L⁻¹ calcium glycerophosphate, 0.15-mol L⁻¹ magnesium acetate, and 0-10 mmol L⁻¹ silver nitrate. After pouring the electrolyte into the electrochemical cell, positive voltage was applied for 8-10 min. The surface morphologies and compositions of the specimens were analyzed using a scanning electron microscope with an energy-dispersive X-ray spectroscopy (SEM/EDS). X-ray diffraction (XRD) was also performed with a diffractometer to identify the crystal structure of the oxide layer. 0.9mass% NaCl solution was used as a simulated body fluid to evaluate the Ag ion release from the MAO-treated specimen. The solution was replaced every 7 d to simulate the refreshment of the body fluid inside a living body. ICP-AES was used to measure the concentration of the Ag ions in the solution.

RESULTS AND DISCUSSION

The specimen after MAO treatment shows porous oxide layer on its surface (Fig.1). The morphology of the porous oxide layer was not changed by the presence of

Ag ions in the electrolyte. However, the voltage was not fully raised when the Ag concentration of the electrolyte exceeded 5 mmol L⁻¹ so that it was unable to form the oxide layer. The EDS results showed that Ag was incorporated in the oxide layer.

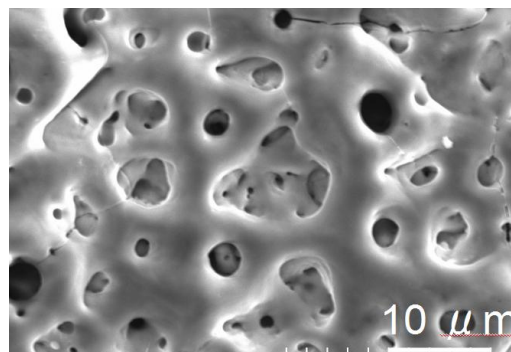


Fig. 1 Porous oxide layer containing Ag formed on Ti after MAO treatment

Figure 2 shows Ag-ion release from the oxide layer during the immersion in simulated body fluid (0.9mass%NaCl aqueous solution). Although the release rate of Ag ion was decreased at the initial stage of the immersion, it was stabilized at a certain value around 5 mg·m⁻²/week. It was confirmed that the incorporated Ag was gradually released from the oxide layer to the environment for long period.

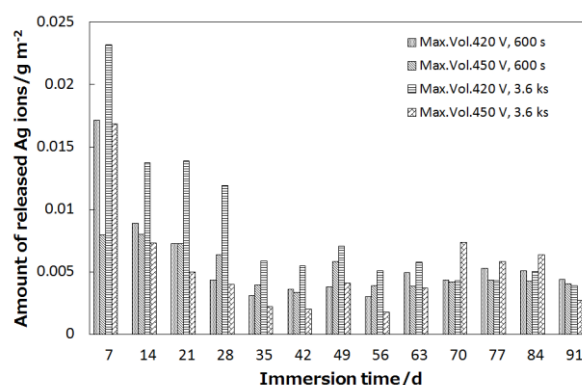


Fig. 2 Change in the Ag-ion release rate from the oxide layers to the simulated body fluid

CONCLUSION

We succeeded to make the Ag-containing porous oxide layer on Ti by MAO treatment. Ag ions were properly released from the sample when it was immersed in a simulated body fluid. Thus, this technique is useful to develop novel biomaterials having both bioactive and antibacterial properties.

Imaging the structure, dissolution, and bone ingrowth into Bioactive Glass scaffolds

Peter D. Lee¹, Taek Bo Kim², Wouter van den Bergh¹, Hua Geng¹, Sheng Yue¹, Christopher Mitchell³, Julian Jones²

¹Diamond-Manchester Collaboration, School of Materials, The University of Manchester, Oxford Rd, Manchester UK

²Department of Materials, Imperial College London, UK

³Centre for Molecular Biosciences, University of Ulster at Coleraine, Coleraine UK

peter.lee@manchester.ac.uk

INTRODUCTION

The success of Bioactive Glass (BG) has been dominated by its controlled chemical degradation in biological systems where it can be applied as a powdered glass inserted into a defect sites, locally stimulating bone regrowth. However, for applications such as repair of long bone defects, a scaffold structure is required to guide growth and ideally provide strength. For over 15 years a number of groups have been producing Bioactive Glass scaffolds, using a range of techniques from sol gel foaming to 3D printing. This development has required not only significant advances in materials processing and chemistry, but also concomitant developments in 3D imaging and image quantification techniques. In this study the developments both in imaging techniques, and quantification techniques, are first reviewed and then the current state of the art laboratory and synchrotron techniques are applied to optimise BG scaffold chemistry and morphology.

Quantification of 3D scaffold architecture is critical in its matching the design criteria to act as both a guide and a stimulus for bone regeneration *in vitro* and then *in vivo* as defined by Jones, Ehrenfried and Hench [1]: a suitable interconnected porous network is important as the pore size and more importantly the interconnect size must be large enough to enable cell migration, fluid exchange and eventually bone ingrowth and vascularisation. Features such as interconnect diameter for vascularised bone ingrowth can now be automatically quantified and plotted using X-ray micro computed tomography (μ CT), as shown in Fig. 1. [2,3]

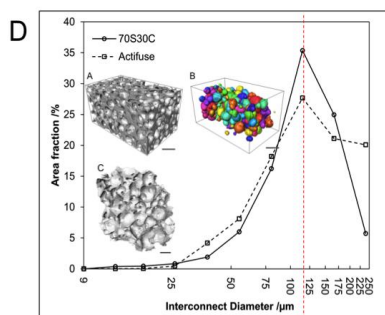


Figure 1. Quantification of a 70S30C sol gel scaffold (A&B) and Actifuse (C) with the distribution of interconnect sizes plotted (D).

EXPERIMENTAL METHODS

Laboratory and synchrotron μ CT was used to image the initial structures and ex vivo bone ingrowth into sol gel and 3D printed BG structures. Both commercial and in house code was then applied to quantify the structures, bone in growth, and scaffold dissolution, allowing a

quantitative comparison of the efficacy of different morphologies and compositions of glasses.

RESULTS AND DISCUSSION

The influence different pre-treatments of a 70S30C scaffold were compared to commercially available products such as Actifuse porous granules, as qualitatively assessed in Midha *et al.* [4]. Using quantitative μ CT quantitative measures of bone ingrowth were obtained. First a model joint was developed (Fig. 2a) and then registered in 3D to ex vivo scans at different time points (Fig. 2b).

The results show that with an effective pretreatment, there is excellent bone regeneration using a 70S30C scaffold (Fig. 2c,d) comparable to Actifuse (Fig. 2g,h), but without the presence of growth across the marrow cavity that occurs under these conditions when Actifuse is used. Without pretreatment ingrowth into the 70S30C scaffold is poor (Fig. 2e,f)

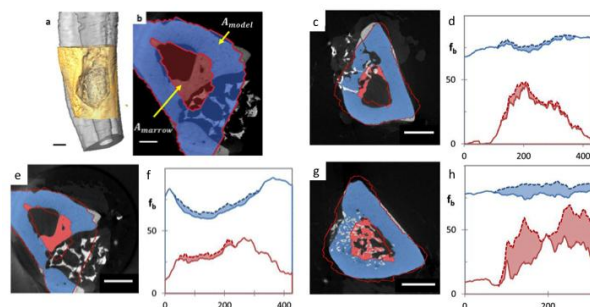


Figure 2. A 'model' joint was developed via statistical averaging (a,b) and then used to quantify the bone in growth into (c,d) 70S30C scaffold pre-conditioned by immersion into media for 3 days; (e,f) 70S30C scaffold with no preconditioning; and (g,h) Actifuse granules in autologous blood.

CONCLUSION

The use of laboratory and synchrotron μ CT allows not only the initial structures of Bioactive Glass scaffolds to be quantified, but also the time dependent in growth of bone, providing effective feedback for the optimisation of both BG chemistry and scaffold morphology.

REFERENCES

1. J.R. Jones, Ehrenfried, Hench, Biomaterials 27 (2006) 964.
2. Jones, J.R., Lee, P.D., and Hench, L.L, Phil Trans Roy Soc A, 364 (1838): 263-281, 2006
3. Yue, S., et al., Acta Biomater, 7 (2011) 2637-2643.
4. S. Midha et al., Acta Biomater. 9 (2013) 9169-82.

ACKNOWLEDGMENTS

Research Complex at Harwell and EPSRC EP/IO21566/1 and EP/IO20861/1.

Bioactive hydrogels supporting angiogenesis produced by EB-irradiation

Bożena Rokita^{1,2}, Sławomir Kadlubowski^{1,2}, Piotr Komorowski^{3,4}, Bogdan Walkowiak^{2,3,4}, Janusz M. Rosiak^{1,2}

¹Technical University of Lodz, Institute of Applied Radiation Chemistry, Wroblewskiego 15. 90-924 Lodz, POLAND,

²Technical University of Lodz, European Centre of Bio and Nanotechnology, Zeromskiego 116. 90-924 Lodz, POLAND,

³Technical University of Lodz, Institute of Materials Science and Engineering, Stefanowskiego 1/15. 90-924 Lodz, POLAND,

⁴BioTechMed Advanced Technology Centre, Stefanowskiego 1/15. 90-924 Lodz, POLAND,
rokitab@mitr.p.lodz.pl

INTRODUCTION

Angiogenesis is the physiological process involving the growth of new blood vessels from pre-existing ones. It is a critical process not only during normal development, but also in pathologic situations, where inadequate vascular evolution contributes to health complications. Angiogenesis is predominantly regulated by local factors that promote or inhibit neovascularization like e.g. AcSDKP (N-acetyl-seryl-aspartyl-lysyl-proline, acetyl-N-Ser-Asp-Lys-Pro)¹ isolated originally from fetal calf bone marrow.

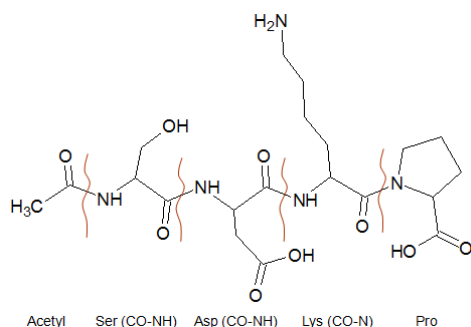


Figure 1. Structure of N-acetyl-Ser-Asp-Lys-Pro

It has been shown that AcSDKP acts as a mediator of angiogenesis which occurs both during embryonic development and in postnatal life. AcSDKP can be used as biologically active supplement in number of different biomaterials². That is why its support in angiogenesis process has been investigated. Because of using ionizing radiation as a method of choice for sterilization, its influence on tetrapeptide has been also studied.

EXPERIMENTAL METHODS

In this work hydrogel matrixes containing polyvinylpyrrolidone – PVP, poly(ethylene glycol) – PEG, agar and tetrapeptide were synthesized using EB-irradiation (25 kGy, 4μs, 50 Hz). Release kinetics of active substance from the hydrogel dressings by high performance liquid chromatography – HPLC and gel swelling kinetics by the gravimetric method were

investigated. The equilibrium swelling degree of hydrogels and gel fraction content were determined. Changes in gene expression of human endothelial cells EA.hy926 (CRL-2922™ ATCC) induced by hydrogel matrix containing AcSDKP were studied using Human Angiogenesis Oligo GEArray System (SABiosciences). Cells were grown, in the presence of hydrogel with AcSDKP, to 80% of confluence. Total RNA was then isolated from the cells. cRNA was obtained in PCR reaction, then it was amplified and labeled with biotin-16-dUTP. The synthesized molecular probe (biotined cRNA) was used for 12 hours of hybridization with oligonucleotide fragments immobilized on microarrays. Chemiluminescent reaction was triggered by an addition of CDP-Star (1,2-dioxetane). Gene expression was determined by the spot darkness analysis on X-ray film (Kodak) by using ImageQuant 300 and ImageQuant TL 8.0 software (GE Healthcare).

RESULTS AND DISCUSSION

It was observed that the amount of active substance released from hydrogel matrix into water at 25 °C reaches the level of 55 - 80% after 6 h. Furthermore, swelling degree of hydrogel matrix in water rises with the amount of active substance and achieves the equilibrium after 160 h swelling. Gel fraction of matrix decreases with increasing amount of AcSDKP. Contact of endothelial cells with hydrogel matrix containing AcSDKP results in a higher level of changes in expression of genes responsible for angiogenesis.

CONCLUSION

Hydrogel based matrix containing acetyl-N-Ser-Asp-Lys-Pro activating angiogenesis process can be synthesized using EB-irradiation technique.

REFERENCES

1. Wang D., *et al.*, AJP-Heart Circ Physiol 287:2099-2105, 2004
2. Fromes Y., *et al.*, Wound Rep Reg 14:306–312, 2006

Nanostructured Organic Layers via Polymer Demixing to Control Mesenchymal Stem Cell Response

Mohammed Khattak^{1,2}, John Hunt¹ and Raechelle A. D'Sa^{2*}

¹Clinical Engineering, Musculoskeletal Biology, Institute of Ageing and Chronic Disease, University of Liverpool, UK

^{2*}Centre for Materials and Structures, School of Engineering, University of Liverpool, UK, r.dsa@liverpool.ac.uk

INTRODUCTION

The initial acceptance or rejection of a biomaterial is controlled by the interface of a material surface with the biological environment. Variations in substratum surface properties such as chemistry, topography, surface energy, etc., affect cell–biomaterial interfacial characteristics, potentially influencing cellular functions.¹ Biological response can be controlled by biomimetic approaches by patterning methods and selective chemical modification schemes.² A cell that comes into contact with a biomaterial will detect the surface chemistry to find suitable sites for adhesion, growth and maturation. Additionally, the 3D topographical environment is also important for cellular response.

We investigated cell–nanotopographic substrata interactions by using cells cultured on polymer-demixed nanotopographies. The nanofabrication system employed involves demixing of two immiscible polymers. The shape of the features is controlled by varying the composition of the polymer mixture. These surfaces were used to evaluate the biological response of mesenchymal stem cells (MSCs). Furthermore, to assess the effect of nanotopography versus surface chemistry, similar topographies with varying polymer combinations were investigated.

EXPERIMENTAL METHODS

In this study, we investigated six different polymer combinations of poly(methyl methacrylate) (PMMA), poly (lactic acid) (PLA), polystyrene (PS) and polycaprolactone (PCL) to produce polymer demixed thin films with varying nanotopographies. Control surfaces were produced using 100% of each of the polymers and each combination set was assessed at 3 different ratios (25:75, 50:50 and 75:25). The topography of each sample was assessed by AFM, while surface chemistry was analysed by FTIR and wettability by contact angle microscopy. Following MSC culture and seeding onto each sample, analysis of cell proliferation, morphology and differentiation by immunostaining (using osteocalcin, collagen II and adiponectin markers) was performed at 7, 14 and 28 days.

RESULTS AND DISCUSSION

The polymer demixed surfaces were predominantly made up of either nanoislands and protrusions or nanopits. Each polymer combination showed a preference for either the substrate or air interface. In the case of PMMA:PS, demixed films from blend solutions with a greater PS dose displayed pitted topographies whereas those with a higher proportion of PMMA were

largely made up of nanoscale protrusions. Such variation was also demonstrated in the PS:PLA group, with PS seemingly preferring the substrate interface and PLA the air interface; this produced pits when the proportion of PS was higher and islands and protrusions when the PLA dose increased. In both cases, higher doses of PMMA and PLA produced an island-dominant topography. Fittingly, the PMMA:PLA group, exhibited topographies that were all made up of interconnecting protrusions, which are even more apparent as the PLA dose increases. PCL appeared to prefer the substrate interface much more than both PMMA and PS. This is because as the proportion of PCL fell and PMMA/PS increased, the surface changed from a predominantly pitted surface to an island-dominant surface. The PCL:PLA group however produced topographies that were all relatively similar; this could be because the surface energies of these two polymers are similar. Representative images of the PS:PLA polymer combination is given in Figure 1.

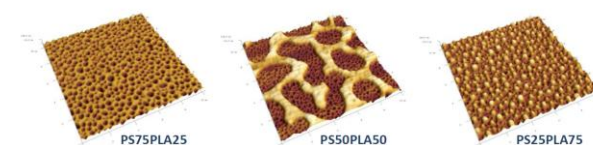


Figure 1: AFM topographical images of PS:PLA films

Cell–substrata interactions were studied by using MSCs cultured on polymer-demixed nanotopographies. The results confirm that both physical and chemical characteristics can influence cell behaviour, specifically in terms of proliferation and differentiation. Cell proliferation was similar on the different samples studied at 7, 14 and 28 days. The morphology of the samples showed a shift from a fibroblast-like MSC morphology at 7 days, to a much more spindle-like morphology by 28 days.

CONCLUSION

Spin cast blends of displayed either nanoislands or nanopits depending on the ratio of the polymer used. It is hypothesized that the pits are a result of an incomplete dewetting process of a polymer blend. Cells not only prefer nanotopographies, but the underlying chemistry also plays a significant role on differentiation.

REFERENCES

1. Anselme, K. *et al.*, J. Adhes Sci Technol. 24: 831-852, 2010.
2. Lord, M.S. *et al.*, Nano Today. 5:66-78, 2010.

Role of Gallium doped phosphate-based glasses in the Management of Periodontitis

Bernadette Lackey¹, Rohan Sahdev¹, Quentin Nunes², Tahera Ansari³, Susan Higham¹, David Fernig⁴, Sabeel Valappil^{1*}

^{1*} Department of Health Services Research, University of Liverpool, UK, S.Valappil@liv.ac.uk

² NIHR Liverpool Pancreas Biomedical Research Unit, Royal Liverpool University Hospital, UK

³ Department of Surgical Research, Imperial College London, UK

⁴ Department of Structural and Chemical Biology, University of Liverpool, UK

INTRODUCTION

This study aimed at evaluating the potential role of gallium, which is incorporated in controlled delivery agent phosphate-based glasses (PBGs)¹, for the management of periodontitis. Periodontitis describes a group of inflammatory diseases of the gingiva and supporting structures of the periodontium. They are initiated by the accumulation of plaque bacteria such as the putative periodontal pathogen *Prophyromonas gingivalis*, but the host immune response is the major contributing factor for destruction of periodontal tissues. Proteins that bind to heparin (HBPs) play important roles in health and disease and interact with each other via networks known as 'heparin interactomes'².

EXPERIMENTAL METHODS

In silico analyses using published datasets were used to construct a putative HBPs using online database resource 'Search Tool for the Retrieval of Interacting Genes' (STRING). *In vitro* study investigated the effect of gallium on matrix metalloproteinase (MMP-2) activity using MMP assay kit. Antibacterial assay of gallium was conducted using disc diffusion assay on *P. gingivalis* ATCC33277. *In vivo* biocompatibility of gallium was evaluated in rats as subcutaneous implants. Student's t-test was used to compare the mean values using GraphPad software (San Diego, CA, USA). P values < 0.05 were considered statistically significant.

RESULTS AND DISCUSSION

In silico analyses using published datasets revealed 25 up-regulated and 23 down-regulated HBPs in periodontitis. *In vitro* study of gallium on MMP-2, which is part of the HBP interactome in periodontitis confirmed that gallium ions released from Ga-PBGs inhibited MMP-2 activity significantly in water (p=0.03) and artificial saliva (p=0.003) media. Antibacterial assay of gallium displayed activity against *P. gingivalis* (22 ± 0.5mm compared with controls 0mm). *In vivo* biocompatibility of gallium evaluated in rats showed a non-toxic and foreign body response after two weeks of implantation (Fig 1).

The network analysis indicates that MMP-2 is an important player in the putative HBP interactome and a potential target for antibacterial gallium in the management of periodontitis. It was reported that the antibacterial effect of gallium was marked in an iron-controlled medium¹ hence Ga-PBG would be more effective in humans, where iron is sequestered by iron-

binding complexes to maintain an extremely low concentration of free iron.

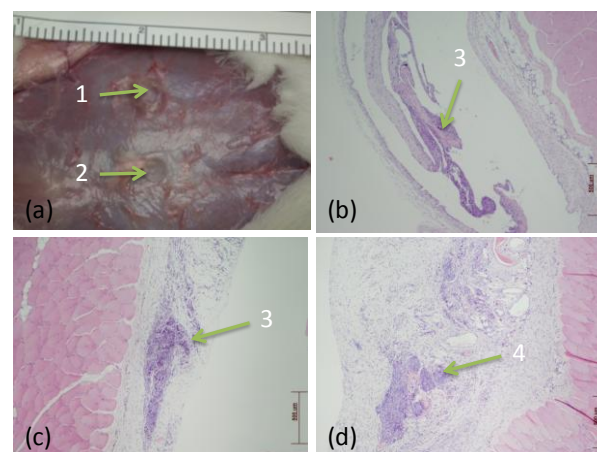


Fig 1. Digital image of two glass discs after two week subcutaneous implantation in SD rats (a). Histological H&E stained sections following two week post implantation showing the biological response of (b) C-PBG (×40), (c) and (d) Ga-PBG (×40). Key: 1; Ga-PBG disc, 2; C-PBG disc, 3; darken area of the capsule shows signs of increased inflammatory cells and 4; lymphoid aggregates (collection of lymphocytes).

CONCLUSION

The results indicate that gallium ions might act on multiple targets of biological mechanisms underlying periodontal disease. Moreover, Ga-PBGs are biocompatible in a rat model evaluated after two weeks of implantation. The findings warrant further investigation into optimisation of gallium release from glass composition that will have important clinical implications in the future treatment and management of periodontal disease.

REFERENCES

1. Valappil SP. *et al.*, Acta Biomater. 8:1957-1965, 2012.
2. Nunes QM. *et al.*, Pancreatolgy. 13:598-604, 2013.

ACKNOWLEDGMENTS

This research was supported by an induction award (University of Liverpool, UK) and a 2009 3MESPE ODRT Research Award (Oral and Dental Research Trust, UK). Rohan Sahdev was funded internally by the University of Liverpool, Department of Biochemistry and Cell Biology. We thank Lee Cooper for artificial saliva preparation and Michael Dixon from Hitachi High-Technologies Europe GmbH for the SEM-EDX analyses.

Antibacterial TiO₂ nanotubes incorporated with silver nanoparticles

Zhijun Guo and Li Zhang*

Research Center for Nano-biomaterials, Sichuan University, China,

*corresponding author: zhangli9111@126.com

INTRODUCTION

Titanium implants are widely used clinically, however, implant associated infection remains one of the most complications. So it is important to attain long-term ability to combat bacterial colonization on the implant¹. Due to the high surface-area-to-volume ratio, TiO₂ nanotubes (Ti-NT) are promising bioactive coating that can induce direct bone-implant bonding with enhanced host defense and serve as carriers for silver particles which is one of most popular antibacterial agents with benefits of lower resistant strains and no-cytotoxicity at suitable doses²⁻³. In this work, we attempt to fabricate silver-incorporated TiO₂ nanotubes. And investigate whether the samples indeed possess long-term antibacterial capability by *S. aureus* and *E. coli*.

EXPERIMENTAL METHODS

The Ti foils (10×10×1mm³) were polished by SiC sandpapers and soaked in mixed acid to remove the oxidation layer and ultrasonically cleaned by acetone, ethanol and deionized water. Afterwards, Ti foil served as the anode electrode and a graphite as counter in ethylene glycol electrolyte containing 0.5wt% NH₄F and 5 vol% deionized water. After anodization, the samples were soaked in AgNO₃ solutions with different concentration (0.5, 1, 1.5 and 2M) for 2 hours. Afterwards, they were cleaned with deionized water, dried, and irradiated with UV light for 2 hours. The samples were denoted as NT-Ag0.5, NT-Ag1.0, NT-Ag1.5, NT-Ag2.0.

RESULTS AND DISCUSSION

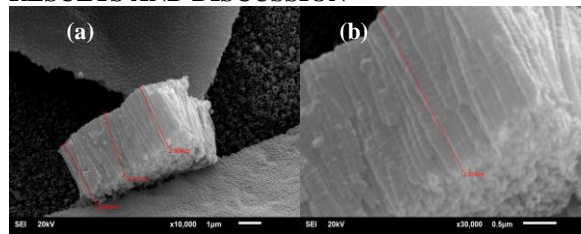


Fig.1 (a) SEM images of TiO₂ nanotubes anodized for 5h at 40V in 0.5% NH₄F ethylene glycol and (b) high magnification of a TiO₂-NTs formed by anodization of a Ti foil at 40 V for 5 h, which is a optimized anodization conditions, have a typical inner diameter of about 130 nm, outer diameter of 160 nm and length of about 2.8μm. (Fig.1). TiO₂-NTs perpendicular to the substrate and separated from each other, were open at the top and closed at the bottom.

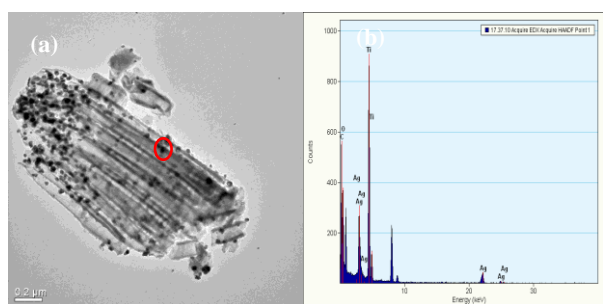
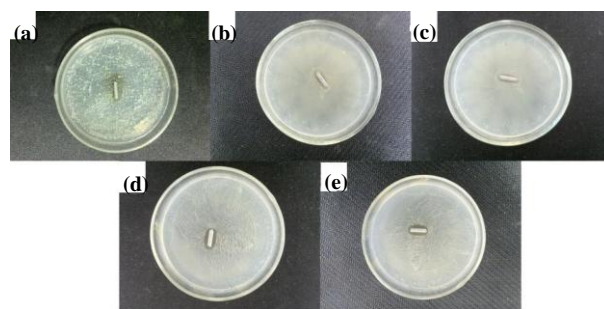


Fig.2 TEM images (a) and EDS (b) of Ag-incorporated TiO₂ nanotubes

The TEM image acquired from the nanotubes taken from NT-Ag0.5 shown in Fig.2. Careful inspection of Fig.2 reveals the Ag nanoparticles incorporated into the nanotubes tightly. The diameter of the Ag nanoparticles varies from 15 to 80 nm, which is related to AgNO₃ concentration. The Ag nanoparticles attached mainly to the inner wall of TiO₂ nanotubes, but also outer side walls and on top edges. The silver particles (black dots) are distributed homogenously in the TiO₂ nanotube layer. EDS analysis further confirms that the random black dots in Fig.2 is Ag nanoparticles.



a: control, b: NT-Ag0.5, c: NT-Ag1.0, d: NT-Ag1.5, e: NT-Ag2.0

Fig.3 photos of bacteriostatic annulus of samples

As shown in Fig.3, the bacteria and samples are cultured together to determine the bacteriostatic effect from zone of inhibition. The results indicated that all silver-loaded Ti-NTs reduced the proliferation of bacterial. In comparison, no zone of inhibition was seen around NT-0.0. Besides, the NT-Ag 1.5 and NT-2.0 have a wider zone of inhibition than other groups. NT-1.5 have high Ag-loaded efficacy than that of NT-2.0, indicating that it is a best choice to realize a better long-term antibacterial effect.

CONCLUSION

In summary, Ag nanoparticles are incorporated into TiO₂ nanotubes on Ti implants using a simple procedure involving AgNO₃ solution immersion and UV irradiation. The Ag nanoparticles adhere strongly to the inner walls of TiO₂ nanotubes, and the size and loaded dose of Ag nanoparticles can be regulated by adjusting the AgNO₃ concentration and immersion time.

The antimicrobial activity of NT-Ag were evaluated by *S. aureus* and *E. coli*. The results indicated that the Ag-loaded TiO₂ nanotubes could prevent the bacteria from adhering to the NT walls dramatically. Thus, the Ti implant with a series of treatment will have excellent antibacterial and osseointegrative abilities and have a great potential to be used in the field of hard tissue repair.

REFERENCES

1. Zhao L, *et al.*, J Biomed Mater Res B Appl Biomater. 91: 470-80, 2009
2. Alt V, *et al.*, Biomaterials. 25: 4383-91, 2004
3. Agata R, *et al.*, Eur. J. Inorg. Chem. 5199-5206, 2012

ACKNOWLEDGMENTS

This work was jointly supported by the National Basic Research Program of China (973 Program, 2012CB933902).



Bone Nodule Formation by Osteoblast-Like Cells Incubated with a Novel Silane Modification of Glass

Sandra Fawcett¹, Nicholas Rhodes¹, John Hunt¹, and Judith Curran²

¹ Clinical Engineering, UKCTE, Department of Musculoskeletal Biology, Institute of Ageing & Chronic Disease, University of Liverpool, UK

² School of Engineering, University of Liverpool, UK fawcett@liv.ac.uk

INTRODUCTION

Modification to biomaterial surface chemistry has been shown to be a useful tool for controlling cell response. More specifically, enriching substrates with groups that are prevalent in the extracellular matrix, *e.g.* $-NH_2$ (amine) can be used as a technique for enhancing the osteogenicity of a biomaterial¹. Whilst this research shows potential, results achieved to date have been variable due to the lack of consideration of the material induced responses at the sub-micron scale. In this work primary human osteoblast-like cells were isolated from human bone and seeded onto a range of $-NH_2$ -modified glass substrates. We fabricated $-NH_2$ -modified substrates with controlled chemical group distribution, surface energy and nanotopography. The optimal combination of these material factors was constructed to produce highly osteoconductive substrates.

EXPERIMENTAL METHODS

A range of $-NH_2$ -silane modified substrates were produced. The exact mechanism of material production is currently undergoing patent protection. All substrates were characterised using a ninhydrin assay (for amine concentration), water contact angle (surface energy), scanning electron microscopy (surface morphology) and atomic force microscopy (nanotopography).

Human osteoblasts (hOBs) were isolated from primary human trabecular bone. When the primary-derived cells had formed a monolayer, cells were trypsinised and seeded onto modified materials (50,000 cells / ml medium in a 24 well culture plate, 1 ml / well) and incubated in basic DMEM media with no exogenous growth factors, for 7, 14 and 28 days. Samples were then fixed and stained using Von Kossa's stain for mineralisation and visualised using light microscopy. In parallel cell-material interactions and formation of matrix was also qualitatively assessed using SEM (Zeiss/Leo 1550). Nodule formation was monitored and size and number were recorded for each test substrate using image analysis software. Quantitative evaluation of the mRNA expression of collagen I, osteopontin, osteocalcin, osteonectin, Cbfa1 and sclerostin was performed using real time polymerase chain reaction (qRT-PCR). All targets were normalised to β -actin and up-regulation of genes of interest calculated using the $\Delta\Delta C_t$ method. For all measurements of nodule size and qRT-PCR expression, a total of 4 repeats were carried out and differences in expression determined by ANOVA.

RESULTS AND DISCUSSION

Viable cell adhesion and general maintenance of the osteogenic phenotype was maintained on all $-NH_2$ -

modified substrates throughout the test period, although changes in $-NH_2$ modification affected the levels of expression observed in a modification-dependant manner. Bone nodules were formed on amine modified substrates with significantly smaller peak heights (sub 20nm) compared with other modified substrates, after 7 days. This material factor was the only significant difference between all tested amine-modified substrates.

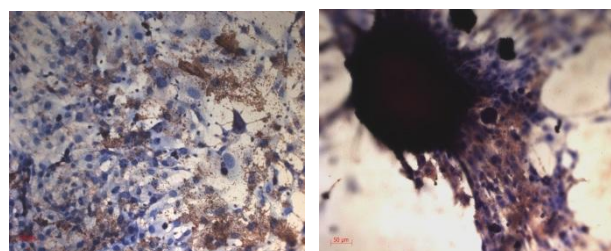


Figure 1 Bone nodule formation by hOBs on sub-20nm peak height amine modifications (right), compared to untreated glass control (left)

There was no significant difference in overall amine concentration or surface energy on all $-NH_2$ -modified substrates tested within the study.

In addition the expression of sclerostin, marker of an osteocyte phenotype, was present on the sub 20nm peak heights after 14 days, but not present on the $-NH_2$ -modified substrates that had an average peak height greater than 20nm. Substrates that had a peak height greater than 100nm did not support nodule formation. Instead, cells cultured on these substrates were flattened and formed a cohesive monolayer, and maintained mRNA profiles that were suggestive of maintenance of the osteoblast phenotype. The expression of osteogenic markers on the surfaces with peak height greater than 100nm was smaller than the other test substrates.

CONCLUSION

Enrichment of a substrate surface with $-NH_2$ modifications is a valid tool for producing cell contacting materials that are osteoconductive. In order to enhance the osteogenic nature of these substrates and control the subtle switches from osteoblast to osteocyte and develop materials that induce matrix remodelling, we must combine changes in surface chemistry with a controlled nanotopography.

REFERENCES

1. Curran, J. Fawcett, S, *et al.*, Biomaterials 34 (2013) 9352-9364.

ACKNOWLEDGMENTS

The authors would like to thank the EPSRC for providing financial support to this project, and Prof. J. Gallager for his help with the primary human tissues.



Manufacturing of AZ91D Implants with Micro-Scale Features by Powder Metallurgy Route

Aydin Tahmasebifar¹, Said Murat Kayhan², Zafer Evis¹, Yusuf Usta³ and Muammer Koç²

¹Engineering Sciences, Middle East Technical University, Turkey, aydin.tahmasebifar@metu.edu.tr

²Industrial and System Engineering, Istanbul Sehir University, Turkey

³Mechanical Engineering, Gazi University, Turkey

INTRODUCTION

Pure Mg and Mg alloys show great potential for application as biomaterial due to their special properties such as light weight, biodegradability, strength under load and the natural decay in the period of 3-4 months in vivo condition which is a perfect time for the integration of bone tissue¹. The number of biomedical applications with porous surfaces in micro scale is increasing especially in orthopedic applications. Micro-porous surfaces improve the integration between implant and bone and increase new bone formation². Porous surfaces also allow to control corrosion rate of an implant by manipulating the porosity. Previous studies showed that both micro-pores and micro-structures are responsible for the adherence of bone cells on implant surface and the acceleration of healing process^{3,4}. Therefore, it is assumed that a micro-textured and porous Mg alloy implant with an achievable porosity can enhance bone attachment and corrosion resistance.

In this study, different surface texture characteristics of AZ91D alloy were studied for the first time.

EXPERIMENTAL METHODS

AZ91D Mg, powders (Grain size: 10% < 50.4 µm, 50% < 177.6 µm and 90% < 614.1µm) were compacted by a Dartec Universal testing machine under different compaction pressures (150 and 200 MPa) at 100 and 150°C. Compacted implants are sintered at temperatures of 380 and 420°C at different periods (40, 60, 120 and 150 >mins) (Table 1). The goal is to determine acceptable windows of pressure, temperature and time to produce Mg implants with acceptable levels of porosity and strength for further biocompatibility and biodegradability tests.

No.	Mold Type	Load (kN)	Load Rate (kN/s)	Compaction Temp. (°C)	Sintering Temp. (°C)	Sintering Time (min)
1	#	360	4	150	420	60
2	#	360	4	300	420	60
3	#	360	4	300	420	120
4	O	360	4	300	420	120
5	O	480	4	300	380	150
6	#	480	4	300	380	150
7	#	480	4	150	420	40
8	O	480	4	150	420	40
9	W	480	4	150	420	120
10	#	480	4	150	420	60

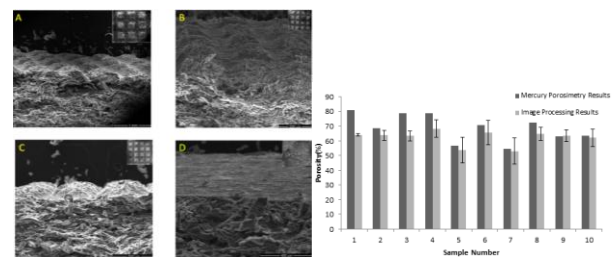
"Table 1 shows experiment conditions."

XRD was used to investigate the presence and amount of the phases of the samples. XRD was performed on Also, the morphology of powder and specimens was investigated by SEM. The density and pore size of the implant were measured by Archimedes and Mercury porosimetry methods, respectively. Electrochemical tests were carried out to measure the electrical

conductivity in Hank's solution, DMEM and DMEM +10%FBS.

RESULTS AND DISCUSSION

The results show that compaction load has a significant effect on the attainable porosity level. Porosity of samples decreases with increasing compaction pressure. During trial experiments, sufficient bonding between particles could not be achieved when metal powders were compacted at temperatures below 100°C. It was also proved that the mold surface type has no significant effect on porosity. Image processing results were highly matched with mercury porosimetry results. The other conclusion from SEM images was that we were able to manufacture a porous surface, which have patterned or smooth surface features. No significant difference was observed between micro-hardness values after sintering in temperatures below eutectic temperature.



"Figure 1 show a) the SEM images of compacted powders; b) porosimetry results"

CONCLUSION

The main purpose of this investigation was to verify the feasibility of manufacturing porous structure of AZ91D alloy with micro surface features.

In summary, porosity can be controlled by manipulating the experiment parameters. The compaction temperature should also be higher than 100 °C in order to achieve strong bonding between particles. Moreover, de-inserting problems generally occur at compaction temperatures below 100 °C. Also, there was no oxidation problem because the working temperatures were relatively low at compaction stage. However, sufficient gas flow should be provided to prevent oxidation of magnesium during heat treatment process. And there is a need for obtaining uniform particles to get better results from image processing technique.

REFERENCES

References must be numbered. Keep the same style.

1. Witte F. *et al.*, *Biomater.* 26:3557-3563, 2005
2. Arifin A *et al.*, *Mat. and Design* 55:165-175, 2014
3. Jiang P. *et al.*, *App. Sur. Sci.* 280:373-380, 2013
4. Lin L *et al.*, *J. of Orth. Trans.* 2:35-42, 2014

ACKNOWLEDGMENTS

"The authors would like to thank the Scientific and Technological Research Council Of Turkey (Grant no: 112M340) for providing financial support to this project."

Nerve Tissue Engineering Using Blends of Polyhydroxyalkanoates

L.R. Lizarraga-Valderrama and Ipsita Roy*

Faculty of Science and Technology, University of Westminster, United Kingdom royi@wmin.ac.uk

INTRODUCTION

Peripheral nerve injury (PNI) affects 2.8% of trauma patients, many of whom suffer life-long disability. For injuries consisting of gaps of more than 5mm the treatment is most commonly attempted using autologous nerve graft repair. This treatment has various limitations including donor site morbidity, scar tissue invasion, lack of donor nerves, inadequate return of function and aberrant regeneration¹. Currently, there are several clinically approved artificial nerve guidance conduits (NGCs) made from various biomaterials that have overcome some of the limitations of nerve autografts. The drawbacks of using NGCs include the difficulty in their application surgically, their tendency to trigger immune responses, to induce scar tissue and to release compounds that are detrimental to the regeneration process¹.

Polyhydroxyalkanoates (PHAs), linear polyesters synthesized by a variety of bacterial species are potential materials to be used in the manufacturing of nerve guidance conduits to assist axonal regeneration. Properties such as: controllable surface erosion; variability in material properties, lower acidity of by-products after degradation and longer stability compared to their synthetic counterparts are of special interest in this field. Currently, poly-3-hydroxybutyrate P(3HB) would appear to be only type of PHA that has been explored for use in nerve regeneration. P(3HB) conduits have been shown to repair nerve gaps of 10mm and 40mm in rat sciatic nerves and rabbit peroneal nerves respectively^{2, 3}. The main objective of this project is to develop an advanced nerve conduit made from PHAs that have never been used before in nerve tissue engineering, such as mcl-PHAs and blends of mcl-PHA with scl-PHA. A key objective will be to determine the ideal mcl/scl PHA blend ratio that provides the desired physical properties and degradation rate for optimal nerve regeneration. This will then be used to produce a range of conduit structures

EXPERIMENTAL METHODS

Short chain length (scl) and medium chain length (mcl) PHAs were produced through bacterial fermentation at shaken flask and fermenter level. The polymers were extracted by using the chloroform-hypochlorite dispersion method and purified by using organic solvents. Chemical structure confirmation was carried out using FTIR, GC-MS, ¹³C and ¹H NMR. Different films made from neat PHAs and PHA blends in various ratios were fabricated using the solvent casting method. DMA was used to measure the mechanical properties of the polymers and the blends. To evaluate the hydrophobicity of the films, contact angle studies were carried-out. The thermal properties of the polymers and

films were analysed by using DSC. Surface study of each polymer was performed using scanning electron microscopy (SEM) and white light interferometry study. The *in vitro* cell culture studies were carried-out on the pure PHA films and their blends using NG108-15 neuronal cells.

RESULTS AND DISCUSSION

Chemical characterization. FTIR, ¹³C and ¹H NMR

The typical bands of the ester carbonyl group (C=O) and C-O stretching of mcl- and scl-PHAs confirmed the chemical nature of the polymers. The carbonyl bands were detected at 1727.15 cm⁻¹ for mcl-PHAs and at 1719.02 cm⁻¹ for scl-PHAs. The C-O stretching bands for mcl- and scl-PHAs were 1160.22 and 1180.14 cm⁻¹ respectively. The corresponding spectra of ¹³C and ¹H NMR of both PHAs (data not shown) verified the chemical structure of these polymers.

DMA, DSC and water contact angle

Young's modulus (E values), elongation at break and tensile strength of the different blends are shown in the Table 1. The results show that Young's modulus values increase as the content of scl-PHA increases in the blend film.

Table 1

Film	E' (MPa)	Tensile strength (MPa)	% Strain
mcl/scl PHA (75:25)	1.06	0.58	91.9
mcl/scl PHA (50:50)	93.44 ± 7.04	15.71 ± 2	48.80 ± 2.37
mcl/scl PHA (25:75)	144.12 ± 6.84	19.40 ± 2.96	39.62 ± 4.54

The mechanical properties of the blend mcl/scl-PHA (75:25) are similar to those found in acellular peripheral nerve suggesting that this blend could be a good base material for the manufacture of NGCs. DSC results (not shown) of blends suggested lack of homogeneity. Water contact angle of the blends (75:25), (50:50) and (25:75) were 95.02 ± 1.24, 84.40 ± 0.50 and 77.83 ± 3.05 ° respectively. As the content of mcl-PHA increased, the hydrophobicity increased because of the longer aliphatic chains present in these polymers.

CONCLUSION

PHA blends have varying properties, which can be tailored to obtain PHA-based materials suitable for nerve tissue engineering.

REFERENCES

1. Babu, P. *et al.*, Indian J. Neurotr. 5 (1): 15-20, 2008.
2. Hart, A.M. *et al.*, Br. J. Plast. Surg. 56 (5): 444-450.
3. Mohanna, P.N. *et al.*, Scand. J. Plast. Reconstr. Surg. Hand Surg. 39 (3): 129-137.

ACKNOWLEDGMENTS

I would like to thank the University of Sheffield and University College of London for their significant collaboration in this work.



Polyethyleneimine-iron oxide hybrid nanomaterials – structure and biocompatibility

Roxana Mioara Piticescu¹, Laura Madalina Popescu^{1*}, Alexandrina Burlacu^{1,2}, Ana-Maria Rosca², Eugeniu Vasile^{1,3},
 Andrea Danani⁴

^{1*}Laboratory of Nanostructured Materials/National R&D Institute for Non-ferrous and Rare Metals, Romania,
mpopescu@imnr.ro

²Laboratory of Stem Cell Biology/Institute of Cellular Biology and Pathology „Nicolae Simionescu”, Bucharest,
 Romania

³Micro and Nanostructured Multifunctional Materials/University POLITEHNICA of Bucharest, Romania

⁴Laboratory of Applied Mathematics and Physics, University of Applied Sciences and Arts of Southern Switzerland,
 Galleria 2, 6928, Manno, Ticino, Switzerland

INTRODUCTION

Iron oxide nanoparticles attracted the interest of researchers working in nanotechnology due to potential biomedical applications, amongst others, in drug and gene delivery, magnetic resonance imaging (MRI) and hyperthermia¹⁻⁶. However, these nanoparticles should be easily dispersible, colloidal stable and biocompatible⁴. For this purpose, various polymers such as dextran, poly(lactic acid), poly(ethylene glycol), chitosan, poly(vinyl alcohol), polyaniline and polyethyleneimine (PEI) have been successfully coated on the surface of iron oxides.

In this paper, we describe a new approach to synthesize hybrid nanostructures based on Fe_3O_4 and PEI.

EXPERIMENTAL METHODS

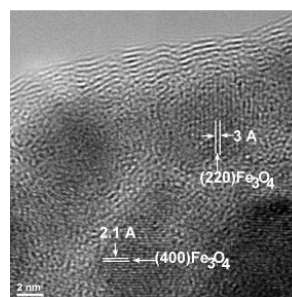
Organic-inorganic hybrid nanostructures were synthesized using hydrothermal method in high pressure and low temperature conditions. Predictive studies concerning interaction of iron oxides with PEI were performed based on computational models. Composition of PEI based hybrids was carried out via FT-IR spectroscopy. The morphology and size of the inorganic particles were characterized with HRTEM analysis. Stable aqueous colloidal suspensions were prepared for in vitro measurements

The biocompatibility of this suspension was evaluated by interaction with mouse bone marrow-derived mesenchymal stem cells (MSC) in culture. The viability, proliferation and morphology of cells in the presence of nanohybrid were followed by MTT assay and phase-contrast microscopy.

RESULTS AND DISCUSSION

HRTEM micrograph presented in the figure below demonstrates the existence of crystalline planes with Miller indexes (220) and (400) corresponding to Fe_3O_4 . Crystallite sizes range between 2.5 and 7 nm. All structures were biocompatible with cells in vitro, in terms of supporting proliferation in complete medium (DMEM supplemented with 10% MSC qualified FBS). Interestingly, the sample having Fe_3O_4 :PEI=1:2 induced a change in MSC morphology resembling brown fat cell specific lipid. Further studies are needed to determine whether vacuoles appeared inside the cells are lipid

loaded and cells are directed towards differentiation into adipose cells.



CONCLUSION

New hybrid nanostructures based on polyethyleneimine and iron oxides were obtained, consisting of small crystallite of magnetite entrapped in organic phase. Biological interaction of these hybrid nanomaterials with MSC cells in vitro showed no cytotoxic effect and preservation of the cells morphology. Surprisingly, one sample having Fe_3O_4 :PEI=1:2 induced a change in MSC morphology and might be promising for their differentiation into adipose cells.

REFERENCES

1. Schweiger G. *et al.*, Int. J. Pharm. 408:130-37, 2011
2. Lam T. *et al.*, Adv. Colloid Interface Sci.199-200:95-113, 2013
3. Prijic S. *et al.*, Biomaterials 33:4379-91, 2012
4. Li J. *et al.*, Biomaterials 35:3666-77, 2014
5. Stojanovic Z. *et al.*, Colloids Surf., B 109: 236-243, 2013
6. Gupta A. K. *et al.*, Biomaterials 26:3995-4021, 2005

ACKNOWLEDGMENTS

“The authors would like to thank the Romanian-Swiss Research project “PPI/PEI dendrimers immobilized iron oxide nanoparticles as contrast agents for cancer detection” ctr. IZERZO_142141 and CTR 4 / RO-CH / RSRP / 2012 for providing financial support to this project”.

Regulation of Sclerostin Expression by ATP and PTH at Different Stages of Human Bone Development

Osman M Azuraiddi, Peter J Wilson, Nicholas P Rhodes and James A Gallagher

Department of Musculoskeletal Biology, Institute of Ageing and Chronic Disease, University of Liverpool L69 3GA, UK, Moht-Azuraidi.Osman@liv.ac.uk

INTRODUCTION

Sclerostin is a glycoprotein expressed by the SOST gene in osteoblast and osteocyte lineage cells¹. Sclerostin has anti-anabolic effects on bone formation through the inhibition of the WNT signalling pathway². The WNT signalling pathway is thought to be a major regulator of bone modelling and remodelling. Precise understanding and modulation of the WNT pathway should result in better control of the bone healing response³. Administration of Parathyroid hormone (PTH) in osteoporosis treatments has been shown to stimulate fracture healing⁴. However, in clinical trials, PTH has been shown to contribute only a limited improvement to bone healing in humans⁵. Consequently, there is much interest in sclerostin as a potential therapeutic target for applications in bone regeneration and healing. The aim of this study was to determine how SOST expression is regulated by ATP and PTH at different stages of osteoblastic development.

EXPERIMENTAL METHODS

We investigated the effect of ATP and PTH on the expression of sclerostin in three human osteosarcoma cell lines representing different stages of osteoblast differentiation, MG-63 the least differentiated, TE-85 intermediate and SaOS-2 the most mature. All cell lines were grown in DMEM + 10% FCS in 6 wells plate until 90% confluent. Cells were serum deprived for 48 hours with serum-free DMEM before treatment. Cells were treated with 10 μ M ATP, 10ng/ml PTH and 10 μ M ATP + 10ng/ml PTH respectively and incubated at 37°C for 17 hours. mRNA was extracted and reverse transcribed to cDNA. Expression of specific sclerostin was monitored by qRT-PCR using an iCycler iQ. Results were analysed using a Kruskal-Wallis test and Mann-Whitney with Bonferroni Correction.

RESULTS AND DISCUSSION

The gene expression profile in the three cells lines was consistent with the previously reported differentiation status. In control/untreated cells, SaOS-2 cells had the highest expression of sclerostin ($p < 0.05$) compared to MG63 and TE85 (Figure 1). Expression of sclerostin was intermediate in TE85 cells but significantly higher than MG63 ($p < 0.05$). One of the most striking differences between the cell lines was the expression of sclerostin in MG-63 cells, which was barely detectable, and that in SaOS-2 cells which was abundantly expressed. Sclerostin transcripts were present in TE85 cells but at an order of magnitude less than in SaOS-2 cells. In both TE85 and SaOS-2 cells, treatment with 10 μ M ATP, 10ng/ml PTH and 10 μ M ATP + 10ng/ml PTH caused a decrease in the expression of sclerostin.

However, the inhibition of sclerostin was not significant ($p > 0.05$) in all treatments in both cell lines compared to the control group.

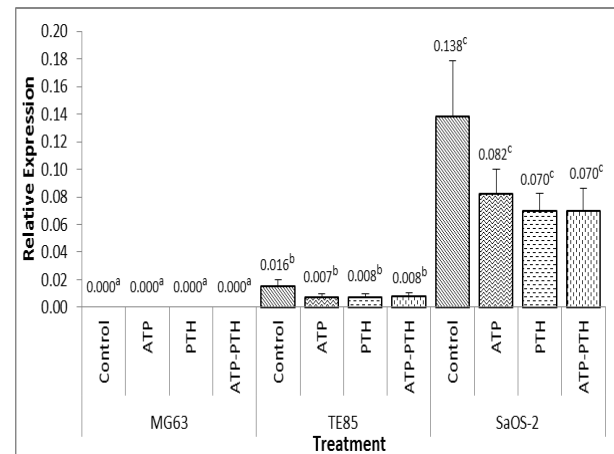


Figure 1 Relative expression of sclerostin in response to ATP and PTH treatments in MG63, TE85 and SaOS-2 cells

CONCLUSION

The results reinforce previous reports on the relative differentiation status of these commonly used osteoblastic cell models. The robust expression of sclerostin in SaOS-2 confirms that this cell line represents a mature stage of the osteoblast / osteocyte lineage. However, the findings of this study show that inhibition of sclerostin by ATP and PTH occurred at all stages of bone development. Better understanding of the regulation of sclerostin should contribute to the development of new therapeutic approaches to the regeneration of bone in degenerative diseases, trauma and surgery and metabolic bone conditions.

REFERENCES

1. Agholme F. *et al.*, Journal of Orthopaedic Research. 32:471–476, 2014.
2. Bezooijen R. L. *et al.*, Cytokine & Growth Factor Reviews. 16:319–327, 2005.
3. Chen Y. *et al.*, PLoS Medicine. 4:e249, 2007.
4. Nakajima A. *et al.*, Journal of Bone and Mineral Research. 17:2038–2047, 2002.
5. Aspenberg P. *et al.*, Journal of Bone and Mineral Research. 25:404–414, 2010.

ACKNOWLEDGMENTS

The authors would like to thank the Ministry of Education Malaysia and Universiti Putra Malaysia for providing financial support to this project.

Hemocompatible Biomaterial Based on Fibrin Coatings

Ondřej Kaplan, Tomáš Riedel, Milan Houska, and Eduard Brynda

Department of Biomaterials and Bioanalogous Systems/ Institute of Macromolecular Chemistry, Academy of Sciences of the Czech Republic, v.v.i., Czech Republic, kaplan@imc.cas.cz

INTRODUCTION

Various biomaterials have been synthesized for the manufacture of blood vessels prostheses and cardiovascular implants such as stents or aortic valves. However, no synthetic material has been capable of substituting the active functions of blood vessel endothelium. Thus, surface modifications are searched which could prevent an acute thrombus formation and encourage the subsequent endothelialisation on the cardiovascular implants.

Recently developed technique¹ has allowed us to coat materials, e.g. glass, nitinol, polystyrene, poly(ethyleneterephthalate), poly(lactide), poly(caprolactone), poly(hydroxyethyl methacrylate), and collagen, with fibrin networks growing from their surfaces. The coatings promoted the in vitro formation of confluent layers of vessel endothelium cells seeded on their surfaces². In the presented work we reached a decrease in thrombogenicity after coating glass surface with fibrin networks and immobilized heparin.

EXPERIMENTAL METHODS

Fibrin network was prepared on a glass surface by catalytic action of surface-attached thrombin on ambient fibrinogen solution². The fibrin structures were observed by SEM, AFM and confocal microscopy. The anticoagulant effect of the coating was characterized by the measurement of coagulation time after the recalcification of human blood plasma.

RESULTS AND DISCUSSION

Thickness of the surface fibrin gels was controlled within a range from 20 nm to 180 µm. The coagulation time of the recalcified human blood plasma increased from several minutes to couple of hours after coating of the surface with fibrin gel containing immobilized heparin depending on the gel thickness and heparin content.

CONCLUSION

The coatings can be applied on objects of various shape, structure, and materials. Potentially, they can encourage the endothelialisation of vessel prostheses lumen and other cardiovascular implants before thrombi are formed on their surface.

REFERENCES

1. Riedel T. *et al.*, J. Biomed Mater Res A 88(2):437-4, 2009
2. Chlupáč J. *et al.*, Physiol Res. 2014

ACKNOWLEDGMENTS

This work was supported by Ministry of Education, Youth and Sports of the Czech Republic (Grant no: EE2.30.0029)

Inflammation-modulating biomaterial impacts neutrophil-monocyte juxacrine and paracrine regulation

Hannah Caitlin Cohen,¹ Tyler Jacob Lieberthal,² W. John Kao (PI, wjkao@wisc.edu)^{1,2}

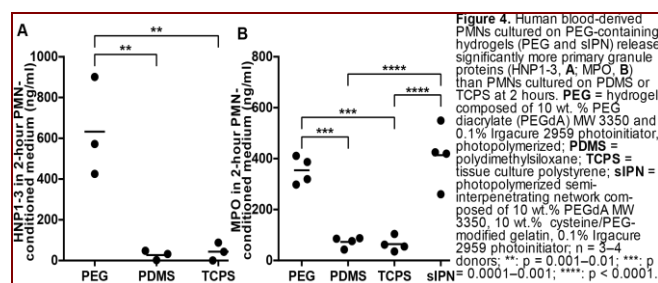
¹Pharmaceutical Sciences Division, School of Pharmacy, University of Wisconsin-Madison, Madison, Wisconsin 53705

²Department of Biomedical Engineering, University of Wisconsin-Madison, Madison, Wisconsin 53705

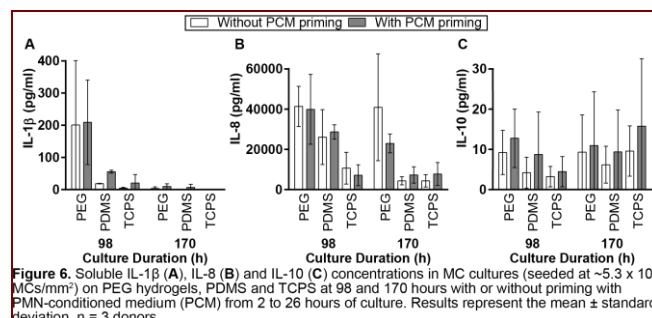
Statement of Purpose: The extend and the duration of the host inflammatory response have a predictive impact on wound healing outcome and material biocompatibility. Material-mediated polymorphonuclear leukocyte (PMN) and monocyte/macrophage (MC) paracrine and juxacrine regulation is not well understood. A mechanistic understanding of this will result in novel material engineering strategies.

Methods: Whole blood was collected from human donors and PMN and MC were isolated using a gradient method.² PEG hydrogels, PDMS and gelatin-PEG hydrogels were prepared as previously described,^{3,4} and cultured with PMN and/or MC with or without Src or PI3K γ inhibitors. Cellular viability, MPO as a primary granule marker and MMP-9 as a tertiary granule marker were measured. PMN conditioned medium was utilized to study the effect on MC migration in a Boyden chamber and cytokine expression. Experiments were repeated for four donors.

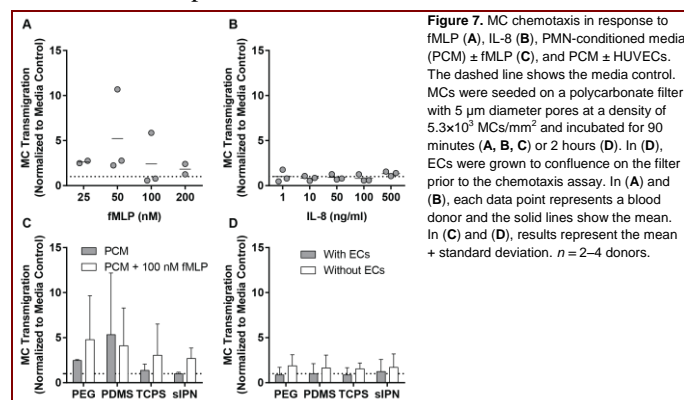
Results: There were no significant differences in adherent viable or necrotic cell densities among biomaterials. PEG-containing hydrogels had significantly higher MPO expression where MMP9 levels were comparable. Src was ubiquitously important for degranulation but PI3K γ dependent pathway was crucial only in PMN primary granule degranulation mediated by PEG and gelatin-PEG hydrogels.



To determine the downstream effect of PMN degranulation on MC function, MC were treated with material-specific PMN conditioned medium. We found that PMN-MC paracrine and juxacrine interactions minimally influenced PMN and/or MC viability and adhesion as well as cytokine expression (ie. IL-1 β , IL-8, IL-10)



Furthermore, no downstream effect on MC transmigration was observed when MC were treated with material-specific PMN conditioned medium either with or without endothelial cells present.



Conclusions: The incorporation of ECM-derived component gelatin to a PEG matrix resulted in an effected inflammation-modulating construct that mediated normal inflammatory response that quickly attenuated with more pro-healing MC phenotype. This minimalistic but yet robust material design bypass the complexity of employing biomolecules such as IL4 in regulating the host inflammatory response.

Acknowledgements: Funded in part by a National Defense Science and Engineering fellowship and National Institutes of Health

References: 1. Soehnlein O. et al. Trends Immunol. 2009;30:546-556. 2. Waldeck H. et al. Biomaterials 2012;33:29-37. 3. Cohen H.C. et al. Am. J. Pathol. 2013;182:2180-2190. 4. Xu K.D. et al. Acta Biomater. 2012;8:2504-2516.

A Heterotypic Microfluidic Model of PDAC Microenvironment for Investigating Stroma-Tumor Interactions and Therapeutic Evaluations

Cole Drifka,^{ab} Kevin Eliceiri,^{abc} Agnes Loeffler,^{cd} Sharon Weber,^{cd} W. John Kao (PI, wjkao@wisc.edu)^{a-d}

^aDepartment of Biomedical Engineering, ^bLaboratory for Optical and Computational Instrumentation, ^cPaul P. Carbone Comprehensive Cancer Center, ^dSchool of Medicine and Public Health, University of Wisconsin, Madison, WI, USA

Introduction: Pancreatic ductal adenocarcinoma (PDAC) is nearly 100% fatal. The interplay between cancer cells, stromal cells, and the collagen-rich extracellular matrix (ECM) during progression to aggressive metastasis is critical but not fully understood.¹ Greatly limiting this understanding is the lack of a PDAC model that recapitulates key features of the *in vivo* stromal microenvironment while maintaining robust physical control with imaging and therapeutic accessibility. Additionally, traditional 2D culture formats may not accurately predict *in vivo* tumor responses due to neglected stromal contributions and may therefore limit the translation of new therapeutics. We have bioengineered a microfluidic model of the PDAC stroma-cancer axis incorporating clinically-isolated multicellularity, ECM components, and a spatially-defined 3D architecture.² The model's utility is supported by validating key features against clinically-evaluated human tissues, the ability to modulate ECM structure and monitor live cell-ECM interplay, and the potential to evaluate therapeutics in a microenvironment context.

Methods: Primary pancreatic stellate cells (PSCs) and cancer cells (PCCs) were isolated and characterized from clinically-evaluated PDAC tissue specimens. Microfluidic devices were fabricated via polydimethylsiloxane (PDMS) lithography. PSCs and PCCs, suspended in a collagen-based ECM, were patterned as 3D trilayers within devices. Void space created on each side of the trilayer was used to change media and administer therapeutic agents via capillary action. Second Harmonic Generation (SHG) imaging was used to visualize and quantify collagen structure and reorganization patterns in 111 pathology-reviewed human PDAC tissues and in different ECM formulations within the model. Microfluidic models were established, treated with increasing doses of paclitaxel for 48 hr, and assayed for cytotoxicity and culture compactness.

Results: Primary PSCs and PCCs pattern as a 3D trilayer due to laminar flow. PSC contraction of the ECM away from the PDMS sidewalls results in a compressed trilayer culture with void space flanking each side that can be used to exchange fluid via capillary action for *in situ* media changes or therapeutic administration (Fig 1).

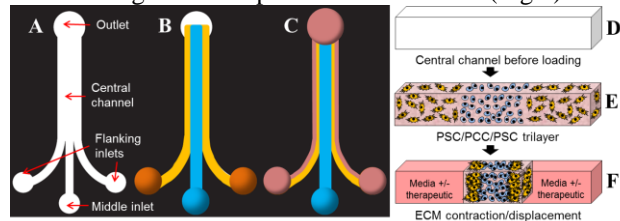


Fig 1 (A,D) Empty device (B,E) PSC-PCC-PSC trilayer in 3D ECM (C,F) contracted trilayer with media +/- therapeutics in flanking void space.

Additionally, the trilayer emulates the spatial histological relationship of dense stromal components (PSCs and collagen) encompassing disseminating cancer cells *in vivo* (Fig 2A). After ECM contraction, the interface between PSCs and PCCs can be resolved and provides a unique opportunity to parse out cell-ECM interactions as a function of cell type (Fig 2C). Compared to normal pancreas, we show that collagen fibers in PDAC tissue are significantly longer (21.02 vs 18.56 μm , $p < 0.001$) and more aligned (0.36 vs 0.27, $p < 0.001$). In the model, *in vivo* collagen fiber lengthening and alignment can be represented by modulating the initial ECM formulation and allowing the intrinsic contractile behavior of PSCs to remodel the collagen network (Fig 2D). This establishes a platform to study the unclear role collagen architecture has on PDAC cell behaviors. Additionally, paclitaxel treatment reduces cell viability and culture compactness in a dose-dependent manner, suggesting that both cell and ECM responses to therapeutics can be analyzed (Fig 3).

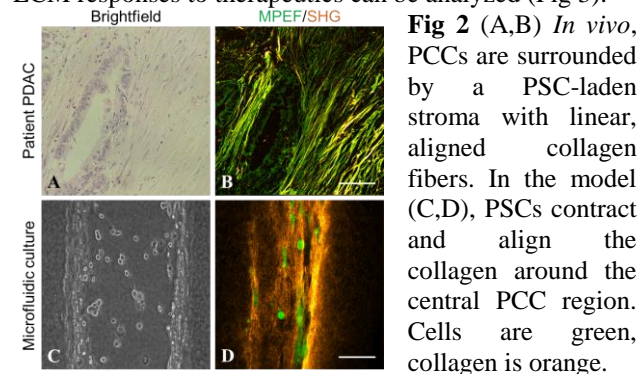


Fig 2 (A,B) *In vivo*, PCCs are surrounded by a PSC-laden stroma with linear, aligned collagen fibers. In the model (C,D), PSCs contract and align the collagen around the central PCC region. Cells are green, collagen is orange.

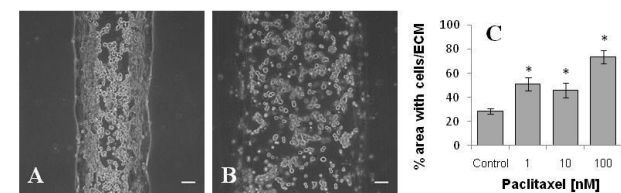


Fig 3 Trilayer culture compactness after treatment with (A) vehicle control (B) 100 nM paclitaxel. (C) Quantified cell/ECM area as an indication of trilayer compactness. Data shows mean \pm SEM, * $p < 0.05$ vs. control for $n = 3$ devices. Scale bars = 100 μm .

Conclusions: We have developed and characterized a human tissue-based PDAC model to study underlying pathological mechanisms and to assess new therapeutic approaches, which are needed to improve PDAC prognosis. The use of patient-derived tissue components, ability to introduce therapeutics, and power to modulate and quantify cell and ECM changes support the model's value to PDAC translational research.

References: [1] Erkan *et al.* Nat Rev Gastroentero 2012; 9:454-67 [2] Drifka *et al.* Lab Chip 2013;13:3965-75.

Enhanced migration of Mesenchymal stem cell spheroids towards glioma

Smruthi Suryaprakash¹ and Hon Fai Chan¹ and Kam W Leong^{2*}

¹Department of Biomedical Engineering, Duke University, USA

^{2*}Department of Biomedical Engineering, Duke University, ss515@duke.edu

INTRODUCTION

Glioblastoma is one of the most aggressive forms of brain cancer. Each year 18,000 people are diagnosed with glioblastomas with an average survival of 10 to 12 months. MSC are an attractive candidate for cell based therapy since they can be easily isolated, manipulated and have no immune rejection. MSC transduced with TRAIL are capable of migrating towards the tumor cells and kill the tumor cells due to bystander effect¹. However for cell based therapy migration, survival and retention are the major factors. MSC in spheroidal form has shown to have increased expression of CXCR4 which is critical for migration towards tumor cells². The spheroidal form also might help the cells to survive for longer and prevent it from getting washed out due to the extracellular matrix surrounding the cells and larger size respectively.

Hence MSC in spheroidal created using a microfluidic platform was used for cell based therapy to treat glioma

EXPERIMENTAL METHODS

Preparing the chip

Microfluidic device was prepared using soft lithography techniques. Silicon mold was patterned using SU-8 3025 to be of 200um in height. PDMS prepolymer and curing agent was then poured onto the silicon mold and cured. The PDMS mold was peeled and holes were punched in the inlet and the outlet. The device was bonded to a cover slip using oxygen plasma treatment. To make the second chip hydrophilic a two-step sol-gel coating procedure was followed.

Preparing the MSC spheroids

Cell culture medium supplemented with 0.3% pluronic F-127 and 10 million cells/ml was used as the inner phase. The oil phase used was HFE-7500 supplemented with Pico-Surf 1 surfactant. The outer aqueous phase comprised culture medium supplemented with Pluronic F-127 (2.5 wt%). The Flow rate of the inner phase was 4ul/min, middle phase was 13ul/min and outer phase 30ul/min.

RT-PCR for CXCR4

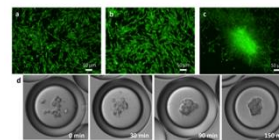
MSC single cells and MSC spheroids were cultured for 3days. mRNA was extracted and RT-PCR was performed using CXCR4 and GAPDH primers. A 2% agarose gel was used to run the cDNA.

MSC Migration assay

IBIDI cell culture insert was used to culture MSC/MSC spheroid and U87 on either side of a 500um gap

RESULTS AND DISCUSSION

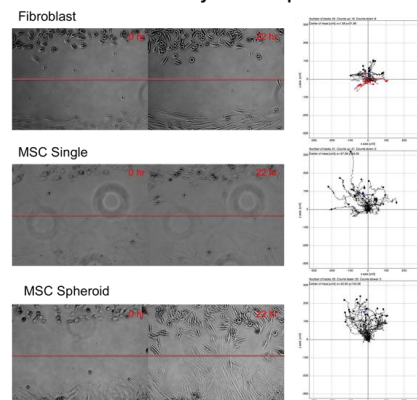
Rapid formation of MSC spheroids



Enhanced CXCR4 expression in MSC spheroids



Enhanced directionality of MSC spheroids



Using the microfluidic device the MSC spheroids were prepared in as fast as 4hrs. RT-PCR showed enhanced expression of CXCR4 which is crucial for MSC migration towards tumor cells. The migration assay demonstrated that MSC in spheroidal form moved greater distance and was more directional towards the tumor cell compared to single MSC cells.

CONCLUSION

MSC spheroids were prepared using a microfluidic device in as small as 4 hrs. These MSC spheroids showed higher expression of CXCR4 and enhanced migration towards tumor cells. Hence MSC in spheroidal form are an excellent candidate for treating glioblastomas. In the future these spheroids will be transduced with TRAIL and evaluated as a potential drug carrier for treating glioblastomas.

REFERENCES

1. Sasportas, L. S. *et al.* Assessment of therapeutic efficacy and fate of engineered human mesenchymal stem cells for cancer therapy. *Proc. Natl. Acad. Sci. U.S.A.* **106**, 4822–4827 (2009).
2. Bartosh, T. J. *et al.* Aggregation of human mesenchymal stromal cells (MSCs) into 3D spheroids enhances their antiinflammatory properties. *Proc. Natl. Acad. Sci. U.S.A.* **107**, 13724–13729 (2010).

ACKNOWLEDGMENTS

Smruthi Suryaprakash was supported by Schlumberger faculty for the future award.

A Novel Soft Tissue Model for Biomaterial-Associated Infection and Inflammation – Bacteriological, Morphological and Molecular Observations

Sara Svensson^{1,2}, Margarita Trobos^{1,2}, Maria Hoffman^{1,2}, Birgitta Norlindh^{1,2}, Sarunas Petronis^{1,3}, Jukka Lausmaa^{1,3}, Felicia Suska^{1,2} and Peter Thomsen^{1,2}

¹BIOMATCELL VINN Excellence Center of Biomaterials and Cell Therapy, Sweden

²Department of Biomaterials, Sahlgrenska Academy at University of Gothenburg, Sweden

³SP Technical Research Institute of Sweden, Sweden, sara.svensson@biomaterials.gu.se

INTRODUCTION

Infection is one of the main risks for implant failure, resulting in severe patient suffering and high treatment costs. Biofilm-producing bacteria are a great concern and a “race for the surface” between bacteria and host tissue cells has been postulated¹. However, little is known about the initial events *in vivo* during biomaterial-associated infection and the role of specific surface characteristics. In the present study an infection model in soft tissues focusing on the initial events between host defence cells and bacteria on and adjacent to biomedical implants was developed. A primary aim was to analyse the biological events in three interconnected “sub-compartments”: the implant surface, the peri-implant exudate and the tissue. A secondary aim was to investigate the role of noble metal chemistry versus nanotopography *in vivo*.

EXPERIMENTAL METHODS

A biofilm-producing strain of *Staphylococcus epidermidis* (10^6 CFU) was inoculated to implant and sham (no biomaterial) sites in subcutaneous pockets in rats. Very smooth titanium disks (sTi), nanostructured Ti disks (nTi), noble metal coated (silver, gold and palladium) nanostructured Ti disks (nNoble) and sham sites were analysed with respect to number of viable bacteria; amount, viability and gene expression of host cells; as well as with different morphological techniques on the implant surfaces, the surrounding exudate and the tissue after 4 h, 24 h and 72 h. Control rats were inoculated with saline. Results were evaluated with Wilcoxon signed rank test, Mann-Whitney U test and paired samples t-test ($n=7-8$).

RESULTS AND DISCUSSION

The results showed a low and transient inflammatory response in both sham and implant sites without bacteria, as demonstrated by a peak of infiltrating inflammatory cells at 24 h, a low degree of cell death and early but transient gene expression levels of tumour necrosis factor- α (TNF- α), interleukin-6 (IL-6), IL-8, Toll-like receptor 2 (TLR2), TLR4 and elastase (ELA2). Administration of *S. epidermidis* to the sham and implant sites resulted in a significantly higher recruitment of inflammatory cells with a predominance of polymorphonuclear cells (PMN), higher and continuous cell death and an overall higher gene expression of TNF- α , IL-6, IL-8, TLR2 and ELA2. Very few viable *S. epidermidis* were detected at 4 h, but increased significantly to 24 h. Relatively lower levels (10^1-10^3 CFU) of *S. epidermidis* were detected on the implants compared with the exudates (10^2-10^4). At

all time points, *S. epidermidis* was predominantly located in the interface zone, both extra- and intracellularly (Figure 1). The results suggest that an efficient immune response was elicited at all sites, as judged by the extra recruitment and higher activity of inflammatory cells at infected sites, the PMN predominance and the distribution of inflammatory cells at the interface. Small differences were found between the different materials, but a trend towards an increased inflammatory response and a reduced amount of viable bacteria was seen for nNoble implants, demonstrating a role of the noble metal chemistry. However, the access to and the presence of bacteria on the implant surface may shift the race for the surface in favour of *S. epidermidis*, emphasizing the need for long-term studies

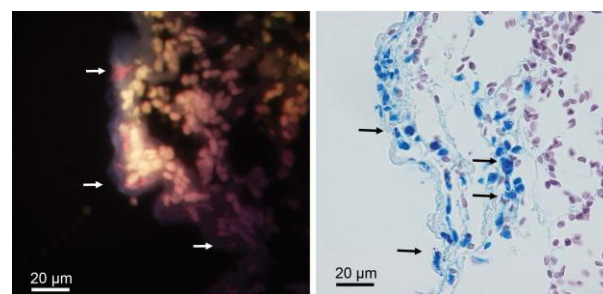


Figure 1. Tissue sections labelled by a coagulase-negative-specific FISH-probe (left) and stained with May-Grünwald Giemsa (right) showed *S. epidermidis* localised extra- and intracellularly of host defence cells in the interface zone between the implant and the tissue.

CONCLUSION

This experimental model allows detailed analysis of early events in inflammation and infection in relation to biomaterials *in vivo* and may lead to insights of host defence mechanisms in biomaterial-associated infections.

REFERENCES

1. Gristina AG *et al.*, Med. Prog. Technol. 14:205-24, 1988

ACKNOWLEDGMENTS

The noble metal coating was performed by Bactiguard AB, Sweden. Financial support was provided from the BIOMATCELL Vinn Excellence Center of Biomaterials and Cell Therapy, the Swedish Research Council (grant K2012-52X-09495-25-3), the Hjalmar Svensson Foundation, the IngaBritt and Arne Lundberg Foundation, the Wilhelm and Martina Lundgren Research Fund and the Felix Neubergh Foundation.



Pore Structure and Imaging of Collagen- and Elastin-based Scaffolds for Vascular Grafts

H. Frank*, J. Shepherd, S. Best, R. Cameron

Department of Materials Science and Metallurgy, University of Cambridge, United Kingdom

*hef30@cam.ac.uk

INTRODUCTION

Vascular grafts are needed to treat atherosclerosis, the single biggest cause of death in the developed world. Autografts such as the internal mammary artery or the saphenous vein are commonly used, but their main problem is with availability. Collagen- and elastin-based scaffolds used as vascular grafts are advantageous as they mimic the extracellular matrix of blood vessels (~30% collagen, ~7% elastin)¹. Previous studies have used SEM and histology to characterise collagen- and elastin-based scaffolds² but here confocal microscopy is laid out as an improvement to histology.

In this study, collagen- and elastin-based scaffolds have been created by freeze drying. They were visualised using SEM in order to determine the effects of elastin on the pore structure of the scaffold. Confocal microscopy was used as a new technique for clearly distinguishing between and elucidating the distribution of the two proteins.

EXPERIMENTAL METHODS

The experimental procedure used was detailed by Pawelec *et al.*³. Briefly, a 1 wt% slurry of protein in acetic acid was prepared. The protein was a mixture of collagen and elastin (ranging from 20:80 to 100:0 collagen:elastin). The slurry was degassed under vacuum and lyophilised in a mould made of stainless steel and PTFE. Scaffolds were then cross-linked using EDC and NHS.

SEM and confocal microscopy were used to image the interaction between collagen and elastin. Samples imaged using SEM were coated with gold while those observed using confocal microscopy had been stained with acriflavine, a non-specific fluorescent dye.

RESULTS AND DISCUSSION

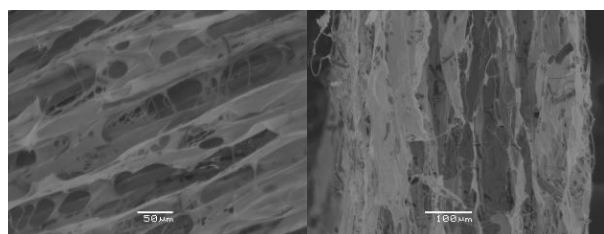


Figure 1. SEM images of mixed collagen and elastin scaffolds. Left: collagen:elastin = 75:25. Right: collagen:elastin = 25:75.

The SEM images (figure 1) clearly show the pore structure of freeze dried collagen and elastin scaffolds. In both cases the pores are elongated, with sheets of collagen separating the pores. However, differences in the proportions of collagen and elastin cannot be seen clearly.

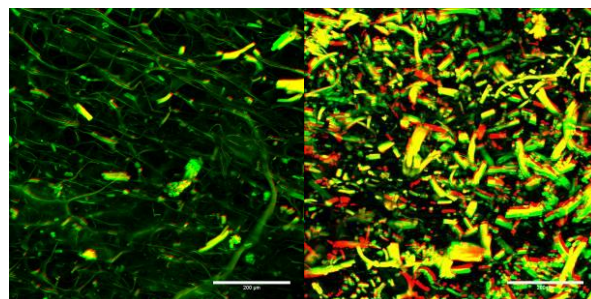


Figure 2. Confocal images of mixed collagen and elastin scaffolds. Left: collagen:elastin = 80:20. Right: collagen:elastin = 20:80. Green = collagen, red/yellow = elastin. Scale bars are 200 μm.

The images from figure 2 clearly show the differing concentrations of collagen and elastin in the two scaffolds, and can lead to a calculation of a quantitative value of collagen and elastin concentrations. The left hand image shows sheets of collagen in green, with large fibres of elastin distributed across the scaffold. This challenges a previous study which shows a more integrated structure of collagen and elastin². The right hand image confirms the even distribution of large elastin fibres across the scaffold.

CONCLUSION

The proportion of collagen and elastin within a freeze dried scaffold does not noticeably affect the pore structure of the scaffold, as shown by SEM. In all cases, collagen sheets are formed with differing amounts of elastin fibres on, depending on initial elastin concentration. These elastin fibres could affect mechanical or biological properties of the scaffolds.

A mixture of SEM and confocal microscopy should be used when determining the structure of mixed collagen and elastin scaffolds. SEM clearly shows the pore structure of scaffolds, while confocal microscopy gives an indication of the distribution of collagen and elastin across the scaffolds, along with a quantitative measure of the collagen and elastin concentrations. This will aid in creating scaffolds with a collagen/elastin concentration gradient which will better mimic the extra cellular matrix of blood vessels.

REFERENCES

1. Ozolanta I. *et al.*, Med. Eng. Phys. 20:523-533, 1998.
2. Buijtenhuijs P. *et al.*, Biotechnol. Appl. Bioc. 39:141-149, 2004.
3. Pawelec K. *et al.*, J. R. Soc. Interface. 11:1-9, 2014.

ACKNOWLEDGMENTS

The authors would like to acknowledge EPSRC for the funding of a PhD studentship and European Research Council for Advanced Grant 320598.



Sustained Release of Naproxen Sodium from Electrospun Aligned PLLA/PCL Scaffold for Tendon Tissue Regeneration

Yuan Siang LUI^{1,2}, Mark P. LEWIS³, Joachim Say Chye LOO^{1*}

¹School of Materials Science and Engineering, Nanyang Technological University, Singapore

²Institute for Sports Research, Nanyang Technological University, Singapore

³School of Sport, Exercise and Health Sciences, Loughborough University, United Kingdom

*Email: joachimloo@ntu.edu.sg

INTRODUCTION

Tissue engineering (TE) emerges as a promising approach in promoting tendon regeneration. However, unfavourable post-surgical adhesion formations restrict adequate tendon healing through the TE approach. Naproxen sodium (NPS), a non-steroidal anti-inflammatory drug (NSAID), has been demonstrated to prevent adhesions through inhibiting inflammatory response. In this work, polymer compositions (i.e. different poly-L-lactic acid (PLLA) to polycaprolactone (PCL) ratios) and percentage of water (H₂O) to hexafluoroisopropanol (HFIP) as co-solvent were varied to understand how these factors can influence the release of NPS from electrospun scaffolds.

EXPERIMENTAL METHODS

NPS was loaded into 8wt% PLLA/PCL blends with different polymer ratios and different HFIP/H₂O ratios. These varying formulations were electrospun into aligned scaffolds. Morphological assessment of these scaffolds was done through Scanning Electron Microscopy (SEM). *In vitro* drug release was carried out and the distribution of NPS within the electrospun fibers was determined by using X-ray photon spectrometry (XPS). *In vitro* cell culture studies were conducted by using L929 murine fibroblasts to assess the biocompatibility of NPS-loaded aligned scaffolds.

RESULTS AND DISCUSSION

PLLA/PCL-NPS were successfully electrospun into well-aligned fibers with beadless morphology. *In vitro* drug release profiles of the scaffolds with different PCL to PLLA ratios (Fig. 1A) and different amount of H₂O (Fig. 1B) were shown in Fig. 1. By adjusting the amount of H₂O as the co-solvent, NPS could be released sustainably for as long as two weeks.

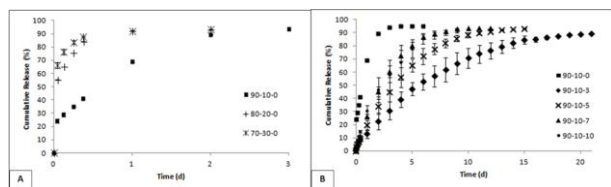


Fig. 1: Cumulative NPS release of the scaffolds prepared from (A) different PCL to PLLA ratio and (B) different H₂O to HFIP ratio

In XPS data (Fig. 2), the presence of NPS was indicated by the Na 4s characteristic peak (binding energy = 1071 eV). More NPS was detected on the fiber surface when no water was added (90-10-0, solid line), while lower

NPS amount was detected on the fiber surface when 3 vol% of H₂O was used (dash-dot line), indicating that more NPS resided in the core of the fiber (Sch. 1). However, further increasing H₂O content resulted in having more NPS on the fiber surface, yielding a peak with an intermediate area that lies between 90-10-0 (no H₂O) and 90-10-3 (3 vol% H₂O).

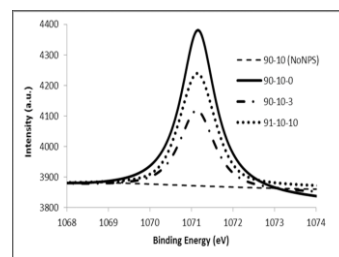
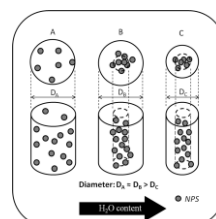


Fig. 2: The XPS analysis of the scaffolds with and without NPS



Sch. 1: Possible NPS distribution within fibers with different H₂O contents

Live/Dead staining showed that L929 cells were able to proliferate healthily and arrange themselves according to the fibers alignment on day 7 of culturing (Fig. 3).

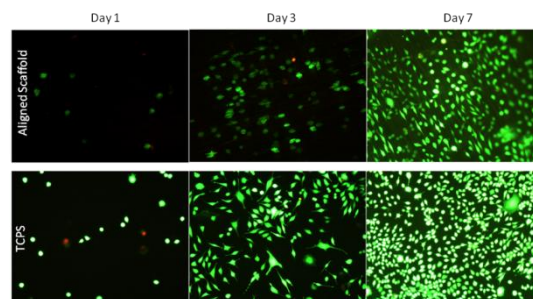


Fig. 3: Fluorescence microscopy images of L929 cultured samples over 7 days.

CONCLUSION

In this work, NPS was loaded into electrospun PLLA/PCL scaffolds with aligned, beadless and continuous fibrous morphology. By adjusting the H₂O content, a two-week sustained release could be achieved. *In vitro* cell studies showed that L929 cells could proliferate and align to the fiber orientation. These optimized PLLA/PCL scaffolds possess both sustained NPS releasing ability and desirable tendon TE characteristics, and could have good potential in achieving better tendon regeneration.

ACKNOWLEDGMENTS

The authors would also like to acknowledge the financial support from the Institute for Sports Research.

Analysis of cells proliferation after dynamic culture on cross-linked synthetic collagen peptide based microcarriers

M. La Marca and Suzan van Dongen

Fujifilm Manufacturing Europe, The Netherlands, margherita_la_marca@fujifilm.eu

INTRODUCTION

Nowadays, non-satisfying therapies for musculoskeletal injuries exist, above all for larger defect. Tissue engineering is a possible solution to restore the morphology and functions in bone disease¹.

During the last years different tissue engineering strategies including degradable porous scaffolds of natural or synthetic biomaterial, were proposed.

Interrogating the biological micro-world in a continuous and non-invasive manner is one of the most critical aspects which may limit the understanding of the biological complexity.

In this study synthetic collagen peptide (SCP) based microcarriers were prepared, , To mitigate the nutrient concentration gradients at the surface of the scaffolds, we used the spinner flasks. In this 3D, dynamic culture system, we investigate the proliferation and differentiation of C2C12 cell line.

EXPERIMENTAL METHODS

SCP microcarriers were prepared by an emulsification method and cross linked by DHT method. Cultispher G® was use as a reference.

Sterile spinner flasks were filled up with medium containing, microcarriers and C2C12 cells. The speed of the stirrer was set up and the cells were then cultured at 37°C, 5% CO₂ in a humidified incubator.

After day 1, 7, 14 and 21, SEM, dapi, live/dead and DNA content analysis were performed.

Data are expressed as mean \pm S.D., and statistical significance has been evaluated by Student's t-test or one-way ANOVA. Data were considered statistically significant when $p < 0.05$.

RESULTS AND DISCUSSION

SEM and dapi analysis were performed to verify the morphology of the cells, furthermore to have a quality results of cells proliferation.

Live/Dead assay showed that cells are viable up to 21 days.

DNA content analysis performed using the PicoGreen® assay, showed a linear increase of DNA content during the three weeks of the experiment. So we can assume a linear proliferation of the cells in our system. Moreover, we observed an improved proliferation on the SCP based microcarriers than in the commercial (shown in figure 1).

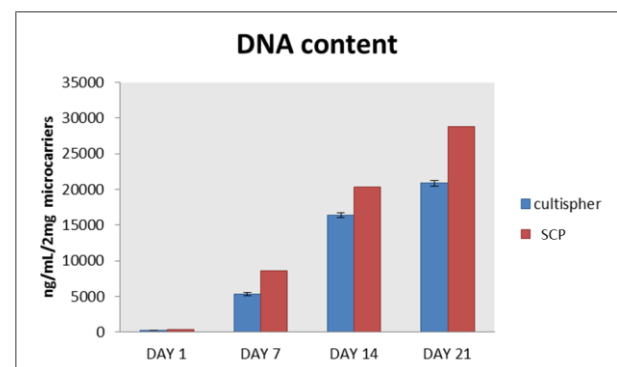


Figure 1 shows the DNA content results after day 1, 7, 14 and 21.

CONCLUSION

SCP based microcarriers show promising cell attachment and proliferation results and seem to be very suitable for cell culturing. On the basis of obtained results, we will further optimize the SCP microcarriers using the same dynamic system, in order to improve cell proliferation and differentiation.

REFERENCES

1. Hofmann *et al.*, Biomaterials 28:1152-1162, 2007

ACKNOWLEDGMENTS

The work leading to these results has received funding from the European Commission within the 7th Framework Programme.

Cell Response on the Ti-15Mo alloy Surface after Nanotubes Growth

Ana Paula Rosifini Alves Claro¹, André Luiz Reis Rangel¹, Nathan Trujillo², Ketul C. Popat²

¹ UNESP - Univ Estadual Paulista, Faculty of Engineering, Materials and Technology Department, Guaratinguetá Campus, São Paulo, Brazil

² Department of Mechanical Engineering, Colorado State University, Fort Collins, CO 80523, USA

INTRODUCTION

Titanium and its alloys have been widely used for biomedical applications due to their excellent properties and biocompatibility. However, these materials are considered bioinerts, i.e., they cannot bond chemically to the surrounding bone. Surface modification techniques have been studied to promote the chemical bond and better osseointegration [1-5].

EXPERIMENTAL METHODS

Ti-15Mo alloys were produced from sheets of commercially pure titanium and molybdenum in an arc-melting furnace under an argon atmosphere. The ingots were remelted and then homogenized under vacuum at 1000 °C for 86.4 ks. They were cold worked by swaging into bars (10 mm of diameter). Discs with 3 mm of thickness were cut for analysis.

Prior anodization, samples were grinded with emery papers and polished. TiO₂ nanotubes were obtained by anodizing method at room temperature in an electrolyte with 0.25 %NH₄F and glycerol at a constant anodic potential of 20 V. Annealing of nanotubes was performed at 450 °C for 1 hour. The morphology was observed by field emission scanning electron microscopy (FE-SEM; XL 30 FEG, Philips). Crystal structure was analysed by wide-angle X-ray diffraction. A contact angle goniometer was used to evaluate the wettability by sessile water-drop method.

Fibroblasts functionality was investigated by cellular adhesion, viability and morphology after 1, 4 and 7 days of culture. Cellular adhesion was investigated by fluorescence microscope imaging using calcein-AM live stain. Short-term cellular viability was investigated using MTT assay kit after 1, 4 and 7 days. Fibroblast morphology on Ti-15Mo alloy substrates was examined after 1, 4 and 7 days of culture using SEM.

RESULTS AND DISCUSSION

Figure 1 shows SEM micrographs of Ti15Mo after electrochemical anodic oxidation. Nanotubes highly ordered and vertically oriented were formed on surface alloy (Fig.1). Results indicate nanotube dimensions of approximately 60 nm in diameter and 160 nm in height. Surface exhibited super-hydrophilic behaviour after anodization.

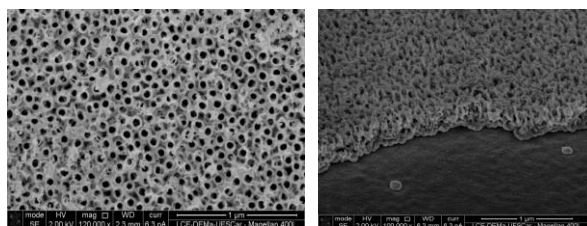


Figure 1 – SEM images of the Ti-15Mo alloy surface morphologies after anodization: (a) top view ; (b) cross-section of TiO₂ nanotubes

MTT assay was used to evaluate the cell viability and results indicate that the cells are viable on nanotubular titania surfaces as well as on titanium alloy surfaces. The similarity between the absorbance values suggests that the cells are healthy and viable on all surfaces.

Fluorescence microscopy images of fibroblasts cells on Ti15Mo alloy before and after anodization are show in Fig.2a and Fig 2b, respectively. The images suggest that the cells are viable on these surfaces after 7 days of culture. SEM images (Fig. 3) show the morphology of cells on nanotubular surfaces after 7 days of culture.

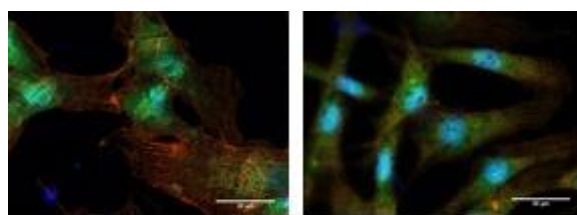


Figure 2- Immunofluorescence images of the morphology of the fibroblasts cell on Ti15Mo alloy (a) and Ti15Mo (NT) groups (b) after 7 days of culture

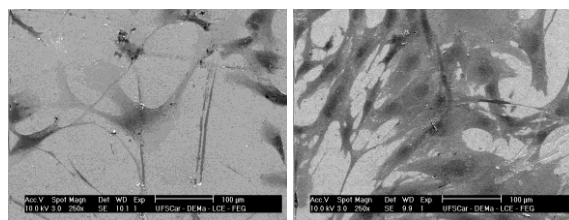


Figure 3 – SEM observation of cells after 7 days of culture : (a) Ti-15Mo alloy; (b) Ti15Mo alloy after anodization

CONCLUSIONS

In this study, nanotubular formation was obtained on the Ti15Mo alloy surface by using anodization technique. The growth of TiO₂ nanotubes on the Ti-15Mo alloy surface lead to decrease of contact angle and a superhydrophilic behaviour was observed. Also a good interaction cell-material was verified after cell culture.

REFERENCES

1. Capellato P *et al.*, Materials Science and Engineering C 32: 2060–2067, 2012.
2. Escada ALA *et al.*, Nanoscience and Nanotechnology Letters 5: 510-512, 2013.
3. Popat, KC. *et al.* Biomaterials 28: 3188–3197, 2007.

ACKNOWLEDGMENTS

The authors would like to thank the FAPESP 2010/10174-8 ad 2013/00317-4 for providing financial support to this project.

Elaboration of degradable PCL-based shape memory materials

Thomas Defize¹, Raphaël Riva¹, Jean-Michel Thomassin¹, Michaël Alexandre¹, Bernard Gilbert² and Christine Jérôme^{1*}

^{1*}Center for Education and Research on Macromolecules (CERM), University of Liege, Belgium

²Laboratory of Raman Spectroscopy, University of Liege, Belgium

c.jerome@ulg.ac.be

INTRODUCTION

Shape memory polymers (SMPs) are smart materials presenting the remarkable property to switch from a temporary shape (stressed) to a permanent shape (relaxed) upon exposure to a stimulus, such as heat or light. SMPs raised a lot of interest, especially for biomedical applications, for the elaboration of suture wires and stents.^{1,2} In the last few years, biodegradable aliphatic polyesters, typically poly(ϵ -caprolactone) (PCL) and poly(lactide) (PLA) were widely studied for the synthesis of SMPs.^{3,4}

This communication aims at reporting a new concept for the synthesis of PCL-based SMPs. In order to meet the increasingly stringent requirements of biomedical applications, a metal-free process is proposed occurring at relatively low temperature, which can be compatible with the presence of a drug during implementation.⁵⁻⁷

EXPERIMENTAL METHODS

Shape memory properties were measured with a DMA Q800 (TA Instruments) using the tensile film clamp in controlled force mode. The sample was first equilibrated at 65°C for 5 min then a tensile stress ramp was applied to 0.6 MPa. The sample was then cooled down under stress at 3°C/min to 0°C and kept at 0°C for 5 min. The stress was then released and the sample was reheated at to 65°C. The process was repeated 4 times.

RESULTS AND DISCUSSION

According a Diels-Alder (DA) mechanism, two types of SMP, presenting reversible (furan) or non-reversible (anthracene) crosslinking, were synthesized in order to determine the influence of the crosslinking strategy on the shape memory properties. Typically, 4-arm star-shaped PCLs bearing either a diene (furan or anthracene) or a dienophile (maleimide) at their chain-ends were melt blended at 125°C before being cross-linked at 65°C. Shape memory properties were studied by Dynamical Mechanical Analysis (DMA) and the results are presented in Figure 1.

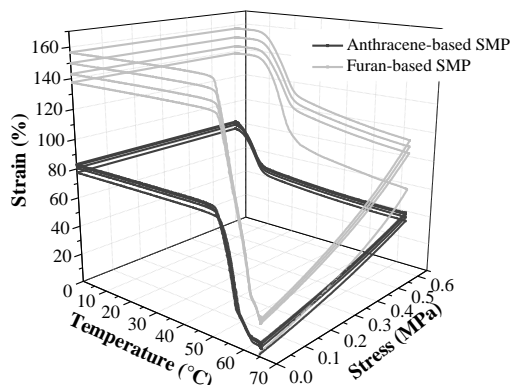


Figure 1: Dynamical mechanical analysis (DMA) of the PCL-based SMPs

When comparing the two curves, two main differences were observed between furan and anthracene strategies. Firstly, a higher strain for the furan-based is measured in addition of a steady increase in strain from cycle to cycle, which is not observed for the anthracene-based SMP. The first observation can be related to the crosslinking density, which is smaller for the furan-based SMP, due to the lower reactivity of furan with maleimide leading to a lower conversion yield and, in this way, of the crosslinking nodes density. The second observation can also be related to the occurrence of retro DA reactions under stress, leading creep of the material. From cycle to cycle, the sample is therefore less and less cross-linked, leading to larger ductility upon stress application, corresponding to a not pure elastic deformation. In case of the anthracene-based SMP, this phenomenon was not observed, corresponding to a pure elastic deformation. High fixity and recovery values were observed for each sample, about 99% and 98%, respectively). Moreover, upon cooling under constant stress, between 15°C and 0°C, a large increase of the sample strain was observed, due to the oriented crystallization of the PCL chains⁸, a behaviour that can promote so-called two-way shape memory property. Since anthracene-based SMP exhibit pure elastic deformation, two-way shape memory behaviour was successfully observed.

CONCLUSION

Owing to the different crosslinking strategies, reversible or not, the resulting SMPs exhibit marked differences in their shape memory properties. However, for each SMP, excellent recovery and fixity were observed as assessed by DMA. Moreover, the higher stability under stress of anthracene-based SMP allows considering its application for the elaboration of a material presenting remarkable two-way shape memory behaviour.

REFERENCES

1. Tamai H. *et al.*, Circulation 102:399-404, 2000.
2. Ormiston J. A. *et al.*, Lancet 371:899-907, 2008.
3. Lendlein A. *et al.*, PNAS. 98:842-847, 2001.
4. Lendlein A. *et al.*, Science 296:1673-1676, 2002.
5. Defize T. *et al.*, Macromol. Rapid Commun. 32:1264-1269, 2011.
6. Defize T. *et al.*, Macromol. Chem. Phys. 213:187-197 2012.
7. Defize T. *et al.*, Macromolecules 2014, *submitted*.
8. Zhao Y. *et al.*, Macromolecules 32:1218-1225, 1999.

ACKNOWLEDGMENTS

The authors are grateful to F.R.S.-F.N.R.S and to University of Liege for their financial support.

Surface immobilization of a green fibronectin-like protein onto cold plasma modified polystyrene substrates

O. M. Ba¹, A. Ponche², O. Gallet³, P. Marmey⁴, A.C. Duncan¹, K. Anselme²

¹Laboratoire PBS UMR 6270 CNRS-BRICS, Faculté des sciences & techniques, Université de Rouen, Bâtiment Dulong, 76130 Mont Saint Aignan, France.

²Institut de Science des matériaux de Mulhouse (IS2M) – UMR CNRS 7361, 15 rue de Jean Starcky B.P. 2488, 68057 Mulhouse cedex, France.

³Equipe de Recherche sur les Relations Matrice-Extracellulaire/Cellule (ERRMECe) EA 1391, Université de Cergy-Pontoise, 95302 Cergy-Pontoise cedex, France.

⁴Pôle Ingénierie Biologique et Médicale, Centre de transfert de technologie du Mans, 20 rue Thalès de Milet, 72000 Le Mans, France.

karine.anselme@uha.fr

INTRODUCTION

Fibronectin (FN), a large glycoprotein found in body fluids and in the extracellular matrix, plays a key role in numerous cellular behaviours and particularly in cell adhesion¹. In recent work we were able to extract from pea plants a glycoprotein (called “green fibronectin” or gFN) with very high homology compared to plasma fibronectin (pFN). The gFN is purified by the method described by Pellenc et al.². It was also shown that the gFN has a higher percentage of glycosylation (70%) than pFN³ (5%). In view of its homology to pFN, it seemed appropriate to investigate its potential to elaborate cell and bacteria adhesive substrates as a substitute to pFN. Such strategies would enable to be free from the drawbacks associated with the use of human or animal plasma derived proteins. In this first study, we propose to graft the gFN to nitrogen plasma treated polystyrene surfaces (PSN₂) or via its sugar moieties.

EXPERIMENTAL METHODS

1 ml of a 20 µg/ml FN solution in PBS buffer (0.15 M, pH 7.4) was transferred to the plasma treated PSN₂ wells. The plates were then incubated at the desired adsorption temperature (37 °C) in a convection oven for the required adsorption time. We developed and optimized grafting of the FN via its sugar moieties to the aminated surfaces by reductive amination. The wells were sequentially washed with 3 rinses in PBS buffer. This step was followed by 3 rinses in 1% SDS aqueous solutions in the case of the desorption experiments. The amount of protein before and after the various rinses was determined using a BCA assay.

The amounts of grafted and adsorbed gFN were quantitatively compared to those for the pFN (the model protein) before and after SDS rinsing.

RESULTS AND DISCUSSION

The amount of adsorbed gFN was 0.85 ± 0.05 µg/cm² and more than 85% of the adsorbed protein was desorbed after three 1% SDS rinses. For pFN adsorption, the amount of adsorbed protein was 0.68 ± 0.02 µg/cm² of which 100 % was desorbed after 1% SDS rinsing. In the same conditions of temperature and protein time exposure to the surface, the amount of

proteins immobilized via our grafting method was 0.69 ± 0.03 µg/cm² and 0.58 ± 0.06 µg/cm² for gFN and pFN, respectively. The amounts remaining after 1% SDS rinses were 0.43 ± 0.03 µg/cm² and 0.19 ± 0.09 µg/cm² for gFN and pFN, respectively. The protein fractions remaining on the surface after three 1% SDS rinses were thus 68 ± 3 % and 38 ± 3 % for gFN and pFN, respectively. This result suggests that the amount of protein remaining on the surface was considerably higher for the gFN compared to that of the pFN protein. This result is consistent with a higher fraction of more tightly bound protein for the gFN compared to that of the pFN likely due a higher relative amount of sugar moieties on the gFN as described above.

CONCLUSION

These results are promising in that they validate our described grafting method approach for this “green” protein and likely for many other types of “green” proteins.

REFERENCES

1. Vitronectin alters fibronectin organization at the cell–material interface; Cristina González-García, Marco Cantini, David Moratal, George Altankov, Manuel Salmerón-Sánchez; *Colloids and Surfaces B: Biointerfaces* 2013, 111,618–625.
2. Purification of plant cell wall fibronectin-like adhesion protein involved in plant response to salt stress, D. Pellenc, E. Schmitt and O. Gallet., *Protein Expression and Purification* 2004, 34, 208-214.
3. Comparative adherence to human A549 cells, plant fibronectin-like protein, and polystyrene surface of four *Pseudomonas fluorescens* strains from different ecological origin ; E. Cossard, O. Gallet and P. Di Martino; *Can. J. Microbiol.* 2005, 51, 811-815.

ACKNOWLEDGMENTS

The authors would like to thank the ANR (Grant GreenFib n° 2010 BLAN 1530) for providing financial support to this project.

Peptide-Polysaccharide Based Injectable Hydrogel for Sustained Delivery of Active Agents

Cem Bayram^{1*}, Ekin Çelik² and Emir Baki Denkbaş³

^{1*} Chemistry Department, Aksaray University, Turkey, cembayram@gmail.com

² Bioengineering Department, Hacettepe University, Turkey

³ Chemistry Department, Hacettepe University, Turkey

INTRODUCTION

In recent years, low molecular weight building blocks and their ability to form self assembled gels and applications via noncovalent interactions have attracted a great interest. These molecular hydrogels have been reported as biocompatible and exhibit a protective environment for bioactive molecules such as enzymes and proteins¹.

However, there is a limitation in use of these hydrogel structures as matrix due to low mechanical properties. For example, frequently used Fmoc-peptides lose their stability and mechanical integrity at pH levels above 6.5. This situation makes them difficult to be used inside human body. A recent approach to enhance the mechanical properties of these structures is to mix them with polymeric additives and better fracture resistances have been observed than in cases when two mixing structures used alone. The conjugation of self-assembled gel structures of polysaccharides with low molecular weight molecules are also known as suitable and stable compositions for drug delivery and tissue culture applications².

EXPERIMENTAL METHODS

The lyophilized peptide (Fmoc-Phe-Phe-OH) were dissolved in 0.1M NaOH to obtain 20mM peptide solution. Then the mixture was separated into 1 mL aliquots, and GdL (glucono-d-lactone) was added to each specimen with, 20 mM concentration to start gelation. Meanwhile, another set of peptides were dissolved in 0.1 M NaOH containing 0.1% – 0.5% w/v alginate solutions and then gelated as mentioned above. The resulting gels were characterized morphologically, chemically and mechanically. Imaging of specimen were carried out with Scanning Electron Microscopy after freeze drying of the gels and chemical characterization was analyzed with Fourier Transform Infrared Spectroscopy. Rheological measurements were performed by rheometer system with cone-plate geometry (34 mm scale, 4°) at 25°C.

For sustained release studies, the gelation solutions were incorporated with varying concentrations (0.5%, 1.5% and 2.5%) of vancomycin. HCl. Release experiments were performed with simply injection of hydrogels into Phosphate Buffer Saline release media (pH:7.4)

RESULTS AND DISCUSSION

Stable transparent gels were obtained after standing overnight at room temperature. The SEM images revealed that the structure of resulting gel systems, – both Fmoc-Phe-Phe-OH only, and with alginate – resembles each other with slight differences. Matrices made from peptide only shows highly entangled fibers with approximately 30 nm diameter; whereas composite scaffolds have these nanofibers homogenously dispersed through alginate leaflet structures.

FTIR analyses exhibits the peaks around 3310 – 3290 cm⁻¹, 1650 – 1630 cm⁻¹ and 1540 – 1530 cm⁻¹ indicating the N-H stretching (amide A), >C=O stretching (amide I) and N-H bending (amide II), respectively. In addition to these peaks, carboxylic acid functionality can be observed in composite gels.

The rheological analysis of the gels were done with 0.1% deformation ratio at 0.01-10 Hz frequency with frequency- sweep scanning, The elastic modulus (G') of gels were calculated higher than viscous modulus (G'') with the data evaluated from rheometry analyses, which means that all systems are solid gels.

The most effective parameter on vancomycin release was found as alginate concentration.

CONCLUSION

A Fmoc-Phe-Phe-OH hydrogel was prepared by self assembly of peptides alone and in presence of alginate. Alginate incorporation improved the mechanical integrity and stability respect to peptide only gel structure. The sustained release time of vancomycin also was found to be prolonged by managing incorporated alginate amount. The resulting peptide-polysaccharide composite gel system is a promising material for injectable and biodegradable hydrogel.

REFERENCES

1. Baral A. *et al.*, Langmuir. 30:929-936, 2014.
2. Huang R. *et al.*, Soft Matter. 7:6222-6230, 2011.

ACKNOWLEDGMENTS

“The authors would like to thank the Hacettepe University Scientific Research Projects Coordination Office (Grant no: 1136) for providing financial support to this project”.

Characterisation of Freeze-Dried Collagen-Fibrinogen Constructs

Jennifer Shepherd^{1*}, Charlotte Rasser¹, Serena Best¹, Ruth Cameron¹

¹Department of Materials Science and Metallurgy, University of Cambridge, UK, *jhr37@cam.ac.uk

INTRODUCTION

A promising route for tissue repair is via the implantation of a scaffold structure that enables infiltration and proliferation of a patient's own cells, leading to production of extra-cellular matrix and regeneration of native tissue characteristics. Collagen is a common material of choice, but a high degree of cross-linking is typically required in order to avoid rapid degradation *in vivo*. This degree of cross-linking can affect the bioactivity¹. The addition of another biologically relevant material within the system may impart additional biological cues to, for example promote a particular cell type or cell response. In a freeze-dried structure it is important to be able to characterise the effect of multi-composition on structure as well as understanding the distribution of the different materials within the structure.

This work considers the freeze-drying of 50:50 collagen: fibrinogen materials. Fibrinogen has been demonstrated to promote cell migration^{2,3} and thus appears a promising additive to a collagen based scaffold. Structures were imaged using SEM, micro-computed tomography and confocal microscopy.

EXPERIMENTAL METHODS

A 1wt% collagen slurry in 0.05M acetic acid (insoluble type I collagen derived from bovine dermis) was produced and acriflavine, a non-specific fluorescent dye (excited at 488 nm) added in trace amount. Fibrinogen (derived from human blood plasma and depleted of plasminogen) was dissolved to form a 1wt% solution in deionised water and a Fibrinogen - Alexa Fluor 647 conjugate added in a ratio 50:1 fibrinogen: fibrinogen conjugate. The collagen suspension and fibrinogen solution were then combined and gently mixed before being poured into silicone moulds.

Freeze-drying was carried out in an AdVantage Virtis Freeze-dryer using a freezing temperature of -30°C and primary drying temperature of 0°C. Confocal imaging could then be carried out dry without any post-lyophilisation processing. A Leica SP2 confocal system was used with excitation at 488 and 633 nm. SEM (JEOL JSM-5510) and Micro-computed Tomography (Skyscan 1172) were also considered in order to analyse pore structure in 2 and 3 dimensions.

RESULTS AND DISCUSSION

The use of two fluorescent stains with widely separated excitation and emission wavelengths enable fibrinogen and the acriflavine staining to be clearly detected independently (*Figure 1*). The conjugated fibrinogen (red on the images) appeared uniformly distributed and despite the relatively low ratio of conjugate to standard fibrinogen, provided thorough staining of the material.

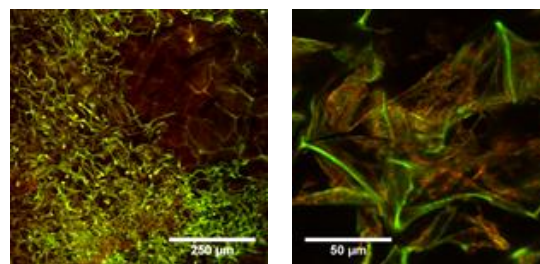


Figure 1: Confocal images at low and high magnification demonstrating the distribution of the fibrinogen alexa-fluor conjugate through the structure

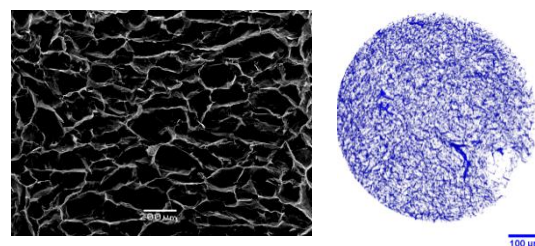


Figure 2: Pore structure imaged with (a) SEM and (b) a volume rendered model derived from micro-CT

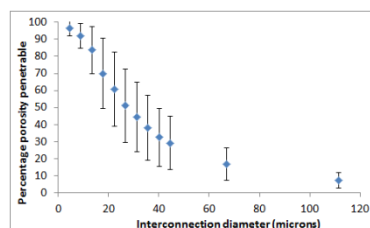


Figure 3: Using a shrink wrap analysis in CT-Analyser (Bruker Micro-CT) interconnection diameters could be investigated.

A combination of SEM and micro-CT allowed for both a qualitative and quantitative analysis of the pore structure (*Figures 2 and 3*). Analysis showed the addition of fluorophores to have no significant effect on pore structure.

CONCLUSION

Addition of a non-specific fluorescent stain and the Fibrinogen - Alexa Fluor conjugate to the initial slurries, enabled confocal microscopy to be used as a means of analysing chemical distribution, without any post-lyophilisation processing. Although confocal imaging allowed some investigation of pore structure, SEM and micro-CT provided additional qualitative and quantitative information.

ACKNOWLEDGMENTS

The authors would like to thank the European Research Council for their Advanced Grant 320598.

REFERENCES

1. Powell and Boyce, *Biomaterials* (2006), 27, 5821-5827
2. Ahmed et al, *Cell Motil Cytoskel* (2000) 46, 6-16
3. McManus et al, *J Biomed Mat Res A* (2007) 81, 299-309

Nanosized grooves controlling neuronal cell-organization and axonal outgrowth for cochlear implant optimization

Alexey Klymov¹, Joost te Riet², John A Jansen¹ and X Frank Walboomers¹

¹ Department of Biomaterials, Radboud University Medical Center, Nijmegen, The Netherlands

² Department of Tumor Immunology, Radboud Institute for Molecular Life Sciences, Radboud University Medical Center, Nijmegen, The Netherlands

INTRODUCTION

The loss of hair cells ultimately leads to sensorineural deafness. This is due to the resulting lack of stimulation of up to 30000 neuronal cells (spiral ganglion cells, SGCs) of the auditory nerve. Preferentially these hearing deficits are treated by placement of cochlear implants (CI), circumventing the hair cells by direct SGCs stimulation [1]. While being able to return the ability to perceive abstract sound, the modern CI cannot return the patients high fidelity hearing. This is mainly due to the lack of direct interaction between the SGCs and the CI electrode, leading to a strong decrease in separation of electrical stimuli. While the attraction of SGCs to the electrode surface can be achieved by use of neurotrophins[2], the interaction between cells and electrode-surfaces could be optimized by utilization of surface topographies [3]. This may allow a more organized cell-electrode contact.

EXPERIMENTAL METHODS

A silicon master featuring five different grooved patterns (pitch sized between 150 nm and 1000 nm) and a smooth control, were used for replication of the surfaces into tissue culture plastic polystyrene by solvent casting (Figure 1). The substrates were used for culture of rat pheochromocytoma derived neuron-like PC12 cells. The cells were analyzed after 7 days of cell culture by light microscopy and scanning electron microscopy. Cell body orientation, axon orientation and axonal outgrowth have been assessed.

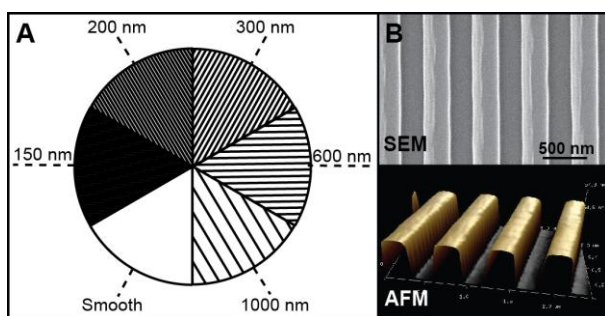


Figure 1: Multi-patterned culturing replicate. A) Silicon wafers with smooth and grooved surfaces (pitches between 150 nm and 1000 nm) were combined to one silicon master mold for solvent casting of polystyrene surfaces. B) The substrates were analyzed by SEM and AFM for quality control (600 nm pitch pattern shown).

RESULTS AND DISCUSSION

Axonal outgrowth was significantly stimulated by all grooved patterns compared to the smooth control (Figure 2). A threshold was found for cell-body alignment on grooves with a pitch size of 300 nm, while axons already aligned to grooves with a pitch size of

200 nm (Figure 3). The interaction of the axons has been found to be primarily based on contact with the ridge regions, rather than with the groove region on the substrates.

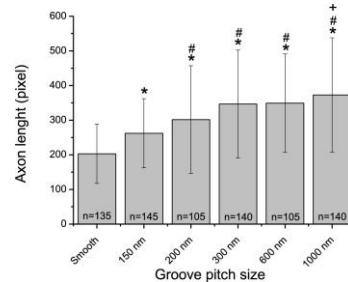


Figure 2: Differences in axon-outgrowth of neuronal cells as a response to differently patterned substrates.

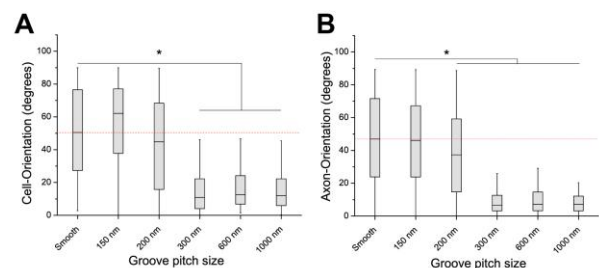


Figure 3: Cell-body and axon orientation on smooth and grooved topographies.

CONCLUSION

Nanogrooves can be used to manipulate neuronal cell behavior by increasing the axonal outgrowth and direct the alignment of cell bodies and axons. For optimization of CI electrodes a starting point can be the threshold of grooves having a 300 nm pitch, as this is the smallest pattern that could induce significant cell body and axon orientation.

REFERENCES

1. Wilson, B.S. and M.F. Dorman, Hearing Research, 2008. 242(1-2): p. 3-21.
2. Miller, J.M., et al., Journal of Neuroscience Research, 2007. 85(9): p. 1959-1969.
3. Klymov, A., et al., Biomaterials Science, 2013. 1(2): p. 135-151.

ACKNOWLEDGMENTS

This work was supported by a grant from the Dutch government to the Netherlands Institute for Regenerative Medicine (NIRM, grant No. FES0908).

The effectiveness of tetra sodium EDTA as an anti-biofilm agent for use in biomaterials

Steven L Percival^{1,2} and Peter Kite²

¹Institute of Ageing and Chronic Disease, University of Liverpool, Liverpool, UK

²Surface Science Research Centre, University of Liverpool, Liverpool, UK

INTRODUCTION

EDTA is regarded as a 'potentiator' of other antimicrobials¹. Consequently EDTA *per se* has not generally been recognised as an important antimicrobial in its own right. Conversely tetra sodium EDTA has been found to be a very effective antimicrobial on biofilms in catheters². In spite of this recent research there is a significant lack of available data on the effectiveness of TEDTA on biofilms. Biofilms are microcolonies of microorganisms encased in an extracellular polymeric matrix. Biofilms are reported to be associated with 80% of all known human infections and 65% of hospital acquired infections. It is well documented that microorganisms growing within the biofilm lack susceptibility to antimicrobials when compared to their planktonic counterparts. It is therefore imperative that any antimicrobial agent used, and developed for use on and within biomaterials, is effective on biofilms. The purpose of this study was to determine the minimum biofilm eradication concentration (MBEC) of tetra sodium ethylenediaminetetraacetic acid (TEDTA) on the clinical isolates *Staphylococcus lentus*, *Staphylococcus simulans*, *Staphylococcus aureus*, *Staphylococcus aureus* (MRSA), *Klebsiella ornitholytica*, *Escherichia coli* and *Acinetobacter baumannii* using the an MBEC biofilm model.

EXPERIMENTAL METHODS

- A starting suspension for each microorganism was prepared to a McFarland standard of 1.0 in Mueller-Hinton Broth. The starting suspension was diluted to obtain a working inoculum of 10⁷ cfu/ml.
- 150 µl of the working inoculum was placed in each test well in the designated column of the MBEC plate (University of Calgary, Calgary, Canada).
- Columns were set up to test a maximum of 8 isolates per plate, with one well for growth control and six EDTA concentrations in duplicate.
- Using a 96 well tissue culture plate, the challenge plate was prepared.
- The concentrations of TEDTA prepared and tested were 0, 5, 10, 20 and 40 mg/ml.
- The peg lids were transferred to the challenge plates and incubated at 35°C for 1, 3, 6, 12 and 24 hours.
- Pegs from the challenge plates were rinsed in saline for approximately 1 minute, transferred to recovery media plates and then sonicated in a

sonicating water bath on high for 5 minutes to dislodge the surviving biofilm.

- The challenge plate was used to determine minimum inhibitory concentration (MIC) values for TEDTA.
- The turbidity, determined on a plate reader, in the wells of the challenge plate was used to determine the MIC for the planktonic bacteria shed from the biofilm during the challenge incubation.
- The MBEC for each TEDTA concentration and time was obtained by reading the turbidity or re-growth on the recovery plate.
- A 3 log drop was defined as being the MBC (Minimum Bactericidal Concentration) of tetra sodium EDTA.

RESULTS AND DISCUSSION

For *Staphylococcus aureus* maximal log reductions of 2.67 were seen in 5 and 10 mg/ml of TEDTA at 24 hours. With *S. simulans* the maximal reduction in colony forming units was reached at 2 hours at a concentration of 5 mg/ml (2.38 log reduction). *S. aureus* was reduced by 3 logs after 6 hours. *S. lentus* was reduced by >3 logs after 6 hours for all the concentrations of TEDTA investigated. With *A. baumannii* the MBC was reached at 3 hours with 40 mg/ml of TEDTA. For *E.coli* a 3 log reduction was achieved after only 1 hour for all concentrations of TEDTA investigated. For *K. ornitholytica* all TEDTA concentrations resulted in a 3 log reduction after 3 hours.

CONCLUSION

More work is needed to elucidate the importance of these findings and the potential role of TEDTA as an antimicrobial agent for use in both clinical and environmental situations.

REFERENCES

1. Brown, M.R.W. and R.M.E. Richards. 1965. Effect of ethylenediamine tetraacetate on the resistance of *Pseudomonas aeruginosa* to antibacterial agents. *Nature* 20: 1391-1393.
2. Kite, P., K. Eastwood, S. Sugden and S.L. Percival. 2004. Use of *in vivo*-generated biofilms from hemodialysis catheters to test the efficacy of a novel antimicrobial catheter lock for biofilm eradication *in vitro*. *J Clin Microbiol.* 42:3073-6.



Composite scaffolds from gelatin and elastin-like block polypeptides for tissue engineering

Duc H. T. Le¹, Tatsuya Okubo¹, Ayae Sugawara-Narutaki²

¹Department of Chemical System Engineering, The University of Tokyo, Japan

²Department of Crystalline Materials Science, Nagoya University, Japan, voltrapp@chemsys.t.u-tokyo.ac.jp

INTRODUCTION

Severe burn injuries, which cause large and deep damage to the skin dermis, are a major health problem due to their resulting physical and psychological traumas. Collagen, with its favourable physical and biological functions, shows promising use as dermal substitutes for severe burn treatments. However, successful wound healing without skin contraction still remains a challenge due to insufficient elasticity of the materials.^[1] Elastin, despite its small proportion in skin dermis, plays an important role in skin elasticity. This is because elastin assembles into elastic fibers interwoven among collagen bundles to convey elasticity to the whole structure.^[1]

Recently, we have constructed a novel elastin-like polypeptide (ELP) by mimicking the localization of hydrophobic domains in native elastin molecule.^[2] The polypeptide, named **GPG**, contains a proline-rich (VPGXG)₂₅ (X: V or F) sandwiched by two glycine-rich (VGGVG)₅ (Figure 1). **GPG** is able to assemble into beaded nanofibers with flexibility and well dispersibility in water by temperature trigger or in 10–30% (v/v) trifluoroethanol (TFE) aqueous solutions. These obtained nanofibers can be used to mimic the elastin structure in skin dermis. In this study, scaffolds composed of **GPG** fibers and gelatin, a hydrolyzed form of collagen, are fabricated by electrospinning method to resemble the composite fibrous structures in skin dermis, where elasticity is effectively tuned by a small amount of elastin fibers.

MKL-(VGGVG)₅-LWLGSGL-[(VPGVG)₂VPGFG(VPGVG)₂]₅-KL-(VGGVG)₅-LWLEHHHHHH

Figure 1. The amino acid sequence of **GPG**.

EXPERIMENTAL METHODS

A suspension of **GPG** fibers formed in 30% (v/v) TFE was mixed with a gelatin solution (30% TFE) to produce a homogeneous mixture of **GPG** fibers and gelatin. The concentration of gelatin was 12.5 wt%. The proportions of **GPG** fibers toward gelatin were 0, 0.5, and 1.0 wt%. The mixtures were loaded into syringes and electrospun in the optimized conditions as follows: voltage supply 25 kV, air gap distance 13 cm, feed rate 0.5 mL/h. Electrospun scaffolds were cross-linked by glutaraldehyde vapour in 16 h. Cross-linked matrices were immersed in glycine solution to remove unreacted glutaraldehyde, and then washed repeatedly by water. For the tensile test, all samples were cut into a dumbbell-shape and soaked in phosphate buffer saline prior to the measurement.

RESULTS AND DISCUSSION

Figure 1a–c shows SEM images of the as-spun gelatin and **GPG**/gelatin composite fibers. Formation of gelatin fibers with an average diameter of about 100 nm

was observed in Figure 1a. Blending of gelatin with small amounts of **GPG** fibers did not alter the morphologies of the electrospun fibers (Figure 1b, c). The elastic moduli of cross-linked scaffolds are shown in Figure 1d. The **GPG**/gelatin composite shows a decrease in elastic modulus when 1.0 wt% of **GPG** fibers were added into gelatin. The modulus of 1.0 wt% **GPG**/gelatin matrix is 1.20 ± 0.50 MPa. As a control experiment, elastic modulus of a composite sample composed of 1.0 wt% (VPGXG)₂₅, the middle block component of **GPG**, and gelatin was also examined. The elastic modulus of the control sample is 3.17 ± 0.82 MPa, which shows no decrease compared to one of the gelatin scaffolds. Noteworthy, (VPGXG)₂₅ only assembled into nanoparticles but not fibers in 30% TFE. The result suggests that the assembled structures of **GPG** may affect the elastic modulus of the composite materials. Studies of cell attachment and proliferation on the constructed scaffolds are in progress.

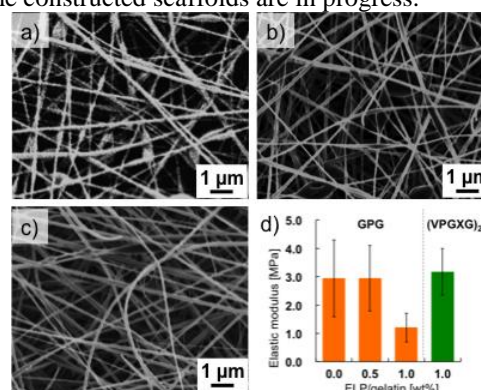


Figure 1. SEM images of as-spun fibers of (a) gelatin, (b,c) **GPG**/gelatin composite scaffolds with **GPG**/gelatin ratio: (b) 0.5 wt%, (c) 1.0 wt%. (d) Elastic moduli of cross-linked scaffolds.

CONCLUSION

GPG/gelatin composite scaffolds were successfully constructed by electrospinning method. The elastic modulus of **GPG**/gelatin scaffolds decreases at 1.0 wt% addition of **GPG** fibers. Works to adjust elastic moduli of the composite scaffolds close to one of skin dermis (0.08 MPa)^[1] are on-going.

REFERENCES

1. Rnjak-Kovacina J. *et al.*, Acta. Biomater. 8:3714–22, 2011
2. Le D. H. T. *et al.*, Biomacromolecules 14:1028–34, 2013

ACKNOWLEDGMENTS This work was supported by a Grant-in-Aid for Scientific Research (No. 22107005) on the Innovative Areas: “Fusion Materials” (Area no. 2206), MEXT and a Grant-in-Aid for Young Scientists from JSPS, Japan. We thank Prof. Atsushi Hotta, Keio University, for the tensile test.

Pelvic Floor Repair Materials Releasing Vitamin C to Promote Extracellular Matrix Production

Naside Mangir^{1,2}, Anthony J Bullock¹, Sabiniano Roman¹, Nadir Osman^{1,2}, Christopher Chapple², Sheila MacNeil¹

¹Department of Materials Science Engineering, KROTO Research Institute, University of Sheffield, United Kingdom

²Royal Hallamshire Hospital, Urology Clinic, Sheffield, United Kingdom, n.mangir@sheffield.ac.uk

INTRODUCTION

Non-absorbable synthetic meshes (polypropylene) currently used in surgical treatment of Stress Urinary Incontinence (SUI) and Pelvic Organ Prolapse (POP) are associated with serious complications such as exposure and erosion¹.

We hypothesize that slowly degrading synthetic matrices, which stimulates cell infiltration and extracellular matrix (ECM) production, may overcome these complications leading to a better integration into patient's native tissues. The aim of this study was to develop a pelvic floor repair material from poly-lactic acid (PLA) scaffold releasing vitamin C which was assessed for fibroblast attachment and proliferation, ECM production and mechanical properties.

EXPERIMENTAL METHODS

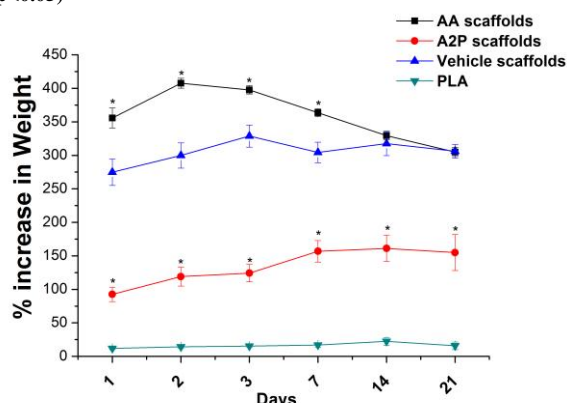
The technique of emulsion electrospinning was used to construct a core-shell morphology of vitamin C and PLA for achieving continuous release of the hydrophilic bioactive factor from the hydrophobic polymer. The electrospun PLA fibres contained Ascorbic Acid (AA), the naturally occurring active form, or Ascorbate-2-Phosphate (A2P), the synthetic long acting form, or distilled water (Vehicle). The surfactant Span80® was used to obtain a stable water in oil emulsion with a water/oil phase ratio of 1:40. The release of both drugs was measured by spectrophotometric methods. Then, a total of 500,000 human dermal fibroblasts were seeded on 1 cm² sized scaffolds and cultured for 2 weeks. Cell attachment and viability were evaluated by Resazurin assay and DAPI staining. Total collagen production was assessed using Sirius red staining. Mechanical properties (ultimate tensile strength, strain and Young's Modulus) of scaffolds were evaluated in dry and wet states using BOSE electroforce tensiometer.

RESULTS AND DISCUSSION

No significant differences were observed between emulsion electrospun scaffolds and pure PLA scaffolds in terms of fibre diameter and pore size. The successful release of both AA and A2P was demonstrated with a burst release of 20-25%. Both AA and A2P containing scaffolds and Vehicle scaffolds were significantly more hydrophilic (Figure 1) and stronger in both dry and wet states compared to pure PLA scaffolds. We observed a positive correlation between the water uptake and the

strength of the scaffolds (Pearson's $r=0.66$; $p<0.005$). Fibroblasts showed higher metabolic activity and produced more total collagen on scaffolds containing either AA or A2P compared to cells grown on control PLA scaffolds (Figure 2).

Figure 1. Diagram showing water uptake (percent increase in weight after incubation in PBS compared to dry state) of scaffolds (*: $p<0.05$)

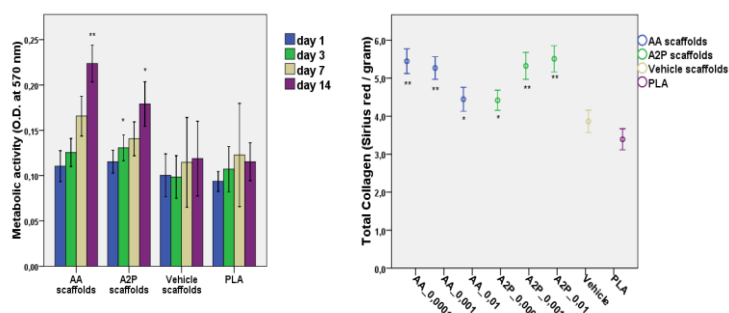


These results showed that incorporation of a surfactant and other bioactive factors can significantly improve the hydrophilicity and mechanical properties of PLA scaffolds as well as the cellular response to them. This study is the first to compare the effect of AA and A2P in 3D on collagen production and mechanical properties of biomaterials. These findings are in line with previous studies showing increased collagen production of fibroblasts in 2D and 3D culture conditions upon stimulation with various forms vitamin C.

CONCLUSION

One strategy in developing a pelvic floor repair material for treatment of SUI and POP can be to incorporate bioactive factors for stimulating cell infiltration and ECM production from host tissues leading to a good integration of the material into the native tissues.

Figure 2. Metabolic activity (left) and collagen production of fibroblasts grown on scaffolds (right) [$**p<0.005$ and $*p<0.05$ compared to Vehicle scaffolds; numbers after letters show grams of AA or A2P per gram of PLA]



REFERENCES

1. FDA statement, 2011 (www.fda.gov/MedicalDevices/Safety/AlertsandNotices/ucm262435.htm)



Synthetic collagen peptide based microspheres/ hydrogel hybrid system for bone growth factor delivery

L. de Miguel^{1*}, G. van Osch² and S.G.J.M. Kluijtmans¹

¹Fujifilm Life Sciences, P.O. Box 90156 Tilburg, Netherlands

²Departments of Orthopaedics and Otorhinolaryngology, Erasmus Medical Center, Rotterdam, Netherlands
laura_de_miguel@fujifilm.eu

INTRODUCTION

Bone fractures and other orthopaedic related injuries constitute a major health problem nowadays, with more than 500,000 bone graft procedures being performed annually¹. For bone regeneration purposes, bone morphogenetic proteins (BMP) have attracted much attention in the past years.

BMP-2 is one of the most powerful osteoinductive factors for bone regeneration in ectopic and orthotopic sites, including critical size defects. It is involved in the recruitment of endogenous mesenchymal stem cells from adjacent tissues and in their stimulation towards osteogenic differentiation, resulting in bone tissue formation. BMP-2 is clinically used in association with a collagen scaffold for spinal fusion surgery and tibial fracture healing. However, both its supraphysiological doses needed to be efficacious and its animal origin results in side effects. Increased stability and controlled release of BMP-2 have shown to enhance bone formation². Therefore, many efforts have been directed to the use of carriers that could provide a controlled release and protect the BMP from the rapid degradation by proteolytic enzymes. Hybrid systems have shown to be a useful approach to achieve better controlled protein release⁴.

Synthetic collagen peptide (SCP) is a new animal-free material, which is fully bio-degradable and bio-absorbable.

The final aim of this work is to design a hybrid system consisting of BMP-2 loaded-SCP microspheres included into a hydrogel for controlled BMP-2 release.

EXPERIMENTAL METHODS

SCP was produced at Fujifilm by recombination techniques. SCP microspheres were prepared by an emulsification process and further crosslinked by different methods. SCP microspheres were characterized in terms of size and morphology by diffraction particle size analysis and scanning electron

microscopy. The degree of crosslinking was quantified by the 2, 4, 6-trinitrobenzenesulfonic acid (TNBS) assay. A model protein, FITC-lysozyme and BMP-2 were loaded onto the microspheres by diffusional loading at different doses and protein release studied in PBS in presence and absence of collagenases. These microspheres were further included into a hydrogel and protein release studies were performed.

RESULTS AND DISCUSSION

Microspheres had a size of ~50 µm and a spherical morphology with a rough surface. The degree and type of crosslinker of the SCP microspheres were shown to influence protein retention and release. Their inclusion onto a hydrogel contributed to a better controlled protein release.

CONCLUSION

SCP microspheres could be easily obtained by emulsification techniques and stabilized by further crosslinking. The ability of the hybrid SCP microspheres/hydrogel system to control protein release was shown SCP microspheres are therefore considered as promising candidates for the delivery of growth factors in bone regeneration applications.

REFERENCES

1. Laurencin C, Khan Y, E.-A. S. *Expert Rev. Med. Devices* 3(1):49-57 (2006).
2. Oju Jeon Su Jin Song et al. *Biochem. Biophys. Res. Commun.* 369, 774–780 (2008).

ACKNOWLEDGMENTS

Authors acknowledge the Analytical Support and Development Department at Fujifilm for their contribution to this work.

The authors would like to acknowledge the PEOPLE Work Programme, Marie Curie Actions (Grant no: 607051, BIOINSPIRE project) for providing financial support to this project.

Development of a Novel Composite Polymer Material to Facilitate Regeneration of Chronic Non-Healing Wounds

Alma Akhmetova^{1*}, Matthew Illsley², Timur Saliev¹, Gulsim Kulsharova³, Talgat Nurgozhin¹, Sergey Mikhlovsky², Iain Allan²

¹*Department of Translational Medicine, Longevity and Global Health/Center for Life Sciences, Nazarbayev University, Kazakhstan, alma.akhmetova@nu.edu.kz

²School of Pharmacy and Biomolecular Sciences, University of Brighton, UK

³School of Engineering, Nazarbayev University, Kazakhstan

INTRODUCTION

Chronic wound represents a complex environment that requires multipurpose approach. The healing process consists of several phases. The prolonged inflammation stage, indicative of chronic wounds, damages the surrounding healthy cells and tissues. This phase is associated with uncontrolled secretion of pro-inflammatory cytokines from macrophages, neutrophils and T-cells, and decrease of growth factors required for re-epithelialization and formation of granulation tissue. As a consequent result, the wound is prevented from the tissue repair and closure.

In order to remove inflammatory cytokines, macrophages, necrotic tissue, and bacteria we decided to increase adsorbing properties of the wound dressing. For this purpose activated carbon (AC) was chosen as the main adsorbing agent. Today's market is full of activated charcoal dressings, where a thick layer of charcoal is used. While, in this novel dressing we propose reduction of AC particles through their even distribution in the polymer. For this purpose, agarose (AGR) was selected as a promising biomaterial for wound healing applications. It does not require additional crosslinking agents and forms a gel at the room temperature. The transparent nature of this polysaccharide can allow monitoring of the wound state. Absence of toxicity and inertness of agarose may prevent unnecessary reactions at the wound site. Its slow degradation rate is beneficial for the end product properties such as longer shelf life.

Three various gels (hydrogels, cryogels, and double cryogels) with or without incorporated AC particles were prepared for comparison of physical and mechanical properties and to identify the best option.

EXPERIMENTAL METHODS

To prepare agarose cryogels, agarose powder was dissolved in distilled water which was brought to boil. AGR solutions of 0.5%, 1%, 1.5%, 2% (w/v) were poured into glass tubes and placed in cryobath at -12°C for two hours. Then, tubes were extracted and left at room temperature to thaw. To prepare AGR solution with incorporated AC particles, AC was added to AGR powder and the above steps were repeated.

AGR hydrogels with or without AC were used as control. To prepare hydrogels, AGR solution after boiling was placed at the room temperature to form a gel.

The inner structure of gels was analyzed by confocal microscope. Gels were assessed for sorption capacity, porosity, flowrate and permeability. Adsorption

capacity of AC within agarose gels was tested using crystal violet as a model small molecule.

RESULTS AND DISCUSSION

Assessment of gels demonstrated successfully formed cryogels and hydrogels. In comparison to hydrogels, cryogels possessed larger pores, evenly distributed AC particles in pore walls, high moisture, and better physical-mechanical properties. Larger pores can allow absorption of necrotic tissue and bacteria from the wound. Adsorption by AGR-AC cryogels was stably increasing and did not reach equilibrium in contrast to AGR-AC hydrogels.

ELISA analysis showed that AC particles effectively remove TNF-alpha, IL-6, and IL-8. The adsorption profile was proportional to the size of molecules. IL-8 as a smaller cytokine was absorbed more efficiently than TNF, although there was not a significant difference.

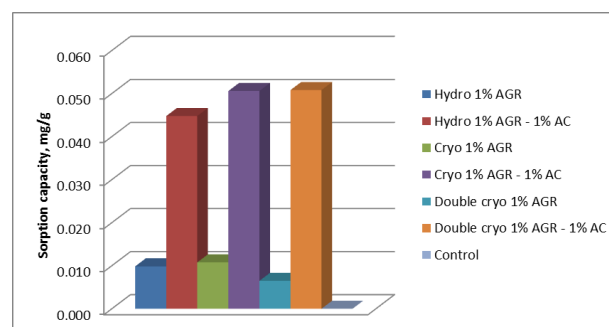


Figure 1. Adsorption of small model molecule –crystal violet by agarose and agarose-activated carbon cryogels, hydrogels, and double cryogels.

CONCLUSION

The obtained results indicate that AGR-AC cryogel is a potential wound dressing material that is not prone to bacterial spoilage, provides moist environment, has high sorption capacity, large pores, and is able to remove inflammatory cytokines from the wound exudate to facilitate wound healing process. We hypothesize that removal of inflammatory cytokines, bacteria, and necrotic tissue will assist chronic wounds to escape from the inflammation phase and proceed to regeneration of tissues.

ACKNOWLEDGMENTS

Funded by the Ministry of Education and Science of the Republic of Kazakhstan.

The Effect of Amphiphilic and Anionic β -sheet Peptides on Blood Clotting

Ziv Azoulay¹ and Hanna Rapaort^{1,2*}

¹ Avram and Stella Goldstein-Goren Department of Biotechnology Engineering, Ben-Gurion University of the Negev, Beer - Sheva, Israel

^{2*} Ilse Katz Institute for Nano-Science and Technology (IKI), Ben-Gurion University of the Negev, Beer - Sheva, Israel, hannarap@bgu.ac.il

INTRODUCTION

In the past decade there has been an increasing interest in developing blood coagulation inducers. β -sheet amphiphilic zwitterionic peptides were recently reported to accelerate bleeding arrest in induced in-vivo bleeding models².

In this study, we characterized the influence of an amphiphilic and anionic β -sheet peptide on blood clotting and bleeding arrest. In-vitro rheological, spectral and microscopic assays were utilized to assess the peptide's effect on swine blood plasma coagulation.

EXPERIMENTAL METHODS

Peptides: The amphiphilic and anionic β -sheet peptide Pro-Asp-(Phe-Asp)₅-Pro and its scrambled analog Asp-(Phe)2-Pro-(Asp)2-Pro-Phe-Asp-(Phe)2-(Asp)2, denoted P-FD-5 and Sc-PFD respectively were custom synthesized and supplied as lyophilized powders.

Thromboestograph (TEG): Peptide aqueous solutions were mixed with freshly re-calcified platelets poor swine plasma (PPP) in a standard TEG cup (360 μ L) to a final concentration of 10 mM Ca²⁺ and 0.17 % w/v (1 mM) peptide. The slope of the curve and the level of the plateau are a measure of the coagulation kinetics and the strength of the clot, respectively.

Circular dichroism (CD): Spectra of P-FD-5 peptide, purified human fibrinogen and purified human thrombin solutions were taken separately and after mixing combinations of 1:3400 (molar ratio) of each protein to peptide. The CD signals of the mixtures were compared to the calculated sum of the individual ones to indicate whether interactions between the peptide and the proteins led to conformational changes.

Confocal microscopy: Human fibrinogen (1-10% fluorescently labelled) was first mixed with human thrombin and CaCl₂ as described elsewhere¹ and latter mixed with peptide solutions or injected beside P-FD-5 hydrogel³ on a confocal plate. Samples were left to interact for 1 h at 37° C and saturated humidity.

RESULTS AND DISCUSSION

According to TEG measurements P-FD-5 inhibited the coagulation kinetics and weakened the clot strength (compare curves a and c, Figure 1). This effect could have been attributed to reduce in calcium concentrations interacting with the peptides; However, increase in Ca²⁺ concentrations did not alleviate the effect (not shown). Based on the smaller effects of Sc-PFD on the coagulation (curve b Figure 1) it could be deduced that the inhibitory effect of the P-FD-5 peptide is both related to the amino acids composition, i.e. the anionic charge, and to the β -sheet conformation.

CD analysis revealed a distinct conformational change for P-FD-5 in the presence of thrombin suggesting enzyme inhibition by the peptide (Figure 2). This effect wasn't seen for P-FD-5 and fibrinogen mixtures (not shown).

At elevated P-FD-5 concentration (4% w/v) the peptide which forms a hydrogel was found to have little effect on fibrin fibres formation at its proximity as could be deduced by the confocal images (Figure 3).

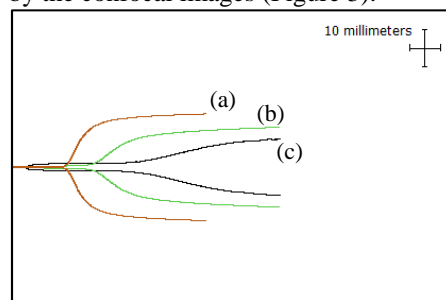


Figure 1: Representative TEG curves tracking the coagulation in swine's recalcified PPP, supplemented with: (a) Tris buffer as a control, 0.17% w/v (1mM) Sc-PFD (b) and P-FD-5 (c). Y axes correlative to storage modulus G'

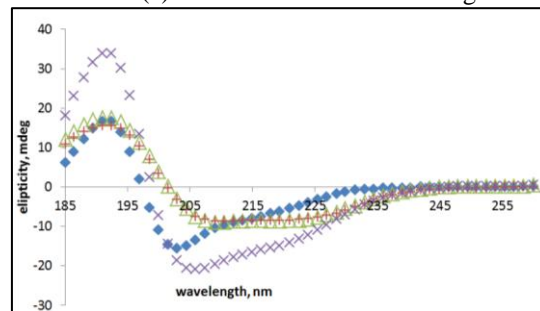


Figure 2: CD spectra of P-FD-5 0.3 mM (diamonds), Thrombin, 1 U/ml (triangles) and their mixture in DIW (+, same concentrations) and a curve of the calculated sum of the peptide and the protein (x).

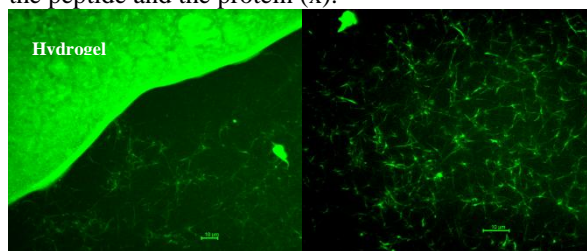


Figure 3: Confocal microscopy images indicative of fibrin fibres formation at the proximity of 4% w/v P-FD-5 hydrogel (right) and in absence of the hydrogel (left).

CONCLUSION

In summary, the amphiphilic and anionic β -sheet peptide P-FD-5 inhibits plasma clotting when soluble, and appears to have little effect when in gel state on fibrin fibres formation.

REFERENCES

1. Chernysh I.N. *et al.*, Sci. Rep. 2:879, 1-6, 2012
2. Ellis-Behnke R.G. *et al.*, Nanomedicine 2:207-215, 2006.
3. Rapaort H. *et al.*, Adv. Funct. Mater. 18:2889-2896, 2008.

Processing and Mechanical Properties of Biodegradable β TCP-15Fe15Mg Composites

Sanjaya K. Swain, Irena Gotman, Elazar Y. Gutmanas

Department of Materials Science and Engineering, Technion, Haifa, 32000, Israel, swains@technion.ac.il

INTRODUCTION

Due to their similarity to bone mineral, calcium phosphate (CaP) ceramics are considered materials of choice for bioresorbable (β -tricalcium phosphate, TCP) and non-resorbable (hydroxyapatite, HA) bone graft substitutes. The brittle nature of these ceramics, however, limits their use to low load bearing applications. To improve mechanical behavior, CaPs are combined with biodegradable polymers (PLA, PGA, PCL). Typical CaP-polymer composites are produced by hot pressing and contain low volume fractions ($< 20\%$) of the ceramic phase¹. As a result, the strength of such composites is close to that of the polymer matrix. Significantly higher strength values combined with measurable ductility were reported for β TCP-PLA nanocomposites that comprised large ($\geq 60\%$) volume fraction of the CaP phase². To achieve even better mechanical properties, the PLA component in the reported work was substituted with a biodegradable Mg-Fe alloy, all while retaining the high volume fraction of β TCP. Both Mg and Fe based alloys are increasingly studied as potential materials for temporary medical implants³. Still, the corrosion of Mg in the physiological environment is too rapid for most implant applications whereas that of Fe is considered too slow⁴. Combining Fe and Mg in a nanocomposite is expected to result in an acceptable degradation rate, in between Mg and Fe.

MATERIALS AND METHODS

β TCP nanopowder was prepared by chemical precipitation followed by calcination at 750°C . 50Fe50Mg (vol.%) nanocomposite blend was prepared by attrition milling of Fe ($\sim 2\ \mu\text{m}$) and Mg ($< 44\ \mu\text{m}$) powders for 4 h, in dry hexane under Ar at 20:1 stainless steel balls-to-powder ratio. 30 vol.% of the prepared 50Fe50Mg powder was blended with 70 vol.% of β TCP powder and milled for additional 4 h to yield β TCP-15Fe15Mg composition. Dense β TCP-15Fe15Mg disks 10 mm in diameter were produced by high pressure consolidation in a rigid die at 2.5 GPa, at T_{room} . Some specimens were annealed at 400°C for 4 h. The density of consolidated specimens was measured and mechanical properties tested in an Instron machine. The microstructure and phase composition of the composites were characterized employing x-ray diffraction (XRD) and scanning electron microscopy (SEM/EDS).

RESULTS AND DISCUSSION

The density of all high pressure consolidated specimens was above 98 % of the theoretical. XRD patterns of dense β TCP-15Fe15Mg specimens are shown in Fig. 1. Only the peaks of β -TCP and Fe are present, the absence of the Mg peaks suggesting amorphization (at least partial) of Mg during attrition milling. After annealing at 400°C , a small peak of Mg appears in the pattern suggesting crystallization of the Mg component.

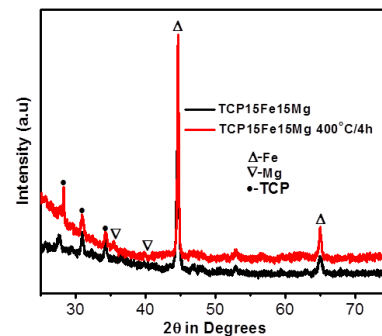


Fig.1: XRD patterns of as-consolidated and annealed (400°C , 4 h) β TCP-15Fe15Mg composites.

SEM image in Fig. 2(A) demonstrates uniform phase distribution in β TCP-15Fe15Mg composite; the absence of pores confirms that the material is near fully dense.

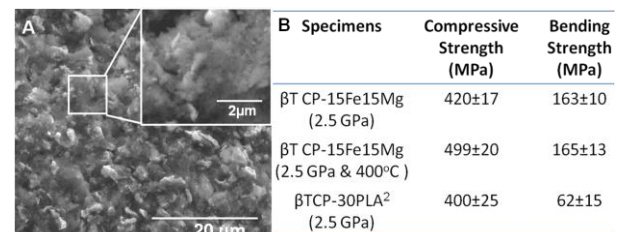


Fig.2: Mechanical properties (A) and SEM images of the fracture surface (B) of β TCP-15Fe15Mg specimen annealed at 400°C for 4 h.

Fig. 2(B) presents the strength of β TCP-15Fe15Mg specimens compared to β TCP-30PLA nanocomposite. In bending, β TCP-15Fe15Mg is almost 3 times stronger than β TCP-30PLA and approaches the bending strength of compact bone. Such a significant increase of bending strength is achieved owing to the much higher strength of the metallic phase compared to the PLA polymer. Annealing at 400°C did not affect bending strength of β TCP-15Fe15Mg but resulted in an increase of the compressive strength.

CONCLUSION

β TCP-15Fe15Mg composites possess attractive mechanical properties and can be considered as candidate materials for load bearing orthopedic applications. Further work will concentrate on degradation studies and fabrication of porous 3D scaffolds.

REFERENCES

1. Ignjatovic N. *et al.*, *Biomater.* 20:809-16, 1999
2. Rakovsky A. *et al.*, *J. Mech. Behav. Biomed. Mater.* 18:37-46, 2013
3. Schinhammer M. *et al.*, *Acta Biomater.* 6:1705-13, 2010
4. Kraus T. *et al.*, *Acta Biomater.* 10:3346-53, 2014

ACKNOWLEDGMENTS

This work was supported by Israel Science Foundation-ISF through research grant No. 1326/11.

Economical Production of Medium Chain Length Polyhydroxyalkanoates

Yiingos Psaras

Faculty of Science and Technology, University of Westminster, United Kingdom, y.psaras@my.westminster.ac.uk

INTRODUCTION

The plastics industry is being increasingly criticized concerning the nature of its products. Although used in an extensive variety of products, one third of all plastics serve the function of packaging and are inevitably discarded². Being non-biodegradable, their disposal raises the issue of pollution and toxic hazard to wildlife, the environment and humans. The economical burden of processing landfill waste and the finite amount of petroleum require that traditional plastics be replaced.

Polyhydroxyalkanoates (PHAs) are produced as intracellular storage compounds by bacteria under nutrient limiting-induced growth stress¹. Their wide range of properties makes these polymers suitable replacements for traditional oil-derived plastics; the polymers present additional features that extend their applications into the biomedical field. Conversely, high production costs hurdle their large-scale industrial and biomedical application³.

The objective of this study was to address the issue by investigating the production of polymer by *Pseudomonas mendocina* via the utilization of cheap sources for carbon and nitrogen; biodiesel waste, glucose and corn steep liquor were used and compared with sodium octanoate.

EXPERIMENTAL METHODS

Production:

PHAs were produced at shaken flask level using a two-stage seed culture of *P. mendocina* (no. 10542, strain CH20). First seed cultures, prepared in nutrient broth (10% by volume of the second seed culture), cultured for 24 hours were used to inoculate the second stage mineral salt media (MSM) seed culture (10% by volume of the final production media), which was cultured until the optical density reached 1.6 or the incubation time reached 24 hours. This was then used to inoculate the final production media cultured for 48 hours. All media were autoclaved separately and flasks were inoculated simultaneously with the same inoculum under sterile conditions and incubated at 200 rpm and 30°C. Experiments were carried out in triplicate. Growth profile curves were constructed by measuring the optical density at 450nm, pH and nitrogen concentration of the production media in samples retrieved every three hours. For the estimation of nitrogen, 0.2ml of phenol nitroprusside (pH 12) and 0.3ml alkaline hypochlorite were added to 0.5 ml of culture sample supernatant (centrifuged at 15600 relative centrifugal force (rcf) for 10 min and diluted a hundredfold), followed by incubation in the absence of direct light for 45 minutes at room temperature and spectrophotometric measurement at 635nm.

Extraction

Harvested cultures were freeze-dried at -47°C and 0.32mbar. Sodium hypochlorite and chloroform were used in a 5:22.5 ratio for every 0.3g of dry cells. The mixture was incubated at 30°C and 200rpm for 2 hours followed by centrifugation at 6260 rcf for 18 minutes, condensation on a rotary distillator at 37°C, filtration and precipitation in approximately 10 volumes of ice-cold 50% absolute ethanol-50% absolute methanol.

Characterization

Carbon-13 and Proton Nuclear Magnetic Resonance (NMR), Differential Scanning Calorimetry (DSC) and Dynamic Mechanical Analysis (DMA) were carried out for the polymer produced with sodium octanoate. Fourier Transform Infrared Spectroscopy (FTIR) was carried out for all polymers.

RESULTS AND DISCUSSION

Utilization of sodium octanoate in the production media produced a medium chain length PHA (MCL-PHA), identified as poly(3-hydroxyoctanoate), to a yield of 14.2%. This polymer had glass transition temperature of -34°C, melting temperature of 52°C and a Young's modulus value of 3.63MPa. By comparison, utilization of biodiesel waste gave a yield of 2.1% and the mixture of corn steep liquor and glucose gave a yield of 11.3%. These polymers were confirmed to have been MCL-PHAs but were not further characterized.

We report the use of simple, low-cost production at shaken flask level in contrast to fed batch and stirred fermentation, which are known to confer higher yield, as reported in previous studies.

CONCLUSION

Economic production of MCL-PHAs can be achieved with the use of cheap sources. Moreover, it is evident that yields achieved with cheap sources can rival those produced with the use of laboratory reagents, as seen on utilization of glucose and corn steep liquor, which approached the yield achieved with sodium octanoate.

REFERENCES

1. Basnett P. and Roy I., Cur. Res. Tech. Ed. App. Micro. Micro Biotech. 1405-1415, 2010
2. Thompson R.C. *et al.*, Phil. Trans. Roy.Soc. 364:1973-1976, 2009
3. Williams S.F., *et al.*, Int. J. Bio. Macro. 25:111-121, 1998

ACKNOWLEDGMENTS

The author would like to thank Dr Ipsita Roy and Dr Pooja Basnett for their help in this research and the University of Westminster FST Undergraduate Bursary Scheme for providing financial support.



A New Method to Rapidly Retrieve Encapsulated Cells from Alginate Hydrogels using Pyrophosphate

David C. Bassett* and Pawel Sikorski

Department of Physics, Norwegian University of Science and Technology, Norway

*david.bassett@ntnu.no

INTRODUCTION

Alginate hydrogels have a long and successful application in pharmacy, medicine and biomedical sciences¹ and are routinely used to encapsulate various types of cells to provide a synthetic extracellular matrix (ECM), provide immunoprotection, or transport cells to the point of injury^{2,3}. In our laboratory, we routinely encapsulate mammalian cells in alginate microbeads for 3D *in vitro* cell culture studies. In order to study the cells post encapsulation, it is often necessary to remove the cells from the alginate. Typically this is achieved using a calcium chelator such as citrate ions or Ethylenediaminetetraacetic acid (EDTA) and while effective at removing crosslinking Ca^{2+} , ourselves⁴ and others⁵ have observed high toxicity when using these reagents, which is detrimental to studies of this nature. Therefore we sought to test alternative chemical treatments in an attempt to improve the outcome of such experiments. Here we present our initial findings towards the development of a new protocol which is both rapid and cell compatible. This highly promising approach would appear to have great utility in extracting viable cells from alginate.

EXPERIMENTAL METHODS

Alginate microbeads were prepared as previously described⁶. Briefly, aqueous sodium alginate (2%, Protanal LF 2005, FMC Biopolymer) was extruded through a narrow needle (0.35 mm) into a bath of calcium chloride (50 mM) under an electrostatic accelerating voltage of 7 kV. The alginate was prepared with or without cells (MC3T3-E4 pre osteoblasts, 1×10^6 cells mL^{-1}). A known mass of alginate beads were de-gelled by the addition of 100 mM solutions of EDTA, sodium citrate and sodium pyrophosphate (PPI) at a range of pHs adjusted by the addition of NaOH or HCl. De-gelling was monitored visually and with the aid of a light microscope. Food colouring was added to cell-free alginate to aid observation that was found to not interfere with de-gelling. Cells were retrieved by centrifugation and washed in cell media prior to infiltration with toluidine blue and counting using an automated cell counter (Countess®, Life Technologies).

RESULTS AND DISCUSSION

Electrostatically generated microbeads were well formed spheres and had a narrow size distribution. ($\varnothing = 405 \pm 18 \mu\text{m}$). Phytic acid, EDTA, citrate and PPI were evaluated for their ability to chelate Ca^{2+} ions and de-gel Ca-alginate hydrogels. Phytic acid showed no de-gelling activity, even after prolonged periods of exposure and high concentrations. EDTA and sodium citrate were effective Ca chelators and performed well, however PPI appeared to react very rapidly with the Ca-

alginate (Figure 1). The rate of de-gelling was found to be dependant on pH: rates at pH 8-10 were significantly faster than rates at pH 6-7 for PPI. At pH 8, 1 mL volume of alginate beads could be completely de-gelled in approx. 2 ½ minutes. EDTA and citrate achieved similar and much slower rates in the range of pHs tested and were less affected by pH, although significant differences were found between them at the extremes of pH 6 and pH 10. Cell integrity following de-gelling using the Ca chelators at pH 8 and 100 mM concentration was measured by toluidine blue infiltration. Cell viability of $83 \pm 2\%$ was recorded for cells recovered from alginate using PPI, compared to $61 \pm 8\%$ and $64 \pm 10\%$ using EDTA and citrate respectively.

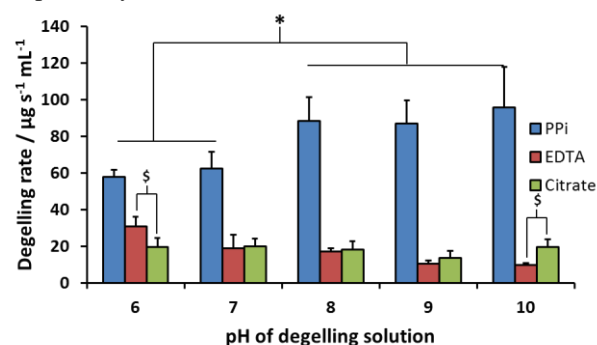


Figure 1: Rates of alginate microbead de-gelling as a function of pH for the indicated chelators. Sig. differences: * $P < 0.05$ 1 way ANOVA with Holm-Sidak test. \$ $P < 0.02$ Mann-Whitney t-test. N=6.

CONCLUSION

PPI would appear to be an effective reagent for the purpose of retrieving encapsulated cells from alginate hydrogels. Both the rate of de-gelling and viability of retrieved cells were enhanced compared to conventionally used reagents. A possible limitation of this technique is that PPI will tend to crystallise with Ca, though in our experiments this only occurred at prolonged times (hours).

REFERENCES

1. Augst AD *et al*, *Macromol.Biosci.*6(8): 623-33; 2006
2. Kuo C.K. and Ma P.X. *Biomat.* 22(6): 511-521; 2001
3. Rokstad AMA. *et al.* *Adv. Drug. Deliv. Rev.* 67-68: 111-130; 2014
4. Westhrin M. Master's Thesis, NTNU; 2011.
5. Cohen J. *et al.* *J. Biomed. Mater. Res. A.* 96(1): 93-99; 2011
6. Strand BL *et al*, *J.Microencapsul.* 19(5):615-30;2002

ACKNOWLEDGMENTS

The Research Council of Norway is acknowledged for financial support to DCB and PS through the FRINATEK program (project 214607).



Stable Electrospun Hyaluronan Matrices: Production and In Vitro Characterization for the Evaluation as Skin Substitute

Annalisa La Gatta¹, Marcella Cammarota¹, Antonella D'Agostino¹, Agata Papa¹, Stefano Guido², Chiara Schiraldi¹

¹Department of Experimental Medicine, Second University of Naples, Italy, annalisa.lagatta@unina2.it

²Department of Chemical Engineering, University Federico II of Naples, Italy

Please download and read the instruction sheet to ensure all necessary formatting and abstract criteria are adhered to.

INTRODUCTION

Glycosaminoglicans, as native constituents of human tissues, are widely employed for tissue engineering purposes including the fabrication of skin substitutes for wound healing (1). The use of GAGs has been recently combined with electrospinning process in order to produce nanofibrous, highly porous matrices mimicking not only the composition but also the architecture of the extracellular matrix (ECM). In particular hyaluronan (HA) and chondroitin sulfate (CS) have been electrospun, usually in combination with collagen or gelatin and proposed as active analogs of native ECM. The presence of proteins in the matrix was reported to be necessary in order to achieve proper stability in physiological environment (2,3). Here, novel stable membranes were produced by HA electrospinning and subsequent crosslinking. No other macromolecules than HA were introduced in the final networks. Developed materials were characterized to assess their potential as skin substitutes.

EXPERIMENTAL METHODS

HA (M_w equal to 1400kDa, M_w/M_n equal to 1,4) was dissolved in DMF/water (1/1v/v) at 0.9% w/v. Newtonian viscosity of the solution, measured at 40°C was equal to 10.4 ± 0.2 Pa's. The solution was electrospun by using a blowing-assisted electrospinning apparatus.

Electrospun HA was crosslinked using 1-Ethyl-3- (3-dimethylaminopropyl) carbodiimide (EDC), EDC/1-Hydroxybenzotriazole (HOBt) or EDC/HOBt in the presence of Lysinemethyl ester in heterogeneous conditions. Morphology of the unmodified matrix, the same after reaction and after reaction and swelling in aqueous medium was observed by SEM. Swelling degree of crosslinked materials was measured by means of gravimetric measurements. Stability was evaluated in Phosphate buffered saline and in DMEM by quantitative determination of HA soluble fraction (carbazole assay). The most stable material was tested for biological response using human keratinocyte (HaCaT)/human dermal fibroblasts (HDF) co-culture in

a time-lapse experiment over 96h. Morphology of adherent cells was observed by SEM.

RESULTS AND DISCUSSION

SEM observation of electrospun HA revealed the attainment of nanofibers with a high interconnected porosity and pore dimension considered useful as a barrier against infection. After chemical modification by treatment in heterogeneous conditions with EDC, EDC/HOBt or EDC/HOBt in the presence of Lysine methyl ester, materials proved insoluble in aqueous medium and, as indicated by SEM analyses, the nanometric porous architecture was preserved during crosslinking. Swelling studies demonstrated membranes high water uptake capacity suggesting their appropriateness to maintain a moist environment at wound interface. Matrices stabilized by ester bonds completely dissolved in phosphate buffer saline solution (pH 7.4) within three weeks while, when diamine was used, the nano-matrices remained stable over two months, also in DMEM. Results showed that the chemistry here applied prompted the formation of tunable degrading nano(fibers)scaffold. Materials elicited a rather good biological response.

CONCLUSION

In conclusion, nanofibrous HA based matrices exhibiting outstanding stability were produced; characterization highlighted features suggesting membranes as interesting materials in skin repair.

REFERENCES

1. Wang *et al.*, Biomaterials 2006, 27: 5689-5697
2. Xu *et al.*, Polymer 2009, 50: 3762-3769
3. Zhong *et al.*, Materials Science & Engineering C 27: 262-266

ACKNOWLEDGMENTS

Authors would like to acknowledge Dr. Maria Assunta Frezza for her precious technical support.

Collagen and PNIPAM Hydrogels: An Injectable Solution to Repair the Knee

Amanda Barnes¹, J Lapworth², Mark Coles³, Stephen Rimmer² and Paul Genever¹
amanda.barnes@york.ac.uk

¹Biomedical Tissue Research Group, University of York, UK, ²Department of Chemistry, University of Sheffield, UK
³Centre for Immunology and Infection, University of York, UK

INTRODUCTION

Cartilage defects in the knee are commonly treated by surgical interventions such as micro-fracture and autologous chondrocyte implantation (ACI), to regenerate the damaged tissue. Although the newly formed cartilage may histologically resemble native cartilage, it lacks the mechanical properties. Treatments utilising biomaterials alongside micro-fracture or ACI could improve the quality of the regenerated cartilage. Furthermore the use of a thermo-responsive hydrogel will permit non-invasive surgery, as the biomaterials could be delivered via injection. Both collagen I and poly(N-isopropylacrylamide) (PNIPAM) hydrogels undergo gelation at physiological temperatures and are biocompatible. Individually as scaffolds they can be less than ideal for tissue engineering, collagen gels are mechanically weak, whilst PNIPAM gels are prone to syneresis during gelation and can be non-cell adhesive. Combining these two materials can overcome these limitations and exploit the biocompatibility of collagen and the mechanical strength of PNIPAM within one scaffold.

EXPERIMENTAL METHODS

Poly(NIPAM-co-styrene)-graft-poly(N-vinylpyrrolidone) (NSN) was synthesised as previously described [1]. Whilst collagen I was extracted from rat-tail tendon and solubilised in acetic acid. Hybrid gels were created by mixing NSN and collagen I at 4°C and subsequently gelling by incubation at 37°C. To combine the hybrid gels with mesenchymal stromal cells (MSCs), a cell pellet was directly suspended in the hydrogel liquid at 4°C prior to gelation.

RESULTS AND DISCUSSION

To assess the varying material properties of the hydrogels SEM imaging, rheological and syneresis measurements were performed. Collagen content was maintained at 0.3 wt% within the hybrid gels, whilst NSN was varied between 0.25 – 5 wt%. At concentrations below the minimum gelation concentration of NSN (approximately 2 wt%), collagen dominated the overall properties of the hydrogel, where the reverse was observed in gels with NSN concentrations of 2.5 wt% upwards. Acellular collagen gels did not exhibit syneresis after gelation, whilst gels of 5 wt% NSN shrank down to 30% of their original volume. Syneresis in blends of collagen and NSN reduced with decreasing concentrations of NSN. The highest mechanical properties observed from the gels upon application of shear force, was observed in the NSN only gels, where the shear moduli increased with increasing NSN concentration. Collagen only gels had a

low shear modulus of 0.16 kPa, addition of up to 5 wt% of NSN hydrogel increased this to 11.3 kPa.

The microstructure of the hydrogels also varied with NSN concentration, revealing the differences in the hydrogel properties. Collagen only gels contained a homogenous network of collagen fibrils. Inclusion of NSN, resulted in gels with increased porosity and the appearance of NSN globules coating the fibrils. The collagen fibrils were less visible as the NSN concentration was increased. It is this interaction between the two hydrogel components that is believed to result in the variable mechanical properties and syneresis behaviour.

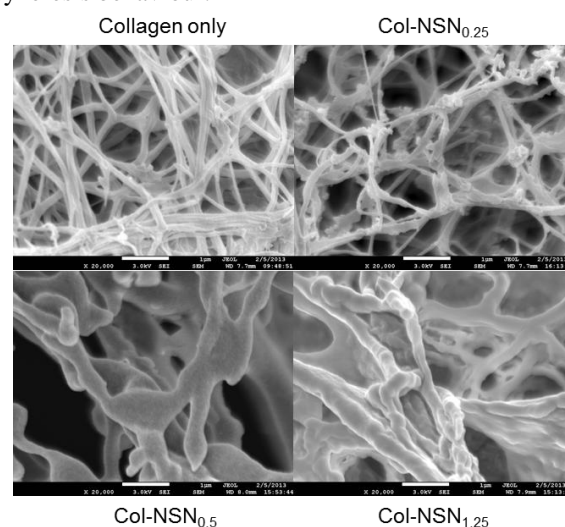


Figure 1. Internal structure of collagen-NSN hybrid gels

Mesenchymal stromal cells (MSCs) encapsulated within the hybrid gels were found viable and uniformly distributed throughout the gels after 7 days of culture.

CONCLUSION

By varying the composition of collagen and NSN in the blends a series of hydrogels was produced, which have variable mechanical properties and microstructures. The hydrogels are easily fabricated and uniformly encapsulate MSCs. To progress this work, the chondrogenic potential of MSCs and chondrocytes within the different blends will be examined.

REFERENCES

1. Lapworth J W *et al.*, Interface. 9:362-75. 2012

ACKNOWLEDGMENTS

We thank the EPSRC for funding this research through the White Rose DTC in TERM and E-TERM landscape fellowship.

Antimicrobial efficacy and biocompatibility of silver-including nanocomposite carbon coatings

Dorota Bociaga^{1*}, Piotr Komorowski^{2,3)}, Witold Jakubowski²⁾, Anna Jędrzejczak¹⁾, Anna Olejnik¹⁾

1) Division of Biomedical Engineering and Functional Materials, Institute of Materials Science and Engineering, Lodz University of Technology, Poland, dorota.bociagal@gmail.com

3) Division of Biophysics, Institute of Materials Science and Engineering, Lodz University of Technology, Poland

3) BioNanoPark Laboratories of Lodz Regional Park of Science and Technology, Lodz, Poland

INTRODUCTION

The formation of bacteria biofilm on the surface of the medical products, nowadays, is a major clinical issue. Highly adaptive ability of bacteria to colonize the surface of biomaterials causes a lot of infections. This study evaluates samples of the AISI 316 LVM with special nanocomposite silver-including carbon coatings prepared by hybrid RF/MS PACVD (Radio Frequency/Magnetron Sputtering Plasma Assisted Chemical Vapour Deposition) deposition technique in order to improve the physicochemical and biological properties of biomaterials, adding new features, such as antibacterial properties.

The aim of the present work was to evaluate antimicrobial efficacy and biocompatibility of gradient a-C:H/Ti coatings in relation to the physicochemical properties of the surface and chemical composition of coating.

EXPERIMENTAL METHODS

For this purpose, samples were tested in live/dead test using two cell strains: human endothelial cells (Ea.hy 926) and osteoblasts-like cells (Saos-2). For testing bactericidal activity of the coatings, an exponential growth phase of *E. coli* strain DH5 α was used as a model microorganism. In order to evaluate the surface condition and estimate its physicochemical properties in connection with biological results, the structure and morphology were investigated using scanning electron microscopy (SEM), surface characteristics were determined using atomic force microscopy (AFM) and chemical composition of coatings were tested using X-Ray photoelectron spectroscopy (XPS). The mechanism of reactions was analysed also in reference to mechanical properties (hardness, modulus, adhesion) which were evaluated by means of the nanoindentation

technique and revealed very good mechanical characteristic of silver doped carbon coating

RESULTS AND DISCUSSION

Examined coatings showed an uniformity of silver ions distribution in the amorphous DLC matrix, good biocompatibility in contact with mammalian cells and the increased level of bactericidal properties. Additionally, if we take into consideration very good mechanical parameters of these Ag including gradient a-C:H/Ti coatings, they constitute a very good material for biomedical application, e.g. orthopaedics or dental.

CONCLUSION

Summarizing, a carbon coatings being manufactured by the RF/MS RFPACVD method modified by Ag ion enables to obtain biomaterial which limits the growth of bacteria and, at the same time, has a limited impact to the human cells.

REFERENCES

References must be numbered. Keep the same style.

1. Love C.A., *et al.*, Tribology International 63:141–150, 2013
2. Ohgoe Y., *et al.*, Surface & Coatings Technology 207:350–354, 2012
3. Hauert R., Diamond and Related Materials 12: 583–589, 2003

ACKNOWLEDGMENTS

This work has been supported by the National Centre for Research and Development under grant no. M-ERA.NET/2012/02/2014 and LIDER/040/707/L-4/12/NCBR/2013.

UKSB

POSTER PRESENTATIONS

The Impact of Serum, Plasma, and Platelet-Rich Plasma Derived After Exposure to Exercise, Altitude and Recombinant Human Erythropoietin (rHuEpo) on Mesenchymal Stem Cells

C. Coombs, P. Watt, A. Guildford, G. Bruinvels, Y. Pitsiladis

Brighton Centre for Regenerative Medicine, University of Brighton, United Kingdom.

C.V.Coombs@brighton.ac.uk

INTRODUCTION

Mesenchymal stem cells (MSC) have been widely used in tissue regeneration due to their multipotent ability, immunomodulatory functions and capacity to secrete a range of bioactive molecules¹. Consequently MSCs have been used therapeutically for: cardiovascular², inflammatory bowel and liver disease³ and type one³ and two diabetes^{4,5}.

Exercise has been reported as a stimulus for stem cell proliferation, migration and incorporation into damaged tissue⁶ and therefore has a potential role in promoting tissue regeneration. However, a systematic investigation of exercise-induced perturbations of blood-derived fractions on mesenchymal stem cells has not been conducted.

Therefore the aim of the current investigation is to provide baseline data to inform future studies in this area of research. It will assess the impact of serum, plasma, and platelet-rich plasma derived from a variety of exercise modalities, exposure to altitude and administration of recombinant human erythropoietin (rHuEpo) on the behaviour of MSCs *in vitro*.

EXPERIMENTAL METHODS

Pre- and post-exercise blood-derived fractions were isolated from recreationally active males who completed eccentric or concentric exercise protocols in a randomised cross-over design. On a separate occasion blood derived fractions were isolated from 24 well-trained athletes (19 males, 5 females) exposed to altitude for periods ranging from 2-4 weeks (n=10) and microdose rHuEpo injections ranging from 20 to 40 IU·kg⁻¹ body mass for 7 weeks before, during and 3 weeks after administration. Repeated sprint ability and maximal oxygen uptake ($\dot{V}O_{2max}$) were measured pre and post administration (n=14).

RESULTS

Preliminary data has shown that eccentric exercise, altitude and rHuEpo have an effect on a number of exercise variables. It is predicted that they will impact upon the behaviour of MSC *in vitro*.

CONCLUSION

Results obtained from this investigation have the potential to provide mechanistic evidence to construct interventions aimed at exploiting MSCs to promote tissue regeneration and repair.

REFERENCES

1. Wang S. *et al.*, J. Hematol. Oncol. 5:19, 2012.
2. Chen S. *et al.*, Am J. Cardiol. 94:92-95, 2004.
3. Bernardo M. *et al.*, Bone Marrow Transplant. 47:164-171, 2012.
4. Si Y. *et al.*, Diabetes. 6:1616-25, 2012.
5. Zhao Y. *et al.*, Autoimmun. Rev. 2:137-42, 2011.
6. Fizua Lucas C. *et al.*, Physiology. 5:330-358, 2013.

Towards a 3-Dimensional Model of Neural Tissue with Integrated Recording Sites

H. Lancashire*, C. Pendegrass, A. Vanhoostenberghe and G. Blunn

Institute of Orthopaedics and Musculoskeletal Science, University College London, UK

*henry.lancashire.10@ucl.ac.uk

INTRODUCTION

In vitro systems are typically limited to 2D, particularly for recording from neural cells¹. New techniques emerging include spike arrays for recording from *ex vivo* culture², and 3D electrode arrays for recording from primary neuronal cultures¹.

The aim of this study is to develop a layered collagen/silicone construct, in which the silicone layer has windows to allow interconnection of the collagen in 3D, and has an embedded microelectrode array for *in vitro* neuronal recording. We present proof of concept experiments demonstrating the construction of cellular and acellular constructs using an example mouse fibroblast cell line.

EXPERIMENTAL METHODS

Recording electrodes were manufactured as sheets using a Nd:YAG laser cutter. Poly(4-styrene sulfonic acid) (Aldrich) was spin coated onto glass slides. A 30 μm layer of PDMS (Sylgard 184, Dow Corning) was spin coated and partially cured. 316L Stainless Steel (12.5 μm thick, Advent Research Materials, UK) was placed over the PDMS and patterned using the laser cutter. A second layer of PDMS was spin coated, fully cured, and windows and electrode pads were opened using the same laser cutter. **Collagen gels** were formed using protocols previously described³. L929 cells (mouse fibroblasts from subcutaneous adipose tissue, ECACC, UK) were dispersed in the gels uniformly. Cells were cultured in DMEM + 10% FBS. After 7 days *in vitro* (DIV) constructs were fixed with 10% formal saline. **Constructs** were formed by layering recording electrode sheets between collagen gels. Layered constructs were plastically compressed³. **Four treatment groups** were considered: Acellular Collagen; 0.5 million cells/mL; 1 million cells/mL; and Control electrode sheets without collagen. **Impedance Spectroscopy** of electrodes ($n=9$) was measured before construct formation, and after 7 DIV, in 0.9% saline using a Wayne Kerr 6500B Impedance Analyser (0 A bias current, 200 mV p-p). Absolute impedance, $|Z|$, and phase angle, θ , were measured from 20 Hz to 10 kHz. **Statistical significance** was determined at the $p \leq 0.05$ level using non-parametric statistical tests. Values are expressed as mean \pm standard deviation.

RESULTS AND DISCUSSION

Cellular and acellular constructs were successfully formed with feature sizes down to 100 μm (track widths). Of $N=36$ electrodes 1 failed (<3% failure) during manufacture. Cells remained viable throughout the culture period. Fig. 1 shows plots of mean electrode impedance. After 7DIV 1 kHz electrode impedance fell

in the control group from $2.0 \pm 0.2 \text{ k}\Omega$ to $1.4 \pm 0.2 \text{ k}\Omega$ (p

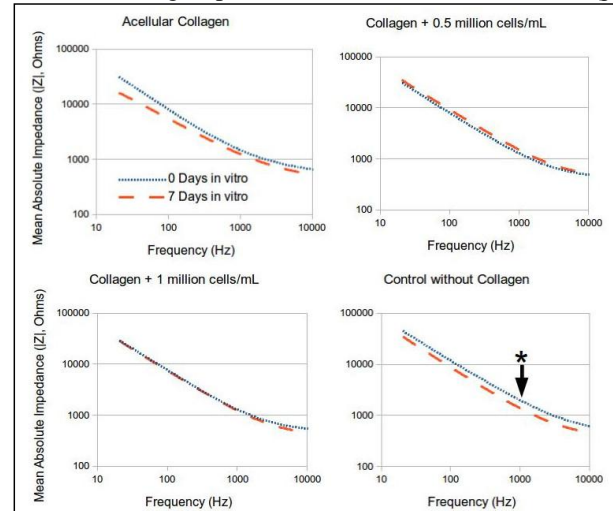


Fig. 1: Plots of mean electrode impedance. Significant differences in 1kHz impedance are marked (*).

< 0.001), this may be a spurious change due to air bubble formation following immersion in saline. Electrode impedance did not significantly change after 7DIV for constructs with acellular and cellular collagen gels ($p \geq 0.198$). After 7DIV 1 kHz electrode impedances were not significantly different between groups ($p = 0.272$), mean impedance was $1.4 \pm 0.4 \text{ k}\Omega$.

Continuation of this research includes: increasing electrode sheet transparency; electrophysiology of cells *in vitro*; and further minaturisation to increase electrode number and allow the use of modified tissue culture well plates. New designs (not yet tested) have reduced interelectrode distance from 5 mm to 500 μm and electrode diameter from 1 mm to 60 μm .

CONCLUSION

This work demonstrates a 3D tissue model with integrated recording sites. Over 7DIV cell number does not significantly alter 1 kHz electrode impedance.

REFERENCES

1. Musick K. *et. al.*, Lab Chip 9(14):2036-42, 2009.
2. Kibler A.B. *et. al.*, J. Neurosci. Meth. 204(2):296-305, 2012.
3. Brown R.A. *et. al.*, Adv. Funct. Mater. 15:1762–1770, 2005.

ACKNOWLEDGMENTS

The authors would like to thank the EPSRC (UK) for providing financial support for this project through grant EP/G036675/1. The authors would like to thank Dr. U Cheema (UCL) for assistance with collagen gels.

Indirect Prototyped Polyurethane Urea Scaffolds for Cardiac Tissue Engineering

Roberto Hernandez-Cordova¹, Donna A Mathew², Alberto Ceballos-Villanueva¹, Hugo J Carrillo-Escalante¹,
Araida Hidalgo-Bastida^{2*}, Fernando Hernandez-Sanchez¹

¹Centro de Investigacion Cientifica de Yucatan (CICY), Merida, Mexico

²Manchester Metropolitan University, Manchester, UK, *a.hidalgo@mmu.ac.uk

INTRODUCTION

Multi-layered scaffolds with honeycomb-like micro-architecture could provide suitable scaffolds for cardiac tissue engineering. Such scaffolds require a completely interconnected micro-structure and an elastomeric-like behaviour to match the characteristics of the native tissue. Our aim was to fabricate these by indirect prototyping, using a porogen of polyvinyl alcohol (PVA) and injecting a poly-urethane urea (PUU).

EXPERIMENTAL METHODS

PUU was synthesized by two step method¹ from polycaprolactone-diol ($M_n \sim 2,000$), 4,4'-Methylenebis(cyclohexyl isocyanate) (HMDI) and 1,4-butanediol (BDA) as chain extender (Sigma Aldrich). Sn-octate was used as catalyser and N,N-Dimethylformamide (DMF) as solvent to carry the synthesis. The Replicator®3D printer, and a 1.7 mm PVA filament (MakerBot Industries) were used to fabricate a 3D porogen using a wood pile (grid) fibre arrangement. CAD model was obtained using OpenSCAD. We controlled the PVA fibre diameter and spaces between fibres through fabrication parameter to achieve different pore size on scaffold at the end of the process. A solution 25% p/V of PUU dissolved in DMF at 100°C during 3 hours was used to inject in porogen by a nitrogen gas injecting system. Specimens (5x10 mm, HxØ) were cut and placed in vacuum at 60 °C during 24 hours to allow solvent evaporation. Dried specimens were placed in distilled water during three days with two water change daily to dissolve PVA and then dried at 60°C overnight. SEM was used to assess micro-architecture. Elastic modulus at compression mode was determined in dried and wet (70% ethanol) samples. Biocompatibility was assessed by culturing human cardiomyocytes (Promocell, Germany) in 2D and 3D.

RESULTS AND DISCUSSION

PVA porogens of different filament cross-sectional area (300µm, 400µm and 500µm) were fabricated and used to obtain PUU scaffolds labelled as PUUS300, PUUS400 and PUUS500 (300µm, 400µm and 500µm equivalent pore diameter). Honeycomb-like micro-architecture (Fig. 1C) presents tubular channels which are controlled by dissolved PVA filaments. Pores are completely interconnected, which allow incursion of cells in all internal scaffold micro-architecture during cell culture. PUU scaffolds possess an elastomeric behaviour under compressive stress (Fig 1D) with elastic modulus of 11.16 kPa, 10.55 kPa and 16.03 kPa, PUU300, PUU400 and PUU500 respectively; similar to natural cardiac tissue (20-500 kPa)². We assessed scaffolds mechanical behaviour in wet condition to approximate scaffolds performance during cell culture.

Softening of scaffolds is showed as a decrease in elastic modulus, a notable advantage in this material³. Higher modulus in PUUS500 is due to higher distance between PVA filaments (Fig. 1A, B) producing a thicker wall in scaffolds. Furthermore, scaffolds demonstrated to be biocompatible with human cardiomyocytes *in vitro*.

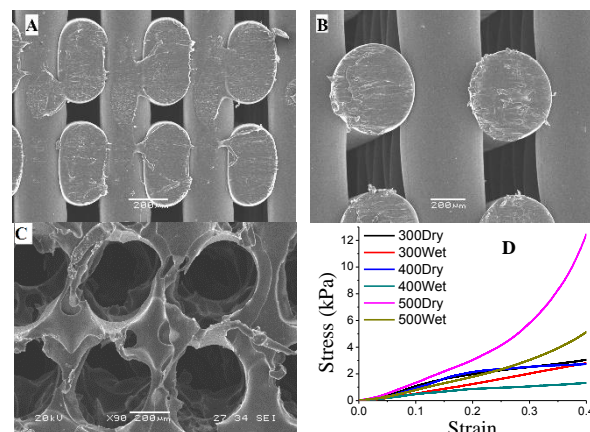


Fig. 1. A) and B) PVA porogen of 300µm and 500µm cross-sectional area. C) PUUS300 showing micro-architecture. D) Stress-Strain curve of PUU scaffolds.

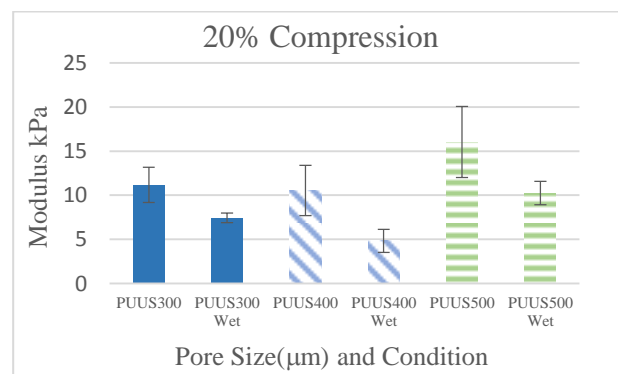


Fig. 2. Modulus of PUU scaffolds in compressive mode for 300µm, 400µm and 500µm pore size.

CONCLUSION

Indirect prototyped method can be a reliable processing approach for PUU scaffolds, resulting in structures with mechanical behaviour and micro-architecture similar to cardiac tissue, showing its potential for this application.

REFERENCES

1. L. May-Hernández, et al. Jour. of App. Pol. Sci. Vol. 119: 2093 – 2104 (2011).
2. Chen, Qi-Zhi, et al. Biomaterials 29: 47–57 (2008).
3. Zdrachala RJ et al. J Biomater Appl. 2(4):544-61 (1988).

ACKNOWLEDGMENTS

This research was funded by CONACYT-Mexico.

RF Magnetron Sputtering of Multicomponent Ion Doped Phosphate Glasses

Bryan Stuart¹, M. Gimeno-Fabra², D. Grant³, I. Ahmed⁴ and J. Segal⁵

¹Department of Mechanical, Materials and Manufacturing Engineering, University of Nottingham, England, epxbs4@nottingham.ac.uk

INTRODUCTION

Phosphate glasses have the ability to fully resorb in aqueous solution by reacting to form hydroxyl groups and leached ionic by-products. For biomedical applications these glasses have been used for tissue scaffolds and to produce glass fibres for biodegradable polymer composites. Currently their applications in this field are expanding to coatings and bone fixation devices (1).

This research utilises RF magnetron sputtering to create thin films of ion doped phosphate glass. We focus on understanding the relationship between the nature of sputtering target and the generated substrate's composition for a given set of sputtering parameters.

The phosphate network former combined with metal network modifying ions creates a complex quaternary oxide, consisting of varying strength covalent and ionic bonds, similar to the network depicted in Fig. 1. When bombarded with charged argon particles, atoms are preferentially ejected from the glass structure (2); a relationship termed "sputtering yield".

The purpose of this research is to understand this phenomenon by the use multicomponent oxide targets. The as-produced thin films are resorbable and potentially bioactive, with applications as coatings for implant devices, acting as slow release doping agents for improved osseointegration.



Figure 1. Tertiary phosphate glass structure (3).

EXPERIMENTAL METHODS

Quaternary phosphate glass targets, produced by melt-quenching have been applied using RF magnetron sputtering on commercially pure titanium discs and borosilicate cover slides. The phosphate glass coated titanium discs have been studied using SEM/EDX for deposition rate and compositional analysis.

RESULTS AND DISCUSSION

We have found that P40 coatings at 60 watts are deposited amorphous at $\approx 3.17 \text{ nm min}^{-1}$ (Fig.2 sample after coating for 4 hours). At higher powers of 120 watts, temperature increases and crystallisation occurs of both the target and sputtered coating. Preferential sputtering is related to the bonding strength of the oxide constituents, therefore as the network connectivity increases, deposition rate is reduced and sputtering yield is in favour of the network modifying ions. Network modifier ions are prone to preferential sputtering in comparison to the covalently bonded network forming the phosphate backbone. Furthermore, the sputtering of network modifying ions is related to reactivity, atomic mass and the oxide binding energy.

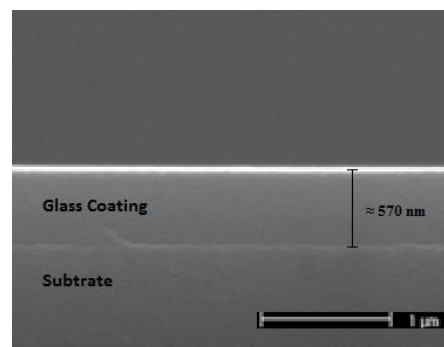


Figure 2. Cross sectional SEM of an applied ion doped phosphate glass by RF magnetron sputtering.

CONCLUSION

Thin film quaternary phosphate glass targets can be applied via RF magnetron sputtering to form coatings at low deposition rates between $1\text{--}5 \text{ nm min}^{-1}$. With careful consideration of the target's composition and the sputtering parameters, accurate predictions of the composition and thickness of the resulting thin films can be drawn.

REFERENCES

1. Knowles JC. Phosphate based glasses for biomedical applications. *Journal of Materials Chemistry*. 2003;13(10):2395-401.
2. Stan GE, Marcov DA, Pasuk I, Miculescu F, Pina S, Tulyaganov DU, et al. Bioactive glass thin films deposited by magnetron sputtering technique: The role of working pressure. *Applied Surface Science*. 2010 Sep 15;256(23):7102-10. PubMed PMID: WOS:000279592200029. English.
3. Jones JEC, Alexis (Editor). *Bio-Glasses : An Introduction*: John Wileys and Sons Ltd; 2012

Manufacture of Bioresorbable Fibre Reinforced Composites for Fracture Fixation Devices

Fernando Barrera Betanzos, Miquel Gimeno-Fabra, Joel Segal, David Grant and Ifty Ahmed

Department of Materials, Mechanics and Structures, Faculty of Engineering, University of Nottingham, UK
emxfb@nottingham.ac.uk

INTRODUCTION

Femoral diaphyseal fractures are one of the most common long bone fractures affecting the lower extremities. Due to the high vascularity and soft tissue volume associated with the femur, traumas within this region often require surgical intervention¹. Intramedullary (IM) nailing represents the best option to reduce and stabilise bone fragments in virtue of its inherent advantages over similar fixation devices, including minor tissue tethering, and reduced infection risk¹. In spite of these benefits, current IM nails remain metal-based devices, thus can potentially elicit a series of detrimental conditions such as inflammatory cascades and bone atrophy secondary to stress shielding, coupled with the possible need for removal after bone healing¹. Therefore, the prospect fabrication of an implant from materials with bone matching properties, capable of providing immediate fracture stabilisation while gradually transferring the load to the healing tissue, and eventually resorbing *in vivo*, becomes really attractive. Accordingly, this study focus on the manufacture of bioresorbable composites = from phosphate glass fibres (PGF) and polylactic acid (PLA)^{2,3}.

EXPERIMENTAL METHODS

Continuous glass fibres were produced using an in-house melt-draw transverse fibre spinning facility. The glass with theoretical composition of $45\text{P}_2\text{O}_5\text{-}16\text{CaO-}13\text{Na}_2\text{O-}24\text{MgO-}2\text{Fe}_2\text{O}_3$ (mol%) was synthesised from reagent grade precursors, batched and melted in a platinum crucible at 1150 °C.

A series of unidirectional (UD) composites with three volume fractions (~0.8, ~0.15, ~0.25) were fabricated by compression moulding at 180 °C for 10 minutes of a stack encompassing alternate layers of UD fibre mats and PLA films made by pressing batches of PLA pellets (NatureWorks 3251 D). A pure PLA plate was also produced by the same process for control purposes.

The plates were then cut into small pieces ($4 \times 1.5 \times 0.2$) cm³ for flexural properties measurement (n=9) using a Hounsfield Series S testing machine with a cross-head speed of 1 mm min⁻¹, and a 5 kN load cell in accordance with BS EN ISO 14125:1998. The results reported here are the mean value coupled with the standard error.

RESULTS AND DISCUSSION

Initial results confirm the reinforcing effect of PGF in PLA mechanical properties. Blank PLA samples had a flexural modulus and strength of 2.78 ± 0.06 GPa and 68.1 ± 1.02 MPa respectively. In the case of the 0.25 Vf specimen, the average strength values exceed 200 MPa, being superior or, at the least comparable to those previously reported (Fig. 1)³. Nevertheless, it should be

noted that the composite's flexural modulus (11.33 ± 0.57 GPa) is lower than the predicted using the rule of mixtures (16.65 GPa), requiring fibre contents in the order of 0.5 Vf to reach the upper limit of cortical bone modulus. Since the flexural modulus is highly sensible to the laminate stacking sequence, it can be anticipated that change in such parameter by piling up thinner laminae, will certainly improve the composite properties.

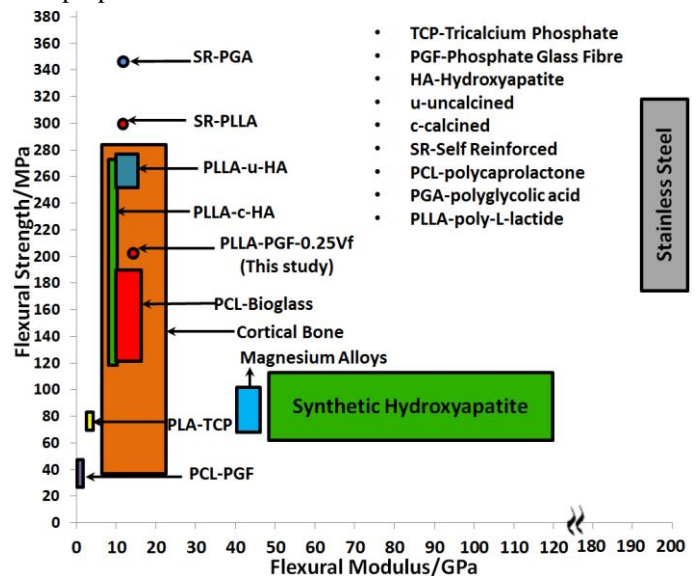


Figure 1. Flexural properties comparison of proposed composite systems and common biomaterials for fixation devices³.

CONCLUSION

Effective bioresorbable implants can be fabricated by compression moulding of PLA and PGF. Further efforts will focus on the close control of fibre orientation and laminating sequence, as we have demonstrated that these parameters are essential to optimise the final mechanical properties of the composite without compromising *in vivo* performance.

REFERENCES

1. Trompeter A. *et al.*, Orthopaedic and Trauma 5:322-331, 2013
2. Harper L.T. *et al.*, J. of the Mechanical Behaviour of Biomedical Materials 15:13-23, 2012
3. Felfel R., PhD thesis, University of Nottingham, 2013

ACKNOWLEDGMENTS

The authors would like to thank the EPSR-Centre for Innovative Manufacturing in Medical devices, the University of Nottingham and the CONACyT for providing financial support for this project.

Development of a Soft Tissue *in vitro* Model for Ameloblastoma

T. Eriksson¹, S. Fedele¹, R. Day², V. Salih³

¹Eastman Dental Institute, University College London, UK

²Applied Biomedical Engineering, University College London, UK,

³Plymouth University Peninsula School of Medicine & Dentistry, UK; t.eriksson.11@ucl.ac.uk

INTRODUCTION

Ameloblastoma is a rare odontogenic tumour with great infiltrative capacity. It accounts for around 1% of oral tumours and occurs mainly in the jaw bones. Surgery is the main treatment option, however recurrent tumours occasionally occur¹. These recurrences sometimes invade the soft tissue surrounding the jaw bone. Recurrences in the gingivae are most common, but tumours growing into the sinonasal passages, eyes and brain have also been reported². Soft tissue spread of the tumour is difficult to stop, as no non-invasive therapies are currently available³. By creating an *in vitro* three-dimensional model of the tumour using tissue-engineering techniques, we aim to assess the interactions of the tumour cells with the surrounding stroma and the invasion mechanisms the tumour cells use to infiltrate the soft tissue. The model can also be used to test anti-infiltrative agents to stop the growth of the tumour. Here, we present work towards developing an *in vitro* model able to support the inclusion of ameloblastoma tumour cells.

EXPERIMENTAL METHODS

Gingival fibroblast cells (GF) were added to pH neutralised collagen type I gels to create a three-dimensional model. In order to mimic the tissue stroma and ground substance, growth factor-reduced Matrigel (BD Biosciences) was added to half of the gels (2:1 collagen to Matrigel). Plastic compression was then performed to improve the mechanical properties of the scaffold⁴. The optimum cell density was determined by seeding increasing cell concentrations in the gels and measuring contraction over time. Gels were cultured for 14 days and assessed for cell viability with Live/Dead confocal staining using 2uM calcein AM and 4uM EthD-1 (Life Technologies) in PBS. Samples were examined with haematoxylin and eosin staining on formalin-fixed paraffin-embedded sections and transmission electron microscopy (TEM) on resin-embedded samples. Several methods to incorporate cells from the AM-1 cell line into the scaffold were also explored.

RESULTS AND DISCUSSION

Fibroblasts were shown to exert major contractile forces on the scaffolds (fig.1). For further studies a cell concentration which results in minimal contraction, but does not compromise scaffold remodelling will be used. Fibroblasts remain alive and proliferate in both scaffolds during the two-week culture period (fig. 2). The cells were shown to remodel the scaffold and produce extracellular factors seen as large vesicles through TEM.

Further characterisation of the two scaffold types will be carried out using SEM to assess differences in scaffold appearance.

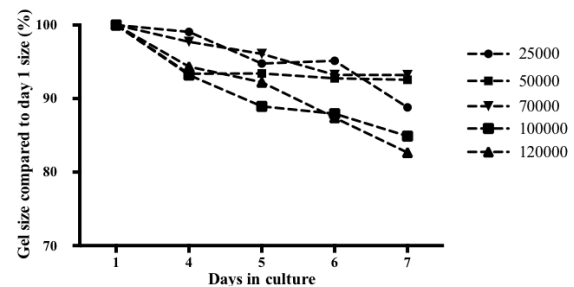


Figure 1: Cell induced collagen gel contraction. Increasing the cell density (displayed per ml of collagen gel) caused increased contraction in compressed gels.

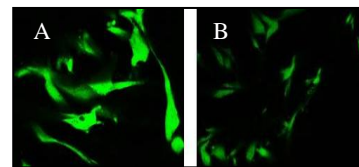


Figure 2: Live/Dead staining of fibroblasts A) Matrigel and collagen; B) collagen-only scaffold on day 14. Green = live cells.

CONCLUSION

These models form the basis for a soft tissue scaffold into which an ameloblastoma tumour model made with the AM-1 cell line will be incorporated. The ability of the scaffold to maintain AM-1 cells will initially be assessed with single-cell culture in decellularised collagen scaffolds. Once incorporated, the ameloblastoma cells in the 3D co-culture scaffold will be analysed both for interactions with the scaffold itself and with fibroblasts, protein production and infiltrative potential. This will allow for identification of any pathways the tumour cells use for tissue destruction. This may lead to development of non-invasive therapies.

REFERENCES

1. Reichart PA. *et al.*, Oral Oncol 31B(2):86-99, 2004
2. DeVilliers J. *et al.*, Dental Research 90:463-9, 2011
3. Gomes CC. *et al.*, J Pathology 232(5):488-91, 2014
4. Brown R. *et al.*, Adv Funct Mat 15:1762-70, 2005
5. Harada H. *et al.*, J Oral Pathol Med 27(5):207-12, 1998

ACKNOWLEDGMENTS

This study is funded by a UCL Impact Scholarship through the UCL Development Fund and sponsorship from the Biss-Davies charitable trust.

Porous Electrospun PCL Fibres for Osteo-Differentiation

Selene Alcantara-Barrera¹, Zandra Flores², Ricardo Vera-Graziano¹, Alfredo Maciel- Cerda¹, L. Araida Hidalgo-Bastida^{2*}

¹ Centro de Biomateriales, Universidad Nacional Autonoma de Mexico, Mexico

² Manchester Metropolitan University, Manchester, UK, *a.hidalgo@mmu.ac.uk

INTRODUCTION

Electrospinning has been used with different natural and synthetic polymers, to produce nanofibres as scaffolds for regenerative medicine. Polycaprolactone (PCL), a FDA approved semi-crystalline biodegradable polymer, presents good mechanical properties, compatible with both strong and soft tissues. However, the PCL hydrophobicity inhibits cell attachment and growth. Our aim in this work was to fabricate porous PCL nanofibres with glucose on the surface, to decrease their hydrophobicity and to promote osteo-differentiation.

EXPERIMENTAL METHODS

Solutions of PCL (Aldrich®) 12% wt were prepared dissolving in chloroform and in the solvents system dichloromethane: N,N-dimethylformamide (80:20). The solutions were electrospun with the following parameters: flow rate 1.0 ml/h, voltage 8 kV, distance (syringe tip-collector) 25 cm. For solutions of PCL with glucose (Sigma-Aldrich®), glucose content was 10% wt respect to PCL, with the solvent system THF: DMF: H₂O (86.5:4.5:9). The scaffolds were analysed by SEM with a JEOL field emission JSM-7600F microscope using a backscattered electrons detector (LABE). The mechanical tests were conducted according to the ASTM D1708-96 norm, using a universal testing machine Instron 5500R at 10 mm/min and 25 °C. The glucose solution in water was prepared with a concentration of 10% wt. Cellular adhesion was evaluated by seeding mesenchymal stem cells (Promocell, Germany) and quantified via Alamar blue and Live/Dead stain (Life Technologies, UK).

RESULTS AND DISCUSSION

The fibre diameter and relative porosity of the scaffolds are shown in Table 1. It was observed that the fibres generated from chloroform solution exhibited larger diameters, 0.5-1.0 µm pores along the fibres (Fig. 1 A).

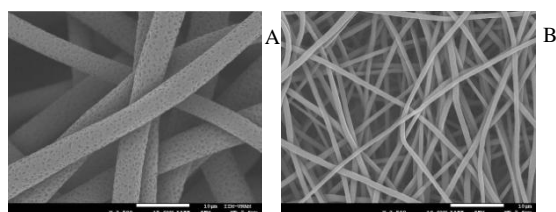


Fig. 1. SEM micrographs of PCL fibres showing A)Porous fibres:chloroform, B)Non-porous fibres: dichloromethane / N,N dimethylformamide.

The scaffolds obtained with the DCM: DMF (80:20) resulted in thinner fibres without pores (Fig. 1 B). In order to modify the hydrophobicity of these scaffolds, a glucose solution was sprinkled on the surface of both materials, and subsequently compared with PCL. Finally, the solution of PCL containing glucose generates a scaffold constituted by rough fibres with diameter slightly bigger than in the case of DCM: DMF system (Table 1).

The mechanical behaviour of the electrospun scaffolds indicated that porous fibres exhibited a lower tensile value compared to the non-porous fibres; although the porous fibres presented a higher Young modulus than the non-porous scaffolds (Table 1). Fibre's porosity and glucose presence also affected the cellular response (data not shown), although further studies need to be conducted.

SCAFFOLD	FIBRE DIAMETERS (µm)	RELATIVE POROSITY (%)	TENSION (MPa)	YOUNG MODULUS (MPa)
PCL/CF	5.36 ± 0.633	22.79	1.23	11.16
PCL/DC M-DMF	0.91 ± 0.146	29.44	3.48	5.36
(PCL/CF) + gluc	5.36 ± 0.633	< 10	1.23	11.16
(PCL/DC M-DMF) + gluc	0.91 ± 0.146	7.73	3.48	5.36
PCL-gluc/THF-DMF-H ₂ O	1.37 ± 0.41	22.37	NA	NA

Table 1. Fibre diameter, relative porosity and mechanical properties of the electrospun scaffolds.

CONCLUSIONS

The solvent system used in solution is crucial in the final electrospun scaffold morphology, and contributes to the microstructure and porosity of the fibres. This ultimately has an effect on mechanical properties and cellular response, both for biocompatibility and osteo-differentiation.

REFERENCES

1. Pham, Q.P., Sharma, U., & Mikos, A.G. (2006). Tissue Engineering, 12(5),1197-1211.
2. Reed, C.R. (2009). Annals of Plastic Surgery, 62(5), 505-512.

ACKNOWLEDGMENTS

The authors would like to thank CONACYT-Mexico for providing financial support to this project.

Atomic Layer Deposition of Silver on High Aspect Ratio Structures for Medical Implants

Zahra Golrokhi

Department of Materials Science and Engineering, University of Liverpool, Liverpool L69 3GH, UK

E-mail: golrokhi@liv.ac.uk

INTRODUCTION

Silver nanoparticles are one of the interesting research topics in recent years. There has been growing interest toward silver nanoparticles use as antimicrobial coatings. Silver nanoparticles release a low level of silver ions to supply defence against bacteria. In this study, we present the synthesis of silver nanoparticles via liquid injection atomic layer deposition (ALD) with precise thickness control by using the saturated growth rate at relatively low substrate temperatures (<130°C).

The characteristic to ALD is a saturated film growth rate which allows conformality and uniformity on high aspect ratio structures [1, 2].

EXPERIMENTAL METHODS

Silver thin films were deposited in the Aixtron AIX 200FE which is a liquid injection ALD designed for various oxide materials on different types of substrates. The flow of the Argon as a carrier gas is controlled by a mass flow controller. The 0.1M silver precursor ((hexafluoroacetylacetonato)silver(I)(1,5cyclooctadiene)) [Ag(hfac)(COD)] was dissolved in anhydrous toluene in a nitrogen glove box. The substrates were Si (100) wafer and soda lime glass (75 × 25 mm²) at the same time for each growth experiment. Silver thin films were deposited at growth temperature of 125-128°C.

Elemental compositions of the surface, morphology and crystal structures of the films were analyzed by XPS, AFM and XRD respectively.

RESULTS AND DISCUSSION

Figure 1 shows the effect of [Ag(hfac)(COD)] dose by varying the dose between 0 and 6s at a growth temperature of 125°C with 2s propanol doses as a co-reactant. The growth rate rapidly increased between 0-2s doses to 0.013 nm/cycle and then saturated above 3s. This confirms that [Ag(hfac)(COD)] is a self-limiting precursor for ALD growth which provides large area uniformity, and the thickness uniformity on high aspect ratio structures.

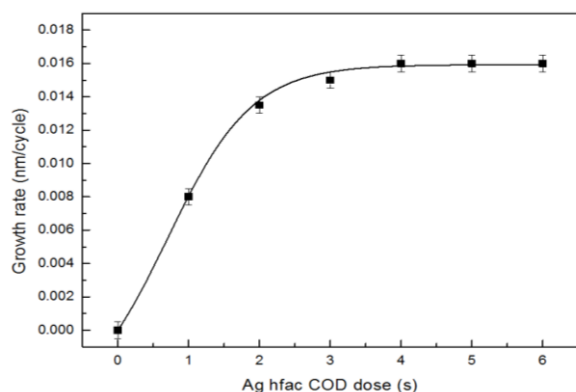


Figure1. Growth rate as a function of [Ag(hfac)(COD)] dose for propanol (2s) based ALD at 125°C on Silicon.

Figure 2 shows scanning electron microscope images deposited from (hfac) Ag (1,5-COD) as a function of doses on silicon. As the silver dose is increased from 1s to 6s, the silver NPs on the surface reached saturation and consistency.

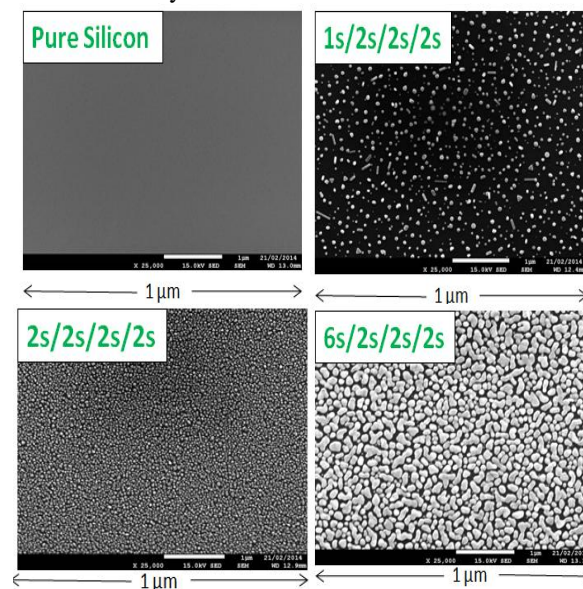


Figure2. SEM micrographs at different silver doses on silicon substrate at 125°C.

CONCLUSION

Silver NPs were deposited by liquid injection atomic layer deposition technique using pulses of ((hexafluoroacetylacetonato)silver(I)(1,5cyclooctadiene)) [Ag(hfac)(COD)] dissolved in 0.1M toluene solution and pulses of propan-1-ol as a co-reactant.

There has been a significant resurgence of interest in silver NPs due to its diagnostic and antibacterial applications. Current research aimed to develop antibacterial coatings for bio-compatible medical implants with atomic layer deposition technique. However, several related facts were not investigated in detail, and the work is to be continued.

REFERENCES

- George, S. M. Chem. Rev. 110, 111–131, 2010
- Ritala, M.; Niinistö, J. In Chemical Vapour Deposition: Precursors, Processes and Applications; Royal Society of Chemistry. 158_206, 2008.

ACKNOWLEDGMENTS

The authors are grateful to the Stryker for financial support.

Characteristics and Cytocompatibility of Novel Borophosphate Glasses

Chenkai Zhu¹, Ifty Ahmed¹, Xiaoling Liu¹, Andy Parsons¹, Jingsong Liu², Chris Rudd¹

¹ Division of Materials, Mechanics and Structures, Faculty of Engineering, University of Nottingham, UK,

² Sinoma Science & Technology Co., Ltd. Jiangning District, Nanjing, China,

eaxcz4@nottingham.ac.uk

INTRODUCTION

Bioresorbable phosphate-based glasses have been investigated for varying tissue engineering applications¹. The degradation rate of these glasses can be tailored by doping with varying metal ions such as Mg, Fe, Ti, and B². In this study, boron was added at varying quantities in place of phosphate. The effect of boron addition on the glass thermal properties, chemical durability and cytocompatibility was investigated.

EXPERIMENTAL METHODS

Glasses with three different compositions were produced, denoted as P48B12, P45B15 and P40B20. The thermal processing window T_{pw} (i.e. onset of crystallisation temperature T_{con} minus glass transition temperature T_g) of the glasses was investigated via Differential Thermal Analysis. The chemical durability was characterised in phosphate buffer saline at 37°C for 60 days. The cytocompatibility of the glasses was studied by culturing the human osteosarcoma cell line (MG63) directly onto the glass surface for 14 days.

RESULTS AND DISCUSSION

The thermal properties of the glasses in Table 1 revealed that T_{con} and T_c values decreased with the addition of B₂O₃, whilst only slight increases were observed for the T_g values. The thermal processing window (T_{pw}) was observed to decrease with increasing boron content, thus increased glass crystallisation tendency and reduced thermal stability³.

Table 1: thermal properties of glasses with B₂O₃ variation.

Glass code	$T_g/^\circ\text{C}$	$T_{con}/^\circ\text{C}$	$T_{pw}/^\circ\text{C}$	$T_c/^\circ\text{C}$
P48B12	545	800	255	860
P45B15	550	780	230	825
P40B20	555	750	195	770

The degradation study revealed the dissolution rate of P48B12 glass at $3.64 \times 10^{-5} \text{ kg cm}^{-2} \text{ hr}^{-1}$, which increased to $4.23 \times 10^{-5} \text{ kg cm}^{-2} \text{ hr}^{-1}$ for P45B15 and then have a further increase to $5.92 \times 10^{-5} \text{ kg cm}^{-2} \text{ hr}^{-1}$ for P40B20 (Figure 1). The decrease of chemical durability with boron addition was suggested to be due to the P₂O₅ content being replaced by B₂O₃, boron units BO₃ and BO₄ introduced into glass system while BO₃ units were not as resistance as BO₄ units⁴. For all three glasses, the metabolic activity of MG63 cell line (Figure 2) was seen to increase throughout the 14 days culture period. The metabolic activity of cells on P48B12 glasses and

P40B20 glasses were significantly close to tissue culture plastic (TCP).

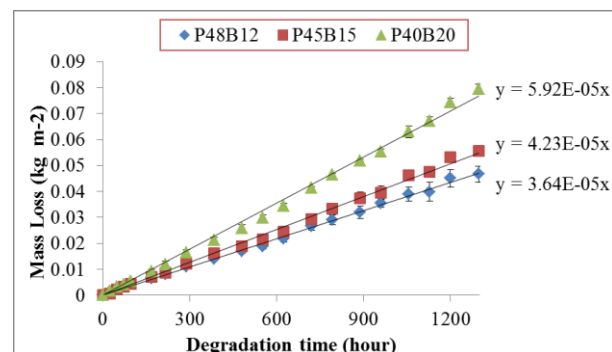


Figure 1: Weight loss vs time for glass compositions investigated.

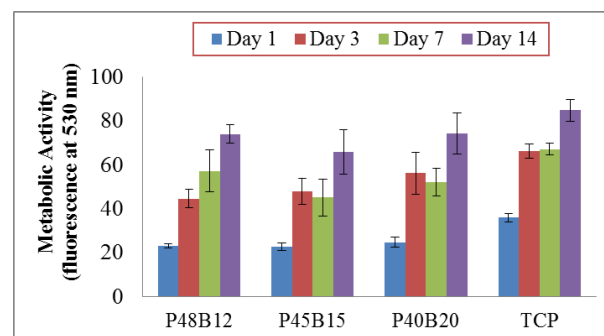


Figure 2: Metabolic activity of MG63 cells, (Alamar Blue assay).

CONCLUSIONS

Thermal stability and chemical durability of borophosphate glass decreased with the addition of boron in place of phosphate. Cell culture studies suggested all glasses produced had good cytocompatibility with the MG63 cell line.

REFERENCES

1. Ahmed I. *et al.*, JB, 25: 501-507,2004.
2. Sharmin N. *et al.*, Biomed Res Int, 2013: 1-2, 2013.
3. Massera, J., *et al.*, J Non Cryst Solids, 357: 3623–30, 2011.
4. ElBatal H. *et al.*, Mater. Chem. Phys, 110: 352-362, 2008.

ACKNOWLEDGMENTS

The author would like to thank University of Nottingham, providing Inter-Campus PhD Scholarship for this project, and Sinoma Science & Technology Co., Ltd. for technical formulation.